

# 27th European Conference on Biomaterials



[www.esb2015.org](http://www.esb2015.org)

## FINAL PROGRAMME AND BOOK OF ABSTRACTS

# ESB2015

30 August–3 September  
Kraków, Poland



# Honorary Patronage & Partners



## Financially Supported by:



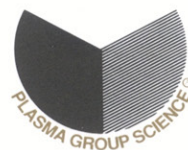
Ministry of Science  
and Higher Education

Republic of Poland

## Sponsors & Exhibitors



**Anton Paar**



**UNI-EXPORT**



**THE ROYAL SOCIETY  
PUBLISHING**

**IOP Publishing**



# Table of Contents

<b>FINAL PROGRAMME</b>	<b>1</b>
• <b>Welcome Address</b>	<b>3</b>
• <b>ESB President's Address</b>	<b>4</b>
• <b>Committees</b>	<b>6</b>
Local Organizing Committee	6
International Advisory Committee	6
Local Advisory Committee	8
• <b>General Information</b>	<b>9</b>
• <b>ICE Congress Centre Floor Plans</b>	<b>13</b>
• <b>Programme at a Glance</b>	<b>18</b>
• <b>Plenary Speakers</b>	<b>20</b>
• <b>Keynote Speakers</b>	<b>28</b>
• <b>Awards Winners</b>	<b>36</b>
International Award	36
Jean Leray Award	37
George Winter Award	38
• <b>Other Awards</b>	<b>39</b>
• <b>Special Sessions</b>	<b>40</b>
Young Scientists Forum	40
Special Fellows Session	41
Translational Research Symposium	43
Session on Surface Charge	45
Science for Industry	46
• <b>Additional Meetings</b>	<b>48</b>
• <b>Social Events</b>	<b>49</b>
• <b>Detailed Scientific Programme</b>	<b>51</b>
• <b>Oral Presentations</b>	<b>57</b>
Sunday, 30 <sup>th</sup> August	57
Monday, 31 <sup>st</sup> August	58
Tuesday, 1 <sup>st</sup> September	70
Wednesday, 2 <sup>nd</sup> September	83
Thursday, 3 <sup>rd</sup> September	96
• <b>Rapid Fire Presentations</b>	<b>104</b>
• <b>Poster Presentations</b>	<b>107</b>
• <b>Authors Index</b>	<b>140</b>
• <b>Exhibitors</b>	<b>165</b>
 <b>BOOK OF ABSTRACTS</b>	 <b>174</b>
• <b>Plenary Lectures</b>	<b>L1 - L8</b>
• <b>Keynotes</b>	<b>K1 - K16</b>
• <b>Oral Presentations</b>	<b>1 - 277</b>
• <b>Rapid Fire Presentations</b>	<b>278 - 315</b>
• <b>Poster Presentations</b>	<b>316 - 811</b>
• <b>Special Sessions</b>	



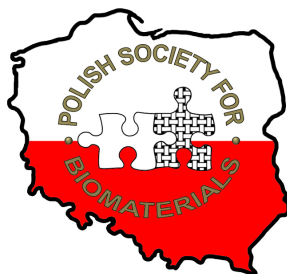
# FINAL PROGRAMME



## Address of the Organizing Committee

Polish Society for Biomaterials  
AGH University of Science and Technology  
Faculty of Materials Science and Ceramics  
Department of Biomaterials

Al. Mickiewicza 30  
30-059 Krakow, Poland



© Copyright by the Polish Society for Biomaterials, Kraków 2015

Printed in Poland

**ISBN 978-83-63663-63-6**

Issue: 1000

## Publishing:



Scientific Publishing House „Akapit”, Kraków, Poland  
phone 48 608 024 572; [www.akapit.krakow.pl](http://www.akapit.krakow.pl)  
e-mail: [wn@akapit.krakow.pl](mailto:wn@akapit.krakow.pl)



# Welcome Address



On behalf of the Organizing Committee, I would like to warmly welcome all of you to the 27<sup>th</sup> European Conference on Biomaterials. It is also my great pleasure to welcome you to the Royal Capital City of Kraków.

Kraków is often considered as one of the most beautiful cities in the Eastern Europe, and a historic and cultural heart of Poland. The unique places are the Main Market Square, Cloth Hall, St. Mary's Basilica and Wawel Castle - the seat of Polish kings from 11<sup>th</sup> to the early 17<sup>th</sup> century. Nowadays, Kraków is a modern city with increasing number of conference and congress centres hosting world's most prestigious scientific and cultural events. Our conference is organized in newly opened Congress Centre ICE, localized nearby Old Town with beautiful view of Royal Wawel Castle.

The ESB2015 is in many ways a very special Conference. It is the first time when we all gather in the middle east of Europe, in a unique city filled not only with proud history and tradition but also with modern spirit. Kraków is well known for its great universities like the Jagiellonian University and my home university - AGH University of Science and Technology. I am sure that the academic spirit of the city will support scientific discussions.

The main motto of the ESB2015 conference is: *"Balancing the needs for basic research and translation in a time of limited resources"*. The theme of our conference covers variety of different topics, in which we bring up traditional biomaterials issues, novel manufacturing and modification techniques, most current research on stem cells, cell instructive materials, angio- and vasculogenesis, and many more. In addition to our exciting scientific programme, we are pleased to host also some special sessions like e.g. Young Scientist Forum or Special Fellows Session.

We are extremely grateful to the European Society for Biomaterials for giving us this wonderful opportunity to organize the ESB conference. We appreciate all those who have helped us during almost two years of preparation. We would like to thank our Honorary Patronage and Partners, and the Conference Sponsors and Exhibitors.

Once more I would like to express our warmest welcome to participants from all over the world, to experienced and young researchers, to industrial partners - thank you all for coming. I hope that after those few days, you will leave Kraków feeling inspired by the scientific atmosphere of the Conference and delighted by the cultural beauty of our Royal City.



**Jan Chłopek**

*Chair of the ESB2015 Organizing Committee*

*President of the Polish Society for Biomaterials*





# ESB President's Address



Dear Members and Friends of the ESB,

During the last few months our Secretary, Prof Marc Bonher and his team have gone through the hard work of digitalisation of the vast, 40 years-old archive of the ESB. Noticeably, the very first paper of this archive is a letter of intent drafted by the founders of our Society and dated 3<sup>rd</sup> October 1975, a year before the establishment of the ESB.

It is a concise letter that powerfully encapsulates their great vision, a vision that is still at the core of our mission today after so many years. A sentence in this letter is particularly meaningful today:

*"All the gentlemen being present at this meeting will undertake a promotional work and try to find potential new members in their own countries, also raising the interest of institutions in the matter".*

I am sure that our founders would be very proud to see that after 40 years the ESB is still holding that vision and determination.

On 30<sup>th</sup> August 2015 Eastern Europe will open, for the first time, its doors to the ESB through the excellent work of our colleagues of the Polish community and in particular through the leadership of the conference chairman Prof Jan Chlopek, the co-chair Prof Elzbieta Pamula and the whole local organising committee.

The ESB Council and I are very grateful to them for their professional approach to the organisation. Throughout the time of preparation they have meticulously looked at all the aspects of the conference giving demonstration of a true collaborative spirit and passionate dedication to the cause of the ESB. The choice of a beautiful venue, the finesse with which the scientific programme has been articulated and the care for the legacy of this conference has been exemplar.

Prof Chlopek and his team will open the doors with generous hospitality, but also with a decisive statement that concerns us all:

*"Balancing the needs for basic research and translation in a time of limited resources".*

This hospitality and this statement echo the vision set for our Society 40 years ago; we are invited to look at new outreaches and at the interest of all parties involved in biomaterial R&D and we are asked to do so at a time of limited financial resources. Indeed, balancing the needs of researchers, industry, clinicians and patients is more than ever a shared effort where all the stakeholders involved have to have their voice and input. While we are challenged by a shortage of financial resources, we are growing stronger and stronger in our human capital and it is our duty to nourish it, particularly valuing the contribution of our Young Scientist Forum. To this end, in the last 12 months the ESB has been pursuing concerted actions in collaboration with the Presidents of the national societies and the European Commission; we will present this initiative to you all at the General Assembly.



In this occasion we will also give our farewell to three friends who will be ending their mandate as ESB Council members, Prof Lucy Di Silvio, Prof Michael Doser and Prof Pedro Granja. They have been pillars of our Council for many years contributing to the launch of the YSF, to the strengthening of our links with industry and to the re-organisation of the ESB administration. They leave behind a strong legacy that will not be forgotten and we count on their advice and support for the years to come. At the same time, we will welcome the new elected members of the Council. Their names will also be announced at the General Assembly and a new exciting page of our long history will be written through the integration of their talents.

Beside all that, when attending the oral and poster sessions of this exciting programme, let us stand proud for the value of the knowledge we are capable of generating and let us earnestly assess the costs and benefits that our work bring to our society. Above all, let us ponder for a while on the views of those who may not be attending the conference, in particular let us look at things with the eyes of our patients.

It is an invitation to us all, but it is a particular exhortation for our young scientists. The ability of balancing pure scientific knowledge with societal responsibility will define the future; that is their future.



**Matteo Santin**

*President of the European Society for Biomaterials*





# Committees

## Local Organizing Committee

Chair: Prof. Jan Chłopek

Vice-Chair: Prof. Elżbieta Pamuła

Katarzyna Trała

Barbara Szaraniec

Karol Gryń

Anna Morawska-Chochół

Małgorzata Krok-Borkowicz

Patrycja Domalik-Pyzik

Krzysztof Pietryga

Katarzyna Reczyńska

Łucja Rumian

## International Advisory Committee

Kazunari Akiyoshi (Japan)

Eben Alsberg (United States)

Luigi Ambrosio (Italy)

Guillermo Ameer (United States)

James Anderson (United States)

Karine Anselme (France)

Iulian Antoniac (Romania)

Conrado Aparicio (United States)

Lucie Bacakova (Czech Republic)

Rolando Barbucci (Italy)

Yves Bayon (France)

Serena Best (United Kingdom)

Manus Biggs (Ireland)

Nicolas Blanchemain (France)

Aldo Boccaccini (Germany)

Marc Bohner (Switzerland)

Assunta Borzacchiello (Italy)

Adrian Boyd (United Kingdom)

John Brash (Canada)

Arie Bruinink (Switzerland)

Darren Burke (United Kingdom)

Neil Cameron (Australia)

Jose M Cervantes-Uc (Mexico)

Jiang Chang (China)

Guoping Chen (Japan)

Roberto Chiesa (Italy)

Jan Chłopek (Poland)

Wojciech Chrzanowski (Australia)

Daniel Cohn (Israel)

Sally-Ann Cryan (Ireland)

Fu-Zhai Cui (China)

Guy Daculsi (France)

Matthew Dalby (United Kingdom)

Kenneth Dalgarno (United Kingdom)

Antonio H. De Aza (Spain)

Loredana De Bartolo (Italy)

Joost De Bruijn (Netherlands)

Roberto De Santis (Italy)

Sanjukta Deb (United Kingdom)

Aranzazu Del Campo (Germany)

Lynn Dennany (United Kingdom)

Lucy Di Silvio (United Kingdom)

Michael Doser (Germany)

Timothy Douglas (Belgium)

Denis Dowling (Ireland)

Peter Dubruel (Belgium)

Nicholas Dunne (United Kingdom)

Christine Dupont-Gillain (Belgium)

Peter Edelman (United States)

Mirosława El Fray (Poland)

Elisabeth Engel (Spain)

Håkan Engqvist (Sweden)

Matthias Eppe (Germany)

John Fisher (United States)



Michael Gelinsky (Germany)  
Roberto Giardino (Italy)  
Floreille Gindraux (France)  
Manuela Gomes (Portugal)  
Enrique Gomez-Barrena (Spain)  
Isabel Goñi (Spain)  
Irina Gotman (Israel)  
Francisco M. Goycoolea (Germany)  
Pedro Granja (Portugal)  
Dirk Grijpma (Netherlands)  
Bernd Grimm (Netherlands)  
George Grobe (United States)  
Zhongwei Gu (China)  
Jerome Guicheux (France)  
Marilo Gurruchaga (Spain)  
Pamela Habibovic (Netherlands)  
Vasif Hasirci (Turkey)  
Paul Hatton (United Kingdom)  
Håvard Haugen (Norway)  
John Haycock (United Kingdom)  
Andreas Heise (Ireland)  
Christophe Helary (France)  
Rocio Herrero-Vanrell (Spain)  
Jons Hilborn (Sweden)  
Yan Yan Shery Huang (United Kingdom)  
John Hunt (United Kingdom)  
Dietmar Hutmacher (Australia)  
Anita Ignatius (Germany)  
Kazuhiko Ishihara (Japan)  
John Jansen (Netherlands)  
Julian Jones (United Kingdom)  
John Kao (United States)  
Kazunori Kataoka (Japan)  
Paul Kemp (United Kingdom)  
Garry Kerch (Latvia)  
Soo Hyun Kim (Korea)  
Charles James Kirkpatrick (Germany)  
Joachim Kohn (United States)  
Sotirios Korossis (Germany)  
Damien Lacroix (United Kingdom)  
Sander Leeuwenburgh (Netherlands)  
Didier Letourneur (France)  
Małgorzata Lewandowska-Szumieł (Poland)  
Andrew Lloyd (United Kingdom)  
Matthias Lutolf (Switzerland)

Ravikumar Majeti (United States)  
Diego Mantovani (Canada)  
Alexandra Marques (Portugal)  
Ivan Martin (Switzerland)  
Dimosthenis Mavrilas (Greece)  
Todd Mcdevitt (United States)  
Brian Meenan (United Kingdom)  
Gordon Meijs (Australia)  
Antonio Merolli (Italy)  
Claudio Migliaresi (Italy)  
Véronique Migonney (France)  
Yannis Missirlis (Greece)  
Manuel Monleon Pradas (Spain)  
Lorenzo Moroni (Netherlands)  
Antonella Motta (Italy)  
John Nicholson (United Kingdom)  
Elżbieta Pamuła (Poland)  
Abhay Pandit (Ireland)  
Triantafillos Papadopoulos (Greece)  
Ana Paula Pego (Portugal)  
Erhan Pişkin (Turkey)  
Josep Planell (Spain)  
Laura Poole-Warren (Australia)  
Stefan Przyborski (United Kingdom)  
Malcolm Purbrick (United Kingdom)  
Michael Raghunatyh (Singapore)  
Murugan Ramalingam (India)  
Stefan Rammelt (Germany)  
John Ramshaw (Australia)  
Heinz Redl (Austria)  
Nick Rhodes (United Kingdom)  
Geoff Richards (Switzerland)  
Lia Rimondini (Italy)  
José Carlos Rodríguez-Cabello (Spain)  
Julio San Roman (Spain)  
Paul Santerre (Canada)  
Matteo Santin (United Kingdom)  
Etienne Schacht (Belgium)  
Dieter Scharnweber (Germany)  
Katja Schenke-Layland (Germany)  
Michael Sefton (Canada)  
Dror Seliktar (Israel)  
Francesco Serino (Italy)  
Prasad Shastri (Germany)  
Neil Smart (United Kingdom)



Dimitrios Stamatialis (Netherlands)  
Molly Stevens (United Kingdom)  
Yasuhiko Tabata (Japan)  
Elizabeth Tanner (United Kingdom)  
Mariacristina Tanzi (Italy)  
Johnna Temenoff (United States)  
Pentti Tengvall (Sweden)  
Peter Thomsen (Sweden)  
Joanne Tipper (United Kingdom)  
Matthew Tirrell (United States)  
Klemens Trieb (Austria)  
Hasan Uludag (Canada)

Gianluca Vadalà (Italy)  
Sandra Van Vlierberghe (Belgium)  
Michel Vert (France)  
William Wagner (United States)  
Beat Walpoth (Switzerland)  
Christine Wandrey (Switzerland)  
Anthony (Tony) Weiss (Australia)  
Jerome Werkmeister (Australia)  
Rachel Williams (United Kingdom)  
Joyce Wong (United States)  
Dimitrios Zeugolis (Ireland)

## Local Advisory Committee

Piotr Augustyniak  
Maciej Ambroziak  
Grzegorz Bajor  
Romuald Będziński  
Marta Błażewicz  
Stanisław Błażewicz  
Dorota Bociąga  
Maria Borczuch-Łączka  
Tomasz Ciach  
Beata Cwalina  
Jan Ryszard Dąbrowski  
Jarosław Deszczyński  
Piotr Dobrzyński  
Justyna Drukała  
Grażyna Ginalska  
Jacek Grabarczyk  
Zbigniew Jaegermann  
Leopold Jeziorski  
Janusz Kasperczyk  
Ireneusz Kotela  
Elżbieta Krasicka-Cydzik  
Roman Kustos  
Marek Langner  
Jadwiga Laska  
Małgorzata Lewandowska  
Bogusław Major

Paweł Małydyk  
Jan Marciniak  
Jarosław Markowski  
Stanisław Mazurkiewicz  
Stanisław Mitura  
Zbigniew Nawrat  
Piotr Niedzielski  
Maria Nowakowska  
Czesława Paluszkiewicz  
Zbigniew Paszenda  
Jan Pilch  
Stanisław Rumian  
Daniel Sabat  
Jerzy Silberring  
Piotr Silmanowicz  
Alina Sionkowska  
Emil Staszków  
Barbara Surowska  
Mikołaj Szafran  
Hieronim Szymanowski  
Anna Ślósarczyk  
Beata Świeczko-Żurek  
Wojciech Świąszkowski  
Bogdan Walkowiak  
Tadeusz Wierchoń  
Ewa Zuba-Surma



# General Information

## CONFERENCE VENUE

The conference is being held at the ICE Kraków Congress Centre, 17 Marii Konopnickiej Street. This modern centre was designed to meet the highest, world class requirements and it was opened less than a year ago. Excellent location of the venue, its contemporary interiors and finest technical solutions make it a perfect setting for the organization of international conferences, as well as prestigious cultural and social events.

Password-free **Wi-Fi** is available for the Conference Delegates. However, because of the large number of users, Wi-Fi should not be used for large file exchanges.

## TRANSPORT INFORMATION

The Conference venue is located close to the City Center - it is only a 15-min walk.

It is also possible to use different forms of public and private transportation to get to the venue, e.g. bus, tram or taxi.

ICE Kraków Congress Centre Access Information can be found here:

**<http://www.icekrakow.com/information/access>**

Public transport connections can be found here:

**<http://krakow.jakdojade.pl/?locale=en>**

To avoid overcharging and for safety reasons, Delegates are advised to use only licensed taxis (there are over dozen of licensed taxi companies in Kraków) - full list of those is available here:

**<http://cracow.travel>**

## REGISTRATION DESK

The Registration Desk is located in Main Foyer on Level 0.

Opening times are as follows:

Sunday, 30 <sup>th</sup> August	12:00 - 20:00
Monday, 31 <sup>st</sup> August	07:30 - 18:00
Tuesday, 1 <sup>st</sup> September	08:00 - 19:30
Wednesday, 2 <sup>nd</sup> September	08:00 - 18:00
Thursday, 3 <sup>rd</sup> September	08:00 - 15:00

Social event and optional tours tickets can be bought at the Registration Desk. The Staff will be also happy to give extra tourist information and make travel or transport arrangements.

## BADGES

Name badges will be issued to all delegates upon registration. **Attendees must wear the official conference badge at all times and present it to enter the Conference venue and all ESB2015 social events.**



## ORGANIZING COMMITTEE INFORMATION DESK

Organizing Committee members can be found at the Information Desk on Level 0. Please do not hesitate to contact us with all the enquiries.

## CLOAKROOMS

Cloakrooms are located on Level 0 (on the left from the main entrance) and are free of charge. It is also possible to leave travel luggage there.

Opening times are as follows:

Sunday, 30 <sup>th</sup> August	12:00 - 20:30
Monday, 31 <sup>st</sup> August	08:00 - 19:00
Tuesday, 1 <sup>st</sup> September	08:00 - 20:00
Wednesday, 2 <sup>nd</sup> September	08:00 - 18:00
Thursday, 3 <sup>rd</sup> September	08:00 - 15:00

## CONFERENCE HALLS

There will be six parallel sessions in Halls: 1, 2, 3A, 3B, 4A, 4B.

Hall 1 can be entered from level 0 and 1.

Hall 2 can be entered from level 0 and 1.

Halls 3A, 3B, 4A, 4B are located on level 3.

Please refer to the Conference venue levels maps for the exact locations of the halls.

## POSTER AREA

Poster Area is located on Level -1. Either lifts or staircases might be used to get there. Please note that the lifts close to Halls 3A, 3B, 4A, 4B can be used only to get to the Poster & Lunch Area (other levels are not available). The lifts in the Foyer go to each level.

In case of any troubles with finding the right way, please ask Technical Support or Organizing Committee members for help.

## EXHIBITION AREA

The Exhibition is located on Level 0 and Level 1 (Sponsor). Please refer to exhibition map for names and exact location of the Exhibitors' booths.

## COFFEE BREAKS

Coffee together with other refreshments and sweet pastries will be served on Levels 0 and 1 and will be a perfect opportunity to join the Exhibition.

Please note: On Sunday, 30<sup>th</sup> August coffee break for Delegates participating in the Young Scientists Forum Workshop and IUSBSE Committee Meeting will be held on Level 2.

## LUNCH AREA

Lunch will be served on Level -1. Either lifts or staircases might be used to get there. Please note that the lifts close to Halls 3A, 3B, 4A, 4B can be used only to get to the Poster & Lunch Area (other levels are not available). The lifts in the Foyer go to each level.

In case of any troubles with finding the right way, please ask Technical Support or Organizing Committee members for help.



## SPEAKER READY ROOM

**All presentations (.ppt or .pptx) should be brought to the Speaker Ready Room (level 0, near the Registration Desk) no later than 16:00 on the day prior to presentation.**

Speakers are advised to check with technicians if the presentation or embedded videos run properly. The system is PC-based, thus Mac users should also ensure PowerPoint compatibility of their presentation.

Speaker Ready Room hours:

Sunday, 30 <sup>th</sup> August	12:00 - 17:45
Monday, 31 <sup>st</sup> August	07:30 - 18:00
Tuesday, 1 <sup>st</sup> September	08:00 - 18:00
Wednesday, 2 <sup>nd</sup> September	08:00 - 16:30
Thursday, 3 <sup>rd</sup> September	08:00 - 11:00

## ORAL PRESENTATIONS

To ensure that all the sessions run smoothly, Oral Presenters are kindly requested to read the following instructions.

- Speakers should check the conference programme carefully for the scheduled session time and presentation order.
- Use of personal laptops to run the presentation will not be possible. Speakers must upload their presentations (.ppt or .pptx) in the Speaker Ready Room no later than 16:00 on the day prior to their allocated session.
- Speakers should arrive to their assigned session hall 5 minutes before the start of their session in order to introduce themselves to the Session Chairs and familiarize with the hall arrangement.
- In each hall, there is a speaker podium with two microphones and a slide changer/laser pointer for use in the presentation.
- Oral presentations should last no longer than 12 min, and then there should be 3 min for discussion. With six parallel sessions it is crucial to keep strictly to the timetable; it is also a sign of respect to Session Chairs, other Speakers and fellow Delegates. All Oral Presenters are kindly requested not to exceed their time, otherwise their presentation will be interrupted by the Chair, whose responsibility is to keep the session on schedule.
- Technical support and audiovisual operators are ready to attend any problem during presentations. In case of such an event, Speakers should continue their presentation; the problem will be fixed as quickly as possible.

## DISCUSSION

After each presentation there should be enough time for longer or shorter discussion.

Numbered microphone stands have been prepared in Hall 1 and Hall 2. Delegates wishing to ask a question or make a comment, should stand next to the closest microphone stand (queue if necessary) and wait for the permission from the Session Chair.

In all the other halls (Hall 3A, Hall 3B, Hall 4A, Hall 4B), there will be a Technical Support person ready to hand the microphone, so one should just raise a hand or stand up to make a clear sign that is willing to take part in the discussion.

Delegates are kindly asked not to speak without the microphone, since it might be hard for the presenter or the audience to hear.





## RAPID FIRE PRESENTATIONS

There are three Rapid Fire Sessions planned - each of them during the Poster Session and lunch time. Special Rapid Fire Area was arranged on Level -1, next to the Poster Area. Rapid Fire Presentations start at 13:30 on Monday, Tuesday and Wednesday.

Rapid Fire Presenters are kindly requested to read the following instructions.

- Speakers should check in the Final Programme time and order of the presentation.
- Use of personal computers will not be possible. All Rapid Fire Presentations (maximum 4-5 slides, .ppt or .pptx) should be uploaded in the Speaker Ready Room no later than 16:00 on the day prior to scheduled presentation.
- Speakers should arrive to the Rapid Fire area 5 minutes before the start of their session.
- Rapid Fire Presentation must not exceed 4 minutes. The timing should be kept strictly.
- Speakers will be provided with a wireless microphone and a slide changer/laser pointer for use in the presentation.

## POSTER SESSIONS

Poster Presenters are kindly requested to attach their poster (1189 mm (tall) x 841 mm (wide), Portrait style (A0 Size)) to their assigned poster panel on Sunday, 30<sup>th</sup> August (12:00 - 17:45) or on Monday morning, 31<sup>st</sup> August. Posters will be arranged numerically and organized by topics. Please check the Final Programme for the assigned poster number.

Poster Sessions will be held on the Level -1 next to the Lunch Area. All posters will be exposed during the whole Conference. Poster Presenters are encouraged to be present at their posters on:

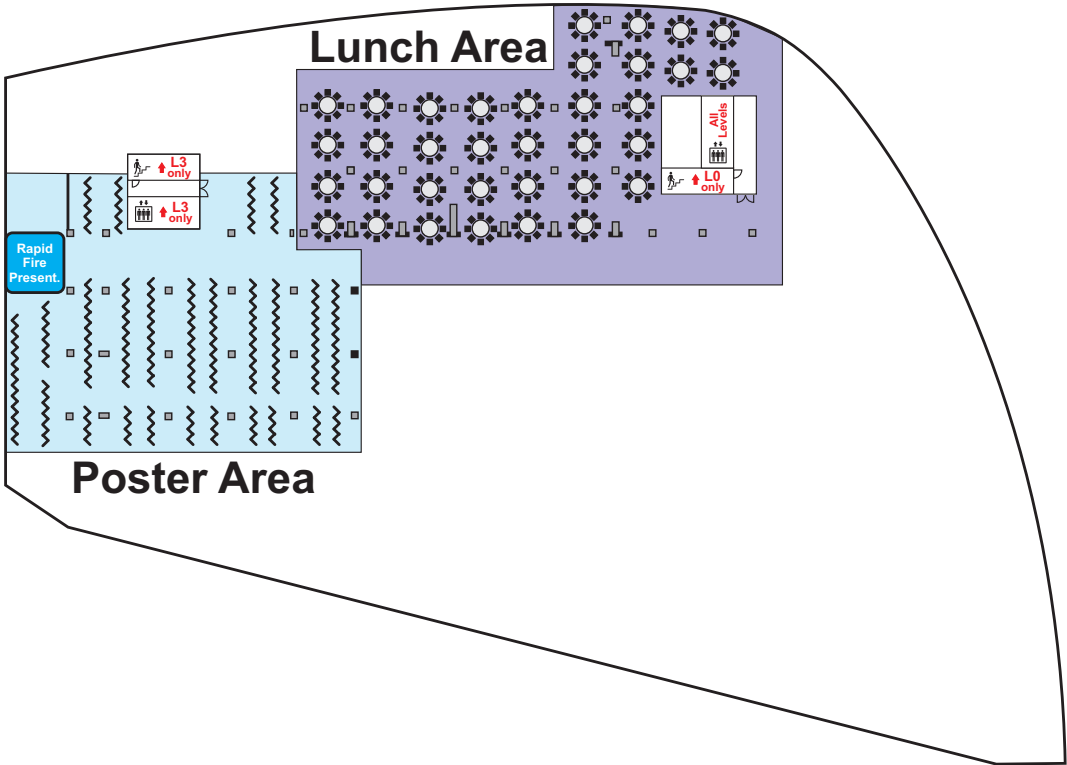
Monday, 31 <sup>st</sup> August	13:15 - 14:45
Tuesday, 1 <sup>st</sup> September	13:00 - 14:30
Wednesday, 2 <sup>nd</sup> September	13:00 - 14:30

Posters must be removed until 18:00 on Wednesday, 2<sup>nd</sup> September. After that time, all the remaining posters will be taken off and gathered at the Organizing Committee Information Desk, where it would be possible to collect them. Any posters not collected by 14:00 on Thursday, 3<sup>rd</sup> September will be discarded.



# ICE Congress Centre Floor Plan

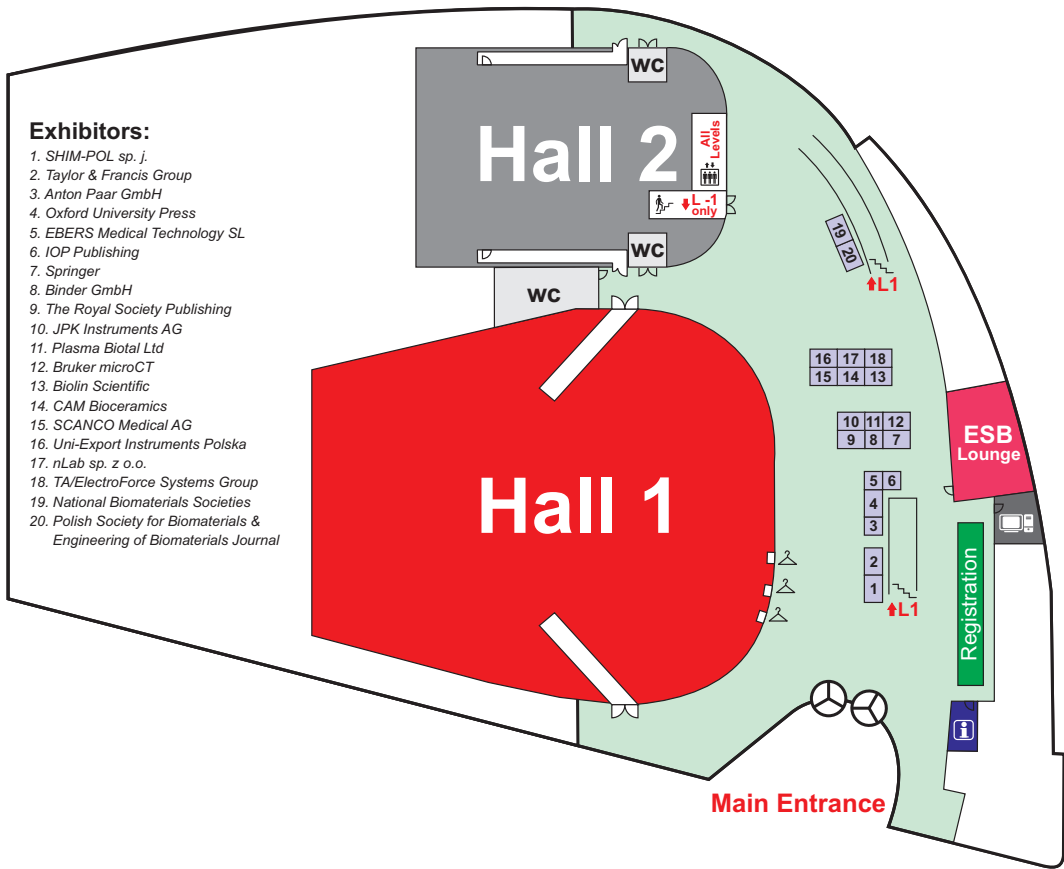
## Level -1





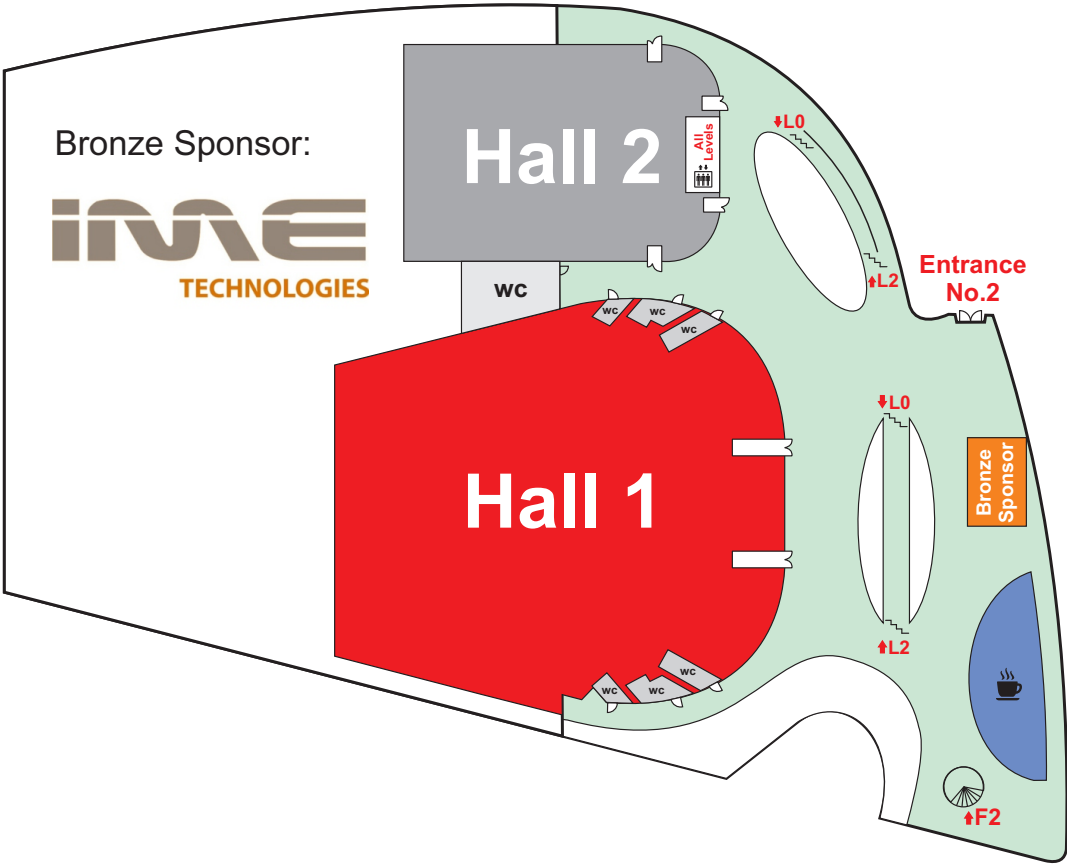
# ICE Congress Centre Floor Plan

## Level 0



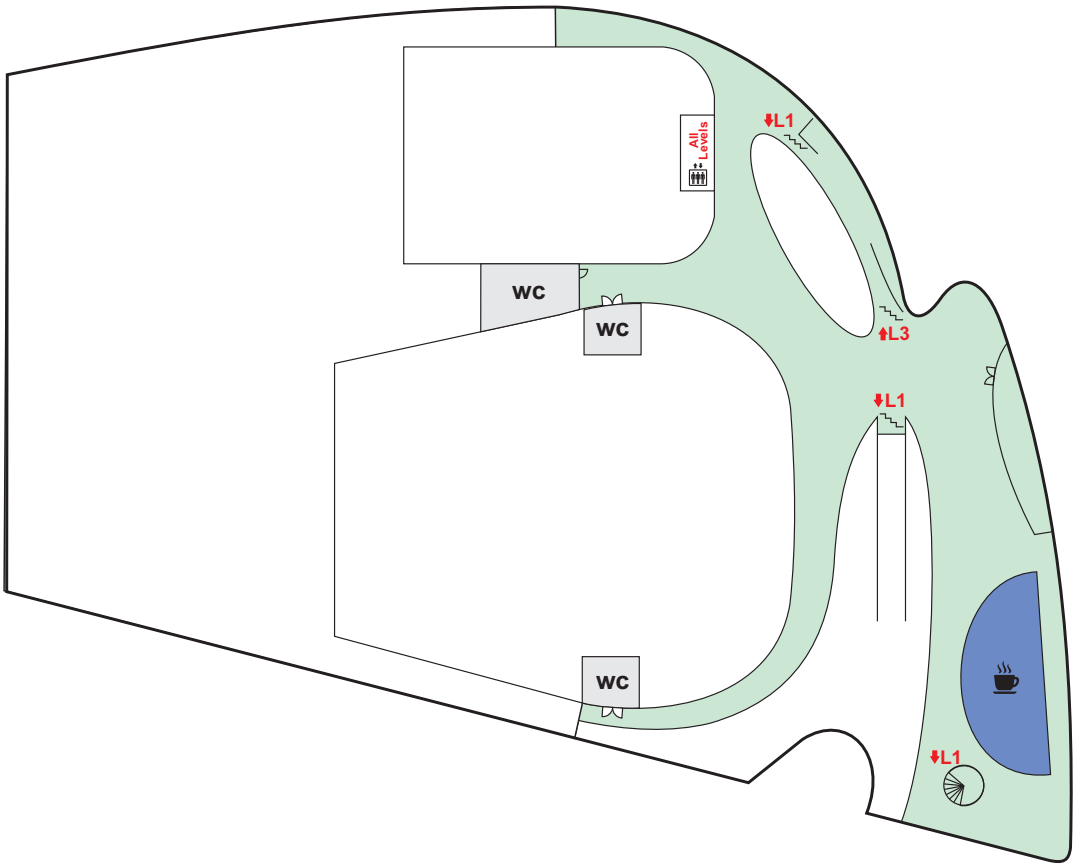
# ICE Congress Centre Floor Plan

## Level 1



# ICE Congress Centre Floor Plan

## Level 2



# ICE Congress Centre Floor Plan

## Level 3



# Programme at a Glance

	Sunday, 30th Aug	Monday, 31st Aug	Tuesday, 1st Sept	Wednesday, 2nd Sept	Thursday, 3rd Sept	
8						8
9		Opening Ceremony	International Award Nicholas Peppas	Plenary Lecture (L6) Kazunori Kataoka	George Winter Award Luigi Ambrosio	9
10		Plenary Lecture (L1) Joachim Kohn	Plenary Lecture (L4) Geoff Richards	Break	Plenary Lecture (L8) Abhay Pandit	10
11		Plenary Lecture (L2) Maria Siemionow	Break	32 33 34 35 36	Break	11
12		Coffee Break Exhibition	TRS 18 19 20 21 22	SFI 47 48 49 50 51 52		12
13		1 2 3 4 5 6	Coffee Break Exhibition	Coffee Break Exhibition	Coffee Break Exhibition	13
14		Break	TRS 23 24 25 26 Sch	37 38 39 40 41 SFI	53 54 55 56 57 58	14
15	YSF Young Scientists Forum Workshop	Poster Session Rapid Fire Presentations Lunch	Poster Session Rapid Fire Presentations Lunch	Poster Session Rapid Fire Presentations Lunch	JMS:MM Editorial Board Meeting and Lunch	15
16	Coffee Break Exhibition	Plenary Lecture (L3) James Kirkpatrick	ESB General Assembly	Jean Leray Award J. Miguel Oliveira	Closing Ceremony	16
17	YSF Young Scientists Forum Workshop	Coffee Break Exhibition	Plenary Lecture (L5) Michael Sefton	Plenary Lecture (L7) Małgorzata Lewandowska-Szumieł		17
18		13 14 15 16 17	Coffee Break Exhibition	Coffee Break Exhibition		18
19		ESB Council and Presidents of the National Societies for Biomaterials Meeting	TRS 27 28 29 30 31	42 43 44 45 46 SFI		19
20	Welcome Reception (Level 3)	Concert in St. Mary's Basilica	Acta Biomaterialia Anniversary Reception (Level 1)	18:00-23:00 Gala Dinner Wieliczka Salt Mine		20
21		20:30-22:00 Keynotes & Chair- persons Dinner	20:30-3:00 YSF Social Event			21



## Special Sessions:

YSF - Young Scientists Forum

Fellows Session (ICF-BSE) - Special Fellows Session on Biomaterials Education

TRS - Translational Research Symposium

Sch - Surface Charge for Biomaterial Characterization

SFI - Science for Industry: Bioresorbable Materials for Medical Applications

## Sessions:

1. Bone Tissue Engineering 1
2. Cartilage Tissue Engineering 1
3. Drug Delivery 1
4. Surface Modification 1
5. Cell Instructive Materials 1
6. Advanced Manufacturing 1
7. Osteointegration 1
8. Neural Regeneration 1
9. Drug Delivery 2
10. Surface Modification 2
11. Cell Instructive Materials 2
12. Cell Encapsulation and Delivery 1
13. Bioactive Materials
14. Stem Cells 1
15. Antimicrobial Surfaces and Materials 1
16. Gene Delivery
17. Biointerfaces 1
18. Smart Biomaterials 1
19. Wound Healing 1
20. Surface Modification 3
21. Cartilage Tissue Engineering 2
22. Cell Encapsulation and Delivery 2
23. Bone Tissue Engineering 2
24. Stem Cells 2
25. Surface Modification 4
26. Cell Instructive Materials 3
27. Bone Tissue Engineering 3
28. Angio- and Vasculogenesis
29. Antimicrobial Surfaces and Materials 2
30. Bioimaging and Biosensing
31. Biointerfaces 2
32. Cancer Therapy
33. Soft Tissue Engineering
34. Cardiovascular Applications 1
35. Antimicrobial Surfaces and Materials 3
36. Advanced Manufacturing 2
37. Drug Delivery 3
38. Composite Scaffolds
39. Cardiovascular Applications 2
40. Neural Regeneration 2
41. Cell Instructive Materials 4
42. Bone Tissue Engineering 4
43. Cellular Response
44. Wound Healing 2
45. Bone Cements
46. Nanoparticles
47. Neural Regeneration 3
48. Bone Tissue Engineering 5
49. Clinical Trials
50. Antimicrobial Surfaces and Materials 4
51. Biomimetic Materials
52. Osteointegration 2
53. Advanced Manufacturing 3
54. Bone Tissue Engineering 6
55. Cardiovascular Applications 3
56. Surface Modification 5
57. Smart Biomaterials 2
58. Drug Delivery 4



# Plenary Speakers



## Joachim KOHN

*The New Jersey Center for Biomaterials  
UNITED STATES*

### L1

**Title: “Bioactive Materials for the Treatment of Major Injuries: Opportunities and Challenges”**

**Monday, 31<sup>st</sup> August  
9:00 - 9:45, Hall 1**

Joachim Kohn, PhD, Board of Governors, Professor of Chemistry and Chemical Biology at Rutgers University, is a research entrepreneur, a multi-disciplinary translational scientist, and a national leader in the development of polymeric biomaterials for drug delivery, tissue engineering, and regenerative medicine. In 1997, Kohn founded the New Jersey Center for Biomaterials, which has grown into a collaborative network spanning 25 institutions and 40 laboratories. As a translational scientist, Kohn has 58 issued US Patents on novel biomaterials and seven companies have licensed his technologies. He has raised about \$100M in research funding at Rutgers and helped four licensees to raise about \$200M in private capital.

In 2014, Professor Kohn was inducted into the National Academy of Inventors. He is the recipient of numerous awards and honors, including the prestigious Thomas Alva Edison Patent Award for best patent in New Jersey in the category of medical research, and the Clemson Award from the Society for Biomaterials. He is a Fellow of AIMBE and serves as the Chair of the International College of Fellows of Biomaterials Science and Engineering. Since 2008, he is the Director and Principal Investigator of the Rutgers-Cleveland Clinic Consortium of the Armed Forces Institute of Regenerative Medicine, a \$60 Million research project funded by the Department of Defense.

Professor Kohn’s scientific expertise ranges from synthetic polymer chemistry and materials science to drug delivery, cell biology, tissue engineering, and regenerative medicine. He pioneered the use of combinatorial and computational methods for the optimization of biomaterials for specific medical applications. He discovered „pseudo-poly(amino acid)s” - a new class of polymers that combine the non-toxicity of individual amino acids with the strength and processability of high-quality engineering plastics. Medical devices using these materials are being developed by several companies, have been approved in the USA and Canada, and have been implanted in more than 50,000 patients.







## **Maria SIEMIONOW**

*University of Illinois at Chicago  
Department of Orthopaedics  
UNITED STATES*

### **L2**

**Title: “Regenerative Transplantation -  
from Experimental Laboratory to Clinical Applications”**

**Monday, 31<sup>st</sup> August  
9:45 - 10:30, Hall 1**

Dr. Siemionow, a world-renowned scientist and microsurgeon, is Professor of Orthopedics and Director of Microsurgery Research at The University of Illinois at Chicago. She earned her medical degree from Poznan Medical Academy in her native Poland. Prior to her UIC appointment, she was Director of Plastic Surgery Research and Head of Microsurgical Training for Cleveland Clinic’s Department of Plastic Surgery. She specializes in microsurgery, hand surgery, peripheral nerve surgery, transplantation, and microsurgery research. She is pioneering development of new technology for minimal immunosuppression in transplantation and enhancement of nerve regeneration.

Currently President of the American Society for Reconstructive Transplantation, Dr. Siemionow is Past President of the International Hand and Composite Tissue Allotransplantation Society and the American Society for Peripheral Nerve. Additionally, she is a member of the academic-industry team, Warrior Restoration Consortium, focusing on development of clinical therapies and new treatments for wounded soldiers as part of the second phase of the Armed Forces Institute for Regenerative Medicine (AFIRM II).

She has received numerous honors, including high praise as Principal Investigator for the world’s first, her Composite Facial Allograft Transplantation protocol; in 2008, she led the team that performed the first near-total face transplantation in the United States.

Author of more than 330 scientific publications, she twice has been honored with the James Barrett Brown Award for the best publication in a plastic surgery journal, and earned the Folkert Belzer Award in Transplantation for her work on transplantation and tolerance. Dr. Siemionow also received Outstanding Achievement in Clinical Research Award from the Plastic Surgery Educational Foundation (2010); the 2011 American Society of Plastic Surgeons’ Board of Trustees Special Achievement Award and in 2013 Casimir Funk National Science Award and the Honoris Causa Doctorat awarded by Poznan University of Medical Sciences. In 2014, Dr Siemionow received the Great Immigrants Award from the Carnegie Foundation of New York.







## **C. James KIRKPATRICK**

*Institute of Pathology, University Medical Center  
Johannes Gutenberg University of Mainz  
GERMANY*

### **L3**

**Title: “In vitro Models & Nanobiointerfaces:  
A Multidisciplinary Challenge”**

**Monday, 31<sup>st</sup> August  
14:45 - 15:30, Hall 1**

C. James Kirkpatrick has a triple doctorate in science and medicine (MD, PhD, DSc) from the Queen’s University of Belfast (N. Ireland) and since 1993 is Professor and Chairman of Pathology at the Johannes Gutenberg University (JGU) in Mainz, Germany. He has a special interest in human cell culture techniques to study cell-biomaterial interactions, and has pioneered complex co-culture systems in three-dimensions. His “REPAIR-lab”, is a member of the European Institute of Excellence on Tissue Engineering and Regenerative Medicine. He is a former President of both the German and the European Society for Biomaterials and was the latter’s recipient of the George Winter Award in 2008. In 2010 he was awarded the Chapman Medal from the Institute of Materials, Minerals & Mining, London, UK for “Distinguished research in the field of biomedical materials”. Since 2013 he is an Honorary Member of the German Society for Biomaterials, and in 2014 he received the TERMIS-EU Career Achievement Award (awarded in Genova, Italy). He also holds visiting professorships in China, Singapore and Sweden.

He is author/coauthor of 486 publications in peer-reviewed journals and has an h-index of 54 (Web of Science). He is a former Associate Editor of the Journal of Pathology (2001-2006) and a current Associate Editor of Biomaterials (since 2002) as well as a member of the Editorial Advisory Board of several journals in the biomaterials and regenerative medicine fields. He is a member of the Scientific Advisory Board of a number of research institutes, centres of excellence and companies in biomaterials and regenerative medicine in Europe, as well as the German Federal Institute for Drugs & Medical Devices (BfArM) (since 2007).

Current research is on nanoparticle interactions with the air-blood and blood-brain barriers, as well as on adult stem cells and inflammatory processes in vascularization of tissue engineered constructs.





## **Geoff RICHARDS**

AO Research Institute Davos  
SWITZERLAND

### **L4**

**Title: “Medical Translational Research:  
A Different Route to Fundamental Research”**

**Tuesday, 1<sup>st</sup> September  
9:00 - 9:45, Hall 1**

Since 1991 Prof Richards has been based at the AO Research Institute Davos performing R&D of fracture fixation devices. In 2009, Prof Richards became Director of the Institute. Currently he holds an honorary Professorship at Cardiff University, Wales and also one at Aberystwyth University, Wales. He has been a member of European Society of Biomaterials since 1993 and co-organised ESB2009 in Lausanne, Switzerland (with Marc Böhner and Christine Wandrey). 1201 attendees participated (highest ESB registration at that time). Prof Richards holds a Life Honorary Member Swiss Society for Biomaterials after being in many functions including president. He was involved in helping set up statutes of the Romanian Society for Biomaterials and helped them (and later) the Polish Society for Biomaterials affiliate to ESB. In 2004 he was awarded the ESB Jean Leray Award. He is a Fellow of Biomaterials Science and Engineering (FBSE).

In 1999 Prof Richards co-founded eCM journal ([www.ecmjournal.org](http://www.ecmjournal.org)), one of the first online open access journals in the world (before “open access” was used). He is Editor-in-Chief, webmaster and webeditor. eCM initiated the first transparent review process in 1999 (now known as open peer review) including a transparent route to becoming a member of the eCM International Review Panel. He has organised annual eCM conferences since 1999. Prof Richards is an executive Committee member European Orthopaedic Research Society (organised EORS2010 in Davos) and an elected member European & World Council for Tissue Engineering & Regenerative Medicine International Society (TERMIS). He will organise TERMIS-EU in 2017 in Davos. In 2014 after helping set up the charter of International Combined Orthopaedic Research Societies (ICORS), he became a Member of the executive committee. He is author on 120 peer reviewed papers, 4 patents, more than 400 abstracts and 11 book chapters. He has supervised 10 PhD's, 15 masters thesis's, 4 medical thesis's and 2 diplomas.





## **Michael V. SEFTON**

*Institute of Biomaterials and Biomedical Engineering  
University of Toronto  
CANADA*

### **L5**

**Title: “Vascularization in Tissue Engineering:  
Alternative Foreign Body Responses”**

**Tuesday, 1<sup>st</sup> September  
15:30 - 16:15, Hall 1**

Michael V. Sefton is University Professor and Michael E. Charles Professor in the Department of Chemical Engineering and Applied Chemistry and the Institute of Biomaterials and Biomedical Engineering, University of Toronto. He was Director of the Institute of Biomaterials and Biomedical Engineering at the University of Toronto from 1999-2005 and President of the US Society for Biomaterials in 2006.

He received the Albright and Wilson Americas Award of the Canadian Society for Chemical Engineering (CSChE) in 1988, named University Professor in 2003 and elected a Fellow of the Royal Society of Canada in 2005. He has also received the Founders Award of the US Society for Biomaterials and the Killam Prize in Engineering of the Canada Council. In 2011 he received the Acta Biomaterialia Gold award and more recently received the RS Jane Award of the CSChE (2012), the Professional Engineers Ontario Gold Medal (2013) and the Canadian Council of Professional Engineering Gold Medal in 2014.

He has been active in the preparation of blood compatible materials through heparinization, the microencapsulation of mammalian cells in synthetic polymers and various strategies for vascularizing tissue constructs.





## **Kazunori KATAOKA**

*Department of Materials Engineering  
University of Tokyo  
JAPAN*

### **L6**

***Title: “Targeted Chemo- and Molecular-therapy  
by Self-assembled Supramolecular Nanosystems”***

***Wednesday, 2<sup>nd</sup> September  
8:30 - 9:15, Hall 1***

Kazunori Kataoka, Ph.D. is Professor of Biomaterials at Graduate School of Engineering, the University of Tokyo, Japan. He has been appointed joint position since 2004 from Graduate School of Medicine, the University of Tokyo as Professor of Clinical Biotechnology at Center of Disease Biology and Integrative Medicine. He received B.Eng. (1974) and Ph.D. (1979) from the University of Tokyo.

Dr. Kataoka received several awards, including the Society Award from the Japanese Society for Biomaterials (1993), the Society Award from the Society of Polymer Science, Japan (2000), Clemson Award from the Society for Biomaterials USA (2005), Founder’s Award from the Controlled Release Society (2008), the Science and Technology Prize awarded by the Minister of Education, Culture, Sports, Science and Technology, Japan (2010), Humboldt Research Award (2012), Leo Esaki Prize (2012) and Lif-time Achievement Award for Journal of Drug Targeting.

He served as a president of the Society of Polymer Science, Japan (2010-12), and a president of the Controlled Release Society (2012-13). He has been elected as a Fellow of the American Institute of Medical and Biological Engineering (AIMBE) (1999-), and a Fellow of the International Union of Societies for Biomaterials Science and Engineering (IUSBSE) (2004-). He has been on the editorial board of twelve international journals, including Journal of Biomaterials Science, Polymer Edition (Editor) and Biomaterials (Associate Editor).

His current major research interest is supramolecular materials for nanobiotechnology, particularly focusing on drug and gene targeting, and has published more than 500 papers with h-index: 108.





## Małgorzata LEWANDOWSKA-SZUMIEŁ

Center for Biostructure Research  
Medical University of Warsaw  
POLAND

**L7**

**Title: "Cell-made or Man-made Materials for Bone Reconstruction?"**

**Wednesday, 2<sup>nd</sup> September**

**15:30 - 16:15, Hall 1**

Małgorzata Lewandowska-Szumieł PhD, DSc - professor and a Head of the Tissue Engineering Laboratory, Department of Histology and Embryology, Centre for Preclinical Research and Technology (CePT), Medical University of Warsaw, Poland.

Her major scientific Interest is focused on: tissue engineering, adult stem cells in regenerative medicine, biomaterials and scaffolds for cell transplantation, cell behavior in contact with implantable materials (biocompatibility in vitro), cell response toward physical factors.

She was graduated from the Warsaw University of Technology, Department of Materials Science and Engineering (M.Sc., Eng.) and her further education and scientific career was connected with the Medical University of Warsaw (Ph.D. in medicine with honors, thesis: "Aluminium releasing from alumina based bioceramics under in vivo conditions", Post-doctoral degree (habilitation) in medicine, thesis: "Potential of in vitro systems in biocompatibility studies of implantable materials for bone reconstruction".

She holds the honorary status of „Fellow, Biomaterials Science and Engineering” (FBSE) from International Union of Societies of Biomaterials Science and Engineering and was awarded by the Polish Academy of Sciences for a series of works on the interaction of cells with implantable materials.

She is an author and co-author of over 50 papers published in peer-review journals and five patents (at various stages of the patent process) concerning original systems for cell culture and cell-based systems for bone reconstruction. She served as a Polish expert for the EU negotiations on the Regulation of The European Parliament and of the Council on advanced therapy medicinal products.







## **Abhay PANDIT**

*Network of Excellence for Functional Biomaterials  
National University of Ireland, Galway  
IRELAND*

### **L8**

**Title: “Biological-basis for Designing Biomaterials for the Injured and Degenerated Host - Examples in the Neural Space”**

**Thursday, 3<sup>rd</sup> September  
9:00 - 9:45, Hall 1**

Prof Abhay Pandit is the Director of the newly formed Center for Research in Medical Devices (CURAM) that is funded by Science Foundation Ireland. Prior to this he founded and directed the Network of Functional Biomaterials (NFB), a Science Foundation Ireland funded Strategic Research Cluster at the National University of Ireland, Galway. Prof Pandit has over twenty-five years of experience in the field of biomaterials. After a seven-year stint in industry he began working in academia. His research programme at the National University of Ireland, Galway hosts several patented technology platforms associated with the development of bioinspired materials, which are responsive to their environment and trigger the smart release of the biomolecule at the desired target site. These platforms have been developed for musculoskeletal, cardiovascular, soft tissue repair and neural targets with a number of others targets currently under investigation. He is the author of 4 granted patents with 18 patent applications pending. He has published 165-refereed journals and has authored 484 papers at both national and international conferences. He is an Associate Editor of Biomaterials journal and also serves on the editorial board of 13 journals, a referee for 77 journals, a Grant Panellist for 8 funding agencies, and an expert Grant Reviewer for 37 funding agencies.

Prof Pandit hosted the Tissue Engineering Regenerative Medicine International Society Conference – EU Meeting in 2010 and hosted The European Society for Biomaterials Conference in 2011 – the first group to host these prestigious conferences in consecutive years. In recognition of his services to the research community Prof Pandit was inducted as an International Fellow in Biomaterials Science and Engineering by the International Union of Societies for Biomaterials Science and Engineering (IUSBSE)-the first Irish academic to be inducted as a fellow. He has been elected as a Council Member of the Tissue Engineering and Regenerative Medicine (2010-2013) and as a Council Member of the International Society and European Society for Biomaterials (2013-2017).



# Keynote Speakers



## **Matthias EPPLÉ**

*Institute of Inorganic Chemistry  
University of Duisburg-Essen  
GERMANY*

### **K1**

**Title: “Antimicrobial Effects of Biomaterials:  
Silver Ions, Silver Nanoparticles and Antimicrobial Peptides”**

**Monday, 31<sup>st</sup> August  
16:00 - 16:30, Hall 3B**

Matthias Epplé is a Professor of Inorganic Chemistry at the University of Duisburg-Essen (Germany). After completion of his PhD at the Technical University of Braunschweig, he did research at the University of Washington (Seattle, USA), the University of Hamburg (Germany), and the Royal Institution (London, U.K.). In 2000, he became Professor at the University of Bochum and in 2003, he moved to the University of Duisburg-Essen. His research interests are concentrated on the chemistry of solid biomaterials, e.g. the properties of calcium phosphate ceramics and their composites, inorganic and polymeric nanoparticles for drug and gene delivery, and the synthesis of metallic nanoparticles and their biological actions. He is the past President of the German Society for Biomaterials.



## **Zhongwei GU**

*National Engineering Research Center for Biomaterials  
Sichuan University  
CHINA*

### **K2**

**Title: “Bioinspired Design of Dynamic Macromolecular  
for Gene Delivery”**

**Monday, 31<sup>st</sup> August  
16:00 - 16:30, Hall 4A**

Professor Zhongwei Gu has thrice being the chief scientist of the National Basic Research Program of China (the 973 program) since 1999, director of the National Engineering Research Center for Biomaterials at Sichuan University, vice-chairman of the Chinese Society for Biomaterials (CSBM), executive member of the council of the Chinese Materials Research Society(C-MRS) and Chinese Society for Biomedical Engineering (CSBME) and is a Fellow of international Biomaterials Science and Engineering (FBSE). His current research activities focus on the molecular design and controlled preparation of novel biomedical polymers, self-assembled biomaterials and nano-biomaterials, polymeric carriers and controlled drug/gene delivery systems, and biomaterials for molecular diagnosis. He has published more than 280 papers and received ~25 patents, composes/ translates ~14 books and chapters, and is the invited speaker in many international and domestic conferences.





## **Satoru KIDOAKI**

*Institute for Materials Chemistry and Engineering  
Kyushu University  
JAPAN*

### **K3**

**Title: “Manipulation of Cell Mechanotaxis by Designing Curvature of the Elasticity Boundary on Hydrogel Matrix”**

**Monday, 31<sup>st</sup> August  
16:00 - 16:30, Hall 4B**

Satoru Kidoaki, Ph.D, a professor of Laboratory of Biomedical and Biophysical Chemistry, Institute for Materials Chemistry and Engineering (IMCE), Kyushu University, Japan. He graduated from Nagoya University, Japan in 1998, and earned his Ph.D. degree on physical chemistry on first-order phase transition of giant duplex DNAs. From 1998 to 2000, he worked at National Cardiovascular Research Center in Japan as a post-doc researcher, where he investigated direct measurement of molecular and surface forces acting on the biomedical devices. After another one-year pos-doc position, he was employed in 2001 as an associate professor of Division of Biomedical Engineering, Graduate School of Medicine, Kyushu University, Japan. He started the researches on mechanics of biomolecules, biosurfaces, and cells and tissues for development of tissue engineering devices and regenerative medicine. Since 2006, he has been in the present position, and promoting the studies on mechanobio-materials to manipulate cell behaviors.



## **Yasuhiko TABATA**

*Institute for Frontier Medical Sciences  
Kyoto University  
JAPAN*

### **K4**

**Title: “Dual Release of a Macrophages Recruitment Agent and Growth Factor for Bone Regeneration”**

**Tuesday, 1<sup>st</sup> September  
11:30 - 12:00, Hall 2**

Dr. Yasuhiko Tabata is the Professor and Chairman of the Department of Biomaterials at the Institute for Frontier Medical Sciences, Kyoto University and serves as adjunctive professor at 14 different universities. He received his BD in Polymer Chemistry (1981), Ph.D. (1988) in Technology, D.Med. Sc. (2002), and D.Pharm. (2003) all at Kyoto University. He received the Young Investigator Award (1990), the Scientific Award from the Japanese Society for Biomaterials (2002), the Scientific Award from the Japan Society of Drug Delivery System (2011), and several awards. He has published 1,280 scientific papers including 120 book chapters and review articles, and has 130 patents. Dr. Tabata is the Board Governor of 5 Japanese Academic Societies or an associate member of the Science Council of Japan, Cabinet Office and the Editorial Board of 7 scientific journals. Specific research interests include biomaterials, drug delivery system (DDS), tissue engineering, stem cell technology, and medical diagnostics.







## Véronique MIGONNEY

Laboratory of Biomaterials and Specialty Polymers  
Université Paris 13  
FRANCE

### K5

**Title: "Contributions of Adhesive Proteins to the Cell Response to Bioactive Polymers and Surfaces"**

**Tuesday, 1<sup>st</sup> September**  
**11:30 - 12:00, Hall 3B**

Véronique Migonney is Professor of Chemistry and Biomaterials at the Institut Galilée, University Paris 13, France. She has been appointed as Director of the research laboratory Chemistry, Structures and Properties of Biomaterials and Therapeutic Agents by the CNRS. She received Materials Eng. Diploma (1981) and Ph.D. (1986). She served as associated director of the Institut Galilée (1998-2004), director of the Master Degree in Biomaterials (2004-), president and past-president of the French Society of Biomedical Engineering (2011-) and vice-president of the Alliance for Biomedical Engineering (2014-). She has been elected as Fellow of the International Union of Societies for Biomaterials Science and Engineering (IUSBSE) (2012). She has been Editor in chief and on the editorial board of IRBM, JBSMM. Her major research interest is the synthesis and grafting of bioactive polymers onto biomaterials surfaces to control the host response. She has published > 90 papers and 22 patents.



## Dieter SCHARNWEBER

Max Bergmann Center of Biomaterials  
Technische Universität Dresden  
GERMANY

### K6

**Title: "Glycosaminoglycan Derivatives – Promising Candidates for the Design of Functional Biomaterials"**

**Tuesday, 1<sup>st</sup> September**  
**11:30 - 12:00, Hall 4A**

Prof. Scharnweber is head of the group „Biomaterial-Development“ at the Max Bergmann Center of Biomaterials at the Institute of Materials Science, Technische Universität Dresden (TU Dresden). He is local speaker of the DFG-Transregio 67 „Functional biomaterials for controlling healing processes in bone and skin – from material science to clinical application“. His major scientific interests are on biomaterials focusing on (i) composition-structure-property relationships of oxide layers on titanium-based materials, (ii) techniques for surface-engineering of biomaterials, (iii) matrix-engineering, i.e. the design of artificial extracellular matrices mimicking the native cellular microenvironment, and (iv) the design and combination of defined biochemical and physical microenvironments for applications in tissue engineering and regenerative therapies. Dieter Scharnweber has studied chemistry at the TU Dresden with a PhD in physical chemistry. After a habilitation on biomaterials in 2002 he is professor at the TU Dresden since 2008.





## **Rui L. REIS**

*3B's Research Group - Biomaterials, Biodegradables and Biomimetics*  
*University of Minho*  
 PORTUGAL

**K7**

**Title: „Hydrogels and Scaffolds of Natural Origin as Support for Stem Cells in the Regeneration of Different Tissues”**

**Tuesday, 1<sup>st</sup> September**  
**16:45 - 17:15, Hall 2**

Professor Rui L. Reis, PhD, DSc, Hon. Causa MD, 48 years old, is the Vice-Rector for R&D of University of Minho (UMinho) in Portugal, Director of the 3B's Research Group on Biomaterials, Biodegradables and Biomimetics ([www.3bs.uminho.pt](http://www.3bs.uminho.pt)) and of the ICVS/3B's Associate Laboratory (around 430 researchers), of UMinho. He is the CEO of the European Institute of Excellence on Tissue Engineering and Regenerative Medicine (TERM), the President and CSO of the company Stematters, the President-elect of Global TERMIS and the editor-in-chief of the Journal of Tissue Engineering and Regenerative Medicine. He is co-author of 870 ISI listed publications (710 full papers in scientific journals), around 210 book chapters, 30 patents and 6 books. He has around 1650 communications in international conferences. He is PI of projects totalizing around 30 MEuros, including the very prestigious ERC Advanced Grant and an ERA Chairs. He runs a research group of around 175 researchers with more than 70 PhD holders. He was been awarded several major national and international scientific and innovation awards in Europe and the USA, including the Jean Leray and George Winter awards from ESB and the Clemson Award for Contributions to the Literature from SFB.



## **Wojciech CHRZANOWSKI**

*Faculty of Pharmacy*  
*The University of Sydney*  
 AUSTRALIA

**K8**

**Title: “Bionano Characterization - Beyond Imaging with Scanning Probe Microscopy”**

**Tuesday, 1<sup>st</sup> September**  
**16:45 - 17:15, Hall 4A**

Dr Wojciech Chrzanowski joined the University of Sydney in 2010 and he has established the Bio-interface group and Bio-nano-characterisation laboratory within the Faculty of Pharmacy. His research is balanced between basic and translation science and it develops new examination approaches to interrogate biological responses at nano level to inform the design of new biologically active materials for implantable devices and drug delivery. For a series of publications describing significant advances in nanobiomedical sciences and biointerfaces he was invited to present over 50 seminars, and lectures at Universities in the USA, Japan, Australia, UK, and Korea. He received two invitational fellowships to Tokyo University and Chubu University funded by Japan Society of Promotion of Science. Dr Chrzanowski published excess of 100 peer-reviewed publications (last 10 years). His publications attracted 1100 citations and his h-index is 20. He is also an inventor on 4 patents.





## Lucie BACAKOVA

Institute of Physiology  
Academy of Sciences of the Czech Republic  
CZECH REPUBLIC

**K9**

**Title: "Endothelial Cells on Biofunctionalized Polymeric Materials for Vascular Tissue Engineering"**

**Wednesday, 2<sup>nd</sup> September**

**9:30 - 10:00, Hall 3A**

Lucie Bacakova, MD, PhD, Assoc. Prof. graduated from the Charles University, Faculty of General Medicine, Prague, Czech Republic, and received the PhD degree in Physiology and Pathophysiology of Humans and Animals in 1992. Then she did research at the Institute of Physiology, Academy of Sciences of the Czech Republic. In 1996, she was a Research Fellow at the University of Washington, Department of Vascular Biology and Pathology, Seattle, WA, U.S.A. (Prof. S.M. Schwarz), and in 2000-2001, at the University of Pennsylvania, Biophysical Engineering & NanoBio-Polymers Lab, Philadelphia, PA, U.S.A. (Prof. D.E. Discher). Since 2005, she is the Head of the Department of Biomaterials and Tissue Engineering at the Institute of Physiology, Acad. Sci. CR. In 2013, she became Associated Professor at the 2<sup>nd</sup> Medical Faculty, Charles University, Prague, CR. She has published about 150 papers in international impacted journals (h-index 26). Her main interests include the cell-material interaction *in vitro* and engineering of bone, vascular and skin tissue.



## Sandra VAN VLIERBERGHE

Polymer Chemistry & Biomaterials Group  
Ghent University  
BELGIUM

**K10**

**Title: "3D Printing of Crosslinkable Gelatins: Overcoming the Mechanical Boundaries"**

**Wednesday, 2<sup>nd</sup> September**

**9:30 - 10:00, Hall 4A**

Prof. Sandra Van Vlierberghe is active within the Polymer Chemistry & Biomaterials Group (PBM) at Ghent University (UGent, Belgium) and holds a 10% professorship at the Faculty of Engineering of the Vrije Universiteit Brussel (VUB, Belgium). She has acquired expertise related to the synthesis, the modification and the processing of (bio)polymers including polyesters, proteins and polysaccharides for a plethora of applications in the fields of regenerative medicine and optical applications. She received her PhD in Sciences in 2008 at Ghent University. She authored more than 65 Web of Science Core Collection cited papers and she is promoter of 11 PhD's, edited a book, authored 5 chapters in books and was invited speaker at several international conferences. She currently is spokesperson of the 'Young Scientists Forum (YSF)' and editorial board member of the Biomaterials Network. Finally, she also holds a 10% professorship at the University of Antwerp (Belgium) for teaching polymer-related courses.







## **Neil CAMERON**

*Department of Materials Science and Engineering  
Monash University  
AUSTRALIA*

### **K11**

**Title: “Polypeptide Nanoparticles for Ocular Drug Delivery”**

**Wednesday, 2<sup>nd</sup> September**

**11:30 - 12:00, Hall 1**

Prof. Neil Cameron is the Monash Warwick Alliance Professor of Polymer Materials, based at Monash University. His research is focused on novel polymeric biomaterials, in particular scaffolds for 3D cell culture and tissue engineering, self-assembling polypeptides and sugar-containing polymers (glycopolymers). His research to date has led to >125 papers and he has given >130 invited lectures. He was awarded a DTI SMART Award (2001), the Macro Group UK Young Researcher’s Medal (2003), an ICI Strategic Fund Award (2004), a Durham University Christopherson/Knott Fellowship (2008) and he was a member of the team that won the RSC’s Rita and John Cornforth award (2011). He serves/has served on the Scientific Advisory Boards of the Centre of Excellence in Polymeric Materials (PoliMat) and Reinnervate Ltd, the Editorial Board of the journal Polymer Chemistry and the Editorial Advisory Board of the journal Polymer. He is currently Chairman of the Macro Group UK.



## **Laura POOLE-WARREN**

*Graduate School of Biomedical Engineering  
University of New South Wales  
AUSTRALIA*

### **K12**

**Title: “Tissue-engineered Electrodes for Neural and Cardiovascular Applications”**

**Wednesday, 2<sup>nd</sup> September**

**11:30 - 12:00, Hall 3B**

Laura Poole-Warren is a Professor in Biomedical Engineering at the University of New South Wales (UNSW Australia). Her research group focuses on incorporating functional biological molecules into hydrogels and electroactive polymers for application to medical devices. Specific interests are in cell and drug delivery in neural and cardiovascular applications. She has published over 100 papers and has had grant funding of approximately \$4 million over the past 10 years. She has also held appointments as visiting research professor at Rutgers University in the USA and as a preclinical scientist in the biomedical industry working on development of implantable devices including wound dressings and embolic agents for cancer treatment. For 10 years up to 2012, she was a member of the Australian Commonwealth Government statutory Advisory Committee on Medical Devices which is concerned with advising the Therapeutic Goods Administration on the safety of medical devices.





## **Che CONNON**

*Institute of Genetic Medicine  
Newcastle University  
UNITED KINGDOM*

### **K13**

**Title:** „*Bio-fabrication and Physiological Self-release of Tissue Equivalents using Smart Peptide Amphiphile Templates*”

**Wednesday, 2<sup>nd</sup> September**

**11:30 - 12:00, Hall 4A**

Che Connon obtained a PhD in Biophysics from the Open University Oxford Research Unit in 2000, during which time he investigated corneal wound healing and transparency. He subsequently obtained a JSPS post-doctoral fellowship to work in Kyoto, Japan for two years studying corneal stem cell transplantation. Upon his return to the UK he was awarded a Royal Society Fellowship to investigate the nanostructure of amniotic membrane used in ocular therapeutics. Since 2013 he has held the position of Professor of Tissue Engineering at Newcastle University.

Professor Connon's research team seeks to engineer functional replacement and temporary 'bridge' tissues using a modular approach while also developing model systems to study physiological and pathophysiological corneal tissue formation. Of current interest is the application of self-assembling peptide amphiphiles to control cell behavior and direct tissue formation.



## **Roberto DE SANTIS**

*Institute of Polymers, Composites and Biomaterials  
National Research Council of Italy  
ITALY*

### **K14**

**Title:** “*3D Fiber Deposition and Stereolithography Techniques for the design of Multifunctional Nanocomposite Magnetic Scaffolds*”

**Thursday, 3<sup>rd</sup> September**

**11:30 - 12:00, Hall 1**

Roberto De Santis was born in Naples, Italy, in 1966. He received the mechanical engineering degree in 1994, the PhD in Biotechnology of Dental Materials in 1997 and the Master in Biomaterials in 2001. He is researcher at the Institute of Polymers, Composites and Biomaterials of the Italian National Research Council from 2001. He is adjunct professor of Science and Technology of Dental Materials at the School of Dentistry, Faculty of Medicine of Naples “Federico II”. He is leader of the “Biomaterials and Tissue Engineering” unit of the Department of Chemical Science and Materials Technology. He is part of the board member of the SIB Italian Society of Biomaterials and of the SIBOT Italian Society of Biomechanics in Orthopadics and Traumatology. He is author of more than 70 papers published on international and national journals, 10 book chapters, 5 patents, 1 trade mark, and more than 100 international congress presentations.





## **Lorenzo MORONI**

Maastricht University, MERLN Institute  
Department of Complex Tissue Regeneration  
THE NETHERLANDS

### **K15**

**Title: “Polymer Brush-Assisted Fabrication of Protein Gradients inside of 3D Microporous Scaffolds”**

**Thursday, 3<sup>rd</sup> September**  
**11:30 - 12:00, Hall 2**

Dr. Moroni studied Biomedical Engineering at Polytechnic University of Milan, Italy, and Nanoscale Sciences at Chalmers Technical University, Sweden. He received his Ph.D. cum laude in 2006 at University of Twente on 3D scaffolds for osteochondral regeneration, for which he was awarded the European Doctorate Award. In 2007, he worked at Johns Hopkins University as a post-doctoral fellow in the Elisseeff lab, focusing on hydrogels and stem cells. In 2008, he was appointed the R&D director of the Musculoskeletal Tissue Bank of Rizzoli Orthopedic Institute, where he investigated the use of stem cells from alternative sources for cell banking, and the development of novel bioactive scaffolds for skeletal regeneration. From 2009 till 2014, he joined again University of Twente, where he worked in the Tissue Regeneration Dept. Since 2014, he holds an associate professor position at the MERLN Institute. His research group interests aim at developing biofabrication technologies to generate libraries of 3D scaffolds able to control cell fate. In 2014, he received the prestigious Jean Lera Award for outstanding young principal investigators from the ESB and the ERC starting grant.



## **Mirosława EL FRAY**

Division of Biomaterials and Microbiological Technologies  
Polymer Institute, West Pomeranian University of Technology  
POLAND

### **K16**

**Title: “Elastomeric Materials of Enhanced Mechanical Performance for Implantable Artificial Heart”**

**Thursday, 3<sup>rd</sup> September**  
**11:30 - 12:00, Hall 3A**

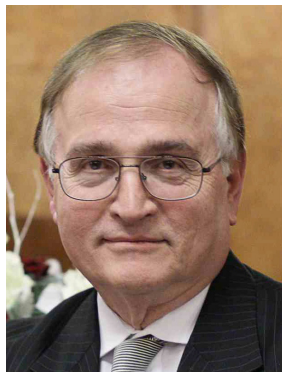
Head of the Division of Biomaterials and Microbiological Technologies and director of the Nanotechnology Centre for Education and Research, and director of Polymer Institute. She graduated from Szczecin University of Technology, where she also received her PhD in 1996. She was a post-doc at the Technical University Hamburg-Harburg, and scientific researcher at the University Bayreuth, Germany (2000-2003). She received her habilitation (DSc) at the Warsaw University of Technology in 2004. She received the Royal Society fellowship in 2005 at the Imperial College London, UK. She is an author and co-author of over 250 scientific papers. Her scientific background is on the polymer synthesis and characterization, biodegradation and modification towards specific biomedical applications (including polymers for artificial heart, heart patches, elastomeric and photocurable networks, and nanocomposites). Currently, she is employed as full professor at the West Pomeranian University of Technology, Szczecin, contributing to research and education in the field of polymer chemistry, nanotechnology, including nanocomposites, and polymeric biomaterials.





# Awards Winners

## International Award



### **Nicholas A. PEPPAS**

*Biomedical Engineering Department  
The University of Texas at Austin  
UNITED STATES*

***Tuesday, 1<sup>st</sup> September  
8:30 - 9:00, Hall 1***

Nicholas A. Peppas is the Cockrell Family Distinguished Chaired Professor in the Departments of Chemical, Biomedical Engineering and Pharmacy, and Chairman of the Department of Biomedical Engineering of the University of Texas at Austin. His work in biomaterials, polymer physics, drug delivery and bionanotechnology follows a multidisciplinary approach by blending modern molecular and cellular biology with engineering principles to design the next-generation of medical systems and devices for patient treatment. Over the past 40 years he has set the fundamentals and rational design of biomedical hydrogels and drug delivery systems and developed models of drug and protein diffusion in controlled release devices and biological tissues.

In 2012 he received the Founders Award of the National Academy of Engineering, the highest recognition of the Academy, for these contributions to the field. In 2008, AIChE named him one of the One Hundred Chemical Engineers of the Modern Era. Peppas is a member of the National Academy of Engineering, the National Academy of Medicine, the National Academy of Inventors, the National Academy of France, the Royal Academy of Spain, the Academy of Athens and the Academy of Texas. He has been recognized with awards from AIChE (Founders Award, William Walker Award, Institute Lecture, Jay Bailey Award, Bioengineering Award, Materials Award), the Biomedical Engineering Society (Distinguished Scientist Award), the American Institute of Medical and Biological Engineering (Galletti Award), the Society for Biomaterials (Founders, Clemson and Hall Awards), the Controlled Release Society (Founders, Heller and Eurand Awards) and other societies.

He is President of the International Union of Societies of Biomaterials Science and Engineering, and Past-Chair of the Engineering Section of the American Association for the Advancement of Science, and the Council of BME Chairs. Previously, he served as President of SFB and the Controlled Release Society. He has supervised the research of 100 PhDs and about 180 postdocs and visiting scientists. Peppas holds a Dipl. Eng. from the NTU of Athens (1971), a Sc.D. from MIT (1973), honorary doctorates from the Universities of Ghent, Parma, Athens, Patras and Ljubljana, and an Honorary Professorship from Sichuan University.



## Jean Leray Award



### **Joaquim Miguel OLIVEIRA**

*3B's Research Group - Biomaterials, Biodegradables and Biomimetics  
University of Minho  
PORTUGAL*

**Wednesday, 2<sup>nd</sup> September**

**14:30 - 15:00, Hall 1**

J. Miguel Oliveira BSc, PhD (Portuguese, M, 37 years old) is a Principal Investigator “Investigador FCT 2012” at the PT Government Associate Laboratory ICVS/3B's (<http://www.3bs.uminho.pt/users/migueloliveira>). He is the Director of Pre-Clinical Research at the FIFA MEDICAL CENTER, Estádio do Dragão, Porto, PT since Feb. 2013. Currently, he is a Lecturer in Doctoral Program in Tissue Engineering, Regenerative Medicine and Stem Cells (TERM&SC) at UMinho, PT (since Dec. 2013). He is also an Invited lecturer at the Faculty of Medicine, U. Porto (since Sept. 2013) and Dept. of Polymer Eng., UM, PT (2009-present). Along the years he has focused his work on the field of biomaterials for tissue engineering, nanomedicine, stem cells and cell/drug delivery. More recently, he set-up a new research line within the ICVS/3B's on 3D in vitro models for cancer research. As result of his proficiency, he has published so far more than 100 scientific contributions in scientific journals with referee, being 3 of those review papers produced under invitation.

Miguel Oliveira was approved 7 patents, published 2 books, 1 special issue in scientific journals, and more than 40 book chapters in books with international circulation. He has participated in more than 140 communications in national/international conferences and has been invited/keynote speaker in more than 30 plenary sessions. He has an h-index of 20, i10 of 35 and received more than 1800 citations. He has been the responsible for developing and licensing a patent on gellan gum-based polysaccharides (Mimsys® G) to Stematters, the first product commercialized by this spin-off of 3B's. He has been awarded several prizes and he is very active on the elaboration and scientific coordination of several PT and international funded projects.

In addition, he is member of the advisory board of the Journal of Materials Science: Materials in Medicine, International Journal of Tissue Engineering, Journal ISRN Biomaterials, The Journal of Experimental Orthopaedics, Journal “Recent Patents on Corrosion Science”, and referee in more than 30 international journals.



# George Winter Award



## Luigi AMBROSIO

*Chemical Sciences & Materials Technology Department  
National Research Council  
ITALY*

**Thursday, 3<sup>rd</sup> September  
8:30 - 9:00, Hall 1**

Luigi Ambrosio is Director of Chemical Sciences & Materials Technology Department, National Research Council of Italy.

He received the doctoral degree in Chemical Engineering (1982) from University of Naples "Federico II". He was Research Associate at University of Naples (1983-1985), Research Associate at University of Connecticut, USA (1985-1986), and Visiting Scientist at Kontron Medical Inc., USA (1986- 1988). Adjunct Professor of University of Connecticut, USA (1997-2003) and of University of Naples "Federico II" (1997-2010). Director of Institute of Composites and Biomedical Materials, National Research Council of Italy (2008-2012). Visiting Professor at Instituto de Química/UFRGS, Porto Alegre, Brazil (since 2012). Distinguished Professor at Nanjing Normal University, China (since 2013).

He is member of Advisory Board and Guest Editor of International and National Scientific Journals, Vice-President of the Italian Society of Biomaterials (2006-2013), and President of the European Society for Biomaterials (2006-2013), Past President since 2013.

Board Committee Member of: - IMAST Scarl., (2002-2008), CRdC - Campania Region (since 2004), IBEC, Barcelona, Spain (2007-2013), ALS srl (2006-2015). CIRA S.C.p.A (2012-2014), CNCCS Scarl (since 2012), Dhitec Scarl (Since July 2014), INAIL (Since July 2014).

He has been nominated Fellow of the American Institute for Medical and Biological Engineering (March 2001), and Fellow of Biomaterials Science and Engineering (May 2004) and APA Distinguished Award (2014).

Member of the European Commission Advisory Group of the FP7-NMP (2006-2008) and Member of High Level Group - *Key Enabling Technologies* - European Commission (since 2009).

Research interests include design and characterisation of polymers and composites for medical applications and tissue engineering, rheology of biological fluids, structural properties of natural tissue, properties and processing of polymers and composites and nanostructures, hydrogels and biodegradable polymers.

Publications include over 300 papers on international scientific journals and book, 18 patents, over 500 presentations at international and national conferences and over 100 invited lectures.



## Other Awards

### Translational Award

This award is established to recognise, encourage and stimulate outstanding translational research contributions to the field of biomaterials. The award is attributed to a postdoctoral scientist presenting the best contribution in translational research at the Biomaterials conference of the Society. Among the numerous applications for the Translational Award 7 candidates were selected. Their oral presentations are scheduled on Tuesday, 1<sup>st</sup> September, at 16:45 – 18:30 during Translational Research Symposium. The winner announcement will take place during the Closing Ceremony on Thursday, 3<sup>rd</sup> September, at 13:15.

### European Doctoral Award

This award is established to recognise, encourage and stimulate outstanding translational research contributions to the field of biomaterials. The candidate applies for and completes his/her Ph.D. according with the rules of his/her own country and university. This award demonstrate that the winners have all received high standard research education and training at a European level in the fields of Biomaterials and Tissue Engineering, and that they are also able to produce scientific results deserving recognition by being published and accepted in high quality journals and conferences. The EDA awardees are: Ana Puga, Andrada Serafim, Cristina Gonzalez Garcia, Israel Gonzalez de Torre, Jose Ballester, Małgorzata Krok, Martina Lorenzetti, Michael Monaghan, Riccardo Levato, Shane Browne and Tiziano Serra. EDA awardees presentation will be during Young Scientists Forum on Wednesday, 2<sup>nd</sup> September, at 15:00.

### Rudolf Cimdins Scholarship Awards (Travel Awards)

The ESB supports student participation at the ESB Annual conference through the travel award scheme. Candidates apply to the ESB Council and the award covers a contribution to registration and travel. The winners still need to pay their registration etc, but they will get the money reimbursed by the ESB Treasurer after the conference. It should be noted that the awards are normally given to candidates who would not otherwise be able to attend the ESB conference as they come a long way/ come from a poorly funded country/group. Recipients will be announced at the Closing Ceremony on Thursday, 3<sup>rd</sup> September, at 13:15.

### Best Student Oral/Poster Presentations

All candidates must be students, must have an accepted abstract as presenting author and should have indicated on the registration form their desire to be considered for these awards. Oral presentations and posters will be assessed by the Conference Award Committee. Winners will be announced during the Closing Ceremony on Thursday, 3<sup>rd</sup> September, at 13:15.

### Best Rapid Fire Presentations

Springer, international publisher specialising in science, technology and medicine, is awarding two Best Rapid Fire Presentation Prizes. The winners will receive Springer book voucher worth 250 €.



# Special Sessions

## Young Scientists Forum

Sunday, 30<sup>th</sup> August  
13:00 - 17:00, Hall 2



### “From Creative Thinking Towards Product Commercialization: The Complete Value Chain”

#### Organizers:

Sandra Van Vlierberghe, Lorenzo Moroni, Giuseppe Cama, Anna Finne Wistrand, Izabela Stancu

#### Supported by:

Young Scientists Forum @ ESB

The YSF workshop in Kraków, Poland will aim to cover the entire value chain ranging from idea creation towards commercialization of a developed product.

#### Programme:

- 13:00**    **Prof. Abhay Pandit**, National University of Ireland, Galway, Ireland  
*“Creative Thinking – How to Come up with New Ideas”*
- 13:35**    **Prof. Fabrizio Barberis**, University of Genoa, Italy  
*“How to Get Money to Work out your Idea”*
- 14:10**    **Prof. Paul Santerre**, University of Toronto, Canada  
*“You Received Funding – What’s Next – How to Survive in Research Land”*
- 14:45**    Coffee break
- 15:15**    **Prof. Joachim Kohn**, The New Jersey Center for Biomaterials, United States  
*“How to Advance Research Results Towards the Development of a Medical Product”*
- 15:50**    **Dr. Lechosław F. Ciupik**, LfC-Medical, Poland  
*“R&D in Creation of Bio-Engineering Product; Researcher Responsibility”*
- 16:25**    **Panel discussion**

In addition to PhD students, the workshop will also focus on topics relevant for post-doctoral researchers as well as PIs.

The workshop will be closed with a round table discussion during which delegates can share their opinion and exchange ideas to create an excellent networking opportunity.





# Special Fellows Session

Monday, 31<sup>st</sup> August  
16:00 - 17:45, Hall 1



## “Biomaterials Education is not Ready for the Challenges of the Future”

### Session Chair and Organizer:

**Joachim Kohn**, PhD, FBSE

*Chair, International College of Fellows*

*Board of Governors Professor and Director, New Jersey Center for Biomaterials*

*Rutgers - The State University of New Jersey, USA*

The “Special Fellows Session” is organized by the International College of Fellows of Biomaterials Science and Engineering (IUS-BSE). Special Fellows Sessions explore important and sometimes controversial topics. A group of six prominent Fellows will highlight the perceived strengths and weaknesses of the way most universities educate and train the next generation of biomaterials scientists. Three Fellows will argue in favor of the current status of biomaterials education, while three other Fellows will provide provocative and stimulating arguments highlighting the weaknesses of current biomaterials education. One key point of the debate will be an exploration to which extent the careers of young scientists are impacted by a lack of skills needed to translate laboratory research into products within an industrial setting. Another key point relates to the fact that current biomaterials education prioritizes breadth over depth, producing “generalists” who are not well-trained in any one field. The changing job market for biomaterials scientists (especially at the PhD level), and global challenges and perspectives will also be discussed. Together, the six presenters will provide the audience with a deep and multifaceted understanding of the strength and weaknesses of the way many young biomaterials scientists are educated and prepared for their careers. Special Fellows Sessions are designed to be interactive: the audience will have an opportunity to participate in the debate and will vote on the issues.

Previous “Special Fellows Sessions” examined the utility of animal experiments (WBC Amsterdam, 2008), explored whether we will ever be able to regenerate a complete human arm (WBC Chengdu, 2012), looked at the tension between basic research and translational research (ESB Liverpool, 2014) and the competition between material science approaches and biology-based approaches in developing the next generation of regenerative therapies (US Society for Biomaterials, Charlotte NC, 2015).





## Speakers:

### **Kristi S. Anseth, PhD**

*Distinguished Professor, Tisone Professor, Associate Professor of Surgery,  
and Howard Hughes Medical Institute Investigator*

Chemical and Biological Engineering

University of Colorado, Boulder, USA

### **David W. Grainger, PhD, FBSE**

*University Distinguished Professor and George S. & Dolores Doré Eccles  
Presidential Endowed Chair of Pharmaceutics and Pharmaceutical Chemistry*

Department of Bioengineering

University of Utah, USA

### **Dietmar Hutmacher, PhD, FBSE**

*Professor, Science and Engineering Faculty,*

Queensland University of Technology, Brisbane, Australia

### **Lynne C. Jones, M.S., PhD, FBSE**

*Director, Center for Osteonecrosis Research and Education*

*Associate Professor of Orthopaedic Surgery*

Johns Hopkins University

Baltimore, MD, USA

### **Laura Poole-Warren, PhD, FBSE**

*Professor and Pro Vice-Chancellor for Research Training, Dean of Graduate Research  
Graduate School of Biomedical Engineering,*

University of New South Wales

Sydney, Australia

### **Elizabeth Tanner, PhD, FBSE**

*Professor of Biomedical Materials*

*Department of Biomedical Engineering*

University of Glasgow, Scotland, UK



# Translational Research Symposium

Tuesday, 1<sup>st</sup> September

10:00 - 11:00

11:30 - 13:00

16:45 - 18:30

Hall 1



## “Innovating in the Medical Device Industry – Challenges & Opportunities”

### Organizers:

Yves Bayon, Marc Bohner, David Eglin, Geoff Richards, Dimitrios Zeugolis

### Supported by:

DSM Biomedical, Netherlands

The ESB 2015 Translational Research Symposium will focus on **“Innovating in the Medical Device Industry – Challenges & Opportunities”**. It will include invited lectures from the medical device innovation stakeholders, i.e. medical device industry, academic translational centres, customers and medical device regulatory experts. The Translational Research Symposium will also offer open sessions for sharing translational research initiatives both from academia and industry. This event will be of interest to a wide audience from large medical device producers to academics and entrepreneurs and promoters of biomaterial technologies for medical applications. The program includes significant time for networking during coffee breaks, lunch and is also synchronized with other ESB2015 sessions throughout the day allowing the delegates to view other interesting lectures during the event.

### Session 1 (10.00-11.00)

#### Invited Speakers:

**Philip Procter**, Medical Device Industry Consultant, France

*“Clinical Needs Based Biomaterial Strategy: Reducing the Risk that Innovation is “Lost in Translation” in Products for Poor Quality Bone”*

**Nils Reimers**, Manager R&D, Global Funding & Reimbursement,  
Stryker Trauma & Extremities, Germany

*“Best Practice for Registration Trials of Biodegradable Implants”*

**Xiang Zhang**, Lucideon Ltd., Royal Society Industry Fellow at University of Cambridge, UK

*“New Concept of Hybrid Polymer Composites for Implant Applications”*

**Ipsita Roy**, University of Westminster, London, UK

*“Novel Biodegradable and Biocompatible Polymers for Medical Applications”*



## Session 2 (11.30-13.00)

### **Invited Speakers:**

**Jan Weber**, Sr Research Fellow, Corporate Research, Boston Scientific Corporation, USA  
*"Insights into Collaboration and Innovation for Early Stage Medical Device Development"*

**Jens Thies**, Director Science and Innovation, DSM Biomedical, Netherlands  
*"From Biomaterials Supplier to Device Development Partner – Supporting Medical Device Companies in De-Risking Medical Products"*

**Herbert De Breuck**, Manager R&D, Luxilon, Wijnegem, Belgium  
*"Next Generation of Fibers for Medical Devices: Biopolymers and Functionalized Coatings"*

## Session 3 (16.45-18.30)

### **Oral presentations of Candidates for Translational Research Award:**

**Antoine Alves**, NAMSA, Chasse/Rhône, France  
*"FTIR Microscopy Contribution for Comprehension of Poly-L-Lactic Acid (PLA) Degradation Mechanisms"*

**Mikhail Durymanov**, Institute of Gene Biology of the RAS, Russia  
*"Possible Approach to Improve Systemic Gene Delivery to Tumour Using Polyplex Nanoparticles"*

**Beata Butruk-Raszeja**, Warsaw University of Technology, Poland  
*"Endothelialization of Polyurethanes: Immobilization of REDV Peptide"*

**Inês Gonçalves**, INEB - Instituto de Engenharia Biomédica, Universidade do Porto, Portugal  
*"Helicobacter Pylori-Binding Small Chitosan Microparticles that Penetrate Gastric Mucosa"*

**Stephen Swioklo**, Institute for Genetic Medicine, Newcastle University, United Kingdom  
*"Leaving Cells Out in the Cold: Hydrogel Encapsulation for the Improved Hypothermic Preservation of Stem Cells"*

**Daniel Rodriguez**, Technical University of Catalonia (UPC-BarcelonaTECH), Barcelona, Spain  
*"Antibacterial Coatings on Titanium Surfaces: a Comparison Study Between In Vitro Single-species and Multispecies Biofilm"*

**Elisabeth Engel**, Institute for Bioengineering of Catalonia (IBEC), Barcelona, Spain  
*"The Proangiogenic Potential of a Novel Poly(Lactic) Based Composite Membrane for Guided Bone Regeneration"*



# Surface Charge for Biomaterial Characterization

Tuesday, 1<sup>st</sup> September  
11:30 - 13:00  
Hall 4B



## Speakers:

Dr. Christine Körner, Anton Paar GmbH, Graz, Austria

Dr. Martina Lorenzetti, Jožef Stefan Institute, Ljubljana, Slovenia

## Sponsored by:

Anton Paar, Austria

The session “Surface Charge for Biomaterial Characterization” focuses on the role of zeta potential analysis as a surface sensitive technique for the characterization of biomaterial surfaces. The zeta potential is an interfacial parameter which describes the charge that a surface assumes when it gets in contact with a liquid. As the zeta potential is sensitive to the outermost surface layer, it furthermore enables time-resolved adsorption studies of biological compounds on solid surfaces. It thus combines the clear visualization of the interaction between biomaterials and their environment with the validation of the chemistry of the adsorbed layer. This enables the optimization of solid surface properties of biomaterials.

The surface charge of solid materials is best assessed by means of zeta potential analysis performed directly at the solid/water interface using the streaming potential technique. Zeta potential analysis is applicable to all classes of materials used for biomaterial applications, i.e. metals, polymers and ceramics.

The first part of the session introduces the basic principles and benefits of zeta potential analysis. The state-of-the-art instrument for zeta potential analysis on solids, SurPASS Elektrokinetic Analyzer, will be presented. Together with its wide range of measuring cells, SurPASS allows for the analysis of biomaterial samples of different shape and geometry over a wide pH range and at different electrolyte compositions.

The second part of the session focuses on recent research on modified titanium-based substrates (TiO<sub>2</sub>-coated by nanocrystals or nanotubes) used for hard tissue replacement. Influences of the topography of the surface (roughness and size of nanostructures), the substrate nature, and the material behaviour in contact with different biologically relevant electrolytic solutions on the surface charge are discussed. The information obtained by zeta potential analysis allowed for a better understanding of the behavior of such coatings in physiological conditions.

The session “Surface Charge for Biomaterial Characterization” is interesting for scientists and researchers searching for a direct method for biomaterial/environment interface analysis and a state-of-the-art technique for solid surface analysis to successfully promote the development of biomaterials.



# Science for Industry: Bioresorbable Materials for Medical Applications

Wednesday, 2<sup>nd</sup> September

9:30 - 11:00

11:30 - 13:00

16:45 - 17:45

Hall 4B



**ReBioStent**

Reinforced Bioresorbable Biomaterials for Therapeutic Drug Eluting Stents



## Organizers:

Xiang Zhang, Ipsita Roy, Kadem Al-Lamee, Stuart Maclachlan, Maria Joao Barros, Nial Bullett, Mark Taylor

## Supported by:

- ReBioStent project, grant agreement n° 604251 from the European Union's Seventh Programme for research, technological development and demonstration (FP7)
- ARTERIUS, United Kingdom

## Chairs:

Dr Xiang Zhang, *Principal Consultant, Lucideon Limited, and Royal Society Industry Fellow at University of Cambridge*

Dr Ipsita Roy, *Reader, Head of Applied Biotechnology Research Group, Department of Life Sciences, Faculty of Science and Technology, University of Westminster*

Materials for medical applications take many forms, from metallic to synthetic and natural polymers, composites and materials of biological origin. The ultimate goal of an implantable device is for it to be unrecognised by the body, to allow for stable long term lifetime of the device. One strategy for this is for the devices to be bioresorbable – to disappear after their initial function is no longer needed as healing has occurred. Permanent implants may cause complications many years after initial healing has occurred and their presence in the body is no longer necessary.

Bioresorbable materials have applications in a wide range of medical indications, such as sutures, coronary and peripheral vascular scaffolds, bone pins and anchors, tissue fixation screws, drug delivery coatings and microspheres and surgical meshes and matrices. The bioresorbable materials may include polymers, metals, ceramics, glasses, composites and materials of biological origin such as natural collagen, and may allow for drug elution and delivery as well as performing a mechanical function.

Bioresorbable sutures have been available for over 40 years, yet recent innovations have expanded the market for bioresorbable implants to include cardiovascular, orthopaedic and general surgery. This has demanded increased performance from polymers, with increased strength and control over degradation being necessary.



### Session 1 (9.30-11.00)

- 9:30** **Welcome and Introduction: Dr Xiang Zhang, Dr Ipsita Roy**
- 9:50** **Dr Kadem Al Lamee, Arterius Limited**  
*"Commercial needs for bioresorbable materials, transfer from laboratory and barriers and gaps in the technology"*
- 10:15** **Prof. Oskar Hoffmann, University of Vienna**  
*"Production and Evaluation Platforms for Preclinical Assessment of Novel Biomaterials for Non-Healing Bone Lesions"*
- 10:40** **Dr Ipsita Roy, University of Westminster**  
*"Bioresorbable Systems: Polymers and Metals"*

### Session 2 (11.30-13.00)

- 11:30** **Prof. Aldo R. Boccaccini, University of Erlangen-Nuremberg**  
*"Bioresorbable Systems: The Role of Inorganic Fillers in Composites"*
- 11:50** **Dr Iban Quintana, IK4 - Tekniker**  
*"Bioresorbable Systems: The Role of Surface Functionalisation"*
- 12:10** **Prof. Atul Bhaskar, University of Southampton**  
*"Bioresorbable Systems: The Role of Modelling and Simulation in Performance Assessment of Bio-Structures and Implants"*
- 12:30** **Dr Gianluca Giavaresi, Istituto Ortopedico Rizzoli, Bologna**  
*"Bioresorbable Systems: The Role of Preclinical Testing"*
- 12:50** **Bioresorbable Systems: Discussion**
- 13:00** **Lunch including networking and posters**

### Session 3 (16:45 – 17:45)

- 16:45** **Welcome back and overview of morning's proceedings: Dr Xiang Zhang, Dr Ipsita Roy**
- 16:55** **Elena Boccardi, University of Erlangen-Nuremberg**  
**Zein Azhari, Cambridge University**  
*"Research into Bioresorbable Systems"*
- 17:15** **Panel discussion and overview of proceedings with speakers from the Bioresorbable System Session**





# Additional Meetings



## **IUSBSE Committee Meeting**

**The Annual Meeting of the Delegates to the International Union of Societies for Biomaterials Science and Engineering**

**Sunday, 30<sup>th</sup> August**

**12:00 - 17.00**

**Hall 4C, Level 3**

**(14:45 – 15:15 Coffee break, Level 2)**



## **ESB Council and Presidents of the National Societies for Biomaterials Meeting**

**Monday, 31<sup>st</sup> August**

**17:45 - 18:45**

**ESB Lounge, Level 0**



## **Fellows Business Meeting and Lunch**

**(FBSE - “Fellow, Biomaterials Science and Engineering”)**

**Tuesday, 1<sup>st</sup> September**

**13:00 - 14:30**

**Hall 4C, Level 3**



## **Editorial Board Meeting and Lunch**

**Journal of Materials Science: Materials in Medicine**

**Wednesday, 2<sup>nd</sup> September**

**13:00 - 14:30**

**ESB Lounge, Level 0**



# Social Events

## Welcome Reception

**ICE Congress Centre, Level 3**

**Sunday, 30<sup>th</sup> August**

**18:00 - 20:00**

Begin your ESB2015 journey at the appealing Welcome Reception! Say hello to your biomaterials community friends and meet new ones. Get exclusive opportunity to experience traditional Polish song and dance performance of “Małe Słowianki” group. Enjoy delicious food and drinks and get a first taste of famous Polish hospitality.

## Concert

**St. Mary’s Basilica, Main Market Square - Rynek Główny**

**Monday, 31<sup>st</sup> August**

**19:30 - 20:15**

After a day filled with a scientific programme, come to the St. Mary’s Basilica, magnificent gothic church, famous for its wooden altarpiece carved by Wit Stwosz, for the soothing and relaxing classical music concert.

## Keynotes & Chairpersons Dinner *(by invitation only)*

**Cloth Hall - National Museum, Main Market Square - Rynek Główny**

**Monday, 31<sup>st</sup> August**

**20:30 - 22:00**

To show our appreciation to all those who have helped us with the ESB2015 Conference organization. The Keynotes&Chairpersons Dinner is an exclusive event and the Cloth Hall is truly a unique place, perfectly tailored to this occasion.

## YSF Social Event

*(Limited number of tickets – on a first come first served basis!)*

**The Club “Under the Lizards” – “Pod Jaszczurami”, Main Market Square - Rynek Główny**

**Monday, 31<sup>st</sup> August**

**20:30 - 03:00**

**Ticket: 30€/person**

**Haven’t bought the ticket, yet? Do this ASAP at the Registration Desk.**

The exciting YSF Social Event in one of the oldest students club in Kraków, the Club “Under the Lizards”, for all those feeling young at heart. The unique atmosphere, the exceptional climate, great music, food and drinks - Under the Lizards has it all. Let’s have fun and get to know each other better!



## Acta Biomaterialia Anniversary Reception

ICE Congress Centre, Level 1  
Tuesday, 1<sup>st</sup> September  
18:30 - 19:30

*Acta* BIOMATERIALIA



Do not miss the opportunity to celebrate wonderful 10<sup>th</sup> anniversary of Acta Biomaterialia, the Elsevier Journal! Feel welcomed by the Acta Bio Editor-in-Chief, prof. William R. Wagner and enjoy food and drinks. Remember to toast for Acta Biomaterialia superb achievements!

### Gala Dinner

*(Limited number of tickets – on a first come first served basis!)*

**Wieliczka Salt Mine - 125 m underground!**

**Wednesday, 2<sup>nd</sup> September**

**18:00 - 21:00**

**Ticket: 100€/person, available also at the Registration Desk**

The Wieliczka Salt Mine is one of the most valuable monuments of material and spiritual culture in Poland. Each year it is visited by more than one million tourists from all over the world. It is also a world class monument, featuring among twelve objects on the UNESCO's World Cultural and Natural Heritage List.

The ESB2015 Conference Gala Dinner will be organized in the chamber "Warszawa", located 125 m underground.

For the Gala Dinner Participants, transport from the Conference Venue to the Wieliczka Salt Mine will be provided. Bus will depart at 18:00 from a parking located in front of the ICE Congress Centre. The journey to Wieliczka will take about half an hour. Before the Dinner, a sightseeing tour in the underground part of the museum is planned. The tour begins with a walk down exactly 380 wooden steps, and thus appropriate walking shoes are recommended (after the Dinner, the way upward will be with the lift). Also, please note that the air temperature in the salt mine chambers is only about 14-16°C (57-61°F).



# **DETAILED SCIENTIFIC PROGRAMME**



# Sunday, 30<sup>th</sup> August

	Hall 1	Hall 2	Hall 3A	Hall 3B	Hall 4A	Hall 4B	
12	12:00 Registration opens						12
13		Young Scientists Forum Workshop (1) Abhay Pandit Fabrizio Barberis Paul Santerre					13
14							14
15	Coffee Break, Exhibition (Level 2)						15
16		Young Scientists Forum Workshop (2) Joachim Kohn Lechosław F. Ciupik					16
17							17
18	18:00-20:00 Welcome Reception (Level 3)						18



# Monday, 31<sup>st</sup> August

	Hall 1	Hall 2	Hall 3A	Hall 3B	Hall 4A	Hall 4B	
8	7:30 Registration opens						8
	Opening Ceremony						
9	Plenary Lecture (L1) Joachim Kohn						9
10	Plenary Lecture (L2) Maria Siemionow						10
	Coffee Break, Exhibition (Level 0, 1)						
11	1. Nakamura 2. Guerrero 3. Suzuki 4. Lewandowska-Łańcucka	5. Gelinsky 6. Belamie 7. Bochyńska 8. Zykwińska	9. de Oliveira 10. Tolle 11. Lynge 12. Nelsen	13. Huang 14. Baum 15. Deschrevel 16. Vallejo Giraldo	17. Vilaboa 18. Nakano 19. Dupin 20. Loebel	21. Sohier 22. Clarke 23. Brüggemann 24. Massera	11
	1. Bone Tissue Eng. 1	2. Cartilage	3. Drug Delivery 1	4. Surface Mod. 1	5. Cell Inst. Mat. 1	6. Adv. Manuf. 1	
12	Break						12
	25. Wing Yuk 26. Zhao 27. Pavon 28. Cieřlik-Górna	29. Serrano 30. Ganesh 31. Laska 32. Olayo	33. Mao 34. Ouerghemmi 35. Song 36. Russo	37. Pflaum 38. Wakelin 39. Daumann 40. Sowa	41. Yang 42. Włodarczyk-Biegun 43. Ibáñez-Fonseca 44. Arias	45. Pereira 46. Cano 47. Best 48. Reys	
13	7. Osteointeg. 1	8. Neural Reg. 1	9. Drug Delivery 2	10. Surface Mod. 2	11. Cell Inst. Mat. 2	12. Cell Encap. Del. 1	13
14	Poster Session, Rapid Fire Presentations (1) Lunch (Level -1)						14
15	Plenary Lecture (L3) James Kirkpatrick						15
	Coffee Break, Exhibition (Level 0, 1)						
16	Special Fellows Session on Biomaterials Education Chair: Joachim Kohn  Kristi S. Anseth David W. Grainger Dietmar Hutmacher Lynne C. Jones Laura Poole-Warren Elizabeth Tanner	49. Boccaccini 50. Yamaguchi 51. Gutmanas 52. Arcos 53. Clarkin 54. Hupa 55. El-Meliegy	56. Łos 57. Gaspar 58. Canton 59. Im 60. Shariatzadeh 61. Guarino 62. Zuba-Surma	15. Antimicrobial Surf. Mat. 1 K1. Epple 63. Lisboa-Filho 64. Pokrowiecki 65. Su 66. Trzcńska 67. Mas-Moruno	K2. Gu 68. Heo 69. Piña 70. Zhao 71. Gomes 72. McCarthy	K3. Kidoaki 73. Pauthe 74. Nash 75. Huber 76. Dupont-Gillain 77. Golda-Cepa	16
17	13. Bioactive Materials	14. Stem Cells 1	16. Gene Delivery	17. Biointerfaces 1			17
18							18
19	19:30 - 20:15 Concert in St. Mary's Basilica (Main Market Square)						19
	20:30 - 22:00 Keynotes & Chairpersons Dinner (Cloth Hall - National Museum, Main Market Square)			20:30 - 3:00 YSF Social Event ("Under the Lizards" – "Pod Jaszczurami", Main Market Square)			





# Tuesday, 1<sup>st</sup> September

	Hall 1	Hall 2	Hall 3A	Hall 3B	Hall 4A	Hall 4B	
8	8:00 Registration opens						8
	International Award Nicholas Peppas						
9	Plenary Lecture (L4) Geoff Richards						9
	Break						
10	Translational Research Symposium (TRS) Philip Procter Nils Reimers Xiang Zhang Ipsita Roy	18.Smart Biomater. 1 78. Urciuolo 79. Matloubigha-ragozloo 80. Stamatialis 81. Boisselier	19. Wound Heal. 1 82. Ma 83. Franz 84. Pal 85. Ullm	20.Surface Mod. 3 86. Naganuma 87. Sukhorukova 88. Deligianni 89. Trembecka-Wójciga	21.Cartilage 2 90. Adekanmbi 91. Murakami 92. Pina 93. Réthoré	22.Cell Encap. Del. 2 94. Evangelista 95. Matsumura 96. Zhang 97. Malheiro	10
11	Coffee Break, Exhibition (Level 0, 1)						11
12	Translational Research Symposium (TRS) Jan Weber Jens Thies Herbert De Breuck	23.Bone Tissue Eng. 2 K4. Tabata 98. Pazarcevrein 99. Chróścicka 100. Terzopoulou 101. Brauer	24.Stem Cells 2 102. Beloti 103. McLister 104. Al Tawil 105. Peters 106. Brunelli 107. Filipowska	25.Surface Mod. 4 K5. Migonney 108. Thissen 109. Royer 110. Melo Rodriguez 111. Jarosz	26.Cell Inst. Mat. 3 K6. Scharnweber 112. Rodrigues Araújo 113. Nazir 114. Marquis 115. Szczubiátka	Session on Surface Charge for Biomaterials Characterisation Christine Körner Martina Lorenzetti	12
13	Poster Session, Rapid Fire Presentations (2) Lunch (Level -1)						13
14							14
15	ESB General Assembly						15
16	Plenary Lecture (L5) Michael Sefton						16
	Coffee Break, Exhibition (Level 0, 1)						
17	116. Alves 117. Durymanov 118. Butruk-Raszeja 119. Gonçalves 120. Swioklo	27.Bone Tissue Eng. 3 K7. Reis 123. Raucci 124. Nkhwa 125. Davidenko	28.Angio- Vasculogenesis 128. Verdenelli 129. Cheng 130. Kulanthaivel 131. Dew 132. Chatzinikolaïdou 133. Dye 134. Shiroasaki	29.Antimicrobial Surf. Mat. 1 135. Duckworth 136. Douglas 137. Flores 138. Gallagher 139. Larreta Garde 140. Sardon 141. Posadowska	30.Bioimaging and Biosensing K8. Chrzanowski 142. Yamaoka 143. Madsen 144. Plawinski 145. Koivisto 146. Nilebäck	31.Biointerfaces 2 147. Zeugolis 148. Castano 149. Gand 150. Knopf-Marques 151. Li 152. Kemper 153. Palmquist	17
18	121. Rodriguez 122. Engel	126. Alagoz 127. Gallo					18
	18:30 - 19:30 Acta Biomaterialia Anniversary Reception (Level 1)						



# Wednesday, 2<sup>nd</sup> September

	Hall 1	Hall 2	Hall 3A	Hall 3B	Hall 4A	Hall 4B	
8	8:00 Registration opens						8
	Plenary Lecture (L6) <b>Kazunori Kataoka</b>						
9	Break						9
10	154. Aguilar	160. Fernandez	34.Cardiovascular Appl. 1	K9. Bacakova	170. Hook	K10. Van Vlierberghe	<a href="#">Science for Industry</a> Bioresorbable Materials for Medical Applications  <b>Kadem Al-Lamee</b> <b>Oskar Hoffmann</b> <b>Ipsita Roy</b>
	155. You	161. Bektas			171. Prymak		
	156. Carvalho	162. Spanoudes			172. Levato		
	157. Nešporová	163. Bushkalova			173. Seabra		
	158. Amorim	164. Roy			174. Buxadera Palomero		
	159. Łapok	165. Flores-Merino			175. Islas	179. Wysocki	
	32.Cancer Therapy	33.Soft Tissue Eng.		35.Antimicrobial Surf. 3	36.Adv. Manuf. 1		
11	Coffee Break, Exhibition (Level 0, 1)						11
12	K11. Cameron	184. Harley	39.Cardiovascular Appl. 2	190. Aussel	K12. Poole-Warren	K13. Connon	<a href="#">Science for Industry</a> Bioresorbable Materials for Medical Applications  <b>Aldo R. Boccaccini</b> <b>Iban Quintana</b> <b>Atul Bhaskar</b> <b>Gianluca Giavaresi</b>
		185. Demitri		191. Boccafroschi			
		186. Tarantili		192. Giol			
		187. Gorodzha		193. Basnett			
		188. Moreno Gomez		194. Mizuta			
	180. Menzel	189. Salma-Ancane		195. Gonsior	196. Samal	200. Cortella	
	181. Eglin				197. Kohn	201. Major	
	182. Araújo				198. Frey	202. Sayin	
	183. Farbod				199. Aregueta Robles	203. Navarro	
	37.Drug Delivery 3	38.Composite Scaffolds		40. Neural Reg. 2	41.Cell Inst. Mat. 4		
13	Poster Session, Rapid Fire Presentations (3) Lunch (Level -1)						13
14							14
	Jean Leray Award <b>Joaquim Miguel Oliveira</b>						
15	Young Scientists Forum						15
	Plenary Lecture (L7) <b>Małgorzata Lewandowska-Szumieł</b>						
16	Coffee Break, Exhibition (Level 0, 1)						16
17	204. Yuan	208. Babensee	44. Wound Heal. 2	212. Pompe	216. Lode	220. Gao	<a href="#">Science for Industry</a> <b>Elena Boccardi</b> <b>Zein Azhari</b>
	205. Tetteh	209. Foerster		213. San Roman	217. Cox		
	206. Covarrubias	210. Bax		214. Witte	218. Pielichowska		
	207. Vargas-Becerril	211. Rumiński		215. Lombardi	219. Palmer		
	42.Bone Tissue 4	43.Cellular Resp.		45. Bone cements	46.Nanoparticles	221. Siatkowska	
						222. Oliveira	
						223. Benko	
18	18:00 - 23:00 Gala Dinner - Wieliczka Salt Mine (Departure from ICE Congress Centre)						18



# Thursday, 3<sup>rd</sup> September

	Hall 1	Hall 2	Hall 3A	Hall 3B	Hall 4A	Hall 4B	
8	8:00 Registration opens						8
9	George Winter Award Luigi Ambrosio						9
	Plenary Lecture (L8) Abhay Pandit						
Break							
10	47. Neural Reg. 3 224. Alekseeva 225. Liu 226. Buzanska 227. Mobasserri	48.Bone Tissue 5 228. Hanawa 229. Antoniac 230. Aydin 231. Gryń	49.Clinical Trials 232. Ai 233. Klimecs 234. Merolli 235. Daculsi	50.Antimicrobial 4 236. Rodrigues 237. Durrieu 238. Fernandes 239. Kyziot	51.Biomimetic Mat. 240. Chappell 241. Abdul Rahman 242. Ishikawa 243. Zyman	52. Osteointeg. 2 244. Faré 245. Guichaoua 246. Langford 247. Hendrikx	10
11	Coffee Break, Exhibition (Level 0, 1)						11
12	53Adv. Manuf. 5 K14. De Santis 248. Montufar 249. Cama 250. Ciofani 251. Claeyskens	54.Bone Tissue Eng. 6 K15. Moroni 252. O'Doherty 253. Uklejewski 254. De Mones 255. Petersen	55.Cardiovascular Appl. 3 K16. El Fray 256. Kimura 257. Mavrilas 258. Cohn 259. Cauich-Rodriguez	56.Surface Mod 5 260. Dugan 261. Moseke 262. Lorenzetti 263. Guillem-Marti 264. Hoene 265. Bociaga	57.Smart Biomater. 2 266. Martin Saavedra 267. Zheng 268. Ohya 269. Pentlavalli 270. Nagase 271. Chen	58.Drug Delivery 4 272. Texier 273. Smejkalova 274. Borzacchiello 275. Karewicz 276. Giugliano 277. Schumacher	12
13	Break						13
	Closing Ceremony and Travel&Conference Awards						



# Oral presentations

Sunday, 30<sup>th</sup> August

Sunday, 30<sup>th</sup> Aug

<b>Hall 2</b>	<b>Young Scientists Forum Workshop (1)</b> Organizers: Sandra Van Vlierberghe, Lorenzo Moroni, Giuseppe Cama, Anna Finne Wistrand, Izabela Stancu
13:00	<b>Creative Thinking – How to Come up with New Ideas</b> <u>Prof. Abhay Pandit</u> <i>National University of Ireland, Galway, Ireland</i>
13:35	<b>How to Get Money to Work out your Idea</b> <u>Prof. Fabrizio Barberis</u> <i>University of Genoa, Italy</i>
14:10	<b>You Received Funding – What’s Next – How to Survive in Research Land</b> <u>Prof. Paul Santerre</u> <i>University of Toronto, Canada</i>

<b>Hall 2</b>	<b>Young Scientists Forum Workshop (2)</b> Organizers: Sandra Van Vlierberghe, Lorenzo Moroni, Giuseppe Cama, Anna Finne Wistrand, Izabela Stancu
15:15	<b>How to Advance Research Results Towards the Development of a Medical Product</b> <u>Prof. Joachim Kohn</u> <i>The New Jersey Center for Biomaterials, United States</i>
15:50	<b>R&amp;D in Creation of Bio-Engineering Product; Researcher Responsibility</b> <u>Lechosław F. Ciupik</u> <i>LfC-Medical, Poland</i>
16:25	<b>Panel Discussion</b>



Hall 1	Plenary Lecture 1	
9:00	L1	<b>Bioactive Materials for the Treatment of Major Injuries: Opportunities and Challenges</b> <u>Joachim Kohn</u> <i>The New Jersey Center for Biomaterials, United States</i>  Chairs: Elżbieta Pamuła, AGH University of Science and Technology, Poland Jan Chłopek, AGH University of Science and Technology, Poland Matteo Santin, University of Brighton, United Kingdom

Hall 1	Plenary Lecture 2	
9:45	L2	<b>Regenerative Transplantation - from Experimental Laboratory to Clinical Applications</b> <u>Maria Siemionow</u> <i>University of Illinois at Chicago, Department of Orthopaedics, United States</i>  Chairs: Elżbieta Pamuła, AGH University of Science and Technology, Poland Jan Chłopek, AGH University of Science and Technology, Poland Matteo Santin, University of Brighton, United Kingdom

Session 1	Bone Tissue Engineering 1	
Hall 1	Chairs: Despina Deligianni, University of Patras, Greece Zhongwei Gu, Sichuan University, China Gifty Tetteh, University of Sheffield, United Kingdom (YSF Chair)	
11:00	1	<b>Osteocyte Function in Regulating Osteoclast Differentiation on Ceramic Biomaterials</b> <u>Miho Nakamura</u> , Teuvo Hentunen, Jukka Salonen, Naoko Hori, Kimihiro Yamashita <i>Tokyo Medical and Dental University, Japan</i>
11:15	2	<b>Pannexin 1 and Pannexin 3 Regulated Osteoblastic Differentiation of Human Bone Marrow Mesenchymal Stem Cells in a Three Dimensional Macroporous Scaffold</b> <u>Julien Guerrero</u> , Hugo Oliveira, Rachida Aid, Reine Bareille, Didier Letourneur, Yong Mao, Joachim Kohn, Joelle Amedee <i>INSERM U1026, France</i>
11:30	3	<b>Hydrolysis of Octacalcium Phosphate Co-Precipitated Gelatin Composite and Osteoblastic Cell Response</b> Yushi Ezoe, Takahisa Anada, Hajime Yamazaki, Tetsu Takahashi, <u>Osamu Suzuki</u> <i>Tohoku University, Japan</i>
11:45	4	<b>Novel Bioactive Hydrogel-Nanosilica Hybrid Materials as a Potential Injectable Scaffold for Bone Tissue Engineering</b> <u>Joanna Lewandowska-Łańcucka</u> , Sylwia Fiejdasz, Łucja Rodzik, Marcin Koziół, Maria Nowakowska <i>Jagiellonian University, Poland</i>





## Session 2 Hall 2

Chairs: Lucy Di Silvio, *King's College London Guy's Hospital, United Kingdom*  
Dietmar Hutmacher, *Queensland University of Technology, Australia*  
Christoph Tondera, *Helmholtz-Zentrum Dresden-Rossendorf, Germany* (YSF Chair)

11:00	5	<b>Anisotropic Bilayered Alginate Hydrogels with Channel-Like Pores for Osteochondral Regeneration</b> Kathleen Schütz, Florian Despang, Giuseppe Filardo, Alice Roffi, Annapaola Parilli, Maria Sartori, Francesca Salamanna, Elizaveta Kon, <u>Michael Gelinsky</u> <i>TU Dresden, Germany</i>
11:15	6	<b>Induction of Mesenchymal Stem Cell Differentiation and Cartilage Formation by Cross-Linker-Free Collagen Microspheres</b> <u>Emmanuel Belamie</u> , Marc Mathieu, Sylvain Vigier, Marie-Noëlle Labour, Christian Jorgensen, Danièle Noël <i>Institut Charles Gerhardt Montpellier, France</i>
11:30	7	<b>Biodegradable Glues for Meniscus Repair in a Full-Thickness Explant Model</b> <u>Agnieszka Bochynska</u> , Gerjon Hannink, Tony van Tienen, Dirk Grijpma, Pieter Buma <i>Radboud UMC / University of Twente, Netherlands</i>
11:45	8	<b>A Bioactive Bacterial Exopolysaccharide from Deep-Sea Environment: Modification, Characterization and Chondrogenic Potential for Cartilage Regenerative Medicine</b> <u>Agata Zykwińska</u> , Nathalie Chopin, Corinne Sinquin, Jacqueline Ratiskol, Jean Le Bideau, Boris Halgand, Claire Vinatier, Jérôme Guicheux, Pierre Weiss, Sylvia Collic-Jouault <i>Ifremer, France</i>

## Session 3 Hall 3A

Chairs: Nicholas Peppas, *The University of Texas, United States*  
Wojciech Chrzanowski, *The University of Sydney, Australia*  
Katarzyna Krukiewicz, *Silesian University of Technology, Poland* (YSF Chair)

11:00	9	<b>Functionalized Poly(Vinyl Alcohol) Membranes for the Thermal and Photochemical Nitric Oxide Delivery</b> Sarah Lourenço, <u>Marcelo G. de Oliveira</u> <i>University of Campinas, Brazil</i>
11:15	10	<b>Smart Polymer Nanoparticles for Triggered Drug Releases</b> Christian Tolle, Jan Riedel, Dagmar Wirth, Henning Menzel <i>Braunschweig University of Technology, Germany</i>
11:30	11	<b>Polymer Coatings with Liposomal Drug Deposits towards Substrate-Mediated Drug Delivery</b> <u>Martin E. Lyngé</u> , Marie Baekgaard Laursen, Marina Fernandez-Medina, Brigitte Städler <i>Aarhus University, Denmark</i>
11:45	12	<b>PLGA/Calcium Phosphate Composite Nanoparticles as Efficient Carriers of Hydrophilic Drugs (Nucleic Acids, Proteins)</b> <u>Jens Nelsen</u> , Gregor Dördelmann, Diana Kozlova, Sarah Karczewski, Rosario Lizio, Silko Grimm, Jessica Mueller-Albers, Shirley Knauer, Matthias Eppler <i>University Duisburg-Essen, Germany</i>



## Session 4 Hall 3B

### Surface Modification 1

Chairs: Iulian Antoniac, *University Politehnica of Bucharest, Romania*  
Veronique Larreta Garde, *University of Cergy Pontoise, France*  
Yi-Shiang Huang, *University of Liege, Belgium* (YSF Chair)

- |       |    |  |
|-------|----|--|
| 11:00 | 13 | <b>Human Bone Marrow Mesenchymal Stem Cells Responses to Titanium Surface Coated with Type I Collagen Using Natural Cross-Linker Genipin</b><br>Ying-Sui Sun, <u>Her-Hsiung Huang</u> , Kai-Chun Chang<br><i>National Yang-Ming University, Taiwan</i>   |
| 11:15 | 14 | <b>Inspired by Snake - Impulses for Surface Design of Biomaterials, a Biotribological Perspective</b><br>Martina Baum, Lars Heepe, Stanislav Gorb<br><i>University of Kiel, Germany</i>  |
| 11:30 | 15 | <b>Molecular Weigth of Hyaluronan Immobilized on the Surface of a Porous Asymetric Scaffold Strongly Affects the Behavior of Co-Cultured Mesenchymal Stem Cells and Colorectal Cancer Cells</b><br>Elias Al Tawil, Alexandre Monnier, Yusra Kassim, Quang Trong Nguyen, <u>Brigitte Deschrevel</u><br><i>University of Rouen, France</i> |
| 11:45 | 16 | <b>Topographical and Biochemical Functionalized PEDOT films as Coating Strategies for Improved Neuroelectrode Functionality</b><br><u>Catalina Vallejo-Giraldo</u> , Marc Fernandez-Yague, Abhay Pandit, Eilís Dowd, Manus Jonathan Paul Biggs<br><i>National University of Ireland, Galway, Ireland</i>                                 |

## Session 5 Hall 4A

### Cell Instructive Materials 1

Chairs: Christine Dupont-Gillain, *Université Catholique de Louvain, Belgium*  
Satoru Kidoaki, *Kyushu University, Japan*  
Beatriz Palla Rubio, *University of The Basque Country (UPV/EHU), Spain* (YSF Chair)

- |       |    |   |
|-------|----|---|
| 11:00 | 17 | <b>Structural Features of Biomaterials Influence the Paracrine Relationships that Mesenchymal Stem Cells Establish with Osteoblasts and Endothelial Cells</b><br>Lara Crespo, Francisco Martín-Saavedra, Laura Saldaña, Enrique Gomez-Barrena, <u>Nuria Vilaboa</u><br><i>Hospital Universitario La Paz-IdiPAZ, Spain</i> |
| 11:15 | 18 | <b>Strategy for Providing the Preferential Alignment of Osteoblasts and Extracellular Matrix for Bone Replacement</b><br>Takayoshi Nakano, Aira Matsugaki, Takuya Ishimoto<br><i>Osaka University, Japan</i>  |
| 11:30 | 19 | <b>Injectable and Self-Healing Supramolecular Hydrogel for Tissue Engineering Applications</b><br><u>Damien Dupin</u> , Pablo Casuso, Natividad Díaz, Adrián Pérez-San Vicente, Iraida Loinaz, Ibon Odriozola<br><i>IK4-CIDETEC, Spain</i>  |
| 11:45 | 20 | <b>Tailoring of DMTMM Conjugated Ha-Tyr Allows Precise Control of Cellular Environment</b><br><u>Claudia Loebel</u> , Tino Stauber, Matteo D'Este, Mauro Alini, Marcy Zenobi-Wong, David Eglin<br><i>AO Research Institute, Switzerland</i>   |



## Session 6 Hall 4B

### Advanced Manufacturing 1

Chairs: Sandra Van Vlierberghe, *Ghent University, Belgium*  
Dimitrios Stamatialis, *University of Twente, Netherlands*  
Artur Pinto, *LEPABE and INEB, Portugal (YSF Chair)*

- |       |    |  |
|-------|----|--|
| 11:00 | 21 | <b>Jet-Sprayed Hybrid Nanofibrillar Matrices with Controlled Deposition and Delivery of Nanoparticles</b><br>Nermin Keloglu, Bernard Verrier, Dominique Sigaudou-Roussel, Thomas Trimaille, <u>Jerome Sohier</u><br><i>UMR CNRS 5305, France</i>                               |
| 11:15 | 22 | <b>Microstereolithography &amp; Plasma Polymerisation Coating of Nerve Guidance Conduits</b><br>James Clarke, Adam Harding, Fiona Boissonade, John Haycock, Frederik Claeysens<br><i>The University of Sheffield, United Kingdom</i>   |
| 11:30 | 23 | <b>Smart Biomaterials from Extruded Biopolymer Nanofibres</b><br>Mohammad Raoufi, Neda Aslankoochi, Sarah Young, Joachim P. Spatz, <u>Dorothea Brüggemann</u><br><i>MPI for Intelligent Systems, Germany</i>   |
| 11:45 | 24 | <b>Borophosphate Glasses/Fibers and their In-Vitro Properties</b><br><u>Jonathan Massera</u> , Yaroslav Shpotyuk, Thierry Jouan, Catherine Boussard-Plédel, Bruno Bureau, Laeticia Petit, Miina Ojansivu, Susanna Mietinen<br><i>Tampere University of Technology, Finland</i> |

## Session 7 Hall 1

### Osteointegration 1

Chairs: Pamela Habibovic, *Maastricht University, Netherlands*  
Tomasz Ciach, *Warsaw University of Technology, Poland*  
Caitlin Langford, *Monash University, Australia (YSF Chair)*

- |       |    |  |
|-------|----|--|
| 12:15 | 25 | <b>In Vivo Study on the Biodegradation Behaviour of Mg-Based Alloys for Orthopaedic Application</b><br>Sau Shun Wong, <u>Wing Yuk Ip</u> , Luen Chow Chan, Chi Ping Lai<br><i>The University of Hong Kong, Hong Kong</i>   |
| 12:30 | 26 | <b>A Comparative Tribocorrosion Study Between TiN- and DLC- Coated Titanium for Loading Bearing Biomedical Applications</b><br><u>Guohua Zhao</u> , Nuria Espallargas, Ragnhild E. Aune<br><i>KTH Royal Institute of Technology, Sweden</i>  |
| 12:45 | 27 | <b>In vitro Biological Studies of Porous Titanium Obtained by Two Different Powder Metallurgy (PM) Techniques: Loose Sintering and Space Holder</b><br><u>Juan Pavón</u> , Ana Civantos, Viviana Ramos, Jose A Rodriguez, Yadir Torres, Jose Lopez-Lacomba<br><i>University of Antioquia, Colombia</i> |
| 13:00 | 28 | <b>"Bridging of Spine" – Comparison of Titanium and Dynamic Polymer Stabilization</b><br>Lechosław Ciupik, Agnieszka Kierzkowska, Jacek Sterna, Edward Słoiński, <u>Monika Cieřlik-Górna</u><br><i>Institute of Bioengineering and Medical Technologies, Poland</i>                                    |



## Session 8 Hall 2

### Neural Regeneration 1

Chairs: Yuichi Ohya, *Kansai University, Japan*

Michael Doser, *Institute for Textile Research and Process Engineering, Germany*

Chaoyu Liu, *The University of Hong Kong, Hong Kong (YSF Chair)*

- 
- |       |    |   |
|-------|----|---|
| 12:15 | 29 | <b>Interfacing 3D Graphene Oxide Scaffolds with the Injured Rat Spinal Cord</b><br>Ankor González-Mayorga, Elisa López-Dolado, Jorge E. Collazos-Castro, María Luisa Ferrer, Francisco del Monte, María Concepción Gutiérrez, <u>María Concepción Serrano</u><br><i>Hospital Nacional de Paraplégicos, Spain</i>  |
| <hr/> |    |   |
| 12:30 | 30 | <b>Dual Peptide Functionalised Intraluminal Collagen Fibre Conduits Regulates Neurite Outgrowth of Primary Neurons</b><br><u>Sahana Ganesh</u> , William Daly, Abhay Pandit<br><i>National University of Ireland, Galway, Ireland</i>   |
| <hr/> |    |   |
| 12:45 | 31 | <b>Characterization of Polyurethane/Poly lactide Blends in Terms of their Applicability as Biomaterials Supporting Nerve Regeneration</b><br><u>Jadwiga Laska</u> , Paulina Bednarz, Anna Lis, Jakub Grzesiak, Krzysztof Marycz, Dariusz Szarek<br><i>AGH University of Science and Technology, Poland</i>  |
| <hr/> |    |   |
| 13:00 | 32 | <b>Spinal Cord Injury Recovery of Rhesus Monkey Implanted with PPy/I Plasma Polymer</b><br>Ayayacatl Morales-Guadarrama, Hermelinda Salgado-Ceballos, Israel Grijalva, Juan Morales-Corona, Camilo Rios, Guillermo J. Cruz, Araceli Diaz-Ruiz, Maria-Guadalupe Olayo, Laura Alvarez-Mejia, Rodrigo Mondragón-Lozano, Alejandra Ibáñez-Contreras, Braulio Hernández-Godínez, Omar Fabela-Sánchez, Stephanie Sánchez-Torres, <u>Roberto Olayo</u><br><i>Instituto Nacional de Investigaciones Nucleares, Mexico</i> |
- 

## Session 9 Hall 3A

### Drug Delivery 2

Chairs: Anna Karewicz, *Jagiellonian University, Poland*

David Grainger, *University of Utah, United States*

María Rosa Aguilar, *Spanish National Research Council, Spain (YSF Chair)*

- 
- |       |    |   |
|-------|----|---|
| 12:15 | 33 | <b>Cell Membrane Capsules for Encapsulation of Chemotherapeutic and Cancer Cell Targeting <i>in Vivo</i></b><br><u>Zhengwei Mao</u> , Yuanhong Zhang, Lihua Peng, Jianqing Gao<br><i>Zhejiang Univeristy, China</i>   |
| <hr/> |    |   |
| 12:30 | 34 | <b>Electrospun Triclosan-Loaded Chitosan Nanofibres for Potential Drug Delivery Application</b><br><u>Safa Ouerghemmi</u> , Stéphanie Degoutin, Nicolas Tabary, Frédéric Cazaux, Ludovic Janus, Nicolas Blanchemain, Bernard Martel<br><i>UMET, France</i>  |
| <hr/> |    |   |
| 12:45 | 35 | <b>Dual Release and Antibacterial Effects of Chlorhexidine and Silver Released from Electrospun Chitosan/Poly(Ethylene Oxide) Nanofibres</b><br><u>Jiankang Song</u> , Stefan S. Remmers, Carla J.M. Bartels, Jinlong Shao, Eva Kolwijck, Sander C.G. Leeuwenburgh, John A. Jansen, Fang Yang<br><i>Radboud University Medical Centre, Netherlands</i>    |
| <hr/> |    |   |
| 13:00 | 36 | <b>Collagen/Hyaluronic Acid-Based Hydrogels for Brain Applications: the Role of Hyaluronic Acid Molecular Weight</b><br>Marta Tunesi, Armando Chierchia, Luca Barbieri, <u>Teresa Russo</u> , Lucia Boeri, Annalisa Grimaldi, Roberto De Santis, Luigi Ambrosio, Antonio Gloria, Diego Albani, Carmen Giordano<br><i>National Research Council, Italy</i> |
- 



## Session 10 Hall 3B

### Surface Modification 2

Chairs: Triantafillos Papadopoulos, *University of Athens, Greece*  
Stanisław Błażewicz, *AGH University of Science and Technology, Poland*  
Elena Diana Giol, *Ghent University, Belgium* (YSF Chair)

- |       |    |  |
|-------|----|--|
| 12:15 | 37 | <b>Endothelialisation of Titanium Dioxide Coated Gas Exchange Membranes for the Development of a Bioartificial Lung</b><br><u>Michael Pflaum</u> , Marina Kauffeldt, Bettina Wiegmann, Sabrina Schmeckebeier, Daniele Dipresa, Sotirios Korossis, Jochen Schein, Axel Haverich<br><i>Hannover Medical School, Germany</i>      |
| 12:30 | 38 | <b>Orthopaedic Bio-activation of PEEK using Plasma Immersion Ion Implantation</b><br><u>Edgar Wakelin</u> , Giselle Yeo, Alexey Kondyurin, Michael Davies, David McKenzie, Anthony Weiss, Marcela Bilek<br><i>University of Sydney, Australia</i>  |
| 12:45 | 39 | <b>Alginate Hydrogels, Coated with Calcium Phosphate Nanoparticles by an Electrophoretic Deposition Method</b><br><u>Sabrina Daumann</u> , Katrin Wallat, Michael Gepp, Ronan Le Harzic, Heiko Zimmermann, Frank Stracke, Matthias Eppler<br><i>University of Duisburg-Essen, Germany</i>                                      |
| 13:00 | 40 | <b>Calcium- and Phosphorus-Rich Oxide Coatings on Tantalum Obtained by Plasma Electrolytic Oxidation</b><br><u>Maciej Sowa</u> , Maja Woszczak, Grzegorz Dercz, Andrey I. Kukharensky, Danila M. Korotin, Ernst Z. Kurmaev, Seif O. Cholak, Wojciech Simka, Marcin Basiaga<br><i>Silesian University of Technology, Poland</i> |

## Session 11 Hall 4A

### Cell Instructive Materials 2

Chairs: Sander Leeuwenburgh, *Radboudumc Biomaterials, Netherlands*  
Rachel Williams, *University of Liverpool, United Kingdom*  
Anna Diez-Escudero, *Technical University of Catalonia (UPC), Spain* (YSF Chair)

- |       |    |   |
|-------|----|---|
| 12:15 | 41 | <b>Human E-Cadherin Fusion Protein Matrix Improving the Proliferation and Hepatic Differentiation of Human Mesenchymal Stem Cells</b><br><u>Jun Yang</u> , Jinbin Xu, Yan Zhang, Toshihiro Akaike<br><i>Nankai University, China</i>  |
| 12:30 | 42 | <b>Silk-Collagen Inspired Artificial Proteins for 3D Cell Culture Study</b><br><u>Małgorzata Włodarczyk-Biegun</u> , Kambiz Farbod, Marc Werten, Frits de Wolf, Jeroen van den Beucken, Sander Leeuwenburgh, Marleen Kamperman, Martien Cohen Stuart<br><i>Wageningen UR, Netherlands</i> |
| 12:45 | 43 | <b>Fluorescent Hydrogel for Improved Traceability of Biomedical Devices In Vivo</b><br><u>Arturo Ibáñez-Fonseca</u> , Francisco Javier Arias, José Carlos Rodríguez-Cabello<br><i>Bioforge Group, Universidad de Valladolid, Spain</i>  |
| 13:00 | 44 | <b>Self-Gelling Elastin and Silk-Elastin Recombinamers for Ophthalmic Applications</b><br>Alicia Fernández-Colino, Daniela Quinteros, José Bermúdez, Santiago De Palma, José Carlos Rodríguez-Cabello, <u>Francisco Javier Arias</u><br><i>University of Valladolid, Spain</i>            |





**Session 12**  
**Hall 4B**

**Cell Encapsulation and Delivery 1**

Chairs: Pedro Granja, *University of Porto, Portugal*  
Elżbieta Pamuła, *AGH University of Science and Technology, Poland*  
Juhi Samal, *National University of Ireland, Galway, Ireland (YSF Chair)*

- |       |    |  |
|-------|----|--|
| 12:15 | 45 | <b>A Functional Macromolecular Gradient Hydrogel System as a Platform to Model Tissue-to-Tissue Interfaces</b><br>Diana Pereira, Joaquim Oliveira, Rui Reis, Abhay Pandit<br><i>3B's Research Group, Portugal</i>  |
| 12:30 | 46 | <b>Cell-Laden Microparticles for Microtissue Assembling: a Bottom-Up Approach for Bone Tissue Engineering</b><br>Irene Cano-Torres, Riccardo Levato, Miguel A. Mateos-Timoneda, Elisabeth Engel<br><i>Institute for Bioengineering of Catalonia, Spain</i>                             |
| 12:45 | 47 | <b>Enhanced <math>\beta</math>-cell Pancreatic Islet Formation Using Carboxybetaine-Functionalised Chitosan Nanobeads</b><br>Mark Best, Valeria Perugini, Gary Phillips, Anna Guildford, Adrian Bone, Wendy MacFarlane, Matteo Santin<br><i>University of Brighton, United Kingdom</i> |
| 13:00 | 48 | <b>Assessing the Potential of Fucoidan-Based Microparticles for Biomedical Application</b><br>Lara L. Reys, Simone S. Silva, Nuno Oliveira, Diana Soares da Costa, João F. Mano, Tiago H. Silva, Rui L. Reis<br><i>3B's Research Group, Portugal</i>                                   |

**Hall 1**  
**Plenary Lecture 3**

- |       |    |   |
|-------|----|---|
| 14:45 | L3 | <b>In Vitro Models &amp; Nanobiointerfaces: a Multidisciplinary Challenge</b><br>C. James Kirkpatrick<br><i>Institute of Pathology, University Medical Center, Johannes Gutenberg University of Mainz, Germany</i><br><br>Chairs: Michael Doser, <i>Institute for Textile Research and Process Engineering, Germany</i><br>Pedro Granja, <i>University of Porto, Portugal</i> |
|-------|----|---|

**Hall 1**  
**Special Fellows Session**  
**"Biomaterials Education is not Ready for the Challenges of the Future"**

Chair: Joachim Kohn, *The New Jersey Center for Biomaterials, United States*

- |       |  |
|-------|--|
| 16:00 | <b>Speakers:</b><br>Kristi S. Anseth, <i>University of Colorado, United States</i><br>David W. Grainger, <i>University of Utah, United States</i><br>Dietmar Hutmacher, <i>Queensland University of Technology, Brisbane, Australia</i><br>Lynne C. Jones, <i>Johns Hopkins University, United States</i><br>Laura Poole-Warren, <i>University of New South Wales, Sydney, Australia</i><br>Elizabeth Tanner, <i>University of Glasgow, Scotland, United Kingdom</i> |
|-------|--|



## Session 13      Bioactive Materials

### Hall 2

Chairs: Guy Daculsi, *INSERM LIOAD UMR 791, France*  
 Hasan Uludag, *University of Alberta, Canada*  
 Andrada Serafim, *University Politehnica of Bucharest, Romania (YSF Chair)*

16:00	49	<b>Influence of Calcium Salt Addition on Bioactive Glass Nanospheres</b> Kai Zheng, Qiang Chen, Nicola Taccardi, V. R. Reddy Marthala, Martin Hartmann, <u>Aldo Boccaccini</u> <i>University of Erlangen-Nuremberg, Germany</i>
16:15	50	<b>Bioactive Ti Metal Able to Release Ga Ions: Preparation by Chemical and Heat Treatments</b> <u>Seiji Yamaguchi</u> , Shekhar Nath, Yoko Sugawara, Tomiharu Matsushita, Tadashi Kokubo <i>Chubu University, Japan</i>
16:30	51	<b>High Strength <math>\beta</math>-TCP-Fe-Ag Nanocomposites and Porous Scaffolds for Bone Repair</b> <u>Elazar Gutmanas</u> , Sanyaja Kumar Swain, Irena Gotman <i>Technion, Israel</i>
16:45	52	<b>Tailoring the Bioactivity of Mesoporous Bioglasses: the Role of the Structure Directing Agents</b> Natividad Gómez-Cerezo, Isabel Izquierdo-Barba, <u>Daniel Arcos</u> , María Vallet-Regí <i>Universidad Complutense de Madrid, Spain</i>
17:00	53	<b>Novel Bioactive Glass Composites for Soft Tissue Applications</b> <u>Owen Clarkin</u> , Dermot F. Brougham, Bing Wu, Catriona Lally <i>Dublin City University, Ireland</i>
17:15	54	<b>Thermal and In Vitro Properties of SrO and ZnO Containing Bioactive Glasses</b> Johan Sangder, Susanne Fagerlund, <u>Leena Hupa</u> <i>Åbo Akademi University, Finland</i>
17:30	55	<b>Bioresorbable Chitosan- Bioglass Nanocomposite Scaffolds for Drug Delivery Applications</b> <u>Emad El-Meliigy</u> , Sara Ali <i>National Research Centre, Egypt</i>



# Session 14 Hall 3A

Chairs: Maria Siemionow, *University of Illinois at Chicago, United States*  
Joaquim Miguel Oliveira, *3B's Research Group - University of Minho, Portugal*  
Minkle Jain, *Japan Advanced Institute of Science and Technology, Japan (YSF Chair)*

- |       |    |   |
|-------|----|---|
| 16:00 | 56 | <b>Generation of Limbal Epithelial Cell Progenitors by Two Methods: by Differentiation form iPS Cells and by Direct Trans-differentiation form Human Dermal Fibroblasts</b><br>Artur Cieřlar-Pobude, Viktoria Knořlach, Saeid Ghavami, <u>Marek Łos</u><br><i>Linköping University, Sweden</i>  |
| 16:15 | 57 | <b>A Multifactorial Approach Towards Enhanced Extracellular Matrix Deposition and Maintenance of Mesenchymal Stem Cell Phenotype Using Macromolecular Crowding and Low Oxygen Tension</b><br>Diana Gaspar, Daniela Cigognini, Pramod Kumar, Abhigyan Satyam, Senthil Alagesan, Clara Sanz-Noguéz, Matthew Griffin, Timothy O'Brien, Abhay Pandit, Dimitrios Zeugolis<br><i>National University of Ireland, Galway, Ireland</i>                      |
| 16:30 | 58 | <b>Cryptic Cell Cycle Stasis of Human Pluripotent Stem Cells Revealed by Culture in a Biocompatible Thermoresponsive Copolymer Gel</b><br>Irene Canton, Nicholas J. Warren, Richard Weightman, Andrew Wood, Harry Moore, Steve P. Armes<br><i>University of Sheffield, United Kingdom</i>   |
| 16:45 | 59 | <b>Co-Transplantation of VEGF-Transfected Adipose Derived Stromal Cells to Enhance Bone Regeneration and Neovascularization from Bone Marrow Stromal Cells</b><br>Mi Lan Kang, Ji Eun Kim, <u>Gun-Il Im</u><br><i>Dongguk University Ilsan Hospital, Republic of Korea</i>  |
| 17:00 | 60 | <b>Effect of Mechanical Stimulation on Osteogenesis of Self-Assembled Collagen-Cell Seeded Microspheres</b><br><u>Maryam Shariatzadeh</u> , Cecile Perrault, Damien Lacroix<br><i>University of Sheffield, United Kingdom</i>   |
| 17:15 | 61 | <b>5-Azacytidine Mediated hMSC Behaviour On Electrospun Scaffolds to Induce Myogenesis</b><br>Ines Fasolino, <u>Vincenzo Guarino</u> , Valentina Cirillo, Marica Marrese, Luigi Ambrosio<br><i>Institute of Polymers, Composites and Biomaterials, CNR, Italy</i>   |
| 17:30 | 62 | <b>Microvesicles Derived from Stem Cells as a Novel Effective Tool for Transferring of Bioactive Molecules to Mature Primary Cells - Future Implications for Tissue Regeneration</b><br>Sylwia Bobis-Wozowicz, Katarzyna Kmiotek, Małgorzata Sekula, Sylwia Kedracka-Krok, Elżbieta Kamycka, Urszula Jankowska, Jacek Kolcz, Dariusz Boruczkowski, Buddhadeb Dawn, Zbigniew Madeja, <u>Ewa Zuba-Surma</u><br><i>Jagiellonian University, Poland</i> |



## Session 15 Hall 3B

## Antimicrobial Surfaces and Materials 1

Chairs: Dieter Scharnweber, *Technische Universität Dresden, Germany*  
Mirosława El Fray, *West Pomeranian University of Technology, Poland*  
Hanna Tiainen, *University of Oslo, Norway* (YSF Chair)

16:00	K1	<b>Keynote</b> <b>Antimicrobial Effects of Biomaterials: Silver Ions</b> <u>Matthias Epple</u> , Svitlana Chernousova, Kateryna Loza, Oleg Prymak, Maria A. Surmeneva, Roman Surmenev <i>University of Duisburg-Essen, Germany</i>
16:30	63	<b>Influences of the pH on the Adsorption Properties of an Antimicrobial Peptide on Titanium Surfaces</b> Yendry Corrales-Ureña, Linda Wittig, Matheus Vieira Nascimento, Juliano Faccioni, <u>Paulo Lisboa-Filho</u> , Klaus Rischka <i>São Paulo State University (UNESP), Brazil</i>
16:45	64	<b>Titanium Modified with Silver Nanoparticles for Oral Implantology</b> <u>Rafał Pokrowiecki</u> , Barbara Szaraniec, Tomasz Zaręba, Tomasz Szponder, Krzysztof Pałka, Jan Chłopek, Stefan Tyski <i>Jagiellonian Medical University, Poland</i>
17:00	65	<b>Bio-Inspired Antimicrobial Surfaces for Titanium Implant</b> Ting Dju, Terje Sjöström, Leanne Fisher, Angela Nobbs, Howrad Jenkinson, Max Ryadnov, Monica Tsimbouri, Matt Dalby, <u>Bo Su</u> <i>University of Bristol, United Kingdom</i>
17:15	66	<b>Antimicrobial Titanium Surfaces</b> <u>Zuzanna Trzcińska</u> , Fabien Brouillet, David Grossin, Cedric Charvilat, Anna Peacock, Artemis Stamboulis <i>University of Birmingham, United Kingdom</i>
17:30	67	<b>Novel Biosensor for Detecting and Preventing Periodontal Disease</b> M. Hoyos-Nogués, S. Brosel-Oliu, N. Abramova, A. Bratov, <u>C. Mas-Moruno</u> , F.J. Gil <i>Technical University of Catalonia, Spain</i>

Monday, 31<sup>st</sup> Aug



# Session 16 Hall 4A

Chairs: Neil Cameron, *Monash University, Australia*  
 Henning Menzel, *University of Technology Braunschweig, Germany*  
 Bernhard Neuhaus, *Universität Duisburg-Essen, Germany (YSF Chair)*

16:00	K2	<b>Keynote</b> <b>Biointspired Design of Dynamic Macromolecular for Gene Delivery</b> <u>Zhongwei Gu</u> <i>Sichuan University, China</i>
16:30	68	<b>Biostable Gold-Installed Nanocomplexes as siRNA Carriers for Improved In Vivo Tumor Targeting</b> <u>Roun Heo</u> , Jueun Jeon, Jae Hyung Park <i>Sungkyunkwan University, Korea</i>
16:45	69	<b>ELR Devices for Breast Cancer Gene Delivery</b> <u>Maria Jesus Piña</u> , Alessandra Girotti, Mercedes Santos, Jose Carlos Rodríguez-Cabello, Francisco Javier Arias <i>Universidad Valladolid, Spain</i>
17:00	70	<b>Ion-Doped Hydroxyapatite Nanoparticles as Potential Vectors in Gene Therapy</b> <u>Zhitong Zhao</u> , Montserrat Espanol, Maria-Pau Ginebra <i>Universitat Politècnica de Catalunya, Spain</i>
17:15	71	<b>Tuning Transfection Efficiency by Modulating the Biodegradation Rate of Trimethyl Chitosan Nanoparticles</b> <u>Carla Gomes</u> , Aida Varela-Moreira, Maria Gomez-Lazaro, Pedro Moreno, Ana Pêgo <i>INEB - Instituto Engenharia Biomédica, Portugal</i>
17:30	72	<b>Cell-Penetrating Peptide Mediated Gene Delivery via Polymeric Microneedles; A Platform for DNA Vaccination</b> <u>Helen McCarthy</u> , Ahlam Ali, Joanne McCaffrey, John McBride, Adrien Kissenpfennig, Ryan Donnelly <i>Queen's University Belfast, United Kingdom</i>





## Session 17 Hall 4B

### Biointerfaces 1

Chairs: Dimitrios Zeugolis, *National University of Ireland, Galway, Ireland*  
Krzysztof Szczubiałka, *Jagiellonian University, Poland*  
Rongquan Duan, *University of Twente, Netherlands (YSF Chair)*

16:00	K3	<b>Keynote</b> <b>Manipulation of Cell Mechanotaxis by Designing Curvature of the Elasticity Boundary on Hydrogel Matrix</b> <u>Satoru Kidoaki</u> , Ayaka Ueki <i>Kyushu University, Japan</i>
16:30	73	<b>Nanotemplated and Fibronectin Based-Polyelectrolytes Films as Bioactive Delivery Systems</b> Adeline Gand, Coline Chat, Mathilde Hindie, Paul Van Tassel, <u>Emmanuel Pauthe</u> <i>University of Cergy-Pontoise, France</i>
16:45	74	<b>Mapping Interactions between MMP1 and Collagen Substrate: from Crystal Structure to Molecular Dynamics with Meta-Dynamics</b> Anthony Nash, Laurent Bozec, Helen Birch, Nora de Leeuw <i>University College London, United Kingdom</i>
17:00	75	<b>Protein-Adsorption and Blood-Interaction Studies on Nanotopography Gradients</b> <u>Rebecca Huber</u> , Katharina Maniura, Nicholas Spencer <i>ETH Zürich/ EMPA St.Gallen, Switzerland</i>
17:15	76	<b>Heterogeneous Polymer Surfaces with Organized Collagen Layers Influence Preosteoblasts Behavior</b> Emilienne Zuyderhoff, <u>Christine Dupont-Gillain</u> <i>Université Catholique de Louvain, Belgium</i>
17:30	77	<b>Nanoroughness and Oxygen Functional Groups on Parylene C Coating: Towards Anti-Infective and Biocompatible Implants Surface</b> <u>Monika Gołda-Cepa</u> , Monika Brzychczy-Włoch, Minna Hakkarainen, Klas Engvall, Andrzej Kotarba <i>Jagiellonian University, Poland</i>



Hall 1      Plenary Lecture 4

9:00      L4      **Medical Translational Research: A Different Route to Fundamental Research**  
Geoff Richards  
AO Research Institute Davos, Switzerland

**Chairs:** Joelle Amedee, INSERM, U1026, France  
Marc Bohner, RMS Foundation, Switzerland

Hall 1      Translational Research Symposium (1)

Organizers: Yves Bayon, Marc Bohner, David Eglin, Geoff Richards, Dimitrios Zeugolis

- 10:00      TRS1      **Clinical Needs Based Biomaterial Strategy: Reducing the Risk that Innovation is “Lost in Translation” in Products for Poor Quality Bone**  
Philip Procter  
Medical Device Industry Consultant, France
- 10:20      TRS2      **Best Practice for Registration Trials of Biodegradable Implants**  
Nils Reimers  
Manager R&D, Global Funding & Reimbursement, Stryker Trauma & Extremities, Germany
- 10:40      TRS3      **New Concept of Hybrid Polymer Composites for Implant Applications**  
Xiang Zhang  
Lucideon Ltd., Royal Society Industry Fellow at University of Cambridge, United Kingdom
- TRS4      **Novel Biodegradable and Biocompatible Polymers for Medical Applications**  
Ipsita Roy  
University of Westminster, London, United Kingdom

Session 18      Smart Biomaterials 1  
Hall 2

**Chairs:** Che Connon, Newcastle University, United Kingdom  
Pedro Granja, INEB - University of Porto, Portugal  
Giuseppe Cama, University of Ghent, Belgium (YSF Chair)

- 10:00      78      **Overcoming Transport Limitation in 3D Cell Culture by Using a New Class of Oxygen Delivery Systems**  
Antonio Paciello, Giuseppe Amalfitano, Alessandro Garziano, Francesco Urciuolo, Paolo Antonio Netti  
Istituto Italiano di Tecnologia, Italy
- 10:15      79      **Tunable Biodegradable Polyurethane with Thermal Activation Cues at Human Body Temperature**  
Maziar Matloubigharagozloo, V. Prasad Shastri  
Hermann Staudinger Institute of Macromolecular Chemistry, Germany
- 10:30      80      **Mixed Matrix Membranes for Removal of Protein-Bound Toxins from Human Plasma**  
Esmee van Geffen, Denys Pavlenko, Karin Gerritsen, Dimitrios Stamatiadis  
University of Twente, Netherlands
- 10:45      81      **Glucose Delivery System Based-Hydrogel Composite Scaffold for Enhancing MSC Survival**  
Julie Boisselier, Joseph Paquet, Laurent Bidault, Michael Deschepper, Elodie Lefebvre, Charline Gossart, Julie Dubois, Adeline Gand, Delphine Logeart-Avramaglou, Veronique Larreta Garde, Emmanuel Pauthe, Hervé Petite  
University of Cergy-Pontoise, France



## Session 19 Hall 3A

### Wound Healing 1

Chairs: Julio San Roman, *Institute of Polymer Science and Technology, CSIC, Spain*  
Miriam V. Flores-Merino, *Autonomous University of The State of Mexico, Mexico*  
Peter Duckworth, *University of Bristol, United Kingdom (YSF Chair)*

- |       |    |   |
|-------|----|---|
| 10:00 | 82 | <b>In Situ Skin Regeneration by the Gene-Activated Materials</b><br><u>Lie Ma</u> , Luyan Li, Xing Liu, Rui Guo, Changyou Gao<br><i>Zhejiang University, China</i>  |
| 10:15 | 83 | <b>Modulation of Inflammatory Macrophage Activation by StarPEG–Heparin Based Hydrogels to Improve Impaired Wound Healing</b><br>Nadine Lohmann, Wandel Elke, Inka Forstreuter, Lucas Schirmer, Uwe Freudenberg, Carsten Werner, Jan Simon, <u>Sandra Franz</u><br><i>University Leipzig, Germany</i>                      |
| 10:30 | 84 | <b>Nano-Microfibrous Scaffold for Burn-Wound Healing</b><br><u>Pallabi Pal</u> , Pavan Srivas, Prabhash Dadhich, Bodhisatwa Das, Santanu Dhara, Arun Achar<br><i>Indian Institute of Technology, India</i>  |
| 10:45 | 85 | <b>Expression Pattern of Tissue Transglutaminase in the Response to Gelatin based Hydrogels <i>In Vitro</i> and <i>In Vivo</i></b><br><u>Sandra Ullm</u> , Christoph Tondera, Robert Wodtke, Tim Gebauer, Axel Neffe, Andreas Lendlein, Reik Löser, Jens Pietzsch<br><i>Helmholtz-Zentrum Dresden-Rossendorf, Germany</i> |

## Session 20 Hall 3B

### Surface Modification 3

Chairs: Håvard Haugen, *University of Oslo, Norway*  
Véronique Migonney, *Université Paris 13, France*  
Catalina Vallejo Giraldo, *National University of Ireland, Galway, Ireland (YSF Chair)*

- |       |    |  |
|-------|----|--|
| 10:00 | 86 | <b>Functionalization of Scaffold Surfaces: Role of Ce Valence States of Cerium Oxide Nanoparticles in Control of Cell Proliferation</b><br><u>Tamaki Naganuma</u><br><i>National Institute for Materials Science (NIMS), Japan</i>                             |
| 10:15 | 87 | <b>Antibacterial Jet Bioactive Surfaces</b><br><u>Irina Sukhorukova</u> , Alexander Sheveyko, Philipp Kiryukhantsev-Korneev, Natalya Gloushankova, Sergey Ignatov, Dmitry Shtansky<br><i>National University of Science and Technology, Russian Federation</i> |
| 10:30 | 88 | <b>Differential Response of Human Bone Marrow Cells on Aligned vs Randomly Oriented Carbon Nanotubes</b><br>Anthoula Kroustalli, <u>Despina Deligianni</u><br><i>University of Patras, Greece</i>  |
| 10:45 | 89 | <b>Bioinspired Thin Films Materials for Direct Blood Contact</b><br><u>Klaudia Trembecka-Wojciga</u> , Roman Major, Juergen M. Lackner, Hanna Plutecka, Boguslaw Major<br><i>Institute of Metallurgy and Materials Science PAS, Poland</i>                     |



## Session 21 Hall 4A

### Cartilage Tissue Engineering 2

Chairs: Michael Gelinsky, *Technische Universität Dresden, Germany*

Yasuhiko Tabata, *Kyoto University, Japan*

Judith Hahner, *Leibniz-Institute für Polymerforschung Dresden, Germany (YSF Chair)*

- 
- |       |    |  |
|-------|----|--|
| 10:00 | 90 | <b>Mechanical &amp; Degradation Characterisation of AZ31 Magnesium (Mg) for Use in Paediatric Tracheal Stents</b><br><u>Isaiah Adekanmbi</u> , K. Elizabeth Tanner, Haytham Kubba, Helen Lu<br><i>Glasgow University, United Kingdom</i>         |
| <hr/> |    |  |
| 10:15 | 91 | <b>Superior Lubrication Ability of Artificial Hydrogel Cartilage</b><br><u>Teruo Murakami</u> , Seido Yarimitsu, Kazuhiro Nakashima, Tetsuo Yamaguchi, Yoshinori Sawae, Nobuo Sakai, Atsushi Suzuki<br><i>Kyushu University, Japan</i>           |
| <hr/> |    |  |
| 10:30 | 92 | <b>Sr- and Zn-Substituted Calcium Phosphates-Based Composites for Osteochondral Tissue Engineering Scaffolding</b><br><u>Sandra Pina</u> , Joaquim M. Oliveira, Rui L. Reis<br><i>University of Minho, Portugal</i>                              |
| <hr/> |    |  |
| 10:45 | 93 | <b>Si-HPMC and Si-Chitosan Hydrogel for Cartilage Tissue Engineering</b><br><u>Gildas Réthoré</u> , Cécile Boyer, Amadou Touré, Fabienne Jordana, Olivier Gauthier, Jérôme Guicheux, Pierre Weiss<br><i>LIOAD - Université de Nantes, France</i> |
- 

## Session 22 Hall 4B

### Cell Encapsulation and Delivery 2

Chairs: Mariacristina Tanzi, *Politecnico di Milano, Italy*

Roman Major, *Institute of Metallurgy and Materials Science PAS, Poland*

Solène Passemard, *Ecole Polytechnique Fédérale de Lausanne, Switzerland (YSF Chair)*

- 
- |       |    |  |
|-------|----|--|
| 10:00 | 94 | <b>Response of Human Macrophages to Cytokine Induction under Three-Dimensional (3D) Artificial Extracellular Matrix (ECM) Mimicking Conditions</b><br><u>Marta Evangelista</u> , Alexandru Gudima, Vladimir Riabov, Martin Pravda, Julia Kzhyskowska, Nihal Engin Vrana<br><i>PROTIP MEDICAL, France</i> |
| <hr/> |    |  |
| 10:15 | 95 | <b>2D Cell Monolayer and 3D Cell Construct Cryopreservation by Slow Vitrification</b><br><u>Kazuaki Matsumura</u> , Keiko Kawamoto, Suong-Hyu Hyon<br><i>Japan Advanced Institute of Science and Technology, Japan</i>   |
| <hr/> |    |  |
| 10:30 | 96 | <b>Interaction of Sub-Compartmentalized Microreactors with Hepatocytes</b><br><u>Yan Zhang</u> , Brigitte Städler<br><i>Aarhus University, Denmark</i>   |
| <hr/> |    |  |
| 10:45 | 97 | <b>Macrophage-Laden 3D Fibrin Gels: Effect of Fibrinogen Concentration on Inflammation</b><br><u>Katharina Maniura</u> , Arie Bruinink, <u>Vera Malheiro</u><br><i>EMPA, Switzerland</i>   |
- 



## Hall 1 Translational Research Symposium (2)

Organizers: Yves Bayon, Marc Bohner, David Eglin, Geoff Richards, Dimitrios Zeugolis

11:30	TR55	<b>Insights into Collaboration and Innovation for Early Stage Medical Device Development</b> <u>Jan Weber</u> <i>Sr Research Fellow, Corporate Research, Boston Scientific Corporation, United States</i>
12:00	TR56	<b>From Biomaterials Supplier to Device Development Partner – Supporting Medical Device Companies in de-Risking Medical Products</b> <u>Jend Thies</u> <i>Director Science and Innovation, DSM Biomedical, Netherlands</i>
12:30	TR57	<b>Next Generation of Fibers for Medical Devices: Biopolymers and Functionalized Coatings</b> <u>Herbert De Breuck</u> <i>Manager R&amp;D, Luxilon, Wijnegem, Belgium</i>

## Session 23 Hall 2 Bone Tissue Engineering 2

Chairs: Pamela Habibovic, Maastricht University, Netherlands

William Wagner, University of Pittsburgh McGowan, United States

Christy Thomas, University of Westminster, United Kingdom (YSF Chair)

11:30	K4	<b>Keynote</b> <b>Dual Release of a Macrophages Recruitment Agent and Growth Factor for Bone Regeneration</b> Yang-hee Kim, <u>Yasuhiro Tabata</u> <i>Institute for Frontier Medical Sciences, Kyoto University, Japan</i>
12:00	98	<b>Fabrication and Characterization of Clinoptilolite/PCL-PEG-PCL Composite Scaffolds for Bone Tissue Engineering</b> <u>Ahmet Engin Pazarçeviren</u> , Ayşen Tezcaner, Özge Erdemli <i>Middle East Technical University, Turkey</i>
12:15	99	<b>Osteoinductive Dental Ring for Vertical Bone Regeneration with Simultaneous Introduction of Dental Implants</b> <u>Anna Chróścicka</u> , Piotr Wychowński, Ewa Jankowska-Steifer, Marek Kujawa, Małgorzata Lewandowska-Szumieł <i>Medical University of Warsaw, Poland</i>
12:30	100	<b>Novel N-(2-Carboxybenzyl)Chitosan Bionanocomposites for Tissue Scaffolding Applications</b> Maria Nerantzaki, Zoi Terzopoulou, Maria Anastasopoulou, Michalis Karakassides, Iro Koliakou, Aldo Boccaccini, Dimitrios Bikiaris <i>Aristotle University of Thessaloniki, Greece</i>
12:45	101	<b>BMP-2 stimulation Affects Structure and Mechanical Properties of Newly Synthesized ECM In Vitro</b> <u>Erik Brauer</u> , Aaron Herrera, Petra Knaus, Georg Duda, Ansgar Petersen <i>Julius Wolff Institute, Germany</i>





## Session 24 Hall 3A

## Stem Cells 2

Chairs: Josep A. Planell, *Universitat Oberta de Catalunya, Spain*

Ewa Zuba-Surma, *Jagiellonian University, Poland*

Maryam Shariatzadeh, *University of Sheffield, United Kingdom (YSF Chair)*

- |       |     |   |
|-------|-----|---|
| 11:30 | 102 | <b>Aging Reduces Osteogenic and Increases Adipogenic Potential of Mesenchymal Stem Cells Grown on Titanium</b><br>Rodrigo Abuna, Camila Stringhetta-Garcia, Rita Dornelles, Adalberto Rosa, <u>Marcio Beloti</u><br><i>University of Sao Paulo, Brazil</i>  |
| 11:45 | 103 | <b>Controlled Release of Amorphous Calcium Phosphate from Titania Nanostructures Induces Osteoblastic Differentiation in Human Mesenchymal Stem Cells</b><br><u>Robert McLister</u> , Mura McCafferty, George Burke, Brian J. Meenan<br><i>Ulster University, United Kingdom</i>  |
| 12:00 | 104 | <b>Chondrogenesis of Umbilical Cord Mesenchymal Stem Cells in a Porous Asymmetric Scaffold of Poly(Lactic Acid) Functionalized with Hyaluronan: Deposition of a Hyaline Cartilaginous Matrix</b><br>Elias Al Tawil, Alexandre Monnier, Quang Trong Nguyen, Jean-Pierre Vannier, Brigitte Deschrevel<br><i>University of Rouen, France</i> |
| 12:15 | 105 | <b>Characterization of In Vitro-Spheroids from Human Mesenchymal Stem Cells under Osteogenic and Adipogenic Differentiation</b><br>Geneviève Schmid, Heike Paape, Ellen Schmuhl, Stefanie Adam, Nicole Herzmann, Juliane Meyer, Achim Salamon, Susanne Meyer, <u>Kirsten Peters</u><br><i>Rostock University Medical Center, Germany</i>  |
| 12:30 | 106 | <b>Investigation of the Effect of Different Velocities and Surface Treatments on hMSCs Seeding Efficiency and Mechanical Characterization of 3D Insert PCL Scaffolds Undergoing Compression Loading</b><br><u>Marzia Brunelli</u> , Cecile M. Perrault, Damien Lacroix<br><i>University of Sheffield, United Kingdom</i>                  |
| 12:45 | 107 | <b>Osteogenic Effects of Short, Steady Media Perfusion in hBMSC 3D Cultures Depend on Cell Culture and Cell Differentiation Stage and a Scaffold Type</b><br><u>Joanna Filipowska</u> , Justyna Pawlik, Katarzyna Cholewa-Kowalska, Maria Laczka, Anna M. Osyczka<br><i>Jagiellonian University, Poland</i>                               |



## Session 25 Hall 3B

### Surface Modification 4

Chairs: Christine Dupont-Gillain, *Université Catholique de Louvain, Belgium*  
Dorota Bociąga, *Lodz University of Technology, Poland*,  
Luis Rojo, *King's College London, United Kingdom* (YSF Chair)

11:30	K5	<b>Keynote</b> <b>Contributions of Adhesive Proteins to the Cell Response to Bioactive Polymers and Surfaces</b> Helena Felgueiras, Meg Evans, <u>Véronique Migonney</u> <i>Université Paris 13, France</i>
12:00	108	<b>Prebiotic Chemistry Inspired Coatings for Biomedical Applications</b> Helmut Thissen, Mario Salwiczek, Christopher D. Easton, Aylin Koegler, Richard A. Evans <i>CSIRO Manufacturing Flagship, Australia</i>
12:15	109	<b>Grafting of Bioactive Molecules on PET to Recruit Endothelial Progenitors Cells and Enhance Adhesion of Endothelial Cells</b> <u>Caroline Royer</u> , Laurent Plawinski, Gaétan Laroche, Marie-Christine Durrieu <i>Hôpital Saint-François d'Assise, France</i>
12:30	110	<b>Functionalization of Biomedical Surfaces by Peptide Aptamers</b> Gabriela Melo Rodriguez, James Bowen, Artemis Stamboulis <i>University of Birmingham, United Kingdom</i>
12:45	111	<b>Nanoporous Anodic Titanium Dioxide Layers as Scaffolds for Cell Growth</b> <u>Magdalena Jarosz</u> , Anna Pawlik, Justyna Syguda-Cholewińska, Tomasz Sawoszczuk, Danuta Jarocho, Marcin Majka, Grzegorz D. Sulka, Marian Jaskuła <i>Jagiellonian University, Poland</i>



## Session 26 Hall 4A

### Cell Instructive Materials 3

Chairs: John Jansen, *Radboud University, Netherlands*

Timothy Douglas, *Ghent University, Belgium*

Jennifer Ashworth, *University of Cambridge, United Kingdom (YSF Chair)*

11:30	K6	<b>Keynote</b> <b>Glycosaminoglycan Derivatives – Promising Candidates for the Design of Functional Biomaterials</b> <u>Dieter Scharnweber</u> , Linda Hübner, Sandra Rother, Ute Hempel, Ulf Anderegg, Sergey A. Samsonov, M. Teresa Pisabarro, Lorenz Hofbauer, Matthias Schnabelrauch, Sandra Franz, Jan C. Simon, Vera Hintze <i>TU Dresden, Germany</i>
12:00	112	<b>Glycosaminoglycan Mimicking Surfaces Trigger Distinct Response of Stem Cells via Fibronectin Adsorption</b> <u>Ana Rodrigues Araujo</u> , D. Soares da Costa, S. Amorim, RL Reis, RA Pires, I. Pashkuleva <i>3B's Research Group, Portugal</i>
12:15	113	<b>Collagen-GAGs Based Interpenetrating Polymer Networks (IPNs) as Tissue Engineered Heart Valve (TEHV)</b> <u>Rabia Nazir</u> , Arne Bruyneel, Carolyn Carr, Jan Czernuszka <i>Oxford University, United Kingdom</i>
12:30	114	<b>Biofunctional Microassemblies Based on Renewable Resources - Microfluidic Generation and Release Applications</b> <u>Mélanie Marquis</u> , Agata Zykawska, Corinne Sinquin, Jacqueline Ratiskol, Stéphane Cuenot, Bernard Cathala, Denis Renard, Sylvia Collic-Jouault <i>INRA, France</i>
12:45	115	<b>Glycosaminoglycans as Biomaterials, Drugs and Pathogens</b> Kamil Kamiński, Bartłomiej Kałaska, Anna Mikulska, Joanna Filipowska, Anna Osyczka, Shin-Ichi Yusa, Małgorzata Kajta, Andrzej Mogielnicki, Maria Nowakowska, <u>Krzysztof Szczubiatka</u> <i>Jagiellonian University, Poland</i>

## Hall 4B

### Surface Charge for Biomaterial Characterization

Sponsored by: Anton Paar

11:30	SCh1	<b>Zeta Potential for Biomaterial Surface Characterization</b> <u>Christine Körner</u> , Thomas Luxbacher <i>Anton Paar GmbH, Graz, Austria</i>
12:15	SCh2	<b>TiO<sub>2</sub>-Coated Ti-Alloys for Body Implants &amp; Surface Charge: Expectations on the Bio-Response</b> <u>Martina Lorenzetti</u> , Mukta Kulkarni, Aleš Iglič, Thomas Luxbacher, Spomenka Kobe, Saša Novak <i>Jožef Stefan Institute, Ljubljana, Slovenia</i>



## Hall 1 Plenary Lecture 5

- 15:30 L5 Vascularization in Tissue Engineering: Alternative Foreign Body Responses**  
Michael V. Sefton  
*Institute of Biomaterials and Biomedical Engineering, University of Toronto, Canada*
- Chairs:** Abhay Pandit, *National University of Ireland, Galway, Ireland*  
 Małgorzata Lewandowska-Szumieł, *Medical University of Warsaw, Poland*

## Hall 1 Translational Research Symposium (3)

Organizers: Yves Bayon, Marc Bohner, David Eglin, Geoff Richards, Dimitrios Zeugolis

- 16:45 116 FTIR Microscopy Contribution for Comprehension of Poly-L-Lactic Acid (PLA) Degradation Mechanisms**  
 Yves Bayon, Antoine Alves, Carol Grossiord, Céline Brunon  
*NAMSA, Chasse/Rhône, France*
- 17:00 117 Possible Approach to Improve Systemic Gene Delivery to Tumour Using Polyplex Nanoparticles**  
Mikhail Durymanov, Alexei Yartukin, Andrey Rosenkranz, Alexander Sobolev  
*Institute of Gene Biology of the RAS, Russia*
- 17:15 118 Endothelialization of Polyurethanes: Immobilization of REDV Peptide**  
Beata Butruk-Raszeja, Magdalena Dresler, Aleksandra Kuźmińska, Tomasz Ciach  
*Warsaw University of Technology, Poland*
- 17:30 119 Helicobacter pylori-Binding Small Chitosan Microparticles that Penetrate Gastric Mucosa**  
 Patrícia C. Henriques, Paula Sampaio, Maria Lázaro, André Maia, António Gouveia, José Manuel Lopes, Ana Magalhães, Celso A. Reis, M. Cristina L. Martins, Paulo Costa, Inês C. Gonçalves  
*Universidade do Porto, Portugal*
- 17:45 120 Leaving Cells Out in the Cold: Hydrogel Encapsulation for the Improved Hypothermic Preservation of Stem Cells**  
 Stephen Swiokło, Che Connon  
*Newcastle University, United Kingdom*
- 18:00 121 Antibacterial Coatings on Titanium Surfaces: a Comparison Study Between In Vitro Single-Species and Multispecies Biofilm**  
 Maria Godoy-Gallardo, Zhejun Wang, Ya Shen, José M. Manero, F. Javier Gil, Carlos Mas-Morun, Daniel Rodríguez, Markus Haapasalo  
*Technical University of Catalonia, Spain*
- 18:15 122 The Proangiogenic Potential of a Novel Poly(lactic) Based Composite Membrane for Guided Bone Regeneration**  
 Hugo Oliveira, Nadège Sachot, Sylvain Catros, Sylvie Rey, Joan Martí, Oscar Castano, Joëlle Amedee, Elisabeth Engel  
*Institute for Bioengineering of Catalonia (IBEC), Spain*



## Session 27 Hall 2

### Bone Tissue Engineering 3

Chairs: Joelle Amedee, *INSERM, U1026, France*

Małgorzata Lewandowska-Szumieł, *Medical University of Warsaw, Poland*

Claudia Loebel, *AO Research Institute Davos, Switzerland (YSF Chair)*

- |       |     |  |
|-------|-----|--|
| 16:45 | K7  | <b>Keynote</b><br><b>Hydrogels and Scaffolds of Natural Origin as Support for Stem Cells in the Regeneration of Different Tissues</b><br><u>Rui Reis</u><br><i>3B's Research Group - University of Minho, Portugal</i>   |
| 17:15 | 123 | <b>Organic and Inorganic Bioactive Signals to Prepare Biomimetic Chitosan Based Scaffolds for Bone Tissue Regeneration</b><br><u>Maria Grazia Raucci</u> , Daniela Giugliano, Antonella Giuri, Vincenzo De Benedictis, Christian Demitri, Alessandro Sannino, Luigi Ambrosio<br><i>National Research Council of Italy, Italy</i> |
| 17:30 | 124 | <b>Polyvinyl Alcohol/Alginate Dual Network Hydrogels for Tissue Engineering</b><br><u>Shathani Nkhwa</u> , Sanjukta Deb<br><i>King's College London Dental Institute, United Kingdom</i>   |
| 17:45 | 125 | <b>Analysis of Integrin-Binding Dependent Cell Attachment on Collagen-Based Scaffolds</b><br>Carlos Schuster, Richard Farndale, Samir Hamaia, Serena Best, Ruth Cameron,<br><u>Natalia Davidenko</u><br><i>Cambridge University, United Kingdom</i>  |
| 18:00 | 126 | <b>A Novel Biological Polyester Based Wet Spun Scaffold for Bone Tissue Engineering</b><br><u>Ayse Selcen Alagoz</u> , Jose Carlos Rodriguez-Cabello, Nesrin Hasirci, Vasif Hasirci<br><i>BIOMATEN METU Center of Excellence in Biomaterials and Tissue Engineering, Turkey</i>  |
| 18:15 | 127 | <b>Resorption of Calcium Phosphate Bone Substitutes: an In Vitro Study</b><br><u>Marta Gallo</u> , Solène Tadier, Sylvain Meille, Marc Bohner, Aldo Boccaccini, Rainer Detsch, Jérôme Chevalier<br><i>INSA, France</i>   |





## Session 28 Hall 3A

## Angio- and Vasculogenesis

Chairs: Abhay Pandit, *National University of Ireland, Galway, Ireland*

Michael Sefton, *University of Toronto, Canada*

Sonia Zia, *Hannover Medical School, Germany (YSF Chair)*

16:45	128	<b>Induction of Endothelial Cell Sprouting by Poly (<math>\epsilon</math>-Lysine) Dendron Tethered with an Angiopoietin-1-mimicking Peptide</b> <i>Maria Elena Verdenelli, Steven Meikle, Gary Phillips, Matteo Santin</i> <i>University of Brighton, United Kingdom</i>
17:00	129	<b>Sustained Release of Adipose-Derived Stem Cells by Thermosensitive Chitosan-Gelatin Hydrogel for Therapeutic Angiogenesis</b> <i>Nai-Chen Cheng, Tai-Horng Young</i> <i>National Taiwan University Hospital, Taiwan</i>
17:15	130	<b>Cobalt Doped Proangiogenic Hydroxyapatite for Bone Tissue Engineering Application</b> <i>Senthilguru Kulanthaivel, Krishna Pramanik, Indranil Banerjee</i> <i>National Institute of Technology, India</i>
17:30	131	<b>Development of a Synthetic Pseudovascular Network to Investigate Neovascularisation for Tissue Engineering Applications</b> <i>Lindsey Dew, Ilida Ortega, Adam Kelly, Frederik Claeysens, Sheila MacNeil</i> <i>University of Sheffield, United Kingdom</i>
17:45	132	<b>Angiogenic Response on Chitosan-Graft-Poly (<math>\epsilon</math>-Caprolactone) Copolymer in vitro, enhanced by Wharton's Jelly-derived Mesenchymal Stromal Cells</b> <i>Evi Mygdali, Maria Kaliva, Maria Vamvakaki, Charalampos Pontikoglou, Maria Chatzinikolaidou</i> <i>University of Crete, Greece</i>
18:00	133	<b>Vasculogenesis and Accelerated Healing through the Emergent Design of an Hierarchically Structured Scaffold</b> <i>Julian F Dye, Giuseppe Scionti, Elizabeth A Wahl, Tomas Egana, Maroun Khoury</i> <i>Dept LHCS, The Open University, United Kingdom</i>
18:15	134	<b>Repair of "Burr Holes" Using Chitosan-Siloxane Porous Hybrids</b> <i>Yuki Shirotsaki, Motomasa Furuse, Takuji Asano, Yoshihiko Kinoshita, Toshiki Miyazaki, Satoshi Hayakawa, Akiyoshi Osaka, Toshihiko Kuroiwa</i> <i>Kyushu Institute of Technology, Japan</i>



## Session 29 Hall 3B

## Antimicrobial Surfaces and Materials 2

Chairs: Matthias Epple, *University of Duisburg-Essen, Germany*  
Barbara Szaraniec, *AGH University of Science and Technology, Poland*  
Riccardo Levato, *Institute for Bioengineering of Catalonia (IBEC), Spain* (YSF Chair)

- |       |     |   |
|-------|-----|---|
| 16:45 | 135 | <b>A Nanocomposite Wound Dressing with Potential to Sustain Active Chlorhexidine on a Wound Bed</b><br><u>Peter Duckworth</u> , Sarah Maddocks, Gareth Robinson, Sameer Rahatekar, Michele Barbour<br><i>University of Bristol, United Kingdom</i>  |
| 17:00 | 136 | <b>Enrichment of Enzymatically Mineralized Gellan Gum Hydrogels with Polyphenol-Rich Ecklonia Cava Extract Seanol® to Endow Antibacterial Properties</b><br><u>Timothy Douglas</u> , Gilles Brackman, Katarzyna Reczynska, Agnieszka Dokupil, Krzysztof Pietryga, Peter Dubrue, Tom Coenye, Elzbieta Pamula<br><i>Ghent University, Belgium</i> |
| 17:15 | 137 | <b>Development of an Antibacterial Hybrid Sponge (Chitosan/Hydroxyapatite) for Bone Regeneration</b><br><u>Claudia Flores</u> , Jean Christophe Hornez, Feng Chai, Gwenael Raoul, Nicolas Tabary, Frédéric Cazaux, Joel Ferri, Hartmunt F. Hildebrand, Bernard Martel, Nicolas Blanchemain<br><i>University of Lille, France</i>                |
| 17:30 | 138 | <b>Antimicrobial Properties of a Novel Hydrogel Bandage Lens Material</b><br><u>Andrew Gallagher</u> , Mal Horsburgh, Jamal Alorabi, Don Wellings, Rachel Williams<br><i>University of Liverpool, United Kingdom</i>  |
| 17:45 | 139 | <b>Ephemeral Biogels to Control Anti-Biofilm Agent Delivery</b><br><u>Véronique Larreta Garde</u> , Elodie Lefebvre, Damien Seyer<br><i>University of Cergy Pontoise, France</i>  |
| 18:00 | 140 | <b>Broad-Spectrum Antimicrobial Polycarbonate Hydrogels for Wound Dressing Applications</b><br><u>Haritz Sardon</u> , Ana Pascual, Jeremy Tan, James Hedrick, Yi YanYang<br><i>University of the Basque Country, Spain</i>  |
| 18:15 | 141 | <b>Injectable Gellan Gum-Based Nanoparticle-Loaded System for the Local Delivery of Vancomycin in Osteomyelitis Treatment</b><br><u>Urszula Posadowska</u> , Monika Brzychczy-Włoch, Elzbieta Pamula<br><i>AGH University of Science and Technology, Poland</i>   |



## Session 30 Hall 4A

## Bioimaging and Biosensing

Chairs: Didier Letourneur, *Inserm U1148 Cardiovascular Bioengineering, France*

Tomasz Ciach, *Warsaw University of Technology, Poland*

Magdalena Ziabka, *AGH University of Science and Technology, Poland (YSF Chair)*

16:45	K8	<b>Keynote</b> <b>Bionano Characterization - Beyond Imaging with Scanning Probe Microscopy</b> <u>Wojciech Chrzanowski</u> <i>The University of Sydney, Australia</i>
17:15	142	<b>Long-Term and Bioinert Labeling of Mesenchymal Stem Cells with Polymeric-Gd Conjugates and MRI Monitoring of the Cell Behaviour in Ischemic Rats</b> <u>Tetsuji Yamaoka</u> , Yoichi Tachibana <i>National Cerebral and Cardiovascular Center Research Institute, Japan</i>
17:30	143	<b>Nile Blue-Based Nano-Sized pH Sensors for Simultaneous Far-Red and Near-Infrared Live</b> <u>Jeppe Madsen</u> , Irene Canton, Nicholas J. Warren, Efrosyni Themistou, Adam Blanz, Burcin Ustbas, Xiaohu Tian, Russell Pearson, Giuseppe Battaglia, Andrew L. Lewis, Steven P. Armes <i>University of Sheffield, United Kingdom</i>
17:45	144	<b>Phenotypic and Functional Sensing of Cell Microvesicles Using an Immobilized Chemosensor</b> Catherine Belle, Sylvain Nlate, Marie-Christine Durrieu, Eduardo Angles-Cano, <u>Laurent Plawinski</u> UMR 5248, CNRS, Bordeaux University, <i>France</i>
18:00	145	<b>Mass Transport Study with Fluorescent Dextran Molecules in Gellan Gum Hydrogel</b> Ana M. Soto, <u>Janne Koivisto</u> , Jenny E. Parraga, Jari Hyttinen, Minna Kellomäki, Edite Figueiras <i>University of Tampere, Finland</i>
18:15	146	<b>The Effect of Biomolecular Interaction and Chondrocyte Adhesion to Surface Grafted Hyaluronan Layers</b> <u>Erik Nilebäck</u> , Noomi Altgärde, Angelika Kunze, Lars Enochson, Laura de Battice, Iva Pashkuleva, Jana Becher, Stephanie Möller, Matthias Schnabelrauch, Rui L. Reis, Anders Lindahl, Sofia Svedhem <i>Biolin Scientific, Sweden</i>



## Session 31 Hall 4B

## Biointerfaces 2

Chairs: Yannis Missirlis, *University of Patras, Greece*  
Alina Sionkowska, *Nicolaus Copernicus University, Poland*  
Judit Buxadera Palomero, *Technical University of Catalonia, Spain* (YSF Chair)

- |       |     |  |
|-------|-----|--|
| 16:45 | 147 | <b>Surface Topography: Is It Clinically Relevant?</b><br>Andrew English, Ayesha Azeem, Manus Biggs, Abhay Pandit, <u>Dimitrios Zeugolis</u><br><i>National University of Ireland, Galway, Ireland</i>  |
| 17:00 | 148 | <b>Cell-Material Interaction Enhanced by Hybrid Covalent Coated Nanofibers</b><br>Joan Marti, Nadege Sachot, <u>Oscar Castano</u> , Miguel Mateos-Timoneda, Aldrik Velders, Malgorzata Lewandoska, Josep A. Planell, Elisabeth Engel<br><i>Institute for Bioengineering of Catalonia (IBEC), Spain</i>         |
| 17:15 | 149 | <b>Fibronectin Based Thin Films: Description of a Novel Growth Mechanism and Influence on Cell Behavior</b><br><u>Adeline Gand</u> , Coline Chat, Alysée Barraux, Guy Ladam, Paul R Van Tassel, Emmanuel Pauthe<br><i>University of Cergy-Pontoise, France</i>   |
| 17:30 | 150 | <b>Primary Macrophage Phenotype Control by IL-4 Releasing, Self-Crosslinking PLL/HA-Aldehyde Derivative Multilayer Coatings</b><br><u>Helena Knopf-Marques</u> , Sonali Singh, Lucie Wolfowa, Vladimir Velebny, Pierre Schaaf, Amir Ghaemmaghami, Nihal Engin Vrana, Philippe Lavalle<br><i>INSERM, France</i> |
| 17:45 | 151 | <b>Biointerfaces through Continuous Electrojet-Writing</b><br><u>Zhaoying Li</u> , Yan Yan Shery Huang, Xia Li<br><i>University of Cambridge, United Kingdom</i>   |
| 18:00 | 152 | <b>Bioactive Helical Nanomaterials and their Influence on Stem Cell Differentiation</b><br><u>Gregor Kemper</u> , Laurent Plawinski, Emilie Pouget, Shawn Wettig, Reiko Oda, Marie-Christine Durrieu<br><i>CBMN UMR 5248, CNRS, Bordeaux University, France</i>  |
| 18:15 | 153 | <b>Case Study of a Retrieved Trans-Femoral Bone Anchored Amputation Prosthesis</b><br><u>Anders Palmquist</u> , Sara Windahl, Birgitta Norlindh, Rickard Brånemark, Peter Thomsen<br><i>University of Gothenburg, Sweden</i>   |



Hall 1		Plenary Lecture 6
8:30	L6	<b>Targeted Chemo- and Molecular-Therapy by Self-Assembled Supramolecular Nanosystems</b> <u>Kazunori Kataoka</u> <i>Department of Materials Engineering, University of Tokyo, Japan</i>  <b>Chairs:</b> Maria Siemionow, <i>University of Illinois at Chicago, United States</i> Michael Sefton, <i>University of Toronto, Canada</i>

Session 32 Hall 1		Cancer Therapy
		<b>Chairs:</b> Kazunori Kataoka, <i>University of Tokyo, Japan</i> Hasan Uludag, <i>University of Alberta, Canada</i> Joana Silva-Correia, <i>3B's Research Group, University of Minho, Portugal (YSF Chair)</i>
9:30	154	<b>Multitargeting Theranostic Nanoparticles for the Treatment of HER2-Positive Breast Cancer</b> Raquel Palao-Suay, <u>Maria Rosa Aguilar</u> , Francisco Parra-Ruiz, Susan N. Thomas, Nathan Rohner, Samarendra Maji, Richard Hoogenboom, Julio San Roman <i>ICTP-CSIC, Spain</i>
9:45	155	<b>ROS-Generating Titanium Oxide-Based Nanoparticles for Non-Invasive Cancer Surgery</b> <u>Dong Gil You</u> , V.G. Deepagan, Wooram Um, Sangmin Jeon, Ich Chan Kwon, Kwangmeyung Kim, Jae Hyung Park <i>Sungkyunkwan University, Korea</i>
10:00	156	<b>Investigation of Dendrimer-Based Nanoparticles Cellular Uptake and Cell Tracking in a Semi-Automated Microfluidic Platform</b> <u>Mariana Carvalho</u> , Fátima Maia, Rui Reis, Miguel Oliveira <i>3B's Research Group, Portugal</i>
10:15	157	<b>Effects of SPION Loaded Hyaluronan Polymeric Micelles on Gene Expression in Normal and Cancer Cells</b> <u>Kristina Nešporová</u> , Vojtěch Pavlík, Daniela Šmejkalová, Vladimír Velebný <i>Contipro Biotech, Czech Republic</i>
10:30	158	<b>Molecular Weight of Surface Immobilized Hyaluronic Acid Influences CD44-Mediated Adhesion of Gastric Cancer Cells</b> <u>Sara Amorim</u> , Diana Soares da Costa, Daniela Freitas, Ana Magalhães, Celso Reis, Rui Reis, Iva Pashkuleva, Ricardo Pires <i>3B's Research Group - University of Minho, Portugal</i>
10:45	159	<b>Novel Halogenated Phthalocyanines as Photosensitizers for Photodynamic Therapy for Cancer</b> <u>Łukasz Łapok</u> , Arkadiusz Gut, Małgorzata Cyza, Mariusz Kępczyński, Dorota Jamróż, Grzegorz Szewczyk, Tadeusz Sarna, Alexandr Gorski, Jędrzej Solarski, Tadeusz Waluk, Maria Nowakowska <i>Jagiellonian University, Poland</i>



## Session 33 Hall 2

## Soft Tissue Engineering

Chairs: Julia Babensee, *Georgia Institute of Technology, United States*  
Lorenzo Moroni, *Maastricht University, Netherlands*  
Andrew Gallagher, *University of Liverpool, United Kingdom (YSF Chair)*

- |       |     |  |
|-------|-----|--|
| 9:30  | 160 | <b>The Role of Electrical Stimulation in Tendon Maintenance and Repair: Electrospun PVDF-TrFE/Boron Nitride Nanotubes as Bioactive Scaffold for Promoting Tendon Regeneration</b><br><u>Marc Fernandez</u> , Gemma Orpella, Ghazal Tadayyon, Matteo Palma, Abhay Pandit, Dimitrios Zeugolis, Manus Biggs<br><i>National University of Ireland, Galway, Ireland</i> |
| 9:45  | 161 | <b>Patterned Thermoresponsive pNIPAM-pHEMA Hydrogels for Corneal Repair</b><br><u>Cemile Bektas</u> , Vasif Hasirci<br><i>Middle East Technical University, Turkey</i>   |
| 10:00 | 162 | <b>Macromolecular Crowding in Corneal Fibroblasts Culture Accelerates the Production of Extracellular Matrix-rich Supramolecular Assemblies</b><br>Pramod Kumar, Abhigyan Satyam, <u>Kyriakos Spanoudes</u> , Abhay Pandit, Dimitrios Zeugolis<br><i>National University of Ireland, Galway, Ireland</i>   |
| 10:15 | 163 | <b>Elaboration and Evaluation of Alginate Foam Scaffolds for Soft Tissue Engineering</b><br><u>Raya Bushkalova</u> , Caroline Ceccaldi, Christophe Tenailleau, Benjamin Duployer, Philippe Bourin, Daniel Cussac, Angelo Parini, Brigitte Sallerin, Sophie Girod-Fullana<br><i>INSERM UMR 1048, France</i>   |
| 10:30 | 164 | <b>Polyhydroxyalkanoates, a Family of Natural Polymers and Their Application in Cardiac Tissue Engineering</b><br><u>Ipsita Roy</u> , Andrea Bagdadi, Prachi Dubey, Ranjana Rai, Jonathan Knowles, Aldo R. Boccaccini, Mohan Edirisinghe, Sian Harding<br><i>University of Westminster, United Kingdom</i>   |
| 10:45 | 165 | <b>Fabrication of a Biosynthetic Hydrogel Scaffold for Skin Repair</b><br>Mario Flores-Reyes, Jaime Flores-Estrada, Ma. Victoria Dominguez-García, <u>Miriam V. Flores-Merino</u><br><i>Research Center in Medical Sciences, Uaem, Mexico</i>  |

## Session 34 Hall 3A

## Cardiovascular Applications 1

Chairs: Ana Paula Pego, *INEB - Instituto de Engenharia Biomédica, Portugal*  
Mirosława El Fray, *West Pomeranian University of Technology, Poland*  
Lindsey Dew, *University of Sheffield, United Kingdom (YSF Chair)*

- |       |     |   |
|-------|-----|---|
| 9:30  | K9  | <b>Keynote</b><br><b>Endothelial Cells on Biofunctionalized Polymeric Materials for Vascular Tissue Engineering</b><br><u>Lucie Bacakova</u> , Jaroslav Chlupac, Elena Filova, Jana Musilkova, Katarina Novotna, Tomas Riedel, Vladimir Proks, Ilya Kotelnikov, Ognen Pop-Georgievski, Eduard Brynda, Frantisek Rypacek, Laurence Bordenave<br><i>Academy of Sciences of the Czech Republic, Czech Republic</i> |
| 10:00 | 166 | <b>Evaluation of a Pro-Healing Polydopamine-Coated Stent on In-Stent Restenosis Using a Rat Model</b><br><u>Adrien Hertault</u> , Blandine Maurel, Feng Chai, Mickael Maton, Joël Lyskawa, Jonathan Sobocinski, Stephan Haulon, Nicolas Blanchemain<br><i>INSERM U1008, Research Group on Biomaterials, France</i>  |
| 10:15 | 167 | <b>Anti-Thrombogenic Effects Of Bioactive CoCr Surfaces for Cardiovascular Applications</b><br>Maria Isabel Castellanos, Jordi Guillem-Martí, Carlos Mas-Moruno, Maribel Díaz-Ricart, Ginés Escolar, Francisco Javier Gil, José María Manero, <u>Marta Pegueroles</u><br><i>Technical University of Catalonia (UPC), Spain</i>  |
| 10:30 | 168 | <b>Improving the Biocompatibility of Intravascular Devices</b><br><u>Guillaume Le Saux</u> , Laurent Plawinski, Sylvain Nlate, Marie-Christine Durrieu<br><i>CBMN, France</i>   |
| 10:45 | 169 | <b>Nanomaterials for Cardiovascular Applications: Quo Vadimus?</b><br><u>Iwona Cicha</u> , Christoph D. Garlich, Christoph Alexiou<br><i>University Hospital Erlangen, Germany</i>  |





**Session 35**  
**Hall 3B**

**Antimicrobial Surfaces and Materials 3**

Chairs: Nicolas Blanchemain, *Université de Lille, France*

Fabrizio Barberis, *Università di Genova, Italy*

Zuzanna Trzcńska, *University of Birmingham, United Kingdom* (YSF Chair)

9:30	170	<b>High Throughput Methods for the Discovery of Materials that Resist Bacterial Adhesion</b> <u>Andrew Hook</u> <i>University of Nottingham, United Kingdom</i>
9:45	171	<b>Physicochemical Properties and Cell-Biological Action of Alloyed Silver-Gold Nanoparticles</b> <u>Oleg Prymak</u> , Simon Ristig, Svitlana Chernousova, Wolfgang Meyer-Zaika, Matthias Epple <i>University of Duisburg-Essen, Germany</i>
10:00	172	<b>Enzymatic Disassembly of Biofilm Extracellular Matrix by Smart Nanoparticles to Eradicate Bacterial Infections</b> <u>Riccardo Levato</u> , Aida Baelo, Esther Julian, Joan Gavalda, Elisabeth Engel, Eduard Torrents, Miguel Angel Mateos-Timoneda, Anna Crespo <i>Institute for Bioengineering of Catalonia, Spain</i>
10:15	173	<b>Anti-Helicobacter Pylori Activity of Nanoparticles Loaded with a Polyunsaturated Fatty Acid</b> <u>Catarina L. Seabra</u> , Cláudia Nunes, Marta Correia, José C. Machado, Celso A. Reis, Inês C. Gonçalves, Salette Reis, M. Cristina L. Martins <i>Universidade do Porto, Portugal</i>
10:30	174	<b>Antifouling Coatings as a Platform for Antimicrobial Peptide Immobilization</b> <u>Judit Buxadera-Palomero</u> , Patricia Carrasco, Cristina Canal, Carles Mas-Moruno, F. Xavier Gil, Daniel Rodríguez <i>Technical University of Catalonia, Spain</i>
10:45	175	<b>Modified PVC Urinary Catheters to Prevent Bacterial Adhesion</b> <u>Luisa Islas</u> , Guillermina Burillo, Carmen Alvarez-Lorenzo, Angel Concheiro <i>Universidad Nacional Autonoma de Mexico, Mexico</i>



## Session 36 Hall 4A

## Advanced Manufacturing 2

Chairs: Roberto De Santis, *National Research Council of Italy, Italy*  
Karol Gryń, *AGH University of Science and Technology, Poland*  
Robin Rajan, *Japan Advanced Institute of Science and Technology, Japan (YSF Chair)*

9:30	K10	<b>Keynote</b> <b>3D Printing of Crosslinkable Gelatins: Overcoming the Mechanical Boundaries</b> Jasper Van Hoorick, Heidi Declercq, Maria Cornelissen, Hugo Thienpont, Aleksandr Ovsianikov, Peter Dubrue, <u>Sandra Van Vlierberghe</u> <i>Ghent University, Belgium</i>
10:00	176	<b>3D Bioprinting of Functional Fibrin-Based Skin Equivalents</b> Nieves Cubo, Marta García, Diego Velasco, Juan Cañizo, Jose Luis Jorcano <i>Universidad Carlos III, Spain</i>
10:15	177	<b>A New Laser-Based Approach for Native Silk Structuring</b> Anastasia Brif, Chris Holland, Frederik Claeysens <i>University of Sheffield, United Kingdom</i>
10:30	178	<b>Development of Porous PLLA Micro-Cylinders for Tissue Engineering Applications</b> Antonio Castro, John Jansen, Jeroen van den Beucken, Fang Yang <i>RadboudUMC, Netherlands</i>
10:45	179	<b>Cell Proliferation Controlled by Selective Laser Melting (SLM) Process Parameters</b> Bartłomiej Wysocki, Joanna Idaszek, Wojciech Świążkowski, Krzysztof Kurzydłowski <i>Warsaw University of Technology, Poland</i>

## Hall 4B

## Science for Industry (1)

## Bioresorbable Materials for Medical Applications

Organizers: Xiang Zhang, Ipsita Roy, Kadem Al-Lamee, Stuart MacLachlan, Maria Joao Barros, Nial Bullett, Mark Taylor

9:30	<b>Welcome and Introduction</b> Xiang Zhang, Ipsita Roy
9:50	<b>Commercial Needs for Bioresorbable Materials, Transfer from Laboratory and Barriers and Gaps in the Technology</b> Kadem Al-Lamee <i>Arterius Limited, United Kingdom</i>
10:15	<b>Production and Evaluation Platforms for Preclinical Assessment of Novel Biomaterials for Non-Healing Bone Lesions</b> Oskar Hoffmann <i>University of Vienna, Austria</i>
10:40	<b>Bioresorbable Systems: Polymers and Metals</b> Ipsita Roy <i>University of Westminster, United Kingdom</i>



## Session 37 Hall 1

### Drug Delivery 3

Chairs: Wojciech Chrzanowski, *The University of Sydney, Australia*  
Izabela-Cristina Stancu, *University Politehnica Bucharest, Romania*  
Martin Lynge, *Aarhus University, Denmark (YSF Chair)*

11:30	K11	<b>Keynote</b> <b>Polypeptide Nanoparticles for Ocular Drug Delivery</b> <u>Neil Cameron</u> <i>Monash University, Australia</i>
12:00	180	<b>Micro and Nano Hydrogel Carrier Systems for Controlled Drug Delivery of Therapeutic Proteins</b> Henning Menzel, Andreas Bertz, Nils Poth, Wibke Dempwolf, Jan-Erik Ehlers, Karl-Heinz Gericke, Peter P. Müller, Gerhard Gross, Stefanie Wöhl-Bruhn, Heike Bunjes <i>University of Technology, Germany</i>
12:15	181	<b>Peptide Binding Dendrimer Decorated Injectable Hyaluronan Hydrogels Modulate the Controlled Release of BMP-2 and TGF-<math>\beta</math>1</b> Ryan Seelbach, Peter Fransen, Miriam Royo, Fernando Albericio, Mauro Alini, Alvaro Mata, <u>David Eglin</u> <i>AO Research Institute Davos, Switzerland</i>
12:30	182	<b>Co-Deliver of Glucagon-Like Peptide-1 and Dipeptidyl Peptidase 4 Inhibitor for Treatment of Type 2 Diabetes</b> <u>Francisca Araújo</u> , Neha Shrestha, Mohammad-Ali Shahbazi, Dongfei Liu, Bárbara Herranz-Blanco, Ermei Mäkilä, Jarno Salonen, Jouni Hirvonen, Pedro L. Granja, Bruno Sarmento, Hélder A. Santos <i>INEB, Portugal</i>
12:45	183	<b>Controlled Release of Platinum-Bisphosphonate Complexes from Injectable Calcium Phosphate Cements for Treatment of Bone Tumors</b> Kemal Sariibrahimoglu, <u>Kambiz Farbod</u> , Astghik Hayrapetyan, Jan N. W. Hakvoort, Michele Iafisco, Nicola Margiotta, Joop G. C. Wolke, Jeroen J. J. P. van den Beucken, John A. Jansen, Sander C. G. Leeuwenburgh <i>Radboud University Medical Center, Netherlands</i>



## Session 38 Hall 2

## Composite Scaffolds

Chairs: Luigi Ambrosio, *National Research Council, Italy*

Ki Dong Park, *Ajou University, Korea*

Sungho Lee, *Nagoya Institute of Technology, Japan* (YSF Chair)

11:30	184	<b>Structurally-Graded Collagen Biomaterials for Osteotendinous Repair</b> Laura Mozdzen, William Grier, Ashley Moy, Steven Caliari, <u>Brendan Harley</u> <i>University of Illinois, United States</i>
11:45	185	<b>Biomaterialized Cellulose-PEGDA Scaffolds for Bone Tissue Regeneration</b> <u>Christian Demitri</u> , Maria Grazia Raucci, Antonella Giuri, Vincenzo Maria De Benedictis, Daniela Giugliano, Alessandro Sannino, Luigi Ambrosio <i>University of Salento, Italy</i>
12:00	186	<b>Preparation and Characterization of Silicone Elastomer Composites for Biomedical Prosthetic Applications</b> <u>Petroula Tarantili</u> <i>National Technical University of Athens, Greece</i>
12:15	187	<b>High-Resolution Synchrotron X-Ray Analysis of Bioglass-Enriched Hydrogels</b> <u>Svetlana Gorodzha</u> , Timothy Douglas, Sangram Samal, Katarzyna Cholewa-Kowalska, Kevin Braeckmans, Andre Skirtach, Venera Weinhardt, Tilo Baumbach, Maria Surmeneva, Roman Surmenev <i>National Research Tomsk Polytechnic University, Russian Federation</i>
12:30	188	<b>Computational and Experimental Study of the Degradation Behaviour of CaCO<sub>3</sub>-PLGA Composites</b> <u>Ismael Moreno Gomez</u> , Xiang Zhang, Serena Best, Ruth Cameron <i>University of Cambridge, United Kingdom</i>
12:45	189	<b>Development of Nanostructured Composites Based on ε-Polylysine and Apatite</b> <u>Kristine Salma-Ancane</u> , Liga Stipniece, Inga Narkevica <i>Rudolfs Cimdins Riga Biomaterials Innovation and Development Centre, Latvia</i>



## Session 39 Hall 3A

## Cardiovascular Applications 2

Chairs: Elisabeth Engel, *Institut for Bioengineering of Catalonia, Spain*

Paul Santerre, *University of Toronto, Canada*

Agnieszka Piegat, *West Pomeranian University of Technology, Poland (YSF Chair)*

11:30	190	<b>Chitosan Based Hydrogels for Vascular Applications: In Vitro and In Vivo Hemocompatibility Evaluation</b> <u>Audrey Ausseil</u> , Xavier Berard, Sandro Cornet, Vincenzo Brizzi, Marlène Durand, Alexandra Montembault, Laurent David, Rachida Aid, Didier Letourneur, Laurence Bordenave <i>INSERM U1026, France</i>
11:45	191	<b>Enriched Decellularized Matrices for Tissue Engineering: Effects of Des-Acyl Ghrelin on Vascular Cells</b> <u>Francesca Boccafroschi</u> , Margherita Botta, Luca Fusaro, Martina Ramella, Francesco Copes, Mario Cannas <i>University of Piemonte Orientale, Italy</i>
12:00	192	<b>Biomimetic Strategy to Improve Haemo- and Biocompatibility of PET</b> <u>E. Diana Giol</u> , Ronald Unger, Sandra van Vlierberghe, C. James Kirkpatrick, Peter Dubruel <i>Ghent University, Belgium</i>
12:15	193	<b>Synthesis of Porous Polyhydroxyalkanoate (PHA) Fibres by Pressurized Gyration Process and their Evaluation as Tissue Engineering Scaffolds</b> <u>Pooja Basnett</u> , Suntharavathanan Mahalingam, Barbara Lukasiewicz, Sian Harding, Mohan Edirisinghe, Ipsita Roy <i>University of Westminster, United Kingdom</i>
12:30	194	<b>Enhanced Interfacial Strength of Surgical Sealants Composed of Hydrophobically Modified, Cod-Derived Gelatins with Different Hydrocarbon Chain Length</b> <u>Ryo Mizuta</u> , Temmei Ito, Keiko Yoshizawa, Toshimasa Akiyama, Katsuhiro Kamiya, Tetsushi Taguchi <i>National Institute for Materials Science, Japan</i>
12:45	195	<b>Athrombogenic Diffusive Layers as the Biomaterial for Blood Contact Applications in the Dynamic High Shear Stresses Conditions</b> <u>Małgorzata Gonsior</u> , Tadeusz Wierzchoń, Roman Kustosz, Maciej Darlak, Magdalena Kościelniak-Ziemniak <i>Foundation for Cardiac Surgery Development, Poland</i>



**Session 40**  
**Hall 3B**

**Neural Regeneration 2**

Chairs: Michael Doser, *Institute for Textile Research and Process Engineering, Germany*  
Leonora Buzanska, *Mossakowski Medical Research Centre PAS, Poland*  
Sahana Ganesh, *National University of Ireland, Galway, Ireland (YSF Chair)*

11:30	K12	<b>Keynote</b> <b>Tissue-Engineered Electrodes for Neural and Cardiovascular Applications</b> <u>Laura Poole-Warren</u> , Josef Goding, Ulises Aregueta-Robles, Alexander Patton, Penny Martens, Rylie Green <i>University of New South Wales, Sydney, Australia</i>
12:00	196	<b>Delivery of Neurotrophic Factors to the Brain Using Fibrin-Based Hollow Microsphere Reservoirs</b> <u>Juhi Samal</u> , Deirdre Hoban, Carol Naughton, Ruth Concannon, Eilis Dowd, Abhay Pandit <i>National University of Ireland, Galway, Ireland</i>
12:15	197	<b>Amine-Functionalized Oligomer-Cross-Linked Gelatin-Based Conduits for Nerve Regeneration</b> <u>Caroline Kohn</u> , Julia M. Mehnert, Christian Kascholke, Michaela Schulz-Siegmund, Matthias Brandenburger, Michael C. Hacker <i>University of Leipzig, Germany</i>
12:30	198	<b>A Dual-Layered Microfluidic System for the Controlled In Situ Delivery of Anti-inflammatory Factors in Chronic Neural Implants</b> <u>Laura Frey</u> , Su Ryon Shin, Kevin O'Kelly, Ali Khademhosseini <i>Harvard Medical School, United States</i>
12:45	199	<b>Schwann Cell Behavior in Degradable PVA-Tyramine Hydrogels</b> <u>Ulises Aregueta Robles</u> , Khoon Lim, Penny Martens, Laura Poole-Warren, Nigel Lovell, Rylie Green <i>University of New South Wales, Sydney, Australia</i>





## Session 41 Hall 4A

### Cell Instructive Materials 4

Chairs: Guy Daculsi, *INSERM LIOAD UMR 791, France*

Maria Chatzinikolaidou, *University of Crete, Greece*

Ana Rita Rodrigues Araújo, *3B's Research Group - University of Minho, Portugal (YSF Chair)*

11:30	K13	<b>Keynote</b> <b>Bio-Fabrication and Physiological Self-Release of Tissue Equivalents Using Smart Peptide Amphiphile Templates</b> <u>Che Connon</u> , Ricardo Gouveia, Valeria Castelletto, Ian Hamely <i>Newcastle University, United Kingdom</i>
12:00	200	<b>Cellular Alignment in Response to Direct Laser Interference Patterning on Polyurethane Surfaces</b> <u>Lucas Cortella</u> , Denise Langheinrich, Idágene Cestari, Andrés Lasagni, Ismar Cestari <i>University of São Paulo, Brazil</i>
12:15	201	<b>Correlation of Mechanical Properties of Bio-Imitating Coatings with the Life Processes of Human Cells</b> <u>Roman Major</u> , Juergen M. Lackner <i>Institute of Metallurgy and Materials Science PAS, Poland</i>
12:30	202	<b>Effect of Osteogenic Growth of Adipose Derived Stem Cells And Human Osteoblasts on the Mechanical Properties of Protein Based Films with Microchannels</b> <u>Esen Sayin</u> , Rosti Hama Rashid, Ahmed Elsheikh, José Carlos Rodríguez-Cabello, Erkan Türker Baran, Vasif Hasirci <i>Center of Excellence in Biomaterials and Tissue Engineering, Turkey</i>
12:45	203	<b>Vasculogenesis by a Maleimide Cross-Linked PEG Hydrogel Containing Calcium Phosphate Glass Particles</b> <u>Claudia Navarro</u> , Jessica Weaver, Óscar Castaño, Amy Clark, Jose Garcia, Soledad Pérez-Amodio, Dennis Zhou, Douglas Clift, Andres J. García, Elisabeth Engel <i>Institute for Bioengineering of Catalonia, Spain</i>

## Hall 4B

### Science for Industry (2)

#### Bioresorbable Materials for Medical Applications

Organizers: Xiang Zhang, Ipsita Roy, Kadem Al-Lamee, Stuart MacLachlan, Maria Joao Barros, Nial Bullett, Mark Taylor

11:30	<b>Bioresorbable Systems: The Role of Inorganic Fillers in Composites</b> <u>Aldo R. Boccaccini</u> <i>University of Erlangen-Nuremberg, Germany</i>
11:50	<b>Bioresorbable Systems: The Role of Surface Functionalisation</b> <u>Iban Quintana</u> <i>IK4-TEKNIKER Ultra - Precision Processes Unit, Spain</i>
12:10	<b>Bioresorbable Systems: The Role of Modelling and Simulation in Performance Assessment of Bio-Structures and Implants</b> <u>Atul Bhaskar</u> <i>University of Southampton, United Kingdom</i>
12:30	<b>Bioresorbable Systems: The Role of Preclinical Testing</b> <u>Gianluca Giavaresi</u> <i>Istituto Ortopedico Rizzoli, Italy</i>
12:50	<b>Bioresorbable Systems: Discussion</b>



## Hall 1

## Plenary Lecture 7

- 15:30 L7 **Cell-Made or Man-Made Materials for Bone Reconstruction?**  
Małgorzata Lewandowska-Szumieł  
*Center for Biostructure Research, Medical University of Warsaw, Poland*
- Chairs:** Kazunori Kataoka, *University of Tokyo, Japan*  
Peter Dubruel, *Ghent University, Belgium*

## Session 42 Hall 1

### Bone Tissue Engineering 4

**Chairs:** Michael Gelinsky, *Technische Universität Dresden, Germany*  
Peter Dubruel, *Ghent University, Belgium*  
Marianne Sommer, *ETH Zurich Complex Materials, Switzerland (YSF Chair)*

- 16:45 204 **Ectopic Bone Formation by Commercial Calcium Phosphate Bone Graft Substitutes**  
Rongquan Duan, Davide Barbieri, Xiaoman Luo, Joost de Bruijn, Huipin Yuan  
*Xpand Biotechnology BV, Netherlands*
- 17:00 205 **In Vivo and In Vitro Characterization of Porous Polyurethane-Hydroxyapatite Scaffolds as a Bone Substitute**  
Gifty Tetteh, Maksym Pogorielov, Ihtesham U. Rehman, Gwendolen C. Reilly  
*University of Sheffield, United Kingdom*
- 17:15 206 **Preparation and Bioactivity of Nanocomposite Scaffolds Based on Biodegradable Polyurethane Foams and Bioactive Glass Nanoparticles**  
Cristian Covarrubias, Amaru Aguero, Monserrat Cádiz, Mario Díaz, Mehrdad Yazdani-Pedram, Juan Pablo Rodríguez, Carla Urra, Juan Cahuich, Juan M. Cervantes  
*University of Chile, Chile*
- 17:30 207 **Influence of Hydroxyapatite on Degradation Behaviour of PLA Fibres Scaffold**  
Nancy Vargas-Becerril, Lucia Téllez-Jurado, Octavio Álvarez-Fregoso, Manuel Hipólito-García, Luis María Rodríguez-Lorenzo, José Arturo Fernández-Pedrero, Marco Antonio Álvarez-Pérez  
*Autonome National University of Mexico, Mexico*



## Session 43 Hall 2

## Cellular Response

Chairs: Ana Paula Pego, *INEB - Instituto de Engenharia Biomédica, Portugal*  
Lucy Di Silvio, *King's College London Guy's Hospital, United Kingdom*  
Małgorzata Krok-Borkowicz, *AGH University of Science and Technology, Poland (YSF Chair)*

- |       |     |   |
|-------|-----|---|
| 16:45 | 208 | <b>Biomaterial Systems for Delivery or Education of Immunosuppressive Dendritic Cells to Ameliorate Multiple Sclerosis in a Murine Model</b><br>Aline Thomas, Sangeetha Srinivasan, Jennifer Blanchfield, Aaron M. Rosado, Andres Garcia, Brian Evavold, <u>Julia Babensee</u><br><i>Georgia Institute of Technology, United States</i> |
| 17:00 | 209 | <b>Microdialysis and Proteomics – New Approaches to Analyse the Early Stages of Fracture Repair in Bone Defects</b><br><u>Yvonne Förster</u> , Johannes Schmidt, Sven Baumann, Ute Hempel, Martin von Bergen, Stefan Kalkhof, Stefan Rammelt<br><i>Technische Universität Dresden, Germany</i>  |
| 17:15 | 210 | <b>Cellular Recognition of Collagen Based Scaffolds</b><br><u>Daniel Bax</u> , Natalia Davidenko, Richard Farndale, Ruth Cameron, Serena Best<br><i>University of Cambridge, United Kingdom</i>   |
| 17:30 | 211 | <b>Multicellular Spheroids and 3D Scaffold Cultures Up-Regulate Different Events in Osteogenic Differentiation of Adipose-Derived Mesenchymal Stem Cells</b><br><u>Sławomir Rumiński</u> , Adam Zalewski, Małgorzata Lewandowska-Szumiel<br><i>Medical University of Warsaw, Poland</i>   |

## Session 44 Hall 3A

## Wound Healing 2

Chairs: Antonio Merolli, *The Catholic University Gemelli Medical School, Italy*  
Marc Bohner, *RMS Foundation, Switzerland*  
Patrycja Domalik-Pyzik, *AGH University of Science and Technology, Poland (YSF Chair)*

- |       |     |   |
|-------|-----|---|
| 16:45 | 212 | <b>Balancing Fibroblast Differentiation in a Biomimetic Wound Healing Model</b><br>Jiranuwat Sapudom, Michael Ansorge, Marina Chkolnikov, Katja Franke, Ulf Anderegg, <u>Tilo Pompe</u><br><i>Universität Leipzig, Germany</i>  |
| 17:00 | 213 | <b>New Bilayered Biodegradable Polymeric Systems. A Feasible Approach for Skin Lesions</b><br>Noemi Santurce, Álvaro González-Gómez, Raul Rosales, Marcela Martin del Campo-Fierro, Blanca Vazquez, <u>Julio San Roman</u><br><i>Institute of Polymers CSIC and CIBER-BBN, Spain</i>  |
| 17:15 | 214 | <b>Fluorescent Activated Cell Sorting (FACS) as a Tool to Quantify the Immune Cell Response to Intramuscular Implanted Materials in Rats</b><br>Tanja Schmidt, Zienab Kronbach, Marie Heinze, Susann Krummsdorf, Marcel Geilling, <u>Frank Witte</u><br><i>Berlin-Brandenburg Center For Regenerative Medicine, Germany</i> |
| 17:30 | 215 | <b>Endogenous Human Dermal Equivalent in Vitro Model to Study Wound Healing Process</b><br><u>Bernadette Lombardi</u> , Costantino Casale, Giorgia Imparato, Francesco Urciuolo, Paolo Netti<br><i>Istituto Italiano di Tecnologia, Italy</i>   |



## Session 45 Hall 3B

### Bone Cements

Chairs: Heinz Redl, *Ludwig Boltzmann Institute for Experimental and Clinical Traumatology, Austria*  
Zbigniew Jaegermann, *Institute of Ceramics and Building Materials, Poland*  
Anton Goncharenko, *V.N. Karazin Kharkiv National University, Ukraine (YSF Chair)*

- |       |     |  |
|-------|-----|--|
| 16:45 | 216 | <b>Modification of Calcium Phosphate Bone Cements with Biologically Active Metal Ions: In Vitro and In Vivo Characterization</b><br><i>Anja Lode, Anne Bernhardt, Barbe Rentsch, Claudia Rentsch, Martha Geffers, Mandy Quade, Stefan Rammelt, Uwe Gbureck, Michael Gelinsky</i><br><i>Technische Universität Dresden, Germany</i> |
| 17:00 | 217 | <b>Development of Novel Implants with Embedded Therapeutics</b><br><i>Sophie Cox, Hany Hassanin, Moataz Attallah, Duncan Shepherd, Owen Addison, Uwe Gbureck, Liam Grover</i><br><i>University of Birmingham, United Kingdom</i>   |
| 17:15 | 218 | <b>The Influence of Phase Change Materials Based on Poly(Ethylene Glycol) on the Properties of Acrylic Bone Cements</b><br><i>Kinga Pielichowska, Katarzyna Filipek</i><br><i>AGH University of Science and Technology, Poland</i>   |
| 17:30 | 219 | <b>Marine Collagen Reinforcement of Calcium Phosphate Bone Cements: A Biological Assessment</b><br><i>Iwan Palmer, John Nelson, Wolfgang Schatton, Nicholas Dunne, Fraser Buchanan, Susan Clarke</i><br><i>Queen's University, United Kingdom</i>  |

## Session 46 Hall 4A

### Nanoparticles

Chairs: Josep A. Planell, *Universitat Oberta de Catalunya, Spain*  
Aneta Frączek-Szczypta, *AGH University of Science and Technology, Poland*  
Hyeyoun Chang, *Korea University of Science and Technology, Korea (YSF Chair)*

- |       |     |   |
|-------|-----|---|
| 16:45 | 220 | <b>Cellular Uptake and Degradation of Poly(Lactide-co-Glycolide) Nanoparticles and its Influences on Cell Functions</b><br><i>Dahai Yu, Pengfei Jiang, Zhengwei Mao, Changyou Gao</i><br><i>Zhejiang University, China</i>  |
| 17:00 | 221 | <b>Evaluation of Biological Effects of Nanomaterials on Human Cell Line, EA.hy926</b><br><i>Małgorzata Siatkowska, Tomasz Wasiak, Paulina Sokołowska, Joanna Rywaniak, Katarzyna Działoszyńska, Sylwia Kotarba, Kinga Kądzioła, Nina Bartoszek, Marta Kamińska, Agnieszka Kołodziejczyk, Piotr Komorowski, Krzysztof Makowski, Bogdan Walkowiak</i><br><i>Lodz University of Technology, Poland</i> |
| 17:15 | 222 | <b>Gellan-Gum Coated Gold Nanorods as Intracellular Drug Release System for Osteogenic differentiation</b><br><i>Stephanie Vial, Silvia Vieira, Fatima Maia, Mariana Carvalho, Rui Reis, Pedro Granja, Joaquim Oliveira</i><br><i>3Bs Research Group, Portugal</i>  |
| 17:30 | 223 | <b>On the Influence of Various Physiochemical Properties of the CNTs Layers on the Cell's Reaction In Vitro</b><br><i>Aleksandra Benko, Elzbieta Menaszek, Marek Nocurń, Marta Błażewicz, Aneta Frączek-Szczypta</i><br><i>AGH University of Science and Technology, Poland</i>   |



Science for Industry (3)  
Bioresorbable Materials for Medical Applications

Organizers: Xiang Zhang, Ipsita Roy, Kadem Al-Lamee, Stuart Maclachlan, Maria Joao Barros,  
Nial Bullett, Mark Taylor

16:45	<b>Welcome back and overview of morning's proceedings</b> Xiang Zhang, Ipsita Roy
16:55	<b>Research into Bioresorbable Systems</b> <u>Elena Boccardi</u> , <i>University of Erlangen-Nuremberg, Germany</i> <u>Zein Azhari</u> , <i>Cambridge University, United Kingdom</i>
17:15	<b>Panel discussion and overview of proceedings with speakers from the Bioresorbable System Session</b>



Hall 1		Plenary Lecture 8
9:00	L8	<b>Biological-Basis for Designing Biomaterials for the Injured and Degenerated Host - Examples in the Neural Space</b> <u>Abhay Pandit</u> <i>Network of Excellence for Functional Biomaterials, National University of Ireland, Galway, Ireland</i>  <b>Chairs:</b> Laura Poole-Warren, <i>University of New South Wales, Sydney, Australia</i> Jadwiga Laska, <i>AGH University of Science and Technology, Poland</i>

Session 47 Hall 1		Neural Regeneration 3
		<b>Chairs:</b> Jadwiga Laska, <i>AGH University of Science and Technology, Poland</i> Serena Best, <i>University of Cambridge, United Kingdom</i> Caroline Kohn, <i>Universität Leipzig, Germany</i> (YSF Chair)
10:00	224	<b>Novel Collagen Type I-Hyaluronic Acid Bi-Phasic Conduit for Peripheral Nerve Repair: an In Vivo Study</b> <u>Tijna Alekseeva</u> , Phoebe E. Roche, Amos Matsiko, Amro Widaa, William A. Lackington, Alan Ryan, Alan J. Hibbitts, Garry Duffy, Fergal J. O'Brien <i>Royal College of Surgeons in Ireland, Ireland</i>
10:15	225	<b>Sustained Biochemical Signalling and Contact Guidance Provided by Electrospun Bicomponent Scaffolds for Enhancing Nerve Regeneration</b> <u>Chaoyu Liu</u> , Min Wang <i>The University of Hong Kong, Hong Kong</i>
10:30	226	<b>The “Micro” and “Macro”- Scale Approach in Building Up Neural Stem Cell Microenvironments for Developmental and Toxicity Studies</b> <u>Leonora Buzanska</u> , Marzena Zychowicz, Krystyna Pietrucha, Martyna Podobinska, Jose Luis Gerardo Nava, Gary Brook <i>Mossakowski Medical Research Centre PAS, Poland</i>
10:45	227	<b>Pre-Clinical Investigation of a Novel Biodegradable Polymer Based Medical Device for Peripheral Nerve Regeneration</b> <u>Atefeh Mobasser</u> i, Giorgio Terenghi, Adam Reid, Julie Gough, David Richards <i>University of Manchester, United Kingdom</i>





## Session 48 Hall 2

### Bone Tissue Engineering 5

Chairs: Aldo Boccaccini, *University of Erlangen-Nuremberg, Germany*  
Rui Reis, *3B's Research Group - University of Minho, Portugal*  
Thomas Paterson, *University of Sheffield, United Kingdom (YSF Chair)*

10:00	228	<b>Decrease of MRI Artifact in Spinal Instruments of Zirconium Alloy</b> <u>Takao Hanawa</u> , Naoyuki Nomura, Maki Ashida, Yusuke Tsutsumi, Hisashi Doi, Peng Chen, Manabu Itoh <i>Tokyo Medical and Dental University, Japan</i>
10:15	229	<b>Investigation of Degradation Behavior and Corrosion of Magnesium Alloys for Orthopedic Implants</b> <u>Iulian Antoniac</u> , Ana Blajan, Aurora Antoniac <i>University Politehnica of Bucharest, Romania</i>
10:30	230	<b>Polyurethane-Ceramic Matrices as Orbital Implants</b> Semih Sahan, Pezhman Hosseinian, Deniz Ozdil, Mustafa Turk, <u>Halil Murat Aydin</u> <i>Hacettepe University, Turkey</i>
10:45	231	<b>Bioresorbable Multifunctional Composite Devices – Practical Aspects of Miniplates for Osteosynthesis</b> <u>Karol Gryń</u> , Barbara Szaraniec, Maja Kuś, Kamil Dudziński, Jan Chłopek <i>AGH University of Science and Technology, Poland</i>

## Session 49 Hall 3A

### Clinical Trials

Chairs: Dimosthenis Mavrilas, *University of Patras, Greece*  
Ryszard Uklejewski, *Casimir the Great University, Poland*  
Shahram Ghanaati, *Medical Center of the Goethe University Frankfurt, Germany (YSF Chair)*

10:00	232	<b>Clinically Used Dextran Coated Iron Oxide Nanoparticles and Their Induced Macrophage Autophagy</b> Rongrong Jin, Jiuju Du, James Anderson, <u>Hua Ai</u> <i>Sichuan University, China</i>
10:15	233	<b>Radiodensitometric Assessment Long Time after Dental Periimplantitis Defect Filled with “Pure” Synthetic HAp Bioceramics</b> <u>Vadims Klimecs</u> , Girts Salms, Andrejs Skagers, Aleksandrs Grishulonoks, Laura Neimane, Liga Berzina-Cimdina, <i>Institute of Stomatology, Latvia</i>
10:30	234	<b>Debris of a Carbon-Fibre-Reinforced Polymers (CFRP) Wrist Plate Led to a Destructive Synovitis in Human</b> <u>Antonio Merolli</u> , Lorenzo Rocchi, Alessandro Morini, Luigi Mingarelli, Paolo Scialabba D'Amico, Francesco Fanfani <i>The Catholic University of Rome, Italy</i>
10:45	235	<b>Clinical Performance of Moldable Bioceramic for Bone Regeneration in Maxillofacial Surgery</b> <u>Guy Daculsi</u> , Thomas Miramond, Pascal Borget, Elodie Seris <i>Inserm UMRS 791 Lioad, France</i>



## Session 50 Hall 3B

### Antimicrobial Surfaces and Materials 4

Chairs: Pentti Tengvall, *University of Gothenburg, Sweden*

Lukasz Major, *Institute of Metallurgy and Materials Science PAS, Poland*

Bora Onat, *Middle East Technical University, Turkey (YSF Chair)*

- 
- |       |     |   |
|-------|-----|---|
| 10:00 | 236 | <b>Antibacterial Effect of Bioactive Starch-Based Scaffolds Functionalized with Silanol Groups</b><br><u>Ana Rodrigues</u> , Albina Franco, Fernando Rodrigues, António Castro, Isabel Leonor, Rui Reis<br><i>3Bs Research Group, Portugal</i>                        |
| <hr/> |     |   |
| 10:15 | 237 | <b>Bioactive Orthopaedic Devices Preventing Biofilm Formation and Local Infection</b><br>Loïc Pichavant, Hélène Carrié, Laurent Plawinski, Jocelyne Caillon, Gilles Amador,<br>Valérie Héroguez, <u>Marie-Christine Durrieu</u><br><i>Université Bordeaux, France</i> |
| <hr/> |     |   |
| 10:30 | 238 | <b>Anti-Bacterial Borosilicate Glass Formulations for Bone Tissue Engineering Applications</b><br><u>João S. Fernandes</u> , Margarida Martins, Nuno N. Neves, Ricardo A. Pires, Rui L. Reis<br><i>3Bs Research Group, Portugal</i>                                   |
| <hr/> |     |   |
| 10:45 | 239 | <b>Alginate/Chitosan-Based Materials with Bioactive Functionalities</b><br><u>Agnieszka Kyzioł</u> , Anna Regiel-Futyr, Aleksandra Mazgala, Justyna Michna,<br>Małgorzata Kus-Liśkiewicz, Silvia Irueta<br><i>Jagiellonian Univeristy, Poland</i>                     |
- 

## Session 51 Hall 4A

### Biomimetic Materials

Chairs: Sanjukta Deb, *King's College, United Kingdom*

Anna Ślósarczyk, *AGH University of Science and Technology, Poland*

Nina Henry, *INSERM, France (YSF Chair)*

- 
- |       |     |  |
|-------|-----|--|
| 10:00 | 240 | <b>First Principles Modelling to Establish the Thermodynamically Most Favourable Form and Position of Silicon in Bone Mineral</b><br><u>Helen Chappell</u> , Ravin Jugdaohsingh, Jonathan Powell<br><i>MRC Human Nutrition Research, United Kingdom</i>  |
| <hr/> |     |  |
| 10:15 | 241 | <b>Modification of Living Diatom, <i>Thalassiosira weissflogii</i> by Calcium Precursor as a Sacrificial Template for Development of Next Generation of Structural Biomaterials</b><br><u>Asrizal Abdul Rahman</u> , Syed Ansar Md. Tofail, Abhay Pandit<br><i>National University of Ireland, Galway, Ireland</i>   |
| <hr/> |     |  |
| 10:30 | 242 | <b>Fabrication and Histological Evaluation of Carbonate Apatite Coated Calcite</b><br><u>Kunio Ishikawa</u> , Kanji Tsuru, Masako Kobayashi, Youji Miyamoto<br><i>Kyushu University, Japan</i>   |
| <hr/> |     |  |
| 10:45 | 243 | <b>Crystallization and Thermal Evolution of Pyrophosphate Polymorphs and Prospective Biomaterials with a Metastable <math>\alpha</math>1-Calcium Pyrophosphate from Amorphous Calcium Phosphates with an Initial CaP Ratio of 1:1</b><br>Zoltan Zyman, Matthias Epple, Anton Goncharenko, Dmytro Rokhmistrov<br><i>V.N. Karazin Kharkiv National University, Ukraine</i> |
- 



## Session 52 Hall 4B

### Osteointegration 2

Chairs: Jerome Guicheux, *INSERM U791 LIOAD, France*  
Helmut Thissen, *CSIRO Manufacturing Flagship, Australia*  
Monika Golda-Cępa, *Jagiellonian University, Poland (YSF Chair)*

- |       |     |  |
|-------|-----|--|
| 10:15 | 244 | <b>Functionally Graded Hybrid Scaffolds for Osteo-Chondral Defect Repair: Scaffold Design</b><br>Serena Bertoldi, Masoumeh Meskinfam, Paola Petrini, Alessandro Cerri, Nicolò Albanese, MariaCristina Tanzi, <u>Silvia Farè</u><br><i>Politecnico di Milano, Italy</i>                                       |
| 10:30 | 245 | <b>Formation of Hybrid Materials Based on Calcium Phosphate Deposit on Carbon Fiber Scaffold</b><br>Quentin Picard, <u>Lise Guichaoua</u> , Sandrine Delpoux, Nathalie Rochet, Jérôme Chancolon, Franck Fayon, Fabienne Warmont, Sylvie Bonnamy<br><i>Université d'Orléans, France</i>                       |
| 11:00 | 246 | <b>Emulsion Templating: a Versatile Route to the Preparation of Biodegradable and Biocompatible Scaffolds for Tissue Engineering</b><br>Caitlin Langford, David Johnson, Neil Cameron<br><i>Monash University, Australia</i>   |
| 11:15 | 247 | <b>Cross-Linked, Macroporous Hybrid Glass Implants of Defined Architecture for Bone Regeneration</b><br><u>Stephan Hendrixx</u> , Christian Kascholke, Tobias Flath, Christian Raack, Mathias Gressenbuch, Peter Schulze, Michael C. Hacker, Michaela Schulz-Siegmund<br><i>Universität Leipzig, Germany</i> |

## Session 53 Hall 1

### Advanced Manufacturing 3

Chairs: Jérôme Sohier, *CNRS Institute of Biology and Chemistry of Proteins, France*  
Tomasz Goryczka, *University of Silesia, Poland*  
Barbara Lukasiewicz, *University of Westminster, United Kingdom (YSF Chair)*

- |       |     |   |
|-------|-----|---|
| 11:30 | K14 | <b>Keynote</b><br><b>3D Fiber Deposition and Stereolithography Techniques for the Design of Multifunctional Nanocomposite Magnetic Scaffolds</b><br><u>Roberto De Santis</u> , Ugo D'Amora, Teresa Russo, Alfredo Ronca, Antonio Gloria, Luigi Ambrosio<br><i>IPCB-CNR Institute of Polymers, Composites and Biomaterials – Naples, Italy</i> |
| 12:00 | 248 | <b>Tailoring Porosity from the Nano- to the Macroscale of Low-Temperature Consolidated Robocasted Scaffolds</b><br><u>Edgar B. Montufar</u> , Yassine Maazouz, Borja Gonzalez, Ladislav Celko, Jozef Kaiser, Maria-Pau Ginebra<br><i>Technical University of Catalonia, Spain</i>   |
| 12:15 | 249 | <b>Development of Bioactive and Antimicrobial 3D Plotted PCL Scaffolds for Bone Tissue Engineering</b><br>Giuseppe Cama, Myriam Gomez Tardajos, Peter Dubruel<br><i>Ghent University, Belgium</i>   |
| 12:30 | 250 | <b>Two-Photon Polymerization ofOrmocomp® 3D Structures Doped with Piezoelectric Barium Titanate Nanoparticles</b><br>Attilio Marino, Jonathan Barsotti, Massimiliano Labardi, Barbara Mazzolai, Virgilio Mattoli, Gianni Ciofani<br><i>Italian Institute of Technology, Italy</i>   |
| 12:45 | 251 | <b>Additive Manufacturing of Poly-High Internal Phase Emulsion Scaffolds with Tuneable Mechanical Properties for Bone Tissue Engineering</b><br>Robert Owen, Colin Sherborne, Gwendolen Reilly, <u>Frederik Claeysens</u><br><i>The University of Sheffield, United Kingdom</i>   |



## Session 54 Hall 2

### Bone Tissue Engineering 6

Chairs: Elizabeth Tanner, *University of Glasgow School of Engineering, United Kingdom*  
Serena Best, *University of Cambridge, United Kingdom*  
Anna Donesz-Sikorska, *Wrocław University of Technology, Poland (YSF Chair)*

- |       |     |  |
|-------|-----|--|
| 11:30 | K15 | <b>Keynote</b><br><b>Polymer Brush-Assisted Fabrication of Protein Gradients Inside of 3D Microporous Scaffolds</b><br>Andrea Di Luca, Michel Klein Gunnewiek, Hermen Bollemaat, Clemens van Blitterswijk, Julius Vancso, Edmondo Benetti, <u>Lorenzo Moroni</u><br><i>University of Maastricht, Netherlands</i>                                 |
| 12:00 | 252 | <b>Osteogenic Potential of Self-Assembling Bioceramic Nanoparticles</b><br><u>Michelle O'Doherty</u> , Sreekanth Pentlavalli, Philip Chambers, Marine Chalanqui, Helen McCarthy, Nicholas Dunne<br><i>Queen's University Belfast, United Kingdom</i>   |
| 12:15 | 253 | <b>Results of Pilot Experimental Studies in 10 Animals on Prototype of the Multispiked Connecting Scaffold with Thermo-Electrochemically Ca-P Modified Surface for Non-Cemented Biofixation of RA Endoprostheses</b><br>Ryszard Uklejewski, Piotr Rogala, Mariusz Winiecki, Wanda Stryła<br><i>Casimir the Great University, Poland</i>          |
| 12:30 | 254 | <b>Analysis of Osteoinductive Properties of Combinations of Macroporous Ceramic (MBCP+™), Simvastatin, rhBMP-2, and BMSC in a Femoral Critical Size Induced Membrane Model in Rats</b><br><u>Erwan de Mones</u> , Silke Schlaubitz, Reine Bareille, Lionel Couraud, Jean-Christophe Fricain<br><i>INSERM U1026, France</i>                       |
| 12:45 | 255 | <b>The Influence of Calcium Phosphate Microparticle Incorporation in Highly Orientated Macroporous Collagen Scaffolds on the Mechanism of Bone Defect Healing</b><br><u>Ansgar Petersen</u> , Hans Leemhuis, Andreas Hoess, Agnes Ellinghaus, Berthold Nies, Ingo Heschel, Georg N. Duda<br><i>Charité – Universitätsmedizin Berlin, Germany</i> |

## Session 55 Hall 3A

### Cardiovascular Applications 3

Chairs: Lucie Bacakova, *Academy of Sciences of the Czech Republic, Czech Republic*  
Kinga Pielichowska, *AGH University of Science and Technology, Poland*  
Claudia Navarro, *Institute for Bioengineering of Catalonia, Spain (YSF Chair)*

- |       |     |   |
|-------|-----|---|
| 11:30 | K16 | <b>Keynote</b><br><b>Elastomeric Materials of Enhanced Mechanical Performance for Implantable Artificial Heart</b><br>Agnieszka Piegat, <u>Mirosława El Fray</u><br><i>West Pomeranian University of Technology, Szczecin, Poland</i>   |
| 12:00 | 256 | <b>Preparation of a Small Diameter Decellularized Blood Vessel Covered with SPU Fibers by Electrospinning</b><br><u>Tsuyoshi Kimura</u> , Hiroko Morita, Pingli Wu, Naoko Nakamura, Kwangwoo Nam, Toshiya Fujisato, Akio Kishida<br><i>Tokyo Medical and Dental University, Japan</i>   |
| 12:15 | 257 | <b>Blend Electrospinning of Biodegradable Chitosan/Polycaprolactone Fibers as a Process to Create Scaffolds for Cardiovascular Tissue Engineering</b><br>Alexandros Repanas, Birgit Glasmacher, Alexandra Theodoropoulou, <u>Dimosthenis Mavrilas</u><br><i>University of Patras, Greece</i>  |
| 12:30 | 258 | <b>Designing Novel Polymeric Endovascular Devices</b><br>Daniel Cohn, Randa Abbas, Fany Widlan, Matthew Zarek, Ram Malal, Allan Bloom<br><i>The Hebrew University of Jerusalem, Israel</i>  |
| 12:45 | 259 | <b>Mechanical Characterization of Small Diameter Grafts Made of Segmented Polyurethanes Based on Alkaline Aminoacids</b><br>Omar Castillo-Cruz, Francis Aviles, Rossana F. Vargas-Coronado, Jose Manuel Cervantes-Uc, <u>Juan Valerio Cauich-Rodriguez</u> , Lerma Hannaiy Chan-Chan<br><i>Centro de Investigación Científica de Yucatán, Mérida, Yucatán, Mexico</i> |



**Session 56**  
**Hall 3B**

**Surface Modification 5**

Chairs: Kunio Ishikawa, *Kyushu University, Japan*

Tomasz Moskaiewicz, *AGH University of Science and Technology, Poland*

Aleksandra Benko, *AGH University of Science and Technology, Poland (YSF Chair)*

11:30	260	<b>Patterning of Neuron Adhesion and Differentiation on Diamond-Like Carbon by Pulsed Laser Ablation</b> <u>James Dugan</u> , Frederik Claeysens <i>University of Sheffield, United Kingdom</i>
11:45	261	<b>Electrochemically Assisted Deposition of Strontium Modified Magnesium Phosphate on Titanium Surfaces</b> Markus Meininger, Julia Zerweck, Cornelia Wolf-Brandstetter, Uwe Gbureck, Jürgen Groll, <u>Claus Moseke</u> <i>University of Würzburg, Germany</i>
12:00	262	<b>Hydrothermally-Treated Nano-Crystalline TiO<sub>2</sub> Coatings Boost the "Race for the Surface" Towards Osteogenesis rather than Bacterial Adhesion</b> <u>Martina Lorenzetti</u> , Iztok Dogša, David Stopar, Katrin Susanne Lips, Reinhard Schnettler, Mitjan Kalin, Spomenka Kobe, Saša Novak <i>Jožef Stefan Institute, Slovenia</i>
12:15	263	<b>Covalent Attached Fibronectin Fragment-PLDLLA Nanofibers on Titanium for Guiding Osteoblast Behaviour</b> <u>Jordi Guillem-Marti</u> , Gerard Boix-Lemonche, Dencho Gugutkov, George Altankov, Francisco Javier Gil, Jose Maria Manero <i>Technical University of Catalonia (UPC), Spain</i>
12:30	264	<b>Morphometric Examination of Local Tissue Reactions following Implantation of Ti<sub>6</sub>Al<sub>4</sub>V Plates Coated with Anti-Adhesive Plasma-Fluorocarbon-Polymer Films in Rats</b> <u>Andreas Hoene</u> , Birgit Finke, Holger Testrich, Silke Lucke, Uwe Walschus, Karsten Schröder, Jürgen Meichsner, Maciej Patrzyk, Michael Schlosser <i>University Medical Center Greifswald, Germany</i>
12:45	265	<b>Evaluation of Biological Response of Implants Modified by Carbon Coatings with Si (Si-DLC)</b> <u>Dorota Bociaga</u> , Jacek Grabarczyk, Joanna Piasecka-Zelga, Jan Skowroński, Piotr Niedzielski <i>Lodz University of Technology, Poland</i>



**Session 57**  
**Hall 4A**

**Smart Biomaterials 2**

Chairs: Manus Biggs, *National University of Ireland, Galway, Ireland*

Helen Chappell, *MRC Human Nutrition Research Biominerals Research, United Kingdom*

Valentina Bonfrate, *University of Salento, Italy (YSF Chair)*

11:30	266	<b>Biodegradable Semiconductor Hydrogels for the Photothermal Control of Growth Factor Bioavailability</b> <u>Francisco Martín-Saavedra</u> , Martín Prieto, Manuel Arruebo, Jesús Santamaría, Nuria Vilaboa <i>La Paz University Hospital-IdiPAZ, Spain</i>
11:45	267	<b>Nanoporous Bead and Monolith Adsorbents for Haemoperfusion Applications</b> Yishan Zheng, Susan Sandeman, Ganesh Ingavle, Carol Howell, Sandeep Kumar, Matthew Pope, Michal Kowalski, Kolitha Basnayake, Steve Tension, Sergey Mikhailovsky <i>University of Brighton, United Kingdom</i>
12:00	268	<b>Biodegradable Temperature-Responsive Injectable Polymer Formulation Convenient at Clinical Scene</b> <u>Yuichi Ohya</u> , Yasuyuki Yoshida, Akihiro Takahashi, Akinori Kuzuya <i>Kansai University, Japan</i>
12:15	269	<b>Mechanical and Cytotoxic Evaluation of a Novel Hydrogel with Potential to Deliver Bioceramic Nanoparticles</b> <u>Sreekanth Pentlavalli</u> , Michelle O'Doherty, Philip Chambers, Marine Chalanqui, Helen McCarthy, Nicholas Dunne <i>Queen's University, United Kingdom</i>
12:30	270	<b>Thermally Modulated Mesenchymal Stem Cell Separation Using Thermoresponsive Cationic Copolymer Brush</b> <u>Kenichi Nagase</u> , Yuri Hatakeyama, Tatsuya Shimizu, Katsuhisa Matsuura, Masayuki Yamato, Naoya Takeda, Teruo Okano <i>Tokyo Women's Medical University, Japan</i>
12:45	271	<b>Biopolymer Mediated Uptake of Sugar Molecules for Cell Preservation and Therapy</b> <u>Rongjun Chen</u> , Andrew Lynch, Liwei Wu, Zhenlu Hu, Nigel Slater <i>Imperial College London, United Kingdom</i>





**Session 58  
Hall 4B**

**Drug Delivery 4**

Chairs: David Eglin, *AO Research Institute Davos, Switzerland*  
Henning Menzel, *University of Technology Braunschweig, Germany*  
Jiankang Song, *Radboud University, Netherlands (YSF Chair)*

11:30	272	<b>Lipid Nanoparticles Loaded into Biopolymer-Based Hydrogels; Materials for Controlled Rate of Drug Delivery</b> Lisa Racine, Rachel Auzély-Velty, <u>Isabelle Texier</u> <i>Université Grenoble Alpes, CEA/DTBS, France</i>
11:45	273	<b>Selective In Vitro Anticancer Effect of Hyaluronan Polymeric Micelles Loaded with SPIONs</b> Daniela Smejkalova, Kristina Nesporova, Gloria Huerta-Angeles, Jakub Syrovatka, Andrea Galisova, Daniel Jirak, Vladimir Velebny <i>Contipro Pharma, Czech Republic</i>
12:00	274	<b>Injectable Hydrogel Based on a Novel Amphiphilic Hyaluronic Acid Derivative for Controlled Drug Release</b> Assunta Borzacchiello, Luisa Russo, Fabio Salvatore Palumbo, Stefano Agnello, Giovanna Pitarresi, Gaetano Giammona, Luigi Ambrosio <i>Institute for Composite and Biomedical Materials IMCB-CNR, Italy</i>
12:15	275	<b>Polysaccharide-Based Nanomicrosystems for Controlled Delivery of Anti-Inflammatory Agents</b> <u>Anna Krawiec</u> , Agnieszka Rojewska, Marta Baster, Elena Iruin Amatriain, Michał Rączy, Maria Nowakowska <i>Jagiellonian University, Poland</i>
12:30	276	<b>Combination of Different BMP2- Peptide Release Mechanisms from Natural Polymeric Systems</b> <u>Daniela Giugliano</u> , Maria Grazia Raucci, Luigi Ovaleo Pandolfo, Alessandra Sorinte, Luigi Ambrosio <i>Institute of Polymers, Composites and Biomaterials – National Research Council of Italy, Italy</i>
12:45	277	<b>Mesoporous Bioactive Glass/CaP Bone Cement Composites for the Delivery of the Growth Factor BDNF</b> <u>Matthias Schumacher</u> , Katrin S. Lips, Michael Gelinsky <i>Technische Universität Dresden, Germany</i>



# Rapid Fire Presentations (1)

Monday, 31<sup>st</sup> August (start at 13:30)

278	<b>Development of Novel Bioresorbable Iron-silver Materials and their in vitro Degradation Behavior</b> <u>Sanjaya K. Swain</u> , David Starosvetsky, Irena Gotman, Elazar Y. Gutmanas <i>Israel</i>
279	<b>Dissolution Behaviours of MgO-P<sub>2</sub>O<sub>5</sub>-TiO<sub>2</sub>/Nb<sub>2</sub>O<sub>5</sub> Glasses in MgO-rich Region</b> <u>Sungho Lee</u> , Hiroataka Maeda, Akiko Obata, Kyosuke Ueda, Takayuki Narushima, Toshihiro Kasuga <i>Japan</i>
280	<b>Development of Structurally Analogous Cryoprotective Synthetic Polyampholytes and Elucidation of Mechanism</b> <u>Robin Rajan</u> , Kazuaki Matsumura <i>Japan</i>
281	<b>Shear- Thinning Soft Bionanocomposites Based on Laponite and Poly-L-Lysine for Cell Delivery Purposes</b> <u>Minkle Jain</u> , Kazuaki Matsumura <i>Japan</i>
282	<b>Viscoelastic Behaviour of Embroidered Scaffolds for the Tissue Engineering of Ligaments</b> <u>Judith Hahner</u> , Claudia Hinüber, Annette Breier, Gert Heinrich <i>Germany</i>
283	<b>Exploring the Limits of Scaffold Interconnectivity for Cell Type Specific Invasion</b> <u>Jennifer Ashworth</u> , Marco Mehr, Paul Buxton, Serena Best, Ruth Cameron <i>United Kingdom</i>
284	<b>The Impact of Thrombocytes on the Cell Proliferation within the 3D Scaffolds</b> <u>Kateřina Pilařová</u> , Věra Jenčová, Jana Horáková, Jakub Erben, Jiří Chvojka, David Lukáš <i>Czech Republic</i>
285	<b>Development of a Valved Conduit for Venal Reconstruction</b> <u>Sonia Zia</u> , Lucrezia Morticelli, Karsten Grote, Igor Tudorache, Sergei Cebotari, Andres Hilfiker, Birgit Glasmacher, Axel Haverich, Sotirios Korossis <i>Germany</i>
286	<b>Biocompatible Collagen Paramagnetic Scaffold for Controlled Drug Release</b> <u>Valentina Bonfrate</u> , Simona Bettini, Luca Salvatore, Marta Madaghiele, Ludovico Valli, Gabriele Giancane, Alessandro Sannino <i>Italy</i>
287	<b>Uptake of Nanoparticles by Macrophage Cell Line Predicts In Vivo Clearance by Reticuloendothelial System</b> <u>Hyeoun Chang</u> , Ick Chan Kwon, Kwangmeyung Kim <i>Republic of Korea</i>
288	<b>Development of Novel Biomaterials, Natural Polymers, Polyhydroxyalkanoates (PHAs), for Biomedical Applications</b> <u>Barbara Lukasiwicz</u> , Pooja Basnett, Ipsita Roy <i>United Kingdom</i>
289	<b>Does Ascorbic Acid Modified Polyurethanes May be Suitable Candidates for Soft Tissue Engineering?</b> <u>Iga Gubanska</u> , Justyna Kucinska-Lipka, Marta Pokrywczynska, Tomasz Drewa, Helena Janik <i>Poland</i>
290	<b>Thermal Crystallization and Phase Evolution in the Amorphous Calcium Phosphate Powders with a Ca/P Ratio of 1:1</b> <u>Anton Goncharenko</u> , Matthias Eppler, Zoltan Zyman, Dmytro Rokhmistrov <i>Ukraine</i>



# Rapid Fire Presentations (2)

Tuesday, 1<sup>st</sup> September (start at 13:30)

291	<b>Methodological Evaluation of Quantitative <i>in Vivo</i> MRI Volume Measurements of Hydrogels by <i>ex Vivo</i> CT Imaging</b> <u>Christoph Tondera</u> , Sandra Ullm, Sebastian Meister, Tim P. Gebauer, Axel T. Neffe, Andreas Lendlein, Jens Pietzsch <i>Germany</i>
292	<b>Intraocular Lenses with Surfaces Functionalized by Biomolecules in Relation with Lens Epithelial Cell Adhesion</b> <u>Yi-Shiang Huang</u> , Virginie Bertrand, Dimitriya Bozukova, Christophe Pagnoulle, Edwin De Pauw, Marie-Claire De Pauw-Gillet, Marie-Christine Durrieu <i>Belgium</i>
293	<b>Introducing Controlled Nano-Roughness in 3D Silk Fibroin Scaffolds for Bone Tissue Engineering</b> <u>Marianne R. Sommer</u> , Ralph Müller, Sandra Hofmann, André R. Studart <i>Switzerland</i>
294	<b>Effect of Calcium Phosphate Ceramic Substrate Geometry on Cell Organization and Behaviour</b> <u>A. Hayrapetyan</u> , E.R. Urquia Edreira, J.G.C. Wolke, J.A. Jansen, J.J.J.P. van den Beucken <i>Netherlands</i>
295	<b>Novel Approach Towards Osseointegration: Surface Functionalization on Zirconia</b> <u>Carlos Caravaca</u> , Liu Shi, Sandra Balvay, Pascaline Rivory, Emmanuelle Laurenceau, Yann Chevolot, Daniel Hartmann, Laurent Gremillard, Jérôme Chevalier <i>France</i>
296	<b>Novel Enzymatically Cross-linked Silk Fibroin Hydrogel with Potential Applications as Suppressor of Angiogenesis and Tumor Progression</b> Viviana Ribeiro, <u>Joana Silva-Correia</u> , Vera Miranda-Gonçalves, Le-Ping Yan, Ana L. Oliveira, Rui M. Reis, Rui L. Reis, Joaquim M. Oliveira <i>Portugal</i>
297	<b>Electrophoretic Deposition of Composite Coatings Based on ZnO Nanoparticles on Ti6Al7Nb Alloy</b> <u>Joanna Karbowniczek</u> , Luis Cordero-Arias, Aleksandra Czyrska-Filemonowicz, Aldo R. Boccacini <i>Poland</i>
298	<b>Bioactivation of SiO<sub>2</sub> Sol-gel Coatings as a Modification Method of Metallic Implants</b> <u>Anna Donesz-Sikorska</u> , Justyna Krzak, Jerzy Kaleta, Małgorzata Krok-Borkowicz, Elżbieta Pamuła <i>Poland</i>
299	<b>Multimodal Image Registration for Assessment of Bone Formation in Porous Metal Implants</b> <u>Hua Geng</u> , Taek Bo Kim, Aine Devlin, Naomi Todd, Kamel Madi, Julian R. Jones, Christopher Mitchell, Chris Sutcliffe, Sarah Cartmell, Peter D. Lee <i>United Kingdom</i>
300	<b>Injectable Hydroxyapatite Enriched Hyaluronate Gels for Versatile Tissue Engineering Applications</b> <u>Cecilia De León</u> , Elvira Estella, L. Téllez-Jurado, M.A. Álvarez-Pérez, Julio San Román, Luis M. Rodríguez-Lorenzo <i>Spain</i>
301	<b>Bone Induction by Surface Modified Calcium Phosphate Ceramics</b> <u>Rongquan Duan</u> , Davide Barbieri, Xiaoman Luo, Florence de Groot, Huipin Yuan, Joost D. de Bruijn <i>Netherlands</i>
302	<b>Optical Coherence Tomography as a Complementary Method to X-ray Computed Tomography in Dental Diagnosis</b> Marcin Strąkowski, Milena Supernak-Marczewska, <u>Paulina Strąkowska</u> , Ewa Kowalska, Maciej Kraszewski, Małgorzata Ryniec-Wilczyńska, Michał Trojanowski, Violetta Szyzik <i>Poland</i>
303	<b>Molecular Basis of the Gp36 MPER Fusogenic Activity</b> <u>Anna Maria D'Ursi</u> , Agostino Bruno, Mario Scrima, Manuela Grimaldi, Grazia Della Sala, Vittorio Limongelli <i>Italy</i>



# Rapid Fire Presentations (3)

Wednesday, 2<sup>nd</sup> September (start at 13:30)

304	<b>Engineering PEGylated Alginate Hydrogels for Cell Microencapsulation</b> <u>Solène Passemard</u> , François Noverraz, Virginia Crivelli, Redouan Mahou, Françoise Borcard, Sandrine Gerber-Lemaire, Christine Wandrey <i>Switzerland</i>
305	<b>Study of Biodegradation Impact on PLA/Graphene-Nanoplatelets Biocomposites Mechanical and Biological Properties</b> <u>Artur M. Pinto</u> , Carolina Gonçalves, Inês C. Gonçalves, Fernão D. Magalhães <i>Portugal</i>
306	<b>Osteoinductive and Antibacterial Coatings for Dental Implants</b> <u>Beatriz Palla</u> , Francisco Javier Romero, Mar Fernández, Julio Suay, Mariló Gurruchaga, Isabel Goñi <i>Spain</i>
307	<b>On-Demand Release of Dexamethasone from Conjugated Polymer Matrix</b> <u>Katarzyna Krukiewicz</u> , Artur P. Herman, Sławomir Boncel, Jerzy K. Żak <i>Poland</i>
308	<b>Mesoporous Silica Nanofibers as Drug Delivery Systems for Intervertebral Disc Regenerative Medicine: Analysis of Protein-Silica Interactions</b> <u>Nina Henry</u> , Johann Clouet, Catherine Le Visage, Eric Gautron, Bernard Humbert, Jérôme Guicheux, Jean Le Bideau <i>France</i>
309	<b>Regulation of Inflammatory Gene Expression by Functionalized Calcium Phosphate Nanoparticles with Different Delivery Strategies to the Gut</b> <u>Bernhard Neuhaus</u> , Annika Frede, Astrid Westendorf, Matthias Eppe <i>Germany</i>
310	<b>How the Interfacial Shear Strength in PLGA Fibre-Reinforced Brushite Cements Affects the Composites Mechanical Properties</b> <u>Stefan Maenz</u> , Max Hennig, Mike Mühlstädt, Elke Kunisch, Raimund W. Kinne, Frank Plöger, Jörg Bossert, Klaus D. Jandt <i>Germany</i>
311	<b>Heparinization of Calcium Phosphates: Towards Enhancing Biological Performance</b> <u>Anna Díez-Escudero</u> , Montserrat Espanol, Maria-Pau Ginebra <i>Spain</i>
312	<b>Intercellular Delivery of Self-Assembling Osteogenic Nanoparticles: Fate and Effect</b> <u>Philip Chambers</u> , Sreekanth Pentlavalli, Michelle O'Doherty, Marine Chalanqui, Helen O. McCarthy, Nicholas Dunne <i>Northern Ireland</i>
313	<b>Porous Particles as Cell Delivery Vehicles for Bone Tissue Engineering</b> <u>Thomas Paterson</u> , James Dugan, Colin Sherborne, Chia-Cheng Chen, Nicola Green, Gwendolen Reilly, Frederik Claeyssens <i>United Kingdom</i>
314	<b>Biodegradable SCL-PHA Composite Scaffolds for Bone Tissue Engineering</b> <u>Christy Thomas</u> , Aldo. R. Boccaccini, Ipsita Roy <i>United Kingdom</i>
315	<b>Multifunctional Anti-Adhesive Films Prepared by Layer-by-Layer Formation of Zwitterionic Micelles</b> <u>Bora Onat</u> , Vural Bütün, Sreeparna Banerjee, İrem Erel-Göktepe <i>Turkey</i>



# Poster Presentations

316	<b>Production of Spray Dried Calcium Phosphate-Gelatin Composite and The Impact of Cross-linking Agent on Composite Structure and Bioactivity in Simulated Body Fluid</b> <u>Tugba Basargan Ozsagioglu</u> , Gülhayat Nasun Saygili <i>Turkey</i>
317	<b>Preparation of Polycaprolactone-Polyethylene Glycol-Casein Bioblends using Spray Dryer</b> <u>Erhan Ozsagioglu</u> , Yuksel Avcibasi Guvenilir <i>Turkey</i>
318	<b>3D-Powder-Printing of Strontium Modified Magnesium Phosphate Cements for Bone Augmentation</b> Emilie März, Claus Moseke, Uwe Gbureck, Jürgen Groll, <u>Elke Vorndran</u> <i>Germany</i>
319	<b>Selection and Optimization of Hydroxyapatite and Chlorapatite Powders for 3D-printing</b> Zeinab Salary, Parastoo Parastoo Jamshidi, <u>Zuzanna Trzcíńska</u> , David Grossin, Ghislaine Bertrand, Olivier Marsan, Cédric Charvillat, Imane Demnati, Moataz Moataz Attallah, Artemis Stamboulis <i>United Kingdom</i>
320	<b>Zirconia-Ceria Hydroxide Sol-Gel Synthesis: Colloid Processing and Powders Preparation for Potential Biomedical Application</b> <u>Damian Nakonieczny</u> , Zbigniew Paszenda, Tomasz Radko <i>Poland</i>
321	<b>Influence of the Colloid System pH for the Phase Composition and Morphology of Cerium Oxide Doped Zirconia Powders – Properties Evaluation</b> <u>Damian Nakonieczny</u> , Zbigniew Paszenda, Sabina Drewniak, Tomasz Radko <i>Poland</i>
322	<b>Synthesis of MTA Powder by Spray-Pyrolysis</b> Jeong-Cheol Lee, Seung-Hoon Um, Bong Kyu Choi, <u>Sang-Hoon Rhee</u> <i>Republic of Korea</i>
323	<b>Direct Fabrication of Porous Titanium Implant via 3D Printing</b> <u>Pavan Kumar Srivas</u> , Kausik Kapat, Prabhash Dadhich, Pallabi Pal Pal, Bodhisatwa Das, Santanu Dhara <i>India</i>
324	<b>Preparation of Electroconductive Titania Scaffolds for Bone Tissue Regeneration</b> <u>Inga Narkevica</u> , Jurijs Ozolins <i>Latvia</i>
325	<b>A Novel Model of Nonalcoholic Fatty Liver Disease in a 3D Liver-on-Chip Device</b> <u>Manuele Gori</u> , Maria Chiara Simonelli, Luca Businaro, Marcella Trombetta, Alberto Rainer <i>Italy</i>
326	<b>Stainless Steels Alloyed with Molybden for Medical Applications</b> <u>Victor Geanta</u> , Ionelia Voiculescu <i>Romania</i>
327	<b>New Titanium Alloys for Medical Applications</b> <u>Ionelia Voiculescu</u> , Victor Geanta <i>Romania</i>
328	<b>A Novel Pluronic/Alginate Scaffold for 3D Liver Cell Culture</b> <u>Manuele Gori</u> , Sara Maria Giannitelli, Pamela Mozetic, Marcella Trombetta, Alberto Rainer <i>Italy</i>
329	<b>As-cast Biodegradable MgCa Alloys –Structure, Mechanical and Corrosion Properties</b> <u>Sonia Boczkal</u> , Michał Karaś, Anna Kozik, Dawid Kapinos, Marzena Lech-Grega <i>Poland</i>
330	<b>Bone Tissue Engineering Using Combined Additive Manufacturing and Microtomography with FEM Verification</b> <u>Jakub Kamiński</u> , Maciej Śniechowski, Sebastian Wroński, Janusz Malinowski, Jacek Tarasiuk <i>Poland</i>



331	<b>Investigating Neovascularization in Rat Decellularized Intestine - an in vitro Platform for Studying Angiogenesis</b> <u>Lindsey Dew</u> , Giulia Gigliobianco, Chuh Chong, Sheila MacNeil <i>United Kingdom</i>
332	<b>Development of a Bioengineered Vascular Niche for the Treatment of Type 1 Diabetes Mellitus</b> Valeria Perugini, <u>Mark Best</u> , Anna Guildford, Gary Phillips, Wendy Macfarlane, Adrian Bone, Matteo Santin <i>United Kingdom</i>
333	<b>Capture Antibodies to Biofunctionalize Vascular Prosthesis</b> Sven Liebler, Fritz Grunert, John Thompson, <u>Burkhard Schlosshauer</u> <i>Germany</i>
334	<b>Utilization of Biocompatible and Biodegradable Polymers in Stem Cell Research and Biomedical Applications</b> Malgorzata Sekula, <u>Patrycja Domalik-Pyzik</u> , Anna Morawska-Chochół, Jakub Czuchnowski, Zbigniew Madeja, Ewa Zuba-Surma, Jan Chłopek <i>Poland</i>
335	<b>High Throughput Materials Discovery of Polymers Resistant to Staphylococcus Epidermidis</b> <u>Andrew Hook</u> <i>United Kingdom</i>
336	<b>Fabrication of Antibacterial Multi-function Materials on Bioactive Micro Arc Oxidized TiO<sub>2</sub></b> Tzer-Min Lee, Yu-Pu Chu, Yen-Ting Liu <i>Taiwan, Province of China</i>
337	<b>Silver-Containing Bioceramics Based on Hydroxyapatite</b> <u>Zoltan Zyman</u> , Mykola Tkachenko, Tatiana Babkina <i>Ukraine</i>
338	<b>Antimicrobial and Toxicological Studies of Novel Chlorhexidine-Hexametaphosphate Nanoparticles for Coating Central Venous Catheters</b> Helena Grady, Sarah Maddocks, Margaret Saunders, Andrew Collins, Michele Barbour <i>United Kingdom</i>
339	<b>Anti-Biofilm Effects of Poly-epsilon-Lysine Dendrons and their Interactions with Bacterial Membranes</b> <u>Orode Aniejurengho</u> , Mariagemiliana Dessi, Steve Meikle, Matteo Santin <i>United Kingdom</i>
340	<b>Influence of Silver Additive on the Physicochemical Properties of the New Cement Type Biomaterials</b> <u>Dominika Siek</u> , Joanna Czechowska, Aneta Zima, Anna Ślósarczyk <i>Poland</i>
341	<b>In vitro Studies of Antibacterial Activity of Sol-Gel Bioglasses Containing Mg, Sr and Au</b> <u>Lidia Ciolek</u> , Andrzej Olszyna, Ewa Zaczyńska, Anna Czarny <i>Poland</i>
342	<b>Bone Allograft with Antibacterial Coating for Therapeutic Application</b> <u>István Hornyák</u> , Edit Madácsi, Pálma Kalugyer, Zsombor Lacza <i>Austria</i>
343	<b>Antimicrobial Efficiency and Bacterial Damage on Copper Surfaces</b> <u>Claudia Hahn</u> , Michael Hans, Frank Muecklich, Ralf Moeller, Reinhard Wirth, Guenther Reitz, Petra Rettberg <i>Germany</i>
344	<b>Antibacterial Sol-Gel Coating of Ceramic TiO<sub>2</sub> Scaffolds for Bone Regeneration</b> <u>David Wiedmer</u> , Cedric Bossard, Hanna Tiainen, Håvard Haugen <i>Norway</i>
345	<b>Metallic Copper as an Antimicrobial Agent for Infection Prevention</b> <u>Michael Hans</u> , Claudia Hahn, Marc Solioz, Ralf Möller, Frank Muecklich <i>Germany</i>
346	<b>Interaction and Miscibility of Biodegradable Polymers with Biologically Active Molecules</b> <u>Eva Sanchez-Rexach</u> , Inger Martínez de Arenaza, Emilio Meaurio, Jose-Ramon Sarasua <i>Spain</i>





347	<b>Bactericidal Behaviour of a New Biodegradable and Biocompatible PLDA/Mg Composite</b> Miguel Ángel Pacha-Olivenza, Juan Pablo Fernández-Hernán, Amparo María Gallardo-Moreno, José Luis González-Carrasco, Sandra Carolina Cifuentes, <u>María Luisa González-Martín</u> <i>Spain</i>
348	<b>Development and in vitro Testing of Gelatin-Based Antibacterial Burn Wound Dressings</b> Birgit Stubbe, <u>Sandra Van Vlierberghe</u> , Gilles Brackman, Mohaddeseh Amiri Aref, Henk Hoeksema, Stan Monstrey, Frank Vanhaecke, Piet Van Espen, Karolien Dewael, Tom Coenye, Peter Dubruel <i>Belgium</i>
349	<b>Improvement of the Antibacterial Properties of Hydroxyapatite Coatings</b> <u>Alina Vladescu</u> , Mariana Braic, Mihaela Badea, Adrian Kiss, Viorel Braic <i>Romania</i>
350	<b>A 17-mer Membrane-Active MSI-78 Derivative with Improved Selectivity Towards Bacterial Cells</b> Claudia Monteiro, Marina Pinheiro, Mariana Fernandes, Sílvia Maia, Catarina L. Seabra, Frederico Ferreira-da-Silva, Salette Reis, Paula Gomes, <u>M. Cristina L. Martins</u> <i>Portugal</i>
351	<b>Comparative Study of the Bactericidal and Chemical Properties of Oxidized Regenerated Cellulose and Oxidized Cellulose Topical Absorbable Hemostats</b> <u>Douglas B Johns</u> , Shubhangi Bhende, Sheri Baker, Benjamin D Fitz, Stephen Rothenburger <i>United States</i>
352	<b>Biological Response To Titanium-Silver Alloys Produced by Powder Metallurgy</b> <u>Barbara Szaraniec</u> , Elżbieta Menaszek, Tomasz Goryczka, Rafał Pokrowiecki, Tomasz Zaręba <i>Poland</i>
353	<b>Silver and Gold Nanoparticle-Based Composites with Chitosan as Efficient and Biocompatible Materials for Antimicrobial Therapy</b> Anna Regiel-Futyr, Małgorzata Kus-Liśkiewicz, Victor Sebastian, Sílvia Irueta, Manuel Arruebo, Agnieszka Kyzioł, Grażyna Stochel <i>Poland</i>
354	<b>Facile Biosynthesis of Silver Nanoparticles Using Tilia Tomentosa Leaf Extract: its Characterization and Antimicrobial Activity</b> <u>Fatih Duman</u> , Murat Kaya, Ismail Ocsoy, Fatma Ozturk Kup, Fatih Dogan Koca <i>Turkey</i>
355	<b>Mg Ions Effect on Staphylococcus epidermidis Strain</b> <u>Jesús Rodríguez-Sánchez</u> , Miguel Ángel Pacha-Olivenza, María Luisa González-Martín <i>Spain</i>
356	<b>Thin Film as an Enzyme Release System for Antimicrobial Applications</b> <u>Andreza Ribeiro</u> , Michaela Müller <i>Germany</i>
357	<b>Bacteria, Biofilms and Mass Spectroscopy: Following the Bacteria's Footprints</b> <u>E. Peter Magennis</u> , Andrew Hook, Paul Williams, David Barrett, Morgan Alexander <i>United Kingdom</i>
358	<b>Bacteria-Instructed Synthesis of Polymers for Self-Selective Microbial Binding and Labelling</b> <u>E. Peter Magennis</u> , Francisco Fernandez-Trillo, Cheng Sui, Sebastian Spain, David Bradshaw, David Churchley, Giuseppe Mantovani, Klaus Winzer, Cameron Alexander <i>United Kingdom</i>
359	<b>Microbial Adhesion On Nanostructured Biomaterials Surfaces</b> <u>Carolin Dewald</u> , Claudia Lüdecke, Martin Roth, Jörg Bossert, Klaus Jandt <i>Germany</i>
360	<b>Design of Ag@SiO<sub>2</sub> Nanorattles for Antimicrobial Implant Coatings</b> <u>Sarah-Luise Abram</u> , Katharina Fromm <i>Switzerland</i>
361	<b>Synthesis of Poly(N-Isopropylacrylamide)-Silver Nanocomposite for Biomedical Applications</b> <u>Milene Tan</u> , Katharina Fromm <i>Switzerland</i>



362	<b>Multilayer Coating of a Nonwoven Polyester Textile for Antibacterial Wound Dressing</b> François Aubert-Viard, Oumaira Rahmouni, Adeline Martin, Feng Chai, Nicolas Tabary, Christel Neut, Bernard Martel, Nicolas Blanchemain <i>France</i>
363	<b>PVCL-based Nanogels as Multi-Drug Delivery System for Hybrid Imaging</b> Andrea Götz, Wa'el Rawashdeh, Andrij Pich, Fabian Kiessling <i>Germany</i>
364	<b>MP-SPR New Characterization Method for Interactions and Ultrathin Films</b> Niko Granqvist, Annika Jokinen, Willem Albers, Janusz Sadowski <i>Finland</i>
365	<b>Quantitative Characterization of Adhesion and Mechanics of Single Cells and Their Interactions with Biomaterials by AFM</b> Torsten Müller, Dimitar Stamov, Jörg Barner, Anne Hermsdörfer, Carmen Pettersson, Torsten Jähne <i>Germany</i>
366	<b>Modular Polymeric Substrate System for Printable Biosensors</b> Peter Sobolewski, Agata Goszczyńska, Agata Niemczyk, Ewa Mijowska, Jacek Podolski, Mirosława El Fray <i>Poland</i>
367	<b>Investigative Method for Clarifying the Allergizing Effect of Substance in Antigen Presentation</b> Melinda Szalóki, Laura Kustos, Csaba Hegedűs <i>Hungary</i>
368	<b>Nanoparticles Sensing on Endothelial Cells by Means of Atomic Force Microscopy and Nanoindentation with an AFM Tip</b> Agnieszka Kołodziejczyk, Sylwia Kotarba, Kinga Kądzioła, Nina Bartoszek, Małgorzata Siatkowska, Paulina Sokołowska, Tomasz Wasiak, Joanna Rywaniak, Katarzyna Działoszyńska, Marta Kamińska, Piotr Komorowski, Krzysztof Makowski, Bogdan Walkowiak <i>Poland</i>
369	<b>Nanomagnetite Composite Implants in Magnetic Resonance Imaging</b> Katarzyna Nowicka, Anna Krak, Henryk Figiel, Krzysztof Turek <i>Poland</i>
370	<b>Rotational Dual-Chamber Bioreactor Designed for Tissue Engineered Interfaces</b> Raphaël F. Canadas, Alexandra P. Marques, Joaquim M. Oliveira, Rui L. Reis <i>Portugal</i>
371	<b>Nanocrystalline Hydroxyapatite Effects on M1 and M2 Macrophage Populations</b> Javier Linares, Ana Belén Fernández, María José Feito, María Concepción Matesanz, Sandra Sánchez-Salcedo, Daniel Arcos, María Vallet-Regí, José María Rojo, María Teresa Portolés <i>Spain</i>
372	<b>Probing Endothelial Cell Behaviour on Extracellular Matrix Mimetic Supported Lipid Bilayers</b> Gulistan Kocer, Pascal Jonkheijm <i>Netherlands</i>
373	<b>Magnesium Implant Degradation Influenced by Blood and Cells</b> Nezha Ahmad Agha, Frank Feyerabend, Boriana Mihailova, Hans-Peter Wendel, Daniel Laipple, Regine Willumeit-Römer <i>Germany</i>
374	<b>Surface-Dependent Mechanical Stability of Adsorbed Human Plasma Fibronectin on Ti6Al4V</b> Virginia Vadiello-Rodríguez, Jose M. Bruque, Amparo M. Gallardo-Moreno, M. Luisa González-Martín <i>Spain</i>
375	<b>Electrophoretic Deposition of Free Standing Collagen Films</b> David Barrett, Terance Hart, Serena Best, Ruth Cameron <i>United Kingdom</i>
376	<b>Determination of Foreign Body Giant Cells after Implantation of Different Biodegradable Materials into Rats</b> Silke Lucke, Uwe Walschus, Andreas Hoene, Jens-Wolfgang Pissarek, Matthias Schnabelrauch, Birgit Finke, Karsten Schröder, Maciej Patrzyk, Michael Schlosser <i>Germany</i>



377	<b>Long Term Stability of Proteins in Contact with Solid Surfaces</b> <u>Tongtong Huang</u> , Karine Anselme, Segolene Sarrailh, Arnaud Ponche <i>France</i>
378	<b>The Bone-Implant Interface – Are Osteocytes at the Implant Surface Responsible for Mechanical Load Transfer?</b> <u>Furqan Ali Shah</u> , Xiaoyue Wang, Peter Thomsen, Kathryn Grandfield, Anders Palmquist <i>Sweden</i>
379	<b>The Distribution of Apatite Nanoparticles Decide the Biological Interaction of Gelatin-Alginate Hydrogels</b> Sergiu Cecoltan, Daniela-Geta Petre, Catalin Tucureanu, Aurora Salageanu, Eugeniu Vasile, Mircea Istodorescu, Dan Laptoiu, Rodica Marinescu, Marius Petrusescu, <u>Izabela-Cristina Stancu</u> <i>Romania</i>
380	<b>A Porous Membrane to Reconstitute Tissue-Tissue Interfaces in a Biomechanical Environment in vitro</b> <u>Ina Prade</u> , Kristin Trommer, Michael Meyer <i>Germany</i>
381	<b>Strontium Folate, a New Alternative for the Treatment of Osteoporosis and Other Bone Diseases</b> <u>Luis Rojo</u> , Sofia Radley-Searle, Cristina Abradelo, Sanjukta Deb, Julio San Roman <i>United Kingdom</i>
382	<b>The Use of Microporous Hydroxyapatite Material in Regenerative Treatment of Periodontal Tissues in Dogs</b> <u>Izabella Polkowska</u> , Anna Ślósarczyk, Aleksandra Sobczyńska-Rak, Magdalena Gołyńska, Tomasz Szponder, Beata Żylińska <i>Poland</i>
383	<b>Bone Substitute from Mineralized Phosphate Prestructured Gelatine – Cell Culture and Mechanical Characterization</b> Benjamin Krupke, Christiane Heinemann, Jana Farack, Hartmut Worch, <u>Thomas Hanke</u> <i>Germany</i>
384	<b>Innovative Bioresorbable Intramedullary Nail for Fixation of Long Bone Fractures, Preliminary Research</b> Jarosław Deszczyński, <u>Tomasz Ciach</u> , Łukasz Nagraba, Tomasz Mitek, Artur Stolarczyk <i>Poland</i>
385	<b>Biomimetic Composites of Chitosan Mineralized with CaCO<sub>3</sub> for Bone Regeneration</b> <u>Timothy Douglas</u> , Sangram Keshari Samal, David Schaubroeck, Kevin Braeckmans, Andre Skirtach <i>Belgium</i>
386	<b>Development of Boron Doped Hydroxyapatite by Biomimetic Method</b> <u>Ekin Ozge Tuncay</u> , Tolga Tugrul Demirtas, Menemse Gumusderelioglu <i>Turkey</i>
387	<b>Intra-molecular Glucosepane Cross-linking of Type I Collagen, Determination of the Site Specificity and its Effect on the Biological and Mechanical Function</b> Thomas Collier, <u>Anthony Nash</u> , Laurent Bozec, Helen Birch, Nora de Leeuw <i>United Kingdom</i>
388	<b>PBSu-based Composite Scaffolds Containing Micro-Bioactive Glass and Nano-Hydroxyapatite for Bone Reconstruction</b> Maria Nearantzaki, Ioanna Koumentakou, <u>Iro Koliakou</u> , Evangelia Siska, Martha Kaloyanni, Dimitrios Bikiaris <i>Greece</i>
389	<b>Microfluidics in Biomaterials For Bone Tissue Engineering Applications</b> Eleftheria Babaliari, George Petekidis, <u>Maria Chatzinikolaidou</u> <i>Greece</i>
390	<b>Porosity Determination in Pure and Hydroxyapatite Reinforced Calcium Phosphate Cements Using <math>\mu</math>CT Images</b> <u>Triantafillos Papadopoulos</u> , Efstathia Tsetsenekou, Stamatia Rokidi, Nikolaos Bouropoulos <i>Greece</i>
391	<b>Effect of Powder/Liquid Ratio on the Strength of Mechano-Chemically Modified <math>\beta</math>-tricalcium Phosphate Cement</b> <u>Yumika Ida</u> , Ji-Young Bae, Kazumitsu Sekine, Fumiaki Kawano, Kenichi Hamada <i>Japan</i>



392	<b>A Dual Crosslinking Strategy for Reinforcing Gelatine-Methacrylamide Hydrogels for Cartilage Repair</b> Ferry Melchels, Kaj Blokland, <u>Riccardo Levato</u> , Jos Malda <i>Spain</i>
393	<b>Design and Characterization of a Composite Material Based on Sr(II)-Loaded Clay Nanotubes Included within a Biopolymer Matrix</b> Stefano Del Buffa, Massimo Bonini, Francesca Ridi, Mirko Severi, Paola Losi, Silvia Volpi, Tamer Al Kayal, <u>Giorgio Soldani</u> , Piero Baglioni <i>Italy</i>
394	<b>Assessment of Magnesium Biodegradability by Micro-CT Platform</b> <u>Ivana Ročňáková</u> , Edgar B. Montufar, Miroslava Horynová, Tomáš Zikmund, Karel Novotny, Ladislav Celko, Lenka Klakurkova, Jozef Kaiser <i>Czech Republic</i>
395	<b>In-vitro Evaluation of Bioactivity of Chemically Treated Titanium Metals in the Presence of Proteins</b> <u>Weitian Zhao</u> , Jacques Lemaître, Paul Bowen <i>Switzerland</i>
396	<b>Artificial Extracellular Matrices with Sulfated Glycosaminoglycans Promote the Osteogenic Differentiation of Osteoblast Precursor Cells</b> <u>Sarah Vogel</u> , Ute Hempel, Stephanie Möller, Matthias Schnabelrauch, Vera Hintze, Dieter Scharnweber <i>Germany</i>
397	<b>In situ Setting Calcium Magnesium Phosphate Bone Cements as Drug Carrier System</b> Andreas Hoess, Anna Schmidt, Theresa Christel, Berthold Niess, Jürgen Groll, Uwe Gbureck, <u>Elke Vorndran</u> <i>Germany</i>
398	<b>MgCO<sub>3</sub> and (Mg/Ca)CO<sub>3</sub> Microparticles for Bone Regeneration: Synthesis, Characterization and Applications</b> <u>Katarzyna Reczyńska</u> , Timothy E.L. Douglas, Agata Łapa, Krzysztof Pietryga, Andre G. Skirtach, Elżbieta Pamuła <i>Poland</i>
399	<b>Mechanical and Biological Characterization of Brushite/PCL Scaffolds</b> <u>Alberto Lagazzo</u> , Claudia Fabbi, Giuseppe Cama, Fabrizio Barberis, Marco Capurro <i>Italy</i>
400	<b>Brushite-Aminoacid Composite Materials: Properties and Interactions at a Molecular Level</b> <u>Alberto Lagazzo</u> , Fabrizio Barberis, Elisabetta Finocchio <i>Italy</i>
401	<b>In vitro Performance of Biomimetic Hydroxyapatite: Unravelling the Effect of Ionic Exchange</b> <u>Joanna Maria Sadowska</u> , Jordi Guillem Marti, Maria Pau Ginebra Molins <i>Spain</i>
402	<b>Collagen Gel in Hip Cartilage Repair, the in vivo Preliminary Study</b> <u>Anna Bajek</u> , Joanna Skopińska-Wiśniewska, Aldona Rynkiewicz, Arkadiusz Jundziłł, Magdalena Bodnar, Andrzej Marszałek, Tomasz Drewa <i>Poland</i>
403	<b>Osteointegration of a Macroporous Cement Designed to Repair Large Cancellous Bone Defects</b> Bruno Cimatti, Wendell Barboza, Marcelo Nogueira-Barbosa, <u>Edgard Engel</u> <i>Brazil</i>
404	<b>In vitro Cytotoxicity and in vivo Acute Toxicity of Porous Cements Based on Polymethylmethacrylate and Castor Oil Polyurethane</b> Mariana Santos, Bruno Cimatti, Maria Sol Brassesco, Laura Okano, <u>Edgard Engel</u> <i>Brazil</i>
405	<b>Phosphate-Hydroxyapatite Cements: Mechanical Stress Analysis and Osteoblastic Induction</b> Toshimi Kano, Stamatia Rokidi, Eumorphia Remboutsika, Dionysios Mouzakis, Stefanos Zaoutsos, Nikolaos Bouropoulos, <u>Eleni Douni</u> <i>Greece</i>
406	<b>Functionalized Polymeric Composite Nano-Fibrous Scaffold for Bone Tissue Engineering</b> Prabhash Dadhich, Bodhisatwa Das, Pavan Srivas, <u>Pallabi Pal</u> , Joy Dutta, Sabyasachi Ray, Santanu Dhara <i>India</i>



407	<b>Biodegradable Mg-Alloys with Ultra-Fine Grain Structure for Orthopaedic Applications</b> <u>Eva Jablonská</u> , Peter Minárik, Jan Lipov, Tomáš Ruml <i>Czech Republic</i>
408	<b>Cytocompatibility of Novel PLDA/Mg Composites as Biodegradable Implants for Bone Repair</b> Sandra Cifuentes, Fatima Bensiamar, Tim Osswald, José Luis González-Carrasco, Eduardo García-Cimbrelo, Nuria Vilaboa, <u>Laura Saldaña</u> <i>Spain</i>
409	<b>Local Recovery of Bone Tissue in Osteoporotic Rabbit Hip after Implantation of HAP/TCP Bioceramic Granules</b> <u>Ilze Salma</u> , Sandris Petronis, Mara Pilmane, Andrejs Skagers, Vita Zalite, Janis Locs <i>Latvia</i>
410	<b>Multinucleated Giant Cell Formation in Different Xenogeneic Bone Substitute Materials, Preclinical and Clinical Studies</b> <u>Jonas Lorenz</u> , Mike Barbeck, Charles J. Kirkpatrick, Robert Sader, Shahram Ghanaati <i>Germany</i>
411	<b>Mechanical and in vitro Properties of Stereocomplex Polylactide Coatings on Porous Bioactive Glass Scaffolds for Bone Regeneration</b> <u>Peter Uppstu</u> , Simon Engblom, Saara Inkinen, Leena Hupa, Carl-Eric Wilén <i>Finland</i>
412	<b>The Osteogenic Effect of Alginate Nanoparticles Contained Bone Morphogenetic Proteins-2 on Bone Marrow Stromal Cells</b> <u>Ho Yun Chung</u> , Hyun Ju Lim, Jae Bong Kim, Eun Jung Oh, Tae Jung Kim, Jin Hyun Choi <i>Republic of Korea</i>
413	<b>Space-Maker Membrane Modified with Ceramic Nanoparticles</b> <u>Ewa Stodolak-Zych</u> , Katarzyna Medrela <i>Poland</i>
414	<b>Evaluation of the Biofuncionality of Internal Fixation Plates for Small Animals</b> <u>Barbara Szaraniec</u> , Karol Gryń, Tomasz Szponder, Aleksandra Wąsik <i>Poland</i>
415	<b>The Influence of Poly(Ethylene Glycol) with Different Molecular Weight on the Properties of Acrylic Bone Cements</b> <u>Klaudia Król</u> , <u>Kinga Pielichowska</u> <i>Poland</i>
416	<b>Optimizing Tibial Fractures Treatment With Carbon-Plate Fixator – CARBOELASTOFIX</b> <u>Maciej Ambroziak</u> , Jan Chłopek, <u>Anna Morawska-Chochół</u> , Wojciech Zakiewicz <i>Poland</i>
417	<b>The Influence of Chain Extender on Properties of Polyurethane-Based Composites as Potential Injectable Bone Substitutes</b> <u>Piotr Szczepańczyk</u> , Kinga Pielichowska, Jan Chłopek <i>Poland</i>
418	<b>Human Amniotic Membrane for Bone Regeneration of Calvaria Defects in Mice</b> Mathilde Fénelon, Claudine Boiziau, Reine Bareille, Olivier Chassande, Sylvie Rey, Hélène Boeuf, Florelle Gindraux, Zoran Ivanovic, <u>Jean-Christophe Fricain</u> <i>France</i>
419	<b>The Influence of Synthesis Environment on Thermal Properties Of Chitosan-Based Nanocomposites</b> <u>Krzysztof Pazdan</u> , Kinga Pielichowska, Jan Chłopek <i>Poland</i>
420	<b>Why Incorporation of Poly(Ethylene Glycol) into Polyurethane Chain is an Attractive Way to Improve its Physicochemical Properties for Bone Regeneration?</b> <u>Michalina Marzec</u> , Justyna Kucinska-Lipka, Helena Janik <i>Poland</i>
421	<b>Construction of a Funtional Bone Implant to Direct the Biomineralization Process</b> <u>Inas Özcan</u> , Kursad Kazmanlı, Fatma Nese Kok <i>Turkey</i>





422	<b>Mechanically Robust and Sterilizable, Biosignalling Surfaces for Metallic and Polymer Orthopedic Implants</b> Marcela Bilek, Wojciech Chrzanowski, <u>Edgar Wakelin</u> , Giselle Yeo, Alexey Kondyurin, David McKenzie, Anthony Weiss <i>Australia</i>
423	<b>Exploring Osteoclastogenesis in a Co-Culture System</b> <u>Sabine Schulze</u> , Peter Dieter, Ute Hempel <i>Germany</i>
424	<b>Chondrogenic Differentiation of Mesenchymal Stem Cells Derived from Osteoarthritic Patients on Pure or Chitosan-Coated Poly(L-Lactic Acid) Scaffolds</b> <u>Joana Magalhães</u> , Cristina Álvarez-Martínez, Elena F. Burguera, Cristina Ruiz-Romero, José Luís Gómez-Ribelles, Francisco J. Blanco <i>Spain</i>
425	<b>Resorbable Scaffolds with Sodium Alendronate Loaded Microparticles for the Treatment of Bone Tissue Defects</b> <u>Małgorzata Krok-Borkowicz</u> , Urszula Posadowska, Karolina Tos, Elżbieta Pamuła <i>Poland</i>
426	<b>Composition Structure Relationships in the Anomaly Range of a Tertiary Borate Glass</b> <u>Kathleen MacDonald</u> , Margaret Hansen, Daniel Boyd <i>Canada</i>
427	<b>Artificial Bones for Laboratory Tests on Dentistry Devices</b> <u>Elisa Rossi</u> , Alberto Lagazzo, Fabrizio Barberis <i>Italy</i>
428	<b>Alginate-Based Magnetic Electrospun Matrixes for Potential Hyperthermia Treatment</b> Yen-Hsuan Chen, Wan-Ju Chang, Tzer-Min Lee, Chi-Hui Cheng, <u>Jui-Che Lin</u> <i>Taiwan, Province of China</i>
429	<b>Antitumor Effects for Osteosarcoma Cells by Carbon Nanotubes</b> <u>カオリ Aoki</u> , Masanori Okamoto, Seiji Takanashi, Shinsuke Kobayashi, Hiroki Nomura, Manabu Tanaka, Takashi Takizawa, Hiroyuki Kato, Yuki Usui, Hisao Haniu, Naoto Saito <i>Japan</i>
430	<b>Electrically-Triggered Delivery System for Regional Chemotherapy</b> <u>Katarzyna Krukiewicz</u> , Magdalena Cichy, Barbara Bednarczyk-Cwynar, Piotr Ruszkowski, Tomasz Jarosz, Mieczysław Łapkowski, Jerzy Żak <i>Poland</i>
431	<b>Targeted Cancer Therapy</b> <u>Monika Dzieciuch-Rojek</u> , Mariusz Kępczyński, Maria Nowakowska, Marcin Majka <i>Poland</i>
432	<b>miRNA Treatment for Bone Metastasis Inducing Prostate Cancer</b> <u>Marine Chalanqui</u> , Sreekanth Pentlavalli, Stephen Loughran, Michelle O'Doherty, Philip Chambers, Nicholas Dunne, Helen McCarthy <i>United Kingdom</i>
433	<b>Development of a Polymeric Conjugate Foreignizing Tumor Cells for Targeted Immunotherapy in Vivo</b> Hong Yeol Yoon Yoon, Young-Ho Lee, <u>Jung Min Shin</u> , Tae Woo Kim, Jae Hyung Park <i>Republic of Korea</i>
434	<b>Electrochemistry and Thin-Layer Spectroelectrochemistry of PDT Active Phthalocyanines</b> <u>Łukasz Łapok</u> , Arkadiusz Gut, Maria Nowakowska <i>Poland</i>
435	<b>Alginate-Based Matrices as 3D in vitro Model to Investigate EMT and its Reversion</b> <u>Silvia Bidarra</u> , Sara Rocha, Patrícia Oliveira, Carla Oliveira, Cristina Barrias <i>Portugal</i>
436	<b>Modelling of Antimetastatic Agent NAMI-A Fate After Serum Administration</b> <u>Klaudyna Śpiewak</u> , Małgorzata Brindell <i>Poland</i>





437	<b>Alginate/Protein Hybrid Hydrogels for Vascular Grafts: Effects on Human Vascular Cell Attachment and Growth</b> Raminder Singh, Bapi Sarker, Raquel Silva, Rainer Detsch, Aldo R. Boccaccini, <u>Iwona Cicha</u> <i>Germany</i>
438	<b>Nanotopography of TiN Produced on Plasma Region under Glow Discharge Conditions Enhances Endothelial Cells Adhesion</b> <u>Agnieszka Sowińska</u> , Elżbieta Czarnowska, Joanna Bierła, Tomasz Borowski, Tadeusz Wierchoń <i>Poland</i>
439	<b>Electrospun Polylactide-Polycaprolactone Copolymer for Vascular Tissue Engineering</b> <u>Jana Horakova</u> , Petr Mikes, Ales Saman, Michal Ackermann <i>Czech Republic</i>
440	<b>Combination of Vinpocetine and AcSDKP for Developing Drug-Eluting Stent with Anti-Inflammatory Function</b> Seong Ho Seo, Kwang-Sook Park, Samy Gobaa, Yoon Ki Joung, Ik Hwan Kim, <u>Dong Keun Han</u> <i>Republic of Korea</i>
441	<b>Capture of Late Endothelial Progenitor Cell by anti-CD146 Antibody Immobilization on Nano-Filamentous Silicone Coated Stent</b> Sung Nam Kang, Yoon Ki Joung, <u>Dong Keun Han</u> <i>Republic of Korea</i>
442	<b>Magnetic Susceptibility and Hardness of Alloys of Au and Group V Elements (Nb, Ta) for MRI Artifact-Free Biomedical Applications</b> <u>Kenichi Hamada</u> , Shihoko Inui, Emi Uyama, Eiichi Honda <i>Japan</i>
443	<b>Magnetic Susceptibility and Hardness of Alloys of Au and Group IV Elements (Ti, Zr) for MRI Artifact-free Biomedical Applications</b> <u>Shihoko Inui</u> , Emi Uyama, Eiichi Honda, Kenichi Hamada <i>Japan</i>
444	<b>Dissolution &amp; Mechanical Properties of Bioresorbable Glass Fibres for use in Paediatric Stents</b> <u>Isaiah Adekanmbi</u> , K Elizabeth Tanner, Haytham Kubba, Helen Lu <i>United Kingdom</i>
445	<b>A Combined Method for Bilayered Vascular Graft Fabrication</b> Tamer Al Kayal, Devid Maniglio, Walter Bonani, Paola Losi, Claudio Migliaresi, <u>Giorgio Soldani</u> <i>Italy</i>
446	<b>Circulating Cell-Capturing Technology for Rapid Neointima Formation and Excellent Patency of Acellular Vascular Grafts with 2mm ID and 30cm Length</b> <u>Tetsuji Yamaoka</u> , Marina Kitai, Maria Munisso, Naoki Kobayashi, Shota Somekawa, Yoshiaki Hirano, Yuichi Ohya, Atsushi Mahara <i>Japan</i>
447	<b>Interaction Of Nanocomposites Containing Carbon Fillers With Different Degradation Media</b> <u>Agnieszka Piegat</u> , Zygmunt Staniszewski, Mirosława El Fray <i>Poland</i>
448	<b>Scanning Electron Microscopy Assessment of the Silicon Endocardial Extracted Leads</b> <u>Magdalena Ziabka</u> , Barbara Malecka, Andrzej Zabek, Krzysztof Boczar <i>Poland</i>
449	<b>Investigation into Surface Characteristics of Coronary Stents</b> <u>Sarah Morgan</u> , Richard.A Black, Christopher McCormick <i>United Kingdom</i>
450	<b>Influence of Preservative on the Tensile Strength of the Tissue of Porcine Circulatory System</b> <u>Alicja Stanisławska</u> , Kinga Dawidowska <i>Poland</i>
451	<b>Encapsulation of Anti-Inflammatory Drug into PCL Based Electrospun Fibres for Nerve Regeneration</b> Valentina Cirillo, <u>Vincenzo Guarino</u> , Annunziata Cummaro, Olimpia Oliviero, Luigi Ambrosio <i>Italy</i>



452	<b>Preparation of Biomedical Poly(<math>\epsilon</math>-caprolactone) via Ring Opening Polymerization Catalyzed by <i>Candida Antarctica</i> Lipase B In Ionic Liquids</b> <u>Urszula Piotrowska</u> , Marcin Sobczak, Ewa Olędzka <i>Poland</i>
453	<b>The Biomimetic Hydrogel Matrix for Long-term Cell Culturing</b> <u>Agata Stefanek</u> , Tomasz Ciach <i>Poland</i>
454	<b>Microencapsulation and Nano coating of Pancreatic Beta Cells</b> <u>Niusha Nikraves</u> , Gurpreet Chouhan, Anita Ghag <i>United Kingdom</i>
455	<b>Design of a 3D Bone Cell Co-Culture System Using Mineralised Alginate Microbeads</b> David Bassett, Sabrina Ehnert, Andreas Nussler, Pawel Sikorski <i>Norway</i>
456	<b>Design of Polymeric Membranes for the Encapsulation of Pancreatic Islets</b> <u>Anna Cavallo</u> , Ugo Masullo, Francesca Gatti, Amilcare Barca, Marta Madaghiele, Alessandro Sannino <i>Italy</i>
457	<b>Cell-Based Therapy for Targeted Treatment of Lung Injury</b> Sally Yunsun Kim, Hak-Kim Chan, Janette Burgess, Hak-Kim Chan, <u>Wojciech Chrzanowski</u> <i>Australia</i>
458	<b>Development of Limonene Compositd Lipid Nanocarriers of Tretinoin for Dermal Delivery</b> <u>Ponwanit Charoenputtakun</u> , Praneet Opanasopit, Theerasak Rojanarata, Tanansait Ngawhirunpat <i>Thailand</i>
459	<b>Gene Activated Matrix For Mesenchymal Stem Cells – Application To Cartilage Regeneration</b> <u>Sophie Raisin</u> , Marc Mathieu, Danièle Noël, Christian Jorgensen, Jean-Marie Devoisselle, Emmanuel Belamie, Marie Morille <i>France</i>
460	<b>Skin Penetration Enhancement of Hydrophilic Macromolecules using Microneedles Combination with Electroporation and Sonophoresis: Effect of Molecular Weight on Skin Permeation</b> <u>Maleenart Petchsangjai</u> , Praneet Opanasopit, Theerasak Rojanarata, Tanasait Ngawhirunpat <i>Thailand</i>
461	<b>Poly-L-lysine Based Covalently Crosslinked Bionanocomposites with Controlled Drug Release and Cell Adhesion Properties</b> <u>Jain Minkle</u> , Kazuaki Matsumura <i>Japan</i>
462	<b>New Macromolecular Conjugates of Camptothecin - Synthesis, Characterization and in Vitro Evaluation</b> Marcin Sobczak, Ewa Olędzka, Paweł Horeglad, Urszula Piotrowska, Andrzej Plichta, Joanna Kolmas, Grzegorz Nałęcz-Jawecki <i>Poland</i>
463	<b>Preparation and Therapeutic Effect of Calcium Phosphate Nano-Capsules Enclosing DNA/PEI/Hyaluronic Acid Complex for Durable Gene Expression</b> <u>Tomoko Ito</u> , Yoshiyuki Koyama, Masazumi Eriguchi, Makoto Otsuka <i>Japan</i>
464	<b>Thermally Responsive Core-Shell Nanocapsules with Independent Dual Drug Release Profiles for Combined Therapy of Osteoarthritis</b> <u>Mi Lan Kang</u> , Ji Eun Kim, Gun-Il Im <i>Republic of Korea</i>
465	<b>Combined Scaffold Composed of Hydroxyapatite/Biodegradable Polymer and Pamidronate as a Model Drug for the Therapy of Bone Tumour</b> <u>Ewa Oledzka</u> , Marcin Sobczak, Joanna Kolmas, Grzegorz Nałęcz-Jawecki <i>Poland</i>
466	<b>Poly(Lactic-co-Glycolic Acid)-Based Nanoparticles as Drug Delivery Systems for Doxycycline Hyclate and Simvastatin for the Treatment of Inflammation-Caused Bone Resorption</b> <u>Manuel Schweikle</u> , Hanna Tiainen, Håvard Haugen <i>Norway</i>



467	<b>Upsalite: Novel Mesoporous Drug Delivery System</b> Peng Zhang, Teresa Zardán Gómez de la Torre, Johan Forsgren, Maria Strømme <i>Sweden</i>
468	<b>Morphological and Biomechanical Analysis of Biodegradable Electrospun Scaffolds for Drug Delivery</b> Alexandros Repanas, Panagiotis Kalozoumis, <u>Sofia Andriopoulou</u> , Sotirios Korossis, Birgit Glasmacher <i>Germany</i>
469	<b>Controlled Release of Acyclovir from Cytosine-Modified Polymer Matrix</b> Katarzyna Klysik, <u>Anna Karewicz</u> , Aneta Pietraszek, Krzysztof Szczubiałka, Maria Nowakowska <i>Poland</i>
470	<b>Biological Assessment of Polymeric Micelles-Based Powders for Pulmonary Administration of Biopharmaceutics</b> Fernanda Andrade, José das Neves, Pedro Fonte, <u>Francisca Araújo</u> , Petra Gener, Simó Schwartz, Mafalda Videira, Domingos Ferreira, Mireia Oliva, Bruno Sarmento <i>Portugal</i>
471	<b>Developing Stable Chitosan Microspheres for Biomedical Applications</b> Ewelina Kozikowska, <u>Monika Bil</u> , Wojciech Świążkowski <i>Poland</i>
472	<b>Plasma-Grafted Intraocular Lenses for Controlled Release of Moxifloxacin</b> Ana Vieira, Andreia Pimenta, Patrícia Alves, Patrícia Coimbra, Helena Gil, José Mata, Ana Serro, <u>António Guiomar</u> <i>Portugal</i>
473	<b>Bioengineering of Spider Silk Protein to Modify its Affinity for Drugs</b> Kamil Kucharczyk, Katarzyna Jastrzebska, Ewelina Dondajewska, Andrzej Mackiewicz, <u>Hanna Dams-Kozłowska</u> <i>Poland</i>
474	<b>Functionalized Bioengineered Spider Silk for CpG-siRNA Delivery</b> Anna Kozłowska, Maciej Smialek, Anna Florczak, Andrzej Mackiewicz, Marcin Kortylewski, <u>Hanna Dams-Kozłowska</u> <i>Poland</i>
475	<b>Encapsulation and Controlled Release of L-Ascorbic Acid via Bioblends</b> <u>Erhan Ozsagioglu</u> , Yuksel Avcibasi Guvenilir <i>Turkey</i>
476	<b>Silicone Stabilized Liposomes as Novel Nanostructural Drug Carriers</b> <u>Joanna Lewandowska-Łańcucka</u> , Katarzyna Mystek, Maria Nowakowska <i>Poland</i>
477	<b>Design of Biodegradable pH-Responsive Microgels as Efficient Targeted Drug Delivery System</b> Damien Dupin, Adrián Pérez-San Vicente, Pablo Casuso, Natividad Díaz, Iraidia Loinaz <i>Spain</i>
478	<b>Partially Oxidized Alginate Grafted with <math>\beta</math>-CyD: A Potential Release System for Biomedical Molecules</b> <u>Line Aa. Omtvedt</u> , Marianne Ø. Dalheim, Thorbjørn T. Nielsen, Kim L. Larsen, Berit L. Strand, Finn L. Aachmann <i>Norway</i>
479	<b>Increased Cellular Uptake of Exosomes via Active Macropinocytosis Induction</b> <u>Ikuhiko Nakase</u> , Nahoko Bailey Kobayashi, Tomoka Takatani-Nakase, Tetsuhiko Yoshida <i>Japan</i>
480	<b>Electrospraying of Aliphatic Polyesters for Drug Delivery Systems</b> <u>Aleš Šaman</u> , Jana Horáková, Kateřina Pilařová, Petr Mikeš <i>Czech Republic</i>
481	<b>Injectable Platforms Containing Functionalised Mesoporous Silica Nanoparticles for Controlled Release of Chemotherapeutics</b> <u>Assunta Borzacchiello</u> , Luisa Russo, Andrea Salis, Luca Medda, Maura Monduzzi, Gerardino D'Errico, Luigi Paduano, Luigi Ambrosio <i>Italy</i>
482	<b>Visible Light-Curable, Nanoparticles Created Hydrogel for in situ Useable Drug Delivery System</b> <u>József Bakó</u> , Farkas Kerényi, Edit Hrubí, Lajos Daróczy, Beatrix Dienes, Csaba Hegedűs <i>Hungary</i>



483	<b>Liposomal Formulations as Treatment for Facial Erythema of Rosacea</b> Anca N Cadinoiu, <a href="#">Lacramioara Ochiuz</a> , Delia M Rata, Oana M Daraba, Vasile Burlui, Marcel Popa <i>Romania</i>
484	<b>Tetracycline - Loaded Chitosan/Pectin Hydrogels for the Treatment of Periodontitis</b> Delia M Rata, Anca N Cadinoiu, Oana Daraba, Vasile Burlui, <a href="#">Lacramioara Ochiuz</a> , Marcel Popa <i>Romania</i>
485	<b>The Quantification of Doxorubicin and Lipids in Liposomal Doxorubicin Formulation</b> <a href="#">Jan Procek</a> , Maciej Łukawski, Magdalena Przybyło, Marek Langner <i>Poland</i>
486	<b>Lactic Acid Photocrosslinkable Adhesives to be Used as Transdermal Delivery Systems</b> <a href="#">João Santos</a> , Filipe Aguiar, Fernando Cruz, Cristina Baptista <i>Portugal</i>
487	<b>Pitavastatin Loaded Calcium Phosphate Foams for Enhanced Mineralization and Vascularization</b> Kanupriya Khurana, Jordi Guillem-Marti, <a href="#">Cristina Canal</a> , Maria-Pau Ginebra <i>Spain</i>
488	<b>Stability Enhanced Gold-Cross-Linked Polymeric Nanocarriers</b> <a href="#">Sangmin Jeon</a> , Hong Yeol Yoon, Dong Gil You, Hwa Seung Han, Ick Chan Kwon, Kwangmeyung Kim, Jae Hyung Park <i>Republic of Korea</i>
489	<b>Brushite/Alginate Microbeads for Sustained Drug Delivery</b> <a href="#">Alberto Lagazzo</a> , Laura Pastorino, Noemi Frisina, Fabrizio Barberis, Marco Capurro <i>Italy</i>
490	<b>High Intensity Focused Ultrasound-Mediated Doxorubicin Delivery Using Thermosensitive Liposome: Induced Drug Bursting Release by Mild Hyperthermia</b> <a href="#">Wooram Um</a> , Dong Gil You, Ju Eun Jeon, Jae Hyung Park <i>Republic of Korea</i>
491	<b>Photothermal Treatment to Remotely Control Drug Release from Plasmonic Lipogels</b> <a href="#">Francisco Martín-Saavedra</a> , Martín Prieto, Manuel Arruebo, Jesús Santamaría, Gert Storm, Wimm Hennik, Eduardo Ruiz-Hernández, Nuria Vilaboa <i>Spain</i>
492	<b>Determination of Liposomal Doxorubicin Concentration in Blood by Fluorescence Spectroscopy</b> <a href="#">Maciej Łukawski</a> , Magdalena Przybyło, Marek Langner <i>Poland</i>
493	<b>Capability of Polymer Ceramics Drug Delivery System</b> <a href="#">Ewa Stodolak-Zych</a> , Barbara Samolej, Alicja Rapacz-Kmita <i>Poland</i>
494	<b>Hydrolysis of Crosslinked Poly(Ester Anhydride) Networks in Different pH Conditions</b> <a href="#">Sanja Asikainen</a> , Harri Korhonen, Jukka Seppälä <i>Finland</i>
495	<b>Ceramic Scaffolds Containing Gentamicin Sulphate Loaded Poly(Lactic-co-Glycolic Acid) Microparticles for Bone Tissue Engineering</b> <a href="#">Łucja Rumian</a> , Hanna Tiainen, Urszula Posadowska, Monika Brzychczy-Włoch, Håvard J. Haugen, Elżbieta Pamuła <i>Poland</i>
496	<b>Influence of Degradation of D,L-PLGA on the Release of Risperidone</b> Artur Turek, <a href="#">Aleksandra Borecka</a> , Katarzyna Jelonek, Janusz Kasperczyk, Henry Janeczek, Agata Skibińska-Zuber, Piotr Dobrzyński, Marcin Libera <i>Poland</i>
497	<b>FOL-PEG-g-PEI-g-PLGA Polymeric Vector for Gene Delivery: Synthesis and Characterization</b> <a href="#">Chaoyu Liu</a> , Min Wang <i>Hong Kong</i>
498	<b>Assessment of Drug Incorporation and Release from a Novel Coronary Stent Coating</b> <a href="#">Craig Martin McKittrick</a> , Simon Dixon, Christopher McCormick <i>United Kingdom</i>



499	<b>BMP-2 Release from Collagenous Particles</b> <u>Didem Mumcuoglu</u> , Laura de Miguel, Gerjo van Osch <i>Netherlands</i>
500	<b>Functionalized Hydrophilic Nanogels for Endogenous Radiotherapy</b> <u>Smriti Singh</u> , Natascha Drude, Felix M. Mottaghy, Agnieszka Morgenroth, Martin Moeller <i>Germany</i>
501	<b>Advanced Poly-(ε)-Lysine Dendrons as Functional Non Viral Macromolecules to Target Pancreatic β Cells</b> <u>Mariagemiliana Dessi</u> , Valeria Perugini, Gary Phillips, Matteo Santin <i>United Kingdom</i>
502	<b>Silica Particles for the Design of Smart Delivery Nanotools</b> Rafał Mech, <u>Beata Borak</u> , Katarzyna Łuszczzyk, Daniel Lewandowski, Agnieszka Baszczuk, Marek Jasiorski, Jerzy Kaleta <i>Poland</i>
503	<b>Cell Penetrating Peptide Constructs: Novel Drug Delivery to the Eye</b> <u>Felicity de Cogan</u> , Lisa J Hill, Peter J Morgan-Warren, Anna FA Peacock, Robert AH Scott, Ann Logan <i>United Kingdom</i>
504	<b>Inhibiting Pathogenous Processes by siRNA Releasing Polymer Coatings</b> <u>Diane Zengerle</u> , Olivia König, Christian Schlensak, Tobias Walker, Hans-Peter Wendel, Andrea Nolte-Karayel <i>Germany</i>
505	<b>Synthesis and Characterization of Poloxamer-Based Theranostic Vehicles</b> <u>Karolina Morawska</u> , Anna de la Fuente, Sandra Van Vlierberghe, Frank Roesh, Peter Dubruel <i>Belgium</i>
506	<b>Injectable Extracellular Matrix Hydrogels as Scaffolds for Spinal Cord Injury Repair</b> <u>Sarka Kubinova</u> , Dmitry Tukmachev, Serhiy Forostyak, Kristyna Zaviskova, Zuzana Koci, Eva Sykova <i>Czech Republic</i>
507	<b>Nerve Guidance Channels of Synthetic Biodegradable Polymers with Internal Hydrogel Scaffold of Radiation-Crosslinked Polysaccharide</b> <u>Radosław Wach</u> , Jarosław Cala, Karolina Kowalska-Ludwicka, Charito Aranilla, Agnieszka Adamus, Alicja Olejnik, Zbigniew Pasięka, Janusz Rosiak, Piotr Ulanski <i>Poland</i>
508	<b>A Potential Advantage of Alginate and Poly(3,4ethylenedioxythiophene): Poly(styrenesulfonate) (PEDOT:PSS) Blended for Neurite Outgrowth</b> <u>Pichaya Srisuk</u> , Nandita Singh, Jonathan Hanley, Sameer Rahatekar <i>United Kingdom</i>
509	<b>Polyurethane/Polylactide Electrospun Nonwovens for Neural Tissue Engineering</b> Anna Lis, Jakub Grzesiak, Ryszard Fryczkowski, Dariusz Szarek, Krzysztof Marycz, Włodzimierz Jarmundowicz, Jadwiga Laska <i>Poland</i>
510	<b>Alginate-Based Hydrogels as Artificial Extracellular Matrix for Central Nervous System Regeneration</b> Anna Lis, Jakub Grzesiak, Joanna Mastalska- Popławska, Dariusz Szarek, Krzysztof Marycz, Włodzimierz Jarmundowicz, Jadwiga Laska <i>Poland</i>
511	<b>Poly Glycerol Sebacate for Use as a Neuronal Biomaterial</b> <u>Dharaminder Singh</u> , John Haycock, Frederik Claeysens <i>United Kingdom</i>
512	<b>Ease and Inexpensive Technique for Manufacturing Chitosan Scaffolds for Neuronal Tissue Engineering</b> Danilo Akio Kakazu, <u>Sonia Maria Malmonge</u> <i>Brazil</i>
513	<b>Surface Properties of Sterilized Polyurethane/Polylactide Films</b> Paulina Bednarz, Mateusz Marzec, <u>Jadwiga Laska</u> <i>Poland</i>
514	<b>Development of Microstructured Collagen-Based Nerve Guides for Peripheral Nerve Regeneration</b> <u>Hans Leemhuis</u> , Leon Olde Damink, Lizette Eummelen, Frank Schügner, Sabien van Neerven, Norbert Pallua, Ahmet Bozkurt <i>Germany</i>





515	<b>Shape Memory Polymeric Scaffolds in Tendon Regeneration</b> <u>Ghazal Tadayyon</u> , Gemma Orpella-Aceret, Manus Jonathan Paul Biggs <i>Ireland</i>
516	<b>Electrochemical Study of Uncemented Hip Endoprosthesis Cups</b> <u>Wojciech Kajzer</u> , Anita Kajzer, Jacek Semenowicz, Adam Mroczka, Ola Grzeszczuk <i>Poland</i>
517	<b>Synthetic, pH-Responsive Glycopolypeptides and their Interactions with Lectins</b> <u>Katharina Haak</u> , Robert Mildner, Henning Menzel <i>Germany</i>
518	<b>Biological Properties of Oxynitrided Layers on NiTi Shape Memory Alloy Produced under Glow Discharge Conditions</b> <u>Justyna Witkowska</u> , Agnieszka Sowińska, Elżbieta Czarnowska, Tomasz Borowski, Tadeusz Wierchoń <i>Poland</i>
519	<b>Thiolated Chitosan: Biomaterial of Electrospun Nanofiber Mats for Mucoadhesive Drug Delivery</b> <u>Wipada Samprasit</u> , Ruchadaporn Kaomongkolgit, Prasert Akkamongkolporn, Theerasak Rojanarata, Tanasait Ngawhirunpat, Praneet Opanasopit <i>Thailand</i>
520	<b>Zwitterionic Polyampholyte as a Novel Inhibitor of Lysozyme Aggregation</b> <u>Robin Rajan</u> , Kazuaki Matsumura <i>Japan</i>
521	<b>pH Dependence of Disruption of Liposomal Membranes by Artificial Lytic Peptide</b> <u>Ayumi Kashiwada</u> , Masaki Mizuno, Iori Yamane, Jun-ichi Hashimoto <i>Japan</i>
522	<b>Synthetic Biphasic Scaffold Composed of Polylactic Acid (PLA) and PLA / Bioactive Glass (G5) - Guided Vascularization Induced by Multinucleated Giant Cells</b> Mike Barbeck, <u>Patrick Booms</u> , Tiziano Serra, Robert Sader, Charles James Kirkpatrick, Melba Navarro, Shahram Ghanaati <i>Germany</i>
523	<b>Biosynthesis of CdS Quantum Dots by Leaf Extract of Water Mint (Mentha aquatica L.)</b> <u>Fatih Duman</u> , Hakan Colak, Fatih Dogan Koca, Goksel Sezen <i>Turkey</i>
524	<b>Design of Multilayer Collagen-Based Systems for in situ Drug and/or Cell Release</b> <u>Diogo Lopes Rodrigues</u> , Teresa Russo, Ugo D'Amora, Olimpia Oliviero, Antonio Gloria, Roberto De Santis, Luigi Ambrosio <i>Italy</i>
525	<b>How Synthesis Method Affects Bioglass Properties?</b> Michał Dziadek, Barbara Zagajczuk, Kamil Karwat, Justyna Pawlik, Maria Łączka, <u>Katarzyna Cholewa-Kowalska</u> <i>Poland</i>
526	<b>Preparation of Chitosan Hydrogel Modified with Xanthan Gum</b> <u>Bożena Tyliszczak</u> , Katarzyna Gaca, Katarzyna Bialik-Was, Dagmara Malina, Agnieszka Sobczak-Kupiec <i>Poland</i>
527	<b>Study of Hydrogels Containing Magnetic Nanoparticles</b> <u>Bożena Tyliszczak</u> , Katarzyna Gaca, Katarzyna Bialik-Was, Dagmara Malina, Agnieszka Sobczak-Kupiec <i>Poland</i>
528	<b>Development of Biodegradable Derivatives of Hyaluronic Acid for Cross-Linking Nanofibers and Nanomicelles</b> <u>Gloria Huerta-Angeles</u> , Martina Brandejsova, Martina Hermannova, Vladimír Velebný <i>Czech Republic</i>
529	<b>Thermoresponsive Anionic Copolymer Brush on Porous Monolithic Silica Rod For Separation of Basic Biomolecules</b> <u>Kenichi Nagase</u> , Jun Kobayashi, Akihiko Kikuchi, Yoshikatsu Akiyama, Hideko Kanazawa, Teruo Okano <i>Japan</i>





530	<b>The Effect of Chemical Structure of Polyesters with Shape Memory on Release Kinetics of Bioactive Molecules</b> <u>Joanna Idaszek</u> , Monika Bil, Wojciech Świąszkowski <i>Poland</i>
531	<b>Tissue-Adhesive Hydrogel for Hemostasis Comprising Water-Swellable Poly(acrylic Acid)/Poly(Vinylpyrrolidone) Complex</b> <u>Yoshiyuki Koyama</u> , Tomoko Ito, Shingo Yamaguchi, Yoichi Kurachi, Masazumi Eriguchi <i>Japan</i>
532	<b>An Engineered Double Network Based Composite Hydrogel for a Synthetic OOKP Skirt</b> <u>Ganesh Ingavle</u> , Venkata Avadhanam, Yishan Zheng, Sandeep Kumar, Christopher Liu, Susan Sandeman <i>United Kingdom</i>
533	<b>MMP Sensitive Artificial Extracellular Matrix Based on a Clickable Elastin-Like Recombinamer</b> <u>Doriana Orbanic</u> , Istraél González deTorre, Javier Francisco Arias Vallejo, José Carlos Rodríguez-Cabello <i>Spain</i>
534	<b>Investigation of the Influence of Different Process Parameters on Hydroxyapatite Powder Production</b> <u>Azade Yelten</u> , Suat Yilmaz <i>Turkey</i>
535	<b>Degradation and Cellular Compatibility of Poly(Hydroxy Acid)-Based Segmented Polyurethanes</b> <u>Maziar Matloubigharagozloo</u> , Nils Blumenthal, V. Prasad Shastri <i>Germany</i>
536	<b>Photo-Responsive Fluoropolymer Coated Surface for Cell Adhesion Control</b> <u>Masamichi Nakayama</u> , Tomonori Kanno, Akihiko Kikuchi, Teruo Okano <i>Japan</i>
537	<b>The Effect of the Vesicle Diameter on the Bending Rigidity of POPC and DOPC Lipid Bilayers</b> <u>Dominik Drabik</u> , Magdalena Przybyło, Marek Langner <i>Poland</i>
538	<b>Engineered Microenvironment for Regulating 3D-Encapsulated Cell Behaviors</b> <u>Youn-Mook Lim</u> , Young Min Shin, Jong-Seok Park, Hui-Jeong Gwon, Sung In Jeong, Sohyoun Lee <i>Republic of Korea</i>
539	<b>Biodegradable Thermoplastic Shape-Memory Polymers for Potential Biomedical Applications</b> <u>Monika Bil</u> , Natalia Wojas, Marcin Heljak, Joanna Idaszek, Wojciech Świąszkowski <i>Poland</i>
540	<b>Towards an Embedded Integrated Measurement System for the in vitro Monitoring of Biomedical Impedance Related to Fibrosis Phenomenon</b> <u>Mehdi Terosiet</u> , Aymeric Histace, Olivier Romain, Michel Boissiere, Sabrina Kellouche, Franck Carreiras, Emmanuel Pauthe <i>France</i>
541	<b>Preparation of Beetosan</b> Bożena Tyliśzczak, Katarzyna Z. Gaca, Katarzyna Bialik-Was, Dagmara Malina, <u>Agnieszka Sobczak-Kupiec</u> <i>Poland</i>
542	<b>Preparation of Chitosan Hydrogel Modified with <i>Salvia officinalis</i></b> Bożena Tyliśzczak, Katarzyna Z. Gaca, Katarzyna Bialik-Was, Dagmara Malina, <u>Agnieszka Sobczak-Kupiec</u> <i>Poland</i>
543	<b>Light-Responsive Polymeric Materials for Biomedical Applications</b> Anna Mikulska, Joanna Filipowska, Agnieszka Iwanowska, Anna Osyczka, Maria Nowakowska, <u>Krzysztof Szczubiałka</u> <i>Poland</i>
544	<b>Hyaluronic Acid Modified as <math>\alpha,\beta</math>-Unsaturated Aldehyde - Biopolymer Suitable for Tissue Engineering and Drug Delivery</b> Radovan Buffa, Ivana Basarabová, Petra Šedová, Martina Dvořáková, Lucie Wolfová, Vladimír Velebný <i>Czech Republic</i>
545	<b>Gelatin Methacrylamide: Poly(Ethylene Glycol) Composite Hydrogels with Tunable Mechanical Properties to Control Mesenchymal Stromal Cell Differentiation</b> <u>Jeroen Rouwkema</u> , Ajaykumar Vishwakarma, Ali Khademhosseini <i>Netherlands</i>



546	<b>Toxic Chemical Crosslinker-Free Chitosan Cryosponge for Cartilage Tissue Engineering</b> <u>Takayuki Takei</u> , Hiroki Yoshitomi, Kohei Fukumoto, Yoshihiro Ozuno, Masahiro Yoshida <i>Japan</i>
547	<b>Development of a New Confinement System for Controlled Release of Active Species in Biomaterial</b> <u>François Aubert-Viard</u> , Adeline Gand, Michel Boissière, Véronique Larreta-Garde, Emmanuel Pauthe <i>France</i>
548	<b>PFKFB3-Expression Pattern Distinguishes Between Induced-Pluripotent Stem Cells and Cancer-Stem Cells</b> Artur Cieślak-Pobuda, Mayur V. Jain, Gunnar Kratz, Joanna Rzeszowska-Wolny, Saeid Ghavami, <u>Emilia Wiecheć</u> <i>Sweden</i>
549	<b>Extracellular Vesicles From Induced Pluripotent Stem Cells: A Promising Source of Cell-Based Therapy</b> <u>Marta Adamiak</u> , Sylwia Bobis-Wozowicz, Elżbieta Karnas, Michał Sarna, Zbigniew Madeja, Ewa Zuba-Surma <i>Poland</i>
550	<b>New Concept of Stem Cells Differentiation - Graphene-Based Substrate as a Promising Tool in Biomedical Applications</b> <u>Małgorzata Sekuła</u> , Magdalena Baran, Katarzyna Kmiotek, Joanna Jagiełło, Elżbieta Karnas, Zbigniew Madeja, Ludwika Lipińska, Ewa Zuba-Surma <i>Poland</i>
551	<b>Mesenchymal Stem Cell Culture Evaluation by CVD Graphene-Transferred PDMS Substrates</b> <u>Masahito Ban</u> , Hiroki Sunada, Masatou Ishihara, Masataka Hasegawa <i>Japan</i>
552	<b>Very Small Embryonic-Like Stem Cells are Activated by Acute Tissue Injury in vivo and Participate in Regeneration of Ischemic Tissue</b> <u>Anna Labedz-Masłowska</u> , Elżbieta Kamycka, Tomasz Brzozowski, Mariusz Z. Ratajczak, Zbigniew Madeja, Ewa K. Zuba-Surma <i>Poland</i>
553	<b>Human Adipose Stem Cells on Ti-6Al-4V Alloy with Various Surface Modifications</b> <u>Nikola Krocilova</u> , Lucie Bacakova, Martin Parizek, Jana Havlikova, Hooman Motarjemi, Martin Molitor, Roman Gabor <i>Czech Republic</i>
554	<b>Genome Editing of HLA Locus Using Zinc Finger Nucleases</b> <u>Ken-ichi Tezuka</u> , Shunji Chikusa, Shota Ishii, Ken Sugiyama, Tomoko Kawaguchi-Takeda <i>Japan</i>
555	<b>Human Mesenchymal Stem Cells Expansion under Xeno-Free Conditions for Regenerative Therapies</b> <u>Maura Cimino</u> , Ewa Bauman, Raquel Goncavels, Francisco Belda, Cristina Barrias, Cristina Martins <i>Portugal</i>
556	<b>Wollastonite Fibers-Reinforced Calcium Sulfate Composites with Enhanced Bioactivity</b> <u>Yaser Greish</u> , Abdel-Hamid Mourad, Nuha Attia <i>United Arab Emirates</i>
557	<b>Functionalization of Hydrogels for Cells Encapsulation</b> <u>François Noverraz</u> , Solène Passemard, Virginia Crivelli, Françoise Borcard, Redouan Mahou, Sandrine Gerber, Christine Wandrey <i>Switzerland</i>
558	<b>The Comparison of Wettability and Surface Energy of Biomaterials and Bone Tissue</b> <u>Anita Kajzer</u> , Wojciech Kajzer, Ewa Kieruzel <i>Poland</i>
559	<b>Combination of Pro-Angiogenic and Bone Cell Attracting Coatings on Titanium Implants</b> <u>Cornelia Wolf-Brandstetter</u> , René Beutner, Claus Moseke, Dieter Scharnweber <i>Germany</i>
560	<b>Surface Properties of Chitosan Mixtures with Hyaluronic Acid and Collagen as Materials Designed for Biomedical Applications</b> <u>Alina Sionkowska</u> , Katarzyna Lewandowska, Sylwia Grabska <i>Poland</i>



561	<b>Alendronate Self Assembling Monolayers. A Bioactive Bonding Agent on Titanium Surfaces</b> <u>Luis Rojo</u> , Borzo Gharibi, Sanjukta Deb <i>United Kingdom</i>
562	<b>Bio- Mimetic, Smart Coatings for Medical Tools Application</b> <u>Lukasz Major</u> , Juergen M. Lackner, Boguslaw Major <i>Poland</i>
563	<b>Novel Silica-Enriched Bioactive Coatings for Titanium Implants</b> <u>Amanda Bartkowiak</u> , Katarzyna Suchanek, Barbara Szaraniec, Marta Marszałek <i>Poland</i>
564	<b>Composite Sol-gel Bioactive Glass/Chitosan Coatings Deposited on Ti13Zr13Nb Alloy</b> <u>Dawid Jugowiec</u> , Katarzyna Cholewa-Kowalska, Michał Dziadek, Łukasz Cieniek, Tomasz Moskalewicz <i>Poland</i>
565	<b>Deposition and Characterisation of Microporous Sol-gel Bioactive Glass/PEEK 704 Coating on Near-β Titanium Alloy</b> <u>Anita Sak</u> , Łukasz Cieniek, Katarzyna Cholewa-Kowalska, Agnieszka Radziszewska, Marcin Kot, Alicja Łukaszczyk, Tomasz Moskalewicz <i>Poland</i>
566	<b>Influence of PEEK 704 Coating on Tribological Properties of Ti13Zr13Nb Alloy</b> <u>Anita Sak</u> , Sławomir Zimowski, Marcin Kot, Beata Dubiel, Tomasz Moskalewicz <i>Poland</i>
567	<b>Influence of Electrophoretic Deposition Parameters on Chitosan Coatings Quality</b> <u>Dawid Jugowiec</u> , Tomasz Moskalewicz <i>Poland</i>
568	<b>Surface Modification of Ti-Nb-Sn Alloy Controlling OCP Precipitation by Electron Cyclotron Resonance Plasma Oxidation</b> <u>Hiroshi Masumoto</u> , Mayumi Oikawa, Yusuke Orie, Takahisa Anada, Osamu Suzuki, Keiichi Sasaki <i>Japan</i>
569	<b>Influence of Purified ECM Components on Corneal Epithelial Cells Cultivated on Silk Fibroin</b> <u>Thomas Hogerheyde</u> , Shuko Suzuki, Sally-Anne Stephenson, Damien Harkin, Laura Bray, Neil Richardson <i>Australia</i>
570	<b>Change in Mechanical Performance of Biomedical Titanium Alloys Subjected to Mechanical Surface Modifications</b> <u>Akahori Toshikazu</u> , Yurie Oguchi, Tomokazu Hattori, Hisao Fukui <i>Japan</i>
571	<b>Evaluation of the Possibilities of Affecting the Interspike Structural-Osteoconductive Potential of Additively Manufactured Prototypes of the Multispiked Connecting Scaffold for Hip Resurfacing Anrthroplasty Enoprostheses</b> Ryszard Uklejewski, <u>Mariusz Winiecki</u> , Piotr Rogala, Adam Patalas <i>Poland</i>
572	<b>Thin Nanostructured RF-Magnetron Sputter-Deposited Hydroxyapatite Coatings on Metals</b> <u>Roman Surmenev</u> , Maria Surmeneva, Irina Selezneva, Matthias Eppe <i>Russian Federation</i>
573	<b>Electrochemical Immobilisation of Doxycycline on Titanium Surfaces</b> <u>Sebastian Geissler</u> , Hanna Tiainen, Håvard Haugen <i>Norway</i>
574	<b>Injectable Lubricants for Prosthetic Joints</b> <u>Rishikesan Sankaranarayanan</u> , Kirsi Pakkanen, Seunghwan Lee <i>Denmark</i>
575	<b>pH Triggered Aggregation of Structurally Disordered Proline-Rich Polypeptide</b> <u>Hanna Tiainen</u> , Sebastian Geissler, Reidar Lund, Håvard J Haugen <i>Norway</i>
576	<b>Stability of Oxygen Plasma Treatment of Parylene C Biomedical Coating</b> <u>Monika Golda-Cepa</u> , Klas Engvall, Andrzej Kotarba <i>Poland</i>



577	<b>Synthesis and Characterization of Thermo-Sensitive Poloxamer 407/Chitosan-Functionalized Carbon Nanotubes Hydrogel</b> <u>Jun Ou</u> , Li Zhen, Jin-Min Zhao, Qing H. Qin, Zbigniew H. Stachurski <i>China</i>
578	<b>Technology of Bioactive Coatings on Porous, Non-Toxic Titanium Alloy Ti13Nb13Zr</b> <u>Milena Supernak-Marczewska</u> , Agnieszka Ossowska, Paulina Strąkowska, Tomasz Seramak, Andrzej Zielinski <i>Poland</i>
579	<b>Low Temperature Atomic Layer Deposition Technology for Low Thermal Resistance Polymer Surface Modification</b> <u>Li-Chun Wang</u> , Hsin-Chih Lin, Kai-Chiang Yang, Miin-Jang Chen, Yin-Yi Han <i>Taiwan, Province of China</i>
580	<b>Electrochemical Methods of Stainless Steel 316L Surface Modification for Biocompatibility Improvement</b> <u>Paulina Trzaskowska</u> , Marta Trzebińska, Aleksandra Poniatowska, Tomasz Ciach <i>Poland</i>
581	<b>The Effect of Surface Modification on Biofunctional Properties of AISI 440B Martensitic Stainless Steel</b> <u>Magdalena Łepicka</u> , Małgorzata Grądzka-Dahlke <i>Poland</i>
582	<b>An Electrically Conducting Composite Scaffold for Bone Tissue Engineering</b> <u>Izabella Rajzer</u> , Monika Rom, Elżbieta Menaszek <i>Poland</i>
583	<b>Biocomposite Materials Based on Poly(Butylene Succinate) with Modified Hemp Fibers</b> Zoe Terzopoulou, Vasileios Nikolaidis, Konstantinos Triantafyllidis, <u>Dimitrios Bikiaris</u> <i>Greece</i>
584	<b>Impact of Sterilisation in Ethylene Oxide on Electrochemical Characteristics of Drawn Steel Wires Used as Urological Guidewires</b> <u>Joanna Przendziona</u> , Witold Walke, Marek Tkocz <i>Poland</i>
585	<b>Photopolymerisation Preparation of Chitosan Hydrogel Containing Iron (II, III) Oxide Nanoparticles</b> Bożena Tyliszczak, <u>Katarzyna Z. Gaca</u> , Katarzyna Bialik-Wąs, Dagmara Malina, Agnieszka Sobczak-Kupiec <i>Poland</i>
586	<b>Change in Mechanical Strength of Newly Developed Ti-Cr System Alloy Subjected to Heat Treatment and Surface Modification Processing</b> <u>Kentaro Niwa</u> , Toshikazu Akahori, Tomokazu Hattori, Mitsuo Niinomi, Masaaki Nakai <i>Japan</i>
587	<b>High Mechanical Functionalization of Biomedical Ti Alloys Subjected to Air Oxidation Processing</b> <u>Yoshiki Tsujimura</u> , Toshikazu Akahori, Tomokazu Hattori <i>Japan</i>
588	<b>Surface Modification Layer and Mechanical Properties of Biomedical Titanium Alloys Subjected to HAp Fine Particle Bombarding</b> <u>Akinori Ban</u> , Toshikazu Akahori, Tomokazu Hattori, Koichiro Nambu, Shoichi Kikuchi <i>Japan</i>
589	<b>Development of New Polymer-Liposome Complexes of Poly(Acrylic Acid) for Controlled Drug Delivery</b> <u>Patrícia Alves</u> , Manuela Carvalheiro, M. Manuela Gaspar, Jorge Coelho, Eugénia Cruz, M. Helena Gil, Pedro Simões <i>Portugal</i>
590	<b>Magnetron Sputtering of Modular Targets for the Deposition of Silver-Doped Titanium Coatings</b> <u>Tobias Schmitz</u> , Franziska Warmuth, Jürgen Groll, Uwe Gbureck, Claus Moseke <i>Germany</i>
591	<b>Co-Localization of RGD and PHSRN Peptides on Titanium to Guide Stem Cell Behaviour and Enhance Implant Osteointegration</b> Roberta Fraioli, José Maria Manero, Javier Gil, <u>Carlos Mas-Moruno</u> <i>Spain</i>
592	<b>Surface Modification of PEEK-carbon Composites to Induce Apatite Formation in Body Environment</b> <u>Toshiki Miyazaki</u> , Chisato Matsunami, Yuki Shiroaki <i>Japan</i>



593	<b>Controlled Growth of Smooth Muscle Cells to Provide Biomaterial with Blood Vessel-Like Properties</b> <u>Aldona Mzyk</u> , Roman Major, Jan Marczak, Bogusław Major <i>Poland</i>
594	<b>Growth and Tribological Performance of Cr-based Nitrides and Oxynitrides Multilayers</b> <u>Alina Vladescu</u> , Mihaela Dinu, Mariana Braic, Mihai Balaceanu, Viorel Braic <i>Romania</i>
595	<b>Dual Modal Superparamagnetic Iron Oxide Nanoparticles with Surface Attached Gadolinium Complexes</b> <u>Witold Prendota</u> , Agnieszka Szpak, Sylwia Fiejdasz, Tomasz Strączek, Kamil Goc, Czesław Kapusta, Janusz Szmyd, Maria Nowakowska, Szczepan Zapotoczny <i>Poland</i>
596	<b>On the Cytocompatibility of Ti6Al4V Thermally Oxidized by Means of Laser Shock Processing</b> Lara Crespo, Margarita Hierro-Oliva, Sandra Barriuso, Virginia Vadillo-Rodríguez, M <sup>a</sup> Ángeles Montealegre, Laura Saldaña, Enrique Gomez-Barrena, José Luis González-Carrasco, María Luisa González-Martín, <u>Nuria Vilaboa</u> <i>Spain</i>
597	<b>Cell Adhesion to Plasma Treated and Fluorinated Collagen Surfaces</b> <u>Ina Prade</u> , Frauke Junghans, Michael Meyer <i>Germany</i>
598	<b>Enhancement of Osseointegration of Ti Based Alloy by Bioactive Calcium Phosphate Coatings</b> <u>Cosmin Cotrut</u> , Irina Titorencu, Adrian Kiss, Mihai Tarcolea, Florin Miculescu, Diana Vranceanu, Alina Vladescu <i>Romania</i>
599	<b>Permanent Implant Surfaces Equipped with the Cell Adhesive Plasma Polymer Film PPAAM</b> Birgit Finke, Henrike Rebl, Uwe Walschus, <u>Michael Schlosser</u> , Carolin Gabler, Carmen Zietz, Rainer Bader, Klaus-Dieter Weltmann, Barbara Nebe <i>Germany</i>
600	<b>Structure and Biological Response of Multi-layers Deposited on NiTi Shape Memory Alloy</b> <u>Tomasz Goryczka</u> , Karolina Dudek, Agnieszka Szurko, Beata Swieczko-Zurek <i>Poland</i>
601	<b>Electrochemical Properties of CrSi-based Oxynitrides Deposited on NiCr and CoCr Dental Alloys</b> <u>Mihai Tarcolea</u> , Mihaela Dinu, Ana Gherghilescu, Diana Vranceanu, Raluca Comaneanu, Cosmin Cotrut <i>Romania</i>
602	<b>Dynamics of Motion and Agglomeration of Magnetic Nanoparticles in Suspensions under Applied Magnetic Field</b> <u>Kamil Goc</u> , Tomasz Strączek, Jakub Jurczyk, Witold Prendota, Czesław Kapusta, Agnieszka Szpak, Szczepan Zapotoczny, Maria Nowakowska, Janusz Szmyd, Stanisław Rumian <i>Poland</i>
603	<b>Carbon Nanomaterials Coatings as Potential Substrates for Nerve Cells Stimulation</b> <u>Aneta Fraczek-Szczypta</u> , Alicja Wedel, Justyna Grzonka <i>Poland</i>
604	<b>Stainless Steel Surface Coating: Problems with Surface Pre-Treatment</b> <u>Paulina Trzaskowska</u> , Tomasz Ciach <i>Poland</i>
605	<b>Seamless Electronic-Tissue Interfaces</b> <u>Tobias Schmitz</u> , Maren Jannasch, Tobias Weigel, Sabine Gätzner, Jan Hansmann <i>Germany</i>
606	<b>Improvement of Bioactivity of Vanadium-Free Titanium Alloy using Plasma Electrolytic Oxidation</b> <u>Maciej Sowa</u> , Magdalena Piotrowska, Magdalena Widziołek, Grzegorz Dercz, Grzegorz Tylko, Tadeusz Gorewoda, Anna M. Osyczka, Wojciech Simka <i>Poland</i>
607	<b>Ti-Alloy with Nanotubular Surface Modification for Orthopaedic Applications</b> <u>Eva Jablonská</u> , Penelope Tsimbouri, Jaroslav Fojt, Matthew Dalby, Jan Lipov, Tomáš Ruml <i>Czech Republic</i>





608	<b>Surface Functionalization Strategies for Cardiovascular Applications</b> <u>E Diana Giol</u> , Sandra Van Vlierberghe, Peter Dubrue <i>Belgium</i>
609	<b>The Influence of NiTi-Alloy Surface Passivation on Biofilm Formation by <i>Desulfovibrio desulfuricans</i> Bacteria</b> <u>Beata Cwalina</u> , Weronika Dec, Joanna Michalska, Marzena Jawoska-Kik, Wojciech Simka <i>Poland</i>
610	<b>Dynamics of Biofilm Formation by <i>Desulfovibrio desulfuricans</i> Bacteria on Grinded Surface of NiTi-Alloy</b> <u>Beata Cwalina</u> , Weronika Dec, Joanna Michalska, Marzena Jawoska-Kik, Wojciech Simka <i>Poland</i>
611	<b>An Electrically Conductive Non-Woven Web Made of Microfibrinous Poly(L-Lactic Acid) and Poly(3,4-Ethylenedioxythiophene)</b> Xufeng Niu, Mahmoud Rouabhia, Nicolas Chiffot, Martin King, <u>Ze Zhang</u> <i>Canada</i>
612	<b>Electroless Deposition of Calcium-Phosphate Coatings on Ti6Al4V and Their Biological Response</b> <u>Ena A. Aguilar-Reyes</u> , Benito Jacinto-Diaz, Carlos A. Leon-Patino <i>Mexico</i>
613	<b>Microhardness of the Polylactide Sheets Modified by Laser</b> <u>Magdalena Tomanik</u> , Bogusz Stępak, Jarosław Filipiak, Arkadiusz Antończak, Krzysztof Abramski, Celina Pezowicz <i>Poland</i>
614	<b>The Metal Implants Covered with Hydroxyapatite Coatings and Nanometals Supplements</b> <u>Beata Świeczko-Żurek</u> <i>Poland</i>
615	<b>Zinc Oxide and Titanium Dioxide-Chitosan Nanocomposites for UV-light Protection</b> <u>Anna Regiel-Futrya</u> , Małgorzata Kus-Liśkiewicz, Szymon Wojtyła, Grażyna Stochel, Wojciech Macyk <i>Poland</i>
616	<b>Polymer Coating as a Method of Cytocompatibility Improvement of Magnesium Alloy ZM21</b> <u>Agnieszka Witecka</u> , Akiko Yamamoto, Wojciech Swieszkowski <i>Poland</i>
617	<b>Influence of Plasma Nitriding Process on Multi-Layer Coatings Produced by MW CVD Technique for Hip Prosthesis Applications</b> <u>Agnieszka Kyzioł</u> , Łukasz Kaczmarek, Marek Klich, Karol Kyzioł <i>Poland</i>
618	<b>Topographic Nanostructures for the Regulation of Cell Adhesion</b> <u>Patrick Elter</u> , Thomas Weihe, Jan Gimsa, Ulrich Beck <i>Germany</i>
619	<b>The Effect of TiN and DLC Surface Modification on Wear of AISI 440B Martensitic Stainless Steel Surgical Drill Bits</b> <u>Magdalena Łepicka</u> , Małgorzata Grądzka-Dahlke <i>Poland</i>
620	<b>Surface Engineering by Means of a Toolbox of Biodegradable 3-Armed Macromers</b> <u>Benno M Müller</u> , Rudi Loth, Peter-Georg Hoffmeister, Michael C Hacker, Michaela Schulz-Siegmund <i>Germany</i>
621	<b>Tribocorrosion of Ca-P Doped TiO<sub>2</sub> Nanotubes</b> <u>Ana Almeida</u> , Carlos Laurindo, Paulo Soares <i>Brazil</i>
622	<b>Adsorption Reaction of L-Cysteine on the Au Nanoparticle Precovered with PC Molecules</b> <u>Chie Tsukada</u> , Takuma Tsuji, Koichi Matsuo, Toyokazu Nomoto, Takaaki Murai, Toyonari Yaji, Toshiaki Ohta, Hirofumi Nameki, Satoshi Ogawa, Tomoko Yoshida, Shinya Yagi <i>Japan</i>
623	<b>Sol-Gel Siloxane-Gelatine Coatings for Improving Titanium's Osseointegration: Synthesis, Characterization and Biological Assessment</b> <u>Maria Martinez-Ibañez</u> , Yong Mao, Julio Suay, Mariló Gurruchaga, Isabel Goñi, Joachim Kohn <i>Spain</i>





624	<b>Functionalised Dextran Nanoparticles for Drug Delivery to the Brain</b> <u>Daniel Ibegbu</u> , Eugen Barbu, John Tsibouklis <i>United Kingdom</i>
625	<b>TiO<sub>2</sub> Mesoporous Layers of Tunable Chemical Composition and Morphology</b> <u>Paolo Canepa</u> , Sureeporn Uttiya, Ilaria Solano, Gianluca Gemme, Ranieri Rolandi, Maurizio Canepa, Ornella Cavalleri <i>Italy</i>
626	<b>Surface Modification by a Catalyst Free Covalent Layer-by-Layer Approach of Clickable Elastin-Like Recombinamers</b> <u>Israel González de Torre</u> , Luis Quintanilla, Matilde Alonso, José Carlos Rodríguez-Cabello <i>Spain</i>
627	<b>Paired Cyclodextrin Polyelectrolytes Multilayer Coatings onto a Textile Support for Prolonged Drug Delivery of Model Molecules</b> Jatupol Junthip, <u>Nicolas Tabary</u> , Bernard Martel, Laurent Leclercq, Feng Chai, Nicolas Blanchemain <i>France</i>
628	<b>Spatial Arrangements of Carboxylate-Derived Ti6Al4V Alloy for Medical Applications</b> Abraham Rodríguez-Cano, Anna Zdziennicka, <u>Margarita Hierro-Oliva</u> , María Luisa González-Martín, Reyes Babiano, Pedro Cintas, Bronisław Jańczuk <i>Spain</i>
629	<b>Structural Characterization of Silver-Organic Complexes on Ti6Al4V</b> Abraham Rodríguez-Cano, Anna Zdziennicka, <u>M Luisa González-Martín</u> , Pedro Cintas, Reyes Babiano, M Coronada Fernández-Calderón, Bronisław Jańczuk <i>Spain</i>
630	<b>Pulse Current Cathodic Deposition of Hydroxyapatite on Type 316L Stainless Steel</b> <u>Sayaka Miyabe</u> , Naoya Asakura, Takuya Nakao, Shinji Fujimoto <i>Japan</i>
631	<b>Evaluation of Biometals Modified by UV Nanosecond Nd:YVO4 Laser. Effects on Cell Viability</b> Elena Burguera, Paula Fiorucci, L. Gato-Calvo, <u>Joana Magalhaes</u> , Ana de Jesus López, S. Pozo-Antonio, Francisco Blanco, Alberto Ramil <i>Spain</i>
632	<b>Cell Attraction, Repulsion and Sorting by Submicron and Nano-Topographies</b> <u>Alexey Klymov</u> , Remco Doodkorte, John A. Jansen, X. Frank Walboomers <i>Netherlands</i>
633	<b>Innovative Nanostructured Medical Devices - A Risk of Nanoparticles Release</b> <u>Laëtitia Salou</u> , Engin Vrana, Anne Piscitelli, Pierre Layrolle, Guy Louarn, Valérie Dumay <i>France</i>
634	<b>Chitosan Nanofibers for Peripheral Nerve Applications</b> Cristiana Carvalho, Albino Martins, Nuno Neves, Rui Reis, <u>Joaquim Miguel Oliveira</u> <i>Portugal</i>
635	<b>The Concurrent-Electrospinning of Polylactide and Gelatine Fibres as a Way of Obtaining Advanced Hybrid Materials</b> <u>Anna Magiera</u> , Stanisław Błazewicz <i>Poland</i>
636	<b>Bone Marrow MSC Systemic Administration for in vivo IVD Regeneration</b> <u>Carla Cunha</u> , Maria I. Almeida, Catarina R. Almeida, Sofia Lamas, Andreia M. Silva, Maria Molinos, Catarina L. Pereira, Graciosa Q. Teixeira, Susana G. Santos, Raquel M. Gonçalves, Mário A Barbosa <i>Portugal</i>
637	<b>Evaluation of the Efficiency of Mechanical Agitation Method in Heart Decellularization Process</b> Ana Paula Brandão, <u>Jonathas Haniel</u> , Betânia Soares, Rosana Cruz, Marcos Pinotti <i>Brazil</i>
638	<b>Vascularization of Biphasic Calcium Phosphate Biomaterials: Correlation with Monocyte Pre-Seeding, but not with Foreign Body Giant Cell Reaction or Granule Size</b> <u>Mike Barbeck</u> , Michel Dard, Maria Kokkinopoulou, Juergen Markl, Patrick Booms, Robert Sader, Charles James Kirkpatrick, Shahram Ghanaati <i>Germany</i>



639	<b>Design and Development of Device for Decellularization Process of Heart</b> <u>Jonathas Haniel</u> , Ana Paula Brandão, Betânia Soares, Rosana Cruz, Marcos Vale, Marcos Pinotti <i>Brazil</i>
640	<b>Mechanical Properties of Chitosan/Collagen Composites Modified by Sodium Alginate</b> <u>Alina Sionkowska</u> , Beata Kaczmarek, Marta Michalska <i>Poland</i>
641	<b>Biophysical, Biochemical and Biological Tools for Tendon Repair and Regeneration</b> D Gaspar, K Spanoudes, A Satyam, P Kumar, D Cigognini, A Pandit, <u>DI Zeugolis</u> <i>Ireland</i>
642	<b>Adhesion/Proliferation of Cells on TiO<sub>2</sub> under UV Irradiation</b> <u>Masato Ueda</u> , Yasuka Yoshida, Masahiko Ikeda, Aira Matsugaki, Takayoshi Nakano <i>Japan</i>
643	<b>Evaluation of Poly (ε-Caprolactone) / Sodium Alginate Nanofibrous Patch for Cardiac Tissue Engineering</b> <u>Rouhollah Mehdinavaz Aghdam</u> , Seyed Hossein Ahmadi Tafti <i>Iran</i>
644	<b>Biofunctional Microassemblies Based on an Exopolysaccharide Produced by a Deep-Sea Hydrothermal Bacterium for Tissue Engineering Applications</b> <u>Agata Zykwinska</u> , Mélanie Marquis, Corinne Sinquin, Jacqueline Ratiskol, Stéphane Cuenot, Denis Renard, Sylvia Collic-Jouault <i>France</i>
645	<b>Evaluation of Transport Properties of Poly(ε-Caprolactone) Membranes in a Bioreactor for Tissue Engineering</b> Beatriz Gomez, <u>Nazely Diban</u> , Inmaculada Ortiz, Ana María Urtiaga <i>Spain</i>
646	<b>In situ Forming and H<sub>2</sub>O<sub>2</sub>-Generating Gelatin Hydrogels via Glucose Oxidase- and Horseradish Peroxidase-Catalyzed Reaction</b> Bae Young Kim, Jin Woo Bae, Yunki Lee, Dong Hwan Oh, <u>Ki Dong Park</u> <i>Republic of Korea</i>
647	<b>Controlling Macro-Porosity in Hydrogels with Sacrificial Fibres Prepared from Melt Electrospinning Writing</b> <u>Jodie Haigh</u> , YaMi Chuang, Brooke Farrugia, Richard Hoogenboom, Paul Dalton, Tim Dargaville <i>Australia</i>
648	<b>Mechanical Properties of Collagen/Hydroxyapatite Based Materials</b> <u>Justyna Kozłowska</u> , Alina Sionkowska <i>Poland</i>
649	<b>Chitosan Solution as the Effective Liquid Phase for Composite-Type Bone Cements</b> <u>Joanna Czechowska</u> , Aneta Zima, Dominika Siek, Anna Ślósarczyk <i>Poland</i>
650	<b>New Biodegradable Bone Implant Materials Based on Calcium Phosphates and Calcium Sulphate</b> <u>Dominika Siek</u> , Joanna Czechowska, Aneta Zima, Anna Ślósarczyk <i>Poland</i>
651	<b>Effect of Liquid Phase on the Basic Properties of Chemically Bonded Material</b> <u>Joanna Czechowska</u> , Dominika Siek, Aneta Zima, Anna Ślósarczyk <i>Poland</i>
652	<b>Cement-Type Implant Material Based on Ca and Mg Phosphates with Adjustable Setting Time and Improved Resorption</b> <u>Aneta Zima</u> , Joanna Czechowska, Dominika Siek, Anna Ślósarczyk <i>Poland</i>
653	<b>Modified Citrus Pectin and Silk Fibroin Based Scaffolds for Bone Tissue Engineering Applications</b> Sibel Ataol, Akın Akdag, Dilek Keskin, <u>Aysen Tezcaner</u> <i>Turkey</i>
654	<b>Fabrication Methods of Porous Biomaterials for Dental and Orthopedic Applications Using the Selective Laser Sintering Technique</b> <u>Zaneta Anna Mierzejewska</u> , Jarosław Sidun, Bartłomiej Wonsewicz <i>Poland</i>



655	<b>Mechanical Properties and Degradation of a Co(Poly-Lactide-epsilon-Caprolactone) Braided Scaffold for ACL Tissue Engineering</b> <u>Blandine Landrieu</u> , Cedric Laurent, Rachid Rahouadj <i>France</i>
656	<b>Sulfation of Textile Chitosan Scaffolds Enhances Adhesion, Proliferation and Osteogenic Differentiation of Human Bone Marrow Stromal Cells</b> Christiane Heinemann, Susanne Höhne, Annette Breier, Frank Simon, Hans Peter Wiesmann, <u>Thomas Hanke</u> <i>Germany</i>
657	<b>Reconstruction of a Dog Mandibular Resection Defect by Octacalcium Phosphate Collagen Composite</b> <u>Tadashi Kawai</u> , Keiko Matsui, Yushi Ezoe, Yuji Tanuma, Hidenori Tanaka, Fumihiko Kajii, Atsushi Iwai, Tetsu Takahashi, Osamu Suzuki, Shinji Kamakura <i>Japan</i>
658	<b>The Biological Evaluation of Ultra-Fine Titanium with Improved Mechanical Strength for Tissue Engineering</b> <u>Lucie Ostrovska</u> , Lucie Vistejnova, Jan Dzigan, Egor Ukraintsev, Dana Kubies, Milena Kralickova, Marie Hubalek-Kalbacova <i>Czech Republic</i>
659	<b>The Effect of Alendronate-Loaded Polycaprolactone Scaffolds for the Enhancement of Osteogenic Differentiation in vitro and Bone Regeneration in vivo</b> <u>Kwang-Won Park</u> , Sung-Eun Kim, Young-Pil Youn, Hae-Ryong Song <i>Republic of Korea</i>
660	<b>New Fibrin-Polymer Interpenetrating Networks: a Potential Support for Human Skin Construct</b> <u>Véronique Larreta Garde</u> , Marie Deneufchatel, Laurent Bidault, Mathilde Hindié, Cedric Vancaeyzeele, Odile Fichet <i>France</i>
661	<b>A New Light Comes up in the World of Periodontal Therapy- P11 Peptides and their in vitro Evaluation on Human Hard and Soft Tissue Cells</b> <u>Franziska Koch</u> , Uwe Pieleles, Stephanie Mathes, Ursula Graf <i>Switzerland</i>
662	<b>Evaluation of Bone Formation Using Solid Freeform Fabrication-Based PCL/PLGA Scaffolds Containing Bone Morphogenetic Protein-2</b> Sung-Eun Kim, Kwang-Won Park, Young-Pil Yun, Hae-Ryong Song <i>Republic of Korea</i>
663	<b>Chitin Nanofibers as Structural and Functional Units in Genipin-Cross-Linked Chitosan Foams for Regenerative Nanomedicine</b> Verónica Zubillaga, Asier Salaberria, Jalel Labidi, Susana Fernandes, Ana Alonso-Varona, <u>Teodoro Palomares</u> <i>Spain</i>
664	<b>Effect of Solvent Type on Material Properties of Solution-cast Poly(epsilon-Caprolactone) Films</b> <u>Michał Dziadek</u> , Barbara Zagrajczuk, Katarzyna Cholewa-Kowalska <i>Poland</i>
665	<b>Materials Determinants of Biological Activity of New Polymer-Based Composites Modified by Gel-Derived Bioglasses</b> <u>Barbara Zagrajczuk</u> , Michał Dziadek, Justyna Pawlik, Joanna Filipowska, Amadeusz Bryła, Katarzyna Cholewa-Kowalska, Anna Maria Osyczka, Maria Łączka <i>Poland</i>
666	<b>Pulp-Dentin Complex Regeneration by Boron Doped Biomimetic Nano Hydroxyapatite Coated Chitosan Scaffolds</b> <u>Farzin Asghari Sana</u> , Gokce Kaynak, Merve Capkin Yurtsever, Ozge Ekin Tuncay, Arlin Kiremitci, Menemse Gumusderelioglu <i>Turkey</i>
667	<b>Humoral Immune Response against Poly(L-Lactide-co-D/L-Lactide) after Implantation in Rats</b> <u>Uwe Walschus</u> , Silke Lucke, Andreas Hoene, Maciej Patrzyk, Matthias Schnabelrauch, Michael Schlosser <i>Germany</i>
668	<b>Toolbox of Gelatin-Poly(Vinylpyrrolidone) Layers with Various Architecture for Skin Regeneration</b> <u>Andrada Serafim</u> , Sergiu Cecoltan, Eugeniu Vasile, Izabela-Cristina Stancu <i>Romania</i>



669	<b>Biological Response of Biocomposites Based on Wharton's Jelly, Bioceramic and Bioglass in Bone Regeneration</b> Carlos A. Fernandez, Cristian A. Martinez, Andrés Ozols, <a href="#">Dagnija Loca</a> , Miguel O. Prado, Daniel Olmedo <i>Latvia</i>
670	<b>Porcine-Based Collagen Membranes and Matrices Induce Different Tissue Reaction Depending on Origin: Vascularization and Inflammatory Response in Preclinical and Clinical Studies</b> <a href="#">Shahram Ghanaati</a> , Mike Barbeck, Jonas Lorenz, Patrick Booms, Robert A. Sader, C. James Kirkpatrick <i>Germany</i>
671	<b>Cultivation of Mesenchymal Stem Cells on Collagen-Based Scaffolds Cross-Linked by EDC/NHS or Genipin</b> <a href="#">Pavla Sauerova</a> , Martina Verdanova, Tomas Suchy, Monika Supova, Sarka Ryglova, Margit Zaloudkova, Zbynek Sucharda, Marie Hubalek Kalbacova <i>Czech Republic</i>
672	<b>Remineralization of Demineralized Bone Matrix in Critical Size Cranial Defects in Rats: A Six Months Follow-up Study</b> Dénés Horváthy, Dora Polsek, Gabriella Vác, István Hornyák, <a href="#">Zsombor Lacza</a> <i>Austria</i>
673	<b>Development of a Bioactive and Biodegradable Poly(<math>\epsilon</math>-Caprolactone)-Based Prosthetic Ligament</b> Geraldine Rohman, Amélie Auge, Gabriela Radu-Bostan, Roger Guillard, Bernard Brulez, <a href="#">Véronique Migonney</a> <i>France</i>
674	<b>Dental Caries: Biomimetic Mineralization Model Development</b> <a href="#">Lucy Kind</a> , Christian Mangeng, Sabrina Stevanovic, Benjamin Bellon, Stefan Winkler, Iwona Dziadowiec, Hans Deyhle, Bert Müller, Uwe Piele <i>Switzerland</i>
675	<b>Glycomer™ 631 in Tendon Tissue Engineering: An Old Material in New Ventures</b> Kyriakos Spanoudes, Geoffrey Hanley, Yves Bayon, Abhay Pandit, Dimitrios Zeugolis <i>Ireland</i>
676	<b>Efficacy of Platelet Rich Plasma in Treatment of Plantar Fasciopathy</b> <a href="#">Łukasz Nagraba</a> , Tomasz Mitek, Jarosław Deszczyński, Artur Stolarczyk <i>Poland</i>
677	<b>Development and Characterisation of a Decellularised Porcine Mitral Valve Scaffold</b> <a href="#">Sofia Andriopoulou</a> , Lucrezia Morticelli, Michael Harder, Andres Hilfiker, Igor Tudorache, Sergei Cebotari, Axel Haverich, Sotirios Korossis <i>Germany</i>
678	<b>Advanced Biocompatible Scaffolds Obtained Through Stereolithography for Bone Tissue Engineering</b> <a href="#">Roberto De Santis</a> , Alfredo Ronca, Sara Ronca, Giuseppe Forte, Ugo D'Amora, Antonio Gloria, Teresa Russo, Luigi Ambrosio <i>Italy</i>
679	<b>Scaffolds for the Bone Tissue Engineering Combining Micro and Nano Fibers</b> Jakub Erben, Katerina Pilarova, Filip Sanetrník, Jiri Chvojka, Jana Horakova, Lenka Blazkova, Eva Kostakova, Jiri Havlicek, Petr Mikes, David Lukas, Vera Jencova, <a href="#">Martin Pelc</a> <i>Czech Republic</i>
680	<b>Biophysical, Biochemical and Biological Properties of Nano-textured Collagen Fibres</b> Anna Sorushanova, Anne Maria Mullen, <a href="#">Abhay Pandit</a> , Dimitrios Zeugolis <i>Ireland</i>
681	<b>Multifactorial Approaches on Cell Phenotype Maintenance and Function</b> Christina Ryan, <a href="#">Manus Biggs</a> , Abhay Pandit, Dimitrios Zeugolis <i>Ireland</i>
682	<b>Stimulating Cellular Response via Cross-linking in Tissue Engineering Scaffolds</b> <a href="#">Kendell M. Pawelec</a> , Gloria Ramírez-Rodríguez, Monica Sandri, Simone Sprio, Suzan van Dongen, Bas Kluijtmans <i>Netherlands</i>
683	<b>Control over Anisotropic Permeability in Aligned Tissue Engineering Scaffolds</b> <a href="#">Kendell M. Pawelec</a> , Huib van Boxtel, Bas Kluijtmans <i>Netherlands</i>



684	<b>Biocompatibility of Dental Pulp Stem Cells onto PLA Scaffolds Synthetize by Air Jet Spinning Technique.</b> <u>José Luis Suárez-Franco</u> , Nancy Vargas-Becerril, Lucía Téllez-Jurado, Octavio Álvarez-Fragoso, Manuel Hipólito-García, José Arturo Fernández-Pedrero, Marco Antonio Álvarez-Pérez <i>Mexico</i>
685	<b>Characterization of Cellulose/Hydroxyapatite Scaffolds for Bone Tissue Engineering</b> <u>Jolanta Liesiene</u> , Odeta Baniukaitiene, Povilas Daugela, Arturas Stumbras, Mindaugas Pranskunas, Gintaras Juodzbaly <i>Lithuania</i>
686	<b>Effect of Different Nanoparticles on the Mechanical and Biological Properties Of Poly(<math>\epsilon</math>-Caprolactone): A Comparative Study</b> <u>Maria Nerantzaki</u> , Iro Koliakou, Dimitrios Bikiaris <i>Greece</i>
687	<b>Rheology of Alginate Gels Containing Modified Alginate: Gels with Tunable Properties</b> Marianne Ø. Dalheim, <u>Line Aa. Omtvedt</u> , Finn L. Aachmann, Berit L. Strand <i>Norway</i>
688	<b>Quality and Quantity of Growth Factors Released from Processed Bone Matrix</b> <u>Katarzyna Włodarczyk</u> , Ilona Kalaszczyńska, Artur Kamiński, Małgorzata Lewandowska-Szumieł <i>Poland</i>
689	<b>Modulation of Cell Microenvironments with Oxygen Tension and Macromolecular Crowding: A Multifactorial Approach Towards in vitro Organogenesis</b> Abhigyan Satyam, Pramod Kumar, <u>Diana Gaspar</u> , Abhay Pandit, Dimitrios Zeugolis <i>Ireland</i>
690	<b>Reconstituted Fibrillar Collagen II - Chondroitin Sulphate for Cartilage Tissue Engineering</b> <u>Narjes Rashidi</u> , Jan Czernuszka <i>United Kingdom</i>
691	<b>Collagen Hydrogels Cross-linked by Squaric Acid</b> <u>Joanna Skopinska-Wisniewska</u> , Anna Bajek, Małgorzata Maj, Marta Ziegler-Borowska, Alina Sionkowska <i>Poland</i>
692	<b>Synthesis and Characterization of Biodegradable Genipin-cross-Linked Chitosan Scaffold for Bone Tissue Engineering</b> <u>Simona Dimida</u> , Vincenzo Maria De Benedictis, Nadia Cancelli, Francesca Gervaso, Francesca Scalera, Barbara Palazzo, Christian Demitri, Alessandro Sannino <i>Italy</i>
693	<b>Towards the Regeneration of Gastric Epithelium Using a Tissue Engineering Approach</b> <u>Yaser E. Greish</u> , Sunitha Polikott, Sneha Ann Thomas, Abdel Hamid Mourad, Sherif Karam <i>United Arab Emirates</i>
694	<b>Polytetrafluoroethylene Scaffolds for Cell Technologies</b> <u>Daria Chernobrovkina</u> , Ekaterina Shishatskaya, Egor Proskurin, Victor Lazarenko <i>Russian Federation</i>
695	<b>Novel Nanofibrillar Composite Matrices of Multiple Polymers and Improved Properties for Peri-Implantitis</b> Malika Ould Aklouche, Kerstin Gritsch, Brigitte Grosgeat, <u>Jerome Sohier</u> <i>France</i>
696	<b>Mechanical Characterization of Artificial Materials to Mimic Liver Tissue</b> Valeria Baronti, Alberto Lagazzo, Fabrizio Barberis, Marco Capurro, Rodolfo Repetto <i>Italy</i>
697	<b>Effects of Strontium on Physicochemical and Biological Properties of Hydroxyapatite Gel Materials for Periodontal Tissue Regeneration</b> <u>Maria Grazia Raucci</u> , Daniela Giugliano, Marco Antonio Alvarez-Perez, Christian Demitri, Vincenzo De Benedictis, Luigi Ambrosio <i>Italy</i>
698	<b>Osteoblast Response to Novel Zinc and Silicon Co-Substituted Hydroxyapatite</b> Robert Friedrichs, <u>Helen Chappell</u> , David Shepherd, Roger Brooks, Serena Best <i>United Kingdom</i>





699	<b>Incorporation of the Chondroitin Sulfate into Collagen Scaffolds to Create a Biomimetic Niche with Neurally Committed Human Induced Pluripotent Stem Cells</b> <u>Krystyna Pietrucha</u> , Marzena Zychowicz, Justyna Augustyniak, Martyna Podobinska, Leonora Buzanska <i>Poland</i>
700	<b>Hybrid Scaffolds of Collagen Modified by Dialdehyde Cellulose with iPS-Derived Neural Precursor Cells</b> <u>Krystyna Pietrucha</u> , Marzena Zychowicz, Justyna Augustyniak, Martyna Podobinska, Leonora Buzanska <i>Poland</i>
701	<b>Study of Poly(Lactic Acid) Hybrid Systems for Preparation of Interconnected Porous Scaffolds</b> Ioanna-Georgia Athanasoulia, Maria Kanidi, <u>Petroula Tarantili</u> <i>Greece</i>
702	<b>Solution Blow Spun Polyurethane Nanofibers: Tailoring Properties and Biocompatibility Evaluation</b> <u>Michał Wojasiński</u> , Małgorzata Bieniak, Tomasz Ciach <i>Poland</i>
703	<b>Integration of Biphasic Calcium Phosphate Bioceramics Mixed with Autologous Mesenchymal Cells in Osteoporotic Rabbit's Jaw</b> <u>Aleksandrs Grishulonoks</u> , Inese Chakstina, Arvids Jakovlevs, Vita Zalite, Andrejs Skagers, Ilze Salma, Vadims Klimets <i>Latvia</i>
704	<b>Evaluation of Graphene Based Composite Films for Biomedical Applications</b> <u>Christian Demitri</u> , Maria Grazia Raucci, Anna Moscatello, Daniela Giugliano, Vincenzo Maria De Benedictis, Alessandro Sannino, Luigi Ambrosio <i>Italy</i>
705	<b>In situ Investigation of Chemical Composition, Morphology, Gelling and Mineralisation Kinetics in Hydrogel/Mineral Composites</b> Sindre Hove Bjørnøy, David Bassett, Stefan Mandaric, Pawel Sikorski <i>Norway</i>
706	<b>Fabrication of co-Axial Electrospinning Nanofibrous Mats for Bone Tissue Engineering</b> <u>Katarzyna Zalewska-Wierzbicka</u> , Joanna Idaszek, Ewa Kijeńska, Manfred Zinn, Wojciech Swieszkowski <i>Poland</i>
707	<b>Crystal Structure of Calcium Carbonates Influence Osteoclasts Stimulation – Potential Importance of Similarity to the Bone Mineral</b> <u>Małgorzata Kolodziejczyk</u> , Zbigniew Jaegermann, Jarosław Sadło, Małgorzata Lewandowska-Szumiel <i>Poland</i>
708	<b>Shark Collagen/Hydroxyapatite Scaffolds Envisaging Biomedical Applications</b> Gabriela S. Diogo, Estefania López, Pio González, Julia Serra, Ricardo I. Martin, Carmen G. Sotelo, Tiago H. Silva, <u>Joana Moreira-Silva</u> , Rui L. Reis <i>Portugal</i>
709	<b>Macrophage Polarization on Composites Based on Silica, Collagen and Calcium Phosphate Phase</b> <u>Sina Rößler</u> , Christiane Heinemann, Thomas Hanke <i>Germany</i>
710	<b>Linear Polyglycerol Derivatives with Adjustable LCST and Good Biocompatibility</b> <u>Daniel Stöbener</u> , Silke Heinen, Tobias Becherer, Qiang Wei, Rainer Haag, Marie Weinhart <i>Germany</i>
711	<b>Long-Term Propagation of Cells in 3D Culture Effects Cell Morphology and Behaviour</b> Alisha Chhatwal, <u>Stefan Przyborski</u> <i>United Kingdom</i>
712	<b>Electrospinning of a Chitosan Based Artificial GAG for Tissue Engineering Application</b> <u>Safa Ouerghemmi</u> , Stéphanie Degoutin, Nicolas Tabary, Frédéric Cazaux, Ludovic Janus, Nicolas Blanchemain, Bernard Martel, Feng Chai <i>France</i>
713	<b>Electrospun Piezoelectric P(VDF-TrFE) Scaffolds and the Effect of Electrical Stimulation for Tendon Tissue Regeneration</b> <u>Gemma Orpella</u> , Marc Fernandez, Matteo Palma, Dimitrios Zeugolis, Abhay Pandit, Manus Biggs <i>Ireland</i>





714	<b>Highly Porous Silica Aerogel-Based Bioactive Composite Materials as Potential Scaffolds for Bone Regeneration</b> <u>Farkas Kerényi</u> , Andre Kuttor, István Tombác, Ágnes Baráthné Szabó, István Lázár, Csaba Hegedűs <i>Hungary</i>
715	<b>Fabrication and Evaluation of <math>\beta</math>-TCP/ZrO<sub>2</sub>-Doped-Phosphate Bioglass Scaffolds for Bone Tissue Engineering</b> <u>Ena A. Aguilar-Reyes</u> , Criseida Ruiz-Aguilar, Carlos A. Leon-Patino, Ana E. Higareda-Mendoza <i>Mexico</i>
716	<b>Biocompatibility Study of Polylactide Composites with Iron Oxide Nanoparticles</b> <u>Katarzyna Nowicka</u> , Anna Wiecheć, Marta Błażewicz <i>Poland</i>
717	<b>In situ Patterning of Collagen by Laser-Assisted Bioprinting Guides HUVECs Alignment and Promotes the Creation of Capillary-Like Structures</b> Olivia Kérouédan, Jérôme Kalisky, Murielle Rémy, Emeline Pagès, Joëlle Amédée, <u>Jean-Christophe Fricain</u> , Sylvain Catros, Raphaël Devillard <i>France</i>
718	<b>Influence of Strontium on the Synthesis and Degradation Behaviour of Biphasic Calcium Phosphate Ceramics</b> <u>Līga Stipniece</u> , Kristine Salma-Ancane, Dagnija Loca <i>Latvia</i>
719	<b>Different Crosslinking Systems Enable of Hydrogels Preparation Based on Hyaluronan-Tyramine Conjugates</b> <u>Lenka Kohutová</u> , Lucie Wolfová, Martin Pravda, Ivana Ščigalková, Vladimír Velebný, Julie Bystroňová <i>Czech Republic</i>
720	<b>Graphene-Based Tissue Engineering Scaffolds Prepared by 3D Printing</b> <u>Harri Korhonen</u> , Le Hoang Sinh, Nguyen Dang Luong, Jukka Seppälä <i>Finland</i>
721	<b>Decidual Mesenchymal Stem Cells and Ceramic-Based Graft Substitutes as Constructs for Bone Tissue Engineering</b> <u>Gema Vallés</u> , Fatima Bensiamar, Laura Saldaña, Ana Flores de la Cal, Almudena de Laiglesia, Rosa M Gonzalo-Daganzo, Jose Cordero, Nuria Vilaboa, Enrique Gómez-Barrena <i>Spain</i>
722	<b>Characterization of Human Neural Networks Cultured on Hydrogel Matrix</b> <u>Tiina Joki</u> , Laura Ylä-Outinen, Susanna Narkilahti <i>Finland</i>
723	<b>Functionally Graded Hybrid Scaffolds for Osteo-Chondral Defect Repair: Osteogenic Differentiation of Human Placenta-Derived Cells (hPDC)</b> Valentina Spoldi, Gabriela Kmieciak, Silvia De Munari, Patrizia Bonassi Signoroni, Roberta Gentilini, Antonietta Silini, <u>Silvia Farè</u> , Ornella Parolini <i>Italy</i>
724	<b>Synthesis and Characterization of Hydroxyapatite/Polyvinyl Alcohol Nanocomposite Hydrogels</b> Marta Branka, <u>Dagnija Loca</u> , Marina Sokolova, Agnese Pura <i>Latvia</i>
725	<b>Synthesis and Characterization of Chitosan-Modified Montmorillonite Nanoparticles for Tissue Engineering Applications</b> <u>Zahra Rezvani</u> , Masoud Mozafari <i>Iran</i>
726	<b>How Chitosan Addition Affects the Characteristics of Polyvinyl Alcohol Nanofibrous Scaffolds</b> <u>Zahra Rezvani</u> , Masoud Mozafari <i>Iran</i>
727	<b>New Biomimetic Multi-Substituted Hydroxyapatite Phases for Bone Regeneration Assisted by Antibacterial Effect</b> <u>Alberto Ballardini</u> , Andrea Ruffini, Simone Sprio, Anna Tampieri <i>Italy</i>
728	<b>Influence of Implant Surfaces on Osseointegration</b> <u>Żaneta Mierzejewska</u> <i>Poland</i>



729	<b>Treatment of Osteonecrosis of Femoral Head (ONFH) with Co-transplantation of Adipose-Derived Stromal Cells and Bone Marrow Stromal Cells in Minipig Model</b> <u>Woo-Lam Jo</u> , Mi Lan Kang, Ji Eun Kim, Eun Ah Kim, Soon-Yong Kwon, Gun-Il Im <i>Republic of Korea</i>
730	<b>Bioengineering of Mandibular Reconstruction in Cancer Surgery</b> <u>Camille Ehret</u> , Thomas Sagardoy, Rachida Aid, Robin Siadous, Reine Bareille, Damien Le Nihouanen, Jérôme Kalisky, Stanislas Pechev, Leatitia Etienne, Didier Letourneur, Jean-Christophe Fricain, Erwan De Mones, Joëlle Amedee <i>France</i>
731	<b>iPS-Derived Neural Cells in a 3D Collagen Scaffold as a Tool for Investigating Interrelations Between Biomaterials and Nerve Tissue</b> <u>Marzena Zychowicz</u> , Jose Luis Gerardo Nava, Krystyna Pietrucha, Hanna Winiarska, Martyna Podobińska, Gary Brook, Leonora Bużańska <i>Poland</i>
732	<b>Carbon Nanofiber Scaffolds for Cartilage Tissue Engineering</b> <u>Anna Magiera</u> , Joanna Konko, Jaroslaw Markowski, Jan Pilch, Elzbieta Menaszek, Marta Blazewicz <i>Poland</i>
733	<b>Collagen and Carboxymethyl Cellulose Bilayers for Skin Tissue Repair</b> <u>Cemile Kilic Bektas</u> , Ilgin Kimiz, Aylin Sendemir Urkmez, Vasif Hasirci, Nesrin Hasirci <i>Turkey</i>
734	<b>In vitro Studies of Novel PLDA/Mg Composites Processed by Injection Moulding</b> <u>Sandra Cifuentes</u> , Marcela Lieblich, Rosario Benavente, José Luis González-Carrasco <i>Spain</i>
735	<b>Quantification of Cell Migration on Culture Substrates—the Effect of the Surrounding Cells on Direction of Chondrocyte Migration</b> <u>Yotaro Nakane</u> , Kumpei Sano, Kenji Isshiki, Akihisa Otaka, Kazuya Takahashi, Katsura Kojima, Yasushi Tamada, Naohide Tomita <i>Japan</i>
736	<b>Quantification of Cell Migration on Culture Substrates—Proposal of New Parameters for Co-Migration</b> <u>Hirotaaka Nakamura</u> , Kumpei Sano, Akihisa Otaka, Kazuya Takahashi, Yotaro Nakane, Oki Shimizu, Katsura Kojima, Yasushi Tamada, Naohide Tomita <i>Japan</i>
737	<b>Wet Spun Scaffolds of PHA-PLA Blend for Bone Tissue Engineering</b> <u>Ayşe Selcen Alagoz</u> , Jose Carlos Rodriguez-Cabello, Nesrin Hasirci, Vasif Hasirci <i>Turkey</i>
738	<b>Bone Formation in a Rat Tibial Defect Model Using Carboxymethyl Cellulose/BioC/Bone Morphogenic Protein-2 Hybrid Materials</b> <u>Young-Pil Yun</u> , Sang-Heon Song, Hak-Jun Kim, Kyeongsoon Park, Sung Eun Kim, Hae-Ryong Song <i>Republic of Korea</i>
739	<b>Acellular Periodontal Ligament Matrix for Artificial Tooth Implant</b> <u>Naoko Nakamura</u> , Tsuyoshi Kimura, Ai Ito, Toshiya Fujisato, Takashi Tsuji, Akio Kishida <i>Japan</i>
740	<b>Extracellular Matrix Hydrogels from CNS and Non-CNS Tissues Developed for Neural Tissue Repair</b> <u>Karel Vyborný</u> , Zuzana Koci, Oleg Lunov, Eva Sykova, Sarka Kubinova <i>Czech Republic</i>
741	<b>A Novel Human Plasma-Derived Medium Supplement for Xeno-Free Culture of hMSC</b> <u>Ewa Bauman</u> , Cristina C. Barrias, Arantxa Blázquez, José M Díez, Rodrigo Gajardo, Salvador Grancha <i>Portugal</i>
742	<b>In vitro Hemolysis Assay and Platelet Aggregation Test of PEG Hydrogels for Tissue Engineering Applications</b> Alondra Escudero-Castellanos, Jaime Flores-Estrada, Victoria Domínguez-García, Blanca Elí Ocampo-García, Miriam V. Flores-Merino <i>Mexico</i>



743	<b>Elastin-like Recombinamer and Allogeneic Mesenchymal Stem Cells for Repair of Rotator Cuff Injury in Infrapinatus Tendon Rabbit Animal Model</b> <u>Alessandra Girotti</u> , Matilde Alonso, Arturo Ibañez, José María Trigueros Larrea, Aurelio Vega Castrillo, Ana Sánchez García, Ángel Luis Gato, Francisco J. Santos Martín, Jose Carlos Rodríguez-Cabello <i>Spain</i>
744	<b>Porous Microfiber Structures with Changeable Stiffness</b> <u>Jason Bolderson</u> , Maggie Cusack, Matthew Dalby, Huabing Yin <i>United Kingdom</i>
745	<b>Gradiently Mineralised Polysaccharide Hydrogels for the Treatment of Osteochondral Lesions</b> <u>Krzysztof Pietryga</u> , Katarzyna Reczyńska, Jonas Wengenroth, Håvard Haugen, Elżbieta Pamuła <i>Poland</i>
746	<b>Ceramic Materials for Dental Prosthetics – Optical and Microstructural Properties of Zirconia Ceramics</b> <u>Zbigniew Jaegermann</u> , Zdzisław Wiśniewski, Artur Oziębło, Robert Michalik <i>Poland</i>
747	<b>The Implementation of a Novel Process for the Preparation of Colored Zirconia Blocks for Dental Prosthetics</b> <u>Zbigniew Jaegermann</u> , Zdzisław Wiśniewski, Artur Oziębło, Robert Michalik <i>Poland</i>
748	<b>3D Printing of Artificial Nerve-Guides may be Clinically Effective and may Bring Ethical Benefit</b> <u>Antonio Merolli</u> , Paolo Scialabba D'Amico <i>Italy</i>
749	<b>Implementation and Commercialization Process of the New Polish Extracorporeal Ventricular Assist Device</b> <u>Małgorzata Gonsior</u> , Roman Kustosz, Artur Kapis, Agnieszka Szuber, Paweł Jurkowski, Zenon Narojek <i>Poland</i>
750	<b>Evaluation of Angiogenic Effect of Drug-Loaded Poly (DL-Lactic Acid) Porous Matrix Film for Wound Dressing Application by CAM Assay</b> <u>Sasiprapa Chitrattha</u> , Thawatchai Phaechamud <i>Thailand</i>
751	<b>Bilayered Scaffolds Incorporated with Gold Nanoparticles: Fabrication, Characterization and Toxicological Evaluation as Potential Skin Substitutes</b> Omer Akturk, <u>Dilek Keskin</u> <i>Turkey</i>
752	<b>Sulfated Glycosaminoglycan Derivatives Affect the Bioactivity of Angiogenic Growth Factors</b> <u>Linda Huebner</u> , Vera Hintze, Stephanie Moeller, Matthias Schnabelrauch, Dieter Scharnweber <i>Germany</i>
753	<b>Electrospun Fibrous Scaffolds for Wound Dressing of Mucous Membranes</b> <u>Gerlind Schneider</u> , Ralf Wyrwa, Sibylle Voigt, Katja Otto, Matthias Schnabelrauch <i>Germany</i>
754	<b>Impact of Biomimetic 3D Microenvironments on Macrophage Polarization</b> Katja Franke, Liv Kalbitzer, Jiranuwat Sapudom, Sandra Franz, <u>Tilo Pompe</u> <i>Germany</i>
755	<b>Surface Modification of Chitosan Hydrogels</b> Bożena Tyliszczak, <u>Katarzyna Z. Gaca</u> , Katarzyna Bialik-Wąs, Dagmara Malina, Agnieszka Sobczak-Kupiec <i>Poland</i>
756	<b>Synthesis, Functionalization and Characterization of UV-Curable Oligomers to be Used as Bioadhesive</b> Stacy Morgado, João Santos, Tiago Correia, Ilídio Correia, Cristina Baptista, Maria Gil, <u>Paula Ferreira</u> <i>Portugal</i>
757	<b>Hybrid Dressing of Highly Absorbent Polyurethane Foam and PVA Nano Fiber with Adipose-derived Stem Cell promotes Wound Healing</b> <u>Ho Yun Chung</u> , Hyung Min Sung, Eun Jung Oh, Tae Jung Kim, Jin Hyun Choi <i>Republic of Korea</i>



758	<b>Antimicrobial Activity of Silver Nanoparticles Incorporated in a Cryogel Matrix</b> Matthew Illsley, Cressida Bower, <u>Alma Akhmetova</u> , Gulsim Kulsharova, Timur Saliev, Talgat Nurgozhin, Sergey Mikhalevsky <i>Kazakhstan</i>
759	<b>Design of a Functional Degradable Wound Dressing for Acute Injuries</b> Beren Sen, <u>Ayşe Buse Özdebak</u> , Alper Tunga Akarsubası, Fatma Nese Kok <i>Turkey</i>
760	<b>Design of a Functional Degradable Wound Dressing System for Effective Pain Relief</b> <u>Beren Sen</u> , Ayşe Buse Özdebak, Fatma Nese Kok <i>Turkey</i>
761	<b>Dental Lessons from the Past: Ultrastructure of Teeth from Recent and Extinct Sharks, Plesiosaurs and Dinosaurs</b> <u>Alwina Lübke</u> , Joachim Enax, Oleg Prymak, Helge Fabritius, Dierk Raabe, Matthias Epple <i>Germany</i>
762	<b>Testing Stress Relaxation Process of a Pig's Skin</b> <u>Aneta Liber-Kneć</u> , Sylwia Łagan <i>Poland</i>
763	<b>Relationship between Solution Treatment and Mechanical Properties of Newly Developed Ag-Pd-Cu-Au System Alloy</b> <u>Yushi Hoshiya</u> , Toshikazu Akahori, Tomokazu Hattori, Hisao Fukui <i>Japan</i>
764	<b>Physical Properties and Toxic Potential of Dental Composites Containing a Triazol-Monomer</b> Torbjørn Knarvang, Jan T. Samuelsen, Hilde Kopperud <i>Norway</i>
765	<b>Structures of Chosen Degradation Byproducts Originating from Alkali Treatment of Hyaluronan Oligosaccharides</b> <u>Ondrej Kotland</u> , Kristina Nesporova, Radovan Buffa, Petra Liskova, Daniela Smejkalova, Martina Hermannova, Marek Kuzma, Vladimir Velebný, Tereza Silova <i>Czech Republic</i>
766	<b>SEM Evaluation on Adaptation of Various Materials Interface under Composite Sandwich Restorations</b> <u>Sam'an Malik Masudi</u> , Ninin Sukminingrum <i>Malaysia</i>
767	<b>Microleakage in Open-Sandwich Class II Dental Restorations</b> <u>Sam'an Malik Masudi</u> , Ninin Sukminingrum <i>Malaysia</i>
768	<b>Microscopy Analysis of Cement-Enamel Junction in Teeth</b> <u>Urszula Stachewicz</u> , Wojciech Kożuch, Aleksandra Czyrska-Filemonowicz <i>Poland</i>
769	<b>Influence of Precipitation Conditions on Cytocompatibility of Hydroxyapatite Substrates</b> <u>Sophie Cox</u> , Parastoo Jamshidi, Richard Williams, Liam Grover, Kajal Mallick <i>United Kingdom</i>
770	<b>Characterisation of Bioresorbable Composite Performance for Validation of New On-Line Process Monitoring Technology</b> Mark Billham, Darren Whitaker, Marion McAfee, <u>Nicholas Dunne</u> , Fraser Buchanan <i>Ireland</i>
771	<b>Silica Nanoparticles Stability in Model Biological Media</b> <u>Beata Borak</u> , Błażej Poźniak, Rafał Wiglus, Robert Pązik <i>Poland</i>
772	<b>Direct Contact Cytotoxicity Evaluation of Three Different Tricalcium Silicate Cements Used in Dentistry – An in vitro Study</b> <u>Sivaprakash Rajasekharan</u> , Heidi Declercq, David Schaubroeck, Peter De Coster, Luc Martens <i>Belgium</i>
773	<b>Gene Expression Profiling and Molecular Signalling of Dental Pulp Cells in Response to Tricalcium Silicate Cements: A Systematic Review</b> <u>Elanagai Rathinam</u> , Sivaprakash Rajasekharan, Ravi Teja Chitturi, Luc Martens, Peter De Coster <i>Belgium</i>



774	<b>Porous Ca-Deficient Hydroxyapatite/Biodegradable Polymer Composites</b> <u>Marina Sokolova</u> , Janis Locs, Aleksandrs Mirošnikovs <i>Latvia</i>
775	<b>Modulation of A<math>\beta</math>(25-35) Conformation: Curcumin and Curcumin Derivatives Effects</b> <u>Anna Maria D'Ursi</u> , Manuela Rodriguez, Maria Carrano, Manuela Grimaldi, Rosario Randino <i>Italy</i>
776	<b>Novel Environmental Use of Polyhydroxyalkanoates – Controlled Release Fertilizers</b> <u>Katarzyna Gorazda</u> , Ipsita Roy, Agnieszka Makara <i>Poland</i>
777	<b>Comparative Study of Mechanical Properties of the Selected Bioresorbable Thread Used in Orthopedics</b> <u>Magdalena Tomanik</u> , Sylwia Szotek, Anna Nikodem <i>Poland</i>
778	<b>Influence of Processing Methods on Biological Behaviour of Polylactide and Its Composites</b> <u>Anna Morawska-Chochół</u> , Jan Chłopek, Danuta Paluch <i>Poland</i>
779	<b>Analysis of the Biodegradable Miniplates Deformation. Finite Elements Method vs. Uniaxial Tensile Test</b> <u>Kamil Dudziński</u> , Robert Karńtoch, Karol Gryń <i>Poland</i>
780	<b>Water Loss of Surface Treated Glass-Ionomer Cements</b> <u>Elizabeth Bent</u> , John Nicholson <i>United Kingdom</i>
781	<b>Imaging of in-vitro Plaque Removed From Titanium Using Cavitation</b> <u>Emilia Pecheva</u> , Nina Vyas, Judith Brown, Gareth Price, Rachel Sammons, Damien Walmsley <i>United Kingdom</i>
782	<b>Degradation Processes of Ti6Al4V Alloy by Fretting and Fretting-Corrosion</b> Marcin Klekotka, <u>Jan Ryszard Dąbrowski</u> <i>Poland</i>
783	<b>Effects of Surface Characteristics of Orthodontic Adhesives on Multi-Species Biofilm</b> <u>Jung-Sub An</u> , Kyung Sun Kim, So Ha Jo, Sug-Joon Ahn <i>Republic of Korea</i>
784	<b>Hydrazide Modified Dextran as Scavengers for Carbonylated Proteins</b> <u>Ming Gao</u> , Tobias Larsson, Tim Bowden <i>Sweden</i>
785	<b>Preparation of Substituted Hydroxyapatite for Tooth Enamel Remineralization</b> <u>Vita Zalite</u> , Janis Locs <i>Latvia</i>
786	<b>Shape and Surface Chemistry Effects on the Cytotoxicity and Cellular Uptake of Metallic Nanorods and Nanospheres</b> Pelagie Favi, Mariana Morales, Paul Elliot, Alejandro Restrepo, Ming Gao, Hanchen Huang, <u>Juan Pavon</u> , Thomas Webster <i>Colombia</i>
787	<b>Chitosan-Based Hydrogels Modified with Silk Fibres for Cartilage Tissue Regeneration</b> <u>Magdalena Koziol</u> , Kinga Pielichowska, Jan Chłopek <i>Poland</i>
788	<b>Stable Pluronic Gel Formation by Incorporating Graphene Oxide</b> Da-Ae Won, Manse Kim, <u>Giyoong Tae</u> <i>Republic of Korea</i>
789	<b>Nanotoxicity Studies of Nanodiamond on 2D and Magnetically Bioprinted 3D Scaffold-Free Liver Model</b> <u>Dipesh Khana</u> , Dong Fu, Iqbal Ramzan, Wojciech Chrzanowski <i>Australia</i>
790	<b>Investigation of a Novel Bioresorbable Polymer Coated Drug-Eluting Scaffold</b> <u>Tamara Mahmood</u> , David Scurr, Nial Bullett, Kadem Al-Lamee, Morgan R. Alexander, Clive J. Roberts <i>United Kingdom</i>





791	<b><i>In vitro</i> Degradation Study of Calcium Phosphate Glass-Ceramic Exhibiting Angiogenic Properties</b> <u>Anna Matras</u> , Agata Roguska, Małgorzata Lewandowska, Marc Batista, Elisabeth Engel, Oscar Castano <i>Poland</i>
792	<b>Potential for Bio-Inspired Eggshell-derived Hydroxyapatite/Collagen Scaffolds for Osteochondral Tissue Engineering</b> <u>Cristian Parisi</u> , Luca Salvatore, Neelam Gurav, Sanosh Kunjalukkal Padmanabhan, Francesca Gervaso, Marta Madaghiele, Antonio Licciulli, Alessandro Sannino, Lucy Di Silvio <i>United Kingdom</i>
793	<b>Biomimetic Scaffolds Based on Biopolymers and Calcium Phosphates for Bone Tissue Engineering</b> <u>Liliana Verestiuc</u> , Florina Ivan, Maria Butnaru <i>Romania</i>
794	<b>Porosity Related Mechanical Response of Calcium Phosphate Bone Cements</b> <u>Dionysios Mouzakis</u> , Stefanos Zaoutsos, Stamatia Rokidi, Nikolaos Bouropoulos <i>Greece</i>
795	<b>Antioxidant Enzymes Immobilized on Biocompatible SPIONs for Cardiovascular Applications</b> <u>Liliana Verestiuc</u> , Lacramioara Lungoci, Vera Balan, Maria Butnaru, Ovidiu Bredetean <i>Romania</i>
796	<b>Regeneration the Urethral with Collagen Scaffold in Stricture Urethral Induced the Heat</b> Christian Acevedo-García, Jorge Jaspersen, Guillermo Soria, Jorge García, Saulo Mendoza, Luis Molina, Jaime Sanchez, Benjamin León, Cristina Piña, Gabriela Gutierrez-Reyes <i>Mexico</i>
797	<b>Insitu Nanoindentation of Dentine and Enamel Treated with 45S5 Bioactive Glass</b> <u>Richard Langford</u> , Jonathan Earl, John J. Melcholsky <i>United Kingdom</i>
798	<b>Effect of Crystallinity of Carbonated Hydroxyapatite on Bone Repair</b> Suelen Sartoretto, Marcelo Uzeda, Adriana Alves, Rodrigo Resende, José Calasans-Maia, Mônica Calasans-Maia, <u>Alexandre Rossi</u> , José Mauro Granjeiro <i>Brazil</i>
799	<b>Production of HA Scaffolds via Conversion of 3D Printed Gypsum Structures</b> <u>Alan Dantas</u> , Andrea Ferraz, Amanda Barbosa, Debora Scalabrin, Márcio Fredel, Jens Günster, Cynthia Gomes <i>Germany</i>
800	<b>Repeatability of Surgical Implantation of Biomaterials. Radiological Analysis of a-TCP Localization in Critical Sized Femoral Metaphysis Defect in Rabbits</b> Nikolaos Papaioannou, Triantafillos Papadopoulos, <u>Christos Zafeiris</u> , Nikitas Schizas, Aikaterini – Anna Neri, Cleopatra Nacopoulos, Ismini Donta <i>Greece</i>
801	<b>Formation and Structure of Silica-Rich Gel Layer in Na/H-exchanged 45S5 Bioglass: MD Models</b> <u>Antonio Tilocca</u> <i>United Kingdom</i>
802	<b>Physical and Mechanical Characterization of Hybrid Scaffolds Based on b-TCP and Collagen</b> Isadora Deschamps, Gabriel Magrin, Aguedo Aragonés, Cesar Benfatti, Ricardo Magini, <u>Júlio Souza</u> , Márcio Fredel <i>Brazil</i>
803	<b>Combined Effect of Magnesia and Zirconia on the Bioactivity of Calcium Silicate Ceramics at C/S ratio Less Than Unity</b> <u>Emad Ewais</u> , Amira Amine, Yasser Ahmed, Eman Ashor, Ulrike Hess, Kursch Rezwan <i>Egypt</i>
804	<b>Lanyu Minipig is a Better Model System for Studying Wound Healing</b> Ting-Yung Kuo, Ming-Jen Lin, Lih-Ren Chen, <u>Lynn L.H. Huang</u> <i>Taiwan, Province of China</i>
805	<b>Scanning Electron Microscope in Evaluation of Biomedical Materials – Own Experiences</b> Jacek Składzień, Agnieszka Wiatr, Katarzyna Zagórska-Swieży, <u>Maciej Wiatr</u> <i>Poland</i>





806	<b>Stem Cells Differentiation in Osteoblasts Lineage Using Bioactive Surfaces Mimicking Bone Microenvironment</b> Laurence Padiolleau, <a href="#">Laurent Plawinski</a> , Gaëtan Laroche, Marie-Christine Durrieu <i>France</i>
807	<b>Textile-Based Silk Scaffolds for Bone Tissue Engineering Applications</b> Viviana Ribeiro, Alain Morais, Vítor Correlo, Alexandra Marques, Ana Ribeiro, Carla Silva, Nuno Durães, Graça Bonifácio, Rui Sousa, Joaquim Oliveira, Rui Reis, <a href="#">Ana Oliveira</a> <i>Portugal</i>
808	<b>Impact of the Micro-scale Distribution of RGD/BMP-2 Peptides on hMSCs Osteogenesis</b> Ibrahim Bilem, Pascale Chevallier, Laurent Plawinski, Eli Sone, <a href="#">Marie-Christine Durrieu</a> , Gaëtan Laroche <i>France</i>
809	<b>Controllable Synthesis and Characterization of Multifunctional Poly(Lactic-co-Glycolic Acid) Nanoparticles for Tissue Engineering Applications</b> <a href="#">Masoud Mozafari</a> , Katayoun Nazemi, Fathollah Moztarzadeh <i>Iran</i>
810	<b>Tissue-engineered Poly (L-lactide-co-<math>\beta</math>-malic acid) Bone Scaffolds Functionalized with Forsterite Nanoparticles</b> Sina Moztarzadeh, Fuzhan Rahmadian, Fathollah Moztarzadeh, <a href="#">Masoud Mozafari</a> <i>Iran</i>
811	<b>Organ Decellularization: Design and Construction of a Device for Obtaining 3D Scaffolds, The Beginning of Bioartificial Organs in México</b> Héctor Martínez-Hernández, Benjamín León Mancilla, <a href="#">María-Cristina Piña-Barba</a> <i>Universidad Nacional Autónoma de México, Mexico</i>



# Authors Index

## A

- Aachmann Finn L. 478, 687  
Abbas Randa 258  
Abdul Rahman Asrizal 241  
Abradelo Cristina 381  
Abram Sarah-Luise 360  
Abramova N. 67  
Abramski Krzysztof 613  
Abuna Rodrigo 102  
Acevedo Garcia Christian 796  
Achar Arun 84  
Ackermann Michal 439  
Adam Stefanie 105  
Adamiak Marta 549  
Adamus Agnieszka 507  
Addison Owen 217  
Adekanmbi Isaiah 90, 444  
Agnello Stefano 274  
Aguero Amaru 206  
Aguiar Filipe 486  
Aguilar Maria Rosa 154  
Aguilar-Reyes Ena A. 612, 715  
Ahmad Agha Nezha 373  
Ahmadi Tafti Seyed Hossein 643  
Ahmed Yasser 803  
Ahn Sug-Joon 783  
Ai Hua 232  
Aid Rachida 2, 190, 730  
Akahori Toshikazu 586, 587, 588, 763  
Akaike Toshihiro 41  
Akarsubasi Alper Tunga 759  
Akdag Akin 653  
Akhmetova Alma 758  
Akiyama Toshimasa 194  
Akiyama Yoshikatsu 529  
Akkamongkolporn Prasert 519  
Akturk Omer 751  
Al Kayal Tamer 393, 445  
Al Tawil Elias 15, 104  
Alagesan Senthil 57  
Alagoz Ayse Selcen 126, 737  
Albanese Nicolò 244  
Albani Diego 36  
Albericio Fernando 181  
Albers Willem 364  
Alekseeva Tijna 224  
Alexander Cameron 358  
Alexander Morgan 357, 790  
Alexiou Christoph 169  
Ali Ahlam 72  
Ali Sara 55  
Alini Mauro 20, 181  
Al-Lamee Kadem 790  
Almeida Ana 621  
Almeida Catarina R. 636  
Almeida Maria I. 636  
Alonso Matilde 626, 743  
Alonso-Varona Ana 663  
Alorabi Jamal 138  
Altankov George 263  
Altgärde Noomi 146  
Álvarez-Fregoso Octavio 207, 684  
Álvarez-Lorenzo Carmen 175  
Álvarez-Martínez Cristina 424  
Álvarez-Mejia Laura 32  
Álvarez-Pérez Marco Antonio 207, 300, 697, 684  
Alves Adriana 798  
Alves Antoine 116  
Alves Patrícia 472, 589  
Amador Gilles 237  
Amalfitano Giuseppe 78  
Ambrosio Luigi 36, 61, 123, 185, 274, 276, 451, 481, 524, 678, 697, 704, K14  
Ambroziak Maciej 416  
Amédée Joëlle 2, 122, 717, 730  
Amine Amira 803  
Amorim Sara 112, 158  
An Jung-Sub 783  
Anada Takahisa 3, 568  
Anastasopoulou Maria 100  
Anderegg Ulf 212, K6  
Anderson James 232  
Andrade Fernanda 470  
Andriopoulou Sofia 468, 677  
Angles-Cano Eduardo 144  
Aniejurenghe Orode 339  
Ann Thomas Sneha 693  
Anselme Karine 377  
Ansorge Michael 212  
Anthony Weiss 422  
Antoniac Aurora 229  
Antoniac Iulian 229  
Antończak Arkadiusz 613  
Aoki Kaoru 429  
Aragones Aguedo 802  
Aranilla Charito 507  
Araujo Ana 112  
Araújo Francisca 182, 470  
Arcos Daniel 52, 371  
Aref Mohaddeseh Amiri 348  
Aregueta-Robles Ulises 199, K12  
Arias Francisco Javier 43, 44, 69  
Arias Vallejo Javier Francisco 533  
Armes Steven P. 58, 143  
Arruebo Manuel 266, 353, 491  
Asakura Naoya 630  
Asano Takuji 134  
Asghari sana Farzin 666  
Ashida Maki 228  
Ashor Eman 803  
Ashworth Jennifer 283  
Asikainen Sanja 494  
Aslankoohi Neda 23  
Ataol Sibel 653  
Athanasoulia Ioanna-Georgia 701



Attallah Moataz 217  
 Attia Nuha 556  
 Aubert-Viard François 362, 547  
 Auge Amélie 673  
 Aune Ragnhild E. 26  
 Aussel Audrey 190  
 Auzély-Velty Rachel 272  
 Avadhanam Venkata 532  
 Avcibasi Guvenilir Yuksel 317, 475  
 Aviles Francis 259  
 Aydin Halil Murat 230  
 Azeem Ayesha 294

## B

Babaliari Eleftheria 389  
 Babensee Julia 208  
 Babiano Reyes 628, 629  
 Babkina Tatiana 337  
 Bacakova Lucie K9, 553  
 Badea Mihaela 349  
 Bader Rainer 599  
 Bae Jin Woo 646  
 Bae Ji-Young 391  
 Baelo Aida 172  
 Bagdadi Andrea 164  
 Baglioni Piero 393  
 Bailey Kobayashi Nahoko 479  
 Bajek Anna 402, 691  
 Baker Sheri 351  
 Bakó József 482  
 Balaceanu Mihai 594  
 Balan Vera 795  
 Ballardini Alberto 727  
 Balvay Sandra 295  
 Ban Akinori 588  
 Ban Masahito 551  
 Banerjee Indranil 130  
 Banerjee Sreeparna 315  
 Baniukaitiene Odeta 685  
 Baptista Cristina 486, 756  
 Baran Erkan Türker 202  
 Baran Magdalena 550  
 Baráthné Szabó Ágnes 714  
 Barbeck Mike 410, 522, 638, 670  
 Barberis Fabrizio 399, 400, 427, 489, 696  
 Barbieri Davide 204, 301  
 Barbieri Luca 36  
 Barbosa Amanda 799  
 Barbosa Mário A. 636  
 Barbour Michele 135, 338  
 Barboza Wendell 403  
 Barbu Eugen 624  
 Barca Amilcare 456  
 Bareille Reine 2, 254, 418, 730  
 Barner Jörg 365  
 Baronti Valeria 696  
 Barraux Alysée 149  
 Barrett David 357, 375  
 Barrias Cristina 435, 555, 741  
 Barriuso Sandra 596  
 Barsotti Jonathan 250

Bartels Carla J.M. 35  
 Bartkowiak Amanda 563  
 Bartoszek Nina 221, 368  
 Basarabová Ivana 544  
 Basargan Ozsagiroglu Tugba 316  
 Basiaga Marcin 40  
 Basnayake Kolitha 267  
 Basnett Pooja 193, 288  
 Bassett David 455, 705  
 Baster Marta 275  
 Baszczuk Agnieszka 502  
 Batista Marc 791  
 Battaglia Giuseppe 143  
 Baum Martina 14  
 Bauman Ewa 555, 741  
 Baumann Sven 209  
 Baumbach Tilo 187  
 Bax Daniel 210  
 Bayon Yves 116, 675  
 Becher Jana 146  
 Becherer Tobias 710  
 Beck Ulrich 618  
 Bednarczyk-Cwynar Barbara 430  
 Bednarz Paulina 31, 513  
 Bektas Cemile 161  
 Belamie Emmanuel 6, 459  
 Belda Francisco 555  
 Belle Catherine 144  
 Bellon Benjamin 674  
 Beloti Marcio 102  
 Benavente Rosario 734  
 Benetti Edmondo K15  
 Benfatti Cesar 802  
 Benko Aleksandra 223  
 Bensiamar Fatima 408, 721  
 Bent Elizabeth 780  
 Berard Xavier 190  
 Bermúdez José 44  
 Bernhardt Anne 216  
 Bertoldi Serena 244  
 Bertrand Ghislaine 319  
 Bertrand Virginie 292  
 Bertz Andreas 180  
 Berzina-Cimdina Liga 233  
 Best Mark 47, 332  
 Best Serena 125, 188, 210, 283, 375, 698  
 Bettini Simona 286  
 Beutner René 559  
 Bhende Shubhangi 351  
 Bialik-Wąs Katarzyna 526, 527, 541, 542, 585, 755  
 Bidarra Silvia 435  
 Bidault Laurent 81, 660  
 Bieniak Małgorzata 702  
 Bierla Joanna 438  
 Biggs Manus 16, 294, 160, 515, 681, 713  
 Bikiaris Dimitrios 100, 388, 583, 686  
 Bil Monika 471, 530, 539  
 Bilek Marcela 38, 422  
 Bilem Ibrahim 808  
 Billham Mark 770  
 Birch Helen 74, 387



Bjørnøy Sindre Hove 705  
 Black Richard.A 449  
 Blajan Ana 229  
 Blanazs Adam 143  
 Blanchemain Nicolas 34, 137, 166, 362, 627, 712  
 Blanchfield Jennifer 208  
 Blanco Francisco 424, 631  
 Blazkova Lenka 679  
 Blázquez Arantxa 741  
 Blokland Kaj 392  
 Bloom Allan 258  
 Blumenthal Nils 535  
 Błażewicz Marta 223, 716, 732  
 Błażewicz Stanisław 635  
 Bobis-Wozowicz Sylwia 62, 549  
 Boccaccini Aldo 49, 100, 127, 164, 297, 314, 437  
 Boccafoschi Francesca 191  
 Bochynska Agnieszka 7  
 Bociąga Dorota 265  
 Boczar Krzysztof 448  
 Boczkal Sonia 329  
 Bodnar Magdalena 402  
 Boeri Lucia 36  
 Boeuf Hélène 418  
 Bohner Marc 127  
 Boisselier Julie 81  
 Boissière Michel 540, 547  
 Boissonade Fiona 22  
 Boix-Lemonche Gerard 263  
 Boiziau Claudine 418  
 Bolderson Jason 744  
 Bollemaat Hermen K15  
 Bonani Walter 445  
 Bonassi Signoroni Patrizia 723  
 Boncel Sławomir 307  
 Bone Adrian 47, 332  
 Bonfrate Valentina 286  
 Bonifácio Graça 807  
 Bonini Massimo 393  
 Bonnamy Sylvie 245  
 Booms Patrick 522, 638, 670  
 Borak Beata 502, 771  
 Borcard Françoise 304, 557  
 Bordenave Laurence 190, K9  
 Borecka Aleksandra 496  
 Borget Pascal 235  
 Borowski Tomasz 438, 518  
 Boruckowski Dariusz 62  
 Borzacchiello Assunta 274, 481  
 Bossard Cedric 344  
 Bossert Jörg 310, 359  
 Botta Margherita 191  
 Bourin Philippe 163  
 Bouropoulos Nikolaos 390, 405, 794  
 Boussard-Plédel Catherine 24  
 Bowden Tim 784  
 Bowen James 110  
 Bowen Paul 395  
 Bower Cressida 758  
 Boyd Daniel 426  
 Boyer Cécile 93  
 Bozec Laurent 74, 387  
 Bozkurt Ahmet 514  
 Bozukova Dimitriya 292  
 Brackman Gilles 136, 348  
 Bradshaw David 358  
 Braeckmans Kevin 187, 385  
 Braic Mariana 349, 594  
 Braic Viorel 349, 594  
 Brandão Ana Paula 637, 639  
 Brandejsova Martina 528  
 Brandenburger Matthias 197  
 Brånemark Rickard 153  
 Branka Marta 724  
 Brassesco Maria Sol 404  
 Bratov A. 67  
 Brauer Erik 101  
 Bray Laura 569  
 Bredetean Ovidiu 795  
 Breier Annette 282, 656  
 Brif Anastasia 177  
 Brindell Małgorzata 436  
 Brizzi Vincenzo 190  
 Brook Gary 226, 731  
 Brooks Roger 698  
 Brosel-Oliu S. 67  
 Brougham Dermot F. 53  
 Brouillet Fabien 66  
 Brown Judith 781  
 Brüggemann Dorothea 23  
 Bruinink Arie 97  
 Brulez Bernard 673  
 Brunelli Marzia 106  
 Bruno Agostino 303  
 Brunon Céline 116  
 Bruque Jose M. 374  
 Bruyneel Arne 113  
 Bryła Amadeusz 665  
 Brynda Eduard K9  
 Brzozowski Tomasz 552  
 Brzychczy-Włoch Monika 77, 141, 495  
 Buchanan Fraser 219, 770  
 Buffa Radovan 544, 765  
 Bullett Nial 790  
 Buma Pieter 7  
 Bunjes Heike 180  
 Bureau Bruno 24  
 Burgess Janette 457  
 Burguera Elena 631  
 Burillo Guillermina 175  
 Burke George 103  
 Burkhard Schlosshauer 333  
 Burlui Vasile 483, 484  
 Bushkalova Raya 163  
 Businaro Luca 325  
 Butnaru Maria 793, 795  
 Butruk-Raszeja Beata 118  
 Bütün Vural 315  
 Buxadera-Palomero Judit 174  
 Buxton Paul 283  
 Bużańska Leonora 226, 731  
 Bystroňová Julie 719



## C

- Cadinoiu Anca N 483, 484  
 Cádiz Monserrat 206  
 Cahuich Juan 206  
 Caillon Jocelyne 237  
 Cala Jaroslaw 507  
 Calasans-Maia José 798  
 Calasans-Maia Mônica 798  
 Caliarì Steven 184  
 Cama Giuseppe 249, 399  
 Cameron Neil K11, 246  
 Cameron Ruth 125, 188, 210, 283, 375  
 Canadas Raphaël F. 370  
 Canal Cristina 174, 487  
 Cancelli Nadia 692  
 Canepa Maurizio 625  
 Canepa Paolo 625  
 Cañizo Juan 176  
 Cannas Mario 191  
 Cano-Torres Irene 46  
 Canton Irene 58, 143  
 Capkin Yurtsever Merve 666  
 Capurro Marco 399, 489, 696  
 Caravaca Carlos 295  
 Carlos Rodríguez-Cabello José 202  
 Carr Carolyn 113  
 Carrano Maria 775  
 Carrasco Patricia 174  
 Carreiras Franck 540  
 Carrié Hélène 237  
 Cartmell Sarah 299  
 Carvalheiro Manuela 589  
 Carvalho Cristiana 634  
 Carvalho Mariana 156, 222  
 Casale Costantino 215  
 Castano Oscar 122, 148, 203, 791  
 Castellanos Maria Isabel 167  
 Castelletto Valeria K13  
 Castillo-Cruz Omar 259  
 Castro António 178, 236  
 Casuso Pablo 19, 477  
 Cathala Bernard 114  
 Catros Sylvain 122, 717  
 Cauich-Rodriguez Juan Valerio 259  
 Cavalleri Ornella 625  
 Cavallo Anna 456  
 Cazaux Frédéric 34, 137, 712  
 Cebotari Sergei 285, 677  
 Ceccaldi Caroline 163  
 Cecoltan Sergiu 379, 668  
 Celko Ladislav 248, 394  
 Cerri Alessandro 244  
 Cervantes Juan 206  
 Cervantes-Uc Jose Manuel 259  
 Cestari Idágene 200  
 Cestari Ismar 200  
 Chai Feng 137, 166, 362, 627, 712  
 Chakstina Inese 703  
 Chalanqui Marine 252, 269, 312, 432  
 Chambers Philip 252, 269, 312, 432  
 Chan Hak-Kim 457  
 Chan Luen Chow 25  
 Chan-Chan Lerma Hannaiy 259  
 Chancolon Jérôme 245  
 Chang Hyeyoun 287  
 Chang Kai-Chun 13  
 Chang Wan-Ju 428  
 Chappell Helen 240, 698  
 Charoenputtakun Ponwanit 458  
 Charvillat Cédric 66, 319  
 Chassande Olivier 418  
 Chat Coline 73, 149  
 Chatzinikolaïdou Maria 132, 389  
 Chen Chia-Cheng 313  
 Chen Lih-Ren 804  
 Chen Miin-Jang 579  
 Chen Peng 228  
 Chen Qiang 49  
 Chen Rongjun 271  
 Chen Yen-Hsuan 428  
 Cheng Chi-Hui 428  
 Cheng Nai-Chen 129  
 Chernobrovkina Daria 694  
 Chernousova Svitlana 171, K1  
 Chevalier Jérôme 127, 295  
 Chevallier Pascale 808  
 Chevolot Yann 295  
 Chhatwal Alisha 711  
 Chierchia Armando 36  
 Chiffot Nicolas 611  
 Chikusa Shunji 554  
 Chitraththa Sasiprapa 750  
 Chitturi Ravi Teja 773  
 Chkolnikov Marina 212  
 Chlupac Jaroslav K9  
 Chłopek Jan 64, 231, 334, 416, 417, 419, 778, 787  
 Choi Bong Kyu 322  
 Choi Jin Hyun 412, 757  
 Cholakh Seif O. 40  
 Cholewa-Kowalska Katarzyna 107, 187, 525, 564, 565, 664, 665  
 Chong Chuh 331  
 Chopin Nathalie 8  
 Chouhan Gurpreet 454  
 Christel Theresa 397  
 Chróścicka Anna 99  
 Chrzanowski Wojciech K8, 422, 457, 789  
 Chu Yu-Pu 336  
 Chuang YaMi 647  
 Chung Ho Yun 412, 757  
 Churchley David 358  
 Chvojka Jiří 284, 679  
 Ciach Tomasz 118, 384, 453, 580, 604, 702  
 Cicha Iwona 169, 437  
 Cichy Magdalena 430  
 Cieniek Łukasz 564, 565  
 Cieślak-Pobuda Artur 56, 548  
 Cieślak-Górna Monika 28  
 Cifuentes Sandra 347, 408, 734  
 Cigognini Daniela 57, 641  
 Cimatti Bruno 403, 404  
 Cimino Maura 555  
 Cintas Pedro 628, 629  
 Ciofani Gianni 250  
 Ciolek Lidia 341





Cirillo Valentina 61, 451  
 Ciupik Lechostaw 28  
 Civantos Ana 27  
 Claeysens Frederik 22, 131, 177, 251, 260, 313, 511  
 Clark Amy 203  
 Clarke James 22  
 Clarke Susan 219  
 Clarkin Owen 53  
 Clift Douglas 203  
 Clouet Johann 308  
 Coelho Jorge 589  
 Coenye Tom 136, 348  
 Cohen Stuart Martien 42  
 Cohn Daniel 258  
 Coimbra Patrícia 472  
 Colak Hakan 523  
 Collazos-Castro Jorge E. 29  
 Collic-Jouault Sylvia 8, 114, 644  
 Collier Thomas 387  
 Collins Andrew 338  
 Comaneanu Raluca 601  
 Concannon Ruth 196  
 Concheiro Angel 175  
 Connon Che K13, 120  
 Copes Francesco 191  
 Cordero Jose 721  
 Cordero-Arias Luis 297  
 Cornelissen Maria K10  
 Cornet Sandro 190  
 Corrales-Ureña Yendry 63  
 Correia Ilídio 756  
 Correia Marta 173  
 Correia Tiago 756  
 Correlo Vitor 807  
 Cortella Lucas 200  
 Costa Paulo 119  
 Cotrut Cosmin 598, 601  
 Couraud Lionel 254  
 Covarrubias Cristian 206  
 Cox Sophie 217, 769  
 Crespo Anna 172  
 Crespo Lara 17, 596  
 Crivelli Virginia 304, 557  
 Cruz Eugénia 589  
 Cruz Fernando 486  
 Cruz Guillermo J. 32  
 Cruz Rosana 637, 639  
 Cubo Nieves 176  
 Cuenot Stéphane 114, 644  
 Cummaro Annunziata 451  
 Cunha Carla 636  
 Cusack Maggie 744  
 Cussac Daniel 163  
 Cwalina Beata 609, 610  
 Cyza Małgorzata 159  
 Czarnowska Elżbieta 438, 518  
 Czarny Anna 341  
 Czechowska Joanna 340, 649, 650, 651, 652  
 Czernuszka Jan 113, 690  
 Czuchnowski Jakub 334  
 Czyrska-Filemonowicz Aleksandra 297, 768

**D**  
 D'Este Matteo 20  
 D'Errico Gerardino 481  
 Daculsi Guy 235  
 Dadhich Prabhaskar 84, 323, 406  
 Dalby Matthew 65, 607, 744  
 Dalheim Marianne Ø. 478, 687  
 Dalton Paul 647  
 Daly William 30  
 Damink Leon Olde 514  
 D'Amora Ugo 524, 678, K14  
 Dams-Kozłowska Hanna 473, 474  
 Dantas Alan 799  
 Daraba Oana 483, 484  
 Dard Michel 638  
 Dargaville Tim 647  
 Darlak Maciej 195  
 Daróczy Lajos 482  
 Das Bodhisatwa 84, 323, 406  
 das Neves José 470  
 Daugela Povilas 685  
 Daumann Sabrina 39  
 David Laurent 190  
 Davidenko Natalia 125, 210  
 Davies Michael 38  
 Dawidowska Kinga 450  
 Dawn Buddhadeb 62  
 Dąbrowski Jan Ryszard 782  
 de Battice Laura 146  
 De Benedictis Vincenzo 123, 185, 692, 697, 704  
 De Breuck Herbert TRS7  
 de Bruijn Joost 204, 301  
 de Cogan Felicity 503  
 De Coster Peter 772, 773  
 de Groot Florence 301  
 de la Fuente Anna 505  
 de Laiglesia Almudena 721  
 de Leeuw Nora 74, 387  
 de Leon Cecilia 300  
 de Miguel Laura 499  
 de Mones Erwan 254, 730  
 De Munari Silvia 723  
 de Oliveira Marcelo 9  
 De Palma Santiago 44  
 De Pauw Edwin 292  
 De Pauw-Gillet Marie-Claire 292  
 De Santis Roberto K14, 36, 524, 678  
 de Wolf Frits 42  
 Deb Sanjukta 124, 381, 561  
 Dec Weronika 609, 610  
 Declercq Heidi 772, K10  
 Deepagan V.G. 155  
 Degoutin Stéphanie 34, 712  
 Del Buffa Stefano 393  
 del Monte Francisco 29  
 Delcassian Derfogail 1624  
 Deligianni Despina 88  
 Della Sala Grazia 303  
 Delpoux Sandrine 245  
 Demirtas Tugrul Tolga 386  
 Demitri Christian 123, 185, 692, 697, 704





Demnati Imane 319  
 Dempwolf Wibke 180  
 Deneufchatel Marie 660  
 Dercz Grzegorz 40, 606  
 Deschamps Isadora 802  
 Deschepper Michael 81  
 Deschrevel Brigitte 15, 104  
 Despang Florian 5  
 Dessi Mariagemiliana 339, 501  
 Deszczyński Jarosław 384, 676  
 Detsch Rainer 127, 437  
 Devillard Raphaël 717  
 Devlin-Mullin Aine 299  
 Devoisselle Jean-Marie 459  
 Dew Lindsey 131, 331  
 Dewael Karolien 348  
 Dewald Carolin 359  
 Deyhle Hans 674  
 Dhara Santanu 84, 323, 406  
 Di Luca Andrea K15  
 Di Silvio Lucy 792  
 Díaz Mario 206  
 Díaz Natividad 19, 477  
 Díaz-Ricart Maribel 167  
 Diaz-Ruiz Araceli 32  
 Diban Nazely 645  
 Dienes Beatrix 482  
 Dieter Peter 423  
 Diez José M 741  
 Díez-Escudero Anna 311  
 Dimida Simona 692  
 Dinu Mihaela 594, 601  
 Diogo Gabriela S. 708  
 Dipresa Daniele 37  
 Dixon Simon 498  
 Dju Ting 65  
 Dobrzyński Piotr 496  
 Dogša Iztok 262  
 Doi Hisashi 228  
 Dokupil Agnieszka 136  
 Domalik-Pyzik Patrycja 334  
 Domínguez-García Victoria 165, 742  
 Dondajewska Ewelina 473  
 Donesz-Sikorska Anna 298  
 Donnelly Ryan 72  
 Donta Ismini 800  
 Doodkorte Remco 632  
 Dördelmann Gregor 12  
 Dornelles Rita 102  
 Douglas Timothy 136, 187, 385, 398  
 Douni Eleni 405  
 Dowd Eilís 16, 196  
 Drabik Dominik 537  
 Dresler Magdalena 118  
 Drewa Tomasz 289, 402  
 Drewniak Sabina 321  
 Drude Natascha 500  
 Du Jiuju 232  
 Duan Rongquan 204, 301  
 Dubey Prachi 164  
 Dubiel Beata 566  
 Dubois Julie 81

Dubruel Peter 136, 192, 249, 348, 505, 608, K10  
 Duckworth Peter 135  
 Duda Georg 101, 255  
 Dudek Karolina 600  
 Dudziński Kamil 231, 779  
 Duffy Garry 224  
 Dugan James 260, 313  
 Duman Fatih 354, 523  
 Dumay Valérie 633  
 Dunne Nicholas 219, 252, 269, 312, 432, 770  
 Dupin Damien 19, 477  
 Duployer Benjamin 163  
 Dupont-Gillain Christine 76  
 Durães Nuno 807  
 Durand Marlène 190  
 Durrieu Marie-Christine 109, 144, 152, 168, 237, 292, 806, 808  
 D'Ursi Anna Maria 303, 775  
 Durymanov Mikhail 117  
 Dutta Joy 406  
 Dvořáková Martina 544  
 Dye Julian F 133  
 Dziadek Michał 525, 564, 664, 665  
 Dziadowiec Iwona 674  
 Działoszyska Katarzyna 221, 368  
 Dzieciuch-Rojek Monika 431  
 Dzugan Jan 658

## E

Earl Jonathan 797  
 Easton Christopher D. 108  
 Edirisinghe Mohan 164, 193  
 Egana Tomas 133  
 Eglin David 20, 181  
 Ehlers Jan-Erik 180  
 Ehnert Sabrina 455  
 Ehret Camille 730  
 El Fray Mirosława K16, 366, 447  
 Ellinghaus Agnes 255  
 Elliot Paul 786  
 El-Meliegy Emad 55  
 Elsheikh Ahmed 202  
 Elter Patrick 618  
 Enax Joachim 761  
 Engblom Simon 411  
 Engel Edgard 403, 404  
 Engel Elisabeth 46, 122, 148, 172, 203, 791  
 English A 294  
 Engvall Klas 77, 576  
 Enochson Lars 146  
 Epple Matthias K1, 12, 39, 171, 243, 290, 309, 572, 761  
 Erben Jakub 284, 679  
 Erdemli Özge 98  
 Erel-Göktepe İrem 315  
 Eriguchi Masazumi 463, 531  
 Escolar Ginés 167  
 Escudero-Castellanos Alondra 742  
 Espallargas Nuria 26  
 Espanol Montserrat 70, 311  
 Estella Elvira 300  
 Etienne Leatitia 730  
 Eummelen Lizette 514  
 Evangelista Marta 94



Evans Meg K5  
Evans Richard A. 108  
Evavold Brian 208  
Ewais Emad 803  
Ezoe Yushi 3, 657

## F

Fabbi Claudia 399  
Fabela-Sánchez Omar 32  
Fabritius Helge 761  
Faccioni Giuliano 63  
Fagerlund Susanne 54  
Fanfani Francesco 234  
Farack Jana 383  
Farbod Kambiz 42, 183  
Farè Silvia 244, 723  
Farndale Richard 125, 210  
Farrugia Brooke 647  
Fasolino Ines 61  
Favi Pelagie 786  
Fayon Franck 245  
Feito María José 371  
Felgueiras Helena K5  
Fenelon Mathilde 418  
Fernandes João S. 238  
Fernandes Mariana 350  
Fernandes Susana 663  
Fernández Ana Belén 371  
Fernandez Carlos A. 669  
Fernandez Mar 306  
Fernandez Marc 160, 713  
Fernández-Calderón M Coronada 629  
Fernández-Colino Alicia 44  
Fernández-Hernán Juan Pablo 347  
Fernandez-Medina Marina 11  
Fernández-Pedrero José Arturo 207, 684  
Fernandez-Trillo Francisco 358  
Fernandez-Yague Marc 16  
Ferraz Andrea 799  
Ferreira Domingos 470  
Ferreira Paula 756  
Ferreira-da-Silva Frederico 350  
Ferrer María Luisa 29  
Ferri Joel 137  
Feyerabend Frank 373  
Fichet Odile 660  
Fiejdasz Sylwia 4, 595  
Figiel Henryk 369  
Figueiras Edite 145  
Filardo Giuseppe 5  
Filipek Katarzyna 218  
Filipiak Jarosław 613  
Filipowska Joanna 107, 115, 543, 665  
Filova Elena K9  
Finke Birgit 264, 376, 599  
Finocchio Elisabetta 400  
Fiorucci Paula 631  
Fisher Leanne 65  
Fitz Benjamin D 351  
Flath Tobias 247  
Florczak Anna 474  
Flores Claudia 137

Flores de la Cal Ana 721  
Flores-Estrada Jaime 165, 742  
Flores-Merino Miriam V. 165, 742  
Flores-Reyes Mario 165  
Fojt Jaroslav 607  
Fonte Pedro 470  
Forostyak Serhiy 506  
Forsgren Johan 467  
Förster Yvonne 209  
Forstreuter Inka 83  
Forte Giuseppe 678  
Fraczek-Szczypta Aneta 603  
Fraïoli Roberta 591  
Franco Albina 236  
Franke Katja 212, 754  
Fransen Peter 181  
Franz Sandra 83, 754, K6  
Frączek-Szczypta Aneta 223  
Frede Annika 309  
Fredel Márcio 799, 802  
Freitas Daniela 158  
Freudenberg Uwe 83  
Frey Laura 198  
Fricain Jean-Christophe 254, 418, 717, 730  
Friederichs Robert 698  
Frisina Noemi 489  
Fromm Katharina 360, 361  
Fryczkowski Ryszard 509  
Fu Dong 789  
Fujimoto Shinji 630  
Fujisato Toshiya 256, 739  
Fukui Hisao 570, 763  
Fukumoto Kohei 546  
Furuse Motomasa 134  
Fusaro Luca 191

## G

Gabler Carolin 599  
Gabor Roman 553  
Gaca Katarzyna Z. 526, 527, 541, 542, 585, 755  
Gajardo Rodrigo 741  
Galisova Andrea 273  
Gallagher Andrew 138  
Gallardo-Moreno Amparo María 347, 374  
Gallo Marta 127  
Gand Adeline 73, 81, 149, 547  
Ganesh Sahana 30  
Gao Changyou 82, 220  
Gao Jianqing 33  
Gao Ming 784, 786  
García Andres J. 203, 208  
Garcia Jorge 796  
Garcia Jose 203  
García Marta 176  
García-Cimbrelo Eduardo 408  
Garlichs Christoph D. 169  
Garziano Alessandro 78  
Gaspar Diana 57, 641, 689  
Gaspar M. Manuela 589  
Gato-Calvo L. 631  
Gatti Francesca 456  
Gätzner Sabine 605



- Gauthier Olivier 93  
 Gautron Eric 308  
 Gavalda Joan 172  
 Gbureck Uwe 216, 217, 261, 318, 397, 590  
 Geanta Victor 326, 327  
 Gebauer Tim 85, 291  
 Geffers Martha 216  
 Geilling Marcel 214  
 Geissler Sebastian 573, 575  
 Gelinsky Michael 5, 216, 277  
 Gemme Gianluca 625  
 Gener Petra 470  
 Geng Hua 299  
 Gentilini Roberta 723  
 Gepp Michael 39  
 Gerardo Nava Jose Luis 226, 731  
 Gerber Sandrine 557  
 Gerber-Lemaire Sandrine 304  
 Gericke Karl-Heinz 180  
 Gerritsen Karin 80  
 Gervaso Francesca 692, 792  
 Ghaemmaghami Amir 150  
 Ghag Anita 454  
 Ghanaati Shahram 410, 522, 638, 670  
 Gharibi Borzo 561  
 Ghavami Saeid 56, 548  
 Gherghilescu Ana 601  
 Giammona Gaetano 274  
 Giancane Gabriele 286  
 Giannitelli Sara Maria 328  
 Gigliobianco Giulia 331  
 Gil Francisco Javier 67, 121, 167, 174, 263, 591  
 Gil Maria 472, 589, 756  
 Gimsa Jan 618  
 Gindraux Florelle 418  
 Ginebra Maria-Pau 70, 248, 311, 487  
 Ginebra Molins Maria Pau 401  
 Giol E Diana 192, 608  
 Giordano Carmen 36  
 Girod-Fullana Sophie 163  
 Girotti Alessandra 69, 743  
 Giugliano Daniela 123, 185, 276, 697, 704  
 Giuri Antonella 123, 185  
 Glasmacher Birgit 257, 285, 468  
 Gloria Antonio 36, 524, 678, K14  
 Gloushankova Natalya 87  
 Gobaa Samy 440  
 Goc Kamil 595, 602  
 Goding Josef K12  
 Godoy-Gallardo Maria 121  
 Golda-Cepa Monika 77, 576  
 Gołyńska Magdalena 382  
 Gomes Carla 71  
 Gomes Cynthia 799  
 Gomes Paula 350  
 Gomez Beatriz 645  
 Gomez Tardajos Myriam 249  
 Gomez-Barrena Enrique 17, 596  
 Gomez-Lazaro Maria 71  
 Gómez-Ribelles José Luís 424  
 Gonçalves Carolina 305  
 Gonçalves Inês C. 119, 173, 305  
 Gonçalves Raquel 555, 636  
 Goncharenko Anton 243, 290  
 Goñi Isabel 306, 623  
 Gonsior Małgorzata 195, 749  
 Gonzalez Borja 248  
 González de Torre Israel 533, 626  
 González Pio 708  
 González-Carrasco José Luis 347, 408, 596, 734  
 González-Gómez Álvaro 213  
 González-Martín María Luisa 347, 355, 374, 596, 628, 629  
 González-Mayorga Ankor 29  
 Gonzalo-Daganzo Rosa M 721  
 Gorazda Katarzyna 776  
 Gorb Stanislav 14  
 Gorewoda Tadeusz 606  
 Gori Manuele 325, 328  
 Gorodzha Svetlana 187  
 Gorski Alexandr 159  
 Goryczka Tomasz 352, 600  
 Gossart Charline 81  
 Goszczyńska Agata 366  
 Gotman Irena 51, 278  
 Götz Andrea 363  
 Gough Julie 227  
 Gouveia António 119  
 Gouveia Ricardo K13  
 Gómez-Barrena Enrique 721  
 Gómez-Cerezo Natividad 52  
 Grabarczyk Jacek 265  
 Grabska Sylwia 560  
 Grady Helena 338  
 Graf Ursula 661  
 Granchar Salvador 741  
 Grandfield Kathryn 378  
 Granja Pedro 182, 222  
 Granjeiro José Mauro 798  
 Granqvist Niko 364  
 Grądzka-Dahlke Małgorzata 581, 619  
 Green Nicola 313  
 Green Rylie 199, K12  
 Greish Yaser 556, 693  
 Gremillard Laurent 295  
 Gressenbuch Mathias 247  
 Grier William 184  
 Griffin Matthew 57  
 Grijalva Israel 32  
 Grijpma Dirk 7  
 Grimaldi Annalisa 36  
 Grimaldi Manuela 303, 775  
 Grimm Silko 12  
 Grishulonoks Aleksandrs 233, 703  
 Gritsch Kerstin 695  
 Groll Jürgen 261, 318, 397, 590  
 Grosgeat Brigitte 695  
 Gross Gerhard 180  
 Grossin David 66, 319  
 Grossiord Carol 116  
 Grote Karsten 285  
 Grover Liam 217, 769  
 Grunert Fritz 333  
 Gryń Karol 231, 414, 779  
 Grzesiak Jakub 31, 509, 510



Grzeszczuk Ola 516  
 Grzonka Justyna 603  
 Gu Zhongwei K2  
 Guarino Vincenzo 61, 451  
 Gubanska Iga 289  
 Gudima Alexandru 94  
 Guerrero Julien 2  
 Gugutkov Dencho 263  
 Guich Lise 245  
 Guicheux Jérôme 8, 93, 308  
 Guillard Roger 673  
 Guildford Anna 47, 332  
 Guillem-Marti Jordi 167, 263, 401, 487  
 Guiomar António 472  
 Gumusderelioglu Menemse 386, 666  
 Günster Jens 799  
 Guo Rui 82  
 Gurav Neelam 792  
 Gurruchaga Mariló 306, 623  
 Gut Arkadiusz 159, 434  
 Gutiérrez María Concepción 29  
 Gutierrez Reyes Gabriela 796  
 Gutmanas Elazar 51, 278  
 Gwon Hui-Jeong 538

## H

Haag Rainer 710  
 Haak Katharina 517  
 Haapasalo Markus 121  
 Hacker Michael C. 197, 247, 620  
 Hahn Claudia 343, 345  
 Hahner Judith 282  
 Haigh Jodie 647  
 Hakkarainen Minna 77  
 Hakvoort Jan N W 183  
 Halgand Boris 8  
 Hamada Kenichi 391, 442, 443  
 Hamaia Samir 125  
 Hamely Ian K13  
 Han Dong Keun 440, 441  
 Han Hwa Seung 488  
 Han Yin-Yi 579  
 Hanawa Takao 228  
 Haniel Jonathas 637, 639  
 Haniu Hisao 429  
 Hanke Thomas 383, 656, 709  
 Hanley Geoffrey 675  
 Hanley Jonathan 508  
 Hannink Gerjon 7  
 Hans Michael 343, 345  
 Hansen Margaret 426  
 Hansmann Jan 605  
 Harder Michael 677  
 Harding Adam 22  
 Harding Sian 164, 193  
 Harkin Damien 569  
 Harley Brendan 184  
 Hart Terance 375  
 Hartmann Daniel 295  
 Hartmann Martin 49  
 Hasegawa Masataka 551

Hashimoto Jun-ichi 521  
 Hasirci Nesrin 126, 733, 737  
 Hasirci Vasif 126, 161, 202, 733, 737  
 Hassanin Hany 217  
 Hatakeyama Yuri 270  
 Hattori Tomokazu 570, 586, 587, 588, 763  
 Haugen Håvard 344, 466, 495, 573, 575, 745  
 Haulon Stephan 166  
 Haverich Axel 37, 285, 677  
 Havlicek Jiri 679  
 Havlikova Jana 553  
 Hayakawa Satoshi 134  
 Haycock John 22, 511  
 Hayrapetyan Astghik 183, 294  
 Hedrick James 140  
 Heepe Lars 14  
 Hegedús Csaba 367, 482, 714  
 Heinemann Christiane 383, 656, 709  
 Heinen Silke 710  
 Heinrich Gert 282  
 Heinze Marie 214  
 Heljak Marcin 539  
 Hempel Ute 209, 396, 423, K6  
 Hendriks Stephan 247  
 Hennik Wimm 491  
 Henning Max 310  
 Henriques Patrícia 119  
 Henry Nina 308  
 Hentunen Teuvo 1  
 Heo Roun 68  
 Herman Artur 307  
 Hermannova Martina 528, 765  
 Hermsdörfer Anne 365  
 Hernández-Godínez Braulio 32  
 Héroguez Valérie 237  
 Herranz-Blanco Bárbara 182  
 Herrera Aaron 101  
 Hertault Adrien 166  
 Herzmann Nicole 105  
 Heschel Ingo 255  
 Hess Ulrike 803  
 Hibbitts Alan J. 224  
 Hierro-Oliva Margarita 596, 628  
 Higareda-Mendoza Ana E. 715  
 Hildebrand Hartmunt F. 137  
 Hilfiker Andres 285, 677  
 Hill Lisa J 503  
 Hindie Mathilde 73, 660  
 Hintze Vera 396, 752, K6  
 Hinüber Claudia 282  
 Hipólito-García Manuel 207, 684  
 Hirano Yoshiaki 446  
 Hirvonen Jouni 182  
 Histace Aymeric 540  
 Hoban Deirdre 196  
 Hoeksema Henk 348  
 Hoene Andreas 264, 376, 667  
 Hoess Andreas 255, 397  
 Hofbauer Lorenz K6  
 Hoffmeister Peter-Georg 620  
 Hofmann Sandra 293



Hogerheyde Thomas 569  
 Höhne Susanne 656  
 Holland Chris 177  
 Honda Eiichi 442, 443  
 Hoogenboom Richard 154, 647  
 Hook Andrew 170, 335, 357  
 Horáková Jana 284, 439, 480, 679  
 Horeglad Paweł 462  
 Hori Naoko 1  
 Hornez Jean Christophe 137  
 Hornyák István 342, 672  
 Horsburgh Mal 138  
 Horváthy Dénes 672  
 Horynová Miroslava 394  
 Hoshiya Yushi 763  
 Hosseinian Pezhman 230  
 Howell Carol 267  
 Hoyos-Nogués M. 67  
 Hrubí Edit 482  
 Hu Zhenlu 271  
 Huang Hanchen 786  
 Huang Her-Hsiung 13  
 Huang Lynn L.H. 804  
 Huang Tongtong 377  
 Huang Yan Yan Shery 151  
 Huang Yi-Shiang 292  
 Hubalek-Kalbacova Marie 658, 671  
 Huber Rebecca 75  
 Hübner Linda 752, K6  
 Huerta-Angeles Gloria 273, 528  
 Humbert Bernard 308  
 Hupa Leena 54, 411  
 Hyon Suong-Hyu 95  
 Hyttinen Jari 145

**I**  
 Iafisco Michele 183  
 Ibañez Arturo 743  
 Ibáñez-Contreras Alejandra 32  
 Ibáñez-Fonseca Arturo 43  
 Ibegbu Daniel 624  
 Ida Yumika 391  
 Idaszek Joanna 179, 530, 539, 706  
 Iglič Aleš SCh2  
 Ignatov Sergey 87  
 Ikeda Masahiko 642  
 Illsley Matthew 758  
 Im Gun-Il 59, 464, 729  
 Imperato Giorgia 215  
 Ingavle Ganesh 267, 532  
 Inkinen Saara 411  
 Inui Shihoko 442, 443  
 Ip Wing Yuk 25  
 Iruin Amatriain Elena 275  
 Irusta Silvia 239, 353  
 Ishihara Masatou 551  
 Ishii Shota 554  
 Ishikawa Kunio 242  
 Ishimoto Takuya 18  
 Islas Luisa 175  
 Isshiki Kenji 735

Istodorescu Mircea 379  
 Ito Ai 739  
 Ito Temmei 194  
 Ito Tomoko 463, 531  
 Itoh Manabu 228  
 Ivan Florina 793  
 Ivanovic Zoran 418  
 Iwai Atsushi 657  
 Iwanowska Agnieszka 543  
 Izquierdo-Barba Isabel 52

**J**  
 Jablonská Eva 407, 607  
 Jacinto-Díaz Benito 612  
 Jaegermann Zbigniew 707, 746, 747  
 Jagiełło Joanna 550  
 Jähnke Torsten 365  
 Jain Mayur V. 548  
 Jain Minkle 281  
 Jakovlevs Arvids 703  
 Jamróz Dorota 159  
 Jamshidi Parastoo 769  
 Jandt Klaus 310, 359  
 Janeczek Henry 496  
 Janik Helena 289, 420  
 Jankowska Urszula 62  
 Jankowska-Steifer Ewa 99  
 Jannasch Maren 605  
 Jansen John 35, 178, 183, 294, 632  
 Janus Ludovic 34, 712  
 Jańczuk Bronisław 628, 629  
 Jarmundowicz Włodzimierz 509, 510  
 Jarocho Danuta 111  
 Jarosz Magdalena 111  
 Jarosz Tomasz 430  
 Jasiorski Marek 502  
 Jaskuła Marian 111  
 Jaspersen Jorge 796  
 Jastrzebska Katarzyna 473  
 Jawoska-Kik Marzena 609, 610  
 Jelonek Katarzyna 496  
 Jenčová Věra 284, 679  
 Jenkinson Howrad 65  
 Jeon Ju Eun 68, 490  
 Jeon Sangmin 155, 488  
 Jeong Sung In 538  
 Jiang Pengfei 220  
 Jin Rongrong 232  
 Jirak Daniel 273  
 Jo So Ha 783  
 Jo Woo-Lam 729  
 Johns Douglas B 351  
 Johnson David 246  
 Joki Tiina 722  
 Jokinen Annika 364  
 Jones Julian R 299  
 Jonkheijm Pascal 372  
 Jorcano Jose Luis 176  
 Jordana Fabienne 93  
 Jorgensen Christian 6, 459  
 Jouan Thierry 24





Joung Yoon Ki 440, 441  
Jugdaohsingh Ravin 240  
Jugowiec Dawid 564, 567  
Julian Esther 172  
Jundziłł Arkadiusz 402  
Junghans Frauke 597  
Junthip Jatupol 627  
Juodzbalyš Gintaras 685  
Jurczyk Jakub 602  
Jurkowski Paweł 749

## K

Kaczmarek Beata 640  
Kaczmarek Łukasz 617  
Kaiser Jozef 248, 394  
Kajii Fumihiko 657  
Kajta Małgorzata 115  
Kajzer Anita 516, 558  
Kajzer Wojciech 516, 558  
Kakazu Danilo Akio 512  
Kalaszczyńska Ilona 688  
Kalbitzer Liv 754  
Kaleta Jerzy 298, 502  
Kalin Mitjan 262  
Kalisky Jérôme 717, 730  
Kaliva Maria 132  
Kalkhof Stefan 209  
Kaloynni Martha 388  
Kalozoomis Panagiotis 468  
Kalugyer Pálma 342  
Kałaska Bartłomiej 115  
Kamakura Shinji 657  
Kamińska Marta 221, 368  
Kamiński Artur 688  
Kamiński Jakub 330  
Kamiński Kamil 115  
Kamiya Katsuhiro 194  
Kamperman Marleen 42  
Kamycka Elżbieta 62, 552  
Kanazawa Hideko 529  
Kang Mi Lan 59, 464, 729  
Kang Sung Nam 441  
Kanidi Maria 701  
Kanno Tomonori 536  
Kano Toshimi 405  
Kańtoch Robert 779  
Kaomongkolgit Ruchadaporn 519  
Kapat Kausik 323  
Kapiński Dawid 329  
Kapis Artur 749  
Kapusta Czesław 595, 602  
Karakassides Michalis 100  
Karam Sherif 693  
Karaś Michał 329  
Karbowniczek Joanna 297  
Karczewski Sarah 12  
Karewicz Anna 275, 469  
Karnas Elżbieta 549, 550  
Karwat Kamil 525  
Kascholke Christian 197, 247  
Kashiwada Ayumi 521  
Kasperczyk Janusz 496  
Kassim Yusra 15  
Kasuga Toshihiro 279  
Kataoka Kazunori 16  
Kato Hiroyuki 429  
Kauffeldt Marina 37  
Kawaguchi-Takeda Tomoko 554  
Kawai Tadashi 657  
Kawamoto Keiko 95  
Kawano Fumiaki 391  
Kaya Murat 354  
Kaynak Gokce 666  
Kazmanlı Kursad 421  
Kądzioła Kinga 221, 368  
Kedracka-Krok Sylwia 62  
Kellomäki Minna 145  
Kellouche Sabrina 540  
Kelly Adam 131  
Keloglu Nermin 21  
Kemper Gregor 152  
Kerényi Farkas 482, 714  
Kérourédan Olivia 717  
Keskin Dilek 653, 751  
Kępczyński Mariusz 159, 431  
Khademhosseini Ali 198, 545  
Khanal Dipesh 789  
Khoury Maroun 133  
Khurana Kanupriya 487  
Kidoaki Satoru 13  
Kieruzel Ewa 558  
Kierzkowska Agnieszka 28  
Kiessling Fabian 363  
Kijerńska Ewa 706  
Kikuchi Akihiko 529, 536  
Kikuchi Shoichi 588  
Kilic Bektas Cemile 733  
Kim Bae Young 646  
Kim Eun Ah 729  
Kim Hak-Jun 738  
Kim Ik Hwan 440  
Kim Jae Bong 412  
Kim Ji Eun 59, 464, 729  
Kim Kwangmeyung 155, 287, 488  
Kim Kyung Sun 783  
Kim Manse 788  
Kim Sung-Eun 659, 662, 738  
Kim Tae Jung 412, 757  
Kim Tae Woo 433  
Kim Taek Bo 299  
Kim Yang-hee 14  
Kimiz Ilgin 733  
Kimura Tsuyoshi 256, 739  
Kind Lucy 674  
King Martin 611  
Kinne Raimund W. 310  
Kinoshita Yoshihiko 134  
Kiremitci Arlin 666  
Kirkpatrick C. James 13, 192, 410, 522, 638, 670  
Kiryukhantsev-Korneev Philipp 87  
Kishida Akio 256, 739  
Kiss Adrian 349, 598





Kissenpfennig Adrien 72  
 Kitai Marina 446  
 Klakurkova Lenka 394  
 Klein Gunnewiek Michel K15  
 Klekotka Marcin 782  
 Klich Marek 617  
 Klimecs Vadims 233, 703  
 Kluijtmans Bas 682, 683  
 Klymov Alexey 632  
 Kłysik Katarzyna 469  
 Kmiecik Gabriela 723  
 Kmiolek Katarzyna 62, 550  
 Knapp David TR55  
 Knarvang Torbjorn 764  
 Knauer Shirley 12  
 Knaus Petra 101  
 Knoflach Viktoria 56  
 Knopf-Marques Helena 150  
 Knowles Jonathan 164  
 Kobayashi Jun 529  
 Kobayashi Masako 242  
 Kobayashi Naoki 446  
 Kobayashi Shinsuke 429  
 Kobe Spomenka 262, Sch2  
 Koca Fatih Dogan 354, 523  
 Kocer Gulistan 372  
 Koch Franziska 661  
 Koci Zuzana 506, 740  
 Koegler Aylin 108  
 Kohn Caroline 197  
 Kohn Joachim L1, 2, 623  
 Kohutová Lenka 719  
 Koivisto Janne 145  
 Kojima Katsura 735, 736  
 Kok Fatma Nese 759, 760  
 Kokkinopoulou Maria 638  
 Kokubo Tadashi 50  
 Kolcz Jacek 62  
 Koliakou Iro 100, 388, 686  
 Kolmas Joanna 462, 465  
 Kolodziejczyk Małgorzata 707  
 Kolwijck Eva 35  
 Kołodziejczyk Agnieszka 221, 368  
 Komorowski Piotr 221, 368  
 Kon Elizaveta 5  
 Kondyurin Alexey 38, 422  
 König Olivia 504  
 Konko Joanna 732  
 Kopperud Hilde 764  
 Korhonen Harri 494, 720  
 Körner Christine Sch1  
 Korossis Sotirios 37, 285, 468, 677  
 Korotin Danila M. 40  
 Kortylewski Marcin 474  
 Kostakova Eva 679  
 Kościelniak-Ziemniak Magdalena 195  
 Kot Marcin 565, 566  
 Kotarba Andrzej 77, 576  
 Kotarba Sylwia 221, 368  
 Kotelnikov Ilya K9  
 Kotland Ondrej 765  
 Koumentakou Ioanna 388  
 Kowalska Ewa 302  
 Kowalska-Ludwicka Karolina 507  
 Kowalski Michał 267  
 Koyama Yoshiyuki 463, 531  
 Koziel Marcin 4  
 Kozik Anna 329  
 Kozikowska Ewelina 471  
 Koziol Magdalena 787  
 Kozlova Diana 12  
 Kozłowska Anna 474  
 Kozłowska Justyna 648  
 Kożuch Wojciech 768  
 Krak Anna 369  
 Kralickova Milena 658  
 Kraszewski Maciej 302  
 Kratz Gunnar 548  
 Krocilova Nikola 553  
 Krok-Borkowicz Małgorzata 298, 425  
 Kronbach Zienab 214  
 Kroustalli Anthoula 88  
 Król Klaudia 415  
 Krukiewicz Katarzyna 307, 430  
 Krummsdorf Susann 214  
 Kruppke Benjamin 383  
 Krzak Justyna 298  
 Kubba Haytham 90, 444  
 Kubies Dana 658  
 Kubinova Sarka 506, 740  
 Kucharczyk Kamil 473  
 Kucinska-Lipka Justyna 289, 420  
 Kujawa Marek 99  
 Kukhareno Andrey I. 40  
 Kulanthaivel Senthilguru 130  
 Kulkarni Mukta Sch2  
 Kulsharova Gulsim 758  
 Kumar Pramod 57, 162, 641, 689  
 Kumar Sandeep 267, 532  
 Kumar Sanyaja 51  
 Kunisch Elke 310  
 Kunjalukkal Padmanabhan Sanosh 792  
 Kunze Angelika 146  
 Kuo Ting-Yung 804  
 Kurachi Yoichi 531  
 Kurmaev Ernst Z. 40  
 Kuroiwa Toshihiko 134  
 Kurzydłowski Krzysztof 179  
 Kus Maja 231  
 Kus-Liśkiewicz Małgorzata 239, 353, 615  
 Kustos Laura 367  
 Kustos Roman 195, 749  
 Kuttor Andre 714  
 Kuzma Marek 765  
 Kuzuya Akinori 268  
 Kuźmińska Aleksandra 118  
 Kwon Ick Chan 155, 287, 488  
 Kwon Soon-Yong 729  
 Kyziol Agnieszka 239, 353, 617  
 Kyziol Karol 617  
 Kzyshkowska Julia 94



## L

- L. Seabra Catarina 350  
 Labardi Massimiliano 250  
 Labedz-Maslowska Anna 552  
 Labidi Jalel 663  
 Labour Marie-Noëlle 6  
 Lackington William A. 224  
 Lackner Juergen M. 89, 201, 562  
 Lacroix Damien 60, 106  
 Lacza Zsombor 342, 672  
 Laczka Maria 107  
 Ladam Guy 149  
 Lagazzo Alberto 399, 400, 427, 489, 696  
 Lai Chi Ping 25  
 Laipple Daniel 373  
 Lally Catriona 53  
 Lamas Sofia 636  
 Landrieu Blandine 655  
 Langford Caitlin 246  
 Langford Richard 797  
 Langheinrich Denise 200  
 Langner Marek 485, 492, 537  
 Laptoiu Dan 379  
 Laroche Gaétan 109, 806, 808  
 Larreta-Garde Véronique 81, 139, 547, 660  
 Larsen Kim L. 478  
 Larsson Tobias 784  
 Lasagni Andrés 200  
 Laska Jadwiga 31, 509, 510, 513  
 Laurenceau Emmanuelle 295  
 Laurent Cedric 655  
 Laurindo Carlos 621  
 Laursen Marie Baekgaard 11  
 Lavalle Philippe 150  
 Layrolle Pierre 633  
 Lázár István 714  
 Lazarenko Victor 694  
 Lazaro Maria 119  
 Le Bideau Jean 8, 308  
 Le Harzic Ronan 39  
 Le Nihouanen Damien 730  
 Le Saux Guillaume 168  
 Le Visage Catherine 308  
 Lech-Grega Marzena 329  
 Leclercq Laurent 627  
 Lee Jeong-Cheol 322  
 Lee Peter D. 299  
 Lee Seunghwan 574  
 Lee Sohyoun 538  
 Lee Sungho 279  
 Lee Tzer-Min 336, 428  
 Lee Young-Ho 433  
 Lee Yunki 646  
 Leemhuis Hans 255, 514  
 Leeuwenburgh Sander 35, 42, 183  
 Lefebvre Elodie 81, 139  
 Lemaître Jacques 395  
 Lendlein Andreas 85, 291  
 Leon Benjamin 796  
 Leonor Isabel 236  
 Leon-Patino Carlos A. 612, 715  
 Letourneur Didier 2, 190, 730  
 Levato Riccardo 46, 172, 392  
 Lewandowska Katarzyna 560  
 Lewandowska Małgorzata 148, 791  
 Lewandowska-Łańcucka Joanna 4, 476  
 Lewandowska-Szumieł Małgorzata 17, 99, 211, 688, 707  
 Lewandowski Daniel 502  
 Lewis Andrew L. 143  
 Li Luyan 82  
 Li Xia 151  
 Li Zhaoying 151  
 Libera Marcin 496  
 Liber-Kneć Aneta 762  
 Licciulli Antonio 792  
 Liebler Sven 333  
 Lieblich Marcela 734  
 Liesiene Jolanta 685  
 Lim Hyun Ju 412  
 Lim Khoon 199  
 Lim Youn-Mook 538  
 Limongelli Vittorio 303  
 Lin Hsin-Chih 579  
 Lin Jui-Che 428  
 Lin Ming-Jen 804  
 Linares Javier 371  
 Lindahl Anders 146  
 Lipińska Ludwika 550  
 Lipov Jan 407, 607  
 Lips Katrin 262, 277  
 Lis Anna 31, 509, 510  
 Lisboa-Filho Paulo 63  
 Liskova Petra 765  
 Liu Chaoyu 225, 497  
 Liu Christopher 532  
 Liu Dongfei 182  
 Liu Xing 82  
 Liu Yen-Ting 336  
 Lizio Rosario 12  
 Loca Dagnija 669, 718, 724  
 Locs Janis 409, 774, 785  
 Lode Anja 216  
 Loebel Claudia 20  
 Logan Ann 503  
 Logeart-Avramaglou Delphine 81  
 Lohmann Nadine 83  
 Loinaz Iraidia 19, 477  
 Lombardi Bernadette 215  
 Lopes José Manuel 119  
 Lopes Rodrigues Diogo 524  
 Lopez-Lacomba Jose 27  
 Lorenz Jonas 410, 670  
 Lorenzetti Martina 262, Sch2  
 Löser Reik 85  
 Losi Paola 393, 445  
 Loth Rudi 620  
 Louarn Guy 633  
 Loughran Stephen 432  
 Lourenço Sarah 9  
 Lovell Nigel 199  
 Loza Kateryna K1  
 López Ana de Jesus 631



López Estefania 708  
 López-Dolado Elisa 29  
 Lu Helen 90, 444  
 Lübke Alwina 761  
 Lucke Silke 264, 376, 667  
 Lüdecke Claudia 359  
 Luis Gato Ángel 743  
 Lukáš David 284, 679  
 Lukasiewicz Barbara 193, 288  
 Lund Reidar 575  
 Lungoci Lacramioara 795  
 Lunov Oleg 740  
 Luo Xiaoman 204, 301  
 Luong Nguyen Dang 720  
 Luxbacher Thomas Sch1, Sch2  
 Lynch Andrew 271  
 Lynge Martin E. 11  
 Lyskawa Joël 166  
 Łagan Sylwia 762  
 Łapa Agata 398  
 Łapkowski Mieczysław 430  
 Łapok Łukasz 159, 434  
 Łączka Maria 525, 665  
 Łępicka Magdalena 581, 619  
 Łos Marek 56  
 Łukaszczyk Alicja 565  
 Łukawski Maciej 485, 492  
 Łuszczczyk Katarzyna 502

## M

Ma Lie 82  
 Maazouz Yassine 248  
 MacDonald Kathleen 426  
 MacFarlane Wendy 47, 332  
 Machado José C. 173  
 Mackiewicz Andrzej 473, 474  
 MacNeil Sheila 131, 331  
 Macyk Wojciech 615  
 Madácsi Edit 342  
 Madaghiele Marta 286, 456, 792  
 Maddocks Sarah 135, 338  
 Madeja Zbigniew 62, 334, 549, 550, 552  
 Madi Kamel 299  
 Madsen Jeppe 143  
 Maeda Hirotaka 279  
 Maenz Stefan 310  
 Magalhães Ana 119, 158  
 Magalhães Fernão 305  
 Magalhães Joana 424, 631  
 Magennis E. Peter 357, 358  
 Magiera Anna 635, 732  
 Magini Ricardo 802  
 Magrin Gabriel 802  
 Mahalingam Suntharavathanan 193  
 Mahmood Tamara 790  
 Mahou Redouan 304, 557  
 Maia André 119  
 Maia Fátima 156, 222  
 Maia Sílvia 350  
 Maj Malgorzata 691  
 Maji Samarendra 154

Majka Marcin 111, 431  
 Major Bogusław 89, 562, 593  
 Major Łukasz 562  
 Major Roman 89, 201, 593  
 Makara Agnieszka 776  
 Mäkilä Ermei 182  
 Makowski Krzysztof 221, 368  
 Malal Ram 258  
 Malda Jos 392  
 Malecka Barbara 448  
 Malheiro Vera 97  
 Malina Dagmara 526, 527, 541, 542, 585, 755  
 Malinowski Janusz 330  
 Mallick Kajal 769  
 Malmonge Sonia Maria 512  
 Mancilla Benjamín León 811  
 Mandarin Stefan 705  
 Manero José M. 121, 167, 263, 591  
 Mangeng Christian 674  
 Maniglio Devid 445  
 Maniura Katharina 75, 97  
 Mano João F. 48  
 Mantovani Giuseppe 358  
 Mao Yong 2, 623  
 Mao Zhengwei 33, 220  
 Marczak Jan 593  
 Margiotta Nicola 183  
 Marinescu Rodica 379  
 Marino Attilio 250  
 Markl Juergen 638  
 Markowski Jarosław 732  
 Marques Alexandra P. 370, 807  
 Marquis Mélanie 114, 644  
 Marrese Marica 61  
 Marsan Olivier 319  
 Marszałek Andrzej 402  
 Marszałek Marta 563  
 Martel Bernard 34, 137, 362, 627, 712  
 Martens Luc 772, 773  
 Martens Penny 199, K12  
 Marthala V. R. Reddy 49  
 Martí Joan 148  
 Martí Joan 122  
 Martin Adeline 362  
 Martin del Campo-Fierro Marcela 213  
 Martin Ricardo I. 708  
 Martinez Cristian A. 669  
 Martínez de Arenaza Inger 346  
 Martínez-Hernández Héctor 811  
 Martinez-Ibañez Maria 623  
 Martins Albino 634  
 Martins Cristina 119, 173, 350, 555  
 Martins Margarida 238  
 Martín-Saavedra Francisco 17, 266, 491  
 Marycz Krzysztof 31, 509, 510  
 März Emilie 318  
 Marzec Mateusz 513  
 Marzec Michalina 420  
 Mas-Moruno Carlos 67, 121, 167, 174, 591  
 Massera Jonathan 24  
 Mastalska- Popławska Joanna 510



Masudi Sam'an Malik 766, 767  
 Masullo Ugo 456  
 Masumoto Hiroshi 568  
 Mata Alvaro 181  
 Mata José 472  
 Mateos-Timoneda Miguel A. 46, 148, 172  
 Matesanz María Concepción 371  
 Mathes Stephanie 661  
 Mathieu Marc 6, 459  
 Matloubigharagzloo Maziar 79, 535  
 Maton Mickael 166  
 Matras Anna 791  
 Matsiko Amos 224  
 Matsugaki Aira 18, 642  
 Matsui Keiko 657  
 Matsumura Kazuaki 95, 280, 281, 461, 520  
 Matsunami Chisato 592  
 Matsuo Koichi 622  
 Matsushita Tomiharu 50  
 Matsuura Katsuhisa 270  
 Mattoli Virgilio 250  
 Maurel Blandine 166  
 Mavrilas Dimosthenis 257  
 Mazgala Aleksandra 239  
 Mazzolai Barbara 250  
 McAfee Marion 770  
 McBride John 72  
 McCafferty Mura 103  
 McCaffrey Joanne 72  
 McCarthy Helen 72, 252, 269, 312, 432  
 McCormick Christopher 449, 498  
 McKenzie David 38, 422  
 McKittrick Craig Martin 498  
 McLister Robert 103  
 Meaurio Emilio 346  
 Mech Rafał 502  
 Medda Luca 481  
 Medrela Katarzyna 413  
 Meenan Brian J. 103  
 Mehdinavaz Aghdam Rouhollah 643  
 Mehnert Julia M. 197  
 Mehr Marco 283  
 Meichsner Jürgen 264  
 Meikle Steven 128, 339  
 Meille Sylvain 127  
 Meininger Markus 261  
 Meister Sebastian 291  
 Melchels Ferry 392  
 Melcholsky John J. 797  
 Melo Rodriguez Gabriela 110  
 Menaszek Elżbieta 223, 352, 582, 732  
 Mendoza Saulo 796  
 Menzel Henning 10, 180  
 Menzel Henning 517  
 Merolli Antonio 234, 748  
 Meskinfam Masoumeh 244  
 Meyer Juliane 105  
 Meyer Michael 380, 597  
 Meyer Susanne 105  
 Meyer-Zaika Wolfgang 171  
 Michael Frank 345

Michalik Robert 746, 747  
 Michalska Joanna 609, 610  
 Michalska Marta 640  
 Michna Justyna 239  
 Miculescu Florin 598  
 Mierzejewska Żaneta 654, 728  
 Mietinen Susanna 24  
 Migliaresi Claudio 445  
 Migonney Véronique K5, 673  
 Mihailova Boriana 373  
 Mijowska Ewa 366  
 Mikeš Petr 439, 480, 679  
 Mikhlovsky Sergey 267, 758  
 Mikulska Anna 115, 543  
 Mildner Robert 517  
 Minárik Peter 407  
 Mingarelli Luigi 234  
 Minkle Jain 461  
 Miramond Thomas 235  
 Miranda-Gonçalves Vera 296  
 Mirosnikovs Aleksandrs 774  
 Mitchell Christopher A. 299  
 Mitek Tomasz 384, 676  
 Miyabe Sayaka 630  
 Miyamoto Youji 242  
 Miyazaki Toshiki 134, 592  
 Mizuno Masaki 521  
 Mizuta Ryo 194  
 Moataz Attallah Moataz 319  
 Mobasser Atefeh 227  
 Moeller Martin 500  
 Moeller Ralf 343  
 Moeller Stephanie 752  
 Mogielnicki Andrzej 115  
 Molina Luis 796  
 Molinos Maria 636  
 Molitor Martin 553  
 Möller Ralf 345  
 Möller Stephanie 146, 396  
 Mondragón-Lozano Rodrigo 32  
 Monduzzi Maura 481  
 Monnier Alexandre 15, 104  
 Monstrey Stan 348  
 Montealegre Ángeles 596  
 Monteiro Claudia 350  
 Montembault Alexandra 190  
 Montufar Edgar B. 248, 394  
 Moore Harry 58  
 Morais Alain 807  
 Morales Mariana 786  
 Morales-Corona Juan 32  
 Morales-Guadarrama Ayayacatl 32  
 Morawska Karolina 505  
 Morawska-Chochół Anna 334, 416, 778  
 Moreno Gomez Ismael 188  
 Moreno Pedro 71  
 Morgado Stacy 756  
 Morgan Sarah 449  
 Morgan-Warren Peter J 503  
 Morgenroth Agnieszka 500  
 Morille Marie 459



Morini Alessandro 234  
 Morita Hiroko 256  
 Moroni Lorenzo K15  
 Morticelli Lucrezia 285, 677  
 Moscatello Anna 704  
 Moseke Claus 261, 318, 559, 590  
 Moskalewicz Tomasz 564, 565, 566, 567  
 Motarjemi Hooman 553  
 Mottaghy Felix M. 500  
 Mourad Abdel-Hamid 556, 693  
 Mouzakis Dionysios 405, 794  
 Moy Ashley 184  
 Mozafari Masoud 725, 726, 810, 809  
 Mozdzen Laura 184  
 Mozetic Pamela 328  
 Moztarzadeh Fathollah 810, 809  
 Moztarzadeh Sina 810  
 Mroczka Adam 516  
 Muecklich Frank 343  
 Mueller-Albers Jessica 12  
 Mühlstädt Mike 310  
 Mullen Anne Maria 680  
 Müller Benno M 620  
 Müller Bert 674  
 Müller Michaela 356  
 Müller Peter P. 180  
 Müller Ralph 293  
 Müller Torsten 365  
 Mumcuoglu Didem 499  
 Munisso Maria 446  
 Murai Takaaki 622  
 Murakami Teruo 91  
 Musilkova Jana K9  
 Mygdali Evi 132  
 Mystek Katarzyna 476  
 Mzyk Aldona 593

## N

Nacopoulos Cleopatra 800  
 Naganuma Tamaki 86  
 Nagase Kenichi 270, 529  
 Nagraba Łukasz 384, 676  
 Nakai Masaaki 586  
 Nakamura Hirotaka 736  
 Nakamura Miho 1  
 Nakamura Naoko 256, 739  
 Nakane Yotaro 735, 736  
 Nakano Takayoshi 18, 642  
 Nakao Takuya 630  
 Nakase Ikuhiko 479  
 Nakashima Kazuhiro 91  
 Nakayama Masamichi 536  
 Nakonieczny Damian 320, 321  
 Natęcz-Jawecki Grzegorz 462, 465  
 Nam Kwangwoo 256  
 Nambu Koichiro 588  
 Nameki Hirofumi 622  
 Narkevica Inga 189, 324  
 Narkilahti Susanna 722  
 Narojek Zenon 749  
 Narushima Takayuki 279

Nash Anthony 74, 387  
 Nasun Saygılı Gülhayat 316  
 Nath Shekhar 50  
 Naughton Carol 196  
 Navarro Claudia 203  
 Navarro Melba 522  
 Nazemi Katayoun 809  
 Nazir Rabia 113  
 Nearantzaki Maria 388  
 Nebe Barbara 599  
 Neffe Axel 85, 291  
 Neimane Laura 233  
 Nelsen Jens 12  
 Nelson John 219  
 Nerantzaki Maria 100, 686  
 Neri Aikaterini Anna 800  
 Nese Kok Fatma 421  
 Nešporová Kristina 157, 273, 765  
 Netti Paolo Antonio 78, 215  
 Neuhaus Bernhard 309  
 Neut Christel 362  
 Neves Nuno N. 238, 634  
 Ngawhirunpat Tanasait 458, 460, 519  
 Nguyen Quang Trong 15, 104  
 Nicholson John 780  
 Niedzielski Piotr 265  
 Nielsen Thorbjørn T. 478  
 Niemczyk Agata 366  
 Nies Berthold 255, 397  
 Niinomi Mitsuo 586  
 Nikodem Anna 777  
 Nikolaidis Vasileios 583  
 Nikraves Niusa 454  
 Nilebäck Erik 146  
 Niu Xufeng 611  
 Niwa Kentaro 586  
 Nkhwa Shathani 124  
 Nlate Sylvain 144, 168  
 Nobbs Angela 65  
 Nocuń Marek 223  
 Noël Danièle 6, 459  
 Nogueira-Barbosa Marcello 403  
 Nolte-Karayel Andrea 504  
 Nomoto Toyokazu 622  
 Nomura Hiroki 429  
 Nomura Naoyuki 228  
 Norlindh Birgitta 153  
 Novak Saša 262, SCh2  
 Noverraz François 304, 557  
 Novotna Katarina K9  
 Novotny Karel 394  
 Nowakowska Maria 4, 115, 159, 275, 431, 434, 469, 476, 543, 595, 602  
 Nowicka Katarzyna 369, 716  
 Nunes Cláudia 173  
 Nurgozhin Talgat 758  
 Nussler Andreas 455

## O

O'Brien Fergal J. 224  
 O'Kelly Kevin 198





Obata Akiko 279  
 O'Brien Timothy 57  
 Ocampo-García Blanca Elí 742  
 Ochiuz Lacramioara 483, 484  
 Ocsoy Ismail 354  
 Oda Reiko 152  
 O'Doherty Michelle 252, 269, 312, 432  
 Odriozola Ibon 19  
 Ogawa Satoshi 622  
 Oguchi Yurie 570  
 Oh Dong Hwan 646  
 Oh Eun Jung 412, 757  
 Ohta Toshiaki 622  
 Ohya Yuichi 268, 892  
 Oikawa Mayumi 568  
 Ojansivu Miina 24  
 Okamoto Masanori 429  
 Okano Laura 404  
 Okano Teruo 270, 529, 536  
 Olayo Maria-Guadalupe 32  
 Olayo Roberto 32  
 Oledzka Ewa 465  
 Olejnik Alicja 507  
 Ołędzka Ewa 452, 462  
 Oliva Mireia 470  
 Oliveira Ana 296, 807  
 Oliveira Carla 435  
 Oliveira Hugo 2, 122  
 Oliveira Joaquim M. 45, 92, 156, 222, 296, 370, 634, 807  
 Oliveira Nuno 48  
 Oliveira Patrícia 435  
 Oliviero Olimpia 451, 524  
 Olmedo Daniel 669  
 Olszyna Andrzej 341  
 Omtvedt Line Aa. 478, 687  
 Onat Bora 315  
 Opanasopit Praneet 458, 460, 519  
 Orbanic Doriana 533  
 Orii Yusuke 568  
 Orpella Gemma 160, 713  
 Orpella-Aceret Gemma 515  
 Ortega Ilida 131  
 Ortiz Inmaculada 645  
 Osaka Akiyoshi 134  
 Ossowska Agnieszka 578  
 Osswald Tim 408  
 Ostrovska Lucie 658  
 Osyczka Anna 107, 115, 543, 606, 665  
 Otaka Akihisa 735, 736  
 Otsuka Makoto 463  
 Otto Katja 753  
 Ou Jun 577  
 Ouerghemmi Safa 34, 712  
 Ould Aklouche Malika 695  
 Ovaleo Pandolfo Luigi 276  
 Ovsianikov Aleksandr K10  
 Owen Robert 251  
 Ozcan Inas 421  
 Ozdabak Ayse Buse 759, 760  
 Ozdil Deniz 230  
 Oziębło Artur 746, 747

Ozolins Jurijs 324  
 Ozols Andrés 669  
 Ozsagiroglu Erhan 317, 475  
 Ozturk Kup Fatma 354  
 Ozuno Yoshihiro 546

## P

Paape Heike 105  
 Pacha-Olivenza Miguel Ángel 347, 355  
 Paciello Antonio 78  
 Padiolleau Laurence 806  
 Paduano Luigi 481  
 Pagès Emeline 717  
 Pagnoulle Christophe 292  
 Pakkanen Kirsi 574  
 Pal Pallabi 84, 323, 406  
 Palao-Suay Raquel 154  
 Palazzo Barbara 692  
 Palla Beatriz 306  
 Pallua Norbert 514  
 Palma Matteo 160, 713  
 Palmer Iwan 219  
 Palmquist Anders 153, 378  
 Palomares Teodoro 663  
 Paluch Danuta 778  
 Palumbo Fabio Salvatore 274  
 Pałka Krzysztof 64  
 Pamuła Elżbieta 136, 141, 298, 398, 425, 495, 745  
 Pandit Abhay L8, 16, 30, 45, 57, 294, 160, 162, 196, 241, 641, 675, 680, 681, 689, 713  
 Papadopoulos Triantafillos 390, 800  
 Papaioannou Nikolaos 800  
 Paquet Joseph 81  
 Parastoo Jamshidi Parastoo 319  
 Parilli Annapaola 5  
 Parini Angelo 163  
 Parisi Cristian 792  
 Parizek Martin 553  
 Park Jae Hyung 68, 155, 433, 488, 490  
 Park Jong-Seok 538  
 Park Ki Dong 646  
 Park Kwang-Sook 440  
 Park Kwang-Won 659, 662  
 Park Kyeongsoon 738  
 Parolini Ornella 723  
 Parraga Jenny E. 145  
 Parra-Ruiz Francisco 154  
 Pascual Ana 140  
 Pashkuleva I. 112  
 Pashkuleva Iva 146, 158  
 Pasieka Zbigniew 507  
 Passemard Solène 304, 557  
 Pastorino Laura 489  
 Paszenda Zbigniew 320, 321  
 Patalas Adam 571  
 Paterson Thomas 313  
 Patrzyk Maciej 264, 376, 667  
 Patton Alexander K12  
 Pauthe Emmanuel 73, 81, 149, 540, 547  
 Pavlenko Denys 80  
 Pavlík Vojtěch 157





Pavón Juan 27, 786  
 Pawelec Kendall M. 682, 683  
 Pawlik Anna 111  
 Pawlik Justyna 107, 525, 665  
 Pazarçeviren Ahmet Engin 98  
 Pazdan Krzysztof 419  
 Pązik Robert 771  
 Peacock Anna 66, 503  
 Pearson Russell 143  
 Pechev Stanislas 730  
 Pecheva Emilia 781  
 Pêgo Ana 71  
 Pegueroles Marta 167  
 Pelcl Martin 679  
 Peng Lihua 33  
 Pentlavalli Sreekanth 252, 269, 312, 432  
 Pereira Catarina L. 636  
 Pereira Diana 45  
 Pérez-Amodio Soledad 203  
 Pérez-San Vicente Adrián 19, 477  
 Perrault Cecile M. 60, 106  
 Perugini Valeria 47, 332, 501  
 Petchsangsa Maleenart 460  
 Petekidis George 389  
 Peters Kirsten 105  
 Petersen Ansgar 101, 255  
 Petit Laetitia 24  
 Petite Hervé 81  
 Petre Daniela-Geta 379  
 Petrini Paola 244  
 Petronis Sandris 409  
 Petrutescu Marius 379  
 Pettersson Carmen 365  
 Pezowicz Celina 613  
 Pflaum Michael 37  
 Phaechamud Thawatchai 750  
 Phillips Gary 47, 128, 332, 501  
 Piasecka-Zelga Joanna 265  
 Picard Quentin 245  
 Pich Andrij 363  
 Pichavant Loïc 237  
 Piegat Agnieszka 447, K16  
 Pieleś Uwe 661, 674  
 Pielichowska Kinga 218, 415, 417, 419, 787  
 Pietraszek Aneta 469  
 Pietrucha Krystyna 226, 731  
 Pietryga Krzysztof 136, 398, 745  
 Pietzsch Jens 85, 291  
 Pilařová Kateřina 284, 480, 679  
 Pilch Jan 732  
 Pilmane Mara 409  
 Pimenta Andreia 472  
 Piña Maria Jesus 69  
 Pina Sandra 92  
 Piña-Barba María-Cristina 796, 811  
 Pinheiro Marina 350  
 Pinotti Marcos 637, 639  
 Pinto Artur 305  
 Piotrowska Magdalena 606  
 Piotrowska Urszula 452, 462  
 Pires Ricardo A. 112, 158, 238  
 Pisabarro M. Teresa K6

Piscitelli Anne 633  
 Pissarek Jens-Wolfgang 376  
 Pitarresi Giovanna 274  
 Planell Josep A. 148  
 Plawinski Laurent 109, 144, 152, 168, 237, 806, 808  
 Plichta Andrzej 462  
 Plöger Frank 310  
 Plutecka Hanna 89  
 Podobirńska Martyna 226, 731  
 Podolski Jacek 366  
 Pogorielov Maksym 205  
 Pokrowiecki Rafał 64, 352  
 Pokrywczyńska Marta 289  
 Polikkot Sunitha 693  
 Polkowska Izabella 382  
 Polsek Dora 672  
 Pompe Tilo 212, 754  
 Ponche Arnaud 377  
 Poniatowska Aleksandra 580  
 Pontikoglou Charalampos 132  
 Poole-Warren Laura K12, 199  
 Popa Marcel 483, 484  
 Pope Matthew 267  
 Pop-Georgievski Ognen K9  
 Portolés María Teresa 371  
 Posadowska Urszula 141, 425, 495  
 Poth Nils 180  
 Pouget Emilie 152  
 Powell Jonathan 240  
 Pozo-Antonio S. 631  
 Poźniak Błażej 771  
 Prade Ina 380, 597  
 Prado Miguel O. 669  
 Pramanik Krishna 130  
 Pranskunas Mindaugas 685  
 Pravda Martin 94, 719  
 Prendota Witold 595, 602  
 Price Gareth 781  
 Prieto Martín 266, 491  
 Procek Jan 485  
 Procter Philip TRS1  
 Proks Vladimir K9  
 Proskurin Egor 694  
 Prymak Oleg 171, 761, K1  
 Przondziona Joanna 584  
 Przyborski Stefan 711  
 Przybyło Magdalena 485, 492, 537  
 Pura Agnese 724

## Q

Qin Qing H. 577  
 Quade Mandy 216  
 Quintanilla Luis 626  
 Quinteros Daniela 44

## R

Raabe Dierk 761  
 Racine Lisa 272  
 Radko Tomasz 320, 321  
 Radley-Searle Sofia 381  
 Radu-Bostan Gabriela 673  
 Radziszewska Agnieszka 565



Raeck Christian 247  
 Rahatekar Sameer 135, 508  
 Rahmanian Fuzhan 810  
 Rahmouni Oumaira 362  
 Rahouadj Rachid 655  
 Rai Ranjana 164  
 Rainer Alberto 325, 328  
 Raisin Sophie 459  
 Rajan Robin 280, 520  
 Rajasekharan Sivaprakash 772, 773  
 Rajzer Izabella 582  
 Ramella Martina 191  
 Ramil Alberto 631  
 Rammelt Stefan 209, 216  
 Ramos Viviana 27  
 Ramzan Iqbal 789  
 Ramírez-Rodríguez Gloria 682  
 Randino Rosario 775  
 Raoufi Mohammad 23  
 Raoul Gwenael 137  
 Rapacz-Kmita Alicja 493  
 Rashid Rosti Hama 202  
 Rashidi Narjes 690  
 Rata Delia M 483, 484  
 Ratajczak Mariusz Z. 552  
 Rathinam Elanagai 773  
 Ratiskol Jacqueline 8, 114, 644  
 Raucci Maria Grazia 123, 185, 276, 697, 704  
 Rawashdeh Wa'el 363  
 Ray Sabyasachi 406  
 Rączy Michał 275  
 Rebl Henrike 599  
 Reczyńska Katarzyna 136, 398, 745  
 Regiel-Futyra Anna 239, 353, 615  
 Rehman Ihtesham U. 205  
 Reid Adam 227  
 Reilly Gwendolen 205, 251, 313  
 Reimers Nils TRS2  
 Reis Celso 119, 158, 173  
 Reis Rui L. K7, 45, 48, 92, 112, 146, 156, 158, 222, 236, 238, 296, 370, 634, 708, 807  
 Reis Rui M. 296  
 Reis Salette 173, 350  
 Reitz Guenther 343  
 Remboutsika Eumorphia 405  
 Remmers Stefan S. 35  
 Rémy Murielle 717  
 Renard Denis 114, 644  
 Rentsch Barbe 216, 82  
 Rentsch Claudia 216  
 Repanas Alexandros 257, 468  
 Repetto Rodolfo 696  
 Resende Rodrigo 798  
 Restrepo Alejandro 786  
 Réthoré Gildas 93  
 Rettberg Petra 343  
 Rey Sylvie 122, 418  
 Reys Lara L. 48  
 Rezvani Zahra 725, 726  
 Rezwan Koursch 803  
 Rhee Sang-Hoon 322  
 Riabov Vladimir 94  
 Ribeiro Ana 807  
 Ribeiro Andreza 356  
 Ribeiro Viviana 296, 807  
 Richards David 227  
 Richards Geoff L4  
 Richardson Neil 569  
 Ridi Francesca 393  
 Riedel Jan 10  
 Riedel Tomas K9  
 Rios Camilo 32  
 Rischka Klaus 63  
 Ristig Simon 171  
 Rivory Pascaline 295  
 Roberts Clive J. 790  
 Robinson Gareth 135  
 Rocchi Lorenzo 234  
 Rocha Sara 435  
 Roche Phoebe E. 224  
 Rochet Nathalie 245  
 Ročňáková Ivana 394  
 Rodrigues Ana 236  
 Rodrigues Fernando 236  
 Rodríguez Daniel 121, 174  
 Rodriguez Jose A 27  
 Rodríguez Juan Pablo 206  
 Rodríguez-Cabello José Carlos 43, 44, 69, 126, 533, 626, 737, 743  
 Rodríguez-Cano Abraham 628, 629  
 Rodríguez-Lorenzo Luis María 207, 300  
 Rodríguez-Sánchez Jesús 355  
 Rodriguez Manuela 775  
 Rodzik Łucja 4  
 Roesch Frank 505  
 Roffi Alice 5  
 Rogala Piotr 253, 571  
 Roguska Agata 791  
 Rohman Geraldine 673  
 Rohner Nathan 154  
 Rojanarata Theerasak 458, 460, 519  
 Rojewska Agnieszka 275  
 Rojo José María 371  
 Rojo Luis 381, 561  
 Rokhmistrov Dmytro 243, 290  
 Rokidi Stamatia 390, 405, 794  
 Rolandi Ranieri 625  
 Rom Monika 582  
 Romain Olivier 540  
 Romero Francisco-Javier 306  
 Ronca Alfredo 678, K14  
 Ronca Sara 678  
 Rosa Adalberto 102  
 Rosado Aaron M. 208  
 Rosales Raul 213  
 Rosenkranz Andrey 117  
 Rosiak Janusz 507  
 Rossi Alexandre 798  
 Rossi Elisa 427  
 Rößler Sina 709  
 Roth Martin 359  
 Rothenburger Stephen 351  
 Rother Sandra K6  
 Rouabhia Mahmoud 611



Rouwkema Jeroen 545  
 Roy Ipsita 164, 193, 288, 314, 776, TRS4  
 Royer Caroline 109  
 Royo Miriam 181  
 Ruffini Andrea 727  
 Ruiz-Aguilar Criseida 715  
 Ruiz-Hernándezchool Eduardo 491  
 Ruiz-Romero Cristina 424  
 Rumian Łucja 495  
 Rumian Stanisław 602  
 Rumiński Sławomir 211  
 Ruml Tomáš 407, 607  
 Russo Luisa 274, 481  
 Russo Teresa 36, 524, 678, K14  
 Ruskowski Piotr 430  
 Ryadnov Max 65  
 Ryan Alan 224  
 Ryan Christina 681  
 Ryglova Sarka 671  
 Ryniec-Wilczyńska Małgorzata 302  
 Rynkiewicz Aldona 402  
 Rypacek Frantisek K9  
 Rywaniak Joanna 221, 368  
 Rzeszowska-Wolny Joanna 548

## S

Sachot Nadège 122, 148  
 Sader Robert 410, 522, 638, 670  
 Sadlo Jarosław 707  
 Sadowska Joanna Maria 401  
 Sadowski Janusz 364  
 Sagardoy Thomas 730  
 Sahan Semih 230  
 Saito Naoto 429  
 Sak Anita 565, 566  
 Sakai Nobuo 91  
 Salaberria Asier 663  
 Salageanu Aurora 739  
 Salamanna Francesca 5  
 Salamon Achim 105  
 Salary Zeinab 319  
 Saldaña Laura 17, 408, 596, 721  
 Salgado-Ceballos Hermelinda 32  
 Saliev Timur 758  
 Salis Andrea 481  
 Sallerin Brigitte 163  
 Salma Ilze 409, 703  
 Salma-Ancane Kristine 189, 718  
 Salms Girts 233  
 Salonen Jarno 182  
 Salonen Jukka 1  
 Salou Laëtitia 633  
 Salvatore Luca 286, 792  
 Salwiczek Mario 108  
 Samal Juhi 196  
 Samal Sangram 187  
 Samal Sangram Keshari 385  
 Saman Ales 439, 480  
 Sammons Rachel 781  
 Samolej Barbara 493  
 Sampaio Paula 119  
 Samprasit Wipada 519

Samsonov Sergey A. K6  
 Samuelsen Jan T. 764  
 San Roman Julio 154, 213, 300, 381  
 Sánchez García Ana 743  
 Sánchez Jaime 796  
 Sanchez-Rexach Eva 346  
 Sánchez-Salcedo Sandra 371  
 Sánchez-Torres Stephanie 32  
 Sandeman Susan 267, 532  
 Sandri Monica 682  
 Sanetnik Filip 679  
 Sangder Johan 54  
 Sankaranarayanan Rishikesan 574  
 Sannino Alessandro 123, 185, 286, 456, 692, 704, 792  
 Sano Kumpei 735, 736  
 Santamaría Jesús 266, 491  
 Santin Matteo 47, 128, 332, 339, 501  
 Santos Hélder A. 182  
 Santos João 486, 756  
 Santos Mariana 404  
 Santos Martín Francisco J. 743  
 Santos Mercedes 69  
 Santos Susana G. 636  
 Santurdes Noemi 213  
 Sanz-Noguéz Clara 57  
 Sapudom Jiranuwat 212, 754  
 Sarasua Jose-Ramon 346  
 Sardon Haritz 140  
 Sariibrahimoglu Kemal 183  
 Sarker Bapi 437  
 Sarmento Bruno 182, 470  
 Sarna Michał 549  
 Sarna Tadeusz 159  
 Sarrailh Segolene 377  
 Sartoretto Suelen 798  
 Sartori Maria 5  
 Sasaki Keiichi 568  
 Satyam Abhigyan 57, 162, 641, 689  
 Saueroava Pavla 671  
 Saunders Margaret 338  
 Sawae Yoshinori 91  
 Sawoszczuk Tomasz 111  
 Sayin Esen 202  
 Scalabrín Debora 799  
 Scalera Francesca 692  
 Schaaf Pierre 150  
 Scharnweber Dieter K6, 396, 559, 752  
 Schatton Wolfgang 219  
 Schaubroeck David 385, 772  
 Schein Jochen 37  
 Schirmer Lucas 83  
 Schizas Nikitas 800  
 Schlaubitz Silke 254  
 Schlensak Christian 504  
 Schlosser Michael 264, 376, 599, 667  
 Schmeckebier Sabrina 37  
 Schmid Geneviève 105  
 Schmidt Anna 397  
 Schmidt Johannes 209  
 Schmidt Tanja 214  
 Schmitz Tobias 590, 605  
 Schmuhl Ellen 105



- Schnabelrauch Matthias 146, 376, 396, 667, 752, 753, K6  
 Schneider Gerlind 753  
 Schnettler Reinhard 262  
 Schröder Karsten 264, 376  
 Schügner Frank 514  
 Schulze Peter 247  
 Schulze Sabine 423  
 Schulz-Siegmund Michaela 197, 247, 620  
 Schumacher Matthias 277  
 Schuster Carlos 125  
 Schütz Kathleen 5  
 Schwartz Simó 470  
 Schweikle Manuel 466  
 Scialabba D'Amico Paolo 234, 748  
 Ščigalková Ivana 719  
 Scionti Giuseppe 133  
 Scott Robert 503  
 Scrima Mario 303  
 Scurr David 790  
 Seabra Catarina L. 173  
 Sebastian Victor 353  
 Šedová Petra 544  
 Seelbach Ryan 181  
 Sefton Michael L5  
 Sekine Kazumitsu 391  
 Sekuła Małgorzata 62, 334, 550  
 Selezneva Irina 572  
 Semenowicz Jacek 516  
 Sen Beren 759, 760  
 Sendemir Urkmez Aylin 733  
 Seo Seong Ho 440  
 Seppälä Jukka 494, 720  
 Serafim Andrada 668  
 Seramak Tomasz 578  
 Seris Elodie 235  
 Serra Julia 708  
 Serra Tiziano 522  
 Serrano María Concepción 29  
 Serro Ana 472  
 Severi Mirko 393  
 Seyer Damien 139  
 Sezen Goksel 523  
 Shah Furqan Ali 378  
 Shahbazi Mohammad-Ali 182  
 Shao Jinlong 35  
 Shariatzadeh Maryam 60  
 Shastri V. Prasad 79, 535  
 Shen Ya 121  
 Shepherd David 698  
 Shepherd Duncan 217  
 Sherborne Colin 251, 313  
 Sheveyko Alexander 87  
 Shi Liu 295  
 Shimizu Oki 736  
 Shimizu Tatsuya 270  
 Shin Jung Min 433  
 Shin Su Ryon 198  
 Shin Young Min 538  
 Shirosaki Yuki 134, 592  
 Shishatskaya Ekaterina 694  
 Shpotyuk Yaroslav 24  
 Shrestha Neha 182  
 Shtansky Dmitry 87  
 Siadous Robin 730  
 Siatkowska Małgorzata 221, 368  
 Sidun Jarosław 654  
 Siek Dominika 340, 649, 650, 651, 652  
 Siemionow Maria L2  
 Sigaudou-Roussel Dominique 21  
 Sikorski Paweł 455, 705  
 Silini Antonietta 723  
 Silova Tereza 765  
 Silva Andreia M. 636  
 Silva Carla 807  
 Silva Raquel 437  
 Silva Simone S. 48  
 Silva Tiago H. 48, 708  
 Silva-Correia Joana 296  
 Simka Wojciech 40, 606, 609, 610  
 Simões Pedro 589  
 Simon Frank 656  
 Simon Jan C. 83, K6  
 Simonelli Maria Chiara 325  
 Singh Dharaminder 511  
 Singh Nandita 508  
 Singh Raminder 437  
 Singh Smriti 500  
 Singh Sonali 150  
 Sinh Le Hoang 720  
 Sinquin Corinne 8, 114, 644  
 Sionkowska Alina 560, 640, 648, 691  
 Siska Evangelia 388  
 Sjöström Terje 65  
 Skagers Andrejs 233, 409, 703  
 Skibińska-Zuber Agata 496  
 Skirtach Andre G. 187, 385, 398  
 Składzień Jacek 805  
 Skopińska-Wisniewska Joanna 402, 691  
 Skowroński Jan 265  
 Slater Nigel 271  
 Słoński Edward 28  
 Smejkalova Daniela 157, 273, 765  
 Smialek Maciej 474  
 Soares Betânia 637, 639  
 Soares da Costa Diana 48, 112, 158  
 Soares Paulo 621  
 Sobczak Marcin 452, 462, 465  
 Sobczak-Kupiec Agnieszka 526, 527, 541, 542, 585, 755  
 Sobczyńska-Rak Aleksandra 382  
 Sobocinski Jonathan 166  
 Sobolev Alexander 117  
 Sobolewski Peter 366  
 Sohler Jerome 21, 695  
 Sokolova Marina 724, 774  
 Sokołowska Paulina 221, 368  
 Solano Ilaria 625  
 Solarski Jędrzej 159  
 Soldani Giorgio 393, 445  
 Solioz Marc 345  
 Somekawa Shota 446  
 Sommer Marianne 293  
 Sone Eli 808  
 Song Hae-Ryong 659, 662, 738  
 Song Jiankang 35



- Song Sang-Heon 738  
 Soria Guillermo 796  
 Soriente Alessandra 276  
 Sorushanova Anna 680  
 Sotelo Carmen G. 708  
 Soto Ana M. 145  
 Sousa Rui 807  
 Souza Júlio 802  
 Sowa Maciej 40, 606  
 Sowińska Agnieszka 438, 518  
 Spain Sebastian 358  
 Spanoudes Kyriakos 162, 641, 675  
 Spatz Joachim P. 23  
 Spencer Nicholas 75  
 Spoldi Valentina 723  
 Sprio Simone 682, 727  
 Srinivasan Sangeetha 208  
 Srisuk Pichaya 508  
 Srivas Pavan 84, 323, 406  
 Stachewicz Urszula 768  
 Stachurski Zbigniew H. 577  
 Städler Brigitte 11, 96  
 Stamatialis Dimitrios 80  
 Stamboulis Artemis 66, 110, 319  
 Stamov Dimitar 365  
 Stancu Izabela-Cristina 379, 668  
 Stanisławska Alicja 450  
 Staniszewski Zygmunt 447  
 Starosvetsky David 278  
 Stauber Tino 20  
 Stefanek Agata 453  
 Stephenson Sally-Anne 569  
 Sterna Jacek 28  
 Stevanovic Sabrina 674  
 Stępak Bogusz 613  
 Stipniece Liga 189, 718  
 Stöbener Daniel 710  
 Stochel Grażyna 353, 615  
 Stodolak-Zych Ewa 413, 493  
 Stolarczyk Artur 384, 676  
 Stopar David 262  
 Storm Gert 491  
 Stracke Frank 39  
 Strand Berit L. 478, 687  
 Strączek Tomasz 595, 602  
 Strąkowska Paulina 302, 578  
 Strąkowski Marcin 302  
 Stringhetta-Garcia Camila 102  
 Strømme Maria 467  
 Stryła Wanda 253  
 Stubbe Birgit 348  
 Studart André 293  
 Stumbras Arturas 685  
 Su Bo 65  
 Suárez-Franco José Luis 684  
 Suay Julio 306, 623  
 Suchanek Katarzyna 563  
 Sucharda Zbynek 671  
 Suchy Tomasz 671  
 Sugawara Yoko 50  
 Sugiyama Ken 554  
 Sui Cheng 358  
 Sukhorukova Irina 87  
 Sukminingrum Ninin 766, 767  
 Sulka Grzegorz D. 111  
 Sun Ying-Sui 13  
 Sunada Hiroki 551  
 Sung Hyung Min 757  
 Supernak-Marczewska Milena 302, 578  
 Supova Monika 671  
 Surmenev Roman 187, 572, K1  
 Surmeneva Maria A. 187, 572, K1  
 Sutcliffe Chris 299  
 Suzuki Atsushi 91  
 Suzuki Osamu 3, 568, 657  
 Suzuki Shuko 569  
 Svedhem Sofia 146  
 Swain Sanjaya Kumar 278  
 Swiokło Stephen 120  
 Syguła-Cholewińska Justyna 111  
 Sykova Eva 506, 740  
 Syrovatka Jakub 273  
 Szalóki Melinda 367  
 Szaraniec Barbara 64, 231, 352, 414, 563  
 Szarek Dariusz 31, 509, 510  
 Szczepańczyk Piotr 417  
 Szczubiałka Krzysztof 115, 469, 543  
 Szewczyk Grzegorz 159  
 Szmyd Janusz 595, 602  
 Szotek Sylwia 777  
 Szpak Agnieszka 595, 602  
 Szponder Tomasz 64, 382, 414  
 Szuber Agnieszka 749  
 Szurko Agnieszka 600  
 Szycik Violetta 302  
 Ślósarczyk Anna 340, 382, 649, 650, 651, 652  
 Śniechowski Maciej 330  
 Śpiewak Klaudyna 436  
 Świeczko-Żurek Beata 600, 614  
 Świąszkowski Wojciech 179, 471, 530, 539, 616, 706

## T

- Tabary Nicolas 34, 137, 362, 627, 712  
 Tabata Yasuhiko K4  
 Taccardi Nicola 49  
 Tachibana Yoichi 142  
 Tadayyon Ghazal 160, 515  
 Tadier Solène 127  
 Tae Giyoong 788  
 Taguchi Tetsushi 194  
 Takahashi Akihiro 268  
 Takahashi Kazuya 735, 736  
 Takahashi Tetsu 3, 657  
 Takanashi Seiji 429  
 Takatani-Nakase Tomoka 479  
 Takeda Naoya 270  
 Takei Takayuki 546  
 Takizawa Takashi 429  
 Tamada Yasushi 735, 736  
 Tampieri Anna 727  
 Tan Jeremy 140  
 Tan Milene 361  
 Tanaka Hidenori 657  
 Tanaka Manabu 429





- Tanner K Elizabeth 90, 444  
 Tanuma Yuji 657  
 Tanzi MariaCristina 244  
 Tarantili Petroula 186, 701  
 Tarasiuk Jacek 330  
 Tarcolea Mihai 598, 601  
 Teixeira Graciosa Q. 636  
 Téllez-Jurado Lucía 207, 300, 684  
 Tenailleau Christophe 163  
 Tennsion Steve 267  
 Terenghi Giorgio 227  
 Terosiet Mehdi 540  
 Terzopoulou Zoe 100, 583  
 Testrich Holger 264  
 Tetteh Gifty 205  
 Texier Isabelle 272  
 Tezcaner Ayşen 98, 653  
 Tezuka Ken-ichi 554  
 Themistou Efrosyni 143  
 Theodoropoulou Alexandra 257  
 Thienpont Hugo K10  
 Thies Jens C. TR56  
 Thissen Helmut 108  
 Thomas Aline 208  
 Thomas Christy 314  
 Thomas Susan N. 154  
 Thompson John 333  
 Thomsen Peter 153, 378  
 Tiainen Hanna 344, 466, 495, 573, 575  
 Tian Xiaohu 143  
 Tilocca Antonio 801  
 Titorencu Irina 598  
 Tkachenko Mykola 337  
 Tkocz Marek 584  
 Todd Naomi M 299  
 Tofail Syed Ansar 241  
 Tolle Christian 10  
 Tomanik Magdalena 613, 777  
 Tombácz István 714  
 Tomita Naohide 735, 736  
 Tondera Christoph 85, 291  
 Torrents Eduard 172  
 Torres Yadir 27  
 Tos Karolina 425  
 Toshikazu Akahori 570  
 Touré Amadou 93  
 Trembecka-Wojciga Klaudia 89  
 Triantafyllidis Konstantinos 583  
 Trigueros Larrea José María 743  
 Trimaille Thomas 21  
 Trojanowski Michał 302  
 Trombetta Marcella 325, 328  
 Trommer Kristin 380  
 Trzaskowska Paulina 580, 604  
 Trzcińska Zuzanna 66, 319  
 Trzebińska Marta 580  
 Tsetsenekou Efstathia 390  
 Tsibouklis John 624  
 Tsimbouri Monica 65  
 Tsimbouri Penelope 607  
 Tsuji Takashi 739  
 Tsuji Takuma 622  
 Tsujimura Yoshiki 587  
 Tsukada Chie 622  
 Tsuru Kanji 242  
 Tsutsumi Yusuke 228  
 Tucureanu Catalin 379  
 Tudorache Igor 285, 677  
 Tukmachev Dmitry 506  
 Tuncay Ozge Ekin 386, 666  
 Tunesi Marta 36  
 Turek Artur 496  
 Turek Krzysztof 369  
 Turk Mustafa 230  
 Tyliczszak Bożena 526, 527, 541, 542, 585, 755  
 Tylko Grzegorz 606  
 Tyski Stefan 64
- ## U
- Ueda Kyosuke 279  
 Ueda Masato 642  
 Ueki Ayaka K3  
 Uklejewski Ryszard 253, 571  
 Ukraintsev Egor 658  
 Ulanski Piotr 507  
 Ullm Sandra 85, 291  
 Um Seung-Hoon 322  
 Um Wooram 155, 490  
 Unger Ronald 192  
 Uppstu Peter 411  
 Urciuolo Francesco 78, 215  
 Urquia Edreira E.R. 294  
 Urta Carla 206  
 Urtiaga Ana María 645  
 Ustbas Burcin 143  
 Usui Yuki 429  
 Uttiya Sureeporn 625  
 Uyama Emi 442, 443  
 Uzeda Marcelo 798
- ## V
- Vác Gabriella 672  
 Vadillo-Rodríguez Virginia 374, 596  
 Vale Marcos 639  
 Vallejo-Giraldo Catalina 16  
 Vallés Gema 721  
 Vallet-Regí María 52, 371  
 Valli Ludovico 286  
 Vamvakaki Maria 132  
 van Blitterswijk Clemens K15  
 van Boxel Huib 683  
 van den Beucken Jeroen 42, 178, 183, 294  
 van Dongen Suzan 682  
 Van Espen Piet 348  
 van Geffen Esmee 80  
 Van Hoerick Jasper K10  
 van Neerven Sabien 514  
 van Osch Gerjo 499  
 Van Tassel Paul 73, 149  
 van Tienen Tony 7  
 Van Vlierberghe Sandra K10, 192, 348, 505, 608  
 Vancaeyzeele Cedric 660  
 Vancso Julius K15  
 Vanhaecke Frank 348





Vannier Jean-Pierre 104  
 Varela-Moreira Aida 71  
 Vargas-Becerril Nancy 207, 684  
 Vargas-Coronado Rossana F. 259  
 Vasile Eugeniu 379, 668  
 Vazquez Blanca 213  
 Vega Castrillo Aurelio 743  
 Velasco Diego 176  
 Velders Aldrik 148  
 Velebný Vladimír 150, 157, 273, 528, 544, 719, 765  
 Verdanova Martina 671  
 Verdenelli Maria Elena 128  
 Verestiuc Liliana 793, 795  
 Verrier Bernard 21  
 Vial Stephanie 222  
 Videira Mafalda 470  
 Vieira Ana 472  
 Vieira Nascimento Matheus 63  
 Vieira Silvia 222  
 Vigier Sylvain 6  
 Vilaboa Nuria 17, 266, 408, 491, 596, 721  
 Vinatier Claire 8  
 Vishwakarma Ajaykumar 545  
 Vistejnova Lucie 658  
 Vladescu Alina 349, 594, 598  
 Vogel Sarah 396  
 Voiculescu Ionelia 326, 327  
 Voigt Sibylle 753  
 Volpi Silvia 393  
 von Bergen Martin 209  
 Vorndran Elke 318, 397  
 Vrana Engin 633  
 Vrana Nihal Engin 94, 150  
 Vranceanu Diana 598, 601  
 Vyas Nina 781  
 Vyborny Karel 740

## W

Wach Radosław 507  
 Wahl Elizabeth A 133  
 Wakelin Edgar 38, 422  
 Walboomers X. Frank 632  
 Walke Witold 584  
 Walker Tobias 504  
 Walkowiak Bogdan 221, 368  
 Wallat Katrin 39  
 Walmsley Damien 781  
 Walschus Uwe 264, 376, 599, 667  
 Waluk Tadeusz 159  
 Wandel Elke 83  
 Wandrey Christine 304, 557  
 Wang Li-Chun 579  
 Wang Min 225, 497  
 Wang Xiaoyue 378  
 Wang Zhejun 121  
 Warmont Fabienne 245  
 Warmuth Franziska 590  
 Warren Nicholas J. 58, 143  
 Wasiak Tomasz 221, 368  
 Wąsik Aleksandra 414  
 Weaver Jessica 203  
 Weber Jan TRS5

Webster Thomas 786  
 Wedel Alicja 603  
 Wei Qiang 710  
 Weigel Tobias 605  
 Weightman Richard 58  
 Weihe Thomas 618  
 Weinhardt Venera 187  
 Weinhart Marie 710  
 Weiss Anthony 38  
 Weiss Pierre 8, 93  
 Wellings Don 138  
 Weltmann Klaus-Dieter 599  
 Wendel Hans-Peter 373, 504  
 Wengenroth Jonas 745  
 Werner Carsten 83  
 Werten Marc 42  
 Westendorf Astrid 309  
 Wettig Shawn 152  
 Whitaker Darren 770  
 Wiatr Agnieszka 805  
 Wiatr Maciej 805  
 Widaa Amro 224  
 Widlan Fany 258  
 Widziółek Magdalena 606  
 Wiecheć Emilia 548  
 Wiecheć Katarzyna 716  
 Wiedmer David 344  
 Wiegmann Bettina 37  
 Wierzchoń Tadeusz 195, 438, 518  
 Wiesmann Hans Peter 656  
 Wigłusz Rafał 771  
 Wilén Carl-Eric 411  
 Williams Paul 357  
 Williams Rachel 138  
 Williams Richard 769  
 Willumeit-Römer Regine 373  
 Windahl Sara 153  
 Winiarska Hanna 731  
 Winiński Mariusz 253, 571  
 Winkler Stefan 674  
 Winzer Klaus 358  
 Wirth Dagmar 10  
 Wirth Reinhard 343  
 Wiśniewski Zdzisław 746, 747  
 Witecka Agnieszka 616  
 Witkowska Justyna 518  
 Witte Frank 214  
 Wittig Linda 63  
 Włodarczyk-Biegun Małgorzata 42  
 Włodarczyk Katarzyna 688  
 Wodtke Robert 85  
 Wöhl-Bruhn Stefanie 180  
 Wojas Natalia 539  
 Wojasiński Michał 702  
 Wojtyła Szymon 615  
 Wolf-Brandstetter Cornelia 261, 559  
 Wolfová Lucie 150, 544, 719  
 Wolke Joop G C 183, 294  
 Won Da-Ae 788  
 Wong Sau Shun 25  
 Wonsewicz Bartłomiej 654  
 Wood Andrew 58



Worch Hartmut 383  
Woszczak Maja 40  
Wroński Sebastian 330  
Wu Bing 53  
Wu Liwei 271  
Wu Pingli 256  
Wychowański Piotr 99  
Wyrwa Ralf 753  
Wysocki Bartłomiej 179

## X

Xu Jinbin 41

## Y

Yagi Shinya 622  
Yaji Toyonari 622  
Yamaguchi Seiji 50  
Yamaguchi Shingo 531  
Yamaguchi Tetsuo 91  
Yamamoto Akiko 616  
Yamane Iori 521  
Yamaoka Tetsuji 142, 446  
Yamashita Kimihiro 1  
Yamato Masayuki 270  
Yamazaki Hajime 3  
Yan Le-Ping 296  
Yang Fang 35, 178  
Yang Jun 41  
Yang Kai-Chiang 579  
YanYang Yi 140  
Yarimitsu Seido 91  
Yarutkin Aleksei 117  
Yazdani-Pedram Mehrdad 206  
Yelten Azade 534  
Yeo Giselle 38, 422  
Yilmaz Suat 534  
Yin Huabing 744  
Ylä-Outinen Laura 722  
Yoon Hong Yeol Yoon 433, 488  
Yoshida Masahiro 546  
Yoshida Tetsuhiko 479  
Yoshida Tomoko 622  
Yoshida Yasuyuki 268, 642  
Yoshitomi Hiroki 546  
Yoshizawa Keiko 194  
You Dong Gil 155, 488, 490  
Youn Young-Pil 659  
Young Sarah 23  
Young Tai-Horng 129  
Yu Dahai 220  
Yuan Huipin 204, 301  
Yun Young-Pil 662, 738  
Yunsun Kim Sally 457  
Yusa Shin-Ichi 115

## Z

Zabek Andrzej 448  
Zaczyńska Ewa 341  
Zafeiris Christos 800  
Zagórska-Świeży Katarzyna 805  
Zagrajczuk Barbara 525, 664, 665  
Zalewska-Wierzbicka Katarzyna 706  
Zalewski Adam 211  
Zalite Vita 409, 703, 785  
Zaloudkova Margit 671  
Zaoutsos Stefanos 405, 794  
Zapotoczny Szczepan 595, 602  
Zardán Gómez de la Torre Teresa 467  
Zarek Matthew 258  
Zaręba Tomasz 64, 352  
Zaviskova Kristyna 506  
Zdziennicka Anna 628, 629  
Zengerle Diane 504  
Zenobi-Wong Marcy 20  
Zerweck Julia 261  
Zeugolis Dimitrios 57, 294, 160, 162, 641, 675, 680, 681, 689, 713  
Zhang Peng 467  
Zhang Xiang 188, TRS3  
Zhang Yan 41, 96  
Zhang Yuanhong 33  
Zhang Ze 611  
Zhao Guohua 26  
Zhao Jin-Min 577  
Zhao Weitian 395  
Zhao Zhitong 70  
Zhen Li 577  
Zheng Kai 49  
Zheng Yishan 267, 532  
Zhou Dennis 203  
Zia Sonia 285  
Ziabka Magdalena 448  
Ziegler-Borowska Marta 691  
Zielinski Andrzej 578  
Zietz Carmen 599  
Zikmund Tomáš 394  
Zima Aneta 340, 649, 650, 651, 652  
Zimmermann Heiko 39  
Zimowski Sławomir 566  
Zinn Manfred 706  
Zuba-Surma Ewa 62, 334, 549, 550, 552  
Zubillaga Verónica 663  
Zuyderhoff Emilienne 76  
Zychowicz Marzena 226, 699, 700, 731  
Zykwinska Agata 8, 114, 644  
Zyman Zoltan 243, 290, 337  
Żak Jerzy 307, 430  
Żakiewicz Wojciech 416  
Żylińska Beata 382



# EXHIBITORS



**Bronze Sponsor:**

**IME TECHNOLOGIES**

**Hall 2**

**Hall 1**

**WC**

**Entrance No. 2**

**Bronze Sponsor**

**Level 1**

**Level 1**

**Exhibitors:**

1. SHIM-POL sp. j.
2. Taylor & Francis Group
3. Anton Paar GmbH
4. Oxford University Press
5. EBERS Medical Technology SL
6. IOP Publishing
7. Springer
8. Binder GmbH
9. The Royal Society Publishing
10. JPK Instruments AG
11. Plasma Biotat Ltd
12. Bruker microCT
13. Biolin Scientific
14. CAM Bioceramics
15. SCANCO Medical AG
16. Uni-Export Instruments Polska
17. nLab sp. z o.o.
18. TA/ElectroForce Systems Group
19. National Biomaterials Societies
20. Polish Society for Biomaterials & Engineering of Biomaterials Journal

**Hall 2**

**Hall 1**

**Main Entrance**

**Registration**

**ESB Lounge**

**WC**

**All Levels**

**L1 only**

**16 17 18**  
**15 14 13**

**10 11 12**  
**9 8 7**

**5 6**  
**4**  
**3**  
**2**  
**1**

**L1**

# Exhibitors

## BRONZE SPONSOR - Level 1

### IME Technologies

[www.imetechnologies.nl](http://www.imetechnologies.nl)



IME Technologies is a successful electrospinning OEM that develops, manufactures and sells state-of-the-art electrospinning equipment. IME Technologies specifically serves academic institutes and innovative customers in the biomedical industry all over the world. With our products and supporting services we help our customers to improve the efficiency of their electrospinning research, product development and manufacturing, thereby shortening their time-to-market for new nanofiber applications.

## Stand 1

### SHIM-POL A.M. BORZYMOWSKI

[www.shim-pol.pl](http://www.shim-pol.pl)



SHIM-POL A. M. BORZYMOWSKI is an exclusive representative of a SHIMADZU-KRATOS corporation and a service centre for Poland. We offer UHPC, HPLC and GC chromatographs; MS systems: GC-MS(MS), LC-MS(MS), LCMS-IT-TOF, MALDI-TOF-TOF; UV-VIS, FTIR spectrophotometers; TOC analysers; ESCA-XPS, SIMS, ISS and Auger spectrometers, and fluorescence analysers (EDX); additional equipment: PHENOMENEX, CHROMACOL, generators, PIKE - accessories, HORIZON TECHNOLOGY.

## Stand 2

### Taylor & Francis Group

[www.taylorandfrancisgroup.com](http://www.taylorandfrancisgroup.com)



**Taylor & Francis Group**  
an informa business

Taylor & Francis partners with world-class authors, from leading scientists and researchers, to scholars and professionals operating at the top of their fields. Together, we publish in all areas of the Humanities, Social Sciences, Behavioural Sciences, Science, Technology and Medicine sectors. We are one of the world's leading publishers of scholarly journals, books, eBooks, text books and reference works.



### Stand 3

**Anton Paar**

[www.anton-paar.com](http://www.anton-paar.com)



Anton Paar develops, produces and distributes highly accurate laboratory instruments and process measuring systems, and provides custom-tailored automation and robotic solutions. It is the world leader in the measurement of density, concentration and CO<sub>2</sub> and in the field of rheometry. Anton Paar GmbH is owned by the charitable Santner Foundation.

### Stand 4

**Oxford University Press**

[global.oup.com](http://global.oup.com)



Oxford University Press is a department of the University of Oxford. It furthers the University's objective of excellence in research, scholarship, and education by publishing worldwide. We publish in many countries, in more than 40 languages, and in a variety of formats - print and digital. Our products cover an extremely broad academic and educational spectrum, and we aim to make our content available to our users in whichever format suits them best.

### Stand 5

**EBERS Medical Technology SL**

[www.ebersmedical.com](http://www.ebersmedical.com)



EBERS Medical Technology SL designs, manufactures and commercializes of tissue engineering bioreactors, mechanical testing machines for biological samples and biomaterials, microfluidic devices for cell culture under physiological conditions and oxygen sensors.





## Stand 6

**IOP Publishing**

[www.ioppublishing.org](http://www.ioppublishing.org)

**IOP Publishing**

IOP Publishing provides a range of journals, magazines, websites, books and services that enable researchers to reach the widest possible audience for their research.

Visit our stand at ESB to find out what IOP Publishing can offer to our authors.

## Stand 7

**Springer**

[www.springer.com](http://www.springer.com)



Our business is publishing. With more than 2,900 journals and 200,000 books, Springer offers many opportunities for authors, customers and partners. Throughout the world, we provide scientific and professional communities with superior specialist information – produced by authors and colleagues across cultures in a nurtured collegial atmosphere of which we are justifiably proud.

## Stand 8

**BINDER GmbH**

[www.binder-world.com](http://www.binder-world.com)



**Best conditions for your success**

BINDER is the world's largest specialist in simulation chambers for the scientific and industrial laboratory. More than 22,000 units leave our plant in Tuttlingen, Germany annually. Our products: CO<sub>2</sub> incubators, incubators, growth chambers, ultra-low temperature freezers, drying/heating ovens, temperature test chambers, vacuum drying ovens, safety drying ovens, and climate chambers.



## Stand 9

### Royal Society Publishing

[www.royalsocietypublishing.org](http://www.royalsocietypublishing.org)

## THE ROYAL SOCIETY PUBLISHING

J R Soc Interface and Interface Focus regularly publish high quality content in the area of biomaterials. For more information about the scope and editorial procedures of our journals, please come and have a chat with our representative Dr Tim Holt at the Royal Society's booth.

## Stand 10

### JPK Instruments AG

[www.jpk.com](http://www.jpk.com)

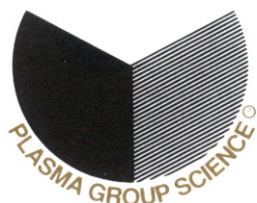


JPK Instruments, is a world-leading manufacturer of Atomic Force Microscopes and optical tweezers systems. From the beginning applying AFM technology, JPK has recognized the opportunities within nanotechnology for life sciences and soft matter research. This led to JPK's success in uniting the worlds of nanotechnology tools and life science applications.

## Stand 11

### Plasma Biototal Ltd

[www.plasma-biototal.com](http://www.plasma-biototal.com)



Manufacturer of Calcium Hydroxylapatite (Captal® Grades) and Beta TriCalcium Orthophosphate powders for use in manufacturing orthopaedic composites, ceramic products and coatings. Provision of coating services to orthopaedic device manufacturers on a global basis. Company holds relevant ISO quality management accreditations and FDA compliant Masterfiles for products.



## Stand 12

### BRUKER microCT

[www.bruker-microct.com](http://www.bruker-microct.com)



Bruker microCT formerly known as SkyScan develops and manufactures microtomography and nanotomography systems for non-destructive 3D imaging. The company provides the leading imaging and analytical X – ray microCT.

## Stand 13

### Biolin Scientific

[www.biolinscientific.com](http://www.biolinscientific.com)



Biolin Scientific is a leading Nordic instrumentation company with roots in Sweden, Denmark and Finland. Our customers include companies working with pharmaceuticals, energy, chemicals, and advanced materials, as well as academic and governmental research institutes. Our precision instruments help discover better drugs faster, develop better solutions for energy and materials, and perform research at the frontiers of science and technology. Biolin Scientific proprietary systems are based on nanotechnology and advanced measurement techniques. They have earned leadership in several industries through our commitment to scientific excellence and continuous product development. Today, Biolin Scientific provides products and services in more than 70 countries around the world.

## Stand 14

### CAM Bioceramics B.V.

[www.cambioceramics.com](http://www.cambioceramics.com)



CAM Bioceramics is a contract manufacturer of orthobiologic ceramics. We use our experience and production capabilities to enable orthopedic and dental OEMs develop and manufacture a wide range of bioceramics. CAM develops orthobiologic ceramics and manufactures them in compliance with the industry quality standards.



## Stand 15

**SCANCO Medical AG**

[www.scanco.ch](http://www.scanco.ch)

**SCANCO**  
MEDICAL

SCANCO Medical is a Swiss company that specializes in the development of state-of-the-art micro-computed tomography systems. These systems integrate high-quality imaging with powerful 3D analysis tools. We provide long-term support to our customers that includes technical assistance, maintenance, updates and training. Leading academic, industrial and healthcare institutions worldwide employ SCANCO Medical microCT systems in a wide range of applications.

## Stand 16

**UNI-EXPORT INSTRUMENTS**

[www.uni-export.com.pl](http://www.uni-export.com.pl)

**UNI-EXPORT**  
Instruments Polska

UNI-EXPORT INSTRUMENTS Polska operates on a market of specialized research and measurement equipment for more than 10 years. We are an authorised (and in most cases exclusive) distributor of some leading equipment manufacturers from the USA and Europe.

## Stand 17

**nLab sp. z o.o.**

[www.nlab.pl](http://www.nlab.pl)

 **nLab**  
Spółka z o.o.

Since 1998 nLab delivers advanced research instrumentation. We specialize in the field of electrochemistry, corrosion research, electrochemical energy sources, tensiometry, studies of surface properties, surface plasmon resonance (SPR and L-SPR), scanning electrochemical microscopy (SECM), physico-chemical and analytical studies. We are the exclusive representative in Poland of well-known brands: Metrohm-Autolab, KSV-NIMA, Attension, Biolin Scientific, BioNavis, KEInstruments, Sensolytics, Insplorion. For all these products we also provide the service.



## Stand 18

**TA/ElectroForce**

[www.bose-electroforce.com](http://www.bose-electroforce.com)



Your success is our mission at TA/ElectroForce®. We provide mechanical testing, characterization, and tissue growth solutions to researchers worldwide. Our ElectroForce® zero-friction motor technology provides exceptional performance and simplicity for sterile and non-sterile applications. Visit our booth to learn more about our biomedical instruments, including the NEW 3DCulturePro™ bioreactor.

## Stand 19

**National Biomaterials Societies**

**WBC2016** [www.wbc2016.org](http://www.wbc2016.org)

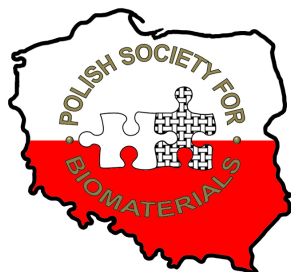
**ESB2017** [www.esb2017.org](http://www.esb2017.org)



## Stand 20

**Polish Society for Biomaterials &  
Engineering of Biomaterials Journal**

[www.biomat.krakow.pl](http://www.biomat.krakow.pl)





# BOOK OF ABSTRACTS





# Plenary Lectures



## Bioactive Materials for the Treatment of Major Injuries: Opportunities and Challenges

Joachim Kohn, PhD.

Distinguished Professor and Director  
The New Jersey Center for Biomaterials  
Rutgers, the State University of New Jersey  
[kohn@dls.rutgers.edu](mailto:kohn@dls.rutgers.edu)

### HISTORIC PERSPECTIVE

This presentation addresses recent advances in the treatment of major tissue evulsions, stemming from trauma, disease, or aging. In the USA and Europe, the large number of war veterans returning from the recent military conflicts in Afghanistan and Iraq heightened the willingness of the Government to invest in regenerative medicine. The goal of this effort is the development of fundamentally new therapies that can restore “form and function” to patients who suffered very significant injuries, including devastating injuries to the face, massive 3<sup>rd</sup> degree burns, and loss of limbs due to blast injuries. As these new therapies are perfected, they will undoubtedly revolutionize the treatment of major injuries and will benefit not only military personnel but the civilian population as well. Biomaterials science in combination with cell-based therapies and new bioactives is at the center of these research efforts.

### BIOACTIVE MATERIALS – A NEW FRONTIER

There is a strong and growing emphasis on using synthetic biomaterials in combination with cells (in particular stem cells). Recently, the profound influence of biology on the development of biomaterials became evident with the search for bioactive materials, e.g., materials that can be used to direct the cellular response toward predictable and desirable outcomes. Achieving “bioactivity” by a synthetic, engineering approach has been an elusive goal. Nobody has so far been able to create an engineered construct that mimics all the functions of natural extracellular matrix (ECM) perfectly. To develop materials with ECM-like properties, two approaches are being explored concurrently: The “engineering approach” starts from simple, but readily available (usually synthetic) materials that can be decorated with various biologically active signaling moieties in such a way that key cellular responses such as attachment, migration, proliferation, and differentiation can be driven towards a desired outcome. In contrast, the “biological approach” starts from living tissue. The main goal of the biological approach is to simplify the tremendous complexity of natural tissues by removing most cellular components and their associated antigens without destroying the fine structure of ECM and without significant damage to the many sensitive signaling moieties that give ECM its characteristic biological activity. Since these two approaches come from opposite directions, it is very likely that the next generation of synthetic, bioactive scaffolds will compete with ECM-derived allograft products or products derived from de-cellularized tissues.

### BIOMATERIALS-ENABLED THERAPIES

Major injuries can be treated in three ways: By replacing lost limbs or tissues with prosthetic devices (examples: artificial legs, arms, total hip replacement), by replacing lost tissue with allografts (example: face transplant, organ transplant), or by regenerative approaches where bioactive scaffolds and cells are used to generate the lost tissue de novo. The quest to regenerate a living human ear is an illustrative example for a biomaterials-enabled therapy. The first attempt at creating a living human ear replacement goes back to the early 1990's when a crudely shaped scaffold seeded with chondrocytes was implanted under the skin of nude mice. This research concept was recently developed further, using the latest techniques in biomaterials science and biology, resulting for the first time in a promising prototype that may be useful in the clinic. Another example is the development of nerve conduits for regeneration of large gaps in peripheral nerves, using a bioactive polymer that intrinsically supports neurite growth better than other synthetic materials. Recent work on the first bioactive scaffolds for the regeneration of the osteochondral interface of major joints represents yet another example of a biomaterials-enabled cell therapy.

### CURRENT LIMITATIONS AND CHALLENGES

In spite of significant progress, the field of biomaterials science still faces significant challenges that are best presented in three distinct groups:

*Fundamental science challenges* include (1) our inability to overcome mass transfer limitations (nutrient transport) in tissues sized for human patients; (2) our inability to generate innervated tissues, mostly muscle; (3) our inability to engineer micro-vascular beds and fully vascularized tissue; (4) the lack of regenerative approaches to treat traumatic brain injury or degenerative brain disorders. *Technology challenges* include our bottlenecks around (1) cell sourcing, (2) problems relating to the scale up of production, sterilization, shelf life, and (3) the lack of an efficient FDA regulatory approval processes. Finally, a major challenge relates to the *assembly of complex tissue constructs*. While we can grow muscle, bone, tendons, and ligaments separately in the lab, we cannot grow a fully assembled joint, and we cannot regenerate whole limbs or whole organs (other than skin and bladder). This specific challenge is due to our inability to recapitulate in the lab the natural processes that occur during embryonic development.

### ACKNOWLEDGMENTS

This is an overview based on the work of the entire biomaterials research community. The author acknowledges the countless scientists who contributed to the research advances described in this lecture.



## Regenerative Transplantation - from Experimental Laboratory to Clinical Applications

Maria Siemionow

Department of Orthopaedics, University of Illinois at Chicago, USA  
[siemiom@hotmail.com](mailto:siemiom@hotmail.com)

### **Introduction**

The presentation will outline cellular therapies which are currently developed in the Microsurgery Laboratory at University of Illinois at Chicago. These therapies represent four different regenerative medicine approaches of combining naturally occurring nerve scaffolds with stem cells of allogeneic origin as well as novel chimeric cell therapy for transplant tolerance. These scaffold based therapies are targeted for restoration of limb function by application of new nerve conduits, epineural jackets and epineural patches. Introduction of new, safer, chimeric cell therapies will support transplantation of solid organ and vascularized composite allografts (VCA) such as hand and face transplants. Summary of scaffold and stem cell based approaches is briefly outlined below.

### **Epineural Nerve Conduits for Restoration of Nerve Defects**

We have introduced a new naturally occurring epineural sheath conduit supported with bone marrow stromal cells for enhancement of nerve regeneration over long 6 cm nerve gaps. These conduits are of allogeneic nerve origin and after decellularization constitutively express Laminin B and VEGF which are growth factors supporting nerve regeneration.

These nerve conduits were tested in 2 and 6 cm nerve defects in small - rat and large-sheep animal models respectively and confirmed nerve regeneration comparable to autologous controls.

### **Epineural Sheath Patches for Support of Nerve Regeneration**

To protect nerve regeneration in unfavourable wound conditions, including diabetic wounds, we have developed an epineural patch to cover the neural tissues after nerve trauma such as crush or traction injury, as well as following peripheral nerve decompression and decompression of the spinal cord. We are also introducing a new technology of epineural sheath jackets for prevention and treatment of painful neuromas.

### **Chimeric Cell Therapies for Tolerance Induction**

There is a need for development of new anti-rejection therapies for solid organ and vascularized composite allografts (VCA) such as face and limb transplants to eliminate side effects of currently available immunosuppressive protocols. We have developed a novel tolerance inducing therapy by fusion of bone marrow cells of Donor and Recipient origin and creating Donor-Recipient Chimeric Cells. These cells are recognized by transplant recipient as "Self" and support organ survival. We will introduce Chimeric Cells as supportive therapy for face and limb transplants which will reduce side effects, cost and the need for lifelong immunosuppression.

The other approach we are taking as a continuation of Chimeric Cell therapy application is to create a universal chimera which will serve as universal bone marrow transplantation with direct application to the wounded warrior in case of a nuclear bomb attack. We are currently developing a second and third generation of Chimeric Cells leading to ultimate goal of creating universal Chimeric Cells. We also are testing cryopreservation methods for Chimeric Cell storage and propose to introduce a Universal Chimera Bank for civilians and military applications.



## ***In Vitro* Models and Nanobiointerfaces: a Multidisciplinary Challenge**

Charles James Kirkpatrick<sup>1,2</sup>

<sup>1</sup>Department of Biomaterials, Sahlgrenska Academy, University of Gothenburg, Sweden

<sup>2</sup>REPAIR-lab, Clinic for Oral & Cranio-Maxillofacial Surgery, Goethe University Frankfurt, Germany

[cjkirkpatrick@biomaterials.gu.se](mailto:cjkirkpatrick@biomaterials.gu.se); [james.kirkpatrick@kgu.de](mailto:james.kirkpatrick@kgu.de)

### **INTRODUCTION**

Cellular testing systems begin with relatively simple 2D models for most of biomaterial development, with the lowest level of complexity being permanent cell lines, usually tumour cells, for simple cytotoxicity testing (direct & indirect tests). A greater challenge is to conceive 2D cellular models which give relevant read-outs of biomaterial-associated functionality of a primary cell type of human origin, for example osteoblasts or endothelial cells (EC). The subsequent step to sophisticated heterotypic co-culture systems, in which cells of different phenotypes interact with each other, represents a major element in simulating the *in vivo* situation and is essential for the study of non-bound nanoparticle (NP) systems developed, for example, for drug and gene delivery. Such models are required for the important biological barriers in the body, which would be the natural nanobiointerfaces encountered in clinical translation, depending on the mode of NP application (e.g. inhalation, injection, oral ingestion).

### **EXPERIMENTAL MODELS**

In the past years we have set up mono- and especially co-culture models of important biological barriers both of the lower (air-blood barrier, ABB) and upper respiratory tract (bronchial model)[1-3], as well as of the blood-brain barrier (BBB)[4-6]. Further models are of the intestinal and the skin barrier. All of these, with the exception of the BBB, can be established in a human system, and most readily using suitable permanent cells lines, with the primary cells being the benchmark. The lack of availability of fresh human brain tissue with preservation of capillary EC, pericytes and astrocytes, all of which are required for a genuine BBB, make alternatives necessary. This can be achieved, for example, with porcine cells. In the barrier models for NP interaction special physiological and biological methodologies are necessary to elucidate barrier function as well as the uptake, intracellular transport, distribution and possible storage and secretion of NPs following cellular contact. This usually requires tracer entities, which in the case of fluorescent probes can enable both *in vitro* and *in vivo* follow-up.

For NP uptake across the ABB, various NPs based on silica have been studied in comparison with polyorganosiloxane NPs [7]. The influence of NP characteristics, such as diameter and surface chemistry have been investigated, and cellular uptake mechanisms appear to involve clathrin- and caveolin-independent pathways, for example, via flotillins [8,9]. A further level of complexity in the ABB is the presence of surfactant in the alveoli. This has been found to change NP cytotoxicity [10].

### **FUTURE DEVELOPMENTS**

The described models represent static systems. For more relevance to the *in vivo* situation there is a need to introduce biomechanical factors operating in the niche under consideration. Currently, the role of stretch and contraction forces, which are highly complex and continuously operative in the alveoli, is now being studied [11]. An immunologically relevant triple culture system has also been established for the bronchial model by adding dendritic cells (DCs), and for the air-blood barrier by adding different macrophage phenotypes [12], as these immunocompetent cells are important in barrier defence mechanisms. In addition to these double and triple co-culture systems further developments in the future must include multi-parametric, high throughput micro-systems to permit screening. Moreover, the real life situations in which a nanobiointerface would arise are more complex still, as in most cases there can be different intensities and types of inflammation, hypoxia and the possible stimulating or inhibiting effects of medication [13]. These phenomena will impinge on nano-bio-interactions and must be reflected in the assay systems we establish, especially if the latter are to have predictive function.

### **REFERENCES**

1. Hermanns MI *et al.* Lab Invest 2004; 84, 736-752
2. Hermanns MI *et al.* J R Soc Interface 2010; 7, S41-S54
3. Pohl C *et al.* Eur J Pharm Biopharm 2009; 72: 339-349
4. Freese C *et al.* Part Fibre Toxicol 2012; 9: 23
5. Freese C *et al.* PLoS One 2014; 9(3): e91003
6. Freese C *et al.* Biomater Sci 2013; in press
7. Kasper J *et al.* Part Fibre Toxicol 2011; 8: 6
8. Kasper J *et al.* Arch Toxicol 2013; 87: 1053-1065
9. Kasper J *et al.* Eur J Pharm Biopharm 2013; 84: 275-287
10. Kasper J *et al.* Beilstein J Nanotechnol 2015; 6: 517-528
11. Freese C *et al.* Part Fibre Toxicol 2014; 11: 68
12. Kasper J *et al.* JTERM 2015 ; in press
13. Kirkpatrick CJ. Tissue Eng A 2014; 20:1355-1357

### **ACKNOWLEDGMENTS**

Supported by various EU projects, and research grants in Germany from the DFG, BMBF/DAAD German-Chinese Cooperation in Regenerative Medicine, and the German Defense Ministry (BMVg).



## Medical Translational Research: A Different Route to Fundamental Research

R. Geoff Richards

AO Research Institute Davos, Clavadelerstrasse 8, 7270 Davos, Switzerland ([www.aofoundation.org/ari](http://www.aofoundation.org/ari))  
[geoff.richards@aofoundation.org](mailto:geoff.richards@aofoundation.org)

### INTRODUCTION

The AO Research Institute Davos has had over 50 years of experience in translation of ideas to improved surgical techniques for patient care in the field of fracture fixation<sup>1</sup> with the largest world-wide trauma surgeon network for appropriate clinical guidance. These patent protected financially exploitable innovations were either licenced attaining royalty fees or sold to industry.

Despite this long-term successful record in translation, the need for fracture fixation moves now towards faster repair along with treatment of major co-morbidities such as infection at the same time as the economics of the field are driven downwards by many factors including increasing medical approval hurdles and associated costs. The need for cartilage and disc clinical functionality moves more towards regeneration, as a first step to increase the time of use before possible replacement. The policy makers, healthcare providers, insurance companies and patient groups additionally add their demands to the demands and wishes of the surgeons and the industrial producers. From an idea to help a patient's clinical problem to an actual clinical protocol or approved implant at the bedside costs massive resources in knowhow beyond the preclinical research that we are used to as scientists. Clinical guidance is essential at every major step in medical translation research to make sure the idea has any chance in the operation room.

For the preclinical side, accreditation of R&D processes and facilities is important (ISO for an Institute overall and GLP and AAALAC for a preclinical facility) and the team must have a mix of academic and more development oriented members in various fields. In medical translational research it is also extremely important to know very early on (before large investments into the preclinical research) What the current situation on the market is? What is the current clinical solution (or workaround)? What is the financial cost and market for such a clinical problem (regional and world-wide) What are the regulatory hurdles to such a solution? (regionally they may vary); What is the current patent situation for this area and is your idea really novel? (the search cannot be just European, a patent in an individual country can easily kill your patent application many years down the line (and after significant costs). Based upon this, are the estimated R&D costs worthwhile to get a chance of return on investment?

Once you have performed such searches and intend to protect your idea, the project needs to be differentiated from fundamental research projects. PhD's and postdocs

need to publish for their careers while a real medical translational research project needs to be kept confidential at minimum until patent protection is submitted. This can delay academic recognition, yet helps make the idea tradable after filing the patent. Since patent protection is not cheap, initial studies to test your hypothesis are recommended before patent filing, but must not be made public and therefore need to be under the project lead of Research Associates or higher with technician support (whose careers are not based only upon academic publications). Medical translational research projects need special routes and rules and different targets and milestones for the project leaders compared to fundamental research projects. For these project leaders, a balance in fundamental and translational research projects is required, since certainly not all translational projects will be successful.

Despite the professional set up to nurture, approve and expose medical translation projects, key areas of the translation cycle are still missing where the dependence lies with industrial partnerships of the AO Research Institute. As the AO Research Institute has moved more towards biology, tissue engineering and regenerative medicine this century, the steps from bench to bedside are exponentially more difficult than for a simple biomaterial fracture fixation device. There is an increasing clinical demand for the targeted and controlled delivery of active molecules (or cells) to specific parts of the body which requires good extremely well characterised biomaterial delivery platforms e.g. for localised delivery of antibiotics to infection sites or release of stimulants for local tissue regeneration. The biomaterials ideally should be biocompatible, biodegradable and allow controlled temporal release of the active substances. This involves a lot of developmental controls and after proof of concept at the preclinical research level, costs and legal hurdles for the jump from this to get a product to the bedside are enormous. What should one insource and what should one outsource? Many companies no longer will buy a proof of concept. Technology transfer and licencing to industry, certification (e.g. CE), regulatory issues, GLP and GLM for tissue engineering are all areas that have to be considered for this question. This presentation will attempt to show how we at the AO Research Institute Davos are trying to solve these issues of Intellectual Property for technology transfer.

### REFERENCES

1. Richards RG. AO Research Institute Davos within the AO Foundation: A model for translation of science to the clinics. *Journal of Orthopaedic Translation*. (2013) 1, 11-18.





## Vascularization in Tissue Engineering: Alternative Foreign Body Responses

Michael V. Sefton

Institute of Biomaterials and Biomedical Engineering, University of Toronto, Canada  
[michael.sefton@utoronto.ca](mailto:michael.sefton@utoronto.ca)

### INTRODUCTION

The foreign body response is the classic response to an implanted biomaterial or device, resulting in a fibrotic tissue response intending to “wall off” the foreign body and protect the host. We are exploring alternative foreign body responses which result in vascularized rather than fibrotic tissue. A critical issue associated with creating large tissues is the difficulty of supplying nutrients to all the cells in a thick segment of tissue beyond the limits of Fick's law; such vascularized responses are expected to circumvent this issue.

### MODULAR TISSUE ENGINEERING

A three-phase construct containing of endothelial cells (EC), mesenchymal stromal cells (MSC) and collagen using modular components drives a remodelling process that results in a perfusable vasculature. *In vivo*, modules are initially hypoxic and this drives a remodeling process involving the host response (including host macrophages), angiogenesis and pericyte recruitment, among other processes. This remodeling produces, within ~21 days, a mature chimeric and functional vascular supply composed of graft EC (that migrated from the modules) and host EC recruited to the construct as part of the host response<sup>1,2</sup>.

Vascularization depends on the host response to modules in SCID/bg mice (although immune-compromised, they still mount an inflammatory response) or tacrolimus treated rats (allogeneic transplants). Clodronate depletion of macrophages (iv + sc) reduced vessel number suggesting that macrophages are needed for vessel formation. Conversely, GR1<sup>+</sup> neutrophils in the NSG mouse appeared to interfere with vessel formation; antibody depletion restored vessel formation. We have isolated macrophages from the explanted tissue and characterized their phenotype by flow cytometry. Inflammatory cell number (CD45<sup>+</sup>) decreased from day 3 to day 7, while the proportion of CD206<sup>+</sup> M2 cells increased; the presence of adMSC had no substantive effect on these results. We have also begun to assess circulating cells and noted that module injection did increase the levels of various sub-populations which we are still analysing.

Our goal is to engineer a well vascularized subcutaneous niche to support cell transplantation. We need to significantly accelerate mature, functional vessel formation to perfuse transplanted cells as quickly as possible and prevent ischemia. Generating robust, mature vessels at early times is still an unmet challenge, which we believe requires new tools to control the host response.

### ANGIOGENIC BIOMATERIAL

A 45 mole % methacrylic acid copolymer (with MMA) in the form of beads caused a significant increase in the

number of vascular structures in a rat skin graft model that also lead to enhanced ‘take’ of the graft; similar results were obtained in diabetic mice wound healing. This vascularization is a consequence of the host wound healing response.

Gene analysis indicated that upregulation of Sonic Hedgehog (Shh) in the wound is a factor in this angiogenic effect<sup>3</sup>. In order to identify which cells are producing Shh, large (1.5x1.5 cm) full thickness wounds were created on the dorsum of non-diabetic transgenic animals in which Shh and Ptch1 (Shh receptor) were co-expressed with two reporter genes, GFP and lacZ respectively. Hair follicles may be an important source of Shh in this context.

Macrophage-like cells (dTHP1) incubated on smooth 40% MAA films (copolymerized with isodecyl acrylate, IDA) for 96 hours increased the expression of angiogenic genes HIF1 $\alpha$  and SDF1 $\alpha$ , and of inflammatory genes IL1 $\beta$ , IL6 and TNF $\alpha$ , while decreasing the expression of osteopontin. Gene expression changes were more significant above a threshold between 30 to 40% MAA.

Plasma/serum protein adsorption showed that the adsorbed protein on MAA biomaterials and particularly complement levels may be an upstream influence on the wound healing and vascularisation environment while sonic hedgehog is a downstream consequence of that cell-material interaction.

How these separate elements link together to explain why MAA containing materials (and not other materials) cause the profound angiogenic response continues to be a mystery. We are continuing to unravel complexities in how a simple material (a MAA copolymer) has such a profound *in vivo* effect.

### CONCLUSION

MAA is an example of a regenerative biomaterial – a material with regenerative effect without cells or drugs. Like modules, it exploits an alternative foreign body response, that uses *in vivo* remodelling to result in vascularised tissue. We suggest that there are many other biomaterials and devices that can exploit similar host responses to functional benefit.

### REFERENCES

1. Chamberlain MD et al, *Tiss Eng Pt A*. 285-94, 2012.
2. Ciucurel EC et al. *Tiss Eng Pt A*. 1235-52, 2014.
3. Fitzpatrick LE et al *Biomaterials*. 5297-5307. 2012.

### ACKNOWLEDGMENTS

The author would like to thank his many students and collaborators for their contributions to this work as well as the financial support of the Canadian and Ontario governments.





## Targeted Chemo- and Molecular-Therapy by Self-Assembled Supramolecular Nanosystems

Kazunori Kataoka<sup>1,2</sup>

<sup>1</sup> Departments of Materials Engineering and Bioengineering, Graduate School of Engineering,  
The University of Tokyo, Tokyo, Japan

<sup>2</sup> Center for Disease Biology and Integrative Medicine, Graduate School of Medicine,  
The University of Tokyo, Tokyo, Japan  
[kataoka@bmw.t.u-tokyo.ac.jp](mailto:kataoka@bmw.t.u-tokyo.ac.jp)

Nanosystems with 10 to 100 nm in size can be prepared by programmed self-assembly of block copolymers in aqueous entity. Most typical example is polymeric micelles with distinctive core-shell architecture. Several micellar formulations of antitumor drugs have been intensively studied in preclinical and clinical trials, and their utility has been demonstrated<sup>1,2</sup>. Compared with conventional formulations, such as liposomes, polymeric micelles have several advantages, including controlled drug release, tissue penetrating ability and reduced toxicity. Critical features of the polymeric micelles as drug carriers, including particle size, stability, and loading capacity and release kinetics of drugs, can be modulated by changing the chemical composition of the constituent block copolymers<sup>3</sup>. The development of smart polymeric micelles that dynamically change their properties due to sensitivity to chemical or physical stimuli is the most promising trend toward nanomedicines, directing to the targeting therapy with high efficacy and ensured safety. Notable anti-tumor efficacy against intractable cancer, including pancreatic cancer, of antitumor drug-incorporated polymeric micelles with pH-responding property was demonstrated to emphasize a promising utility of nanosystems for the cancer treatment<sup>4-6</sup>. Furthermore, polymeric micelles loaded with platinum-based anti-cancer reagents successfully treated systemic metastasis even from the early stage of pre-angiogenic micrometastatic niches associated with inflammation<sup>7,8</sup>.

Versatility in drug incorporation is another feasibility of polymeric micelles. Recently, we have succeeded to incorporate proteasome inhibitor, MG132 into polymeric micelles through acid-labile linkage, and verified the micelle efficacy against xenograft tumor model by systemic injection<sup>9</sup>. Notably, selective release of MG132 in acidic endo/lysosomal compartments of tumor cells was observed in time- lapse manner under fluorescent microscopy by the use of fluorescent dye-tagged polymeric micelles loaded with MG132. This result demonstrates the promising features of polymeric micelles as platform nanoformulation for tumor-selective delivery of a variety of molecular-targeted drugs with issues on physicochemical properties, such as solubility, and toxicity against normal tissues and organs.

The success in gene and nucleic acid delivery indeed relies on the development of the safe and effective devices to transport them into target cells. In this regard, polyion complex (PIC) micelles, which are formed between nucleic acid and PEG-polycation block copolymers, have a great promise due to their small size (<100 nm) and excellent biocompatibility.

This presentation will also focus on the development of PIC micelles for systemic delivery of gene, mRNA, and oligonucleotides, including siRNA<sup>10-12</sup>.

### REFERENCES

1. K. Kataoka; A. Harada; Y. Nagasaki, *Adv. Drug Deliv. Rev.*, 2012, 64, 246.
2. H. Cabral and K. Kataoka, *J. Contrl. Rel.*, 2014, 190, 465.
3. H. Cabral; N. Nishiyama; K. Kataoka, *Acc. Chem. Res.*, 2011, 44, 999.
4. Y. Mochida; H. Cabral; Y. Miura; F. Albertini; S. Fukushima; K. Osada; N. Nishiyama; K. Kataoka, *ACS Nano*, 2014, 8, 6724.
5. H. Cabral; Y. Matsumoto; K. Mizuno; Q. Chen; M. Murakami; M. Kimura; Y. Terada; M. R. Kano; K. Miyazono; M. Uesaka; N. Nishiyama; K. Kataoka, *Nature Nanotech.*, 2011, 6, 815.
6. H. Cabral; M. Murakami; H. Hojo; Y. Terada; M. R. Kano; U. -I. Chung; N. Nishiyama; K. Kataoka, *Proc. Natl. Acad. Sci. USA.*, 2013, 110, 11397.
7. M. Rafi; H. Cabral; M. R. Kano; P. Mi; C. Iwata; M. Yashiro; K. Hirakawa; K. Miyazono; N. Nishiyama; K. Kataoka, *J. Contrl. Rel.*, 2012, 159, 189.
8. H. Wu; H. Cabral; K. Toh; P. Mi; Y.-C. Chen; Y. Matsumoto; N. Yamada; X. Liu; H. Kinoh; Y. Miura; M. R. Kano; H. Nishihara; N. Nishiyama; K. Kataoka, *J. Contrl. Rel.*, 2014, 189, 1.
9. S. Quader; H. Cabral; Y. Mochida; T. Ishii; X. Liu; K. Toh; H. Kinoh; Y. Miura; N. Nishiyama; K. Kataoka, *J. Contrl. Rel.*, 2014, 188, 67.
10. K. Miyata; N. Nishiyama; K. Kataoka, *Chem. Soc. Rev.*, 2012, 41, 2562.
11. M. Baba; K. Itaka; K. Kondo; T. Yamasoba; K. Kataoka, *J. Contrl. Rel.*, 2015, 201, 41.
12. H.-J. Kim; H. Takemoto; Y. Yi; M. Zheng; Y. Maeda; H. Chaya; K. Hayashi; P. Mi; F. Pittella; R. J. Christie; K. Toh; Y. Matsumoto; N. Nishiyama; K. Miyata; K. Kataoka, *ACS Nano*, 2014, 8, 8979.



## Cell-Made or Man-Made Materials for Bone Reconstruction?

Malgorzata Lewandowska-Szumiel

Tissue Engineering Lab, Department of Histology and Embryology,  
Centre for Preclinical Research and Technology, Medical University of Warsaw, Poland  
[mszumiel@wum.edu.pl](mailto:mszumiel@wum.edu.pl)

The history of use of biomaterials in bone is probably the oldest comparing to other tissues. Coconut shells, wood and ivory were found to be used for bone and teeth repair already in ancient times. Years of research in modern medical sciences resulted in a huge offer of biomaterials used in bone surgery, including metals, polymers, ceramics and composites.

Regardless of the fact we have the plethora of the biomaterials for bone reconstruction, the research oriented towards developing the new materials and improving the existing ones remains still an open platform. It is illustrated by permanently growing number of scientific publications, grants and patents in the field as well as the continuing interest of biomedical enterprises and pharma.

The modern biomaterials are designed especially to integrate with host bone as well as to promote bone organization and remodeling, but they are non-viable and they are recognized by host tissues as “foreigners”. Even the most biomimetic man-made material will be far from the excellence of the natural extracellular matrix (ECM).

ECM provides a perfectly organized structure which is, by nature, an ideal environment able to keep equilibrium with its resident cells and to control cell migration, proliferation, differentiation and specialized function. Currently, after years of intensive work on new man-made materials, this very basic statement is full force spotted. Such an issue attracted significant interest in creating tissue substitutes based on biological scaffolds derived from the decellularized tissues and eventually repopulated with living cells. During the past decade many biomedical products based on this idea have been proposed. The history of using processed ECM in bone is even longer, as the osteogenic properties of demineralized bone matrix was discovered by Urist in 1965. Relating to the title of this lecture, such materials should be classified as the cell-made. However, decellularized ECM is not the only one concept of cell-made biomaterial.

In vitro-generated ECM is an intriguing and promising alternative. The knowledge and experience gained over more than two decades of tissue engineering research performed in cell culture resulted in working out sophisticated culture systems. They are based on different 3D constructions for cells distribution supported by regulated stiffness as well as by multi-cell co-cultures. There is more and more evidence of the successful construction of in vitro cell-made ECM constructs designed directly for transplantation to injured tissues. Even more exiting results indicate high usefulness of such systems as a niche for stem cells as well as a tool in directing cells differentiation into specialized immunophenotypes. Their potential use in regenerative medicine seems apparent.

Therefore, cell-made materials hold a promise perspective in bone reconstruction. The real “taste” of such systems is that they are of biological origin, alive but at the same time perfectly controlled.

Better control of cell-made ECM-based biomaterials needs well-orchestrated engineering job and basic research, which is an issue indicated as critical in the majority of leading opinions in the field.

Several examples of the original research performed in this direction, coming both from the literature and from the experience of our lab, will be given in the lecture. In particular, tissue engineered products obtained via replacement of the degrading scaffold by cell-produced ECM in vitro, similarity of cell-produced mineral to the native one as well as the role of the materials stiffness and architecture in regulating cell fate will be addressed.

Those promising examples are intended to settle the title key issue in favor of cell-made materials.

But even if so, the question still remains - who is an engineer who organizes and controls the production? Hopefully, the answer opens a very nice space for research in a fascinating field of biomaterials.

## Biological-Basis for Designing Biomaterials for the Injured and Degenerated Host - Examples in the Neural Space

Abhay Pandit

Centre for Research in Medical Devices (CÚRAM),  
National University of Ireland Galway, Ireland  
[Abhay.pandit@nuigalway.ie](mailto:Abhay.pandit@nuigalway.ie)

Biomaterials are no longer considered innate structures and using functionalisation strategies to modulate a desired response whether it is a host or implant is currently an important focus in current research paradigms. Fundamentally, a thorough understanding the host response will enable to design proper functionalisation strategies. The input from the host response needs to be weighed in depending on the host disease condition. In addition biomaterials themselves provide immense therapeutic benefits which needs to be accounted for when using functionalisation strategies. Using functionalisation strategies such as enzymatic and hyperbranched linking systems, we have been able to link biomolecules to different structural moieties. The programmed assembly of biomolecules into higher-order self-organized systems is central to innumerable biological processes and development of the next generation of functionalized scaffolds. Recent design efforts have utilized a bottom-up approach toward both understanding and engineering supramolecular protein assemblies. These include functionalisation of micro and nanoparticles with biomolecules that include designed peptide motifs, growth factors and a multitude of gene vector systems. Structural moieties have taken a variety of different forms such as nanofibers and nanoparticulate. In addition, nature itself has abundant structural complexity that can be harnessed for targeted clinical applications. This talk will elucidate some of these ongoing strategies in our laboratory.

### References

- Rethore, G. and **Pandit, A.** 'Use of Templates to Fabricate Nanoscale Spherical Structures for Defined Architectural Control.' *Small*. 2010: 6(4): 488-498.
- Rooney, P., Srivastava, A., Watson, L., Quinlan, L. and **Pandit, A.** 'Hyaluronic Acid Decreases IL-6 and IL-8 Secretion and Permeability in an Inflammatory Model of Interstitial Cystitis.' *Acta Biomaterialia*. 2015: (In Press)
- Samal, J., Hoban, D.B., Naughton, C., Concannon, R., Dowd, E. and **Pandit, A.** 'Fibrin-based Microsphere Reservoirs for Delivery of Neurotrophic Factors to the Brain.' *Nanomedicine*. 2015: 10(5): 765-783.
- Thomas, D., Fontana, G., Chen, X., Sanz-Nougés, C., Zeugolis, D., Dockery, P., O'Brien, T. and **Pandit, A.** 'A Shape-controlled Tuneable Microgel Platform to Modulate Angiogenic Paracrine Responses in Stem Cells.' *Biomaterials*. 2014: 35(31): 8757-66.
- Newland, B., Aied, A., Pinoncelly, A.V., Zheng, Y., Zhao, T., Zhang, H., Niemeier, R., Dowd, E., **Pandit, A.** and Wang, W. 'Untying a Nanoscale Knotted Polymer Structure to Linear Chains for Efficient Gene Delivery in Vitro and to the Brain.' *Nanoscale*. 2014: 6(13): 7526-7533.
- Lang, Y., del Monte, F., Collins, L., Rodriguez, B.J., Thompson, K., Dockery, P., Finn, D.P. and **Pandit, A.** 'Functionalization of the Living Diatom *Thalassiosira weissflogii* with Thiol Moieties.' *Nature Communications*. 2013: 4: 3683
- Hoban, D., Newland, B., Moloney, T., Howard, L., **Pandit, A.** and Dowd, E. 'The Reduction in Immunogenicity of Neurotrophin Overexpressing Stem Cells after Intra-Striatal Transplantation by Encapsulation in an In Situ Gelling Collagen Hydrogel.' *Biomaterials*. 2013: 2013: 34(37): 9420-9429.
- Mathew, A., Parkan, J.M., Collin, E., Wang, W., McDermott, K., Fitzgerald, U., Reynolds, R. and **Pandit, A.** 'An Ex-vivo Multiple Sclerosis Model of Inflammatory Demyelination using Hyperbranched Polymer.' *Biomaterials*. 2013: 34: 5872-5882.



# Keynotes



## Antimicrobial Effects of Biomaterials: Silver Ions, Silver Nanoparticles and Antimicrobial Peptides

Matthias Eppe<sup>1</sup>, Svitlana Chernousova<sup>1</sup>, Kateryna Loza<sup>1</sup>, Oleg Prymak<sup>1</sup>, Maria A. Surmeneva<sup>3</sup> and Roman Surmenev<sup>2,3</sup>

<sup>1</sup>Institute for Inorganic Chemistry and Center for Nanointegration (CeNIDE), University of Duisburg-Essen, Germany

<sup>2</sup>Fraunhofer Institute for Interfacial Engineering and Biotechnology IGB, Germany

<sup>3</sup>Theoretical and Experimental Physics Department, Tomsk Polytechnic University, Russia

[matthias.eppe@uni-due.de](mailto:matthias.eppe@uni-due.de)

### INTRODUCTION

The fight against bacterial infections is a very hot topic in current biomedicine, possibly of even higher importance than a good biocompatibility towards the tissue surrounding the implant. If bacterial colonies are formed on the surface of an implant, e.g. as a biofilm, they are very difficult to combat and may cause the failure of the implant. We will discuss two approaches: First: the application of silver nanoparticles and of silver ions. Second: The application of silver-containing films of calcium phosphate by magnetron sputtering. Third: The genetic transfection of an antimicrobial peptide (defensin) by calcium phosphate nanoparticles

### RESULTS AND DISCUSSION

The biological effect of silver nanoparticles and of silver ions was compared in extensive experiments with eukaryotic cells and bacteria. The toxic nature of silver nanoparticles is due to their slow dissolution with the release of silver ions. These, however, are reacting with components of biological media, e.g. chloride ions and proteins. The active species in silver-containing media are silver chloride nanoparticles as it was demonstrated by extensive physicochemical and cell-biological studies. The therapeutic window of silver, e.g. the difference in toxicity towards bacteria and eukaryotic cells, is smaller than typically assumed.

Silver nanoparticles can be applied to surfaces by different methods. One possibility is the electrophoretic deposition, followed by magnetron-sputtering of a thin layer of calcium phosphate. It is also possible to add silver ions to a layer of calcium phosphate if the sputtering target contains silver.

A completely different approach is the introduction of DNA into cells of the surrounding tissue by transfection with calcium phosphate nanoparticles. If the DNA encodes the formation of the antimicrobial peptide defensin, the cells will start to produce this peptide. The possibilities of this approach will be discussed, based on cell-culture experiments.

### CONCLUSION

Silver offers possibilities to combat infections in the vicinity of an implant, but care must be taken with respect to damage of the surrounding tissue and to the development of bacterial resistance. A silver coating must assure a sufficiently high silver concentration. Transfection of the surrounding tissue offers new possibilities, but the fact that the proteins or peptides are expressed inside a cell restricts this approach.

### REFERENCES

1. S. Chernousova, M. Eppe, "Silver as antibacterial agent: Ion, nanoparticle, and metal", *Angew. Chem. Int. Ed.* 52:1636-1653, 2013
2. K. Loza, J. Diendorf, C. Sengstock, L. Ruiz-Gonzalez, J. M. Gonzalez-Calbet, M. Vallet-Regi, M. Köller, M. Eppe, "Dissolution and biological effects of silver nanoparticles in biological media", *J. Mater. Chem. B* 2:1634-1643, 2014
3. C. Greulich, D. Braun, A. Peetsch, J. Diendorf, B. Siebers, M. Eppe, M. Köller, "The toxic effect of silver ions and silver nanoparticles towards bacteria and human cells occurs in the same concentration range", *RSC Adv.* 2:6981-6987, 2012
4. A.A. Ivanova, R.A. Surmenev, M.A. Surmeneva, T. Mukhametkaliyev, K. Loza, O. Prymak, M. Eppe, "Hybrid biocomposite with a tunable antibacterial activity and bioactivity based on rf magnetron sputter deposited coating and silver nanoparticles", *Appl. Surf. Sci.* 329:212-218, 2015





Zhongwei Gu<sup>1</sup><sup>1</sup>National Engineering Research Center for Biomaterials, Sichuan University, P.R. China  
[Zhongwei.Gu@scu.edu.cn](mailto:Zhongwei.Gu@scu.edu.cn)

## INTRODUCTION

The lack of safe and efficient gene delivery systems is a major obstacle to achieve successful human gene therapy. With the growing understanding the mechanisms of non-viral gene delivery, and inspired by the viral structures and functions, much effort has been directed to the development of intelligent macromolecular based bioinspired gene delivery systems. Supramolecular self-assembly of dendrimers is a promising approach to engineer advanced vectors for gene delivery. Such as peptide dendrimers coupled with linear peptides spontaneously assembled into well-defined viral capsid like nanostructure<sup>1</sup>, and the bioinspired supramolecular hybrid strategy<sup>2</sup>. Meanwhile, the dynamic polyplexes based on disulfide linkage modified hyaluronic acid (HA) envelop and diselenide conjugated oligoethylenimine (OEI) caspid were designed for mimicking the delivery functions and structures of viral particles for gene delivery<sup>3,4</sup>.

## EXPERIMENTAL METHODS

Synthesized compounds were structurally characterized by <sup>1</sup>HNMR, GPC and mass spectrophotometer. The biophysical properties, cytotoxicity, cellular association, transfection *in vitro* and *in vivo* of nanovehicles were systematically investigated. Data were expressed as means  $\pm$  SD. Statistical significance ( $p < 0.05$ ) was computed by SPSS version 13.0 software.

## RESULTS AND DISCUSSION

With a rational design, dual-functionalized low generation peptide dendrons self-assemble onto inorganic nanoparticles via coordination interactions to generate supramolecular hybrid dendrimers (SHDs).

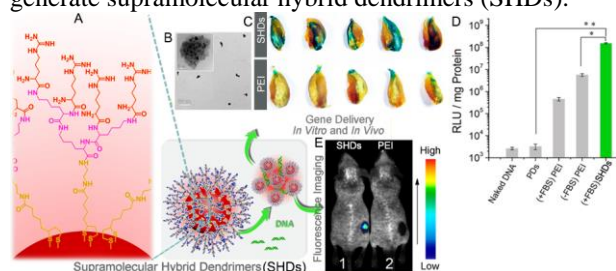


Figure 1. (A) Schematic illustrations for self-assembly of SHDs; (B) TEM of the SHDs/DNA complex; (C) Transfection efficacy of pCMV- $\beta$ -gal in mouse muscles after intramuscular injection; (D) Luciferase activity in HepG2 cells; (E) Fluorescence images of nude mice with HepG2 tumor xenografts after intratumoral injection.

As expected, the bioinspired supramolecular hybrid strategy largely enhances the gene transfection efficiency of SHDs approximately 50000-fold as compared to single dendrons at the same R/P ratio. *In vivo* animal experiments demonstrate that SHDs offer considerable gene transfection efficiency in muscles

and real-time bioimaging capabilities. These SHDs will likely stimulate studies on bio-inspired supramolecular hybrid dendritic systems for biomedical applications.

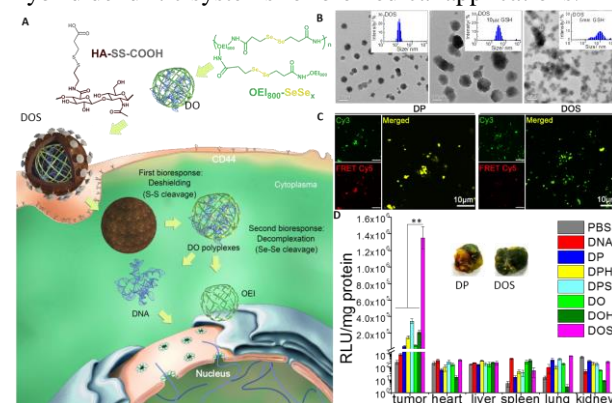


Figure 2. (A) Schematic of DOS for gene delivery; (B) TEM of DOS with GSH; (C) FRET images of DOS on HepG2 cells; (D) Transfection efficacy of pCMV-Luc or pORF-LacZ (insert) after intratumoral treatment.

A new concept of “reduction-controlled hierarchical unpacking” is proposed for developing virus-mimicking gene delivery system. Disulfide linkage modified HA was deposited to the surface of diselenide-conjugated OEI /DNA (DO) to form DNA/OEI-SeSex/HA-SS-COOH (DOS) ternary polyplexes. The cleavage of disulfide linkage in HA envelop and diselenide linkage in OEI-SeSex caspid is triggered by different levels of GSH at tumor site and in the cell, which is confirmed by TEM and FRET. Gene transfection of DOS in nude mice with HepG2 cells xenograft tumor showed significantly enhancement as compared to PEI.

## CONCLUSION

Thus, the intelligent macromolecular based bioinspired design nanovehicles achieved high gene expression *in vitro* and *in vivo*, which provide an encouraging strategy to further develop synthetic gene transfer systems.

## REFERENCES

- Gu Z. *et al.*, Angew. Chem. Int. Ed. 51:3184-3187, 2012
- Gu Z. *et al.*, ACS Nano 8:9255-9264, 2014
- Gu Z. *et al.*, Biomaterials 35:1657-1666, 2014
- Gu Z. *et al.*, Adv. Mater. 26:1534-1540, 2014

## ACKNOWLEDGMENTS

The authors would like to thank the National Science Foundation of China (NSFC, 51133004 and 81361140343), National Basic Research Program of China (National 973 program, 2011CB606206), and Joint Sino-German Research Project (GZ756 and GZ905) for providing financial support to this project.



# Manipulation of Cell Mechanotaxis by Designing Curvature of The Elasticity Boundary on Hydrogel Matrix

Satoru Kidoaki<sup>1</sup>, Ayaka Ueki<sup>2</sup>

<sup>1</sup>Institute for Materials Chemistry and Engineering, Kyushu University, Japan

<sup>2</sup>Graduate School of Engineering, Kyushu University, Japan

[kidoaki@ms.ifoc.kyushu-u.ac.jp](mailto:kidoaki@ms.ifoc.kyushu-u.ac.jp)

## INTRODUCTION

Directional cell migration induced by the stiffness gradient of cell culture substrates is known as a subset of the mechanical-cue-induced taxis, so-called mechanotaxis. To establish the general conditions of biomaterials to manipulate the mechanotaxis, the effect of the shape of the elasticity transition boundary on mechanotaxis should be systematically determined as well as the conditions of elasticity gradient strength. In this report, we focus on the curvature of the elasticity boundary as a simplified factor of expressing variations in the shape of the elasticity boundary in living tissues. Photolithographic microelasticity patterning of gelatinous gels was employed to systematically prepare elasticity boundaries with various curvatures, and the efficiency of mechanotaxis of fibroblast cells around each curved boundary was examined. The curvature of the elasticity boundary was found to markedly affect the efficiency of induction and the direction of mechanotaxis. The mechanism responsible for this phenomenon and the implication for the curvature effect in *in vivo* systems are discussed.

## EXPERIMENTAL METHODS

Photocurable styrenated gelatin (StG) was used for photolithographic microelasticity patterning of the gel, which was synthesized according to the method previously reported by our group<sup>1,2</sup>. StG sol solution was spread between vinylated glass and a normal glass substrate, then irradiated with a custom-built, reduction-projection-type photolithographic system. The elastically-alternating patterns of concentric circles with Rs of 250, 500, 750, and 1000  $\mu\text{m}$ , and semicircles with Rs of 50 and 100  $\mu\text{m}$  were prepared. The surface elasticity of the gels was determined by AFM nanoindentation analysis. The migratory behavior of 3T3 fibroblast cells on the gels was monitored using an automated all-in-one microscope with a temperature- and humidity-controlled cell chamber (BIO REVO BZ-9000; Keyence Corporation, Osaka, Japan). Phase-contrast images of cells were captured every 15 min for 24 h. Moving trajectories of 22–58 isolated cells on 3–6 gel samples were determined using ImageJ software (ImageJ 1.46r, <http://rsbweb.nih.gov/ij/>).

## RESULTS AND DISCUSSION

Cell migrations were observed on the microelastically-patterned gels for 24 h and the trajectories of the cells interacting with the elasticity boundaries were monitored for 12 h (Fig.1).

Firstly for the control linear boundary, usual mechanotaxis behaviors could be seen (Fig.1c). Degree of the biased migrations in the control condition was weak as planned to easily detect curvature effect. Secondary for the convex boundary (Fig.1a), biased

time-dependent migrations toward the hard region were confirmed for boundaries with Rs of 50, 100, and 250  $\mu\text{m}$ , while no biased migrations were detected for the boundaries with larger Rs (500, 750, and 1000  $\mu\text{m}$ ). The convex boundary with an R of 100  $\mu\text{m}$  displayed the largest bias of migration. Thirdly for the concave boundaries

(Fig.1b), biased migrations toward the hard region were confirmed for Rs of 750 and 1000  $\mu\text{m}$ , while biased migrations toward the soft region, i.e., “negative” mechanotaxis, were observed for concave boundaries with Rs of 50 and 100  $\mu\text{m}$ .

Interestingly, as R in convex boundary got larger to 1000  $\mu\text{m}$ , mechanotaxis was not observed, however, when R approached to infinite, i.e., linear boundary, weak mechanotaxis was observed. Then after, in the reversed curvature condition of R of 1000  $\mu\text{m}$  in the concave boundary, force of mechanotaxis was enhanced. Such enhancement also appeared in the condition of R of 750  $\mu\text{m}$  in the concave boundary. This trend suggests that the concave boundary with optimized R is preferable to induce efficient mechanotaxis<sup>3</sup>.

## CONCLUSION

Highly efficient usual durotaxis was induced on a convex boundary with R 100  $\mu\text{m}$  and on a concave boundary with R 750  $\mu\text{m}$ . Biased migration toward soft regions of the gel, i.e., inverse durotaxis, or “negative mechanotaxis” was first observed for concave boundaries with Rs of 50  $\mu\text{m}$  or 100  $\mu\text{m}$ .

## REFERENCES

1. Kidoaki S and Matsuda T., J. Biotechnol. 133:225-230, 2011.
2. Kawano T. and Kidoaki S., Biomaterials, 32: 2725-2733, 2011.
3. Ueki A. and Kidoaki S., Biomaterials, 41: 45-52, 2015.

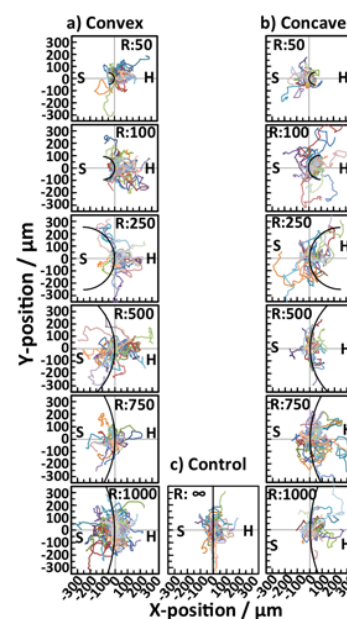


**Fig 1.** The starting position-superimposed cell trajectories around the elasticity boundaries with different curvatures. The black curves indicate the elasticity boundaries. H and S indicate hard and soft region, respectively.

# Dual Release of a Macrophages Recruitment Agent and Growth Factor for Bone Regeneration

Yang-Hee Kim, [Yasuhiko Tabata](mailto:Yasuhiko.Tabata)

Department of Biomaterials, Institute for Frontier Medical Sciences, Kyoto University, Japan

[yasuhiko@frontier.kyoto-u.ac.jp](mailto:yasuhiko@frontier.kyoto-u.ac.jp)

## INTRODUCTION

The process of bone healing can be classified into four histologically distinguishable stages: inflammation, fibrous, callus, and bone formation. Inflammation is the initial and the most vital stage from the viewpoint of bone regeneration. Macrophages are typical inflammatory cells, which infiltrate into injured and defect sites and have a key role in the modulation of the inflammatory response. Recently, it has been demonstrated that the decreased number of macrophages generally implicates their dysfunction of dead cell clearance, the phagocytosis of apoptotic cells, and the up-regulation of pro-inflammatory cytokines<sup>1,2</sup>. This may induce inflammation and delayed tissue repair.

Therefore, as one trial to positively regulate the inflammation and repairing processes, we considered to enhance recruitment macrophages to the defect site by a macrophage recruitment agent release. In addition, we have developed the controlled release technology of platelet rich plasma (PRP) and bone morphogenetic protein (BMP)-2 from gelatin hydrogels to enhance tissue regeneration<sup>3,4</sup>. The purpose of this study is to evaluate the effect of dual release of a macrophage recruitment agent and PRP or BMP-2 from gelatin hydrogels on the modulation of inflammation and bone regeneration.

## EXPERIMENTAL METHODS

A macrophage recruiting agent, SEW2871(SEW) of a sphingosine-1 phosphate agonist, and PRP or BMP-2 were used. The non-water soluble SEW was solubilized in water through micelles formation with L-lactic acid grafted gelatin, and the resulting micelles with PRP or BMP-2 were incorporated into gelatin hydrogels. To investigate their effect on bone regeneration, a bone defect model of rat ulna was prepared, and the bone formation ability was evaluated by histological, radiological, and micro-computed tomographic ( $\mu$ -CT) examinations. In addition, we examined the expression levels of inflammatory cytokines and osteoprotegerin (OPG) of osteoclastogenesis inhibitory factor genes after implantation of the gelatin hydrogels.

## RESULTS AND DISCUSSION

Mixed SEW-micelles and PRP or BMP-2 were released from gelatin hydrogels in a controlled fashion both in vitro and in vivo. The culture of macrophages with a growth factor induced to increase the production of anti-inflammatory cytokines compared with macrophages without a growth factor.

When applied to a bone defect of rats, the hydrogels incorporating mixed SEW-micelles and PRP or BMP-2 recruited a higher number of macrophages than those of hydrogels incorporating either SEW or a growth factor. In addition, the SEW and a growth factor incorporated

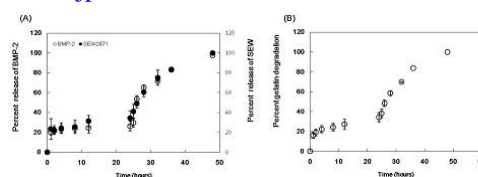


Fig. 1 Time profiles of SEW and BMP-2 release from gelatin hydrogels and their degradation in vitro.

into hydrogels enhanced the level of tumor necrosis factor (TNF)- $\alpha$  and interleukin (IL)-6 of pro-inflammatory cytokine, 3 days after application, while pro-inflammatory responses coupled with a significant increase in the expression level of OPG and IL-10 and transforming growth factor (TGF)- $\beta$ 1 of anti-inflammatory cytokine were observed 7 or 10 days postoperatively.

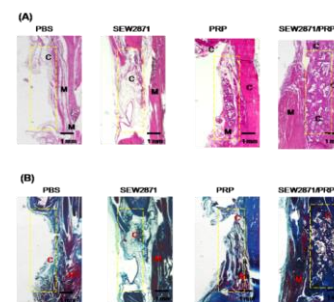


Fig. 2 Histological images of bone regenerated in defects after implantation of hydrogels incorporating SEW and PRP

The hydrogels incorporating mixed SEW-micelles and PRP or BMP-2 promoted bone regeneration to a significant great extent compared with those incorporating PBS and either SEW-micelles or growth factor, such as PRP or BMP-2. This suggests that growth factor stimulated the macrophages recruited and triggered their activation and the production of anti-inflammatory cytokines, which are associated with tissue regeneration. Consequently, the dual release of SEW and growth factor, PRP or BMP-2 would accelerate bone regeneration.

## CONCLUSION

We experimentally demonstrated that the dual release of a macrophage recruitment agent, SEW and PRP or BMP-2 in a controlled fashion from the gelatin hydrogels recruited higher number of macrophages into the bone defects compared with hydrogels incorporating either SEW or a growth factor. In addition, dual release of SEW and PRP or BMP-2 modulated inflammatory responses thereat, resulting in promoted bone regeneration.

## REFERENCES

1. Kharraz Y., et al. *Inflamm.* 2013;49:1497, 2013
2. Herold S., et al. *Front Immunol.* 2:65,2011
3. Matsui M., et al. *Acta Biomater.* 8:1792-801, 2012
4. Takahashi Y., et al. *Biomaterials* 26:4856-65, 2005

## ACKNOWLEDGMENTS

The research was supported by a grant from Japan society for Promotion of Science (JSPS).



## Contributions of Adhesive Proteins to the Cell Response to Bioactive Polymers and Surfaces

Helena Felgueiras<sup>1</sup>, Margaret D. M. Evans<sup>2</sup>, [Véronique Migonney](mailto:veronique.migonney@univ-paris13.fr)<sup>1</sup>

<sup>1</sup>Laboratory of Biomaterials and Specialty Polymers, LBPS-CSPBAT CNRS UMR 7244, Université Paris 13, SPC UNIVERSITY France

<sup>2</sup>CSIRO Biomedical Materials Program, Manufacturing Flagship, Sydney, NSW Australia  
[veronique.migonney@univ-paris13.fr](mailto:veronique.migonney@univ-paris13.fr)

### ABSTRACT

Fantastic progress has been made during the last decades in biomaterials science due to improvements in macromolecular chemistry and biology as well as in materials science and surgical techniques. Despite this, the failure rate of biomedical implants remains too high. The underlying causes of failure can largely be attributed to inadequate control of the biological response to the implant leading to a foreign body response and/or infection.

Materials used in the field of implantable medical devices and scaffolds ideally have to present properties of 'perfect compatibility' to the living systems to become accepted in the host (biointegrated). However, such perfection is extremely hard to achieve. The compatibility of an implantable material in the fully operant biological context is directly related to its structural and surface properties and also requires an understanding of the biology of the surrounding tissues. The mechanisms underlying implant failure must be better understood and this must be the constant objective of biomaterials research.

Amongst those mechanisms, the study of protein/surface interactions represents one of the most important since the adsorption of proteins is the very first event to occur when a material is implanted into living tissue [1-3]. The functionalization of polymers and surfaces to make them bioactive is the starting point in controlling the protein/surface interactions which dictates events that follow and may lead to integration or failure of the implant. Failure can involve infection and/or the foreign body response mounted by the immune system of the host [4]. Various strategies have been employed to control protein adsorption including the synthesis of polymers bearing chemical groups capable of modulating the biological response or the functionalization of implant surfaces using those same functional groups to create bioactive surfaces suitable for implant.

These strategies are exemplified by the optimisation of bioactive polymers to control the adsorption of cell adhesive proteins for target tissues such as the adhesion and integration of osteoblast cells and the functionalization of titanium alloy surfaces using bioactive polymers to modulate the protein and cell responses [5-10]. Polymers bearing anionic sulfonate groups have been shown to stimulate osteoblastic differentiation in addition to preventing bacterial adhesion. Poly(sodium styrene sulfonate) that is highly stable in physiological environments and resistant to

enzymatic degradation has been successfully grafted onto Ti6Al4V model surfaces. The distribution of the sulfonate groups from poly(sodium styrene sulfonate) has been found to instigate specific protein adsorption patterns that favor a positive cell response. Examination of the role of fibronectin and vitronectin in the initial attachment and spreading of osteoblast cells to poly(sodium styrene sulfonate) grafted Ti6Al4V surfaces and the role of collagen in the maturation of osteoblast cell on those surfaces has been correlated to results from animal models. Together, outcomes demonstrate that the competitive protein binding behaviour which occurs at the protein-surface interface makes a significant contribution to cellular responses observed both *in vitro* and *in vivo*.

### REFERENCES

1. Anderson JM *et al.* Biomaterials. 1984 5(1):5-10.
2. R. A. Latour Biomaterials: Protein-surface interactions, Encyclopedia of Biomaterials and Biomedical Engineering 2005
3. Ratner B. D. The biocompatibility manifesto: biocompatibility for the twenty-first century, J Cardiovasc Transl Res. 2011 4(5):523-7.
4. El Kadhali, *et al.* Biomacromolecules 2002 3(1) : 51-56
5. 4. Latz C, *et al.*, Biomacromolecules. 4:766-71, 2003.
6. Michiardi A, *et al.*, Acta Biomater. 6:667-75, 2010.
7. Migonney V *et al.*, in Bone Repair Biomaterials, Ed by Planell JA, Best S, Lacroix D, Merolli A Woodhead Publishing in Materials, 2009, pp309-23
8. Felgueiras H, *et al.*, Langmuir. 30:9477-83, 2014.
9. Zorn G, *et al.*, Langmuir 2011 27(21):13104-12.
10. DM Vasconcelos, *et al.*, *Materials Science and Engineering: C*, 2014, (45) 1 :176-183



## Glycosaminoglycan Derivatives – Promising Candidates for the Design of Functional Biomaterials

Dieter Scharnweber<sup>1</sup>, Linda Hübner<sup>1</sup>, Sandra Rother<sup>1</sup>, Ute Hempel<sup>2</sup>, Ulf Anderegg<sup>3</sup>, Sergey A. Samsonov<sup>4</sup>, M. Teresa Pisabarro<sup>4</sup>, Lorenz Hofbauer<sup>5</sup>, Matthias Schnabelrauch<sup>6</sup>, Sandra Franz<sup>3</sup>, Jan Simon<sup>3</sup>, Vera Hintze<sup>1</sup>

<sup>1</sup>Institute of Materials Science, Max Bergmann Center of Biomaterials, TU Dresden; <sup>2</sup>Institute of Physiopathological Chemistry, Medical Department, TU Dresden; <sup>3</sup>Department of Dermatology, Venerology and Allergology, Leipzig University; <sup>4</sup>Structural Bioinformatics, BIOTEC TU Dresden; <sup>5</sup>Division of Endocrinology, Diabetes and Bone Diseases, Department of Medicine III, TU Dresden Medical Center; <sup>6</sup>Biomaterials Department, INNOVENT e.V. Jena, all Transregio 67 ([www.trr67.de](http://www.trr67.de)), Germany  
[Dieter.Scharnweber@tu-dresden.de](mailto:Dieter.Scharnweber@tu-dresden.de)

### INTRODUCTION

Numerous biological processes such as tissue formation, remodelling and healing are strongly influenced by the composition and the biochemical properties of the cellular microenvironment. Glycosaminoglycans (GAGs), as major component of the native extracellular matrix (ECM), e.g. in the form of proteoglycans can be chemically functionalized and thereby modified in their binding profiles, both for direct cell interaction<sup>1</sup> and for interaction with mediator proteins (e.g. growth factors)<sup>2</sup>. Thus GAGs and their derivatives are promising candidates for the design of functional biomaterials to control healing processes in healthy and health-compromised patients<sup>3</sup>.

### EXPERIMENTAL METHODS

GAG derivatives based on hyaluronic acid (HA) and chondroitin sulfate (CS) are characterized in their interaction properties with mediator proteins (BMP-2, BMP-4, TGF- $\beta$ 1, and OPG) using surface plasmon resonance (SPR; Biacore<sup>TM</sup>T100), receptor binding studies, immunochemical methods and molecular modelling. The biological property profiles of selected GAG derivatives, either alone or being a component of collagen type I-based artificial ECM (aECM) are studied *in vitro* with cells relevant for healing processes in bone and skin (human mesenchymal stromal cells (hMSC), osteoblasts, osteoclasts, osteocytes, fibroblasts).

### RESULTS AND DISCUSSION

Biophysical studies show that the interaction profiles between growth factors and GAG derivatives are strongly influenced by the (i) sulfation degree, (ii) the sulfation pattern, and (iii) the composition and structure of the GAG backbone. For most mediator proteins HA-based derivatives demonstrate a higher binding strength for the same degree of sulfation compared to CS. These results are in line with biological effects of the respective GAG derivatives, either in solution or incorporated in collagen I-based aECMs, on cells relevant for wound healing processes.

These aECMs are characterized in their GAG association and release behaviour as well as in their GAG-depending biodegradation by matrix metalloproteinases. Prominent effects are (i) an anti-inflammatory, immunomodulatory effects on macrophages and dendritic cells, (ii) enhanced osteogenic differentiation of hMSC, (iii) an altered differentiation of fibroblasts to myofibroblasts, (iv) a reduced osteoclast activity and (v) an

improved osseointegration of aECM coated scaffolds in animal models.

Joint results from biophysical interaction and *in vitro* studies as well as molecular modelling simulations reveal that pre-bound GAGs influence the interaction of growth factors with their respective receptors having major consequences on their bioactivity. For example, results on TGF- $\beta$ 1/GAG complex formation with TGF-receptors indicate that the complex is biologically inactive (Fig. 1).

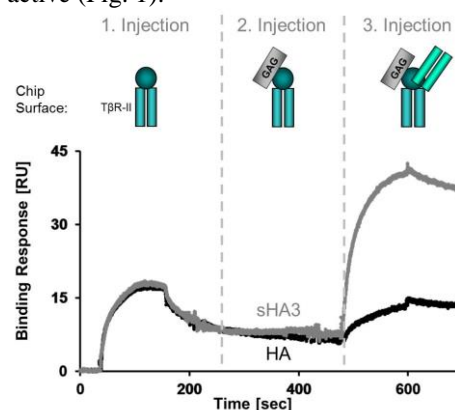


Fig. 1: SPR response curves for the sequential interaction of immobilized TGF-receptor II with solute TGF- $\beta$ 1 (green circle), followed by solute GAG and TGF-receptor I. GAGs: native HA in comparison to sulfated HA (sHA3) with a sulfation degree of 3.

### CONCLUSION

The presented results contribute to improved understanding on biological interaction profiles of mediator proteins with GAG derivatives. The resulting knowledge on structure-function-relationships of GAGs will enable the design of functional biomaterials to selectively control and promote bone and skin regeneration.

### REFERENCES

1. Klimt *et al.* J Proteome Res. 12:378-89, 2013
2. Hintze *et al.* Biomacromolecules 15:3083-92, 2014.
3. Schulz *et al.* J Mater Sci Mater Med. 25:247-58, 2014.

### ACKNOWLEDGMENTS

The authors would like to thank the DFG grant TRR67, (A2, A3, A7, B1, B2, B3, B4) for providing financial support to this project.





## Hydrogels and Scaffolds of Natural Origin as Support for Stem Cells in the Regeneration of Different Tissues

Rui L. Reis<sup>1,2</sup>

<sup>1</sup> Director of the 3B's Research Group - Biomaterials, Biodegradables and Biomimetics, Univ. Minho, Headquarters of the European Institute of Excellence on Tissue Engineering and Regenerative Medicine, AvePark, 4806-909 Taipas- Guimarães, Portugal

<sup>2</sup> Director of the ICVS/3B's - PT Associate Laboratory, Braga/Guimarães, Portugal  
[rgreis@dep.uminho.pt](mailto:rgreis@dep.uminho.pt)

### INTRODUCTION

The selection of a scaffold material is both a critical and a difficult choice that will determine the success of failure of any tissue engineering and regenerative medicine (TERM) strategy. We believe that natural origin polymeric biomaterials are the best choice for many approaches. We have working with this type of systems for the past 20 years. In addition, we have been developing an all range of processing methodologies to produce adequate scaffolds and hydrogels for different TE applications. Furthermore an adequate cell source should be selected. In many cases efficient cell isolation, expansion and differentiation methodologies should be developed and optimized. In our research group we have developed many different strategies to deal with these issues.

### EXPERIMENTAL METHODS

We have been using different human cell sources namely: mesenchymal stem cells from bone marrow, mesenchymal stem cells from human adipose tissue, human cells from amniotic fluids and membranes and cells obtained from human umbilical cords. The potential of each type of cells, to be used to develop novel useful regeneration therapies has been studied. Their uses and their interactions with different natural origin degradable scaffolds and distinct nano and micro-carriers, and smart release systems has been assessed.

### RESULTS AND DISCUSSION

In our research a great focus is given to the different sources of stem cells, the isolation of distinct sub-populations, ways of differentiating them, as well as their interactions with different 3D architectures and materials for culturing them. The use of bioreactors to control cell differentiation, as well as the surface modification of the materials in order to control cell adhesion and proliferation has also been studied in great detail. Several examples of biomimetic and novel hydrogels to combine with adequate stem cells will be described.

### CONCLUSION

Several 3D-architectures, novel hydrogel systems, biomimetic and nanotechnology based strategies to engineer different types of tissues were developed. Some examples to be presented are based on bone, cartilage, osteochondral, skin, neurological tissues, intervertebral disk (IVD) and meniscus.

### ACKNOWLEDGMENTS

The author would like to acknowledge the ERC Advanced Grant 321266, ComplexiTE for partially funding this research.



<sup>1</sup>The Faculty of Pharmacy, The University of Sydney, Australia<sup>2</sup>Department of of Nanobiomedical Science and WCU Nanobiomedical Science Research Center, Dankook University, Cheonan 330-715, Republic of Korea  
[wchrzanowski@sydney.edu.au](mailto:wchrzanowski@sydney.edu.au)

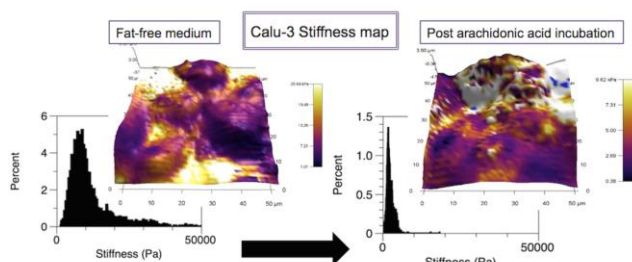
## INTRODUCTION

Scanning probe microscopy (SPM) techniques have gained immense popularity in the field of biomedical engineering due to their ability to characterise material properties at nano and atomic level. While the imaging capability of these techniques is the most established, more recently several new approaches based on the SPM platform have been developed. Many of these techniques allow probing different material properties, interactions of materials, their degradation and oxidation. Importantly these techniques are typically combined with the imaging capability, thus allow the quantitative imaging. Furthermore, many of these methods is fully applicable for biological samples (cell, tissues, and bacteria) allowing characterisation of material-cell or material-bacteria interactions and probing their properties. Of particular interest for biomaterials are colloidal force probing, force spectroscopy and amplitude modulated force spectroscopy, thermal probe and Lorenz contact resonance spectroscopy.

## EXPERIMENTAL METHODS

Nanomechanical properties of cells.

Cell stiffness is directly related to cell functionality and cell type. Hence, the examination of the cell mechanics is considered as an effective way to interrogate cell interactions with biomaterials, drugs, nanoparticles and it enables studying the impact of these materials on cell fate. Furthermore, cell mechanics is a measure of progression or regression of a disease. Here, effects of cell stiffness on a drug uptake were examined. Cell stiffness was regulated by the incubation with fatty acids (arachidonic acid, AA) and the stiffness was



measured using molecular force probe (MFP-3D-Bio). Figure 1 Effects of incubation of lung tissue model with fatty acids on cell stiffness.

Particle-particle interactions.

A metered-dose inhaler (MDI) is the most commonly used delivery system for treating asthma, chronic obstructive pulmonary disease (COPD) and other respiratory diseases. The ability to disperse given dose of the drug is highly dependent on drug particle interactions. To study single drug particle interactions

(i.e. energy of adhesion, repulsion and attraction forces) colloidal probe nanoscopy was employed. Custom made colloidal probe were fabricated and particle-particle interactions were measured using instantaneous and dwelled forces – Figure 2.

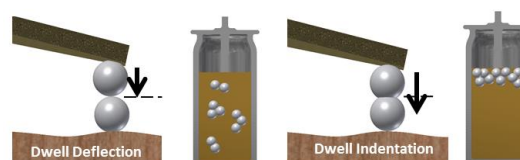


Figure 2 Particle-particle interactions measurement.

High resolution nanomechanical properties mapping.

Amplitude modulated force microscopy (AMFM) and Lorenz contact resonance spectroscopy (LCR) are emerging techniques that enable high resolution mapping of mechanical properties. These techniques were used to study the peptide-induced remineralisation of tooth structure (enamel and dentine). The effect of peptides on remineralisation was evidenced by the measurement of Young's modulus and dissipation energy (AMFM), and viscoelasticity (LCR) – Figure 3.

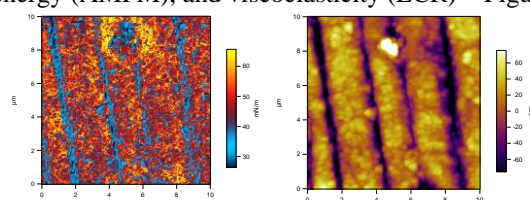


Figure 2 Map of stiffness and corresponding topography of dentine structure.

## RESULTS AND CONCLUSION

Cell mechanics – it was demonstrated that cell stiffness is directly correlated with the drug uptake and cell incubated with AA were softer and drug uptake was significantly upregulated Figure 1.

Particle-particle interactions – the energy and force of adhesion measured between the particles enable the optimisation of the particles morphology (roughness and porosity) and resulted in the design of more effective drug formulation.

Mapping of nanomechanical properties – AMFM and LCR allowed real time measurement of remineralisation of the tooth structure, and demonstrated the effects of peptides on this process.

## REFERENCES

1. Chrzanowski W., Dehghani F.: Standardised chemical analysis and testing of biomaterials; Woodhead Publishing Ltd, Cambridge, UK, 2013
2. D'Sa D, Chan H-K, Chrzanowski W. Predicting physical stability in pressurized metered dose inhalers via dwell and instantaneous force colloidal probe microscopy. European Journal of Pharmaceutics and Biopharmaceutics. 2014;88(1):129-35.



## Endothelial Cells on Biofunctionalized Polymeric Materials for Vascular Tissue Engineering

Lucie Bacakova<sup>1</sup>, Jaroslav Chlupac<sup>1</sup>, Elena Filova<sup>1</sup>, Jana Musilkova<sup>1</sup>, Katarina Novotna<sup>1</sup>, Tomas Riedel<sup>2</sup>, Vladimir Proks<sup>2</sup>, Ilya Kotelnikov<sup>2</sup>, Ognjen Pop-Georgievski<sup>2</sup>, Eduard Brynda<sup>2</sup>, Frantisek Rypacek<sup>2</sup>, Laurence Bordenave<sup>3</sup>

<sup>1</sup>Institute of Physiology, Academy of Sciences of the Czech Republic, Prague, Czech Republic

<sup>2</sup>Institute of Macromolecular Chemistry, Academy of Sciences of the Czech Republic, Prague, Czech Republic

<sup>3</sup>Inserm U577, Université Victor Segalen, Bordeaux, France

[lucy@biomed.cas.cz](mailto:lucy@biomed.cas.cz)

### INTRODUCTION

Synthetic polymers endowed with ligands for cell adhesion receptors are promising materials for vascular tissue engineering. These ligands can be attached to the polymers in two forms, i.e. (1) as entire protein molecules or (2) as oligopeptides derived from these proteins, recognized by cell adhesion receptors. These oligopeptides can also ensure binding of extracellular matrix molecules, which are necessary for replacing degradable materials with newly-formed tissue.

### EXPERIMENTAL METHODS

In the first set of experiments, knitted polyethylene terephthalate (PET) vascular prostheses (diameter 6 mm), impregnated with type I collagen (PET/Co), were modified in their lumen by coating them with a network of fibrin (Fb), i.e. a provisional matrix molecule participating in tissue regeneration, and they were seeded with primary human saphenous vein endothelial cells ( $15 \times 10^4/\text{cm}^2$ ). The cells were cultured for 72 h in a static culture system, and then they were exposed to laminar shear stress  $15 \text{ dyn/cm}^2$  for 120 min, generated by a custom-built hemodynamic chamber<sup>1</sup>.

In the second set of experiments, anti-fouling polydopamine-polyethylene oxide (pDOPA-PEO) films, suitable for deposition on PET, were functionalized with an RGD-containing peptide (azidopentanoyl-GGGRGDSGGGY-NH<sub>2</sub>) and a collagen-derived QRQVVGLOGQRGERGFOGLOG-NH<sub>2</sub> peptide binding fibronectin, referred to as Col. These peptides were used either alone or in combination (RGD+Col, ratio 1:1), and in concentrations of  $90 \text{ fmol/cm}^2$  or  $700 \text{ fmol/cm}^2$ . Vascular endothelial CPAE cells ( $17 \times 10^3/\text{cm}^2$ ) were cultured on these surfaces in a static system for 24 hours, and then in a dynamic system Mini Orbital Shaker SSM1 (Stuart) for 7 days.

### RESULTS AND DISCUSSION

After 3-day cultivation in the static system, the numbers of endothelial cells were similar on prostheses with and without an Fb coating. However, after dynamic cultivation, the cell population density on PET/Co dropped to 61%, while the cells on PET/Co+Fb did not show significant detachment (Fig. 1). This result is positive, especially considering the fact that fibrin can be isolated in autologous form from the patient's blood. One day after seeding, the number of cells adhering to surfaces with lower peptide concentrations was very low. On surfaces with RGD+Col, it did not even exceed the number obtained on bioinert pDOPA-PEO surfaces. However, at higher peptide concentrations, the number of cells on all functionalized surfaces approached the value on standard cell culture polystyrene dishes.

Moreover, the cells on surfaces with the RGD+Col combination showed the highest resistance to detachment during dynamic cultivation (Fig. 2).

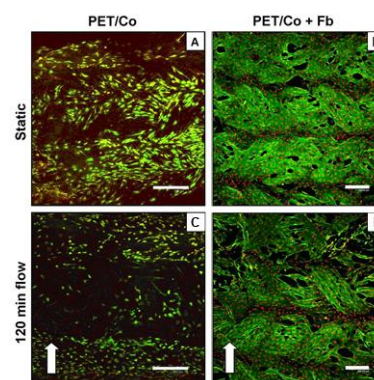


**Fig. 1.** Human saphenous vein endothelial cells on PET/Co (A, C) and PET/Co + Fb (B, D) 72 h after seeding in static conditions (A, B), and after subsequent application of 120 min of flow (C, D). The flow direction is indicated by the arrows.

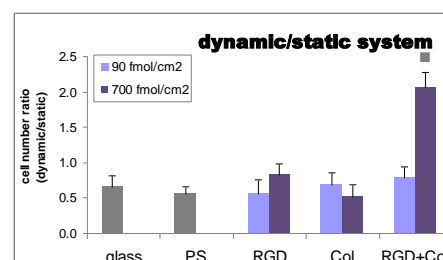


**Fig. 2.** The ratio of the cell numbers obtained in dynamic and static cell culture systems on day 7 after seeding on glass, on polystyrene dishes (PS), and on PEO surfaces with RGD, Col, or with a combination of RGD+Col in concentrations of  $90 \text{ fmol/cm}^2$  or  $700 \text{ fmol/cm}^2$  for each peptide. Mean  $\pm$  S.E.M. from 3 experiments. ANOVA, Student-Newman-Keuls method. <sup>##</sup> $P < 0.001$  compared to the other samples.

### CONCLUSION

The surfaces functionalized with a fibrin network or with a combination of an RGD-containing peptide with a collagen-derived peptide binding fibronectin showed the highest retention of the endothelial cells under dynamic stress. These modifications are suitable for endothelialization of vascular prostheses.

### REFERENCES

1. Chlupac J. *et al.*, Physiol. Res. 63: 167-177, 2014.

### ACKNOWLEDGMENTS

The authors would like to thank the Grant Agency of the Czech Republic (P108/12/G108) for providing financial support for this project.



### 3D Printing of Crosslinkable Gelatins: Overcoming the Mechanical Boundaries

Jasper Van Hoorick<sup>1</sup>, Heidi Declercq<sup>2</sup>, Maria Cornelissen<sup>2</sup>, Hugo Thienpont<sup>1,3</sup>, Aleksandr Ovsianikov<sup>4</sup>, Peter Dubrue<sup>1</sup>,  
Sandra Van Vlierberghe<sup>1,3</sup>

<sup>1</sup>Department of Organic and Macromolecular Chemistry, Ghent University, Belgium

<sup>2</sup>Tissue Engineering Group, Department of Basic Medical Sciences, Ghent University, Belgium

<sup>3</sup>Brussels Photonics Team, Department of Applied Physics and Photonics, Vrije Universiteit Brussel, Belgium

<sup>4</sup>Institute of Materials Science and Technology, Vienna University of Technology, Austria

[Sandra.VanVlierberghe@UGent.be](mailto:Sandra.VanVlierberghe@UGent.be)

## INTRODUCTION

Two Photon polymerization (2PP) is a rapid prototyping technique which benefits from the two photon absorption principle, resulting in the production of scaffolds characterized by a very high resolution with nearly no structural limitations. Gelatin is an ideal scaffolding material due to the presence of RGD peptides which render this protein very cell-interactive.<sup>1</sup> However, currently applied photo-crosslinkable gelatin derivatives lack sufficient mechanical properties for 2PP processing in adequately diluted conditions to enable metabolite and nutrient transfer. To overcome these limitations, the present work aims to develop gelatin-based hydrogels with tunable mechanical properties which reach beyond the capabilities of conventionally applied methacrylamide-modified gelatin (gel-MOD).

## EXPERIMENTAL METHODS

In a first part, the free amines present in gelatin B were functionalized using 2.5 equivalents methacrylic anhydride in a phosphate buffered solution (pH 7.3) (10 w/v%) to obtain gel-MOD with a degree of substitution (DS) of 97%. Additional crosslinkable functionalities were introduced via reaction of the carboxylic acids in gel-MOD with 2 aminoethylmethacrylate (AEMA) (2 equivalents) via conventional EDC/NHS coupling in DMSO under inert atmosphere ( $DS_{COOH} = 30\%$ ). Via film casting, 10 w/v% solutions of gel-MOD (DS 97%) and gel-MOD-AEMA containing 2 mol% of Irgacure 2959 were crosslinked by applying UV-light (365 nm) for 30 minutes. The obtained hydrogels were characterized using DSC, gel fraction/swelling tests, rheology and (HR-MAS) <sup>1</sup>H-NMR spectroscopy. Finally, the biocompatibility was assessed via live/dead staining experiments and a proof-of-concept for 2PP processing was established.

## RESULTS AND DISCUSSION

A first remarkable finding, in contrast to non-modified gelatin and gel-MOD was the solubilization of the gel-MOD-AEMA hydrogel precursors at room temperature. To investigate this phenomenon in depth, DSC experiments were performed which displayed a drop in UCST together with a significant reduction in the associated energy concomitant with this phase transition. Both gel fraction tests as well as HR-MAS <sup>1</sup>H NMR spectroscopy indicated a higher crosslinking efficiency for the AEMA derivatives developed. Real-time rheological monitoring of the crosslinking reaction

further supported the proposed hypothesis. The gel-MOD-AEMA derivative exhibited a storage modulus roughly twice the value of the gel-MOD derivative (see Figure 1). Furthermore, live/dead staining experiments revealed a comparable biocompatibility for both derivatives.

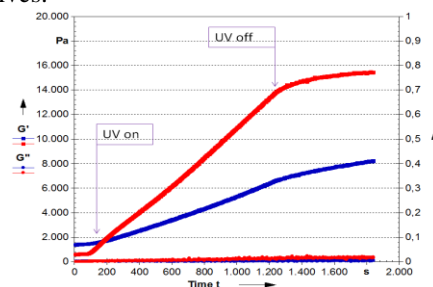


Figure 1: Rheological properties of gel-MOD (blue) and gel-MOD-AEMA (red) during UV crosslinking.

In a final part, preliminary 2PP processing experiments illustrated the potential of the novel hydrogels with respect to reproducibility and structural integrity of the scaffolds developed as gelatin solutions with concentrations of 10 w/v% and below could be processed. The latter is of crucial importance since low concentrations enable superior diffusion of oxygen and metabolites through the scaffolds.<sup>2</sup> The porous scaffolds are currently also being evaluated as cell carriers for tissue engineering purposes.

## CONCLUSIONS

The incorporation of additional crosslinkable functionalities through the reaction of the carboxylic acids present in gel-MOD using AEMA provides an excellent method to increase the structural integrity of gelatin-based hydrogels. Furthermore, the derivatization does not affect the material cytocompatibility. The results further increase the potential of 2PP starting from gelatin-based hydrogel building blocks to yield optimal, mechanically tailored hydrogel scaffolds for soft tissue engineering applications.<sup>1</sup>

## REFERENCES

- 1.Ovsianikov, A. *et al.*, *Biomacromolecules* 12:851-858, 2011
- 2.Billiet, T *et al.*, *Biomaterials* 35:49-62, 2014

## ACKNOWLEDGMENT

The authors would like to acknowledge the Research Foundation Flanders for financial support.



## Polypeptide Nanoparticles for Ocular Drug Delivery

Neil R. Cameron

Department of Materials Engineering, Monash University, Clayton 3800, Victoria, Australia

[Neil.cameron@monash.edu](mailto:Neil.cameron@monash.edu)

### INTRODUCTION

Polypeptides are ideal materials for ocular drug delivery vehicles due to their biocompatibility and biodegradability [1]. Polypeptides of desired molecular weight possessing tunable properties, can be synthesized from amino acid building blocks in a controlled manner using ring-opening polymerization (ROP) of *N*-carboxyanhydride (NCA) monomers. In this work, peptide-based nanostructures for ocular drug delivery have been prepared from polypeptides which were synthesized by controlled ROP of NCAs, using modified previously described procedures [2, 3].

### EXPERIMENTAL METHODS

Block copolypeptides were prepared by sequential monomer addition without intermediate purification steps. Different target molecular weights and block ratios were obtained by varying the monomer to (macro)initiator ratio. Example procedure: *N*-Benzyltrimethylsilylamine in DMF (127  $\mu$ L) was added to NCA 1 (0.38 mmol) in 1.5 mL of dry DMF in a Schlenk tube pre-filled with nitrogen, and allowed to stir for 24 h. NCA 2 (0.38 mmol) was then added to the reaction mixture. After 24 h of additional stirring the solution was poured into a 20-fold excess of diethyl ether with stirring. The precipitated solid was collected by centrifugation to afford the block copolypeptide (yield 184 mg, 91%) as a white powder.

Self-assembly into nanoparticles was performed as follows: polymers were first dissolved in THF at a concentration of 1.0 mg mL<sup>-1</sup>. Filtered MilliQ water was added to the solution and it was stirred overnight, allowing the THF to evaporate. If necessary, the solutions were finally filtered through a 0.45  $\mu$ m filter. The final polymer concentration in water was 1.0 mg mL<sup>-1</sup>.

### RESULTS AND DISCUSSION

A range of amphiphilic polypeptide block copolymers was prepared by sequential ring-opening polymerisation of NCAs. Representative data are presented in Table 1. Polymerisations were controlled giving molecular weights that agreed well with predicted values, and narrow dispersities.

Table 1. Characterisation Data for Polypeptide Block Copolymers

Sample	Expected $M_n$ [Da]	Obtained $M_n$ [Da]	$\bar{D}_M$
PBnE <sub>30</sub> - <i>b</i> -ZK <sub>30</sub>	14,700	15,800	1.17
PBnE <sub>30</sub> - <i>b</i> -ZK <sub>15</sub>	10,607	14,500	1.17
PBnE <sub>50</sub> - <i>b</i> -ZK <sub>50</sub>	24,157	30,500	1.27
PBnE <sub>50</sub> - <i>b</i> -ZK <sub>25</sub>	17,607	20,400	1.28

BnE =  $\gamma$ -benzyl-L-glutamic acid NCA; ZK =  $\epsilon$ -carbobenzyloxy-L-lysine NCA; subscript denotes block length.

Block copolypeptides were assembled into nanostructures (micelles or vesicles, depending on copolymer composition) by the solvent evaporation method. Nanostructure characterisation was performed by TEM and dynamic light scattering. The diameter of the nanostructures obtained varied from around 40nm to around 200nm.

Nanoparticles were loaded with dexamethasone (Dx), an anti-inflammatory drug used in treating ocular diseases. Repeated preparation of the Dx-loaded nanoparticles showed excellent reproducibility, giving an average particle diameter of around 180 nm. The release of Dx was then monitored at 37 °C over 16 days (polymer:Dx = 20:1). The Dx loading was 5.5 wt% (HPLC) and loading efficiency was 90%. Around 20% burst release of dexamethasone was observed in the first 24 hours, after which the release was steady over the remaining period of the study. After 16 days, 94% of the loaded dexamethasone had been released (Figure 1).

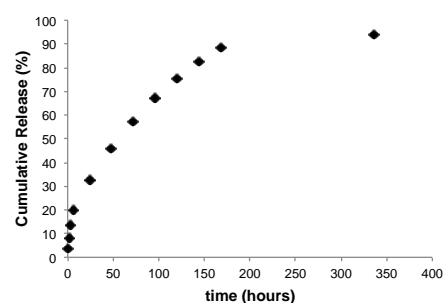


Figure 1. Release of dexamethasone from PE<sub>50</sub>-*b*-ZK<sub>25</sub> nanoparticles.

### CONCLUSION

Nanoparticles composed of block copolypeptides have been prepared and shown to be capable of releasing the ocular drug dexamethasone over 16 days.

### REFERENCES

1. J.V. González-Aramundis, *et al.*, Expert Opin. Drug Deliv. 9:183-201, 2012.
2. H. Lu, *et al.*, J. Am. Chem. Soc. 130:12562-12563, 2008.
3. T. Stukenkemper, *et al.* Macromol. Biosci. 15:138-145, 2015.

### ACKNOWLEDGMENTS

We thank the EC for funding under the FP7 programme (NMP4-SL-2010-246180)





Laura Poole-Warren<sup>1</sup>, Josef Goding<sup>1</sup>, Ulises Aregueta-Robles<sup>1</sup>, Alexander J. Patton<sup>1</sup>, Penny Martens<sup>1</sup>, Rylie A. Green<sup>1</sup>

<sup>1</sup>Graduate School of Biomedical Engineering, UNSW Australia  
[l.poolewarren@unsw.edu.au](mailto:l.poolewarren@unsw.edu.au)

## INTRODUCTION

Soft biomedical electrodes open up new frontiers for neural applications. Fabricated by growth of conducting polymers (CPs) within hydrogels, soft conducting hydrogel (CH) electrodes support integration of living cells. The concept is based on encapsulating living cells within biosynthetic hydrogels designed to overlay the CH as shown in Figure 1. Such tissue-engineered electrodes will deliver the capacity for more direct, physiological stimulation of target neural tissues<sup>1</sup>.

CHs are typically formed on metal electrode substrates to produce robust adhesive coatings (Fig 1). Although this approach is suitable for neural applications using metal electrodes, development of standalone soft conductive materials will support applications where electrode compliance is critical. An example is in soft electroactive cardiovascular patches. The primary aim of this research was to investigate robust approaches for fabricating CH coatings and standalone CHs. Glial cell responses to the CH and to encapsulation within biosynthetic hydrogel constructs were also examined.

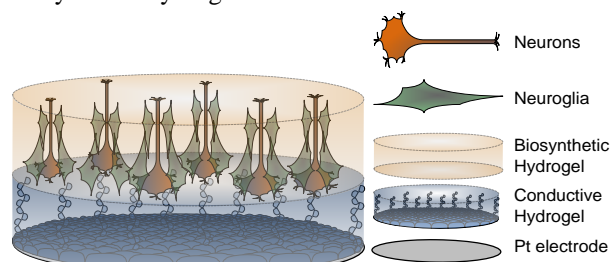


Figure 1. Schematic of tissue engineered electrode.

## EXPERIMENTAL METHODS

Nucleation of CP growth within hydrogels was achieved using two key approaches. The first was modification of 16kDa poly(vinyl alcohol) (PVA) hydrogel backbone with taurine, a low molecular weight (MW) sulphonic acid designed to act as an immobilised dopant. The second approach was blending dispersions of chemically synthesised poly(3,4-ethylene dioxithiophene): poly(styrenesulfonate) (PEDOT:PSS; Orgacon<sup>TM</sup>) with PVA hydrogels<sup>4</sup>. Following cross-linking of hydrogels at polymer concentrations up to 20 wt% via UV photo-polymerisation, electrodeposition of PEDOT within EDOT loaded hydrogels was conducted<sup>2</sup>. Characterisation of electrical properties was conducted by cyclic voltammetry and impedance spectroscopy. Cytotoxicity of modified PVA hydrogels was assessed via contact inhibition studies using primary astrocyte enriched glial cell (GC) cultures. Degradable hydrogels were fabricated based on tyramine modified 16kDa PVA (see Lim *et al*<sup>3</sup>) and Schwann cell (SC) response was studied after encapsulation for up to 21 days.

## RESULTS AND DISCUSSION

Robust CH coatings and standalone CH were successfully fabricated. CH coatings had smooth hydrogel-like surfaces (Fig 2a) in contrast with typical rough and friable electrodeposited PEDOT/PSS. Electrical properties of both CH materials were comparable with control conducting polymers based on PEDOT/PSS.

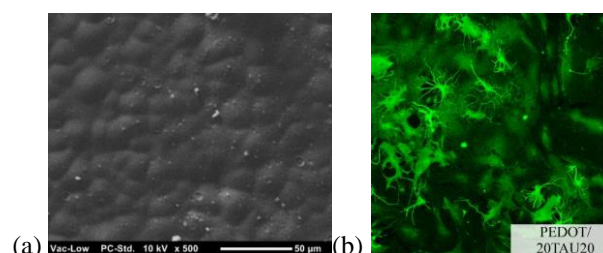


Figure 2. (a) SEM of CH based on 20%PVA modified with ~10 taurine/chain (b) GC cultures following contact with PVA-taurine CH.

Contact inhibition studies showed that GC survived 14 days contact with CH (see Fig 2b). SC encapsulated in the “overlay” degradable PVA hydrogel showed significant growth and matrix production over 21 days *in vitro*. These results confirm that the concept of a layered tissue-engineered construct is feasible.

## CONCLUSION

Elegant strategies confirmed for incorporating dopants into hydrogels included low MW dopant immobilisation on the polymer backbone and blending high MW CP plus dopant into the hydrogel. The capacity to fabricate CH as adhesive coatings or as standalone CH was also demonstrated. *In vitro* studies showed these materials have utility for biomedical device applications. These findings show that this flexible platform is a significant step towards realising standalone tissue engineered electrodes for neural and cardiovascular applications.

## REFERENCES

1. Aregueta-Robles *et al*, Front Neuroeng. 2014, 27; 7:15
2. Green *et al*, Macromol. Biosci. 2012, 12, 494–501
3. Lim *et al*, Biomaterials, 2013, 34(29): p. 7097-7105
4. Patton *et al*. APL Materials, 3, 014912 (2015); <http://dx.doi.org/10.1063/1.4904820>

## ACKNOWLEDGMENTS

Funding by Ramaciotti Foundation Establishment Grant ES2012/0106 and Australian Research Council (ARC) Special Research Initiative (SRI) in Bionic Vision Science and Technology grant to Bionic Vision Australia (BVA) are acknowledged.



Che J. Connon<sup>1</sup>, Ricardo M. Gouveia<sup>1</sup>, Valeria Castelletto<sup>2</sup>, and Ian W. Hamley<sup>2</sup><sup>1</sup>Faculty of Medicine, Newcastle University, United Kingdom<sup>2</sup>School of Chemistry, Food and Pharmacy, University of Reading, United Kingdom[che.connon@newcastle.ac.uk](mailto:che.connon@newcastle.ac.uk)

## INTRODUCTION

One of the main challenges in tissue engineering is the creation of a suitable *in vitro* environment in which cells derived from native tissue (such as stem cells) can be seeded, grown, and induced to differentiate as they do *in vivo*<sup>1</sup>. There are numerous examples in the literature and in the clinic of artificial environments that provide such a milieu of factors and conditions including smart or intelligent scaffolds that respond to cells with culture progression. Peptide amphiphiles (PAs) constitute a notable example of such self-assembling materials<sup>2</sup>.

This smart coating was formed from a self-assembling peptide amphiphile comprising a protease-cleavable sequence contiguous with a cell-attachment and signaling motif. This multi-functional material was subsequently used not only to instruct human corneal or skin fibroblasts to adhere and deposit discrete multiple layers of native extracellular matrix, but also govern their own self-directed release from the template solely via the action of endogenous metalloproteases (MMP).

## EXPERIMENTAL METHODS

C16-TPGPQG↓IAGQRGDS peptide amphiphile was custom-synthesized by CS Bio (Menlo Park, USA) and spotted and dried on to low-attachment tissue culture plastic at an initial concentration range of  $1 \times 10^5$ - $10^2$  M. After washing, human fibroblasts were cultured on the PA coatings in serum conditions initially in the presence of retinoic acid (RA) to suppress endogenous MMP expression<sup>3</sup> for 90 days followed by 3 days in the absence of RA to illicit MMP derived cleavage of the PA coating and tissue detachment (n=12). Subsequent reattachment of the newly formed tissues onto fresh PA coatings was repeated 3 times (Fig 1). Characterization of the tissue at a gene, protein and ultra structural level was undertaken by qPCR, immuno-blotting, confocal and electron microscopy and compared against normal tissue (skin and cornea) values.

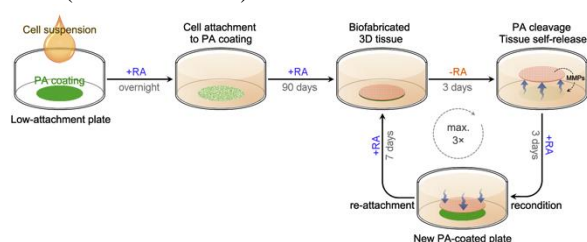


Fig 1. Schematic depicting how cells isolated from human donors were seeded and grown on MMP sensitive PA coatings in RA supplemented media. Lifted tissues were then easily recoverable for repeated reattachment and re-lifting processes.

## RESULTS AND DISCUSSION

The newly-shaped tissues governed their own release from the template via the action of endogenous proteases. Tissues recovered through this physiologically relevant process were carrier-free, and structurally and phenotypically equivalent to their natural counterparts (Fig 2). The tissues were shown to be functional (via contraction assay) (Fig 3).

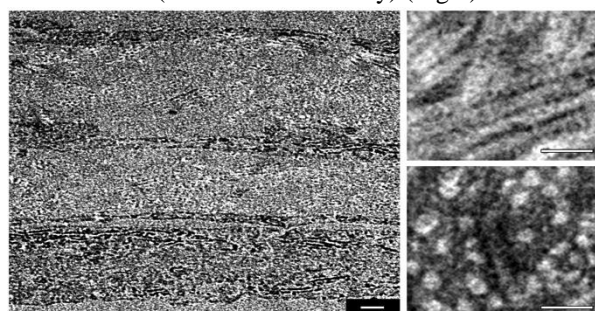


Fig 2. Transmission electron microscopy, evidencing the multi-layered organization of the tissue, with intercalating layers of fibroblasts and deposited ECM comprised of densely-packed collagen fibrils. Scale bars 500nm (left), 100nm (right).

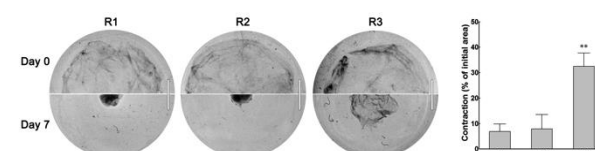


Fig 3 Myofibroblastic activity of fibroblasts from self released tissues after incubation in serum-containing medium following 3x reattachment (R1-3) at day 0 and day 7. Quantification of tissue contraction expressed as ratio between final and initial area of tissue.

## CONCLUSION

The resulting technology contributes to a new paradigm in regenerative medicine whereby materials are able to actively direct and respond to cell behavior. The novel application of materials as a template coating, directing the formation and detachment of complex tissues solely under physiological conditions, will undoubtedly have broad use in future cell and tissue therapies.

## REFERENCES

1. Griffith, LG *et al.* Nat. Rev 7:211-224, 2006
2. Boekhoven, J & Stupp, SI Adv. Mat 2014
3. Gouveia, RM *et al.* IOVS 54:7483-7491, 2013

## ACKNOWLEDGMENTS

BBSRC, UK (I008187/1) for financial support

### 3D Fiber Deposition and Stereolithography Techniques for the Design of Multifunctional Nanocomposite Magnetic Scaffolds

Roberto De Santis, Ugo D'Amora, Teresa Russo, Alfredo Ronca, Antonio Gloria, Luigi Ambrosio

Institute of Polymers, Composites and Biomaterials, National Research Council of Italy, V. le J.F. Kennedy 54 - Pad. 20,  
Mostra d'Oltremare, 80125 Naples, Italy

[rosantis@unina.it](mailto:rosantis@unina.it)

#### INTRODUCTION

The concept of magnetic guidance usually spans from drug delivery and hyperthermia treatment of tumors, to magneto-mechanical stimulation/activation of cell constructs and mechanosensitive ion channels such as magnetic cell seeding procedures and controlled cell proliferation and differentiation. The possibility to extend these concepts to tissue engineering has opened an exciting wide research area of interest.<sup>1-4</sup> The aim of the present work was to assess morphological, mechanical, magnetic and biological performances of nanocomposite magnetic scaffolds obtained through rapid prototyping techniques (RP).

Among all the RP techniques, 3D fiber deposition and stereolithography may provide a morphologically controlled and tailored structure with interconnected pores of specific scale. Furthermore, a superparamagnetic scaffold should provide the fascinating possibility to magnetically "switch-on/switch-off" it in order to deliver biofactors and stem cells, or to stimulate cell adhesion, proliferation and differentiation.

#### EXPERIMENTAL METHODS

Firstly, 3D well-organized cylindrical poly( $\epsilon$ -caprolactone) (PCL) and poly( $\epsilon$ -caprolactone)/magnetic nanoparticles (PCL/MNPs) nanocomposite magnetic scaffolds were manufactured through 3D fiber deposition technique by alternatively plotting fibers along 0°/90° lay-down pattern. Successively, 3D mathematically defined porous polyethylene glycol diacrylate/magnetic nanoparticles (PEGDA/MNPs) scaffolds with a diamond architecture were prepared through stereolithography technique. To this aim, MNPs were mixed in different amount with a solution of PEGDA as photocrosslinkable oligomers, Lucirin TPO-L as biocompatible UV photo initiator, and Orasol Orange G as dye.

The performances of the designed scaffolds were assessed by means of experimental/theoretical *in vitro* investigations. In particular, morphological studies were performed through micro-computed tomography (Micro-CT) and scanning electron microscopy (SEM). Nano-, Micro- and Macro-mechanical analyses were carried out through nanoindentation, tensile and compression tests, respectively.

Human mesenchymal stem cells (hMSCs) were statically seeded on 3D cylindrical scaffolds in order to study the effect of a static and a time-dependent magnetic stimulation on cell adhesion and spreading. Cell viability/proliferation was assessed by using

Alamar Blue assay, whilst cell differentiation was evaluated by ALP activity.

#### RESULTS AND DISCUSSION

Micro-CT and SEM analyses highlighted that 3D fiber deposition and stereolithography are able to manufacture morphologically-controlled scaffolds.

Results from compression and tensile tests showed that beyond a specific limit of MNP amount, by further increasing the nanoparticle concentration, the mechanical performances of the nanocomposite scaffolds decrease because the nanoparticles act as "weak points" instead of reinforcement for the polymeric matrix. In order to locally map mechanical properties, nanoindentation tests were performed showing interesting results in terms of hardness and reduced modulus. Magnetic analysis revealed a superparamagnetic behavior of these materials.

Results obtained from the biological analyses showed that prolonged exposure time to the static or dynamic magnetic field seems to negatively affect cell viability. It is worth noting that in terms of cell viability/proliferation there were some differences between magnetically and not magnetically stimulated scaffolds. Confocal analyses highlighted interesting results in terms of cell adhesion and spreading. An increase in adhered number and a more evident spreading of hMSCs were evidenced. On the other hand, the Alamar Blue assay and ALP/DNA measurements provided a quantitative evaluation of cell viability/proliferation and differentiation, respectively over the culture time.

#### CONCLUSION

3D nanocomposite magnetic scaffolds obtained through RP techniques should be considered as a potential alternative to bone graft substitute with attractive new performances.

#### REFERENCES

1. De Santis R., et al., J. Appl. Polym. Sci., 122: 3599–3605, 2011.
2. Gloria A. et al., J. R. Soc. Interface. 80 (10): 1, 2013.
3. Russo T. et al., Procedia Eng., 59: 233 – 239, 2013.
4. De Santis R. et al., J. Biomed. Nanotech. 11: 1236-1246, 2015.

#### ACKNOWLEDGMENTS

The authors would like to thank MAGISTER project (NMP3-LA-2008-214685), and FIRB MERIT project (GAE: P0000570) for providing financial support.





## Polymer Brush-Assisted Fabrication of Protein Gradients inside of 3D Microporous Scaffolds

Andrea Di Luca<sup>1</sup>, Michel Klein Gunnewiek<sup>2</sup>, Hermen Bollemaat<sup>2</sup>, Clemens van Blitterswijk<sup>1,4</sup>, Julius Vancso<sup>2</sup>, Edmondo Benetti<sup>2,3</sup>, [Lorenzo Moroni](mailto:l.moroni@maastrichtuniversity.nl)<sup>1,4</sup>

<sup>1</sup>Department of Tissue Regeneration, University of Twente, The Netherlands

<sup>2</sup>Department of Materials Science and Technology of Polymers, University of Twente, The Netherlands

<sup>3</sup>Department of Materials, ETH Zurich, Switzerland

<sup>4</sup>Department of Complex Tissue Regeneration, University of Maastricht, The Netherlands

[l.moroni@maastrichtuniversity.nl](mailto:l.moroni@maastrichtuniversity.nl)

### INTRODUCTION

Regenerative medicine holds the promise to create continuous body-part replacements through the combination of cells, biological factors, and scaffolds. First generation products consisted of cells in solution, combined with injectable hydrogels, or seeded on 3D fleeces. Although the initial response to these treatments showed excellent results, long-term follow-ups revealed the formation of fibrotic-like tissue with lower functionality compared to the targeted tissue to regenerate. One of the current viable alternative imply the use of stem cells. Yet, a better control over cell-material interactions need to be achieved to transform this promise into better performing and long-lasting products. In particular, it is still critical to control stem cell differentiation into 3D scaffolds. In our bodies stem cell differentiation is ruled by physical and chemical gradients. Therefore, the design of next scaffold generation should take into account how these phenomena can be actively controlled. In this study, we present a new technique to produce three-dimensional (3D) gradients of protein concentrations within microporous, biodegradable scaffolds.

### EXPERIMENTAL METHODS

The 3D supports were manufactured by fused deposition modeling (SysENG, Germany) of poly-ε-caprolactone (PCL), forming a regularly layered network of microfibers with diameter ( $d_1$ ) = 250 μm, spacing ( $d_2$ ) = 650 μm, layer thickness ( $d_3$ ) = 150 μm. From these values the theoretical porosity (~50%) of the scaffold was calculated.

Uniform coating of the scaffold surface with “grafted-from” poly[oligo(ethylene glycol) methacrylate] (POEGMA) brush was adapted from previously published studies on two-dimensional substrates [1]. The coating allowed covalent immobilization of proteins from solution and the formation of 3D protein gradients within the supports. POEGMA brushes on PCL scaffolds were activated by placing them in a dry DMSO solution containing 200 mM of DSC and DMAP. Later on, the samples were incubated in a protein solution containing either 0,4 μM fluorescently labeled BSA or 0,1 μM fibronectin (FN), 10 μM bone morphogenetic protein-2 (BMP2), or 10 μM transforming growth factor β1 (TGF-β1).

Bone marrow derived human mesenchymal stromal cells (hMSCs) were seeded at a density of 500,000 cells in 40 μL per scaffold. After 4 hours, cell culture media was added and cultures were maintained for up to 10 days. Cell adhesion was observed by microscopy, while cell differentiation by polymerase chain reaction and

biochemical assays for the expression and production of specific osteogenic and chondrogenic markers.

### RESULTS AND DISCUSSION

The hydrophilic character of thin brush coatings (10-50 nm thick) strongly affected surface energy and capillary forces within the microporous structure, consequently allowing the controlled diffusion of protein solutions inside the pores. Additionally, the multifunctional character of POEGMA brush enabled the efficient and stable bio-conjugation of proteins via covalent linkages. 3D axial and radial protein gradients were, thus, fabricated enabling a variation of the functional group distribution by varying diffusion time and volume of diffusing solution (Figure 1). Finally, we fabricated different gradients of brush-supported FN, BMP-2, and TGF-β1. The subsequent seeding with hMSCs showed spatially determined cell immobilization and to a certain extent differentiation within the 3D support according to the protein gradient.

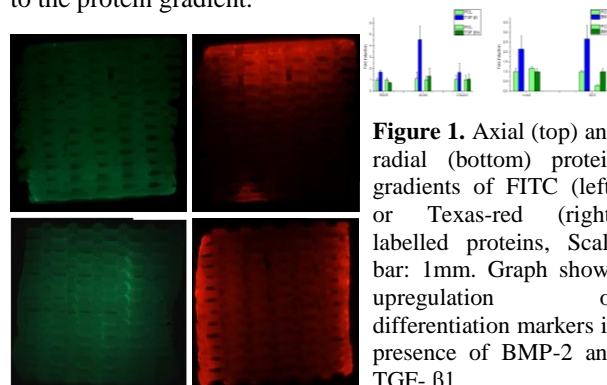


**Figure 1.** Axial (top) and radial (bottom) protein gradients of FITC (left) or Texas-red (right) labelled proteins, Scale bar: 1mm. Graph shows upregulation of differentiation markers in presence of BMP-2 and TGF-β1.

### CONCLUSION

We have developed a versatile method to present different configuration of protein gradients, which showed to effectively control spatial cell distribution and hold potential to further control cell differentiation.

### REFERENCES

1. Klein Gunnewiek M. *et al.*, J. Austral Chem. 29:1384-52, 2013

### ACKNOWLEDGMENTS

This work was financially supported the Technology foundation STW (STW, 11135). Some of the materials employed in this work were provided by the Texas A&M Health Science Center College of Medicine Institute for Regenerative Medicine at Scott & White through a grant from NCRR of the NIH (Grant # P40RR017447).



Agnieszka Piegat, Mirosława El Fray

West Pomeranian University of Technology, Polymer Institute,  
 Division of Biomaterials and Microbiological Technologies, Al. Piastów 45, Szczecin, Poland  
[mirfray@zut.edu.pl](mailto:mirfray@zut.edu.pl)

## INTRODUCTION

Thermoplastic elastomers (TPE) belongs to high performance polymers with good solvent resistance, elasticity, tear strength and flex fatigue. They already found a wide range of applications in medicine such as medical tubing or equipment parts. Selected TPEs are also used for implant applications [1]. Polyurethane TPU are already used as “gold standard” in blood contacting medical devices, including artificial heart. Their major problem, however, is mechanical instability under cyclic dynamic loading [2] due to environmental cracking. However, there are no literature data reporting how much of the total organic carbon is extracted from PU what could shade the light on their performance. This paper will discuss the static mechanical and dynamic fatigue properties of medical grade polyurethane (PCU) and new segmented polyester TPE containing dimerized fatty acid (PET-DLA), proposed as alternative material to PCU. We will try to find dependence between mechanical performance in simulated body fluid (SBF) and total organic carbon (TOC) extracted from the materials.

## METHODS

Static mechanical testing was performed with Instron 3366 according ISO 527-1:1998. Fatigue testing was carried out using a servo-hydraulic test machine with a digital controller (Instron Electropulse), equipped with a 200-N load cell, a 10 kN cylinder and an environmental chamber. For all tests, the load ratio  $R = \sigma_{\min}/\sigma_{\max}$  was held constant at 0.1. The strain was measured as the real-time clamp displacement. The possible phase shift between the stress and strain signals were minimized below 20  $\mu$ s by the experimental set-up. Testing in simulated body fluid (SBF) was carried out at 24 and 37°C. Testing was carried out using the SILT (Stepwise Increasing Load Test) and SLT (Single Load Test) methods [3]. Water extraction was carried out on material previously purified by solvent extraction. Polymer granules were immersed in water at 37°C for 3, 7, 14, 21 and 28 days in shaking incubator. As reference material, commercially available PCU was used. Water extracts were used for determination of total organic carbon (TOC), turbidity, conductivity and total dissolved solids.

## RESULTS AND DISCUSSION

PET-DLA material containing 60wt% hard segments showed static mechanical properties comparable to medical grade PCU (Table 1). The stepwise increasing load test has been performed for 12K cycles and then, single load test has been performed for 1 mln cycles at ambient temperature (24°C) and in SBF and at 37°C. PCU experienced tremendous dynamic creep ( $\Delta\epsilon$ ), especially at

body temperature (37°C). PET-DLA copolymer showed very good stability of mechanical properties during long term testing. Such different behaviour in PU and PET-DLA can be interpreted based on Takahara's *et al.* [4] suggestions regarding the fatigue of segmented polyurethanes that under the cyclic deformation, the destruction of the hard segment domain and/or intermixing of the hard and soft segments can take place. Interestingly, PCU showed much higher total organic carbon content derived from water extracts as compared to PET-DLA (Fig. 1). This indicates again, much higher chemical stability of PET-DLA as compared to PCU.

**Table 1** Comparison of mechanical properties

Material	$\sigma$ (MPa)	$\epsilon$ (%)	$\Delta\epsilon$ @ 24°C (%)	$\Delta\epsilon$ @ 37°C (%)
PCU	$54.3 \pm 3.2$	$435.9 \pm 26.6$	20.9	217.3
PET-DLA	$24.1 \pm 2.9$	$566.7 \pm 42.1$	3.2	6.5

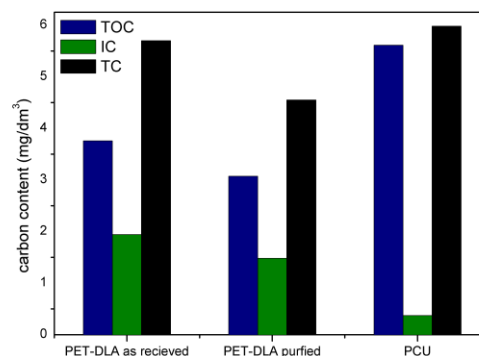


**Figure 1:** The carbon content in water extracts from materials.

## CONCLUSIONS

The hysteresis method seems to be a useful new method to evaluate the dynamic behavior of elastomeric biomaterials. From this method, and from the extraction results, it can be concluded that PET-DLA showed improved dynamic fatigue properties and higher chemical stability as compared to PCU material.

## REFERENCES

1. G. Holden, et al, *Thermoplastic Elastomers*, 2<sup>nd</sup> Ed., Hanser Publishers, Munich Vienna New York, 1996
2. Hayashi, K. et al. (1985) *Biomaterials*, **6** (2), pp. 82-88
3. M. El Fray, V. Altstaedt, *Polymer*, (2003), **44**, 4635-4642
4. A. Takahara, et al, *J. Biomed. Mater. Res.* (1985) **19**, 13-34

## ACKNOWLEDGEMENTS

Financial support by research grant no: PBS1/A5/2/2012 is acknowledged.



# Oral Presentations



## Osteocyte Function in Regulating Osteoclast Differentiation on Ceramic Biomaterials

Miho Nakamura<sup>1</sup>, Teuvo Hentunen<sup>2</sup>, Jukka Salonen<sup>2</sup>, Naoko Hori<sup>1</sup> and Kimihiro Yamashita<sup>1</sup>

<sup>1\*</sup>Institute of Biomaterials and Bioengineering, Tokyo Medical and Dental University, Japan

<sup>2</sup>Institute of Biomedicine/Cell Biology and Anatomy, University of Turku, Finland  
[miho.bcr@tmd.ac.jp](mailto:miho.bcr@tmd.ac.jp)

### INTRODUCTION

Ceramic biomaterials are used for clinical applications as bone grafts to reconstruct bone tissue in defects. Both bone-forming osteoblasts and bone-resorbing osteoclasts play prominent roles in bone formation surrounding the implanted ceramic biomaterials. Osteoclast formation are regulated by osteocytes embedded in bone matrix through the expression of receptor activator of nuclear factor- $\kappa$ B ligand (RANKL)<sup>1</sup>.

We designed the osteocyte-stimulating biomaterials without addition of any growth factors. Osteocytes are most abundant cells in bone, buried in the mineralized bone matrix. Although the osteocytes are used for the evidence for the osteoblast differentiation from the osteoblast progenitors, there are few studies on the interaction between the osteocytes and ceramic biomaterials. In the present study, the interactions of osteocytes with bone marrow cells through the cell-to-cell communications on various types of ceramic biomaterials, were investigated.

### EXPERIMENTAL METHODS

**Cell culture:** Osteocyte-like cells<sup>2</sup> (MLO-Y4, kindly gifted from Prof. Bonewald) were co-cultured with bone marrow cells (BMC) isolated from mouse femurs (C57Bl/6J, male, 10-week-old) on the synthesized ceramic biomaterials such as hydroxyapatite (HA), carbonate apatite (CA) and bone slices as a control.

The fixed cells were also stained for tartrate-resistant acid phosphatase (TRAP) to confirm the differentiation of BMC into osteoclasts. The cells adhered to the samples were stained with rhodamine-phalloidin and Hoechst. After removing the cells, the resorption pits were observed using scanning electron microscope and quantified using laser microscope.

**Implantation into rat femurs:** The ceramic biomaterials were surgically implanted in the femoral diaphysis of Wistar rats (13-week-old, male). At 7 d after the implantation surgery, the femurs were extracted and immersed in 4% paraformaldehyde. After fixation, each sample was decalcified with 10% neutralized ethylenediamine tetraacetic acid (EDTA), dehydrated in an ascending gradient of ethanol concentrations, cleared in xylene, embedded in paraffin, and cut into 5- $\mu$ m sections. Each section was deparaffinized with xylene, rehydrated with ethanol, and stained with hematoxylin and eosin (HE) and for TRAP using standard methods.

### RESULTS AND DISCUSSION

The giant cells with multiple nuclei were formed both on the synthesized CA and bone slices after a co-culture of MLO-Y4 with BMC. These cells were positively stained for TRAP, which indicated that they were differentiated from BMC into osteoclastic cells without any added differentiation factors. Actin rings, which are specific markers for activated osteoclasts to resorb the substrata, were formed in osteoclasts on the CA and bone slices. As a result, the resorption pits were formed on CA and bone slices. The possible explanations of the enhanced differentiation and activation of osteoclastic cells on the CA are the cell-to-cell interactions and secretion of differentiation factors from MLO-Y4 cells.

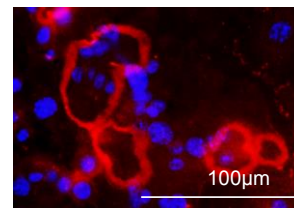


Fig. Actin rings were formed on the synthesized CA after co-culture of osteocyte-like cells with bone marrow cells without any differentiation factors.

After the implantation of ceramic biomaterials for 7 d into the rat femur, most of the HA surfaces were covered with fibrous tissue layers containing nucleated spherical and flattened fibroblastic cells. Newly formed bones were also found in the regions approximately 100–200  $\mu$ m away from the implanted CA5. Giant and multinuclear osteoclastic cells were found near the implanted CA5 and on the newly formed bone in bone marrow.

### CONCLUSION

TRAP-positive and multinuclear cells with actin ring structures were formed by the interaction with osteocyte-like cells and BMC. The formation of mature and activated osteoclasts was enhanced on the CA compared to HA.

### REFERENCES

1. Nakashima T, *et al.*, Nat Med 11: 1231-1234, 2011
2. Kato Y. *et al.*, J Bone Miner Res 12: 2014-2023, 1997

### ACKNOWLEDGMENTS

The authors would like to thank the Shiseido Female Researcher Science Grant and the Murata Science Foundation for providing financial support to this project.

## Pannexin 1 and Pannexin 3 Regulated Osteoblastic Differentiation of Human Bone Marrow Mesenchymal Stem Cells in a Three Dimensional Macroporous Scaffold

Julien Guerrero<sup>1</sup>, Hugo Oliveira<sup>1</sup>, Rachida Aid<sup>2</sup>, Reine Bareille<sup>1</sup>, Didier Letourneur<sup>2</sup>, Yong Mao<sup>3</sup>, Joachim Kohn<sup>3</sup>, Joëlle Amédée<sup>1</sup>

<sup>1</sup>Inserm, U1026, Tissue Bioengineering, University of Bordeaux, Bordeaux, France

<sup>2</sup>Inserm, U1148, Cardiovascular Bioengineering, University Paris 13, Paris, France

<sup>3</sup>The New Jersey Center for Biomaterials, Department of Chemistry and Chemical Biology, Rutgers – The State University of New Jersey, Piscataway, New Jersey, United States

[julienp.guerrero@gmail.com](mailto:julienp.guerrero@gmail.com)

### INTRODUCTION

The multicellularity has required the development of forms of communication and interaction, in order to allow the complex coordination of groups of cells. The intricate control of cell differentiation and synchronization, which occurs during tissue development, is mediated by the intercellular diffusion of signaling molecules through gap junctions. In this context, connexin43 (Cx43), a component of gap junctions, has been found in several types of bone cells and also in mesenchymal stem cells. The importance of Cx43 for osteogenesis and bone formation has been demonstrated *in vitro*<sup>1</sup> and *in vivo*<sup>2</sup>. Interestingly, another family of membrane proteins named pannexins (Panxs) was recently described to present similar characteristics to connexins<sup>3</sup>. Despite the evidence supporting the key role of pannexins in cell communication and function, only a few studies have examined their implication in human cells<sup>4,5</sup> and on human physiology or disease<sup>6,7</sup>. Indeed, no study has yet focused on the implication of pannexins in the osteoblastic differentiation of human bone marrow mesenchymal stem cells (HBMSCs), when in a 3D environment that would favor bone regeneration.

### EXPERIMENTAL METHODS

HBMSCs, isolated from human bone marrow samples, were seeded in 6 mm diameter pullulan/dextran 75:25 (pullulan, MW 200,000, Hayashibara Inc; Dextran, MW 500,000, Sigma) matrix disks at  $4 \times 10^5$  cells/disk and cultured for 1 and 4 days in  $\alpha$ -MEM medium supplemented with 10% (v/v) FCS, with and without the use of Panx1 specific inhibitors probenecid and <sup>10</sup>panx1. At designated time points samples were processed for mRNA and protein extraction, or for immunocytochemistry evaluation. Gene expression of Panx1, Panx3, CaSR, ALP, Cbfa1/runx2, OCN and Cx43 was evaluated by qPCR. Semi quantitative Panx1, Panx3 and Cx43 protein expression was assessed by Western blot analysis. Additionally, scaffolds seeded with HBMSCs were implanted in dorsal subcutaneous sites of 12-week-old NOG mice and explanted at 3 and 8 weeks for histological analysis.

### RESULTS AND DISCUSSION

Here we show that Panx1 is involved in 3D cell-cell organization of human stem cells, demonstrated by the use of the inhibitory drug Probenecid and the mimetic peptide <sup>10</sup>panx1, which specifically block Panx1 channels. Panx1 is involved in the compaction of the cellular aggregates induced by the 3D organization.

Furthermore, our study demonstrates that culturing HBMSCs within 3D scaffolds induces Panx1 and Panx3 expression. Inhibition of Panx1 lead to a reduced expression of osteogenic markers in HBMSCs when in 2D culture, but had a minimal effect on HBMSCs when in 3D, suggesting specific roles of Panx1 in osteogenesis. We also show that the Panx3 gene expression profile correlates with those of osteoblastic markers.

Taken together, our data indicate that Panx1 and Panx3, likely in conjunction with Cx43, may act on HBMSCs cultured in 3D, by improving cellular communication within the dense cellular aggregates and supporting their differentiation towards the osteoblastic phenotype. This study demonstrates that Panx1 and Panx3 are expressed and involved in human bone tissue formation *in vitro* and *in vivo*.

Future studies will focus on the mechanism of how Panx1 impacts on the HBMSCs actomyosin cytoskeleton and how it may regulate cell differentiation towards an osteoblastic phenotype. Additionally, the use of Panx3 specific inhibitors will allow to identify the role of this pannexin in this intricate cell communication process.

### CONCLUSION

This study opens new avenues in the establishment of novel conditions to promote osteogenic differentiation of multipotent MSCs without the addition of external stimuli (i.e. differentiation medium or mechanical stimulus).

### REFERENCES

- Guillotin B. *et al.*, Bone. 42:1080-91, 2008
- Chaible LM. *et al.*, Toxicol Pathol. 39:1046-55, 2011
- Panchin Y. *et al.*, Curr Biol. 10:R473-4, 2000
- Alvarez CL. *et al.*, PLoS One. 9:e96216, 2014
- Ohbuchi T. *et al.*, Physiol Rep. 2:e00227, 2014
- Penuela S. *et al.*, Biochem J. 461:371-81, 2014
- Velasquez S. *et al.*, Front Physiol. 5:96, 2014

### ACKNOWLEDGMENTS

This work was supported by Grants from INSERM (National Institute for Health and Medical Research), from University of Bordeaux, Universities of Paris 7 and Paris 13, and by Grants from the French Research National Agency (ANR-10-EMMA-009-01 MATRI+; ANR-12-TecSan-0011 INEOV). Thanks to the New Jersey Center for Biomaterials (NJCB), Rutgers – the State University of New Jersey, USA for all their help.





## Hydrolysis of Octacalcium Phosphate Co-Precipitated Gelatin Composite and Osteoblastic Cell Response

Yushi Ezoe<sup>1,3</sup>, Takahisa Anada<sup>1</sup>, Hajime Yamazaki<sup>2</sup>, Tetsu Takahashi<sup>3</sup>, Osamu Suzuki<sup>1</sup>.

<sup>1</sup>Division of Craniofacial Function Engineering, Tohoku University Graduate School of Dentistry, Japan

<sup>2</sup>The Forsyth Institute, Center for Biomaterialization, Department of Applied Oral Sciences, USA

<sup>3</sup>Division of Oral and Maxillofacial Surgery, Tohoku University Graduate School of Dentistry, Japan  
[suzuki-o@m.tohoku.ac.jp](mailto:suzuki-o@m.tohoku.ac.jp)

### INTRODUCTION

We have previously found that octacalcium phosphate (OCP), if synthesized in a specific condition, shows a higher osteoconductive property than hydroxyapatite (HA), while it is hydrolyzed *in situ* into apatitic phase in critical-sized rat calvaria defects, and that the partial hydrolysis of the OCP material increases its osteoconductivity further in rat tibia defects<sup>1-3</sup>. The osteoconductivity of OCP in rat calvaria defects is more enhanced if OCP is combined with one of natural polymer gelatin (Gel) matrices through co-precipitation, which also exhibits a higher bone regenerative property and biodegradable property<sup>4</sup>. However, the effect of the OCP hydrolysis in the OCP/Gel composite has not been examined yet. The present study was designed to investigate the material characteristics and bioactivity of the OCP/Gel composites *in vitro*.

### EXPERIMENTAL METHODS

OCP was synthesized by introducing calcium and phosphate salts in a gelatin-containing solution under a supersaturated condition with respect to HA and OCP<sup>4</sup>. The resultant composite contained 40wt% of OCP<sup>4</sup>. Hydrolyzed OCP/Gel composites were obtained by a conversion from the synthesized OCP/Gel slurry<sup>3</sup> at 70°C with constant stirring for 6 to 40 h. The hydrolysis rate was compared with that of OCP alone up to 40 h. The hydrolyzed OCP/Gel composites were then lyophilized in a mold to obtain disks with a 9 mm diameter and 1 mm thickness, and then underwent dehydrothermal treatment at 150°C for 24 h in a vacuum drying condition. The resultant composites, having a spongy porous structure<sup>4</sup>, were characterized by chemical analyses, X-ray diffraction (XRD), Fourier transform infrared spectroscopy (FTIR), scanning electron microscopy (SEM), transmission electron microscopy (TEM) and selected area electron diffraction (SAED). Mouse bone marrow stromal ST-2 cells were seeded and incubated on OCP/Gel disks. The cell attachment at 6 h, and the proliferation and the differentiation into osteoblastic cells (the activity of alkaline phosphatase, ALP) were determined up to 21 days. In addition, the effect of co-presence of Gel molecules on the OCP hydrolysis was analysed. Pre-precipitated OCP was hydrolyzed in the presence of Gel with various concentrations (up to 0.45%) at 70°C with constant stirring up to 12 h.

### RESULTS AND DISCUSSION

Transformation of OCP into HA was confirmed by XRD and FTIR. The plate-like morphology of OCP was observed even after the hydrolysis by SEM and TEM. The analysis by SAED suggested that the structure of OCP is still retained even in the most hydrolyzed

product. Ca/P molar ratio of OCP in the composite progressively increased with the advancement of the hydrolysis, but did not reach the stoichiometric HA composition, as seen in the previous hydrolysis study with OCP alone<sup>5</sup>. The presence of Gel in the composite, obtained by the co-precipitation, affected the hydrolysis rate. The OCP/Gel composites tended to hydrolyze faster than OCP alone. Furthermore, an analysis of the hydrolysis of the pre-precipitated OCP in the presence of Gel indicated that OCP hydrolysis tended to advance with increasing the Gel concentration. The results suggest that Gel molecules may interact with OCP crystal surfaces and regulate the rate of the hydrolysis.

The number of attached ST-2 cells on each composite was compatible to that on the Gel disk (without calcium phosphate crystals) at 6 h. ST-2 cells proliferated and reached the same level between all composites and Gel disk until 21 days. The ALP activity of ST-2 cells increased with the incubation time on all composites and was comparable to that on the Gel disk (without calcium phosphate crystals) at 21 days. The results suggest that the OCP/Gel composites with various degree of hydrolysis could have a similar bioactivity with the gelatin material that is widely used as an implantable biomaterial, using a bone marrow derived stromal ST-2 cell line.

### CONCLUSION

The present study provided evidence that the presence of Gel molecules accelerates the OCP hydrolysis. The hydrolyzed OCP/Gel composites show a similar bioactivity with Gel alone in terms of the osteoblastic cellular response. *In vivo* analysis of the hydrolyzed OCP/Gel composites is under way to elucidate the potential effect of the hydrolysis of OCP within the Gel matrix on bone regenerative properties as previously seen in the hydrolysis of OCP without Gel<sup>3</sup>.

### REFERENCES

1. Suzuki O *et al.*, Biomaterials 27:2671-2681, 2006
2. Kobayashi K *et al.*, ACS Appl Mater Interfaces 6:22602-22611, 2014
3. Miyatake N *et al.* Biomaterials 30:1005-14, 2009
4. Handa T *et al.* Acta Biomater 8:1190-1200, 2012
5. Suzuki O *et al.*, Cells Mater 5:45-54, 1995

### ACKNOWLEDGMENTS

This study was supported in part by Grants-in-aid (23106010, 25670829, 26670846, 26282133 and 26293417) from the MEXT, Japan.



## Novel Bioactive Hydrogel-Nanosilica Hybrid Materials as a Potential Injectable Scaffold for Bone Tissue Engineering

Joanna Lewandowska-Łańcucka<sup>1</sup>, Sylwia Fiejdasz<sup>1</sup>, Łucja Rodzik<sup>1</sup>, Marcin Kozieł<sup>1</sup>, Maria Nowakowska<sup>1</sup>

<sup>1</sup>Faculty of Chemistry, Jagiellonian University, Poland  
[lewandow@chemia.uj.edu.pl](mailto:lewandow@chemia.uj.edu.pl)

### INTRODUCTION

Biomaterials play an important role in bone tissue engineering, since they mimic the structure and composition of human tissue and provide mechanical stability<sup>1,2</sup>. The biodegradable biopolymers like chitosan and collagen serve often as the scaffolds in the development of hybrid materials for bone replacement and regeneration<sup>3</sup>. It was also reported that addition of silica can improve the bioactivity and biocompatibility of the polymeric materials<sup>4</sup>. In this study we have presented the preparation and studies of bioactivity of the novel hybrid organic-inorganic materials based on collagen, collagen-chitosan and chitosan hydrogels containing silica nanoparticles<sup>5</sup>. These materials can be considered as potentially useful injectable scaffolds for bone tissue regeneration. The effect of such parameters as: the type of hydrogel matrix used, the presence of SiNP in the hybrid material, the size of added NPs on promotion of apatite-like mineral structures formation under physiological conditions (incubation in a simulated body fluid, (SBF) was evaluated and discussed.

### EXPERIMENTAL METHODS

The silica nanoparticles were prepared *in situ* by Stöber method. Dynamic light scattering (DLS) and zeta potential measurements were carried out to determine their size and zeta potential values. The silica nanoparticles (SiNP) of two different sizes (S1-210 nm and S2-440 nm) were next dispersed in collagen (Col), collagen-chitosan (ColCh) or chitosan (Ch) sols. These sols were then subsequently crosslinked with genipin. Taking into account the potential application of hybrid organic-inorganic systems as a potential injectable scaffold for bone tissue engineering the *in vitro* experiments with simulated body fluid (SBF) treatment were carried out. For that purpose the samples were incubated in SBF for 21 days. After incubation in SBF the structures of the resulting mineral were examined using scanning electron microscopy (SEM), energy dispersive X-Ray spectroscopy (EDS), and X-ray diffraction (XRD) techniques. In order to demonstrate the usefulness of the presented materials for biomedical applications their cytotoxicity was investigated with Primary Dermal Fibroblasts using colorimetric assay (XTT tests).

### RESULTS AND DISCUSSION

Novel organic-inorganic hybrids composed of biopolymer matrix based on collagen, collagen-chitosan or chitosan with incorporated silica nanoparticles of two different sizes were obtained. By monitoring the gelation process using the anisotropy fluorescence probe technique it was demonstrated that these

materials might be applied as injectable hydrogels. The *in vitro* experiments carried out under SBF conditions have shown that the prepared materials induce the mineralization. The rate of that process can be adjusted by the composition of the material. SEM images revealed mineral phase formation in majority of the obtained hybrid materials while they were exposed to SBF. Applying EDS analysis it was proven that these mineral phases are mainly composed of calcium and phosphorus. The XRD studies confirmed that mineral phases formed during SBF incubation of hybrid materials based on the collagen are bone-like apatite minerals. It was shown that the silica nanoparticles present in hydrogels promote mineralization. Furthermore addition of silica nanoparticles to the sol before the material gelation resulted in occurrence of mineralization not only at the surface but also in the bulk of the material. That is especially important for preparation of scaffolds for bone tissue engineering. It was also demonstrated that silica nanoparticles influenced the viability of the fibroblast cells *in vitro*. In all samples studied they have shown the positive effect, increasing the number of metabolic active cells cultured at these materials.

### CONCLUSION

Novel bioactive organic-inorganic hybrid materials which can serve as injectable hydrogel systems for bone tissue regeneration were successfully obtained. Studies on mineralization process under simulated body fluid (SBF) conditions confirmed the bioactivity of prepared materials. *In vitro* studies on fibroblast cells viability indicated that the hybrid materials are biocompatible. The ability of these materials to undergo *in situ* gelation under physiological temperature, their biocompatibility and bioactivity make them potentially useful candidates for bioactive injectable systems for bone tissue repair.

### REFERENCES

1. Belluci D. et al., Mater. Sci. Eng. C 33: 1091-1101, 2013
2. Dreifke M B. et al., J. Biomed. Mater. Res. Part A 101A: 2436-2447, 2013
3. Leonor I B. et al., Acta Biomater. 4: 1349-1359, 2008
4. Madhumathi K. et al., Int. J. Biol. Macromol. 45: 289-292, 2009
5. Lewandowska-Łańcucka et al., Biomedical Materials, 2015, in press

### ACKNOWLEDGMENTS

Project operated within the Foundation for Polish Science Team Programme co-financed by the EU European Regional Development Fund, PolyMed, TEAM/2008-2/6



## Anisotropic Bilayered Alginate Hydrogels with Channel-like Pores for Osteochondral Regeneration

Kathleen Schütz<sup>1</sup>, Florian Despang<sup>1</sup>, Giuseppe Filardo<sup>2</sup>, Alice Roffi<sup>2</sup>, Annapaola Parrilli<sup>2</sup>, Maria Sartori<sup>2</sup>, Francesca Salamanna<sup>2</sup>, Elizaveta Kon<sup>2</sup>, Michael Gelinsky<sup>1</sup>

<sup>1</sup>Centre for Translational Bone, Joint and Soft Tissue Research, Technische Universität Dresden, Germany

<sup>2</sup>Rizzoli Orthopaedic Institute, Bologna, Italy

[michael.gelinsky@tu-dresden.de](mailto:michael.gelinsky@tu-dresden.de)

### INTRODUCTION

Regeneration of deep articular cartilage defects remains a challenging task because of the low self-healing capacity of this tissue. To overcome limitations of autologous grafting such as limited availability as well as donor-site morbidity, many biomaterials have been investigated as synthetic alternative. We have developed an anisotropic bilayered alginate-based scaffold mimicking osteochondral tissue<sup>1</sup>. The material fabrication can be completely conducted under sterile conditions, allowing the easy integration of living cells into the chondral layer. The present study describes differences between embedding of human chondrocytes (hCh) and mesenchymal stem cells (hMSC) as well as the results of a first animal pilot study, performed in sheep.

### EXPERIMENTAL METHODS

Scaffolds were fabricated applying the principle of diffusion-controlled directed ionotropic gelation of alginate. The bony layer consists of a composite made of alginate and hydroxyapatite (HAP), the chondral layer of alginate and hyaluronic acid (HYA). During gelation, channel-like pores are formed which run through the whole length of the scaffold. The two layers are tightly fused together, leading to biphasic but mechanically stable monolithic scaffolds<sup>1</sup>. Either hCh or hMSC were embedded into the chondral layer in the course of the gelation process. Cells were either cultured in presence or absence of chondrogenic supplements over a period of 3 weeks. Viability was analysed by live dead staining as well as measurement of the LDH activity. Chondrogenic differentiation was proven by means of collagen type II ELISA and gene expression analysis of chondrogenic markers. In an *in vivo* pilot study, 8 bilayered hydrogel scaffolds not containing cells were press-fit implanted in osteochondral defects 7 mm in diameter and 5 mm in depth, made in the medial and lateral femoral condyle of 4 Merinos-Sarda sheep. The animals were sacrificed 6 months after implantation and  $\mu$ -CT as well as histological analyses were carried out. Equally sized empty defects served as control.

### RESULTS AND DISCUSSION

Live/dead analysis one day after completed gelation revealed a high viability of both hMSC and hCh embedded into the chondral part of the bilayered scaffolds indicating that the gelation process does not strongly affect the viability. Viability of chondrogenically induced hMSC and hCh was superior compared to that of non-induced hMSC over a period of 21 d, as shown by measurement of LDH activity. The data indicates that the induction of chondrogenesis is crucial for survival of cells embedded in this type of hydrogel matrix. Successful chondrogenic (re)differentiation of induced

hMSC and hCh could be confirmed by gene expression of the chondrogenic markers COL2A1, ACAN and COMP. Additionally, strong deposition of collagen II was verified. The material allowed easy press-fit implantation in osteochondral defects, made in the knee joint of sheep. Micro-CT as well as histological investigations revealed a high biocompatibility and good integration of the hydrogel scaffolds. In most of the explants, regeneration of the chondral tissue layer was observed whereas the bony part of the defects was not yet completely healed 6 months after implantation.

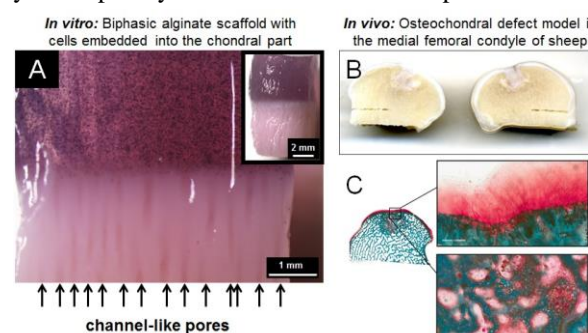


**Fig. 1:** **A** – Photographs showing the bilayered hydrogel scaffolds; bottom: alginate/HAP composite, top: alginate/HYA layer with embedded hCh (dark spots, stained with MTT dye). **B** – Macroscopic view of sectioned femoral condyle of sheep. **C** – Histological images of the implantation site. **B & C:** 6 months after implantation of cell-free biphasic hydrogels.

### CONCLUSION

The developed scaffolds exhibit a structure that partly mimics the complex hierarchical architecture of natural osteochondral tissue. Our data indicate that the bilayered hydrogels are suitable for embedding of hMSC and hCh, respectively, into the chondral part. The superior viability of chondrogenically induced cells within the hydrogel highlights that a successful chondrogenic (re)differentiation is crucial for survival of the embedded cells. The pilot animal study, performed in sheep, yielded the high biocompatibility and stimulating effect of the biomimetic composite scaffold, especially for healing of the chondral part of osteochondral defects.

### REFERENCES

- Schütz K. *et al.*, J. Tissue Engin. Regen. Med. 2014 (in press, DOI 10.1002/term.1879)

### ACKNOWLEDGMENTS

Authors want to thank the European Commission (Collaborative project consortium OPHIS) and the German Research Foundation (DFG) for funding.





## Induction of Mesenchymal Stem Cell Differentiation and Cartilage Formation by Cross-Linker-Free Collagen Microspheres

Emmanuel Belamie<sup>1,2</sup>, Marc Mathieu<sup>3,4</sup>, Sylvain Vigier<sup>1,2</sup>, Marie-Noëlle Labour<sup>1,2</sup>, Christian Jorgensen<sup>3,4</sup>, Danièle Noël<sup>3,4</sup>

<sup>1</sup>Ecole Pratique des Hautes Etudes, Paris, France

<sup>2</sup>Institut Charles Gerhardt, UMR 5253, Equipe MACS, Ecole Nationale Supérieure de Chimie, Montpellier, France,

<sup>3</sup>Inserm, U1183, Hôpital Saint-Eloi, Montpellier, France

<sup>4</sup>Université Montpellier, UFR de Médecine, Montpellier, France

[Emmanuel.Belamie@enscm.fr](mailto:Emmanuel.Belamie@enscm.fr)

### INTRODUCTION

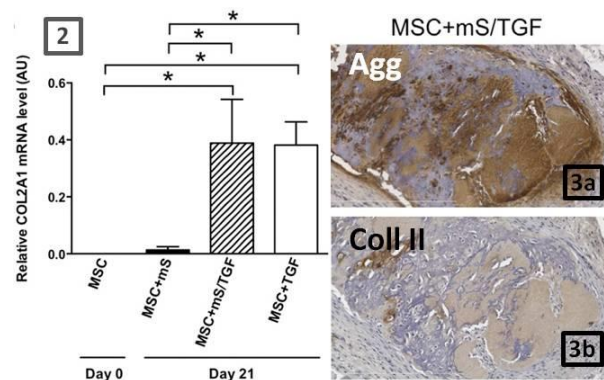
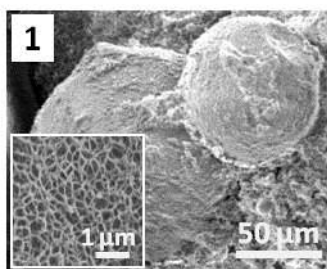
Because of a poor self-healing ability, joint cartilage undergoes progressive degradation in the course of aging or following traumatic injuries. One promising therapeutic approach is the use of mesenchymal stem cells (MSC), which have the potential to differentiate into chondrocytes. However, anchorage of MSC to the sites of injury and their differentiation *in situ* require combining cells with a biomaterial releasing a differentiation factor such as TGF $\beta$ 3. Our objective was to design and test a new injectable and active scaffold to support chondrogenic differentiation of human MSC.

### EXPERIMENTAL METHODS

An emulsion-based process was designed to prepare the microspheres using an acidic type I collagen solution and perfluorated oil, stabilized by a surfactant. Spherical microparticles of fibrillar collagen were obtained through a sol-gel transition induced in aqueous droplets in contact with ammonia vapors, in the absence of chemical cross-linkers. Microspheres were impregnated with TGF $\beta$ 3 and release of this factor was measured using a reporter gene assay. Impregnated microspheres were combined with human MSC and cultivated *in vitro* or subcutaneously injected into immunodeficient mice. Expression of chondrocyte markers was monitored by RT-qPCR and immunohistochemistry.

### RESULTS AND DISCUSSION

Microspheres (Fig.1) are constituted by a gel of striated collagen fibrils and are  $300 \pm 67$   $\mu$ m in diameter. Fibrils occupy ca. 5% of the total volume, forming an entangled network with pores of 1-10  $\mu$ m. After MSC adhesion onto the microspheres and *in vitro* culture for 21 days, they differentiate into chondrocytes expressing the specific markers, such as aggrecan and collagen type II (Fig. 2), as assessed by RT-qPCR. The type I collagen matrix is progressively degraded and replaced by the cartilaginous matrix. *In vivo*, MSC form a tissue histologically resembling cartilage which stain positive for aggrecan (Fig.3a) and collagen II (Fig.3b).



Recently, we have successfully adapted the microspheres synthesis to a microfluidic-based process, which widens the possibility for scaffold modifications, as well as control over morphology and mechanical properties. The relatively versatile scaffold processing and association of cells makes it amenable to a wide variety of therapeutic indications.

### CONCLUSION

Here, we demonstrated the feasibility of a novel potential cartilage engineering approach based on MSC and self-cross-linked collagen microspheres carrying TGF- $\beta$ 3. In the present proof of principle study, we were able to successfully induce chondrogenic differentiation *in vitro* and the formation of a tissue resembling cartilage *in vivo*. However, induction of hypertrophy and calcification is an issue that needs to be addressed in future studies. The interest of these collagen microspheres resides in the versatility of the simple impregnation method used for loading the differentiation factor, ease of handling, and potentially rapid transfer to the clinic thanks to the nature and structure of this injectable scaffold which does not require differentiation of MSC prior to implantation.

### REFERENCES

1. Mathieu M. *et al.*, *Eur. Cells Mater.* 28:82-97, 2014

### ACKNOWLEDGMENTS

This study was supported by funding from the CNRS (Programme Interdisciplinaire « Longévité & Vieillesse », the program “Bonus de l’Université de Montpellier I de Soutien à la Recherche” and the Agence de la Biomédecine.

## Biodegradable Glues for Meniscus Repair in a Full-thickness Explant Model

Agnieszka I. Bochyńska<sup>1,2</sup>, Gerjon Hannink<sup>1</sup>, Tony G. van Tienen<sup>1</sup>, Dirk W. Grijpma<sup>2,3</sup>, Pieter Buma<sup>1</sup>

<sup>1</sup>Orthopaedic Research Laboratory, Department of Orthopaedics, Radboud UMC, Nijmegen, The Netherlands

<sup>2</sup>Department of Biomaterials Science and Technology, University of Twente, Enschede, The Netherlands

<sup>3</sup>Department of Biomedical Engineering, UMC Groningen, University of Groningen, Groningen, The Netherlands

[Agnieszka.Bochyńska@radboudumc.nl](mailto:Agnieszka.Bochyńska@radboudumc.nl)

### INTRODUCTION

Meniscus tears are common knee injuries. They directly result in pain, swelling and locking of the knee joint, and may eventually lead to osteoarthritis. Current repair techniques are associated with both short and long term problems. Therefore, there is an unmet clinical need for new solutions to repair a torn meniscus. Tissue adhesives are considered promising materials for this purpose, since they are easy to apply and cause minimal tissue trauma. However, to date, the development of a strong and biocompatible adhesive material has not been accomplished.

We previously reported that isocyanate-terminated copolymers based on poly (ethylene glycol) (PEG), trimethylolpropane ethoxylate (TMPE) and trimethylene carbonate (TMC) can be successfully used as tissue adhesives. Particularly, the 3-armed structures showed better adhesive properties than analogous linear ones [1]. The aim of this study was to assess novel hyper-branched amphiphilic copolymers as tissue adhesives for meniscus repair. Their interfacial shear stress on meniscus tissue and potential cytotoxicity was compared with the properties of the 3-armed structures.

### EXPERIMENTAL METHODS

Oligomers were synthesized by ring opening polymerization of TMC using linear PEG or three-armed TMPE as initiator. Subsequently, excess of PEG-based oligomer was reacted with citric acid (CA) to introduce branching. Reactive copolymers were synthesized by functionalizing the terminal hydroxyl groups of the oligomers with hexamethylene diisocyanate (HDI). In order to assess the effect of curing time of adhesive materials, a well established push-out test was performed after 1, 4, 8 and 24 hours after application on fresh bovine meniscus tissue [2]. The interfacial shear stress between surfaces of the glued meniscus was tested with BOSE ElectroForce using full thickness cylinder-shaped explants (Figure 1).

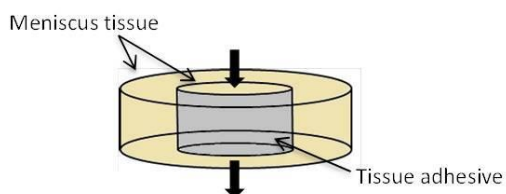


Figure 1. Push-out adhesion test using a full-thickness cylindrical bovine meniscus explant model. The area marked in grey is covered with the adhesive material.

The potential cytotoxicity was assessed by adding the adhesives in a trans-well system to bovine meniscus cells. Alamar Blue and live/dead assays were used to determine cells' viability. Moreover, in order to assess

the tissue reaction after contact with adhesives, glued meniscus explants were cultured *in vitro* for 7 days, after which haematoxylin and eosin (H&E) staining was performed.

### RESULTS AND DISCUSSION

The shear adhesive strength of the copolymers significantly increased with the curing time. The adhesive strength measured in the push-out test increased during 24 hours from 10 to 60 kPa for the 3-armed adhesive and from 50 to 140 kPa for the hyper-branched composition (Figure 2). Although the maximum bonding strength was obtained after 24 hours, attachment to the tissue was observed already after 1 hour. The hyper-branched copolymer performed better in the adhesion test than the analogous 3-armed structure, probably due to higher number of reactive isocyanate groups, which can covalently attach to the tissue. Histological inspection of the explants revealed no severe tissue response to none of the two glues. After 1 week of culture vital meniscus fibroblasts were present in the rim area of the tissue directly contacting the glue. This is a confirmation of the *in vitro* culture test, in which we showed that cell viability was not significantly affected by physiological amounts of glue.

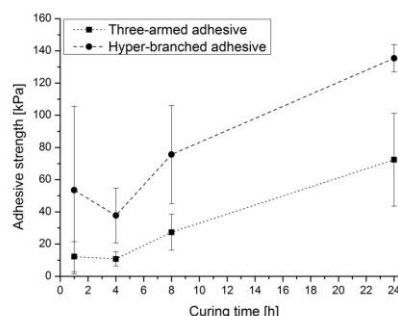


Figure 2. Results of the push-out adhesion test of the 3-armed and hyper-branched adhesive materials as a function of their curing time.

### CONCLUSION

The proposed copolymers, particularly the hyper-branched structure, appear to be suitable candidates for resorbable tissue adhesives for meniscus repair. They are biocompatible and able to attach to tissue already after 1 hour and full bonding strength is obtained after 24 hours. Further optimization of the system to decrease curing time still needs to be performed.

### REFERENCES

- [1] Bochyńska, A.I., *et al.*, Macromol. Symp., 2013. 334(1): p. 40-48, [2] Hennerbichler, A., *et al.*, Osteoarthritis and Cartilage, 2007. 15(9): p. 1053-1060

### ACKNOWLEDGMENTS

This research is supported by Reumafonds, the Dutch Arthritis Foundation



## A Bioactive Bacterial Exopolysaccharide from Deep-Sea Environment: Modification, Characterization and Chondrogenic Potential for Cartilage Regenerative Medicine

Agata Zykwinska<sup>1</sup>, Nathalie Chopin<sup>1,2</sup>, Corinne Sinquin<sup>1</sup>, Jacqueline Ratiskol<sup>1</sup>, Jean Le Bideau<sup>2</sup>, Boris Halgand<sup>3</sup>, Claire Vinatier<sup>3</sup>, Jérôme Guicheux<sup>3</sup>, Pierre Weiss<sup>3</sup> and Sylvia Collic-Jouault<sup>1</sup>

<sup>1</sup>Ifremer, EM<sup>3</sup>B Laboratoire des Ecosystèmes Microbiens et Molécules Marines pour les Biotechnologies, Nantes, France

<sup>2</sup>Institut des Matériaux Jean Rouxel (IMN), Université de Nantes, CNRS UMR 6502, France

<sup>3</sup>INSERM U791, Laboratoire d'Ingénierie Ostéo-Articulaire et Dentaire (LIOAD), Université de Nantes, France

[Agata.Zykwinska@ifremer.fr](mailto:Agata.Zykwinska@ifremer.fr)

### INTRODUCTION

In cartilage tissue engineering, differentiation of mesenchymal stem cells into chondrocytes is crucial to obtain successful cartilage regeneration. Differentiation can be promoted by various biological agents, including polysaccharides. In particular, glycosaminoglycans (GAG) were shown to participate in many biological processes likely through interaction with proteins, such as growth factors, proteases and chemokines<sup>1,2</sup>. Sulfate and carboxylic groups in GAG structure are key factors for interaction setting<sup>1</sup>. Marine bacteria producing exopolysaccharides (EPS) were recently shown to be a promising source of new GAG-like molecules useful for cartilage repair<sup>3,4</sup>. In order to enhance the biological activity of the marine EPS and to provide GAG mimetic compounds, structural modifications are however required.

### EXPERIMENTAL METHODS

GY785 exopolysaccharide (EPS) was produced by *Alteromonas infernus*, a deep-sea hydrothermal bacterium by the fermentation process<sup>5</sup>. In the next step, native high molecular weight (HMW) GY785 EPS was depolymerized to obtain low molecular weight (LMW) derivatives (DR). GY785 DR were therefore sulfated either in dimethylformamide, DMF leading to GY785 DRS-DMF or in ionic liquid (IL), 1-butyl-3-methylimidazolium chloride, BMImCl leading to GY785 DRS-IL. Molecular weight,  $M_w$  before and after sulfation was determined by HPSEC-MALS and sulfur content (wt% S) by HPAEC chromatography. ATR-FTIR and NMR spectroscopy were used to assess the efficiency of sulfation reaction. Cell viability in the medium supplemented with sulfated derivatives was studied by MTS assays. Chondrogenic differentiation of stem cells is currently being assessed.

### RESULTS AND DISCUSSION

In the present study, a new one-step sulfation process was developed in order to design GAG-mimetic compounds able to enhance the chondrogenic differentiation of mesenchymal stem cells, considered as an attractive source of cells for cartilage engineering<sup>3-5</sup>. The effect of EPS molecular weight and sulfur content on chondrogenesis was evaluated.

In the first step, native HMW GY785 EPS of low sulfate content (up to 3 wt%) was depolymerized to obtain LMW GY785 derivatives (GY785 DR). The obtained derivatives were then oversulfated in ionic liquid (IL), considered as a new class of solvent for

carbohydrate chemistry. In comparison, the sulfation was also performed in DMF, a classical organic solvent. The use of IL as solvent allows the sulfation to be carried out in a homogeneous medium in one-step process, whereas, in DMF, an additional step is necessary to obtain the pyridinium salt of EPS in order to improve its solubility prior to sulfation. GY785 DR were efficiently sulfated, as the sulfur content increased from 3 wt% before sulfation to 10-15 wt% after sulfation in either IL (GY785 DRS-IL) or in DMF (GY785 DRS-DMF). The sulfation was devoid of side effects, e.g. depolymerization and degradation.

In the next step, cell viability was evaluated using MTS assay. Stem cells from adipose tissue were cultured in control medium in the absence or in the presence of GY785 DR and GY785 DRS-IL, and GY785 DRS-DMF at different concentrations. It was observed that oversulfated derivatives improved the cell viability *in vitro* and that for some concentrations, GY785 DRS-IL showed better results than GY785 DRS-DMF. To correlate MTS activity with cell proliferation, the number of viable cells was also estimated and revealed that GY785 DRS increased stem cells proliferation in comparison to the control condition. The effect of the presence of GY785 oversulfated derivatives on chondrogenic differentiation is in progress.

### CONCLUSION

The present work describes a new one-step chemical sulfation process based on ionic liquid, BMImCl, as a reaction medium. The sulfation of highly branched anionic heteropolysaccharide from marine origin was shown to be devoid of undesired structure degradation. The potential of new derivatives obtained as GAG-mimetic compounds for cartilage regeneration is being assessed.

### REFERENCES

1. Rapraeger, J. Cell Biol. 149:995-998, 2000
2. Rabenstein, Nat. Prod. Rep. 19:312-331, 2002
3. Merceron *et al.*, Stem Cells 30:471-480, 2012
4. Merceron *et al.*, Patent WO 2012/126824
5. Chopin *et al.*, BioMed Res. Int. 1-9, 2014

### ACKNOWLEDGMENTS

The authors would like to thank the BIOREGOS network and IONIBIOGEL ANR Blanc SIMI 9 for providing financial support to this work.



## INTRODUCTION

Nitric oxide (NO) is an endogenously found radical species, which plays important roles in many physiological processes, including the control of vascular tone. Microcirculatory disorders associated with the depletion of endogenous NO production are the underlying causes of ischemic diseases and chronic wounds and have demanded biomaterials capable of delivering NO locally to tissues in a controlled manner. Poly(vinyl alcohol), PVA, is a biocompatible hydroxylated polymer already used for medical purposes, which allows chemical modification through condensation reactions with carboxylic acids<sup>1</sup>. In this study we used mercaptosuccinic acid (MSA) to prepare SH-containing, crosslinked PVA membranes (PVA-SH) capable of being further S-nitrosated to release NO locally through thermal and photochemical pathways.

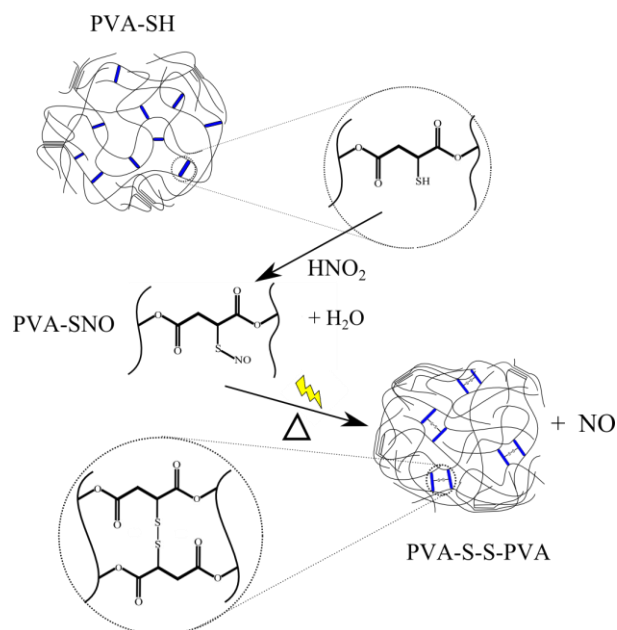
## EXPERIMENTAL METHODS

PVA was esterified with MSA in aqueous HCl-acidified medium under stirring and reflux, followed by removal of half of the water content under heating in an open flask. The membranes were cast by precipitation of the polymeric solutions, through their immersion in acetone, followed by washing with water and acetone, dried by lyophilization and subsequently S-nitrosated with nitrous acid. The dry membranes were characterized regarding their thermal, crystallographic and morphological properties. The S-nitrosated membranes (PVA-SNO) were characterized regarding their NO-releasing properties and ability to promote skin vasodilation in topical application, protected from light and under irradiation with visible light.

## RESULTS AND DISCUSSION

Functionalization of PVA with MSA was confirmed by IR spectroscopy. The PVA-SH membranes displayed a reduced crystallinity degree, as reflected in their X-ray diffraction pattern and DSC thermogram. This result was assigned to the reduction in the number and size of PVA crystallites due to the chemical crosslinking obtained in the esterification reaction. As a consequence, the membranes displayed a swelling degree higher than 600% in water, what makes them suitable for wound dressing. Morphological analysis by SEM showed that the membranes are highly porous. Real time chemiluminescence measurements showed that the S-nitrosated membranes can be charged with up to 90 nmol NO/mg and are capable of releasing NO thermally over more than 3 h after their immersion in water at 37 °C. Irradiation of the hydrated PVA-SNO membranes with visible light led to an increase of ca. 10-fold in the first order rate constant of NO a release. These NO-release properties were shown to lead to

local vasodilation and erythema formation after topical application of the membranes on the forearm of health volunteers, as measured by laser Doppler Flowmetry. In addition, irradiation of the topically applied membranes led to a significant increase in the local vasodilation.



Scheme showing the structure of the sulphydrylated PVA membranes (PVA-SH) and a detail of the MSA ester bridges, which are S-nitrosated yielding PVA-SNO groups. These, undergo thermal and photochemical decomposition releasing free NO, leading to a double crosslinked structure with sulphur bridges.

## CONCLUSION

PVA-SNO membranes can be used for the local delivery of NO on the skin and their rate of NO-release can be modulated through the irradiation with visible light. Therefore, PVA-SNO membranes have potential to be used as NO-releasing biomaterials for the treatment of tissues affected by impaired endogenous NO production.

## REFERENCES

1. Marcelli RHM, de Oliveira MG, Colloids Surf. B: Biointerfaces. 116:643-651, 2014

## ACKNOWLEDGMENTS

SDML was supported by a fellowship from CAPES. This work was supported by grants from CNPq (proj. 309390/2011-7) and FAPESP (project 2008/57560-0).

## Smart Polymer Nanoparticles for Triggered Drug Releases

Christian Tolle<sup>1</sup>, Jan Riedel<sup>2</sup>, Dagmar Wirth<sup>2</sup>, Henning Menzel<sup>1</sup>

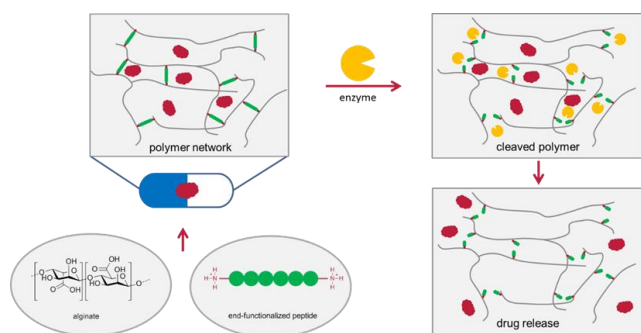
<sup>1</sup>Institute for Technical Chemistry, Braunschweig University of Technology, Germany

<sup>2</sup>Helmholtz Centre for Infection Research, Braunschweig, Germany

[c.tolle@tu-bs.de](mailto:c.tolle@tu-bs.de)

### INTRODUCTION

The adhesion of bacteria and formation of biofilms is an important issue for implants. The bacterial films can lead to severe infections and might result in revision surgeries. This problem might be overcome with nanoparticles immobilized on the implant surface which can release antibacterial drugs triggered by the infection. Recent studies have shown that nanoparticles based on polysaccharides like chitosan or alginate provide an excellent approach for drug delivery applications.<sup>1,2,3</sup> As the conventional systems lack infection triggered drug release mechanisms the objective of this work is to render the nanoparticles degradable by specific enzymes which are released upon inflammation or infection.



Scheme 1: Schematic overview of nanoparticle preparation and subsequent degradation upon addition of enzyme.

### EXPERIMENTAL METHODS

The nanoparticles were prepared by ionotropic gelation. The characterization with regard to particle diameter and zeta potential was performed by dynamic light scattering (DLS). A simple spray-coating process was applied to coat titanium substrates with the nanoparticle suspension. Surface characterization was carried out by means of ellipsometry, X-ray photoelectron spectroscopy (XPS) and scanning electron microscope (SEM) measurements. During the particle preparation process interferon- $\beta$  was encapsulated. Corresponding encapsulation efficiencies were calculated based on a luciferase assay.

### RESULTS AND DISCUSSION

Two different nanoparticle systems were prepared by ionotropic gelation. Negatively charged alginate was reacted with either positively charged poly-L-lysine or an aggrecanase-labile peptide with lysine sequences as positively charged end groups. According to Dynamic Light Scattering measurements the particles exhibit well-defined particle size and zeta potential. Successful deposition of alginate/peptide layers was proven by ellipsometry, XPS and SEM. Moreover encapsulation and release experiments were undertaken with the antiviral and antitumoral drug interferon- $\beta$ <sup>4</sup>, which could be easily incorporated in the particles.

### CONCLUSION

Ionotropic gelation of alginate with a peptide having lysine-sequences at both ends results in well-defined nanoparticles. Deposited nanoparticle films on titanium can be characterized by surface analytics. In addition the loading with interferon- $\beta$  has been performed to indicate the particles great potential as drug delivery system.

### REFERENCES

1. Wang J. J. *et al.*, Int J Nanomedicine 6:765-774, 2011.
2. Tønnesen H. H. *et al.*, Drug Development and Industrial Pharmacy. 28:621-630, 2002.
3. Bhattarai A. *et al.*, Chron Young Sci 2:192-196, 2011.
4. Garbe C. *et al.*, J Invest Dermatol 95:231S-237S, 1990.

### ACKNOWLEDGMENTS

This research project has been supported by the President's Initiative and Networking Funds of the Helmholtz Association of German Research Centers (HGF) under contract number VH-GS-202.

## Polymer Coatings with Liposomal Drug Deposits towards Substrate-Mediated Drug Delivery

Martin E. Lyng<sup>1</sup>, Marie Baekgaard Laursen<sup>1</sup>, Marina Fernandez-Medina<sup>1</sup> and Brigitte Städler<sup>1</sup>

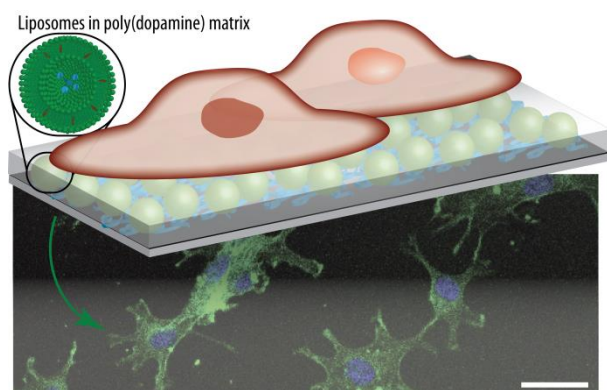
<sup>1</sup>Interdisciplinary Nanoscience Center, iNANO, Aarhus University, Denmark  
[mlynge@inano.au.dk](mailto:mlynge@inano.au.dk)

### INTRODUCTION

Implantable substrates modified with a drug-loaded polymer coating, such as stents or intrauterine devices, are emerging as an efficient tool to administer therapeutic cargo locally. However, challenges with the retention of small hydrophobic molecules or the activity of structurally dependent biomolecules remain. To this end, we report liposomal drug deposits as carriers of both hydrophobic and hydrophilic cargo embedded in a polymer matrix. The liposomes have been immobilized in the polymer film either through the layer-by-layer technique<sup>1</sup> or co-immobilized with poly(dopamine)<sup>2-4</sup> (scheme 1). The interactions between cells and the substrates were assessed with regards to capping layer thickness, types of liposome (e.g. embedding of a lipophilic dopamine conjugate or different charge).

### EXPERIMENTAL METHODS

The assembly of the films containing intact liposomes was monitored with quartz-crystal microbalance with dissipation measurements (QCM-D). Microscopy imaging and flow cytometry were used to assess the cell adhesion and uptake/association of fluorescent lipids embedded in the liposomes as model cargo while cell viability measurements were conducted with the use of cell counting kit-8 and multiwell-plate reader.



Scheme 1. Schematic representation of liposomal drug deposits embedded in a poly(dopamine) matrix for substrate-mediated drug delivery to adhering cells, scale bar 50  $\mu\text{m}$ .

### RESULTS AND DISCUSSION

QCM-D revealed that intact liposomes could be embedded in the polymer film and by using polymer separation layers, a second liposome layer was found capable of adsorbing. Myoblasts, hepatocytes, macrophages and endothelial cells were all found to adhere to the liposome-containing films as confirmed with microscopy. The adhesion was found to be independent of liposome charge with the exception of

endothelial cells which could only adhere to films containing negative liposomes. The cells were observed to be able to take up the fluorescent lipid embedded in the liposomes. The uptake depended on initial dopamine concentration, separation layers, liposome charge and number of liposome deposition steps. The successful delivery of active cargo to adhering cells was demonstrated by incorporating a cytotoxic and hydrophobic molecule, thiocoraline, into the liposomes and measuring the viability of the adhering cells. The uptake pathway was determined to be clathrin-mediated by treating adhering myoblasts with inhibitors against distinct endocytosis pathways. In an attempt to mimic the dynamic environment *in vivo*, microfluidic channels, coated with the mixed films, were connected to a pump which would exert a shear stress on adhering endothelial cells. The cell/substrate interactions were found to be affected by the shear stress as revealed by a decrease in cell mean fluorescence.

### CONCLUSION

Based on the presented results, liposomes have been shown to act as intact drug deposits in a cell adhesive polymer matrix which can be tailored for a controlled cargo delivery. In summary, the various approaches to design liposome-containing polymer films can have great potential in the field of substrate-mediated drug delivery.

### REFERENCES

1. M. E. Lyng, M. Baekgaard Laursen, L. Hosta-Rigau, B. E. B. Jensen, R. Ogaki, A. A. A. Smith, A. N. Zelikin and B. Städler, *ACS Applied Materials & Interfaces*, 2013, 5, 2967-2975.
2. M. E. Lyng, R. Ogaki, A. O. r. Laursen, J. Lovmand, D. S. Sutherland and B. Städler, *ACS Applied Materials & Interfaces*, 2011, 3, 2142-2147.
3. M. E. Lyng, B. M. Teo, M. B. Laursen, Y. Zhang and B. Städler, *Biomaterials Science*, 2013, 1, 1181-1192.
4. M. E. Lyng, M. Fernandez-Medina, A. Postma and B. Städler, *Macromolecular Bioscience*, 2014, 14, 1677-1687.

### ACKNOWLEDGMENTS

This work was financed through a Sapere Aude Starting Grant from the Danish Council for Independent Research, Technology and Production Sciences, Denmark.



## PLGA/Calcium Phosphate Composite Nanoparticles as Efficient Carriers of Hydrophilic Drugs (Nucleic Acids, Proteins)

Jens Nelsen<sup>1</sup>, Gregor Dördelmann<sup>1</sup>, Diana Kozlova<sup>1</sup>, Sarah Karczewski<sup>2</sup>, Rosario Lizio<sup>3</sup>, Silko Grimm<sup>4</sup>, Jessica Mueller-Albers<sup>4</sup>, Shirley Knauer<sup>2</sup> and Matthias Eppe<sup>1</sup>

<sup>1</sup>Inorganic Chemistry and Center for Nanointegration Duisburg-Essen (CeNIDE), University of Duisburg-Essen, Universitätsstr. 5-7, 45117 Essen, Germany

<sup>2</sup>Molecular Biology, Center for Medical Biotechnology (ZMB), University of Duisburg-Essen, Universitätsstr. 5, 45117 Essen, Germany

<sup>3</sup>Evonik Industries AG, Rodenbacher Chaussee 4, 63457 Hanau, Germany

<sup>4</sup>Evonik Industries AG, Kirschenallee, 64293 Darmstadt, Germany

[jens.nelsen@uni-due.de](mailto:jens.nelsen@uni-due.de)

### INTRODUCTION

A challenge in modern drug delivery is the transportation of negatively charged and hydrophilic biomolecules like DNA or siRNA, e.g. for transfection or gene silencing in gene therapy.<sup>[1]</sup> For such compounds, the biocompatible and biodegradable polymer poly(D,L-lactide-co-glycolide) (PLGA) was often used as a nanoparticulate carrier system. However, it is difficult to encapsulate hydrophilic molecules into a PLGA matrix by classical emulsion techniques, because they tend to diffuse into the continuous aqueous phase during the synthesis. Thus, the encapsulation efficiency for such compounds is rather low. Therefore, a drug delivery system consisting of calcium phosphate (high affinity to nucleic acids and proteins) and PLGA nanoparticles was developed, to increase the encapsulation efficiencies of hydrophilic biomolecules into PLGA nanoparticles.<sup>[2, 3, 4]</sup> The high affinity of polar biomolecules to calcium phosphate should thereby strongly increase their incorporation into the hydrophobic matrix of PLGA.

### EXPERIMENTAL METHODS

To form calcium phosphate nanoparticles (loaded with anti-eGFP-siRNA or eGFP-DNA, a rapid precipitation method was used. For the incorporation of either eGFP-DNA- or siRNA-functionalized calcium phosphate nanoparticles into PLGA nanoparticles, a water-in-oil-in-water ( $W_1/O/W_2$ ) double emulsion solvent evaporation method was applied in a second synthesis step. To encapsulate FITC-BSA into the nanoparticles, a modified  $W_1/O/W_2$  emulsion solvent evaporation method according to Tang *et al.*<sup>[5]</sup> was used. The nanoparticles were characterized by dynamic light scattering (DLS), scanning electron microscopy (SEM), cell culture experiments (cell uptake studies by confocal laser scanning microscopy (CLSM), transfection and gene silencing experiments as well as cell viability tests). Furthermore, the encapsulation efficiency was determined by UV/Vis spectroscopy.

### RESULTS AND DISCUSSION

The resulting calcium phosphate/PLGA nanoparticles, loaded with either proteins or nucleic acid had a diameter of about 200 nm and a negative zeta potential of -26 mV. The addition of calcium phosphate into the

inner aqueous phase increased the encapsulation efficiency of siRNA, DNA and FITC-BSA by a factor of 3 to 10 compared to PLGA nanoparticles without calcium phosphate. To improve the cellular uptake of these nanoparticles, an outer layer of either chitosan or polyethyleneimine (PEI) was added to reverse the negative zeta potential to  $>+30$  mV. In cell uptake studies, the cationic nanoparticles showed an improved cellular uptake and induced the proton sponge effect as shown by CLSM. Nanoparticles loaded with eGFP-DNA showed good transfection efficiencies in transfection experiments with HeLa cells. In gene silencing experiments, anionic nanoparticles gave knockdown efficiencies of 53%, and cationic nanoparticles (chitosan- or PEI-coated) gave knockdown efficiencies of 68% and 89%, respectively.

### CONCLUSION

The encapsulation efficiency of hydrophilic and anionic biomolecules (siRNA, plasmid DNA and FITC-BSA) into PLGA nanoparticles was strongly increased by the addition of calcium phosphate, probably due to a better adsorption of these hydrophilic biomolecules onto the surface of calcium phosphate nanoparticles. An increased loading, as well as a positive surface charge lead to higher efficiencies in intracellular drug delivery.

### REFERENCES

- [1] V. Sokolova, M. Eppe, *Angew. Chem., Int. Ed.*, 2008, **47**, 1382-1395.
- [2] B.D. Ulery, L.S. Nair *et al.*, *J. Polym. Sci., Part B: Polym. Phys.*, 2011, **49**, 832-864.
- [3] C. Perez, A. Sanchez, D. Putnam *et al.*, *J. Controlled Release*, 2001, **75**, 211-224.
- [4] V. Sokolova, O. Rotan *et al.*, *J. Nanopart. Res.*, 2012, **14**, 910.
- [5] J. Tang, J. Y. Chen *et al.*, *Int. J. Pharm.*, 2012, **431**, 210-221.

### ACKNOWLEDGMENTS

This work was supported by Evonik Industries, Darmstadt and by the Deutsche Forschungsgemeinschaft (DFG) in the framework of the Collaborative Research Center "Supramolecular Chemistry on Proteins" (SFB 1093).





# Human Bone Marrow Mesenchymal Stem Cells Responses to Titanium Surface Coated with Type I Collagen Using Natural Cross-linker Genipin

Ying-Sui Sun<sup>1</sup>, Her-Hsiung Huang<sup>1</sup>, Kai-Chun Chang<sup>2</sup>

<sup>1</sup>Department of Dentistry, National Yang-Ming University, Taipei, Taiwan

<sup>2</sup>Institute of Oral Biology, National Yang-Ming University, Taipei, Taiwan  
[hhuang@ym.edu.tw](mailto:hhuang@ym.edu.tw)

## INTRODUCTION

Various surface treatments have been focused on coating bioinert metallic implants with biomolecular in order to regulate the functions of cells on implant surfaces<sup>1</sup>. Type I collagen, the most abundant protein in the bone matrix, has been used to improve the biological activity on implant surfaces<sup>2</sup>. This study sought to immobilize the type I collagen to biologically inert titanium surface through the use of the nontoxic, natural cross-linker genipin. Surface characterizations and cell responses of the treated titanium surfaces for dental implant application were investigated.

## EXPERIMENTAL METHODS

We selected type I collagen for the biomolecular coating. For the sake of simplicity and low cost, we used the nontoxic natural cross-linker genipin as the medium with which to immobilize type I collagen to the machined titanium surface designated TiGC. The untreated machined titanium surface was used as control designated Ti. Surface characterizations, including the morphology, chemistry, hydrophilicity, and roughness, of the test materials were analyzed. Human bone marrow mesenchymal stem cells (hBMSCs) responses, including the adhesion, migration, proliferation, mineralization, and differentiation, to the test materials were performed. At least five samples were used for each test group. Statistical analysis was performed using Student's t-test with alpha of 0.05.

## RESULTS AND DISCUSSION

X-ray photoelectron spectroscopy analysis results demonstrated that the genipin could successfully immobilize the type I collagen to titanium surface. Scanning electron spectroscopy (SEM) analysis results showed that the thickness of the type I collagen coated on titanium surface could be controlled at a nanoscale. The resulting surface of TiGC included a mixture of reticular submicro- and nanostructures (Figure 1(b)) and displayed high hydrophilicity (water contact angle < 22°). Following few months of storage at 4°C, the type I collagen on titanium surface still presented good bonding and functionality, which promoted the mineralization of hBMSCs. Cell responses analysis revealed that the type I collagen coating promoted the adhesion (Figure 2(b)), migration, and osteogenesis of hBMSCs as well as the mineralization of the extracellular matrix (ECM). Compared to the untreated Ti, the type I collagen-coated TiGC had higher expression levels of osteogenic markers, in terms of osteopontin (Figure 3(a)), bone sialoprotein, and osteocalcin (Figure 3(b)).

## CONCLUSION

The use of the natural cross-linker genipin as the medium to immobilize type I collagen to titanium surface promoted the adhesion, migration, and osteogenesis of hBMSCs as well as the mineralization of the ECM. The proposed surface treatment technique is a simple low-cost process that can be potentially employed for titanium dental implant.

## REFERENCES

1. Park J.W. *et al.*, Acta Biomater. 7:3222-9, 2011.
2. Schliephake H. *et al.*, Clin. Oral Implants Res. 20:31-7, 2009.

## ACKNOWLEDGMENTS

The authors would like to thank the financial support from Ministry of Science and Technology, Taiwan (MOST101-2314-B-010-052-MY3). Thanks are also due to Dr. S.H. Chiou from Taipei Veterans General Hospital, Taiwan, for kindly providing us with the cells.

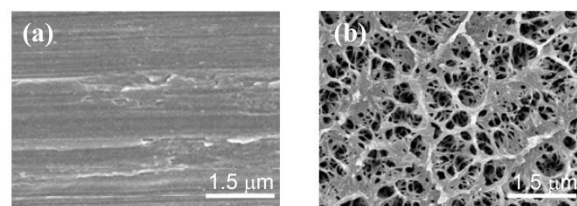


Figure 1 SEM micrographs of test materials: (a) Ti; (b) TiGC.

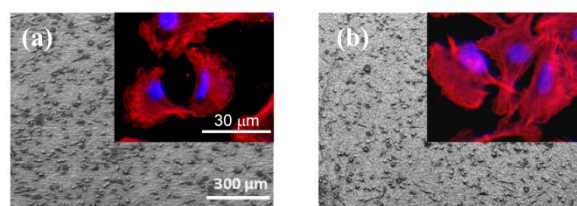


Figure 2 SEM and immunofluorescent staining micrographs of test materials: (a) Ti; (b) TiGC.

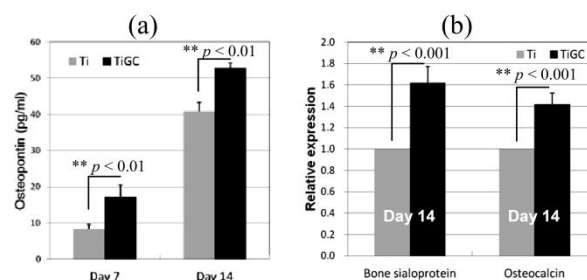


Figure 3 Expression levels of osteogenic markers, in terms of osteopontin (a), bone sialoprotein, and osteocalcin (b), of test materials Ti and TiGC.

## INTRODUCTION

The legless locomotion of snakes has tremendous tribological consequences for the ventral body side [1]. We focused on the influence of microstructures found on ventral scales of the California King Snake (*Lampropeltis getula californiae*) on friction behaviour of the skin. Snake-inspired anisotropic microstructured polymer surfaces (SIMPS) (Figure 1) and other microstructured surfaces with isotropic and anisotropic geometry were compared [2].

In biomedical applications, like in many technical systems, appearance of the stick-slip phenomenon is undesirable due to an increase of abrasion [3], which can reduce the lifetime of e. g. joint implants with negative implications for patients' health and healthcare costs.

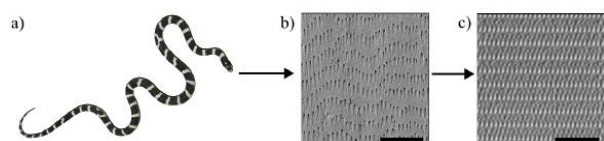


Figure 1 From snake to SIMPS, a) Photograph of the California King Snake (*L. g. californiae*). SEM micrograph of b) snake ventral scale and c) SIMPS. Scale bars: 10 µm.

## EXPERIMENTAL METHODS

The frictional coefficient was measured by a microtribometer. The frictional signal was analysed by performing fast Fourier transformations (FFT), allowing to describe the stick-slip motion in a quantitative way. To exclude the influence of physico-chemical variations, all friction measurements were performed on identical epoxy polymer. For details please see [4].

## RESULTS AND DISCUSSION

The ventral microstructures of the snake skin and the SIMPS do not only possess anisotropic frictional properties, but also reduce stick-slip vibrations during sliding. Furthermore, our experimental data did not confirm the previous statement that frictional coefficient correlates with the stick-slip occurrence [5]. It can be assumed, that snakes are able to alter frictional properties of their ventral body surface by the variation of body stiffness and thereby their effective elastic modulus. The observed reduction of stick-slip motion of the skin indicates that the ventral body surface is not only optimised towards frictional properties, but also towards abrasion reduction. Therefore, snake skin is a

very attractive biological model for optimizing technical surfaces under tribological stress.

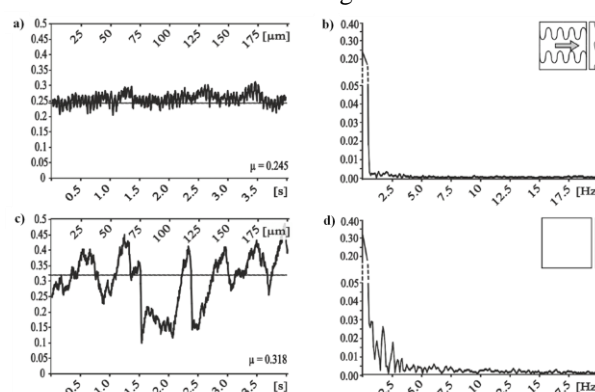


Figure 2 Frequency analysis of frictional coefficient on (a, b) SIMPS, (c, d) smooth surface. Frictional coefficient signal (a, c) in frequency domain after FFT (b, d). (Only exemplary data, for more data see [4]).

## CONCLUSION

Snake skin is a highly optimized tribological system, which shows anisotropic frictional properties and reduced wear, as well as a reduction in stick-slip vibration, which by itself is known to increase abrasion between sliding partners. We were able to transfer these properties to artificial polymer surfaces (SIMPS).

The investigation of the effects of surface texturing on the frictional coefficient and stick-slip motion in biological surfaces may represent a short cut towards frictional systems with reduced stick-slip vibrations. Additionally, this approach of surface modification by surface texturing opens up the possibility for tribological optimization of state of the art biomaterials, e. g. for implant design.

## REFERENCES

1. Baum M. *et al.*, Tribol. Lett. 54:139-150, 2014
2. Baum M. *et al.*, Beilstein J. Nanotech. 5:1091-1103, 2014
3. Popov V. Contact mechanics and friction, 2010
4. Baum M. *et al.*, Beilstein J. Nanotech. 5:83-97, 2014
5. Urbakh M. *et al.*, Nature 430:525-528, 2004

## ACKNOWLEDGMENTS

This work was funded by the Federal Ministry of Education and Research, Germany within the BIONA program (01 RB 0812A) to SNG.

## Molecular Weigh of Hyaluronan Immobilized on the Surface of a Porous Asymetric Scaffold Strongly Affects the Behavior of Co-Cultured Mesenchymal Stem Cells and Colorectal Cancer Cells

Elias Al Tawil<sup>1</sup>, Alexandre Monnier<sup>1</sup>, Yusra Kassim<sup>2</sup>, Quang Trong Nguyen<sup>1</sup>, Brigitte Deschrevel<sup>1</sup>

<sup>1</sup>Laboratory "Polymères, Biopolymères, Surfaces" (PBS), UMR 6270, Normand Institute of Molecular, Medicinal and Macromolecular Chemistry, FR 3038, CNRS – University of Rouen, F-76821 Mont-Saint-Aignan Cedex, France

<sup>2</sup> Laboratory "MicroEnvironnement et Renouvellement Cellulaire Intégré" (MERCi), EA 3829, University of Rouen, 22 Bd Gambetta, F-76183 Rouen Cedex, France

[brigitte.deschrevel@univ-rouen.fr](mailto:brigitte.deschrevel@univ-rouen.fr)

### INTRODUCTION

In recent years, we elaborated new porous asymmetric scaffolds for tissue engineering. The scaffolds are made of poly(lactic acid) (PLA) and their surface are entirely functionalized by a nanolayer of hyaluronan (HA). Scaffolds show a tridimensional structure with interconnected macro- and micropores. Diameter of pores opened to the surface can be controlled and ranges from 80 to 185  $\mu\text{m}$ . These PLA-HA scaffolds have proved to be well-adapted for adhesion and proliferation of different cell types including mesenchymal stem cells (MSC) and cancer cells like HT-29 colorectal cancer cells. Interestingly, we showed that functionalization of scaffold surface by HA can be performed as much efficiently whatever the HA chain molecular weight. This enables us to use these new scaffolds to investigate the effect of HA molecular weight on cell behavior in a tridimensional environment. Since it is known that both HA is involved in cancer progression<sup>1</sup> and MSC are recruited to tumoral sites<sup>2</sup>, we used our biomaterials for mimicking a tumor microenvironnement: we studied the influence of the molecular weight of HA chains immobilized on the scaffold surface on the interactions between MSC and HT-29.

### EXPERIMENTAL METHODS

Biomaterial discs (16 mm diameter) were placed in 24-well plates. Each disc was seeded with  $10^6$  cells in 2 mL of culture medium ( $\alpha$ -MEM or HDMEM). Cultures were incubated at 37°C under 5 %  $\text{CO}_2$  during 12 days. For each set of experimental conditions, cell culture and analysis were performed in triplicate. Cell proliferation was measured using WST-1 test. To observe cell behavior by video microscope, cells were previously labeled with a blue fluorescent tracer (7-amino-4-chloromethylcoumarin) for MSC and a green fluorescent tracer (5-chloromethylfluorescein diacetate) for HT-29 cells. Membrane antibody arrays were used to detect the expression of proteins in co-culture media. Cytokines in co-culture media and VEGFR-2 in cell lysates were quantified by ELISA.

### RESULTS AND DISCUSSION

Separate cultures of MSC (in  $\alpha$ -MEM) and HT-29 (in HDMEM) showed that proliferation was maximum for both cell types in scaffold with mean pore diameter of 160  $\mu\text{m}$ . When co-cultured, proliferation of cells was significantly dependent on the ratio of seeded cells. The best ratio, 2:1 (MSC:HT-29), was used for all the following experiments. MSC and HT-29 were co-cultured on scaffolds covered with either high

molecular weight HA (HMW-HA,  $3.10^6 \text{ g.mol}^{-1}$ ) or low molecular weight HA (LMW-HA,  $880 \text{ g.mol}^{-1}$ ). In both cases, HT-29 form spheroids (Figure 1) with a necrotic center which reflects the structure of *in vivo* solid tumor. However, co-cultures of the two cell types showed great differences in behavior according to HA molecular weight. In the presence of HMW-HA, there was no evidence of physical interaction between MSC and HT-29 (Figure 1A) whereas MSC came to surround the voluminous HT-29 spheroids in the presence of LMW-HA (Figure 1B). Moreover, with HMW-HA the microenvironnement was found to be proinflammatory, with increased secretion of interleukin 6 and macrophage migration inhibitory factor, while an increased secretion of angiogenic cytokines such as vascular endothelial growth factor and metalloproteases (MMP9) were observed with LMW-HA.

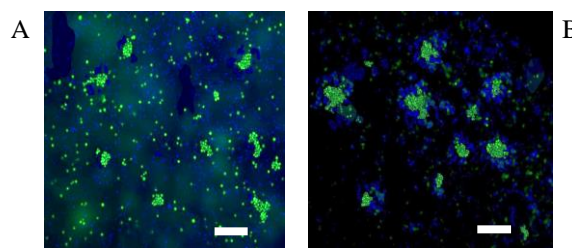


Figure 1: Organisation of MSC (blue) and HT-29 (green) co-cultured in PLA-HA scaffold in the presence of  $\alpha$ -MEM medium as observed by video microscope; A, HMW-HA and B, LMW-HA. Bar corresponds to 100  $\mu\text{m}$ .

### CONCLUSION

The results clearly show that interactions between MSC and HT-29 strongly depend on HA molecular weight and they suggest that these interactions induce different MSC differentiation pathways. This study also indicates that our new biomaterials may constitute useful tools in the field of tumor engineering.

### REFERENCES

1. Toole B.P. *et al.*, J Biol Chem 277:4593-4596, 2002
2. Hogan N.M. *et al.*, Biochem Biophys Res Comm 435:574-579, 2013

### ACKNOWLEDGMENTS

We are grateful to the French Research and Technology Ministry for the fellowship granted to E. Al Tawil and A. Monnier.





## Topographical and Biochemical Functionalized PEDOT Films as Coating Strategies for Improved Neuroelectrode Functionality

Catalina Vallejo-Giraldo<sup>1</sup>, Marc Fernandez-Yague<sup>1</sup>, Abhay Pandit<sup>1</sup>, Eilís Dowd<sup>2</sup>, Manus Jonathan Paul Biggs<sup>1</sup>

<sup>1</sup> Network of Excellence for Functional Biomaterials (NFB), <sup>2</sup>Pharmacology, National University of Ireland, Galway  
[c.vallejogiraldo@nuigalway.ie](mailto:c.vallejogiraldo@nuigalway.ie)

### INTRODUCTION

Studies with conducting polymers (CPs) as functional electrode coatings have shown to enhance tissue/electrode integration and electrode performance in situ. Current strategies in this field have focused on reducing impedance and the presentation of neurotropic moieties to enhance the integration with brain milieu and to help with cell attachment properties<sup>1</sup>. The use of biochemical functionalization of CPs surfaces is an increasingly utilized mechanism to present biologically active dopants to promote or inhibit specific biological interaction with brain cells. However, a remarkable disruption of the polymer's physio-electrical properties is observed by the incorporation of structural ligands or peptides on the CPs surfaces<sup>2</sup>. This study investigates a range of physical, electrical and biological properties of a conventional conducting polymer PEDOT with dual functionalization by means of micro and nanotopographical modification (nanoimprinting) and entrapped mimetic polysialic acid peptide (PSA) to support the electrode stability and electrical properties via sustained neural integration within the PEDOT electrode coating film.

### EXPERIMENTAL METHODS

**Topographical modification:** PEDOT films were polymerized galvanostatically on platinum coated glass, and characterized by FTIR, EIS, AFM and SEM. PEDOT films were then thermally nanoimprinted using photolithography fabricated Ni masters.

**Bioactive-polymer-composite synthesis:** PEDOT/mimetic molecule films were polymerized galvanostatically on platinum coated glass. The cytocompatibility of the functionalized PEDOT films is evaluated by culturing isolated rat ventral mesencephalon (VM) cells on the polymeric films by alamar blue™, live and dead assay and fluorescent microscopy for adherent cell counting and quantitative immunostaining of relevant neural biomarkers and neural outgrowth.

### RESULTS AND DISCUSSION

The results from an optimization study performed using dissociated hippocampal primary cells as a proof of concept of primary cell viability cultured on pristine PEDOT films indicated the cytocompatibility of this material and no toxicity was detected (Fig.1a). SEM results depicted in Fig.1b show the topographical modification of PEDOT polymeric films after imprinting an ordered array of 1µm wide/deep pits. Also, the mimetic PSA peptide was successfully entrapped during electrodeposition and it preserved biofunctionality as assessed by the preliminary promotion of ventral mesencephalon (VM) cells on PEDOT electrode coating films up to a period of five

days in culture. Furthermore, the polymeric films treated with a combined functionalization of both imprinted films with mimetic PSA peptide incorporation show promotion of VM cells and slightly disruption of the stability and electrical performance of the PEDOT films compared to controls.

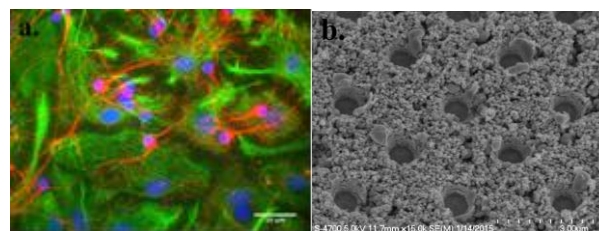


Fig.1.a.Fluorescent micrograph of immunostained hippocampal primary cells cultured on pristine PEDOT film formed with 0.4 mA/cm<sup>2</sup> current density. Red β tubulin III, green GFAP and blue Hoeschst, Scale bar = 50µm. b. Scanning electron micrograms (SEM) of a nanoimprinted PEDOT film formed with 0.4 mA/cm<sup>2</sup> current density

### CONCLUSION

Designing an optimized electrode coating material will require a trade-off between desired electrical, morphological, chemical and biological properties. The development of bioactive conductive polymers through biological dopants addresses the cell interaction, selection and attachment when using polymers. However, this only goes part of the way as to solving biological interface interaction as the physio- electrical material properties significantly get disrupted by biological dopants. An alternative approach used to functionalize conducting polymers involves creating polymers with multiple functionalities. The presence of a dual functionalization in the context of both topographical and biochemical modifications presented here, significantly show to be a great enhancement of the PEDOT polymeric films with a promotion of healthy ventral mesencephalon cell population up to a period of five days in culture and with a close preservation of physico-electrical film's properties compared to controls.

### REFERENCES

- 1.Green RA, Lovell NH, et al. Biomaterials. 2008;29:3393-9.
- 2.Green, RA., Lovell NH, et al. Acta Biomater. 2010;6.1: 63-71.

### ACKNOWLEDGMENTS

This work was funded through Science Foundation Ireland 11/SIRG/B2135.



## Structural Features of Biomaterials Influence the Paracrine Relationships that Mesenchymal Stem Cells Establish with Osteoblasts and Endothelial Cells

Lara Crespo<sup>1,2</sup>, Francisco Martín-Saavedra<sup>2,1</sup>, Laura Saldaña<sup>1,2</sup>, Enrique Gomez-Barrena<sup>3</sup>, Nuria Vilaboa<sup>1,2</sup>

<sup>1</sup>Hospital Universitario La Paz-IdiPAZ, Spain

<sup>2</sup>CIBER de Bioingeniería, Biomateriales y Nanomedicina (CIBER-BBN), Spain

<sup>3</sup>Departamento de Cirugía, Universidad Autónoma de Madrid, Spain

[nuria.vilaboa@salud.madrid.org](mailto:nuria.vilaboa@salud.madrid.org)

### INTRODUCTION

Cellular-based approaches in bone tissue engineering involve culturing human mesenchymal stem cells (hMSC) on three-dimensional scaffolds, which provide support structures<sup>1</sup>. Upon implantation of the intermediate tissue in the bone defect site, transplanted hMSC may establish paracrine relationships with host cells located at their vicinity. Multiple studies have addressed the cross-talk between hMSC and osteoblasts or endothelial cells using conventional co-cultures in which the studied cell types do not establish direct contact. However, it is unknown whether these relationships are affected by the structural features of the substrates that harbor hMSC. To this aim, hMSC from bone marrow were seeded in porous or flat biomaterials and then co-cultured with human osteoblasts (hOB) obtained from bone explants or human umbilical vein endothelial cells (HUVEC), using a transwell insert system that allows humoral contact of both cell types without direct cell contact.

### EXPERIMENTAL METHODS

hMSC were seeded in highly porous scaffolds made of polystyrene or Ti6Al4V, or encapsulated in fibrin hydrogels. As controls, hMSC were seeded in polyester membrane cell culture inserts, which were used as flat permeable supports. In addition, hMSC were seeded on flat Ti6Al4V samples, which surfaces were polished to get a mirror-like finish. hOB or HUVEC were seeded in tissue culture plastic. hMSC seeded in porous or flat substrates were co-cultured with hOB or HUVEC using a transwell system. Co-cultures were incubated in DMEM medium containing fetal bovine serum. In some experiments, media were supplemented with dexamethasone, ascorbic acid and  $\beta$ -glycerolphosphate. Cell viability was assessed using the alamarBlue assay. Secretion of procollagen type I, OPG, soluble RANKL (sRANKL), M-CSF, VEGF and Flt-1 were measured in culture media while levels of TGF- $\beta$  were quantified in cell layers, using ELISA kits. Alkaline phosphatase activity (ALP) was measured in cell layers. Gene expression analyses were carried out by real-time quantitative RT-PCR assays. A scratch assay was used to study changes in HUVEC migration. Tubule formation was assessed in HUVEC seeded on Matrigel-GFR, which were incubated with conditioned media from hMSC cultures.

### RESULTS AND DISCUSSION

Compared to isolated cultures, hOB viability was not affected when co-cultured with hMSC seeded in polystyrene or polyester substrates, but was impaired

when MSC had been seeded in flat Ti6Al4V or encapsulated in fibrin hydrogels. Interestingly, hOB viability increased in co-cultures with hMSC seeded in porous Ti6Al4V. Levels of *COL1A1* and *ALPL* mRNAs were higher in hOB co-cultured with hMSC seeded in porous polystyrene scaffolds than in hOB co-cultured with hMSC seeded on flat polyester substrates. This effect correlated with increased levels of procollagen type I in co-cultures of hOB and hMSC seeded on porous surfaces, as well as with higher osteoblastic ALP activity. The degree of cell layer mineralization and *BGLAP* mRNA levels were lower in hOB co-cultured with hMSC seeded in porous polystyrene than in flat polyester substrates. The OPG/sRANKL ratio in co-culture media was substantially lower when hMSC were seeded in polystyrene scaffolds, while M-CSF levels increased. Compared to hOB co-cultured with MSC seeded in flat polyester substrates, levels of TGF- $\beta$  were diminished in hOB co-cultured with hMSC seeded in polystyrene scaffolds.

Compared to isolated cultures, HUVEC viability and migration ability increased when co-cultured with hMSC seeded in all tested substrates except fibrin hydrogels. The increases were higher in those co-cultures in which hMSC were seeded on porous substrates. Tubule formation was enhanced when HUVEC were incubated with conditioned media from hMSC cultured in polystyrene scaffolds. The paracrine effects of hMSC co-cultured in porous substrates were not mediated through secretion of VEGF or its receptor Flt-1, which mRNA levels were not either sensitive to the substrate features.

### CONCLUSION

The paracrine interactions that hMSC establish with hOB and HUVEC are strongly influenced by the structural features of substrates. Upon implantation of a tissue intermediate, the chemical and topographical characteristics of the scaffold may influence the control of transplanted hMSC on the behaviour of neighbouring osteoblasts and endothelial cells.

### REFERENCES

1. Kneser U *et al.*, J. Cell. Mol. Med. 2006 10:7-19.

### ACKNOWLEDGMENTS

This work was supported by grants PI12/01698 (FIS, Spain), S2013/MIT-2862 (Comunidad de Madrid, Spain), MAT2012-37736-C05-05 (MINECO, Spain) and fellowship BES-2010-034989 (MINECO) to LC.





Takayoshi Nakano<sup>1</sup>, Aira Matsugaki<sup>1</sup> and Takuya Ishimoto<sup>1</sup><sup>1</sup>Division of Materials and Manufacturing Science, Graduate School of Engineering, Osaka University, Japan  
[nakano@mat.eng.osaka-u.ac.jp](mailto:nakano@mat.eng.osaka-u.ac.jp)

## INTRODUCTION

Bone tissue has well-organized hierarchical structure at various scale levels. Original intact bone exhibits specific oriented architecture derived from biological apatite (BAP) crystallite orientation that is closely related to the arrangement of collagen fibrils. Preferential alignment of anisotropic BAP crystallites/collagen fibrils in typical cortical and spongy bones, for example, alters depending on the bone shape, *in vivo* stress distribution, and bone turnover. The preferential alignment of BAP *c*-axis, in particular, tends to arrange along the stress distribution in the original bones, indicating anisotropy of mechanical properties.

In contrast, recovery of anisotropic BAP alignment strongly depends on the portion and period of regeneration process, which is insufficient to reach the original level, while bone mineral density (BMD) is almost improved to its original value [1,2].

The purpose of this study is to develop some strategies which can control the preferential alignment of osteoblasts and the resultant formation of normal anisotropic extracellular matrix (ECM).

## EXPERIMENTAL METHODS

Primary osteoblasts were subjected to various anisotropic environments involving stress field, substrates with step patterning or with aligned collagen fibers. The preferential orientation of osteoblasts and the BAP *c*-axis were analysed. The BAP orientation in secreted ECM, especially, is evaluated by various  $\mu$ XRD systems with collimators that are several dozen or hundreds of micrometers in diameter. The BAP orientation is roughly related to the direction of collagen matrix secreted by cells.

## RESULTS AND DISCUSSION

Control of cellular alignment is one of the methodologies for arranging the oriented ECM of tissue. Figure 1 shows the aligned osteoblasts along the slip traces caused by dislocation gliding. Dislocations are introduced into  $\alpha$ -titanium single crystals by plastic deformation of the prism slip system, which induces a step-like structure with acute angles between the normal surface and the slip plane. The topographical properties of step patterning could be controlled by variation of the compressive plastic strain. The step geometry introduced by plastic deformation strongly influences osteoblast elongation along the slip traces. Cellular alignment is very important because anisotropic control of bone structural formation *in vitro* can be established by organizing cell alignment and the following BAP/collagen preferential orientation [3].

Anisotropic architecture of bone is derived from the collagen fiber scaffold and the related osteoblast

alignment. The oriented collagen scaffolds were fabricated by a hydrodynamic method. Osteoblast orientation is regulated by the degree of the scaffold collagen orientation, with preferential alignment along the collagen molecular orientation. The directional secretion and fibrogenesis of collagen matrix and BAP crystallite formation, which has preferential *c*-axis orientation along the cell direction, is shown in Figure 2. The degree of BAP orientation deposited by osteoblasts depends on the directional distribution of osteoblasts cultured on the oriented collagen scaffolds.

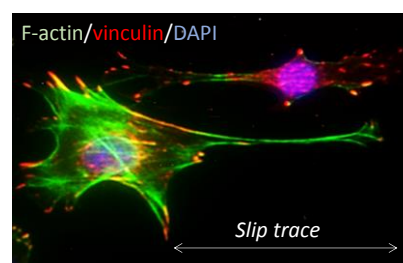


Figure 1 Fluorescent image of osteoblasts aligned along slip traces (10% compressive strain).

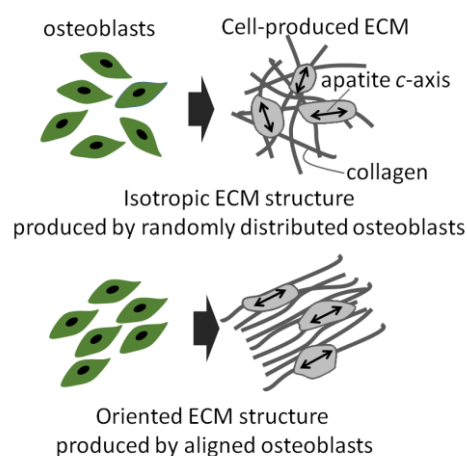


Figure 2 Osteoblasts orientation determines the secreted bone matrix alignment.

## CONCLUSION

The appropriate anisotropic ECM structure which enables its proper function can be controlled by surface morphology and the chemical and/or physical environment surrounding the constituent cells.

## REFERENCES

1. Nakano T. *et al.*, Bone. 51:741–747, 2012
2. Ishimoto T. *et al.*, JBMR. 28:1170–1179, 2013
3. Matsugaki A. *et al.*, Biomaterials. 37:134–143, 2015

## ACKNOWLEDGMENTS

This work was supported by Grants-in-Aid for Scientific Research (S) from the Japan Society for Promotion of Science (JSPS).

## Injectable and Self-Healing Supramolecular Hydrogel for Tissue Engineering Applications

Damien Dupin, Pablo Casuso, Natividad Díaz, Adrián Pérez-San Vicente and Iraida Loinaz

Biomaterials Unit, Materials Department, IK4-CIDETEC, Spain

[ddupin@cidetec.es](mailto:ddupin@cidetec.es)

### INTRODUCTION

In-situ forming hydrogel systems have attracted considerable interest as injectable scaffolds for tissue engineering and drug delivery due to their easy applications and minimally invasive injection procedure.<sup>1,2</sup>

Our research group has recently developed a new family of injectable supramolecular hydrogels based on low molecular-weight Au (I) and Ag (I) thiolates.<sup>3,4</sup> Here we present a new family of polymeric hydrogel with self-healing properties and adjustable mechanical properties.<sup>5,6</sup>

### EXPERIMENTAL METHODS

*Hydrogels were prepared* by mixing an aqueous solution of polymer at 10 wt.% with an aqueous solution containing metal salt. *Dynamic rheology* measurements were performed using a TA Instruments AR G2 temperature-controlled rheometer with 20 mm diameter plate geometry.

### RESULTS AND DISCUSSION

Supramolecular polymeric hydrogels were obtained by mixing an aqueous solution of salt metals ( $\text{Ag}^+$  or  $\text{Au}^+$ ) with a solution of thiolated poly(ethylene glycol) [PEG] polymer at physiological pH. The instantaneous gel formation by means of metal-thiolate centres allows its application as injectable hydrogel (Figure 1).

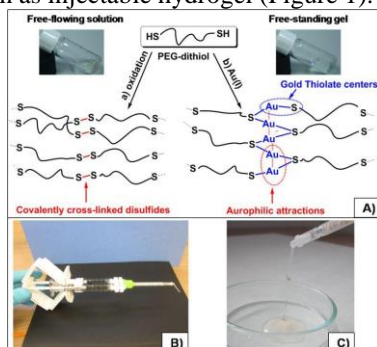


Figure 1. (A) Schematic representation of the metal-thiolate cross-linking and (B,C) its injection using a double barrel syringe.

The supramolecular hydrogel exhibits self-healing (Figure 2a). Varying the amount of metallophilic cross-linker allows tuning the mechanical properties of the hydrogel as judged by reology studies. Moreover, the variation of  $G'$  over  $G''$  indicates the hardening of the material under high frequencies. MTS assay confirmed that the hydrogel is not cytotoxic to cells.

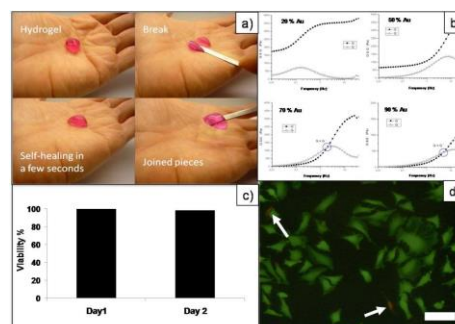


Figure 2. (a) Self-healing behaviour and (b) dynamic mechanical properties of the supramolecular hydrogel. (c, d) MTS assay of the viability of the hydrogel.

Judicious adjustment of the hydrogel concentration and the amount of gold added allowed the use of this material for musculoskeletal applications as a substitute of the synovial fluid or nucleus pulposus for patient suffering arthritis or intervertebral disc degeneration.

### CONCLUSION

The supramolecular hydrogel appears to be an excellent candidate for tissue engineering due to its facile injection and positive cell viability. Thanks to the permanent interchange of metal-thiolate, the supramolecular hydrogel exhibits self-healing properties at physiological conditions. Moreover, the hydrogels could also be designed for different application like viscosupplement material or nucleus pulposus replacement.

### REFERENCES

1. Burkoth A. K. *et al.*, Biomaterials 21:2395-2399, 2000
2. Klouda L., *et al.*, Eur. J. Pharm. Biopharm. 68:34-45, 2008
3. Casuso P., *et al.*, Org. Biomol. Chem. 8:8455-8458, 2010.
4. Odriozola I., *et al.*, Org. Biomol. Chem. 9:5059-5061, 2011
5. Patent number EP11382365
6. Casuso P., *et al.*, Chem. Comm. 50:15199-15201, 2014

### ACKNOWLEDGMENTS

The authors would like to thank the ETORTEK Program [biomaGUNE11(E11-301) and biomaGUNE12(E12-332)] as well as the INNPACTO Program [Hueso Injectable(IPT-2012-0745-300000)] for providing financial support to this project.

# Tailoring of DMTMM Conjugated HA-Tyr Allows Precise Control of Cellular Environment

Claudia Loebel<sup>1,2</sup>, Tino Stauber<sup>2</sup>, Matteo D'Este<sup>1</sup>, Mauro Alini<sup>1</sup>, Marcy Zenobi-Wong<sup>2</sup>, David Eglin<sup>1</sup>

<sup>1</sup>AO Research Institute Davos, Switzerland

<sup>2</sup>Cartilage Engineering + Regeneration, Department of Health, Science and Technology ETH Zurich, Switzerland  
[claudia.loebel@aofoundation.org](mailto:claudia.loebel@aofoundation.org)

## INTRODUCTION

Tyramine modified hyaluronic acid (HA-Tyr) hydrogels have shown great potential in tissue engineering and regenerative medicine<sup>1</sup>. The bio-orthogonal cross-linked mechanism enables independent tuning of mechanical properties and gelation rate of HA-Tyr by varying the hydrogen peroxide (H<sub>2</sub>O<sub>2</sub>) and horseradish peroxidase (HRP) concentration, respectively. Recently, we have shown that using 4-(4,6-dimethoxy-1,3,5-triazin-2-yl)-4-methylmorpholinium chloride (DMTMM) as conjugating agent allows to precisely tailor the tyramine functionality and the rheological features of the HA-Tyr hydrogels at constant HRP and H<sub>2</sub>O<sub>2</sub> concentrations<sup>2</sup>.

To answer major questions on how mechanical factors may lead to changes in cell behaviour, it is of paramount importance to provide a precise tailored extracellular environment. However, there is little data on the effect of encapsulated cells, in particular human mesenchymal stromal cells (hMSCs), on bulk mechanical properties of HA-Tyr hydrogels.

In the first part of this study, a modified strategy of DMTMM mediated HA-Tyr synthesis was used to improve rheological properties of the cross-linked matrices. Then, HA-Tyr hydrogels were explored as matrices for encapsulated hMSCs and their impact on bulk visco-elastic hydrogel properties was investigated.

## EXPERIMENTAL METHODS

HA-Tyr was prepared by optimizing a recently described protocol<sup>2</sup>. Briefly, amidation of the carboxylic acid groups of HA with the amine groups of Tyr was conducted in water (dH<sub>2</sub>O) at room temperature (RT) and 37 °C. Degree of tyramine substitution (DS<sub>mol</sub>) was calculated using UV-vis spectrophotometry. hMSCs (Freiburg, EK-326/08) or polystyrene beads (15 µm) were encapsulated in HA-Tyr (2.5% (w/v)) precursor solution containing HRP and H<sub>2</sub>O<sub>2</sub>. Evolution of network formation and visco-elastic properties were monitored in situ by rheology. Live-dead staining and confocal imaging documented viability and spreading of encapsulated hMSCs.

## RESULTS AND DISCUSSION

Coupling of HA-Tyr in dH<sub>2</sub>O reaches significantly higher yields compared to the previously shown synthesis in MES pH 5.5 (Figure 1A). It does not require accurate pH control or shift during reaction. Visco-elastic properties (Figure 1B) of cross-linked HA-Tyr matrices can be controlled by DS<sub>mol</sub>. Thus, DMTMM mediated HA-Tyr synthesis in dH<sub>2</sub>O extends the range of tunable mechanical properties of HA-Tyr hydrogels without affecting H<sub>2</sub>O<sub>2</sub> and HRP concentrations.

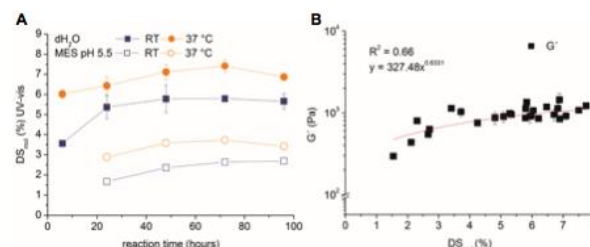


**Figure 1** A DS<sub>mol</sub> of HA-Tyr conjugates and B elastic modulus (G') of 2.5% (w/v) HA-Tyr (0.5 U/ml HRP/ 0.34 mM H<sub>2</sub>O<sub>2</sub>; n=3, mean ± SD).

Encapsulation of hMSCs reduces G' of HA-Tyr hydrogels about 300 Pa +/- 50 Pa compared to pure HA-Tyr hydrogels (Figure 2A). Notably, the effect is more pronounced in HA-Tyr hydrogels with low DS<sub>mol</sub>. Replacing the cells with polystyrene beads prolongs evolution of G' without changing final G' (Figure 2A). These results indicate that encapsulated hMSCs may participate in the crosslinking of HA-Tyr hydrogels and therefore reduce bulk mechanical properties of the matrix. Live-dead staining of encapsulated hMSCs demonstrates 90-95% cell viability after 5 days in culture (Figure 2B).

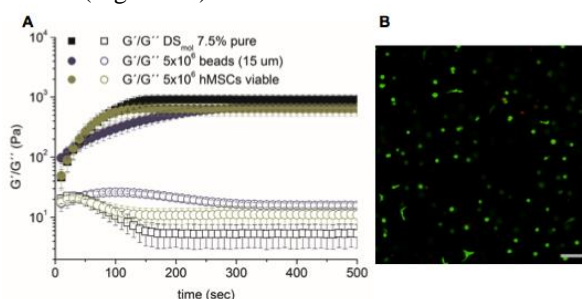


**Figure 2** A Time-sweep of cellular HA-Tyr and beads compared to pure HA-Tyr with PBS only (n=3, mean ± SD). B Live-dead staining (day 5) 5x10<sup>6</sup> hMSCs/ml cultured in DMEM/10% FBS, 1% P/S (scale bar 100 µm)

## CONCLUSION

Here we present an optimized conjugation strategy for DMTMM mediated HA-Tyr conjugation. Higher yields while maintaining precise control of DS<sub>mol</sub> and the physical characteristics provide a precise tailored 3D environment for encapsulated hMSCs without affecting H<sub>2</sub>O<sub>2</sub>/HRP concentrations.

## REFERENCES

- <sup>1</sup>Darr A & Calabro A, J.Mater.Sci.Mater.Med., 2009
- <sup>2</sup>Loebel C *et al.*, Carbohydr. Polym., 2015

## ACKNOWLEDGMENTS

The authors would like to thank the COST Action 1005 NAMABIO for providing financial support.





Nermin Keloglu<sup>1</sup>, Bernard Verrier<sup>1</sup>, Dominique Sigaudou-Roussel<sup>1</sup>, Thomas Trimaille<sup>2#</sup>, Jérôme Sohier<sup>1#</sup><sup>1</sup>Laboratory of Tissue Biology and Therapeutic Engineering (LBTI), UMR CNRS 5305, Lyon, France<sup>2</sup>Aix-Marseille University, UMR CNRS 7273, Marseille, France ; # Equal contributors[jerome.sohier@ibcp.fr](mailto:jerome.sohier@ibcp.fr)

## INTRODUCTION

Biodegradable polymer nanofibrillar structures that mimic native extracellular matrix fibers are extensively studied in tissue engineering. Aside from nanofibrillar architecture, the supportive matrices should as well provide an optimal environment to the cells, modulated along tissue formation through delivery of specific growth factors or bioactive molecules.

The use of biodegradable nanoparticles (NP) to localize and temporally control the delivery of encapsulated or adsorbed biomolecules represents therefore a valuable approach when combined to nanofibrillar (NF) matrices. Although different approaches have been proposed for such combination, a need remains to provide matrices that efficiently incorporate bioactive and homogeneously distributed NP, which can subsequently be released from the NF in a controlled and orchestrated fashion.

While bioactive NP can be safely obtained by nano-precipitation, jet-spraying has been described as a successful way of creating highly porous nanofibrillar scaffolds that allow extensive cell colonisation and tissue formation, unlike electrospinning<sup>1</sup>. Jet-spraying being based on the projection of a polymer solution to create nanofibers, we hypothesised that NP could be directly and permanently deposited onto the NF surface during their formation by co-projection. In addition, we postulated that electrostatic interactions could allow NP post-adsorption and controlled release from the highly porous NF matrices.

To investigate these hypotheses, we synthesized poly(lactic acid) (PLA) fluorescent NP and co-projected them during jet-spraying of poly(lactic-co-glycolic acid) (PLGA) NF. Alternatively, we incubated NP solutions with poly(lactic acid) (PLA) jet-sprayed matrices, either blank or pre-coated with poly-lysine (PLL). The two different approaches were compared in regards of efficiency, safety and distribution of the resulting NF/NP association, while NP release was determined.

## EXPERIMENTAL METHODS

Fluorescent PLA (MW 100000 g/mol) NP were prepared by nano-precipitation, coumarin-6 being dissolved in the acetone phase. Resulting NP size and zeta potential were determined by DLS. NF structures were obtained by jet-spraying PLGA (50/50, MW 80000 g/mol) and PLA (MW 100000 g/mol). Co-projection was achieved by simultaneously spraying NP in water and polymer solutions on the same collection point. Incubation of NP with blank or PLL coated NF matrices (discs of 18 x 1 mm thick) was performed in water solutions for 2 hours at room temperature. Scanning electron microscopy and fluorescence quantitation were used to characterize the hybrid NF/NP structures and determine NP release on matrices discs.

## RESULTS AND DISCUSSION

The produced fluorescent NP were of average 254nm in diameter with a very narrow distribution (Ip 0.05) and a negative zeta potential (-67 mV). Co-projection of NP during jet-spraying of PLGA allowed to efficiently deposit NP on the fibre surface as droplets-like structures. The amount of deposited NP appeared related to the quantity of projected NP and full covering of the nanofibers could be achieved, reaching an amount of 305 µg/mg of nanofibrillar matrix (fig. 1). Interestingly, the resulting nanofibrillar matrix remained visually of high porosity and interconnection.

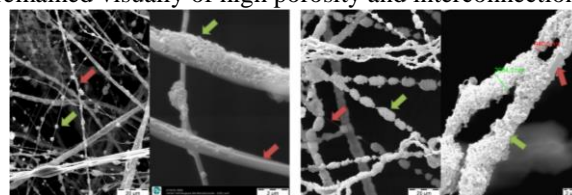


Fig. 1. Co-projection of NP during jet-spraying of PLGA results in deposition of NP (green arrows) on NF (red arrows), in varying amounts.

Incubation of the negatively charged NP with jet-sprayed PLA nanofibrillar matrices either blank (negative surface charge) or pre-coated with poly-lysine (positive surface charge) resulted in a complete and homogeneous covering of each fibre. Although the amount of NP associated by incubation was lower than for co-projection (respectively 38 and 83 µg/mg for blank and PLL coated NF), it permitted to modulate NP release by electrostatic interaction with PLL, unlike co-projection where NP remained bound to the NF (fig.2).

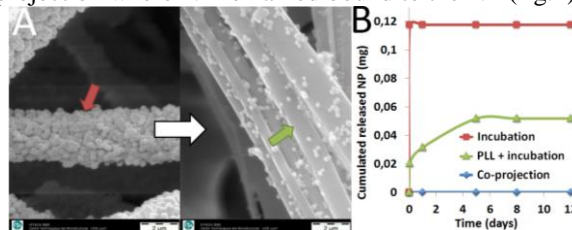


Fig. 2. Post-incubation of NP with jet-sprayed NF results in homogeneous NP coating (A) which can be released in a controlled fashion (B).

Overall, these results present novel and efficient approaches to associate NP with nanofibrillar matrices and release them in a controlled way. Ongoing experiments with protein-loaded NP will further confirm their safety and resulting bioactivity.

## CONCLUSION

The possibility to associate and release NP from NF matrices in a controlled way is promising to provide defined functionality and bioactivity to inert NF structures.

## REFERENCES

- Sohier J, Corre P, et al. Tiss. Eng. Part C, Methods. 20(4), 285-96, 2014.

## Microstereolithography & Plasma Polymerisation Coating of Nerve Guidance Conduits

James Clarke<sup>1</sup>, Adam Harding<sup>2</sup>, Fiona Boissonade<sup>2</sup>, John W Haycock<sup>1</sup> and Frederik Claeysens<sup>1</sup>

<sup>1</sup>Kroto Research Institute, Department of Materials Science & Engineering, The University of Sheffield, United Kingdom

<sup>2</sup>School of Clinical Dentistry, The University of Sheffield, United Kingdom

[mtp12jc@sheffield.ac.uk](mailto:mtp12jc@sheffield.ac.uk)

### INTRODUCTION

Nerve Guidance Conduits (NGC) are increasingly used in surgical peripheral nerve repair. Improving NGC performance is challenging as existing FDA approved materials are bio-inert. Both microtopographical features and surface functionalisation have been proposed to improve neuroregeneration with these materials<sup>1-2</sup>. In this study we focus on both the inclusion of organised micro geometries and plasma polymer surface coating to improve their effectiveness at stimulating nerve regeneration.

### EXPERIMENTAL METHODS

**Microstereolithography ( $\mu$ SL)** - NGC were produced from photocurable polycaprolactone (PCL) or polyethylene glycol (PEG) by microstereolithography ( $\mu$ SL). Photocurable PCL was produced from PCL triol ( $M_n \approx 900$  g/mol) by dissolving in dichloromethane (DCM) and adding triethylamine (TEA) and methacrylic anhydride (MAA) to attach methacrylate end groups. DCM, TEA and excess MAA were removed by precipitating methacrylated PCL in methanol.

The  $\mu$ SL setup consisted of a 405 nm laser and digital micromirror device (DMD). The required image was loaded onto the DMD and the laser light reflected from this, then focused onto the surface of the liquid prepolymer causing it to crosslink. 3D shapes were produced by lowering a stage within the prepolymer (figure 1).

**Plasma Treatment** - Plasma chambers were used to air etch and coat substrates with either acrylic acid (AAc), allylamine (AAm) or maleic anhydride (MA).

**in vitro Experiments** - NG108-15 neuronal cells and RN22 Schwann cells were cultured on surfaces. MTT assay was used to confirm cell viability.

After 72 hours, cells were fixed and labelled with phalloidin-TRITC (actin filaments) and DAPI (nuclei). Cells were imaged by confocal microscopy and neurite growth analysed using ImageJ software.

**in vivo Experiments** - Grooved and smooth NGCs were implanted in *thy-1-YFP-H* mouse common fibular nerve and compared with nerve graft. Regeneration was assessed by confocal-like microscopy.  $n = 5$  for each condition, results are shown as average  $\pm$  SEM.

### RESULTS AND DISCUSSION

Guidance features with dimensions less than 100  $\mu$ m were created on the inner surfaces of the NGC (figure 1). Plasma coating was achieved evenly on the inner

surfaces of NGCs <1 mm internal diameter with a length of 5 mm. Preliminary results show increased cell viability and neurite growth on AAc coated surfaces. Cells adhered well to other coated surfaces but neurite growth was less extensive. Micro geometries showed significantly improved regeneration than smooth NGC and were comparable to autograft.

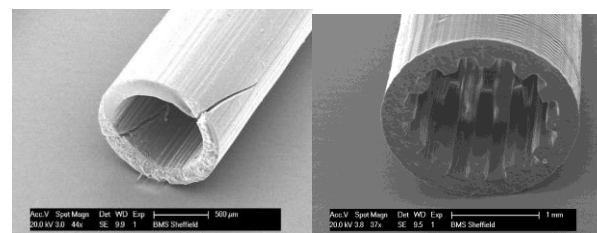


Fig. 1 Micrographs of NGC produced by  $\mu$ SL

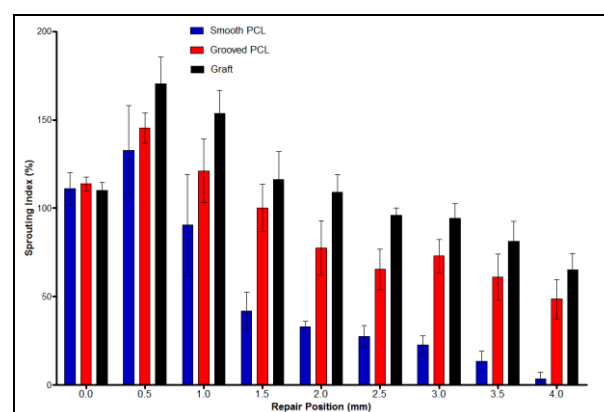


Fig. 2 Sprouting index of *thy-1-YFP-H* mouse common fibular nerve repair

### CONCLUSION

We have produced NGC with user-defined topography and surface chemistry. Plasma treatment may be used to enhance neuronal and Schwann cell responses to otherwise bio-inert materials. Topographical features enhance peripheral nerve regeneration in an animal model.

### REFERENCES

1. Annu. Rev. Biomed. Eng. 2010, 12:203-231.
2. Tissue Eng., Part B. 2012, 18:2 116-128.

### ACKNOWLEDGMENTS

The authors would like to thank the EPSRC for DTA funding and the National EPSRC XPS User's Service (NEXUS) at Newcastle University. Confocal microscopy was performed at the Kroto Research Institute Confocal Imaging Facility.





Mohammad Raoufi<sup>1,2</sup>, Neda Aslankoochi<sup>1,2</sup>, Sarah Young<sup>1,2</sup>, Joachim P. Spatz<sup>1,2</sup>, Dorothea Brüggemann<sup>1,2</sup>

<sup>1</sup> Department of New Materials and Biosystems, Max Planck Institute for Intelligent Systems, D-70569 Stuttgart, Germany

<sup>2</sup> Department of Biophysical Chemistry, University of Heidelberg, D-69120 Heidelberg, Germany  
[brueggemann@is.mpg.de](mailto:brueggemann@is.mpg.de)

## INTRODUCTION

Nanofibrous biopolymer scaffolds hold great potential for many biomedical applications, such as tissue engineering, wound dressings and drug delivery, as they closely mimic the natural extracellular matrix (ECM).<sup>1</sup> Three main techniques are currently used to prepare biopolymeric nanofibres: self-assembly, phase separation and electrospinning.<sup>2</sup> These methods often have restrictions in terms of scalability and yield or the use of toxic solvents and electric fields, which can interfere with the biological activity of many biopolymers.<sup>3,4</sup> Here, we present a new approach to prepare protein and polysaccharide nanofibre assemblies, involving extrusion of a biopolymer solution through nanopores, which overcomes such limitations and employs physiological buffers.

## EXPERIMENTAL METHODS

Nanoporous anodic aluminium oxide (AAO) membranes with varying pore diameters were prepared from aluminium by anodisation in polyprotic acids. Different ECM proteins and polysaccharides were dissolved in physiological buffers and extruded through the AAO nanopores and collected on glass substrates for further analysis. Prior to extrusion the substrates were functionalised with 0.1 % (w/v) poly-L-lysine in H<sub>2</sub>O. To detect the presence of nanofibres and their hierarchical assembly into microscopic structures confocal fluorescence microscopy was used. The size and morphology of the extruded nanofibres were analysed by scanning electron microscopy (SEM).

## RESULTS AND DISCUSSION

Using our custom-built extrusion setup we showed for the first time that a large variety of ECM proteins including collagen, fibronectin, fibrinogen, elastin and laminin could be extruded into nanofibres. We also succeeded in the extrusion of various polysaccharides, like hyaluronan, chitosan and chondroitin sulphate, into nanofibres. SEM analysis of the different biopolymer nanofibres revealed that they either assembled into highly aligned micron-sized fibre bundles up to millimetre length or into randomly oriented, porous meshes of single nanofibres (see Fig. 1). Our novel technique also facilitated the first-time preparation of extruded nanofibrous composites consisting of different proteins and/or polysaccharides within single nanofibres, which for instance contained blends of collagen/elastin or collagen/hyaluronan. When we extruded fluorescently labelled proteins in an aqueous environment we observed that the structure of the nanofibrous assemblies did not change over several hours (see Fig. 2). By varying the AAO nanopore diameter and the concentration of the

different biopolymer solutions we could precisely adjust the diameter of the extruded nanofibres between 15 and 200 nm.

Compared to existing methods for the fabrication of nanofibres, we could apply our extrusion technique to a large variety of biopolymers in aqueous environment, which will support their biological functionality. The possibility to reproducibly control the fibre diameter and composition in extruded protein fibres will form the basis for very interesting future cell culture studies on these novel nanofibrous scaffolds.

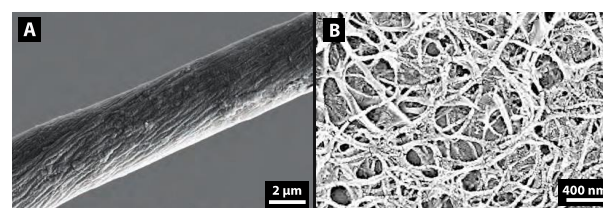


Fig. 1: SEM images of (A) highly aligned chitosan nanofibres assembled into a micron-sized bundle and (B) a randomly oriented mesh of collagen nanofibres.

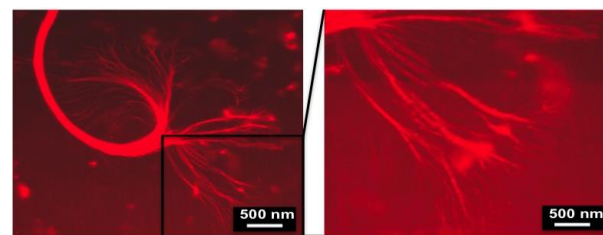


Fig. 2: Fluorescence microscopy image of an extruded fibrinogen bundle labelled with Alexa Fluor 647.

## CONCLUSION

Our novel extrusion approach holds great potential for the convenient and well-controlled fabrication of a novel class of biopolymer nanofibres under physiological conditions. In future, this simple and one-step technique can be used to develop smart, nanofibrous protein-based biomaterials for various biomedical applications.

## REFERENCES

1. P. X. Ma, *Adv Drug Deliver Rev*, 2008, **60**, 184–198
2. R. Vasita and D. S. Katti, *Int J Nanomedicine*, 2006, **1**, 15
3. S. G. Kumbar *et al.*, *Biomed. Mater.*, 2008, **3**, 034002
4. C. P. Barnes *et al.*, *Adv Drug Deliv Rev*, 2007, **59**, 1413–1433

## ACKNOWLEDGMENTS

This project was financially supported by the Max Planck Society and the European Research Council under the EU's 7<sup>th</sup> Framework Programme (FP/2007-2013) / ERC Grant Agreement no. 294852.

## Borophosphate Glasses/Fibers and their in-vitro Properties

Jonathan Massera<sup>a,b</sup>, Yaroslav Shpotyuk<sup>c</sup>, Thierry Jouan<sup>c</sup>, Catherine Boussard-Plédel<sup>c</sup>, Bruno Bureau<sup>c</sup>, Laeticia Petit<sup>d</sup>, Miina Ojansivu<sup>b</sup>, Susanna Miettinen<sup>b</sup>

a. Tampere University of Technology, Department of Electronics and Communications Engineering, Tampere, Finland

b. BioMediTech, Tampere, Finland

c. University of Rennes, Equipe Verres et Céramiques, UMR-CNRS 6226, Rennes, France

d. nLIGHT corp., Lohja Finland

[jonathan.massera@tut.fi](mailto:jonathan.massera@tut.fi)

### INTRODUCTION

Fibers based on bioactive glasses can be used for reinforcement in composite [1] or biosensing [2]. Due to their biocompatibility, silica-based glasses such as 45S5 [3] and S53P4 [4] are well-known candidates for different biomedical applications including bone-grafting but they cannot be drawn into fibers [5]. Phosphate glasses have been found to be good alternatives as they are also suitable glasses for biomedical purposes, such as for example bone repair and reconstruction [6]. Recently, boron was found to accelerate the formation of hydroxyapatite layer and bond to bone [7] and SrO was found to enhance gingival fibroblasts adhesion and proliferation.

In this paper, we present our study on the effect of B<sub>2</sub>O<sub>3</sub> addition on the thermal, structural and bioactive properties of phosphate glasses in the P<sub>2</sub>O<sub>5</sub> - CaO - SrO - Na<sub>2</sub>O glass system as well as on the attachment and proliferation of human adipose stem cells. We also show that fibers can be drawn from those glasses.

### EXPERIMENTAL METHODS

The thermal properties of the glasses were assessed using a DTA. Structural properties were determined by FTIR and Raman spectroscopy as well as NMR. In vitro testing was performed in simulated body fluid (SBF). Glass particles were analysed after immersion in SBF using EDX/SEM and FTIR. The solution was also analysed using ICP-OES. Finally human adipose stem cells were plated at the surface of polished glasses and fibers. Viability test was performed.

### RESULTS AND DISCUSSION

The glass transition ( $T_g$ ) and the onset of crystallization ( $T_x$ ) increase with an increase in B<sub>2</sub>O<sub>3</sub> content indicating an increase in the glass connectivity.  $\Delta T = (T_x - T_g)$ , which provides a gauge of the resistance to crystallization is larger than 100°C for all the investigated glasses suggesting that the glasses can be drawn into fiber with good quality. Fibers were successfully processed from the glass with 2.5mol% of boron. In vitro testing was performed in simulated body fluid. All glasses/fibers started to precipitate a calcium phosphate layer at their surface upon immersion in SBF already after 72h. Here, we show that the addition of B<sub>2</sub>O<sub>3</sub> led to a decrease in the phosphate chains length using Raman and FTIR spectroscopy and confirmed by NMR. Such decrease in chains length decreases the rate at which the glass reacts in SBF. With increasing B<sub>2</sub>O<sub>3</sub> content the layer formation was further delayed. The degradation of the fiber was found to be similar to

the degradation of the parent glass. Human adipose stem cells were plated at the surface of the glasses and the fibers. While it was found that the cells did not attach properly at the glass surface, the cells grew at the bottom of the well indicating that the dissolution products from all the glasses are not cytotoxic. The reason for the improper adhesion of the cells at the surface of the glass could be attributed to the too fast glass dissolution and too slow reactive layer formation leading to a surface that does not permit cells to find proper nucleation sites.

### CONCLUSION

The addition of B<sub>2</sub>O<sub>3</sub> in borophosphate bioactive glasses led to a shortening of the phosphate chains reducing the rate at which CaP is formed at the surface of the glasses. Fibers were successfully drawn into fibers. Human adipose stem cells were plated at the surface of the glasses and fibers. While the cells had difficulties to attach to the material due to a too rapid glass resorption, the dissolution products were beneficial and promoted cell growth and proliferation. With this study, we show that those new borophosphate glasses are good candidates as bioresorbable fiber to reinforce composites.

### REFERENCES

1. Pirhonen E. *et al.*, J. Mater. Sci., 41: 2031-2036, 2006.
2. Clupper D.C. *et al.*, Transactions of the Society for Biomaterials, Tampa, FL, 2002.
3. Hench L.L. *et al.*, Bioactive glasses. In: An introduction to bioceramics. June Wilson; 1993.
4. Andersson O.H. *et al.*, Corrosion of bioactive glass under various in vitro conditions. Advance in Biomaterials No 8. Amsterdam: Elsevier; 1990.
5. Massera J. *et al.*, J. Am. Ceram. So., 95:607-613, 2012.
6. Clement J., *et al.*, J. Mater. Sci.- Mater. Med., 10:729-732, 1999.
7. Liang W. *et al.*, J. Non-Cryst. Solids, 357:958-962, 2011

### ACKNOWLEDGMENTS

A part of the research leading to these results has received funding from the European Union Seventh Framework Programme FP7/2007-2013 under grant agreement n°264526 through the GlaCERCo Marie-Curie ITN project. The Academy of Finland is gratefully acknowledged for the financial support of J.M.



## ***In Vivo* Study on the Biodegradation Behaviour of Mg-Based Alloys for Orthopaedic Application**

Sau Shun Wong<sup>1</sup>, Wing Yuk Ip<sup>1</sup>, Luen Chow Chan<sup>2</sup>, Chi Ping Lai<sup>2</sup>

<sup>1</sup> Department of Orthopaedics and Traumatology, University of Hong Kong, Hong Kong SAR, China

<sup>2</sup> Department of Industrial and Systems Engineering, Hong Kong Polytechnic University, Hong Kong SAR, China  
[wyiphkucc@yahoo.com.hk](mailto:wyiphkucc@yahoo.com.hk)

### **INTRODUCTION**

Biodegradable implants can eliminate the need for implant removal procedures and reduce the chances of surgical infections<sup>1</sup>. Magnesium (Mg)-based alloys are popular materials for use in orthopaedic biodegradable implants because of their desirable strength and biocompatibility<sup>2</sup>. Zinc (Zn) and manganese (Mn) are chosen as the alloying elements for pure magnesium to enhance the corrosion and mechanical properties<sup>3</sup>. X-ray microtomography (Micro-CT) can be used to perform continuous non-destructive *in vivo* monitoring and is gaining more attention in Mg implant research<sup>4</sup>.

This paper presents the micro-CT reconstruction findings regarding *in vivo* implantation for pure Mg and two Mg-based alloys. The objective is to investigate the differences in their degradation behaviours by online imaging and to analyse the consequences for bone healing.

### **EXPERIMENTAL METHODS**

**Sample preparation:** Pure Mg, Mg-5Zn-1Mn and Mg-1Zn-1Mn alloys were produced in forms of rods of 4mm long and 1.6mm diameter by extrusion and wire-cutting. Eighteen Sprague Dawley rats (Female, 9 weeks old, 250-300 gram) were divided into three groups of six animals each. Each rat received one implant (99.999% Pure Mg, Mg-1Zn-1Mn, Mg-5Zn-1Mn) on its right femur. The 6-month implantation period was monitored by micro-CT scans at sixteen time points (day 0, week 1, 2, 3, 4, 5, 6, 8, 10, 12, 14, 16, 18, 20, 22, 24). At the experimental endpoint, the femurs were extracted for examination.

### **RESULTS AND DISCUSSION**

3D reconstructions of the implants at day 0, week 6 and week 24 are shown in Figure 1. The unalloyed pure Mg shrank and degraded for a substantial volume. The 5Zn implant fragmented within 6 weeks, which was too fast to provide sufficient mechanical support. The 1Zn implant gradually thinned and was able to remain intact for optimal bone healing.

Figure 2 shows that both the Pure Mg implant and 5Zn implant degraded and were no longer observed on the surfaces of the femurs. On the other hand, a large portion of the 1Zn implant seemed to remain intact and observable on the surface of the extracted femur.

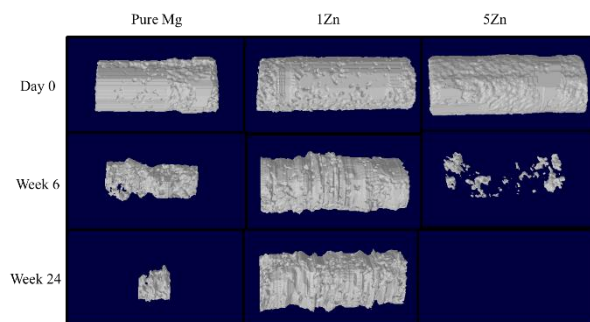


Figure 1. Micro-CT 3D reconstructions of the implants at day 0, week 6, and week 24.

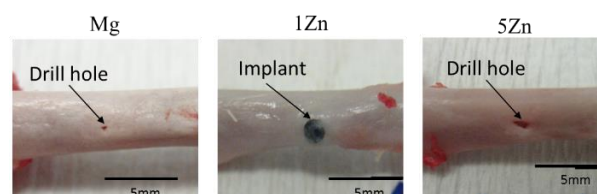


Figure 2. Images of the extracted femurs at the experimental endpoint. The implant or the drill holes can still be seen clearly on the femurs.

### **CONCLUSION**

Micro-CT monitored the degradation process of the degradable Mg-based alloys effectively. The difference between the modes of degradation was illustrated clearly by the 3D reconstructions.

The relatively steady and slow biodegradation of 1Zn alloy made it a better candidate for orthopaedic applications with these samples. A long-term implantation is suggested so that its complete degradation can be observed. Alloys of similar composition can also be produced and compared. Toxicity measurement should also be carried out.

### **REFERENCES**

1. Beaupre G.S. *et al.*, J Orthop Trauma 10(2):87-92, 1996
2. Staiger M.P. *et al.*, Biomaterials 27:1728:34, 2006
3. Rosalbino F. *et al.*, J Mater Sci Mater Med 21: 1091-8, 2010
4. Dziuba D. *et al.*, Acta Biomater 9: 8548-60, 2013

### **ACKNOWLEDGMENTS**

This project was partially supported by project funding from the University of Hong Kong (Project No. 201308176011) and grants from the Innovation and Technology Fund of the HKSAR, China (Project No. ITP/041/12NI).

## A Comparative Tribocorrosion Study Between TiN- and DLC- coated Titanium for Loading Bearing Biomedical Applications

Guohua Zhao<sup>1,3</sup>, Nuria Espallargas<sup>2</sup> and Ragnhild E. Aune<sup>3</sup>

<sup>1</sup>Dept. of Materials Science and Engineering, KTH Royal Institute of Technology, Sweden

<sup>2</sup>Dept. of Engineering Design and Materials, NTNU Norwegian University of Science and Technology, Norway

<sup>3</sup>Dept. of Materials Science and Engineering, NTNU Norwegian University of Science and Technology, Norway  
[guohua@kth.se](mailto:guohua@kth.se)

### INTRODUCTION

Medical grade titanium and its alloys are today commonly used in different biomedical components as a result of their excellent corrosion resistance and relatively low weight<sup>1,2</sup>. The orthopaedic biomaterials are required to possess high strength, good wear and corrosion resistance as well as biocompatible to bone and tissues. Titanium nitride (TiN) is one of the refractory transition metal nitrides, and it has been used as a coating on the heads of hip prostheses to improve their wear and fatigue resistance<sup>3,4</sup>. Recently, Diamond-like Carbon (DLC) coating has been proven to secure the combining benefits of high hardness, low wear rate, low friction coefficient, and the coating is biocompatible<sup>5,6</sup>. In other words, both TiN and DLC are promising surface modifications/ coatings for load bearing implants.

In this work the electrochemical and tribocorrosion behaviours of a surface modified medical grade titanium substrate, under the combining effects of sliding wear and corrosion, has been studied. The surface modifications used were TiN and a DLC coating. Furthermore, the degradation mechanisms of the different surfaces were evaluated.

### EXPERIMENTAL METHODS

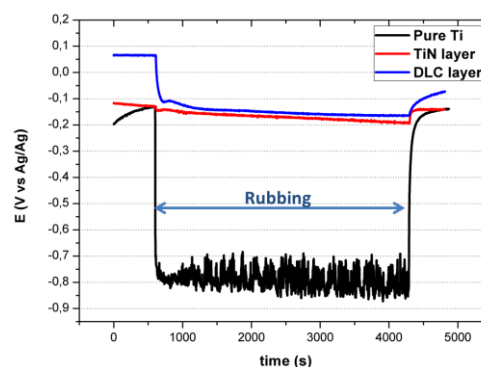
The medical grade pure Ti was cut and polished to mirror-like surfaces before further treatments. The plasma nitriding treatments were performed in a vacuum furnace at a temperature of 550°C, and in an atmosphere containing more than 66 wt% nitrogen. The taC DLC coatings were prepared by using a special arc physical vapour deposition system. The taC DLC coating has the sp<sup>3</sup> fraction of 80-95% with the electric resistivity of 107- 109 μΩcm.

The corrosion resistance of the samples was evaluated by polarization measurements in Phosphate Buffer Solution (PBS) with pH value 7.4 at room temperature. The tribocorrosion properties of the modified materials were evaluated with a linear reciprocating ball-on-plate tribometer, and the tests were performed at open circuit potential conditions. The corrosion potential changes during the wear were recorded by a potentiostat.

### RESULTS AND DISCUSSION

The XRD patterns of the TiN layer exhibited the crystalline peaks that are originated from the TiN (111) and (220) planes, while the DLC coating showed an amorphous background without crystalline peaks. A carbon layer with the thickness of 1.8 μm was observed from the cross-section SEM image. It was established,

from the potentiodynamic polarization measurements, that the TiN and DLC coated titanium substrate lost its passive property and exhibited higher corrosion potential than the pure titanium substrate. In the dry wear tests, however, the DLC coated material showed the lowest friction coefficient (0.12), and the TiN produced the smallest wear track which indicated it has the best wear resistance against the rubbing movement of the alumina ball under dry conditions.



The figure above exhibits the corrosion potential changes during the tribocorrosion measurements. As onset of rubbing, a significant potential drop was observed from the pure Ti sample, followed by a plateau where the potential remains at the lower level. After the rubbing stops, the potential was immediately restored to the initial OCP value. Comparatively, the rubbing did not influence the corrosion potential of TiN and DLC samples. The present results imply that sliding wear may accelerate the corrosion process of passive metal due to the galvanic coupling effect.

### CONCLUSION

The TiN coated titanium substrate exhibited the best wear resistance under dry condition. The DLC coated titanium substrate did, however, prove to have the best wear resistance in the PBS solution. It also proved to have a low friction coefficient, as well as high hardness. Furthermore, passive metals should be avoided in a tribocorrosion environment.

### REFERENCES

1. J. Narayan. *et al.*, Mater. Sci. Engi. B 25: 5-10, 1994
2. C. Elias. *et al.*, JOM. March: 46-49, 2008
3. X. Liu. *et al.*, Mater. Sci. Engi. R 47: 49-121, 2004
4. S. Akamaru. *et al.*, Mater. Tran. 49: 1638-1643, 2008
5. T. Manhabosco, *et al.*, Tribol Lett. 33: 193-197, 2009
6. E. Arslan, *et al.*, Proc. Orga. Coat. 74: 768-771, 2012



## ***In Vitro* Biological Studies of Porous Titanium Obtained by Two Different Powder Metallurgy (PM) Techniques: Loose Sintering and Space Holder**

Juan Pavón<sup>1</sup>, Ana Civantos<sup>2</sup>, Viviana Ramos<sup>2</sup>, José L. López-Lacomba<sup>2</sup>, José A. Rodríguez<sup>3</sup>, Yadir Torres<sup>3</sup>

<sup>1</sup>Group of Advanced Biomaterials and Regenerative Medicine, BAMR, Program of Bioengineering, University of Antioquia, Colombia

<sup>2</sup>Center of Biofunctional Studies, Complutense University of Madrid, Spain

<sup>3</sup>Department of Materials Engineering and Transport, University of Seville, Spain

[juan.pavon@udea.edu.co](mailto:juan.pavon@udea.edu.co)

### **INTRODUCTION**

The proper osseointegration of titanium implants is one of the most important factors for their clinical success<sup>1</sup>. Loose sintering and space holder are techniques frequently used that allow to obtain titanium implants, among others. In the present work, these two different methods were evaluated through *in vitro* assays to study how porous titanium surfaces can be modulated to influence the cell adhesion and cell proliferation of different cell lines.

### **EXPERIMENTAL METHODS**

**Samples processing.** Details are described in a previous work of the authors<sup>2</sup>. Commercially pure Titanium (cp Ti, ASTM F67-00, GIV, SE-JONG Materials Co. Ltd., Korea) was used. Space holder used was NaCl (Panreac, purity 99.5%), 30 vol.%. Loose-sintering (LsTi) process was applied to porous cpTi powder that was vibrated for 2 min. Samples were heated to 1250 °C for 2 h ( $5 \times 10^{-5}$  mbar). Space-holder technique (SaTi) used consisted of mixing of titanium and NaCl powders, compaction step with 800 MPa; NaCl was dissolved in distilled water (50–60 °C), and sintering as before. **Cell culture assays.** MC3T3 cell line (CRL 2593, American Type Culture Collection, Manassas, Virginia) was used for a routine passaging of the cell line. Samples were placed into a 24-well plate, and trypsinized cells were seeded at a density of 30.000 cells/cm<sup>2</sup>. Afterwards, 800 µL of pre-warmed culture medium was added, and culture plates were kept at 37°C in a humidified 5 % CO<sub>2</sub> atmosphere. To follow cell adhesion and proliferation it was used C2C12 cell line (CRL 1772 obtained from ATCC). **Cell proliferation.** AlamarBlue® (Invitrogen) was used to assess cell proliferation and cell viability. After incubation, samples were removed and culture medium was exposed to fluorescent read on microplate reader (Biotek FL-600). **Immunocytostaining assay.** Cytoskeletal organization was analyzed using protocols from Texas red phalloidin (Molecular Probes). A two-way ANOVA was performed using Graph Path Prism 6 software, and a value of  $p < 0.05$  was considered significant.

### **RESULTS AND DISCUSSION**

**Fig. 1** shows images in/at real time of C2C12-GFP growing on the samples; these were taken every day to observed differences of cells behavior. C2C12-GFP cells appear well attached to all samples. However, some cells appear widely spread on titanium samples with increased roughness (LsTi and SaTi), with respect to the smooth one (panel A, cpTi).

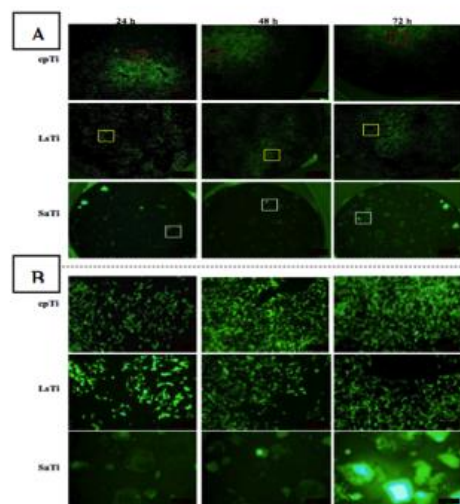


**Fig 1.** Images of C2C12-GFP cells seeded onto titanium samples at 24 h, 48 h and 72 h, followed by fluorescent microscope. Panel A, 2x, and panel B, 10X.

Alamarblue assessed cell proliferation at 24 h, 48 h and 72 h. It was observed the increase of cell proliferation due to a higher metabolic activity. At 24 h, the metabolic activity was lower comparing to other days. At 48 h and 72 h, the fluorescent levels are similar in all samples and, thus, correspond to cells that are in a proliferative phase. The lowest metabolic activity levels were found in SaTi which contains higher porosity, around 30%. At 72 h, MC-3T3 cells were fixed and immuno-staining was performed.

### **CONCLUSION**

These two methods to obtain different titanium surfaces allow cell adhesion and proliferation, comparing with conventional Ti surfaces, being possible to be used as techniques that can improve the success of titanium implants.

### **REFERENCES**

1. Abarrategi A. *et al.*, Biomacromolecules. 9 (2): 711-18, 2008.
2. Torres Y. *et al.*, J Mater Sci. 47:6565–6576, 2012.

### **ACKNOWLEDGMENTS**

Authors would like to thank to Junta de Andalucía, Spain, for the Excellence Grant P12-TEP-1401.



## “Bridging of Spine” – Comparison of Titanium and Dynamic Polymer Stabilization

L.F.Ciupik<sup>1</sup>, A.Kierzkowska<sup>1</sup>, J.Sterna<sup>2</sup>, E.Słonski<sup>1</sup>, M.Cieslik-Gorna<sup>3</sup>

<sup>1</sup>LfC-Medical, Poland

<sup>2</sup>Department of Clinic of Small Animal Diseases, Warsaw University of Life Sciences SGGW, Poland

<sup>3</sup>Institute of Bioengineering and Medical Technologies, Poland  
[monika.cieslik3@gmail.com](mailto:monika.cieslik3@gmail.com)

### INTRODUCTION

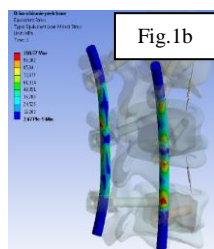
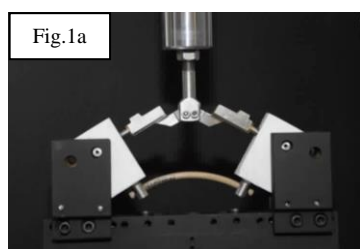
The development of material bioengineering and deepening medical knowledge cause the need of extending the biomaterials functionality. Currently trends in spinal implants are designed to improve the properties of dynamic stabilization.

Dynamic stabilization (**DS**) is intended to allow the transfer of loads in an elastic-flexible way by mechanical system - implants. However, only the analysis of relationship between DS with elements of bone-muscle-ligament system and formation of the bio-dynamic stabilization (**bDS**) is the basis for evaluation of its safety and suitability for surgical treatment.

The aim of the study was evaluation of dynamism of support beams (made of polyetheretherketone PEEK Optima and Ti6Al4V alloy) for “bridging” posterior spine column by experimental implementation and with the use of model engineering tools. The work also includes the aspect of biocompatibility in *in vivo* animals tests and the safety and clinical conditions.

### EXPERIMENTAL METHODS

In the work several aspects influencing dynamism of spinal rods with diameter 6 mm were analyzed, among others; kind of biomaterial (PEEK and Ti-alloy), the length, shape of rod (straight, with a defined curvature). Strength properties were evaluated in static and fatigue (5 million cycles) tests on MTS MiniBionix (Fig. 1a). The experimental evaluation was supported by FEM simulations - Ansys 14.0 (Fig.1b). Tissue response to biomaterial was evaluated post-mortem approx. 6M after animal tests on the basis of macroscopic observations and histopathological (HP) analysis.

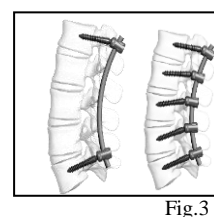
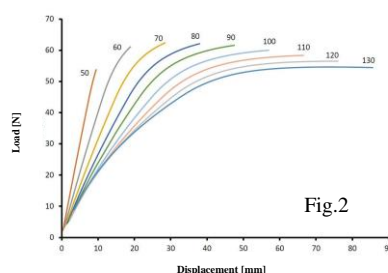


### RESULTS AND DISCUSSION

DS is characterized by a usage of PEEK polymer rods which dynamism is dependent on the angle of curvature and the length of rod (Fig.2). Static and dynamic characteristics of PEEK rods have beneficial dependence hysteresis “load-deformation”. In destructive tests the material flow was observed with maintenance of structural integrity, which is a good indicator of the functional safety.

Polymer rod elements transfer dynamic loads well (5 million cycles). This feature gives the possibility of designing DS, control dynamic properties with the comprehensive clinical factors related to the disease, the extent of stabilization, the number of screws-support “bridging” the spine (Fig.3), which have been taken into account.

HP analysis of tissues adjacent to the PEEK and Ti-alloy indicated that these materials are bioacceptable. Tissue adhesion to the polymer surface shows no osseointegration, which proves its beneficial properties as a “non-fusion” implants. Much better osseointegration was obtained for Ti-alloy, which is a desirable element for “fusion” stabilization.



### CONCLUSION

- 1) Creation of bio-dynamic spinal stabilization is a combination of stabilizer’s mechanical properties with the biomechanical properties of the bone-muscle-ligament system.
- 2) “Dynamics” can be achieved by a suitable choice of biomaterial and/or through construction features.
- 3) Polymer supporting beam has the potential for controlled “dynamism” in the creation of spinal stabilization bDS.
- 4) Introducing bDS stabilization healing processes can be safely promoted by, e.g.:
  - acceleration of bone overgrowth in the area of dysfunction by micro movements presence,
  - offload/regeneration of disc structures and joints,
  - reduction of adverse “stiffness” outside of the stabilization area (e.g. the ASD effect - *Adjacent Segment Degeneration*).
- 5) Obtained results have been confirmed by two years clinical follow up.

### ACKNOWLEDGMENTS

In this paper, we used the results of research financed by the European Regional Development Fund under the Operational Programme Innovative Economy, 2007-2013 (POIG.01.04.00-08-001/08).

## Interfacing 3D Graphene Oxide Scaffolds with the Injured Rat Spinal Cord

Ankor González-Mayorga<sup>1,a</sup>, Elisa López-Dolado<sup>1,a</sup>, Jorge E. Collazos-Castro<sup>1</sup>, María Luisa Ferrer<sup>2</sup>, Francisco del Monte<sup>2</sup>, María C. Gutiérrez<sup>2</sup>, M. Concepción Serrano<sup>1</sup>

<sup>a</sup>These authors contributed equally to this work

<sup>1</sup>Hospital Nacional de Paraplégicos, Servicio de Salud de Castilla La Mancha, Spain

<sup>2</sup>Instituto de Ciencia de Materiales de Madrid, Consejo Superior de Investigaciones Científicas, Spain

[mslopezterradas@sescam.jccm.es](mailto:mslopezterradas@sescam.jccm.es)

### INTRODUCTION

Limitations associated with the treatment of spinal cord injury (SCI), a lesion with an increasing prevalence and high sanitary costs associated, are acting as a fuel to encourage experts in different fields to explore new avenues for neural repair<sup>1</sup>. In this context, graphene and its derivatives (GDM) are attracting significant attention<sup>2</sup>, although their toxicity and biocompatibility *in vivo* is still unclear<sup>3</sup>. Based on our previous findings *in vitro* with 3D flexible and porous scaffolds composed of partially reduced graphene oxide (rGO)<sup>4</sup>, we herein explore the acute tissue response to the implantation of these scaffolds in the injured rat spinal cord to evaluate their feasibility to be part of a guiding platform for neural regeneration in SCI patients. Early responses were thoroughly investigated at the major organs (kidney, liver, lung, and spleen) and the site of implantation (injured spinal cord at C6) by both histological and immunofluorescence studies.

### EXPERIMENTAL METHODS

**Preparation of 3D porous rGO scaffolds:** Samples were fabricated by ISISA as previously described<sup>4</sup>.

**Surgical procedures:** Lesions consisted on a complete hemisection at the right side of C6 on adult male Wistar rats. All experimental protocols adhered to the regulations of the European Commission (directives 2010/63/EU and 86/609/EEC) and the Spanish government (RD53/2013). Treatment groups were: control (C, n = 3), injury (I, n = 6) and injury + scaffold (I+SC, n = 6). Rats were sacrificed at 10 postoperative (PO) days by a perfusion-fixation protocol and the different organs and neural tissue carefully extracted.

**Tissue processing and histology:** Fixed tissues were quick-frozen in OCT compound and cut in sagittal sections (10- $\mu$ m) by using a Microm HM550 cryostat. Samples were examined using hematoxylin-eosin and hematoxylin-van Giesson stainings.

**Immunofluorescence studies:** Spinal cord samples were examined for the presence of map-2, tau, vimentin, glial fibrillary acidic protein (GFAP), ED1, platelet-derived growth factor receptor  $\beta$  (PDGFR $\beta$ ), and Ki67. Cell nuclei were labelled with Hoechst. Fluorescence images were calibrated and processed with ImageJ.

**Statistics:** Values were expressed as mean  $\pm$  standard deviation. Comparisons were done by ANOVA. The significance level was  $p < 0.05$  in all comparisons.

### RESULTS AND DISCUSSION

Organ weight in I and I+SC groups remained unaltered at 10 PO days compared to control. A thorough inspection of major organs revealed no significant

damage or inflammation signals, in agreement with previous work after oral and intraperitoneal injection<sup>5</sup>. No alterations were identified in non-lesion areas close to the injury for the markers studied. At the injury site in both I and I+SC, the amount of cells significantly increased with respect to areas with no lesion, likely indicating the activation of both cell migration and proliferation. Markers for neurons (*e.g.*, map-2 and tau) were totally absent inside the injured area (**Figure**). On the contrary, vimentin was strongly positive in injured areas of both I and I+SC, as well as ED1 and PDGFR $\beta$  (**Figure**). A discrete but evident internalization of GFAP<sup>+</sup> cells into the scaffold was observed in 3 out of 6 animals. Finally, we confirmed the presence of a significant percentage of actively proliferating cells at the injury site in both I and I+SC, contrary to control.

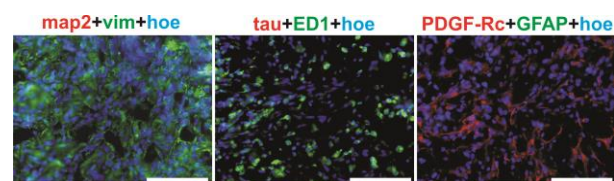


**Figure.** Representative immunofluorescence images of the injured spinal cord in I+SC group. Scale: 100  $\mu$ m.

### CONCLUSION

The absence of systemic and local toxic responses, along with positive signs found at the lesion site (*e.g.*, complete scaffold colonization by cells, discrete sprouting of GFAP<sup>+</sup> cells inside the scaffold) encourage further investigation of GDM as promising components of more efficient material-based platforms for neural regeneration in the CNS.

### REFERENCES

1. Hyun J.K. and Kim H.K. J. Tissue Eng. Article 650857, 2010
2. Feng L. *et al.*, Adv. Mater. 25:168-186, 2013
3. Seabra A.B. *et al.*, Chem. Res. Toxicol. 27:159-168, 2014
4. Serrano M.C. *et al.*, J. Mater. Chem. B 2:5698-5706, 2014
5. Yang K. *et al.*, Biomaterials 34:2787-2795, 2013

### ACKNOWLEDGMENTS

The authors would like to thank the *Instituto de Salud Carlos III-MINECO* (Grant no: CP13/00060) and *MINECO* (Grant no: MAT2011-25329 and MAT2013-43299-R) for financial support to this project. A.G.M. and M.C.S. acknowledge the *Instituto de Salud Carlos III-MINECO* for respective contracts.



# Dual Peptide Functionalised Intraluminal Collagen Fibre Conduits Regulates Neurite Outgrowth Of Primary Neurons

Sahana Ganesh, William Daly, Abhay Pandit

Network of Excellence for Functional Biomaterials, National University of Ireland, Galway, Ireland

[sahanag.29@gmail.com](mailto:sahanag.29@gmail.com)

## INTRODUCTION

The process of repair following peripheral nerve injury occurs at the molecular level and the regenerative responses are specific to the biomaterial used to bridge the intraneural gap. Proteomic analysis following implantation of intraluminal collagen fibre conduit in a sciatic nerve injury model identified a number of molecules that are intrinsic to repair, one of them being Myristoylated alanine rich C-kinase substrate (MARCKS) [1]. MARCKS is critical to neurite outgrowth and is dependent on its interaction with Polysialic acid (PSA) on NCAM [2]. Hence we hypothesise that intraluminal fibre conduits functionalised with MARCKS and PSA will enhance nerve repair and functional recovery in sciatic nerve injury model and the specific objective of the present study is to assess the loading efficiency, release profile and to test the bioactivity of MARCKS and PSA functionalised conduit using embryonic rat dorsal root ganglion cells (DRGs).

## EXPERIMENTAL METHODS

Type I bovine atellocollagen (3mg/ml) was mixed with MARCKS (KKKKKRFSFKKSFKLSGFSFKKNKK) (80µg) and intraluminal fibres were fabricated using fibre extrusion method [1]. Loading efficiency of MARCKS was assessed using amino acid analysis. Collagen conduit was fabricated as described in [1] and was functionalised with PSA mimetic peptide (NTHTDPYIYPID) (200µg/ml) by incubating the conduit in loading buffer containing PSA for 24 hours. The loading efficiency was calculated using micro BCA assay. The functionalised fibres were placed in release buffer in the absence and presence of collagenase for a period of 14 days. At specific time points release buffer was collected to assess the release profile of MARCKS using micro BCA assay. The functionalised conduit was placed in release buffer in the absence and presence of collagenase for a period of 14 days and at specific time points release buffer was collected to assess the release profile of PSA using micro BCA assay. Bioactivity of the released MARCKS and PSA in comparison to scramble MARCKS peptide (KKKKKRASAKK-SAKLSGASAKKNKK) and scramble PSA (TNYDITPPHDIYC) was tested by neurite outgrowth analysis using  $\beta$ -III tubulin staining in DRGs.

## RESULTS AND DISCUSSION

Amino acid analysis of the functionalised fibres showed that approximately 70 percent of MARCKS was loaded. In the absence of collagenase less than 20% of MARCKS was released over 14 days however in the presence of collagenase it increased to up to 78%. On the other hand, around 66 percent of PSA was loaded.

into the conduit. In the absence and presence of collagenase the release of PSA over 14 days was 5 and 42% respectively. Preliminary results show that the released peptides are bioactive following neurite outgrowth analysis in DRGs.

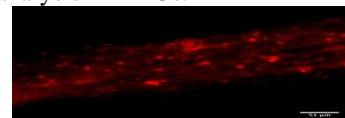
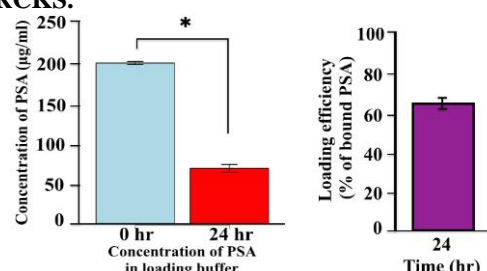
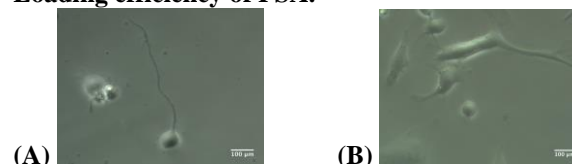


**Fig 1. Fluorescent image of fibre functionalised with MARCKS.**



**(A) (B)**  
**Fig 2. A) Concentration of PSA measured in supernatant at 0 and 24 hr, n=3, p<0.001. B) Loading efficiency of PSA.**



**(A) (B)**  
**Fig 3. Light microscopic images of DRGs showing neurite outgrowth in the presence of (A) PSA loaded conduit (B) no neurite outgrowth with scramble PSA loaded conduit after 24 hrs.**

## CONCLUSION

An intraluminal fibre conduit functionalised with MARCKS and PSA has been fabricated in the present study. The release kinetics of both the peptides from the fibre/conduit was found to be mainly governed by collagen degradation. Preliminary results show that both the peptides retained their bioactivity upon release in vitro and resulted in neurite outgrowth in DRGs. The current results will allow for optimisation of future in vitro studies and also will involve implantation of MARCKS-PSA functionalised fibre conduit in a rat sciatic nerve injury model.

## REFERENCES

1. Daly B, (Doctoral thesis, NUI Galway), 154-201, 2014.
2. Theis T et al. J Biol Chem, 288(9), 6726-42, 2013.

## ACKNOWLEDGMENTS

The authors would like to acknowledge TIDA (Grant No: 14/TIDA/2410) for funding this project.



## Characterization of Polyurethane/Poly lactide Blends in Terms of Their Applicability as Biomaterials Supporting Nerve Regeneration

Jadwiga Laska<sup>1</sup>, Paulina Bednarz<sup>2</sup>, Anna Lis<sup>1</sup>, Jakub Grzesiak<sup>3</sup>, Krzysztof Marycz<sup>3</sup>, Dariusz Szarek<sup>4</sup>

<sup>1</sup>AGH University of Science and Technology, Faculty of Materials Science and Ceramics, Dept. of Biomaterials, Poland

<sup>2</sup>State Higher Vocational School in Tarnow, Institute of Technology, Poland

<sup>3</sup>Electron Microscopy Laboratory, University of Environmental and Life Sciences, Poland

<sup>4</sup>Department of Neurosurgery, Lower Silesia Specialist Hospital of T. Marciniak. Emergency Medicine Centre, Poland

[jlaska@agh.edu.pl](mailto:jlaska@agh.edu.pl)

### INTRODUCTION

Reconstruction of injured nerves is one of the most demanding processes in regenerative medicine. Even mild injuries can lead to motor or sensory deficits. Natural and synthetic polymers are potential solution for grafting the severed nerve<sup>1</sup>. *In vitro* and *in vivo* studies with the use of neural cells and animals show encouraging results for the application of new synthetic materials. Several polymers have been found as the most promising. Among them polylactide, polycaprolactone and polyesterurethane<sup>2,3</sup>.

In our study a biodegradable polyurethane (PU) based on hexamethylene diisocyanate, poly( $\epsilon$ -caprolactone) and dianhydro-D-sorbitol as a chain extender was investigated. It was blended with polylactide to modify its mechanical properties and degradation rate. Alginate fibers and hydrogels were also applied used to support nerve regeneration. Full characterisation of the materials, *in vitro* cell culture, and *in vivo* studies were performed.

### EXPERIMENTAL METHODS

Blends of polylactide (Purac) and polyurethane (Bayer) were tested. Both polymers were of biomedical grade and used without further purification. PU/PLA blends with various weight ratios (9/1, 8/2, 7/3, 6/4, and 5/5) were prepared. Samples for biological examination were sterilised with the use of the H<sub>2</sub>O<sub>2</sub> cold plasma technique (Sterradyl, ASP, J&J, USA).

The water contact angle, surface roughness, tensile strength, Young's moduli, and elongation at break ( $\epsilon$ ) of the blends were determined. Morphology of the samples was investigated using scanning electron microscopy. *In vitro* assessment of the biomaterials was performed with the use of glial cells. Rat sciatic nerve regeneration was observed *in vivo* after implantation of PU/PLA tubes.

### RESULTS AND DISCUSSION

In our search for a material enabling to fabricate a scaffold for regenerating axons we focused on blending two polymers with very different mechanical properties, i.e. rigid polylactide and elastic polyurethane. Both polymers were biodegradable but differing with the rate of degradation. We found that the morphology and mechanical properties of investigated materials could be easily regulated through mixing different ratios of PU and PLA. Optimal properties for surgical handiness were achieved this way. Porous films and sponges were fabricated by salt leaching. Porosity improves the

communication between cells and facilitates the exchange of metabolites. Moreover, surface roughness and wettability of particular biomaterials has been reported as an important factor responsible for cell adhesion and proliferation. We found that roughness of our investigated biomaterials may be increased through addition of PLA to the pure PU. Roughness of PU/PLA blend was  $5,52 \pm 0,62 \mu\text{m}$ . Water contact angle for pure PU was  $88,6^\circ \pm 2,6$ , whereas for PLA  $80,4^\circ \pm 2,2$ . The PU/PLA blends, however, exhibited the water contact angle of  $95,4^\circ \pm 2,3$ . The pure PLA showed the Young's modulus over 3000 MPa, which resulted in high rigidity and disadvantaged surgical manipulations. Mixing PLA with elastic PU strongly and positively influenced all mechanical properties.

Glial cells were cultured on pure polyurethane and the various blends. After 24 hrs. the cells cultured on pure PU showed decrease in proliferative activity, in relation to the control polystyrene cultures. In contrary, PU/PLA blend slightly increased proliferative activity of glial cells after the first day, what can be an effect of the presence of PLA. After seven days, culture cells on the PU sample still showed decreased PF value in relation to control, while the PU/PLA sample showed the PF value slightly above 1. In pure PLA sample, the proliferative activity of glial cells was considerably decreased. In PU/PLA blend cells showed proper morphology, significant number of p75-positive cells was observed, and the presence of a bipolar shape in fibroblast-like cells.

For *in vivo* evaluation PU/PLDL tubular implants were prepared. They were flexible and compression-resistant with a good shape memory and surgical handiness. Empty tubes and tubes filled with calcium alginate fibers were implanted into a lesion in a rat's sciatic nerve. The latter proved to be especially promising because of the additional stimulus of calcium ions on the regenerating axons.

### REFERENCES

1. Wang S., Cai L., Int. J. Polymer Sci Article ID 138686 (2010)
2. Lis. A. *et al.*, Polimery w medycynie 43:59-80 (2013)
3. Ciardelli G., Chiono V., Macromol. Biosci. 6: 13-26 (2006)

### ACKNOWLEDGMENTS

This research was financially supported by National Science Center, Poland (grants no: 2011/01/B/STB8/07795)





## Spinal Cord Injury Recovery of Rhesus Monkey Implanted with PPy/I Plasma Polymer

Axayacatl Morales-Guadarrama<sup>1,2</sup>, H. Salgado-Ceballos<sup>5,6</sup>, Israel Grijalva<sup>5,6</sup>, Juan Morales<sup>3</sup>, Camilo Ríos<sup>6</sup>, Guillermo J. Cruz<sup>7</sup>, Araceli Díaz-Ruiz<sup>6</sup>, María-Guadalupe Olayo<sup>7</sup>, L. Alvarez-Mejía<sup>2</sup>, R. Mondragón-Lozano<sup>2</sup>, A. Ibáñez-Contreras<sup>6</sup>, B. Hernández-Godínez<sup>6</sup>, O. Fabela-Sánchez<sup>2</sup>, S. Sánchez-Torres<sup>4</sup>, Roberto Olayo<sup>3</sup>

<sup>1</sup>Centro Nacional de Investigación en Imagenología e Instrumentación Médica (CI<sup>3</sup>M), <sup>2</sup>Departamento de Ingeniería Eléctrica, <sup>3</sup>Departamento de Física, <sup>4</sup>Depto. Biología Celular, Universidad Autónoma Metropolitana Iztapalapa

<sup>5</sup>Unidad de Inv. Médica en Enfermedades Neurológicas, Centro Médico Nacional Siglo XXI

<sup>6</sup>Centro de Investigación, Proyecto CAMINA, A.C, Unidad de Primates; Ciudad de México

<sup>7</sup>Departamento de Neuroquímica, Instituto Nacional de Neurología y Neurocirugía Manuel Velasco Suárez S.S.A.

<sup>8</sup>Departamento de Física, Instituto Nacional de Investigaciones Nucleares

[oagr@xanum.uam.mx](mailto:oagr@xanum.uam.mx)

### INTRODUCTION

Traumatic spinal cord injury (SCI) has a great medical and socioeconomic impact, due to a severe neurological disability<sup>1</sup>. Polymers synthesized by plasma derived of pyrrole and implanted in adult rats with SCI by transection, favor protection of the nervous tissue adjacent to the lesion and the functional recovery of the animals, significantly<sup>2,3</sup>. Animal studies have contributed greatly to a better understanding of the pathophysiology of SCI. However, it has not been possible to translate these findings effectively to improve treatments for SCI human. Therefore, to facilitate the translation of advances made in the laboratory to the clinic it is recommended the use of non-human primates (NHP). Magnetic Resonance Imaging (MRI) enables us to obtain morphometric information of the lesion area and the state of the affected tissue<sup>4,5</sup>. Diffusion tensor MRI (DTI) can be used in order to determinate the white matter microstructure. In this work the evolution of SCI in NHP is evaluated, both, with and without implant, *in vivo* using MRI.

### EXPERIMENTAL METHODS

Polymeric materials used to prepare the implants were synthesized, and analysed according to previous works<sup>2,3</sup>.

#### Spinal Cord Injury and functional evaluations

NHP Rhesus female were used, they underwent to transection SCI, one was implanted with the polymer (NHP-C) and the other one was only injured (NHP-I). The NHPs were treated to our institutions ethics and to "National Institutes of Health Guide for the Care and Use of Laboratory Animals". The 9th spinous process was extirpated. Then a laminectomy was done. Reflex recovery and locomotor behaviour were assessed once a week, for 12 weeks. Reflexes were evaluated with the animal seated in a restrainer.

#### Magnetic Resonance Imaging

MRI studies were taken with a 3T scanner *in vivo* and a 7T scanner *ex vivo*. The studies *in vivo* were carried out: pre-SCI; the SCI day ( $t_0$ ); 4, 8, and 12 ( $t_f$ ) weeks post-SCI; at last *ex vivo* studies were performed.

The animals were euthanized 12 weeks post-injury, for histological studies.

### RESULTS AND DISCUSSION

Functional evaluation after SCI shows recovery comparing both subjects. The withdrawal reflex present in NHP-I is highlighted. MRI in the NHP-I shows the spinal cord decreased to 81% at  $t_0$  and recovered to 91% at  $t_f$  from its baseline. The PPy/I decreased, this is consistent with the experience obtained in rats where the material tends to disintegrate it and allow tissue to grow through it<sup>4</sup>. DTI shows different behaviour between the subjects in the epicentre of the lesion as  $t_f$ : in the PNH-C a rostral and caudal separation exists, while the PNH-I shows transversal spinal cord reconnection of the diffusion (Fig1). The MRI data are concordant with the histological studies.

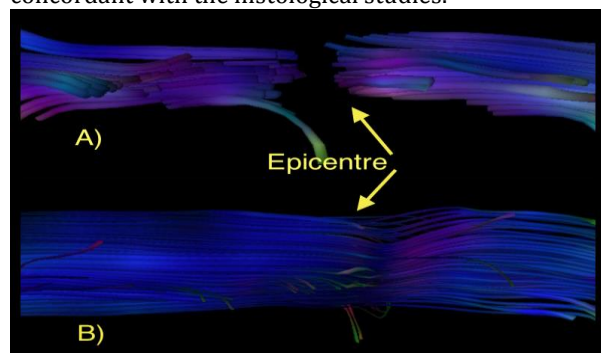


Fig1. Tractography for non-human primate implanted at the day of SCI (A) and 12 weeks after SCI (B). Shows transversal spinal cord reconnection of the diffusion.

### CONCLUSION

The monkey implanted with the plasma polypyrroles after spinal cord transection are capable of slight voluntary movements, also the implant contribute to the conservation of the histoarchitecture near the lesion epicentre, and promotes tissue growth through it. The results were consistent according to the experiences in rats, indicating that it is possible to reduce the paralysis when are implanted immediately after the SCI. With MRI is possible to monitor the *in vivo* state of the surrounding tissue to the area of SCI in a model of NHP.

### REFERENCES

1. Strauss *et al.*, Arch Phys Med Reh 89:572–576, 2008.
2. Olayo *et al.*, J Mater Sci:Mat Med. 19:817–826, 2008.
3. Cruz *et al.*, J Mater Sci: Mater Med. 23:2583–2592, 2012
4. Morales-Guadarrama *et al.*, RMIB 34:145–155, 2013.
5. Kozlowski *et al.*, J. Neurotrauma 25:653–676, 2008.



# Cell Membrane Capsules for Encapsulation of Chemotherapeutic and Cancer Cell Targeting *in vivo*

Zhengwei Mao<sup>1\*</sup>, Yuanhong Zhang<sup>1</sup>, Lihua Peng<sup>2</sup>, Jianqing Gao<sup>2</sup>

<sup>1</sup> MOE Key Laboratory of Macromolecular Synthesis and Functionalization, Department of Polymer Science and Engineering, Zhejiang University, P.R. China

<sup>2</sup> Institute of Pharmaceutics, College of Pharmaceutical Sciences, Zhejiang University, P.R.China

[zwmao@zju.edu.cn](mailto:zwmao@zju.edu.cn)

## INTRODUCTION

Systemic administration of chemotherapeutic agents results in indiscriminate drug distribution and severe toxicity. Until now, encapsulation and targeting of drugs have typically relied on synthetic vehicles, which cannot minimize clearance by the renal system and may also increase the risk of chemical side effects. Cell membrane capsules (CMCs) provide a generic and far more natural approach to the challenges of drug encapsulation and delivery *in vivo*.

## RESULTS AND DISCUSSION

Here aptamer AS1411, which can recognize and bind over-expressed nucleolin on cancer cell membrane, was chemically conjugated onto CMCs. As a result, AS1411 modified CMCs showed enhanced ingestion in certain cancer cells *in vitro* and accumulation in mouse cancer xenografts *in vivo*. Chemotherapeutics and contrast agents with therapeutically significant concentrations can be packaged into CMCs by reversible permeating their plasma membranes. The systematic administration of cancer targeting CMCs loaded with doxorubicin can significantly inhibit tumor growth in mouse xenografts, with significantly reduced toxicity compare to free drug. These findings suggest that cancer targeting CMCs may have considerable benefits in drug delivery and cancer treatment.

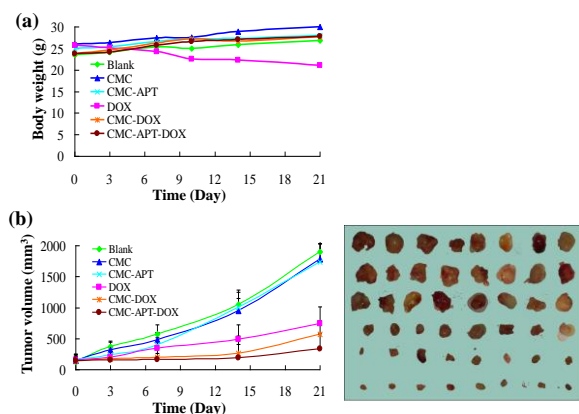


**Figure 1.** (a) Body weight and (b) tumor volume of BALB/c nude mice with xenograft tumors as a function of culture time after first treatment. Digital images show tumors harvested from mice treated with different groups for three weeks (from top to bottom: blank/saline, CMCs, Apt-CMCs, free DOX, CMCs/DOX, and Apt-CMCs/DOX groups).

## CONCLUSION

In this study, biocompatible cell membrane capsules were prepared from human endothelial cells with preserved membrane structure and functions. Cancer cell targeting aptamer AS1411 was conjugated onto the CMCs, resulted in enhanced ingestion of CMCs in certain cancer cells and accumulation of CMCs in mouse tumor xenografts. Chemotherapeutics and contrast agents can be packaged into the CMCs by reversible permeating their plasma membranes. The systematic administration of cancer targeting CMCs loaded with doxorubicin can inhibit tumor growth in mouse xenografts, with significantly reduced toxicity compare to free drug. These findings suggest that targeting CMCs may have considerable benefits in drug delivery and cancer treatment.

## REFERENCES

1. Mao Z. *et al.*, Nano letters 2011, 11, 2152-2156.
2. Peng L. *et al.*, Biomaterials 2014, 35, 5605-5618.

## ACKNOWLEDGMENTS

We thank Prof. Changyou Gao for valuable discussion. This study was supported by the Natural Science Foundation of China (51120135001), “Qianjiang” outstanding researcher funding of Zhejiang Province (2011R10047), and Zhejiang Provincial Program for the Cultivation of High-Level Innovative Health Talents.

## Electrospun Triclosan-loaded Chitosan Nanofibres for Potential Drug Delivery Application

Safa Ouerghemmi<sup>1</sup>, Stéphanie Degoutin<sup>1</sup>, Nicolas Tabary<sup>1</sup>, Frédéric Cazaux<sup>1</sup>, Ludovic Janus, Nicolas Blanchemain<sup>2</sup> and Bernard Martel<sup>1</sup>

<sup>1</sup>Unité Matériaux et Transformations (UMET) UMR CNRS 8207, University of Lille, France

<sup>2</sup>INSERM U1008, Controlled Drug Delivery Systems and Biomaterials, University of Lille, France

[safa.ouergemmi@ed.univ-lille1.fr](mailto:safa.ouergemmi@ed.univ-lille1.fr)

### INTRODUCTION

Electrospinning is a widely used technique for the preparation of nanofibrous materials. Due to its high surface to volume ratio and microporous structure, its potential for biomedical applications is increasing, especially for tissue engineering and drug delivery system. In fact, thanks to its flexibility, this technique provides different strategies for drug loading, such as the one step strategy that consists on electrospinning the polymer-drug mixture, or the two steps strategy where the electrospun membrane is afterwards dipped into a drug solution [1]. In this study, the first strategy was adopted. A first system was obtained from the electrospinning of a chitosan-triclosan solution (CHT-TCL system). The release of TCL and the antibacterial activity of the loaded mats were studied. As an improvement of this system, a second one including cyclodextrin (CD) is proposed.

### EXPERIMENTAL METHODS

**Preparation of CHT based solutions:** 3.5wt% of CHT/polyethylene oxide (PEO) mixtures (ratio 9:1) were dissolved in 90% acetic acid aqueous solution. In order to stabilise nanofibrous mats in aqueous medium, 0.05wt% and 0.1wt% of genipin (a biosourced crosslinker) was added into the electrospun solution and obtained membranes were then exposed to water saturated atmosphere at 37°C in order to activate genipin-CHT reaction [2]. 5%, 10% and 20% (with respect to total polymer concentration 3.5wt %) of TCL were also added into the polymer solution.

**Electrospinning conditions:** the following parameters were optimized for the preparation of nanofibres: 0.8mm for the inner diameter of the needle, 0.3ml/h for the flow rate, 13kV for the applied voltage and 200mm for the tip to-collector distance. Temperature and relative humidity were kept at 23°C and 30% respectively.

**Drug release study:** CHT based nanofibres loaded with TCL were immersed in PBS and incubated at 37°C for 10 days. The amount of released triclosan was measured by UV-vis spectroscopy at 280nm (n=3).

**Microbiological evaluation:** The Kirby-Bauer disk diffusion method was carried out to determine the antibacterial properties of the CHT based nanofibres, containing or not TCL, against Gram-positive bacteria (*S.aureus*) and Gram-negative bacteria (*E.coli*) after 24h of incubation (n=3).

### RESULTS AND DISCUSSION

CHT nanofibres blended with PEO were successfully developed by electrospinning. The fibres diameters are in the range of 100 - 250 nm (figure 1.a).

The stability of membranes in aqueous medium was improved by a genipin crosslinking. The membranes collapse completely without genipin (figure 1.b)

whereas they are not affected with genipin (figure 1.c).

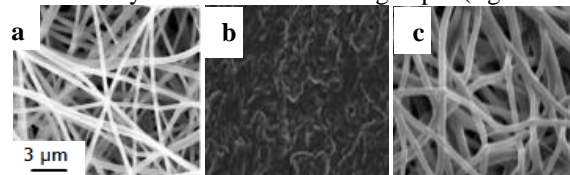


Figure 1: SEM observations of chitosan based nanofibres (a) in aqueous medium without (b) and with genipin treatment (c). The release profile (figure 2.A) shows a *burst* effect for all the TCL loaded nanofibres, and then a sustained release. The time of release increases with the drug loading of the mats.

According to the antibacterial assays, all tested membranes displayed an inhibition on both bacteria whose diameter varied with the initial TCL loading (figure 2.B).

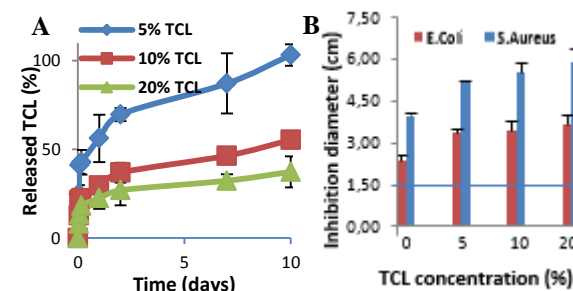


Figure 2: A) The release profile and B) Antibacterial activity of TCL loaded nanofibrous membranes.

The next part of this work is to limit the *burst* effect and to improve the sustained release. Therefore, we are developing new systems consisting on mixing CDs/TCL inclusion complexes, in order to control more efficiently the TCL release. Nanofibres of 150 to 280 nm diameter were obtained. Release study and antimicrobial assays will be attempted in order to demonstrate the expected effect of those CDs based nanofibrous systems.

### CONCLUSION

Nanofibres were successfully prepared by electrospinning a CHT/PEO/TCL solution. The release study has shown that this strategy did not allow to obtain a sufficient sustained release. Though, considering our former works in this field, the perspective of using cyclodextrin-TCL complex is a promising path for improving the sustained release performances.

### REFERENCES

- [1] D.-G. Yu, *Health (N. Y.)* 1: 67-75, 2009.
- [2] E. Mirzai et al, *Nanomed. J.* 1: 137-146, 2014

### ACKNOWLEDGMENTS

Region Nord-Pas-de-Calais, University of Lille and federation Chevreul are acknowledged for their supports.



## Dual Release and Antibacterial Effects of Chlorhexidine and Silver Released from Electrospun Chitosan/Poly(ethylene Oxide) Nanofibres

Jiankang Song<sup>1</sup>, Stefan S. Remmers<sup>1</sup>, Carla J.M. Bartels<sup>2</sup>, Jinlong Shao<sup>1</sup>, Eva Kolwijck<sup>2</sup>, Sander C.G. Leeuwenburgh<sup>1</sup>, John A. Jansen<sup>1</sup> and Fang Yang<sup>1\*</sup>

<sup>1</sup>Department of Biomaterials, Radboud University Medical Centre, Nijmegen, The Netherlands

<sup>2</sup>Department of Medical Biology, Radboud University Medical Centre, Nijmegen, The Netherlands

[jiankang.song@radboudumc.nl](mailto:jiankang.song@radboudumc.nl)

### INTRODUCTION

The traditional strategy for the treatment of implant-related infection involves systemic administration of high doses of antibiotics. This strategy is, however, associated with systemic toxicity and may result into antibiotic resistance [1]. Therefore, local and sustained delivery of multiple bacteria susceptible antiseptics, e.g. silver and chlorhexidine (CHX), is advocated as a new treatment modality. Besides, synergistic antibacterial effects could be achieved by combining release of Ag<sup>+</sup> and CHX. To achieve a controlled delivery, chitosan-based nanofibres have been widely used as carriers due to their high drug encapsulation efficiency, superior biocompatibility, and ease of processing [2]. Consequently, the objective of this study was to develop a chitosan-based nanofibrous drug carrier system containing silver nanoparticles (AgNPs) for the dual release of Ag<sup>+</sup> and CHX.

### EXPERIMENTAL METHODS

Nanofibrous matrices containing AgNPs were prepared by one-step electrospinning of a chitosan/poly(ethylene oxide) (PEO) (75:25) solution containing different amounts of AgNO<sub>3</sub> without any other reductive reagents. In situ formation of AgNPs was investigated by cryo-transmission electronic microscopy (TEM) and energy dispersive X-ray microscopy (EDX). CHX was loaded onto the matrix through a post-diffusional loading method and the release of CHX was detected by high performance liquid chromatography. Long-term release of Ag<sup>+</sup> was monitored by inductively coupled plasma mass spectrometry. Antibacterial effects of the membrane were confirmed by a zone of inhibition test against *S. aureus*.

### RESULTS AND DISCUSSION

Uniform, defect free nanofibres were obtained (Figure 1A). AgNPs were formed and distributed homogeneously throughout the fibres (Figure 1 B, C, D and E), which is attributed to the self-reductive ability of the chitosan solution. Compared to other methods for the preparation of electrospun nanofibres containing AgNPs, no reductive agent or other reductive treatment (e.g. UV) was used in this study. Besides, no AgNPs were observed using TEM when 0.1 wt% AgNO<sub>3</sub> (ratio to polymer) was added into chitosan/PEO solution, and the AgNPs became visible when the amount of AgNO<sub>3</sub> was equal or higher than 1 wt%, which corresponds to the lowest amount of AgNO<sub>3</sub> required in this system to form TEM-detectable AgNPs.

Burst release was observed for CHX, irrespective of the amount of CHX loaded (Figure 2A), which

indicated that there was no interaction between CHX and the nanofibres. In contrast, Ag<sup>+</sup> was released in a sustained manner for more than 28 days (Figure 2B). Moreover, identical patterns of release of Ag<sup>+</sup> from matrix with or without CHX were obtained (Figure 2B), which indicated that the loading of CHX on the nanofibres had no influence on the release of Ag<sup>+</sup>.

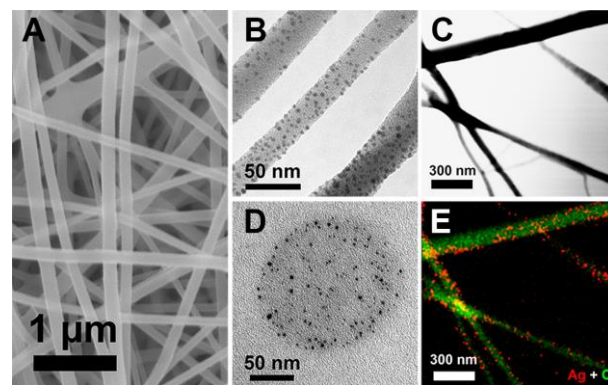


Figure 1 Characterization of chitosan/PEO nanofibers containing 5 wt% AgNO<sub>3</sub>. Scanning electron micrograph (A), transmission electron micrograph of the fibres (B) and fibre cross-section (D), TEM-EDX pictures of the nanofibers in bright field (C) and elemental distribution of silver and carbon (E).

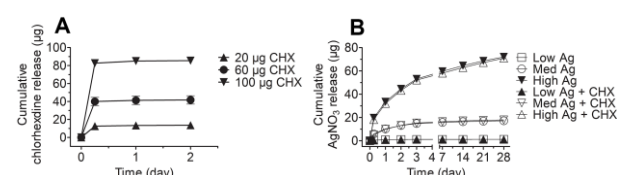


Figure 2 Release kinetics of chlorhexidine (A) and Ag<sup>+</sup> (B) from chitosan/PEO electrospun nanofibrous matrix.

### CONCLUSION

A simple one-step electrospinning procedure was developed for the formation of nanofibrous chitosan/PEO matrices containing AgNPs without addition of any other reductive reagent. The AgNPs were distributed homogeneously throughout the fibres. Burst-type release of CHX at the early stage and sustained release of Ag<sup>+</sup> at the later stage were obtained. This drug delivery system has strong potential great for the treatment of implant-associated infections.

### REFERENCES

- [1] Zhang *et al.*, Int J Nanomedicine, 9: 3027-36, 2014.
- [2] Ding *et al.*, Nanoscale, 6:9477-93, 2012.

### ACKNOWLEDGMENTS

This work was financially supported by Fonds NutsOhra (project no. 1303-024).





## Collagen/Hyaluronic Acid-based Hydrogels for Brain Applications: the Role of Hyaluronic Acid Molecular Weight

Marta Tunesi<sup>1,2</sup>, Armando Chierchia<sup>3</sup>, Luca Barbieri<sup>1</sup>, Teresa Russo<sup>4</sup>, Lucia Boeri<sup>3</sup>, Annalisa Grimaldi<sup>5</sup>, Roberto De Santis<sup>4</sup>, Luigi Ambrosio<sup>4</sup>, Antonio Gloria<sup>4</sup>, Diego Albani<sup>3</sup>, Carmen Giordano<sup>1,2</sup>

<sup>1</sup>Department of Chemistry, Materials and Chemical Engineering “G. Natta”, Politecnico di Milano, Milan, Italy

<sup>2</sup>Unità di Ricerca Consorzio INSTM, Politecnico di Milano, Milan, Italy

<sup>3</sup>Department of Neuroscience, IRCCS-Istituto di Ricerche Farmacologiche “Mario Negri”, Milan, Italy

<sup>4</sup>Institute of Polymers, Composites and Biomaterials, National Research Council, Naples, Italy

<sup>5</sup>Department of Structural and Functional Biology, University of Insubria, Varese, Italy

[teresa.russo@unina.it](mailto:teresa.russo@unina.it)

### INTRODUCTION

Hydrogels made from a number of natural and synthetic polymers have been studied for their ability to deliver therapeutics directly into the central nervous system<sup>1</sup>. In particular, hyaluronic acid (HA)-based gels have been used to deliver trophic factors<sup>2</sup> or cells into the injured spinal cord<sup>3</sup>. Type I collagen (COLL) is also an appealing candidate for neural tissue regeneration. In fact it self-assembles to form a fibrillar structure at physiological conditions and interacts with cells to guide their adhesion, migration, survival, proliferation, and differentiation<sup>4</sup>.

The aim of the present work has been designing and characterizing injectable COLL/HA acid-based semi-interpenetrating polymer networks (semi-IPNs) for the delivery of neuroprotective proteins (e.g. 70 kDa-heat shock proteins, Hsp70) or cells in the treatment of Alzheimer's and Parkinson's diseases, focusing on the role of HA molecular weight.

### EXPERIMENTAL METHODS

COLL and COLL/HA-based gels differing from the molecular weight of HA (100 or 1600 g·mol<sup>-1</sup>, COLL-LMW HA or COLL-HMW HA, respectively) were designed and characterized.

Their dynamic moduli were evaluated as a function of frequency (0.1-10 Hz) by small amplitude oscillatory shear tests and their viscosity was assessed as a function of shear rate (0.01-100 s<sup>-1</sup>) by steady shear measurements, while their injectability was confirmed by an INSTRON 5566 testing machine mounting a syringe with a 30 G needle. Hydrogel morphology was observed by scanning electron microscopy (SEM) and transmission electron microscopy (TEM). Hydrogel biological behavior was assessed both *in vitro* and *in vivo*. SH-SY5Y human neuroblastoma cell line were embedded within gels and their metabolic activity was quantified by MTS assay on days 1, 4 and 7. LMW HA, HMW HA and the semi-IPNs were injected in mouse striatum. After 7 days, the inflammatory response was evaluated by glial fibrillary acidic protein (GFAP) and CD11b staining on 30 µm-thick coronal sections. In particular, the quantitative evaluation of both GFAP and CD11b reactivity was performed by recording the number and the area covered by positive cells at 20X magnification.

### RESULTS AND DISCUSSION

Small amplitude oscillatory shear tests have shown that COLL and COLL-HA share a gel-like behavior, with

the storage modulus  $G'$  that is always greater than the loss modulus  $G''$ . In particular, for COLL-LMW HA  $G'$  is lower than for COLL-HMW HA gels. Steady shear tests have shown a shear thinning behavior and the viscosity of COLL-LMW HA is always lower than for COLL-HMW HA gels. Regarding the injectability tests, the values of maximum and plateau loads for COLL-HMW HA are almost double than for COLL-LMW HA matrices. TEM images have shown that COLL fibrils are coated by HA in COLL-LMW HA, while HA does not seem to follow the fibrillar network of COLL in COLL-HMW HA gels. MTS assays has indicated that cell metabolic activity increases with time, suggesting that SH-SY5Y cells may proliferate within gels. Results from *in vivo* injections have shown that the inflammatory response elicited by LMW HA is negligible (Fig.1).

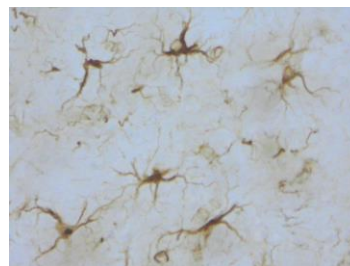


Fig.1: GFAP staining after LMW HA injection

### CONCLUSION

The available results have suggested that the rheological and preliminary biological properties shown by both the proposed collagen/hyaluronic acid-based gels are suitable for brain applications.

Future studies will focus on the suitability of COLL-HA gels for the delivery of Hsp70.

### REFERENCES

1. Khaing ZZ. *et al.*, Materials Today. 17:332-3401, 2014
2. Kang CE. *et al.*, Tissue Eng Part A. 15:595-604, 2009
3. Mothe AJ. *et al.*, Biomaterials. 34:3775-3783, 2013
4. Tunesi M. *et al.*, Int J Artif Organs. 36:762-774, 2013

### ACKNOWLEDGMENTS

The authors would like to thank Fondazione Cariplo (Grant no: 2011-0335) for providing financial support to this project and Altegon Italia for providing technical information about LMW HA and HMW HA.

## Endothelialisation of Titanium Dioxide Coated Gas Exchange Membranes for the Development of a Bioartificial Lung

Michael Pflaum<sup>1,3</sup>, Marina Kauffeldt<sup>5</sup>, Bettina Wiegmann<sup>1,3,4</sup>, Sabrina Schmeckebeier<sup>1,3</sup>, Daniele Dipresa<sup>1,3</sup>,  
Sotirios Korossis<sup>1,2,3,4</sup>, Jochen Schein<sup>5</sup>, Axel Haverich<sup>1,2,3,4</sup>

<sup>1</sup>Department of Cardiothoracic, Transplantation and Vascular Surgery (HTTG), Hannover Medical School, Germany

<sup>2</sup>Lower Saxony Centre for Biomedical Engineering, Implant Research and Development (NIFE), Hannover, Germany

<sup>3</sup>Leibniz Research Laboratories for Biotechnology and Artificial Organs, (LEBAO), Hannover, Germany

<sup>4</sup>Member of the German Center for Lung Research

<sup>5</sup>University of Federal Armed Forces, Munich, Germany

[pflaum.michael@mh-hannover.de](mailto:pflaum.michael@mh-hannover.de)

### INTRODUCTION

Currently, the use of extra corporeal membrane oxygenation (ECMO) devices, which is indicated for patients awaiting lung transplantation, is limited to a few weeks only, due to thrombus formation and deposition of blood components within the device. Therefore, the basic idea is to improve the haemocompatibility by endothelialisation of the poly-4-methyl-1-pentene gas exchange membranes (PMP), which necessitates the development of coating techniques for the mediation of endothelial cell adhesion to the hydrophobic polymers. The pulsed vacuum cathodic arc plasma deposition (PVCAPD) technique has been shown to enable the coating of thermosensitive polymers. Hence the eligibility of titaniumdioxide (TiO<sub>2</sub>) deposited on PMP using PVCAPD as an effective coating technique for enabling the endothelialisation was assessed.

### EXPERIMENTAL METHODS

PMP film samples were coated with TiO<sub>2</sub> via PVCAPD and characterised by SEM, contact angle measurement and oxygen transfer rate assessment. Umbilical cord blood derived endothelial cells (hCBECs) were seeded on such samples and incubated for 24 h. Established monolayers were investigated for the expression of activation-relevant marker genes and subjected to a leucocyte adhesion assay. The integrity of the monolayer was investigated by immunofluorescence staining for the adherence junction protein VE-Cadherin as well as the focal adhesion protein vinculin. Flow resistance and self-healing capacity of the established EC-monolayer were assessed in a parallel plate laminar flow chamber applying 30 dyne/cm<sup>2</sup> for 24 h.

### RESULTS

SEM analysis confirmed the homogeneous deposition of a thin layer consisting of nanoscale TiO<sub>2</sub> particles, which resulted in a decrease in the oxygen transfer rate by 22%. The coating increased the wettability of the PMP surface, which was detected by contact angle measurements (uncoated PMP: 82,79°, TiO<sub>2</sub> coated PMP: 57,48°).

hCBECs exclusively adhered to areas of the PMP film coated with TiO<sub>2</sub>. Gene expression analysis revealed that hCBECs seeded on TiO<sub>2</sub> coated surface retained the non-activated state, additionally confirmed by a leucocyte adhesion assay. The integrity of the cell layer was confirmed by the detection of the adherence junction protein VE-Cadherin, homogeneously expressed at sites of cell-cell contacts. The cell-substrate contacts could be detected by immunofluorescence staining of the focal adhesion protein vinculin. Furthermore, the established monolayer was resistant to a high physiologic shear rate of 30 dyne/cm<sup>2</sup>, for 24h. Besides planar PMP, the coating technique was successfully applied to 3D hollow fibres.

### CONCLUSION

This study demonstrated that TiO<sub>2</sub> coating via PVCAPD is a promising technique for coating thermosensitive PMP gas exchange membranes, enabling the generation of a non-activated, flow-resistant and integer EC monolayer.

### ACKNOWLEDGMENTS

This work was supported by the German Research Foundation (DFG), by the Cluster of Excellence (REBIRTH), and the German Center for Lung Research (DZL). The authors would like to thank the core facility for Scanning Electron Microscopy of the Laser Zentrum Hannover e.V. (LZH).





# Orthopaedic Bio-activation of PEEK using Plasma Immersion Ion Implantation

Edgar Wakelin<sup>1</sup>, Giselle Yeo<sup>2,3,4</sup>, Alexey Kondyurin<sup>1</sup>, Michael Davies<sup>5</sup>, David McKenzie<sup>1</sup>, Anthony Weiss<sup>2,3,4</sup>, Marcela Bilek<sup>1</sup>

<sup>1</sup>Applied and Plasma Physics, University of Sydney, Australia; <sup>2</sup>School of Molecular Bioscience, University of Sydney, Australia; <sup>3</sup>Charles Perkins Centre, University of Sydney, Australia; <sup>4</sup>Bosch Institute, University of Sydney, Australia; <sup>5</sup>Translational and Bioengineering Group, Heart Research Institute, Australia

[edgarw@physics.usyd.edu.au](mailto:edgarw@physics.usyd.edu.au)

## INTRODUCTION

Orthopaedic implantable devices encounter two major obstacles to long-term stability: the dual demands for biological and mechanical compatibility. Current implantable devices made of titanium are biologically benign, but are too rigid and lead to bone degradation via stress shielding<sup>[1]</sup>. Attempts to alter the elastic moduli of implantable devices to values similar to bone have met with limited success<sup>[2]</sup>. Polyether ether ketone (PEEK) is a promising candidate for the next generation of orthopaedic implants because of its tensile similarity to bone. However, PEEK produces a bone-implant interface strength that is inferior to titanium<sup>[3]</sup> – a critical determinant for orthopaedic implantation. In this study we use Plasma Immersion Ion Implantation (PIII) to activate a surface layer of PEEK by introducing radicals that covalently bind proteins to improve bone-implant interface strength and integration.

## EXPERIMENTAL METHODS

**PIII treatment:** PEEK (Victrex, UK) was treated using a 100 W nitrogen plasma at a pressure of  $2 \times 10^{-3}$  Torr. Ions were accelerated towards the surface with a pulsed bias of -20 kV, a current of 1.4 mA, and pulse length of 20  $\mu$ s at 50 Hz. **EPR:** Spectra were obtained using a Bruker EMX Xband spectrometer with a centre field of 3485 G, sweep width of 100 G, a microwave frequency of 9.76 GHz and power of 8 mW at 21°C. The receiver gain was set to  $1 \times 10^5$ , with modulation amplitude of 5 G, a time constant of 82 ms and sweep time of 83 s. **FTIR:** Spectra were obtained using a Digilab FTS 7000 spectrometer fitted with an attenuated total-reflection trapezium germanium crystal at an angle of incidence of 45°. Spectra were averaged over 50 scans with a resolution of 4 cm<sup>-1</sup>. Covalent protein attachment was determined by washing in a 5% SDS solution in PBS at 80°C for 60 minutes. **Cell attachment:** PEEK samples were incubated in tropoelastin solutions varying from 2–50  $\mu$ g/ml in PBS for 12 hours at 4°C, and then blocked with denatured BSA for 60 minutes. SAOS-2 osteosarcoma cells were seeded ( $13.2 \times 10^4$  cells/cm<sup>2</sup>) onto the surface for 60 minutes. Bound cells were then fixed, stained and quantified.

## RESULTS AND DISCUSSION

EPR measurements (Figure 1) show that radicals are created within the PIII treated surface. The concentration of radicals increases with treatment time, and decreases with aging time. The radicals produced are long-lived, enabling an activated surface with a long shelf life.

Figure 2A shows the fraction of tropoelastin remaining on PEEK samples after SDS washing as a function of the coated protein concentration. The removal of nearly all tropoelastin from the untreated PEEK indicates that

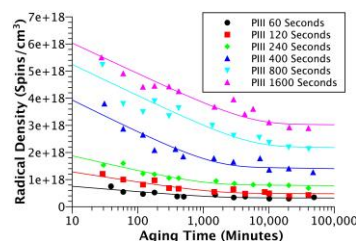


Figure 1 Density of radicals created by PIII treatment of PEEK as a function of aging time.

the protein is simply physically adsorbed to the surface. In contrast, the high protein retention on the PIII treated PEEK indicates that the majority of tropoelastin molecules are covalently bound to the surface. Figure 2B shows attachment of SAOS-2 cells to PEEK as a function of protein coating concentration. Untreated and PIII treated PEEK coated with tropoelastin concentrations  $\geq 5$   $\mu$ g/mL show similarly high cell attachment activity, in contrast to BSA-blocked PEEK. Tropoelastin retains osteoconductivity when covalently bound to the treated surface (data not shown).

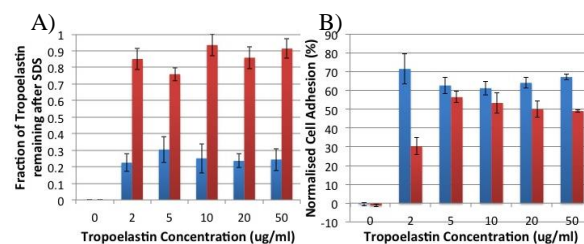


Figure 2A: Tropoelastin was covalently bound to PIII treated (red) but not untreated (blue) PEEK, as shown by protein retention after SDS washing. 2B: Tropoelastin bound to PIII treated PEEK (red) supports high levels of bone cell attachment.

## CONCLUSION

Plasma Immersion Ion Implantation modifies the surface of PEEK by introducing radicals. The radicals are capable of covalently binding proteins in a robust and reliable way. The immobilised protein retains its biological activity and cannot be displaced through vigorous washing. The treatment produces a surface that can cloak the underlying PEEK structures so that bound proteins can interact favourably with cells to improve the bone-implant interface.

## REFERENCES

1. M.M. Bilek *et al.*, *PNAS*, 108: 14405-14410, 2011
2. M. Geetha *et al.*, *Prog. Mater. Sci.*, 54: 397-425, 2009
3. C.M. Han *et al.*, *Biomaterials*, 2010, 31, 13

## ACKNOWLEDGMENTS

Project funding provided by the Australian Research Council. EW (PhD Student) was supported by an Australian Postgraduate Award.



# Alginate Hydrogels, Coated with Calcium Phosphate Nanoparticles by an Electrophoretic Deposition Method

Sabrina Daumann<sup>1</sup>, Katrin Wallat<sup>1</sup>, Michael Gepp<sup>2</sup>, Ronan Le Harzic<sup>2</sup>,  
Heiko Zimmermann<sup>2,3</sup>, Frank Stracke<sup>2</sup>, Matthias Eppe<sup>1</sup>

<sup>1</sup>Institute for Inorganic Chemistry and Center for Nanointegration Duisburg-Essen (CeNIDE),  
University of Duisburg-Essen, Essen, Germany

<sup>2</sup>Fraunhofer Institute for Biomedical Engineering IBMT, St. Ingbert, Germany

<sup>3</sup>Department of Molecular and Cellular Biotechnology, Saarland University, Saarbrücken, Germany  
[sabrina.berger@uni-due.de](mailto:sabrina.berger@uni-due.de)

## INTRODUCTION

Electrophoretic deposition (EPD) can be used to coat different surfaces with (nano)particles to enhance their bioactivity. The coating of implants by EPD is a versatile technique in modern biomaterials science.<sup>[2]</sup> Nanoparticles can be used for the transport of drugs and nucleic acids because they are easily taken up by cells and no other transport vectors are necessary.<sup>[1]</sup> Alginate, a hydrogel derived from marine brown algae, is a highly suitable matrix to immobilize nanoparticles. Alginate is often used for cell encapsulation and easy to modify according to specific cell characteristics and applications.<sup>[3]</sup> Here we report on the coating of alginate hydrogels with calcium phosphate nanoparticles which had been previously deposited on a silicon surface.

## EXPERIMENTAL METHODS

Three kinds of calcium phosphate nanoparticles were used for EPD. All nanoparticles were stabilized with polyethylenimine (PEI). Spherical nanoparticles were synthesized by precipitation, followed by functionalization. The particles can be functionalized with fluorescent molecules like tetramethylrhodamine (TRITC) and also with biomolecules like DNA or proteins and synthetic drugs. In addition, calcium phosphate nanorods (Ostim<sup>®</sup>)<sup>[4]</sup> were dispersed in water with PEI. After redispersion of the nanoparticles in ethanol, a high voltage can be applied for EPD. In aqueous dispersion, however, a low voltage is necessary (Table 1).

Table 1. Parameters for EPD of calcium phosphate nanoparticles on silicon from different dispersion media.

Dispersion medium	Ethanol	Water
Voltage	50 V, DC	2 V, DC
Deposition Time	30 s to 2 min	30 min to 5 h

Alginate beads were produced with an air-jet droplet generator as described in Refs.<sup>[3, 5]</sup> Alginate beads were coated with the calcium phosphate nanoparticles by rolling them over a nanoparticle-coated silicon surface.

## RESULTS AND DISCUSSION

Fig. 1 shows typical results of electrophoretically-deposited calcium phosphate nanorods on silicon. Fig. 2 shows an alginate bead, coated with red-fluorescing nanoparticles. The transfer of the nanoparticles to the alginate bead was highly efficient as it is evident from the strong fluorescence intensity. As indicator of the changed surface properties of alginate, introduced by coating with calcium phosphate nanoparticles, the attachment of fibroblasts was quantified after 24 h. 76±21% of the cells attached to nanoparticle-coated alginate hydrogels, while only 1.8±2.2% of the cells

were attached to native alginate hydrogel surfaces. This demonstrates the increased affinity of the very hydrophilic alginate surface to cells after coating with calcium phosphate nanoparticles.

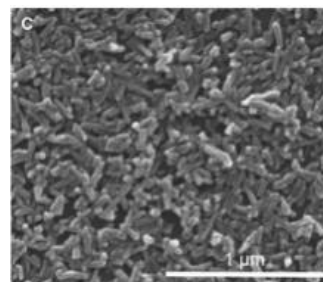


Fig. 1. SEM image of a calcium phosphate nanorod-coated silicon surface.

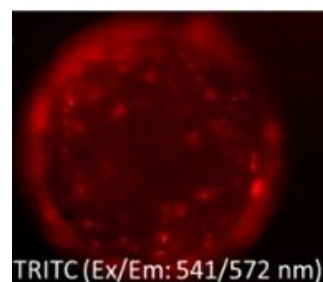


Fig. 2. An alginate bead, coated with TRITC-labelled (red) calcium phosphate nanoparticles.

## CONCLUSION

Calcium phosphate nanoparticles were deposited by electrophoretic deposition onto silicon and transferred to alginate beads by rolling. The adhesion of fibroblasts to the coated alginate beads was much higher than to the native alginate surface.

## REFERENCES

- [1] V. Sokolova, M. Eppe, *Angew. Chem. Int. Ed.* **2008**, 47, 1382-1395.
- [2] A. R. Boccaccini, S. Keim, et al., *J. Roy. Soc. Interface* **2010**, 7, 581-613.
- [3] H. Zimmermann, S.G. Shirley, et al., *Curr Diab Rep.* **2007**, 7, 314-320.
- [4] J. Klesing, S. Chernousova, et al., *J. Mater. Chem.* **2010**, 20, 6144-6148.
- [5] H. Zimmermann, F. Ehrhart, et al., *Appl. Phys. A.* **2007**, 89, 909-922.

## ACKNOWLEDGMENTS

This work was supported by the Deutsche Forschungsgemeinschaft (DFG, SPP 1327).



## Calcium- and Phosphorus-Rich Oxide Coatings on Tantalum Obtained by Plasma Electrolytic Oxidation

Maciej Sowa<sup>1</sup>, Maja Woszczak<sup>1</sup>, Grzegorz Dercz<sup>2</sup>, Andrey I. Kukhareno<sup>3,4</sup>, Danila M. Korotin<sup>3</sup>, Ernst Z. Kurmaev<sup>3</sup>, Seif O. Cholak<sup>4</sup>, Marcin Basiaga<sup>5</sup>, Wojciech Simka<sup>1</sup>

<sup>1</sup>Faculty of Chemistry, Silesian University of Technology, Poland

<sup>2</sup>Institute of Materials Science, University of Silesia, Poland

<sup>3</sup>Institute of Metal Physics, Russian Academy of Sciences-Ural Division, Russia

<sup>4</sup>Ural Federal University, Russia

<sup>5</sup>Faculty of Biomedical Engineering, Silesian University of Technology, Poland

[maciej.sowa@polsl.pl](mailto:maciej.sowa@polsl.pl)

### INTRODUCTION

Tantalum-based implants were known to be successful since the research conducted by Burke<sup>1</sup> in 1940's. Although its relatively high cost effectively impedes the widespread application of this biocompatible metal there are some attempts to bring this material into affordable price-range with the use of porous structures. Additional advantage of such approach is reduction of implant's weight and enlarging its surface area<sup>2,3</sup>.

Bioactive coatings on valve metals such as titanium or tantalum (mainly enriched with Ca and P) can be obtained by a myriad of ways<sup>4</sup>. Plasma electrolytic oxidation (PEO) presents relatively inexpensive yet effective method of formation of thick oxide coatings with an ability to introduce electrolyte components into the oxide layers<sup>5</sup>. Manipulation of process parameters such as voltage, current density or electrolyte composition gives control over coatings' parameters<sup>6</sup>. Herein, a study of bioactive behaviour of PEO coatings obtained on tantalum in Ca and P containing solutions is described. The coatings were characterised in terms of their surface morphology, thickness, chemical and phase compositions, corrosion resistance and *in vitro* bioactivity.

### EXPERIMENTAL METHODS

Anodic oxide coatings were obtained by anodising (Kikusui 800H DC power supply) tantalum workpiece (discs -  $\phi$ : 9 mm; height: 5 mm; BIMO metals) in  $\text{Ca}(\text{H}_2\text{PO}_2)_2$ ,  $\text{Ca}(\text{HCOOH})_2$ ,  $\text{Mg}(\text{CH}_3\text{COOH})_3$ ,  $\text{Na}_2\text{SiO}_3$  and  $(\text{NH}_4)_3\text{PO}_4$  solutions with different compositions and voltages (200-500 V). Surface morphology of the tantalum specimens was investigated using SEM/EDX (Hitachi S-3400N / Thermo Noran), their phase composition by XRD (X-Pert Philips PW 3040/60) and chemical composition by XPS (PHI XPS Versaprobe 5000). Corrosion resistance of the samples was assessed in Ringer's solution at 37°C with the use of potentiostat (Parstat 4000) and bioactivity of the coatings was studied by SBF soaking. Adhesion of the coatings was assessed using Micro-Combi-Tester (CSM).

### RESULTS AND DISCUSSION

Surfaces of anodic oxide coatings were determined to be composed mainly from Ca and P (calcium hypophosphite and calcium formate bath) or Ca, P and Mg (calcium hypophosphite and magnesium acetate bath) as was determined with EDX analysis. Tantalum was present in small amount. Furthermore, only little Si

and Na was incorporated into tantalum oxide layers at low voltages in the case of sodium silicate/ammonium phosphate baths, however, at higher voltages the oxide layer was covered with relatively thick amorphous silica layer. It was shown that anodising voltage increases the amount of electrolyte species introduced into the oxide layer. Higher concentration of electrolyte components in the anodisation bath increases this percentage as well. Upon anodising at 500 V additional surface features were observed in the case of all anodised samples. These were identified as highly crystalline with (depending on the choice of bath) calcium tantalate, hydroxyapatite and tricalcium phosphate species within their structure. Increase of anodisation voltage increased the adhesion of the obtained coatings. Corrosion resistance of tantalum in Ringer's solution was significantly improved by anodisation, regardless of the process conditions. SBF soaking tests revealed that the proposed method of surface modification induces precipitation of calcium phosphates (apatites) on the immersed surfaces. The effect is more pronounced in the case of calcium- and phosphorus-rich oxide layers.

### CONCLUSION

Plasma electrolytic oxidation of tantalum in solutions containing Ca, P, Mg and Si was investigated as a potential method of improvement of bioactivity of the bare Ta. Results suggest that the properties of the coatings can be easily tuned by means of process conditions and yield different amounts of electrolyte species incorporated into oxide layers. These layers protect the metal from corrosion and induce apatite formation after immersion in SBF for 4 weeks. *In vitro* biological tests are the next step in the assessment of bioactivity of anodised tantalum.

### REFERENCES

1. Burke G.L. Can Med Assoc J 43:125, 1940
2. Bobyn J.D. *et al.* J Bone Joint Surg Br 81:907, 1999
3. Wauthle R *et al.* Acta Biomater 14:217, 2015
4. Bächle M. *et al.* Clin Oral Impl Res 15:683, 2004
5. Krzakała A. *et al.* R Soc Chem Adv 3:19725, 2013
6. Yerokhin A.L. *et al.* Surf Coat Tech 122:73, 1999

### ACKNOWLEDGMENTS

The authors would like to thank the Polish Ministry of Science and Education under "Diamond Grant" programme, research project no. DI 1212 024142 for providing financial support to this project".





## Human E-cadherin Fusion Protein Matrix Improving the Proliferation and Hepatic Differentiation of Human Mesenchymal Stem Cells

Jun Yang<sup>1</sup>, Jinbin Xu<sup>1</sup>, Yan Zhang<sup>1</sup>, Toshihiro Akaike<sup>2</sup>

<sup>1</sup>College of Life Sciences, Nankai University, Tianjin 300071, China

<sup>2</sup>Department of Biomolecular Engineering, Tokyo Institute of Technology, Yokohama 226-8501, Japan  
[yangjun106@nankai.edu.cn](mailto:yangjun106@nankai.edu.cn)

### INTRODUCTION

The development of novel biomaterials constitutes a major challenge for materials science and regenerative medicine. The functional bioactive materials present various microenvironmental cues and ultimately determine cell behaviour by eliciting specific intracellular signalling response. Proteins were known as mainly inter-related signaling molecules in the interface between biomaterials and cells for regulating cell adhesion, proliferation and in some cases differentiation. New biological materials of recombinant protein are now being developed using common genetic engineering to create well-defined, multifunctional materials. In recent years, the recombinant protein materials with tissue engineering applications have been studied including structural protein, growth factor and cell-bind protein. In this study, a fusion protein consisting of human E-cadherin extracellular domain and the immunoglobulin G Fc region (hE-cadherin-Fc) was biosynthesized and used as a cell-cell adhesion biomimicking matrix for the expansion and differentiation of human mesenchymal stem cells (hMSCs) *in vitro*.

### EXPERIMENTAL METHODS

The hE-cadherin-Fc fusion protein was expressed and purified by the Free-Style MAX 293 Expression System was analyzed by western blotting. The purified hE-cadherin-Fc solution was added to a 96-well PS plate at various concentrations. After incubating at 4°C overnight, the plates were washed with PBS three times and used for cell culture. The immobilization of hE-cadherin-Fc was determined with ELISA assay, AFM and water contact angle (WCA) measurements.

Human bone marrow mesenchymal stem cells (hMSCs) (HUXMA-01001, Cyagen Biosciences, China) were cultured with OriCell™ Human Mesenchymal Stem Cell Growth Medium (HUXMA-90011, Cyagen Biosciences, China) containing 10% (v/v) fetal bovine serum, glutamine and the antibiotics penicillin and streptomycin under 5% (v/v) CO<sub>2</sub> at 37°C and 95% air humidity. The hMSCs between passages 3 and 6 were used in all experiments. The adhesion and proliferation of hMSCs were MTT assay and cell cytoskeleton staining. The mRNA and protein expression of stem cell feature were characterized by RT-PCR and western blotting.

Statistical significance was assessed with two-way ANOVA ( $P \leq 0.05$ ,  $P \leq 0.01$ ,  $P \leq 0.001$ ) using GraphPad Prism Version 5.0 software (GraphPad, San Diego, CA). All results were reported as the mean  $\pm$  SD.

### RESULTS AND DISCUSSION

Water contact angles (WCA) and Atomic Force Microscope (AFM) showed that the hE-cadherin-Fc was stably immobilized onto hydrophobic surface and enhanced the surface wettability and topography. The hE-cadherin-Fc matrix markedly promoted the cell adhesion and proliferation of hMSCs comparing with the tissue culture-treated plate (TC-PS) and gelatin. The expanded hMSCs on the hE-cadherin-Fc were positive for CD105, showing the hE-cadherin-Fc matrix could maintain the undifferentiation of hMSCs. The expressions of E-cadherin and  $\beta$ -catenin in the hMSCs were improved on the hE-cadherin-Fc matrix, suggesting that the cell-cell adhesion junctions were substituted by the interactions between the hE-cadherin-Fc matrix and the hMSCs at the initial culture stage in the absence of cell-cell interactions.

Compared with TC-PS and gelatin, the hE-cadherin-Fc matrix effectively stimulated the hMSCs to progress toward the polygonal morphology of hepatocyte, upregulated hepatocyte-specific genes (ALB, CK18 and HNF4) and live-specific functions (the glycogen storage, ICG uptake, albumin secretion and urea production) after 4 weeks of hepatic differentiation culture. These results show hE-cadherin-Fc may be a promising artificial extracellular matrix for the hMSCs differentiation via the homophilic interaction of hE-cadherin and the synergy between cell adhesion molecular and growth factors.

### CONCLUSION

hE-cadherin-Fc was successfully prepared as a cell-cell adhesion biomimicking matrix which can be used for the surface modification of hydrophobic materials effectively. The hE-cadherin-Fc fusion protein matrix could enhance the adhesion and proliferation of the hMSCs, and improve the hepatic differentiation of hMSCs by the synergy of adhesion junction and cell growth factors. The hE-cadherin-Fc was shown to be a promising artificial ECM for hMSCs.

### REFERENCES

1. Nagaoka M. *et al.*, Annals of Biomedical Engineering 38(3):683-693, 2010.
2. Xu J. *et al.*, Colloids and surf. B: Biointerfaces 109:97-102, 2013.
3. Xu J. *et al.*, Chinese Journal of Biomedical Engineering 32(6):27-34, 2013.

### ACKNOWLEDGMENTS

This study was supported by the National Natural Science Foundation of China (Grant Nos. 31070855, 31370965), the 973 Program (Grant No. 2011CB606202).



## Silk-Collagen Inspired Artificial Proteins for 3D Cell Culture Study

Małgorzata Włodarczyk-Biegun<sup>1</sup>, Kambiz Farbod<sup>3</sup>, Marc Werten<sup>2</sup>, Frits de Wolf<sup>2</sup>, Jeroen van den Beucken<sup>3</sup>, Sander Leeuwenburgh<sup>3</sup>, Martien Cohen Stuart<sup>1</sup>, Marleen Kamperman<sup>1</sup>

<sup>1</sup>Laboratory of Physical Chemistry and Colloid Science, Wageningen University, The Netherlands

<sup>2</sup>Wageningen UR Food and Biobased Research, The Netherlands

<sup>3</sup>Department of Biomaterials, Radboud UMC Nijmegen, The Netherlands

[gosia.wlodarczyk-biegun@wur.nl](mailto:gosia.wlodarczyk-biegun@wur.nl)

### INTRODUCTION

Recombinant DNA technology enables the synthesis of artificial proteins with highly controlled structure and properties [1-2]. In our group we designed, produced and characterized a silk- and collagen- inspired block copolymer (CSC) [3], which forms self-assembled, pH-responsive hydrogel networks. Additionally, we produced a protein variant that is rich in integrin-binding (RGD) domains (CSC-RGD). The main aim of this study was to obtain scaffolds from artificial proteins and study their 3D cell culture performance.

### EXPERIMENTAL METHODS

Silk-collagen- inspired proteins (CSC) and RGD-modified CSC proteins were obtained in the process of *P. pastoris* fermentation and purified by selective precipitation.

Cell culture scaffolds were prepared by dissolving protein at low pH and subsequently increasing the pH to physiological values to induce gelation. Scaffolds, made of pure CSC protein, CSC mixed with 50% CSC-RGD and pure CSC-RGD protein at total protein concentration 1%, 2% and 4%, were prepared in cell culture inserts (ThinCerts™). For 7 days, MG63 cells were cultured inside the gels and cell behaviour was analysed with AlamarBlue assay, DAPI/actin staining and LIVE/DEAD assay (data not shown).

### RESULTS AND DISCUSSION

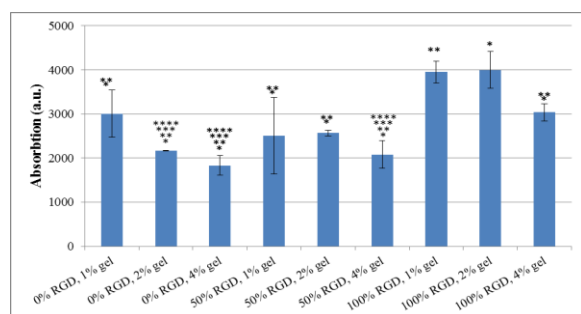


Figure 1. AlamarBlue assay after 7 days of cell culture; sign.diff. ( $p < 0.05$ ) in comparison to: \* - 100% RGD, 1% gel, \*\* - 100% RGD, 2% gel, \*\*\* - 100% RGD, 4% gel, \*\*\* - 0% RGD, 1% gel

An alamarBlue assay was used to estimate cell activity (fig.1.). Based on the results we conclude that cells were most active in the RGD functionalized gels containing low protein concentrations.

This observation was confirmed by image analysis using confocal microscopy (fig.2.). After 7 days of culture, cells spread much better in the gels with high RGD content and low protein concentration. At higher protein concentrations cells could not spread, regardless of the high RGD content.

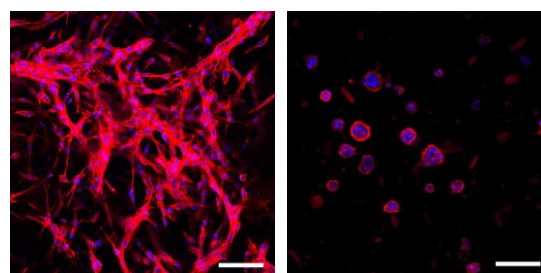


Figure 2. Cells after 7 days of culture in 100% RGD, 1% gel (left) and 100% RGD, 4% gel (right); scale bars = 100µm

The results indicated that for improved cell behaviour RGD functionality is not the sole requirement. The gel matrix needs to exhibit the right mechanical properties and architecture for cells to grow. For example, studies show that by introducing porosity cell performance can be enhanced [4]. We improved the architecture of our scaffolds by decreasing the protein concentration, thereby creating more space for cells in the gel matrix and making the network more deformable.

### CONCLUSION

We synthesized hydrogel scaffolds from artificial protein polymers and performed a 3D cell culture. Optimum cell behaviour was obtained by incorporation of RGD-domains in the proteins and decreasing protein concentration.

### REFERENCES

1. Petka WA et al., Science. 1998; 281(5375): 389-92.
2. Sengupta D, Helishorn SC, Tissue Eng Part B Rev. 2010; 16(3):285-93
3. Włodarczyk-Biegun MK et al., Acta Biomater. 2014; 10(8):3620-9
4. Sun J et al., Biomaterials. 2014; 35(17):4759-68

### ACKNOWLEDGMENTS

The authors would like to thank the Netherlands Institute for Regenerative Medicine (NIRM) and ERC (Advanced Grant 267254 “BioMate”) for providing financial support to this project.





## Fluorescent Hydrogel for Improved Traceability of Biomedical Devices *in Vivo*

Ibáñez-Fonseca A., Arias F.J., Rodríguez-Cabello J.C.

BIOFORGE, CIBER-BBN, Universidad de Valladolid, Spain  
[aibanez@bioforge.uva.es](mailto:aibanez@bioforge.uva.es)

### INTRODUCTION

The increasing applications of genetically engineered materials, such as elastin-like recombinamers, in the field of biomedicine have led to the developing of different devices for tissue engineering, e.g. biocompatible and bioactive hydrogels used as scaffolds that simulate extracellular matrix, with a transition temperature below 37°C allowing its usage as an injectable solution<sup>1</sup>.

One of the issues regarding these devices is the correct and certain traceability of the material when implanted or introduced in an organism. For the purpose of addressing this problem, a silk-elastin-like recombinamer (SELR)<sup>2</sup> fused to enhanced green fluorescent protein (EGFP)<sup>3</sup> by recombinant DNA technology has been developed. This recombinamer is able to form nanoparticles at low concentrations and physically cross-linked hydrogels at higher ones, increasing the potential applications of this material.

### EXPERIMENTAL METHODS

SELR synthesis was done by molecular biology recombinant DNA techniques, assessed by agarose gel electrophoresis, and expression in *E. coli* analyzed by SDS-PAGE and fluorescence measurement. Characterization of the obtained material included MALDI-TOF mass spectrometry, amino acid composition by HPLC, differential scanning calorimetry (DSC) to determine transition temperature (T<sub>t</sub>), dynamic light scattering (DLS) to evaluate particle size, zeta potential measurement and rheology. *In vitro* cell cultures were performed in human fibroblasts (HFF-1 cell line). Fluorescence was studied qualitatively by fluorescence microscopy and quantitatively in a fluorometer.

### RESULTS AND DISCUSSION

Results regarding physicochemical characterization of the recombinamer showed a right molecular weight according to theoretical data. Transition temperature was observed at 16.8°C in physiological solution, allowing a gel phase when implanted *in vivo*. Furthermore, fluorescence was assured at different pH conditions and concentrations of the material, determining the non-influence of the SELR backbone on the correct folding of the EGFP, even observing fluorescent bacteria while expressing the recombinamer. Zeta-potential was -25mV because of the glutamic acid residues included in the elastin derived amino acid sequences.

Dual particles were also achieved through the covering of the fluorescent nanoparticles with another ELR with cell-adhesive properties positively charged by the presence of lysine residues, taking advantage of the electrostatic interaction with the negatively charged EGFP recombinamer, resulting in a positive zeta-potential and larger nanoparticles. These particles showed cell interaction and even internalization, being observed by fluorescent microscopy, suggesting bioactivity and biocompatibility.

Hydrogels made of the fluorescent recombinamer were formed at 150mg/mL showing stability through time and mechanical properties desirable for different applications in the field of biomedicine. Their fluorescence was assessed qualitatively and results showed high intensity, suggesting that a minimum amount of this material could lead to a successful traceability when implanted *in vivo* combined with other bioactive materials.

### CONCLUSION

A fluorescent and hydrogel-forming material has been successfully developed. *In vitro* cell cultures showed other applications working as nanoparticles and good biocompatibility. Its properties make it a potential candidate to be included in biomedical devices allowing hydrogel traceability and determination of the biodegradation and migration *in vivo*. Non-expensive instruments can be used for these purposes, taking advantage of the 2-photon fluorescence.

### REFERENCES

1. Rodríguez-Cabello J.C *et al.*, Nanomedicine. 6:111-122, 2011.
2. Fernández-Colino A. *et al.*, Biomacromolecules, 15(10):3781-93, 2014
3. Shimomura O. *et al.*, J. Cell Comp. Physiol., 59:223-239, 1962.

### ACKNOWLEDGMENTS

Authors would like to thank THE GRAIL project included in the FP7 European funding. (Grant no: 278557) for providing financial support to this project.



## Self-gelling Elastin and Silk-Elastin Recombinamers for Ophthalmic Applications

Alicia Fernández-Colino<sup>1</sup>, Daniela Quinteros<sup>2</sup>, José Bermudez<sup>3</sup>, Santiago de Palma<sup>2</sup>, José Carlos Rodríguez-Cabello<sup>1</sup>,  
Francisco Javier Arias<sup>1</sup>

<sup>1</sup> BIOFORGE Research Group, University of Valladolid, CIBER-BBN, Spain

<sup>2</sup> UNITEFA-CONICET, Faculty of Chemical Sciences, National Univ. of Cordoba, Argentina

<sup>3</sup>Facultad de Ingeniería, Instituto de Investigaciones para la Industria Química (INIQUI-CONICET), Universidad Nacional de Salta, Argentina

[arias@bioforge.uva.es](mailto:arias@bioforge.uva.es)

### INTRODUCTION

The development of topical ophthalmic formulations for the treatment of eye diseases such as glaucoma, present a challenge<sup>1</sup>, since most drugs are hardly absorbed, having bioavailabilities from 1-10%. Among other factors, such low bioavailability is consequence of a rapid and extensive loss of the formulation from the pre-corneal area due to the turnover of the lacrimal drainage. An alternative to increase the residence time of formulations in the area of application is the use of bioadhesive systems. Taking this into account, here we developed an elastin-like and a silk-elastin like recombinamers<sup>2,3</sup>, named respectively as ELR and SELR, for their incorporation in an ophthalmic formulation against glaucoma. Our hypothesis is that due to the thermo-sensitive behavior of these materials, the formulation could be administered topically as drops, and once sensing the temperature of the eye, suffer a shift to a gel system, which could help to prolong the permanence of the formulation in the eye, and therefore, could enhance the therapeutic effect.

### EXPERIMENTAL METHODS

The recombinamers were obtained by molecular biology standard techniques. Rheological tests were performed to assess the thermogelling properties of both systems. Circular dichroism (CD) and FTIR analysis were carried out evaluate conformational changes on the differences in the rheological behavior. *In vivo* studies were performed on New Zealand rabbits. Each formulation was placed into the conjunctival fornix and the intraocular pressure (IOP) was measure by a Tonovet tonometer.

### RESULTS AND DISCUSSION

Both recombinamers display clearly differences on the rheological properties. Concretely, the SELR show a dual physical gelation process, as consequence of the presence of the silk domains intercalated with amphiphilic engineering elastin-blocks, whereas the ELR displays a single gelation step. Such differences in the reological behavior were consequence of different conformational features of both materials, as verified by CD and FTIR.

Relative to their pharmacological application, it should be pointed that the self-assembly nature of both recombinamers allowed facile encapsulation of the therapeutics within the gel. *In vivo* tests evidenced that formulations containing the recombinamers further decreased the IOP when compared with the control formulation (without any of the recombinamers). Furthermore, SELR-formulation was found to be more effective that its counterparts ELR-formulation, which agrees with the enhanced mechanical properties provided by the presence of the silk moieties.

### CONCLUSIONS

These results evidenced that the self-gelling ELR and SELR have great potential for its use as components of ophthalmic pharmaceutical formulations.

The initial liquid-like state of the recombinamers allows easy topical administration with ulterior gelification as consequence of the thermosensitive properties. *In vivo* studies show an enhanced reduction in IOP provided by the presence of the recombinamer, which was more accentuated in the case of SELR. Finally, the crosslinking mechanism based on self-assembly makes its preparation biologically friendly and very simple.

### REFERENCES

1. Knight O J *et al.*, Curr Opin Ophthalmol. 25(2):112-7.2014
2. Arias F. J, *et al.*, A. Current Topics in Medicinal Chemistry, 14, 2014
3. Fernández-Colino A, *et al.*, Biomacromolecules. 13;15(10):3781-93, 2014

### ACKNOWLEDGMENTS

The authors would like to thank MINECO Project PRI-PIBAR-2011-1403, and European Social Founding, Operative Programme of "Castilla y Leon" and JCyL, through "Consejería de Educación" for providing financial support to this project.



# A Functional Macromolecular Gradient Hydrogel System as a Platform to Model Tissue-to-Tissue Interfaces

D.R. Pereira<sup>1,3</sup>, J.M. Oliveira<sup>1,2</sup>, R.L. Reis<sup>1,2</sup>, Abhay Pandit<sup>3</sup>

<sup>1</sup>3B's Research Group - Biomaterials, Biodegradables and Biomimetics, Univ. Minho, Headquarters of the European Institute of Excellence on Tissue Engineering and Regenerative Medicine, AvePark, S. Cláudio de Barco, 4806-909 Taipas, Guimarães, Portugal;

<sup>2</sup>ICVS/3B's - PT Government Associate Laboratory, Braga/Guimarães, Portugal;

<sup>3</sup>Network of Excellence for Functional Biomaterials, National University of Ireland Galway, Ireland

[diana.pereira@dep.uminho.pt](mailto:diana.pereira@dep.uminho.pt)

## INTRODUCTION

One of the critical challenge facing tissue engineering strategies relate to simultaneous generation of multiple tissues and its functional assembly that lead to complex organ systems[1]. The gradient of structural and mechanical properties present in tissues have led to engineering strategies that focus on this interface. The tissue-to-tissue interface is the most crucial parameter in the approach to multitissue repair. Tissue interfaces present a chemical hierarchical structure leading to different mechanical properties. The interface is the transition between two adjacent tissues as it presents a highly heterogenous structure of chemical and biological organization[2,3]. The hypothesis in this study is that differential functional properties can be engineered by modulation of macromolecules gradient in a cell seeded three-dimensional hydrogel system. Specifically, differential paracrine secretory profiles can be engineered using hBMS. Hence, the specific objectives of this study are to: assemble the macromolecular gradient from natural materials (gellan gum, hyaluronic acid and collagen); to evaluate whether the gradient is suitable for hMSC encapsulation by cellular viability assesment; and screen the paracrine secretion of hBMS over time within this gradient hydrogel system.

## EXPERIMENTAL METHODS

Three different solutions of methacrylated gellan-gum (GG-MA) and hyaluronic acid (HA) were assembled keeping GG-MA constant at 15mg/ml while HA was incorporated at different ratios (5, 2.5 and 0.5 mg/ml). A similar approach was used for GG-MA – Collagen I (Col I) but with different ratios of Col I (2, 1 and 0.1mg/ml). The gradient hydrogels were fabricated into cylindrical silicon moulds with higher ratio solutions assembled at the bottom of the mould and adding the two solutions consecutively on top of each other. Crosslinking was performed by phosphate buffer solution (PBS). PBS cations interact only with GG-MA chains allowing the chains to get closer and create the crosslinked network. Controls of GG-MA (15mg/ml) were also fabricated. FITC-labelling HA and Col I was used to confirm the fabrication of the gradient. AFM was used to assess the differential mechanical properties. Human Bone Marrow Stem Cells (hBMS) at passage three (P3) were loaded into each batch solution at  $10^6$  cells/ml solution and gradient hydrogels were produced as previously described. The hBMS were observed under confocal microscopy after staining with Calcein AM and Propidium Iodide (PI). Secretory cytokine measurement for pro-inflammatory factors was carried out using ELISA.

## RESULTS AND DISCUSSION

The gradient hydrogel was successfully constructed and validated by fluorescent emission of FITC labelled HA and Col I (Figure 1 (B) Additionally,

AFM analysis demonstrated a different stiffness for two distinct regions of the gradient.

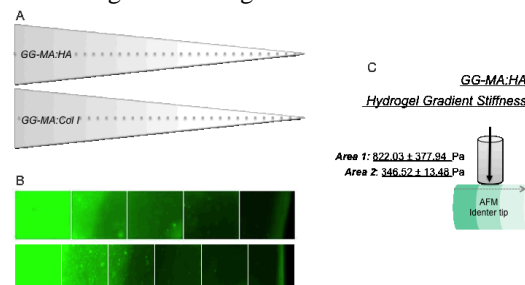


Figure 1: **A:** Schematic representation of hydrogel gradients; **B:** FITC-Fluorescent labeling macromolecules (HA/COL) incorporating the hydrogel gradient; **C:** Stiffness by AFM analysis of GG-MA: HA gradient hydrogel across layers.

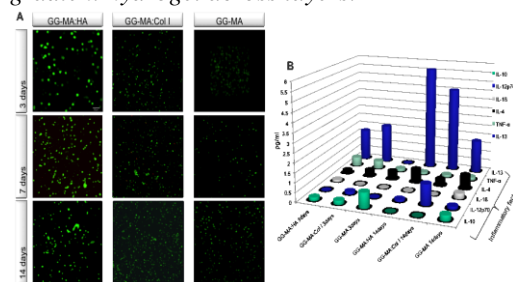


Figure 2: Gradient hydrogel microenvironment alters hMSC viability and protein expression. **A:** Confocal images from Live/Dead staining (Calcein Am/PI) showing hBMS cells viability of encapsulated cells within gradient hydrogels up to 14 days. **B:** Multiplex ELISA protein expression of hMSCs on the gradient hydrogel controlled for 3 and 14 days timepoint.

Viability of hBMS was studied by the green emission of Calcein AM conversion on the membrane of live cells. There is a positive effect on cell viability of both macromolecules (HA and Col I) on the overall gradient. Preliminary results from protein analysis show significant differences in the levels of cytokine production in the HA and Col I gradient hydrogels when compared to those of the control and over time.

## CONCLUSION

The macromolecular gradient hydrogel systems were successfully achieved combining either HA or Col I with GG-MA demonstrating differentially secretion of pro-inflammatory factors by encapsulated hBMS within the gradient hydrogel systems.

## REFERENCES

1. Phillips, JE. Et al., Proc Natl Acad Sci USA, 26:12170-5, 2008
2. Lienemann, PS. Et al., Integr Biol (Camb), 7:101,2014
3. Karpiv, JV. Et al., Adv Mater, 24:1466-70, 2012

## ACKNOWLEDGMENTS

Portuguese Foundation for Science and Technology (FCT) (doctoral scholarship SFRH/BD/81356/2011).



Irene Cano-Torres<sup>1</sup>, Riccardo Levato<sup>1</sup>, Miguel A. Mateos-Timoneda<sup>2,1</sup>, Elisabeth Engel<sup>1,2,3</sup>

<sup>1</sup>Institute for Bioengineering of Catalonia (IBEC), Barcelona, Spain

<sup>2</sup>CIBER en Bioingeniería, Biomateriales y Nanomedicina (CIBER-BBN), Barcelona, Spain

<sup>3</sup>Technical University of Catalonia (UPC), Barcelona, Spain

[icano@ibecbarcelona.eu](mailto:icano@ibecbarcelona.eu)

## INTRODUCTION

*Ex vivo* generation of functional tissues and organs still faces challenging limitations particularly concerning construct size and matrix composition. Mass transfer and oxygen diffusion into the inner space represent two of the major constraints. Additionally, designing and engineering suitable scaffolds is an arduous task due to the complexity and dynamic composition of the native cellular niches. To this aim, bottom-up strategies wherein microtissue blocks are assembled to form a macroscopic tissue are gaining ground<sup>1</sup>.

In our study, microtissues are directly obtained from rat mesenchymal stromal cells seeded on biodegradable poly-(lactic) acid (PLA) microparticles (MP). This strategy overcomes low seeding efficiencies and poor cell distributions. Besides, MP facilitate cell expansion, and induces osteogenic phenotype<sup>2</sup>. In the end, to avoid nutrient and oxygen diffusion issues during *ex vivo* matrix deposition, cell-laden MP are transferred to a chamber in a perfusion system allowing the formation of a clinical-relevant construct.

## EXPERIMENTAL METHODS

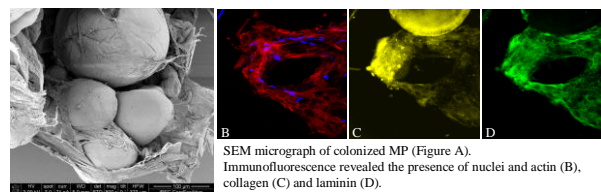
PLA MP are obtained following a solution jet break-up polymer precipitation technique, using Ethyl Lactate as environmental-friendly solvent<sup>3</sup>. Adhesion and proliferation studies are performed on collagen-I covalently coated MP. Experiments are performed both in static and dynamic culture, using a spinner flask bioreactor. Cell morphology is evaluated using Confocal and Scanning Electron Microscopy (SEM). Cell-laden MP are then transferred into a transparent chamber connected to a perfusion system for the formation of a 3D scaffold. In this, cell proliferation and survival are evaluated by constitutive expression of luciferase and bioluminescence emission. Scaffold size, cell survival, matrix composition are evaluated at different time points for 14 days.

## RESULTS AND DISCUSSION

The obtained MP dimensions, ranging between 60 and 120  $\mu\text{m}$ , allow cell-cell interactions for the formation of the extracellular matrix (ECM). Several approaches have used diverse MP sizes such as 20-60  $\mu\text{m}$ <sup>4</sup> and 400-700  $\mu\text{m}$ <sup>5</sup>. They reported the deposition of a dense matrix on the outer region of the construct, matching our results. Static conditions for cell culture showed a positive and constant proliferation rate over a week, and then became steady. On the contrary, others<sup>6</sup> reported constant increases within 30 days, proving the importance for macroporous surfaces on the MP.

Immunofluorescence after 21 days revealed the presence of collagen, laminin and fibronectin within the matrix (Figures B, C, and D). ECM distribution was evaluated by SEM micrographs (Figure A) and a dense matrix entrapping the MP was observed. Cells penetrated 0.75mm from the scaffold surface, which stays within the limits previously reviewed<sup>7</sup>. However, deeper invasion faces mass transfer constraints.

In order to facilitate cell distribution throughout the construct, spinner flask bioreactor was used for a homogenous microsphere initial colonization. After 8h of dynamic stirring, 80% of MP were uniformly colonized. Afterwards, cell-laden MP were transferred into a chamber, and culture medium was perfused through the circuit. Non-invasive bioluminescence is used to assess cell growth, survival, and distribution in the perfused system. Moreover, further decellularization techniques will be evaluated by this means.



## CONCLUSION

These results state the bases for the production of cell-derived ECM using PLA MP. Cells are able to proliferate and secrete their own and specific ECM. Macrotissue formation following this bottom-up strategy entails diverse applications which include the formation of functional tissues to repair or substitute damaged ones. Furthermore, this methodology can aid in the expansion of cells which are unable to maintain their phenotype *ex vivo*, creating a suitable niche. As well as to create biological models for *in vitro* testing to limit the use of animal models.

## REFERENCES

1. Chen M. *et al.*, Biomaterials. 32:7532-42, 2011
2. Sam S. *et al.*, Biotechnol Prog. 29:1354-66, 2013
3. Levato R. *et al.*, Macromol Biosci. 12:557-66, 2012
4. Tour G. *et al.*, Tissue Eng. 17:127-137, 2011
5. Tour G. *et al.*, J Biomed Mater Res Part A. 101:2826-37, 2013.
6. Yuan Y. *et al.*, J Tissue Eng Regen Med. 8:210-225, 2014.
7. Yeatts AB. *et al.*, Bone. 48:171-181, 2011.



## Enhanced $\beta$ -cell Pancreatic Islet Formation Using Carboxybetaine-Functionalised Chitosan Nanobeads

Mark Best, Valeria Perugini, Gary Phillips, Anna Guildford, Adrian Bone, Wendy Macfarlane, Matteo Santin

Brighton Centre for Regenerative Medicine, Department of Pharmacy and Biomolecular Sciences,  
University of Brighton, UK  
[m.best2@brighton.ac.uk](mailto:m.best2@brighton.ac.uk)

### INTRODUCTION

Type I diabetes mellitus (T1DM) is a condition in which the body cannot adequately control glucose levels in the blood due to a reduction in the ability of  $\beta$ -cells to produce the insulin. T1DM is a chronic condition requiring drugs and insulin therapy to manage the disease. However, current methods of disease management cannot fully prevent the development of long term health complications associated with the disease. Transplantation of insulin producing  $\beta$ -islet cells offers promise as a minimally invasive, long-term solution to regain normoglycaemia. However, a shortage of suitable donors together with sub-optimal islet engraftment and loss of cell mass due to the host's immune response limit the procedures success. Chitosan has been exploited as a successful drug delivery vehicle and is now being explored as a microencapsulation material to prevent the immune attack on the transplanted  $\beta$ -cells. As an extension of this approach, this work reports the use of chitosan nanobeads with carboxybetaine (CB) functionalities to facilitate the tethering of nanobeads with  $\beta$ -cell glycocalyx. The aim was to increase the number of viable cells available for transplantation, by forming bioengineered pancreatic pseudo-islets from single  $\beta$ -cells using functionalised nanobeads as biocompatible scaffolds.

### EXPERIMENTAL METHODS

#### Nanobead synthesis

Chitosan was dissolved in acetic acid and diluted 1:1 with methanol before *N*-succinylating with 14% (w/v) succinic anhydride in acetone solution. Ionic gelation at a 1:1 mass ratio with 1mg/mL sodium tripolyphosphate in dH<sub>2</sub>O was used to form nanobeads, the surface of which was cross-linked with CB, activated through reaction with 10x Molar excess N-(3-dimethylaminopropyl)-N'-ethylcarbodiimide hydrochloride (EDC) and 25x Molar excess N-hydroxysuccinimide (NHS) in 0.1M MES buffer pH 6.0. Beads were desalted into dH<sub>2</sub>O using dialysis with 3.5kDa MWCO cellulose tubing and syringe filtered at 0.45 $\mu$ m before lyophilising. Characterisation was carried out using Fourier transform infrared spectroscopy (FTIR), scanning electron microscopy (SEM) and dynamic light scattering (DLS).

#### In vitro experimentation

MIN-6 mouse pancreatic  $\beta$ -cells were cultured in Dulbecco's Modified Eagle Medium (DMEM) at low glucose, with 10% fetal calf serum. Cells were seeded in 24 well cell culture plates at a density of 4.0 x 10<sup>4</sup> cells/cm<sup>2</sup> and incubated with or without nanobeads at 24 and 48 hours. Cells were stained with 70 $\mu$ L of

90%:5%:5% (v/v) growth media: propidium iodide: Hoechst stain and incubated at 37°C for 5 minutes and analysed for live/apoptotic cells within the populations using UV microscopy.

### RESULTS AND DISCUSSION

Bioengineered pancreatic pseudo-islets were only formed from single MIN-6  $\beta$ -cells grown as monolayers when incubated with *N*-succinylated chitosan nanobeads functionalised with CB. These pseudo-islets, formed after 48 hours incubation at nanobead concentrations exceeding 0.3mg/mL and were larger in diameter than those formed using Matrigel™ (Fig 1). Aggregates of nanobeads were visible at the periphery of pseudo-islet structures, with no indication of significant cell death.

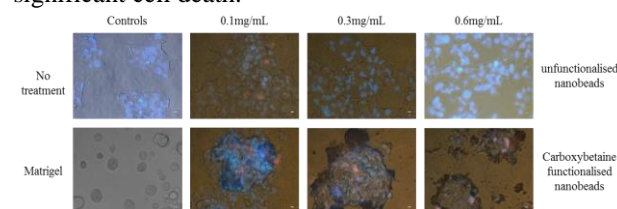


**Figure 1:** MIN-6  $\beta$ -cells incubated with *N*-succinylated chitosan nanobeads after 48h incubation (n=3). Scale bar = 100 $\mu$ m.

### CONCLUSION

The data suggests that 3D clustering of MIN-6  $\beta$ -cells is enhanced due to the aggregation of chitosan nanobeads which allows anchoring of the cells. Functionalisation with CB is thought to improve this process by exploiting superior anti-fouling properties of the zwitterionic surface coating, resulting in larger, rougher nanobead aggregates that promote enhanced cell adhesion and improved cell viability. These bioengineered pancreatic pseudo-islets show superior morphology more representative of *in situ* islet of Langerhans structures. Further studies are underway to confirm the cells ability to produce and release insulin.

### REFERENCES

1. Major and Chronic diseases: Diabetes [Online] Brussels, European Commission, 2014. Available online: [http://ec.europa.eu/health/major\\_chronic\\_disease/s/diseases/diabetes/index\\_en.htm](http://ec.europa.eu/health/major_chronic_disease/s/diseases/diabetes/index_en.htm) [accessed 19/12/2014].

### ACKNOWLEDGMENTS

Project funded by the European Commission Seventh Framework Programme. Project number 602235: Nano Engineering for Cross Tolerance (NEXT).





## Assessing the Potential of Fucoidan-Based Microparticles for Biomedical Application

Lara Reys<sup>1,2</sup>, Simone Silva<sup>1,2</sup>, Nuno Oliveira<sup>1,2</sup>, Diana Soares da Costa<sup>1,2</sup>, João Mano<sup>1,2</sup>, Tiago Silva<sup>1,2</sup> and Rui Reis<sup>1,2</sup>

<sup>1</sup>3B's Research Group - Biomaterials, Biodegradables and Biomimetics, University of Minho, Headquarters of the European Institute of Excellence on Tissue Engineering and Regenerative Medicine. Avepark - Parque de Ciência e Tecnologia, 4805-017 Barco GMR, Portugal

<sup>2</sup>ICVS/3B's- PT Government Associated Laboratory, Braga/Guimarães, Portugal

[lara.reys@dep.uminho.pt](mailto:lara.reys@dep.uminho.pt)

### INTRODUCTION

Marine organisms are rich in a variety of materials with potential use in Tissue Engineering and Regenerative Medicine. One important example is fucoidan (Fu), a sulphated polysaccharide extracted from the cell wall of the brown seaweeds, with higher solubility in water<sup>1</sup>. Fucoidan is composed by L-fucose and glucuronic acid including sulphate groups and have important bioactive properties such as antioxidative, anticoagulant, anticancer and in the reduction of blood glucose<sup>1,2</sup>. In this work, the biomedical potential of fucoidan was assessed by processing modified fucoidan (MFu) into microparticles by photocrosslinking using superamphiphobic surfaces and visible light<sup>3,4</sup>. Biological performance on the developed constructs was further explored.

### EXPERIMENTAL METHODS

To design the materials structures, fucoidan was modified by methacrylation reaction<sup>3</sup>. Briefly, 4% (wt/v) of Fu aqueous solution was mixed with methacrylated anhydride (MA) in volumes of 8% (MFu1) and 12% (MFu2) (v/v) at 50°C to react for 6h. The modified fucoidan was dialyzed against water and purified by washing it with acetone to remove the unreacted material. Further, both MFu1, 2 were processed as micro-particles using superamphiphobic surfaces and then photocrosslinked with visible light<sup>4</sup>. Microparticles were characterized by FTIR, <sup>1</sup>HNMR, quantification of sulphate degree and zeta potential. The ability of the developed materials to support adhesion and proliferation of cells was assessed by suspension culture of L929 cells (3.5x10<sup>5</sup> cells/ml) in contact with MFu microparticles up to 14 days.

### RESULTS AND DISCUSSION

The chemical modification performed on Fu was confirmed by the presence of vinyl and methyl peaks in the <sup>1</sup>HNMR of modified fucoidan. The mentioned peaks do not appear in Fu spectrum. Methacrylated fucoidan was obtained with different methacrylation degree, (Table1) which depended on the reaction conditions. This fact could indicate that methacrylation reaction is not selective and sulphate groups may be involved in the reaction. Differences on sulphate degree were evidenced (Table1). In addition, the zeta potential measurement confirmed the anionic charge of fucoidan. These findings also revealed that the zeta potential decrease after modification. This result could be related to the introduction of methacrylated groups. The results (Fig.1A, B) show that produced fucoidan porous particles have round shape and average diameter between 1.42 mm and 1.53mm, in dry state (Fig.1C). The direct contact assay demonstrated (Fig.1D) that the

MFu particles are not cytotoxic for L929 cells. The results (MTS and DNA) also revealed a good adhesion, viability and proliferation. The cells show a spindle-like shape and are able to migrate into the particles core during the culture period studied (Fig. 1D).

Samples	Methacrylation degree (%)	Sulphation degree (%)	Zeta potential (mV)
Fu	-----	38.60 ± 6.97	-30.40
MFu1	2.78	14.62 ± 3.66	-32.98
MFu2	6.50	24.24 ± 5.38	-62.10

Table 1: Properties of modified fucoidan obtained by different techniques.

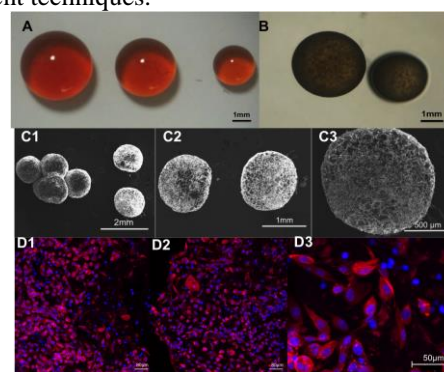


Figure 1: A, B) Modified fucoidan-particles, C1,C2,C3) SEM images of porous MFu particles and D1,D2,D3) confocal microscopy images of L929 cells seeded onto MFu1 after 7 days in culture; staining of actin (red) and nuclei (blue).

### CONCLUSION

This work demonstrates the successful production of fucoidan-based-microparticles with a versatile mechanical, physical and biological performance. The proposed technology based on the methacrylation of fucoidan, using visible light and superamphiphobic surfaces, may result in a method to obtain particles and partial insoluble fucoidan in water, which can be applied alone in tissue engineering applications.

### REFERENCES

1. Silva T.H. et al, Biomater, 2(4): 278-289, 2012
2. Sezer Alidemir et al, Springer Ber. Heid., ch(67):377-406, 2011.
3. Mihaila S. et al, Adv. Hel. Mat.; 2(6)895-907, 2013
4. Rial Hermida I. et al, Act. Biom., 10(10):4314-4322.

### ACKNOWLEDGMENTS

This work was partially funded by projects 0687\_NOVOMAR\_1\_P (POCTEP), CarbPol\_u\_Algae (EXPL/MAR-BIO/0165/2013) and POLARIS (FP7-REGPOT-CT2012-316331). Portuguese Foundation for Science and Technology is also gratefully acknowledged for doctoral grant of N. Oliveira and post-doc grants of S.S. Silva and D. Soares da Costa.

## Influence of Calcium Salt Addition on Bioactive Glass Nanospheres

Kai Zheng<sup>1</sup>, Qiang Chen<sup>1</sup>, Nicola Taccardi<sup>2</sup>, V. R. Reddy Marthala<sup>3</sup>, Martin Hartmann<sup>3</sup>, Aldo R. Boccaccini<sup>1</sup>

<sup>1</sup>Institute of Biomaterials, University of Erlangen-Nuremberg, Germany

<sup>2</sup>Institute of Chemical Reaction Engineering, University of Erlangen-Nuremberg, Germany

<sup>3</sup>Erlangen Catalysis Resource Center, University of Erlangen-Nuremberg, Germany

[aldo.boccaccini@ww.uni-erlangen.de](mailto:aldo.boccaccini@ww.uni-erlangen.de)

### INTRODUCTION

Bioactive glass nanospheres (BGNs) are of interest for bone regeneration application due to their high bioactivity, osteoconductivity and osteoinductivity<sup>[1]</sup>. The ionic dissolution products of bioactive glasses play a critical role in the properties related to osteogenesis and angiogenesis<sup>[2]</sup>. Among the ionic dissolution products,  $\text{Ca}^{2+}$  favours osteoblast proliferation, differentiation, mineralization of the extracellular matrix, and stimulates the expression of growth factors<sup>[3]</sup>.

The Stöber method is the most convenient way to synthesize BGNs. However, the introduction of  $\text{Ca}^{2+}$  into BGNs by using calcium salts as precursors could lead to severe agglomeration and irregular shapes. Moreover, the addition manner of calcium precursors could also affect the  $\text{Ca}^{2+}$  distribution on the BGNs.

The aim of this study is to understand the influence of calcium nitrate addition timing on the morphology, dispersity and  $\text{Ca}^{2+}$  distribution of BGNs.

### EXPERIMENTAL METHODS

BGNs were synthesized by a modified Stöber method<sup>[4]</sup>. To investigate the addition timing on BGNs, calcium nitrate was added 0, 10, 30 or 60 min after the induction of Stöber reaction. The corresponding synthesized samples were labelled as BGN-0, BGN-10, BGN-30, and BGN-60, respectively. The as-synthesized BGNs were calcinated at 700 °C to remove catalyst, solvent and nitrate groups.

The morphology and dispersity were studied using transmission electron microscopy (TEM), field emission scanning electron microscopy (FE-SEM) and zeta potential measurement.

$\text{Ca}^{2+}$  distribution in BGNs was studied using inductively coupled plasma (ICP), solid-state nuclear magnetic resonance (MAS-NMR), Energy-dispersive X-ray spectroscopy (EDS) and auger electron spectroscopy (AES).

### RESULTS AND DISCUSSION

Figure 1 shows the BGNs synthesized under different calcium nitrate addition timing. It can be seen that monodispersed BGNs can be synthesized by adding calcium precursor >30 min after the induction of Stöber reaction. However, the incorporated amount of calcium decreased with the increasing of time gap between induction and calcium precursor addition. According to the ICP results, the composition of BGN-0 was similar to the pre-determined nominal composition, while BGN-60 contained the least amount of calcium.

The MAS-NMR results showed that more Q2 and Q3 structures were in BGN-0 compared with other

samples. In BGN-30 and BNG-60, only limited Q2 or Q3 structures could be found compared with the samples synthesized under the same conditions except for addition of calcium nitrate. All the above results indicated that only limited  $\text{Ca}^{2+}$  could enter the silicate network of monodispersed BGNs. In addition, the ICP results showed that  $\text{Ca}^{2+}$  was not released continuously together with  $\text{Si}^{2+}$ . This phenomenon combined with the MAS-NMR results could suggest that most of  $\text{Ca}^{2+}$  was only distributed on the surface but not incorporated in the silicate network.

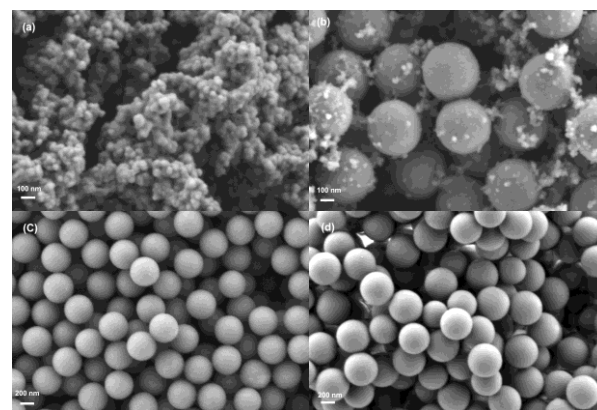


Figure 1 SEM images of (a) BGN-0; (b) BGN-10; (c) BGN-30; (d) BGN-60.

### CONCLUSION

In summary, monodispersed BGNs were synthesized by optimizing the addition timing of calcium nitrate in a modified Stöber process. A critical point that more  $\text{Ca}^{2+}$  was incorporated while the monodispersed spherical morphology was maintained could be determined. Moreover, incorporated  $\text{Ca}^{2+}$  was mainly distributed on the surface of BGNs, while only limited  $\text{Ca}^{2+}$  could enter the silicate network.

### REFERENCES

- [1] M. Erol-Taygun, Kai Zheng and AR. Boccaccini, *International Journal of Applied Glass Science*, 4, 136-148 (2013).
- [2] A. Hoppe, NS. Güldal, and AR. Boccaccini, *Biomaterials*, 32, 2757-2774 (2011).
- [3] O. Tsigkou, S. Labbaf, JR. Jones et al, *Advanced Healthcare Materials*, 3, 115-125 (2013).
- [4] T. Zheng, Q. Zhang, J. Ge et al, *The Journal of Physical Chemistry C*, 113, 3168-3175 (2009).

### ACKNOWLEDGMENTS

K. Z. would like to acknowledge the scholarship of the China Scholarship Council (CSC NO.201206740003).

## Bioactive Ti Metal Able to Release Ga Ions: Preparation by Chemical and Heat Treatments

Seiji Yamaguchi<sup>1\*</sup>, Shekhar Nath<sup>1</sup>, Yoko Sugawara<sup>1</sup>, Tomiharu Matsushita<sup>1</sup> and Tadashi Kokubo<sup>1</sup>

<sup>1</sup>Department of Biomedical Sciences, Chubu University, Japan

<sup>1\*</sup> Department of Biomedical Sciences, Chubu University, Japan, [sy-esi@isc.chubu.ac.jp](mailto:sy-esi@isc.chubu.ac.jp)

### INTRODUCTION

Titanium (Ti) metal is widely used in orthopedic and dental fields because of its good biocompatibility and high mechanical strength. However, it does not bond to living bone. The present authors earlier showed that Ti metal bonded to living bone through an apatite layer formed on their surfaces in a living body, when a Ca-deficient calcium titanate layer had been produced on the metals by NaOH, CaCl<sub>2</sub>, heat and water (Ca-heat) treatments [1]. Recently, it has been found that along with Ca ions, various other kinds of metallic ions such as Sr, Mg can be incorporated on the surface of Ti metal by modifying the Ca-heat treatment [2].

Gallium (Ga) is known for its inhibitory effect on calcium release from bone tissue, thus effective for preventing bone resorption. Gallium has also shown clinical efficacy in suppressing osteolysis and bone pain and has been suggested as a treatment for osteoporosis [3].

In the present study, Ga ion incorporation was attempted on the surface of Ti metal by the modified Ca-heat treatment. Apatite formation on the surface of the resultant product in a simulated body fluid (SBF) and release of Ga ions in a phosphate-buffered solution (PBS) are discussed in terms of the surface structure.

### EXPERIMENTAL METHODS

Ti metal with the size of 10 × 10 × 1 mm<sup>3</sup> were soaked in 5 M NaOH aqueous solution at 60 °C for 24 h, then subsequently in 100 mM GaCl<sub>3</sub> or a mixed solution of 99.95 mM CaCl<sub>2</sub> and 0.05 mM GaCl<sub>3</sub> at 40 °C for 24 h. They were heated at 600 °C for 1 h, and then soaked in hot water at 80 °C for 24 h. Then the samples were washed by flowing ultra-pure water for 30 sec after each solution treatment.

Surfaces of the samples were examined by a field emission scanning electron microscope (FE-SEM) equipped with energy dispersive X-ray analyzer (EDX), thin-film X-ray diffractometer (TF-XRD), and laser Fourier Transform Raman spectrometer (FT-Raman). Apatite formation on the samples were examined by soaking in SBF with ion concentrations (Na<sup>+</sup> 142.0, K<sup>+</sup> 5.0, Ca<sup>2+</sup> 2.5, Mg<sup>2+</sup> 1.5, Cl<sup>-</sup> 147.8, HCO<sub>3</sub><sup>-</sup> 4.2, HPO<sub>4</sub><sup>2-</sup> 1.0, and SO<sub>4</sub><sup>2-</sup> 0.5 mM) nearly equal to those of human blood plasma at 36.5 °C [4] for 3 days. The samples subjected to the chemical and heat treatments were soaked in 2 ml of PBS at 36.5 °C. After soaked in PBS for various periods up to 3 days, Ca and Ga ion concentrations in PBS were measured by inductively coupled plasma emission spectroscopy (ICP).

### RESULTS AND DISCUSSION

FE-SEM observation showed that nano-scaled network structures had been produced on the surface of Ti metal by the initial NaOH treatment, and it was maintained even after the subsequent solution and heat treatments. EDX analysis revealed that the Ca enriched surface layer containing 1.9 % Ca and 1.1 % Ga was produced on the metal when the metal was soaked in the mixed solution of 99.95 mM CaCl<sub>2</sub> and 0.05 mM GaCl<sub>3</sub> following the NaOH treatment. In contrast, 7.7 % Ga was incorporated into the surface of the metal when the metal was soaked in 100 mM GaCl<sub>3</sub> instead of the mixed solution. TF-XRD and FT-Raman analysis revealed that former produced Ga-containing calcium titanate, rutile and anatase on its surface by the subsequent heat treatment, whereas latter formed gallium titanate in addition to the rutile and anatase. These crystalline phases were not changed even after the final water treatment.

When the treated metals were soaked in SBF, both of them formed apatite fully on their surfaces within 3 days. When they were soaked in PBS, the metal with the Ga-containing calcium titanate slowly released Ga ions up to 0.3 ppm within 3 days, whereas the metal with the gallium titanate released 1.3 ppm. The difference of released amount of Ga ions might be due to Ga contents in the surface layer.

It was reported that significant inhibition was observed on osteoclastic resorption activity of rabbit bone cells by adding 0.7 – 7 ppm of Ga ions to a culture medium [5].

Based on these results, it is expected that the treated metal with the gallium titanate layer in the present study could prevent osteoclastic resorption so as to prevent bone resorption by releasing Ga ions, and tightly bond to bone through an apatite formed on its surface.

### CONCLUSION

Ti metal with gallium titanate layer able to release Ga ions was prepared by the chemical and heat treatments.

It is expected that the treated metal might bond even to osteoporotic bone, since it releases Ga ions in a living body to prevent bone resorption and induces apatite formation on its surface.

### REFERENCES

1. Fukuda A. *et al.*, Acta Biomater. 7:1379-1386, 2011
2. Yamaguchi S. *et al.*, Acta Biomater 10:2282–2289, 2014
3. Warrell RP Jr, in Handbook of Metal Ligand Interactions in Biological Fluids, Bioinorganic Medicine (Berthon G ed) vol 2, pp 1253–1265, 1995, Marcel Dekker, New York.
4. Kokubo T. *et al.*, Biomaterials 27:2907-2915, 2006
5. Verron E. *et al.*, Br J Pharmacol. 159:1681-1692, 2010





## INTRODUCTION

Calcium phosphates (CaP) are attractive osteoconductive materials for healing bone defects however brittleness and low flexural strength limit their application to non-load-bearing sites<sup>1</sup>. The mechanical behavior of CaP scaffolds is further compromised by high porosity required for bone ingrowth. The load-bearing properties of CaP can be improved by forming a composite material, through addition of a ductile second phase. An attractive combination of strength and ductility was reported for  $\beta$ -tricalcium phosphate ( $\beta$ -TCP) reinforced with 30-40 vol.% polylactic acid (PLA)<sup>2</sup>. Even better mechanical properties can be achieved if the weak polymer component is replaced with a stronger and tougher metal, e.g. iron. Fe is slowly resorbed in the body and its corrosion can be accelerated by dispersing silver nanoparticles that are cathodic towards Fe matrix. An additional benefit of Ag is its recognized antimicrobial activity<sup>3</sup>. In this work, we report the preparation of strong  $\beta$ -TCP-30 vol.% (Fe-Ag) composites and macroporous scaffolds by attrition milling, high pressure consolidation and a modified particulate leaching method<sup>3</sup>.

## MATERIALS AND METHODS

$\beta$ -TCP nanopowder was prepared by chemical precipitation and calcination. Fe powder ( $\sim 2 \mu\text{m}$ ) was mixed with 10, 20 and 30 vol.% silver oxide ( $\text{Ag}_2\text{O}$ ) powder ( $< 2 \mu\text{m}$ ) by high energy attrition milling for 4 h in hexane under Ar, at 20:1 balls-to-powder ratio. 30 vol.% of the obtained Fe-Ag blend was admixed to  $\beta$ -TCP and milled for additional 4 h.  $\beta$ -TCP-Fe-Ag blends were compacted at 400 MPa and annealed at  $450^\circ\text{C}$ , 1 h in  $\text{H}_2$ -flow to reduce  $\text{Ag}_2\text{O}$ . The compacts were then high pressure consolidated at 2.5 GPa, at  $T_{\text{room}}$  and annealed at  $400^\circ\text{C}$  for 4 h. To produce 3-D scaffolds,  $\beta$ -TCP-Fe-Ag compacts were crushed and sieved to produce small (100-200)  $\mu\text{m}$  and large (200-300)  $\mu\text{m}$  non-dense granules that were then mixed with 50-80 vol.%  $\text{Na}_2\text{SO}_4$  porogen of comparable size. The blends were consolidated at 2.5 GPa and porogen removed in water. The final scaffolds were 11 mm in diameter and 3 mm thick. Dense composites and scaffolds were examined in a scanning electron microscope (SEM) and tested in bending and/or compression. Scaffolds permeability was measured by the Darcy test.

## RESULTS AND DISCUSSION

The density of all high pressure consolidated  $\beta$ -TCP-30(Fe-Ag) specimens, before and after annealing, was  $\geq 95\%$  TD. SEM examination revealed a homogeneous distribution of submicron metal phase in  $\beta$ -TCP matrix. Strength characteristics of dense specimens are shown in Fig. 1. Both the compressive ( $\sigma_c$ ) and bending ( $\sigma_b$ ) strengths increase with increasing Ag content. The strength is significantly improved by annealing,

presumably due to enhanced bonding integrity of  $\beta$ -TCP-metal interfaces. For all the  $\beta$ -TCP-30(Fe-Ag) compositions,  $\sigma_c$  and  $\sigma_b$  are several-fold higher than the 320 and 62 MPa reported for  $\beta$ -TCP-30PLA<sup>2</sup>.

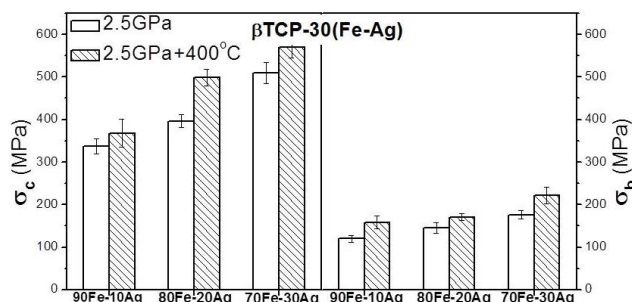


Fig.1: Bending and compressive strengths of  $\beta$ -TCP-30 vol.% (Fe-Ag) composites before and after annealing at  $400^\circ\text{C}$ .

All the produced  $\beta$ -TCP-30(Fe-Ag) scaffolds had an interconnected pore structure, Fig. 2. Increasing the porosity decreased compressive strength ( $\sigma_c$ ) and increased permeability ( $k$ ), Table 1. The scaffolds exhibited good combination of compressive strength and permeability comparable to trabecular bone.

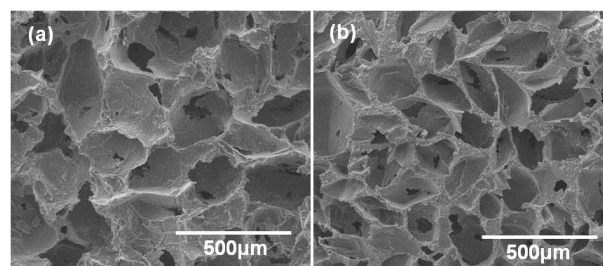


Fig.2: SEM images of  $\beta$ -TCP-30(Fe-20Ag) scaffolds: a - 80% porosity, large porogen; b - 70% porosity, small porogen.

Table 1. Properties of  $\beta$ -TCP-30(Fe-20Ag) scaffolds prepared using small (100-200)  $\mu\text{m}$  granules and porogen

Porosity, %	50	60	70	80
$\sigma_c$ , MPa	17.1	7.6	4.8	3.3
$k$ ( $\times 10^{10}$ ), $\text{m}^2$	1.5	2.4	4.7	6.2

## CONCLUSION

The developed  $\beta$ -TCP-(Fe-Ag) composites and porous scaffolds prepared by the modified salt leaching method offer an attractive combination of properties and should be further tested as potential bone repair materials.

## REFERENCES

1. Bohner M. *et al.*, Biomater 26:6423-9, 2005
2. Rakovsky A. *et al.*, J. Mech. Behav. Biomed. Mater. 18:37-46, 2013
3. Rakovsky A. *et al.*, *ibid.* 32:89-94, 2014

## ACKNOWLEDGMENTS

This work was supported by Israel Science Foundation-ISF through research grant No. 1326/11.

## Tailoring the Bioactivity of Mesoporous Bioglasses: the Role of the Structure Directing Agents

Natividad Gómez-Cerezo<sup>1,2</sup>, Isabel Izquierdo-Barba<sup>1,2</sup>, Daniel Arcos<sup>1,2</sup>, María Vallet-Regí<sup>1,2</sup>

<sup>1</sup> Dpto. Química Inorgánica y Bioinorgánica, Universidad Complutense de Madrid, Instituto de Investigación Sanitaria Hospital 12 de Octubre i+12, Spain

<sup>2</sup> CIBER de Bioingeniería, Biomateriales y Nanomedicina (CIBER-BBN), Spain

[arcosd@ucm.es](mailto:arcosd@ucm.es)

### INTRODUCTION

Mesoporous bioactive glasses (MBGs) are a new generation of bioceramics intended for regenerative therapies of bone<sup>1</sup>. They comprise the bone bonding capabilities of melt-derived and sol-gel bioactive glasses<sup>2</sup>, as well as the porous structure of SiO<sub>2</sub> based mesoporous materials<sup>3</sup>.

The synthesis of MBGs requires the addition of a structure directing agent (SDA). In most of the cases, the SDA is an amphiphilic molecule with self-organizing properties at the supramolecular level. The SDA determine the textural properties of MBGs, such as porous structure, pore volume, pore size and also the surface area. However, very little is known about the local atomic environment within the pore walls of MBG, and how it affects their bioactive behaviour. In this work we demonstrate that by adding the appropriated SDA we can tailor the bioactivity of MBG by controlling both, textural properties and local atomic environment.

### EXPERIMENTAL METHODS

MBGs of composition SiO<sub>2</sub> 85-CaO 10-P<sub>2</sub>O<sub>5</sub> 5 (% mol) were synthesized by the evaporation induced self-assembly (EISA) method. For this aim, Pluronic P123, F68 and F127 were used as structure directing agents. Tetraethyl orthosilicate (TEOS), triethyl phosphate (TEP) and calcium nitrate were used as SiO<sub>2</sub>, P<sub>2</sub>O<sub>5</sub> and CaO sources, respectively. The MBGs characterization has been carried out by XRD, FTIR spectroscopy, N<sub>2</sub> adsorption porosimetry, solid-state NMR and HR-TEM. Assessments of in vitro bioactivity were carried out soaking the MBGs into simulated body fluid (SBF). The evolution of the glass surface was analysed by FTIR spectroscopy and TEM.

### RESULTS AND DISCUSSION

Figure 1 shows the HR-TEM of the SiO<sub>2</sub> 85-CaO 10-P<sub>2</sub>O<sub>5</sub> 5 mesoporous glass prepared with F68. The images evidence an excellent porous arrangement that corresponds to a 2D hexagonal symmetry with a *p6mm* planar group. Mesoporous orderings were also obtained in MBGs prepared with P123 and F127.

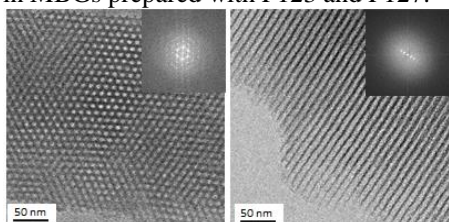


Figure 1. HR-TEM images of MBG prepared with F68

The pore size of the mesoporous glasses can be easily tailored as a function of the surfactant size. In addition, the local atomic environment can be controlled as evidenced by the evolution of the SiO<sub>2</sub> network

connectivity (*NC*) as a function of the SDA used. These data are collected in the table below.

MBG (SDA used)	Structure	Pore size	<i>NC</i> (SiO <sub>2</sub> )
MBG-F68	<i>p6mm</i>	3.36	3.79
MBG-P123	<i>p6mm</i>	5.92	3.80
MBG-F127	<i>p6mm</i>	7.18	3.96

The in vitro bioactivity tests demonstrate that after 6 hours in SBF, only the MBG prepared with F68 developed hydroxyapatite onto the surface, as evidenced by the doublet at 585 and 604 cm<sup>-1</sup> in the FTIR spectra and TEM-ED studies (figure 2).

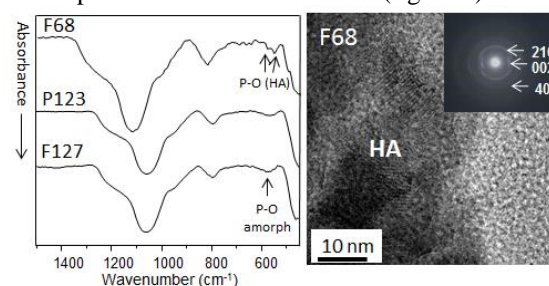


Figure 2. FTIR spectra after 6 hours in SBF (left); TEM image of MBG-F68 after 6 hours in SBF. HA indicates newly formed hydroxyapatite (right).

MBG-F68 exhibits the lowest *NC* among MBGs studied. High silica *NC*, like that observed for MBG-P123 and MBG-F127, indicates that Ca<sup>2+</sup> cations are not acting as SiO<sub>2</sub> network modifiers required to initiate the bioactive process. <sup>31</sup>P NMR studies evidenced that in these cases Ca<sup>2+</sup> cations are sequestered as calcium phosphate (CaP) heterogeneities. MBGs with small pore size, like MBG-F68, contain a low amount of CaP heterogeneities, indicating that the formation of these clusters is also conditioned by steric factors. Consequently there is more Ca<sup>2+</sup> available to react with the SBF and thus the bioactive response is enhanced.

### CONCLUSION

The porosity and atomic environment of MBGs can be controlled by adding the appropriated SDA. The bioactivity of these biomaterials can be adjusted to be faster or slower. These results open new possibilities for tailoring mesoporous bioactive glasses as bone grafts for each specific clinical case.

### REFERENCES

1. Yan X. *et al.* Angew. Chem. 43:43:5980-8, 2004
2. Arcos D. *et al* Acta Biomaterialia 6:2874-88, 2010
3. Vallet-Regí M. *et al.* Angew. Chem. 46:7548-58, 2007

### ACKNOWLEDGMENTS

This study was supported with the projects MAT2012-35556, MAT2013-43299-R) and Ageing Network of Excellence (CSO2010-11384-E).



## Novel Bioactive Glass Composites for Soft Tissue Applications

Owen M. Clarkin<sup>1</sup>, Dermot F. Brougham<sup>2</sup>, Bing Wu,<sup>2</sup> Catriona Lally<sup>1</sup>

<sup>1</sup>School of Mechanical and Manufacturing Engineering, Dublin City University, Ireland

<sup>2</sup>School of Chemical Sciences, Dublin City University, Ireland

[Owen.Clarkin@dcu.ie](mailto:Owen.Clarkin@dcu.ie)

### INTRODUCTION

From the age of 30 years onwards all human tissue progressively deteriorates<sup>1</sup>. Due to extending life expectancies, redevelopment of human tissues *via* tissue engineering is no longer an option but a requirement. In the 1960s Hench developed Bioglass<sup>®</sup>, which was shortly followed by Wilson who developed the glass ionomer cement<sup>2</sup>. These developments marked early moves from the use of bioinert to bioactive biomaterials for medical implants. Since these early developments of bioactive glasses, progress to new applications has been slower. Today the field has transitioned from bioactive material implants to tissue engineering materials and regenerative medicine.

Bioactive glass compositions can rapidly regenerate trabecular bone. However, to-date bioactive glasses have been largely limited to hard tissue engineering applications. This study focuses on the application of bioactive glasses in soft tissue engineering applications. The authors have developed a novel glass formulation that can control the setting of a flexible hydrogel composite, producing a material ideal for minimally invasive soft tissue applications or tissue engineering constructs. The glass examined is based on a glass ionomer cement formulation wherein neurotoxic aluminium is replaced by gallium. Alginate forms the surrounding hydrogel matrix.

### EXPERIMENTAL METHODS

Four CaO-Ga<sub>2</sub>O<sub>3</sub>/Al<sub>2</sub>O<sub>3</sub>-SiO<sub>2</sub>-P<sub>2</sub>O<sub>5</sub>-CaCl<sub>2</sub> glasses were produced with varying Al<sub>2</sub>O<sub>3</sub>/Ga<sub>2</sub>O<sub>3</sub> ratios from 0 to 1. Differential thermal analysis (Stanton Redcroft STA 1640, Rheometric Scientific, UK) was carried out at a heating rate of 10 °C min<sup>-1</sup>, to 900 °C. The structure of the glasses was analysed using Si<sup>29</sup> and Al<sup>27</sup> Magic Angle Spinning Nuclear Magnetic Resonance (MAS-NMR). These glasses were then mixed with glucono-delta-lactone and a polymeric alginate solution to form composite hydrogels. Working and setting times of each glass were analysed using methods modified from ISO9917. The aluminium free gel was freeze dried at time points of 10 seconds, 60 seconds, 5 minutes, 60 minutes and 24 hours after mixing. The chemistry of the setting reaction was analysed using Fourier Transform Infrared (FTIR) spectroscopy between 4000 and 400 cm<sup>-1</sup>. Compression samples were produced (9.00 mm, height 15.00 mm) and stored in 20 ml of Dulbecco's modified eagle medium containing 1 vol.% penicillin streptomycin before being loaded, at a rate of 2 mm/min until failure, using a Zwick BT1-FR005TN test machine fitted with a 500N load cell.

### RESULTS AND DISCUSSION

Glass transition temperatures were in the range of 732-764 °C, with no significant difference across the glass series. The high T<sub>g</sub> values indicate high network connectivity (NC) and their limited variability suggests similar NC across the series. Al<sup>27</sup> MAS-NMR analysis indicated a predominantly tetrahedral coordination of the aluminium containing glasses, with minimal octahedral and pentavalent coordination. Si<sup>29</sup> MAS-NMR exhibited a typical broad peak, which centred around -80 ppm, indicating a Q<sub>2</sub>/Q<sub>3</sub> structure. No shift in Si<sup>29</sup> MAS-NMR was observed across the glass series, regardless of Al<sub>2</sub>O<sub>3</sub>/Ga<sub>2</sub>O<sub>3</sub> ratio, which indicates no substantial alteration in the network. The NMR analysis strongly suggests that gallium is also predominantly tetrahedrally coordinated.

FTIR results indicate that, with time, the characteristic band of the carbonyl stretching of the free carboxylic acid groups at 1780 - 1710 cm<sup>-1</sup> disappears and is replaced by weaker C=O stretching bands at 1640-1690 cm<sup>-1</sup>, indicating that alginate is becoming increasingly complexed with cations released from the glass phase. Substitution of aluminium for gallium lengthened working times and shortened setting times (242%, 24% respectively), which is beneficial for many minimally invasive procedures where a 'snap' set is required. Compressive strength was shown to increase with Ga/Al ratio and strength continued to increase over 7 days.

### CONCLUSION

A novel glass hydrogel was produced, based on ionomer cement glasses, where neurotoxic aluminium was replaced with gallium. It was shown that like aluminium, gallium adopts a charge balanced tetrahedral coordination resulting in a high network connectivity glass with long working time, snap set properties, and exhibiting increased compressive strength (244%). Strength continues to increase over up to 7 days of incubation (130%).

### REFERENCES

1. Hench, L. L., NJGC, 3:67-73, 2013.
2. Wilson, A.D., Kent, B.E., J. App. Chem. Biotech. 21 (11):313, 1971.

### ACKNOWLEDGMENTS

The authors would like to thank the Irish Research Council (Grant no: PD/2011/2167) and Enterprise Ireland (Grant no: CF/2013/3364) for providing financial support for this project.



# Thermal and In Vitro Properties Of SrO and ZnO Containing Bioactive Glasses

Johan Sangder<sup>1</sup>, Susanne Fagerlund<sup>1,2</sup>, [Leena Hupa](mailto:leena.hupa@abo.fi)<sup>1</sup>

<sup>1</sup>Johan Gadolin Process Chemistry Centre, Åbo Akademi University, Finland

<sup>2</sup>Paroc Group Oy, Finland

[leena.hupa@abo.fi](mailto:leena.hupa@abo.fi)

## INTRODUCTION

Porous scaffolds based on bioactive glass are intensively studied for various tissue engineering applications<sup>1,2</sup>. When fabricated from melt-derived bioactive glasses the hot-working conditions must be optimized to avoid crystallization of the glass<sup>3,4</sup>. In addition, the release rate of inorganic ions from the glass must be controlled to provide the desired tissue healing or regeneration capacity in the body. Today, the biological response of several inorganic ions in the interfacial solution of the biomaterial is known<sup>5</sup>. In this work we report the effect of partial substitution of ZnO and SrO for MgO and CaO on the thermal and in vitro properties of bioactive glass 1-98. Implants of 1-98 have shown positive effects on osteogenesis<sup>6</sup>. ZnO and SrO enhance bone formation, and ZnO also shows anti-inflammatory effects<sup>5</sup>. The effect of these oxides on the properties of bioactive glasses is not well established.

## EXPERIMENTAL METHODS

Bioactive glass 1-98 (in mol-%: 53.8SiO<sub>2</sub>, 5.9Na<sub>2</sub>O, 7.1K<sub>2</sub>O, 7.6MgO, 23.9 CaO, 0.9 P<sub>2</sub>O<sub>3</sub>, and 0.9 B<sub>2</sub>O<sub>3</sub>) and two experimental glasses, Zn2Sr4 and Zn4Sr2, were melted in-house as described previously<sup>7</sup>. The glass codes give their ZnO and SrO contents in mol-%. ZnO and SrO were substituted for MgO and CaO, respectively in glass 1-98. The annealed glasses were cut into plates or crushed and sieved to give particles of various size ranges. The thermal properties were measured using differential thermal analysis (TGA-DTA/DSC, Netzsch STA 449F1 Jupiter) and hot stage microscopy (HSM/ODHT, Misura, Expert System Solutions). The ion dissolution was measured for glass plates in static simulated body fluid, SBF up to 168h. The ion release in dynamic conditions was measured for a fresh SBF fed through glass particles<sup>7,8</sup>. The pH and ion concentrations (ICP-OES, Optima 5300 DV, Perkin Elmer) in SBF were measured at selected time points. Formation of silica rich and hydroxyapatite layers at the glass surfaces were studied using SEM-EDX (LEO 1530 Gemini, EDXA from Thermo Electron Corp.). All measurements were done for 3-5 parallel samples.

## RESULTS AND DISCUSSION

In static conditions, the pH of SBF for all glasses increased. However, for 1-98 a constant value was reached at 78 h, while for Zn2Sr4 and Zn4Sr2 the increase was less and did not reach a stable value during 168 h. Similarly, in dynamic conditions 1-98 gave clear pH changes, while only minor effects were recorded for Zn2Sr4 and Zn4Sr2. This suggests that ZnO and SrO decrease the in vitro bioactivity.

ZnO and SrO had only minor effects on the crystallization temperature ( $T_p$ ), while they clearly decreased the sintering range,  $T_{si}-T_{xi}$  (Table 1). The

glass transition temperature,  $T_g$  was lowest for Zn2Sr4. Melting of crystals,  $T_{xf}$  started at the lowest temperature for glass Zn2Sr4. The results suggest that ZnO and/or SrO slightly increase the hot-working range of 1-98.

Table 1. Characteristic hot-working temperatures

Glass Code	$T_g$ ( $\pm 3^\circ\text{C}$ )	$T_p$ ( $\pm 3^\circ\text{C}$ )	$T_{si}$ ( $\pm 3^\circ\text{C}$ )	$T_{xi}$ ( $\pm 5^\circ\text{C}$ )	$T_{xf}$ ( $\pm 5^\circ\text{C}$ )
1-98	609	1001	681	827	1028
Zn2Sr4	593	998	663	850	1013
Zn4Sr2	605	996	669	831	1030

The release of silicon was highest for 1-98. For this glass, the phosphorous concentration decreased most with increasing immersion time. Zinc was released only in modest amounts. For Zn4Sr2 the zinc concentration was 0.34 mg/l at 168 h. In contrast, strontium concentration reached around 10 mg/l at 168 for Zn2Sr4. These results suggest that Zn is strongly bonded in the glass network, while Sr acts as a network modifier and dissolves more easily than Zn.

SEM images show reaction layers at each time point only at 1-98, while layers with a measurable thickness were detected only after 168 h at the two other glasses.

## CONCLUSION

Partial substitution of MgO and CaO for ZnO and SrO, respectively in bioactive glass 1-98 resulted in minor increase in the hot-working range. ZnO and SrO decreased the in vitro reactivity expressed as rate of HAP layer formation. Only minor concentrations of Zn were measured in the solution, while Sr concentrations showed levels that may be of interest for tissue engineering scaffolds based on bioactive glass.

## REFERENCES

1. Fu, Q. *et al.*, Adv. Funct. Mater. 23:5461–5476, 2013
2. Gerhardt, L.C. *et al.*, Mater. 3: 3867–3910, 2010
3. Arstila, H. *et al.*, J. Non-Cryst. Solids 354:722–728, 2008
4. Arstila, H. *et al.*, Glass Technol. 46: 138–141, 2005
5. Hoppe, A. *et al.*, Biomaterials 32:2757–2774, 2011
6. Itälä, A. *et al.*, J. Biomed. Mater. Res. 62:404–411, 2002
7. Fagerlund, S. *et al.*, J. Am. Ceram. Soc. 95:3130–3137, 2012
8. Fagerlund, S. *et al.*, Acta Biomater. 9:5400–5410, 2013

## ACKNOWLEDGMENTS

This work is part of the activities at the Johan Gadolin Process Chemistry Centre, a Centre of Excellence financed by Åbo Akademi University.



## Bioresorbable Chitosan- Bioglass Nanocomposite Scaffolds for Drug Delivery Applications

Emad El-Meliegy<sup>1</sup> and Sara Ali<sup>2</sup>

<sup>1,2</sup>Department of biomaterials, National Research Centre, Cairo, Egypt  
[emadmeliagy@hotmail.com](mailto:emadmeliagy@hotmail.com)

### INTRODUCTION

Tissue engineering is a promising technology that has the potential to create tissues and organs. It involves in vitro seeding of human cells onto porous bioresorbable scaffolds by attachment. Once the scaffolds are implanted, the human cells proliferate, migrate and differentiate into specific tissues. 1

Synthetic biodegradable nanocomposite scaffolds based on biopolymers and bioglasses have excellent tissue compatibility and safety profiles critical for their successful utility in the human body. A wide variety of drugs and supplementary therapies can be encapsulated into nanocomposite scaffolds for easy delivery to specific human cells. In order for the produced scaffolds to guarantee effective delivery of drugs, the structure of the scaffolds should show control over pore size distribution and have networked interconnected pores. 2

Thus, the objective is to generate scaffolds with effective 3D interconnected pore structure that would allow cells to migrate deep into the scaffold for drug delivery applications. The pore size distribution and the in vitro cytotoxicity will be evaluated.3

### EXPERIMENTAL METHODS

This work involved the synthesis of bioglass nanoparticles, and chitosan-bioglass nanocomposite scaffolds therefrom by freeze drying of bioglass/chitosan nanodispersions at a temperature at -75°C. The nanoparticles and nanocomposites were characterized by XRD and DTA, SEM and TEM.

The pore size distribution of the prepared scaffolds was tested using HG- Porosimeter. The biodegradability of the scaffolds was evaluated in vitro in SBF and distilled water. Furthermore, the cytotoxicity of the scaffolds was tested to evaluate the cell viability.

### RESULTS AND DISCUSSION

The results showed that the particle size of bioglass nanoparticles is found to be 6-12nms. The XRD and

DTA of bioglass heat treated up to 700°C showed no signs of crystallization.

The prepared scaffolds have shown porous structure with >70% porosity and interconnected pore morphology. Pores ranges in size between 200-400µm, which is preferred in hosting various living cells and supplementary drugs. The results of degradation in SBF and distilled water indicated controlled degradation profiles over weeks of time.

The results of cytotoxicity indicated no toxicity and in role, showed effective cell viability, growth and proliferation, the fact that enhance the potential of nanocomposite scaffolds for drug delivery applications.

### CONCLUSION

Nanocomposite 3D scaffolds based on chitosan- nano-bioglass with higher pore volume and interconnected pore structure were developed. The results proved that the scaffolds have excellent bioresorbability, no toxicity and effective cell viability indicating their potential for biomedical applications.

### REFERENCES

1. E. El-Meliegy, J. Mats. Sci.: Mats. in Med., 23:2069-80, 2012
2. D. M. Cruz et al., J. Biomed. Mat. Res. A, 95A, [4]:1182-93, 2010
3. Z. Zhang, et al., Adv. Drug Delivery Reviews, 64: 1129-41, 2012

### ACKNOWLEDGMENTS

The authors would like to thank *STDF: Science & Technology Development Fund in Egypt* for providing the financial support



## Generation of Limbal Epithelial Cell Progenitors by Two Methods: by Differentiation from iPS Cells and by Direct Trans-differentiation from Human Dermal Fibroblasts

Artur Cieřlar-Pobuda<sup>1,2,3</sup>, Viktoria Knořlach<sup>1,3</sup>, Saeid Ghavami<sup>4</sup>, Marek Łos<sup>1,3</sup>

<sup>1</sup> Department of Clinical and Experimental Medicine (IKE), Division of Cell Biology, Linköping University, 58185 Linköping, Sweden

<sup>2</sup> Biosystems Group, Institute of Automatic Control, Silesian University of Technology, Akademicka 16, 44-100 Gliwice, Poland

<sup>3</sup> Integrative Regenerative Medicine Center (IGEN), Linköping University, 58185 Linköping, Sweden

<sup>4</sup> Department of Human Anatomy and Cell Science, University of Manitoba, Manitoba, Canada  
[marek.los@liu.se](mailto:marek.los@liu.se)

The corneal epithelium is maintained by a small pool of tissue stem cells located at the limbus. Through certain injuries or diseases this pool of stem cells may get depleted. This leads to visual impairment. Standard treatment options include autologous or allogeneic limbal stem cell transplantation, but graft rejection and chronic inflammation lowers the success rate over long time. Induced pluripotent stem (iPS) cells have opened new possibilities for treating various diseases with patient specific cells, eliminating the risk of immune rejection. In recent years, several protocols have been developed, aimed at the differentiation of iPS cells into the corneal epithelial lineage by mimicking the environmental niche of limbal stem cells. However, the risk of teratoma formation associated with the use of iPS cells hinders most applications from lab into clinics.

Here we show that the differentiation of iPS cells into corneal epithelial cells results in the expression of corneal epithelial markers showing a successful differentiation, but the level of gene expression for the pluripotency markers does not vanish completely and Klf4 is expressed at very high levels, probably due to transgene activation. Therefore, we have tested a direct transdifferentiation approach to circumvent the intermediate state of pluripotency (iPS-stage). The resulting cells exhibited corneal epithelial cell morphology and expressed corneal epithelial markers (please see the attached figure). We show for the first time a direct transdifferentiation of human dermal fibroblasts into the corneal epithelial lineage. Thus, easily-obtainable autologous human dermal fibroblasts may serve as progenitors for the production of corneal epithelial cells for transplantation approaches.

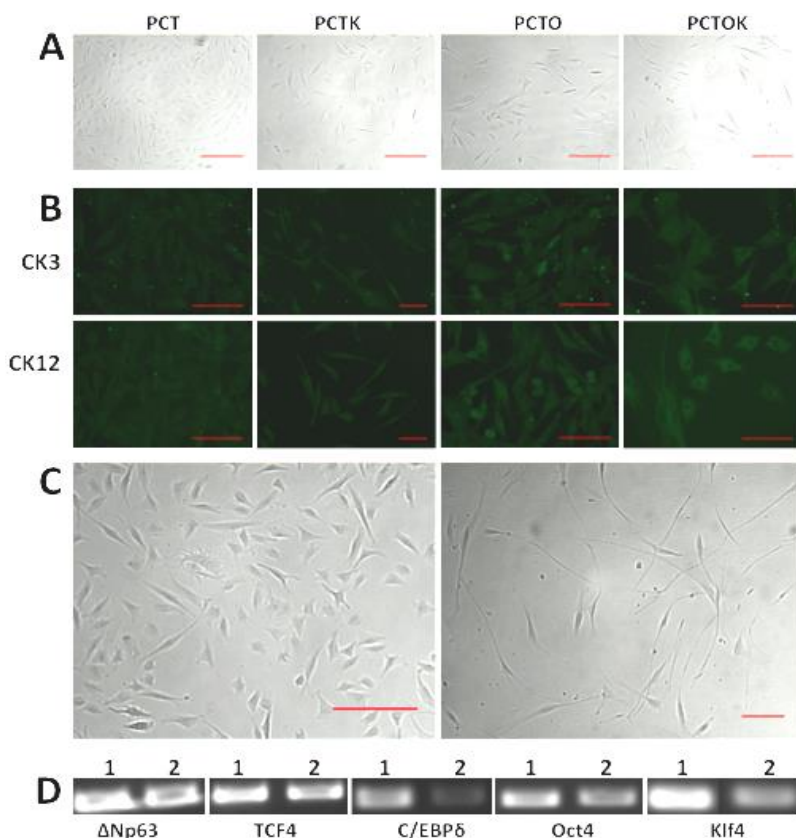


**Figure legend: Direct transdifferentiation of human fibroblasts into corneal epithelial lineage.** (A): Bright field images of transdifferentiated fibroblasts 7 days post infection either with PCT, PCTK, PCTO or PCTOK (explained in the text). Note the heterogeneous cell morphology of the infected cells. Scale bar: 200  $\mu$ m. (B): Immunocytochemistry analysis of transdifferentiated fibroblasts infected with PCT, PCTK, PCTO or PCTOK for the expression of CK3 and CK12. Cells were analyzed on day 7 post infection. Scale bar: 100  $\mu$ m. (C): Bright field images of transdifferentiated cells (left, 7 days post infection) and uninfected fibroblasts (right). Scale bar: 200  $\mu$ m. (D): RT-PCR for transduction efficiency analysis. 1: transfection of HEK-293 for virus production. 2: transduction of human dermal fibroblasts with virus. Abbreviations: PCT, lentivirus cocktail containing  $\Delta$ Np63, C/EBP $\delta$  and TCF4 lentiviruses; PCTK, lentiviruses cocktail containing PCT plus Klf4; PCTO, lentiviruses cocktail containing PCT plus Oct4; PCTOK, lentivirus cocktail containing PCT plus Oct4 and Klf4.



## A Multifactorial Approach Towards Enhanced Extracellular Matrix Deposition and Maintenance of Mesenchymal Stem Cell Phenotype Using Macromolecular Crowding and Low Oxygen Tension

Diana Gaspar<sup>1\*</sup>, Daniela Cigognini<sup>1\*</sup>, Pramod Kumar<sup>1</sup>, Abhigyan Satyam<sup>1</sup>, Senthil Alagesan<sup>2</sup>, Clara Sanz-Nogués<sup>2</sup>, Matthew Griffin<sup>2</sup>, Timothy O'Brien<sup>2</sup>, Abhay Pandit<sup>1</sup>, Dimitrios Zeugolis<sup>1</sup>

\*These authors share first authorship

<sup>1</sup>Network of Excellence for Functional Biomaterials (NFB), National University of Ireland, Galway, Ireland

<sup>2</sup>Regenerative Medicine Institute (REMEDI), National University of Ireland, Galway, Ireland

Corresponding Author: [dimitrios.zeugolis@nuigalway.ie](mailto:dimitrios.zeugolis@nuigalway.ie)

### INTRODUCTION

Cell-based tissue engineering strategies have limited clinical applicability due to delayed extracellular matrix (ECM) deposition and consequent prolonged production time. Scaffold-free tissue production *in vitro* can be enhanced by macromolecular crowding (MMC)<sup>1</sup>, a biophysical phenomenon that governs the intra- and extra-cellular milieu of multicellular organisms<sup>2</sup>. Although MMC has been proven to be an effective tool in enhancing ECM deposition in permanently differentiated cells<sup>1</sup>, its effectiveness in mesenchymal stem cell (MSC) culture has still to be fully assessed. It is hypothesised that MSCs cultured under MMC and low oxygen tension (2%)<sup>3</sup> conditions will maintain their phenotype and function, resulting in multipotent and ECM-rich cell sheets for a variety of clinical targets.

### EXPERIMENTAL METHODS

Human bone marrow MSCs were cultured for 7 and 14 days with 100 µg/ml of carrageenan (MMC) at 20% and 2% oxygen tension at 37°C and 5% CO<sub>2</sub> in a humidified atmosphere. Collagen I deposition was assessed using sodium dodecyl sulphate polyacrylamide gel electrophoresis (SDS-PAGE). Phenotypic assessment was performed by flow cytometry for the expression of cell surface markers CD90, CD105, CD73, CD44 and lack of expression of CD34, CD11b, CD19, CD45 and HLA-DR. Staining for Oil Red O, Alizarin Red S and Safranin O / Fast green was used to assess adipogenic, osteogenic and chondrogenic differentiation.

### RESULTS AND DISCUSSION

**Figure 1:** Under MMC conditions, collagen I deposition was significantly increased at both 20% and 2% oxygen tension, as compared to the non-crowded control (CTR) counterparts at both time points.

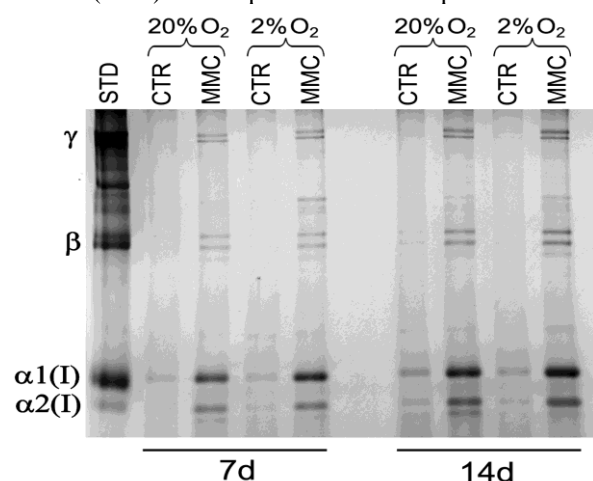


**Figure 2:** Expression of positive cell surface markers evaluated by flow cytometry represented in the form of median fluorescence intensity (MFI). Graphs show fold increase over the appropriate isotype control for 7 and 14 days and except for CD105, MMC and low oxygen tension (2%) did not affect the expression of positive surface markers, indicating maintenance of the multipotent phenotype.

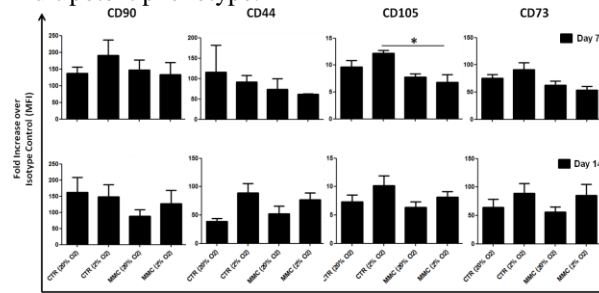
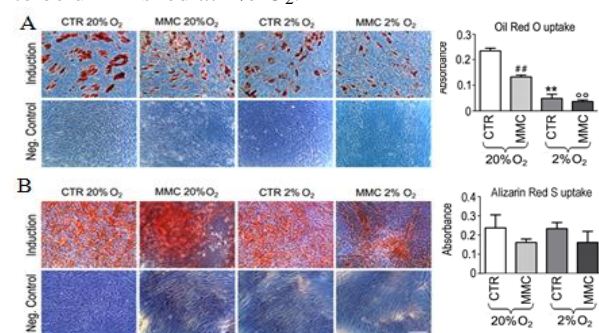


**Figure 3:** Oil Red O staining of hMSCs (A) and Alizarin Red S staining (B) and respective quantification shows that the cells still maintained their multidifferentiation potential, after exposure to MMC and 20% or 2% O<sub>2</sub> tension; adipogenic potential seems to be diminished at 2% O<sub>2</sub>.



### CONCLUSION

MMC and low oxygen tension can be used effectively to enhance extracellular matrix deposition in human MSC culture, without detrimental effect on cell phenotype and function. This multifactorial approach paves the ways for the development of scaffold-free cell therapies for various clinical targets.

### REFERENCES

1. Satyam A. *et al*, Adv Mat, 26:3024-3034, 2014
2. Chen C. *et al*, Adv Dr Del Rev 63: 277-290, 2011
3. Mohyeldin A. *et al*, Cell Stem Cell, 7:150-161, 2010

### ACKNOWLEDGMENTS

The authors would like to acknowledge the Irish Research Council and Health Research Board for financial support.





## Cryptic Cell Cycle Stasis of Human Pluripotent Stem Cells Revealed by Culture in a Biocompatible Thermo-responsive Copolymer Gel

Irene Canton,<sup>1,3</sup> Nicholas J. Warren,<sup>3</sup> Richard Weightman<sup>1</sup>, Andrew Wood,<sup>1</sup> Harry Moore,<sup>1\*</sup> and Steven P. Armes<sup>3\*</sup>

<sup>1</sup>The Centre for Stem Cell Biology, and <sup>2</sup>The Centre for Membrane Interactions and Dynamics (CMIAD), Department of Biomedical Science, The University of Sheffield, Western Bank, Sheffield, S10 2TN, United Kingdom. <sup>3</sup>Department of Chemistry, University of Sheffield, Brook Hill, Sheffield, S3 7HF, United Kingdom, [i.canton@sheffield.ac.uk](mailto:i.canton@sheffield.ac.uk)

### INTRODUCTION

The physicochemical interaction between stem cells and the extracellular milieu is crucial for determining their fate. The routine maintenance of human pluripotent stem cells *in vitro* (PSCs; embryonic and induced pluripotent) usually involves rapid proliferation after adherence to extracellular matrix, resulting in cells displaying a short cell cycle (16-18 h) characterized by a rapid G<sub>1</sub> phase (~ 2.5 h) and complete absence of any arrest at the G<sub>0</sub> stage<sup>1</sup>. However, pre-implantation embryos in certain mammals (e.g. marsupials) exhibit cellular arrest or diapause *in utero* for days or months while preserving pluripotent capacity<sup>2</sup>. Although there is no evidence of diapause-like processes in many mammals including humans, recent evidence shows that diapause can be induced in certain species that do not naturally undergo this process<sup>3</sup>.

Here we describe induction of cell cycle stasis on human PSCs colonies and blastocysts in a wholly synthetic thermo-responsive gel comprising poly(glycerol monomethacrylate)-poly(2-hydroxypropyl methacrylate) [PGMA-PHPMA] diblock copolymer worms<sup>4</sup>.

### EXPERIMENTAL METHODS

PGMA-PHPMA diblock copolymer worm gels were synthesized by RAFT polymerization in physiological buffers. The polymers were extensively dialyzed and freeze dried prior to assessment of cell biocompatibility by MTT assay. Human PSCs were suspended in 6% PGMA-PHPMA-polymer cell medium solution at 5 °C and gelation was triggered by incubation at 37 °C. Cell colonies were kept for extended periods of time in the thermo-responsive gels (7, 14 and 21 days) and recovered by simply cooling at 5 °C. Live (Syto9)/Dead(PI) imaging staining was used to investigate PSCs viability while in the gels. Total DNA quantification over time was used to assess proliferation. Immunolabelling of the cell proliferation marker (ki-67) and the stasis marker, (nuclear envelope statin) were used to investigate quiescence. Stem cell markers (oct-4, Tra-1-60, SSEA-4 and SSEA-1) were monitored by flow cytometry and immunolabeling.

### RESULTS AND DISCUSSION

The non-adherent gel culture system preserved the viability and pluripotency of PSCs in non-proliferative G<sub>0</sub> quiescence and without passage for up to three weeks. Cooling to 5 °C causes degelation via a worm-to-sphere transition, which in principle enables facile cell harvesting. The isolated cell colonies spontaneously re-enter the cell cycle within hours and resume

proliferation while maintaining the expression of stem cell markers. Human blastocysts in Matrigel fragmented after just two days, whereas those within the worm gels were stable for up to 8 days (embryo development day 14) (Figure 1E and 1B). Furthermore, blastocysts within worm gels were positive for the expression of nuclear envelope statin, indicating stasis (Figure 1C).

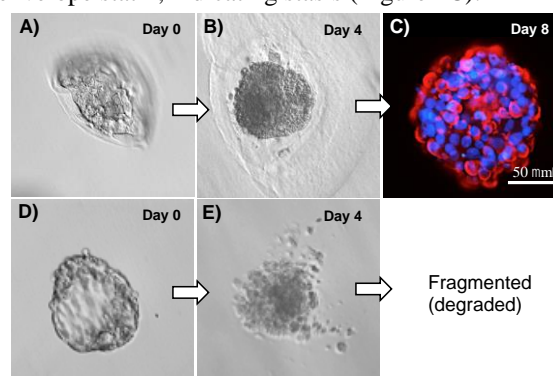


**Figure 1. Human blastocysts gelled in PGMA-PHPMA gels or in Matrigel.** Hatched human blastocysts at 6-day embryo development (A and D) were gelled in PGMA-PHPMA gels or Matrigel<sup>TM</sup>. On day 4 after gelation (10-day embryo development), matrigel embryos fragmented (E), whereas PGMA-PHPMA embryos appeared non-fragmented (B). PGMA-PHPMA embryos were kept up to 8 days in the gels (14-day embryo development) and they were stained for nuclear envelope statin (C, red: nuclear envelope statin; C, blue: nuclei).

### CONCLUSION

The discovery of a cryptic cell arrest mechanism for PSCs serves to illustrate the importance and prevalence of quiescence in homeostasis. Far from remaining merely passive, the 3D niche actively influences adult stem and PS cells. The design of novel synthetic stem cell niches may provide solutions for new therapeutic avenues, from facilitating short-term storage to arresting disease processes or promoting regeneration.

### REFERENCES

1. Kapinas et al., J Cell Physiol. 228: 9–20, 2013
2. Renfree et al., Int J Dev Biol. 58:175-81, 2014
3. Ptak et al., PLoS ONE 7:e33027, 2012
4. Blanazs et al. J Am Chem Soc, 134: 9741-9748, 2012

### ACKNOWLEDGMENTS

The authors thank EPSRC (EP/L024160/1) for providing financial support to this project and Prof. E. Wang (Univ. of Louisville, KY, USA) for kindly donating the nuclear envelope statin antibody. The human embryo work was carried out under licence from the HFEA (R0192-1-A). This work is IP protected and industrial collaboration is in place with GE healthcare UK and GEO Speciality Chemicals UK.

## Co-transplantation of VEGF-transfected Adipose Derived Stromal Cells to Enhance Bone Regeneration and Neovascularization from Bone Marrow Stromal Cells

Mi Lan Kang, Ji Eun Kim, Gun Il Im\*

\*Department of Orthopaedics, Dongguk University Ilsan Hospital, Korea  
[gunil@duih.org](mailto:gunil@duih.org)

### INTRODUCTION

Because of the strong angiogenic property of ADSCs<sup>1</sup>, the addition ADSCs to BMSCs can enhance the revascularization of implanted BMSCs for bone regeneration. However, considering the lower osteogenic potential of ADSCs compared to BMSCs<sup>2</sup>, we thought about ways to decrease the proportion of ADSCs while further enhancing angiogenic and osteogenic effect as a further step. More potent angiogenic ADSCs that is effective even when treated in a small number can further advance the combined cell therapy.

Vascular endothelial growth factor (VEGF) has been identified as one of the most potent inducer of angiogenesis and lymphangiogenesis, being a highly specific mitogen for endothelial cells<sup>3</sup>. Treatment with exogenous VEGF has been shown to promote fracture healing<sup>4,5</sup>.

In this study, we devised a potent angiogenic ADSC by the transfection of VEGF gene using electroporation system and tested the in vitro angiogenesis and osteogenesis and in vivo repair of critical size defect when combined in various proportion to BMSCs. The aim of this study was to evaluate the potential of VEGF-transfected ADSCs (ADSCs<sup>VEGF</sup>) to direct formation of a vascular network, and thereby promoting bone regeneration when added in small proportion to BMSCs.

### EXPERIMENTAL METHODS

ADSCs were transfected with pEGFP-C1 vector containing human VEGF gene using electroporation. ADSCs/VEGF was added to BMSCs and cocultured in variable proportion (BMSCs : ADSCs/VEGF ratio of 0.025~0.5). In vitro osteogenesis was evaluated by ALP and Alizarin Red S staining, calcium quantification, real-time qPCR and ELISA for osteogenic makers. In vitro angiogenesis was evaluated by tube formation assay of human umbilical cord vascular endothelial cell. In vivo angiogenesis was assessed by subcutaneous transplantation of BMSCs and ADSCs<sup>VEGF</sup> with fibrin in nude mice. In vivo bone regeneration and neovascularization were carried out with critical sized defect in rat calvarias by co-transplantation of BMSCs and ADSCs/VEGF.

### RESULTS AND DISCUSSION

ADSCs<sup>VEGF</sup> produced 27-fold greater level of VEGF as compared to untransfected ADSC. ADSCs<sup>VEGF</sup> or ADSCs<sup>VEGF</sup> with BMSCs (BMSCs : ADSCs<sup>VEGF</sup> ratio of 0.025~0.5) induced significantly greater number of tube formation in human umbilical vein endothelial cells than untransfected ADSCs. Higher VEGF release

seems to have caused greater number of tube formation of HUVEC with ADSCs<sup>VEGF</sup> when compared with untransfected ADSCs.

The coculture of BMSCs and ADSCs<sup>VEGF</sup> at the ratio of 1: 0.025~ 0.1 showed significantly greater in vitro osteogenic differentiations and mineralization than BMSCs alone. These findings suggest that ADSCs<sup>VEGF</sup> can exert synergistic osteogenic effect even when treated in small number.

The vascular structure counting from CD31 IHC of cutaneous tissues showed that ADSCs<sup>VEGF</sup>, either by themselves or implanted with BMSCs, induced significantly more vascular structures than BMSCs alone.

When critical size calvarial defects in rats were implanted with mixture of BMSCs and ADSCs<sup>VEGF</sup> along with hydroxyapatite/beta-tricalcium phosphate granules, BMSCs and ADSCs<sup>VEGF</sup> at the ratio of 1:0.05 showed significantly greater bone area, volume and mineral density on the regenerated defect than BMSCs alone. The results of current study are in line with the previous reports that VEGF-A gene transfer enhances mineral density in bone fracture healing<sup>4,5</sup>.

VEGF has an activity in promoting vascularization during endochondral bone formation, as well as multifarious activities including regulation of the survival and activity of endothelial, chondrogenic and osteogenic cells in bone development<sup>6</sup>. Both microvessel density and staining intensity counts of CD31 demonstrated that ADSCs<sup>VEGF</sup> alone or co-transplantation of BMSCs/ADSCs<sup>VEGF</sup> at 1:0.5 induced significantly higher CD31 expression than those of BMSCs alone ( $p < 0.05$ ) while BMSCs/ADSCs<sup>VEGF</sup> at 1:0.05 induced increase only in signalling densities.

### CONCLUSION

Our results demonstrated that ADSCs/VEGF enhanced neovascularization and angiogenesis as well as mineral density in bone regeneration.

### REFERENCES

1. Kokai LE et al. J Lab Clin Med 2014;163:399-408.
2. Im GI et al. Osteoarthritis Cartilage 2005;13:845-53.
3. Hoeber A et al. Pharmacol Rev 2004;56:549-80.
4. Mayer H et al. J Cell Biochem 2005;95:827-39.
5. Tarkka T et al. J Gene Med 2003;5:560-6.
6. Coultas L et al. Nature 2005;438:937-45.

### ACKNOWLEDGMENTS

The authors would like to thank the National Research Foundation of Korea (Grant no: 2013R1A1A2062978) for providing financial support to this project.



## Effect of Mechanical Stimulation on Osteogenesis of Self-Assembled Collagen-Cell Seeded Microspheres

Maryam Shariatzadeh, Cécile M. Perrault, Damien Lacroix

INSIGNEO Institute for in silico medicine, Mechanical Engineering Department, University of Sheffield, UK  
[m.shariatzadeh@sheffield.ac.uk](mailto:m.shariatzadeh@sheffield.ac.uk)

### INTRODUCTION

Mechanical forces and 3D topological environment can be used to control differentiation of Mesenchymal Stem Cells (MSCs)<sup>1, 2</sup>. However, the effects of physical and mechanical cues of the microenvironment on MSC fate determination have not yet been fully understood. This study investigates and compares the effect of mechanical stimulations on soft cellular microspheres when subjected to dynamic fluid compression in 3 different in-vitro systems: microfluidic chamber, compression bioreactor and orbital shaker. It is hypothesised that dynamic compressive strains influence cell morphology and expression of osteogenic cell marker heMSCs.

### EXPERIMENTAL METHODS

Microspheres were produced by gelation of bovine collagen type I with concentrations of 2 mg/ml and 2500-3200 heMSC cells per 5µl droplet. Three loading conditions were studied: (1) the microspheres were forced to flow through the chamber (D=0.7mm) at a flow rate of 200 µl/min for 3 cycles/day for 5 days; (2) 10% dynamic compression strain was applied by a Bose biodynamic bioreactor for 15 and 40 min/day for 5 and 10 days; (3) fluid shear stress was applied by an orbital shaker at 50 rpm for 40 min/day for 10 days. All experiments started at day 6 post-encapsulation. Cell viability and proliferation, alkaline phosphatase activity and mineralization were monitored and compared with free floating control samples.

### RESULTS AND DISCUSSION

Low concentration of bovine collagen was shown to be an efficient microenvironment for cellular growth which supported cell proliferation and viability up to 28 days post-encapsulation, as shown by DNA pico green assay (Fig. 1). ALP activity level increased steadily from day 6 post-encapsulation up to day 28 with a slight drop at day 21 for most conditions (Fig. 2). All samples showed a peak for ALP activity at day 28 post-encapsulation with the highest level for free floating (0.0014) and 5 days controls (0.0013). Microfluidics condition manifested the lowest ALP level at day 21 among other experiment groups (> 0.0003). Also deposition of calcium and mineralisation were confirmed in all samples from day 14 post-encapsulation onward by alizarin red staining (ARS). The highest ARS colour intensity was reported in cyclic compression group but calcium deposition could not be detected due to the very low cell number and mineral expression level. Rotation of collagen microspheres through microfluidic chamber and shaker experiment may cause nonhomogeneous transfer of fluid flow shear stress and compression forces to the cells. Therefore,

cells in different areas of a microsphere may experience more random mechanical forces.

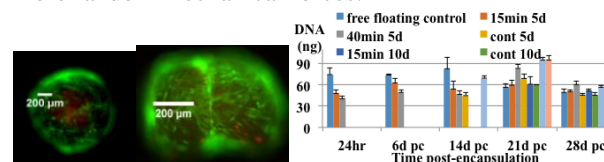


Fig. 1: Fluorescent staining of live / dead heMSCs day 7 and day 28 post encapsulation (left), heMSCs cell proliferation (right).

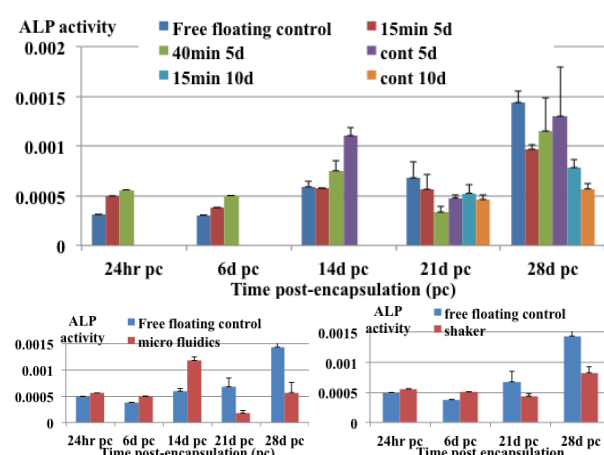


Fig. 2: ALP activity of cyclic compression samples compare to the free floating controls (top), Microfluidic experiment (lower left) and fluid shear stress experiment (lower right).

### CONCLUSION

Mechanical forces can stimulate the differentiation of mesenchymal progenitors in micro-environment. Our results showed that despite similar cell viability, on average the level of ALP activity in 5 days dynamic compression regime was nearly two times higher than 10 days compression. Also, free floating samples presented the highest cell number and ALP activity compare to other conditions. Application of compression cycles on heMSC cells could be used as a model to study the effect of mechanostimulation on osteogenesis. Future work will assess qPCR and gene expression to identify the role of osteogenesis marker genes and new gene / protein pathways in heMSCs mineralization.

### REFERENCES

1. Chan, B. P. *et al.*, Biomaterials. 28:4652-66, 2007
2. Delaine-smith R.M. *et al.*, Vitam Horm. 87:417-480, 2011

### ACKNOWLEDGMENTS

Financial support from the European Research Council (258321) is acknowledged



## 5-Azacytidine Mediated hMSC Behaviour on Electrospun Scaffolds to Induce Myogenesis

Ines Fasolino, Vincenzo Guarino, Valentina Cirillo, Marica Marrese, Luigi Ambrosio

Institute for Polymers, Composites and Biomaterials, Department of Chemical Sciences & Materials Technology, National Research Council of Italy, V.le Kennedy 54, Naples, Italy

[vincenzo.guarino@cnr.it](mailto:vincenzo.guarino@cnr.it)

### INTRODUCTION

Incomplete regeneration after traumatic muscle injury or muscular dysfunction is a common problem in regenerative medicine. The main goal in skeletal muscle engineering is to replicate the structure and function of skeletal muscle tissue *in vitro* and *in vivo* to obtain a therapeutic implantable device.

For this purpose, it is required to design bio-inspired platforms which convey all the main features of native extracellular matrix - i.e., morphological and biochemical signals - and to properly address muscle cells towards myotube differentiation and maturation. According to current pharmacological therapies, they have to assure the efficient interaction of cells with selected drugs, such as 5-Azacytidine (5-AZA) - a DNA-methylation inhibitor just known for promoting up-regulation of muscle genes and hMSC differentiation - thus promoting the formation of *in vitro* tissues with functional contraction<sup>1</sup>.

Here, we investigate the *in vitro* response of human mesenchymal stem cells (hMSC) on electrospun fibres made of Polycaprolactone (PCL) or PCL and Gelatin (PCL/Gel). Firstly, we demonstrate the ability of hMSCs to differentiate in mature myofibres under specific conditions. Then, we evaluate the effects of 5-azacytidine on myotubes generation thus underlining the contribution of 3D fibre network on the pharmacological activity of protein in the myogenic regeneration process.

### EXPERIMENTAL METHODS

PCL and PCL/Gel fibres were produced by using an electrospinning equipment (Nanon01, MECC, Japan) as reported elsewhere<sup>2,3</sup>. SEM, TEM, AFM in Tapping Mode (TM) were employed to obtain more information on morphological features of electrospun fibres and defects (i.e., beads, branched fibres). Bone marrow hMSCs (passages 4-6) were grown in myogenic culture medium [high-glucose DMEM supplemented with 10% fetal bovine serum (FBS; GIBCO), 5% horse serum (HS; GIBCO), non essential amino acids (LONZA) and 100 mM 2-mercaptoethanol (GIBCO)] in a humidified incubator (37°C, 5% CO<sub>2</sub>).

Cells plated onto electrospun PCL and PCL/Gel were treated with 5-AZA (1 and 5 µM) from 7 to 28 days. 5-AZA was added to myogenic medium and culture medium was replaced twice a week. Skeletal muscle differentiation was assessed by YIP-1B - a muscle specific protein - expression whereas cellular morphology by SEM. Skeletal muscle cells formation was analyzed by Azan Mallory stain.

### RESULTS AND DISCUSSION

In order to produce PCL/Gelfibres, lower polymer concentration and a high polar solvent have been used respect to PCL ones. This determines a reduction of average fibres diameter to  $(0.71 \pm 0.15) \mu\text{m}$ , also minimizing the formation of beads due to the stronger interaction of polar solvent with the electric field forces. Moreover, TEM images showed a preferential exposure of protein along the fibre surface also confirmed by roughness ( $R_q$ ) measurement calculated by AFM. The addition of Gelatin in PCL fibres determines an increase of  $R_q$  value to  $(22.3 \pm 5.15) \text{ nm}$ , in comparison with PCL fibres  $(16 \pm 2.72) \text{ nm}$ . According with peculiar morphological and biochemical features of fibres, we have recognized some differences in hMSC behaviour mediated by 5-AZA. In particular, 5-AZA significantly increases YIP-1B expression (index of myogenic differentiation) both in the presence of PCL and PCL/Gel fibres compared to plate control (5-AZA 1 µM alone). Most interestingly, an effect of drug concentration on hMSC activity may be recognized. Indeed, for higher amounts of 5-AZA (5 µM), YIP-1B expression does not change in the presence of PCL fibres, even showing a decay in the case of PCL/Gel ones. Accordingly, SEM images indicate a higher stretching of hMSC after 5-AZA treatment, so resembling to myotubes, whereas Azan Mallory staining confirms the hMSCs differentiation in skeletal muscle cells.

### CONCLUSION

Summarizing, we verified that hMSCs *in vitro* differentiate after treatment with 5-azacytidine, so forming mature myofibres. In particular, 3D fibre network concurs to corroborate the biological effect of 5-azacytidine protein, mainly amplifying the pharmacological activity of protein during the *in vitro* process of myogenic regeneration.

### REFERENCES

1. Karalaki M. *et al.*, *In vivo*. 23(5): 779-96, 2009
2. Guarino V. *et al.*, *J. Bioact Comp Pol.* 26: 144, 2011
3. Guarino V. *et al.*, *Macromol. Biosci.* 11 (12):1693, 2011

### ACKNOWLEDGMENTS

This work has been financially supported by MERIT (RBNE08HM7T) and REPAIR (PON01-02342). Scanning Electron Microscopy was supported by the Transmission and Scanning Electron Microscopy Labs (LAMEST) of the National Research Council.





## Microvesicles Derived from Stem Cells as a Novel Effective Tool for Transferring of Bioactive Molecules to Mature Primary Cells - Future Implications for Tissue Regeneration

Sylwia Bobis-Wozowicz<sup>1</sup>, Katarzyna Kmietek<sup>1</sup>, Malgorzata Sekula<sup>1,2</sup>, Sylwia Kedracka-Krok<sup>3</sup>, Elzbieta Kamycka<sup>1</sup>, Urszula Jankowska<sup>2,3</sup>, Jacek Kolcz<sup>4</sup>, Dariusz Borucki<sup>5</sup>, Buddhadeb Dawn<sup>6</sup>, Zbigniew Madeja<sup>1</sup>,  
Ewa K Zuba-Surma<sup>1,\*</sup>

<sup>1</sup>Department of Cell Biology, Faculty of Biochemistry, Biophysics and Biotechnology, Jagiellonian University, Krakow, 30-387, Poland

<sup>2</sup>Malopolska Centre of Biotechnology, Jagiellonian University, Krakow, 30-387, Poland

<sup>3</sup>Department of Physical Biochemistry, Faculty of Biochemistry, Biophysics and Biotechnology, Jagiellonian University, Krakow, 30-387, Poland

<sup>4</sup>Department of Pediatric Cardiac Surgery, Polish-American Children's Hospital, Krakow, 30-663, Poland

<sup>5</sup>Polish Stem Cell Bank, 00-131, Warsaw, Poland

<sup>6</sup>Division of Cardiovascular Diseases, Cardiovascular Research Institute, University of Kansas Medical Center, Kansas City, KS 66160, USA

[ewa.zuba-surma@uj.edu.pl](mailto:ewa.zuba-surma@uj.edu.pl)

### INTRODUCTION

Microvesicles (MVs) are membrane-enclosed particles shed into the extracellular environment by direct budding from the cell plasma membrane or may be derived from the endosomal compartment. MVs may carry bioactive components of cell cytoplasm and membrane including mRNAs, miRNAs, proteins and lipids and may act as mediators of cell-to-cell communication by transferring such content from parent to target cells.

In this study, for the first time, we examined phenotype and bioactive content of MVs derived from human induced pluripotent stem cells (iPS) produced in our laboratory. We also investigated the transfer of selected miRNAs and mRNAs by such iPS-MVs to mature cardiac cells. We examined functional impact of the transferred components on selected functions of primary heart cells including metabolic activity, viability and survival in hypoxia as well as angiogenic and cardiac differentiation potential *in vitro*.

### EXPERIMENTAL METHODS

MVs were isolated by ultracentrifugation from conditioned media harvested from iPS cells cultured in novel optimized feeder layer-, serum-, and xeno- free conditions. The level of selected several transcripts including genes related to cardiac and angiogenic differentiation was examined in donor iPS cells and iPS-MVs by real-time RT-PCR. Multiantigenic profile of iPS cells and iPS-MVs including the expression of selected markers related to stemness as well as angiogenic and cardiomyogenesis was examined by classical and high-sensitivity cytometry (ApoGee). Moreover, extended regulatory microRNA profile was evaluated by employing microarray assays by real time RT-PCR,

while global proteome was examined by mass spectroscopy.

### RESULTS AND DISCUSSION

We established that several bioactive transcripts including mRNAs and microRNAs as well as proteins expressed in iPS cells are transferred to iPS-MVs. Moreover, we found that MVs may carry and transfer the bioactive content to primary mature cardiac cells. Importantly, we found significant impact of such transfer on selected functions of target cells including metabolic activity, survival as well as angiogenic differentiation potential *in vitro*.

### CONCLUSION

The data indicate that iPS- derived MVs may represent natural nanocarriers of several proangiogenic, cardiomyogenic and antiapoptotic agents to mature heart cells. Such iPS-MVs may potentially represent important carriers enforcing both function and survival of mature heart cell when delivered into ischemic myocardium. Thus, this report suggests the potential future role of microvesicles including iPS-MVs in heart repair that represents an example of a novel rising approach in applications of stem cells and their derivatives in tissue regeneration.

### ACKNOWLEDGMENTS

This work was supported in part by TEAM-2012/9-6 grant from the Foundation for Polish Science (FNP) to EZS and POIG.01.01.02-00-109/09 project.





## Influences of the pH on the Adsorption Properties of an Antimicrobial Peptide on Titanium Surfaces

Yendry Corrales Ureña<sup>1,2</sup>, Linda Wittig<sup>2</sup>, Matheus Vieira Nascimento<sup>2,3</sup>, Juliano Luiz Faccioni<sup>2,4</sup>, Paulo Noronha Lisboa Filho<sup>5</sup>, Klaus Rischka<sup>2</sup>.

<sup>1</sup> São Paulo State University (UNESP), POSMAT, Bauru, São Paulo, Brazil

<sup>2</sup> Fraunhofer Institute for Manufacturing Technology and Advanced Materials (IFAM), Bremen, Germany

<sup>3</sup> Federal University of Ceará, Fortaleza, Ceará, Brazil

<sup>4</sup> Federal University of Rio Grande do Sul, Porto Alegre – RS, Brazil

<sup>5</sup> São Paulo State University (UNESP), Bauru, São Paulo, Brasil

[plisboa@fc.unesp.br](mailto:plisboa@fc.unesp.br)

### INTRODUCTION

Antimicrobial peptides have recently been investigated for their broad antimicrobial activity against gram-positive and gram-negative bacteria [1] as well as for their immunomodulatory properties [2]. In this study the immobilization of antimicrobial peptides on titanium alloy surfaces have been studied to improve the antibacterial properties of the surface. The peptide studied is the Tet-124 sequence KLWWMIRRW, which was previously synthesized by Hilpert *et al.* [3]. The immobilization strategy is based on the electrostatic interactions of the peptide with a titanium alloy surface and the modification of both N- and C-terminus with glycine-3,4-dihydroxyphenylalanine-glycine (G-DOPA-G). The DOPA amino acid was added to the sequences to promote adhesion to titanium alloy surfaces by the catechol moiety due the possible formation complexes with the metal and metal oxide surface [4].

### EXPERIMENTAL METHODS

Quartz crystal micro balance with dissipation (QCM-D, Q-Sense E4, Sweden) was used to evaluate the adsorption on titanium coated quartz crystals with peptides solutions at pH=4.75 (acetate buffer 0.1 M, 0.3mg/ml) and 6.9 (deionized water, 0.18mg/ml).

The attachment of *Escherichia coli* (*E.coli*, DSM 10290, 4 h in contact) and fibroblast (cells L929) on 1cm<sup>2</sup> Ti-6Al-4V substrates modified with Tet-124-G-DOPA-G and unmodified (control) was evaluated.

### RESULTS AND DISCUSSION

The adsorption due to the crystal contact with the peptide solution was monitored in real time for all the overtones (n=1, 3, 5, 7...) at a temperature of 25°C. Figure 1 A and B shows the frequency changes due to the mass adsorption crystal in contact with the Tet-124 and Tet 124-G-DOPA-G respectively. The peptides show similar adsorption rate behavior. No desorption upon rinsing with buffer is detected. Also rigid layers were formed on the surface accordingly with the changes on the dissipation coefficient (data not shown).

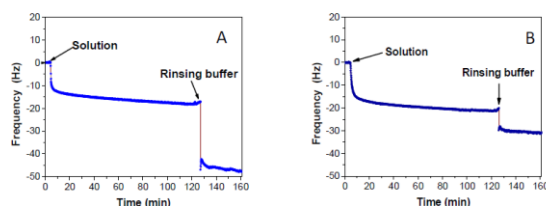


Figure 2. Frequency changes A) Tet-124 B) Tet-124-G-DOPA-G, 0.33 mg/ml in acetate buffer 0.1 M.

Figure 2. A shows lower adsorption rate and mass of the Tet-124 in comparison with Tet124-G-DOPA-G at pH=6.9

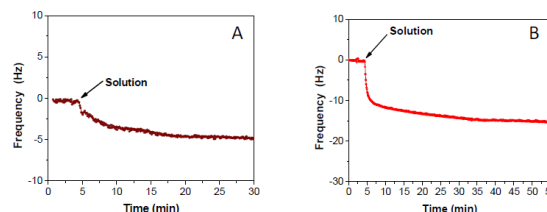


Figure 2 Frequency changes A) Tet-124 B) Tet-124-G-DOPA-G, 0.18 mg/ml deionized water.

### CONCLUSIONS

The layer formation at pH 4.75 of the Tet-124 and both Tet-124-DOPA specimen is related to the electrostatic interaction with the negatively charged titanium oxide layer. At pH 6.9 the influence of the DOPA moieties enhance the adlayer formation due to the Ti(IV) catechol complexes formation. This study shows that it is possible to change the mass adsorption coverage of the antimicrobial peptide layer on the surface depending the pH and salt concentration. The modification of the Ti-6Al-4V with the Tet-124-G-DOPA-G does not change the attachment of *E.coli* bacteria to its surface; however. The results indicate also indicate that the surface modification does not influence the biocompatibility and cell attachment of fibroblast to the surface. The G-DOPA-G N and C terminal sequence modification peptide can be used as immobilization strategies of antimicrobial peptides on titanium alloy surfaces.

### REFERENCES

1. Yoshinari, M. *et al.* Biofouling 26: 103–110, 2010.
2. De la Fuente, C. *et al.* Antimicrob Agents Chemother 56: 2696–2704, 2012.
3. Hilpert, K. *et al.* Chemistry & Biology 13: 1101–1107, 2006.
4. Ye, Q. *et al.* Chem Soc Rev 40: 4244–4258, 2011.

### ACKNOWLEDGMENTS

The authors thank to Science without Borders (Ciência sem Fronteiras, proc: 88888.015774/2013-00, 88888.020073/2013-00), FAPESP 2013/07296-2 and Consejo Nacional para Investigaciones Científicas y Tecnológicas de Costa Rica (CONICIT) for the funding. Prof. Dr. Bernd Mayer, Prof. Dr. Andreas Hartwig and Dr. Ingo Grunwald for the support and advices.



## Titanium Modified with Silver Nanoparticles for Oral Implantology

Rafał Pokrowiecki<sup>1</sup>, Barbara Szaraniec<sup>2</sup>, Tomasz Zaręba<sup>3</sup>, Tomasz Szponder<sup>4</sup>, Krzysztof Pałka<sup>5</sup>,  
Jan Chłopek<sup>2</sup>, Stefan Tyski<sup>3</sup>

<sup>1</sup>Department of Oral Surgery, Jagiellonian Medical University, Montelupichst., 4, 31-155 Cracow, Poland

<sup>2</sup>Department of Biomaterials, Faculty of Materials Science and Ceramics, AGH University of Science and Technology,  
30 Mickiewicza Ave., 30-059 Cracow, Poland

<sup>3</sup>Department of Antibiotics and Microbiology, National Health Institute, Chełmska 30/34 st., 00-725 Warsaw, Poland

<sup>4</sup>Department and Clinic of Veterinary Surgery, Faculty of Veterinary Medicine, University of Life Sciences in  
Lublin, Akademicka 13 st., 20-950 Lublin, Poland

<sup>5</sup>Lublin University of Technology, Department of Materials Engineering, Nadbystrzycka St. 36, 20-618 Lublin  
[pokrowiecki@gmail.com](mailto:pokrowiecki@gmail.com)

### INTRODUCTION

Titanium and its alloys are commonly used in regenerative surgery protocols in oral and maxillofacial surgery. Despite high success rate ranging up to 98%, biological complications such as *periimplant mucositis* and *periimplantitis* are still possible threat for implant treatment and may be diagnosed in 28- 56% patients in their implant sites 12-43%. Despite a variety of therapeutic options infected implants are difficult to treat and often require removal. Therefore, one of proposed strategies to prevent implant infection rate is to decrease bacterial adhesion, while maintaining material biocompatibility. Nanosilver is a material which gained much attention in biomedical science in last decade. It is assumed that silver nanoparticles (AgNPs) in controlled amounts exhibit sufficient antimicrobial properties and present little or non-toxic effect on hosts tissue. The aim of this study was to evaluate a potential applicability of silver nanoparticles modified titanium for oral implantology.

### EXPERIMENTAL METHODS

Commercially pure titanium Grade 2 in shape of discs, 10 mm in diameter were used. Surface of all samples was pre-treated by the authors formula- triple surface etching (TSE). In order to provide incorporation of AgNPs onto titanium surface, Tollens reagents formula was adapted. Incubation in Tollens reagents solution were performed for 10, 5, 2 minutes and 30 seconds respectively. Surface roughness, wettability, silver ion release and *in vitro* bioactivity were evaluated. The antibacterial behaviour was estimated by observing the sample ability to stop bacterial proliferation around it (zone of inhibition- ZOI). Seven clinical strains of each: *Streptococcus mutans*, *Streptococcus salivarius*, *Streptococcus oralis* and *Streptococcus mitis* as well as *P. Gingivalis* (ATCC 33227). For evaluation of osseointegration, 6 titanium sinter implants [2] pre-treated for 30s with aforementioned formula with AgNPs, were tested *in vivo* in healthy 6 New Zealand white rabbits. Each Rabbit received a total of 2 implants: implant coated with AgNPs in one leg and reference implants (pure sintered titanium) in the other. The implant retrieval was performed after 12 weeks. All statistical analyses were performed by Anova with the student t- test. A *p*-value of 0,05 was considered statistically significant.

### RESULTS AND DISCUSSION

AgNPs deposition by Tollens method influenced mean surface Ra only marginally. SEM observations revealed that AgNPs did not affect surface nanofeatures. However, they significantly influenced the surface wettability. In the PBS buffers surfaces continuously released silver ions with characteristic burst release during first 24 hours of incubation. Also a moderate surface enrichment in calcium and phosphate after 6 weeks of incubation was noticed.

Antimicrobial assay confirmed high antimicrobial properties of all titanium specimens with AgNPs against oral *streptococci* species as well as *P. Gingivalis* inhibition halos were > 1mm (*p*<0,05). Time of surface treatment with AgNPs did not have a statistically significant influence on antimicrobial activity (*p*>0,05). However, there were a statistically significant differences between mean ZOIs for tested bacteria. The most susceptible species to AgNPs were *P. Gingivalis* followed by *S. mitis*. *S. mutans* was the least susceptible. All animals reached the endpoint of the study. Histopathological and radiographic findings confirmed full osseointegration of the titanium sinters with AgNPs comparably to the control group (*p*>0,05).

### CONCLUSION

Tollens method for silver incorporation may exert a diversified effect on physicochemical properties of titanium surface. Incorporation of AgNPs provides an efficient antimicrobial properties against both: early (oral *streptococci*) and late (*P. Gingivalis*) colonizers of the dental implant. *In vivo* biocompatibility tests confirmed a good biotolerance of titanium implants modified with nanosilver thus such materials may find clinical application in oral implantology.

### REFERENCES

1. Szaraniec B. *et al.* Eng. Biom. 81–84: 49-52, 2008
2. Pałka K. *et al.* Eng. Biom. 112: 26–30, 2012
3. Pokrowiecki R *et al.* Eng. Biom. 124: 2-10, 2014

### ACKNOWLEDGMENTS

This work was financed by statutory research 11.11.160.616 of Faculty of Material Science and Ceramics AGH University of Science and Technology.



## Bio-Inspired Antimicrobial Surfaces for Titanium Implant

Ting Diu<sup>1</sup>, Terje Sjöström<sup>1</sup>, Leanne Fisher<sup>1</sup>, Angela Nobbs<sup>1</sup>, Howrad Jenkinson<sup>1</sup>,  
Max Ryadnov<sup>2</sup>, Monica Tsimbouri<sup>2</sup>, Matt Dalby<sup>3</sup> and Bo Su<sup>1</sup>

<sup>1</sup>School of Oral & Dental Sciences, University of Bristol, UK

<sup>2</sup>National Physical Laboratory, UK

<sup>3</sup>Centre for Cell Engineering, University of Glasgow, UK

[b.su@bristol.ac.uk](mailto:b.su@bristol.ac.uk)

### INTRODUCTION

Infection at the implant surface is one of the biggest challenges in biomaterial research. Reducing the risk of infection during and after surgery, without using antibiotics, would be of great benefit to both patients and the healthcare system. It has recently been suggested that nanotopographies found in nature, act as bactericidal surfaces by physically damaging bacteria<sup>1</sup>. By mimicking such topographies on relevant materials, it may be possible to create antimicrobial implant surfaces. In this work we have produced nanowire surfaces on Ti alloy substrates which are capable of killing bacteria while maintaining mammalian cell functionality<sup>2</sup>.

### EXPERIMENTAL METHODS

Two fabrication methods, hydrothermal synthesis and controlled thermal oxidation, were used to produce nanowires on pure Ti and Ti-6Al-4V (Ti64) surfaces. Hydrothermal synthesis was carried out in NaOH solution at 240°C for 2-3 h on Ti substrates, followed by ion exchange and crystallisation. Ti64 samples were heated to 850°C in a tube furnace under Ar atmosphere. At the final temperature, acetone vapour was introduced at 500sccm for 45 minutes, and finally the furnace was allowed to cool under Ar. The substrates were then annealed in air at 600°C for 1h to remove carbon residue. *Pseudomonas aeruginosa* and *Staphylococcus aureus* were cultured on smooth (control) and nanowire surfaces at 37°C for 1h. The cells were then either stained for LIVE/DEAD and examined using fluorescence and confocal laser microscopy, or cultured with assays to examine cell viability.

### RESULTS AND DISCUSSION

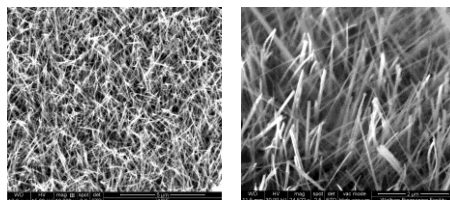


Figure 1. Side view SEM of nanowires grown on Ti (left) and Ti64 (right) substrates.

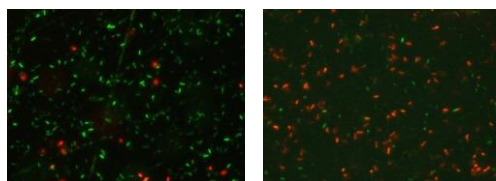


Figure 2. Fluorescence microscopy images of LIVE/DEAD stained *P. aeruginosa* on smooth Ti64 (left) and nanowire Ti64 (right). Green = live cells. Red = dead cells.

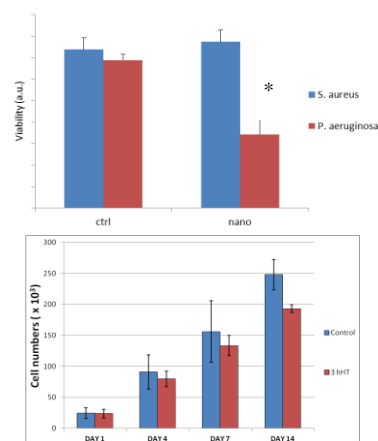


Figure 3. Cell viability measured with AlamarBlue, of *S. aureus* and *P. aeruginosa* on smooth Ti64 and nanowire Ti64. \*  $P < 0.05$ .

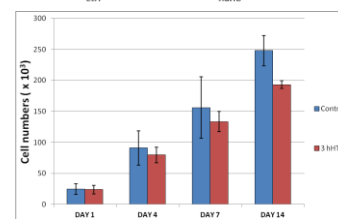


Figure 4. 14 day viability plot of MG-63 cells seeded on Control, hydrothermal TiO<sub>2</sub> nanowire (3 hHT) surfaces by absorbance reading of the PrestoBlue stain and converted into cell population.

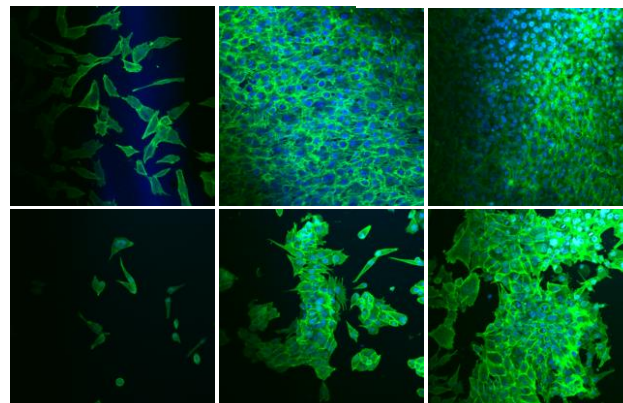


Figure 5. Confocal images showing the cell coverage on two different surfaces from day 1, 4 to 7 (from left to right). The cells on the Control surface (first row) have already established a monolayer coverage by day 4 (top, middle) and multilayers were formed by day 7 (top, right). The cells on hydrothermal TiO<sub>2</sub> nanowires (second row) were quite sparse at day 1 but the cells appeared to have formed clusters by day 4, instead of an even monolayer spread. The clusters were still evidence by day 7 but in larger numbers. The cell morphology were elongated but possessed a much flatter, spread morphology, which were rounder in shape (not as spread out).

### CONCLUSION

Sharp nanowire features were produced on Ti and Ti64 alloys by hydrothermal and controlled thermal oxidation methods. The nanowires were able to kill Gram-negative bacteria by physical means but can maintain the cell viability. These surfaces have potential for antimicrobial surfaces for orthopaedic implants.

### REFERENCES

- Ivanova, E.P. *et al.*, Small 8:2489-94, 2012
- Diu, T. *et al.* Sci. Rep. 4, 7122, 2014

### ACKNOWLEDGMENTS

The authors would like to acknowledge the EPSRC (EP/K035142/1) for providing financial support and a CASE studentship (TD) to this work.



Zuzanna Trzcińska<sup>1</sup>, Fabien Brouillet<sup>2</sup>, David Grossin<sup>1,3</sup>, Cedric Charvilat<sup>3</sup>, Anna Peacock<sup>4</sup>, Artemis Stamboulis<sup>1</sup>

<sup>1</sup>School of Metallurgy and Materials, University of Birmingham, United Kingdom

<sup>2</sup>CIRIMAT, UPS-INPT-CNRS, Faculté de Pharmacie, Université de Toulouse, France

<sup>3</sup>CIRIMAT, UPS-INPT-CNRS, ENSIACET, Université de Toulouse, France

<sup>4</sup>School of Chemistry, University of Birmingham, United Kingdom

[zxt166@bham.ac.uk](mailto:zxt166@bham.ac.uk)

## INTRODUCTION

Postsurgical infections are one of the causes of implant rejection and prolonged healing of the implantation sites. Functionalization of surfaces with Antimicrobial Peptides (AMPs) can be a tool which is more effective against bacterial infection than the currently used methods such as antibiotics administration.

AMPs are short molecules, which have a broad spectrum of antibacterial, antifungal and antiviral properties.<sup>1</sup> They can act by interaction with bacterial membranes leading to their destruction, while they do not affect eukaryotic cell membranes.<sup>1</sup>

Attachment of AMP molecules on the surface of materials with the use of an adhesive polymer, such as polydopamine<sup>2</sup> could provide a successful method to introduce antimicrobial properties to medical surfaces.

## EXPERIMENTAL METHODS

Fluorescently labelled and unlabelled AMPs were synthesised using Solid Phase Peptide Synthesis (SPPS), followed by purification with High Pressure Liquid Chromatography (HPLC) and mass characterisation with Mass Spectroscopy (MS).

The effect of AMPs on the bacterial and eukaryotic cell membrane was tested with Circular Dichroism Spectroscopy (CD) in dodecylphosphocholine (DPC) and sodium dodecylsulphate (SDS) micelle environment that mimics eukaryotic and bacterial cell membranes.

Polished titanium alloy (Ti6Al4V) plates were coated with the adhesive polymer via a dip coating method.

Peptides were then conjugated to the polymer coated on the Ti6Al4V by using Schiff base chemistry.

The thickness of the polymer-AMP layer was measured by Atomic Force Microscopy (AFM) and Ellipsometry.

Hydrophobicity changes of coated and uncoated surface of Ti6Al4V were measured by Water Contact Angle.

Scanning Electron Microscopy (SEM) images were used to analyse the coating of the polymer on the surface of Ti6Al4V plates.

Plates prepared with fluorescent label were analysed under fluorescence microscopy to visualise the coating of AMPs on the surface of titanium.

## RESULTS AND DISCUSSION

Synthesised AMPs were purified to give  $\geq 95\%$  purity and the MS showed agreement of peptides molecular weights with the theoretical molecular weights.

The Ellipsometry and AFM studies showed the polymer-AMP coating thickness to increase with increasing coating time (Table 1).

The water droplet angles showed decrease of hydrophobicity of Ti6Al4V surface when the polymer

and polymer-AMP were coated on the surface (coating time 72 h) (Table 2).

**Table 1:** Adhesive polymer-AMPs thickness changes with increasing time of coating.

Time	24 h	48 h	72 h
Thickness of Coating	5.2±1.1 nm	32.8±5.1 nm	50.4±7.0 nm

**Table 2:** Changes of the water contact angle with the applied coating.

Surface	Ti6Al4V	Ti6Al4V polymer	Ti6Al4V polymer - AMPs
Water contact angle	82 ± 10°	60 ± 6°	54 ± 11°

SEM images and fluorescence microscopy images showed uniform coatings of polymer and polymer-AMPs on the surface of Ti6Al4V plates (Figure 1a and b).

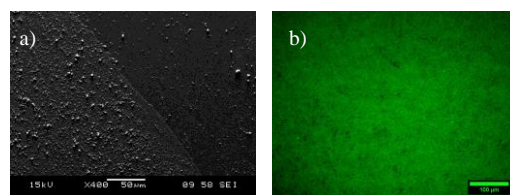


**Figure 1:** a) SEM image of a boundary between polymer coated surface and uncoated surface of Ti6Al4V, b) Fluorescence microscopy image of AMPs linked on the surface of Ti6Al4V via an adhesive polymer.

## CONCLUSION

The functionalization of Ti6Al4V surfaces with polymer and polymer-AMPs resulted in a coating of nanosize thickness which depends on the time of polymerization. The coverage of coating was shown to be uniform. Functionalization of the surface with the coating caused a decrease in hydrophobicity which can have an effect on the attachment of bacterial and mammalian cells.

## REFERENCES

1. Pasupuleti M. *et al.*, Critical reviews in Biotechnology. 32, 143 2012
2. Luo R. *et al.*, Colloid. Surf. B-Biointerfaces 2013, 106, 66

## ACKNOWLEDGMENTS

The authors would like to thank the EPSRC for funding the project and COST NEWGEN – STSM for funding the mobility of ZT to CIRIMAT Toulouse.



## Novel Biosensor for Detecting and Preventing Periodontal Disease

M. Hoyos-Nogués<sup>1,2,3</sup>, S. Brosel-Oliu<sup>4</sup>, N. Abramova<sup>4</sup>, A. Bratov<sup>4</sup>, C. Mas-Moruno<sup>1,2,3</sup>, F.J. Gil<sup>1,2,3</sup>

<sup>1</sup>Biomaterials, Biomechanics and Tissue Engineering Group, Technical University of Catalonia, Spain

<sup>2</sup>Biomedical Research Networking Centre in Bioengineering, Biomaterials and Nanomedicine (CIBER-BBN), Spain

<sup>3</sup>Centre for Research in Nano Engineering, Technical University of Catalonia, Spain

<sup>4</sup>BioMEMS Group, Centre Nacional de Microelectrònica (IMB-CNM, CSIC), Spain

[carles.mas.moruno@upc.edu](mailto:carles.mas.moruno@upc.edu)

### INTRODUCTION

Peri-implantitis, an inflammation caused by biofilm formation, constitutes a major cause of implant failure in dentistry[1]. Thus, the detection of bacterial pathogens at the early steps of biofilm growth represents a very powerful strategy to prevent from implant-related infections. Among different methods to detect pathogenic bacteria, electrochemical biosensors, especially impedance-based systems (EIS), present key advantages in terms of miniaturization, improvement in sensitivity and low cost.

In this regard, antimicrobial peptides (AMPs), which are highly sensitive and active towards are well-known components of the immune system and display a broad range of bacteria [2], can be used to develop highly effective biological recognition elements. Thus, the aim of the present study is to combine the use of miniaturized and integrated EIS and the ability of AMPs as robust biorecognition moieties to obtain biosensors with high sensitivity, specificity and low detection limits for pathogenic bacteria.

### EXPERIMENTAL METHODS

**1. Synthesis of hLf1-11:** The hLf1-11 peptide (Lys-(Ahx)<sub>3</sub>-GRRRRSVQWCA-NH<sub>2</sub>), a potent AMP derived from the human lactoferrin, was synthesized by solid-phase chemistry (Figure 1)

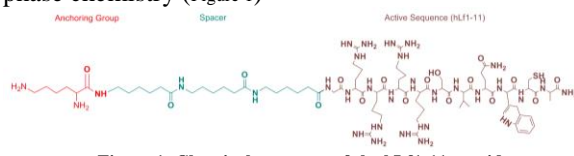


Figure 1: Chemical structure of the hLf1-11 peptide

**2. Sensor biofunctionalization.** a) *Production of the electrodes:* The planar interdigitated electrode and the three dimensional interdigitated electrode arrays (3D-IDEA) were produced by microfabrication technique [3]. b) *Silanization:* The electrodes were silanized with epoxysilane either via gas or liquid-phase and the AMP hLf1-11 in a PBS solution immobilized on the surface.

**3. Characterization of the surfaces.** a) *Chemical characterization:* The immobilization method was characterized and optimized by X-ray photoelectron spectroscopy to obtain the highest density of peptide attachment. b) *Impedance characterization:* Characterization of functionalization of the surface was also performed by impedance measurements in a 100 Hz to 1 MHz frequency range.

**4. Bacterial Adhesion Assays:** Bacterial detection assays were performed using *S.sanguinis* as model of oral bacteria. Functionalized sensors were incubated with bacterial suspensions at different concentrations in bacterial culture broth or synthetic/human saliva, and the presence of bacteria analyzed by impedance measurements, microscopy and live/dead methods.

### RESULTS AND DISCUSSION

**Chemical characterization of the surface:** The atomic composition of all surfaces was analyzed by means of XPS. The coating of planar sensors with peptide by physical adsorption and covalent immobilization resulted in significant increases in the percentages of carbon and nitrogen, and reductions in the detectable amounts of TaSi<sub>2</sub>. Gas-phase silanization with GPTES and peptide immobilization at pH=8 resulted in the highest extent of peptide attachment on the biosensors.

**Bacterial Adhesion Assays:** The presence of the hLf1-11 peptide on the electrodes surface resulted in an increase in the adhesion of *S.sanguinis* within the first 2 hours of incubation, followed by a reduction of bacterial adherence after 4 h, most likely due to the bactericidal effect of the hLf1-11 peptide. This effect was more pronounced when the peptide was covalently attached to the sensors (Figure 2). Thus, these results illustrate that impedance-based sensors coated with AMPs can effectively detect bacterial colonization on the surfaces.

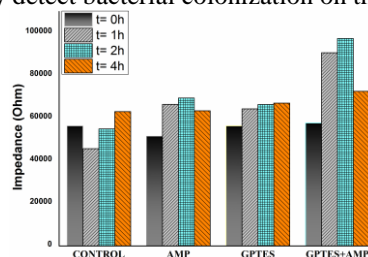


Figure 2: Bacterial Adhesion and Detection Assay

Moreover, the detection limits, stability and selectivity of the biosensors, as well as experimental data on bacteria determination in synthetic and human saliva, will be presented.

### CONCLUSION

The interaction of bacteria with the AMP on the sensor surface provoked changes in the impedance spectra, which were univocally associated with the presence of bacteria. Results of this work suggest that our approach can be effective in preventing the formation of biofilms due to an early detection of primary colonizers and their reduction by therapeutic means.

### REFERENCES

- [1] A. Lee *et al.*, *Implant Dent.*, 19(5):387–93, 2010;
- [2] M. Godoy-Gallardo *et al.*, *Acta Biomater.*, 10(8):3522–34, 2014;
- [3] A. Bratov *et al.*, *Electroanalysis*, 24(1):69–75, 2012

### ACKNOWLEDGMENTS

M. Hoyos thanks *Ministerio de Educación, Cultura y Deporte* for the research support.





# Biostable Gold-Installed Nanocomplexes as siRNA Carriers for Improved *In Vivo* Tumor Targeting

Roun Heo<sup>1</sup>, Jueun Jeon<sup>2</sup>, Jae Hyung Park<sup>1,2,\*</sup>

<sup>1</sup>Department of Health Science and Technology, SAIHST, Sungkyunkwan University, Republic of Korea

<sup>2</sup>School of Chemical Engineering, Sungkyunkwan University, Republic of Korea

[virtuousie@naver.com](mailto:virtuousie@naver.com)

## INTRODUCTION

Small interfering RNA (siRNA) has become a potent next-generation medical breakthrough, since it has excellent gene silencing effects and has no side effects<sup>1</sup>. So far, diverse carrier systems have been developed for siRNA delivery. Meanwhile, current delivery systems have been challenged in using siRNA for clinical applications<sup>2</sup>. The main issues, related with nanocarriers for siRNAs, are their poor stability and lack of tumor targetability *in vivo*. To address these needs, we developed biostable gold-installed nanocomplexes (GICs) as siRNA carriers for enhanced tumor targeting.

## EXPERIMENTAL METHODS

The GICs were prepared using the layer-by-layer method. For growth of gold nanoparticles (AuNPs) on the complexes, gold chloride solution as slowly added to the complex solution. The stability of GICs was evaluated in a 50% serum solution. The gold-deficient complexes (GDCs) and free siRNA were used as controls. The complexes were incubated with rat serum solution at 37°C. An aliquot was removed from the samples at predetermined time points. The released siRNAs were visualized by electrophoresis. Melanoma cell line (B16F10) and embryo fibroblast cell line (NIH3T3) were dispersed into a 6-well plate at  $5 \times 10^4$  cells/well and incubated for 24 h at 37 °C. siRNA was labelled with YOYO-1 dye ( $\lambda_{ex} = 491$ ,  $\lambda_{em} = 509$ ). The cells were treated with serum-free medium containing free siRNA, GICs or GDCs for 3h. After washing and fixation, the cells were visualized using a confocal LSM 700 microscope. Tumor-bearing mice were prepared by subcutaneously injecting a suspension of  $1 \times 10^6$  SCC7 cells into the left flank of mice. The Cy5.5-labeled complexes (10  $\mu$ g of siRNA/mouse) were injected into the tail vein of the mice ( $n = 3$  for each group). The time-dependent *in vivo* biodistribution of the complexes was observed with a whole-body animal imaging system. The statistical significance among the groups was analysed using one-way ANOVA. The figure, marked with an asterisk, was considered significant if  $p$ -value was less than 0.05.

## RESULTS AND DISCUSSION

In order to obtain GICs, gold was installed on the PEI/siRNA complexes by growing AuNPs through reduction of HAuCl<sub>4</sub>, followed by surface coating with PEGylated hyaluronic acid (HA). As shown in Table 1, the hydrodynamic size of PEI/siRNA, GDCs and GICs increased gradually and finally present negatively charged. This implies that the complexes were efficiently coated with PEGylated HA.

Sample	Size (nm)	$\zeta$ (mV)
PEI/siRNA complexes	$213.0 \pm 5.56$	$44.4 \pm 2.46$
GDCs	$247.6 \pm 1.63$	$-5.58 \pm 0.18$
GICs	$327.6 \pm 10.2$	$-7.58 \pm 0.81$

Table 1. Characteristics of the PEI/siRNA complexes, GDCs and GICs.

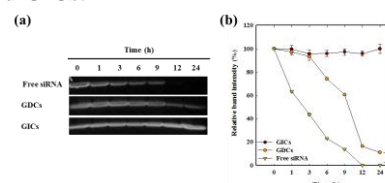


Figure 1. Stability of free siRNA, GDCs and GICs (a) Gel images (b) Relative intensity graph of bands.

The GICs showed remarkable stability compared to the GDCs or free siRNA in the presence of serum as shown in Fig 1.

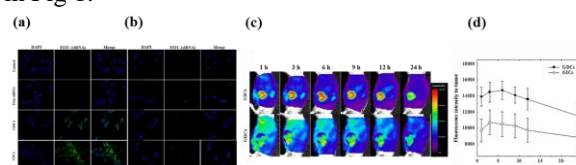


Figure 2. *In vitro* cellular uptake of complexes (a) B16F10 (b) NIH3T3 cells. The scale bar represents 20  $\mu$ m. *In vivo* (c) Whole body images of the mice. (d) Relative fluorescence intensity of tumor ROI.

For the CD44-overexpressed B16F10 cells, strong fluorescent signals were observed, whereas no detectable signals were found for the CD44-deficient NIH3T3 cells (Fig 2a and b). Finally the GICs selectively accumulated at the tumor site after systemic administration into tumor-bearing mice ( Fig 2c and d).

## CONCLUSION

GICs were prepared and investigated as siRNA carriers for efficient delivery. The results suggested that GICs had outstanding stability and high tumor targetability through receptor-mediated endocytosis. Consequently, the GICs exhibited excellent *in vivo* gene silencing efficiency.

## REFERENCES

1. Daniel H. *et al.*, Nat. Rev. Genet. 8:173-84, 2007
2. Kathryn A. *et al.*, Nat. Rev. Drug Discov. 8:129-38, 2009

## ACKNOWLEDGMENTS

The authors would like to thank the Global Ph.D. Fellowship Program (2012) for providing financial support to this project

Maria Jesus Piña, Alessandra Girotti, Mercedes Santos, Jose Carlos Rodríguez-Cabello, Francisco Javier Arias

BIOFORGE Research Group, University of Valladolid, CIBER-BBN, Spain  
[mjpina@bioforge.uva.es](mailto:mjpina@bioforge.uva.es)

## INTRODUCTION

Elastin-like recombinamers are natural elastin derived polypeptides with growing applications in the biomedicine fields<sup>1-3</sup>. The use of genetic engineering techniques allow the total control over their chemical and physical features such as surface charge, polydispersity, self-assembly and biocompatibility. The design of positively charged ELR to complex plasmatic DNA is essential to trigger the formation of structures called polyplexes. MUC1 glycoprotein is aberrantly overexpressed in breast cancer<sup>4</sup>. In this study, the functionalization of polyplexes with MUC1 aptamers is carried out and their ability to target MUC1 expressing tumor cells is tested.

## EXPERIMENTAL METHODS

Genetic engineering techniques were utilized to design the ELR whereas production and purification methods were used as described elsewhere<sup>5</sup>. The incorporation of aptamers to polyplex was assessed at different ratios N/P/Pap by size, zeta potential and TEM analysis. Biocompatibility assays were accomplished with MCF-7 (MUC1 +) and HepG2 (MUC1 -) tumor cell line and transfection assays were accomplished also with normal cells such as MSC, HUVEC and HFF-1.

## RESULTS AND DISCUSSION

The ELR was designed, produced in *E. coli* and characterized by chemical and physical methods. MUC1 aptamers were bound to the polyplexes at different ratios where the size and zeta potential was measured. The selected ratio for the polyplex-aptamer complexes had a highly positive zeta potential and an appropriate size for cell uptake.

These complexes were tested *in vitro* in terms of biocompatibility in tumoral cells (MCF-7 and HepG2) and transfection in tumoral and normal cells. The results showed a polymeric based device able to transfect in a specific manner breast cancer cells (Fig.1) and maintain a protective effect over the human normal cells.

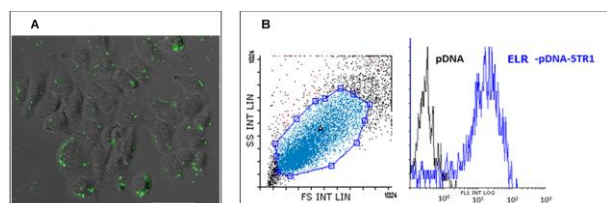


Fig.1. Cellular uptake of polyplexes-aptamer with fluorescein-labeled pDNA. (A) Fluorescence microscopy image of MCF-7 treated with polyplexes-aptamer nanoparticles labelled with FITC. Scale Bar corresponds to 50  $\mu$ m. (B) Flow cytometry analysis of treated MCF-7 cells. Black line corresponds to cells incubated with pDNA and blue with polyplexes-aptamer.

## CONCLUSION

We have developed a non-viral gene delivery device formed by ELR and MUC1 aptamers. The resulting polyplexes showed specific uptake in breast cancer cells besides of cytotoxic effect when a plasmid containing the p53 transgene was used. The ELR-aptamer device constitutes a promising strategy in the delivery of therapeutic genes of interest targeted to breast tumor cells.

## REFERENCES

1. Arias F. *et al.* Curr Top Med Chem. 14(6):819-36, 2014.
2. Garcia-Arevalo C. *et al.* Mol Pharm. 10(2):586-97, 2013.
3. de Torre I. *et al.* Acta Biomaterialia 12:146-55, 2015.
4. Duraisamy S. *et al.* Int J Oncol. 31(3):671-7, 2007.
5. Girotti A. *et al.* J Mater Sci Mater Med. 15(4):479-84, 2004.

## ACKNOWLEDGMENTS

“The authors would like to thank the financial support from the EU through European Social Fund (FSE), Operative programme of Junta of Castilla and Leon (JCyL) through Consejería de Educación, the European regional development fund (ERDF), from the MINECO (MAT2013-41723-R, MAT2013-42473-R, PRI-PIBAR-2011-1403, and MAT2012-38043), the JCyL (Projects VA155A12, VA152A12, and VA244U13), the CIBER-BBN, the JCyL, and the Instituto de Salud Carlos III under the Network Center of Regenerative Medicine and Cellular Therapy of Castilla and Leon.

<sup>1</sup>Biomaterials, Biomechanics and Tissue Engineering Group, Technical University of Catalonia, Spain<sup>2</sup>Centre for Research in Nanoengineering, Technical University of Catalonia, Spain<sup>3</sup>Biomedical Research Networking Centre in Bioengineering, Biomaterials and Nanomedicine, Spain  
[zhao.zhitong@upc.edu](mailto:zhao.zhitong@upc.edu)

## INTRODUCTION

Hydroxyapatite (HA) nanoparticles (NPs) have gained intense interest as carriers for gene delivery due to their excellent biocompatibility and good affinity to DNA molecules<sup>1</sup>. Since gene delivery is dependent on cellular uptake, assessment of the interaction of HA NPs with cells is of key concern. Although ionic substitution into HA bulk materials has shown such a vast range of improvements over pure HA in orthopaedic applications<sup>2</sup>, there is very limited data on the effect of HA NPs on cell behaviour for cellular internalization applications. Thus, the main goal of our work is to evaluate the effect of ionic substitution on cell behaviour and ensure optimal design of HA NPs for gene delivery.

## EXPERIMENTAL METHODS

**NPs preparation and characterization:** HA NPs were synthesized at 40°C mixing 100ml of 2.475g Ca(OH)<sub>2</sub> suspension with H<sub>3</sub>PO<sub>4</sub> (0.2mol/L) that was added dropwise (1mL/min) to the above suspension until the pH value was 8. The solution was left overnight for maturation. The precipitate was then washed with milliQ water and freeze dried. To prepare ion-doped HA NPs, the salt of interest (SrCl<sub>2</sub>·6H<sub>2</sub>O, ZnCl<sub>2</sub> or FeCl<sub>3</sub>·6H<sub>2</sub>O) was first mixed with Ca(OH)<sub>2</sub> or H<sub>3</sub>PO<sub>4</sub> (e.g. tetraethyl orthosilicate (TEOS)) before titration. Various salt concentrations ranging from 1-20wt% were explored. Characterization of the NPs comprised X-ray diffraction (XRD), transmission electron microscopy (TEM), Fourier infrared spectroscopy, He pycnometry, N<sub>2</sub> adsorption.

**In vitro cytotoxicity test:** Osteoblast-like MG63 cells and rat mesenchymal stem cells (rMSCs) were seeded onto 96 well plates at a cell density of  $1 \times 10^4$  cells/well and incubated at 37 °C in 5% CO<sub>2</sub> atmosphere for 24h. Afterwards, cells were exposed to NPs (100µg/mL) for 24h in cell culture medium containing or excluding 10% of foetal bovine serum (FBS). Lactate dehydrogenase (LDH) assay was performed to assess cell viability.

## RESULTS AND DISCUSSION

The XRD patterns indicated that all NPs were phase pure as only peaks corresponding to HA were detected (Fig.1). The diffraction peaks showed a gradual shift to higher or lower 2θ angles depending on the degree of substitution and the doping ion, proving their incorporation. TEM images (Fig.1) showed that doping had little influence on the morphology of NPs as in all cases they kept their needle like structure.

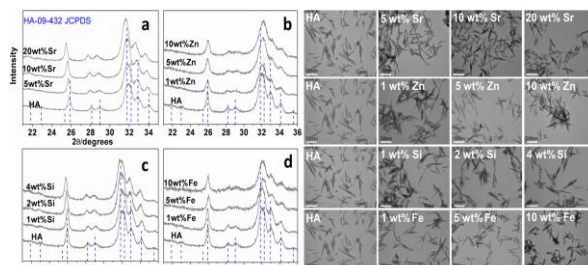


Fig.1 XRD patterns and TEM images of the different NPs.

LDH results showed that the various ion-doped HA NPs did not produce any cytotoxic effect in MG63 cells if FBS was present in the culture medium (Fig. 2). However, when FBS was excluded, Zn- and Fe-doped HA NPs induced a significant increase in MG63 cells proliferation, while Sr-doped HA caused a slight decrease in the cells viability. Interestingly, unlike for MG63 cells, there were no significant differences in rMSCs cells viability that could be attributed to the presence of the different ions (Fig. 3).

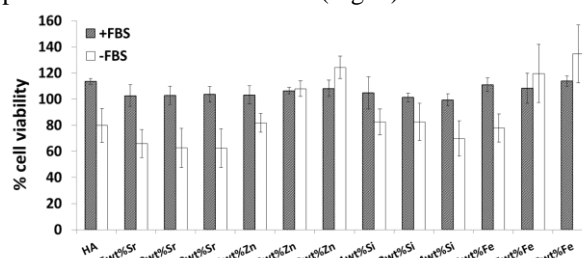


Fig. 2 Cytotoxic effects of NPs on MG63.

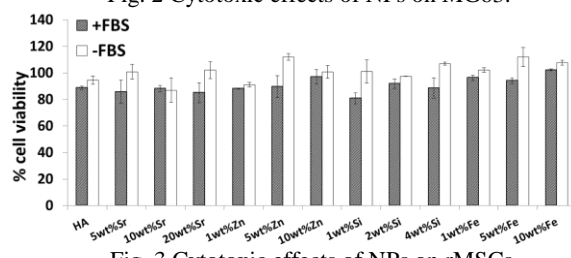


Fig. 3 Cytotoxic effects of NPs on rMSCs.

## CONCLUSIONS

Ionic substitutions in HA NPs have been shown to play a major role in cell behaviour depending on cell type. The noticeable increase in cell proliferation for Zn- and Fe-doped NPs can be foreseen to have great potential for gene delivery.

## REFERENCES

1. TN. Do. *et al.*, Ther. Deliv.3:623, 2012
2. E. Boanini. *et al.*, Acta Biomater.6:1882, 2010

## ACKNOWLEDGMENTS

This study was supported by the Spanish Government through project MAT2012-38438-003-01.



## Tuning Transfection Efficiency by Modulating the Biodegradation Rate of Trimethyl Chitosan Nanoparticles

Carla Pereira Gomes<sup>1,2,3\*</sup>, Aida Varela-Moreira<sup>1,2,4\*</sup>, Maria Gomez-Lazaro<sup>1,2</sup>, Pedro M. D. Moreno<sup>1,2</sup>, Ana Paula Pêgo<sup>1,2,3,5</sup>  
<sup>1</sup>INEB – Instituto de Engenharia Biomédica, Universidade do Porto (UPorto), Portugal; <sup>2</sup>I3S – Instituto de Investigação e Inovação em Saúde, UPorto, Portugal; <sup>3</sup>Faculdade de Engenharia, UPorto, Portugal; <sup>4</sup>Faculdade de Medicina, UPorto, Portugal; <sup>5</sup>ICBAS – Instituto de Ciências Biomédicas Abel Salazar, UPorto, Portugal  
[carla.gomes@ineb.up.pt](mailto:carla.gomes@ineb.up.pt); \*Equal contribution

### INTRODUCTION

Trimethyl chitosan (TMC) has been described as a promising gene delivery vector for biomedical applications<sup>1</sup>. In the design of non-viral vectors for gene therapy, biomaterial degradation and the fate of the resulting by-products are important features that must be taken into consideration. TMC enzymatic biodegradation occurs between acetylated monomers and is mostly affected by the degree of acetylation (DA)<sup>2</sup>. In this work, we investigated the impact of the DA on the enzymatic degradation and biological performance of TMC-based nanoparticles, exploring top-notch bioimaging techniques as imaging flow cytometry.

### EXPERIMENTAL METHODS

TMC with 43.3 kDa, 11% DA and 30% degree of quaternization (TMC<sub>11</sub>) was used as starting material. TMC<sub>11</sub> was deacetylated and subsequently re-acetylated to achieve polymers with different DAs<sup>3</sup>. TMC:pDNA nanoparticles with different N/P ratios (moles of quaternized amines:moles of phosphate groups) were prepared in 20 mM HEPES buffer with 5% (w/v) glucose at pH 7.4. To evaluate TMC nanoparticle enzymatic degradation, an enzymatic competition assay was performed, where chitosan with the same molecular weight was used as control<sup>3</sup>. Nanoparticles internalization profile, as well as nanoparticle-loaded vesicles (NLVs) and pDNA nuclear localization were evaluated by imaging flow cytometry between 0.5 to 24 h of incubation with ND7/23 cells (neuronal cell line). Data has been confirmed by TEM (transmission electron microscopy) analysis (TMC being labeled with quantum dots and DNA with gold nanoparticles). Finally, the impact of nanoparticles biodegradation rate on transfection efficiency was assessed 72 h post-transfection, using eGFP as reporter gene.

### RESULTS AND DISCUSSION

TMC<sub>11</sub> was successfully deacetylated (DA 2%, TMC<sub>2</sub>) and subsequently re-acetylated (DA 17%, TMC<sub>17</sub>), with no significant alteration to the polymer molecular weight (confirmed by GPC). TMC:pDNA complexes were efficiently prepared (>95% of complexation efficiency), with an average diameter of 200 nm at physiological conditions, irrespectively of the N/P ratio and polymer DA. No major differences were observed between the different TMC nanoparticles in terms of internalization profile, neither in the number of particles bounded to the cell membrane or cytoplasm localized

nanoparticles. However, when considering the number of NLVs per cell or the percentage of pDNA nuclear localization one observed significant differences between TMC's. TMC<sub>11</sub> nanoparticles are present in a higher amount of vesicles in the initial time-points and then the number NLVs decreases significantly, suggesting that these nanoparticles are being released to the cytoplasm (confirmed by TEM). Regarding nuclear pDNA localization, a significant difference was seen between TMC's, with TMC<sub>11</sub> and TMC<sub>17</sub> mediating the delivery of a higher quantity of pDNA to the cell nucleus. In terms of transfection efficiency, TMC<sub>11</sub>-based nanoparticles promoted the higher transfection efficiency (>20% of transfected cells). These results suggest that the biodegradation rate of these nanoparticles affects their intracellular trafficking and pDNA protection capacity and, consequently, their efficiency to transfect cells. Taking this into account, we are currently characterizing the nanoparticle intracellular track conducting confocal microscopy studies in which we labeled both nanoparticles (polymer and pDNA) and vesicles from the endocytic pathway (endosomes/lysosomes) to further dissect the mechanisms ruling nanoparticle mediated pDNA delivery.

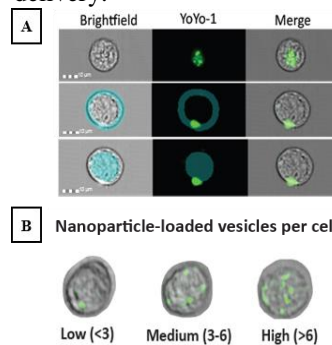


Figure 1. Representative images from imaging flow cytometry - ImageStream<sup>X</sup>. (A) pDNA from nanoparticles was labeled with YoYo-1. In blue are represented masks defined by the user that identify the cell membrane and cell cytoplasm; (B) Quantification of Nanoparticle-loaded vesicles per cell.

### CONCLUSION

TMC nanoparticle biodegradation is influenced by the polymers DA. The 24 h bioimaging study of the nanoparticles intracellular route disclosed important data about the process of intracellular trafficking indicating that biodegradation, hence associated DNA availability, is a key feature for the overall transfection process.

### REFERENCES

1. MRS Bulletin 39 (01): 60-70, 2014; 2. Biomaterials 30 (18): 3129-35, 2009; 3. Nanomedicine 6: 1499-512, 2011.

### ACKNOWLEDGMENTS

FCT grants (SFRH/BD/79930/2011, PTDC/CTM-NAN/115124/2009) and Marie Curie Action (PIEF-GA-2011-300485).



# Cell-Penetrating Peptide Mediated Gene Delivery via Polymeric Microneedles; A Platform for DNA Vaccination

Helen O. McCarthy<sup>1</sup>, Ahlam A. Ali<sup>1</sup>, Joanne McCaffrey<sup>1</sup>, John W. McBride<sup>1</sup>, Adrien Kissenpfennig<sup>2</sup>, Ryan F. Donnelly<sup>1</sup>

<sup>1</sup>School of Pharmacy, Queen's University Belfast, Northern Ireland

<sup>2</sup>Centre for Infection and Immunity, Queen's University Belfast, Northern Ireland

[h.mccarthy@qub.ac.uk](mailto:h.mccarthy@qub.ac.uk)

## INTRODUCTION

Cervical cancer has the second highest mortality rate amongst women worldwide, despite the production of recombinant protein HPV vaccines. Limited access in poorer regions, the prophylactic nature of current vaccines and poor patient compliance contribute to a rising incidence. Furthermore, the current vaccine is not effective for those patients with pre-existing HPV lesions. There is a critical need for a more potent vaccine that can be self-administered. DNA vaccination evokes both therapeutic and prophylactic responses.<sup>1</sup> The bottleneck in the DNA vaccination market lies in an effective delivery technology. The 'solution' to this problem is in the two-pronged approach of our technology; i) a peptide delivery system, termed RALA, that is able to wrap the DNA into nanoparticles, protect the DNA from degradation, enter cells, disrupt endosomes and deliver the DNA to the nucleus ii) a microneedle patch (MN) that will house the nanoparticles within the polymer matrix, painlessly breach the skin's stratum corneum barrier and dissolve upon contact with skin interstitial fluid thus releasing the nanoparticles into the skin to the antigen presenting cells. Using our novel technology platform we have created a DNA vaccine for cervical cancer in a dissolvable microneedle patch. More specifically the MN patch is loaded with RALA/E6-E7 nanoparticles and this study demonstrates stability, functionality and a prophylactic and therapeutic response to cervical cancer tumours *in vivo*.

## EXPERIMENTAL METHODS

The RALA/E6/E7 nanoparticles were characterized in terms of gel retardation, size and zeta-potential analysis and transmission electron microscopic imaging. The functionality of the RALA/E6-E7 nanoparticles within the polymeric microneedle matrix was assessed by analysis of transfection efficacy in fibroblast NCTC cells via western blot analysis. Cellular toxicity was also assessed via WST-1 assay. Balb-C mice were immunized with the RALA-E6/E7 in a prime-boost-boost regimen and blood serum was isolated to measure specific IgG responses and IFN- $\gamma$  levels via ELISAs. Balb-C mice were also immunised with the MN-RALA/E6-E7 patches and challenged with cervical cancer. A therapeutic response study was performed *in vivo*. Finally the RALA/E6-E7 nanoparticles were lyophilised to increase the dose that can be loaded into the MN patch. This was also evaluated *in vivo*.

## RESULTS AND DISCUSSION

The RALA/E6-E7 nanoparticles had a positive zeta-potential, particle diameter <50 nm and TEM

confirmed their spherical shape. These are all optimal characteristics for successful cellular transfection. These DNA-containing nanoparticles were combined with a rapidly dissolving poly(vinylpyrrolidone) polymeric microneedle delivery platform. Results proved that RALA was essential for stability of the E6-E7 DNA in PVP (Fig.1) and that MN-RALA/E6-E7 evokes a more consistent humoral mediated immune response (Fig. 2). Tumour challenge studies indicate the MN-RALA/E6-E7 vaccine patch is preventing the uptake of tumours and treating established tumours. Lyophilisation studies are ongoing and the dose that can be delivered from one patch is currently at 50  $\mu$ g.

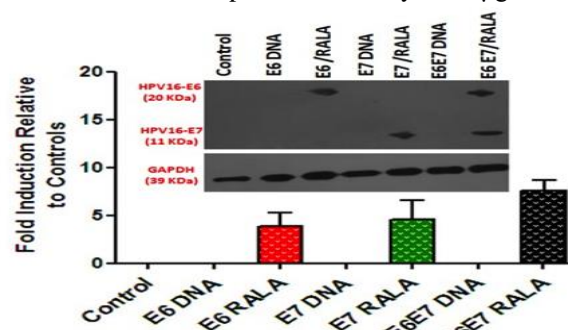


**Fig. 1.** Functionality of the RALA/E6-E7 following release from 20% PVP MNs. MNs were dissolved and added to NCTC cells. 24 h later protein was analysed.

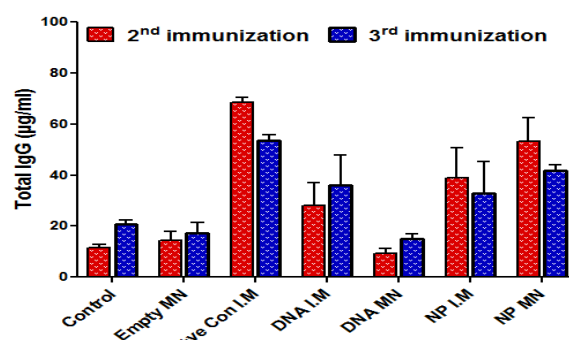


**Fig. 2.** Detection of E6/E7 specific IgG levels following booster immunisations in Balb-C mice. (Naked E6/E7, NPs delivered IM or via MN patches)

## CONCLUSION

We have created a fully functional prototype MN/RALA/E6-E7 DNA vaccine for cervical cancer.

## REFERENCES

1. Aly HA. J Immunol Methods. 382:1-23, 2012.
2. McCarthy HO *et al.* J Control Release. 189:141-9 2014.
3. Donnelly RF *et al.* J Pharm Pharmacol. DOI: 10.1111, 2014.

## ACKNOWLEDGMENTS

This project was funded by Invest Northern Ireland Proof of Concept Award (PoC330).





Adeline Gand<sup>1</sup>, Coline Chat<sup>1</sup>, Mathilde Hindie<sup>1</sup>, Paul Van Tassel<sup>2</sup>, Emmanuel Pauthe<sup>1</sup><sup>1</sup>Biomaterial for Health Group, ERRMECe, Department of Biology, University of Cergy-Pontoise, France<sup>2</sup>Department of Chemical and Environmental Engineering, Yale University, New Haven, USA[emmanuel.pauthe@u-cergy.fr](mailto:emmanuel.pauthe@u-cergy.fr)

## INTRODUCTION

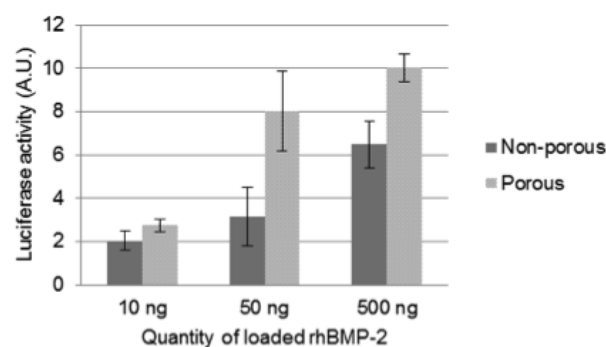
Biomaterials capable of both enhancing cell adhesion and delivering controlled quantities of bioactive agents, while maintaining mechanical integrity, represent a significant challenge, but also an excellent opportunity toward a variety of cell contacting applications. We propose two new thin film biomaterials, one that contains a reservoir for biomolecules, such as growth factors, for an efficient local and controlled release of biomolecules, and one that is formed from biomolecules from the extracellular matrix, such as fibronectin, in order to mimic the extracellular environment and promote cell behavior.

## EXPERIMENTAL METHODS

Thin films are formed by the layer-by-layer assembly of poly(L-lysine) and poly(L-glutamic acid) or Fibronectin. Carboxy-functionalized latex nanoparticles (25 nm) are incorporated as template. Films are cross-linked (EDC/NHS) to increase mechanical rigidity. Tetrahydrofuran (THF) is used to dissolve nanoparticles and create porous films to enable loading of bioactive species, as BMP2.

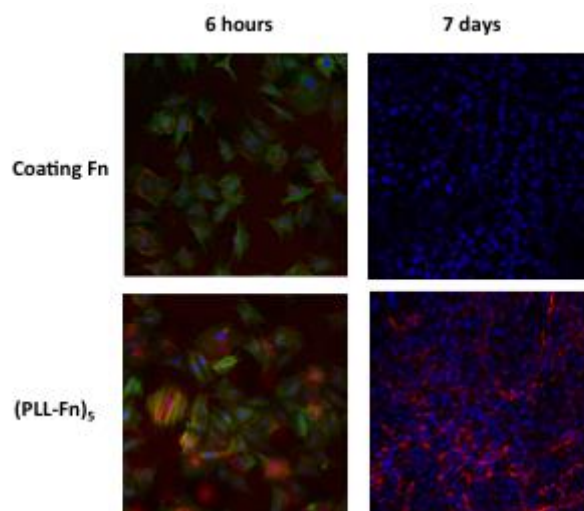
## RESULTS AND DISCUSSION

We describe here two strategies to control cell behavior. First, a nanotemplating strategy toward porous, polyelectrolyte-based thin films capable of controlled biomolecular loading and release is presented. Films are formed via the layer-by-layer assembly of charged polymers and nanoparticles, chemically cross-linked to increase mechanical rigidity and stability, and finally exposed to tetrahydrofuran to dissolve the NP and create an intra-film porous network<sup>1</sup>. We report here on the loading and release of the growth factor bone morphogenetic protein 2 (BMP-2), and the influence of BMP-2 loaded films on contacting murine C2C12 myoblasts.



We observe nanotemplating to enable stable BMP-2 loading throughout the thickness of the film, and find the nanotemplated film to exhibit comparable cell adhesion, and enhanced cell differentiation, compared to a non-porous cross-linked film (where BMP-2 loading is mainly confined to the film surface)<sup>2</sup>.

The second strategy involves the direct incorporation of the extracellular matrix protein Fibronectin (Fn) during film construction, in order to mimic the extracellular environment and influence the cell behavior. Fn serves as the anionic polymer during layer-by-layer assembly. We investigate the influence of Fn on film construction and physicochemical and mechanical properties, and the influence of Fn containing films on pre-osteoblastic cells. We observe Fn-based thin films to enhance cell adhesion, spreading and proliferation compared to a Fn monolayer, and Fn present in the films to be structurally reorganized by contacting cells.



## CONCLUSION

We engineer, design and construct bioactive thin films biomaterials able to direct the behavior of contacting cells. Nanotemplated polyelectrolyte films can be employed to spatially and temporally release bioactive molecules, such as as BMP2. Fn incorporation within layer-by-layer films leads to Fn-rich films, which enhance cell adhesion, spreading and proliferation compared to a standard 2D Fn layer.

## REFERENCES

1. Wu *et al.*, Adv. Funct. Mat. 23, 66-74, 2013.
2. Gand *et al.*, Biomatter, 4, 8231-8239, 2014.

# Mapping Interactions between MMP1 and Collagen Substrate: from Crystal Structure to Molecular Dynamics with Meta-Dynamics

Anthony Nash<sup>1</sup>, Laurent Bozec<sup>2</sup>, Helen Birch<sup>3</sup>, Nora de Leeuw<sup>1,4</sup>

<sup>1</sup>Department of Chemistry, University College London, UK

<sup>2</sup>Eastman Dental Institute, University College London, UK

<sup>3</sup>Institute of Orthopaedics & Musculoskeletal Science, University College London, UK

<sup>4</sup>School of Chemistry, University of Cardiff, UK

[a.nash@ucl.ac.uk](mailto:a.nash@ucl.ac.uk)

## INTRODUCTION

Matrix Metalloproteinases (MMPs) are a family of zinc-dependent endoproteinases found within the extracellular matrix of vertebrates<sup>1-3</sup>. Besides their physiological role in degrading major structural tissues, they have been linked to pathological processes such as arthritis<sup>4</sup> and skin ulceration<sup>5</sup>. Although the specific catalytic bond scissile mechanism is understood, crystallographic data suggest that the active site is too narrow to encompass a collagen protein. Either MMP adjusts to encompass the width of the collagen protein<sup>6</sup> or the collagen protein uncoils locally near the active site to facilitate insertion and cleavage<sup>7</sup>. We present a Molecular Dynamics (MD) study on the structural properties of a full MMP1-collagen crystallographic structure (4AUO)<sup>8</sup>, whilst exploring the thermodynamic properties of *opening* the active site entrance with and in the absence of collagen. Finally, we map the Free Energy Surface (FES) of the collagen along a set of collective variables (CV) used to facilitate uncoiling and insertion of collagen into the active site.

## EXPERIMENTAL METHODS

The crystallographic geometry was parameterised using the Amberff99SB force field and implemented into Gromacs. The collagen-MMP1 complex was fully solvated and maintained a neutral charge. Partial charges on the two zinc atoms and coordinating side chains were derived from electron structural calculations using PyRED. The collagen-MMP1 complex was equilibrated following a steepest descent energy minimisation by progressively reducing protein backbone restraints over 10 ns. Restraints were removed and the system was allowed to evolve for 50 ns. Meta-dynamics were performed using PLUMED. Gaussian potentials were added over a set of collective variables every 500 MD steps.

## RESULTS AND DISCUSSION

Our MD trajectory demonstrates a stable MMP1 secondary structure with little in the way of deviation from the initial crystal structure. We observed two distinct polar ridges on the MMP1 active site, which are seen to interact with the collagen backbone and thought to keep the substrate bound. Distance based CVs were used to encourage sampling of an *open* active site conformation. After 30 ns, a converged lone deep energy-well in the FES (Figure 1.) of unbound MMP1 suggests a preferable *neutral* active site conformation. Furthermore, when collagen was introduced, an

independent calculation yielded a similar singular FES energy-well also suggesting a preferable *neutral* conformation. Upon observation, as the cavity widens in sync with the increase in free energy, potential hydrogen-bonds separate resulting in a clear disruption to collagen binding. Finally, coercion of collagen local to the active site to uncoil and insert into the cavity along CVs is considered to be energetically favourable.

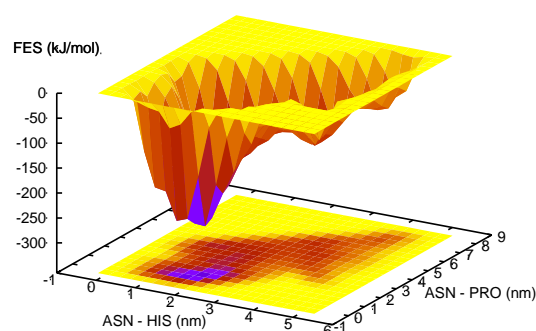


Figure 1. FES of unbound MMP1 along two distance CVs defined at the entrance of the active site.

## CONCLUSION

Our work is the first to map potential hydrogen-bond interactions between collagen and MMP1 from an MD trajectory of the crystal structure. We observed persistent interactions between enzyme and substrate and a single conformation for the active site. The insertion of a lone collagen peptide into a *neutral* active site may further the argument for a localised uncoiling mechanism.

## REFERENCES

1. Overall M, *et al.*, Nat Rev Cancer. 2:657-672, 2002.
2. Vihinen P, *et al.*, Int J Cancer. 99:157-166, 2002.
3. Chaudhary A, *et al.*, J Biomed Sci. 17:1-13, 2010.
4. Mitchell P, *et al.*, J Clin Invest. 97:761-768, 1996.
5. Sekhon S, Res Reports Biol. 1:1-20, 2010.
6. Bode W, Structure. 3:527-530, 1995.
7. Chung L, *et al.*, EMBO J. 23:3020-3030, 2004.
8. Manka W, *et al.*, CA Cancer J Clin. 54:9-29, 2004.

## ACKNOWLEDGMENTS

The authors would like to thank BBSRC (Grant no: BB/K007785) for funding and the Research Computing Platform, UCL, for the use of Legion.



## INTRODUCTION

The success of a surgical implant is dependent on an appropriate biological response to the implant surface<sup>1</sup>. Wound healing around implants is a complex process in which water molecules from the surrounding blood first come in contact with the surface. In the next step, ions and blood proteins adsorb and a fibrin network is formed, before osteoblastic cells respond to the protein-covered surface<sup>2</sup>.

Blood protein adsorption and blood coagulation are greatly influenced by the topography of titanium surfaces<sup>3,4</sup>, which may further impact the eventual adhesion, migration and differentiation of primary human osteogenic cells on a titanium implant. It is therefore of major importance for implantology to understand the early interaction between blood and the implant and how this further steers osseointegration.

Roughness gradients are a very promising tool to investigate the effect of surface topography on a biological system, as a wide range of parameters can be explored in a single experiment. Additionally, homogenous conditions are ensured during all measurements<sup>5,6</sup>.

## EXPERIMENTAL METHODS

To study the effect of nano-roughness on protein adsorption and blood coagulation, nanoparticle density gradients were fabricated. The gradients were exposed to protein mixtures or single protein solutions. The adsorption of specific proteins in the solution was studied by fluorescent labelling of individual proteins (albumin, fibrinogen or fibronectin). To achieve an easy and rapid data read-out, a fluorescence micro-array scanner was used to map all adsorbed proteins.

In the second step, the same gradients were used to study blood coagulation by incubation of the gradients for 2 to 10 min with partially heparinized (0.5 IU/ml) whole human blood from healthy volunteers. The formation of the blood clot was investigated by scanning electron microscopy and fluorescence microscopy.

## RESULTS AND DISCUSSION

Gradients with particles of different sized diameters (12, 39 and 72 nm) were tested. The protein-adsorption experiments showed no significant influence of nano-features on protein adsorption for gradients with 39 and 72 nm nanoparticles. On the contrary for 12 nm gradients, fibrinogen in competition with albumin and fibronectin or serum, showed a higher adsorption in the high-particle-density region of the gradient (see Figure 1).

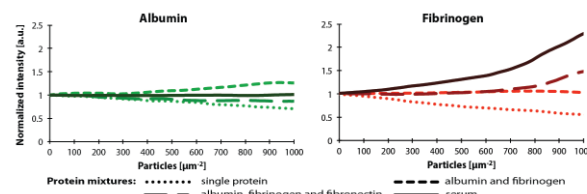


Fig. 1: Albumin and fibrinogen adsorption on 12 nm gradient.

In Figure 2 SEM images taken every 2 mm along a 12 (a) and 39 (b) nm nanoparticle density gradient following a 5 min blood-incubation experiment are presented. It is clearly visible that the appearance of the blood-surface interaction changes along the particle-density gradient. For the 39 nm gradient, coagulation/fibrin formation was observed everywhere on the sample, a denser fibrin network could be detected towards the high-density end of the gradient. For the 12 nm gradient, a similar trend but in an earlier stage of fibrin network formation is visible. High-density nanostructures seem to have an accelerating effect on the fibrin-network forming process.

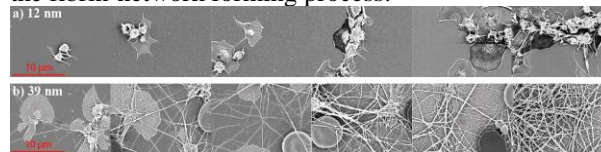


Fig. 2: SEM images taken every mm along nanoparticle density gradient. a) 12 nm gradient and b) 39 nm gradient after incubation for 5 min in whole human blood.

## CONCLUSION

Nanostructures were shown to enhance blood coagulation, but appear to have only little influence on protein adsorption from solutions. This study suggests that implant surfaces with a high-density nanostructure show improved blood clot formation and should therefore enhance osseointegration.

## REFERENCES

1. C.J. Wilson *et al.*, Tissue engineering 11, Nr. 1/2 (2005): 1-18
2. B. Kasemo, Surface Science 500 (2002): 656-677
3. M.S. Lord *et al.*, Nano Today 5, Nr.1 (2010): 66-78
4. Hong J *et al.*, Biomaterials 20 (1999): 603-11.
5. S. Morgenthaler *et al.*, Soft Matter 4 (2008): 419-434.
6. C. Zink *et al.*, Biomaterials 33 (2012): 8055-8061

## ACKNOWLEDGMENTS

We would like to thank the ScopeM of ETH Zurich for their skillful SEM support. The Swiss National Science Foundation (SNF, Grant no: CR31I3\_146468) is gratefully acknowledged for funding.



## INTRODUCTION

The extracellular matrix (ECM), which provides physical and (bio)chemical cues for the regulation of cell behavior, presents a complex structure on the micro- and nanoscales. The creation of environments mimicking the ECM is a challenge of importance in biomaterials science and tissue engineering. Type I collagen, a self-assembling protein, is one of the main components of ECM, and provides adhesion signals to cells. The supramolecular organization of collagen at interfaces is known to depend of the physico-chemical properties of the substrate, including its wettability<sup>1</sup>. The aim of the present work is to create a variety of biointerfaces with different supramolecular organizations of type I collagen, obtained by collagen adsorption on chemically heterogeneous substrates. Then, the behavior of preosteoblasts cultured on the designed biointerfaces is investigated.

## EXPERIMENTAL METHODS

**Preparation of organized collagen layers:** Polymer demixing upon spin-coating was used to create surfaces containing hydrophobic inclusions in a more hydrophilic matrix or conversely, to further create heterogeneity in the supramolecular organization of adsorbed collagen. The immiscible polymers used for demixing were polystyrene (PS) and poly(methyl methacrylate) (PMMA). Several polymer concentration ratios and solvents were tested to obtain a range of substrates showing different nanoheterogeneities. Collagen adsorption was then performed on homogeneous and heterogeneous substrates by immersion for 2 h in 30 µg/ml collagen solution in phosphate buffer. The topography of the surfaces obtained before and after collagen adsorption was assessed by atomic force microscopy (AFM), while their surface chemical composition was determined using X-ray photoelectron spectroscopy.

**Cell culture:** A murine osteoprogenitor cell line, MC3T3-E1, was cultured on the created protein layers. Cell morphology and density were investigated after 4h and 6 days in serum-containing medium, using fluorescence microscopy (actin, nucleus and vinculin labeling).

## RESULTS AND DISCUSSION

After spin-coating of several PS/PMMA blends, four interesting substrates were identified: substrates with PMMA inclusions in a PS matrix, and conversely, substrates with PS inclusions in a PMMA matrix, the inclusions being either under the form of pits or islands. The obtained surface morphologies could be linked to the respective solubility of the polymers in the solvents used.

The organisation of collagen layers was different

depending on the nature of the polymer substrate (Figure 1): the layer was quite smooth on pure PMMA, while large assemblies were found on pure PS. Collagen adsorption on heterogeneous substrates led to surfaces presenting a heterogeneous distribution of collagen. The more the substrate contained PS, the more the collagen layer contained fibrils. Moreover, when PS domains size was lower than ~600 nm, assemblies larger than the ones observed on pure PS were formed<sup>2</sup>.

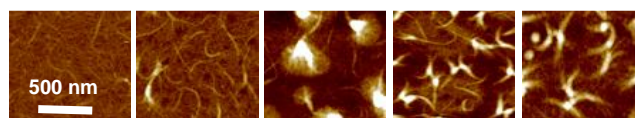


Figure 1. AFM images showing collagen organization on PS/PMMA blends, in function of PS surface fraction (from left to right: 0, 15, 21, 64 and 100 % PS)

MC3T3-E1 cells adhered on all collagen-coated surfaces. Cell density remarkably increased on heterogeneous surfaces compared to homogeneous ones, especially when very large collagen fibrils were present. Besides, the observed cell morphologies were also different depending on the biointerface architecture. Quite small and round cells were found on the smooth collagen layer formed on PMMA, while cells were bigger and more elongated on the collagen fibrils found on PS. Intermediate cell morphologies were observed on the heterogeneous PS/PMMA surfaces after collagen adsorption.

After 6 days, remodeling of the collagen layer probably occurs, and while a strong effect of substrate heterogeneity is still observed, the same effect is also found on the naked substrates, in absence of collagen.

## CONCLUSION

The present work demonstrates that chemical and topographical nanoheterogeneities, obtained by polymer demixing, interfere with collagen adsorption. The protein layer organization (smooth layers vs supramolecular assemblies; size of assemblies) is indeed altered by the presence of domains of different chemical nature (PMMA vs PS) at the surface of the substrate used for adsorption. Culture of preosteoblasts highlights major differences between cell behaviors observed on the different biointerfaces obtained by collagen adsorption on pure PMMA, PS/PMMA heterogeneous surfaces, and pure PS. A better control of cell-material interaction may thus be obtained through tailoring of ECM protein layers.

## REFERENCES

1. Dupont-Gillain C. Colloids Surf B 124:87-96, 2014.
2. Zuyderhoff E. *et al*; Langmuir 28:2007-2014, 2012.

## Nanoroughness and Oxygen Functional Groups on Parylene C Coating: Towards Anti-infective and Biocompatible Implants Surface

Monika Gołda-Cępa<sup>1</sup>, M. Brzywczy-Włoch<sup>2</sup>, M. Hakkarainen<sup>3</sup>, K. Engvall<sup>4</sup>, A. Kotarba<sup>1</sup>

<sup>1</sup>Faculty of Chemistry, Jagiellonian University, Krakow, Poland,

<sup>2</sup>Department of Microbiology, Medical College, Jagiellonian University, Krakow, Poland

<sup>3</sup>Department of Fibre and Polymer Technology, KTH Royal Institute of Technology, Stockholm, Sweden

<sup>4</sup>Department of Chemical Engineering and Technology, KTH Royal Institute of Technology, Stockholm, Sweden.

[golda@chemia.uj.edu.pl](mailto:golda@chemia.uj.edu.pl)

**The oxygen plasma functionalization of parylene C implant coating leads to nanoroughness generation and insertion of oxygen groups. It is a tool for tuning the physicochemical properties, biocompatibility and provides the possibility of further biofunctionalization. The oxygen plasma treatment significantly influenced the chemistry and physical properties of the polymer becoming an effective tool in surface preparation for the better osteoblast-like cells adhesion. At the same time it did not stimulate bacterial growth.**

### INTRODUCTION

Parylene C is an excellent protective coating material for metal implants due to its *in vivo* compatibility, mechanical properties and stability in body fluids<sup>1</sup>. However, for better adhesion of the osteoblast-like cells, parylene C surface must be modified via insertion of functional groups<sup>2</sup>. Low pressure oxidative/reductive plasmas are considered as a universal tool for such surface treatment<sup>3</sup>. Moreover, by precise adjustment of the plasma parameters (power, exposition time, oxygen partial pressure), the surface can be modified in a controlled way<sup>2</sup>. The aim of this study was to investigate the influence of oxygen plasma treatment on the surface functional properties of parylene C coating. The general strategy of preparation of the multilayer therapeutic coating based on functionalized parylene C is presented in Fig.1. The polymer coating was thoroughly characterized in terms of structure and nanoscale morphology (XRD, AFM, E-SEM), surface composition (XPS, LDI-MS, contact angle, TG/DTA) and biofunction such as biocompatibility (MG-63 cells) and microbiological tests (*S. aureus*, *S. epidermidis*, *P. aeruginosa*).

### EXPERIMENTAL METHODS

Parylene C films were prepared by CVD technique (ParaTech Coating Scandinavia AB). In order to modify the parylene C surface, the oxygen plasma treatment was carried out using a Diener electronic Femto plasma system. The morphology of the samples was investigated using E-SEM (Quanta 3D FEG) and AFM (Park Scientific Instrument Autoprobe CP II). The changes in chemical composition were observed using XPS (XPS-UHVS with SES R4000, Al K $\alpha$ ) and LDI-MS (Bruker UltraFlex TOF with SCOUT-MTP).

### RESULTS AND DISCUSSION

The strong effect of oxygen plasma treatment on parylene C topography and chemical composition was observed. The unmodified parylene C is smooth, but after the plasma exposure it becomes

corrugated with large irregularities of the order 40-60 nm in depth and 200-300 nm in width as revealed by AFM and E-SEM. The XPS and LDI-MS results clearly indicate the insertion of oxygen into the parylene C surface after the plasma treatment. The identified oxygen-containing groups were -COOH, -COH, -OH. The observed changes have significant impact on the wettability and surface free energy of parylene C. The water contact angle ( $\theta_w$ ) of the unmodified parylene C is  $\sim 90 \pm 2^\circ$ , immediately after plasma modification the  $\theta_w = 0^\circ$  and after 24h it slowly grows up to  $\theta_w = 50^\circ \pm 5^\circ$ , never reaching the value of the untreated, hydrophobic samples. In order to evaluate the biological response of the obtained surface, MG-63 cells and microbiological tests were carried out. There was a significant increase in the number of adhered cells and their surface area on the oxygen plasma modified parylene C. It was found, that the most suitable for cells adhesion is the surface exposed to oxygen plasma with the optimized parameters ( $p = 0.2$  mbar,  $P = 50$  W and  $t = 10$  min). The microbiological results did not indicate any significant changes in the bacteria attachment between the unmodified and the oxygen plasma treated parylene C.

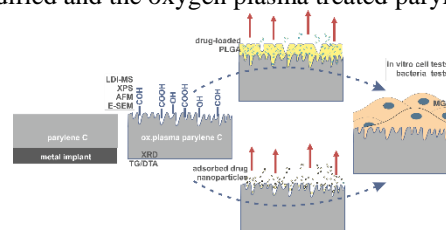


Fig. 1 The general strategy pathways of the preparation with dedicated experimental methods of the multilayer therapeutic coating based on functionalized parylene C

### CONCLUSION

Oxygen plasma treatment is an efficient technique for the surface functionalization of parylene C protective films. The oxygen insertion into the polymer surface provides a suitable platform for the osteoblast-like cells and further functionalization such as bonding of drug-loaded nanoparticles or biodegradable polymer

### REFERENCES

1. Cieřlik M., *et al.*, Mater Sci Eng C, 32:2431-2435, 2012.
2. Gołda-Cępa M., *et al.*, RSC Adv, 4: 26240-26243, 2014.
3. Gołda M., *et al.*, Mater Sci Eng C, 33:4221-4227, 2013

### ACKNOWLEDGMENTS

The authors would like to thank the Polish National Science Centre decision number DEC-2012/05/N/ST8/ for providing financial support to this project.





Antonio Paciello<sup>2</sup>, Giuseppe Amalfitano<sup>2</sup>, Alessandro Garziano<sup>1,2</sup>, Francesco Urciuolo<sup>2</sup>, Paolo Antonio Netti<sup>1,2</sup><sup>1</sup>University of Naples Federico II, Naples, Italy<sup>2</sup>Istituto Italiano di Tecnologia (iit), Naples, Italy[francesco.urciuolo@iit.it](mailto:francesco.urciuolo@iit.it)

## INTRODUCTION

The main challenge for tissue engineering is to produce 3D tissue equivalent of macroscopic dimension. The greater problem related to it, is due to oxygen supply within three-dimensional cell culture system in order to obtain no necrotic zone inside the final tissue equivalent. In an effort to enhance oxygen delivery, we report the feasibility of using a new oxygen depot capable to release oxygen under hypoxic conditions by conjugating of human haemoglobin (Hb) to gelatine microspheres.

## EXPERIMENTAL METHODS

Biodegradable gelatine micro-beads (GM) were obtained by an emulsion process [REF]. To realize the Hb-based oxygen micro carriers (HbOC), the Hb were conjugated to GM by means of two-step reaction: (i) firstly a polyurethane spacer was added to GM surface and then (ii) Hb was linked to the spacer. GM functionalization has been studied by means of FTIR and HPLC and UV-vis analysis. In order to study the oxygen storage/release capability of the HbOC in *in vitro* 3D tissue culture, HbOC were loaded in rat tail collagen / NIH system and cultured statically for up to 72 h. Three experimental configurations has been explored: (a) collagen / NIH; (b) collagen / NIH / GMs; (b) collagen / NIH / HbOC. Cells viability profile and cell proliferation rate were evaluated by immunofluorescence and used as index of HbOC functionality in the 3D cell culture.

## RESULTS AND DISCUSSION

Prior to be used in 3D cell culture we demonstrated the capability of HbOC to work as a system able to catch oxygen from the surrounding saturated environment. HbOC was then able to release the captured oxygen when kept under hypoxic environment until equilibrium condition. Static 3D cell culture was used as model to assess the capability of the HbOC to work in hypoxic biological environments. The cell viability profile within the systems Collagene/NIH, Collagene/NIH/GMs and Collagene/NIH/HBOCs, was evaluated. In Fig. 1 are reported the reconstructed sections (0.4mm x 2mm) of the Collagen/NIH system at 0h and 72 h (A-B), and Collagen/NIH/HBOC (C-D). At 0h it was observed a uniform cell distribution and low amount of died cells, compared with the number of living cells. The fraction of living cell ( $\phi$ ), as a function of the thickness (Fig. 2), was used to compare the cell viability profiles at each culture time (0, 24, 48, 72h). At time 0, no variation of  $\phi$  was observed along the sample thickness (100% viability) and no differences were found between the three experimental configurations. For the other time points, in both

systems Collagen/NIH and Collagen/NIH/GM, no difference are detected, while for the Collagen/NIH/HBOC system, the cell viability fraction was found to be statistically higher than in the control systems (Collagen/NIH and Collagen/NIH/GM). The decrease in the cell viability in the system Collagen/NIH/HBOC was due to the total cell proliferation. Indeed, in the Collagen/NIH and Collagen/NIH/GM system, cell density reached a plateau value. In contrast, in the Collagen/NIH/HBOC system the cell density continued to increase up to 72h. Such increase in the total cell number led to an increase in the metabolic request and the cell viability decreased due to insufficient oxygen supply.

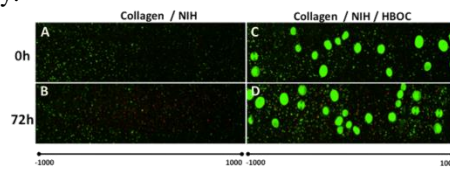


FIG.1 3D cell culture in collagen gel: Coll + NIH3T3 (left); Coll + NIH3T3 + HBOC (right)

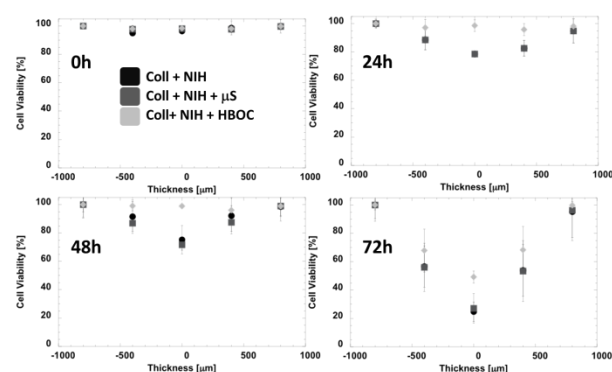


FIG.2 Cell viability profile within 3D cell culture at different culture time

## CONCLUSION

In this work we demonstrated the capability to develop an hemoglobin-based oxygen carrier able to overcome the oxygen transport limitations in 3D static culture up to 72h. Such oxygen releasing microcarriers can be either loaded inside hydrogel scaffolds or can be sintered to build up a oxygen releasing porous scaffold.

## REFERENCES

- [1] Cittadini A, Monti MG, Petrillo V, Esposito G, Imparato G, Luciani A, et al. European Journal of Heart Failure 2011;13:1264-74.
- [2] Guaccio A, Borselli C, Oliviero O, Netti PA. Biomaterials 2008;29:1484-93.
- [3] Magazu S, Calabro E, Campo S. The journal of physical chemistry B 2010;114:121

Maziar Matloubi<sup>1</sup> and V. Prasad Shastri<sup>1,2</sup><sup>1</sup>Institute of Macromolecular Chemistry, University of Freiburg, Germany<sup>2</sup>BIOSS - Centre for Biological Signaling Studies, University of Freiburg, Germany[maziar.matloubi@makro.uni-freiburg.de](mailto:maziar.matloubi@makro.uni-freiburg.de)

## INTRODUCTION

Biocompatible Polyurethane (PU) is used routinely in biomedicine and tissue engineering as heart valves, blood contacting catheters and bio membranes due its excellent tissue and blood compatibility<sup>1</sup>. To ensure patency in any given application biodegradation, elasticity and responsiveness to physiological cues such temperature, pH needs to be optimized and continues to remain a significant challenge.

In this work we introduce a family of segmented polyurethanes (SPUs) that incorporate many of the aforementioned properties in a single system. A high degree of customization in properties was achieved by judicious choice and chemical tailoring of hard segments derived from biodegradable poly(hydroxy acid) (PHA), in combination with an inorganic polymer that imparts flexibility and elasticity<sup>2</sup>. Using this novel polymer architecture, properties such as shape change in physiological temperature range, and mechanical properties that match natural cardiovascular tissue components could be realized.

## EXPERIMENTAL METHODS

**Polymer Synthesis:** The SPUs were synthesized by polycondensation of PHAs of well-defined MW and narrow polydispersity with hexamethylene diisocyanate. PHAs were synthesized by ring opening polymerization (ROP) of either lactide or glycolide using inorganic polymer initiator blocks.

**Analytical Techniques:** *Nuclear Magnetic Resonance* (NMR) (<sup>1</sup>H and <sup>13</sup>C) and *Fourier Transform Infra-red Spectroscopy* (FTIR) were used to confirm the chemical structure and incorporation of different segments in the polymer backbone. *Thermogravimetric Analysis* (TGA) and *Differential Scanning Calorimetry* (DSC) were used to determine thermal stability, processing temperature, and glass transition temperature (*T<sub>g</sub>*) respectively. Elastic modulus and elongation at breakage were determined using tensile test. *Atomic Force Microscopy* (AFM): Cryo-fractured interface of SPU block were analyzed using tapping mode AFM.

## RESULTS AND DISCUSSION

The chemical architecture of the SPU was confirmed using <sup>1</sup>H- and <sup>13</sup>C-NMR. Additionally, the vibrational and stretching bands associated with the PHA and inorganic domains were confirmed by FTIR. By using PHA segments of different molecular weights (initiator:lactide ratio 1:1, 1:1.5 and 1:2) SPUs that exhibit phase-separated microstructure were realized. The Atomic force micrograph of 1:1 SPU (**Figure 1**) revealed a bulk phase-separated microstructure. These

SPUs show high thermal stability up to 300 °C making them suitable for melt processing. By optimizing the

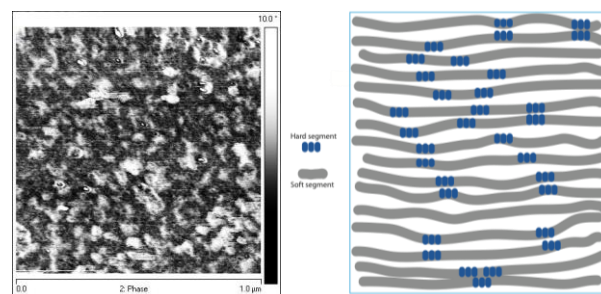


**Figure 1:** AFM image of a typical SPU surface showing phase

PHA and inorganic polymer component in the polymer backbone, SPUs with glass transition temperatures at, below and above 37 °C could be synthesized, thus making them suitable for manipulation in physiological conditions. By controlling the lactide composition the mechanical properties of the SPUs could also be tuned

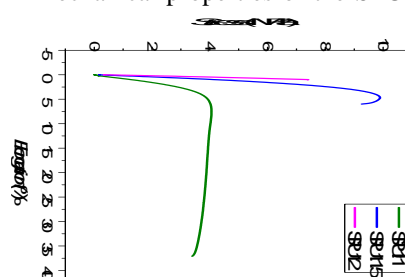


**Figure 2:** Tunability of mechanical properties in SPUs

(**Figure 2**). SPUs investigated having Young's modulus in the range of 80 – 800 MPa, with elongation at break as high 37%. Ongoing degradation studies have shown that these SPUs undergo

degradation in physiological conditions while retaining their mechanical properties.

## CONCLUSION

Degradable, thermoplastic polymers with high-content (≥ 50 weight %) PHA, showing excellent mechanical and elastic properties has been synthesized. Currently, they are being optimized for implementation in temperature triggered cardiovascular implants.

## REFERENCES

1. Chen Q. *et al.*, Prog. Polym. Sci. 38.3 (2013)
2. Matloubighargozloo M. and Shastri V.P., European Patent Application (2015)

## ACKNOWLEDGMENTS

This study was supported by Excellence Initiative of the German federal and state government (EX 294) and land Baden-Württemberg.

## Mixed Matrix Membranes for Removal of Protein-Bound Toxins from Human Plasma

Esmée van Geffen<sup>1,2</sup>, Denys Pavlenko<sup>1</sup>, Karin Gerritsen<sup>2</sup>, [Dimitrios Stamatialis<sup>1</sup>](mailto:d.stamatialis@utwente.nl)

<sup>1</sup>Department of Biomaterials Science and Technology/MIRA Institute, Twente University, The Netherlands

<sup>2</sup>Department of Nephrology and Hypertension/ University Medical Center Utrecht, The Netherlands

[d.stamatialis@utwente.nl](mailto:d.stamatialis@utwente.nl)

### INTRODUCTION

Protein-bound toxins are difficult to remove by conventional dialysis, while their accumulation plays an important role in uremic complications, in particular in cardiovascular disease.

Previously we showed that protein-bound toxin removal can be improved by use of a mixed matrix membrane (MMM)<sup>1</sup>. This membrane consists of 2 layers: an outer layer with adsorptive particles incorporated in a porous polymer and a particle-free hemocompatible inner layer (see figure 1). The double layer concept of MMM combines benefits of adsorption and diffusion and thus boosts removal of uremic toxins. The first generation MMM showed a potential for improved protein bound toxin removal, but had relatively large dimensions with a diameter of 984  $\mu\text{m}$ .

In this study we develop new generation MMM with diameter comparable to conventional dialysis membranes, with improved mass transfer characteristics.

smaller modules with excellent clearance of uremic toxins can be produced.

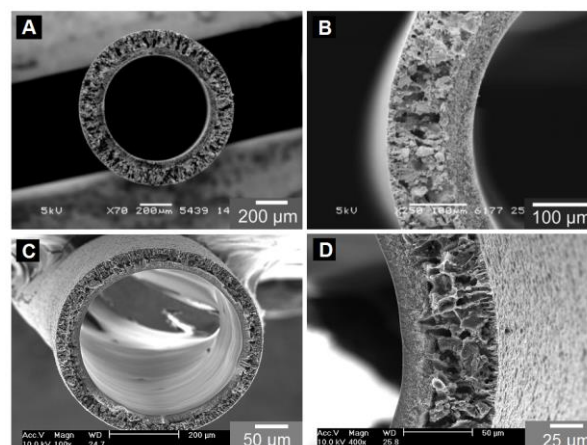


Figure 1 – A and B show first generation MMM. C and D show new fibers with reduced diameter.

### EXPERIMENTAL METHODS

The inner and outer layer of hollow fiber MMM were produced from a polyethersulfone / polyvinylpyrrolidone polymer blend. Activated carbon was loaded in the outer polymer matrix layer for adsorption of protein-bound toxins. The membranes were characterized by scanning electron microscopy (SEM) and clean water flux and dialysis/adsorption experiments were with plasma spiked with uremic concentrations of the protein-bound toxins indoxyl sulfate (IS) and p-cresyl sulfate (pCS), and ultrapure water dialysate.

### RESULTS AND DISCUSSION

By optimizing spinning conditions we produced fibers with an inner diameter of 450  $\mu\text{m}$  and inner membrane layer thickness of 21  $\mu\text{m}$  (Figure 1C and 1D), which is markedly smaller than previously reported MMM fibers (Figure 1A and 1B). Clean water permeability of the newly fabricated is close to the permeability of conventional low flux dialysis membranes, and 20 times lower than first generation MMM. The adsorption of IS and pCS per gram of membrane is ~3-4 times than that of previously reported MMM. These results suggest that

### CONCLUSION

Due to lower mass transport resistance, smaller diffusion length and increased surface to volume ratio new MMM with smaller diameter and thinner inner membrane layers show improved removal of protein-bound toxins.

### REFERENCES

1. Tijink M. *et al.*, Biomaterials. 34(32):7819-28, 2013.

### ACKNOWLEDGMENTS

The authors would like to thank the EU Marie Curie ITN BIOART for providing financial support to this project.

## Glucose Delivery System Based-Hydrogel Composite Scaffold for Enhancing MSC Survival

Julie Boisselier<sup>1\*</sup>, Joseph Paquet<sup>2\*</sup>, Laurent Bidault<sup>1</sup>, Michael Deschepper<sup>2</sup>, Elodie Lefebvre<sup>1</sup>, Charline Gossart<sup>1</sup>, Julie Dubois<sup>1</sup>, Adeline Gand<sup>1</sup>, Delphine Logeart-Avramaglou<sup>2</sup>, Véronique Larreta Garde<sup>1#</sup>, Emmanuel Pauthe<sup>1#</sup>, Hervé Petite<sup>2#</sup>  
Argentina

<sup>1</sup>Biomaterial for Health Group, ERRMECe, Department of Biology, University of Cergy-Pontoise, France

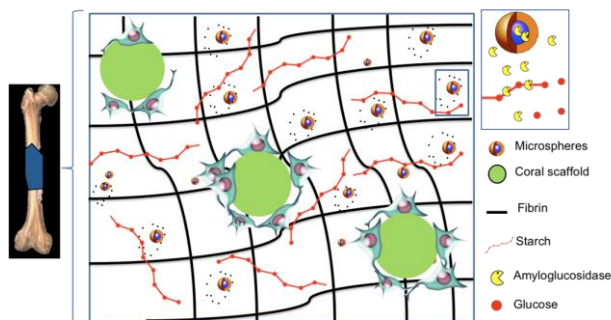
<sup>2</sup>Laboratory of Osteo-articular Bioengineering and Bioimaging, University of Paris Diderot, Paris, France.

\*JB & JP contributed equally to the manuscript, # VLG, EP & HP contributed equally to the supervision of the project

[julie.boisselier@u-cergy.fr](mailto:julie.boisselier@u-cergy.fr)

### INTRODUCTION

Constructs developed for tissue engineering present very limited potential due to massive death of transplanted cells after engraftment into the tissue-construct. This issue can be overcome by *in situ* supplying glucose that acts as the main metabolic fuel for Mesenchymal Stem Cells (MSCs) in severe hypoxia and significantly enhances their survival<sup>1</sup>. In this study, a composite construct is engineered to provide sufficient level of glucose to MSCs and to enhance their survival and function when transplanted in the ischemic milieu *in vivo*. Two combined strategies are developed. The glucose leakage outside the tissue construct is limited/delayed by increasing the intrinsic viscosity of the aqueous phase of the fibrin hydrogels by supplementation with starch. The starch polysaccharide alternatively serves as the main reservoir and source of glucose. The long-term (weeks) supply of glucose is achieved by designing, preparing and using gels with  $\alpha$ -amyloglucosidase (AMG)-containing poly(lactic-co-glycolic acid) (PLGA) nanoparticles. Sustained delivery of  $\alpha$ -amyloglucosidase into the starch-loaded fibrin gel provides continuous production of glucose *in situ* via the enzymatic hydrolysis of starch.



Schematic representation of the composite construct.

### EXPERIMENTAL METHODS

hMSCs were isolated from the bone marrow samples obtained as discarded tissue during routine bone surgery at the Lariboisiere Hospital (Paris, France) as previously described. AMG-containing PLGA nanoparticles (NPe) are prepared using a double emulsion technique previously described<sup>2</sup>. Gels are prepared as follow. Starch, human fibrinogen, AMG-containing PLGA nanoparticles, and hMSCs are mixed together. Human thrombin is subsequently added. The polymerization is carried out during 1h at 37°C. Hydrogels are fully characterized, followed and used for *in vitro* and *in vivo* experiments.

### RESULTS AND DISCUSSION

Hydrogels containing fibrin, starch and AMG (free or encapsulated) are self-supported and present a storage moduli superior to 1 kPa. Glucose production and glucose release diffusion kinetics are in accordance with the amount required by the cells for their survey and growth over a month.

Models demonstrated that AMG diffusion outside the gel is non-negligible after 5 days. Entrapping the enzyme into nanoparticles is a suitable way to maintain the enzyme inside the composite.

PLGA particles prepared by double emulsion technique where nearly monodisperse, with nanometric size (average of 280 nm), and a highly efficient encapsulation rate of AMG (~65%). Enzymes containing-nanoparticles are able to progressively produce glucose over a month and allow sustained glucose delivery inside hydrogels.

After 7 days of *in vitro* culture, in the presence of glucose-containing medium, the viability of hMSC was increased 6-fold compared to cells cultured w/o glucose. In presence of both starch and AMG (either within or w/o NP) cell viability was similar than in presence of glucose. In absence of AMG, the hMSC viability dramatically decreased after 14 days of implantation *in vivo* (0.3 to 0.5-fold compare to the signal at day 1). In comparison, in presence of AMG, the hMSC did not only survive but also proliferated within the hydrogels over the 14 day-period of implantation. Incorporation of the enzyme within the NPs further (2-fold) improved the hMSC proliferation.

### CONCLUSION

This work is a proof of concept that an innovative-engineered construct, based on a starch hydrogel containing  $\alpha$ -amyloglucosidase is able to deliver glucose *versus* time. It also represents a highly pertinent system to enhance Human Mesenchymal Stem Cells survival in cell constructs for up to 14 days *in vivo*.

### REFERENCES

- Deschepper M. *et al.*, Stem Cells, 31, 526-535, 2013
- Steinbach J. *et al.*, J. of Controlled Release 162, 102–110, 2012.

### ACKNOWLEDGMENTS

We would like to thank the French Agence Nationale pour la Recherche for providing financial support.



## In Situ Skin Regeneration by the Gene-Activated Materials

Lie Ma, Luyan Li, Xing Liu, Rui Guo, Changyou Gao

MOE Key Laboratory of Macromolecular Synthesis and Functionalization, Department of Polymer Science and Engineering, Zhejiang University, Hangzhou 310027, China

[liema@zju.edu.cn](mailto:liema@zju.edu.cn)

### INTRODUCTION

Skin loss caused by trauma, burn and chronic diseases has become one of the most serious problems in clinic. Recent advances in regenerative medicine have developed diverse methods for skin repair and regeneration<sup>1</sup>. However, there are still many obstacles, such as angiogenesis, hypertrophic scar, and loss of appendix organs, should be overcome to realize the full regeneration as the living skin<sup>2</sup>.

As an important aspect of regenerative medicine, tissue engineering has been brought ever closer to achieve its potential as life-saving and life-improving option for patients. As a general principle of tissue engineering, the scaffold, acting as the artificial extracellular matrix (ECM), should present well-designed multiple chemical, physical and biological cues to build a suitable cellular microenvironment to achieve proper tissue function and regeneration. The spatial and temporal delivery of bioactive molecules (including low molecular weight drugs, peptides, growth factors, cytokines, and mediators for gene therapy) mediated by the scaffold has been the subject of intensive researches<sup>3</sup>. Compared to the instability and high cost of cell growth factors, the gene-activated materials (GAM) which is prepared by loading of functional plasmid DNAs into the scaffolds, can locally transfect cells and produce the required cell growth factors at the wound site<sup>4</sup>. In this study, the gene-activated strategy was applied in the design of the materials for skin regeneration.

### EXPERIMENTAL METHODS

TMC was applied to form nano-sized complexes with pDNA or siRNA. The influence of N/P ratio on particle size, binding affinity and serum stability was assessed by DLS and polyacrylamide gel electrophoresis (PAGE). The TMC/pDNA complexes were then loaded into collagen/chitosan scaffold through physical adsorption. By using Ribogreen staining and PAGE, the release profile of pDNA from scaffold was examined. The successful uptake of the complexes by HDFs in scaffold was confirmed by fluorescent staining. For in vivo study, the gene-loaded scaffold was combined with a silicone membrane to build a bilayer dermal equivalent (BDE) and then transplanted into full-

thickness incisional wounds in a porcine model. Gross observation was performed and tissue samples were harvested on pre-determined time points post-surgery. The levels of the key growth factors were tested by immunohistochemistry, RT-PCR and Western-Blotting.

### RESULTS AND DISCUSSION

Two kinds of gene-activated scaffolds were reported, which were fabricated by incorporating pDNA-VEGF and siRNA-TGF- $\beta$ 1 with the collagen-chitosan scaffold to enhance the angiogenesis and inhibit the scar formation, respectively. Firstly, a gene vector derived from chitosan-trimethyl chitosan was synthesized and used to accelerate the transfection of pDNA and gene-silence of siRNA, respectively. By in vitro and in vivo tests, the properties of enhanced angiogenesis and inhibited scar of the gene-activated scaffold were evaluated. By the combination of gene technologies and stem cells therapy, the possibility of the regeneration of skin appendages by the gene-activated material was investigated.

### CONCLUSION

A gene functionalized bilayer dermal equivalent is fabricated for skin regeneration, with capabilities to up/down-regulate targeted tissue regeneration-related factors and yield a repaired full-thickness skin in pig model with enhanced angiogenesis, successful scarring inhibition and the regeneration of skin appendages.

### REFERENCES

1. MacNeil S. *et al.*, Nature. 445(7130): 874-880, 2007
2. Lim C. *et al.*, Wiley Interdisciplinary Reviews: Nanomedicine and Nanobiotechnology. 2(5): 510-525, 2010
3. Shea L. D. *et al.*, Advanced Drug Delivery Reviews. 59:292-307, 2007
4. Pandit A. *et al.*, Advanced drug delivery Review. 63:197-201, 2011

### ACKNOWLEDGMENTS

The authors would like to thank the National Basic Research Program of China (2011CB606203) and the Natural Science Foundation of China (51322302) for providing financial support to this project.





## Modulation of Inflammatory Macrophage Activation by StarPEG–Heparin Based Hydrogels to Improve Impaired Wound Healing

Nadine Lohmann<sup>1,3</sup>, Elke Wandel<sup>1,3</sup>, Inka Forstreuter<sup>1,3</sup>, Lucas Schirmer<sup>2,3</sup>, Uwe Freudenberg<sup>2,3</sup>, Carsten Werner<sup>2,3</sup>, J.C. Simon<sup>1,3</sup>, Sandra Franz<sup>1,3</sup>

<sup>1</sup> Department of Dermatology, Venerology and Allergology, Leipzig University, Germany

<sup>2</sup> Leibniz Institute of Polymer Research Dresden, Max Bergmann Center of Biomaterials Dresden, Center for Regenerative Therapies Dresden, Germany

<sup>3</sup> Collaborative Research Center (SFB-TRR67) Matrixengineering, Leipzig and Dresden, Germany  
[sandra.franz@medizin.uni-leipzig.de](mailto:sandra.franz@medizin.uni-leipzig.de)

### INTRODUCTION

Impaired wound healing is a problem of immense clinical and economic relevance. Persistent inflammation in impaired wound healing is primarily driven by unresisted inflammatory M1 macrophage (infM1) activation. Therefore, hydrogel-biomaterials capable to bring unopposed inflammation under control by repressing infM1 activity and thus enabling inflammatory resolution represent a promising approach as wound dressings for the treatment of non-healing wounds<sup>1</sup>. Since cellular functions are known to be influenced by physicochemical and biomolecular cues of the extracellular matrix (ECM) hydrogels that are capable to modulate such extracellular signals are of great interest within this context<sup>2</sup>.

Here, we use biohybrid hydrogels composed of four-armed (star-shaped) poly(ethylene glycol) (starPEG) and heparin derivatives varying in their sulfation pattern. Heparin acts as multifunctional cross-linker allowing functionalization of the hydrogels through biomimetic presentation of growth factors. Delivery of pro-angiogenic factors FGF-2 and VEGF by starPEG-heparin hydrogels was shown to encourage angiogenesis<sup>4</sup>. Since both reduction of uncontrolled inflammation and induction of vascularization are suggested to improve an impaired healing response, we tested different starPEG-heparin-based hydrogels with respect to their immunomodulating capacity on infM1.

### EXPERIMENTAL METHODS

Biohybrid hydrogels were prepared by reacting the carbodiimide/N-hydroxysulfosuccinimide (EDC/s-NHS)-activated carboxylic acid group of heparin with amine-functionalized starPEG. Different heparin derivatives were utilized including standard heparin (SH) and two selectively desulfated heparins: N-desulfated heparin (N-DSH) and 6-O/N-desulfated heparin (6ON-DSH). RGD peptides were covalently attached to the hydrogels to provide cell adhesion sites. Inflammatory M1 macrophages were derived from human CD14<sup>+</sup> monocytes by differentiation with GM-CSF for 6 days and subsequently seeded on the different starPEG-heparin-based hydrogels. After 3 days culture on the hydrogels survival (XTT cell viability assay) and adhesion of infM1 were assessed and inflammatory functions (cytokine response) upon stimulation with LPS were determined (ELISA, qPCR). Additionally, interaction of the hydrogels with infM1-derived mediators was analysed in a cytokine adsorption assay.

### RESULTS AND DISCUSSION

StarPEG-heparin-based hydrogels functionalized with RGD adhesion sites promote survival and adhesion of infM1. Inflammatory activation of infM1 was modulated by starPEG-heparin-based hydrogels via two mechanisms: i) downregulation of cytokine expression and release in infM1, and ii) binding of cytokines released from infM1. Interestingly, modulation of the cytokine response is determined by the sulfation level of heparin. Hydrogels based on standard heparin predominantly bind and sequester inflammatory mediators including TNF, IL-12p40, IL-23, IL-8 and MCP-1 released from infM1. In contrast hydrogels based on desulfated heparin derivatives predominantly downregulate production of pro-inflammatory cytokines in infM1 as seen by reduced expression and release of TNF, IL-12p40, IL-23 and MCP-1. However they did not induce expression and release of IL-10, which represents a crucial cytokine for inflammatory resolution.

### CONCLUSION

From these results we conclude that starPEG-heparin-based hydrogels exert anti-inflammatory effects on infM1 and are capable to modulate the cytokine environment of infM1. The immunomodulating capacities of the hydrogels may be fine-tuned by usage of heparin derivatives with adjusted levels of sulfation. We suggest that starPEG-heparin-based hydrogels are capable to modulate unopposed infM1 activity in conditions of chronic inflammation. Inflammatory resolution may be additionally enhanced by delivery of mediators (IL-10/IL-4) promoting regulatory macrophage phenotypes through these hydrogels. We are currently testing immunomodulating effects of starPEG-heparin-based hydrogels in different settings in vivo mice models of impaired wound healing.

### REFERENCES

- References must be numbered. Keep the same style.
1. Franz S. *et al.*, *Acta Biomater.* 9:5621-9, 2013
  2. Franz S. *et al.*, *J. Biomaterials.* 32:6692-709, 2011
  3. Zieris A. *et al.*, *Biomacromolecules* 15:4439-46, 2014
  4. Zieris A. *et al.*, *J. Control Release* 156:28-36, 2011

### ACKNOWLEDGMENTS

The authors thank Deutsche Forschungsgemeinschaft (SFB-TR67/A10 and B3) for financial support.



## Nano-Microfibrous Scaffold for Burn-Wound Healing

Pallabi Pal<sup>1</sup>, Pavan Kumar Srivas<sup>1</sup>, Prabhash Dadhich<sup>1</sup>, Bodhisatwa Das<sup>1</sup>, Santanu Dhara<sup>1</sup>  
Arun Achar<sup>2</sup>

<sup>1</sup>Biomaterial and Tissue Engineering Laboratory, School of Medical Science and Technology, Indian Institute of Technology Kharagpur, India

<sup>2</sup>Midnapore Medical College and Hospital, India  
[pallabipal@yahoo.com](mailto:pallabipal@yahoo.com)

### INTRODUCTION

Patients with 50 per cent Total Body Surface Area (TBSA) full-thickness burn wounds have only 50 per cent of undamaged skin left which could be used for split-thickness skin harvesting. Donor sites would add to the total wound size resulting in a wound area covering 100 per cent of the body. Donor sites also heal with some scarring and may be very painful; hence an additional analgesic pharmacological load is required. Moreover, depending on the thickness of the dermis, only three to four split-thickness skin harvests are possible from the same site and re-cropping is delayed by the time necessary for re-epithelialization. Alternative life-saving approaches in the treatment of extensive burn wounds, where donor sites for SSG harvesting are not available, include the use of bioengineered skin substitutes.

The basement membrane of a human skin is a specialized extracellular matrix providing compartmentalization along with cell attachment and signaling factors. The dermal layer comprises mostly of nano/microfibrous collagens while the epidermal layer is a compact sheet of cell layer. For successful development of skin graft, it is important to reciprocate the nano/microscalar architecture of tissue matrix as well as its biological cell recognition character. Nanofiber morphology facilitates good cellular response owing to their high surface area, interconnected pore, simplicity, environmentally friendly nature, cost-effectiveness, scalability and tailorable mechanical properties

### EXPERIMENTAL METHODS

In this study, chitosan/PCL/collagen nano-microfibers were fabricated followed by crosslinking resulting in a highly porous dermal equivalent. The microstructures of samples were evaluated by scanning electron microscopy (SEM). FTIR spectroscopy, mechanical properties, swelling behavior, biodegradation kinetics of matrices was studied for their suitability as skin regenerating scaffold. Normal human fibroblast and keratinocyte were culture and cell adhesion properties were observed through SEM and Rhodamine-DAPI.

Healing of burn wound was tested on rat by wound area closure rate and histochemical analysis

### RESULTS AND DISCUSSION

SEM results showed formation of nanofibrous layer of PCL/chitosan with collagen. The matrices showed swelling of upto 200%, slower degradation rate, high mechanical strength and contact angle of nanofiber is 90°. SEM results showed good cell attachment on nanofiber layer. MTT assay Rhodamine-DAPI staining, assay indicated cytocompatibility of the scaffold. Animal experiment revealed faster healing of burn wound with proper formation of skin tissue with its appendages.

### CONCLUSION

Incorporation of chitosan and collagen increased hydrophilic as well as well degradation rate of the scaffold. Results using primary keratinocyte and fibroblast showed, non-toxic and cytocompatible nature of the matrix. Material characterization yielded definite results proving the scaffolds potential for tissue engineering application specially for healing extensive burn wound.

### REFERENCES

1. Fabrication and biocompatibility of novel bilayer scaffold for skin tissue engineering applications. R.A. Franco, et al, J Biomater Appl, 2013, 27(5):605-615

### ACKNOWLEDGMENTS

Authors would like to thank Council for Scientific and Industrial Research and IIT Kharagpur for financial assistance



# Expression Pattern of Tissue Transglutaminase in the Response to Gelatin Based Hydrogels *in Vitro* and *in Vivo*

Sandra Ullm<sup>1,2\*</sup>, Christoph Tondera<sup>1,2</sup>, Robert Wodtke<sup>1,2</sup>, Tim P. Gebauer<sup>3,4</sup>, Axel T. Neffe<sup>3,4</sup>, Andreas Lendlein<sup>3,4</sup>, Reik Löser<sup>1,2</sup>, Jens Pietzsch<sup>1,2</sup>

<sup>1\*</sup>Helmholtz-Zentrum Dresden-Rossendorf, Institute of Radiopharmaceutical Cancer Research, Department of Radiopharmaceutical and Chemical Biology, Dresden, Germany

<sup>2</sup>Technische Universität Dresden, Department of Chemistry and Food Chemistry, Dresden, Germany

<sup>3</sup>Institute of Biomaterial Science and Berlin-Brandenburg Centre for Regenerative Therapies, Helmholtz-Zentrum Geesthacht, Teltow, Germany

<sup>4</sup> Helmholtz Virtual Institute "Multifunctional Biomaterials for Medicine", Teltow and Berlin  
[s.ullm@hzdr.de](mailto:s.ullm@hzdr.de)

## INTRODUCTION

Tissue transglutaminase (TGase 2) is known as enzyme with versatile functions depending on its location and conformation, mediating, e.g., crosslinking of proteins through its  $\text{Ca}^{2+}$ -dependent transamidase activity or enhancement of interactions between fibronectin, integrins, and syndecan-4 via its role as scaffold protein. Both functions are proposed to be important for biomaterial-cell or -tissue interactions. Additionally, TGase 2 is a key player during the development of fibrosis. Consequently, TGase 2 is a potential target for the improvement and visualization of tissue regeneration following biomaterial implantation. Here, we studied the expression pattern of TGase 2 in the response to novel gelatin-based hydrogels with tailorable elastic properties and degradation behavior due to different degrees of crosslinking with lysine diisocyanate ethyl ester.

## EXPERIMENTAL METHODS

Solutions of 10 wt.-% gelatin were crosslinked with 3- (G10\_LNCO3) or 8-fold (G10\_LNCO8) excess of isocyanate groups of lysine diisocyanate ethyl ester compared to amino groups of gelatin. Primary human aortic endothelial cells (HAEC) and human leukemia THP-1 and HL-60 cells, differentiated to macrophages ( $\text{M}\phi$ ) or granulocytes ( $\text{G}\phi$ ), were seeded either directly on the hydrogel films or cultivated with material eluates in order to simulate hydrolytic or enzymatic hydrogel degradation *in vivo*. Expression levels of intracellular and secreted TGase 2 were quantified via Western blotting. Additionally, hydrogels were implanted subcutaneously in immunocompetent, hairless SKH-1 mice. TGase 2 expression at the implantation site was detected *ex vivo* by immunohistochemistry at several time points up to 112 days after implantation.

## RESULTS AND DISCUSSION

HAEC showed high expression and secretion of TGase 2, independent from hydrogel contact. THP-1  $\text{M}\phi$  highly expressed TGase 2, and increased its secretion only after direct hydrogel contact. In contrast, HL-60  $\text{M}\phi$  and  $\text{G}\phi$  exhibited enhanced expression of TGase 2 after direct contact to the hydrogels, without secreting TGase 2. These results demonstrate that TGase 2 expression and secretion by  $\text{M}\phi$  and  $\text{G}\phi$  are influenced by contact to the hydrogel surface structure and not by hydrogel degradation products. Additionally, the hydrogels with higher content of diurea lysine

junction units (G10\_LNCO8) induced higher effects than G10\_LNCO3. It should be noted that the two hydrogels differ in elasticity, with G10\_LNCO8 having a Young's modulus of  $55 \pm 11$  kPa and G10\_LNCO3 of  $13 \pm 3$  kPa. *Ex vivo* analysis of tissue sections by immunohistochemistry revealed enhanced expression levels of TGase 2 around the hydrogels 14 and 21 days after implantation (Figure 1), indicating a role of TGase 2 in hydrogel integration and tissue remodelling.

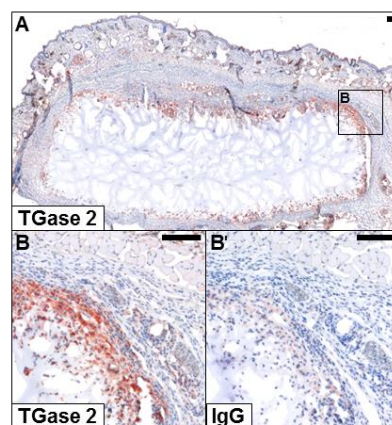


Figure 1: TGase 2 expression 14 days after implantation of G10\_LNCO8 in SKH-1 mice visualized by immunohistochemical staining. (A) TGase 2 expression in a cross section of the mouse skin with the implant. (B) Detailed location of TGase 2 around the implant and in immigrating cells. (B') Detail with control staining (IgG). Scale bars represent 200  $\mu\text{m}$ .

## CONCLUSION

Our results revealed that contact to the gelatin-based hydrogels influenced TGase 2 expression and secretion by  $\text{M}\phi$  and  $\text{G}\phi$  *in vitro*, as well as TGase 2 expression *in vivo*. This underlines TGase 2 to be a promising theranostic target during biomaterial integration processes. Nevertheless, the subcellular location of TGase 2 and its functionality remain to be elucidated to gain further insights into the exact role of this enzyme.

## ACKNOWLEDGMENTS

The authors thank the Helmholtz Association for funding of this work through Helmholtz-Portfolio Topic "Technologie und Medizin - Multimodale Bildgebung zur Aufklärung des In-vivo-Verhaltens von polymeren Biomaterialien". Sandra Ullm was recipient of a fellowship by Europäische Sozialfonds (ESF) from 2012 until 2014.

## Functionalization of Scaffold Surfaces: Role of Ce Valence States of Cerium Oxide Nanoparticles in Control of Cell Proliferation

Tamaki Naganuma<sup>1\*</sup>

<sup>1\*</sup> Smart Biomaterials Group, Nano-Life Field, Biomaterials Unit, International Centre for Materials Nanoarchitectonics,  
National Institute for Materials Science (NIMS), Japan  
[Naganuma.Tamaki@nims.go.jp](mailto:Naganuma.Tamaki@nims.go.jp)

### INTRODUCTION

A fundamental understanding of the interaction between cells and biomaterial surfaces is essential for the design of scaffold and artificial niche surfaces in tissue engineering. Functionalized biomaterial surfaces play a significant role in control of cell adhesion, proliferation and differentiation. Our research has focused on use of cerium oxide nanoparticles (CNPs) in functionalization of scaffold material, because CNPs have a capability to enhance cell proliferation.<sup>1</sup> The mechanism of cellular interaction with extracellular CNPs is, however, unclear. As for the therapeutic ability of CNPs, e.g. scavenging of reactive oxygen species in cells, it is known that  $\text{Ce}^{3+}$  and  $\text{Ce}^{4+}$  ions in CNPs mimic the enzyme activities of superoxide dismutase and catalase, respectively.<sup>2-3</sup>  $\text{Ce}^{3+}$  ions in CNPs also show the potential to inhibit redox-dependent apoptosis.<sup>4</sup> For these reasons, we hypothesised that Ce valence states in CNPs also correlate with proliferation behaviour of adherent cells. This study investigated the influence of Ce valence states of CNP surfaces on cell proliferation.<sup>5</sup> To evaluate the interaction between adherent cells and CNPs with  $\text{Ce}^{3+}$  and  $\text{Ce}^{4+}$ , we created CNP layers (CNPLs) with dominant  $\text{Ce}^{3+}$  and  $\text{Ce}^{4+}$  ions on poly-L-lactide acid substrates.<sup>5-7</sup> We utilized these CNPLs to investigate cell adhesion, migration and proliferation behaviour on the  $\text{Ce}^{4+}$  and  $\text{Ce}^{3+}$  regions of CNPLs.

### EXPERIMENTAL METHODS

In brief, typical CNPs with dominant  $\text{Ce}^{4+}$  ions were deposited on PL surfaces as a nano-ordered layer ( $\text{Ce}^{4+}$ -CNPLs). Ar ion irradiation was used to partially form a region of high  $\text{Ce}^{3+}$  concentration on the CNPLs ( $\text{Ce}^{3+}$ -CNPLs).<sup>5-7</sup> Cell proliferation behaviour of osteoblast-like cells (MG63) and human mesenchymal stem cells (hMSCs) was observed onto the surfaces of  $\text{Ce}^{3+}$ - and  $\text{Ce}^{4+}$ -CNPLs. Morphology of cells migrating between the  $\text{Ce}^{3+}$  and  $\text{Ce}^{4+}$  regions of CNPLs was also observed. To compare cell adhesion levels, single cell force spectroscopy was used to measure cell detachment force from CNPL surfaces.

### RESULTS AND DISCUSSION

Fig. 1a shows proliferation behaviour of MG63 cells on  $\text{Ce}^{4+}$  and  $\text{Ce}^{3+}$  regions at 3 days after seeding. Interestingly, cells rapidly proliferated on  $\text{Ce}^{4+}$  regions, whereas proliferation on  $\text{Ce}^{3+}$  regions was slow (Fig. 1a).<sup>5</sup> Most cells attached to both  $\text{Ce}^{3+}$ - and  $\text{Ce}^{4+}$ -CNPLs survived. It is noteworthy that even spherical shaped cells on  $\text{Ce}^{3+}$  CNPLs also survived. In addition, a comparison of cell attachment force on each  $\text{Ce}^{4+}$  and  $\text{Ce}^{3+}$  region was carried out by single cell force spectroscopy (Fig. 1b). Detachment force of a cell from the  $\text{Ce}^{4+}$ -CNPLs was clearly higher than that involving  $\text{Ce}^{3+}$ -CNPLs.<sup>5</sup> This result suggests that the strong

interaction of cells with  $\text{Ce}^{4+}$  regions promotes proliferation, while the weak  $\text{Ce}^{3+}$  region interaction inhibits proliferation.

After immersion in culture medium, surface characteristics of all CNPLs: (i) converted to negatively-charged and (ii) became moderately-hydrophilic.<sup>5</sup> Although CNPLs immersed in culture medium display phosphorus adsorption only on  $\text{Ce}^{3+}$  regions, the total amount of protein and BSA adsorption on both  $\text{Ce}^{4+}$ - and  $\text{Ce}^{3+}$ -CNPLs was similar.<sup>5</sup> It appears that these surface characteristics slightly affect cell proliferation behaviour on  $\text{Ce}^{4+}$ - and  $\text{Ce}^{3+}$ -CNPLs. These findings suggest that the Ce valence states of CNPLs influence, at least indirectly, cell proliferation.

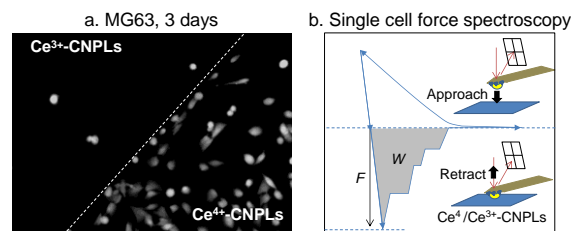


Figure 1 (a) Cell proliferation behaviour on the  $\text{Ce}^{4+}$  and  $\text{Ce}^{3+}$  regions and (b) schematic drawing of single cell force spectroscopy to evaluate detachment force of a single cell from substrate surfaces.

### CONCLUSION

The influence of Ce valence states of CNPLs on cell proliferation was investigated. It was determined that the valence states of  $\text{Ce}^{4+}$ - and  $\text{Ce}^{3+}$  ions on CNPLs, at least indirectly, promote or inhibit cell proliferation. Findings in this study may be utilized in the design and development of biomaterials (e.g. scaffolds and artificial niches) to control cell proliferation in tissue engineering.

### REFERENCES

1. Mandoli C *et al.*, Adv Funct Mater. 20:1617-24, 2010.
2. Korsvik C *et al.*, Chem Commun. 10:1056-8, 2007.
3. Pirmohamed T *et al.*, Chem Commun. 46:2736-8, 2010.
4. Celardo I *et al.*, ACS Nano. 5:4537-49, 2011.
5. Naganuma T *et al.*, Biomaterials. 35:4441-53, 2014.
6. Naganuma T *et al.*, Nanoscale. 4:4950-3, 2012.
7. Naganuma T *et al.*, Nanoscale. 6: 6637-45, 2014.

### ACKNOWLEDGMENTS

This work was supported, in part, by the World Premier International (WPI) Research Centre Initiative Program. Technical support by the Bio-Organic Materials Facility in the Nanotechnology Innovation Station (NIMS) is acknowledged.





Irina Sukhorukova<sup>1</sup>, Alexander Sheveyko<sup>1</sup>, Philipp Kiryukhantsev-Korneev<sup>1</sup>,  
Natalya Gloushankova<sup>2</sup>, Sergey Ignatov<sup>3</sup>, Dmitry Shtansky<sup>1</sup>

<sup>1</sup>National University of Science and Technology "MISIS", Leninsky prospect 4, Moscow 119049, Russia

<sup>2</sup>N.N. Blokhin Russian Cancer Research Centre of RAMS, Kashirskoe shosse 24, Moscow 115478, Russia

<sup>3</sup>State Research Center for Applied Microbiology and Biotechnology, Obolensk, Moscow Region 142279, Russia  
[irina\\_btnn@mail.ru](mailto:irina_btnn@mail.ru)

## INTRODUCTION

Biocompatible materials with antibacterial yet bioactive surfaces are continuing to attract attention of the medical and materials science communities, nevertheless no “dream material” has been developed so far. The present study aims to establish the optimal range of Ag concentration and its state of agglomeration in bioactive nanocomposite TiCaPCON films which would provide a strong bactericidal effect without compromising the material biocompatibility and bioactivity.

## EXPERIMENTAL METHODS

Different Ag contents and distributions were achieved by two different methods: sputtering of composite  $\text{TiC}_{0.5}\text{-Ca}_3(\text{PO}_4)_2$  target followed by  $\text{Ag}^+$  ion implantation (sample denoted as F1) and magnetron co-sputtering of composite  $\text{TiC}_{0.5}\text{-Ca}_3(\text{PO}_4)_2$  and Ag targets (F3). Both types of films were additionally treated by ion etching to remove an Ag rich surface layer (F2 and F4, correspondingly).

The films were characterized using different analytical techniques including X-ray diffraction, scanning and transmission electron microscopy, glow discharge optical emission spectroscopy, atomic force microscopy, Fourier transform infrared spectroscopy, inductively coupled plasma mass-spectrometry.

The antibacterial effect of the Ag-doped TiCaPCON films was evaluated against clinically isolated *Escherichia coli* O78 (*E. coli*). The influence of the surface chemistry on spreading, proliferation, and early stages of MC3T3-E1 osteoblastic cell differentiation was also studied.

## RESULTS AND DISCUSSION

The as-deposited TiCaPCON-Ag films were characterized by the presence of numerous Ag nanoparticles with a diameter of 5-10 nm.  $\text{Ar}^+$  ion etching resulted in partial (ion implantation) or complete (co-deposition) removal of Ag nanoparticles. Depending on the preparation method, the films demonstrated different  $\text{Ag}^+$  ion release behavior. Film F3 demonstrated rapid initial and stable continuous

$\text{Ag}^+$  ion release during 5 days. Ion etching didn't change the kinetics of  $\text{Ag}^+$  ion release. Films F1 was characterized by relatively slow ion release rate, which further slows down after ion etching. The strongest antibacterial effect (100%) against *E. coli* bacteria was observed for F3 films. After additional ion etching, the antibacterial effect was less pronounced. Films F1 and F4 exhibited a strong antibacterial activity toward *E. coli* bacteria already after 24 h. After the preliminary incubation of all the tested samples in PBS for 7 days, the antibacterial activity was markedly increased. Cytocompatibility tests showed that films F1 and F2 provided good adhesion, spreading, and proliferation of osteoblastic cells. In contrast, MC3T3-E1 cells were poorly attached and spread on the surface of films F3 and F4. Proliferation of osteoblastic cells on the surface of sample F3 was slightly retarded, whereas film F4 showed a toxic effect. We did not find any statistically significant differences in the level of alkaline phosphatase activity between MC3T3-E1 cells cultivated on the surface of Ag-doped and Ag-free films F1-F3. In the case of film F4, a drastic decrease of the ALP activity of MC3T3-E1 cells was observed.

## CONCLUSION

Bactericidal yet bioactive TiCaPCON-Ag films were successfully produced on titanium alloys by sputtering of composite  $\text{TiC}_{0.5}\text{-Ca}_3(\text{PO}_4)_2$  target followed by  $\text{Ag}^+$  ion implantation using a magnetron sputtering process. Under optimal conditions in terms of Ag content and agglomeration, the Ag-doped TiCaPCON films are highly efficient against *E. coli* bacteria and, at the same time, provide good adhesion, spreading, proliferation and differentiation of osteoblastic cells which reflect high level of biocompatibility and bioactivity of the films.

## ACKNOWLEDGMENTS

The work was supported by the Russian Foundation for Basic Research (Grant №13-03-12081) and the Ministry of Education and Science of the Russian Federation (Agreement 14.578.21.0086).





# Differential Response of Human Bone Marrow Cells on Aligned vs Randomly Oriented Carbon Nanotubes

Anthoula Kroustalli and Despina Deligianni

Department of Mechanical Engineering & Aeronautics, University of Patras, Greece  
[deligian@mech.upatras.gr](mailto:deligian@mech.upatras.gr)

## INTRODUCTION

Studies on the interaction of cells with carbon nanotubes have been receiving increasing attention owing to their potential for various applications. Through mediation of integrin clustering, their nano-scale surface structure directly affects cell binding and subsequent behaviour<sup>1,2</sup>. In this work, interactions between human bone marrow mesenchymal cells (hBMSCs) and multi-walled carbon nanotube (MWCNT) films were investigated and focused on how morphological structures of MWCNT films affected cellular behavior.

## EXPERIMENTAL METHODS

The pristine MWCNTs were obtained from Nanothinx, Nanomaterials, and Nanotechnology R&D (purity 98.3%), who also prepared the aligned, vertically oriented MWCNT films. Randomly oriented MWCNT films were prepared by filtration in the lab. Substrates were observed with SEM

hMSCs, obtained by aspiration from the marrow of femoral diaphysis of healthy patients, undergoing hip surgery after trauma, were cultured in specific conditions to form osteoblasts.

Cell spreading, proliferation, differentiation, cytotoxicity and integrin mediated adhesion were quantified after 1, 3, and 7 days of incubation, either cultured on MWCNTs films or on TCP (control). LDH expression (using the standard protocol for a commercially available colorimetric proliferation assay), intracellularly or in the culture medium, was used to quantify cell proliferation or cytotoxicity, respectively. ALP enzyme activity of hMSCs was quantified by the specific conversion of p-nitrophenyl phosphate into p-nitrophenol. For cytoskeletal organization, cells were observed under an inverted confocal microscope at 60x magnification, after being stained for nucleus, F-actin and FAK.

Data were collected from three separate experiments and analyzed statistically using SPSS software. Overall differences between groups were assessed by ANOVA and individual paired comparisons were analyzed post hoc with Scheffé's test.

## RESULTS AND DISCUSSION

Cells settled and extended earlier on both MWCNT surfaces than on TCP, toward a polygonal shape. On TCP cells have a more fibroblastic appearance. The results of cell adhesion and proliferation for 1, 3, and 7 days are shown in Fig. 1. The cells attached and proliferated on all surfaces and a statistically significantly ( $p < 0.01$ ) increased number of attached cells in all days was observed on aligned MWCNTs surfaces in relation to the other substrates.

ALP/cell number of the cells cultured on both

MWCNTs films was lower than that on control (aligned < randomly oriented < TCP) at each culture time point, suggesting that when hBMSCs increase their proliferation, their differentiation is delayed<sup>2</sup>.

On aligned MWCNTs, the numbers of FAK-positive focal adhesions increased continuously from the 1<sup>st</sup> day, whereas on randomly oriented, the respective numbers were lower.

Aggregated CNTs were observed on the randomly oriented MWCNT films in the SEM images, increasing film roughness. Further work is necessary to elucidate whether surface roughness or the more structured topography is the main contributor to the cells response.

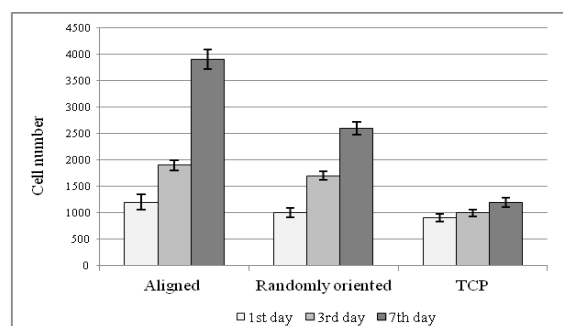


Fig.1. hMSCs proliferation after 1, 3, and 7 days of culture on the three substrates.

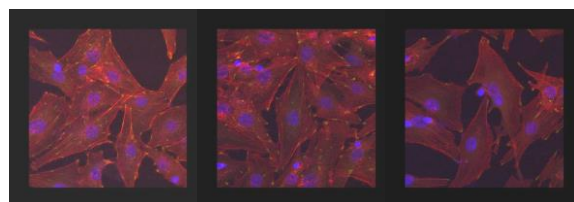


Fig. 2. Fluorescent staining of the f-actin (red), DNA (blue) and FAK (green), after 7days in culture on aligned, randomly oriented MWCNTs and TCP.

## CONCLUSION

Despite literature evidence supporting the nano-structures' ability to be both osteoconductive and osteoinductive, there is still disparity regarding how nanostructures regulate the progression towards an osteoblastic phenotype. It is necessary to explore various architectures, to understand how they initiate osteoinductive or proliferating signals. Further work is require to define the specific mechanisms operative in proliferating cells that allow for increased phenotypic alterations and the signals that promote progressive differentiation of the hBMSCs.

## REFERENCES

1. Kroustalli A. *et al.*, Ann Biomed Eng 41:2655-2665, 2013.
2. Deligianni D, Cell Adh Migr 3:487-492, 2014.

Klaudia Trembecka-Wojciga<sup>1</sup>, Roman Major<sup>1</sup>, Juergen M. Lackner<sup>2</sup>, Hanna Plutecka<sup>3</sup> and Boguslaw Major<sup>1</sup>

<sup>1</sup> Institute of Metallurgy and Materials Science Polish Academy of Sciences, 25 Reymonta Street, 30-059 Cracow, Poland

<sup>2</sup> JOANNEUM RESEARCH Forschungsges.m.b.H., Institute of Surface Technologies and Photonics, Functional Surfaces, Leobner Strasse 94, 8712 Niklasdorf, Austria

<sup>3</sup> Department of Medicine, Jagiellonian University Medical College, 8 Skawinska Street, 31-066 Cracow, Poland  
[k.trembecka@imim.pl](mailto:k.trembecka@imim.pl)

## INTRODUCTION

Progress in the field of biomedical engineering solutions can effectively combine materials science with alive cells <sup>1</sup>. The essence of the work is novel coated surfaces with self-assembling topography mimicking the cellular niches, formed by the controlled share of the residual stress and focused on the stem cell capturing from the whole flowing blood <sup>2</sup>. At this stage of the work the coating structure was developed and optimized towards the haemocompatible properties.

## EXPERIMENTAL METHODS

The medical grade PU has been covered by different types of coatings by using PVD technique. The layer structure and the mechanisms of the coating anchoring to the substrate were analysed using electron microscopy techniques. The cross section study was performed by the transmission electron microscopy equipped with field emission gun <sup>3</sup>. The physical surface structuring was done using plasma based techniques. The blood- material interaction analysis was done in arterial flow condition simulator with whole human blood. Blood used in test was collected from healthy male volunteer. The blood collected from above the sample was mixed with the antibodies CD61-PerCP, CD62P, PAC-1 in order to estimate platelet activation upon contact with the material. The platelet activation was analysed using flow cytometry technique and scanning confocal microscopy.

## RESULTS AND DISCUSSION

Microstructure analysis confirmed by electron diffraction revealed amorphous structure of the thin coatings deposited on PU substrate (Fig. 1). When exposed on physiological like conditions, blood components were activated which may result in platelets and leukocytes adhesion to the surface of biomaterials. The quality of the blood after the dynamic interaction with the tested material is presented in Fig.2. The active blood cells attached to the surface (Fig. 3) were considered as CD 62 (blood clotting cascade activation- active platelets) and CD 45 (immune response activation- active leucocytes) positive.

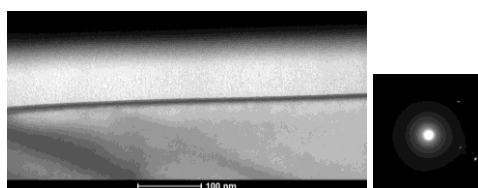


Fig. 1 TEM microstructure of the deposited coatings

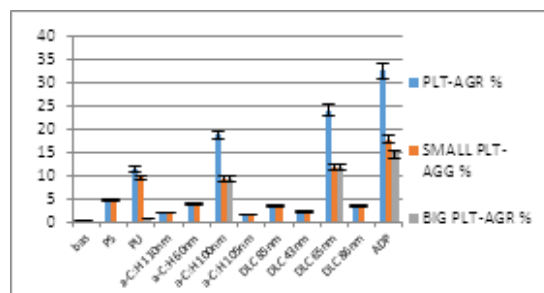


Fig. 2. Flow cytometric analysis of the blood: PLT-AGR- platelets aggregates, considered as two platelets- SMALL and over two platelets BIG

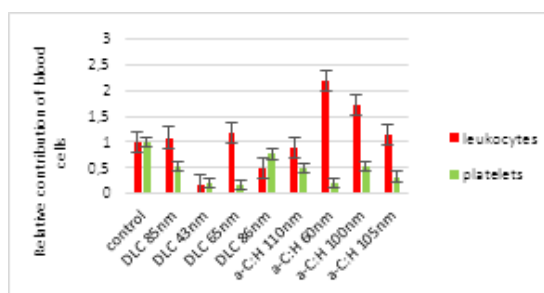


Fig. 3. Confocal laser scanning microscopy analysis of active platelets and leukocytes on the surface

## CONCLUSION

Coatings based on amorphous carbon and diamond-like coating resulted in improved haemocompatible performance. It was found the strong dependence of the microstructure on the blood-material interaction. Different topography of coatings have direct influence on blood-material interactions.

## REFERENCES

1. Lackner J.M., Waldhauser W., Major R., Major L., Hartmann P., Surface & Coatings Technology. 215:192-198, 2013
2. Major R., Journal of Material Science Materials in Medicine; Springer. 24: 725-733, 2013
3. Major L., Janusz M., Kot M., Lackner J. M. and Major B., RSC Adv., 5: 9405-9415, 2015

## ACKNOWLEDGMENTS

This research was financially supported by project 2011/03/D/ ST8/04103 "Self-assembling, biomimetic porous scaffolds in terms of inhibiting the activation of the coagulation system" of the Polish National Center

## Mechanical & Degradation Characterisation of AZ31 Magnesium (Mg) for Use in Paediatric Tracheal Stents

Isaiah Adekanmbi<sup>1</sup>, K.Elizabeth Tanner<sup>1</sup>, Haytham Kubba<sup>2</sup>, Helen Lu<sup>3</sup>

<sup>1</sup>Biomedical Engineering Division, School of Engineering, University of Glasgow, UK

<sup>2</sup>ENT Paediatric Surgery, Royal Hospital for Sick Children, Yorkhill, Glasgow, UK

<sup>3</sup>Biomedical Engineering, School of Engineering and Applied Science, Columbia University, USA

[Isaiah.adekanmbi@glasgow.ac.uk](mailto:Isaiah.adekanmbi@glasgow.ac.uk)

### INTRODUCTION

The trachea (windpipe) consists of rigid cartilage rings in a soft tissue network. In infant airways, deficiency of these supportive structures (Tracheomalacia) may occur at 1.3 affected per million children below the age of 16, predisposing airway constriction (tracheal stenosis)<sup>1</sup> and leading to significant problems with breathing. Current treatment options involve reconstructive surgery. However when this fails a cardiovascular balloon expandable stent is used in the trachea<sup>2</sup>.

The stent is required to provide mechanical support for a minimum of 18 months to allow maturation of the dysfunctional tracheal cartilage<sup>3</sup>. Issues arise however with commercially available permanent metallic airway stent materials (Nitinol or stainless steel) which require multiple surgical procedures for surveillance, removal, resectioning and possible reconstruction of the airways. Mg alloys have received attention for use as medical implants, but until now have not been clinically approved for use in airway stents. In this study the degradation behaviour and associated changes in mechanical properties with *in vitro* degradation of AZ31 Mg alloys was used to test the hypothesis that a biodegradable metallic tracheal expansion stent with appropriate mechanical and degradation characteristics can be developed for use in neonates.

### EXPERIMENTAL METHODS

**Degradation test:** AZ31 Magnesium alloy specimens were immersed in 4000ml of Phosphate Buffered Saline (PBS) and incubated at 37°C for 1, 3, 6 months and the degradation media was renewed every 2-5 days (1 cycle). After each immersion cycle the specimens were cleaned with acetone, rinsed in water, dried and weighed to calculate average mass change and degradation rate. The pH of the degradation media was adjusted to 7.5 at the start of each immersion cycle and recorded at the end.

**Mechanical Tests:** An Instron 5984 was used to perform uniaxial tension tests to failure (at 0.033s<sup>-1</sup>) on dumbbell shaped AZ31 Mg specimens (150x60x2mm) at 0, 1, 3 and 6 months (n=5 per time point) *in vitro* degradation. Force-displacement data was used to calculate stress-strain graphs and to compare ultimate strength, strain at failure and modulus at each time point. Fatigue and four point bend tests (MTS810) were used to evaluate the ability of the stent material to accommodate tracheal dilatation and on going cyclic loading.

**Statistical techniques:** Significance tests (Student's t-test) were performed using Prism v.5 (GraphPad Software, La Jolla, CA). \*Indicates statistically significant differences between groups, p < 0.05.

### RESULTS AND DISCUSSION

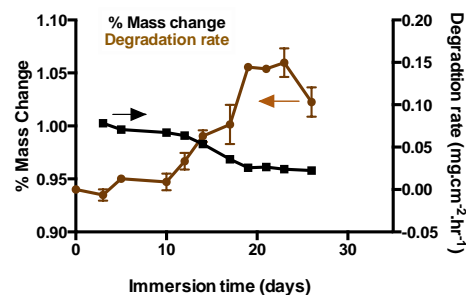


**Fig1:** Average percentage mass change & degradation rate of AZ31 samples over 1 month in PBS

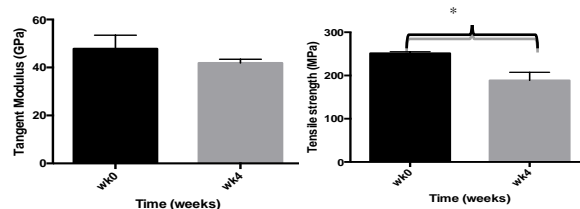


**Fig2:** Mean tangent modulus and tensile strength of AZ31 Mg specimens at 0 and after 1 month degradation

A slow, but continuous, mass loss was observed from day 3 (total <3% in a month). Degradation rate (DR) of AZ31 varied with time showing an initial drop after 3 days and a steady rise to a maximum of 0.1445 mg cm<sup>2</sup> hr<sup>-1</sup>, reflecting a well established pattern<sup>4</sup>. This material when subject to *in vitro* degradation for 4 weeks showed a trend towards a slow reduction in mechanical properties.

### CONCLUSIONS

The results demonstrate that AZ31 Mg alloy offers sufficient mechanical properties for at least one month in an aggressive degradation environment similar to that presented by bodily fluids. AZ31 Mg therefore represents a promising biomaterial candidate for use in airway stents counteracting tracheal stenosis in infants and eradicating the requirement for multiple life threatening surgical procedures.

### REFERENCES

1. Zopf *et al* *Ort Head Neck Surg.* 140:66-71, 2014
2. Furman *et al* *Ort Head Neck Surg.* 125:203-207, 1999
3. Luff *et al* *J Biom Mat Res.* 102A:611-620, 2014
4. Ren *et al* *Front Mater Sci.* 1:401-404, 2007

### ACKNOWLEDGMENTS

The authors would like to thank Action Medical Research and Yorkhill Children's Charity for providing financial support to this project.

## Superior Lubrication Ability of Artificial Hydrogel Cartilage

Teruo Murakami<sup>1</sup>, Seido Yarimitsu<sup>1</sup>, Kazuhiro Nakashima<sup>2</sup>, Tetsuo Yamaguchi<sup>2</sup>, Yoshinori Sawae<sup>2</sup>, Nobuo Sakai<sup>3</sup>, Atsushi Suzuki<sup>4</sup>

<sup>1</sup>Research Center for Advanced Biomechanics, Kyushu University, Japan

<sup>2</sup>Department of Mechanical Engineering, Kyushu University, Japan

<sup>3</sup>Department of Applied Science for Integrated System Engineering, Kyushu Institute of Technology, Japan

<sup>4</sup>Department of Materials Science, Yokohama National University, Japan

[tmura@mech.kyushu-u.ac.jp](mailto:tmura@mech.kyushu-u.ac.jp)

### INTRODUCTION

Total joint prostheses composed of ultra-high molecular weight polyethylene (UHMWPE) and metal or ceramics have been widely applied. The crosslinking, addition of vitamin E and phospholipid coating to UHMWPE have reduced wear and extended the life of joint prostheses. However, wear problems have not yet been completely solved under severe conditions, where direct contacts can occur in mixed or boundary lubrication. Therefore, another method to establish no wear and low friction is required. The application of poly(vinyl alcohol) (PVA) hydrogel with high water content as biomimetic compliant artificial cartilage is expected to reproduce similar multimode lubrication mechanism to natural synovial joints<sup>1</sup>. In this study, the friction and wear behaviors in PVA hydrogels prepared by three kinds of methods were evaluated.

### EXPERIMENTAL METHODS

As artificial hydrogels, three kinds of PVA hydrogels were prepared using the repeated freeze-thawing (FT) method<sup>1</sup>, the cast-drying (CD) method<sup>2</sup> and hybrid method<sup>3</sup> with a layered structure as CD on FT, which are physically crosslinked with hydrogen bonding but differ in terms of structure and mechanical properties. CD gel has lower permeability than FT gel. The reciprocating tests were conducted for sliding pair of an ellipsoidal PVA hydrogel with 2 mm thickness and flat glass plate. Lubricants were saline solution and simulated synovial fluid (0.5 wt% hyaluronate (HA) solution containing 1.4 wt% albumin, 0.7 wt% gamma-globulin and 0.01 wt% L alpha-dipalmitoyl phosphatidylcholine). Molecular weight of HA is  $9.2 \times 10^5$  Da. The sliding speed, stroke length and load were 20 mm/s, 35 mm, and 2.94 N respectively. The extent of wear was observed by optical microscopy.

### RESULTS AND DISCUSSION

In saline solution, three kinds of hydrogels exhibited very different frictional behaviors as hybrid < CD < FT as shown in Fig.1. It is noteworthy that the hybrid gel maintained very low friction until the end of test. The CD gel showed slightly higher friction with gradual increase. Meanwhile, the FT gel showed initial medium friction and a gradual increase over 0.25 at final stage. Slight wear features were observed in all gels. In contrast, in simulated synovial fluid containing main lubricating constituents, friction levels were remarkably decreased for all PVA hydrogels, but the order of

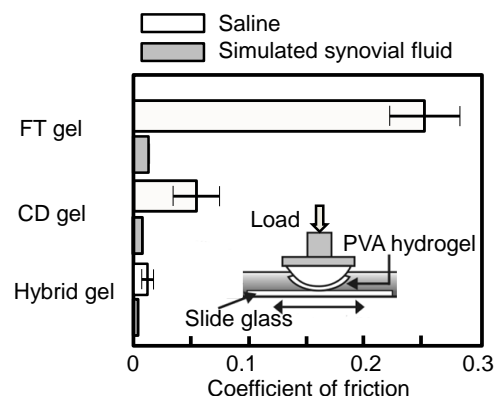


Fig.1 Frictional properties of three kinds of PVA hydrogels (Error bars: standard deviation, n = 3)

coefficients of friction were same as hybrid < CD < FT (Fig.1). On CD gel surface which was smooth surface, some scratchings were observed, but little wear was noticed on hybrid and FT gels. As described above, hybrid gel showed very low friction and minimum wear in similar environment to human joint. This is attractive hydrogel for clinical application as artificial cartilage. It is considered that at initial stage the biphasic lubrication is more effective for hybrid gel than for CD gel as evaluated by biphasic finite element analysis, but with repetition of rubbing, the superior surface lubricity of hybrid gel plays an important role.

### CONCLUSION

Hybrid PVA hydrogel as layered structure of CD gel on FT gel for artificial cartilage had a superior lubricity with very low friction and minimum wear in simulated synovial fluid in reciprocating test.

### REFERENCES

1. Murakami T. et al., Proc. IMechE, Part H: J. Engineering in Medicine. 212:23-35, 1998
2. Otsuka E. and Suzuki A., Journal of Applied Polymer Science. 114: 10-16, 2009
3. Suzuki A. et al., Extended Abstract for World Tribology Congress 2013, Torino, in USB, 2013

### ACKNOWLEDGMENTS

The authors would like to thank the JSPS Grant-in-Aid for Specially Promoted Research (23000011) for providing financial support to this project.



## Sr- and Zn-Substituted Calcium Phosphates-Based Composites for Osteochondral Tissue Engineering Scaffolding

Sandra Pina<sup>1,2</sup>, Joaquim M. Oliveira<sup>1,2</sup>, Rui L. Reis<sup>1,2</sup>

<sup>1</sup> 3B's Research Group – Biomaterials, Biodegradables and Biomimetics, University of Minho, Headquarters of the European Institute of Excellence on Tissue Engineering and Regenerative Medicine, Guimarães, Portugal

<sup>2</sup> ICVS/3B's - PT Government Associate Laboratory, Braga/Guimarães, Portugal

[sandra.pina@dep.uminho.pt](mailto:sandra.pina@dep.uminho.pt)

### INTRODUCTION

The repair and regeneration of osteochondral (OC) defects has been increasing owing the high number of trauma related injuries or osteoarthritis. Although current clinical options are effective for the treatment of the OC defects, new therapeutic options are necessary for the complete regeneration of the damaged articular cartilage which has a limited healing capacity. The main purpose for OC tissue engineering is to recreate a biomimetic scaffold consisting of a cartilaginous layer and an underlying osseous layer, for regeneration of cartilage and bone, respectively, involving different combinations of materials, morphologies and properties in both parts of the scaffolds<sup>1</sup>. Composite scaffolds composed of biopolymers (silk fibroin) and calcium phosphates incorporating different ions (Sr, Zn), for the simultaneous repair/ regeneration of cartilage and bone are herein developed. These scaffolds present great bioresorbability and osteointegration, and high mechanical strength<sup>2</sup>. In particular, Sr and Zn plays vital roles in the formation, growth, and repair of bone, thus it can promote osteogenesis and angiogenesis<sup>3</sup>. Besides, these elements can lend controlled degradation and increase the mechanical strength of the biomimetic materials.

### EXPERIMENTAL METHODS

Sr- and/or Zn-substituted calcium phosphate powders were prepared by aqueous precipitation from  $\text{Ca}(\text{NO}_3)_4 \cdot 4\text{H}_2\text{O}$ ,  $(\text{NH}_4)_2\text{HPO}_4$ ,  $\text{Sr}(\text{NO}_3)_2$ , and  $\text{Zn}(\text{NO}_3)_2 \cdot 6\text{H}_2\text{O}$ , with  $(\text{Ca}+\text{Sr})/\text{P}=1.48$ , followed by heat treatments at 800-1000 °C and milling. Silk fibroin (SF) was extracted from *Bombyx mori* cocoons.

Porous composite scaffolds with distinct cartilage and bone sides were produced through solvent casting and particulate-leaching technique, followed by freeze-drying. Cartilage layer was engineered using 100 wt.% SF, and bone layer was obtained by combining 85 wt.% SF with 15 wt.% Sr-, Zn-doped powders.

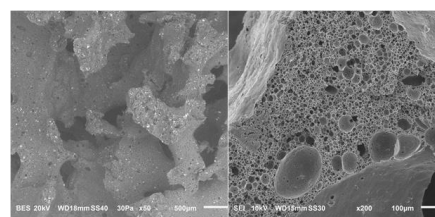
XRD, FTIR, SEM/EDS and  $\mu$ -CT techniques were employed to characterize the starting powders and scaffolds. Current studies are on-going to evaluate the scaffolds *in vitro* degradation and ions release profiles, and mechanical properties.

### RESULTS AND DISCUSSION

Rietveld analysis of XRD patterns of the powders heat-treated at 1000 °C, confirmed the incorporation of the ionic-dopants into calcium phosphate structure by the changes in lattice parameters, resulting in a phase

composition of 92 wt.% doped  $\beta$ -tricalcium phosphate (TCP) and of 8 wt.% calcium pyrophosphate.

SF/Sr-, Zn-doped  $\beta$ -TCP composite scaffolds presented macroporosity highly interconnected and microporosity with sizes around 500  $\mu\text{m}$ , and 1-10  $\mu\text{m}$ , respectively, with TCP powder well distributed throughout the scaffolds as shown in Figure 1.



The microstructure of the scaffolds was quantitatively studied by  $\mu$ -CT, as presented in Table 1.

Structure	Porosity (%)	Mean pore size ( $\mu\text{m}$ )	Mean trabecular thickness ( $\mu\text{m}$ )	Interconnectivity (%)	SrTCP (%)
SF/SrTCP	69.8	491.7	260.3	85.2	12

### CONCLUSION

The present work demonstrates the feasibility of formulating porous composite scaffolds incorporating Sr and Zn, with promising applications in OC tissue engineering.

### REFERENCES

- Oliveira JM. *et al.*, Biomater. 27:6123-37, 2006.
- Pina S. *et al.*, Adv Mater. 2015.
- Pina S. *et al.*, Eur Cell Mater. 20:162-77, 2010.

### ACKNOWLEDGMENTS

The authors would like to thank the European Union's Seventh Framework Program (FP7/2007-2013) under grant agreement n° REGPOT-CT2012-316331-POLARIS, and QREN (ON.2 – NORTE-01-0124-FEDER-000016) cofinanced by North Portugal Regional Operational Program (ON.2 – O Novo Norte), under the National Strategic Reference Framework (NSRF), through the European Regional Development Fund (ERDF) for providing financial support to this project. The FCT distinction attributed to J.M. Oliveira under the Investigator FCT program (IF/00423/2012) is also greatly acknowledged.





## Si-HPMC And Si-Chitosan Hydrogel For Cartilage Tissue Engineering

Réthoré Gildas<sup>1</sup>, Boyer Cécile<sup>1</sup>, Amadou Touré<sup>1</sup>, Fabienne Jordana<sup>1</sup>, Olivier Gauthier<sup>1</sup>, Guicheux Jérôme<sup>1</sup>, Weiss Pierre<sup>1</sup>

<sup>1</sup> Laboratoire d'Ingénierie OstéoArticulaire et Dentaire (LIOAD), UMR5791, Centre Hospitalier Universitaire de Nantes, Université de Nantes, INSERM, ONIRIS, Nantes, France

[gildas.rethore@univ-nantes.fr](mailto:gildas.rethore@univ-nantes.fr)

### INTRODUCTION

It was believed that biomaterial selection was performed based on its macroporosity, biocompatibility and degradability properties but recently its ability to withstand biomechanical stress has also been considered. Discher et al. [1] have indeed shown that material stiffness induces critical effects on cell behaviour and differentiation. Therefore, we have recently embarked on the development of mechanically-competent hydrogels for bone and cartilage tissue engineering. We prepared a cellulose based polymer capable of self cross-linkage (Si-HPMC) to avoid any toxicity issues resulting from using cross-linking chemicals or photo cross-linking. Therefore, LIOAD has been working on the development of hydrogels as ECM for bone and cartilage regeneration. The objectives of the present work are to modulate the physico-chemical and biological properties of our hydrogels by mixing two silated polysaccharides Si-HPMC and Si-Chitosan.

### EXPERIMENTAL METHODS

The self cross-linkable polymer (Si-HPMC) was prepared according to an already published method developed in LIOAD [2]. Silanol groups were linked to amine moieties of the chitosan via thio-urea bond.

**Hydrogel characterizations:** Hydrogels and reinforced hydrogels were characterized physico-chemically to determine their elastic moduli using MARS rheometer ( $G'$ ), Dynamic Mechanical Analysis ( $E'$ ) and microscopy.

Biological investigations have been done with human nasal chondrocytes by determining the cell viability in 2D using MTS, 3D by confocal microscopy after Live&Dead staining.

In vivo investigations have been performed in subcutaneous sockets in nude mice, in rat calvaria defects and in knee focal defects in rabbit.

### RESULTS AND DISCUSSION

The characterizations showed that adding Si-Chitosan within Si-HPMC hydrogels increases the elastic moduli without interfering with the biocompatibility. Indeed, all the constructs that we used in this study showed no toxicity both in 2D and 3D (as shown in figure 1). Culturing cells in 3D within our hydrogel containing Si-Chitosan

also induces cell adhesion onto the matrix as I can be observed on confocal micrograph in figure 2.

It is worth noted that after 5 weeks of implantation, the chondrocytes showed a good viability and still express a chondrocyte phenotype. Moreover, during the surgery, due to the presence of chitosan, our constructs showed good adhesion behaviour onto the cartilage focal defect.

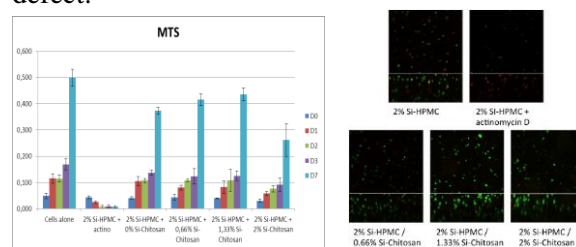


Fig 1: left: 2D hASCs viability in contact with Si-HPMC/Si-Chitosan hydrogels (Positive control : cells alone, control for cell death : actinomycin D). Right: Confocal micrograph showing living cells (green) and dead cells (red) after 7 days of culture inside hydrogels.

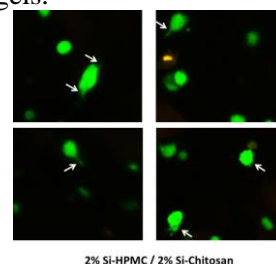


Fig 2: Confocal micrographs showing cell adhesions after 7 days culture in Si-HPMC/Si-Chitosan hydrogel.

### CONCLUSION

The study demonstrates the feasibility of our approach to modulate our self-setting hydrogel while keeping them biocompatible.

### REFERENCES

1. ENGLER AJ, SEN S, SWEENEY HL, DISCHER DE. Cell, 126, 677-689, 2006.
2. BOURGES X, WEISS P, DACULSI G, LEGEAY G. Advances in Colloid and Interface Science, 99,3, 215-228, 2002.

### ACKNOWLEDGMENTS

We would like to acknowledge ANR (ANR-09-PIRI-0004-01) and Pays de la Loire council for their funding and technical support.



## Response of Human Macrophages to Cytokine Induction under Three-Dimensional (3D) Artificial Extracellular Matrix (ECM) Mimicking Conditions

Marta B. Evangelista<sup>1</sup>, Alexandru Gudima<sup>2</sup>, Vladimir Riabov<sup>2</sup>, Martin Pravda<sup>3</sup>, Julia Kzhyshkowska<sup>2</sup>, Nihal Engin Vrana<sup>1</sup>

<sup>1</sup>Protip Medical, France

<sup>2</sup>Institute of Transfusion Medicine and Immunology, Medical Faculty of Mannheim, University of Heidelberg, Germany

<sup>3</sup>Contipro, Czech Republic

[m.evangelista@protipmedical.com](mailto:m.evangelista@protipmedical.com)

### INTRODUCTION

Macrophages (Mφs) were initially recognized by Elie Metchnikoff as phagocytic cells responsible for pathogen elimination and housekeeping functions in a wide range of organisms<sup>1</sup>. Mature macrophages are virtually present in every tissue of the body. Macrophages are key innate immune cells with multiple immunoregulatory functions that include clearance of pathogens and apoptotic cells, regulation of ECM turn over, initiation and control of inflammatory reaction by activation of various cell types of innate and adaptive immunity<sup>2,3</sup>. Macrophages are activated in a specific way during anti-bacterial, anti-parasitic and allergic responses, as well as during wound healing and implantation<sup>4,5</sup>.

Macrophages develop tissue specific phenotypes (osteoclasts in bone tissue, microglia in CNS<sup>6</sup>.) Frequently the devices aiming to provide a newer solution for a specific problem face the host's foreign-body response<sup>4</sup>. In this work we have studied the survival and response to cytokine induction of macrophages in order to control macrophage phenotype in 3D conditions. Reported work is being performed with the immobilization of macrophages. For that, naïve human monocytes have been immobilized within gelatin and modified with hyaluronic acid molecules gelatin gels, mimicking ECM components to investigate the behaviour of these cells within an ECM-like environment.

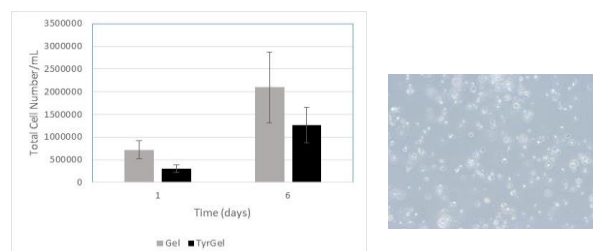
### EXPERIMENTAL METHODS

CD14<sup>+</sup> monocyte cells were isolated from human peripheral blood. Cells were immobilized within 6 wt-% gelatin gels and 4% tyraminated hyaluronic acid (TyrHA)/gelatin gels both enzymatically crosslinked with 10 wt-% transglutaminase (TG) and HRP at a density of 6 million cells/mL of material. Cells were cultured up to six days in a 5% CO<sub>2</sub>:7% O<sub>2</sub> atmosphere at 37° C with macrophage-SFM and physiological levels of dexamethasone (10<sup>-8</sup> M) with the addition of M2-like phenotype inducing cytokines. At a given timepoint samples were analysed for cell viability and cell proliferation using CASY® Cell Counter and Particle Analyzer (Scharfe Systems, Germany) and reactive oxygen species (ROS) production using CellROX® Orange Reagent (Life Technologies).

### RESULTS AND DISCUSSION

We have observed an increase in total cell number over the six days of the culture, in both gel conditions. As the proliferation of naïve macrophages was not

observed by us and other groups in 2D experiments, additional experiments are necessary to elaborate on the underlying mechanism in this increase<sup>7</sup>.



“Figure 1. A) The total number of cells after gel dissolution of naïve monocytes immobilized within gelatin and Tyraminated HA Gelatin 3D gels; B) phase contrast image in Gelatin hydrogel”

Moreover it was detected that ROS production is not significantly different between Gelatin. TyrHA/gelatin gels both at day 1 and day 6. In addition, two different conditions were compared (no LPS, lipopolysaccharide, and stimulated with LPS) with no major differences detected. These results show that human macrophages can be immobilized and that they can be differentiated in M2-like cells *in vitro*. Further analysis were carried out such as ELISA analysis of cytokines (TNF-α (M1, non-detectable) and CCL-18 (M2, present in small amounts produced by human macrophages).

### CONCLUSION

Gelatin and Tyraminated gelatin promote higher cell survival as well as prevent production of reactive oxygen species. This system can be used for controlling macrophage phenotype in 3D conditions.

### REFERENCES

1. Martinez *et al.*, Annu. Rev. Immunol. 27:451-483, 2009
2. Nagata S. *et al.*, Cell. 140:619-630, 2010
3. Martinez and Gordon, F1000Prime Rep. 6:1-13, 2014
4. Grainger DW, Nat. Biotech. 31:507-509, 2013
5. Gratchev *et al.* Immunobiology. 211:473-486, 2006.
6. Ginhoux F, Jung S, Nat. Rev. Immunol. 14:392-404, 2014
7. Brown *et al.*, PLOS One. 3:e3664, 2008

### ACKNOWLEDGMENTS

We acknowledge the European Project “IMMODGEL” (Contract number 602694) for financial support. The authors are most grateful to Ajinomoto Co. Inc. (TG)



## 2D Cell Monolayer and 3D Cell Construct Cryopreservation by Slow Vittrification

Kazuaki Matsumura<sup>1</sup>, Keiko Kawamoto<sup>1</sup>, Suong-Hyu Hyon<sup>2</sup>

<sup>1</sup>School of Materials Science, Japan Advanced Institute of Science and Technology, Japan

<sup>2</sup>Center for Fiber and Textile Science, Kyoto Institute of Technology, Japan

[mkazuaki@jaist.ac.jp](mailto:mkazuaki@jaist.ac.jp)

### INTRODUCTION

Cryopreservation is used for long-term preservation of biological materials containing cells. Two primary techniques of cryopreservation are slow freezing and vitrification, in which water transition directly to the glassy state without crystallization. Slow freezing methods, which utilize 10% dimethyl sulfoxide (DMSO) as a cryoprotectant, are effective for numerous cell lines. However, the method is not acceptable for the effective cryopreservation of large volume cell such as oocyte or 2D or 3D cell constructs.

Vitrification methods have been developed with the advent of preservation techniques for oocytes and embryos, primarily in the field of reproductive medicine. We previously utilized carboxylated poly-L-lysine (COOH-PLL) [1], a novel polymer cryoprotectant as a component of vitrification solution of human iPS cells by using its recrystallization inhibition property [2].

In this study, we reported the development of slow vitrification technique for the effective cryopreservation of 2D and 3D cell constructs by using novel cryoprotectants.

### EXPERIMENTAL METHODS

We previously reported the synthesis of the polymeric cryoprotectant, COOH-PLL[1]. We prepared a vitrification solution (VS) based on 6.5 M ethylene glycol (EG, Wako) and 0.75 M sucrose (Wako) in PBS. COOH-PLL was added to the solution at 10% w/v to evaluate the effect of the polymer. A DAP213 solution [2 M DMSO, 1 M acetamide and 3 M propylene glycol (all from Wako), in PBS] was used as control.

One mL of VS was added on the human mesenchymal stem cells (MSCs) sheet cultured in the dish. And after 5 min, the VS was removed by aspiration and held various distance above the surface of liquid nitrogen. The temperature of the MSC monolayer was monitored with the thermocouple attached on the monolayer. After 20 min, the vitrified MSC monolayer sheet was soaked into liquid nitrogen. The MSC monolayers were warmed on the same day by gently addition of the pre-warmed medium (2mL) and after 3min, monolayer was washed with DMEM twice for 5min each. The cell viability was evaluated by Live/Dead assay kit.

To compare stabilities of the glassy states among these vitrification solutions, thermal analysis was performed using a differential scanning calorimeter (DSC).

### RESULTS AND DISCUSSION

The freezing speed could be varied from 0.58-0.08 degree/sec by changing the distance between the bottom of MSC culturing dish and surface of liquid nitrogen. Cell viability of MSC sheets after thawing with

vitrification through various freezing speed was shown in Fig.1. The live/dead assay results of thawed MSC sheets after vitrification through 0.58 and 0.08 degree/sec were shown Fig.2. From these results, COOH-PLL addition was very effective on the vitrification with low freezing speed. The mechanisms might be related with the ice crystallization inhibition and inhibition of de-vitrification properties of COOH-PLL, which were evaluated by DSC measurements. And also our vitrification system could be applied for 3D cell constructs and tissue-engineered skin vitrification successfully.

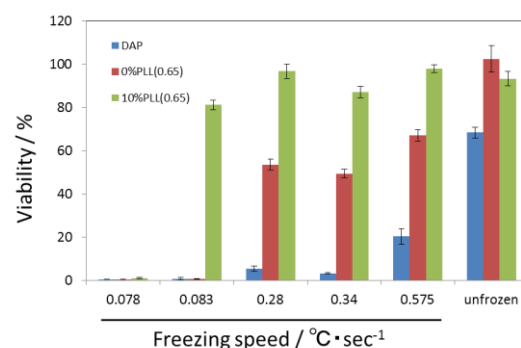


Fig.1 Cell viability after vitrification of MSC sheets with various vitrification solution through various freezing speed.

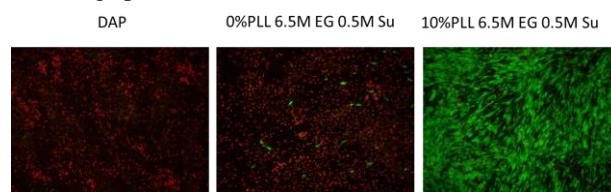


Fig.2 Microphotographs of MSC sheets by Live/Dead assay after vitrification with various vitrification solutions at a freezing speed of 0.08 degree/sec.

### CONCLUSION

It was shown that COOH-PLL improved effectively the vitrification properties of current vitrification system due to its inhibition of recrystallization property. From our results, tissue constructs can be cryopreserved in glassy state at relatively slow freezing speed such as 0.08 degree/sec.

### REFERENCES

1. Matsumura K. et al., *Biomaterials* 30:4842-49, 2009.
2. Matsumura K. et al., *Cryobiology* 63:76-83, 2011.

### ACKNOWLEDGMENTS

"The authors would like to thank the Grant-in-Aid for Scientific Research(A), MEXT, (Grant no: 25242050) for providing financial support to this project.

## Interaction of Sub-Compartmentalized Microreactors with Hepatocytes

Yan Zhang<sup>1</sup>, Brigitte Städler<sup>1</sup>

<sup>1</sup>iNANO Interdisciplinary Nanoscience Centre, Aarhus University, Denmark  
[yanzhang@inano.au.dk](mailto:yanzhang@inano.au.dk)

### INTRODUCTION

Microreactors have the potential to become a desirable method to maximize the efficacy of therapeutic treatments in numerous ways, because they can synthesis and release their contents by responding to external triggers or biomarkers [1]. Microreactor could be used for encapsulation of enzymes, substrate, catalyst, gene and peptide cargo [2, 3]. Sub-compartmentalized microreactors are of particular interest, since they mimic the hierarchical structure of cells, allowing for the co-encapsulation of multiple cargo and for triggered activity. [6] Although therapeutic cell mimicry is an interesting approach which the potential to substitute for missing or lost cellular function, most of the research has so far been done in cell-free environment. The objective of this work is to understand, if microreactors co-cultured with hepatocytes can induce a (positive) effect in the growing cell sheet. Therefore, it was investigated whether soft alginate (Alg) particles and hard polystyrene (PS) particles could be co-culture with hepatocytes for assembling interacting cell-particle constructs. Further, the Alg particles were equipped with trypsin loaded liposomes as a model microreactor and its activity was assessed in cell culture.

### EXPERIMENTAL METHODS

Alg particles (~41 µm diameter) without and with different enzyme-loaded liposomes were prepared by droplet microfluidics. Alg particles and PS particles (~41 µm diameter) were coated with poly (L-lysine), cholesterol-modified poly (methacrylic acid, (PMA<sub>c</sub>) or (PMA), co-cultured with hepatocytes (HepG2) and their interaction was analyzed at different time points. The enzyme trypsin was trapped in the liposomal subunits and the enzymatic activity was assessed using bisamide substrate of rhodamine 110 as substrate which can be converted into a fluorescent product by trypsin.

### RESULTS AND DISCUSSION

When bare PS particles were co-cultured with hepatocytes, the particles were only badly incorporated into the cell sheet. After surface modification of the particles, the PLL and PMA<sub>c</sub> coated particles were found to be suitable for the assembly of particle-cell constructs when co-culture with hepatocytes for up to 10 days. A similar trend has been observed for the Alg particles. The coated particles were better incorporated into the hepatic tissue. Further, tested particles did not negatively affect the cell viability.

In order to assemble a microreactor, different amounts of liposomes were loaded into Alg particles yielding increasing fluorescence intensity with increasing amount the fluorescence liposomes. Trypsin was loaded

in liposomes and the conversion of the substrate occurred in a temperature controlled manner. The enzyme loaded liposome-containing Alg particles were co-cultured with hepatocytes, and after incubating with the substrate, the cells became fluorescence, which showed that the product was released from Alg particles.

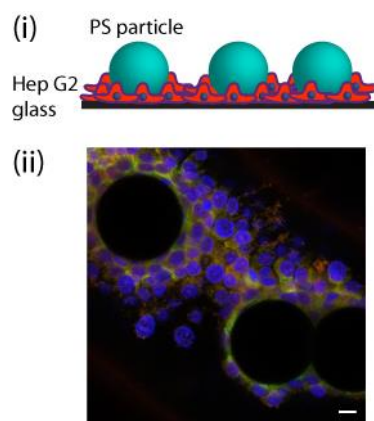


Figure 1. (i) Scheme of a PS particle- hepatocytes cell construct. (ii) Representative CLSM image of PS particles co-cultured with hepatocytes for 7 days. The scale bar is 10 µm.

### CONCLUSION

We demonstrated that subcompartmentalized enzyme loaded Alg particles can be incorporated into the growing hepatocyte cell sheet and that the product produced by the microreactor could be internalized by the cells. These findings are a major step towards the assembly of bionic tissue – a combination of biological and synthetic entities.

### REFERENCES

1. Ju X. J. et al., Expert Opin. Ther. Pat. 2009, 19: 683, 2009
2. Bäuml H. et al., Biomacromolecules, 11: 1480, 2010
3. Hosta-Rigau L. et al., ACS Appl. Mater. Interfaces., 6: 12771, 2014
4. Palankar R. et al., Small, 5: 2168, 2009
5. Raemdonck K. et al. Adv. Funct. Mater., 18: 993, 2008
6. Zelikin A.N. et al., Small, 6(20): 2201, 2010

### ACKNOWLEDGMENTS

The authors would like to thank the Lundbeck Foundation for providing financial support to this project.



## Macrophage-Laden 3D Fibrin Gels: Effect of Fibrinogen Concentration on Inflammation

Vera Malheiro<sup>1</sup>, Arie Bruinink<sup>1</sup>, Katharina Maniura<sup>1</sup>

<sup>1</sup>Biointerfaces, EMPA Swiss Federal Laboratories for Materials Science and Technology, Switzerland  
[vera.malheiro@empa.ch](mailto:vera.malheiro@empa.ch)

### INTRODUCTION

Fibrin is the first temporary matrix at the tissue-implant interface. Its primary role is to stabilize the wound site and provide the matrix through which cells can migrate to the implant surface. As such, fibrin is inherently related to healing. Changes in its structure can interfere with cell function and resultant tissue repair [1]. Fibrin is formed from the conversion of fibrinogen to an insoluble matrix through a complex natural polymerization mechanism. The properties of fibrin are affected by fibrinogen concentration [2], which varies in human plasma due to disease, demographic and environmental factors [3]. Macrophages are the predominant cell type at the wound site by 48-72 hours post-injury and thus potentially responsive to variations in the fibrin-rich extracellular matrix.

In the current work we have encapsulated macrophages onto 3D fibrin gels and examined whether gels produced from non-physiological concentrations of fibrinogen interfere with the cell viability and inflammatory response.

### EXPERIMENTAL METHODS

Macrophages encapsulation onto fibrin gels was achieved by mixing a fibrinogen solution with a macrophage cell suspension and a Tris- buffered saline solution containing 2 IU/mL of thrombin and 5 mM CaCl<sub>2</sub>. Complete gelification was achieved following 1 h incubation at 37 °C.

THP-1 monocytic leukemia cell line was used as cell model. Macrophage viability was examined by live & dead staining and LDH release. Macrophage distribution in the gel was analysed by confocal laser scanning microscopy, whereas its morphology and adhesion to the fibrin gel was examined by scanning electron microscopy. As a measure of inflammatory response, the secretion of the inflammatory cytokine TNF- $\alpha$  was determined by an enzyme-linked immunosorbent assay.

### RESULTS AND DISCUSSION

Typical gels architecture are illustrated by the scanning electron micrographs (SEM) shown in Fig. 1. Whilst all gels show similar random fibre orientation, the frequency of fibres with a smaller diameter and the fibre and branch-point density seems to increase as the fibrinogen concentration increases.

Macrophages were homogeneously distributed within the fibrin matrix, and showed direct contact with fibrin fibres. Macrophage viability within fibrin gels was comparable to that on tissue culture treated polystyrene (TCP) control, except for fibrin gels produced with supra-physiological concentrations

where a decrease of viability was noted on day 3 in culture (Fig.2 (a)). TNF-alpha release was increased in fibrin gels in comparison to TCP negative control (Fig.2 (b)), with a maximum value detected for fibrin gels produced with supra-physiological concentrations of fibrinogen. LPS treated cultures served as positive control.

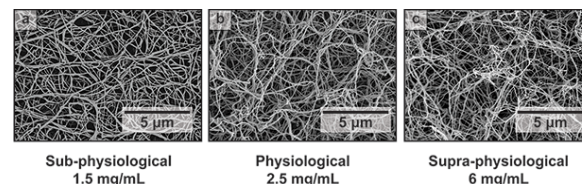


**Fig. 1:** SEM images of fibrin gels formed with a concentration of fibrinogen increasing from (a) sub-physiological, to (b) physiological and (c) supra-physiological levels.

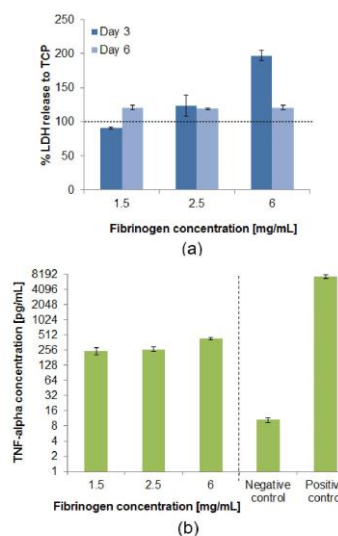


**Fig. 2:** Effect of fibrinogen concentration on (a) Lactate dehydrogenase (LDH) and (b) TNF-alpha release from macrophages encapsulated onto fibrin gels. TNF-alpha release was determined after 6 days in culture and is presented in the logarithmic scale.

### CONCLUSION

Macrophages can be successfully encapsulated in fibrin gels. Higher concentration of fibrinogen affects macrophage viability. TNF-alpha release is increased by macrophages encapsulated in fibrin gels.

### REFERENCES

- [1] Shiu HT, Goss B, Lutton C, Crawford R, Xiao Y. Tissue Eng Part B Rev 2014;20:697–712.
- [2] Ryan EA, Mockros LF, Weisel JW, Lorand L. Biophys J 1999;77:2813–26.
- [3] DE MAAT MPM. Ann N Y Acad Sci 2001;936:509–21.

### ACKNOWLEDGMENTS

The authors would like to thank the Marie Curie Co-funding programme (COFUND) for providing financial support to this project.





## Fabrication and Characterization of Clinoptilolite/PCL-PEG-PCL Composite Scaffolds for Bone Tissue Engineering

Pazarceviiren, Ahmet Engin<sup>1</sup>, Özge Erdemli<sup>2</sup>, Dilek Keskin<sup>1,3</sup>, Ayşen Tezcaner<sup>1,3</sup>

Department of Engineering Sciences, <sup>1</sup>Middle East Technical University, Turkey

<sup>2</sup>Laboratory of Physical Chemistry and Microbiology for the Environment, University of Lorraine, France

<sup>3</sup>Center of Excellence in Biomaterials and Tissue Engineering, Middle East Technical University, Turkey

### INTRODUCTION

Biodegradable synthetic polymers such as poly ( $\epsilon$ -caprolactone) (PCL) and poly (ethylene glycol) (PEG) have been frequently used for scaffolding in tissue engineering studies because of their biocompatibility, non-cytotoxic degradation products, easily tailored degradation rates and porosity<sup>1,2</sup>. PEG has been utilized to form various block copolymers with PCL<sup>3</sup>. Extensively, ring opening polymerization is applied to form PCL and PEG block copolymers having various thermoplasticity, degradability and hydrophilicity<sup>4</sup>. Clinoptilolite is an aluminosilicate mineral which has  $(Ca, Fe, K, Mg, Na)_3-6Si_3OAl_6O_{72} \cdot 24H_2O$  as general formula<sup>5</sup>. While showing good mechanical properties, clinoptilolite can also be used as a protein adsorbent<sup>6</sup>. In this study, highly porous and interconnective Clinoptilolite/ PCL-PEG-PCL composite scaffolds were fabricated by particulate leaching method and also it was hypothesized that they can enhance bone tissue growth and induce osseointegration by providing a controlled and sustained release of protein or growth factors.

### EXPERIMENTAL METHODS

PCL-PEG-PCL triblock copolymer was synthesized from  $\epsilon$ -caprolactone (pure >99%) and PEG ( $M_n=4000$ , pure 99%) by ring opening polymerization under 140 °C for 24 hours. Obtained triblock copolymer was characterized spectroscopically by <sup>1</sup>H NMR and FTIR analyses. Furthermore, DSC and TGA analyses were conducted for thermal characterization of triblock copolymer. Clinoptilolite mineral having overall size between 1  $\mu m$  and 50  $\mu m$  was sintered at 250 °C for 24 hours. In addition, clinoptilolite was analysed for protein adsorption capacity using Bovine Serum Albumin (BSA) 0.1 M PBS at pH 7.4 for various time intervals (10, 30, 60, 360 and 1440 min). Finally, clinoptilolite, PCL-PEG-PCL triblock copolymer and sodium bicarbonate (< 50  $\mu m$ , pure >95%) were mixed at various ratios. Mixtures were obtained by disperser (15000 rpm, 5 min) utilizing ethanol (pure, 99%) in order to powder and form homogenous mixture while averting use of any organic solvent. Homogenous mixture was vacuumed overnight under 40 °C overnight to remove ethanol and powder was compressed under 250 MPa for 3 min at 25 °C and scaffolds having 13 mm diameter and 6 mm thickness were obtained. Scaffolds were observed under SEM to investigate surface and cross-sectional porosity as well as analysing the overall pore sizes. Porosities of scaffolds were calculated through Archimedes' Principle and compressive mechanical properties were obtained by uniaxial compression under 2.5 kN load cell at a rate of 3 mm/min up to 25% strain.

### RESULTS AND DISCUSSION

From the spectroscopic analysis by <sup>1</sup>H NMR, it was shown that the PCL-PEG-PCL triblock copolymer was synthesized successfully (Fig 1). FTIR, DSC and TGA analyses were also complementary to NMR results.

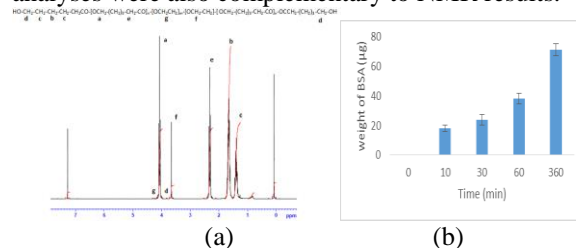


Figure 1. (a) <sup>1</sup>H NMR results for PCL-PEG-PCL triblock copolymer. (b) Protein adsorption onto 25 mg clinoptilolite powder samples

SEM images indicated that upper, lower and side surfaces and cross-sections were highly porous while overall pore size ranged between 10 to 50  $\mu m$ . Scaffolds with highest sodium bicarbonate concentration showed 55% porosity (3:1 salt to copolymer) and with lowest salt concentration show 35% porosity (1:1 salt to copolymer). Corresponding to porosities, scaffold compressive strengths ranged between 1.8 MPa for most porous scaffold to 4.8 MPa for least porous scaffold. Moreover, it was shown that clinoptilolite presence increased the compressive moduli when compared with non-clinoptilolite groups which were used as control groups.

### CONCLUSION

Porous, interconnective and mechanically stable composite PCL-PEG-PCL scaffolds were developed successfully. Clinoptilolite was shown to absorb large amounts of protein ( $q_e=4$  mg/g clinoptilolite) so that clinoptilolite will enable composite scaffolds to be used for the delivery of bioactive molecules both in vivo and in vitro. Furthermore, bioactivity, direct and indirect cytotoxicity and differentiation studies for developed scaffolds are under study..

### REFERENCES

1. Bose et al., 2012. Trends Biotech. 30(10), 546–54.
2. Kutikov et al., 2013. Acta Biomater. 9(9), 8354–64.
3. Sosnik and Cohn, 2003. Polymer. 44(23), 7033-42.
4. Huang et al., 2004. J Biomed. Mat. 69(3), 417–27
5. Uyumaz et al., 2011. Key Eng. Mat. 493-494.
6. Akgül et al., 2008. Hac. J Biol. & Chem. Eng. 36(1), 21-9.

### ACKNOWLEDGMENTS

“The authors would like to thank the Middle East Technical University Coordinatorship of Scientific Research Projects (Grant no: BAP-03-10-2014-001) for providing financial support to this project.

# Osteoinductive Dental Ring for Vertical Bone Regeneration with Simultaneous Introduction of Dental Implants

Anna Chróścicka<sup>1,2</sup>, Piotr Wychowański<sup>3</sup>, Ewa Jankowska-Steifer<sup>1</sup>, Marek Kujawa<sup>1</sup>,  
Małgorzata Lewandowska-Szumiel<sup>1,2</sup>

<sup>1</sup>Department of Histology and Embryology, Centre for Biostructure Research, Medical University of Warsaw, Poland

<sup>2</sup>Centre for Preclinical Research and Technology, Poland

<sup>3</sup>Department of Oral Surgery, Medical University of Warsaw, Poland

[anna.chroscicka@wum.edu.pl](mailto:anna.chroscicka@wum.edu.pl)

## INTRODUCTION

Bone augmentation is one of the most important problems in dental implantology. Only recently proposed, so called bone ring technique allows bone augmentation and the implant placement to be performed in a single operation [1, 2]. For this purpose, either autologous bone grafts or pre-fabricated bone rings of processed allogenic donor bone are currently in use. In order to avoid well-known limitations connected with tissue transplantation, in this study we have evaluated and verified at the pre-clinical level, the alternative original system based on use of the ceramic rings - either enriched with osteogenic cells or not.

## EXPERIMENTAL METHODS

Commercially available blocks of HA/ $\beta$ TCP (Maxresorb®), with open porosity of 80% were used. The ring-shape samples with an internal diameter of 3.3mm, outer diameter of 10mm, high to 5mm were cut and prepared for the implantation. In order to mimic the ring technique, the animal model was developed. The rings were implanted into the mandible of Göttingen minipigs and were fixed by commercially available dental implants. There were two experimental groups. In one group the rings were pre-soaked in cell culture medium, seeded with autologous pig adipose derived stem cells (ADSC) at the density of 700000cells/ring and put to the *in vitro* culture for 14 days. Before implantation cell viability was examined in the XTT assay. In the second group, rings pre-soaked in a medium but without ADSC were prepared.

Two rings were implanted into each animal: one seeded and the other one non-seeded with ADSCs. Individual rings were implanted on the right and left side of a mandible in parallel. Six weeks after implantation the animals were euthanized and the rings together with a surrounding tissues were excised. The excised rings were fixed in 10% buffered formalin solution and prepared to histological analysis: the Hematoxylin and Eosin (HE) and Sirius Red staining were used. Moreover, stability of the implants fixation was measured immediately after implantation and at the end of the experiment.

## RESULTS AND DISCUSSION

As confirmed by XTT test, ADSC seeded on the ceramic rings were alive at the time of implantation. Six weeks after implantation there were no macroscopic differences between cell-seeded and non-seeded rings. All rings were overgrown by tissue and stably embedded in a mandible bone with no intervening soft tissue layer or signs of inflammation. The mean implant

stability was about 70 ISQ, with no significant differences between the groups. The histological analysis revealed the presence of well vascularized and well organized connective tissue in the pores of the rings. Numerous bone trabeculae were observed. They were organized mainly at the internal surface of pores. Interestingly, the amount of the new bone tissue present inside the ceramic rings was significantly higher in the scaffolds non-seeded with ADSC before implantation. Similar results were previously presented, by F.G. Lyons et al. [3] who found that the cell-seeded groups of scaffolds showed poor bone infiltration as compared to the unseeded groups (studies on critical-sized rat cranial defect). The differences may be related to the higher activity of M1 (pro-inflammatory) macrophages in the cell-seeded implants as well as the more beneficial localization of M2 (pro-repair) macrophages in the unseeded ones.

The legitimacy of the use of cell-containing implants is an important issue for the further development of tissue engineering. We believe that our research brings an interesting contribution to this discussion and gives a good basis for further investigations.

Regardless of the issues related to the role of the cells in bone tissue engineered products, our results encourage the use of ceramic implants instead of bone grafts in a ring technique of simultaneous bone augmentation and dental implant placement. If rings without prior-to-implantation-cell-seeding are good enough or even better than those enriched with cells, then off-the-shelf man-made rings can be offered for reconstruction of vertical bone losses.

## CONCLUSION

Synthetic rings prepared from a porous ceramic material and as such, free from the limitations associated with using bone grafts, can replace bone rings currently used in dental surgery. HA/ $\beta$ TCP rings are capable of simultaneous reconstruction of a vertical bone loss and introduction of implants in dental surgery. Addition of cells to the ceramic rings may worsen their overgrowth with bone tissue.

## REFERENCES

1. Stevens M.R. *et al.*, J. Oral Implantol. 36 (1):69-74, 2010;
2. Giesenhausen B. *et al.*, From Practitioner to Practitioner 29 (3): 244-254, 2013;
3. Lyons F.G. *et al.*, Biomaterials 31: 9232-9243, 2010

## ACKNOWLEDGMENTS

This work was supported by National Centre for Research and Development grant NR13-0008-10/2010



## Novel N-(2-Carboxybenzyl)chitosan Bionanocomposites for Tissue Scaffolding Applications

Maria Nerantzaki<sup>1</sup>, Zoe Terzopoulou<sup>1</sup>, M.D. Anastasopoulou<sup>2</sup>, Michalis Karakassides<sup>2</sup>, Iro Koliakou<sup>3</sup>, Aldo Boccacini<sup>4</sup>, Dimitrios Bikiaris<sup>1</sup>

<sup>1</sup>Department of Chemistry, Aristotle University of Thessaloniki, Greece

<sup>2</sup>Department of Materials Science & Engineering, University of Ioannina

<sup>3</sup>Department of Biology, Aristotle University of Thessaloniki, Greece

<sup>4</sup>Institute of Biomaterials University of Erlangen-Nuremberg

[terzoe@gmail.com](mailto:terzoe@gmail.com)

### INTRODUCTION

N-(2-Carboxybenzyl)chitosan (CBCS) is a chitosan derivative which presents a wide range of properties that make it appropriate for tissue engineering applications, such as non-toxicity, biodegradability, biocompatibility, antibacterial and antifungal activity, water solubility (which can be controlled by the degree of substitution), high viscosity, large hydrodynamic volume and ability to form pH sensitive hydrogel. Moreover, various studies demonstrate that by combining bioactive materials with bioresorbable polymers, composites of tailored physical, biological, and time-dependant mechanical properties can be produced, allowing new tissue, as it grows naturally, to take over its load-bearing capability<sup>1</sup>. Hence in this work, CBCS foams containing either microsilicized bioglass or nanosized titania (CBCS/TiO<sub>2</sub>) were prepared by freeze-drying technique and studied as potential tissue engineering scaffolds. In Regenerative Medicine cytocompatible scaffolds for cell therapies are commonly used. Cytotoxicity, stability, cell adhesion, proliferation and spreading are factors that influence effectively the regenerative medicine applications<sup>2</sup>.

### EXPERIMENTAL METHODS

In this work 0.5, 2.5 and 5% TiO<sub>2</sub> nanoparticles and 2.5% Bioglass 45S5 (BG45S5) were added during the carboxyalkylation reaction, in order to obtain different CBCS composites. The scaffolds were prepared by freezing and lyophilizing CBCS solutions. The sample tubes employed had an inner diameter of 1.5 cm and a 1.2 mm wall thickness. For comparison purposes, chitosan xerogel was also prepared with the same method. The porous structure of scaffolds was obtained by freeze-drying technique and characterized using SEM. Compression test (n=5 per condition) were performed using an Instron 3344 with a crosshead speed of 5 mm min<sup>-1</sup>. The swelling, degradation and in-vitro biomineralization of the composite scaffolds were also studied. Mesenchymal stem cells are collected by enzymatic digestion of Wharton's Jelly. Prior to cell seeding, the scaffolds were incubated with culture medium and the mesenchymal stem cells were placed dropwise on to the top of the scaffold. Cell attachment studies, proliferation assays of cells on the scaffolds were evaluated using fluoresce microscopy. Furthermore viability of cells on the scaffolds was evaluated using MTT (3-(4,5-dimethylthiazol-2-yl)-2,5-diphenyltetrazolium bromide) assay. Finally the morphology of cells on the scaffolds was evaluated by using SEM, TEM and photonic microscopy.

### RESULTS AND DISCUSSION

SEM micrograph of composite scaffolds showed that scaffolds were macroporous in nature with interconnected pore system, important for cell loading in tissue engineering and cell in-growth in tissue induction. Pore size varied from 150–300 µm. Very few agglomerates appear on the walls of the pores, which may constitute fragments that were formed during the cross-section process.

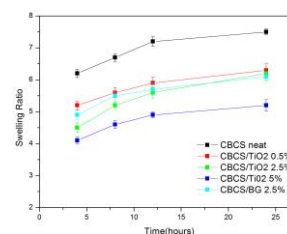


Figure 1: Swelling ratio of the scaffolds

In addition, the swelling test results (Figure 1) suggest that the composite scaffolds indicated increased swelling ratio, with increase of the concentration of the inorganic fillers. Compressive strength values verified that the modification of chitosan backbone in combination with the presence of inorganic fillers can attribute significant mechanical stiffness to the chitosan scaffold, too. The in vitro biomineralization test confirmed that all the samples are bioactive as mineral deposits were detected after incubation in SBF, using X-ray diffractometry. The cells appeared to attach around the pores and most of the pores are filled with cells. Cells keep their morphology, proliferate and migrate across the scaffold and show consistent and proved cytocompatibility.

### CONCLUSION

All studied composites have high cytocompatibility and maintain the biological properties of the seeded cells. So these could be appropriate for tissue regeneration.

### REFERENCES

1. Henc L. *et al.*, Science 295:1014-1017, 2002
2. Costa-Pinto A. *et al.* Tissue Eng Part B 17:331-347, 2011

### ACKNOWLEDGMENTS

The author wishes to acknowledge co-funding of this research by IKY (Greece) and DAAD (Germany), Action "IKYDA 2013.



## BMP-2 Stimulation Affects Structure and Mechanical Properties of Newly Synthesized ECM *In Vitro*

Erik Brauer<sup>1,2,3</sup>, Aaron Herrera<sup>1,3</sup>, Petra Knaus<sup>2,3</sup>, Georg Duda<sup>1,2,3</sup>, Ansgar Petersen<sup>1,3</sup>

<sup>1</sup> Julius Wolff Institute, Charité - Universitätsmedizin Berlin, Germany

<sup>2</sup> Freie Universität Berlin – Institut für Chemie und Biochemie, Germany

<sup>3</sup> Berlin-Brandenburg Center and School for Regenerative Therapies, Germany

[erik.brauer@charite.de](mailto:erik.brauer@charite.de)

### INTRODUCTION

The mechanical microenvironment is known to have a fundamental influence on cell behaviour and might be decisive for tissue regeneration. BMP growth factors are potent inducers of bone formation with known effects on cellular processes such as differentiation and migration<sup>(1)</sup>. Aside of their impact on cell fate, less is known about how BMP affects structural and mechanical properties of the extracellular matrix (ECM) in the process of tissue regeneration<sup>(2)</sup>. We hypothesize that BMP stimulation alters ECM formation in a 3D *in vitro* environment, which serves as a model for the early phase of wound healing in bone.

### EXPERIMENTAL METHODS

Microtissues were created by culturing primary human dermal fibroblasts inside macroporous porcine collagen I scaffolds in expansion medium containing 2% FBS and 1.36 mM ascorbic acid. Biochemical stimulation was performed with 500 ng/ml rhBMP-2 for 6, 24 and 72h (gene expression) and 14 days (histology and mechanical testing). Gene expression was quantified via q-RT-PCR from mRNA isolated from the microtissues. Newly formed collagen I inside the scaffold pores was visualized via immunohistochemistry (IHC). To quantify structural properties, microtissue mechanical properties were analysed via a monoaxial compression test after 2 weeks of stimulation.

### RESULTS AND DISCUSSION

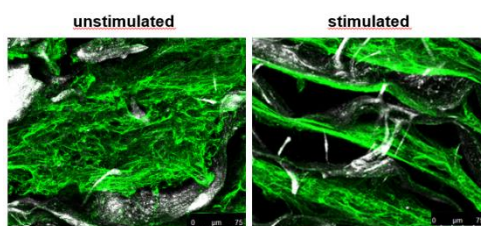


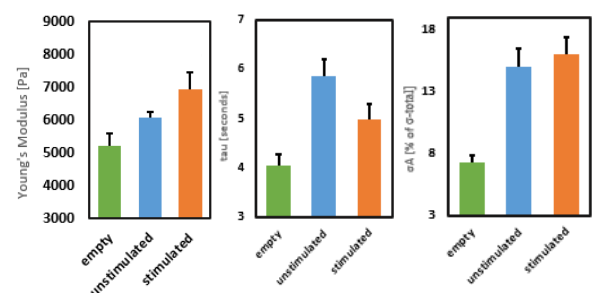
Figure 1: IHC for newly synthesized collagen I (green) and scaffold by SHG (white).

We started to investigate the gene expression of the main fibrillar component of bone extracellular matrix, collagen I with and without BMP-2 stimulation over a time course of 3 days (data not shown). No significant differences were found in the expression patterns but significant differences in collagen network structure of the ECM were found after 2 weeks with highly condensed collagen fibres in stimulated vs. more loose networks in controls (Figure 1).

Structural properties showed an increase in stiffness after 2 weeks of stimulation (Figure 2). Microtissues exhibit viscoelastic material properties, thus we

furthermore analysed stress relaxation succeeding mechanical compression. Experimental data was fitted with an exponential decay function ( $\sigma(t) = \sigma_0 + \sigma_A \cdot e^{(-t/\tau)}$ ). While we didn't observe changes in the amplitude  $\sigma_A$  of stress relaxation, analysis of relaxation time constant,  $\tau$ , revealed a clearly altered relaxation dynamics upon BMP-2 stimulation (Figure 2).

Figure 2: Analysis of mechanical properties after 2



weeks of culture, comparison of BMP-2 stimulated and unstimulated to empty scaffold. Left: Young's Modulus; middle: stress relaxation time constant  $\tau$ ; right: Amplitude  $\sigma_A$  [%] of relaxation.  $p < 0.05$ ,  $n = 4$

### CONCLUSION

We analysed the changes in mechanical properties of microtissues upon BMP-2 stimulation to better understand the influence of the ligand on ECM formation in the early phase of wound healing. Our data indicates, that BMP-2 not only drives fracture healing by induction of osteogenic differentiation of mesenchymal stem cells, but also guides early steps of wound healing and tissue formation. The observed differences in structure and mechanical properties of the collagen network may play an additional role in the invasion of stem cells and their differentiation in order to restore tissue function. Thus our data may hold clues for the future design of bioartificial environments supporting bone regeneration.

### REFERENCES

1. Sieber et al. *Cytokine & growth factor reviews* 2009, **20**(5-6): 343-355.
2. Kopf et al. *BioFactors* 2013. doi: 10.1002/biof.1137

### ACKNOWLEDGEMENTS

This work has been partially funded by the DFG research group "FOR 2165 – Regeneration in Aged" and by the DFG Graduate School 203 "Berlin-Brandenburg School for Regenerative Therapies".



## Aging Reduces Osteogenic and Increases Adipogenic Potential of Mesenchymal Stem Cells Grown on Titanium

Rodrigo P. F. Abuna<sup>1</sup>, Camila T. Stringhetta-Garcia<sup>2</sup>, Rita C. M. Dornelles<sup>2</sup>, Adalberto L. Rosa<sup>1</sup>, Marcio M. Beloti<sup>1</sup>

<sup>1</sup>Cell Culture Laboratory, School of Dentistry of Ribeirão Preto, University of São Paulo, Brazil

<sup>2</sup>Department of Basic Sciences, Araçatuba Dental School, Universidade Estadual Paulista, Brazil

[mmbeloti@usp.br](mailto:mmbeloti@usp.br)

### INTRODUCTION

Titanium (Ti) is the gold standard biomaterial used to produce dental implants thanks to its physical properties and superior ability to osseointegrate<sup>1</sup>. In addition to the implant characteristics, the clinical success of this treatment is also related to patient health conditions and local bone quality and quantity, both affected by aging. As elderly is the main population that needs dental implants, it is of relevance to understand how aging affects bone/implant interactions. Thus, the aim of this study was to evaluate the effect of aging on osteoblastic differentiation of mesenchymal stem cells (MSCs) grown on Ti.

### EXPERIMENTAL METHODS

Discs of commercially pure Ti (12 mm in diameter and 1.5 mm thick) were polished using 320 and 600 grit silicon carbide, cleaned by sonication, sterilized and air-dried. Bone marrow MSCs were obtained from the femurs of 1-month (young) and 21-month (old) male Wistar rats and were cultured in growth medium until reaching subconfluence. Then, MSCs were cultured in osteogenic medium on Ti discs for periods of up to 21 days. During the culture period, cells were incubated at 37°C in a humidified atmosphere of 5% CO<sub>2</sub>, and the medium was changed every 3 days. Cell proliferation was evaluated at days 4, 7 and 10 with 3-(4,5-dimethylthiazol-2-yl)-2,5-diphenyltetrazolium bromide (MTT). At the same time-points, alkaline phosphatase (ALP) activity was determined by measuring the release of thymolphthalein from thymolphthalein monophosphate using a commercial kit. Extracellular matrix mineralization was detected at day 21 by alizarin red staining and calcium content was measured by a colorimetric method. Quantitative real-time polymerase chain reaction (PCR) was performed at day 10 to evaluate the gene expression of the osteoblast markers, runt-related transcription factor 2 (RUNX2), osterix (OSX), ALP, bone sialoprotein (BSP), osteocalcin (OC) and osteopontin (OPN), and adipocyte markers, peroxisome proliferator-activated receptor gamma (PPARγ), adipocyte protein 2 (aP2) and resistin (RTN). The data obtained in three time-points were analyzed using two-way ANOVA followed by Student Newman Keuls post-test and in one time-point using Student's t-test. For all experiments the level of significance was set at  $p \leq 0.05$ .

### RESULTS AND DISCUSSION

Cell proliferation was higher in cultures from 1-month compared with 21-month rats at all evaluated time-points ( $p < 0.001$  for all time-points). Besides, the cell

number increased ( $p < 0.001$ ) over time in cultures from 1-month rats, while no significant difference ( $p = 0.127$ ) was observed between 7 and 10 days in cultures from 21-month rats. Cells from 1-month rats showed higher ALP activity compared with cells from 21-month rats at 7 and 10 days ( $p < 0.001$  for both time-points), while no significant difference ( $p = 0.561$ ) was observed at 4 days. In addition, the ALP activity increased ( $p < 0.001$ ) over time in cultures from 1-month rats, while no significant difference ( $p > 0.050$ ) was observed between 4, 7 and 10 days in cultures from 21-month rats. Mineralized extracellular matrix was detected on Ti discs irrespective of cell source, with cells from 1-month rats producing the most dense and regularly distributed matrix. Additionally, the calcium content was higher ( $p < 0.001$ ) in cultures from 1-month compared with 21-month rats. The gene expression of all evaluated osteoblast markers, RUNX2, OSX, ALP, BSP, OPN and OC was higher ( $p < 0.001$  for all genes) in cultures from 1-month compared with 21-month rats. On the other hand, the gene expression of all evaluated adipocyte markers, PPARγ ( $p < 0.007$ ), aP2 ( $p < 0.050$ ) and RTN ( $p < 0.001$ ) was higher in cultures from 21-month compared with 1-month rats.

These findings indicate that aging reduces osteoblast differentiation of cells cultured on Ti as described elsewhere<sup>2</sup>. Additionally, it was observed that this reduction is associated with an increased adipogenic differentiation.

### CONCLUSION

Our results showed that the reduced osteogenic potential of MSCs derived from aging rats goes along with the increased adipogenic potential in cultures grown on Ti. As a consequence, the development of therapies to recover the balance between osteoblast and adipocyte differentiation, which could be associated with dental implant treatment in the elderly population, is of great interest.

### REFERENCES

1. Albrektsson T. *et al.*, Acta Orthop. Scand. 52:155-170, 1981.
2. Olivares-Navarrete R. *et al.*, J. Bone Miner. Res. 27:1773-1783, 2012.

### ACKNOWLEDGMENTS

Fabiola S. Oliveira, Milla S. Tavares and Roger R. Fernandes are acknowledged for their technical assistance. State of São Paulo Research Foundation (FAPESP, Brazil, #2012/01291-6) is acknowledged for providing financial support to this study.





# Controlled Release of Amorphous Calcium Phosphate from Titania Nanostructures Induces Osteoblastic Differentiation in Human Mesenchymal Stem Cells

Robert McLister, Mura McCafferty, George Burke, Brian J. Meenan

Biomaterials and Tissue Engineering Research Group, University of Ulster, Northern Ireland

[mc\\_lister-r@email.ulster.ac.uk](mailto:mc_lister-r@email.ulster.ac.uk)

## INTRODUCTION

It is well established that sputter deposited amorphous CaP coatings have osteoconductive properties that can be advantageous for directing cell response (1). This non-crystalline form of CaP is highly soluble in aqueous cell culture media and its controlled release in combination with key topographical features could be beneficial for encouraging osteoblastic differentiation of human mesenchymal stem cells (hMSCs) without the use of osteogenic media. In this work, the response of hMSCs to sputtered CaP coatings deposited onto titanium substrates with various nanoscale topographies has been determined. The focus of the work is on the role that specific forms of titania nanotopography can have in controlling CaP dissolution and how this subsequently influences hMSCs *in vitro*. The response of hMSC that have been cultured in osteogenic media prior to exposure to the surfaces is also reported.

## EXPERIMENTAL METHODS

Titania Nanotube (TiNT) surfaces were created by electrochemical anodisation of titanium coupons at 20V for 120 minutes in a solution of ethylene glycol with 0.3% wt NH<sub>4</sub>F and 3% wt DI H<sub>2</sub>O. Polycrystalline titania surfaces with nanostructured features were prepared by RF magnetron sputtering from titanium (98.9%) targets onto the same titanium coupons. Both types of surface were then coated with an amorphous CaP coating via RF magnetron sputtering from hydroxyapatite surfaces was carried out at a source power of 50 watts for 9 hours. A number of samples were annealed at 500°C to increase their relative crystallinity. Dissolution studies were undertaken by immersion in 2ml of DI H<sub>2</sub>O at 37°C for 7 days. XPS (Kratos Axis Ultra DLD spectrometer) was used to detect changes in the CaP coating after dissolution. *In vitro* cell studies were carried out using passage 5 hMSCs cultured in high glucose DMEM media with 10% foetal bovine serum (FBS). Osteogenic media was created by supplementing normal media with 10nm dexamethasone, 50µm ascorbic acid-2-phosphate and 10nM β glycerophosphate. Pico green and alkaline phosphatase (ALP) assays were carried out at days 1, 3, 7, 14, 21 to determine cell viability and osteoblastic differentiation, respectively. RNA extraction and qPCR analysis was undertaken at days 7, 14, 21 and 28 to assess Runx2, BMP and osteocalcin gene expression.

## RESULTS AND DISCUSSION

Figure 1 shows the high resolution Ca<sub>2p</sub> and P<sub>2p</sub> XPS spectra for sputtered deposited amorphous CaP coatings on titania nanotubes after 7 days dissolution. The percentage change in each element is indicated in the histogram for before (blue) and after (red) dissolution.

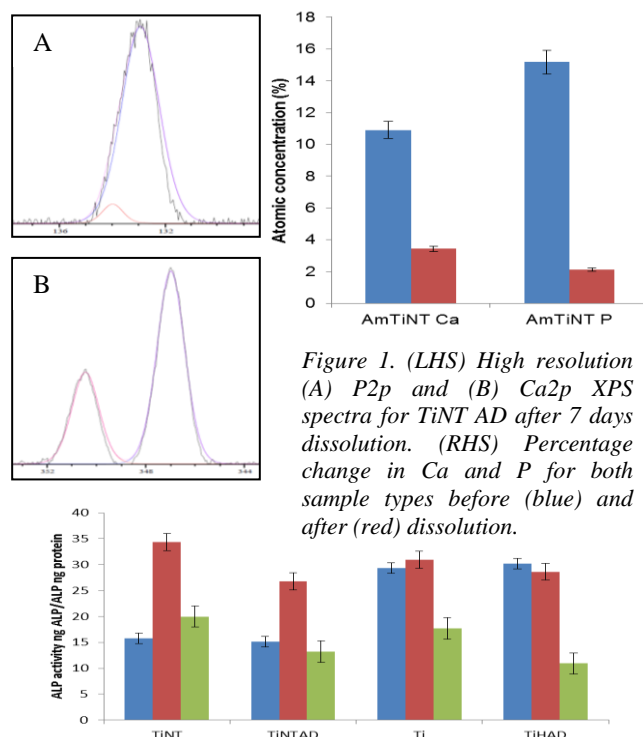


Figure 1. (LHS) High resolution (A) P<sub>2p</sub> and (B) Ca<sub>2p</sub> XPS spectra for TiNT AD after 7 days dissolution. (RHS) Percentage change in Ca and P for both sample types before (blue) and after (red) dissolution.

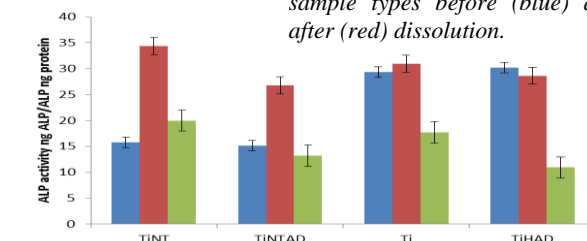


Figure 2. ALP expression at days 7, 14 and 21 from hMSCs cultured on titania nanotube surfaces (TiNT), titania nanotube with Am CaP after 7 days dissolution (TiNT AD), polycrystalline titanium coating (Ti) and polycrystalline coating with Am CaP after 7 days dissolution (TiHAD).

PicoGreen assay indicates the presence of viable cells on all surfaces at each time point. ALP expression from hMSCs cultured in normal media indicates their differentiation to an osteoblastic lineage with the highest expression observed at days 7 and 14. A significant decrease then occurs at day 21. qPCR data for hMSCs cultured in normal media shows osteocalcin at day 28 for CaP on both types of nanotopography after dissolution for 7 days.

## CONCLUSIONS

XPS shows that the dissolution of sputtered CaP is influenced by titania nanotopography. ALP assay data indicates that all the surfaces studied can promote differentiation of hMSC to osteoblastic lineage. qPCR confirms osteocalcin expression at day 28 from hMSCs cultured on a combination of nanoscale topography and amorphous CaP without the use of osteogenic media.

## REFERENCES

(1) I. Mutreja, D. Kumar, A. R. Boyd, B. J. Meenan. Titania nanotube porosity controls dissolution rate of sputter deposited calcium phosphate (CaP) thin film coatings. RSC Advances. 2013;3(28).

## ACKNOWLEDGMENTS

Financial support from the Department for Employment and Learning NI by way of a PhD studentship to RMcL is gratefully acknowledged.



# Chondrogenesis of Umbilical Cord Mesenchymal Stem Cells in a Porous Asymmetric Scaffold of Poly(lactic acid) Functionalized with Hyaluronan: Deposition of a Hyaline Cartilaginous Matrix

Elias Al Tawil<sup>1</sup>, Alexandre Monnier<sup>1</sup>, Quang Trong Nguyen<sup>1</sup>, Jean-Pierre Vannier<sup>2</sup>, Brigitte Deschrevel<sup>1</sup>

<sup>1</sup>Laboratory "Polymères, Biopolymères, Surfaces" (PBS), UMR 6270, Normand Institute of Molecular, Medicinal and Macromolecular Chemistry, FR 3038, CNRS – University of Rouen, F-76821 Mont-Saint-Aignan Cedex, France

<sup>2</sup>Laboratory "MicroEnvironnement et Renouvellement Cellulaire Intégré" (MERCi), EA 3829, University of Rouen, 22 Bd Gambetta, F-76183 Rouen Cedex, France

[elias-al-tawil@etu.univ-rouen.fr](mailto:elias-al-tawil@etu.univ-rouen.fr)

## INTRODUCTION

Articular cartilage is an avascular tissue whose ability to self-repair is extremely low. Even minor injuries may thus lead to painful osteoarthritic damages. Cartilage tissue engineering is one of the most promising approach for treatment of these damages. It is henceforth clear that this approach requires constructs associating at least a matrice scaffold and cells<sup>1</sup>. Among the several cell sources, mesenchymal stem cells (MSC) provide the greatest advantages<sup>1,2</sup>. Scaffold for cartilage tissue engineering should satisfied many requirements including biocompatibility, bioresorbability, porosity, and bioactivity<sup>2</sup>. Although there have been significant advances in cartilage tissue engineering, it remains challenges to overcome such as deposition of a hyaline rather than a fibrocartilaginous matrix<sup>1,2</sup>. Using an inversion phase process we prepared porous asymmetric scaffolds made of poly(lactic acid) which show a tridimensional architecture with interconnected macro- and micro-pores. Macropore mean diameter can be controlled and ranges between 80 and 185  $\mu\text{m}$ . Scaffold surface was entirely functionalized by a nanolayer of hyaluronan which is known to play an important role in hyaline cartilaginous matrix<sup>1,2</sup>. In this context, our work aims to study adhesion, proliferation and differentiation of umbilical cord MSC in our new biomaterials.

## EXPERIMENTAL METHODS

Biomaterial discs (16 mm diameter) were placed in 24-well plates. Each disc was seeded with  $10^6$  MSC in 2 mL of supplemented HDMEM culture medium containing  $0.15 \text{ ng.mL}^{-1}$  TGF- $\beta$ 3. Cultures were incubated at  $37^\circ\text{C}$  under 5 %  $\text{CO}_2$  during 42 days. For each set of experimental conditions, cell culture and analysis were performed in triplicate. Cell proliferation was measured using WST-1 test. Cell viability was quantified with the Vybrant<sup>TM</sup> Apoptosis assay using Alexia Fluor 488 annexin V as probe for apoptotic cells and propidium iodide as probe for necrotic cells. Cell profile was characterized by flow cytometry using fluorescent monoclonal antibodies. Gene expression of SOX-9, collagens I and II was analysed by RT-PCR.

## RESULTS AND DISCUSSION

MSC proliferated in the scaffold when its surface was covered with HA. However proliferation was significantly higher in scaffold with mean pore diameter of 160  $\mu\text{m}$  than in those with mean pore diameters of 130 and 185  $\mu\text{m}$ . This clearly shows that pore diameter strongly influences cell behavior. On the basis of this result, scaffold with mean pore diameter of 160  $\mu\text{m}$  was selected for following experiments. All along the 42-

days of culture, more than 90 % cells stayed alive, less than 10 % were apoptotic cells and no necrotic cell were detected indicating that our biomaterial does not cause cellular stress. We used the simple enzymatic method we developed to retrieve large numbers of viable cells for phenotypic analysis. Flow cytometry analysis showed that expressions of CD 90, CD 105 and CD 166 receptors<sup>3</sup> on cell surface strongly decreased after day 7 whereas expression of CD 49c and CD 151 receptors<sup>4</sup> strongly increased from day 14 to day 42. For each receptor, the level reached at day 42 was very closed to that measured for P2 chondrocytes. This change in phenotypic profil revealed MSC differentiation into chondrocytes<sup>3,4</sup>. Figure 1 shows RT-PCR analysis results. While the expression of SOX-9 and collagen I indicated the chondrogenesis condensation phase, that of collagen II revealed the maturation phase with deposition of a hyaline cartilaginous matrix<sup>5</sup>.

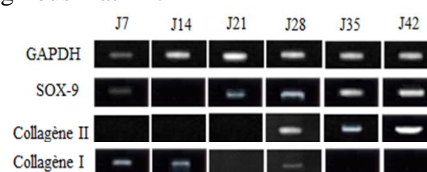


Figure 1: RT-PCR analysis of the expression of SOX-9, collagens I and II by cells during the 42 days of culture. GAPDH was used as negative control.

## CONCLUSION

Our new scaffold functionalized with hyaluronan is well-adapted to MSC adhesion and proliferation. In the presence of a chondrogenic medium, it allows MSC to differentiate into mature chondrocytes with deposition of a hyaline cartilaginous matrix. Our biomaterial is thus a good candidate for cartilage tissue engineering.

## REFERENCES

1. Jhonstone B. *et al.*, Eur Cell Mater 25:248-267, 2013
2. Matsiko A. *et al.*, Materials 6:637-668, 2013
3. Pittenger M.F. *et al.*, Science 5411:143-147, 1999
4. Hamada T. *et al.*, J Med Sci 75: 101-111, 2013
5. Demoor M. *et al.*, BBA 1840:2414-2440, 2014

## ACKNOWLEDGMENTS

We are grateful to the French Research and Technology Ministry for the fellowship granted to E. Al Tawil and A. Monnier and to the Haute-Normandie Agency of Innovation, SEINARI, for providing financial support to this project.



## Characterization of *in vitro*-Spheroids from Human Mesenchymal Stem Cells under Osteogenic and Adipogenic Differentiation

Geneviève Schmid<sup>1</sup>, Heike Paape<sup>2</sup>, Ellen Schmuhl<sup>2</sup>, Stefanie Adam<sup>1</sup>, Nicole Herzmann<sup>1</sup>, Juliane Meyer<sup>1</sup>, Achim Salamon<sup>1</sup>, Susanne Meyer<sup>2</sup>, Kirsten Peters<sup>1</sup>

<sup>1</sup>Department of Cell Biology, Rostock University Medical Center, Germany

<sup>2</sup>Bioserv GmbH, Rostock, Germany

[kirsten.peters@med.uni-rostock.de](mailto:kirsten.peters@med.uni-rostock.de)

### INTRODUCTION

Multipotent mesenchymal stem cells (MSC) are a promising source for cell based therapies. Cultivation conditions can have a strong impact on differentiation characteristics of MSC. Three-dimensional (3D) culture systems have the basic idea of a higher similarity to the physiological environment of cells in the body than conventional two-dimensional (2D) cultures, as the cells can undergo increased cell-cell and cell-matrix interactions. Moreover, spheroids do not adhere to cell culture surfaces and are thus injectable without pre-treatment.

In this study we characterized 3D-spheroids of human MSC from adipose tissue (adipose tissue-derived MSC/adMSC) compared to adMSC in 2D grown on tissue culture polystyrene. The characterization was done non-stimulated as well as under specific osteogenic and adipogenic stimulation. Furthermore, the two different cell culture models were examined for the release of the pro-inflammatory cytokine interleukin-6 (IL-6), the basic fibroblast growth factor (bFGF) and the vascular endothelial growth factor (VEGF).

### EXPERIMENTAL METHODS

We used human adMSC in passage 4 and cultivated them under 2D (standard cultivation) and 3D/spheroid cultivation conditions. Seeding density was 20,000 cells/cm<sup>2</sup> for 2D- and 12,5000 cells/cm<sup>2</sup> for 3D-culture. Spheroid formation was attained by seeding in low attachment plates (Corning). Cultivation was performed for a period of up to three weeks.

Specific stimulation of differentiation was induced by standard reagents (osteogenic stimulation: dexamethasone, ascorbic acid, glycerophosphate; adipogenic stimulation: dexamethasone, indomethacin, IBMX, insulin).

Characterization of osteogenic differentiation potential was by detection of alkaline phosphatase activity and mineralization. Adipogenic differentiation was examined by oil red O. Cytokines and growth factors were quantified by ELISA (R&D-Systems).

### RESULTS AND DISCUSSION

Spheroid formation occurred within 1-2 days after seeding (Fig. 1). Whereas unstimulated (US) and osteogenically stimulated (OS) spheroids disintegrated within the period of observation for the most part, adipogenically stimulated (AS) spheroids were stable (Fig.1).

Adipogenic differentiation after specific stimulation took place in 2D and 3D culture (Fig. 2). The comparative quantification of lipid amount is pending.

The release of bFGF was upregulated in 3D cultures whereas the release of VEGF was downregulated in 3D compared to 2D (Table 1). Quantification of the pro-

inflammatory IL-6 revealed a downregulation in 3D spheroids (Table 1), which might be an important feature for the use of spheroids in regenerative medicine.

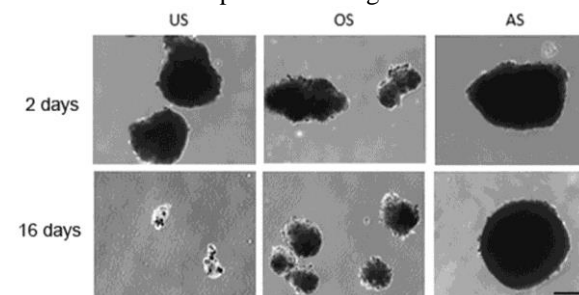


Fig. 1: Phenotype of spheroids after 2 and 16 days of cultivation under non-stimulated (US), osteogenically stimulated (OS) and adipogenically stimulated (AS) conditions (scale bar: 200 µm).

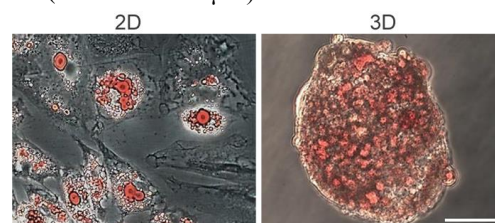


Fig. 2: Lipid detection in 2D and 3D culture after 21 days of adipogenic stimulation (scale bar: 50 µm).

Table 1: Growth factor and cytokine quantification in cell culture supernatants after 2 and 7 days in unstimulated (US) and adipogenically stimulated (AS) 2D and 3D cultures of adMSC.

time/stimulation		b-FGF		VEGF		IL6	
		2D	3D	2D	3D	2D	3D
		[µg/ml]		[µg/ml]		[µg/ml]	
2 d	US	-	29.46	266.59	-	2201.64	189.82
	AS	-	-	108.41	-	1067.09	84.36
7 d	US	-	23.75	1084.77	-	1778	494.36
	AS	-	65.18	435.68	-	1230.73	370.73

### CONCLUSION

Due to the successful adipogenic differentiation of spheroids and the clear reduction of pro-inflammatory cytokine release in 3D, spheroid cultures should be further examined for future application in cell-based therapies and tissue engineering.

### REFERENCES

1. Bara J.J. *et al.*, Stem Cells. 32:1713-23, 2014

### ACKNOWLEDGMENTS

This work was financially supported by the federal state Mecklenburg-Vorpommern and the EU (grant numbers ESF/IV-WM-W340001/11;ESF/IV-WM-B34-0013/11).



# Investigation of the Effect of Different Velocities and Surface Treatments on hMSCs Seeding Efficiency and Mechanical Characterization of 3D Insert PCL Scaffolds Undergoing Compression Loading

Marzia Brunelli, Cecile M. Perrault, Damien Lacroix

INSIGNEO Institute for in silico medicine, Department of Mechanical Engineering, University of Sheffield, UK  
[mep12mb@sheffield.ac.uk](mailto:mep12mb@sheffield.ac.uk)

## INTRODUCTION

The study of mechanically-induced cell differentiation in a scaffold requires a preliminary understanding of the cellular distribution in the scaffold and the distribution of the mechanical load throughout the structure. A good cell seeding efficiency and distribution can be achieved by dynamically perfusing cells at appropriate rate<sup>1</sup> or statically seeding cells on structures modified by surface plasma<sup>2</sup> or collagen bulk treatments<sup>3</sup>. The objectives of this study were (1) to study the bioreactor conditions of a custom microfluidic system in term of surface/bulk treatments and flow rate in order to achieve uniform cell distribution in 3D PCL scaffolds seeded statically and dynamically, and (2) to measure the compressive mechanical properties of 3D PCL scaffolds and test their suitability in bearing cyclic loads.

## EXPERIMENTAL METHODS

**Microfluidic system.** Devices were developed using polydimethylsiloxane (PDMS) and drilling holes to accommodate 3 scaffolds in series. Air plasma treatment was applied to achieve glass-PDMS bonding. hMSCs were pumped at 0.01 and 0.1 mm/s and DNA assay was performed after 1, 2, 3 and 24 h.

**PCL scaffold seeding.** Air plasma was applied. Treated and non-treated 3D Insert PCL scaffolds (3D Biotek, USA) were seeded by dropping 20  $\mu$ l of cell suspension with or without collagen bovine 1 (Gibco). Presto Blue and DNA assays were performed after 24 h.

**PCL mechanical properties.** Scaffold area (A) was calculated as  $A = a \cdot (h/h + d)$  where  $h$  is the initial height,  $a$  is the area calculated as  $h = 1.5$  mm, and  $d$  is the displacement. A 14% compressive strain was maintained constant for 150 min. Then, samples were loaded with cyclic ramps at 5% strain and apparent modulus ( $E$ ) was calculated as average stress over strain at 25, 30 and 37°C.

## RESULTS AND DISCUSSION

Scaffolds seeded at 0.1 mm/s showed low attachment with an initial peak of 14% reduced to 6% after 24 h. The microfluidic system at low velocities is subject to the gravitational action requiring a pre-cycle at 0.1 mm/s before setting a constant velocity of 0.01 mm/s in order to obtain the same seeding efficiency among samples. Static seeding showed enhanced attachment on treated scaffolds due to a more active surface (Fig.1A). Collagen allows a steep increase of efficiency up to 60%. Scaffolds present a high variability for strain above 2.5% suggesting a strong dependence of the mechanical properties on scaffold orientation and fiber alignment (Fig.1B). For strain values below 1%, the change in slope due to contact and stabilization of the structure is noticeable. Between 1 and 2.5% strain

scaffolds show a linear behaviour resulting in an apparent modulus of  $5.5 \pm 1.5$  MPa at 25°C.  $E$  decreases progressively with temperature up to  $2.5 \pm 1.1$  MPa at 37°C. The maximum stress at 37°C acting on samples loaded with 5% strain amounts to  $0.31 \pm 0.09$  MPa.

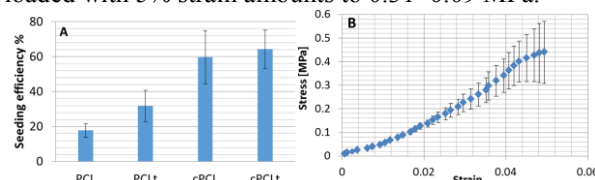


Fig.1: (A) Viability of plasma treated (PCLt), collagen embedded (cPCL) and treated collagen embedded (cPCLt) samples after 24 h; (B) Loading stress/strain curve of PCL scaffolds.

## CONCLUSION

The multi-chamber perfusion system presents a uniform distribution of cells at high flow rates but the excessive shear stress prevents a significant seeding efficiency. At low flow rates, gravity prevents a uniform cellular distribution among scaffolds and applying high rate pre-cycles have negative effects on cell adhesion capabilities. A simple configuration based on a single chamber is preferred to minimize the effect of gravity and flow variability between the chambers. Static seeding is improved by embedding collagen within plasma treated scaffolds as the viscosity of the gel prevents cells from drifting out the structure and the plasma treatment allows uniform spreading of collagen and cells. Following relaxation, PCL scaffolds do not show significant viscoelastic effects. The stiffness measured on this PCL scaffold show consistent values with repeated cyclic compression and are of sufficient magnitude to provide an initial stabilization for osteochondral or bone repair applications.

## REFERENCES

- Wendt, D., Marsano, J.M., Heberer, M. & Martin, I. *Biotechnol. Bioeng.* 84, 205–14 (2003).
- Declercq, H., Desmet, T., Berneel, E.E.M., Dubruel, P. & Cornelissen, M.J. *Acta Biomater.* 9, 7699–708 (2013).
- Aydin, H. M. *et al. Adv.Eng.Mater.* 11, 83–88 (2009).
- Rauh, J., Milan, F., Günther, K.P. & Stiehler, M. *Tissue Eng. Part B. Rev.* 17, 263–80 (2011).

## ACKNOWLEDGEMENTS

Funding from the European Research Council (FP7-258321) is acknowledged.

## DISCLOSURE

The author has nothing to disclose.



## Osteogenic Effects of Short, Steady Media Perfusion in hBMSC 3D Cultures Depend on Cell Culture and Cell Differentiation Stage and a Scaffold Type

Joanna Filipowska<sup>1\*</sup>, Justyna Pawlik<sup>2</sup>, Katarzyna Cholewa-Kowalska<sup>2</sup>, Maria Laczka<sup>2</sup> & Anna M. Osyczka<sup>1</sup>

<sup>1</sup>Dept. Cell Biology & Imaging, Faculty of Biology & Earth Sci., Jagiellonian University, 9 Gronostajowa Str., 30-387 Kraków, Poland

<sup>2</sup>Dept. Glass Tech. & Amorphous Coatings, Faculty of Ceramics & Materials Engineering, University of Science & Technology AGH, 30 Mickiewicza Av., 30-059 Kraków, Poland

[joanna.filipowska@uj.edu.pl](mailto:joanna.filipowska@uj.edu.pl)

### INTRODUCTION

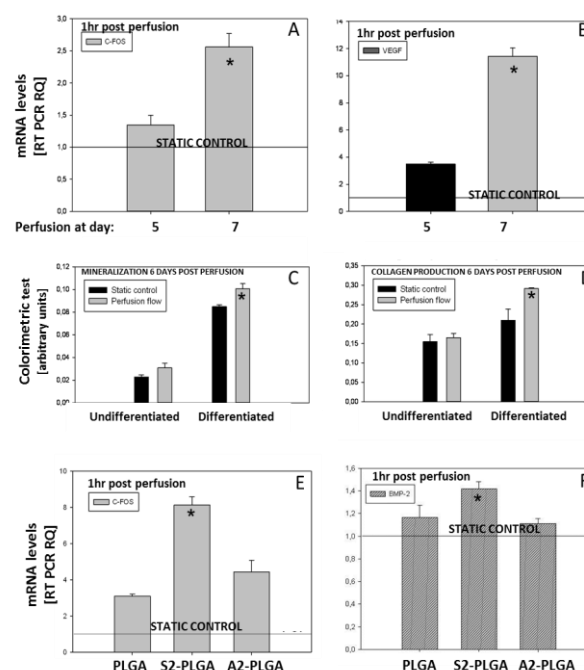
Perfusion of culture media through cell-seeded 3D scaffolds may provide several benefits to cells growing within the scaffold pores. Recently, Keogh et al. showed that a short flow perfusion effectively stimulates osteogenesis in 3D osteoprecursors culture<sup>1</sup>. We have examined whether a short, one-directional media perfusion through porous 3D scaffolds can enhance *in vitro* osteogenesis of human bone marrow-derived osteoprogenitor cells (hBMSC). hBMSC are commonly used in cell-based bone therapies and hBMSC dynamic cultures become an important part of bone tissue engineering with these cells. We show that a short, steady, one-directional media perfusion through the scaffold pores may enhance hBMSC osteogenic response, but this depends on cell culture and cell differentiation stage as well on scaffold chemistry.

### EXPERIMENTAL METHODS

hBMSC<sup>2</sup> were seeded on either gelatine-coated polyurethane (PU)<sup>3</sup> or on composite scaffolds made of PLGA and gel-derived bioactive glass (i.e. high silica S2 or high calcium A2)<sup>4</sup>. Cells were stimulated with osteoinducers (i.e. dexamethasone or rhBMP-2) or left untreated. Some hBMSC were pre-treated with osteoinducers in 2D cultures (differentiated) and compared to undifferentiated cells. Media perfusion was applied at 2.5ml/min for 2h in EBERS 1000TEB bioreactor. Perfusion stimulated cultures were compared to corresponding static controls. Data were collected in triplicates. Statistical analyses were performed in Sigma 11.0 software and  $p \leq 0,05$  was considered significant.

### RESULTS AND DISCUSSION

We found that a single perfusion session is sufficient to enhance hBMSC response, but this depends on a culture stage the perfusion is applied. Perfusion at day 7 resulted in increased *c-Fos* and *VEGF* mRNA levels compared to perfusion at day 5 (Fig. 1A, B). This suggested increased mechanical and angiogenic response of hBMSC, respectively. Perfusion at day 7 also enhanced mRNA levels of *RUNX-2* and *BMP-2* that are important for initiation of osteogenesis (data not shown). When hBMSC were pre-differentiated in 2D cultures, the effects of perfusion were more profound compared to respective static controls. Perfusion applied at day 7 of 3D cultures significantly enhanced collagen deposition and matrix mineralization in differentiated (Fig. 1C, D). Finally, when hBMSC were



cultured on bioactive composite scaffolds, the scaffolds chemistry seemed to determine their response to perfusion. hBMSC cultured on

composite S2-PLGA scaffolds and subjected to perfusion, expressed significant mRNA levels of mechanoresponsive *c-Fos* and pro-osteogenic *BMP-2* compared to PLGA or A2-PLGA (Fig 1E, F). Thus, the chemical composition of the scaffolds should be taken into account when dynamic culture is applied.

### CONCLUSIONS

Our data indicate that a short stimulation of 3D hBMSC cultures with media perfusion may find a broad application in bone tissue engineering on either bioinert or bioactive scaffolds, but culture conditions and cell delivery constructs must be carefully optimized to achieve beneficial perfusion effects.

### REFERENCES

1. Keogh MB et al. *Biotechnol Bioeng.* 2011;108(5):1203-10.
2. Osyczka AM et al. *Calcif. Tissue Int.* 2002;71(5):447-58.
3. Sittichokechaiwut A et al. *Eur Cell Mater.* 2010 21;20:45-57.
4. Filipowska J et al. *Biomed Mater.* 2014;9(6):065001

### ACKNOWLEDGEMENTS

This work was supported by the Polish National Science Centre Grants no B/NZ4/00664 and DEC-2014/13/B/ST8/02973.





Helmut Thissen<sup>1</sup>, Mario Salwiczek<sup>1</sup>, Christopher D. Easton<sup>1</sup>, Aylin Koegler<sup>1</sup>, Richard A. Evans<sup>1</sup>

<sup>1</sup>CSIRO Manufacturing Flagship, Bayview Avenue, Clayton Victoria 3168, Australia  
[Helmut.Thissen@csiro.au](mailto:Helmut.Thissen@csiro.au)

## INTRODUCTION

Prebiotic chemistry is the study of the chemistry associated with the origin of life<sup>1</sup>. HCN derived polymers have been studied for many years in this context as possible sources for the precursors of proteins and nucleic acids<sup>2</sup>. However, the application of these polymers in the field of materials science has not been reported. Here, we have investigated the polymerization of the HCN trimer aminomalononitrile as a simple generic surface coating method. Our results suggest that the resulting rich surface chemistry is highly suitable for biomedical applications<sup>3</sup>.

## EXPERIMENTAL METHODS

Aminomalononitrile p-toluenesulfonate (AMN) was used as a precursor material. PBS buffer solutions containing AMN were adjusted to pH 8.5 using sodium hydroxide to initiate polymerization. Copolymerization reactions were carried out both during coating formation and via secondary immobilization reactions, while metallization experiments were carried out after coating deposition. Surface analysis was carried out XPS, AFM, SEM and contact angle measurements. Cell culture experiments were carried out using L929 mouse fibroblasts. Biofilm assays were carried out using *S. Epidermidis* and *P. Aeruginosa* strains.

## RESULTS AND DISCUSSION

Aminomalononitrile polymerizes spontaneously to give a brown protein-like polymer. We found that this polymerization reaction, when carried out in simple aqueous buffer solutions, can be used to produce adherent coatings on a wide range of organic and inorganic substrate materials (Figure 1).

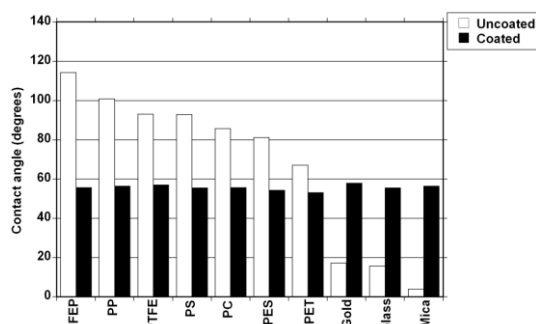


Figure 1. Contact angles determined on a range of materials before and after AMN coating deposition.

We also demonstrated that the robust, non-cytotoxic AMN coatings provide cell attachment equivalent to tissue culture polystyrene (TCPS), thereby providing access to a range of biomedical applications (Figure 2).

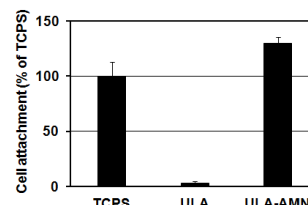


Figure 2. L929 cell attachment after 24 h on Corning Ultra-low attachment surface (ULA) before and after AMN coating in comparison to TCPS.

In addition, the nitrogen-rich coating chemistry allows the covalent immobilization of compounds carrying suitable complementary functional groups such as aldehydes both during coating formation and via secondary immobilization reactions. Furthermore, AMN coatings can be used for metallization. This can be exploited for the formation of antimicrobial coatings via the release of silver ions (Figure 3).

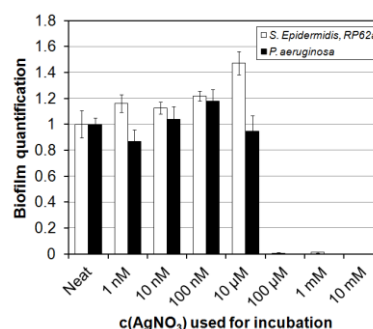


Figure 3. AMN polymer coatings are effective in preventing the formation of biofilms after electroless silver deposition.

## CONCLUSION

We have demonstrated that prebiotic chemistry inspired coatings derived from AMN can be deposited on a wide range of substrate materials. These coatings combine excellent biocompatibility with a rich surface chemistry, allowing the immobilization of bioactive signals and the complexation of metal ions. Combined with an extraordinarily simple coating process, it is expected that these coatings will be translated into a number of biomedical applications.

## REFERENCES

1. Miller S.L., Science 117:528, 1953; Bada, J.L., Chem. Soc. Rev. 42, 2186, 2013.
2. Matthews C.N. *et al.*, Nature, 215:1230, 1967; Matthews C.N. *et al.*, Faraday Discuss. 133:393, 2006.
3. Thissen H. *et al.*, WO 2013/170308 A1.

## Grafting of Bioactive Molecules on PET to Recruit Endothelial Progenitors Cells and Enhance Adhesion of Endothelial Cells

Caroline Royer<sup>1,2</sup>, Laurent Plawinski<sup>1</sup>, Gaétan Laroche<sup>2,3</sup> and Marie-Christine Durrieu<sup>1</sup>

<sup>1</sup>Institute of Chemistry & Biology of Membranes & Nanoobjects (UMR5248 CBMN), France

<sup>2</sup>Laboratoire d'Ingénierie de Surface, Centre de recherche du CHU de Québec, Hôpital Saint-François d'Assise, Canada

<sup>3</sup>Département de génie des mines, de la métallurgie et des matériaux, Centre de Recherche sur les Matériaux Avancés, Canada

[caroline.royer.1@ulaval.ca](mailto:caroline.royer.1@ulaval.ca)

### INTRODUCTION

Over the last three decades, the envisaged strategies to develop biocompatible vascular materials have considerably evolved. Nowadays, several research group objectives are targeted towards the development of bioactive materials. It is expected that these materials would promote specific interactions with the endothelial progenitors cells. The main strategy used in our work is the co-immobilization of two different bioactive molecules onto biomaterial surface in order to improve cell recruitment, adhesion and differentiation. Accordingly, sitagliptine<sup>1</sup> and RGDS peptide are covalently conjugated on PET to recruit these cells and promote their adhesion, respectively. They were micropatterned by photolithography process<sup>2</sup> to mimic the extracellular matrix. This technique consists of the transfer of a specific pattern to a photosensitive material (a photoresist) by selective exposure to a radiation source. This allows enhancing the biocompatibility of the so-called biomaterial<sup>3</sup>. The present work focuses on characterizing the grafting of these bioactive molecules on PET.

### EXPERIMENTAL METHODS

Sitagliptine, was from Biovision, Milpitas, CA. RGDS and RGDS-TAMRA peptides were purchased from Genecust, Luxembourg.

#### Bioactive molecule grafting:

PET films were subjected to ethanol washing under sonication before use. The first grafting step consisted in hydrolysing PET ester groups to get carboxylic acid moieties onto the polymer surface<sup>4</sup>. These –COOH groups were then converted into activated esters through reaction with NHS and EDC grafting. This step allowed further peptide grafting. Fluorescent peptide (RGDS-TAMRA) was used in order to characterize the homogenous and patterned functionalization of PET.

#### Characterization:

All the samples were analysed with XPS, AFM (data not shown). Epifluorescence microscopy (Leica DM5500B, Germany) was used to characterize

grafting of RGD-peptide. Optical profilometer (VEECO NT9080) was used to study size and spacing of the lines of pattern (Fig3). Various patterns will be used. After the reaction, the amount of COOH grafted onto the film was determined using the toluidine blue-O method. The density of the carboxyl groups is determined with a calibration plot containing several samples with different carboxyl group concentrations.

### RESULTS AND DISCUSSION

As we expected the experiment shows (Fig 4) that the density of carboxyl groups increase with the oxidation step, which is normal because of the breakage of the polymer chains it expose more COOH groups on its surface. The

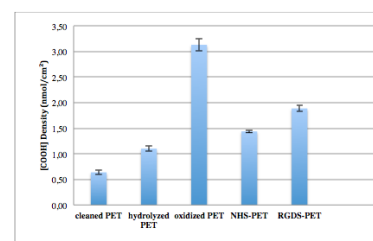


Fig4 : Carbonyl group density of the different steps of functionalization of PET

decreasing of COOH density after NHS grafting proves NHS is covalently grafted by COOH functions onto PET surface. The PET sample functionalized with the peptide shows a higher density due to carboxyl groups in its structure. Fluorescent microscopy permitted to validate homogeneous RGDS peptides (Fig5) grafting onto PET surfaces, and patterned RGDS peptides and sitagliptine grafting

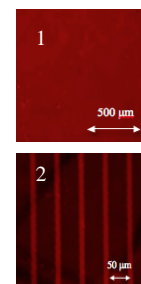


Fig5 : RGDS-TAMRA peptides homogeneously grafted onto PET surfaces (1) RGDS-TAMRA peptides and sitagliptine patterned on PET (2)

### CONCLUSION

Bioactive molecules were successfully grafted onto the surface of PET. These molecules were selected to promote the recruitment of endothelial progenitor cells as well as their adhesion, proliferation, and differentiation. Further experiments will be done in order to study the recruitment effect of sitagliptine on EPCs and adhesive properties of RGD peptide. Impact of surface grafting homogeneously and patterned with different geometry will be study on endothelial progenitor cell.

### REFERENCES

- (1) S. Chua et al., *Cytotherapy*. 15: 1148e1163, 2013.
- (2) C. Chollet et al., *Colloid Surface B*. 75:107-114, 2010.
- (3) C. Chollet et al., *Biomaterials*. 30:711-720, 2009.
- (4) B.M. Boxus et al., *Polym Adv Technol*. 589-98,1996.

### ACKNOWLEDGMENTS

The authors thanks the « Région Aquitaine » for financial support.

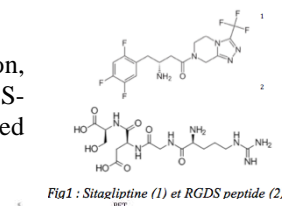


Fig1 : Sitagliptine (1) et RGDS peptide (2)

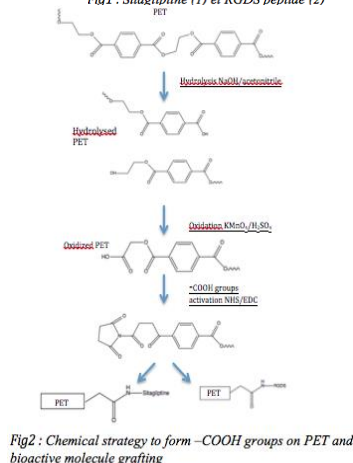


Fig2 : Chemical strategy to form -COOH groups on PET and bioactive molecule grafting

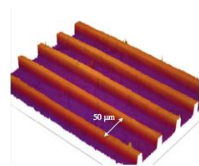


Fig3 : Optical profil of micropatterned PET after photolithography

## INTRODUCTION

Titanium (Ti) and Ti alloys are largely used in different clinical areas for example in orthopaedics, craniofacial, dental and bone replacement<sup>1</sup> due to their exceptional mechanical properties tensile strength, stiffness, fracture toughness and corrosion resistance<sup>2</sup>. It is well known that Ti and their alloys have an amphoteric oxide layer<sup>3</sup> and by increasing the thickness of this oxide layer can improve adsorption of biomolecules<sup>4</sup>. Synthetic peptides are developed to be used as non-pathogenic and -cytotoxic scaffolds for drug delivery, tissue repair and engineering<sup>5</sup>. In this study a peptide aptamer is electrostatically adsorbed onto modified Ti surfaces. The interaction of a range of peptide aptamer sequences with modified Ti6Al4V surfaces of different roughness is explored. The aim is the formation of a stable and homogeneous layer of peptide aptamers, to explore the possibility of adding functionalities to Ti-based medical surfaces.

## EXPERIMENTAL METHODS

Solid-phase peptide synthesis (SPPS) principles were used to synthesise the Ti-hydroxyapatite (Ti-HA) aptamer KKLPDAKKLPDAEEEEEEEEEE labelled with 5(6)-carboxyfluorescein (5-FAM) for posterior tracking. Ti6Al4V plates of medical grade and of dimensions 0.01m x 0.01m were dip coated in PBS buffer pH 7.4 with 1, 5 and 10 $\mu$ M of peptides and without peptide as control. The surfaces were characterized by SEM, white light interferometry, and fluorescence microscopy.

## RESULTS AND DISCUSSION

The TiO<sub>x</sub> layer obtained after different chemical treatments with 30wt% aqueous H<sub>2</sub>O<sub>2</sub> was analysed by SEM (Figure 1). The roughness was measured by interferometry to investigate the effect of etching time on the topography of the samples (Table 1).

**Table 1.** Surface roughness of titanium plates after etching with H<sub>2</sub>O<sub>2</sub> 30 wt% aqua solution for 0, 1, 3, 6, 13, 24 and 48 hours.

Etching time (h)	S <sub>a</sub> (average roughness, nm)	S <sub>y</sub> (peak to valley, $\mu$ m)
0	13 $\pm$ 9	0.22 $\pm$ 0.08
1	37 $\pm$ 3	1.14 $\pm$ 0.14
3	29 $\pm$ 1	1.57 $\pm$ 0.12
6	78 $\pm$ 4	1.23 $\pm$ 0.04
13	33 $\pm$ 3	2.6 $\pm$ 0.31
24	197 $\pm$ 7	2.38 $\pm$ 0.37
48	128 $\pm$ 2	3.35 $\pm$ 0.41

Etching with H<sub>2</sub>O<sub>2</sub> increased electrostatic interactions according with the literature<sup>4</sup>. An increase in roughness also had an effect on the electrostatic interactions and quality of the Ti-HA peptide coating as shown clearly in Figure 2. This observation is in good agreement with previous work<sup>4</sup>. This suggests that both the roughness and composition of Ti surfaces are important for improved bioactivity<sup>1-4</sup>.

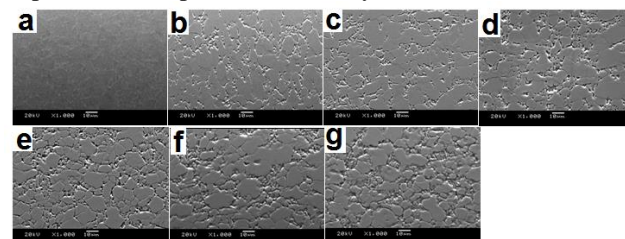


**Figure 1.** Micrographs of (a) Ti mirror polished surface, (b) Ti mirror polished surface etched for 1h, (c) 3h, (d) 6h, (e) 13h, (f) 24h and (g) 48h.

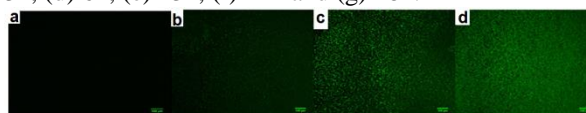


**Figure 2.** Fluorescence intensity of (a) control (b) 1 $\mu$ M Ti-HA peptide on etched Ti6Al4V, (c) 5 $\mu$ M Ti-HA peptide on etched Ti6Al4V and (d) 10 $\mu$ M Ti-HA peptide on etched Ti6Al4V.

## CONCLUSION

Ti6Al4V was etched with H<sub>2</sub>O<sub>2</sub> to increase hydroxyl groups on the surface. The oxide layer became thicker with increasing the etching time resulting in a simultaneous increase in roughness that allowed better adsorption of peptide aptamers on the Ti surface. A homogeneous surface coating was achieved.

## REFERENCES

- de Jonge, L.T., et al., Pharm. Res. **25**: 2357-2369, 2008.
- Liu, X.Y., P.K. Chu, and C.X. Ding, Mater. Sci. Eng. R. **47**: 49-121, 2004.
- Hanawa, T., Corrosion Rev. **21**: 161-181, 2003.
- Sano, K.-I. and K. Shiba, J. Am. Chem. Soc.. **125**: 14234-14235, 2003.
- Holmes, T.C., Trends Biotechnol.. **20**: 16-21, 2002.

## ACKNOWLEDGMENTS

The authors acknowledge Birmingham Science City: Innovative Uses for Advanced Materials in the Modern World (West Midlands Centre for Advanced Materials Project 2), supported by Advantage West Midlands (AWM) and part funded by the European Regional Development Fund (ERDF).

## Nanoporous Anodic Titanium Dioxide Layers as Scaffolds for Cell Growth

Magdalena Jarosz<sup>1</sup>, Anna Pawlik<sup>1</sup>, Justyna Syguła-Cholewińska<sup>2</sup>, Tomasz Sawoszczuk<sup>2</sup>, Danuta Jarocho<sup>3</sup>, Marcin Majka<sup>3</sup>, Grzegorz D. Sulka<sup>1</sup>, Marian Jaskuła<sup>1</sup>

<sup>1</sup>Department of Physical Chemistry & Electrochemistry, Jagiellonian University, Ingardena 3, 30-060 Krakow, Poland

<sup>2</sup>Department of Microbiology, Faculty of Commodity Science, Cracow University of Economics, Rakowicka 27, 31-510 Krakow, Poland

<sup>3</sup>Department of Transplantation, Collegium Medicum of the Jagiellonian University, Wielicka 265, 30-663 Kraków  
[jarosz@chemia.uj.edu.pl](mailto:jarosz@chemia.uj.edu.pl)

### INTRODUCTION

Recently, the most commonly used materials for bone-implants are titanium and its alloys. It is due to their good biocompatibility, high strength to weight ratio and an excellent corrosion resistance [1]. Unfortunately, there are some drawbacks connected with titanium implants, such as their inertness and long-term osseointegration via the natural oxide (TiO<sub>2</sub>) existing on Ti surface. Therefore, nanoporous materials on Ti surfaces become a novel solution for bone implants [2]. One of the materials proposed as a potential nanostructured material for that purpose are nanoporous anodic titanium dioxide (ATO) layers on Ti formed by electrochemical anodization [3]. The main advantage of such materials is a direct growth of TiO<sub>2</sub> on Ti surface, using a simple and cost-effective method of anodic oxidation. Anodization allows to precisely control nanopore size and structure porosity, which have a great impact on cell growth [4]. Nanoporous layer guarantees an excellent inertness of its surface, allowing it to readily heal into the bone tissue. Such surfaces may be also modified with antibacterial and anti-inflammatory compounds, that could help with the healing process.

### EXPERIMENTAL METHODS

ATO layers on Ti foil were prepared via a three-step anodization in glycol ethylene based solutions under a constant voltage of 40 V and temperature 20 °C. As-prepared ATO layers were then annealed at two different temperatures in order to obtain polymorphic structures of TiO<sub>2</sub> (anatase and a mixture of anatase and rutile). Some of the TiO<sub>2</sub> layers were modified with Ag nanoparticles for increased antibacterial properties. Moreover, two kinds of drugs, ibuprofen and gentamicin, were loaded inside ATO pores. The drug release profiles were made. Afterwards, non-modified and modified samples were used for cell and microbial growth examinations. The MG63 osteoblast cell line was used for cell viability and proliferation tests. *Staphylococcus aureus* and *Pseudomonas aeruginosa* bacteria were used for evaluation of the inhibition of microorganisms growth and possibility of a biofilm formation on various nanoporous TiO<sub>2</sub> surfaces.

### RESULTS AND DISCUSSION

ATO layers on Ti substrate formed by anodization process allow to obtain a well-organized nanoporous structure with a well-defined pore diameter and oxide thickness. Furthermore, the presence of porous structure enables to load small compounds inside the pores. Both,

silver nanoparticles and drug compounds were successfully loaded inside pores. ATO layers enriched with either ibuprofen or gentamicin exhibits an extended release profiles. This may suggest that ATO layers may be used as a drug delivery systems, especially in implantology. Microbiological tests showed that gentamicin completely inhibits growth of bacteria on TiO<sub>2</sub> surface. Silver nanoparticles also show antibacterial properties but to a lesser extent. The cell growth on ATO layers is enhanced. Dependently on a crystallographic structure, osteoblast like cells grow differently. The best surface for cell growth seems to be an anatase phase.

### CONCLUSION

ATO layers presents a new and promising alternative for the osteoblast like cell growth. Due to the presence of the nanoporous dioxide on Ti substrate, there is a possibility to enrich ATO layers with antibacterial and anti-inflammatory compounds. Nanoporous TiO<sub>2</sub> on Ti foil enhances cell growth and at the same time inhibits bacteria expansion.

### REFERENCES

1. K.M. Buettner, A.M. Valentine, Chem. Rev., 112 (2012) 1863-1881
2. M. Stigter, J. Bezemer, K. de Groot, P. Layrolle, J. Control. Release, 99 (2004) 127-137
3. M. Pisarek, M. Lewandowska, A. Roguska, J. Kurzydowski, M. Czachor, Mater. Chem. Phys., 104 (2007) 93-97
4. G.D. Sulka in: Nanostructured Materials in Electrochemistry, Wiley-VCH 2008, pp. 1-116

### ACKNOWLEDGMENTS

Magdalena Jarosz acknowledges the financial support from the project Interdisciplinary PhD Studies "Molecular sciences for medicine" (co-financed by the European Social Fund within the Human Capital Operational Programme).

The project was founded by the National Science Center on the grounds of the decision no. DEC-2013/11/N/ST5/01640.





# Glycosaminoglycan Mimicking Surfaces Trigger Distinct Response of Stem Cells via Fibronectin Adsorption

AR Araújo<sup>1,2</sup>, D Soares da Costa<sup>1,2</sup>, S. Amorim<sup>1,2</sup>, RL Reis<sup>1,2</sup>, RA Pires<sup>1,2</sup> and I. Pashkuleva<sup>1,2\*</sup>

<sup>1</sup>3B's Research Group - Biomaterials, Biodegradables and Biomimetics, University of Minho, Headquarters of the European Institute of Excellence on Tissue Engineering and Regenerative Medicine, AvePark, 4806-909 Taipas, Guimarães, Portugal

<sup>2</sup>ICVS/3B's PT Government Associate Laboratory, Guimarães/Braga, Portugal

[anarita.araujo@dep.uminho.pt](mailto:anarita.araujo@dep.uminho.pt)

## INTRODUCTION

Glycosaminoglycans (GAGs) are main building elements of the extracellular matrix where they act in synergism with proteins and are equally critical for the development, growth, function or survival of an organism[1]. GAGs are anionic linear polysaccharides made of repeating disaccharide units, whose negative charge is due to the presence of sulfate groups. These charge units have a crucial role in GAG interaction with proteins and therefore in key biochemical/signalling processes related to cell functionality and survival. In a previous work we have developed a platform that is based on self-assembled monolayers (SAM) and allow precise control on the surface exposed sulfonic groups (-SO<sub>3</sub>H)[2]. We proved that those surfaces are reliable tools to study GAGs interactions with proteins (basic fibroblast growth factor, FGF-2) or cells[2, 3]. Herein, we have used the same SAM platform to investigate the influence of sulfonic functional groups on the interactions with fibronectin and the impact of these interactions on the adhesion and morphology of human adipose derived stem cells (ASCs).

## EXPERIMENTAL METHODS

SAMs were prepared by adsorption of HS(CH<sub>2</sub>)<sub>11</sub>OH or HS(CH<sub>2</sub>)<sub>11</sub>SO<sub>3</sub>H on gold coated glass slides or QCM crystals to obtain -OH or -SO<sub>3</sub>H functionalised surfaces respectively. The interaction between these surfaces and fibronectin (FN) was studied in situ by quartz crystal microbalance with dissipation (QCM-D). Live-imaging and QCM-D were used to follow in situ the cell adhesion on SAMs surfaces with or without adsorbed fibronectin. Immunofluorescence was employed to assess the effect of surface chemistry and protein adsorption on cell morphology.

## RESULTS AND DISCUSSION

FN has an acidic isoelectric point and thus, we were expecting some repulsion between the negatively charges sulfonic groups on -SO<sub>3</sub>H surfaces and this protein. However, QCM-D data showed that more FN adsorbs on -SO<sub>3</sub>H surfaces in comparison to the uncharged -OH functionalised ones. Unexpectedly, the adsorbed protein had negative influence on the cell adhesion: ASCs adhere significantly faster on -SO<sub>3</sub>H surfaces in the absence of FN (Fig. 1A). Opposite effect was observed for the -OH surfaces: adsorbed FN shortens significantly the adhesion time in this case. Different cell morphology was also observed: cells spread after 7h on -SO<sub>3</sub>H surfaces and on -OH surfaces when coated with FN (Fig. 1B). The analysis of cell motility (Fig. 1C) showed that cells have longer

migration paths on -OH surfaces suggesting weakest ASC adhesion on those surfaces.

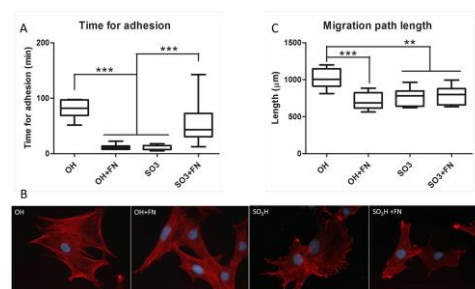


**Figure 1.** Time of adhesion (A), morphology (B) and migration paths (C), obtained from the live imaging analysis (A and C) and immunofluorescence (B).

These results suggested different mechanism of adhesion on both studied surfaces. Live-imaging analysis and QCM-D confirmed this hypothesis. The presence of fibronectin causes an opposite effect on the studied surfaces – it delays cell adhesion on -SO<sub>3</sub>H functionalised surfaces and accelerates it on -OH ones. The protein causes formation of ASCs clusters on -SO<sub>3</sub>H surfaces, i.e. the cell adhesion depends on previous adherent cells on the surface.

## CONCLUSION

Based on these results, we propose a model according to which positively charged amino acids from FN interact electrostatically with the underlying -SO<sub>3</sub>H groups causing both passivation of the surface by neutralisation of its charge and irreversible change in the conformation of the protein. As a result the protein is not active in further interactions with cells. The FN adsorption on -OH is based on weaker interactions that do not restrict the protein flexibility in the following interactions with ASCs.

## REFERENCES

1. Pashkuleva I and RL Reis, Sugars: burden or biomaterials of the future? *J Mat Chem* 2010, 20: 8803-8818.
2. Soares da Costa D et al., Sulfonic groups induce formation of filopodia in mesenchymal stem cells. *J Mat Chem* 2012, 22: 7172-7178.
3. Amorim S et al., Interactions between exogenous FGF-2 and sulfonic groups: in situ characterization and impact on the morphology of human adipose-derived stem cells. *Langmuir* 2013, 29: 7983-7992.

## ACKNOWLEDGMENTS

The FP7 project POLARIS (REGPOT-2012-2013-1-316331) is acknowledged.





Rabia Nazir<sup>1</sup>, Arne Bruyneel<sup>2</sup>, Carolyn Carr<sup>2</sup> and Jan Czernuszka<sup>1</sup>

<sup>1</sup>Department of Materials, University of Oxford, Parks Road, Oxford, OX1 3PH, UK.

<sup>2</sup>Department of Physiology, Anatomy and Genetics, University of Oxford, Parks Road, Oxford, OX1 3PT, UK  
[rabia.nazir@materials.ox.ac.uk](mailto:rabia.nazir@materials.ox.ac.uk)

## INTRODUCTION

Natural polymer derived scaffolds for use in tissue engineering of heart valves have been seen as the ultimate devices proposed by heart surgeons for replacing diseased heart valves. Interpenetrating polymer networks (IPNs) can provide an even better way of building natural polymer based TEHVs with properties matching those of native heart valves. The characteristic interlocking structure of two polymers in an IPN is expected to enhance the mechanical integrity and in-vitro degradation resistance of resulting TEHVs. Collagen and glycoaminoglycans (GAGs) are the most abundant polymers found in human heart valve accounting for 60% and 20% by weight respectively [1]. Hyaluronic acid (HA)-collagen system has found applications in reconstruction of different tissues in the body such as skin and eye etc [2-4]. In the current study, the fundamentals of this approach have been extended to utilize HA-collagen for the development of novel TEHVs.

## EXPERIMENTAL METHODS

HA-Collagen based full IPNs were prepared by combining different proportions of HA and collagen hydrogels. Parent hydrogels (i.e. HA and collagen) with varying crosslinking densities were synthesized using freeze drying method followed by carboiimide crosslinking chemistry. In the next stage, collagen hydrogels (primary network) were penetrated by HA chains (secondary network) followed by HA chain crosslinking in the presence of collagen network. HA hydrogel, collagen hydrogel and resulting IPNs were characterized by Fourier transform infrared spectroscopy (FTIR), nuclear magnetic resonance (NMR) and scanning electron microscopy (SEM) to estimate the effect of crosslinking on chain structure and pore size. The effect of concentration of crosslinking agent on crosslinking densities and swelling ratio were studied. Degradation behaviour of hydrogels was studied in Phosphate buffer saline (PBS) at 37°C. To assess the biocompatibility of IPNs, scaffolds were cultured with cardiosphere derived cells (CDCs) from rats.

## RESULTS AND DISCUSSION

Peak analysis performed on FTIR spectra of hydrogels confirmed the modified polymer chain structure. Degree of modification was calculated around 30% for HA hydrogel. Swelling studies indicated that swelling ratio decrease with increase in concentration of crosslinking agent for both HA and collagen hydrogels. Image analysis of SEM micrographs revealed that pore size tends to decrease with an increase in crosslinking density for primary networks i.e. Collagen. The

degradation profile of HA hydrogels at pH4.0 and pH 7.4 indicates that crosslinking density contribute significantly to the degradation resistance. For instance, HA hydrogels showed higher weight loss (50% wt) in neutral media as compared to acidic media (30% wt). However, in contrast, Collagen did not show any appreciable weight loss under different conditions. This feature can be manipulated for tailored degradation rates of IPNs under physiological conditions. HA hydrogels only respond to specific cell receptors such as CD44, when combined with collagen which is capable of interacting with wide spectrum of cells, cell attachment can be enhanced on HA-collagen IPNs. Percentage reduction in AlmarBlue assay on CDCs cultured cross-linked collagen hydrogels suggested that degree of cell attachment decreases with increase in crosslinking density and the rate of cell proliferation was found to be independent of the extent of crosslinking density.

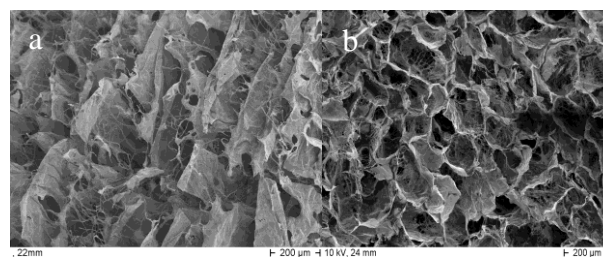


Figure showing scanning electron micrographs (SEM) of (a) HA hydrogel (b) Cross-linked collagen network at 100X.

## CONCLUSION

HA and collagen could be the ideal natural polymers for the construction of TEHV. A unique experimental route based on a chemical crosslinking technique to fabricate the HA-collagen based full IPN structures has been demonstrated. The emerging 3D constructs have shown great potential for mimicking the healthy heart valve in terms of mechanical and in-vitro biological compatibility.

## REFERENCES

- [1] K. Kunzelman, R. Cochran, S. Murphree, W. Ring, E. Verrier, R. Eberhart, The Journal of heart valve disease 2 (1993) 236.
- [2] Y. Guo, T. Yuan, Z. Xiao, P. Tang, Y. Xiao, Y. Fan, X. Zhang, J. Mater. Sci. Mater. Med. 23 (2012) 2267.
- [3] F. Lee, M. Kurisawa, Acta biomaterialia 9 (2013) 5143.
- [4] N. Shanmugasundaram, P. Ravichandran, P.N. Reddy, N. Ramamurthy, S. Pal, K.P. Rao, Biomaterials 22 (2001) 1943.

## ACKNOWLEDGMENTS

The authors would like to thank COMSATS Institute of Information Technology (CIIT), Pakistan for their financial assistance

## Biofunctional Microassemblies Based on Renewable Resources - Microfluidic Generation and Release Applications

Mélanie Marquis,<sup>1</sup> Agata Zykwska,<sup>2</sup> Corinne Sinquin,<sup>2</sup> Jacqueline Ratiskol,<sup>2</sup> Stéphane Cuenot,<sup>3</sup> Bernard Cathala,<sup>1</sup> Denis Renard<sup>1</sup> and Sylvia Collic-Jouault<sup>2</sup>

<sup>1</sup>INRA, UR1268 Biopolymères Interactions Assemblages, Nantes, France

<sup>2</sup>Ifremer, EM<sup>3</sup>B Laboratoire des Ecosystèmes Microbiens et Molécules Marines pour les Biotechnologies, Nantes, France

<sup>3</sup>Institut des Matériaux Jean Rouxel (IMN), Université de Nantes, CNRS UMR 6502, Nantes, France

[Melanie.Marquis@nantes.inra.fr](mailto:Melanie.Marquis@nantes.inra.fr)

[Agata.Zykwska@ifremer.fr](mailto:Agata.Zykwska@ifremer.fr)

### INTRODUCTION

During the past decade, multicompartiment and anisotropic assemblies with complex architectures have received significant attention due to their novel morphologies and diverse potential applications<sup>1</sup>. Microassemblies with complex architectures are more desired due to their unique properties such as anisotropic responses to external force, large surface area and building blocks for hierarchical superstructures formation. For the biological and medical areas, shape-controlled biocompatible and biodegradable hydrogel microassemblies can be applied as drug delivery<sup>2</sup> and cell immobilization<sup>3</sup> systems.

We firstly describe microfluidic devices for the generation of monodisperse anisotropic microparticles and microfibers based on plant or marine polysaccharides. Secondly, we demonstrate the ability of these renewable resources microassemblies to control the release of a model protein.

### EXPERIMENTAL METHODS

Low-methoxyl citrus pectin was purchased from Cargill France SAS. Alginate was obtained from FMC biopolymer (U.S.A.). HE800 exopolysaccharides (EPS) was produced by *Vibrio diabolicus* hydrothermal bacterium by fermentation process<sup>4</sup>. Gel formation was set by the ability of cross-linking between the carboxylic groups of uronic acids present in these polysaccharide structures and divalent cations. Flow-focusing devices were designed to structure pectin, alginate or HE800 into complex anisotropic microparticles (Janus and rose-shape morphologies) or microfibers. Polysaccharide gelation was initiated in the chip by diffusion-controlled ionic cross-linking. Morphological characteristics were studied by confocal scanning laser microscopy (CSLM) and scanning electron microscopy (SEM). Encapsulation of fluorescein isothiocyanate labelled bovine serum albumin (BSA-FITC) was investigated. The distribution of labelled BSA was studied by CSLM and/or fluorescence spectrophotometry.

### RESULTS AND DISCUSSION

In a first step, microfluidic technology was applied to elaborate microassemblies based on natural polysaccharides, namely pectin and alginate. Janus microparticles made of pectin-pectin (homo Janus) and pectin-alginate (hetero Janus) of perfectly controlled size and composition were produced. The microparticles of a high monodisperse diameter of 90µm were shown to be stable in calcium solution. The

efficiency of formation of the two hemispheres was then investigated by CSLM. The Janus structure was also confirmed by subjecting each microparticle hemisphere to specific enzymatic degradation. As a proof of concept, free labelled-BSA or labelled-BSA grafted with dextran, were encapsulated in each hemisphere of the hetero Janus microparticles<sup>5</sup>.

In a second step, microfluidic was used for the first time to structure HE800 EPS. This polysaccharide displays an interesting glycosaminoglycan (GAG)-like structure and can thus be considered as an innovative compound to design biomaterials for tissue engineering. We took advantage of microfluidic tool to generate either stable cylindrical stream or emulsion to elaborate, respectively, microfibers and microparticles. Microfibers of 1-5 mm in length and 90 µm in diameter were structured in layers with a smooth surface. The convective intermixing inside the droplets led to microparticles of rose-shape structure composed of rolled up layers. Microparticles had a diameter of 90µm. Both microassemblies were shown to be stable in copper solution. In order to evaluate the potential of the microassemblies formed as delivery systems, encapsulation of labelled-BSA was assessed. The protein release was studied in different buffers and culture media.

### CONCLUSION

This study demonstrates the use of microfluidic to generate complex microassemblies based on natural polysaccharides, which can further be used as controlled release systems. Microfluidic tools offer high control, of the size, the shape and the composition of microassemblies. The encapsulation using microfluidic devices is highly advantageous since all active compound is integrated within microassemblies formed.

### REFERENCES

1. Du *et al.*, Chem. Soc. Rev., 40: 2402–2416, 2011
2. Dai *et al.*, Colloids Surf., B, 41(2-3): 117–120, 2005
3. Siracusa *et al.*, Trends Food Sci. Technol. 19 (12) : 634-643, 2008
4. Raguénès *et al.*, Int. J. Syst. Bacteriol. 47 : 989-995, 1997
5. Marquis *et al.*, Carbohydr. Polym. 116 : 189-199, 2015

### ACKNOWLEDGMENTS

We would like to thank J. Davy for her technical assistance in CSLM and SEM microscopy.



## Glycosaminoglycans as Biomaterials, Drugs and Pathogens

Kamil Kamiński<sup>1</sup>, Bartłomiej Kałaska<sup>2</sup>, Anna Mikulska<sup>1</sup>, Joanna Filipowska<sup>3</sup>, Anna Osyczka<sup>3</sup>, Shin-Ichi Yusa<sup>4</sup>, Małgorzata Kajta<sup>5</sup>, Andrzej Mogielnicki<sup>2</sup>, Maria Nowakowska<sup>1</sup>, and Krzysztof Szczubiałka<sup>1</sup>

<sup>1</sup>Faculty of Chemistry, Jagiellonian University, Poland

<sup>2</sup>Department of Pharmacodynamics, Medical University of Białystok, Poland

<sup>3</sup>Department of Biology and Cell Imaging, Jagiellonian University, Poland

<sup>4</sup>Department of Materials Science and Chemistry, University of Hyogo, Japan

Institute of Pharmacology, Polish Academy of Sciences, Poland

[szczubia@chemia.uj.edu.pl](mailto:szczubia@chemia.uj.edu.pl)

### INTRODUCTION

Glycosaminoglycans (GAGs) are a class of anionic polysaccharides, most of them being more or less sulfated<sup>1</sup>. GAGs perform many structural and physiological functions such as regulating hemostasis, morphogenesis and immune response, and take part in a multitude of pathological processes. They are also anatomical components of many structures on different levels, e.g., cellular receptors, extracellular matrix (ECM), cartilage, tendons, cornea, and many others.

### RESULTS AND DISCUSSION

In our studies GAGs played three different roles:

**1. GAGs as biomaterials.** Using the LbL technique we have obtained ultrathin multi-layered cell culture supports<sup>2</sup>. The polycation used to fabricate the supports was diazoresin while heparin, chondroitin sulfate and hyaluronic acid (the only nonsulfated GAG) were used as polyanions. Irradiation of the supports resulted in photocrosslinking of the multilayer and increased its stability. We found that human mesenchymal stem cells (hMSC) grew on these supports much faster than on the commercial tissue culture plastic (TCP) supports. Moreover, the hMSC monolayers spontaneously detached from the support so that no trypsinization was necessary. The supports could be regrown by new cell layers relatively early during culture indicating that the supports were not modified by the growing cells.

**2. GAGs as drugs.** Heparin is a GAG commonly used as an anticoagulant in thrombotic disorders and cardiac surgeries. In emergency (e.g., hemorrhage), its anticoagulative action has to be interrupted by the administration of protamine, which is, however, a hypotensive and immunogenic protein and may trigger life-threatening reactions. Therefore, searching for a safer heparin antidote, we have obtained a series of cationic polymers, both synthetic and of natural origin, which have been proved to inhibit heparin both *in vitro* and *in vivo*<sup>3</sup>. Some of them have been found to be superior to protamine.

**3. GAGs as pathogens.** As mentioned above, GAGs are essential components of human body. However, the disorders in their metabolism may result in serious diseases, such as the Sanfilippo disease, a rare genetic and so far incurable disease caused by the excessive storage of heparan sulfate in all body cells, ultimately leading to death in the second decade of life. Some isoflavone compounds, such as daidzein, are known to

decrease level of GAGs. Unfortunately, poorly soluble daidzein shows very low bioavailability. To overcome this problem we have developed drug delivery systems based on the complex of cationized  $\alpha$ -cyclodextrin with daidzein. The cationic cyclodextrin was shown to be efficiently taken up by murine nervous cells and by normal human dermal fibroblasts (HDFs) and its complex with daidzein decreased the level of GAGs in HDFs<sup>4</sup>. Moreover, the cationic cyclodextrin was found to be mucoadhesive suggesting the possibility of its oral administration.

### CONCLUSIONS

Glycosaminoglycans are an important yet apparently underappreciated class of biopolymers. A better understanding of their structure, physicochemical properties and mechanism of action is needed to fully exploit their great potential as biomaterials and drugs and to treat GAG-related pathologies.

### REFERENCES

1. Kuberan B et al, (Eds.). Glycosaminoglycans. Chemistry and Biology Series: Methods in Molecular Biology, Vol. 1229, Springer, 2015.
2. Mikulska A, Filipowska J, Osyczka AM, Szuwarzyński M, Nowakowska M, and Szczubiałka K. Photocrosslinked ultrathin anionic polysaccharide supports for accelerated growth of human mesenchymal stem cells. *Cell Prolif.* **2014**, *47*, 516–526.
3. Kałaska B, Kamiński K, Sokółowska E, Czaplicki D, Kujdowicz M, Stalińska K, Bereta J, Szczubiałka K, Pawlak D, Nowakowska M, Mogielnicki A. Nonclinical Evaluation of Novel Cationically Modified Polysaccharide Antidotes for Unfractionated Heparin *PLoS ONE*, **2015**, accepted.
4. Kamiński K, Kujdowicz M, Kajta M, Nowakowska M, Szczubiałka K. Enhanced delivery of daidzein into fibroblasts and neuronal cells with cationic derivatives of gamma-cyclodextrin for the control of cellular G. *Eur.J.Pharm.Biopharm.* **2015**, accepted.

### ACKNOWLEDGMENTS

Polish National Science Centre grants UMO-2013/09/D/ST5/03864, UMO-2011/03/B/NZ7/00755, UMO-2012/05/N/ST5/01495 and Foundation for Polish Science grant co-financed by the EU European Regional Development Fund, PolyMed, TEAM/2008-2/6 are gratefully acknowledged.



Bayon Yves<sup>1</sup>, Alves Antoine<sup>2</sup>, Grossiord Carol<sup>3</sup> and Brunon Céline<sup>3</sup>

<sup>1</sup> Covidien, Trévoux, France <sup>2</sup> NAMS, Chasse/Rhône, France <sup>3</sup> Science et Surface, Ecully, France  
[yves.bayon@covidien.com](mailto:yves.bayon@covidien.com)

## INTRODUCTION

PLA and related polymers are widely used materials in medical devices because of their biocompatible and biodegradable properties. The history and changes of such polymers after implantation as medical devices should be characterized since they condition their tissue repair functions by providing mechanical and/or scaffolding properties.

In this study, PLA degradation has been investigated, in particular, in terms of molecule transformation and crystallinity evolution, after subcutaneous implantation in rabbits. The extent and mapping of PLA degradation within selected medical devices was documented by a novel approach combining FTIR spectroscopy and image analysis, from tissue explant sections.

## MATERIALS AND METHODS

18 New Zealand White male rabbits were included in this study. Each rabbit received 8 subcutaneous implants: 4 PLLA test meshes and 4 control meshes (TIGR® Matrix Surgical (made of copolymers of lactic acid, glycolic acid and trimethylene carbonate - Novus Scientific). The follow-up period was 4, 26 and 52 weeks (n=6 animals per time-period). Both the test and control meshes were implanted in 3 configurations: original state, partially pre-degraded and highly pre-degraded state in terms of residual molecular weight, gravimetric mass and manipulability by controlled accelerated hydrolysis. The tissue explants were paraffin-embedded and the glass slide histological sections (9 µm thickness) were prepared before dewaxing.

FTIR (Fourier Transform Infra-Red) measurements were made directly on the tissue sections using Spotlight 400 (Perkin-Elmer) microspectrometer. FTIR mapping was performed in ATR (Attenuated Total Reflection) mode using the ATR-imaging accessory with Ge crystal. The scanned area was 400 x 400 µm<sup>2</sup> with lateral resolution of 1.56 µm. The MCT (?) detector covered the range from 720 to 4000 cm<sup>-1</sup> with a spectral resolution of 8 cm<sup>-1</sup>.

Standard histology staining on serial tissue sections were carried out in parallel.

## RESULTS

FTIR analysis of reference PLA fibers (non-degraded PLA and PLA pre-degraded during 120 h) revealed peak shifts and intensity changes for bands at 1209 cm<sup>-1</sup> and 1130 cm<sup>-1</sup> (Fig. 1). These bands are related respectively to the asymmetric C-O-C stretching ( $\nu_{as}COC$ ) and asymmetric CH<sub>3</sub> rocking ( $\nu_{as}CH_3$ ) vibrations<sup>1</sup>. The intensity of these bands is linked to the crystallinity of PLA, increasing with lower

molecular weights of PLA as a result of hydrolysis progression.

FTIR maps of PLA fibers from tissue explant sections have been processed and the ratio R1 (1209 cm<sup>-1</sup> band intensity / 1181 cm<sup>-1</sup> band intensity) was imaged in false colors, in the overall tissue sections (≈10 x 20 mm<sup>2</sup>) as illustrated in Fig. 2.

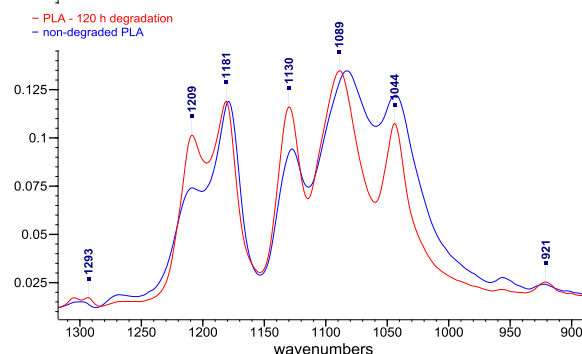


Fig. 1. FTIR spectra of non-degraded (blue) and degraded PLA (red).

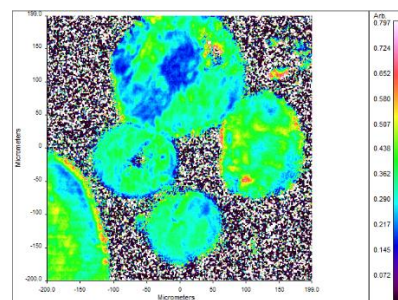


Fig. 2. FTIR mapping of the PLLA mesh 26 weeks post-operatively. In red, degraded PLA (high R1 ratio) and in blue non-degraded PLA (low R1 ratio).

## DISCUSSION AND CONCLUSIONS

FTIR microscopy has been used to image the degradation of PLA from explanted tissues. It precisely mapped out the progression of degradation of PLA and related polymers in meshes and inside yarns. This helped in better understanding the foreign body reaction kinetics and tissue repair throughout the in vivo life of the degradable polymers, by confronting FTIR and standard histology results.

## REFERENCES

- 1 Bourque et al. Langmuir 2001, 17, 5842
- 2 Krikorian & Pochan Macromolecules 2005, 38, 6520

## ACKNOWLEDGMENTS

This work was partially supported by the Rhône-Alpes Region and the Fonds Unique Interministériel program (REVAMED collaborative project).



## Possible Approach to Improve Systemic Gene Delivery to Tumour Using Polyplex Nanoparticles

Mikhail Durymanov<sup>1</sup>, Alexei Yarutkin<sup>2</sup>, Andrey Rosenkranz<sup>1,2</sup>, and Alexander Sobolev<sup>1,2</sup>

<sup>1</sup> Laboratory of Molecular Genetics of Intracellular Transport, Institute of Gene Biology of the RAS, Russia

<sup>2</sup> Department of Biophysics, Lomonosov Moscow State University, Russia

[mdurymanov@gmail.com](mailto:mdurymanov@gmail.com)

### INTRODUCTION

Systemic nanoparticle gene delivery has a great potential for cancer therapy but its application still limited mostly due to low efficacy of gene delivery<sup>1</sup>. Basing on our previous data<sup>2</sup>, we hypothesized that low transfection is a result of poor extravasation and permeation of gene delivery nanoparticles. In an attempt to improve the tumour accumulation of PEI-PEG-based polyplexes, their *in vivo* application was combined with three different physiologically active agents including nitroglycerin (generates NO which causes disruption of adherens junction between endotheliocytes and improves tumour vasculature leakiness<sup>3</sup>), losartan (inhibits angiotensin signaling in cancer-associated fibroblasts that leads to suppression of collagen I production and enhancement of extracellular matrix permeability<sup>4</sup>) and angiotensin-II (induces mild hypertension and increases convective influx<sup>5</sup>).

### EXPERIMENTAL METHODS

**Intravital microscopy.** Murine Cloudman S-91, clone M-3 or B16F1 melanoma cells were inoculated subcutaneously in DBA/2 and C57 black mice bearing dorsal skinfold chamber (DSC), respectively. For intravital microscopy, mice (3 per group) were anesthetized and stably mounted onto a platform above the objective (10x) of Zeiss LSM 510 microscope. Blood vessels were visualized by 0.5 mg of 150 kDa FITC-dextran i.v. injected, and polyplexes (80 µg of quantum dot labeled plasmid DNA per mouse) were injected i.v. immediately after FITC-dextran. Sequential 3D 96-µm stacks were obtained for up to 4 hours after polyplex administration.

**Polyplex application and gene expression analysis.** M-3 or B16F1 mouse melanoma tumours were established in female DBA/2 or C57 black mice, respectively. Polyplexes containing firefly luciferase as a reporter gene under CMV promoter were i.v. injected when tumour size was 200 mm<sup>3</sup>. The mice were treated with three different physiologically active agents (5 mice per group): nitroglycerin (NG), angiotensin-II (AT-II) and losartan (LS). NG ointment was applied locally onto the skin overlying tumour at doses of 0.5-1.0 mg/tumour 20 min before polyplex injection. For AT-induced hypertension, AT-II was continuously infused at a rate of 3 µg/kg/min immediately after polyplex injection and maintained for 30 min. The last group of mice was treated with LS (30 mg/kg i.p.) each day for 7 days before polyplex administration. Control mice were injected with the same polyplexes without any treatments. At 24 hours post-injection tumours were harvested and luciferase activity was measured.

### RESULTS AND DISCUSSION

Mixing plasmid DNA with PEI-PEG-MC1SP (at N/P=20) resulted in formation of positively charged ( $\zeta$ -potential 22.7±1.0 mV) polyplex nanoparticles with average hydrodynamic diameter of 41.2±4.0 nm. Previously, it has been shown that the major part of extravasated polyplex nanoparticles reside in close proximity to the blood vessels<sup>2</sup>. We have found that LS potentiates systemic gene delivery in a greater extent than other physiologically active agents (Figure 1) and causes 3-6-fold increase in reporter gene expression. Visualization of fluorescently labelled polyplex distribution using intravital microscopy has shown that enhanced gene expression turned out to be a result of improved polyplex extravasation.

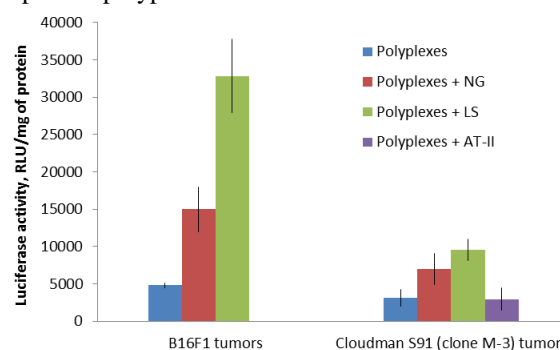


Figure 1 shows luciferase activity in B16F1 and Cloudman S91 (clone M-3) melanoma tumours at 24 hours after polyplex i.v. injection combined with physiologically active agents. Results are means ± S.E.M.

### CONCLUSION

Our results have shown that polyplex accumulation in tumour tissue may be enhanced using safe physiologically active agents resulting in superior systemic gene delivery.

### REFERENCES

- Hendricks W. *et al.* Nanomedicine (Lond). 9: 1121-4, 2014
- Durymanov M. *et al.* Biomaterials. 34: 10209-16, 2013
- Seki T. *et al.* Cancer Sci. 100: 2426-30, 2009
- Chauhan V. *et al.* Nat. Commun. 4: 2516, 2013
- Li C. *et al.* Br. J. Cancer. 67: 975-80, 1993

### ACKNOWLEDGMENTS

This work was supported by the Russian Foundation for Basic Research grant no. 13-04-01282-a.





## Endothelialization of Polyurethanes: Immobilization of REDV Peptide

Beata Butruk-Raszeja<sup>1</sup>, Magdalena Dresler<sup>1</sup>, Aleksandra Kuźmińska<sup>1</sup>, Tomasz Ciach<sup>1</sup>

<sup>1</sup>Faculty of Chemical and Process Engineering, Warsaw University of Technology, Warsaw, Poland  
[b.butruk@ichip.pw.edu.pl](mailto:b.butruk@ichip.pw.edu.pl)

### INTRODUCTION

The challenge for cardiovascular tissue engineers is to design hemocompatible biomaterials that promote neo-tissue formation. Despite many years of intensive research materials used to fabricate synthetic implants still cause formation of clots in the bloodstream, which can have fatal consequences for the patient. Under physiological conditions, the process of blood clotting is controlled by endothelial cells. These cells constantly and actively prevent thrombosis by releasing a number of substances. Synthetic materials are not able to release certain substances due to limited capacity. Thus, the most promising strategy to fabricate non-thrombogenic materials is covering the implant surface with a layer of endothelial cells.

### EXPERIMENTAL METHODS

The aim of this research was to improve hemocompatibility of polyurethane (PU) surface by REDV peptide sequence immobilization. The study included REDV peptide chemical immobilization to the polyurethane surface, peptide presence on the material confirmation and the material hemocompatibility analysis. Peptide presence was confirmed by BCA assay and contact angle measurement. Hemocompatibility analysis included anti-fibrinogen ELISA assay and SEM observation (platelet adhesion). Endothelial cells adhesion was also evaluated.

### RESULTS AND DISCUSSION

Studies have shown that the modified materials have a higher wettability compared to the unmodified PU. BCA assay confirmed successful immobilization of the peptide molecules. Modification resulted in decrease in serum-derived fibrinogen (fig.1). SEM analysis confirmed decreased adhesion of platelets to the peptide-modified surface compared the non-modified one. Hypothesis that REDV peptide immobilization improves hemocompatibility of polyurethane materials has been confirmed.

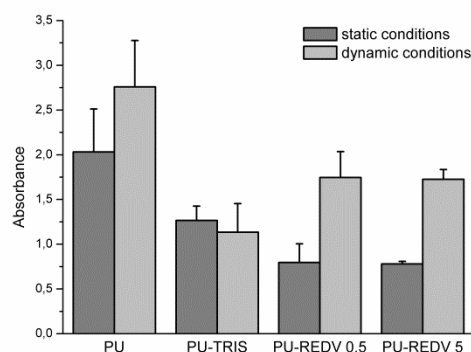


Fig. 1: Surface-adsorbed fibrinogen on unmodified polyurethane (PU) and polyurethane modified with REDV peptide (PU-REDV 0.5, PU-REDV 5).

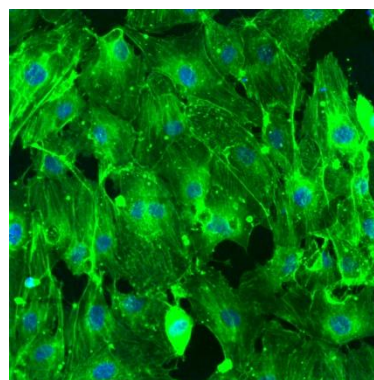


Fig. 2: Growth of endothelial cells on polyurethane modified with REDV peptide.

### CONCLUSION

Hypothesis that REDV peptide immobilization improves hemocompatibility of polyurethane materials has been confirmed.

### ACKNOWLEDGMENTS

Research funded by the National Science Centre on the basis of the decision DEC-2011/03/N/ST5/04443.

## ***Helicobacter pylori*-Binding Small Chitosan Microparticles that Penetrate Gastric Mucosa**

Patrícia C. Henriques<sup>1,2</sup>, Paula Sampaio<sup>3</sup>, Maria Lázaro<sup>1</sup>, André Maia<sup>3</sup>, António Gouveia<sup>4,5</sup>, José Manuel Lopes<sup>4,5</sup>, Ana Magalhães<sup>4</sup>, Celso A. Reis<sup>4</sup>, M. Cristina L. Martins<sup>1</sup>, Paulo Costa<sup>6</sup>, Inês C. Gonçalves<sup>1</sup>

<sup>1</sup> INEB - Instituto de Engenharia Biomédica, Universidade do Porto, Portugal

<sup>2</sup> Faculdade de Engenharia, Universidade do Porto, Portugal

<sup>3</sup> IBMC – Instituto de Biologia Molecular e Celular, Universidade do Porto, Portugal

<sup>4</sup> IPATIMUP – Instituto de Patologia e Imunologia Molecular da Universidade do Porto, Portugal

<sup>5</sup> Faculdade de Medicina, Universidade do Porto & Centro Hospitalar São João, Portugal

<sup>6</sup> Faculdade de Farmácia, Universidade do Porto, Portugal

[icastro@ineb.up.pt](mailto:icastro@ineb.up.pt)

### **INTRODUCTION**

*Helicobacter pylori* (*H. pylori*), a gram-negative bacterium, is the only known organism able to survive and colonize the human gastric mucosa, infecting over 50% of the world's population and causing several gastric disorders from gastritis to gastric cancer.<sup>1</sup> Current treatments rely on antibiotic-based therapies, but are still inefficient in 20% of the cases, thus leaving around 140 million patients worldwide without alternative treatment.<sup>2</sup> Chitosan microspheres have recently been proposed as a promising *H. pylori*-binding system, mainly due to their antimicrobial/mucoadhesive properties.<sup>3,4</sup> After oral administration, these particles should bind *H. pylori* present in the mucosa and remove them through the gastrointestinal tract. Chitosan particles with 170  $\mu\text{m}$  can adhere to *H. pylori*<sup>3</sup> in the mucus layer, but are too big to penetrate the human gastric foveola (stomach invaginations) where *H. pylori* is also present, which are around 70  $\mu\text{m}$  wide. This work aims to produce smaller chitosan particles (diameters < 50  $\mu\text{m}$ ), characterize them and evaluate their interaction with *H. pylori* and mice and human gastric mucosa.

### **EXPERIMENTAL METHODS**

Chitosan microparticles (Mics) were produced by ionotropic gelation into a sodium tripolyphosphate solution using an aerodynamically assisted spraying system, varying parameters such as chitosan degree of acetylation (DA) (6% and 16%), concentration (0.5 and 1% (w/v)), flow rate (0.25, 0.33, 0.5 and 1ml/min), air pressure (205 and 525mbar) and nozzle diameter (0.25 and 0.5mm). Mics were then crosslinked with genipin (10mM, 45min) to avoid dissolution in gastric pH, followed by lyophilisation. Particles size, morphology and area were evaluated using laser diffractometry (Mastersizer, MS), high-throughput microscopy (IN Cell Analyzer, ICA) and imaging flow cytometry (ImageStream, IS).

Mics ability to adhere *H. pylori* was assessed by confocal microscopy (CM) and IS after incubating Mics with FITC-labelled *H. pylori* ( $1 \times 10^7$  CFU/ml) at pH 6.0 for 2h. The ability of Mics to enter into gastric foveolae was evaluated by incubating Mics with fresh mice (C57BL/6) and human stomach samples at pH 6.0. Gastric mucosa was either labelled with CellMask™ Deep Red plasma membrane stain and immediately assessed by CM or frozen in OCT medium, cryosectioned into 50 $\mu\text{m}$  slices and analysed by ICA.

### **RESULTS AND DISCUSSION**

Mics size was found to decrease with increase of chitosan DA and air pressure and with decrease of chitosan concentration and nozzle diameter; flow rate did not influence particle size. The optimization of the production process revealed 6% DA chitosan at 0.5% (w/v), flow rate of 0.5 ml/min, 525 mbar and 0.25 mm nozzle diameter as the optimal conditions to obtain particles with the required size.

Size distribution was obtained by MS, which revealed that 50% of Mics (Dv50) presented a diameter below 55.2  $\mu\text{m}$ . The lyophilisation process was found to reduce the particles size and to make them more irregular: ICA showed a reduction in the circular diameter from 43.8  $\mu\text{m}$  to 29.8  $\mu\text{m}$ , in the maximum chord from 55.8  $\mu\text{m}$  to 43.3  $\mu\text{m}$  and in the area from 1725.6  $\mu\text{m}^2$  to 786.9  $\mu\text{m}^2$ . IS corroborated this reduction in the particles size.

CM and IS showed the ability of FITC-labelled *H. pylori* to adhere throughout the surface, although not inside Mics.

Regarding *ex-vivo* Mics penetration studies, both CM and ICA revealed the presence of Mics in different depths of the mice and human gastric mucosa, thus indicating their ability to enter into gastric foveola.

### **CONCLUSION**

Chitosan microparticles with 29.8  $\mu\text{m}$  circular diameter were successfully produced using an extremely fast system that can be used for large scale production. These Mics are able to adhere *H. pylori* and penetrate the foveola from mice and human gastric mucosa, revealing to be very promising to fight *H. pylori* infection and thus potentially preventing gastric cancer.

### **REFERENCES**

1. Wroblewski LE *et al.* Clin Microbiol Rev. 2010; 23 (4): 713–39;
2. Gonçalves IC *et al.* Expert Rev Anti Infect Ther. 2014; 12 (8): 981–92;
3. Fernandes M *et al.* Int J Pharm 2013;454:116–24.
4. Gonçalves IC *et al.* Acta Biomater. 2013; 9 (12): 9370–8.

### **ACKNOWLEDGMENTS**

FEDER and FCT for financial support through Programa Operacional Factores de Competitividade (COMPETE): PEst-C/SAU/LA0002/2013, NORTE-07-0124-FEDER-000005, EXPL/CTM-BIO/0762/2013.



Swioklo<sup>1</sup>, Stephen; Connon, Che<sup>1</sup><sup>1</sup>Institute for Genetic Medicine, Newcastle University, United Kingdom  
[Stephen.Swioklo@newcastle.ac.uk](mailto:Stephen.Swioklo@newcastle.ac.uk)

## INTRODUCTION

The clinical application of cell-based therapeutics is ever accelerating with an emergence of approved cell therapy products (CTPs) to the market. One of the major bottlenecks for CTPs, however, is in the short-term storage of cells for quality, safety and efficacy testing, and their distribution from the donor or bank, to sites of processing, and back to the clinic<sup>1</sup>. To meet this need, we have developed an alginate-based encapsulation system for cell storage at hypothermic temperatures (0–32°C) allowing the preservation of cell viability and function for extended time periods, obviating the need for cryogenic storage.

## EXPERIMENTAL METHODS

**Cell encapsulation.** Human adipose-derived stem cells (hASCs) ( $0.5 \times 10^6$  cells/mL) were encapsulated in 0.5mL 1.2% calcium alginate discs as previously described<sup>2</sup> before transferring to sealed cryovials containing medium and storing for up to 3 weeks at a specified temperature (see figure 1 for schematic).

**Assessment of viable cell recovery.** Cells were extracted from alginate discs and viable cell number was assessed by Calcein-AM staining before counting using a Countess II FL automated cell counter.

**Assessment of cell attachment.** Cells were seeded at 20,000 cells/cm<sup>2</sup> and incubated for 24 hours at 37°C, 5% CO<sub>2</sub> before assessing the attached cell number by methylene blue staining as previously described<sup>3</sup>.

**Statistical analysis.** Differences between groups were assessed by unpaired T-test (viable recovery) and one-way ANOVA (cell attachment) analyses.  $n = 3$ .

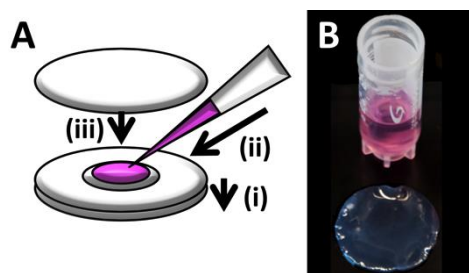


**Figure 1. Encapsulation of cells in alginate discs.** A: Discs were formed in filter paper moulds saturated in calcium chloride. Two filter paper rings were placed upon a filter paper disc (i) before pipetting 500µL cell/alginate suspension into the aperture (ii). A second filter paper disc was placed on top of the mould to allow initial gelation before transfer to a calcium chloride bath to complete gelation. B: Alginate disc for cell storage.

## RESULTS AND DISCUSSION

Alginate encapsulation improved viable cell recovery following 72 hours storage at a range of temperatures. These included 4 and 17°C where encapsulation affected a significantly higher viable cell recovery compared to control (non-encapsulated cells) at both temperatures.

Viable cell yield was, however, temperature dependent with 15°C storage resulting in a greater number of viable cells compared to 4°C in all samples, with encapsulated samples yielding 86±6% of viable cells loaded (figure 2). The protective effect of alginate encapsulation was observed for up to 3 weeks of storage.

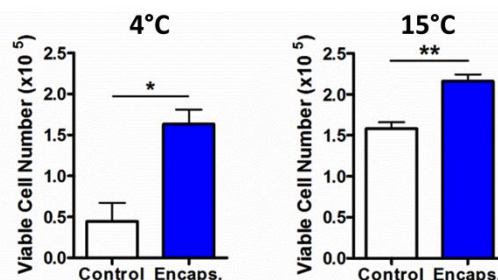


**Figure 2. The protective effect of encapsulation at multiple storage temperatures.** hASCs were stored for 72 hours at either 4°C or 15°C. Values are expressed as means ± SEM (\*\* $p < 0.01$ ; \* $p < 0.05$ ;  $n = 3$ ).

As well as promoting viability, alginate encapsulation also preserved cell function following release from storage, including the ability for cells to attach and proliferate. Whilst control samples exhibited a significant decrease in attached cell number compared to the non-stored control (NSC), encapsulated cells exhibited no significant decrease, rather a significantly higher number of attached cells were apparent compared to the control with normal morphological characteristics (figure 3). Subsequently, cells regained metabolic activity, proliferative potential, and differentiation capacity.

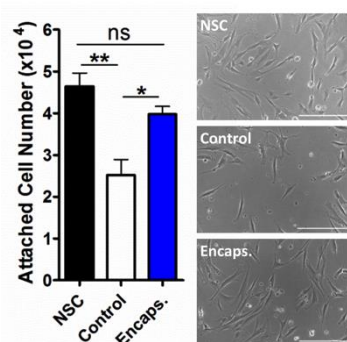


**Figure 3. Preservation of cell attachment by encapsulation.** hASCs were stored for 5 days at 15°C before assessing attachment 24 hours after seeding. NSC, non-stored control. Values are expressed as means ± SEM (\*\* $p < 0.01$ ; \* $p < 0.05$ ;  $n = 3$ ). Scale bars = 500µm

## CONCLUSION

We present a simple and cost-effective method to preserve stem cell viability and function during hypothermic storage which could be of great benefit in counteracting the short time windows associated with cell-based therapeutic manufacture and distribution.

## REFERENCES

1. Robinson *et al.*, Biotechnol. Lett. 36:201-209, 2014
2. Chen *et al.*, Tissue Eng. Pt.C-Meth 19:568-576, 2013
3. Oliver *et al.*, J. Cell Sci. 92: 513-518, 1989



## Antibacterial Coatings on Titanium Surfaces: a Comparison Study Between *In Vitro* Single-Species and Multispecies Biofilm

Maria Godoy-Gallardo<sup>2,3</sup>, Zhejun Wang<sup>4</sup>, Ya Shen<sup>4</sup>, José M. Manero<sup>2,3</sup>, F. Javier Gil<sup>1,2,3</sup>, Carlos Mas-Moruno<sup>2,3</sup>,  
Daniel Rodríguez<sup>1,2,3</sup>, Markus Haapasalo<sup>4</sup>

<sup>1</sup>Escola Universitaria d'Enginyeria Tècnica Industrial de Barcelona, Consorci Escola Industrial de Barcelona, Technical University of Catalonia (UPC-BarcelonaTECH), Barcelona, Spain

<sup>2</sup>Biomaterials, Biomechanics and Tissue Engineering Group, ETSEIB, Technical University of Catalonia (UPC), Spain

<sup>3</sup>CIBER de Bioingeniería, Biomateriales y Nanomedicina (CIBER-BBN), Spain

<sup>4</sup>Department of Oral Biological and Medical Sciences, University of British Columbia, Canada

[daniel.rodriguez.rius@upc.edu](mailto:daniel.rodriguez.rius@upc.edu)

### INTRODUCTION

Dental plaque is a biofilm that causes dental caries, gingivitis and periodontitis. Most of the studies in antibacterial coatings have been conducted by *in vitro* single-species biofilm formation but oral biofilm involves more than 500 different bacterial species that are able to interact.<sup>1,2</sup> Therefore, new studies are focused on *in vitro* multispecies biofilm model that mimic *in vivo* biofilms.<sup>3,4</sup> This work has two main goals: (1) to investigate the efficiency of five antibacterial coatings on titanium and (2) to compare the antibacterial properties of these coatings on single species and multispecies oral biofilms.

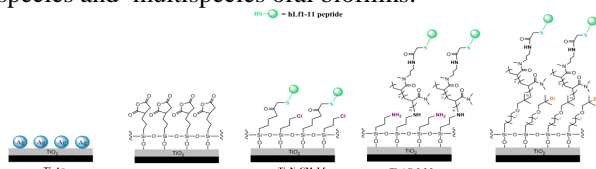


**Figure 1.** Schematic representation of the applied surface treatments.

### EXPERIMENTAL METHODS

Smooth titanium (Ti) samples were coated with five different conditions: silver electrodeposition, TESPSA silane coating, hLf1-11 peptide binding with CPTES silane and polymer brush based (ATRP) peptide binding with two different chemical routes. Surfaces were characterized by contact angle measurements, white-light interferometry and X-ray photoelectron spectroscopy (XPS). Cellular viability and proliferation were studied by LDH assay with human fibroblasts. The *in vitro* antibacterial properties of the modified surfaces were tested with single biofilm and oral plaque biofilm by means of bacterial adhesion assay at 2 h and evolution of biofilm formation after 24 h, 1, 2 and 3 weeks.

### RESULTS AND DISCUSSION

The success of each coating process was evaluated by means of XPS studies. Silver was deposited onto titanium surfaces and silanization with covalent attachment of the Lhf1-11 onto Ti was successfully performed. Surface roughness was not affected by these treatments. Cell viability and proliferation evaluated with LDH assays were not affected by the modified surfaces. The treated titanium samples displayed a promising reduction in bacterial adhesion. Overall, the results showed a reduction of bacterial attached on all

modified surfaces, thus confirming the efficacy of the antibacterial coatings.

Finally, the focus in the experiments was placed on the long-term antibacterial properties and biofilm formation onto modified coatings (**Figure 2**). These experiments showed that after 4 weeks of incubation the treated surfaces still showed a reduction in bacterial viability. These results are of great interest because they demonstrate that distinct mono-species biofilms show differences in bacterial adhesion and long-term biofilm evolution. Besides, disparities are also obtained when oral plaque biofilm was used. Thus, bacterial strains exhibit different sensitivities to the activity of antibacterial and/or antifouling treatment.

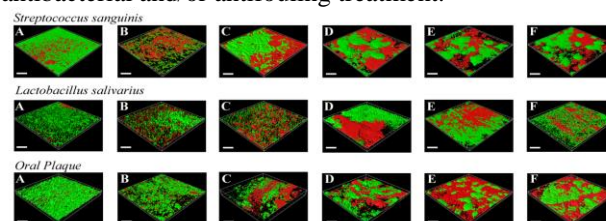


**Figure 2.** Live/dead staining of *S. sanguinis*, *L. salivarius* and oral plaque after 4 weeks of incubation at 37°C. (A) Ti, (B) Ti\_Ag, (C) Ti\_N\_TSP, (D) Ti\_N\_CM\_Lf, (E) Ti\_ACoI\_Lf and (F) Ti\_BCoI\_Lf

### CONCLUSION

Two different *in vitro* biofilm models were used to study the antibacterial properties of five different titanium surface coatings. A higher decrease was measured when a single-species bacteria model was used, especially for *S. sanguinis*. The *in vitro* multispecies biofilm model is a promising strategy to study the properties of antibacterial coatings because it more realistically mimics the complex microflora of peri-implantitis.

### REFERENCES

1. Foster J.S. *et al.*, Appl. Environ. Microbiol. 70:4340-4348, 2004
2. Kolenbrander P. E. *et al.*, Microbiol. Mol. Biol. Rev. 66: 486–505, 2002
3. Shen Y. *et al.*, Endod. 37:657–661, 2011
4. Shen Y. *et al.*, J. Endod. 35:981–985, 2009

### ACKNOWLEDGMENTS

This study was supported by the Ministry of Economy and Competitiveness (MINECO) of the Spanish Government (Proj. MAT2009-12547, MAT2012-307).



# The Proangiogenic Potential of a Novel Poly(lactic) Based Composite Membrane for Guided Bone Regeneration

Hugo Oliveira<sup>1</sup>, Nadège Sachot<sup>2,3</sup>, Sylvain Catros<sup>1</sup>, Sylvie Rey<sup>1</sup>, Joan Martí<sup>2,3</sup>, Oscar Castano<sup>2,3,4</sup>, Joëlle Amedee<sup>1</sup>,  
Elisabeth Engel<sup>2,3,4</sup>

<sup>1</sup>Inserm, U1026, Tissue Bioengineering, University Bordeaux Segalen, Bordeaux Cedex 33076, France,

<sup>2</sup>Institute for Bioengineering of Catalonia (IBEC), Barcelona, Spain, <sup>3</sup>CIBER-BBN, Zaragoza, Spain, <sup>4</sup>Dpt. Materials Science and Metallurgical Engineering, Universitat Politècnica de Catalunya, Barcelona, Spain;

[eengel@ibecbarcelona.eu](mailto:eengel@ibecbarcelona.eu)

## INTRODUCTION

In current bone tissue engineering strategies the obtaining of sufficient angiogenesis during tissue regeneration is still a major limitation in order to attain construct integration and tissue functionality. This drawback is further relevant when considering large bone defects, where the amount of oxygen required for cell survival is limited to a diffusion distance between 150-200  $\mu\text{m}$  from the supplying blood vessels. Several strategies have been described to tackle this problem, mainly by the use of angiogenic factors or endothelial progenitor cells. However, when facing a clinical scenario these approaches are inherently complex and present a high cost. As such, more cost effective approaches are awaited. We have recently demonstrated that the increased local concentration of calcium ions ( $\text{Ca}^{2+}$ ) could induce the migration, maturation and organization of endothelial progenitors<sup>1</sup>. Moreover, a composite biomaterial of poly(lactic acid) (PLA) and Ca phosphate glass has shown to elicit proangiogenic and chemotactic properties on endothelial precursor cells *in vitro*<sup>2</sup>. Here, we tested electrospun PLA fiber-based materials, containing different ratios of calcium phosphate glass nanoparticles, subcutaneously in mice. These distinct formulations allowing different  $\text{Ca}^{2+}$  release kinetics to the vicinity of the matrix expect to improve vessel formation into the biomaterial.

## EXPERIMENTAL METHODS

Aligned electrospun PLA nanofibers containing glass ceramic nanoparticles (CaP) at a mass ratio of 0, 10, 20 and 30% (i.e. PLA, NP10, NP20 and NP30, respectively) were prepared as previously described<sup>3</sup>. One cm diameter membrane disks were cut and sterilized by UV. The biomaterials were implanted subcutaneously in the dorsal pouch of swiss strain female mice (3 month, n=6). At 1 and 4 weeks post implantation animals were sacrificed and materials, together with the surrounding tissue, were recovered. Samples were fixed in 4% paraformaldehyde for 24 hrs at 4°C and then processed for cryosection. Sequential 8  $\mu\text{m}$  sections were performed; samples were then processed for HE staining or immunohistochemistry for CD31 and the assessment of the macrophage density and phenotype. The same implantation procedure was equally performed for 3 weeks of implantation, samples were recovered, snap frozen and homogenized for total protein extraction. A dot blot array of angiogenic factors (Abcam) was used to assess the different composites.

## RESULTS AND DISCUSSION

All constructs tested showed augmented cellular penetration with increased time of implantation. An increase on microvessel formation was observed in the

case of the constructs containing glass ceramic nanoparticles, when compared with PLA alone, at both 1 and 4 weeks post implantation.

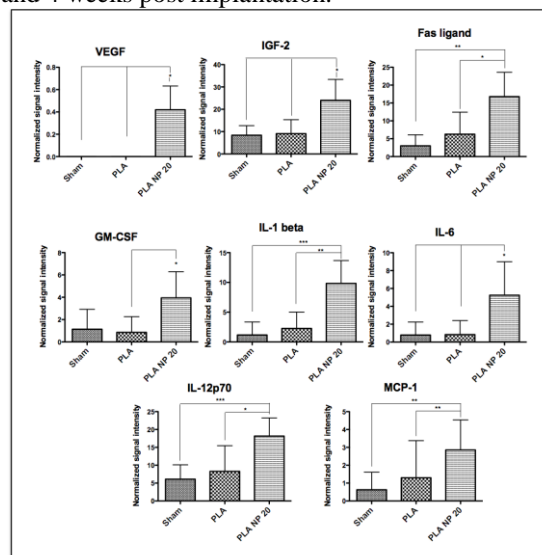


**Figure 1-** Relative quantification of angiogenic factor expression within the tissue of the implanted matrices of electrospun poly(lactic acid) (PLA) alone, containing 20% of calcium phosphate nanoparticles (NP) or sham operated animals, at 21 days (n=4, average $\pm$ SD).

Additionally, this effect was shown to correlate with their mass ratio and their  $\text{Ca}^{2+}$  release profile. Angiogenic factor array assessment, at 3 weeks post implantation, revealed an increased expression of key pro-angiogenic and chemotactic factors for the 20% composite materials in comparison with PLA alone or sham-operated animals (Fig.1). Macrophage density and profile evaluation allow us to postulate on a mechanism of chemotaxis mediated by the released  $\text{Ca}^{2+}$ , leading to the mediation of endothelial cell recruitment and increased angiogenesis. Additionally, the evaluation of selected materials in a bone orthotopic site in a rat critical size defect model is underway and will shed light on their impact for bone regeneration strategies.

## CONCLUSION

The developed composite materials have the ability, *in vivo*, to increase the vessel formation into the implanted structures. This approach, due to its simplicity, presents an attractive strategy for clinical musculoskeletal repair.

## REFERENCES

1. Aguirre A. *et al.* Biochem Biophys Res Comm. 393(1): 156-61, 2010
2. Aguirre A. *et al.* Cells and Mater. 24: 90-106, 2012
3. Sachot N. *et al.* J R Soc Interface. 10: 88, 2013

## ACKNOWLEDGMENTS

This work was supported by funding from the European Commission; PI11/03030, NANGIOFRAC, and the MINECO (Project MAT2011-29778-C02-01).





## Organic and Inorganic Bioactive Signals to Prepare Biomimetic Chitosan Based Scaffolds for Bone Tissue Regeneration

<sup>1</sup>M.G. Raucci, <sup>1</sup>D. Giugliano, <sup>2</sup>A. Giuri, <sup>2</sup>V.M. De Benedictis, <sup>2</sup>C. Demitri, <sup>2</sup>A. Sannino, <sup>1,3</sup>L. Ambrosio

<sup>1</sup>Institute of Polymers, Composites and Biomaterials – National Research Council of Italy. Mostra d'Oltremare Pad.20 - Viale Kennedy 54, 80125- Naples, Italy.

<sup>2</sup>Department of Engineering for Innovation, University of Salento, Via Monteroni, 73100 Lecce, Italy.

<sup>3</sup>Department of Chemicals Science and Materials Technology, National Research Council of Italy (DSCTM-CNR), P.le Aldo Moro 7, 00185 – Rome, Italy.  
[mariagrazia.raucci@cnr.it](mailto:mariagrazia.raucci@cnr.it)

### INTRODUCTION

Current tissue engineering strategies are focused on the restoration of pathologically altered tissue architecture by transplantation of cells in combination with supportive scaffolds and biomolecules. In recent years, considerable attention has been given to chitosan (CS)-based materials and their applications in the field of orthopaedic tissue engineering. Interesting characteristics that render chitosan suitable for this purpose are a minimal foreign body reaction, an intrinsic antibacterial nature, and the ability to be molded in various geometries and forms such as porous structures, suitable for cell ingrowth and osteoconduction. Due to its favourable gelling properties chitosan can deliver morphogenic factors and pharmaceutical agents in a controlled fashion [1]. Here, we reported the possibility to compare two different approaches based on inorganic and organic bioactive signals used to obtain biomimetic chitosan scaffolds.

### EXPERIMENTAL METHODS

Chitosan scaffolds were prepared by using a foaming method based on physical foaming combined with microwave curing. In the first step of the process, a stable physical foaming was induced using a surfactant (i.e. Pluronic) as blowing agent of a homogeneous blend of Chitosan (CS) and Polyethylene glycol diacrylate (PEGDA700) solutions. In the second step, the porous structure of the foaming was chemically stabilized by radical polymerization induced by homogeneous heating of the sample in a microwave by using a thermoinitiator (TI). The biomimetic scaffolds were obtained by using two different approaches based on inorganic and organic compounds, respectively. The first one was based by treating the scaffolds with a supersaturated SBF solution (5SBF); the treatment is able to create an hydroxyapatite coating on the surface and into the porous wall in few days (7days). The second approach is based by using a bioactive peptide of Bone Morphogenetic Protein (BMP-2). The 67-87 residue of the “knuckle” epitope of hBMP-2 (NSVNSKIPKACCVPTLSAI) was synthesized by microwave-assisted Fmoc solid phase peptide synthesis (SPPS). The physicochemical, morphological and mechanical properties of materials, before and after treatments, have been evaluated. Furthermore, biological analysis by using hMSC cells to estimate the effect of the two different biomimetic approaches on cellular behaviour were performed.

### RESULTS AND DISCUSSION

In this study, the combination of foaming method and

biomimetic approaches has a great potential as process of production of chitosan based scaffold for bone tissue regeneration. The *in vitro* degradation tests showed a gradual dissolution of the foam over time, but maintaining their 3-D morphology and integrity even after 6 week of incubation. The surface morphology of the scaffolds after biomimetic treatment was observed using SEM-EDS analyses that demonstrated the presence apatite coating after few days of treatment. This data was confirmed by ATR-IR that also demonstrated the interactions between the polymeric matrix and peptide sequence. The kinetic release showed a sustained release in the time with a good effect on osteogenic differentiation of hMSC.

The biological tests performed in basal medium without osteogenic factors demonstrated that the cell proliferation increases with time during the *in vitro* culture period suggesting that the materials are nontoxic, not affecting the cell proliferation and showed good biocompatibility. Moreover, for scaffold materials after inorganic and organic biomimetic approaches, an early osteogenic differentiation was observed, demonstrating that a layer of apatite and/or BMP-2 peptide are bioactive solid signals for cells.

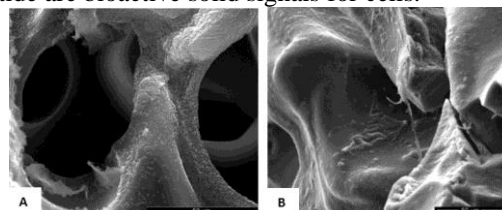


Fig.1 SEM images of Chitosan scaffold after 7days of SBF treatment (A) and after 21days of hMSC cell culture (B).

### CONCLUSION

This study has demonstrated the possibility to generate biomimetic structures with an highly interconnected and homogeneous structure with pores of different size in agreement with the dimensional characteristics required for bone regeneration scaffold. The presence of bioactive signals on the scaffold surface allows to obtain an osteoinductive effect on hMSC, making chitosan a promising candidate scaffold material for bone tissue regeneration.

### REFERENCES

[1] Ana R. Costa-Pinto *et al.* Biomacromolecules 2009, 10, 2067.

### ACKNOWLEDGMENTS

This study was supported through *funds* provided by the PNR-CNR Aging Program 2012-2014. The authors also thank Mrs. Cristina Del Barone for facilitating microscopy analysis.



## INTRODUCTION

Hydrogels are three-dimensional, hydrophilic, polymeric networks that have the ability to retain substantial amounts of water/biological fluids that typically exhibit physico-chemical properties reminiscent of the cell microenvironment. Thus, hydrogels can provide essential cues to cells and form an important class of biomaterials for tissue engineering. However, single hydrogel networks are mechanically weak and exhibit large dimensional changes on fluid uptake that has led to several new platform technologies, such as formation of multi-component, interpenetrating and double-networks and some nanocomposite hydrogels<sup>1</sup>.

Polymer blending of polyvinyl alcohol (PVA) and sodium alginate (SA) have been attempted to combine mechanical and biological properties. Although high water absorption and hydrophilicity are important parameters this also limits cell adhesion. In this study we report the formation of dual networks PVA and SA to elucidate the effect on mechanical properties and swelling behaviour. Furthermore, these hydrogel networks can be designed to entrap fluids such as platelet rich plasma, growth factors, blood, cells, marrow and proteins, which make them potential candidates for tissue engineering.

## EXPERIMENTAL METHODS

Briefly a solution of PVA 10%(w/v) was prepared and subjected to 1, 2, and 3 cycles of freeze thawing (FT) in a (VirTis SP Scientific) freeze dryer at -59.4°C, vacuum 17mT for 24hrs. The FT-PVA xerogels were swollen in SA until equilibrium and chelated with calcium chloride. The gels formed were then subjected to 1 cycle of FT or air-drying (AD) and FT (AD+1FT). Hydrogels were characterised by FTIR, EWC, mechanical testing and thermal properties determined using a differential scanning calorimetry (DSC).

## RESULTS AND DISCUSSION

PVA-alginate dual networks were successfully formed and the methodology optimised. FTIR spectra of the dual networks exhibited characteristic peaks corresponding to the stretching of the hydroxyl group along with alkyl groups in PVA, and carboxylate groups present in both the guluronic and mannuronic acid units in alginate. The EWC of dual networks was significantly lower than that of PVA hydrogels ( $P < 0.001$ ), indicating the formation of a tight network, which consisted of the PVA network with the entangled alginate fibrils that was chelated with calcium chloride (Table 1). It was interesting to note that 3FT PVA used for dual network formation did not lower EWC or enhance UTS, which may be attributed to the limited ingress of the alginate fibrils in the first network. The PVAFT/alg-1FT derived from the 2FT-PVA cycles

exhibited significantly higher UTS than the other dual networks ( $P < 0.001$ ) (Table 2) and much higher than PVA-alginate ( $\sim 0.19\text{MPa}$ )<sup>2</sup> blends.

Hydrogel system	PVA Freeze-thaw cycles	EWC (%)	Degree of swelling
PVA	1	$82.07 \pm 0.47$	$4.58 \pm 0.15$
	2	$76.80 \pm 1.02$	$3.32 \pm 0.18$
	3	$74.27 \pm 0.40$	$2.89 \pm 0.06$
PVAFT/alg-1FT	1	$53.63 \pm 2.56$	$1.16 \pm 0.12$
	2	$56.89 \pm 2.01$	$1.32 \pm 0.11$
	3	$53.86 \pm 1.96$	$1.17 \pm 0.09$
PVAFT/alg-AD+1FT	1	$55.59 \pm 1.64$	$1.25 \pm 0.08$
	2	$57.49 \pm 2.08$	$1.36 \pm 0.11$
	3	$57.74 \pm 0.59$	$1.37 \pm 0.03$

Table1: EWC and degree of swelling of PVA, PVA/Alg hydrogels subjected to different cycles of freeze thawing as well as AD+1FT

Hydrogel system	PVA: Freeze thaw cycles	Ultimate tensile strength (MPa)	Glass transition Tg(°C)
PVAFT/alg-1FT	1	$0.45 \pm 0.07$	$155.2 \pm 3.0$
	2	$0.73 \pm 0.12$	$164.3 \pm 4.6$
	3	$0.48 \pm 0.08$	$158.7 \pm 5.8$
PVAFT/alg-AD+1FT	1	$0.58 \pm 0.06$	$169.3 \pm 2.2$
	2	$0.48 \pm 0.09$	$176.6 \pm 2.6$
	3	$0.50 \pm 0.10$	$177.4 \pm 2.3$

Table 2: Glass transition (Tg) and Ultimate tensile strength (UTS) of PVA, PVA/Alg hydrogels with the 1<sup>st</sup> PVA network subjected to different cycles of freeze thawing and a FT or AD+1FT post alginate chelation

The Tg of the dual networks, also indicated the dense network formation and the influence of the second network formed within the first network.

## CONCLUSION

Insoluble dual networks were formed with PVA and alginate resulting in a dense network structure with reduced swelling, EWC and good mechanical properties, which suggest that the hydrogel maybe better suited to cell adhesion and be explored as orthobiologic bone grafts.

## REFERENCES

- Annabi, N., et al., Adv. Mater., 2014, 26: 85-124
- Xie, L., et al., J. Appl. Polym. Sci, 2012, 124: 823-831

## ACKNOWLEDGMENTS

SN would like to thank the University of Botswana for her PhD scholarship.



## Analysis of Integrin-Binding Dependent Cell Attachment on Collagen-Based Scaffolds

Natalia Davidenko<sup>1</sup>, Carlos Schuster<sup>1</sup>, Richard Farndale<sup>2</sup>, Samir Hamaia<sup>2</sup>, Serena Best<sup>1</sup>, Ruth Cameron<sup>1</sup>

<sup>1</sup>Department of Materials Science and Metallurgy, University of Cambridge, United Kingdom

<sup>2</sup>Department of Biochemistry, University of Cambridge, United Kingdom

[nd313@cam.ac.uk](mailto:nd313@cam.ac.uk)

### INTRODUCTION

Despite improvements in the management of coronary artery disease, a need exists to develop procedures to repair damaged heart tissue. Intensive research has recently been conducted in our group towards creating tailor-made 3D scaffolds, based on Collagen (Col) and Gelatin (Gel), for myocardial tissue repair and regeneration. Biopolymer scaffolds, mimicking the function of ECM, should not only possess the appropriate morphology, physical properties and mechanics, but also supply correct signals for cell activity<sup>1</sup>. Studies of cell attachment to collagen-based materials often ignore the details of the binding mechanisms - be they integrin mediated or non-specific. In this work we have used a range of cells which express different integrins and have measured cell adhesion in order to probe the nature of integrin binding sites as a function of collagen type, degree of crosslinking, composition and two or three dimensional architecture of the substrate.

### EXPERIMENTAL METHODS

Protein scaffolds (Col, Gel and Col/Gel=50/50) were obtained by freeze-drying, and cross-linked (XL) with carbodiimide (EDC) in combination with succinimide. EDC concentration 11.5mg/ml was taken as standard (100%) and was varied in the interval 1 – 200%. Films of ~8µm thickness were prepared by drying the corresponding 0.5% suspension of protein directly in 96-well plates used for cell attachments. Treated surfaces were obtained by deposition of 1µg/well of different types of Col (I, II or III) or Col-Gel compositions from 10µg/ml solutions. Studies of cell adhesion were made on the following cell lines: HT 1080 (fibroblast from human sarcoma, expressing  $\alpha_2\beta_1$  integrin), RUGLI (derived from a rat glioma, expressing  $\alpha_1\beta_1$ ), C2C12 (mouse myoblast, expressing  $\alpha_v\beta_3$  and  $\alpha_5\beta_1$ ) and L3, transfected C2C12- $\alpha_2+$ , which in addition expresses  $\alpha_2\beta_1$  integrin. Cell adhesion in the presence of  $Mg^{+2}$  (integrin mediated) and EDTA (non-specific) was assessed by calorimetric assay.

### RESULTS AND DISCUSSION

Static adhesion on treated surfaces showed very similar behaviour for HT1080 and Rugli cells for all Col types (I, II and III) and for all Col-Gel-based compositions. Examples of adhesion profiles of HT1080 are displayed in (Fig.1a). Adhesion was integrin-dependent and increased linearly with initial cell concentration (from 0.5 to  $2 \times 10^5$  cells/ml) for all systems studied. The incorporation of Gel to Col decreased adhesion of both cell lines. It is known that Col possesses the high affinity triple-helical motif GFOGER which interacts with cells via specific  $\beta_1$ -integrins, especially  $\alpha_1\beta_1$ ,  $\alpha_2\beta_1$ ,  $\alpha_{10}\beta_1$ ,  $\alpha_{11}\beta_1$ . Gel's main recognition motif is RGD

which signals to integrins, mainly  $\alpha_5\beta_1$  and  $\alpha_v\beta_3$ . The presence of Gel should decrease the cell receptor sites and, hence, cell adhesion. Adhesion values of HT1080 and RUGLI cells similarly depend on Col type: Col I  $\approx$  Col II > Col III, possibly due to the different affinity of Col motifs to  $\alpha_2\beta_1$  and  $\alpha_1\beta_1$  integrins. C2C12 cells did not adhere to any type of Col or to mixed surfaces due to lack of Col binding integrins in these cells. L3, transfected with  $\alpha_2\beta_1$  integrin, showed the same adhesion behaviour as HT1080 and Rugli cells.

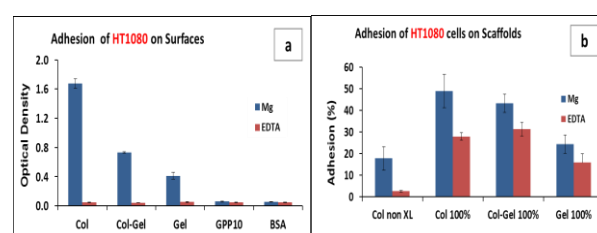


Fig.1 HT1080 cell adhesion on surfaces (a) and scaffolds (b)

Static adhesion on films and scaffolds depends on composition and XL status. For films, adhesion decreased with increase in XL due to decrease in cell-binding sites consumed in EDC-mediated bond-formation. Surprisingly, EDC treatment significantly increased adhesion of all cell lines studied on all scaffolds (Fig.1 b), suggesting that 3D properties and mechanics (spatial structural strength) strongly influence cell behaviour. Cell adhesion on 100%-XL matrices depends on composition and cell lines: a decrease with increasing of Gel content for both HT1080 and RUGLI cell lines; similar values shown for Col and Gel for L3 and maximum values for Gel for C2C12. These results may be explained by availability and affinity of cell-binding sites on the scaffolds of different compositions.

### CONCLUSION

Focusing on the nature and extent of integrin binding in cell adhesion, studies on treated surfaces, 2D films and 3D scaffolds provides a simple and effective way of assessing separately the influence of the availability of cell binding sites, material properties and 3D architecture on cell adhesion. This assessment should assist in the tailoring of the biological activity of scaffolds for specific TE applications.

### REFERENCES

1. Chen O. *et al.*, Mat Sci Eng R. 59:1-37, 2008
2. Barczyk M. *et al.*, Cell Tissue Res 339:269-81, 2010

### ACKNOWLEDGMENTS

The authors gratefully acknowledge the financial support of ERC Advanced Grant 320598 3D-E and of the British Heart Foundation Grant NH/11/1/28922.





# A Novel Biological Polyester Based Wet Spun Scaffold for Bone Tissue Engineering

Ayşe Selcen Alagoz<sup>1</sup>, Jose Carlos Rodriguez-Cabello<sup>5</sup>, Nesrin Hasirci<sup>2,3,4</sup>, Vasif Hasirci<sup>1,2,4</sup>

Depts. of <sup>1</sup>Biological Sciences, <sup>2</sup>Biotechnology, <sup>3</sup>Chemistry, METU, Turkey

<sup>4</sup>BIOMATEN- Center of Excellence in Biomaterials and Tissue Engineering, METU, Turkey, <sup>5</sup>Department of Condensed Material, Universidad de Valladolid, Spain

[selcen.alagoz@metu.edu.tr](mailto:selcen.alagoz@metu.edu.tr)

## INTRODUCTION

In this study, poly(3-hydroxybutyrate-co-3-hydroxyvalerate), PHBV, a biodegradable, natural polymer, was used as an alternative for the petroleum based polyesters to fabricate a wet spun scaffold for bone tissue engineering. VEGF and an elastin like recombinamers (ELR) with REDV sequences specific for endothelial cells<sup>1</sup> were introduced to the scaffold to make it attractive for endothelial cells so that it can be vascularized as needed in a thick implant which otherwise cannot maintain the viability of the cells that have penetrated deep into the scaffold.

## EXPERIMENTAL METHODS

PHBV scaffolds prepared by wet spinning were characterized under compression, and fiber morphology and porosity were determined by SEM and micro CT. Surface of the fibers was coated with ELR by exposing PHBV film with oxygen plasma (50 W, 5 min) and then immersing into ELR solution. Toluidine Blue staining and FTIR-ATR analysis were used to show of protein on the surface. AFM was used to study the influence of the treatments used in the binding process. PHBV nanocapsules loaded with BSA were produced by the double emulsion. BSA was used as a model protein instead of VEGF. Size distribution of PHBV nanocapsules was determined by using the Zeta Potential and Mobility Measurement System. These PHBV nanocapsules were incorporated to scaffold fibers by adsorption from a solution. Scaffold was examined with fluorescence microscope and SEM to study final form ready for in vitro studies.

## RESULTS AND DISCUSSION

The ultimate compressive strength of dry scaffolds under compression (5 mm/min) was  $4.65 \pm 0.69$  MPa, which showed compressive strength adequate for substituting human cancellous bone ( $\sim 2$ -12 MPa) not the native human cortical bone ( $\sim 100$ -230 MPa)<sup>2</sup>. The average fiber diameter was about 90  $\mu\text{m}$  and porosity of scaffolds was measured as 75% by using both SEM micrographs processed with NIH Image J program and micro CT data (Figure 1). Blue spots on the surface of ELR attached PHBV films were observed after Toluidine Blue staining. FTIR-ATR showed that upon treatment with O<sub>2</sub> plasma new peaks at around 1530 cm<sup>-1</sup> and 1650 cm<sup>-1</sup> was observed due to stretching of carbonyl groups. After ELR attachment, these peaks became more intense. This was probably due to the amide I and amide II groups of ELR attached onto the PHBV film<sup>3</sup>. AFM micrographs showed that surface roughness decreased upon oxygen plasma treatment

from 343.4 nm to 160.0 nm and increased to 280.3 nm after ELR attachment.

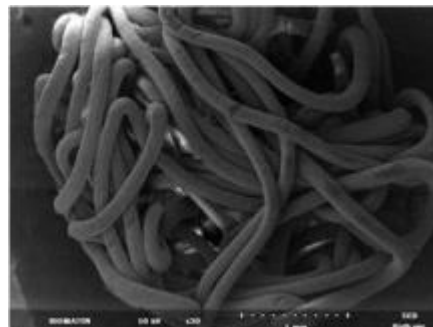


Figure 1: SEM image of the PHBV scaffold

PHBV capsules were found to have an average diameter of 340 nm, with particle size in the range 190-530 nm. SEM images showed that PHBV nanocapsules were attached on PHBV fibers (Figure 2).

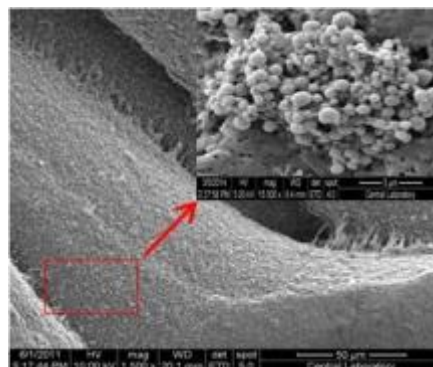


Figure2: SEM image of PHBV fibers and VEGF loaded PHBV nanocapsules

## CONCLUSION

In this study a biological polyester PHBV, which is an alternative to petroleum based polyesters was used to design a novel cell carrier. It was treated with an endothelial cell attractive ELR and VEGF loaded nanocapsules were attached. Thus, a novel multifunctional scaffold with appropriate mechanical and physical properties could be prepared.

## REFERENCES

1. Garcia et al., Tissue Engineering. 15(4): 887-899, 2009.
2. Sopyana et al., Science and Technology of Advanced Materials. 8: 116-123, 2007.
3. Serrano et al., Biophysical Journal. 93:2429-2435, 2007.

## Resorption of Calcium Phosphate Bone Substitutes: an *In Vitro* Study

Marta Gallo<sup>1</sup>, Solène Tadier<sup>1</sup>, Sylvain Meille<sup>1</sup>, Marc Böhner<sup>2</sup>, Aldo R. Boccaccini<sup>3</sup>, Rainer Detsch<sup>3</sup>, Jérôme Chevalier<sup>1</sup>

<sup>1</sup>Université de Lyon, INSA-Lyon, Université Lyon 1, MATEIS CNRS UMR 5510, 69621 Villeurbanne Cedex, France

<sup>2</sup>RMS Foundation, Bischmatstrasse 12, 2544 Bettlach, Switzerland

<sup>3</sup>Institute of Biomaterial, University of Erlangen-Nuremberg, Cauerstrasse 6, 91058 Erlangen, Germany

[marta.gallo@insa-lyon.fr](mailto:marta.gallo@insa-lyon.fr)

### INTRODUCTION

Traumatic or disease-caused bone defects, account annually for at least 2.2 million procedures worldwide. At present mainly autografts and allografts are used during surgeries, but the interest towards synthetic grafts has constantly grown. Synthetic bone substitutes not only avoid risks of rejection and of disease transmission, but might also degrade gradually and be replaced by natural bone when they are resorbable (such as calcium phosphates, CaP). At the moment, however, these resorption phenomena (including both acellular and cellular related aspects) are still partially unclear. In the same way, although several kinds of metal ions-doped CaP have been investigated, the consequences of these chemical modifications have been evaluated in terms of their impact on cell vitality and differentiation, more than on the resorption process of the material itself. The aim of the present work is, therefore, to develop an experimental method to assess mechanisms and kinetics of degradation of some CaP bone substitutes (some of which doped).

### EXPERIMENTAL METHODS

$\beta$ TCP ( $\beta$ -tricalcium phosphate,  $\beta$ -Ca<sub>3</sub>(PO<sub>4</sub>)<sub>2</sub>) dense samples, pure and doped (5% mol. Mg), were produced in cylindrical shape ( $\varnothing$ =9 mm, h=4 mm). The initial powders were first uniaxially, then isostatically pressed (by means of Cold Isostatic Pressing) and finally sintered at high temperature (1050°C). *In vitro* cellular tests were performed with the aim of evaluating the influence of Mg-doping on the resorption process. For this purpose murine RAW 264.7 cells were cultured in RPMI medium enriched with growth factors (MCSF and RANKL) and then seeded on the surface of the  $\beta$ TCP and Mg- $\beta$ TCP samples. After 2-4-7 days respectively, samples and cells were fixed and analysed (SEM, fluorescence, TRAP staining, WST).

Another part of the study was devoted to assess the relationship between acellular degradation, mechanical, physico-chemical and structural properties. For this purpose micro-porous  $\beta$ TCP and DCPD (dicalcium phosphate dihydrate, CaHPO<sub>4</sub>·2H<sub>2</sub>O) samples underwent dissolution tests *in vitro* (PBS and TRIS-buffer solutions, static and dynamic conditions, from 30' to 2 months). Particular attention was paid to the mechanical properties which were assessed by the use of a "non-conventional" micro-indentation technique<sup>1</sup>.

### RESULTS AND DISCUSSION

Preliminary tests have shown how RAW 264.7 cells grown directly on  $\beta$ TCP samples hardly differentiate into osteoclast-like cells. This behaviour, also according to previous studies<sup>2</sup>, could be caused by the strong release of Ca ions induced by  $\beta$ TCP. In order to overcome this problem, in the present work, RAW 264.7 cells were not directly seeded on the samples, but first incubated for some days in well-plates with growth factors (RANKL, MCSF). The first results have showed no substantial differences between cells incubated on  $\beta$ TCP and Mg- $\beta$ TCP. Cell viability and morphology, in fact, seemed to be comparable in both cases.

The dissolution tests performed on micro-porous  $\beta$ TCP and DCPD samples, have displayed how the chosen medium and conditions (static/dynamic) influence the degradation phenomena and the precipitation of new CaP phases. Although with differences, both for  $\beta$ TCP and DCPD, the degradation process seemed to start at the interface between liquid and sample and induced a gradient of properties between the surface and the inner part of the specimen. Thanks to the use of micro-indentation it was possible to assess a strong decrease of mechanical properties localised on the outer part of the specimen, while only smaller changes were measured in the inside.

### CONCLUSION

All in all this study showed that the Mg doping didn't seem to affect radically the cellular behaviour.

As far as acellular tests of dissolution were concerned, the evolution of mechanical properties was correlated both to the changes observed in the chemistry (precipitation of new CaP phases, mostly on DCPD) and in the microstructure (increase of porosity, above all in  $\beta$ TCP) of the samples.

### REFERENCES

1. P. Clément, *et al.*, Acta Materialia, 61:6649-6660, 2013
2. R. Detsch, *et al.*, J Biomater Appl, 00:1-22, 2010

### ACKNOWLEDGMENTS

The authors would like to acknowledge the European Commission funding under the 7<sup>th</sup> Framework Program (Marie Curie Initial Training Networks; grant number: 289958, Bioceramics for bone repair).





# Induction of Endothelial Cell Sprouting by Poly ( $\epsilon$ -Lysine) Dendron Tethered with an Angiopoietin-1-mimicking Peptide

Maria Elena Verdenelli, Steven Meikle, Gary Phillips, Matteo Santin

BrightSTAR Group, School of Pharmacy and Biomolecular Sciences, University of Brighton, UK

[M.E.Verdenelli@brighton.ac.uk](mailto:M.E.Verdenelli@brighton.ac.uk)

## INTRODUCTION

Coronary heart disease and stroke are leading causes of mortality in Europe, resulting in a loss of function of the affected tissue<sup>1</sup>. The challenge is to restore the tissue functionality using growth-factors mimicking peptides to stimulate the development of pre-existing blood vessels and enhance tissue regeneration.

In this research, poly ( $\epsilon$ -lysine) dendrons of different branching generations (Gx) will be used as molecular scaffold to present, at their uppermost branching generation, the Angiopoietin-1 (Ang-1) mimicking peptide, QHREDGS, previously shown to be able to promote blood vessel formation and stabilisation<sup>2</sup>.

## EXPERIMENTAL METHODS

G2 and G3 dendrons were synthesised by solid-phase peptide synthesis (SPPS) with a manual method. G2 and G3 were designed starting from a molecular root of two phenylalanine residues (FF) and branching up the molecule by addition of lysine monomers to expose either 8 (G2) or 16 (G3) active amino groups. Finally, G3 and G2 dendrons were functionalised, using the same SPPS method, with the bioactive peptide sequence, QHREDGS, mimicking Ang-1. Non-functionalised and functionalised dendrons were analysed by both analytical HPLC and micro-time-of-flight mass spectrometry (TOF-MS). The *in vitro* cytotoxicity effect of G2 and G3 functionalised with the Ang-1-mimicking peptide was evaluated as cell viability in a 2D culture model using human umbilical vein endothelial cells (HUVEC). Cells were seeded at  $22 \times 10^3$  cells  $\cdot$  well<sup>-1</sup> using 1 mL of F12 K medium supplemented with 10 vol% of foetal bovine serum, 0.05 g  $\cdot$  mL<sup>-1</sup> heparin and 0.1 g  $\cdot$  mL<sup>-1</sup> ECG. A linear QHREDGS sequence was used as control. After 24 hours in culture, cells were stained for their vitality with Hoerscht Propidium Iodide and for their cytoskeleton organization by Rhodamine-Phalloidin staining. HUVEC were analysed by confocal microscope.

## RESULTS AND DISCUSSION

Generation two and three poly ( $\epsilon$ -lysine) dendrons were characterised successfully: peaks (G2  $MH^+ = 402.30$ ; 549.37 and G3  $MH^+ = 914.69$ ; 970.74) generated through MS analysis correspond to different dendron generation and HPLC chromatograms showed that the increased molecular weight led to a decrease in peak retention time from 9 min to 8min. Laser confocal images with Phalloidin-Rhodamine staining show the effect of the linear and branched Ang-1-mimicking peptides. Indeed, while in the control cells grew as a monolayer (Fig. 1 A); the QHREDGS linear peptide appeared to induce their organization into 2D branched patterns (Fig. 1B). The spiking with non-functionalised

G2 dendron generated more dense branched 2D patterns (Fig. 1C), but the Ang-1 peptide-functionalised G2 dendrons clearly induced the formation of a network of endothelial sprouting where cells appeared to establish connections also in a 3D fashion (Fig 1,D). The results shown in Fig 1, C and D seem to demonstrate the synergistic action played by the dendron branched structure and by the QHREDGS sequence in guiding the 3D organization of the endothelial sprouting. G3 dendrons presenting a higher number of QHREDGS led to the formation of small 3D cell clusters unable to sprout (data not shown).

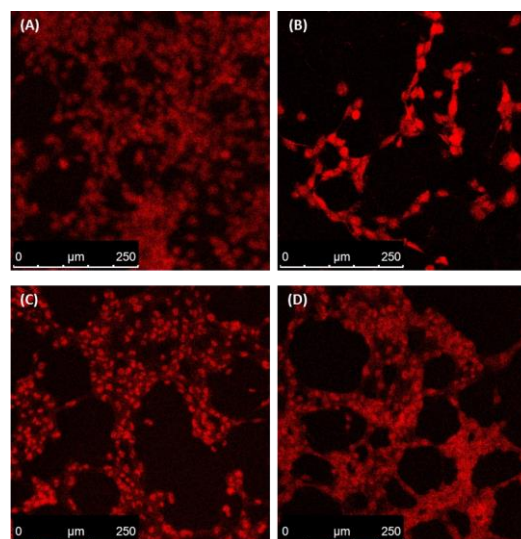


**Fig.1.** Effect of linear Ang-1 peptide and dendron Ang-1 on HUVEC in a 2D model at 24h. (A) Control, (B) linear Ang-1 peptide, (C) G2 dendron, (D) dendron Ang-1.

## CONCLUSION

The present study for the first time unveils a novel biomaterial approach to stimulate angiogenesis through nano-structured biomaterials and emphasise the need for a finely spaced presentation of the relevant peptide sequence to obtain established endothelial sprouting.

## REFERENCES

1. M. Nichols, N. Townsend. *European Cardiovascular disease statistics*. University of Oxford, 2012
2. Dallabrida SM, Ismail N, et All. *Angiopoietin-1 promotes cardiac and skeletal myocyte survival through integrins*. Circ Res 2005;96:e8-e24

## ACKNOWLEDGMENTS

“This work was funded by the EC FP7 Marie Curie ITN, AngioMat, grant agreement n. 317304.”



## Sustained Release of Adipose-Derived Stem Cells by Thermosensitive Chitosan-Gelatin Hydrogel for Therapeutic Angiogenesis

Nai-Chen Cheng<sup>1</sup>, Tai-Horng Young<sup>2</sup>

<sup>1</sup> Department of Surgery, National Taiwan University Hospital and College of Medicine, Taipei, Taiwan

<sup>2</sup> Institute of Biomedical Engineering, National Taiwan University, Taipei, Taiwan

[naichenc@gmail.com](mailto:naichenc@gmail.com)

### INTRODUCTION

Recent studies showed that adipose tissue exhibits mesenchymal stem cells, referred as adipose-derived stem cells (ASCs). These cells are multipotent and can be applied for tissue engineering or regenerative medicine. However, transplantation of isolated ASCs frequently resulted in cell death quickly, so a good carrier is required to deliver these cells *in vivo*. The carrier is expected to have good biocompatibility and easy to handle. Because thermosensitive hydrogels are liquid at room temperature or 4°C, ASCs can be mixed with the gels and delivered by injection in a minimally-invasive fashion. Once *in vivo*, the hydrogels solidify and retain the injected ASCs in the target area.<sup>1</sup> This study aimed to develop a thermosensitive hydrogel capable of sustained releasing ASCs for therapeutic angiogenesis.

### EXPERIMENTAL METHODS

We blended gelatin in the chitosan/glycerophosphate hydrogel system, and we estimated the release pattern of gelatin *in vitro*. Human ASCs were then encapsulated in the chitosan-based temperature-sensitive hydrogels and perform *in vitro* culture. The characteristics of ASCs encapsulated in hydrogels, including proliferation activity, were investigated. *In vitro* migration assay and *in vitro* tube formation assay were performed. Moreover, the chick embryo chorioallantoic membrane (CAM) assay,<sup>2</sup> a well-established *in vivo* assay for studying angiogenesis, was performed by injecting ASC-encapsulated hydrogels into chick embryos.

### RESULTS AND DISCUSSION

We were able to add gelatin in the mixed solution of chitosan/glycerophosphate and maintained the temperature-sensitive property. By immersing chitosan-gelatin hydrogels into PBS, sustained release of gelatin from the composite hydrogel was found. After ASC encapsulation, we also detected sustained release of ASCs from the chitosan-gelatin hydrogel. By performing live/dead assay, death of a significant portion of the encapsulated cells was observed in pure chitosan hydrogel, but the cell survival improved significantly after blending gelatin in the chitosan/glycerophosphate hydrogel (Fig 1).

Moreover, *in vitro* wound healing could be significantly facilitated by co-culturing fibroblast (Hs68) with ASCs encapsulated in chitosan-gelatin hydrogel. In terms of angiogenesis, co-culturing endothelial cells (SVEC4-10) with ASC-encapsulated chitosan-gelatin hydrogel revealed SVEC4-10 cells forming tube-like structures, indicating the potential of the hydrogel in promoting angiogenesis. In the CAM assay, quantification of the capillary density in the chorioallantoic membrane showed that ASC-encapsulated chitosan-gelatin

hydrogel significantly promoted angiogenesis comparing to pure chitosan hydrogel (Fig 2).

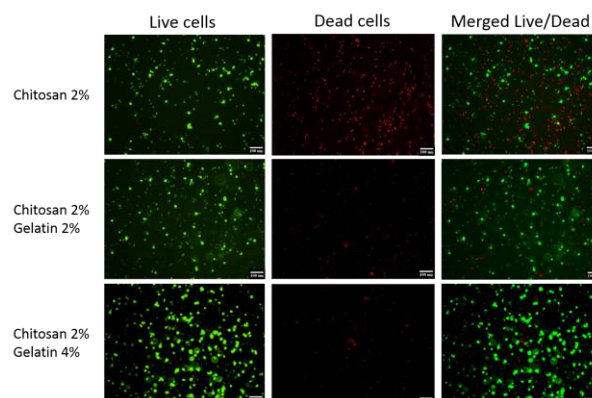


Figure 1. After 5 days of *in vitro* culture, more live cells (green) were observed if gelatin was mixed in the chitosan/glycerophosphate hydrogel.

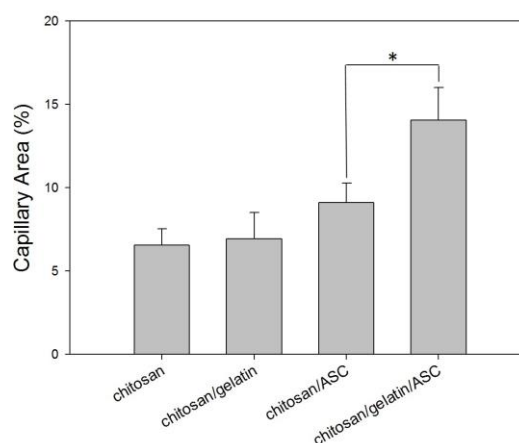


Figure 2. The CAM assay revealed significantly larger area consisting of capillary when chitosan-gelatin hydrogel was injected. (\* $p < 0.05$ )

### CONCLUSION

Chitosan-gelatin-based temperature-sensitive hydrogel not only can provide a niche to maintain ASC survival, it also enables sustained release of ASCs for application in therapeutic angiogenesis.

### REFERENCES

- Richardson SM. *et al.*, Biomaterials 29:85-93, 2008
- Wang CH. *et al.*, Biomaterials 34:4223-4234, 2013

### ACKNOWLEDGMENTS

The study was supported by National Taiwan University Hospital and E-Da Hospital- National Taiwan University Hospital Joint Research Program.



## Cobalt Doped Proangiogenic Hydroxyapatite for Bone Tissue Engineering Application

Senthilguru Kulanthaivel, Krishna Pramanik, Indranil Banerjee\*

Department of Biotechnology and Medical Engineering, National Institute of Technology,  
Rourkela-769008, Odisha, India.

[senthilgurubt@gmail.com](mailto:senthilgurubt@gmail.com), [Indraniliti@gmail.com](mailto:Indraniliti@gmail.com)

### INTRODUCTION

In bone tissue engineering success of any implant is ensured by early angiogenesis after implantation. Angiogenesis is crucial for active transport of oxygen and nutrients to the cells where the implant size is considerably larger than diffusional limit (150-200  $\mu\text{m}$ ) of solutes<sup>1</sup>. Existing methodologies involve the application of growth factors like Vascular Endothelial Growth Factor (VEGF)<sup>2</sup> and other micro-patterning techniques to induce angiogenesis which may limit the processing and commercial availability of implant. Interestingly, cobalt bivalent ions can induce angiogenesis through Hypoxia Inducible Factor 1 alpha (HIF-1 $\alpha$ ). Synthetic hydroxyapatite, a well known biomaterial for decades has more flexibility and stability over incorporation of bivalent metal ions. The present study describes the synthesis of cobalt doped HAp and its physico-chemical and biological characterisation.

### EXPERIMENTAL METHODS

Cobalt doped hydroxyapatite (Co-HAp) (different doping percentage) were prepared by the ammoniacal precipitation method. X-ray Diffraction (XRD) and FT-IR (Fourier transformed infrared spectroscopy) analysis were performed to study the structural properties of doped HAp. Extent of doping and release of Co<sup>2+</sup> ions were estimated by ICP-OES analysis. Osteogenic property of doped HAp were accessed by performing analysis pertaining to cell proliferation (cell viability assay), Cell cycle progression (Flow cytometry) and expression of differentiation markers (Runx2 and Osterix) (Immunocytochemistry) in MG-63cells cells. Angiogenic property of the material was analyzed by checking the expression of HIF-1 $\alpha$  (Western blot analysis) and VEGF (ELISA) in MG-63 cells<sup>3</sup>. Finally, tube formation assay was performed with human umbilical vein endothelial cells (HUVEC) to confirm the pro-angiogenic potential of the material.

### RESULTS AND DISCUSSION

Hydroxyapatites, doped with varying concentration of cobalt were successfully prepared by ammoniacal precipitation method and extent of doping was measured by ICP-OES. Crystalline structure of doped hydroxyapatite was confirmed by XRD (Fig. 1a) and FTIR (Fig. 1b) studies which showed slight deformation in the patterns with respect to doping nature. Analysis pertaining to the effect of doped hydroxyapatite on cell proliferation (Fig. 1c) and cell cycle progression (Fig. 1d) of MG-63cells revealed that the doping of cobalt supported the cell viability and proliferation up to a threshold limit. Such level of doping also induced differentiation of osteoblast cells, which was evident from the higher expression of differentiation markers (Runx2 and Osterix) and better nodule formation (SEM study). Western blot analysis (Fig. 1e) in conjugation

with ELISA study (Fig. 1f) confirmed that the doped HAp samples significantly increased the expression of HIF-1 $\alpha$  and VEGF in MG-63 cells. Tube formation assay (Fig. 1g) well supported the western blot and ELISA analysis, where the doped HAp samples induced better tube formation compared to pure HAp.

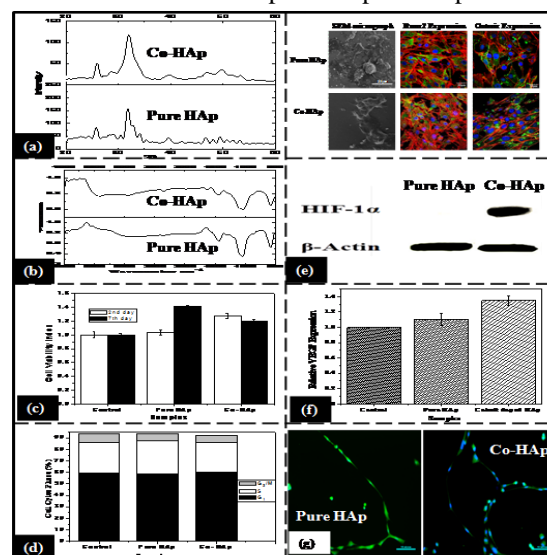


**Fig. 1 Characterization of cobalt (Co<sup>2+</sup>) doped HAp**

### CONCLUSION

The present study confirmed that doping of HAp with bivalent cobalt ions imported an excellent angiogenic property. These studies clearly proved that bivalent cobalt ion doped HAp may be a potential alternative to the prevailing methodologies for inducing angiogenesis in bone tissue engineering. Furthermore, *in vivo* studies and HAp desorption profiling in the presence of osteoclast are required to confirm the pro-angiogenic and osteogenic properties of cobalt doped hydroxyapatite.

### REFERENCES

1. M.W. Laschke, Y. Harder, M. Amon, I. Martin, J. Farhadi, A. Ring, N. Torio-Padron, R. Schramm, M. Rücker, D. Junker, Tissue engineering, 12 (2006) 2093-2104.
2. F. Yang, S.-W. Cho, S.M. Son, S.R. Bogatyrev, D. Singh, J.J. Green, Y. Mei, S. Park, S.H. Bhang, B.-S. Kim, Proceedings of the National Academy of Sciences, 107 (2010) 3317-3322.
3. C. Wu, Y. Zhou, W. Fan, P. Han, J. Chang, J. Yuen, M. Zhang, Y. Xiao, Biomaterials, 33 (2012) 2076-2085.

### ACKNOWLEDGEMENT

1. SAIF IIT Madras for ICP-OES analysis.
2. DBT, Govt of India (RGYI scheme project no. BT/PR6230/GBD/27/391/2012)
3. DBT, Govt of India (RGYI scheme project no. BT/PR6227/GBD/27/390/2012)
4. Institute Funding, NIT Rourkela.



## Development of a Synthetic Pseudovascular Network to Investigate Neovascularisation for Tissue Engineering Applications

Lindsey Dew<sup>1</sup>, Ilida Ortega<sup>2</sup>, Adam Kelly<sup>1</sup>, Frederik Claeyssens<sup>1</sup>, Sheila MacNeil<sup>1</sup>

<sup>1</sup>Kroto Research Institute, Department of Materials Science and Engineering, University of Sheffield, UK

<sup>2</sup>The School of Clinical Dentistry, University of Sheffield, Sheffield, UK.

[l.dew@sheffield.ac.uk](mailto:l.dew@sheffield.ac.uk)

### INTRODUCTION

One of the greatest challenges currently faced in Tissue Engineering (TE) is the incorporation of vascular networks within tissue engineered constructs. Generally, TE grafts thicker than 400  $\mu\text{m}$  will need the presence of vasculature for avoiding necrosis and allowing diffusion of nutrients and gases<sup>1,2</sup>. Knowledge of the major factors that drive vascular ingrowth is key to overcoming this hurdle.

**AIM** To develop a technique for producing a perfusable, cell friendly model of vascular structures which can be used to study the factors affecting angiogenesis.

### EXPERIMENTAL METHODS

Electrospun mats were produced by dissolving PHBV in a mixture of dichloromethane (DCM) and methanol. Optimal concentrations of 10% w:w of PHBV (containing 10% w:w of methanol) was prepared and electrospun for 1 hour using four 5 ml syringes with 0.6mm ID blunt tip at a rate of 40  $\mu\text{l}/\text{min}$  and a voltage of 17 kV. Using these parameters nanofibres with diameters of  $0.70 \pm 0.05 \mu\text{m}$  were obtained. Alginate paste was printed on top of the mat by placing inside a syringe barrel attached to a dispensing system whilst a 3D printer was used to hold the dispensing arm and print the alginate at a feed rate of 8.3cm/s and extrusion rate of 0.025cm<sup>3</sup>/s. Electrospinning was then carried out again to cover the alginate. To remove the alginate the scaffolds were submerged in 0.5M EDTA solution overnight. Removal of the sacrificial substrate was studied by both SEM and fluorescence microscopies. The suitability of the constructs as synthetic vascular networks was then explored by seeding the structures with proliferating human dermal microvascular endothelial cells (HDMECs) alone and in combination with human dermal fibroblasts (HDFs). Briefly,  $0.5 \times 10^6$  HDMECs were infused through a cannula into the hollow structures and allowed to attach overnight at 37°C. The scaffolds were then flipped and this process was repeated before culturing for 5 days. To observe the effect of HDFs as a potential 'helper' cells this process was repeated but this time  $0.5 \times 10^6$  HDFs were seeded onto both sides of the scaffold and cultured for 5 days. Samples were fixed, cryosectioned and stained for CD31 and DAPI.

### RESULTS AND DISCUSSION

Upon removal of the alginate substrate nanofibrous hollow networks ranging from 0.5-2mm were created (Fig. 1). These networks were perfusable which enabled the recellularisation of the hollow channels. Both HDMECs and HDFs were found to adhere well to

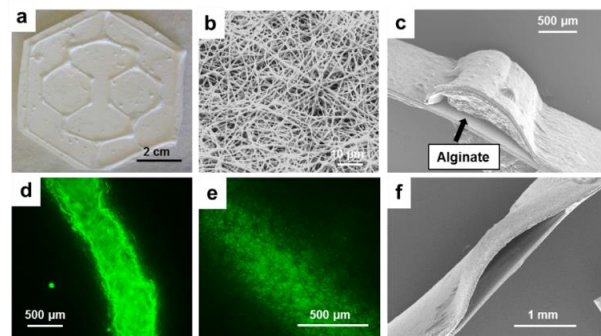


Figure 1. Image of PHBV artificial electrospun vascular network (a); High magnification SEM image of PHBV fibres in the vascular construct (b); SEM image of vascular conduit containing the alginate sacrificial substrate (c); Fluorescence image of alginate loaded with Eosin-Y after printing (d); Fluorescence image of alginate loaded with Eosin-Y after spinning (e); SEM image of vascular conduit after removing the alginate sacrificial substrate (f).

the PHBV material attaching to both the curved and flat surfaces. When the channels were reseeded with HDMECs alone, cell coverage was found to be irregular. However when using a co-culture of HDMECs and HDFs coverage was found to be continuous throughout the internal channel (Fig. 2) implying the need for a 'helper' cell.

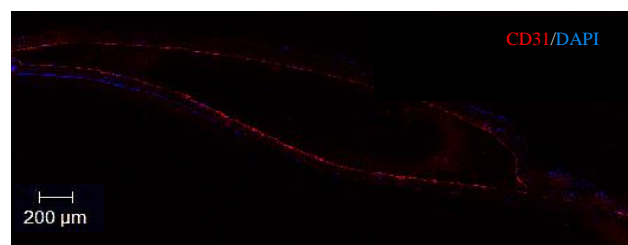


Figure 2 – Fluorescence image showing CD31 positive cells (red) with DAPI counterstaining (blue) throughout a cross section of the scaffold using a co-culture of HDMECs and HDFs.

### CONCLUSION

We have developed a technique for the fabrication of bespoke constructs with applications in the study of angiogenesis. We have demonstrated that HDMECs attach uniformly to our constructs when co-cultured with HDFs and that we can tune our scaffolds in terms of chemical nature, size and morphology.

### REFERENCES

1. Auger FA *et al.*, Annual review of biomedical engineering. 177-200, 2013
2. Nguyen LH *et al.*, Tissue engineering. Part B. 363-382, 2012.

### ACKNOWLEDGMENTS

We thank the EPSRC DTC Tissue Engineering Regenerative Medicine programs for funding this research.



# Angiogenic Response on Chitosan-graft-Poly ( $\epsilon$ -Caprolactone) Copolymer, *in Vitro*, Enhanced by Wharton's Jelly-Derived Mesenchymal Stromal Cells

Evdokia Mygdali<sup>1,3</sup>, Maria Kaliva<sup>1,2</sup>, Maria Vamvakaki<sup>1,2</sup>, Charalampos Pontikoglou<sup>4</sup>,  
Maria Chatzinikolaïdou<sup>1,2</sup>

<sup>1</sup> University of Crete, Dept. of Materials Science and Technology, 71003 Heraklion, Greece,

<sup>2</sup> IESL-FORTH, 71110 Heraklion, Greece,

<sup>3</sup> University of Crete, Dept. of Biology, 71003 Heraklion, Greece,

<sup>4</sup> University of Crete, Dept. of Hematology, School of Medicine, 71003 Heraklion, Greece

[mchatzin@materials.uoc.gr](mailto:mchatzin@materials.uoc.gr)

## INTRODUCTION

Enhanced vascularisation is critical for the treatment of ischemic tissues and the engineering of new tissues and organs [1]. Paracrine factors from Wharton's Jelly-derived Mesenchymal Stromal cells (WJ-MSCs) could act as a stimulant for the vascular formation [1, 2].

In this study we report on the strong adhesion of Human Umbilical Vein Endothelial Cells (HUVECs) on a chitosan-graft-poly ( $\epsilon$ -caprolactone) (CS-g-PCL) copolymer [3], which is used as a biodegradable matrix for the formation of angiogenic sprouting induced by the Conditioned Medium (CM) from WJ-MSCs.

We investigate the cellular adhesion and viability of HUVECs, as well as the production of Platelet Derived Growth Factor (PDGF BB), a characteristic marker of endothelial "tip cell" which leads the angiogenic sprouting [1,3].

## EXPERIMENTAL METHODS

The copolymer was synthesized by grafting the modified PCL-COOH onto a chitosan backbone as described previously [4]. Spin-coated films of the grafted copolymer were prepared on round glass substrates. We investigated the cellular adhesion of HUVECs on the films by means of Scanning Electron Microscopy (SEM), their viability by the AlamarBlue® assay, and their focal adhesion points by confocal microscopy. We examined the expression of secreted PDGF BB by means of indirect ELISA after incubation with CM from WJ-MSCs.

## RESULTS AND DISCUSSION

Successful seeding of HUVECs on CS-g-PCL surfaces led to strong adhesion and cellular proliferation (Fig. 1). Treatment of the cells with CM from WJ-MSCs resulted in higher cell viability and increased the expression of the characteristic angiogenic marker PDGF BB (Fig. 2). Ongoing experiments focus on the expression of the angiogenic genes DLL4, VEGFR2, ANGPT2, SPROUTY2, PDGFBB and MMP2 by means of semi-quantitative PCR.

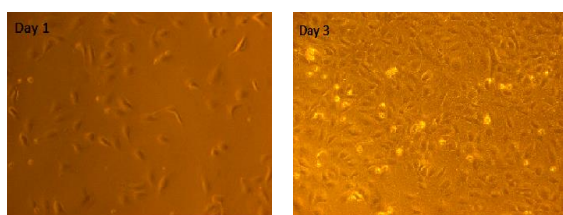


Figure 1: Optical microscopy images illustrating the viability of HUVECs on CS-g-PCL substrates on day 1 (left), and their growth after 3 days (right) using Endothelial Growth Medium+2% FBS

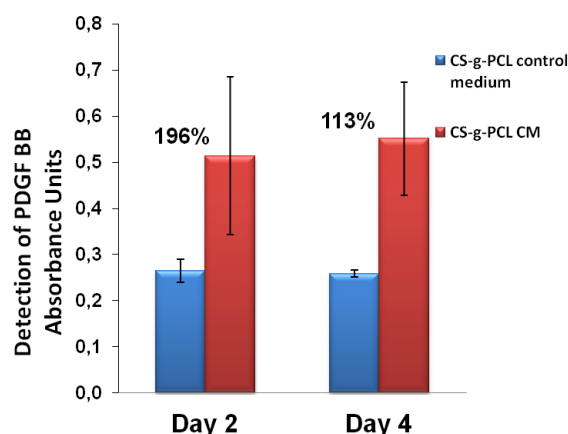


Figure 2: Higher levels of PDGF BB are secreted by HUVECs cultured on CS-g-PCL with CM after 2 and 4 days compared to the control medium. Bars represent averages of triplicates with standard deviation.

## CONCLUSION

We show that the copolymer CS-g-PCL strongly supports the adhesion and proliferation of HUVECs, which is increased in the presence of the Conditioned Medium from WJ-MSCs. Moreover, HUVECs angiogenic response is significantly induced in the presence of the CM, suggesting the potential of the copolymer as an inductive substrate for blood vessel regeneration and vascularized tissue.

## REFERENCES

1. Patel ZS. *et al.*, Journal of Biomaterials Science, Polymer Edition 15:701-26,2004.
2. Batsali A. *et al.*, Cytotherapy 16:S73-S4,2014.
3. De Smet F. *et al.*, Arterioscl Throm Vas 29:639-49,2009.
4. Chatzinikolaïdou M. *et al.*, Curr Pharm Design 20:2030-9,2014.

## ACKNOWLEDGEMENTS

"The authors acknowledge the Greek General Secretariat for Research and Technology Excellence Grant 'Aristeia II Osteobiomimesis 3438' for financial support."



Julian F Dye<sup>1</sup>, Giuseppe Scionti<sup>2</sup>, Elizabeth A Wahl<sup>3</sup>, Tomas Egana<sup>3</sup> & Maroun Khoury

<sup>1</sup>LHCS, The Open University, UK

<sup>2</sup>Cells-4-Cells, Santiago, Chile

<sup>3</sup> Dept Plastic Surgery & Hand Surgery, Klinikum rechts der Isar, Technische Universität München, Germany

[Julian.Dye@open.ac.uk](mailto:Julian.Dye@open.ac.uk)

## INTRODUCTION

The prospect for patients with chronic ulcers is challenging, they face protracted treatment and management of underlying primary pathology to attain wound healing by secondary intent. Recent gains in understanding wound pathologies and the introduction of an increasingly diverse range of advanced wound and synthetic skin technologies has resulted in only marginal improvements in healing rate and health economic benefits<sup>1</sup>

Bio-intelligent biomaterial scaffolds are an integrative modality which can provide cell adhesive signals, a reservoir of activators and or signals for, or modulators of, tissue reconstruction, a proteolytic environment, a source of cryptic or released regulators, or delivery system for complex biological therapies.

This work investigates the potential for fibrin-based materials to be used in stem cell therapy for chronic wounds.

## EXPERIMENTAL METHODS

Fibrin/alginate scaffolds were prepared from a foam mixture by glutaraldehyde cross-linking, reduction, washing and lyophilisation. Adipose-MSC were used with permission to assess cell infiltration in vitro. Samples were fixed, stained with Texas red-X phalloidin/To-Pro3(white) for laser confocal microscopy visualisation against green scaffold autofluorescence at each scaffold depth (xz section). Integration of scaffolds was assessed in porcine acute full thickness or delayed partial burn excision defects, by punch biopsy histology over a 6 week time course. Histology was stained for vWF to observe vascularisation. Collagen based materials, Integra and Matrigel, were used as controls.

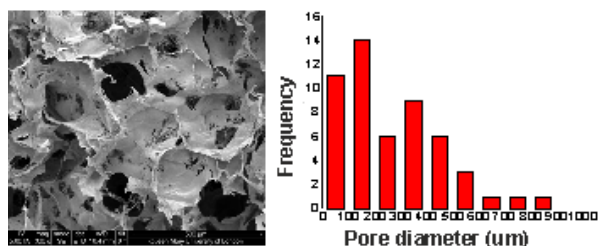


Figure 1. SEM of fibrin alginate scaffold and pore size distribution. Scalebar = 500 um.

## RESULTS AND DISCUSSION

Fibrin alginate scaffolds form an hierarchical interconnected pore structure from fibrin nanofibre mesh (Fig 1). 24 h infiltration of MSC occurs throughout the depth of the fibrin scaffold whereas MSC density is heavily polarised to the seeding surface of Integra scaffold (fig 2) with similar cell viability.

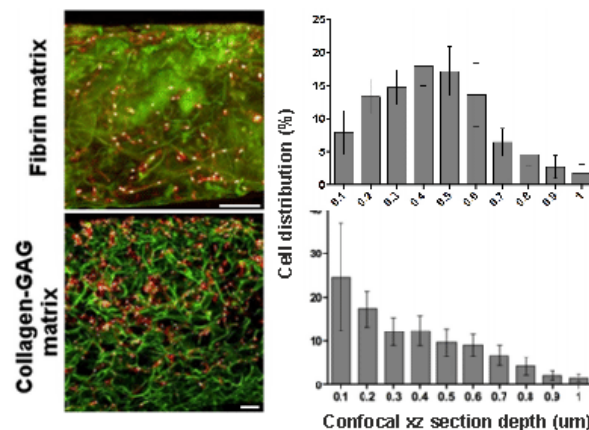


Figure 2. MSC ingress into fibrin/alginate & Integra.

In acute wounds fibrin/alginate scaffolds gave rapid cellularisation & neovascularisation via vasculogenesis through the scaffold depth within 7 days. This allowed single step reconstruction with a split thickness overgraft. Matrigel integrated via rapid resorption without vasculogenesis (fig 3). In the delayed wound model, tissue scaffolds increased the healing response and achieved integration at 7 days. The fibrin/alginate scaffold resulted in greater neo-dermal organisation.

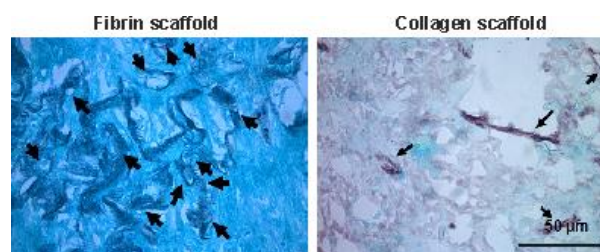


Figure 3. vWF staining of tandem 7d wound biopsies.

Fibrin-alginate scaffolds were designed to optimise porosity to support rapid cellular vascularisation, tissue formation and subsequent remodelling. Support of MSC corroborates previous data on fibroblasts<sup>2</sup>. This material may be additionally suited to cell therapy potentiation.

## CONCLUSION

This work demonstrates an emergent scaffold design with pro-vascular integration properties, with potential for accelerating delayed wound healing.

## REFERENCES

1. Snyder DL, Tech Ass Rep: 2012.
2. Garetta-Garcia, E et al, BioRes 2,6 1-9:2014

## ACKNOWLEDGMENTS

The authors acknowledge the support of DoH LINK grant HTD247, Kirby Lang Foundation, RAFT and The Worshipful Company of Firefighters.

## Repair of “Burr Holes” Using Chitosan-Siloxane Porous Hybrids

Yuki Shirosaki<sup>1</sup>, Motomasa Furuse<sup>2</sup>, Takuji Asano<sup>3</sup>, Yoshihiko Kinoshita<sup>3</sup>, Toshiki Miyazaki<sup>4</sup>, Satoshi Hayakawa<sup>5</sup>, Akiyoshi Osaka<sup>5</sup>, Toshihiko Kuroiwa<sup>2</sup>

<sup>1</sup>Frontier Research Academy for Young Researchers, Kyushu Institute of Technology, Japan

<sup>2</sup>Department of Neurosurgery, Osaka Medical College, Japan, <sup>3</sup>Nikkiso Co., Ltd., Japan

<sup>4</sup>Graduate School of Life Science and Systems Engineering, Kyushu Institute of Technology, Japan

<sup>5</sup>Graduate School of Natural Science and Technology, Okayama University, Japan

[yukis@lsse.kyutech.ac.jp](mailto:yukis@lsse.kyutech.ac.jp)

### INTRODUCTION

Chitosan-siloxan porous hybrids prepared via sol-gel method have high potential as scaffolds as for the several tissues [1-3]. In addition, the incorporation with calcium chloride into the hybrids deposited hydroxyapatite on their surface into the simulated body fluid (SBF) [1]. However, the hybrids must wash with sodium hydroxide solution before soaking in SBF because neutralization of the remained acetic acid in to their matrix. Recently, we have tried to soak the hybrids into alkaline phosphate solution to deposit apatite and remove the acid simultaneously. In this study, we report that the apatite formation of the hybrids into alkaline phosphate solution and implantation them into the skull defect, named “bull hole”.

### EXPERIMENTAL METHODS

Chitosan (0.5 g, high molecular weight, deacetylation: 79.0%, Aldrich®, USA) was dissolved in aqueous acetic acid (0.25 M, 25 mL). GPTMS (Lancaster, Lancashire, UK) and calcium chloride (Nacalai Tesque, Kyoto, Japan) were added to give a molar ratio of chitosan to GPTMS (ChG) of 1:0.5 or chitosan to GPTMS :to CaCl<sub>2</sub> (ChGCa) of 1.0 : 0.5 : 1.0. The mixtures were stirred for 1 h at room temperature and a fraction of each resultant sol was poured into a polystyrene container and frozen at -20°C for 24 h. The frozen hybrids were then transferred to a freeze dryer (FDU-506, EYELA, Tokyo, Japan) for 12 h until dry. The resultant porous ChG and ChGCa hybrids were then washed with NaOH (0.25 M) and distilled water to neutralize remaining acetic acid and were again lyophilized. Some ChGCa hybrids were instead soaked in aqueous Na<sub>2</sub>HPO<sub>4</sub> (0.01 M, pH8.8) at 80°C for 3 days (ChGCa\_HAp). The hybrids were then washed with distilled water and lyophilized.

The surface analyses of the samples were examined by thin film X-ray diffraction (TF-XRD), Fourier transform infrared spectroscopy (FT-IR) and scanning electron microscopy (SEM).

The hybrids were sterilized with  $\gamma$ -ray irradiation. Adult female beagles were used for in vivo animal test. Four 14-mm burr holes were created to evacuate the liquefied hematoma and then the hybrids were inserted into each burr hole. The commercial bone cement was also implanted as a control. After implantation period, specimens of the parietal bones including the cranioplasty were harvested and examined histologically.

### RESULTS AND DISCUSSION

The low crystalline hydroxyapatite deposited on the hybrids surfaces in alkaline phosphate solution. Their porous structure was maintained after apatite deposition.

The hybrids fitted the burr holes and blood infiltrated the pores, but did not overflow. Following implantation, all beagles survived with no wound infection or automutilation. The chitosan-siloxane porous hybrid induced new bone formation in their matrix. Every hybrid degraded and disappeared within 12 months of implantation. In the case of ChG, many osteoblasts were on the hybrid and many blood vessels with havers canals formed in the new tissue. There are some reports that a pore sizes smaller than 100  $\mu$ m is not sufficient for cell migration; however in this work, the chitosan-siloxane hybrids induced new bone and blood vessel formation even at a pore size of around 100  $\mu$ m.

Incorporation of calcium ions (ChGCa) and modification of hydroxyapatite (ChGCa\_HAp) accelerated bone formation. Osteoblasts were also present at the interface of the pre-existing bone and newly formed osteoid tissue. Calcifications were found in the osteoid tissue easily. In particular, Azan staining showed the strong calcifications in the osteoid tissue. In the present work, we could not find osteoclasts around the new bone. In this case, we observed them only 12 months after implantation and the hybrids had already disappeared. The osteoclasts may be present in the early stages after implantation.

### CONCLUSION

After 12 months implantation, no inflammation occurred and the hybrids were degraded and disappeared completely. In the hybrid groups, the new bone formation occurred the site of the implantation and there were many osteoblast and blood vessels with havers canals. Hydroxyapatite coating accelerated the calcification. The chitosan-siloxane porous hybrids are useful for the new scaffold of “burr holes” in cranioplasty.

### REFERENCES

1. Shirosaki *et al.*, Chem. Eng. J. 137:122-128, 2008
2. Amado *et al.*, Biomaterials 29:4409-4419, 2008
3. Shirosaki *et al.*, Int. J. Mater. Chem., 3:1-7, 2013

### ACKNOWLEDGMENTS

This work was supported in part by the programs in “Improvement of Research Environment for Young Researchers (Kojinsenbatsu)”, Ministry of Education Culture, Sports, Science and Technology (MEXT) and the Foundation for the Promotion Ion Engineering.



## A Nanocomposite Wound Dressing with Potential to Sustain Active Chlorhexidine on a Wound Bed

Peter F. Duckworth<sup>1,2</sup>, Sarah E. Maddocks<sup>3</sup>, Gareth M. Robinson<sup>4</sup>, Sameer S. Rahatekar<sup>1</sup> and Michele E. Barbour<sup>2</sup>

<sup>1</sup>Advanced Composites Centre for Innovation and Science (ACCIS), University of Bristol (UoB), UK,

<sup>2</sup>Oral Nanoscience, UoB, UK, <sup>3</sup>Cardiff School of Health Sciences, Cardiff Metropolitan University, UK

<sup>4</sup>Biological, Biomedical and Analytical Sciences, University of the West of England (UWE), UK

[Peter.Duckworth@Bristol.ac.uk](mailto:Peter.Duckworth@Bristol.ac.uk)

### INTRODUCTION

Chronic wounds are susceptible to infection and are increasing in prevalence. 14 days application of topical antiseptic is the initial recommended treatment.<sup>1</sup> An antiseptic eluting wound dressing which could deliver active antiseptic to the wound bed over two weeks would greatly aid in this bioburden management.

Chlorhexidine (CHX) is a topical antiseptic widely used in wound care due to its broad spectrum antimicrobial effect, rapid mechanism of action and low cytotoxicity.<sup>2</sup>

The purpose of this study is to investigate the feasibility of encasing novel antiseptic CHX-hexametaphosphate nanoparticles (CHX-NPs)<sup>3</sup> within an alginate matrix – widely used in wound dressings – to provide a sustained release of CHX and the impact this may have on the bioburden of a chronic wound.

### EXPERIMENTAL METHODS

#### CHX-NPs synthesis<sup>3</sup>

10 mM aqueous solutions of CHX digluconate and sodium hexametaphosphate were combined (1:1 ratio).

#### CHX-NPs alginate nanocomposite

Powdered alginate was dissolved in the diluted CHX-NPs to give doping of 6, 3 & 0 wt%. These solutions were cast (55g alginate per m<sup>2</sup>), and the water allowed to evaporate (RT, 3 days). These thin films were cross-linked in CaCl<sub>2</sub> (aq) (0.18 M) for 25 min, washed with distilled water and air dried. Disks (ø = 10 mm) were cut from this material and used in subsequent work.

#### CHX elution

One alginate disk was immersed in distilled water (2.25 mL) and the [CHX]<sub>(aq)</sub> monitored ( $\lambda = 255$  nm) over two weeks (n=15 for each CHX-NPs doping; 6, 3 & 0 wt%).

#### Microbial growth inhibition

Single alginate disks were placed on an agar plate seeded with a bacterium (methicillin-resistant *S. aureus* (MRSA), *P. aeruginosa*, *E. coli*, *K. pneumoniae* or *A. baumannii*) by the spread plate method. The zone of inhibition was measured following 24 h incubation at 37°C (n=9 for each CHX-NPs doping; 6, 3 & 0 wt%).

#### Bioluminescent imaging<sup>4</sup>

Single alginate disks were placed on a petri dish seeded with *E. coli*, modified with the *Photobacterium luminescens lux* operon, by the spread plate method. Light output across the petri dish was recorded for 16 h using an Andor iXon EM+ DU-897 back-illuminated EMCCD camera with a Tamron SP AF 17-35 mm F/2.8-4 lens.

### RESULTS AND DISCUSSION

CHX elution was sustained over two weeks with the material tailorable with respect to delivery dose (Fig 1).

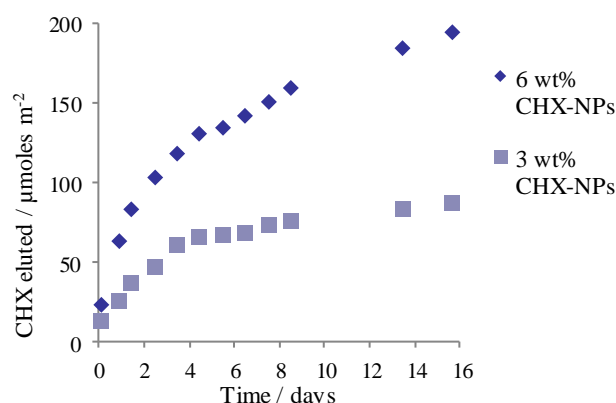


**Fig 1.** Alginate nanocomposite thin films at two CHX-NPs dopings sustain CHX elution for two weeks.

The initial CHX release (25.5 & 62.6 µmoles m<sup>-2</sup> for 3 & 6 wt% CHX-NPs respectively at 21 h) was found to be effective against five common wound infecting microorganisms (Fig 2).



**Fig 2.** Inhibition zones (MRSA) produced by alginate thin film disks (ø = 10 mm) containing a wt% CHX-NPs

Video imaging of bioluminescent *E. coli* allowed visualisation of the antiseptic effect in real time *in situ*.

### CONCLUSION

CHX-NPs impregnated alginate facilitates the tailorable release of antiseptic at therapeutic concentrations, effective against common infecting microorganisms. *In vitro* cytotoxicity studies are planned on fibroblast cell lines which will provide an indication of any effect upon the healing pathways of a wound.

### REFERENCES

1. Best Practice Statement: The use of topical antiseptic/antimicrobial agents in wound management, *Wounds UK*, Aberdeen, 2010.
2. A. Drosou, *et al.*, *Wounds*, 2003, 15, 149.
3. M. E. Barbour *et al.*, *Int. J. Nanomed.*, 2013, 8, 3507.
4. G. M. Robinson, *et al.*, *Antimicrob. Agents Chemother.*, 2011, 55, 5214.

### ACKNOWLEDGMENTS

The EPSRC and the Bristol centres; ACCIS and NSQI.





## Enrichment of Enzymatically Mineralized Gellan Gum Hydrogels with Polyphenol-Rich *Ecklonia cava* Extract Seanol® to Endow Antibacterial Properties

Timothy E.L. Douglas<sup>1,2</sup>, Gilles Brackman<sup>3</sup>, Katarzyna Reczyńska<sup>4</sup>, Agnieszka Dokupil<sup>4</sup>, Krzysztof Pietryga<sup>4</sup>, Peter Dubrue<sup>1</sup>, Tom Coenye<sup>3</sup>, Elżbieta Pamuła<sup>4</sup>

<sup>1</sup>Polymer Chemistry and Biomaterials group, Department Organic Chemistry, Ghent University, Belgium

<sup>2</sup>Nano & Biophotonics group, Department Molecular Biotechnology, Ghent University, Belgium

<sup>3</sup>Laboratory of Pharmaceutical Microbiology, Ghent University, Belgium

<sup>4</sup>Department of Biomaterials, AGH University of Science and Technology, Krakow, Poland

Timothy.Douglas@UGent.be

### INTRODUCTION

Antibacterial properties are highly desirable for materials for bone regeneration. Hence, biomaterial enrichment with antimicrobial agents is advantageous. Polyphenols are organic chemicals containing phenol structural units. Phlorotannins are a subset of polyphenols occurring in brown seaweeds such as *Ecklonia cava*. They possess antibacterial<sup>1</sup> and anti-inflammatory activity<sup>2</sup>. Brown seaweed extracts such as Seanol® are widely used as food supplements thanks to their antioxidant properties, but their use as biomaterial components to endow antibacterial activity remains unexplored. Seanol® is an *E. cava* extract of which <95% consists of polyphenols. In this study, Seanol® was incorporated into hydrogels consisting of gellan gum (GG), which were enzymatically mineralized with calcium phosphate (CaP) using alkaline phosphatase (ALP) as in previous work<sup>3</sup> in order to further improve their suitability for bone regeneration. It was hypothesized that Seanol® would inhibit biofilm formation of Methicillin-resistant *Staphylococcus aureus* (MRSA) on hydrogels, both before and after mineralization with CaP.

### EXPERIMENTAL METHODS

Hydrogels containing 0.7% GG (sterilized by ethylene oxide) and 0.03% CaCl<sub>2</sub> (w/v) with Seanol® and ALP concentrations described in Table 1 were fabricated as described in Figure 1 under sterile conditions. Hydrogel cylinders of diameter 6 mm and height 10 mm were incubated in a 0.1 M CaGP solution-suspension for 7 d to induce mineralization with CaP in GG/S2.5/ALP samples. To evaluate ability of Seanol®-loaded GG hydrogels to inhibit biofilm formation, 6 cylinders of GG/S2.5 and GG/S2.5/ALP were placed on a silicone disc and incubated with 10<sup>4</sup> Colony Forming Units (CFU) of MRSA. After 24 h incubation at 37°C, the number of sessile bacteria present on both the silicone disc and the hydrogel cylinders were determined by plating. Physicochemical characterization was also performed. Dry mass percentage (mass percentage attributable to polymer and CaP and not water) served as a measure of CaP formed. Compressive modulus was determined. For all measurements, n = 3.

Table 1: Composition of sample groups

Sample group	Conc. Seanol®	Conc. ALP
GG/S2.5	2.5 mg/ml	0 mg/ml
GG/S2.5/ALP	2.5 mg/ml	2.5 mg/ml

### RESULTS AND DISCUSSION

Both GG/S2.5 and GG/S2.5/ALP samples strongly inhibited biofilm formation on hydrogel samples (Figure 2). Inhibition of biofilm formation on silicone discs was similar (data not shown). Hydrogel incubation

in 0.1 M CaGP caused a reduction in antibacterial activity, presumably due to release of Seanol®.

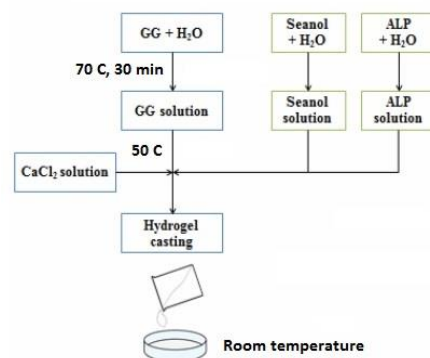


Figure 1: Schematic description of hydrogel production

However, biofilm formation on GG/S2.5/ALP samples was significantly lower than on controls, indicating retention of antibacterial activity. This may be due to CaP formation, inhibiting complete loss of Seanol®. Seanol® also increased CaP formation and compressive modulus: values for GG/S2.5/ALP samples were significantly higher than those for GG/ALP samples.

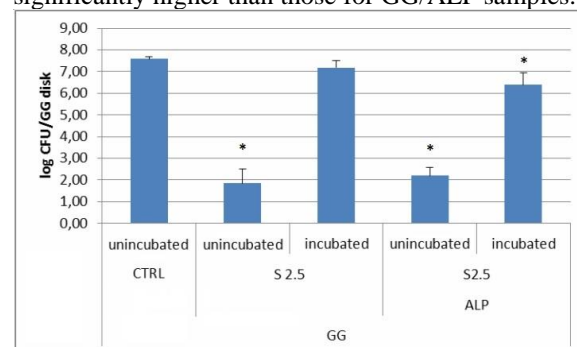


Figure 2: Biofilm formation on hydrogels, which were either incubated in 0.1 M CaGP for 7 days prior to testing or unincubated. \* p<0.05 compared to CTRL (GG hydrogels without ALP or Seanol®).

### CONCLUSION

Incorporation of Seanol® in GG hydrogels inhibits MRSA biofilm formation, even after mineralization.

### ACKNOWLEDGMENTS

T.E.L.D. thanks FWO, B for a postdoctoral fellowship. Trey MacPhee, JP Renew Distributors LLC, USA is thanked for providing Seanol®.

### REFERENCES

1. Lopes G. *et al.*, PLoS One, 2012, 7(2), e31145.
2. Choi J-G. *et al.*, Foodborne Pathog. Dis., 2010, 7(4), 435-41
3. Douglas T. *et al.*, J Tissue Eng Regen Med. 2014, 8(11),906-18.

## Development of an Antibacterial Hybrid Sponge (Chitosan/Hydroxyapatite) for Bone Regeneration

Claudia Flores<sup>1</sup>, Jean Christophe Hornez<sup>2</sup>, Feng Chai<sup>1</sup>, Gwenael Raoul<sup>1</sup>, Nicolas Tabary<sup>3</sup>, Frédéric Cazaux<sup>3</sup>, Joel Ferri<sup>1</sup>, Hartmut F. Hildebrand<sup>1</sup>, Bernard Martel<sup>3</sup>, Nicolas Blanchemain<sup>1</sup>

<sup>1</sup>INSERM U1008, Biomaterials Research Group, University Lille 2, France.

<sup>2</sup>EA2443, LMCPA, Université de Valenciennes Hainaut Cambrésis, France

<sup>3</sup>UMET, UMR-CNRS8207, Ingénierie des Systèmes Polymères, Université Lille 1, France

[claudia.floresvilca@univ-lille2.fr](mailto:claudia.floresvilca@univ-lille2.fr)

### INTRODUCTION

The surgical disciplines involved in the bone replacement (osteolysis, osteosarcoma) raise multiple problems, in particular infection (1-2%), which can lead to dramatic consequences for the patient (re-interventions, amputation, fistulisation, *etc.*); and the need of vascularisation. Hydroxyapatite (HA) is largely used for bone tissue regeneration due to its excellent biocompatibility, bioactivity and osteoconduction properties<sup>1,2</sup>. Chitosan is a biopolymer known for its antibacterial, haemostatic properties and its ability to form hydrogel networks, *i.e.* through the reaction with an anionic polymer (*e.g.* cyclodextrin) to form a polyelectrolyte complex. The aim of this project is to develop an antibacterial spongy hybrid (chitosan/HA), obtained by the physical gelation of chitosan and polymer of cyclodextrin. After freeze-drying, the rheological and biological properties of this hybrid material were determined, and the antibiotics release profile and antibacterial properties were assessed by loading the ciprofloxacin on the hybrid.

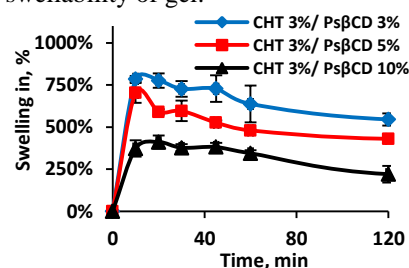
### EXPERIMENTAL METHODS

The hydrogel was prepared by dissolving chitosan (CHT, 3% w/v, 75-85% deacetylated), and polymer of cyclodextrin (PCD, 3; 5 or 10% w/v) in an acetic acid solution (1% v/v) with or without HA particles (80  $\mu$ m; 30% w/v). At the end of the process, the hydrogels were freeze dried (-60°C, 0.06mbar) and stored at room temperature. Their swelling ratio was determined by immersing 20 mg of hybrid in 10 mL of ultrapure water and/or phosphate buffer saline (PBS, 0.1M; pH 7.4).

Cell vitality was evaluated by the Alamar blue method with pre-osteoblast cells (MC3T3/E1) according to the ISO 10993-5 standards. Scanning electron microscope (SEM, S-4000 Hitachi, Krefeld, Germany) was used to observe the microstructure of the sponge. Rheological studies were carried out on rheometer (MCR301-Anton-Paar). The storage modulus ( $G'$ ) and loss modulus ( $G''$ ) of the hydrogels were carried out with a controlled shear stress ( $\gamma=1\%$ ,  $T=25^\circ\text{C}$ , and  $\omega=10\text{s}^{-1}$ ). For drug sorption and drug release studies, 20 mg of sponge was impregnated in 10 mL of ciprofloxacin (CFX, Kabi®, 200 mg/100 mL) at room temperature. The drug loading was then determined by UV spectrophotometer at 271 nm by desorption of drug in NaOH 0.1 N overnight. The release profile of CFX was determined under dynamic condition with a USP4 apparatus (Sotax®, 37°C, 30 mL/min). Finally the antibacterial activity of the CFX-loaded sponge was determined by Kirby-Bauer method

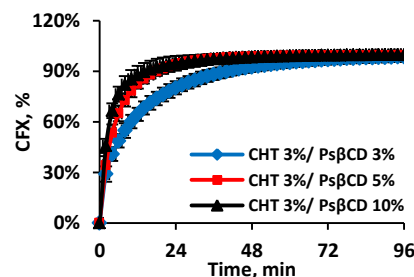
### RESULTS AND DISCUSSION

Fig. 1 shows that the swelling rates increase to reach a maximal value (up to 800%), and then decreased and stabilized after 120 minutes. Increasing PCD ratios in the formulations provoked the decrease of the swellability of gel.



**Figure 1:** Swelling behaviour of the hydrogel at different proportion of PCD in PBS (0.1M, pH7.4)

After impregnation of the sponge in CFX solution, the drug sorption (25 mg/g) did not increase with the PCD ratio, but the release profile was prolonged with decrease of PCD ratio. These results were also confirmed by the microbiological evaluation, which revealed antibacterial activity on *E. coli* and *S. aureus*. Rheological studies of the gel displayed the elasticity of the gels the storage modulus  $G'$  was always superior to the loss modulus  $G''$ , the ratio  $G'/G'' \approx 2$ . The evaluation cell vitality test showed an excellent cytocompatibility (>80% of osteoblast vitality).



**Figure 2:** Kinetic release of CFX in mg/g of hydrogel at different proportion of PCD in PBS(0.1M, pH7.4)

### CONCLUSION

We demonstrated the prospect of preparing a well characterized HA incorporated CHT/PCD spongy hybrid. The gel structure can be fine-tuned by varying the ratio of PCD to CHT. Increasing PCD resulted in the stiffer gels, but didn't improve the reservoir property. The HA particles can improve osteoblastic proliferation on the hydrogel and PCD could carry CFX to prevent infections. Moreover, other therapeutic agents could also be applied in future.

### REFERENCES

1. Meurice *et al.*, JECS32 :2673-2678, 2012
2. Cox *et al.*, MSEC 47: 237-247, 2015

### ACKNOWLEDGMENTS

The authors thank the region Nord-Pas-de-Calais for providing financial support (ARCir-BioCerMed).



## Antimicrobial Properties of a Novel Hydrogel Bandage Lens Material

Andrew Gallagher<sup>1,3</sup>, Mal Horsburgh<sup>2</sup>, Jamal Alorabi<sup>2</sup>, Don Wellings<sup>3</sup> and Rachel Williams<sup>1</sup>

<sup>1</sup>Eye and Vision Science/Institute of Ageing and Chronic Disease, University of Liverpool, England

<sup>2</sup>Functional and Comparative Genomics/Institute of Integrative Biology, University of Liverpool, England

<sup>3</sup>Spheritech Ltd, Runcorn, England

[andy.gallagher@spheritech.com](mailto:andy.gallagher@spheritech.com)

### INTRODUCTION

Corneal bandage lenses have an important role to play in the treatment of corneal infection and disease<sup>1</sup>. Corneal ulcers are of particular interest as current treatment involves the topical administration of antibiotics, of which only 1 - 7 % is absorbed to the site of infection<sup>2</sup>. This inefficiency allows a lot of scope to improve the delivery of drugs to the surface of the eye.

This study aimed to investigate the natural antimicrobial activity of a novel hydrogel as well as observing differences in activity when compounds such as additional poly-ε-lysine (Pεk) and penicillin G (pen G) were covalently or ionically coupled to the hydrogel.

### EXPERIMENTAL METHODS

Peptide gels were synthesised from poly-ε-lysine and crosslinked with suberic acid with a density of 0.071 g/cm<sup>3</sup> and 45%, 60% or 75% crosslinking. Some of the hydrogel surfaces were modified to bind additional poly-ε-lysine using an EDCI/NHS mediated crosslinking technique and/or the β-lactam antibiotic penicillin G by soaking in an ionic solution of the antibiotic. Hydrogel samples were incubated with *E.coli* or *S.aureus* inoculum ( $5 \times 10^5$  cells/ml) for 2 h, 4 h and 18 h before being removed and washed in PBS (x5). An alamar blue metabolic assay coupled with serial dilution plate counts were used to determine the bacterial burden on the surface of the hydrogel materials.

### RESULTS AND DISCUSSION

The degrees of crosslinking had no significant difference on alamar blue reduction between the hydrogels and performed similarly to the LB agar control which suggests the variation in amine groups at these concentrations had little effect on antimicrobial activity. A significant difference in antimicrobial activity was obtained by altering the surface properties of the hydrogel material with either additional poly-ε-lysine or penicillin G compared to the LB agar control. The *S.aureus* experiment control (28 % resazurin after 18 h) was significantly less ( $P < 0.001$ ) than values for poly-ε-lysine (90 %), penicillin G (96 %) and poly-ε-lysine + penicillin G (96 %) (figure 1). Results for *E.coli* were similar, the resazurin in the control was significantly ( $P < 0.001$ ) reduced (30 % resazurin after 18 h) when compared to values for poly-ε-lysine (80 %), penicillin G (99 %) and poly-ε-lysine + penicillin G (99 %) (figure 2). These data demonstrate

the potential to modify the hydrogel material in such a way that enables an increase in antimicrobial activity. This may allow for the tailoring of the hydrogel to target other pathogens utilising alternative antimicrobial compounds bound to the surface.

Figure 1: Metabolic Activity of *S. aureus* Newman Incubated with the Hydrogel Variants

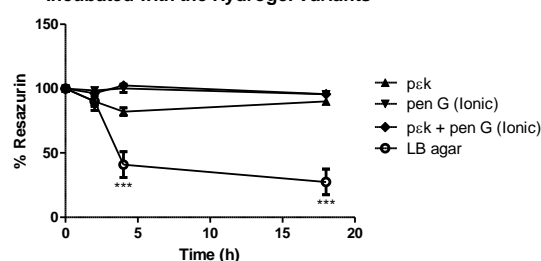
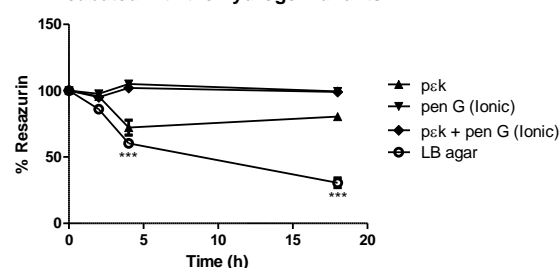


Figure 2: Metabolic Activity of *E. coli* MC1061 Incubated with the Hydrogel Variants



### CONCLUSION

Crosslinked poly-ε-lysine hydrogel alone was not antimicrobial to *E.coli* or *S.aureus* however binding poly-ε-lysine or penicillin G to the free amine groups on the crosslinked hydrogel caused a significant antimicrobial effect. These modified hydrogels could have a role as bandage contact lenses in the treatment of corneal ulcers.

### REFERENCES

- Willoughby C. *et al.*, Surv Ophthalmol. 47:174-182, 2002
- Ciolino J. *et al.*, Invest. Ophthalmol. Vis. Sci. 50: 3346-3352

### ACKNOWLEDGMENTS

The authors would like to thank Spheritech Ltd. for providing financial support for this project.



## Ephemeral Biogels to Control Anti-Biofilm Agent Delivery

Véronique Larreta-Garde, Elodie Lefebvre, Damien Seyer

Biology Department/ERRMECe, University of Cergy-Pontoise, France

[veronique.larreta-garde@u-cergy.fr](mailto:veronique.larreta-garde@u-cergy.fr)

### INTRODUCTION

Over the past 15 years, the impact of biofilms on persistent infections and their potential role on chronic wounds have been extensively documented<sup>1</sup>. However, up to now, no efficient system to deliver anti-biofilm agents has been described<sup>2</sup>.

The aim of this study was to create a biogel system entrapping and releasing various agents to allow eradication of bacteria in biofilms. The anti-biofilm strategy combined destruction of bacteria and disruption of the biofilm matrix, expecting a biomass decrease by at least 5 log. The biomaterial here elaborated was conceived to control the delivery of active compounds and tested on monospecies and mixed biofilms from *Pseudomonas aeruginosa* and *Staphylococcus aureus*.

### EXPERIMENTAL METHODS

**Biogels:** Gelatin 5 to 7% (W/V) solutions containing PHMB (from  $5 \cdot 10^{-2}$  to  $8 \text{ mg.mL}^{-1}$ ), EDTA (20mM) without and with Esperase ( $6$  to  $9 \text{ U.mL}^{-1}$ ) are turned to gels under the action of transglutaminase ( $1 \text{ U.mL}^{-1}$ ). The mechanical properties of the biogels are measured through rheology.

**Biofilms:** *Pseudomonas aeruginosa* and *Staphylococcus aureus* biofilms were grown for 24h, then treatments (contact with the active biogel) were applied for 24 to 48 h and the viable biofilm bacteria quantified on agar.

### RESULTS AND DISCUSSION

The combination of a commercial antiseptic (PHMB, low concentration), and an ion chelator able to inhibit MMPs (EDTA) in solution was first tested on biofilms. The mixture was proven efficient with a very high anti-bacterial effect ( $> 99.999\%$ ) against both *P. aeruginosa* and *S. aureus* biofilms. The addition of EDTA potentialized the effect of PHMB, showing an efficient synergistic effect of the two compounds.

The two active compounds were then entrapped together into a 5% gelatin gel. Unfortunately, the efficiency of this gel against biofilms was largely reduced compared to the antiseptic solution. The PHMB concentration was then increased to  $8 \text{ mg.mL}^{-1}$ , but this induced a large decrease of the mechanical properties of the gel. The 5% gelatin gel entrapping PHMB was 7 times less elastic than the control gel. Using a more concentrated gelatin solution (7%) allowed obtaining satisfactory elastic properties, the gel containing the antiseptic compounds being handeable.

However, in these conditions, a diffusion limitation of the chosen antiseptic was evidenced. Only 4% of the

initial PHMB concentration included in the gel diffused in the surrounding medium within 24h, limiting its efficiency against biofilms.

To overcome this diffusion limitation, an innovative drug delivery system, developed in our laboratory<sup>3</sup> and allowing a gelatin gel formation followed by a controlled-time resolubilization was elaborated. This gel is based on the action of two antagonistic enzymes, one generating and the other cleaving covalent bonds, respectively a transglutaminase and a protease. The use of this ephemeral gel, named Enzgel leads to enhanced and controlled molecular release<sup>4</sup>.

Thus, a protease, Esperase, was added to the gelatin solution containing the treatment; a gel was first formed which later re-solubilized. The network hydrolysis was complete after about 2 days. This system promoted molecule diffusion from the gel to the surrounding medium allowing their anti-biofilm activity to express. After 24 h contact, the biomass was reduced by 5 logarithms for *S. aureus* biofilm and by 7 logarithms for *P. aeruginosa* biofilm, an improvement of 40 and 11 times compared to the gel without protease. After 48h contact, both monospecies biofilms and a mixed biofilm were totally eradicated. The efficiency rates fixed in the project were thus largely overcome.

### CONCLUSION

In the United States, 8 million people are affected by chronic wounds which lead to a cost of 20 billion dollars per year. The presence of biofilm may extend the healing delay. Our strategy to limit or eradicate biofilms was based on two major points: destabilize the biofilm and its matrix and eliminate pathogenic bacteria by the use of an antiseptic. In this study, we have conceived and elaborated an active biogel, able to control the bacteria level in various biofilms. This biomaterial is very promising for wound care and will be developed in the near future.

### REFERENCES

1. James GA. *et al.* Wound Repair and Regeneration 16: 37–44.2008.
2. Ammons MC. Drug Discovery, 5-1:10-17, 2010.
3. Giraudier S. and Larreta Garde V., patent WO 2006/056700 A2
4. Klak MC. *et al* Soft Matter, 8 : 4750-4755, 2012.

### ACKNOWLEDGMENTS

The authors would like to thank the french National Agency for Research (ANR-10-TECS-019) for providing financial support to this project and C. Vighetto for efficient technical assistance.



## Broad-Spectrum Antimicrobial Polycarbonate Hydrogels for Wound Dressing Applications

Haritz Sardon<sup>1</sup>, Ana Pascual<sup>1</sup>, Jeremy P. K. Tan<sup>2</sup>, James L. Hedrick<sup>3</sup>, Yi Yan Yang<sup>2</sup>

<sup>1</sup> POLYMAT, University of the Basque Country UPV/EHU Joxe Mari Korta Center, Avda. Tolosa 72, 20018 Donostia-San Sebastián, Spain.

<sup>2</sup> Institute of Bioengineering and Nanotechnology, 31 Biopolis Way, Singapore 138669, Singapore

<sup>3</sup> IBM Almaden Research Center, 650 Harry Road, San Jose, CA 95120, USA

[haritz.sardon@ehu.es](mailto:haritz.sardon@ehu.es)

**In this study, a new family of broad-spectrum antimicrobial polycarbonate hydrogels has been successfully synthesized and characterized. *In vitro* antimicrobial studies revealed that quaternized hydrogels exhibited broad-spectrum antimicrobial activity against *Staphylococcus aureus* (Gram-positive), *Escherichia coli* (Gram-negative), *Pseudomonas aeruginosa* (Gram-negative), and *Candida albicans* (fungus).**

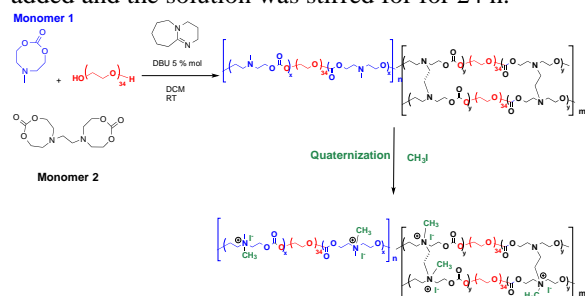
### INTRODUCTION

Wound treatments have a major impact on quality of life. It is believed that the treatment of chronic wounds will become an important challenge to healthcare systems worldwide due to an aging society. Despite these urgent needs, wound dressing technology still has a long way to go probably due to the intrinsic complexity of the wound healing process.<sup>1</sup>

In the last decade, polymeric hydrogels have been studied and used as alternative to gauze dressing materials in wound dressing applications. Hydrogels have the ability to maintain wound occlusion, creating a more conducive environment for tissue regeneration than exposed wounds. The main problem in using hydrogels for wound care is the high risk of infection as the moist environment in the hydrogels allows pathogen to proliferate and colonize. The goal of this study is to design a hydrogel that fast degrades and prevents bacterial infection. In this sense, aliphatic polycarbonates were chosen not only due to their ability to degrade fast under physiological condition but also their activity against multidrug resistant bacteria.<sup>2</sup>

### EXPERIMENTAL METHODS

**Synthesis of polycarbonate hydrogels** A 20 mL glass vial containing a magnetic stir-bar was charged with monomer 1, monomer 2, PEG<sub>1500</sub> in DCM. DBU was added and the solution was stirred for 24 h.



DBU was quenched with an excess of benzoic acid. The resulting hydrogel was washed by immersion in DCM to remove catalyst and soluble fractions, and dried under vacuum. (Yield: 0.40 g, 89 %) Finally, the gel was immersed in methyl iodide (CH<sub>3</sub>I) for 48 h at room temperature under N<sub>2</sub>. (Scheme 1)

**Antibacterial activity** The quaternized hydrogel was cut into 5 x 5 mm square and placed into a 1.7 mL micro-centrifuge tube. TSB or YMB (100  $\mu$ L) was added into the tube before an equal volume of microbe suspension ( $3 \times 10^5$  CFU/mL) was added. After the hydrogel treatment, the samples were taken for a series of tenfold dilution, and plated onto agar plates. The plates were incubated for 24 h at 37 °C for bacterial samples or 42 h at room temperature for *C. albicans* before the number of colony-forming units (CFU) was counted.

### RESULTS AND DISCUSSION

The antimicrobial activity of different hydrogels was evaluated against Gram-positive bacteria *S. aureus*, Gram-negative bacteria *E. coli* and *P. aeruginosa*, and fungi *C. albicans*. After treating the microbes with the hydrogels, the growth of the microbes was completely suppressed with killing efficiency of at least 99.999%. Furthermore, the CFU counts after 18 h of treatment showed that the hydrogels were bactericidal to a wide range of microbes. There was a 6 – 10 log reduction in colony counts. Meanwhile, the unquaternized gels did not show any significant activity towards the microbes. All hydrogels demonstrated similar antimicrobial activity against all microbes tested. These hydrogels were chemically cross-linked as thin transparent films, making them desirable for wound healing applications.

### CONCLUSION

Quaternized polycarbonate hydrogels exhibited high ability to kill Gram-positive and Gram-negative bacteria as well as fungi. Therefore, these materials have potential applications in wound healing and medical implants for the prevention of infections.

### REFERENCES

1. F. Nederberg et al. *Nat Chem*, 2011, 3, 409-414.
2. V. W. L. Ng et al. *Advanced Drug Delivery Reviews*, 2014, 78, 46-62.

### ACKNOWLEDGMENTS

Hartiz Sardon gratefully acknowledges financial support in the form of a postdoctoral grant (DKR) from the Basque Government.



## Injectable Gellan Gum-Based Nanoparticle-Loaded System for the Local Delivery of Vancomycin in Osteomyelitis Treatment

Urszula Posadowska<sup>1\*</sup>, Monika Brzychczy-Włoch<sup>2</sup>, Elżbieta Pamuła<sup>1</sup>

<sup>1</sup>AGH University of Science and Technology, Faculty of Materials Science and Ceramics,  
Department of Biomaterials, Poland

<sup>2</sup>Jagiellonian University, Medical College, Department of Microbiology, Poland  
[uposadow@agh.edu.pl](mailto:uposadow@agh.edu.pl)

### INTRODUCTION

Conventionally elimination of pathogens from musculo-skeletal environment involves surgical removal of necrotic tissue, osseous repair and antibiotherapy for 4 – 6 weeks<sup>1,2</sup>. The procedure applied is often inefficient and harmful to the patients. Alternative solution that seems to be less complicated and more accurate is the usage of drug releasing degradable implants placed exclusively into the infected tissue (preferentially via non-invasive way<sup>3,4</sup>). Thus, here we present application of gellan gum-based biomaterial enriched with nanoparticles loaded previously with antimicrobial agent (vancomycin) for local elimination of musculoskeletal infection that leads to chronic bone disease, i.e. osteomyelitis.

### EXPERIMENTAL METHODS

Vancomycin was encapsulated in poly(L-lactide-co-glycolide) (PLGA, 85:15, Mn = 80 kDa, d = 1.8) nanoparticles (Vanc-NPs) via double-emulsification. Vanc-NPs were characterized with dynamic light scattering (DLS), capillary electrophoresis, atomic force microscopy (AFM); fluorescence spectroscopy (OPA assay) was used to assess loading and encapsulation efficiencies. In order to obtain injectable drug delivery system, Vanc-NPs were suspended in gellan gum (Gelzan<sup>TM</sup>) and cross-linked with Ca<sup>+2</sup> (GG-Vanc-NPs). The systems obtained were evaluated with respect to injectability, rheology, drug release and morphology (SEM). Then, they were studied *in vitro* via an indirect way. Extracts performed to cell culture medium (37 °C, 24 h) were examined on osteoblast-like MG-63 cells. Cells were evaluated with respect to their metabolic activity (Alamar Blue test), viability (live-dead test) and morphology. For the antimicrobial activity agar-diffusion tests via Kirby-Bauer method were conducted. Bone inhabiting pathogens causing osteomyelitis *Staphylococcus spp.*, both referential strains and strains isolated from infected joints were used.

### RESULTS AND DISCUSSION

DLS studies showed that size of Vanc-NPs was in nanometric range (250 – 380 nm). Analysis of morphology by AFM showed their spherical shape. Laser electrophoresis demonstrated negative zeta potential connected with the ionized carboxyl end group of PLGA. Results of solubilization revealed encapsulation efficiency of 55.2 ± 0.5% and drug loading of 8.4 ± 0.1%. Injectability studies performed in

compression mode (cross-head speed 50 mm/min) showed that extrusion force from the standard 18G needle was lower than 15 N and the force increased upon Vanc-NPs addition. Rheological evaluations showed that despite Vanc-NPs addition gellan gum matrix had good mechanical properties ( $G'$  - storage modulus 7.4 kPa,  $G''$  - loss modulus 0.4 kPa). The  $G'$  and  $G''$  moduli were lower than for unloaded system. The structure exhibited ability to self-organize after disruption by strain sweep deformation. Drug release studies of GG-Vanc-NPs showed short burst release followed by long sustained release phase. Regarding *in vitro* studies, comparable values of Alamar Blue reduction by MG-63 cells were obtained when cells were incubated in culture medium or in GG-Vanc-NPs extracts. Incubating *S. aureus* and *S. epidermidis* with GG-Vanc-NPs resulted in inhibition of microbes growth. The inhibition zones had diameters in the range 24 – 29 mm, what indicated sensitivity of the tested strains.

### CONCLUSION

Our systems based on vancomycin loaded nanoparticles suspended in gellan gum matrix: i) were found to be syringeable and easy to administer (injectable), ii) reassembled their structure after disruption by strain sweep deformation, iii) ensured local vancomycin delivery, iv) did not affect osteoblast-like cells viability, and v) demonstrated antimicrobial activity against *Staphylococcus spp.* referential as well as the clinical isolates. The results show the promising potential of developed injectable systems for the local elimination of microbial infections leading to osteomyelitis.

### REFERENCES

1. Xie Z. *et al.*, J Contr Release 139:118-126, 2009
2. Makarov C. *et al.*, Eur J Pharm Sci 62:49-56, 2014
3. Balmayor E. *et al.*, Carbohydr Polym 87:32-39, 2012
4. Chaisri W. *et al.*, Colloids Surf B: Biointerfaces 84:508-514, 2011

### ACKNOWLEDGMENTS

National Science Centre in Poland (Grant no: 2012/05/B/ST8/00129) provided financial support to this project. The authors would like to thank FYSKO group at Wageningen University for the possibility to conduct rheology studies.





## Long-Term and Bioinert Labeling of Mesenchymal Stem Cells with Polymeric-Gd Conjugates and MRI Monitoring of the Cell Behaviour in Ischemic Rats

Tetsuji Yamaoka\*, Yoichi Tachibana

Department of Biomedical Engineering, National Cerebral and Cardiovascular Center Research Institute, Japan  
[yamtet@ncvc.go.jp](mailto:yamtet@ncvc.go.jp)

### INTRODUCTION

There is an increasing interest in stem cell transplantation therapy, and autologous mesenchymal stem cells (MSCs) have received much attention in treating limb ischemia, infarcted myocardium, brain injury, and so on. Although the detailed mechanisms of MSC actions in vivo remain unclear, recent studies have focused on paracrine mechanisms. It is also reported that the transplanted MSCs decrease within 2 to 3 weeks according to the histological analysis, that is a semi-quantitative method and cannot distinguish whether the cells died or migrated elsewhere. To clarify the behaviour of transplanted MSCs quantitatively, we have developed novel magnetic resonance imaging (MRI) cell tracking system. There are two important factors to achieve long-term cell tracking; the stable retentivity of the contrast agent in the cells and the elimination of the free contrast agents when they leak out of the cells upon cell death.

We have been studying the water-soluble gadolinium (Gd)-based MRI contrast agent for cell labeling and tracking for the first time<sup>1-4</sup>. Gd-chelate molecules were conjugated to the side hydroxyl groups of water soluble carrier such as poly(vinyl alcohol) (PVA) or dextran. The novel polymeric-Gd, was delivered under a mild condition system to various types of cells. In the present study the migration and survival of MSCs in rat ischemia model will be discussed.

### EXPERIMENTAL METHODS

Polymeric-Gd was synthesized by recently reported method<sup>5</sup>. First, rMSCs were cultured at a concentration of  $5 \times 10^5$  cells/dish for 1 day, washed with PBS three times, and suspended in culture medium without serum. Polymeric-Gd or low molecular weight contrast agent ProHance® at a final Gd concentration of 10 mM was added to the culture medium. Electrical pulses were applied to cells using a CUY-21 electroporator (NEPPA GENE, Tokyo, Japan). Rectangular electrical pulses (field strength, 300 V/cm; number of pulses, 10; pulse duration, 5 ms) were applied to cells using two parallel electrodes with a 5-mm gap, resulting in the cell labelling with the Gd with very low cytotoxicity.

Male rats (8 weeks old) were anesthetized with isoflurane (1.5% in air) and the left femoral artery and vein and their branches were ligated and completely excised through a skin incision. The Gd-labeled MSCs were injected intramuscularly.

MR imaging was conducted using T1-weighted images obtained with a 1.5-T compact MRI system (MRmini, Dainippon Sumitomo Pharma, Osaka, Japan)

with a repetition time (TR) of 2000 ms and an echo time (TE) of 9 ms.

The recovery of blood flow in ischemic limbs 輪 measured by using a Laser Doppler Perfusion Imager (LDPI). The amount of [Gd(III)] retained in the cell, accumulated in the tissue, and excreted to the urine was measured by the inductively coupled plasma atomic emission spectroscopy (ICP-AES) (Model 7510, Shimadzu Co., Kyoto, Japan).

### RESULTS AND DISCUSSION

Polymeric-Gd did not show any cytotoxicity in the tried condition and did not affect the growth or differentiation of the MSC, indicating that they are safe and could be translated for use in clinical cell therapy

Polymeric-Gd was retained in the cytosolic compartment of MSCs higher than 90% at 1 month post labelling. In vivo T1-weighted images of rMSCs revealed that rMSCs are eliminated with time from the site of transplantation within two weeks even when the stem cells are seeded and trapped in the porous gelatin scaffold, Spongel®.

### CONCLUSION

Our system is very effective to quantify the cell survival by noninvasively visualizing them with MRI. These cell tracking system will be a powerful tool for studying the lifespan of transplanted cells and developing the most effective transplantation methods for stem cell therapy.

### REFERENCES

1. Tachibana Y. *et al.*, Contrast Media Mol. Imaging 5, 309-317, 2010.
2. Agudelo CA. *et al.*, Tissue Eng. Part A 17, 2079-2089, 2011
3. Agudelo CA. *et al.*, Biomaterials 33, 2439-2448, 2012
4. Agudelo CA. *et al.*, J Biomater Appl, 28(3):473-80, 2013
5. Tachibana Y. *et al.*, Bioconjug Chem. 25(7):1243-51, 2014

### ACKNOWLEDGMENTS

This work was supported by grants-in-aid from the Ministry of Health, Labour and Welfare of Japan (Health and Labour Sciences Research Grants, research on Nanotechnical Medical). This work was also supported by a Research Grant for Cardiovascular Diseases (18A-2) from the Ministry of Health, Labour and Welfare of Japan..





# Nile Blue-Based Nano-Sized pH Sensors for Simultaneous Far-Red and Near-Infrared Live

Jeppe Madsen<sup>1,2</sup>, Irene Canton<sup>1</sup>, Nicholas J. Warren<sup>2</sup>, Efrosyni Themistou<sup>2</sup>, Adam Blanz<sup>2</sup>, Burcin Ustbas<sup>1</sup>, Xiaoho Tian<sup>1</sup>, Russell Pearson<sup>1</sup>, Giuseppe Battaglia<sup>1</sup>, Andrew L. Lewis<sup>3</sup>, Steven P. Armes<sup>2</sup>

<sup>1</sup>Department of Biomedical Sciences, University of Sheffield, Sheffield, S10 2TN, UK

<sup>2</sup>Department of Chemistry, Dainton Building, University of Sheffield, Sheffield, S3 7HF, UK

<sup>3</sup>Biocompatibles UK Ltd., Farnham Business Park, Weydon Lane, Farnham, GU9 8QL, UK

[p.madsen@sheffield.ac.uk](mailto:p.madsen@sheffield.ac.uk)

## INTRODUCTION

Fluorescent probes are widely used for imaging in cell biology. Increasingly, they are also being utilized as chemosensors to diagnose specific pathological conditions and report on cellular events<sup>1-3</sup>. There is considerable interest in designing nanoparticles that report on physiologically relevant species such as hydrogen ions<sup>4,5</sup> because such sensors provide attractive cell and tissue uptake kinetics and distribution.

## EXPERIMENTAL METHODS

Monomers, Nile Blue methacrylamide (NBM) and Nile Blue 2-(methacryloyloxy)ethyl carbamate (NBC) were prepared from Nile Blue (NB). pH-responsive diblock copolymers based on (2-(methacryloyloxy)ethyl phosphorylcholine) [MPC] and 2-(diisopropylamino)ethyl methacrylate [DPA], PMPC-PDPA labelled with Nile Blue derivatives were synthesised using Atom Transfer Radical Polymerisation (ATRP). Polymer toxicity on HDF cells was assessed using an MTT assay. Uptake and intracellular distribution of polymer nanoparticles was studied on Human Dermal Fibroblast (HDF) cells using confocal microscopy and conventional subcellular markers. 3D Multicellular tumour spheroids (MCTS) of MDA-MB-231 breast cancer cells were cultured according to literature<sup>6</sup>. Hypoxia-induced pH change of live spheroids was monitored using an optical microscope and the results were compared to results obtained using a control marker for hypoxia (Glut-1). Full experimental details can be found in reference 7.

## RESULTS AND DISCUSSION

Absorption and emission properties of two Nile Blue derivatives were found to be pH-sensitive around physiological pH. These dyes were found to attach themselves to polymers through a radical mechanism. PMPC-PDPA diblock copolymers were easily labelled with NB, NBM or NBC (Figure 1B). The resulting polymers were found to exhibit pH-responsive absorption characteristics as shown in Figure 1A. The pH-responsive absorption was used to monitor hypoxia in tumours (see Figure 1C). In addition, such polymers are known to be rapidly incorporated into many different cell types and are distributed inside intracellular organelles<sup>8</sup>. Therefore, it was possible to simultaneously monitor lysosomes and early endosomes by exploiting the pH-induced change in the fluorescence emission wavelength.

## CONCLUSION

PMPC-PDPA-based pH-responsive nanoparticle probes

report clinically-relevant pH-changes in tumors and cell organelles thus enabling pH sensing both at the interstitial level and also at the sub-cellular level.

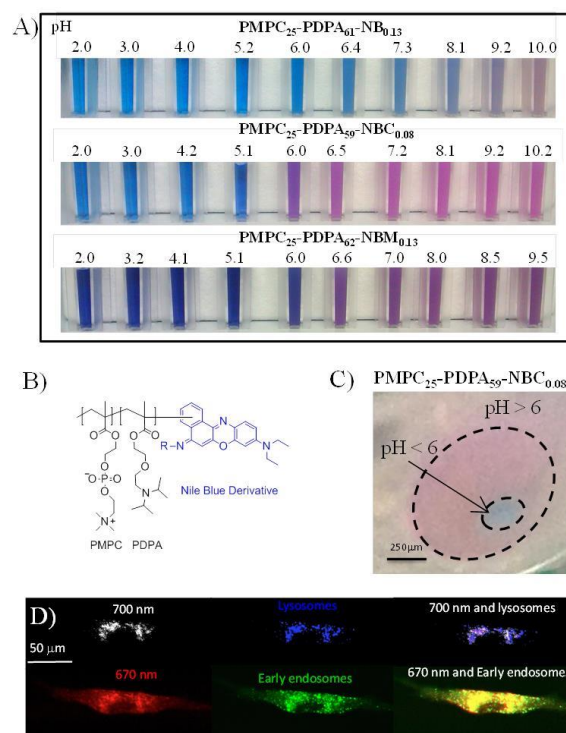


Figure 1: A) pH-dependent absorption of three PMPC-PDPA block copolymers labelled with NB dyes. B) Structure of PMPC-PDPA. C) Picture of an MCTS treated with PMPC-PDPA-NBC. D) Confocal fluorescence microscopy pictures of HDF cells treated with PMPC<sub>25</sub>-PDPA<sub>59</sub>-NBC<sub>0.08</sub> measured at 700 nm and 670 nm.

## REFERENCES

- Nadler, A. *et al.*, Angew.Chem.Int.Ed. 52:2408, 2013
- Schäferling, M. Angew.Chem.Int.Ed. 51:3532, 2012
- Lee *et al.*, N. S. Adv. Mater. 21:1344, 2009
- Wang, X.-d. *et al.*, J.Am.Chem.Soc. 134:17011, 2012
- Benjaminsen, R. V. *et al.*, ACS Nano 5:5864, 2011
- Vinci, M. *et al.*, BMC Biology 2012, 10:29
- Madsen, J. *et al.*, J.Am.Chem.Soc. 135:14863, 2013
- Massignani, M. *et al.*, Small 5:2424, 2009

## ACKNOWLEDGMENTS

EPSRC are acknowledged for funding of Post-doctoral fellowships for J. Madsen. Prof. Armes acknowledges an ERC Advanced Investigator grant. YCR is acknowledged for funding B. Ustbas. Mr. Adrian Joseph and Prof. Matthew Holley are acknowledged for their help.



# Phenotypic and Functional Sensing of Cell Microvesicles Using an Immobilized Chemosensor

Catherine Belle<sup>a</sup>, Sylvain Nlate<sup>b</sup>, Marie-Christine Durrieu<sup>b</sup>, Eduardo Angles-Cano<sup>c</sup> and Laurent Plawinski<sup>b</sup>

<sup>a</sup> UMR 5250, CNRS University Grenoble Alpes, F-38000 Grenoble, France

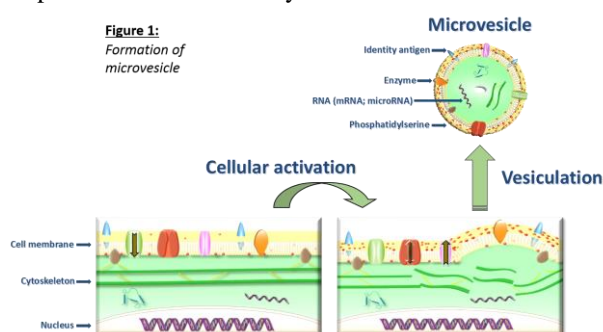
<sup>b</sup> UMR 5248, CNRS, Bordeaux University, F-33607 Pessac, France

<sup>c</sup> U1140, Inserm, University Paris Descartes, F-75006 Paris, France

[l.plawinski@cbmn.u-bordeaux.fr](mailto:l.plawinski@cbmn.u-bordeaux.fr)

## INTRODUCTION

Circulating platelets and blood cells (leucocytes, red cells) as well as endothelial cells are capable of releasing membrane microvesicles under the influence of a variety of stimuli (fig 1). Variations in the relative amount of one or the other microvesicles may be characteristically found in specific pathologies including atherosclerotic vascular disease, diabetes, cancer, rejection of cardiac transplants and inflammatory diseases<sup>1</sup>.



In addition to exposure of phosphatidylserine at the surface of the membrane, microvesicles convey surface identity antigens and/or contain biomolecules that allow their identification and functional characterization. Accordingly, detection of microvesicles and their specific functional properties open new horizons for clinical applications including patients' follow-up and treatment monitoring. Here, we propose a chemosensor capture assay based on recognition of phosphatidylserine at the surface of microvesicle by two type of functionalized synthetic dinuclear zinc complexes (fig 2).

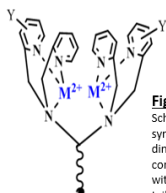


**Figure 2:** Schema of synthetic dinuclear zinc complexes with varying tail length.

## EXPERIMENTAL METHODS

To prove the concept, we first immobilized two types of chemosensors by activated 96 well-plates with polyglutaraldehyde. Secondly, microvesicles of human endothelial cell origin were incubated for 1h at room temperature. At last, the captured microvesicles were revealed by 2 techniques: immunoassay (using antibodies directed against CD105 present at the endothelial-derived microvesicle membrane) and enzyme analytic assay. This one is based on the ability of microvesicles to activate 1μM of plasminogen in the presence of a chromogenic substrate selective for plasmin (CBS 0065). Plasminogen is converted in plasmin by plasminogen activators bound at the surface of microvesicles. Thus, plasmin cleaves the chromogenic substrate and the released p-nitroaniline is detected by measuring A405nm as a function of time.

## RESULTS AND DISCUSSION

**Antigenic detection.** In fig 3, we observe a dose-dependent response, using an increasing number of microvesicles for our two types of chemosensors.

However, we observed a signal saturation with the first chemosensor (short tail; dark bar).

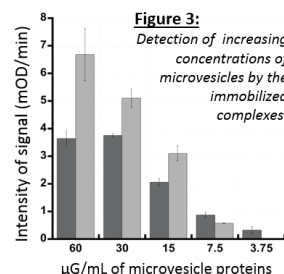
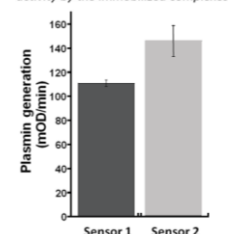


**Figure 4:** Detection of microvesicles fibrinolytic activity by the immobilized complexes



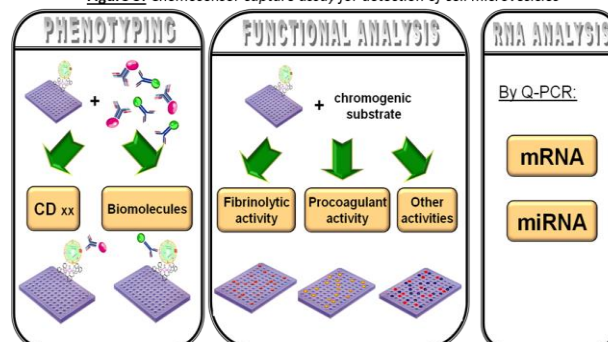
**Functional detection.** Two types of chemosensors were tested with plasminogen chromogenic assay. Fig 4 shows a better functional detection of captured microvesicles with the second chemosensor (long tail; grey bar).

## CONCLUSION

The innovation of the technology we propose is that we have identified a novel synthetic ligand (dinuclear zinc complex) for phosphatidylserine that **allows capture, origin identification** (using specific antibodies) **and functional analysis** (including fibrinolytic activity) **of microvesicles**. Our experimental development indicates no interaction of the immobilized complex with added antibodies or reagents thus ensuring specific signal detection and high sensitivity. This is a major advance as there is currently no technological procedure that may allow this versatility. The expected product (fig 5) is a kit assay in a 96-well microplate format where the functionalized complex allows (i) capture of microvesicles from plasma or other biological fluids, and (ii) their identification and characterization with provided reagents. This will be the first test assay<sup>2</sup> available for routine clinical practice that allows microvesicle characterization and can thereby be applied to the study of a number of pathologies where microvesicles are implicated.

## REFERENCES

**Figure 5:** Chemosensor capture assay for detection of cell microvesicles



1. Maule et al, *Circ Res.* 2010;107:1047-1057

2. Plawinski L et al. MPsZn2 probe Patent n°B100507FRA.

## ACKNOWLEDGMENTS

The authors thanks the U919-Inserm for financial support.

# Mass Transport Study with Fluorescent Dextran Molecules in Gellan Gum Hydrogel

Ana M. Soto<sup>1,3\*</sup>, Janne Koivisto<sup>2,3,4\*</sup>, Jenny E. Parraga<sup>2,3</sup>, Jari Hyttinen<sup>1,3</sup>, Minna Kellomäki<sup>2,3</sup>, Edite Figueiras<sup>1,3</sup>

<sup>1</sup> Computational Biophysics and Imaging Group, ELT Dept., Tampere University of Technology, Finland,

<sup>2</sup> Biomaterials and Tissue Engineering Group, ELT Dept., Tampere University of Technology, Finland,

<sup>3</sup> BioMediTech - Institute of Biosciences and Medical Technology, Finland,

<sup>4</sup> Heart Group, BMT Dept., University of Tampere, Finland,

\*equal contribution

[janne.t.koivisto@tut.fi](mailto:janne.t.koivisto@tut.fi)

## INTRODUCTION

Porosity and polymer network architecture are very important properties for hydrogels in tissue engineering and cell culture applications as cell proliferation, migration and nutrient diffusion are all dependent on pore structure<sup>1</sup>. If hydrogel is transparent, optical methods can be used for analysis of physical properties and pore structure.

In previous work, we have compared the diffusion properties of bioamine cross-linked gellan gum (GG) hydrogels using confocal microscopy technique fluorescence recovery after photobleaching (FRAP)<sup>2</sup>. The spermine (SPM) bioamine is an attractive choice to replace  $\text{Ca}^{2+}$  as cross-linker, due to the reduced interference with cellular electrophysiology. In this work we use optical projection tomography (OPT)<sup>3</sup> in the fluorescent mode to image the fluorescent dextran-FITC molecule mass transport through GG hydrogel. This technique can be used to study diffusion in mesoscopic scale to complement the more local diffusion measurement done with FRAP<sup>2</sup>.

## EXPERIMENTAL METHODS

GG and cross-linker stock solutions were made in 10 % sucrose water solutions and sterilized by filtration. The used cross-linker concentrations are 0.6 & 1.1 % -w/w SPM and 2.5 mM  $\text{Ca}^{2+}$ . The hydrogel samples were made by mixing the reagents at +37 °C inside disposable polystyrene cuvettes.

The penetration of dextran inside the hydrogel was imaged using fluorescence emission illumination mode of an in-house built OPT-system<sup>3</sup>, using only one projection. The samples were excited using a collimated LED with 470 nm (M470L3, Thorlabs) and the detection system consisted of a 5x objective, a band pass filter with center wavelength of 520 nm, tube lens and a sCMOS camera (ORCA-Flash 4.0, Hamamatsu). Images were collected every minute with an exposure time of 0.04 seconds. Dextran-FITC with molecular weights 20 kDa and 2000 kDa, 10mg/mL, were used as model diffusing agents. The imaged area is the upmost 3 mm of the hydrogel with 100  $\mu\text{L}$  of dextran solution applied on top and image acquisition started 1 min before applying the dextran. The image acquisition time was 120 min for 20 kDa and 250 min for 2000 kDa.

## RESULTS AND DISCUSSION

In Figure 1 (a), (b), and (c) can be seen the penetration of 2000 kDa dextran at 1, 111 and 250 min time points. In parallel sample Figure 1 (d), the detected fluorescence is not uniform throughout the hydrogel,

indicating that the diffusion is affected by the pore structure and the heterogeneity showed by the hydrogel.

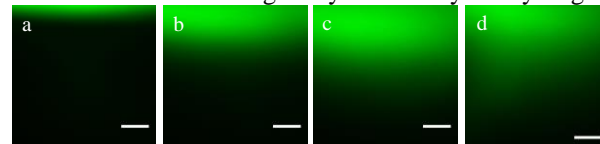


Figure 1. From a) to c): time series of dextran-FITC spreading inside the GG- $\text{Ca}^{2+}$ -hydrogel, d) example of uneven penetration at 250 min in parallel sample. Scale bar is 500  $\mu\text{m}$ .

The change in average pixel intensity at ~1.5 mm depth is plotted in Figure 2, showing penetration of dextran deeper into the hydrogel. The  $\text{Ca}^{2+}$  cross-linked GG has the highest diffusion speed and 1.1 % SPM the lowest, so their pore structure is hypothesized to be different.

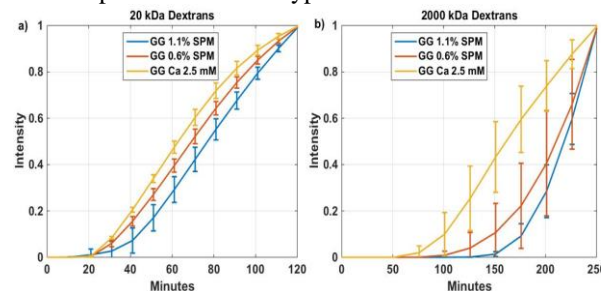


Figure 2. Normalized average pixel intensity along the middle pixel row of the image over time, a) 20 kDa, b) 2000 kDa.

The different diffusion properties can be due to different pore number, size and interconnectivity, which can also be interpreted as the density of the microstructure of the polymer network. Diffusion of the largest dextran also varies between parallel samples, indicating a threshold molecular weight, which can pass through this hydrogel easily, to be lower than 2000 kDa.

## CONCLUSION

Our study demonstrates that fluorescent molecules of known size can be used for studying the mass transport and porosity of hydrogel in an OPT setup. In this study we show how used cross-linker and its concentration affect diffusion of differently sized dextran molecules.

## REFERENCES

1. Annabi, N., *et al*, Adv Mater **26**: 85-124 2014.
2. Koivisto, J., *et al*. ESB Conference 2014.
3. Figueiras, E., *et al*, Biomed.Opt.Express **5**: 3443-3449 2014.

## ACKNOWLEDGMENTS

The authors would like to thank the Human Spare Parts project of Tekes – Finnish Funding Agency for Innovation, the Jane and Aatos Erkko Foundation and Finnish Cultural Foundation for financial support.





# The Effect of Biomolecular Interaction and Chondrocyte Adhesion to Surface Grafted Hyaluronan Layers

Erik Nilebäck<sup>1</sup>, Noomi Altgärde<sup>2</sup>, Angelika Kunze<sup>2</sup>, Lars Enochson<sup>3</sup>, Laura de Battice<sup>2</sup>, Iva Pashkuleva<sup>4,5</sup>, Jana Becher<sup>6</sup>, Stephanie Möller<sup>6</sup>, Matthias Schnabelrauch<sup>6</sup>, Rui L Reis<sup>4,5</sup>, Anders Lindahl<sup>3</sup>, Sofia Svedhem<sup>2</sup>

<sup>1</sup> Biolin Scientific, Sweden

<sup>2</sup> Dept. Applied Physics, Chalmers University of Technology, Sweden

<sup>3</sup> Dept. of Clinical Chemistry and Transfusion Medicine, Sahlgrenska Academy, Gothenburg University, Sweden

<sup>4</sup> 3Bs Research Group-Biomaterials, Biodegradables and Biomimetics, University of Minho, Portugal

<sup>5</sup> ICVS/3B's—PT Government Associate Laboratory, Portugal

<sup>6</sup> Biomaterials Dept., INNOVENT e.V., Jena, Germany

[erik.nileback@biolinscientific.com](mailto:erik.nileback@biolinscientific.com)

## INTRODUCTION

Hyaluronan (HA) is an important component in the extracellular matrix of cartilage and other tissues. It is widely used as a scaffold material and can be found in many synthetically engineered forms. Here, model HA surfaces were developed for biomolecular and cell interaction studies using surface sensitive techniques.

## EXPERIMENTAL METHODS

Biotinylated HA was immobilized to streptavidin-modified sensors compatible with quartz crystal microbalance with dissipation monitoring (QCM-D) and surface plasmon resonance (SPR).<sup>1</sup> The obtained HA surfaces were subjected to either hyaluronidase or aggrecan under liquid flow and changes of properties at/near the surface were detected by QCM-D or SPR. Hyaluronidase degradation was also studied using high-performance liquid chromatography (HPLC). QCM-D and light microscopy were combined using a dedicated measurement module to study cell attachment of chondrocytes to biotinylated HA.

## RESULTS AND DISCUSSION

HA of different degree of biotinylation was tested for enzymatic degradation by hyaluronidase with QCM-D (Fig. 1):

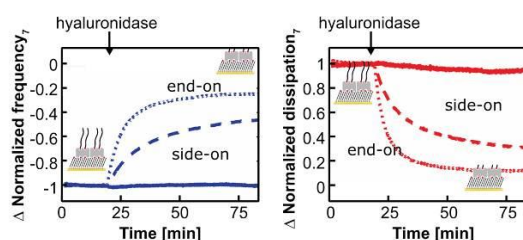


**Fig. 1:** Hyaluronidase degradation of biotinylated HA bound in a side-on (dashed, solid) or end-on (dotted) orientation. -1 to 0 in normalized  $\Delta f$  is equivalent to complete degradation.<sup>2</sup>

The HA biotinylation procedure was crucial for retained biofunctionality of the immobilised HA, where only the end-on orientation allowed for almost complete degradation. This dependency on biotinylation degree was also verified separately in bulk degradation by HPLC.

The end-on biotinylated HA was further used for cell interaction studie, including chondrocytes from human cartilage (Fig. 2):

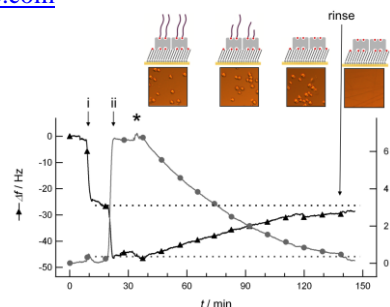


**Fig. 2:** QCM-D  $\Delta f$  and  $\Delta D$  shifts for the addition chondrocytes (marked by \*) to immobilized HA. (i) Addition of streptavidin, (ii) addition of HA. Top row: the suggested degradation process and microscopy images taken during the QCM-D experiment during incubation with cells and after rinsing with media.<sup>3</sup>

In Fig. 2 the addition of chondrocytes induced a positive  $\Delta f$  equal to removal of the HA layer. By simultaneous microscopy it could be verified that the cells were present on the sensor. Thus, QCM-D could be used to study the cell-interface interactions without the disturbance of the relatively large cellular mass.

## CONCLUSION

Control of the degree of biotinylation is crucial for retaining the functionality of surface grafted HA. End-on biotinylated HA was proven to have the most retained biofunctionality with respect to enzymatic degradation by hylauronidase. Taking a QCM-D based approach to study chondrocyte-HA interaction, it was shown that the cells degrade HA in a similar way as for the hyaluronidase study.

## REFERENCES

1. Nilebäck E. *et al*, Biosensors and Bioelectronics 28:407-413, 2011
2. Altgärde N. *et al*, Acta Biomater., 9:8158-8166, 2013
3. Nilebäck E. *et al*, Analyst, 21:5350-5350, 2014

## ACKNOWLEDGMENTS

The research leading to these results has received significant funding from the European Union Seventh Framework Programme (FP7/2007-2013) under grant agreement no NMP4-SL2009-229292 ("Find & Bind") and from the Swedish Research Council through the Linneaus program SUPRA.





## Surface Topography: Is It Clinically Relevant?

A English, A Azeem, M Biggs, A Pandit, DI Zeugolis\*

Network of Excellence for Functional Biomaterials (NFB)  
National University of Ireland Galway (NUI Galway), Galway, Ireland  
[dimitrios.zeugolis@nuigalway.ie](mailto:dimitrios.zeugolis@nuigalway.ie)

### INTRODUCTION

Two- and three- dimensional scaffold fabrication technologies (e.g. electro-spinning, fibre extrusion, isoelectric focusing and imprinting) have been at the forefront of scientific and technological research and innovation to recapitulate native tissue extracellular matrix (ECM) supramolecular assemblies. Although fibrous constructs can maintain permanently differentiated cell phenotype and to differentiate stem cells towards specific lineages *in vitro* and to induce acceptable regeneration in preclinical models, none of these technologies offers precise control over the spatial distribution of the fibres. Imprinting technologies, on the other hand, have demonstrated a diverse effect on a range of permanently differentiated and stem cell functions, including adhesion, orientation, secretome expression and lineage commitment. Despite these advancements, a comprehensive study on the influence of surface topography over different scales, ranging from nano- to micron-level, on cell function *in vitro* and on tissue response *in vivo* has yet to be elucidated.

### EXPERIMENTAL METHODS

In the present study, we employed imprinting lithography technologies to create anisotropically grooved substrates with constant width and spacing and varying depth and we subsequently assessed the influence of anisotropic topography, as opposed to isotropic topography, on tenocyte (1) and on osteoblast (2) function *in vitro* and on host tissue response *in vivo*.

### RESULTS AND DISCUSSION

**Figure 1:** DAPI (blue) and rhodamine conjugated phalloidin (red) indicates that tenocytes aligned parallel to the substrate topography on substrates with groove depths of ~317 nm and ~1988 nm. A random morphology was observed on isotropic substrates and substrates with groove depth of ~37 nm (A).

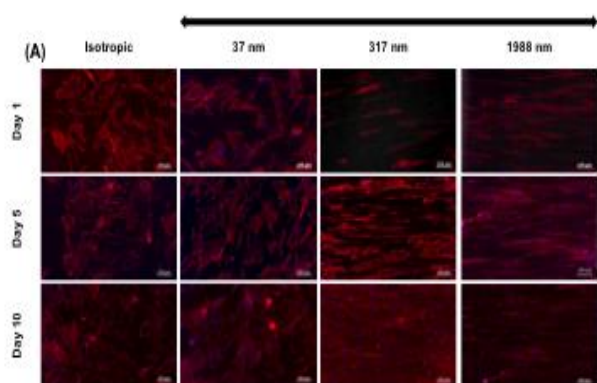
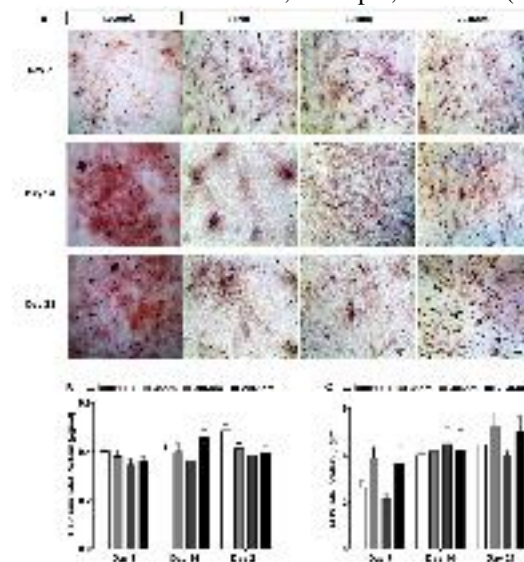


**Figure 2:** Only substrates with groove depth of ~2046 nm induced aligned mineralised matrix by day 21 (A). No significant difference between the groups was observed in calcium deposition (B). At day 7, ALP activity was significantly increased on ~35 nm and

~2046 nm in groove depth substrates, as compared to ~306 nm in depth, control and isotropic substrates (C). At day 14 and 21, no significant difference was observed in ALP activity between all structured substrates and the control, isotropic, substrate (C).



### FUTURE WORK & CONCLUSION

Topographical features in the middle nano-range (~300 nm) and low micron-range (~2000 nm), rather than in the low nano-scale (~30 nm) groove depth, induce cellular and matrix alignment and upregulation of tenogenic / osteogenic markers *in vitro*. However, these topographical features did not translate *in vitro* contact guidance, directional cell growth and matrix alignment into enhanced interfacial integration and directional neotissue formation *in vivo* in a tendon model in a bone model and in a subcutaneous study.

### REFERENCES

1. A English, A Azeem, M Biggs, E Jones, B Tripathi, N Basu, N Rooney, G Riley, A O'Riordan, G Cross, D Huttmacher, A Pandit, D Zeugolis. Biomater, Submitted
2. A Azeem, A English, P Kumar, A Satyam, M Biggs, E Jones, B Tripathi, N Basu, J Henkel, C Vaquette, N Rooney, G Riley, A O'Riordan, G Cross, S Ivanovski, D Huttmacher, A Pandit, D Zeugolis. Nanomedicine (Future in Medicine), In Press

### ACKNOWLEDGMENTS

The authors would like to acknowledge: EU FP7 Marie Curie, IAPP, Tendon Regeneration; EU FP7, NMP, Green Nano Mesh; Science Foundation Ireland; Health Research Board; Irish Research Council; Enterprise Ireland; Collaborative Centre for Applied Nanotechnology.

### DISCLOSURES

The authors declare no conflict of interest.

## Cell-Material Interaction Enhanced by Hybrid Covalent Coated Nanofibers

Joan Martí<sup>1,2</sup>, Nadège Sachot<sup>1,2</sup>, Oscar Castano<sup>1,2,4</sup>, Miguel Mateos-Timoneda<sup>1,2</sup>, Aldrik Velders<sup>5</sup>,  
Malgorzata Lewandowska<sup>6</sup>, Josep A. Planell<sup>1,2,3</sup> and Elisabeth Engel<sup>1,2,3</sup>

<sup>1</sup>Biomaterials for Regenerative Therapies, Institute for Bioengineering of Catalonia (IBEC), Spain

<sup>2</sup>Centro de Investigación Biomédica en Red en Bioingeniería, Biomateriales y Nanomedicina (CIBER-BBN), Spain

<sup>3</sup>Materials Science and Metallurgy Engineering, Universitat Politècnica de Catalunya (UPC), Spain

<sup>4</sup>Materials Science and Metallurgical Engineering, Universitat de Barcelona (UB), Spain

<sup>5</sup>BioNano Technology, Wageningen University (WU), Netherlands

<sup>6</sup>Faculty of Materials Science and Engineering, Warsaw University of Technology (WUT), Poland

[ocastano@ibecbarcelona.eu](mailto:ocastano@ibecbarcelona.eu)

### INTRODUCTION

Hybrid 3D scaffolds in regenerative medicine are used to combine the organic phase as a mechanical supporting constituent and the inorganic phase to promote bioactivity. Their potential is very promising, although several studies report some dramatically weak points, such as the fragile interaction between components which can lead to an undesirable collapse of the structure. Another problem is that the bioactive phase is often masked by the organic matrix, leading to inefficient contact with cells<sup>1</sup>.

Recently, our group found that calcium ions released by the degradation of glasses are effective angiogenic promoters because of their stimulation of a cell-membrane calcium sensing receptor (CaSR)<sup>2</sup>. Based on this, other focused tests on angiogenesis have found that Bioglasses® also have potential as angiogenic promoters even with high contents of silicon (80%); however, their slow degradation is still a problem, as the levels of silicon cannot be decreased any lower than 45%<sup>3</sup>. In this work, we propose a new generation of hybrid organically modified glass coatings (ormoglasses) that allows the Si content to be reduced, therefore speeding up the degradation process, the direct contact with cells and efficient polymer-ormoglass contact, thanks to a covalent bond. Using electrospinning as an accurate way of mimicking the extracellular matrix (ECM), we successfully produced hybrid fibrous mats with different Si, Ca and P contents and thus different calcium ion release rates and degradation.

### EXPERIMENTAL METHODS

PLA nanofibers were made by the electrospinning technique. Ormoglass nanoparticles were prepared using two composition ratios within the system SiO<sub>2</sub>:CaO: P<sub>2</sub>O<sub>5</sub> (60 S60 and 40% Si S40) by a partial hydrolyzed sol-gel method using alkoxide precursors. PLA nanofibers were coated with ormoglass nanoparticles using APTES as coupling agent. Material characterization included EDS, FE-SEM, Z-potential, contact angle, FTIR, tensile-strain assays, AFM, TGA, DSC and Ca<sup>2+</sup> release and pH evaluation. Biological characterization involved rMSCs and rEPCs adhesion and proliferation assays.

### RESULTS AND DISCUSSION

The production of different PLA coatings with two different ormoglass composition was successful. Mechanical properties, surface roughness and

hydrophilicity of coated samples increased compared to pure PLA samples, as Si content was increased.

The coated samples induced successful rMSCs and rEPCs adhesion. The 40% Si sample showed the best results in agreement with the previous blending results published by our group<sup>4</sup>. The lower the Si content, the higher the release rate of calcium and the more constant the sustained decrease at higher time points. 40% Si sample showed the best cell-material interaction (figure 1). However, the proliferation was slightly increased when the Si content was increased.

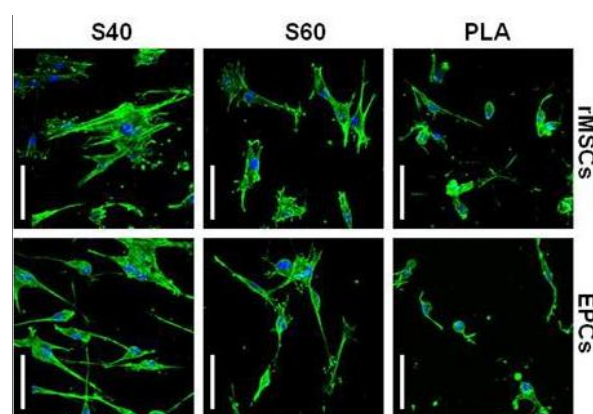


Figure 1: Adhesion after 1 day

### CONCLUSION

The total exposure of the bioactive phase to the media is possible using this novel hybrid-coating protocol. Controlling the Si content in ormoglasses allows the tailoring of important parameters such as the mechanical properties, degradability, surface roughness and layer thickness, modulating cell response.

### REFERENCES

1. N. Sachot et al. *Curr Org Chem.* 18, 18, 2299-2314 (2014)
2. Aguirre, A. et al., *Eur. Cells Mater.* 24:90-106 (2012)
3. N. Sachot et al. *J. Roc. Soc. Interface.* 10(88), 20130684. (2013)
4. O. Castano et al. *ACS Appl. Mater. Interfaces*, 28;6(10):7512-7522 (2014)

### ACKNOWLEDGMENTS

The authors would like to thank the nAngiofrac (PI11/03030) and MINECO (MAT2011-29778-C02-01) projects.



# Fibronectin Based Thin Films: Description of a Novel Growth Mechanism and Influence on Cell Behavior

Adeline Gand<sup>1</sup>, Coline Chat<sup>1</sup>, Alysée Barraux<sup>1</sup>, Guy Ladam<sup>2</sup>, Paul R Van Tassel<sup>3</sup> and Emmanuel Pauthe<sup>1</sup>

<sup>1</sup>Biomaterial for Health Group, ERRMECe, Department of Biology, University of Cergy-Pontoise, France

<sup>2</sup>Lab Biophys & Biomat La2B, MERCI, Univ Rouen, Ctr Univ Evreux, France

<sup>3</sup>Department of Chemical and Environmental Engineering, Yale University, New-Haven, CT 06520-8286, USA  
[adeline.gand@u-cergy.fr](mailto:adeline.gand@u-cergy.fr)

## INTRODUCTION

Thin films formed *via* the Layer-by-Layer (LbL) assembly of oppositely charged macromolecules are finding widespread application in energy, sensing, and biomedicine. LbL films are particularly attractive for applications involving cell-material contact, as they are easy to fabricate, can be used to modify the surface of many types of materials, irrespective of shape, and possess physicochemical properties that are readily controllable.

A key goal in the engineering of thin films is to direct the cell behavior of contacting cells. Biocompatibility and bioactivity can be improved through surface-adsorbed or film embedded macromolecules. Of particular interest is to recreate the cell micro-environment through the surface modification or functionalization with components of the extracellular matrix. Fibronectin (Fn) is an extracellular matrix protein known to play a key role in cell adhesion, spreading, migration, differentiation and proliferation<sup>1</sup>. Previous studies have demonstrated that multilayer films can be functionalized via the adsorption of Fn on a positively charged terminated layer, and promote cell adhesion and spreading<sup>2</sup>.

Here we investigate the direct incorporation of Fn as the anionic polymer during film assembly, in order to generate a thin film enriched in Fn that could better mimic the extracellular environment. We investigate the influence of Fn on a (PLL-Fn) film construction and physicochemical and mechanical properties, as well as the influence on pre-osteoblastic cells.

## EXPERIMENTAL METHODS

Film assembly is achieved by alternate dipping in polyelectrolyte solutions of opposite charge. The polyelectrolytes are poly-L-Lysine (PLL) as the polycation, and either poly-L-glutamic acid (PGA) or Fn as the polyanion (Fn is net negatively charged under near-neutral pH).

Film assembly is followed by ATR-FTIR and Quartz Crystal Microgravimetry (QCM). Information about the surface charge (zeta potential) is assessed using an electrokinetic analyzer for solid surface. Pre-osteoblastic MC3T3-E1 cells attachment and proliferation are observed by LCSM and cell counting. Fn reorganization is observed by LCSM using fluorescently labeled Fn.

## RESULTS AND DISCUSSION

The buildup process of (PLL-Fn) is followed by ATR-FTIR and QCM-D. The amide I' band area (FTIR-ATR) and the mass (QCM-D) are observed to increase with layer number, confirming the layer-by-layer growth of PLL-Fn thin films. However, film growth

appears to stall after a few layers (Figure 1). Cessation of layer-by-layer assembly is unusual – multilayer films generally follow either linear or exponential growth<sup>3</sup>.

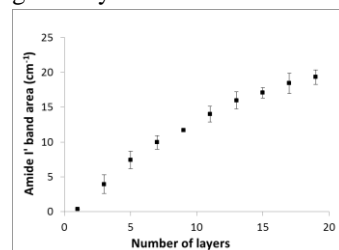


Figure 1 : Evolution of the amide I' band measured by ATR-FTIR during (PLL-Fn)<sub>10</sub> film

Our finding may suggest a new growth mechanism, with a terminated-growth regime.

Layer-by-layer assembly generally involves a charge overcompensation following each layer placement. Here we find that after a few

layers, the surface charge is not modified after PLL or Fn adsorption, comforting the hypothesis of a terminated growth for (PLL-Fn) films.

We next assess the influence of PLL-Fn thin films on pre-osteoblastic cells behavior, compared to a simple Fn monolayer. Fn coatings are known to enhance cell adhesion, spreading and proliferation. PLL-Fn films are seen to exhibit similar initial adhesion, and enhanced cell proliferation, compared to the Fn monolayer (Figure 2).

Using fluorescently labelled Fn, we find cells are able to reorganize Fn into fibrils in both

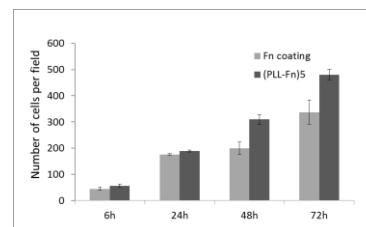


Figure 2 : Cell adhesion and proliferation monolayer coatings and PLL-Fn films. Interestingly, fibrils consume all the Fn within a monolayer following 48h, whereas unassembled Fn remains in the (PLL-Fn)<sub>5</sub> thin film even after 7 days.

## CONCLUSION

We demonstrate here the possibility of thin films enriched in Fn by direct incorporation of Fn during layer-by-layer assembly. These films present a novel growth regime that can be described as terminated growth.

Fn-based films show enhanced cell proliferation, possibly due to the extended availability of Fn for fibril formation.

## REFERENCES

1. Yamada K. *et al.*, Cold Spring Harbor Symp. Quant. Biol., LVII, 203-212, 1992
2. Wittmer C.R. *et al.*, Biomaterials, 28(5):851-860, 2007
3. Lavallo P. *et al.*, Macromolecules, 35, 4458-4465, 2002





# Primary Macrophage Phenotype Control by IL-4 Releasing, Self-Crosslinking PLL/HA-Aldehyde Derivative Multilayer Coatings

Helena Knopf-Marques<sup>1,2</sup>, Sonali Singh<sup>3</sup>, Lucie Wolfowa<sup>4</sup>, Vladimir Velebny<sup>4</sup>, Pierre Schaaf<sup>1</sup>, Amir M. Ghaemmaghami<sup>4</sup>, Nihal Engin Vrana<sup>5</sup>, Philippe Laval<sup>1,2</sup>

<sup>1</sup> INSERM UMR 1121, 11 rue Humann, 67085 Strasbourg, France

<sup>2</sup> Faculté de Chirurgie Dentaire, Université de Strasbourg, 3 rue Sainte Elisabeth, 67000 Strasbourg, France

<sup>3</sup> School of Life Sciences, University of Nottingham, Queen's Medical Centre, Nottingham, NG7 2UH, UK

<sup>4</sup> Contipro Biotech S. R. O, Dolni Dobrouc 401 561 02 Dolni Dobrouc, Czech Republic

<sup>5</sup> PROTIP MEDICAL, 8 Place de l'Hôpital, 67000 Strasbourg, France

Hyaluronic acid (HA) is a major intracellular component of connective tissues where it plays an important role in cell differentiation and growth. Although it has been widely used for tissue engineering applications, it does not support cell attachment and spreading and needs chemical modification to support cellular adhesion. In the present study, polyelectrolyte multilayer films of HA and Poly-L-lysine (PLL) were built up by layer-by-layer method, which is of particular interest for tissue engineering and surface functionalization. The principle is based on the assembly of polyanion/polycation constituting a layer pair [1-2]. The main objective was to optimize the polyelectrolyte multilayer film growth and controlled cytokine release via controlling the crosslinking of HA component. The aim is to decrease the implant and medical device failure due to adverse immune reactions by developing an innovative immunomodulatory system.

Hyaluronic acid (HA), HA-Tyramine derivative and HA-Aldehyde were produced and characterized by CONTIPRO. HA contains functional groups along its backbone that can be used to introduce functional domains. HA-Tyramine has been synthesized with tyramine moiety attached to the polymer backbone via aliphatic linker; it could be crosslinked to amino groups by a horseradish peroxidase mediated reaction. HA-aldehyde is crosslinked by hydrolytically labile imine bond between amino groups of one polymer and aldehydic derivative of HA. The polyelectrolyte (PLL/HA's) films were built by consecutive deposition of oppositely charged polyelectrolytes with a dipping robot system.

The build-up process of the multilayered films was monitored *in situ* by quartz crystal microbalance-dissipation. In first approximation, changes in the resonance frequency can be associated with a variation of the mass adsorbed on the crystal. The evolution of the thickness and of the adsorbed mass with the number of deposited layers is exponential for all of the films (Fig.1).

Confocal laser scanning microscope section images of (PLL/HA)<sub>24</sub>PLL-FITC-HA multilayer deposited on glass slides are presented in Figure 2. Confocal sections demonstrated a homogeneous fluorescence of PLL-FITC throughout the entire film thickness for all the obtained films. This may be attributed to the diffusion of mobile PLL-FITC chains in and out of the film due to interlayer mixing of HA and PLL-FITC.

In order to study the release behavior of the multilayered films, the FITC-labeled bovine serum albumin (FITC-BSA) was loaded on the top of the

films. By confocal analysis, it was observed that there is no difference on FITC-BSA adsorption for the PLL/HA's films. However, the kinetics of FITC-BSA release from the multilayered films, investigated by fluorimetry, seem to be dependent on the film crosslinking. A rapid release was observed for PLL/HA-tyramine crosslinked. On the other hand, PLL/HA-aldehyde, which presents the most rigidity property (Young Modulus ~ 38kPa), is the one that presents the lowest amount of FITC-BSA released. This is hypothesized that it is due to the denser nature of the PLL-HA-aldehyde films.

The cytocompatibility of the films has been checked with a human monocytic cell line (THP-1). HA derivatives did not cause any significant cytotoxic effect compared to PLL/HA controls.

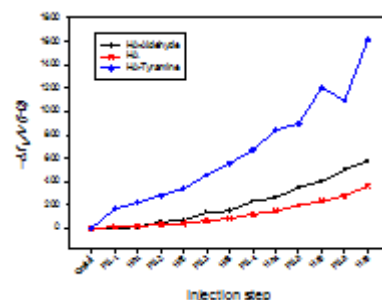


Figure 1 - Buildup (PLL/HA)<sub>6</sub> multilayer film on a SiO<sub>2</sub>-coated crystal followed by QCM-D.

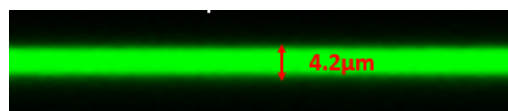


Figure 2 - Confocal cross-section image of a (PLL/HA)<sub>24</sub>PLL-FITC-HA multilayer.

The results confirmed the hypothesis that polyelectrolyte multilayer made of PLL and HA-derivatives can be successfully deposited onto the biomaterials surface. Biofunctionalization of these films can be envisioned by introducing bioactive molecules. Moreover, drug release behavior could be modulated in function of the physical property of the films. Our current focus is to use the controlled release capacities for the delivery of immunomodulatory cytokines such as IL-4 and quantification of its effect on primary macrophages.

## REFERENCES

[1] Laval, P. *et al.* Adv. Mater. 2011, 23, 1191-1221.

[2] Vrana, N.E. *et al.* J. Mater. Chem. B. 2014, 2, 999-1008.

**ACKNOWLEDGMENTS:** "This project has received funding from the European Union's Seventh Framework Programme for research, technological development and demonstration under grant agreement no. 60269.



## Biointerfaces through Continuous Electrojet-Writing

Zhaoying Li<sup>1</sup>, Xia Li<sup>1,2</sup> and Yan Yan Shery Huang<sup>1</sup>

<sup>1</sup>Department of Engineering, University of Cambridge, UK

<sup>2</sup>Department of Physics, University of Cambridge, UK

[yysh2@cam.ac.uk](mailto:yysh2@cam.ac.uk)

**We report continuous electrojet writing (cEJW) of geometrical cues for guided cell motility. cEJW allows direct-writing commonly used tissue cultureware material into controlled architectures over tens of centimetres squared. The fibre resolution can be tuned crossing three orders of magnitude, from 100nm to 100s of microns, where the combination of resolution and process flexibility is unique amongst existing bio-microfabrication.**

### INTRODUCTION

The complex, but well-defined extracellular matrix consists of topographical and adhesive features ranging from nanometres to micrometres [1]. Leveraging the control of nano- micro-topography in a biointerface, which recapitulates the intricate ECM features, opens up numerous possibilities: these range from investigating the fundamentals of mechanobiology, to elucidating cancer drug targets under well-defined laboratory conditions. However, fabricating biointerface geometries in a scalable and adaptable manner remains a challenge [2] which critically limits the translation of interface engineering for the use in day-to-day cell culture studies.

### EXPERIMENTAL METHODS

Our configuration of cEJW is processed under two distinct jetting modes for depositing fibres based on polystyrene, a standard cultureware material. Fibre deposition is achieved by a stable jet string initiated from an electrified droplet of solution material at a syringe tip. The cross-sectional profile can be controlled to either circular using N,N-Dimethylformamide (DMF) or ribbon-like using tetrahydrofuran (THF) under room temperatures and humidity. A 1D fibril-guided cell migration assay and a 3D cell scaffold were demonstrated.

### RESULTS AND DISCUSSION

#### 1. cEJW

With a continuous jet initiation mechanism, cEJW achieves large area patterning by mitigating solvent drying at the jetting nozzle. Interface patterning is facilitated over areas of tens of centimeters, even for fast-solidifying solutions. Two distinct jetting modes yield two types of building blocks: a fibril structure with a nano-wrinkled surface and a ribbon structure with a smooth surface. The 1D fibrils show both topographical and mechanical mimicry to the naturally occurring type-I collagen fibrils. The 3D scaffolds are formed by interconnected ribbon structures. The associated framework exhibits high optical transparency, providing a high quality platform for evaluating cellular behavior at different sample depths.

#### 2. Culture Models for Cancer Niche

The cellular migration on the 1D polystyrene fibrils was found to exhibit a persistent migration speed of  $\sim 65 \mu\text{m/hr}$ ; in comparison to  $\sim 36 \mu\text{m/hr}$  found for the migration taken place on a featureless PDMS surface. Compared to studies performed by Doyle *et al.* [3], who showed that fibroblasts interfacing with tracks of fibronectin less than  $2 \mu\text{m}$  width would induce a 1D migratory behavior resembling 3D, our data suggests that a similar phenotype can also be spontaneously triggered by the polystyrene fibril topology with non-specific adhesion. It may be plausible that the nano-wrinkled surface texture may have enhanced the cell-fibril interaction.

The 3D ribbon scaffold has an ultrastructure providing inter-connected channels for cell migration and penetration. Using MB231 cancer cells as a model, we observed cell attachment to the ribbon surface, as well as cell-bridging between the layer inter-space. Closer study of the cancer cells presented in different layers in show strikingly different cellular morphologies. The images also indicated a vastly heterogeneous vinculin expression across different cells within the same layer.

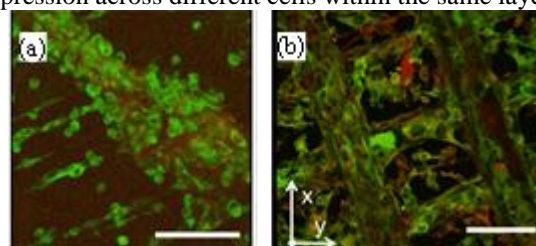


Figure 1. (a) Fibril guided cell migration; (b) a cancer niche supported by interconnected ribbons. Scale bar=100 $\mu\text{m}$ .

### CONCLUSION

In this work, we have demonstrated cEJW as a versatile and precise technique for biointerface engineering in the size regime critical for cellular geometry and topography sensing. Using polystyrene as a scaffold material, tailored architecture can be designed for different *in vitro* studies compatible with conventional culturing techniques.

### REFERENCES

1. Stevens & George, Science (2005) 310, 1135.
2. Kim *et al.* Ann. Biomed. Eng. (2012) 40, 1339.
3. Doyle *et al.* J Cell Biol. (2009) 184, 481.

### ACKNOWLEDGMENTS

X.L. acknowledges the funding support from China Scholarship Council; Y.Y.S.H. acknowledge financial support from Engineering and Physical Sciences Research Council (EPSRC, UK; EP/M018989/1)



Gregor Kemper<sup>1</sup>, Laurent Plawinski<sup>1</sup>, Emilie Pouget<sup>1</sup>, Shawn Wettig<sup>2</sup>, Reiko Oda<sup>1</sup>, Marie-Christine Durrieu<sup>1</sup>

<sup>1</sup> Institut of Chemistry & Biology of Membranes & Nanoobjects (CBMN UMR 5248, CNRS), Bordeaux University, European Institute of Chemistry and Biology, 2 Rue Robert Escarpit, 33607 Pessac, France

<sup>2</sup> University of Waterloo School of Pharmacy, 10A Victoria Street South, Kitchener ON, Canada N2G 1C5

[gregor.kemper@u-bordeaux.fr](mailto:gregor.kemper@u-bordeaux.fr)

## INTRODUCTION

Elucidation of the cues that control fate decisions of stem cells is critical in the understanding of normal development and repair, and can be utilized in tissue engineering and regeneration applications that require stem cells to be directed towards specific cell fates [1].

In fact, both biochemical and physical cues in the natural extracellular matrix (ECM) are known to play important roles in directing the differentiation of mesenchymal stem cells (MSCs) [2], [3].

In this study, we focus on how MSC adhesion and differentiation are influenced by nanohelices (with the same periodicity as Collagen I functionalized or not with RGD and BMP-2 mimetic peptides and grafted onto glass surfaces. Nanohelices presenting different lengths were used in this work.

## EXPERIMENTAL METHODS

Chiral structures with nanometric periodicity are synthesized by silica transcription of organic precursors made by auto-assembly of enantiomerically pure gemini surfactant tartrate and functionalized or not with cell adhesion peptide (RGD peptides) or/and BMP-2 mimetic peptides (Figure 1). Human mesenchymal stem cells are cultivated on these substrates and examined using scanning electron and fluorescence microscopy. Materials without peptide and/or helices act as reference surfaces.

(functionalized or not with RGD and BMP-2 mimetic peptides) and grafted onto glass surfaces.

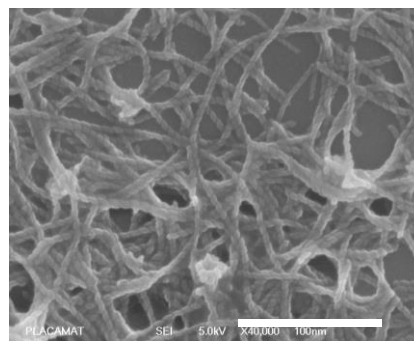


Figure 2: SEM image of helical ribbons without peptide functionalization grafted onto glass surface. Scaling bar 1  $\mu$ m.

## CONCLUSION

Helices mimicking the periodic geometry of collagen have been synthesized and functionalized. Materials grafted with these helices were synthesized.

Perspectives: Future work is going to include the evaluation of the impact of MSC differentiation using bare glass, peptide-grafted glass and helices with and without peptide functionalization grafted onto glass.

The present study also provides a tool to promote hMSC osteogenic capacity, which may be exploited in a 3D scaffold for bone tissue engineering and repair.

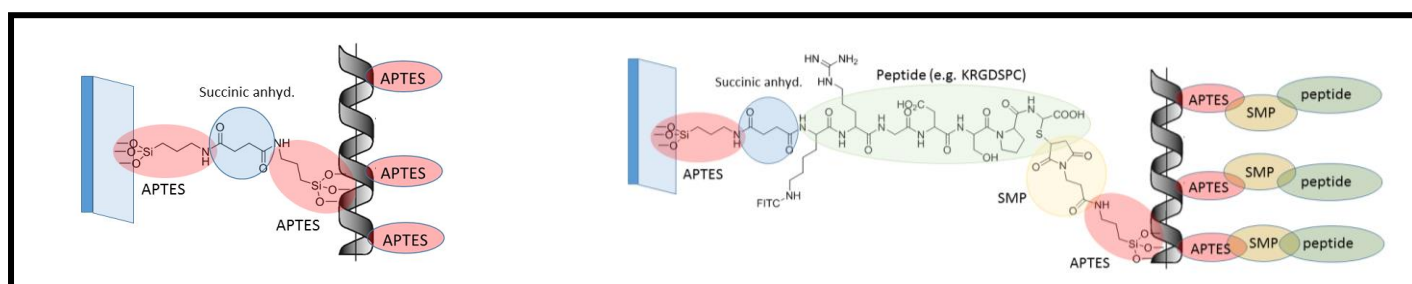


Figure 1: Grafting of unfunctionalized (left) and RGD peptide functionalized (right) helices to glass surfaces.

## RESULTS AND DISCUSSION

Each surface type was characterized by AFM, XPS, fluorescent microscopy using fluorescent peptides and SEM to validate our grafting process. Successful grafting of helical ribbons (periodicity 63.5 nm) without (Figure 2) and with peptide functionalization [4] was confirmed by fluorescence microscopy and SEM. Ongoing work focusses on the behaviour of MSC seeded on nanohelices presenting different lengths

## REFERENCES

- [1]. Huebsch N. and Mooney D. J., Nature 462: 426-432 2009
- [2]. Huebsch N. *et al.*, Nat. Mater. 9: 518-526, 2010
- [3]. Engler A. J. *et al.*, Cell 126: 677-689, 2006
- [4]. Das *et al.*, ACS Nano, 2013, 7 (4), pp 3351–3361

## ACKNOWLEDGMENTS

This project is funded by the Erasmus Mundus IDSfunmat program and takes place in cooperation with the University of Waterloo School of Pharmacy.

## Case Study of a Retrieved Trans-Femoral Bone Anchored Amputation Prosthesis

Anders Palmquist<sup>1,2</sup>, Sara H. Windahl<sup>3</sup>, Birgitta Norlindh<sup>1,2</sup>, Rickard Brånemark<sup>2,4</sup> and Peter Thomsen<sup>1,2</sup>

<sup>1</sup> Department of Biomaterials, Sahlgrenska Academy at University of Gothenburg, Göteborg, Sweden

<sup>2</sup> BIOMATCELL VINN Excellence Center of Biomaterials and Cell Therapy, Gothenburg, Sweden

<sup>3</sup> Centre for Bone and Arthritis Research, Department of Internal Medicine, Sahlgrenska Academy at University of Gothenburg, Göteborg, Sweden

<sup>4</sup> Department of Orthopaedics, Sahlgrenska Academy at University of Gothenburg, Göteborg, Sweden

[anders.palmquist@biomaterials.gu.se](mailto:anders.palmquist@biomaterials.gu.se)

### INTRODUCTION

The established treatment of trans-femoral amputees is the use of a socket-prosthesis. Mismatch in the fit between the socket and the remaining stump is a frequent problem. A solution would be to transfer the loads directly to the remaining skeleton rather than via the soft tissues. In the dental field, osseointegrated titanium implants are regarded as a routine treatment and could potentially be used in orthopaedic applications. A prospective study of 51 patients treated with an osseointegrated titanium fixture for the anchorage of an amputation prosthesis in the residual femoral limb has shown promising results.<sup>1</sup> To date, more than 100 patients have been treated with good results both in terms of function and quality of life.<sup>2</sup> In order to understand the maintenance of osseointegration in high load applications and long-term use, analysis of clinically retrieved materials is required.

### CASE HISTORY

The current case,<sup>3</sup> a female patient born 1960, suffered a high transfemoral amputation due to tumor at the age of 17. At the age of 33 she was enrolled for treatment using bone anchored prosthesis (Fig 1A). The titanium fixture suffered a fracture in 1998, however, as the majority of the fixture remained stable, a custom-made abutment was fitted to the fixture and the patient could continue to use the prosthesis. In 2004, the fixture suffered yet another fatigue fracture and it was decided to remove it. The fixture was removed with a thin collar of bone by trephine burring and immersed in formalin. The patient received a new fixture.

### EXPERIMENTAL METHODS

After formalin fixation, the sample was dehydrated and plastic embedded. A ground-section was prepared for histology and histomorphometry, and the remaining block was used for ultrastructural evaluation by scanning electron microscopy and micro-CT.

### RESULTS AND DISCUSSION

Large amount of cortical bone tissue was observed around the implant (Fig 1B-E), while predominantly trabecular bone was seen in the hollow apical region. The histomorphometric quantification of bone showed a bone-implant contact of 81% and bone area of 87% when averaging for the 29 intact threads of the ground-section. The results showed morphological evidence of osseointegration of the titanium implant from a patient

with trans-femoral amputation and demonstrates similar high amount of bone implant contact as previously observed for oral<sup>4</sup> as well as in the upper extremity.<sup>5</sup> This shows that the concept of osseointegration could be transferred to the lower extremity as well. This taken together with published studies on the quality of life for patients treated with osseointegrated amputation prosthesis<sup>6</sup> suggests that osseointegration is a promising long-term treatment option for amputees.

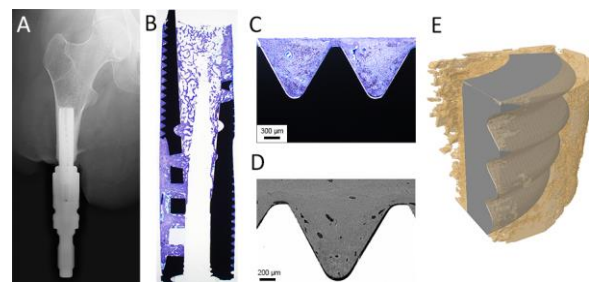


Figure 1: A) Clinical x-ray of the patient. B) Overview of the ground-section. C) Two threads filled with bone in light optical microscopy. D) One thread filled with bone in BSE. E) Segmented micro-CT image of bone surrounding the implant.

### CONCLUSION

These observations support that the osseointegration concept could be extended from the head and oral cavity to high load femoral sites, for long-term treatment of amputees.

### REFERENCES

1. Brånemark *et al.*, Bone Joint J. 96:106, 2014
2. Hagberg *et al.*, J Rehabil Res Dev. 46:331, 2009
3. Palmquist *et al.*, Acta Orthop. 85:442, 2014
4. Sennerby *et al.*, Clin Oral Impl Res. 2:103, 1991
5. Palmquist *et al.*, Acta Orthop. 79:78, 2008
6. Hagberg *et al.*, Prosthet Orthot Int. 32:29 2008

### ACKNOWLEDGMENTS

The study was supported by the Swedish Research Council (grant K2012-52X-09495-25-3), the LUA grant (ALFGBG-11128), BIOMATCELL VINN Excellence Center of Biomaterials and Cell Therapy (VINNOVA and Region Västra Götaland), IngaBritt and Arne Lundberg Foundation, Promobilia Foundation and Dr Felix Neuberghs Stiftelse, which are all gratefully acknowledged.



## Multitargeting Theranostic Nanoparticles for the Treatment of HER2-Positive Breast Cancer

Raquel Palao-Suay<sup>1,2</sup>, María Rosa Aguilar<sup>1,2</sup>, Francisco J. Parra-Ruiz<sup>1,2</sup>, Susan N. Thomas<sup>3</sup>, Nathan Rohner<sup>3</sup>, Samarendra Maji<sup>4</sup>, Richard Hoogenboom<sup>4</sup>, and Julio San Román<sup>1,2</sup>

1. Grupo de Biomateriales. Instituto de Ciencia y Tecnología de Polímeros, ICTP-CSIC. Madrid, Spain
2. Centro de Investigación Biomédica en Red, Biomateriales, Bioingeniería y Nanomedicina, CIBER-BBN, Spain
3. Thomas Lab. Georgia Institute of Technology, Atlanta, Georgia, USA
4. Supramolecular Chemistry Group. Department of Organic Chemistry. University of Ghent, Belgium  
[mraguilar@ictp.csic.es](mailto:mraguilar@ictp.csic.es)

### INTRODUCTION

Approximately 30% of breast cancers overexpress HER2 receptor that contributes to the metastatic potential and resistance to many drugs. Additionally, actual cancer therapies are highly toxic and, therefore, research is focused on the development of new treatments that selectively target cancer cells. In this sense,  $\alpha$ -TOS is considered a potent mitocan (mitochondrially targeted anticancer compound) that selectively induces apoptosis of tumor and proliferating cells [1]. For that reason, the main objective of this project was the synthesis, characterization and biological evaluation of new multi-targeting polymeric nanovehicles based on  $\alpha$ -TOS that target specifically the mitochondria of cancer cells (figure 1).

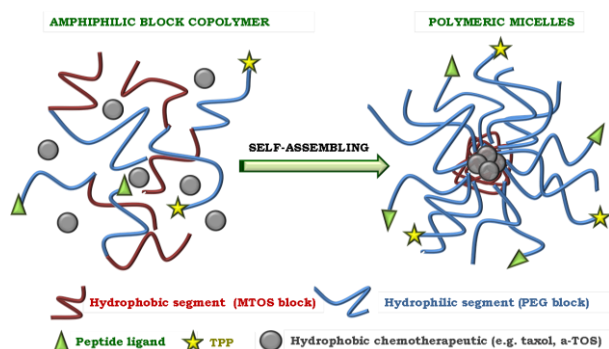


Figure 1: Scheme of new multi-targeting polymeric nanovehicles

For this purpose, block copolymers of a hydrophilic segment (PEG) and a hydrophobic segment (based on a methacrylic derivative of vitamin E, MTOS) were obtained by RAFT polymerization. The amphiphilic nature of the macromolecules and their structural homogeneity allowed to obtain self-assembled NP. Additionally, specific functional groups (triphenyl phosphonium TPP, heptamethine NIR dye IR-780 or peptide ligand LTVSPWY) were incorporated in the molecular structure of the polymers in order to target the mitochondria of HER2-positive breast cancer cells.

### EXPERIMENTAL METHODS

NP bearing targeting molecules were prepared by Self-Organized Precipitation method (SORP). These self-assembled NP were characterized by Dynamic Light Scattering and microscope techniques. Fluorescence properties of IR780-NP were measured using a microplate reader ( $\lambda_{exc}$  = 770 nm and  $\lambda_{emis}$  = 810 nm). HER2-positive breast cancer cells (MDA-MB-453) were cultured following the instructions of the manufacturer. Cell viability (Alamar Blue) in the presence of NP was tested in order to evaluate the effect of the modifications with different targeting molecules.

The endocytosis of coumarin-6 loaded NP was monitored and co-localization of NP into the mitochondria of cancer cells was performed using mitotracker green. *In vivo* biodistribution of NP was evaluated on orthotopic mammary MDA-MB-453 cells growing in athymic nude mice.

### RESULTS AND DISCUSSION

Nanoparticles bearing different targeting molecules were successfully prepared by SORP with sizes between 80 and 200 nm. TPP and IR780 modified NP had positive charge, crucial to target mitochondria. IR780-NP were fluorescent with excellent optical properties for *in vitro* and *in vivo* applications.

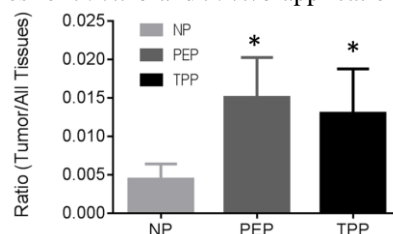


Figure 2: Comparative biodistribution [Ratio(Tumor/all Tissues)] of NP unmodified or bearing peptide ligand (PEP) and TPP.

*In vitro* biological results demonstrated a higher activity of the targeting NP in comparison to unmodified NP. Additionally, TPP and PEP decorated NP entered the cells faster than unmodified NP and preferentially localized in the mitochondria. Finally, *in vivo* biodistribution results indicated that NP with TPP and PEP had a higher accumulation in tumor in comparison to unmodified NP (figure 2).

### CONCLUSION

New block copolymers based on PEG and MTOS were obtained and multi-micellar nanoparticles were prepared with targeting moieties (TPP, IR-780 and peptide) attached to the PEG segment. Targeting molecules significantly increased *in vitro* biological activity of the NP and significantly enhanced *in vivo* NP accumulation in orthotopic breast tumor. Moreover, IR780-NP allowed visualization of NP *in vivo*.

### REFERENCES

- [1] *Journal of Controlled Release*. 2014, 182, 33-44.

### ACKNOWLEDGMENTS

The authors would like to thank the CIBER BBN-ECO program and MAT2010-14558 for providing financial support to this project.





## ROS-Generating Titanium Oxide-Based Nanoparticles for Non-Invasive Cancer Surgery with High Intensity Focused Ultrasound

Dong Gil You<sup>a,b</sup>, V.G. Deepagan<sup>a</sup>, Wooram Um<sup>b,c</sup>, Sangmin Jeon<sup>a,b</sup>,  
Ick Chan Kwon<sup>b</sup>, Kwangmeyung Kim<sup>b</sup>, Jae Hyung Park<sup>a,c,\*</sup>

<sup>a</sup> School of Chemical Engineering, Sungkyunkwan University, Suwon 440-746, Republic of Korea

<sup>b</sup> Center for Theragnosis, Korea Institute of Science and Technology, 39-1 Hawolgok-dong, Seongbuk-gu, Seoul 136-791, Republic of Korea

<sup>c</sup> Samsung Advance Institute for Health Sciences and Technology, Sungkyunkwan University, Suwon 440-746, Republic of Korea

[dbehdrf1234@naver.com](mailto:dbehdrf1234@naver.com)

### INTRODUCTION

Traditionally, surgery has been the only cure for tumour. Technological advances have catalysed a shift from open surgery towards less invasive techniques, such as radiotherapy, laser ablation and high intensity focused ultrasound (HIFU)<sup>1,2</sup>. The clinical applications of photodynamic therapy (PDT), however, have been frustrated because laser cannot reach deep tissues in the body<sup>3</sup>. Ultrasound, being widely used for diagnostic imaging, has emerged as the therapeutic modality in combination with drugs. Particularly, since ultrasound is non-invasive and permeable to the deep tissue. In this study, we designed hydrophilized TiO<sub>2</sub> nanoparticle (HTiO<sub>2</sub> NPs) which could be activated by HIFU to generate reactive oxygen species (ROS) *in vivo*. We have shown that our system can suppress the tumor growth in liver tumour model. These results prove the feasibility of using TiO<sub>2</sub> nanoparticles as sonodynamic agents for non-invasive cancer surgery.

### EXPERIMENTAL METHODS

HTiO<sub>2</sub> nanoparticles were prepared in two steps; dopamine was dissolved in deionized water (0.192 mg/ml). TiO<sub>2</sub> anatase nanoparticles were dispersed in formamide (10mg/5ml). 100 µl of dopamine solution was added and the suspension was stirred for 6 hr and purified by centrifugation and washing with formamide. For the activation of carboxylic acid group, 200 mg of carboxymethyl dextran (CMD) was dissolved in 20 ml of formamide to which 76.7 mg 1-ethyl-3-(3-dimethylaminopropyl)carbodiimide and 57.5 mg N-hydroxysuccinimide were added and stirred overnight. The activated CMD was added into 2 ml of dopamine TiO<sub>2</sub> solution and stirred for 10 hr. The HTiO<sub>2</sub> NPs were obtained after dialysis against sodium borate buffer (pH 8.6) and deionized water for 48 hr.

### RESULTS AND DISCUSSION

HTiO<sub>2</sub> NPs have a hydrodynamic radius of 188.6±39.4 nm with a zeta potential value of -15.8 mV. The TEM image and the FT-IR data confirm the presence of polymer coating around the nanoparticles. Even after 24 hours incubation in presence of fetal bovine serum, the HTiO<sub>2</sub> NPs did not show drastic increase in the size. The HIFU treated HTiO<sub>2</sub> NPs produce ROS in dose-dependent manner *in vitro*. And also, the long circulating HTiO<sub>2</sub> NPs were activated by HIFU to generate ROS *in vivo* (Figure 1). The HIFU activated HTiO<sub>2</sub> nanoparticles can up-regulate the pro inflammatory cytokines to several folds and

significantly suppress the tumour growth in a dose-dependent manner. Also, we evaluated the effectiveness of our system in treating tumor in deep region. The HIFU activated HTiO<sub>2</sub> nanoparticles can suppress the tumor growth by at least 15 folds in liver tumour model when compared with the controls (Figure2).

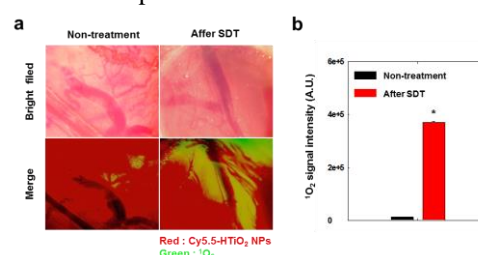


Figure 1. *In vivo* ROS generation with SDT.

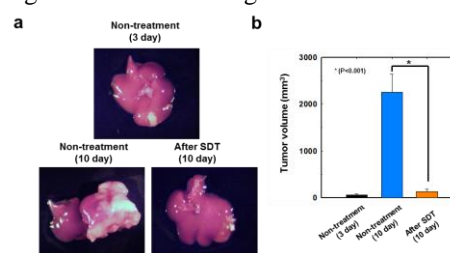


Figure 2. Anti-tumour efficacy in liver tumour model.

### CONCLUSION

In this study, we demonstrated extensive evaluation of sonodynamic cancer therapy using HTiO<sub>2</sub> NPs for the first time. Sonodynamic therapy could be a potential alternative for cancer photodynamic therapy, especially for treating deeply set tumours. With our HTiO<sub>2</sub> NPs can activate the immune-response to cancer and destroyed the tumour vessels. These results make the HTiO<sub>2</sub> NPs a suitable candidate as sonosensitizer for non-invasive cancer surgery.

### REFERENCES

1. Kennedy, J. E.; Nat Rev Cancer. 2005, 5, 321-327.
2. Kennedy, J. E., ter Haar, G. R. & Cranston, D.; Brit J Radiol. 2003, 76, 590-599.
3. Wilson, B. C.; Canadian journal of gastroenterology. 2002, 16, 393-396 (2002).

### ACKNOWLEDGMENTS

This study was funded by the GRL Project (NRF-2013K1A1A2A02050115).



## Investigation of Dendrimer-Based Nanoparticles Cellular Uptake and Cell Tracking in a Semi-Automated Microfluidic Platform

Mariana Carvalho<sup>1,2</sup>, F. Raquel Maia<sup>1,2</sup>, Rui L. Reis<sup>1,2</sup>, J. Miguel Oliveira<sup>1,2</sup>

<sup>1</sup> 3B's Research Group - Biomaterials, Biodegradables and Biomimetics, University of Minho, Headquarters of the European Institute of Excellence on Tissue Engineering and Regenerative Medicine, AvePark, 4806-909 Taipas, Guimarães, Portugal; <sup>2</sup> ICVS/3B's - PT Government Associate Laboratory, Braga/Guimarães, Portugal  
[mariana.carvalho@dep.uminho.pt](mailto:mariana.carvalho@dep.uminho.pt)

### INTRODUCTION

A microfluidic device such as Kima Pump and Vena8 biochip is able to realize functions that are not easily imaginable in conventional biological analysis, such as highly parallel, sophisticated high-throughput analysis and single-cell analysis in a well-defined manner [1].

Cancer cell tracking within the microfluidic model will be achieved by grafting fluorescent label probe Fluorescein-5(6)-isothiocyanate (FITC) to dendrimer nanoparticles allowing cell visualization by immunofluorescent staining followed by fluorescence microscopy. In this study, synthesis and physicochemical characterization of Carboxymethyl-chitosan/poly(amidoamine) dendrimer nanoparticles (CMChT/PAMAM NP's) were performed[2]. Several cancer cell lines such as a HeLa (cervical carcinoma cell line), HTTC-116 (Colon Carcinoma) and Glioblastoma cell line (GBM) were exposed to different concentrations of CMChT/PAMAM dendrimer nanoparticles over a period of 7d. After finding the adequate NP concentration, the internalization efficiency was tested, as well as cellular trafficking, in static and dynamic conditions (Kima Pump bioreactor).

### EXPERIMENTAL METHODS

CMChT/PAMAM NP's were synthesized and labelled with fluorescein isothiocyanate (FITC) according to Oliveira *et al.* [3].

To access internalization efficiency, semi-automated microfluidic platform, Vena8 Endothelial+ biochips (Cellix®, Dublin, Ireland) was used to mimic physiological flow conditions. Biochips were coated with fibronectin (Sigma, Germany) into each microchannel and placed at 4°C for overnight coating, followed by cell seeding. A solution of FITC-CMChT/PAMAM NP's at a concentration of 0.4 mg.mL<sup>-1</sup> was prepared in a complete culture medium and then transferred to Kima Pump. Perfusion was performed for 24 hrs and 48 hrs at a flow rate of 2 µL/min for 2 min. (Period I) followed by 20 min of pause (Period II).

### RESULTS AND DISCUSSION

CMChT/PAMAM NP's were successfully synthesized as shown by <sup>1</sup>H-NMR analyses. Moreover, they exhibited good physicochemical properties, with a consistent nanosphere-like shape and a diameter of ~30 nm, as shown by TEM, DLS and AFM analysis. Fluorescent-probe labelled CMChT/PAMAM NP's were found to be internalized with high efficiency by all cell types, either in conventional static conditions and when seeded and

grown in a biochip under perfusion with Kima Pump. It was found that the best flow rate was 2 µL/min (Period I), followed by a pause of 20 min. (Period II). Kima Pump bioreactor permits reaching cell confluence in dynamic conditions in just 3 hours consisting in a faster way to perform assays with lower consumption of reagents. Fluorescent probe labelled nanoparticles were found to be internalized with high efficiency in several cancer cell lines (Fig.1), either in conventional static conditions and when seeded and grown in a biochip under perfusion with Kima Pump.

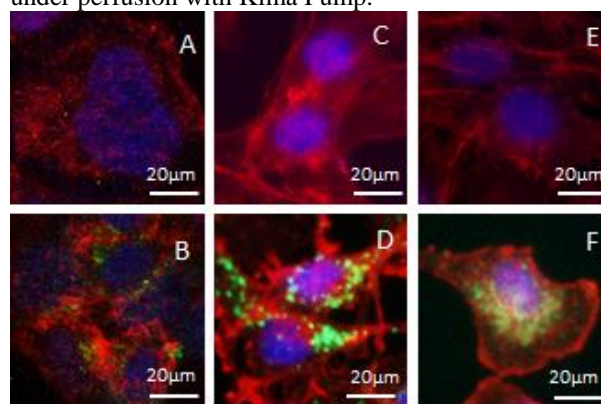


Figure 1 - Fluorescence microscopy images of HTTC-116 cells (B), GBM (D) and HeLa (F) in the presence of FITC-labelled CMChT/PAMAM NP's 0.4mg.mL<sup>-1</sup> (green) in dynamic conditions. A), C) and E) represent the same cell lines cultured in complete DMEM medium.

### CONCLUSION

CMChT/PAMAM NP's were successfully synthesized. The microfluidic platform allowed investigating the uptake of the CMChT/PAMAM NPs by different tumour cells (2D cultures) and monitor its fate in real-time. Another feature to be considered is high-resolution, real-time imaging and the possibility of *in vitro* analysis of biochemical, genetic and metabolic activities of living cells in the tumor context. The promising results encourages us to develop relevant 3D models of disease on a chip for both TE and cancer research.

### REFERENCES

- [1] Xiong B. *et al.*, Adv. Mater. 26:5525-32, 2014
- [2] Oliveira JM. *et al.*, Prog. Polym. Sci. 35:1163-94, 2010
- [3] Oliveira JM. *et al.*; Adv. Funct. Mater. 18:1840-53, 2008

### ACKNOWLEDGMENTS

The authors acknowledge the Portuguese Foundation for Science and Technology (FCT) through the project PEst-C/SAU/LA0026/201.



## Effects of SPION Loaded Hyaluronan Polymeric Micelles on Gene Expression in Normal and Cancer Cells

Kristina Nešporová<sup>1,2</sup>, Vojtěch Pavlík<sup>1,3</sup>, Daniela Šmejkalová<sup>1</sup>, Vladimír Velebný<sup>1</sup>

<sup>1</sup>Contipro Biotech, Dolní Dobrouč, Czech Republic

<sup>2</sup>Institute of Experimental Biology, Faculty of Science, Masaryk University, Brno, Czech Republic

<sup>3</sup>Department of Dermatology, Third Faculty of Medicine, Charles University in Prague, Prague, Czech Republic  
[kristina.nesporova@contipro.com](mailto:kristina.nesporova@contipro.com)

### INTRODUCTION

Superparamagnetic Iron Oxide Nanoparticles (SPIONs) are in biology and medicine utilized mostly as biocompatible contrasting and tracking agent for organs, single cells or even implanted material. For most preparations only minimal effects on cellular physiology have been reported (mainly increased oxidative stress). Hyaluronan based polymeric micelles loaded with SPIONs intended for theranostic development showed in vitro specific antitumorigenic properties on several cancer cell lines while primary cells remained viable<sup>1</sup>. For this reason mechanism of this effect was studied and gene expression analysis brought interesting results in both cancer (HT-29 cell line) and normal primary cells (dermal fibroblasts).

### EXPERIMENTAL METHODS

SPION loaded polymeric micelles (HA-SPION) were prepared by previously described method<sup>1</sup>. MTT assay and flow cytometry was used for cytotoxicity and cell death analysis. Whole human genome expression microarray (Agilent) was used for the differential analysis in control and HA-SPION treated samples. Statistical analysis was done with R (R Development Core Team) using package limma. Gene ontology terms of the significantly changed transcripts were investigated in online annotation database DAVID.

### RESULTS AND DISCUSSION

Occurrence of necrosis in cancer cells after HA-SPIONs treatment correlated with previously published data<sup>1</sup>. Normal fibroblasts showed no significant effects in both viability and cell death frequency. No effect of SPIONs themselves and HA derivatives on either cell type viability was observed. This finding is in agreement with general knowledge about iron nanoparticles, which are considered significantly less damaging to cells than for example gold nanoparticles<sup>2</sup>.

At the cellular level one of the adverse effects of iron nanoparticles might be oxidative stress. In both normal and cancer cells no increase of the concentration of ROS was detected. Interestingly, overall gene expression of proinflammatory genes (including CXCL1, IL6, CXCL2 and CCL8) even decreased in fibroblasts. Only small number of upregulated genes was detected in normal cells. Cancer cells, on the other hand, showed upregulation in lipid and steroid synthesis and metabolism (including genes like HMGCR,

CYP51A1, SCD, UGCG, ACACA, HMGCS1, LSS, SREBF1, LDLR, INSIG1, PCSK9 and ABCA1). However, these changes might be attributed to oleyl chains in HA-SPION composition. The most significant decrease was in genes of metal metabolism (metallothioneins MT1L, MT2A, MT1E, MT1B, MT1H, MT1X and MT1F) and DNA replication and repair (histons, RFC5, RPA3, PRIM1, MSH6, DTL, UNG, TIPIN, MLH1, GTF2H5, TTC5, RAD54L, RAD51, NSMCE1, RAD54B, PARP1, CCNO, NTHL1 and RTEL1).

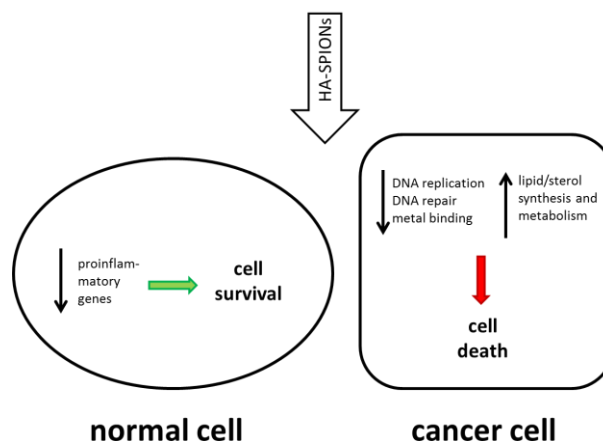


Figure 1. Different effect of SPION loaded HA polymeric micelles (HA-SPIONs) on gene expression pattern in normal and cancer cells

### CONCLUSION

Cytotoxic effect of HA-SPIONs on cancer cells is accompanied by gene expression changes in both metal binding and DNA replication and repair. This suggests that HA-SPIONs cause the impairment of iron homeostasis, crucial for DNA processing enzymes, which results in significant reduction of viability of the rapidly proliferating cells.

### REFERENCES

References must be numbered.

- Šmejkalová D. *et al.*, Biomacromolecules. 15:4012-20, 2014
- Markides H. *et al.*, J Nanomater. 2012:Article ID 614094, 2012



## Molecular Weight of Surface Immobilized Hyaluronic Acid Influences CD44-mediated Adhesion of Gastric Cancer Cells

Sara Amorim<sup>1,2</sup>, Diana Soares da Costa<sup>1,2</sup>, Daniela Freitas<sup>3</sup>, Ana Magalhães<sup>3</sup>, Celso Reis<sup>3</sup>, Rui Reis<sup>1,2</sup>, Iva Pashkuleva<sup>1,2</sup> and Ricardo Pires<sup>1,2</sup>

<sup>1</sup>3B's Research Group - Biomaterials, Biodegradables and Biomimetics, University of Minho, Headquarters of the European Institute of Excellence on Tissue Engineering and Regenerative Medicine, AvePark, 4806-909 Taipas, Guimarães, Portugal

<sup>2</sup>ICVS/3B's - PT Government Associate Laboratory, Braga/Guimarães, Portugal

<sup>3</sup>Institute of Molecular Pathology and Immunology of the University of Porto – IPATIMUP  
[sara.amorim@dep.uminho.pt](mailto:sara.amorim@dep.uminho.pt)

### INTRODUCTION

CD44, a transmembrane glycoprotein, is the major cell surface receptor for hyaluronic acid (HA).<sup>1</sup> HA is a negatively charged polysaccharide composed of repeating disaccharides of D-glucuronic acid and N-acetyl-D-glucosamine and is a naturally occurring glycosaminoglycan. It has been studied as a targeting motif in drug delivery systems for cancer therapy because several tumor cells are known to overexpress CD44.<sup>2</sup> CD44 cell surface marker is reported to have increased expression in AGS and MKN-45 gastric cell lines.<sup>3</sup> The influence of HA molecular weight (Mw) on the HA-CD44 interaction has been reported for solubilized HA.<sup>4</sup> However, this Mw influence has not been reported for surface immobilized HA, e.g. by Layer-by-Layer (LbL). In this study, the adhesion of AGS and MKN-45 cells and the influence of the HA Mw on the CD44 expression were evaluated on LbL constructs obtained through the sequential adsorption of HA and Poly-L-Lysine (PLL).

### EXPERIMENTAL METHODS

**LbL construction and CD44 adsorption:** the sequential adsorption (10 layers) of HA (6.4 kDa, 752 kDa or 1.5 MDa) and PLL (30-70 kDa), as well as the subsequent adsorption of recombinant CD44 (onto the constructs presenting HA as top layer) was monitored using Quartz Crystal Microbalance with Dissipation (QCM-D). Surpass Electrokinetic Analyzer were used to measure the Zeta potential of the complete LbL systems. **Immunostaining:** AGS and MKN-45 cells were cultured onto the LbL constructs presenting different HA Mws in the surface and the cellular CD44 expression was evaluated. Nuclei were counterstained with DAPI. **Statistical Analysis:** Shapiro-Wilk normality tests followed by Kruskal-Wallis with Dunn's Post hoc test. \*\*\* Significant differences (<0.001).

### RESULTS AND DISCUSSION

We evaluated the LbL deposition, the stability of the systems, and their capacity to adsorb CD44 as a function of HA Mw. The QCM-D data shows that the CD44 adsorption is directly dependent on the HA Mw (higher adsorption observed for higher Mws, Fig. 1b). The adhesion of MKN-45 and AGS cells to the LbL constructs (produced with the different HA Mws) presents significant differences in the number of adherent cells after 24h (Fig. 2a). Surprisingly, and in contrast with the QCM-D adsorption study, the cellular CD44 expression and the number of adherent cells was

higher for the surfaces presenting HA with lower Mw, i.e. 6.4kDa, for both AGS and MKN-45 cell lines.

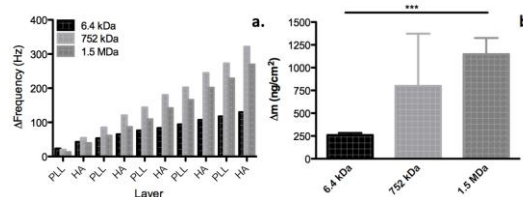


Fig. 1. LbL buildup executed using different HA Mws (a); and quantification of CD44 adsorption as a function of the HA Mws on the surface of the LbL constructs (b).

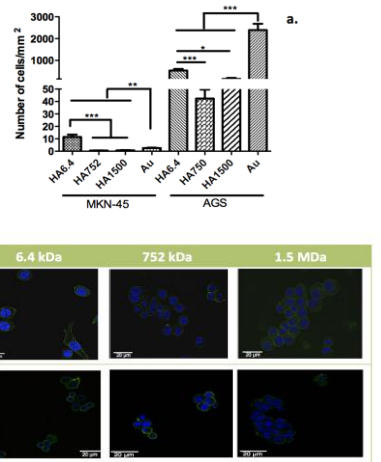


Fig. 2. Adhesion of AGS and MKN-45 after 72h (a). Immunostaining for CD44 expression (blue - nucleus; green - CD44) (b).

### CONCLUSION

Adhesion of AGS and MKN-45 cells is affected by HA Mw. AGS cells adhere faster than MKN-45, but AGS spread more in contact with 6.4 kDa HA. In the surfaces that present higher Mws the adhesion of AGS and MKN-45 depend on previously adhered cells, resulting in the formation of clusters and round-shaped cells, as well as, in a delayed CD44-independent cell adhesion.

### REFERENCES

1. Wolny *et al.*, *J. Biol. Chem.* **285**:30170–80, 2010
2. Choi *et al.*, *J. Mater. Chem.* **19**:4102, 2009
3. Takaishi *et al.*, *Stem Cells* **27**: 1006-20, 2009
4. Fuchs *et al.*, *Cell Death Dis.* **4**:e819, 2013

### ACKNOWLEDGMENTS

The authors would like to thank to EU's FP7 (FP7/2007-2013) under grant agreement n° REGPOT-CT2012-316331-POLARIS, for financial support.





# Novel Halogenated Phthalocyanines as Photosensitizers for Photodynamic Therapy for Cancer

Łukasz Łapok<sup>1</sup>, Arkadiusz Gut<sup>1</sup>, Małgorzata Cyza<sup>1</sup>, Mariusz Kępczyński<sup>1</sup>, Dorota Jamróz<sup>1</sup>, Grzegorz Szewczyk<sup>2</sup>,  
Tadeusz Sarna<sup>2</sup>, Alexandr Gorski<sup>3</sup>, Jędrzej SolarSKI<sup>3</sup>, Tadeusz Waluk<sup>3</sup>, Maria Nowakowska<sup>1</sup>

<sup>1</sup>Faculty of Chemistry, Jagiellonian University, Ingardena 3, 30-060 Kraków, Poland

<sup>2</sup>Department of Biophysics, Jagiellonian University, Gronostajowa 7, 30-387 Krakow, Poland

<sup>3</sup>Institute of Physical Chemistry, Polish Academy of Science, 44/52 Kasprzaka, 01-224 Warsaw, Poland

[lapok@chemia.uj.edu.pl](mailto:lapok@chemia.uj.edu.pl)

## INTRODUCTION

Conventional cancer treatment strategies, such as chemotherapy, radiotherapy, hormone therapy and surgery, result in severe side-effects including systemic toxicity or damage to healthy organs<sup>1</sup>. There is a need for less invasive cancer treatment technologies with significantly reduced side effects. A promising therapeutic procedures for the management of a variety of tumors is photodynamic therapy (PDT). PDT relies on the cytotoxicity of singlet oxygen (<sup>1</sup>O<sub>2</sub>) and other reactive oxygen species like O<sub>2</sub><sup>•-</sup>, OH<sup>•</sup> or HO<sub>2</sub><sup>•</sup> generated upon light-induced activation of photosensitizers. Most of the photosensitizers with established utility in PDT are macrocyclic compounds from the class of porphyrins, chlorins and corroles (e.g. Photofrin, Tookad, Foscan, Purytin, Lutrin and Levulan). Recently, photosensitizers that belong to the class of phthalocyanines (Pcs), attracted considerable attention. Phthalocyanines are organic dyes structurally related to the porphyrins. Pcs are well known for their distinct physicochemical properties such as: absorption of light in the range 600 – 700 nm, high molar extinction coefficient, usually good photochemical/chemical stability, as well as, the ability to photogenerate singlet oxygen and other reactive oxygen species (ROS).

## EXPERIMENTAL METHODS

MgPcI<sub>4</sub> was prepared from 4-iodophthalonitrile. ZnPc(t-Bu)<sub>4</sub>I<sub>4</sub> was prepared from 6-*tert*-butyl-4-iodo-1,3-diiminoisoindoline, while ZnPc(t-Bu)<sub>4</sub>(CF<sub>3</sub>)<sub>4</sub> was obtained from 5-*tert*-butyl-3-(trifluoromethyl) phthalonitrile. Compounds were characterized by <sup>1</sup>H-NMR, <sup>13</sup>C-NMR, UV-Vis, IR, MALDI-TOF-MS and elemental analysis. The quantum yield of singlet oxygen formation (Φ<sub>Δ</sub>) was determined by two methods, viz. by measuring time-resolved phosphorescence at 1270 nm and by using chemical quenchers. The interaction between Pcs and lipid bilayer in an aqueous liposomal suspension was studied using a laser scanning confocal microscopy, fluorescence technique and the atomic-scale molecular dynamics.

## RESULTS AND DISCUSSION

Challenges associated with the synthesis of Pc photosensitizers will be discussed along with spectroscopic characterization. Moreover, photophysical properties of the synthesized Pcs that are

important from the PDT perspective were evaluated and presented in Table 1. Photostabilities and photosensitization efficiencies were determined.

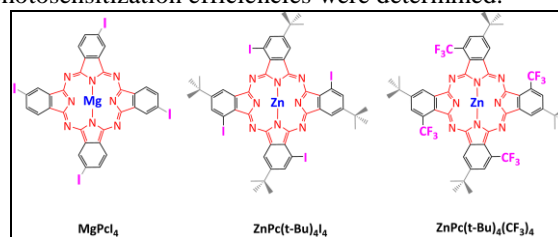


**Table 1.** Summary of photophysical and photochemical data of photosensitizers (in DMF).

Compound	$\lambda_{abs}$ (nm)	$\epsilon$ (M <sup>-1</sup> cm <sup>-1</sup> )	$\Phi_f$	$\Phi_\Delta$	$\tau_T$ ( $\mu$ s)	$\tau_f$ (ns)
MgPcI <sub>4</sub>	678	223 872	0.063	0.95	-	-
ZnPc(t-Bu) <sub>4</sub> I <sub>4</sub>	689	295 177	0.015	0.76	3.3	-
ZnPc(t-Bu) <sub>4</sub> (CF <sub>3</sub> ) <sub>4</sub>	664	157 881	0.139	0.63	131	2.5

In view of potential clinical applications, the photosensitizers were encapsulated in the liposomal carriers. The position and orientation of the Pcs molecules within the lipid bilayer and their tendency to migrate from one leaflet to the other were assessed by atomic-scale molecular dynamic simulations.

## CONCLUSION

Novel photosensitizers were developed and studied as potential PDT active agents. The halogen substituents present in the structure of Pcs induced efficient singlet-to-triplet intersystem crossing (heavy atom effect), which resulted in high quantum yields of singlet oxygen (Φ<sub>Δ</sub>). MgPcI<sub>4</sub> is among the Pcs with the highest Φ<sub>Δ</sub> ever reported for this class of compounds, viz. 0.95 ± 0.01. MgPcI<sub>4</sub> possesses limited photostability, which is advantageous in PDT therapy of cancer as rapid breakdown and clearance of photosensitizers from the patient's system after treatment is desirable<sup>2</sup>. All synthesized Pcs can be administered in liposomal formulations.

## REFERENCES

1. Krantz F. *et al.*, Drug Delivery in Oncology, Vol. 1-3, Wiley-VCH GmbH & Co. KGaA, 2012.
2. Łapok Ł. *et al.*, J. Photochem. Photobiol. A: Chemistry 286:55-63, 2014.

## ACKNOWLEDGMENTS

Work supported by NCN grant, DEC-2011/03/D/ST5/05910.



# The Role of Electrical Stimulation in Tendon Maintenance and Repair: Electrospun Poly (vinylidene fluoride-co-trifluoroethylene) /Boron Nitride Nanotubes as Bioactive Scaffold for Promoting Tendon Regeneration

Marc A. Fernandez-Yague<sup>1</sup>, Gemma Orpella-Aceret<sup>1</sup>, Ghazal Tadayyon<sup>1</sup>, Matteo Palma<sup>2</sup>, Abhay Pandit<sup>1</sup>, Dimitrios Zeugolis<sup>1</sup> and Manus J.P Biggs<sup>1</sup>

<sup>1</sup>Network of Excellence for Functional Biomaterials (NFB), National University of Ireland, Galway

<sup>2</sup>Department of Chemistry, School of Biological and Chemical Sciences, Queen Mary, London

[m.fernandez2@nuigalway.ie](mailto:m.fernandez2@nuigalway.ie)

## INTRODUCTION

Artificial scaffolds mimicking the morphology, mechanical properties and biochemical complexity of natural tissues are of vital importance for tissue engineering applications. Tendonous tissues are comprised of aligned collagen fibrils providing topographical guidance for cells and mechanical strength; however, an often-overlooked physical property of collagenous tissues is an inherent piezoelectric response, which is speculated as having a functional role in musculoskeletal homeostasis<sup>1,2</sup>.

Piezoelectric materials can exploit the loading capacity of tendon tissue to produce stimulating current, which, is important for tissue repair. In this study, a piezoelectric fibrous scaffold is developed from Poly (vinylidene fluoride-co-trifluoroethylene) P(VDF-TrFE), a material capable of generating electrical charges under mechanical loading in physiological conditions to maintain cell tenogenic phenotype. In addition, fiber alignment for adequate topographic guidance of the cells and piezoelectric properties are controlled through the incorporation of Boron Nitride Nanotubes (BNNT) which have same structure as MWCNT but present piezoelectricity.

## EXPERIMENTAL METHODS

P(VDF-TrFE) is dissolved in DMF/Acetone and electrospun into fine fibers by changing the voltage, mandrel rotation speed and the distance between tip and collector with a constant flow rate. To improve the mechanical and electrical properties, BNNT are coated with amphiphilic polyvinyl pyrrolidone (PVP) using an ultrasonication process and incorporated into the matrix. The scaffold morphology is observed by FESEM and the electrical properties in response to cyclic loading are assessed with piezoresponse microscopy (PFM) and an in-house oscilloscope/dynamic loading system. Primary Human Tenocytes are isolated and cultured for 1, 3, 7 and 14 days onto the scaffolds under static and mechanical loading conditions. Samples are stained for focal adhesions (FA) using an anti-vinculin antibody. The number of FA and its length is counted using confocal microscopy and analyses by means of software (ImageJ 1.49c). Proliferation of cells is assessed via Alamar blue® and gene expression is evaluated by RT-PCR using different markers such as Osterix, Osteocalcin, Collagen Type I and GAPDH.

## RESULTS

PFM measurements show that the incorporation of 0,1% w/w of BNNT result in an increase on the piezoelectric behaviour. Thus, the coercive voltage after

incorporation of BNNT is 3,8 V rather than 1,2 V for pristine polymer. The results show that PDVF-TrFE/BNNT scaffolds have no cytotoxicity and stimulate differentiation; attachment and growth of tenocytes on scaffolds. In addition, the results show that cell morphology and focal adhesion distribution in cells cultured on composite scaffold are distinctly different from those on pristine scaffold. Tenocytes grown on the composite scaffolds exhibited a more elongated and spread morphology while cells on pristine scaffolds are not well-spread.

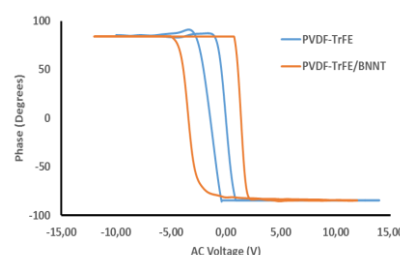
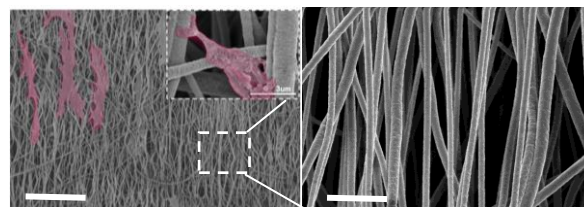


Figure 1 a) show PVDF-TrFE scaffold guiding cells b) Hysteresis loop showing higher coercive voltage for PVDF-TrFE/BNNT sample.

## CONCLUSION

This study shows that the physical properties of piezoelectric PVDF-TrFE/BNNT fibers can be readily controlled by incorporation of BNNT by electrospinning. Moreover, the tenocyte phenotype is maintained up to 14 days under mechanical loading on these fibres.

## REFERENCES

1. Lee B. *et al.*, Nature Nanotechnology 7, 351–356, 2012
2. Denning, D. *et al.*, B. J.. Acta Biomater, 8, 3073–3079, 2012

## ACKNOWLEDGMENTS

Science Foundation Ireland, Starting Investigator Research Programme, 11/SIRG/B2135; (FP7/2007-2013), PCIG13 GA-2013-61886



# Patterned Thermoresponseive pNIPAM-pHEMA Hydrogels for Corneal Repair

Cemile Bektas<sup>1,2</sup> and Vasif Hasirci<sup>1,2,3</sup>

Departments of <sup>1</sup>Biological Sciences and <sup>2</sup>Biotechnology METU, Turkey

<sup>3</sup>BIOMATEN, Center of Excellence in Biomaterials and Tissue Engineering, METU, Turkey

[kcemile@metu.edu.tr](mailto:kcemile@metu.edu.tr)

## INTRODUCTION

The cornea is the most exterior protective barrier of the eye and serves as the principal optical element of the eye by refracting 70% of the incoming light<sup>1</sup>. Cornea has a layered structure consisting of 200-400 lamellae that are orthogonal to each other forming a plywood-like structure<sup>2</sup>. It is very difficult to mimic the natural organization with the various approaches tested until now due to the thickness and orthogonal arrangement which is not possible with sheets or fibers<sup>3</sup>. This study aims to construct a cornea by combining cell sheet engineering to mimic the natural micro environment of the cornea by using thermo-responsive surfaces created by poly(N-isopropylacrylamide) (pNIPAM) with tissue engineering approach by using photoresponsive methacrylated gelatin (GelMA) hydrogels to surround the aligned cell sheets for higher stability and integration. Micropatterned NIPAM-HEMA films were used as the micropatterning tool for the cell sheets produced and swelling properties against temperature were studied. Methacrylated gelatin was synthesized and gelation under UV in 1 min. was achieved.

## EXPERIMENTAL METHODS

Micropatterned NIPAM-HEMA films were prepared by UV crosslinking in the presence of ethylene glycol dimethylacrylate (EGDMA) as the crosslinker and azobisisobutyronitrile (AIBN) as the photoinitiator onto a micropatterned silicon wafer with ridge-valley patterns (Figure 1). Micropatterns were clearly visible under the stereomicroscope. The temperature response (swelling) of the pNIPAM-pHEMA discs were studied in the temperature range 20-37 °C gravimetrically. Methacrylated gelatin (GelMA) was synthesized from type A porcine skin gelatin by dissolving in PBS and crosslinking under UV in the presence of photoinitiator (2-(hydroxyl)-4-(2-hydroxyethoxy)-2-methylpropiophenone).

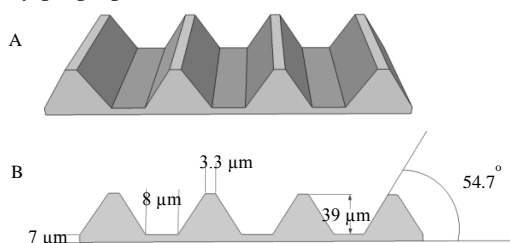


**Figure 1:** Template for patterned films. A) Schematic representation of the surface of the template and B) dimensions of the template.

## RESULTS AND DISCUSSION

In order to produce micropatterned pNIPAM films various isopropanol:water ratios (1:1 to 9:1) were used. Pattern sharpness was enhanced when isopropanol proportion was increased and 9:1 ratio yielded the best patterns but made them brittle. In order to improve the handling and strength of the film poly(2-hydroxyethyl

methacrylate) (pHEMA) (1 to 5% wrt NIPAM) was added to the composition. Higher pHEMA decreased the water contents of the hydrogels (Figure 2) but did not affect the diameter change. The swelling difference was almost 14 fold with pure NIPAM and the lowest change was 8 fold with NH5 at RT. The rate of change from hydrophilic to hydrophobic was not very rapid. All the samples reached equilibrium swelling within 60 min. With higher pHEMA content suturability was better but flexibility was lower. As a result NH3 was chosen as the optimum property product. Meanwhile, to be used at the final step of production of cornea substitute to cover the aligned cell sheets, methacrylated gelatin was synthesized. Gelation took place in 1.5 min for 5% and in 8% GelMA hydrogels in PBS. Results were promising in the way of creating a full thickness cornea.

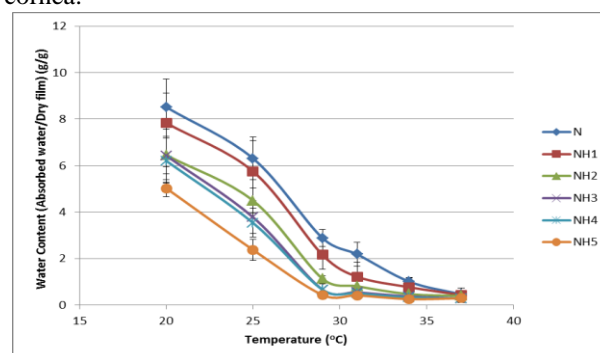


**Figure 2:** Degree of swelling of the pNIPAM-pHEMA films at different temperatures. pHEMA fraction in the composition was shown as NH1 to represent 1% HEMA and so on.

## CONCLUSION

In this current study it was aimed to construct a cornea by using tissue engineering and cell sheet engineering approaches. Temperature responsive NIPAM-HEMA surfaces were created to obtain cell sheets. Characterization of these surfaces showed that increasing pHEMA concentration in the composition leading to decreased swelling properties but enhanced the durability of the hydrogels as understood from the suturability tests. To cover the aligned cell sheets GelMA hydrogels were created 1 min crosslinking times was achieved under UV with 8% GelMA.

## REFERENCES

- 1- Liu, Z. et al., *The British Journal of Ophthalmology*, 83:774–778, 1999.
- 2- Ruberti J. W. et al., *Principles of tissue engineering* (third edition) (pp. 1025-1047), 2007.
- 3- Lawrence B. D. et al., *Biomaterials*, 30(7):1299-1308,2009

## ACKNOWLEDGMENTS

The authors would like to acknowledge to BIOMATEN and the financial support from METU BAP-01-08-2013-003 and BAP08-11-DPT-2011-K120350 projects and TÜBİTAK for the BİDEB 2211 Scholarship.





## Macromolecular Crowding in Corneal Fibroblasts Culture Accelerates the Production of Extracellular Matrix-rich Supramolecular Assemblies

Pramod Kumar, Abhigyan Satyam, Kyriakos Spanoudes, Abhay Pandit and Dimitrios I. Zeugolis

Network of Excellence for Functional Biomaterials, National University of Ireland Galway Ireland

[dimitrios.zeugolis@nuigalway.ie](mailto:dimitrios.zeugolis@nuigalway.ie)

### INTRODUCTION

Therapeutic strategies based on tissue engineering by self-assembly put forward the notion that functional regeneration can be achieved by utilising the inherent capacity of cells to create highly sophisticated supramolecular assemblies similar to the native tissue. However, very few products have reached the clinic, due to the prolong culture time required to develop an implantable device<sup>1</sup>. Corneal stromal cells require 35-84 days in culture to build a cohesive stromal substitute, which is poor in extracellular matrix (ECM) and thinner than the native tissue<sup>2,3</sup>. Macromolecular crowding (MMC), the addition of inert macromolecules in culture media, can significantly accelerate the cell specific ECM deposition within two days of culture, without any phenotypic changes<sup>4</sup>. Herein, the role of MMC on human corneal fibroblasts (HCFs) culture was assessed.

### EXPERIMENTAL METHODS

HCFs cultured under MMC (100  $\mu$ g/ml dextran sulphate (DxS); 37.5mg/ml Ficoll™ 70 and 25mg/ml Ficoll™ 400; and 75  $\mu$ g/ml Carrageenan (CR)) for 2-6 days. ECM deposition was analysed by SDS-PAGE, immunocytochemistry (ICC), atomic force microscopy (AFM) and proteomic analysis. Gene expression was assessed using the qRT-PCR. Intact HCFs cell sheets were developed using NIPAAM/n-tert butyl acrylamide (65% + 35%) thermal responsive polymer and characterised using van-Geison/Masson's trichrome staining, ICC and absorbance assay at visible light.

### RESULTS AND DISCUSSION

ECM is one of the most vital elements of tissue engineering and plays an active role of scaffold and growth factor reservoir in scaffold free cell based therapy. The MMC of HCFs with DxS, CR and FC significantly increase the collagen type I deposition ( $p < 0.005$ ). The immunofluorescence further confirmed the more aligned organization of ECM in the presence of MMC. The higher ECM deposition also promotes the development of cell sheet which show good light transmittance behaviour. Thus, the deposited ECM does not compromise the transmittance of the cell sheet<sup>5,6</sup>.

**Table 1:** Significant increase in several ECM peptides and total proteins deposition was observed at day 6 of FC treatment, whilst,  $\alpha$ -SMA, a myofibroblast marker remains unchanged.

Peptides	Change
Total proteins, Histone H4, Fibronectin, Collagen $\alpha$ -1(I), Collagen $\alpha$ -2(I), Collagen $\alpha$ -3(VI), Collagen $\alpha$ -1(VI)	Significant increase
$\alpha$ -SMA, Vimentin	No change

**Figure 1:** Densitometric analysis of SDS-PAGE (A), immunocytochemistry (B, E), van-Geison staining (C) and Trichrome's staining (D) demonstrate enhanced ECM deposition in the presence of MMC.

Light transmittance assay (F) and AFM analysis (G) confirmed the ECM rich nature of developed cell sheet without affecting the light transmittance.

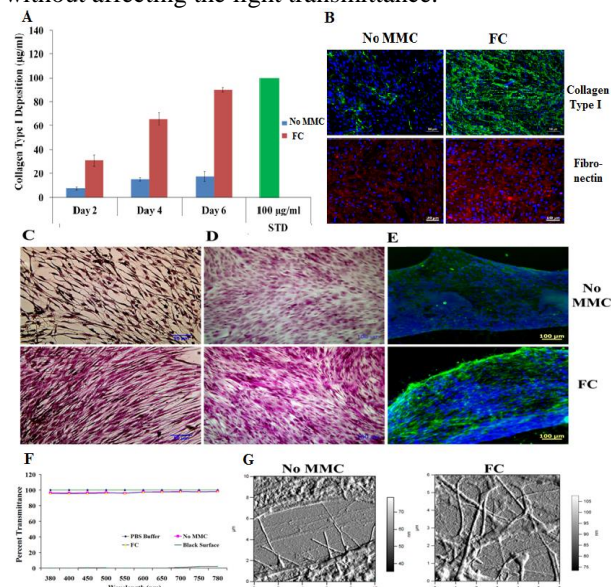
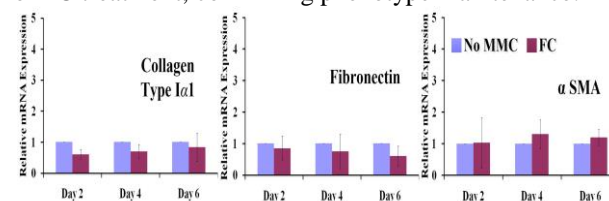


**Figure 2:** No change in mRNA expression for collagen type I, fibronectin or  $\alpha$ -SMA was evidenced up to day 6 of FC treatment, confirming phenotype maintenance.



### CONCLUSIONS

MMC significantly accelerates corneal specific ECM deposition and favours the development of ECM rich HCFs cell sheets. Thus, MMC provides an alternative approach in the field of cell-based therapies for corneal stromal repair with considerable clinical implications.

### REFERENCES

1. Peck M. *et al.*, Mater. Today, 14:218-224, 2011
2. Proulx S. *et al.*, Mol. Vis. 16:2192-2201, 2010
3. Vrana N. *et al.*, Invest. Ophthalmol. Vis. Sci. 49:5325-5331, 2008
4. Satyam A. *et al.*, Adv. Mat. 26:3024-3034, 2014
5. Kumar P. *et al.*, Tissue Eng. Part- C In Press
6. Kumar P. *et al.*, Sci. Rep. In Press

### ACKNOWLEDGMENTS

College of Engineering and Informatics, National University of Ireland Galway, Ireland & Science Foundation of Ireland for providing the financial support (Grant-07/IN1/B031& 09/ RFP/ENM2483).

### DISCLOSURES

The authors have no financial interests to declare.



## Elaboration and Evaluation of Alginate Foam Scaffolds for Soft Tissue Engineering

Raya Bushkalova<sup>1,2</sup>, Caroline Ceccaldi<sup>1,2</sup>, Christophe Tenailleau<sup>2</sup>, Benjamin Duployer<sup>2</sup>, Philippe Bourin<sup>3</sup>, Daniel Cussac<sup>1,4</sup>, Angelo Parini<sup>1,4,5</sup>, Brigitte Sallerin<sup>1,4,5</sup> and Sophie Girod-Fullana<sup>2</sup>.

<sup>1</sup>INSERM UMR 1048, Toulouse, 31432 France

<sup>2</sup>Institut Carnot CIRIMAT, Université Paul Sabatier, Toulouse, 31062 France

<sup>3</sup>Etablissement Français du Sang, Laboratoire de Thérapie Cellulaire, Toulouse, 31027 France

<sup>4</sup>Université Paul Sabatier, Faculté des Sciences Pharmaceutiques, Toulouse, 31062 France

<sup>5</sup>CHU Toulouse, Pôle Pharmacie, Toulouse, 31432 France

[raya.bushkalova@inserm.fr](mailto:raya.bushkalova@inserm.fr)

### INTRODUCTION

Recent studies have demonstrated the benefits of polymeric 3D scaffolds seeded with various cell types for the regeneration of heart<sup>1</sup>, kidney<sup>2</sup> and liver<sup>3</sup>. Since the past decades, there is a growing interest in the use of bone marrow mesenchymal stem cells (MSCs) to regenerate tissues after acute and chronic diseases through the secretion of paracrine factors<sup>4</sup>. MSC delivery to the targeted organ via a 3D biomimetic scaffold may present several advantages in comparison with direct cell injection, including cell retention on the injury site and improved viability and secretion. The success of this therapeutic strategy lies on the scaffold design, as its biocompatibility and architecture influence host's reaction and implanted cells fate. In this context, we describe here the design of alginate foam scaffolds specifically tailored for MSC immobilization and improvement of their therapeutic effects on soft tissues.

### EXPERIMENTAL METHODS

Alginate foams were produced by mixing alginate solution with a pore-forming agent and various surfactants acting as foam stabilizers. After cross-linking, rinsing and lyophilisation, macroporous sponges were obtained and characterized by Fourier-Transformed Infra-Red spectroscopy (FTIR), scanning electron microscopy (SEM) and micro-computed tomography (micro-CT). Their mechanical and rheological properties were also studied in order to evaluate their accordance with soft tissue characteristics. Cell seeding within scaffolds and quantification of cell metabolic activity was evidenced by Live/Dead<sup>®</sup> and AlamarBlue<sup>®</sup> assays, respectively. Finally, cell secretion function was investigated by the quantification of HGF, FGF-2 and VEGF released in the supernatant of MSC-loaded scaffolds.

### RESULTS AND DISCUSSION

Whatever the formulation tested, highly interconnected porous scaffolds (fig. 1A) were obtained, with pore sizes suitable for 3D cell culture (100-230  $\mu\text{m}$  on

surface and in cross-section, determined by micro-CT). All scaffolds exhibited storage moduli higher than their loss moduli, thus confirming a well-structured polymeric network. Their mechanical properties were in the range of the elastic moduli of soft tissues (alginate foams: 10-27 kPa; soft tissues: 1-20 kPa). FTIR analysis confirmed the efficacy of the rinsing steps, warranty of alginate scaffolds' preserved biocompatibility. The generated porosity allowed an efficient cell seeding in-depth (fig. 1B), and the metabolic activity of the seeded MSCs was maintained during 14 days showing the good in vitro biocompatibility of all the scaffolds. In addition, the MSC secretion level measurements revealed that growth factors release was globally improved in comparison with control alginate scaffolds (VEGF:  $p < 0.05$ ; HGF and FGF2:  $p > 0.05$ ).

### CONCLUSION

Our work presents for the first time a comparative study of the use of various surfactants associated with alginate to generate highly porous (foam-based) scaffolds with tunable properties for soft tissue engineering with MSCs. By varying the surfactant type, various microarchitectures were generated, together with different secretion profiles of the seeded MSCs, which could give rise to different biological effects in vivo. Associating MSCs with alginate foam-based scaffolds appears as a promising strategy to improve soft tissues cell therapy.

### REFERENCES

1. Ceccaldi C. *et al.*, Cell Transplant. 21:1969-84, 2011
2. Trouche E. *et al.*, Cell Transplant. 19:1623-33, 2010
3. Dvir-Ginzberg M. *et al.*, FASEB J. 22:1440-9, 2008
4. Mias C *et al.*, Stem Cells. 27:2734-43, 2009
5. Leor J. *et al.*, Ann N Y Acad Sci. 1015:312-9, 2006

### ACKNOWLEDGMENTS

This work was supported by CNRS, Région Midi-Pyrénées and INSERM grants.

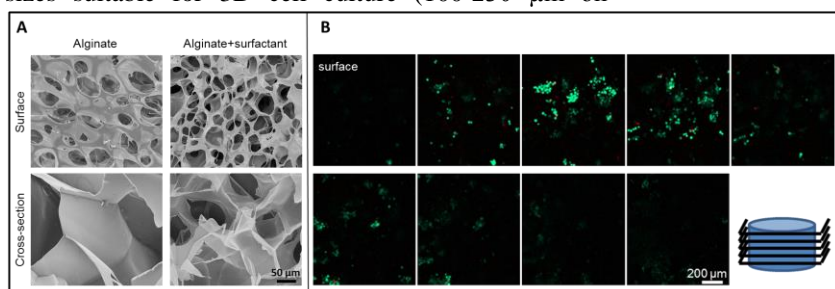


Fig.1 A) SEM images of the surface and cross-section porosity of a foam scaffold in comparison with a control alginate scaffold. B) Confocal z-planes of a MSC-seeded foam scaffold after a Live/Dead staining (live cells appearing in green and dead cells in red).

## Polyhydroxyalkanoates, a Family of Natural Polymers and their Application in Cardiac Tissue Engineering

Ipsita Roy<sup>1</sup>, Andrea Bagdadi<sup>1</sup>, Prachi Dubey<sup>1</sup>, Ranjana Rai<sup>1</sup>, Jonathan Knowles<sup>2</sup>, Aldo R. Boccaccini<sup>3</sup>, Mohan Edirisinghe<sup>4</sup> and Sian Harding<sup>5</sup>

<sup>1</sup>School of Life Sciences, University of Westminster, London, UK

<sup>2</sup>Division of Biomaterials and Tissue Engineering, UCL EDI, London, UK

<sup>3</sup>Department of Materials Science and Engineering, University of Erlangen-Nuremberg, Germany

<sup>4</sup>Department of Mechanical Engineering, UCL, London, UK

<sup>5</sup>National Heart and Lung Institute, Imperial College, London, UK

[royi@wmin.ac.uk](mailto:royi@wmin.ac.uk)

### INTRODUCTION

Polyhydroxyalkanoates (PHAs) are water-insoluble storage polymers which are polyesters of hydroxyalkanoic acids, produced by a variety of bacterial species<sup>1</sup>. They are biodegradable and biocompatible, exhibit thermoplastic properties and can be produced from renewable carbon sources<sup>1</sup>. In this work we have focussed on the use of PHAs in cardiac tissue engineering applications. Myocardial infarction (MI) and congestive heart failure (CHF) are the main cardiovascular diseases. Cardiac patches aim to facilitate the normal functioning of the heart muscle by providing repair and support to the infarcted tissue; post MI. The main objective of this study was to fabricate cardiac patches using Poly(3-hydroxyoctanoic acid), P(3HO), which would be able to mimic the structure and functionality of the cardiac muscle.

### EXPERIMENTAL METHODS

The production, characterisation and production of P(3HO) solvent cast films were carried out as in Rai *et al.*, 2010<sup>2</sup>. Surface functionalized porous patches were developed using the particle leaching method and electrospinning. Cell culture involved the use of the specific cell line and proliferation was measured using the MTT Assay.

### RESULTS AND DISCUSSION

**Production and characterisation of P(3HO):** P(3HO) was successfully produced, extracted and purified. GC-MS and NMR results confirmed that the PHA produced was Poly(3-hydroxyoctanoate), i.e. P(3HO).

#### Material Characterisation:

The  $T_g$  and  $T_m$  for P(3HO) were  $-34.86^\circ\text{C}$  and  $45.62^\circ\text{C}$  respectively. The Young's modulus, % elongation at break and the tensile strength, was  $3.7 \pm 0.3\text{MPa}$ ,  $299 \pm 29\%$  and  $2.8 \pm 0.1\text{MPa}$ , respectively. Porous patches and surface functionalised patches with electrospun fibres, VEGF and RGD peptide were produced.

#### Biocompatibility Studies:

*In vitro* studies using C2C12 cells were conducted on these patches. The porous patches containing random fibres on the surface showed the highest cell proliferation rate. Also, the % proliferation of C2C12 cells in the VEGF and RGD peptide modified P(3HO) patches was found to be much higher as compared to only VEGF or only RGD peptide containing patches.

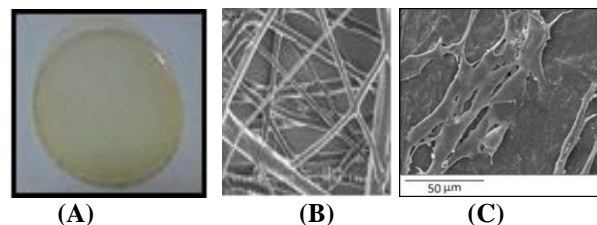


**Figure 1:** P(3HO) (A) neat patch (B) with fibres (C) C2C12 cells proliferation on the P(3HO) patch

Adult ventricular cardiomyocytes were seeded on P(3HO) films, the cells survived well and their contractile parameters were maintained.

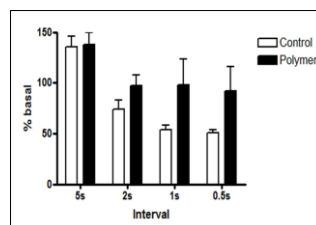


**Figure 2:** Contraction amplitude of adult ventricular cardiomyocytes stimulated to beat at different intervals on glass and P(3HO).

Human induced pluripotent stem cells derived cardiomyocytes (hiPSC-CM) were seeded on P(3HO) and gelatin (control). The cardiomyocytes were live and healthy on the P(3HO) constructs. The beating rate on the control was  $33 \pm 1.53$  beats/min while that on P(3HO) construct was  $42.0 \pm 2.52$  beats/min.

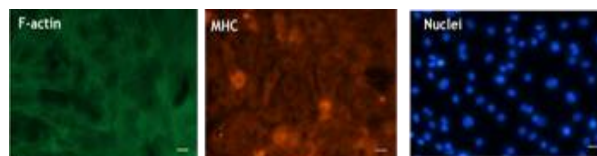


**Figure 3:** Immunohistochemistry analysis for P(3HO)

Immunohistochemistry analysis for F-actin, MHC and nuclei showed similar results for both gelatin and P(3HO).

### CONCLUSION

In conclusion, the MCL-PHA, P(3HO) has been confirmed as a new emerging material with great potential in cardiac tissue engineering.

### REFERENCES

1. Valappil *et al.*, 2006, Expert Review of Medical Devices 3(6):853-68.
2. Rai *et al.*, 2010, 2010, Biomacromolecules 12 (6), p2126–2136.

### ACKNOWLEDGMENTS

Authors thank the University of Westminster and the BHF funded Cardiovascular Centre, Imperial College for providing financial support to this project.



## Fabrication of a Biosynthetic Hydrogel Scaffold for Skin Repair

M. Flores-Reyes<sup>1</sup>, J. Flores-Estrada<sup>2</sup>, M.V. Dominguez-Garcia<sup>3</sup>, M.V. Flores-Merino<sup>3</sup>

<sup>1</sup>Faculty of Medicine, Autonomous University of the State of Mexico, Mexico

<sup>2</sup>Faculty of Chemistry, Autonomous University of the State of Mexico, Mexico

<sup>3\*</sup>Research Center in Medical Sciences, Autonomous University of the State of Mexico, Mexico

[mvfloresm@uaemex.mx](mailto:mvfloresm@uaemex.mx)

### INTRODUCTION

Hydrogels are polymeric materials with a wide range of advantages such as: good biocompatibility, high water content, adjustable architecture, high permeability etc...<sup>1</sup> These properties make them ideal materials for tissue engineering applications<sup>2</sup>. However single polymeric systems are not able to mimic all tissue properties, for example poly(ethylene glycol) is cell repellent in spite of being highly biocompatible<sup>3</sup>. Therefore, combination of synthetic and biological polymers can overcome limitations of single polymer hydrogels and it can be a solution for the design of functional scaffolds.

In this study a novel biosynthetic hybrid scaffold comprised of poly (ethylene glycol) and chitosan was obtained by UV polymerization. Their physicochemical properties were studied and analyzed for their potential use as skin substitute.

### EXPERIMENTAL METHODS

**Synthesis of biosynthetic hydrogel scaffold.** First, a microwave-assisted method was used to obtain poly(ethylene glycol) dimethacrylate (PEGDM). Briefly, linear PEG polymer (MW = 4000 g.mol<sup>-1</sup>; Polioles, MX) and methacrylic anhydride (Sigma-Aldrich, USA) were mixed, then acrylation was carried out for 6 minutes (700 Watts). Biosynthetic Hydrogel was fabricated by free radical polymerization of a homogenous solution of PEGDM, chitosan (Sigma-Aldrich, USA) and a UV initiator (Sigma-Aldrich, USA) in a PTFE mold. Samples were washed with de-ionized water several times in order to remove any unreacted initiator.

**Physicochemical characterization.** Chemical structure of the biosynthetic scaffold was analyzed by FTIR, the test was done by triplicate. Swelling behavior was studied by gravimetry of previously dried cylindrical samples of (n = 12) until equilibrium was reached in a phosphate buffer saline solution (PBS; pH = 7.4). Scanning electron Microscopy (SEM) was used to analyze pore structure of samples.

### RESULTS AND DISCUSSION

PEG hydrogels are widely used because of their lack of toxicity, however the non-adhesive properties of its polymeric chains are a drawback for tissue engineering applications. For this reason, a chitosan polymer, well known for its adhesive characteristics, was combined with a PEG network in a simultaneous way. Physicochemical properties were compared for both: the single PEG network and the PEG-Chitosan biosynthetic hydrogel. It was shown, that maximum swelling ratio (Qw) of biosynthetic hydrogel (3.90±0.09) has a lower value than the PEG network by

its own (5.60±0.78). The PBS uptake in the biosynthetic scaffold decreases due to the introduction of chitosan polymeric chains. Although the PEG-Chitosan hydrogel has a lower Qw compared with the PEG network, it still can uptake 3 fold their own weight in PBS (Fig. 1) and it can provide a moist environment in skin wounds.

SEM analysis shows an average pore size of approximately 30 µm in previously lyophilized samples of biosynthetic hydrogel (Fig.1). For regeneration of adult mammalian skin a pore size between 20–125 µm have been reported to be the optimal, therefore this material can be expected to promote cell proliferation of fibroblast.

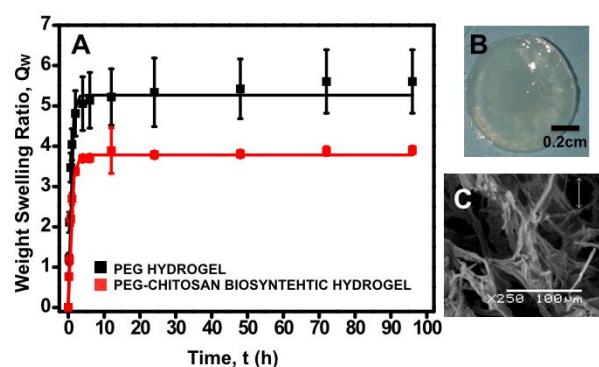


Figure 1. A. Weight swelling behavior in PBS of dried cylindrical samples at room temperature (n=9, sigmoidal fit:  $R^2=0.99$ ), B. PEG-chitosan hydrogel y C. SEM micrograph of biosynthetic hydrogel of PEG-Chitosan.

### CONCLUSION

Physicochemical characterization is the first step to assess performance of tissue-engineered scaffolds. Although, it does not replace other studies such as cell or animal models, it helps to have a better prediction of their *in vivo* behaviour. Here, the swelling and pore structure indicates that the biosynthetic material has potential use as skin substitute.

### REFERENCES

1. Fichman G. and Gazit E. Acta Biomaterialia. 10: 671–1682, 2014
2. Zhu J. and Marchan R.E. Expert Rev Med Devices. 8(5): 607–626, 2011
3. Zhu J. Biomaterials. 31(17): 4639–4656, 2010

### ACKNOWLEDGMENTS

The authors would like to thank PROMEP (Grant no: 103.51/13/6535) for providing financial support to this project and Dr. Blanca Elí Ocampo-García (ININ, México) for SEM micrographs.





## Evaluation of a Pro-Healing Polydopamine-Coated Stent on In-Stent Restenosis Using a Rat Model

Adrien Hertault<sup>1</sup>, Blandine Maurel<sup>1</sup>, Feng Chai<sup>1</sup>, Mickaël Maton<sup>1</sup>, Joël Lyskawa<sup>2</sup>, Jonathan Sobocinski<sup>1</sup>, Stephan Haulon<sup>1</sup>, Nicolas Blanchemain<sup>1</sup>,

<sup>1</sup> INSERM U1008, Research Group on Biomaterials, University of Lille, France

<sup>2</sup> UMET – Engineering of Polymeric Systems, UMR CNRS 8207, University of Lille, France

[Adhertault@gmail.com](mailto:Adhertault@gmail.com)

### INTRODUCTION

In-stent restenosis (ISR) is induced by an uncontrolled smooth muscular cells (SMC) proliferation after stent implantation. It is associated with recurrence of symptoms and additional health costs. Drug-eluting stents have demonstrated efficiency on ISR, but induce a high risk of late acute thrombosis due to a delayed struts reendothelialization<sup>1</sup>. Polydopamine (PDA), a biocompatible polymer inspired from mussels byssus, has been reported to promote endothelial cells (EC) and SMC proliferation *in-vitro*<sup>2,3</sup>, thus suggesting a potential pro-healing effect on the vascular wall. This study aimed to evaluate the impact of a pro-healing PDA-coated stent on in-stent restenosis (ISR) and on the quality of the struts re-endothelialization *in-vivo* using a rat model.

### EXPERIMENTAL METHODS

Chemical oxidation of Cobalt-Chromium (CoCr) plates was achieved using a “piranha” solution mixture. PDA coating was performed by dip coating in a 2mg/mL dopamine solution, followed by rinsing in deionized water and thermal treatment at 150°C<sup>4</sup> for one hour. Surface morphologies were assessed on PDA-coated CoCr plates by scanning electron microscopy (SEM). Ten Wistar rats received the implantation of 2.5mm CoCr coronary stent in aortic position (5 bare metal stents (BMS), 5 PDA stents, prepared according to the same protocol) and then sacrificed on the 28<sup>th</sup> day. Eight rats were used to estimate ISR in optic microscopy with quantification of the neointima/media (n/m) ratio after eosin/hematoxylin coloration<sup>5</sup>. Quality of the struts reendothelialization was analyzed in the two remaining rats with transmission electron microscopy (TEM).

### RESULTS AND DISCUSSION

Visual aspect of PDA-coating appears smooth and homogeneous, however SEM analyses with a scratch test revealed a rough surface of around 50 nm in depth (Figure 1).

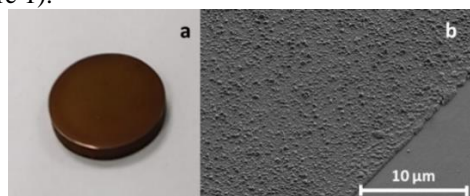


Figure 1: Typical aspect of PDA-coated CoCr plates after thermal treatment (a) and PDA coating aspect in SEM (b).

On the ten rats, one died of bleeding complications after stent implantation in the BMS group. The aspect of rats aortas is presented in Figure 2. PDA stents demonstrated a significant reduction in ISR compared to bare metal stents (ratio n/m = 0.48 (+/- 0.26) versus 0.83 (+/- 0.42),  $p < 0.001$ ). TEM analyses confirmed the presence of neointima surrounding the struts in each group, and revealed a thinner neointima layer in the PDA-stent group compared to BMS (Figure 2), with similar ultrastructures of the cells facing the arterial lumen.

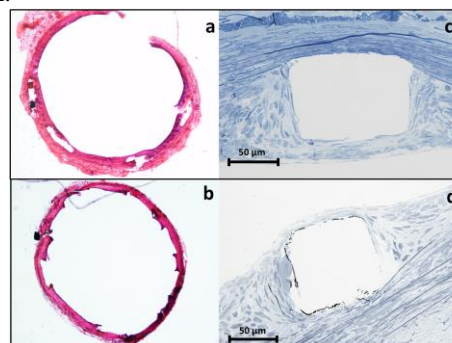


Figure 2: Morphology of the aortic wall 28 days after stent implantation of BMS (a) and PDA-stents (b) with optic microscopy. TEM analyses confirmed re-endothelialization of BMS (c) and PDA-stents (d). The neointima layer appeared thinner with PDA-stents (or in the PDA-stent group).

### CONCLUSION

The pro-healing effect expected of PDA-coating on the arterial wall seems to be confirmed in this *in-vivo* model. This biocompatible polymer could intrinsically limit in-stent restenosis. Additionally, it also offers the possibility to immobilize many relevant drugs on its surface through amine functions providing potential synergistic effects.

### REFERENCES

1. Finn AV. et al., Circulation. 2005;112:270-83;
2. Ding Y. et al., J. Mater. Chem. B, 2014;2:3819;
3. Yang Z. et al., Adv. Healthcare Mater. 2012;1:548–559;
4. Sobocinski J et al., ACS Appl Mater Interfaces, 2014;12 ;6(5) :3575-86;
5. Hyvelin JM et al., J Vasc Surg. 2010;51(2):417-28

### ACKNOWLEDGMENTS

The authors would like to thank the Abbott Company who provided the vascular stents, and the French Society of Vascular Surgery (SCV) for providing financial support to this project.



## Anti-Thrombogenic Effects of Bioactive CoCr Surfaces for Cardiovascular Applications

Maria Isabel Castellanos<sup>1,2,3</sup>, Jordi Guillem-Martí<sup>1,2,3</sup>, Carlos Mas-Moruno<sup>1,2,3</sup>, Maribel Díaz-Ricart<sup>4</sup>, Ginés Escolar<sup>4</sup>, Francisco Javier Gil<sup>1,2,3</sup>, Jose María Manero<sup>1,2,3</sup>, Marta Pegueroles<sup>1,2,3</sup>

<sup>1</sup> Biomaterials, Biomechanics and Tissue Engineering group (BBT), Technical University of Catalonia (UPC), Barcelona, Spain.

<sup>2</sup> Biomedical Research Networking Centre on Bioengineering, Biomaterials and Nanomedicine (Ciber-BBN), Spain

<sup>3</sup> Centre for Research in NanoEngineering (CRnE), Spain

<sup>4</sup> University of Barcelona, Hospital Clinic, Department of Hemotherapy and Hemostasis, IDIBAPS, Spain

[marta.pegueroles@upc.edu](mailto:marta.pegueroles@upc.edu)

### INTRODUCTION

In recent years, there is a growing interest in the immobilization of bioactive molecules on the surface of biomaterial implants<sup>1</sup>. In this regard, the coating of stents with bioactive sequences to prevent restenosis after percutaneous transluminal angioplasty is of particular therapeutic relevance<sup>2</sup>. For this purpose, it is essential that the stent enhances the adhesion of endothelial cells to facilitate healing of the blood vessel and also prevents restenosis and thrombosis. However, the optimal sequences and their combinations remain to be elucidated. We aimed to investigate the biological effects of bioactive CoCr surfaces on endothelial cells adhesion, vascularization, pro-thrombosis and anti-thrombosis processes through gene expression studies<sup>3</sup>. A further step is presented here with the study of platelet cell adhesion response to evaluate anti-thrombogenic effects.

### EXPERIMENTAL METHODS

CoCr alloy (ASTM F90) polished discs were etched with 5M NaOH 2h to activate the surface, previous to silanization with 3-chloropropyltriethoxysilane, and functionalized with cell adhesive peptides –containing the active sequences RGDS (RGD), YIGSR (Lam) - with aminohexanoic acid as spacer units - and their combination (Mx). Plain surfaces were used as control (CT). Real time polymerase chain reaction (RT-qPCR) gene expressions for selected genes of adhesion (ICAM-1, VCAM-1), vascularization (VEGFA, VEGFR-1, VEGFR-2), pro-thrombogenic (vWF) and anti-thrombogenic (eNOS, TPA) in HUVEC cultured on the different surfaces for 24h, 48h and 72h were determined.  $\beta$ -actin was used as housekeeping gene. Thrombogenicity was evaluated through platelet adhesion and aggregation, by circulating human blood onto TCPS coated surfaces - RGD, Lam and Mx - using a flat chamber perfusion at 75 ml/min during 5 min and 37°C to then, stain by immunofluorescence. ANOVA tables with Fisher's multiple comparison tests were obtained to determine statistically significant differences ( $p < 0.005$ ).

### RESULTS AND DISCUSSION

CoCr surface functionalized with RGD, Lam, or Mx sequences influenced the expression of anti-coagulatory genes of HUVECs and the adhesion and aggregation of platelets. Moreover, differences have been detected if the biomolecules are simply adsorbed or covalently adhered to the surface. HUVEC cells cultured on CoCr surfaces with the peptides RGD, Lam or Mx physisorbed did not show differences in the expression

of ICAM-1 (Figure 1) and VCAM-1 genes after 24h and 72h. Conversely, gene expression was enhanced on RGD and Lam silanized CoCr surfaces after 72h where Mx surfaces overexpressed ICAM-1 and VCAM-1. This can be explained by the higher immobilization of peptides RGD, Lam and Mx onto CoCr surfaces via silanization compared to physisorption, which effectively guides cell adhesion response.

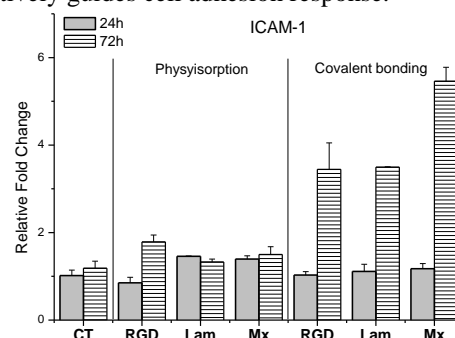


Figure 1. Gene expression of ICAM-1 on all different surfaces by RT-qPCR

vWF factor, related to pro-thrombogenic events, decreased its gene expression over time in all studied surfaces, thereby suggesting a lower blood clot formation on the mentioned surfaces.

Interestingly, tPA and eNOS were overexpressed on silanized Mx CoCr series after 72h compared to all surfaces, indicating lower thrombogenic properties on this surface and a better prevention of platelet aggregation. A blood *in vitro* assay confirmed this behaviour, where all CoCr surfaces with immobilized bioactive sequences presented a lower platelet adhesion and aggregation compared to CT surfaces. This effect was noticeable for RGD and Mx coated surfaces, which resulted in a lower thrombogenicity.

### CONCLUSION

Coating of CoCr surfaces with the combination of RGDS and YIGSR bioactive sequences influences HUVEC's adhesion and inhibits platelet adhesion and aggregation. These biomaterials may have a great potential for arteries recover.

### REFERENCES

1. Heng B.C. *et al.*, Biointerphases 5(3):FA53-FA62, 2010
2. Castellanos M.I. *et al.*, Colloids Surf., B 127:22-32, 2015
3. Verheul H. *et al.*, Nat. Rev. Cancer 7:475-485, 2007

### ACKNOWLEDGMENTS

The authors would like to thank the Spanish Science Ministry project MAT 2012-30706, and the Government of Catalonia Government of Catalonia (2014 SGR 1333 and FI-2011) for providing financial support.



Guillaume Le Saux<sup>1\*</sup>, Laurent Plawinski<sup>1</sup>, Sylvain Nlate<sup>1</sup> and Marie-Christine Durrieu<sup>1</sup><sup>1\*</sup> Institute of Chemistry & Biology of Membranes & Nano-objects, Université de Bordeaux, France  
[guillaume.le-saux@u-bordeaux.fr](mailto:guillaume.le-saux@u-bordeaux.fr)

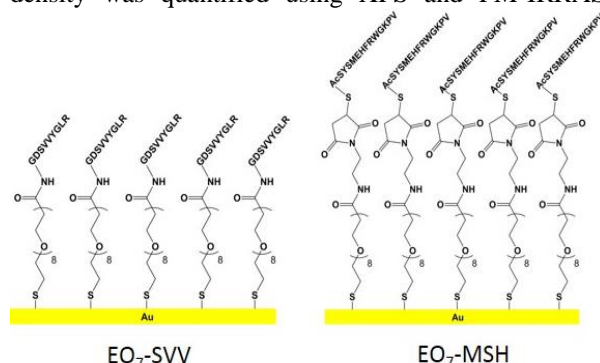
## INTRODUCTION

Continuous glucose monitoring is an efficient method for the management of diabetes and in limiting the complications induced by large fluctuations in glucose levels. For this, intravascular systems may be useful in producing more reliable and accurate devices. However, biocompatibility remains the key issue to be addressed for optimal performance<sup>1</sup>. In particular, inflammation and neo-vascularization are key factors to be addressed. Currently, the most commonly used method to overcome these obstacles is the use of drug releasing implants<sup>2</sup>. We believe that this paradigm should be reconsidered in view of their limited lifetime. In this scope, the perennial modification of the surface of a gold-based implant with pro-angiogenic and/or anti-inflammatory principles holds some promise. Gold is widely used in medical devices due to its excellent biocompatibility.

The objective of this study is to investigate the impact of surface modified with the anti-inflammatory molecule  $\alpha$ -Melanocyte Stimulating Hormone<sup>3</sup> ( $\alpha$ -MSH) as well as the pro-angiogenic peptide sequence GDSVVYGLR<sup>4</sup> on Human Umbilical Vein Endothelial Cell (HUVEC) behavior *in vitro*.

## EXPERIMENTAL METHODS

**Functionalization** – Our model is based on self-assembled monolayers (SAMs) of thiol-bound carboxyethyl terminated hepta(ethylene oxide) (EO<sub>7</sub>-COOH) on gold. Following this,  $\alpha$ -MSH is grafted using a thiol-maleimide bond, thus yielding EO<sub>7</sub>-MSH surfaces, while GDSVVYGLR is coupled by peptide linkage to obtain EO<sub>7</sub>-SVV surfaces. Peptide surface density was quantified using XPS and PM-IRRAS.



Schematic diagram of the bioactive modified gold surfaces used in this study.

**Biological studies** – HUVEC proliferation was investigated after 96h. To discriminate the effect of surface grafted SVVYGLR from Vascular endothelial Growth Factor (VEGF), experiments were performed in cell culture media containing either 0.1% or 0% VEGF. Finally, ERK1/2 signaling was investigated.

HUVEC inflammatory response was assessed by quantifying the impact of the EO<sub>7</sub>-MSH surfaces on the production of the pro-inflammatory cytokine IL-6. A

comparative study of the effect of soluble versus immobilized  $\alpha$ -MSH on IL-6 production was also performed.

## RESULTS AND DISCUSSION

**Surface characterisation** – Using XPS and PM-IRRAS we found that the EO<sub>7</sub>-COOH surfaces are compact, homogeneous and have a structure analogous to crystalline poly(ethylene oxide). EO<sub>7</sub>-SVV and EO<sub>7</sub>-MSH were successfully produced with surface densities of SVVYGLR and  $\alpha$ -MSH of 1.6 and 3.5 pmol/mm<sup>2</sup> respectively.

**Proliferation** – HUVECs proliferated more on the EO<sub>7</sub>-SVV surfaces, regardless of VEGF concentration. Importantly, in VEGF deprived conditions, surface grafted SVV was able to maintain adhesion and proliferation *via* activation of the ERK1/2 signaling pathway.

**Inflammation** – We observed that IL-6 production was significantly reduced on the EO<sub>7</sub>-MSH surface. In addition surface bound  $\alpha$ -MSH was found to be as efficient as physiological levels of soluble  $\alpha$ -MSH in reducing IL-6 expression.

## CONCLUSION

**Summary** – Bioactive gold surfaces with controlled surface density were produced and characterized. These were used to assess HUVEC response with regards to proliferation and inflammation. We found that HUVECs respond to the presence of bioactive molecules by proliferating on surfaces presenting the SVVYGLR peptide, *via* activation of a pro-angiogenic pathway. We also observed that surface bound  $\alpha$ -MSH is beneficial in limiting HUVEC inflammation and that it is as potent as equivalent levels in solution in reducing inflammation.

**Perspectives** – Future work includes simultaneously modifying gold surfaces with both anti-inflammatory and pro-angiogenic molecules and to test their effect on cell behavior *in vitro*, with ultimately the prospect of an *in vivo* study.

## REFERENCES

1. Onuki, Y. *et al.*, J. Diabetes Sci. Technol. 2:1003-1015, 2008
2. 3. Norton, L.W. *et al.*, J. Control. Release 146:341-348, 2010
3. He, W. *et al.*, Adv. Mater. 19:3529-3533, 2007
4. Lei, Y. *et al.*, PLOS ONE. 7:e41163, 2012

## ACKNOWLEDGMENTS

“This work was supported by the French Government under the LabEx AMADEus program (reference ANR-10-LABX-0042-AMADEus), managed by the French National Research Agency under the initiative of excellence IdEx Bordeaux program (reference n°ANR-10-IDEX-0003-02).”

## Nanomaterials for Cardiovascular Applications: Quo Vadimus?

Iwona Cicha<sup>1</sup>, Christoph D. Garlich<sup>2,3</sup>, Christoph Alexiou<sup>1</sup>

<sup>1</sup>Cardiovascular Nanomedicine Unit, SEON, University Hospital Erlangen, Germany

<sup>2</sup>Department of Cardiology and Angiology, University Hospital Erlangen, Germany

<sup>3</sup>Internal Medicine Clinic, Diako-Hospital, Flensburg, Germany

[Iwona.Cicha@uk-erlangen.de](mailto:Iwona.Cicha@uk-erlangen.de)

### INTRODUCTION

Cardiovascular diseases, including ischemic heart disease and stroke, are collectively responsible for 25% of all deaths worldwide. Globally, their prevalence continues to increase, in spite of enormous progress in diagnostics and therapy. For therapeutic and regenerative purposes, biomaterials constitute a solution with multiple advantages over synthetic materials. In this work, we focus on the directions for the current and future development of (nano)biomaterials for cardiovascular applications.

### EXPERIMENTAL METHODS

The current literature regarding (nano)biomaterials for cardiovascular medicine was reviewed based on the Medline bibliographic database.

### RESULTS AND DISCUSSION

**Vascular grafts:** One of the most addressed, but thus far unanswered needs in cardiovascular tissue engineering is the development of small-diameter vascular grafts which would mimic anti-thrombogenic effect of an autologous vessel. Promising results were recently obtained with biodegradable polymers (e.g. poly (caprolactone) (PCL); poly(lactic-co-glycolic) acid (PLGA)) and their blends with proteins (silk fibroin, elastin, collagen, gelatin) electrospun to fabricate tubular scaffolds with nanometer-range fibre diameter mimicking native-like topology. To improve endothelialisation and prevent thrombosis, surface modifications of nanofibres, as well as incorporation of cell attachment-supporting peptide sequences or nitric oxide donors into the scaffolds were proposed<sup>1</sup>. Aspirin-loaded electrospun PCL tubular scaffold were also suggested as anti-thrombotic drug-releasing graft for small-diameter vessel replacement. Apart from electrospinning, several rapid prototyping techniques, including submerged bioprinting, have been recently developed to improve the mechanical stability of the biofabricated tubular constructs.

**Vascular bioresorbable stents:** Recent advances in bioresorbable metal and polymer materials enable the design of stents, which are aimed at scaffolding the vessel only temporarily after coronary interventions. Following revascularization and restoration of vessel function, the stents are progressively resorbed to eliminate the drawback of an unnecessary permanent metallic implant. This new concept of vascular regenerative therapy utilizes nanoparticulate drug delivery systems in combination with bioresorbable polymers (e.g. PLA, PLGA), or bioabsorbable metal stents based on iron or magnesium alloys that use a controlled corrosion by body fluids as mechanism of degradation<sup>2</sup>.

**Cardiac patches:** Abnormal heart formation or heart tissue damage often require placement of a cardiac patch to repair the defect, but the available polymeric materials obstruct the transfer of electrical signals between cardiomyocytes, which can cause arrhythmias. Novel myocardial patches based on hydrogels containing conductive nanoparticles (e.g. alginate hydrogels with gold nanowires, or chitosan/gelatin-hydrogels with single-walled carbon nanotubes) are now proposed that provide the native-like extracellular matrix environment for cardiac cells, but also support the electrical conductivity necessary for cardiomyocyte function.

**Nanoparticles for cardiovascular imaging and drug delivery:** PLGA<sup>3</sup> and chitosan are commonly used as nanocarriers, due to their favourable safety profiles. To highlight but a few novel biomaterial-based nanosystems with the best potential for use in clinical applications<sup>4</sup>, glycol chitosan-gold nanoparticles were successfully tested in mice as contrast agents for thrombus detection with CT. Chitosan nano-tPA gene plasmids and urokinase-coated, self-assembled chitosan and tripolyphosphate nanoparticles were used to prevent thrombus formation in dog and rabbit models respectively. Nanoparticulate drug-delivery was also proposed for the regeneration of myocardial infarction-induced injury, utilizing e.g. chitosan-alginate nanoparticles loaded with cardioprotective placental growth factor, or PLGA nanoparticles conjugated with insulin-like growth factor-1. PLGA nanoparticles containing active superoxide dismutase were also tested in an animal model of stroke, showing considerable protection against ischemia and reperfusion injury.

### CONCLUSIONS

The potential clinical impact of tissue-engineering, biofabrication and nanotechnology in terms of cardiovascular disease management is enormous. Clinically-driven needs give the precise directions for further improvement of existing, and development of novel nano(bio)materials that can be translated into the clinical trials.

### REFERENCES

1. Ercolani E. et al., *J Tissue Eng Regen Med.*, 2013
2. Foin N. et al., *Int J Cardiol.* 177:800-808, 2014
3. Danhier F. et al., *J Control Release.* 161:505-522, 2012
4. Cicha I. et al., *Eur J Nanomed.* 6:63-87, 2014

### ACKNOWLEDGMENTS

The authors thank the Emerging Field Initiative of the University of Erlangen-Nuremberg (TOPbiomat) and the DGF (CI 162/2-1 and SPP1681) for support.



Andrew L. Hook<sup>1</sup>,<sup>1</sup>Laboratory of Biophysics and Surface Analysis, University of Nottingham, UK  
[andrew.hook@nottingham.ac.uk](mailto:andrew.hook@nottingham.ac.uk)

## INTRODUCTION

Biofilm formation leads to a 1000 times increase in antibiotic tolerance compared with planktonic bacteria and is associated with 80% of hospital acquired infections. New materials that prevent biofilm formation would offer enormous benefits to the health industry and improve patient welfare. However, the limited understanding of bacteria-material interactions restricts the rational design of such materials. Polymer microarrays are a key enabling technology for the discovery of new biomaterials<sup>1</sup> and have been utilised to identify novel polymers that resist bacterial attachment.<sup>2,3</sup> The hundreds of polymer-bacteria interactions observed on a microarray can be used to elucidate the structure-function relationship underpinning the ability of a material to resist bacterial attachment.<sup>4</sup>

## EXPERIMENTAL METHODS

Polymer microarrays were formed using a XYZ3200 pin printing workstation (Biodot) onto poly(hydroxyethyl methacrylate) coated slides. Printing was carried out using slotted metal pins. Polymerisation solution was composed of 75% (v/v) monomer, 24% (v/v) DMF and 1% (w/v) photoinitiator 2,2-dimethoxy-2-phenylacetophenone. After printing polymers were UV cured and vacuum extracted. A bacterial attachment assay was developed using green fluorescing protein (GFP) tagged bacterial strains (*Pseudomonas aeruginosa* PAO1, *Staphylococcus aureus* 8325-4, Uropathogenic *Escherichia coli* (UPEC)) where the attachment of bacteria to each material was quantified by measuring the fluorescence after incubation.

## RESULTS AND DISCUSSION

Polymer microarrays were used for the discovery of novel materials that resist bacterial attachment. A multi-generation approach was used to search the chemical space represented by polymerised commercially available acrylates. First generation arrays were designed to represent a large chemical diversity whilst subsequent generations utilised copolymers to explore 'hit' formulations in greater detail. Using this approach over 1200 unique materials were screened to identify a hit formulation that was able to reduce bacterial attachment by up to 99% compared with silicone.<sup>2,3</sup> The 'hit' material was able to reduce infection *in vivo* on subcutaneous implants within a mouse model (Fig. 1). The materials with the lowest bacterial attachment were homologues as they each contained a hydrophilic ester group, associated with the acrylate functionality, and a bulky hydrophobic pendant group. Each of the materials was, thus, amphiphilic.

To explore structure-function relationships, a new array

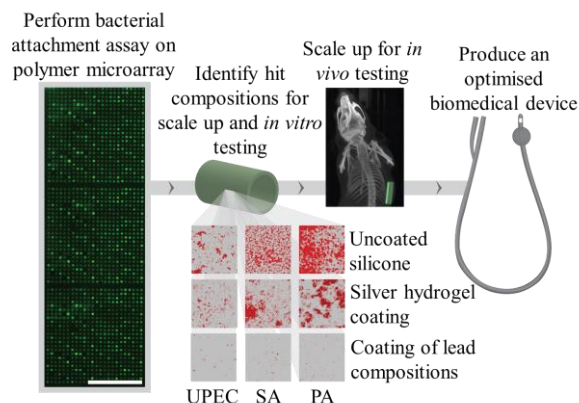


Figure 1 – Summary of high throughput method to discover a material resistant to bacterial attachment, from the polymer microarray to *in vivo* application.

was prepared containing copolymers with pendant groups derived from the *tert*-butyl cyclohexyl moiety. Bacterial attachment to these materials was found to correlate with a composite parameter representing both molecular flexibility and hydrophobicity (Fig. 2).

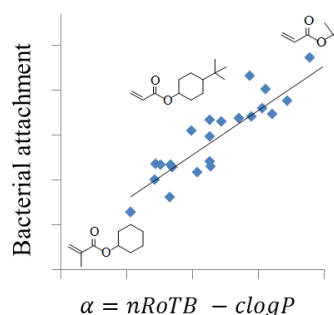


Figure 2 - For weak amphiphiles, bacterial attachment was found to correlate with the combination of a rigid hydrophobic pendant group.

## CONCLUSION

Polymer microarrays were successfully applied to discover new materials resistant to bacterial attachment. This was achieved without the requirement for a comprehensive understanding of the underlying material-biological interactions, however, this understanding was developed subsequently from the biological responses observed on microarrays.

## REFERENCES

1. Hook, A. L. *et al. Biomaterials*, 31:187-198, 2010.
2. Hook, A. L. *et al. Adv. Mater.*, 25:2542-2547, 2013.
3. Hook, A. L. *et al. Nat. Biotech.*, 30:868-875, 2012.
4. Sanni, O. *et al. Adv. Healthcare Mater.*, Early view, 2015.

## ACKNOWLEDGMENTS

The authors would like to thank the Wellcome Trust (Grant no: 085245) for providing financial support to this project.



Oleg Prymak, Simon Ristig, Svitlana Chernousova, Wolfgang Meyer-Zaika, Matthias Eppele\*

Institute of Inorganic Chemistry and Center for Nanointegration Duisburg-Essen (CeNIDE),  
University of Duisburg-Essen, Essen, Germany  
[oleg.prymak@uni-due.de](mailto:oleg.prymak@uni-due.de)

## INTRODUCTION

Silver nanoparticles as antibacterial agent in biomedicine with unfortunately a rather narrow therapeutic window<sup>[1-3]</sup> and biologically inert gold nanoparticles for the use in tumor therapy, drug delivery or imaging applications<sup>[4,5]</sup> recently became a prominent subject in scientific studies. Alloyed silver-gold nanoparticles are promising candidates to combine and tune the properties of both metals, e.g. their optical characteristics or their toxicity towards cells or bacteria.

## EXPERIMENTAL METHODS

The alloyed Ag:Au nanoparticles with different compositions of silver and gold were prepared in aqueous media by co-reduction of silver nitrate and tetrachloroauric acid with a mixture of citrate and tannic acid and subsequently functionalized by the addition of polyvinylpyrrolidone (PVP).<sup>[6]</sup> For comparison, pure gold and silver nanoparticles were synthesized with the same reaction parameters. After colloidal stabilization and physicochemical characterization, the nanoparticles were purified by multiple ultracentrifugation steps for further cell-biological experiments with HeLa cells and human mesenchymal stem cells.

## RESULTS AND DISCUSSION

The presented synthesis is well suited for the generation of monodisperse bimetallic Ag:Au nanoparticles with different molar compositions (with the molar ratios of Ag:Au ranging from 90:10 to 10:90). Characterization with X-ray powder diffraction (XRD), transmission electron microscopy (TEM), differential centrifugal sedimentation (DCS), UV-Vis and atomic absorption spectroscopy (AAS) showed spherical monodisperse and colloiddally stable silver-gold nanoparticles with diameters of ~7 nm (see Fig. 1) with the actual molar metal compositions very close to the theoretical values.

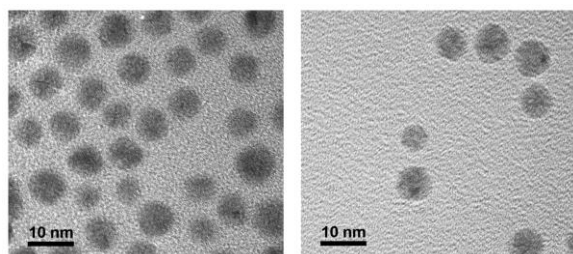


**Figure 1:** Representative transmission electron micrographs (TEM) of synthesized Ag:Au-30:70 (left) and Ag:Au-60:40 (right) nanoparticles with an average particle diameter of 7 nm.

Examination of the nanoparticle cytotoxicity towards HeLa cells and human mesenchymal stem cells (hMSCs) showed that the toxicity increases non-linearly with increasing silver content. Nanoparticles with a molar Ag:Au composition of 80:20 showed the highest cytotoxicity. It is possible that a passivating effect from the alloyed gold is responsible for this effect.

## CONCLUSION

The presented one-pot synthesis of alloyed Ag:Au nanoparticles in aqueous medium can easily be modified to gain size control over the final particle diameter and the stabilizing agents without affecting the resulting purity or stability. The cytotoxicity towards HeLa cells and hMSCs increases with growing silver fractions in the nanoparticles with a maximum at Ag:Au=80:20. This may permit to reduce the dose of silver for the antibacterial action.

## REFERENCES

- [1] Liu H.L., Dai S.A., Fu K.Y., Hsu S.H., *Int. J. Nanomed.* 5 (2010) 1017
- [2] Chernousova S., Eppele M., *Angew. Chem. Int. Ed.* 52 (2013) 1636
- [3] Kittler S., Greulich C., Köller M., Eppele M., *Mat.-wiss. u. Werkstofftech.* 40 (2009) 258
- [4] Homberger M., Simon U., *Phil. Trans. R. Soc. A* 368 (2010) 1405
- [5] Huang X., Neretina S., El-Sayed M.A., *Adv. Mater.* 21 (2009) 4880
- [6] Mahl D., Diendorf J., Ristig S., Greulich C., Li Z.A., Farle M., Köller M., Eppele M., *J. Nanopart. Res.* 14 (2012) 1153

## ACKNOWLEDGMENTS

We thank the *Deutsche Forschungsgemeinschaft* (DFG) for generous support within the Priority Program BioNanoResponses (SPP 1313) and Kerstin Brauner and Veronika Hiltenkamp for AAS measurements.

# Enzymatic Disassembly of Biofilm Extracellular Matrix by Smart Nanoparticles to Eradicate Bacterial Infections

Riccardo Levato<sup>1</sup>, Aida Baelo<sup>2</sup>, Esther Julian<sup>3</sup>, Anna Crespo<sup>2</sup>, Joan Gavalda<sup>4</sup>, Elisabeth Engel<sup>1,5,6</sup>, Eduard Torrents<sup>2</sup>, Miguel Angel Mateos-Timoneda<sup>5,1</sup>

<sup>1</sup>Biomaterials for regenerative therapies and <sup>2</sup>Bacterial infections and antimicrobial therapies group, Institute for Bioengineering of Catalonia, Spain; <sup>3</sup>Dept. of Genetics and Microbiology, Autonomous University of Barcelona, Spain;

<sup>4</sup>Infectious Diseases Research Lab, Vall d'Hebron Research Institute, Spain; <sup>5</sup>CIBER en bioingeniería, biomaterials y nanomedicina, Spain; <sup>6</sup>Dept. of Materials Science and Metallurgy, Technical University of Catalonia, Spain

[rlevato@ibecbarcelona.eu](mailto:rlevato@ibecbarcelona.eu)

## INTRODUCTION

Biofilm-forming bacteria are a major treat to hospitalized patients and the main cause of chronic obstructive pulmonary disease and pulmonary infections, which are the third cause of death worldwide. There is an urgent necessity for novel therapeutic approaches, since current antibiotic delivery fails to eliminate biofilm-protected bacteria. Biomaterial carriers designed to improve such drug release need to overcome the biological barrier that is the biofilm extracellular matrix (ECM), a mesh made of proteins, polysaccharides and extracellular DNA (eDNA)<sup>1</sup>. In this work we propose to target bacterial ECM with enzyme-activated NPs, able to disassemble the biofilm matrix and boost the efficacy of antibiotic treatment. Polylactic-co-glycolic acid nanoparticles (PLGA NPs) loaded with ciprofloxacin (CPX) were prepared and coated with DNase to degrade the eDNA that stabilizes the biofilm structure. Such NPs were evaluated against established *P. aeruginosa* biofilm, under static and dynamic conditions.

## EXPERIMENTAL METHODS

NPs were prepared co-dissolving 1.5% w/v PLGA (Purasorb PLG 5010, Purac) and 700 µg/mL CPX in the green solvent ethyl lactate. The mixture was added to a water bath, and NPs formed by nanoprecipitation. Polylysine (PL)-coated NPs were obtained adding 70 µg/mL of PL to the water bath. DNase-coated NPs were produced grafting DNase I on the ε-aminogroups of PL via carbodiimide chemistry. NPs size and surface charge were studied by dynamic light scattering, and their morphology by scanning electron microscopy. DNA degradation by DNase-NPs was quantified via gel electrophoresis. CPX content and release kinetics at 37°C were measured by high performance liquid chromatography. Cytotoxicity was tested on J774 murine macrophages. Antimicrobial activity of NPs was first assessed against planktonic *P. aeruginosa* PAO1 and the minimum inhibitory concentration of each NPs type was determined. NP efficacy against 48h-old mature *P. aeruginosa* biofilm was evaluated *in vitro*. NP treatment was applied either once or repeatedly (1 dose/day for 3 days) and surviving biofilm-forming bacteria were counted. NP antibiofilm activity was also studied under dynamic conditions in a microfluidic flow chamber. 96h-old biofilms were subjected to a single dose NP treatment, stained (LIVE/DEAD assay), and analysed by confocal laser scanning microscopy.

## RESULTS AND DISCUSSION

Spherical and monodispersed NPs encapsulating CPX,

were synthesized with a size between 200 and 300 nm. Z-potential can be tuned as PLGA NPs had negative surface charge and PL-coated NPs (with and without DNase) showed a positive charge. PL-coating also enabled a simple way to graft bioactive molecules on the NPs surface. For all NPs formulations CPX release kinetics had a biphasic behaviour, with an initial burst in the first hour, followed by a slower sustained release. NPs were non-cytotoxic for mammalian cells, enhanced CPX antimicrobial activity against planktonic *P. aeruginosa* and prevented biofilm formation. More importantly, administration of DNase-NPs delivering CPX concentrations as low as 0.0078 µg/mL against 2-days old mature biofilms successfully reduced the living bacteria by >95%, outperforming free-soluble CPX (cell reduction <40%). Higher doses of DNase-coated NPs, as well as repeated administrations over 3 days, were able to completely eradicate the established biofilm, which was not possible with CPX alone or uncoated NPs. In the flow chamber assay, a model closer to the *in vivo* milieu, DNase-NPs kept their activity also under dynamic flow. Both living biomass density and biofilm thickness were reduced, indicating the contextual disassembly of the biofilm ECM and bacteria elimination due to the improved antibiotic delivery (Fig. 1).

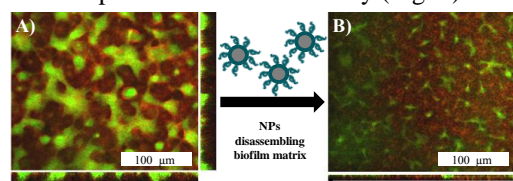


Figure 1: Flow chamber biofilm (A) untreated and (B) after DNase-NPs treatment. Bacterial cells: green (live), red (dead)

## CONCLUSION

PLGA NPs encapsulating CPX, with size suitable for airway delivery, were successfully prepared and endowed with functional DNase activity as smart drug delivery devices that target and disassemble the biofilm ECM. Such NPs enhance antibiotic penetration into the biofilm and eradicate persistent infections *in vitro*. Enzyme-activated NPs are proposed as novel antimicrobial agents, and these results provide fundamental clues to design the next generation of drug delivery devices to treat biofilm infections.

## REFERENCES

1. Gloag ES. *et al.*, PNAS. 110:11541-6, 2013.

## ACKNOWLEDGMENTS

RL acknowledges the Spanish MECD for financial support (FPU AP2010-4827). ET was supported by the Ramón y Cajal and I3 program (Spanish MICINN).



# Anti-*Helicobacter pylori* Activity of Nanoparticles Loaded with a Polyunsaturated Fatty Acid

Catarina L. Seabra<sup>1,2,3,4</sup>, Cláudia Nunes<sup>5</sup>, Marta Correia<sup>1,3</sup>, José C. Machado<sup>1,3,6</sup>, Celso A. Reis<sup>1,3,4,6</sup>, Inês C. Gonçalves<sup>1,2</sup>, Salette Reis<sup>5</sup>, M. Cristina L. Martins<sup>1,2,3</sup>

<sup>1</sup>Instituto de Investigação e Inovação em Saúde, Universidade do Porto, Portugal

<sup>2</sup>INEB - Instituto de Engenharia Biomédica, Universidade do Porto, Portugal

<sup>3</sup>IPATIMUP – Instituto de Patologia e Imunologia Molecular da Universidade do Porto, Portugal

<sup>4</sup>ICBAS- Instituto de Ciências Biomédicas Abel Salazar, Universidade do Porto, Portugal

<sup>5</sup>REQUIMTE, Laboratório de Química Aplicada, Faculdade de Farmácia, Universidade do Porto, Portugal

<sup>6</sup>Faculdade de Medicina, Universidade do Porto, Portugal

[catarina.seabra@ineb.up.pt](mailto:catarina.seabra@ineb.up.pt)

## INTRODUCTION

*Helicobacter pylori* (*Hp*) colonizes the stomach of more than 50% of the World's population<sup>1</sup>. *Hp* infection recommended treatment is based in a combination of two antibiotics and a proton pump inhibitor<sup>2</sup>. However, this therapy fails in 20% of patients especially due to bacterial resistance<sup>3</sup>. Therefore, it is urgent to develop new antibacterial agents that can effectively eradicate *Hp* with minimum drug resistance. We have previously demonstrated that docosahexaenoic acid (DHA), a polyunsaturated fatty acid present in fish oil, has antibacterial activity against *Hp* growth *in vitro* in a dose-dependent way and inhibits mice gastric colonization *in vivo*. However, up to 40% of infected mice remain colonized by *Hp* after DHA treatment<sup>4</sup>. This might be explained by low residence time of DHA on mice stomach and/or low penetration of DHA through the stomach mucus layer, leading to insufficient concentration of DHA to eradicate *Hp* at the infection site. The main goal of this work is to develop a DHA gastric delivery system to improve its efficacy in the treatment of *Hp* infection.

## EXPERIMENTAL METHODS

DHA (0, 1, 2 and 2.5% v/v in solution) was incorporated into nanostructured lipid carriers (NLC) by hot homogenization technique using a mixture of solid lipids/liquid lipid/stabilizer<sup>5</sup>. Nanoparticles were characterized in terms of size and  $\xi$ -potential by electrophoretic light scattering and DHA incorporation was quantified using UV-Vis spectroscopy (200-400nm) after dissolution in ethanol. Nanoparticles physical stability was evaluated by examining changes of mean particle size and charge during storage conditions for 1 month at RT.

The effect of DHA-NLC (prepared with 2% v/v) on *Hp* J99 strain growth ( $\sim 1 \times 10^7$  bacteria/ml) was evaluated in Brucella broth (150rpm, 37°C) with different concentrations of NLCs and DHA-NLCs (10, 25, 50, 100, 500  $\mu$ M). DHA in solution was used as control. Samples of bacteria cultures were collected every 3h for 24h and plated on *Hp* selective medium. Number of viable bacteria was determined by colony forming units (CFU) counting.

Cytotoxicity of different concentrations of NLCs and DHA-NLC (10, 25, 50, 100  $\mu$ M) towards MKN45 gastric carcinoma cell line ( $\sim 5 \times 10^5$  cells/well) was performed using LDH and MTT assays by measuring optical density at 490 and 630 nm and at 590 and 630 nm, respectively, using a microplate reader.

## RESULTS AND DISCUSSION

The maximum of DHA incorporation into nanoparticles was obtained using at least 2% v/v DHA in solution ( $2.0 \pm 0.2$  mM/ml). After incorporation of DHA, the size of NLCs increased from  $151 \pm 16$  nm to  $214 \pm 31$  nm, independently of DHA concentration. All nanoparticles have a negative  $\xi$ -potential ( $\sim -30$  mV), demonstrating that DHA did not change the particle charge. All nanoparticles were stable during storage conditions at room temperature.

Encapsulation of DHA improves its bactericidal effect against *Hp*, since all DHA-NLCs used, even at lower concentration (10  $\mu$ M) are bactericidal in opposite to DHA in solution that did not kill *Hp* at concentrations lower than 100  $\mu$ M. Also, NLCs without DHA have an inhibitory effect on *Hp* and are able to kill it after 12h. Cytotoxicity studies revealed that all nanoparticles tested are non-cytotoxic for gastric cells at concentrations that kill *Hp*.

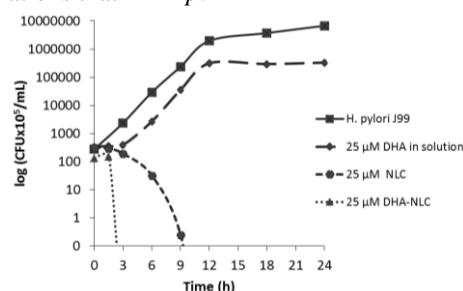


**Figure 1.** Effect of soluble DHA, NLCs and DHA-NLCs (25  $\mu$ M) on *Hp* J99 growth during 24 hours.

## CONCLUSION

The inhibitory and bactericidal activity of unloaded and DHA-loaded NLCs nanoparticles, respectively, in treating *Hp* infection, was demonstrated. These nanoparticles are not cytotoxic against gastric cells at bactericidal concentrations. DHA-loaded NLC should therefore be considered as an alternative to the current treatment of *Hp*.

## REFERENCES

1. Wroblewski *et al.*; Microbiol Rev. 23:713-39, 2010
2. Malfertheiner *et al.*; Gut. 61:646-64, 2012
3. Vakil; Am J Gastroenterol. 101:497-9, 2006
4. Correia *et al.*; PLoS One.7: e35072, 2012
5. Neves *et al.*; Int J Nanomedicine.8:177-187, 2013

## ACKNOWLEDGMENTS

FEDER funds through COMPETE and Portuguese FCT (Fundação Ciência e a Tecnologia) in the project PTDC/CTM-BPC/121149/2010 and grant SFRH/BD/89001/2012.



# Antifouling Coatings as a Platform for Antimicrobial Peptide Immobilization

Judit Buxadera-Palomero<sup>1,3,4</sup>, Patricia Carrasco<sup>1,4</sup>, Cristina Canal<sup>2,3,4</sup>, Carles Mas-Moruno<sup>2,3,4</sup>, F. Javier Gil<sup>2,3,4</sup>, Daniel Rodríguez<sup>1,3,4</sup>

<sup>1</sup>Biomaterials, Biomechanics and Tissue Engineering Group, E. U. d'Enginyeria Tècnica Industrial de Barcelona, Technical University of Catalonia (UPC), C/ Comte d'Urgell 187, 08036 Barcelona, Spain

<sup>2</sup>Biomaterials, Biomechanics and Tissue Engineering Group, E. T. S. d'Enginyeria Industrial de Barcelona, Technical University of Catalonia (UPC), Av. Diagonal 647, 08028 Barcelona, Spain

<sup>3</sup>Biomedical Research Networking Centre in Bioengineering, Biomaterials and Nanomedicine (CIBER-BBN), Spain

<sup>4</sup>Center for Research in nanoEngineering (CRnE), UPC, Spain

[judit.buxadera@upc.edu](mailto:judit.buxadera@upc.edu)

## INTRODUCTION

Dental implants are a common solution to overcome the problem of tooth loss. Despite their high rate of success, however, such implants can fail due to different factors, e.g. poor quantity and quality of the bone, defective implant placement, or infection. Among them, infection has been described to play a key role in mid- and long-term implant failure<sup>1</sup>. Thus, different approaches to avoid peri-implant infection have been studied, including loading of antibiotics, antibacterial polymeric coatings or immobilization of antimicrobial peptides (AMPs).

In this study, a combination of an antifouling coating (polyethylene glycol, PEG) and an AMP has been developed on Ti surfaces. Two different AMPs have been tested: Lactoferrin 1-11 (LF1-11) and Magainin-2 (MG-2), to compare the biological performance of the coatings in terms of biocompatibility and bacterial adhesion.

## EXPERIMENTAL METHODS

Samples of polished titanium (Ti) grade 2, cleaned with ethanol, acetone and water were activated with argon plasma (0.40mbar, 100W, 5min).

PEG-amine electrodeposition was done with an electrolyte containing 2% PEG-amine and 0.3M of NaCl. The potential was applied with a constant sweep rate of  $-0.1\text{Vs}^{-1}$  and maintained at  $-5.0\text{V}_{\text{SCE}}$ . Process optimization was studied for electrodeposition time (5, 15, 30min) and pulsed or non-pulsed regime.

Amine-functionalized PEG (PEG-amine) surfaces were treated by either crosslinking with N-Succinimidyl 3-maleimido-propionate (SMP) or carboxylic acid activation with EDC/sulfo-NHS to bond the AMP to the PEG. Coatings were characterized by sessile drop contact angle, white light interferometry, ATR-FTIR and XPS. Bacterial adhesion assays were done by immersion of the samples in culture medium with bacteria (*Staphylococcus aureus* and whole dental plaque) for 2h. Bacteria presence was measured by seeding and CFU counting, as well as by staining with a life/dead kit and analysing with a confocal fluorescence microscope. Cell adhesion and cytotoxicity LDH assays were done with human fibroblasts. Polished titanium surfaces were used as controls.

## RESULTS AND DISCUSSION

Water contact angle measurements showed an increase in the surface hydrophilicity due to the presence of the PEG-amine coating. ATR-FTIR measurements showed the presence of PEG-amine and peptide in all the samples.

Based on the XPS results (table 1), a higher amount of

carbon, nitrogen and sulphur was detected on the samples coated with AMPs, sign of a successful immobilization process.

Table 1. Atomic concentration of the control and treated samples

	C 1s	O 1s	N 1s	Ti 2p	S 2p
Ti	23.4±1	59.6±1	0.6±0	16.3±0	0.0±0.0
PEG-amine	28.1±1	47.1±1	0.9±0	34.5±0	0.0±0.0
LF crosslinker	49.1±7	33.1±6	11.9±1	5.2±2	0.7±0.0
MG crosslinker	51.4±6	32.8±5	9.6±1	5.6±1	0.5±0.0
LF (EDC/NHS)	51.4±6	33.7±3	8.3±1	6.3±1	0.2±0.0
MG (EDC/NHS)	50.2±9	35.9±5	7.4±1	6.2±4	0.1±0.0

Cytotoxicity assays showed a cell survival rate higher than 80%, demonstrating the biocompatibility of the coating *in vitro*, while the cell adhesion was not significantly affected by the presence of PEG or PEG plus AMP.

Bacterial adhesion assays (figure 1) showed a decrease on the bacterial adhesion with the presence of PEG-amine. This antibacterial effect was further increased with the presence of the AMP. In this regard, a similar behaviour was observed between MG-2 and LF1-11.

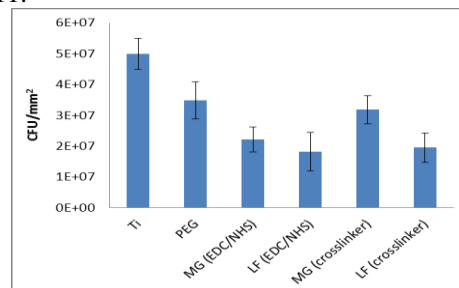


Figure 1. Bacterial adhesion on the treated samples

## CONCLUSION

Titanium surface has been functionalized with a PEG-amine antifouling coating by an electrodeposition method. This coating has been used as a platform for the immobilization of AMP as antibacterial agents. The bonding of AMP to PEG-amine was successfully established with both SMP and EDC/NHS. The coatings showed a good biocompatibility and a significant decrease on the bacterial adhesion.

## REFERENCES

1. Porter JA. *et al.*, *General Dentistry*, 53:423-46, 2005

## ACKNOWLEDGMENTS

The authors acknowledge financial support from the UPC and Fundación Ramón Areces, project MAT2012-30706, co-funded by the EU through European Regional Development Funds, and COST action MP1101.





## Modified PVC Urinary Catheters to Prevent Bacterial Adhesion

Luisa Islas<sup>1</sup>, Guillermina Burillo<sup>1</sup>, Carmen Alvarez-Lorenzo<sup>2</sup>, Angel Concheiro<sup>2</sup>.

<sup>1</sup>Instituto de Ciencias Nucleares, Universidad Nacional Autónoma de México, México

<sup>2</sup>Departamento de Farmacia y Tecnología Farmacéutica, Universidad de Santiago de Compostela, Spain

[leislal@gmail.com](mailto:leislal@gmail.com)

### INTRODUCTION

In hospitals, nearly 20% of patients use a urinary catheter, which increases the risk of developing a urinary tract infection (UTI)<sup>1</sup>. Health care related UTIs are due to the formation of a bacterial biofilm on the surface of the catheter<sup>2</sup>. In this study, modified poly(vinyl chloride) urinary catheters, with a binary graft of acrylic acid and poly(ethylene glycol) methacrylate, were submitted to cytocompatibility testing, drug loading and release studies, and bacterial inhibition and adhesion tests, to see whether the binary graft could successfully prevent the formation of a biofilm.

### EXPERIMENTAL METHODS

Ciprofloxacin loading and release studies were carried out using pieces of pristine and modified catheters (1 cm). The samples were left to swell in an aqueous ciprofloxacin solution and the amount of drug absorbed was calculated by monitoring the solution's absorbance at 271 nm. The drug-loaded catheters were then placed in an artificial urine solution, and the drug release was calculated by monitoring the absorbance at 273 nm. Cytocompatibility tests were conducted *in vitro* using BALB 3T3 mouse fibroblast clone A31 cells (ATCC<sup>®</sup> CCL-163<sup>™</sup>, Manassas, VA, USA) following the ROCHE© protocol. All experiments were carried out in triplicate. For the bacterial inhibition tests, drug-loaded catheters (1 cm) were placed in an agar Petri dish that had been seeded with *Staphylococcus aureus* (ATCC 25923) or *Escherichia coli* (ATCC 11229). The plates were kept at 37°C for 24 h, and then the inhibition rings were measured. For the bacteria adhesion tests, the samples were placed in 2 mL of an *Escherichia coli* solution in trypticase soy broth ( $8 \times 10^8$  CFU/mL) and cultured at 37°C for 3 h under static conditions. Afterwards, the samples were washed with phosphate buffer (PBS), placed in 2 mL of a sterile PBS, and sonicated for 5 min. The suspensions were then spread on TSA plates, and the colony forming units (CFUs) were measured after 24 h of incubation at 37°C.

### RESULTS AND DISCUSSION

Catheters grafted with PEGMA or the binary graft improved the cell viability and had better cytocompatibility for longer periods of time (Table 1).

Table 1: Cytocompatibility of pristine and modified catheters after 24 and 48 h.

	Cell viability (%)	
	24 h	48 h
PVC	94 ± 7	73 ± 4
PVC-g-PEGMA(40%)	99 ± 1	83 ± 8
PVC-g-AAc(44%)	67 ± 5	69 ± 2
[PVC-g-PEGMA(10%)]-g-AAc(14%)	98 ± 16	92 ± 8

The catheters that were grafted with AAc were able to absorb ciprofloxacin; however, catheters grafted solely with PEGMA did not significantly absorb the drug, as was the case with pure PVC (Fig 1).

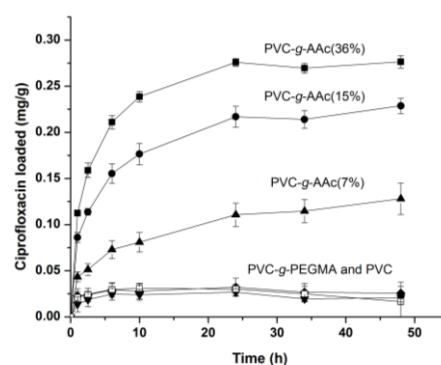


Fig 1: Ciprofloxacin absorbed by PVC, PVC-g-AAc, and PVC-g-PEGMA.

The catheters grafted with PEGMA proved better than PVC-g-AA and binary grafted catheters at preventing bacterial growth (not shown) and adhesion (Fig 2).

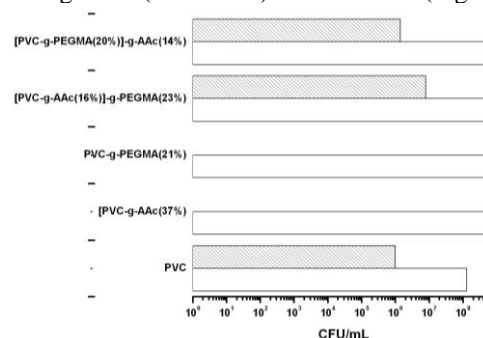


Fig 2: CFU/mL of *Escherichia coli* upon pristine and modified catheters that were loaded with drug (shaded region) and not loaded with drug (white).

### CONCLUSION

Catheters grafted with PEGMA could prevent bacteria growth and adhesion better than PVC, PVC-g-AAc, or the binary grafted catheters.

### REFERENCES

- Allegranzi B. *et al.*, Report on the Burden of Endemic HCAI Worldwide. WHO 2011.
- Spellbergh B. *et al.*, Clin Infect Dis. 26:13-17, 2012

### ACKNOWLEDGMENTS

This work was supported by CONACYT-CNPq174378 Mexico, MICINN (SAF2011-22771) Spain and FEDER. The authors thank A. Ortega, F. Garcia and B. Leal of the ICN-UNAM, and M.I. Rial, L. Pereiro, and B. Blanco of USC for their technical assistance.



### 3D Bioprinting of Functional Fibrin-Based Skin Equivalents

Nieves Cubo<sup>1</sup>, Marta García<sup>1,2</sup>, Diego Velasco<sup>1</sup>, Juan Cañizo<sup>3</sup>, J.L. Jorcano<sup>1,2</sup>

<sup>1</sup>Department of Bioengineering and Space Engineering, Universidad Carlos III de Madrid, Spain

<sup>2</sup>Department of Regenerative Medicine (CIEMAT), Spain

<sup>3</sup>Pavilion of Experimental Medicine and Surgery, Hospital Universitario Gregorio Marañón, Spain

[ncubo@ing.uc3m.es](mailto:ncubo@ing.uc3m.es)

#### INTRODUCTION

Over the past several years, the development of sophisticated laboratory-grown skin substitutes containing dermal and epidermal components has gained intensive interest in skin tissue engineering. In particular, plasma-based skin equivalents<sup>1</sup> have been used extensively for the treatment of extensive skin injuries since they can be produced as complete autologous scaffolds. However, limitations in the process of skin generation such as the use of specialized personnel combined with a high demand of artificial skin, necessitate the development of new methods that allow the automation and the reduction of production costs of the entire process. In this sense, 3D bioprinting, has emerged as a flexible tool in regenerative medicine and provides a platform to address these needs. 3D bioprinting allows for the construction of artificial tissues or organs, either autologous or allogeneic by printing cells, soluble factors and biomaterials in a desired pattern with the help of high-precision Cartesian robots. In this approach, we were able to build 400 cm<sup>2</sup> of functional skin in 45 - 60 min.

#### EXPERIMENTAL METHODS

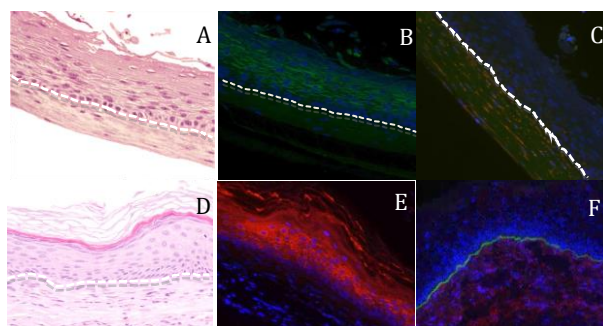
Skin equivalents consisted of two layers, the inner layer (dermis) which was composed by human fibroblasts embedded in a plasma-derived fibrin matrix and the upper layer (epidermis) which was formed by human primary keratinocytes seeded on the top of the fibrin scaffold. These equivalents were deposited using a bioprinter in two different ways: six transwells prepared to differentiate in the incubator (*in vitro* test) and a p100 cell culture dish to be transplanted into a mouse (*in vivo* test). When the process was carried out *in vivo*, the upper layer of keratinocytes differentiated in the mouse. In this case, the equivalents were manually detached from the p100 cell culture dish and placed on the backs of athymic mice (4 immunodeficient *nu/nu* female mice). To characterize the *in vitro* and *in vivo* differentiated printed skin, biopsies from the *in vitro* equivalents and grafted mice were collected. It was performed histologies and immunofluorescence analysis using human specific antibodies against markers of epidermal differentiation (K5, K10, vimentin).

#### RESULTS AND DISCUSSION

***In vitro* test:** The histological staining of printed skin equivalent was able to give rise to all the different strata

found in a normal skin. The histology obtained from these equivalents was very similar to the real skin (Fig. A). The immunostaining also showed that all the cells and the main layers of the skin were in the bioengineered final tissue (Fig. B and C).

***In vivo* test:** The quality recovery of the epidermal phenotype was analyzed (Fig. D). There was a strong suprabasal expression of keratin K10 as it is found in the normal mature skin (Fig. E). The correct epidermal-dermal junction of the skin was confirmed by labeling with an anticollagen VII antibody (Fig. F).



**Histology of engineered human skin reconstructed by bioprinting differentiated *in vitro* 17 days (A,B,C) and on an immunodeficient mouse 6 weeks postgrafting (D,E,F).** A: Hematoxylin and eosin staining. B: Human K10 immunofluorescence (green). C: Human vimentin (red). D: Histologic appearance of the regenerated human skin. E: Human K10 immunofluorescence (red). F: Human vimentin (red) and collagen type VII (green).

(These are only a sample of the obtained results).

#### CONCLUSION

In this work, a new method to print human skin equivalents has been developed. It was also demonstrated that these equivalents maintained a similar functionality compared to the real human skin.

#### REFERENCES

1. Sara G. Llames *et al.*, Transplantation., 77(3), 350-5, 2004.

#### ACKNOWLEDGMENTS

The authors acknowledge financial support of this work by Universidad Carlos III de Madrid, and the plasma supplied by the Centro Comunitario de Sangre y Tejidos in Asturias.



# A New Laser-Based Approach for Native Silk Structuring

Anastasia Brif<sup>1</sup>, Chris Holland<sup>2</sup> and Frederik Claeysens<sup>1</sup>

<sup>1</sup>Department of Materials Science and Engineering, The Kroto Research Institute, North Campus, University of Sheffield, Broad Lane, Sheffield, S3 7HQ, UK

<sup>2</sup>Department of Materials Science and Engineering Sir Robert Hadfield Building, Mappin Street, Sheffield, S1 3JD, UK  
[abrif1@sheffield.ac.uk](mailto:abrif1@sheffield.ac.uk)

## INTRODUCTION

Silk is undergoing a renaissance, especially garnering researcher's interest in the fields of biomaterials and tissue regeneration [1]. Applications of silk-based biomaterials range from templating controlled crystal growth [2] to complex drug delivery systems [3] and even a substrate for transient biodegradable electronics [4]. Yet despite this impressive diversity of applications the manufacturing processes for silks are yet to be fully exploited and call for the development of simple, fast and low-cost silk structuring routes. Currently, most of the silk structuring techniques involve a complex multi-stage process of silk solution production, prior to any structuring [5]. In this research, we present a more direct route for laser silk structuring using photocurable *Bombyx mori* native silk feedstock. Microfabrication techniques including direct laser writing (DLW) and Digital Micromirror Device (DMD) based micro-stereolithography ( $\mu$ SL) were used for the fabrication of various microstructures down to a few microns in scale.

## EXPERIMENTAL METHODS

**Photocurable silk solution preparation:** Native silk feedstock was extracted from posterior section of the middle division of the silk glands from final instar *B. mori* silkworms and diluted in Type II water silk so that the concentration varied from 0.3 to 1.5 wt%. Photocurable silk solution was produced by addition of 1 wt% of Rose Bengal (Sigma-Aldrich) for DLW  $\mu$ SL or of 0.02 wt% Riboflavin (Sigma-Aldrich) for the DMD-based  $\mu$ SL as required.

**Preparation of silk structures by DLW  $\mu$ SL:** A passively Q-switched DPSS Nd-YAG microchip laser with integrated second harmonic generator, with a sub-ns pulse duration was used. This laser emits at wavelengths 1064 and 532 nm (45 kHz repetition rate, Alphas laser). The laser output was expanded by Galilean beam expander to  $\sim 8$  mm beam diameter, reflected by a silver mirror and focused through a 10 $\times$  objective lens (NA 0.3) into a sample holder mounted on a high precision xyz stage. 10  $\mu$ l of the silk solution was dispersed on a glass slide. The patterns were written *via* focusing the laser just above the glass-silk interface.

**Preparation of silk structures by DMD  $\mu$ SL:** A 405 nm violet diode laser was used (150 mW, Vortran laser technology). The laser output was expanded to a 5 mm diameter beam and was reflected from a DMD. The reflected image was directed by a silver coated mirror onto a glass slide covered with photocurable silk solution. The laser power was 100 mW and projection time varied from 10 sec to 10 min.

## RESULTS AND DISCUSSION

The results of this research clearly indicate that native silk solution down to 0.3 wt% can be laser structured by combining with Rose Bengal and Riboflavin photo-

absorbents. By applying a  $\mu$ SL fabrication technique, micrometre-sized complex silk structures were produced by DLW (fig. 1a) and DMD (fig. 1c). In addition, we noticed alignment of silk structures *outside* sections exposed by the laser writing direction. This created an additional sub-micron grooved pattern (fig. 1b) which may have potential use for tissue engineering.

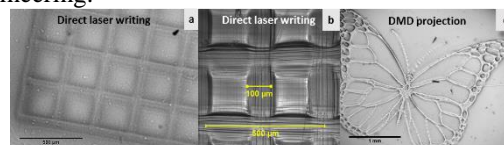


Figure 1: Native silk structuring by a,b) DLW and c) DMD  $\mu$ SL

To better understand the mechanism of silk photocuring, silk structures were analysed by ATR-FTIR. A clear shift in the amide I peak position [6] confirmed the partial structural conversion/solidification of the silk solution (fig. 2). A methanol wash of the structured silk resulted in a full conversion of native silk to cocoon-like structure.

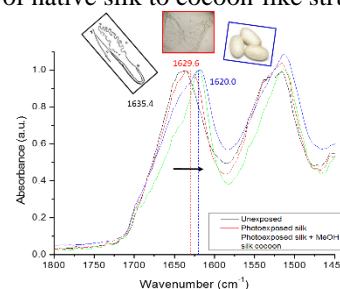


Figure 2: ATR-FTIR spectra of native silk conversion under laser illumination

## CONCLUSION

The innovative results of this study indicate that native silk conversion can be achieved by laser light illumination. Complex structure were fabricated by laser structuring techniques for various biomedical and tissue engineering application.

## REFERENCES

1. N. Kasoju, U. Bora, *Adv. Healthc. Mater.* 1, 393–412, 2012
2. X. D. Kong, *et al.*, *J. Cryst. Growth.* 270, 197–202, 2004
3. H. Tao *et al.*, *Proc. Natl. Acad. Sci.* 111, 17385–17389, 2014
4. S. W. Hwang *et al.*, *Sci.* 337, 1640–1644, 2012
5. D. N. Rockwood *et al.*, *Nat. Protoc.* 6, 1612–1631, 2011
6. M. Boulet-Audet, *et al.*, *Acta Biomater.* 10, 776–84, 2014

## ACKNOWLEDGMENTS

The authors would like to thank Pete Laity for help with the FTIR data collection and Nicola Green for the confocal imaging. For funding we thank the EPSRC (EP/K005693/1) and the University of Sheffield.





A.G.B. Castro, John A Jansen, Jeroen JJP van den Beucken, Fang Yang

Department of Biomaterials, Radboud University Medical Center, Philips van Leydenlaan 25 6525 EX, Nijmegen, The Netherlands

[antonio.goncalvesdebritocastro@radboudumc.nl](mailto:antonio.goncalvesdebritocastro@radboudumc.nl)

## INTRODUCTION

Non-spherical microparticles, as for example micro-cylinders, have presented interesting features such as a high surface area to volume, sustainable drug release<sup>[1]</sup>, reduced immune clearance<sup>[2]</sup> and good internalization by cells<sup>[3]</sup>, making them suitable for drug delivery and tissue engineering applications. Such structures can be developed using physical processes such as lithography, stretching techniques and cryo-sectioning of microfibers or chemical-based strategies. Compared to the other approaches, the chemical-based strategies present the advantages as a lower cost, more mild conditions and a better control of the properties present in the final product. A promising chemical approach to produce micro-cylinders is aminolysis, by which an amine reagent reacts with the polymeric material, e.g. polymeric microfibers, resulting in their controlled sectioning<sup>[4]</sup>. More importantly primary amine groups are attached to its surface, leading to an increase in hydrophilicity and serving as linking points to the immobilization of different compounds.

The aim of this work is to produce micro-cylinders that present a high porosity, surface area to volume and are functionalized with reactive amine groups at their surface. In order to achieve such goal electrospun Poly(L-lactic acid) (PLLA) microfibers were subjected to an aminolysis process.

## EXPERIMENTAL METHODS

PLLA fibers were prepared by dissolving the polymer in different solvents; hexafluoro-2-propanol (HFIP), a dichloromethane (DCM)/chloroform mixture or a dichloromethane/water emulsion and subjected to electrospinning. Micro-cylinders were prepared by an aminolysis procedure, using a 5% ethylenediamine solution, and further characterized by Scanning Electron Microscopy (SEM), X-Ray Diffraction (XRD), Fourier Transform Infrared Spectroscopy (FT-IR), nitrogen adsorption BET method, Differential Scanning Calorimetry and Thermogravimetric Analysis (DSC-TGA) techniques. Primary amines present in the micro-cylinders were quantified by a TNBS (2,4,6-trinitrobenzene sulfonic acid) colorimetric assay. Statistical evaluation of the results was performed using two-way analysis of variance (ANOVA) significance test.

## RESULTS AND DISCUSSION

Morphological evaluation has shown that the use of HFIP generated fibers with a smooth surface while the use of DCM as a solvent lead to the formation of porous fibers after electrospinning (Fig 1a and b). Porosity of the fibers increased by using a DCM and water emulsion (Fig 1c).

After aminolysis the porous morphology of the different materials was maintained (Fig 1d, e and f). Micro-cylinders with different dimensions were obtained, being their length dependant of the time of aminolysis.

The results obtained from the morphological evaluation and XRD analysis show that aminolysis lead to the sectioning of the fibers and that such process occurs mainly in their amorphous regions, resulting in the maintenance of the more crystalline domains in the final product.

Quantification of primary amines detected the presence of such groups in the samples subjected to aminolysis, being their amount proportional to the time of aminolysis.

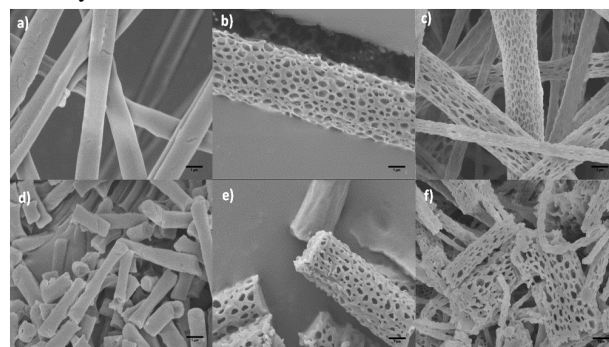


**Fig 1** Electrospun fibers prepared with a) HFIP b) DCM/Chloroform c) DCM+H<sub>2</sub>O. Microcylinders after 3 hours of aminolysis (d; e and f).

## CONCLUSION

The results obtained suggest that the structural and morphological properties of PLLA electrospun fibers can be modified using different solvents. Micro-cylinders of different porosity and lengths were obtained by tuning the aminolysis treatment conditions. Primary amines immobilization was achieved, enabling the functionalization of these structures with compounds relevant for biomedical applications.

## REFERENCES

1. Christian, D.A., et al., *Flexible Filaments for in Vivo Imaging and Delivery: Persistent Circulation of Filicelloses Opens the Dosage Window for Sustained Tumor Shrinkage*. *Molecular Pharmaceutics*, 2009. **6**(5): p. 1343-1352.
2. Muro, S., et al., *Control of endothelial targeting and intracellular delivery of therapeutic enzymes by modulating the size and shape of ICAM-1-targeted carriers*. *Molecular Therapy*, 2008. **16**(8): p. 1450-1458.
3. Gratton, S.E.A., et al., *The effect of particle design on cellular internalization pathways*. *Proceedings of the National Academy of Sciences of the United States of America*, 2008. **105**(33): p. 11613-11618.
4. Kim, T.G. and T.G. Park, *Biodegradable polymer nanocylinders fabricated by transverse fragmentation of electrospun nanofibers through aminolysis*. *Macromolecular Rapid Communications*, 2008. **29**(14): p. 1231-1236.

## ACKNOWLEDGMENTS

This work was supported by a grant from the Dutch government to the Netherlands Institute for Regenerative Medicine (NIRM, grant No. FES0908).



# Cell Proliferation Controlled by Selective Laser Melting (SLM) Process Parameters

Bartłomiej A. Wysocki<sup>1</sup>, Joanna Idaszek<sup>1</sup>, Wojciech Świążkowski<sup>1</sup>, Krzysztof J. Kurzydłowski<sup>1</sup>

<sup>1</sup>Faculty of Materials Science and Engineering, Warsaw University of Technology, Poland  
[bartlomiej.wysocki@inmat.pw.edu.pl](mailto:bartlomiej.wysocki@inmat.pw.edu.pl)

## INTRODUCTION

The usage of laser 3d printers is very perspective in fabrication of solid and porous implants from various polymers, metals and its alloys. The Selective Laser Melting (SLM) process, where consolidated powders are fully melted on each layer, gives possibility of fabrication structures with interconnected pores like scaffolds for bone tissue engineering basing on CAD model. During SLM fabrication on 3d printer, depending on used system, there is possibility for setting amount of energy density [ $\text{J}/\text{mm}^3$ ] transferred to the consolidated powders thus controlling contact angle and roughness of created implants surface. In this study, we are controlling energy density delivered to titanium powder by setting various laser power, exposure time and exposure point distance. This study allowed us to determine the optimal laser parameters for cell proliferation on CP titanium alloy substrates.

## EXPERIMENTAL METHODS

The sets of disks with dimensions of 12 mm diameter and 2 mm thickness were fabricated from CP titanium powder on Realizer SLM50 3d printer. The average size of titanium powder was  $40\text{ }\mu\text{m}$ . The energy density used for powder consolidation was in range from 4 to  $45\text{ J}/\text{mm}^3$ . The energy density values were changed by laser power, exposure time and point distance in range 1000-1800 mA, 20-80  $\mu\text{s}$  and 20-60  $\mu\text{m}$  respectively. The selectively laser melted disks morphology was observed using Scanning Electron Microscope (Hitachi SU8000). The surface roughness was measured using optical profilometer (Wyko NT9300), contact angle was measured using Contact Angle System OCA, the Archimedes method and Radwag XA 110 were used for theoretical density calculations. The proliferation of human mesenchymal stem cells (hMSC, Lonza, passage 4) on discs fabricated with various parameters was evaluated by means of MTS assay after 24h and 7 days of culture.

## RESULTS AND DISCUSSION

The cells proliferation after one-day incubation was similar for all samples irrespectively from parameters used during fabrication. The differences in cells proliferation were clearly seen after 7 days incubation (Fig. 1). We have observed that growing energy density from 4 to  $23\text{ J}/\text{mm}^3$  had positive influence on cell proliferation. Higher values of energy density, delivered for powder consolidation, than  $23\text{ J}/\text{mm}^3$  caused proliferation decrease. The cells proliferation had the lowest value for samples with fully hydrophilic or close to hydrophobic surface. There was not found Ra parameter influence on samples cell adhesion. Samples Ra parameter was in range from  $6.2$  to  $37\text{ }\mu\text{m}$  and there

was no direct connection between Ra parameter and cell proliferation. In our study we report also that hydrofluoric (HF) acid treatment, positive for unmelted titanium particles removal, had negative influence on cell proliferation on fabricated samples. The titanium surface treatment with hydrofluoric acid concentration from 1 to 5% decreased cell proliferation more than 50% in comparison to untreated surfaces.

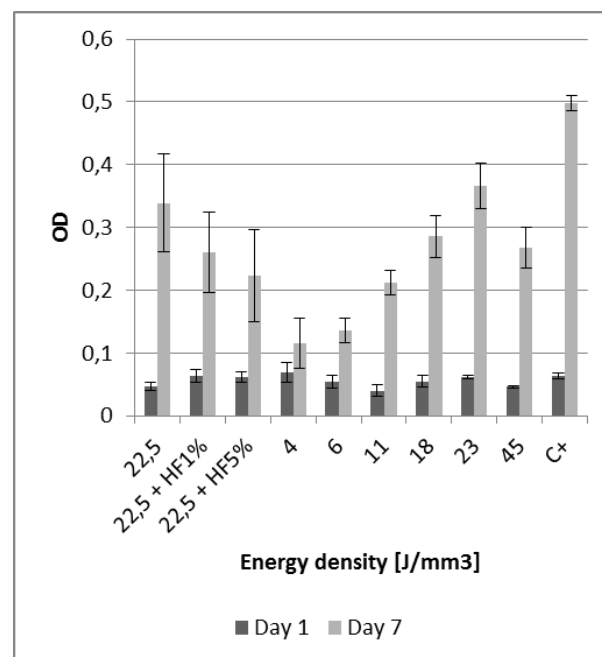


Fig. 1. The Energy density [ $\text{J}/\text{mm}^3$ ] and HF treatment influence on cells proliferation on selectively laser melted CP titanium implants.

## CONCLUSION

The cell proliferation on titanium implants fabricated by laser 3d printer can be controlled by amount of delivered energy density [ $\text{J}/\text{mm}^3$ ]. The energy density should be set carefully by various laser work parameters (laser power, exposure time, point distance) to avoid obtaining a fully hydrophilic or hydrophobic surface. Unmelted fully particles should be removed in as low as possible hydrofluoric acid concentrations to avoid cell proliferation decrease.

## ACKNOWLEDGMENTS

The authors would like to thank the NCBiR (National Center for Research and Development) for providing financial support to PBS project LasIMP (The innovative additive shaping laser technology LENS for cementless hip implants geometry modification and surface layer biofunctionalization).

Henning Menzel<sup>1</sup>, Andreas Bertz<sup>1</sup>, Niels Poth<sup>1</sup>, Wibke Dempwolf<sup>1</sup>, Jan-Erik Ehlers<sup>2</sup>, Karl-Heinz Gericke<sup>2</sup>, Peter P. Müller<sup>3</sup>, Gerhard Gross<sup>3</sup>, Stefanie Woehl-Bruhn<sup>4</sup>, Heike Bunjes<sup>4</sup>

<sup>1</sup>Institute of Technical Chemistry, Braunschweig University of Technology, Germany

<sup>2</sup>Institute of Physical Chemistry, Braunschweig University of Technology, Germany

<sup>3</sup>Helmholtz Centre for Infection Research, Braunschweig, Germany

<sup>4</sup>Institute of Pharmaceutical Technology, Braunschweig University of Technology, Germany

[h.menzel@tu-braunschweig.de](mailto:h.menzel@tu-braunschweig.de)

## INTRODUCTION

Therapeutic proteins have a high potential for pharmaceutical applications. Drug delivery systems are needed to protect these proteins from *in-vivo* degradation. Furthermore, the proteins can induce unwanted side effects, e.g. an immunogenic response. A local administration close to the diseased area and a slow drug release can minimize these effects. Hydrogels are well suited as drug delivery systems. To investigate the relation between network structure and release hydroxyethyl starch modified with polyethylene glycol-methacrylate was used to obtain bulk hydrogels or injectable hydrogel microspheres.

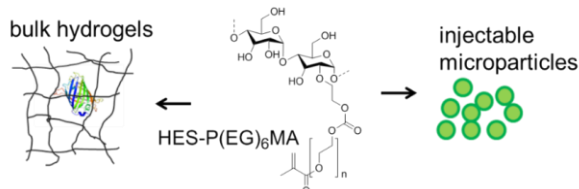


**Figure 1:** Hydroxyethylstarch derivatives can be used to prepare bulk hydrogels or injectable hydrogel micro-particles

## EXPERIMENTAL METHODS

Hydroxyethylstarch was modified with polymerizable methacrylate groups via ester or carbonate linkers, respectively (see Figure 1), and with different degrees of substitution.<sup>1</sup> These prepolymers can be cross-linked as aqueous solutions in the presence of proteins using photoinitiators and encapsulate proteins with high efficiency. By a water-in-water emulsion technique microgels are accessible.<sup>1</sup> Several model proteins e.g. green fluorescent protein (GFP), but also antibody fragments have been incorporated. The release and mobility of the proteins was studied. Furthermore, nanogel suspensions were prepared by ionotropic gelation of chitosan with a degree of deacetylation of 58% with tripolyphosphate in the presence of bone morphogenetic protein 2 (BMP-2). The suspensions were used to coat implants. The coatings were investigated *in-vitro* and *in-vivo*.

## RESULTS AND DISCUSSION

Green fluorescent protein (GFP) loaded hydrogels have been analyzed by fluorescence methods with two-photon excitation.<sup>2</sup> Via fluorescence anisotropy the inner rotational motions can be studied. The results suggest an unrestricted GFP rotation within the hydrogel (see Figure 2).<sup>2</sup> Fluorescence recovery after photo-bleaching gives information about the

translational diffusion. Here the data indicate that translational mobility of GFP is strongly restricted in the hydrogel.<sup>2</sup>

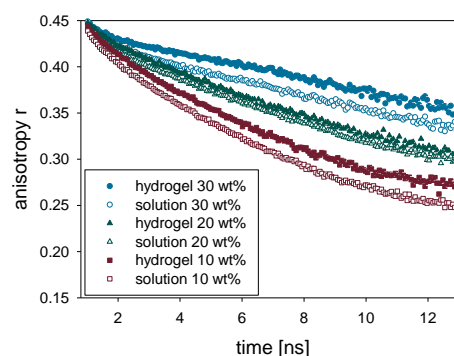


**Figure 2:** Decay of the fluorescence anisotropy of eGFP in solutions and hydrogels prepared with HES-P(EG)<sub>6</sub>MA<sup>2</sup>

The release of the proteins was investigated and correlated with the mesh size.<sup>1</sup> These *in-vitro* results were compared with *in-vivo* release experiments carried out with an *in vivo* imaging system (IVIS 200).<sup>3</sup> Entrapment of BMP-2 in chitosan and tripolyphosphate nanogels was highly efficient. Release is slow and depends on the degradation of the nanogel. The BMP-2 released from the nanogel shows biological activity *in-vitro* and *in-vivo*.<sup>4</sup>

## CONCLUSION

Hydrogels prepared from hydroxyethylstarch derivatives and chitosan/tripolyphosphate nanogels are systems well suited for the delivery of therapeutic proteins. The release can be adjusted by the crosslinking density and the degradability of the hydrogel as well as the interaction of the proteins with the polymer forming the hydrogel.

## REFERENCES

1. A. Bertz, et al., J. Biotechnol. 2013, 163, 243.
2. A. Bertz, et al., Macromol. Biosci. 2013, 13, 215.
3. S. Wöhl-Bruhn, et al., J. Controlled Release 162, 127 (2012)
4. N. Poth, et al., Biomolecules 2015, 5, 3.

## ACKNOWLEDGMENTS

This work was supported by the German Research Foundation (DFG) via the collaborative research centres CRC 578 "From Gene to Product" and CRC 599 "Bioresorbable and Permanent Implants".



# Peptide Binding Dendrimer Decorated Injectable Hyaluronan Hydrogels Modulate the Controlled Release of BMP-2 and TGF- $\beta$ 1

Ryan Seelbach<sup>1,2</sup>, Peter Fransen<sup>3</sup>, Miriam Royo<sup>4</sup>, Fernando Albericio<sup>3</sup>, Mauro Alini<sup>2</sup>, Alvaro Mata<sup>5</sup>, David Eglin<sup>2</sup>

<sup>1</sup>Department of Nanotechnology, University of Barcelona, Spain

<sup>2</sup>AO Research Institute Davos, Switzerland

<sup>3</sup>Institute of Research in Biomedicine, Spain

<sup>4</sup>Combinatorial Chemistry Unit, Barcelona Science Park, Spain

<sup>5</sup>Department of Materials Science and Engineering, Queen Mary, University of London, United Kingdom

[david.eglin@aofoundation.org](mailto:david.eglin@aofoundation.org)

## INTRODUCTION

The potential of affinity binding peptide functionalized dendrimers to modulate the release and availability of growth factors important for musculoskeletal regeneration therapies, in combination with thermoresponsive hyaluronan hydrogels was assessed. Dendrimers were synthesized and characterized by HPLC, LC-MS and NMR. The BMP-2 and TGF- $\beta$ 1 released from injectable hydrogels were measured by ELISA assay in the presence and the absence of orthogonally synthesized dendrimers bearing BMP-2 or TGF- $\beta$ 1 affinity binding peptides.

## EXPERIMENTAL METHODS

Thermoresponsive hyaluronan conjugates (HpN) were synthesized as reported with thermoresponsive segments, poly(*N*-isopropylacrylamide) (pN) of Mw equal to 16 and 21 kDa, and an identical degree of substitution 4.4 molar % measured by <sup>1</sup>H NMR [1]. Dendrimers bearing BMP-2 or TGF- $\beta$ 1 binding epitopes, YPV and LPL respectively, were synthesised, characterized and grafted onto hyaluronan as assessed by amino-acid analysis<sup>1</sup>. The purified and lyophilized polymers were reconstituted in PBS to 15% wt/vol (13% wt/vol Hyal-pN and 2% wt/vol dendrimer modified hyaluronic acid).

*In vitro* release studies of loaded hydrogels were quantified by ELISA. Statistical significance was calculated with a mixed design analysis of variance (ANOVA) model.

## RESULTS AND DISCUSSION

The dendrimers combined with poly(*N*-isopropylacrylamide) hyaluronan (HpN) conjugates do not significantly influence their gelation temperature 28°C  $\pm$  0.5°C and 30°C  $\pm$  0.5°C and elastic modulus at 37°C, 0.4 and 2 kPa respectively for HpN16 and HpN21 with and without dendrimers. In physiological mimicking conditions, the compositions loaded with either BMP-2 or TGF- $\beta$ 1 show that in the presence of dendrimers a statistically significant lower amount ( $p < 0.0005$ ) of BMP-2 and TGF- $\beta$ 1 is released (Figure 1). The peptide bearing dendrimers attenuate the protein release from HpN depots, causing a sharp decrease in the burst phase as well as a lower final concentration at 7 days. The specificity of the synthesized peptide epitopes was also performed by loading BMP-2 into depots containing TGF- $\beta$ 1 binding hyaluronan, and vice

versa. Interestingly in all scenarios, the dendrimers are at least similarly efficacious in retaining growth factors suggesting that the binding behavior of these peptides are not specific to BMP-2 and TGF- $\beta$ 1 in our experimental set-up.

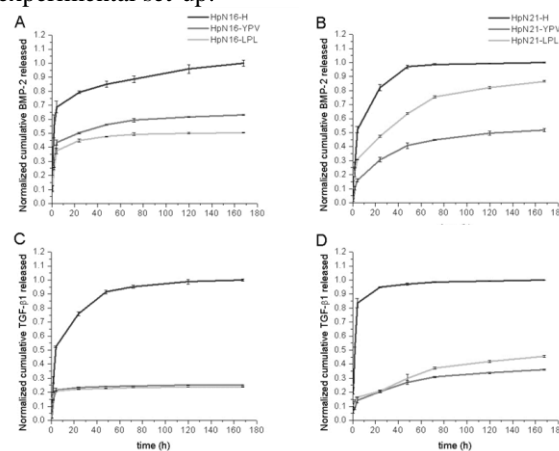


**Figure 1.** Normalized cumulative protein release from loaded hydrogels showing the relative amounts of BMP-2 released from (A) HpN16 and (B) HpN21, and TGF- $\beta$ 1 released from (C) HpN16 and (D) HpN21.

## CONCLUSION

We have designed, developed and characterized unique nanoscale tools called dendrimers which have been augmented with terminal peptide binding sequences. We found that the peptide binding dendrimers attenuate the release of the GFs, but their binding was non-specific to either tested epitope. This study highlights the potential of incorporating these unique nanotools into a biomaterial platform with the goal to control the scaffold functionality with nanoscale precision.

## REFERENCES

1. Seelbach R. *et al.* Acta Biomater. 10:4340-50, 2014

## ACKNOWLEDGMENTS

The authors would like to acknowledge the financial support from the AO Foundation (grant number C10-60S), the Spanish Ministry of Economy and Competitiveness (SAF2011-30508-C02-01), the Generalitat de Catalunya (2009SGR 1024), CIBER-BBN and La Caixa social program.



## Co-Deliver of Glucagon-like Peptide-1 and Dipeptidyl Peptidase 4 Inhibitor for Treatment of Type 2 Diabetes

Francisca Araújo<sup>1,2,3</sup>, Neha Shrestha<sup>3</sup>, Mohammad-Ali Shahbazi<sup>3</sup>, Dongfei Liu<sup>3</sup>, Bárbara Herranz-Blanco<sup>3</sup>, Ermei Mäkilä<sup>3,4</sup>, Jarno Salonen<sup>4</sup>, Jouni Hirvonen<sup>3</sup>, Pedro L. Granja<sup>1,2</sup>, Bruno Sarmento<sup>1,5</sup>, Hélder A. Santos<sup>3</sup>

<sup>1</sup>INEB – Instituto de Engenharia Biomédica, 4150-180 University of Porto, Portugal,

<sup>2</sup>ICBAS – Instituto Ciências Biomédicas Abel Salazar, 4150-180 University of Porto, Portugal,

<sup>3</sup>Division of Pharmaceutical Chemistry and Technology, Faculty of Pharmacy, FI-00014 University of Helsinki, Finland,

<sup>4</sup>Laboratory of Industrial Physics, FI-20014 University of Turku, Finland,

<sup>5</sup>INFACTS - Instituto de Investigação e Formação Avançada em Ciências e Tecnologias da Saúde, Instituto Superior de Ciências da Saúde-Norte, CESPU, 4585-116 Gandra, Portugal.

[francisca.araujo@ineb.up.pt](mailto:francisca.araujo@ineb.up.pt)

### INTRODUCTION

The clinical use of glucagon like peptide-1 (GLP-1) is in the pipeline of type 2 diabetes Mellitus (T2DM) therapy. It acts in a glucose-dependent way stimulating insulin production [2]. Nevertheless, GLP-1 has to be administrated by parenteral route which is not well accepted by patients [3]. To achieve an efficient oral release and permeability of active GLP-1, GLP-1 was loaded into different nanoparticles (NPs).

### EXPERIMENTAL METHODS

Poly(lactic-co-glycolic acid) (PLGA) and porous silicon (PSi) NPs were prepared and coated with chitosan [3]. Cell-penetrating peptide conjugation was made using EDC/NHS chemistry. Afterwards, GLP-1 loaded NPs were coated with a pH-sensitive polymer HPMCAS-MF and loaded with DPP4 inhibitor using a microfluidics technique. The system was then characterized.

### RESULTS AND DISCUSSION

The particles presented a regular and round shape with the maintenance of their integrity at pH below 6.0 (gastric conditions). When the pH increased (small intestine conditions), the polymer degraded, and the NPs were released (Fig. 1).

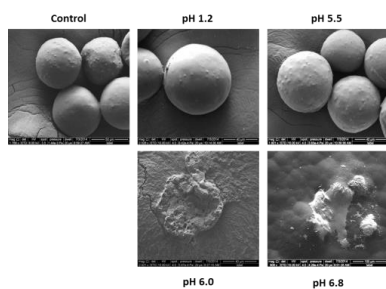


**Fig. 1.** SEM images of the enteric-coated NPs in different pH conditions.

The *in vitro* release profiles of GLP-1 from the nanosystems were evaluated at pH 1.2 to mimic the gastric conditions and in fasted state simulated intestinal fluid (FaSSiF) (pH 6.8) to mimic the intestinal conditions. The release profiles showed that the enteric coating was successful, protecting the release of GLP-1 in acidic conditions, while in FaSSiF it reached 40% release after 6 h.

The cell viability studies showed that all nanosystems were compatible with the gastric AGS cells for 3 h and

with the intestinal cell lines HT29-MTX and Caco-2 for 12 h, presenting viability higher than 80% (results not shown). The interaction between the NPs and the intestinal co-culture cells showed that there was a clear increase in the interaction between the modified NPs with the cells, compared to the control and to the unmodified NPs.

The activity results of DPP4 enzyme after the contact with the inhibitor showed that its activity is extremely lower in comparison with cells without any contact with the inhibitor.

### CONCLUSION

A multisystem was developed using a microfluidic technique using modified NPs as a nanomatrix. These systems were sensitive to different pH, protecting the release of GLP-1 at low pH. They showed to be viable systems to interact in a closer way with intestinal cells and allow the co-delivery of two drugs in a single formulation. The very low activity of DPP4 enzyme is expected to prolong GLP-1's half-life, thus decreasing the blood glucose levels for a long time.

### REFERENCES

1. Hosseiniinasab, S. *et al.*, Chem. Biol. Drug Des. 84:307-15, 2014.
2. Araújo, F. *et al.*, Curr. Pharm. Biotechnol. 15:609-19, 2014.
3. Araújo, F. *et al.* Biomaterials. 35:9199-207, 2014.

### ACKNOWLEDGMENTS

The European Regional Development Fund through the Programa Operacional Factores de Competitividade – COMPETE, by the Portuguese funds through Fundação para a Ciência e a Tecnologia (FCT) in the framework of the project PEst-C/SAU/LA0002/2013, and co-financed by the North Portugal Regional Operational Programme (ON.2 – O Novo Norte) in the framework of the project SAESCTN-PIIC&DT/2011, under the National Strategic Reference Framework, is acknowledged. F. Araújo thanks FCT for financial support (SFRH/BD/87016/2012). Dr. H.A. Santos acknowledges financial support from the Academy of Finland (decision no. 252215), the University of Helsinki Research Funds, the Biocentrum Helsinki, and the Finnish Center for International Mobility (grant no TM-13-9048).



## Controlled Release of Platinum-Bisphosphonate Complexes from Injectable Calcium Phosphate Cements for Treatment of Bone Tumors

Kemal Sariibrahimoglu<sup>1</sup>, Kambiz Farbod<sup>1</sup>, Astghik Hayrapetyan<sup>1</sup>, Jan N W Hakvoort<sup>1</sup>, Michele Iafisco<sup>2</sup>, Nicola Margiotta<sup>3</sup>, Joop G C Wolke<sup>1</sup>, Jeroen J J P van den Beucken<sup>1</sup>, John A Jansen<sup>1</sup>, Sander C G Leeuwenburgh<sup>1</sup>

<sup>1</sup>Department of Biomaterials, Radboud University Medical Center, Nijmegen, The Netherlands

<sup>2</sup>Institute of Science and Technology for Ceramics (ISTEC), National Research Council (CNR), Faenza, Italy

<sup>3</sup>Department of Chemistry, Università degli Studi di Bari Aldo Moro, Bari, Italy

[kambiz.farbod@radboudumc.nl](mailto:kambiz.farbod@radboudumc.nl)

### INTRODUCTION

Injectable, self-setting calcium phosphate cements (CPCs) have been developed as synthetic bone substitutes in view of their similarity to the mineral component of bone. CPCs that maintain a high local concentration of drug would represent ideal therapeutic strategies<sup>1</sup> after tumor resection. During the last decade, nanotechnology has emerged as an additional tool to improve the efficacy of drug delivery for cancer therapies. Iafisco et al. (2012)<sup>2</sup> recently developed hydroxyapatite nanoparticles for local delivery of two chemotherapeutic platinum-bisphosphonate complexes<sup>3,4</sup>: (bis-{ethylenediamineplatinum(II)}-2-amino-1-hydroxyethane-1,1-diyl-bisphosphonate and bis-{ethylenediamineplatinum(II)}-medronate (Fig.1). Both complexes were developed to target traditional cisplatin-based drugs to bone tissue. The presence of bisphosphonate ligands allowed for efficient loading of these complexes onto hydroxyapatite nanoparticles. The results revealed a high loading capacity of hydroxyapatite nanoparticles for the complexes, while the release of chemotherapeutically active Pt was shown to proceed in a sustained manner. Nevertheless, drug-loaded nanoparticles cannot be injected directly into bone defects, due to the risk of excessive leakage of nanoparticles into the surrounding tissues.

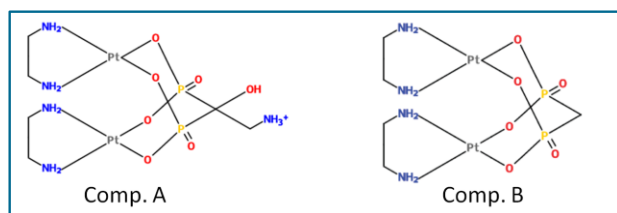


**Fig.1:** Sketches of Complex A: bis-{ethylenediamineplatinum(II)}-2-amino-1-hydroxyethane-1,1-diyl-bisphosphonate and Complex B: bis-{ethylenediamineplatinum(II)}-medronate

Herein, we present a novel method to confine drug-loaded hydroxyapatite nanoparticles inside apatitic CPCs in an attempt to develop CPCs with a sustained chemotherapeutic efficacy.

### EXPERIMENTAL METHODS

Hydroxyapatite nanoparticles loaded with platinum-bisphosphonate complexes were added to the cement powder phase at different amounts ranging from 5–20wt% (Table 1). The morphology and crystal phases of the drug-loaded cements were studied using Scanning Electron Microscopy and X-Ray Diffraction, respectively. The release profiles of the complexes were investigated *in vitro* by soaking drug-loaded cements

into phosphate buffered saline (PBS) followed by quantification of Ca and Pt release for up to four weeks using Inductively Coupled Plasma-Optical Emission Spectroscopy (ICP-OES).

Abbreviations	$\alpha$ -TCP (wt%)	PLGA (wt%)	HA (wt%)
CPC1	55	40	5
CPC2	55	40	5 (+Complex)
CPC3	50	40	10 (+Complex)
CPC4	40	40	20 (+Complex)
CPC5	40	40	20
CPC6	95	-	5 (+Complex)
CPC7	80	-	20 (+Complex)
CPC8	95	-	5

**Table 1:** Abbreviations and compositions the various CPCs

### RESULTS AND DISCUSSION

ICP-OES results revealed that release of  $\text{Ca}^{2+}$  from all CPCs increased with incubation time, while Pt release increased with increasing the amount of drug-loaded HA NPs in CPC; however, the type of complex had a more significant effect (Fig.2). Furthermore, it was observed that incorporation of PLGA MPs into CPCs did not affect the release rate of Pt.

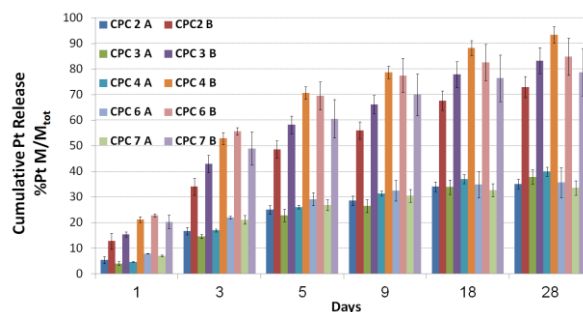


**Fig.2:** Cumulative release of Pt as a function of soaking time in Hepes buffer

### CONCLUSION

This study demonstrated that platinum-bisphosphonate complexes can be released in a sustained manner at rates which can be controlled by varying the hydroxyapatite-binding affinity of the complexes as well as the amount of drug-loaded hydroxyapatite nanoparticles.

### REFERENCES

1. Lopez-Heredia MA et al., Biomaterials, 32:5411–5416, 2011
2. Iafisco M et al., Nanoscale, 4:206–217, 2012
3. Margiotta N et al., Dalton Trans., 29:3131–3139, 2007
4. Palazzo B et al., Adv. Funct. Mater., 17:2180–2188, 2007

## Structurally-Graded Collagen Biomaterials for Osteotendinous Repair

Laura Mozdzen<sup>1</sup>, William Grier<sup>1</sup>, Ashley Moy<sup>1</sup>, Steven Caliar<sup>1</sup>, Brendan Harley<sup>1,2</sup>

<sup>1</sup> Chemical and Biomolecular Engineering, University of Illinois at Urbana-Champaign, USA

<sup>2</sup> Carl R. Woese Institute for Genomic Biology, University of Illinois at Urbana-Champaign, USA

[bharley@illinois.edu](mailto:bharley@illinois.edu)

### INTRODUCTION

Injuries to spatially-ordered tissues in the musculoskeletal system present unique challenges to the field of tissue engineering. The osteotendinous interface connects tendon to bone via a complex insertional zone. The inability to regenerate this interface after injury leads to poor healing and high re-failure rates. A long-term objective in our lab is to develop biomaterials that address current barriers to osteotendinous regeneration. Our efforts concentrate on collagen biomaterials to direct mesenchymal stem cell (MSC) differentiation down multiple osteotendinous lineages in a spatially-selective manner. Such a construct could be seeded with the patient's own stem cells then implanted to regenerate the interface. Here we describe a model collagen-GAG (CG) scaffold containing gradients of mineral content and structural alignment can locally modulate how MSCs respond to cyclic strain using an in vitro bioreactor. Further, given the mechanical strength of the scaffold is a critical design requirement for preclinical testing, we report the use of 3D printing to generate fiber-reinforced CG constructs to better balance strength and bioactivity requirements.

### EXPERIMENTAL METHODS

**Scaffold fabrication.** Single and multi-compartment scaffolds were fabricated from CaP-mineralized (CGCaP) and non-mineralized (CG) collagen suspensions via lyophilization. Directional solidification was used to create geometrically anisotropic scaffold.<sup>1</sup> ABS fibers (straight, 1 mm sinusoidal amplitude, 2 mm sinusoidal amplitude) were printed using a MakerBot Replicator 2X (MakerBot Industries, Brooklyn, NY). ABS fiber-reinforced scaffolds were created by embedding fiber variants into liquid CG suspensions prior to lyophilization. ABS fiber-reinforced scaffolds were characterized via mechanical tensile testing.

**Assessing bioactivity.** Scaffolds were subjected to strain by immobilization into plastic end blocks that were subsequently loaded into a custom built bioreactor. Scaffolds were then seeded with hMSCs and subsequently subjected to various levels of cyclic strain for up to 72 hours. Western blot, RT-PCR, ELISA, and histological analysis were used to evaluate hMSC differentiation and activity.

### RESULTS AND DISCUSSION

Uniaxial stretching of hMSC seeded scaffolds shows an immediate down-regulation in ROCK1 expression as well as a time-dependent relationship between the activation of ERK 1/2 and p38 MAP kinases. ERK 1/2, linked to cyclic strain-induced collagen production, is maximally activated within 10 minutes of strain, then decreases with activation of p38 MAPK by 30 minutes of strain. Short-term stretching was sufficient to induce

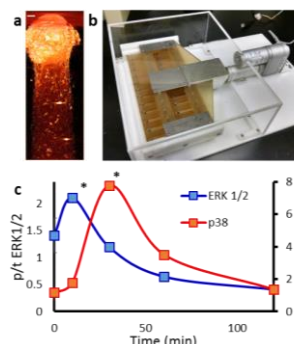


**Fig. 1.** (A) Model osteotendinous scaffold with integrated mineral (top) and aligned (bottom) zones. (B) 24-well tensile bioreactor. (C) Time-dependent ERK1/2 and p38 MAPK activation with 10% cyclic strain.

compartment specific mechanotransduction and integrin subunit ( $\beta 1$ ,  $\beta 3$ ) expression profiles. Increased expression of osteogenic genes (BSP, OCN) is seen in the mineralized compartment while expression of COL1 and the tendon marker SCX in the aligned non-mineral compartment is upregulated with the addition of strain.

The elastic modulus ( $\sim 70$ -fold;  $15.05 \pm 1.73$  MPa) and toughness ( $\sim 55$ -fold) of fiber-reinforced scaffolds increased significantly versus non-reinforced scaffold controls. Further, covalent immobilization of PDGF to the ABS fibers led to significant increase in cell viability within the fiber-scaffold composite.

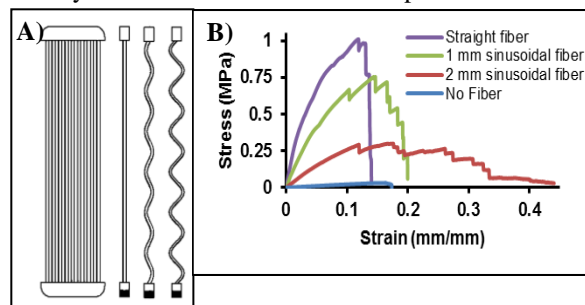


**Fig. 2.** (A) Schematic of fiber reinforcement. (B) Stress-strain curves for fiber-reinforced scaffolds vs. control scaffold.

### CONCLUSION

We describe the use of uniaxial cyclic strain to elicit spatially and strain-dependent hMSC responses (activation and osteotendinous lineage specification) within a model CG scaffolds for osteotendinous repair. We report use of 3D printing to create scaffold-fiber composites with enhanced mechanical properties as well as the use of the fiber to present growth factors (PDGF) to enhance cell activity within the composite.

### REFERENCES

1. Caliar S. *et al.*, Adv. Healthc. Mater. 2015.

### ACKNOWLEDGMENTS

The authors would like to thank the U.S. National Institutes of Health (Grant R21AR063331) for funding.



## Biomaterialized Cellulose-PEGDA Scaffolds for Bone Tissue Regeneration

C. Demitri<sup>1</sup>, M.G. Raucci<sup>2</sup>, A. Giuri<sup>1</sup>, V.M. De Benedictis<sup>1</sup>, D. Giugliano<sup>2</sup>, A. Sannino<sup>1</sup>, L. Ambrosio<sup>3</sup>

<sup>1</sup>Department of Engineering for Innovation, University of Salento, Via Monteroni, 73100 Lecce, Italy.

<sup>2</sup>Institute of Polymers, Composites and Biomaterials – National Research Council of Italy. Mostra d'Oltremare Pad.20 - Viale Kennedy 54, 80125- Naples, Italy.

<sup>3</sup>Department of Chemicals Science and Materials Technology, National Research Council of Italy (DSCTM-CNR), P.le Aldo Moro 7, 00185 – Rome, Italy.

[christian.demitri@unisalento.it](mailto:christian.demitri@unisalento.it)

### INTRODUCTION

In this work, interconnected porous scaffolds have been obtained by an innovative foaming method based on the combination of both physical and chemical foaming stabilization. [1]. Microwaving curing allows the foam formation, employing short reaction times [2]. Current efforts are focused on improving the bioactivity and biological properties of cellulose scaffolds through the incorporation of bioceramics such as hydroxyapatite (HA). Here, we have used a facile biomimetic treatment with the aim to improve the bioactivity and biological properties on scaffold surface.

### EXPERIMENTAL METHODS

Different mixtures of sodium salt of carboxymethylcellulose (CMCNa) and polyethylene glycol diacrylate (PEGDA) were cured in a laboratory microwave oven into silicone vessels. Azobis(2-methylpropionamide) dihydrochloride was used as thermoinitiator (TI). CMCNa and PEGDA mixtures were prepared with different PEG/CMCNa ratios in order to investigate the effect of the concentration on the final material properties. The biomimetic scaffolds were obtained by treating the scaffolds with a supersaturated SBF solution (5SBF); the treatment is able to create an hydroxyapatite coating on the surface and into the porous wall in few days (7days). The rheological properties for each mixture before the curing process were evaluated by viscosity measurements (ARES Rheometric Scientific). The influence of different ratios of PEG/CMCNa in the final product was evaluated by different techniques. Firstly, chemical properties of each sample have been evaluated by spectroscopy analysis FT-IR, before and after curing in order to maximize reaction yield, and optimize the kinetic parameters (i.e. time curing, microwave power). The mechanical properties of the final product were evaluated by the calculation of the elastic modulus. Porous structure and surface analysis were characterized by SEM. Water absorption capacity and stability of materials was evaluated by means of in-vitro degradation test in PBS media. Finally, preliminary biological characterization was carried out with the aim to evaluate the effect of biomaterialization on cellular behaviour in terms of proliferation and early osteogenic differentiation.

### RESULTS AND DISCUSSION

During the foaming procedure, the solutions increased in volume at least by 100% of the initial volume after addition of Pluronic. All the foams with a lower PEG/CMCNa ratios are homogeneous and stables due

to an increased viscosity, resulting in more stable foam. Based on spectroscopy analysis FT-IR, it is evident that the reaction is not complete. Therefore it was added a post-cure in oven at 45°C for 12 h that has improved reaction yield. Mechanical properties of the foam increase by increasing the CMCNa concentration. This is mainly due to the presence of physical entanglements resulting in a higher degree of cross-linking. Fig. 1a shows the SEM image of a biomimetic foam. It is evident a hierarchical structure with open pores of different size and a presence of hydroxyapatite deposits on the scaffold surface.

The response of human mesenchymal stem cells cultured onto the cellulose scaffolds before and after biomimetic treatment showed that the materials are not cytotoxic and have good biocompatibility. The Fig.1B demonstrated a good proliferation. The potential of differentiation of hMSC cells were evaluated by expression of early marker of osteogenic differentiation like Alkaline Phosphatase (ALP) and our results showed that the hydroxyapatite deposits improve the differentiation in the early 3days of incubation evaluated by using a media without osteogenic factors. After 21 days, the majority of the areas of biomaterialized scaffolds were covered by layers of cells as demonstrated by SEM images (Fig.1B).

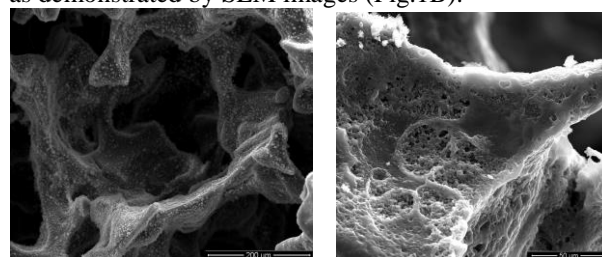


**Figure 1.** SEM images of biomimetic scaffold before (left) and after 21 days of hMSC cell culture (right).

### CONCLUSION

This work demonstrated that physical foaming followed by thermo-polymerization induced by microwave is a solid method to create structures with interconnected open porosity. The suitability to use a biomimetic treatment to increase the cell proliferation has been successfully evaluated. Moreover, the preliminary biological analysis demonstrated the excellent biocompatibility profile.

### REFERENCES

- [1] Demitri C. *et al.*, Interface Focus, 4-1: 20130053, 2014
- [2] Brent Tisserat *et al.*, Journal of Applied Polymer Science 125:3429–3437, 2012.



## INTRODUCTION

Silicones have been used in medical science for a variety of prosthetic applications, because of their unique properties, such as biocompatibility, weather resistance, low chemical reactivity, oxidation resistance and low toxicity. However, in some cases SR does not organically unite with tissues leading, in some cases, to inflammation and foreign-body reaction after long term implantation. Many attempts have been made to further improve SR's biocompatibility and bioactivity and to overcome the above drawbacks, including the incorporation of inorganic bioactive nanoparticles as a modifying additive<sup>1</sup>.

## EXPERIMENTAL METHODS

Polydimethylsiloxane (PDMS), composites reinforced with organically modified montmorillonite (OMMT: Cloisite 20A, Cloisite 30B), hydroxyapatite (HA), silica (Aerosil R972) nanoparticles and bioactive glass (Bonalive) particles were prepared using the sonication technique and subsequently characterized by differential scanning calorimetry (DSC) and thermogravimetric analysis (TGA), whereas their tensile and tear properties were also tested. An "in-vitro" assay of bioactivity was carried out by soaking PDMS hybrids in Simulated Body Fluid (SBF) at pH 7.4 for 7, 21 and 40 days<sup>2</sup>. The formation of hydroxyapatite was evaluated by FTIR-ATR spectroscopy and SEM/EDAX analysis.

## RESULTS AND DISCUSSION

The incorporation of reinforcement increases the rate of curing of PDMS, assessed by viscosity and DSC measurements, in all the examined systems. The introduction of all types of fillers used in this work, decreases the temperature of "cold" crystallization of PDMS, whereas the glass transition and melting temperatures remain intact.

The addition of Cloisite 20A to polysiloxane leads to higher increase in tensile strength compared with that of composites with bioactive glass, silica and Cloisite 30B while hydroxyapatite does not present any reinforcing effect (Table 1).

Table 1. Mechanical properties of PDMS and 5 phr loaded PDMS composites.

Material type	Tensile strength MPa	Mod. of elastic. (MPa)	Tear strength (Nt/mm)
PDMS	0.32	1.27	0.114
CI20A/PDMS	0.92	1.79	0.274
CI30B/PDMS	0.53	1.51	0.261
Silica/PDMS	0.63	1.48	0.122
HA/PDMS	0.34	1.30	0.103
BG/PDMS	0.70	1.27	0.147

The modulus of elasticity increases by the incorporation of the two types of montmorillonite as well as with silica, but remains almost stable by the addition of hydroxyapatite and bioactive glass. Resistance to tearing was increased in almost all the examined composites except those reinforced with hydroxyapatite (Table 1).

After 21 days and especially after 40 days of immersion in SBF, a large number of microparticles were detected on the surface of all the examined specimens by SEM. Using the EDAX technique, the percentage weight of Ca and P and then the molar ratio of Ca/P were calculated (Table 2). Ca and P are present at low percentage up to 21 days and their presence become significant after 40 days of immersion. Within this period of immersion, the Ca/P ratio is close to 1.67, which corresponds to hydroxyapatite. Deviations from this value were attributed to the formation of some defects during apatite growth.

Table 2. The quantitative results using EDAX analysis on the examined PDMS composites (5 phr), after 40 days immersion in SBF.

Material type	w% Ca	w% P	Ca/P
PDMS	28.14	13.6	1.60
CI20A/PDMS	30.24	14.16	1.65
CI30B/PDMS	11.17	7.34	1.18
Silica/PDMS	29.87	14.52	1.59
HA/PDMS	28.84	13.68	1.39
BG/PDMS	28.24	16.70	1.31

## CONCLUSION

The use of the appropriate type of montmorillonite (Cloisite 20A) as biomedical silicone filler might ensure high mechanical strength as well as biocompatibility similar to that provided by other bioactive fillers (hydroxyapatite and bioactive glass).

Bioactive glass (BG) is a new alternative for the modification of biomedical prosthetic silicone elastomers and despite the fact that it does not significantly improve the mechanical behaviour, seems to enhance biocompatibility of polysiloxane matrix.

## REFERENCES

1. Tarantili P.A., in "Concise Encyclopedia of High Performance Silicones", WILEY-Scrivener Publisher, USA, 2014
2. Kokubo T., Biomaterials 12:155-163, 1991

## ACKNOWLEDGMENTS

Author should acknowledge Dr. S. Vasilakos, I.-G. Athanasoulia and G. Gotsis for their significant contribution to the experimental part of this work.



## High-Resolution Synchrotron X-Ray Analysis of Bioglass-Enriched Hydrogels

Svetlana Gorodzha<sup>1,7</sup>, Timothy E.L. Douglas<sup>2</sup>, Sangram K. Samal<sup>3</sup>, Katarzyna Cholewa-Kowalska<sup>4</sup>, Kevin Braeckmans<sup>3</sup>, Andre G. Skirtach<sup>2</sup>, Venera Weinhardt<sup>5,6,7</sup>, Tilo Baumbach<sup>6,7</sup>, Maria A. Surmeneva<sup>1</sup>, Roman A. Surmenev<sup>1</sup>

<sup>1</sup>Dept. Theoretical and Experimental Physics, National Research Tomsk Polytechnic University, Russia

<sup>2</sup>Nano & Biophotonics group, Department Molecular Biotechnology, Ghent University, Belgium

<sup>3</sup>Laboratory of General Biochemistry & Physical Pharmacy, Ghent University, Belgium

<sup>4</sup>Dept. Glass Technology and Amorphous Coatings, AGH University of Science and Technology, Poland

<sup>5</sup>Centre for Organismal Studies, University of Heidelberg, Germany

<sup>6</sup>Laboratory for Applications of Synchrotron Radiation, Karlsruhe Institute of Technology, Germany

<sup>7</sup>ANKA/Institute for Photon Science and Synchrotron Radiation, Karlsruhe Institute of Technology, Germany

[surmenev@tpu.ru](mailto:surmenev@tpu.ru)

## INTRODUCTION

Hydrogels-inorganic particle composites are gaining interest as materials for bone regeneration. Enrichment with inorganic particles improves hydrogels' mechanical properties and mineralizability and biological properties, e.g. bioactivity and adhesion, proliferation and differentiation of bone-forming cells, while maintaining injectability. Knowledge of the size and distribution of particles/particle agglomerates in the hydrogel is desirable. High-resolution techniques (e.g. SEM) require drying. Distribution in the dry state is not representative of the wet state. Techniques in the wet state (histology,  $\mu$ CT) are of lower resolution.

In this study, self-gelling, injectable composites of Gellan Gum (GG) hydrogel and bioactive glass (bioglass) particles were analysed in the wet state using Synchrotron X-ray radiation to determine size and spatial distribution of bioglass particles with high resolution. To our best knowledge, this is the first report on use of this technique to study hydrogel-particle composites in the biomaterials field.

## EXPERIMENTAL METHODS

Bioglass preparation S2 was produced by a sol-gel technique (1) (see Table 1 for composition). Self-gelling GG-bioglass composites (1% w/v bioglass, 0.7% w/v GG) were generated as in previous work (2). Cylindrical composite samples of height 1 cm and diameter 6 mm in 0.5 ml vessels filled with water to prevent evaporation were subjected to X-ray imaging at the Topo-Tomo beamline, ANKA light source facility, Karlsruhe Institute of Technology, Germany. From the spectrum of the bending magnet (white beam) 10 keV monochromatic X-ray beam was selected by a double multilayer monochromator. The detector system consisted of Andor Neo camera (sensor size 5.5 megapixels, 6.5  $\mu$ m pixel size), BAM microscope 3.6x and the scintillator LAG 50  $\mu$ m thickness resulting in the effective pixel size of 1.8  $\mu$ m and field of view of 10x6.7 mm. Volumes were obtained by X-ray computed tomography: 1501 projection images were taken over an angular range of 360° with an exposure time of 2 ms per projection. Dark current of the camera and reference images without sample were taken to reduce artefacts.

S2 particles were also suspended in water for zeta potential and particle size distribution measurements.

Table 1: composition of bioactive glass S2

component	SiO <sub>2</sub>	CaO	P <sub>2</sub> O <sub>5</sub>
Molar %	80	16	4

## RESULTS AND DISCUSSION

A 3D reconstruction of the GG-S2 composite is presented in Figure 1. Predominantly, homogeneously distributed agglomerations of approximate diameter 90  $\mu$ m were observed. Larger agglomerations were also seen. Analysis of particle size distribution confirmed this. The most commonly occurring agglomerates were of volume 20000  $\mu$ m<sup>3</sup>, corresponding to an approximate diameter of 90  $\mu$ m. Numerous agglomerations with approximate diameters in the range 90-240  $\mu$ m were detected. The largest agglomerations had an approximate diameter of 900  $\mu$ m. Flow cytometry revealed that the average diameter of S2 particles in solution is 1  $\mu$ m, proving that agglomeration took place. Zeta potential was -4.25 mV. Agglomeration might be caused by both particle-particle interactions and hydrophobic interactions with the negatively charged GG polymer.

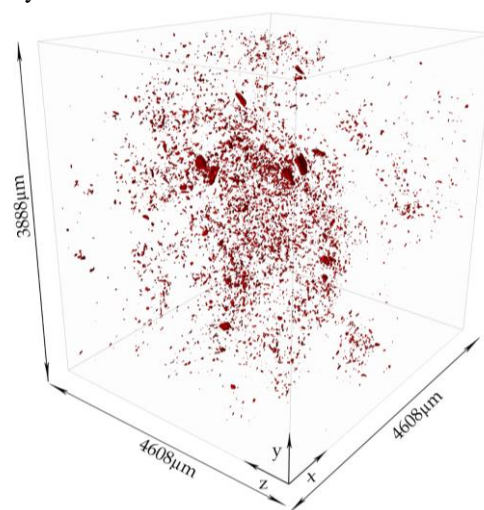


Figure 1: Image showing distribution of S2 bioglass (red) in GG hydrogel based on synchrotron X-ray data.

## CONCLUSION

Synchrotron X-ray radiation is a novel and powerful tool to visualize size and spatial distribution of inorganic particles in hydrogel biomaterials. Bioglass particles aggregate upon incorporation in GG hydrogels.

## REFERENCES

1. Laczka M *et al.* J Biomed Mater Res 52:601-12, 2000.
2. Douglas T *et al.* Biomed Mater 9:045014, 2014

## ACKNOWLEDGMENTS

T.E.L.D. thanks FWO, B for a postdoctoral fellowship. We thank Roman Shkarin for his assistance with the data visualisation and ANKA facility for the beamtime.

Ismael Moreno-Gomez<sup>1</sup>, Xiang Zhang<sup>2</sup>, Serena Best<sup>1</sup> and Ruth Cameron<sup>1</sup>  
<sup>1</sup>Department of Materials Science & Metallurgy, University of Cambridge, UK  
<sup>2</sup>Lucideon Ltd., UK  
[im380@cam.ac.uk](mailto:im380@cam.ac.uk)

## INTRODUCTION

Significant differences in degradation behaviour of similar composites made from biodegradable polymer (poly- $\alpha$ -hydroxy-acids) and calcium-based ceramic (tricalcium phosphate, hydroxyapatite) have been reported<sup>1,2</sup>. The simultaneous phenomena and the interactions of the different factors affecting the degradation are not yet fully understood. In the present study a combined computational-experimental approach is used to investigate the degradation behaviour of CaCO<sub>3</sub>-PLGA composites and gain insight into the degradation mechanisms.

## EXPERIMENTAL METHODS

### Computational model

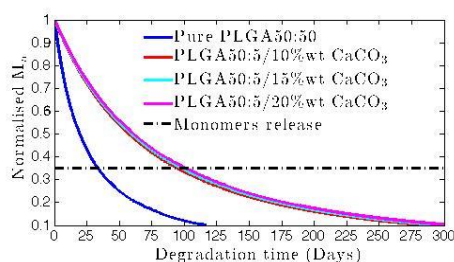
The computational model was implemented in C++ based on an existing degradation model for TCP composites<sup>3</sup>. The model uses three sets of equations: a set of differential equations to characterize the polymer, another set for the ceramic and a third set to represent the interactions between both. The model outputs amongst other things the evolution of the average molecular weight of the polymer and the ceramic content.

### Composite material

Composites were fabricated with 50:50 molar ratio poly(D,L-lactide-co-glycolide) (trade name PLGA50:50 5E) from Lakeshore Biomaterials<sup>TM</sup>, Evonik Industries as matrix and calcium carbonate cubic particles of 80 nm and 150 nm from Shiraishi Calcium Kaisha, Ltd.

The CaCO<sub>3</sub> particles and the polymer were stirred separately in acetone. Then both mixtures were blended and stirred further. The composite mix was cast in shallow moulds. The resulting films were injection moulded into rods. The rods were cut into cylinders with a diameter of 3 mm and a height of 2 mm. Pure injection-moulded polymer was used as control for the degradation study. The degradation protocol has been previously reported in literature<sup>4</sup>.

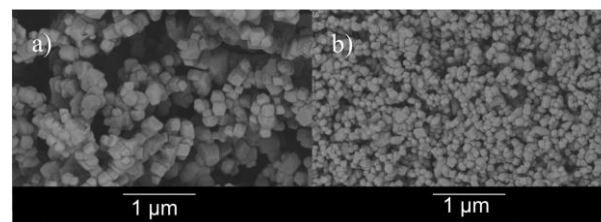
## RESULTS AND DISCUSSION



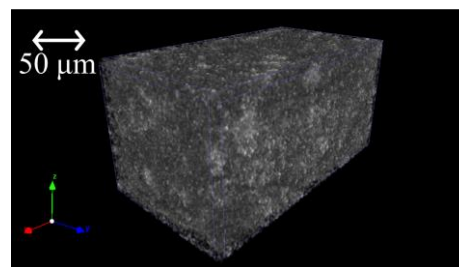
**Figure 1:** Predicted evolution of the average matrix Mn (number-averaged molecular weight) during the degradation study.

Figure 1 depicts an example of the computational predictions. It shows a reduction in hydrolytic degradation rate due to the buffering effect of the ceramic particles and the influence of the CaCO<sub>3</sub> quantity in the reduction. These predictions agree with experimental data published in the literature<sup>5</sup>.

Figure 2 illustrates the size consistency of the CaCO<sub>3</sub> particles and figure 3 shows the good dispersion of the particles in the composite.



**Figure 2:** SEM of two sizes of CaCO<sub>3</sub> cubic particles (a) cubes of 155 nm ± 28 nm (b) cubes of 84 ± 19 nm (mean ± standard deviation).



**Figure 3:** 3D micro-CT reconstructions of a section of the injection-moulded rod.

## CONCLUSION

The use of a combined computational and experimental approach is a promising tool to gain insight into the degradation behaviour of the composites. The comparison between the predicted and the actual behaviour will highlight the depth of the actual understanding and will point new factors to be considered for the degradation process.

## REFERENCES

1. Yang F. *et al.*, Polym Degrad Stabil 91.12: 3065-3073, 2006
2. Barrett C.E. *et al.*, Polymer 55:4041-4049, 2014
3. Pan J. *et al.*, Biomaterials, 32(9), 2248-2255, 2011.
4. Hurrell S. *et al.*, J. Mater. Sci.: Mater. Med. 14.5: 457-464, 2003.
5. Tsunoda, M. Dent Mater J 22(3): 371-382, 2003

## ACKNOWLEDGMENTS

I. Moreno-Gomez acknowledges Lucideon and O. S. “La Caixa” for the provision of funding towards this project and M. Ueda for supplying the nanoparticles.

## Development of Nanostructured Composites Based on $\epsilon$ -Polylysine and Apatite

Kristine Salma-Ancane<sup>1</sup>, Liga Stipniece<sup>1</sup>, and Inga Narkevica<sup>2</sup>

<sup>1</sup>Rudolfs Cimdins Riga Biomaterials Innovation and Development Centre, Riga Technical University, Latvia

<sup>2</sup>Institute of General Chemical Engineering, Riga Technical University, Latvia

[kristine.salma-ancane@rtu.lv](mailto:kristine.salma-ancane@rtu.lv)

### INTRODUCTION

In recent years, fabrication of inorganic–organic composites mimicking the composite nature of bone has attracted research interest in the field of bone regeneration<sup>1</sup>. Over the last decade, nanosized and nanocrystalline apatite (Ap) has been of special interest to dentistry, the orthopedic industry and nanomedicine because of their excellent performance<sup>2</sup>.  $\epsilon$ -Polylysine ( $\epsilon$ -PL) is non-toxic, biodegradable, water soluble natural homopolymer with potential applications in medicine<sup>3</sup>.  $\epsilon$ -PL is a cationic surface active agent due to its positively charged amino group in water. In last decade experimental work has been done investigating the interactions of various macromolecules of acidic amino acids with hydroxyapatite<sup>4</sup>. In this study, novel bioactive nanostructured composites for bone tissue engineering were developed based on  $\epsilon$ -PL and apatite (Ap). This composite biomaterial would combine the chemical and biological functionality of  $\epsilon$ -PL and bioactivity of Ap.

### EXPERIMENTAL METHODS

Ap/ $\epsilon$ -PL containing nanostructured composites were processed by spray drying technique using slurry of *in situ* synthesized Ap in 5% (w/v)  $\epsilon$ -PL aqueous solution. *In situ* synthesis of Ap was realized by precipitation method using  $\text{Ca}^{2+}$  and  $\text{PO}_4^{3-}$  ions sources as starting reagents with molar ratio of  $\text{Ca/P} = 1.67$  in order to obtain spray-dried products containing Ap and  $\epsilon$ -PL at the 50/50 and 70/30 wt.%. The obtained slurry was spray dried by using a tabletop spray dryer with nozzle of 1.4 mm diameter at a temperature 200°C. The collected spray-dried composite powders were structurally characterized using X-ray diffraction (XRD), Fourier transform infrared spectroscopy (FT-IR), Field emission-scanning microscopy (FE-SEM) and differential thermal analysis (DTA).

### RESULTS AND DISCUSSION

FE-SEM studies of obtained spray-dried products confirmed the formation of spherical composites with diameter in the range 2–8  $\mu\text{m}$  (Figure 1). FT-IR analysis demonstrated formation of Ca-deficient apatite which incorporates the  $\epsilon$ -PL macromolecules. The XRD

results suggested that *in situ* synthesis in  $\epsilon$ -PL produces a nanocrystalline apatite. Accordingly,  $\epsilon$ -PL influences apatite crystal nucleation and growth, allow for chemical functionalization of the inorganic phase.

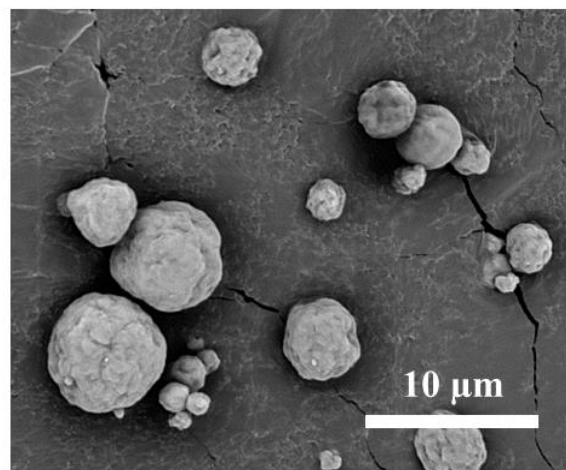


Figure 1: FE-SEM micrograph of spray-dried spherical composites based on Ap/  $\epsilon$ -PL (50/50 wt.%).

### CONCLUSION

The development of bioactive nanostructured apatite and  $\epsilon$ -polylysine containing composites was done. Obtained spherical composites can be used as ideal carriers in drug delivery and bone fillers in tissue engineering.

### REFERENCES

1. Zhou H. *et al.*, *Acta Biomater.* 8:1999-2016, 2012
2. Dorozhkin S.V. *et al.*, *Acta Biomater.* 6:715–734, 2010
3. Shukla S.C. *et al.*, *Biochem. Eng. J.* 65:70-81, 2012

### ACKNOWLEDGMENTS

This work has been supported by the National Research Programme No. 2014.10-4/VPP-3/21 “Multifunctional Materials and Composites, Photonics and Nanotechnology (IMIS<sup>2</sup>)” Project No. 4 “Nanomaterials and Nanotechnologies for Medical Applications”.



Audrey Aussel<sup>1,2</sup>, Xavier Bérard<sup>3</sup>, Sandro Cornet<sup>3</sup>, Vincenzo Brizzi<sup>3</sup>, Marlène Durand<sup>1,2,3</sup>,  
Alexandra Montembault<sup>4</sup>, Laurent David<sup>4</sup>, Rachida Aid<sup>5</sup>, Didier Letourneur<sup>5</sup>, Laurence Bordenave<sup>1,2,3</sup>

<sup>1</sup>Univ. Bordeaux, Bioingénierie tissulaire, U1026, University of Bordeaux, F-33000 Bordeaux, France

<sup>2</sup>INSERM, U1026, University of Bordeaux, F-33000 Bordeaux, France

<sup>3</sup>CHU de Bordeaux, CIC, F-33000 Bordeaux, France

<sup>4</sup>IMP, CNRS UMR 5223, Université Claude Bernard Lyon 1, F-69000 Lyon, France

<sup>5</sup>INSERM, U 1148, University of Paris 13, F-75000 Paris, France

[audrey.aussel@u-bordeaux.fr](mailto:audrey.aussel@u-bordeaux.fr)

## INTRODUCTION

Resorbable biomaterials play central roles in modern strategies for vascular tissue engineering (TE). Chitosan is a linear polysaccharide obtained industrially from deacetylation of chitin and particularly interesting for TE applications. We have shown that the physical and biological properties of chitosan physical hydrogels can be modulated by acting on chitosan concentration, acetylation degree (DA) and gelation route, inducing differential *in vivo* responses after subcutaneous implantation<sup>1</sup>. Here, these hydrogels were screened *in vitro* (direct contact of blood with chitosan, suture retention) and *in vivo* (arterial wall repair with chitosan patch) for hemocompatibility evaluation.

## EXPERIMENTAL METHODS

**Materials.** Chitosan (450,000 g/mol) was purchased from Mahtani Chitosan, purified and structurally characterized<sup>2</sup>. Hydrogels (Chitosan concentration 5%w/w and 10%w/w, Ch5% and Ch10% respectively both with 5% DA) were prepared following two physical gelation routes: the hydro-alcoholic and the aqueous routes, respectively<sup>1</sup>. Gel membranes were obtained.

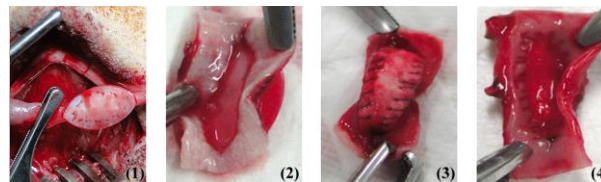
***In vitro* testing.** According to standards ISO and ASTM, the following tests were performed after contact of Ch5% with human blood and in comparison with negative and positive controls: partial thromboplastin time (PTT), hemolysis, CH50 (complement consumption) and C5b-9 (final anaphylatoxin produced by both activation pathways). Suture retention (n = 3) was evaluated according to previous studies<sup>3</sup>.

***Surgical procedure.*** Procedure and animal treatment both complied with Principles of Laboratory Animal Care. Anesthetized sheep<sup>4</sup> underwent a common carotid artery exposure through a longitudinal incision in the mid neck. The arteries were cross clamped after a heparin bolus (0.5mg/kg) was administrated intravenously. A longitudinal 1 cm arteriotomy was performed on the anterior wall of the artery and then repaired with either a chitosan patch, or a polyester urethane (PU) vascular patch (control, n = 6) (B Braun, Germany). The patches were cut out from a hydrogel membrane or PU in a suitable shape and a slightly larger than the vascular wall defect then fixed with a Prolene 6/0 running suture. All surgical procedures were performed by the same 2 surgeons. Patency was assessed peroperatively and every 30 min by carotid doppler ultrasound (US) exam. Animals were sacrificed at 2h. Measurements of fibrinogen, cell counts, hematocrit and hemoglobin content were performed.

Tissues including patches were harvested for scanning electron microscopy (SEM) and histology.

## RESULTS AND DISCUSSION

***In vitro* testing:** a minimal contact activation of the intrinsic pathway of blood coagulation was observed in the presence of Ch5% (84% of negative control) and Ch 5% did not induce *in vitro* hemolysis, nor complement activation. Suture retention values were 51 and 162 gF for Ch5%, Ch10%, respectively, the latter being consistent with native vessels<sup>5</sup>. ***In vivo* testing:** the Ch5% patch (n = 3) was not strong enough to sustain the stitches and was partially lacerated by the thread. It is the reason why Ch10% was manufactured and implanted (n = 7), showing a greatly improved strength to sustain the suture. Time required to complete implantation was 25 and 7 min for chitosan and PU patches, respectively. Figure below shows fixed Ch10% *in situ* (1), Ch5% once harvested on luminal side (2), harvested control PU on external side (3) and luminal side (4).



US showed no flow obstruction inside carotids repaired by Ch5%, Ch10% or PU patches at 2h. SEM results indicated a lower fibrin deposition and platelet aggregation on Ch5% than on PU. Histology of Ch5% revealed an absence of thrombus in 2 out of 3 sheep.

## CONCLUSION

*In vitro* and *in vivo* results are promising for vascular TE. Blood flowing platelets are of great importance in inducing a thrombus, because of their immediate reaction<sup>5</sup>, they do not seem here to be activated after blood-material contact. Tube elaboration optimization as well as their endothelialization ability are ongoing.

## REFERENCES

1. Rami L. *et al.* J.Biomed.Mater.Res.10:3666-76, 2014
2. Montembault A. *et al.* Biomaterials 26: 933-43, 2005
3. Chaouat M. *et al.* Adv.Funct.Mater.18:2855-61, 2008
4. Rémy M. *et al.*, Biomaterials, 34:9842-9852, 2013
5. van Oeveren W., Scientifica 2-14, 2013

## ACKNOWLEDGMENTS

Agence Nationale de la Recherche for financial support (Chitoart). LEMI for hemocompatibility testing *in vitro*.





## Enriched Decellularized Matrices for Tissue Engineering: Effects of Des-Acyl Ghrelin on Vascular Cells

Francesca Boccafroschi<sup>1</sup>, Margherita Botta<sup>1</sup>, Luca Fusaro<sup>1</sup>, Martina Ramella<sup>1</sup>, Francesco Copes<sup>1</sup>, Mario Cannas<sup>1</sup>

<sup>1</sup>Dipartimento di Scienze della Salute, Università del Piemonte Orientale, Italia

[francesca.boccafroschi@med.uniupo.it](mailto:francesca.boccafroschi@med.uniupo.it)

### INTRODUCTION

Vascular calcification is a common finding in many cardiovascular diseases, such as hypertension, atherosclerosis, diabetes mellitus, chronic renal failure, prosthetic valve replacements, aortic stenosis, and aging (1). It causes decreased aortic compliance and elastic recoil, which, in severe cases, results in ischemia due to significantly impaired reverse arterial flow and organ perfusion (2). Blood vessels repair and replacement is one of the most challenging issues for biomedical research and, in particular, arterial bypass graft remains the primary surgical approach for patients with advanced cardiovascular diseases. Recently, decellularization of native tissue has gained a significant attention in vascular tissue engineering and this method is used to obtain biological scaffolds that are expected to closely mimic the complex three dimensional structure, preserving the biomechanical properties of the native tissues. After decellularization, the biological substitutes can be enriched with several molecules and be repopulated with different cell types and in order to optimize the repair, growth and remodeling *in vivo*.

Ghrelin is a 28-amino acid peptide present in two major forms: n-Octanoyl-modified Ghrelin and Des-Acyl Ghrelin (DAG). The two peptides differ for the third amino acid serine which is not acylated (3). Recently, Ghrelin role in cardiovascular functionality has been studied. Our work is focused on the effects of DAG on vascular smooth muscle cells (VSMCs) and endothelial cells (ECs). DAG has been even used for decellularized matrix enrichment and the biological effects have been studied. In particular, we focused on the role of DAG on cell proliferation, differentiation, with particular attention on the anti-calcifying effect on VSMCs.

### EXPERIMENTAL METHODS

VSMCs and ECs were isolated from porcine aorta and treated with  $10^{-7}$ M DAG. Western Blot analyses were performed in order to evaluate the expression of proliferation and differentiation cell markers (PCNA, Myogenin and eNOS). Moreover, a Real Time PCR was performed to evaluate the expression of Osteocalcin gene (BGLAP). The anticalcifying effect was also evaluated through a calcein assay on VSMCs cultured in calcifying medium with and without  $10^{-7}$ M DAG. Decellularized and enriched matrices have been characterized by XPS and FT-IR analysis. To evaluate the inflammatory response, decellularized and grafted materials were seeded with monocytes and a cytokine assay was performed. Also, materials were seeded with platelet and analyzed using scanning electron microscope. *In vivo* tests have been performed in order to evaluate the biological response of the decellularized matrices as tissue substitutes.

### RESULTS AND DISCUSSION

Western Blot analysis showed the ability of DAG in controlling VSMCs' proliferation while the expression of PCNA on ECs was not affected by DAG. VSMCs contractile phenotype was not affected by the presence of DAG while eNOS resulted up-regulated by the presence of DAG. The expression of BGLAP gene decreased in presence of DAG with respect to control. Calcein assay confirmed the results. These data show a role of DAG as anticalcifying agent on vascular cells. Decellularized enriched matrices show an excellent biocompatibility *in vitro* and *in vivo*.

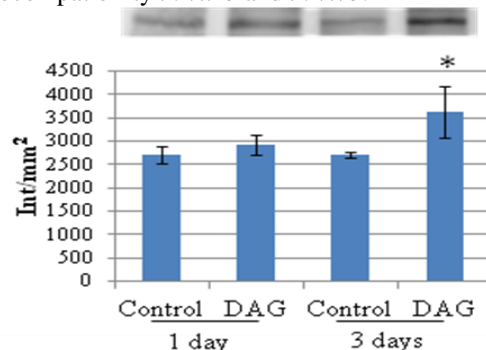


Fig.1 eNOS expression is enhanced in ECs after 3 days of culture in medium with DAG  $10^{-7}$ M. ( $p < 0.05$ )

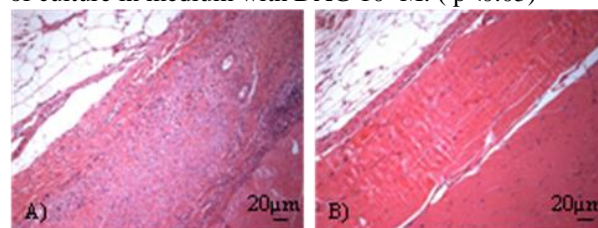


Fig. 2 A) Decellularized matrix after 28 days of intraperitoneal implant in mice B) Decellularized and enriched matrix after 28 days of intraperitoneal implant, no inflammatory response is present at the implant site.

### CONCLUSION

Our work showed that DAG has an anticalcifying effect on VSMCs and ECs.

Moreover, DAG can be grafted on a decellularized biological matrix and create innovative substitutes for vascular tissue engineering. Thus, enriched decellularized matrices may represent an excellent solution to guide tissue regeneration.

### REFERENCES

- Burke AP et al., Herz 26: 239-244, 2001.
- Wallin R, et al., Med Res Rev, 21(4):274– 301, 2001.
- Sato et al., J Biochem. 151(2):119-28, 2012.

### ACKNOWLEDGMENTS

We would like to thank Assut Europe s.p.a for providing financial support to this project.

# Biomimetic Strategy to Improve Haemo- and Biocompatibility of PET

E. Diana Giol<sup>1</sup>, Ronald Unger<sup>2</sup>, Sandra Van Vlierberghe<sup>1,3</sup>, C. James Kirkpatrick<sup>2</sup> and Peter Dubrue<sup>1</sup>

<sup>1</sup>Polymer Chemistry and Biomaterials Research (PBM) Group, Ghent University, Belgium;

<sup>2</sup>REPAIR LAB, Johannes Gutenberg University Mainz, Germany;

<sup>3</sup>Brussels Photonics Team, Vrije Universiteit Brussel, Belgium

[elenadiana.giol@ugent.be](mailto:elenadiana.giol@ugent.be)

## INTRODUCTION

Nature continuously amazes the scientific world with its highly complex or straightforward solutions to a given problem. For example, mussels adhere to a wide range of surfaces (i.e. ship hulls, stones, wood and shells) independent of environmental media *via* the so-called mussel adhesion proteins (MAPs). Dopamine coatings<sup>1</sup> mimic the structure of MAPs and are capable of adhering to a variety of substrates including metals, ceramics and polymers upon incubation in aqueous alkaline media. The precise adhesion mechanism is not completely unravelled, but non-toxicity and non-inflammatory responses of dopamine-coated materials have already been reported in the literature, rendering them suitable for a vast range of applications in the biomedical field<sup>2,3</sup>.

Polyethylene terephthalate (PET) is an ideal candidate for medical use due to its good mechanical and thermal properties together with its inertness, but its poor surface properties induce poor cell-interactions and thrombus formation upon contact with blood<sup>4</sup>. In this study, we propose a straightforward biomimetic method suitable to covalently immobilize a cell-interactive protein (e.g. gelatin)<sup>5</sup> on PET for cardiovascular applications. A comparative study between these chemically and physically modified PET surfaces was initiated and preliminary haemo-compatibility and cell-interaction investigations were performed.

## EXPERIMENTAL METHODS

PET samples (0.5 cm x 2 cm, Goodfellow) were ultrasonically cleaned with disinfectol for 15 min prior to the surface modification. A dopamine-based coating procedure<sup>1</sup> (2g/L in Tris-HCl buffer, pH=8.5, 24h) was used to facilitate the subsequent covalent immobilization of gelatin type B (5 w%, GelB). In parallel with thus obtained chemically modified PET surfaces, physically modified surfaces were obtained by dip-coating procedures.

Gelatin-modified PET films were characterized in depth using static contact angle (SCA), atomic force microscopy (AFM) and X-ray photoelectron spectroscopy (XPS) combined with radiolabelling. Whole blood to assess preliminary haemocompatibility and HUVEC cells (passage 2-3) to investigate preliminary cell-biomaterial interactions were applied on all investigated samples.

## RESULTS AND DISCUSSION

The successful coating of PET was confirmed by XPS, AFM and SEM measurements. Improved homogeneity of the protein coating was observed for the chemical approach and the coating stability was investigated by an I<sup>125</sup> radiolabelling technique. Clear differences were observed after only 72 hours incubation (in PBS, at 37 °C), with remaining labelled protein amounts of 19 ng/mm<sup>2</sup> and 120 ng/mm<sup>2</sup> for physical and chemical immobilization respectively. Interestingly, minimal platelet activation was observed for chemically modified PET, while HUVEC cell adhesion tests demonstrated the importance of a stable coating (see Figure 1).

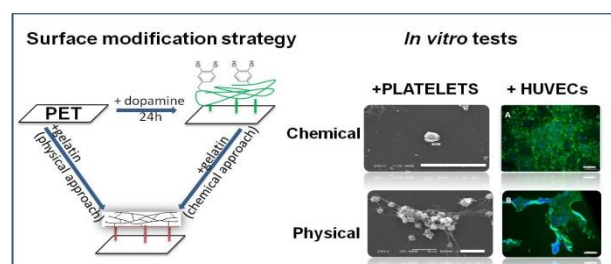


Figure 1. Overview of the surface modification strategy (left) and *in vitro* testing *via* platelet adhesion and HUVEC cell adhesion (right). The scale bars are 5  $\mu$ m for platelet images and 100  $\mu$ m for HUVEC immunostaining images. A clear delamination process can be observed for the latter.

## CONCLUSION

Stability and toxicity issues were avoided by using a 100 % organic solvent-free method inspired from nature in order to surface modify PET for cardiovascular applications. The importance of a covalent coating was shown to play an essential role in both haemo- and biocompatibility.

## REFERENCES

1. Haeshin L. *et al.*, Science. 318:426-430, 2007;
2. Ku S.H. *et al.*, Biomaterials. 31(9):2535-2541, 2010;
3. Joddar B. *et al.*, Acta Biomater. 9(5):6753-6761, 2013.
4. Chen H. *et al.*, Prog Polym Sci. 33(11):1059-1087, 2008.
5. Van Vlierberghe S. *et al.*, Polymers 3(1):114-130, 2011.

## ACKNOWLEDGMENTS

The authors would like to thank Ghent University and the Research Foundation Flanders (FWO) for the financial support.

# Synthesis of Porous Polyhydroxyalkanoate (PHA) Fibres by Pressurized Gyration Process and Their Evaluation as Tissue Engineering Scaffolds

Pooja Basnett<sup>1</sup>, Suntharavathanan Mahalingam<sup>2</sup>, Barbara Lukasiewicz<sup>1</sup>, Sian Harding<sup>3</sup>, Mohan Edirisinghe<sup>2</sup>, Ipsita Roy<sup>1</sup>

<sup>1</sup>Faculty of Science and Technology, University of Westminster, London, UK

<sup>2</sup>Department of Mechanical Engineering, University College London, UK

<sup>3</sup>National Heart and Lung Institute, Imperial College, London, UK

[p.basnett@my.westminster.ac.uk](mailto:p.basnett@my.westminster.ac.uk)

**INTRODUCTION:** An ideal tissue engineering scaffold (TES) is considered to have a (i) three dimensional, porous, inter-connected structure which facilitates cell growth, (ii) have biocompatibility and biodegradability properties that mimic the cell properties and (iii) possess surface topography that enhance cell attachment and proliferation<sup>1</sup>. Polymer fibres due to their high surface area have emerged as a new class of biomaterials for tissue engineering applications. In this project, we have used the pressurized gyration process (PGP) to produce polyhydroxyalkanoate (PHA) fibres. It is a robust, reliable, cost-effective and a novel method that produces fibres of desired properties<sup>2</sup>. PHA, which is the chosen polymer for this study, are hydrophobic storage polymers that are polyesters of 3-, 4-, 5- and 6-hydroxyalkanoic acids produced by bacterial species under nutrient-limiting conditions. They are biodegradable, biocompatible and exhibit thermoplastic properties<sup>3</sup>. In this study, we have focused on the production of PHAs, synthesis of random and aligned porous PHA fibres using PGP and their evaluation as TES.

**EXPERIMENTAL METHODS:** Production and characterisation of PHAs: PHAs were produced by bacterial fermentation of *Cupriavidus necator* in bioreactors using edible oil as a sole carbon source. The PHA produced was extracted, purified and characterised using Gas chromatography-Mass Spectrometry (GC-MS) and Nuclear magnetic Resonance (NMR). Synthesis and characterisation of PHA fibres: Purified PHA was used to generate fibres using PGP as described in Fig1.

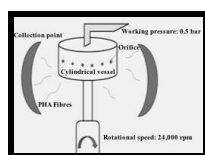


**Figure 1:** Experimental set up of the pressurized gyration process. PHA fibres were viewed under the scanning electron microscope (SEM) to determine their size. In vitro biocompatibility studies: Human microvascular endothelial cells (HMEC-1) were seeded on to these fibres for 1, 3 and 7 days. Cell viability studies were carried out using MTT assay. Confocal imaging as well as the SEM was done after the Live versus Dead assay. These experiments were also carried out on the 5wt% PHA films for comparative study.

**RESULTS AND DISCUSSION:** Production and characterisation of the PHA produced: PHA was successfully produced, extracted and purified. GC-MS and NMR results confirmed that the PHA produced was poly(3-hydroxybutyrate) or P(3HB). Synthesis and characterisation of PHA fibres: P(3HB) fibres, both random and aligned were successfully synthesized

using PGP as shown in Fig 2. SEM images revealed interconnected porous fibres of  $9 \pm 2.6 \mu\text{m}$  and  $3.0 \pm 0.8 \mu\text{m}$  width for random and aligned fibres respectively.

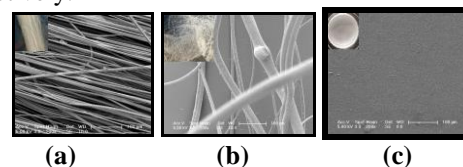


**Figure 2:** SEM images of the (a) Aligned P(3HB) fibres (b) random P(3HB) fibres (c) P(3HB) film.

Cell proliferation studies: Results of these studies have been summarised in Fig 3. Cell attachment and proliferation was found to be the highest on the aligned fibres compared to the random fibres, the P(3HB) film and tissue culture plastic which was used as the positive control.

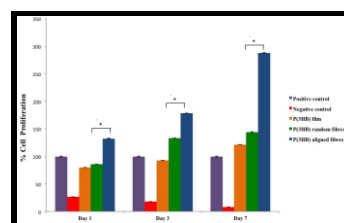


**Figure 3:** Cell proliferation study on P(3HB) fibres and film samples.

Live Vs Dead staining: Confocal images revealed that cells were alive at the end of the 7<sup>th</sup> day of incubation in both random and aligned fibres. However, the HMEC-1 cells on the aligned fibres grew in an aligned fashion.

SEM: SEM images further confirmed that the HMEC-1 cells attached, proliferated and grew in an aligned manner in contrast to that on the random fibres and the film as shown in Fig 4.

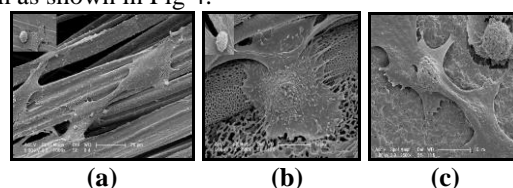


**Figure 4:** SEM images of HMEC-1 cells on (a) aligned fibres and (b) random fibres and (c) P(3HB) film.

**CONCLUSION:** Cell adhesion, proliferation and alignment were significantly higher on aligned fibres and hence, proved to be an ideal biomaterial for TE applications.

**REFERENCES:** 1. Huttmacher D. W., *Biomater* 24:2529-2543, 2000. 2. Mahalingam S. *et al.*, *Macromolecular rapid Communications* 14: 1134-1139, 2013. 3. Basnett P. *et al.*, *Adv. Eng. materials* 6: 330-343, 2012.

**ACKNOWLEDGMENTS:** We would like to thank University of Westminster and University College London for their support.



## Enhanced Interfacial Strength of Surgical Sealants Composed of Hydrophobically Modified, Cod-Derived Gelatins with Different Hydrocarbon Chain Length

Ryo Mizuta<sup>1,2</sup>, Temmei Ito<sup>1,2</sup>, Keiko Yoshizawa<sup>1</sup>  
Toshimasa Akiyama<sup>3</sup>, Katsuhiro Kamiya<sup>3</sup>, Tetsushi Taguchi<sup>1,2\*</sup>

<sup>1</sup>Graduate School of Pure and Applied Science, University of Tsukuba, Japan

<sup>2</sup>Biomaterials Unit, National Institute for Materials Science, Japan

<sup>3</sup>Senko Medical Instrument Manufacturing Co., Ltd., Japan

[TAGUCHI.Tetsushi@nims.go.jp](mailto:TAGUCHI.Tetsushi@nims.go.jp)

### INTRODUCTION

For the treatment of pulmonary air leaks and anastomotic sites between living tissues, surgical sealants have been widely used in clinical field. Fibrin sealant is a typical sealant which consists of human blood components and has excellent biocompatibility and versatile, however, it does not possess sufficient sealing effect because of its low interfacial bonding strength to tissues. Therefore, the molecular design of a tissue sealant is required for the sealant to adhere onto a living tissue and organs under wet environment during surgery. In our previous study, we have shown that tissue adhesives containing hydrophobically modified porcine-derived gelatins showed excellent bonding strength onto fresh vascular media compared with non-modified gelatin<sup>1,2</sup>. However, porcine-derived gelatin solution with high concentration has low fluidity at room temperature because of its high contents of imino acids and is required heat treatment before using sealant.

In this study, we have chosen cod-derived gelatins (cGltN) instead of porcine-derived gelatin as a base material for surgical sealants because it has low transition temperature due to its low contents of imino acids. We synthesized various hydrophobically modified cGltNs (Hm-cGltN) with different hydrophobic groups and introduction ratios and evaluated their sealing effects on wet tissues by combining Hm-cGltNs with polyethylene glycol-based 4-armed crosslinker (4S-PEG)<sup>3</sup>.

### EXPERIMENTAL METHODS

Modification of cGltN with hydrophobic groups was carried out by nucleophilic substitution reaction of the amino group with fatty acid chlorides (Hydrocarbon chain length : C3~18) in dimethyl sulfoxide. Modification ratio of hydrophobic groups was calculated by determination of residual amino group using trinitrobenzensulfonic acid. The measurement of burst strength for the porcine blood vessel was performed according to the method reported as ASTM (F2392-04). As shown in Figure 1, the sealant composed of Hm-cGltNs and 4S-PEG was fixed diameter and thickness. The burst strength was then measured by running a saline from the lower portion of the tissue at a flow rate of 2 ml/min at 37 °C.

Sealing effects for lung tissues were also evaluated by using rat lungs. The test sample was prepared by sealing on the air leak of a rat lung wound. Air leak pressures of Hm-cGltN-based sealants for rat lungs were measured by flowing air from the trachea at a flow rate of 1 ml/s.

Biodegradability of Hm-cGltN based sealants was observed by implanting in subcutaneous tissues of mice.

### RESULTS AND DISCUSSION

Hm-cGltNs were successfully synthesized by the method as we reported previously<sup>1,2</sup>. Propanoyl chloride (Pro:C3) and Hexanoyl chloride (Hx:C6), Lauroyl chloride (Lau:C12), Stearoyl chloride (Ste:C18) were used as fatty acid chlorides. By changing initial concentrations of fatty acid chlorides, each Hm-cGltN with three different modification ratios of hydrophobic groups was obtained.

The burst strengths of all Hm-cGltN-based sealants against blood vessel were higher than that of original cGltN (Org-cGltN)-based sealant. Highest burst strength of Hm-cGltN-based sealant was 10-fold higher than that of fibrin sealant and 3-fold higher than that of Org-cGltN-based sealant. This result indicated that the introduction of hydrophobic groups effectively enhanced the tissue penetration of sealants and, increased the interfacial strength between tissue and sealant. Furthermore, the burst strengths of Lau and Ste-cGltN-based sealant were higher than those of Pro and Hx-cGltN-based sealant. This result indicated that the bulk strength as well as interfacial bonding strength of sealants significantly affects the burst strength.

From the measurement of sealing effects of sealants against rat lungs, the burst strength of 9.6Ste-cGltN-based sealant was 2.1-fold higher than that of fibrin sealant and 1.6-fold higher than that of Org-cGltN-based sealant.

After subcutaneous implantation of sealants, 9.6Ste-cGltN-based sealant was completely degraded within 8 weeks. Cell infiltrations into 9.6Ste-cGltN-based sealants were also observed after 4 weeks.

### CONCLUSION

We developed surgical sealant which has a high interfacial strength by combining Hm-cGltN with 4S-PEG. Hm-cGltN-based sealant was completely degraded within 8 weeks in subcutaneous tissues. Therefore, our sealants can be applied in the field of thoracic surgery as well as cardiovascular surgery.

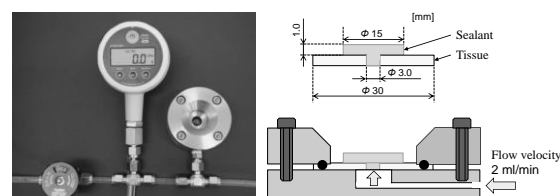


Figure1. Images of ASTM (F2392-04) burst strength test system

### REFERENCES

- 1) Matsuda, M. et al., *J. Bioact. Compat. Polym.*, 27(5), 481-498, **2012**.
- 2) Matsuda, M. et al., *Colloids Surf. B.*, 91, 48-56, **2012**.
- 3) Taguchi, T. et al., *Biomaterials*, 26, 1247-1252, **2005**.



# Athrombogenic Diffusive Layers as the Biomaterial for Blood Contact Applications in the Dynamic High Shear Stresses Conditions

Małgorzata Gonsior<sup>1</sup>, Tadeusz Wierzchoń<sup>2</sup>, Roman Kustos<sup>1</sup>, Maciej Darlak<sup>1</sup>, Magdalena Kościelniak-Ziemniak<sup>1</sup>

<sup>1</sup>Artificial Heart Laboratory (AH Lab), Foundation for Cardiac Surgery Development (FCSD), Poland

<sup>2</sup>Material Engineering Department (ME Dept.), Warsaw University of Technology (WTU), Poland  
[gosiag@frk.pl](mailto:gosiag@frk.pl)

## INTRODUCTION

The innovative implantable ventricular assist device, rotary blood pump called ReligaHeart ROT, has been developed in Poland<sup>1,2</sup>. An appropriate titanium surface engineering has to be developed, to reduce shear stress induced platelet activation on blood contacting pump elements.

The athrombogenic diffusive TiN layers have been applied for blood pump's house and rotor. The innovative process of plasma glow discharge technology and detail appropriate surface structure and topography has been developed and confirmed in laboratory testing<sup>3</sup>. The haemolytic properties as well as platelets activation and adhesion in the blood after contact with diffusive layers were analyzed in vitro, at high shear stress conditions.

## EXPERIMENTAL METHODS

The titanium nitride layers were formed in ME Dept. WTU (Warsaw, Poland). Different diffusive layers: TiN+Ti<sub>2</sub>N+αTi(N) and TiO<sub>2</sub>+TiN+Ti<sub>2</sub>N+αTi(N) were formed in plasma space within glow discharge on titanium samples. The process parameters were as following: temperature - 830°C (TiN) and 650°C (TiO<sub>2</sub>), treating time - 6 h, pressure - 2,5hPa (TiN) and 1,6hPa (TiO<sub>2</sub>). Titanium samples were polished before nitriding process to obtain different roughness: Ra=0,63μm, 0,16μm and 0,08μm.

The microstructure of diffusive layers was analyzed utilizing electron scanning microscopes, surface topography and morphology were analyzed using AFM microscope and optical scanning profile meter, wear resistance was examined in compliance with PN-83/H-04302 and tribological properties - PN-EN ISO 145771. Examinations were completed by ME Dept. WTU team. The special physical model, to evaluate the diffusive layers thrombogenic and hemolytic properties, was developed in AH Lab FCSD (Zabrze, Poland). The chamber with rotating biomaterial disk simulates the rotary pump rotor moving in close distance (0,05 to 0,3mm) to pump house wall. The shear stress exposed thrombocytes activity was determined in the dynamic conditions of different rotor-pump wall distance and disk rotation speed, under controlled blood flow through the chamber (1 to 15ml/min).

## RESULTS AND DISCUSSION

Tribological and mechanical tests showed that surface roughness and stoichiometric TiN presence are very important factors increasing material properties. TiN+Ti<sub>2</sub>N+αTi(N) layer formed in plasma space with the thicker TiN+Ti<sub>2</sub>N area has the best mechanical and tribological properties.

Surface topography of diffusive layers formed in

plasma space within glow discharge on titanium samples is more homogenous than surface of diffusive layers formed in cathode's potential. The best surface properties was achieved for layers produced on titanium polished at Ra level 0,08μm.

The experiments performed with fresh blood have confirmed the proper haemolytic properties of all examined diffusive layers. All tested diffusive layers have caused similar level of platelet aggregates on the biomaterial surface after contact with fresh blood under dynamic high shear stress conditions.

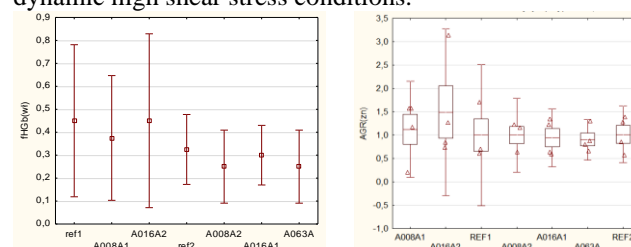


Fig.1. Hemolytic properties and platelets aggregates

Ref1 and Ref2 – titanium Grade 2 with Ra=0,08μm; A008A1 – TiN layer (cathodes' potential) with Ra=0,08μm; A016A2 – TiN layer (cathodes' potential) with Ra=0,16μm; A008A2 – TiN layer (plasma potential) with Ra=0,08μm; A016A1 – TiN layer (plasma potential) with Ra=0,16μm; A063A – TiN layer (plasma potential) with Ra=0,63μm

## CONCLUSION

The thrombogenicity and hemolytic examinations results analysis demonstrated that diffusive TiN+Ti<sub>2</sub>N+αTi(N) and TiO<sub>2</sub>+TiN+Ti<sub>2</sub>N+αTi(N) layer produced on titanium surface does not cause erythrocytes damage and platelets adhesion in the dynamic high shear stress conditions. Results obtained in reported research promise good properties of new developed layers for application in blood contacting elements of rotary blood pumps, where blood velocity and shear stresses are very high and increase the risk of thrombosis. The detail examinations will be done in order to choose the best diffusive layers for rotary blood elements implementation.

## REFERENCES

1. M. Darlak, *et al.*, ISBN 978-83-63310-12-7: 463-533, 2013
2. M. Gawlikowski, *et al.*, ISBN 978-83-63310-12-7: 534-565, 2013
3. T. Wierzchoń, *et al.*, Applied Surface Science (2014), <http://dx.doi.org/10.1016/j.apsusc.2014.08.071>

## ACKNOWLEDGMENTS

The authors would like to thank the National Centre for Research and Development (Grant no: PBS1/A5/20/2012) for providing financial support to this project.



# Delivery of Neurotrophic Factors to the Brain using Fibrin-Based Hollow Microsphere Reservoirs

Juhi Samal<sup>1</sup>, Deirdre B. Hoban<sup>2</sup>, Carol Naughton<sup>2</sup>, Ruth Concannon<sup>2</sup>, Eilis Dowd<sup>1,2</sup>, Abhay Pandit<sup>1\*</sup>

<sup>1</sup>Network of Excellence for Functional Biomaterials,

<sup>2</sup>Pharmacology and Therapeutics, National University of Ireland, Galway

[juhisamal@gmail.com](mailto:juhisamal@gmail.com)

## INTRODUCTION

*In vivo* therapeutic potential of neurotrophic factors to modify neuronal dysfunctions is limited by their short half-life. A biomaterials-based intervention, which protects these factors and allows a controlled release, is therefore required. Fibrin as a biomaterial offers the advantage of being an autologous substrate where the rate of polymerization and degradation can be well controlled. The hypothesis of this study is to establish that template charge manipulation can lead to fabrication of hollow fibrin microspheres as a reservoir for controlled delivery of the neurotrophins *in vivo*. Specific objectives were to fabricate and characterize the fibrin based reservoir system, investigate interaction with cells, impact of neurotrophin encapsulation on its bioactivity and *in vivo* characterisation in rodent model.

## EXPERIMENTAL METHODS

Hollow fibrin microspheres were fabricated by template charge manipulation method<sup>1</sup>. The hollow microspheres were physically characterized and protein loading and release from the microspheres was demonstrated using NGF as a model neurotrophin. Impact of fibrin microspheres on rat mesenchymal stem cells (rMSCs), PC-12 and fetal ventral mesencephalon (VM) cells was shown using alamar Blue<sup>TM</sup> and live/dead assay. Bioactivity of released NGF was demonstrated by neuronal outgrowth assay in PC-12 cells followed by *in vivo* assessment for NGF release and host response. Statistical analysis was performed using two-tailed Student t-test ( $p < 0.05$ ).

## RESULTS AND DISCUSSION

Hollow fibrin spheres fabricated using the manipulation of electrostatic interactions showed high loading efficiency (>80%) with no adverse impact on cell viability. Neurotrophin encapsulation into the microspheres did not alter its bioactivity (Fig.1). Controlled release of NGF was observed from hollow fibrin spheres in the *in vivo* study (Fig. 2). The immune response obtained in response to NGF, spheres and NGF- loaded spheres was comparable.

## CONCLUSION

Fibrin hollow microspheres act as a suitable delivery platform for neurotrophic factors with tunable loading efficiency and maintaining their bioactive form after release. When tested qualitatively *in vivo*, fibrin spheres did not elicit any adverse immune response in the host and obtained a sustained release of NGF.

## REFERENCES

1. Browne S., Fontana G., Rodriguez B.J., Pandit A. *Mol Pharm* (2012), 9:3099-3106.

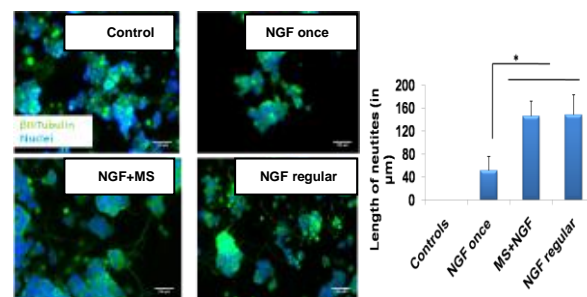


Fig.1. (A) Neuronal outgrowth in PC12 cells following culture with NGF-loaded spheres ( $\beta$ -III Tub staining (green) of differentiated cells). (B) Quantification of neurite outgrowth using Image J ( $n=30$  neurites/group).

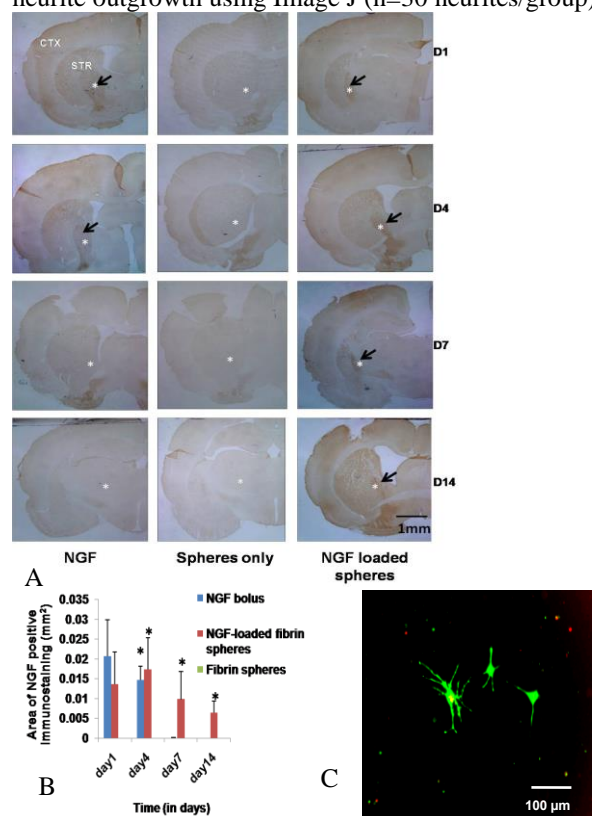


Fig.2. (A) Immunohistochemical analysis showing that the experimental group treated with NGF-loaded fibrin spheres had a sustained NGF release over a period of 14 days. (B) Quantification of NGF-positive immunostaining area using Image J ( $n=6$ ), (CTX: cortex, STR: striatum). (C) Live/dead assay showing no significant toxicity of microspheres on fetal VM cells.

## ACKNOWLEDGMENTS

Hardiman Fellowship and CÚRAM (13/RC/2073), National University of Ireland, Galway. Baxter Healthcare, Vienna for fibrin.



## Amine-Functionalized Oligomer-Cross-Linked Gelatin-Based Conduits for Nerve Regeneration

Caroline Kohn<sup>1</sup>, Julia M. Mehnert<sup>2</sup>, Christian Kascholke<sup>1</sup>, Michaela Schulz-Siegmund<sup>1</sup>,  
Matthias Brandenburger<sup>2</sup>, Michael C. Hacker<sup>1</sup>

<sup>1</sup> Institute of Pharmacy, Pharmaceutical Technology, University of Leipzig, Germany

<sup>2</sup> Fraunhofer Research Institution for Marine Biotechnology EMB, Lübeck, Germany

[caroline.kohn@uni-leipzig.de](mailto:caroline.kohn@uni-leipzig.de)

### INTRODUCTION

The clinical performance of artificial nerve guidance conduits (NGCs) is unsatisfying compared to the functional recovery obtained with the autologous gold standard<sup>1</sup>. With advanced bioengineered materials, topographical modifications and biochemical cues the next generation of NGCs is expected to mimic internal physiology to improve peripheral nerve repair<sup>2</sup>. Our gelatin-based conduits combine a natural, cell-adhesive polypeptide that is cross-linked by a multifunctional, tunable oligomer<sup>3,5</sup>. The composition allows for simple fabrication of artificial NGCs, adjustment of viscoelastic properties and chemical functionalization with biochemical factors or small amines that generate positively charged surfaces for improved neuronal outgrowth<sup>4</sup>.

### EXPERIMENTAL METHODS

The cross-linker oPNMAx was copolymerized from pentaerythritol diacrylate monostearate (P), N-isopropylacrylamide (N) and maleic anhydride (MA) in a molar feed ratio of P:(N+MA) = 1:(20-x)<sup>5</sup>. oPNMAx (x=7.5;10;12.5) were used to cross-link free amine functions of the collagen-hydrolyzate Collagel® (COL) (Gelita, Germany) to form a stable hydrogel network (cGEL)<sup>3</sup>. Hydrogel formation occurred when precursor solutions were mixed in presence of non-nucleophilic base (10% V/V) (triethylamine (TEA) or N-methylpiperidin-3-ol (NMPO)). The gelation step and resulting cGEL-discs were kinetically and mechanically characterized by oscillation rheology to identify suitable formulations for the fabrication of single-lumen cGEL conduits (cGEL-NGCs). A static mixing device and templating concept with tubular molds was developed to fabricate cGEL-NGCs of various lengths (≤50mm) and diameters (≤5mm). Furthermore, covalent derivatization of oPNMAx (x=7.5; 10; 12.5) in precursor solution was conducted prior to cross-linking. Predetermined equivalents of intact MA (MA<sub>eq</sub>=2.5) were amidated with N,N-diethylethylenediamine (DEED) for up to 4 h to produce a positively charged surface (cGEL<sup>+DEED</sup>). Evaluation of the derivatization was performed using established titration protocols and oscillation rheology<sup>3</sup>. Prenatal neurons from dorsal root ganglia (DRG) were used to examine neuronal outgrowth on cGEL- and cGEL<sup>+DEED</sup>-matrices.

### RESULTS AND DISCUSSION

The established gelation protocol was adopted with regard to gelation technique, base type and -concentration<sup>3</sup>. The fraction of TEA or NMPO was lowered from 10 down to 2% to promote slower gelation kinetic. This allowed for an injection-molding

technique and the reproducible fabrication of cGEL-NGCs. The tubes exhibited a high degree of flexibility, superior bending properties and elasticity. In the following step, chemical functionalization of oPNMAx was considered to promote neuronal outgrowth on cGEL<sup>+DEED</sup>-matrices. The initial coupling reaction was analyzed to quantify derivatization efficiency, constitution of MA and viscoelastic properties of resulting cGEL<sup>+DEED</sup>-matrices. The covalent incorporation of DEED and consumption of reactive MA groups decreased the cross-linking efficiency of oPNMAx resulting in reduced elastic modulus of cGEL<sup>+DEED</sup>. For oPNMAx x= 7.5 the cross-linking speed decreased over time; whereby for x=10 and 12.5 the gelation kinetic accelerated. We hypothesize that besides covalent cross-linking electrostatic forces contribute to the formation of cGEL<sup>+DEED</sup>-network. Based upon this, the derivatization time was reduced down to 2 h and oPNMA12.5 was preferred to fabricate cGEL<sup>+DEED</sup>-NGCs with sufficient mechanical properties complying with requirements for *in vivo* application. In addition, neurite-supporting behavior on cGEL- and cGEL<sup>+DEED</sup>-matrices was determined. Outgrowth of DRG neurons was found on cGEL<sup>+DEED</sup>. This validates the assumption that DEED-derivatization and occurring surface charge qualify cGEL<sup>+DEED</sup> as biomaterial for nerve repair.

### CONCLUSION

Tunable oPNMAx and base variations were used to modify cGEL fabrication and allow for a novel tubular injection-molding concept to produce flexible, elastic cGEL-NGCs. Pre-derivatization of oPNMAx with DEED was performed to functionalize cGEL-matrices to cGEL<sup>+DEED</sup>. Formulations were optimized for a suitable balance between cross-linking efficiency, mechanical properties and chemical composition through optimization of derivatization conditions. Preliminary results confirmed that neurite outgrowth was observed on cGEL<sup>+DEED</sup>-matrices, which makes these oligomer-cross-linked gelatin-based materials candidates for next generation NGCs.

### REFERENCES

1. Pabari A. *et al.*, J Plast Reconstr Aesthet Surg, 63: 1941–1948, 2010
2. Jiang X. *et al.*, Exp Neuro, 223:86-101, 2010
3. Loth T. *et al.*, Biomacromolecules, 15: 2104-18, 2014
4. Tu Q. *et al.*, Analyst, 139: 105-115, 2014
5. Loth T. *et al.*, React Funct Polym, 73:1480-92, 2013

### ACKNOWLEDGMENTS

German Research Foundation (DFG; TRR67/A1) funded parts of this project.





## A Dual-Layered Microfluidic System for the Controlled *In Situ* Delivery of Anti-Inflammatory Factors in Chronic Neural Implants

Laura Frey<sup>1,2,3†</sup>, Su Ryon Shin<sup>2,3,4†</sup>, Kevin O'Kelly<sup>1\*</sup>, Ali Khademhosseini<sup>2,3,4\*</sup>.

<sup>1</sup>Trinity Centre for Bioengineering, TBSI, Trinity College Dublin, Ireland

<sup>2</sup>Harvard-MIT Division of Health Sciences and Technology, Massachusetts Institute of Technology, Cambridge, USA

<sup>3</sup>Center for Biomedical Engineering, Department of Medicine, Brigham and Women's Hospital, Harvard Medical School, 65 Landsdowne Street, Cambridge, MA 02139, USA.

<sup>4</sup>Wyss Institute for Biologically Inspired Engineering, Harvard University, Boston, MA 02139, USA.

\* These authors contributed equally as corresponding author to this work. † These authors contributed equally as first author to this work.

[lauracfrey@gmail.com](mailto:lauracfrey@gmail.com)

### INTRODUCTION

Considerable advancements have been made using neural electrodes to minimise the effects of motor neurone disease, Parkinson's disease, epilepsy and to overcome paralysis<sup>1,2</sup>. These electrodes need to be implanted chronically (long-term) into the brain which has proven to be problematic, with most electrodes failing after 5-6 months<sup>3</sup>. Failure is mainly attributed to the formation of an inhibitory glial scar around the electrode, either due to the acute insertion-associated injury<sup>4</sup>, the chronic local inflammation of the neural tissue<sup>2</sup> or damage caused by micro-motion of the electrode<sup>2</sup>. The Trinity College Dublin (TCD) group is developing an alternative strategy using highly localized cooling paired with an MIT designed long term drug delivery system which we believe will significantly reduce the formation of a glial scar and extend the lifetime and efficacy of these probes.

### EXPERIMENTAL METHODS

Microfluidic channels of <100µm diameter were fabricated in a photocrosslinkable methacrylated gelatin (GelMA) hydrogel system and covered with a PDMS membrane with micropores. This system was dried (as it would be for insertion into the body) and reswollen. Drug and pro-healing cytokine diffusion rates were calculated using fluorescently labelled markers. The effects of the release of drugs and cytokines were tested *in vitro* on monocytes in order to determine macrophage behaviour over a period of 4 weeks. These monocytes were encapsulated in GelMA hydrogel crosslinked under UV light that was devised to have similar mechanical properties to brain tissue.

### RESULTS AND DISCUSSION

Microfluidic channels of <100µm diameter were successfully created in a hydrogel system using a sacrificial microfiber and maintained their integrity in a 37°C environment over a period of weeks.

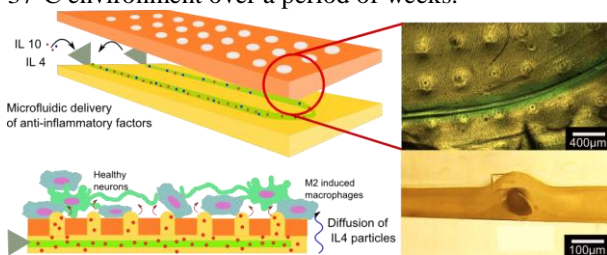


Fig 1: Top view and cross-section of microchannel filled with dye and covered by PDMS porous membrane.

The hydrogel was optimised to have the desired mechanical properties and swelling ratios to reduce micromotion once inserted into the brain without causing undue pressure on the surrounding tissue. The hydrogel system was coupled with a PDMS membrane that was shown to slow down diffusion of particles into the *in vitro* brain model and reduce hydrogel degradation over time. As well as this, the PDMS allowed the anchorage of an inlet/outlet system that enabled the channels to be filled, emptied and refilled with a series of drugs and cytokines as required. These active particles significantly reduced the presence of inflammatory markers such as 27E10 and IL6 in monocytes and increased the presence of anti-inflammatory markers such as CD206 and CD163 which implies that a larger proportion of monocytes have differentiated to form M2 macrophages which are associated with healing. This implies that, in an *in vivo* environment, chronic drug delivery could potentially reduce the body's immune response against the implants and ensure they function better during long term implantation.

### CONCLUSION

The utilisation of a double layered coating system with incorporated microchannels allowed the controlled release of drugs from a biocompatible material with adequate mechanical properties. The swelling properties of the hydrogel were also shown to increase the stability of the implants and reduce micromotion. The release of anti-inflammatory drugs and cytokines from this system was shown to increase the presence of pro-healing macrophages in our *in vitro* brain model. This system could be repeatedly filled with different drugs or cytokines allowing for the design of an adaptable drug profile to reduce the formation of scar tissue. Combined with the use of cooling instead of electrical stimulation as a therapeutic method, this system could increase the long term efficacy of these implants in patients.

### REFERENCES

1. Massia *et al.* J Biomed Mater Res 68A, 2004
2. Polikov *et al.* J. Neurosci. Methods, 148, 2005
3. Green *et al.* Biomaterials, 2008
4. Yu *et al.* J Materials Today, 11, 2008

### ACKNOWLEDGMENTS

Prof. Shane O'Mara, TCIN, Trinity College Dublin  
Fulbright Ireland  
Funded by HEA(PRTL15) GREP Programme





# Schwann Cell Behavior in Degradable PVA-Tyramine Hydrogels

Ulises A. Aregueta-Robles<sup>1</sup>, Khoon S. Lim<sup>2</sup>, Penny J. Martens<sup>1</sup>, Laura A. Poole-Warren<sup>1</sup>, Nigel H. Lovell<sup>1</sup>, Rylie A. Green<sup>1</sup>

<sup>1</sup>Graduate School of Biomedical Engineering, University of New South Wales, Australia.

<sup>2</sup>Department of Orthopaedic Surgery & Musculoskeletal Medicine, University of Otago, New Zealand

[u.areguetarobles@student.unsw.edu.au](mailto:u.areguetarobles@student.unsw.edu.au)

## INTRODUCTION

Tissue engineered electrodes<sup>1</sup> aim to stimulate neural tissues through synapse formation between cells within the tissue engineered electrode and those in target tissue. A major challenge in this research is to deliver functional neural networks capable of synapse formation. To address this issue, it is critical to understand the conditions required to support glia such as Schwann cells (SC), as they will in turn provide neurons with the appropriate niche. This study will examine SC encapsulation, survival and growth in a degradable biosynthetic hydrogel. Little research has been conducted on SC encapsulation from the point of view of developing SC into functional glia. Key design criteria for the supporting hydrogel include matching glial tissue stiffness (1-10 kPa) and delivery of appropriate biological cues to promote development and extracellular matrix (ECM) deposition by SC. Tyramine functionalized poly(vinyl alcohol) (PVA-tyr) supports covalent incorporation of non-modified tyrosine rich proteins within synthetic hydrogels<sup>2</sup> and can be tailored to mimic the biological environment while providing mechanical support. SC culture is well understood on two dimensional substrates, however there is little research on optimal three dimensional matrices that meet key design criteria. The aim of this research was to explore SC responses to encapsulation in PVA-tyr/sericin/gelatin hydrogels (PVA-T/S/G).

## EXPERIMENTAL METHODS

PVA-tyr (8 wt%) hydrogel was crosslinked with gelatin (1 wt%) and sericin (1 wt%) using previously described methods<sup>2</sup>. Gelatin was used to provide cellular attachment cues and sericin provided radical scavenging. Hydrogels were prepared with or without SC (SCL4.1/F7, 10 x 10<sup>6</sup> cells/ml). Samples were immunostained for S100 (mature SC marker), laminin (ECM deposition) and counterstained with bisbenzimidazole (nuclei). Cellular viability was tracked by live/dead staining. Hydrogel stiffness was measured by compression testing using a 50N load cell at a crosshead speed of 0.5 mm min<sup>-1</sup>. All the tests were performed at 1, 3, 5, 10 and 21 days. Hydrogel degradation was tracked to the point of reverse gelation.

## RESULTS AND DISCUSSION

Embedded cells remained viable at all the time points. S100 staining results showed that embedded SC were predominantly spherical at all the time points, however, cells localized at the upper surface of the gel were able to spread out processes. At day 21, embedded cells adopted bipolar morphologies and presented laminin on the cell surface (see Figure 1). These outcomes suggest that the PVA-T/S/G hydrogel provides sufficient support for SC differentiation.

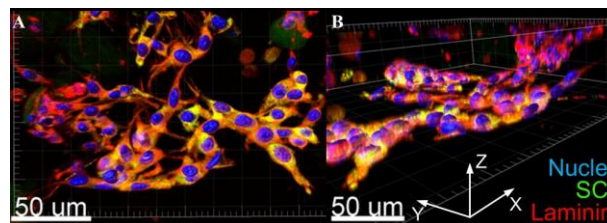


Figure 1. SC embedded in PVA-T/S/G hydrogel at 21 days. A. Top view. B. Side view. Nuclei (blue). S100 (green), laminin (red), laminin/S100 overlap (yellow).

Hydrogel degradation produced ~10fold decrease in bulk stiffness from 41.5 ± 4.6 at 1 day to 4.83 ± 0.8 kPa at 21 days. The day 21 modulus is similar to glial tissue elastic modulus<sup>3</sup>. Hydrogels without cells were stiffer than those with cells at the 3-10 day time points. However, at 21 days, hydrogels with cells were significantly stiffer than those without (see Figure 2). These results suggest that although initial stiffness was similar in gels with and without cells, the presence of cells resulted in greater persistence of gel structure over extended time periods. Reverse gelation was observed at 27 days in gels without cells. Gels with cells had a modulus of ~2.7 kPa at the same time point.

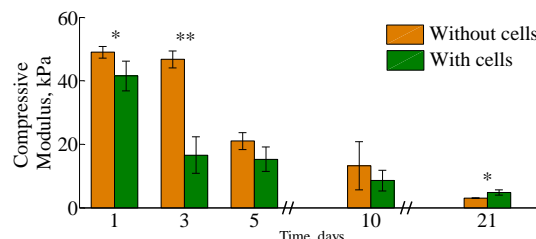


Figure 2. Compressive modulus of gels with and without cells \*(p < 0.05). \*\*(p < 0.001).

## CONCLUSION

SC growth within hydrogels has an impact on hydrogel stiffness most likely mediated by changes in gel degradation kinetics and ECM formation. Future studies will test different mesh sizes and cellular densities to assess whether faster degradation or denser cell-cell interactions will enhance SC development resembling tissue *in vivo*.

## REFERENCES

- Green R.A., *et al.*, EMBC, 35th Annual International Conference of the IEEE. 2013: 6957-6960.
- Lim, K.S., *et al.*, Biomaterials, 2013. 34(29): p. 7097-7105
- Lacour, S.P., *et al.*, MBEC, 2010. 48(10): p. 945-954

## ACKNOWLEDGMENTS

This research was supported by the Australian Research Council (ARC) through its Special Research Initiative (SRI) in Bionic Vision Science and Technology grant to Bionic Vision Australia (BVA).



# Cellular Alignment in Response to Direct Laser Interference Patterning on Polyurethane Surfaces

Lucas Cortella<sup>1</sup>, Denise Langheinrich<sup>2</sup>, Idágene Cestari<sup>1</sup>, Andrés Lasagni<sup>2</sup>, Ismar Cestari<sup>1</sup>

<sup>1</sup>Bioengineering Department / Heart Institute, University of São Paulo, Brazil

<sup>2</sup>Fraunhofer Institute for Material and Beam Technology (IWS), Dresden, Germany

[lucas.cortella@hc.fm.usp.br](mailto:lucas.cortella@hc.fm.usp.br)

## INTRODUCTION

Polyurethanes (PU) are used in a wide variety of implantable biomedical devices. A favorable aspect of PU chemistry is the broad range of physical and biological properties that can be achieved with this polymer<sup>1</sup>. A promising technology which permits direct fabrication of periodic micro structured surface patterns on solid materials such as PU is Direct Laser Interference Patterning (DLIP)<sup>2</sup>. Topographic patterns have been shown to induce cell alignment, a phenomenon called contact guidance<sup>3</sup>. In this study we evaluated cellular orientation in response to surface modifications produced by DLIP on vegetal oil based PU.

## EXPERIMENTAL METHODS

### *Vegetal oil based polyurethane and DLIP technique*

A high-power pulsed (pulse duration: 10 ns; repetition rate: 10 Hz), frequency quadrupled Nd:YAG (laser wavelength 266 nm) was used to fabricate periodic line like surface structures onto PU disc samples (5,6 mm of diameter and 1 mm of thickness). Spatial periods (distance between two ridges,  $\Lambda$ ) of 1  $\mu\text{m}$  and 10  $\mu\text{m}$  were achieved by adjusting the intercepting angle between the beams. The laser fluences chosen were 1000  $\text{mJ}/\text{cm}^2$  and 700  $\text{mJ}/\text{cm}^2$  to obtain high quality ridges with groove depth of 1  $\mu\text{m}$  ( $\Lambda$  1  $\mu\text{m}$ ) and 0,5  $\mu\text{m}$  ( $\Lambda$  10  $\mu\text{m}$ ) respectively.

### *Cell growth on DLIP modified PU*

Abdominal adipose tissue was collected from adult male Wistar rats and incubated with collagenase to obtain the stromal vascular fraction. After removal of blood and fat components, the remaining cells were cultured at 37 °C under static condition in a moisturized atmosphere with 5%  $\text{CO}_2$ . Following 5 subculture cycles, cells were seeded (140 cells/ $\text{mm}^2$ ) on control and DLIP-modified PU discs and incubated under the same culturing conditions as above ( $N = 3$ ; quadruplicates). The experimental groups were as follows: 1) unmodified PU (control), 2)  $\Lambda = 1 \mu\text{m}$  and 3)  $\Lambda = 10 \mu\text{m}$ .

### *Scanning electron microscopy (SEM)*

Three hours after the initial seeding cells were fixed with 4% paraformaldehyde and imaged with a Hitachi TM 3000.

### *Quantification of cell orientation*

SEM images of individual cells ( $n=100$ ) were analyzed using the *ImageJ* software (NIH). The angle between the major axis of the cell and the axis of the PU groove was obtained and cells considered aligned when this angle was less than 10°. For controls, the angle between

the major axis of the cell and the arbitrary image x-axis was measured.

### *Statistical analysis*

Statistical comparison between groups was performed by the Mann-Whitney Rank Sum Test. Statistical significance was accepted at  $P < 0.001$ .

## RESULTS AND DISCUSSION

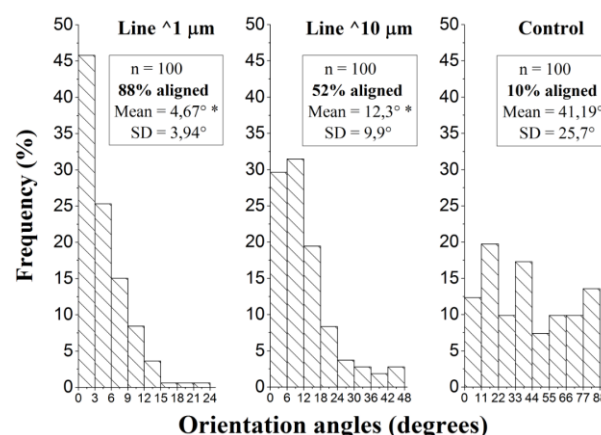


Figure. Frequency distribution of orientation angles. Text boxes indicate mean values of three similar experiments carried out in quadruplicate for each group. SD = standard deviation. (\*) denotes statistical significance ( $P < 0.001$ ) versus control.

Various cell types display contact guidance when cultured on groove and ridge patterns with dimensions in the micrometer range<sup>3</sup>. The 1  $\mu\text{m}$   $\Lambda$  pattern showed higher cell alignment (88%) than the 10  $\mu\text{m}$   $\Lambda$  pattern (52%) ( $P < 0.001$ ).

## CONCLUSION

Our results show that high quality micrometer surface patterns can be produced by DLIP on PU surfaces. Also, the data reveal that line like micro structures generated onto PU surfaces by DLIP technique induced cell alignment along the groove direction which was dependent on fluence, groove depth and spatial period.

## REFERENCES

- Guelcher S., Tissue Engineering. 14:3-17, 2008
- Langheinrich D. *et al.*, J. Pol. Sci. 50:415-422, 2012
- Flemming R. *et al.*, Biomaterials. 20:573-588, 1999

## ACKNOWLEDGMENTS

The authors would like to thank FAPESP (Grant n° 12/50283-6) for providing financial support to this project.



<sup>1</sup> Institute of Metallurgy and Materials Science Polish Academy of Sciences, 25 Reymonta Street, 30-059 Cracow, Poland

<sup>2</sup> JOANNEUM RESEARCH Forschungsges.m.b.H., Institute of Surface Technologies and Photonics, Functional Surfaces, Leobner Strasse 94, 8712 Niklasdorf, Austria

[r.major@imim.pl](mailto:r.major@imim.pl)

## INTRODUCTION

The structure of the blood vessel can be imitated by conventional surface engineering techniques, or haemocompatible coating by applying the concept of a tissue analogue, it means the substrate- promoting controlled angiogenesis process of proper blood vessels in tissue colonization. Bioactive materials should assist the body in regeneration of the natural hierarchical systems of cells to rebuild tissues. Angiogenesis is the process of creating new microvascular structures from existing vessels. This process is crucial in the embryonic development <sup>1</sup>. In healthy adult bodies the process is tightly restricted to a few organs <sup>2</sup>.

## EXPERIMENTAL METHODS

Porous coatings with varying degrees of rigidity modulated by the cross-linking were elaborated as a cell culture substrate. They were deposited using a layer-by-layer technique. Interaction of cells with the substrate was analysed for non-cross-linked and cross-linked EDC and NHS polyelectrolyte coatings with varying degrees of stiffness. The coatings were modified by physical vapour deposition in order to extend the life time duration and to improve biocompatibility. Rigidity of materials was determined by a micro hardness test using the Berkovich indenter geometry. Analysis revealed an effect of the temperature variation depending on stiffness of the porous coating. The performed bioassays used vascular endothelial cells. Materials were analysed in a dynamic system simulating the aortic flow of whole blood.

## RESULTS AND DISCUSSION

The temperature-dependent behaviour in polyelectrolyte multilayers was observed for native polyelectrolyte layers and layers subjected to the cross-linking in using confocal microscopy. The results are presented in Fig.1. The top polyelectrolyte layer was conjugated with FITC green fluorescent marker. A plot of fluorescence distribution along a line confirms that the is distributed not uniformly on the surface. Fluorescence intensity analysis confirmed local incensement in light fluorescence intensity for the non-cross-linked coating (native). On the surface endothelium was cultured as the natural layer to inhibit clot formation (Fig. 2). The more efficient growth of endothelial cells was observed on rigid, cross-linked coatings.

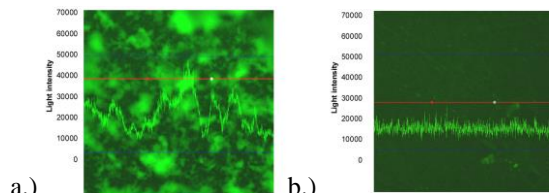


Fig. 1. Level of fluorescence a.) the surface of the non-cross-linked polymer materials b.) cross-linked polyelectrolytes

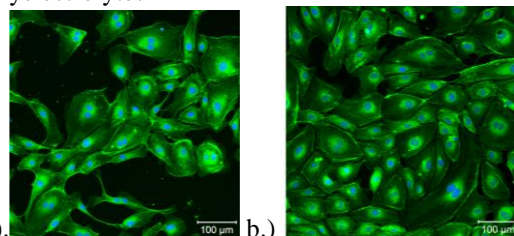


Fig. 2. The efficiency of endothelial monolayers formation a.) on non-cross-linked polymer materials b.) for cross-linked polyelectrolytes

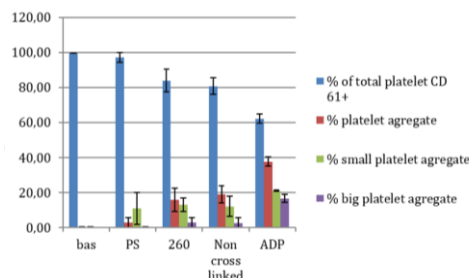


Fig. 3. Blood material interaction in the function of the applied material with deposited endothelium

## CONCLUSION

Stiff coatings enabled the more efficient endothelial cell growth, which resulted better cell growth and faster confluent formation on the top of the coating thus the better inhibition of the coagulation system

## REFERENCES

1. B. D. Ratner, A. S. Hoffman, F. J. Schoen, J. E. Lemons, editors. Biomaterials Science. An introduction to materials in medicine. 201–218, 2004
2. Major R., Journal of Material Science Materials in Medicine; Springer. 24: 725-733, 2013

## ACKNOWLEDGMENTS

This research was financially supported by project 2011/03/D/ST8/04103 “Self-assembling, biomimetic porous scaffolds in terms of inhibiting the activation of the coagulation system” of the Polish National Center of Science.



# Effect of Osteogenic Growth of Adipose Derived Stem Cells and Human Osteoblasts on the Mechanical Properties of Protein Based Films with Microchannels

Esen Sayin<sup>1,2,5</sup>, Rosti Hama Rashid<sup>3</sup>, Ahmed Elsheikh<sup>3</sup>, José Carlos Rodríguez-Cabello<sup>4</sup>, Erkan Türker Baran<sup>2</sup>, Vasif Hasirci<sup>1,2,5,\*</sup>

<sup>1</sup>METU Departments of <sup>1</sup>Biotechnology, <sup>2</sup>Biological Sciences, Turkey,

<sup>3</sup>School of Engineering, University of Liverpool, UK, <sup>4</sup>BIOFORGE, Centro I+D, Universidad de Valladolid, Spain,

<sup>5</sup>METU BIOMATEN, Center of Excellence in Biomaterials and Tissue Engineering, Turkey

[esayin@metu.edu.tr](mailto:esayin@metu.edu.tr)

## INTRODUCTION

Bone grafts are required for the treatment of injuries, tumors, infections and diseases such as osteoporosis and osteoarthritis. Bone is composed highly aligned collagen fibers and inorganic compounds which contribute to its tensile and compressive strength. In this study, microchannel patterned films of collagen and fibroin were prepared to guide anisotropic tissue formation. ELP was added to the blend to study accumulation of hydroxyapatite (HAP) owing to its functional DDDEEKFLRRIGRFG sequence [1]. The importance of cell type on the mechanical properties of microchanneled collagen – fibroin – elastin like recombinant polymer (ELP) blend films were investigated.

## EXPERIMENTAL METHODS

Stem cells derived from human adipose (ADSCs) and human osteoblasts (HOBs) were seeded on micropatterned films which were produced by solvent casting of collagen-fibroin-ELP solution on silicone elastomer mold. Protein films were crosslinked with 1-ethyl-3-[3-dimethylaminopropyl] carbodiimide hydrochloride (EDC) and *N*-hydroxysulfosuccinimide (NHS). In order to strengthen the films CaP was precipitated on the films using successive treatments with  $\text{NaNH}_4\text{HPO}_4$  and  $\text{CaCl}_2$  solutions. ADSCs were cultured in growth medium for 1 week and subsequently in osteogenic medium for 3 weeks. After 28 days ultimate tensile strength (UTS) of films ( $n=3-5$ ) were determined in wet state. Orientation of HOB and ADSC in microchannels were assessed using the SEM micrographs. Mineral deposition was analyzed with EDAX and calcium content of films was determined with o-cresol phthalein complexone and 8-hydroxyquinone assay. Statistical analysis was carried out for UTS, Young's modulus, elongation at break, and calcium determinations with ANOVA followed by Tukey's test and significant differences between groups were determined for  $p \leq 0.05$ .

## RESULTS AND DISCUSSION

CaP formed *in situ* on the protein films led to the highest UTS, Young's modulus and calcium amounts (Table 1). However, SEM results showed that ADSC was not found on the CaP precipitated surface after 28 days of cell culture. ADSCs covered native film surface and gave the second best mechanical strength and Ca amount. On the contrary, HOB seeded samples led to the lowest mechanical strength and highest elongation at break. Possible explanation can be matrix

metalloproteinase-2 (MMP-2) secretion by HOBs *in vitro* [2] while its downregulated during osteogenic differentiation of ADSCs [3]. Although mineral deposition was observed on each type of film, only *in situ* CaP formed films had Ca/P ratio close to tricalcium phosphate as shown by EDAX.

**Table 1.** Ultimate tensile strength (UTS) and Young's modulus (E) of unseeded (control) and cell seeded films (\* represents statistically significant difference between HOB seeded and other samples.).

Sample	UTS (MPa)	E (MPa)
HOB, day 28	$0.13 \pm 0.06$	$0.41 \pm 0.11$
ADSC, day 28	$0.32 \pm 0.15$	$1.21 \pm 0.42^*$
CaP/ADSC, day 28	$0.33 \pm 0.06$	$1.28 \pm 0.38^*$
Control, day 1	$0.18 \pm 0.05$	$0.58 \pm 0.13$
Control, day 28	$0.28 \pm 0.07$	$1.19 \pm 0.33^*$

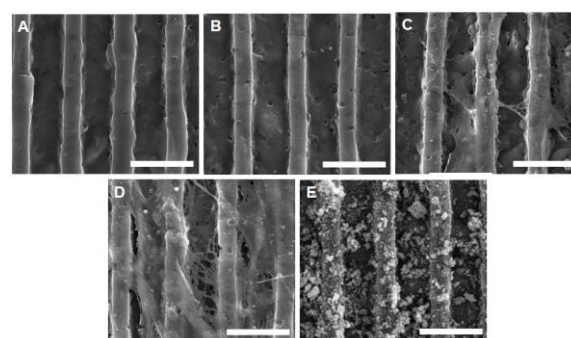


**Fig. 1.** SEM micrographs of (a) unseeded film on Day 1, (b) unseeded film on Day 28, (c) HOB seeded film on Day 28, (d) ADSC seeded film on Day 28, and (e) CaP formed films with ADSC seeding on Day 28 (x5000). Scale bar: 20  $\mu\text{m}$ .

## CONCLUSION

Mechanical properties of blend film were improved by ADSCs growth unlike HOBs. *In situ* CaP deposition enhanced tensile strength but decreased cell adhesion.

## REFERENCES

- Prieto S. *et al.*, Biomacromolecules. 12:1480–6, 2011
- Rifas L. *et al.*, J. Clin. Invest. 84:686-94, 1989
- Egusa H. *et al.*, Tissue Eng. 13:2589-600, 2007

## ACKNOWLEDGMENTS

The authors would like to thank METU (BAP-07.02.2013.101) and State Planning Organization for the financial support to this project.





# Vasculogenesis by a Maleimide Cross-Linked PEG Hydrogel Containing Calcium Phosphate Glass Particles

Claudia Navarro<sup>1,2</sup>, Jessica Weaver<sup>4,5</sup>, Óscar Castaño<sup>1,2,3</sup>, Amy Clark<sup>4,5</sup>, Jose García<sup>4,5</sup>, Soledad Pérez-Amodio<sup>1,2</sup>, Dennis Zhou<sup>4,5</sup>, Douglas Clift<sup>1,2</sup>, Andrés J. García<sup>4,5</sup>, Elisabeth Engel<sup>1,2,3</sup>

<sup>1</sup>Institute for Bioengineering of Catalonia (IBEC), Barcelona, Spain. <sup>2</sup>CIBER de Bioingeniería, Biomateriales y Nanomedicina (CIBER-BBN), Barcelona, Spain. <sup>3</sup>Dpt. Materials Science and Metallurgical Engineering, Technical University of Catalonia (UPC), Barcelona, Spain. <sup>4</sup>Woodruff School of Mechanical Engineering, Georgia Institute of Technology, Atlanta, GA. <sup>5</sup>Petit Institute for Bioengineering and Bioscience, Atlanta, GA

[cnavarro@ibecbarcelona.eu](mailto:cnavarro@ibecbarcelona.eu)

## INTRODUCTION

Achieving vascularization of implanted materials is critical for an effective integration and the success of many regenerative medicine strategies. Typically, the angiogenic effect has been pursued through the delivery of cells and growth factors but these present significant limitations, such as sourcing issues, high cost of production, and regulatory challenges. Polyethylene glycol (PEG) hydrogels have emerged as promising biomaterials due to their structural similarity to extracellular matrices and the ability to functionalize them in precise and versatile ways. Recently, calcium phosphate based glasses (CaP) have shown to stimulate an angiogenic effect both *in vitro*<sup>1</sup> and *in vivo*<sup>2</sup>. The aim of this work was to test the angiogenic properties of a new material based on the combination of a PEG hydrogel and calcium phosphate particles.

## EXPERIMENTAL METHODS

**Material fabrication and characterization.** Two types of particles were fabricated with the sol-gel method: a CaP glass with fast calcium ( $\text{Ca}^{2+}$ ) release (FRP), and a glass-ceramic with slow release (SRP). The size of the particles was measured from FE-SEM images and their atomic composition with EDS.  $\text{Ca}^{2+}$  release into cell media was determined with a colorimetric method. The hydrogels were synthesized from 4-arm PEG-maleimide macromers (20 kDa, 4.5 polymer wt%) functionalized with the cell adhesive site RGD and a protease-cleavable cross-linker. Hydrogels containing 0.1%, 0.5% and 1% (w/v) of each particle were used.

**In vitro studies.** Cytotoxic effects were tested with hydrogels containing human mesenchymal stem cells (hMSC) in a live-dead assay. Angiogenic effects were studied through quantification of VEGF released in the media from hMSC embedded in the materials and a network formation assay with a co-culture of hMSC and human umbilical vein endothelial cells (HUVEC).

**In vivo study.** Vascularization *in vivo* was studied by implanting the gels containing luciferase-expressing hMSC in the epididymal fat pad (EFP) in immunocompromised mice. Three groups were examined: hydrogels + 0.5% SRP, hydrogels + VEGF (10 µg/ml) and empty gels. Six animals were used per condition with one precast gel implanted per fat pad. Bioluminescence was imaged with IVIS at several time points. Two weeks after material implantation, animals were injected fluorescently labelled lectin to stain functional vasculature and were humanely euthanized. Tissues were explanted and processed for histology and immunostaining.

## RESULTS AND DISCUSSION

SRP have a diameter of approximately 5 µm and a sustained daily release of Ca of 0.125 mM/mg for up to 8 days. FRP are 66.20 ± 11.41 nm in diameter and release  $\text{Ca}^{2+}$  in a burst of 2.25 mM/mg during the first 2h. No cytotoxic effects were observed for any of the conditions tested. Significant differences were detected in *in vitro* endothelial cell network formation for 0.5% SRP compared to cells in particle-free gels and regular media, but not for VEGF secretion into the media. IVIS images showed significantly higher signal for the hydrogel + 0.5% SRP compared to VEGF-containing and empty gels on days 2 and 7 post-implantation, indicating enhanced cell survival. Moreover, images taken on the EFP functional vasculature presented thicker vessels for the hydrogels containing 0.5% SRP and VEGF compared to empty gels (Fig.1). Detailed histological and immunostaining analyses are ongoing to confirm the presence of a more mature vasculature.

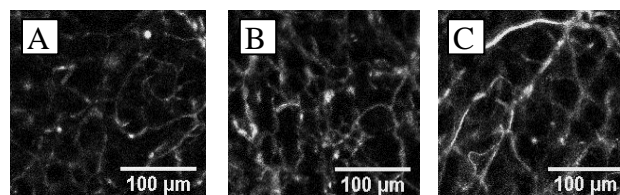


**Figure 1.** Vasculature of the fat pad tissue present in the area of implantation of the empty gel (A), the gel + 0.5% SRP (B) and the gel with VEGF (C) after lectin staining and tissue fixation.

## CONCLUSION

This study shows the fabrication of a new biomaterial based on the combination of a PEG hydrogel and glass-ceramic particles and its vasculogenic effect. The stimulation of the cells implanted in the hydrogel with the release of the particles promotes an angiogenic effect both *in vitro* and *in vivo*, although further studies should be performed to confirm this. The use of bioactive glasses instead of biological cues to stimulate angiogenesis in implanted materials can be a great contribution in tissue regeneration.

## REFERENCES

1. Aguirre A *et al.* Biochem Biophys Res Comm. 393(1):156-61. 2010.
2. Vila OF *et al.* J Biomed Mater Res A. 101(4):932-41. 2013.

## ACKNOWLEDGMENTS

The authors would like to thank the Spanish MINECO (FPU grant ref. AP-2012-5310) and MAT2012-38793 for providing financial support to this project.

# Ectopic Bone Formation by Commercial Calcium Phosphate Bone Graft Substitutes

Rongquan Duan<sup>1,2</sup>, Davide Barbieri<sup>1,2</sup>, Xiaoman Luo<sup>1,2</sup>, Joost D. D de Bruijn<sup>1,2</sup>, Huipin Yuan<sup>1,2,3</sup>

<sup>1</sup>Biomaterial Science and Technology, MIRA, University of Twente, the Netherlands;

<sup>2</sup>Xpand Biotechnology BV, Bilthoven, the Netherlands;

<sup>3</sup>College of Physical Science and Technology, Sichuan University, Chengdu, China

[h.yuan@utwente.nl](mailto:h.yuan@utwente.nl)

## INTRODUCTION

Due to the chemical similarity to the inorganic component of bone and bone bonding properties, calcium phosphate (CaP) ceramics are widely used as synthetic bone graft materials and many commercial CaP ceramics are available. It has been shown that the physicochemical properties (e.g. chemistry and surface structure) of CaP ceramics affect their bone forming ability and play an important role in their effectiveness in bone regeneration<sup>1</sup>. Since commercially available CaP ceramics have different physicochemical properties, their bone forming ability might vary. Using a well-established canine model<sup>2,3</sup>, we compared the ectopic bone forming ability of seven CaP ceramic products (i.e. BioOss, Actifuse, Bi-Ostetic, MBCP, OSferion, Vitoss and Chronos), as well as an experimental CaP ceramic (TCP-S).

## EXPERIMENTAL METHODS

Commercial CaP ceramics (Table 1) were purchased and used as supplied. The materials were subjected to XRD analysis and SEM observation. Mercury intrusion was used to evaluate strut microporosity (volume percentage of pores smaller than 10µm), micropore size and surface area. One cc of each material (n=4) was intramuscularly implanted in the dorsal muscle of 4 beagles for 12 weeks. Experimental osteoinductive (TCP-S) and non-osteoinductive tri-calcium phosphate ceramic (TCP-B) were implanted in cylinder form (Ø9x6mm) as positive and negative control<sup>2,3</sup>. TCP-S particles (1-2mm) were implanted to allow a comparison to commercial CaP ceramics in particulate form. After 12 weeks, the incidence and volume of de novo bone formation were investigated by histology and histomorphometry.

## RESULTS AND DISCUSSION

Table 1 and figure 1 show the main physicochemical characteristics of the different CaP ceramics. They are chemically different, have various surface structures (strut microporosity, micropore size and grain size) and different specific surface areas.

**Table 1. Physicochemical properties of CaP ceramics**

Materials	Supplier	Chemistry	Granules size [mm]	Strut Porosity [%]	Pore Size [µm]	Surface Area [m <sup>2</sup> /g]	Grain size [µm]
BioOss	Geistlich Pharma AG	HA	0.25-1.0	43.03	n/a	n/a	n/a
Actifuse	Apatech, Baxter	Si-HA	1-2	22.03	1.3	0.3	1.0±0.4
Biostetics	Berkeley Advanced Biomaterials	45HA/55TCP	1.4-2.8	53.67	1.5	2.7	1.8±0.3
MBCP	Biomatante	55HA/45TCP	0.5-1	40.53	0.4	1.4	1.4±0.4
OSferion	Olympus	TCP	1-3	51.90	0.9	1.4	2.7±0.9
Vitoss	Orthovita, Stryker		1-4	42.69	2.5	0.4	1.9±0.7
Chronos	Synthes		1.4-2.8	31.52	0.9	0.4	10.0±3.8
TCP-S granules	Xpand BV		1-2	45.09	0.5	1.4	0.8±0.2

The canine osteoinduction model was validated with the evidence of bone formation in TCP-S cylinders (bone in 4 out of 4 samples, 31.0±8.8%) and the absence of bone in all TCP-B cylinders. Ectopic bone formation in the commercially available CaP ceramics varied (Figure 2-3). No bone was formed in BioOss, Vitoss, Bi-Ostetic

and Chronos; limited amount of bone (<0.1%) was seen in 2 out of 4 Actifuse implants; whereas TCP-S granules (21.6±4.5%), OSferion (9.4±3.2%) and MBCP (2.1±1.4%) gave rise to bone formation in all 4 implants.

Due to the differences in chemistry, strut microporosity, micropore size, grain size and surface area, it is difficult to attribute the bone forming potential to a single physicochemical parameter, but literature indicates that grain size, micropore size and microporosity all play important roles in material-directed osteoinduction<sup>1</sup>.

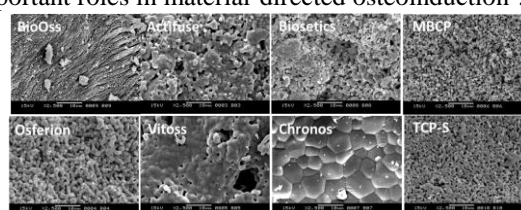


**Figure 1.** SEM images showing the surface structure of the materials

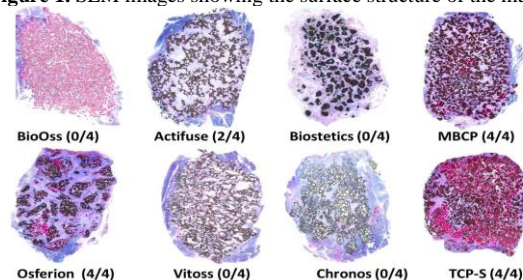


**Figure 2.** Histological overview of implants (un-decalcified sections stained with methylene blue and basic fuchsin) harvested from dorsal muscle of canines after 12 weeks of implantation

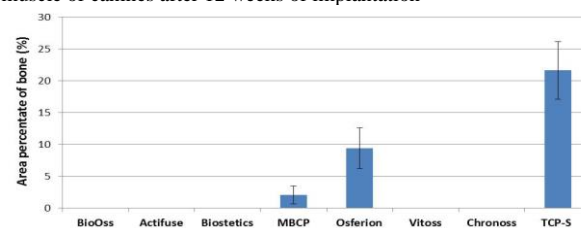


**Figure 3.** Percentage of bone in the available space of the implants (12 weeks after the intramuscular implantation)

## CONCLUSION

These results show that commercially available CaP ceramics have different bone forming potentials in the canine ectopic bone formation model. Although these differences cannot be ascribed to one physicochemical parameter, we show that an experimental CaP can be developed with superior ectopic bone formation potential. This warrants the evaluation of its bone regeneration potential in large bone defects.

## REFERENCES

- Yuan *et al.*, PNAS 107:13614-19, 2010
- Zhang *et al.*, Acta Biomaterialia 10:3254-3263, 2014
- Davison *et al.*, Biomaterials 35:5088-5097, 2014

## ACKNOWLEDGMENTS

The authors would like to thank the Netherlands Institute for Regenerative Medicine (NIRM) and Rapid Prototyping of Custom-Made Bone-Forming Tissue Engineering Constructs (Rapidots) project for their financial support to this project.



# ***In Vivo* and *in Vitro* Characterization of Porous Polyurethane-Hydroxyapatite Scaffolds as a Bone Substitute**

Gifty Tetteh<sup>1,2</sup>, Maksym Pogorielov<sup>3</sup>, Ihtesham U. Rehman<sup>1</sup>, & Gwendolen C. Reilly<sup>1,2</sup>

<sup>1</sup> Kroto Research Institute, University of Sheffield, Sheffield, UK S3 7HQ

<sup>2</sup> INSIGNEO Institute for *in silico* Medicine, University of Sheffield, Sheffield, UK S1 3JD,

<sup>3</sup> Sumy State University, Medical Institute, 40018, Sumy, Ukraine

[gifty.tetteh@sheffield.ac.uk](mailto:gifty.tetteh@sheffield.ac.uk)

## **INTRODUCTION**

Synthetic bone-graft substitutes may provide a better alternative to autografts and allografts, as they eliminate donor-site morbidity and reduce immune response. Hydroxyapatite (HA) has been extensively investigated due to its excellent bioactivity, osteoconductivity and its similarity to the main mineral component of bone. However, its poor compressive strength and fatigue failure limits its applicability to low or non-load-bearing sites<sup>1</sup>. Polyurethane (PU) presents with desirable properties of greater elasticity, viscoelastic behaviour and higher mechanical strength associated with its versatile chemistry<sup>2,3</sup>. Although PU is a promising material for scaffold fabrication, the lack of bone-bonding bioactivity limits its use in bone. Therefore, the aim is to develop a biocompatible and osteoconductive PU-HA composite with optimal mechanical properties and beneficial bioactivity to enhance bone remodelling and growth.

## **EXPERIMENTAL METHODS**

Using a novel layer-by-layer particulate leaching technique, scaffolds were fabricated with 15%wt PU dissolved in 70/30 DMF/THF solvent and NaCl particles (~250 µm). Composite scaffolds with nano or micro hydroxyapatite particles were fabricated in a ratio of 3 PU: 1 HA. Scaffold morphology, pore size and pore interconnectivity were accessed with SEM and Micro-CT imaging, whereas chemical characterisation was done with Raman and PAS-FTIR spectroscopy. Scaffolds were mechanically tested in compression and biologically characterised *in vitro* with MLO-A5 osteoblastic mouse cells and assayed over a 21-day culture period for cell attachment, viability, depth penetration and matrix deposition. For *in vivo* biocompatibility studies, 36 rats were subcutaneously implanted with scaffolds and were sacrificed on Day 7 and 45 after implantation.

## **RESULTS AND DISCUSSION**

With an average pore size of  $190 \pm 75$  µm, composite scaffolds with nHA particles had the highest Young's Modulus and yield strength of  $0.671 \pm 0.080$  MPa and  $0.040 \pm 0.014$  MPa, respectively. These were significantly higher than that of PU scaffolds without HA (PU-only) which had the highest pore size of  $236 \pm 67$  µm. The presence of hydroxyl, phosphate and phosphate bending peaks in FTIR characterization confirmed the presence of HA in all composite scaffolds<sup>3</sup>, with Raman spectroscopy also confirming the presence of HA after autoclaving. Micro-CT imaging showed good pore interconnectivity in all

scaffolds, with a porosity of 89.38% for PU-only scaffolds being significantly higher than that of micro-HA composites at 83.19%. Confocal, SEM and histology demonstrated that all scaffolds supported cell attachment, proliferation and the deposition of calcified matrix. Interestingly, mHA composites with an average pore size of  $187 \pm 66$  µm had the highest cell viability and collagen matrix deposition. This was significantly higher than that of composites with nHA particles and PU-only scaffolds. After 45 days of *in vivo* studies, tissue in-growth was present in all composites with HA particles, but was not observed in PU-only scaffolds emphasising the need for HA in bone-matrix formation.<sup>1</sup>

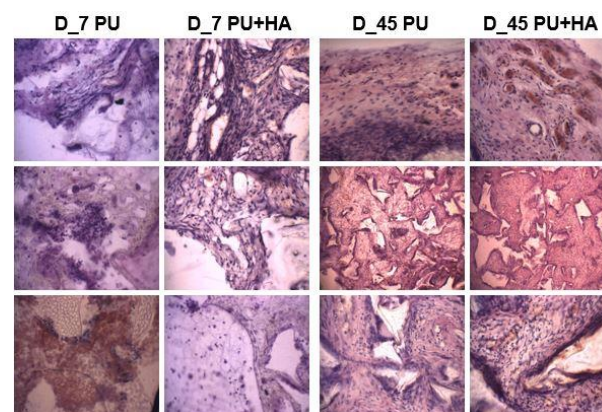


Fig. 1: H&E staining of PU-only and HA composite scaffolds on Day 7 & 45 after *in vivo* implantation x360 (Above): Superficial Zone (Middle); Intermediate Zone (Below): Deep Zone

## **CONCLUSION**

We have developed novel PU-HA composites that mimic the composition of natural bone and have good mechanical properties in relation to their highly interconnected porosity. The fabricated scaffolds support bone matrix formation *in vivo* and *in vitro* and are promising constructs for bone-graft substitutes.

## **REFERENCES**

1. Li Z. *et al* JMS: Materials in Medicine, 16 (3): 213-219, 2005
2. Boissard C. *et al*, Acta biomaterialia, 5:3316-3327, 2009
3. Tetteh *et al*. (2014), JMBBM 39C:95-110

## **ACKNOWLEDGMENTS**

The authors would like to thank the Ghana Education Trust Fund for providing financial support to this project.



## Preparation and Bioactivity of Nanocomposite Scaffolds Based on Biodegradable Polyurethane Foams and Bioactive Glass Nanoparticles

Cristian Covarrubias<sup>1</sup>, Amaru Agüero<sup>1</sup>, Monserrat Cádiz<sup>1</sup>, Mario Díaz<sup>1</sup>, Merhadd Yazdani-Pedram<sup>1</sup>, Juan P. Rodríguez<sup>2</sup>, Carla Urrea<sup>2</sup>, Juan V. Cahuich-Rodríguez<sup>3</sup>, Juan M. Cervantes<sup>3</sup>,

<sup>1</sup>Laboratory of Nanobiomaterials, INCO, Faculty of Dentistry, University of Chile, Santiago, Chile.

<sup>2</sup>Laboratory of Cell Biology, INTA, University of Chile, Santiago, Chile.

<sup>3</sup>Centro de Investigación Científica de Yucatán A.C, Mérida, México.

[ccovarru@u.uchile.cl](mailto:ccovarru@u.uchile.cl)

### INTRODUCTION

Bioactive glass nanoparticles (nBG) and mesoporous bioactive glass nanospheres (nMBG) have demonstrated to have improved bioactivity properties [1,2]. However, the use of these nanosized particles in bone tissue engineering (TI) requires their incorporation in suitable polymer scaffold matrices. Bionanocomposite scaffolds combine the bioactivity of nanoparticles with the supporting properties of the polymeric matrix. Biodegradable polyurethane (PU) are of particular interest in TI due its excellent mechanical properties. In this work, an *in situ* method for the preparation bionanocomposites based on biodegradable PU synthesized with non-toxic aliphatic diisocyanate, and nanosized BG particles is presented.

### EXPERIMENTAL METHODS

nBG was synthesized by using sol-gel technique following a modified procedure reported for us [1]. nMBG synthesis was carried according to the method reported by Wu et al. [2]. PU nanocomposites were prepared by adding dropwise a suspension of 13.2 mL of isophorone diisocyanate (IPDI) containing the BG nanoparticles to 24.3 mL of castor oil under constant stirring. Then, stannous octoate catalyst was added. Prepolymer was formed after 25 min at room temperature, after which 0.435 mL of butanediol and 0.6 mL of water were added. The foaming process was completed after 1 hour at 120 °C. Nanoparticles were characterized by high-resolution electron microscopy (HRTEM), X-ray diffraction and attenuated total reflectance with Fourier transform infrared spectroscopy (ATR - FTIR). Composites were examined by using scanning electron microscopy (SEM). Bioactivity was assessed in simulated body fluid (SBF) and citocompatibility by using alamarBlue® assay with fibroblast cultures.

### RESULTS AND DISCUSSION

The particle size of nBG and nMBG was of 70 and 100 nm, respectively (Fig. 1). nMBG exhibited the characteristic hexagonal close-pack array of nanopores of around 4 nm. nBG/PU scaffolds presented a more open macroporosity than those prepared with nMBG (Fig. 2). Microsized agglomerations of nMBG particles were also detected on the scaffold surface. Both, nBG and nMBG composites induced the formation of apatite on their surface after short time of immersion in SBF (3 days), which was not observed on the neat PU (Fig. 2)

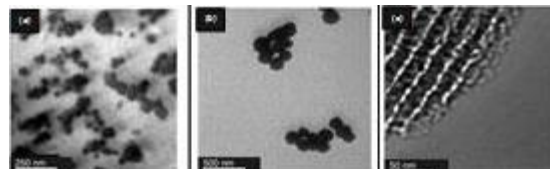


Fig. 1 HRTEM images of nBG (a) and nMBG (b,c) particles.

Higher apatite crystallization was detected on the surface of nMBG/PU. Cell viability was not reduced when cultured in the presence of the nanocomposites. Previous works of PU impregnated with microsized BG report apatite formation after more prolonged incubation times [3]. In the current work, nanometric dimensions of BG particles having higher dissolution rate, accelerate the apatite crystallization process.

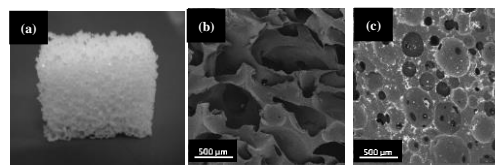


Fig. 2 Photograph of typical nanocomposite scaffold (a), and SEM images of nBG/PU (b) and nMBG/PU.

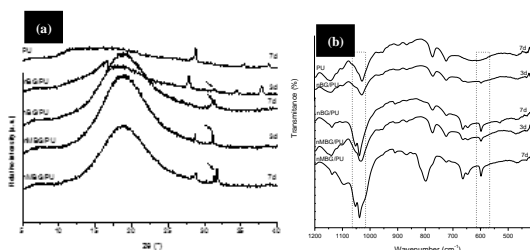


Fig. 3 XRD (a) and ATR-FTIR (b) analysis of neat PU and nanocomposites after immersion in SBF.

### CONCLUSION

Nanodimensional BG particles significantly improve the *in vitro* bioactivity of aliphatic PU scaffolds.

### REFERENCES

1. F Valenzuela, Covarrubias C, *et al.* J Biomed Mater Res Part B Appl Biomater 100:1672–1682, 2012.
2. Wu C, Fanb W, *et al.*, J Mater Chem B1:2710–2718, 2013.
3. F. Bairo F, E. Verné, *et. al.*, J Mater Sci Mater Med. 20:2189-95, 2009.

### ACKNOWLEDGMENTS

FONDECYT 1130342 (CONICYT) and U-Redes NanoBioMat (VID-University of Chile) Projects.





## Influence of Hydroxyapatite on Degradation Behaviour of PLA Fibres Scaffold

Nancy Vargas-Becerril<sup>1</sup>, L. Téllez-Jurado<sup>2</sup>, O. Alvarez-Fregoso<sup>3</sup>, M. Hipólito-García<sup>3</sup>, L.M. Rodriguez-Lorenzo<sup>4</sup>, J.A. Fernández-Pedrero<sup>1</sup>, M.A. Álvarez-Pérez<sup>1</sup>

<sup>1</sup>Laboratorio de Bioingeniería de Tejidos; DEPeI, Facultad de Odontología, UNAM, 04510, México DF, México

<sup>2</sup>Departamento de Ingeniería Metalúrgica y de Materiales E.S.I.Q.I.E.-I.P.N, 07738, México DF, México

<sup>3</sup>Instituto de Investigaciones en Materiales, UNAM, 04510, México DF, México

<sup>4</sup>Grupo de Biomateriales ICTP-CSIC, Juan de la Cierva No. 3, 28006, Madrid, España

[nancyvb09@gmail.com](mailto:nancyvb09@gmail.com)

### INTRODUCTION

Biodegradable materials have received great interest in tissue engineering research. Usually these materials are synthesized into porous, fibre or film scaffolds, which can provide a biomimetic structure and biological functions as the extracellular matrix of several tissues. Polylactic acid (PLA) is one of these biodegradable materials commonly applied in surgery, medicine and tissue regeneration because it is biocompatible with bone tissue and its biodegraded products are nontoxic and could be absorbed by the body [1]. Degradation of PLA depends on the molecular weight, crystallinity, purity, pH, temperature, doped by nanoparticles, water permeability and the presence of terminal carboxyl or hydroxyl groups [2]. It occurs in two stages: the first one starts with the water diffusion into the amorphous zones of PLA, breaking the ester bonds. The second stage starts when the degradation of amorphous zones increases [3]. The aim of this study was evaluated the degradation behaviour of PLA scaffolds doped with hydroxyapatite nanoparticles prepared by air jet spinning, using three different concentrations of PLA 6, 7 and 10 % for bone tissue regeneration.

### EXPERIMENTAL METHODS

Hybrid fibers of poly(lactic-acid)-hydroxyapatite PLA-HA were synthesized by air jet spinning and subject to degradation test with PBS, Trypsin and collagenase enzymes at 1, 3, 5, 7, 14 and 21 days at 37 °C and with an atmosphere controlled with 5% of CO<sub>2</sub>. Characterization of hybrid fibres were carried out by infrared spectroscopy, X-ray diffraction and electron scanning microscopy. The results from degradation test were obtained by FITR and the pH was monitored during the test, for observe the changes as result from degradation of fibres.

### RESULTS AND DISCUSSION

PLA-HA fibers were obtained by air jet spinning; Figure 1 displays the hybrid fibre micrograph. It can see HA nanoparticles into the PLA fibres. Rugosity and diameter size of the fibres change when HA nanoparticles were incorporated into the fibres. HA nanoparticles contained into the PLA fibres could play an important role on the physic-chemical properties of the PLA and its degradation behaviour under some enzymes. First results obtained of the degradation test

showed that degradation accelerate on the fibres when they are subject to interaction with the trypsin, since, the fibres are complete solubilized at 5 days. While, with PBS and collagenase, they still are not complete degraded.

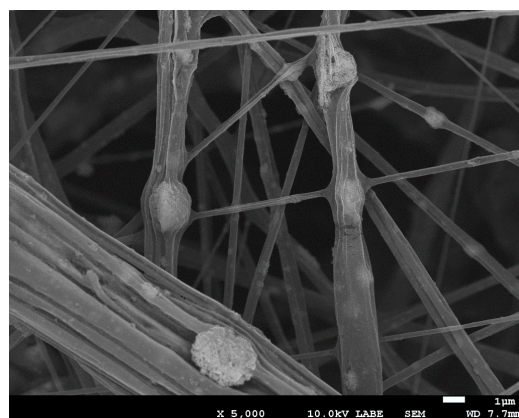


Figure 1. Micrograph of the PLA-HA hybrid fibres.

### CONCLUSION

Hydroxyapatite has an effect on PLA fibres scaffold and also the degradation test showed that trypsin enzyme accelerate the degradation behaviour of the scaffold. However, more studies are need for understanding the degradation process by the enzyme.

### REFERENCES

1. Jinglu Chen et. al, Journal of Biomedical Materials Research Part A DOI 10.1002/jbm.a
2. K. M. Nampoothiri et al, Biosource Technology 101 (2010) 8493-8501.
3. E. L. Sambha'a et al, Polym Environ. 18 (2010) 532-538.

### ACKNOWLEDGMENTS

Authors want to thank to UNAM-DGAPA for postdoctoral scholarship supporting to NVB during the course of this study. This research were financially supported by funds from the UNAM-DGAPA: PAPIIT project IN213912 and PAPIIT project IN210815.

# Biomaterial Systems for Delivery or Education of Immunosuppressive Dendritic Cells to Ameliorate Multiple Sclerosis in a Murine Model

Aline M. Thomas<sup>1</sup>, Sangeetha S. Srinivasan<sup>1</sup>, J. Lori Blanchfield<sup>2</sup>, Aaron M. Rosado<sup>1</sup>, Andres J. García<sup>3</sup>, Brian D. Evavold<sup>2</sup>, [Julia E. Babensee<sup>1</sup>](mailto:julia.babensee@bme.gatech.edu)

<sup>1</sup>Wallace H. Coulter Department of Biomedical Engineering, Georgia Institute of Technology, USA

<sup>2</sup>Department of Microbiology and Immunology, Emory University, USA

<sup>3</sup>Department of Mechanical Engineering, Georgia Institute of Technology, USA

[julia.babensee@bme.gatech.edu](mailto:julia.babensee@bme.gatech.edu)

## INTRODUCTION

Multiple Sclerosis (MS) is an autoimmune inflammatory disease characterized by axonal demyelination in the central nervous system (CNS) and resultant neurological deficits. The autoimmune attack includes an imbalance between inflammatory auto-reactive T cells and tolerance inducing regulatory T cells which is mirrored in the dendritic cell (DC) phenotype. Biomaterial-based strategies are being pursued to 1) pre-program antigen-specific and immunosuppressive DCs *in vitro* for their delivery within an injectable polyethylene glycol (PEG) hydrogel or 2) *in situ* education of recruited DC precursors using controlled release of immunomodulators and antigen from an implanted agarose scaffold (AgSc). Applicability of these complementary approaches for MS attenuation is being considered in a murine Experimental Autoimmune Encephalomyelitis (EAE) disease model.

## EXPERIMENTAL METHODS

**PEG hydrogel for delivery of immunosuppressive DCs:** Murine bone marrow (BM)-derived DCs from C57BL/6 mice were obtained upon treatment with GM-CSF and IL-4 (6 days)<sup>1</sup>, followed by treatment with IL-10 (2 days), and EAE antigen conditioning using MOG<sub>35-55</sub>. Subsequently, DCs were incorporated into PEG hydrogel [5% (w/v) PEG-4MAL; 20 kDa MW; with 2 mM RGD] at a pH of 7.4, on ice, with 1 mM TEA buffer and hydrogel crosslinked via Michael-type addition using a cysteine-flanked protease-degradable peptide VPM<sup>2</sup>. **AgSc with gelatin microparticles (GelMPs) for immunomodulator delivery:** GelMPs (10 wt%, gelatin type B) were prepared by emulsification-solvent extraction, differentially crosslinked with glutaraldehyde and washed with 25mM glycine solution<sup>3</sup>. Freeze-dried gelMPs were diffusionally-loaded with rmGM-CSF (1.54µg/ml), DEX (24µg/ml), or PGN (120µg/ml) or without DEX/PGN but with rmIL-10 (4°C, 12 hr). Appropriate numbers of each type of loaded-gelMPs were mixed into 1.5% agarose solution which was frozen (-30°C, 1hr) followed by controlled rate thawing in a cryostat<sup>4</sup>. BM precursors were treated with AgSCs with gelMPs loaded separately with DEX and PGN (GM-CSF in culture medium) for 8 days. As needed, harvested DCs were treated with MOG<sub>35-55</sub> for antigen-specificity. Phenotype and functionality of derived DCs was assessed using flow cytometric analysis of surface markers, intracellular cytokine expression and an antigen presentation assay. **Amelioration of EAE:** PEG hydrogel-encapsulated

MOG-specific DC10s (1x10<sup>6</sup> in two 50 µl injections) were delivered to the flank or neck at the time of EAE induction and EAE disease scores recorded<sup>5</sup>.

## RESULTS AND DISCUSSION

Immunosuppressive DCs were derived upon treatment with soluble IL-10 (as used in PEG hydrogels) or upon treatment with DEX/PGN released from gelMPs in AgSCs (or soluble controls) as determined by surface marker expression and enhanced IL-10 and lower IFN-γ intracellular expression, compared to mature DCs. Using an MS antigen-specific presentation assay, DCs treated with soluble IL-10 or DEX+PGN or with DEX+PGN from GelMPs in AgSCs, resulted in lower levels of MOG-dependent proliferation of 2D2 T cells. Hydrogel delivery of pre-cultured MOG-specific

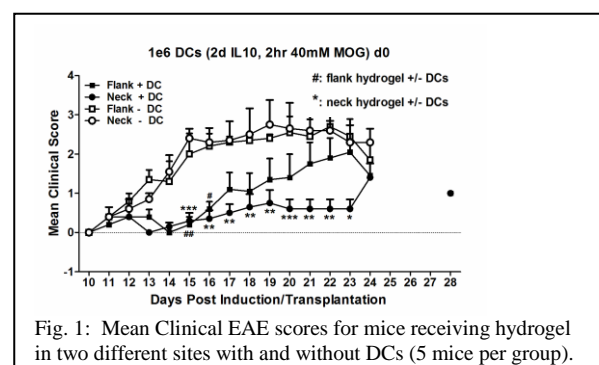


Fig. 1: Mean Clinical EAE scores for mice receiving hydrogel in two different sites with and without DCs (5 mice per group).

immunosuppressive DC10s attenuated EAE symptoms, particularly when delivered to the neck region (Fig. 1).

## CONCLUSION

Two biomaterial-based approaches demonstrate promise in adjusting the excessive pro-inflammatory autoimmune situation to tolerance through the delivery of antigen-specific immunosuppressive DCs or inducing their phenotype using controlled release technologies.

## REFERENCES

1. Banchereau J. *et al.*, Nature 392:245-252, 1998.
2. Phelps E. *et al.*, Adv. Mater. 24:64-70, 2011.
3. Bratt-Leal A. *et al.*, Biomaterials 32:48-56, 2011.
4. Loznsky VI. *et al.*, J. App. Poly. Sci. 108:3046-3062, 2008.
5. Bettini M. *et al.*, J. Neuroimmunol. 213:60-68, 2009.

## ACKNOWLEDGMENTS

Financial support by the NIH (T90DK097787-01/ILET2, UL1TR000454/ACTSI, REM Seed Grant).



Yvonne Förster<sup>1</sup>, Johannes Schmidt<sup>2</sup>, Sven Baumann<sup>3</sup>, Ute Hempel<sup>4</sup>, Martin von Bergen<sup>2,3</sup>, Stefan Kalhof<sup>2</sup>, Stefan Rammelt<sup>1</sup>

<sup>1</sup>University Center of Orthopaedics and Trauma Surgery, University Hospital Carl Gustav Carus at Technische Universität Dresden, Germany

<sup>2</sup>Department of Proteomics, Helmholtz-Centre for Environmental Research – UFZ, Leipzig, Germany

<sup>3</sup>Department of Metabolomics, Helmholtz-Centre for Environmental Research – UFZ, Leipzig, Germany

<sup>4</sup>Institute of Physiological Chemistry, Faculty of Medicine, Technische Universität Dresden, Germany  
[yvonne.foerster@uniklinikum-dresden.de](mailto:yvonne.foerster@uniklinikum-dresden.de)

## INTRODUCTION

Healing of bone defects is a complex process which is regulated by internal and external factors. However, the knowledge about this process at the actual fracture site is still limited. This is caused by a general lack of methods for *in situ* sampling of such extracellular factors, metabolites, and proteins. Microdialysis is a minimally invasive method for continuously sampling cytokines, growth factors and other mediators from the site of injury.<sup>1</sup> In combination with proteomics this is one of the promising approaches to get comprehensive and time-resolved data to characterize the wound fluid in the fracture hematoma directly after the injury.<sup>2</sup>

## EXPERIMENTAL METHODS

In the femur of adult male Wistar rats a 5 mm defect was created and stabilized with an internal fixator. The microdialysis catheter was placed within the defect and the wound fluid was collected continuously under anaesthesia for 24 h. Samples were collected in 3 h intervals and used to quantify cytokines and growth factors by ELISA. Metabolites were analysed by mass spectrometry. At the end of experiment the microdialysis catheters were explanted, the proteins adsorbed to the membrane of the microdialysis catheter were extracted and were analysed after separation by 1D gel electrophoresis by nano-HPLC/nano-ESI-MS/MS. The functional annotation clustering was performed using the software packages PANTHER and DAVID.

## RESULTS AND DISCUSSION

Analysis of wound fluid by ELISA resulted in concentration profiles for 9 different cytokines and growth factors. For example, the detailed studies of potentially relevant chemokines like chemokine (C-X-C motif) ligand 4 (CXCL4) and CXCL7 showed a rapid decrease of the concentration of these proteins immediately after injury suggesting the release of these proteins by activated platelets (Figure 1A).

More than 600 proteins were detected at the membrane of the microdialysis catheter which were previously discussed as direct biomarker candidates such as matrix metalloproteases, oxidative stress markers, serin proteases, as well as complement factors. Cytokines or chemokines were not detected within the adsorbed proteins, but more than 50 proteins related to inflammation could be found.

In addition, we are also able to assign the identified proteins to more than 100 different pathways which

seem to be activated in the early stage of wound healing in bone defects. Major protein clusters were “response to wounding” (63 proteins), “homeostatic process” (58), “proteolysis” (57), “regulation of apoptosis” (57), “defense/ inflammatory response” (55), vesicle-mediated transport (40), “acute inflammatory response” (25), and “response to oxidative stress” (24).

Interestingly, 60 extracellular proteins could be allocated to at least one of the processes related to wound healing (Figure 1B).

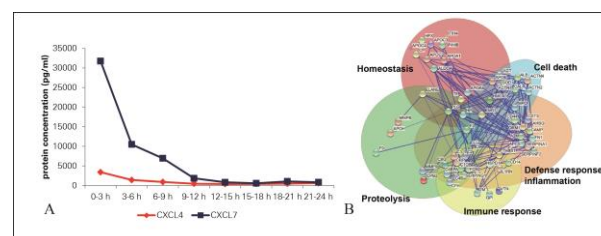


Fig. 1: A) Protein concentration of CXCL4 (n=3) and CXCL7 (n=5) in the microdialysate. B) Functional clustering of the proteins related to wounding.

## CONCLUSION

Microdialysis and proteomics provide a promising approach for detailed and direct insight into the local extracellular microenvironment of a bone defect. It is possible to collect, enrich and purify proteins in a sufficient amount for a detailed analysis of selected cytokines and growth factors and a comprehensive proteome analysis of the wound fluid to gain complementary and time-resolved information of the same defect.

## REFERENCES

1. Förster Y. *et al.*, Acta Othop. 84:76-81, 2013
2. Kalkhof S *et al.*, Biomed. Res. Int. 2014:934848, 2014

## ACKNOWLEDGMENTS

The authors would like to thank the Deutsche Forschungsgemeinschaft for financial support (Transregio 67, subprojects B1, B5, and Z4). We thank C. Preissler and J. Kobelt for technical assistance.

Ethical statement: The animal study has been licensed by the local animal care committee (24-9168.11-1/2010-22). All animals were cared for according to the European guidelines for care and use of laboratory animals



## Cellular Recognition of Collagen Based Scaffolds

D.V. Bax<sup>1\*</sup>, N.Davidenko<sup>1</sup>, R.W. Farndale<sup>2</sup>, R.E. Cameron<sup>1</sup>, S.M. Best<sup>1</sup>

<sup>1</sup>Department of Materials Science and Metallurgy, University of Cambridge, UK

<sup>2</sup>Department of Biochemistry, University of Cambridge, UK

[dvb24@cam.ac.uk](mailto:dvb24@cam.ac.uk)

### INTRODUCTION

Collagen I is a key structural component of the extracellular matrix, providing resilience to tissues. As such it has been heavily utilized as a major structural component for a wide variety of biomaterial applications. In addition to its structural role collagen interacts with cell receptors such as the heterodimeric integrins  $\alpha_1\beta_1$  and  $\alpha_2\beta_1$ . This collagen-integrin interaction occurs through a major cell-binding motif (GFOGER) contained within the triple helical structure of collagens [1]. Through these interactions collagen influences many cellular functions such as attachment, spreading and proliferation.

Ice templating is well-established method for the fabrication of 3-dimensional (3D) porous collagen scaffolds. This involves the sublimation of an interpenetrating network of ice crystals from frozen collagen slurries. Stabilisation of these scaffolds often involves carbodiimide based chemical crosslinking strategies that bond carboxylic acid to amine containing amino acid side chains. As the interaction of integrins with collagen requires one such acidic side chain, the E of GFOGER, we have examined if carbodiimide crosslinking affects integrin-mediated cell interactions with collagen-based biomaterials.

### EXPERIMENTAL METHODS

**Collagen film preparation:** 0.5% w/v insoluble collagen was homogenised then dried onto plates. NHS/EDC crosslinking was performed as [2] (100% = 1.150g EDC:0.276g NHS:1g scaffold) then washed exhaustively in deionised H<sub>2</sub>O.

**Cell attachment;**  $5 \times 10^4$  of HT1080 cells were added to collagen films in 96 well plates for 45 min. Loosely bound cells were removed and bound cells were quantified using a phosphatase detection substrate.

**Cell spreading;**  $2.5 \times 10^4$  of HT1080 cells were added to collagen films for 60 min. After fixation cell spreading was quantified by phase contrast microscopy.

**Annexin V staining;**  $5 \times 10^4$  of HT1080 cells were added to collagen films for 60 min. These were stained using an Annexin V-FITC apoptosis detection kit (abcam) following the manufacturers protocol.

**Cell expansion;**  $1 \times 10^4$  of HT1080 cells were added to collagen films in 96 well plates. After 5 days in culture the number of cells per field of view was counted by phase contrast microscopy using a 20X objective lens.

**Purified integrin I domain binding;** 10 $\mu$ g/ml of GST tagged recombinant integrin I domain was added to collagen films for 60min. Bound I domain was detected using an anti-GST-HRP antibody.

### RESULTS AND DISCUSSION

Integrin  $\alpha_2\beta_1$  dependent HT1080 adhesion and spreading to collagen films was inhibited with increasing degrees of carbodiimide crosslinking (fig.

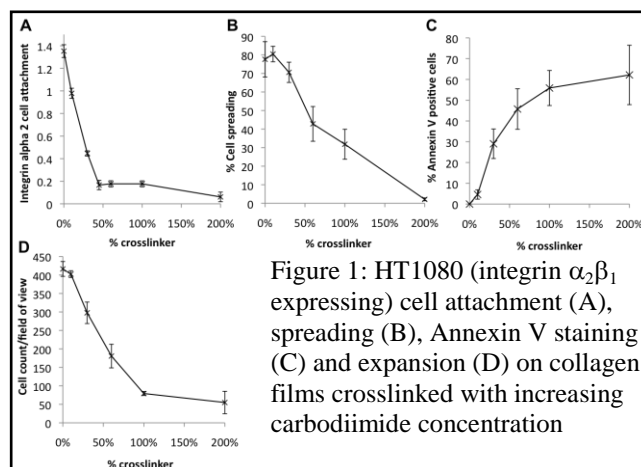


Figure 1: HT1080 (integrin  $\alpha_2\beta_1$  expressing) cell attachment (A), spreading (B), Annexin V staining (C) and expansion (D) on collagen films crosslinked with increasing carbodiimide concentration

1a,b). The number of apoptotic cells, as measured by Annexin V staining, increased dose dependently with increasing carbodiimide treatment of the collagen films (fig. 1c). Consistent with this increase in apoptosis, after 5 days in culture, the degree of cell expansion decreased with increasing carbodiimide crosslinking (fig. 1d). Together these data show that cellular engagement by collagen biomaterials is reduced with carbodiimide crosslinking. This results in decreased collagen dependent cell function.

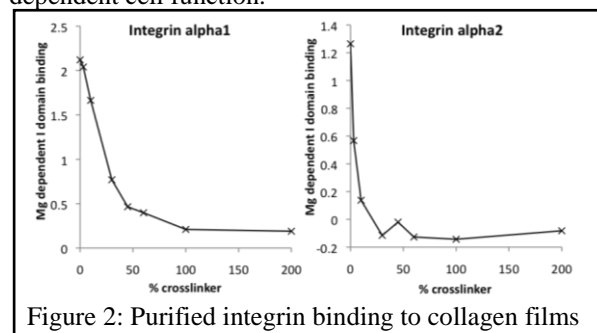


Figure 2: Purified integrin binding to collagen films

Integrin  $\alpha_1\beta_1$  and  $\alpha_2\beta_1$  interact with collagen via an inserted A domain (I domain) contained within the  $\alpha$  subunit [1]. Purified integrin  $\alpha_1$  and  $\alpha_2$  I domain binding to collagen was found to be sensitive to the degree of carbodiimide crosslinking (fig.2).

### CONCLUSION

We propose that carbodiimide reaction with integrin binding motifs inhibit integrin-mediated biofunction on collagen-based biomaterials.

### REFERENCES

1. Emsley J *et al.*, Cell 101:47-56, 2000
2. Davidenko N *et al.*, Acta Biomater. 6:3957-68, 2010

### ACKNOWLEDGMENTS

Funding was provided by the IKC PoC and ERC Advanced Grant 320598 3D-E. D.Bax is funded by the Peoples Programme of the EU 7<sup>th</sup> Framework Programme (RAE no: PIIF-GA-2013-624904).





## Multicellular Spheroids and 3D Scaffold Cultures Up-Regulate Different Events in Osteogenic Differentiation of Adipose-Derived Mesenchymal Stem Cells

Śławomir Rumiński<sup>1,2,3</sup>, Adam Zalewski<sup>1,2</sup>, Małgorzata Lewandowska-Szumieł<sup>1,2</sup>

<sup>1</sup>Department of Histology and Embryology, Centre for Biostructure Research, Medical University of Warsaw, Poland

<sup>2</sup>Centre for Preclinical Research and Technology, Poland

<sup>3</sup>Postgraduate School of Molecular Medicine, Medical University of Warsaw, Poland

[slawomir.ruminski@wum.edu.pl](mailto:slawomir.ruminski@wum.edu.pl)

### INTRODUCTION

Adipose-derived mesenchymal stem cells are routinely cultured in standard polystyrene plates in a form of a monolayer. However, mesenchymal stem cells *in vivo* are embedded in a spatially arranged environment composed of extracellular matrix proteins and other cells. It was shown that ADSC cultured in a form of multicellular aggregates displayed up-regulation of “stemness” transcription factors and increased pro-angiogenic properties [1]. ADSC cultured in 3D spheroids produced a mineralized matrix containing extracellular matrix proteins- collagen type I and osteopontin [2]. In this study, we aimed to describe the differences in ADSC osteoblast differentiation process in standard monolayer cultures and two different 3D culture systems- multicellular spheroids and scaffolds. The study also addressed the role of exogenous attachment substrate in differentiation, which is provided in the 3D scaffolds but not in multicellular spheroids.

### EXPERIMENTAL METHOD

ADSC cells were detached from monolayer cultures with trypsin. Cellular spheroids were generated with the hanging drop method [3] with ADSC in osteogenic medium used for spheroid generation. ADSC were also seeded onto Alvetex® 3D polystyrene scaffolds and into standard polystyrene culture plates. Osteogenic medium was composed of DMEM with 10% FBS, 1% antibiotics, 50µg/ml ascorbic acid phosphate, 10nM dexamethasone and 3mM NaH<sub>2</sub>PO<sub>4</sub>. After 2 days, the formed spheroids were transferred to non-culture treated dishes and cultured in osteogenic medium for another 5 days on a rotary shaker. Live/Dead fluorescent staining was performed to qualitatively assess cell viability. The cultures were lysed with 0.1% triton buffer for DNA quantification with Picogreen assay and alkaline phosphatase (ALP) assay. The ALP activity was normalized to DNA quantity. Cells were also lysed in RLT buffer for RNA isolation and quantification of Runx2, Osterix and collagen type I α1 gene expression with Real-Time PCR.

### RESULTS AND DISCUSSION

ADSC cells maintained high viability in all three culture systems for 7 days as was judged from Live/Dead fluorescent staining. Cells cultured on standard polystyrene plates had higher proliferation rate than cells cultured in spheroids as could be seen by a much higher increase in DNA quantity between day 2 and day 7 of culture. ALP activity increased at 2 days in

all three osteogenic culture systems compared to undifferentiated cells but the activity was the highest in spheroids compared to both monolayer and scaffold cultures. Expression of collagen was up-regulated in monolayer and scaffold osteogenic cultures at 2 days but dropped below control in monolayer at 7 days. After 7 days of culture expression of collagen was 1.5-, 2.9- and 4.8-fold up-regulated in monolayer, spheroid and scaffold cultures respectively. The expression of Runx2 and Osterix genes was higher in spheroids compared to scaffolds (5.7 vs. 2.1 and 3.4 vs. 0.2, respectively). The expression level of those genes in monolayer culture did not increase over control (Fig. 1). These results suggest that the presence of exogenous attachment surface in Alvetex® scaffolds results in increased collagen I expression. On the other hand, enhanced cell-to-cell communication in spheroids is likely to potentiate differentiation signals resulting in elevated expression of osteogenic transcription factors.

### CONCLUSION

The results of this study confirmed that culture in 3D systems up-regulates osteogenic differentiation processes. However, the characteristics of different 3D systems may influence the differentiation events. Therefore biomaterials can be potentially used both to provide an increased cell attachment surface and enhanced cell-to-cell contacts in order to improve ADSC differentiation, which is an important factor to consider for successful bone regeneration with the use of mesenchymal stem cells isolated from adipose tissue.

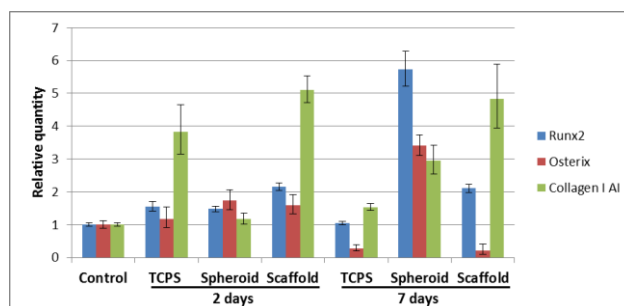


Fig. 1. Gene expression analysis

### REFERENCES

- Cheng, N.C., et al., Stem Cells Transl Med, 2013. 2(8): p. 584-94.
- Hildebrandt, C., H. Buth, and H. Thielecke, Tissue Cell, 2011. 43(2): p. 91-100.
- Foty, R., J Vis Exp, 2011(51).

## Balancing Fibroblast Differentiation in a Biomimetic Wound Healing Model

Jiranuwat Sapudom<sup>1</sup>, Michael Ansorge<sup>1</sup>, Marina Chkolnikov<sup>1</sup>, Katja Franke<sup>1</sup>, Ulf Anderegg<sup>2</sup>, Tilo Pompe<sup>1</sup>

<sup>1</sup>Institute of Biochemistry, Universität Leipzig, Germany

<sup>2</sup>Department of Dermatology, Venereology and Allergology, Universitätsklinikum Leipzig, Germany  
[tilo.pompe@uni-leipzig.de](mailto:tilo.pompe@uni-leipzig.de)

### INTRODUCTION

Dermal wound healing requires the coordinated interaction of several cell types including fibroblasts and macrophages. Involved processes like migration, infiltration, proliferation and differentiation of these cells are regulated not only by soluble autocrine and paracrine signalling molecules (e.g. TGF- $\beta$ 1, IL-10), but furthermore, by the characteristics of the surrounding extracellular matrix (ECM). Especially, the 3D context and mechanical characteristics of the physiological situation has to be observed in relevant studies. In order to gain a better understanding of the regulation of scarless wound healing and dysregulation, like hypertrophy, 3D models are required for high-resolution *in vitro* studies.

Here, we set up a 3D ECM context of a wound healing model, based on fibrillar collagen, fibronectin und glycosaminoglycans at defined microstructure and composition. We asked on the subtle interplay of ECM parameters and temporal stimuli by the paracrine signals TGF- $\beta$ 1 and IL-10 on the differentiation of dermal fibroblasts (dFb) into myofibroblasts (MFb). The setup should simulate an intermediate stage of wound healing. By that we envision to reveal key factors in the homeostasis of fibroblast phenotypes under the control of IL-10 secreting regulatory macrophages.

### EXPERIMENTAL METHODS

Fibroblast from the human foreskin were cultured on collagen I matrices (2 mg/ml collagen concentration) of defined microstructure and mechanics<sup>1</sup>, optionally functionalized with fibronectin (FN) and sulfated or non-sulfated hyaluronic acid at different concentrations. The dFb were stimulated with TGF- $\beta$ 1 for 4 d at 5 ng/mL to induce MFb differentiation. To address the impact of paracrine IL-10 on dFb fate, cells were treated with IL-10 at different time points and doses (0...20 ng/mL). Wst-1 assay was performed to assess cell proliferation and viability. The MFb differentiation was analyzed by immunocytochemical staining of actin cytoskeleton and alpha-SMA, as well as gene expression using qPCR of  $\alpha$ -smooth muscle actin ( $\alpha$ SMA), collagen I ( $\alpha$ 1) (Coll I) and EDA variant of FN (EDA-FN). Additionally, cell invasion depth into the collagen matrices was quantified.

Besides global delivery of paracrine signals, a set of experiments used local secretion of TGF- $\beta$ 1 and IL-10 from protein-laden hydrogel microbeads, providing a short-range gradient over several days. Local changes in dFb phenotype were investigated by immunofluorescence inside the matrices and single cell tracking of cell migration and proliferation.

### RESULTS AND DISCUSSION

The dFb responded sensitively to FN functionalization in a dose-dependent manner. At increasing FN amount, an increase in cell invasion depth into collagen matrices could be observed. This behaviour was correlated with a reduced cell proliferation, while gene expression of  $\alpha$ SMA, EDA-FN and Coll I was unchanged. By inducing MFb phenotype using TGF- $\beta$ 1, characteristic genes ( $\alpha$ SMA, EDA-FN, Coll I) were expressed at higher levels and cell proliferation was increased compared to untreated cells. Cell invasion depth was found to be decreased. alpha-SMA staining confirmed the differentiation of dFb to MFb by TGF- $\beta$ 1. The results suggest that FN bound to the 3D collagen matrices regulates adhesion and migration and down-regulates proliferative capacity of dFb, but not MFb. Moreover, we found that MFb rearranged collagen fibrils in FN-functionalized matrices, which compares well to tissue contraction at early wound healing *in vivo*.

A subsequential stimulation by IL-10 did not influence proliferation and invasion of dFb and MFb. However, down-regulation of MFb genes was found. Furthermore, IL-10 treated MFb showed similar morphology to dFb and a reduction in actin stress fibres and  $\alpha$ SMA could be observed pointing to a de-differentiation of MFb into dFb triggered by IL-10.

Single cell tracking and immunofluorescence analysis inside matrices with local, cell-sized delivery of IL-10 could directly visualize the local, paracrine effect of MFb de-differentiation.

### CONCLUSION

We found that matrix-bound FN plays an important role in wound healing, by regulating migratory, proliferative and differentiation capacity of dFb. The results demonstrate that IL-10 is a cytokine to terminate new tissue formation by de-differentiation of MFb controlling scar formation at later stages of wound healing. Current studies in our lab ask on ECM stimuli to control macrophage function in the regulation of local and temporal IL-10 levels.

### REFERENCES

1. Franke *et al.*, Acta Biomaterialia 10:2693 (2014).

### ACKNOWLEDGMENTS

The authors thank EFRE, ESF 'European Social Funds' and Free State of Saxony (SAB 100144684, SAB 100140482) and Deutsche Forschungsgemeinschaft (SFB-TR67/B4 and B10, INST 268/293-1 FUGG) for financial support.



## New Bilayered Biodegradable Polymeric Systems. A Feasible Approach for Skin Lesions

Noemi Santurdes,<sup>1</sup> Álvaro González-Gómez,<sup>1,2</sup> Raúl Rosales-Ibáñez,<sup>3</sup> Marcela Martín del Campo-Fierro,<sup>3</sup>  
Blanca Vázquez-Lasa,<sup>1,2</sup> Julio San Román<sup>1,2</sup>

<sup>1</sup>Institute of Polymer Science and Technology, CSIC, Spain

<sup>2</sup>CIBER-BBN, Spain

<sup>3</sup>Faculty of Stomatology, Autonomous University of San Luis Potosi, México

[jsroman@ictp.csic.es](mailto:jsroman@ictp.csic.es)

### INTRODUCTION

A variety of wound dressings and devices are currently used to treat different dermal lesions such as burns, chronic ulcers, etc.<sup>1</sup> Among them, biologic-synthetic dressings are bilayered systems formed by a synthetic polymer as the top layer and a bioactive and biologically derived material as the bottom layer.

This work reports the preparation and characterization of a bi-layered system with potential application as a wound dressing. A series of poly( $\epsilon$ -caprolactone) (PCL) based polyesterurethanes (PEUR) containing polyethyleneglycol (PEG) or Pluronic F127 were synthesized for the external layer and a gelatin (G) hydrogel was prepared for the internal bioactive layer.

### EXPERIMENTAL METHODS

Three types of PEURs were obtained containing PEG of  $M_n$  1000 or 10000, or Pluronic F127, which were labelled PEUR-1, PEUR-10 and PEUR-F127 respectively. The PEURs were synthesized in solution following a two-step approach according to Scheme 1.

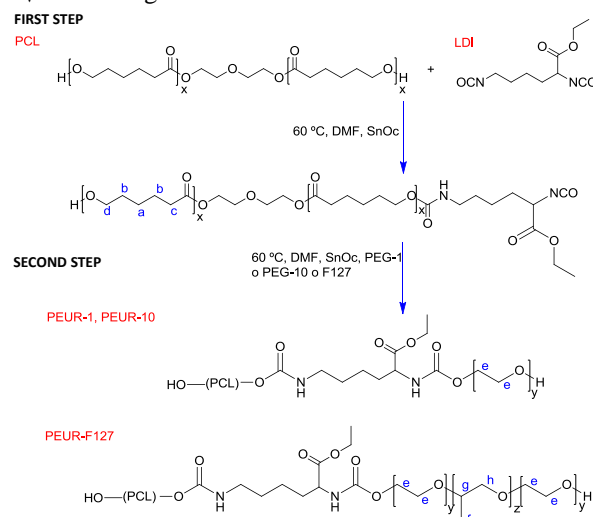
PEUR membranes were obtained by the solvent casting method. G hydrogels were prepared from G aqueous solutions (3 wt-%) in the presence of genipin (GP) (5 wt-%) at room temperature for 48 h. The system was characterized by <sup>1</sup>H-NMR, ATR-FTIR, SEC, SEM, DSC, TGA, DMTA and microindentation assays. Swelling and stability behaviour was studied *in vitro*. Cellular behaviour was evaluated with human fibroblasts and HUVEC through MTT and Alamar Blue assays. Finally *in vivo* experiments were performed on wounds experimentally created on the back of Wistar rats.

### RESULTS AND DISCUSSION

<sup>1</sup>H-NMR and ATR-FTIR spectroscopy analysis of PEUR samples confirmed the expected chemical structure shown in Scheme 1. Chemical composition was determined from <sup>1</sup>H-NMR spectra from the intensities of the signal at 3.6 ppm due to oxyethylene protons ( $H_e$ ) and the signal at 4.1 ppm pertaining to PCL ( $H_d$ ) (see assignment in Scheme 1 and results in Table 1).

The ATR-FTIR spectrum of G xerogel showed changes in the bands of amide I and amide II, compared to that of native G, attributed to the formation of new covalent amide bonds between the  $-NH_2$  groups of G and the carboxylic groups of GP during the crosslinking reaction. From DSC studies values of melting temperature ( $T_m$ ) of PEURs were around 57 °C, attributed to melting of PCL which is the predominant component. Thermal stability of PEURs was lower than that of PCL mainly at the initial stages with lower  $T_{5\%}$  and  $T_{50\%}$  values. Storage moduli of PEURs obtained by DMTA were between 320 and 420 MPa, and

microhardness ( $H_v$ ) between 33 and 67 MPa, whereas  $H_v$  of G xerogel was 206 MPa.



Scheme 1. Synthesis of PEURs.

Table 1. Molar fraction ( $f_m$ ) of PCL, PEG and Pluronic F127, number average molecular weight ( $M_n$ ) and polydispersity index (P. I.) of the PEURs.

Sample	$f_m(\text{PCL})$	$f_m(\text{PEG/F127})$	$M_n$ (kDa)	P. I.
PEUR-1	0.990	0.010	118	1.36
PEUR-10	0.873	0.127	125	1.32
PEUR-F127	0.858	0.142	125	1.31

Swelling of PEURs was between 6 and 10% whereas that of G hydrogel was 274%. All samples were not cytotoxic in a standard MTT test. *In vivo* results after 4 weeks of implantation showed that the PEUR-10/G hydrogel system promotes wound healing (see Figure 1).

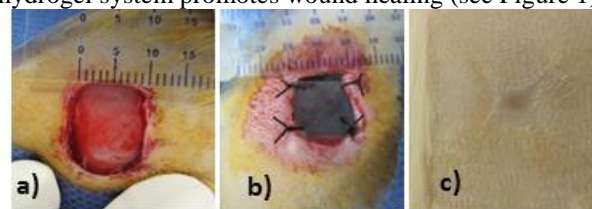


Fig.1. a) and b): Implantation of PEUR-10/G hydrogel. c) After 30 days.

### CONCLUSION

The bilayered PEUR-10/G system proved to be an effective tissue-engineered construct that can promote the healing of full-thickness skin lesions. With the support of further clinical trials, this procedure could be an alternative to wound healing for patients with partial- and full-thickness burns.

### REFERENCES

1. Boateng J. S. *et al.*, J. Pharm. Sci. 97:2892-2923, 2008

### ACKNOWLEDGMENTS

Authors thank CIBER-BBN for financial support.

## Fluorescent Activated cell Sorting (FACS) as a Tool to Quantify the Immune Cell Response to Intramuscular Implanted Materials in Rats

Tanja Schmidt<sup>1</sup>, Zienab Kronbach<sup>2</sup>, Marie-Christin Heinze<sup>1</sup>, Susann Krummsdorf<sup>1</sup>, Marcel Geiling<sup>1</sup>, Frank Witte<sup>1</sup>

<sup>1</sup>Berlin-Brandenburg Center for Regenerative Therapies, and Julius Wolff Institut, Charité'-Universitätsmedizin Berlin, Germany

<sup>2</sup>Botiss, Germany

[frank.witte@charite.de](mailto:frank.witte@charite.de)

### INTRODUCTION

Biodegradable implants based on magnesium offer several advantages mainly the lack of the need for a second surgery for implant retrieval. However, negative effects of the degradation products can reduce the biocompatibility of those materials. Currently, the inflammatory reaction to implants mainly is analysed by histology which does not allow for quantification of the different cells involved in the foreign body reaction. Therefore, our group established a FACS immune cell panel for rat species as a standard animal model to characterize and compare the inflammatory reaction of degradable versus non degradable implants and to compare between the local response formed in the capsule and the systemic response in the blood by single cell analysis on a quantitative level.

### EXPERIMENTAL METHODS

One implant (round shape, 0.8cm) made from PEEK (negative control) or polystyrene (PS, positive control) or pure magnesium (MG) was implanted intramuscular (i.m.; M. gluteus) in 60 female 12 weeks old Lewis rats. After 1, 3, 7 and 14 days (21 days in case of magnesium; n=4) animals were sacrificed and the capsules around the implants were harvested. Blood samples were taken at the day of surgery and sacrificing. Tissue was digested with collagenase buffer. Blood was prepared with RBC lysis buffer (eBioscience) to remove red blood cells. Samples were stained for CD45, CD3, CD4, CD8 and granulocytes (HIS48) as well as a marker for ED2 tissue macrophages (HIS 36; only capsule samples) following the instructions of the manufacturer (eBioscience). FACS analysis was performed on MACSQuant. Cell counting results are presented in % of all cells (CD45+) resp. in % on CD45+ cells. Blood cell counts were normalized to the values of the day of surgery. Statistics: Kruskal Wallis Test, Man Whitney U Test, p0.05.

### RESULTS AND DISCUSSION

From day one to day 14 CD45+ immune cells (Fig A) significantly increased ( $p \leq 0.05$ ) in all groups. Granulocytes significantly decreased (Fig. B,  $p \leq 0.05$ ) in

all groups from day one to day 14. In Magnesium group also CD4 helper-cells significantly increased from day 1 to day 14 ( $p=0.029$ ). In PS also T-helper and T-killer-cells significantly increased from day 1 to 14 ( $p \leq 0.05$ ) Macrophages increased from day one to day 7 and decreased from day 7 to day 14 in all groups.

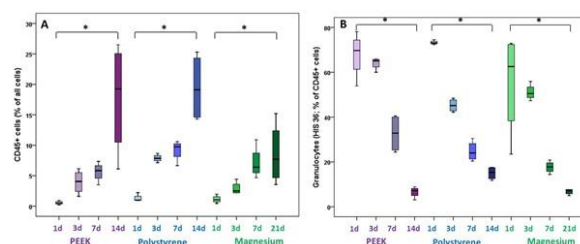


Fig A: Shows the results from CD45+ cell analysis

Fig B: Shows the results from granulocyte cell analysis.

MG implants showed signs of corrosion from day one. In one animal gas bubbles were found around the implant after 21 days (Fig C). Blood cell analysis showed no statistic differences.



Fig C: Shows PS (1,2) and MG implants (3,4) at day 14 resp 21

### CONCLUSION

The established FACS panel is a good tool to quantify the inflammatory response to implants in rats. The results show a moderate, local foreign body response to the implants. In the blood, no signs for systemic reactions were found. The degradation of pure magnesium did not increase the number of inflammatory cells indicating a good biocompatibility.

### ACKNOWLEDGMENTS

The authors acknowledge the financial support of Helmholtz Virtual Institut - MetBioMat and DFG project WI 2109/10-1.



## Endogenous Human Dermal Equivalent *in Vitro* Model to Study Wound Healing Process

Bernadette Lombardi<sup>1,2</sup>, Costantino Casale<sup>1,2</sup>, Giorgia Imparato<sup>1,2</sup>, Francesco Urciuolo<sup>1,2</sup>, Paolo Netti<sup>1,2</sup>

<sup>1</sup> Center for Advanced Biomaterials for HealthCare@CRIB Istituto Italiano di Tecnologia, Largo Barsanti e Matteucci n. 53, 80125 Napoli, Italy

<sup>2</sup>Interdisciplinary Research Centre on Biomaterials (CRIB), University of Naples Federico II, P.le Tecchio 80, 80125 Naples, Italy

[bernadette.lombardi@iit.it](mailto:bernadette.lombardi@iit.it)

### INTRODUCTION

Wounds represent a significant and increasing burden on healthcare systems globally and new therapies and wound management approaches are urgently required. Numerous difficulties are associated to use of small animal models, for this reason *in vitro* wound models using human cells in two- and three-dimensional (2D and 3D) environments have been developed to delineate the molecular mechanisms of cellular repair [1].

Skin equivalents have already been developed to investigate *in vitro* wound healing. Although these studies extensively described the reepithelialization process, and the state of keratinocyte's differentiation during healing [2], to the best of our knowledge a few of information on dermal healing are reported in literature. In order to provide a model more closely resembles the *in vivo* system, the present study was carried out to describe the dermal wound healing process and the related ECM response. In this perspective, a new 3D human dermal equivalent (3D-HDE) [3], based on endogenous ECM, was used as model.

### EXPERIMENTAL METHODS

The 3D-HDE was prepared as reported by Palmiero C. *et al.* (2010) [3]. Sterile scalpel was used to create full thickness wounds. During 18 days of standard culture condition wound was monitored by using time-lapse microscopy. Morphological analysis was performed on histological section at 10, 16 and 20 days. Nucleus detections was assessed by using Sytox Green staining and alfa smooth muscle actin ( $\alpha$ SMA) was detected by using anti- $\alpha$ SM actin antibody. HA was detected by using an Alcian blue-P.A.S kit.

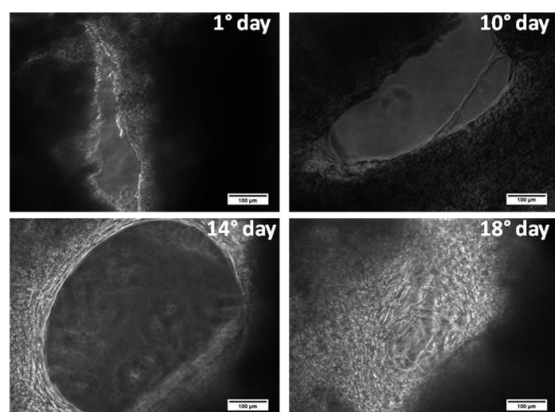


Figure 1. cut evolution in human dermis model.

### RESULTS AND DISCUSSION

The figure 1 showed the evolution of the wound during 20 days. It is evident a significant changing in geometry of the edge of the wound and an activation state and migratory abilities of the fibroblast. Thus, the results displayed a complete healing of the dermal wound in 18 days with a mean closure velocity of  $0.053 \text{ h}^{-1}$ .

In figure 2  $\alpha$ SMA (stained in red) and HA production during dermal healing are reported in the left and right column, respectively. We found that both  $\alpha$ SMA and HA signals presented the strongest signal at 16 days (fig. 2b). According to the literature,  $\alpha$ SMA expression was transient and it was not detectable at 20 days (fig. 2c). At this time HA levels was present (fig. 2f) but decreased compared to 16 days (fig. 2e). Taken together these results demonstrate that some of typical proteins involved in the wound healing process *in vivo*, are induced in our model following the same timing existing *in vivo*.

### CONCLUSION

In conclusion with our 3D-HDE *in vitro* model we can demonstrate the relationship between cell migration, differentiation marker and ECM production during the wound healing process (fig. 2).

We believe that our 3D-HDE wound model could be a starting point for a novel platform to test dermal wound therapies. As a fact, future developments could provide a complete model that will put the healthcare research into a better defined frame and more closely resembles the *in vivo* system.

### REFERENCES

- David J. Geer *et al.*, Tissue Engineering 7/8, 2004
- Yan Xie *et al.*, Tissue Engineering 5, 2005
- Palmiero C. *et al.*, Acta Biomaterialia 6, 2010

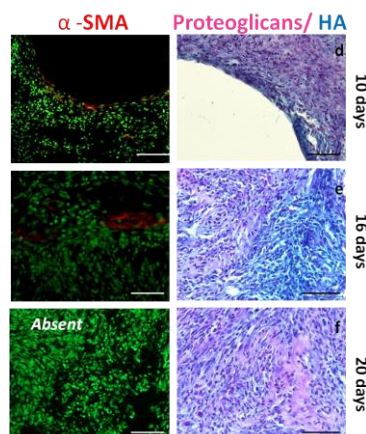


Figure 2. Immunofluorescence of the  $\alpha$ SMA at 10-16-20 days (a, b and c, respectively) and Alcian blue-P.A.S. staining for proteoglycans production at 10-16-20 days (d, e and f, respectively). a,d Scale bar = 100  $\mu\text{m}$ ; b,c,e,f, Scale bar 50  $\mu\text{m}$ .

## Modification of Calcium Phosphate Bone Cements with Biologically Active Metal Ions: *In Vitro* and *In Vivo* Characterization

Anja Lode<sup>1</sup>, Anne Bernhardt<sup>1</sup>, Barbe Rentsch<sup>1,2</sup>, Claudia Rentsch<sup>2</sup>, Martha Geffers<sup>3</sup>, Mandy Quade<sup>1</sup>, Stefan Rammelt<sup>2</sup>, Uwe Gbureck<sup>3</sup>, Michael Gelinsky<sup>1</sup>

<sup>1</sup>Centre for Translational Bone, Joint and Soft Tissue Research, Technische Universität Dresden, Dresden, Germany

<sup>2</sup>University Centre for Orthopaedics and Trauma Surgery, University Hospital *Carl Gustav Carus*, Dresden, Germany

<sup>3</sup>Department of Functional Materials in Medicine and Dentistry, University of Würzburg, Würzburg, Germany

[anja.lode@tu-dresden.de](mailto:anja.lode@tu-dresden.de)

### INTRODUCTION

Various studies have demonstrated that metal ions are capable to affect different cell types and biological processes essential for bone regeneration<sup>1-4</sup>. Therefore, a promising strategy to stimulate remodeling and new bone formation is the incorporation of such ions into the implant material. In this study, we have modified a brushite-forming calcium phosphate cement with various metal ions ( $\text{Cu}^{2+}$ ,  $\text{Co}^{2+}$ ,  $\text{Cr}^{3+}$ ) and investigated the impact of these modifications on biocompatibility, resorption and new bone formation.

### EXPERIMENTAL METHODS

Brushite cements were produced by mixing  $\beta$ -TCP powder, which was sintered with the according amount of metal nitrates, in a molar ratio of 0.8 with dicalcium phosphate anhydrous ( $\text{Ca}(\text{H}_2\text{PO}_4)_2$ ). Afterwards, the powder was mixed with 0.1 M phytic acid in a powder to liquid ratio of 2 g/ml. Ion release from the cements was investigated during immersion in cell culture medium which was collected at different time points and analyzed by inductively coupled plasma mass spectrometry (ICP-MS).

Cytocompatibility was studied with human mesenchymal stem cells (hMSC) in indirect culture as well as in direct contact over 21 days. Osteogenic differentiation of hMSC was induced by addition of dexamethasone,  $\beta$ -glycerophosphate and ascorbic acid-2-phosphate to the cell culture medium. Osteoclast formation and activity was investigated in direct contact to the cement surface. Human monocytes were seeded onto the samples and cultivated in the presence of RANKL and M-CSF over 16 days. Resorption of the cements as well as new bone formation was studied in unloaded cylindrical defects in the tibia head of rats 3 and 6 months after implantation.

### RESULTS AND DISCUSSION

The phase composition of the set cements was not influenced by the different metal ions. Every cement formulation has formed brushite with a certain amount of unreacted  $\beta$ -TCP. During immersion in cell culture medium,  $\text{Cu}^{2+}$  and  $\text{Co}^{2+}$  were released with an initial burst followed by a sustained release, however, the concentrations in the release solution was always far below the cytotoxic threshold. In contrast, nearly no  $\text{Cr}^{3+}$  was released from the cements.

Indirect culture of hMSC revealed a higher cell proliferation and viability in the presence of extracts obtained from  $\text{Cu}^{2+}$  and  $\text{Cr}^{3+}$  modified cement samples compared to the reference cement. In addition, slightly higher values of alkaline phosphatase (ALP) activity indicated a positive effect of these modifications on osteogenic

differentiation. Cultivation of hMSC directly on the cement samples demonstrated a clear improvement of the cytocompatibility of brushite by incorporation of  $\text{Cr}^{3+}$ , but not of  $\text{Cu}^{2+}$  and  $\text{Co}^{2+}$ .

Multinuclear osteoclasts were formed from monocytes on reference cements as well as on  $\text{Co}^{2+}$  and  $\text{Cr}^{3+}$  modified cements. In contrast, monocytes did barely survive on the surface of  $\text{Cu}^{2+}$  modified cements. Highest osteoclast number as well as highest activity of the osteoclast-specific enzymes tartrate-resistant acid phosphatase (TRAP) and carbonic anhydrase II (CAII) were found on  $\text{Cr}^{3+}$  cements.

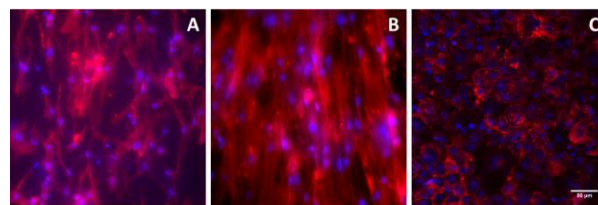


Figure 1: hMSC (day 14) on unmodified (A) and on  $\text{Cr}^{3+}$  modified brushite cements (B); osteoclasts (day 16) on  $\text{Cr}^{3+}$  modified brushite cements (C)

Compared to unmodified brushite cements, the addition of  $\text{Cr}^{3+}$  stimulated bone remodeling *in vivo* as indicated by an increased cellular activity and a significantly enhanced bone resorption after 3 and 6 month of implantation. The addition of  $\text{Cu}^{2+}$  and  $\text{Co}^{2+}$  showed no stimulating effect. Both, the *in vitro* and *in vivo* experiments indicate a positive effect of the  $\text{Cr}^{3+}$ -modification.

### CONCLUSION

The incorporation of metal ions into implant materials can influence their biocompatibility and resorption as well as the bone remodeling process. Data of our study demonstrated that the modification of a brushite cement with  $\text{Cr}^{3+}$ -ions could improve its performance.

### REFERENCES

- Gerard C. *et al.*, Biomaterials 31:824-831, 2010
- Patntirapong S. *et al.*, Biomaterials 30:548-555, 2009
- Niki Y. *et al.*, Biomaterials 24:1447-1457, 2003
- Mourino V. *et al.*, J R Soc Interface 9:401-419, 2012

### ACKNOWLEDGMENTS

The authors would like to thank the German Research Society (DFG; Grant no: GE1133/13-2) for providing financial support to this project. We thank Anja Henss and Markus Rohnke (Justus Liebig University Giessen, Germany) for TOF-SIMS analyses.

## Development of Novel Implants with Embedded Therapeutics

Sophie C. Cox<sup>1</sup>, Hany Hassanin<sup>2</sup>, Moataz M. Attallah<sup>2</sup>, Duncan E.T. Shepherd<sup>3</sup>, Owen Addison<sup>4</sup>, Uwe Gbureck<sup>5</sup>, Liam M. Grover<sup>1</sup>

<sup>1</sup>School of Chemical Engineering, University of Birmingham, UK; <sup>2</sup>School of Metallurgy and Materials, University of Birmingham, UK; <sup>3</sup>School of Mechanical Engineering, University of Birmingham, UK; <sup>4</sup>School of Dentistry, University of Birmingham, UK; <sup>5</sup>Department of Functional Materials in Medicine and Dentistry, University of Wurzburg, Germany.

[s.c.cox@bham.ac.uk](mailto:s.c.cox@bham.ac.uk)

### INTRODUCTION

Metallic implants are used throughout the body, particularly for the repair of orthopaedic and craniofacial defects. Irrespective of surgical domain, there are three inherent problems associated with such implants that are yet to be addressed: (1) relatively high rates of infection (5% in US<sup>1</sup>), (2) lack of customisation of fit to the tissue defect, and (3) a mismatch of mechanical properties between the implant and patient's bone. These issues compromise implant functionality. For example, the high stiffness of metals, such as Ti-6Al-4V, compared with bone may lead to localised resorption of native tissue and ultimately loosening of the implant.

This project aims to address the deficiencies associated with current metallic implants by using an additive layer manufacturing (ALM) method, to create customised implants with a defined internal porosity that may be infiltrated with a second phase that: (1) is of lower stiffness than the metal, and (2) may carry a biologically active molecule that may modify the tissue healing response or prevent infection altogether.

This study describes how cold-setting brushite cements have been modified for injection into a demonstration metal part (*Fig 1*), manufactured using selective laser melting (SLM). The physiochemical properties of the materials were evaluated using scanning electron microscopy, X-Ray diffraction, compression testing, and pycnometry. Furthermore, the efficacy of the cement as a release reservoir infiltrated into the

minutes. Selected samples were analysed via XRD ( $2\theta=5-60^\circ$ ) to determine the conversion rate to brushite and cylinders ( $h = 12 \text{ mm}$ ,  $d = 6 \text{ mm}$ ) were manufactured to assess microstructural development via SEM, compressive strength ( $n=10$ ; 1 mm/min), and porosity. Test SLM parts were designed using *Solidworks* (*Fig 1*), converted to STL format, and manufactured using a *Concept M2 Cusing System*.

### RESULTS AND DISCUSSION

SEM micrographs demonstrated significant morphological and average particle size variation (MCPM: 8.3 – 192  $\mu\text{m}$ ;  $\beta$ -TCP: 27.4 – 67.5  $\mu\text{m}$ ) between different reagent suppliers. Brushite cements produced at the same PLR and using the same liquid phase but using reagents from different suppliers exhibited significant differences in setting time and injectability. For example, at a PLR 3.0 using 1000 mM citric acid the setting time varied 62-223 minutes and injectability through a 15G needle was between 0 and 94%. Eight formulations were determined to exhibit an injectability >80% and setting time 10-30 minutes. Interestingly, no samples formed using orthophosphoric acid met this criteria, which was due to setting times either being too fast or samples with appropriate setting times having a high PLR and therefore poor injectability. The conversion rate to brushite for these 8 formulations varied between 77 and 92%. A positive correlation between conversion rate and injectability was observed ( $R^2=0.6$ ), suggesting that minimising the amount of unreacted  $\beta$ -tricalcium phosphate may facilitate minimally invasive delivery of the cement paste. The maximum compressive strength of uncompacted cements was <20 MPa and samples exhibited porosities from 49 to 64%. Surprisingly, no obvious correlation was observed between maximum compressive strength and porosity. Although this may be explained by other factors, such as the maximum pore diameter, which are known to influence strength.

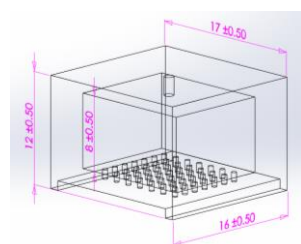


*Fig 1*: CAD of part manufactured by SLM (dimensions in mm)

structure was evaluated by determining antibacterial potency and endothelial cell tubule formation.

### EXPERIMENTAL METHODS

Cement reagents were purchased from various suppliers and manufactured at powder to liquid ratios 2.0, 3.0, and 4.0 using water, 500 mM/1000mM citric acid or 500/1000 mM trisodium citrate as the liquid phase. Cement pastes were prepared by hand mixing the relevant powder and liquid phases for 30 s. The ease of injecting the cements pastes through a 5 mL syringe and a 15G hypodermic needle as well as setting time were determined. Formulations to inject into metal parts were then selected according to a criteria of >80% injectability and a setting time between 10 and 30

### CONCLUSIONS

This study demonstrates the ability to infiltrate brushite cements loaded with a therapeutic agent into customised metal parts; highlighting the potential of this strategy to impact on current orthopaedic and craniofacial implant design.

### REFERENCES

1. National Healthcare Safety Database

### ACKNOWLEDGMENTS

The authors would like to thank the EPSRC (EP/L020815/1) for providing financial support.





## The Influence of Phase Change Materials Based on Poly(Ethylene Glycol) on the Properties of Acrylic Bone Cements

Kinga Pielichowska, Katarzyna Filipek

Faculty of Materials Science and Ceramics, Department of Biomaterials,  
AGH University of Science and Technology, Poland

[kingapie@agh.edu.pl](mailto:kingapie@agh.edu.pl)

### INTRODUCTION

Commercial acrylic bone cements (mainly based on poly(methyl methacrylate) (PMMA)) have been used in total joint arthroplasty since late 1950s [1]. Acrylic bone cements are composed of solid and liquid phase. The solid phase consists of PMMA or its copolymers, initiator and radiological contrast ( $\text{ZrO}_2$  or  $\text{BaSO}_4$ ), while the liquid component is methyl methacrylate monomer, an activator and an inhibitor to avoid premature polymerization [2]. Now, PMMA-based bone cements are widely used in orthopaedic surgery, mainly for fixation of prostheses, but also for stabilizing compressive vertebral fractures or filling bone defects [3]. The major problem with the use of acrylic cement is thermal necrosis of surrounding bone tissue due to the high heat generation during curing process. Polymerization of the acrylic bone cement is an exothermal process, which can give a local temperature peak ranging from 50 to 120°C [4]. In this work we propose modification of acrylic bone cement with poly(ethylene glycol) as phase change materials (PCM) able to store thermal energy in the form of latent heat to decrease the maximum curing temperature.

### EXPERIMENTAL METHODS

Acrylic bone cement was modified by PEG with molecular weight of 1450 in amounts of 2.5, 5, 10, 15, 20%. The setting time was measured using the Gillmore needle method while maximum curing temperature  $T_{\text{max}}$  and setting time  $t_{\text{set}}$  were measured in accordance with ISO 5833 standard. Thermal properties were investigated using DSC and TG methods; mechanical properties were tested using compression tests and ultrasonic non-destructive method. Microstructure was observed using SEM. Moreover, samples were incubated at 37 °C according to EN ISO 10993-13 for 14 weeks in Ringer solution and in PBS. The pH, conductivity, and mass change were measured during incubation.

### RESULTS AND DISCUSSION

Results of setting time and temperature measurements during curing of acrylic bone cement with different PEG content are presented in Fig. 1. As it can be observed, the setting time of modified acrylic bone cements slightly increase with increasing PEG content. However, for all samples it does not increase above 15 min and is still consistent with ISO 5833:2002.

It can be also seen a significant decrease in maximum temperature in curing process – maximum temperature decreased from 71°C for unmodified cement to 60°C for cement with 15% of PEG that undergo melting during curing of acrylic bone cement due to large exothermal effect, and it stores thermal energy in form of latent heat of phase transition [5, 6].

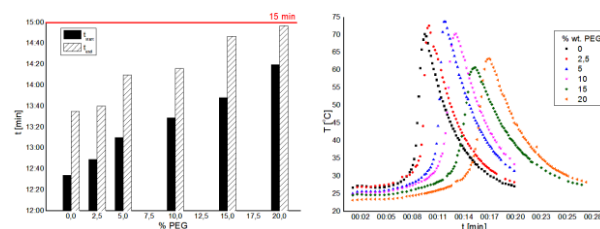


Fig. 1. Setting time (left) and temperature (right) as a function of time for different PEG contents

Major changes in microstructure have been observed by SEM analysis – Fig. 2.

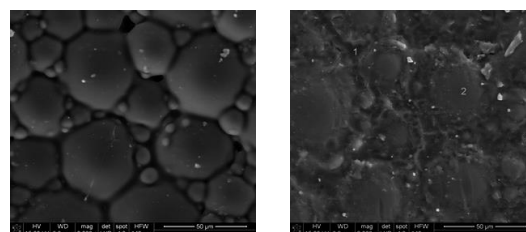


Fig. 2. SEM microphotographs of unmodified acrylic bone cement (left) and modified with 20% of PEG

### CONCLUSIONS

Modification of acrylic bone cement using PCM strongly influences the maximum setting of acrylic cement and can significantly reduce the temperature. The maximum temperature of curing process gets lower with an increase of the amount of PCM in cement. With an increase of PCM content, cement setting time is longer, but it is still below 15 min. As modification with PCMs influences cement's microstructure, some changes in the mechanical properties and in vitro stability have been observed.

### REFERENCES

1. J. Charnley. Anchorage of the femoral head prosthesis to the shaft of the femur, *J Bone Joint Surg Br*, 1960, 42B, 28-30.
2. J. Charnley. Acrylic cement in orthopaedic surgery. *British Journal of Surgery*, 1970, 57, 874-874.
3. M. Stańczyk, B. van Rietbergen. Thermal analysis of bone cement polymerisation at the cement–bone interface, *Journal of Biomechanics*, 2004, 37, 1803-1810.
4. M.A. Puska, L.V.J. Lassila, A.J. Aho, A. Yli-Urpo, P.K. Vallittu, I. Kangasniemi. Exothermal Characteristics and Release of Residual Monomers from Fiber-reinforced Oligomer-modified Acrylic Bone Cement, *Journal of Biomaterials Applications*, 2005, 20, 51-64.
5. K. Pielichowska, K. Pielichowski. Phase change materials for thermal energy storage, *Progress in Materials Science*, 2014, 65, 67-123.
6. K. Pielichowska, S. Błazewicz. Acrylic bone cement/Akrylanowy cement kostny, Polish patent application P.406713, 2013.

### ACKNOWLEDGMENTS

This work was financed by statute fund of Faculty of Materials Science and Ceramics AGH-UST under contract No. 11.11.160.616.





## Marine Collagen Reinforcement of Calcium Phosphate Bone Cements: A Biological Assessment

Iwan Palmer<sup>1</sup>, John Nelson<sup>2</sup>, Wolfgang Schatton<sup>3</sup>, Nicholas J Dunne<sup>1</sup>, Fraser J Buchanan<sup>1</sup>, Susan A Clarke<sup>4</sup>

<sup>1</sup>School of Mechanical & Aerospace Engineering, Queen's University Belfast, UK

<sup>2</sup>Institute for Global Food Security, School of Biological Sciences, Queen's University Belfast, UK

<sup>3</sup>Klinipharma GmbH, Frankfurt am Main, Germany

<sup>4</sup>School of Nursing & Midwifery, Queen's University Belfast, UK

[i.palmer@qub.ac.uk](mailto:i.palmer@qub.ac.uk)

### INTRODUCTION

Induction of *in vivo* responses by implanted biomaterials is of great interest in the medical device field. Calcium phosphate bone cements (CPCs) can potentially promote natural bone remodelling and ingrowth *in vivo* and, as such are becoming more common place in a range of orthopaedic procedures. However, concerns remain regarding their mechanical and handling properties. Compressive modulus and fracture toughness of CPCs can be improved, without compromising injectability and setting time, through the incorporation of bovine collagen fibres<sup>1</sup>. Incorporation of marine derived collagen fibres has also yielded similar improvements<sup>2</sup>. It is hypothesised that, due to its role in bone formation and function, that incorporation of collagen in CPCs will also result in biological benefits.

### EXPERIMENTAL METHODS

$\alpha$ -tricalcium phosphate and 5 wt%  $\text{Na}_2\text{HPO}_4$  in  $\text{dH}_2\text{O}$  were mixed at a liquid/powder ratio of 0.35 mL/g to produce a CPC ( $\alpha$ -TCP-CPC). Bovine (BC-CPC) and Marine (MC-CPC) collagen-CPC composites were produced by adding 1 wt% collagen into the powder and liquid phases respectively. A CPC based on a commercial formulation<sup>3</sup> (Merck-CPC) and a clinically used injectable poly(methyl methacrylate) bone cement (VP-PMMA - Vertebroplastic® Radiopaque Resinous Material, DePuy) were used as controls.

Human bone marrow stromal cell cytotoxicity, proliferation and differentiation were assessed *in vitro* using lactate dehydrogenase (LDH), PicoGreen and alkaline phosphatase (ALP) activity assays respectively.

New Zealand white rabbits were used as an *in vivo* model. Conical cement samples (8 mm long and 4 mm base diameter) were press fit into defects created in the distal femoral condyles; retrieval for analysis took place at 5 and 10 weeks. Bone apposition (BA) onto the implants and mineral apposition rate (MAR) were evaluated and tartrate resistant acid phosphatase (TRAP) staining was used to assess osteoclast activity in the implanted region.

### RESULTS AND DISCUSSION

Relatively low (< 15 %) levels of cytotoxicity were associated with each of the cements. Increased cell death was associated with collagen incorporation, but only to the extent observed for hydroxyapatite<sup>4</sup>, another common orthopaedic biomaterial. Cellular proliferation occurred on all cements, but the most notable variation between formulations was in induction of osteoblastic differentiation (Figure 1). ALP activity was significantly higher on each of the CPCs than on

VP-PMMA. Activity was similar on the collagen-CPCs at each time point; however, by Day 21 ALP activity was significantly higher on both unaugmented CPCs when compared to BC-CPC. This is likely to be due to the increased surface roughness of BC-CPC, which has been associated with delayed differentiation<sup>5</sup>.

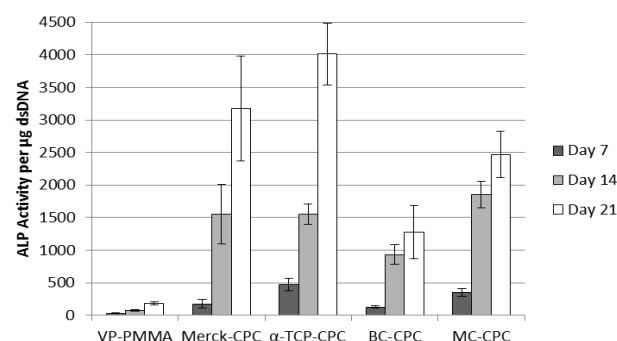


Figure 1: ALP activity per  $\mu\text{g}$  dsDNA associated with each cement formulation.

All formulations were well tolerated *in vivo*. CPCs induced higher BA than VP-PMMA, though BA was unaffected by collagen incorporation. MAR was unchanged, suggesting little influence on bone growth rate at the times considered. Osteoclastic activity within CPC cracks was indicated by TRAP staining and bone growth within cracks also suggests that small scale cement remodelling occurred.

### CONCLUSION

The biological properties of  $\alpha$ -TCP-CPC were largely unchanged by the incorporation of marine derived collagen. However, as a result of significant improvements to the mechanical properties, its incorporation may still result in a suitable alternative to some commercially available bone cements.

### REFERENCES

1. Dunne N. J. *et al.*, 6<sup>th</sup> World Congress of Biomechanics, pp 1173-1176, Springer.
2. O'Hara R. (2010), *Injectable Calcium Phosphate Cements for Spinal Repair*, PhD Thesis, Queen's University Belfast.
3. Ooms E. *et al.*, J. Biomed. Mater. Res. 61:9-18, 2002.
4. Skelton K. L. *et al.*, Acta Biomater. 3:563-572, 2007.
5. Deligianni D. D. *et al.*, Biomaterials. 22:87-96, 2000.

### ACKNOWLEDGMENTS

The authors would like to thank the Engineering and Physical Sciences Research Council for providing financial support to this project.



## Cellular Uptake and Degradation of Poly(Lactide-co-Glycolide) Nanoparticles and its Influences on Cell Functions

Dahai Yu, Pengfei Jiang, Zhengwei Mao, Changyou Gao\*

MOE Key Laboratory of Macromolecular Synthesis and Functionalization, Department of Polymer Science and Engineering, Zhejiang University, Hangzhou 310027, China  
[cygao@zju.edu.cn](mailto:cygao@zju.edu.cn)

### INTRODUCTION

The polymeric nanoparticles (NPs) have been widely used in biological and biomedical fields such as drug/gene carriers, contrast agents, photo-thermal therapeutic materials, etc. However, the interaction between these NPs and cells, such as internalization process, intracellular fate and influence on cell functions, is still not fully addressed. This study is focused on the internalization processes and intracellular fate of functional polymeric NPs, especially poly(lactide-co-glycolide) (PLGA) NPs, and their influences on cells.

### EXPERIMENTAL METHODS

The polymeric NPs with different physiochemical properties such as charge, ligands, and stiffness were prepared. Their cellular uptake kinetics and pathways as well as intracellular transportation were studied by in vitro cell culture. The alternation of particle structures and functions inside cells was investigated via fluorescence resonance energy transfer (FRET) technique. The influences of particles on cell functions and phenotypes were also determined.

### RESULTS AND DISCUSSION

The physiochemical properties of particles significantly influenced particle-cell interactions. For example, endothelial cells preferred to ingest positively charged PLGA-PEI particles than negatively charged PLGA-BSA particles. Both types of particles were internalized into the cells via macropinocytosis and clathrin-mediated endocytosis pathways. Ingestion of the positively charged particles caused apparently a decrease in cell viability, proliferation, cell adhesion and migration, as well as wound healing ability. By contrast, uptake of negatively charged particles caused much less influence on cell functions. Uptake of the stiffer PLGA NPs enhanced the osteogenic differentiation of mesenchymal stem cells as evidenced by the higher expression of ALP activity and collagen type I and osteocalcin.

The PLGA-PEI particles were further covalently modified via grafting of fluorescein isothiocyanate (FITC), dimethyl 3,3'-dithiobispropionimidate (DTBP), amino-ended polyethyleneglycol (PEG), and tetramethylrhodamineisothiocyanate (TRITC), as shown in Figure 1. The Fluorescence resonance energy transfer (FRET) could be observed and the intensity ratio between 520 nm and 570 nm was used to evaluate the dissociation of disulfide bonds on the surface of PLGA particles. The dissociation of fluorescent dyes in the cells was significantly slower than that in simulated phosphate buffered saline (PBS) containing the same

concentration of reduction agent glutathione, revealing the difference of particle dissociation behaviors.

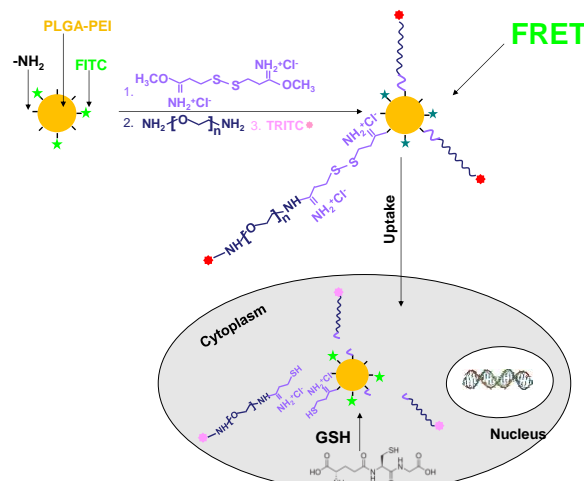


**Figure 1** Preparation of PPFDP particles and their FRET change caused by GSH reduction.

### CONCLUSION

The particle physiochemical properties can modulate cell uptake and cell functions such as viability, adhesion, migration and differentiation. The alternation of particle structures and functions in cells can be significantly different than that in simulated buffer, which should be taken into consideration for design of those intracellular delivery vehicles.

### REFERENCES

1. Yu DH, Zhang YY, Mao ZW, Gao CY. *Macromolecular Bioscience*, 2013, 13(10): 1413-1421.
2. Yu DH, Zhang YY, Zhou XY, Mao ZW, Gao CY. *Biomacromolecules*, 2012, 13(10): 3272-3282.
3. Liu WJ, Zhou XY, Mao ZW, Yu DH, Wang B, Gao CY. *Soft Matter*, 2012, 8(35): 9235-9245.
4. Zhang YY, Hu L, Yu DH, Gao CY. *Biomaterials* 2010, 31: 8465-8475.

### ACKNOWLEDGMENTS

The authors would like to acknowledge the financial supports by the Natural Science Foundation of China (51120135001) and European FP7 project NANOSOLUTIONS (309329).

## Evaluation of Biological Effects of Nanomaterials on Human Cell Line, EA.hy926

Małgorzata Siatkowska<sup>1,2</sup>, Tomasz Wasiak<sup>1</sup>, Paulina Sokołowska<sup>1</sup>, Joanna Rywaniak<sup>1</sup>, Katarzyna Działoszyńska<sup>1</sup>, Sylwia Kotarba<sup>1</sup>, Kinga Kądzioła<sup>1</sup>, Nina Bartoszek<sup>1</sup>, Marta Kamińska<sup>2</sup>, Agnieszka Kołodziejczyk<sup>1</sup>, Piotr Komorowski<sup>1,2</sup>, Krzysztof Makowski<sup>1</sup>, Bogdan Walkowiak<sup>1,2</sup>

<sup>1</sup>Department of Biophysics, Institute of Materials Science and Engineering, Lodz University of Technology

<sup>2</sup>Laboratory of Molecular and Nanostructural Biophysics, Lodz Regional Science and Technology Park Ltd., Poland, 93-465 Lodz, 114/116 Dubois Street

[m.siatkowska@technopark.lodz.pl](mailto:m.siatkowska@technopark.lodz.pl)

### INTRODUCTION

In the last decades the field of nanotechnology becomes the main focus of numerous research centers over the world. Nanomaterials are being used in rapidly increasing applications and many products in nano-scale have already been launched on the market. However, despite of new, unique and alternative properties of nanomaterials comparing to their bulk counterparts, the level of risk towards human health is still unclear and not fully examined<sup>1</sup>. In the view of above, the use of commercial products in biomedical applications raises big concerns – due to the investigated short- or long-term toxicity of nanoparticles and potential hazardous influence on human body<sup>2,3</sup>. In the present study, we investigated the biological effects of three commercially available nanoproducts: polyamidoamine dendrimers (PAMAMs) of 4.0 generation, silver nanopowders (SNPs) and multi-walled carbon nanotubes (MWCNTs) on EA.hy926 endothelial cell line. Owing to the extensive scope of this work it was possible to assess changes in endothelial cells on the structural as well as the molecular level.

### EXPERIMENTAL METHODS

After seeding on culture plates, endothelial cells were cultured in DMEM medium at 37°C for 24h in a fully humidified atmosphere of 5% CO<sub>2</sub>. Cells were then stimulated with examined nanoparticles for 24h. For assessment of morphological changes scanning electron microscope (Quanta FEG 250 FEI) working in high vacuum at accelerating voltage of 10 kV, 15 kV or 20 kV was used. To evaluate the cytotoxic potential of nanoparticles, LIVE/DEAD test was performed using Accuri C6 Flow Cytometer (Becton-Dickinson). For transcriptomic analysis, Agilent SuperPrint G3 Human GE 8×60K V2 oligonucleotide microarrays were used. Total RNA from EA.hy926 cell was isolated using TRI Reagent (Molecular Research), purified, labelled and hybridized for 17h at 65°C with a rotation speed 10 rpm. Gene Spring GX 12.6.1 (Agilent) Software was used to analyze gene expression data. For assessment of the whole proteome of endothelial cells, differential in-gel electrophoresis DIGE was used. Samples were labeled with Cy3, Cy5, isofocused on 18cm long DryStrip gels, pH 4-7 using IPGphor III (GE Healthcare) and separated in second dimension in Ettan DALTsix system (GE Healthcare). Obtained data were analyzed with ImageMaster 2D Platinum 7.0 DIGE (GE

Healthcare). Proteins under changed expression were identified with MALDI-TOF/TOF spectrometer (UltrafleXtreme Smartbeam II, Bruker Daltonics) and identification was performed via MASCOT search engine against Swiss Prot database.

### RESULTS AND DISCUSSION

Using scanning electron microscopy, we reported the differences in cell morphology under experimental conditions comparing to control, particularly apparent for SNP. It was observed that cells internalized SNP after 24h of incubation period what consequently might affect cell morphology and proliferation. These findings are correlated with flow cytometry analysis – we demonstrated increased value of SSC parameter for SNP and altered viability of cells for all nanomaterials compared to control. What is more, cytotoxic effect manifested by increased population of dead cells, is dose-dependent for SNP, while for PAMAM dendrimers and MWCNT the tendency was not clear and not statistically significant.

DIGE analysis revealed changes in the expression of a number of distinct proteins. In response to nanoparticle incubation, among almost 900 proteins expressed in cells at average for each nanomaterial and control, statistically significant changes were addressed to SNP for 100 proteins (including 74 down-regulation, 26 up-regulation), to MWCNT – 41 proteins (31 down-regulation, 10 up-regulation) and to PAMAM dendrimers – 50 proteins (29 down-regulation, 21 up-regulation). Transcriptomic analysis showed that more than 400 genes were in changed expression. We also observed that only several proteins identified by mass spectrometry corresponded to changes in genes' expression.

### CONCLUSION

Our findings highlight changes on both – structural and molecular level - in EA.hy26 cells due to exposure to nanoparticles at various concentrations. As these issues are crucial for commercial use of nanoproducts, it should be regarded with more attention and further studies must be carried out to achieve better knowledge in this field.

### REFERENCES

1. Agarwal M. *et al.*, Int J Curr Microbiol App Sci 2(10): 76-82, 2013
2. Kim J. S. *et al.* Part Fibre Toxicol., 7(20): 1-11, 2010
3. Buzea C. *et al.*, Biointerphases. 2(4): 17-71, 2007



## Gellan-Gum Coated Gold Nanorods as Intracellular Drug Release System for Osteogenic Differentiation

S. Vial<sup>1,2</sup>, S. Vieira<sup>1,2,3</sup>, F. R. Maia<sup>1,2</sup>, M. Carvalho<sup>1,2</sup>, R. L. Reis<sup>1,2</sup>, P. L. Granja<sup>3</sup>, J. M. Oliveira<sup>1,2</sup>.

1- 3B's Research Group - Biomaterials, Biodegradables and Biomimetics, University of Minho, Headquarters of the European Institute of Excellence on Tissue Engineering and Regenerative Medicine, AvePark, 4806-909 Taipas, Guimarães, Portugal

2- ICVS/3B's - PT Government Associate Laboratory, Braga/Guimarães, Portugal

3- INEB – Instituto de Engenharia Biomedica, Universidade do Porto, Rua do Campo Alegre, 823, 4150-180 Porto, Portugal

[miguel.oliveira@dep.uminho.pt](mailto:miguel.oliveira@dep.uminho.pt)

### INTRODUCTION

Recently, gold nanoparticles have shown to have interesting features to stimulate the osteogenic differentiation of mesenchymal stem cells as well as osteoblast-like cell toward osteoblast formation.<sup>1,2</sup> Due to their remarkable physicochemical properties, gold nanorods (AuNR) gain a lot of interest to be used for diagnosis, cell tracking, thermal therapy and drug delivery system (DDS) for regenerative medicine.<sup>3</sup> However, their surface modification is primordial in order to improve their biocompatibility and stability under biological conditions, while enable the controlled release of drugs/bioactive agents. In this purpose, the coating of gold nanorods within hydrogel as Gellan Gum (GG), a biodegradable and biocompatible natural-based polymers<sup>4</sup>, was performed and allowed to greatly fulfill the requirement needed to develop an efficient DDS for osteogenic differentiation.

### EXPERIMENTAL METHODS

Gold nanorods were prepared following the seed-mediated growth method and then, were pre-coated with a bilayer of polyelectrolytes. Subsequently, a solution of “Gelzan” Gellan Gum was previously heated at 90°C to allow dissolution. The nanorods were added to the GG solution and the mixture was stirred overnight at room temperature. The GG-coated nanorods (AuNR@GG) have been characterized by UV-visible spectrometry, zeta potential measurements and Transmission electron microscopy (TEM). The cell viability has been performed in normal and osteogenic media after 1, 3, 7 and 14 days of culture using MTS assay in SAOs-2 and rabbit adipose stem cell, and human adipose-derived stem cell. The internalization was characterized by TEM. The dexamethasone, osteogenic precursor, have therefore been adsorbed into gold nanorods suspension and then the mixture was added the GG solution for one night.

### RESULTS AND DISCUSSION

Gold nanorods were successfully coated with ~10 nm layer of gellan gum, as shown in figure 1. The AuNR@GG exhibited better stability than crude AuNRs and polyelectrolyte-modified AuNRs (data not shown) in different concentrations of salt and pH. The cell viability assays have shown that AuNR@GG are no cytotoxic after 14 days of culture in normal and osteogenic media in three different cell lines. Moreover, the particles have been uptaken inside cells, aggregated in vesicles (Figure 2). The incorporation of dexamethasone, and the stability of the drug-functionalized nanoparticles are significantly improved

in presence of the gellan gum (data not shown).

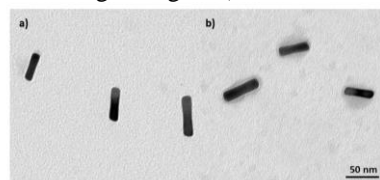


Figure 1. TEM images of A) pre-coated AuNR and B) AuNR@GG

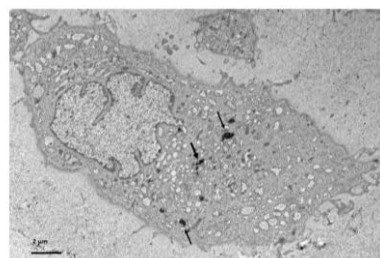


Figure 2. TEM image of internalized AuNR@GG inside adipose stem cell

### CONCLUSION

In this study, we report the successful coating of individual gold nanorods within gellan gum and the ability to improve the drug loading yield. The proposed system has shown interesting features for osteogenesis, and further will be extended for cancer therapy and tissue engineering studies.

### REFERENCES

- [1] Yi, C. *et al.*, ACS Nano. 4 : 6439–6448, 2010
- [2] Heo, D.N. J. *et al.*, Chem. Mater. 2: 1584-1593, 2014
- [3] Huang X *et al.*, Adv. Mater. 21:4880-4910, 2009
- [4] Dhar S. *et al.*, Nanoscale 3 :575-580, 2011

### ACKNOWLEDGMENTS

The authors would like to thank the European Union's Seventh Framework Program (FP7/2007-2013) under grant agreement n° REGPOT-CT2012-316331-POLARIS, and QREN (ON.2 – NORTE-01-0124-FEDER-000016) co-financed by North Portugal Regional Operational Program (ON.2 – O Novo Norte), under the National Strategic Reference Framework (NSRF), through the European Regional Development Fund (ERDF) for providing financial support to this project. The FCT distinction attributed to J.M. Oliveira under the Investigator FCT program (IF/00423/2012) is also greatly acknowledged.





## On the Influence of Various Physiochemical Properties of the CNTs Layers on the Cell's Reaction *in Vitro*

Aleksandra Benko<sup>1</sup>, Aneta Frączek-Szczypta<sup>1</sup>, Elżbieta Menaszek<sup>2</sup>, Marek Nocuń<sup>1</sup>, Marta Błażewicz<sup>1</sup>

<sup>1</sup> AGH University, Faculty of Materials Science and Ceramics, Krakow, Poland

<sup>2</sup> Department of Cytobiology, Collegium Medicum, Jagiellonian University, Medyczna 9, 30-068 Krakow, Poland  
[abenko@agh.edu.pl](mailto:abenko@agh.edu.pl)

### INTRODUCTION

Extremely high mechanical properties, good thermal and electrical conductivity, combined with reported potential to stimulate cell's growth, differentiation and proliferation are major factors of an increased scientific interest in applying carbon nanotubes (CNTs) to various biomedical systems [1, 2]. However, within the literature, large discrepancies, concerning CNTs biocompatibility, can be found. In some studies, a cytotoxic reaction is reported [3], whereas in others, a successful application with no adverse effects can be found [4].

Most of the biocompatibility studies are focused on the impact of the various physiochemical properties of the CNTs dilutions on their outcome toxicity and are aimed to answer the question whether the CNTs are good candidates for targeted therapies [5]. However, different type of cellular reaction is expected when the cells are contacted with the CNTs surfaces.

The aim of the presented study is to reveal the correlation between the physiochemical properties of the CNTs layers and their outcome biocompatibility.

### EXPERIMENTAL METHODS

Functionalized multiwalled carbon nanotubes were either obtained from the producer (CNT\_OH) or fabricated from the pure CNTs via chemical reflux (CNT\_ox). The materials were supplied by NanoAmor, Inc. (stock # 1249YJF and 1213NMGS, respectively). Thin layers of CNTs were deposited through the EPD process. Physiochemical evaluation included wettability measurement, SEM observation, and the XPS study. Influence on cells was studied on the L929 cell line (mouse fibroblasts). In long-term *in vitro* experiments, cell apoptosis, lysis and viability was evaluated after being grown on materials. Simultaneously, cell adhesion was evaluated and spreading was observed under a fluorescence microscope.

### RESULTS AND DISCUSSION

CNT\_OH and CNT\_ox were found to differ majorly in terms of type and amount of functional groups. Consequently, these were found to affect the morphology and wettability of the obtained layers.

Finally, the study revealed that all of the presented factors have major influence on the outcome cell's reaction towards the materials.

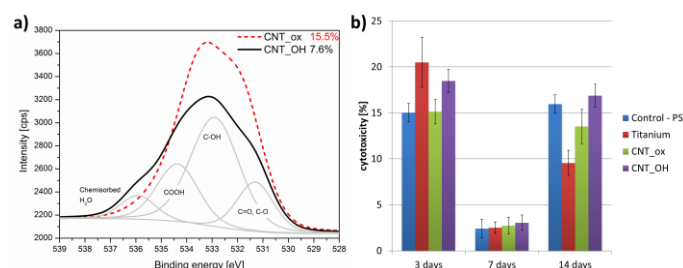


Fig. 1 reveals correlation between a) chemical composition revealed during an XPS study and c) cell's reaction towards the material

### CONCLUSION

Within the presented study, numerous analytical techniques were applied in order to evaluate influence of various physiochemical properties of the CNTs layers on the outcome cells' response. Presented results imply that outcome biocompatibility of the CNTs depends not only on their size and shape, but also – on the type and amount of different functional groups present on their outer sidewalls.

### REFERENCES

1. B.S. Harrison, *et al.*, *Biomaterials*, 28:344–353, 2007
2. X. Li, *et al.*, *Biomed. Mater.*, 5 (2010) 022001.
3. O. Vittorio, *et al.*, *Nanomedicine: Nanotechnology, Biology and Medicine*, 5:424-431, 2009.
4. J. Wang, *et al.*, *Carbon*, 47:1752-1760, 2009.
5. P. Wick, P. *et al.*, *Toxicol. Lett.*, 168:121-131, 2007.

### ACKNOWLEDGMENTS

This research has been supported by the National Center of Science (NCN) under grants: UMO-011/01/B/ST/5/06424 and UMO-2013/11/N/ST8/01357.

# Novel Collagen Type I-Hyaluronic Acid Bi-Phasic Conduit for Peripheral Nerve Repair: An *In Vivo* Study

Tijna Alekseeva, Phoebe E. Roche<sup>1</sup>, Amos Matsiko, Amro Widaa, William A. Lackington, Alan Ryan, Alan J. Hibbitts, Garry Duffy, Fergal J. O'Brien

Tissue Engineering Research Group, Department of Anatomy and

<sup>1</sup>Department of Otolaryngology, Royal College of Surgeons in Ireland, Ireland

[tijnaalekseeva@rcsi.ie](mailto:tijnaalekseeva@rcsi.ie)

## INTRODUCTION

Peripheral nerve (PN) injuries usually require surgical intervention associated with multiple risks and inferior functional outcomes<sup>1</sup>. Coupled with the diminishing capacity for regeneration associated with age<sup>2</sup> and underlying conditions such as diabetes<sup>3</sup>, there is a considerable demand for alternative treatments. A novel bi-phasic conduit for PN repair was developed in the Tissue Engineering Research Group at RCSI, Ireland, consisting of the outer collagen type I based conduit and inner hyaluronic based luminal filler (Fig.1A). This conduit is bio-compatible and bio-degradable, has an aligned porous microstructure and supports neuro- and gliogenesis *in vitro*. It was hypothesised that nerve conduit will support nerve regeneration across critical size defect *in vivo* (Fig.1B).

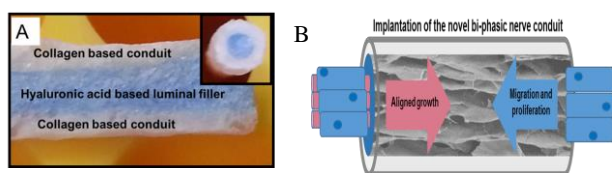


Fig.1: (A) Gross morphology of the novel nerve conduit. Colour is used to highlight bi-phasic composition. (B) Cellular response to the novel nerve conduit following PN injury

Here we present the encouraging results of a pilot *in vivo* study investigating the pro-regenerative capacity of the novel conduit in the critical size PN defect rat model.

The overall aim of this study was to assess the pro-regenerative performance of the nerve conduit *in vivo* in a critical length peripheral nerve injury model.

## EXPERIMENTAL METHODS

The conduits were implanted into a 10 mm sciatic nerve gap within Sprague Dawley rats (n=9) following approval from the RCSI Ethics Committee. At 8 weeks post-implantation, functional assessment of regeneration through the conduit was performed by measuring nerve conductivity across the regeneration site and the force of the motor response to the nerve stimulation. These data were compared to the contralateral uninjured control or negative control (10 mm injury, no treatment, n=9). Nerve regeneration was assessed morphologically by histomorphological analysis of the excised tissue using immunostaining.

## RESULTS AND DISCUSSION

Significant recovery of nerve functionality was achieved 8 weeks after implantation of the novel conduit. No functional recovery was detected in the negative control group confirming absence of

spontaneous regeneration and highlighting the role of the nerve conduit in recovery of the nerve function after injury. Functional recovery data were supported by the histomorphological analysis of the excised tissue showing aligned ingrowth of axons across the conduit (Fig.2 A, B) and into the distal nerve (Fig. 2C), using axonal marker neurofilament (shown in red)

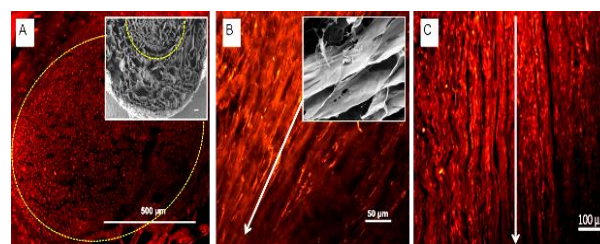


Fig.2 Immunofluorescent images of the transverse (A) and longitudinal (B) sections of the nerve conduit after 8 weeks *in vivo*. Longitudinal section of the nerve distal to the site of implantation is shown in (C). Inserts show scanning electron microscopy images of the conduit prior to implantation. Demarcation between the outer conduit and luminal filler is indicated by dashed line. Arrows indicate the direction of axonal alignment.

Further histomorphological analysis demonstrated that explanted conduits were repopulated by the host SCs expressing SC-specific marker, S100 $\beta$  and myelin marker, Myelin Basic Protein, indicating regeneration of the normal PN morphology. Moreover, infiltrating SCs were able to lay down basal lamina proteins fibronectin and laminin, further highlighting pro-regenerative role of the nerve conduit.

## CONCLUSIONS

- Implantation of the novel bi-phasic conduit restored nerve functionality after 8 weeks.
- The conduit was capable of guiding axons across the injury site with a high degree of alignment.
- Furthermore, the conduit supported migration and pro-regenerative functional behaviour of Schwann cells.
- Future work involves further enhancement of the regenerative capacity of the conduit by incorporation of neuro-inductive growth factors and progenitor cells.

## REFERENCES

1. Deumens, R. *et al.*, Prog Neurobiol, 92(3):245-76, 2010
2. Painter, M. W. *et al.*, Neuron, 83(2):331-43, 2014
3. Ebenezer, G. J. *et al.*, Brain, 134(6):1853-63, 2011

## ACKNOWLEDGMENTS

This publication has emanated from research conducted with the financial support of Science Foundation Ireland (SFI) Grant Number SFI/13/TIDA/B2655

## Sustained Biochemical Signalling and Contact Guidance Provided by Electrospun Bicomponent Scaffolds for Enhancing Nerve Regeneration

Chaoyu Liu, Min Wang

Department of Mechanical Engineering, The University of Hong Kong, Pokfulam Road, Hong Kong  
[jamesliu@hku.hk](mailto:jamesliu@hku.hk)

### INTRODUCTION

Repairing severely injured peripheral nerves requires suitable devices for bridging the nerve and guiding axon growth. Electrospun fibrous scaffolds offer distinctive advantages and have gained popularity in nerve tissue repair. Nanofibrous scaffolds provide favourable conditions including high surface-area-to-volume ratio and structural similarity with extracellular matrix for Schwann cell migration and neurite outgrowth<sup>1</sup>. On the other hand, controlled local delivery of nerve growth factor (NGF) and/or glial cell line-derived growth factor (GDNF) promotes peripheral nerve regeneration. It was also shown that electrospun aligned fibres provided contact guidance, leading to elongation and alignment of cultured cells<sup>2</sup>. In this investigation, bicomponent scaffolds composed of random or aligned nanofibers which were incorporated with NGF and GDNF were fabricated for providing sustained biochemical signal and contact guidance for peripheral nerve regeneration.

### EXPERIMENTAL METHODS

Using dual-source dual-powder electrospinning (DSDP-ES)<sup>3</sup>, emulsion electrospinning (E-ES) and a drum collector rotating at different speeds, new bicomponent scaffolds composed of random or aligned fibers were made, incorporating NGF in poly(D,L-lactic acid) (PDLLA) fibers and GDNF in poly(lactic-co-glycolic acid) (PLGA) fibers. PDLLA emulsions (15 or 20% w/v) and PLGA emulsions (12 or 15% w/v) were used in electrospinning. The ratio of NGF/PDLLA fibers to GDNF/PLGA fibers in scaffolds was varied. The morphological and structural properties of scaffolds were assessed using SEM and TEM. *In vitro* release profiles of NGF and GDNF were studied using ELISA kit assay. For biological investigations, PC12 cells were seeded on scaffolds and cultured for up to 7 days. MTT assay was used for cell proliferation study. F-actin and neurofilament were stained at day 4 and day 7 for investigating cell differentiation using laser scanning confocal microscopy (LSCM). Neurite length and alignment were measured using an image analysis tool.

### RESULTS AND DISCUSSION

Robust GDNF/PLGA and NGF/PDLLA fibers with core-shell structures (Fig.1) were produced via E-ES. Through DSDP-ES, both types of nanofibers were evenly distributed in bicomponent scaffolds and desirable fiber ratios (and hence GF ratios) could be achieved (Fig.2). Within a 42-day release test period, GFs from bicomponent scaffolds showed an initial burst release within 24 h, followed by a sustained release. Both NGF and GDNF from scaffolds with various fiber ratios exhibited similar release profiles but different release amounts (Fig.3). The bioactivity of released NGF and GDNF was preserved at maximum. MTT

results showed that novel scaffolds had significant enhancement in PC12 cell proliferation as compared with the control group. It was shown that GF-containing scaffolds significantly enhanced cell differentiation in terms of neurite outgrowth and branching of PC12 cells (Fig.4). Larger GF release amounts led to higher differentiation levels. The synergetic effect of dual delivery of NGF and GDNF on cell differentiation occurred at the 2:1 ratio of NGF/PDLLA to GDNF/PLGA fibres for bicomponent scaffolds. Longer neurite outgrowth and alignment of PC12 cells were observed on scaffolds with aligned fibres.

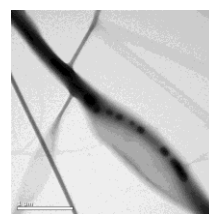


Fig.1 TEM image

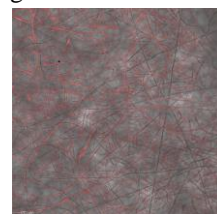


Fig.2 Confocal Image

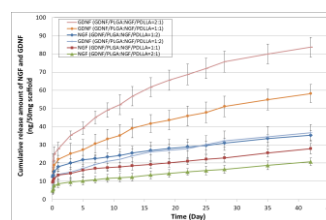


Fig. 3 Release profile

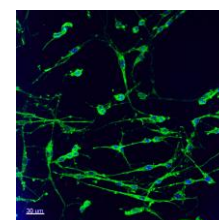


Fig. 4 Cell Morphology

### CONCLUSION

Novel bicomponent scaffolds composed of aligned fibers containing designed amounts of NGF and GDNF could be made via DSDP-ES with E-ES. Good post-release bioactivity and sustained release of both GFs were achieved. Compared with the control group, bicomponent scaffolds containing GFs induced much enhanced PC12 cell differentiation. Furthermore, growth factors released from bicomponent scaffolds at a certain fiber ratio promoted cell differentiation in a synergetic manner and aligned fibers predominantly provided contact guidance, resulting in the elongation and alignment of cells. These scaffolds are promising for peripheral nerve regeneration.

### REFERENCES

1. Wang HB, *et al.*, Acta Biomaterialia, 6:2970-78,2010
2. Schnell E, *et al.*, Biomaterials, 28(19):3012-25, 2007
3. Wang C, *et al.*, J. Mater.Sci.-Mater.Med., 23:2381-97, 2012

### ACKNOWLEDGMENTS

This work was supported by the Hong Kong Research Grants Council via a GRF grant (7177/13E). CY.Liu thanks HKU for providing him with a PhD scholarship.





## The “Micro” and “Macro”- Scale Approach in Building up Neural Stem Cell Microenvironments for Developmental and Toxicity Studies

Leonora Buzanska<sup>1,2</sup>, Marzena Zychowicz<sup>1,2</sup>, Krystyna Pietrucha<sup>3</sup>, Martyna Podobinska<sup>1,2</sup>, Jose Luis Gerardo-Nava<sup>4</sup>, Gary Brook<sup>4</sup>

<sup>1</sup> Stem Cell Bioengineering Unit, Mossakowski Medical Research Centre, Polish Academy of Sciences, Warsaw, Poland

<sup>2</sup> Department of Biotechnology, Wrocław Research Centre EIT+, Wrocław, Poland

<sup>3</sup> Department of Material and Commodity Sciences and Textile Metrology, Lodz University of Technology, Lodz, Poland

<sup>4</sup> Institute for Neuropathology, RWTH Aachen University, Aachen, Germany

[buzanska@imdik.pan.pl](mailto:buzanska@imdik.pan.pl)

### INTRODUCTION

Combining advances in stem cell research with emerging technologies of the stem cell niche bioengineering, allows the creation of paradigms that mimic *in vivo*-microenvironments. There are two different strategies to create such advanced “biomimetic” research systems *in vitro*. The first is to establish “microscale” environments to test cell behaviour, even at the single cell resolution<sup>1</sup>. The second approach is to provide a “macroscale” structural 3D template<sup>2</sup> for cell differentiation and function that allows the growth of complicated human tissues and organoids.

In this report we are presenting both, “micro” and “macro”- scale culture systems used by our group for developmental and toxicity studies of human neural stem cells derived from cord blood and neurally committed induced pluripotent stem cells (iPSC).

### EXPERIMENTAL METHODS

Human umbilical cord blood-derived neural stem cells (HUCB-NSC)<sup>3</sup> and virus-free, feeder-free human umbilical cord blood-derived iPSC (hiPSC, Life Technologies) were cultured and harvested at different stages of neuronal development. The cells were seeded on: 1) matrigel-coated plates, 2) different microprinted or microspotted patterns of extracellular matrix domains functionalized with signalling proteins (Shh, Wnt3a, Dkk1, Jagged1, CNTF)<sup>4</sup> and 3) chemically modified collagen scaffolds<sup>2</sup>. The last approach was to co-culture collagen scaffold/hiPSC hybrids with rat dissociated dorsal root ganglia neurons and organotypic spinal cord slices<sup>5</sup>, testing for cell migration and axonal growth between dissociated cells/slices and the seeded and non-seeded scaffold.

The “micro-scale” culture systems were obtained by soft lithography, microcontact printing of different biomolecules, mainly ECM proteins and by piezoelectric microspotting of ECM alone or combined with signalling proteins<sup>4</sup>. Collagen scaffolds were prepared from porcine collagen dispersion using a lyophilization technique to obtain 3D, porous scaffolds. Scaffolds cross-linking with carbodiimide ensured mechanical and thermal properties. Differentiation potential of neural stem cells was tested by immunocytochemical staining and real time PCR of developmental stage dependent markers. Microscopy was performed using an AxioScope with associated AxioCamMRC5 camera as well as a confocal LSM 510 system (Carl Zeiss, Germany).

### RESULTS AND DISCUSSION

Microcontact printing allows easy fabrication of complex patterns with one type of biomaterial for studying stem cell migration and differentiation on

different geometries. Micro-spotting is a versatile tool for depositing different biomolecules on the same chip, allowing rapid screening of the effects of multiple biomolecules at different concentrations on stem cell fate. We have shown that the potential to differentiate of HUCB-NSC and hiPSC depends on the type of functional domain and its geometry and that “smart” biodomains with signalling molecules can direct stem cell fate into neuronal or glial lineage. In macro-scale conditions, cells were seeded onto collagen scaffolds or forced for the self assembly into embryoid bodies in matrigel. The control cultures of hiPSC under neural-differentiating protocol revealed all typical changes from pluripotent to neuronal and glial phenotypes. RT-PCR and immunocytochemical analyses revealed that pluripotent markers (e.g. Oct4, Sox2 and Nanog) are gradually lost while neural markers (e.g. nestin, MAP-2,  $\beta$ -tubulin, GFAP) are acquired. The iPSC cells seeded on matrigel can form 3D aggregates/organoid spheres with cells representing three germ layers, which in proper differentiating conditions can obtain advanced neuronal markers MAP-2, Dbc, Synapsin, TH as well as glial markers: PDGFR $\alpha$ , GFAP and GalC.

Co-culture of iPSC-seeded collagen scaffolds with organotypic slices revealed only uni-directional migration/extension of cells and neural processes from the slice into the cell seeded scaffold.

### CONCLUSION

The micro-scale experimental approach such as cell culture platforms with microprinted and microspotted biofunctional domains can be used to test molecular mechanisms of neuronal differentiation while macro-scale systems, such as scaffolds colonized by stem cells and self-assembled tissue structures are more suitable for tracing of neuro-developmental processes and toxicological studies. The macro-scale approach allows us to build up a hybrid testing platform for medium/long term cultures of neural stem cells with a range of host tissues.

### REFERENCES

1. Zychowicz M. *et al.*, *Tox in Vitro* 28: 76–87, 2014
2. Pietrucha K. *Med & Biol Eng & Comp* (JIFMBE) 14: 3369–3372, 2007
3. Buzanska L. *et al.*, *Stem Cells Dev* 15:391–406, 2006
4. Buzanska L. *et al.*, *Toxicology* 270: 35–4, 2010
5. Gerardo-Nava J. *et al.*, *Biomaterials* 35(14):4288–96, 2014

### ACKNOWLEDGMENTS

The research was supported by Wrocław Research Centre EIT+ under the project „Biotechnologies and advanced medical technologies” – BioMed (POIG.01.01.02-02-003/08) financed from the European Regional Development Fund (Operational Programme Innovative Economy, 1.1.2); EC JRC “NanoBiotech for Health” and statutory funds to Mossakowski Medical Research Centre PAS.





## Pre-Clinical Investigation of a Novel Biodegradable Polymer Based Medical Device for Peripheral Nerve Regeneration

Atefeh Mobasser<sup>1</sup>, David Richards<sup>1</sup>, Giorgio Terenghi<sup>2</sup>, Adam Reid<sup>2</sup>, Julie Gough<sup>1</sup>

<sup>1</sup>Material Sciences Centre, School of Materials, University of Manchester, Manchester, United Kingdom.

<sup>2</sup>Blond McIndoe Laboratories, Centre for Tissue Injury and Repair, Institute of Inflammation & Repair, University of Manchester, Manchester, United Kingdom

[Atefeh.mobasser@manchester.ac.uk](mailto:Atefeh.mobasser@manchester.ac.uk)

### INTRODUCTION

Damage to the peripheral nerve is a global clinical problem and can result in loss of function and considerable morbidity and affect patient's quality of life. Nerve guide conduits have emerged as a promising approach for the management of peripheral nerve injuries and a potential alternative to the autografts. We have developed the biodegradable-based nerve guide conduits made of poly caprolactone/ poly lactic acid with a micro-structured intraluminal surface (1). The grooved PCL/PLA conduits outperformed non-grooved conduits and showed comparable experimental outcomes to autografts during short and long term *in vivo* experiments (2).

To translate the developed medical device to the clinic and human applications several requirements should be fulfilled. The medical grade sterilisation method and its effect and limitation are one of the important factors that need to be assessed. The present study evaluated the outcome of two sterilisation methods including gamma radiation and E-beam on the PCL/PLA conduits. Several different radiation doses (15-45KGy) were used to identify the suitable dose for sterilisation of PCL/PLA conduits.

### EXPERIMENTAL METHODS

PCL/PLA conduits were sterilised with gamma and E-beam with 15, 20, 25, 30, 35, 40, 45 KGy (Synergy, UK). To analyse the mechanical properties, instron1122 was used to measure maximum stress, strain and Young Modulus. Differential scanning calorimetry (DSC) were used to assess the melting point temperature and crystallinity. Molecular weight of the samples was measured by gel permeable chromatography (GPC). Surface structure and grooves morphology were imaged and assessed by Scanning electron microscopy (SEM). One-way ANOVA was used to analyse the differences between groups of samples (Prism 6, GraphPad).  $P < 0.05$  was set as a threshold for significant difference.

### RESULTS AND DISCUSSION

Following sterilisation, surface structure and specifically grooved structure remained unaffected. The mechanical properties analysis showed no significant difference in the maximum stress of non-irradiated films, gamma and E-beam irradiated films with the highest dose (45KGy). However E-Beam radiation with the higher doses (40 and 45 KGy) decreased the maximum strain significantly ( $88.80 \pm 15.01\%$  and  $54.60 \pm 5.55\%$  for non-irradiated and 45KGy-irradiated films, respectively) ( $p < 0.05$ ). Furthermore, DSC analysis showed no significant differences in melting temperature ( $T_m$ ) and Glass transition temperature ( $T_g$ ), however the radiation with high dose (40 and 45KGy) increased the crystallinity of PCL/PLA samples.

### CONCLUSION

Choosing the suitable sterilisation method is essential for the development of medical device and specifically polymer-based biomaterial. The sterilisation process should be optimised to reduce its drawback on the material properties. In the present study we showed that gamma radiation and E-beam could be used as the potential sterilisation process for PCL/PLA conduits. However it is necessary to optimise the relevant radiation dose to minimise molecular scission and linkage and hence mechanical and chemical properties.

### REFERENCES

1. Mobasser SA. *et al.*, Mater Sci Mater Med. 24(7):1639-47, 2013
2. Mobasser SA. *et al.*, Tissue Eng Part A 21(5-6):1152-62, 2015

### ACKNOWLEDGMENTS

The authors would like to thank the NIHR, invention for innovation (i4i) programme for providing financial support to this project.



# Decrease of MRI Artifact in Spinal Instruments of Zirconium Alloy

Takao Hanawa<sup>1</sup>, Naoyuki Nomura<sup>2</sup>, Maki Ashida<sup>1</sup>, Yusuke Tsustumi<sup>1</sup>, Hisashi Doi<sup>1</sup>, Peng Cheng<sup>1</sup>, Manabu Itoh<sup>3</sup>

<sup>1</sup>Institute of Biomaterials and Bioengineering, Tokyo Medical and Dental University, Japan

<sup>2</sup>Department of Materials Science and Engineering, Tohoku University, Japan

<sup>3</sup>Hokkaido Medical Center, National Hospital Organization, Japan

[hanawa.met@tmd.ac.jp](mailto:hanawa.met@tmd.ac.jp)

## INTRODUCTION

Magnetic resonance imaging (MRI) is used as an important diagnostic tool for whole-body. However, images of organs and tissue are disturbed around metallic implants and artifacts occur in intense magnetic field of MRI instruments. On the other hand, over 70% of implant devices consist of metals because of their high strength, high toughness and good durability, while magnetic susceptibility of metals is still relatively large. Therefore, metals show a low magnetic susceptibility or antimagnetic materials are required for medical devices. Among various pure metals, Zr possesses low magnetic susceptibility compared to Ti, Co and Fe alloys. We have developed Zr-based alloys, showing low magnetic susceptibility, high strength and corrosion resistance<sup>1-5</sup>. The magnetic susceptibilities of Zr alloys are almost one-third that of Ti-6Al-4V and one-seventh of Co-Cr alloy. In this study, we have attempted large-amount melting of Zr-1mass%Mo alloy and investigated mechanical properties, crystal phase, and magnetic susceptibility, for the commercialization of the alloy. Finally, MRI artifact of spinal instruments consisting of the alloy and implanted in sheep spine was observed.

## EXPERIMENTAL METHODS

Zr-1mass%Mo alloy was employed in this study because tensile strength was the largest among Zr-Mo alloys<sup>3</sup>. Cold crucible induction melting of Zr-1Mo alloy was attempted. Zr rods were sandwiched between Mo flakes lapped by Zr foil, layer by layer, and 5-kg ingot was obtained. The ingot was cast to rods with 30 mm in diameter. Test specimens were produced from the rod. Composition analysis, tensile test, X-ray diffraction, SEM-EBSD, TEM observation, and measurement of magnetic susceptibility were performed. Finally, pedicle screws, spinal cage, and rod were implanted in spine of sheep and observed with 3T MRI.

## RESULTS AND DISCUSSION

The large amount melting was succeeded because molybdenum in the alloy existed in a range of 1.06-1.14mass% in all region of the rod. XRD revealed that the phase was almost  $\alpha$ . Mass magnetic susceptibility was  $0.98 \times 10^{-6} \text{ cm}^3 \text{ g}^{-1}$  as low as the previous study<sup>3</sup>. Results of the tensile test were summarized in Table 1. Elongation to fracture of the alloy was 23% and much larger than that of Ti-6Al-4V. Crystal structure of the alloy was identified as follows. Regions with a width of 3  $\mu\text{m}$  where dislocation density was low were surrounded by a network (Fig. 1). The former consisted of  $\alpha$  phase contributing to plasticity and the latter consisted of  $\beta$  and  $\omega$  phases contributing to strength.

Artifact less than 2 mm was observed on 3T MRI image of the spinal instruments and the vertebral canal appeared (Fig.2).

Table 1 0.2% yield strength (YS), tensile strength (TS) and Elongation to fracture (EL) of Zr-1Mo and Ti-6Al-4V alloys.

	YS(MPa)	TS (MPa)	EL(%)
Zr-1Mo (top)	612	676	23
Zr-1Mo (bottom)	602	672	23
Ti-6Al-4V (cast)	791	845	11
Ti-6Al-4V (rough)	863	963	18

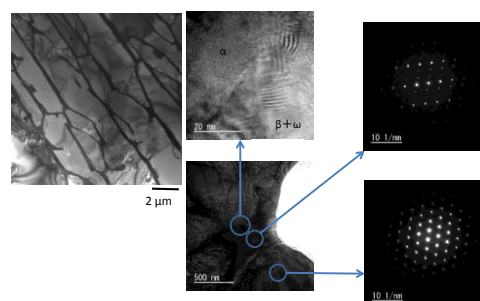


Fig. 1 TEM image and electron diffraction pattern.

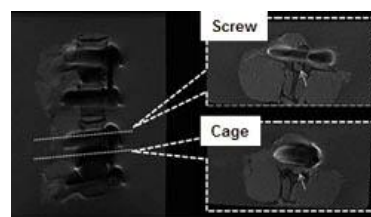


Fig.2 MRI images of the screw and cage.

## CONCLUSION

Zr-1Mo alloy after large-amount melting showed large strength and elongation and low magnetic susceptibility. 3T MRI artifact of spinal instruments consisting of the alloy and implanted into sheep spine occupied in 2 mm and the vertebral canal appeared. Therefore, this alloy is a candidate of MRI compatible alloy.

## REFERENCES

1. Nomura N. *et al.*, Mater. Trans. 50: 2466-2472, 2009
2. Suyalatu *et al.*, Act. Biomater. 6: 1033-1088, 2010
3. Suyalatu *et al.*, Act. Biomater. 7: 4259-4266, 2011
4. Kondo R. *et al.*, Mater. Sci. Eng. C31: 900-905, 2011
5. Kondo R. *et al.*, Act. Biomater. 9: 5795-5801, 2013

## ACKNOWLEDGMENTS

The authors would like to thank JST S-Innovation Program "Biofunctionalization of Metallic Biomaterials -A vital point of supporting long healthy life in musculoskeletal medicine-" for providing financial support to this project.



Iulian Antoniac<sup>1</sup>, Ana Blajan<sup>1</sup>, Aurora Antoniac<sup>1</sup>

<sup>1</sup>Materials Science and Engineering Faculty, University Politehnica of Bucharest, Romania  
[antoniac.iulian@gmail.com](mailto:antoniac.iulian@gmail.com)

## INTRODUCTION

Studies regarding biodegradable materials have shown that magnesium is a potential biomaterial for orthopedic application due to its major advantage to biodegrade in biological medium<sup>1</sup>. Different alloying element play an important role for experimental biodegradable magnesium alloys not just in term of properties but also considering that the degradation products are expected to be non-toxic<sup>2</sup>. Because the hydrogen release is a crucial fact in potentially using of these alloys as orthopedic biomaterials, we evaluate the hydrogen release in different testing media for all experimental magnesium alloys. Also, this work evaluates the degradation behavior and corrosion of different magnesium alloys (from the systems Mg-Zn-Zr or Mg-Ca) in different simulated biological medium through the evaluation of biodegradability and corrosion products. We take in consideration the application of these alloys as orthopedic biomaterials.

## EXPERIMENTAL METHODS

Different magnesium alloys from the systems Mg-Zn-Zr and Mg-Ca systems was used as experimental material. Experimental samples of circular shape and 2mm x10mm size were polished on metallographic papers and washed with ethanol. For immersion and corrosion tests were used three different mediums: Phosphate buffer solution (PBS), Hanks' Balanced Salt Solution (HBSS) and Dulbecco Modified Eagle Medium supplemented with fetal bovine serum (DMEM + 10% FBS). During immersion tests, the experimental samples were immersed in 50 ml solution each (total surface area to volume of solution = 314mm<sup>2</sup>:50mL) at 37 °C for 3, 7, and 21 days. The samples were weighted before and after the immersion and the hydrogen evolution was monitored. For microstructural characterization of experimental samples was used an Olympus BX51 optical microscope and a Philips XL30-ESEM scanning electron microscope. Also, scanning electron microscopy was used for surface analysis of the samples after immersion and corrosion tests. The surface of all experimental samples was analyzed in the terms of chemical composition using an energy dispersive X-ray (EDX) spectrometer. The experimental values were analyzed using the Student's t-test and expressed by the mean values  $\pm$  standard deviation (SD). A P-value(0.05) was considered statistically significant.

## RESULTS AND DISCUSSION

Immersed samples show different patterns of degradation depending on the magnesium alloy composition and type of medium, showing an accelerated degradation process with increasing immersion time. In the case of phosphate buffered solution (PBS) it can be noticed a fine crystals deposit

on the surface. For the samples tested in Hanks' Balanced Salt Solution (HBSS) we observed a different pattern of degradation with rapid accumulation of corrosion products and loss of integrity up to the end of the test. When we used Dulbecco Modified Eagle Medium supplemented with fetal bovine serum (DMEM + 10% FBS) we observed that the proteins seems to form a passivation layer on top.

In figure 1 we present an example of experimental results obtained using SEM coupled with EDS for an Mg-0,8Ca alloy samples after immersion in different testing medium (PBS, HBSS, DMEM) for 21 days.

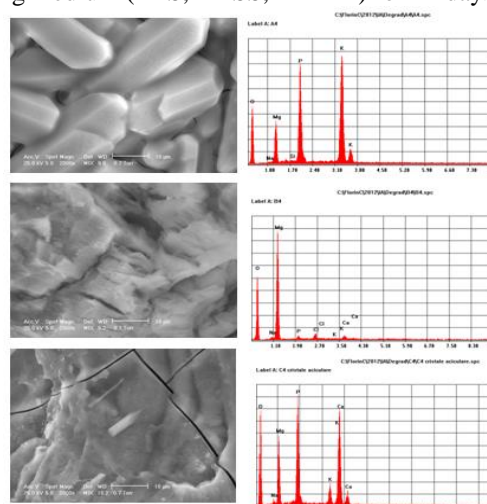


Fig. 1. SEM micrographs and EDS result of Mg-0,8Ca alloy samples after immersion in PBS, HBSS and DMEM after 21 days.

## CONCLUSION

The aim of this study was to evaluate the effects of different mediums on magnesium alloys and to determine the optimal degradation medium. Regarding this issue it have been used both phosphate-based and cell culture medium to observe the influence of amino acids and vitamins and also proteins present in the added amount of fetal bovine serum. This cell culture condition was introduced for simulate a more physiological corrosion environment. We demonstrate that the alloying elements from magnesium alloys influence the surface morphology, degradation and corrosion pattern.

## REFERENCES

1. M. Salahshoor *et al.*, Materials 5:135-155, 2012.
2. M. Staiger *et al.*, Biomaterials 27:1728-1734, 2006.

## ACKNOWLEDGMENTS

The authors would like to thank the fundung agency UEFISCDI, programme PN II-Partnerships in Priority Areas (Contract No. 271/2014) for providing financial support to this project.

## Polyurethane-Ceramic Matrices as Orbital Implants

Semih Sahan<sup>1</sup>, Pezhman Hosseinian<sup>2</sup>, Deniz Ozdil<sup>1</sup>, Mustafa Turk<sup>3</sup>, Halil Murat Aydin<sup>1,4</sup>

<sup>1</sup>BMT Calsis Health Technologies Co., Turkey

<sup>2</sup>Nanotechnology and Nanomedicine Division, Hacettepe University, Turkey

<sup>3</sup>Biology Department, Kirikkale University, Turkey

<sup>4</sup>Environmental Engineering Department & Bioengineering Division and Centre for Bioengineering, Hacettepe University, Turkey

[hmaydin@hacettepe.edu.tr](mailto:hmaydin@hacettepe.edu.tr)

### INTRODUCTION

The loss of an eye is found to be a significant issue for an individual from both an aesthetic and psychological point of view. Medically, the off-the-shelf orbital implants currently used unfortunately do not have a holistic regenerative approach. With current implants, those materials used which are commonly reported and currently on the market, are hydroxyapatite, porous polyethylene and silicone. During implantation extraocular muscles directly attach to either the implant or the ring and with this the implant attempts to simultaneously mimic the natural movement of the other eye<sup>1,2</sup>. In this study, the application of a porous polyurethane<sup>3</sup>/beta-tricalcium phosphate composite as an implant different to those in the literature has been investigated.

### EXPERIMENTAL METHODS

The orbital implant presented in this study is composed of polyurethane and ceramic components. As the degradable component, commercially available beta-tricalcium phosphate particles (1-2 mm, BMT Calsis Co., Turkey) were used. The polyurethane was synthesised with a prepolymer and polyol reaction. Methylene diisocyanate, caprolactone monomer, catalyst (3,6,9-triazaundecamethylenediamine) (all Sigma, Germany) and d.i.-water was used in the preparation of the polyurethane. The molar ratio of the reactants was calculated to give a product in which all NCO groups are reacted. The ceramic particles were introduced in to the mixture obtained before it set, and the whole mixture was then allowed to set over 24 hours in an orbital implant-shaped mould. The resulting structure was then analysed using differential scanning calorimetry (DSC), scanning electron microscopy (SEM) and micro-computerized tomography ( $\mu$ -CT). Cytotoxicity tests were performed to reveal biocompatibility.

### RESULTS AND DISCUSSION

The analyses revealed 96.93 % porosity within the composites. Mechanical compression testing found the Young's Modulus of the material to be 43.2 MPa. DSC and FTIR analyses confirmed the chemical structure and that all the NCO groups were consumed. Figure 1 displays the SEM image of the samples prepared.

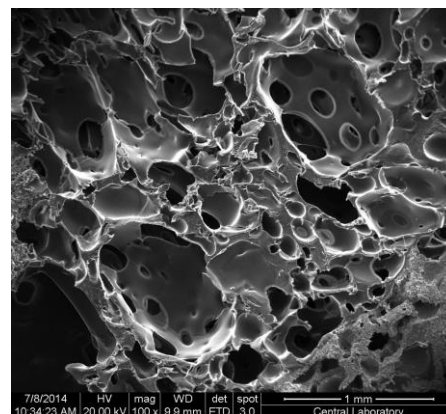


Figure 1. A representative SEM micrograph of PU/TCP composites.

The WST-1 test used to determine the cytotoxicity have shown that the samples were highly biocompatible. Apoptosis and necrosis phenomena were investigated. The material was found to pose no negative effects on the cells.

### CONCLUSION

In this study, a new composite material that has the potential for used as an orbital implant has been proposed. This matrix, with a biocompatible, porous and lightweight structure, and with both suitability for tissue infiltration and incorporation potential, holds great promise. A material with enhanced integration through the fully biodegradable ceramic particles that remain within its structure post-implantation has been prepared.

### REFERENCES

1. Custer P. L. *et al.*, Ophthalmology, 110:2054-2061, 2003.
2. Mengher L. S. *et al.*, Orbit, 27:37-40, 2007.
3. Zdrahala R. J. & Zdrahala I. J., J. Biomater. Appl.mech., 14(1):67-90, 1999

### ACKNOWLEDGMENTS

The authors would like to thank TUBITAK-TEYDEB Programme (Grant no: 7131048) and BMT Calsis Co. for providing financial support to this project.



Karol Gryń, Barbara Szaraniec, Maja Kus, Kamil Dudzinski, Jan Chlopek

Department of Biomaterials, Faculty of Material Science and Ceramics,  
AGH University of Science and Technology, Krakow, Poland

[kgryn@agh.edu.pl](mailto:kgryn@agh.edu.pl)

## INTRODUCTION

The use of bioresorbable miniplates could offer many benefits as compared with commonly used metallic devices for osteotomies. Among them there are: no risk of corrosion, no need for reoperation, translucency for radiological diagnostics. The main advantage of the proposed composite is its multifunction - it means that the implant not only stabilizes fragments of the bone in the position but also resorbs and loses the strength during the polymer matrix degradation. The load is transferred to the healed bone, thus the bone tissue receives signals to remodel the structure according to the Wolff's law [1,2]. Additionally, nanoadditives realised from the polymer matrix have contact with the growing tissue, activating cells and enhancing osteointegration [3]. Regrettably, resorbable polymers such PLA, PGLA, PLLA, PLDL are rather weak and brittle, hence their clinical application is limited to the areas of moderate loads. Furthermore, it is crucial to establish their mechanical limits, especially the factors that may cause the damage of the plate during the implantation surgery.

This report summarizes the research on the development, mechanical and structural description and FEM simulations of the multifunctional miniplates made of PLLA- and PLLA-based composite with bioactive ceramic nanoadditives.

## EXPERIMENTAL METHODS

Three types of materials were prepared. Polymer poly(L-lactide) PLLA (Purasorb PL38, Purac) and two composites consisting of PLLA matrix and the following additives: nanosized TCP (Chema-Elektromed, Lublin, Poland) and both TCP and HAP (Chema-Elektromed, Lublin, Poland) in adequate volumes. Injection molding machine ( $T=200^{\circ}\text{C}$ ) was used to fabricate miniplates. Different shapes of implants were obtained (Fig.1).



Fig. 1 Miniplates - variability of types and shapes

Mechanical properties were examined on the universal testing machine Zwick 1435 in various tests: uniaxial tension (2 mm/min), 3pts (2 mm/min,  $d = 50\text{mm}$ ), 4pts bending (2 mm/min,  $d = 60\text{ mm}$ ,  $b = 22\text{ mm}$ ). During the fixation procedure two important

factors needed to be taken under consideration: the maximum tightening torque, which can be applied to the miniplate and the permissible deformation without damage. Tightening torque was determined with digital dynamometric screwdriver (Poltorque PRO, Poland). Deformation was measured in "single-side" bending test.

Number of stress cycles that a specimen sustains before failure was verified in fatigue tests, including cyclic dynamic uniaxial stretching (100.000 cycles, 30% of  $\epsilon_{\text{max}}$ ; both in normal and in simulated body fluids conditions (Ringer solution,  $37^{\circ}\text{C}$ ) and creeping tests (80-20%  $R_m$ ).

The material's microstructure was observed using optical and SEM microscope

Additionally, FEM analysis and simulations were performed (ABAQUS CEA).

## DISCUSSION

It is vital to investigating the mechanical aspects of resorbable miniplates used for bone fixation – the particular shapes not only normative samples. Such miniplates are more brittle than metallic ones, thus more prone to destruct during or shortly after implantation. It is very important to describe a variety of factors influencing implantation process and causing potential danger. The conducted research also verified mechanical stability of osteosynthesis. Both FEM simulation and the actual tensile and bending tests were analyzed. Maps of stresses and deformations gave information and helped to understand the mechanisms and the nature of the internal deformation of analyzed shapes and geometries of miniplates.

This data made it possible to determine safe values of tightening torque and the range deformation while fitting the composite miniplates to the bone so as to assure the stable and properly functioning osteosynthesis.

## REFERENCES

1. R.M. Loughlin *et al.*: J Oral Maxillof Surg 65:89-96, 2007
2. B. Szaraniec, K. Gryń, T. Szponder *et al.* Engineering of Biomaterials 125: 30-36, 2014
3. Y. Shikinami, M. Okuno: Biomaterials 22 (2001) 3197–3211

## ACKNOWLEDGMENTS

This research was financially supported by the research project No: 5.23.160.254 financed by the Ministry of Science and Higher Education with cooperation with MEDGAL Company.

# Clinically Used Dextran Coated Iron Oxide Nanoparticles and Their Induced Macrophage Autophagy

Rongrong Jin<sup>1</sup>, Jiuju Du<sup>1</sup>, James M. Anderson<sup>3,4</sup> Hua Ai<sup>1,2</sup>

<sup>1</sup> National Engineering Research Center for Biomaterials, Sichuan University, PR China

<sup>2</sup> Department of Radiology, West China Hospital, Sichuan University, PR China

<sup>3</sup> Department of Biomedical Engineering, Case Western Reserve University, Cleveland, OH 44106, USA

<sup>4</sup> Department of Pathology, Case Western Reserve University, Cleveland, OH 44106, USA

[huaai@scu.edu.cn](mailto:huaai@scu.edu.cn)

## INTRODUCTION

Superparamagnetic iron oxide nanoparticles (SPION) are excellent MR contrast agents, which are widely used in disease diagnosis and therapy<sup>1</sup>. However, side effects have been reported<sup>2</sup>. Recently, nanoparticles are considered as a new class of autophagy activator (Fig. 1)<sup>3</sup>. And it has been found that SPION are mainly recognized and eliminated by macrophages in RES (reticuloendothelial system) organs such as liver, lymph node, spleen, etc. In this study, we used clinically approved SPION to explore the relationship between their potential safety risks and autophagy effects in macrophage cells.

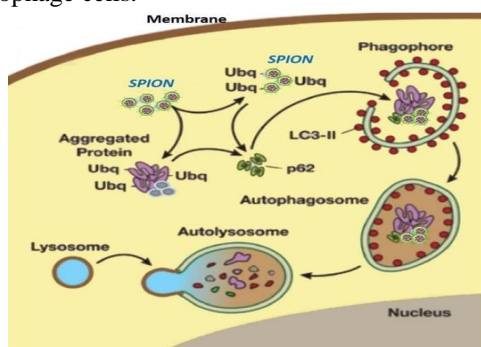


Fig. 1 Possible mechanisms of SPION induced autophagy.<sup>3</sup>

## EXPERIMENTAL METHODS

1. Western blot of nanoparticle induced autophagy was detected with transformation of LC3 I to LC3 II and up-regulation of P62. RIPA lysis of cells were loaded into 13.2 % SDS-PAGE for immune blot assay;
2. Cytokine secretion in cell culture supernatants was measured by ELISA, according to the manufacturer's standard protocol (DAKEW systems). Absorbance was measured at 450 nm on a microplate reader;
3. Data was analysed using Student's paired t-test and  $p < 0.05$  was considered statistically significant;

## RESULTS AND DISCUSSION

As shown in Fig. 2, clinically used MRI contrast agent Resovist and Feraheme can induce obvious variations of autophagy flux (LC3 transformation and p62 up-regulation) in macrophage cells including BMDM (bone marrow derived macrophage) (Fig. 2a), mouse macrophage cell lines Raw264.7 (Fig. 2b) and Ana-1 (data not shown). However, they could not induce autophagy in other cell lines such as Hela (Fig. 2c) and 293T cells (data not shown). The autophagy were mainly caused by iron oxide cores of nanoparticles other than its surface coating of dextran or excipient mannitol (Fig. 2d). At the same time, we found that macrophages treated with SPIONs secreted more inflammatory cytokines (IL-6, IL-1 $\beta$ , TNF- $\alpha$ ) than macrophages alone (Fig. 3).

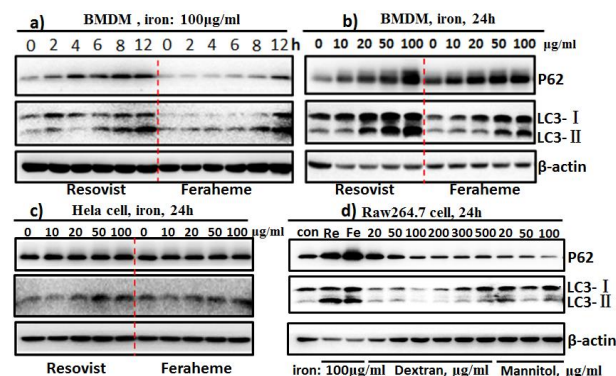


Fig. 2 Iron oxide cores of SPION could induce macrophage autophagy. Cultured cells were treated with nanoparticles at indicated time points and concentrations. Cell lysis were collected for immune blot assay of LC3 transformation and p62 up-regulation.  $\beta$ -actin were detected as loading control. (abbreviation in Fig. 2d: Re: Resovist, Fe: Feraheme)

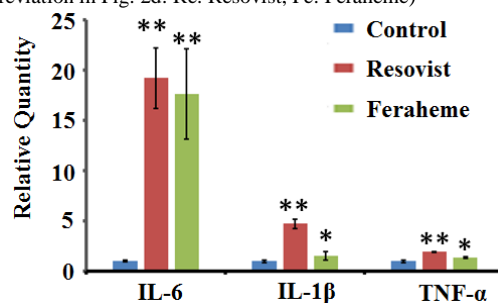


Fig. 3 SPION could induce inflammatory responses of macrophage. Macrophages were treated with 100  $\mu$ g/ml nanoparticles for 24 h. The production of cytokine was analysed by ELISA (IL-6, TNF- $\alpha$ ) or western blot (IL-1 $\beta$ ). (\*\*,  $P < 0.01$ , \*,  $P < 0.05$ ) (control: cells w/o Resovist or Feraheme treatment.)

These results demonstrated that iron oxide cores of SPION could induce autophagy and minimal inflammation in macrophages. And our data showed that macrophages treated with nanoparticles didn't exhibit proliferation inhibition and apoptosis. Most likely, the inflammatory response was regulated by autophagy and will be investigated in our future work.

## CONCLUSIONS

Iron oxide cores of clinically used SPION can induce autophagy of macrophages but not in unphagocytosed cells. The nanoparticles could induce macrophage activation and cytokine release; i.e. inflammatory responses.

## REFERENCES

1. Jin, R et al. *Curr Opin Pharmacol* 2014; 18; 18-27
2. Morteza et al. *Chem. Rev.* 2012; 112; 2323-2338
3. Stern et al. *Particle and Fibre Toxicology* 2012; 9; 20

## ACKNOWLEDGMENTS

The work was supported by National Key Basic Research Program of China (2013CB933903).



## Radiodensitometric Assessment Long Time after Dental Periimplantitis Defect Filled with “Pure” Synthetic HAp Bioceramics

Vadims Klimecs<sup>1</sup>, Girts Salms<sup>1</sup>, Andrejs Skagers<sup>1</sup>, Aleksandrs Grishulonoks<sup>1</sup>, Laura Neimane<sup>2</sup>, Liga Berzina-Cimdina<sup>3</sup>

<sup>1</sup>Department of Oral and Maxillofacial Surgery, Institute of Stomatology, Riga Stradins University, Latvia

<sup>2</sup>Department of Diagnostic Radiology, Institute of Stomatology, Riga Stradins University, Latvia

<sup>3</sup>Rudolph Cimdins Biomaterials Innovation and Development Center, Riga Technical University, Latvia  
[vadims.klimecs@gmail.com](mailto:vadims.klimecs@gmail.com)

### INTRODUCTION

Periimplantitis is a loss of bone tissue correctly joined to dental implants after period of normal osseointegration in cases of 1 – 45 % going to implant loss in many cases<sup>1</sup>. In surgical periimplant treatment materials efficient is xenogenic Bio-Oss with manual debridement and resorbable barriers<sup>2</sup>.

### EXPERIMENTAL METHODS

From 2009 to 2015 years 0,5 1,0 mm of granules HAp produced in Riga Technical University, Rudolph Cimdins Biomaterials Innovation and Development Center as biphasic calcium phosphate bioceramic materials "pure" form was used in periimplantitis treatment on 29 patients. At least after 5 years clinical examination and 3D CT (iCAT) radiodensitometry was carried out in the same program in 9 points - 1 point crystal implantation center, 2 points with 2mm step in meiodistal direction, 2 points with 2mm step on the periapical and crone from the center, as well as 2 points with 2mm step in buccally-lingual direction Housfield (HU) units<sup>3</sup>.

### RESULTS AND DISCUSSION

The measurements in HU were as follows: in the central point - 734.0/514.6. meiodistal direction - from 648.6/422.6 to 632.3/388.0; periapical – crone - from 673.6/487 to 580.3/341; and buccal-lingual from - 665,6/422 to 666.0/520.3.

### CONCLUSION

Indicators of radiodensitometry after 5 years in the place after periimplantite treatment by HAp was minimally different from the patient's bone measurements; the difference of less than 10%, it could indicate a high degree of mineralization after HAp crystals implantation.

### REFERENCES

1. Derks J. *et al.*, J Clin Periodontol, 12 Dec,2014
2. Esposito M..J Oral Implantol.5 Suppl.: 21-41,2012
3. De Vos W., Int J Maxillofac Surg . 38:609-625,2009.

## Debris of a Carbon-Fibre-Reinforced Polymers (CFRP) Wrist Plate Led to a Destructive Synovitis in Human

Antonio Merolli, Lorenzo Rocchi, Alessandro Morini, Luigi Mingarelli, Paolo Scialabba, Francesco Fanfani

Gemelli Medical School, The Catholic University in Rome, Italy

[antonio.merolli@gmail.com](mailto:antonio.merolli@gmail.com)

### INTRODUCTION

Composite materials are largely applied in aerospace and car industry, where an accurate modelling of the possible strains and stresses endured by the artefact is possible. The more complex is the geometry and load-cycle of an artefact, the more difficult (and expensive) will be the design and production by composites. Application of CFRP artefacts in humans has been promoted in Orthopaedic and Trauma Surgery. A prominent advantage is their X-ray transparency. Literature documents the biocompatibility of materials used, namely carbon fibres and poly-ether thermoplastics, like poly-ether-ether-ketone (PEEK) and poly-ether-imide (PEI). Actually, the interface with living tissues is the matrix polymer alone, since the carbon fibres should remain deeply embedded.

In the past, literature showed that, sometimes, carbon fibres can be exposed to a direct contact with soft or hard tissues. In this case an inflammatory reaction may ensue because of the fibre geometry, regardless of the biologically inert character of the material [1-3]. A properly designed and accurately implanted composite artefact should not expose its fibres during or after surgery: however this may happen. We had the chance to document a case of severe destructive synovitis in a distal radius fracture treated by a CFRP wrist plate.

### EXPERIMENTAL METHODS

A white Caucasian woman of 64 years of age came to our attention 11 months after surgery for a right distal radial fracture. She had a CFRP plate in place (CarboFix™ Orthopaedics Ltd., Israel). A painful swelling was evident on the volar wrist 3 months after surgery, and it kept worsening. After 4 months she was unable to flex the thumb and soon afterwards she experienced inability in flexing the index finger and DIP joint of the third finger. She had normal active MCP flexion (thanks to intrinsic muscles); no instrumental evidence of neurological disorders; no laboratory evidence of Rheumatoid Disease. An ultrasound examination showed a massive synovitis.

### RESULTS AND DISCUSSION

We surgically explored the site. An aggressive erosive flexor tendons synovitis was present and there were eroded stumps of flexor tendons with loss of substance: we judged the damage beyond repair. We retrieved the CFRP plate which appeared positioned correctly and secured with screws in proper way. Histopathology showed granulomatous fibrogenic process with many black carbon fibres engulfed inside multinucleated giant cells. After surgical debridement we planned a second surgery

and performed a tendon transfer to the recover thumb-to-digits pinch.

We would like to discuss the point that biocompatibility of phase materials alone cannot suffice for the application of CFRP artefacts in humans. Complex geometries, like a wrist plate, may result in overwhelming difficulties in designing and producing an artefact which do not expose fibres, at a reasonable developing cost. Another occurrence may be that a CFRP implant may require an out-of-ordinary care in surgical technique to avoid the exposure of fibres. In any case, all of these seem major disadvantages.

### CONCLUSIONS

Our discussion is not focused on clinical reports, past and present. We advocate that if there is a key theoretical limit in a technology, this should be a permanent warning, regardless any initial report of short fail-safe clinical series. We should not wait a massive number of failures to uncover a problem which is supposed to be known “from the drawing-board”. We are aware that it is not easy to publish on sporadic adverse reactions. We ourselves underestimated the danger of carbon fibres as we reported on an adverse reaction in animals but we embedded this finding in an otherwise positive paper on the good biocompatibility of PEI [1]. We have no evidence that the retrieved plate was badly implanted. However, even if this would have been the case (despite provision from the firm of a leaflet of good surgical practice) this will not reduce our reluctance about implanting CFRP artefacts. It is our opinion that no demanding technique will ever bring a real progress in surgery, as it will always be a relative risk for the patient. It is likely that it will be abandoned as soon as a simpler technique will appear [4].

### REFERENCES

- 1-Merolli A, et Al. Response to polyetherimide based composite materials implanted in muscle and in bone. **J Mater Sci Mater Med** 1999, 10:265-268
- 2-Ali MS, et Al. Carbon fibre composite bone plates. Development, evaluation and early clinical experience. **J Bone Joint Surg Br** 1990, 72(4):586-591
- 3-Tayton K, Phillips G, Ralis Z. Long term effects of carbon fibre on soft tissues. **J Bone Joint Surg Br** 1982, 64B(1):112-114
- 4-Merolli A, Rocchi L. A discussion on the limits of carbon-fibres reinforced polymers prompted by a case of destructive synovitis in the wrist. **Injury** 2014 doi: 10.1016/j.injury.2014.12.011.





## Clinical Performance of Moldable Bioceramic for Bone Regeneration in Maxillofacial Surgery

Daculsi Guy<sup>1</sup>, Miramond Thomas<sup>2</sup>, Borget Pascal<sup>2</sup>, Seris Elodie<sup>2,3</sup>

<sup>1</sup> INSERM U791 LIOAD; Nantes University, Nantes France

<sup>2</sup> BIOMATLANTE SA, rue E. Belin, 44360, France

<sup>3</sup> CIC INSERM BioDiMI, CHU and Bordeaux University, France  
[thomasmiramond@biomatlante.com](mailto:thomasmiramond@biomatlante.com)

### INTRODUCTION

The development of implantology, required bone augmentation, bone reconstruction. To overcome autograft limits, several bone substitutes are proven the efficacy, however it remains numerous difficulties in the handling, and resorption capacity. Bioactive injectable bioceramics, are particularly devoted to these applications. In this clinical study we used a combination of CaP microporous granules and hydrogel for maxillofacial bone regeneration [1]. The non-interventional study) was to assess the safety and performance of the In'Oss<sup>TM</sup> bioceramic/hydrogel bone substitute in maxillofacial surgery. Specifically, the biomaterial was evaluated clinically and radiographically in healed extraction sockets filled with putty (In'Oss<sup>TM</sup>) in combination with a resorbable porcine collagen membrane ((EZ Cure) to protect the implantation site after the implantation.

### EXPERIMENTAL METHODS

In'Oss<sup>TM</sup> putty (Biomatlante SA) was constituted of MBCP<sup>TM</sup> granules with hydrosoluble hydrogel. Suspension was contained in syringe, ready to use, the putty is a non-hardening injectable biomaterial. The putty ensures bonding of the mineral phase with high permeability and suitable rheological property. In'Oss<sup>TM</sup> putty was CE mark and FDA approval. EZ Cure collagen membrane is crosslink porcine high purified collagen matrix. EZ Cure was used to protect the site of implantation,

The clinical study was classified "Case Analysis". Six international clinical centers were involved (USA, Korea, Europe) with 37 surgeons. The study comply with Institutional Review Board and Ethics committee requirements.

The 78 patients needed a single tooth extraction and would benefit from prosthetic reconstruction with a dental implant. Tooth sockets were filled with In'Oss<sup>TM</sup> putty and closed using the resorbable collagen membrane EZ<sup>TM</sup> for preservation of the alveolar ridge following tooth extraction. Five to 6 months post filling, a dental implant will be placed. The subjects were followed about 6 additional weeks. The followed up was performed at 1 and 3 months, recording clinical and radiological features. The efficacy for mucosa healing using EZ Cure resorbable collagen membrane for closing the site of implantation was assessed at 1 months and 3 months by clinical aspect taking in account the mucosa aspect with or without inflammation

In 11 patients, we have performed analysis of biopsies taken during the dental implantation sequence, (between 5 to 10 months). Micro CT, Scanning electron

microscopy, light microscopy and image analysis were performed. Resorption and bone ingrowth at the expense of the composite were analyzed by micro CT, Scanning electron microscopy, light microscopy and image analysis.

All data were expressed as averages and standard error. Differences were evaluated by analysis of variance (ANOVA) with Fisher's probability least significant difference (PLSD) post-hoc test. Differences were considered significant for  $p < 0.05$ .

### RESULTS AND DISCUSSION

The safety of the procedure using bioceramic putty and collagen membrane for implantation site closure was evidenced in more of 93% of the cases. 78 patients showed no major complications in 93%. One failure was listed, which was due to gingivitis and required reopening of the site. The post-filling follow-up of patients at 1 and 3 months indicated no inflammation/infection in more than 89% and 98% of the patients, respectively. The EZ Cure membrane was efficient in combination with the putty, preventing exposure and expulsion of the granules.

The post-filling follow-up of patients at 1 and 3 months indicated a completely radio-dense area at the bone-biomaterial interface in 61% and 77% of the cases respectively.

Classical follow-up and radiographical examinations revealed resorption and absorption of the composite after only 4 months. Also, interconnected bone trabeculae were progressively found to replace the biomaterials. During drilling for dental implantation, the density was similar to natural bone trabecula, and implant stability was perfect in more than 90% of the cases.

Bone histomorphometry revealed the resorption and absorption of the putty and bioceramic granules. In fact, at 6 months, 95% of the putty was resorbed and replaced by physiological bone.

### CONCLUSION

Taken together, the clinical, radiological, and histological data from this non-interventional clinical study have demonstrated the safety and efficacy of the In'Oss<sup>TM</sup> (bioceramic/hydrogel) bone substitute in bone regeneration during maxillofacial surgery.

### REFERENCES

Weiss Pet al, 2007, Biomaterials 28:3295-305

### ACKNOWLEDGMENTS

European Union's 7th Framework Program (grant number FP7-HEALTH-2009-241879; REBORNE) supported by Biomatlante.



## Antibacterial Effect of Bioactive Starch-Based Scaffolds Functionalized with Silanol Groups

Ana I. Rodrigues<sup>1,3</sup>, Albina R. Franco<sup>1,3</sup>, Fernando Rodrigues<sup>2,3</sup>, António G. Castro<sup>2,3</sup>, Isabel B. Leonor<sup>1,3</sup>, Rui L. Reis<sup>1,3</sup>

<sup>1</sup>3B's Research Group – Biomaterials, Biodegradables and Biomimetics, Headquarters of the European Institute of Excellence on Tissue Engineering and Regenerative Medicine, University of Minho, AvePark - Parque de Ciência e Tecnologia, Zona Industrial da Gandra, 4805-017 Barco, Guimarães, Portugal

<sup>2</sup> Life and Health Sciences Research Institute, School of Health Sciences, University of Minho, Braga, Portugal.

<sup>3</sup>ICVS/3B's – PT Government Associate Laboratory, Braga/Guimarães, Portugal

[ana06rodrigues@gmail.com](mailto:ana06rodrigues@gmail.com)

### INTRODUCTION

Bacterial infections are a significant issue on post-transplant and surgery since bacteria can readily colonize the surface of implants<sup>1</sup>. The antibacterial potential of silicon-based biomaterials as well as their application in bone regeneration has been studied, suggesting that the presence of silicon (Si) can decrease bacterial activity<sup>2</sup>. Also, in a previous study it was demonstrated that starch-based scaffolds functionalized with silanol (Si-OH) groups sustain human adipose stem cells (hASC) osteogenic features in vitro<sup>3</sup>. However the antibacterial properties of these scaffolds are still unknown. Thus, this study aims to investigate the potential application of these scaffolds as antibacterial surfaces for biomedical implants by studying their effects against *Escherichia coli* (Gram negative) and *Staphylococcus aureus* (Gram positive).

### EXPERIMENTAL METHODS

Scaffolds were produced by wet-spinning using a blend of corn-starch with polycaprolactone (30/70 wt.%, SPCL) dissolved in chloroform. Two coagulation baths were used: methanol for SPCL scaffolds (control) and a calcium silicate solution for SPCL-CaSi scaffolds. The surface composition of the scaffolds was characterized by X-ray photoelectron spectroscopy (XPS). Scaffolds potential to sustain and improve hASC proliferation and osteogenic differentiation was evaluated by DNA and ALP quantification, respectively. The antibacterial properties of the scaffolds were evaluated against *E. coli* DH5 $\alpha$  and *Staphyl. aureus* ATCC 29213 through radial diffusion assay. Also, bacterial growth and viable bacteria counts (CFU mL<sup>-1</sup>) were evaluated. Biofilm formation and distribution were analysed by scanning electron microscopy (SEM). Each experiment was performed in triplicate. Statistical analysis was performed using a one-way ANOVA test, differences were considered statistically significant if  $p < 0.05$ .

### RESULTS AND DISCUSSION

XPS results demonstrate the effective incorporation of the ions on the surface of the produced scaffolds. Results showed that hASC readily proliferated on both scaffolds and expressed higher ALP activity when cultured on SPCL-CaSi scaffolds. The radial diffusion assay showed the formation of an inhibition zone on the

SPCL-CaSi scaffolds for *E. coli*. The number of viable bacteria counts of *E. coli* and *Staphyl. aureus* significantly decreased in the SPCL-CaSi scaffolds after 4h and 6h of incubation when

compared to both controls (bacteria alone and SPCL scaffolds) (Figure 1A). Bacteria adhesion and biofilm formation significantly decreased after 4h of incubation on SPCL-CaSi scaffolds, when compared to the control (Figure 1B). No biofilm formation was observed after 24h incubation. Results suggest that SPCL-CaSi scaffolds have an antibacterial effect, i.e. the capacity to prevent the bacteria adhesion.

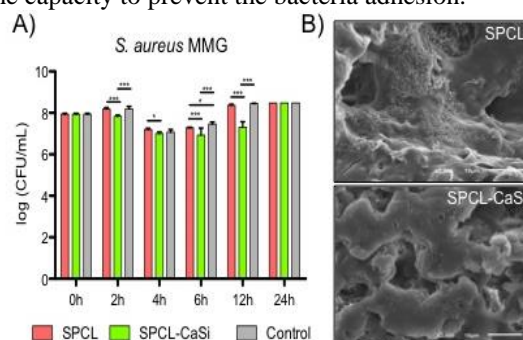


Figure 1-Number of viable *S. aureus* in Minimal medium with 0.4% glucose (MMG) (A) and SEM images of *S. aureus* cultured on SPCL and SPCL-CaSi scaffolds for 6h in MMG (B).

### CONCLUSION

The outcomes of this study suggest that SPCL scaffolds functionalized with Si-OH groups inhibited the formation of bacterial biofilm and adhesion to the scaffold surface. Moreover, it also demonstrates the positive effect of the presence of Ca and Si ions in preventing biofilm formation. The functionalized scaffolds could pose as a new strategy to device biomaterials capable of preventing bacterial proliferation associated to infections problems on prosthetic joints as well as a supporting matrix for hASC osteogenic differentiation.

### REFERENCES

1. Hess A et al. Diagn Microbiol Infect Dis. 2014 (79:73-76)
2. Mortazavi V et al. J Biomed Mater Res A. 2010 (94:160-168)
3. Rodrigues A et al. Acta Biomater. 2012 (8:3765-3776)

### ACKNOWLEDGEMENTS

A.I. Rodrigues thank the Portuguese Foundation for Science and Technology (FCT) for providing a PhD scholarship (SFRH/BD/69962/2010). This work was partially supported by national funds through the FCT under the scope of the project PTDC/CTM-BIO/0814/2012 and PTDC/BBB-BIO/0827/2012. Authors thank European Union's Seventh Framework Programme (FP7/2007-2013) under grant agreement n° REGPOT-CT2012-316331-POLARIS.



Loïc Pichavant<sup>1,2,‡</sup>, Hélène Carrié<sup>1,2,‡</sup>, Laurent Plawinski<sup>2</sup>, Jocelyne Caillon<sup>3</sup>, Gilles Amador<sup>3</sup>, Valérie Héroguez<sup>1</sup> and Marie-Christine Durrieu<sup>2</sup>

<sup>1</sup> CNRS UMR5629, Laboratoire de Chimie des Polymères Organiques, IPB-ENSCBP, Université de Bordeaux, France

<sup>2</sup> Institute of Chemistry & Biology of Membranes & Nanoobjects (UMR5248 CBMN), Bordeaux University, France

<sup>3</sup> Université de Nantes, Faculté de Médecine, EA3826, 1, rue Gaston Veil, F-44035 Nantes, France

<sup>‡</sup> These authors contributed equally to this work

[marie-christine.durrieu@inserm.fr](mailto:marie-christine.durrieu@inserm.fr)

## INTRODUCTION

Bacterial infections are the most current complication which could occur during the fitting of prosthesis in orthopaedic surgery. They can be the cause of morbidity and mortality and take place in 0.7 to 2.2% of the cases despite antibioprophyllaxis. Bacteria responsible for this kind of infections are *Staphylococcus epidermidis* or *Staphylococcus aureus* and mostly, it happens in per-operative conditions. Even if antibioprophyllaxis considerably decreases the rate of per-operative infections, it presents risks of allergy, side effects or bacteria resistance. Moreover, standard antibiotic protocols present little efficiency because of immunocompetent zone around implant, reduced sensitivities of bacteria growing in a biofilm and difficulties of achievement of the drug at the site of infection.

In a recent contribution to this field, we have presented a new biomaterial having applications as implant in orthopaedic surgery and allowing the release of an antibiotic (Gentamicin Sulphate, GS) only in case of infection [1, 2]. In order to optimise our material, we decided to investigate two strategies. In our first strategy, we increased the gentamicin density using a polymer capable of higher functionalization. In our second strategy, we explored a new route using another antibiotic grafted onto titanium (without possible release): Vancomycin (VAN).

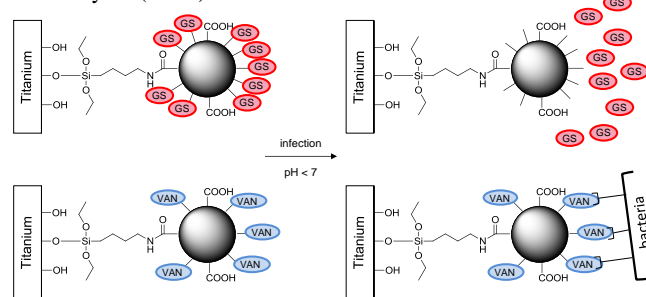


Fig. 1. Representation of the bioactive biomaterial

## EXPERIMENTAL METHODS

$\alpha$ -norbornenyl poly(ethylene oxide) and  $\alpha$ -norbornenyl poly(ethylene oxide)-*block*-polyglycidol macromonomers were synthesized by anionic ring-opening polymerization of ethylene oxide or copolymerization of ethylene oxide and glycidol successively. Those macromonomers were  $\omega$ -functionalized with a carboxylic acid, with GS linked by an imine bond<sup>1</sup> or with VAN linked by an amide bond.

Characterisations were done by <sup>1</sup>H NMR, Size Exclusion Chromatography (SEC) and MALDI TOF. Nanoparticles were obtained by Ring-Opening Metathesis coPolymerization (ROMP) of norbornene with functionalized macromonomers in dispersed medium. Their colloidal stabilities were shown by Dynamic Light Scattering measurements. Nanoparticles

were grafted onto titanium discs ( $\varnothing = 5$  mm ;  $h = 3$  mm) functionalized with amine groups using aminosilane molecules (APTES). The grafting was characterized by Scanning Electron Microscopy (SEM) and fluorescence microscopy. The *in vitro* evaluations were carried out by Minimum Inhibitory Concentration (MIC), Minimum Bacterial Concentration (MBC) and bacterial survival measurements.

## RESULTS AND DISCUSSION

Well defined  $\alpha$ -norbornenyl macromonomers were obtained with a size of about 5000 g.mol<sup>-1</sup> for VAN-functionalized macromonomer and about 8000 g.mol<sup>-1</sup> for GS  $\omega$ -functionalized macromonomer and a narrow distribution (PDI < 1.1).

Nanoparticles were synthesized with total monomer and macromonomers conversions and diameters were about 350 nm for VAN-functionalized particles and 550 nm for GS-functionalized particles.

Controlled densities of NPs were anchored on biomaterial surfaces and those densities were measured by scanning electron microscopy observations.

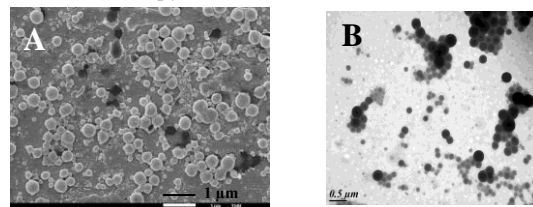


Fig. 2. SEM observation of VAN-functionalized biomaterial (A). TEM observation of GS-functionalized particles (B).

The efficiency of vancomycin and gentamicin functionalized biomaterials was proved by *in vitro* bacterial inhibition tests using *Staphylococcus aureus* as bacterial strain.

## CONCLUSION

In this work was presented the synthesis of different types of bioactive biomaterials and their characterization. We equally demonstrated the *in vitro* activity of such materials. *In vivo* experiments on rabbits are now in progress.

## REFERENCES

- 1 Pichavant L.; Bourget C.; Durrieu M.C.; Héroguez V. Macromol. 44:7879-87, 2011
- 2 Pichavant, L.; Amador, G.; Jacqueline, C.; Héroguez, V., Durrieu, M.C. J. Controlled release, 162:373-81, 2012

## ACKNOWLEDGMENTS

The authors would like to thank the TTO Aquitaine Science Transfert for providing financial support.





## Anti-Bacterial Borosilicate Glass Formulations for Bone Tissue Engineering Applications

João S. Fernandes<sup>1,2</sup>, Margarida Martins<sup>1,2</sup>, Nuno N. Neves<sup>2</sup>, Ricardo A. Pires<sup>1,2</sup>, Rui L. Reis<sup>1,2</sup>

<sup>1</sup>3Bs Research Group – Biomaterials, Biodegradable and Biomimetics, University of Minho, Headquarters of the European Institute of Excellence on Tissue Engineering and Regenerative Medicine, AvePark, 4806-909 Taipas, Guimarães, Portugal

<sup>2</sup>ICVS/3Bis - PT Government Associate Laboratory, Braga/Guimarães, Portugal

[joao.fernandes@dep.uminho.pt](mailto:joao.fernandes@dep.uminho.pt)

Bioactive glasses (BGs), including 45S5 glass, have been widely investigated in Bone Tissue Engineering (BTE) for more than three decades. They have been regarded as relevant materials for the repair and replacement of bone defects. However, the majority of BG particles show slow degradation rates and present no effect against bacterial infections<sup>1, 3</sup>. The Borosilicate matrix is known to possess a faster degradation rate, increases the formation of hydroxyapatite (HA) and presents an enhanced release of specific cations (e.g.: Ca, Sr and Mg)<sup>2</sup>. Such of those cations are known for their influence in the cell proliferation and differentiation, as well as, for their antimicrobial character. The aim of this study was to assess if borosilicate BGs are able to present antimicrobial properties for BTE applications.

### EXPERIMENTAL METHODS

Borosilicate glass compositions of general formula  $0.20\text{B}_2\text{O}_3 : 0.40\text{SiO}_2 : x\text{MgO} : y\text{CaO} : (0.35-x-y)\text{SrO} : 0.05\text{Na}_2\text{O}$  (molar ratio, where  $x, y = 0.35$  or  $0.00$ , and  $x \neq y$ ) were synthesized by melt quenching ( $T \approx 1450^\circ\text{C}$ ) and ground to obtain particles with a size  $< 63 \mu\text{m}$ .

The capacity to form calcium phosphate layer was tested after immersion of the BG samples into simulated body fluid (SBF) for 7 days.

Microbial susceptibility was measured using standardized inocula of *Pseudomonas aeruginosa*, *Escherichia coli*, *Staphylococcus aureus* and *Staphylococcus epidermidis* in contact with the BG samples. Disk diffusion (DD) and broth dilution (BD) methods were adapted to BG samples, testing known amounts of glass particles.

The cytotoxicity of the glass particles was assessed by direct contact with human osteosarcoma cell line during 7 days of incubation ( $37^\circ\text{C}$  and  $5\% \text{CO}_2$ ). Cell proliferation (DNA) and metabolic activity (MTS) profiles were followed along the culture time.

### RESULTS AND DISCUSSION

The BG samples were successfully obtained by melt quenching, ground and presented non-toxic effects up to 3 days.

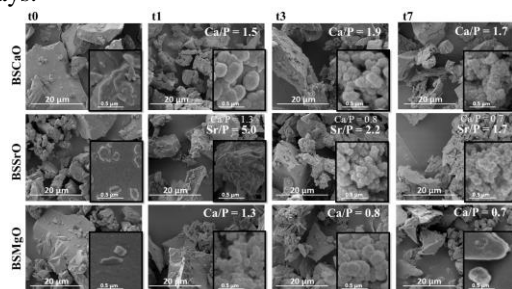


Figure 1 - SEM images of BG samples after 1, 3 and 7 days of immersion in SBF solution. The Ca/P ratio on the glass surface, obtained by EDS, is presented on the top right corner.

After the immersion of BG samples into SBF, Ca- (BSCaO) and Sr-containing glasses (BSSrO) revealed the presence of bone-like apatite structures at their

surface, although at different stages of crystallization. However, after 7 days of immersion, the BSCaO glass displayed an increase in apatite-like deposition with a Ca/P ratio of  $\approx 1.67$ , similar to HA (Figure 1).

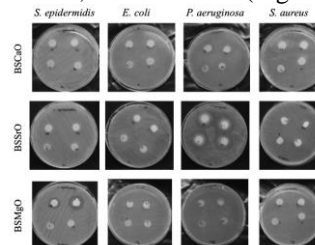


Figure 2 - Example of disc diffusion assay of the samples BSCaO, BSSrO, BSMgO (at different concentrations: 9, 18, 36, 72 mg/mL) in contact with *S. aureus*, *P. aeruginosa*, *E. coli* and *S. epidermidis* respectively.

The DD data demonstrate that the Mg-containing (BSMgO) and the BSSrO glasses inhibited the growth of bacteria *S. epidermidis* and *P. aeruginosa* respectively. Clear halos appeared around the glass-loaded agar discs. The inhibition zone for each bacterial strain is shown in Figure 2.

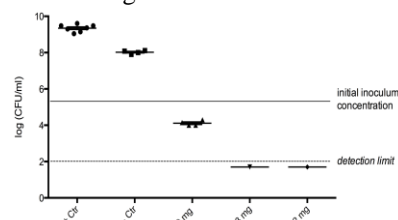


Figure 3 - Broth dilution assay of the BSSrO sample in Mueller Hinton culture medium (+Ctr.) in contact with *P. aeruginosa* (-Ctr. is Bioglass 45S5).

Moreover, BD data (Figure 3) showed a concentration dependent effect of BSSrO glasses against *P. aeruginosa* (e.g.: BSSrO\_18mg exhibiting a reduction of  $\approx 4 \log_{10}\text{CFU/ml}$ ).

### CONCLUSION

We were able to synthesise borosilicate-based glasses by melt quenching, and we observed no cytotoxic effects up to 3 days culture. Chemical characterization supported the high reactivity and their bioactivity (BSCaO sample with a Ca/P  $\approx 1.67$ ).

Bacterial tests with different concentrations (9, 18, 36 and 72 mg/ml of BG) indicate that BSMgO and BSSrO glasses have antibacterial activity against *S. epidermidis* and *P. aeruginosa* respectively. Moreover BSSrO glasses have specific bactericidal activity against *P. aeruginosa* for quantities equal or higher than 18 mg/ml. Results also revealed a concentration dependence on the anti-bacterial properties.

### REFERENCES

1. Hailuo Fu et al, *Journal of Materials Science: Materials in Medicine*, 23 (2012), 1181-91.
2. Mohamed N. Rahaman et al, *Acta Biomaterialia*, 7 (2011), 2355-73.
3. Christian Vassena et al, *International Journal of Antimicrobial Agents*, 44 (2014), 47-55.

### ACKNOWLEDGMENTS

Portuguese Foundation for Science and Technology (Ph.D. grant BD/73162/2010) and the European Union's Seventh Framework Programme (FP7/2007–2013) under Grant No. REGPOT-CT2012-31633-POLARIS. M. Martins is financed by the project "Tissue engineering of connective tissues" (Ref. RL3 – TECT - NORTE-01-0124-FEDER-000020) co-financed by North Portugal Regional Operational Programme (ON.2 – O Novo Norte), under the National Strategic Reference Framework (NSRF), through the European Regional Development Fund (ERDF).

Authors have nothing to disclose



Agnieszka Kyziol<sup>1</sup>, Anna Regiel-Futyr<sup>1</sup>, Aleksandra Mazgala<sup>1</sup>, Justyna Michna<sup>1</sup>, Małgorzata Kus-Liśkiewicz<sup>2</sup>, Silvia Irusta<sup>3,4</sup>

<sup>1</sup>Faculty of Chemistry, Jagiellonian University, Poland

<sup>2</sup>Faculty of Biotechnology, Biotechnology Centre for Applied and Fundamental Sciences, University of Rzeszów, Poland

<sup>3</sup>Department of Chemical Engineering and Nanoscience Institute of Aragon (INA), University of Zaragoza, Spain

<sup>4</sup>Networking Research Center on Bioengineering, Biomaterials and Nanomedicine, CIBERBBN, Spain

[kyziol@chemia.uj.edu.pl](mailto:kyziol@chemia.uj.edu.pl)

## INTRODUCTION

The bacteria, when present in the wound, begin to produce biofilm in response to reduction of nutrients, increased levels of reactive oxygen species, change in pH, and under influence of immune cells or antibiotics. Biofilm is a community of either single or multiple bacterial species enclosed in a self-produced extracellular polymeric substance (EPS), consisting of polysaccharide, protein and DNA<sup>1</sup>. Bacterial biofilms are adherent to an inert or living surfaces and in the latter case cause serious and persistent infections.

Treatment of chronic wounds is a major problem, not only in medical but also economic terms. Lack of an effective method of the bacterial biofilm destruction leads to a significant prolongation and complication of the medical treatment. Literature data show that the killing dose for any given antibiotic is more than 1000 times higher for biofilm forming bacteria than for planktonic bacteria of the same strain<sup>2</sup>. The poor efficacy of antibiotics against bacteria embedded in the biofilm is mainly associated with inefficient penetration of the antibiotic through the biofilm matrix either due to specific adsorption by polymeric matrix of biofilm or to physical barriers.

## EXPERIMENTAL METHODS

### Materials preparation

Alginate/chitosan (AL/ChS) beads were prepared using the emulsification/ionic gelation modified method described by Silva *et al.*<sup>3</sup>. Electrospun AL fibers with ChS sheath were prepared using procedure described by Bonino *et al.*<sup>4</sup> with some modifications. AL cores were loaded with a model drug *i.e.* ciprofloxacin or ibuprofen, while on ChS shells an appropriate lytic enzyme was immobilized.

### Materials characterization

Size and zeta potential were studied by nanoparticle tracking analysis (NTA) and dynamic light scattering technique (DLS), respectively. The presence of ChS layer on AL core was confirmed by FTIR analysis. Morphology of the resulting materials was investigated with SEM and TEM. Drug loading efficiency and cumulative drug release profiles were evaluated by UV-Vis analysis. Enzymatic activity of free and immobilized enzymes was measured by hydrolysis of a relevant substrate according to the supplied protocols. Cytotoxic activity *in vitro* on human lung adenocarcinoma epithelial cell line (A549) and mouse fibroblast cell line (NIT3T3) was determined by MTT assay. Antibacterial activity was evaluated against two

biofilm forming bacterial strains: Gram-negative *Pseudomonas aeruginosa* and Gram-positive *Staphylococcus aureus*.

## RESULTS AND DISCUSSION

Spherical in shape AL/ChS beads loaded with ciprofloxacin were successfully synthesized. Cumulative drug release studies revealed the extended over time antibiotic release profiles. The maximum of enzymatic activity of the immobilized lysozyme was observed after *ca.* 40 min. of beads incubation with enzyme.

AL fibers were electrospun and coagulated with ChS with co-axial technique application. The resulting fibers exhibited a core-sheath structure that was revealed by TEM analysis. The average diameter of the AL/ChS fibers ranged from 140 to 180 nm depending on the composition and electrospinning parameters.

The cytotoxic and antibacterial activity of obtained materials were studied *in vitro*. No significant cytotoxic effect on A549 and NIT3T3 cell lines was observed. Antibacterial experiments are in progress.

## CONCLUSION

The presented research was focused on preparation and characterization of AL/ChS materials, constructed of polymeric core loaded with antibiotic and polymeric shell with immobilized lytic enzyme. Proposed materials were designed for the biofilm structure degradation in order to facilitate a biocidal agent penetration and enable its antimicrobial activity.

## REFERENCES

1. Hoiby, N. *et al.*, International Journal of Antimicrobial Agents 35:322-332, 2010
2. Olson, M.E. *et al.*, The Canadian Journal of Veterinary research 66:86-92, 2002
3. Silva, C.M. *et al.*, The AAPS Journal 7:903-913, 2006
4. Bonino, Ch.A. *et al.*, Carbohydrate Polymers 85:111-119, 2011

## ACKNOWLEDGMENTS

The authors would like to thank The Foundation for Polish Science (Grant no: POMOST/2013-7/7 "Alginate/chitosan core-shell beads with bioactive functionalities") for providing financial support to this project.



# First Principles Modelling to Establish the Thermodynamically Most Favourable Form and Position of Silicon in Bone Mineral

Helen Chappell<sup>1</sup>, Ravin Jugdaohsingh<sup>1</sup>, Jonathan J Powell<sup>1</sup>

<sup>1</sup>MRC Human Nutrition Research Unit, University of Cambridge, UK

[Helen.chappell@mrc-hnr.cam.ac.uk](mailto:Helen.chappell@mrc-hnr.cam.ac.uk)

## INTRODUCTION

An important role for silicon in connective tissues has long been proposed<sup>1</sup>, although its biochemical function remains a matter of investigation. Recent work has shown that silicon is present in both the collagenous and mineral phase of bone<sup>2</sup> and indeed silicon is used in a number of commercial bone graft materials, which have enhanced biocompatibility compared to Si-free biomaterials. However, the form and position of silicon within the bone structure at the atomic level remains unclear. Previous simulations by one of the authors (HC) have shown that Si can substitute for phosphorus in a thermodynamically favourable way<sup>3</sup> but simulations looking at different positions and charge states have not before been carried out. In this work we simulated the substitution of silicon for phosphorus and compared it to the inclusion of ortho-silicic acid ( $H_4SiO_4$ ) as both a substitution for a phosphate ion and as a neutral interstitial molecule. The objective was to assess the thermodynamic stability of the various silicon substitutions and to predict, therefore, the most feasible interaction of silicon within the mineral phase of bone.

## EXPERIMENTAL METHODS

Bone mineral was approximated using a phase-pure hydroxyapatite (HA) unit cell. Substitutions were made in this unit cell and optimization was carried out using the Density Functional Theory, plane-wave code CASTEP<sup>4</sup>. Convergence testing determined a cut-off energy of 430 eV and a 3x3x3 Monkhorst Pack k-point grid. Formation energies were calculated upon optimization via Equation 1,

$$E_f = E_{HA\_Sub} - (E_{HA} - \mu_{PO4} + \mu_{H_4SiO_4}) \quad (1)$$

where  $E_{HA\_Sub}$  is the energy of the substituted HA unit cell,  $E_{HA}$  the energy of a phase-pure HA unit cell,  $\mu_{PO4}$  the chemical potential of a phosphate ion and  $\mu_{H_4SiO_4}$  the chemical potential of a single molecule of ortho-silicic acid. This equation was varied depending on the substitution being made. The test substitutions were:

1. Si for P
2.  $H_4SiO_4$  as an interstitial molecule
3.  $H_4SiO_4$  for  $PO_4$

The final substitution of  $H_4SiO_4$  for  $PO_4$  required charge compensation and 4 different compensation mechanisms were tried, which gave very similar results.

## RESULTS AND DISCUSSION

Figure 1 shows the disrupted structure predicted with interstitial  $H_4SiO_4$  and Table 1 provides the formation energies and lattice parameters of all the unit cells.

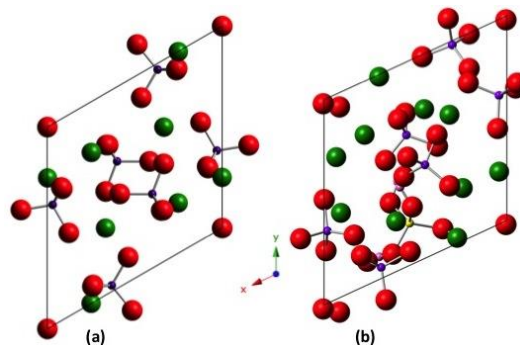


**Figure 1.** Phase-pure (a) and optimised  $H_4SiO_4$  substituted (b) HA unit cells. Oxygen shown in red, hydrogen pink, calcium green, phosphorus purple and silicon yellow.

Substitution	$x / \text{\AA}$	$y / \text{\AA}$	$z / \text{\AA}$	$E_f / \text{eV}$
HA	9.477	9.477	6.851	-
Si for P	9.410	9.497	6.900	-2.05
$H_4SiO_4$	9.365	9.378	9.192	2.86
$H_4SiO_4$ for $PO_4$	9.685	9.595	6.861	17.70

**Table 1.** Lattice data and formation energies for the different substitutions in comparison with phase-pure HA. The favourable  $E_f$  is shown in green and the unfavourable values in red.

The results show that silicon substitution for phosphorus (i.e. silicate for phosphate) is the only thermodynamically favourable way to include silicon in the unit cell. The other substitutions are energetically unfavourable and cause a large degree of physical distortion to the unit cell. Although silicon is likely to exist as ortho-silicic acid during and following absorption, it seems that the inclusion of silicon in bone mineral may occur only after chemical changes to the  $H_4SiO_4$  molecule.

## CONCLUSION

Inclusion of silicon as neutral ortho-silicic acid is unlikely from a thermodynamic perspective. This raises questions about the mechanism by which silicon enters bone mineral and its chemical speciation therein.

## REFERENCES

1. Carlisle E.M., Science. 178:619-21, 1972
2. Jugdaohsingh, R. et. al., Bone Reports, 1: 9-15, 2015
3. Chappell H.F. et al, Mater. Sci. Mater. Med. 18: 829-837, 2007
4. Clark S.J. et al., Z. Kristallogr. 220:267, 2005

## ACKNOWLEDGMENTS

The authors wish to thank the University of Cambridge Supercomputing Facility, and the MRC for funding.



## Modification of Living Diatom, *Thalassiosira weissflogii* by Calcium Precursor as a Sacrificial Template for Development of Next Generation of Structural Biomaterials

Asrizal Abdul Rahman<sup>1</sup>, Syed Ansar Md. Tofail<sup>2</sup>, Abhay Pandit<sup>1</sup>

<sup>1</sup>Network of Excellence for Functional Biomaterials, National University of Ireland, Galway

<sup>2</sup>Materials and Surface Science Institute, University of Limerick, Ireland

[a.abdulrahman2@nuigalway.ie](mailto:a.abdulrahman2@nuigalway.ie)

### INTRODUCTION

Diatoms, have the potential to be novel bio-functional materials as they display a diversity of patterns, and a unique micro- and nanostructure. Diatoms consist largely of amorphous silica<sup>1</sup>, a structure that is versatile and flexible for surface modification and has many functions that can be utilised for biomaterial platforms. Existing devices directly use the original structure of the bio-silica frustules, which limits the potential of the diatoms. Therefore, to fully utilize their application, alteration of the chemical composition of this intricate structure is essential<sup>2,3</sup>. The hypothesis of the study is that calcium can be up taken by the living diatom using the same mechanism as silica without altering the topography of its unique three-dimensional structure. The specific objective of this study is to optimize the incorporation of calcium hydroxide into the diatom during the frustule synthesis and monitor the effects toward the architectural parameter with surface analysis. Additionally, the amount of calcium incorporated will be investigated using bulk analysis.

### EXPERIMENTAL METHODS

Axenic *Thalassiosira weissflogii* cultures were grown in artificial seawater. Cultures were silica depleted for a minimum of 48 hours before inoculation with the calcium precursor and were inoculated at  $1 \times 10^4$  cells/mL in a final volume of 200 mL in a polystyrene tissue culture flask. Sodium metasilicate ( $\text{Na}_2\text{SiO}_3$ ) or calcium hydroxide (CaOH) was added to cultures and grown at a 14 hour:10 hour light:dark cycle at a light intensity of 3000 lux and temperature range of 16–22°C. Multiple additional cultures received further additions of  $\text{Na}_2\text{SiO}_3$  or CaOH at 48, 96, and 144 hours. Cultures were collected at 192 hours post-inoculation and cleaned of organic matter. Cell density was monitored during growth using a haemocytometer. The silica and calcium formation was studied using PDMPO-Rhodamine 123 and Calcium Green staining. The morphology of the frustule walls was investigated by SEM, TEM, AFM and the amounts of calcium were quantitatively determined by ICP-MS. To obtain further structural information, FTIR and XPS were used.

### RESULTS AND DISCUSSION

Fluorescence microscopy and XPS analysis confirmed that Ca was incorporated into the frustule of CaOH-modified *T. weissflogii* (Figure 1,2). This amount was dependent on the dosing regimen of Ca that the culture received. No adverse effect was observed on the topography of the modified diatom.

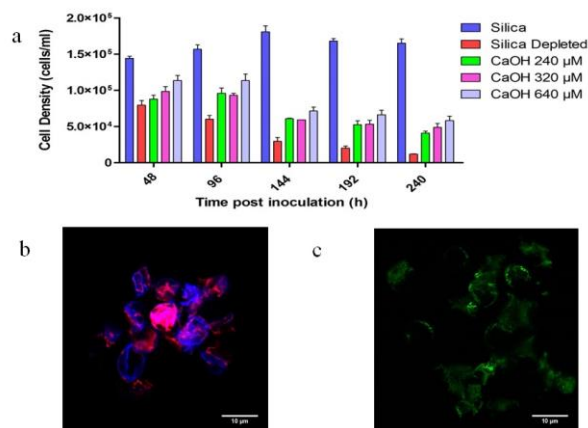


Figure 1. a) Growth profile of *T. weissflogii* for unmodified and CaOH-modified diatom. Two way ANOVA revealed an effect of time and treatment, statistical significant with  $** p < 0.01 (n = 3)$ . b) Staining of the silica valve using dual marker PDMPO-Rhodamine c) Staining of Ca from diatom valve using Calcium Green

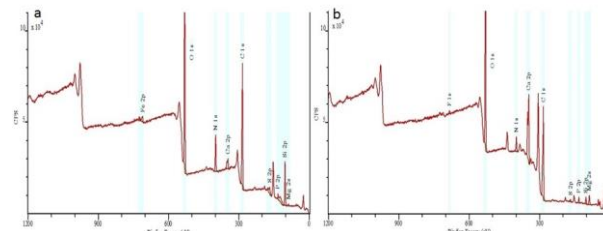


Figure 2. Quantitative analysis of diatom using XPS. a) Spectra of unmodified *T. weissflogii*, b) Spectra of CaOH-modified *T. weissflogii*. Result show that an increase ratio of ca peak has been observed in the CaOH-modified diatom compare to unmodified diatom.

### CONCLUSION

The modification of the diatom frustule with calcium has been achieved and the characteristic architectural features were unaltered.

### REFERENCES

1. Hildebrand, M. Chemical Review. 108:4855-4874, 2008
2. Lang, Y. Scientific Reports. 3:3205, 2013
3. Lang, Y. Nature Communications. 4:2683, 2013

### ACKNOWLEDGMENT

Majlis Amanah Rakyat (Grant no: R0115969) for providing financial support to this project.





## Fabrication and Histological Evaluation of Carbonate Apatite Coated Calcite

Kunio Ishikawa<sup>1</sup>, Kanji Tsuru<sup>1</sup>, Masako Kobayashi<sup>2</sup>, Youji Miyamoto<sup>2</sup>

<sup>1</sup>Department of Biomaterials/Faculty of Dental Science, Kyushu University, Japan

<sup>2</sup>Department of Oral Surgery/Institutes of Health Bioscience, The University of Tokushima, Japan  
[ishikawa@dent.kyushu-u.ac.jp](mailto:ishikawa@dent.kyushu-u.ac.jp)

### INTRODUCTION

Although bone apatite is known as carbonate apatite (CO<sub>3</sub>Ap), it decomposes to other calcium phosphates at high temperature required for sintering process. Therefore, sintered hydroxyapatite (HAp) has been used as artificial bone substitute since 1970's. We have proposed fabrication method of CO<sub>3</sub>Ap by compositional transformation reaction based on dissolution-precipitation reaction using a precursor such as calcite<sup>1</sup>. CO<sub>3</sub>Ap thus fabricated was found to up-regulate differentiation of osteoblastic cells when compared to sintered HAp. Histological studies also revealed that CO<sub>3</sub>Ap shows higher osteoconductivity than sintered HAp. In the present study, CO<sub>3</sub>Ap coated calcite (CO<sub>3</sub>Ap/CaCO<sub>3</sub>) was fabricated and its tissue response was evaluated by implanting CO<sub>3</sub>Ap/CaCO<sub>3</sub> granular in the bone defect of rabbit femur.

### EXPERIMENTAL METHODS

CO<sub>3</sub>Ap/CaCO<sub>3</sub> granular was fabricated by immersing 300-600 µm CaCO<sub>3</sub> granular, which was made by exposing Ca(OH)<sub>2</sub> compact to CO<sub>2</sub>, into 1 mol/L Na<sub>2</sub>HPO<sub>4</sub> solution at 40°C, 60°C and 80°C up to 20 hours. Compositional analysis was made by powder x-ray diffraction and EDAX. Morphology of the granular was observed by SEM. Bone defects made at the femur of rabbits were reconstructed with CO<sub>3</sub>Ap, 10% CO<sub>3</sub>Ap/CaCO<sub>3</sub>, 30% CO<sub>3</sub>Ap/CaCO<sub>3</sub> and CaCO<sub>3</sub>. The µ-CT images and histological analysis were made 4 and 8 weeks after implantation.

### RESULTS AND DISCUSSION

Calcite transformed to CO<sub>3</sub>Ap with time when immersed in Na<sub>2</sub>HPO<sub>4</sub> solution. Transformation was faster in the Na<sub>2</sub>HPO<sub>4</sub> solution with higher temperature as shown in Fig. 1. EDAX analysis of the cross section granular revealed that surface of the granular was CO<sub>3</sub>Ap and inside was CaCO<sub>3</sub> indicating that dissolution-precipitation reaction occurred from surface to inside. Immersion of CO<sub>3</sub>Ap/CaCO<sub>3</sub> in the Na<sub>2</sub>HPO<sub>4</sub> solution at 60°C for 4 hours and 16 hours result in the fabrication of 10% CO<sub>3</sub>Ap/CaCO<sub>3</sub> and 30% CO<sub>3</sub>Ap/CaCO<sub>3</sub>, respectively.

The µ-CT images and histological analysis made 4 weeks after implantation of rabbit femur defect revealed largest amount of bone formation in the case of 10% CO<sub>3</sub>Ap/CaCO<sub>3</sub> granular followed by 30% CO<sub>3</sub>Ap/CaCO<sub>3</sub>, CO<sub>3</sub>Ap and CaCO<sub>3</sub> (Fig. 2). After 8 weeks, amount of the new formed bone around the granular increased to reach the same level in the case of CO<sub>3</sub>Ap, 10%CO<sub>3</sub>Ap/CaCO<sub>3</sub>, and 30%CO<sub>3</sub>Ap/CaCO<sub>3</sub>. In contrast, new bone formed around the granular decreased when compared to 4 weeks in the case of CaCO<sub>3</sub>. This decrease is thought to be caused by the dissolution of CaCO<sub>3</sub>.

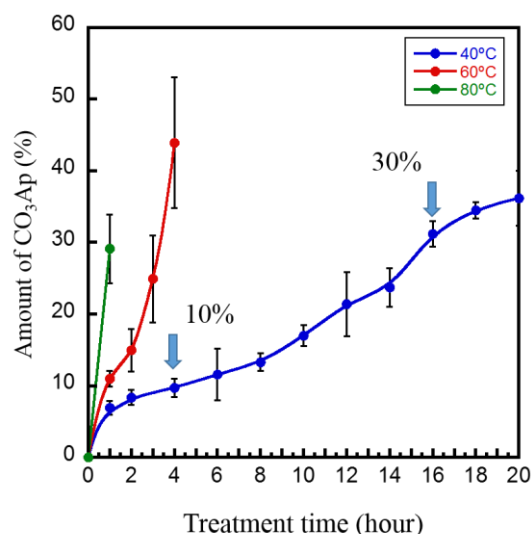


Fig. 1 Conversion of calcite to CO<sub>3</sub>Ap as a function of time when immersed in 1 mol/L Na<sub>2</sub>HPO<sub>4</sub> solution at 40, 60 and 80°C.

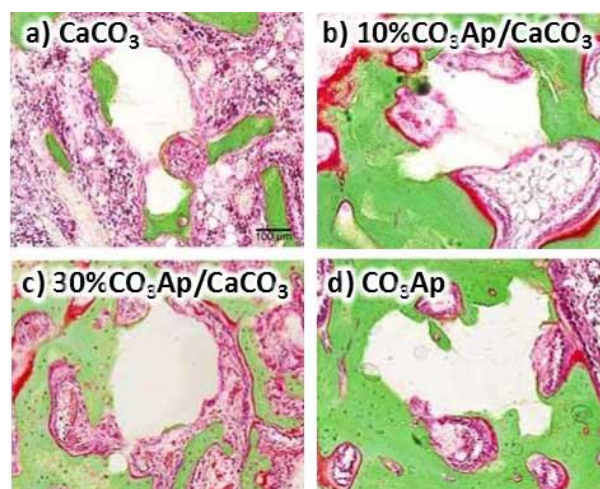


Fig. 2 Four weeks histological pictures of specimens when used to reconstruct bone defect made at the femur of rabbits.

### CONCLUSION

CO<sub>3</sub>Ap/CaCO<sub>3</sub> was found to be fabricated by regulating the reaction temperature and duration of immersion time of CaCO<sub>3</sub> in Na<sub>2</sub>HPO<sub>4</sub> aqueous solution. 10% CO<sub>3</sub>Ap/CaCO<sub>3</sub> demonstrated higher osteoconductivity than CO<sub>3</sub>Ap.

### REFERENCES

1. Ishikawa K., Materials 3:1138-1155, 2010.

### ACKNOWLEDGMENTS

This study was supported, in part, by the Strategic Promotion of Innovative Research and Development Program, Japan Science and Technology Agency, Japan



# Crystallization and Thermal Evolution of Pyrophosphate Polymorphs and Prospective Biomaterials with a Metastable $\alpha^1$ -calcium Pyrophosphate from Amorphous Calcium Phosphates with an Initial Ca/P Ratio of 1:1

Zoltan Zyman<sup>1</sup>, Matthias Eppler<sup>2</sup>, Anton Goncharenko<sup>1</sup>, Dmytro Rokhmistrov<sup>1</sup>

<sup>1</sup> Physics of Solids Department, V.N. Karazin Kharkiv National University, Ukraine;

<sup>2</sup> Institute of Inorganic Chemistry and Center for Nanointegration Duisburg-Essen (CeNIDE), University of Duisburg-Essen, Germany

[intercom@univer.kharkov.ua](mailto:intercom@univer.kharkov.ua); [solids@karazin.ua](mailto:solids@karazin.ua)

## INTRODUCTION

Biomaterials based on hydroxyapatite  $\text{Ca}_{10}(\text{PO}_4)_6(\text{OH})_2$ , HA, tricalcium phosphate  $\text{Ca}_3(\text{PO}_4)_2$ , TCP (in  $\alpha$ - and  $\beta$ -forms), and octacalcium phosphate  $\text{Ca}_8(\text{HPO}_4)_2(\text{PO}_4)_4 \cdot 5\text{H}_2\text{O}$ , OCP, can be prepared from amorphous calcium phosphate, ACP [1].

Calcium pyrophosphate  $\text{Ca}_2\text{P}_2\text{O}_7$ , CPP, known in  $\alpha$ -,  $\beta$ -,  $\gamma$ -forms [2], has not yet been widely considered as a biomaterial. Nevertheless, it was recently found that porous  $\beta$ -CPP has the potential to be used as a prospective biomaterial because it was more incorporated into newly formed bone and more rapidly resorbed than porous HA in vivo [3].

CPP is normally prepared by calcination of crystalline dicalcium phosphate dihydrate, brushite,  $\text{CaHPO}_4 \cdot 2\text{H}_2\text{O}$  (DCPD), or dicalcium phosphate anhydrous, monetite,  $\text{CaHPO}_4$  (DCPA).  $\gamma$ -CPP is formed at relatively low temperatures,  $\beta$ -CPP – at intermediate temperature, and  $\alpha$ -CPP is the high-temperature phase. Here we aim to reveal the crystallization peculiarities and thermal evolution of the CPP polymorphs and the formation conditions of a metastable calcium pyrophosphate,  $\alpha^1$ -CPP, depending on the structural state (amorphous and /nanocrystalline) of DCPA prepared from ACP with an initial Ca/P ratio of 1.

## EXPERIMENTAL METHODS

The preparation of the initial ACP powder was based on the fast precipitation variety of the nitrous synthesis. The solutions of stock salts ( $\text{Ca}(\text{NO}_3)_2$  and  $(\text{NH}_4)_2\text{HPO}_4$ ) were rapidly mixed at a molar Ca/P ratio of 1, pH 10-11 and 5°C. The vessel with the mixture was shaken (1 min) and put into a freezer (-25°C, 24 h). The obtained friable powders were used unwashed or after 3- or 6- times washing with aqueous ammonia (pH 10-11, 5°C) and repeated lyophilization. The powders are designated as UW, 3W- and 6W in the following, respectively. Powder samples were examined as-prepared and upon heating in air in the range of 25 to 980°C by XRD, TG-DTA, IR and mass spectrometric thermal analysis, MSTA.

## RESULTS AND DISCUSSION

All initial powder samples were X-ray amorphous. The UW samples were converted at 600-640°C into a metastable pyrophosphate,  $\alpha^1$ -CPP, which by composition and structure was similar to the high-temperature polymorph  $\alpha$ -CPP (normally occurring above 1200°C).  $\alpha^1$ -CPP was stable to about 780°C (a small amount of the medium-temperature polymorph  $\beta$ -

CPP was also present). Above 800°C,  $\alpha^1$ -CPP gradually transformed to  $\beta$ -CPP, and only  $\beta$ -CPP was detected at 980°C. The temperature phase evolution in the 3W and 6W samples was qualitatively similar. The washed samples crystallized in a somewhat higher temperature range of 680-730°C into a four-phase mixture:  $\alpha^1$ -TCP,  $\beta$ -TCP,  $\beta$ -CPP and  $\alpha^1$ -CPP;  $\alpha^1$ -TCP is a metastable analogue of the high-temperature polymorph  $\alpha$ -TCP (normally occurring above 1150°C); the relative amount of the phases decreased in this order. The phase composition was preserved until 800°C. Above this temperature,  $\alpha^1$ -TCP and  $\alpha^1$ -CPP gradually transformed into  $\beta$ -TCP and  $\beta$ -CPP, respectively, and a biphasic mixture of  $\beta$ -TCP and  $\beta$ -CPP was detected in the samples upon heating to 980°C.

The occurrence of the two metastable phases,  $\alpha^1$ -CPP and  $\alpha^1$ -TCP is associated with the Ostwald effect. The increase of the Ca/P ratio to a value that ensured the crystallization of the TCP phases with a notably higher Ca/P ratio (1.5:1), than that in the mother liquor (1:1), is mainly attributed to the hydrolyses of initially present amorphous monetite and partly to the carbonate substituting for hydrogen phosphate ( $\text{CO}_3^{2-}$  ions were detected in the washed samples) during the washing process.

## CONCLUSION

1. Novel calcium phosphate biomaterials, including a low-temperature metastable pyrophosphate, can be prepared using the results of this study by simple, fast and inexpensive processing routes.
2. The observed increase of the Ca/P ratio in an ACP precipitate during washing (ageing) implies that a precursor for bioapatite formation may have a small Ca/P ratio as 1:1. Therefore, the suggested ACP precursor with Ca/P = 1.5:1 (Posner's version) might be formed on a later stage of the biomineralization process.

## REFERENCES

1. Campana V. *et al.*, J. Mater. Sci.: Mater. Med. 25:2455-61, 2014.
2. Cornilsen B.C. *et al.*, J. Inorg. Nucl. Chem. 41:602-5, 1979.
3. Lee JH. *et al.*, Key Eng. Mater. 240-242:399-402, 2003.

## ACKNOWLEDGMENTS

The authors would thank the German Academic Exchange Service (DAAD) providing financial support to this project.



## Functionally Graded Hybrid Scaffolds for Osteo-Chondral Defect Repair: Scaffold Design

Serena Bertoldi<sup>1,2</sup>, Masoumeh Meskinfam<sup>1,3</sup>, Paola Petrini<sup>1,2</sup>, Alessandro Cerri<sup>1</sup>, Nicolò Albanese<sup>1</sup>, M. Cristina Tanzi<sup>2</sup>  
Silvia Farè<sup>1,2</sup>

<sup>1</sup>Department of Chemistry, Materials and Chemical Engineering “G. Natta”, Politecnico di Milano, Italy

<sup>2</sup> INSTM Local Unit Politecnico di Milano, Italy

<sup>3</sup>Islamic Azad University Lahijan branch, Lahijan, Iran

[silvia.fare@polimi.it](mailto:silvia.fare@polimi.it)

### INTRODUCTION

Articular cartilage defects are a major clinical problem for orthopedic surgeons. Among them, osteo-chondral lesions affect active young and over sixty years old patients as well, and lead to a progressive but relentless joint mechanical instability<sup>1,2</sup>.

Scaffolds for osteo-chondral regenerative medicine should have both load-bearing properties, able to mimic the bone structure, and more flexible ones, mimicking the physiology of cartilage ECM<sup>3</sup>.

Our research activity is aimed at designing and developing a novel functionally-graded hybrid (FGHY) scaffold where the load-bearing structure is a PU foam, CaPs with a graded composition represent the biomimetic component, and pectin gel is used as cell carrier (Fig. 1). This FGHY scaffold should be able to support MSCs proliferation and promote their differentiation for osteo-chondral defect repair.

The present work was aimed at designing the FGHY scaffold and at optimizing the materials processing techniques.

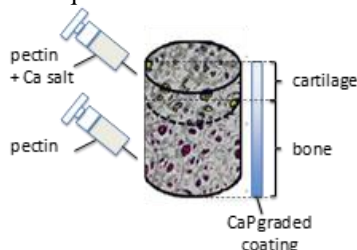


Fig. 1: an open-pore PU foam is the matrix graded-coated and/or loaded with CaPs, perfused with pectin gel as cell carrier

### EXPERIMENTAL METHODS

A PU foam (PU) was synthesized by one-step process, using MDI prepolymer (Bayer), an ad hoc polyether-polyol mixture, FeAA as catalyst and water (2% w/w<sub>polyol</sub>) as expanding agent<sup>4</sup>. Different coating approaches were performed to obtain through the foam the presence of Ca ions necessary to induce pectin gelification<sup>6</sup>. The foam was interpenetrated with  $\beta$ -TCP using a novel vacuum-assisted procedure (VAC, [approach 1](#)). Two strategies (NUCL-SBF and NUCL) were investigated to obtain the precipitation and nucleation of CaPs. In particular, a uniform HA layer on the surface of PU pores was obtained both in NUCL-SBF by using different salt solutions and 1.5 SBF ([approach 2](#)), and in NUCL due to a chemical reaction between Ca and P ions ([approach 3](#)).

Low methoxyl citrus pectin (PECT) was used to obtain the gel coating onto the PU foam previously treated with CaPs.

SEM, FTIR, and XRD analysis were performed on the CaP-based coatings. FGHY scaffolds were characterized by SEM, water uptake (37°C, PBS),

compression mechanical properties, and *in vitro* tests with human placenta-derived stem cells (hPDCs)<sup>7</sup>.

### RESULTS AND DISCUSSION

After characterization, VAC approach was selected due to the presence of a CaP gradient (Fig. 1) and a higher quantity of CaPs available for pectin gelification, compared to NUCL-SBF and NUCL. SEM images of PU/VAC/PECT showed a thin continuous layer of pectin gel, homogeneously distributed on all the surfaces (Fig.2a). Compression mechanical tests showed a  $\sigma_{max}$  higher for PU/VAC/PECT than PU matrix ( $p < 0.05$ ), indicating that the mechanical strength resistance increased for interpenetrated samples (Fig.2b). Compared to PU matrix, PU/VAC/PECT showed a significantly different creep/recovery behaviour in terms of residual strain, indicating that the pectin gel influenced the viscoelastic behavior of the PU matrix.

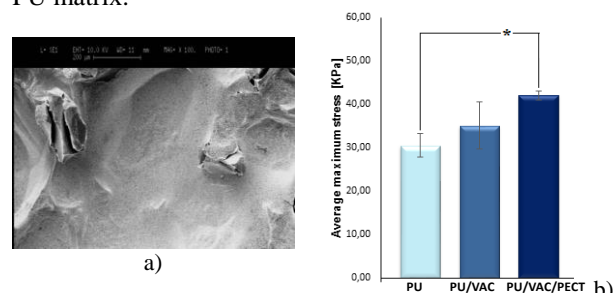


Fig. 2: a) SEM image of PU/VAC/PECT (scale bar 200  $\mu$ m); b)  $\sigma_{max}$  in compression mechanical test

### CONCLUSION

These novel FGHY scaffold displayed morphology and mechanical properties suitable for osteo-chondral defect repair and resulted adequate for hPDCs adhesion, and differentiation<sup>7</sup>. *In vivo* experimentation of FGHY scaffolds on the rabbit model will be the focus of future work.

### REFERENCES

1. Martin I. *et al.*, J Biomech. 40(4):750-65, 2007
2. Hangody L. *et al.*, Injury. 39 Suppl 1:S32-S39, 2008
3. Noeaid P. *et al.*, J Cell Mol Med. 16:2247-70, 2012
4. Zanetta M. *et al.*, Acta Biomater. 5:1126-36, 2009
5. Bertoldi S. *et al.*, J Mater Sci Mat Med.21:1005,2010
6. Munarin F. *et al.*, Biomacromol. 12:568-577, 2011
7. Spoldi V. *et al.*, abstract submitted to the ESB 2015

### ACKNOWLEDGMENTS

The authors would like to thank the Cariplo Foundation 2012 Programme (Grant no: 2012-0842) for providing financial support to this project.

## Formation of Hybrid Materials Based on Calcium Phosphate Deposit on Carbon Fiber Scaffold

Q. Picard<sup>1</sup>, L. Guichaoua<sup>1</sup>, S. Delpoux<sup>1</sup>, N. Rochet<sup>2</sup>, J. Chancolon<sup>1</sup>, F. Fayon<sup>3</sup>, F. Warmont<sup>1</sup>, S. Bonnamy<sup>1</sup>

<sup>1</sup> ICMN (ex-CRMD), CNRS / University of Orléans, 1B rue de la Férollerie, 45071 Orléans Cedex 2, France

<sup>2</sup> Institut de biologie Valrose INSERM/BIPOA, 06107 Nice Cedex 2, France

<sup>3</sup> CEMHTI, CNRS, 1D Avenue de la Recherche Scientifique, 45071 Orléans Cedex 2, France  
[lise.guichaoua@cnrs-orleans.fr](mailto:lise.guichaoua@cnrs-orleans.fr)

### INTRODUCTION

Due to their breathability, specific mechanical properties, i.e. high flexural and fatigue strength relative to their weight ratio and biocompatibility, activated carbon clothes (ACC) have previously been considered for hard and soft tissue implanting. However, their poor biological activity restricts their extensive use in medical applications and therefore needs to be enhanced<sup>1,2,3</sup>. Thanks to their excellent biocompatibility, osteoconductivity and bioactivity, calcium phosphate (CaP) ceramics, especially hydroxyapatites (HA), have received much attention in the biomedical materials field and have been clinically applied in orthopaedics<sup>3</sup>. So, carbon fiber-reinforced HA composites, combining the highly biocompatible CaP matrix with the properties of carbon fibers, are promising bioceramic materials, which could be particularly useful in the reconstruction of bone defects<sup>3</sup>.

### EXPERIMENTAL METHODS

To get bioactive hybrid materials to be further used as scaffolds, CaP coatings are deposited on activated carbon substrates by a sono-electrodeposition process. A mixture of  $\text{Ca}(\text{NO}_3)_2$ ,  $4\text{H}_2\text{O}$  and  $\text{NH}_4\text{H}_2\text{PO}_4$  is used as electrolyte. A three electrode system connected with a potentiostat-galvanostat is used to apply a cathodic polarization at the carbon electrode. The influence of electrochemical parameters is connected to the quantity, microtexture, structure and chemical composition of CaP phases.

The biocompatible properties of materials were determined by culturing human osteoblast-cells (HOST) in contact with CaP/ACC hybrid materials.

### RESULTS AND DISCUSSION

Data show that polarization duration influences the deposit thickness: from 500 nm to 5  $\mu\text{m}$ . The mass uptake tends to a limit corresponding to the decrease of nucleation sites. The current density influences the CaP deposit quantity, morphology and chemical composition. Indeed, at low regime, the quantity of deposit is proportional to the applied current density. During CaP deposition, two phenomena occur due to water electrolysis:  $\text{H}_2$  release at working electrode surface leads to a more or less homogeneous coating and the electrolyte pH decrease along polarization leads to CaP re-dissolution. The carbonate amount in CaP ceramics is controlled by addition of carbonate salt in the electrolyte. SEM, TEM and FTIR characterizations show that the coating consists in a mixture of plate-like

octocalcium phosphate and carbonated calcium phosphate phases for low current densities and needle-like carbonated calcium deficient HA (cdHA) together with calcium carbonates allotropic forms for high current densities.  $^1\text{H}$  and  $^{31}\text{P}$  NMR MAS performed on deposits confirm the presence of carbonated cdHA and underline the presence of minority disordered CaP phases.

Concerning biological experiments, first results have shown evidence of biocompatibility of hybrid materials (Fig. 1). Osteoblasts culture is employed in order to assess the *in vitro* viability and bioactivity of our hybrids biomaterials.

Mechanical tests are in progress to assess the adhesion properties between cloth and deposit.

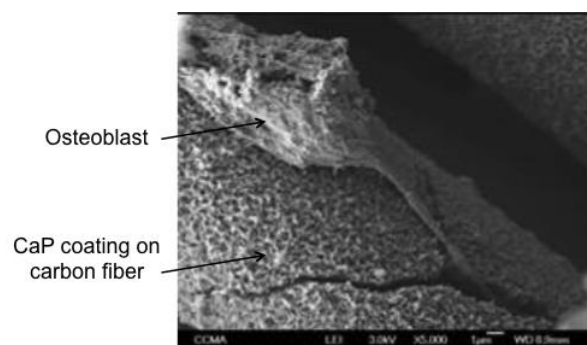


Figure 1: SEM images of human osteoblasts cultured for 7 days in the presence of CaP/ACC hybrid material obtained at low current density.

### CONCLUSION

The sono-electrodeposition process consists in a co-precipitation of calcium and phosphate ions with hydroxides ions provided by water electrolysis. It is an efficient method to obtain a controlled thickness, morphology (platelets or needles) and chemical composition of CaP deposits. Preliminary *in vitro* studies of HOST interaction with CaP/ACC material show a good biocompatibility whatever CaP morphologies.

### REFERENCES

1. Han HM. *et al.*, New Carbon Mat. 22:121-125, 2007
2. Stoch A. *et al.*, J. Mol. Struct. 651-3: 389-396, 2003
3. Kuo MC. *et al.*, Mat. Sci. Eng. C 20:153-160, 2002

### ACKNOWLEDGMENTS

This work was supported by AAPrégion-IR : bioactive hybrid materials for bone reconstruction. 2014-2016 MatBioReOs.

## Emulsion Templating: A Versatile Route to the Preparation of Biodegradable and Biocompatible Scaffolds for Tissue Engineering

Caitlin R Langford<sup>1</sup>, David W. Johnson<sup>2</sup>, Neil R Cameron<sup>1</sup>

<sup>1</sup>Department of Materials Engineering, Monash University, Clayton 3800, Victoria, Australia

<sup>2</sup>Department of Chemistry, Durham University, Durham, DH1 3LE, UK

[Caitlin.langford@monash.edu](mailto:Caitlin.langford@monash.edu)

### INTRODUCTION

The emulsion templating process, offers a route to highly porous polymers with well-defined morphologies<sup>1</sup>. The process, whereby the continuous phase of a high internal phase emulsion (HIPE) is polymerized, results in materials referred to as polyHIPEs. Recent developments in the photo-initiated polymerization of HIPEs have allowed for the preparation of polyHIPE polymers from monomers which form highly unstable emulsions, such as multifunctional thiol and alkene (typically acrylate) monomers<sup>2</sup>. The resulting polymers are biodegradable and have been found to be biocompatible in initial cell culture studies<sup>3</sup>. The surface chemistry of these materials can be altered by a variety of post-polymerization functionalization techniques<sup>4,5</sup>.

### EXPERIMENTAL METHODS

Biodegradable polyHIPEs were prepared by radically initiated network formation between combinations of thiols and acrylates where the combined functionality of the monomers is at least 5. Example procedure: The HIPE oil phase, consisting of a trithiol (10.0 mmol), triacrylate (10.0 mmol), solvent (7 ml), surfactant (3 wt% of organic phase), and photoinitiator (7 wt% of monomer content) were combined in a 2-neck round bottom flask with continuous stirring at 350 rpm from an overhead stirrer fitted with a D shaped PTFE paddle. Water (80 wt% of total emulsion) was added dropwise to form the HIPE. The HIPE was then poured into a mould and cured by passing under a UV lamp. The resulting polyHIPE is then washed by immersion in acetone and dried under reduced pressure.

### RESULTS AND DISCUSSION

A range of biodegradable polyHIPE polymers can be prepared by the described method. Typical monomers used are shown in Figure 1.

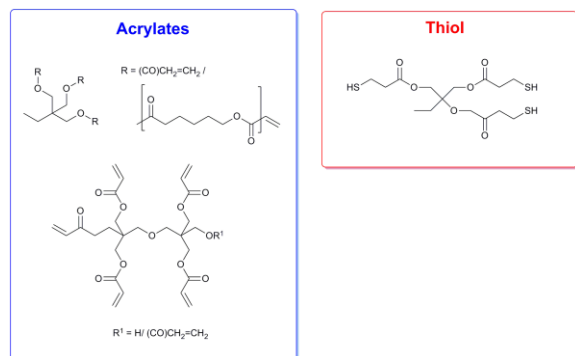


Figure 1. Acrylate and thiol monomers used in thiol-acrylate polyHIPE synthesis.

The above monomers are sufficiently hydrophobic to produce an emulsion kinetically stable enough for photopolymerization to occur without significant emulsion collapse (Figure 2.)

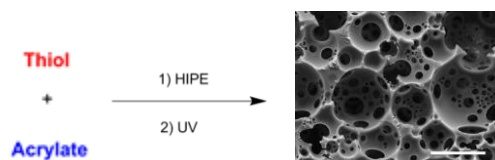


Figure 2. Synthesis of thiol-acrylate polyHIPE. Scale bar = 50  $\mu$ m.

The resulting polyHIPE materials have well-defined and interconnected porosities, allowing for cell penetration into the polymer. A variety of cell lines have been successfully cultured on such thiol-acrylate polyHIPEs for periods of up to 7 days (Figure 3), indicating they are biocompatible.

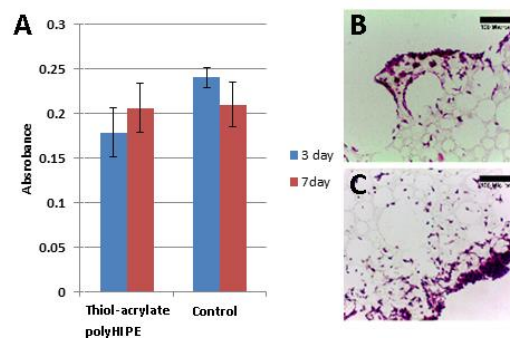


Figure 3. a) MTT assay of cultured cell line on thiol-acrylate polyHIPE vs control. b, c) Micrographs of H&E stained sections of thiol-acrylate polyHIPE after 3 (b) and 7 (c) days of culture. Scale bar = 100  $\mu$ m.

### CONCLUSION

PolyHIPEs have been prepared from multifunctional thiol and acrylate monomers by emulsion templating. These polymers have been shown to be biodegradable and biocompatible in initial cell culture studies.

### REFERENCES

1. Cameron N. R., Polymer, 46:1439-1449, 2005
2. Lovelady E., *et al.*, Polym. Chem., 2:559-562, 2011
3. Caldwell S., *et al.*, Soft Matter, 8:10344-10351, 2012
4. Kircher L., *et al.*, Polymer, 54:1755-1761, 2013
5. Langford C. R., *et al.*, Polym. Chem., 5:6200-6206

### ACKNOWLEDGMENTS

The authors thank the European Commission (Grant no: FP7-SME-2008-2-243542) and Monash University for providing financial support to this project.



## Cross-Linked, Macroporous Hybrid Glass Implants of Defined Architecture for Bone Regeneration

Stephan Hendriks<sup>1</sup>, Christian Kascholke<sup>1</sup>, Tobias Flath<sup>2</sup>, Mathias Gressenbuch<sup>3</sup>, Christian Raeck<sup>4</sup>, Peter Schulze<sup>2</sup>, Michael C Hacker<sup>1</sup>, Michaela Schulz-Siegmund<sup>1</sup>

<sup>1</sup> Institute of Pharmacy, Pharmaceutical Technology, Universität Leipzig, Germany

<sup>2</sup> Faculty of Mechanical and Energy Engineering, Leipzig University of Applied Sciences, Germany

<sup>3</sup> DMG Chemie GmbH, Germany

<sup>4</sup> Intelligent Fluids<sup>®</sup>, bubbles and beyond GmbH, Germany

[stephan.hendriks@uni-leipzig.de](mailto:stephan.hendriks@uni-leipzig.de)

### INTRODUCTION

Regeneration of bone defects with the aid of artificial macroporous implants is a complex task, because the implants have to withstand mechanical stress on the one hand and, on the other hand, provide high macroporosity to allow for tissue ingrowth, remodelling and vascularisation. Moreover, materials need to be biocompatible and bioactive with regards to the formation of a mechanically stable bone-implant interface. Last but not least the production costs of these implants should be reasonable and the technology should allow for easy up-scaling at reproducible product quality.<sup>1</sup>

We developed an organic-inorganic hybrid material based on a silicate glass produced via the sol-gel route, reinforced with organic cross-linkers. Furthermore, we present a templating technique for scaffold generation based on a mold produced by rapid prototyping that allows for the generation of macroporous scaffolds with defect-specific architecture.

### EXPERIMENTAL METHODS

We produced macroporous hybrid-glass scaffolds by cross-linking a silica sol, derived from tetraethoxysilane (TEOS), with silane functionalized trimethylolpropane-ethoxylate (TMPEO) of different molecular weights. This hybrid sol was cast into molds printed from polycaprolactone, (PCL) using a melt extrusion print head (Bioscaffolder<sup>®</sup>, Syseng). The molds had a closed outer structure and stacked grids of 200 µm wide PCL strands forming double layers alternating in orientation by 90°. We systematically modified the silica sol with TMPEO of molecular weights of 170 (T170), 450, 730 and 1014 g/mol and crosslinker contents from 1 to 40% and evaluated the mechanical strength of the scaffolds. To this end, 6 scaffolds of each composition were compressed between two parallel plates until failure (crosshead speed 1 mm/min, 50 kN load cell). Scaffold morphology was examined by scanning electron microscopy (SEM). To determine the biological activity of the hybrid scaffolds, we seeded Saos-2 cells on 4 scaffolds each and determined the proliferation, mineralisation and the cells' distribution throughout the scaffold over 14 days of dynamic culture with osteogenic medium.

### RESULTS AND DISCUSSION

SEM imaging revealed a uniform pore structure with tubular pores and interconnect sizes of at least 120 to 140 µm. Compression testing showed good mechanical compatibility of the implants to cancellous bone. We

observed compressive strengths up to 32 MPa for the T170 hybrid and could cover a wide range of compressive moduli from 24 MPa to 568 MPa, while maintaining good mechanical strength. These values fall within the range of the values for cancellous bone which are 2-12 MPa for the compressive strength and 50-500 MPa for compressive modulus<sup>2</sup>. Systematic variation of the cross-linker content revealed a maximum strength for 20-30% of TMPEO in the silica sol whereas at higher organic contents the organic cross-linker dominated over the influence of the silica phase, leading to softer materials with higher elasticity. Concerning the influence of cross-linker molecular weight, we found decreasing mechanical strength with increasing Mr likely due to a lower crosslinking degree at constant cross-linker mass content in the hybrid.

Cell culture tests showed a good attachment of Saos-2 cells on the scaffolds. We observed proliferation in the first seven days and mineralization of the cells as well as the scaffolds until day 14. Microscopic analysis of cryosections revealed that the cells spread homogeneously through the pores and also mineralized throughout the scaffold. They formed a tight cell layer on the material surface, which indicates effective nutrient and oxygen supply, even in the inner pores of the scaffolds.

### CONCLUSION

We fabricated macroporous hybrid glass scaffolds using rapid prototype templates. By using this templating technique, we were able to produce hybrids of a wide variety of compositions. In addition, the templating technique allows for modification of the scaffolds' pore size and geometry as well as for an individualization of size and shape of the implant, while a high reproducibility is guaranteed.

### REFERENCES

1. Jones J. *et al.*, Biomaterials 7:964-973, 2006
2. Hench L. *et al.*, An Introd. to Bioceramics, 1993

### ACKNOWLEDGMENTS

The authors thank Prof. Rieger (HTWK Leipzig, Germany) for access to the compression testing equipment. The authors would also like to thank the AiF Projekt GmbH (Grant no: KF2734502MU1), the Saxon ministry for science and arts (Grand no: 4-7531.60/64/18) and the German Research Council (DFG SFB/Transregio 67) for financial support.



Edgar B. Montufar<sup>1,2,3</sup>, Yassine Maazouz<sup>1,2</sup>, Borja Gonzalez<sup>1</sup>, Ladislav Celko<sup>3</sup>, Jozef Kaiser<sup>3</sup>, Maria-Pau Ginebra<sup>1,2</sup>

<sup>1</sup>Biomaterials, Biomechanics and Tissue Engineering Group, Technical University of Catalonia, Barcelona, Spain

<sup>2</sup>Biomedical Research Networking Centre in Bioengineering, Biomaterials and Nanomedicine, Spain

<sup>3</sup>Central European Institute of Technology, Brno University of Technology, Czech Republic

[edgar.benjamin.montufar@upc.edu](mailto:edgar.benjamin.montufar@upc.edu)

## INTRODUCTION

Recently, a new generation of self-setting inks were developed, which avoid the high temperature treatments commonly needed to consolidate robocasted ceramic scaffolds<sup>1</sup>. These inks are based on the hydrolysis of alpha tricalcium phosphate ( $\alpha$ -TCP) into calcium deficient hydroxyapatite (CDHA) and incorporate a hydrogel as printing additive. Nonetheless, until now the influence of the hydrolysis process on the properties of such scaffolds has not been studied. This work explores the influence of several hydrolysis conditions on the nano/microstructure, composition and mechanical strength of robocasted scaffolds. Furthermore, different hydrolysis conditions were combined with different printed patterns to tailor in an independent manner the macro and nano/micro structure of the scaffolds.

## EXPERIMENTAL METHODS

$\alpha$ -TCP powder was obtained as described elsewhere<sup>1</sup>. This powder was mixed with poloxamer F127 solution (20 wt%) at liquid to powder ratio of 0.5 mL/g. Cylindrical scaffolds (6 mm  $\varnothing$  x 12 mm height) were fabricated using a customized robocasting device (Fundacio CIM). The paste was dispensed with 250  $\mu$ m tapered tips following three different patterns: honey comb (HC), orthogonal (O) and orthogonal rotated at 45 degrees (OR). In all cases the material infill was set up at 45 %. Printed scaffolds were then consolidated either by autoclaving (hydrothermal condition at 121 °C for 30 min) or by immersion in deionized water at 37 °C for 7 days (biomimetic condition). For hydrothermal consolidation two alternatives were studied i) samples immersed in deionized water and ii) samples exposed to a moisture atmosphere (MA). X-ray powder diffraction (XRD) was performed to quantify the crystalline phases present; scanning electron microscopy (SEM) was used to observe sample microstructure; uniaxial compressive strength (CS) was determined in the parallel direction of the axes of the cylindrical sample, at a rate of 1 mm.s<sup>-1</sup>; mercury intrusion porosimetry (MIP) was employed to quantify the entrance pore size distribution; and X-ray computed microtomography ( $\mu$ CT; GE v|tome|x L 240) scans of voxel size 25  $\mu$ m were acquired to assess the architecture of the macroporosity.

## RESULTS AND DISCUSSION

Fig. 1 shows  $\mu$ CT reconstructions of the printed scaffolds together with their CS and macroporosity (mP: free spaces between scaffold strands) when consolidated at 37 °C. In congruence with its lowest mP, HC structure was the most resistant. In contrast, OR structure, with similar mP than HC, presented the lowest CS. O structure, with the highest mP, presented an intermediate CS, which evidenced a higher load bearing efficiency in comparison with OR. Since all

samples were consolidated in the same condition, the nano/microporosity ( $\mu$ P: spaces within the scaffold strands) can be considered to be the same (~30 % in all cases). Fig. 1 also shows the pore entrance size distribution and the microstructure of the strands for three consolidation conditions. Clear differences were observed, not only in terms of microstructure but also in the amount of  $\mu$ P and pore size distribution. Hydrothermal-MA led to the lowest  $\mu$ P, and XRD showed only a partial conversion of  $\alpha$ -TCP to CDHA together with a partial allotropic transformation to  $\beta$ -TCP. SEM images revealed low crystal entanglement, which can be the cause of a low mechanical strength for these type of materials. In contrast, the conversion to CDHA was complete in the other two methods. However, whereas the transformation took only 30 min in the autoclave with the samples immersed in water, in the biomimetic condition it took 7 days. The microstructure was very different, with needle-like crystals in the autoclaved samples and plate-like crystals in the biomimetic method, which resulted in scaffolds 1.3 times stronger than the former.

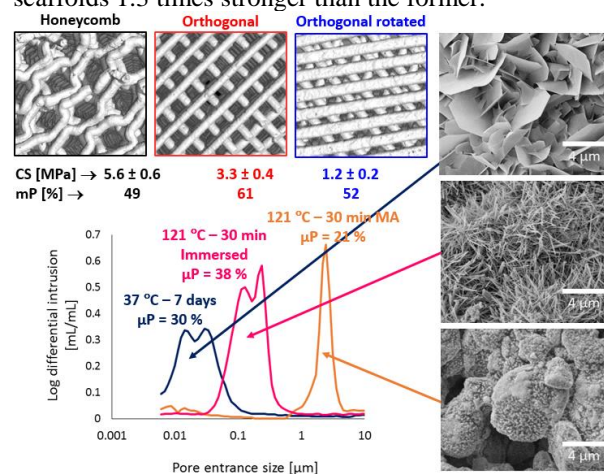


Fig. 1:  $\mu$ CT reconstructions, CS, mP, pore entrance size distribution and microstructure of studied scaffolds.

## CONCLUSION

Varying consolidation conditions allows tailoring  $\mu$ P and microstructure, while varying the printed pattern allows tailoring the mP content and architecture, all essential parameters to induce specific cell responses in future applications of these scaffolds in bone tissue engineering.

## REFERENCES

<sup>1</sup>Y. Maazouz, *et al.*, *J Mater Chem B* 2:5378-86, 2014.

## ACKNOWLEDGMENTS

To the Spanish Government (MAT2012-38438-C03-01), FPU scholarship of YM and ICREA Academia prize by the Generalitat de Catalunya of MPG.



## Development of Bioactive and Antimicrobial 3D Plotted PCL Scaffolds for Bone Tissue Engineering

Giuseppe Cama, Myriam Gomez Tardajos, Peter Dubruel

Polymer Chemistry and Biomaterials Research Group,  
Ghent University, Krijgslaan 281, 9000 Ghent, Belgium  
[giuseppe.cama@ugent.be](mailto:giuseppe.cama@ugent.be)

**INTRODUCTION** The treatment of “critical” bone defects (i.e. bone deficiency that precludes the spontaneous healing of the natural tissue leading to severe functional impairments) represents a challenge for orthopaedic and oral-maxillofacial surgeons due to the lack of therapeutic approaches that are able to fully restore the lost bone<sup>1</sup>.

A way of reducing the drawbacks of the conventional treatments is to use bone graft substitutes with a tailored porosity, suitable to ensure nutrient and metabolic waste transport to and from the core of the scaffold, a critical issue for proper vascularization and new bone tissue formation. To this purpose rapid prototyping techniques have been developed in order to fabricate 3D polymeric layered grids with the desired thread size and thread spacing as well as with different orientations of the grids between one layer and the other. Poly-ε-caprolactone (PCL) is a biocompatible polymer extensively employed to fabricate 3D plotted structures due to its easy processability. However, it is not properly a bioactive material (i.e. able to bond to the living bone tissue) and it does not show antimicrobial activity. This latter property is highly required for a material to be used for the treatment of bone defect considering that infections associated with implantation of bone graft substitutes represent a challenging problem for surgeons and patients alike<sup>2</sup>. The aim of this work is to overcome the PCL limitations by coating 3D plotted PCL structures with bioactive calcium phosphate (CaP) crystals and chitosan (CH) functioning as antimicrobial agent.

**EXPERIMENTAL METHODS** 3D plotted PCL (Sigma-Aldrich, Mw 70.000–90.000 g/mol) scaffolds with a cubic shape (l=10mm) and square shaped pores (l= 300 μm) were fabricated using a Bioscaffolder® (Sys-Eng, Germany) device. Briefly, PCL in form of granules (d~3mm) was melted at a temperature of about 120 °C and extruded through a 27-gauge needle. The pressure during extrusion was maintained at 5 bar. The plotted structures were subjected to 30 seconds of Argon plasma treatment and then functionalised by grafting Methacrylic acid N-hydroxysuccinimide ester (NHSMA) by immersion in a solution with a molar concentration equal to 0.5M. The polymerization was carried out for 30 minutes under UV-C. Subsequently, the samples were chitosan coated by placing them overnight in a 2% wt of chitosan solution at pH 5. Then, the scaffolds were CaP coated by immersion in Milli-Q water where CaCl<sub>2</sub> and disodium hydrogen phosphate (Na<sub>2</sub>HPO<sub>4</sub>) (molar ratio of Ca/P equal to 1.67) powders were let to dissolve and precipitate onto the PCL struts.

**RESULTS AND DISCUSSION** A qualitative preliminary investigation showed the precipitation of a

CaP phase onto the PCL struts (Figure 1). FTIR analysis reported brushite (DCPD: CaHPO<sub>4</sub>·2H<sub>2</sub>O) as the precipitated phase (Figure 2). The acid pH value (pH=4.5±0.1) measured immediately after the immersion of the reactants powders could be the main cause that drove the precipitation process towards the formation of brushite, which is the CaP phase generally found in acid aqueous solution<sup>3</sup>.

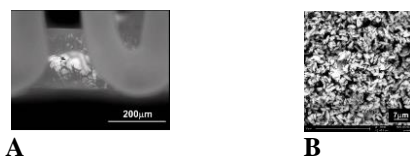


Figure 1 A: Optical image (200x) of a 3D plotted PCL coated with brushite. B: SEM analysis of the precipitated brushite crystals.

PCL was functionalized by grafting a methacrylate containing succinimide functionality (NHSMA) after plasma activation. Subsequently, the NHS groups of the grafting were used to coat native chitosan as shown in Figure 2.

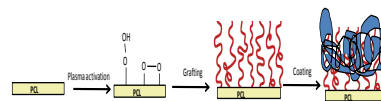


Figure 2: scheme of functionalization method of PCL using NHSMA for the subsequent immobilization of native chitosan.

Preliminary XPS analysis showed the presence of the peak of nitrogen on the grafted surface and an increase of the %N after the chitosan coating. Qualitative changes of the contact angle were also observed in the different steps of the process.

**CONCLUSION** Coating 3D plotted PCL scaffolds with chitosan and calcium phosphate crystals could be considered as a potential strategy to produce biologically improved materials for bone tissue engineering applications. Antimicrobial tests will be performed and reported on during the meeting.

**REFERENCES** 1. Lee K. *et al.* Journal of Biomedical Materials Research Part B: 89B: 252-263, 2008  
2. Hu H. *et al.* Acta Biomaterialia. 8:904-915, 2012  
3. Mekmene O. *et al.* Dairy Sci. Technol. 89:301-316, 2009

**ACKNOWLEDGMENTS** The work had the financial support of Nano3Bio project funded by the European Union. Grant agreement n° 613931.





## Two-Photon Polymerization of Ormocomp® 3D Structures Doped with Piezoelectric Barium Titanate Nanoparticles

Attilio Marino<sup>1,2</sup>, Jonathan Barsotti<sup>1,2</sup>, Massimiliano Labardi<sup>3</sup>, Barbara Mazzolai<sup>1</sup>, Virgilio Mattoli<sup>1</sup>, Gianni Ciofani<sup>1</sup>

<sup>1</sup>Istituto Italiano di Tecnologia, Center for Micro-BioRobotics @SSSA, Viale Rinaldo Piaggio 34, 56025 Pontedera, Italy

<sup>2</sup>Scuola Superiore Sant'Anna, The Biorobotics Institute, Viale Rinaldo Piaggio 34, 56025 Pontedera, Italy

<sup>3</sup>CNR-IPCF, UOS Pisa, Largo Pontecorvo 3, 56127 Pisa, Italy

[gianni.ciofani@iit.it](mailto:gianni.ciofani@iit.it)

### INTRODUCTION

Two photon polymerization (2pp) is a high-resolution photolithographic technique which allows the prototyping of 3D nanostructures suitable for cell-surface interaction investigations, tissue engineering, and regenerative medicine.<sup>1</sup>

The possibility to combine different nanoparticles with traditional photoresists opens new perspectives for the photofabrication of 3D structures characterized by several tunable properties.<sup>2</sup> As an example, piezoelectric materials can be exploited for sensing/actuating purposes, both at cellular and tissue level. In this context, piezoelectric barium titanate nanoparticles (BTNPs) were already successfully exploited for stem cell stimulation.<sup>3</sup>

In this work, we propose for the first time the 2pp of 3D nanocomposite structures prepared with the commercially available Ormocomp® photoresist doped with a high concentration (1:10 mass ratio) of BTNPs.

### EXPERIMENTAL METHODS

#### *Fabrication of nanocomposite 3D structures*

BTNPs were obtained from Nanostructured and Amorphous Materials (Houston, TX, USA) and were homogeneously mixed with the Ormocomp® photopolymer by applying ultrasounds (8 W, 2 min, with a Ultrasonic Homogenizer 7 mini 20, Bandelin). Subsequently, 2pp of the BTNPs dispersion in Ormocomp® was achieved by using a Direct Laser Writing system (Photonic Professional, Nanoscribe GmbH) and a Zeiss microscope equipped with an oil-immersion objective (100x, numerical aperture = 1.4). The photon wavelength was 790 nm and the pulse duration was 120 fs. The 3D structures were fabricated thanks to a layer-by-layer writing approach. At the end of the procedure, the unexposed resist was removed with Ormodev® developer.

#### *Characterization of the polymerized structures*

The nanoparticles were detected on the surface and inside of the polymerized 3D structures thanks to atomic force microscopy (AFM, MultiMode Veeco) and confocal microscopy (C2s, Nikon), respectively. For the confocal scans we exploited the excitation at 642 nm, at which BTNPs resulted detectable without any further labeling.

Furthermore, we combined focused ion beam and scanning electron microscopy (dual beam system, FEI Helios 600) with energy dispersive X-ray spectroscopy (EDX, Bruker) for a deeper characterization of the fabricated structures.

### RESULTS AND DISCUSSION

The successful 2pp of the Ormocomp® photopolymer doped with BTNPs (1:10 mass ratio) into a desired structure (in this case, as an example, the 3D logo of our

institution, IIT) was analyzed (Fig. 1). Fig. 1a is an AFM scan showing the presence of BTNPs on the surface, while Fig. 1b is a confocal z-stack of the whole structure (BTNPs in green) and Fig. 1c the 3D reconstruction of the signal collected by all the z-stacks (pseudo-colors indicate depth).

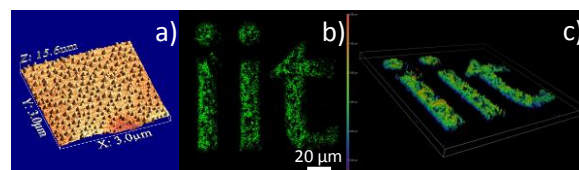


Fig. 1. AFM surface scan (a), single confocal z-stack (b) and 3D reconstruction (c) of the IIT logo obtained by the two-photon polymerization of Ormocomp® doped with barium titanate nanoparticles (BTNPs).

Thanks to the AFM and to the confocal imaging, it is possible to appreciate the high concentration of nanoparticles, which are uniformly dispersed into the 3D structure.

This observation is confirmed by SEM analysis. In particular, after milling the first layers of the structure by using a focused ion beam, a SEM scan (Fig. 2a) revealed the presence of BTNPs in the whole depth of the structure, and the elemental microanalysis (Fig. 2b) demonstrated the presence of barium titanate.

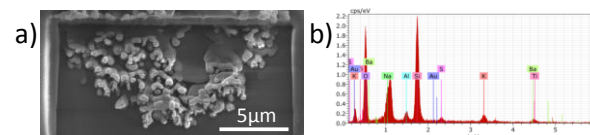


Fig. 2. SEM scan after milling the first layers of the logo by using a focused ion beam (a). Elemental microanalysis of the same area reveals the presence of barium titanate (b).

Collectively, all the analyses not only demonstrated the presence of BTNPs inside the polymerized structure, but also highlighted as the polymerization process was not affected by the presence of the nanoparticles in the photoresist.

### CONCLUSION

Concluding, we obtained for the first time a two-photon polymerized 3D nanocomposite structure based on Ormocomp® doped with piezoelectric nanoparticles.

The exploitation of these structures for the piezoelectric stimulation of cells and tissues could represent an interesting approach in tissue engineering and regenerative medicine, which deserves future deeper investigations.

### REFERENCES

1. Marino A. *et al.*, Nanoscale, on line, 2015
2. Farsari M. *et al.*, J. Opt. 12:124001, 2010
3. Rocca A. *et al.*, Int. J. Nanomed. 10:433–445, 2015



## Additive Manufacturing of Poly-High Internal Phase Emulsion Scaffolds with Tuneable Mechanical Properties for Bone Tissue Engineering

Robert Owen<sup>1</sup>, Colin Sherborne<sup>2</sup>, Gwendolen Reilly<sup>1</sup> and Frederik Claeyssens<sup>2</sup>

<sup>1</sup>Department of Materials Science and Engineering, INSIGNEO Institute for in silico medicine, The Pam Liversidge Building, Sir Frederick Mappin Building, Mappin Street, Sheffield, S1 3JD, United Kingdom

<sup>2</sup>Department of Materials Science and Engineering, The Kroto Research Institute, North Campus, University of Sheffield, Broad Lane, Sheffield, S3 7HQ, United Kingdom

[F.Claeyssens@sheffield.ac.uk](mailto:F.Claeyssens@sheffield.ac.uk)

### INTRODUCTION

An interesting self-assembly route for production of highly porous polymeric materials is emulsion templating via high internal phase emulsions (HIPEs). To form porous polymers from HIPEs typically a dispersed aqueous droplet phase is used with a curable pre-polymer continuous phase. During the curing process a foam is produced in which the pores are interconnected (a polyHIPE).<sup>1</sup> In this paper we report the use of polyHIPEs as a material for additive manufacturing, in particular microstereolithography ( $\mu$ SL). In  $\mu$ SL a laser is scanned through a photocurable resin to build up a 3D objects with micrometre length scale resolution. This enables the production of hierarchical structures based on polyHIPEs where the internal porosity is governed by the emulsion templating process and macroscopic structuring is governed by the  $\mu$ SL process.<sup>2</sup> This study assesses the ability of acrylate based PolyHIPE scaffolds to support bone cells *in vitro* by seeding with immortalised human embryonic stem cells. Scaffolds with different stiffness and surface chemistries are used to evaluate their effects on differentiation.

### EXPERIMENTAL METHODS

3D structured scaffolds with varying mechanical properties have been produced via combining the water-immiscible monomers 2-Ethylhexy acrylate (EHA) and Isobornyl acrylate (IBOA) with a triacrylate crosslinking agent, photoinitiator and a surfactant (see Fig. 1). The HIPE is cured into woodpile structures by scanning the UV light (355 nm) generated by a Nd:YAG microchip laser (0.5 ns pulse duration, 16.6 kHz, 10 mW) over the photocurable resin. The scanning patterns were generated via a computer controlled xyz-stage (Aerotech). 3D structures were produced from polyHIPE with internal porosity ranging from 75 to 90%.

SEM analysis of 4-layer 3D grid arrays produced via  $\mu$ SL were used to assess the porosity and surface features. The tunability of the mechanical properties of PolyHIPE monomer blends was studied via nanoindentation and tensile testing. The surfaces of the scaffolds were rendered hydrophilic via both oxygen plasma treatment and plasma polymerisation of acrylic acid and the scaffolds were tested *in vitro* for cell ingrowth with human embryonic stem cell-derived mesenchymal progenitors (hES-MPs). Resazurin reduction assays were used to assess viability and Alkaline Phosphatase (ALP) and DNA assays for osteogenic differentiation.

### RESULTS AND DISCUSSION

3D structures built from polyHIPEs with a range of mechanical properties and porosities. Young's Moduli of PolyHIPEs ranged from  $0.36 \pm 0.04$  to  $63.01 \pm 9.13$  MPa and Ultimate Tensile Strength ranged from  $0.11 \pm 0.01$  to  $2.03 \pm 0.33$  MPa. 13 mm diameter woodpile scaffolds were made from 0%, 50% and 100% EHA compositions at 80% porosity with a fibre diameter of 350  $\mu$ m and a spacing of 650  $\mu$ m (Fig. 1). All scaffolds supported cells, with an increase in viability over time and no significant differences between compositions. Composition also had no significant effect on differentiation, with the exception of the stiffest scaffold in combination with an acrylic acid plasma treatment which exhibited a significant higher ALP activity.

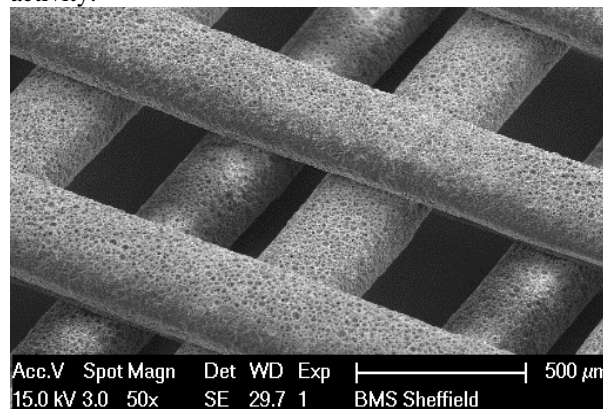


**Figure 1:** PolyHIPE woodpile scaffold showing micro- and macro-porosity

### CONCLUSION

PolyHIPEs can be used to create regular porous structures by microstereolithography with micropores. This hybrid technique addresses the resolution trade-off between macro structuring with micro resolution, while maintaining user control over structural parameters throughout the process. Mechanical properties of these scaffolds can be varied by changing the monomer concentration to provide a range of application specific stiffnesses relevant for bone tissue engineering.

### REFERENCES

1. A. Barbeta, Chem. Comm., 3, 221-222 (2000)
2. Johnson et al., Adv. Mat., 25, 3178-3181 (2013)

### ACKNOWLEDGMENTS

The authors would like to thank BBSRC and the Leverhulme Trust for providing financial support to this project.



## Osteogenic Potential of Self-Assembling Bioceramic Nanoparticles

Michelle O'Doherty<sup>1</sup>, Sreekanth Pentlavalli<sup>1</sup>, Philip Chambers<sup>1</sup>, Marine J. Chalanqui<sup>2</sup>, Helen O. McCarthy<sup>2</sup> and Nicholas Dunne<sup>1</sup>

<sup>1</sup>School of Mechanical & Aerospace Engineering, Queen's University Belfast, UK

<sup>2</sup>School of Pharmacy, Queen's University Belfast, UK

[michelle.odoherty@qub.ac.uk](mailto:michelle.odoherty@qub.ac.uk)

### INTRODUCTION

A major challenge in the repair of joint injuries lies in the reattachment of the soft tissue to the bone<sup>1</sup>. Failure to regenerate these interfaces results in compromised graft stability and poor long-term clinical outcomes<sup>2</sup>. Fabrication of scaffold constructs that promote the formation of bone-to-ligament interfaces is limited<sup>3</sup>. Therefore development of a construct with the ability to promote bone and soft tissue regeneration is a priority.

In this study we propose that the sustained, localized delivery of osteogenic nanoparticles (NPs) from a biomaterial scaffold will promote osteogenesis, enhancing formation of interfacial tissue. A series of *in vitro* tests were performed to determine whether NPs comprised of an amphipathic peptide (RALA) incorporating  $\alpha$ -tri-calcium phosphate ( $\alpha$ -TCP) and the RUNX2 gene, released via thermo-responsive hydrogels, elicited an osteogenic response in human osteoblast cells.

### EXPERIMENTAL METHODS

**Formulation of RALA/ $\alpha$ -TCP NPs:** Particle size and zeta potential (ZP) were measured using a Malvern Zetasizer to determine the optimal formulation. NP stability was tested over time and temp range.

**Cell viability:** The effects of RALA/ $\alpha$ -TCP, RALA/RUNX2 NPs and NP-loaded hydrogel on human osteosarcoma cells MG63 and normal human osteoblasts was assessed every 7 d using MTS, LDH and live/dead cell assays up to 28 d

**RT-PCR analysis:** Cells were cultured with RALA/ $\alpha$ -TCP, RALA/RUNX2 NPs and NP-loaded hydrogels. RNA was extracted up to 28 d post transfection and complementary DNA (cDNA) synthesised. RT-PCR was performed and relative gene expression of osteoblastic markers determined using REST software.

**Immunocytochemistry (ICC) & quantification of osteogenic proteins:** Cells were fixed, permeabilised and blocked prior to incubation with col-I, RUNX2 and osteocalcin (OC) primary antibodies. Following incubation secondary antibodies samples were visualized by fluorescence microscopy. Quantification of col-I, OC and ALP was determined using quantitative colorimetric assays

**Mineralisation Assay:** Mineralisation activity was evaluated using Alizarin red (AR) staining. Cells were fixed and stained with AR at room temperature for 45 min. CPC extraction was performed to quantify staining.

### RESULTS AND DISCUSSION

NPs prepared with a mass ratio of 5:1 were observed to have a size of  $43 \pm 4.5$  nm and a zeta potential of  $26 \pm 4.3$  mV. The NP size and ZP remained consistent for up to 28 d at room temperature and across a broad range of temperatures (4–40°C) (Figure 1.A). Cell viability was seen to decrease 24 h post-transfection with the RALA/ $\alpha$ -TCP NP treatment. However cytotoxicity decreased to a level similar to that observed untreated control group 7 d after transfection (Figure 1.B). ICC staining for collagen I (red) up to 21d post-transfection with RALA/ $\alpha$ -TCP NPs indicated MG63 cells treated with NPs exhibit enhanced col-I expression compared to an untreated control (Figure 1.C). Taken together these data demonstrate that RALA/ $\alpha$ -TCP form stable NPs that elicit an osteogenic response in MG63 cells. ICC and quantification of osteogenic proteins is ongoing.

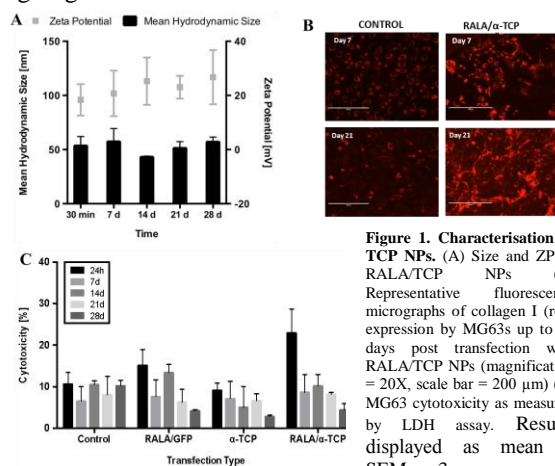


**Figure 1. Characterisation of TCP NPs.** (A) Size and ZP of RALA/TCP NPs (B) Representative fluorescence micrographs of collagen I (red) expression by MG63s up to 21 days post transfection with RALA/TCP NPs (magnification = 20X, scale bar = 200  $\mu$ m) (C) MG63 cytotoxicity as measured by LDH assay. Results displayed as mean  $\pm$  SEM, n=3

### CONCLUSION

We have successfully demonstrated that the RALA peptide was capable of forming NPs with  $\alpha$ -TCP, which were stable across a range of temperatures and over an extended duration. Furthermore these NPs were shown to induce osteogenesis in osteosarcoma cells and osteoblasts, and when loaded into a hydrogel form a potential biomimetic interface between bone and ligament.

### REFERENCES

1. P. Yang *et al.*, Tissue Eng Part B Rev., 2: 127-41, 2009
2. H.H. Lu *et al.*, Ann Biomed Eng., 38: 2142-54, 2010
3. A.R. Amini *et al.*, Crit Rev Biomed Eng.; 40: 363–408, 2012

### ACKNOWLEDGMENTS

MRC:MC\_PC\_12021

EPSRC:EP/K029592/1

## Results of Pilot Experimental Studies in 10 Animals on Prototype of the Multispiked Connecting Scaffold with Thermo-Electrochemically Ca-P Modified Surface for Non-Cemented Biofixation of RA Endoprostheses

Ryszard Uklejewski<sup>1,2</sup>, Piotr Rogala<sup>3</sup>, Mariusz Winiecki<sup>1,2</sup>, Wanda Stryła<sup>4</sup>

<sup>1</sup>Department of Medical Bioengineering Fundamentals, Institute of Technology, Casimir the Great University, Poland

<sup>2</sup>Laboratory of Medical Biomaterials and Bioprocess Engineering, Department of Process Engineering, Institute of Technology and Chemical Engineering, Poznan University of Technology, Poland

<sup>3</sup>Department of Spine Surgery, Oncologic Orthopaedics and Traumatology, Poznan University of Medical Sciences, Poland

<sup>4</sup>Chair and Clinic of Rehabilitation, Poznan University of Medical Sciences, Poland

[uklejew@ukw.ukw.pl](mailto:uklejew@ukw.ukw.pl)

### INTRODUCTION

The current worldwide accepted standard fixation for modern metal-on-metal hip RA (resurfacing arthroplasty) is a hybrid technique using a cemented short-stem femoral component in combination with an uncemented acetabular component (e.g., Birmingham Hip Implant, Cormet 2000 Implant, DePuy ASR Implant, etc.). With our elaborated prototype of the multispiked connecting scaffold (MSC-Scaffold), invented by Rogala<sup>1</sup> and designed, manufactured<sup>2</sup> and tested by our research team<sup>3</sup>, we propose completely non-cemented biofixation of RA endoprostheses. The aim of this contribution is to present the main results of pilot experimental studies in 10 animals on the prototype of the MSC-Scaffold with Ca-P (or HA) modified surface, performed to establish the suitable constructional directives for manufacturing in SLM technology the subsequent prototype of such scaffold for RA endoprostheses. The possibilities of affecting the pro-osteoconduction functionality of the MSC-Scaffold, which is essential for its proper successive osteointegration with the periarticular trabecular bone tissue, has been evaluated in the associated ESB2015 contribution (Uklejewski, Winiecki *et al.*)<sup>4</sup>.

### EXPERIMENTAL METHODS

The prototype of the MSC-Scaffold for non-cemented RA endoprostheses was investigated on its constructional prototype variants (Fig. 1a) with thermo-electrochemically Ca-P (or HA) modified bone contacting surfaces, which were implanted (Fig. 1a,b) in hip and knee joints of 10 animals (swine; breed: Polish Large White) in a veterinary clinic operating room with permission of the Local Ethic Commission. After 6-7 weeks the animals were scarified and the bone-prototypes preparations were made (Fig. 2a) and the bone tissue contacting and surrounding the prototypes was microscopically evaluated in the Pathomorphology Unit of the J. Strus Clinical Hospital of Poznan Medical University.



Fig. 1. a) MSC-Scaffold prototype variant, b) partial knee resurfacing endoprosthesis prototype with the MSC-Scaffold implanted into swine knee joint, c) assisted laboratory biomechanical test on the MSC-Scaffold prototypes (push-in test in periarticular cancellous bone of swine femoral head).

### RESULTS AND DISCUSSION

The exemplary pathomorphological microscopic slides of bone tissue contacting and surrounding the implanted prototypes are presented in Fig. 2a,b. It was found, that the Ca-P (or HA) modification of the MSC-Scaffold significantly improves its osteointegration with the surrounding periarticular bone. Due to the technical difficulties in the bone-prototype microscopic slides preparation, the special 2D X-ray analysis (Fig. 2c) and micro-tomography analysis have been undertaken in cooperation with the COMEF Scientific and Research Equipment Company.

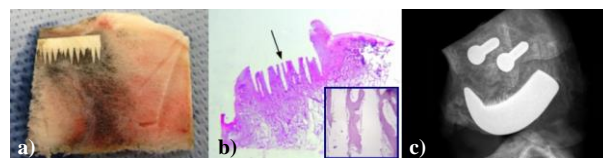


Fig. 2.: a,b) exemplary pathomorphological microscopic slides of bone tissue surrounding the implanted MSC-Scaffold prototypes, c) 2D X-ray radiogram (XPRT 40, Kubtec, USA) of swine knee joint with implanted partial knee resurfacing endoprosthesis prototype with the MSC-Scaffold.

### CONCLUSIONS

On the base of the performed pilot experimental studies in animal models (assisted by the biomechanical push-in test) on the constructional prototype variants of the MSC-Scaffold for RA endoprostheses, and the obtained results, it was possible to establish the suitable constructional directives for the engineering design and manufacturing the prototypes of partial and total RA endoprostheses for knee and hip joints, which – according to the ISO 10993 recommendations – should be verified in the full standard experimental study on animal models (in the planned next research project).

### REFERENCES

1. Rogala P, US/Canada patent nr 5,91,759], 1999/2002.
2. Uklejewski R, *et al.*, Rapid Prototyping J. 17:76, 2011.
3. Uklejewski R, *et al.*, BioMed Res. Int., 2013, doi:10.1155/2013/689089.
4. Uklejewski R, Winiecki M, *et al.*, ESB2015 Conference Proceedings. Abstract ID: ID: 0257\_0303.

### ACKNOWLEDGMENTS

The work supported by the Polish Ministry of Science in the Research Project no. NN518412638: “The thermochemical surface modification of preprototypes of the minimally invasive hip RA endoprostheses and porous intraosseous implants” (Head: R. Uklejewski).



# Analysis of Osteoinductive Properties of Combinations of Macroporous Ceramic (MBCP+™), Simvastatin, rhBMP-2, and BMSC in a Femoral Critical Size Induced Membrane Model in Rats

Erwan de Monès<sup>1,2,3</sup>, Silke Schlaubitz<sup>4</sup>, Reine Bareille<sup>1,2</sup>, Lionel Couraud<sup>4</sup>, Jean-Christophe Fricain<sup>1,2,5</sup>

<sup>1</sup>INSERM U1026, Tissue Bioengineering, 146 rue Léo-Saignat, F-33000 Bordeaux, France

<sup>2</sup>University of Bordeaux, 146 rue Léo-Saignat, F-33000 Bordeaux, France

<sup>3</sup>Department of Otolaryngology, Univ. Bordeaux, Place Amélie Raba Léon, F-33000 Bordeaux, France

<sup>4</sup>Bordeaux University Hospital, CIC, PTIB, Xavier Arnoz Hospital, Avenue Haut Lévêque, F-33000 Bordeaux, France

<sup>5</sup>Department of Dentistry, Univ. Bordeaux, Place Amélie Raba Léon, F-33000 Bordeaux, France

[erwan.de-mones-del-pujol@chu-bordeaux.fr](mailto:erwan.de-mones-del-pujol@chu-bordeaux.fr)

## INTRODUCTION

Induced membrane technique has been first proposed by Masquelet and his collaborators for wide segmental diaphysal bone reconstruction with autologous cancellous bone graft [1]. Historically, a PMMA spacer is placed in a bone defect to prevent fibrous ingrowth into the site and to induce the formation of a cavity surrounded by the induced membrane that can be filled with a graft in a second surgical intervention. Induced membrane technique can be applied for two-staged bone reconstruction in carcinologic context with irradiation. To reduce donor site morbidity following bone harvest, synthetic bone substitutes in combination or not with bone morphogenetic protein 2 (BMP-2) to the graft were proposed. Statins were investigated in numerous studies showing an enhanced expression of BMP-2 mRNA and osteoblastic differentiation *in vitro* and *in vivo*. The aim of this study was to evaluate the osteogenic properties of several combinations of grafts and the osteoinductive capacity of simvastatin in comparison to BMP-2 in an induced membrane filled with a HA/  $\beta$ -TCP bone substitute (MBCP+™) in association with bone marrow allografts in a segmental, critical size femoral rat defect. Furthermore, the stability of a semi-flexible silicone spacer for membrane induction was tested in this model.

## EXPERIMENTAL METHODS

36 Wistar RjHan rats received an osteosynthesis plate that was fixed on the anterior surface of the femur with two cortical screws (all SYNTHES, Solothurn, Switzerland). The osteosynthesis plate was removed, a segmental defect of 6 mm length was created and the silicone spacer (A-H, see table below) was placed in the defect site and stabilized with stiches against the metal plate. Rats of two conditions (E, F) received radiotherapy (50 Gy over 5 weeks). Bone marrow and spongy bone allografts were harvested from long bones and condyles of same strain rats.

Condition	MBCP+™	Total bone marrow	BMP-2 (InductOs®)	Simvastatin	radiotherapy (50Gy)	spongy bone	cavity not filled	no spacer implantation after defect
A	x							
B	x	x						
C	x	x	x					
D	x	x		x				
E	x	x	x		x			
F	x	x		x	x			
G						x		
H							x	
I								x

Bone mineral densities (BMD), as well as the overall stability of the model, were investigated by  $\mu$ CT scanning and X-ray acquisition. The percentages of collagenous and osteoid tissue within the induced membrane were measured with adapted software from histological sections.

## RESULTS AND DISCUSSION

Overall, conditions that received the silicone spacer in the first surgical and MBCP+™ in the second intervention showed the highest stability. Osteosynthesis plates stayed straight and the distance between the screws stayed stable within the group. Only in conditions that were left empty after membrane induction and after defect creation (H and I), osteosynthesis plates bended, so that the distance between the screws was significantly reduced in comparison to the other seven conditions. There was no significant difference in BMD within the six conditions with MBCP+™. Only the non-irradiated condition with BMP-2 (C) showed a significant increase in BMD in comparison to the control conditions (G-I). Measurements of collagenous content within MBCP+™ filled induced membrane indicated a significantly lower percentage for the non-irradiated condition with BMP-2 (C) in comparison to 3 other conditions. When investigating the osteoid percentage, the two conditions with BMP-2 (C, E) showed significantly increases in comparison to the material by itself (A), or associated with total bone marrow (B). In comparison, conditions with simvastatin (D, F) showed more fibrosis and less osteoid tissue, BMD and stability were comparable with BMP-2 containing conditions. Irradiation did not influence the evaluated factors.

## CONCLUSION

Conditions with BMP-2 showed a high stability, the highest mineral content, the lowest fibrosis and a high present of osteoid tissue. In comparison with simvastatin, BMP-2 seems to favour bone regeneration in our segmental femoral model in rats.

## REFERENCES

1. Masquelet *et al.*, The Orthopedic Clinics of North America 2010;41:27–37

## ACKNOWLEDGMENTS

The authors would like to thank the programmes of “Gueules Cassées” (Grant GC27-2011) and “Fondation Avenir” (Grants ET1-632 and ET2-666) for their financial support.





## The Influence of Calcium Phosphate Microparticle Incorporation in Highly Orientated Macroporous Collagen Scaffolds on the Mechanism of Bone Defect Healing

Ansgar Petersen<sup>1</sup>, Hans Leemhuis<sup>2</sup>, Andreas Hoess<sup>3</sup>, Agnes Ellinghaus<sup>1</sup>, Berthold Nies<sup>3</sup>, Ingo Heschel<sup>2</sup>, Georg N. Duda<sup>1</sup>

<sup>1</sup>Julius Wolff Institute and Berlin-Brandenburg Center for Regenerative Therapies,  
Charité – Universitätsmedizin Berlin, Germany

<sup>2</sup>Matricel GmbH, Herzogenrath, Germany

<sup>3</sup>InnoTERE GmbH, Radebeul, Germany

[ansgar.petersen@charite.de](mailto:ansgar.petersen@charite.de)

### INTRODUCTION

Next generation biomaterials supporting bone regeneration are expected to mimic callus properties and guide cell behavior towards functional tissue formation rather than providing properties of intact bone tissue [1]. This study aims at combining A), a previously developed macroporous biomaterial scaffold with a highly orientated pore architecture for guided tissue growth, and B), calcium phosphate (CaP) microparticles for improved bioactivity. The influence of the mechanical and geometrical properties of this biomaterial scaffold as well as the biological response to CaP incorporation were investigated under *in vitro* and *in vivo* conditions.

### EXPERIMENTAL METHODS

Fine  $\alpha$ - and  $\beta$ -tricalcium phosphate (TCP) particles were prepared by solid state synthesis and subsequent milling. Hydroxyapatite (HAp) powder was synthesized via a wet-chemical process. All three calcium phosphates had comparable particle size distributions and mean particle sizes smaller 10 $\mu$ m. Powder X-ray diffraction (XRD) confirmed high phase purity and crystallinity of both  $\alpha$ - and  $\beta$ -TCP, whereas the HAp powder was mainly amorphous. Highly orientated collagen scaffolds were produced by directional solidification, freeze-drying and chemical crosslinking. CaP microparticles were incorporated avoiding any impairment of pore geometry and CaP properties. Structural characteristics of the scaffolds were analyzed via scanning electron microscopy. Using human primary fibroblasts, *in vitro* cell organization and ECM formation inside collagen/CaP hybrid scaffolds were studied longitudinally via (immune)histology and confocal/multiphoton microscopy up to 14 days. Gene expression patterns related to osteogenic differentiation of human mesenchymal stromal cells (hMSCs) were analyzed after 7 days of culture in the scaffold prototypes via real time quantitative PCR. Finally, *in vivo* bone formation in a 5mm critical sized defect in rats was quantified via  $\mu$ -CT analysis (newly formed bone) and histomorphometry (callus composition).

### RESULTS AND DISCUSSION

Mineral particles were uniformly distributed after incorporation in the highly orientated collagen-I scaffolds. No pronounced alteration of scaffold inner architecture (pore size, pore orientation and geometry) was observed while maintaining the high porosity (>98%). Fibroblasts showed an increasing degree of alignment over time resulting in a highly anisotropic

network of newly formed fibronectin at day 14 in the hybrid scaffolds comparable to CaP free collagen scaffolds. However, formation of fibrillar collagen was delayed in hybrid scaffolds as a consequence of the changed microenvironment. Strongest upregulation of osteogenic genes like alkaline phosphatase (ALP), osteocalcin (OC), and osteopontin (OP) was induced by HAp particles compared to  $\alpha$ - and  $\beta$ -TCP and osteogenic medium. This may be attributed to the very high specific surface of HAp (>80m<sup>2</sup>/g) compared to the TCP's (approx. 1m<sup>2</sup>/g), which seemed to outbalance its lower solubility ( $\alpha$ -TCP >  $\beta$ -TCP > HAp). Even though HAp microparticles showed to be effective in enhancing MSC differentiation towards the osteoblast lineage under *in vitro* conditions, no increase in volume of newly formed bone was observed in the bone defect model. At the same time cartilage was completely absent at 6weeks in any of the three hybrid scaffold types in contrast to the pure collagen scaffolds. It was concluded that the bioactivity of CaP particles in the highly orientated collagen scaffold structure favors osteogenic processes but suppresses cartilage formation *in vivo*. Thus the particles seemed to induce a switch in the mechanism of bone tissue formation from endochondral to intramembranous ossification. While the mineralized callus was observed to infiltrate the scaffold material for the pure collagen scaffold, the incorporation of CaP particles leads to a more periosteal bone formation.

### CONCLUSION

The induced alterations in bone formation highlight the role of the concerted interactions between structural, mechanical and chemical signals for healing of large bone defects. The gained knowledge will help to develop biomaterial approaches that mimic the early phases of endogenous callus formation for efficient bone formation. This seems to be a promising alternative to common approaches mimicking the mechanical and chemical properties of intact bone tissue.

### REFERENCES

[1] Willie & Petersen et al., Soft Matter, 2010, 6, 4976-4987.

### ACKNOWLEDGMENTS

The authors acknowledge financial support by the German Federal Ministry of Education and Research (BMBF grants no.13N12154, 13N12152 and 13N12518).



## Preparation of a Small Diameter Decellularized Blood Vessel Covered with SPU Fibers by Electrospinning

Tsuyoshi Kimura<sup>1</sup>, Hiroko Morita<sup>1</sup>, PingLi Wu<sup>1</sup>, Naoko Nakamura<sup>1</sup>, Kwangwoo Nam<sup>1</sup>,  
Toshiya Fujisato<sup>2</sup>, Akio Kishida<sup>1</sup>

<sup>1</sup> Institute of Biomaterials and Bioengineering, Tokyo Medical and Dental University, Japan

<sup>2</sup> Department of Engineering, Osaka Institute of Technology, Japan

[kimurat.mbme@tmd.ac.jp](mailto:kimurat.mbme@tmd.ac.jp)

### INTRODUCTION

Cardiovascular diseases (CVDs) are accounting for nearly one-third of deaths worldwide. For CVDs treatment, it is expected to develop small diameter blood vessels. Previously, the artificial small diameter blood vessels have been developing [1, 2]. Recently, novel small diameter blood vessels were investigated by using tissue-engineering technologies, such as cell sheet engineering, 3D bio-printer and decellularized tissue. Our group also have developing decellularized blood vessel using high hydrostatic pressure (HHP) technology. The in vivo good performance of the HHP-decellularized aorta and carotid artery was demonstrated due to the good preservation of the basement membrane of the HHP decellularized arteries [3,4]. While the HHP decellularized carotid artery is a candidate of small diameter blood vessels, it is short length for clinical usage. In this study, the HHP decellularized aorta was fabricated to make a small diameter blood vessel having long length. The electrospinning technology was used to control the strength of small diameter blood vessels for various applications.

### EXPERIMENTAL METHODS

Fresh porcine aorta was purchased from a local slaughterhouse (Tokyo Shibaura Zouki, Japan). The intima-media (300-500  $\mu$ m) of aorta was peeled and treated with HHP at 10,000 atm for 15 min and washed with saline containing DNase. The decellularization of aortic intima-media was evaluated by hematoxylin and eosin (H & E) staining and residual DNA quantification.

Segmented polyurethane (SPU, Pellethane® 2363-80AE) was used. SPU solution in THF/dioxane of 100/1 was prepared at various concentrations. The decellularized intima-media was rolled onto a mandrel (4 mm diameter, 150 mm length). The mandrel was set on our original rotating collector (Fig. 1). Nanofibers were electrospun to the outside surface of decellularized intima-media. The obtained small diameter decellularized blood vessel covered with electrospun nanofibers was investigated by SEM observation, mechanical strength test.

### RESULTS AND DISCUSSION

The optimal electrospinning condition of SPU was decided and the diameter of SPU fibers with 0.3-1.5  $\mu$ m was obtained. The decellularization of the intima-media of aorta by HHP method was confirmed using H & E stain and DNA quantification. Using our original electrospinning apparatus, the small diameter blood vessel covered with SPU fibers was obtained. Figure 2 shows macro and micro graphs of the small diameter

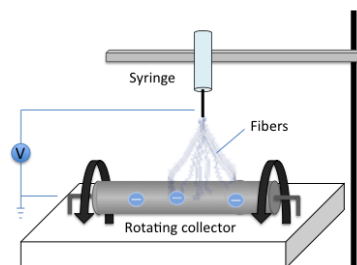


Figure 1. The schematic diagram of electrospinning apparatus for preparation of a small diameter decellularized blood vessel.

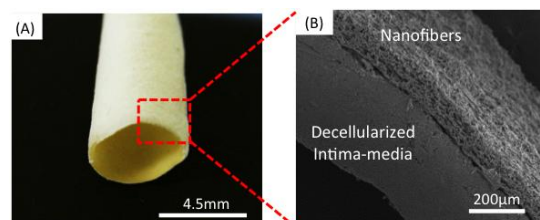


Figure 2 The obtained small diameter decellularized blood vessel. (A) Macro-image and (B) SEM image.

decellularized blood vessel with SPU fibers. The outer and inner layers were SPU fibers and decellularized intima-media, respectively. The SPU fibers were covered on the tissue surface with the homogenous thickness and a porous 3-dimension structure. The physical properties of small diameter decellularized blood vessel were similar to that of native carotid artery when the SPU fibers layer was adjusted (data not shown).

### CONCLUSION

In this study, the small diameter blood vessels composed of decellularized intima-media of aorta and electrospun SPU fibers was obtained.

### REFERENCES

1. Yoneyama T. *et al.*, J. Biomed. Mater. Res. 43:15-20, 1998
2. Bhattacharjee *et al.*, Blood 95:581-585, 2000
3. Fujisato T. *et al.*, Cardiovascular Regeneration Therapies Using Tissue Engineering Approaches, Tokyo: Springer, Tokyo, pp. 83-94, 2005
4. Negishi J. *et al.*, J Artif Organs. 14:223-231, 2011

### ACKNOWLEDGMENTS

The authors would like to thank the Grants-in-Aid (B) from The Ministry of Education, Culture, Sports, Science and Technology (MEXT), Japan for providing financial support to this project.

## Blend Electrospinning of Biodegradable Chitosan/Polycaprolactone Fibers as a Process to Create Scaffolds for Cardiovascular Tissue Engineering

Alexandros Repanas<sup>1</sup>, Birgit Glasmacher<sup>1</sup>, Alexandra Theodoropoulou<sup>2</sup>, Dimosthenis Mavrilas<sup>2</sup>

<sup>1</sup>Institute for Multiphase Processes, Leibniz University Hannover, Germany

<sup>2</sup>Laboratory of Biomechanics & Biomedical Engineering, Mechanical Engineering & Aeronautics, University of Patras, Greece

[mauril@mech.upatras.gr](mailto:mauril@mech.upatras.gr)

### INTRODUCTION

Cardiovascular diseases are the main cause of death worldwide with the cost of treatment for the patients expected to surpass 1.5 trillion dollars only in the USA by 2030 according to the American Heart Association <sup>1</sup>. Besides heart transplantation, there have been developed several therapeutic strategies including the design of biological, polymeric and hybrid bio-artificial scaffolds. These scaffolds can mimic the extra-cellular matrix (ECM) enabling cells to repopulate a site in the heart that has been damaged and new tissue to grow. Electrospinning is a facile and cost-effective technique that can produce 3D biocompatible structures to serve as extracellular matrix (ECM)-like scaffolds where cells can be seeded and proliferate eventually forming a hybrid bio-artificial tissue <sup>2</sup>. Fibrous mats, tubes and more complex 3D shapes can be successfully engineered not only to induce cell proliferation but also to release in a controllable manner biomolecules (e.g. proteins, growth factors) that can further support tissue formation <sup>3</sup>.

### EXPERIMENTAL METHODS

Polycaprolactone (PCL) and chitosan (CS) were dissolved as a blend in 99.8% acetic acid (AAC) at concentrations of 190 mg/ml and 12.5 mg/ml respectively. Electrospinning was performed at a custom made apparatus, at temperature and relative humidity of  $23 \pm 1$  °C and  $35 \pm 5\%$ , respectively. Structural and morphological analysis of the collected fiber mats was performed by scanning electron microscopy (SEM) while the samples were previously sputter-coated with gold for better quality imaging. Cyclic sinusoidal uniaxial mechanical tests were performed with an electroforce dynamic tensile testing system by BOSE®, equipped with a 200 N load cell. Rectangular, 15x10 mm strips were cut and tested at 0-30% strain, 1 cycle/sec, RT, dry conditions. The applied force and the local principal strain were monitored and stress/strain data was computed. Mechanical properties like Young's modulus (the elastic modulus at high slope - post transition phase - linear portion of stress/strain curve) were evaluated<sup>4</sup>. A nano-indentation system based on an atomic force microscope (AFM) apparatus with a special tip was used to examine the hardness of the samples and the Young's modulus. Each sample was tested in 15 different sites using 100 & 500 µN force. Static water contact angle experiments were performed to study the nature of the fibers' surface and its hydrophilicity. Chemical characterization including Fourier-Transformed Infrared Spectroscopy (FTIR) and X-rays diffraction (XRD) was carried out in order to

determine the physicochemical state of the polymeric compounds in the fibers. Statistical analysis was performed using Origin Pro 8.5 and IBM SPSS Statistics v.21 (One-way ANOVA with post-hoc Tukey/Bonferroni) and statistical differences were considered significant if  $p < 0.05$ .

### RESULTS AND DISCUSSION

Structural and morphological analysis indicated that the created fibers have a smooth, "spaghetti-like" shape with an average diameter of  $2.42 \pm 0.38$  µm and an average pore size of  $8.27 \pm 0.83$  µm<sup>2</sup> with random orientation. The average values of Young's modulus and stiffness calculated from the nano-indentation studies were  $31.55 \pm 1.52$  MPa and  $3.76 \pm 0.11$  MPa when the applied force was 500µN and  $61.29 \pm 4.25$  MPa and  $6.28 \pm 0.63$  MPa for the 100µN applied force. The hysteresis ratio  $h$  was  $0.46 \pm 0.10$  revealing the viscoelastic nature of the fibers. The surface of the fiber-mats can be considered relatively hydrophilic as the static water contact angle was  $74.5 \pm 2.5$  °. FTIR and XRD data lead to the conclusion that PCL and CS interact in the blend, possibly forming non-covalent bonds with PCL being in a semi-crystalline state and CS in an amorphous form in the fibers.

### CONCLUSION

The experimental results showed that the polymeric fiber mats can be considered as suitable candidates for bio-artificial scaffolds in order to enable cell seeding, proliferation and repopulation of a damaged tissue after a cardiovascular incident.

### REFERENCES

1. Go A.S. et al. Circulation 2013;127:143-152
2. Szentivanyi A. et al. International Journal of Artificial Organs 2011;34(10):986-997
3. Szentivanyi A. et al. Advanced Drug Delivery Reviews 2011;63:209-220.
4. Mavrilas D. et al., Journal of Biomechanics 2005; 38:761-768

### ACKNOWLEDGMENTS

The authors like to thank Prof. Dr.-Ir. Willem F. Wolters from the Institute for Multiphase Processes for his contribution to the analysis of the FTIR data. This study was partially granted by the Deutsche Forschungsgemeinschaft (DFG German Research Foundation) by the Cluster of Excellence REBIRTH (From Regenerative Biology to Reconstructive Therapy, DFG EXC 62/1).



Daniel Cohn<sup>1</sup>, Randa Abbas, Fany Widlan, Matthew Zarek, Ram Malal, Allan Bloom<sup>2</sup>

<sup>1</sup>Institute of Chemistry, The Hebrew University of Jerusalem, Jerusalem, Israel

<sup>2</sup>Vascular and Interventional Radiology, Hadassah University Medical Center, Jerusalem, Israel

[dcohn18@gmail.com](mailto:dcohn18@gmail.com)

## INTRODUCTION

The formation of aneurysms is an extremely dangerous degenerative pathology of arterial tissues, especially common in adult and elderly populations, whereby the wall of the artery weakens locally and largely expands. Aortic Abdominal Aneurysms (AAA), are the most common and fatal type of aneurysms.

Until 1991, the only treatment available entailed an open surgical procedure, whereby the dilated segment of the artery was replaced by an artificial vascular graft. In the early nineties, endografts consisting of a modified vascular prosthesis mounted on a stent and deployed intra-luminally at the aneurysmal site using a balloon, were introduced. Unfortunately, several factors restrict significantly the use of these devices. Most importantly, anatomical constraints that largely limit the access to the aneurismal site often prevent the use of the endograft.

This lecture introduces a polymeric device for AAA treatment that is deployed intra-luminally at the aneurismal site and then expanded so it tightly attaches to the aorta, proximally and distally to the aneurysm.

The implantation of these devices is divided into two parts: {a} the insertion through the iliac artery, the navigation to the site and the expansion stages, during which flexibility is critical, and {b} its performance at the aneurismal site, where the device is required to display appropriate mechanical properties.

Two strategies were pursued: (1) The device is thermally softened using a balloon filled with warm saline, so it can be easily expanded, followed by its firm and conformable attachment to the arterial wall, proximally and distally to the aneurysm. While in its expanded configuration, the endograft is then cooled down to 37°C and attains the mechanical properties required. (2) The endograft consists of an Expandable Component (EC) and a “Smart” Component (SC), with the latter being present within the former. The SC is a low molecular weight, polymerizable or crosslinkable precursor that fulfills two different roles: {a} It acts as a plasticizer of the EC during the early stages of the procedure (navigation and expansion), rendering it with the required flexibility, and, {b} It stiffens the device after its expansion and attachment to the vessel wall, once it polymerizes or crosslinks, imparting to the endograft the necessary mechanical properties.

## EXPERIMENTAL METHODS

PEU thermoplastic elastomers softening between 50 and 60 degrees were used when following the first strategy, while poly(meth)acrylates and PEsUs performed as the EC, and methacrylates such as hydroxyethyl methacrylate

(HEMA) were used as the SC. The various polymers were characterized by NMR, DSC, GPC and their mechanical properties were determined using an Instron Universal Testing Machine. Their ex-vivo performance was assessed in a cadaveric pig aorta segments and the acute *in vivo* feasibility of the device was evaluated by implanting it in a pig for eight hours.

## RESULTS AND DISCUSSION

Following the basic working concept of this study, various expandable conduits were generated, differing in their composition, their mechanical properties, their expandability ratio, and the technique used to produce them. As an example, an elastomeric PEsU was blended with hydroxyethyl methacrylate (HEMA) at different concentrations. HEMA molecules soften the PEsU EC during the early stages of the procedure, and remarkably stiffen it when polymerization takes place (Fig. 1), after the device is expanded and tightly attached to the aortic wall, proximally and distally to the aneurismal sac.

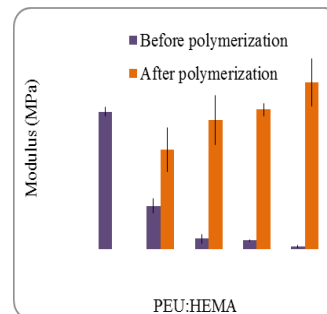


Figure 1. Mechanical behavior of a PEsU/HEMA device.

The expandability of the devices created was demonstrated in both cadaveric pig aorta sections and in an acute *in vivo* experiment in a pig. This was also demonstrated by measuring the displacement force required to pull out our device (~45N), well above devices presently in clinical use (4.5-25 N)<sup>1</sup>.

## CONCLUSION

The *in vivo* Proof of Principle of these devices, namely their ability to be deployed and inflated at the aneurismal site, following minimally invasive procedures that are routinely used in the clinic, and generate a stable and safe conduit, was demonstrated *in vitro* and acutely (eight hours) in the abdominal aorta of pigs

## REFERENCES

1. Resch, T. et al Eur. J. Vasc. Endovasc. Surg., 2000, 20, 190-195.



## Mechanical Characterization of Small Diameter Grafts Made of Segmented Polyurethanes Based on Alkaline Aminoacids

O. Castillo-Cruz<sup>1</sup>, F. Avilés<sup>1</sup>, R. Vargas-Coronado<sup>1</sup>, J. M. Cervantes-Uc<sup>1</sup>, J. V. Cauich-Rodríguez<sup>1</sup>, L. H. Chan-Chan<sup>2</sup>

<sup>1</sup>Centro de Investigación Científica de Yucatán, Mérida, Yucatán, México

<sup>2</sup>Departamento de Física, Universidad de Sonora-Cátedras-CONACYT, Hermosillo, Sonora, México  
[jvcr@cicy.mx](mailto:jvcr@cicy.mx)

### INTRODUCTION

Cardiovascular related diseases such as coronary artery disease, cardiomyopathy, valvular disease, etc. are currently the main cause of death worldwide. However, nowadays there is no effective biomaterial to treat these diseases, especially as small-diameter (<6 mm) bypass grafts<sup>1</sup>. Among the synthetic polymers used in the cardiovascular area, segmented polyurethanes (SPUs) have played a significant role due to their excellent mechanical properties as well as relatively good biocompatibility<sup>2</sup>. However, when used as small diameter vascular graft one of the key factors that need to be considered is the matching of their mechanical properties with the host artery/vein in order to avoid hyperplasia in the anastomoses. In turn, thrombosis of vascular grafts results in a change of mechanical properties promoting early graft failure<sup>3</sup>. Therefore, an artificial vascular graft device has to comply with either ISO 7198 or ANSI/AAMI VP20-1994 standards for vascular graft prosthesis<sup>4</sup>. Recently, our group reported that the use of segmented polyurethanes based on amino acids promotes the growth of endothelial cells<sup>5</sup>. In order to fully assess their performance, in this study we present the mechanical characterization of small diameter vascular grafts made of SPUs based on alkaline amino acids.

### EXPERIMENTAL METHODS

SPUR and SPUK were synthesized by the reaction of poly ( $\epsilon$ -caprolactone) diol (PCL) with an excess of 4,4'-methylene-bis-cyclohexyl diisocyanate (HDMI) in the first step and then extended with L-Arginine (R) or L-Lysine (K) respectively<sup>5</sup>. Small diameter vascular grafts were obtained after wrapping an SPU film around 5.5 mm diameter mandrel. Films and small caliber vascular grafts were characterized by FTIR, DSC, TGA and AFM while their mechanical properties were assessed following ISO 7198 in terms of longitudinal and circumferential tensile strength, probe burst strength and suture retention strength. Tecoflex™ (LifeSciences) was used for comparison purposes.

### RESULTS AND DISCUSSION

FTIR showed urethane group absorptions at 3300 cm<sup>-1</sup> (NH) and at 1525 cm<sup>-1</sup> (-NHCOO-) <sup>1</sup> and C=O from the PCL at 1730 cm<sup>-1</sup>. Through DSC these polymers exhibited Tm=49.6°C and 47.8°C for SPUR and SPUK respectively. TGA thermograms indicate that the first mass loss occurs at 348°C and 426°C for SPUK and SPUR whereas a second decomposition occurred at 455°C and 520°C, respectively. AFM showed that the internal surfaces of SPUK and Tecoflex have a higher roughness than the outer surface of the vascular grafts. In general, films' elastic moduli were similar (6.4, 6.3

and 6.2 MPa for SPUR, SPUK and Tecoflex) but a difference was observed in their longitudinal (Table 1) and circumferential (Table 2) modulus (E) and strength ( $\sigma_{break}$ ). These values are higher than the iliac artery (0.4-0.77 MPa) and iliac vein (1.8-5.3 MPa) for longitudinal tension but similar to iliac vein (1.3-4.8 MPa) and iliac artery (4.8-6.3 MPa) for circumferential tension. In addition, probe burst strength was higher in Tecoflex (25.5±5.60 N) than SPUR (9.9±4.95 N) but similar to SPUK (24.4±4.45). Finally, SPUK exhibited lower suture retention strength than SPUR (18 N vs 14 N) but this was higher compared to the resistance to suture in native arteries 2.7 N<sup>6</sup>. These values also depended on the type of suture material. In general it was lower when 3-0 silk was used instead of 2-0 nylon.

**Table 1 Longitudinal tensile properties of SPUR and SPUK**

Sample	E (MPa)	$\sigma_{break}$ (MPa)	$\epsilon_{max}$ (%)
PUUR	5.53 ± 0.99	7.90 ± 1.97	564 ± 60
PUUK	4.34 ± 0.55	1.70 ± 0.19	339 ± 82
Tecoflex	6.65 ± 1.25	11.1 ± 1.95	563.7 ± 39

**Table 2 Circumferential tensile properties of SPUR and SPUK**

Sample	E (MPa)	$\sigma_{break}$ (MPa)	$\epsilon_{max}$ (%)
PUUR	3.76 ± 0.77	985 ± 352	679 ± 43
PUUK	4.44 ± 1	673 ± 245	396 ± 142
Tecoflex	4.22 ± 1.34	1730 ± 380	862 ± 130

### CONCLUSION

Small diameter vascular grafts were made from PUs based on amino acids of L-Arginine and L-Lysine. The mechanical properties of the synthetic grafts showed differences between the longitudinal and transverse directions, suggesting anisotropy. These findings in addition to good endothelial cell biocompatibility suggest them as good candidates for use as vascular grafts.

### REFERENCES

1. Wise, S. G. *et al.* *Acta biomater* 7, 295–303, 2011.
2. Han, J. *et al.* *J Biomed Mater Res Part A* 96, 705–14, 2011.
3. Puskas, J. E. *et al.* *American Chemical Society* 5, 2004.
4. Barron, V. *et al.* *Annals of Biomedical Engineering* 31, 1017–1030, 2003.
5. Chan-Chan, L. H. *et al.* *J Mater Sci: Mater Med* 24, 1733–44 (2013).
6. Niklason, L. E. *et al.* *Science* 284, 489–93, 1999.

### ACKNOWLEDGMENTS

The authors wish to thank CONACYT for financial support (Grant 79371).



James Dugan and Frederik Claeysens

Department of Materials Science and Engineering, The University of Sheffield, Sheffield, UK.

[j.dugan@sheffield.ac.uk](mailto:j.dugan@sheffield.ac.uk)

## INTRODUCTION

The development of electrodes for direct interface with the brain has the potential to greatly improve prostheses to aid victims of spinal injury or similar disablement. However, the development of such electrodes relies on careful engineering of the biological-electronic interface with control of scarring, cell phenotype and tissue organisation. Diamond-like-carbon (DLC) may be an ideal material for coating electrodes as it has flexible electrical properties, it is extremely stable *in vivo* and is already used as a coating for orthopaedic implants<sup>1</sup>. Chemical modification is essential, however, to control and promote adhesion, differentiation and organisation of neurons and glia. A combination of atom transfer radical polymerisation (ATRP) and pulsed laser ablation was used to modify the surface properties of DLC with a high degree of spatial control.

## EXPERIMENTAL METHODS

DLC was coated on silicon by chemical vapour deposition. The surface chemistry of the DLC was modified by atom transfer radical polymerization (ATRP) in order to produce PEG-coated non-cell-adhesive surfaces. Patterns were generated by pulsed laser ablation using a sub-nanosecond pulsed Nd YAG DPSS laser focused onto the sample surface which was translated using a programmable three-axis translation stage. The functionalised and ablated DLC surfaces were characterised by contact angle measurement, XPS and Raman spectroscopy.

NG108 neuron-like cells were seeded to the DLC samples and allowed to differentiate for 7 days. Rat neural stem cells (NSCs) were isolated from E18 embryos and cultured in the presence of bFGF and EGF before being seeded to the DLC samples. Growth factors were withdrawn and spontaneous differentiation was allowed for 25 days in Neurobasal/B27 medium. Morphology, phenotype and neuritogenesis were investigated using immunocytochemistry.

## RESULTS AND DISCUSSION

Upon functionalisation with PEG brushes the DLC became more hydrophilic. The modified surfaces were non-fouling and resisted the adsorption of laminin from solution. Pulsed laser ablation removed the top layer of material from the region directly irradiated by the laser. In addition, a region surrounding the ablated region (the heat affected zone) was also modified and ceased to be non-fouling. Polyornithine and laminin were then adsorbed onto the ablated regions, allowing subsequent cell adhesion.

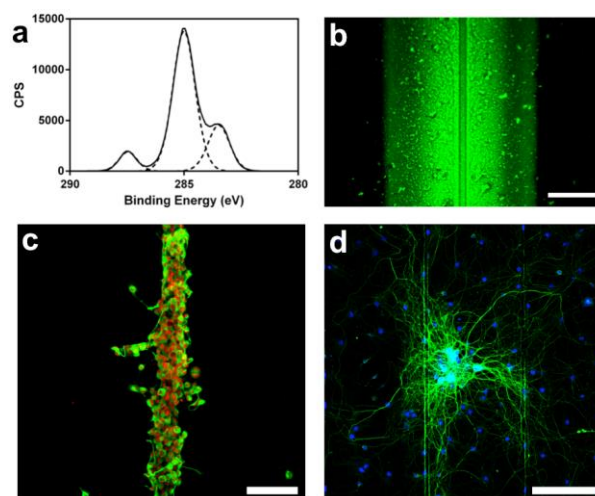


Fig.1 – (a) XPS C 1s spectrum of DLC functionalised with PEG brushes by ATRP. (b) Fluorescence micrograph of FITC-labelled laminin adsorbed on ablated track. Scale = 25  $\mu\text{m}$  (c) Differentiating NG108 cells stained for  $\beta 3$ -tubulin (green) and TOPRO3 (red). Scale = 200  $\mu\text{m}$  (d) Differentiating rat NSCs stained for  $\beta 3$ -tubulin (green) and DAPI (blue). Scale = 100  $\mu\text{m}$ .

NG108 cells and NSCs adhered onto ablated tracks and adopted oriented morphologies. Upon differentiation the NG108s expressed  $\beta 3$ -tubulin and remained confined to the ablated tracks. In contrast, over time the NSCs differentiated but broke free of the ablated tracks and populated the entire ablated region. However, extremely long neurites were observed to follow the topographical cues from the ablated tracks over several hundred micrometres.

## CONCLUSION

Spatial control over neuron cell adhesion and differentiation was achieved on DLC using a combination of ATRP and pulsed laser ablation. Both NG108s and NSCs were constrained within ablated tracks and adopted elongated morphologies. Over 25 days the NSCs differentiated and spread over the DLC surface, although long neurites tracked along the ablated features over long distances demonstrating the potential for preparing *in vitro* neural networks on DLC with a great degree of control.

## REFERENCES

1. Regan, EM *et al.* Biomaterials (2010), 31, 2, 207-215.

## ACKNOWLEDGMENTS

We are grateful to the Engineering and Physical Sciences Research Council (EPSRC) for funding this project.

# Electrochemically Assisted Deposition of Strontium Modified Magnesium Phosphate on Titanium Surfaces

Markus Meininger<sup>1</sup>, Julia Zerweck<sup>1</sup>, Cornelia-Wolf-Brandstetter<sup>2</sup>, Uwe Gbureck<sup>1</sup>, Jürgen Groll<sup>1</sup>, Claus Moseke<sup>1</sup>

<sup>1</sup>Department for Functional Materials in Medicine and Dentistry, University of Würzburg, Germany

<sup>2</sup>Institute of Materials Science, Max Bergmann Center of Biomaterials, Technische Universität Dresden, Germany

[claus.moseke@fmz.uni-wuerzburg.de](mailto:claus.moseke@fmz.uni-wuerzburg.de)

Electrochemically assisted deposition (ECAD) (see Figure 1) was utilized to produce dense struvite coatings on titanium. The coatings were modified by incorporation of strontium ions and characterized regarding their physicochemical properties, ion release kinetics, and biocompatibility.

## INTRODUCTION

Despite the generally good success rates of enossal implants concerning healing and retention time there is still a need for further improvements, particularly for use in more challenging situations, e.g. in the case of a weakened osseous bed, caused by systemic diseases like osteoporosis. The aim of this study was the functional modification of biocompatible struvite coatings on titanium discs with strontium ions, in order to reduce osteoclast activity in affected bone regions.

## EXPERIMENTAL METHODS

The aqueous coating electrolytes for struvite deposition were composed of 1.9167 g ammonium dihydrogen phosphate, 1.0075 g magnesium oxide, and 3.3 g nitric acid, dissolved in a total volume of 500 ml. Doping with Sr ions was achieved by addition of various amounts of strontium nitrate (0.0135-2.706 g) to the electrolyte. In addition, the total amount of deposited struvite was adjusted by variation of the coating parameters current density and deposition time.

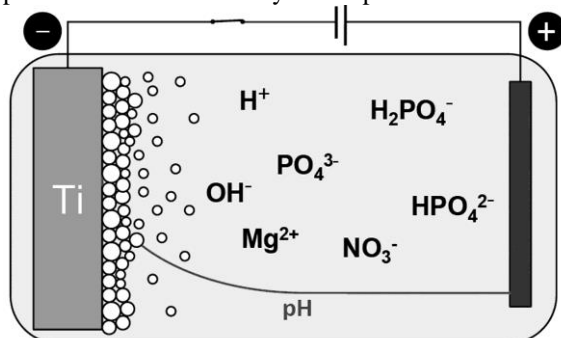


Figure 1: Principle of ECAD in aqueous electrolyte.

The resulting coatings were characterized by scanning electron microscopy (SEM) with a Zeiss DSM 940 regarding their surface morphology. Phase analysis was performed by X-ray diffraction (XRD) with a Siemens D5005 powder diffractometer in Bragg-Brentano geometry using  $\text{CuK}_\alpha$  radiation with a voltage of 40 kV and a current of 40 mA. The Sr content of the deposited struvite was determined by dissolving the coatings in nitric acid and elemental analysis by inductively coupled plasma mass spectrometry (ICP-MS). ICP-MS was also used to examine the release kinetics of Mg, Sr,

and phosphate ions as well as the chemical behaviour in synthetic body fluid (SBF).

## RESULTS AND DISCUSSION

A total coating mass of  $1.3 \text{ mg/cm}^2$  was achieved with a current density of  $-3.8 \text{ mA/cm}^2$  being applied for 25 min. Sr contents up to 14.4 wt.% could be reached. Sr ions were released from the doped coatings over 14 days of immersion in SBF with a total released amount of about  $25 \mu\text{g}$  (about 55 % of the absolute strontium content in the coating). XRD and SEM analysis before and after immersion revealed the transformation of the struvite to dense coatings with hydroxyapatite-like morphology (Figure 2).

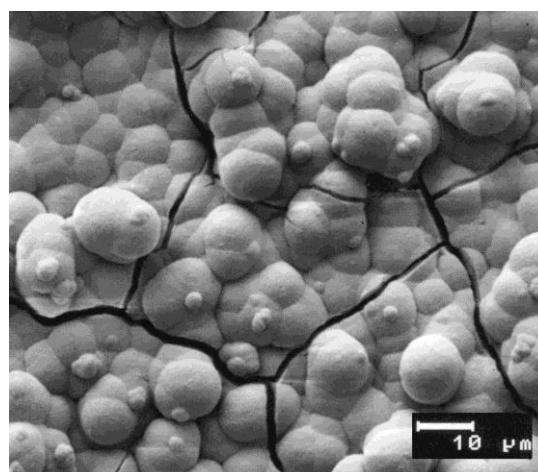


Figure 2: SEM image of Sr-doped struvite coating after 10 days immersion in SBF.

## CONCLUSION

Strontium ions were successfully co-deposited with struvite on titanium substrates. Content as well as the release kinetics of Sr ions could be varied in a wide range, which makes this method a most promising technique for the fabrication of biocompatible implant coatings with tailored and beneficial properties regarding the regulation of osteoclasts in bone tissue adjacent to the functionalized orthopaedic implant.

## REFERENCES

1. Moseke *et al.*, Adv. Eng. Mater 11(3):B1-B6, 2009

## ACKNOWLEDGMENTS

The authors wish to thank the Deutsche Forschungsgemeinschaft for their financial support (DFG MO 1728/2-1).



## Hydrothermally-Treated Nano-Crystalline TiO<sub>2</sub> Coatings Boost the “Race for the Surface” Towards Osteogenesis rather than Bacterial Adhesion

Martina Lorenzetti<sup>1</sup>, Iztok Dogša<sup>2</sup>, David Stopar<sup>2</sup>, Katrin Susanne Lips<sup>3</sup>, Reinhard Schnettler<sup>3</sup>, Mitjan Kalin<sup>4</sup>, Spomenka Kobe<sup>1,5</sup>, Saša Novak<sup>1,5</sup>

<sup>1</sup>Department of Nanostructured Materials, Jožef Stefan Institute, Ljubljana, Slovenia

<sup>2</sup>Biotechnical Faculty, University of Ljubljana, Ljubljana, Slovenia

<sup>3</sup>Laboratory for Experimental Trauma Surgery, University-Hospital of Giessen and Marburg, Giessen, Germany

<sup>4</sup>Faculty of Mechanical Engineering, University of Ljubljana, Ljubljana, Slovenia

<sup>5</sup>Jožef Stefan International Postgraduate School, Ljubljana, Slovenia

[martina.lorenzetti@ijs.si](mailto:martina.lorenzetti@ijs.si)

### INTRODUCTION

Immediately after surgery, a “race for the surface”<sup>1</sup> between cells and bacteria occurs on the exterior of body implants. Since the outcome depends on the physico-chemical properties of the inserted material, in the last few decades a lot of research has been addressed on surface modifications of Ti-based body implants. The aim is to improve the quality of the natural passivation layer, made of amorphous titanium dioxide (TiO<sub>2</sub>), by creating a higher protective interlayer at the implant-tissue interface.

### EXPERIMENTAL METHODS

The synthesis of fully-dense and stable nanocrystalline TiO<sub>2</sub>-anatase coatings can be achieved by hydrothermal treatment (HT) of different Ti-based bone implants. Such coatings showed superior topographical, mechanical and electrochemical surface properties than the bare Ti-substrates<sup>2</sup>, as well as higher hydrophilicity, especially after photo-activation by UV irradiation<sup>3</sup>.

In the present work, coatings with different crystals morphology, wettability and surface charge were used both in non-irradiated and UV pre-irradiated state, in comparison with the non-treated titanium (Ti NT).

The HT TiO<sub>2</sub>-coatings were analysed in terms of biological interactions at the biointerface.

Firstly, primary human mesenchymal stem cells (hMSCs) were cultured on the HT TiO<sub>2</sub>-coatings up to 28 days (study approved by the Local Ethics Commission, Ref. no: 245/13). The alkaline phosphatase (ALP) production and Ca<sup>2+</sup> uptake from the culture medium were probed to evaluate the cell activity and the osteogenesis process. Fluorescence and scanning electron (SEM) microscopy were also applied to observe the cell morphology and spreading.

Next, the estimation of adhesion of a green fluorescent protein-expressing *Escherichia coli* strain on the TiO<sub>2</sub>-coatings was performed after 1h of incubation in contact with the surfaces. The fraction of alive and dead bacteria adhered to the surface was estimated.

### RESULTS AND DISCUSSION

An extensive physico-chemical characterization of the HT TiO<sub>2</sub>-coating properties was performed prior any *in vitro* assessment, in order to correlate the surface properties to the biological response.

The hMSCs studies revealed the cell ability to proliferate and differentiate into osteoblasts, once

seeded upon the HT-coatings. Also, the UV pre-irradiated samples showed a significant increase in the amount and rate of osteogenesis, as demonstrated by the higher cell activity, enhanced uptake of calcium ions and formation of a well-developed mineral phase and bone-like nodules. More extended actin filament network and cell spreading were also observed. Therefore, the UV photo-induced wettability proved to be the key factor which positively influenced the cell development<sup>4</sup>.

On the other hand, the adhesion of *E. coli* in contact with the HT-substrates was largely affected by surface micro-topography, surface charges, and, least, wettability. In particular, the presence of anatase nanocrystals resulted in micro-asperities with specific width, which prevented the adhesion of *E. coli* by allowing only “contact-point” interactions with the TiO<sub>2</sub> coating. Oppositely, machined non-treated titanium surfaces provided a high surface contact area, which increased bacterial adhesion by “interlocking” effect<sup>5</sup>.

### CONCLUSION

The results suggested that the hydrothermally synthesized TiO<sub>2</sub>-anatase coatings, with adequate morphology and surface properties, stimulate the osseointegration, especially after photo-activation, and significantly reduce the bacterial adhesion on the implant surface. Therefore, hydrothermally grown TiO<sub>2</sub>-coatings have a large potential to be applied on medical devices to positively boost the bio-events at the implant interface.

### REFERENCES

1. Gristina AG., Science. 237:1588-95, 1987.
- 2 Lorenzetti M. *et al.* Materials. 7:180-194, 2014
- 3 Lorenzetti M. *et al.* Mat Sci Eng C. 37:390-8, 2014
- 4 Lorenzetti M. *et al.* J Biomater Appl. 0:1-14, 2015
- 5 Lorenzetti *et al.* ACS Appl Mater Interfaces. 7:1644–51, 2015

### ACKNOWLEDGMENTS

Funding by the European Commission within the framework of the FP7-ITN network BioTiNet (FP7-PEOPLE-2010-ITN-264635) is acknowledged.

The authors would like to thank Mrs. Olga Dakischew, Dr. Katja Trinkaus, Ms. Tjaša Stošicki for the provided support with cell cultures and bacteria experiments, respectively.





# Covalent Attached Fibronectin Fragment-PLDLLA Nanofibers on Titanium for Guiding Osteoblast Behaviour

Jordi Guillem-Martí<sup>1,2,3</sup>, Gerard Boix-Lemonche<sup>1,2,3</sup>, Dencho Gugutkov<sup>4</sup>, George Altankov<sup>4</sup>, Francisco Javier Gil<sup>1,2,3</sup>, José María Manero<sup>1,2,3</sup>.

<sup>1</sup>Biomaterials, Biomechanics and Tissue Engineering Group (BBT), Department of Materials Science and Metallurgical Engineering, Technical University of Catalonia (UPC), Barcelona, Spain.

<sup>2</sup>Biomedical Research Networking Center in Bioengineering, Biomaterials and Nanomedicine (CIBER-BBN), Spain.

<sup>3</sup>Center for Research in nanoEngineering (CRnE), Technical University of Catalonia (UPC), Barcelona, Spain.

<sup>4</sup>ICREA and Institute for Bioengineering of Catalonia (IBEC), Barcelona, Spain

[jordi.guillem.marti@upc.edu](mailto:jordi.guillem.marti@upc.edu)

## INTRODUCTION

Titanium (Ti) is the most widely used material for bone substitution due to its biomechanical properties. However, in some cases the osseointegration is not achieved due to Ti poor biological activity, ending with implant failure. Hence, several surface modifications have been proposed to improve the cellular interactions. These interactions rely on fundamental processes such as protein adsorption and ligand-receptor interactions which determine the subsequent cellular response. In order to mimic the natural interaction of cells with the extracellular matrix (ECM), several strategies are being developed. In this respect, the covering with micro- and nanofibers (NFs) produced by electrospinning are gaining interest because they mimic the spatial distribution of ECM providing ECM-like stimuli<sup>1</sup>. Polylactic acid (PLA) and their derivatives are of special interest because they are biocompatible, biodegradable and also easy to prepare. However, the cellular interaction with these materials is low and their biological improvement is required.

The aim of this study was to modify the Ti surface by generating an ECM-like structure composed of PLA derivative NFs with ECM-derived protein incorporated in order to improve the bone cell response.

## EXPERIMENTAL METHODS

Titanium discs (10 mm diameter) were polished using Al<sub>2</sub>O<sub>3</sub> suspension (0.05 µm). Then, surfaces were activated by plasma treatment and silanized using APTES aminosilane. Fibronectin Cell Attachment Site (CAS) fragment containing the type III<sub>8-10</sub> domains (which contains RGD and PHSRN cell adhesive motifs) was synthesized using recombinant protein methods. Poly(L-lactide-co-D,L-lactide) (PLDLLA) was dissolved in hexafluoroisopropanol at 20 mg/mL at room temperature and was mixed with CAS fragment obtaining a final concentration of 4% PLDLLA and 100 µg/mL of CAS. NFs of PLDLLA or PLDLLA/CAS were randomly deposited onto silanized titanium discs for covalently attachment by electrospinning the polymer solution for 2 min. The applied voltage was 20–25 kV, the distance between the needle tip and the collector was 125 mm, and the pump flow rate was 0.3 mL/h. Non silanized titanium samples were used as control. Distribution of NFs was observed by SEM. NFs chemical stability was evaluated fluorometrically after depositing FITC-labelled CAS containing NFs and incubating for 5, 24 and 72h. In addition, stability of covalent attached NFs was also evaluated after 5 min sonication. Osteoblastic cells (SaOS-2) were seeded in

serum-free conditions on the different samples and cell adhesion (LDH and immunofluorescence evaluation), proliferation (LDH) and differentiation (ALP) were quantified after 4h and 7, 14 and 21 days.

## RESULTS AND DISCUSSION

Random and aligned NFs were obtained with similar diameters ( $331 \pm 77$  nm). The silanization process increased the stability of CAS-PLDLLA NFs compared to the PLDLLA NFs due to the covalently interaction between silane and CAS, even after sonication process. Although there were no statistically significant differences in the number of cells adhered, cells were well spread when the CAS recombinant fragment was present in PLDLLA NFs compared to plain PLDLLA NFs, where cells were rounded and no actin filaments were developed (Figure 1). In addition, proliferation and also differentiation was improved when cells were cultured on CAS-PLDLLA NFs.

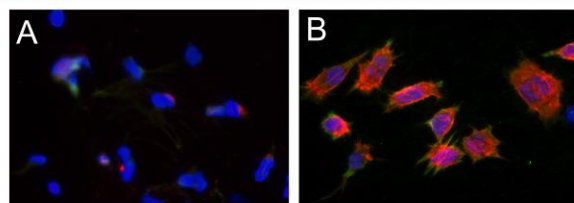


**Figure 1.** Immunofluorescence images showing cell spreading on PLDLLA NFs (A) and CAS-PLDLLA NFs (B).

## CONCLUSION

The development of a NF network for improving the biocompatibility of Ti implants is a novel and interesting approach. Herein, we seek to further improve the biological activity of PLDLLA NFs by incorporating a fibronectin recombinant fragment before the fabrication of NFs, which allows the presence of the protein fragment at the NFs surface. Being relatively stable for several days under physiological conditions, CAS-PLDLLA NFs were well recognized by osteoblastic cells, presumably generating ECM-like stimuli that triggered osteoblasts proliferation and also differentiation.

## REFERENCES

1. Gugutkov D. *et al.*, Langmuir, 25(18):10893-10900, 2009.

## ACKNOWLEDGMENTS

Financial support was provided by the MINECO MAT2012-30706 project and co-funded by the EU through European Regional Development Funds.



## Morphometric Examination of Local Tissue Reactions Following Implantation of Ti6Al4V Plates Coated with Anti-Adhesive Plasma-Fluorocarbon-Polymer Films in Rats

Andreas Hoene<sup>1</sup>, Birgit Finke<sup>2</sup>, Holger Testrich<sup>3</sup>, Silke Lucke<sup>4</sup>, Uwe Walschus<sup>4</sup>,  
Karsten Schröder<sup>2</sup>, Jürgen Meichsner<sup>3</sup>, Maciej Patrzyk<sup>1</sup>, Michael Schlosser<sup>4\*</sup>

<sup>1</sup>Department of Surgery, University Medical Center Greifswald, Germany

<sup>2</sup>Leibniz Institute for Plasma Science and Technology (INP), Greifswald, Germany

<sup>3</sup>Institute of Physics, Ernst Moritz Arndt University of Greifswald, Greifswald, Germany

<sup>4</sup>Department of Medical Biochemistry and Molecular Biology, University Medical Center Greifswald, Germany  
[\\*schlosse@uni-greifswald.de](mailto:schlosse@uni-greifswald.de)

### INTRODUCTION

Titanium (Ti) is widely used in orthopaedic surgery for permanent bone replacement implants and for temporary stabilization devices like screws or external fixators in osteosynthesis. For the latter application, the device has to be removed after successful fracture healing. While sufficient cell colonization is needed for long-term anchorage of permanent implants, the cell-material interface firmness for temporary devices should remain limited to facilitate uncomplicated removal.

therefore, anti-adhesive coatings could inhibit cell attachment onto the Ti surface. This can be achieved with plasma-fluorocarbon-polymer (PFP) films created by low-temperature plasma processes<sup>1</sup>. This study aimed at examining the influence of PFP films on the time course of local tissue response after intramuscular implantation in rats.

### EXPERIMENTAL METHODS

**Implants and PFP film preparation.** PFP films were created on Ti6Al4V plates (5×5×1mm) by (1) microwave discharge plasma (MW; 2.45 GHz, 500-1200W, 10-50Pa, 300-1000s; C<sub>3</sub>F<sub>8</sub>/ H<sub>2</sub> or C<sub>6</sub>F<sub>6</sub>/ H<sub>2</sub> mix) or (2) capacitively coupled radiofrequency discharge plasma (RF; 13.56 MHz, 20-150W, 20-60Pa, 20-1000s; C<sub>3</sub>F<sub>8</sub>/ H<sub>2</sub> mix)<sup>1</sup>. The three PFP sample series were designated as MW-C3F8, MW-C6F6 and RF-C3F8, respectively. Plates without PFP film served as controls.

**In vivo study.** One sample from each series was simultaneously implanted i.m. into the neck of male Lewis rats (n=24). Tissue containing the implants was retrieved from each 8 animals after 7, 14 and 56 days.

**Histological examination.** Following careful removal of Ti plates from the shock-frozen tissue and filling of the pockets with Cryomatrix™, cryosections were stained for CD68<sup>+</sup> macrophages/ monocytes (ED1), CD163<sup>+</sup> macrophages (ED2), T lymphocytes (R73), IL-2R<sup>+</sup> cells (OX39), antigen-presenting cells (OX6) and activated NK cells (ANK61) with the APAAP system. Mast cells were detected by toluidine blue staining. Morphometric results (ImageJ) were expressed as percentage of stained area or cells per mm<sup>2</sup> for low cell numbers (R73, OX39, ANK61, toluidine blue).

**Statistics.** The non-parametric Mann-Whitney test was used for data analysis.

### RESULTS AND DISCUSSION

The tissue reactions were influenced by either the PFP films itself (PFP vs. controls), by precursor chemistry (C<sub>3</sub>F<sub>8</sub> vs. C<sub>6</sub>F<sub>6</sub>) or by the process technology (MW vs.

RF). For CD68<sup>+</sup> macrophages/ monocytes (Fig. 1A), MW-C3F8 had a significantly stronger reaction than controls on day 14, while MW-C6F6 demonstrated a similar trend on day 14 and a significantly stronger reaction on day 56. In contrast, RF-C3F8 did not differ from controls on any day. For CD163<sup>+</sup> macrophages (Fig. 1B) and antigen-presenting cells (Fig. 1C), MW-C3F8 and MW-C6F6 had a significant higher response than controls on day 14 while no difference was observed on day 56. However, the antigen-presenting cells on day 56 were increased for MW-C6F6 compared to controls, MW-C3F8 and RF-C3F8. T lymphocytes (Fig. 1D) were increased for all three PFP series on day 56 compared to controls, significantly for RF-C3F8 and MW-C3F8. A similar outcome was observed for the IL-2R<sup>+</sup> cells, indicating T lymphocyte activation. For activated NK cells and mast cells, MW-C6F6 had a significant higher reaction than controls on day 14.

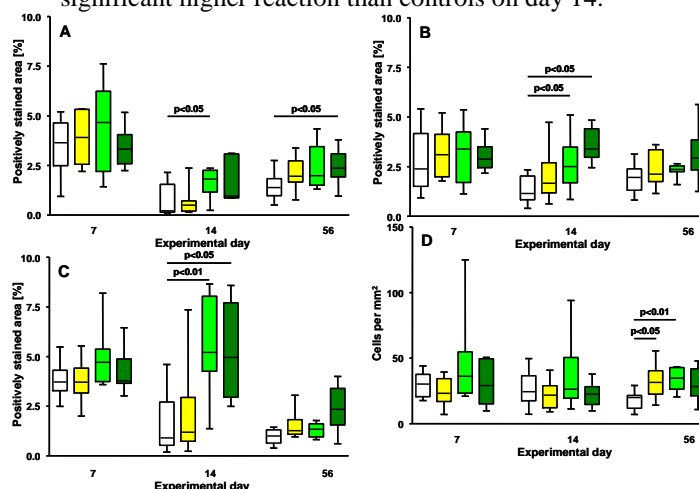


**Figure 1:** Response of CD68<sup>+</sup> macrophages/ monocytes (A), CD163<sup>+</sup> macrophages (B), antigen-presenting cells (C) and T lymphocytes (D) for Ti6Al4V controls (□) or Ti6Al4V plates with RF-C3F8 (■), MW-C3F8 (■) and MW-C6F6 (■) films

### CONCLUSION

The results demonstrate that PFP films, particularly RF-C3F8, have no negative effects on local inflammatory reactions. However, further studies regarding choice of plasma technology, precursor chemistry and process parameters are needed to optimize the in vivo response.

### REFERENCES

1. Finke B. *et al.*, Mater Sci Forum 783-786:1238, 2014

### ACKNOWLEDGMENTS

The study was supported by the Federal Ministry of Education & Research in the Campus PlasmaMed (project PlasmaImp).



## Evaluation of Biological Response of Implants Modified by Carbon Coatings with Si (Si-DLC)

Dorota Bociaga<sup>1</sup>, Jacek Grabarczyk<sup>1</sup>, Joanna Piasecka-Zelga<sup>2</sup>, Jan Skowronski<sup>3</sup>, Piotr Niedzielski<sup>1</sup>

<sup>1</sup> Division of Biomedical Engineering and Functional Materials, Institute of Materials Science and Engineering, Lodz University of Technology, Poland

<sup>2</sup> Nofer Institute of Occupational Medicine in Lodz, Poland

<sup>3</sup> The Medical University of Bialystok Clinical Hospital, Bialystok, Poland  
[dorota.bociaga@p.lodz.pl](mailto:dorota.bociaga@p.lodz.pl)

### INTRODUCTION

Among numerous different approaches, diamond-like carbon (DLC) layers are the most frequently applied solution due to the combination of highly desirable properties in the context of biomedical applications<sup>1-2</sup>. DLC coatings exhibit high biocompatibility confirmed in both *in vitro* and *in vivo* studies<sup>3-4</sup>. However, the usability of DLC coatings is limited by certain disadvantages, such as low thermal stability<sup>5</sup> and high internal stress leading to insufficient adhesion<sup>5-6</sup>.

Various studies have shown that those issues may be solved by the incorporation of particular elements into the DLC matrix, such as Si, which improves the thermal stability<sup>7</sup> of DLC layers and increases the adhesion strength<sup>8</sup>. Furthermore, also other useful parameters of carbon coatings, including cell behaviour and body reaction towards the DLC surface, can be tailored through the addition of different elements<sup>9</sup>. For instance, the introduction of Ti and Si results in better mechanical and tribological characteristics<sup>10-11</sup>. As far as biological properties are concerned, for elements such as Ti or Si the enhanced osseointegration was observed with the simultaneous reduction in the bone resorption<sup>10,12</sup>.

### EXPERIMENTAL METHODS

Round samples, commercial screws and regular implants made of AISI316L stainless steel and Ti6Al4V alloy were modified by Si-DLC coatings and used for all conducted tests. In order to evaluate the physicochemical and mechanical properties the fabricated coatings were tested using AFM, Raman, XPS, nanoindentation technique. The *in vitro* evaluation was conducted on the osteoblast Saos-2 cells and endothelial cells line EA.hy 926. The proliferation and cytotoxicity were checked using "live/dead" test. For *in vivo* model the rabbits and guinea pigs were used to obtain results with reference to irritation, intradermal reactivity, sensitization, local effects after implantation with the histopathological examination after 1, 3, 6, 9, 12-months of observation. The clinical trials were conducted on two kinds of bone implants modified by carbon coating with Si: proximal femoral intramedullary nail (GAMMA type) and volar plate for distal radius fixation.

### RESULTS AND DISCUSSION

XPS results have shown that the silicon content for each group of samples, both steel and titanium alloy, was about 3, 4 and 5%. Tests revealed that addition of silicon in the range of 3-5% does not negatively affect

the mechanical and structural properties of the modified surface and from this point of view, all the criterion of strength. Performed studies confirmed good mechanical properties of Si-DLC coatings too. *In vitro* studies indicated the optimal concentration of silicon in the coating, where the material is biocompatible. Biocompatibility was also confirmed by irritation and sensitization testing in the *in vivo* model. Bone screws coated by Si-DLC had no negative impact on the morphological and biochemical indices of blood and the surrounding tissues. The results of clinical trials indicate a high medicinal values and biocompatibility of coated implants. Radiological monitoring of fractures suggests a slightly earlier (a few days) adhesion fractures treated using coated plates.

Obtained results indicated the positive influence of Si-DLC coating for biological response, improve mechanical properties and can enhance the fractures healing processes.

### CONCLUSION

The Si-DLC coatings can be apply for medical devices in order to improve their biocompatibility and mechanical properties ensuring a proper work in living organism as a commercial product.

### REFERENCES

1. Love C.A. *et al.*, Tribology Inter. 63:141-150, 2013
2. Hauert R. *et al.*, Surface and Coatings Technology 233:119-130, 2013
3. Chai F. *et al.*, Acta Biomaterialia 4: 1369-1381, 2008
4. Bociaga D. *et al.*, DRM 17:1410-1415, 2008
5. Grill A. *et al.*, DRM 8:428-434, 1999
6. Morshed, M.M. *et al.*, Journal of Mat Proc Techn 143-144: 922-926, 2003
7. Camargo Jr S.S. *et al.*, DRM 7: 1155-1162, 1998
8. Bendavid, A. *et al.*, DRM 16:1616-1622, 2007
9. Hauert R. DRM 12:583-589, 2003
10. Bendavid, A. *et al.*, DRM 16:1616-1622, 2007
11. Cui J. *et al.*, App Surf Sc 258:5025- 5030, 2012
12. Francz G. *et al.*, Surf and Interf Anal 28:3-7, 1999

### ACKNOWLEDGMENTS

The authors would like to thank the National Centre for Research and Development – NCBiR (Grant no: INNOTECH-K1/IN1/18/156542/NCBR/12, LIDER/040/707/L-4/12/NCBR/2013 and M-ERA.NET/2012/02/2014) for providing financial support to this research”.



Francisco Martín-Saavedra<sup>1,2</sup>, Martín Prieto<sup>3</sup>, Manuel Arruebo<sup>3,1</sup>, Jesús Santamaría<sup>3,1</sup>, Nuria Vilaboa<sup>2,1</sup><sup>1</sup>Networking Center in Bioengineering, Biomaterials and Nanomedicine, CIBER-BBN, Spain<sup>2</sup>La Paz University Hospital-IdiPAZ, Spain<sup>3</sup>Aragon Institute of Nanoscience, Zaragoza University, Spain[fco.martin.saavedra@gmail.com](mailto:fco.martin.saavedra@gmail.com)

## INTRODUCTION

Copper sulphide nanoparticles (CuSNPs) provide an alternative to gold nanoparticles (AuNPs) in converting optical energy into thermal energy. As semiconductor, CuSNPs exhibit strong optical absorption at near infrared (NIR) wavelengths (650-1100 nm) originated from the d-d transitions of copper (Cu) ions and hence are not sensitive to size, shape or solvents. CuSNPs are not dependent on the dielectric constant of the surrounding matrix to absorb NIR light and can be metabolized, thus overcoming the major drawbacks of AuNPs in photothermal therapy protocols. CuSNPs biodegradation, which involves a slow release of Cu ions, can account for attractive bioeffects in regenerative medicine. For example, Cu ions are involved in the activity of transcription factors and enzymes required for cell proliferation and matrix remodeling; and can bind to cell membrane complexes to facilitate growth factor release from producing cells. In this work, CuSNPs were added as fillers within *in situ* polymerized fibrin hydrogels (CuSNPs-hydrogels). These matrices were used to encapsulate cells, derived from a mesenchymal multipotent C3H/10T/1/2 cell line, which harbors a transgene controlled by a heat-activated and rapamycin-dependent gene switch. We tested the extent to which optical properties of CuSNPs-hydrogels can be used to control transgene expression and growth factor delivery after NIR-irradiation in the presence of rapamycin. Furthermore, we investigated the bioactive effect of CuSNPs biodegradation on the cellular component included in NIR-responsive cell-constructs.

## EXPERIMENTAL METHODS

CuSNPs were synthesized according to a previously reported method<sup>1</sup> with the slight modification of adding 400  $\mu\text{L}$  of the  $\text{Na}_2\text{S}$  (320  $\text{mg mL}^{-1}$ ) solution to increase the stability of the resulting nanoparticles. C3H/10T/1/2-fLuc and C3H/10T/1/2-BMP2 clonal cell lines were obtained after stable transfection of C3H/10T/1/2 cells with a heat-activable, rapamycin-dependent gene switch for the control of firefly Luciferase (fLuc) or Bone Morphogenetic Protein 2 (BMP2), respectively. Fibrin-based hydrogels filled with CuSNPs were prepared after mixing 10  $\text{mg mL}^{-1}$  bovine fibrinogen (fbg), 0.03-0.25  $\text{mg mL}^{-1}$  CuSNPs and 2 NIH units  $\text{mL}^{-1}$  thrombin in a final volume of 250  $\mu\text{L}$  of Dulbecco's Modified Eagle's Medium. Cells were added to the mixture at a final concentration of  $1 \times 10^6$  cells  $\text{mL}^{-1}$ . For fibrinolysis assays, the polymerization mixture was supplemented with 30  $\mu\text{g mL}^{-1}$  of fbg-Alexa Fluor 546. Scaffolds polymerized at 37°C in a  $\text{CO}_2$  incubator for 1 h. Concentration of  $\text{Cu}^{2+}$  in culture media was determined by inductively coupled plasma mass spectrometry. Hydrogels were irradiated with an 808 nm laser diode at 37-44  $\text{mW mm}^{-2}$  for 5-15

min. Cell viability was evaluated after NIR-irradiation, using the alamarBlue assay. Induced target gene activity was evaluated by bioluminescence imaging assay and ELISA using a specific immunoassay for BMP2. For confocal laser scanning microscopy examination, cell constructs were fixed and stained with Phalloidin-TRITC and Hoechst. Gene expression profiling of cells encapsulated in CuSNPs-hydrogels was analyzed by real-time quantitative RT-PCR assays.

## RESULTS AND DISCUSSION

IR-thermal imaging of NIR-irradiated fibrin hydrogels showed a rapid temperature increase in matrices containing CuSNPs. Temperature in the hydrogels increased as a function of the amount of CuSNPs embedded in the fibrin network. Entrapment of CuSNPs in the fibrin matrix did not negatively affect the viability of cells encapsulated within the hydrogel, demonstrating the good biocompatibility of the system. NIR-irradiation in the presence of rapamycin triggered 3-dimensional patterns of transgene expression that matched the illuminated areas of CuSNPs-hydrogels loaded with C3H/10T/1/2-fLuc cells. In the presence of rapamycin, laser treatment of CuSNPs-hydrogels encapsulating C3H/10T/1/2-BMP2 cells led to robust secretion of BMP2 into the culture medium. Compared to hydrogels lacking CuSNPs, we observed a sustained release of  $\text{Cu}^{2+}$  ions into the culture media as well as an increase of cell-mediated fibrinolysis in CuSNPs-hydrogels, regardless of NIR irradiation and drug treatment. These effects were accompanied with changes in the shape of cells that arranged in cord-like structures within the scaffold. Finally, we observed that expression profile of genes related to vasculogenesis and extracellular matrix remodeling changed significantly in C3H10T-1/2 cells that populate CuSNPs-hydrogels.

## CONCLUSION

Optical properties of CuSNPs-hydrogels efficiently enabled photothermal regulation of transgene expression to control growth factor bioavailability. Biodegradation of CuSNPs embedded in fibrin matrices resulted in a sustained release of  $\text{Cu}^{2+}$  ions which promoted phenotypic changes in multipotent cells that dramatically affected the dynamics of scaffold remodeling.

## REFERENCES

1- Ramadan, S.; *et al. Small* **2012**, 8, 3143-3150.

## ACKNOWLEDGMENTS

This work was supported by grant PI12/01698 from Fondo de Investigaciones Sanitarias (FIS, Spain) to NV and by grant MAT2011-24988 (MICINN) to MA.





## Nanoporous Bead and Monolith Adsorbents for Haemoperfusion Applications

Yishan Zheng<sup>1</sup>, Susan Sandeman<sup>1</sup>, Ganesh Ingavle<sup>1</sup>, Carol Howell<sup>1</sup>, Sandeep Kumar<sup>1</sup>, Matthew Pope<sup>2</sup>,  
Michal Kowalski<sup>3</sup>, Kolitha Basnayake<sup>2</sup>, Steve Tennison<sup>3</sup>, Sergey Mikhalevsky<sup>1,4</sup>

<sup>1</sup> Biomaterials and Medical Devices Research group, Huxley Building, University of Brighton, Brighton, BN2 4GJ, UK

<sup>2</sup> Brighton & Sussex University Hospitals NHS Trust, Clinical Investigation and Research Unit, Brighton, BN2 5BE, UK

<sup>3</sup> MAST Carbon International Ltd., Jays Close, Viabes, Basingstoke, Hampshire RG22 4BA, UK

<sup>4</sup> School of Engineering, Nazarbayev University, Kabanbay Batyr Avenue, Astana 010000, Kazakhstan

[yz9@brighton.ac.uk](mailto:yz9@brighton.ac.uk)

### INTRODUCTION

Phenolic resin derived activated carbon adsorbent biomaterials with advanced nanoporous domains have a range of biomedical applications related to adsorption of protein bound and high molecular weight biotoxins which are difficult to remove by other methods. For example, haemodialysis and peritoneal dialysis are life-saving treatments for patients with kidney failure but fail to remove high molecular weight and protein bound toxins which drive pathophysiology. The removal of such molecules is only possible by adsorption and remains a major issue in the optimisation of these systems [1, 2]. Our group has developed bead and monolith adsorbents with nanoporosity optimised for broad spectrum biotoxin removal [3-5]. The haemocompatibility and adsorptive properties of blood contacting synthetic, nanoporous activated carbon was investigated comparing bead and monolith forms to overcome issues created by packed bed columns such as undesirable high column back pressure and cross-column pressure drop during haemoperfusion [6]. The potential use of this ACM as an adjunct to improve the current HD treatment regime was explored.

### EXPERIMENTAL METHODS

#### 1. Material physical characterisations

Mercury porosimetry and scanning electron microscopy (SEM) imaging were used to study the material porosity and internal structure.

#### 2. *in vitro* adsorption of biotoxins

The efficacy of the nanoporous activated carbon beads (ACB) and monoliths (ACM) were determined by their capability in adsorbing selected protein bound and high molecular weight toxin markers p-cresyl sulphate (PCS), indoxyl sulphate (IS) and interleukin (IL6). Small scale batch adsorption study were

#### *ex vivo* haemocompatibility assessment

ACB and ACM were pre-conditioned by circulating 20 ml of NaCl (0.9%) solution at a flow rate of 5 ml/min for 30 min. Then freshly drawn healthy donor blood (20 ml) was perfused through the monolith at a rate of 1 ml/min. A tubing only control was also included. Blood samples were collected before perfusion, after first pass, 30 and 60 min of perfusion.

**Complement activation** was evaluated by ELISA measurement of C3a concentration in plasma using lithium heparin anticoagulant and a Zymosan A complement activation positive control.

**Platelet activation** was assessed by flow cytometry using citrated blood samples stained with fluorophore conjugated antibodies PE/CD61, APC /D62P, and FITC/PAC-1. Adenosine 5'-diphosphate sodium salt

(ADP) was used as positive control.

**T cell activation** was analysed by flow cytometry using EDTA anticoagulated donor blood and measurement of phosphorylated cell-signalling protein Stat3 and STAT signalling pathway activation following T-cell activation (BD Phosflow T cell Activation Kit). Cytokine IL6 was used as a positive controls for Stat3 phosphorylated protein expression

### RESULTS AND DISCUSSION

Within 60 minutes of *in vitro* plasma direct contact, both ACB and ACM showed efficient removal of the spiked toxin markers from the plasma indicating adsorptive capacity for these toxins and the potential application of these nanoporous carbon materials. The *ex vivo* haemocompatibility studies indicated no additional stimulation of complement, platelet and T-cell activation compared to tubing only controls and a marked increase in the positive activation controls compared to the monolith filtration samples

### CONCLUSION

It is shown the first time *in vitro* study that both ACB and ACM were capable of removing marker key uraemic target toxins from a circulating spiked plasma pool. In addition, the *ex vivo* perfusion of healthy donor whole blood through the ACM did not trigger excessive complement activation, platelet activation or T cell activation, confirming haemocompatibility of the adsorbent and potential use as an adjunct to improve current HD therapy. This makes them very useful for treatment of range of conditions where biotoxins cause problems - sepsis, liver and kidney failure.

### REFERENCES

1. Naka T., et al., Contrib Nephrol, 2010.
2. Liabeuf S. et al., Toxins (Basel), 2011.
3. Mikhalevsky S. et al., Biodefence. 2009.
4. Sandeman, S. et al., Biomaterials, 2008.
5. Zheng, Y., et al., ACS Appl Mater Interfaces, 2012.
6. Cooney D. et al., Artif Organs, 1983.

### ACKNOWLEDGMENTS

The authors would like to thank National Institute for Health Research i4i ADEPT project and FP7 PEOPLE MCA IAPP ACROBAT project for the financial support.



Yuichi Ohya<sup>1,2</sup>, Yasuyuki Yoshida<sup>1</sup>, Akihiro Takahashi<sup>2</sup>, Akinori Kuzuya<sup>1,2</sup><sup>1</sup>Department of Chemistry and Materials Engineering, Kansai University, Japan<sup>2</sup>ORDIST, Kansai University, Japan[yohya@kansai-u.ac.jp](mailto:yohya@kansai-u.ac.jp)

## INTRODUCTION

Biodegradable polymers exhibiting temperature-responsive sol-gel transition between room temperature and body temperature are expected to be applied as injectable polymer (IP) systems in biomedical applications. IP solution containing drugs or living cells can be injected by simple syringe injection at the target site in the body to form a hydrogel acting as sustained drug releasing depot or scaffold for tissue regeneration. For example, Lee and coworkers reported ABA-type triblock copolymer of poly(lactide-co-glycolide) and poly(ethylene glycol), PLGA-*b*-PEG-*b*-PLGA, as biodegradable injectable polymer exhibiting temperature-responsive sol-gel transition between room temperature and body temperature<sup>1</sup>. We also reported several biodegradable IP systems exhibiting temperature-responsive sol-gel transition and relatively high mechanical strength in gel state using block copolymers of polylactide and branched PEG<sup>2,3</sup>. However, these copolymers are usually sticky paste in dry state at room temperature, and inconvenient for storage and weighing. Moreover, it takes a long time (usually more than 5 hours) to be dissolved in aqueous solution. On these issues, Jeong *et al.* reported solidification of the triblock copolymers containing poly( $\epsilon$ -caprolactone), PCL-*b*-PEG-*b*-PCL, exhibiting temperature-responsive sol-gel transition<sup>4</sup>. However, the copolymers must be heated above melting temperature upon dissolution. In this study, in order to provide convenient IP system for instant use at clinical scene, which is solid state in dry condition and can be dissolved in short time, we synthesized a triblock copolymer of poly( $\epsilon$ -caprolactone-co-glycolide) and PEG, PCGA-*b*-PEG-*b*-PCGA, and investigated the effect of some additives on dissolution time of IP formulation. Then, we succeeded to develop an IP formulation quickly preparative at room temperature<sup>5</sup>.

## EXPERIMENTAL METHODS

A series of triblock copolymer of poly( $\epsilon$ -caprolactone-co-glycolide) and PEG, PCGA-*b*-PEG-*b*-PCGA, was synthesized by ring-opening polymerization of  $\epsilon$ -caprolactone and glycolide using PEG and Sn(Oct)<sub>2</sub> as an initiator and a catalyst, respectively. Temperature-responsive sol-gel transition behavior of PCGA-*b*-PEG-*b*-PCGA solution was investigated by a test tube inverting method and by a dynamic rheometer (HAAKE, Thermo HAAKE RS600). Then, we investigated the effect of additives (hydrophilic polymers or saccharides) on the dissolution time and sol-gel transition for the mixture of PCGA-*b*-PEG-*b*-PCGA and these additives in aqueous solution.

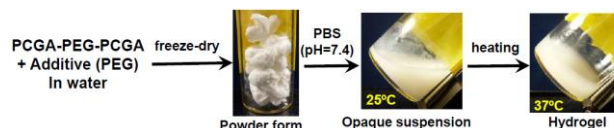


Figure 1. Preparation of PCGA-*b*-PEG-*b*-PCGA + additive (PEG) formulation: from powder form in dry state, to PBS solution (suspension) at 25°C, and then to the hydrogel form at 37°C.

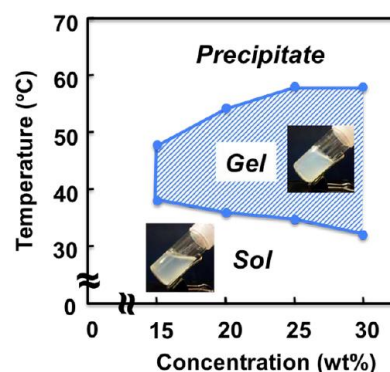


Figure 2. The phase diagrams of PCGA-*b*-PEG-*b*-PCGA solution at various temperature and concentrations.

## RESULTS AND DISCUSSION

The obtained PCGA-*b*-PEG-*b*-PCGA could be freeze-dried to show powder form morphology in dry state at room temperature (Fig. 1). Its aqueous solution exhibited temperature-responsive sol-gel transition between room temperature and body temperature (Fig. 2). We found that formulations composed of PCGA-*b*-PEG-*b*-PCGA and PEG as additives could be distributed in PBS to give suspension within 1 min at room temperature (Fig. 1). The obtained suspension was opaque, but could be sucked by syringe, and exhibited temperature-responsive sol-gel transition between room temperature and body temperature.

## CONCLUSION

We found instantly preparative IP/additive system, which can be distributed in PBS within 1 min. This system should be convenient for instant preparation of IP formulation at clinical scene.

## REFERENCES

1. Lee D. S. *et al.*, *Macromol. Rapid. Commun.* 22:587-592, 2001
2. Nagahama K. *et al.*, *React. Funct. Polym.* 73:452-460, 2013
3. Nagahama K. *et al.*, *Adv. Funct. Mater.* 18:1220-1231, 2008
4. Jeong B. *et al.*, *Macromolecules* 38:5260-5265, 2005.
5. Yoshida Y. *et al.*, *Polym. J.* 46:632-635, 2014

# Mechanical and Cytotoxic Evaluation of a Novel Hydrogel with Potential to Deliver Bioceramic Nanoparticles

Sreekanth Pentlavalli<sup>1</sup>, Michelle O'Doherty<sup>1</sup>, Philip Chambers<sup>1</sup>, Marine Chalanqui<sup>2</sup>, Helen .O. McCarthy<sup>2</sup> and Nicholas Dunne<sup>1</sup>

<sup>1</sup>School of Mechanical & Aerospace Engineering, Queen's University Belfast, UK

<sup>2</sup>School of Pharmacy, Queen's University Belfast, UK

[s.pentlavalli@qub.ac.uk](mailto:s.pentlavalli@qub.ac.uk)

## INTRODUCTION

The development of localised drug delivery systems (DDSs) represents a valuable option to overcome the typical drawbacks associated with conventional systemic administration, which is not directed to the target organ or tissue<sup>1</sup>. In this context, injectable polymer dispersions have emerged as a superior, non-surgical alternative for tissue regeneration<sup>2</sup>. For example Tan *et al* (2012) developed alginate based injectable hydrogel for tissue engineering<sup>3</sup>. However these studies have limited success due to lack of high mechanical strength and tedious synthetic procedures.

In this study, we propose the use of novel thermo-responsive poly(Alginate-g-N-isopropylacrylamide) (P(Alg-g-NIPAAm)) hydrogel with the aim of identifying a system that meets all necessary requirements for soft tissue repair, i.e. biocompatibility, biodegradability and adequate mechanical strength. In addition, this study assessed the effect of the lower critical solution temperature (LCST) and cytotoxicity of the hydrogel with and without drug loading.

## EXPERIMENTAL METHODS

**Preparation of hydrogel:** Sodium alginate (Alg) and poly (N-Isopropylacrylamide) (PNIPAAm) were coupled via free radical polymerisation to form P(Alg-g-NIPAAm) hydrogel of various ratios. All copolymers were characterised by <sup>1</sup>H NMR and FTIR. Rheological measurements were performed during the process of sol-gel transformation with a constant shear rate (6.283 rad/s). Temperature sweep experiments from 20 to 50°C were conducted at a heating rate of 3°C/min.

**Formulation of RALA/GFP plasmid NPs:** The RALA/GFP plasmid nanoparticles (NPs) were formed by self-assembly via electrostatic interactions. Particle size and zeta potential (ZP) was measured using a Malvern Zeta sizer Nano ZS.

**Drug Delivery:** Fluorescein sodium salt was loaded in a 5% hydrogel solution and the release profile was assessed at 37°C in PBS at pH. 7.4. The samples were collected at regular intervals and measured the fluorescence (Ex at 480nm and Em at 520 nm).

**DNA Delivery:** 5% P(Alg-g-NIPAAm) was loaded with RALA/GFP plasmid. Hydrogel-NP constructs were placed in trans-wells adapted for 24-well plate and immersed in water at 37°C. The release profile was assessed by sampling the supernatant at different time points and measuring nucleic acid content using Picogreen<sup>®</sup> assay.

**Cell viability:** MG63 cells were co-cultured with the hydrogel for up to 28 d. The biocompatibility of the

P(NIPAAm-co-Alg) hydrogel was assessed every 7 d using MTS assay.

## RESULTS AND DISCUSSION

The P(Alg-g-NIPAAm) hydrogels exhibited a drastic increase in the viscosity of the gels around 32-34°C, which is the low critical solution temperature of P(Alg-g-NIPAAm) polymer. At LCST the free flowing aqueous solutions were transformed to gel like material. Consequently, the storage modulus ( $G'$ ) and loss modulus ( $G''$ ) of a 5% w/w P(Alg-g-NIPAAm) hydrogel increased from 32-34°C onwards. This change in the storage modulus is also reflected on the mechanical strength of the P(Alg-g-NIPAAm), which was approx. 800 Pa at 37°C.

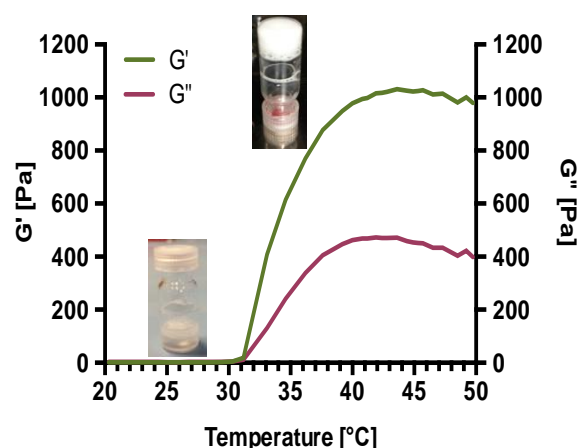


**Figure 1.** a) Storage modulus ( $G'$ ) and loss modulus ( $G''$ ) of 5% P(NIPAAm-co-Alg) solution in PBS. pH:7.4 (insert: the LCST behaviour of polymer solution).

## CONCLUSION

We have successfully produced a thermo-responsive polymer with the potential to behave as both a scaffold and delivery vehicle. Furthermore, we have demonstrated delivery of small molecules and NPs via thermo-responsive hydrogel.

## REFERENCES

1. Harsha S. et al., *Int J Pharm* 380:127-32, 2009
2. Tan R. et al., *Carbohydr. Polym.* 87: 1515-1521, 2012

## ACKNOWLEDGMENTS

We would like to thank the US-Ireland Grant (Grant no: 3568) and the Medical Research Council (Grant no: 1294) for providing financial support for this project



Kenichi Nagase<sup>1</sup>, Yuri Hatakeyama<sup>2</sup>, Tatsuya Shimizu<sup>1</sup>, Katsuhisa Matsuura<sup>1</sup>, Masayuki Yamato<sup>1</sup>,  
Naoya Takeda<sup>2</sup>, Teruo Okano<sup>1</sup>

<sup>1</sup> Institute of Advanced Biomedical Engineering and Science, Tokyo Women's Medical University, Japan

<sup>2</sup> Department of Life Science and Medical Bioscience, Waseda University, Japan

[nagase.kenichi@twmu.ac.jp](mailto:nagase.kenichi@twmu.ac.jp)

## INTRODUCTION

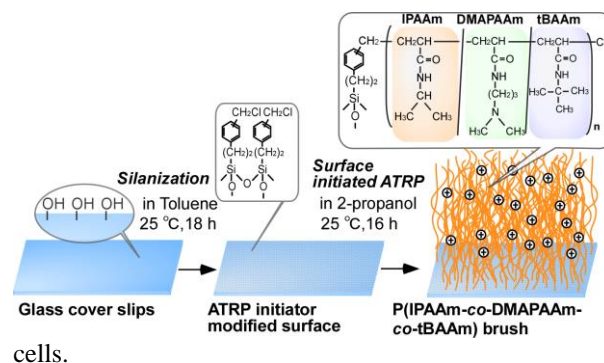
In regenerative medicine, an effective cell separation method that can provide adequate purity, yield, and function have been needed for fabricating transplantable tissues.<sup>1</sup> In the present study, poly(*N*-isopropyl acrylamide (IPAAm)-*co-N,N*-dimethylaminopropyl acrylamide(DMAPAAm)-*co-N-tert*-butylacrylamide (tBAAm)) brush grafted surfaces were prepared through surface-initiated atom transfer radical polymerization (ATRP). Temperature-dependent adhesion and detachment behaviour of human bone marrow mesenchymal stem cell (hbmMSC) was observed for investigating the possibility of the copolymer brush surface as a cell separating materials.

## EXPERIMENTAL METHODS

An ATRP initiator, 2-(*m/p*-chloromethylphenyl) ethyltrimethoxysilane, was modified on glass coverslips (Fig. 1). Copolymerization of IPAAm (75mol%), DMAPAAm(5mol%), and tBAAm(20mol%) was performed through surface-initiated ATRP for 16 h at 25 °C using CuCl/Me<sub>6</sub>TREN as a catalyst and 2-propanol as reaction solvent.<sup>2</sup> In the polymerization,  $\alpha$ -chloro-*p*-xylene was added as free initiator and brush length was estimated using the prepared copolymer in the reaction solution. Cell adhesion and detachment behaviour of hbmMSC and other human bone marrow derived cells were observed at 37 and 20 °C.

## RESULTS AND DISCUSSION

Prepared cationic copolymer brush was characterized by ATR/FT-IR, GPC measurement and zeta potential measurement. As result, amount of grafted copolymer and graft density were 1.51  $\mu\text{g}/\text{cm}^2$  and 1.04 chains/nm<sup>2</sup>, respectively. Zeta potential of copolymer brush was 19.8 mV. These result indicated that densely packed cationic copolymer brush was formed on glass substrate. Cells adhesion and detachment properties on copolymer brush were observed using hbmMSC and other bone marrow derived cells. hbmMSC adhered on the cationic copolymer brush at 37 °C, while other bone marrow cells did not adhered (Fig.2). With reducing temperature to 20 °C, adhered hbmMSC detached from cationic copolymer brush. Using this properties, purification of hbmMSC was performed simply by changing temperature. Mixture of hbm derived cells were seeded on cationic copolymer brush and hbmMSC adhered on cationic copolymer brush (Fig.3). Subsequently, temperature reduced to 20 °C, and purified hbmMSC was successfully recovered from the copolymer brush. The result indicated that thermoresponsive cationic copolymer brush would be useful tool for purification of hbmMSC from other



cells.

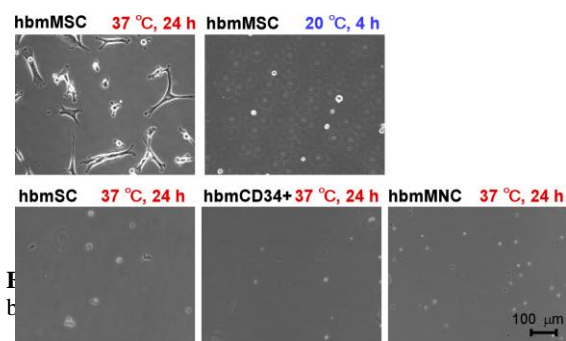


**Fig.2** hbm derived cells adhesion and detachment behaviour on thermoresponsive cationic copolymer brush

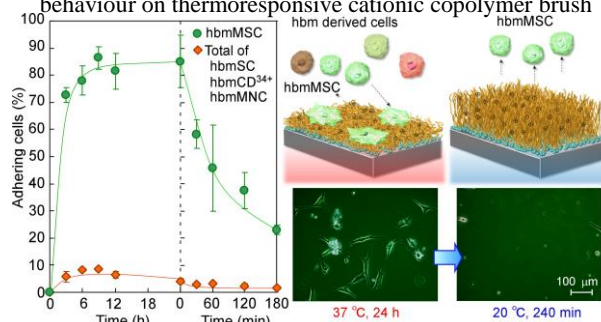


**Fig.3** Purification of hbmMSC from human bone marrow derived cells using thermoresponsive copolymer brush

## CONCLUSION

Thermoresponsive cationic copolymer brush can selectively adhered and detach hbmMSC. Thus, the thermoresponsive cationic copolymer brush would be useful for purification of hbmMSC simply by changing temperature.

## REFERENCES

- Diogo MM. *et al.*, Biotech. Bioeng., 109: 2699-2709, 2012
- Nagase K *et al.*, Biomacromolecules, 10.1021/bm5015



## Biopolymer Mediated Uptake of Sugar Molecules for Cell Preservation and Therapy

Rongjun Chen<sup>1</sup>, Andrew Lynch<sup>2</sup>, Liwei Wu<sup>1</sup>, Zhenlu Hu<sup>1</sup>, Nigel K.H. Slater<sup>2</sup>

<sup>1</sup>Department of Chemical Engineering, Imperial College London, South Kensington Campus, London SW7 2AZ, UK

<sup>2</sup>Department of Chemical Engineering and Biotechnology, University of Cambridge, Cambridge CB2 3RA, UK  
[rongjun.chen@imperial.ac.uk](mailto:rongjun.chen@imperial.ac.uk)

### INTRODUCTION

Successful preservation of mammalian cells builds the foundation for cell therapy that relies on delivery of new live cells into a tissue of a patient, such as blood transfusion, stem cell transplantation, and fertility preservation<sup>1,2</sup>. Currently cryopreservation is the only technology that allows for reliable long-term storage of most cells. Cryopreservation is usually accomplished utilising high concentrations of toxic cryoprotectants, such as DMSO. Therefore, significant interest exists in development of alternative protectants, such as sugars, most notably trehalose that is a hydrophilic disaccharide accumulated in a variety of freezing- and desiccation-tolerant organisms<sup>3,4</sup>.

As sugar molecules are normally impermeable to the cell membrane, the primary obstacle to the realisation of viable mammalian cell preservation using sugars is the requirement of the high concentrations not only around but also within cells for optimum bioprotection<sup>3,5</sup>. A few techniques have been investigated for delivering trehalose into cells for biopreservation. However, the methods yielding sufficient intracellular trehalose for cell preservation have utilised hazardous materials, such as mutant bacterial toxins<sup>3</sup>, or have lacked scalability, such as the use of microinjection<sup>5</sup>. Low concentrations of trehalose (15 mM) have been introduced into human red blood cells using a safer liposomal delivery system<sup>6</sup>, below a threshold intracellular trehalose concentration range of 100 – 200 mM for bioprotection development in mammalian cells<sup>3,5,7</sup>.

This presentation will cover our recent efforts in the precise control of cell membrane permeabilisation using non-toxic, biocompatible and cell-permeating synthetic biopolymers to improve the loading of sugars into cells. These amphipathic polymers, which incorporate weakly ionisable carboxyl groups and hydrophobic side chains, were designed to mimic viral peptide structure and membrane permeabilising activity<sup>8</sup>. They can undergo a conformational change from extended charged chains to aggregated hydrophobic structures as pH drops below their pKa, facilitating interaction with the hydrophobic interiors of lipid bilayers and subsequent cell membrane permeabilisation<sup>8-11</sup>.

### EXPERIMENTAL METHODS

The linear poly(L-lysine *iso*-phthalamide) backbone-derived biopolymers were synthesised according to the procedure which we have published previously<sup>8,9</sup>. Cells such as erythrocytes were incubated with trehalose and polymer of selected concentrations in PBS buffer. The

intracellular trehalose concentrations were tested based on the anthrone method. The cells with loaded trehalose were preserved using two methods: cryopreservation (in a –80 °C freezer or in liquid nitrogen) and desiccation (vacuum drying) respectively. Percent cell survival after freeze/thaw or desiccation/rehydration was measured based on the haemolysis assay. Cells were imaged by confocal microscopy and atomic force microscopy<sup>12,13</sup>.

### RESULTS AND DISCUSSION

These biomimetic biopolymers reversibly increased the cell membrane permeability, yielding trehalose loading dependent on polymer structure, polymer concentration, pH, external trehalose concentration, incubation time and temperature (intracellular trehalose concentration up to  $251 \pm 6$  mM). The trehalose loading resulted in  $83 \pm 3\%$  erythrocyte survival after freeze-thaw processes, an improvement of  $20.4 \pm 5.6\%$  in cryosurvival over the unloaded erythrocytes. This improvement indicates that extracellular trehalose alone is insufficient for optimum cryoprotection. Trehalose uptake in cells also facilitated an increase in the membrane integrity of vacuum dried cells by a factor of  $9 \pm 1$  and reduced the extent of haemoglobin oxidation in dried cells from  $66 \pm 1\%$  to  $23 \pm 3\%$ . Herein, the intracellular loading of other sugar molecules and the resulting effects on mammalian cell preservation were compared against trehalose. The mechanism of the biopolymer-mediated delivery of sugar molecules was also elucidated.

### CONCLUSION

The non-toxic biopolymers can deliver sugar molecules into cells efficiently without causing cell damage. The results provide a foundation for the cryopreservation and desiccation of a wide variety of mammalian cells and stem cells using non-toxic sugars and an important step towards viable cell lyophilisation and cell therapy.

### REFERENCES

1. Stacey GN *et al.*, Nat. Biotechnol., 32:320-2, 2014.
2. Tournaye H *et al.*, Lancet, 384:1295-301, 2014.
3. Eroglu A *et al.*, Nat Biotechnol., 18:163-7, 2000.
4. Guo *et al.*, Nat Biotechnol., 18:168-71, 2000.
5. Eroglu A *et al.*, Fertil. Steril., 77:152-8, 2002.
6. Holovati JL *et al.*, Cryobiology, 58:75-83, 2009.
7. Chen T *et al.*, Cryobiology, 43:168-81, 2001.
8. Chen R *et al.*, J. Mater. Chem., 19:4217-24, 2009.
9. Chen R *et al.*, Biomacromolecules, 10:2601-8, 2009.
10. Chen R *et al.*, Biomaterials, 30:1954-1961, 2009.
11. Zhang S *et al.*, Langmuir, 27:8530-8539, 2011.
12. Lynch AL *et al.*, Biomaterials, 31:6096-6013 2010.
13. Lynch AL *et al.*, Biomaterials, 32:4443-4449, 2011.



# Lipid Nanoparticles Loaded into Biopolymer-Based Hydrogels; Materials for Controlled Rate of Drug Delivery

L. Racine<sup>1,2</sup>, R. Auzély-Velty<sup>2</sup>, I. Texier<sup>1</sup>

<sup>1</sup> Université Grenoble Alpes, F-38000 Grenoble, France ; CEA-LETI MINATEC/ DTBS, 17 avenue des Martyrs, F-38054 Grenoble Cedex 9, France

<sup>2</sup> Centre de Recherches sur les Macromolécules Végétales (CERMAV-CNRS), Université Joseph Fourier, Institut de Chimie Moléculaire de Grenoble, BP53, 38041 Grenoble Cedex 9, France  
[isabelle.texier-nogues@cea.fr](mailto:isabelle.texier-nogues@cea.fr)

## INTRODUCTION

Biopolymer-based hydrogels find widespread applications in the field of regenerative medicine and drug delivery<sup>1</sup>. Hydrogels are able to provide local delivery of hydrophilic therapeutic agents, but the diffusion of agents from the hydrogels can be rapid and not easily time-controllable. On the other hand, nano-sized objects are being increasingly investigated for *in vivo* drug delivery<sup>2</sup>. In this regard, we have developed lipid nanoparticles (LNPs) as promising carriers for lipophilic drugs and therapeutic biomolecules<sup>3</sup>. This work deals with designing original hybrid biomaterials composed of LNPs entrapped within hydrogels in view of their application for drug sustained release. In particular, we selected two biocompatible polysaccharides which are currently used in pharmaceutical and biomedical applications: carboxymethylcellulose (CMC) and chitosan, which are negatively and positively-charged respectively.

## EXPERIMENTAL METHODS

CMC-PEG and chitosan-PEG hydrogels were chemically cross-linked using photo-induced thiol-ene chemistry<sup>4</sup>. Fluorescently labelled LNPs (50 nm diameter) with different surface charge were prepared using a previously described sonication process<sup>3</sup>, characterized by Dynamic Light Scattering (NanoSizer ZS, Malvern), and suspended into the polysaccharide solution before cross-linking to achieve the particle-loaded biomaterials. The physico-chemical properties (swelling ratio, rheological properties (AR2000 rheometer, TA Instruments)) of the obtained hydrogels and the release kinetics of the LNPs (fluorescence titration (LS50B fluorimeter, Perkin Elmer) were evaluated according to the surface charge and the concentration of LNPs entrapped into the hydrogels.

## RESULTS AND DISCUSSION

The presence and the homogeneous distribution of the labelled LNPs within the hydrogels were confirmed by confocal laser scanning microscopy observations. The LNP loading, up to a concentration of 50% (w/w<sub>polymer</sub>), did not prevent the gel formation, nor significantly modify the rheological and swelling properties of the obtained materials (Figure 1). Similarly, particle hydrodynamic diameter and polydispersity index after their recovery from the digested material were not affected for a few weeks after material loading. LNPs were slowly released from the hydrogels immersed in NaCl 154 mM (Figure 2). Interestingly, significant differences in the release kinetics were observed depending on the surface charge properties of the LNPs.

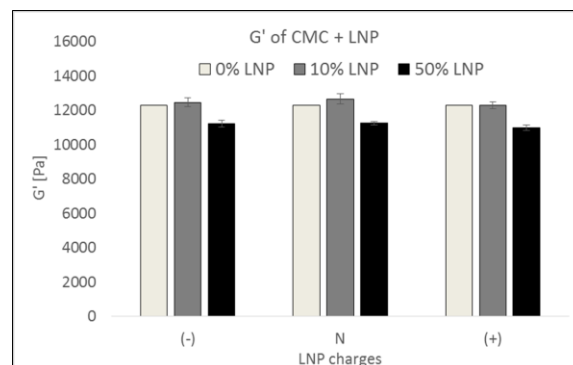


Figure 1. Elastic moduli ( $G'$ ) of the CMC-PEG materials obtained after loading of negative (-), neutral (N), or positive (+) LNPs with different payloads.

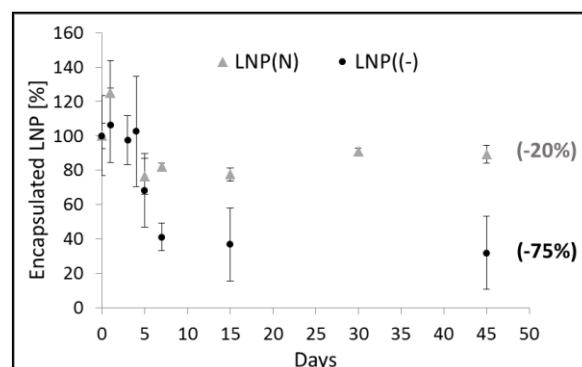


Figure 2. Kinetics of release of negative (-) and neutral (N) LNPs loaded at 50% (w/w<sub>polymer</sub>) in CMC-PEG hydrogels.

## CONCLUSION

LNPs were included in CMC-PEG and chitosan-PEG matrices with high payloads while not affecting material properties. Release of the particles and their lipophilic drug content is sustained in time and easily tuneable with particle design.

## REFERENCES

1. Van Vlierberghe S. *et al.*, Biomacromol. 13:1818-1827, 2012.
2. Natajaran J. V. *et al.*, J. Control. Release 193:122-138, 2014.
3. Delmas T. *et al.*, J. Colloid Interf. Sci. 360:471-481, 2011.
4. Hachet E. *et al.*, Biomacromol. 13:1818-1827, 2012.

## ACKNOWLEDGMENTS

LETI/DTBS is part of the Arcane Labex program, funded by the French National Research Agency (ARCANE project n° ANR-12-LABX-003).



## Selective *in Vitro* Anticancer Effect of Hyaluronan Polymeric Micelles Loaded with SPIONs

Daniela Šmejkalová<sup>1</sup>, Kristina Nešporová<sup>1,2</sup>, Gloria Huerta-Angeles<sup>1</sup>, Jakub Syrovátka<sup>1</sup>, Daniel Jiráček<sup>3,4</sup>, Andrea Gálisová<sup>3</sup>, Vladimír Velebný<sup>1</sup>

<sup>1</sup>Contipro Pharma, Dolní Dobrouč 401, 561 02 Dolní Dobrouč, Czech Republic

<sup>2</sup>Institute of Experimental Biology, Faculty of Science, Masaryk University, Kotlářská 267/2, 611 37 Brno, Czech Republic

<sup>3</sup>MR Unit, Department of Diagnostic and Interventional Radiology, Institute for Clinical and Experimental Medicine IKEM, Vídeňská 1958/9, 140 21 Prague, Czech Republic

<sup>4</sup>Institute of Biophysics and Informatics, 1<sup>st</sup> Medicine Faculty, Charles University, Salmovská 1, 120 00 Prague, Czech Republic

[daniela.smejkalova@contipro.com](mailto:daniela.smejkalova@contipro.com)

### INTRODUCTION

Superparamagnetic Iron Oxide Nanoparticles (SPIONs) are of great interest in biomedical applications because of their characteristic magnetic properties exhibited only in the magnetic field. SPIONs are hydrophobic nanoparticles and for this reason they tend to aggregate in bloodstream through van der Waals interactions and are more likely to be removed by the RES. To prevent this, SPIONs usually undergo surface modification. One way of elegant SPION modification can be represented by SPION loading in drug delivery vehicle. SPIONs are usually considered to be inert imaging agents without intended pharmacological functions. However, we have noticed that SPIONs may be selectively cytotoxic when they are encapsulated in polymeric micelle made from hydrophobized hyaluronic acid<sup>1</sup>.

### EXPERIMENTAL METHODS

SPIONs (5-20 nm) were incorporated in acylated hyaluronan (HAC6, HAC8, HAC10, HAC18, HAC18:0-HAC18:3) by sonication. The obtained polymeric micelles loaded with SPIONs were characterized by DLS, TEM, ICP-OES and NMR relaxometer. MTT assay and flow cytometry were performed for *in vitro* cell cytotoxicity evaluation.

### RESULTS AND DISCUSSION

All of the tested hydrophobized (acylated) hyaluronic acid samples (HAC6-HAC18:3) were able to form self-assembled particles while loading SPIONs. As observed by TEM, multiple SPIONs were clustered in the micelle cores and the mean diameter of SPION loaded HA particles was about 100 nm. The loading capacity was 1-2 %wt. and the encapsulation efficiency was about 30-40%. A good stability of loaded micelles was indicated by high absolute value of zeta potential (around -40 mV). There was no detected aggregation of loaded micelles within 5 days after their dispersion in aqueous medium. The estimated relaxivity around 200 mM<sup>-1</sup>S<sup>-1</sup> at 1 T was comparable to some of the commercial SPION compositions and indicates good potential to serve as contrast agent for *in vivo* applications.

The cytotoxicity of SPION loaded HA polymeric micelles was tested using control (normal human dermal fibroblasts (NHDF), murine 3T3 Swiss fibroblasts) and cancer cell lines (human cancer cell lines: A2058, A549, C3A, Caco-2, HCT-116, HT-29, MDA-MB231 and MCF-7). Except for A2058, there

was a significant inhibition of cancer cell line viability, while the growth of control cells was positively affected. Comparing the tested samples, the most prominent difference in viabilities between control and cancer cells was observed for HAC18:1-SPION (Figure 1). This sample even showed selective inhibition of cell growth when it was incubated with a mixture of NHDF and HT-29 cells. According to our data, the selective cytotoxicity cannot be connected with an enhanced CD44 uptake or ROS formation, but rather with a different way of SPION intracellular release from the HA micelle.

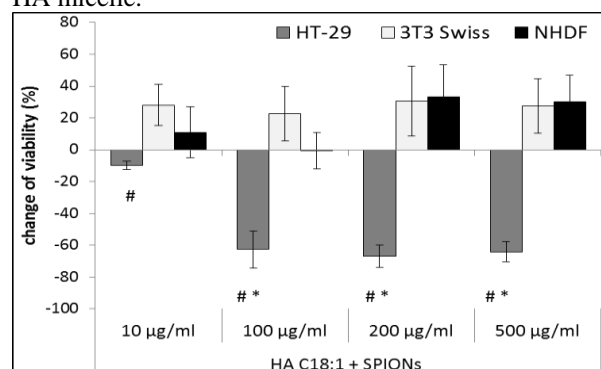


Figure 1. Cell growth inhibition of HAC18:1-SPIONs on NHDF and 3T3 Swiss and HT-29 cell lines.

### CONCLUSION

HA-SPION polymeric micelles are highly cytotoxic towards some cancer cell lines, while at the same time they are harmless towards healthy cell lines and primary cells. The selective *in vitro* behaviour was observed even when HA-SPION was incubated with a mixture of healthy and cancerous cell line. The current explanation of such behaviour failed to be connected with an enhanced CD44 uptake or ROS formation. It is rather connected with different release mechanism of SPIONs from HA micelles in the cells.

### REFERENCES

- Šmejkalová D. *et al.*, Biomacromolecules 15:4012-20, 2014

### ACKNOWLEDGMENTS

The authors would like to thank MH CR-DRO (Institute for Clinical and Experimental Medicine IKEM, IN00023001) for providing financial support.



## Injectable Hydrogel Based on a Novel Amphiphilic Hyaluronic Acid Derivative for Controlled Drug Release

A. Borzacchiello<sup>1</sup>, L. Russo<sup>1</sup>, F. S. Palumbo<sup>2</sup>, S. Agnello<sup>2</sup>, G. Pitarresi<sup>2</sup>, G. Giammona<sup>2</sup> and L. Ambrosio<sup>1,3</sup>

<sup>1</sup>Institute for Composite and Biomedical Materials IMCB-CNR, Italy

<sup>2</sup>Dipartimento di Scienze e Tecnologie Biologiche Chimiche e Farmaceutiche, Sezione di Chimica e Tecnologie Farmaceutiche, Università degli Studi di Palermo, Italy

<sup>3</sup>Department of Chemical Science and Materials Technology DCSMT- CNR, Italy

[bassunta@unina.it](mailto:bassunta@unina.it)

### INTRODUCTION

In the treatment of arthritis, drug delivery systems are of mayor interest since they ensure a controlled release of the active substance in the region of interest. Moreover one possible and often used treatment of osteoarthritis is by intra-articular injection of hyaluronic acid (HA) in order to restore the elastic and viscous properties of the synovial fluid<sup>1</sup>. A significant research effort has been devoted to alter the HA physic-chemical and viscoelastic properties by chemical modification. The idea of this study was to combine viscosupplementation approach with the controlled delivery of an anti-inflammatory drug *in situ*. In this work we tested the potential use of chemically modified HA as viscosupplementation agent and at the same time able to control the release of a hydrophobic drug. To this aim, modified HA samples were characterized from a rheological point of view. The solubility of a hydrophobic drug was studied and its *in vitro* drug release kinetics was evaluated.

### EXPERIMENTAL METHODS

A HA derivative bearing respectively ethylenediamino (EDA) and octadecyl pendant groups (HA-EDA-C<sub>18</sub>) was obtained as elsewhere reported<sup>2</sup>. As anti-inflammatory drug dexamethasone (DM) (Sigma-Aldrich), was chosen. HA-EDA-C<sub>18</sub> based samples were prepared at different polymer concentrations (1%, 3% and 5% w/v) in bidistilled water (DDW) and Dulbecco's Phosphate-Buffered Saline (DPBS). To improve the solubility of both HA-EDA-C<sub>18</sub> and DM, also  $\beta$ -CD (Sigma-Aldrich), at different concentrations (1%, 2% w/v) were used. The viscoelastic properties of the samples were evaluated on a rotational rheometer (Mars HAAKE III, Thermoscientific, Germany) at 25°C.

HA-EDA-C<sub>18</sub> samples were subjected to small amplitude frequency sweep tests to evaluate the dependence of the elastic and viscous moduli,  $G'$  and  $G''$  upon frequency. Solubility tests were carried out by dissolving DM (0.05%), HA-EDA-C<sub>18</sub> and  $\beta$ -CD in DDW and DPBS.

DM release from HA-EDA-C<sub>18</sub> samples was studied by loading the gel in dialysis membranes (molecular cut off: 25 kDa), which were immersed in DPBS at 37 °C. At different time points, the release medium was withdrawn and analyzed by UV.

### RESULTS AND DISCUSSION

HA-EDA-C<sub>18</sub> samples showed a rheological behavior typical of a weak gel. The mechanical spectra was characterized by a elastic modulus  $G'$  greater than loss modulus  $G''$  in all frequency range. In particular for the sample characterized by HA-EDA-C<sub>18</sub> concentration of 3% w/v and  $\beta$ -CD of 1% w/v, at a frequency of 1 Hz,  $G'$  was about 185 Pa and  $G''$  about 50 Pa. Furthermore the viscoelastic properties of HA-EDA-C<sub>18</sub> samples were dependent upon polymer concentration. The increase in HA-EDA-C<sub>18</sub> concentration lead to an increase of both  $G'$  and  $G''$ . They have behaved as weak gel.

The drug solubility tests showed that the presence of hydrophobic groups on HA influenced the drug solubilization positively.

The release tests have shown that the presence of HA-EDA-C<sub>18</sub> leads to an increase of the percentage of drug released until reaching a plateau after one week.

### CONCLUSION

Amphiphilic HA derivative was able to solubilize hydrophobic drug and showed rheological properties of weak gel suitable for viscosupplementation applications. Moreover it was able to sustain the release of an anti-inflammatory drug for at least one week.

### REFERENCES

- 1) Borzacchiello A et al. Effect of hyaluronic acid amide derivative on equine synovial fluid viscoelasticity. Journal of biomedical materials research. Part A 92(3):1162-70, 2010 Mar 1.
- 2) Palumbo FS et al. In situ forming hydrogels of hyaluronic acid and inulin derivatives for cartilage regeneration Carbohydrate Polymers 10.1016/j.carbpol.2014.11.002



Anna Karewicz<sup>1</sup>, Agnieszka Rojewska<sup>1</sup>, Marta Baster<sup>1</sup>, Elena Iruin Amatriain<sup>2</sup>, Michał Rączy<sup>1</sup>, Maria Nowakowska<sup>1</sup>

<sup>1</sup> Nanotechnology of Polymers and Biomaterials Group, Faculty of Chemistry, Jagiellonian University, Cracow, Poland

<sup>2</sup> on leave from Faculty of Chemistry, University of the Basque Country, San Sebastián, Spain

[karewicz@chemia.u.edu.pl](mailto:karewicz@chemia.u.edu.pl)

## INTRODUCTION

Chronic inflammation may lead to a number of serious illnesses such as e.g. atherosclerosis, rheumatoid arthritis, cancer. It is also believed to be active in many other diseases such as asthma, chronic peptic ulcer, tuberculosis, or chronic active hepatitis. Therefore the effective treatment of inflammation is a subject of intense studies. One of the vital problems is the limited solubility of the most effective anti-inflammatory drugs, such as corticosteroids. Some of the promising candidates for anti-inflammatory drugs (e.g. curcumin) are also highly hydrophobic. This leads to their low bioavailability which either totally prevents the effective application or implies the use of high doses, resulting in serious side-effects<sup>1</sup>. One of possible solutions is to design a biocompatible, polymeric delivery system which allows for controlled, sustained delivery of the anti-inflammatory agent in its place of action<sup>3</sup>. Here we propose and compare two different approaches, both based on natural polysaccharides: microspheres encapsulating active agent and drug-releasing conjugate. Two model compounds were tested: dexamethasone<sup>2</sup> (DEX, potent corticosteroid) and curcumin<sup>3</sup> (CUR, highly promising natural agent). The release profiles in physiological conditions were measured and optimized. The influence of the microsphere's size, preparation methodology, pH and additional coating was also studied.

## EXPERIMENTAL METHODS

Sodium alginate/hydroxypropyl cellulose (ALG/HPC) microspheres were obtained either by cross-linking in microemulsion or by injecting of the polymer solution into the cross-linker (calcium chloride) solution under the stream of inert gas. The chitosan-DEX conjugate was synthesized in the three-step process, including ionic modification of the polymer followed by introduction of the spacer and binding of the drug to the polymeric chain. The products were characterized using FTIR, <sup>1</sup>H NMR, mass spectrometry and elemental analysis. Release profiles were obtained in physiological conditions (buffered aqueous media, 37°C), all measurements were done at least in triplicate. The release of CUR was followed by UV-Vis spectrophotometry, while DEX was assessed using HPLC with DAD detection using Waters C<sub>18</sub> column and acetonitrile/acetic buffer (65:35) mixture as eluent.

## RESULTS AND DISCUSSION

Both active compounds, CUR and DEX, were successfully encapsulated in polysaccharide-based microspheres. In order to increase the encapsulation

efficiency, prior to introduction into the polymeric matrix, curcumin was solubilized into micelles formed by Pluronic P-123<sup>®</sup>. This synthetic, biocompatible copolymer forms micelles at relatively low concentrations facilitating incorporation of the hydrophobic compound into the hydrophilic microspheres. Through injection into calcium chloride solution the particles of significantly larger sizes, in the range of hundreds of micrometers, were obtained. Cross-linking performed in water/cyclohexane emulsion, on the other hand, gave microspheres in the range of tens of micrometers.

DEX was modified using succinic anhydride to obtain water soluble product DEX-SA. Product identity was confirmed using mass spectrometry and FTIR spectroscopy. SA additionally functioned as a linker in the conjugate. Chitosan was first modified using glycidyltrimethylammonium chloride in order to increase its solubility in aqueous media. Finally DEX-SA was conjugated with cationic chitosan and the final product was characterised using NMR and FTIR spectroscopies and elemental analysis. Release studies for conjugate were performed after it was cross-linked with genipin forming gel. The influence of pH on the release profiles for both: microspheres and conjugate was studied.

## CONCLUSION

Two different polymeric systems were developed and studied as a possible solution for the optimized delivery of highly hydrophobic anti-inflammatory agents: CUR and DEX. Both compounds were successfully incorporated into ALG/HPC microparticles. The preparation procedure was optimized by using small amounts of Pluronic P-123, adjusting size of the particles and improving control of the release process. The influence of pH on the release profiles for both types of systems was studied. Both systems proved to be promising for defined areas of applications.

## REFERENCES

1. Anand P. *et al.* Mol. Pharmaceutics 4(6):807-818, 2007
2. Karewicz A. *et al.* Colloids Surf. B 88 231-239, 2011
3. Urbańska J. *et al.* Life Sciences 96:1-6, 2014

## ACKNOWLEDGMENTS

Authors would like to thank The National Centre for Research and Development (NCBiR) for the financial support in the form of grant no. K/NCB/000013 obtained in the frame of the INNOTECH Programme.



Daniela Giugliano<sup>1\*</sup>, Maria Grazia Raucci<sup>1</sup>, Luigi Ovaleo Pandolfo<sup>1</sup>, Alessandra Soriente<sup>1</sup>, Luigi Ambrosio<sup>1,2</sup>

<sup>1</sup>Institute of Polymers, Composites and Biomaterials of National Research Council of Italy (IPCB-CNR), Viale Kennedy, 54 Mostra d'Oltremare pad. 20-80125 Napoli

<sup>2</sup>Department of Chemical Science and Materials Technology of National Research Council of Italy (DSCTM-CNR)  
[daniela.giugliano@unina.it](mailto:daniela.giugliano@unina.it)

## INTRODUCTION

Recent advances in biotechnology to the production of various clinically useful peptides and proteins. Sustained peptide delivery can be established through different non-covalent retention mechanisms including physical entrapment, absorption and complexation, or in a covalent manner, using coupling agents. Current work employs a porous gelatin scaffold for the sustained delivery of an human BMP-2 derived-peptide, already applied clinically in bone regeneration for its high osteoinduction activity [1]. One strategy which has been used to produce a quite stable interactions is polyion complexation, in which release from a biodegradable and charged polymeric carrier may occur by electrostatic interactions. The consecutive treatment to guarantee a release in a long time, is the chemical immobilization of peptide into the scaffold [2]. However, because biodegradation of the carrier matrix would be the more likely mechanism of release, it is possible to control drug release kinetics by adjusting the rate of polymeric carrier degradation. In this work, we consider a gelatin (IEP of 5 or IEP of 9) as a polymeric matrix in order to realize a new gelatin crosslinked scaffold used as a vehicle for BMP2 release. Moreover, the combination of chemical immobilization and polyion complexation of peptide with matrix were done to obtain a release able to guarantee an appropriate biological response from human mesenchymal stem cells for bone tissue regeneration.

## EXPERIMENTAL METHODS

BMP-2 modified peptide (IEP of 8.59) (PM=2041.3Da H-NSVNSKIPKASSVPTLSAI-amide), was synthesized by Fmoc chemistry solid phase synthesis, using a microwave synthesizer (Initiator, Biotage). For the synthesis, Tentagel-S NH<sub>2</sub> resin functionalized by Rink Amyde Linker was used to obtain an amide peptide, with only C-terminal extremity with a carboxyl group. In our system, peptide immobilization occurs between COOH<sub>gelatin</sub> and NH<sub>2BMP2-mod</sub>; to induce this reaction, carboxylic acid groups of gelatin (Gel-COOH) were activated by adding EDC [EDC:Gel-COOH of 1.0:1.0] and amino groups of peptide by NHS [NHS:BMP2-mod-NH<sub>2</sub> of 0.2:1.0], both in 0.05M MES-buffer (pH 5.60) 2%w/v. The peptide amount is related to the free carboxyl acid groups in the gelatin crosslinked scaffold tested by titration analysis. Meanwhile, the polyion complexation was obtained by rehydrating crosslinked gelatin (IEP = 5) scaffold with BMP2 solution (50-200µM), and treated in incubator at 37°C for 2hrs.

## RESULTS AND DISCUSSION

Herein, the strategy was based on the design of a

crosslinked gelatin scaffold as controlled delivery vehicle for BMP-2 peptide. The high purity and molecular weight of BMP-2 (>95%) was verified by reverse phase HPLC chromatogram and mass spectrometry analysis.

Crosslinked gelatin scaffolds were prepared starting to a gelatin solution; freeze-drying technology produce a three-dimensional structure with interconnected pores. Titration and FTIR tests were used to analyze the crosslinking degree and peptide immobilization. In particular FTIR analysis, spotting the presence of amide band, confirms the occurred bond. For these systems, there seemed to be a rapid initial release of peptide (burst effect caused by peptide residues not linked at scaffold), followed by modulate release induced by electrostatic and chemical interaction between matrix and peptide.

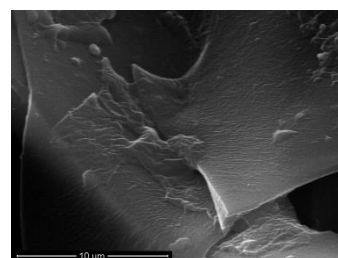


Figure 1: SEM analysis of gelatin scaffold after 28 days of hMSC cell culture in basal medium.

Already after 3 days, the burst effect induces an higher alkaline phosphatase (ALP) activity in basal medium than the plate control ones in the first days of incubation. The trend of biological response remains optimal due to the subsequent modulate release in time, as shown in figure 1.

## CONCLUSION

This work demonstrated that by two different release mechanisms, polyion complexation and peptide immobilization, is possible to obtain a controlled release system. The optimized crosslinked gelatin structure and BMP-2 peptide concentration, induce an early osteogenic differentiation in basal medium.

## REFERENCES

- [1] Gittens SA, Uludag H. *J Drug Target* 2001;9:407.
- [2] Young S, Wong M, Tabata Y, Mikos AG. *J Control Release* 2005;109:256.

## ACKNOWLEDGMENTS

This study was supported by MERIT n.RBNE08HM7T from the Ministero dell'Università e della Ricerca. The authors also thank Mrs S. Zeppetelli for facilitating biological analysis and Mrs C. Del Barone for microscopy investigations.

Matthias Schumacher<sup>1</sup>, Katrin S. Lips<sup>2</sup>, Michael Gelinsky<sup>1</sup><sup>1</sup>Centre for Translational Bone-, Joint- and Soft Tissue Research, Technische Universität Dresden, Germany<sup>2</sup>Laboratory for Experimental Trauma Surgery, Justus Liebig University Gießen, Germany[matthias.schumacher@tu-dresden.de](mailto:matthias.schumacher@tu-dresden.de)

## INTRODUCTION

The loading of growth factors (GF) into biomaterials and tissue engineering scaffolds has become focus of research in the last years since the local delivery of GF into a specific bone defect could help to increase defect healing via recruitment of bone-specific precursor cells as well as stimulation of their differentiation and activity. Low targeting efficiency and general side effects could be overcome by avoiding the systemic administration. Hydroxyapatite-forming calcium phosphate (CaP) bone cements, in particular, could be ideal carriers for growth factor delivery since they are highly biocompatible and resorbable, possess mild setting conditions and can easily be modelled into any bone defect. Since the direct integration of a sensitive GF may still deteriorate the protein structure and unspecific protein binding to the CaP allows only very limited control of its release kinetics, a carrier system entrapping and gradually releasing the GF is of interest.

Therefore, we investigated the applicability of sol-gel derived mesoporous bioactive glass (MBG) particles and granules as GF-loaded component in CaP bone cements. Besides bovine serum albumin (BSA) and lysozyme (LYZ) as model substances we investigated the applicability of the CaP/MBG system to gradually release the *brain derived neurotrophic factor* (BDNF) that has recently been demonstrated to also stimulate bone cells and thus new bone formation [1] and therefore could be an interesting GF in bone regeneration applications.

## EXPERIMENTAL METHODS

A sol-gel approach based on tetraethyl-orthosilicate was used to obtain MBG with intrinsic pores of approx. 5 nm diameter as described by Zhu et al. [2]. The MBG was ground to obtain a 50-150 µm powder fraction. Furthermore, a three channel 3D plotting system, developed by the Fraunhofer IWS (Dresden, Germany) on the basis of the Nano-Plotter<sup>TM</sup> device from GeSiM (Großerkmannsdorf, Germany) was employed to obtain 100-200 µm MBG granules via single-drop deposition into an silicone oil bath (Wacker Chemie, Germany). MBG was characterised by SEM and TEM. 10 wt-% MBG and granules were intermixed with an  $\alpha$ -tricalcium phosphate-based CaP cement (InnoTERE, Germany). After setting in humid atmosphere [3] porosity (He-pycnometry) and compressive strength were evaluated. BSA, LYZ and BDNF loading of MBG was performed by co-immersion in PBS for 30 min, followed by freeze-drying. BSA, LYZ and BDNF release from MBG and CaP/MBG composites was quantified by Bradford, Lysozyme assay and ELISA, respectively. *In vitro* cytocompatibility of GF-free composites was

investigated using primary human mesenchymal stem cells. Furthermore, the biologic activity of BDNF released from MBG was tested using primary human osteoprogenitor cells.

## RESULTS AND DISCUSSION

Characterisation of MBG powders and granules revealed a high intrinsic porosity and meso-pores in the range of 5 nm diameter. Granules had a regular spherical morphology (Fig. 1A). Compressive strength of the composites did not differ significantly from the unmodified CaP cement. No cytotoxic effect of the MBG modification on hMSCs could be detected. BSA (Fig. 1B) and LYZ release from pure MBG powders was shown to depend on the total loading and was fast compared to BDNF, where only ~3% of the initially loaded GF (30 ng/sample) was released within 48 h. Still, *in vitro* tests revealed a positive influence of the BDNF-modification on the adherence of bone precursor cells and thus proof the release of biologically active protein from the composite.

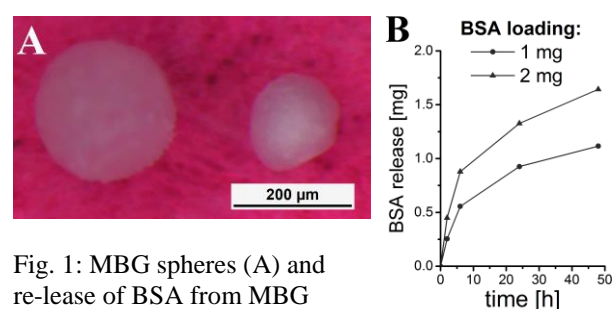


Fig. 1: MBG spheres (A) and re-release of BSA from MBG powder (B).

## CONCLUSION

CaP/MBG composites offer the possibility to deliver controlled amounts of biologically active, sensitive GF molecules into a specific defect location and thus could help in the regeneration of bone defects.

## REFERENCES

1. Kajiya M. *et al.*, J. Biol. Chem. 283:16259-67, 2008
2. Zhu, Y. *et al.*, Micropor. Mesopor. Mat. 112:494-503, 2008
3. Schumacher, M. *et al.*, Acta Biomater. 9: 7536-44, 2013

## ACKNOWLEDGMENTS

The authors thank O. Dakischew, L. Reither and M. May for excellent technical support and the German Research Foundation (Deutsche Forschungsgemeinschaft, DFG; grant SFB/Transregio 79) for providing financial support.

# **Rapid Fire Presentations**





## Development of Novel Bioresorbable Iron-Silver Materials and their *in Vitro* Degradation Behavior

Sanjaya K. Swain, David Starosvetsky, Irena Gotman, Elazar Y. Gutmanas

Department of Materials Science and Engineering, Technion, Haifa, 32000, Israel

[swains@technion.ac.il](mailto:swains@technion.ac.il)

### INTRODUCTION

Bioresorbable implants are increasingly considered for applications in orthopedic and cardiovascular surgery as an attractive alternative to permanent prosthetic devices. The limited load-bearing capacity of biodegradable polymers has led to strong interest in resorbable metals<sup>1</sup>. Iron-based alloys have high strength and can corrode in the body, albeit too slowly for most prospective applications. Thus, current research activities on bioresorbable Fe are focused on accelerating its degradation rate. One approach is to uniformly disperse nanoparticles that are cathodic towards Fe matrix to generate multiple galvanic nanocouples<sup>2</sup>. Silver (Ag) nanoparticles seem especially attractive, both due to their high electrode potential and recognized antimicrobial activity<sup>3</sup>. Here, we report the preparation of dense Fe-Ag specimens with different volume fractions of Ag by attrition milling and high pressure consolidation, their mechanical properties and corrosion behavior.

### MATERIALS AND METHODS

Fe powder ( $\sim 2 \mu\text{m}$ ) was mixed with 10, 20 and 30 vol.% silver oxide ( $\text{Ag}_2\text{O}$ ) powder ( $< 2 \mu\text{m}$ ) by attrition milling for 4 h in hexane under Ar, at 20:1 balls-to-powder ratio. The obtained powder blends were compacted at 400 MPa and annealed at  $450^\circ\text{C}$ , 1 h in  $\text{H}_2$ -flow to reduce  $\text{Ag}_2\text{O}$ . The compacts were then high pressure consolidated at 2.5 GPa, at  $T_{\text{room}}$  to the final dimensions of 10 mm diameter by  $\sim 1.2$  mm thickness. A part of specimens were annealed at  $600^\circ\text{C}$ , 2 h and repressed at 3 GPa. The density of the specimens was measured by the Archimedes method and their mechanical properties tested in an Instron machine. The microstructure and phase composition of the composites were characterized by x-ray diffraction (XRD) and scanning electron microscopy (SEM/EDS). The corrosion/degradation behavior was assessed in Ringer's solution by immersion and electrochemical tests.

### RESULTS AND DISCUSSION

According to XRD analysis, partial reduction of  $\text{Ag}_2\text{O}$  to metallic silver occurred already during attrition milling. Following  $\text{H}_2$ -treatment, the oxide was completely reduced to Ag as indicated by the disappearance of  $\text{Ag}_2\text{O}$  peaks from the XRD patterns. For all the compositions, SEM examination revealed a homogeneous distribution of submicron Ag in Fe matrix. High pressure consolidation resulted in  $\geq 95$  % density which was further increased 1-3 % after annealing and repressing. In Fig. 2, the 3-point bending strength of different Fe-Ag specimens is presented. The already high value of  $\sim 400$  MPa achieved by high pressure consolidation was increased 2.5-4 fold after annealing, with or without repressing. The behaviour of Fe-10Ag specimen after the  $600^\circ\text{C}$  anneal is especially

noteworthy: it exhibited a very high yield stress of 1450 MPa coupled with large ductility.

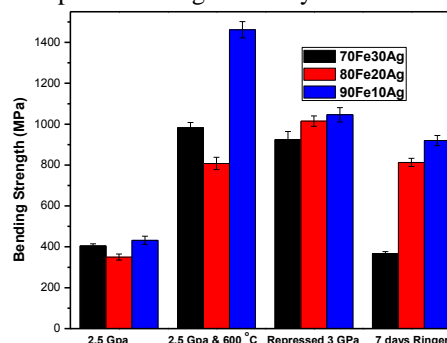


Fig. 1: Three-point bending strength of Fe-Ag (10, 20 and 30 %) after different processing steps, and after 7 days immersion in Ringer's solution (repressed specimens).

In corrosion experiments, Fe-30Ag behaved similarly to pure Fe, Fig. 2. In contrast, Fe-10Ag showed the highest corrosion current density indicating that the corrosion rate also increased. Following one week in Ringer's solution, Fe-10Ag specimens lost  $\sim 12\%$  of strength (less than the other compositions). Some acidification of immersion medium around Fe-10Ag (vs. pH increase for Fe-20/30Ag) is attributed to faster Fe dissolution.

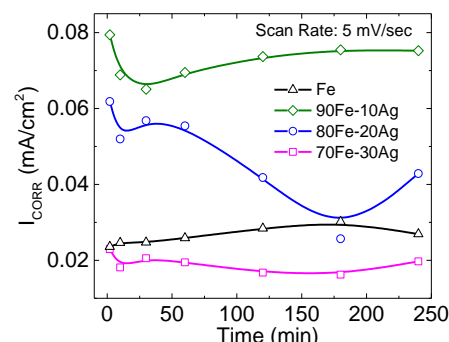


Fig. 2: Corrosion current density of Fe-Ag (10, 20 and 30 %) and pure Fe as a function of time.

### CONCLUSION

Dense and strong Fe-Ag specimens were produced by attrition milling of powders followed by high pressure consolidation. Fe-10vol.% Ag composites exhibited high bending strength, large ductility and faster dissolution rate as compared to pure Fe, making them a promising biodegradable material for medical applications.

### REFERENCES

1. Liu B. *et al.*, Acta Biomater. 7:1407-20, 2011
2. Schinhammer M. *et al.*, Acta Biomater. 6:1705-13, 2010
3. Rai M. *et al.*, Biotechnol Adv. 27:76-83, 2009

### ACKNOWLEDGMENT

This work was supported by Israel Science Foundation-ISF through research grant No. 1326/11.

# Dissolution Behaviours of MgO-P<sub>2</sub>O<sub>5</sub>-TiO<sub>2</sub>/Nb<sub>2</sub>O<sub>5</sub> Glasses in MgO-rich Region

Sungho Lee<sup>1</sup>, Hirotaka Maeda<sup>1</sup>, Akiko Obata<sup>1</sup>, Kyosuke Ueda<sup>2</sup>, Takayuki Narushima<sup>2</sup>, Toshihiro Kasuga<sup>1</sup>

<sup>1</sup> Department of Frontier Materials, Nagoya Institute of Technology, Gokiso-cho, Showa-ku, Nagoya 466-8555, Japan

<sup>2</sup> Graduate School of Engineering, Tohoku University, 6-6-02 Aoba, Aramaki, Aoba-ku, Sendai 980-8579, Japan

[kasuga.toshihiro@nitech.ac.jp](mailto:kasuga.toshihiro@nitech.ac.jp)

## INTRODUCTION

Calcium phosphate invert glasses (Ca-IGs), which consist of short phosphate chains such as ortho- and pyrophosphate, have been focused in our group<sup>1</sup>. Ca-IGs show *in vitro* and *in vivo* bioactivity<sup>2</sup>. Niobium-containing Ca-IGs showed a small amount of Nb<sup>5+</sup> ion, i.e., 0.04 ~ 0.06 mM, dissolved from the glasses enhanced ALP activity<sup>3</sup>. Magnesium-containing phosphate invert glasses showed excellent glassification in our previous work<sup>4</sup>. Mg<sup>2+</sup> ions accelerate osteoblasts' adhesion and enhance their cell proliferation and differentiation<sup>5,6</sup>. In this work, magnesium/titanium- or niobium-containing phosphate invert glasses with the compositions of MgO > 60 mol% were prepared and their dissolution behaviours and structures were characterized.

## EXPERIMENTAL METHODS

Magnesium/titanium- or niobium-containing glasses with the compositions of  $x\text{MgO} \cdot (90 - x)\text{P}_2\text{O}_5 \cdot 10\text{TiO}_2$  (mol%,  $x = 60$  to 66, nominal composition) and  $y\text{MgO} \cdot (94.5 - y)\text{P}_2\text{O}_5 \cdot 5.5\text{Nb}_2\text{O}_5$  (mol%,  $y = 66$  to 69, nominal composition) were prepared by a conventional melt-quenching method (1500°C). Glass transition temperature ( $T_g$ ) and crystallization temperature ( $T_c$ ) were estimated from differential thermal analysis (DTA; heating rate 5 K/min) and glassification degree<sup>7</sup> ( $(T_c - T_g)/T_g$ ; in K/K) was calculated. The glasses structure was examined by Raman spectra and <sup>31</sup>P magic angle spinning nuclear magnetic resonance (MAS-NMR). Their dissolution behaviours in Tris buffer solution (37 °C, 1 to 7 days) were evaluated by inductively coupled plasma atomic emission spectroscopy (ICP-AES).

## RESULTS AND DISCUSSION

Glassification degrees of the samples decreased with increasing Mg/P ratio in the glasses. Raman spectra showed the peak intensities corresponding to orthophosphate (980 cm<sup>-1</sup>), TiO<sub>4</sub> (830 cm<sup>-1</sup>) and NbO<sub>4</sub> (830 cm<sup>-1</sup>) increases, and TiO<sub>6</sub> (660 cm<sup>-1</sup>) and NbO<sub>6</sub> isolated (915 cm<sup>-1</sup>) decreased with increasing Mg/P ratio in the glasses. Fig.1 shows the peak area fractions of orthophosphate ( $Q^0$ ) and pyrophosphate ( $Q^1$ ) groups, estimated from <sup>31</sup>P MAS-NMR spectra.  $Q^0$  fraction increased with increasing Mg/P ratio in glasses, and the glasses of Mg/P > 1.25 indicated the  $Q^0$  fraction was larger than  $Q^1$  one. With the increase in the fraction of  $Q^0$  in the glasses, intermediate oxides such as TiO<sub>2</sub> and Nb<sub>2</sub>O<sub>5</sub> act as network formers, and they take the form of TiO<sub>4</sub> or NbO<sub>4</sub> tetrahedral in the glasses. Mg<sup>2+</sup> and P<sup>5+</sup> ions amounts dissolved from the glasses increased with increasing Mg/P ratio in glasses. Mg<sup>2+</sup> ion of 1 to 2 mM, which may enhance cell adhesion, dissolved from the glasses in day 3. 1.8 mM of Mg<sup>2+</sup> ion were reported to

promote cell adhesion<sup>5</sup>. In cases of titanium and niobium, no significant differences in ion dissolution amounts were observed between 1.00 and 1.24 of Mg/P ratios in the glasses. In the glasses of Mg/P = 1.36, the dissolution amount of Ti<sup>4+</sup> and Nb<sup>5+</sup> ions decreased, since gel layer may form on the glass surface. Magnesium/titanium- or niobium-containing glasses showed lower chemical durabilities compared with Ca-IGs, since Mg<sup>2+</sup> ion coordinates preferentially with phosphate groups and inhibits the formation of P-O-Ti/Nb bonds, which improve the chemical durability of phosphate glasses.

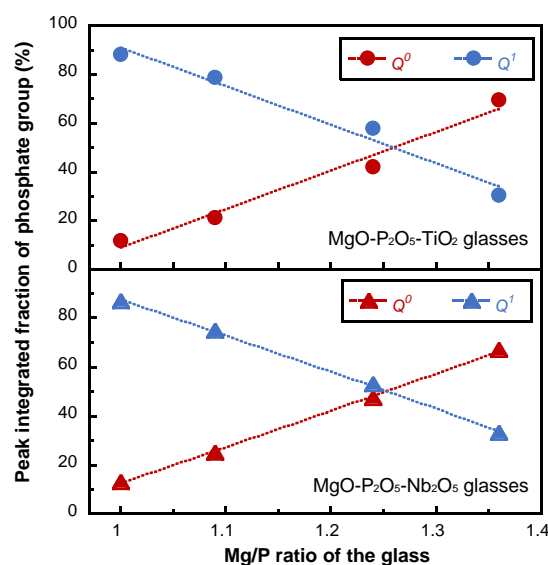


Fig. 1 Contents of  $Q^n$  groups in the glass.

## CONCLUSION

Calcium-free phosphate invert glasses were prepared. With increasing Mg/P ratio in the glasses, the chemical durability of the glasses decreased, since Mg<sup>2+</sup> ions predominantly bond with phosphate groups and inhibit to make bonds between intermediate oxides and phosphate groups. MgO-P<sub>2</sub>O<sub>5</sub>-TiO<sub>2</sub>/Nb<sub>2</sub>O<sub>5</sub> glasses may be used for coating layer on Ti or Ti-alloys for enhancing cell adhesion owing to Mg<sup>2+</sup> ions dissolved from the glasses.

## REFERENCES

1. T. Kasuga *et al.*, J. Non-Cryst. Solids, 243:70, 1999
2. T. Kasuga *et al.*, Phosphorus Res. Bull., 26:8, 2012
3. A. Obata *et al.*, ACS Appl. Mater. Interfaces, 4:5684, 2012
4. H. Morikawa *et al.*, J. Non-Cryst. Solids, 380:53, 2013
5. M. Takeichi *et al.*, Exptl. Cell Res., 74:51, 1972
6. A. Saboori *et al.*, Mater. Sci. Eng., 29:335, 2009
7. M. Ouchetto *et al.*, Phys. Chem. Glasses. 32:22, 1991



Robin Rajan, Kazuaki Matsumura

School of Materials Science, Japan Advanced Institute of Science and Technology, Japan  
[robinrajan2004@gmail.com](mailto:robinrajan2004@gmail.com)

## INTRODUCTION

Cryopreservation of cells refers to storing of cells under very low temperature for a long time. The conventional cryoprotectants (CPAs) like dimethyl sulfoxide (DMSO) and glycerol have many problems and need to be replaced with newer CPAs for various biomedical purposes.<sup>1</sup> In this research; structurally analogous novel synthetic polyampholytes were synthesized via living radical polymerization and examined for their propensity to cryopreserve cells. These Polyampholytes surprisingly exhibited disparate cryoprotective properties.<sup>2</sup> And we believe this structure activity relationship study of polyampholytes could lead us further towards elucidation of molecular mechanism which is crucial for its employment in regenerative medicines and more efficient design of CPAs in the future. The interaction of the different synthetic polymers with cell membrane and their mode of action during freezing, i.e., the mechanism of cryopreservation were evaluated for the first time ever and it revealed that cryoprotective polyampholytes inhibit the recrystallization of ice and forms an irreversible matrix which protects cells from freezing damage.

## EXPERIMENTAL METHODS

Various polymers were synthesized via reversible addition fragmentation chain transfer (RAFT) polymerization. Polymer kinetics and control of its living nature was studied by using  $^1\text{H}$ -NMR and gel permeation chromatography. Interaction of polyampholytes with cell membrane was analysed by using liposome as a cell membrane mimic and various physicochemical analysis like infrared spectroscopy, differential scanning calorimetry, leakage experiment, electron spin resonance (ESR), etc. were carried out. Behaviour of polymer solution during freezing was examined using cryomicroscopy and  $^1\text{H}$  and  $^{23}\text{Na}$  solid state NMR under magic angle spinning conditions.

## RESULTS AND DISCUSSION

Copolymer of methacrylic acid and 2-dimethylaminoethylmethacrylate, poly-(MAA-DMAEMA), showed excellent cryoprotective properties and incorporation of hydrophobicity enhanced cell viability significantly. On the other hand, poly-carboxymethylbetaine (poly-CMB) didn't show any such property, whereas poly-sulfobetaine (poly-SPB), showed intermediate cryoprotective properties. Cooling splat assay demonstrated that poly-(MAA-DMAEMA) inhibits the recrystallization of ice during freezing to the maximum extent as compared to other polymers and thus prevents cell death caused by growth of ice crystals and, introduction of hydrophobicity inhibited ice recrystallization almost completely (Fig. 1). ESR

studies revealed that the polyampholytes' penetration inside the cell membrane has a strong influence on its cryoprotective behaviour.

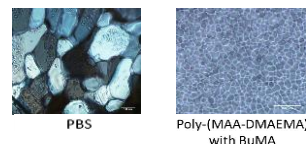


**Figure 1** Micrographs of poly-nucleated ice crystals after 30 minutes annealing at  $-6^\circ\text{C}$  (scale bars =  $100\mu\text{m}$ )

FTIR and DSC studies unveiled the chemical nature of interaction of the polyampholytes with the membrane and its effect on the phase transition temperature of the membrane after freezing. Solid state  $^1\text{H}$  NMR studies of the polyampholytes showed lower molecular motion in poly(MAA-DMAEMA) during freezing, which means that poly-(MAA-DMAEMA) forms a matrix around the membrane during freezing, thus preventing its damage from ice crystals (Fig. 2).  $^{23}\text{Na}$  NMR showed that polymers trap ions during freezing which protects it from osmotic stress.

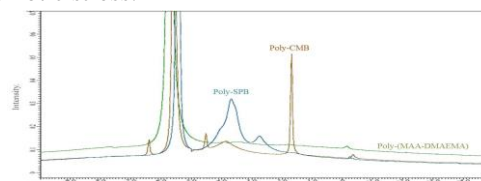


**Figure 2** Solid state  $^1\text{H}$ -NMR spectra of polyampholytes in saline solutions at  $-20^\circ\text{C}$ .

## CONCLUSION

Synthetic polymers can efficiently cryopreserve various types of cells and addition of a small amount of hydrophobicity can significantly enhance its cryopreservation potential. Moreover, the polyampholyte structure is crucial for its cryoprotective property. Cryoprotective polyampholytes act by inhibiting the recrystallization of ice and they have more interaction with the cell membrane which is characterized by their membrane penetration. Also they protect cells from stresses such as drastic changes in soluble space size and osmotic pressure.

## REFERENCES

1. Matsumura K. et al., *Biomaterials* 30:4842-49, 2009.
2. Rajan R. et al., *J. Biomater. Sci. Polym. Ed.* 24:1767-80, 2013

## ACKNOWLEDGMENTS

"The authors would like to thank the Grant-in-Aid for Young Scientists (B), MEXT, (Grant no: 25870267) for providing financial support to this project.



Minkle Jain, Kazuaki Matsumura

School of Materials Science, Japan Advanced Institute of Science and Technology, Japan  
[s140151@jaist.ac.jp](mailto:s140151@jaist.ac.jp)

## INTRODUCTION

For ages the ideal component required to formulate the tissue engineering constructs includes cells, growth factors and scaffolds that results in regenerative response. In order to recapitulate the features pre-existing in nature, currently various nanoceramics such as synthetic silicates<sup>1</sup> and nano-hydroxyapatite are used. Injectable hydrogels that can be applied with minimally applied pressure that is with shear thinning<sup>2</sup> property has opened the new avenues in the field of tissue engineering. In this current study we have focused on the development of new polymer –nanocomposites with novel inorganic/ organic network structures based on laponite (XLG) and succinylated poly-L-lysine (PLL-SA). Previously, our group has reported that poly-L-lysine based polyampholytes are potent cryoprotectants<sup>3</sup> and it can be formulated into hydrogel with cryoprotective property<sup>4</sup>. Our main goal of this study is to develop such a system in which cells can be cryopreserved by the use of PLL-SA and then after thawing this can be converted to gel by physical crosslinking of the polymer and laponite. Here PLL-SA has been used to synthesise physically crosslinked polymer-laponite based hydrogel with tunable mechanical property.

## EXPERIMENTAL METHODS

PLL-SA was synthesised by reacting PLL aqueous solution with succinic anhydride in different mole ratios from 0-80% against  $\text{NH}_2$  group. This differently succinylated PLL was then mixed with laponite in appropriate amounts to formulate the hydrogel. Various parameters were varied to tune the mechanical properties like polymer and laponite concentration, pH and succination ratio. These hydrogels were analysed by XRD and ATR-IR. Dynamic mechanical analysis (DMA) was also carried out.

## RESULTS AND DISCUSSION

XRD data reveals that due to anisotropic distribution of charges in laponite and polyampholytes, intercalation of the polymer is taking place. It also demonstrates that intercalation of the polymer can be tailored by varying pH and degree of substitution of succination in PLL. This unique interaction of the polymer and the laponite leads to the development of smart hydrogels, which have different mechanical properties ranging from 500 Pa to 10 kPa (Figure 1). They exhibit thixotropic property through autonomic reconstruction of crosslinks across damaged interface (Figure 2). The biomedical relevance of this system can be seen through the cell adhesion and proliferation on their surface. Cryopreservation of mouse preosteoblasts cells MC3T3

was successfully carried out using 65% succinylated PLL (PLL-SA (0.65)). It shows excellent post thaw survival efficiency. These results indicate that cryopreserved cells with PLL-SA could directly form hydrogel by mixing with laponite just after thawing to apply as an injectable hydrogel.

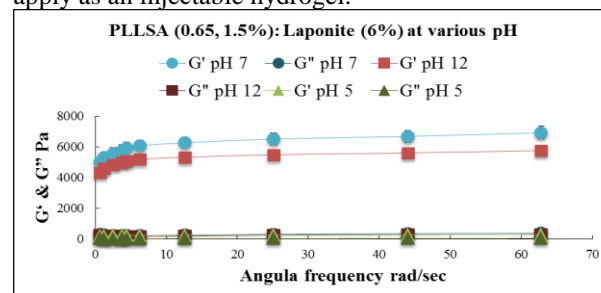


**Figure 1** Tuning of mechanical strength of gel by pH variation

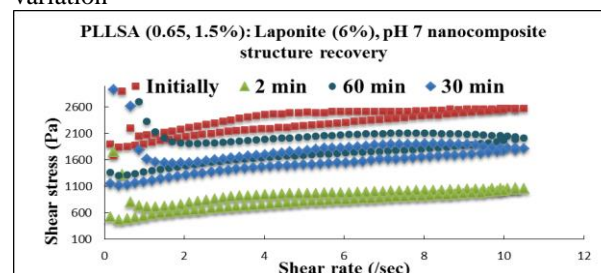


**Figure 2** Shear-thinning property of gel by DMA

## CONCLUSION

The current study clearly demonstrates that PLL-SA-laponite based system exhibit tunable mechanical property and they are suitable candidates for the smart hydrogels. This system can be used as injectable hydrogels that can be employed with minimally applied pressure due to shear thinning property. Thus, these hydrogels can serve as scaffolds with thixotropic and cryoprotective properties that also provide structural integrity to tissue constructs.

## REFERENCES

1. Gharwar A.K. *et al.*, ACTA BIOMATER. 7:568-577, 2011.
2. Gharwar A.K. *et al.*, ACS NANO. DOI: 10.1021/nn503719n (in press).
3. Matsumura K. *et al.*, Biomaterials, 30:4842-4849, 2009.
4. Jain M. *et al.*, Biomater. Sci. 2:308-317 (2014).

## ACKNOWLEDGMENTS

“The authors would like to thank the Grant-in-Aid for Young Scientists (B), MEXT, (Grant no: 25870267) for providing financial support to this project.



## INTRODUCTION

The rupture of the anterior cruciate ligament (ACL) is the most frequent injury of the knee joint with 47%. The reconstruction with autologous tissue from patellar or hamstring tendons has proven its worth despite various risks, such as differing biomechanics or donor site morbidity.

Tissue engineering represents a potential alternative. Biocompatible scaffolds with defined biomechanical properties are required. As one of the textile production processes, embroidery technology facilitates the variation and control of the mechanical characteristics.

## EXPERIMENTAL METHODS

Embroidery technology was used to fabricate three-dimensional (3D) scaffolds (Fig. 1A) from absorbable filaments of poly-L-lactic (PLA, multifilament, 155 dtex) and poly(lactic-co-ε-caprolactone) (PLA-CL, monofilament, 100 dtex).

Scaffolds consisted of 3 two-dimensional layers each with one upper and lower thread, which were stacked and locked to build up a 3D structure according to the dimensions of lapin ACL (10 mm×4 mm×2 mm). Scaffolds were manufactured on water soluble polyvinylalcohol nonwoven, which was washed out in water after the locking process. Scaffolds were rinsed with pure ethanol for 30 min in preparation for the degradation study. Two types of embroidered structures (n=5) were analysed, *MOCO* (mono-component) with PLA as upper and lower thread as well as *BICO* (bi-component) consisting of PLA-CL as upper and PLA as lower thread.

Hydrolytic degradation was performed under physiological conditions in culture medium. The mechanical properties (Fig. 1B) of three different test groups were evaluated at different degradation time points with a tensile testing machine. Results were represented as mean ± standard deviation.

## RESULTS AND DISCUSSION

The influence of hydrolytic degradation on viscoelastic behaviour of embroidered scaffolds was investigated

and compared to lapin ACL. Embroidered scaffolds demonstrated the ability to adapt the biomechanical properties by configuring the embroidery pattern and the material combination<sup>1</sup>.

The intensity of relaxation decreased with previous hysteresis loading for both scaffold types. The relaxation behaviour was more pronounced for *BICO* compared to *MOCO*. However the relaxation behaviour of *BICO* and *MOCO* was comparable to lapin ACL (Fig. 1C)<sup>2</sup>.

The ultimate tensile properties showed no significant differences for both scaffold types whether the scaffolds were unloaded or preloaded by relaxation and/or hysteresis. There were no measurable degradation effects on the mechanical properties after 28 days in culture medium.

In addition to the promising mechanical properties, Hoyer et al. investigated ACL cell adherence and activity on embroidered collagen hybrid scaffolds and demonstrated the potential of this reconstruction strategy<sup>3</sup>.

## CONCLUSION

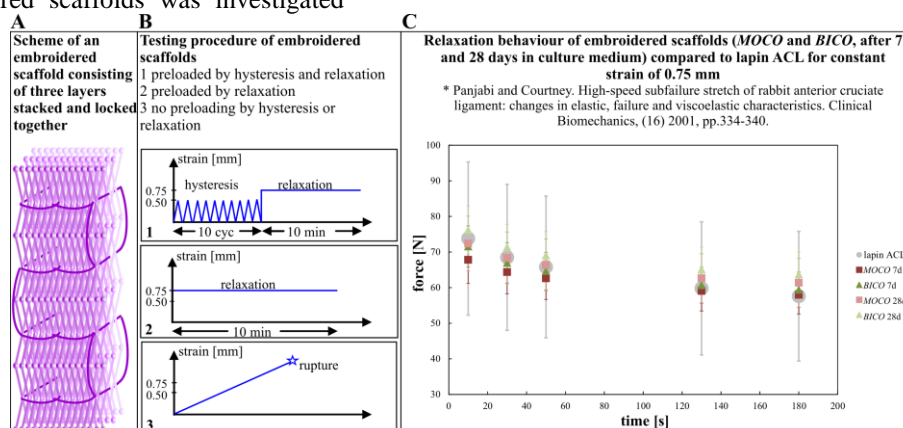
The qualitative and quantitative characterisation of the mechanical properties of embroidered scaffolds was investigated to find an optimal adjustment to native ligament tissue. The viscoelastic behaviour of embroidered scaffolds is comparable to lapin ACL either in dry state or under hydrolytic degradation.

## REFERENCES

1. Hahner J. *et al.*, Text Res J., DOI: 10.1177/0040517514566107, 2015
2. Panjabi M. Clin Biomech. 16:334-340, 2001
3. Hoyer M. *et al.*, Mat Sci Eng C, 43:290-299, 2014

## ACKNOWLEDGMENTS

The authors thank the Deutsche Forschungsgemeinschaft (HE 4466/22-1) for providing financial support.



## Exploring the Limits of Scaffold Interconnectivity for Cell Type Specific Invasion

Jennifer Ashworth<sup>1</sup>, Marco Mehr<sup>2</sup>, Paul Buxton<sup>2</sup>, Serena Best<sup>1</sup>, Ruth Cameron<sup>1</sup>

<sup>1</sup>Cambridge Centre for Medical Materials, University of Cambridge, UK

<sup>2</sup>Geistlich Pharma AG, Wolhusen, Switzerland

[jca35@cam.ac.uk](mailto:jca35@cam.ac.uk)

### INTRODUCTION

Structural cues in collagen scaffolds have great potential for influencing the characteristics of cell invasion.<sup>1</sup> Since accessibility to cells is a necessity for tissue engineering scaffolds, it is vital that the relationship between scaffold structure and cell invasion is well understood. However, there are still gaps in this understanding. In particular, the link between cell invasion and scaffold interconnectivity is obscured by the difficulties involved in interconnectivity characterisation.<sup>2</sup> In this study, we demonstrate how new Micro-CT analysis can allow interconnectivity parameterisation and correlation to the invasion behaviour of various cell types. This method has the potential to provide new criteria for scaffold design, allowing invasion control according to cell type.

### EXPERIMENTAL METHODS

Scaffolds were fabricated by freeze-drying a 1% w/v suspension of insoluble type I bovine collagen from Achilles tendon. Systematic control of scaffold interconnectivity at constant pore size was achieved by variation of fabrication parameters including suspension medium and freezing temperature. X-ray Micro-Computed Tomography (Micro-CT) analysis allowed assessment of pore structure. Scaffold interconnectivity was parameterised by measurement of percolation diameter,  $d_c$ : the largest spherical object able to travel through an infinitely large scaffold. For the cell invasion tests, periodontal ligament fibroblasts (PDLF), MC3T3 or HT1080 cells were seeded onto the scaffold surfaces at 64,000 cells per 1 cm<sup>2</sup>. After 3 days of culture, Phalloidin-staining, cross-sectioning and confocal microscopy allowed assessment of cell invasion. Median cell position was then measured to quantify invasion distance. Mean  $\pm$  standard error is displayed for both  $d_c$  (n=3) and invasion distance (n=6).

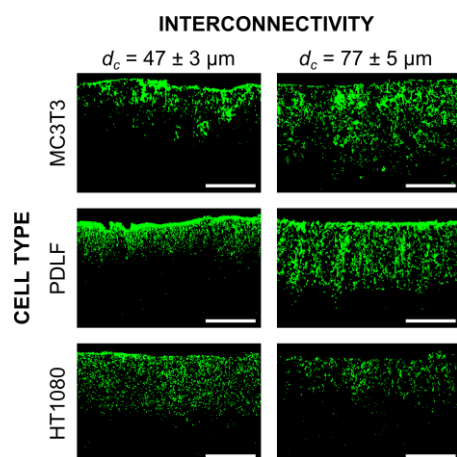


**Figure 1:** Representative Phalloidin-stained scaffold sections showing cell position at day 3. Scale bar 1 mm.

### RESULTS AND DISCUSSION

Representative cross-sections in figure 1 show that scaffold interconnectivity has a variable influence on invasion, according to cell type. At a constant pore size of 70  $\mu$ m, an increase in  $d_c$  from 47 to 77  $\mu$ m allowed both MC3T3 and PDLF cells to invade at visibly greater efficiency. Conversely, there was no clear correlation between scaffold structure and invasion of fibrosarcoma HT1080 cells, which instead showed erratic behaviour that may be explained by their origin. Extension of the range of scaffolds under investigation as in figure 2 revealed a sharp increase in PDLF invasion efficiency as interconnectivity exceeds  $d_c > 40$   $\mu$ m. Combined with the results from figure 1, this indicates the existence of a critical interconnectivity threshold between  $40 < d_c < 50$   $\mu$ m for PDLF invasion, with a similar threshold for MC3T3 cells. The comparatively enhanced HT1080 invasion at low  $d_c$ , however, suggests a lower critical interconnectivity threshold for these cells. Previous studies in microfluidic channels indicate that cells alter their migration behaviour in channels of widths close to that of a single cell.<sup>3</sup> Here we have demonstrated that by quantitative interconnectivity characterisation, similar structure-function correlations may be identified in natural polymer scaffolds.

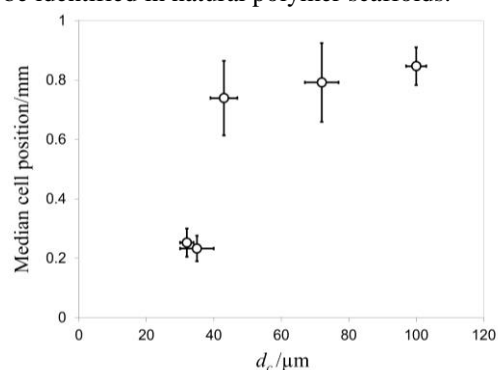


**Figure 2:** Plot of median cell position against  $d_c$  for PDLF cells after three days culture.

### CONCLUSION

Parameterisation of scaffold interconnectivity has identified a critical interconnectivity threshold required for efficient cell invasion, which varies with cell type. This result indicates future potential for directing cell type specific invasion by control of scaffold design.

### REFERENCES

1. Harley B. *et al.*, Biophys. J. 95:4013-4024, 2008
2. Ashworth J. *et al.*, Mater. Technol. 29:281-295, 2014
3. Mills R. *et al.*, Tissue Eng. Pt. C 17:999-1010, 2011

### ACKNOWLEDGMENTS

The authors acknowledge financial support of EPSRC, ERC Advanced Grant 3D-E and Geistlich Pharma AG.



## The Impact of Thrombocytes on the Cell Proliferation within the 3D Scaffolds

Kateřina Pilařová<sup>1</sup>, Věra Jenčová<sup>1</sup>, Jana Horáková<sup>1</sup>, Jakub Erben<sup>1</sup>, Jiří Chvojka, David Lukáš<sup>1</sup>

Department of Nonwovens and Nanofibrous Materials, Technical University of Liberec, Czech Republic  
[katerina.pilarova1@tul.cz](mailto:katerina.pilarova1@tul.cz)

Thrombocytes are well known to be involved in blood coagulation and hemostasis. But they also play an important role in inflammatory and immune responses, cardiovascular diseases and wound healing and many others. They possess number of different granules with a large variety of molecules including chemokines, cytokines, adhesive molecules and immune receptors, which can be secreted when the platelets are activated. Due to all these factors, platelets could help cell proliferation and migration within different scaffolds.

### INTRODUCTION

The platelets possess many good features<sup>1</sup>, among others, they contain a number of active molecules as cytokines, chemokines, adhesive molecules and immune receptors<sup>2</sup>. They are able to attach other cells and stimulate their proliferation<sup>3</sup>. Thus, it would be advantageous to support the cell growth on the scaffolds naturally by these molecules produced by platelets. In our experiments, platelets were able to adhere to our scaffolds and even they supported the cell proliferation and migration into the inner structure of the material.

### EXPERIMENTAL METHODS

The 3D scaffolds made from PCL (Sigma) by combination of melt-blown and electrospinning method<sup>4</sup> were used for in vitro experiments. The samples were analysed by SEM, followed by image analysis.

The scaffolds were treated with platelets for 2 hours prior to cell seeding. Scaffolds were seeded by 3T3 mice fibroblasts ( $1 \times 10^4$  / well) for evaluation of the rate of cell adhesion and proliferation. Controls were taken as follows: scaffolds treated only by platelets, scaffolds seeded only with cells.

Scaffolds were tested for platelet adhesion and activation and cell adhesion and proliferation by fluorescent (anti-CD41-FITC and propidium iodide, respectively) and scanning electron microscopy and by MTT assay. Scaffold were tested 2 hours after platelets treatment and at day 1, 3, 7 and 14 after cell seeding.

### RESULTS AND DISCUSSION

The 3D scaffolds were made from PCL by melt-blown technology and electrospinning. The average electrospun fiber diameter was  $732 \pm 292$  nm, the average meltblown fiber diameter was  $6,5 \pm 4,4 \mu\text{m}$ . The porosity of scaffolds was 95%. Scaffolds were seeded with cells, thrombocytes and cells or thrombocytes only. Our results from fluorescent microscopy as well as from SEM show, that our scaffolds are capable of thrombocytes adhesion (Fig. 1).

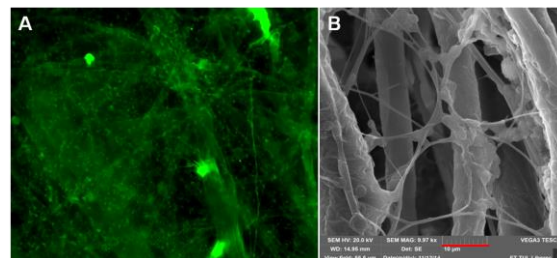


**Fig. 1:** Fluorescent microscopy, magnification 400x (A) and SEM (B) of adhered thrombocytes after 2h of incubation. Scale bar: 10  $\mu\text{m}$ .

From the MTT assay results it is obvious that scaffolds treated with thrombocytes prior to cell seeding show higher proliferation rate than cells only (Fig. 2). Thus, thrombocytes' treated scaffolds support the growth of 3T3 mice fibroblast better than melt-blown scaffolds alone.

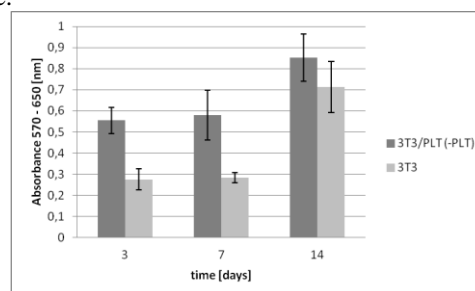


**Fig. 2:** MTT assay results after day 3, 7 and 14 after cell seeding.

### CONCLUSION

Our results show that the melt-blown scaffolds are capable for platelets' adhesion. According to the MTT assay the scaffolds treated with platelets show higher proliferation rate of 3T3 mice fibroblasts.

### REFERENCES

1. Thushara R. M. *et al.*, Crit. Rev. Oncol. Hematol., 2014
2. Tamagawa-Mineoka R., J. Dermatol. Sci., 2014
3. Gawaz M. *et al.*, Blood 122:2550-2554, 2013
4. Erben J. *et al.*, Mater. Lett. 143:172-176, 2015

### ACKNOWLEDGMENTS

The authors would like to thank the Regional Hospital in Liberec for providing us the thrombocytes.

## Development of a Valved Conduit for Venal Reconstruction

Sonia Zia<sup>1</sup>, Lucrezia Morticelli<sup>1</sup>, Karsten Grote<sup>2</sup>, Igor Tudorache<sup>1</sup>, Sergei Cebotari<sup>1</sup>, Andres Hilfiker<sup>1</sup>, Birgit Glasmacher<sup>3</sup>, Axel Haverich<sup>1</sup>, Sotirios Korossis<sup>1</sup>

<sup>1</sup>Department of Cardiothoracic, Transplantation and Vascular Surgery, Hannover Medical School, Germany

<sup>2</sup>Department of Cardiology and Angiology, Hannover Medical School, Hannover, Germany

<sup>3</sup>Institute for Multiphase Processes, Leibniz Universität Hannover, Hannover, Germany

[zia.sonia@mh-hannover.de](mailto:zia.sonia@mh-hannover.de)

### INTRODUCTION

Chronic venous insufficiency has an incidence of 0.3-3% in Western Europe and North America<sup>1</sup>. Usually, dysfunctional veins are replaced by synthetic grafts that, however, lead to early infection, as well as to degeneration, dilation and calcification. Decellularised native valved venal grafts have the potential to offer a promising solution for venal reconstructions that can overcome the limitations of current alternatives<sup>1,2</sup>. The aim of this study was to develop a decellularised porcine saphenous vein scaffold suitable for venal reconstruction.

### EXPERIMENTAL METHODS

Saphenous veins were isolated from 6-9 months pigs and tested within 4 hours of animal slaughter. Valved venal samples were treated with a protocol incorporating sodium dodecyl sulphate (SDS) and Triton X-100. Treated samples, together with native veins were assessed histologically, biochemically and immunohistochemically. The cellular content and gross histoarchitecture of treated and untreated veins were determined by haematoxylin & eosin (H&E), DAPI and collagen IV staining, whereas collagen and elastin were visualised by Masson's trichrome and Van Gieson stain, respectively. Total collagen content was determined by hydroxyproline (HXP) quantification, and glycosaminoglycan (GAG) content by papain digestion. The cytotoxicity of the decellularised scaffolds was assessed by contact and extract cytotoxicity tests, according to ISO 10993-5. The results were analysed by Student's t-test for comparison of two group means and one-way ANOVA for more than two groups at the 95% confidence interval.

### RESULTS AND DISCUSSION

Histology and immunohistochemistry confirmed the complete removal of the cells and the preservation of extracellular matrix (ECM) in the decellularised scaffolds. Collagen IV was observed in the media and basement membrane of both the native and decellularised tissue with no apparent differences. As previously reported, an intact basement membrane is beneficial for the effective graft endothelialization<sup>3</sup>. Furthermore, no significant difference was found in the total collagen level between the native vein and decellularised scaffold. On the other hand, the GAG content was significantly reduced in the treated samples compared to the native tissue. The *in vitro*

biocompatibility assessment indicated that the treated tissue did not induce any cytotoxic effects to L929 murine fibroblasts.

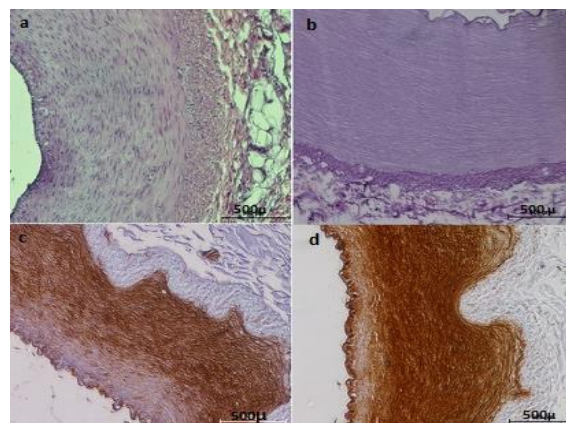


Figure 1. (a) Fresh porcine saphenous vein stained with H&E. (b) Decellularised vein stained with H&E. (c) Fresh vein stained for collagen IV. (d) Decellularised vein stained for collagen IV.

### CONCLUSION

This work successfully developed a non-cytotoxic decellularised saphenous vein valved scaffold, which grossly maintained its natural histoarchitecture and biochemical composition. Future work will focus on the assessment of the  $\alpha$ -gal content of the decellularised scaffolds, as well as on the assessment of its biomechanical and haemodynamic performance.

### REFERENCES

1. Teebken OE. *et al.*, Eur. J. Vasc. Endovasc. Surg. 4:305-12, 2003
2. Luo J. *et al.*, Tissue Eng. Part A. 21-22:2963-74, 2014
3. Brown B. *et al.*, Tissue Eng. 3:519-26, 2006

### ACKNOWLEDGMENTS

This work was supported by the Lower Saxony Centre for Biomedical Engineering, Implant Research and Development (NIFE) and the REBIRTH Cluster of Excellence.



# Biocompatible Collagen Paramagnetic Scaffold for Controlled Drug Release

Valentina Bonfrate<sup>1\*</sup>, Simona Bettini<sup>2</sup>, Luca Salvatore<sup>1</sup>, Marta Madaghiele<sup>1</sup>, Ludovico Valli<sup>2</sup>, Gabriele Giancane<sup>3</sup>, Alessandro Sannino<sup>1</sup>

<sup>1\*</sup> Department of Engineering for Innovation, University of Salento, Italy

<sup>2</sup> Department of Biological and Environmental Sciences and Technologies, DISTEBA, University of Salento, Italy

<sup>3</sup> Department of Cultural Heritage, University of Salento, Italy

[valentina.bonfrate@unisalento.it](mailto:valentina.bonfrate@unisalento.it)

## INTRODUCTION

Porous and biocompatible hydrogels able to deliver hydrosoluble drugs, cells or active compounds have been largely employed in biomedicine<sup>1</sup>. The major problems with the use of these biomaterials are related to a difficult control of the release kinetics of the loaded drugs. The mesh size of hydrogels, which depends on the crosslinking reaction, is a powerful means to tune the diffusion of molecules within the polymeric matrix<sup>2</sup>. Collagen is a natural polymer can be molded into various forms of scaffolds and/or drug delivery systems for a number of biomedical applications. One the most effective chemical crosslinker for collagen is the formaldehyde but is well known as being strongly toxic which limits its use for *in vivo* experiments and applications<sup>3</sup>. In this work, non-toxic magnetite nanoparticles (NPs) are proposed and used in a double role: NPs can work as effective crosslinkers for porous hydrogel matrices and can also provide the matrix with a sharp and accurate sensitivity to an external trigger. The paramagnetic behavior of NPs permits to use an external stimulus, i.e. the application of a magnetic field, to induce and control the release of any loaded substance from the gel matrix. It is worth noting that the interaction among nanoparticles and collagen fibers can also guarantee the magnetite NPs stabilization, preventing their aggregation and oxidation.

## EXPERIMENTAL METHODS

**Synthesis of porous collagen gel (CG).** An aqueous suspension of 0,5% w/v Type I collagen from bovine dermis was prepared by mixing for 5-6 hours at 10°C. Following casting, freeze-drying and dehydrothermal crosslinking treatment (DHT) porous collagen gel was obtained. **Crosslinking by Formaldehyde (CGFA).** Hydrated CG samples were immersed in a 0,4% (v/v) FA aqueous solution for 2h. **Fabrication of Porous Paramagnetic Collagen Gel (NPsCG).** The NPs aqueous solution was added to the collagen slurry while stirring. The suspension was then treated as for CG porous matrices.

**Characterization experiments.** FTIR Analysis, SEM, TG Analysis and Swelling studies were carried out. Release properties were studied by means of fluorescence spectroscopy. The cytotoxicity of all the samples was assessed *in vitro* using a 3T3 cell line, by means of MTT assay.

## RESULTS AND DISCUSSION

A biocompatible cross-linker represented by paramagnetic NPs was used to create a collagen-based gel able to retain water-soluble molecules and then activate their release in the presence of an external magnetic field. By means of infrared spectrometry, the interactions between collagen fibers and NPs were

studied. N-H group vibrations, both stretching and bending modes, and the absorption band of C=O and C-N groups of amide I and amide III drastically change in the presence of the paramagnetic nanoparticles, suggesting the formation of a network among the collagen fibers. The role of NPs was confirmed by scanning electron microscopy that showed a porous matrix with an average pore dimension of 50  $\mu$ m, comparable to that one observed when using formaldehyde as the crosslinker. In addition, to ensuring biocompatibility, paramagnetic nanoparticles allowed to use an external stimulus, the magnetic field, to induce the release of a substance loaded in the gel matrix. Fluorescein was used as the model compound. Release of fluorescein from the MNPs-collagen gel was clearly triggered and controlled by consecutive magnet applications, as demonstrated by means of fluorescence spectroscopy (Figure 1). The preliminary MTT assay seemed to suggest that, not only CG and NPsCG are not cytotoxic, but also the potential degradation products (mainly free NPs) do not affect cell viability.

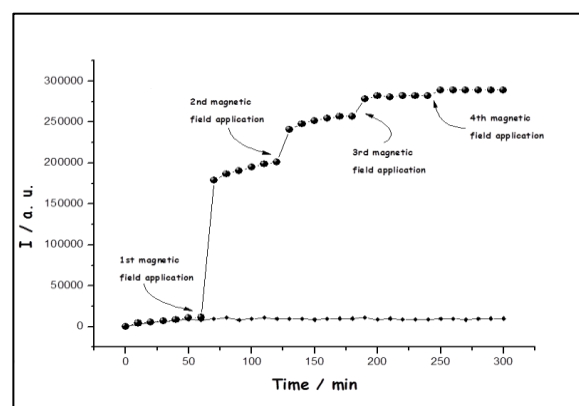


Figure 1. Release of fluorescein from NPsCG

## CONCLUSION

The results obtained in this study suggest the possibility to use the paramagnetic iron oxide NPs-collagen hybrid matrix as a smart scaffold for the controlled release of drugs and other biologically active substances.

## REFERENCES

1. Nair L.S. *et al.*, Small, 9:9-10, 2013
2. Lin C.C. *et al.*, Adv Drug Deliv Rev, 58:1379-1408, 2006
3. Songur A. *et al.*, Rev Environ Contam, 203:105-118, 2010

## ACKNOWLEDGMENTS

The authors acknowledge the Italian Ministry of Education, University and Research for providing partial financial support.



## INTRODUCTION

Polymer-based nanoparticles have been studied extensively for their use in tumour-targeted drug delivery. Leaky vasculature and damaged lymphatic drainage in solid tumours allow appropriately sized nanoparticles to selectively accumulate in the tumour.<sup>1</sup> The tumour-targeting ability of nanoparticles, however, is not only dependent on their sizes, but also on their biological behaviours. Some types of nanoparticles are more likely than others to be cleared by the reticuloendothelial system (RES) when entered the body, leaving low accumulation in the tumour and high accumulation in the RES organs, such as the liver.<sup>2</sup> The unintended RES accumulation of nanoparticles not only lowers the availability of nanoparticles to be accumulated in the tumour, but also increases toxicity. The chemical structure and other physicochemical properties of the base materials may provide reliable means to predict stability, solubility, drug loading efficacy, and cytotoxicity of nanoparticles. However, it has remained impractical to predict the relative level of RES clearance of nanoparticles *in vivo* without a direct testing on animals. Consequently, we have developed an *in vitro* system based on differential uptake of nanoparticles by macrophages that enables the prediction of RES accumulation of nanoparticles *in vivo*.

## EXPERIMENTAL METHODS

Five types of nanoparticles with different base materials (polystyrene, carboxymethyl dextran titanium dioxide, dextran sulphate, hyaluronic acid, and glycol chitosan) were prepared to have a mean diameter of approximately 250 nm.<sup>3,4</sup> The hydrodynamic sizes of the nanoparticles were measured by dynamic light scattering. The zeta potentials of the nanoparticles dispersed in distilled water were determined by electrophoretic light scattering. The morphologies of the nanoparticles were observed by using transmission electron microscopy. The structural rigidities were evaluated by conducting a filtration test.<sup>4</sup> Murine macrophage cell line (RAW 264.7) and squamous cell carcinoma cells (SCC7) were fed with NIRF dye-labelled nanoparticles for two hours to observe the uptake level. Confocal laser scanning microscopy was used to detect the fluorescence signals. SCC7 cells were subcutaneously injected to the left flank of inbred female C3H/HeJ mice to establish tumour xenografts (n=15). The nanoparticles were injected intravenously and their distributions *in vivo* were scanned by an optical imaging module. *Ex vivo* imaging and histological analyses were followed after 24 h of real-time *in vivo* imaging.

## RESULTS AND DISCUSSION

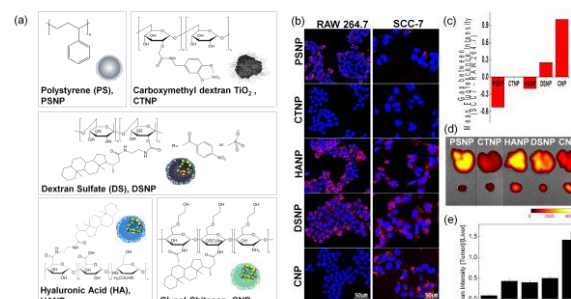


**Figure 1.** (a) Chemical structures and illustrations of the nanoparticles. (b) Cellular uptake of the nanoparticles by macrophage cell line and squamous carcinoma cell line. (c) Differences in the cellular uptake efficiencies in the two different cell lines. A higher value indicates a better uptake of the nanoparticles by SCC7 cells than by RAW 264.7 cells. (d) Fluorescence signals from the excised livers and the tumours at 24h post-injection. (e) Signal intensities from the tumour compared to those from the liver. A higher value indicates more accumulation in the tumour and less accumulation in the liver.

The nanoparticles that shared similar physicochemical properties showed different levels of cellular uptake by macrophages and by cancer cells. The affinities of the nanoparticles to cancer cells or to macrophages were closely related to their distribution *in vivo*. The nanoparticles with a high tumour cell affinity accumulated in the tumour, and those with a high macrophage affinity accumulated in the liver. Furthermore, these nanoparticles were observed co-localized with the resident macrophages in the liver.

## CONCLUSION

The strong correlation between the *in vitro* macrophage uptake and the *in vivo* distribution of the nanoparticles provides evidence to the viability of using this *in vitro* system to predict the *in vivo* fate of nanoparticles. The significance of this finding is that it may decrease the number of sacrificed animals during the development of a nanoparticle-based cancer drug delivery system.

## REFERENCES

1. Maeda H., Adv. Enzyme Regul. 41:189-207, 2001.
2. Sadauskas E. *et al.*, Part. Fibre Toxicol. 4:10, 2007.
3. Choi K. *et al.*, J. Mater. Chem. 19:4102-4107, 2009.
4. Na J. H. *et al.*, J. Control. Release 163:2-9, 2012.

## ACKNOWLEDGMENTS

The authors would like to acknowledge the financial support from the Global Research Laboratory Project (NRF-2013K1A1A2A02050115).

## Development of Novel Biomaterials, Natural Polymers, Polyhydroxyalkanoates (PHAs), for Biomedical Applications

Barbara Lukasiewicz, Pooja Basnett, and Ipsita Roy

Department of Molecular and Applied Biosciences, University of Westminster, London, UK

[barbara.lukasiewicz@my.westminster.ac.uk](mailto:barbara.lukasiewicz@my.westminster.ac.uk)

### INTRODUCTION

Polyhydroxyalkanoates (PHAs) are natural biopolymers produced by various microorganisms as a reserve of carbon and energy under nutrient limiting condition with excess of carbon<sup>1</sup>.

PHAs are promising materials for biomedical applications because they are biodegradable, non-toxic and biocompatible. Homopolymers, random copolymers and block copolymers of PHAs can be produced depending on the bacterial species and growth conditions. Physical properties of PHAs are defined by the number of carbon atoms in a monomer unit<sup>2</sup>.

Due to their characteristics, biodegradable polymers can be used in a variety of applications including medicine, pharmacy, implants, packaging, chemical industry, food industry, cosmetology and photography<sup>3</sup>. However, one of the greatest potential applications of PHAs are in the area of medicine, which includes wound management, nerve regeneration, drug delivery systems, stents, repair of soft tissue and hard tissue and heart tissue engineering<sup>4</sup>.

In this study we have presented results obtained from screening experiments using several bacterial strains and various carbon sources for PHA production with special emphasis on *scl-mcl*-PHA copolymers.

### EXPERIMENTAL METHODS

PHAs were produced using *Pseudomonas* sp., *Cupriavidus* sp. and *Comamonas* sp. Various carbon sources were introduced, such as: fatty acids, oils, carbohydrates and waste materials. Bacterial cultures were grown on mineral salt media under nutrient limitation with excess of carbon source. Different fermentation strategies were used. After cultivation time, obtained biomass was freeze dried. Polymer was extracted by solvent dispersion method. Pure polymer were analysed by Fourier Transformed Infrared Spectroscopy (FTIR), Nuclear Magnetic Resonance (NMR) and Gas Chromatography – Mass Spectrometry (GC-MS).

### RESULTS AND DISCUSSION

The examples of obtained PHAs are presented in Table 1. All tested bacterial strains were able to produce PHAs. Preferences towards each group of PHAs (*mcl/scl*) depend on the carbon source and bacterial metabolic pathway.

Bacterial strain	Carbon source	Polymer yield (% dcw)	GC-MS results	PHA type
<i>Pseudomonas</i> sp.	Sodium octanoate	24.0	P(3HO-3HD)	<i>Mcl</i> -PHA
	Sucrose	4.0	P(3HB-3HV-3HD)	<i>Scl-mcl</i> PHA copolymer
	sucrose+valeric acid	15.4	P(3HB-3HV)	<i>Scl</i> -PHA copolymer
	glucose+butyric acid	25.6	P(3HO-3HD-3HDD)	<i>Mcl</i> -PHA copolymer
	hexanoic acid +glucose	4.8	P(3HB-3HO-3HD)	<i>Scl-mcl</i> -PHA copolymer
	sucrose+ sodium octanoate	4.5	P(3HO-3HD)	<i>Mcl</i> -PHA copolymer
	Butyric acid+sodium octanoate	5.5	P(3HO-3HD)	<i>Mcl</i> -PHA copolymer
	Waste frying oil	38.9	P(3HO-3HD-3HDD)	<i>Mcl</i> -PHA copolymer
<i>Comamonas</i> sp.	1,4-butandiol	6.0	P(3HB-3HO)	<i>Scl-mcl</i> -PHA
	$\gamma$ -butyrolactone + sodium propionate	2.98	P(3HB-3HV)	<i>Scl</i> -PHA copolymer
<i>Cupriavidus</i> sp.	$\gamma$ -butyrolactone + sodium propionate	3.8	P(3HB)	<i>Scl</i> -PHA
	$\gamma$ -butyrolactone	6.70	P(3HB)	<i>Scl</i> -PHA

Table 1: Chemical characterisation of PHAs obtained from various carbon sources.

*Pseudomonas* sp. mainly produced *mcl*-PHAs, whereas *Cupriavidus* sp. mainly produced only P(3HB) polymer. Exploratory work towards more novel copolymers is in progress.

### CONCLUSION

PHAs were successfully produced from various carbon sources. *Mcl*-PHAs, *scl*-PHAs, *mcl*-PHA copolymers, *scl*-PHA copolymers and *mcl-scl*-PHA copolymers were obtained. Copolymers are more attractive materials than homopolymers, because of their intermediate properties as well as better processability.

### REFERENCES

1. S.Y. Lee, *Biotechnol Bioeng*, 49:1–14, 1996.
2. He W. N. *et al.*, *Acta Polym Sin.*, 6:709–714, 1999.
3. Chen G. Q., *Chem Soc Rev.*, 38:2434–2446, 2009.
4. Misra S.K. *et al.* *Biomaterials*, 31: 2806-2815, 2010.

### ACKNOWLEDGMENTS

“The authors would like to thank Dr Rinat Nigmatullin from University of Westminster and Dr Abil Aliev from University College London for the help with polymer characterisation”



## Does Ascorbic Acid Modified Polyurethanes May be Suitable Candidates for Soft Tissue Engineering?

Iga Gubanska<sup>1</sup>, Justyna Kucinska-Lipka<sup>1</sup>, Marta Pokrywczynska<sup>2</sup>, Tomasz Drewa<sup>2,3</sup>, Helena Janik<sup>1</sup>

<sup>1</sup>Department of Polymers Technology, Faculty of Chemistry, Gdansk University of Technology, Poland

<sup>2</sup>Chair of Regenerative Medicine, Ludwik Rydygier Medical College in Bydgoszcz, Nicolaus Copernicus University in Torun, Karłowicza 24 Street, 85-092 Bydgoszcz, Poland

<sup>3</sup>Department of Urology, Nicolaus Copernicus Hospital, Batory 17-19 Street, 87-100 Torun, Poland  
[iga.gubanska@gmail.com](mailto:iga.gubanska@gmail.com)

### INTRODUCTION

Polyurethanes (PU) are synthetic polymers, which properly designed may be biocompatible and biodegradable. Due to this characteristic, they have found wide spectrum of applications in biomedical field<sup>1</sup>. In this study, we tried to improve biological properties of obtained materials by ascorbic acid addition into PU matrix. Ascorbic acid was used due to its antioxidative property and large influence on tissue regeneration. To evaluate the results of this procedure we performed the indirect cytotoxicity test with the use of MTT [3-(4,5-dimethyl-2-thiazolyl)-2-5-diphenyl-tetrazolium bromide] assay according to ISO 10993-5 standard.

### EXPERIMENTAL METHODS

**Synthesis.** Unmodified polyurethanes were obtained with the use of oligomeric  $\alpha,\omega$ -dihydroxy(ethylene-butylene adipate)diol, 1,6-hexamethylene diisocyanate (HDI) or 4,4'-methylene (biscyclohexyl diisocyanate) (HMDI) and 1,4-butanediol chain extender. The standard PU synthesis was carried out at 80°C for 4h in the presence of dibutyltin dilaurate (DBTDL) catalyst. Modification was performed as follows: to the prepolymer 2 wt% of ascorbic acid (AA) was added. The mixture was intensively stirred for 1h. After that time PUs were cast into the mold and the synthesis was completed in the drier set at 80°C for 24h. **Cytotoxicity test:** In order to obtain extracts the sterile PU samples were incubated in cell culture medium (Dulbecco's Modified Eagle's Medium, DMEM supplemented with Fetal Bovine Serum, FBS and antibiotics) for 5 days at 37°C. The ratio of the total surface area of samples to the volume of extraction medium was 3 cm<sup>2</sup>/ml. 3T3 cells were incubated with extracts for 24, 48 and 72h. DMEM was used as a negative, non-toxic, control. To determine cell viability the colorimetric MTT metabolic activity assay was used. Each day of the test the MTT was added (0,5 ml) to the wells and incubated for 3h at 37°C. After that time formed insoluble formazan crystals were dissolved using 2 ml of dimethylsulfoxide (DMSO, Sigma D2650 tissue culture grade) and optical densities were measured at a test wavelength of 570 nm at Cecil CE 201 spectrometer. The results were presented as reduction of metabolic activity in percentage when compared to control cells cultured in medium only (100%). All assays were performed in triplicate. The statistical analysis was performed with the use of the Origin Pro 8.5. To evaluate statistical differences the two-way ANOVA ( $\alpha=0,05$ ) and post hoc Tukey test ( $\alpha=0,05$ ) were used.

### RESULTS AND DISCUSSION

Figure 1 presents 3T3 cells viability after incubation with extracts of unmodified (PU/HDI/AA0) and ascorbic acid modified (PU/HDI/AA2) PUs obtained with the use of HDI.

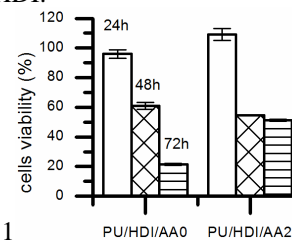


Fig. 1

Figure 2 presents 3T3 cells viability after incubation with extracts of unmodified (PU/HMDI/AA0) and ascorbic acid modified (PU/HMDI/AA2) PUs obtained with the use of HMDI.

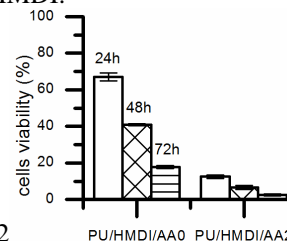


Fig. 2

In case of unmodified and ascorbic acid modified PUs, obtained with the use of HDI, higher cells viability was observed in comparison to unmodified and ascorbic acid modified PUs, obtained with the use of HMDI. These differences were statistically significant ( $p<0.05$ ). In this case the presence of AA provided suitable environment for cells proliferation. In contrary, the application of HMDI diisocyanate and ascorbic acid modification caused severe cytotoxic effect on cells of such PU samples. It could be explained by lower reactivity of HMDI diisocyanate. In that case part of AA, which was not introduced to PU chain, was exposed to the oxygen and AA degradation products may be released and enclosed into PU matrix.

### CONCLUSION

In this study we applied ascorbic acid to improve PUs biocompatibility. In case of PUs, obtained with the use of HDI, this goal was achieved what is in contrary to PU obtained with the use of HMDI. PU obtained with the use of HDI and modified with AA can be suitable candidates for soft tissue engineering.

### REFERENCES

1. Kucinska-Lipka J. *et al.*, Mater Sci Eng C. 46C: 166-176, 2015.



## Thermal Crystallization and Phase Evolution in the Amorphous Calcium Phosphate Powders with a Ca/P Ratio of 1:1

Anton Goncharenko<sup>1</sup>, Matthias Eppe<sup>2</sup>, Zoltan Zyman<sup>1</sup>, Dmytro Rokhmistrov<sup>1</sup>

<sup>1</sup>Physics of Solids Department, Physics Faculty, V.N. Karazin Kharkiv National University, 4 Svoboda Square, 61022 Kharkiv, Ukraine

<sup>2</sup>Institute of Inorganic Chemistry and Center for Nanointegration Duisburg-Essen (CeNIDE), University of Duisburg-Essen, Universitaetsstr. 5-7, D – 45117 Essen, Germany

[gavial88@meta.ua](mailto:gavial88@meta.ua)

### INTRODUCTION

Calcium pyrophosphate,  $\text{Ca}_2\text{P}_2\text{O}_7$ , CPP, results from the thermal decomposition of dicalcium phosphate dihydrate,  $\text{CaHPO}_4 \cdot 2\text{H}_2\text{O}$ , brushite, DCPD, or dicalcium phosphate anhydrous,  $\text{CaHPO}_4$ , monetite, DCPA. CPP normally exists in three polymorphs.  $\gamma$ -CPP is formed from CPDA at relatively low temperatures 300–500 °C,  $\beta$ -CPP– from  $\gamma$ -CPP in the range 600–800 °C, and  $\beta$ -CPP transforms into the high-temperature polymorph  $\alpha$ -CPP above 1200 °C<sup>1</sup>. However, the temperature ranges are not strongly defined. The kinetic parameters of the decomposition have been also actually not ascertained because few data have been obtained and they are contradictory.

It was recently found that ceramics of  $\beta$ -CPP were more bioactive in vivo than of HA<sup>2</sup>. It was also detected that calcination of ACP with an atomic Ca/P ratio of 1:1 prepared by the flame spray synthesis resulted in  $\alpha^1$ -CPP, a metastable medium-temperature polymorph of the high-temperature  $\alpha$ -CPP<sup>3</sup>. However, the synthesis is complex, expensive and has a low yield.

The work reports on the preparation of an ACP powder with Ca/P ratio 1:1 by the known simple, inexpensive and highly productive nitrous synthesis and the examination of crystallization and phase transitions in the ACP powder depending on its processing and heating conditions with the aim of subsequent fabrication of improved CPP ceramics.

### EXPERIMENTAL METHODS

The preparation of initial amorphous DCPA was based on a fast precipitation variety of the nitrous synthesis<sup>4</sup>. A 0.43 M solution of  $(\text{NH}_4)_2\text{HPO}_4$  was rapidly added into a vessel with a 0.43 M solution of  $\text{Ca}(\text{NO}_3)_2$ .

The two solutions before mixing were adjusted by ammonia to pH10–11 and cooled to 5 °C. The vessel with mixture was tightly closed, vigorously shaken and put into a freezer. The whole process from the outset of mixing took about 3 minutes. In another case, before freezing, the slurry in the vessel was six times washed with cold ammoniated water. The vessel was kept in the freezer at – 25 °C. The frozen mass was then taken from the freezer and slowly warmed up to 0 °C. The liquid occurred was removed by a blotting paper. The resultant moist slurry was put back into the freezer and kept there until its weight became stable. Friable products resulted that are hereafter designated as UW (unwashed) and 6W (six times washed) powders. Before examination, the powders were additionally dried in vacuo.

Powder samples were examined as prepared and upon heat treatments in air in the range 25–1000 °C in a

muffle furnace. They were studied by XRD, TG-DTA, and IR.

### RESULTS AND DISCUSSION

Thermal behavior of two kinds of XRD amorphous powders prepared from ACP precipitates with a given Ca/P ratio of 1:1 of the nitrous synthesis was studied.

An UW powder from unwashed precipitate crystallized at 530–640 °C mainly into  $\alpha^1$ -CPP, a metastable polymorph of the high-temperature polymorph  $\alpha$ -CPP, and some admixture of  $\beta$ -CPP. This phase composition slightly changed to 800 °C. Above 800 °C,  $\alpha^1$ -CPP gradually transformed into the stable  $\beta$ -CPP polymorph, so biphasic mixtures with increasing  $\beta$ -CPP/ $\alpha^1$ -CPP ratios were formed from 1:2 at 800 °C to 2:1 at 980 °C.

A 6W powder from six-time washed precipitate consisted of a major part unaffected by the washing procedure and a minor part hydrolyzed during washing to ACP with a Ca/P ratio about that of OCP (1.33). The major part crystallized in the range 620–720 °C mainly into  $\alpha^1$ -CPP with little admixture of  $\beta$ -CPP. Heating above this range exhibited the decomposition of OCP into  $\beta$ -CPP and  $\beta$ -TCP and gradual transformation of  $\alpha^1$ -CPP into  $\beta$ -CPP. As a result, powders upon heating were triphasic of  $\beta$ -CPP,  $\alpha^1$ -CPP and  $\beta$ -TCP with variable phase contents and with the relative amount 3:1:1 at 980 °C. The reason for appearance of TCP (Ca/P = 1.5) from ACP (Ca/P = 1) was discussed.

### CONCLUSION

The activation energy for crystallization of ACP into the metastable polymorph  $\alpha^1$ -CPP was first determined as 165 kJ/mol (39.5 kcal/mol).

The powders are presented as prospective superior biomaterials because they combine effective bioactive phases with a novel metastable  $\alpha^1$ -CPP polymorph. A peculiar feature of the fabricated powders is that they include a metastable  $\alpha^1$ -CPP additionally to the known effective bioactive CPP and CP phases. Biomaterials having such composition is expected to exhibit superior biological behavior compared to that of the HA family.

### REFERENCES

1. Cornilsen BC, *et al.*, J Inorg Nucl Chem. 41:602–5, 1979
2. Lee JH *et al.*, Key Eng Mat. 240–2:399–402, 200
3. Maciejewski M, *et al.*, Thermochim Acta. 468:75–80, 2008.
4. Zyman ZZ, *et al.*, J Mater Sci Mater Med.;21:123–30, 2010



## Methodological Evaluation of Quantitative *in Vivo* MRI Volume Measurements of Hydrogels by *ex Vivo* CT Imaging

Christoph Tondera<sup>1,2\*</sup>, Sandra Ullm<sup>1,2</sup>, Sebastian Meister<sup>1</sup>, Tim P. Gebauer<sup>3,4</sup>, Axel T. Neffe<sup>3,4</sup>, Andreas Lendlein<sup>3,4</sup>, Jens Pietzsch<sup>1,2</sup>

<sup>1\*</sup> Helmholtz-Zentrum Dresden-Rossendorf, Institute of Radiopharmaceutical Cancer Research, Department of Radiopharmaceutical and Chemical Biology, Dresden, Germany

<sup>2</sup> Technische Universität Dresden, Department of Chemistry and Food Chemistry, Dresden, Germany

<sup>3</sup> Institute of Biomaterial Science and Berlin-Brandenburg Centre for Regenerative Therapies, Helmholtz-Zentrum Geesthacht, Teltow, Germany

<sup>4</sup> Helmholtz Virtual Institute "Multifunctional Biomaterials for Medicine", Teltow and Berlin

[c.tondera@hzdr.de](mailto:c.tondera@hzdr.de)

### INTRODUCTION

Hydrogels are often and widely used biomaterials in medical and research applications. Depending on the application there are different hydrogels for, e.g., soft tissue replacement, organ patches, or drug delivery systems. Hence, there is a great interest to investigate the degradation behavior of these materials non invasively *in vivo* in animal models. Because hydrogels mainly consist of water, proton MRI (magnetic resonance imaging), especially T2-weighted sequences, seems to be suitable for hydrogel visualization and quantification. But due to the high water content of the surrounding tissue, there is a need to investigate if the MRI signal correlates with the actual volume of the used hydrogel.

### EXPERIMENTAL METHODS

The hydrogels were synthesized by reacting a 10 wt.-% gelatin solution with 3-fold (G10\_LNCO3) or 8-fold (G10\_LNCO8) molar excess of isocyanate groups of ethyl lysine diisocyanate compared to amino groups of gelatin. Hydrogel samples were implanted subcutaneously in immunocompetent, hairless SKH-1 mice. The volume of implanted hydrogels was determined using dedicated 7 T small animal MRI with a T2-weighted measuring sequence at different time points after implantation *in vivo*. After the measurements the animals were euthanized and material containing tissues were explanted. The tissue samples were dehydrated by incubation in 30, 50 and 70 vol.-% ethanol solution for 1 day each. Afterwards, the samples were incubated for 49 days in 0.3 wt.-% phosphotungstic acid (PTA) in 70 vol.-% ethanol. PTA is a contrast agent for computed tomography (CT) which binds to fibrin and collagen. It is therefore used to visualize different soft tissues. For the *ex vivo* quantification the tissue samples were measured using CT at 55 keV voltage and 600 ms acquisition time. For quantification of both the MRI and CT measurements a voxel-based evaluation method was applied.

### RESULTS AND DISCUSSION

Both hydrogels could clearly be visualized by MRI. Quantification was realized by applying a threshold. Due to their higher amount of water compared to the surrounding tissue a stronger signal intensity of the hydrogels in the T2-weighted measurement could be observed. Interestingly the signal intensity was independent from the crosslinking level.

The PTA stained tissue samples could be visualized similarly. Binding of PTA in hydrogels was higher than in the surrounding tissue. Therefore, a higher X-ray absorption could be detected at the material site.

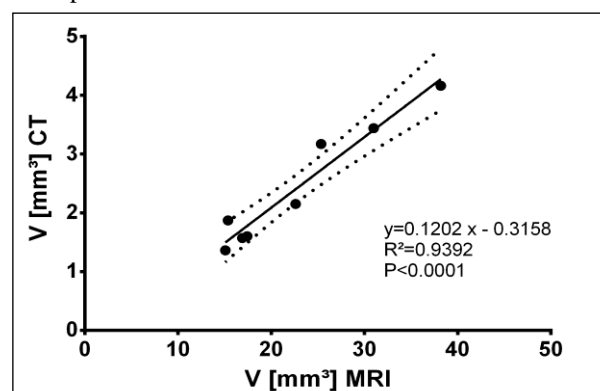


Figure 1: Correlation between MRI and CT measurement based volume quantification.

Both MRI and CT allowed for quantification of hydrogel degradation over the time. However, a much higher volume was observed in the *in vivo* MRI compared to *ex vivo* CT measurements. A strong correlation ( $r=0.9691$ , Pearson correlation coefficient) between both quantification methods could be calculated (Figure 1,  $R^2=0.9392$ ). The MRI quantified volume is higher by a factor of 10 compared to CT quantified volume independent of hydrogel degradation state. The reason for this difference between both volumes lies in the dehydration of the hydrogels for the PTA staining. Because of the high amount of water in the swollen hydrogel the dehydrated volume is much lower.

### CONCLUSION

The *in vivo* MRI volume measurement of hydrogels could be verified by CT contrast agent measurements *ex vivo*. Both methods reflect the hydrogel degradation state. Taken together this imaging study revealed MRI as suitable non invasive method to quantify the volume of gelatin based hydrogels *in vivo*.

### ACKNOWLEDGMENTS

The authors thank the Helmholtz Association for funding of this work through Helmholtz-Portfolio Topic "Technologie und Medizin – Multimodale Bildgebung zur Aufklärung des In-vivo-Verhaltens von polymeren Biomaterialien."



# Intraocular Lenses with Surfaces Functionalized by Biomolecules in Relation with Lens Epithelial Cell Adhesion

Yi-Shiang Huang<sup>1,2</sup>, Virginie Bertrand<sup>1</sup>, Dimitriya Bozukova<sup>3</sup>, Christophe Pagnoulle<sup>3</sup>, Edwin De Pauw<sup>1</sup>, Marie-Claire De Pauw-Gillet<sup>1</sup>, Marie-Christine Durrieu<sup>2</sup>

<sup>1</sup> Mass Spectrometry Laboratory, Department of Chemistry and Mammalian Cell Culture Laboratory, Department of Bio-medical and Preclinical Sciences – GIGA R, University of Liège, Liège, Belgium

<sup>2</sup> CBMN UMR5248, Institute of Chemistry & Biology of Membranes & Nanoobjects, University of Bordeaux, Pessac, France

<sup>3</sup> PhysIOL, Liège,

[pokerface1031@gmail.com](mailto:pokerface1031@gmail.com)

## INTRODUCTION

Posterior capsular opacification (PCO) is the capsule fibrosis developed on implanted intraocular lens (IOL) by the de-differentiation of lens epithelial cells (LECs) undergoing epithelial-mesenchymal transition (EMT). It is generally accepted that the acrylic hydrophilic materials have higher PCO rate than acrylic hydrophobic ones<sup>1</sup>. We recently highlighted their particular properties in terms of adhesion forces, LECs adhesion, and tissue response as indicators of posterior capsular opacification development risk<sup>2</sup>. Our strategy in PCO control is to improve the hydrophilic IOL capsular biocompatibility by creating a higher LEC affinity surface via bioactive peptides (Fig. 1).

## EXPERIMENTAL METHODS

The surfaces of acrylic hydrophilic disks of 25% water content (HA25) were functionalized with cell-adhesion peptides (RGD peptides) and characterized by X-ray photoelectron spectroscopy as well as contact angle measurements. To evaluate the performance against PCO, the *in vitro* LEC culture was performed and compared to acrylic hydrophobic material named GF (glistening free) used as PCO-negative reference. Additionally, in order to ensure that the surface functionalization process does not compromise the material properties, optical and mechanical properties of functionalized polymers were conducted and compared with control materials.

## RESULTS AND DISCUSSION

The surface functionalization process was accomplished by oxygen plasma treatment followed by conjugation, and the washing procedure consisted of consecutive

water extraction in autoclave temperature. The results show the innovative biomaterial improves LEC adhesion, and also exhibits similar optical (light transmittance, contrast sensitivity, dioptre measurement) and mechanical (haptic compression force, IOL injection force) properties comparing to the starting material. In addition, comparing to the hydrophobic IOL material, this bioactive biomaterial exhibits similar abilities in LEC adhesion, morphology maintenance, and EMT biomarker expression. The *in vitro* assay results suggest this biomaterial has the potential to reduce some risk factors of PCO development<sup>3</sup>.

## CONCLUSION

Our pioneering *in vitro* study of the bio-mimicking strategy suggests that the LEC adhesion is promoted and this surface-functionalized IOL material exhibits no detectable effect toward EMT, which is the molecular cell biology mechanism of PCO. This hypothesis still needs to be examined by *in vivo* assays to validate the effectiveness of PCO prevention.

## REFERENCES

1. Bozukova D. *et al.*, Mater. Sci. Eng. R-Rep. 2010; 69: 63–83
2. Bertrand V. *et al.*, J. Cataract Refract. Surg. 2014; 40:1536–1544
3. Huang YS. *et al.*, PLoS ONE 2014; 9(12): e114973

## ACKNOWLEDGMENTS

The authors would like to thank Walloon region, Belgium (Grant no: LINOLA 1117495) for providing financial support to this project.

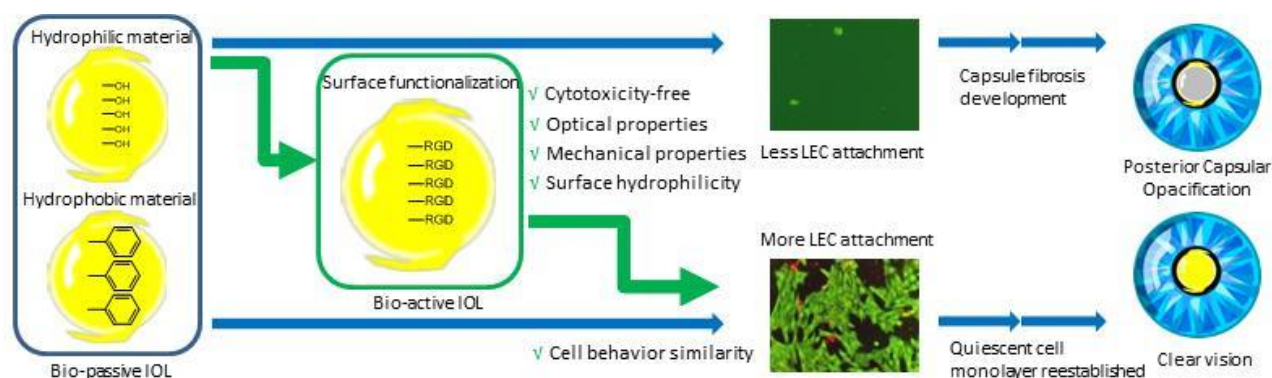


Fig. 1 show that the strategy in PCO control and the tests performed in this study



## Introducing Controlled Nano-Roughness in 3D Silk Fibroin Scaffolds for Bone Tissue Engineering

Marianne R. Sommer<sup>1</sup>, Ralph Müller<sup>2</sup>, Sandra Hofmann<sup>2,3,4</sup>, André R. Studart<sup>1</sup>

<sup>1</sup>Complex Materials, Department of Materials, ETH Zurich, Switzerland

<sup>2</sup>Institute for Biomechanics, ETH Zurich, Switzerland

<sup>3</sup>Orthopaedic Biomechanics, TU Eindhoven, Netherlands

<sup>4</sup>Institute for Complex Molecular Systems, TU Eindhoven, Netherlands

[marianne.sommer@mat.ethz.ch](mailto:marianne.sommer@mat.ethz.ch)

### INTRODUCTION

Submicrometric topography has been shown to influence lineage commitment of human mesenchymal stem cells cultured on flat substrates<sup>1</sup>. Elevated osteogenic gene expression and mineralization was observed in the absence of osteogenic media supplements on substrates with disordered but uniform topography features<sup>1</sup>. However, translating those findings to 3D has so far been difficult, because the nanoroughness created by the usual electrospinning<sup>2</sup> or etching<sup>3</sup> approaches is often heterogeneous. Here we use nanoparticle-decorated porogens as templates to produce silk fibroin scaffolds with nanotopography that can be tuned in size and shape through nanoparticle choice.

### EXPERIMENTAL METHODS

Polycaprolactone (PCL) microparticles with average size of 310  $\mu\text{m}$  were produced by microfluidics. Electrostatic adsorption was used to deposit latex nanoparticles onto those PCL particles using an intermediate positively charged polyelectrolyte layer (see Figure 1a). First, the PCL particles were treated with 1:1 methanol/2M NaOH for 15 minutes and rinsed with water. Then, they were immersed in a 1 % polyallylamine hydrochloride solution for 1 h followed by rinsing with water. Negatively charged polystyrene latex particles were then adsorbed from a 0.25 % suspension overnight and the PCL microparticles rinsed again with water. The decorated PCL particles were afterwards dried, assembled in a mold, subjected to a heat treatment at 57  $^{\circ}\text{C}$ /25 % relative humidity and infiltrated with a 12 % silk fibroin aqueous solution. After complete drying, the scaffolds were placed in methanol for 1 h. The particles were finally leached in dichloromethane for 8 h. Scaffolds were imaged using scanning electron microscopy.

### RESULTS AND DISCUSSION

Negatively charged latex particles of various sizes with both carboxy or sulfate functional groups could be adsorbed onto the polycaprolactone microparticles via a positively charged intermediate polyelectrolyte. Figure 1b shows 1  $\mu\text{m}$  sulfate-functionalized latex adsorbed onto a 310  $\mu\text{m}$  polycaprolactone particle. After infiltration and porogen leaching, imprints of the latex particles could be observed in the silk fibroin pore walls (Figure 1d). Those imprints had diameters of about 55 % of the original latex particle size.

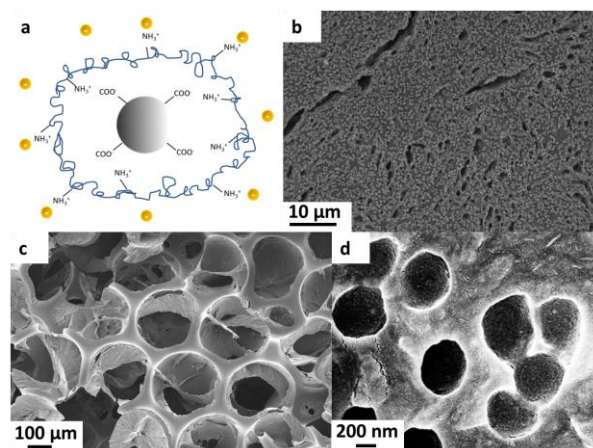


Figure 1: a. Schematics showing the electrostatic adsorption process to create a nanoparticle-decorated porogen for templating. b. 1  $\mu\text{m}$  latex adsorbed onto PCL particles. c. Silk fibroin scaffold d. Imprints made by the latex on the dry silk fibroin scaffold pore wall after template removal.

The presented method offers a simple way of generating tunable random nanotopography in silk fibroin scaffolds. The use of core-shell and monodisperse nanoparticles might enable further control over feature spacing and arrangement.

### CONCLUSION

A simple and versatile route to decorate porogen microparticles with nanoparticles via electrostatic adsorption has been developed. Silk fibroin scaffolds with submicrometric and uniform roughness could be produced using the decorated microparticles as porogens. Future investigations will concentrate on evaluating the effect of such roughness on human mesenchymal stem cell response, both in presence and absence of osteogenic cues in the medium.

### REFERENCES

1. Dalby M.J. *et al.*, Nature Materials. 6:997-1003, 2007
2. Badami A.S. *et al.*, Biomaterials. 27: 596-606, 2006
3. Kumar G. *et al.*, Biomaterials. 33:4022-4030, 2012

### ACKNOWLEDGMENTS

The authors thank Trudel Inc for providing silk cocoons and funding from the European Union's Seventh Framework Programme (FP/2007-2013) / EU Project No. FP7-NMP-2010-LARGE-4: 262948 and grant agreement No. PCIG13-GA-2013-618603.



A. Hayrapetyan, E.R. Urquia Edreira, J.G.C. Wolke, J.A. Jansen, J.J.J.P. van den Beucken

Department of Biomaterials, Radboudumc, The Netherlands

[Astghik.Hayrapetyan@radboudumc.nl](mailto:Astghik.Hayrapetyan@radboudumc.nl)

## INTRODUCTION

Calcium phosphate ceramics in combination with implant surface geometry have been shown to influence biological performance. Ripamonti et al. have extensively investigated the osteoinductive effect of repetitive surface concavities on bulk ceramics and calcium phosphate coated titanium implants<sup>1-3</sup>. These studies have shown that the presence of concavities allows for osteoinductive capacity without loading the ceramic scaffold with osteogenic soluble factors or osteogenic cells.

In our previous study, we tried to rationalize the mineralization process through an *in vitro* test in SBF<sup>4</sup>. Bianchi et al. showed that the mineralization process started preferentially within the concavities in hydroxyapatite (HA) disks sintered at 1200 °C and that concavity size controlled the extent of mineralization.

It is also known that micro- and nano-scale morphology of the calcium phosphate surface can strongly influence osteoblast and stem cell adhesion, proliferation, and differentiation<sup>5-7</sup>. In our current study, we aimed to investigate how cells populate concavities and to what extent concavity size influences cellular mineralization. We hypothesized that surface concavities facilitate cell proliferation and mineralization and that these effects are increased in the smaller concavity due to increased 3D cellular organization.

## EXPERIMENTAL METHODS

Cavity sizes of 440, 800 and 1800 µm were created on the surface of HA disks sintered at 1200°C and cultured with adipose tissue mesenchymal stem cells (AT-MSCs) in osteogenic medium for up to 28 days at 37°C. At selected time points (3, 7, 14, 21, and 28 days), samples were removed and after fixation, cells were fluorescently labeled with phalloidin-Alexa 568 (1:250; molecular probes) for filamentous (F-) actin and DAPI (1:2500) for nuclear staining. Cells were imaged and examined with a confocal laser scanning microscopy (CLSM) Olympus FV1000.

## RESULTS AND DISCUSSION

Immunofluorescence-based three-dimensional (3D) image analysis showed differences in cell number between concavities. The highest number of cell nuclei was found in the 440 µm cavity (Figure 1) and the lowest number in the 1800 µm. Additionally, cells were able to migrate toward the concavities and adhere to their edges and walls. Preferential mineralization was observed inside the concavities. Cells spread over and to the bottom of concavities covering all their volume and creating multilayers on their surfaces.

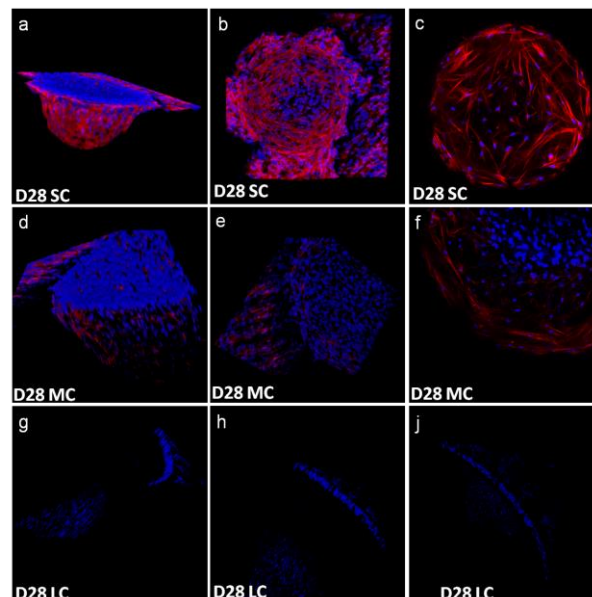


**Figure 1.** 3D reconstruction of confocal microscopy imaging of small, medium, and large concavities after 28 days of culture.

## CONCLUSION

High resolution 3D images gave qualitative and quantitative data on concavity volumes. CaP ceramics with surface concavities induced cell (AT-MSCs) organization within the concavities and were able to create cell multilayers. Results from this study suggest a correlation between concavity size, cellular organization, mineralization and concavity induced osteoinductive properties.

## REFERENCES

1. Ripamonti U. *et al.*, J. Cell. Mol. Med. 13, 2953, 2009
2. Scarano A., *et al.*, Clin. Implant Dent. Rel. Res, 2009
3. Ripamonti U. *et al.*, Biomaterials, 3813, 2012
4. Bianchi M. *et al.*, Acta Biomaterialia, 10, 2012
5. Li B. *et al.*, Acta Biomaterialia, 8, 2012
6. Prodanov L. *et al.*, Biomaterials, 34, 2013
7. Graziano A. *et al.*, PloS One, 2, 2007

## ACKNOWLEDGMENTS

The authors would like to thank the Research Program of the BioMedical Materials Institute (Project P2.04 BONE-IP), co-funded by the Dutch Ministry of Economic Affairs, Agriculture and Innovation for providing financial support and NIRM (Netherlands Institute for Regenerative Medicine).

## Novel Approach Towards Osseointegration: Surface Functionalization on Zirconia

Carlos Caravaca<sup>1</sup>, Liu Shi<sup>2</sup>, Sandra Balvay<sup>1</sup>, Pascaline Rivory<sup>1</sup>, Emmanuelle Laurenceau<sup>2</sup>, Yann Chevolot<sup>2</sup>, Daniel Hartmann<sup>1</sup>, Laurent Gremillard<sup>1</sup> and Jérôme Chevalier<sup>1</sup>

<sup>1</sup> Université de Lyon, UMR CNRS 5510, INSA de Lyon, Université Claude Bernard Lyon 1, France

<sup>2</sup> Université de Lyon, UMR CNRS 5270, École Centrale de Lyon, Institut des Nanotechnologies de Lyon (INL), France  
[carlos.caravaca@insa-lyon.fr](mailto:carlos.caravaca@insa-lyon.fr)

### INTRODUCTION

Bioinert ceramics for orthopaedic devices, such as Zirconia or Alumina, represent a growing market due to their superior performance in dental and joint substitutions. Attempts have been made in the past to improve their interactions with cells by means of roughness, yielding different results. Unfortunately modifying the roughness inevitably creates defects that affect the fracture resistance of ceramics due to their fragility. Another strategy is to modify the chemical composition of the surface without affecting the bulk properties. This would influence the way proteins and cells perceive the surface, without impacting the higher mechanical performance of ceramics. In this way, the development of Self-Assembled Monolayer (SAM) is proven to be an effective and versatile technique of modifying the cell/material interactions<sup>1</sup>. In the present work, we explored a new way of modifying the surface of Zirconia (3Y-TZP) by grafting a Self-Assembled Monolayer (SAM) of 3-aminopropyltrimethoxysilane (APDMES) directly on the surface.

### EXPERIMENTAL METHODS

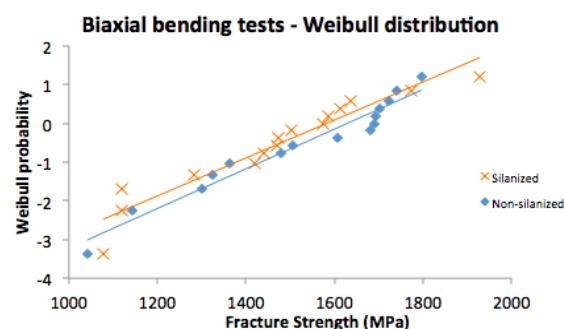
The surfaces of polished zirconia discs were prepared by oxygen plasma and exposed to APDMES in pentane. The modified surfaces were studied by means of XPS, and a modified ADECA method<sup>2</sup> (a colorimetric method allowing the estimation of the density of amine groups on the surface). To study the effect of the treatment on the mechanical performance, 15 treated and 15 untreated discs were tested by 3-ball-on-3-ball biaxial bending in a universal testing machine, and later studied with Weibull probability. Cytotoxicity tests were performed by means of PrestoBlue® assay of MG-63 (osteoblast-like cells) on treated and non-treated surfaces, studying the cell proliferation after 3, 6 and 10 days, and using 5000 cells per well and three samples per condition and repetition.

### RESULTS AND DISCUSSION

Both ADECA and XPS analysis confirmed the presence of amino groups, proving the chemical procedure managed to introduce an APDMES SAM over Zirconia. The estimation of silane density in the surface was  $8.6 \cdot 10^{13}$  molecules per  $\text{cm}^2$ , which is very close to the silanol number ( $4.9 \cdot 10^{13}$  OH per  $\text{cm}^2$ ) given by Zhuravlev corresponding to a fully saturated silica surface<sup>3</sup>.

Mechanical results (figure 1) yielded no evidence of statistical difference between treated and untreated

samples (t-test,  $p \approx 0.5$ ). This proves that neither oxygen plasma nor the liquid-phase silanisation modifies the mechanical behaviour of the material. In regards of the cytotoxicity, results show no difference of cell proliferation between both types of surface, meaning that no traces of toxic solvents remained after the surface modification.



“Figure 1 shows no difference in mechanical behaviour between treated and non-treated samples.”

### CONCLUSION

In the past, researchers have evidenced the potential of SAMs in surface modification<sup>4</sup>. In this work, we demonstrate that a non-silica oxide surface can be directly silanized as well, without the necessity of a silica interlayer. In the future, APDMES could be easily swapped by any other silane with a more interesting functional group, tailoring the surface to specific needs.

We have shown as well that the treatment has no impact whatsoever on the mechanical integrity, making the procedure ideal for orthopaedic devices designed to withstand very high loads. No adverse effects were found on the proliferation of MG-63 cells, which will enable cell adhesion tests as the next step in this research.

### REFERENCES

1. Fauchoux N. *et al.*, *Biomat.* 25(14):2721-30, 2004
2. Yang Z. *et al.*, *Langmuir* 29:1498-509, 2013
3. Zhuravlev L., *Langmuir* 3:316-8, 1987
4. Schickle K. *et al.*, *J. Eur. Ceram. Soc.* 32(12): 3063-71, 2012

### ACKNOWLEDGMENTS

The authors would like to acknowledge the European Commission funding under the 7th Framework Programme (Marie Curie Initial Training Networks; grant number: 289958, Bioceramics for bone repair).



## Novel Enzymatically Cross-linked Silk Fibroin Hydrogel with Potential Applications as Suppressor of Angiogenesis and Tumor Progression

Viviana Ribeiro<sup>1,2</sup>, Joana Silva-Correia<sup>1,2</sup>, Vera Miranda-Gonçalves<sup>2,3</sup>, Le-Ping Yan<sup>1,2</sup>, Ana L. Oliveira<sup>4</sup>, Rui M. Reis<sup>2,3,5</sup>, Rui L. Reis<sup>1,2</sup> and Joaquim M. Oliveira<sup>1,2</sup>

<sup>1</sup>3B's Research Group – Biomaterials, Biodegradables and Biomimetics, University of Minho, Headquarters of the European Institute of Excellence on Tissue Engineering and Regenerative Medicine, AvePark, Guimarães, Portugal;

<sup>2</sup>ICVS/3B's - PT Government Associate Laboratory, Braga/Guimarães, Portugal; <sup>3</sup>ICVS - Life and Health Sciences Research Institute, Braga, Portugal; <sup>4</sup>CBQF—Center for Biotechnology and Fine Chemistry, Portuguese Catholic University, Porto, Portugal; <sup>5</sup>Molecular Oncology Research Center, Barretos Cancer Hospital, Barretos, São Paulo, Brazil  
[joana.correia@dep.uminho.pt](mailto:joana.correia@dep.uminho.pt)

### INTRODUCTION

Angiogenesis, the formation of new blood vessels from pre-existing vascular beds, is essential for tumor growth, invasion and metastasis formation. Thus, the therapeutic suppression of angiogenesis could be the key to prevent tumor progression<sup>1</sup>. We describe the use of injectable, *in situ* cross-linkable SF hydrogels to suppress angiogenic activity and tumor progression, using *in vitro* and *in vivo* models. Recently, it was found that proteins (e.g. silk fibroin) with tyrosine groups can be used to prepare hydrogels *in situ* via an enzyme-mediated cross-linking reaction, using horseradish peroxidase (HRP) and hydrogen peroxide (H<sub>2</sub>O<sub>2</sub>)<sup>2</sup>. Silk fibroin (SF) contains 5 mol% tyrosine groups, which are easily chemically modified, demonstrating the promising application of this protein for the production of injectable systems and non-toxic hydrogels.

### EXPERIMENTAL METHODS

The present work provides a novel route for obtaining enzymatically cross-linked SF hydrogels within a few minutes in physiological conditions, using high concentrate aqueous SF solution (16 wt%), mediated by a HRP/H<sub>2</sub>O<sub>2</sub> complex<sup>3</sup>. The dominant conformation presented by the SF hydrogels was assessed over time, allied to its potential anti-tumoral applications. The  $\beta$ -sheet conformation transition was analyzed by means of Transmission Electron Microscopy (TEM), Thioflavin T and Congo red staining. Human neuronal glioblastoma (U251) and human cervical adenocarcinoma (HeLa) cell lines were encapsulated within the SF hydrogels and cultured for 14 days under standard culture conditions. Cell viability and proliferation were assessed through ATP and DNA quantification assays, respectively. In order to evaluate the *in vivo* biocompatibility of the SF hydrogels, a subcutaneous implantation was performed in mice model for a period of 2 weeks, followed by H&E staining.

### RESULTS AND DISCUSSION

The SF hydrogels presented ionic strength and pH stimuli responsiveness. The  $\beta$ -sheet conformation transition analysis revealed that the fast-formed hydrogels presented mainly an amorphous conformation and transparent appearance during the first week, but a conversion to a dominant  $\beta$ -sheet conformation and opaque appearance was verified from day 7.

Additionally, U251 and HeLa cells were successfully encapsulated within the hydrogels. ATP quantification showed a cell-dependent decrease of cell viability over culture period and from DNA quantification analysis it was possible to conclude a decrease of cell proliferation after 14 days of culture. The *in vivo* results showed that the SF hydrogels did not induce any acute inflammatory reaction after 2 weeks of subcutaneous implantation (Figure 1). The SF hydrogels underwent a  $\beta$ -sheet conformation transition after 7-10 days of *in vitro* cell encapsulation and 2 weeks of *in vivo* implantation, revealing that the observed conformation transition may be responsible for inhibiting cell viability and proliferation.



**Figure 1-** Subcutaneous implantation of the SF hydrogels in mice for 2 weeks. (a-b): Macroscopic images of the explants. (c): H&E staining of the explants (Scale bar: 100  $\mu$ m).

### CONCLUSION

This study provides a straightforward approach to produce injectable SF hydrogels with superior biocompatibility and fast-gelation property to be used as a whole or combined with bioactive agents. Thus, the enzymatically cross-linked SF hydrogels can be a very useful and tunable system for different biomedical applications, including suppressing angiogenesis and tumors progression *in vivo*.

### REFERENCES

1. Liu Y. *et al.*, Tissue Eng. 13(5):1091-101, 2007
2. Sofia S.J. *et al.*, J Macromol Sci A. 39(10):1151-1181, 2002
3. Yan L-P. *et al.*, National Patent Nr. 106041, 06-12, 2011.

### ACKNOWLEDGMENTS

Portuguese Foundation for Science and Technology (FCT) project PEst-C/SAU/LA0026/201. Investigator FCT program IF/00423/2012 and IF/00411/2013 are also greatly acknowledged.





## Electrophoretic Deposition of Composite Coatings Based on ZnO Nanoparticles on Ti6Al7Nb Alloy

Joanna Karbowniczek<sup>1</sup>, Luis Cordero-Arias<sup>2</sup>, Aleksandra Czyrska-Filemonowicz<sup>1</sup>, Aldo R. Boccaccini<sup>2</sup>

<sup>1</sup>Faculty of Metals Engineering and Industrial Computer Science, AGH University of Science and Technology, Al. Mickiewicza 30, 30-059 Krakow, Poland

<sup>2</sup>Institute of Biomaterials, Department of Materials Science and Engineering, University of Erlangen-Nuremberg, Cauerstrasse 6, 91058 Erlangen, Germany  
[jkarbow@agh.edu.pl](mailto:jkarbow@agh.edu.pl)

### INTRODUCTION

Titanium alloys are an important group of materials for orthopedic applications due to their high strength, good corrosion resistance, low weight, low elastic modulus and biocompatibility. Regardless their distinctive properties some problems may occur that could lead to implant failure and revision surgery. One of the risks are surgery-related bacterial infections which prolongs post-implantation patients recovery and may even cause implant rejection. Possible solution to reduce the risk of the infection might be coatings with antibacterial activity<sup>1</sup>. Zinc oxide (ZnO) nanoparticles can release  $Zn^{2+}$  ions which inhibit biofilm formation by affecting bacterial active sugar transport and metabolism<sup>2</sup>. Thus ZnO nanoparticles could be applied as the antibacterial agent in coatings.

### EXPERIMENTAL METHODS

The investigation was performed on two phase ( $\alpha+\beta$ ) Ti6Al7Nb alloy. This alloy was surface treated by electrophoretic deposition (EPD) method, considering a multilayer approach. The first coating was composed of chitosan (Ch). For the second layer polyvinyl alcohol (PVA), alginate (Alg) zinc oxide nanoparticles (nZnO) and bioactive glass particles (45S5 Bioglass®, BG) were used. Two types of suspensions were prepared with composition: PVA-Alg/nZnO and PVA-Alg/nZnO-BG. The suspensions' stability was verified by zeta potential measurements.

Obtained coatings were investigated in terms of their microstructure, chemical composition and wettability by means of SEM, SEM-EDS and static water contact angle measurement. The deposition yield was calculated based on the change of the samples weight before and after deposition.

### RESULTS AND DISCUSSION

Zeta potential values of PVA-Alg/nZnO and PVA-Alg/nZnO-BG suspensions were found to be  $-32.6 \pm 0.4$  mV and  $-35 \pm 1$  mV, respectively. Both suspensions were stable and negatively charged, thus the deposition was anodic. The interlayer of chitosan was found to increase the deposition yield as well as the coatings homogeneity and attachment to the substrate.

Both coatings had hydrophilic surfaces, the wettability measured by contact angle was  $54 \pm 4^\circ$  for PVA-Alg/nZnO and  $61 \pm 4^\circ$  for PVA-Alg/nZnO-BG.

Coatings deposited from PVA-Alg/nZnO-BG suspension were rough with individual, micrometer sized, sharp-edged bioactive glass particles and homogeneously distributed nZnO. However some larger

clusters of zinc oxide particles, not separated during ultrasonication, were also observed in the polymer matrix (Fig. 1).

Coatings deposited from PVA-Alg/nZnO suspensions had similar microstructure as the previous one, with well distributed nanoparticles as well as larger clusters of ZnO in the polymer matrix.

Antibacterial tests against G+ and G- bacteria are in progress, results under evaluation.

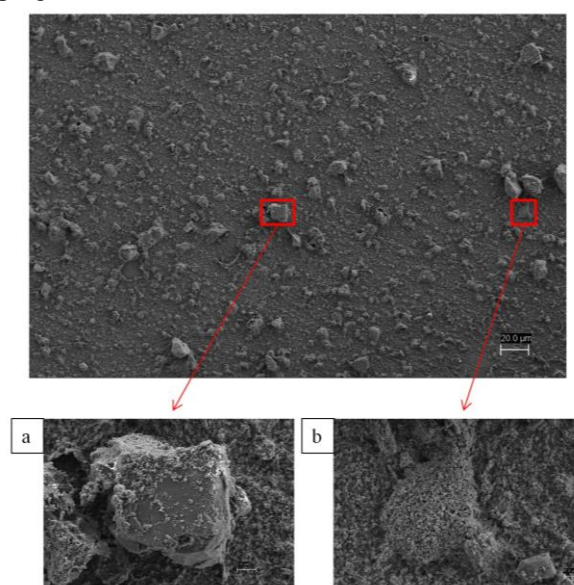


Fig.1. Microstructure of the coating prepared from PVA-Alg/nZnO-BG suspension. Magnified details: a) BG particle, b) cluster of ZnO particles in polymer matrix; SEM-SE images.

### CONCLUSION

EPD is a simple and cost efficient method to modify the surface of different metals by depositing complex coatings. It allows the improvement of the properties of materials to be applied in the medical field. Coatings with antibacterial activity are a promising solution to prevent bacterial adhesion on the surface of the implant and biofilm formation, thus reducing the risk of infection during surgery.

### REFERENCES

1. Simchi A. *et al.*, Nanomed-Nanotechnol 7:22-39, 2011.
2. Sevine B. A., Hanley L., J Biomed Mater Res B 94B:22-31, 2010

### ACKNOWLEDGMENTS

Work was done in the framework of a KMM-VIN fellowship.





Anna Donesz-Sikorska<sup>1</sup>, Justyna Krzak<sup>1</sup>, Jerzy Kaleta<sup>1</sup>, Małgorzata Krok-Borkowicz<sup>2</sup>, Elżbieta Pamuła<sup>2</sup>.

<sup>1</sup>Department of Mechanics, Materials Science and Engineering, Wrocław University of Technology, Poland

<sup>2</sup>Department of Biomaterials, AGH University of Science and Technology, Poland

[anna.donesz-sikorska@pwr.edu.pl](mailto:anna.donesz-sikorska@pwr.edu.pl)

## INTRODUCTION

Metallic materials have found wide application as orthopaedic implants. Nowadays, AISI 316L stainless steel is presumably the most widely used material to produce bone implants due to its high strength, toughness and much lower cost as compared to titanium alloys. However, there is always a concern about corrosion of stainless steel in body fluids and its surface activity which was found to affect cell functions<sup>1</sup>. One of the ways of minimizing corrosion and promoting cells adhesion and growth on metallic surface is applying protective and functional coatings<sup>1,2</sup>.

In this study, authors proposed bioactivation of SiO<sub>2</sub> sol-gel derived coatings on metallic implants by using: osteoinductive factor which plays a crucial role in regeneration process - L-ascorbic acid (LAA), anti-inflammatory drug - salicylic acid (SAL) and neurotransmitter taking part in regulation of bone metabolism - dopamine (DOPA).

## EXPERIMENTAL METHODS

Pure silica coatings (SiO<sub>2</sub>) and SiO<sub>2</sub> coatings doped with active molecules: LAA, SAL and DOPA in adjusted molar ratios: SiO<sub>2</sub>/0.4M LAA, SiO<sub>2</sub>/0.7M SAL, SiO<sub>2</sub>/3.5mM DOPA were prepared by the sol-gel method. Obtained sols were applied on the 316L AISI by dip-coating technique. For the sol-gel synthesis two silica precursors: tetraethoxysilane (TEOS) and n-propyltriethoxysilane (PtEOS) containing different substituents (-C<sub>2</sub>H<sub>5</sub>, -C<sub>2</sub>H<sub>5</sub> and C<sub>3</sub>H<sub>7</sub>, respectively) were used.

The surface morphology, elemental analysis and topography of the coatings were determined using a scanning electron microscope (SEM), EDX analysis and atomic force microscopy (AFM), respectively. Raman spectroscopy measurements were carried out to characterize the chemical structure of obtained materials. Hydrophilicity, water contact angle and surface free energy (SFE) were evaluated by using a drop shape analysis system. The corrosion resistance of coated metal samples was investigated in Ringer's solution. The corrosion characteristics included: corrosion potential ( $E_{CORR}$ ), polarization resistance ( $R_p$ ) and corrosion current density ( $i_{CORR}$ ) which were extracted from the curves, calculated via Stearn-Geary method. Moreover, cytocompatibility of investigated coatings was tested in vitro using osteoblast-like MG-63 cells. Cell adhesion, morphology and distribution were evaluated using fluorescence microscopy after live/dead (calcein AM/propidium iodide) and DAPI/eosin staining. Viability was studied by Alamar Blue test and proliferation factor (PF) was calculated.

## RESULTS AND DISCUSSION

SEM-EDX analysis indicated that all received silica coatings showed characteristic microstructure, without cracks and uniformly covered the metallic substrate (Figure 1); their thickness was about 240 nm.

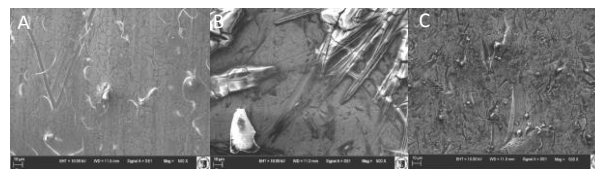


Figure 1. SEM micrographs of functionalised sol-gel derived coatings: SiO<sub>2</sub>/0.4M LAA (A) SiO<sub>2</sub>/0.7M SAL (B) and SiO<sub>2</sub>/3.5mM DOPA (C) applied on AISI 316L stainless steel, at 500x magnification.

AFM measurements revealed differences in nanotopography of the coatings. Moreover significant decrease in roughness parameter ( $R_a$ ) in the case of SiO<sub>2</sub>/0.7M SAL compared to pure silica coatings SiO<sub>2</sub> (TEOS) was observed. Raman spectroscopy showed the characteristic bands for chemical structures forming the silica network. Additionally the spectra analysis confirmed presence of characteristic groups of active molecules in doped SiO<sub>2</sub> coatings. Water contact angle ( $\theta_w$ ) measurements showed that all coated surfaces were hydrophilic ( $\theta_w < 90^\circ$ ); LAA and SAL dopants resulted in significant decrease in  $\theta_w$ . The results of electrochemical analysis indicated that the surface modification by applying sol-gel coatings improved corrosion resistance of the tested biomaterials in Ringer's solution. Biological assays approved that all coatings were cytocompatible with osteoblast-like cells (MG-63) and supported cell adhesion.

## CONCLUSION

Obtained results showed that proposed functionalization procedure of SiO<sub>2</sub> sol-gel derived network with selected active molecules enabled synthesis of bioactive coating materials on metallic substrate, which were cytocompatible and promoted cell adhesion and proliferation. Moreover it can be concluded that immobilization of proper dopant within silica network, enables control of wettability and nano-topography of received coatings using sol-gel route.

## REFERENCES

1. Ma Z. *et al.*, Appl. Surf. Sci. 284:738–744, 2013.
2. Catauro M. *et al.*, J. Mater. Sci. Eng., C 43 375–382, 2014.

## ACKNOWLEDGMENTS

This work has been partly financially supported by Grant no: B40082/W10/K10.

# Multimodal Image Registration for Assessment of Bone Formation in Porous Metal Implants

Hua Geng<sup>1</sup>, Taek Bo Kim<sup>2</sup>, Aine Devlin<sup>3</sup>, Naomi Todd<sup>3</sup>, Kamel Madi<sup>1</sup>, Julian R. Jones<sup>2</sup>, Christopher Mitchell<sup>3</sup>, Chris Sutcliffe<sup>4</sup>, Sarah Cartmell<sup>1</sup>, Peter D. Lee<sup>1</sup>

<sup>1</sup>School of Materials, University of Manchester, Manchester, UK

<sup>2</sup>Department of Materials, Imperial College, London, UK

<sup>3</sup>Centre for Molecular Biosciences, Ulster University, Coleraine, UK

<sup>4</sup>School of Engineering, University of Liverpool, Liverpool, UK

[hua.geng@postgrad.manchester.ac.uk](mailto:hua.geng@postgrad.manchester.ac.uk)

## INTRODUCTION

Histomorphometric analysis is considered the gold standard for analysis of bone formation in tissue scaffolds; however, these 2D sections can bias 3D features. Additionally, the process of fixation, sectioning and polishing can introduce artefacts such as movement and shrinkage (dehydration) of tissue. Micro-computed tomography ( $\mu$ CT) can be readily applied to non-destructively image and quantify bone formation. Combining these techniques can provide multimodal imaging to gain further understanding of tissue growth. In this study,  $\mu$ CT was utilised to non-destructively image and evaluate bone formation in a porous titanium implant, followed by destructive histological sectioning and imaging. Digital registration of  $\mu$ CT and histological images was then performed to compare and contrast the benefits of each method.

## EXPERIMENTAL METHODS

Porous titanium scaffolds with an average porosity of 65 % (1) were fabricated from grade 1 commercially pure titanium using selective laser melting. The scaffolds were implanted in rats, using a 3 mm diameter medial aspect defect in the right tibia. Individual tibial samples were assessed for bone ingrowth at 2, 3, 4 and 6 weeks after implantation. The tibiae were scanned in a laboratory  $\mu$ CT with an isotropic voxel size of 9  $\mu$ m. The tibial specimens were fixed, embedded in resin, sectioned transversely, stained with haematoxylin and imaged optically. A methodology was then developed to register the histology images with the  $\mu$ CT data, with key steps consisting of data segmentation and iterative registration. A comparison study was then performed on the bone ingrowth measured from 3D  $\mu$ CT volume, histology and the corresponding 2D slice in the  $\mu$ CT data. In 3D, the bone ingrowth was further subdivided relative to the surface of the implant (edge, sub-surface and core), allowing quantification of the bone penetration.

## RESULTS AND DISCUSSION

Figure 1 shows new bone successfully formed in the porous scaffold. Good bone contact suggests that the porous implant promotes a stable fixation.

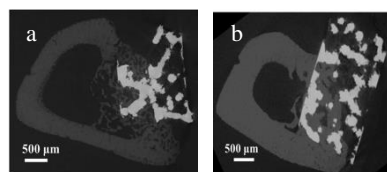


Figure 1.  $\mu$ CT image of implant in the rat tibia after (a) 2 weeks and (b) 6 weeks implantation

Histology provides insight into bone maturity and other cellular information of the bone and surrounding tissue; however, it can also introduce artefacts and is limited in that only a single slice is quantified. Figure 2a shows a 3D  $\mu$ CT volume and 2D histology image of a rat tibia 6 weeks after implanting a Ti scaffold. Due to the size of the Ti scaffold, the histological sections were often taken near the edge of the implant, which biased the results, as shown by comparison to 3D  $\mu$ CT results (Figure 3). Bone ingrowth is fastest near the edge, hence histology has a tendency to overestimate bone ingrowth. Additionally, shrinkage of the histology section during preparation can add errors (Figure 2b).

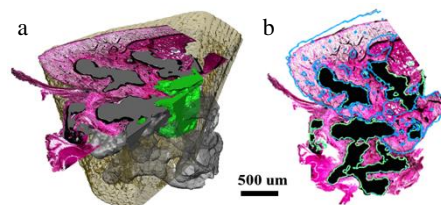


Figure 2. Correlation between 3D  $\mu$ CT and histology, the new bone (green) is observed in the porous titanium scaffold (grey) at 6 week, the old bone is visualised in brown (a), a good correlation was observed in histology and its corresponding 2D  $\mu$ CT slice (blue: bone, green: titanium) (b).

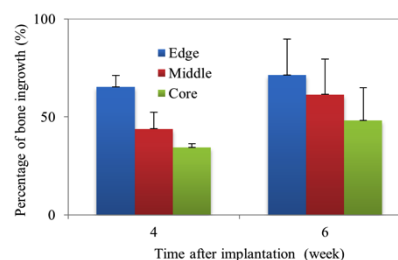


Figure 3. Percentage bone ingrowth from the edge to the core of the implant after 4 and 6 weeks.

## CONCLUSION

Multimodal imaging and registration is a promising hybrid approach to quantify bone formation in scaffolds.  $\mu$ CT removes potential biasing due to histological sectioning near to edge, rather than in the centre, of porous titanium implants.

## REFERENCES

- Kim TB et al. J Mater. Process Technol. 2014 Nov; 214(11): 2706–15.
- Jones AC et al. Biomaterials. 2007; 28(15): 2491–504

## ACKNOWLEDGMENTS

Research Complex at Harwell, Stryker and EPSRC (EP/I02249X/1) for funding.

# Injectable Hydroxyapatite Enriched Hyaluronate Gels for Versatile Tissue Engineering Applications

Cecilia De León<sup>1,2</sup>, Elvira Estella<sup>1,3</sup>, L. Téllez-Jurado<sup>4</sup>, M.A. Álvarez-Pérez<sup>2</sup>, Julio San Román<sup>1,5</sup>,  
Luis M. Rodríguez-Lorenzo<sup>1,5</sup>

<sup>1</sup>Biomaterials Group, ICTP-CSIC, Madrid, Spain

<sup>2</sup>Universidad Nacional Autónoma de México, México DF, México

<sup>3</sup>Universidad Politécnica de Madrid, Madrid, Spain

<sup>4</sup>E.S.I.Q.I.E-I.P.N, México DF, México

<sup>5</sup>Polymeric Biomaterials Group (GBP-CSIC), CIBER-BBN, Madrid, Spain

[ailicec28@yahoo.com](mailto:ailicec28@yahoo.com)

## INTRODUCTION

Colloidal gels are a particularly attractive class of hydrogels for applications in regenerative medicine that allow for a “bottom-up” fabrication of multi-functional biomaterials. Hyaluronic acid (HA) is a biopolysaccharide that has excellent biocompatibility and biodegradability properties and it plays an essential role for bone remodeling. Nanocrystalline apatites exhibit a great ionic mobility, as well as ion exchange and adsorption capacities. They can be surface functionalized with organic molecules including polymers, peptides, proteins or nucleic acids. Hydroxyapatite reinforced hyaluronic acid composite gels may offer a strongly enhanced gel elasticity, shear-thinning and gel stability at high ionic strengths, while chemical, potentially cytotoxic, functionalization may be not necessary to introduce sufficiently strong cohesive interactions. Thus, hydroxyapatite-hyaluronate composites gels may provide with a better control over cell-biomaterials interaction. Bone defects filled with both HA and OHAp demonstrated superior healing compared to defects filled with OHAp alone<sup>1</sup>. Thus, the aim of this work is to establish an appropriate reaction to functionalize apatite with HA and the ability to produce injectable materials.

## EXPERIMENTAL METHODS

Hydroxyapatites have been synthesized through a wet chemistry process by mixing the appropriate proportions of CaCl<sub>2</sub>, H<sub>3</sub>PO<sub>4</sub> and KOH. Some of the batches incorporate also ZnCl<sub>2</sub> to improve the immunological response of the system towards the composite. Hydroxyapatites have been functionalized using three different approaches. For the first one, a hyaluronate solution is added during the synthesis reaction of the hydroxyapatite. For the second one, hyaluronate is added after the synthesis reaction is completed. For the third one, a preliminary step of hyaluronate oxidation is introduced. Hyaluronate-hydroxyapatite composites gels are characterized through FTIR, Raman Spectroscopy, DRX, CHN analysis, TGA, SEM, EDS, specific surface area, zeta potential analysis and rheology measurements.

## RESULTS AND DISCUSSION

Hydroxyapatite formation has been verified by FTIR and XRD. XRD patterns confirm the presence of a single apatitic crystalline phase also for the Zn ions containing samples. No secondary phases have been detected. A decrease on the *a* cell parameter from

9.449 to 9.439 Å, for calcium hydroxyapatite and Zn hydroxyapatite respectively confirms the incorporation of the Zn ion into the apatite structure. A carbon contents in the 1.4-1.6% range and the weight loss observed in the 200-450°C range in the TGA curve confirms the incorporation of 2,4-3,8% hyaluronate on the hydroxyapatite. The method that incorporates hyaluronate after the hydroxyapatite synthesis reaction is completed yields smaller particles that in the case of the incorporation of the apatite during the synthesis reaction. The isoelectrical point disappears for OH-Ap/HA and OH-Ap/oxi-HA and at pH 7 the Z potential decreases from -19 up to -22 and -23 for OHAp, OH-Ap/HA and OH-Ap/oxi-HA respectively. Oxidation of HA has been demonstrated by the appearance of bands at 1737, 2849 and 2918 cm<sup>-1</sup> due to the aldehyde groups in the spectra of oxidized samples that can be attributed to the formation of the aldehyde and it cannot be observed in the spectra of the as received HA. The presence of bands at 2897 and 2984 cm<sup>-1</sup>, attributed to the C-H groups from the HA component are significantly stronger in the spectra for oxidized hyaluronic acid functionalized hydroxyapatite (OH-Ap/oxi-HA), than for the functionalization with hyaluronic acid (OH-Ap/HA) suggesting that the interaction of the oxi-HA acid with the ions of the OHAp is stronger than the interaction of the HA with the OHAp. Suspensions with a 2,7·10<sup>-3</sup>-7,2·10<sup>-3</sup> Pa.s<sup>-1</sup> viscosity can be achieved for gels containing 3.1% and 7.5% hydroxyapatite. These systems can be fully injected with a 5mL syringe.

## CONCLUSION

The preparation of hydroxyapatite/hyaluronate composite gels has been achieved by three different methods. HA does not inhibit the nucleation and crystal growth of OHAp. The interaction of the oxidized hyaluronic acid with the ions of the hydroxyapatite is stronger than the interaction of the HA with the OHAp. The obtained gels are fully injectable materials.

## REFERENCES

1. Khan F. et al., Macromol. Biosci. 13:395-421, 2013

## ACKNOWLEDGMENTS

“The authors would like to thank CIBER-BBN, UNAM-DGAPA: PAPIT Project IN210815 and CONACYT through scholarship 289568 to CLE for providing financial support to this project”.





## Bone Induction by Surface Modified Calcium Phosphate Ceramics

Rongquan Duan<sup>1,2</sup>, Davide Barbieri<sup>1</sup>, Xiaoman Luo<sup>1,2</sup>, Florence de Groot<sup>1</sup>, Huipin Yuan<sup>1,2,3</sup>, Joost D. de Bruijn<sup>1,2</sup>

<sup>1</sup>Xpand Biotechnology B.V., the Netherlands;

<sup>2</sup>MIRA Institute of Biomedical Technology and Technical Medicine, University of Twente, the Netherlands;

<sup>3</sup>College of Physical Science and Technology, Sichuan University, Chengdu, China

[r.duan@utwente.nl](mailto:r.duan@utwente.nl)

### INTRODUCTION

Calcium phosphate (CaP) ceramics are used clinically as bone void fillers and their bone forming capacity depends on physicochemical properties<sup>1</sup>. Dissolution and reprecipitation of a surface apatite layer through epitaxial crystal growth is preceding bone bonding and a submicron surface structure has been reported to allow bone induction by these materials in ectopic sites<sup>2,3</sup>. Herein, we have used a hydrothermal treatment of an otherwise non-osteoinductive calcium phosphate to allow epitaxial crystal growth and investigated in osteogenic differentiation in vitro and in vivo.

### EXPERIMENTAL METHODS

Biphasic calcium phosphate (BCP, 10/90 HA/TCP ratio) was synthesized using a wet precipitation method and sintered at 1200°C for 8 hours. Granules (1-2mm) were prepared and a hydrothermal treatment was applied to obtain epitaxial crystal growth. After characterisation, the biological performance of the BCP granules before and after hydrothermal treatment was investigated in vitro with murine mesenchymal stromal cell (mMSC) at 14 days (basal medium), and in an intramuscular implantation model in dogs for 12 weeks (1cc; n=5).

### RESULTS

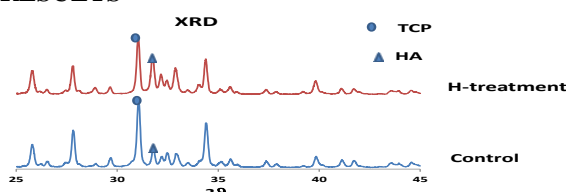


Fig 1. XRD of BCP before and after hydrothermal treatment (note the increase in HA after treatment).

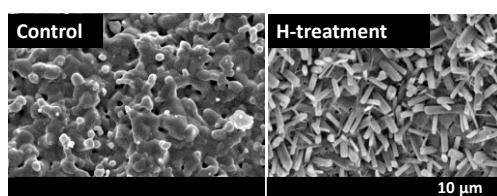


Fig.2 Surface structure of BCP before and after hydrothermal treatment.

Hydrothermal treatment of the BCP resulted in an increase in HA content from 10% to 22% (Fig 1) and the formation of epitaxial polygons on the surface (Fig 2). As a result, the surface was modified from grains with a size of  $2.46 \pm 0.78 \mu\text{m}$  to epitaxial polygons measuring  $1.23 \pm 0.41 \mu\text{m}$ .

The surface modification of BCP did not affect the proliferation and osteogenic differentiation

of cultured mMSCs (Fig 3), while it did affect the bone forming ability in vivo. Bone induction occurred in 4 out of 5 hydrothermally treated BCP implants, while no bone was formed in any of the controls (0 out of 5) (Fig. 4).

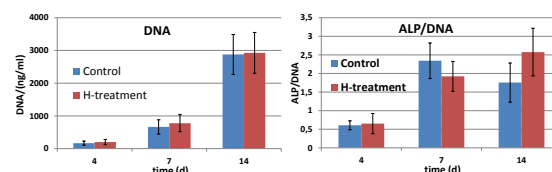


Fig 3. Proliferation and osteogenic differentiation of mMSC grown on BCP before and after surface modification. Culture medium comprised of DMEM supplemented with 10%FBS, 1% sodium pyruvate and 1% Penicillin-Streptomycin.

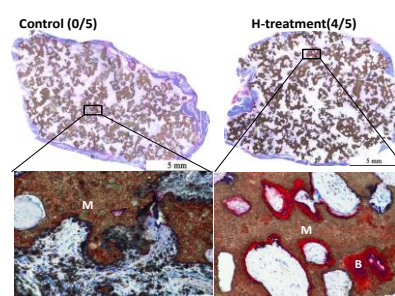


Fig 4. Histology and incidence of bone formation in control and hydrothermally treated BCP implants after a 12-week intramuscular implantation in dogs (undecalcified sections; methylene blue and basic fuchsin staining; M: BCP; B: bone)

### DISCUSSION AND CONCLUSION

The hydrothermal treatment caused the formation of epitaxial polygons on the BCP surface. This resulted in a reduction of surface features from  $2.46 \pm 0.78 \mu\text{m}$  to  $1.23 \pm 0.41 \mu\text{m}$ . Although no in vitro effect was seen, the hydrothermal treatment led to *de novo* bone formation in 4 out of 5 implants. None of the control implants showed any bone formation.

The results present herein indicate that a hydrothermal treatment of BCP granules results in the formation of epitaxial polygons. The resulting material is osteoinductive in canine muscles after 12 weeks of implantation.

### REFERENCES

1. Yuan *et al.*, PNAS 107:13614-19, 2010
2. J. Zhang *et al.*, Acta Biomater 10:3254-3263, 2014
3. N. Davison *et al.*, Biomaterials 35:5088-5097, 2014

### ACKNOWLEDGMENTS

The authors would like to thank the Netherlands Institute for Regenerative Medicine (NIRM) and Rapid Prototyping of Custom-Made Bone-Forming Tissue Engineering Constructs (Rapidos) project for their financial support to this project.





## Optical Coherence Tomography as a Complementary Method to X-ray Computed Tomography in Dental Diagnosis

Marcin Strąkowski<sup>1</sup>, Milena Supernak-Marczewska<sup>2</sup>, Paulina Strąkowska<sup>1\*</sup>, Ewa Kowalska<sup>2</sup>, Maciej Kraszewski<sup>1</sup>, Małgorzata Ryniec-Wilczyńska<sup>2</sup>, Michał Trojanowski<sup>1</sup>, and Violetta Szycik<sup>2</sup>

<sup>1</sup>Dept. of Metrol. and Optoelectr., Faculty of Electronics, Telecom. and Informatics, Gdansk Univ. of Tech., Poland

<sup>2</sup>Vivadental- EUROPEAN DENTAL IMPLANT INSTITUTE, Poland

[\\*pauanton@pg.gda.pl](mailto:pauanton@pg.gda.pl)

### INTRODUCTION

The needs for dental treatment, including standard dental procedures and dental implantology, are very high and they are still growing. Only in Poland the approximately 70 thousands implants are implanted annually (in Germany more than 1 million). Moreover, Polish dental market is one of the fastest growing in the world. Implants have been 18% share in the global dental market calculated the Agency Markets and Markets. Such an advanced and complicated dental implantology procedures require precise, high resolution and reliable diagnosis tools [1]. One of the best and most commonly used methods are based on X-Ray computing tomography (CT). Despite of its awesome features the CT has some limitations in its imaging resolution (hundreds of microns) and exposure time on X-ray radiation. The number of CT measurements is limited in time period. Therefore, we propose to use the optical coherence tomography (OCT) as a complementary method in dental procedures. The OCT is a non-contact and non-invasive optical method, which delivers cross-sectional and 3D images with micrometer resolution. Since the optical radiation is used the OCT is safe for the patient and the diagnosis procedure can be repeated without any limitations [2][3]. Here these two methods, CT and OCT, have been compared.

### EXPERIMENTAL METHODS

For the experiment the IVS-2000 (Santec co., Japan) system has been used. This is the OCT system with polarization sensitive analysis (PS-OCT). Apart from the standard OCT the PS-OCT delivers also information about polarization state of backscattered light. It is useful in teeth diagnostics, since tooth tissue (enamel and dentine) is birefringent and thus changes polarization state of the light. The IVS-2000 PS-OCT system is capable to provide tomographic images with 12  $\mu\text{m}$  of axial resolution and 15  $\mu\text{m}$  in lateral resolution. The measurements have been taken for teeth with and without crowns prosthesis. All samples have been scanned in one hour from their extraction. The teeth without crowns prosthesis were tested from front and rear part of crown and root. The teeth with crowns prosthesis were investigated at the teeth and prosthesis junction. Obtained results have been confirmed with CT measurements.

### RESULTS AND DISCUSSION

In order to express the benefits of using OCT technique in dental procedures the OCT image of the tooth's crown has been compared with CT cross-sections. Obtained results have been presented in Figure 1.

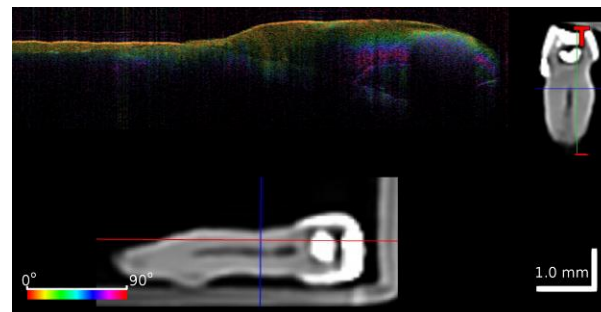


**Figure 1. PS-OCT image of the crown part of tooth compared with CT tomography images.**

The OCT image has been taken by the use of PS-OCT system. This system is capable to evaluate the birefringence of the tooth tissue. The colour of the OCT picture determines polarization state of the backscattered light. However, the pixel intensity referees to the scattering coefficients for the particular points inside tested sample. The presented OCT image express the tooth's crown structure and its local optical anisotropy changes. Comparing the OCT results with CT images (also presented in the Figure 1) the OCT delivers the tomography images with better resolution. Moreover, the useful information on the tooth birefringence can be measured, which cannot be obtained by CT measurements. However, the OCT scanning depth range may reach a few millimetres, while the CT has no such a limitations.

### CONCLUSION

The OCT and its extensions (PS-OCT) can be used in dental diagnosis with success. However, it should be rather a complementary tool to CT than its replacement. The high application potential of this method including standard dental procedures and dental implantology is going to be confirmed fully during conference sessions.

### REFERENCES

1. Resink R.R., Misch C.E., Dental Impl. Prosthetics (Secend edition): 152-158, 2015
2. Fujimoto J.G., Nat. Biotech. 21:1361-1367, 2003
3. Strąkowski M. et al., Acta Phys. Pol. A 120(4): 785-788, 2011
4. Miszczuk K. et al., Protet. Stomatol., LXII 6:428-433, 2012

### ACKNOWLEDGMENTS

This research work has been supported by the NCBR, Poland, under grant no. LIDER/32/205/L-3/11 and DS program of Faculty of ETI PG. The authors would like to thank the Vivadental Institute for providing biological materials, and carried out tests on CT.

## Molecular Basis of the Gp36 MPER Fusogenic Activity

Anna Maria D'Ursi<sup>1</sup>, Agostino Bruno<sup>2</sup>, Mario Scrima<sup>1</sup>, Manuela Grimaldi<sup>1</sup>, Grazia Della Sala<sup>3</sup>, Vittorio Limongelli<sup>2</sup>

<sup>1</sup>Department of Pharmacy, University of Salerno, Via Ponte don Melillo 11c, I-84084 Fisciano, Italy

<sup>2</sup>Department of Pharmacy, University of Naples "Federico II", via D. Montesano, 49, I-80131 Naples, Italy

<sup>3</sup> Department of Neuroscience, Psychology, Drug Research and Child Health NEUROFARBA, University of Florence, Florence ITALY.

[dursi@unisa.it](mailto:dursi@unisa.it)

### INTRODUCTION

Membrane fusion is the process whereby two separate lipid bilayers merge to become one. The energetic barrier for fusion is generally lowered by fusion proteins that, owing to conformational changes, bring membranes into close proximity and destabilize the lipid bilayers by inducing extreme membrane curvature.<sup>1</sup>

The peptide C8 (WEDWVGWI), which corresponds to the membrane proximal external region (MPER) of feline immune deficiency virus (FIV) coat glycoprotein (Gp36) is endowed with fusogenic activity destabilizing the lipid bilayer.<sup>2</sup>

In the present study we elucidate the structural basis of the molecular interaction of C8 with layers made of different composition of zwitterionic and negatively charged phospholipids. The ability of C8 to induce modifications of the membrane curvature and formation of membrane "nipples" is further evaluated by confocal microscopy.

### EXPERIMENTAL METHODS

Solution of lipids in the absence or presence of NBD labelled-C8 peptide was used for confocal microscope imaging. Confocal fluorescence microscopy was performed using an inverted microscope (IX 70, Olympus, Tokyo, Japan) equipped with a spinning disk confocal scanner (CSU10, Yokogawa, Tokyo, Japan) and a krypton argon ion laser (Melles Griot, Carlsbad, CA).

Funnel molecular dynamic simulations, were carried out using the NAMD 2.8 software<sup>3</sup>

<http://www.ks.uiuc.edu/Research/namd/>) and TIP3P as water solvation model. Each C8-bilayer system, was solvated using the vmd autoionize plugin.<sup>4</sup>

<http://www.ks.uiuc.edu/Research/vmd/>

### RESULTS AND DISCUSSION

Fluorescent C8 peptide synthesized by substituting Trp with nitrobenzoxadiazole (NBD) residue was studied on lipidic membranes by imaging 1,2-Dioleoyl-sn-glycero-3-phosphocholine (DOPC), 1,2-dioleoyl-sn-glycero-3-[phospho-*rac*-(1-glycerol)] (DOPG) and DOPC/DOPG (90/10), in absence and presence of C8 peptide. The imaging of DOPC and DOPG vesicles in the presence of NBD labeled C8 evidence the localization of the peptide on the membrane surface. DOPG/DOPG vesicles loaded with labeled C8 peptide show well-extended straight-chain tubular structures

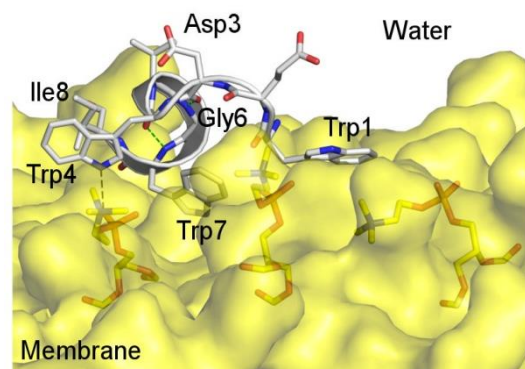


**Figure 1** Selected binding mode for the C8 peptide (white cartoon and sticks) in DOPC-DOPG (90:10) membrane system (highlighted as yellow transparent surface), also, highlighted in yellow stick the DOPC polar heads interacting with C8.

Molecular interpretation of microscopy data using funnel molecular dynamics simulations (FMD) in explicit solvent describes a process where, the binding of C8 to the DOPC-DOPG membrane, induces an expansion of the membrane surface leading to a structural reorganization of the bilayer (Figure 1). Considering the timescale of our calculations it is attractive to suggest that our simulation describes the very early stages of the C8-membrane interaction, which leads in much longer timescale to the macroscopic effects observed by the confocal microscope imaging.

### CONCLUSION

Structural investigation of the fusogenic peptide C8 performed with confocal microscopy and molecular dynamic simulation, allows to elucidate the molecular mechanism that enable C8 to form "nipples" and have fusogenic activity. The comprehension of this mechanism is the basis to design molecular tools capable of modulating this process for therapeutic application.

### REFERENCES

1. Harrison SC., *Nat Struct Mol Biol* 15 690-698, (2008)
2. Giannecchini S et al. *J Virol* 77 3724-3733, (2003)
3. Phillips JC et al. *J. Comput. Chem.* 26, 1781–1802 (2005);
4. Humphrey W et al. *J. Mol. Graph.* 14, 33–38, 27–28 (1996).

## Engineering PEGylated Alginate Hydrogels for Cell Microencapsulation

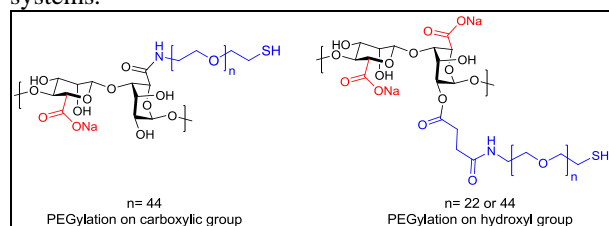
Solène Passemard, François Noverraz, Virginia Crivelli, Redouan Mahou, Françoise Borcard, Sandrine Gerber-Lemaire\*, Christine Wandrey

Ecole Polytechnique Fédérale de Lausanne, 1015 Lausanne, Switzerland

[solene.passemard@epfl.ch](mailto:solene.passemard@epfl.ch)

### INTRODUCTION

Cells microencapsulation is a promising technology to treat a wide range of diseases through cells transplantation. This therapy is an alternative for tissue grafting and engineering and can overcome the problem of graft rejection. The scaffold materials for cells microencapsulation are biocompatible hydrogels which require specific physical properties<sup>1</sup>. The hydrogel network density, stiffness, and hydrophilicity can have a crucial impact on cell proliferation, differentiation, and function. These physical characteristics can be adjusted with covalent modification of the hydrogel materials. Here are investigated several chemical modifications of alginate(alg)-based hydrogels with poly(ethylene glycol) PEG 1000 and 2000 either on hydroxyl or carboxylic groups of the alg backbone (**Scheme 1**). Physical properties of the resulting microspheres (MS) will be reported and compared between the different systems.



**Scheme 1:** PEGylated Na-alg with two different systems.

### EXPERIMENTAL METHODS

#### Synthesis of $\alpha$ -amino- $\omega$ -mercapto PEG1000

-  $\alpha$ -Amino- $\omega$ -mercapto PEG was synthesized starting from commercially available PEG 1000. The unsymmetric alteration was performed through mono-Staudinger reduction as a key step<sup>2</sup>. Thiol functionality was then introduced by copper click reaction.

#### Modification of Na-alginate

- Na-alg was modified by grafting linear  $\alpha$ -amine- $\omega$ -thiol PEG 1000 and 2000 either to the carboxyl or hydroxyl groups up to 5 % of grafting.

#### Microsphere formation

- A BÜCHI Encapsulator B-395 Pro (BÜCHI Labortechnik AG, Switzerland) was used to extrude the polymer solutions into a gelation bath containing  $\text{CaCl}_2$ .

#### Characterization of the polymer solutions

- All polymer solutions were prepared at defined concentrations and characterized by their dynamic viscosity. The osmolality and the pH were adjusted to physiological conditions.

#### Physical characterization of microspheres

- The size of the MS, swelling in different media, and stability were observed by optical microscopy. Water uptake was gravimetrically determined. Mechanical stability, deformability and mechanical resistance to compression were analysed using a TA-XT2i (Stable

micro Systems, Godalming, UK). Ingress diffusion experiments using fluorescence labelled dextran standards (40, 70, 150 kg/mol) served to estimate the permeability.

### RESULTS AND DISCUSSION

The polymer grafting sites and the PEG chain length considerably changed the physical properties of the MS. On the first system, PEG 2000 was inserted on carboxyl functional groups decreasing the available sites needed for electrostatic crosslinking with calcium ions. The second system involving the modification on hydroxyl groups was thus investigated to preserve 100 % of the electrostatic crosslinking. In both systems were observed spontaneous covalent crosslinking through disulfide bond formations. As expected, PEGylation on hydroxyl groups offered a better mechanical resistance to compression and a better stability over time of the MS. A shorter PEG grafted on hydroxyl groups was suitable to modify the polymer network density and consequently the permeability and the mechanical resistance to compression of the MS. Many other parameters such as the degree of grafting can influence the physical properties of the MS.

### CONCLUSION

The combination of electrostatic and covalent crosslinking offers a variety of possibilities to adjust the physical properties of alginate-based MS and to adapt these characteristics to the microencapsulation of specific cell types. The fast electrostatic crosslinking of Na-alg with calcium ions was used to provide a spherical matrix for the simultaneously but slowly occurring covalent crosslinking. Grafting heterobifunctional PEG on Na-alg in such a way that sufficient carboxyl groups remain for fast electrostatic crosslinking also allows reinforcing the MS. The overall advantage of all modifications presented here is the applicability of a one-step MS formation process. Biocompatibility was confirmed for all MS types by *in vitro* and/or *in vivo* experiments including the microencapsulation of different cell types.

### REFERENCES

1. Mahou R. *et al.*, Macromol. Symp. 329:49-57, 2013
2. Passemard S. *et al.*, Bioorg. Med. Chem. Let. 23: 5006–5010, 2013

### ACKNOWLEDGMENTS

The SNSF (205321-116397/1, 205320\_130572/1, 205321\_141286/1), the CTI (138041.1 PFLS-LS) and BÜCHI Labortechnik AG, Switzerland supported this research.



## Study of Biodegradation Impact on PLA/Graphene-Nanoplatelets Biocomposites Mechanical and Biological Properties

Artur M. Pinto<sup>1,2</sup>, Carolina Gonçalves<sup>1</sup>, Inês C. Gonçalves<sup>2</sup>, Fernão D. Magalhães<sup>1</sup>

<sup>1</sup>LEPABE, Faculdade de Engenharia, Universidade do Porto, Rua Dr. Roberto Frias, 4200-465 Porto, Portugal

<sup>2</sup>INEB, Universidade do Porto, Rua do Campo Alegre, 823, 4150-180 Porto, Portugal

[arturp@fe.up.pt](mailto:arturp@fe.up.pt)

### ABSTRACT

Two types of graphene-nanoplatelets (GNPs) were incorporated in PLA (poly(lactic acid)) by melt blending. Materials were biodegraded during 6 months and characterized by XRD, tensile tests, DMA and biocompatibility assays. For both fillers, low loadings (0.25 wt.%) improved mechanical properties and decreased decay until 6 months biodegradation. PLA degradation decreased its toughness (AUC) by 10 fold, while for PLA/GNP-M and C, toughness was only reduced by 3.3 and 1.7 fold, respectively. Comparing with PLA, PLA/GNP-M and C composites presented similar (HFF-1) fibroblasts adhesion and proliferation at the surface and did not released toxic products (6 months).

### INTRODUCTION

A commercial available product, with reduced cost comparing with single layer graphene, GNPs, are constituted by few stacked graphene layers. These materials present high aspect ratio and possess oxygen-containing functional groups in the platelet edges, which may facilitate extensive interfacial interaction with polymer matrices. [1] Some typical composite production techniques like solvent mixing and electrostatic deposition lead to obtainment of toxic materials. [1,2] Thus, melt blending, which assures complete embedding of GNPs in polymer matrix preventing filler leaching, is studied in this work as a green method for production of PLA/GNPs composites.

### EXPERIMENTAL METHODS

PLA 2003D (Natureworks), GNPs (XG Sciences). Composites were prepared by melt blending and moulded in a hot press into thin sheets (0.3-0.5 mm). Samples were immersed in PBS and incubated for 6 months (37 °C, 100 rpm). Tensile properties were measured (Mecmesin Multitest-1d, Mecmesin BF 1000N) using a strain rate of 10 mm min<sup>-1</sup>. Creep/recovery assays were performed using a DMA 242 E Artemis (Netzsch). Biocompatibility of materials was evaluated using HFF-1 cells cultured at the surface of composite films and in direct contact with materials extracts obtained after 6 months degradation. Metabolic activity was determined using resazurin assay.

### RESULTS AND DISCUSSION

#### XRD

GNP-M and C powders present similar XRD spectra, typical of carbon materials. PLA, before (0M) and after 6 months (6M) biodegradation, presents similar spectra, also typical for this polymer. In composites PLA and GNPs peaks were observed. Degradation did not affected spectra.

### Tensile tests

Incorporation of GNP-C and M in PLA increased its Young's modulus by 14 %. Also, tensile strength is increased by 20% for GNP-C and by 6% for GNP-M. After 6 months biodegradation, decreases in tensile strength, elongation at break, and toughness are respectively, for PLA of 2.6, 2.5, and 10 fold, for PLA/GNP-M of 1.6, 1.8 and 3.3 fold, and for GNP-C of 1.4, 1.4 and 1.7 fold.

### Creep/recovery

Figure 1 shows that for undegraded PLA, dL<sub>f</sub> (final, at 6N) after 10 creep/recovery cycles was of 14.2 µm, being of 13.7 and 13.2 µm for PLA/GNP-M and C 0.25 wt.%, respectively. After 6 months degradation, PLA sample ruptured after 4 cycles (1.A) reaching a dL<sub>f</sub> of 56.3 µm. PLA/GNP-M and C 0.25 wt.% did not rupture (1.B,C) and presented only a slight increase in dL<sub>f</sub>, of 16.8 and 16.7 µm, respectively. Materials degradation was confirmed

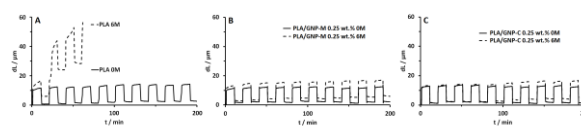


Figure 1. Multi cycle DMA of PLA and composites before and after 6 months degradation.

in terms of molecular weight decrease and changes in surface morphology (results not shown).

### Biocompatibility evaluation

PLA/GNP-M and C 0.25 wt.%, metabolic activity never decreased below 90%, for both composites in comparison with PLA. Composites degradation products are not toxic (24, 48, 72h), comparing with PLA 6M (Figure 2). Also, cell morphology is normal and similar for all conditions tested (images not shown).

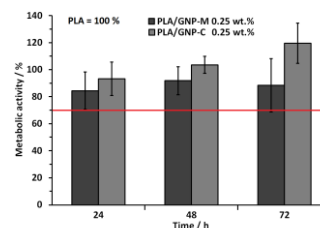


Figure 2. Cytotoxicity of PLA/GNP-M and C 0.25 wt.% 6 months degradation products, comparing with PLA in the same conditions. Assays were performed in triplicate, with 6 replicates for each condition tested. Error bars represent standard deviation. Red line represents cytotoxicity limit of 70%.

### CONCLUSION

GNP-M and GNP-C incorporation in PLA (0.25 wt.%) improved mechanical properties and decreased their decay after 6 months biodegradation. GNPs can be used to tune PLA mechanical performance during biodegradation in biomedical applications, since they did not decrease cell proliferation or cause toxicity.

### REFERENCES

1. Lahiri D. *et al.*, ACS Appl. Mater. Interfaces, 4:2234-2241, 2012.
2. Pinto A.M. *et al.*, Colloids and Surf B Biointerfaces, 111:188-202, 2013.



## Osteoinductive and Antibacterial Coatings for Dental Implants

Beatriz Palla<sup>1</sup>, Francisco Javier Romero<sup>2</sup>, Mar Fernández<sup>3</sup>, Julio Suay<sup>2</sup>, Mariló Gurruchaga<sup>1</sup>, Isabel Goñi<sup>1</sup>

<sup>1</sup>Polymer Science and Technology Department, POLYMAT, University of the Basque Country, Spain

<sup>2</sup>Industrial Systems Engineering and Design Department, Universitat Jaume I, Spain

<sup>3</sup>ICTP-CSIC, Spain

[beatriz.palla@ehu.es](mailto:beatriz.palla@ehu.es)

### INTRODUCTION

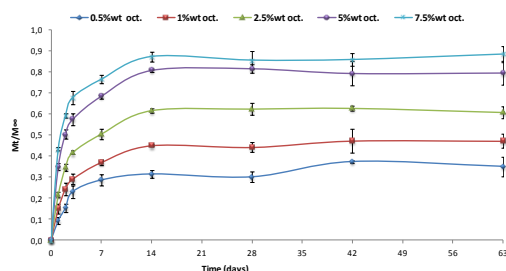
Dental implants in healthy patients have achieved excellent survival and success in the clinic for the recovery of tooth function and aesthetics. However, one of their major limitations is that there is, usually, strict patient selection criterion, because one of the most important requirements that they must achieve is a high capacity for osseointegration<sup>1</sup> in maxilar bone. It is also important, that this capacity of osseointegration include good osteoinduction and osteoconduction ability. The most common and significant problem associated with implantology are infections (peri-implantitis)<sup>2</sup> in association with medical implants and devices which can, in many cases, necessitate surgical removal or intervention and may lead to complications. Moreover, this is particularly the case for dental implants where the prevalence of bone loss induced by inflammation is of increasing importance. Thus, the main goal of this work is getting new active surfaces for dental implants, provided not only with osseointegration properties but also with a strong bactericidal effect through the gradual release of active agents over time.

### EXPERIMENTAL METHODS

Coatings were synthesized by the sol-gel method<sup>3</sup> from specific mixtures of an antimicrobial agent and alcoxysilanes: methyl-trimethoxysilane (MTMOS) and tetraethyl-orthosilicate (TEOS). Thus, the coatings would have a Si content that contributes to bone formation, as we have already demonstrated in previous works<sup>3</sup>, and a bactericidal capacity. Synthesis and characterization for each formulation were thoroughly carried out. After, many experiments were conducted in which both, the releasability of the active agent in time and the effective antibacterial action, were proved. Biocompatibility and antibacterial capabilities of the coatings were studied *in vitro*.

### RESULTS AND DISCUSSION

Figure 1 shows the release ability of the formulation with the bactericidal agent encapsulated over a period of 2 months.



The more antibacterial agent is encapsulated the more agent is released, so the release kinetics and the amount released are load dependent. In all the cases it can be observed that the release is fast at the beginning but followed by a slower, steady release over the time.

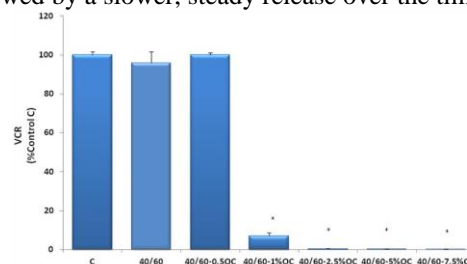


Figure 2 shows the strong bactericidal effect of the coatings charged with different amounts of active agent. As it can be seen, there is an increasing bactericidal effect related to the amount of antibacterial agent in the coating. It can be remarked that this strong bactericidal effect does not affect to the cellular viability.

### CONCLUSION

The excellent results obtained *in vitro* for the sol gel coated implants and the high release of bioactive agent obtained with small amounts containing coatings lead to expect an outstanding behaviour of the coated implants, offering accelerated osseointegration kinetics under infected conditions and as preventive coatings for risk patients. These new coatings present valuable characteristics for their application on orthopaedic and Ti dental implants.

### REFERENCES

1. Majumdar P. *et al.*, Polymer 48: 7499-7509, 2007.
2. Mombelli A. *et al.*, Periodontol.2000, 177:189-28, 2002.
3. Juan-Díaz M.J. *et al.*, Prog.Org.Coat. 77(11):1799-1806, 2014.

### ACKNOWLEDGMENTS

The authors would like to thank the University of The Basque Country (UFI 11/56) and Basque Government (A-Group: IT611-13) and the Spanish Ministry of Economy and Competitiveness through INNPACTO (IPT-2012-0218-090000) for providing financial support to this project.

# On-Demand Release of Dexamethasone from Conjugated Polymer Matrix

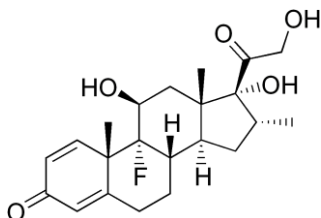
Katarzyna Krukiewicz<sup>1</sup>, Artur P. Herman<sup>2</sup>, Sławomir Boncel<sup>2</sup>, Jerzy K. Żak<sup>1</sup>

<sup>1</sup>Department of Physical Chemistry and Technology of Polymers, Silesian University of Technology, Poland

<sup>2</sup>Department of Organic Chemistry, Bioorganic Chemistry and Biotechnology, Silesian University of Technology, Poland  
[katarzyna.krukiewicz@polsl.pl](mailto:katarzyna.krukiewicz@polsl.pl)

## INTRODUCTION

Dexamethasone is a highly active glucocorticoid drug with anti-inflammatory and immunosuppressant effects. It is frequently used to treat numerous conditions including rheumatologic problems, skin diseases, severe allergies and chronic obstructive lung disease. Because of its efficiency against cerebral edema, it is used to minimize the negative effects of the implantation of neural probes into brain tissue<sup>1</sup>. To prevent the exposition of the whole body to high dosages of dexamethasone, local delivery of drug at the implant / tissue interface is a promising option.



Scheme 1. Chemical structure of dexamethasone

Due to their biocompatibility and ion-exchange properties, selected conjugated polymers can be applied as matrices for localized drug delivery systems<sup>2</sup>. Electrical stimulation is applied to change their reduction-oxidation state, which is followed by the release of a precise amount of drug<sup>3</sup>.

## EXPERIMENTAL METHODS

Poly(3,4-ethylenedioxythiophene), PEDOP, was chosen as a matrix for dexamethasone (Dex) immobilization. The process of Dex incorporation was performed simultaneously with the process of EDOP polymerization by means of cyclic voltammetry. Monomer concentration: 5 mM; Dex concentration: from 0 mM to 100 mM; environment: PBS aqueous solution; potential range: -0.3 V ÷ 0.8 V; number of CV cycles: 25; scan rate: 100 mV·s<sup>-1</sup>.

The process of Dex release was triggered by means of cyclic voltammetry (potential range: -0.5 V ÷ 0.3 V, number of CV cycles: 5, scan rate: 100 mV·s<sup>-1</sup>) and monitored by UV-Vis spectrophotometry.

## RESULTS AND DISCUSSION

Because of the fact that the processes of electrochemical polymerization and Dex immobilization were performed by means of cyclic voltammetry, it was possible to monitor their progress in-situ. CVs collected during electropolymerization of EDOP from solutions of varying Dex concentration (from 0 mM to 100 mM) showed that with the increase

in drug content lower oxidation currents are observed and the polymerization is suppressed.

In order to release Dex from PEDOP/Dex matrix, a cyclic voltammetry was applied in a potential range between -0.5 V and 0.3 V (vs. Ag/AgCl). Selected range of applied potentials is enough to reduce and oxidize PEDOP matrix and to provide the possibility of ion-exchange. To preserve the neutral character of the polymer matrix, together with Dex release, the incorporation of chlorides and phosphates takes place. The absorbance at  $\lambda = 268$  nm, which is characteristic for Dex, was recorded after the procedure of drug release and was the basis to calculate the concentration of released compound. Drug release experiments show that the drug capacity of PEDOP matrix increases with the increase in Dex concentration in the step of matrix synthesis. Because of the fact that higher Dex concentrations suppress the process of polymerization and thinner films are produced, one may conclude that under these conditions Dex is more available and easier to be released.

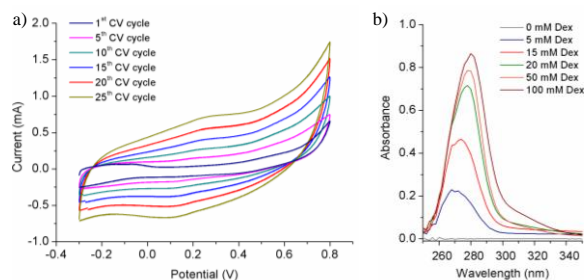


Fig.1. CVs of the process of EDOP (5 mM) polymerization in the presence of Dex (10 mM) in PBS aq solution (a). UV-Vis spectra of Dex released from matrices synthesized under different conditions (b).

## CONCLUSION

In this study, the electrically-triggered release system of dexamethasone from conjugated polymer, PEDOP, was described. It has been proven that by changing the conditions of polymerization, namely the amount of Dex, it is possible to tailor the drug capacity of matrix.

## REFERENCES

1. Wadhwa R. *et al.*, J.Control.Release 110:531-541, 2006.
2. Svirskis D., *et al.*, J.Control.Release 146:6-15, 2010.
3. Krukiewicz K. *et al.*, J.Mater.Sci. 49:5738-5745, 2014.

## ACKNOWLEDGMENTS

The authors would like to thank the Polish National Science Centre (Grant no: 2012/07/N/ST5/01878) for providing financial support to this project.

## Mesoporous Silica Nanofibers as Drug Delivery Systems for Intervertebral Disc Regenerative Medicine: Analysis of Protein-Silica Interactions

Nina Henry<sup>1,2,3</sup>, Johann Clouet<sup>1,3,4,5</sup>, Catherine Le Visage<sup>1,3</sup>, Eric Gautron<sup>2</sup>, Bernard Humbert<sup>2</sup>, Jérôme Guicheux<sup>1,3,6\*</sup>, Jean Le Bideau<sup>2\*</sup>

<sup>1</sup> INSERM, UMRS 791, Center for OsteoArticular and Dental Tissue Engineering (LIOAD), Nantes, France. <sup>2</sup> CNRS, UMR 6502, Institute of Materials Jean Rouxel (IMN), Nantes, France. <sup>3</sup> Université de Nantes, UFR Odontologie, Nantes, France. <sup>4</sup> CHU Nantes, PHU 11 Pharmacie, Pharmacie Centrale, Nantes, France. <sup>5</sup> Université de Nantes, UFR Sciences Biologiques et Pharmaceutiques, Nantes, France. <sup>6</sup> CHU Nantes, PHU 4 OTONN, Nantes, France.

\*Equally contributing authors

[Nina.Henry@univ-nantes.fr](mailto:Nina.Henry@univ-nantes.fr)

### INTRODUCTION

Intervertebral disc (IVD) degeneration is one of the major causes of low back pain<sup>1</sup>. Currently, low back pain is mainly managed by pharmacological treatments and, if unsuccessful, by surgical procedures. New regenerative medicine approaches are considered with great interest since they could offer less invasive and etiological alternatives to spinal reconstructive surgery<sup>2,3</sup>. Stem cells injection associated with a biomaterial to restore the hydration of the nucleus pulposus and provide a favorable 3D microenvironment constitutes an appealing strategy. Sustained release of bioactive growth factors added to the biomaterial could optimize stem cell differentiation and enhance synthesis of an appropriate *in situ* extracellular matrix.

In this context, we used recently designed mesoporous silica nanofibers (NFs)<sup>4</sup> as delivery systems. Lysozyme as a model protein was adsorbed onto the NFs and the protein-silica interactions were analyzed.

### EXPERIMENTAL METHODS

Lysozyme (Sigma-Aldrich) was incubated in presence of NFs under constant stirring in different conditions of (i) pH (4, 7, 10), (ii) time (from 1 to 48 hours) and (iii) concentrations (from 1 to 200 mg/mL) to determine the optimal conditions of adsorption. Analysis of protein-silica interactions were performed with transmission electron microscopy (TEM), attenuated total reflectance infrared (ATR/IR) and thermogravimetric analysis coupled with mass spectrometry (TGA/MS). Lysozyme release assays were then carried out in Phosphate Buffered Saline (PBS), pH 7.2 at 37°C for 20 days. Lysozyme concentration was assessed by a colorimetric method and biological activity was demonstrated by a micrococcus enzymatic assay.

### RESULTS AND DISCUSSION

In this study, we demonstrated that lysozyme could be efficiently adsorbed on NFs. On one hand, the highest amount of adsorbed lysozyme was obtained at pH 10, initial concentration medium of 200 mg/mL and 48h of incubation, corresponding to a 20% adsorption efficiency. On the other hand, we obtained a 100% adsorption efficiency in 1h for low initial concentrations (1 to 10 mg/mL). We thus hypothesized that when in contact with silica fibers, lysozyme would first adsorb very quickly, creating a protein monolayer. Then, additional layers would be stacked on the monolayer. Analysis performed with TEM, ATR/IR, TGA/MS confirmed this hypothesis. Single proteins or

multilayers of proteins onto the surface of NFs have been observed on TEM images. Very precise information was obtained from the IR study by comparison of amides, Si-O-Si, Si-OH and water bands between lysozyme or NFs alone and NFs/lysozyme.

Release experiments under physiological conditions show a burst after 1h of incubation leading to a slow kinetics release for up to 13 days. Although less than 20% of the initial adsorbed amount was released after 13 days from the NFs prepared at concentrations ranging from 1 and 5 mg/mL, up to 80% of lysozyme could be released from NFs prepared at higher concentrations. These kinetics results support the hypothesis that there is a two-step adsorption and thus, two different types of interactions between the protein and the NFs. At all time point, the released lysozyme was enzymatically active, showing that the adsorption phenomenon was not detrimental to the protein.

### CONCLUSION

We have demonstrated the protein adsorption/release capacity of the NFs and obtain precise clues on the protein-silica interactions. These data thus provide us with a better understanding of the adsorption phenomenon involved, as well as a way to control the amount of protein adsorbed and subsequently released. We also show the maintenance of the biological activity of the released protein from this novel biomaterial at any time point. Next steps will focus on Growth Differentiation Factor 5 (GDF5) adsorption and release studies, since GDF5 pivotal role in the differentiation of stem cells into IVD cells has been shown<sup>5</sup>. Its physicochemical properties, close to those of lysozyme, allow us to hypothesize a similar behavior in terms of adsorption/release from NFs.

### REFERENCES

- 1.Colombier P. *et al.*, Joint Bone Spine. 2:125-9, 2013
- 2.Henry N. *et al.* Med Sci. 30:1091–1100, 2014
- 3.Colombier P. *et al.*, Trends Biotechnol.32:433-5, 2014
- 4.Buchtova N. *et al.*, J Mater Sci Mater Med. 24:1875-84, 2013
- 5.Stoyanov J.V *et al.*, Eur Cell Mater. 21:533-47, 2011

### ACKNOWLEDGMENTS

The authors would like to thank Nicolas Stephant, Paul Pilet and Françoise Lary for their contributions. Financial support : FARMA "Etude ET3-683", Région Pays de la Loire "Projet LMA", ANR "Remediv" and FRM Projet DBS20131128442.



## Regulation of Inflammatory Gene Expression by Functionalized Calcium Phosphate Nanoparticles with Different Delivery Strategies to the Gut

Bernhard Neuhaus<sup>1</sup>, Annika Frede<sup>2</sup>, Astrid Westendorf<sup>2</sup>, Matthias Eppe<sup>1,\*</sup>

<sup>1</sup>Institute for Inorganic Chemistry and Center for Nanointegration (CeNIDE), University of Duisburg-Essen, Germany

<sup>2</sup>Institute for Medical Microbiology, University Hospital Essen, Germany

[bernhard.neuhaus@uni-due.de](mailto:bernhard.neuhaus@uni-due.de)

### INTRODUCTION

Due to their size, nanoparticles are taken up by cells via endocytosis. Furthermore they can be functionalized with nucleic acids in order to serve as a transport vehicle over the cellular membrane.<sup>1</sup> Once endocytosed, the nanoparticles can release their cargo into the cytosol. Calcium phosphate nanoparticles are easily synthesized and functionalized with nucleic acids. Furthermore they are biocompatible and non-toxic. If they are functionalized either with pDNA or siRNA, they can be used to interfere with the protein biosynthesis of cells and either induce the expression of specific proteins (transfection by DNA) or induce their downregulation (gene silencing by siRNA).<sup>2, 3</sup>

During chronic inflammatory diseases like Crohn's disease or ulcerative colitis, pro-inflammatory proteins like TNF $\alpha$  are upregulated in the gut. Here we demonstrate how calcium phosphate nanoparticles can be utilized to regulate the expression of pro-inflammatory proteins in the gut.

Since calcium phosphate is dissolved in the acidic pH of the stomach and nucleic acids are degraded in the gastrointestinal tract, the second part of the study focused at delivery strategies of functionalized calcium phosphate nanoparticles to the gut.

### EXPERIMENTAL METHODS

Calcium phosphate nanoparticles were synthesized by rapid precipitation and instantly functionalized with different nucleic acids. Subsequently, the nanoparticles were stabilized by another layer of calcium phosphate and polyethyleneimine (PEI) to yield positively charged particles. The particles were tested *in vitro* on their ability to either silence specific genes or induce protein expression. The influence on protein expression was assessed by qPCR, FACS analysis and fluorescence microscopy.

To deliver the particles to the gut, two strategies were investigated. First, a gelatine capsule was filled with freeze-dried nanoparticles and coated with Eudragit L 100 to survive the acidic conditions in the stomach. Another approach was a suppository dosage form based on the incorporation of freeze-dried particles into a lipid base. The performance of these administration forms was investigated *in vitro*.

### RESULTS AND DISCUSSION

Calcium phosphate nanoparticles were used to influence the protein expression in different cell lines. The model protein eGFP was down-regulated in HeLa cells and the

pro-inflammatory protein TNF $\alpha$  was down-regulated in MODE-K cells.

Both cell lines were also transfected with pDNA by calcium phosphate nanoparticles. After transfection the expression of eGFP was detected in both cell lines. Appropriate delivery strategies of the particles to the gut were developed, i.e. an enteric coated gelatine capsule for oral administration and a nanoparticle-loaded suppository for rectal administration. The gene-delivery effect of the particles from these application forms was investigated *in vitro*.

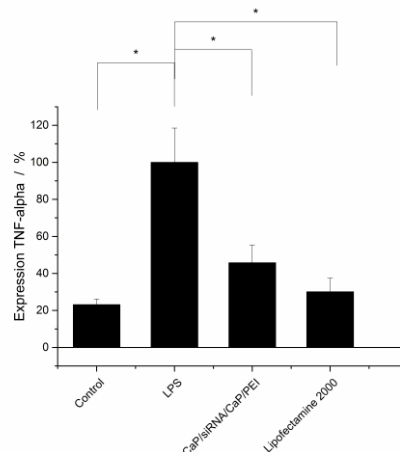


Figure 1: Silencing of TNF $\alpha$  in MODE-K cells

### CONCLUSION

This study demonstrates the feasibility of nanoparticles to regulate the synthesis of inflammatory protein in cells. As it is necessary to transport the nanoparticles to the gut, an acid-resistant gelatine capsule and a suppository were developed as carriers of the nanoparticles.

### REFERENCES

1. I. Canton and G. Battaglia, *Chem. Soc. Rev.*, 2012, **41**, 2718-2739.
2. V. Sokolova, A. Kovtun, O. Prymak, W. Meyer-Zaika, E. A. Kubareva, E. A. Romanova, T. S. Oretskaya, R. Heumann and M. Eppe, *J. Mater. Chem.*, 2007, **17**, 721.
3. V. Sokolova, S. Neumann, A. Kovtun, S. Chernousova, R. Heumann and M. Eppe, *J. Mater. Sci.*, 2010, **45**, 4952-4957.

### ACKNOWLEDGMENTS

We thank the Deutsche Forschungsgemeinschaft (DFG) for providing financial support to this project





## How the Interfacial Shear Strength in PLGA Fibre-Reinforced Brushite Cements Affects the Composites Mechanical Properties

Stefan Maenz<sup>1</sup>, Max Hennig<sup>1</sup>, Mike Mühlstädt<sup>1</sup>, Elke Kunisch<sup>2</sup>, Raimund W. Kinne<sup>2</sup>, F. Plöger<sup>3</sup>, Jörg Bossert<sup>1</sup>, Klaus D. Jandt<sup>1</sup>

<sup>1</sup>Chair of Materials Science, Otto-Schott-Institute of Materials Research, Friedrich Schiller University Jena, Germany

<sup>2</sup>Experimental / Rheumatology Unit, Department of Orthopedics, University Hospital Jena, Waldkrankenhaus "Rudolf Elle", Eisenberg, Germany

<sup>3</sup>BIOPHARM GmbH, Heidelberg, Germany

[stefan.maenz@uni-jena.de](mailto:stefan.maenz@uni-jena.de)

### INTRODUCTION

Injectable calcium phosphate cements (CPCs) are promising materials for the minimal invasive treatment of bone defects. Unfortunately, currently available CPCs have a small mechanical strength and fracture toughness, respectively. One approach to overcome these limitations is the modification of the CPC with reinforcing fibres. The results of a previous study suggest that the interfacial shear strength between matrix and reinforcing poly(l-lactide-co-glycolide) (PLGA) fibres and, therefore, the critical fibre length is of importance for the reinforcing efficiency<sup>1</sup>.

Therefore, the aim of this current study is to control the interfacial strength by different modifications of the reinforcing fibres and to analyse the impact of the interfacial strength on the bulk mechanical properties of fibre-reinforced CPCs.

### EXPERIMENTAL METHODS

PLGA fibres with a diameter of 300 µm were either treated with oxygen plasma or coated with sol-gel layers of different compositions. The modified fibres were then embedded into cylinders of a brushite-forming CPC. The interfacial strength between PLGA and CPC matrix was tested in a single-fibre pull-out test. The fibre surfaces were characterized by SEM, XPS and EDX.

To analyse the impact of the interfacial strength on the bulk mechanical properties of fibre-reinforced CPCs, PLGA fibres with a diameter of 25 µm and a length of 1 mm were surface treated as described above and incorporated into a brushite-forming CPC with different fibre contents. The mechanical properties were determined in a 3-point flexural test.

### RESULTS AND DISCUSSION

The interfacial shear strength between the oxygen plasma treated PLGA fibres as well as the sol-gel coated PLGA fibres and the CPC matrix increased statistically significantly compared to untreated PLGA fibres by up to 100% (see Figure 1).

In the case of the sol-gel coated PLGA fibres we observed that the interfacial shear strength depends on the thickness of the sol-gel coating.

As a result of oxygen plasma treatment of the PLGA fibres their contact angle strongly decreases. Thus, the wettability of the PLGA fibres increases, and in consequence the interfacial shear strength between PLGA fibres and CPC increases.

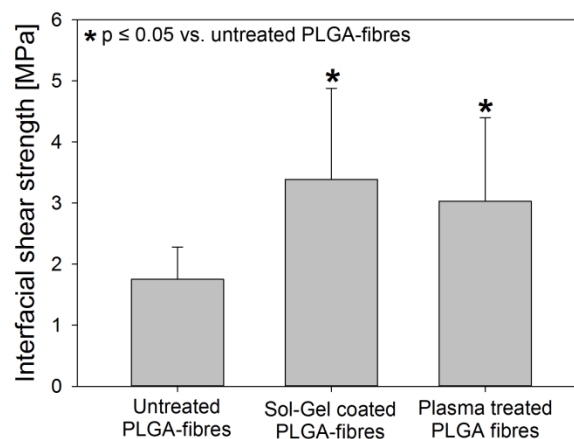


Figure 1: Interfacial shear strength between PLGA-fibres and the brushite-forming CPC.

For the bulk mechanical properties of the fibre-reinforced CPC, we observed only a slightly increase in the flexural strength due to the increased interfacial strength. In contrast, the work of fracture increased strongly as a consequence of the fibre surface modification. The reason for this is a change in the fracture behaviour from a quasi-brittle failure to a more ductile failure.

### CONCLUSION

The present study demonstrates the possibility to improve the mechanical properties of fibre-reinforced CPCs by surface modifications of the reinforcing fibres. Oxygen plasma treatment as well as sol-gel coating resulted in increased interfacial shear strength between PLGA fibres and CPC and, thus, in improved mechanical properties of the composite.

### REFERENCES

1. Maenz S. *et al.*, J. Mech. Behav. Biomed. 39:328-338, 2014.

### ACKNOWLEDGMENTS

We gratefully acknowledge the financial support by the Carl Zeiss Foundation (doctoral candidate scholarship), the German Federal Ministry of Education and Research (BMBF, grant reference 0316205), the partial financial support of the Deutsche Forschungsgemeinschaft (DFG, grant reference INST 275/241-1 FUGG) and the Thüringer Ministerium für Bildung, Wissenschaft und Kultur (TMBWK, grant reference 62-4264 925/1/10/1/01)



## Heparinization of Calcium Phosphates: Towards Enhancing Biological Performance

Anna Díez-Escudero<sup>1,2</sup>, Montserrat Espanol<sup>1,2,3</sup>, Maria-Pau Ginebra<sup>1,2,3</sup>

<sup>1</sup>Biomaterials, Biomechanics and Tissue Engineering Group, Technical University of Catalonia, Spain

<sup>2</sup>Centre for Research in Nanoengineering, Technical University of Catalonia, Spain

<sup>3</sup>Biomedical Research Networking Centre in Bioengineering, Biomaterials and Nanomedicine, Spain  
[anna.diez-escudero@upc.edu](mailto:anna.diez-escudero@upc.edu)

### INTRODUCTION

Calcium phosphates (CaPs) are excellent materials for bone regeneration applications due to their close resemblance to natural bone. However, increasing efforts are being put towards further mimicking the biological environment loading organic moieties such as extracellular matrix components to activate/regulate specific signalling pathways. Collagen accounts for 90-95%wt. of the organic phase of bone, whilst the remaining 5%wt. contains non-collagenous proteins such as growth factors or proteoglycans. It has been demonstrated that proteoglycans are able to bind and regulate several signalling pathways. Specifically, several authors have pointed to the ability of sulphated polysaccharides to form complexes with bone morphogenetic proteins and hence, serve as ligands to their signalling receptors<sup>1</sup>. The present work focuses on the attachment of heparin onto various CaPs both covalent and electrostatically in views of providing materials with enhanced biological performance. Although the use of heparin is not new, little work has been done in the area of CaPs<sup>2</sup>.

### EXPERIMENTAL METHODS

The different CaPs investigated were produced with the same reactants. A solid phase containing 98%  $\alpha$ -TCP and 2% hydroxyapatite was mixed with a liquid phase consisting of water at two liquid to powder ratios, in order to obtain low and high porosities (L/P=0.35 and 0.55 mL/g, respectively). The paste was moulded in 15x2mm discs. Calcium deficient hydroxyapatite (CDHA,  $\text{Ca}_9(\text{PO}_4)_5(\text{HPO}_4)(\text{OH})$ ) was obtained by immersing the discs in water at 37°C for 10 days to complete setting. Stoichiometric hydroxyapatite (HA,  $\text{Ca}_{10}(\text{PO}_4)_6(\text{OH})_2$ ) was obtained through hydrothermal treatment of the unset discs in presence of bicarbonate (2.5wt%  $\text{NaHCO}_3$ ) followed by sintering at 1100°C. Amino functionalization of CaPs was attained by silanisation in 95 v/v% absolute ethanol; 3 v/v% of water was added prior to the incorporation of 2 v/v% of (3-aminopropyl)triethoxysilane (APTES). Silanisation was investigated at different times: 1h, 4h and overnight (o.n.). After amino functionalisation, heparin was covalently immobilized onto CaP surfaces through EDC/Sulfo-NHS amidation. 1 mL of the heparin solution (24 $\mu\text{g/mL}$ ) was poured onto the CaPs discs. Heparinization was performed for 15min, 1h and 2h. Supernatants were collected to quantify the amount of unbound heparin. Heparin quantification was evaluated indirectly through a colorimetric method based in Toluidine Blue dye.

### RESULTS AND DISCUSSION

Silane coupling onto CaPs was performed to allow covalent binding of heparin to CaPs. Fig.1 shows that heparinisation is dependent on the silanisation time for HA discs (L/P=0.55). The efficiency of silanisation was indirectly measured through the amount of heparin remaining in solution. Overnight silanisation led to a lower heparin concentration which translated into a more efficient uptake by the material.

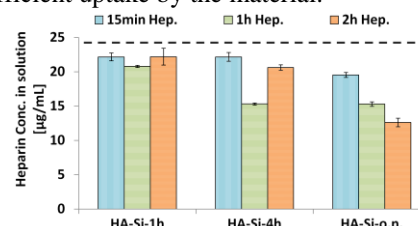


Figure 1. Heparin remaining in the supernatants after soaking samples silanised at different times (1h,4h and overnight). Heparin stock solution (dashed line) was 24 $\mu\text{g/mL}$ .

The effect of material composition, porosity and specific surface area on the immobilization of heparin is depicted in Fig2. Control samples (material without silane) were included. As the porosity (L/P 0.35 vs 0.55 mL/g) and the specific surface area (HA vs. CDHA) increases, higher amount of heparin was bound either electrostatically (control) and covalently (silanised) to the material. Nevertheless, the efficiency of heparin bonding significantly increased with silanisation.

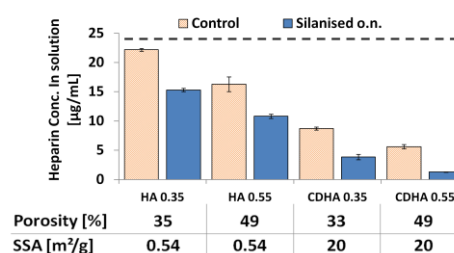


Figure 2. Heparin amount collected from the supernatants after 2h for different L/Ps and different composition of CaPs. Heparin stock solution (dashed line) was 24 $\mu\text{g/mL}$ .

### CONCLUSION

This work proves that silanisation of CaP surfaces is a good method for heparin immobilisation. Porosity, specific surface area and composition of CaPs played an important role on the total heparin immobilised.

### REFERENCES

1. Takada *et al.* J. Biol.Chem. 278 (44):43229-235, 2003.
2. König *et al.* J.Mater Sci: Mater Med 25:607-21,2014.

### ACKNOWLEDGMENTS

The authors thank the Spanish Government (MAT2012-38438-003-01) and Bioiberica S.A. for kindly providing the heparin used in the study.



## Intercellular Delivery of Self-Assembling Osteogenic Nanoparticles: Fate and Effect

Philip Chambers<sup>1</sup>, Sreekanth Pentlavalli<sup>1</sup>, Michelle O'Doherty<sup>1</sup>, Marine Chalanqui<sup>2</sup>, Helen O. McCarthy<sup>2</sup> and Nicholas Dunne<sup>1</sup>

<sup>1</sup>School of Mechanical and Aerospace Engineering, Queen's University Belfast, Northern Ireland

<sup>2</sup>School of Pharmacy, Queen's University Belfast, Northern Ireland

[pchambers07@qub.ac.uk](mailto:pchambers07@qub.ac.uk)

### INTRODUCTION

A major challenge in the repair of joint injuries lies in the reattachment of the soft tissue to the bone<sup>1</sup>. As such much investigation has taken place into the development of a viable method to promote bone and soft tissue regeneration. For example, Li *et al* developed a graded calcium phosphate coating on the surface of electro-spun nanofibres<sup>2</sup>. However, these studies have resulted in limited success<sup>3</sup>.

In this study we propose the use of novel nanoparticles (NPs) comprised of an amphipathic peptide (RALA) and osteogenic hydroxyapatite (HA). The RALA/HA NPs are designed to spontaneously self-assemble via electrostatic interaction, and aim to promote the bioavailability of HA and elicit a potent osteogenic response. Discriminating between HA-NPs and intrinsic cellular granulation is difficult and so the intercellular fate of HA-NPs is not well understood. Therefore, the use of a thiol-reactive fluorophore is proposed for NP intracellular tracking.

### EXPERIMENTAL METHODS

**Formulation of RALA/HA NPs:** NPs were prepared at a range of mass ratios. Particle size and zeta potential (ZP) were measured using a Malvern Zetasizer Nano ZS to determine the optimal formulation. The NPs were tested for stability up to 28 d in addition to the temperature range 4–40°C.

**Cell viability and immunocytochemistry for osteogenic markers:** MG63 osteoblast-like cells were treated with pure HA or transfected with RALA/HA NPs at corresponding doses for 4 h prior to replacement with complete medium. Cell viability was determined by LDH assay. Collagen type I (col-I) expression was determined visually using standard immunocytochemistry method up to 28 d using the MG63 cell line.

**MPTS-functionalized silica-substituted-HA (SiHA-MPTS) fluorophore conjugation:** SiHA-MPTS was prepared as described by Grover *et al*<sup>4</sup>. SiHA-MPTS (6mg) was suspended in phosphate-buffered saline and 7.14 mM stock solution of thiol-reactive Texas Red maleimide (TRM) (Life Technologies Ltd, UK) was added and mixed 2 h at 37°C. The SiHA-MPTS-TRM particles were washed twice with absolute ethanol and five times with double distilled water.

### RESULTS AND DISCUSSION

NPs prepared with a mass ratio of 5:1 exhibited a size of  $57 \pm 9$  nm and a zeta potential of  $17.8 \pm 6.2$  mV. The

size and shape of the NPs was confirmed by TEM (Fig. 1C). The NP particle size and ZP remained consistent up to 28 d (Fig. 1B) at room temperature. Cell viability (Fig. 1A) was seen to decrease 24 h post-transfection with the RALA/HA NP treatment. However by 7 d cytotoxicity decreased to a level similar to that seen in an untreated control group. SiHA-MPTS-TRM NPs were successfully formulated and exhibited fluorescence under excitation at 585 nm.

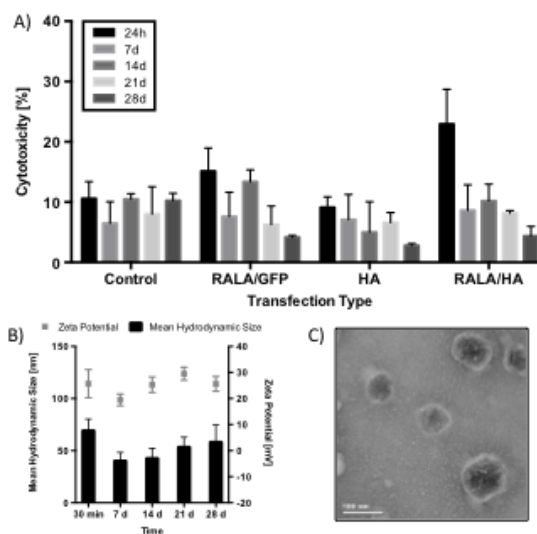


Figure 1. A) MG63 cytotoxicity as measured by LDH assay to evaluate the toxicity of 4 hour transfection with RALA/HA-NPs B) Long term stability (28 d) of RALA/HA-NPs C) TEM image of RALA/HA NPs. Results are displayed as mean  $\pm$  SEM,  $n=3$ , where  $n$  represents the number of independent batches prepared for measurement.

### CONCLUSION

We have successfully demonstrated that RALA peptide is capable of forming biocompatible NPs with HA, which are stable across a range of temperatures and over an extended duration. Transfection of MG63 cells with NPs resulted in increased collagen expression by 21 d indicating the osteogenic properties of the NPs. The formulation of fluorescent SiHA-MPTS-TRM NPs facilitates further analysis of the intracellular trafficking and localisation of internalised SiHA-NPs, by means of particle tracking.

### REFERENCES

1. Yang P. *et al.*, *Tis. Eng Part B Rev.* 2: 127-41, 2009
2. Li X. *et al.*, *Nano. Lett.*, 7: 2763-68, 2009
3. Smith L. *et al.*, *Connect. Tis Res.* 53(2):95-105, 2012
4. Grover L. *et al.*, *J. Mater. Chem. B*, 1: 4370-78, 2013

### ACKNOWLEDGMENTS

US-Ireland Grant (Grant no: 3568)

Medical Research Council (Grant no: 1294)





Thomas Paterson<sup>1</sup>, James Dugan<sup>1</sup>, Colin Sherborne<sup>1</sup>, Chia-Cheng Chen<sup>1</sup>, Nicola Green<sup>1</sup>, Gwendolen Reilly<sup>2</sup>, Frederik Claeysens<sup>1</sup>

<sup>1</sup>Kroto Research Institute, North campus, University of Sheffield, S3 7HQ, Sheffield, United Kingdom

<sup>2</sup>Department of Materials Science and Engineering, INSIGNEO Institute, Pam Liversidge Building, Sheffield, S1 3JD  
[mta08tp@sheffield.ac.uk](mailto:mta08tp@sheffield.ac.uk)

## INTRODUCTION

Particle-based systems have great potential as scaffolds for tissue engineering, since they are injectable, avoiding the need for open surgery [1, 2]. In this study we are investigating the ingrowth of cells into highly porous particles. Specifically how human embryonic stem cell derived mesenchymal progenitor cells (hES-MP) respond to monodisperse porous microparticles. Cells were found to bind the particles together after just a few days into large agglomerations. Differentiated cells were also found to penetrate deep within the porous structure of the particles.

## EXPERIMENTAL METHODS

Porous Poly-High Internal Phase Emulsion (polyHIPE) particles were created by a T-junction set-up in which a small internal diameter (100  $\mu\text{m}$ ) syringe needle injects the photocurable PolyHIPE into a 6 mm diameter silicone tube containing a continuous stream of  $\text{H}_2\text{O}$  (sustained *via* a peristaltic pump) and subsequently curing the spheroidal particles with a UV lamp [3]. Particles were formed with 80% interconnected porosity with a median pore size of 18  $\mu\text{m}$ . Particles were then coated with acrylic acid by plasma treatment. Particles were grown with cells in static culture for 30 days with particles removed at certain time points for analysis. Cells were grown with osteogenic supplements and dexamethasone was added for the positive control to induce osteogenesis. Samples were analysed via histology and confocal microscopy.

## RESULTS AND DISCUSSION

Within the T-flasks, multiple small particle aggregates were formed after a few days, which then increased in size as single particles and other small aggregates combined with each other. After 30 days, only a few very large aggregates remained. Zhang et al. [4] found a similar result using PLGA microspheres and an ovarian cancer cell line (HO8910) cells over 7 days. By the 30 day time point, cells were present within the internal pores of the samples grown in both the positive control (DEX) and within the osteogenic media. There was significantly less cell penetration into particles in the negative control. The scaffold directed the hES-MP's towards an osteoblast lineage without the requirement of DEX. Equally important is that this differentiation allowed cells to penetrate throughout the porous particle. The morphology of the cells within the pores appeared to resemble that of osteocytes (see figure 1) which would be consistent with the expected hypoxic environment within the centre of the cell-particle agglomeration, away from a nutrient supply. There is evidence that the cells within the agglomeration

remained viable as we have seen growth over extended periods of time deep within the particle, indicating the cells could have adapted to the hypoxic environment.

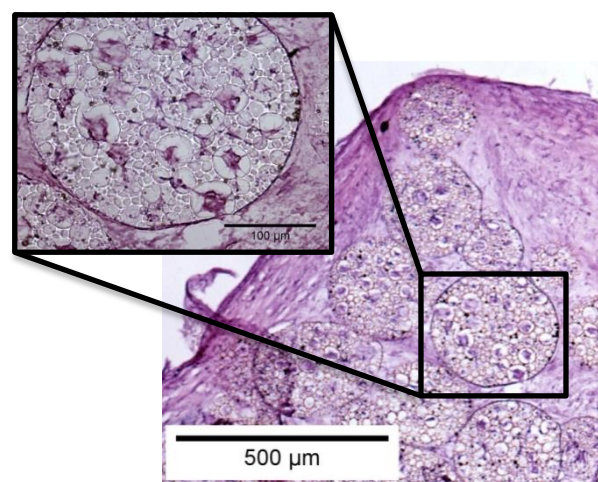


Figure 1: An optical micrograph of 15 $\mu\text{m}$  thick D30 particle slice stained with H&E. It is possible to see cells within the particle's internal porosity linked by cell protrusions. Large quantities of ECM and cells can be seen encircling the microparticles, forming a large cell driven particle agglomeration.

## CONCLUSION

Porous microparticles have been produced in monodisperse populations from 80  $\mu\text{m}$  to 600  $\mu\text{m}$  in size. Particle size was controllable through the production setup. The hES-MP cells grew into the porosity of the particles and also formed anchor points between particles. Evidence currently suggests that the progenitor cells terminally differentiated into osteocyte-like cells. The binding of the particles by cells shows that it will be possible to create a continuous scaffold, with tissue-like properties, from individual particles over a period of time.

## REFERENCES

- [1] Oliveira, M.B. and J.F. Mano, *Biotechnology Progress*. 2011. 27(4): p. 897-912.
- [2] Choi, S.-W., *et al.*, *Journal of Materials Chemistry*, 2012. 22(23): p. 11442-11451.
- [3] Gokmen, M.T. and F.E. Du Prez *Progress in Polymer Science*, 2012. 37(3): p. 365-405.
- [4] Zhang, T.Z., *et al.*, *Colloid surface A*. 2014. 452:115-124.

## ACKNOWLEDGMENTS

The authors would like to thank the EPSRC DTA studentships for TP and CS.





# Biodegradable SCL-PHA Composite Scaffolds for Bone Tissue Engineering

Christy Thomas<sup>1</sup>, Aldo. R. Boccaccini<sup>2</sup>, Ipsita Roy<sup>1</sup>

<sup>1</sup>Department of Life Sciences, Faculty of Science and Technology, University of Westminster, United Kingdom

<sup>2</sup>Department of Materials Science and Engineering, University of Erlangen-Nuremberg, Germany

[christythomas2010@hotmail.com](mailto:christythomas2010@hotmail.com)

## INTRODUCTION

Bone defects raise many challenges in reconstructive surgery. Bone substitute materials made using polymers and composites are preferred over the use of traditional bone grafting methods. Polyhydroxyalkanoates (PHAs) are bacterial derived biopolymers having wide ranging mechanical properties, biocompatibility, surface degradation, as well as biodegradability and hence have more potential than synthetic biopolymers<sup>2</sup>. SCL-PHAs, like P(3HB) have been combined with fillers such as Bioglass<sup>®</sup> and clay to form composites with enhanced mechanical strength, bioactivity and tailored degradability. *Bacillus* spp. fed with different carbon sources and precursors can be used to produce both the homopolymer P(3HB) and the copolymer P(3HB-3HV). Appropriate cell seeding onto the bioactive scaffold can promote the restoration of functional bone. In this study, P(3HB) and P(3HB-3HV) based Cu doped Bioglass<sup>®</sup> composites were fabricated for bone tissue engineering study.

## EXPERIMENTAL METHODS

**Production of P(3HB):** *Bacillus cereus* SPV was grown in Kannan and Rehacek medium with glucose as main carbon source. The cells were harvested after 48 hours.

**Extraction of P(3HB):** P(3HB) was extracted using Soxhlet extraction technique and was precipitated out with chilled methanol and purified.

**Solvent casting technique:** 2D composite films were fabricated, characterised and cut to produce 1cm diameter films for cell culture studies with human bone marrow stromal cells (hMSC).

**Statistical analysis:** A Statistic analytical approach was carried out using a one way ANOVA test in Graph Pad Prism 6 software.

## RESULTS AND DISCUSSION

The homopolymer, P(3HB) was successfully produced using *Bacillus cereus* SPV by utilizing glucose as the main carbon source. Various concentrations in weight percentage of 45S5 and Cu doped Bioglass<sup>®</sup> composites were fabricated using the solvent casting method and characterised. XRD results confirmed the presence Bioglass<sup>®</sup> does not have any impact on the crystalline structure of the polymer (Figure 1). DSC analysis of the neat and composite films showed that the incorporation of Bioglass<sup>®</sup> reduced the crystallization onset temperature of the composites when compared to the neat films. Whereas a decrease in melting onset temperature and a lower glass transition temperature was observed in the Cu<sup>2+</sup>-incorporated 45S5 Bioglass<sup>®</sup>. The surface roughness also increased with the addition of Bioglass<sup>®</sup> which is known to enhance cell adherence.

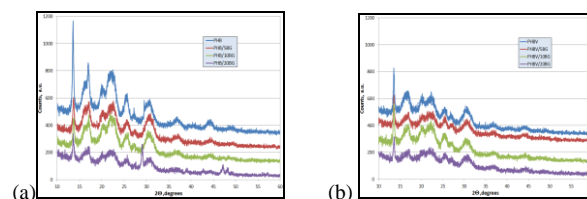


Fig 1: XRD plot showing the crystalline structure of (a) PHB-N, neat P(3HB) with different wt % BG (b) PHBV-N, neat P(3HB-3HV) with different wt % BG.

SEM images of the P(3HB)/Bioglass<sup>®</sup> composites after incubation in simulated body fluid (SBF) are shown in Figure 2. These revealed an increased formation of hydroxyapatite in the case of Cu doped Bioglass<sup>®</sup> composites.

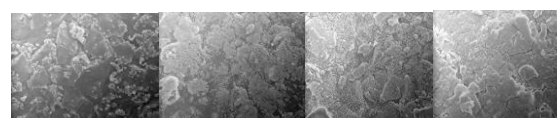


Fig 2: P(3HB)45s-1D P(3HB)Cu-1D P(3HB)45s-7D P(3HB)Cu-7D

Cell culture study on the composites using human bone marrow stromal cells, hMSC, showed the presence of live cells and the expression of osteogenic markers after a 14 day period of study.

## CONCLUSION

P(3HB) was successfully produced and characterised. This was then used to produce 45S5 and Cu doped Bioglass<sup>®</sup> composites. The hydroxyapatite formed after incubation in SBF is known to provide a strong bond to the tissues inside the body. In addition, the release of Cu<sup>2+</sup> from composite scaffolds made of P(3HB) and P(3HB-co-3HV) could enhance vascularization, thereby promoting angiogenesis, without compromising the mechanical stability of the scaffold<sup>1</sup>. Hence, this study provides a potential step forward in bone tissue engineering.

## REFERENCES

1. A. Hoppe, V. Mourino and A. R. Boccaccini, *Biomater. Sci.*, 2013, 1, 254–256.
2. Valappil *et al.*, (2007). Polyhydroxyalkanoate (PHA) biosynthesis from structurally unrelated carbon sources by a newly characterized *Bacillus* spp, *Journal of Biotechnology*, Volume: 127, Issue: 3, Pages: 475-487.

## ACKNOWLEDGMENTS

I would like to thank Dr Ipsita Roy and Prof Aldo Boccaccini for their continuous support, guidance and encouragement throughout my project. I would also like to extend my thanks to Prof Richard Oreffo and Dr Jon Dawson for their guidance, support and for providing a platform for my cell culture studies.



## Multifunctional Anti-Adhesive Films Prepared by Layer-by-Layer Formation of Zwitterionic Micelles

Bora Onat<sup>1</sup>, Vural Bütün<sup>4</sup>, Sreeparna Banerjee<sup>3</sup> and İrem Erel-Göktepe<sup>1,2,5</sup>

<sup>1</sup>Department of Biotechnology, Middle East Technical University, 06800, Ankara, Turkey <sup>2</sup>Department of Chemistry, Middle East Technical University, Çankaya, 06800, Ankara, Turkey

<sup>3</sup>Department of Biological Sciences, Middle East Technical University, Çankaya, 06800, Ankara, Turkey

<sup>4</sup>Department of Chemistry, Eskişehir Osmangazi University, Eskişehir, 26480, Turkey

<sup>5</sup>Department of Polymer Science and Technology, Middle East Technical University, 06800, Ankara, Turkey

[bora.onat@metu.edu.tr](mailto:bora.onat@metu.edu.tr)

### INTRODUCTION

Layer-by-layer self-assembly of polymers show great potential in building multi-layered films on materials due to their flexibility, facile production, ability to respond to multiple stimuli, and incorporate several agents for controlled-release purposes<sup>1</sup>.

Most pathogenic bacteria colonize on surfaces and form biofilms, preventing the penetration of antibiotics. Biofilm-associated bacteria are 100 – 1000 times less susceptible to antibiotics than planktonic bacteria<sup>2</sup>, so alternative methods to controlled-release of antibiotics from surfaces have been designed. One of them is using anti-adhesive surfaces to prevent bacterial adherence and so biofilm formation on surfaces.

Previous studies showed that zwitterionic polymers, including block copolymer-micelles with zwitterionic coronae, showed anti-adhesive property against bacteria<sup>3</sup>.

As much as we know, this is the first study presenting how anti-adhesive property of micelles with zwitterionic coronae gets enhanced when they are in polyelectrolyte multilayered form. Prepared multilayered film is also pH-responsive and was used to release bactericidal agent triclosan; so, it is dual-functional in being anti-adhesive and pH-responsive.

### EXPERIMENTAL METHODS

βPDMA-*b*-PDPA block copolymer, which has zwitterionic and pH-responsive blocks, was previously synthesized and has been used to form polyelectrolyte films with anionic polymers DNA and poly (styrene sulfonate) (PSS). Triclosan was loaded into micelles by self-diffusion at pH 7.5. Glass wafers were base-treated to form negatively-charged SiO<sub>2</sub> layer, so micelle monolayers could be deposited. Other layers are deposited by dip-coating method. Physicochemical properties of micelles and films are determined by electrophoretic light scattering (for zeta potential and nanoparticle size), Ellipsometry, and AFM.

Agar-plating method, Live/Dead Cell Vitality Assay, and light microscopy experiments are carried out to determine bacteria adherence and viability. BSA adherence on wafers is determined by microBCA assay. All of the above bacterial experiments are carried out after incubating wafers in Müller-Hinton Broth containing *Staphylococcus aureus* for 1 h. each.

Statistically, bacteria numbers on coated wafers are compared by the numbers on control samples by Sidak's multiple comparisons test and ANOVA.

### RESULTS AND DISCUSSION

AFM images showed that the fluctuation in the anti-adhesive properties of 1 layered, 3 layered, and 5 layered-films are not significantly dependent on the roughness of film surfaces. The bacteria number is expected to increase with increasing roughness of surfaces, because of the difference in surface area, however 3-layered film of the micelle and PSS showed a lower amount of bacteria adherence, compared to the micelle-covered single-layered surface, and 5-layered surface showed adherence amount as high as the control sample showed. When it came to multilayered-film composed of the micelle and DNA, 5-layered films had lower bacteria adherence than 3-layered films and the degree of adherence was very close to the adherence on single-layered film.

At pH 5.5, triclosan release from surfaces were higher compared to the release at pH 7.5; but there was still diffusion of the bactericidal drug throughout the film at physiological pH.

### CONCLUSION

The main purpose of this investigation was to see if the anti-adhesive property of films incorporating zwitterionic micelles increases as layer number increases. Secondly, to design a multi-layered film which incorporates high amount of hydrophobic drug to be released in mildly acidic conditions, without major loss in the anti-adhesive property. Such pH-responsive systems are highly useful at infection sites around bio-implants, where *in situ* pH is mildly acidic.

We observed the lowest amount of adherence on 3-layered films of micelle and PSS. The drug release was also higher at mildly acidic conditions, but anti-adhesive property decreases at this pH (pH 5.5).

### REFERENCES

1. Tong W. *et al.*, Chemical Society Rev. 41:6103, 2012
2. Saginur R. *et al.*, Antimic. A. Chem. 50: 55-61, 2006
3. Hippus C. *et al.*, Mat. Sci. Eng. C 41:354-362, 2014

### ACKNOWLEDGMENTS

Authors acknowledge the financial support of European Commission Marie Curie International Reintegration Grant (grant number: PIRG07-GA-2010-26830)



# Poster Presentations



## Production of Spray Dried Calcium Phosphate-Gelatin Composite and The Impact of Cross-linking Agent on Composite Structure and Bioactivity in Simulated Body Fluid

Tugba Basargan Ozsagioglu<sup>1</sup>, Gulhayat Nasun Saygili<sup>1</sup>

<sup>1</sup> Chemical Engineering Department, Istanbul Technical University, Turkey  
[basargant@itu.edu.tr](mailto:basargant@itu.edu.tr)

### INTRODUCTION

Calcium phosphates (CaPs) are key factors of biological calcification. Hydroxyapatite ((Ca<sub>5</sub>(PO<sub>4</sub>)<sub>3</sub>(OH)), HAP), has been drawn attraction due to its similarity to the mineral phase of bones and teeth. Among the other crystalline calcium phosphate, phases dicalcium phosphate dihydrate (CaHPO<sub>4</sub>·2H<sub>2</sub>O) is significant to be used in the fabrication of biomaterials and be co-precipitated with other CaPs and/or a product resulted in their transformation. Some researchs showed that they could act as precursors for the calcinification of bone<sup>1</sup>. Hydroxyapatite-Gelatin (HAp-GEL) composites are among the most suitable materials for hard tissue applications due to their similarity to tissues and high osteo-conductivity properties<sup>2</sup>. On the other hand, the usage of gelatin is limited as a result of its rapid degradation in aqua medium. To solve this issue, cross-linking may be applied to GEL. Cross linking of gelatin is not only increasing the mechanical and thermal strength of gelatin, but also, degradation of gelatin gets slower in aqua medium<sup>3</sup>.

The aim of this study is to prepare Ca<sub>2</sub>P<sub>2</sub>O<sub>7</sub>·2H<sub>2</sub>O-Ca<sub>5</sub>(PO<sub>4</sub>)<sub>3</sub>(OH)-GEL (CaPs-GEL) microspheres via spray drying after in one simple step precipitation in the presence of Simulated Body Fluid (SBF) and investigate samples bioactivity in Simulated Body Fluid (SBF). In this content, glutaraldehyde (GA) was used as cross-linking agent.

### EXPERIMENTAL METHODS

CaPs-GEL (weight ratio of 50-50) composites were synthesized in the presence of Simulated Body Fluid. Ca(OH)<sub>2</sub>-SBF solution were added H<sub>3</sub>PO<sub>4</sub>-SBF-GEL solution and mixed at 40 °C. During mixing, pH was maintained around 9 by adding NaOH. The suspension was aged for a night. Next day, it was filtered and washed with distilled water with several times. After distilled water addition, the solution was fed to the spray dryer. The produced microspheres, then, were treated with various ratios of GA (8% and 2%,v/v) after turning into pellets. To dispose of excess GA, the pellets were waited in dilute sodium bisulfate solution for a while. On spray dried composites, XRD, FTIR and SEM analyses were conducted. Lastly, SBF studies were run to evaluate the bioactivity of the selected samples. The samples were soaked in SBF. After immersion in SBF up to 14 days, dried samples were conducted to XRD, FTIR, SEM and SBF absorption measurements. pH measurement was done, as well.

### RESULTS AND DISCUSSION

FTIR analysis of spray dried samples showed a chemical interaction between carboxyl group from GEL and Ca<sup>2+</sup> ion from CaPs. Also, XRD analysis confirmed that composites included Ca<sub>2</sub>P<sub>2</sub>O<sub>7</sub>·2H<sub>2</sub>O-Ca<sub>5</sub>(PO<sub>4</sub>)<sub>3</sub>(OH) structure. After GA addition, it was observed in FTIR analysis C-H stretch bond became sharper in the sample with 8% GA.

In SBF analysis, after 14 days, a pH change of SBF was observed, which might be related with Ca release (pH increase) subsequently followed by apatite formation (pH decrease) on composites. According to pH difference, it was assumed that degradation of sample with 2% was higher than the one with 8%. Also, SBF absorption was calculated based on the Eq. 1.

$$\text{SBF Absorption (\%)} = [(W_s - W_i)/W_i] * 100 \quad (\text{Eq.1})$$

W<sub>i</sub> = Weight os sample before taking in SBF

W<sub>s</sub> = Wet weight of sample after taking of SBF

SBF absorption increased due to GEL presence in the structure and reached around 20%.

SEM analysis (Fig. 1) indicated the production of apatite layer on composites.

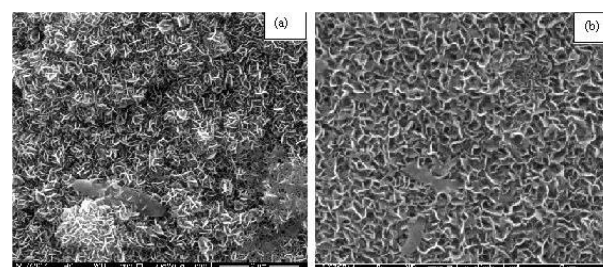


Fig. 1. a) SEM graphs of CaPs-GEL treated with 2% GA, b) 8% GA (14th days)

### CONCLUSION

Analysis conducted confirmed the occurrence of desired CaPs-GEL structure and chemical bonding between CaP and GEL. It was concluded that CaPs-GEL composites may be biocompatible and usable as biomaterials.

### REFERENCES

1. Karampas I.A and Kontoyannis, Vib. Spectrosc. 64: 126–133, 2013
2. Teng S. *et al.*, J. Inorg. Biochem. 101 (4): 686-691, 2007.
3. Touny A. *et al.*, J. Mater. Sci. Mater. Med. 19(10):3193-201, 2008.

### ACKNOWLEDGMENTS

The authors would like to thank the Scientific Research Projects Programme (BAP) for providing financial support to this project.





## Preparation of Polycaprolactone-Polyethylene Glycol-Casein Bioblends using Spray Dryer

Erhan Ozsagiroglu<sup>1</sup>, Yuksel Avcibasi Guvenilir<sup>1</sup>

<sup>1</sup> Chemical and Metallurgical Engineering Faculty, Istanbul Technical University, Chemical Engineering Department, 34469, Maslak-Istanbul/TURKEY.

[ozsagiroglu@itu.edu.tr](mailto:ozsagiroglu@itu.edu.tr)

### INTRODUCTION

Spray drying is the process of contacting an atomized stream to be dried with a gas stream that is at a higher temperature than the liquid stream. The higher temperature of the gas stream causes evaporation of the liquid from the droplets, forming particles. Recently, the use of this process to manufacture hollow, micron and sub-micron particles has also been demonstrated [1]. Furthermore, amorphous solid dispersions, soluble complexes, encapsulated systems, solid self-emulsifying systems and nano-dispersions of poorly soluble drugs prepared by spray drying are primary solubilization strategies [2].

Microspheres based on polycaprolactone (PCL), polyethylene glycol (PEG), and casein (CS) is prepared by spray drying technique. Microparticles are in vitro characterized in terms of yield of production, particle size, morphology, and thermal characterization. The importance of the study is producing of a stable and effective bioblends using ternary polymer mixture by spray dryer. First step of the study is preparation of low particle size, high surface area and homogeneous blend material using spray dryer. Second part is to characterize bioblends using Metasizer, SEM, and TGA. At the end of studies, we achieved minimum  $27.540 \pm 0.656 \mu\text{m}$  particle size with  $0.512 \text{ m}^2/\text{g}$  surface area. In particular, PCL-PEG-CS microspheres can be used for so many areas such as drug delivery systems and tissue engineering applications.

### EXPERIMENTAL METHODS

Polycaprolactone with  $M_n = 10,000 \text{ g/mol}$ ,  $M_w = 14,000 \text{ g/mol}$  and casein from bovine milk are purchased from Sigma-Aldrich. Polyethylene glycol (PEG-6000) is a gift from Ashland Inc. Acetic acid (Merck) and formic acid (Merck) are used as solvent agents for polymer mixtures and used without any further purification.

PCL+PEG+CS polymer mixture solutions are prepared by acetic acid-formic acid solutions with 3:7 (v/v) ratios. The value of 3:7 (v/v) acetic acid:formic acid is determined by previous studies [2]. Polymer contents in all solutions are 10 wt% and all ternary polymer mixtures are prepared by 1:1:1 (wt/wt) ratio.

### RESULTS AND DISCUSSION

Yield and particle size distribution with standard deviation are shown for all studies in Figure 1 and Figure 2, respectively. Due to the Figure 2, Metasizer analyses are done 3 times and particle diameter distribution is determined by standard deviation of the results. Final values demonstrate particle size ( $\mu\text{m}$ ) with standard mean of PCL-PEG-CS microspheres. Figure 1 determines that drying efficiency increase by decreasing of flow rates at  $120^\circ\text{C}$ ,  $135^\circ\text{C}$  and  $150^\circ\text{C}$ . The reason of these results are that increasing drying

temperature resulted in agglomeration of polymer mixture, so contact time with polymer mixture and drying temperature had adversely effect on diameter distribution [20]. Due to these results,  $135^\circ\text{C}$  and  $3 \text{ ml/min}$  are the best drying conditions because the lowest particle diameter and highest surface area are also obtained with  $27.540 \pm 0.656 \mu\text{m}$  particle size with  $0.512 \text{ m}^2/\text{g}$  surface area in this study. Yields are same, compared to the results reported for optimized runs using other laboratory scale spray dryers (Lab Scale Spray Dryer) [21].

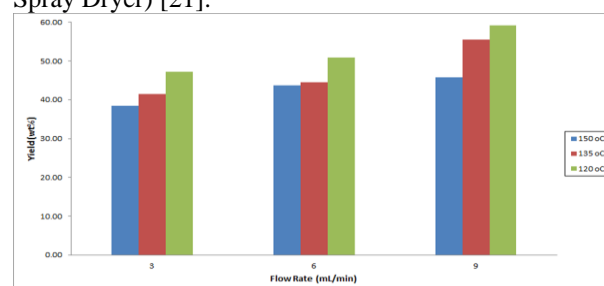


**Figure 1.** Yield (wt%) at different drying temperature ( $^\circ\text{C}$ ) and flow rates (ml/min).

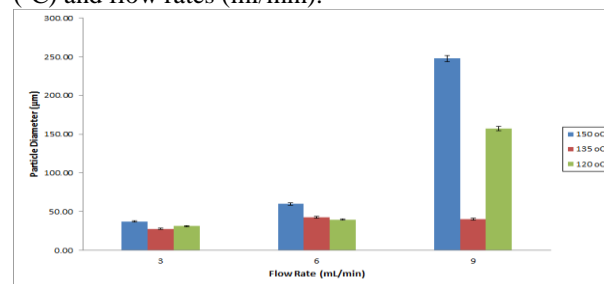


**Figure 2.** Particle diameter ( $\mu\text{m}$ ) with standard deviations at different drying temperature ( $^\circ\text{C}$ ) and flow rates (ml/min).

Furthermore, higher spray rates have been reported to have a negative influence on the yield. Figure 1 shows the tendency of the yield to be higher when the spray rate was low. Additionally, particle size diameters are increased at higher spray rates as seen in Figure 2. It is revealed that we have to avoid higher spray rates because of its reverse effect on encapsulation material.

### CONCLUSION

In comparison the spray dryer method to others, we obtained much more uniform microspheres and lower particle diameters. Significantly, the experimental results indicate that to obtain particle diameter  $27.540 \pm 0.656 \mu\text{m}$  with  $0.512 \text{ m}^2/\text{g}$  surface area does not need to any additive effects during drying process.

### REFERENCES

1. Latorre A. *et al.*, Eur. J. Med. Chem. 82:355-362, 2014.
2. Wu J. *et al.*, Acta. Biomater. 9(7):7410-7419 2013.

### 3D-Powder-Printing of Strontium Modified Magnesium Phosphate Cements for Bone Augmentation

Emilie März, Claus Moseke, Uwe Gbureck, Jürgen Groll, Elke Vorndran

Department for Functional Materials in Medicine and Dentistry, University of Würzburg, Germany  
[elke.vorndran@fmz.uni-wuerzburg.de](mailto:elke.vorndran@fmz.uni-wuerzburg.de)

Magnesium phosphate cement (MgPC) for bone augmentation was processed by 3D-Powder-Printing (3DP) as well as by cement paste formulation. Since strontium (Sr) is known to positively influence the bone metabolism, a modification of the cement with Sr was performed. In this study chemical and physical properties and Sr release kinetic of printed and paste-derived MgPC specimens were investigated.

#### INTRODUCTION

3D-Powder-Printing is an excellent method for the fabrication of bone substitutes for non-load-bearing defects especially in the case of complex defect geometry. The applicability of calcium phosphate cement (CPC) scaffolds produced by 3DP in maxillofacial surgery was recently shown [1]. A new approach is given by the 3DP of struvite forming MgPC, which is biocompatible and shows a faster biodegradation and higher osteoconductive potential compared to CPC [2]. The modification of MgPC with Sr is intended to enhance bone formation and radiopacity and to inhibit bone degradation of peripheral diseased bone tissue by Sr ion release.

#### EXPERIMENTAL METHODS

Raw materials consisted of cement powders with the general composition  $\text{Mg}_{3-x}\text{Sr}_x(\text{PO}_4)_2$  ( $x = 0, 0.33, 0.67, 1.00$ ) and an ammonium phosphate based binder solution. Solidification of the cements was performed by printing the cement materials with a 3DP system (Z510, Z-Corporation) or by manual mixing of the cement powder with the binder in a powder-to-liquid ratio of 5:2. The compressive strength, porosity (Archimedes principle), microstructure (scanning electron microscopy, SEM), chemical composition (X-ray diffraction), radiopacity and Sr release (inductively coupled plasma mass spectrometry, ICP-MS), were analyzed after several time points of elution in a phosphate buffered solution (PBS).

#### RESULTS AND DISCUSSION

Cement raw powders consisted of pure farringtonite ( $\text{Mg}_3(\text{PO}_4)_2$ ) or in the case of Sr modification of a mixture of farringtonite and two unreactive Sr containing MgPC phases ( $\text{Mg}_2\text{Sr}(\text{PO}_4)_2$ ,  $\text{Mg}_3\text{Sr}_2(\text{P}_4\text{O}_{15})$ ). After solidification of the cements, farringtonite was partially converted to struvite ( $\text{MgNH}_4\text{PO}_4 \cdot 6\text{H}_2\text{O}$ ) or in the case of paste formulations to struvite and newberyite ( $\text{MgHPO}_4 \cdot 3\text{H}_2\text{O}$ ). Printed MgPC showed a characteristic high porosity of  $(21 \pm 1) \%$ , which was increased by Sr modification to a maximum of  $(29 \pm 1) \%$ . In contrast, a significant lower porosity of  $(5 \pm 2) \%$  for cement paste formulations was shown, which was increased by Sr addition by a factor of 1.2 –

1.8. In comparison to printed MgPC a significant higher compressive strength, varying between 72 MPa and 47 MPa, was determined for the MgPC paste formulation, which decreased with increasing Sr content (Figure 1). Furthermore the radiopacity could be enhanced by the addition of Sr for both application forms.

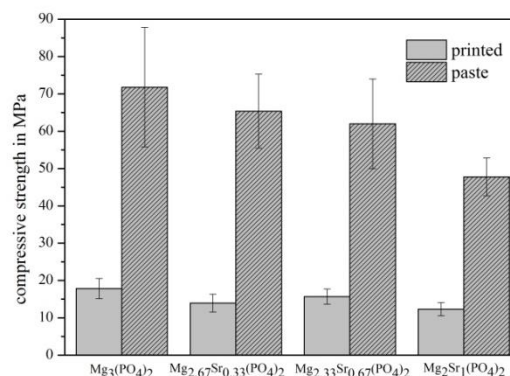


Figure 1: Compressive strength of pure and strontium modified MgPC for printed specimen and paste formulations.

The Sr release was investigated over a period of 14 days. While cement pastes released Sr ions continuously with a rate of approximately 30 – 40  $\mu\text{g}/\text{day}$ , printed specimens showed a first order release kinetic with an accumulated maximal ion release of 45  $\mu\text{g}$  after 14 days.

#### CONCLUSION

MgPC processed by 3DP as well as by cement paste formulations seems to be a promising bone replacement material, since compressive strengths are comparable to proven CPC systems but shows improved osteoconductivity [2]. The Sr content can be adjusted with regard to biological effectiveness and suitable radiopacity without changing the physical or chemical properties of the MgPC system.

#### REFERENCES

1. Klammert U. *et al.*, J. Cranio. Maxill. Surg. 38 (8): 565 – 570, 2010
2. Kanter B. *et al.*, Acta Biomaterialia 10 (7): 3279 – 3287, 2014

## Selection and Optimization of Hydroxyapatite and Chlorapatite powders for 3D-printing

Zeinab Salary (Mona)<sup>1</sup>, Parastoo Jamshidi<sup>1</sup>, Zuzanna Trzcińska<sup>1</sup>, David Grossin<sup>1,2</sup>, Ghislaine Bertrand<sup>2</sup>, Olivier Marsan<sup>2</sup>, Cédric Charvillat<sup>2</sup>, Imane Demnati<sup>2</sup>, Moataz Attallah<sup>1</sup>, Artemis Stamboulis<sup>1</sup>

<sup>1</sup> Biomaterials Group/School of Metallurgy and Materials, University of Birmingham, UK

<sup>2</sup>Phosphates, Pharmacotechnie, Biomaterials /CIRIMAT INPT-UPS-CNRS, Université de Toulouse, France

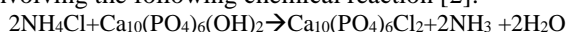
[zxt166@bham.ac.uk](mailto:zxt166@bham.ac.uk)

### INTRODUCTION

The improvement of 3D-printing processes (3DPP) technology in biomedical and tissue engineering has dramatically affected the potential ability of making biomedical implants and scaffolds by applying data of clinical imaging and computer aided designs. Among different types of 3D printing techniques, Selective laser sintering / Melting (SLS/M) and Stereolithography (SLA) are very appropriate for manufacturing highly precise structures which can be used for different biomedical applications such as aids for surgery, scaffolds and body implants. [1] The aim of this work is to select and optimize appropriate hydroxyapatite (HA) or chlorapatite (CIA) powder applied in 3DPP. Different Powders were characterised in order to see the effect of particle size (P.S), flowability and thermal stability for various 3DPP. Synthesis of CIA from HA was described. Also some comparison analysis between CIA and HA were conducted.

### EXPERIMENTAL METHODS

Hydroxyapatite [three different size distributions (0-30µm), (30-50µm) and (50-80µm)] was supplied by TEKNIMED S.A. (France). Expected chlorapatite feedstock was prepared from previous powder HA (50-80µm) using thermal exchange method at 950°C between sublimated NH<sub>4</sub>Cl and commercial HA involving the following chemical reaction [2]:



X-ray diffraction patterns were obtained on Seifert (Cu K $\alpha$  radiation). Fourier-transformed infrared spectroscopy (FTIR) analyses on powders were carried on for complementary phase identification (Nicolet 5700). Raman spectra were recorded, on a Horiba Jobin Yvon HR 800 spectrometer ( $\lambda=632.8$  nm). Thermal stability of starting powder was evaluated by thermogravimetric analyses (TGA) from 30°C to 1400°C under Argon. The flowability was determined as recommended by the European Pharmacopeia. Some Selected powders were applied for fabrication of 3D samples with complexes shape (figure 1) via SLA ( $\lambda=405$  nm using clear resin for making solution) or SLM (Yb-fiber continuous wave  $\lambda=1060$  nm) to see the effect of properties of the powder on the process.



Figure 1: SLA 3D-printed HA

**RESULTS AND DISCUSSION** Figure 2 shows XRD diffraction on raw powder (HA 50-80µm) and obtained powders after chlorination previously described. All peaks in raw powder diffractogram, were indexed using JCPDS 9-432 which prove HA was the only crystalline phase without impurity. For the second diffractogram, all peaks could be attributed to CIA using JCPDS 1-70-1454. This result highlights the full transformation from HA to CIA. These results were confirmed by FTIR and Raman (not show here). The thermal stability of CLA was higher than HA, according to weight loss shown in figure 3, only for HA at  $T > 800^\circ\text{C}$ .

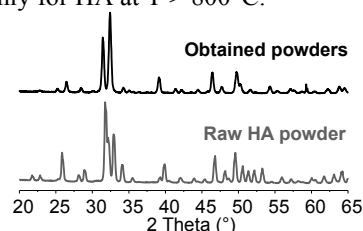


Figure 2: XRD patterns of raw and obtained powders

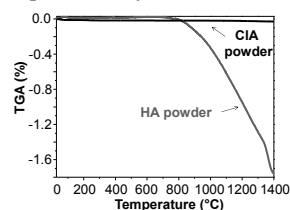


Figure 3: TGA on CIA, HA powders

Flowability and morphology measurement allow selecting appropriate powders for each process. For example, Hausner ratio (HR) measurement allow to reject the use of HA 0-30 ( $1.47 \pm 0.17$ ) because the HR was higher than  $\text{HR}_{\text{limit}} = 1.25$  for SLS/M[3].

### CONCLUSION

According to TGA and XRD characterization CIA has a higher thermal stability than HA which shows that by using CIA we expect better results in both SLS/M and SLA techniques. Also, particles size plays an important role for SLS/M due to the limitation of flowability for this process.

### REFERENCES

1. Melchels F. *et al.*, Biomaterials 31: 6121, 2010
2. Demnati I. *et al.*, Biomed Mater. 7: 054101, 2012
3. Schmid M. *et al.*, Eidgenössische Technische Hochschule Zürich, IWF, 2014

### ACKNOWLEDGMENTS

The authors want to thank COST Action NEWGEN MP1301 for financial support and TEKNIMED S.A. for HA powders.

# Zirconia-Ceria Hydroxide Sol-Gel Synthesis: Colloid Processing and Powders Preparation for Potential Biomedical Application

Damian Nakonieczny<sup>1</sup>, Zbigniew Paszenda<sup>1</sup>, Tomasz Radko<sup>2</sup>

<sup>1</sup>Department of Biomaterials and Medical Device Engineering/Faculty of Biomedical Engineering,  
Silesian University of Technology, Poland

<sup>2</sup>Department of Department of Inorganic, Analytical Chemistry and Electrochemistry/Faculty of Chemistry, Silesian  
University of Technology, Poland  
[damian.nakonieczny@polsl.pl](mailto:damian.nakonieczny@polsl.pl)

## INTRODUCTION

Zirconium Oxide ( $\text{ZrO}_2$ ), because of its promising structural, chemical and thermal properties is used in widespread applications such as manufacturing of gas sensors<sup>1</sup>, corrosion-resistant and thermal barrier's coatings<sup>2</sup> and biomaterials<sup>3</sup>. Pure  $\text{ZrO}_2$  exists in three polymorphic phases namely monoclinic (m), tetragonal (t) and cubic (c). Among these monoclinic phase is stable but tetragonal and cubic phases are metastable. Application of  $\text{ZrO}_2$  as a structural material for biomedical applications and in many other areas depends mostly from synthesis methods and post-synthesis thermal treatment<sup>4</sup>.

The sol-gel method has become a popular method for fabricating wide range of ceramic products including powders and coatings. The main advantage of the sol-gel method is the ability to form inorganic structures at relatively low temperature and to produce with simply process route ceramic powders on large scale.

The goal of the present study was to prepare zirconia-ceria solid solutions ( $0.9\text{ZrO}_2\cdot 0.1\text{CeO}_2$ ) by sol-gel method. The influence of reagents molar ratios and hydrolysis ratio for the macroscopic morphology and the nature of thermal decay of the prepared gels were discussed<sup>5</sup>.

## EXPERIMENTAL METHODS

**Sample preparation:** As a reagents for synthesis were used zirconium *n*-propoxide (ZNP) (Acros) as a zirconia oxide precursor, 2-propanol (PrOH) (analytical grade, Avantor) as organic solvent, acetylacetone (AcAc) as a chelating agent, cerium nitrate hexahydrate (CNH) (Sigma Aldrich) as a ceria oxide precursor, and ultrapure water. Whole sol-gel synthesis and reagent dosing were carried out in nitrogen atmosphere in sealed glass apparatus. Stabilization of the zirconia precursor was achieved by the carefully addition of acetylacetone. Obtained hydroxide gels were dried ( $t = 80^\circ\text{C}$ ,  $\tau = 2,5\text{h}$ ) and calcined. Resultant powders were grinded in hand mortar with pestle. Based on macroscopic observations, the effect of the molar ratios of the ZNP:AcAc and ZNP:H<sub>2</sub>O on homogeneity of gels and powders an morphology. The molar ratios are shown in the table (Table 1).

**Characterization:** The TGA/DTA studies were carried out using a Q 1500D (MOM) in static air with a heating rate of  $10^\circ\text{min}^{-1}$  in the temperature range from 24 to  $1000^\circ\text{C}$ .

## RESULTS AND DISCUSSION

According to our observations, the molar ratios of ZNP: AcAc:H<sub>2</sub>O play an important role in the powders synthesis because they affect on the rate of hydrolysis ratio and same powders macroscopic morphology. Use of lower concentrations of water (in the range of 2÷5) and AcAc (in the range of 0.750÷0.6) resulted in a slow hydrolysis rate and completely foreseeable water addition. Resulting gels were characterized by a very high homogeneity. Obtained powders consisted a large number of big homogeneous agglomerates. Use of water in concentration in the range of 5÷10 and AcAc in the range of 0.4÷0.194 led to inhomogeneous gels, for which water was dosed in extremely gentle drop-by-drop manner. The resulting powders were characterized by considerable heterogeneity and small size of the agglomerates. b

ZNP	AcAc	H <sub>2</sub> O
1	0.750÷0.194	2÷10

Table 1 Used reagents molar ratio range

Noticeable differences was also observed in the TG/DTA spectra under which could be seen an approximate thermal stability of ZNP-AcAc complex. With the increase of complex was observed increase in the obtained powders particle size.

## CONCLUSION

The most satisfying result of applied sol-gel process treatment was observed for high molar ratios of water and low acetyl-acetone concentration which led to small fine grained powders.

## REFERENCES

1. Miura N. *et al.*, Electrochem. Commun. 4:284-87, 2002.
2. Ahmadi-Pidani R. *et al.*, Mat. and Design 57:336-41, 2014.
3. Chevalier J. *et al.*, Coompre. Biomat. 1:95-108, 2011.
4. Cheng-Li W. *et al.*, J. Sol Gel Sci. Technol. 70:428-40, 2014.
5. Nakonieczny D., *et al.*, Mat. Lett. (in review).

## ACKNOWLEDGMENTS

The study was financed from Department of Biomaterials and Medical Device Engineering own funds





## Influence of the Colloid System pH for the Phase Composition and Morphology of Cerium Oxide Doped Zirconia Powders – Properties Evaluation

Damian Nakonieczny<sup>1</sup>, Zbigniew Paszenda<sup>1</sup>, Sabina Drewniak<sup>2</sup>, Tomasz Radko<sup>3</sup>

<sup>1</sup>Department of Biomaterials and Medical Device Engineering/Faculty of Biomedical Engineering, Silesian University of Technology, Poland

<sup>2</sup>Department of Optoelectronics/Faculty of Electrical Engineering, Silesian University of Technology, Poland

<sup>3</sup>Department of Department of Inorganic, Analytical Chemistry and Electrochemistry/Faculty of Chemistry, Silesian University of Technology, Poland  
[damian.nakonieczny@polsl.pl](mailto:damian.nakonieczny@polsl.pl)

### INTRODUCTION

Yttrium oxide doped zirconia is an advanced ceramic used in wide applications in the dental restorations using CAD/CAM techniques and dental implants<sup>1</sup>. Unfortunately use of zirconia in prosthetic dentistry has raised many problems associated with reports of uncontrolled martensitic type phase transformation from the tetragonal ( $\beta$ ) to monoclinic ( $\alpha$ ) in the oral environment and human biomechanics conditions<sup>2,3</sup>. Occurred changes led to increase of zirconia volume and unpredictable prosthetic restorations cracking and irreversible damage<sup>4</sup>. To fully prevent zirconia from unfavorable transformation is doping the zirconia with metal oxides with bigger atomic radius than  $Zr^{4+}$ <sup>5,6</sup>. On the basis of many studies it can be assumed that  $CeO_2$  as a dopant provides complete stability of the  $\beta$  phase and nanoscale grain size<sup>7,8</sup>. Very important for the stabilization of tetragonal zirconia is the method used to prepare the ceramic powders. One of the best preparation process is the sol-gel method because it allows strict control of the chemical composition and the achieving of a homogeneous grain size<sup>8</sup>.

The main objective of this study was to prepare with sol-gel method  $0.9ZrO_2-0.1CeO_2$  (mol%) ceramic powders in different pH conditions to determine that variable for the phase composition and morphology of obtained powders affecting to the final values of zirconia dental ceramics.

### EXPERIMENTAL METHODS

**Sample preparation:** As a starting materials were used zirconium *n*-propoxide (ZNP) (Acros), 2-propanol (PrOH) (analytical grade, Avantor), acetylacetone (AcAc), cerium nitrate hexahydrate (CNH) (Sigma Aldrich), ammonia water (Avantor) and acetic and hydrochloric acids (Sigma Aldrich) as pH agents and ultrapure water. Whole sol-gel synthesis and reagent dosing were carried out in nitrogen. Stabilization of the zirconia precursor was achieved by the addition of acetylacetone as the chelating agent. Obtained hydroxide gels were dried, calcined. Resultant powders were grinded in hand mortar with pestle.

**Characterization:** X-ray diffraction was performed using a Seifert XRD7 diffractometer and  $Co\ K\alpha$  radiation ( $\lambda = 0.179021\text{ nm}$ ). Powders morphology were performed with SEM pictures taken with an FEI INSPECT S50 microscope. The TGA/DTA studies were carried out using a Q 1500D (MOM) in static air with a

heating rate of  $10^\circ\text{ min}^{-1}$  in the temperature range from 24 to  $1000^\circ\text{C}$ .

### RESULTS AND DISCUSSION

Solution of ZNP with PrOH has a pH in the range  $6.5\div 7$ . Therefore it was decided to select four different values of pH: 2, 4, 8 and 10. For the acidic range at 2 resulted powders have a relatively wide range of inhomogeneities and considerable size of the agglomerates. It is noted that, with rise of pH are obtained more dispersed fine-crystal powders. The most homogeneous powders were obtained for pH of 8. It should be stated that the analysis of TG/DTA curves and XRD help confirmed in the range of  $2\div 4$  occurrence of undesirable phase  $\alpha\text{-}ZrO_2$  (the most characteristic peaks of  $2\theta = 28.48, 36.97$ ). In contrast, at pH 8 were found only full tetragonal phase peaks (most characteristic at  $2\theta = 34.99, 40.27$ ). On the basis of the thermograms for obtained powders, samples prepared at pH 8 show only characteristic peaks for crystallization of  $\beta$  phase (sharp peak at  $t = 400\div 420^\circ\text{C}$ ).

### CONCLUSION

In the summary it should be noted that the pH has a significant influence for the phase composition and morphology of the obtained zirconia-ceria powders. The most satisfying result of the applied pH values were obtained for pH = 8.

### REFERENCES

1. Miyazaki T. *et al.*, Aust Dent J. 56(1):97-106, 2011.
2. Lugh V. *et al.*, Dent Mater. 26:807-20, 2010.
3. Cattani-Lorente M. *et al.*, Acta Biomater. 7:858-65, 2011.
4. Keuper M. *et al.*, Acta Biomater. 10:951-59, 2014.
5. Naskar M. K. *et al.*, J Mater Sci. 31:6262-67, 1996.
6. del Monte F. *et al.*, J Am Ceram Soc. 83:628-34, 2000.
7. Chevalier J. *et al.*, J Am Ceram Soc. 92:1901-20, 2009.
8. Trusova E. A. *et al.*, J Eur Ceram Soc. 32:1977-81, 2012.

### ACKNOWLEDGMENTS

The study was financed from Department of Biomaterials and Medical Device Engineering own fund



# Synthesis of MTA Powder by Spray-Pyrolysis

Jeong-Cheol Lee<sup>1</sup>, Seung-Hoon Um<sup>1</sup>, Bong Kyu Choi<sup>2</sup>, and Sang-Hoon Rhee<sup>1</sup>

<sup>1</sup>Department of Dental Biomaterials Science, Dental Research Institute and BK21 HLS, School of Dentistry, Seoul National University, Korea

<sup>2</sup>Department of Oral Microbiology and Immunology, Dental Research Institute and BK21 HLS, School of Dentistry, Seoul National University, Korea  
[rhee1213@snu.ac.kr](mailto:rhee1213@snu.ac.kr)

## INTRODUCTION

The mineral trioxide aggregate (MTA) is a mixture of a refined Portland cement, which is mainly consisted of tricalcium silicate, dicalcium silicate, tricalcium aluminate, gypsum, and bismuth oxide as a radiopacifier.<sup>1</sup>

The MTA has been used for pulp capping, pulpotomy, apexogenesis, apical barrier formation in teeth with open apexes, repair of root perforations, and as a root canal filling material because it is known to be nontoxic, noncarcinogenic, nongenotoxic, biocompatible with the host tissues, insoluble in tissue fluids, and dimensionally stable.<sup>2</sup>

The setting of MTA begins from the hydration of tricalcium silicate, dicalcium silicate, and tricalcium aluminate. Thus, the reaction rate and resultant microstructure are dependent on the size of initial powder. However, the size of powder produced by current method is about tens of micrometers.

The purpose of this experiment is to synthesize sub-micron meter sized MTA powder by spray-pyrolysis method.

## EXPERIMENTAL METHODS

The MTA powder was synthesized by spray pyrolysis. A CaO-SiO<sub>2</sub>-Al<sub>2</sub>O<sub>3</sub> gel solution for spray pyrolysis was prepared by gelation for 1 hour at room temperature after dissolving calcium nitrate tetrahydrate (Aldrich), tetraethyl orthosilicate (Aldrich), and aluminium nitrate nonahydrate (Aldrich) in deionized water followed by adding nitric acid (60%; Aldrich). The CaO-SiO<sub>2</sub>-Al<sub>2</sub>O<sub>3</sub> gel solution was then made into small droplets using an ultrasonic spray generator (1.7 MHz, 17 vibrators) fed into an alumina reaction tube (120 cm in length and 7 cm in diameter) at 1500°C with carrier gas (air) flow rates of 10 L/min, made by a compressor. The droplets were collected in a Teflon<sup>®</sup> filter placed in the exhaust line of the reactor, which was kept at around 100°C to avoid water condensation.

The phase of the powder was evaluated by XRD and microstructure was observed by FE-SEM. The elemental analysis on the sprayed powder was carried out using EPMA.

## RESULTS AND DISCUSSION

The phase analysis using XRD on the powder obtained through spray-pyrolysis was displayed in Fig. 1. It was composed of dicalcium silicate, tricalcium silicate, tricalcium aluminate, and some glass phases. The EPMA analyses showed that the Ca, Si, and Al distributed evenly in a particle. This means that the three major elements of MTA were successfully synthesized through spray-pyrolysis.

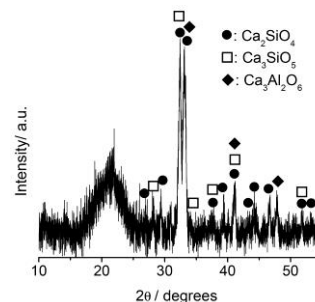


Figure 1. XRD pattern of the MTA powder obtained through spray-pyrolysis at 1500°C at carrier gas flow rate of 10 L/min.

The shape and size of the MTA powder was observed using FE-SEM (Fig. 2). They showed almost spherical shape and the particle size distribution was ranged from about 0.02 to 2.5 μm.

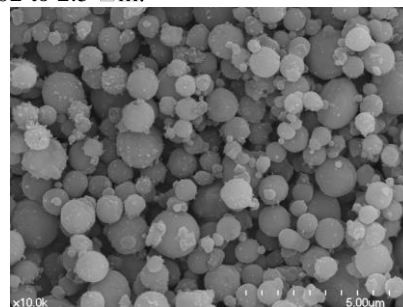


Fig. 2. FE-SEM micrograph of MTA powder obtained through spray-pyrolysis at 1500°C at carrier gas flow rate of 10 L/min.

The results demonstrated that the MTA powder could be synthesized by spray-pyrolysis based on sol-gel method. The final setting of this MTA powder was occurred within 10 min.

## CONCLUSION

The MTA powder was successfully synthesized by spray-pyrolysis based on sol-gel method. Its size and setting time were smaller and faster than those of white Portland cement. This means that it has a potential to be used as a MTA powder.

## REFERENCES

1. Sarkar NK. *et al.*, J. Endo. 31:97-100, 2005
2. Torabinejad M. *et al.*, J. Traumat. 12:161-178, 1996

## ACKNOWLEDGMENTS

“The authors would like to thank the Basic Science Research Program (Grant no: NRF-2013 R1A1A2004752) for providing financial support to this project”.

## Direct Fabrication of Porous Titanium Implant via 3D Printing

Pavan Kumar Srivas<sup>1</sup>, Kausik Kapat<sup>1</sup>, Prabhsh Dadhich<sup>1</sup>, Pallabi Pal<sup>1</sup>, Bodhisatwa Das<sup>1</sup>, Santanu Dhara<sup>1</sup>

<sup>1</sup>Indian Institute of Technology Kharagpur, Kharagpur, West Bengal, India  
[pavansrivas@gmail.com](mailto:pavansrivas@gmail.com)

### INTRODUCTION

There are several techniques for fabrication of porous metallic scaffold like fugitive based technique<sup>1</sup>, direct foaming and casting<sup>2</sup>, freeze drying<sup>3</sup>, extrusion, and rapid prototyping. Amongst all the techniques, additive rapid prototyping technique<sup>4</sup> is an advanced technique to develop 3D physical model by computer controlled sequential transfer of energy and/or material to identified points in space. This technique has been extensively studied to develop customized implants through manipulation of geometrical distribution, modification of mechanical properties and creating porous structures for tissue in-grow as well as better fixation. Amongst all other biomaterial, metals have great potential for long-term load-bearing applications due to its excellent resilience and mechanical strength. Titanium and its alloys exhibit better performance in this aspect.

### EXPERIMENTAL METHODS

For development of titanium lattice, CAD file of 3D model was designed using SolidWorks and the file was saved in 'stl' format and further converted into \*BFB format prior to 3D writing. Using a customized 3D printing machine, titanium slurry was poured into a dispenser and extruded using a compressed air driven extruder through a microtip based nozzle. After each layer of extrusion, the lattice structure was crosslinked to avoid spreading of the filaments and subsequently up to 22 layers were printed. The vacuum dried samples were sintered at 1450 °C under inert atmosphere.

### RESULTS AND DISCUSSION

The titanium lattice structure was successfully sintered under controlled atmosphere and the lattice structure was maintained after sintering. The porosity of the lattice structure, lattice parameters such as diameter of the strand, spacing between strands, number of layers and geometry can be varied based on the design of the CAD model, slurry properties, nozzle diameter etc. The

resultant lattice structure had highly open porous structure and the strands were laminated during printing as well as sintering. This highly open porous structure is most suitable for tissue integration at the interface via tissue in-growth.

### CONCLUSION

The scaffolds showed good compressive strength which is close to natural bone. It also showed promising results in *in vitro* study for 3 days, 5 days and 7 days and bio-compatibility *in vivo*.

### REFERENCES

- [1] O. Lyckfildt and J. M. F. Ferreira, "Processing of Porous Ceramics by Starch Consolidation," J. Eur. Ceram. Soc., 18 131–40 (1998).
- [2] S. Dhara and P. Bhargava, "A simple direct casting route to ceramic foams", J. Am. Ceram. Soc., 86 [10] 1645–50 (2003).
- [3] T. Fukasawa, M. Ando, T. Ohji, and S. Kanzaki, "Synthesis of Porous Ceramics with Complex Pore Structure by Freeze-Dry Processing," J. Am. Ceram. Soc., 84 [1] 230–32 (2001).
- [4] Li, J. P., de Wijn, J. R., Van Blitterswijk, C. a, & de Groot, K. (2006). Porous Ti6Al4V scaffold directly fabricating by rapid prototyping: preparation and in vitro experiment. Biomaterials, 27(8), 122335. doi:10.1016/j.biomaterials.2005.08.033

### ACKNOWLEDGMENTS

The authors acknowledge the Defence Research and Development Organisation for the Funding from Ministry of Defence, India.



## Preparation of Electroconductive Titania Scaffolds for Bone Tissue Regeneration

Inga Narkevica<sup>1</sup>, Jurijs Ozolins<sup>1</sup>

<sup>1</sup> Institute of General Chemical Engineering, Riga Technical University, Latvia  
[inga.narkevica@rtu.lv](mailto:inga.narkevica@rtu.lv)

### INTRODUCTION

Use of scaffolds as sacrificial templates for bone ingrowth is the basis of bone tissue regeneration. The main reasons for using bone scaffolds are to provide an environment for bone formation, maintain the space and at the same time supply mechanical support to the skeleton during healing process<sup>1</sup>. Bone healing can be significantly improved by applying electrical stimuli in the injured region. Thus, electrically active ceramics with three-dimensional porous structure are of interest as bone graft substitute materials<sup>2</sup>. Highly porous TiO<sub>2</sub> ceramic scaffolds has attracted particular attention as a bone substitute material due to its excellent mechanical properties compared to other ceramic materials, biocompatibility and good osteoconductivity<sup>3</sup>. Thus, our research goal was to obtain electroconductive and 3D porous TiO<sub>2</sub> ceramic scaffolds. Such materials could enhance bone healing process by providing electrical stimuli in the regeneration site of bone defects.

### EXPERIMENTAL METHODS

Ceramic scaffolds were produced via polymer foam replica method. Commercially available anatase powder, 5% polyvinyl alcohol solution, ethylene glycol, ammonia solution and deionised water were used as raw materials for ceramic slurry preparation. Homogenisation of the slurry was conducted by stirring for 3 hours at 1000 rpm. Cylindrical polyurethane (PU) foams with fully interconnected pore structure (Fig. 1 (a)) serves as a sacrificial template. PU foam templates were dipped into the ceramic slurry and excess slurry was squeezed out of the foam to ensure that only a thin layer of slurry covered uniformly the entire surface of foam. After drying for 24 h, the polymer was slowly burned out and scaffolds were sintered in air for 30 h at 1500°C temperature. In order to obtain electroconductive TiO<sub>2</sub> ceramic scaffolds, they were additionally thermally treated under high vacuum conditions at 1200°C for 5 h.

Macrostructure and surface morphology was characterized by field emission scanning electron microscopy. Total porosity of the scaffolds was measured by gravimetry. Mechanical strength of the scaffolds was determined by compression test. Electrical resistance was measured using DC Wheatstone bridge.

### RESULTS AND DISCUSSION

Highly porous TiO<sub>2</sub> ceramic scaffolds with fully interconnected and open pore structure were obtained (Fig. 1 (b) and Table 1). Pore size was in the range from 100 to 600 µm that is wide enough to ensure cell migration and vascularisation throughout all scaffold structure.

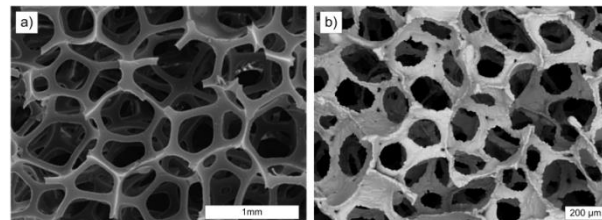


Fig.1. PU foam template (a) and TiO<sub>2</sub> scaffold after thermal treatment in air (b).

Table 1 summarises the main characteristics of obtained scaffolds after thermal treatment in different environments. No significant changes were observed in porosity and mechanical properties of the scaffolds. Electrical conductivity of the scaffolds after sintering in air was very low ( $\sim 3 \cdot 10^{-7}$  µS/m). Thermal treatment under high vacuum conditions caused dramatic increase in electrical conductivity ( $\sim 40$  µS/m). Increased electrical conductivity can be explained by reduction of TiO<sub>2</sub> that results in formation of different crystal lattice defects (oxygen vacancies, Ti<sup>3+</sup> or Ti<sup>4+</sup> interstitials). The reduction changes titanium-oxygen ratio in titanium dioxide. Even a small deviation from stoichiometry results in a significant decrease in electrical resistivity.

Table 1

Thermal treatment environment	Porosity, %	Compressive strength, MPa	Electrical conductivity, µS/m
Air	94±0.5	0.41±0.15	$\sim 3 \cdot 10^{-7}$
Air-Vacuum	93±1.4	0.31±0.05	$\sim 40$

### CONCLUSIONS

Using replica method porous TiO<sub>2</sub> ceramic scaffolds with porosity >90% and pore size >100 µm were obtained. Scaffolds showed fully open and interconnected pore structure. Thermal treatment under high vacuum conditions greatly increased electrical conductivity of the scaffolds. Due to obtained porous structure and electrical conductivity they can be potentially used in bone tissue regeneration to supply electrical stimuli and enhance bone healing process.

### REFERENCES

1. Salgado A.J. *et al.* Macromol. Biosci. 4:743-765, 2004
2. Shahini A. *et al.*, Int. J. Nanomedicine 9:167-181, 2014
3. Haugen H. *et al.*, J. Eur. Ceram. Soc. 24:661-668, 2004
4. Zakrzewska K. *et al.*, Adv. Mater. Res. 2012:1-13, 201



## A Novel Model of Nonalcoholic Fatty Liver Disease in a 3D Liver-on-Chip Device

Manuele Gori<sup>1</sup>, Maria Chiara Simonelli<sup>1</sup>, Luca Businaro<sup>2</sup>, Marcella Trombetta<sup>1</sup>, Alberto Rainer<sup>1,2</sup>

<sup>1</sup>Tissue Engineering Lab, University Campus Bio-Medico of Rome, Rome, Italy; <sup>2</sup>Institute for Photonics and Nanotechnologies, National Research Council (CNR), Rome, Italy

[m.gori@unicampus.it](mailto:m.gori@unicampus.it)

### INTRODUCTION

Nonalcoholic fatty liver disease (NAFLD) is a chronic liver disease, ranging from simple steatosis to nonalcoholic steatohepatitis, which may progress to cirrhosis, leading eventually to hepatocellular carcinoma (HCC). HCC ranks as the third highest cause of cancer-related death globally, requiring an early diagnosis of NAFLD as a potential risk factor<sup>1,2</sup>. However, the molecular mechanisms underlying NAFLD are still under investigation. So far, many *in vitro* studies on NAFLD have been hampered by the limitations of 2D culture systems, in which cells rapidly lose tissue-specific functions. The present liver-on-chip approach aims at filling the gap between conventional *in vitro* models, often scarcely predictive of an *in vivo* condition, and animal models that are potentially biased by their xenogeneic nature.

### EXPERIMENTAL METHODS

Microfluidic devices were fabricated by soft-lithography, starting from a photolithographically-obtained SU-8 master that was used as a mold for replicas in polydimethylsiloxane (PDMS), and seeded with HepG2 cells, a human hepatoblastoma cell line that retains many characteristics of normal differentiated hepatocytes<sup>3</sup>. Cells were cultured in 3D under microfluidic perfusion, through a set of microchannels that mimic the endothelial-parenchymal interface of a liver sinusoid, allowing the necessary diffusion of nutrients<sup>4</sup>. A continuous flow of medium (flow rate: 18  $\mu$ L/day), supplemented with a mixture of Free Fatty Acids (FFAs), namely palmitic and oleic acid at a final concentration of 1mM, was provided. Controls were represented by on-chip and 2D adherent cultures in plain medium. Intracellular lipid accumulation was measured using AdipoRed assay (Lonza). Cell viability was evaluated using LIVE/DEAD assay (Life Technologies), and oxidative stress by analyzing intracellular ROS levels through 2',7'-dichlorodihydrofluorescein diacetate (H<sub>2</sub>DCFDA, Life Technologies).

### RESULTS AND DISCUSSION

Our preliminary data show that on-chip FFA treatment produced a marked intracellular lipid accumulation, with different cytotoxic effects and ROS levels *vs.* 2D controls. Overall, the liver-on-chip system provides a more suitable culture microenvironment, representing a better and more reliable model, close to the *in vivo* liver pathophysiology, for investigating NAFLD pathogenesis.

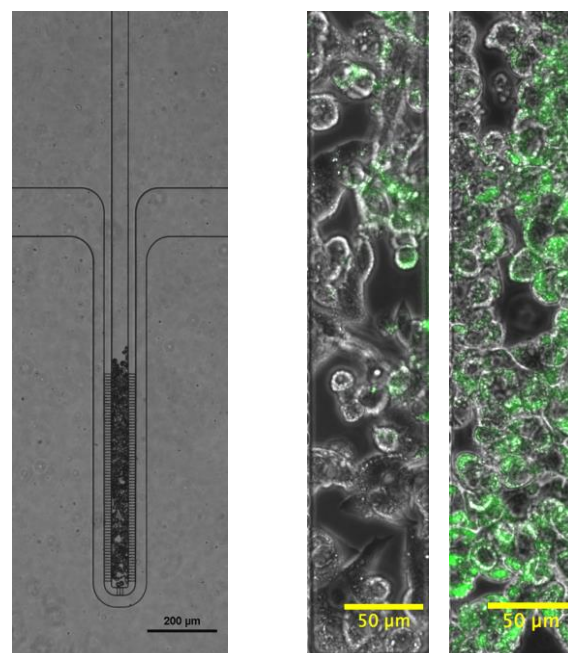


**Figure 1.** Left: Microfluidic liver-on-chip device (scale bar 200  $\mu$ m). Right: The different intracellular lipid accumulation (green fluorescence), evaluated through AdipoRed assay, between control (left panel) and FFA-treated (right panel) HepG2 cells cultured within the microfluidic device (scale bar 50  $\mu$ m).

### CONCLUSION

The liver-on-chip approach constitutes a paradigm shift for developing robust 3D *in vitro* models, representative of *in vivo* liver metabolic disorders, to unveil the molecular basis of NAFLD. In a long-term perspective, liver-on-chip implementation may boost the evaluation of therapeutic effects, selection of tailored treatments and novel therapeutic targets in both NAFLD and other metabolic disorders. This work will be extremely relevant to build a bridge between liver studies and micro-technologies, providing a starting point in genome- or proteome-scale analysis in the framework of metabolic diseases.

### REFERENCES

1. Marra F. *et al.*, Trends Mol. Med. 14:72-81, 2008
2. Starley B.Q. *et al.*, Hepatology 51:1820-32, 2010
3. Javitt N.B. *et al.*, FASEB J. 4:161-168, 1990
4. Lee P.J. *et al.*, Biotechnol. Bioeng. 97:1340-46, 2007

### ACKNOWLEDGEMENTS

Dr. Gori is supported by a “Fondazione Umberto Veronesi” fellowship.



## Stainless Steels Alloyed with Molybden for Medical Applications

Victor Geanta, Ionelia Voiculescu

University Politehnica of Bucharest, Romania  
[victorgeanta@yahoo.com](mailto:victorgeanta@yahoo.com)

### INTRODUCTION

The paper analyses the effect of Mo on microstructure and microhardness of some austenitic stainless steels for medical applications. The addition of one or two percent molybdenum into stainless steels significantly increases the corrosion resistance and the elevated temperature strength. Due to their large atom, molybdenum increases the elevated temperature strength of stainless steels through solid solution hardening<sup>1, 2, 3</sup>.

### EXPERIMENTAL METHODS

The experimental alloys were produced by melting in an argon inert atmosphere of the VAR (vacuum arc remelting) unit, using high purity metallic materials. The alloys composition was conducted from a base of commercial alloy (316L stainless steel), and subsequently 5 experimental stainless steels were obtained, by keeping constant the content of main elements, like Cr and Ni, and changing the content of molybdenum.

### RESULTS AND DISCUSSION

Metallographic analysis revealed microstructure morphology, constituents and different phases, depending on the content of molybdenum. Has been

examined the effects of heat treatment at 1100 °C for 2 hours followed by water quenching, on the evolution of microhardness.

### CONCLUSION

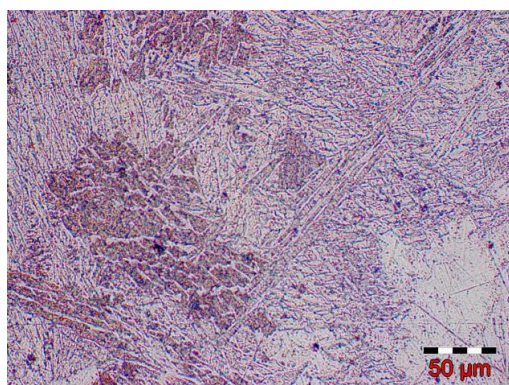
Evolution of microhardness express the hardening effects promoted by increasing molybdenum content in austenitic stainless steel metal matrix.

### REFERENCES

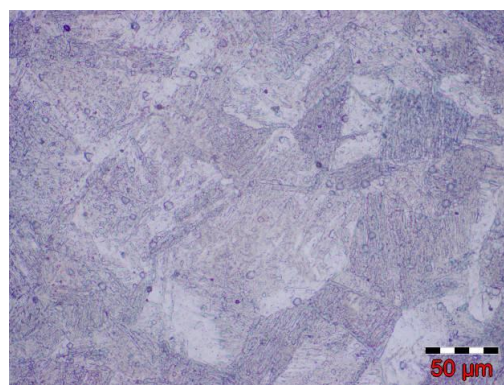
1. H. J. Breme, J. A. Helsen, Chapter 1 "Selection of materials", p. 1-35, in Metals as Biomaterials, 1998.
2. T. Newson, Stainless Steel – A Family of Medical Device Materials, Health & Environment Representative, 2002.
3. ISO 7153-1/1991. Surgical instruments – Metallic materials – Stainless steel.

### ACKNOWLEDGEMENTS

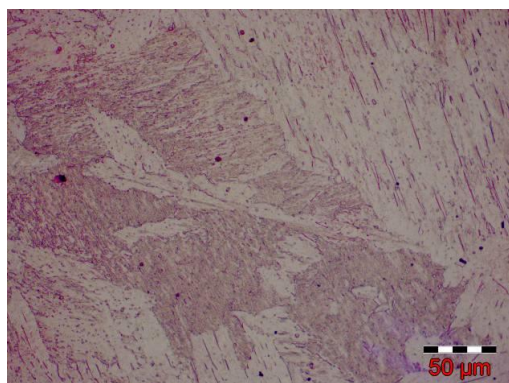
"The authors would like to thank Romanian National Program for Research - Funding Application for Joint Applied Research Projects PN-II-PT-PCCA-2013-4 in the framework of the Project No. PCCA 243/2014 – "Advanced metallic materials for 4R new generation nuclear power plant – NUCLEARMAT" for providing financial support to this project".



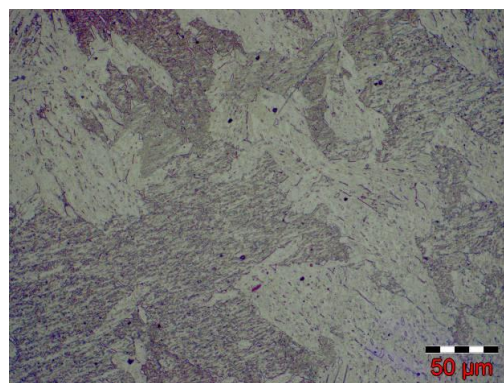
Reference material 316L, 500x



Stainless steel alloyed with 1% Mo, 500x



Stainless steel alloyed with 1.75% Mo, 500x



Stainless steel alloyed with 1.96 %Mo, 500x



## INTRODUCTION

Materials such as pure titanium and its alloys, or those containing Nb and Ta, have high polarization resistance and exhibit an inert behavior in relation to biological fluids. Metallic materials with polarization resistance similar to these, such as 316L and Co-Cr alloys, are covered by a tissue membrane and their long-term behavior is not considered inert<sup>1, 2, 3, 4</sup>.

## EXPERIMENTAL METHODS

In the paper are presented results on obtaining new titanium alloys, like Ti Mn, TiFe and TiAl. Ti, Ta and Nb are reported to be biocompatible due to their capacity to form a protective layer of oxide, which is a semi-conductive or non-conductive oxide. The experimental alloys were produced by melting in an argon inert atmosphere of the RAV unit, using high purity metallic materials and the commercial alloy Ti8Al4V. Were developed, under the same conditions, some binary alloys (Ti9Al, Ti5Fe, Ti3Mn) for highlighting the effects of the singular elements Al, Fe and Mn on the characteristics of titanium alloys.

## RESULTS AND DISCUSSION

Microstructural aspects and micro-hardness values are analyzed in order to estimate the effects promoted by each element separately. Experimental alloys are compared with a commercial technical alloy, Ti6Al4V respectively, against which performance is evaluated in

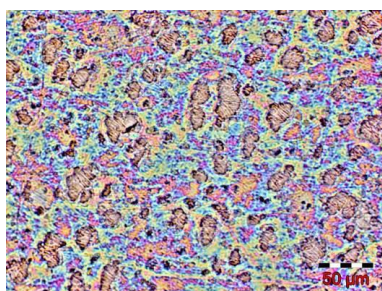
terms of microstructural features and microhardness values.

## CONCLUSION

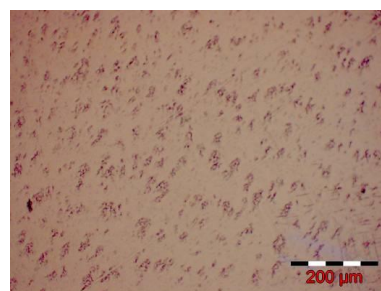
Analyzing the microhardness values has been revealed that items that cause hardening of titanium metal matrix are, in order of decreasing effectiveness, iron, manganese and aluminum. It was found that by combining of certain chemicals we can get an increase in the hardness of titanium metal matrix, such as the simultaneous use of iron and aluminum.

## REFERENCES

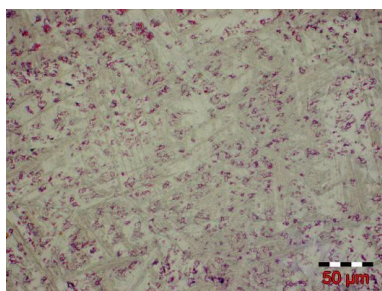
1. M. Niinomi. Recent research and development in titanium alloys for biomedical applications and healthcare goods, Science and Technology of Advanced Materials 4 (2003) pp. 445-454.
2. C. Oldani, A. Dominguez, Titanium as a Biomaterial for Implants, Recent Advanced in Arthroplasty, (2012) pp. 149-162.
3. H. Michelle Grandin, S. Berner, M. Dard, A Review of Titanium Zirconium (TiZr) Alloys for Use in Endosseous Dental Implant, Materials 2012, Vol.5, pp 1348-1360.
4. C.N. Elias, J.H.C. Lima, R.Valiev, M.A. Meyers, Biomedical Applications of Titanium and its alloys, Biological Materials Science, (2008), JOM, pp. 47-49.
5. M. Niinomi, Biologically and Mechanically Biocompatible Titanium Alloys, Materials Transactions, Vol. 49, No 10 (2008) pp.2170-2178.



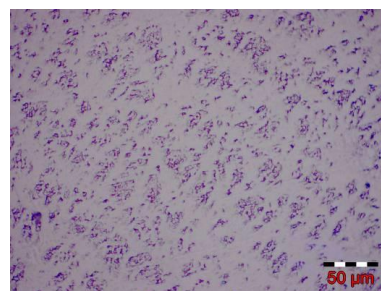
Optical microstructure of commercial Ti8Al4V alloy, 500x



Optical microstructure of experimental Ti8Al alloy, 200x



Optical microstructure of experimental Ti3Mn alloy, 500x



Optical microstructure of experimental Ti5Fe alloy, 500x

Manuele Gori, Sara Maria Giannitelli, Pamela Mozetic, Marcella Trombetta, Alberto Rainer

Department of Engineering, Tissue Engineering Lab, Università Campus Bio-Medico di Roma, via Alvaro del Portillo 21, 00128 Rome, Italy  
[m.gori@unicampus.it](mailto:m.gori@unicampus.it)

## INTRODUCTION

One of the major obstacles to the diffusion of additive manufacturing (AM) in tissue engineering has long been represented by the limited set of available biomaterials that could be directly processed. In this regard, processing of hydrogels represents a main challenge in view of soft tissue engineering applications. Furthermore, direct manufacturing of tissue precursors with a cell density similar to native tissue has the potential to overcome the extensive *in vitro* culture required for conventional cell-seeded scaffolds. Aim of this study was the investigation of hepatic metabolism in a novel composite 3D scaffold, which better approximates the *in vivo* liver conditions compared to a conventional cell culture system. HepG2 cells, a human hepatoblastoma cell line that retains many characteristics of normal differentiated hepatocytes<sup>1</sup>, have been used as a model cell system.

## EXPERIMENTAL METHODS

Pluronic/Alginate scaffolds were fabricated by pressure-assisted deposition using a custom designed AM equipment<sup>2</sup>. A Pluronic/Alginate solution (20 wt% PF127, 2 wt% sodium alginate in diluted DMEM) was loaded into a gel dispensing syringe at 4 °C. The syringe was then heated to 37 °C, leading to gelation, and gel was extruded through a 250 µm nozzle at a pressure of 1.2 bar. Squared scaffolds were obtained by depositing layers of fibers laminated in a 0°/90° pattern. Scaffolds were briefly exposed to a sterile 25 mM CaCl<sub>2</sub> aq. solution to induce alginate crosslinking. Mechanical properties were assessed by unconfined compression tests. Scaffold degradation was measured in terms of weight loss following incubation in PBS. Similarly, cell-laden constructs were prepared by suspending HepG2 cells at a concentration of 2x10<sup>6</sup> cells/mL into ice-cold polymer solution. Afterwards, the gel was extruded at 37 °C using the previously described equipment.

Cell morphology and distribution within the scaffold were assessed by immunofluorescence staining. After 24h, cell viability was determined by Trypan Blue and Vybrant cytotoxicity assay. Proliferation of HepG2 cells on the AM-scaffold, in comparison with a 2D culture plate, was investigated by MTT (3-[4,5-dimethylthiazol-2-yl]-2,5-diphenyl tetrazolium bromide) assay at selected time points (i.e., 1, 4, 7 days). To study the liver-specific functions of the HepG2 cells embedded into the scaffold, secreted albumin and urea levels were determined through specific ELISA assays.

## RESULTS AND DISCUSSION

3D structures with controlled architectures were successfully manufactured starting from a Pluronic/Alginate system, in which Pluronic F127 conferred thermo-sensitive properties, while alginate endowed the formation of a strong gel upon exposure to bivalent cations in aqueous solution. This positive combination led to constructs with precisely defined microarchitectures and enhanced stability.

Embedded HepG2 cells survived the deposition process, homogeneously spread inside the gel phase, and showed albumin and urea production during the culture period.

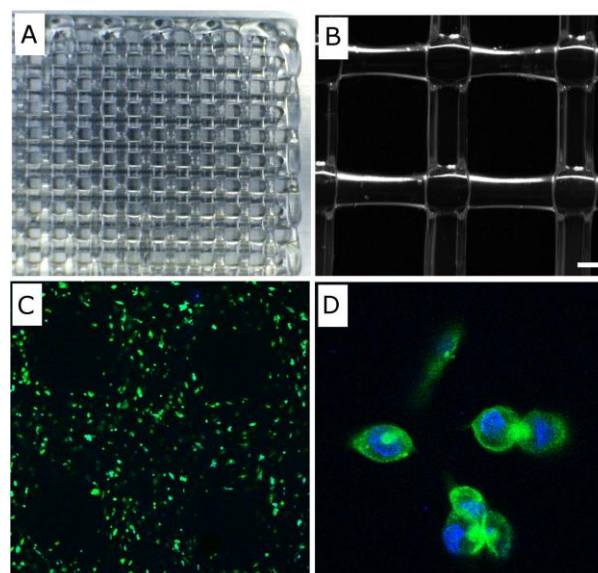


Figure 1: A) Macroscopic image of a four-layered hydrogel scaffold: top view. B) Optical micrograph of scaffold microarchitecture, scale bar: 250 µm. C) Confocal fluorescence microscopy showing distribution of HepG2 cells within the scaffold (magnification 10x). D) Enlarged view of the HepG2 cell morphology (magnification 40x), green (phalloidin) and blue (DAPI) stainings.

## CONCLUSION

Our cell-laden scaffold provides optimal conditions for hepatic cell proliferation as well as a suitable microenvironment for liver-specific metabolic functions. In light of the obtained results, the proposed 3D culture system may represent a novel human hepatic model for drug screening and toxicological studies.

## REFERENCES

1. Javitt N.B., FASEB J. 4:161-168, 1990
2. Smith G. *et al.*, J. Biomech. 2:5-11, 2011



**As-cast Biodegradable MgCa alloys –Structure, Mechanical and Corrosion Properties**

Sonia Boczekal<sup>1</sup>, Michał Karaś, Anna Kozik<sup>1</sup>, Dawid Kapinos<sup>1</sup>, Marzena Lech–Grega<sup>1</sup>

<sup>1</sup>Institute of Non-Ferrous Metals, Light Metals Division, Skawina, Poland  
[sboczekal@imn.skawina.pl](mailto:sboczekal@imn.skawina.pl)

Magnesium plays the fundamental role in the biological system as a component of bone tissue. The yield module and the compressive strength of magnesium with calcium is the closest to the properties of natural bone as compared to other commonly used implants. These alloys are biodegradable in aqueous solutions containing in particular chloride ions. The properties of magnesium alloys predispose them to the study of biocompatibility and biodegradability .

The structure of magnesium alloys containing 1%wt., 2.5%wt. and 5%wt. Ca was examined in as-cast condition. After the casting process, the presence of Mg<sub>2</sub>Ca as eutectic phase at grain boundaries was observed under the scanning electron microscope (SEM) and examined by the X-ray Diffraction (XRD). The quantitative share of the eutectic increased with the

increase of the additive Ca in alloys. Mechanical properties were determined in the compression test at temperatures in the range of 37° C to 420°C. It was found the highest properties were achieved for an alloy containing 5% wt. Ca. The analysis of strength-hardening coefficient in the compressed tests showed that with increasing temperature followed by a rapid decrease in the strengthening value. The strength-hardening coefficient stabilized for the tested alloys at 380°C. This material was subjected to the corrosion test in Ringer solution in order to determine the dissolution kinetics of the alloys at 37°C. The progress of corrosion in MgCa alloys was investigated in the structure observations.

Jakub Kamiński, Maciej Śniechowski, Sebastian Wroński, Janusz Malinowski, Jacek Tarasiuk

Faculty of Physics and Applied Computer Science, AGH University of Science and Technology, Cracow, Poland  
[kaminski@fis.agh.edu.pl](mailto:kaminski@fis.agh.edu.pl)

## INTRODUCTION

X-ray microtomography ( $\mu$ CT) is commonly known as a gold standard for evaluation of bone morphology and microarchitecture in both animal and human models *ex vivo*<sup>1</sup>. It is also being used to study the porous artificial bone replacement structures. Both measured and generated structures can be manufactured in meso- and macro-scale using Additive Manufacturing (AM)<sup>2</sup>. It is an automated technique for direct conversion of 3D data into physical objects using a variety of approaches. Materials for bone-like structures should have properties similar to the bone tissue, while manufactured structures must have certain mechanical properties - both geometry and material is important herein. In the presented study assumptions stated above were the basis for the methodology of AM and  $\mu$ CT for 3D porous structures. Also preliminary validation of the properties using mechanical tests in Finite Element Method (FEM)<sup>3</sup> before and micro-loading with FEM verification after manufacturing was also performed.

## EXPERIMENTAL METHODS

To produce biocompatible porous structures of bones and artificially generated bone-like models in meso- and macro-scale several AM methods were chosen. For each standardized input data in the form of STL files with 3D geometry of the structure were used. Fused Filament Fabrication (FFF) is AM method that uses a plastic filament unwound from a coil to lay down material in layers and produce a part in analogous way to Fused Deposition modeling (FDM). Digital Light Processing (DLP) is AM method that uses a similar process to Stereolithography (SLA) with selective polymerization of model layers in liquid resins with the usage of light source. Selective Laser Sintering (SLS) is AM method that uses a laser as the power source to sinter powdered material to create a solid structure. Selective laser melting (SLM) uses a comparable concept, but in SLM the material is fully melted rather than sintered. 3D structure of porcine cancellous bone from  $\mu$ CT with 10  $\mu$ m voxel was manufactured in ten times enlarged macro-scale resulting in size of 5 cm using FDM (PLA filament), SLS (polyamide powder) and DLP (proprietary resin) methods. Artificially generated 3D heterogeneous porous structures were manufactured in meso-scale resulting in cubic size of 5 mm using SLM (titanium alloy powder) and DLP (proprietary resin). High-resolution  $\mu$ CT measurements of the structures were performed after manufacturing.

## RESULTS AND DISCUSSION

The use of  $\mu$ CT measurements allowed for the acquisition of the 3D structure and inspection of the surface roughness. It also provided the opportunity to use direct three-dimensional methods for the calculation of the morphometrical parameters such as porosity, diameters for the rods and pores, and the degree of anisotropy. Meso-scale artificially generated structures were measured in  $\mu$ CT with voxel size of 3.5  $\mu$ m and also tested in miniature loading machine in linear range. FEM mechanical tests before and after manufacturing were also performed, allowing for the comparative analyses and positive verification of the whole process. The methodology can be illustrated based on the comparison of the input and prepared for AM methods geometries with the reconstructions from  $\mu$ CT scans. These results imply that DLP is currently the most suitable AM method in presented methodology, allowing for the exact reproduction of the geometry and properties of structure both for meso- and macro-scale. Further research may lead to strengthen the mechanical properties, which are actually too small in compare to bone tissue. Designing of the biomaterials paying special attention to fabrication of the geometry of porous structures shall be currently prioritized.

## CONCLUSION

The Advanced techniques for the preparation of porous structures based on AM are becoming increasingly important with the development of new experimental methods. Application of such strategy in conjunction with  $\mu$ CT and FEM opens up new opportunities in designing and study the mechanical properties of more complex materials with well-defined geometrical and precisely measured morphometrical parameters of structures that are impossible to achieve using existing methods and models.

## REFERENCES

1. Stuart R. Stock, MicroComputed Tomography, 2008
2. Gibson I. et al., Additive Manufacturing Tech., 2009
3. Zienkiewicz O.C. et al., The Finite El. Method, 2013

## ACKNOWLEDGMENTS

This work was partially supported by Polish Ministry of Science and Higher Education. One of the authors (J.K.) acknowledge his benefit from Ph.D. scholarships founded by Marian Smoluchowski Cracow Scientific Consortium – KNOW.



Lindsey Dew<sup>1</sup>, Giulia Gigliobianco<sup>1</sup>, Chuh K Chong<sup>1</sup>, Sheila MacNeil<sup>1</sup><sup>1</sup>Kroto Research Institute, Department of Materials Science and Engineering, University of Sheffield, UK  
[L.dew@sheffield.ac.uk](mailto:L.dew@sheffield.ac.uk)

## INTRODUCTION

One of the main challenges currently faced by tissue engineers is the loss of tissues post implantation due to delayed neovascularization upon implantation<sup>1</sup>. Several strategies are under investigation to create vascularized tissue but none have yet overcome this problem. As blood vessel formation is a complex process that is controlled by a large number of interrelated factors it is not surprising that this remains a challenge. To induce vascularization within TE substitutes these same processes will need to occur and therefore an understanding of the basic principles and factors affecting angiogenesis is needed. Many angiogenesis models fail to combine the ability to combine supporting cells, the extracellular matrix and perfusion<sup>2</sup>. In this study we use a detergent treatment to create a natural vascular scaffold from rat intestine that can be used as a platform for angiogenesis studies.

## EXPERIMENTAL METHODS

To produce the natural vascular nets intestine was harvested from fresh rat cadavers. The main vessel of the mesentery was cannulated and flushed with heparin solution before treatment with 1% Triton-X 100 and 0.1% ammonium hydroxide. Distilled water was then circulated to remove residual detergent and the resultant matrix was sterilized using 0.1% peracetic acid. Residual peracetic acid was removed with sterile PBS. Blue dye was injected into the matrix to assess vascular patency. The presence of DNA, GAG, elastin and collagen before and after decellularization were identified through histochemical staining and then quantified. The inherent angiogenic properties of the matrix was analysed using the chick chorioallantoic membrane (CAM) assay cultured for 8 days, with a collagen gel negative control. To recellularize, a co-culture of dermal fibroblasts and human dermal microvascular endothelial cells (HDMECs) were injected through the mesenteric artery of the decellularized intestine and subsequently perfused continuously with cell culture medium for 5 days at 37°C. Samples were taken at days 1 and 5 for histological analysis and fluorescence microscopy.

## RESULTS AND DISCUSSION

A well-defined vascular tree with multiple branching was visible from blue dye injection. Quantitative analyses showed a 97% reduction of DNA upon decellularization. ECM components such as collagen and GAGs were found to be retained whilst almost all elastin was removed by the process. The CAM assay showed good integration of the matrix with the host whilst indicating increased angiogenic properties of the decellularized matrix when compared to the collagen gel control. Upon recellularization, histochemical

analysis showed that the cells attached to the matrix and occupied the blood vessels. Confocal microscopy showed a re-organisation of the HDMECs after 5 days in culture with the cells lining the vessel architecture and showing evidence of sprouting (Fig 1).

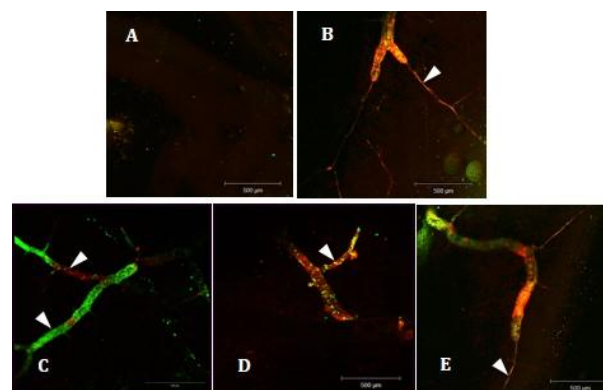


Figure 1 - Representative confocal microscopy images of sections of recellularized jejunum infused with HDMECs (red) and HDFs (green) under static culture with no sign of either cell type occupying the vascular architecture (A) and culture under constant perfusion of media with evidence of cellular adhesion within the vascular structures and vascular sprouting (arrow) (B) after 5 days. After 1 day under perfusion conditions HDMECs and HDFs show the distinct occupation of areas within the native vascular architecture (arrows) (C) reorganizing after 5 days with HDMECs lining the vessels (arrow) (D) and showing evidence of vascular sprouting (arrow) (E).

## CONCLUSION

Histological and quantitative analyses show the almost complete removal of cellular material and the preservation of the native architecture and connective tissue components, whilst recellularization via perfusion through the vascular network shows good cellular adhesion and redistribution and further demonstrates that the inclusion of a stromal cell and of flow lead to new blood vessel formation-not evident in their absence.

## REFERENCES

1. Griffith CK *et al.*, Tissue Engineering, 257-66, 2005
2. Staton CA *et al.*, International Journal of Experimental Pathology. 195-221, 2009

## ACKNOWLEDGMENTS

We thank the EPSRC DTC Tissue Engineering Regenerative Medicine programs for funding this research.



## Development of a Bioengineered Vascular Niche for the Treatment of Type 1 Diabetes Mellitus

Valeria Perugini, Mark Best, Anna Guildford, Gary Phillips, Wendy Macfarlane, Adrian Bone, Matteo Santin

Brighton Centre for Regenerative Medicine, University of Brighton, Brighton, UK

[M.Best2@brighton.ac.uk](mailto:M.Best2@brighton.ac.uk)

### INTRODUCTION

The success of islet transplantation as a treatment for type 1 diabetes mellitus is restricted by various problems such as angiogenesis. Rapid reestablishment of a functional vasculature in transplanted islets is crucial for their survival and function. Functionally, blood vessel endothelium provides a niche essential for the maintenance of  $\beta$ -cell fate. By using vascular endothelial growth factor (VEGF),  $\beta$ -cells attract endothelial cells, which form capillaries with a vascular basement membrane next to them<sup>1</sup>. The proposed mechanism has recently been recapitulated by the development of several synthetic matrices. These matrices have been used to improve current islet culture techniques for islet isolation as well as the design of an artificial immunoprotective islet carrier for transplantation<sup>2</sup>. For example, islets cultured on collagen type I-coated surfaces and those treated with soluble fibronectin exhibited a greater  $\beta$ -cell survival and insulin secretion *in vitro*<sup>3</sup>. However, the control of the cross-talk between  $\beta$ -cells and endothelium vessels is still a significant challenge. The present work aims to investigate the effects of ECM-based substrates on the pancreatic  $\beta$ -cell line Min6 when in co-culture with umbilical vein endothelial cells, HUVECs.

### EXPERIMENTAL METHODS

MIN6  $\beta$ -cells (ATCC, UK) were seeded in a 24 well plate previously coated with 100  $\mu$ l of Matrigel (BD biosciences, UK), in DMEM (Gibco, UK) containing 10%  $\nu$ /<sub>v</sub> FBS (Sigma, UK) in a humidified atmosphere at 37°C and 5% CO<sub>2</sub>. After 24 hour incubation, Min6  $\beta$ -cells were co-cultured with HUVECs (ATCC, UK) at a density of  $3 \times 10^4$  per well with F12-K medium (LGC Ltd., UK) supplemented with 0.1 mg/ml sodium heparin (Fisher Scientific, UK), 0.05 mg/ml ECGS (Sigma, UK) and 10%  $\nu$ /<sub>v</sub> FBS and left for 24 hour under standard culture conditions. MIN6  $\beta$ -cells and HUVECs were also seeded on polystyrene tissue culture plate (TCP) used as a control.

Cells were assessed for their viability and adhesion by Hoescht Propidium Iodide staining (HPI; Sigma, UK). Cytoskeletal actin formation was investigated by staining cells with AlexaFluor 488®-Phalloidin (Invitrogen, UK), after washing with PBS and fixing with 3.7% formaldehyde (Fisher Scientific, UK) for 10 minutes at room temperature. Cellular nuclei were stained with 4',6-diamidino-2-phenylindole (DAPI; Vectashield, UK) and cells were then analysed with a laser scanning confocal microscopy (Leica TCS SP5, UK). Data were expressed as mean cell number/field (standard deviation) from n=6.

### RESULTS AND DISCUSSION

HPI staining revealed that MIN6  $\beta$ -cells were able to attach onto both TCP and Matrigel substrates and to be viable after 24 hour incubation. However, cell adhesion was more pronounced onto Matrigel surfaces ( $72.6 \pm 8.06$  cells/field) compared to the TCP,  $45.7 \pm 7.4$  cells/field suggesting a strong effect of both laminin and collagen IV, the major protein components of Matrigel, on promoting  $\beta$ -cell survival and function. The importance of these ECM proteins was also found to influence cell morphology and indeed cell-cell interaction (Figure 1). On TCP, HUVECs showed a relatively irregular shape with the formation of pointed protrusions indicative of the formation of F-actin extensions likely to facilitate cellular interaction with the MIN6  $\beta$ -cells. On the Matrigel substrate, alongside the expected endothelial sprouting, tight interactions between the two cell populations were observed with pseudo-islets forming in close proximity of the endothelial tubular structures.

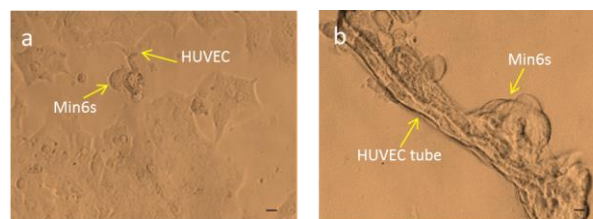


**Figure 1.** Phase contrast images showing a) cell monolayer on TCP; b) Co-culture on Matrigel. Scale bar=50  $\mu$ m.

### CONCLUSION

ECM-based substrates facilitate the *in vitro* organisation of  $\beta$ -cell pseudo-islets and endothelial sprouting into tissue lattices. Such bioengineered tissue units could have a potential in both the treatment and research of Type 1 diabetes through tissue engineering applications and clinically reflective tests.

### REFERENCES

1. Li W. *et al.*, Sci Rep. 4:3, 2863, 2013.
2. Cheung CY. *et al.*, Bioconjug Chem. 17(4):1036-42, 2006.
3. Weber LM. *et al.*, Tissue Eng Part A. 14(12): 1959–1968, 2008.

### ACKNOWLEDGMENTS

This work was supported by the FP7 EC grant NEXT, contract n CP-FP602235-2.





## Capture Antibodies to Biofunctionalize Vascular Prosthesis

Sven S. Liebler<sup>1</sup>, Fritz Grunert<sup>2</sup>, John Thompson<sup>2</sup>, Burkhard Schlosshauer<sup>1</sup>

<sup>1</sup>NMI Natural and Medical Sciences Institute, Reutlingen, Germany

<sup>2</sup>Aldevron Inc., Freiburg, Germany

[schlosshauer@nmi.de](mailto:schlosshauer@nmi.de)

### INTRODUCTION

A major drawback of vascular implants is the thromogenicity of polymer-based prosthesis surfaces. We aim to biofunctionalize the prosthesis biomaterial by capturing blood-born endothelial progenitor cells (EPCs) in situ. Towards this goal monoclonal antibodies were generated against the EPC specific receptor VEGFR-2.

### MATERIALS AND METHODS

Trapping antibodies were generated by genetic immunization and screened by cell-based flow cytometry (FACS). Antigen phosphorylation was monitored by Western blot analysis. Tube formation was microscopically analyzed with human umbilical vein endothelial cells (HUVECs) on matrigel. Cytotoxicity was qualified by fluorescence microcopy. Cell proliferation was determined by metabolic labelling with bromo-deoxy-uridine (BrdU). Uptake of acetylated low-density lipoprotein (ac-LDL-DiI) into HUVECs was investigated by FACS and fluorescence microscopy. Trapping experiments were performed with protein G and the different trapping antibodies. HUVECs were employed under static conditions and in a flow chamber to qualify antibody trapping characteristics.

### RESULTS

Out of 10,200 hybridoma clones eight antibodies specific for all seven VEGFR-2 extracellular domains were selected and affinity purified. All antibodies left cell viability (calcein staining), proliferation (BrdU labelling) and the angiogenic potential of HUVECs unaffected. No side effects were evident with regard to cell differentiation (tube formation capability) and cell functioning (LDL uptake). Antibodies did not significantly modify receptor phosphorylation. The antibodies did neither interfere with growth factor binding nor did they directly activate receptors in a ligand-independent manner indicating that they do not imitate growth factors. Coating of antibodies to microscopic flow chamber surfaces was used to demonstrate the trapping capacity for cells.

We produced antibodies against all seven extracellular domains of the vascular endothelial growth factor receptor 2, which left biological functions of the endothelium essentially unaffected. Different antibodies are specific for pig or human, others crossreact with both species, which aims at combinatorial implantation experiments and finally human applications. One selected rat antibody has already been humanized. Current experiments focus on biofunctionalization of biomaterials and polymer vessels.

Supported by BMBF 13N11679

### DISCUSSION



## Utilization of Biocompatible and Biodegradable Polymers in Stem Cell Research and Biomedical Applications

Małgorzata Sekuła<sup>1,2</sup>, Patrycja Domalik-Pyzik<sup>3</sup>, Anna Morawska-Chochół<sup>3</sup>, Jakub Czuchnowski<sup>1</sup>, Zbigniew Madeja<sup>1</sup>, Ewa Zuba-Surma<sup>1\*</sup>, Jan Chłopek<sup>3\*</sup>

<sup>1</sup> Department of Cell Biology, Faculty of Biochemistry, Biophysics and Biotechnology, Jagiellonian University, Krakow, Poland

<sup>2</sup> Malopolska Centre of Biotechnology, Jagiellonian University, Krakow, Poland

<sup>3</sup> Department of Biomaterials, Faculty of Materials Science and Ceramics, AGH University of Science and Technology, Krakow, Poland  
[pdomalik@agh.edu.pl](mailto:pdomalik@agh.edu.pl)

### INTRODUCTION

Poly( $\alpha$ -hydroxy esters) are one of the most commonly tested materials for tissue engineering applications thanks to their well-characterized biodegradability and Food and Drug Administration (FDA) approval. This polymer family includes e.g. poly(glycolic acid) (PGA), poly(lactic acid) (PLA), their copolymer (PLGA) and polycaprolactone (PCL)<sup>1</sup>. All of those polymers can be easily processed and copolymerized or blended in order to widen spectrum of their application within the field of tissue engineering.

Developing a biocompatible and nontoxic substrate for cells proliferation and differentiation is one of the contemporary challenges of tissue engineering. Mesenchymal stem cells (MSC) are promising cell type which could be utilized in biomedical applications. MSC are multipotent stem cells, which can give rise to different cell lineages. They are characterized e.g. high differentiation potential and low immunogenicity.

The aim of the study was to analyze the potential of polymer surfaces (polycaprolactone and polylactide) for biology and angiogenic differentiation of MSC derived from human umbilical cord Wharton's jelly (hUC-MSC).

### EXPERIMENTAL METHODS

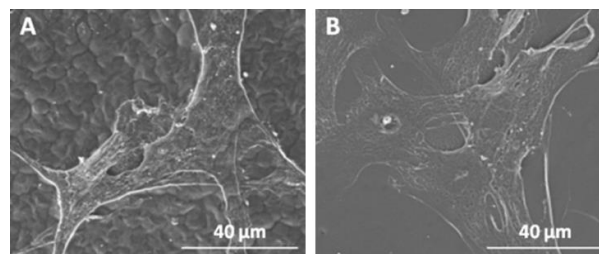
In current study we examined an influence of bioresorbable polymer-based substrate on hUC-MSC phenotype and functions.

5% polymer solutions were prepared by dissolution of PCL (Sigma-Aldrich,  $M_n = 80\ 000$ ) and PLA (Ingeo<sup>TM</sup> 3051D) in glacial acetic acid and dioxane, respectively. Thin layer of the polymer solutions were poured into 24-well plate and left for 96h to evaporate the solvents. The PCL and PLA films were rinsed with alcohol and sterilized under UV radiation, prior to cell culture.

Cells were cultured in standard conditions, in DMEM/F12 medium supplemented with 10% FBS, at 37°C with 5% CO<sub>2</sub>. The analysis of morphology and migratory activity of cells cultured on polymer films were performed by microscopy techniques (conventional light microscopy, fluorescence microscopy and scanning electron microscopy (SEM)). Proliferation rate was assessed for every 24 hrs. To evaluate cells viability and apoptosis flow cytometry analysis was performed. Cell migration and motility was quantitatively examined via on-live movie recording during cell culture. Furthermore, the influence of polymers on hUC-MSC angiogenic differentiation potential was evaluated on gene expression level by real-time PCR.

### RESULTS AND DISCUSSION

The results demonstrated that both analyzed polymers (PCL and PLA) constitute non-toxic culture substrate for hUC-MSC and do not affect cell viability. However, data revealed that proliferation rate was partially reduced. Microscopic analysis of hUC-MSC indicated their slight morphology changes depending on the different type of culture substrate. Figure 1 shows SEM images of hUC-MSC spreading on PCL (A) and PLA (B) substrates. Also, different microstructure of the polymers is visible.



Interestingly, analysis of cells trajectories revealed, that polymers stimulate migratory activity and speed of cells movement. Moreover, we observed, that hUC-MSC, which are cultured on polymers-based substrate are able to spontaneous differentiation into angiogenic cells. We observed expression of genes related to angiogenic differentiation after 8 days of cell culture. This data suggests, that evaluated polymers constitute promising surfaces in stem cell research and regenerative medicine.

### CONCLUSION

Our preliminary data suggested that biodegradable polymers may enhance regenerative properties of selected stem cell populations. However, further studies are necessary to analyze the impact of utilization of stem cells and 3D-composites structures in biomedical applications.

### REFERENCES

1. Buddy D. Ratner (ed.) et al. *Biomaterials Science: An Introduction to Materials in Medicine*. Academic Press. 2012.

### ACKNOWLEDGMENTS

This study was supported by N N302 1773 38 grant from Ministry of Polish Science and Higher Education (MNiSW) to EZS, in part by POIG.01.01.02-00-109/09 project and by the statutory research No 11.11.160.616 of Faculty of Materials Science and Ceramics, AGH University of Science and Technology, Krakow, Poland.



Andrew L. Hook<sup>1</sup>,<sup>1</sup>Laboratory of Biophysics and Surface Analysis, University of Nottingham, UK  
[andrew.hook@nottingham.ac.uk](mailto:andrew.hook@nottingham.ac.uk)

## INTRODUCTION

Modern medicine has been built upon the power of antibiotics to deal with infections. However, antibiotics can no longer be relied upon at a time when the World Health Organisation classifies antibiotic resistance as one of the three greatest threats to human health. Strategies to minimise the risk of infection are of greater importance than ever, yet healthcare associated infections (HAI) have become one of the most serious issues in our health systems today. Annually within Europe 1 million infections are associated with the presence of invasive medical devices. It is clear that better materials must make a contribution to tackling this major problem. In this study high throughput materials discovery using polymer microarrays<sup>1</sup> has been applied to discover new materials resistant to *Staphylococcus epidermidis*. High throughput screening methodologies are relevant when the underlying biological-material interactions are poorly understood. Of particular interest is the production of a coating on metallic substrates such as those employed in fracture victims utilising external fixation devices where a nosocomial infection rate of 20% in the general population increases to 100% for diabetics.<sup>2,3</sup>

## EXPERIMENTAL METHODS

Polymer microarrays were formed using a XYZ3200 pin printing workstation (Biodot) onto poly(hydroxyethyl methacrylate) coated slides. Printing was carried out using slotted metal pins. Polymerisation solution was composed of 75% (v/v) monomer, 24% (v/v) DMF and 1% (w/v) photoinitiator 2,2-dimethoxy-2-phenylacetophenone. After printing polymers were UV cured and vacuum extracted.<sup>4</sup> A bacterial attachment assay was developed using *S. epidermidis* RP62A. After attachment of bacteria to each material bacterial coverage was measured by staining the bacteria with the DNA binding dye DAPI and imaging by confocal microscopy. Protein adsorption to each material was also assessed by incubating the polymer microarray with tetramethyl-rhodamine isothiocyanate labelled albumin and imaging using a fluorescence scanner.

## RESULTS AND DISCUSSION

In order to identify a novel material resistant to bacterial attachment that can function in high protein environments an array of 36 polyacrylates was incubated with protein. Albumin adsorption was quantified by measuring the fluorescence from a rhodamine fluorescence tag (Figure 1A).

Polymer microarrays were also incubated with *S. epidermidis* and the bacterial coverage was measured on each spot (Figure 1B). This enabled the identification of materials that were resistant to both bacterial attachment and protein adsorption (Figure 2).

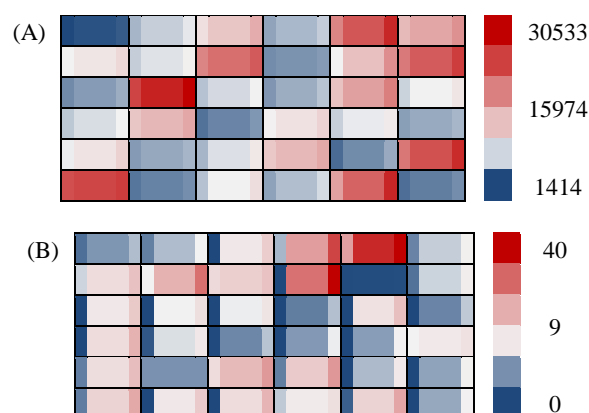


Figure 1 – Quantification of (A) fluorescence of rhodamine labelled albumin or (B) *S. epidermidis* coverage on polymer spots. Within each square the middle region is the average of 6 replicate measurements, whilst the small left and right regions represent  $\pm$  standard deviation unit.

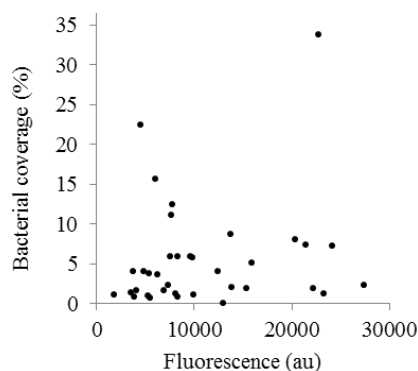


Figure 2 – Fluorescence intensity due to protein adsorption against the bacterial coverage measured for each polymer spot.

## CONCLUSION

A polymer microarray was used to successfully screen for materials that were resistant to both *S. epidermidis* attachment and protein adsorption. The hit materials will be suitable for application to *in vivo* use, particularly for external fixation devices used for fracture victims.

## REFERENCES

1. Hook, A. L. *et al. Biomaterials*, 31:187-198, 2010.
2. Arciola, C. R. *et al. Int. J. Artif. Organs*, 28:1091-1100, 2005.
3. Peleg, A. Y. *et al. Diabetes-Metab. Res.*, 23:3-13, 2007.
4. Hook, A. L. *et al. J. Visual. Exp.*, 59:e3636, 2012.

## ACKNOWLEDGMENTS

The author would like to thank the EMRP (Grant no: IND56) for providing financial support to this project.



Tzer-Min Lee<sup>1,2</sup>, Yu-Pu Chu<sup>2</sup>, Yen-Ting Liu<sup>2</sup><sup>1</sup>School of Dentistry, Kaohsiung Medical University, Taiwan<sup>2</sup>Institute of Oral Medicine, National Cheng Kung University, Taiwan[tmlee@mail.ncku.edu.tw](mailto:tmlee@mail.ncku.edu.tw)

## INTRODUCTION

Titanium and titanium alloys are frequently used in orthopaedic implants because of their good biocompatibility and reliable mechanical properties. After implantation the formation of a bacterial surface biofilm and compromised immunity at the implant/tissue interface may lead to persistent infections on and around titanium implants. Despite this and the contaminated oral surgical field through which they are placed, success rates are reported as being as high as 90-95%. Bacterial infection, extensive inflammation and poor osseointegration have been identified as the major reasons for early orthopaedic implant failures based on titanium (Ti). Some literatures point out that creating implants with drug-eluting properties to locally deliver drugs is an appealing way to address some problems like systemic toxicity of the drugs, reaching deliver drugs locally and continuously.<sup>1</sup>

## EXPERIMENTAL METHODS

In this study, we focuses on the development of a polymer-coated ceramic composite for antimicrobial drug delivery. A micro-arc oxidation (MAO) was used to produce a porous structure comprising calcium acetate hydrate ( $\text{Ca}(\text{CH}_3\text{COO})_2 \cdot \text{H}_2\text{O}$ ) and sodium phosphate monobasic monohydrate ( $\text{NaH}_2\text{PO}_4 \cdot \text{H}_2\text{O}$ ) for improving the biocompatibility of titanium. Using a spray coating method, aqueous drug was loaded into the porous surface. Finally, gamma polyglutamic acid ( $\gamma$ -PGA), a well-known natural hydrophilic biodegradable polymer,<sup>2</sup> Dependent on two types of  $\gamma$ -PGA mixing ratio, water soluble Na<sup>+</sup> type and water insoluble H<sup>+</sup> type, was coated layer-by-layer through spin coating as a barrier to control drug release.<sup>3</sup> The bactericidal effect of antibiotic on the porous surface was evaluated by using *Escherichia coli* (*E. coli*) bacteria(ATCC®PTA-10989™). Additionally, the results obtained from UV-Vis suggested that the drug was successfully filled into coatings and released over time with antibiotic/ $\gamma$ -PGA solution could provide a high bactericidal effect against *E.coli* by the bactericidal effect of antibiotic.

## RESULTS AND DISCUSSION

The morphology of the prepared MAO/Ti substrates was characterized by SEM and is summarized in Fig. 1. These pores are well separated and distributed homogeneously over the surface. The anti-inflammatory, antibiotic was chosen as a test drug to be loaded inside the MAO porous. The deposition of  $\gamma$ -PGA Na<sup>+</sup> type and H<sup>+</sup> type polymers onto drug loaded MAO/Ti by a spin-coating process was evaluated by ESCA characterization. Fig2. Significant changes in the drug release profile were observed as a result of coating

a polymer film on the top of the MAO surface. As expected, the drug release characteristics showed a strong dependence on the mixing ratio of polymer layer. Significantly fewer bacterial colony forming units (CFUs) appeared in samples containing antibiotic modified MAO/Ti prepared with deposition times than were detected in the cp Ti control sample (Figure 3).

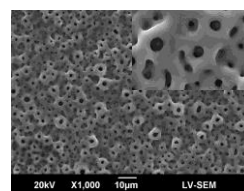


Figure 1. Series of SEM images of MAO fabricated by micro arc oxidation of Ti in Ca/P electrolyte

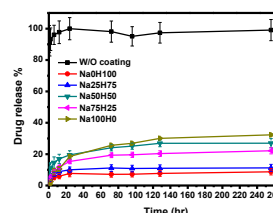


Figure 2. Comparative drug release graphs of anti-inflammatory drug (antibiotic) from polymer coated MAO/Ti.

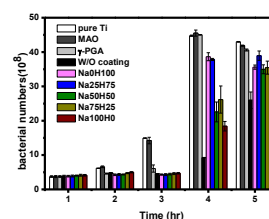


Figure 3. Evaluation of the antimicrobial effects by the antimicrobial susceptibility test against confluent lawns of *Escherichia coli* bacteria. Pure Ti was used as a control compared to duplicate  $\gamma$ -PGA disks treated with antibiotic.

## CONCLUSION

Together, these findings demonstrate that using porous structure with  $\gamma$ -PGA is promising as cost-effective drug delivery formulation for delivering drugs locally and continuously. Further antimicrobial activity demonstrate that the antimicrobial activity of antibiotic toward the growth inhibition of a model bacterium of *E. coli* is not compromised after being loaded into the porous structure. With the reserved drug activity, the porous structure based drug delivery system may find various applications in tissue engineering and pharmaceutical science.

## REFERENCES

1. J.H. Lee, *et al.*, *Acta Odontol Scand.* 71:168–174, 2013
2. A.D. Pye, *et al.*, *J. hosp. infect.* 72: 104-110, 2009
3. Karan Gulati, *et al.*, *Acta Biomater.* 8: 449-456, 2012

## ACKNOWLEDGEMENT

This work was financially supported by the National Science Council, Taiwan (NSC 100-2221-E-006-263)



## INTRODUCTION

Silver-containing hydroxyapatite ceramic is of great medical interest, primarily in terms of its antimicrobial properties. Silver is the bactericidal agent and can be introduced into the ceramic as a dispersed metal phase or as ions replacing calcium ions in the apatite lattice and forming silver-substituted hydroxyapatite. Such ceramics will exhibit different antibacterial properties depending on the localization of silver. In the study, phase composition, microstructure, the effect of silver additives on sintering and physical properties of Ag-containing ceramics were examined.

## EXPERIMENTAL METHODS

An initial powder of hydroxyapatite HA was prepared through the reaction of calcium carbonate,  $\text{CaCO}_3$ , and a solution of the orthophosphoric acid,  $\text{H}_3\text{PO}_4$ . Silver dopants were introduced into the HA powder by soaking the powder in a solution of argentic nitrate,  $\text{AgNO}_3$ , at  $60^\circ\text{C}$  until the solvent was completely evaporated. The concentration of solution was varied so that the amount of silver in the soaked powders was from 0.25–1.5 wt% with a step of 0.25 wt%. Powder compacts as pellets (3 mm height and 8 mm diameter)

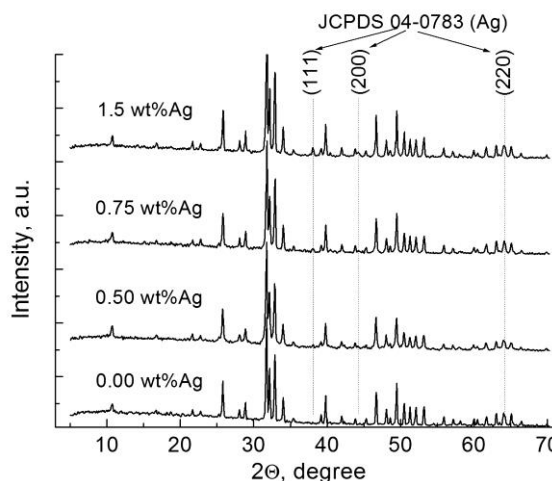


Figure 1. XRD patterns of silver-containing composite ceramics

were prepared in a mold by uniaxial pressing under 120 MPa. The compacts were fired in a muffle in a wet atmosphere at  $1200^\circ\text{C}$  for 2h. The phase composition and microstructure of ceramics were studied by XRD, SEM and IR spectrometry. The density, compressive strength and microhardness of the samples were measured depending on silver concentration by conventional methods.

## RESULTS AND DISCUSSION

XRD analysis (Figure 1) detected that the ceramics are biphasic. One phase is HA, and the other – silver, which results from the decomposition of  $\text{AgNO}_3$ . Silver maxima are reliably identified since an Ag concentration of 0.25 wt%. The lattice constants of HA matrix are faintly dependent on the silver concentration. IR spectra over the entire range of silver additives are consistent with the spectrum of HA. Spectra show the absorptions of  $\text{PO}_4^{3-}$  ions at 566, 602, 962, 1042,  $1090\text{ cm}^{-1}$ . Bands at  $3570$  and  $630\text{ cm}^{-1}$  indicate the presence of  $\text{OH}^-$  groups in the lattice.

SEM examination showed that the ceramics were consisted of HA grains and inclusions of silver nanoparticles on (in) grain boundaries (Figure 2). The density of ceramics slightly increased, the microhardness slightly decreased but the compressive strength slightly increased with increasing silver concentration. Throughout the silver concentrations, the ceramics tended to brittle fracture.

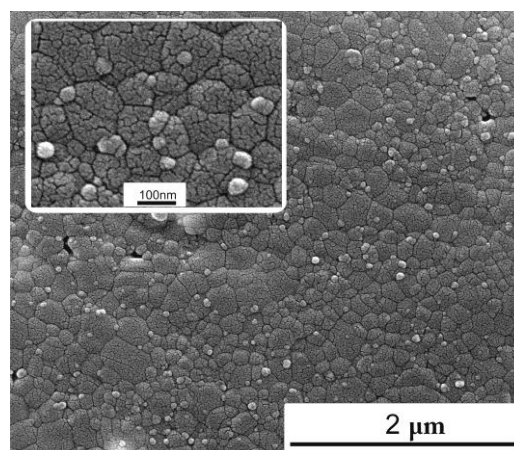


Figure 2. SEM picture of ceramics with 1.5 wt% silver. The inset is an enlarged fragment of the surface

## CONCLUSION

Ceramics based on HA and silver dopants are two-phase composites. One of the phases is (possibly, Ag-substituted) HA, and the other – silver nano-particles. Examined concentrations of the silver additives have no adverse effect on the physical and mechanical properties of the composites.

## ACKNOWLEDGMENTS

The authors would thank the German Academic Exchange Service (DAAD) providing financial support to this project.

# Antimicrobial and Toxicological Studies of Novel Chlorhexidine-Hexametaphosphate Nanoparticles for Coating Central Venous Catheters

Helena J Grady<sup>1,2</sup>, Sarah E Maddocks<sup>3</sup>, Margaret Saunders<sup>4</sup>, Andrew M Collins<sup>1</sup>, Michele E Barbour<sup>2</sup>.

<sup>1</sup>\*Bristol Centre for Functional Nanomaterials, University of Bristol (UoB), UK, <sup>2</sup>Oral Nanoscience, UoB, UK, <sup>3</sup>Cardiff School of Health Sciences, Cardiff Metropolitan University, UK,

<sup>4</sup>BIRCH, Dept of Medical Physics & Bioengineering, UH Bristol NHS FT, UK

[helena.grady@bristol.ac.uk](mailto:helena.grady@bristol.ac.uk)

## INTRODUCTION

With the increasing prevalence of antibiotic-resistant bacteria, there has been a considerable drive to design and fabricate new antimicrobial surfaces to overcome implant-related infections.<sup>1</sup> Here we propose novel chlorhexidine-hexametaphosphate nanoparticles (CHX-NPs)<sup>2,3</sup> as a novel method for coating polyurethane (PU) central venous catheters to reduce bacterial adhesion and biofilm formation.

CHX-NPs act as a slow-release device for the broad-spectrum antimicrobial agent CHX. CHX reacts with negatively charged groups on a bacterial cell wall which causes cytoplasmic membrane disruption and intracellular leakage. This study investigates the antimicrobial efficacy of CHX-NPs against methicillin-resistant *Staphylococcus aureus* (MRSA), *Pseudomonas aeruginosa*, *Escherichia coli* and *Klebsiella pneumoniae*, in addition to preliminary *in vitro* nanoparticle toxicity studies with placental BeWo b30 cells<sup>4</sup> selected as a model to evaluate potential for fetal exposure and damage in women of child-bearing age who may be exposed to CHX-NPs.

## EXPERIMENTAL METHODS

**Nanoparticle synthesis:** 5 mM CHX-NP suspensions were prepared by mixing a 1:1 ratio of aqueous CHX: aqueous hexametaphosphate<sup>2</sup>.

**PU Sample functionalisation:** PU specimens (12 x 15 mm) were immersed in rapidly stirred CHX-NP for 30 s then in deionised water for 10 s before drying in air.

**Total Viable Counts (TVCs):** CHX-NP-functionalised PU specimens, in addition to untreated controls, were inoculated with  $1.5 \times 10^8$  CFU/mL pre-culture of bacteria and incubated at 37 °C for 20 h to allow growth of biofilms. Subsequent TVCs were performed as described by Miles *et al.*,<sup>5</sup> and repeated in triplicate. Results were analysed by 1-way ANOVA with Tukey *post-hoc* test.

**BeWo b30 cell culture:** BeWo b30 cells were cultured in complete medium supplemented with 10% fetal bovine serum<sup>4</sup>, seeded at  $1.75 \times 10^5$  cells/mL and grown until approximately 70 % confluent.

**Cytotoxicity assays:** Cells were treated for 2 and 24 h with 1/100 and 1/1000 dilutions of 5 mM CHX-NPs suspensions, in addition to the same dilutions of 5 mM CHX and 25  $\mu$ M CHX (residual concentration of aqueous CHX in CHX-NPs) controls. Lactate dehydrogenase (LDH) release was measured in culture medium to determine cytotoxicity. Cellular metabolism after NP exposure was assessed using the WST-1 assay. Bicinchoninic acid (BCA) was determined after exposure, to deduce the total cellular protein present. Assays were repeated in triplicate. Results were analysed by 2-way ANOVA with Tukey *post-hoc* test.

## RESULTS AND DISCUSSION

CHX-NP functionalised specimens prevented biofilm

formation of MRSA and *P. aeruginosa*. Growth was observed with *E. coli* and *K. pneumoniae* specimens, however this was significantly less than the untreated controls.

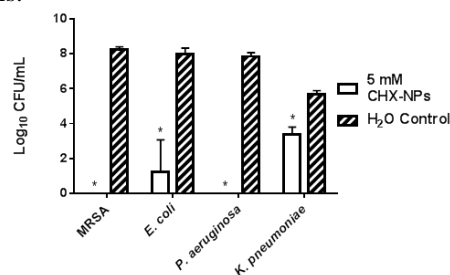


Figure 1. TVCs. \* $p < 0.05$  vs. respective control.

No significant LDH release was observed for 1/1000 CHX-NPs, and cell viability and protein concentration were unaffected. An increase in CHX-NP dose significantly reduced viability over 24 h. Toxicity of CHX-NPs was lower than that of aqueous CHX.

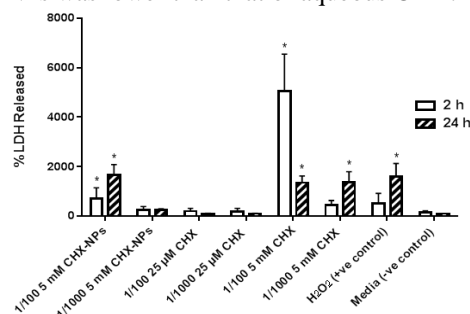


Figure 2. LDH release from BeWo b30 cells exposed to CHX-NPs. \* $p < 0.05$  vs. respective negative control.

## CONCLUSION

CHX-NP functionalised PU fully inhibited MRSA and *P. aeruginosa* under biofilm conditions and significantly reduced growth of *E. coli* and *K. pneumoniae*. CHX-NP toxicity is both concentration and time dependent. At lower CHX-NP levels, cells appear undamaged even after longer exposure times. The nanoparticles, at both dilutions, are significantly less toxic than the equivalent concentrations of aqueous CHX. Further studies are necessary in order to determine the CHX-NP concentration required to dope the PU surfaces, in order to optimise antimicrobial efficacy with the minimum cytotoxicity.

## REFERENCES

1. Hasan, J. *et al.*, Trends Biotechnol. 31: 295-304, 2013.
2. Barbour, M. *et al.*, Int. J. Nanomedicine. 8: 3507-3519, 2013.
3. Wood, N. J. *et al.*, Int. J. Nanomedicine. 9: 4145-4152, 2014.
4. Correia Carreira, S. *et al.*, Nanotoxicology. 1-14, 2013.
5. Miles, A. A. *et al.*, J. Hygiene. 38: 732-49, 1938.

## ACKNOWLEDGMENTS

The authors would like to thank the BCFN and EPSRC for funding this project.



Orode Aniejurengo<sup>1</sup>, Mariagemiliana Dessi<sup>1</sup>, Steve Meikle<sup>1</sup>, Matteo Santin<sup>1</sup>

<sup>1</sup>Brighton Centre for Regenerative Medicine, School of Pharmacy and Biomolecular Sciences, University of Brighton,  
UK

[o.u.aniejurengo@brighton.ac.uk](mailto:o.u.aniejurengo@brighton.ac.uk)

## INTRODUCTION

The increase in the number of multi-drug resistant microorganisms is a critical global problem<sup>1</sup>. Hence, it has become relevant to develop novel antibiotic drugs. Small peptides such as dendrimers are proposed as alternatives to antibiotics, with reports of antimicrobial activity. However, most studies have focused on the efficacy of high generation dendrimers but the smaller units: dendrons have received lesser attention.

This study aimed to clarify if dendrons of similar generations could be used as novel antibacterial agents, also minimising the high immunogenicity associated with dendrimers<sup>2</sup>. The antimicrobial potential of the dendron against *Proteus mirabilis* a significant pathogen and biofilm former in wound infections was performed *in vitro*. The mode of action of these poly-ε-lysine dendrons is currently unknown, hence the interaction between the cationic dendrons and bacterial cell membranes was also investigated.

## EXPERIMENTAL METHODS

### Synthesis/Characterisation of Dendron

An Fmoc-based solid phase peptide synthesis approach was applied to synthesise generation-3 poly (ε-lysine) dendrons (G<sub>3</sub>K)<sup>3</sup>. The dendrons were characterised by Fourier transform infra-red spectroscopy (FTIR), mass spectrometry and analytical high performance liquid chromatography.

### Antimicrobial assay

A microtitre plate assay was used to assess the antimicrobial potential of G<sub>3</sub>K. Different doses of the dendron were administered (0.25 – 2 mg/ml) to clinically significant concentrations of bacteria (10<sup>7</sup> CFU/ml). The effect on biofilm and bacterial cytotoxicity were assessed *via* crystal violet staining and turbidity measurements, at different time points. Anti-biofilm effects were confirmed by light microscopy study. Three replicates per test over 2 different days were performed, and results were analysed with analysis of variance statistical tests.

### Interaction between G<sub>3</sub>K and bacterial cells

Fluorescein-isothiocyanate (FITC) (0.025mmol), was conjugated by solid-phase synthesis to the peripheral amino groups of G<sub>3</sub>K (0.05mmol), and incubated in the dark for 18h. The conjugate (G<sub>3</sub>K-FITC) was characterised by FTIR, UV-Vis and trinitrobenzene sulfonate assay to quantify attached FITC. For cellular interaction studies, G<sub>3</sub>K-FITC and *P. mirabilis* bacterial cells were incubated over 24h. Cells were visualised by confocal microscopy.

## RESULTS AND DISCUSSION

G<sub>3</sub>K showed significant bactericidal effect during the first incubation hours (8 and 16 hours), and reduced the

quantity of adherent bacteria and biofilm extracellular matrix (Fig. 1) by 87% after 48h treatment, whereas the quantity of bacteria in suspension was only reduced by a maximum of 23% up to 16 hours. G<sub>3</sub>K biofilm prevention was time/dose dependent, with dispersal of the biofilm's extracellular matrix at higher doses, which may be due to electrostatic interactions between the negatively charged bacterial cell wall and cationic G<sub>3</sub>K which was also able to target the bacterial cell wall (Fig. 2).

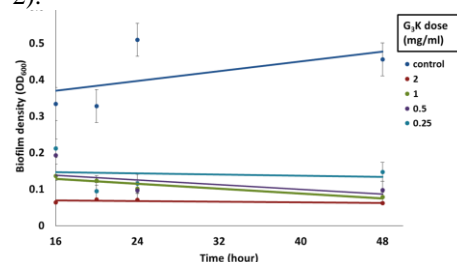


**Figure 1:** Time-Dose Effect of G<sub>3</sub>K on *P. mirabilis* biofilm. The green linear trend-line ( $R^2=0.86$ ) of 1mg/ml G<sub>3</sub>K, showed that G<sub>3</sub>K has time-dose effect on biofilm formation up to 48h

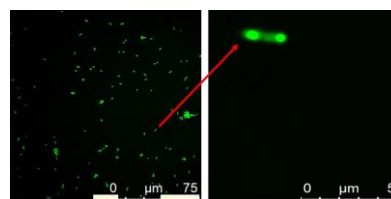


**Figure 2:** Localisation of G<sub>3</sub>K in *P. mirabilis* bacterial cells.

## CONCLUSION

Generation-3 poly (ε-lysine) dendrons were bactericidal at concentrations as low as 0.25 mg/ml and prevented *P. mirabilis* biofilm formation, with preferential localisation at bacterial cell poles, which may impact bacterial cell division/adherence. The cationic/multivalent nature of the dendron could be harnessed for improvement of the anti-biofilm effect. The dendron therefore has potential as an anti-biofilm agent in biofilm related infections such as wounds and nosocomial infections.

## REFERENCES

1. WHO, Global report on surveillance, 2014.
2. Tomalia DJ, dendrimers, dendrons and Dendritic Polymers, 2012
3. Meikle, ST *et al.*, Macromol Biosci. 11:1761–1765, 2011

**ACKNOWLEDGMENTS** This work is supported by a Brighton University PhD studentship

Dominika Siek, Joanna Czechowska, Aneta Zima, Anna Ślósarczyk

Faculty of Materials Science and Ceramics, AGH University of Science and Technology, 30 Mickiewicza Av., 30-059 Krakow, Poland  
[siek@agh.edu.pl](mailto:siek@agh.edu.pl)

## INTRODUCTION

Calcium phosphates (CaPs) are used in many medical applications especially in regeneration and reconstruction of bone tissue. The most common calcium phosphate is hydroxyapatite (HA). The modification of HA structure with Ag ions may influence its physicochemical and biological properties. Incorporation of silver leads to development of the implant materials with antibacterial properties<sup>1</sup>. Calcium sulphate (CS) is well known for its fast resorption after implantation. The combination of hydroxyapatite with CS may provide materials with high surgical handiness and controlled resorption rate in a living organism<sup>2</sup>. The purpose of the study was to evaluate the influence of silver additive (amount and source of Ag ions) on the physicochemical properties of the new cement type bone substitutes.

## EXPERIMENTAL METHODS

Hydroxyapatite doped with silver (1 and 2 wt.%) was synthesized by the wet chemical method. Silver acetate or nitrate served as sources of Ag ions. In order to assess thermal stability of Ag-HA the synthesized powders were heat treated above 1000°C. Non-calcined Ag-HA powders were mixed with calcium sulphate hemihydrate (CSH, Acros Organics). Material based on undoped hydroxyapatite and CSH served as reference. As the liquid phase distilled water was applied. The phase composition (XRD) of modified hydroxyapatite powders as well as final composites after setting and hardening were determined. The setting times (Gillmore Needles), compressive strength (Instron 3345) and open porosity (Auto Pore IV) were checked. The chemical stability of obtained materials were assessed *in vitro*.

## RESULTS AND DISCUSSION

Non-calcined Ag-HA powders showed only hydroxyapatite as a crystalline phase. Heat treatment above 1000°C resulted in the appearance of small amount of  $\beta$ -tricalcium phosphate. Calcined powders demonstrated also a characteristic XRD peak at 38.18° corresponding to the metallic silver (Fig. 1). Developed cements after setting and hardening composed of two phases: hydroxyapatite and calcium sulphate dihydrate (CSD). They set from 6 to 12 minutes. Compressive strength of studied materials was from 5 to 7 MPa. Incorporation of Ag via silver nitrate during the

synthesis of hydroxyapatite slightly decreased compressive strength of the final bodies.

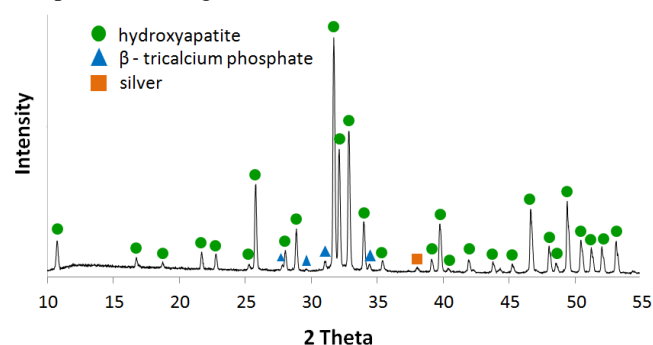


Fig. 1 XRD pattern of heat treated Ag-HA (2 wt.% Ag, source of Ag ions: silver nitrate).

Obtained cements exhibited comparable open porosity (~ 50 vol.%) and pores below 1.5µm with a bimodal pore size distribution. The results of chemical stability of developed materials confirmed gradual release of silver ions during incubation in simulated body fluid. Due to the content of calcium sulphate dihydrate and silver modified hydroxyapatite, they will probably reveal complex (two steps) resorption *in vivo*.

## CONCLUSION

New resorbable cement-type materials based on Ag-HA and CSH were developed and assessed. The results of conducted studies indicated that the obtained cements may not only effectively fill bone defects but also will ensure the local antibacterial treatment. Influence of 1 and 2 wt.% silver additive on the physicochemical properties of the new biomaterials was confirmed. Further studies *in vitro* and *in vivo* are necessary.

## REFERENCES

1. Peng J. *et al.*, J. Dent. 40:531-541, 2012
2. Mamidwar S. *et al.*, Implant. Dent. 17:208-216, 2008

## ACKNOWLEDGMENTS

The work of the first author has been supported by the Polish National Science Centre funds allocated with the decision DEC-2013/09/N/ST8/04171.



## *In vitro* Studies of Antibacterial Activity of Sol-gel Bioglasses Containing Mg, Sr and Au

Lidia Ciolek<sup>1</sup>, Andrzej Olszyna<sup>1</sup>, Ewa Zaczynska<sup>2</sup>, Anna Czarny<sup>2</sup>

<sup>1</sup> Institute of Ceramics and Building Materials, Department of Ceramic Technology, Warsaw, Poland  
Polish Academy of Sciences, Institute of Immunology and Experimental Therapy, 12 Rudolf Weigl Street,  
53-114 Wrocław, Poland

[l.ciolek@icimb.pl](mailto:l.ciolek@icimb.pl)

### INTRODUCTION

The aim of the study was to determine *in vitro* antimicrobial activity of bioglasses doped with Mg, Sr and Au.

The presence of magnesium in the composition of the biomaterial enhances its bioactivity<sup>1</sup>. Strontium improves the proliferation of bone cells<sup>1</sup>. Gold belongs to the group of “ultra elements” which show antibacterial activity and activate metabolism by acting on enzymes<sup>2</sup>. The silane used for the synthesis of sol-gel bioglasses may also increase bioactivity<sup>3</sup>.

Physical and chemical properties of bioglasses containing Mg, Sr and Au produced by sol-gel method as well as its grain morphology and bioactivity in simulated body fluid and the results of *in vitro* cytotoxicity were presented in previous publication<sup>4</sup>.

This paper presents the results of *in vitro* antibacterial activity of these bioglasses.

### EXPERIMENTAL METHODS

Four bioglasses doped with Mg, Sr and Au and undoped bioglass as a reference material were used for the research. Bioglass P5-VS containing 70 wt.% of SiO<sub>2</sub> and 25 wt.% of CaO and 5 wt.% of P<sub>2</sub>O<sub>5</sub> being a reference material was produced using tetraethoxysilane, vinyltriethoxysilane (VS), calcium nitrate tetrahydrate and triethyl phosphate as basic substrates. Bioglasses P5-VS-1\_Mg and P5-VS-1\_Sr with the same composition as P5-VS were obtained by substituting 1 wt.% of CaO by MgO or SrO respectively. In the case of bioglasses P5-VS-Au\_r-r and P5-VS-Au\_nzk nanoparticles of Au in the form of 0,00065 wt.% colloidal solution and 0,002 wt.% nonionic colloidal gold respectively were added.

The process of preparing bioglasses by sol-gel method was carried out according to procedures described in earlier reports<sup>4</sup>.

Studies of antibacterial activity were performed by a dilution method, using precultures of test bacterial strains of *Pseudomonas aeruginosa* and *Staphylococcus aureus* which were deposited on substrates at concentrations of 1,0 mg/ml, 5,0 mg/ml, 10 mg/ml, 20 mg/ml and 50 mg/ml. The 24-wells plates with the bacterial strains were incubated at the temperature (37±1)°C. Antibacterial activity of bioglasses was identified by counting live bacteria population after 24, 48 and 148 h of incubation. The controls consisted of broth cultures of microorganisms without bioglasses.

### RESULTS AND DISCUSSION

Results of *in vitro* antibacterial activity tests carried out with different concentration of bioglasses indicate that all of them lead to reduction of the number of bacteria. The best results were obtained using the highest concentration of bioglass samples. Figure 1 shows the result of antibacterial activity of bioglasses at concentration of 20 mg/ml on selected strains.

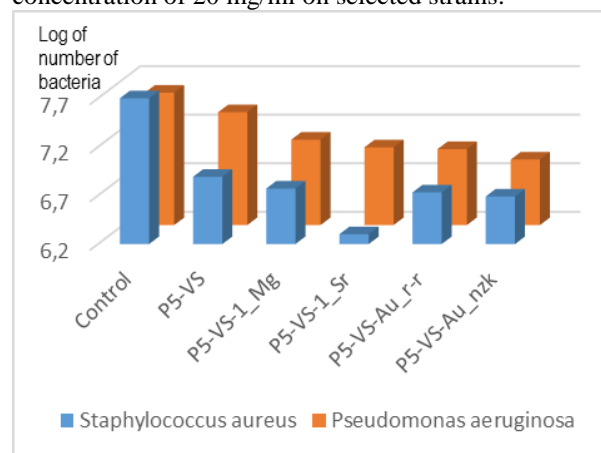


Fig. 1: Survival of strains determined after 148 h at a concentration of 20 mg/ml of bioglasses P5-VS, P5-VS-1\_Mg, P5-VS-1\_Sr, P5-VS-Au\_r-r and P5-VS-Au\_nzk.

### CONCLUSION

*In vitro* studies of antibacterial activity of bioglasses in selected strains of bacteria showed higher activity against strain of *Staphylococcus aureus* than *Pseudomonas aeruginosa*.

Bioglass P5-VS-1\_Sr is the one that inhibits growth of micro-organisms during the tested period most effectively.

### REFERENCES

1. Gorustovich A. A. et al., J. Biomedical Material Research 232:237-92A, 2010,
2. Simon S. et al., J. Materials Science: Material in Medicine 1193:1201-23, 2012.
3. Kim Y., et al., J. Sol-Gel Science and Technology 43:49-45, 2008.
4. Ciolek L. et al., Prace Instytutu Ceramiki i Materiałów Budowlanych 17:28-16, 2014

### ACKNOWLEDGMENTS

The authors would like to thank the Institute of Ceramics and Building Materials in Warsaw for providing financial support to this project.



# Bone Allograft with Antibacterial Coating for Therapeutic Application

István Hornyák<sup>1,2</sup>, Edit Madácsi<sup>1</sup>, Pálma Kalugyer<sup>1</sup>, Zsombor Lacza<sup>1,2</sup>

<sup>1</sup> Tissue Engineering Laboratory, Semmelweis University, Budapest, Hungary.

<sup>2</sup> Lacerta Technologies GmbH, Krems an der Donau, Austria  
[istvan.hornyak@lacertatech.com](mailto:istvan.hornyak@lacertatech.com)

## INTRODUCTION

Use of local antibiotics in connection with bone substitutes has 3 indications: prevention of primary infection, implantation into a contaminated area or the prevention of recurrent infection. These cases all have their requirements in terms of choice of antibiotics and length of release time, so there is no universal coating technique for all cases. We aimed to develop a sustained-release coating for bone allografts, which can achieve long-term characteristics for several antibiotics.

## MATERIALS AND METHODS

Human bone allografts (50±5 mg each) were coated with water-soluble antibiotics amoxicillin, ciprofloxacin or vancomycin. The simple coating methods were soaking (method **A**) or freeze drying (method **B**) using concentrations from 0,1 mg/ml up to 10 mg/ml. The controlled release film coating was prepared in single or double layers. When using one layer, the antibiotics were mixed with 2% chitosan and the coating was freeze dried (method **C**). The preparation of the two layer controlled release coating involved a freeze drying step with the antibiotic followed by a water insoluble film preparation step by using 4% Na-alginate, which was converted with 10% CaCl<sub>2</sub> solution to Ca-alginate (method **D**). Preparations were incubated in 2 ml H<sub>2</sub>O and antibiotic release was measured in the supernatant by spectrophotometry in the specific concentration interval of each antibiotic where the absorbance – concentration ratio was linear. For the antibiotic that we found best, the MIC (minimal inhibitory concentration) was also assessed.

## RESULTS

The antibiotic coating experiments showed that the best concentration was 10 mg/ml using all the antibacterial agents and with method **B**, we were able to enhance the coating compared to the conventional soaking method with every antibiotic. All the antibiotic content was released within 48 hours, so method **A**, **B** and **C** were only suitable for short-term antibiotic release. With method **D** we were able to prepare a coating that released amoxicillin over a 7 day period; ciprofloxacin was released over a 28 day period and vancomycin release exceeded 50 days well over the MIC concentration (0,2 µg/ml).

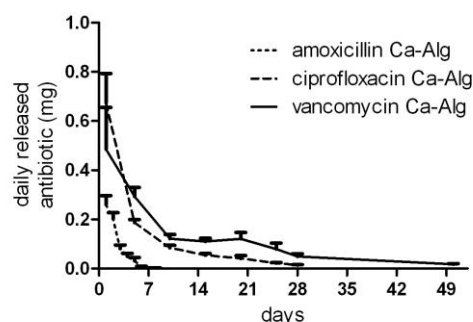


Fig. 1. Antibiotic release into 2 ml volumes.

## DISCUSSION AND CONCLUSIONS

Simply adding antibiotics or freeze-drying them onto the allograft only reaches a 2-day release profile, which is even shorter than the closure time of the surgical wound. Insoluble alginate coating achieved a sustained release of each selected antibiotic to various lengths, depending on the physico-chemical characteristics of the drugs. Amoxicillin may be applicable for primary prevention while ciprofloxacin or vancomycin is suitable for more challenging cases.

## ACKNOWLEDGMENTS

Sponsored by a research grant to Semmelweis University from Lacerta Technologies GmbH

## DISCLOSURES

Dr. Lacza is founder and CEO and Dr. Hornyák is an employee of Lacerta Technologies GmbH, which holds a pending patent of the technology.



## Antimicrobial Efficiency and Bacterial Damage on Copper Surfaces

Claudia Hahn<sup>1</sup>, Michael Hans<sup>2</sup>, Frank Mücklich<sup>2</sup>, Ralf Moeller<sup>1</sup>, Reinhard Wirth<sup>3</sup>, Günther Reitz<sup>1</sup>, Petra Rettberg<sup>1</sup>

<sup>1</sup> Institute of Aerospace Medicine, German Aerospace Center (DLR), Cologne, Germany

<sup>2</sup> Department of Material Science & Engineering, Saarland University, Saarbrücken, Germany

<sup>3</sup> Institute for Microbiology and Archaea Center, University of Regensburg, Regensburg

[claudia.hahn@dlr.de](mailto:claudia.hahn@dlr.de)

### INTRODUCTION

Maintaining human health is a matter of major concern at any time. Under particular conditions, for example in hospitals or during long-term missions in closed habitats such as the ISS (International Space Station), emergence of aggressive multi virulent species is high<sup>1,2</sup>. To address the issue of microbial contamination, several different methods are already in place. However, conventional decontamination methods are too cumbersome for astronauts' to perform on regular basis. The use of antimicrobial surfaces is a promising tool to reduce microbial contaminations in space and even on the Earth. Copper as an antimicrobial metal is also an essential metal and has been used for medical issues and the storage of drinking water for thousands of years<sup>3</sup>. While the toxicity of copper is well known, the exact mechanism is still unclear. In this study the antimicrobial effects of copper ions were tested.

### EXPERIMENTAL METHODS

Type strains of two human-associated microorganisms *Escherichia coli* (DSM 498) and *Staphylococcus cohnii* (DSM 20260) were cultured in LB (Luria-Bertani, *E. coli*) and in TSY medium (Trypticase Soy Broth with Yeast extract, *S. cohnii*) at optimal growth conditions.

Stainless steel (AISI 304: X5CrNi18-10) and copper samples from 99.99% pure rolled copper sheet were cut into 2.25 cm<sup>2</sup> coupons, grounded, polished and sterilized by ethanol.

Wet contact killing experiments have been conducted. Therefore cells in 0.1 PBS (0.7% Na<sub>2</sub>HPO<sub>4</sub> x 2 H<sub>2</sub>O, 0.3% KH<sub>2</sub>PO<sub>4</sub>, 0.4% NaCl, pH 7.5) were exposed on the surfaces for 0, 2 and 4 hours.

For the detection of membrane integrity the Live/Dead staining assay was applied to stainless steel and copper exposed cells. The different fluorescence colours were visualized by the Zeiss AxioImager M2 microscope.

Ex vivo and in vivo DNA and RNA damages were visualized with agarose gel electrophoresis.

The release rate of copper ions was detected by using the ICP-MS 7500 Series, Agilent Technologies. Four hundred µl PBS and cell suspension was exposed for 4 hours. Thereafter, the copper concentration of the whole suspension, in the cells and the supernatant was measured.

### RESULTS AND DISCUSSION

When exposed to metallic copper surfaces high cell inactivation rates have been determined in a concentration depending manner.

A loss in membrane integrity was detectable with the Live/Dead staining. When 10<sup>6</sup> cells/ml were applied for 4 hours on copper surfaces 50% of *S. cohnii* and 75% of *E. coli* cells exhibited a degradation of the cell membrane.

Measurements of the release rate showed that cells indirectly dissolve copper from surfaces and import it.

Despite a relatively high copper concentration inside the cells, the *ex* and *in vivo* studies of the DNA and RNA analysis pointed out that the degradation is much higher under *ex vivo* conditions.

Reasons for the differences in cell survival and membrane integrity can be caused by differences in the cell wall, the uptake and export of copper ions or detoxification effects.

### CONCLUSION

Copper ions are indirectly dissolved from copper surfaces and can be actively taken up by cells. Since in vivo DNA and RNA seem to be protected by cellular components, the damage of the cell membrane appears to be the main target of copper ion toxicity.

For further analysis mechanistic studies on the im- and export are useful targets.

### REFERENCES

1. Ilyin VK (2000) Survey of the microbial contamination knowledge onboard manned Russian space vehicles, ESTEC contract 14254/00/F/TB (Moscow)
2. Pierson DL (2001) Microbial contamination of spacecraft, Gravitational and space biology 14:1-6
3. Dollwet HHA and Sorenson JRJ (1985) Historic uses of copper compounds in medicine Trace Elem Med 2:80-87

### ACKNOWLEDGMENT

This work has been funded by the SpaceLife Graduate School of the Helmholtz association and the German Aerospace Center in Cologne, Germany. The ICP-MS measurements have been kindly provided by Christina Hein and Prof. Dr. Ralf Kautenburger from the Saarland University.



## Antibacterial Sol-Gel Coating of Ceramic TiO<sub>2</sub> Scaffolds for Bone Regeneration

David Wiedmer<sup>1</sup>, Cédric Bossard<sup>1,2</sup>, Hanna Tiainen<sup>1</sup>, Håvard Haugen<sup>1</sup>

Department of Biomaterials, University of Oslo, Norway  
 ENSIACET, National Polytechnic Institute of Toulouse, France  
[d.j.wiedmer@odont.uio.no](mailto:d.j.wiedmer@odont.uio.no)

### INTRODUCTION

Highly porous TiO<sub>2</sub> scaffolds may be used to augment and promote bone regeneration for large bone defects caused by periodontitis or peri-implantitis<sup>1</sup>. However, accumulation of pathogenic bacteria and biofilm deposition can endanger the success of bone regeneration and result in loss of the affected tooth or implant. A crystalline sol-gel coating may add bactericidal properties to the substitute material based on the photocatalytic generation of antimicrobial radicals on the catalyst surface.

### EXPERIMENTAL METHODS

Highly porous TiO<sub>2</sub> scaffolds are produced as previously described elsewhere<sup>1</sup>. The sol-gel coating process steps are illustrated in Figure 1.

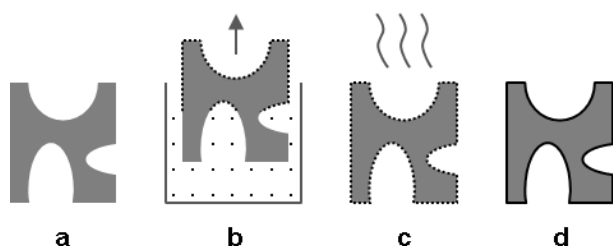


Fig.1: (a) TiO<sub>2</sub> scaffolds were fabricated by polymer sponge method and dipped (b) into a TTIP-HCl-H<sub>2</sub>O-iPrOH system. After a two-step heating treatment (c) a crystalline, thin coating (d) remains on the substrate.

The scaffolds were withdrawn from the solution at a low vertical speed ( $v_{\text{pull}} = 6 \text{ cm} \cdot \text{min}^{-1}$ ). A two-step heating treatment was applied to evaporate the solvent ( $T_{\text{evap}} = 120^\circ\text{C}$ ) and to crystallise the nanoparticle coating ( $T_c = 450^\circ\text{C}$ ). A holding time of 1 h at  $T_c$  was chosen to ensure complete crystallisation. The homogeneity of the coatings was examined by scanning electron microscopy (SEM). UV-vis spectroscopy was used to measure the degradation of the organic dye methylene blue (MB) under UV-irradiation due to the photocatalytic capacity of coated and uncoated TiO<sub>2</sub> scaffolds.

### RESULTS AND DISCUSSION

TiO<sub>2</sub> scaffolds were covered by a thin, homogenous film after sol-gel coating and heat treatment. Only minor flakes or ruptures of the coating were detected for  $v_{\text{pull}} = 6 \text{ cm} \cdot \text{min}^{-1}$ . Higher withdrawal speeds resulted in the agglomeration of microparticles on the 3D structure, incomplete coating of the struts and partly blocked pore windows. Figure 2 shows a randomly picked section of a coated scaffold for  $v_{\text{pull}} = 6 \text{ cm} \cdot \text{min}^{-1}$ .

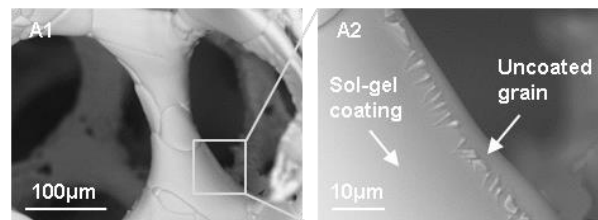


Fig.2: Highly porous and interconnective scaffold (A1) and detailed view (A2) of the applied sol-gel coating.

The dip-coated, amorphous TiO<sub>2</sub> film is crystallised to anatase during the heat treatment at  $T_c = 450^\circ\text{C}$  overlaying the rutile substrate and thereby changing the crystal structure of the scaffold surface. The crystal phase of the substrate is determined by high sintering temperatures ( $\sim 1500^\circ\text{C}$ ) during the fabrication process to obtain appropriate mechanical strength. However, anatase is known to show superior photocatalytic activity compared to rutile when irradiated with UV-light<sup>2</sup>. One explanation for this may be the increased generation of radical oxygen species (ROS), e.g. OH<sup>•</sup> and O<sub>2</sub><sup>•-</sup>, on the catalyst surface. Sol-gel coated scaffolds were found to degrade MB stronger compared to uncoated substrates which also indicates an enhanced generation of ROS. It is the idea to take advantage of this effect and develop a nanoparticle coating with improved bactericidal properties for TiO<sub>2</sub> scaffolds to encounter bacteria-induced inflammation in bone regeneration.

### CONCLUSION

A homogenous, thin sol-gel coating was successfully applied to ceramic TiO<sub>2</sub> scaffolds. A nanoparticle surface with different crystal structure was induced to the substrate while retaining its favourable morphology for osteogenesis. An *in vitro* bacteria study is planned to evaluate the potential antibacterial effect of the coating due to increased generation of oxidising radicals on the TiO<sub>2</sub> surface.

### REFERENCES

1. Tiainen H. *et al.*, J. Mater. Sci. Mater. Med. 21:2783-2792, 2010
2. Su C. *et al.*, Catal. Today 96:119-126, 2004

### ACKNOWLEDGMENTS

This study was supported by EUREKA Eurostars E!8320 NuGel.



## Metallic Copper as an Antimicrobial Agent for Infection Prevention

Michael Hans<sup>1</sup>, Claudia Hahn<sup>2</sup>, Marc Solioz<sup>3</sup>, Ralf Moeller<sup>2</sup>, Frank Mücklich<sup>1</sup>

<sup>1</sup> Functional Materials, Materials Science and Engineering, Saarland University, Saarbrücken, Germany

<sup>2</sup> Institute of Aerospace Medicine, German Aerospace Center (DLR), Cologne, Germany

<sup>3</sup> Department of Plant Physiology and Biotechnology, Tomsk State University, Tomsk, Russian Federation

[michael.hans@mx.uni-saarland.de](mailto:michael.hans@mx.uni-saarland.de)

### INTRODUCTION

Copper-based, antimicrobial materials are extensively discussed as an alternative strategy to antibiotics in order to combat dangerous germs in the healthcare environment. Applications range from bulk copper alloys used as self-decontaminating door knobs to highly functionalized, metallic surfaces employing copper as an additional, antimicrobial agent (e.g. for implants).

It seems to be clear that copper ions act via multiple toxicity mechanisms, which renders them also effective against otherwise multi-resistant microbes and the so called “superbugs” (e.g. methicillin resistant *Staphylococcus aureus*, MRSA).<sup>[1]</sup> Although worldwide field studies already account for the potential to reduce infection risks in hospitals, the actual killing mechanism as well as the linked material and surface properties of copper-based antimicrobial materials are not yet fully understood.

The presentation will give an overview of the ongoing interdisciplinary research project “Antimicrobial copper - Functional surfaces and toxicity mechanisms” (German Research Foundation, MU 959/26-1&2) and include the latest findings of the project.

### EXPERIMENTAL METHODS

An important aspect of the presented project is the generation of model surfaces with tailored properties. As a unique tool for this purpose, Laser Interference Surface Patterning (LISP) by a nanosecond pulsed laser was used to create periodical microstructural, topographical and chemical patterns on the micro- and sub-micrometer scale.<sup>[2]</sup> These patterns were tailored larger, smaller and of the same size as bacteria in order to study possible size effects (see Figure.1).

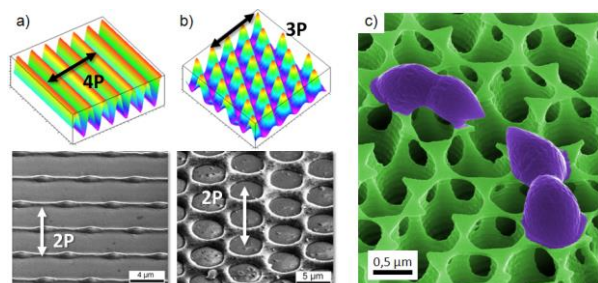


Figure 1: a) and b) intensity distribution (top) of LISP and structured metal surfaces (bottom). c) *E. hirae* bacteria on LISP-surface with periodicity of the same scale.

The nature of the LISP-generated pattern was thoroughly characterized by SEM- and White Light Interferometric (WLI-) techniques and evaluated for their antimicrobial impact and specific interactions with bacteria. Further on, general questions like the impact of surface oxidation on copper or the influence of alloying elements on the antimicrobial behavior were studied.

### RESULTS AND DISCUSSION

Three mayor findings of the project are: By creating inert LISP-arrays on copper surfaces, it was shown that the direct contact between bacteria and metallic copper is a beneficial factor for the killing behavior.<sup>[3]</sup> LISP-generated topographical surface patterns can be used to influence the adhesion of bacteria on metall surfaces. Copper surface oxidation induces different antimicrobial effects depending on the oxide type ( $\text{Cu}_2\text{O}$  or  $\text{CuO}$ ).  $\text{Cu}_2\text{O}$  tends to be more antimicrobially active than  $\text{CuO}$ .<sup>[4]</sup> These findings as well as results of ongoing experiments will be presented in the talk and discussed in the context of biomaterials applications..

### CONCLUSION

The influence of specific materials and surface properties on the killing behavior of metallic copper was studied. The adhesion of bacteria, as one example, can be controlled by LISP surface topography design. Regarding the composition of antimicrobial copper alloys, the formation of  $\text{Cu}_2\text{O}$  should be favored.

### REFERENCES

1. Borkow, G. et al.  
Curr. Med. Chem. 2005, 12, 2163–2175.
2. Mücklich, F. et al.  
Int. J. Mater. Res. 2006, 97, 1–8.
3. Mathews, S. et al.  
Appl. Environ. Microbiol. 2013, 79, 2605–2611.
3. Hans, M. et al.  
Langmuir 2013, 29, 16160–16166.

### ACKNOWLEDGMENT

This work has been funded by the German research Foundation (DFG, MU 959/26-1&2) and the european funding for regional development (EFRE).

## INTRODUCTION

The use of biopolymers for biomedical applications makes smart therapies feasible<sup>1</sup>. In fact, a polymer-drug miscible system is able to release the drug in a controlled way. The purpose of this work is to find out a miscible system based on a biodegradable polymer and a biologically active molecule.

## EXPERIMENTAL METHODS

**Materials.** Poly(DL-lactide) (PDLLA) and poly( $\epsilon$ -caprolactone) (PCL), both biodegradable polymers, were supplied by Purac Biochem. Biologically active molecules, i.e., molecules that kill or inhibit the growth of microbes, erythromycin, thiamphenicol, tetracycline, sulphanilamide, sulfacetamide, sulfachloropyridazine, sulfamethazine trimethoprim, levofloxacin, bronidox and thymol were supplied by Sigma-Aldrich.

**Blend Preparation.** Blends were prepared by two methods: solvent casting and melting the components together for the system PCL/Thymol.

**Differential Scanning Calorimetry (DSC).** Approximately 5-10 mg of each equimolar blend was weighted and sealed in an aluminium pan. Glass transition temperatures ( $T_g$ ) were studied for systems with PDLLA (amorphous) and melting points ( $T_m$ ) for those with PCL (semicrystalline).

**Melting Point Depression.** Specific annealing treatments were conducted under isothermal conditions to obtain the melting point depression values ( $T_m^{mix}$ ).

**Infrared Fourier Spectroscopy (FTIR).** Spectra were taken with a resolution of 2  $cm^{-1}$  and were averaged over 64 scans. Chloroform solutions containing 0.7 % of solute were cast on KBr pellets and evaporated.

## RESULTS AND DISCUSSION

**DSC analysis.** It was studied the miscibility for systems with PDLLA analyzing if the  $T_g$  of the equimolar blend was intermediate between those of the pure components<sup>2</sup>. For blends with PCL, the miscibility was evaluated studying the depression of  $T_m$ .

**Melting point depression.** From the DSC analysis, it was found that PCL/Thymol was susceptible to be a miscible polymer-drug system. Thus, the Flory-Huggins interaction parameter ( $\chi$ ) was estimated adjusting the equation for a polymer-drug system<sup>3</sup> and representing  $(-\Delta H_{thymol}/R)[(1/T_m^{mix}) - (1/T_m^{thymol})] - \ln \phi_{thymol} - \phi_{PCL}$  vs.  $\chi \phi_{PCL}$ , where  $T_m^{mix}$  is the melting temperature of the blend in which the major component is thymol (83-96 %),  $T_m^{thymol}$  is the melting temperature of thymol,  $\Delta H_{thymol}$  is the heat of fusion of thymol,  $\phi_{thymol}$  is the volume fraction of thymol,  $\phi_{PCL}$  is the volume fraction of PCL, and  $R$  is the gas constant. The blends were prepared melting the components together into a closed

bottle inside a heated paraffin bath, in order to avoid thymol volatilization.

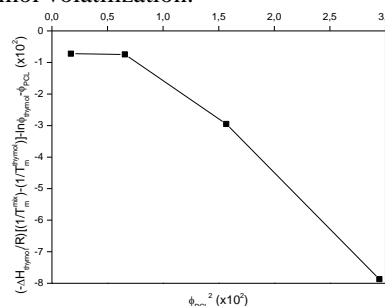


Fig. 1. Flory-Huggins equation plot for PCL/Thymol blends.

The slope of the plot in Figure 1 gives the interaction parameter  $\chi = -2.69$  that confirms that PCL/Thymol is a thermodynamically miscible blend.

## FTIR analysis.

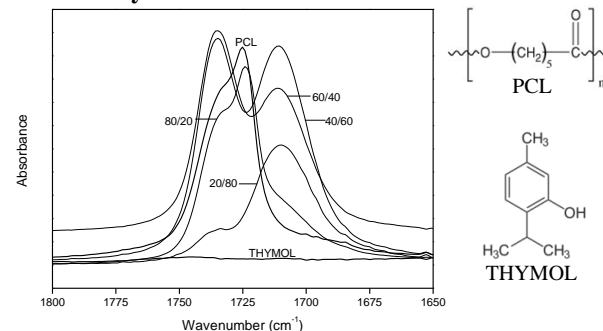


Fig. 2. Carbonyl stretching region for PCL/Thymol blends.

	1735 $cm^{-1}$ Amorphous PCL	1724 $cm^{-1}$ Crystalline PCL	1710 $cm^{-1}$ -C=O...H-O-
PCL	Shoulder	Peak	-
80/20	Shoulder	Peak	-
60/40	Peak	-	Peak
40/60	Peak	-	Peak
20/80	Shoulder	-	Peak

Table 1. Assignment of bands in the spectra for PCL/Thymol blends<sup>4</sup>. Table 1 shows that from a 40 % of thymol in the blend, PCL loses its crystallinity and a new band appears at 1710  $cm^{-1}$ , which can be attributed to hydrogen bonded carbonyl groups (-C=O...H-O-).

## CONCLUSION

A negative interaction parameter ( $\chi = -2.69$ ) indicates miscibility between PCL and thymol. FTIR results show that specific hydrogen bonding interactions are established between PCL and Thymol.

## REFERENCES

1. Rojas M.G. *et al.*, Rev. Ing. e Inv. 28(1):57-71, 2008
2. Meaurio E. *et al.*, Macromolec. 38:1207-1215, 2012
3. Teja S.B. *et al.*, J.Excipients&Food Chem. 4(3), 2013
4. Phillipson K. *et al.*, Thermochim.A. 595:74-82, 2014

## ACKNOWLEDGMENTS

The authors would like to thank Spanish Ministry MINECO (Project MAT2013-4559-P) and EU (COST Action TD 1305) for funds.

## Bactericidal Behaviour of a New Biodegradable and Biocompatible PLDA/Mg Composite

M.A. Pacha-Olivenza<sup>1,2</sup>, J.P. Fernández-Hernán<sup>2</sup>, A.M. Gallardo-Moreno<sup>2,1</sup>, J.L. González-Carrasco<sup>3,1</sup>, S.C. Cifuentes<sup>3,1</sup>,  
M.L. González-Martín<sup>2,1</sup>

<sup>1</sup>Networking Research Center on Bioengineering, Biomaterials and Nanomedicine (CIBER-BBN), Spain

<sup>2</sup>Department of Applied Physics, Faculty of Science, University of Extremadura, Badajoz, Spain

<sup>3</sup>National Centre for Metallurgical Research (CENIM-CSIC), Madrid, Spain

[mlglez@unex.es](mailto:mlglez@unex.es)

### INTRODUCTION

Constrain of current bioresorbable polymers for osteosynthesis are mainly related to their lack of bioactivity and low mechanical properties, which is behind the increasing demand of new bioresorbable materials. Mg and its alloys are among the most interesting options because their suitable mechanical strength and stiffness. However, their use as implants has been limited by their fast degradation rate under physiological conditions. The development of polymer/magnesium composites as new biodegradable and bioresorbable materials for osteosynthesis implants may overcome these problems. The polymeric matrix will benefit from the higher strength and modulus of the Mg particles, whereas Mg will benefit from the surrounded protective polymeric matrix that will control its degradation rate. In this sense, it has been recently reported that incorporation of biodegradable metals such as Mg in a matrix of poly-L-lactic acid improves the hardness of the polymer and its Young's modulus [1].

One of the most important concerns with implants, particularly in elderly people, is related with microbial infections. Most of the infections related to prosthesis are originated during their implantation from the cutaneous flora of the patient, the personnel in charge of performing the implantation and/or the environment of the operating theatre, mainly in the case of *S. epidermidis*.

### EXPERIMENTAL METHODS

#### SUBSTRATES

Two polymeric matrix materials PLDA (acid poly-D-lactide) with different concentrations of Mg (1 wt.% and 10 wt.%) were tested. The polymer PLDA without Mg was used as control.

#### BACTERIA

*Staphylococcus epidermidis* ATCC35983 a gram-positive strain with extracellular polysaccharide substance production were used.

#### BACTERIAL ADHESION TESTS

Samples were located on an orbital shaker with slightly agitation and bacteria were left to deposit mainly by sedimentation for 240 min at 37°C. Quantification of the surface density of bacteria on the surface samples were carried out with an epifluorescence microscope (Leitz DIAPLAN, Leitz Wetzlar, Germany) by staining the adhered microorganisms with the kit Live/Dead BacLight L-7012 (Invitrogen SA, Spain). Bacteria were counted with the software NIS-Elements BR 4.10 (Nikon Instruments INC., Melville, USA).

### RESULTS AND DISCUSSION

The results obtained of the surface density of adhered bacteria on: PLDA, PLDA+1 wt.% and PLDA+10 wt.% surface are shown in Figure 1 for *S. epidermidis*. These results indicate that the adhesion of *S. epidermidis* on the PLDA+1 wt.% and PLDA+10 wt.% surface is similar. However, the adhesion on PLDA+10 wt.% surface decreases in respect to the PLDA surface.

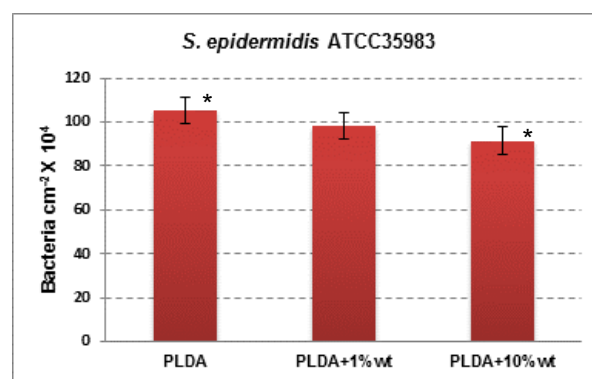


Figure 1. Surface density of *S. epidermidis* bacteria adhered on the samples: PLDA, PLDA+1 wt.% and PLDA+10 wt.%. Asterisks indicate statistical differences ( $p < 0.05$ ) when comparing the specified data using a ANOVA test.

Focusing on the viability of adhered bacteria, all bacteria deposited on the PLDA surface are 100% viable, while bacteria attached to the PLDA+1 wt.% and PLDA+10 wt.% surface show a loss in viability.

### CONCLUSION

The surface of the new biomaterial PLDA+Mg shows bactericidal effect for *S. epidermidis* after 240 min of contact and the adhesion on PLDA+10 wt.% decreases in respect to the PLDA surface without Mg.

### REFERENCES

1. Cifuentes, S.C. *et al.*, M. Materials Letters. 74:239–242, 2012

### ACKNOWLEDGMENTS

Ministerio de Ciencia e Innovación” (MAT2012-37736-C05-01;-03) and “Junta of Extremadura-FEDER: European Regional Development Fund” (GR10149).



## Development and *In Vitro* Testing of Gelatin-based Antibacterial Burn Wound Dressings

Birgit Stubbe<sup>1</sup>, Sandra Van Vlierberghe<sup>1,3</sup>, Gilles Brackman<sup>2</sup>, Mohaddeseh Amiri Aref<sup>3</sup>, Henk Hoeksema<sup>4</sup>, Stan Monstrey<sup>4</sup>, Frank Vanhaecke<sup>5</sup>, Piet Van Espen<sup>3</sup>, Karolien Dewael<sup>3</sup>, Tom Coenye<sup>2</sup>, Peter Dubrue<sup>1</sup>

<sup>1</sup>Polymer Chemistry & Biomaterials Research Group, Ghent University, Belgium

<sup>2</sup>Laboratorium voor Farmaceutische Microbiologie, Ghent University, Belgium

<sup>3</sup>AXES Research Group, University of Antwerp, Belgium

<sup>4</sup>Department of Plastic & Reconstructive Surgery, University Hospital Ghent, Belgium

<sup>5</sup>Department of Analytical Chemistry, Ghent University, Belgium

[Sandra.VanVlierberghe@UGent.be](mailto:Sandra.VanVlierberghe@UGent.be)

### INTRODUCTION

Burns can be considered as a major global health problem. It has been estimated that annually 265,000 people die from the consequences of burn wounds. Moreover, the majority of non-fatal burn wounds results in long hospitalizations, disfigurement and disability.<sup>1</sup> Novel wound dressings accelerating the healing process can tackle these issues.<sup>2</sup> Therefore, the present work is focusing on the development of biopolymer-based wound dressings providing an ideal moist wound environment and antimicrobial activity for the prevention of infections.

### EXPERIMENTAL METHODS

#### Synthesis of photo-crosslinkable gelatin derivatives

Varying photo-crosslinkable functionalities including (meth)acrylamides and vinyl groups were introduced onto the gelatin backbone. The resulting derivatives were characterized via <sup>1</sup>H NMR spectroscopy. Rheology and texturometry were applied to study the cross-linking potential and the final strength of the resulting hydrogel films.

#### Quantification of the incorporated antimicrobial agent and *in vitro* study of the antibacterial activity

In a second part, poly(vinylpyrrolidone)-iodine (PVP-I), one of the most effective and widely used anti-infective agents, was incorporated into the hydrogel films by incubation. The amount of introduced (PVP-)iodine was determined via XRF spectroscopy and electrochemistry. In addition, *in vitro* bacterial tests using *Staphylococcus aureus* were performed to examine the antibacterial effect of the developed hydrogel films.

### RESULTS AND DISCUSSION

In a first step, the cross-linking kinetics and final hydrogel properties of the various gelatin derivatives were compared in order to select the most appropriate strategy for future work. As illustrated by the rheology results in figure 1 (a), gelatin-methacrylamide (gel-MA) with a DS 65% showed the best mechanical properties and was selected for incorporation of PVP-I.

PVP-I was introduced via incubation after UV treatment of the photo-crosslinkable gelatins since chemical cross-linking was shown to be inhibited by the incorporated iodine. PVP-I incorporation was studied via XRF and electrochemistry.

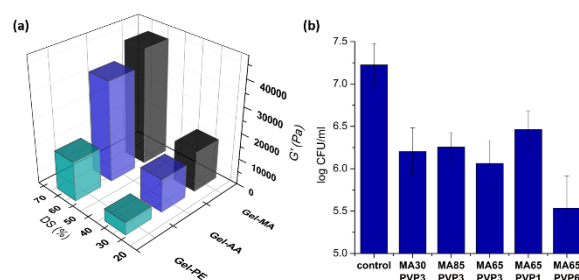


Figure 1 (a) Storage moduli of gelatin-methacrylamide (gel-MA), gelatin-acrylamide (gel-AA) and gelatin-pentenoate (gel-PE) hydrogel films. (b) Amount of bacteria able to form a biofilm (colony-forming unit, CFU) after 24h of incubation with various hydrogels.

Bacterial tests (figure 1b) indicate higher reductions in bacterial count when a larger amount of PVP-I is incorporated. The introduced amount of PVP-I was characterized via XRF and electrochemistry. Interestingly, the cross-linking degree of the hydrogel films appears to have no influence on PVP-I uptake.

### CONCLUSIONS

Gelatin-methacrylamide hydrogels showed the best mechanical properties of all developed derivatives and were selected for incorporation of the antimicrobial agent PVP-I. In addition, microbicidal effectiveness was studied via antibacterial tests indicating increased bacterial count reduction with increasing PVP-I concentration.

### REFERENCES

1. WHO. Fact sheet N°365: Burns. 2014 April 2014 15/01/2015]; Available from: <http://www.who.int/mediacentre/factsheets/fs365/en/>.
2. Hoeksema, H., Brandwonden, in Handboek Wondzorg, I.S. Cordyn, Editor. 2009, Maarsen: Elsevier gezondheidszorg. p. 217-286.

### ACKNOWLEDGMENT

Birgit Stubbe would like to thank the Agency for Innovation by Science and Technology (IWT) Flanders. Sandra Van Vlierberghe would like to acknowledge the Research Foundation Flanders (FWO-Flanders) for financial support under the form of a post-doctoral fellowship and a research grant (Grant no: 1.5.194.12N).





## Improvement of the Antibacterial Properties of Hydroxyapatite Coatings

Alina Vladescu<sup>1</sup>, Mariana Braic<sup>1</sup>, Mihaela Badea<sup>2</sup>, Adrian Kiss<sup>1</sup>, Viorel Braic<sup>1</sup>

<sup>1</sup>National Institute for Optoelectronics (INOE2000), Bucharest-Magurele, Romania

<sup>2</sup>Transilvania University of Brasov, Romania

[alinava@inoe.ro](mailto:alinava@inoe.ro)

### INTRODUCTION

The actual challenge in the dental and orthopedic surgery is to obtain implants with good mechanical, physical, chemical and surface compatibility with the bone and with superior antibacterial properties<sup>1-3</sup>. The main goal of the paper is to obtain osteoconductive and antibacterial coatings in order to enhance the osteoconductive capability and the resistance to the bacteria of the Ti-based alloy. For the present study, hydroxyapatite (HAP) coatings enriched with SiC and Ag were prepared and investigated. SiC was added to enhance film hardness and corrosion resistance, while Ag addition was foreseen to improve the antibacterial properties.

### EXPERIMENTAL METHODS

The reactive magnetron sputtering technique was used to prepare the coatings, by using three cathodes made of HAP, SiC and Ag (99.9% purity, 1 inch diameter, Kurt J. Lesker Company). The base pressure in the deposition chamber was  $1.3 \times 10^{-4}$  Pa. The coatings were deposited in Ar atmosphere at  $6.6 \times 10^{-1}$  Pa. The RF powers on HAP and SiC cathodes were kept constant at 50 W and 15 W, while that on the Ag cathode was varied as 0.6 W, 0.9 W and 1.2 W (SA-1, SA-2 and SA-3). The HAP coating was used as reference coating.

The elemental composition and the chemical binding state of the coatings, close to the film surface, was investigated by energy dispersive X-ray (EDS) and Fourier transform infrared spectroscopies (FTIR), respectively. The phase composition was determined by X-ray diffraction (XRD). Surface topography was examined by AFM, using an INNOVA atomic force microscope. The antimicrobial tests were carried out for antibacterial activity using *Staphylococcus aureus* MRSA. The corrosion resistance was investigated by electrochemical tests in simulated body fluid (SBF) solution, pH=7.2, at  $37 \pm 0.4$  °C, using a VersaSTAT 3 Potentiostat/Galvanostat.

### RESULTS AND DISCUSSION

The EDS results showed that the Ca/P ratios are close to 1.67, which corresponds to a stoichiometric HAP. For all the coatings, XRD diffraction revealed the presence of the HAP crystalline structure, without calcium oxide, calcium phosphate hydroxide or any other calcium phosphate phases such as tricalcium phosphate, tetracalcium phosphate. The FTIR analysis indicated that all bands can be attributed to HAP; the SiC or Ag additions did not have any effect on the chemical bonds in the coating (Fig.1). All coatings improved the corrosion resistance of the Ti-based alloy (Fig.2).

Compared with HAP, the coatings with SiC and Ag exhibited better corrosion behaviour and antibacterial properties. It was shown that the increase in RF power on the Ag target led to an improvement in the antibacterial properties.

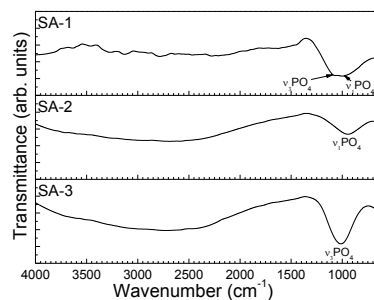


Fig. 1. The FTIR spectra of the HAP coatings with SiC and Ag additions

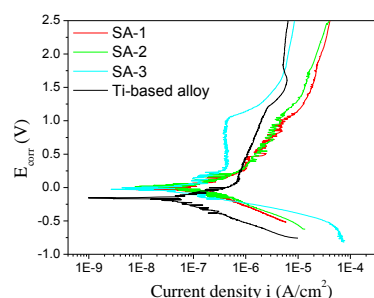


Fig. 2. Potentiodynamic curves of the HAP coatings with SiC and Ag additions

### CONCLUSION

The main conclusion is that Ag addition improves the antibacterial properties without changing the other properties of HAP coatings. The HAP coatings were found to be stoichiometric and no change of stoichiometry by Ag addition was observed. Also, no significant change in phase composition and corrosion resistance with variation of the RF power on Ag cathode was observed. By increasing the Ag content, the antibacterial activity increased.

### REFERENCES

1. Rakhorst G. *et al.*, World Sci. Pub. Co. 2008
2. Yaszemski M.J. *et al.*, Marcel Dekker Inc.41, 2004
3. Brown S.A. *et al.*, ASTM International 45, 1999

### ACKNOWLEDGMENTS

“This work was supported by Partnerships in priority areas program - PN II, developed with support from ANCS, CNDI - UEFISCDI, project no. 212/01.072014 (Osseopromote)”.

## A 17-mer Membrane-Active MSI-78 Derivative with Improved Selectivity Towards Bacterial Cells

Claudia Monteiro<sup>1,2,‡</sup>, Marina Pinheiro<sup>3,‡</sup>, Mariana Fernandes<sup>1,2</sup>, Sílvia Maia<sup>4</sup>, Catarina L. Seabra<sup>1,2,5,6</sup>, Frederico Ferreira-da-Silva<sup>1,7</sup>, Salette Reis<sup>3</sup>, Paula Gomes<sup>4</sup>, M. Cristina L. Martins<sup>1,2,5</sup>

‡These authors contributed equally to this work

<sup>1</sup>I3S, Instituto de Investigação e Inovação em Saúde, Universidade do Porto, Portugal

<sup>2</sup>INEB, Instituto de Engenharia Biomédica, Universidade do Porto, Portugal

<sup>3</sup>UCIBIO, Requimte, Faculdade de Farmácia, Universidade do Porto, Portugal

<sup>4</sup>CIQUP, Departamento de Química e Bioquímica, Faculdade de Ciências, Universidade do Porto, Portugal

<sup>5</sup>Instituto de Ciências Biomédicas Abel Salazar, Universidade do Porto, Portugal

<sup>6</sup>IPATIMUP - Institute of Molecular Pathology and Immunology of the University of Porto, Portugal

<sup>7</sup>IBMC-Instituto de Biologia Celular e Molecular, Unidade de Produção e Purificação de Proteínas, Universidade do Porto, Portugal

[cmartins@ineb.up.pt](mailto:cmartins@ineb.up.pt)

### INTRODUCTION

The increasing emergency to combat resistant bacterial strains has been promoting the development of new generations of antimicrobial agents, being the antimicrobial peptides (AMP) one of the most promising alternatives. However, AMP still present some drawbacks that prevent efficient therapeutic application such as low stability and high toxicity<sup>1</sup>. Therefore, AMP improvement towards high potency and selectivity to bacterial cells is needed. MSI-78 (commercially known as Pexiganan), a highly effective and broad spectrum AMP is one of the most promising AMP for clinical application<sup>2</sup>. In this study, we aimed at designing a shorter derivative of MSI-78 with the aim of improving selectivity, while maintaining antimicrobial activity. Shorter 17-mer derivatives were created by truncating MSI-78 (22-mer) at the N-and/or C-termini, while spanning MSI-78 sequence.

### EXPERIMENTAL METHODS

The 17-mer derivatives were evaluated regarding antimicrobial activity against selected gram-positive *Staphylococcus* strains and the gram-negative *Pseudomonas aeruginosa* (*P. aeruginosa*). Antimicrobial activity was assessed by Minimal Inhibitory Concentration (MIC). The method used to determine MIC was the broth microdilution assay in microtiter plates. Cytotoxicity was assessed by hemolysis assays using human Red Blood Cells (RBC). The mechanism of action, of the most efficient 17-mer was determined using several biophysical assays and simple membrane models that mimic the mammalian and bacterial lipid composition. Secondary structure of the peptides upon interaction with membrane mimetic systems was also determined.

### RESULTS AND DISCUSSION

Despite the truncations made, we found a 17-mer peptide, MSI-78(4-20) (KFLKKAKKFGKAFVKIL), which demonstrated to be as effective as MSI-78 against the gram positive *Staphylococcus* strains tested and against the gram negative *P. aeruginosa*. This shorter derivative was more selective towards bacterial cells as it was less toxic to RBC than MSI-78,

representing an improved version of the lead peptide. Biophysical studies support a mechanism of action for MSI-78(4-20) based on the disruption of the bacterial membrane permeability barrier, which in turn leads to loss of membrane integrity and ultimately to cell death. These features point to a mechanism of action similar to the one described for the lead peptide MSI-78.

### CONCLUSION

In this study, we found a very effective and broad-spectrum AMP, MSI-78(4-20). This MSI-78 derivative is as effective as the lead peptide, while having reduced hemolytic activity, therefore representing an improved version of MSI-78. We can envisage a wide application for this AMP in the field of antimicrobial research.

### REFERENCES

1. Hancock, R. E.; Sahl, H. G. *Nat Biotechnol* **2006**, 24, (12), 1551-7.
2. Lipsky BA, Holroyd KJ, Zasloff M.. Clinical infectious diseases : an official publication of the Infectious Diseases Society of America **2008**, 47:1537-1545.

### ACKNOWLEDGMENTS

This work was financed by FEDER funds through Programa Operacional Factores de Competitividade – COMPETE and by Portuguese funds through FCT – Fundação para a Ciência e a Tecnologia in the framework of project Portugal-China joint Innovation Centre for Advanced Materials (JICAM2013) and the grants: SFRH/BPD/79439/2011 (Claudia Monteiro), SFRH/BPD/99124/2013 (Marina Pinheiro), and SFRH/BD/89001/2012 (Catarina Seabra).

The authors would like to thank to Centro Hospitalar de São João, EPE, Porto, for the human buffy coats.



## Comparative Study of the Bactericidal and Chemical Properties of Oxidized Regenerated Cellulose and Oxidized Cellulose Topical Absorbable Hemostats

Douglas B. Johns<sup>1</sup>, Shubhangi Bhende<sup>1</sup>, Sheri Baker<sup>2</sup>, Benjamin D. Fitz<sup>1</sup>, Stephen Rothenburger<sup>1</sup>

<sup>1</sup>ETHICON, Inc., Somerville, NJ, USA

<sup>2</sup>Durata Therapeutics, Chicago, IL, USA

[djohns@its.jnj.com](mailto:djohns@its.jnj.com)

### INTRODUCTION

Topical absorbable hemostats (TAH) provide several benefits during a surgical procedure, including hemostasis and visualization of the operative field. Oxidized cellulose (OC), and oxidized regenerated cellulose-based (ORC) TAH products have bactericidal properties that occur when an acidic environment is created upon contact between the hemostat and blood or other fluid, a characteristic created through oxidation of the cellulose component. The bactericidal properties of SURGICEL® Original Absorbable Hemostat, an ORC, have been demonstrated in various *in vitro* and *in vivo* evaluations<sup>1</sup>. This study compared SURGICEL® with other ORC and oxidized cellulose products to evaluate the degree of oxidation (carboxyl content) and bactericidal activity against 5 challenge bacteria<sup>2</sup>.

### EXPERIMENTAL METHODS

The carboxyl content was determined by titration, using methodology as described in the United States Pharmacopeia (USP)<sup>3</sup>. Tryptic soy broth was used to measure pH over time. Test articles were challenged *in vitro* with 5 strains identified by the National Healthcare Safety Network as the most common pathogens accounting for health care-associated infections, and bactericidal activity was measured using standard plate count method.

### RESULTS AND DISCUSSION

The USP specification for ORC carboxyl content is 18 – 24 w/w percent. Only one product met the USP criteria (Table 1). It also exhibited the lowest pH at all-time intervals (Figure 1), and showed consistent efficacy against all 5 challenge bacteria evaluated (Table 2). The actual log reduction was 4 logs or more from the initial inoculum within 24 hours for all 5 bacteria tested. All other products exhibited lower levels of oxidation and varying antibacterial activity.

Sample	ORC or OC	pH @ 24 Hours in TSB	COOH (w/w %)
SURGICEL®	ORC	3.31	19.5
BLOODCARE	OC	3.70	15.5
CURACEL®	ORC	3.60	14.1
Equitamp®	ORC	4.68	1.4
GELITACEL®	OC	3.55	15.0
OKCEL®	OC	3.65	15.7
Oxycel	OC	3.53	15.0
Reoxcel®	OC	3.63	13.9
Traumastem	OC	3.38	16.5
RESO-CELL®	ORC	3.49	16.2

Table 1: The pH in TSB of 25 mg/mL at 24 hours with associated test article carboxyl content (COOH)

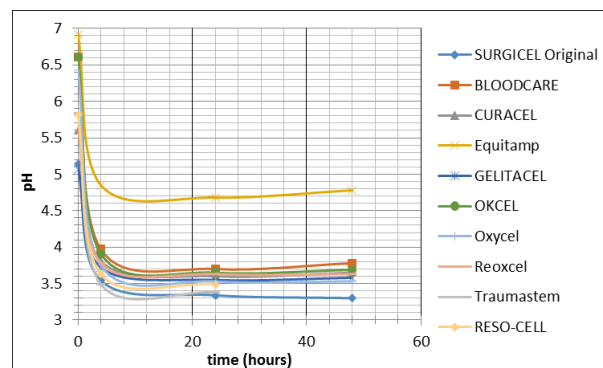


Fig. 1: The pH time-course for test articles in TSB at 25 mg/mL

Sample	MRSA	MRSE	VRE	<i>E. coli</i>	<i>P. aeruginosa</i>
SURGICEL®	>4	>4	>4	>4	>4
BLOODCARE	>4	4	1.0	<1	>4
CURACEL®	>4	3.8	<1	3.2	>4
Equitamp®	1.2	1.0	<1	-2.9	-0.1
GELITACEL®	>4	3.0	<1	<1	>4
OKCEL®	>4	2.8	<1	<1	>4
Oxycel	>4	3.9	>4	1.4	>4
Reoxcel®	>4	4	<1	2.8	>4
Traumastem	>4	>4	2.7	3.2	>4
RESO-CELL®	>4	>4	<1	1.3	>4

Table 2: Log reduction at 24 hours from the initial inoculum for each test article

### CONCLUSION

Only one ORC product met the USP specification for carboxyl content for ORC, and also exhibited the lowest pH at all-time points, and had consistent bactericidal efficacy against all 5 challenge bacteria evaluated. One ORC product within the group actually resulted in increased bacterial count for *E.coli* and *P.aeruginosa*. All other products tested exhibited varying but lesser antibacterial activity against 5 bacterial strains. These results suggest that different processes and oxidation levels may lead to different levels of bactericidal effectiveness.

### REFERENCES

- Spangler D, *et al.*, Surg Infect (Larchmt) 4:255–262, 2003
- Hidron AI, *et al.*, Infect Control Hosp Epidemiol 29:996–1011, 2008
- United States Pharmacopeia (USP 36), 2013



## Biological Response to Titanium-Silver Alloys Produced by Powder Metallurgy

Barbara Szaraniec<sup>1</sup>, Elżbieta Menaszek<sup>2</sup>, Tomasz Goryczka<sup>3</sup>, Rafał Pokrowiecki<sup>4</sup>, Tomasz Zaręba<sup>5</sup>

<sup>1</sup> Department of Biomaterials, Faculty of Materials Science and Ceramics, AGH University of Science and Technology, al. Mickiewicza 30, 30-059 Krakow, Poland

<sup>2</sup> Department of Cytobiology, Collegium Medicum, Jagiellonian University, Krakow, Poland

<sup>3</sup> Institute of Materials Science, University of Silesia, 75 Pułku Piechoty 1A, 40-500 Chorzów, Poland

<sup>4</sup> Department of Oral Surgery, Jagiellonian University Medical College – University Dental Clinic, ul. Montelupich 4, 31-155 Krakow, Poland

<sup>5</sup> Department of Antibiotics and Microbiology, National Health Institute, Warsaw, Poland  
[szaran@agh.edu.pl](mailto:szaran@agh.edu.pl)

### INTRODUCTION

Instead of the widely used titanium titanium-silver can be an alternative group of alloys for medical implants used in dentistry and orthopaedics. Mechanical properties of Ti-Ag produced by powder metallurgy enables obtaining of biocompatible materials with good mechanical properties and with bacteriostatic or bactericidal ability. The aim of this work was to study biological response to Ti-Ag alloys with the silver content lower than 20%at.

### EXPERIMENTAL METHODS

Titanium-silver alloys with nominal chemical composition of silver 3.5at%; 5at.%; 10at.% or 20at.% were manufactured by powder metallurgy. A titanium powder (Atlantic Equipment Engineers) was mixed with silver powder (Nanoamor) and compressed in a hydraulic press with pressure of 8MPa. Cylinder-shaped compacts (10 mm in diameter and 5 mm height) were sintered in vacuum furnace ( $5 \cdot 10^{-4}$  mbar) at 900°C for 10 hours.

*In vitro* tests allowed to evaluate biocompatibility and antimicrobial activity of Ti-Ag alloys. For tests samples with shape in disk were sterilized and placed into 48-well culture plates. Their biocompatibility was tested in fibroblasts cell culture. Murine fibroblasts L-929 (Sigma-Aldrich, Germany) were seeded on surface of samples at a density of  $1.5 \times 10^5$ /ml per well. The interaction of L-929 fibroblasts with Ti-Ag samples: cells adhesion, spreading, viability/proliferation and cytotoxicity were determined after 3 and 7 days from seeding. Adhesion, spreading and proliferation of cells on the surface of biomaterials were observed using a fluorescence microscope (Olympus, Japan). In order to determine cytotoxicity of biomaterials and cells viability/proliferation, a ToxiLight\_BioAssay Kit and ToxiLight™ 100% lysis reagent set (Lonza, USA) were applied.

Susceptibility of bacteria to Ti-Ag alloys were determined from Kirby-Bauer disk diffusion test, carried out according to SNV 195920 standards. The bactericidal effect of materials against *Staphylococcus aureus* and *Escherichia coli* was estimated based on the zone of inhibition around them. The presence of the inhibition zone is a result of diffusion of the antibacterial agent into the solid agar nutrient. An amount of dissolved agent must be therefore sufficient to reach MIC (minimal inhibitory

concentration) or MBC (minimum bactericidal concentration) values for each tested bacterial strain.

### RESULTS AND DISCUSSION

*In vitro* tests proved the good biocompatibility of all studied titanium-silver alloys. The cells on their surface adhered and spread well. The ratio of viability and proliferation was relatively high. Sample fluorescence microphotographs of L-929 cells cultured for 7 days on the surface of titanium-silver alloy (Ti-Ag3,5%) were shown in figure 1.

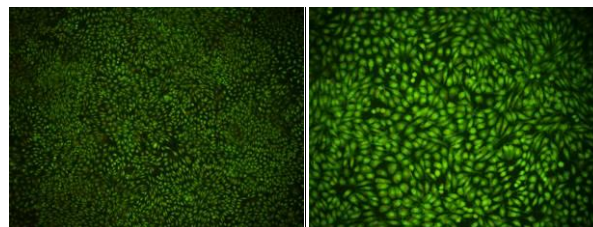


Fig.1 Morphology of L-929 cells seeded on the titanium-silver (3.5at% Ag) after 7 days in culture. Stained with Acridine Orange, Objective magnification: a)10x, b)20x

Antibacterial activity can be determined from the width of the inhibition zone. According to the SNV 195920 standard, the antibacterial behaviour can be defined as good when width of a zone is larger than 1 mm. For all studied alloys bacterial strains were comprised between 1 and 3 mm. Hence, it can be concluded that Ti-Ag surface exhibits significant antimicrobial properties.

### CONCLUSION

Biological response of the Ti-Ag alloys was studied by means of determination of their biocompatibility as well as antimicrobial properties. Obtained results have shown that titanium-silver sinters possess good properties for fibroblasts adhesion, migration and proliferation *in vitro* as well as cells were growing with correct morphology. Moreover, antibacterial test carried out with use of *Staphylococcus aureus* and *Escherichia coli* bacteria proved antibacterial properties of the Ti-Ag alloys.

### REFERENCES

1. Takahashi M. *et al.* Dent Mater J. 21:270-80, 2002

### ACKNOWLEDGMENTS

This work was supported by AGH University of Science and Technology, Faculty of Material Science and Ceramics Grant No. 11.11.160.616.



## Silver and Gold Nanoparticle-Based Composites with Chitosan as Efficient and Biocompatible Materials for Antimicrobial Therapy

Anna Regiel-Futyr<sup>1</sup>, Małgorzata Kus-Liśkiewicz<sup>2</sup>, Victor Sebastian<sup>3</sup>, Silvia Irusta<sup>3,4</sup>, Manuel Arruebo<sup>3,4</sup>, Agnieszka Kyzioł<sup>1</sup>, Grażyna Stochel<sup>1</sup>

<sup>1</sup>Faculty of Chemistry, Jagiellonian University, Poland

<sup>2</sup>Faculty of Biotechnology, Biotechnology Centre for Applied and Fundamental Sciences, University of Rzeszów, Poland

<sup>3</sup>Department of Chemical Engineering and Nanoscience Institute of Aragon (INA), University of Zaragoza, Spain

<sup>4</sup>Networking Research Center on Bioengineering, Biomaterials and Nanomedicine, CIBERBBN, Spain  
[anna.regiel@uj.edu.pl](mailto:anna.regiel@uj.edu.pl)

### INTRODUCTION

Severe bacterial infections has become a major clinical and public health problem. The number of resistant bacterial strains is constantly and rapidly increasing<sup>1</sup>. Biofilm forming bacteria can easily adhere to different surfaces creating attached communities. The isolation from the unfavorable environmental conditions enables bacterial survival even under prolonged antibiotic treatment. Nowadays, additional efforts are needed to develop effective antibacterial materials. The preparation of polymer-metal nanoparticle-based composites is one of the most promising strategies<sup>2,3</sup>. Herein, we present chitosan (CS) based silver and gold nanoparticles (AgNPs, AuNPs) films and their biological activity evaluation.

### EXPERIMENTAL METHODS

The synthesis of chitosan based silver and gold nanoparticles was optimized by factorial design. In both cases CS, a biocompatible polymer, was used as a reducing and stabilizing agent. Three different polymer grades were used, varying in their average molecular weight and deacetylation degree value. The dependence between chitosans properties and obtained NPs features was determined. Several experimental techniques for nanoparticles and nanocomposites characterization were applied: UV-Vis and IR spectroscopy, TG, TEM, XPS, ICP-MS *etc.* Moreover, the biological activity of obtained materials was evaluated. The cytotoxicity was checked by the MTT and LDH assays on selected cell lines (human keratinocytes: HaCaT, mouse fibroblasts: NIH3T3, human lung adenocarcinoma epithelial cell line: A549 and mouse colon fibroblast carcinoma cells: CT26). The antibacterial activity was also examined on Gram-negative (*Pseudomonas aeruginosa*) and Gram-positive (*Staphylococcus aureus*) bacterial strains.

### RESULTS AND DISCUSSION

Chitosan with the medium molecular weight and the highest deacetylation degree appeared to be the most optimum for the silver and gold nanoparticle synthesis providing with an homogeneous particle size and inter-batches reproducibility. A fast reduction of metal ions was favored which consequently leads to smaller nanoparticle formation homogenously dispersed across the film. A complete bactericidal effect towards stationary phase cultures of *Pseudomonas aeruginosa*

and *Staphylococcus aureus* bacterial strains was proven for the most efficient materials. The resulting nanocomposites with AuNPs did not show any cytotoxicity against mammalian somatic (HaCaT, NIH3T3) and tumoral cells (A549, CT26). Films with AgNPs exhibited a negligible toxicity towards somatic cells and a distinct toxicity towards tumoral ones. Both types of materials induced a disruptive effect on the bacteria wall while their internalization was hindered on the eukaryotic cells. This selectivity against bacteria and safety towards eucariotic cells make them potentially applicable as antimicrobial coatings in the biomedical field.

### CONCLUSION

The optimization of silver and gold nanoparticle synthesis allowed obtaining materials with desired properties such as size and NPs distribution in the resulting polymeric film. Chitosan based gold nanocomposites exhibited a significant antibacterial activity and simultaneously low cytotoxicity. For silver containing materials, the bactericidal effect was confirmed. However, significantly higher cytotoxicity towards keratinocyte and fibroblast cell lines was also observed. Presented nanocomposites could be potentially applied in biomedical field as successful antimicrobial materials.

### REFERENCES

1. Levy, S. B., J. of Antimicrob. Chem. 49:25-30, 2002
2. Travan, A. *et al.*, Biomacromol. 10(6):1429-1435, 2009
3. Potara M. *et al.*, Nanotechn. 22:135101, 2011

### ACKNOWLEDGMENTS

The authors would like to thank the National Science Centre (PRELUDIUM2012/07/N/ST5/00157) for providing financial support to this project.



## Facile Biosynthesis of Silver Nanoparticles Using *Tilia tomentosa* Leaf Extract: Its Characterization and Antimicrobial Activity

Fatih Duman<sup>1</sup>, Murat Kaya<sup>2</sup>, Ismail Ocsoy<sup>3</sup>, Fatma Ozturk Kup<sup>1</sup> and Fatih Dogan Koca<sup>1</sup>

<sup>1</sup>Erciyes University, Science Faculty, Biology Department, Kayseri, Turkey

<sup>2</sup>Aksaray University, Science & Art Faculty, Biotech and Molecular Biology, Aksaray Turkey

<sup>3</sup>Erciyes University, Nanotechnology Research Center, Kayseri, Turkey

[fduman@erciyes.edu.tr](mailto:fduman@erciyes.edu.tr)

### INTRODUCTION

Silver nanoparticles (AgNPs) are widely used in pharmaceutical, industrial and medical applications. Using of plant extracts to avoid toxic by-products reveal is very common route to synthesis of AgNPs. It is known that green synthesized AgNPs are environmentally friendly, cheap and safe for medical applications [1, 2]. The size, amount and surface charge on AgNPs vary depending on several parameters such as plant species and volume of extract used. Nowadays, AgNPs are obtained using many different plants extract [3]. However, we could not find any study related to green synthesis of AgNP's using lime (*Tilia tomentosa*) leaf extract and its antimicrobial properties in literature survey. In this study, we aimed to conduct rapid biosynthesis, characterization and antimicrobial activity of AgNP's using a medicinal plant (*T. tomentosa*) extract as reducing and stabilizing agent.

**Keywords:** Biosynthesis; Silver nanoparticle; *Tilia tomentosa*; characterization; antimicrobial activity

### EXPERIMENTAL METHODS

#### Synthesis of AgNP

The leaves of lime were collected from local area of Erciyes University campus. Collected samples were washed thoroughly with distilled water several times to remove dust. The cleaned leaves were shade dried for 10 days. The dried leaves were pulverized in a blender to obtain a fine powder. 10 g of pulverized leaves were boiled in 100 ml of sterile distilled water for 5 min, cooled and filtered through Whatman No. 1 filter paper. This filtrate was used as a reducing and stabilising agent for  $10^{-3}$  M of silver nitrate ( $\text{AgNO}_3$ ). 10 ml of the above filtrate was added to 90 ml of  $10^{-3}$  M  $\text{AgNO}_3$  solution and stirred and incubated at room temperature for 20 min. After incubation the NPs were collected by repeated (3–4 times) centrifugation of the reaction mixture at 10.000g for 10 min.

#### Characterization

Characterization of obtained NP's were conducted by UV-visible spectroscopy, scanning electron microscopy (SEM), X-ray diffraction (XRD), dynamic light scattering (DLS) and Fourier Transform Infra-Red spectroscopy (FTIR).

#### Antimicrobial activity

The agar diffusion method was used for the determination of antimicrobial activities of the AgNP's. *Escherichia coli* O157 was selected as test organism. At the end of the exposure, petri dish was examined for zones of growth inhibition, and the diameters of these zones were measured in millimeters.

### RESULTS AND DISCUSSION

According to SEM image, Ag NPs are spherical with size of  $40 \pm 5$  nm. The weight and atomic percentages of Ag indicated by EDX analysis are about 8.01% and 1.07%, respectively. The FT-IR spectra of *T. tomentosa* extract directed Ag NPs revealed that the O-H bonds (phenolic compounds in plant extract) stretching was observed at  $3389.01 \text{ cm}^{-1}$ . The presence of C=O bonds peak from aldehydes or ketones or ester was found around at  $1620.82 \text{ cm}^{-1}$  with right shift. The vibration bands of aromatic C=O existed at  $1384.73 \text{ cm}^{-1}$ . The vibration band at  $1066.19 \text{ cm}^{-1}$  was attributed to C-O stretching in epoxy. The crystal structure containing peak position and relative intensity of Ag NPs was analyzed by X-ray diffraction technique. The XRD analysis showed the diffraction peaks at  $38.26^\circ$ ,  $46.19^\circ$ ,  $64.85^\circ$  and  $78.35^\circ$  which are relevant to (111), (200), (220) and (311) of the lattice planes of a faced center cubic, respectively. The UV-vis spectrum exhibited a peak at around 292 nm belonging to plant extract while the characteristic absorption peak of Ag NP aqueous solution were absorbed at range of 480–500 nm. The effective diameter of Ag NPs was  $45 \pm 5$  nm. We demonstrated that the Ag NPs was negatively charged with a  $-29.8 \text{ mV}$ . The synthesized AgNPs had significant antimicrobial activity against *E. coli*.

### CONCLUSION

We synthesized an eco-friendly and convenient approach for the synthesis of AgNPs using *T. tomentosa* leaf extract in which no harmful chemical reagent or surfactant template was required. Obtained AgNPs may probably be used as effective antimicrobial agent.

### REFERENCES

1. Schröfel, A., et al., Acta Biomater. 10: 4023-4042, 2014.
2. Rajesh W.R. et al., Curr. Nanosci., 5: 117–122, 2009
3. Mittal, A.K. et al., Biotechnol. Adv. 31: 346-356, 2013



## Mg Ions Effect on *Staphylococcus epidermidis* Strain

Jesús Rodríguez-Sánchez<sup>1,2</sup>, Miguel A. Pacha-Olivenza<sup>2,1</sup>, M. Luisa González-Martín<sup>1,2</sup>

<sup>1</sup> Department of Applied Physics, Faculty of Sciences, University of Extremadura, Avda. Elvas s/n, 06006 Badajoz, Spain

<sup>2</sup> Networking Research Center on Bioengineering, Biomaterials and Nanomedicine, CIBER-BBN, Badajoz, Spain  
[jrs@unex.es](mailto:jrs@unex.es)

### INTRODUCTION

Current biodegradable polymers for osteosynthesis present low mechanical properties and lack of bioactivity<sup>[1]</sup>. Mg and its alloys are among the most interesting options because of their utmost mechanical strength and stiffness although they exhibit a high corrosion rate under physiological fluids. An interesting alternative to these materials is presented as a new approach by the incorporation of Mg and Mg alloys particles into a polymer matrix. The amount of the particles dispersed into the matrix should be high enough to improve the mechanical properties of the polymer, but low enough to avoid the hydrogen accumulation and the subsequent fast increase in pH (caused as a result of the above mentioned behaviour). The degradation process of Mg may damage adjacent tissues<sup>[2]</sup>, and also, metal ions will be released to the blood stream, regulated by the polymer degradation rate, and therefore will interact with the present macromolecules on the surroundings. After surgery, biofilm formation is one of the most important issues. On this work an interaction of the Mg ions with bacteria is proposed as a simulation of the expected release. The study also includes the influence over adhered bacteria onto Ti6Al4V, other well-know biomaterial which hydrophobicity could be modified by UV-light irradiation<sup>[3]</sup>.

### EXPERIMENTAL METHODS

Disks of Ti6Al4V of 25 mm in diameter were kindly supplied by SURGIVAL S.A., Spain. They were mechanically polished with diamond paste, and finished with colloidal silica. Prior to their use, the Ti6Al4V disks were carefully cleaned with DSF disinfectant (DERQUIM DSF 11; Panreac Quimica S.A., Spain), then rinsed and sonicated in deionized water (Milli-Q system), 70% acetone and finally ethanol for periods of 15 min each. Samples used as controls were not subjected to any further treatment. A second set of samples was exposed to an UV-C source for 120 min. This period was sufficient to guarantee the hydrophilization of the surface, as we have recently shown<sup>[3]</sup>.

Mg ions solutions were obtained from the dissolution of metallic Mg alloy particles in the PBS buffer. Final concentrations of ions were determined by mass spectrometry (ICP-MS) as 71 mg L<sup>-1</sup> (named as 1/1).

*S. epidermidis* ATCC35983, gram-positive strain, extracellular polysaccharide substance producer was used in this work.

Static adhesion experiments were carried out with the help of a sterile reusable silicone chamber (flexiPERM, Greiner bio-one, Germany), fixed to the Ti6Al4V surface for 60 min at 37 °C and 20 rpm. Mg ions was used at different concentrations (1/1, 1/2 and 1/4 from the saturated one) were incorporated for 60, 150 and 240 min after static adhesion experiment.

After the adhesion process, the Live/Dead kit BacLight L-7012 (Invitrogen SA, Spain) was used to show out the viability of adhered bacteria to the Ti6Al4V surface before and after being exposed to the UV irradiation.

Also, the pH of the suspensions after the exposure time was measured.

### RESULTS AND DISCUSSION

Slightly differences have been found on the number of adhered bacteria between hydrophobic and hydrophilic Ti6Al4V surfaces. Over the adhered ones, the bactericidal effect of Mg ions follows an increase with both concentration and exposure time but shows no relations with the hydrophobicity of the substrate neither with the pH.

### CONCLUSION

Mg ions have a remarkable antibacterial behaviour. Their controlled-release from the new proposed biomaterial would bring great benefits after implants.

### REFERENCES

1. Maurus PB, *et al.*, Oper. Techn. Sports Med.12: 158, 2004.
2. Witte F *et al.*, Biomaterials 26: 3557, 2005.
3. Pacha-Olivenza MA *et al.* J Colloid Inter. Sci. 320, 117-24, 2008

### ACKNOWLEDGMENTS

The authors acknowledge “Ministerio de Ciencia e Innovación” for financing the project MAT2012-37736-C05-03, “Junta de Extremadura-FEDER” (Grant GR10149) and Networking consortium CIBER-BBN. J.R.-S. would like to thank “Ministerio de Educación, Cultura y Deporte” for his fellowship FPU13/00862.



## INTRODUCTION

Biofilm formation is the critical factor and ultimate cause of persistence in chronic bacterial infections such as implant-associated osteomyelitis<sup>1</sup>, heart valves endocarditis, catheters, among many others<sup>2, 3</sup>. Degradable polymer coatings were mostly considered as tools to improve biocompatibility of the matrixes which exhibited controlled release of therapeutic molecules. Poly (lactic-co-glycolic acid) (PLGA), a biodegradable and biocompatible synthetic polymer was explored in thin film formulation<sup>4</sup>. Alginate (ALG), a natural polymer, has attracted researchers owing to its ease of availability, compatibility with hydrophobic as well as hydrophilic molecules, biodegradability under physiological conditions and the ability to confer sustained release potential<sup>5</sup>. Immobilization of enzymes for antimicrobial strategy has been applied for the protection of biomaterial devices and implantation. Lysozyme (LYS) is the enzyme that has strong antibacterial potential against Gram-positive bacteria<sup>6</sup>. The aim of the present work was to develop and characterize a thin film as a coating system using degradable materials and evaluate the capacity of immobilization and release of LYS.

## EXPERIMENTAL METHODS

### Preparation of thin film by Dip coating

PLGA (50:50) solution (6.25%) (solution A) was prepared through the dissolution in dichloromethane. ALG sodium solution (3%) (solution B) and LYS (12 mg/ml) (solution C) were prepared through the dissolution in 0.1 M phosphate buffer solution pH 6.5. The 0.1 ml of solution B was added to solution C and mixed for 2 min in vortex to form mix D. The 0.8 mL of solution A was added to 0.2 mL of mix D and taken to homogenize using a homogenizer Silentcrusher S at a speed of 45000 rpm for 90 seconds. After the PE sheet substrates (5 cm<sup>2</sup>) were subjected to microwave plasma oxygen treatment on both sides and then was dipped into the mix D, before drying at ambient conditions. For crosslinking the films were immersed for 2 min into a bath consisting of 10 mL of a solution of CaCl<sub>2</sub> (5%) and glycerol (5%). Then, the films were removed from the bath, washed with water. The excess of water was removed with a filter paper and maintained on a support for 4h at room temperature for drying. PLGA/ALG coating was prepared without LYS as control. The thickness of the films was determined in dry state.

### Surface contact angle measurement

The wettability of the films was measured using the sessile drop method using an OCA 40 contact angle system. (n=5)

### Scanning electron microscopy (SEM)

Morphological characterization of the films was done using a field emission SEM.

## ATR-FTIR

FTIR spectra were collected and the LYS secondary structure was analysed during the *in vitro* release test. (n=6)

### *In vitro* release

Lysozyme release was evaluated by immersion of the film (5 cm<sup>2</sup>) into 1.5 ml of 0.1 M HEPES at pH of 7.3 in 2 ml Eppendorf tubes in a thermostatic shaking bath at 37 °C. The amount of LYS released was measured spectrophotometrically at ( $\lambda$ ) 281 nm in samples periodically taken up and placed again into the same tube. (n=6)

## RESULTS AND DISCUSSION

Thin film of PLGA-ALG polymers were successfully produced by dip coating. The SEM micrographs reveal an ordered array of approximately 2  $\mu$ m size pores on the surface<sup>4</sup>. An average thickness of the film is  $\sim$ 5  $\mu$ m. The obtained water contact angle of 80° indicated the relative hydrophobicity of the material. The incorporation of hydrophilic ALG does not affect the proprieties of PLGA structure and can promote modulation of the enzyme release. The results of an *in vitro* lysozyme release assay demonstrated a sustained and prolonged release time for up more to 1 month. The percentage of  $\alpha$ -helices and  $\beta$ -sheets was calculated using the FTIR spectra and confirmed the presence of the secondary structures of LYS.

## CONCLUSION

PLGA-ALG films were prepared using biodegradable polymers and were a suitable platform for incorporated and sustained LYS release. Biodegradable polymers can emerge as an appealing technology platform to functionalize biomaterial surfaces with antimicrobial activities.

## REFERENCES

1. Kazemzadeh-Narbat M. *et al.*, Biomaterials. 31:9519-9526, 2010.
2. Stempel N. *et al.*, Curr Pharm Des. 21:67-84, 2015.
3. Siddiq D.M. *et al.*, Nat Rev Urol. 9:305-314, 2012.
4. Ponnusamy T. *et al.*, Biomater. 2:77-86, 2012.
5. Ahmad Z. *et al.*, Expert Opin Drug Deliv. 5: 1323-1343, 2008.
6. Ma D. *et al.*, J Colloid Interface Sci. 359:399-, 2011.

## ACKNOWLEDGMENTS

This work was support, Brazilian National Research Council, CNPq and the Science without Borders program, Brazil, (Grant 249251/2013-2). The authors would like to thank to Corbion Purac Biomaterials for the kindly donation of PURASORB®PDLG.





## Bacteria, Biofilms and Mass Spectroscopy: Following the Bacteria's Footprints

E. Peter Magennis<sup>1</sup>, Andrew Hook<sup>1</sup>, David Barrett<sup>1</sup>, Paul Williams<sup>2</sup>, Morgan Alexander<sup>1</sup>

<sup>1</sup> Laboratory of Biophysics and Surface Analysis, University of Nottingham, UK

<sup>2</sup> School of Molecular Medical Sciences, University of Nottingham, UK

[peter.magennis@nottingham.ac.uk](mailto:peter.magennis@nottingham.ac.uk)

### INTRODUCTION

Bacteria are a cause of significant acute and chronic disease and their infections can have a serious and detrimental impact upon quality of life and mortality, whilst socio-economic factors associated with infectious diseases have larger impacts. Device related infections are common in modern healthcare and many types of devices are known to become colonized by bacterial biofilms.<sup>1</sup> Bacterial “footprints” including adhesins<sup>2</sup> deposited on surfaces can facilitate attachment but the full range and identity remain unknown. Surface analysis techniques, such as time of flight secondary ion mass spectroscopy (ToF-SIMS) have provided structural information of compounds deposited by microorganisms after culturing and biofilm formation.<sup>3</sup> However, ToF-SIMS analysis supported ambient mass-spectroscopy *before* biofilm development can illuminate a further range of the footprints from bacteria. The differences in these depositions between high-fouling and low-fouling biomaterials can further guide novel material development.

### EXPERIMENTAL METHODS

Known co-polymers resistant to bacterial attachment<sup>4</sup> were synthesised and deposited on glass slides. The coated surfaces were incubated with *Pseudomonas aeruginosa* over a period of 24 hours in RPMI-1640 media and the changes in surfaces were monitored as a function of time. Surfaces were analysed using ToF-SIMS and liquid extraction surface analysis mass spectrometry (LESA-MS).

### RESULTS AND DISCUSSION

Further to incubation with bacteria, principle component analysis of the TOF-SIMS spectra showed that after 24 hours with bacteria significant alteration had occurred to the surface. For example, there was deposition of proteins indicated by the dramatic increase in the  $\text{CN}^-$  and  $\text{CNO}^-$  peaks (figure 1). This change was readily apparent through mass spectroscopy imaging of  $\text{CNO}^-$  (figure 2). However these proteins were less pronounced on the resistant materials after 3 hours of incubation.

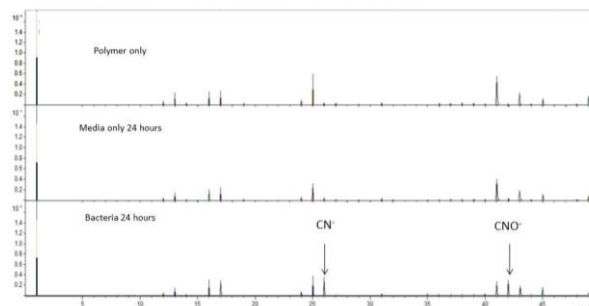


Figure 1. Negative ion ToF-SIMS spectra of polymers before incubation (top) after incubation with media (middle) and after incubation with bacteria (bottom). Highlighted ions  $\text{CN}^-$  [26]<sup>-</sup> and  $\text{CNO}^-$  [42]<sup>-</sup>.

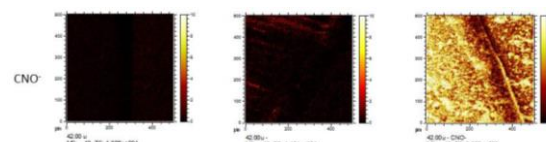


Figure 2. Negative ion ToF-SIMS images of secondary ion  $\text{CNO}^-$  [42]<sup>-</sup> before incubation (left) after incubation with media (centre) and after incubation with bacteria (right). Image area is 500  $\mu\text{m}^2$ .

The use of LESA-MS also provided further information on how the surfaces were altered after exposure to bacterial cultures and facilitated identification of compounds.

### CONCLUSION

Further insight into the deposits of bacteria over time has been explored. Changes in biomaterial surfaces have been demonstrated using mass spectroscopy techniques. Changes include but are not limited to proteins.

### REFERENCES

1. Donlan R. M., *Emerg. Infect. Dis.* 7:277-281, 2001
2. Beloin C *et al.*, *PLoS Biol.* 6:e167, 2008
3. Kaivosoja E. *et al.*, *Eur. Cell Mater.* 24:60-73, 2012
4. Hook, A. *et al.*, *Adv. Mater.* 25:2542-2547, 2013

### ACKNOWLEDGMENTS

The authors would like to thank The Wellcome Trust (Senior Investigator Award ref: 103882) for providing financial support to this project.

# Bacteria-Instructed Synthesis of Polymers for Self-Selective Microbial Binding and Labelling

E. Peter Magennis<sup>1</sup>, Francisco Fernandez-Trillo<sup>2</sup>, Cheng Sui<sup>1</sup>, Sebastian G. Spain<sup>1</sup>, David J. Bradshaw<sup>3</sup>, David Churchley<sup>3</sup>, Giuseppe Mantovani<sup>1</sup>, Klaus Winzer<sup>4</sup>, Cameron Alexander<sup>1</sup>

<sup>1</sup>School of Pharmacy, University of Nottingham, Nottinghamshire, UK

<sup>2</sup>School of Chemistry, University of Birmingham, Edgbaston, UK

<sup>3</sup>GlaxoSmithKline, Weybridge, Surrey, UK

<sup>4</sup>School of Life Sciences, University of Nottingham, Nottinghamshire, UK

[peter.magennis@nottingham.ac.uk](mailto:peter.magennis@nottingham.ac.uk)

## INTRODUCTION

The detection and control of microorganisms is important in a wide range of industries and settings. Traditional antimicrobial agents have been successful but resistance is spreading and alternatives to antibiotics are needed.<sup>1</sup> Non-lethal or cell binding systems include soft-lithography, molecular imprinting and carbohydrate processes.<sup>2-4</sup> However, these techniques have adaptive limitations. The use of hydrophilic co-polymers may be advantageous as they can act as a mimetic of the extracellular matrix (ECM). Such natural systems are operated by bacteria to adapt to their environment and also include redox cascades and metal binding systems. These suggest that, through control of redox processes a synthetic ECM could be produced, capable entombing bacteria in a material of their own design. Using copper mediated ATRP bacterial-instructed ligands could be constructed which are capable of rebinding bacteria targets. The same process could also be applied to a copper-catalysed Huisgen cycloaddition (click-chemistry) to fluorescently tag the bacteria *in situ*.

## EXPERIMENTAL METHODS

Bacterial strains of *E. coli* and *P. aeruginosa* were obtained from stocks held within the University of Nottingham. Bacteria were grown for 24 hours then washed and condensed. Polymers were synthesised by bacteria-activated (b-ATRP) or standard ATRP. For bacterial polymerisations: Monomers were charged into a reaction flask with initiator and bacteria before deoxygenating. The catalyst was degassed separately and added to initiate polymerisation. Polymers were retrieved from bacteria through washing steps. Bacteria-polymer interactions were assessed by cluster analysis. For chemo-labelling of bacteria, a cationic polymer displaying alkynes was incubated with bacteria then an azide-coumarin dye was added which fluoresces after successful "clicking".

## RESULTS AND DISCUSSION

Using novel b-ATRP, polymer constructs were formed which were selective for the microorganism from which they were formed and also compared to control polymers produced by standard ATRP (figure 1). Furthermore, using copper mediated click chemistry, direct fluorescent tagging of bacteria has been demonstrated using a cationic targeting polymer.

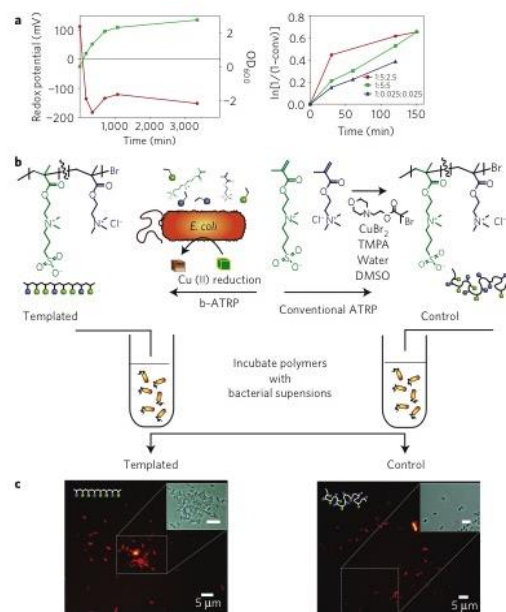


Figure 1. a) Left: Change in redox potential during bacteria growth, Right: Polymerisation kinetics of b-ATRP. b) Schematic of bacteria-instructed synthetic process. c) Fluorescent microscopy of *E. coli* mCherry with bacteria instructed and control polymers.

## CONCLUSION

This work shows that bacterial metabolic processes can be high-jacked for synthetic chemistry. The rebinding by the materials offers a novel approach to bacterial capture. The induction of fluorescence was detectable using a smart phone camera, as potentially simple diagnostic test.

## REFERENCES

1. Bush, K. *et al.*, Nature Rev. Microbiol., 9:894-896, 2011
2. Aherne. *et al.*, Nature J. Am. Chem. Soc., 118:8771-8772, 1996
3. Dickert, F. L. and Hayden, O., Anal. Chem., 74:1302-1306, 2002
4. Disney, M. D. and Seeberger, P. H., Chem. Biol., 11:1701-1707, 2004

## ACKNOWLEDGMENTS

The authors would like to thank GlaxoSmithKline the Biotechnology and Biological Sciences Research Council (BBSRC) and the Engineering and Physical Sciences Research Council (EPSRC) (Grants BB/H53052X/1, EP/H005625/1, EP/G042462/1) for providing financial support to this project.



## Microbial Adhesion on Nanostructured Biomaterials Surfaces

Carolin Dewald<sup>1,2,3</sup>, Claudia Lüdecke<sup>1</sup>, Martin Roth<sup>2,3</sup>, Jörg Bossert<sup>1</sup>, Klaus D. Jandt<sup>1,3</sup>

<sup>1</sup> Chair of Materials Science, Otto Schott Institute of Materials Research (OSIM), Faculty of Physics and Astronomy, Friedrich Schiller University Jena, Löbdergraben 32, 07743 Jena, Germany

<sup>2</sup> Bio Pilot Plant, Leibniz Institute for Natural Product Research and Infection Biology, Hans Knöll Institute (HKI), Beutenbergstrasse 11a, 07745 Jena, Germany

<sup>3</sup> Jena School for Microbial Communication (JSMC), Friedrich Schiller University Jena, Neugasse 23, 07743 Jena, Germany

[carolin.dewald@uni-jena.de](mailto:carolin.dewald@uni-jena.de)

### INTRODUCTION

An increased use of antibiotic drugs has led to the development of numerous multi-resistant microbes in the last years. Due to this medical situation the treatment of biomaterials-associated infections (BAI) with antibiotics is critically discussed. Therefore, a reduced adhesion of microorganisms on biomaterials surfaces is of high interest for preventing BAI<sup>1</sup>. The most frequently isolated fungus from BAI is *Candida albicans*, the pathogen of candidacies and the most frequently isolated bacteria is *Staphylococcus aureus*.

One strategy is the modification of the topographical characteristics of biomaterials surfaces. In a previous work we showed a decreased adhesion of Gram-positive and Gram-negative bacteria on nanorough biomaterials in the range between 2 nm and 6 nm<sup>2</sup>. The aims of this study are [i] to investigate the adhesion of *C. albicans* and *S. aureus* on biomaterials structured physically with nanoparticles and [ii] to identify and understand microbial adhesion mechanisms on these surfaces.

### EXPERIMENTAL METHODS

For reproducible fabrication of gold surfaces physical vapor deposition (PVD) was used. Gold nanoparticles with different size and concentration were used to get different distances between these nanoparticles immobilized on gold surfaces via a chemical reaction pathway. These surfaces were characterized by atomic force microscopy, scanning electron microscopy and contact angle measurements. For microbial adhesion a previously established *in-vitro* testing device was used<sup>3</sup>. For determining the microbial adhesion a confocal laser scanning microscope and focused ion beam scanning electron microscope for cross-sectioning of adhered microbial cells on the surface obtaining the nano-interface between the cells and the biomaterial were used.

### RESULTS AND DISCUSSION

Preliminary results showed an increased microbial adhesion with extending the adhesion time on both the nanostructured surfaces and the control sample without chemically bounded nanoparticles on the surface. On nanostructured biomaterials surfaces the microbial adhesion is reduced compared to the control for each adhesion time. In addition, it is demonstrated that the microbial adhesion on biomaterials surfaces is reduced by decreasing the amount of bounded nanoparticles on the surface. The nanoparticles may act as attachment points for the microbes. By reducing these attachment points the microorganisms need to spread between the

nanoparticles which results in a decreased adhesion on structured surfaces with the lower amount of nanoparticles.

### CONCLUSION

The microbial adhesion of different model organisms can be influenced by modifying the nanostructure of biomaterials surfaces. Therefore, the use of nanoparticles may be a promising antibiotic-free strategy to reduce microbial adhesion on biomaterials surfaces and decrease the risk of BAI.

### REFERENCES

- <sup>1</sup> Campoccia D., Montanaro L., Arciola C.R. (2013): A review of biomaterials technologies for infection-resistance surfaces, *Biomaterials* 34(34): 8533-8554
- <sup>2</sup> Lüdecke C., Bossert J., Roth M., Jandt K.D. (2013): Physical vapor deposited titanium thin films for biomedical applications: Reproducibility of nanoscale surface roughness and microbial adhesion properties, *Applied Surface Science* 280: 578-589
- <sup>3</sup> Lüdecke C., Jandt K.D., Siegesmund D., Kujau M.J., Zang E., Rettenmayr M., Bossert J., Roth M. (2014): Reproducible biofilm cultivation of chemostat-grown *Escherichia coli* and investigation of bacterial adhesion on biomaterials using a non-constant-depth film fermenter, *PloS ONE* 9(1): e84837

### ACKNOWLEDGMENT

We authors thank S. Brunke for providing *C. albicans*. Grateful thanks to M. Cyrlies, K. Perlet and R. Wagner for technical support. This work was funded by the "Jena School for Microbial Communication".



## Design of Ag@SiO<sub>2</sub> Nanorattles for Antimicrobial Implant Coatings

Sarah-Luise Abram<sup>1</sup>, Katharina M. Fromm<sup>1</sup>

<sup>1</sup>Department of Chemistry, University of Fribourg, Switzerland  
[sarah-luise.abram@unifr.ch](mailto:sarah-luise.abram@unifr.ch)

### INTRODUCTION

Medical progress and an ageing world population have led to an increasing use of foreign materials inside the human body. Consequently also the number of infections related to these implants has grown significantly.<sup>1</sup> Antimicrobial coatings that prevent the formation of infectious biofilms on the surface of the implants could make an important contribution to overcome that issue. Silver is known for its good antimicrobial and biocompatible properties and could therefore play an important role in the fight against implant infections, especially if they are caused by antibiotic resistant bacteria.<sup>2</sup>

This project covers the synthesis of silver nanoparticles that are encapsulated inside a protective silica shell in order to prevent aggregation or a too fast release of the antimicrobially active Ag<sup>+</sup> ions. The silica shell provides reactive sites to covalently attach the antimicrobial nanocontainers to the implant surface. Furthermore it enables the functionalization with biosensor units to create a stimuli responsive release of the Ag<sup>+</sup> only in the presence of bacteria.

### EXPERIMENTAL METHODS

Ag colloid:

A variation of the polyol process<sup>3</sup> was used for the synthesis of silver nanoparticles with an average diameter of 24 nm.

Silica coating:

The silver nanoparticles were coated with a silica shell according to a modified Stöber method.<sup>4</sup>

Etching:

The inner part of the silica shell was removed by etching with hot water in presence of PVP<sup>5</sup>.

### RESULTS AND DISCUSSION

The combination of the polyol process for the preparation of a silver colloid with the Stöber method for the synthesis of a silica shell resulted in homogeneously coated Ag@SiO<sub>2</sub> core-shell particles with an average size of 75 nm. The presence of PVP on the particle surface during the following etching procedure allows the selective removal of the inner part of the silica. This creates a hollow container with a shell thickness of about 12 nm. The silver nanoparticles are believed to be freely moveable inside that sphere. Silver ions should be released through the pores of the shell to ensure the antimicrobial properties of the nanorattles. This possibility could be proven by first dissolving the silver cores in nitric acid and then imaging the empty silica containers with TEM.

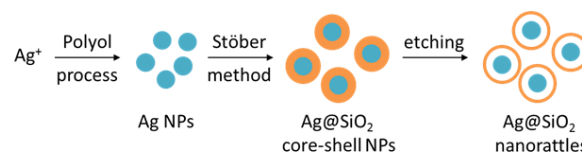
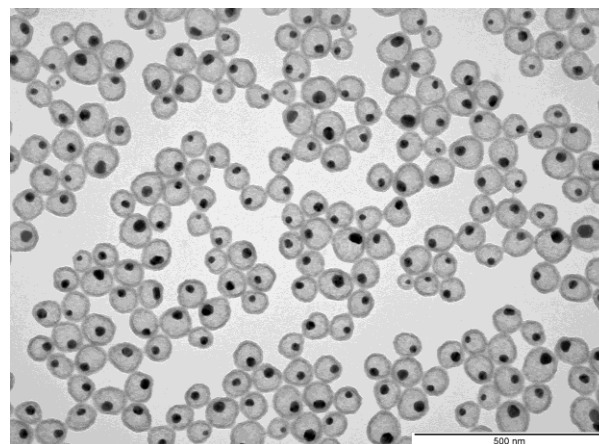


Figure 1: TEM picture and synthesis route to Ag@SiO<sub>2</sub> nanorattles

### CONCLUSION

As a first step in the design of an antimicrobial implant coating we established a reliable synthesis of Ag@SiO<sub>2</sub> nanorattles where just one silver nanoparticle is encapsulated inside a larger hollow silica shell.

A functionalization with amino groups by co-condensation of (3-aminopropyl)trimethoxysilane offers possibilities to coat implant surfaces and for further functionalization in order to obtain an effective and biocompatible antimicrobial material to fight implant infections.

### REFERENCES

1. Veerachamy S. *et al.*, Proc IMechE Part H: J Engineering in Medicine 228:1083-1099, 2014
2. Eckhardt S. *et al.*, Chem. Rev. 113:4708-4754, 2013
3. Silvert P.-Y. *et al.*, J. Mater. Chem. 6:573-577, 1996
4. Li G. L. *et al.*, Polym. Chem. 2:1368-1374, 2011
5. Hu F. *et al.*, small 11:985-993, 2015

### ACKNOWLEDGMENTS

The authors would like to thank the University of Fribourg, the Fribourg Center for Nanomaterials FRIMAT and the Swiss National Research Foundation for the generous funding of the project. It is part of the National Center of Competence in Research “Bio-inspired Materials”.



# Synthesis of Poly(N-Isopropylacrylamide)-Silver Nanocomposite for Biomedical Applications

Milène Tan, Katharina M. Fromm

Department of chemistry, University of Fribourg, Switzerland

[Milene.tan@unifr.ch](mailto:Milene.tan@unifr.ch)

## INTRODUCTION

In the last decades, polymeric materials have attracted a significant interest in the biomedical field especially in their use as implants. With the emergence of new multi-drug resistant bacteria and despite advances sterilization procedures, the contamination of implant surfaces by bacteria is a new challenge to overcome.<sup>1</sup> Then, the design of new surfaces in order to prevent bacterial adhesion and biofilm formation is a serious concern. Silver has already been proved to be effective against bacteria even at low concentrations.<sup>2</sup> Besides, silver in nano-size could present higher efficiency against bacteria over a longer time-activity.<sup>3</sup> For these reasons, silver nanoparticles (NPs) have been exploited in the framework of this project.

Poly(N-isopropylacrylamide) (PNiPAAm) is very suitable for biomedical applications owing to its good biocompatibility and thermosensitivity with a lower critical solution temperature (LCST) close to 32°C. Practically, the polymer is readily soluble under this temperature but above, it becomes insoluble and precipitates out. Furthermore, its synthesis by RAFT polymerization requires a sulfur compound as chain transfer agent, making the polymer very suitable for silver binding.

## EXPERIMENTAL METHODS

Polymer synthesis:

PNiPAAm was obtained by RAFT at 70°C in THF using 2-(Dodecylthiocarbonothioylthio)-2-methylpropionic acid (DMP) and AIBN as RAFT agent and initiator respectively, for a targeted DP of 50. The initial concentration in monomer was established at 3M and with molar ratio [NiPAAm]/[DMP]<sub>0</sub>/[AIBN]<sub>0</sub> 50/1/0.2.

Ag nanoparticles:

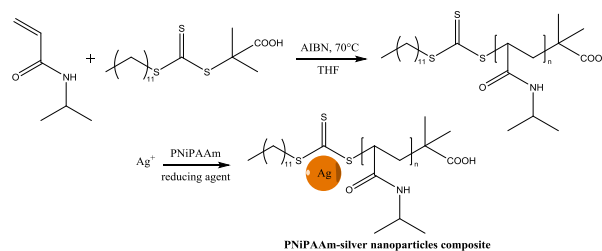
Silver NPs were synthesized by reducing silver nitrate in mild conditions in a solution containing the PNiPAAm.

## RESULTS AND DISCUSSION

As shown in the results presented in the table 1, it obviously appears that the RAFT polymerization leads to the controlled synthesis of the PNiPAAm. Indeed, a good correlation between the theoretical  $M_n$  and the experimental  $M_n$  (obtained by NMR) was observed, as well as a low polydispersity.

Conv (%)	$M_n$ theo (g.mol <sup>-1</sup> )	$M_n$ NMR (g.mol <sup>-1</sup> )	$M_{napp}$ SEC (g.mol <sup>-1</sup> )	PDI
85	4680	4890	4210	1.18

Table 1. Macromolecular parameters of PNiPAAm



Scheme 1 Synthetic route of the nanocomposite

The silver nanoparticles were obtained by reducing the silver ions in the presence of the PNiPAAm in order to prevent their aggregation believed to decrease the antimicrobial properties of the silver.<sup>4</sup> The reduction needs to be done in mild conditions to avoid the reduction of the RAFT end-group of the polymer.

## CONCLUSION

The PNiPAAm was synthesized in a first step by RAFT polymerization known to be an effective and controlled synthetic route to obtain polymers. Besides, the presence of sulphur RAFT end-group in the polymer makes it very suitable for possible silver binding. That kind of nanocomposite provides a biocompatible and effective antimicrobial material for further biomedical applications.

## REFERENCES

- Guo L. *et al.*, Colloids and Surface A : Physiochem. Eng. Aspects, 439:69-83, 2013
- Silver S. *et al.*, J. Ind. Microbiol. Biotechnol., 33:627-634, 2006
- Morones J.R. *et al*, Nanotechnology, 16:2346-53, 2005
- Bae E. *and al.*, Environ. Toxicol. Chem., 29:2154-60, 2010

## ACKNOWLEDGMENTS

The authors would like to thank the University of Fribourg, the Fribourg Center for Nanomaterials FRIMAT and the Swiss National Research Foundation for the generous funding of the project.

# Multilayer Coating of a Nonwoven Polyester Textile for Antibacterial Wound Dressing

François Aubert-Viard<sup>1\*</sup>, Oumaira Rahmouni<sup>1</sup>, Adeline Martin<sup>2</sup>, Feng Chai<sup>1</sup>, Nicolas Tabary<sup>2</sup>, Christel Neut<sup>3</sup>, Bernard Martel<sup>2</sup> and Nicolas Blanchemain<sup>1</sup>

<sup>1\*</sup> INSERM U1008, Biomaterial Research Group, University Lille 2, France,

<sup>2</sup> UMET, Ingénierie des Systèmes Polymères, University Lille 1, Lille

<sup>3</sup> INSERM U995, Laboratoire de Bactériologie, University Lille 2, France

[francois.aubert@univ-lille2.fr](mailto:francois.aubert@univ-lille2.fr)

## INTRODUCTION

Wound healing represents a public health problem with an increase in susceptible populations like geriatric or diabetic patients<sup>1</sup>. The major complication is infection, associated to an increase of morbidity (amputation) or mortality (septicemia). In particular, the infection of the diabetic wounds delays the healing process and progresses to bone destruction<sup>2</sup>. We recently develop a wound dressing functionalized by layer-by-layer system based on chitosan (positive polyelectrolyte, PE+) and cyclodextrin polymer (negative polyelectrolyte, PE-) for synergic bi-therapy with silver or iodide associated to chlorhexidine.

## EXPERIMENTAL METHODS

In a first step, the non woven polyester (PET) is functionalized by chitosan (CHT) crosslinked by citric acid (CTR) to obtain a first charged layer (positive or negative in function of the CTR concentrations) or by genipin to obtain a first positively charged layer only. The textile is characterized by FTIR, SEM and the ionic charge density is evaluated by titration. Then the positively and negatively charged PET-CHT is impregnated in iodine or silver solutions to obtain the first bioactive coating. The drug loading is quantified by elementary analysis and titration. In a second step, the multilayer system is build up on the loaded PET-CHT according to the method develop in our lab<sup>3</sup> using alternatively cyclodextrin polymer (PCD, PE-) and CHT (PE+). In a last step, the multilayer system is impregnated in a chlorhexidine (CHX) solution. The CHX loading and CHX release is measured by HPLC method in function of the number of bilayers. Finally, the kinetic of release of the final wound dressing (PET-CHT-Ag/CHX and PET-CHT-I/CHX) is studied in physiological medium (PBS, pH7.4, 37°C, 80 rpm). The antibacterial activity is evaluated on different bacterial strains (*S. aureus* CIP224; *E. coli* K12; MRSA 07001 and *P. aeruginosa* ATCC 27583) by kill-time method. At each step of the functionalization process, the cytocompatibility is evaluated with epithelial cells (ATCC-CCL5, L132) according to ISO 10993-5 standard.

## RESULTS AND DISCUSSION

The evaluation of the charge density on the functionalized PET with CHT shows the ability of the system to be adapted with the CTR concentrations either with an anionic exchange functions ([CTR] >1%) either with a cationic exchange functions ([CTR] <1%). After impregnation of anionic and cationic PET-CHT in silver and iodine solution, the titration shows a silver loading of 3% and iodine loading of 1600 ppm. *In vitro*,

microbiology evaluation reports the efficiency of the loaded PET-CHT. Indeed, the silver loaded PET-CHT reduces significantly two bacterial population after 24 hours (*S. aureus* : 4 log; *E. coli* : 5 log reduction).

The multilayer system, applies on the loaded PET-CHT, has three functions thanks to the cyclodextrin polymer as previously described<sup>4</sup> i) barrier effect to reduce the release of the cytotoxic silver into the wound ii) gel formation to drain exudates iii) complex-inclusion formation to adsorb other drug. Systems with 5.5, 7.5 and 10.5 bilayers are performed on the PET-CHT-Ag. As show in figure 1a, the presence of silver has no influence on the build-up of the multilayer. Additionally, the figure 1b shows the CHX loading and CHX release depends on the number of bilayers.

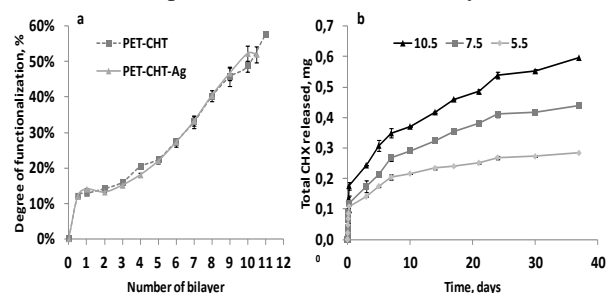


**Fig 1. a. Evolution of weight gain of textiles during the construction of the system. b. Kinetic of release of CHX in function of the number of bilayer (PBS, 80rpm, 37°C) (b).**

The evaluation of cell vitality by the method of the Alamar blue shows an excellent cytocompatibility of the functionalization of the dressings at each stage of the process (vitality rate >70%). Finally, microbiological evaluation confirms the CHX release studies with a prolonged antibacterial effect (>30 days) of the Ag/CHX loaded on wound dressing against *S. aureus* and *E. coli*.

## CONCLUSION

We demonstrate the safety and the prolonged antibacterial effect of a multilayer wound dressing loaded with silver or iodide associated with CHX. The three main characteristics of multilayer system (drug sorption, gel formation, ionic exchange capacity) allow us to obtain a new generation of wound dressing for combined biotherapy.

## REFERENCES

1. Ashcroft GS. *et al.*, Biogerontol. 3:337-345, 2002
2. Abbott CA. *et al.*, Diabet Med. 19:377-384, 2002
3. Martin A. *et al.*, Carbohydr Polym. 93:718-730, 2013
4. Martel B. *et al.*, J Appl Polym Sci, 2005

## INTRODUCTION

In the past two decades, many chemically sophisticated drug delivery systems were developed however, with rather disappointing end results *in vivo*<sup>1</sup>. *N*-Vinylcaprolactam (VCL) based nanogels (NGs) belong to the top candidates to be utilized as drug delivery system due to sizes tunability, biocompatibility<sup>2</sup> and biodegradability. Moreover, they can be functionalized for multiple drug loading<sup>3</sup>. Hence, our scientific goal is to develop degradable, pH-sensitive NGs (< 150 nm) that can be post-modified with a fluorescent dye and covalently bind an antitumor drug. The tumor accumulation and organ biodistribution of these NGs can be monitored non-invasively using hybrid imaging, e.g. combining fluorescence molecular tomography (FMT) with micro computed tomography ( $\mu$ CT), *in vivo*.

## EXPERIMENTAL METHODS

### Nanogel Synthesis

The NGs were synthesized via precipitation copolymerization of VCL with the comonomers itaconic acid dimethyl ester (IADME) and the linear macromonomer (VBA-50)<sup>4</sup> in water. As acid-degradable crosslinker 3,9-divinyl-2,4,8,10-tetraoxa-spiro[5.5]undecane (DTOU) was inserted and for initiation 2,2'-azobis(2-methylpropionamidine)dihydrochloride (AMPA) was used.

### Post-Modification of Nanogels

Via Steglich Esterification thiols were incorporated into the NGs. By thiol-maleimide reaction the NGs were labelled with the fluorescent dye Cyanine7 maleimide (Cy 7) and Mal-DOX was bound covalently. Mal-DOX contains a pH-sensitive hydrazone bond between doxorubicin (DOX) and the maleimide group for pH-sensitive drug release.

### Nanogel Characterization

The NGs were characterized by Raman spectroscopy and H-NMR spectroscopy to confirm the integration of the comonomers and the thiol-functionalization. The size of the NGs was determined by DLS and also degradation of the nanogels was monitored by DLS and AFM.

### Organ Biodistribution Monitoring

Two A431 tumor-bearing mice were injected i.v. with 2 nmol NG-Cy7 in the tail vein. The mice were imaged at 0.25, 3, 6 and 24 h post-injection using a novel imaging protocol of hybrid  $\mu$ CT/FMT (Fig. 3a). NG-Cy7 tumor accumulation and organ biodistribution was quantified for each imaging point using  $\mu$ CT based organ segmentation (Fig. 3b).

## RESULTS AND DISCUSSION

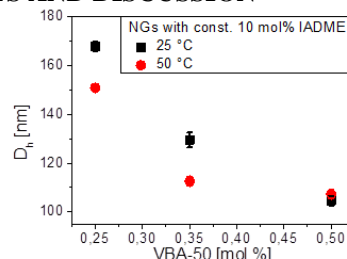


Fig. 1: The desired size range (< 150 nm) of the PVCL-based NGs could be achieved.

Due to the incorporated acid-degradable crosslinker (DTOU) the NGs degrade slowly in acidic medium.

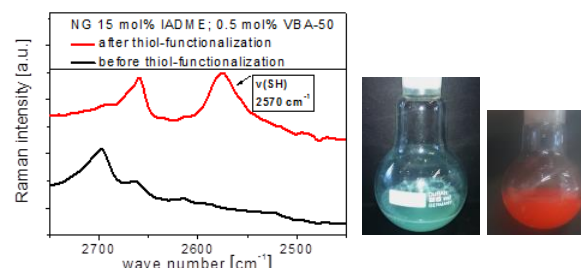


Fig. 2: The thiol-functionalization of the NGs (left) as well as the Cy7 (middle) and Mal-DOX (right) coupling were successful, respectively.

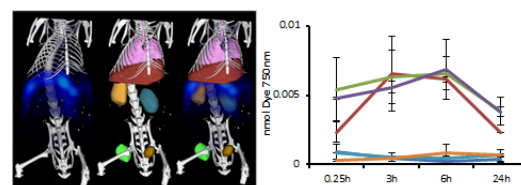


Fig. 3: a) Hybrid  $\mu$ CT/FMT images with organ segmentation: the highest NG-Cy7 accumulation can be seen in the liver (red) and the kidneys (yellow and blue). b) Analysis of organ biodistribution of NG-Cy7 *in vivo*: highest tumor accumulation after 6 h.

## CONCLUSION

The first pilot-study indicated that degradable NG-Cy7 are stable *in vivo* and they accumulate in tumors with minimal renal excretion.

## REFERENCES

1. Lammers T. *et al.* J. Control. Release 161:175-187, 2012.
2. Vihola H. *et al.*, Biomaterials 26:3055-3064, 2005.
3. Schachschal S. *et al.*, Macromolecules, 43:4331-4339, 2010.
4. Pargen S. *et al.*, Macromol. Chem. Phys. 212:1791-1801, 2011.

## ACKNOWLEDGMENTS

The authors would like to thank the Excellence Initiative of the German federal and state governments in the framework of the I<sup>3</sup>TM Seed Fund Program.

Niko Granqvist<sup>1</sup>, Annika Jokinen<sup>1</sup>, Willem M. Albers<sup>1</sup> and Janusz Sadowski<sup>1</sup>

<sup>1</sup>BioNavis Ltd., Finland  
[Janusz.sadowski@bionavis.com](mailto:Janusz.sadowski@bionavis.com)

## INTRODUCTION

Surface Plasmon Resonance (SPR) has been used already for a few decades for label-free detection and characterization of biochemical kinetics and affinities of many different types of analytes. The physical phenomenon is not limited to biochemistry, but is applicable to other nanoscale characterization of thin films<sup>1</sup>.

## EXPERIMENTAL METHODS

Aside of the traditional interactions, Multi Parametric Surface Plasmon Resonance (MP-SPR) can be utilized to determine unique refractive index (*RI*) and thickness (*d*) of ultrathin (*d* 0.5-100 nm) and slightly thicker films (*d* 300 nm- few  $\mu$ m) without prior assumptions of the *RI* of the material. These are important properties not only for thin film coating industries and applications, but also for gaining important knowledge in biomaterials. Two methods utilizing MP-SPR to thickness and *RI* calculations have been introduced, either measuring in two different media (2M) with high *RI* difference, such as air and water<sup>1-3</sup>, or at two or more different wavelengths (2W) of light<sup>2,3</sup> in order to characterize properties of the thin films.

The MP-SPR method also allows study of wide variety of different coatings including plastics, cellulose, lipid layers, minerals and hydrogels. The interactions of different biomolecules towards these coatings can also be characterized using the method.

## RESULTS AND DISCUSSION

MP-SPR is suitable for film deposition *in situ* or *ex situ*, which makes it compatible with several deposition methods and thereby makes it applicable to a wide range of polymers also. Polyelectrolyte multilayer deposition *in situ* was monitored in real-time with MP-SPR. Thickness of each deposited layers was determined utilizing two wavelength method.

Similarly layer thickness and *RI* was determined also for *ex situ* spin coated cellulose layer. MP-SPR was used not only to determine thickness and *RI* of the deposited layer but also for real time monitoring of

other molecules interaction to the cellulose model surface<sup>4,5</sup>.

Recently, MP-SPR was used also to monitor polymer layer structural changes in real time, such as polymer swelling due to pH or electric potential change<sup>6</sup>. At pH = 9 poly (acrylic acid) (PAA) brushes were extended but the brushes collapsed at acidic pH.

The MP-SPR method has also been used in characterizing different materials for their ability to support either lipid bilayer or liposome layer formation<sup>7</sup>. In addition interaction of antimicrobial peptide to lipid bilayers has been studied.

## CONCLUSION

With the ability to characterize both kinetics and nanoscale layer properties, MP-SPR proves to be a versatile tool for nanomaterial, biomaterial and biochemical interactions research, which makes MP-SPR invaluable for multidisciplinary research, where both physical and interaction properties of the materials need to be characterized.

## REFERENCES

1. Albers, Vikholm-Lundin, Chapter4 in Nano-Bio-Sensing, Springer 2010
2. Liang, et al., Sens.Act.B, 149 (1), 2010, 212-220
3. Granqvist et al., Langmuir 29 (27), 2013, 8561-8571
4. Orelma et al., 12 (12), 2011, 4311-4318
5. Kontturi et al., J.Mater. Chem. A, 2013, (ASAP) DOI: 10.1039/C3TA12998E
6. Malmström et al., Macromolecules, 46 (12), 2013, 4955-4965.
7. Granqvist et al. Langmuir 30 (10), 2014, 2799-2809



## Quantitative Characterization of Adhesion and Mechanics of Single Cells and Their Interactions With Biomaterials by AFM

Torsten Müller, Dimitar Stamov, Jörg Barner, Anne Hermsdörfer, Carmen Pettersson, Torsten Jähnke

JPK Instruments AG, Germany

[mueller@jpk.com](mailto:mueller@jpk.com)

Topography, roughness and mechanical properties of biomaterials are crucial parameters influencing cell adhesion/motility, morphology and mechanics as well as the development of stem/progenitor cells [1,2,3,4,5]. Atomic force microscopy is a powerful tool not only to study the morphology in terms of high resolution imaging and roughness measurements, but also to map mechanical and adhesive properties of the sample/cells at high resolution. Combining these remarkable abilities with advanced optical microscopy allows for extensive characterization of biomaterials. The JPK NanoWizard® 3 AFM provides advanced imaging and mapping modes which can be combined with inverted as well as upright optical microscope techniques. Using single cell force spectroscopy (SCFC), cell adhesion can be quantified [6], and the contribution of different components e.g. from the extra cellular matrix, can be assessed [7]. Additionally, based on scanning force microscopy, the nano-indentation technique has emerged as a useful tool to determine elastic properties like the Young's modulus for biological samples. Nano-mechanical analysis of cells increasingly gains in importance in different fields in cell biology like cancer research [8] and developmental biology [9]. We present a strategy to comprehensively characterize biomaterials as well as their interaction with cells and influence on cell behaviour.

### REFERENCES

1. Elter *et al.*, Eur. Biophys. J. 40: 317-327, 2011
2. Docheva *et al.*, Biochem. Biophys. Res. Com. 402:361-366, 2010
3. Engler *et al.*, Cell 126:677-689, 2006
4. Selhuber-Unkel *et al.*, Biophys. J. 98:543-551, 2010
5. Kirmse *et al.*, J. Cell Science 124, 1857-1866, 2011
6. Benoit *et al.*, Nature Cell Biology 2:313 – 317, 2000
7. Puech *et al.*, Journal of Cell Science 118:4199-4206, 2005
8. Cross *et al.*, Nature Nanotechnology 2:780-783, 2007
9. Krieg *et al.*, Nature Cell Biology 10/4:429-436, 2008

### ACKNOWLEDGMENTS

Prof. A. Herrmann and R. Schwarzer, Humboldt-Universität zu Berlin

Dr. J. Friedrichs, Leibnitz Institut für Polymerforschung Dresden

Prof. W. Sand, Universität Duisburg-Essen

Dr. J. Fitreman, CNRS, Université de Toulouse

Dr. R. Kirmse, University of Colorado



Peter Sobolewski<sup>1</sup>, Agata Goszczyńska<sup>1</sup>, Agata Niemczyk<sup>1</sup>, Ewa Mijowska<sup>2</sup>, Jacek Podolski<sup>3</sup>, Mirosława El Fray<sup>1</sup>

<sup>1</sup>Division of Biomaterials and Microbiological Technologies, Polymer Institute

<sup>2</sup>Division of Nanotechnology, Institute of Chemical and Environment Engineering

West Pomeranian University of Technology, Szczecin, Al. Piastów 45, 71-311 Szczecin, Poland

<sup>3</sup>Meditest. Diagnostyka Medyczna. NZOZ, ul. Bronisławy 14d, 71-533 Szczecin, Poland

[a.goszczyńska@zut.edu.pl](mailto:a.goszczyńska@zut.edu.pl)

## INTRODUCTION

There exists a pressing need to develop diagnostic technologies, so-called biosensors, in order to leverage explosion of information provided by the “-omics,” (genomics, proteomics, etc.). Importantly, in addition to sensitivity and specificity, an ideal biosensor platform needs to be fast, affordable, and simple, thus reducing the barrier of entry, especially in the developing world. Graphene nanocomposite inks for ultrasonic, non-contact printing are particularly attractive for achieving these goals. However, successful and low cost application of this technology requires parallel development of suitable substrate platforms.

Here we present a modular polymeric platform, combining the design space flexibility provided by 3D printing with surface optimization enabled by spin coating.

## EXPERIMENTAL METHODS

Basic electrode design (0.63 mm thick) was 3D printed using Zortrax M200 printer and Z-ABS or Z-GLASS polymers.

Surface polymer selection was driven by wettability with ethylene glycol (EG), main component of our graphene nanocomposite ink, and thermal stability up to 170°C. Tested polymers included the family of copolyesters (PET-DLA)<sup>1</sup> consisting of polyethylene terephthalate (PET) hard segments and dilinoleic acid (DLA) soft segments, ranging from 50 to 70% hard segment ratio.

For spin coating, 1 to 15 wt.% of PET-DLA was first allowed to dissolve in hexafluoroisopropanol at room temperature for 24 hours. Next, 1 mL of PET-DLA solution was spread on the 3D printed substrate and spin coated in 4 steps, with a maximum speed of 3000 rpm for 30 sec using Spincoater Spin 3000 (Laurell Technologies).

Surface modification aimed at improving EG wettability and introducing additional functional groups was carried out using 6M NaOH (up to 2 hours) or hydrogen peroxide (30 minutes) at 60°C.

Surfaces wettability with water and EG was evaluated using contact angle goniometer (Krüss DSA100S). Surface printability was tested using graphene/chitosan/EG nanocomposite ink and non-contact ultrasonic microplotter (Sonoplot GIX Microplotter Desktop).

## RESULTS AND DISCUSSION

Basic electrode designs were successfully 3D printed, individually or in triplicate, using both Z-ABS and Z-GLASS. Z-GLASS surfaces tended to be smoother.

PET-DLA copolymers containing at least 50% hard segments possessed suitable thermal properties to resist thermal annealing of graphene nanocomposite ink at 170°C. Contact angle of materials ranging from 50 to 70% hard segments was tested with both water and EG.

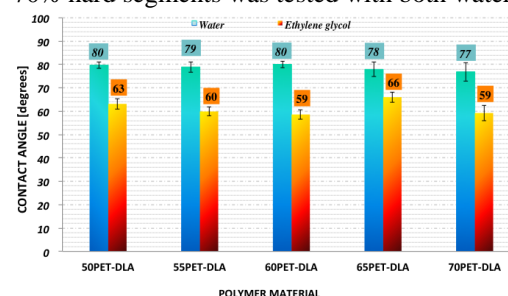
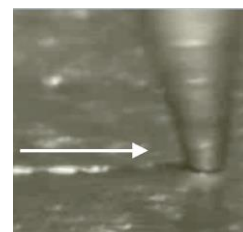


Fig. 1: Contact angle of PET-DLA polymers.

In order to improve EG wettability, PET-DLA copolymers were treated with either NaOH or hydrogen peroxide, resulting in a further ~10° drop in contact angle.

Printing tests with graphene nanocomposite ink determined that 70PET-DLA surfaces were preferable for printing, primarily due to greater hardness.

Fig. 2: Printing graphene nanocomposite ink on 70PET-DLA (60 micron tip).



## CONCLUSION

The combination of 3D printing of supports and spin coating of surfaces allows for a modular design of appropriate polymeric electrodes for inkjet printing with graphene nanocomposite inks.

## REFERENCES

1. Piegat, A et al. *Polymers*. 52:885 (2007).

## ACKNOWLEDGMENTS

The project is financially supported by NCBiR, under Graf Tech programme. The authors thank Z. Staniszewski for useful discussions, K. El Fray for help with 3D printing, and R. Chmielewski for performing preliminary contact angle measurements.

## INTRODUCTION

Some dental materials used by the dentist can cause a hypersensitivity reaction in certain individuals. Potential allergens include the metals, plastics or acrylics in denture, filling materials and different rubber products. According to international data nickel is the most common cause of contact allergy among dental metals<sup>1</sup>. Based on a study the presence of histatins in saliva is responsible for nickel allergy. The histatine-5 (Hst-5) is a histidine-rich (His) protein. N-terminal Asp-Ser-His of Hst-5 is coordinated to the nickel ions<sup>2</sup>. There are some possibilities to detect a wide diversity of biomolecular interactions that may have an important role in the multi-step process of hypersensitivity reaction. The surface plasmon resonance spectroscopy (SPR) is very sensitive technique to recognize label free biomolecular affinity<sup>3</sup>. The formation of self-assembled monolayer (SAM) can ensure the specific binding on sensor chip surface<sup>4</sup>. The main concern of the present study is to investigate the application possibilities of modified SPR sensor chip that can relate to the antigen presentation process. Our aim is to analyse binding affinity of histidine and histidine-nickel complex to different SAM by FT-SPR technique.

## EXPERIMENTAL METHODS

The applied materials are L-histidine (Sigma-Aldrich, Japan), and NiCl<sub>2</sub>·6H<sub>2</sub>O (Sigma-Aldrich, France) in His-Ni binding process. The histidine concentrations are 4, 6, 8, 10, 15 and 20 mM in distilled water (DW) and PBS buffer at three different pH values (pH=3, 7 and 10). The concentration of Ni is 4 mM in distilled water. FT-SPR measurements are carried out using a SPR-100 (GWC Instruments, WI, USA) module coupled with a Nicolet 6700 FT-IR spectrometer (Thermo-Electron, Madison, WI, USA) working in the near infrared (NIR) region which is equipped with a tungsten halogen near-infrared light source, a CaF<sub>2</sub> beam splitter and an InGaAs detector. Two types of SAM are created on SPR gold chip surface. One is amino functionalized by 8-amino-1-octanethiol (AOT; Dojindo, Japan), the other is carboxyl functionalized by 6-mercaptophexanoic acid (MHA; Sigma-Aldrich, USA).

## RESULTS AND DISCUSSION

Based on the measuring it has found the SPR sings shift to lower wavenumbers with increasing His concentration that indicates stronger affinity to sensor chip surface. On the amino functionalized surface (AOT) the histidine binds stronger at acidic pH in the order pH3>pH7>pH10 in distilled water and in PBS too. In the case of carboxyl functionalized surface (MHA) the binding of His is in the order

pH7>pH3>pH10 in distilled water and pH3>pH10>pH7 in PBS. It has showed that the protonated form of histidine binds stronger (at pH=3) in buffer. The shift of SPR sign are detected in real time during the kinetic measurements of the His-Ni binding process. It has found the histidine-nickel complex gives a characteristic sign during the measurement independently of the His concentration. The complex is washable off from the surface.

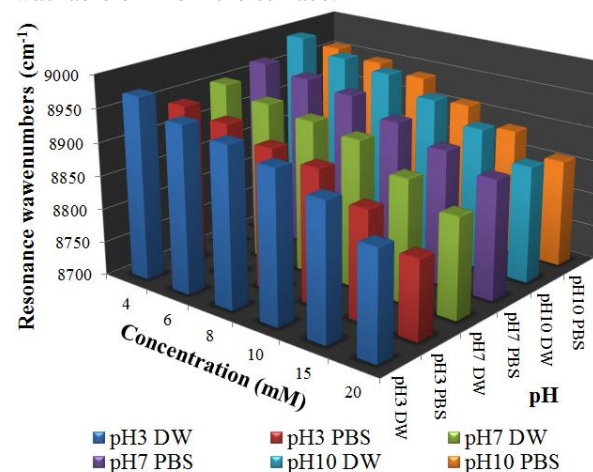


Figure 1 show the histidine bindings on carboxyl functionalized sensor chip surface at different concentration in distilled water (DW) and in PBS buffer at pH=3, pH=7 and pH=10

## CONCLUSION

According to the results it has established that histidine has higher affinity to carboxyl functionalized surface in acidic conditions. Based on this study the SPR is a suitable tool to investigate the binding affinity between amino acids and dental allergens on SAM. These findings can contribute to a better understanding of dental allergen mechanism.

## REFERENCES

- References must be numbered. Keep the same style.
- Schmalz G. *et al.*, Biocompatibility of Dental Materials, Springer, 2009
  - Kurowska E. *et al.*, J. Inorg. Biochem. 105:1220-1225, 2011
  - Gree RJ. *et al.*, Biomater. 21:1823-1835, 2000
  - Love JC. *et al.*, Chem. Rev. 105:1103-1169, 2005

## ACKNOWLEDGMENTS

The authors would like to thank the TÁMOP-4.1.1.C-13/1/KONV-2014-0001 and the TÁMOP 4.2.4. A/2-11/1-2012-0001 'National Excellence Program' for providing financial support to this project.

## Nanoparticles Sensing on Endothelial Cells by Means of Atomic Force Microscopy and Nanoindentation with an AFM Tip

Agnieszka Kołodziejczyk<sup>1</sup>, Sylwia Kotarba<sup>1</sup>, Kinga Kądzioła<sup>1</sup>, Nina Bartoszek<sup>1</sup>, Małgorzata Siatkowska<sup>1,2</sup>, Paulina Sokołowska<sup>1</sup>, Tomasz Wasiak<sup>1</sup>, Joanna Rywaniak<sup>1</sup>, Katarzyna Działoszyńska<sup>1</sup>, Marta Kamińska<sup>2</sup>, Piotr Komorowski<sup>1,2</sup>, Krzysztof Makowski<sup>1</sup>, Bogdan Walkowiak<sup>1,2</sup>

<sup>1</sup>Laboratory of Molecular and Nanostructural Biophysics, Lodz Regional Science and Technology Park Ltd., Poland, 93-465 Lodz, 114/116 Dubois Street

<sup>2</sup>Department of Biophysics, Institute of Materials Science and Engineering, Lodz University of Technology  
[m.siatkowska@technopark.lodz.pl](mailto:m.siatkowska@technopark.lodz.pl)

### INTRODUCTION

It is known that several agents (e.g. drugs, nanoparticles, cytokines) may induce interesting and unexpected changes in cells phenotype – biological and physical parameters, e.g. morphology, cytoskeleton reorganization, intercellular communication or elasticity. Endothelial cells, similarly to muscle or red blood cells, due to their function and location undergo constant squeezing and stretching from the environment. As regards endothelium, elasticity plays a key role in the maintaining vascular pressure regulation. This parameter can be essential in case of evaluation of endothelial cell dysfunction [1] and effectiveness of prospective endothelial drugs [2]. Presented work comprises the study on the influence of three kinds of nanoparticles (NPs): polyamidoamine dendrimers (PAMAMs) of 4.0 generation, silver nanopowders (SNPs) and multi-walled carbon nanotubes (MWCNTs) on EAhy.926 endothelial cell line. Despite dendrimers are intensively studied, their metabolism by the cells, tissues and organs is not well recognized [3]. The comprehensive analysis of nanoparticles influence on cells morphology and elasticity can be useful for understanding of endothelium response during drug and other agent transport by nanoparticles application.

### EXPERIMENTAL METHODS

The endothelial cells were cultured for 24h, and stimulated with examined agents for next 24h. The influence of nanoparticles was investigated for selected concentrations: PAMAM (0.005, 0.012 and 0.024 μM); MWCNT (51.5, 74.1 and 166 μg/ml) and SNP (2.8, 74.8 and 139.6 μg/ml). Atomic force microscopy and nanoindentation with AFM tip were used to characterize the changes in the endothelial cell phenotype. Morphology and elasticity were measured using NTEGRA scanning probe microscope (NT-MDT, Russia) with soft cantilevers (CSG01, with nominal spring constant 0.003 N/m, NT-MDT Probes, Russia). Quantitative morphological cell parameters: volume, surface area and aspect ratio of the central part of the cell (defined as above half of the cells height) were examined for fixed cells in phosphate buffer (pH 7.4). Additionally, the roughness parameters: density of summits (Sds) and texture aspect ratio (Sdr) of the surface were calculated. In order to detect the cell stiffness, the elasticity parameter E (reduced Young's modulus) of the cell central part was measured for live cells in cultured medium in relation to the stimulation agent. The acquired data was compared with the results

obtained at control conditions.

### RESULTS AND DISCUSSION

Precise visualization of the cells morphology confirmed that MWCNTs and SNPs accumulation on the endothelium cell membrane is dose-dependent. Roughness evaluation showed significant increase of Sds value for cells treated with MWCNTs, what may indicate the distinct changes related to actin and myosin fibers reorganization and/or nanotubes accumulation under the cell membrane. Morphological parameters calculation revealed shape changes of the cell central part from longitudinal (control condition) to spherical (incubated with dendrimers). Elasticity results showed the differences for cells incubated with nanoparticles compared to reference sample. Obtained results for NPs indicated the cytotoxicity effects of selected agents, what was confirmed by fluorescent staining and cytometry measurements.

### CONCLUSION

Atomic force microscopy supported with nanoindentation method can be a useful tool for determination of endothelial cells morphology and elasticity changes induced by nanoparticles. Moreover, these methods may help in the evaluation of “endothelium-safe” nanoparticles.

### REFERENCES

- [1] Szczygiel A.M. et al., Elasticity changes anti-correlate with NO production for human endothelial cells stimulated with TNF- $\alpha$ , *European Journal of Physiology*, (2011) 463:487–496
- [2] Kołodziejczyk A.M. et al., Nanomechanical sensing of the endothelial cell response to anti-inflammatory action of 1-methylnicotinamide chloride, *International Journal of Nanomedicine*, (2013) 8: 2757 – 2767
- [3] Sękowski S. et al., Dendrimers in biomedical sciences and nanotechnology, *Postepy Hig Med Dosw.*, 2008; 62: 725-733





## Nanomagnetite Composite Implants in Magnetic Resonance Imaging

Katarzyna Nowicka<sup>1</sup>, Anna Krak<sup>2</sup>, Henryk Figiel<sup>2</sup>, Krzysztof Turek<sup>2</sup>

<sup>1</sup>AGH-University of Science and Technology, Faculty of Material Science and Ceramic, Department of Biomaterials, Krakow, Poland

<sup>2</sup>AGH-University of Science and Technology, Faculty Physics and Applied Computer Science, Department of Medical Physics and Biophysics, Krakow, Poland  
[nowicka@agh.edu.pl](mailto:nowicka@agh.edu.pl)

### INTRODUCTION

The use of implants with magnetic properties in medicine has increased in recent years [1]. Diagnosing of patients treated with such implants requires an individual approach. The Magnetic Resonance Imaging (MRI) is one of the safeties and non-invasive imaging techniques used in medicine [2], however the presence of nanoparticles with magnetic properties incorporated in the implant may induce the deformation of the image [3]. Therefore, it is important to study the visualization process of such implants to obtain proper images and to examine the influence of the magnetic nanoparticle concentration on resulting images. Additionally relationship between the shape of an implant and the quality of the MRI image was investigated.

### EXPERIMENTAL METHODS

For this study composite samples with nanomagnetic particles were prepared. Polylactide (PLA) was a matrix and the nanomagnetite powder was used as the modifier. The samples with three different concentrations were prepared: 0,01wt%; 0,05wt%; 0,5wt%. As a reference PLA (pure polymer) samples were also prepared. Tested materials were shaped in the form of: a) rings of diameter 15 mm, height of 10 mm and the wall thickness 1 mm; b) rollers with a diameter of 9 mm and a height of 10 mm.

Obtained materials were investigated by the MRI technique. The different pulse sequences were tested with the aim to find the optimal sequence for imaging of such materials. In result the spin echo T<sub>1</sub> weighted sequence was chosen for further imaging.

### RESULTS AND DISCUSSION

MRI visualizations allowed to obtain images of the composite samples modified with nanomagnetite. For all three types of composites and for both shapes, the best images were obtained with the spin-echo T<sub>1</sub>-weighted sequence. Analysis of the images showed that increasing the concentration of magnetite in the samples causes more distorted images. Quantitative analysis of number and type of distortions connected with the amount of magnetic modifier were also performed. Images of the highest quality were obtained for the materials with the smallest amount of modifier (0.01wt%). Second type of analysis for this type of

composite was connected with the influence of the sample shape (the ring and the roll) on the quality of the images. It was observed that better results were obtained for the ring-shaped samples and the images were less distorted as compared with the images of roll-shaped samples which were not sharp enough showing less details.

### CONCLUSIONS

The performed analysis have shown that there is a direct connection between the amount of magnetic modifier in the composite and the quality of MRI images.

It was stated in this research that the critical amount of the modifier is 0,5wt%. Addition of such quantity of the modifier made the images very distorted and disqualified them from medical diagnosis. This means that, if a good quality of image is needed, the amount of nanomagnetite particles should be much smaller, the best ~0,01wt%. Another factor affecting the quality of the MRI images is the shape of the samples. For the ring-shaped composite better results were obtained than those for roll-shaped ones.

Based on the presented results it can be concluded, that the use of the spin-echo T<sub>1</sub>-weighted MRI sequence produces the best images of implants with magnetic modifier and can be used for medical diagnosis, but the investigated implants need to have a proper, much less than 0,5wt%, concentration of the nanomagnetite. Furthermore the implants hollow in shape are more preferable than bulk ones, because their images are less distorted.

### REFERENCES

1. Binns C. *Frontiers of Nanoscience* Vol. 6, 217-258 2014
2. Gold M et al., *J Am Coll Cardiol*, 2015
3. Gogola D. et al., *J Magn Magn Mater.*, Vol. 380, 261-265 2015

### ACKNOWLEDGMENTS

This work was financed from statutory works of AGH (No 11.11.160.616 and 11.11.220.01)



# Rotational Dual-Chamber Bioreactor designed for Tissue Engineered Interfaces

Raphaël F. Canadas<sup>1,2</sup>, Alexandra P. Marques<sup>1,2</sup>, Joaquim M. Oliveira<sup>1,2</sup>, Rui L. Reis<sup>1,2</sup>

<sup>1</sup>3B's Research Group – Biomaterials, Biodegradables and Biomimetics, University of Minho, Guimarães, Minho, Portugal <sup>2</sup>ICVS/3B's – PT Government Associate Laboratory, Braga/Guimarães, Minho, Portugal

[miguel.oliveira@dep.uminho.pt](mailto:miguel.oliveira@dep.uminho.pt)

## INTRODUCTION

The use of in vitro platforms presents obvious ethical and cost advantages over in vivo models. Moreover, important scientific benefits in the study of biological mechanisms of action focusing on isolated variables/effects can be obtained. Different 2D and 3D cell culturing systems, static and dynamic (e.g., bioreactors) have been proposed, along the years [1]. However, the lack of suitable physical structures capable of supporting the generation of multilayered tissues has been hampering the tissue engineering (TE) field developing improved models [2]. The existing cell culture technology is not adapted to this need, but new systems are now arising, as adapted bioreactors and 3D well culture plates [1]. With the development of TE tools and cell culture systems, interfaces could be recreated in a more realistic way. In this work a novel bioreactor adapted for multi-layered cell culture was developed [3]. The system can provide a mechanism to enhance cellular homogenization and stratification inside of the 3D construct. So far, the developed system is being tested to create an osteochondral (OC) 3D in vitro model.

## EXPERIMENTAL METHODS

A rotational dual chamber bioreactor capable of improving medium diffusion into 3D layered structures, providing different culture medium to each layer and an homogeneous cell distribution in the scaffolds, as well as of introducing mechanical stimuli by 180° stirring and compression, was fabricated in-house [3]. Two different bilayered sponge-like scaffolds were developed to act as a template for co-culturing rabbit adipose stem cells (rASCs)-derived osteoblasts and chondrocytes. Bilayered low acyl gellan gum (LAGG) 2%w/v-LAGG2%w/v/hydroxyapatite (HAp) 30%w/w structures with and without gelatin (1:1) were produced forming the cartilage- and bone-like layers. The developed cell-scaffolds constructs were cultured in static conditions as control of the dynamic cultures.

## RESULTS AND DISCUSSION

A bioreactor comprising a multiposition magnetic stirred plate on which are connected dual chambers by magnetic attraction has been developed. The dual chambers can have rotational movement, which is horizontal and/or vertical. The size of the scaffold is dependent on the ability of the medium to enter and exit the interior of the 3D structure. By introducing the stirring movement over the cell culture, the diffusion potential increased. This allows the use of bigger 3D scaffold consequently enhancing the ability to produce larger tissues in vitro. Moreover, the multi-chamber bioreactor is adapted for co-culturing different cells types allowing the generation of multi-cell type tissues.

A chamber cap allowing cyclic compression over the respective cell-scaffold construct, creating physical stimuli that intend to mimic the body weight was included. The compartments of the dual chamber allow flowing different culture medium per compartment or the creation of an air-liquid interface.



Figure1. A: Rotational Dual Chamber Bioreactor prototype [3]; B: Bilayered structures of LAGG-LAGG/HAp30% (left) and LAGG/Gelatin-LAGG/Gelatin/HAp30% (right).

The freeze-dried bilayered scaffolds composed of LAGG2%(w/v)-LAGG2%/HAp30% (w/w) and LAGG/Gelatin 1:1 2%(w/v)-LAGG/Gelatin 1:1 2%/HAp30% (w/w) have a gradient of HAp in the bone-like layer that, unlike cartilage-like layer, present a bioactive behavior. The bilayered structures possess about 90% porosity, 500 µm of pore size and 85% interconnectivity as determined by Micro-CT analysis. Swelling and degradation tests revealed that the structures can absorb about 120% of their weight and lost 10% of their mass after 30 days in phosphate buffered saline solution. In vitro studies with rASCs from fat pad are being performed to compare static and dynamic cultures.

## CONCLUSION

The described technology can be used in the development of an in vitro stratified OC tissue model and potentially for developing other interfaces (e.g. epithelia, skin, blood-brain barrier). These can allow decreasing the animal models for basic research and drug screening and efficacy studies.

## REFERENCES

- [1] Ravi, M., V. Paramesh, et al. J Cell Physiol 230(1): 16-26. 2015
- [2] Keeney M, Pandit A. Tissue Eng B: Rev. 2009;15:55–73.
- [3] Canadas RF, Oliveira JM, Marques AP, Reis RL, Patent WO2014141136 A1. 2014.

## ACKNOWLEDGMENTS

Thanks are due to the Portuguese Foundation for Science and Technology and POPH/FSE program for the fellowship grant of Raphaël Canadas (SFRH/BD/92565/2013). The FCT distinction attributed to J.M. Oliveira under the Investigator FCT program (IF/00423/2012) is also greatly acknowledged.



## Nanocrystalline Hydroxyapatite Effects on M1 and M2 Macrophage Populations

Javier Linares<sup>1</sup>, Ana Belén Fernández<sup>1</sup>, María José Feito<sup>1</sup>, María Concepción Matesanz<sup>1</sup>, Sandra Sánchez-Salcedo<sup>2,3</sup>, Daniel Arcos<sup>2,3</sup>, María Vallet-Regí<sup>2,3</sup>, José María Rojo<sup>4</sup>, María Teresa Portolés\*<sup>1</sup>

<sup>1</sup>Department of Biochemistry and Molecular Biology I/Faculty of Chemistry, Universidad Complutense de Madrid, Spain

<sup>2</sup>Department of Inorganic and Bioinorganic Chemistry/Faculty of Pharmacy, Universidad Complutense de Madrid, Instituto de Investigación Hospital 12 de Octubre i+12, Spain

<sup>3</sup>Networking Research Center on Bioengineering/Biomaterials and Nanomedicine, CIBER-BBN, Spain

<sup>4</sup>Department of Cellular and Molecular Medicine/Centro de Investigaciones Biológicas, CSIC, Spain

[portoles@quim.ucm.es](mailto:portoles@quim.ucm.es)

### INTRODUCTION

The success or failure of a biomaterial depends ultimately on the immune response triggered after its implantation. Macrophages are the main components of innate immune system. This cell type presents a remarkable functional plasticity, existing a whole spectrum of populations between the proinflammatory (M1) and reparative (M2) extremes<sup>1</sup>. The M1/M2 balance has been recently related to the capacity of macrophages to play both positive and negative roles in disease processes and tissue remodelling after injury<sup>2</sup>. In the present study, the effects of nanocrystalline hydroxyapatite (nano-HA) and nanocrystalline silicon substituted hydroxyapatite (nano-SiHA) on murine macrophage populations have been evaluated in basal conditions and in the presence of either pro-inflammatory (LPS) or anti-inflammatory (IL-10) stimuli.

### EXPERIMENTAL METHODS

Either RAW 264.7 cells or mouse peritoneal macrophages were cultured for 24 and 72 hours in the presence of 1 mg/ml of nano-HA and nano-SiHA. Specific macrophage surface markers CD80 and CD163 were used to identify M1 and M2 macrophages respectively by flow cytometry and confocal microscopy after immunostaining with phycoerythrin-labelled antibodies. LPS and IL-10 were used as pro-inflammatory and anti-inflammatory stimuli, respectively. Cell viability, proliferation, intracellular reactive oxygen species, IL-6 and TNF- $\alpha$  were also evaluated after treatment with these hydroxyapatites.

### RESULTS AND DISCUSSION

**Figure 1** shows that the treatment of RAW 264.7 macrophages with 1 mg/ml of nano-HA and nano-SiHA produces a significant decrease of the pro-inflammatory M1 (CD80+) population after 72 hours. However, a significant increase of reparative M2 (CD163+) population was observed when compared with control cells in the absence of material. These effects were also obtained after treatment of mouse peritoneal macrophages with these materials in the presence of pro-inflammatory (LPS) or anti-inflammatory (IL-10) stimuli. Different M1 and M2 morphology was observed by confocal microscopy in mouse peritoneal macrophages after 48 hours treatment with LPS and IL-10, in agreement with other authors<sup>3</sup>.

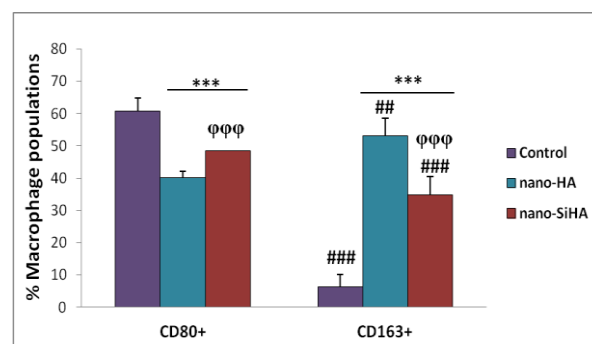


**Figure 1. Effects of nano-HA y nano-SiHA (1mg/ml) on RAW 264.7 macrophage M1 (CD80+) and M2 (CD163+) populations after 72 hours treatment.** Statistical significance: \*\*\*p < 0.005 (compared to the Control without material), ## p < 0.01, ### p < 0.005 (comparison between CD80 and CD163 markers),  $\varphi\varphi\varphi$  p < 0.005 (comparison between nano-HA and nano-SiHA).

### CONCLUSION

The findings of this study allow to conclude that these nanocrystalline hydroxyapatites favour the macrophage polarization toward a M2 reparative phenotype, ensuring an appropriate response in the implantation site of these biomaterials used for bone repair and Tissue Engineering.

### REFERENCES

1. Mosser D.M. *et al.*, Nat. Rev. Immunol. 8:958e69, 2008
2. Brown B.N. *et al.*, Biomaterials 33:3792-3802, 2012
3. McWhorter F.Y. *et al.*, Proc. Natl. Acad. Sci. U S A 110:17253-17258, 2013

### ACKNOWLEDGMENTS

This study was supported by research grants from the Ministerio de Ciencia e Innovación (MAT2012-35556), Ministerio de Economía y Competitividad (MAT2013-43299-R) and Agening Network of Excellence (CSO2010-11384-E). M.C. Matesanz is greatly indebted to MEC for predoctoral fellowship. The authors wish to thank also to the staff of the Centro de Citometría y Microscopia de Fluorescencia of the Universidad Complutense de Madrid (Spain) for the assistance in flow cytometry and confocal microscopy studies.



<sup>1</sup>Laboratory of Bioinspired Molecular Engineering, MESA<sup>+</sup> Institute for Nanotechnology, Department of Science and Technology, University of Twente, The Netherlands  
[g.kocer@utwente.nl](mailto:g.kocer@utwente.nl)

## INTRODUCTION

Endothelial cells are in the centre of angiogenic processes which are crucial for the successful integration of implants in the body<sup>1</sup>. Cell-extracellular matrix (ECM) interactions are essential regulators of these processes. Thus, development of ECM mimetic instructive microenvironments supporting endothelial cell function is important to achieve desired tissue responses upon implantation<sup>1,2</sup>.

Supported lipid bilayers (SLBs), which are readily formed on hydrophilic supports, act as biological interfaces mimicking cellular membranes while retaining their physicochemical properties (i.e. phase behaviour). Their differential phase behaviour enables controlling the mobility of the biomolecules on the surfaces for molecular recognition. Also, by forming non-fouling surfaces using neutral (i.e. PC) lipids, SLB functionalization with synthetic ligands (e.g. RGD of ECM) allows to instruct cell behaviour specifically<sup>3</sup>.

## EXPERIMENTAL METHODS

### Surface Preparation

SLBs were formed via a vesicle fusion method on hydrophilic glass substrates. To prepare bio-functional SLBs, vesicles (either of DOPC (fluid) lipids or DPPC (gel) lipids) were conjugated with defined molar ratios of biotinylated PE lipids and after SLB formation, biotinylated RGD ligands were introduced to the surfaces using neutravidin cross-linkers. In addition, bare (non-functional) bilayers that were formed by unconjugated vesicles and fibronectin coated glass were used as control surfaces.

### Characterization of Cell Behaviour on SLBs

Human umbilical vein endothelial cells (HUVECs) at p5 were seeded at a density of 10 000 cells/cm<sup>2</sup> and cultured for different time points on various surfaces. The cell morphology on the surfaces was monitored using bright-field microscopy.

## RESULTS AND DISCUSSION

Our observations indicate that cells marginally adhered onto non-functional SLBs (data not shown) while cells considerably adhered on ligand presenting bilayers. This difference shows that we could specifically direct endothelial cell attachment by controlling the surface composition. Furthermore, we also observed that cells on the gel state (DPPC) SLBs were spreading after 6 h while cells on fluid state (DOPC) SLBs remained round with a lower extent of attachment. This implies that we could also direct cell behaviour by changing the SLB

properties (i.e. (mobile ligands) fluid vs. (immobile ligands) gel state SLBs) while presenting the same chemical composition in the SLBs (Fig.1).

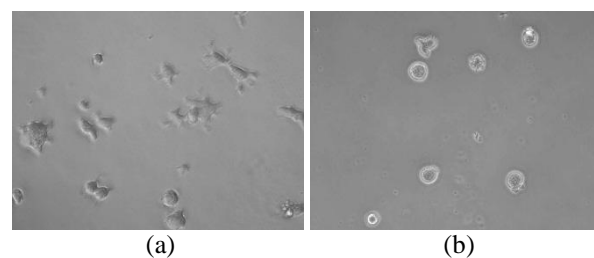


**Fig.1.** HUVECs on 1 mol% ligand presenting (a) DPPC and (b) DOPC based SLBs after 6 h observed with bright-field microscopy (20x magnification, n=3).

Showing the possibility of directing endothelial cell behaviour on these surfaces, understanding the ligand density and time dependent responses in terms of focal adhesion dynamics and cell migration in real time are critical steps that are currently being investigated. Besides, these surfaces introduce a versatile way to present multiple ligands to control endothelial cell behaviour<sup>3</sup>.

## CONCLUSION

In conclusion, our data suggest that endothelial cell behaviour could be directed on SLBs by introduction of ligands on different types of otherwise non-fouling SLB surfaces. In addition, cell contact formation and morphology was dependent on phase behaviour of lipids forming the SLBs. Consequently, our further understanding and exploiting the underlying cellular events will pave the way to develop a biologically active interface for endothelial cells to create smart material coatings on implant surfaces supporting *in vitro* pre-vascularization.

## REFERENCES

1. Rouwkema J., *et al.*, Trends in Biotech., 26:434-441, 2008
2. Rice J.J. *et al.*, Adv. Healthcare Mater., 2:57-71, 2013
3. Yu, C. *et al.*, Med. Biol. Eng. Comput., 48:955-963, 2010

## ACKNOWLEDGMENTS

The authors acknowledge the Netherlands Organisation for Scientific Research (NWO) (NWO-VIDI) for providing financial support.



## Magnesium Implant Degradation Influenced by Blood and Cells

Nezha Ahmad Agha<sup>1</sup>, Frank Feyerabend<sup>1</sup>, Boriana Mihailova<sup>2</sup>, Hans-Peter Wendel<sup>3</sup>, Daniel Laipple<sup>1</sup>,  
Regine Willumeit-Römer<sup>1</sup>

<sup>1</sup>Institute of Material Research, Helmholtz-Zentrum-Geesthacht, Geesthacht, DE

<sup>2</sup>Departments of Earth Sciences, Hamburg University, Hamburg, DE

<sup>3</sup>University of Tübingen, Department of Thoracic and Cardiovascular Surgery, Tübingen, DE  
[regine.willumeit@hzg.de](mailto:regine.willumeit@hzg.de)

### INTRODUCTION

Magnesium and its alloys have a considerable potential for orthopaedic implants. Its degradability *in vivo* is probably the dominating property which indicates its success. However, still not all the involved mechanisms of the degradation process are fully understood. In this *in vitro* study we aim to elucidate the influence of different physiological and biological parameters on the degradation profile. Here, we wish to clarify the differences between short and long-term exposure to whole blood and plasma, respectively. A second aim is to elucidate the possible role of osteoblasts in changing the chemical composition on the interfaced corrosion layer.

### EXPERIMENTAL METHODS

Pure Mg specimens were prepared by permanent mould casting. Disc-shape samples (10mm x 1.5mm) were cleaned in ethanol and sterilized by gamma-irradiation. To elucidate the influence of inorganic and organic parts of blood, samples were exposed to full blood (90 min. and 6 h) and blood plasma (3 d) in an *in vitro* “closed loop” Chandler-loop system. For comparison the specimens were exposed for 72 h to Hank’s balanced salt solution (HBSS) and Dulbecco’s modified Eagle’s medium (DMEM).

The cell influence was verified on samples which were pre-incubated for 24 h under cell culture conditions in cell culture medium (DMEM). 100,000 human primary osteoblasts (OB) were incubated on these discs for 13 days. During that period medium was changed every 2-3 days. After incubation the samples were fixed in 2.5% glutaraldehyde overnight, followed by 1% osmium tetroxide for 0.5 h to stain the cells. Then different washing steps in isopropanol were performed. As final step samples were dried by critical point drying. These samples were examined using scanning electron microscope (SEM). Then micro cuts on these fixed samples were performed by focused ion beam (FIB) on selected cells with the corrosion layer underneath, the cross sections of these cuts was analysed by EDX area mapping and line scans. Corrosion layer composition was analysed by performing electron induced X-ray emission microanalysis spectroscopy and Fourier transform infrared reflection micro-spectroscopy (FTIR) analysis on the whole sample cross section (10 x 1.5) mm.

### RESULTS AND DISCUSSION

Samples immersed in whole blood show mainly  $\text{MgCO}_3$  associated with calcium-phosphate. Whereas samples immersed in plasma show  $\text{Mg}(\text{OH})_2$  as predominate product, with around 20µm thicker corrosion layer as compared to whole blood immersed samples. Cells on samples had further influence on the degradation profile. On one hand by physically covering the material surface they form kind of a biological corrosion protection layer. In addition they alter the chemical composition for the adjacent corrosion layer, which was detected by line EDX scans revealing more calcium and phosphorous elements.

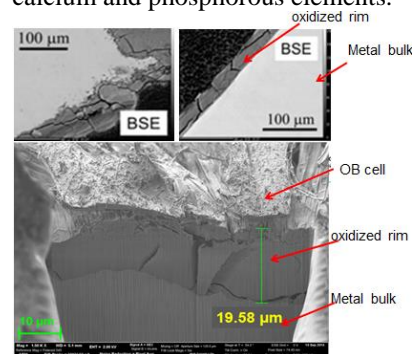


Fig. 1: Up: Back scattered image of corrosion layers after immersing pure magnesium in two different media; left: in plasma for 72 h; right: in whole blood for 6h; down: SEM image for the cross section cut of OB cell on Mg sample

### CONCLUSION

The results highlight the importance of mimicking the biological environment and its complexity. It was shown in blood plasma that the chemical composition of the corrosion layer was significantly altered, which indicate the role of organic components in the corrosion medium. Furthermore, the biological interaction should be carefully considered, as in our study osteoblasts modified the corrosion profile and possibly mediate a biomineralization process which resulted in higher Ca and P contents on the nearby corrosion layer.

### ACKNOWLEDGMENTS

The research leading to these results has received funding from the People Program (Marie Curie Actions) of the European Union's Seventh Framework Program FP7/2007-2013/ under REA grant agreement n° 2891, and Helmholtz Virtual Institute VH-VI-523 (In vivo studies of biodegradable magnesium based implant materials)

<sup>1</sup>Department of Applied Physics and Biomedical Research Networking Center in Bioengineering, Biomaterials and Nanomedicine (CIBER-BBN), University of Extremadura, Badajoz, Spain

[vvadillo@unex.es](mailto:vvadillo@unex.es)

## INTRODUCTION

The spontaneous passivation of Ti6Al4V, one of the most clinically used biomaterials, results on a thin TiO<sub>2</sub> outer surface layer. This layer has recently been shown to confer to Ti6Al4V extraordinary bactericidal properties *in vitro* following its irradiation with UV-C light<sup>1</sup>. The influence of these surface changes on protein adsorption, one of the initial processes that occur upon implantation of a medical device into a body site, has not yet been elucidated at the molecular level. In this study, the structure and mechanical stability of human plasma fibronectin (HFN), a major protein component of blood plasma, is evaluated upon adsorption onto the nonirradiated and irradiated Ti6Al4V through the use of atomic force microscopy (AFM).

## EXPERIMENTAL METHODS

Disks of Ti6Al4V, cut from 25 mm bars supplied by DKSJ Switzerland Ltd., were polished and cleaned as described elsewhere<sup>1</sup>. A set of the samples were exposed to a UV-C source ( $\lambda = 254$  nm) for 15 h receiving an intensity of  $\sim 4.2$  mW/cm<sup>2</sup> prior to experiments. The HFN protein, obtained from Sigma-Aldrich, was suspended in 10 mM PBS at pH 7 to a concentration of 100  $\mu$ g/ml. A volume of 0.5 ml of this solution was allowed to interact with the nonirradiated and irradiated Ti6Al4V samples for 15 min. After the 15 min adsorption time, the protein coated disks were rinsed with PBS and transferred to the AFM.

AFM experiments were performed in PBS using an Agilent AFM 5500 system operating at room temperature and rectangular silicon cantilevers with a tip radius of  $\sim 8$  nm (CSC38 MikroMash). The spring constant of the cantilevers were determined prior to experiments. For each sample, hundreds of force-distance curves were collected at randomly selected locations and used to generate the histograms from which the mean data presented were obtained.

## RESULTS AND DISCUSSION

The mean unfolding force and length obtained upon stretching a single HFN molecule from the nonirradiated Ti6Al4V (Figure 1a) are similar to those obtained by other authors<sup>2</sup>, i.e.  $112 \pm 24$  pN and  $25.6 \pm 3.4$  nm, respectively. These values are typically attributed to the unfolding of the FNIII domains of the protein. The stretching of HFN from the irradiated material, however, reveals a mean unfolding force of  $107 \pm 37$  pN and three different mean unfolding lengths, i.e.  $13.5 \pm 3.2$ ,  $18.1 \pm 1.1$  and  $26.9 \pm 4.8$  nm. These different lengths could be attributed to the unravelling of the FnI, FnII and FnIII domains, assuming

that the disulfide bonds present within the FnI and FnII modules have been likely reduced upon protein adsorption on the irradiated material.

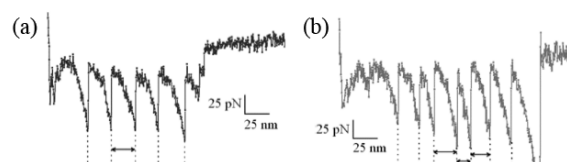


Figure 1. AFM force-plots obtained upon stretching adsorbed HFN from the nonirradiated (a) and irradiated (b) Ti6Al4V

Moreover, a small but significant fraction of the force plots displayed unexpected from transitions (up to three regardless of the substrata) occurring in a stepwise fashion (Figure 2a). Based on the observation that the distance at which the last recorded plateau ends was consistent with the total length of a single molecule, i.e. 160 – 180 nm, it is proposed that the observed behaviour originates from the straitening of a compact molecule (Figure 2b) without the unfolding of its domains. Finally, the mean unravelling forces were found to be lower for the molecules adsorbed on the irradiated than nonirradiated material.

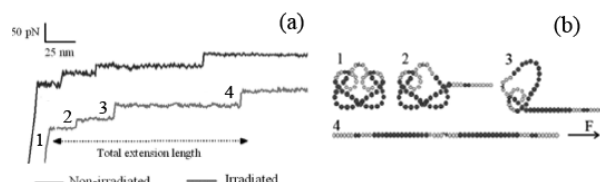


Figure 2. AFM force-plots (a) obtained upon unravelling (b) adsorbed HFN molecules (without the unfolding of its domains) from the nonirradiated and irradiated Ti6Al4V

## CONCLUSION

HFN molecules become structurally looser and mechanically more flexible upon adsorption on the irradiated Ti6Al4V material.

For the first time, force profiles that correlate with the unravelling of a single compact protein without the unfolding of its domains were recorded.

## REFERENCES

1. Gallardo-Moreno, A. M. *et al.*, Biomaterials 31: 5159-5168, 2010
2. Oberhauser, A. F. *et al.*, J. Mol. Biol. 319: 433-447, 2002

## ACKNOWLEDGMENTS

“Ministerio de Ciencia e Innovación” (MAT2012-37736-C05-03 and RYC-2008-03482) and “Junta of Extremadura-FEDER: European Regional Development Fund” (GR10149)

## Electrophoretic Deposition of Free Standing Collagen Films

David Barrett<sup>1</sup>, Terance Hart<sup>2</sup>, Serena Best<sup>1</sup> and Ruth Cameron<sup>1</sup>

<sup>1</sup>Department of Materials Science & Metallurgy, University of Cambridge, UK

<sup>2</sup>Geistlich Pharma AG, Luzern, Switzerland

[db614@cam.ac.uk](mailto:db614@cam.ac.uk)

### INTRODUCTION

Electrophoretic deposition is a widely used technique used to form coatings and structures from a solid suspension and has seen wide applications, mainly in ceramic industries. It allows coatings of complex shapes to be formed quickly and evenly on any conductive substrate<sup>1</sup>.

Recently there has been some interest in applying the technique of electrophoretic deposition to a wider variety of materials, including bioceramics and polymeric biomaterials<sup>2</sup>. In this study we attempted to apply the technique of electrophoretic deposition to forming defect free films of insoluble collagen.

### EXPERIMENTAL METHODS

Insoluble collagen was rehydrated in acetic acid and homogenised until a smooth suspension was achieved. The suspension was then degassed under a vacuum and multiple different suspensions were made up of varying collagen wt%, pH, and water content. The water content of the suspension was varied by addition of acetone and ethanol.

Zeta potential measurements were taken to determine which suspensions allowed the largest charge on the collagen molecules and hence which suspensions would be stable and easily deposited.

The suspension was poured into a cell consisting of two stainless steel electrodes separated by silicone rubber spacers and a voltage pulse sequence was applied. The pulse sequences had periods of 1s to 1ms, with a varied percentage of time at 5V applied and the remaining time at 0V. The pulse sequence was applied for a number of time points before the electrodes were removed and allowed to air dry. The films were massed after drying using a balance.

### RESULTS AND DISCUSSION

Figure 1 shows a graph of zeta potential against pH for a collagen suspension. By varying a range of parameters

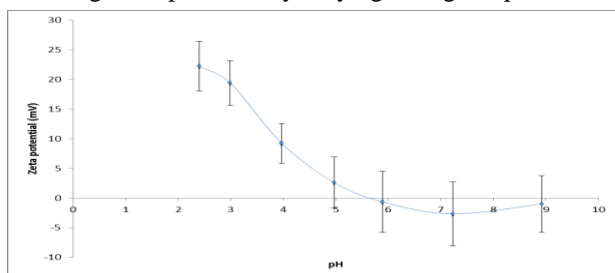


**Figure 1.** Zeta potential vs pH for 0.1wt% collagen in 0.05M acetic acid.

independently it was possible to select a suspension composition that maximised the zeta potential of the collagen and prevented gas bubbles from coalescing due to electrolysis of the aqueous suspension.

Figure 2 shows a fully detached bubble free collagen film produced by electrophoretic deposition of insoluble collagen suspended in an ethanol/water solution.

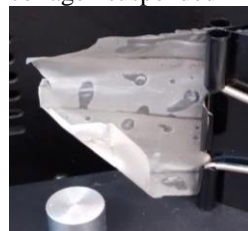


**Figure 2.** A free standing collagen film formed by electrophoretic deposition

### CONCLUSION

This study demonstrated that it is possible to apply the technique of electrophoretic deposition to collagen, allowing the rapid production of smooth, bubble free films of a well-controlled thickness. Additionally the films could be detached from the substrate and used as free standing collagen films.

### REFERENCES

1. Sarkar P. *et al.*, J. Am. Chem. Soc. 79:1987-2002, 1996
2. Ling T. *et al.*, J. Mater. Sci.-Mater. M. 24:2709-2718, 2013

### ACKNOWLEDGMENTS

The authors would like to thank the EPSRC (Grant no: EP/L504920/1) and Geistlich Pharma AG for providing financial support to this project.

# Determination of Foreign Body Giant Cells after Implantation of Different Biodegradable Materials into Rats

Silke Lucke<sup>1</sup>, Uwe Walschus<sup>1</sup>, Andreas Hoene<sup>2</sup>, Jens-Wolfgang Pissarek<sup>3</sup>, Matthias Schnabelrauch<sup>4</sup>, Birgit Finke<sup>5</sup>, Karsten Schröder<sup>5</sup>, Maciej Patrzyk<sup>2</sup>, Michael Schlosser<sup>1\*</sup>

<sup>1</sup>Department of Medical Biochemistry and Molecular Biology, University Medical Center Greifswald, Germany

<sup>2</sup>Department of Surgery, University Medical Center Greifswald, Germany

<sup>3</sup>MBP - Medical Biomaterial Products GmbH, Neustadt-Glewe, Germany

<sup>4</sup>INNOVENT e. V., Biomaterials Department, Jena, Germany

<sup>5</sup>Leibniz Institute for Plasma Science and Technology, Greifswald, Germany

\*schlosse@uni-greifswald.de

## INTRODUCTION

The implantation of medical devices, prostheses and other biomaterials is followed by material-dependent inflammatory reactions, wound healing processes and in the end-stage a foreign body reaction characterized by the occurrence of macrophages and foreign body giant cells (FBGC) formed by fusion of macrophages. Furthermore, FBGC are detectable in the implant surrounding tissue if the implanted material is too large for phagocytosis<sup>1</sup>. Aim of the study was to investigate the occurrence of FBGC after implantation of membranes from different biodegradable materials and of membranes and electrospun fibre meshes of the same material into rats.

## EXPERIMENTAL METHODS

**In vivo study:** In a 1<sup>st</sup> experiment 5×5 mm pieces of a cross-linked acellular porcine dermis collagen matrix (NRX) and Permacol<sup>TM</sup> were implanted intramuscularly into the neck of 24 male Lewis rats. Peri-implant tissue samples of 6 animals for each day were examined 7, 28, 56 and 112 days after implantation. In a 2<sup>nd</sup> series 24 rats received pieces (5×5 mm) of membranes or electrospun meshes from poly(L-lactide-co-D/L-lactide) (PLA) and PLA meshes coated with plasma-polymerized allylamine (PPAAm). After 7, 14 and 56 days peri-implant tissue samples were prepared from 8 animals per experimental day.

**Histological analysis:** Cryosections were stained with Haematoxylin/Eosin (HE) and primary antibodies for CD68<sup>+</sup> macrophages/monocytes (ED1; M1-type) and CD163<sup>+</sup> macrophages (ED2; M2-type), detected using the APAAP system. FBGC were counted in HE-stained slides and calculated as cells per mm<sup>2</sup>.

**Statistical analysis:** The non-parametric Mann-Whitney test and the Wilcoxon matched pairs test were used.

## RESULTS AND DISCUSSION

Day	Permacol <sup>TM</sup>	PLA	NRX
7	0.40 (0.25 – 1.15)	1.00 (0 – 2.00)	0.95 (0.20 – 2.00)
28	0.10 (0 – 0.60)	n.d.	1.85 ** (1.10 – 2.75)
56	0 (0 – 0.10)	0 (0 – 1×10 <sup>-5</sup> )	1.30 ***,++ (0.40 – 3.25)
112	0 (0 – 5×10 <sup>-5</sup> )	n.d.	0.20 (0 – 0.95)

**Tab.1:** Number of FBGC [cells/mm<sup>2</sup>] after implantation of different membranes. Data given as median and interquartile range in brackets; n.d. = not determined; \*\* p<0.05 vs. Permacol<sup>TM</sup>; ++ p<0.05 vs. PLA, Mann-Whitney test

At days 28 and 56 there was a significant higher number of FBGC for NRX membranes compared to Permacol<sup>TM</sup> and at day 56 to PLA, whereas at days 7 and 112 no difference was found. This could either be caused by the material itself and/or by its structure since NRX films are more porous and thicker than Permacol<sup>TM</sup>.

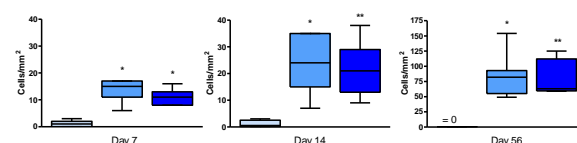


**Fig. 1:** Number of FBGC 7, 14 and 56 days after implantation of PLA membrane (□), PLA mesh (■) and PLA mesh coated with PPAAm (■). \* p<0.05; \*\* p<0.01 vs. PLA membrane, Wilcoxon test

The number of FBGC was significantly higher at all experimental days using both PLA meshes as implant compared to membranes. Thus, an additional surface modification with allylamine did not influence the FBGC reaction. At day 56 for PLA meshes the amount of FBGC was about 4-fold higher than at day 7, whereas using PLA membranes FBGC were no longer detectable.

FBGC were shown to be ED1-positive and ED2-negative, indicating that they are formed by fusion of pro-inflammatory CD68<sup>+</sup> (M1-type) macrophages. This has also been described recently for electrospun polycaprolacton implants<sup>3</sup>.

## CONCLUSION

The foreign body reaction after implantation of biodegradable materials seems to be predominantly influenced by the structure of the implant. Electrospun meshes caused an ongoing stronger reaction compared to membranes of the same material. The FBGC are built by fusion of pro-inflammatory CD68<sup>+</sup> (M1-type) macrophages. This has to be taken into consideration for clinical purposes.

## REFERENCES

1. Anderson JM *et al.*, Sem. Immunol. 20: 86-100, 2008
2. Lucke S *et al.*, Biomed. Res. Int. 2015: ID 938059
3. Duda S *et al.*, Biomed. Res. Int. 2014: ID 835269

## ACKNOWLEDGMENTS

The study was supported by the German state Mecklenburg-Vorpommern (project SYNTERO) and the Federal Ministry of Education & Research (project Campus PlasmaMed).





## Long Term Stability of Proteins in Contact with Solid Surfaces

Tongtong Huang<sup>1,2</sup>, Karine Anselme<sup>1</sup>, Segolene Sarrailh<sup>2</sup> and Arnaud Ponche<sup>1</sup>

<sup>1</sup>Institut de Science des Matériaux de Mulhouse (IS2M), Université de Haute Alsace, France.

<sup>2</sup>Aptar pharma – Route Des Falaises, 27100 Le Vaudreuil, France.

[tongtong9696@gmail.com](mailto:tongtong9696@gmail.com)

### INTRODUCTION

Proteins are widely used in formulation in the pharmaceutical field and play a major role in biological functions. However, as a widespread phenomenon, the adsorption of proteins on solid surface is always observed for a long-term storage, which will result in a reduced dose of active compound or a loss of biological activity<sup>1</sup>. For instance, insulin losses 52% of its biological activity after 5 minutes contacting with glass surface<sup>2</sup>. The interfacial behavior is also known to trigger aggregation phenomena leading to drastic biological inactivation of proteins during long term storage. In this study, several model proteins has been contacted with multiple type of substrates. Parameters including temperature, concentration, adsorption time, rinsing steps and their influence on amount and conformation of adsorbed proteins have been systematically evaluated.

### EXPERIMENTAL METHODS

#### Proteins

Three model proteins were chosen for this study: bovine serum albumin (BSA), lysozyme (LSZ) and myoglobin (MGB).

#### Kinetic of protein adsorption

High performance liquid chromatography (HPLC) coupled with a Zorbax Bio Series GF-250 column with dimensions of 9.4 (i.d.)×250 mm (Agilent Technologies) was used to quantify protein in solution (phosphate buffer saline, pH 7.4) after contact with glass and polydimethylsiloxane (PDMS) surfaces.

#### Protein conformation determination

Attenuated total reflection infrared (ATR-IR) spectroscopy has been adopted for proteins' structure determination. Spectra for protein have been collected with a model IFS66 spectrometer (Bruker Optics).

### RESULTS AND DISCUSSION

#### Kinetic of protein adsorption on glass surface

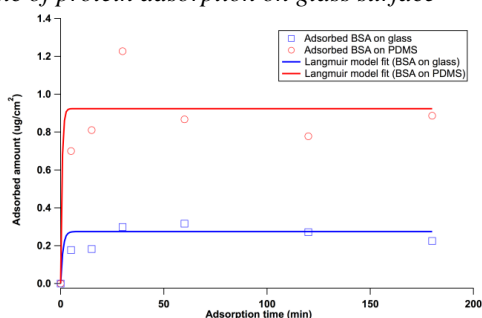


**Figure 1.** Adsorption kinetic curves of BSA on glass surface (blue squares) and on PDMS (red circles).

The three proteins which have different intrinsic properties (such as conformation stability) show

characteristic kinetic curves. These curves can be mathematically fitted with Langmuir or two states models (Figure 1: Langmuir model for BSA adsorption). As a more hydrophobic surface, the amount of BSA adsorbed on PDMS after 3 hrs is fivefold more important than on glass.

#### Conformation study of adsorbed protein

##### 1) Influence of the concentration and time

By peak fitting of amide I band, ATR-FTIR is able to give insight on secondary structures of the adsorbed protein. After a short contact time, adsorbed protein lost about half of the  $\alpha$ -helix structures compared to native protein in solution. By increasing protein concentration, the fraction of  $\alpha$ -helix is maintained close to the solution structure, confirming the protective effect of the concentration over denaturation. But this effect can not be effective over a long time: after 2 hrs of contact, the adsorbed proteins at all concentrations showed similar secondary structures.

##### 2) Influence of rinsing step

Rinsing steps are known in the literature to be one parameter responsible for the lack of reproducibility of protein adsorption studies. It appears indeed to have opposite effects after short or long times of contact. By comparing the protein adsorbed with or without rinsing steps on PDMS, we observe that, after 1 min of contact, the rinsing step exposed more denatured molecules whereas it was the opposite after 2 hrs of contact. The rinsing step will act by removing external layer of weakly adsorbed proteins and it is possible that the organization of the protein layer after 2 hrs is more stable, leading to stronger interaction between less denatured molecules.

After having reviewed the relevant parameters for adsorption of proteins, long term adsorption experiments (over 3 months) are currently under investigation. The first results show that initial adsorption process and nature of the surfaces drive the long term behavior of the protein in the formulation and play a role in initiation of aggregation process.

### CONCLUSION

The interfacial behaviour and conformation of adsorbed proteins are highly dependent on parameters such as sorts of proteins, substrate, temperature, adsorption time, concentration, and the rinsing steps. All these parameters are keypoints to enhance the stability of pharmaceutical formulations containing proteins in contact with multiple surfaces during their life time.

### REFERENCES

- [1] C. J. Burke *et al.*, Int. J. Pharm., 86 : 89–93, 1992.
- [2] C. Petty and N. Cunningham, Anesthesiology, 40, 1974.



Furqan A. Shah<sup>1,2</sup>, Xiaoyue Wang<sup>3</sup>, Peter Thomsen<sup>1,2</sup>, Kathryn Grandfield<sup>3</sup>, Anders Palmquist<sup>1,2</sup>

<sup>1</sup>Department of Biomaterials, Sahlgrenska Academy at University of Gothenburg, Sweden

<sup>2</sup>BIOMATCELL VINN Excellence Center of Biomaterials and Cell Therapy, Göteborg, Sweden

<sup>3</sup>Department of Materials Science and Engineering, McMaster University, Canada

[furqan.ali.shah@biomaterials.gu.se](mailto:furqan.ali.shah@biomaterials.gu.se)

## INTRODUCTION

Osseointegration is controlled by a plethora of cellular mechanisms. However, the long-term maintenance of bone at the bone-implant interface is poorly understood. Of great interest is the role of osteocytes (Ot), which via mechanotransduction are responsible for mechanical loading-based remodelling events in bone. Here, the nanoscale structure of the bone-implant and the bone-Ot interfaces was investigated at laser-modified, human dental implants retrieved after 4 years in function<sup>1</sup>.

## EXPERIMENTAL METHODS

The bone-implant materials were processed for electron microscopy. The Ot network was revealed via resin cast etching and visualised by SEM. TEM samples were prepared by the focused ion beam (FIB) *in situ* lift-out technique. High-angle annular dark field STEM (HAADF-STEM) was used for Z-contrast imaging and chemical analysis. The crystalline orientation of bone apatite was investigated by selected area electron diffraction (SAED). Electron energy loss spectroscopy (EELS) was performed for Ca signal mapping. Electron tomography (ET) allowed 3D imaging of the interfaces.

## RESULTS AND DISCUSSION

Cortical-type osteonal lamellar bone filled the implant threads (Fig 1a). The concentrically configured canalicular network connected the central Haversian canal to the nanotextured implant surface through multiple branching canaliculi traversing up to 50  $\mu\text{m}$ . Direct cell-to-cell communication was also observed (Fig 1b). HAADF-STEM of the bone tissue between the implant surface and the Ot lacuna showed highly ordered collagen fibrils (CF) aligned co-parallel to both surfaces (Fig 1c). SAED revealed the crystallographic *c*-axis of apatite approximately parallel to the CF direction. EELS confirmed apatite ingrowth into the nanostructured surface oxide (Fig 1d). ET showed CF forming an immediate boundary to the lacunar space at the bone-Ot interface (Fig 1e), while the bone-implant interface was structurally graded with apatite interdigitation into the surface oxide layer. However, the general morphology at both interfaces was that of CF exhibiting a unidirectional alignment, exhibiting a rope-like twisting motif.

## CONCLUSION

Through Ot processes, an intimate contact is maintained between bone and nanostructured titanium surfaces, even after four years in function. The bone-implant interface ultrastructure reveals gross similarities to the naturally occurring bone-Ot interface. It is proposed that direct mechanical feedback from the osteocytic

network assists in facilitating adaptive osseointegration over the effective lifetime of bone-anchored implants.

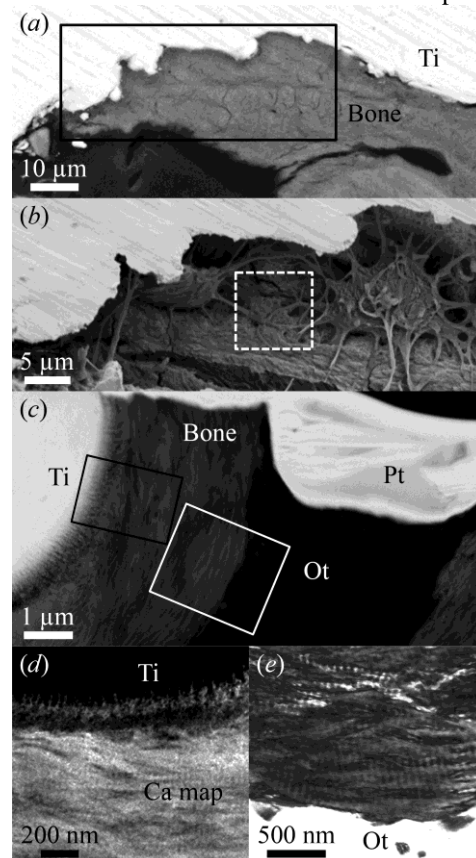


**Fig 1:** (a) The bone-implant interface. (b) Ot at the implant surface, exposed by resin cast etching, showed direct cell-to-cell communication (white box). (c) HAADF-STEM image of a FIB-milled sample prepared across the implant-bone-Ot region. The black and white boxes indicate areas selected for ET. (d) EELS Ca map confirmed apatite formation within the nanostructured surface oxide. (e) ET reconstruction of the bone-Ot interface. CF formed a direct boundary to the Ot lacuna.

## REFERENCES

1. Shah F.A. *et al.*, Nanomedicine. 10:1729-37, 2014.

## ACKNOWLEDGMENTS

Swedish Research Council (grant K2012-52X-09495-25-3), the BIOMATCELL VINN Excellence Center of Biomaterials and Cell Therapy, the Region Västra Götaland, an ALF/LUA grant, the IngaBritt and Arne Lundberg Foundation, the Dr. Felix Neubergh Foundation, Promobilia, the Hjalmar Svensson Foundation, Materials Science Area of Advance at Chalmers and GU Biomaterials, the NSERC Discovery Grant Program, and the Ontario Trillium Scholarship.

## The Distribution of Apatite Nanoparticles Decide the Biological Interaction of Gelatin-Alginate Hydrogels

Sergiu Cecoltan<sup>1</sup>, Daniela Geta Petre<sup>1</sup>, Catalin Tucureanu<sup>2</sup>, Aurora Salageanu<sup>2</sup>, Eugeniu Vasile<sup>3</sup>, Mircea Istodorescu<sup>4</sup>, Dan Laptoiu<sup>4,5</sup>, Rodica Marinescu<sup>5</sup>, Marius Petrutescu<sup>5</sup>, [Izabela-Cristina Stancu](mailto:izabela.cristina.stancu@gmail.com)<sup>1</sup>

<sup>1</sup>Advanced Polymer Materials Group, University Politehnica of Bucharest, Romania

<sup>2</sup>“Cantacuzino” National Institute for Research and Development in Microbiology and Immunology, Bucharest, Romania

<sup>3</sup>METAV Research and Development, Bucharest, Romania

<sup>4</sup>S.C. Medical Ortovit S.R.L., Bucharest, Romania

<sup>5</sup> Clinical Hospital Colentina, Bucharest, Romania

[izabela.cristina.stancu@gmail.com](mailto:izabela.cristina.stancu@gmail.com)

### INTRODUCTION

Composites materials based on biopolymers and apatite represent appealing extracellular matrix- mimicking scaffolds and therefore their microstructure and cell-interaction are intensively investigated for bone regeneration. We developed gelatin-alginate-apatite materials with various compositions and we explored the role of the biopolymers and the role of the apatite-loading methods onto the microstructure of the resulting composites. In addition, we investigated the interaction of the materials with cells.

### EXPERIMENTAL METHODS

A first type of composite materials was obtained through the alternate soaking of the gelatin-alginate hydrogel scaffolds into calcium and phosphate solutions, as previously reported elsewhere<sup>1</sup>. The number of alternating incubation cycles has been varied from one to six.

The second type of materials was synthesized by the incubation of the phosphate-containing hydrogels into calcium-containing baths.

All the composites were characterized with respect to their microstructure and morphology by Scanning and Transmission Electron Microscopy, equipped with X-ray energy dispersive spectrometer (EDX) and X-ray Diffraction (XRD). The stability of the composites in physiologically-relevant simulated media was also evaluated.

The response of cells to the homogeneity of the samples and to the different microstructural features of the scaffolds were explored at 24 hours and after 7 days using MG-63 cells. The corresponding gelatin-alginate hydrogels were used as control samples.

### RESULTS AND DISCUSSION

The synthesis method and the ratio between the raw materials has a strong influence onto the microstructure and morphology of the obtained composites materials.

The alternate soaking in calcium and phosphate solutions leads to materials with homogeneously distributed apatite nanoparticles within the hydrogel

matrix. Increasing the number of incubation cycles from one to six lead to the formation of denser apatite exterior layers that enhance cell interaction.

The second method, based on the incubation of phosphate-containing hydrogels into calcium-containing baths, leads to more homogeneous composites, with no significant differences in the distribution of apatite nanoparticles in the depth of the scaffold. Better stability of the apatite within the matrix was noticed, when compared to the materials obtained by alternate soaking. Intriguingly, low mineralised islands alternating with strongly-mineralised zones were noticed on some materials (despite the homogeneous composition and treatment during the synthesis). In this respect, the mineral-biopolymer compatibility and adhesion phenomena need further investigation.

MG-63 cells strongly adhered to the mineralized scaffolds. The control gelatin-alginate hydrogels did not promote cell adherence. This was very interesting since we expected the presence of gelatin to stimulate cell adherence, view its collagenous nature. The presence of apatite is the decisive factor determining the adherence and proliferation of MG-63 cells on the studied materials. This confirms the potential of the investigated composites to be used in bone regeneration.

### CONCLUSION

Gelatin-alginate-apatite scaffolds are interesting biomaterials that can be used to generate a wide range of scaffolds. These experiments indicated once more that the control over the morphology and microstructure of such composites is not an easy task and it can strongly influence the biological interactions.

### REFERENCES

1. Petre D.G. *et al.*, Key Eng. Mat. 614:26-30, 2014

### ACKNOWLEDGMENTS

The authors would like to acknowledge the financial support from the national research project PCCA Grant no: 183/2012, SmartBIMBBone.



Ina Prade, Kristin Trommer, Michael Meyer

Collagen / Leather / Biopolymers, Forschungsinstitut für Leder und Kunststoffbahnen, Germany  
[ina.prade@filkfreiberg.de](mailto:ina.prade@filkfreiberg.de)

## INTRODUCTION

The cells of the human body are permanently exposed to a variety of mechanical forces, including compression, shear and tensile stress. The importance of this physical microenvironment contributed to an increased demand for new biomimetic systems that more accurately model physiological signals *in vitro*.

In this study we developed a semi-transparent membrane which is optimally adapted to the cultivation of adherent growing cells in a mechanically active environment. The membrane can be colonized on both sides and is porous to allow exchange of signaling molecules and nutrients. Interestingly, it can be used as a barrier for liquid / liquid and gas / liquid interfaces.

## EXPERIMENTAL METHODS

This elastic membrane is made from liquid medical-grade silicone and manufactured on a Mathis Labcoater in a thickness of about 100 microns. The silicone was vulcanized for 4 min at 180 °C. To generate a continuous pore system, PTFE was mixed into the polymer paste and the membrane was stretched after curing. By stretching the polymer tears off the filler, which results in pores with variable diameters. The proportion of the filler is 33 %. In order to promote adhesion of the cells, the membrane was coated with soluble collagen.

## RESULTS AND DISCUSSION

The membrane exhibited good mechanical properties. It has a high elasticity of > 600% and tear strength (> 1.5 N). Importantly, the material is cell compatible as observed in *in vitro* cytotoxicity testing and is tolerated by several different cell types.

The pores of the membrane vary between < 0.5 µm to 15 µm, wherein the filler particles appear in the center of the pores. A migration of cells through the membrane is thus prevented. A complete relaxation of the

membrane leads to the closing of the pores. The membrane must therefore be pre-stretched 1:3.

The cultivation of cells under mechanical strain was examined with the help of a stretching device. For this purpose, the silicone membrane was sterilized with heat, clamped in the device, coated with collagen and seeded with cells. After an incubation period of approximately 16 hours under static conditions, a pulsatile strain at a frequency of 1 Hz was applied.

Cells exhibited significant changes in cell size and shape as it has been described in various cell stretching devices in the literature<sup>1, 2</sup>.

At the moment the membrane is used to mimic the alveolar-capillary interface of a breathing lung. The data indicate that the membrane is suitable to develop biological inspired *in vitro* models.

## CONCLUSION

The successful cultivation of cells demonstrates the suitability of this membrane to generate mechanically active cell culture models.

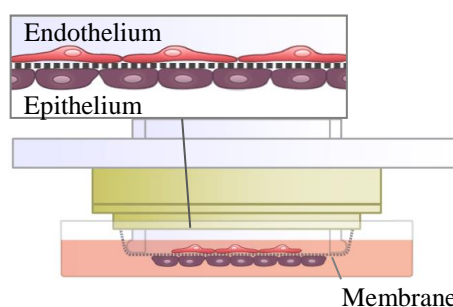
## REFERENCES

1. Hayakawa K. *et al.*, Exp. Cell Res. 268:104-114, 2001
2. Wang JH. *et al.*, J. Biomech. 34:1563-1572, 2001

## ACKNOWLEDGMENTS

The authors gratefully acknowledge the support provided by the German national BMWi / AiF program Innokom-Ost Marktforschung (MF120108).

Sideview



Bottom view

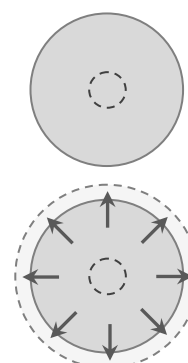


Figure 1. Experimental approach.



Luis Rojo<sup>1</sup>, Sofia Radley-Searle<sup>2,3</sup>, Cristina Abradelo<sup>2</sup>, Sanjukta Deb<sup>1</sup>, Julio San Roman<sup>3</sup>

<sup>1</sup> Division of Tissue Engineering & Biophotonics, King's College London Dental Institute, United Kingdom

<sup>2</sup> San Pablo CEU University, Department of Chemistry and Biochemistry, Faculty of Pharmacy, Spain

<sup>3</sup> Institute of Polymer Science and Technology, and CIBER-BBN, Spain.

[luis.rojo\\_del\\_olmo@kcl.ac.uk](mailto:luis.rojo_del_olmo@kcl.ac.uk)

## INTRODUCTION

Different approaches in osteoporosis treatments include the use of strontium ranelate (SrR), especially indicated in patients unable to tolerate other anti-osteoporotic drugs such as bisphosphonates. However, this treatment presents some long-term safety concerns associated with the risk of blood clots, myocardial infarction and other secondary effects including, disturbances in consciousness, seizures, liver inflammation and reduced number of blood cells<sup>1</sup> leading to severe restriction of the use of this drug by the European Medicines Agency's.<sup>2</sup> Since it is evident that the therapeutic action of SrR is dissociated from the ranelate moiety, we present an alternative compound strontium folate (SrFO) in which the performance of the strontium based drug to stimulate bone formation is enhanced and its capability of skeletal tissue regeneration improved by folate biofunctionality.<sup>3</sup>

## EXPERIMENTAL METHODS

SrFO salt was obtained from folic acid and strontium chloride solutions. Chemical composition of the compound prepared was determined by Mass spectroscopy (MS), elemental analysis (AS) and thermogravimetric analysis (TGA). Structure and coordination mode of folate were elucidated from X-ray diffractograms, infrared and UV-VIS spectroscopy whilst melting point was determined by differential scanning calorimetry (DSC). The same procedure was followed in order to synthesize the calcium based folate derivative (CaFO) as a negative control for *in vitro* tests due to the lack of bone anabolic activity of Ca ions. PEG based scaffolds containing SrFO were prepared and characterised. The *in vitro* behaviour of the folate derivatives were evaluated by standardized MTT and ALP activity assays using osteoblast cell lines (hOb) cultured in presence of SrFO and CaFO salts.

## RESULTS AND DISCUSSION

Pure SrFO and CaFO salts were successfully synthesized in high yield. Spectroscopic analysis indicated that folate crystallized stoichiometrically (1:1) in a bidentate chelating mode of coordination with both Sr and Ca divalent cations through the carboxylate COO<sup>-</sup> groups, presenting four molecules of water of crystallization and thus giving the molecular formulae of SrC<sub>19</sub>N<sub>7</sub>O<sub>10</sub>H<sub>25</sub> (SrFO•4H<sub>2</sub>O, Mw= 599.03 g/mol, Tm = 360 °C) and CaC<sub>19</sub>N<sub>7</sub>O<sub>10</sub>H<sub>25</sub> (CaFO•4H<sub>2</sub>O, Mw= 551.49 g/mol, Tm = 350 °C). Results also indicated that the formation of the folate derivatives do not exhibit the toxic effects related to free Sr<sup>2+</sup> or Ca<sup>2+</sup> ions whilst in the same range the strontium derivative showed an osteogenic activity as indicated by the overexpression of ALP activity.

## CONCLUSION

This study presents for the first time, the synthesis, characterization and the biological behaviour of new strontium folate salts showing evidence of desirable chemical and biological properties with potential as an anti-osteoporotic drug and alternative to the current ranelate based therapies.

## REFERENCES

1. Silverman, S.; Christiansen, C., *Osteoporos Int* 2012, 23 (3), 797-809.
2. Pharmacovigilance Risk Assessment Committee, in EMA/10206/2014, European Medicines Agency, 2014
3. Naharci, I. et al, *Arch. Gerontol. Geriatr* 2012, 54 (3), 469-472.

## ACKNOWLEDGMENTS

"This work has been funded from EU FP7 Marie Curie Actions (PIEF-GA2013-622280) and the Spanish programs PROCUSENS INNPACTO 2011 (IPT-2011-110-900000) and CIBER-BBN"

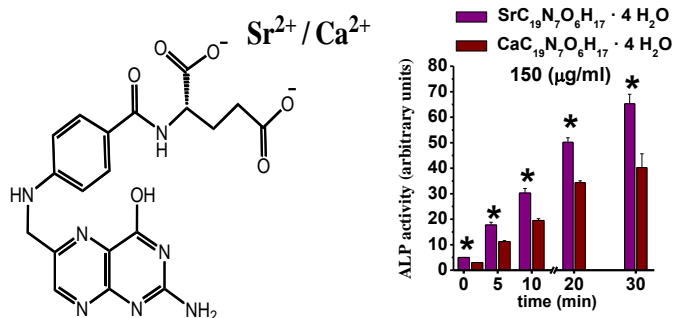


**Figure 1.** Chemical structure of strontium and calcium folate and their ALP activity on hOb cells

## The Use of Microporous Hydroxyapatite Material in Regenerative Treatment of Periodontal Tissues in Dogs.

Izabela Polkowska, Anna Ślósarczyk\*, Aleksandra Sobczyńska-Rak, Magdalena Gołyńska, Tomasz Szponder, Beata Żylińska

Department of Veterinary Surgery, Faculty of Veterinary Medicine,  
University of Life Sciences, 20-612 Lublin, Poland,\*AGH University of Science and Technology, Faculty of Materials  
Science and Ceramics, 30 Mickiewicza Av., 30-059 Krakow, Poland  
[iza.polkowska@tlen.pl](mailto:iza.polkowska@tlen.pl)

### INTRODUCTION

One of the biomaterials used in veterinary dentistry is hydroxyapatite (HAp). It aids the biological process of bone reconstruction and provides the basis on which damaged tissues can be rebuilt. It is also exceptionally biocompatible and bioactive towards bone and other types of tissue. The aim of the present study was to verify the usefulness of hydroxyapatite microporous ceramics for the treatment of periodontal diseases and post-extraction defects. The above material was developed at the Faculty of Materials Science and Ceramics, University of Science and Metallurgy, Krakow, Poland.

### EXPERIMENTAL METHODS

The study was performed on 40 dogs treated at the Department and Clinic of Veterinary Surgery at the University of Life Sciences in Lublin. The dogs were qualified for the in vivo test :-+ 2 study groups and 2 control groups (K1, K2) were created. The first study group comprised 10 dogs diagnosed with moderate to severe gingivitis with 4-8 mm gingival pockets and mobility of mandibular incisors. In order to avoid extraction, hydroxyapatite implantation into the bone pockets was performed. The second study group comprised 10 dogs that required the extraction of mandibular fangs, following which, biomaterial was introduced into the post-extraction cavities. The composition of the control groups reflected that of the respective study groups but without the use of microporous hydroxyapatite.

### RESULTS AND DISCUSSION

In study group 1, considerably better reconstruction of periodontal tissues was observed when compared to the control group K1. The depth of gingival pockets was reduced by 3-4 mm, connective tissue attachment was restored and mobile teeth stabilised. In study group 2, significantly faster healing of bone cavities was stated when compared to the respective control group K2. Moreover, 80% of group K2 patients developed oronasal fistulas while no such cases were observed in the study group.

### CONCLUSION

The study confirmed the validity of using microporous hydroxyapatite granules and shaped blocks in reconstructive periodontal treatment as well as prevention of oronasal fistulas after fang extraction and facilitation of the post-extraction healing process.

### REFERENCES

1. Belcarz A. *et al.*, Engineering of biomaterials 88: 11-15, 2009.
2. Lee JS. *et al.*, J Periodontal Implant Sci 42:50-58, 2012.
3. Oz HS *et al.*, J Biomed Biotechnol doi: 10.1155/2011/754857, 2011.
4. Polkowska I. *et al.*, Med Weter. 68: 436-440, 2012.
5. Shue L. *et al.*, Biomatter 2: 271-277, 2012.

## Bone Substitute from Mineralized Phosphate Prestructured Gelatine – Cell Culture and Mechanical Characterization

Benjamin Kruppke, Christiane Heinemann, Jana Farack, Hartmut Worch, Thomas Hanke

Max Bergmann Center of Biomaterials, Institute of Materials Science, Technische Universität Dresden, Germany, [thomas.hanke@tu-dresden.de](mailto:thomas.hanke@tu-dresden.de)

### INTRODUCTION

Bone substitute materials made from mineralized organic molecules are subject of recent research. The restricted mineralization processes through integration of organic molecules is used as an *in vitro* mimic of natural processes. Gelatine is a partial derivative of collagen and is assumed to be able to restrict mineral formation itself. Therefore, prestructuring of gelatine with phosphate ions and the following mineralization process initiated by adding calcium ions was investigated regarding dental repair material by Kollmann *et al.*<sup>1</sup>. Its transformation to bone substitute materials demands a close look on cellular responses of bone cells. This response was investigated by human mesenchymal stem cell (hMSC) monoculture as well as hMSC and monocyte coculture.

### EXPERIMENTAL METHODS

**Preparation.** Mineralization was performed as batch process. First, phosphate-prestructured (PPS) gelatine was produced. For this, a 6 % w/w gelatine suspension was mixed with 0.1 M Na<sub>2</sub>HPO<sub>4</sub> solution in a volume ratio of 3:17. PPS-suspension was adjusted to pH 7.0. The mineralization solutions (1 M) – CaCl<sub>2</sub>·2H<sub>2</sub>O or SrCl<sub>2</sub>·6H<sub>2</sub>O at pH 7.0 – were added to PPS-suspensions at a rate of 2.5 mL/min. During the entire precipitation process, it has been stirred at 300 rpm. Thereafter, the milky suspension was centrifuged and lyophilized. Finally, the pellets were pulverized by a mixer mill. Precipitates were named PPGC and PPGS for phosphate-prestructured gelatine mineralized with calcium and strontium, respectively. The mineral was compacted with uniaxial compression testing machine (Instron 5566, Darmstadt) with a maximum load of 10 kN (100 mg, o. d. 5 mm, 510 MPa). Selected samples were cross-linked by incubation in 100 mM EDC and 50 mM NHS in 80 vol% ethanol. All samples were sterilized with gamma radiation (25 kGy).

**Characterization.** Mineral precipitates were investigated using X-ray diffraction (XRD), infrared spectroscopy (FTIR) as well as scanning electron microscopy (SEM). Mechanical properties were analysed by ball-on-three-balls test and brazilian test.<sup>2</sup> For that, 400 mg and 100 mg mineral were compressed (510 MPa) to disks of 13 mm or 5 mm diameter and 1.5 mm height. Degradation was determined by static incubation of samples in both simulated body fluid (SBF) and phosphate buffered saline (PBS). During degradation, pH and calcium ion concentrations were determined.

Cell culture experiments were performed with hMSC and human monocytes. hMSC monoculture was performed on non-cross-linked PPGC and PPGS samples over 28 days and compared to polystyrene control. Material and control was cultivated with and without CaCl<sub>2</sub> within the cell culture medium as well as with and without osteogenic additives.

Coculture of hMSC and monocytes was performed on cross linked samples. First, cultivation of hMSCs with and without osteoblast induction were cultivated on samples over 10 days. Monocytes were added to differentiated hMSCs without any additives promoting osteoclastic differentiation according to Heinemann *et al.*<sup>3</sup> Phenotype characterization was performed by biochemical methods (DNA, LDH, ALP, TRAP 5b), light microscopy, confocal laser scanning microscopy, and SEM. Statistical analysis was performed using one-way ANOVA.

### RESULTS AND DISCUSSION

PPGC appears to be brushite and monetite regarding its crystal structure with a platelet morphology. PPGS in contrast has spherical morphology and has a comparable FTIR spectrum to PPGC. Degradation of 4 – 8 weight% during 21 days *in vitro* without cells is an adequate rate. hMSC in monoculture showed a low adhesion, but a high proliferation reaching cell numbers of the control after 28 days. Coculture as well showed a restrained response of hMSCs but revealed an osteoclastic differentiation of monocytes without additives like RANKL or M-CSF during cultivation on PPGC.

### CONCLUSION

In contrast to hydroxyapatite (HAp) with its well known high calcium binding capacity – inhibiting osteoblastic activity – PPGC showed promising properties as loadable material. Additionally its time dependent degradation allows bone remodelling under release of physiological degradation products. For bone regeneration the question arises, which cell type is preferred to seed on degradable / resorbable materials. Induction of an osteoclastic response, leading to an active resorption of the material seems to be favourable for the integration of bone substitutes in remodelling processes.

### REFERENCES

1. Kollmann T. *et al.*, Chem. Mater. 22, 2010
2. Börger A. *et al.*, J. Eur Ceram Soc 22, 2002
3. Heinemann C. *et al.*, eCM Journal. 21, 2011

### ACKNOWLEDGMENTS

We grateful acknowledge the Deutsche Forschungsgemeinschaft Grant TRR79-M03 for financial support.



## Innovative Bioresorbable Intramedullary Nail for Fixation of Long Bone Fractures, Preliminary Research

Jarosław Deszczyński<sup>1</sup>, Tomasz Ciach<sup>2</sup>, Łukasz Nagraba<sup>1</sup>, Tomasz Mitek<sup>1</sup>, Artur Stolarczyk<sup>1</sup>

<sup>1</sup>Orthopaedics and Rehabilitation Department IInd Medical Faculty, Medical University of Warsaw, Poland

<sup>2</sup>Faculty of Chemical and Process Engineering, Warsaw University of Technology, Poland  
[mitek.tomasz@gmail.com](mailto:mitek.tomasz@gmail.com)

### INTRODUCTION

Intramedullary nailing is a standard treatment for patients with long bone shaft fractures. It a very effective way of treatment, that has currently become a gold standard in this type of fractures. Main advantages of the method are: minimal operative approach, limited tissue trauma and good stability of fracture fixation.

Currently all intramedullary fixation devices are made of metal alloy containing: iron, titanium, cobalt, carbon, nickel, vanadium, chrome, molybdenum. Major flaw of those devises is a need to remove implanted material after about a year. This means another surgical procedure for the patient and additional cost of the therapy.

### EXPERIMENTAL METHODS

20-24 sample implants were created in 6 different solutions series (summary of 132 samples). Half of the samples underwent crosslinking.

In each of the series, crosslinked and not, 4 to 6 implants were degraded and the rest used for bending test analysis and SEM investigation. Alterations in mass, length and diameter of the samples were measured in manufacturing process.

### RESULTS AND DISCUSSION

The diameter of implants in drying process altered 60-67%. There was a tendency toward lower alteration of implant diameter in drying process as the amount of ceramic material addition grew. After cross-linking reaction there is a noticeable reduction of diameter.

There was also no significant differences in length in non-ceramic samples compared to samples with addition of hydroxyapatite forming salt. Cross-linking process did not affect the swelling capacity of samples.

During the seven week degradation process, the length of implants remained stable, with only 1-2% alteration from the initial value.

The analysis of degradation process showed that the change in implant length did not depend on cross-linking.

### CONCLUSION

The results of conducted durability study allow us to state that cross-linking process improved mechanical properties of implants with in situ precipitated ceramic material without affecting mechanical properties of implants without ceramic addition.

It would be beneficial to evaluate the influence of order and pace of adding salt to chitosan solution. Further studies should also focus on producing implant of appropriate dimensions and proving the degradation process on animal model.

Implants tested in this study were characterized by good stability of in vivo degradation and satisfactory mechanical properties. The results of sample testing allow us to plan and develop a biodegradable bone implant.

### REFERENCES

References must be numbered. Keep the same style.

1. Nowacki J., Dobrzański L. A., Gustavo F. Implanty śródszpikowe w osteosyn-tezie kości długich. Open Acces Library. 2012, Tom 17, 11.
2. Rezwan K., Chen Q.Z., Blaker J.J., Boccaccini A.R. Biodegradable and bioactive porous polymer/inorganic composite scaffolds for bone tissue engineering. Biomaterials. 2006, 27 18 3413-3431.
3. Yuehuei H.A., Shane K., Woolf R.F. Pre-clinical in vivo evaluation of orthopaedic bioabsorbable devices. Biomaterials. 2000, 21 2635-2652.





# Biomimetic Composites of Chitosan Mineralized with CaCO<sub>3</sub> for Bone Regeneration

Timothy E.L. Douglas<sup>1</sup>, Sangram K. Samal<sup>2</sup>, David Schaubroeck<sup>3</sup>, Kevin Braeckmans<sup>2</sup>, Andre G. Skirtach<sup>1</sup>

<sup>1</sup>Nano & Biophotonics group, Department Molecular Biotechnology, Ghent University, Belgium

<sup>2</sup>Laboratory of General Biochemistry and Physical Pharmacy, Ghent University, Belgium

<sup>3</sup>Center for Microsystems Technology (CMST), ELIS, imec, Ghent, Belgium

[Timothy.Douglas@UGent.be](mailto:Timothy.Douglas@UGent.be)

## INTRODUCTION

Chitosan, a derivative of chitin, the main organic component of the exoskeletons of many marine invertebrates, is a popular biomaterial well known for its cyto- and biocompatibility, antioxidant and antibacterial activity, and its processability into porous scaffolds. Porosity is desirable to facilitate cell and tissue ingrowth. Biomaterials for bone contact should also be bioactive, i.e. capable of forming a direct chemical bond with bone, and also support adhesion and proliferation of bone-forming cells.

In this study, porous chitosan scaffolds were fabricated by a freeze-drying process and subsequently mineralized with calcium carbonate (CaCO<sub>3</sub>) to form composites combining the advantages of the organic and inorganic components. CaCO<sub>3</sub> is the main organic component of many marine invertebrate exoskeletons, hence this approach can be considered to be biomimetic. CaCO<sub>3</sub> has been widely used as a material for bone regeneration and it has performed comparably to the more commonly used materials based on calcium phosphate (CaP). Mineralization with CaCO<sub>3</sub> was expected to lead to mechanical reinforcement with the aim of improving surgical handling and promoting osteogenic differentiation of bone-forming cells. Furthermore, the presence of CaCO<sub>3</sub> is expected to promote bioactivity and adhesion of bone-forming cells. In comparison to pure CaCO<sub>3</sub>, the chitosan-CaCO<sub>3</sub> composites were not expected to be brittle.

Porous scaffolds were fabricated from three different chitosan preparations of varying molecular weight (MW) (low, medium, high) to compare the effect of MW on mineralizability. Mineralization was achieved by alternate soaking of scaffolds in solutions containing calcium and carbonate ions.

## EXPERIMENTAL METHODS

Chitosan of MW 50-190 kD (Low), 190-310 kD (Medium) and > 310 kD (High) were obtained from Sigma-Aldrich. Chitosan was dissolved at 2% (w/v) in 1% (v/v) acetic acid. The solution was frozen at -20° C overnight and lyophilized for 24 h to produce porous scaffolds. Scaffolds were immersed alternately for 10 minutes in 0.333 M CaCl<sub>2</sub> and 0.333 M Na<sub>2</sub>CO<sub>3</sub> solutions. After three alternate soaking cycles, scaffolds were immersed for 24 h in ddH<sub>2</sub>O, weighed, freeze-dried for 24 h and reweighed. Dry mass percentage, i.e. (mass after lyophilization/mass before lyophilization) x 100% served as a measure of mineral formed. Morphology and physicochemical analysis was performed using SEM and ATR-FTIR.

## RESULTS AND DISCUSSION

Calculation of dry mass percentage (Figure 1) revealed that significantly higher amounts of CaCO<sub>3</sub> formed in

scaffolds consisting of high and medium MW chitosan than in low MW chitosan scaffolds. The reasons for this remain unclear at present, however it can be speculated that the medium and MW preparations have a higher affinity for calcium ions.

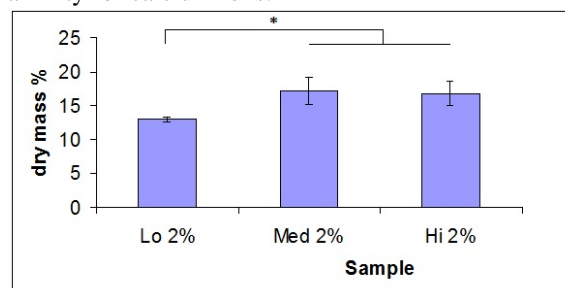


Figure 1: Dry mass percentages after mineralization

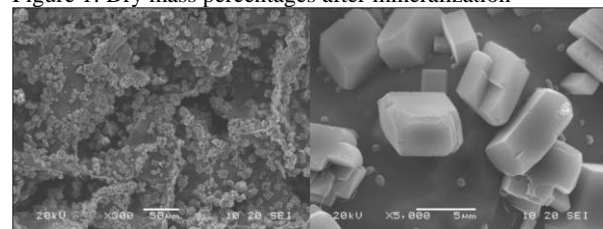


Figure 2: SEM images of medium MW chitosan scaffold mineralized with CaCO<sub>3</sub>. Scale bar: 50 µm (left), 5 µm (right)

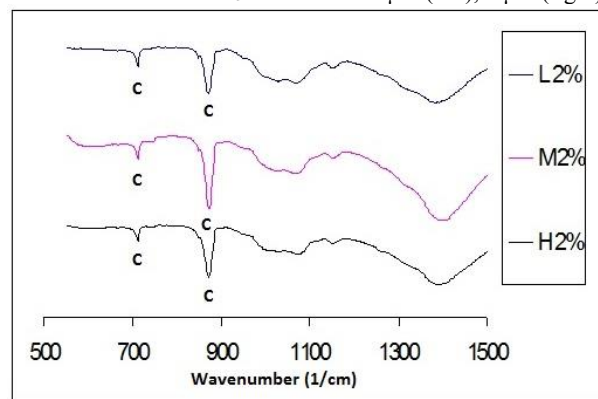


Figure 3: ATR-FTIR spectra. C: band indicating calcite. Calcite, the thermodynamically most stable polymorph of CaCO<sub>3</sub>, was detected in all three chitosan scaffold types. This was confirmed by SEM analysis, which revealed rectangular crystals of calcite homogeneously distributed throughout the scaffold (Figure 2). ATR-FTIR analysis (Figure 3) also proved the presence of calcite. Mechanical strength increased markedly after mineralization. No brittleness was observed.

## CONCLUSION

Mineralization of chitosan scaffolds of different MW with CaCO<sub>3</sub> revealed that extent of mineralization was dependent on MW. These results pave the way for *in vitro* and *in vivo* biological testing

## ACKNOWLEDGMENTS

T.E.L.D. thanks FWO, B for a postdoctoral fellowship.

## Development of Boron Doped Hydroxyapatite by Biomimetic Method

Ekin Ö. Tunçay<sup>1</sup>, Tolga T. Demirtaş<sup>1</sup>, Menemşe Gümüşderelioğlu<sup>1,2</sup>

<sup>1</sup> Department of Bioengineering, Hacettepe University, Turkey

<sup>2</sup>Department of Chemical Engineering and Bioengineering, Hacettepe University, Turkey  
[ekntncy@gmail.com](mailto:ekntncy@gmail.com)

### INTRODUCTION

Boron (B) is a notable trace element in human which has stimulating potential on osteogenesis. Recent findings indicate that dietary boron intake has beneficial effect on  $\text{Ca}^{2+}$  metabolism and thus B affects bone calcification and maintenance [1]. The mineral phase of bone is termed biological apatites which contain significant amounts of various ions such as  $\text{Mg}^{2+}$ ,  $\text{Na}^+$ ,  $\text{Zn}^{2+}$ ,  $\text{F}^-$  and  $\text{Cl}^-$ . Until now, a number of methods such as wet precipitation, hydrothermal and sol-gel synthesis have been developed for the preparation of hydroxyapatite (HAp) and ion-doped HAp in a powder form [2]. In addition, there are very few studies in which B was doped into HAp chemically [3]. The aim of this study is to produce boron doped HAp (B-HAp), using biomimetic method supported by different microwave energies.

### EXPERIMENTAL METHODS

To prepare B-HAp, different amounts of boric acid was added into 10xSBF (simulated body fluid) like solution [4] and pH was adjusted to obtain proper pH value for precipitation. In our previous study, we prepared bone-like HAp precipitated by microwave energy [5]. B-HAp was produced by means of interaction of ions within the boron containing 10xSBF (B-SBF) under microwave energy (Milestone Start, Italy). Characterizations of B-HAp and HAp were carried out by SEM, TEM, ATR-FTIR, ICP-OES, Raman, XRD and elemental analysis.

### RESULTS AND DISCUSSION

B-HAp was precipitated from B-SBF containing 10 mg/mL boric acid ( $\text{H}_3\text{BO}_3$ ) by 600 W microwave power. ICP-OES results demonstrated that B-HAp has  $1.15 \pm 0.11$  % (w/w) B, 1.40 (w/w) Ca/P ratio and  $4.30 \pm 0.07$  % (w/w) carbonate content. In Raman spectrum, the strongest line situated at  $961 \text{ cm}^{-1}$  is attributed to the symmetric stretching  $\nu_1$  mode of  $\text{PO}_4^{3-}$ , the bands at  $429 \text{ cm}^{-1}$  and  $591 \text{ cm}^{-1}$  correspond to the  $\nu_2$  bending vibration and  $\nu_4$  mode of the  $\text{PO}_4^{3-}$  group. In the spectrum of B-HAp, an additional weak peak at  $\sim 910 \text{ cm}^{-1}$  has been assigned to the symmetric stretching  $\nu_1$  mode of the  $\text{BO}_3^{3-}$  groups (Fig.1).

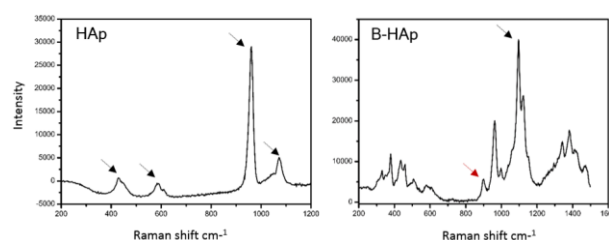


**Fig.1.** Raman spectrum of HAp and B-HAp. Black and red arrows indicate the phosphate and borate groups, respectively.

SEM images of HAp and B-HAp powders are illustrated in Fig. 2. They demonstrate many agglomerations of small spherical particles in nano-scale. Their bulk structure were found similar in size and morphology.

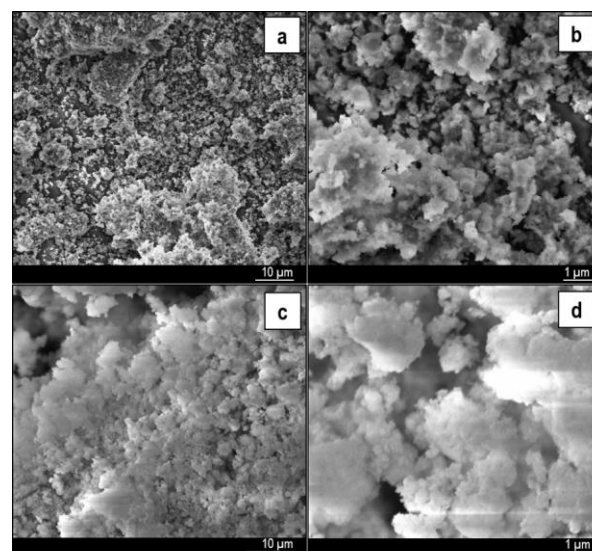


**Fig.2.** SEM images of HAp (a and b) and B-HAp (c and d) particles. b and d are ten times bigger than that of a and c, respectively.

### CONCLUSION

In this study, incorporation of B into hydroxyapatite structure using biomimetic method was achieved by means of microwave irradiation.

In conclusion, B-HAp could be a powerful biomaterial to improve regeneration of bone with synergetic effect of boron and hydroxyapatite for bone tissue engineering.

### REFERENCES

1. Nielsen F.H., J. Trace Elem Med Bio. 28: 383–387, 2014
2. Yang L. *et al.*, Biomaterials 31:2976–2989, 2010
3. Ternane R. *et al.*, J. Alloy Compd 333: 62–71, 2002
4. Mavis B. *et al.*, Acta Biomater 5: 3098–3111, 2009
5. Demirtas T.T. *et al.*, Mater Sci Eng C 49: 713–719, 2015

### ACKNOWLEDGMENT

The authors would like to thank Turkish Scientific and Research Council (Grant no: 112M705) for providing financial support to this project.

<sup>3</sup> Institute of Orthopaedics and Musculoskeletal Science, UCL, RNOH Stanmore Campus, London, United Kingdom.  
[a.nash@ucl.ac.uk](mailto:a.nash@ucl.ac.uk)

A dynamic distance-based criterion search was used to identify lysine and arginine residues within 5 Å of each other within a tropocollagen. Fully atomistic MD simulations, exploiting the D-band periodicity to replicate the dense fibrillar environment, were then conducted under pseudo physiological conditions in AMBER12.<sup>5,6</sup> A site is a likely candidate for glucosepane formation if the total energy of the tropocollagen molecule is lower in the presence of a bound glucosepane cross-link compared to an unbound glucose molecule. Using the candidate cell and matrix interaction domains map of the collagen fibril produced by Sweeney *et al.*,<sup>7</sup> we then transpose our favourable cross-link positions to determine the biological impact of their presence. Constant velocity steered MD simulations were then conducted to calculate changes in the elastic property of collagen.

Of the 24 positions identified based on the distance criteria, only six were found to be energetically favourable (exothermic binding enthalpies) compared to the unbound glucose collagen model. The local environment around the site has a significant effect on the energetics, with the sites within the gap region being more likely to have favourable formation enthalpies (Figure 1). A number of favourable sites may result in potentially huge implications on the biological function of collagen, as they are within sites where key collagen-biomolecule and collagen-cell interactions occur. For example, the formation of glucosepane was found to be energetically favourable within close proximity of the Matrix Metalloproteinase-1 (MMP1) binding site, which could potentially disrupt collagen degradation. Finally the Young's modulus was also found to change as a result of the presence of the cross-link.

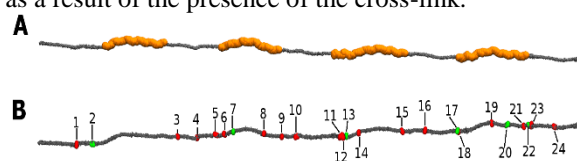


Figure 1. Shows a tropocollagen molecule with A. gap regions highlighted in orange, B. the favourable (green) and unfavourable (red) potential cross-linking sites.

Our 3-dimensional collagen fibril model has identified six likely sites for glucosepane formation within tropocollagen. The positioning of these sites is likely to have a significant effect on tissue function and integrity.

1. Sell D.R. *et al.*, J. Biol. Chem. 280:12310-12315, 2005
2. Wang X *et al.*, Bone, 31:1-7, 2002
3. Zieman S.J. *et al.*, Congest. Hear. Fail. 10:144-151, 2004
4. Gautieri A. *et al.*, Matrix Biology, 13:89-95, 2014
5. Streeter I. *et al.*, J. Phys. Chem. B, 114:13263-13270, 2005
6. Orgel J.P.R.O. *et al.*, Proc. Natl. Acad. Sci. U.S.A., 103:9001-9005, 2006
7. Sweeney S.M. *et al.*, J. Biol. Chem. 283:21187-21197, 2008

**ACKNOWLEDGMENTS**  
The authors would like to thank the BBSRC for financial support (Grant: **BB/K007785**).



## PBSu-based Composite Scaffolds Containing Micro-bioactive Glass and Nano-hydroxyapatite for Bone Reconstruction

Maria Nearantzaki<sup>1</sup>, Ioanna Koumentakou<sup>1</sup>, Iro Koliakou<sup>2</sup>, Evangelia K Siska<sup>3</sup>, Kaloyanni Martha<sup>2</sup>, Dimitrios Bikiaris<sup>1</sup>

<sup>1</sup> Department of Chemistry, Aristotle University of Thessaloniki, Greece

<sup>2</sup> Department of Biology, Aristotle University of Thessaloniki, Greece

<sup>3</sup> Department of Biochemistry, Medical School Aristotle University of Thessaloniki, Greece

[iro.koliakou@gmail.com](mailto:iro.koliakou@gmail.com)

### INTRODUCTION

Poly(butylene succinate) (PBSu), a novel biodegradable aliphatic polyester with excellent processability, is a promising substance for bone and cartilage repair. However, it typically suffers from insufficient bioactivity after implantation into the human body and low mechanical properties, which reduce its application possibilities. Bioactive ceramics include hydroxyapatite (HA), fluorapatite, bioactive glass (BG), and tricalcium phosphate can be either bioactive or bioinert, as they positively affect new bone growth inhibiting resorption and enhancing bone formation<sup>1</sup>. So, in order to overcome this problem, micro-sized bioglass (mBG) or nano-sized hydroxyapatite (nHA) were synthesized and introduced into the polyester via *in situ* polymerization. Regenerative Medicine in orthopedics focuses on research in a wide variety of applications, including bone and cartilage. Biocompatible scaffolds play a key role in successful bone and cartilage regeneration. Cytotoxicity, stability, cell adhesion, proliferation and spreading are factors that influence effectively the use of scaffolds in regenerative medicine applications.

### EXPERIMENTAL METHODS

In this work, indigenous synthetic nano-HA and micro-BG, were developed in the laboratory. Afterwards, PBSu nanocomposites containing 2.5wt% (mBG), 2.5wt% (nHA) and 2.5wt% mBG-nHA were prepared by *in situ* polymerization technique for the first time. We then examine their ability as potential tissue engineering scaffolds. The composites scaffolds were characterized using GPC, SEM, FTIR and XRD. Mechanical testing (Instron 3344) and contact angle measurements were also carried out. Additionally, enzymatic degradation in an aqueous solution containing a mixture of *R. Oryzae* and *P. Cepacia* lipases at 37°C and pH=7.2 and the *in vitro* biomineralization in simulated body fluid (SBF) were studied. Biocompatibility of the composites was assessed using human Mesenchymal stem cells collected by enzymatic digestion of Wharton's Jelly and cultured in osteogenic medium for 28 days. Cell proliferation on the scaffolds was evaluated using fluoresce microscopy. Furthermore MTT (3-(4,5-dimethylthiazol-2-yl)-2,5-diphenyltetrazolium bromide) assay was used in order to assess viability of cells on the scaffolds. Finally the morphology of cells on the scaffolds was evaluated by SEM, TEM and photonic microscopy.

### RESULTS AND DISCUSSION

The presence of the bioceramics in the polymerization mixture, affected the reaction, leading to decrease of the final molecular weight (Mw) of the synthesized polymers. Probably extended reactions took place and branched and/or cross-linked macromolecules were formed, due to the surface hydroxyl groups of the filler, which can act as a multifunctional agent, leading to a partially reduction of Mw<sup>2</sup>. Concerning the tensile test it was proved that the presence of the inorganic fillers in the PBSu matrix led to deterioration of its mechanical properties. This decrease could be attributed not only to very low Mw but also, to the absence of any interaction between the bioceramic and the polyester matrix, as was verified from FTIR spectroscopy and thus the adhesion between the different materials is too low. Additionally, enzymatic hydrolysis revealed that all nanocomposites have higher hydrolysis rates than neat PBSu. The presence of hydroxyl groups in HA makes the nanocomposites more hydrophilic than neat PBSu and hence they absorb more water and subsequently degrade more rapidly. XRD study after biomineralization in SBF indicated the appearance of a crystalline phase of hydroxyapatite. In addition to apatite formation enhancement, both bioceramics can induce osteoblast compatibility. The composites have rougher and more hydrophilic surfaces compared to pristine PBS, thereby causing more osteoblasts to adhere and proliferate on them<sup>1</sup>.

### CONCLUSION

PBSu nanocomposites containing 2.5wt% of (mBG), (nHA) or mBG-nHA were prepared and studied as potential materials for tissue engineering applications. Mechanical properties aggravated for all the composite samples, mainly due to decreased Mw as was verified by GPC analysis. It was also found that nanoadditives can accelerate the enzymatic hydrolysis of PBSu increasing hydrophilicity. Both (mBG) and (nHA) can transform the bioinert PBSu surface into a bioactive one, promoting hydroxyapatite formation in SBF solution. Cell biology studies showed that PBS/(mBG)/(nHA) are biocompatible materials.

### REFERENCES

1. Yuan Y. *et al.*, Materials Science Forum 610:1335-1338,2009
2. Bikiaris D. *et al.* Macromol Rapid Commun 27:1199–205,2006





## INTRODUCTION

In recent years, the clinical demand for bone grafts is extremely large across the population. However, the limited volume of bone grafts and frequent morbidity of patients leads to the need for development of advanced therapeutic strategies for bone regeneration<sup>1,2,3</sup>. The aim of the present work is to study the behavior of pre-osteoblastic MC3T3-E1 cells in a microfluidic system that allows continuous and homogenous feeding of cells, as well as, study of dynamic culture with the use of different biomaterials (gelatin film and collagen fiber networks) inside the microfluidic system.

## EXPERIMENTAL METHODS

### Microfluidic system

The microfluidic system is composed of a pressure pump (Figure 1A) connected with a precisely controlled flow sensor (B) and a chamber (C) including the microfluidic devices. The microfluidic devices are composed of a glass base chip for the cell layer (D) and PMMA chips with PDMS gaskets for loading cells (E) and for flowing fluids across the cells (F).

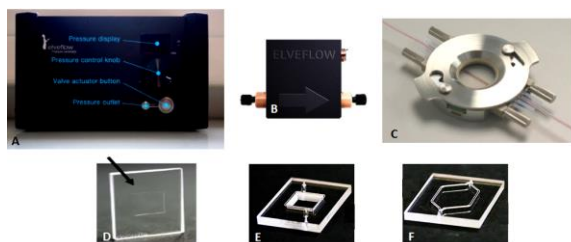


Figure 1: Illustration of the microfluidic system

### Preparation of gelatin films

A 2% w/v gelatin solution was used for coating the glass base chip of the microfluidic system and dried for 2 hours before seeding the cells.

### Preparation of collagen fiber networks

For the generation of collagen fiber networks, a 3 mg/ml collagen solution was used for the chip coating. Gelation was performed by incubating the collagen solution for 48 hours at 4 °C for thick fibers. Thereafter, collagen gel dried for 3 hours, washed with water and PBS and was completely immersed with culture medium overnight in a CO<sub>2</sub> incubator before seeding the cells.

### Cell culture

8x10<sup>4</sup> pre-osteoblastic cells were cultured on the chip of the microfluidic system and investigated under static and flow conditions with flow rates of 30 and 50 µl/min.

### Osteogenic markers response of MC3T3-E1 cells

We determined the alkaline phosphatase (ALP) activity, and the total soluble collagen contents in the culture medium using an enzymatic activity assay and a modified Sirius red assay, respectively.

## RESULTS AND DISCUSSION

The pre-osteoblastic cells strongly attach and show an osteogenic response inside the microfluidic system. Additionally, we observed that under flow conditions cells appear to be oriented along the direction of flow, whereas cells depict a random orientation under static conditions (Figure 2). The ALP activity was similar between static and flow conditions when using gelatin as a substrate for the cells. Interestingly, when we used collagen fiber networks as a substrate, the ALP activity was higher in dynamic cultures under both flow rates of 30 and 50 µl/min compared to statics. Finally, when gelatin was used as a substrate, the collagen produced in the extracellular matrix under a flow rate of 30 µl/min was significantly higher compared to static conditions, with a remarkably significant increase when applying the flow rate of 50 µl/min.

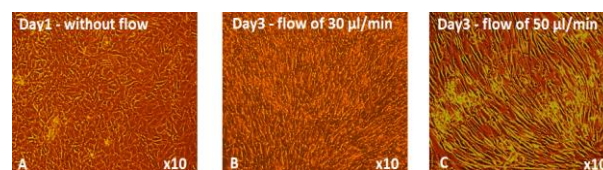


Figure 2: Morphology of MC3T3-E1 cells inside the microfluidic system under static conditions (A), and under flow conditions applying 30 (B), and 50 µl/min (C) using optical microscopy

## CONCLUSION

Our findings are promising for the cell growth and the osteogenic response of pre-osteoblastic cells demonstrating the potential of using microfluidic systems in bone tissue regeneration applications.

## REFERENCES

1. Leclerc E et al., *Biomaterials* 27.4 (2006): 586-595.
2. Bancroft G N et al., *Proceedings of the National Academy of Sciences* 99.20 (2002): 12600-12605.
3. Yu X et al., *Proceedings of the National Academy of Sciences of the United States of America* 101.31 (2004): 11203-11208.

## ACKNOWLEDGMENTS

The authors acknowledge the General Secretariat for Research and Technology Grants: 'Aristeia II, Osteobiomimesis 3438', 'Thales – MIS 380278' and 'GA no 262348, ESMI CP & CSA' for financial support.

Triantafillos Papadopoulos<sup>1</sup>, Efstathia Tsatsenidou<sup>1</sup>, Stamatia Rokidi<sup>2</sup>, Nikolaos Bouropoulos<sup>2</sup>

<sup>1</sup>Department of Biomaterials, School of Dentistry, University of Athens, Greece

<sup>2</sup>Department of Materials Science, University of Patras, 26504 Rio, Patras, Greece

[emailtrpapad@dent.uoa.gr](mailto:emailtrpapad@dent.uoa.gr)

## INTRODUCTION

Porosity is a morphological feature which plays a significant role in new bone generation when bone graft materials are used for filling small or extended bone defects<sup>1</sup>.

Calcium phosphate bone cements (CPBCs) are bone graft materials formed by mixing a powder with a liquid phase. Usually the powder component is  $\alpha$ -TCP whereas the liquid is a sodium phosphate solution. The final product (hardened cement) is composed of calcium deficient apatite. Synthetic hydroxyapatite (HA), a material similar to the basic constituent of bone, has been extensively used in bone tissue regeneration.

The purpose of the present work was to study the effect of HA addition in the initial cement paste on the porosity and pore characteristic of pure and HA reinforced composite CPBCs cements.

## EXPERIMENTAL METHODS

Pure HAP crystals in the form of nanoneedles was prepared by precipitation from aqueous solution using  $\text{CaCl}_2$  0.5M and  $\text{NH}_4\text{H}_2\text{PO}_4$  0.3M as reactants at 70 °C. The pH of the suspension was kept at 9-10 by the addition of concentrated  $\text{NH}_3$ . Preparation of  $\alpha$ -TCP powder, cement setting and hardening was performed using the procedures described elsewhere with slight modifications [2]. Four different CPBCs formulations were prepared: pure  $\alpha$ -TCP cements and cements containing 3, 10 and 20 % HA in the initial paste. X-ray microtomography ( $\mu$ CT) was used to visualize and to quantify pore's size and micro architecture.

The internal microporosity was determined using a  $\mu$ CT equipment (Skyscan 1072), with standard X-ray emission source, where the sample was placed on a rotating base. Images were received with 1024x1024 pixels analysis. Cross-sections ranged between 200-400 in 180 and 360 rotating angle. The following formulations were tested:  $\alpha$ -TCP (control),  $\alpha$ -TCP+HA3%,  $\alpha$ -TCP+HA10%, and  $\alpha$ -TCP + HA20%, expecting to report pore sizes over 80  $\mu\text{m}$ , that are recommended to accelerate and to improve the long in growth within the ceramic<sup>1</sup>. Two cylindrical samples (6mm in diameter and 10mm in height) for each formulation were examined. Five cross-sections, in equal distances, along the sample were received in order to define the mean range of the samples' pore size. The sections were reconstructed in order to determine their inter-connectivity.

## RESULTS AND DISCUSSION

Indicative images ( $\alpha$ -TCP + HAP3%) of microporosity using  $\mu$ CT are presented in Fig 1:

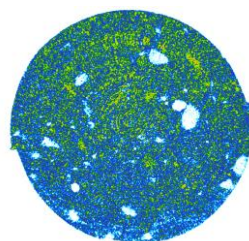


Fig. 1a

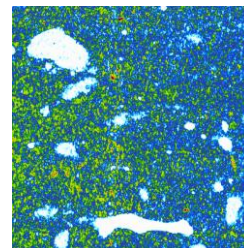


Fig. 1b

Fig.1. Cross-sectional (a) and interconnective (b) microporosity

The percentage porosity is as follows: 1.  $\alpha$ -TCP: 17,20%, 2.  $\alpha$ -TCP+HA3%: 34,80%, 3.  $\alpha$ -TCP+HA10%: 40,30%, 4.  $\alpha$ -TCP + HA20%: 44,40%.

Mean range of the pore size for each sample is between 1.  $\alpha$ -TCP: 20 $\mu\text{m}$ -120 $\mu\text{m}$ , 2.  $\alpha$ -TCP+HA3%: 90 $\mu\text{m}$ -150 $\mu\text{m}$ , 3.  $\alpha$ -TCP+HA10%: 150 $\mu\text{m}$ -490  $\mu\text{m}$ , 4.  $\alpha$ -TCP + HA20%: 230 $\mu\text{m}$  -990  $\mu\text{m}$ .

In oral surgery  $\alpha$ -TCP and HA are useful alternative bone graft substitutes to biologic (autografts etc) and natural materials.  $\alpha$ -TCP cement is more soluble and allows for a larger new bone formation area compared to  $\beta$ -TCP granules<sup>2</sup>. Research data for  $\beta$ -TCP grafts report that recommended pore size >80 $\mu\text{m}$  and optimum interconnection size is >80 $\mu\text{m}$  and <150 $\mu\text{m}$ <sup>1</sup>. The pores' inter-connectivity of the sample was neither homogeneous nor satisfactory.

## CONCLUSION

The majority of pores were larger than 80 $\mu\text{m}$ , but there was lack of pore size homogeneity. Although the percentage of samples' porosity was satisfactory, the pores' inter-connectivity was not. Increasing HA portion increases both the percentage porosity and the mean pore size.

## REFERENCES

1. Galois L and Mainard D, Acta Orthop. Belg. 70:598-603, 2004.
2. Grandi G et al, Mater. Res. 14(1):11-16, 2011.
3. Andriotis O et al, Cryst. Res. Tech. 45(3):239-243, 2009.

## ACKNOWLEDGMENTS

The authors would like to thank the European Union and Greek national funds through the Operational Program "Education and Lifelong Learning" of the National Strategic Reference Framework (NSRF) - Research Funding Program: THALES. (Grant no: MIS 379380) for providing financial support to this project.

Yumika Ida<sup>1</sup>, Ji-Young Bae<sup>1</sup>, Kazumitsu Sekine<sup>1</sup>, Fumiaki Kawano<sup>2</sup> and Kenichi Hamada<sup>1</sup><sup>1</sup>Department of Biomaterials and Bioengineering, <sup>2</sup>Department of Comprehensive Dentistry, Institute of Health Biosciences, Tokushima University, Japan  
[c301251008@tokushima-u.ac.jp](mailto:c301251008@tokushima-u.ac.jp)

## INTRODUCTION

Calcium phosphate cement (CPC) is widely utilized for various clinical applications, such as in bone-substitution materials. The objective of this study was to develop a new CPC with fine injectability, short setting-time, and high strength, and to expand the applications of CPC. Here, we investigated the effect of powder/liquid (P/L) ratio on the properties of CPC.

## EXPERIMENTAL METHODS

$\beta$ -tricalcium phosphate (control TCP; c $\beta$ -TCP) powder was mechano-chemically modified by ball-milling. After milling for 24 h (modified TCP; m $\beta$ -TCP), the powder was mixed with  $\text{CaCl}_2$  solution, and then  $\text{NaH}_2\text{PO}_4$  solution at a P/L ratio of 4:1:1 (R2) or 5:1:1 (R2.5). The P/L ratio for the non-milled c $\beta$ -TCP powder was R2. The mechanical properties of the set cement were measured using the compression strength (CS) test and the diametral tensile strength (DTS) test. The dimensions of the specimens for the CS test were 6 mm in height and 3 mm in diameter, and those for the DTS test were 4 mm in height and 6 mm in diameter. To investigate the initial strength of the cement, CS was measured from 1 to 5 h after mixing. The cement paste was stored for setting in an incubator at 37°C for 14 d, with CS testing at various time points. Fracture surfaces of the specimens stored for 14 d after the DTS test were observed by scanning electron microscopy (SEM).

## RESULTS AND DISCUSSION

The initial CS values from 1 to 5 h after mixing are shown in Fig. 1. The strength of c $\beta$ -TCP cement increased slightly at 3 h after mixing, but showed saturation at 4 h after mixing. m $\beta$ -TCP (R2 and R2.5) cements analysed for more than 1 h after mixing were durable for the tests. The CS of R2 cement increased slightly up to 3 h after mixing, and then increased more substantially between 3 and 4 h after mixing. The CS increased slightly between 4 and 5 h after mixing. R2.5 cement demonstrated significantly higher CS at 1 h after mixing compared to R2 and c $\beta$ -TCP cement. The CS of R2.5 cement continued to increase up to 5 h after mixing. The concomitant acceleration of CS with an increase in setting time might be due to the high dissolution rate of m $\beta$ -TCP powder.

Fig. 2 shows the effect of storage time after mixing on CS in c $\beta$ -TCP and m $\beta$ -TCP cements. R2 and R2.5 cement showed similar CS after 1 d of storage. After 3 d of storage, the CS of R2.5 cement was of higher average value than that of R2 cement. The CS of R2.5 cement showed saturation at more than 3 d of storage, while the CS of R2 cement continued to increase up to 14 d.

Morphology of the fracture surfaces after the DTS test of c $\beta$ -TCP and m $\beta$ -TCP (R2 and R2.5) conducted 14 d after mixing are shown in Fig. 3. Numerous needle-like crystals were observed on the surface of c $\beta$ -TCP, and several pores were observed among the granular structures that resembled urchins. The m $\beta$ -TCP (R2.5) exhibited more clear crystal growth among agglomerate grains than did R2.

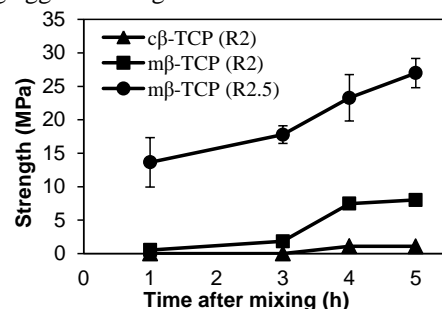


Fig. 1 Initial compression strength of cement

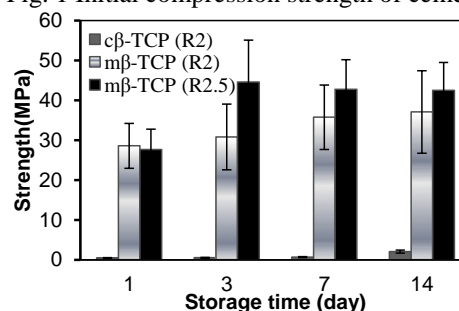


Fig. 2 Compression strength of cements after mixing according to storage time

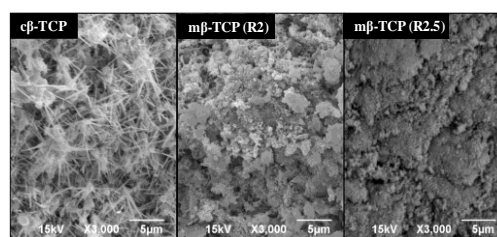


Fig. 3 DTS fracture surfaces of cements 14 d after mixing

## CONCLUSION

These results suggest that the mechano-chemically modified  $\beta$ -TCP powder dissolved rapidly and accelerated hydroxyapatite precipitation, which successfully shortened the cement setting time. Moreover, the m $\beta$ -TCP cement in this study had greater strength at a higher P/L ratio.

## ACKNOWLEDGMENTS

This work was partially supported by the JSPS KAKENHI grant numbers 24592957.



## INTRODUCTION

Hydrogels are promising materials for cell-based cartilage repair, as they provide encapsulated cells with a 3D environment that can stimulate differentiation and tissue formation.<sup>1</sup> However, as their mechanical properties are by far inferior to native cartilage tissue, new strategies are required for the reinforcement of hydrogels without compromising chondrocyte performance. Here, we studied the reinforcement of cell-laden gelatine-methacrylamide (gelMA) gels by thermal ageing prior to UV-crosslinking.

## EXPERIMENTAL METHODS

Gelatine was methacrylamide-functionalised as reported previously.<sup>1</sup> Solutions of 10% or 20% gelMA + 0.1 % Irgacure 2959 photo-initiator were crosslinked into gels by exposure to 15 min UV-A, either in the sol state or after thermal ageing at 20 or 5°C. Compressive moduli were measured after 24 h free swelling at 37°C. Chondrocytes were isolated equine articular cartilage and passaged once before encapsulation in gels at 5·10<sup>6</sup> cells/mL under the same conditions as described above. After 24 h, live/dead and Alamar blue assays were performed. Constructs prepared from 10% gelMA gels thermally aged for 3 h were cultured in chondrogenic medium for 6 weeks, then assayed for DNA and glycosaminoglycan (GAG) content using Picogreen and DMMB, respectively.

## RESULTS AND DISCUSSION

After photo-crosslinking, 10% gelMA gels crosslinked from the sol state had a stiffness of 54 kPa. On the contrary, when thermally aged, the stiffness increased up to 235 kPa after photo-crosslinking, reaching similar values as the 20% gelMA gels crosslinked from the sol state (Figure 1).

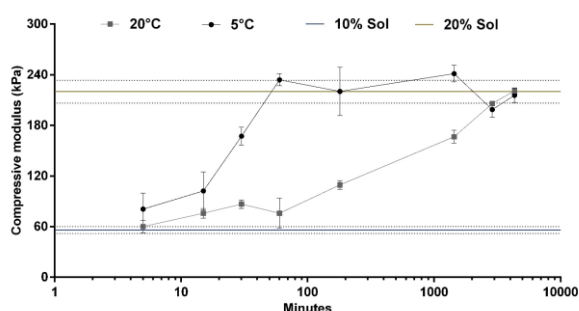


**Figure 1:** Stiffness development in 10% gelMA hydrogels upon thermal ageing at 20 or 5°C prior to UV-crosslinking. The lower and upper lines represent the compressive modulus of 10% and 20% sol UV-crosslinked gels, respectively.

Encapsulated chondrocytes showed a ~40% reduction in metabolic activity, 24 h after 1-6 hr thermal ageing (Figure 2), however cell viability was not affected (~85%).

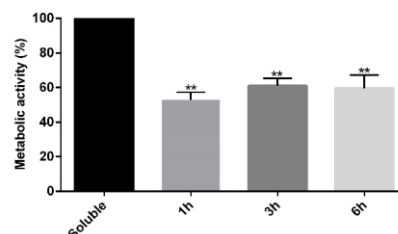


**Figure 2:** Metabolic activity of chondrocytes 24 h after encapsulation, as a function of thermal ageing time prior to UV-crosslinking.

After 6 weeks of culture, overall GAG production was increased in the 10% thermal aged gels compared to both 10% and 20% sol gels (Figure 3 left). This could be explained by the increased proliferation of chondrocytes in this condition, as GAG/DNA was similar for all conditions evaluated.

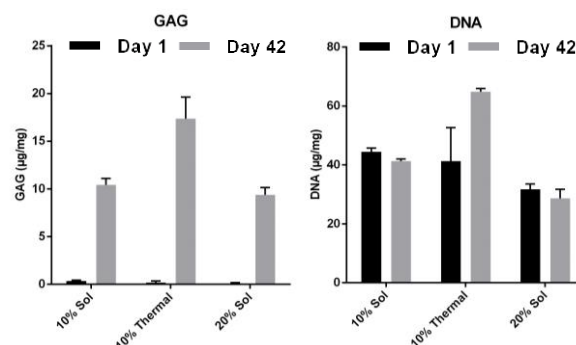


**Figure 3:** GAG production in chondrocyte-laden gelMA gels crosslinked from the sol state or after thermal ageing.

Hydrogels that allow cells to develop new tissue are generally mechanically weak. Here, we present a straightforward method for the reinforcement of cell-laden gelMA gels, which showed both four-fold increase in stiffness and an increased overall GAG production.

## CONCLUSION

Thermal ageing of gelatine-methacrylamide gels prior to UV-initiated crosslinking leads to a fourfold increase in compressive stiffness, while encapsulated chondrocytes remain viable and show proliferation and increased GAG production upon culture.

## REFERENCES

1. Schuurman W *et al.*, Macromol Biosci. 2013, 13, 551

## ACKNOWLEDGMENTS

This research has received funding from the European Union's 7<sup>th</sup> Framework Programme (FP7/2007- 2013) under grant no. 309962 (HydroZONES) and no. 272286 (PrintCART), as well as from the Dutch Arthritis Foundation.



## Design and Characterization of a Composite Material Based on Sr(II)-Loaded Clay Nanotubes Included within a Biopolymer Matrix

Stefano Del Buffa<sup>1,2</sup>, Massimo Bonini<sup>1,2</sup>, Francesca Ridi<sup>1,2</sup>, Mirko Severi<sup>1</sup>, Paola Losi<sup>3</sup>, Silvia Volpi<sup>3</sup>, Tamer Al Kayal<sup>3</sup>, Giorgio Soldani<sup>3</sup> and Piero Baglioni<sup>1,2</sup>

<sup>1</sup> Department of Chemistry “Ugo Schiff”, University of Florence, Italy

<sup>2</sup> CSGI Consortium, Florence, Italy

<sup>3</sup> Institute of Clinical Physiology, National Research Council, Italy

[giorgio.soldani@ifc.cnr.it](mailto:giorgio.soldani@ifc.cnr.it)

### INTRODUCTION

Materials for bone tissue engineering should guide and promote the regeneration of bone tissue. Various biocompatible and biodegradable porous scaffolds have been recently designed, with the aim to provide a temporary substitute which mimics bone extracellular matrix structure. Several materials have been recently suggested in the literature as promising candidates, including bioceramics, bioglasses, and hydroxyapatite particles embedded in polymeric scaffolds. Nevertheless, synthetic scaffolds still display many limitations, boosting the search for materials integrating both osteoconductive and osteoinductive properties<sup>1,2</sup>. In this study we formulated and evaluated the in vitro cytotoxicity of a nanocomposite biomaterial for bone regeneration that integrates the structural properties of Halloysite nanotubes (HNT) and the bioactivity of strontium (Sr(II)) included into a biocompatible and biodegradable 3-polyhydroxybutyrate-co-3-hydroxyvalerate (PHBV) matrix.

### EXPERIMENTAL METHODS

HNT powder (Imerys Minerals Ltd; Auckland, New Zealand) was functionalized with a solution of APTES in ethanol (2.5 %wt). The APTES amount was chosen to cover about 20% of the HNT external surface. To upload Sr(II), 100 mg of HNTs were mixed with 10 ml of a 100 mg/ml SrCl<sub>2</sub>·6H<sub>2</sub>O solution. The dispersion was vigorously mixed for 24 h and then centrifuged. The solid was recollected, dried, and then used for the subsequent preparation of the nanocomposites. HNT dispersions were spin coated by means of a P6700 spin coater (Speciality Coating Systems Inc.) onto the glass previously functionalized with APTES, and then a PHBV chloroform solution (2% wt) was spin coated on top of it. The coating process was carried out at r. t. in two stages at constant rotating speed (1500 and 2500 rpm), separated by an acceleration step. The composite morphology was evaluated after degradation in PBS at 37°C for 28 days by SEM microscopy. The retained amount of loaded Sr(II) in HNT-Sr and HNT-Sr-PHBV was evaluated by inductively coupled plasma-atomic emission spectroscopy. For cytotoxicity evaluation, nanocomposite samples were grinded and suspended in distilled water by a Ultra-Turrax® T25 Basic mechanical homogenizer. L929 fibroblasts (4x10<sup>3</sup> cell/well) were incubated with HNT, HNT-Sr, HNT-PHBV and HNT-Sr-PHBV sample solutions (25, 50 and 100 µg/mL) and cell viability was evaluated by MTT and Trypan blue assay after 72 h of incubation, while cell proliferation by BrdU assay at 48 h.

### RESULTS AND DISCUSSION

SEM image (Fig. 1) of the degraded composite evidenced a random bulk erosion process with an increase of exposed HNT respect the control sample, where HNT was almost completely embedded in PHBV matrix.

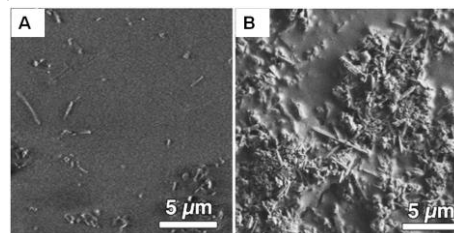


**Figure 1.** SEM image of the nanocomposite A) freshly prepared; B) degraded for 28 days.

The value of retained amount of loaded Sr(II) was similar in HNT-Sr and HNT-Sr-PHBV samples (~ 60% Sr(II) after 28 days) indicating that PHBV did not affect the release of Sr(II) and simply modulated the exposure of HNT to the surrounding medium.

The cytotoxicity and proliferation assays showed a cell viability (>80%) and proliferation (similar to control) of the cells incubated with HNT, HNT-PHBV and HNT-Sr-PHBV at all concentrations, indicating high biocompatibility of HNT, HNT-PHBV and HNT-Sr-PHBV up to 100 µg/mL. However, the HNT-Sr induces a significant viability reduction and proliferation already at 25 µg/mL, suggesting the need for a barrier to modulate its interaction with cells.

### CONCLUSION

In this study we demonstrated the possibility to use a combination of Halloysite nanotubes and PHBV biopolymer for drug delivery of Sr(II). Furthermore, we have prepared for the first time a HNT-PHBV composite capable of effectively uploading and carrying high doses of Sr(II) with a low cytotoxicity modulated by PHBV coating.

### REFERENCES

- McMahon RE. *et al.*, J. Biomed. Mater. Res. Part B., 101B:387–97, 2013
- Peng F. *et al.*, J. Phys. Chem. C, 115:15743–51 2011

### ACKNOWLEDGMENTS

The authors would like to thank Stefano Spezzani (Imerys Tiles Minerals Italia s.r.l.) for kindly providing HNT samples and professor Helmuth Moehwald for the stimulating discussions are gratefully acknowledged.

## Assessment of Magnesium Biodegradability by Micro-CT Platform

Ivana Rocnakova<sup>1</sup>, Edgar B. Montufar<sup>1</sup>, Miroslava Horynova<sup>1</sup>, Tomas Zikmund<sup>1</sup>, Karel Novotny<sup>1</sup>, Ladislav Celko<sup>1</sup>, Lenka Klakurkova<sup>1</sup>, Jozef Kaiser<sup>1</sup>.

<sup>1</sup>Central European Institute of Technology, Brno University of Technology, Czech Republic

[Ivana.rocnakova@ceitec.vutbr.cz](mailto:Ivana.rocnakova@ceitec.vutbr.cz)

### INTRODUCTION

Biodegradable metallic materials for medical applications have received considerable attention in recent years. The reason is that they provide high potential for fabrication of temporal orthopaedic implants such as bone fixation devices and scaffolds. Magnesium (Mg) is an excellent candidate for biodegradable implants due to its biocompatibility and relevance for biological body functions. Unfortunately, the high Mg degradation rate limits its application in medicine. Apart from necessity of decrease in corrosion rate of Mg, there is need of a robust, reproducible, accurate technique for quantification of *in vitro* and *in vivo* Mg biodegradation and also for evaluation of the effect of various surface treatments, performed to decrease its degradation rate. This research is focused on demonstration of X-ray computed microtomography ( $\mu$ CT) as a non-destructive, quantitative and multi-analytical characterization technique to assess the corrosion progress of high-purity-Mg (HP-Mg). The efficacy of the  $\mu$ CT was compared with that of conventional analytical methods which are commonly used for evaluation of Mg degradation.

### EXPERIMENTAL METHODS

HP-Mg (99.9 %, Goodfellow) discs (D = 15 mm, h = 5 mm), cut from an extruded bar, were used in this study. While the surfaces perpendicular to the disc axe were polished up to #1000 sand paper, the disc edge was tested as supplied. The corrosion behaviour of HP-Mg under simulated physiological conditions was studied by immersion test in Hank's solution at 37 °C up to 8 weeks. Mg degradation was monitored by the mass loss of the samples (after removal of corrosion products), pH variations and increase in Mg concentration in the immersion medium, determined by inductively coupled plasma (ICP). Surface morphology and local chemical composition of samples was studied by light microscope, scanning electron microscope (SEM) and X-ray diffraction (XRD).  $\mu$ CT scans of voxel size 25  $\mu$ m were acquired on state-of-art  $\mu$ CT station GE v|tome|x L 240. 3D visualisations and the analysis were completed using VG Studio MAX 2.2 software.

### RESULTS AND DISCUSSION

After immersion test, visual inspection and SEM images showed an evident clay-like corrosion layer on sample surfaces. The extent and thickness of the layer increased with the immersion time. XRD analysis showed that the corrosion layer was mainly composed of  $\text{Mg}(\text{OH})_2$ . The pH of the immersion media increased, reaching a mean value of  $10.3 \pm 0.1$  along the experiment. It is hypothesised that locally, in the sample surface, the increment of pH was even higher to lead on the formation of  $\text{Mg}(\text{OH})_2$ . Fig. 1 shows the  $\text{Mg}^{2+}$  concentration in the immersion medium and the mass loss of the samples determined both gravimetrically and

from  $\mu$ CT (volume loss). There was a constant release of  $\text{Mg}^{2+}$  to the immersion media, leading on a concentration between 150 and 200 mmol/l after every week, suggesting a constant corrosion rate. In general, there was a match between the mass losses determined by the two methods. Just small differences could be observed at the beginning and the end of the experiment. However, these differences were within the experimental variation between samples (around 5 %). In addition to corroborate that samples corroded monotonically ( $r^2 = 0.973$ ),  $\mu$ CT allowed the determination of the corrosion progress. Discs reconstructions in Fig. 1 show that the edge surface corroded faster than the surfaces perpendicular to the disc axes. This could be explained by the differences in microstructure. While the edge consisted of a columnar grain microstructure, the other surfaces had an equiaxial grain microstructure. Even though the mass loss provides information about overall degradation of the sample,  $\mu$ CT also allows the determination of preferential corrosion zones, useful in particular when testing anti corrosion coatings. Furthermore, applying the proper parameters,  $\mu$ CT allows the assessment of the distribution of corrosion products on the sample surface. The limitation of  $\mu$ CT in resolution to observe the microstructure of the corroded layer can be overcome by combining this technique with SEM.

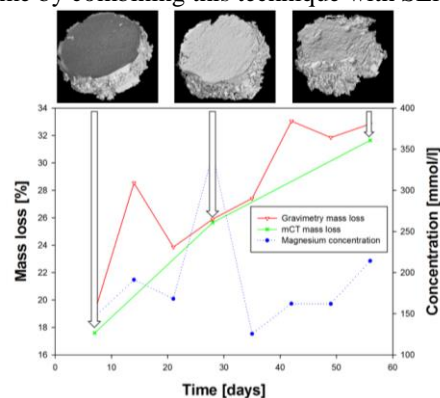


Fig.1:  $\text{Mg}^{2+}$  concentration and mass loss, determined gravimetrically and by means of  $\mu$ CT. Top images show the  $\mu$ CT reconstruction of the samples.

### CONCLUSION

$\mu$ CT can be used for determine Mg corrosion rate and progress. The flexibility and adaptability of the methodology, together with the increasing availability of  $\mu$ CT platforms, make this approach attractive, not only from the scientific aspect, but also in profitability, without losing accuracy in the results.

### ACKNOWLEDGMENTS

To the financial support provided by Czech Science Foundation (GA 107/12/1922) and European Regional Development Fund (CZ.1.05/1.1.00/02.0068).

Weitian Zhao, Jacques Lemaître, Paul Bowen

Powder Technology Laboratory (LTP), École Polytechnique Fédérale de Lausanne (EPFL), Switzerland  
[weitian.zhao@epfl.ch](mailto:weitian.zhao@epfl.ch)

## INTRODUCTION

Artificial materials which have the ability to spontaneously bond to living bone, when implanted into bone defects, are of great interest as implant materials. It is commonly accepted that a spontaneous formation of a hydroxyapatite (HA) layer on the surface of the material under *in-vivo* conditions is the key step for osseointegration<sup>1</sup>. However, compared to the costly and time-consuming *in-vivo* tests, many *in-vitro* test methods have been developed<sup>2</sup>. In these tests, the material is dipped into an artificially prepared solution, referred to as a Simulated Body Fluid (SBF) for the evaluation of its Apatite Forming Ability (AFA). In many cases, it was shown that these results accurately correlate with the material's bioactivity *in-vivo*<sup>2</sup>. However, despite the success, erroneous prediction of the bioactivity also exists<sup>3</sup>. Thus there is still space for improvement and it would be important to gain more fundamental knowledge about various factors determining the AFA under *in-vitro* conditions.

In this work, we tried to approach the problem in two directions. We explored the effects on AFA due to implant surface properties, e.g. crystalline phase, surface roughness etc. In another effort, we investigated the change in AFA with different SBF compositions. We particularly focused on the effect of proteins (e.g. albumin) since these materials are abundant in human blood plasma and could play a role in the kinetics of either apatite nucleation or growth.

## EXPERIMENTAL METHODS

### Preparation of Titanium Discs

Medical grade titanium bars were bought and cut into discs of ~1.5 cm in diameter. These discs were finely polished by sand papers to have a consistent starting surface. The titanium discs were treated with 65% HNO<sub>3</sub> solution for 30 minutes followed by 24h at 60°C in 5M NaOH or 5M HCl aqueous solution. Some of the samples were also annealed under air for 2h at 550°C.

### Preparation of SBF and Procedures of Bioactivity Tests

The SBF used, based on the suggestions of Bohner and Lemaître<sup>3</sup>, consists of NaCl (117.02mM), CaCl<sub>2</sub>·2H<sub>2</sub>O (2.31mM), NaHCO<sub>3</sub> (22.2mM), Na<sub>2</sub>HPO<sub>4</sub>·2H<sub>2</sub>O (1.39mM) and HCl (1.36mM). Bovine Serum Albumin (BSA) was added to some SBFs with a concentration of 5g/L. During the bioactivity tests, each Ti disc was immersed in ~5mL of SBF with the active surface facing down and a CO<sub>2</sub> partial pressure of 5% atm and a temperature of 37°C was maintained. The samples were taken out for observation by SEM after different periods of time. XRD, XPS and profilometry tests were also conducted.

## RESULTS AND DISCUSSION

The experiments were carried out using statistical experimental design. Differences in AFA were observed for samples with different treatments. Particularly, the HCl treated non-annealed sample did not show AFA. However, for the HCl treated and annealed sample, after the test in SBF, hydroxyapatite was found on the surface. This has clearly shown that surface properties play an important role in determining the AFA.

The effect of proteins in the SBF was investigated using the model system NaOH treated Ti discs. The effect of proteins can be seen in the difference in morphology of HA as well as the amount of deposition. Plate-like structures were found for samples without protein, suggesting a growth in preferential crystal orientation. Samples were also characterized using other methods such as IR and XPS, which will be presented and discussed in detail in the presentation.

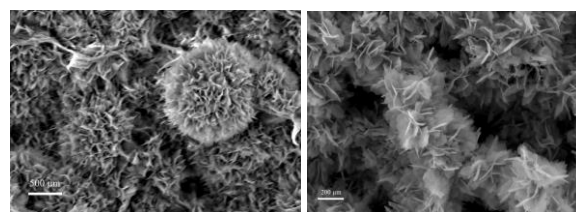


**Fig. 1** SEM images of HA on NaOH-treated Ti surface with BSA (left) and without BSA (right) in SBF.

## CONCLUSION

The surface properties of implant materials were proved to be relevant for the deposition of HA onto the surface. The presence of albumin in the SBF also affects the AFA of active materials. The effect can be seen in SEM as well as with other characterization techniques.

## REFERENCES

1. Kokubo T. *et al.*, Biomaterials 12:155-163, 1991
2. Kokubo T. *et al.*, Biomaterials 27:2907-2915, 2006
3. Bohner M. *et al.*, Biomaterials 30:2175–2179, 2009

## ACKNOWLEDGMENTS

The authors would like to thank Swiss National Science Foundation (Project No: 205321\_150193) for providing financial support for this work.



# Artificial Extracellular Matrices with Sulfated Glycosaminoglycans Promote the Osteogenic Differentiation of Osteoblast Precursor Cells

Sarah Vogel<sup>1</sup>, Ute Hempel<sup>1</sup>, Stephanie Möller<sup>2</sup>, Matthias Schnabelrauch<sup>2</sup>, Vera Hintze<sup>3</sup>, Dieter Scharnweber<sup>3</sup>

<sup>1</sup>Institute of Physiological Chemistry, Medical Faculty Carl Gustav Carus, Technical University Dresden, Germany

<sup>2</sup>INNOVENT e. V., Biomaterials Department, Jena, Germany.

<sup>3</sup>Institute of Material Science, Max Bergmann Center of Biomaterials, Technical University Dresden, Germany

[sarah.vogel@tu-dresden.de](mailto:sarah.vogel@tu-dresden.de)

## INTRODUCTION

In the bone marrow niche, human bone marrow stromal cells (hBMSC) are surrounded by extracellular matrix (ECM) containing inorganic mineral, collagen I (col) and sulfated glycosaminoglycans (sGAG). Synthetically sulfated hyaluronan (sHA) and oversulfated chondroitin sulfate derivatives (sCS) have been shown to support osteogenesis of BMSC<sup>1,2,3</sup> and to inhibit osteoclastogenesis<sup>3</sup>. In this study we describe the pro-osteogenic effect of artificial ECM (aECM) composed of col and sGAG *in vitro*.<sup>4</sup>

## EXPERIMENTAL METHODS

Artificial ECM were prepared from col and sGAG derivatives varying in the degree of sulfation and the position of sulfate groups (Table 1).<sup>1,2</sup>

GAG	DS <sub>s</sub>	position of sulfate group	MW/ g mol <sup>-1</sup>
HA	0	-	1,17 x 10 <sup>6</sup>
sHA1Δ4S	1	GlcNAc6S	26,400
sHA1Δ6S	1	GlcNAc4S	42,600
sHA2	2	GlcNAc6S/GlcA2',3'diS	26,400
sHA3	3	GlcNAc6,4S/GlcA2',3'diS	47,800
sCS1	1	GalNAc4' (70 %),6'S (30 %)	17,900
sCS2	2	GalNAc6',4'S/GlcA2,3diS	23,200
sCS3	3	GalNAc6'/4'S/GlcA2,3diS	19,900

Table 1: Characteristics of GAG derivatives. DS<sub>s</sub> - degree of sulfation per disaccharide repeating unit, MW - molecular weight. GlcNAc - N-acetylglucosamine, GalNAc - N-acetylgalactosamine, Sulfation (S) simultaneously (/) or partially (,).

The aECM were used as a substrate for osteoblast precursor cells and mature osteoblasts. Human BMSC (osteoblast precursors) were obtained from Bone Marrow Transplantation Centre of University Hospital Dresden. The cells were cultured in DMEM with 10 % FCS and osteogenic supplements were added (10 mM β-glycerophosphate, 300 μM ascorbate, 10 nM dexamethasone) from day 4 after seeding.<sup>1,2</sup> The osteosarcoma cell line SaOS-2 (obtained from ATCC) shows features of mature osteoblasts and was cultured in McCoy's 5A medium with 15 % FCS and starting at day 4 after seeding with 10 mM β-glycerophosphate and 300 μM ascorbate.<sup>4</sup>

For characterization, TNAP (tissue-non-specific alkaline phosphatase) activity was determined in cell lysates with p-nitrophenyl phosphate at day 11 after seeding and calcium deposition was quantified with calcium kit (Greiner Diagnostics, Bahlingen, Germany) at day 22.<sup>1</sup>

## RESULTS AND DISCUSSION

Artificial ECM containing sCS2, sCS3, sHA1Δ4S, sHA2 and sHA3 induced a significant increase of

TNAP in hBMSC (Figure 1)<sup>4</sup>. The calcium deposition – a second indicator for osteogenic differentiation – was determined at day 22 and showed the same pattern.

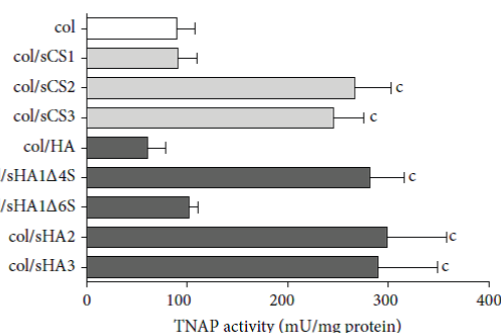


Figure 1: Influence of aECM on specific TNAP activity of hBMSC at day 11 after seeding. Values shown as mean ± standard error of the mean, c (P < 0.001) calculated by one-way ANOVA analysis with Bonferroni's posttest, n = 4.

As seen in figure 1, the pro-osteogenic effect of GAG derivatives was independent of kind of disaccharide unit and the absolute number of sulfate groups. But the C-6 position of the N-acetylglucosamine seems to be necessary. Furthermore, the osteoinduction is specific for osteoblast precursor cells as sGAG did not affect mature osteoblasts SaOS-2 in the same manner.

The molecular mechanism of this specific pro-osteogenic effect is still unknown. However, there are hints that sGAG derivatives interfere with matrix remodelling e.g. by decreasing endogenous col synthesis<sup>5</sup>, reducing formation<sup>5</sup> and activity of matrix metalloproteinases (MMPs) and increasing formation of tissue inhibitors of metalloproteinases (TIMPs).

## CONCLUSION

The manifold effect of sGAG and sGAG containing aECM (e.g. osteoinduction of osteoblast precursor cells, influence on matrix remodelling) makes them to an interesting tool for tissue engineering approaches.

## REFERENCES

- Hempel *et al.*, Acta Biomater. 8: 4064-4072, 2012.
- Büttner *et al.*, J. Cell. Physiol. 288: 330-340, 2012.
- Salbach-Hirsch *et al.*, J. Cell. Biochem. 115: 1101-1111, 2014.
- Hempel *et al.*, BioMed Research Int. 2014.
- Kliemt *et al.*, J. Proteome Res. 12: 378-389, 2013.

## ACKNOWLEDGMENTS

The authors thank Deutsche Forschungsgemeinschaft for financial support (SFB/Tr67 projects B1, A2, A3).





## In Situ Setting Calcium Magnesium Phosphate Bone Cements as Drug Carrier System

Andreas Hoess<sup>2</sup>, Anna Schmidt<sup>1</sup>, Theresa Christel<sup>1</sup>, Berthold Nies<sup>2</sup>, Jürgen Groll<sup>1</sup>, Uwe Gbureck<sup>1</sup>, Elke Vorndran<sup>1</sup>

<sup>1</sup> Department for Functional Materials in Medicine and Dentistry, University of Würzburg, Germany

<sup>2</sup> InnoTERE GmbH, Germany

[elke.vorndran@fmz.uni-wuerzburg.de](mailto:elke.vorndran@fmz.uni-wuerzburg.de)

### INTRODUCTION

Bone augmentation materials should combine both, biodegradation and adequate mechanical properties to provide fast bone regeneration and therefore early rehabilitation of patients. In this context, struvite forming magnesium substituted calcium phosphate cements (CMC) seem to be promising materials due to their biocompatibility, biodegradability and high compressive strength. The aim of this study was to prepare injectable and ready-to-use CMC pastes, which can be shaped as required. Furthermore, the application of such cement pastes as a controlled release system for antibiotics was evaluated.

### EXPERIMENTAL METHODS

CMC pastes (InnoTERE GmbH, Germany) consisted of  $\text{Ca}_x\text{Mg}_{(3-x)}(\text{PO}_4)_2$  powder with  $x=0.5$  or  $x=0.75$ , a biocompatible carrier liquid, and  $3.5\text{M}(\text{NH}_4)_2\text{HPO}_4$  (N-CMC) or a mixture of  $3\text{M}\text{KH}_2\text{PO}_4$  and  $0.5\text{M}\text{K}_2\text{HPO}_4$  (K-CMC) as binder components. The pastes were either applied as 1-component or as 2-component system in which a second aqueous phase was homogeneously mixed with the cement paste at a 1:4 volume ratio by using a static mixing device (Figure 1). For drug elution experiments cement modification with Vancomycin (VHCl) was performed (1) by mixing 1.24wt% solid antibiotic with the paste during manufacturing or (2) by dissolving 10.0 wt.% antibiotic in the aqueous phase of the 2-component system. Samples were prepared by filling the paste into  $6\times6\times12\text{mm}^3$  silicon molds, followed by curing for 24h at  $37^\circ\text{C}$  and  $>90\%$  humidity and subsequent immersion in phosphate buffered solution (PBS). The compressive strength, porosity, microstructure, chemical composition, and drug release were analyzed after several time points.

### RESULTS AND DISCUSSION

The present study demonstrates the preparation of injectable and premixed pastes based on CMC. The cement setting reaction proceeds only in a humid environment due to the substitution of the carrier liquid by water. Depending on the type of phosphate providing salt, different cements were obtained. For N-CMC, cured samples consisted of unreacted raw materials farringtonite and stanfieldite as well as of the reaction products struvite, calciumpyrophosphate and newberyite. Usage of a mixture of potassium phosphates as binding agent (K-CMC) leads to the reduction of struvite content in favor of newberyite. Compressive strength increased during immersion in PBS over 56 days from 8-10 MPa after 5 days to 24 MPa for N-CMC and from 12 MPa to 18 MPa for K-CMC, respectively (Table 1). According to this,

porosity decreased with proceeding immersion time but was independent of chemical composition. Bioactive VHCl was released in a first order kinetic over a period of 28 days for N-CMC and 3 days for K-CMC, respectively. Cement properties like microstructure, porosity, and mechanical strength were not influenced by the addition of the drug. Thus, the different release kinetics may be attributed to differences in the setting reaction and thus final chemical composition of the two cement types.

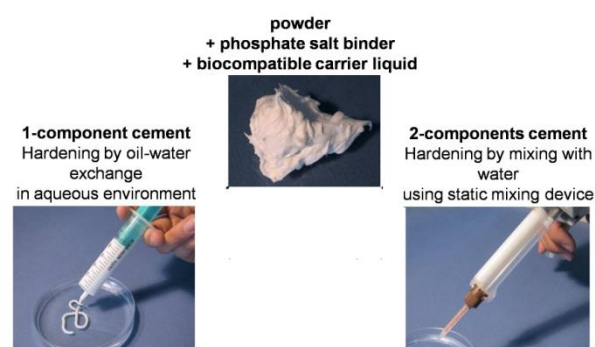


Figure 1: Application and handling of calcium magnesium phosphate cement paste.

Cement paste composition	Compressive strength [MPa]
$\text{Ca}_{0.5}\text{Mg}_{2.5}(\text{PO}_4)_2$ K-CMC 1-component	$18 \pm 3$
$\text{Ca}_{0.5}\text{Mg}_{2.5}(\text{PO}_4)_2$ N-CMC 1-component	$24 \pm 3$
$\text{Ca}_{0.75}\text{Mg}_{2.25}(\text{PO}_4)_2$ N-CMC 1-component	$24 \pm 4$
$\text{Ca}_{0.75}\text{Mg}_{2.25}(\text{PO}_4)_2$ N-CMC 2-components	$10 \pm 2$

Table 1: Compressive strength of drug loaded cement pastes after 56 days in PBS.

### CONCLUSION

The results suggest that premixed CMC pastes are promising bone filling materials with high mechanical stability and drug elution option for the treatment or prevention of osteomyelitis or infection.

### ACKNOWLEDGMENTS

The authors acknowledge financial support by the Federal Ministry of Education and Research (BMBF grants no. 13EZ1208A/B).



# MgCO<sub>3</sub> and (Mg/Ca)CO<sub>3</sub> Microparticles for Bone Regeneration: Synthesis, Characterization and Applications

Katarzyna Reczyńska<sup>1</sup>, Timothy E.L. Douglas<sup>2</sup>, Agata Łapa<sup>1</sup>, Krzysztof Pietryga<sup>1</sup>, Andre G. Skirtach<sup>2</sup>, Elżbieta Pamuła<sup>1</sup>

<sup>1</sup>Department of Biomaterials, AGH University of Science and Technology, Krakow, Poland

<sup>2</sup>Nano & Biophotonics group, Department Molecular Biotechnology, Ghent University, Belgium

[kmr@agh.edu.pl](mailto:kmr@agh.edu.pl)

## INTRODUCTION

Calcium carbonate (CaCO<sub>3</sub>) has been widely applied in scaffold form as a material for bone regeneration. In microparticle form, CaCO<sub>3</sub> is a popular drug delivery vehicle. Magnesium (Mg) has been incorporated in calcium phosphate (CaP)-based materials for bone regeneration to promote bone cell adhesion, proliferation and differentiation *in vitro* as well as integration with surrounding bone *in vivo*. However, Mg-enriched CaCO<sub>3</sub> and magnesium carbonate (MgCO<sub>3</sub>) have attracted far less attention.

In this study, microparticles of MgCO<sub>3</sub>, Mg-enriched CaCO<sub>3</sub> (hereafter referred to as (Mg/Ca)CO<sub>3</sub>) were synthesised and compared to CaCO<sub>3</sub>.

Microparticles were characterized with respect to morphology, both directly after synthesis and after incubation in ddH<sub>2</sub>O. Furthermore, self-gelling, injectable composites for bone regeneration were generated by mixing microparticles with solutions of the polysaccharide Gellan Gum (GG). It is known that GG hydrogels can be formed by crosslinking with calcium (Ca) or Mg ions<sup>1</sup>. We hypothesized that the higher solubility of MgCO<sub>3</sub> and (Mg/Ca)CO<sub>3</sub> compared to CaCO<sub>3</sub> would result in faster gelation.

## EXPERIMENTAL METHODS

MgCO<sub>3</sub>, (Mg/Ca)CO<sub>3</sub> and CaCO<sub>3</sub> microparticles were prepared by mixing equal volumes of solution 1 (consisting of Na<sub>2</sub>CO<sub>3</sub>) and solution 2 (consisting of CaCl<sub>2</sub> and/or MgCl<sub>2</sub>), as shown in Table 1, at room temperature using stirring. Microparticles formed instantly, were isolated by centrifugation, subjected to washing with ddH<sub>2</sub>O and dried in an oven at 38 °C. Particles were also incubated in ddH<sub>2</sub>O for 7 days. Particle morphology was examined by SEM. To produce self-gelling GG-microparticle composites, 0.875% GG was sterilized by autoclaving. Microparticle suspension was mixed into the GG solution to obtain a composite containing 0.7% w/v GG and 0.4% w/v microparticles.

Table 1. Concentrations of solutions mixed to produce microparticles (all values mol dm<sup>-3</sup>)

Microparticle type	Solution 1	Solution 2	
	Na <sub>2</sub> CO <sub>3</sub>	CaCl <sub>2</sub>	MgCl <sub>2</sub>
MgCO <sub>3</sub>	0.333	0.333	0
(Mg/Ca)CO <sub>3</sub>	0.333	0.167	0.167
CaCO <sub>3</sub>	0.333	0	0.333

## RESULTS AND DISCUSSION

Morphology of dried microparticles is shown in Fig. 1. CaCO<sub>3</sub> (fig. 1A) microparticles had a spherical morphology, typical for deposits of the polymorph vaterite. Some cubic deposits of the polymorph calcite were seen. (Mg/Ca)CO<sub>3</sub> microparticles (fig. 1B) were larger and consisted of crystal-like structures of non-uniform morphology. MgCO<sub>3</sub> microparticles had an irregular, non-crystalline morphology. After incubation in ddH<sub>2</sub>O for 7 days, CaCO<sub>3</sub> microparticles (fig. 2A)

converted to calcite, while (Mg/Ca)CO<sub>3</sub> microparticles (fig. 2B) became spherical with a vaterite-like morphology. This may suggest a phase change and Mg release. MgCO<sub>3</sub> microparticles changed after incubation but remained irregular and inhomogeneous.

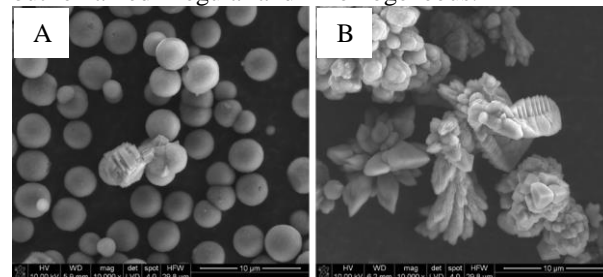


Figure 1: SEM images of CaCO<sub>3</sub> (A) and (Mg/Ca)CO<sub>3</sub> microparticles (B) after drying. Scale bar: 10 µm.

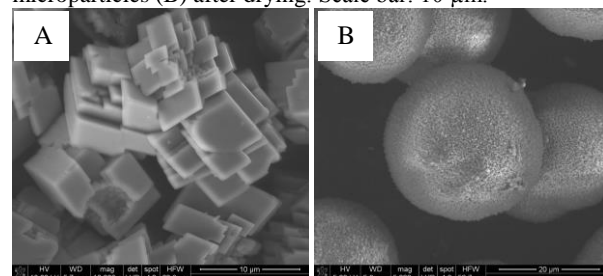


Figure 2: SEM images of CaCO<sub>3</sub> (A) and (Mg/Ca)CO<sub>3</sub> microparticles (B) after incubation in ddH<sub>2</sub>O for 7 days. Scale bar: 10 µm (A), 20 µm (B).

Regarding GG-microparticle composites, addition of MgCO<sub>3</sub> microparticles to GG-solution led to very rapid gelation (within 1 min). Resulting composites were transparent, which may signify dissolution of MgCO<sub>3</sub> microparticles. Addition of (Mg/Ca)CO<sub>3</sub> microparticles to GG-solution led to slower gelation (approx. 3 min) and non-transparent composites. Addition of CaCO<sub>3</sub> microparticles to GG-solution did not cause gelation and resulted in particle sedimentation. Hence, it appears likely that Mg release from microparticles is causing GG hydrogel formation. These self-gelling composites are injectable.

## CONCLUSION

CaCO<sub>3</sub>, (Mg/Ca)CO<sub>3</sub> and MgCO<sub>3</sub> microparticles were synthesized. Addition of microparticles containing Mg to GG solutions induced hydrogel formation, most rapidly in the case of MgCO<sub>3</sub> microparticles. Further work on these self-gelling, injectable materials will focus on their suitability as bone regeneration materials and drug delivery systems, e.g. by incorporation of cells and biologically active molecules, cyto- and biocompatibility testing.

## REFERENCES

1. Douglas T *et al.* Biomed Mater 9:045014, 2014

## ACKNOWLEDGMENTS

T.E.L.D. thanks FWO, B for a postdoctoral fellowship. This study was supported from National Science Centre, Poland (2012/05/B/ST8/00129).



## Mechanical and Biological Characterization of Brushite/PCL Scaffolds

Alberto Lagazzo<sup>1</sup>, Claudia Fabbi, Giuseppe Cama<sup>2</sup>, Fabrizio Barberis<sup>1</sup>, Marco Capurro<sup>1</sup>

<sup>1</sup>Department of Civil, Chemical and Environmental Engineering (DICCA), University of Genoa, Italy.

<sup>2</sup>Polymer Chemistry & Biomaterials Group, University of Ghent, Belgium.

[alberto.lagazzo@unige.it](mailto:alberto.lagazzo@unige.it)

### INTRODUCTION

It has been observed that isolated cells are unable to form new bone tissue with the right mechanical and physiological characteristics. As consequence, tissue engineering involves the use of porous, bioresorbable materials as temporary 3D scaffolds to promote cell attachment, differentiation and proliferation<sup>1</sup>.

Ideally the scaffold would degrade slowly enough to maintain structural support during the initial stages of bone formation, but fast enough to allow space for continuous growth of new bone<sup>2</sup>.

The association of a bone cement based on calcium phosphate (Ca-P) and of biodegradable polymer like PCL (Polycaprolactone) leads to a composite material with improved mechanical properties and a decrease of the intrinsic fragility of bioceramic materials.

### EXPERIMENTAL METHODS

PCL plotted scaffolds, with oriented layer at 0/90° and 45°, diameter of wire 0.3 mm, square pores 0.09mm<sup>2</sup>, were fabricated using a Bioscaffolder® (Sys-Eng, Germany) device. The composites were obtained for infiltration of injectable liquid bone cement based on brushite, with and without plasma oxygen pretreatment, in order to change the hydrophobicity of the PCL and then the wetting with the cement. Putting a small amount of cement on the scaffold surface with a spatula, the fluid paste penetrated for gravity through small hits and finally further amount of cement was spreaded on the scaffold to fill completely the structure. The brushite was prepared by mixing  $\beta$ -TCP (tricalcium phosphate) with MCPM (mono-calcium phosphate monohydrated) in stoichiometric proportion and then adding a water solution of Na-citrate 0.5M (solid-liquid ratio 1.5:1). Mechanical properties of the samples (dynamic tensile and dynamic compression tests) were obtained with a homemade instrument<sup>3</sup>. Also measures of scaffolds and composites degradation (weight loss in water and PBS) and a preliminary biological evaluation (only on the PCL scaffold) were also performed.

A primary human osteoblast cells (HOBs) model was used<sup>4</sup> and proliferation of cells was determined using the Alamar-Blue™ assay (Life technologies), which is a redox indicator that measures proliferation quantitatively. Cells were micro seeded at a total density of 1x10<sup>5</sup> cell per scaffold placed in a 24 well plate. The culture period covered 21 days. The test was performed on days 1, 3, 7, 14 and 21. The cell culture media was changed after 24 h and every 3 days subsequently. Thermanox™ (Nalge NUNC International, Rochester, USA) dishes were used as standard positive controls.

### RESULTS AND DISCUSSION

The Complex Modulus analysis for PCL scaffolds highlights that their mechanical properties are lower than the ones of the trabecular bone in tensile test and even more in compression test. However higher is the solid fraction of the scaffold higher is the storage modulus,  $E'$ . The ox. plasma treatment of the scaffolds leads to an increase of  $E'$  only with the best combination of exposure time and power applied, probably due to a higher interaction between PCL and brushite.

Mechanical tests on PCL/brushite composite show an increase of  $E'$  due to the presence of the ceramic, with a higher improvement in compression test (Tab. 1).

	Solid fract.	Tensile $E'$ (MPa)	Compression $E'$ (MPa)	
		PCL scaffold	Composite	
PCL	61%	112	39	369
PCL ox plasma	68%	118	45	150
PCL (45°)	47%	56	19	178

Table 1.

From the degradation study on PCL/brushite it is possible to observe a real loss of weight after 15 days. PCL scaffold instead has not been affected by the solution during the six weeks of analysis.

The Alamar Blue assay showed an increase in cell number comparing the first and the last time point (21 days). SEM analysis performed after 3 days from the cell seeding showed the ability of the cells to attach and spread onto the fabricated scaffold.

### CONCLUSION

PCL infiltrated with brushite shows an elastic modulus comparable with the one of cancellous bone and very higher than the PCL scaffold. Due to the positive cell tendency to proliferation and a good cell adhesion to a PCL surfaces, combined with the biocompatibility and osteoconductivity of the brushite, the composite PCL/brushite seems promising for applications in bone replacement and repair.

### REFERENCES

1. J. Amy et al., Acta Biomaterialia 7 (2011) 16–30.
2. Y. Lei et al., Mater sci. eng. C 27 (2007) 293–298.
3. L. Seminara et al., Sensor Act. A (2011) 169:49-58
4. L. Di Silvio et al., London, UK: Kluwer Academic Publishers, 2000, vol. ix, pp. 221-241

### ACKNOWLEDGMENTS

The authors would like to thank prof. P. Dubrue and dr. T. Desmet of the University of Ghent (Belgium) and prof. L. DiSilvio of King's College, London (UK).



## INTRODUCTION

Calcium phosphate bone cements are well known biomaterials widely applied in small bone reparation. In particular, brushite phase ( $\text{CaHPO}_4 \cdot 2\text{H}_2\text{O}$ ) is often the best choice to produce a cement paste, which can be injected or moulded to fill damaged bone sites. Its use is also preferred to hydroxiapatite based materials, due to the faster resorption time<sup>1</sup>.

In this work, a series of composite materials was prepared, in which aminoacids have been introduced in the structure following two synthesis methods: i) by impregnation from an aqueous solution on the bone cement after setting and ii) directly by incorporation.

The aim was to understand the interaction between the organic and the inorganic moieties and to evaluate the properties of these new materials.

## EXPERIMENTAL METHODS

Brushite cements were prepared by mixing  $\beta$ -TCP (tricalcium phosphate) with MCPM (mono-calcium phosphate monohydrated) in stoichiometric proportion and then adding a water solution of Na-citrate, 0.1M, used as retardant, according the reaction:



Samples with solid-liquid ratio 2:1 and 1.6:1 were prepared.

Glycine, lysine and proline aminoacids have been chosen as the major components of collagen protein.

Two different methods were adopted to prepare the composite materials: i) by impregnation from an aqueous solution on the bone cement after setting and ii) directly by incorporation of the solid aminoacid with calcium phosphate salts before mixing with the liquid.

All the samples was analysed with FT-IR technique (Nexus Thermo Nicolet FT instrument, OMNIC software).

## RESULTS AND DISCUSSION

FT IR studies show that brushite phase is predominantly produced also in the presence of aminoacids in the solid phase, thus no changes are induced in the solid structure.

The resulting biomaterials show good workability and setting time suitable for mouldable or injectable cement according the solid/liquid rapport. Moreover, the addition of aminoacid could improve the adhesion cell capacity and the bio-degradability of brushite matrix, favouring the bone growth at the exposed surface.

In particular, glycine addition in the solid phase, without adding retardant in the aqueous solution, leads to a cement paste having suitable setting times, possibly due to a coordinating effect of the amino acid towards brushite Ca ions. In fact, FT-IR data (Fig. 1) evidenced changes in shape and position of the NH and C=O stretching modes of the amino and carboxylic groups in glycine structure, suggesting the interaction of the aminoacid with the inorganic matrix mainly through coordination of the carboxylate group (acting as ligand) with inorganic matrix cations<sup>2</sup>.

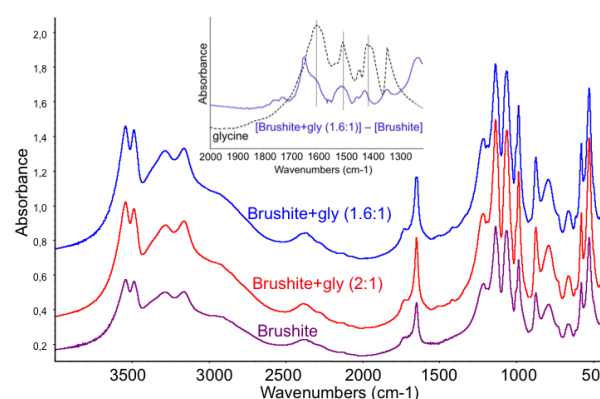


Fig. 1. FT-IR spectra of brushite (reference material) and of the composites Brushite-glycine (glycine in the solid phase). Inset: subtraction spectrum in comparison with pure glycine spectrum.

## CONCLUSION

A retardant effect on setting of calcium phosphate cement due to the interaction between aminoacid and inorganic compound was evidenced. This does not yield to significant changes in the brushite produced, that remain the predominant phase.

## REFERENCES

1. E. Charriere et al, *Biomaterials* 22 (2001) 2937-2945.
2. K. Nakamoto, *Infrared and Raman Spectra of Inorganic and Coordination Compounds*, Wiley (2009).

## ACKNOWLEDGMENTS

The authors would like to thank Pietro Arnaldi and Gianmario Moretto for the experimental contribution to this work during the preparation of their Bachelor's degree thesis.



# In Vitro Performance of Biomimetic Hydroxyapatite: Unravelling the Effect of Ionic Exchange

J.M. Sadowska,<sup>1,2,3</sup> J. Guillem-Martí,<sup>1,2,3</sup> M.P. Ginebra<sup>1,2,3</sup>

<sup>1</sup>Biomaterials, Biomechanics and Tissue Engineering Group, Technical University of Catalonia, Barcelona, Spain.

<sup>2</sup>Center for Research in nanoEngineering, Technical University of Catalonia, Barcelona, Spain.

<sup>3</sup>Biomedical Research Networking Center in Bioengineering, Biomaterials and Nanomedicine, Spain.

[joanna.maria.sadowska@upc.edu](mailto:joanna.maria.sadowska@upc.edu)

## INTRODUCTION

Calcium phosphates obtained by biomimetic routes, such as calcium deficient hydroxyapatite (CDHA), are widely used as bone substitutes due to their similarity with the mineral phase of bone, not only in composition, but also in other relevant properties such as crystallinity, specific surface area and reactivity. However, in spite of exhibiting excellent *in vivo* performance, CDHA has been shown to present poor *in vitro* behaviour<sup>1</sup>. Ionic exchange, which is more pronounced in this material compared to sintered ceramics, due to low crystallinity and high specific surface area, has been pointed out as one of the possible causes, together with the spiky microstructure of these materials<sup>1,2</sup>. However, the role of the two parameters is unclear, due to the difficulty to analyse them separately. The aim of this study was to assess to what extent ionic exchange affected cell response, by performing cell culture studies with different material/cell culture medium ratio. This was an effective way to isolate the effect of ionic exchange from that of surface topography on *in vitro* cell behaviour.

## EXPERIMENTAL METHODS

CDHA discs with different dimensions were prepared by mixing  $\alpha$ -tricalcium phosphate ( $\alpha$ -TCP) powder with an aqueous solution of 2.5 wt.% disodium hydrogen phosphate at liquid/powder ratio of 0.4 mL/g. Rat mesenchymal stem cells (rMSCs) were seeded at a 300 cells/mm<sup>2</sup> density on the CDHA discs using AdvDMEM cell culture medium. Two culture conditions were used: a) Large discs (15 mm  $\varnothing$  x 2 mm height) were immersed in 1 mL medium, b) Small discs (5.5 mm  $\varnothing$  x 300  $\mu$ m height) were immersed in 2.5 mL medium. Thus, the ratio between biomaterial volume and cell culture volume was  $V_B/V_{CM} = 0.35$  and 0.01 respectively for the a) and b) conditions. TCPS with 1 mL and 2.5 mL of medium were used as controls. During cell culture, the  $Ca^{2+}$  and  $P_i$  concentrations as well as protein content were quantified using colorimetric methods, and pH was also monitored. Cell number was determined at 6h, 3, 7 and 14 d by LDH quantification. The differentiation of rMSCs to osteoblastic phenotype in direct contact with the material (condition b), was assessed by measuring gene expression by qRT-PCR. After 6h of adhesion the medium was replaced by osteogenic medium and levels of RUNX2, ALP, COLL I, OC, ON, OPN and BMP-2 were quantified at 6h, 1 and 3d. ACTB was used as housekeeping gene.

## RESULTS AND DISCUSSION

A strong decrease in calcium was observed when  $V_B/V_{CM}$  was 0.35, whereas the levels of calcium remained unaltered, similar to those of tissue culture

plastic, when  $V_B/V_{CM}$  was 0.01 (Fig. 1).

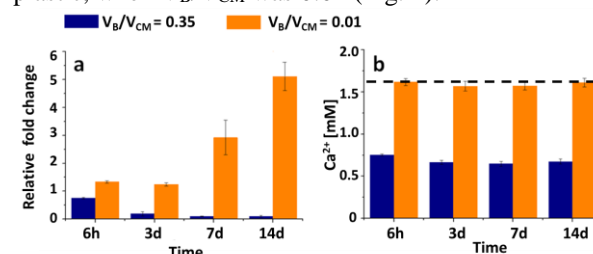


Figure 1. a) Proliferation of rMSCs on CDHA with  $V_B/V_{CM}=0.35$  and  $V_B/V_{CM}=0.01$  b) Evolution of  $Ca^{2+}$  in the cell culture medium. Dashed line indicates experimental values of  $Ca^{2+}$  of AdvDMEM.

Cell behaviour was very different in the two culture conditions (Fig. 1). Although rMSC adhesion on the material was good in the two cases, the number of cells decreased with time when  $V_B/V_{CM}$  was 0.35. In contrast, cells did proliferate when  $V_B/V_{CM}$  was reduced to 0.01. No effect of medium volume (1 mL or 2.5 mL) on cell proliferation in TCPS was observed. Gene expression of rMSCs cultured with  $V_B/V_{CM} = 0.01$  is summarized in Fig 2. An earlier expression of BMP-2, OP, OC and ON was found, with higher levels than the control with osteogenic medium at 6h and 1 day.

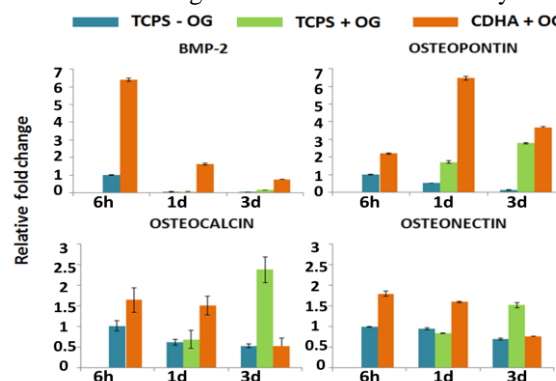


Figure 2. Gene expression levels of rMSCs cultured on TCPS or CDHA with  $V_B/V_{CM}=0.01$ . The presence or absence of osteogenic medium was marked as +OG or -OG, respectively.

## CONCLUSION

The ratio between biomaterial and cell culture volume had a strong influence on proliferation of rMSCs, suggesting a predominant effect of ionic exchange on *in vitro* cell survival. When ionic fluctuations were minimised, cells proliferated, and the overexpression of genes involved in osteogenic processes pointed out the relevance of surface topography on promoting cell differentiation.

## REFERENCES

- Engel E. et al. Tissue Eng A 14, 1341-51, 2008
- Gustavsson J. et al., Acta Biomater. 7, 4242-4252, 2011

## ACKNOWLEDGMENTS

Spanish government (MAT2012-38438-C03-01).



## Collagen Gel in Hip Cartilage Repair, the *In Vivo* Preliminary Study

Anna Bajek<sup>1</sup>, Joanna Skopińska-Wiśniewska<sup>2</sup>, Aldona Rynkiewicz<sup>1</sup>, Arkadiusz Jundziłł<sup>1</sup>, Magdalena Bodnar<sup>3</sup>, Andrzej Marszałek<sup>3</sup>, Tomasz Drewa<sup>1,4</sup>

<sup>1</sup>Chair of Regenerative Medicine, Medical College, Nicolaus Copernicus University, Bydgoszcz, Poland

<sup>2</sup>Chair of Chemistry and Photochemistry of Polymers, Nicolaus Copernicus University, Toruń, Poland

<sup>3</sup>Department of Clinical Pathomorphology, Medical College, Nicolaus Copernicus University, Bydgoszcz, Poland

<sup>4</sup>Department of Urology, Nicolaus Copernicus Hospital, Toruń, Poland

[a\\_bajek@wp.pl](mailto:a_bajek@wp.pl)

### INTRODUCTION

Traumatic injury and age-related degenerative diseases associated with cartilage are major health problems worldwide. The articular cartilage is comprised of a relatively small number of cells, which have a relatively slow rate of turnover. Therefore, damaged articular cartilage has a limited capacity for self-repair<sup>1</sup>. New clinical methods have been designed to achieve better repair of injured cartilage. However, there is no treatment that enables full restoration of it.

The aim of this study was to evaluate how collagen gel with bone marrow mesenchymal stem cells (MSCs) and collagen gel alone will influence on the hip cartilage repair after injury.

### EXPERIMENTAL METHODS

Collagen type I was isolated from rats' tails and cross-linked with N-hydroxysuccinimide in 24-hour process. MSCs were isolated from rats' bone marrow. The experiments were conducted according to the guidelines for animal experiments of Ethics Committee. Fifteen 8-week-old Wistar rats were used in this study. All animals received hip joint surgery with a total of 30 created cartilage defects. Then, animals were randomly divided into three groups and filled, respectively, with collagen gel (group I), collagen gel cultured with MSCs (group II) or left untreated as a control (control group). Immunohistochemistry and radiological evaluation was carried out 11 weeks post implantation.

### RESULTS AND DISCUSSION

It has been proved that the surface of the matrix is non-toxic, and its porosity promotes cell adhesion and growth. However, the *in vivo* regeneration process was poor. We observed the low integration rate of biomaterial. Immunohistochemical evaluation of cartilage

after 11 weeks of treatment showed low II and high X collagen expression in two tested groups in comparison to the control one, in which we observed the high II collagen expression. What is more, after radiological analysis, we observed the best regeneration process in control group. The biomaterial construct and mesenchymal stem cells, as well as the use of the biomaterial itself was not sufficient to regenerate the hip cartilage surfaces.

### CONCLUSION

These results suggest that the collagen gel based biomaterials, even with MSCs, are not satisfactory in repair of hip cartilage defect. However, additional evaluation is needed to confirm these results.

### REFERENCES

1. Qi Y. *et al.*, Knee Surg Sports Traumatol Arthrosc 22:1424-33, 2014

### ACKNOWLEDGMENTS

"The authors would like to thank the National Science Centre (NCN, Poland, Grant no: UMO-2011/03/D/ST8/04600) for providing financial support to this project"



## Osteointegration of a Macroporous Cement Designed to Repair Large Cancellous Bone Defects

Bruno Cimatti<sup>1</sup>, Wendell Monteiro Barboza<sup>1</sup>, Marcelo Henrique Nogueira-Barbosa<sup>2</sup>, Edgard Eduard Engel<sup>1</sup>

<sup>1</sup> Laboratory of Bioengineering, Ribeirão Preto Medical School, University of São Paulo, Brazil

<sup>2</sup> Division of Radiology, Ribeirão Preto Medical School, University of São Paulo, Brazil

[engel@fmrp.usp.br](mailto:engel@fmrp.usp.br)

### INTRODUCTION

Porous cements have been extensively studied for tissue engineering as scaffolds or for small bone defects commonly seen in Dentistry. Large bone defects such as those created after benign bone tumor curettage are usually filled with solid bone cement. The frequent formation of a thin layer of fibrosis around the cement block may cause bone fracture and subsequent arthrosis, mainly when the defect is periarticular<sup>1</sup>. Hirn *et al.* demonstrated that even large bone defects are filled with new bone, but depending on its size, the fracture risk is unacceptable<sup>2</sup>. A bone substitute with large pores that can be molded during surgery, allows bone ingrowth and prevent fracture could be a reasonable alternative<sup>3</sup>.

Polymethylmethacrylate (PMMA) cement mixed to the effervescent components sodium bicarbonate and citric acid, forms large interconnected pores and has physical and mechanical characteristics similar to cancellous bone<sup>3</sup>. The objective of the study was to evaluate the osteointegration capacity of this cement.

### EXPERIMENTAL METHODS

A 15x10mm cylindrical defect was created in 36 sheep tibias and filled with porous PMMA cement in group 1, with solid PMMA cement in group 2 and left empty in group 3. Porous cement was created by adding 20% of effervescent components sodium bicarbonate and citric acid to polymethylmethacrylate cement (PMMA).

Euthanasia was performed 3 months after surgery and the operated region was analyzed with micro-computed tomography scanning ( $\mu$ CT) (high-resolution  $\mu$ CT model 1172, Bruker, Belgium).

### RESULTS AND DISCUSSION

Group 1. In all samples, bone ingrowth could be demonstrated. New bone formation can be seen invading the interconnected pores mainly in the same direction of the mechanical axis.

Group 2. In all samples, a thin layer separates the cement block from bone.

Group 3. Bone ingrowth can be seen in the defect, but it is randomly distributed.

None of the specimens presented fractures of any group.



Figure 1 demonstrates new bone formation in an empty defect of Group 3.

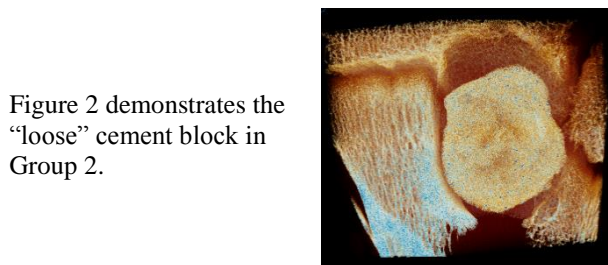
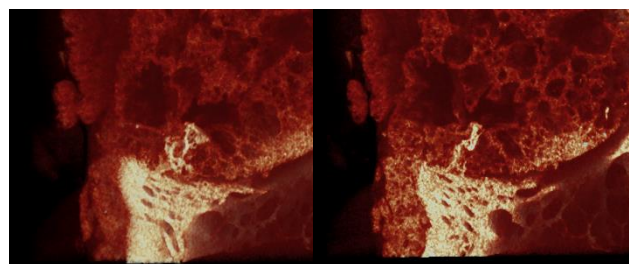


Figure 2 demonstrates the "loose" cement block in Group 2.

Figure 3 demonstrates the bone ingrowth in Group 1.



Clear line in the inferior region of the cement.

### CONCLUSION

PMMA porous bone cement allows bone ingrowth that can be detected 3 months after surgery.

### REFERENCES

1. Hesarak S. *et al.*, J Biomed Mater Res A. 83(1):80–7, 2007
2. Hirn M *et al.* Acta Orthop. 2009;80(1):4–8.
3. Kundu ZS. *et al.*, Indian J Orthop 47(3):295–301, 2013
4. Cimatti B. Ribeirão Preto: Universidade de São Paulo; 2012

### ACKNOWLEDGMENTS

Project supported by FAPESP (São Paulo Research Foundation).

## ***In Vitro* Cytotoxicity and *In Vivo* Acute Toxicity of Porous Cements Based on Polymethylmethacrilate and Castor Oil Polyurethane**

Mariana Avelino dos Santos<sup>1</sup>, Bruno Cimatti<sup>1</sup>, Maria Sol Brassesco<sup>1</sup>, Laura Tiemi Okano<sup>2</sup>, Edgard Eduard Engel<sup>1</sup>

<sup>1</sup> Ribeirão Preto Medical School, University of São Paulo, Brazil

<sup>2</sup> Faculty of Philosophy, Sciences and Letters of Ribeirão Preto, University of São Paulo, Brazil  
[engel@fmrp.usp.br](mailto:engel@fmrp.usp.br)

### **INTRODUCTION**

Large metaphyseal bone defects created after benign bone tumor curettage are usually treated by solid bone cement (PMMA) implantation. Porous and absorbable cements are expected to improve clinical results by lowering incidence of aseptic loosening, heat promoted bone necrosis, mechanical buttress failure and absence of bone integration<sup>1</sup>.

Effervescent components like sodium bicarbonate and citric acid can be mixed to PMMA producing porous cement that fits intraoperative requirements. Furthermore, castor oil polyurethane is a well-known absorbable cement that can be mixed to effervescent components to produce porous and absorbable bone cement<sup>2</sup>.

*In vivo* and *in vitro* toxicity of both products have never been tested to support its clinical use. The spurious production of toxic elements and the effect of citrate, an anticoagulant byproduct of the effervescent components reaction, were analyzed.

### **EXPERIMENTAL METHODS**

#### ***In vitro* experiments**

The three experimental groups consisted of PMMA or one of the two commercially available castor oil polyurethane cements (Poliquil® or Bioosteo®) mixed to the effervescent components specimens. These groups were compared to classic PMMA solid cement specimens. All the elements produced during preparation and incubation of the cements were analyzed by High Efficiency Liquid Chromatography coupled to Mass Spectrometry and Resazurine microplate assay of NIH/3T3 and MRC-5 fibroblasts strains culture.

#### ***In vivo* experiments**

Femoral defects were created in six rabbits per group and filled with PMMA or Poliquil® porous cements or left empty. Magnetic resonance of the limb, histology of the limb, kidneys and liver and coagulation parameters of blood samples collected immediately after and 1, 4 and 7 days after surgery were analyzed.

### **RESULTS AND DISCUSSION**

Castor oil polyurethane of both brands (Bioósteo® and Poliquil®) released 4,4'-diaminodiphenylmethane. The Poliquil® brand released 4,4'-diphenylmethane diisocyanate too. Both compounds are considered toxic and inhalation and ingestion should be avoided<sup>3</sup>. The MRC-5 and NIH3T3 cell strains proliferation was decreased in less than 80% in contact with polyurethane cements and less than 65% with PMMA, compared to the control group. Dilution of the medium diminished

this effect. We believe that the acidity of the medium due to incomplete reaction of the effervescent components may be the cause of this finding.

Liver and kidneys histology showed some slight changes in the same proportion as the control group. We infer that the cements do not cause acute systemic toxicity.

In all groups, histologic analysis of the operated area showed small hematomas and a slight foreign body reaction. Significant inflammatory reaction could not be found in any of the study groups. Citrate formation from the effervescent components reaction seems to not interfere with coagulation. Inflammatory reaction around porous cements is similar to that of classic solid PMMA cement. The cytotoxic effect observed *in vitro*, could not be detected *in vivo*.

Coagulation parameters did not changed at any time after surgery. The evaluation by magnetic resonance imaging confirmed that there was no formation of larger hematomas than in specimens of the control group.

### **CONCLUSION**

Our data suggest that the porous cement produced by mixing effervescent components are well tolerated, produce little inflammatory reaction and do not cause coagulation disorders. However, the reaction of the effervescent components and castor oil polyurethane based cement yields potentially toxic products that deserves a specific investigation.

### **REFERENCES**

1. Miño-Fariña et al. Quantitative analysis of the resorption and osteoconduction of a macroporous calcium phosphite bone cement for the repair of a critical size defect in the femoral condyle. *The Veterinary Journal*. 179:264-72. 2009.
2. Cimatti B. Desenvolvimento e caracterização de um cimento ósseo esponjoso para preenchimento de falhas ósseas. Análise morfológica e ensaio mecânico. Ribeirão Preto: Universidade de São Paulo; 2012.
3. Concise International Chemical Assessment Document 27. DIPHENYLMETHANE DIISOCYANATE (MDI). World Health Organization, Geneva, 2000.

### **ACKNOWLEDGMENTS**

The authors thanks FAPESP (São Paulo Research Foundation) for the financial support of this research.





## Phosphate-Hydroxyapatite Cements: Mechanical Stress Analysis and Osteoblastic Induction

Toshimi Kano<sup>1,2</sup>, Stamatia Rokidi<sup>3</sup>, Eumorphia Remboutsika<sup>4</sup>, Dionysios Mouzakis<sup>5</sup>, Stefanos Zaoutsos<sup>5</sup>, Nikolaos Bouropoulos<sup>3,6</sup> Eleni Douni<sup>1,2</sup>

<sup>1</sup>Department of Biotechnology, Agricultural University of Athens, Greece

<sup>2</sup>Biomedical Sciences Research Center "Alexander Fleming", Athens, Greece

<sup>3</sup>Department of Materials Science, University of Patras, Greece

<sup>4</sup>Department of Pediatrics, University of Athens Medical School, Greece

<sup>5</sup>Department of Mechanical Engineering, Technological Educational Institute of Thessaly, Larissa, Greece

<sup>6</sup>Institute of Chemical Engineering and High Temperature Chemical Processes FORTH, Patras, Greece

[douni@aua.gr](mailto:douni@aua.gr)

### INTRODUCTION

Calcium phosphate biomaterials have been widely used as bone substitute materials in clinical applications due to their good biocompatibility and osteoconduction. However, they are usually plagued by low inherent mechanical properties.

### EXPERIMENTAL METHODS

During this study we synthesized and analyzed nanostructured calcium phosphate bone cements based on  $\alpha$ -tricalcium phosphate ( $\alpha$ -TCP) [1] reinforced with nanoneedles of hydroxyapatite (HAP) (1, 3, 5, 10 and 20%) with strictly controlled porosity so as to optimize both mechanical properties and osteoblast nesting. We further analyzed the ability of the new biocements to induce the proliferation and survival of the pre-osteoblast cell line MC3T3E1 through DNA quantification and cell counting. In addition, cell morphology was observed with Scanning electron microscope (SEM) and fluorescence microscopy. Moreover, the osteoblastic induction was quantified by alkaline phosphatase (ALP) activity measurements and the morphology of the cells with SEM after 14 days of culture in the presence of the osteogenic factors, ascorbic acid and  $\beta$ -glycerophosphate.

### RESULTS AND DISCUSSION

SEM images showed that the surface microstructure of the cements after hardening was composed of plate-like crystals. The compressive strength of pure cements was at  $34.3 \pm 1.7$  MPa while in the case of composite cements is strongly depended upon the HAP content. By increasing the HAP content until 20 % the compressive strength drastically decreased until  $4.9 \pm 0.2$  MPa which was within the cancellous bone ranges

between 1.5 and 45 MPa. As regards the attachment, survival and differentiation of the pre-osteoblast MC3T3E1 cells on the surface of biocements, our results so far indicate that biocements with certain ratio of  $\alpha$ -TCP-HAP composite are tolerated as well as pure  $\alpha$ -TCP with regard to their osteoinductive and osteogenic properties.

### CONCLUSION

In conclusion, pure or HAP loaded calcium phosphate bone cements are suitable for low stress loading locations and display biocompatibility.

### REFERENCES

1. Andriotis O, *et al.*, Cryst. Res. Technol. 45:239-243, 2010.

### ACKNOWLEDGMENTS

This research has been co-financed by the European Union (European Social Fund - ESF) and Greek national funds through the Operational Program "Education and Lifelong Learning" of the National Strategic Reference Framework (NSRF) - Research Funding Program: THALES (grant MIS 379380). Investing in knowledge society through the European Social Fund.



## Functionalized Polymeric Composite Nano-Fibrous Scaffold for Bone Tissue Engineering

Prabhash Dadhich<sup>1</sup>, Bodhisatwa Das<sup>1</sup>, Pavan Kr. Srivas<sup>1</sup>, Pallabi Pal<sup>1</sup>, Joy Dutta<sup>1</sup>,  
Sabyasachi Ray<sup>2</sup>, Santanu Dhara<sup>1</sup>

<sup>1</sup>Biomaterial and Tissue Engineering Laboratory, School of Medical Science and Technology,  
Indian Institute of Technology Kharagpur, Kharagpur, India

<sup>2</sup>Midnapore Medical College and Hospital, Midnapore, India  
[pallabipal@yahoo.com](mailto:pallabipal@yahoo.com)

### INTRODUCTION

To address skeletal defect, several polymeric and composite scaffolds has been developed towards bone graft material. In spite of astounding micro-architecture and fabrication, foreign body reaction during in vivo transplantation is one of the limiting factor with such polymeric scaffolds. The formation of a dense collagenous capsule causes inadequate mass transport and cell communication between scaffold and host. To address such challenges natural origin biopolymer has been functionalized. This functionalized biopolymer (FBP) has zwitterionic properties causing ultra-low-fouling activity, which resist formation of avascular capsule during subcutaneous implantation. FBP further composite with synthetic polymer to develop a bioactive anisotropic 3D scaffold by designing aligned nanofiber sheet through electrospinning and subsequent multi-scalar 3D scaffold formation via micro-fabrication strategy.

### EXPERIMENTAL METHODS

Here, we represent a method for functionalization of natural origin biopolymer. This FBP fabricated into aligned nanofibers sheet via electrospinning. Further, three dimensional multi-scalar scaffold was formed micro-fabrication techniques. Physio-chemical characterization of scaffolds carried out using SEM, EDS, XRD, FTIR, TG-DTA and stereo-zoom microscope. In vitro cells attachment, migration study, proliferation, differentiation studies were performed. Further, in vivo studies were conducted in rabbit animal model.

### RESULTS AND DISCUSSION

Natural sources were successfully used for synthesis of resorbable functionalized polymer, nano-fibrous scaffolds. Natural origin, multiphasic CaP were printed successfully and got highly interconnected multi-scalar porous, fibrous hybrid composite scaffold. As hybrid composite mesenchymal stem cells (MSCs) revealed a higher ALP activity with increased RNA expression of collagen I and osteocalcin. In vivo studies found promising results of bone regeneration after implantation.

### CONCLUSION

In present study, CaP provide high mechanical support and interphase for bone tissue growth, where functionalized polymer act as niche for MSCs differentiation and impart rapid mineralization. Nano-micro architectural hybrid composite scaffolds can be used as a bone graft replacement in a cost effective way using biological waste as raw material.

### REFERENCES

1. US Patent 8652215 B2, Nanofilament Scaffold for Tissue Regeneration. Feb. 2014.
2. US Patent 0154063 A1, Nanofiber Construct and Method of Preparing Thereof. Jul. 2006.
3. Place, E. S., Evans, N. D., & Stevens, M. M. (2009). Complexity in biomaterials for tissue engineering. *Nature Materials*, 8(6), 457–70. doi:10.1038/nmat2441
4. Bose, S., Roy, M., & Bandyopadhyay, A. (2012). Recent advances in bone tissue engineering scaffolds. *Trends in Biotechnology*, 30(10), 546–54.

### ACKNOWLEDGMENTS

This work is partially supported by a grant from the Department of Biotechnology, Government of India and Defense Research & Development Organization (DRDO). IIT Kharagpur has been acknowledged for providing infrastructural facility.



## INTRODUCTION

Degradable orthopaedic implants can be used as temporary fixations e.g. in case of complicated fractures. The gradual degradation eliminates the need of reoperation to remove the implant after bone healing. This means saving costs and reducing risk of surgical complications. Currently used polymers lack sufficient mechanical properties required for orthopaedic applications and therefore, metallic materials, mainly magnesium-based alloys have been extensively developed and studied for these purposes<sup>1</sup>. The main aim is to decrease the corrosion rate using various alloying elements and also by altering the microstructure as the grain size significantly influences the corrosion rate<sup>2</sup>. Equal channel angular pressing (ECAP) is one of the methods of severe plastic deformation leading to ultra-fine grain materials<sup>3</sup>. It was observed that grain refinement of magnesium-based materials can increase<sup>4</sup> as well as decrease<sup>5</sup> the corrosion resistance.

Our aim was to investigate whether the ultra-fine structures of AE42 and LAE442 Mg-alloys achieved by ECAP processing increased the corrosion resistance of the materials and subsequently evaluate the effect of the treatment on changes of their *in vitro* toxicity.

## EXPERIMENTAL METHODS

Commercial Mg-alloys AE42 and LAE442 were extruded and further processed by ECAP by eight or twelve passes, respectively. Three replicates of each sample were used. Corrosion tests were performed in simulated body fluid (SBF). SBF was prepared according to Kokubo *et al.*<sup>6</sup> and samples were incubated for one week at 37 °C in closed vessels at agitation of 125 rpm. Surface to volume ratio was 3.5 mm<sup>2</sup>·ml<sup>-1</sup>. Released ions were measured using AAS. The corrosion rate after extrusion and after additional ECAP was compared. Statistical analysis was conducted with R software. Differences before and after the processing were analyzed using two sample t-test.

## RESULTS AND DISCUSSION

Figure 1 shows concentration of magnesium in extracts of alloys before and after ECAP. Processing through ECAP resulted in significantly reduced corrosion rate in both tested alloys. These results are in accordance with electrochemical measurements. Moreover, the protective corrosion layer on the surface observed by SEM was two times thicker after ECAP treatment<sup>7, 8</sup>. Microstructure characterization by SEM and TEM showed substantial grain refinement due to the ECAP processing that confirms the effect of the microstructure on the degradation rate of these alloys<sup>9</sup>.

Nevertheless, these observations need to be confirmed by *in vitro* experiments using appropriate cell models.

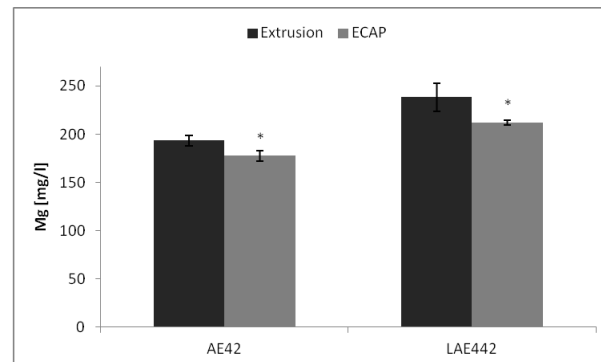


Fig. 1 Mg concentration [mg·l<sup>-1</sup>] in extracts of AE42 and LAE442 before and after ECAP treatment expressed as mean±SSD, n = 3, asterisks indicate p<0.05 in t-test.

Indirect *in vitro* cytotoxicity test will be performed according to ISO 10993-5 standard. Alloys will be incubated in cultivation medium and concentration of ions in extracts will be measured using ICP-MS. Cytotoxicity of extracts will be tested *in vitro* using U-2 OS and L929 cell lines via microculture tetrazolium assay (WST-1).

## CONCLUSION

ECAP treatment reduced corrosion rates of AE42 and LAE 442 magnesium alloys. Cytotoxicity tests need to be performed in order to confirm that decrease in corrosion rate is sufficient for *in vitro* system.

## REFERENCES

1. Chen, Y., *et al.* Acta Biomater. 10:4561-4573, 2014
2. Ralston, K. D. *et al.* Scripta Mater. 63:1201-1204, 2010
3. Furukawa, M., *et al.* J. Mater. Sci. 36:2835-2843, 2001
4. Song D., *et al.* Corros. Sci. 52:481-490, 2010
5. Birbilis N., *et al.* Corros. Eng., Sci. and Technol. 45:224-230, 2010
6. Kokubo, T. *et al.* Biomaterials 27:2907-2915, 2006
7. Minárik, P., *et al.* Acta Phys. Pol. A 122:614-618, 2012
8. Minárik, P., *et al.* Appl. Surf. Sci. 281:44-48, 2013
9. Minárik, P. Doctoral thesis. Prague, 2014, pp. 116.

## ACKNOWLEDGMENTS

Financial support from specific university research (MSMT No 20/2015).

## Cytocompatibility of Novel PLDA/Mg Composites as Biodegradable Implants for Bone Repair

Sandra Cifuentes<sup>1</sup>, Fatima Bensiamar<sup>2,3</sup>, Tim Osswald<sup>4</sup>, José Luis González-Carrasco<sup>1,3</sup>, Eduardo García-Cimbrelo<sup>3,5</sup>, Nuria Vilaboa<sup>2,3</sup>, [Laura Saldaña](mailto:laura.saldana@salud.madrid.org)<sup>2,3</sup>

<sup>1</sup>Centro Nacional de Investigaciones Metalúrgicas, CENIM-CSIC, Spain

<sup>2</sup>Hospital Universitario La Paz-IdiPAZ, Spain

<sup>3</sup>CIBER de Bioingeniería, Biomateriales y Nanomedicina (CIBER-BBN), Spain

<sup>4</sup>Polymer Engineering Center (PEC)- University of Wisconsin-Madison, Madison, USA

<sup>5</sup>Departamento de Cirugía, Universidad Autónoma de Madrid, Spain

[laura.saldana@salud.madrid.org](mailto:laura.saldana@salud.madrid.org)

### INTRODUCTION

Biodegradable polymeric devices for bone repair have been proposed as an alternative to metallic materials since they overcome the need of a second surgical event for removal, especially in pediatric patients. For many years, there have been deep concerns about the weak mechanical properties and rapid degradation of polymeric devices. Moreover, clinical results reveal insufficient osseointegration, adverse tissue reactions and/or osteolysis at the implantation site after almost complete resorption of the biodegradable implant (1). Magnesium (Mg) and its alloys are among the most interesting alternative options to biopolymers because of their mechanical strength and stiffness, which are close to those of natural bone, and good biocompatibility (2). The main concerns regarding the use of Mg biodegradable implants rely on the hydrogen release and the alkalization of the surface. This study investigates the incorporation of Mg particles within a poly-L-D-lactic acid (PLDA) matrix as a way to improve the mechanical properties and biocompatibility of the polymer. We focused on the influence of Mg reinforcement of PLDA on the *in vitro* response of osteoblastic precursors and inflammatory cells.

### EXPERIMENTAL METHODS

PLA 2002D from NatureWorks® was used as the matrix. Commercial purity Mg particles of about 50 µm were provided by Goodfellow. Composites specimens were manufactured in a BOY XS Injection Moulding machine. Mass fractions of 0.2 and 1% Mg were selected to manufacture the composites. Mechanical properties were assessed by compression tests. Mg ion released from the composites into culture medium was quantified by a coupled enzyme assay. Human mesenchymal stem cells (MSCs) and TPA-differentiated THP-1 (dTHP-1) cells were used for cytocompatibility studies. Cell viability was monitored using the AlamarBlue assay and cell morphology was analysed by SEM. Nuclear morphology and actin filaments were revealed after staining MSCs with DAPI or phalloidine-TRITC, respectively. The degree of cell layer maturation was investigated in MSCs cultured in osteogenic medium on the samples or incubated with composite extracts by determination of ALP activity. Soluble factors levels in media of MSCs cultured on the composites or THP-1 exposed to composite extracts were quantified using CBA Flex Sets (BD Biosciences) and ELISA Kits.

### RESULTS AND DISCUSSION

Materials reinforced with Mg particles exhibited higher compressive strength than the neat polymer. PLDA/Mg composites incubated under standard cell culture conditions released Mg into culture medium, and the amount was higher in matrices reinforced with 1% than with 0.2% Mg particles. Viability of MSCs cultured on the composites also increased with Mg content. Confocal images of DAPI-stained MSCs revealed normal nuclear morphologies on all samples. MSCs grown on the materials formed a cell monolayer and exhibited a clearly expanded typically elongated shape. Actin polymerized in a dense meshwork of well-defined stress fibers distributed through the cell body of cells on the three polymer-based materials. Composites induced an increase in FN content and ALP activity in cell layers, being the levels higher on PLDA loaded with 0.2% than with 1% Mg particles. A similar pattern of ALP activity was observed in MSCs cultured in the presence of degradation products of the composites. Compared to unloaded PLDA, MSCs cultured on matrices loaded with 1% Mg particles secreted higher levels of MCP-1 and VEGF. Regarding the effect of composite extracts on inflammatory cytokine release from dTHP-1, our data show that TNF-α and IL-10 secretion were unaffected by degradation products of any of the materials tested. MCP-1 and RANTES secretion levels were also unaffected by composite extracts but increased by degradation products of unloaded PLDA.

### CONCLUSION

Mg reinforcement of PLDA matrices enhances viability and osteoblastic maturation of MSCs as well as secretion of MCP-1 and VEGF. Degradation products of PLDA/Mg composites do not increase levels of inflammatory cytokines released from macrophage-like cells.

### REFERENCES

1. Dhandayuthapani B *et al.* Int J Polym Sci. 1-19, 2011
2. Gu X *et al.* Biomaterials. 30:484-98, 2009

### ACKNOWLEDGMENTS

This work was supported by grants MAT2012-37736-C05-01-05 (MINECO, Spain), CP11/00022 and PI12/01698 (FIS, Spain) and S2013/MIT-2862 (Comunidad de Madrid, Spain).





## Local Recovery of Bone Tissue in Osteoporotic Rabbit Hip after Implantation of HAP/TCP Bioceramic Granules

Ilze Salma<sup>1</sup>, Sandris Petronis<sup>2</sup>, Mara Pilmane<sup>3</sup>, Andrejs Skagers<sup>1</sup>, Vita Zalite<sup>4</sup>, Janis Locs<sup>4</sup>

<sup>1</sup>Department of Oral and Maxillofacial Surgery, Riga Stradins university, Latvia

<sup>2</sup>Department of Doctoral studies, Riga Stradins university, Latvia

<sup>3</sup>Institute of Anatomy and Anthropology, Riga Stradins university, Latvia

<sup>4</sup>Rudolfs Cimdins Riga Biomaterials innovations and development center of Riga Technical University, Latvia

[Ilze.salma@rsu.lv](mailto:Ilze.salma@rsu.lv)

### INTRODUCTION

Biphasic calcium phosphate (BCP) as bone grafting substitute can be used for reinforcement of osteoporotic bone and for promotion of bone healing and bone defect filling<sup>1</sup>. Experimental and clinical data showed bioactivity of BCP<sup>2,3</sup>. In current study the BCP ceramic granules with HAp/b-TCP ratio of 90/10 was selected as appropriate. It is supposed that the minor amount of b-TCP in the composition due to relatively faster resorption rate compared to HAp will ensure the initial burst of releasing calcium and orthophosphate ions into the biological medium, thus seeding new bone formation. The majority of HAp remaining after resorption of b-TCP will act as a tissue scaffold for the complete formation of new bone. Objective of our study was to evaluate by immunohistochemical method local bone tissue response to BCP ceramic granules implanted in experimental animals. Investigation of osteocalcin (OC) and osteopontin (OP) expression helps to understand bone tissue regeneration potential and remodeling after BCP implantation.

### EXPERIMENTAL METHODS

Experimental osteoporosis was induced in 10 female rabbits (age 2 years) by ovariectomy and following injections of methylprednisolone 1 mg/kg daily for 8 weeks<sup>4</sup>. On 6 animals 3mm hole was created in proximal end of the hip bone and filled with a BCP bioceramic granules 1 to 1.4 mm of size, containing hydroxyapatite (HAp) and  $\beta$ -tricalcium phosphate ( $\beta$ -TCP) in ratio 90/10 synthesized in Rudolfs Cimdins Riga Biomaterials innovations and development center of Riga Technical University by aqueous precipitation technique<sup>5</sup>. The control group consisted of 3 rabbits with the analogous defect of osteoporotic bone without implantation of BCP bioceramic granules. After 3 months animals were euthanased and bone samples collected and prepared by routine histological method. Tissue samples were stained according the standart immunohistochemical methods and expression of OC and OP was examined. Distribution of these factors was evaluated semiquantitatively by counting positive structures in the visual field: 0/+ - occasional, + - few, ++ - medium, +++ - many<sup>6</sup>.

### RESULTS AND DISCUSSION

Histological samples from control group showed local bone atrophy proving development of osteoporosis. In experimental group we found partially resorbed granuli

enrolled by osteoclasts and connective tissue capsule. In experimental group bone trabeculae were more developed.

In control group bone formation marker OC was found occasionally in visual field suggesting low bone tissue regeneration potential. In experimental group revealed stable increase of OC expression in all cases. Also OP what is active in bone remodeling was found occasionally in control group and increased in all samples of experimental group, but less obviously as osteocalcin. Probable the difference of OC and OP expression depends on the time of its assessment; greater OP expression happens on early stages of osteogenesis as adhesion of cells on the surface of a biomaterial takes place, OC, in turn, is an indicator of metabolic activity, whose increase would be found in the phase of bone mineralization<sup>7</sup>.

### CONCLUSION

Biphasic calcium phosphate bioceramic granules implanted in osteoporotic bone show good and stable local bone tissue regeneration and remodeling potential by increase of osteocalcin and osteopontin.

### REFERENCES

1. Dorozhkin S.V. *Acta Biomaterialia* 8:963-977, 2012
2. Petronis S. *et al.*, IFMBE Proceed. 38:174-177, 2013
3. Garrido S. *et al.*, *Int J Biomater.* Art ID129727, 2011
4. Li Baofend *et al.*, *Acta Orthop.* 81:396-401, 2000
5. Salma K. *et al.*, *Adv. Mat. Res.* 222:255-258, 2011
6. Pilmane M. *et al.*, *Proc. Latv. Acad. Sci.* 52:144-152, 1998
7. Hoang Q.Q. *et al.*, *Nature* 425(6961):977-980, 2003

### ACKNOWLEDGMENTS

This work has been supported by the National Research Programme No. 2014.10-4/VPP-3/21 "Multifunctional Materials and composites, photonicS and nanotechnology (IMIS<sup>2</sup>)" Project No. 4 "Nanomaterials and nanotechnologies for medical applications".



## Multinucleated Giant Cell Formation in Different Xenogeneic Bone Substitute Materials, Preclinical and Clinical Studies

Jonas Lorenz,<sup>1</sup> Mike Barbeck, MSc,<sup>1,2</sup> Charles J. Kirkpatrick,<sup>2</sup> Robert A. Sader,<sup>1</sup> Shahram Ghanaati<sup>1,2</sup>

<sup>1</sup>Department for Oral, Cranio-Maxillofacial and Facial Plastic Surgery, Medical Center of the Goethe University Frankfurt, Frankfurt am Main, Germany

<sup>2</sup>Institute of Pathology, REPAIR-Lab, University Medical Center, Johannes Gutenberg University Mainz, Germany  
[Jonas.lorenz@kgu.de](mailto:Jonas.lorenz@kgu.de)

### INTRODUCTION

Aim of the presented research was to analyze and compare the tissue reactions to two different xenogeneic bone substitute materials dependent on the different sintering temperatures, preclinically *in vivo* and clinically.

### EXPERIMENTAL METHODS

The two bone substitute materials were implanted subcutaneously in CD-1 mice for up to 60 days additionally to their clinical for sinus augmentation in the upper jaw. Tissue formation, implant bed vascularization and numbers of multinucleated giant cells were investigated histologically and histomorphometrically.

### RESULTS AND DISCUSSION

Both bone substitute materials showed good integration within the peri-implant tissue and no signs of adverse inflammatory effects. In the preclinical *in vivo* study both groups presented an increasing vascularization over the whole study period. Within the implantation bed of the bone substitute of low sintering temperature (LST) few multinucleated giant were obvious on the surface of small sized bone substitute granules in the early integration period, while the tissue reaction to the bigger granules at later stages consisted mainly of mononuclear cells. In contrast, the tissue reaction to the bone substitute material of high sintering temperature (HST) consisted of biomaterial surface associated multinucleated giant cells. The clinical analysis confirmed the different cellular mechanisms

to the investigating biomaterials, mainly differing in the expression of a foreign body giant cell reaction.

### CONCLUSION

The tissue reactions to the investigated low and high sintering temperature bone substitute materials showed distinct differences *in vivo* and clinically, mainly in the formation and migration of multinucleated giant cells. As both biomaterials have the same origin, the observed differences seem to be related to the different processing techniques and the resulting different physico-chemical structures.

### REFERENCES

Barbeck M, Udeabor S, Lorenz J, Schlee M, Grosse Holthaus M, Raetscho N et al. High-temperature sintering of xenogeneic bone substitutes leads to increased multinucleated giant cell formation: *In vivo* and preliminary clinical results. *J Oral Implantol* 2014.

Barbeck M, Udeabor SE, Lorenz J, Kubesch A, Choukroun J, Sader RA et al. Induction of multinucleated giant cells in response to small sized bovine bone substitute (Bio-Oss™) results in an enhanced early implantation bed vascularization. *Ann Maxillofac Surg* 2014; 4(2):150–7.

### ACKNOWLEDGMENTS

The authors would like to thank Mrs. Verena Hoffmann and Mrs. Ulrike Hilbig for their technical assistance.

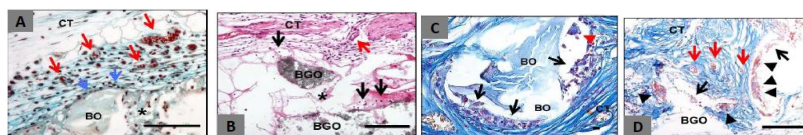


Figure 1 A-D shows tissue reaction to different xenogeneic bone substitute materials 3 (A and B) and 60 days (C and D) after implantation

## Mechanical and *In Vitro* Properties of Stereocomplex Polylactide Coatings on Porous Bioactive Glass Scaffolds for Bone Regeneration

Peter Uppstu<sup>1</sup>, Simon Engblom<sup>1</sup>, Saara Inkinen<sup>1</sup>, Leena Hupa<sup>2</sup>, Carl-Eric Wilén<sup>1</sup>

<sup>1</sup>Centre of Excellence in Functional Materials, Åbo Akademi University, Finland

<sup>2</sup>Johan Gadolin Process Chemistry Centre, Åbo Akademi University, Finland

[peter.uppstu@abo.fi](mailto:peter.uppstu@abo.fi)

### INTRODUCTION

Bioactive glass scaffolds can be favourably used for the regeneration of bone<sup>1</sup>. However, because of the inherent brittleness of glass, polymer/glass composite scaffolds may be better suited for bone regeneration purposes than scaffolds based only on glass, especially in load-bearing sites<sup>2</sup>. Amorphous polylactide (PLA) coating has been shown to considerably increase the compression strength of porous glass scaffolds<sup>3</sup>. PLA stereocomplexes (sc-PLA) are known to increase mechanical properties and retard hydrolytic degradation compared to amorphous PLA or PLA homocrystals<sup>4</sup>. The aim of this study was to evaluate the impact of sc-PLA coatings on mechanical and degradation properties of porous bioactive glass scaffolds. As reference, glass scaffolds were coated with homocrystalline poly(L-lactide) (PLLA) or amorphous poly(D,L-lactide) (PDLLA).

### EXPERIMENTAL METHODS

Porous scaffolds of the bioactive glass 13-93 were manufactured with the foam replication method. The glass scaffolds were dip-coated with amorphous PDLLA, homocrystalline PLLA or an equimolar mixture of PLLA and poly(D-lactide) (PDLA) for stereocomplex formation. After drying the scaffolds were annealed in order to increase the amount of stereocomplex crystals in the coating. In vitro degradation of the scaffolds in simulated body fluid (SBF) was studied for up to 10 weeks. Compression strength was measured both before and after in vitro degradation. Water uptake, mass loss and pH of the SBF were measured. Morphological characterization was performed with SEM to evaluate scaffold porosity and coating thickness. Studies were performed with 5 parallel samples.

### RESULTS AND DISCUSSION

The effect of sc-PLA coatings on compression strength both before and after in vitro degradation, compared to amorphous and homocrystalline PLA coating, will be discussed in detail. The findings are compared to results of amorphous PLA coating of porous glass scaffolds published elsewhere. Mechanical properties and the in vitro degradation properties of the amorphous, homocrystalline and stereocomplex PLA coatings are shown.

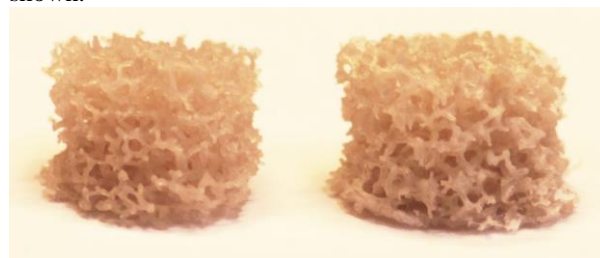


Figure 1. Uncoated (left) and coated (right) glass scaffold.

### CONCLUSIONS

This work gives important insight into the applicability of sc-PLA for adjusting the mechanical and degradation properties of scaffolds for tissue regeneration.

### REFERENCES

1. Fu Q. *et al.*, J. Biomed. Mater. Res. A 93A:1380-1390, 2010
2. Rezwani K. *et al.*, Biomaterials 27:3413-3431, 2006
3. Mantos T. *et al.*, Biomed. Mater. 4:055002, 2009
4. Tsuji H. Macromol Biosci 5:569-597, 2005

### ACKNOWLEDGMENTS

The authors would like to thank Svenska kulturfonden and Stiftelsen för Åbo Akademi for financial support.

## The Osteogenic Effect of Alginate Nanoparticles Contained Bone Morphogenetic Proteins-2 on Bone Marrow Stromal Cells

Ho Yun Chung<sup>1</sup>, Hyun Ju Lim<sup>1</sup>, Jae Bong Kim<sup>1</sup>, Eun Jung Oh<sup>1</sup>, Tae Jung Kim<sup>1</sup>, Jin Hyun Choi<sup>2</sup>

<sup>1</sup>Department of Plastic & Reconstructive Surgery, School of Medicine, Kyungpook National University, Korea

<sup>2</sup>Department of Advanced Materials Science and Engineering, Kyungpook National University, Korea  
[hy-chung@knu.ac.kr](mailto:hy-chung@knu.ac.kr)

### INTRODUCTION

Tissue engineering has greatly benefited from growth factor-based regenerative systems[1,2]. Many matrix-based systems for growth factor delivery[3,4] using natural polymers reported and tried to apply in medical field because their merits such as, safety, easy availability, and. However, long-term efficiency low in natural polymer is a still problem. In this study, we have engineered a delivery system for localized, long-sustained growth factor from alginate nanoparticles containing Bone Morphogenetic Proteins-2(BMP-2) for osteogenesis.

### EXPERIMENTAL METHODS

We observed effect of controlled release BMP-2 from alginate nanoparticles on in vitro osteogenic differentiation of Bone marrow stromal cells (BMSCs), by RT-PCR, western blots, immuno-cell-chemical and several stains. In vivo study, four groups were prepared; fibrin glue for control, fibrin glue with BMSCs, fibrin glue with alginate nanoparticles containing BMP-2 (ANP), and fibrin glue with BMSCs and ANP. These groups were applied in 4mm calvarial defects of nude mice. For evaluation of bone formation effect in each group, the specimens were harvested at 1, 8, and 16 weeks after surgery. The samples were analyzed with micro-CT and histological findings using H&E, von-kossa staining, and immunohistochemistry.

### RESULTS AND DISCUSSION

In vitro data, only BMSCs in culture medium was not expressed osteocalcin in RT-PCR and western blot. BMSCs in osteogenic medium, BMSCs in culture medium with ANP, and BMSCs in osteogenic medium with ANP were expressed osteocalcin in RT-PCR and western blot. Immuno-cell-chemical and several stains were positive in each group respectively except BMSCs in culture medium group.

In vivo study, fibrin glue with BMSCs, fibrin glue with ANP, and fibrin glue with BMSCs and ANP groups were formed bone structure at 8 week. In 16 weeks, bone-forming process kept going in all groups except control. By micro-CT and immunohistochemistry analysis, fibrin glue with BMSCs and ANP group showed most abundant bone formation.

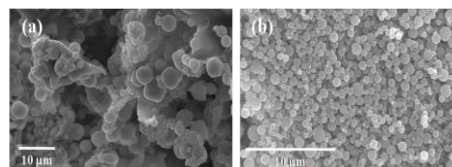


Fig. 1. SEM photographs of the ANP prepared by diffusing water for (a) 10 min and (b) 3 days.

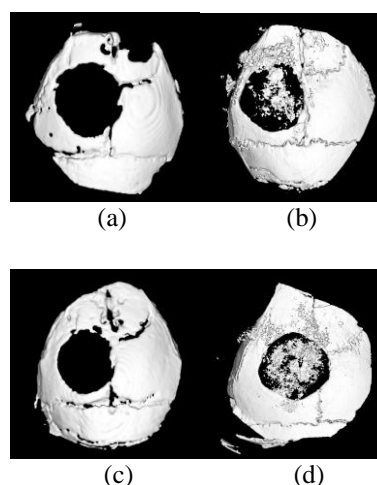


Fig. 2. Micro-computer tomography of critical size calvarial defect model; (a) 1 week, (b) 8 weeks of hBMSCs in fibrin glue group, (c) 1 week, (d) 14 weeks of hBMSCs and ANP in fibrin glue group.

### CONCLUSION

Alginate nanoparticles loaded BMP-2 in this study can be effective to the bone formation by enhanced and long steady release of growth factors. It is expected the application of this delivery system is as a good alternative for osteogenesis in regenerative medicine fields.

### REFERENCES

1. Richardson TP. *et al.*, Nat Biotechnol. 19:1029, 2001
2. Ana J. *et al.*, Biomaterials. 29:1518, 2008
3. Burg KJ. *et al.*, Biomaterials. 21:2347, 2001
4. Geiger M. *et al.*, Adv. Drug Deliv. Rev. 55:1613, 2003

### ACKNOWLEDGMENTS

This research was supported by a grant of the Korea Health Technology R&D Project through the Korea Health Industry Development Institute (KHIDI), funded by the Ministry of Health & Welfare, Republic of Korea (grant number: HI14C3309).



<sup>1</sup> Department of Biomaterials, Faculty of Materials Science and Ceramics, AGH – UST University of Science and Technology, Poland

<sup>2</sup> Multidisciplinary School of Engineering in Biomedicine, AGH-UST University of Science and Technology, Poland  
[stodolak@agh.edu.pl](mailto:stodolak@agh.edu.pl)

## INTRODUCTION

Porous membrane materials allow selective permeability of some nutrients, growth factors and proteins into a tissue defect. These materials also guarantee optimal conditions for cells to adhere and proliferate within the regenerating tissue. For these reasons membranes have been used in stomatology (periodontology), traumatology and orthopedic medicine. In case of a bone defect which size is larger than the critical bone defect a membrane works as a factor stimulating faster bone regeneration. Gradient pores, modification of membrane materials in a bulk (e.g. with ceramic nanoparticles) or at a surface (e.g. with proteins, PRP) are sufficient parameters to create the cellular response [1]. The most popular materials used in forming of membrane implants are synthetic resorbable polymers such as; polylactide (PLA), poliglicolide (PGLA), polycaprolactone (PCL) and their copolymers, or natural polymers such as collagen [2]. When the nanoparticles are present in the polymer matrix such polymer-ceramic composition exhibits novel properties. Bulk modification of the polymer can result in its bioactivity (BG, HAp, TCP), faster degradation (MMT), higher strength (Hap, SiO<sub>2</sub>) and better biocompatibility than the pure polymer. It is a good reason to use the nanocomposite membrane materials as a bone defect separator (e.g. after removal of cysts) or barrier providing optimal conditions for regeneration of a bone defect (e.g. ACL reconstruction).

This work presents results of investigations on polymer-ceramic nanocomposite membranes modified by osteoconductive (SiO<sub>2</sub>) and osteoinductive (TCP) ceramic nanoparticles.

## EXPERIMENTAL METHODS

Porous nanocomposite materials based on resorbable poly-ε-caprolactone (Sigma Aldrich) and ceramic nanoparticles: silica-SiO<sub>2</sub> (5-10 nm, Sigma Aldrich) and tricalcium phosphate-TCP (20-30 nm, Sigma Aldrich) were obtained by the phase inversion method. Porous microstructure of the nanocomposites was investigated using SEM/EDS. Physicochemical properties of the materials surface were investigated by means of wettability and surface energy measurements (DSA 10 Kruss). Mechanical properties of the membranes (strength and Young's modulus) were tested in a stretching test (Zwick 1435). Durability of the materials in *in vitro* conditions was estimated using phosphate buffer solution (PBS). Monitoring of their degradation was performed by the thermal analysis (TG/DSC).

## RESULTS AND DISCUSSION

Microstructures of both manufactured membranes were porous. Size and shape of the pores strongly depended on the applied nanoparticles i.e.; pores in the PCL/SiO<sub>2</sub> membrane were round and had larger diameters (12 - 25 μm) while pores in the PCL/TCP membrane were smaller (7 - 15 μm) and irregular. Additionally, the nanoparticles influenced mechanical properties of the membranes which strength (~140 MPa) and Young's modulus (~14 MPa) were two times larger than those of the pure polymer membrane (Fig 1.). The PCL/SiO<sub>2</sub> as well as the PCL/TCP showed bioactivity because after 3 days in SBF solution on their surface apatite structure could be observed. The membrane with nano-silica apatite structure were observed after 10 days in SBF solution. Degradation test showed that the membrane materials after two weeks of PBS incubation were characterised by larger crystallites than before the test, after 4 weeks the crystallite size of PCL decreased of about 50%, and after 10 weeks the membrane materials collapsed.

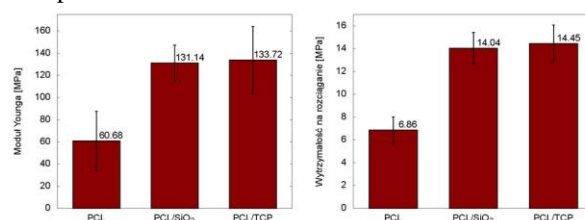


Fig 1. Mechanical properties of the membrane materials

## CONCLUSIONS

Nanocomposite membrane materials based on PCL and modified with SiO<sub>2</sub> or TCP nanoparticles give great possibility to design many materials futures such as: shape and size of pores, bioactivity and wettability. Conventional polymeric membranes lose mechanical properties, but addition of ceramic nanofiller can improve them. It means that the nanocomposite membranes can be potential materials for space-making implant in bone tissue defect regeneration.

## REFERENCES

- [1] Chen F-M. *et al.*, Biomaterials 31, 2010
- [2] Gugala Z. *et al.*, Biomaterials 25, 2004

## ACKNOWLEDGMENTS

This work was financially supported by the Polish Ministry of Science and Higher Education project number: NN 507 401 939

## Evaluation of the Biofunctionality of Internal Fixation Plates for Small Animals

B. Szaraniec<sup>1</sup>, K. Gryń<sup>1</sup>, T. Szponder<sup>2</sup>, A. Wąsik<sup>1</sup>

<sup>1</sup> Department of Biomaterials, Faculty of Materials Science and Ceramics, AGH University of Science and Technology, 30 Mickiewicza Ave., 30-059 Krakow, Poland

<sup>2</sup> Department and Clinic of Veterinary Surgery, Faculty of Veterinary Medicine, University of Life Sciences in Lublin, Lublin, Poland  
[szaran@agh.edu.pl](mailto:szaran@agh.edu.pl)

### INTRODUCTION

There is a big need for broken bone fixation systems targeted at small animals treatment. Metallic plates, which are commonly used for such purpose, have many drawbacks e.g. corrosion, accumulation of metal ions in tissues, too high Young modulus. Degradable plates made of polymer composites reinforced with carbon fibres may offer an interesting alternative. In this work a research on biofunctionality of novel fixation plates made of polylactide based composites are presented.

### EXPERIMENTAL METHODS

Fixation plates were manufactured with two types of forming processes: a hot-press of the prepregs ( $T \sim 200^\circ\text{C}$ ) and an injection moulding ( $T \sim 190^\circ\text{C}$ , system pressure  $80\text{kg/cm}^3$ ). As a matrix the resorbable polylactide Purasorb PLDL 7028 (Purac) was used. Hot-pressed plates were reinforced with 60wt% woven fabric CF2D (Tenax) impregnated with PLDL dissolved in dichlorometane (1/10) (Fig.1a). Continuous carbon fibres CF1D (Tenax) were previously shaped in loops to create a peripheral circumferential reinforcement of injected samples (Fig.1b).

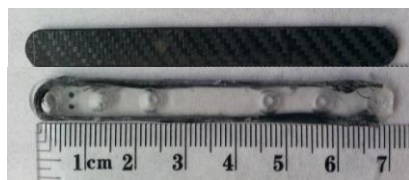


Fig.1 Degradable internal fixation plates:  
a) PLDL/CF2D, b) PLDL/CF1D

Obtained plates were incubated for 6 weeks in distilled water ( $37^\circ\text{C}$ ). Such period of time is suggested in the literature as a minimal for primary ossification. Mechanical testing (3pts bending) of the simulated model allowed to verify biofunctionality of the fixation system. Plates before and after incubation were compared. They were installed with metallic screws to the notched rabbit femoral bones and were bent (Fig.2). Observations of destroyed samples were conducted under stereoscopic microscope. The possibilities of applications of developed plates for veterinary orthopedics were evaluated on analysis of the results.

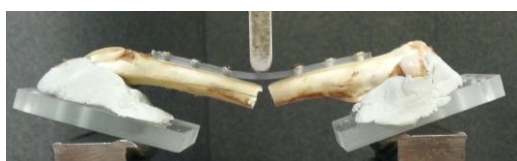


Fig. 2 Three-points bending test - model of simulated fixation system on rabbit femoral bone

### RESULTS AND DISCUSSION

After the mechanical testing it was found that much better results were achieved for PLDL/CF2D samples than for PLDL/CF1D. Introduction of high volume of woven fabric of carbon fibers strongly increased the stiffness of the fixation model and as a result total deformation was much smaller. There was observed an impact of the six-weeks incubation on mechanical properties of the PLDL/CF2D plates (30% decrease of bending strength) in contrary to PLDL/CF1D where such result was not recorded (Fig.3).

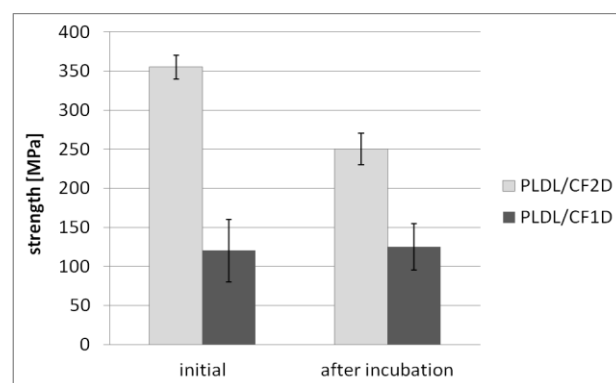


Fig.3 Comparison of bending strength of PLDL/CF plates before and after incubation.

### CONCLUSION

Even though there was a downgrade of bending strength of woven reinforced plates after incubation the value still was twice higher then bending strength of the plate reinforced with carbon fibre circumferential loop. It may indicate that this type of the plate will maintain a high strength and a proper stiffness of the osteosynthesis. It provides the correct amount of strength when necessary. In a presence of body fluids it harmlessly degrades over time and the load can be safely transferred to the healed bone giving the impulse to the bone tissue to remodel the structure according to the Wolff's law.

### REFERENCES

1. B. Szaraniec, K. Gryń, T. Szponder *et al.* Engineering of Biomaterials 125: 30-36, 2014
2. S. Park, K. Kang, H. Park *et al.* Tissue Engineering and Regenerative Medicine 8: 398-405, 2011

### ACKNOWLEDGMENTS

This work was financed by statutory research 11.11.160.616 of Faculty of Material Science and Ceramics AGH University of Science and Technology.

## The Influence of Poly(ethylene glycol) with Different Molecular Weight on the Properties of Acrylic Bone Cements

Klaudia Król, Kinga Pielichowska

Faculty of Materials Science and Ceramics, Department of Biomaterials,  
AGH University of Science and Technology, Poland  
[kingapie@agh.edu.pl](mailto:kingapie@agh.edu.pl)

### INTRODUCTION

Acrylic bone cement is commonly used for orthopaedic prosthesis fixation, since 1958<sup>1</sup>. The main problem that has been noticed with the use of acrylic bone cement is thermal necrosis of surrounding tissues, due to the high amount of heat being generated during the curing process<sup>2</sup>. Many attempts have been made to reduce too high curing temperature of PMMA bone cement. In this study, acrylic bone cement was modified with poly(ethylene glycol) (PEG), well-known, biocompatible phase change material (PCM), to decrease too high temperature of acrylic bone cement<sup>3,4</sup>.

### EXPERIMENTAL METHODS

Acrylic bone cement was modified with 15% of PEG with different molecular weight of 1450 - 10 000. The liquid to powder ratio (L/P ratio) of 0.37 ml/g was used. The setting time was measured using the Gillmore needle test. The curing parameters (maximum temperature  $T_{max}$  and setting time  $t_{set}$ ) were measured in accordance with ISO 5833 standard. The thermal analysis (DSC, TG), mechanical tests (compression testing and ultrasonic testing), microstructure studies (fluorescence microscopy, SEM) were performed to characterize the new material. Moreover, samples were incubated at 37 °C according to EN ISO 10993-13 for 3 months in distilled water. The pH, conductivity, and mass changes were measured during the incubation process.

### RESULTS AND DISCUSSION

The setting time of acrylic bone cements is given in Table 1. Bone cements modified with PEG showed longer setting time than the pure cement. In all cases, the curing process lasted in approximately 30–60s.

Tab. 1 Setting time of acrylic bone cements modified with poly(ethylene glycol) (Gillmore Needle method)

Sample	Setting time	
	Initial time	Final time
Pure cement	7 min 9s	8 min 8s
Cement + PEG 4000	14 min 30s	15min 30s
Cement + PEG 8000	11min 15s	12min 30s
Cement + PEG 10000	12min 30s	13min

An increase in setting time, determined according to ISO 5833:2002 standard, is an evidence for retardation of the polymerization reaction rate, caused by PEG phase change process.

Fig. 1. shows the temperature-time profiles. The maximum polymerization temperature of pure cement was 60.9°C.

A significant decrease in maximum temperature of modified bone cements was observed and it depends on PEG molecular weight. The largest temperature decrease was found for cement containing PEG 4000.

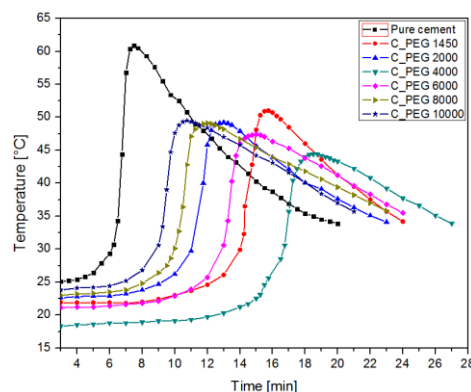


Fig. 1 Polymerization exotherms of acrylic bone cement modified with PEG

PMMA releases large amounts of heat during the polymerization. This thermal energy is utilized by PEG phase change, causing a decrease in the temperature of polymerization and an increase in setting time of acrylic bone cement. Depending on molecular weight of PEG, different amounts of heat can be stored.

### CONCLUSION

The aim of this study was to verify the effect of PEG on polymerization temperature of acrylic bone cement. A considerable decrease in curing temperature together with an increase in the setting time was observed. Importantly, the curing parameters still fulfilled the requirements of ISO 5833 standard.

### REFERENCES

1. R. Vaishya, M. Chauhan, A. Vaish, Bone cement, Journal of Clinical Orthopaedics and Trauma, 2013, 4, 157-163.
2. M. Stańczyk, B. Rietbergen, Thermal analysis of bone cement polymerisation at the cement–bone interface, Journal of Biomechanics, 2004, 37, 1803–1810.
3. K. Pielichowska, K. Pielichowski, Phase change materials for thermal energy storage, Progress in Materials Science, 2014, 65, 67–123.
4. K. Pielichowska, S. Błażewicz, Acrylic bone cement/Akrylanowy cement kostny, patent application P.406713, 2013,

### ACKNOWLEDGMENTS

This work was financed by statute fund of Faculty of Materials Science and Ceramics AGH-UST under contract No. 11.11.160.616.

## Optimizing Tibial Fractures Treatment with Carbon-Plate Fixator – CARBOELASTOFIX

Maciej Ambroziak<sup>1</sup>, Jan Chłopek<sup>2</sup>, Anna Morawska-Chochół<sup>2</sup>, Wojciech Żakiewicz<sup>1</sup>

<sup>1</sup>Chair and Department of Orthopedics and Traumatology of Locomotor System,  
Medical University of Warsaw, ul. Lindleya 4, 02-005 Warszawa, Poland

<sup>2</sup>AGH University of Science and Technology, Faculty of Materials Science and Ceramics,  
Department of Biomaterials, al. Mickiewicza 30, 30-059 Kraków, Poland

### INTRODUCTION

The paper focuses on optimizing the treatment of tibial fractures with a new type of carbon external fixator, named "Carboelastofix" by the design team based on its construction and mechanical properties.

Experimental and clinical research conducted for a number of years at the Clinic of Orthopaedics and Traumatology of the Medical University of Warsaw has shown the advantages of the "Carboelastofix" external fixator in healing tibial fractures.

The authors' main objective was to construct a bone fixation system which lacked the drawbacks of metal constructions. The novel method takes into account the forces transmitted by the fixator and the maximum loading of the fracture healing site at a given stage, which allows to choose the individual initial characteristics of the fixator.

### EXPERIMENTAL METHODS

The innovative external fixator was used to treat tibial fractures (type 42-A1 and 43-A2 according to AO classification) in 30 patients between 2002 and 2006.

All the cases succeeded in fracture healing. Results were based on clinical assessment and conventional X-rays. In addition, the progress of fracture healing was analyzed with ultrasonometry tests and in some cases density analysis of optical digital radiography images.

Fracture healing is a dynamic process and every stage requires different local mechanical and biological conditions. A special measuring device was constructed to assess the stiffness of the fixator - bone interface and it allowed to modify the flexibility (dynamization of fixation) consistently during the course of treatment. As fracture healing progressed and the interfragmentary stiffness increased, the stiffness of the fixator was gradually reduced. Treating fractures with a dynamic method such as these attempts to ensure iso-elasticity of the fixation during the whole healing process, as the principles of orthopaedic trauma suggested for many years to be optimal in achieving bone consolidation.

In addition, as the carbon plates are radiolucent, precise monitoring of fracture site healing and assessment of potential complications is possible.

### CONCLUSION

The presented optimized version of the Polish "Carboelastofix" carbon external fixator and obtained clinical results prove its high effectiveness in treating spiral and oblique tibial fractures. With its mechanical properties (gradual dynamization) and radiolucence this type of fixator has definite advantages over traditional external fixation constructions and may be considered an alternative.





## The Influence of Chain Extender on Properties of Polyurethane-Based Composites as Potential Injectable Bone Substitutes

Piotr Szczepańczyk, Kinga Pielichowska, Jan Chłopek

AGH University of Science and Technology, Faculty of Materials Science and Ceramics, Department of Biomaterials, Poland

[pszczepa@agh.edu.pl](mailto:pszczepa@agh.edu.pl)

### INTRODUCTION

Polyurethanes have potential application in nerve regeneration, cartilage and bone tissue repair, skin and vascular regeneration. Polyurethanes can be fabricated as either rigid or flexible foams. Their interconnected porous structure is beneficial for cell migration and proliferation. Open-celled pores also enable vascularisation and communication between cells. Segmented structure makes it possible to tune their physicochemical, mechanical and biological properties (1). Chain extender influences both structure and properties of the polymer material. For example increasing content of chain extender may cause higher density (2). Molecular weight distribution may be controlled by chain extender concentration (3). Chain extenders influence the elastic modulus and glass transition temperature of the adhesive through the hard/soft segment relationship (4). Their chemical structure also affects the crystallinity (5). Polysaccharide chain extenders such as chitin accelerate the degradation rate. Simultaneously the thermal stability was found to increase with increasing chitin content. Chitin-based polyurethanes exhibited enhanced stiffness, heat resistance, molecular rigidity and strength. The wide range of material properties that were achieved through modifications in chemistry makes these degradable polymers applicable for biomedical applications (6). The aim of this study was to modify polyurethanes reinforced by  $\beta$ -tricalcium phosphate ( $\beta$ -TCP) microparticles by adding chitosan to facilitate biodegradation (7). It has also been proved that polyurethane chains containing either monosaccharides or sugar alcohols do not degrade into toxic by-products (8). The effect of chitosan/1,4-butanediol used as crosslinking agent/chain extender was investigated. The composite foams were synthesized using various amounts of  $\beta$ -TCP. It was found that incorporation of  $\beta$ -TCP and chitosan influenced microstructure of composites.

### EXPERIMENTAL METHODS

The effect of varying  $\beta$ -TCP content and chitosan/1,4-butanediol ratio was investigated using infrared spectroscopy, differential scanning calorimetry, drop shape analysis and microscopic methods. *In vitro* tests

were carried out to study the influence of bioceramics and crosslinking agent/chain extenders on biodegradation as well as a preliminary investigation of the *in vitro* bioactivity.

### RESULTS AND DISCUSSION

Scanning electron microscopy showed presence of the apatites deposition after 4-week incubation in simulated body fluid (Figure 1). Incorporation of  $\beta$ -TCP microparticles improved modulus.

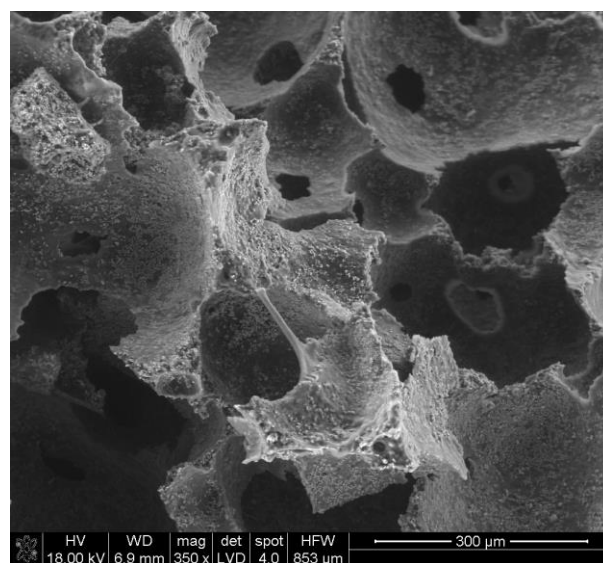


Figure 1 SEM image of PU/ $\beta$ -TCP after SBF incubation

### CONCLUSION

Synthesis of the composites included different  $\beta$ -tricalcium phosphate content and chitosan/1,4-butanediol ratio. The effect of  $\beta$ -TCP and chain extenders was studied by spectroscopic, thermal and microscopic methods. The addition of  $\beta$ -TCP and chitosan influenced thermal stability. Introduction of  $\beta$ -TCP strengthened the hydrophilic nature of polyurethane foams. Both  $\beta$ -TCP and chitosan could be able to tailor properties of the composites so they could be closer to fulfil the requirements of tissue engineering. However, further investigation is necessary to study another factors connected with *in vivo* bone healing.

## Human Amniotic Membrane for Bone Regeneration of Calvaria Defects in Mice

Mathilde Fénelon<sup>1</sup>, Claudine Boiziau<sup>1</sup>, Reine Bareille<sup>1</sup>, Olivier Chassande<sup>1</sup>, Sylvie Rey<sup>1</sup>,  
Hélène Boeuf<sup>2</sup>, Florelle Gindraux<sup>3</sup>, Zoran Ivanovic<sup>4</sup>, Jean-Christophe Fricain<sup>1</sup>

1: INSERM U1026, Laboratory BioTis, Bordeaux University, Bordeaux, France.

2: CNRS UMR 5164, Laboratoire CIRID, Bordeaux University, Bordeaux, France.

3: EA 4268, Franche-Comté University, Besançon, France.

4: French Blood Institute, Aquitaine-Limousin Branch, Bordeaux, France.

[fricainj@aol.com](mailto:fricainj@aol.com)

### INTRODUCTION

The human amniotic membrane (hAM) is a highly abundant and readily available tissue that may be helpful as a support for bone regeneration. Human Amniotic Membrane may be an alternative to induced membrane in the case of critical size bone defects to replace the periosteum. This membrane contains two different cell types: human Amnion Epithelial Cells (hAECs) and human Amnion Mesenchymal Stem Cells (hAMSCs) that have a strong osteoinductive potential<sup>1,2</sup>. Moreover, AEC introduced in tibia bone defect survived in the site of implantation for 45 days and supported consistent bone neoformation<sup>3</sup>. The aim of this project was to analyze bone regeneration potential of hAM implanted in mice calvaria bone defect. We have investigated i) the role of epithelial and mesenchymal layers on bone regeneration efficiency in a model of calvarial critical defect and ii) the consequences of cryopreservation.

### MATERIAL and METHODS

hAM cryopreservation vs fresh membranes: hAM were recovered after elective cesarian surgery and either used as fresh tissue or cryopreserved in RPMI/Glycerol (1/1).

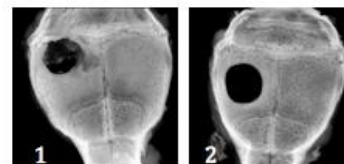
In vivo procedure: Critical bone defects (3.3mm diameter) were performed in adult mice calvaria. Defects remained free or were covered by an hAM fragment, either fresh or cryopreserved in each orientation (hAECs or hAMSCs, n = 8-10 in each group). Sacrifice was performed after 8 weeks and bone regeneration was quantified by X-rays (faxitron). Kruskal & Wallis with Mann & Whitney comparisons were utilized. Decalcified histological analysis was done using trichrome Masson staining.

In vitro: Human Bone Marrow Mesenchymal Stem cells (hBMSCs) were cultured on cryopreserved hAM fragments in basal medium during two weeks; hAM cell survival after cryopreservation and hBMSC viability were analyzed with live/dead staining.

### RESULTS AND DISCUSSION

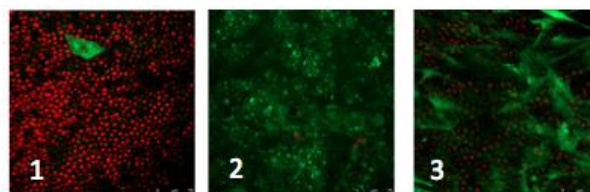
Preliminary results of faxitron analysis showed that no defect was regenerated *ad integrum*. However, mineralized nodule formations were observed, mainly for cryopreserved hAM. Quantitative analysis suggested that cryopreserved hAM (hAECs side)(1) induced mineralized nodule formation with a higher efficiency as compared with fresh hAM or absence of any hAM (2).

Fig 1 : Faxitron showing the defect remaining after 8 weeks of healing.



Histological analysis has shown that hAM did not induced important inflammatory reaction. New bone formation was exceptionally observed at the periphery of the defect.

Live/dead cells viability assays showed very few hAM cells alived after thawing (1). However, after 7 days, dividing cells were detected (AECs and hAMSCs) (2). Preliminary results revealed that hBMSCs could adhere to hAM and survive (3).



### CONCLUSION

hAM alone did not allow regeneration *ad integrum* of critical calvaria bone defect in mice. Cryopreserved hAM with epithelial side in contact with the defect have produced more mineralized nodules than other conditions. In vitro analyses have shown that hAM epithelial side was suitable for hBMSC proliferation. We proposed now to investigate the osteogenic potential of hAM associated with hydroxyapatite in the same model.

### REFERENCES

1. Soncini M & al., J Tissue Eng Regen. 1:296–305, 2007
2. Lindenmair A. & al., Biomaterials. 31:8659-8665, 2010
3. Mattioli M. & al., Cell Biol. Int. 36 :7–19, 2012

### ACKNOWLEDGMENTS

“The authors would like to thank the Fondation des Gueules Cassées and the Fédération de Recherche TecSan for providing financial support to this project”.

Pazdan Krzysztof, Pieliowska Kinga, Chłopek Jan

<sup>1</sup>Department of Biomaterials, Faculty of Materials Science and Ceramics,  
AGH University of Science and Technology, Cracow, Poland  
[kpazdan@agh.edu.pl](mailto:kpazdan@agh.edu.pl)

## INTRODUCTION

The requirements for novel biomaterials for medical applications are still changing and increasing. Apart from bioactivity and appropriate mechanical properties, novel biomaterials should have be biodegradable, have cell immobilization properties and ability to be a drug delivery system for cure of disease or support of healing process, e.g. limit inflammation<sup>1</sup>. Natural based polymers seem to be the best biomaterials to fulfil those requirements. Chitosan is one of them<sup>2</sup>. This polymer is commonly used as a bioresorbable matrix for wound dressing, drug delivery system and as a scaffolds material. It exhibits promising non-toxic, bioactive and cell attachment properties<sup>3</sup>. Synthetic nanoclay commercially named Laponite<sup>®</sup> was used in the research to enhance its properties. Its structure is very similar to commonly used montmorillonite, but synthetic origin guarantees stable and recurrent composition and less content of heavy metal ions in comparison with natural montmorillonite.

## EXPERIMENTAL METHODS

Low molecular weight chitosan was dissolved in three solvents: commonly used acetic acid, ascorbic acid and lactic acid. The concentration of solvents and chitosan were the same, it was 2,5% of chitosan in 2% aqueous acidic solutions. To obtain composites, cross-linker was dispersed first in an aqueous environment and mixed with chitosan. Obtained gels were precipitated in polyphosphate counterions solution to achieve a form of beads. Then, they were air dried and vacuum dried. DSC measurements have been performed using standard procedure 10°C/min in nitrogen atmosphere. Cell culture tests were performed to confirm bioactive properties of the composites.

## RESULTS AND DISCUSSION

The obtained nanocomposites show differences in thermal properties depending on cross-linker concentration and solvent used in the preparation. Significant differences are visible in Figure 1. Curve CL (from chitosan dissolved in ascorbic acid) and LL (from chitosan dissolved in lactic acid) have similar course till 80°C, then there are big differences, especially for chitosan from ascorbic acid solution. Large endothermal

peak is probably caused by evaporation of entrapped water. This suggests that ascorbic acid solution causes stronger water entrapment in chitosan hydrogel structure.

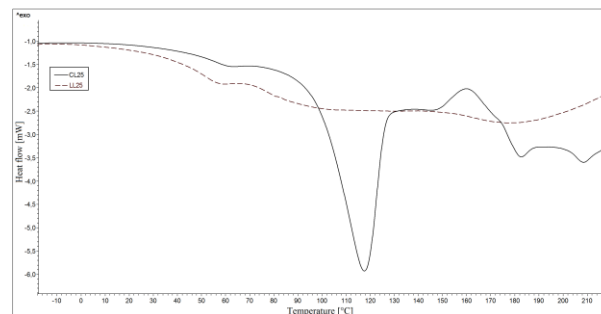


Figure 1. DSC curves of chitosan hydrogels (LL-lactic acid; CL-ascorbic acid).

## CONCLUSION

Synthesis environment is a crucial element influencing properties of obtained material. In DSC curves, there are significant differences in thermal properties chitosan dissolved in aqueous solutions of different organic acids.

## REFERENCES

1. Billström, G. H.; Blom, A. W.; Larsson, S.; Beswick, A. D., Application of scaffolds for bone regeneration strategies: Current trends and future directions. *Tissue Loss and Regeneration: An Update* 2013, 44, Supplement 1 (0), S28-S33.
2. Dash, M.; Chiellini, F.; Ottenbrite, R. M.; Chiellini, E., Chitosan—A versatile semi-synthetic polymer in biomedical applications. *Progress in Polymer Science* 2011, 36 (8), 981-1014.
3. Ravichandran, R.; Sundarajan, S.; Venugopal, J. R.; Mukherjee, S.; Ramakrishna, S., Advances in Polymeric Systems for Tissue Engineering and Biomedical Applications. *Macromolecular Bioscience* 2012, 12 (3), 286-311.

## Why Incorporation of Poly(Ethylene Glycol) into Polyurethane Chain is an Attractive Way to Improve Its Physicochemical Properties for Bone Regeneration?

Michalina Marzec, Justyna Kucińska-Lipka, Helena Janik,

Department of Polymer Technology, Chemical Faculty, Gdansk University of Technology, Poland

[michalina.marzec@pg.gda.pl](mailto:michalina.marzec@pg.gda.pl)

### INTRODUCTION

Polyurethanes (PUs) have unique segmented structure, due to which diverse properties can be obtained using relevant raw materials and additives. Moreover, it is known that PUs undergo calcification when implanted into human body. The ability to promote calcium phosphates (CP) formation is one of the unique properties that stands out PU from other biomaterials and speaks for using PU in bone regeneration. However, calcification occurs only after long-term implantation. In this study, poly(ethylene glycol) (PEG), because of its exceptional properties such as biocompatibility and biodegradability, was chosen to speed up calcification process. We examined the influence of different amount of PEG incorporated into chain on PU properties.

### EXPERIMENTAL METHODS

Five series of PU from poly(ethylene-butylene) adipate diol, poly(ethylene glycol) (PEG), 1,6-hexamethylene diisocyanate and 1,4-buthanediol were synthesized.

*In vitro* calcification was carried out for 80 days. PUs were incubated in Golomb & Wagner's solution. Scanning electron microscope analysis (SEM) was used to examine PU surface before and after incubation. Calcium concentration in solutions after removing samples was measured by atomic absorption spectrometry (AAS). Tensile strength were performed according to PN-EN ISO: 1799 : 2009. The hydrophilic properties were determined by the water contact angle measurement with a sessile drop technique.

### RESULTS AND DISCUSSION

From data presented in table 1 it is clear that incorporation of PEG into PU chain improves mechanical properties, the tensile strength increased from 10 MPa to 26 MPa. The water contact angle decreased with the increase of PEG, what indicates that by PEG incorporation it is possible to obtain more hydrophilic material. Noteworthy, in all series we obtained highly hydrophilic materials. Figure 1 shows that addition of PEG into PU caused calcium phosphate formation already after 16 days of incubation in Golomb & Wagner solution.

Tab. 1 Physical properties of PUs synthesised with different PEG content.

PEG content (wt. %)	0	5	10	20	25
Tensile strength (MPa)	10	17	21	26	22
Water contact angle (°)	15	15	11	10	9

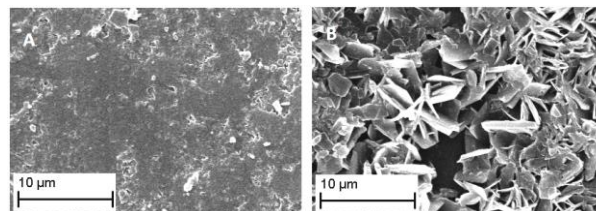


Fig. 1 SEM photographs of the PU surface samples A – PU without PEG, B – PU with 20 wt % of PEG after 16 days of incubation.

The mechanism of calcification is still unknown, but it was discussed in terms of presence of ester and/or ether groups, hydrophilic/hydrophobic properties and hard segment content. In this study we proved that the presence of ether groups and higher isocyanate index enhance calcification, what is in agreement with. However the statement in the literature that hydrophilicity promotes nucleation of CP is not always the case. We found that both materials had comparable contact angles but only sample that possessed ether groups speeded up calcification (Fig. 1, Tab. 1).

### CONCLUSION

Incorporation of poly(ethylene glycol) into polyurethane chain is an attractive way to improve biological properties, mechanical strength and supports formation of new bone. Introducing ether groups speeds up calcification.

### REFERENCES

1. Fu S.H., Meng X.H., Fan J. et al. J. Biomed. Res. Part A 102A: 479-486, 2014
2. Tran R.T., Wang L., Zhang C. et al. J. Biomed. Res. Part A 102A: 2521-2532, 2014
3. Ciobanu G., Ilisei S., Luca C. et al. Prog. Org. Coatings 74: 648-653, 2014
4. Golomb G., Wagner D. Biomater. 12(4):397-405, 1991
5. Vermette P., Griesser H.J., Laroche G., Guidoin R., Tissue engineering intelligence unit 6, Biomedical Applications of Polyurethanes, Landes Bioscience, Georgetown, Texas, U.S.A., 9, 2001
6. Bernacca G.M., Mackay T.G., Wilkinson R. et al. Biomater. 16:279-285, 1995
7. Gorna K., Gogolewski S. J. Biomed. Mater. Res. 60: 592-606, 2002

### ACKNOWLEDGMENTS

The authors would like to thank prof. J. Namiesnik and his team from Department of Analytical Chemistry, Gdansk University of Technology for AAS analysis.



## Construction of a Functional Bone Implant to Direct the Biomineralization Process

Inas Ozcan<sup>1</sup>, Kursad Kazmanli<sup>2</sup>, Fatma Nese Kok<sup>1</sup>

<sup>1</sup>Molecular Biology Genetics and Biotechnology Programme, Istanbul Technical University, Turkey

<sup>2</sup>Metallurgical and Materials Engineering Department, Istanbul Technical University, Turkey

[ins.ozcn@gmail.com](mailto:ins.ozcn@gmail.com)

### INTRODUCTION

The aim of this study is to design a biodegradable, biocompatible hard tissue implant to trigger and direct the biomineralization process. To construct the implant, silk fibroin from *Bombyx mori* and its blend with other polymers such as gelatin and poly(L-lactic acid) (PLLA) was chosen as the main for their superior properties in bone tissue related applications<sup>1-2</sup>. To direct the biomineralization process a short-peptide derived from osteocalcin will be used<sup>3</sup>. As the structure/crystallinity of biominerals are important for their biological activity, the biomineralization process in the constructed implants will be examined by different techniques (SEM-EDC; XPS, etc) both in the absence and the presence of the human fetal osteoblastic cells (fHOB).

### EXPERIMENTAL METHODS

Silk fibroin protein was obtained from *Bombyx mori* cocoons (a modified procedure was adapted from Rockwood et al)<sup>4</sup> with 4-6 % w/v yield (Fig.1). The fibroin solution was aliquoted (5mL), freeze at -20°C overnight and subsequently lyophilized for 48 h. Silk fibroin solutions (2%, 3%, 6% w/v) with or without addition of gelatin (1%; 1:1 v/v) were prepared swelling behavior, porosity and morphology were examined.

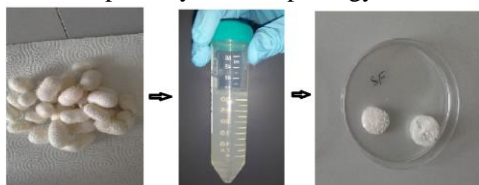


Figure 1. Silk fibroin solution from *B.mori* cocoons and lyophilized-fibroin scaffolds

Silk fibroin scaffolds were cut into 12mm diameter and 6mm thickness were weighted, then immersed in phosphate buffer saline (PBS) at room temperature and weighed again after 1 h, 3h, 5h and 24h. Swelling ratio %S was determined via Ws (swollen scaffold)-Wd (dry scaffold) values and were calculated as follows:

$$\%S = \frac{(W_s - W_d)}{W_d} \times 100$$

Hexane, being a nonsolvent for silk fibroin was used for porosity measurements. The known volume of hexane (V1), hexane-impregnated scaffold along with hexane (V2), the residual hexane volume (V3) were used to calculate the porosity of scaffolds (ε) obtained by:

$$\epsilon(\%) = \frac{V_1 - V_3}{V_2 - V_3} \times 100$$

### RESULTS AND DISCUSSION

Swelling behavior for silk fibroin and silk fibroin/gelatin composite scaffolds were given at Fig.2. It could be noticed that scaffolds with gelatin had low

swelling ratio compared to SF scaffolds. Highest swelling ratio was obtained by 2 and 3% SF scaffolds.

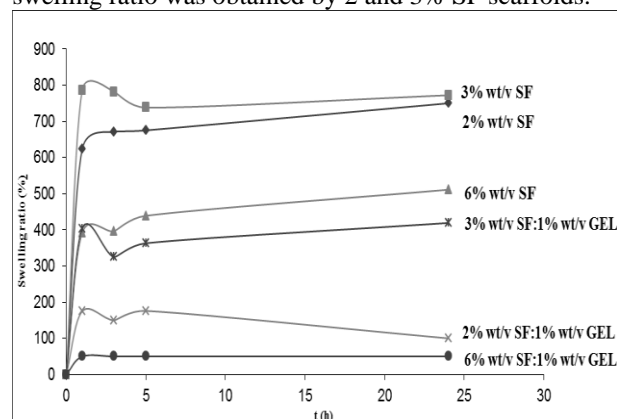


Figure 2. Swelling ratio of SF and SF:GEL scaffolds in PBS

Porosity studies showed that increasing the polymer amount lead to a decrease in porosity for SF implants. Addition of gelatin seems to alter this behavior. All scaffolds had illustrated higher than 60% porosity. Difference in SF amount and addition of gelatin seemed to yield scaffolds with different morphologies (Fig 3).

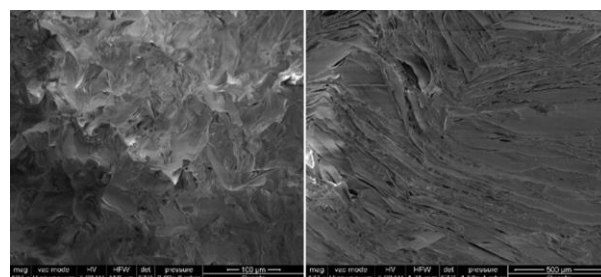


Figure 3. SEM micrographs of the scaffolds

### CONCLUSION

Preparation of silk fibroin/PLLA with different polymer ratios is an ongoing work. After the selection of best candidates, peptides will be immobilized and biomineralization studies will be started.

### REFERENCES

1. Kundu B. *et al.*, Adv. Drug Deliv. Rev. 65:457-470, 2013
2. Agrawal C.M. *et al.*, J Biomed. Mater. Res. 55:141-50, 2001
3. Hosseini S. *et al.*, JBC 28:8:7885-93, 2013
4. Rockwood D. *et al.*, NIH 6:10:1-43, 2011

### ACKNOWLEDGMENTS

The authors would like to thank to Dr. Halime Kenar for her valuable inputs in silk fibroin extraction.

## Mechanically Robust and Sterilizable, Biosignalling Surfaces for Metallic and Polymer Orthopedic Implants

M. Bilek<sup>1</sup>, W. Chrzanowski<sup>2</sup>, E. Wakelin<sup>1</sup>, G. Yeo<sup>3</sup>, A. Kondyurin<sup>1</sup>, DR McKenzie<sup>1</sup>, AS Weiss<sup>3</sup>

<sup>1</sup>Department of Applied Physics, School of Physics; <sup>2</sup>Faculty of Pharmacy; <sup>3</sup>School of Molecular Biosciences;  
University of Sydney, NSW 2006, Australia  
[edgarw@physics.usyd.edu.au](mailto:edgarw@physics.usyd.edu.au)

This paper describes practical surface treatments demonstrated for PEEK and titanium alloy orthopedic implants that significantly improve the osseointegration potential of these materials. The surface treatment provides a biocompatible surface that enables subsequent covalent functionalisation with bioactive molecules. The processes rely on energetic ion bombardment from a plasma to create a nanoscale interfacial layer containing pi-conjugated carbon clusters which serves as a reservoir for radicals. Covalent coupling of tropoelastin molecules by reaction with these embedded radicals is achieved in a one-step application of the biomolecules in buffer solution to the surfaces. The immobilized molecules promote bone cell adhesion and proliferation as observed in assays using MG63 and SAOS cell lines. We take significant steps towards making this a practical treatment with commercial potential by demonstrating 1) sterilization of the tropoelastin-coated devices in packaging without impacting the bioactivity of the protein; 2) robustness of the interlayer against scratching under load, and 3) that the plasma-based processes used can be applied to the complex shaped structures typical of orthopedic implants in a straight-forward way. The utility of the coatings in promoting bone integration is demonstrated by in-vitro cell assays and in-vivo experiments.

### INTRODUCTION

As the population ages and life expectancies continue to increase, the need for orthopedic implants, such as hip and knee replacements and spinal implants, is increasing rapidly. Traditionally titanium alloys have been the preferred materials for such implants. Titanium has a relatively biocompatible surface, which is often modified to help facilitate bone integration using coatings based on hydroxyapatite.

Polyetheretherketone (PEEK) is a polymer whose mechanical properties provide a much better match to bone. It has been introduced as a material for orthopedic implants to combat the problem of stress shielding and has been deployed commercially particularly in spinal implants, however it provides poor integration with surrounding bone tissues. Following improvements of bone integration achieved for titanium by the application of hydroxyapatite (HA) coatings, composites of PEEK with hydroxyapatite (HA) have improved its bioactivity but typically at the expense of the excellent mechanical properties. Coating with titanium has been proposed as a way to improve its ability to integrate with bone tissue.

### EXPERIMENTAL METHODS

Plasma immersion ion implantation in a nitrogen plasma is used to activate the surfaces of polymers, such as PEEK. In this process the sample is immersed in an RF plasma and surrounded by a mesh electrode of appropriate geometry. High voltage negative bias (up to 20kV) pulses are applied to the electrode to accelerate nitrogen ions from the plasma into the surface of the polymer.

For treatment of metals, such as Ti alloys, acetylene and argon are added to the plasma to facilitate deposition of a carbon containing surface layer. The metal workpiece to be modified is connected directly to a high voltage pulsed power supply. Ions accelerated from the plasma provide interface mixing for excellent adhesion as well as creating radicals embedded in the deposited coating.

In each case the treated surface layer is <100nm in thickness and contains sufficient radicals to covalently couple a dense bioactive layer of protein/peptide to the surface by simple contact with a solution containing the biomolecules.

### RESULTS AND DISCUSSION

Mechanical stability of the surfaces was demonstrated by scratching under load and subsequent incubation in heated ionic solutions. The surfaces, as examined under SEM, showed that the modified layer was only removed at the sites where scratched by the indenter. No delamination was observed in surrounding areas.

Covalent immobilisation of bioactive adhesion of signalling proteins and peptides was demonstrated using molecules such as tropoelastin and its derivatives. Resistance to elevated temperature SDS washing showed that the biomolecules were immobilised covalently. Sterilization by gamma irradiation was demonstrated and did not alter the layers' bioactivity.

Cell assays showed that the biomolecules retained their cell adhesive and signalling capabilities when immobilised to these surfaces and significantly enhanced the adhesion and proliferation of cells seeded on them.

Bone cell markers such as alkaline phosphatase showed good bone cell activity and that the surfaces would support bone integration.

### CONCLUSION

We have created a practical and industry scalable platform technology for the bioactivation of surfaces to promote the tissue integration of bone contacting biomaterials.

### ACKNOWLEDGMENTS

Authors acknowledge Linkage funding from the Australian Research Council and LfC



## Exploring Osteoclastogenesis in a Co-Culture System

Sabine Schulze<sup>1</sup>, Peter Dieter<sup>1</sup>, Ute Hempel<sup>1</sup>

<sup>1</sup>Institute of Physiological Chemistry, TU Dresden, Germany  
[Sabine.Schulze1@mailbox.tu-dresden.de](mailto:Sabine.Schulze1@mailbox.tu-dresden.de)

### INTRODUCTION

Bone is a highly dynamic tissue which is characterised by continuous remodelling. Bone mass and bone density are maintained by precise activation and repression of bone-resorbing osteoclasts (OC) and bone-forming osteoblasts (OB). OB secrete M-CSF and RANKL which induce fusion and activation OC precursors. Vice versa, OB are recruited to sites of prior bone resorption by OC-generated factors to refill resorption cavities<sup>1</sup>. For balanced bone formation and resorption it is of great importance to address both cell types in research on implant materials and drugs. Therefore, we established a direct *in vitro* co-culture of OB and OC using a natural OB-derived matrix as a substrate and avoiding any further osteogenic supplements.

### EXPERIMENTAL METHODS

PBMC isolated from buffy coats were seeded on a native extracellular matrix generated by SaOS-2 cells<sup>2</sup> and treated with M-CSF to ensure their survival. Mesenchymal stroma cells (MSC) were incubated with  $\beta$ -glycerophosphate and ascorbic acid. After eight days of predifferentiation MSC were either co-cultured with PBMC or were seeded alone on SaOS-2 matrix. To estimate the impact of cell-cell contact on osteoclastogenesis PBMC medium was supplemented with supernatant from MSC culture. Vice versa, MSC were cultured in medium containing PBMC supernatant. Medium was refreshed twice a week. After two weeks of (co-)culture OC and OB markers were measured. Differentiation of PBMC into OC was verified by resorption pit formation and analysis of the OC marker tartrate-resistant acid phosphatase (TRAP). Osteogenic differentiation of MSC was evaluated by alkaline phosphatase activity.

### RESULTS AND DISCUSSION

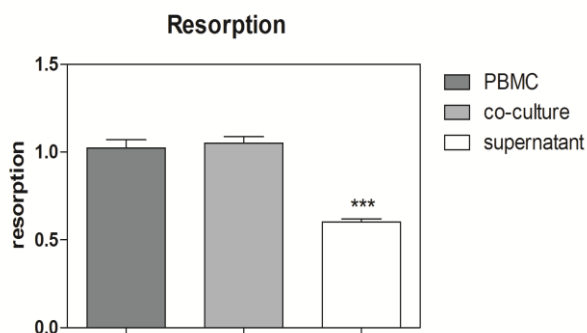


Fig.1: Quantitative resorption assay. PBMC in co-culture with MSC resorbed as much as RANKL-stimulated PBMC. Unstimulated PBMC cultured with MSC supernatant show significantly less resorption.

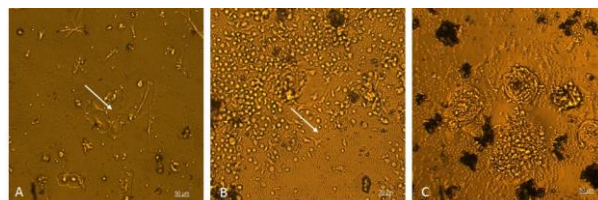


Fig.2: Microscopic images of stimulated PBMC (A), co-culture (B) and PBMC cultured with MSC supernatant (C). Resorption pits are highlighted by white arrows. In PBMC culture with MSC supernatants huge OC occur after PBMC fusion, but no resorption pits are visible.

These data imply that RANKL-dependent bone resorption is enhanced by direct OC-OB contact which enables the exclusive interaction of membrane-bound RANKL (on OB) with its receptor RANK (on OC). In the indirect co-culture system OC are reliant on the release of soluble RANKL by OB which seems to be not sufficient for a OC activity comparable to direct co-culture. Our results confirm previous publications<sup>3,4</sup>.

### CONCLUSION

For actively resorbing osteoclasts cell-cell contact with osteoblasts is essentially required. Therefore, we established a well-tuned co-culture system on a smart calcium phosphate matrix.

### REFERENCES

1. Sheu TJ. *et al.*, J. Biol. Chem. 278:438-43, 2003.
2. Lutter AH. *et al.*, J. Cell. Biochem. 109:1025-32, 2010.
3. Lean JM. *et al.*, Bone, 27:29-40.
4. Nakashima T. *et al.*, Biochem. Biophys. Res. Commun. 275:768-75.

### ACKNOWLEDGMENTS

The authors gratefully acknowledge financial support from TRR67.

## Chondrogenic Differentiation of Mesenchymal Stem Cells Derived from Osteoarthritic Patients on Pure or Chitosan-Coated Poly(L-Lactic Acid) Scaffolds

Joana Magalhães<sup>1,2</sup>, Cristina Álvarez-Martínez<sup>2</sup>, Elena F. Burguera<sup>1,2</sup>, Cristina Ruiz-Romero<sup>1,2</sup>, José Luís Gómez-Ribelles<sup>3</sup>, Francisco J. Blanco<sup>2</sup>

<sup>1</sup>CIBER in Bioengineering, Biomaterials and Nanomedicine, Spain

<sup>2</sup>Tissue Engineering and Cellular Therapy Group (GBTTC-CHUAC). Rheumatology Division. INIBIC. CHUAC. Sergas. UDC. Spain

<sup>3</sup>Centre for Biomaterials and Tissue Engineering, Universitat Politècnica de València, Spain  
[joana.cristina.silva.magalhaes@sergas.es](mailto:joana.cristina.silva.magalhaes@sergas.es)

### INTRODUCTION

The low capacity of articular cartilage for self-repair and regeneration is extremely poor which contributes to the degradation of articular cartilage associated with osteoarthritis (OA).<sup>1</sup> Regenerative medicine offers great potential as an alternative to joint replacement to treat OA patients. We have previously shown the chondrogenic potential of human bone marrow mesenchymal stem cells (BM-MSCs) derived from OA patients in chitosan-coated poly(L-Lactic Acid) (PLLA-CHT) scaffolds after long-term culture.<sup>2</sup> This present study is aimed at analyzing the effect of the physicochemical properties of the scaffolds during the different stages of the chondrogenic differentiation process in order to give better insight of the dependence of the biological response of BM-MSCs on scaffolds' structure and composition.

### EXPERIMENTAL METHODS

Human BM-MSCs ( $2.5 \times 10^5$ ) derived from OA patients, were seeded on pure or chitosan-coated PLLA scaffolds under a defined chondrogenic differentiation medium (CM) composed by DMEM supplemented with knock-out serum (15%), ascorbic acid (10  $\mu$ l/ml), transferrin (6  $\mu$ l/ml), dexamethasone (10  $\mu$ M), retinoic acid ( $10^{-7}$  M) and transforming growth factor beta 3 (TGF- $\beta$ 3, 10 ng/ml), during 7, 14 and 21 days, using a conventional pellet-culture system as control. At each time point the expression of cartilage interest markers at molecular and protein level was studied using rt-PCR and immunohistochemistry (col1a1, col2a1, col10a1, sox9, aggrecan, PRG4, CILP, POSTN and RPL13a as housekeeping gene). The quality of the synthesized extracellular matrix was analyzed by histological staining (toluidine blue (TB), safranin-O (SO)).

### RESULTS AND DISCUSSION

Controlling extraction-gelation parameters allows to create different structures on PLLA-CHT scaffolds, such as hydrogel-(PLLA-CHT1) or fiber-like coatings (PLLA-CHT2) that can directly influence the chondrogenic differentiation process of BM-MSCs. We observed the chondrogenic differentiation of cells and the formation and maturation of an extracellular matrix with deposition of proteoglycans (Fig.1 TB and SO) and zone-specific molecules such as lubricin (PRG4, superficial zone) and cartilage intermediate layer protein (CILP, intermediate zone), although negative for periostin (POSTN, deep layer). Chitosan incorporation negatively affected the chondrogenic

process of BM-MSCs observed at mRNA and protein expression, with a significant decrease on aggrecan and col2a, as well as, PRG4 and CILP, when compared to pure PLLA. A hydrogel-like tissue led to a more heterogeneous tissue whilst fiber-coating to a more homogeneous distribution of the tissue formed. Moreover, the presence of chitosan seems to be accelerating an hypertrophic phenotype, with an early increase on the expression of col10a1, at day 14. The expression of col1a1 remained downregulated at all time points which discards fibrocartilage formation (data not shown).

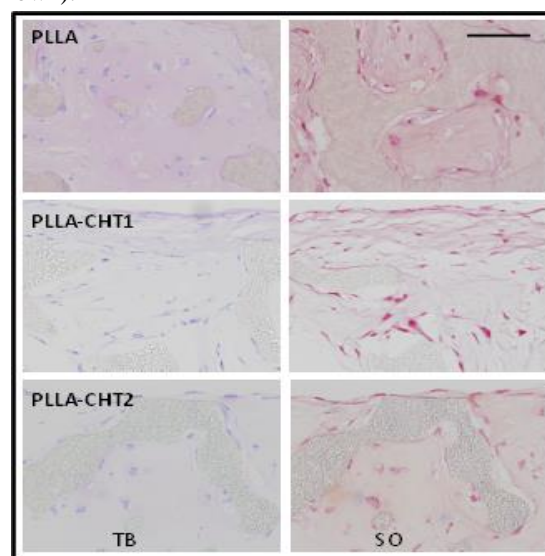


Figure 1. Histological analysis (TB and SO) in cross-sections of pure and CHT-coated PLLA scaffolds (scale bar: 200  $\mu$ m).

### CONCLUSION

BM-MSCs chondrogenic differentiation can be influenced by the composition and structure of pure and CHT-coated PLLA scaffolds, although in our case the composition effect seems to have a higher impact than structural modifications.

### REFERENCES

1. Blanco FJ. *et al.*, Ann Rheum Dis. 72:631-4, 2013
2. Magalhães J. *et al.*, Tissue Eng Part A. 21:3-4, 2015

### ACKNOWLEDGMENTS

The authors would like to thank CIBER-BBN for providing financial support. CIBER-BBN is a national initiative of ISCIII. This study was supported by Galician Network of Biomaterials (R2014/033), from Xunta de Galicia and Consolider Program.





Małgorzata Krok-Borkowicz<sup>1</sup>, Urszula Posadowska<sup>1</sup>, Karolina Toś<sup>1</sup>, Elżbieta Pamuła<sup>1</sup>

<sup>1</sup>AGH University of Science and Technology, Faculty of Materials Science and Ceramics, Department of Biomaterials, Al. A. Mickiewicza 30, 30-059 Krakow, Poland,

[krok@agh.edu.pl](mailto:krok@agh.edu.pl)

## INTRODUCTION

Bone tissue defects, especially those with critical size, are treated with autologous or allogenic grafts or scaffold biomaterials. Designing scaffolds, that mimic structure of bone extracellular matrix (ECM), and provide optimal architecture and chemistry for cell proliferation, migration and differentiation are the goals of many studies<sup>1</sup>. Another approach is the use of drugs that are known to enhance bone growth. In this study we propose to combine both approaches: resorbable scaffolds and drug delivery system based on resorbable microparticles (MPs).

In detail, we prepared poly(L-lactide-co-glycolide) (PLGA) scaffolds and modify them with PLGA MPs containing sodium alendronate (Aln). Our intention was to provide support for osteoprogenitors and osteoblasts adhesion/proliferation/differentiation and concomitantly to inhibit osteoclasts by sustained local delivery of Aln. Aln was chosen because it is widely used for the treatment of several bone diseases like osteoporosis, Paget's disease, bone tumors and recently it has been proposed as osteointegration-enhancing drug<sup>2</sup>.

## EXPERIMENTAL METHODS

PLGA scaffolds were produced by solvent casting/particulate leaching technique. Sodium chloride particles (400 – 600 µm) were used as a porogen. After PLGA dissolution the mixture was transferred into 5-mL syringes and dried. Next the rigid salt/polymer mixture was cut into slices (2 mm) and washed in ultra-high-purity water till conductivity of the water was about 2 µS/cm. Aln-loaded PLGA MPs were prepared by double-emulsification technique. MPs were dispersed in human recombinant collagen solution type I (Collage<sup>TM</sup>, Aldrich, 3 mg/mL) and immobilized on PLGA scaffolds, previously hydrophilized with ethanol, by drop seeding procedure. Morphometric analysis (for empty and Aln-loaded MPs) was done under inverted optical microscope. Scaffolds microstructure was characterized by SEM. Encapsulation and loading efficiencies and drug release kinetics were evaluated by an orthophthaldialdehyde (OPA) assay with the use of fluorescence spectroscopy<sup>3</sup>. Degradation kinetics of MPs in phosphate buffered saline (PBS) was also studied. Cytotoxicity test performed on extracts from scaffolds with MPs was conducted with the use of MG-63 osteoblast-like cells. AlamarBlue (Sigma) and live/dead staining (Aldrich) were used to test proliferation, viability and morphology of the cells<sup>2</sup>.

## RESULTS AND DISCUSSION

Morphometric analysis showed differences between loaded and un-loaded MPs. The average diameters were  $6.8 \pm 2.2$  µm and  $4.2 \pm 2.3$  µm for Aln-MPs and for empty MPs, respectively. The Aln-MPs were characterized by a high solubilization of 90% and drug loading efficiency of  $13.6 \pm 0.3\%$ . Immobilization of MPs on the pore walls with the use of rh-collagen solution was found effective as shown by SEM studies (Fig. 1).

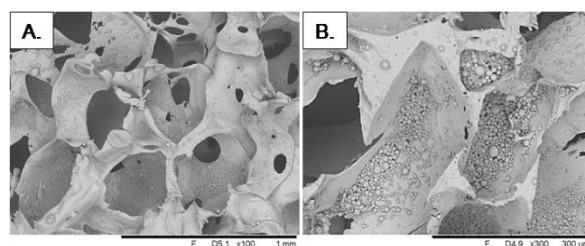


Fig. 1 SEM microphotographs of PLGA scaffolds containing MPs immobilized with rh-collagen type I; mag. 100x (A.) and 300x (B.).

The results of release study show initial slow burst followed by sustained release of Aln; it was correlated with hydrolytic degradation kinetics of MPs. *In vitro* tests confirmed cytocompatibility of PLGA scaffolds modified with Aln-MPs: similar metabolic activity, viability and morphology was found when osteoblast-like MG-63 cells were cultured in the extracts or in pure culture medium.

## CONCLUSION

The study showed that immobilization of MPs loaded with Aln on PLGA scaffolds was successful. Prolonged drug release was achieved and whole system was cytocompatible with osteoblast-like cells. The results suggest that resorbable PLGA scaffolds containing Aln-loaded MPs are promising approach for the treatment of large critical-size bone tissue defects.

## REFERENCES

1. Son J. S. *et al.*, J. Control Release 153:133-140, 2011
2. Harmankaya N. *et al.*, Acta Biomater. 9(6):7064-7073, 2013
3. Posadowska U. *et al.*, Inter J Pharm 485:31-40, 2015

## ACKNOWLEDGMENTS

National Science Centre, Poland (Grant no: 2012/05/B/ST8/00129) provided financial support to this project.

## Composition Structure Relationships in the Anomaly Range of a Tertiary Borate Glass

Kathleen MacDonald<sup>1</sup>, Margaret Hansen<sup>2</sup>, Daniel Boyd<sup>1,3</sup>

<sup>1</sup>School of Biomedical Engineering, Dalhousie University, Canada

<sup>2</sup>Department of Chemistry, Dalhousie University, Canada

<sup>3</sup>Department of Applied Oral Sciences, Dalhousie University, Canada

[kathleen.n.macdonald@dal.ca](mailto:kathleen.n.macdonald@dal.ca)

### INTRODUCTION

Modification of bioactive glasses with strontium oxide has been shown to impart osteoconductive properties through the release of strontium ions in solution, showing potential for use in the treatment of osteoporotic fractures. For use as a biomaterial, a balance must be struck between network disintegration and stability, to provide both ionic release and mechanical stability. Borate based glasses have been shown to be highly tailorable in their degradation, providing potential in this field<sup>1</sup>. Our understanding of borate glass structure however lags behind that of other glass building systems, representing only 2% of publications in the field<sup>2</sup>. Better understanding of the effect of modified content on borate glass structure is needed to understand the changes seen in glass reactivity, specifically in the range of 20-30% modifier additions, where the borate anomaly occurs<sup>3</sup>. This study aims to investigate the effect of compositional changes in a borate glass through the substitution of, therapeutically active SrO, with Na<sub>2</sub>O.

### EXPERIMENTAL METHODS

#### Glass synthesis

Nine tertiary borate glasses were synthesised through equimolar substitution of Na<sub>2</sub>O (0 to 16%) for SrO (30 to 14%). Glass powders were heated to 600°C, for 1 hour, then melted at 1100°C for a further hour before splat quenching. Glass was ground to <45µm and analysed through DSC, XRD (n=3).

#### Structural Analysis

<sup>11</sup>B MAS NMR was performed using a Bruker Avance NMR (11B Larmor frequency = 224.67 MHz) at spinning speeds of 25 and 10 KHz for the centre and sidebands (32 and 4 transients collected respectively).

#### Compositional Analysis

Glass samples were digested using 50 mg of glass powder in 10 ml of 30% ultra trace HCl for 2 hours at 40°C (n=3). Digested glasses were then analysed by ICP-OES for B, Sr and Na content.

### RESULTS AND DISCUSSION

All compositions investigated formed an amorphous glass without evidence of crystallization or APS when analysed through XRD and DSC. While T<sub>g</sub> decreased linearly from 641°C to 520°C with the addition of Na<sub>2</sub>O, significant differences could only be found between the two extremes of the compositional range. The fraction of N4 coordinated boron in the glass network varied from 39.2% to 43.2% in the nine glasses investigated. No definitive effect of the boron anomaly could be seen in the region investigated.

Table 1 shows the post firing compositional changes found in the glass series. A significant change in the borate content was only seen with the 16% strontium composition. Losses of sodium content were greatest in the low sodium glasses; contrary to previous reports of high losses with increasing alkali metal content<sup>3</sup>.

Table 1: Changes in glass composition during glass synthesis expressed in molar percentage

Theoretical Composition			Final Composition		
B <sub>2</sub> O <sub>3</sub>	SrO	Na <sub>2</sub> O	B <sub>2</sub> O <sub>3</sub>	SrO	Na <sub>2</sub> O
70	30	0	67.5	32.5	0
70	28	2	68.4	31.4	0.2
70	26	4	68.9	27.6	3.5
70	24	6	67.8	25.4	6.8
70	22	8	68.5	23.8	7.7
70	20	10	69.2	21.1	9.7
70	18	12	69.7	18.0	12.3
70	16	14	66.0	17.3	16.7
70	14	16	67.4	15.5	17.1

Compositional dependence of glass transition temperature was improved by the use of post firing compositions, shown by regression error mean square values from 8.97 to 6.58. Similarly improvements in linear correlation between boron coordination and composition increased when using for firing compositional analysis with a decrease in regression error mean square values from 1.22 to 1.13.

### CONCLUSION

Significant changes to borate glass composition occur during glass firing process. As glass structure and properties are understood to be composition dependent it is not surprising that these changes affect our ability to predict the relationship between composition, structure and properties. To better understand compositional effects on glass behaviour post fabrication compositional analysis is a valuable tool.

### REFERENCES

1. Hasan S. *et al.*, J Biomed Mater Res Part A 2014;00A: 000-000
2. Mauro J. *et al.*, Int J Appl Glass Sci, 5 [1] 2-15 (2014)
3. Varshneya, Fundamentals of Inorganic Glasses, Elsevier, 1994

### ACKNOWLEDGMENTS

The authors would like to thank the Atlantic Canadian Opportunities Agency for providing financial support to this project.



## INTRODUCTION

An artificial bone for laboratory practices<sup>1</sup> is an advanced composite material that is very useful for many applications such as testing dental implants or orthodontic devices<sup>2</sup>. Three principal advantages can be considered: i) to obtain samples with specific features of trabecular density and cortical thickness that in real bones are subjected to the casualty, ii) to have a bone that maintains its designed properties for long time because it is not subjected to a rapid degrade as in the real case and, finally, iii) to dispose promptly of samples that reproduce the characteristics of different typologies of both animal and human bones.

The first step of this research was to prepare two types of polymeric composites with mechanical properties (flexural and compression elastic modulus) close to the ones of the cancellous and of the cortical human bone. Thereafter bilayer samples - prepared with compact composites polymer and porous polymer, simulating the cortical and the trabecular bone respectively - were evaluated through the measurements of the insertion torque of orthodontic temporary anchorage devices (TADs)<sup>3</sup> and then through their primary stability.

## EXPERIMENTAL METHODS

Trabecular bone was obtained with PMMA polymerized from Methyl Methacrylate monomer (Sigma-Aldrich) and commercial sucrose, 50vol.%, used as porogen. The liquid phase was before added with benzoyl peroxide (4wt.%) used as activator and N,N-methyl-para-toluidine (0.8wt.%) as catalyst and manually mixed with sucrose by mean of a spatula. Then it was inserted in a plastic syringe and compacted and finally maintained at low temperature (4°C) for 24 hours. To remove the porogen, specimens have been leached in hot water for many cycles of low pressure (0.02atm) and atmospheric pressure in order to permit water to penetrate inside the matrix pores.

Compact bone was set with PMMA and alumina trihydrate (ATH), 50vol.%, as reinforcement. To improve the interface between filler and matrix, the manufacturer used an adhesion-promoting additive<sup>4</sup>.

Both the trabecular and compact artificial bone specimens were tested in compression and in flexion with Zwick/Roell Z010 machine (maximum load 10KN), obtaining the stress-strain curve and the elastic modulus of the material.

Final bones samples were prepared spreading a MMA film on the compact bone layer in order to make it adhere to the trabecular specimens. Three kinds of artificial bone with cortical thickness of 1mm, 1.5mm and 2mm were prepared. Inserting torque of TADs on

these samples was evaluated with a digital torsion dynamometer (Cedar, Sugisaki Meter Co. LTD, Japan). Their primary stability was measured with the Zwick/Roell Z0.5 machine (maximum load 500N), after that the bone sample was immobilized to the base of the apparatus, while the TADs abutment was fixed to the mobile head of the machine through a dedicated device. The TADs were submitted to a cycle of load, oscillating at 0.1Hz according to a triangular profile in the range - 5N and +5N. In the meanwhile the TADs displacement was recorded.

## RESULTS AND DISCUSSION

The porous PMMA used as trabecular bone shows an elastic modulus according to the literature values<sup>3</sup>, the 9 samples tested have an mean elastic modulus of 173.0MPa with standard deviation of 39.6.

The composite PMMA-ATH used as compact bone shows an elastic modulus of 10GPa while from literature<sup>5</sup> the mean values are 18.3GPa for mandible and 14.9GPa for maxilla. The mean torque value of the TADs tested is 5Ncm, and their mean value of primary stability is 2.8µm/N as expected.

## CONCLUSION

Artificial bone with porosity and mechanical characteristics comparable to the human bone was prepared. This advanced material also displays a behaviour, evaluated as insertion torque and primary stability of TADs, similar to the one of a natural bone. This material appears therefore very promising as testing bone for mechanical laboratory experiments on TADs.

## REFERENCES

1. Jae-Young Rho *et al.*, Med. Eng. & Phy, 20, 92–102, 1998.
2. M. Migliorati, *et al.*, Europ. J. Orthod., 1–8, 2014.
3. A. Costa *et al.*, Int. J. Adult Orthod. Orthognath. Surg., 13(3), 201–209, 1998.
4. O.A. Stapountzi *et al.*, Composite Sci. Tech., 69, 2015–2023, 2009.
5. W. J. Seong *et al.*, Int. J. Oral Maxillofac. Surg., 38, 1088–1093, 2009.

## ACKNOWLEDGMENTS

The authors are very grateful to Proff. Rodolfo Botter and Marco Capurro for their fundamental suggestions in the preparation of this work.



# Alginate-Based Magnetic Electrospun Matrixes for Potential Hyperthermia Treatment

Yen-Hsuan Chen<sup>1,2</sup>, Wan-Ju Chang<sup>1,2</sup>, Tzer-Min Lee<sup>2,3</sup>, Chi-Hui Cheng<sup>4</sup>, Jui-Che Lin<sup>1,2,3\*</sup>

<sup>1</sup>Department of Chemical Engineering, <sup>2</sup>Medical Device Innovation Center, <sup>3</sup>Institute of Oral Medicine National Cheng Kung University, Taiwan, <sup>4</sup>Chang Gung Memorial Hospital, Chang Gung University, Taiwan  
[jclin@mail.ncku.edu.tw](mailto:jclin@mail.ncku.edu.tw)

## INTRODUCTION

The magnetic electrospun mats were established as an innovative biomaterial for hyperthermia treatment of cancer therapy lately<sup>1,2</sup>. Unlike those surface-modified magnetic nanoparticles that may not firmly adhere onto the tumor site for long-term duration, the magnetic mats with nanofibrous structure can promote cell adhesion and kill the tumor cells directly within an alternating magnetic field (AMF). However, most published magnetic electrospun mats were fabricated using non-biodegradable polymers and organic solvents, which has caused the problem of removal after therapy as well as the suspected biotoxicity issue associated with the residual solvent. Alginate (SA) was utilized in this investigation as the main material for electrospinning because of being biodegradable and water-soluble. The alginate-based electrospun mats were then treated by an ionic or a covalent crosslinking method, then followed by chelation with  $\text{Fe}^{2+}/\text{Fe}^{3+}$  for chemical coprecipitation of  $\text{Fe}_3\text{O}_4$  magnetic nanoparticles. Various qualitative and quantitative analyses for the mats as well as the cytotoxicity and in vitro hyperthermia assay on the  $\text{Fe}_3\text{O}_4$ -SA/PEO (ionic-crosslinked mat) and  $\text{Fe}_3\text{O}_4$ -SA/PVA (covalent-crosslinked mat) were examined.

## EXPERIMENTAL METHODS

SA solution (3%, w/w), PEO solution (4%, w/w) and PVA solution (17%, w/w) were prepared. To prepare two kinds of electrospinning solutions, SA/PEO and GA/SA/PEO/PVA solutions with solid content weight ratios of 1/2.5 and 1.7/1/0.5/2 were used, respectively. For the  $\text{Fe}^{2+}$  ionic crosslinking method, the SA/PEO mat was immersed in  $\text{FeCl}_2 \cdot 4\text{H}_2\text{O}$  and  $\text{FeCl}_3 \cdot 6\text{H}_2\text{O}$  ( $\text{Fe}^{2+}/\text{Fe}^{3+}$  molar ratio: 1/2) for 2 hr in nitrogen purging condition. To prepare the covalently crosslinked mat, the GA/SA/PEO/PVA mat was crosslinked in the presence of  $\text{HCl}(\text{aq})$  vapour in a sealed petri dish at  $45^\circ\text{C}$  for 24 hr. The obtained crosslinked GA/SA/PEO/PVA mat was then immersed in ultrapure water at  $37^\circ\text{C}$  for 3 days to remove most amount of PEO, uncrosslinked SA and PVA, unreacted GA and HCl.

For the fabrication of magnetic electrospun mats, the SA/PEO and the SA/PVA mats were separately immersed in stoichiometric excess amounts of  $\text{FeCl}_2 \cdot 4\text{H}_2\text{O}$  and  $\text{FeCl}_3 \cdot 6\text{H}_2\text{O}$  ( $\text{Fe}^{2+}/\text{Fe}^{3+}$  molar ratio: 1/2) for 2 hr with nitrogen purging. The 37%  $\text{NH}_4\text{OH}$  solution was added drop-wise to the mixture with vigorous stir for 5 min and 30 min, respectively, to form  $\text{Fe}_3\text{O}_4$  *in situ*.

The magnetic electrospun mats were characterized by FTIR, SEM, TEM, thin film X-ray diffraction ICP and

SQUID. The cytotoxicity assay was performed with MTT method. The *in vitro* hyperthermia effect of the samples were carried out in the AMF in which the tube was filled with 0.5 mL culture medium containing  $3 \times 10^5$  A-549 cells. The heating process was performed for 15 min and the temperature was maintained at  $44\text{--}45^\circ\text{C}$ .

## RESULTS AND DISCUSSION

The TEM micrographs as well as the ICP results and XRD pattern of the alginate-based magnetic electrospun mats indicated the successful incorporation of magnetic nanoparticles. In addition, the FTIR results have shown that the PEO added has been removed after immersion in different aqueous solution for electrospun mats. In addition, the ionic crosslinked magnetic electrospun  $\text{Fe}_3\text{O}_4$ -SA/PEO mat started swelling after contacting with the culture medium and cracked into small pieces after 1-day culture. Henceforth, only the covalent crosslinked  $\text{Fe}_3\text{O}_4$ -SA/PVA mat was analyzed for in vitro hyperthermia experiments.

The hyperthermia experiment indicated that the cell viability for all samples containing  $\text{Fe}_3\text{O}_4$  were greatly reduced after the use of AMF heating. (Fig 1)

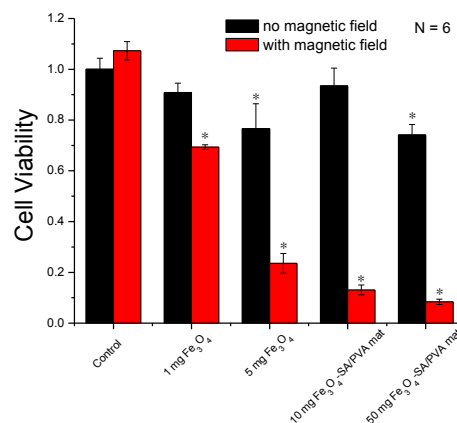


Fig 1. The in vitro hyperthermia effect of the control (PBS only), SA/PVA mat,  $\text{Fe}_3\text{O}_4$  nanoparticles and  $\text{Fe}_3\text{O}_4$ -SA/PVA mat.

## CONCLUSION

The hyperthermia effect showed the  $\text{Fe}_3\text{O}_4$ -SA/PVA mat had greater impact to tumor cells than the  $\text{Fe}_3\text{O}_4$  nanoparticles. Such magnetic mats could effectively lower the viability of tumor cells in the AMF and are of potential for hyperthermic treatment.

## REFERENCES

1. Lin TC *et al.*, Acta Biomater. 8:2704-11, 2012
2. Lin TC *et al.*, J Biomat Sci. Polym Ed 24 1152-63, 2013





## Antitumor Effects for Osteosarcoma Cells by Carbon Nanotubes

Kaoru Aoki<sup>1</sup>, Masanori Okamoto<sup>1</sup>, Seiji Takanashi<sup>1</sup>, Shinsuke Kobayashi<sup>1</sup>, Hiroki Nomura<sup>1</sup>, Manabu Tanaka<sup>1</sup>, Takashi Takizawa<sup>1</sup>, Hiroyuki Kato<sup>1</sup>, Yuki Usui<sup>2</sup>, Hisao Haniu<sup>3</sup>, Naoto Saito<sup>3</sup>.

<sup>1</sup> Department of Orthopaedic Surgery, Shinshu University, Japan

<sup>2</sup> Sports Medical Center of Aizawa Hospital, Matsumoto, Japan

<sup>3</sup> Institute for Biomedical Sciences, Shinshu University Interdisciplinary Cluster for Cutting Edge Research, Japan

[kin29men@shinshu-u.ac.jp](mailto:kin29men@shinshu-u.ac.jp)

### INTRODUCTION

Sarcomas such as osteosarcoma are treated with surgery and chemotherapy by anticancer drugs. The anticancer drugs cause various severe side effects, and prospective enough effects may not be obtained. So-called nano-particles smaller than cells have a property to enter cells and they are expected as drug delivery system (DDS)<sup>1</sup>. We heretofore reported biocompatibility and safety of the carbon nanotubes (CNT)<sup>2, 3</sup>. We report potential as DDS for chemotherapy to osteosarcoma cells with CNTs.

### EXPERIMENTAL METHODS

The 143B cells (human osteosarcoma cell line) were seeded at  $5.0 \times 10^5$  cells/10cm culture plate. After 24 hours, the culture medium was renewed to the medium contained 1  $\mu\text{g/ml}$  or 10  $\mu\text{g/ml}$  multi-walled CNT (MWCNT). Doxorubicin hydrochloride (DOX) (0.1  $\mu\text{M}$ , 1.0  $\mu\text{M}$ , 5.0  $\mu\text{M}$ ) was used as positive control. Each group was  $n=3$ . After more 24 hours, we observed the cells with light microscope and counted the number of 143B cells of each plate.

### RESULTS AND DISCUSSION

In the light microscope images of the 143B cells that we added MWCNTs before 24 hours, the MWCNTs were taken in the cells. In the MWCNT 10  $\mu\text{g/ml}$  group, much MWCNTs were taken in the 143B cells than the MWCNT 1  $\mu\text{g/ml}$  group. The cell number after 24 hours culture was  $23.3 \times 10^5$  cells/plate in control,  $10.3 \times 10^5$  cells/plate in DOX 0.1  $\mu\text{M}$  group,  $5.6 \times 10^5$  cells/plate in 1.0  $\mu\text{M}$  group,  $2.8 \times 10^5$  cells/plate in 5.0  $\mu\text{M}$  group,  $21.3 \times 10^5$  cells/plate MWCNT 1  $\mu\text{g/ml}$  group and  $16.3 \times 10^5$  cells/plate MWCNT 10  $\mu\text{g/ml}$  group (Fig1).

Because CNTs enter into sarcoma cells, we think that CNTs have possibility to improve antitumor effects of chemotherapy as DDS of anticancer drugs.

Number of the 143B cells

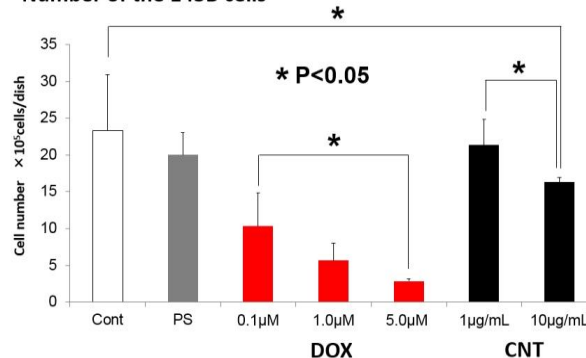


Fig1. Number of the 143B cells. PS; Polysorbate (surfactant). DOX; Doxorubicin. CNT; Multi-walled Carbon nanotube. MWCNTs inhibited the cellular proliferation in concentration-dependency

### CONCLUSION

When the MWCNTs are added to the osteosarcoma cell line; 143B cells, the MWCNTs are taken into the cells and inhibited the cellular proliferation in concentration-dependency. By adhering anticancer drugs to the MWCNTs, we expect to improve invasive efficiency to sarcoma cells of the anticancer drugs, to enhance the chemotherapeutic effect and to reduce the chemotherapeutic side effects

### REFERENCES

1. Wilczewska AZ. *et al.*, Pharmacol Rep. 64:1020-37, 2012
2. Narita N. *et al.*, Nano Lett. 9:1406-13, 2009
3. Hara K, *et al.*, Materials Today. 14:434-440, 2011

### ACKNOWLEDGMENTS

This work was supported by JSPS KAKENHI Grant Number 26861180.



## Electrically-Triggered Delivery System for Regional Chemotherapy

Katarzyna Krukiewicz<sup>1</sup>, Magdalena Cichy<sup>1</sup>, Barbara Bednarczyk-Cwynar<sup>2</sup>, Piotr Ruszkowski<sup>3</sup>,  
Tomasz Jarosz<sup>1</sup>, Mieczysław Łapkowski<sup>1</sup>, Jerzy K. Żak<sup>1</sup>

<sup>1</sup>Department of Physical Chemistry and Technology of Polymers, Silesian University of Technology, Poland

<sup>2</sup> Department of Organic Chemistry, Poznan University of Medical Sciences, Poland

<sup>3</sup> Department of Pharmacology, Faculty of Pharmacy, Poznan University of Medical Sciences, Poland

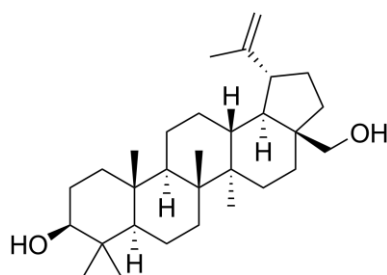
[katarzyna.krukiewicz@polsl.pl](mailto:katarzyna.krukiewicz@polsl.pl)

## INTRODUCTION

Chemotherapy, in which potent drugs are used to destroy cancer cells, carries a high risk of damage to the healthy tissues. The reduction of harmful effects of this method of cancer treatment can be achieved through the use of regional chemotherapy – comprising the administration of anti-cancer agents directly at the tumour site<sup>1</sup>. It is crucial to provide a method of controlled delivery in which both the amount of drug and the time of administration can be regulated.

Conjugated polymers are considered promising materials for use as matrices for drug delivery systems. In contrast to the physical entrapment, conjugated polymers allow controlled, reversible electrostatic immobilisation of a wide range of biologically active compounds<sup>2,3</sup>. Change in their reduction-oxidation state as a result of electrical stimulation is followed by the release of a precise amount of drug<sup>4</sup>.

In this study, we describe the synthesis and performance of conjugated polymer matrix as a reservoir for betulin – naturally occurring triterpene with high anti-cancer activity<sup>5</sup>.



Scheme 1. Chemical structure of betulin.

## EXPERIMENTAL METHODS

Betulin was purchased from “Natchem” company<sup>6</sup>. Cyclic voltammetry (CV) was utilised for the fabrication and in situ analysis of conjugated polymer/betulin composite layers. The release of betulin from the composite was followed by time-resolved UV-Vis spectroscopy. The biological activity of released betulin solutions was determined using chosen cancer cell lines. SEM images were collected and used to track the changes of composite morphology in the process of drug release.

## RESULTS AND DISCUSSION

The in-situ entrapment of betulin into the structure of growing polymer matrix was proven to be an efficient method of immobilization resulting in the formation of conjugated polymer/betulin composite.

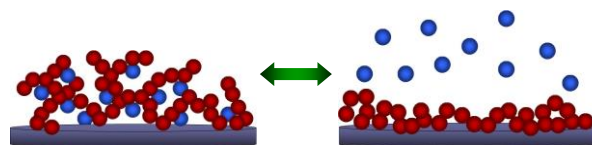


Fig.1. The schematic representation of ion-exchange properties of conjugated polymers.

The release of betulin immobilised in conjugated polymer matrix was performed under spontaneous (passive) and electro-assisted (active) modes in PBS. Through the modification of synthesis conditions it was possible to modify the drug capacity of matrix as well as the proportions of drug released *via* passive and active modes. The range of applied reduction potentials have been optimized – low enough to start the process of release but not too low, to prevent the process of matrix degradation.

## CONCLUSION

Conjugated polymer/betulin composite was shown to be a promising material for electrically-triggered delivery systems applied in regional chemotherapy.

## REFERENCES

1. Fung L.K. Qualtzman W.M., Adv Drug. Deliv. Rev., 26:209–230, 1997.
2. Wadhwa R. Lagenaur C.F., Cui X.T., J. Control. Release 110:531-541, 2006.
3. Krukiewicz K. Zak J.K., J. Mater. Sci. 49:5738-5745, 2014.
4. Alizadeh N., Shamaeli E., Electrochim. Acta 130: 488-496, 2014.
5. Bednarczyk-Cwynar B., Mini Rev. Org. Chem. 11: 251-252, 2015.
6. [www.natchem.pl](http://www.natchem.pl)

## ACKNOWLEDGMENTS

The authors would like to thank the Polish National Science Centre (PRELUDIUM, 2012/07/N/ST5/01878), Foundation for Polish Science together with European Social Fund (INTER'2015, 30/UD/SKILLS/2015).

## Targeted Cancer Therapy

Monika Dzieciuch-Rojek<sup>1</sup>, Mariusz Kępczyński<sup>1</sup>, Maria Nowakowska<sup>1</sup>, Marcin Majka<sup>2</sup>

<sup>1</sup> Faculty of Chemistry, Jagiellonian University, Cracow, Poland

<sup>2</sup>Department of Transplantation, Jagiellonian University, Collegium Medicum, Cracow, Poland  
[dzieciuc@chemia.uj.edu.pl](mailto:dzieciuc@chemia.uj.edu.pl)

### INTRODUCTION

Liposomes are widely studied as drug delivery systems in cancer treatment. The use of drug delivery systems (DDSs) such as liposomes can alter drug pharmacokinetics and biodistribution. The multidrug resistance remains (MDR) a major obstacle of chemotherapy. The resistance mechanism in MDR cells is mainly overexpression of P-glycoprotein (P-gp) on the plasma membrane. Itraconazole (ITZ)- triazole antifungal agent against a broad spectrum of fungal species has potential for modulating MDR [1]. The folate receptor (FR) is often overexpressed in cancers – it has frequently been exploited for the specific delivery of folate-linked drugs into cancer cells.

The aim of our study was to create hybrid drug delivery system: 5-fluorouracil (5-FU, antineoplastic drug) encapsulated in liposomes itraconazole and folic acid modified. The interaction between liposomes and itraconazole was checked using various methods. To evaluate the therapeutic effect of studied hybrid system the biological studies was performed.

### EXPERIMENTAL METHODS

Liposomes were prepared by hydration of the dry lipid film, followed by sonication. The lipid bilayers composed of 2-oleoyl-1-palmitoyl-sn-glycero-3-phosphocholine (POPC) and itraconazole at various molar ratios. Folate-targeted liposomes consisted of 99,5 mole % POPC and 0,5 mole % folate-PEG2000-lipid. Langmuir monolayer experiments and Brewster angle microscopy (BAM) of the POPC/ITZ mixtures displayed the highest content of ITZ in lipid monolayer. Fluorescence methods were used to estimate the position of ITZ in PC bilayer. To check the stability and estimate the size of liposomes with different content of ITZ the dynamic light scattering measurements were used. The morphology of bilayer structures formed in dispersions was inspected using a cryogenic transmission electron microscopy and atomic force microscopy. Encapsulation efficiency of 5-FU in liposomes were determined by spectroscopy Uv-Vis[2]. The cytotoxic activities of hybrid drug delivery system (DDS) in Caco-2 cancer cells were determined by MTS assay. Cellular uptake studies of DDS was measured by fluorescence microscopy.

### RESULTS AND DISCUSSION

Based on the results obtained with the application of BAM microscopy was found that the monolayers containing 10-15 mol% of itraconazole are completely mixes with POPC. At higher concentrations of ITZ the interactions between POPC and itraconazole are unfavorable, which leads to the phase separation and expelling of itraconazole from POPC film. Using fluorescence method and doxil-spin labeled molecules have been shown that the ITZ is located at ca. 13 Å from the center of the bilayer [3]. The ITZ modified liposomes and unmodified liposomes are comparatively stable. The antiproliferative effect of studied DDS in Caco-2 cells is similar to free 5-FU.

### CONCLUSION

In conclusion, we have demonstrated the use of folic acid as a ligand for targeting of liposomes to tumor cells. Incorporating itraconazole into liposomes with 5-fluorouracil could be an attractive approach not only for improving drug efficacy and reduction of side effects but mainly to reverse P-gp- mediated drug resistance.

### REFERENCES

1. Biol.Pharm.Bull. 22 (12) 1355-1359 (1999)
2. Chem. Biol. Drug Des, 2011, 78, 57–72
3. The Journal of Physical Chemistry B 2010, 114, 15483–15494

### ACKNOWLEDGMENTS

Authors acknowledges the financial support from the project Interdisciplinary PhD Studies “Molecular Sciences for Medicine” (co-financed by the European Social Found within the Human Capital Operational Programme).



## miRNA Treatment for Bone Metastasis inducing Prostate Cancer

Marine J. Chalanqui<sup>1</sup>, Sreekanth Pentlavalli<sup>2</sup>, Stephen P. Loughran<sup>1</sup>, Michelle O'Doherty<sup>2</sup>, Philip Chambers<sup>2</sup>, Nicholas Dunne<sup>2</sup> and Helen O. McCarthy<sup>1</sup>.

<sup>1</sup>School of Pharmacy, Queen's University Belfast, Northern Ireland

<sup>2</sup>School of Mechanical and Aerospace Engineering, Queen's University Belfast, Northern Ireland  
[mchalanqui01@qub.ac.uk](mailto:mchalanqui01@qub.ac.uk)

### INTRODUCTION

Prostate cancer (PCa) is one of the most common types of cancer, affecting 15% of the male population worldwide, and a major cause of cancer-related mortality in men<sup>1</sup>. This high rate of mortality is primarily due to metastasis of the primary tumor<sup>2</sup>, 70% of which is primarily localized in the bone.<sup>3</sup>

Metastatic prostate cancer cells have the ability to disrupt the equilibrium of normal bone remodeling processes and can be characterized as either osteolytic or osteoblastic<sup>4</sup>. Metastatic lesions from prostate cancer are predominantly osteoblastic<sup>4</sup>. During osteoblastic bone metastases, the equilibrium between bone resorption and bone formation is disrupted in favor of bone formation<sup>4</sup>. Patients suffer severe bone pain and the poor bone quality often leads to bone fractures<sup>4</sup>. Once tumors metastasise to bone, they are effectively incurable. For patients with bone metastatic disease current therapeutic strategies are limited to palliative treatments to minimise the rate of bone degradation and patient pain<sup>5</sup>.

Aberrant microRNA (miRNA) expression is a common feature of human cancer<sup>5</sup>. miRNA34a (miR-34a) has previously been shown to be down-regulated in PCa cells<sup>6</sup>. Due to its strong anti-tumor and anti-metastatic effects<sup>5</sup>, and consequential potential as a negative regulator of PCa cells, miR-34a represents a promising target to modulate PCa induced-bone metastatic disease.

Therefore up-regulation of miR-34a via nanoparticles (NPs) from a biomaterial scaffold should elicit a therapeutic effect in disseminated PCa. In this study we propose a novel, thermo-responsive alginate-g-PNIPAAm (Alg-g-P(NIPAAm)) hydrogel for non-invasive local delivery of NPs incorporating an amphipathic peptide (RALA) that serves as a delivery vehicle for DNA expressing miR-34a.

### EXPERIMENTAL METHODS

*Preparation of hydrogel:* Alginate (Alg) and NIPAAm were synthesized via free radical polymerisation to form a Alg-g-P(NIPAAm) hydrogel.

*Formulation of RALA/miR-34a NPs:* The RALA/miR-34a NPs are formed by self-assembly via electrostatic interactions. Particle size and zeta potential (ZP) were measured using a Malvern Zetasizer Nano ZS to determine the physiochemical characteristics.

*Clonogenic Assay:* Colony forming assay was performed using the crystal violet method. Confluent

PC-3 prostate cancer cells were transfected with RALA/miR-34a NPs for 6 h then returned to growth media. After 48 h cells were seeded in a 6-well plate at a density of 200 and 500 cells per well. Cells were cultured for 2 weeks before crystal violet staining.

*Drug delivery study:* P(Alg-g-NIPAAm) was loaded with RALA/miR-34a plasmid. These drug delivery systems were placed in trans-wells adapted for 24-well plate and immersed in water or culture media at 37°C. The release profile of the miR-34a was assessed by withdrawing the supernatant at different time points and measuring nucleic acid content using the picogreen assay.

### RESULTS AND DISCUSSION

Preliminary studies demonstrate that the Alg-g-P(NIPAAm) solution exhibits a thermo-responsive behaviour with a lower critical solution transition (LCST) about 32°C. Thus, the hydrogel is liquid at temperatures below 32°C and gels at higher temperatures. Consequently, the hydrogel can be injected into the body and act as a depot for the delivery of the therapeutic NPs. Work is currently ongoing to characterize the size, charge and shape of the RALA/miR-34a NPs. This is necessary to ensure the NPs exhibit optimal physical characteristics to ensure efficient transfection. Release studies are ongoing to determine the NP delivery from the Alg-g-P(NIPAAm) hydrogel. For our therapy we are aiming to have an initial burst release of the NPs, followed by a maintenance effect, ideally for several months. We are also examining the molecular effects of the miR34a therapy on PC-3 tumours.

### CONCLUSION

miR-34a has exhibits a potent anti-cancer effect *in vitro* and *in vivo*. The development of a new formulation for local delivery to bone sites using a thermo-responsive hydrogel presents a therapeutic treatment for those with disseminated prostate cancer.

### REFERENCES

- 1 M.M. Center *et al.*, Eur Urol. 61: 1079-92, 2012
- 2 S. Nandana *et al.*, Am J Clin Exp Urol. 2: 92-101, 2014
- 3 R.E. Coleman *et al.*, Clin Can Res. 12: 6243s-9s, 2006
- 4 Ye *et al.*, J Mol Med. 20)103-111, 2007
- 5 R. Munker *et al.*, Clin Sci. 121: 141-158, 2011
- 6 C. Lui *et al.*, Nat Med. 17: 211-215, 2011

### ACKNOWLEDGMENTS

Funding via MRC Case Award (MR/L015269/1)





# Development of a Polymeric Conjugate Foreignizing Tumor Cells for Targeted Immunotherapy *in Vivo*

Hong Yeol Yoon<sup>1,2</sup>, Young-Ho Lee<sup>3</sup>, Jung Min Shin<sup>1</sup>, Tae Woo Kim<sup>3,\*</sup>, Jae Hyung Park<sup>1,4,\*</sup>

<sup>1</sup>School of Chemical Engineering, Sungkyunkwan University, Republic of Korea

<sup>2</sup>Biomedical Research Institute, Korea Institute of Science and Technology, Republic of Korea

<sup>3</sup>Department of Biochemistry and Molecular Biology, College of medicine, Korea University, Republic of Korea

<sup>4</sup>Department of Health Science and Technology, SAIHST, Sungkyunkwan University, Republic of Korea

[jmabcd@skku.edu](mailto:jmabcd@skku.edu)

## INTRODUCTION

Antigen-specific CD8<sup>+</sup> cytotoxic T lymphocytes (CTLs) are key factors of immunological rejection in transplantation as well as cancer immunotherapy<sup>1</sup>. However, Most of tumors are not immunologically rejected because they have self antigens<sup>2</sup>. In this study, we hypothesized that “foreignizing” tumor cells by delivering non-self foreign antigens into the tumors would result in rejection by foreign antigen-reactive CTLs. In an attempt to demonstrate this hypothesis, we prepared a polymeric conjugate consisting of hyaluronic acid (HA) as the tumor targeting ligand and ovalbumin (OVA) as a model foreign antigen.

## EXPERIMENTAL METHODS

HA-OVA conjugate was prepared by using reductive amination in presence of NaBH<sub>3</sub>CN as a reducing agent. Fluorescein isothiocyanate (FITC) labelled HA-OVA conjugates were used for further experiments.

Cellular uptake behaviour of HA-OVA was monitored using OVA-FITC and HA-OVA-FITC in HPV-16 E7-expressing mouse cervical cancer model (TC-1) cells for 2hr.

*In vitro* antigen presentation and CTL-mediated apoptosis of TC-1 cells were observed using FACS Calibur flow cytometry. *In vivo* biodistribution and anti-tumor efficacy of conjugate were carried out to evaluate *in vivo* effect of HA-OVA conjugate using tumor-bearing mice.

## RESULTS AND DISCUSSION

In this study, OVA were chemically conjugated to HA via reductive amination between the reducing end group of HA and the amino group of OVA in the presence of NaBH<sub>3</sub>CN as a reducing agent.

In cellular uptake experiment, HA-OVA-FITC showed stronger fluorescence signal at the intracellular level than OVA-FITC (figure 1-a). The cellular uptake of conjugate was quantified by using flow cytometry (figure 1-b). These result showed that the HA surface of conjugate accelerated its uptake by TC-1 tumor cells via receptor-mediated endocytosis.

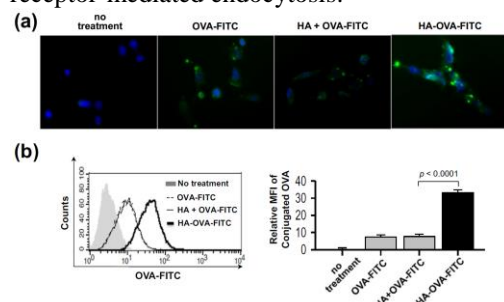


Figure 1. Cellular uptake behavior of the conjugate.

(a) Cellular images were observed by using fluorescence microscopy and (b) the cellular uptake was quantified by flow cytometry.

We carried out whether the delivered OVA could be processed and presented on the TC-1 cell surface (figure 2-a) and whether the conjugate could facilitate OVA-specific CTL-mediated killing of tumor cells (figure 2-b). These results suggest that the *in vitro* delivery of OVA by using conjugated ligand (HA) efficiently provokes CTL-induced apoptotic death of target tumor cells.

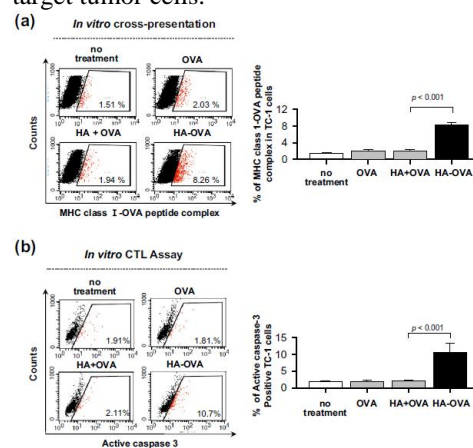


Figure 2. (a) *In vitro* antigen presentation. (b) CTL-mediated apoptosis of TC-1 tumor cells was analysed by flow cytometry.

## CONCLUSION

In this study, we demonstrate that a foreign antigen (OVA) decorated with HA is capable of targeting tumor site and generating anti-tumor effect by provoking immune rejection against tumor that present foreign antigens. This foreign antigen-delivery system may play a role as a platform technology for treatment of various intractable diseases.

## REFERENCES

1. P. Friedl *et al.*, Nat. Rev. Immunol. 5:532-545, 2005
2. N.K. Nanda *et al.*, Cell 82:13-17, 1995

## ACKNOWLEDGMENTS

This research was supported by funding from the National Research Foundation of Korea (20100027955, 2013K1A1A2A02076442, 2013M3A9D3045881, 2012R1A2A2A01007527), and the Korea Healthcare Technology R&D Project (HI11C-0052-030013).

Łukasz Łapok<sup>1</sup>, Arkadiusz Gut<sup>1</sup>, Maria Nowakowska<sup>1</sup><sup>1</sup>Faculty of Chemistry, Jagiellonian University, Ingardena 3, 30-060 Kraków, Poland  
[lapok@chemia.uj.edu.pl](mailto:lapok@chemia.uj.edu.pl)

## INTRODUCTION

Photodynamic therapy (PDT) is a well-established treatment for certain forms of cancer and skin diseases [1]. It is a noninvasive alternative to conventional treatments like surgical tumor resection, chemo- and radiotherapy. Cancerous cells are lysed by the combined action of light, oxygen present in the tissues and dye molecules (photosensitizers) which are administered intravenously or topically. The photosensitizer is activated by a light of a suitable wavelength which after its excitation to the singlet excited state ( $S_1$ ) is followed by intersystem crossing (ISC) resulting in the formation of highly populated triplet state ( $T_0$ ) photosensitizer. The excited triplet state of a given photosensitizer may undergo two different processes. The first process results in the production of singlet oxygen (type II), via energy transfer, while the other leads to the formation of radicals (viz.  $OH^\bullet$ ,  $HO_2^\bullet$ ,  $O_2^{\bullet-}$ ) via electron transfer (Type I and III). Formation of oxygen-containing radicals requires the photosensitizer to undergo oxidation. The knowledge of the ability of the photosensitizer to undergo redox processes (redox potentials) is crucial for the understanding of the photosensitization process.

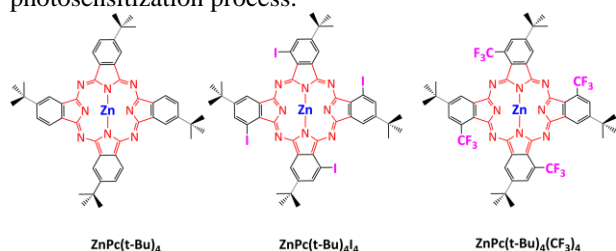


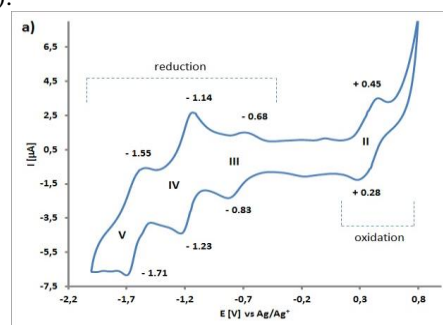
Figure 1. Structures of the studied photosensitizers.

## EXPERIMENTAL METHODS

Two newly synthesized photosensitizers were used, viz. **ZnPc(t-Bu)<sub>4</sub>I** and **ZnPc(t-Bu)<sub>4</sub>(CF<sub>3</sub>)<sub>4</sub>**. Their redox potentials were compared. Cyclic voltammetry (CV) was performed on PalmSens<sup>3</sup> potentiostat/galvanostat and was conducted in deoxygenated dichloromethane or N,N-dimethylformamide. Tetrabutylammonium tetrafluoroborate (TBAF, Fluka,  $\geq 99.0\%$  electrochemical grade) was used as a supporting electrolyte (0.1 M). Cyclic voltammetry experiments were performed on saturated solutions (5 mL) of the respective phthalocyanines (Pcs). The working electrode was either platinum disc (1.6 mm in diameter) or carbon glassy electrode (5 mm in diameter). Spectroelectrochemical experiments were performed in a quartz cell of 0.5 mm optical length with the Pt gauze working electrode, the Pt counter electrode and the Ag/Ag<sup>+</sup> reference electrode (connected to a PalmSens<sup>3</sup>).

## RESULTS AND DISCUSSION

Cyclic voltammograms (CV) of the studied photosensitizers showed a number of one-electron redox processes, all of them being ring-centered events (Fig.2).

Figure 2. Cyclic voltammogram of **ZnPc(t-Bu)<sub>4</sub>I<sub>4</sub>**.

CV measurements of the CF<sub>3</sub> substituted zinc phthalocyanine, viz. **ZnPc(t-Bu)<sub>4</sub>(CF<sub>3</sub>)<sub>4</sub>**, revealed four one-electron reductions and two one-electron oxidations. In general, the CF<sub>3</sub> substituted phthalocyanine is easier to reduce and harder to oxidize than the phthalocyanine counterpart having no CF<sub>3</sub> groups, viz. **ZnPc(t-Bu)<sub>4</sub>**, supporting the notion that trifluoromethyl substituents have a strong electron-withdrawing effect on the phthalocyanine macrocycle. CV measurements of **ZnPc(t-Bu)<sub>4</sub>I<sub>4</sub>** revealed three one-electron reductions and two one-electron oxidations. Spectroelectrochemistry allowed for direct observation of both  $\pi$ -cation and  $\pi$ -anion radicals which formed electrochemically.

## CONCLUSION

CV measurements and spectroelectrochemistry revealed that all studied Pcs undergo only ring-centered redox processes. The  $\pi$ -cations of **ZnPc(t-Bu)<sub>4</sub>(CF<sub>3</sub>)<sub>4</sub>** proved to be stable species, while electrochemical oxidation of **ZnPc(t-Bu)<sub>4</sub>I<sub>4</sub>** resulted in gradual degradation of the phthalocyanine photosensitizer.

## REFERENCES

- O'Connor A. *et al.*, Porphyrin and nonporphyrin photosensitizers in oncology: preclinical and clinical advances in photodynamic therapy, *Photochem. Photobiol.* 85:1053–1074, 2009.
- Nyokong T., Electronic Spectral and Electrochemical Behavior of Near Infrared Absorbing Metallophthalocyanines, *Struct Bond* 135:45–88, 2010.

## ACKNOWLEDGMENTS

Work supported by NCN grant, DEC-2011/03/D/ST5/05910

## Alginate-Based Matrix as 3D *in vitro* Model to Investigate EMT and its Reversion

Sílvia J Bidarra<sup>1,2</sup>, Sara Rocha<sup>3</sup>, Patrícia Oliveira<sup>3</sup>, Carla Oliveira<sup>3</sup>, Cristina C. Barrias<sup>1,2</sup>

<sup>1</sup>IS – Instituto de Inovação em Saúde, Universidade do Porto, Portugal

<sup>2</sup>INEB - Instituto de Engenharia Biomédica, Portugal,

<sup>3</sup>Institute of Molecular Pathology and Immunology of the University of Porto (IPATIMUP), Portugal

[sbidarra@ineb.up.pt](mailto:sbidarra@ineb.up.pt)

### INTRODUCTION

EMT is a biologic process in which epithelial cells (E) lose their polarity and specialized cell-cell contacts, acquiring a mesenchymal phenotype (M) with enhanced migratory and invasion capacity<sup>1</sup>. EMT is crucial for cancer invasion, and reversion of this phenotype is decisive for metastases establishment. Several evidences point to the inter-conversion between E and M states in cancer, with acquisition of a metastable and potentially more aggressive phenotype. The study of such transitions and their implications in cancer progression could greatly benefit from advanced 3D *in vitro* models of EMT. By creating greater similarity with *in vivo* scenarios, such 3D models are likely to generate useful tools to efficiently identify and test anti-cancer therapeutics. Here we propose a new *in vitro* model of EMT and its reversion, combining inducible epithelial cell lines (EpH4) with tunable 3D matrices. Alginate hydrogels modified with cell-adhesion moieties (RGD peptides) were used to partially recapitulate the complexity of the native extracellular matrix (ECM)<sup>2</sup>.

### EXPERIMENTAL METHODS

Near-normal mouse mammary epithelial cells (EpH-4, E cells) were entrapped within 1wt-% RGD-modified alginate hydrogels prepared by internal gelation<sup>3</sup>. To induce EMT, cell-loaded alginate matrices were cultured in the presence of TGF- $\beta$ 1 during 1 week (M cells). As a control, E cells were maintained in cell culture medium without TGF- $\beta$ 1. For reversion, M cells were further cultured for 7 days in culture medium without TGF- $\beta$ 1. To monitor the occurrence of EMT and its reversion in 3D, cell behavior was analysed at different levels, namely in terms of viability (Live/Dead assay); metabolic activity (resazurin assay); proliferation (Ki-67 immunostaining), organization (F-actin staining); phenotype (expression of E markers, E-cadherin; and M markers, fibronectin,  $\alpha$ -SMA); MMPs activity (gelatin zymography). Gene expression of epithelial (CDH1, Occludin) and mesenchymal (CDH2, vimentin) markers, and EMT inducers (Zeb2 and Twist1) was analysed by real-time PCR.

### RESULTS AND DISCUSSION

The mild alginate cross-linking conditions enabled the establishment of 3D cultures with high cell viability. In non-induced cells, E cells proliferated along 7 days in culture (Ki-67 positive) and formed multicellular spheroids. Moreover, E cells expressed E-cadherin at the membrane. After 7 days in culture, several E cells

spheroids showed a central clearing and formation of lumen surrounded by a layer of cells, characteristic of epithelial morphogenesis. On the other hand, induced cells formed smaller cell aggregates and presented lower metabolic activity than E cells. M cells presented E-cadherin delocalization to the cytoplasm and expressed fibronectin and  $\alpha$ -SMA, which are features of mesenchymal-like cells. At the gene level, there were no significant alterations in the expression of epithelial markers, CDH1 and Occludin, between E and M cells. On the other hand, both mesenchymal markers (CDH2 and vimentin) and EMT-related transcription factor Zeb-2 were significantly upregulated in M cells. The ability of induced cells to secrete MMPs was also evaluated. The results showed an enhancement in MMP9 secretion by M cells comparing to E cells at day 7, which has been associated with cell migration and invasion of carcinoma cells. By removing the TGF- $\beta$ 1 stimulus after EMT, i.e. after 7 days of culture, we observed a partial reversion from a mesenchymal to an epithelial-like phenotype with cells presenting an intermediate state between E and M. For instance, we observed E-cadherin presence at cell membrane and  $\alpha$ -SMA expression in the cell cytoplasm and a decrease in MMP9 secretion.

### CONCLUSION

In conclusion, we were able to establish a 3D *in vitro* model of TGF- $\beta$ 1-induced EMT and its reversion, using RGD-modified alginate hydrogels that provide a well-defined and tunable ECM-like microenvironment.

### REFERENCES

- [1] Thiery JP. Epithelial-mesenchymal transition in tumour progression. *Nat Rev Cancer* 2002, 2: 442-54.
- [2] Bidarra SJ, Barrias CC, Granja PL. Injectable alginate hydrogels for cell delivery in tissue engineering. *Acta Biomater* 2014, 10: 1646-62.
- [3] Bidarra SJ, Barrias CC, Fonseca KB, Barbosa MA, Granja PL. Injectable in situ crosslinkable RGD-modified alginate matrix for endothelial cells delivery. *Biomaterials* 2011, 32: 7897-904.

### ACKNOWLEDGMENTS

Portuguese Foundation for Science and Technology (FCT) for post-doctoral grant SFRH/BPD/80571/2011. FundoEuropeu de Desenvolvimento Regional, Programa Operacional Factores de Competitividade-COMPETE, Quadro de Referência Estratégico Nacional, and Fundo Social Europeu [Pest-C/SAU/LA0002/201



# Modelling of Antimetastatic Agent NAMI-A Fate after Serum Administration

Klaudyna Śpiewak, Małgorzata Brindell

Faculty Chemistry, Jagiellonian University of Kraków, Poland  
[klaudyna.spiewak@gmail.com](mailto:klaudyna.spiewak@gmail.com)

## INTRODUCTION

Imidazolium trans-tetrachlorodimethylsulfoxide-imidazolruthenate(III), NAMI-A, a novel antimetastatic ruthenium complex which successfully completed phase I clinical trial<sup>1</sup>. NAMI-A was investigated towards affinity to transferrin (Tf), whether Tf-Ru adducts might be formed after its intravenous injection. Studies were focused on the holotransferrin due to its favoured binding to transferrin receptor. Transferrin receptor can be a targeting molecule for cancer therapy due to its overexpression in rapidly proliferating cells. In this study undermentioned issues were addressed: i) the influence of the iron occupied binding site on the overall association constant and Ru content in ruthenated Tf, ii) the competition in NAMI-A binding to Tf vs. HSA, and finally iii) the effect of low- and high-molecular-mass constituents of human serum on NAMI-A binding to Tf.

## EXPERIMENTAL METHODS

### Spectrofluorimetric titration

Fluorescence measurements were performed on a spectrofluorimeter PerkinElmer LS55. The emission spectra were recorded between 305 and 500 nm upon excitation at 295 nm.

### Separation of protein fractions

The chromatographic system ÄKTA Pure was used for separation. Anion exchanged Mono Q 5/50 GL column was applied to the separation of ruthenated proteins. 0.02 M BIS-TRIS/HCl pH 7.0, A, and 0.02 M BIS-TRIS/HCl, 1 M NaCl pH 7.0, B, were used as eluents. Separation conditions: injection volume: 100 µl, target concentration of B: 50%, gradient length: 20 CV, flow rate: 1 ml/min. CaptureSelect™ Transferrin Affinity Matrix was used for a one-step transferrin purification from human serum. Equilibration buffer: PBS, pH 7.4. 400 µl of sample was injected into the column. Unbound serum components were washed with 5 CV of equilibration buffer. Transferrin was eluted with 5 CV of the elution buffer: 20 mM Tris, 50% (v/v) propylene glycol, 1.0 M NaCl, pH 7.4.

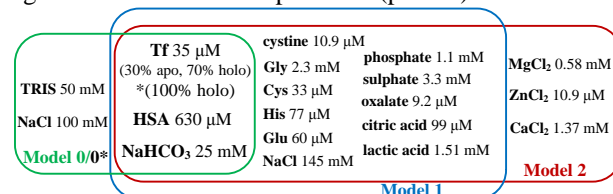
### Determination of protein and ruthenium concentration

The Tf and HSA concentrations in the studied systems were determined using human Tf or HSA ELISA kits, respectively. The total protein concentration in human plasma was measured by Bradford method. The total Ru content in samples was measured by the application of ICP-MS using ELAN 6100 Perkin Elmer spectrometer

## RESULTS AND DISCUSSION

The calculated value of  $K_{SV}$  was found to be  $10\,300 \pm 100\text{ M}^{-1}$  at  $37\text{ }^{\circ}\text{C}$ . The analysis of ruthenium distribution have shown, that both apo- and holo-Tf are able to sequester Ru ions from HSA, though albumin is still the major location of Ru ions.

Fig.1. Serum models compositions (pH 7.4).<sup>2</sup>



Tabele 1. Ru fraction in ruthenated proteins produced after incubation of NAMI-A, Tf and HSA for 24 h at molar ratio at 20:1:18.<sup>2</sup>

Model	Tf saturation	Ru/Tf [mol/mol]	Ru/HSA [mol/mol]
0*	100%	$0.50 \pm 0.08$	$0.50 \pm 0.06$
0	30%	$0.52 \pm 0.07$	$0.51 \pm 0.05$
1	30%	$2.0 \pm 0.2$	$1.2 \pm 0.1$
2	30%	$2.9 \pm 0.5$	$1.1 \pm 0.1$

The addition of low-molecular-weight components of human serum included in Model 1 and 2 gave rise to evident increase in fraction of Ru equivalents in both proteins (Tabele1), while the fraction of free Ru species was negligible. The enhancement of Ru species binding to serum proteins can arise from transformation of NAMI-A into more active Ru species or/and modulation of protein surface making the binding sites more accessible.

## CONCLUSION

Here, we showed that holotransferrin is able to bind NAMI-A as easily as apotransferrin. The presence of physiological concentration of albumin (ca. 18-fold excess over Tf) resulted in a twofold decrease of ruthenium binding to Tf. Interestingly, the introducing of low-molecular-mass components of serum dramatically increased the ruthenation of Tf. Intermolecular competition binding studies between transferrin and albumin showed that both proteins bound similar amount of ruthenium species. Investigation of NAMI-A binding to Tf in human serum showed that this protein was not the major binding partner for Ru complex. However, in spite of many competing proteins still the ruthenation of Tf was observed.<sup>2</sup>

## REFERENCES

- Hartinger CG, *et al.*, J Inorg Biochem 100:891-904, 2006
- Śpiewak K., *et al.*, J Biol Inorg Chem, DOI: 10.1007/s00775-015-1255-5, 2015

## ACKNOWLEDGMENTS

National Science Center (grant no. 2013/09/N/ST5/00858).





## Alginate/Protein Hybrid Hydrogels for Vascular Grafts: Effects on Human Vascular Cell Attachment and Growth

Raminder Singh<sup>1,2</sup>, Bapi Sarker<sup>3</sup>, Raquel Silva<sup>3</sup>, Rainer Detsch<sup>3</sup>, Aldo R. Boccaccini<sup>3</sup>, [Iwona Cicha](mailto:Iwona.Cicha@uk-erlangen.de)<sup>1</sup>

<sup>1</sup>Section of Experimental Oncology and Nanomedicine (SEON), University Hospital Erlangen, Germany

<sup>2</sup>Department of Cardiology and Angiology, University Hospital Erlangen, Germany

<sup>3</sup>Institute of Biomaterials, University of Erlangen-Nuremberg, Erlangen, Germany

[Iwona.Cicha@uk-erlangen.de](mailto:Iwona.Cicha@uk-erlangen.de)

### INTRODUCTION

Lack of adequate venous material for autologous grafts constitutes a common problem in the coronary artery bypass surgery. Developing small vascular grafts with a luminal endothelial surface which would mimic anti-thrombogenic effect of an autologous “living” graft is one of the most urgent tasks in tissue-engineering<sup>1</sup>. In this study, we have investigated the growth of vascular cells on different alginate-based biomatrices to evaluate their potential for vascular scaffolds.

### EXPERIMENTAL METHODS

Different formulations containing alginate solution (2%, w/v) blended with protein solutions (silk fibroin, gelatin, keratin, or elastin) at 1% w/v, were prepared in form of hydrogels and extensively characterized with regard to physico-chemical features<sup>2</sup>. Human umbilical vein endothelial cells (EC), human umbilical artery smooth muscle cells (SMCs) and normal human fibroblasts were seeded on different biomatrices placed in 24-well cell culture plates and cultivated for up to 10 days. Cell growth was monitored microscopically after 3, 7 and 10 days of culture. The numbers of viable cells on each hydrogel were compared by fluorescent staining (calcein/DAPI) and the metabolic activity of the cells was analysed using WST-8 assay. All cell types were investigated in three independent experiments, each with quadruplicate samples.

### RESULTS AND DISCUSSION

Alginate is the biomaterial of choice for various tissue engineering applications due to its ability to form hydrogel. However, alginate has unfavourable degradation characteristics and does not promote the cell adhesion. Our studies show that in comparison to pure alginate hydrogels, vascular cell growth was improved on alginate-protein blend hydrogels. In particular, the alginate-silk fibroin and alginate-keratin<sup>2</sup> provided good surfaces for ECs (Fig. 1), supporting the attachment, growth and spreading of ECs for up to 10 days of culture.

SMCs showed best colonization and growth on alginate-keratin hydrogels, and fibroblasts on silk fibroin, elastin and keratin-containing hydrogels, as shown by actin and calcein staining, as well as WST assay. Interestingly, in contrast to our previous studies with alginate dialdehyde-gelatin crosslinked gels<sup>3</sup>, alginate-gelatin blend provided a less favourable scaffold for fibroblasts growth.

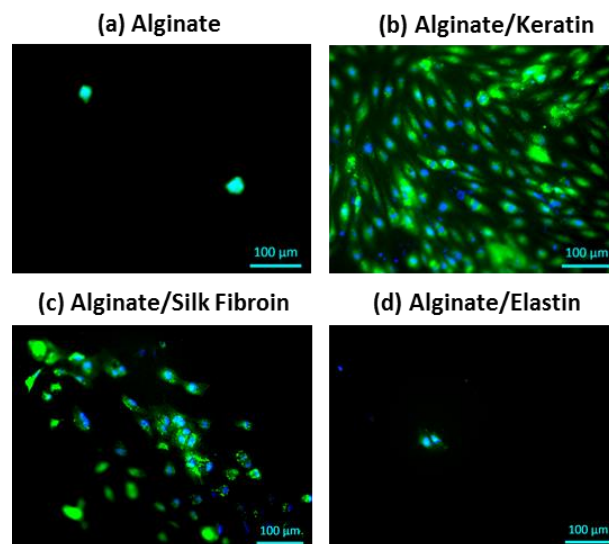


Figure 1. Fluorescent microscopy images of HUVECs on alginate (a), alginate/keratin (b), alginate/silk fibroin (c) and alginate/elastin (d) hydrogel films after 3 days of culture. The cells were stained for calcein (green) and nucleus (blue).

### CONCLUSIONS

Designing a scaffold which supports endothelialisation is an important step for the development of anti-thrombogenic small vascular grafts with improved patency. Due to their good vascular compatibility, alginate-based protein-containing hydrogels constitute good candidates for applications in cardiovascular surgery. Further studies are necessary to evaluate the mechanical stability and behaviour of these scaffolds *in vivo*.

### REFERENCES

1. Niu G. *et al.*, Expert Opin Biol Ther. 14:403-410, 2014
2. Silva R. *et al.*, J Mat Chem B. 2:5441-5451, 2014
3. Sarker B. *et al.*, PLoS ONE 9:e107952, 2014

### ACKNOWLEDGMENTS

This study was supported by Emerging Field Initiative of the University of Erlangen-Nuremberg (Project TOPbiomat), and by the ELAN Fonds of the University Hospital Erlangen (Postdoctoral grant to R. Singh).

## Nanotopography of TiN Produced on Plasma Region Under Glow Discharge Conditions Enhances Endothelial Cells Adhesion

Agnieszka Sowińska<sup>1</sup>, Elżbieta Czarnowska<sup>1</sup>, Joanna Bierła<sup>1</sup>, Tomasz Borowski<sup>2</sup>,  
Tadeusz Wierzchoń<sup>2</sup>

<sup>1</sup>Pathology Department, Children's Memorial Health Institute, Poland

<sup>2</sup>Surface Engineering Faculty, Warsaw University of Technology, Poland

[a.sowinska@czd.pl](mailto:a.sowinska@czd.pl)

### INTRODUCTION

Titanium nitride (TiN) offers particular possibilities for the development of implants with improved haemocompatibility [1, 2]. Data presented in literature shows that nanoscale features of biomaterial surfaces influence on cells response [3, 4]. Materials used so far does not allow to obtain the optimum conditions for adhesion and proliferation of vascular endothelial cells. Thus, recent materials do not promote proper proliferation of endothelial cells.

The aim of study was verified, the effect of the nanocrystalline TiN outer zone of nitrated surface layers with different topography produced under glow discharge conditions in terms biocompatibility with endothelial cells.

### EXPERIMENTAL METHODS

The TiN+Ti<sub>2</sub>N+αTi(N) surface layers (TiN) on Ti6Al4V titanium alloy at low temperature (680°C) under glow discharge nitriding processes at the cathode potential (TiNK) and plasma region (active screen plasma nitriding) (TiNP) were produced.

The TiN surface layers properties in terms of surface roughness and wettability by deionized water were examined using atomic force microscopy (AFM, Veeco) and imaging Nikon Coolpix 4500 and measurement with the use of DROP3 program, respectively.

The biomimetic biofilm was produced on biomaterials surfaces by incubation with albumin and collagen III.

The human umbilical vein endothelial cells (EC) were incubated on biomaterials samples, than fixed cells, and stained with antibody anti-human vinculin and Alexa Fluor 488, TRITC-conjugated Phalloidin, and DAPI were investigated under confocal microscope and morphometrically analyzed using Cell Sense program (both, Olympus). Results were expressed as mean ± SD and statistically analyzed using a Student's t-Test.

### RESULTS AND DISCUSSION

Studies have shown a lower roughness of TiNP in range of parameters Ra, Rq, Rt than TiNK and wettability comparable to TiNK. This was followed by enhance vascular cells adhesion on TiNP (Fig.1, 2). Images documented presence on TiNP large, polymorphic EC with numerous focal adhesion forming discs on cell membrane in contact with the material surface. EC on TiNK in contrast to those on TiNP were much smaller, mostly spindle-shaped with focal adhesions located on the cell edges. In addition, actin in EC on TiNP formed cytoskeleton fibers arranged parallel to the cell border,

while in cells on TiNK the cytoskeleton was blurred distributed in accordance with the cell axis.

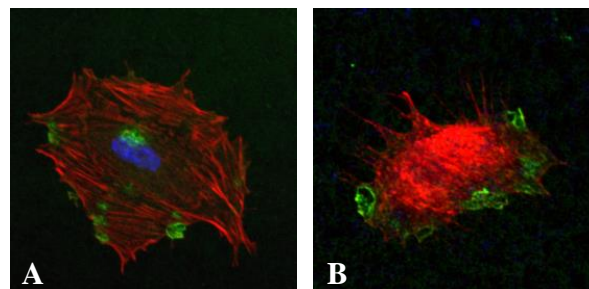


Fig.1. Endothelial cells morphology on TiNP (A) and TiNK (B) surface layers. F-actin stained in red, vinculin –green, and nuclei – blue. Mag.40x zoom 4.

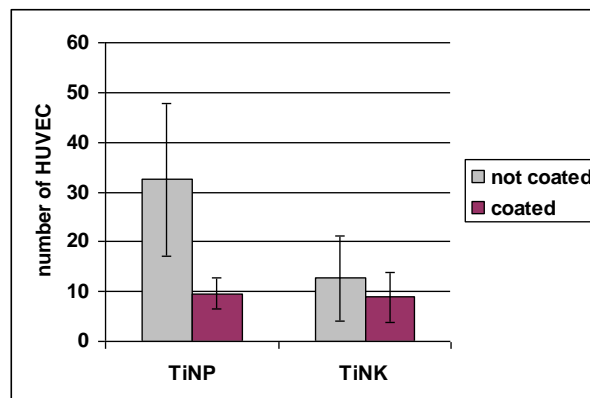


Fig.2. Analysis of endothelial cells number adhered on TiNP and TiNK.

### CONCLUSION

This study results suggest TiNP promising properties for cardiovascular applications by demonstrating strong positive effect of its surface nanotopography, however with additive interaction of produced biofilm.

### REFERENCES

1. Dion I., *et al.*, Int J Artif. Organs, 15:617-621, 1992
2. Sowińska A., *et al.* Inż Mat, 3:202-205, 2012
3. Dalby M.J., *et al.*, Int J Biochem Cell Biol, 36:2005-2025, 2004
4. Yim E.K.F., *et al.*, Biomaterials 26:5405-5413, 2005

### ACKNOWLEDGMENTS

This study was supported by the NSC [grant 2011/01/D/ST8/02931]  
ERDFIEP POIG.02.01.00-14-05

## Electrospun Polylactide-Polycaprolactone Copolymer for Vascular Tissue Engineering

Jana Horakova<sup>1</sup>, Petr Mikes<sup>1</sup>, Ales Saman<sup>1</sup>, Michal Ackermann<sup>2</sup>

<sup>1</sup>Department of Nonwovens and Nanofibrous Materials/Technical University of Liberec, Czech Republic

<sup>2</sup>Department of Applied Mechanics/Technical University of Liberec, Czech Republic

[jana.horakova@tul.cz](mailto:jana.horakova@tul.cz)

Small diameter vascular grafts were produced by electrospinning of polylactide and polycaprolactone copolymer (PLC). The morphology of resulting fibers was uniform with fiber diameter about 1  $\mu\text{m}$ . Scaffolds were mechanically tested showing very good strength and elasticity. The scaffold supports endothelial cell growth on the surface.

### INTRODUCTION

There is a pressing need to develop vascular grafts that can replace failed small diameter arteries. Synthetic vascular grafts made from ePTFE, Dacron, or polyurethane work well as replacements for large diameter vascular grafts (>6 mm) with high blood flow<sup>1</sup>. However, they often fail when used to replace small diameter vessels due to acute thrombogenicity, anastomotic intimal hyperplasia, and aneurysm formation<sup>2</sup>. Biodegradable polymers, such as poly- $\epsilon$ -caprolactone or poly-L-lactic acid have been successfully used for tissue engineering applications, including vascular replacement<sup>3,4</sup>.

### EXPERIMENTAL METHODS

Small diameter vascular grafts were produced by electrospinning of PLC solution. Fibers were collected on rotating mandrel to obtain tubular scaffold. The structure was analyzed by scanning electron microscopy (SEM) and image analysis.

Mechanical properties of the tubular scaffold were measured using tensile tester. The graft was clamped to the tensile tester and stretched until break. Stress-strain curves were recorded for each tested graft ( $n=3$ ). Scaffolds made from PLC were seeded with human umbilical vein endothelial cells. Adhesion and proliferation of the cells was evaluated after 1, 3, 7 and 14 days using MTT test, fluorescence and SEM.

### RESULTS AND DISCUSSION

Tubular scaffolds with inner diameter in range from 1 to 6 mm were produced by electrospinning. The diameter of PLC fibers was  $1.09 \pm 0.40 \mu\text{m}$ . Wall thickness of vascular graft was controlled by time of electrospinning to obtain the thickness of 100  $\mu\text{m}$ .

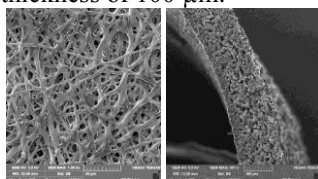


Fig.1: SEM photo of outer site of PLC vascular graft (a), cross section of vascular graft (b).

Copolymer PLC showed excellent mechanical properties in terms of stress and strain as depicted in Figure 2.

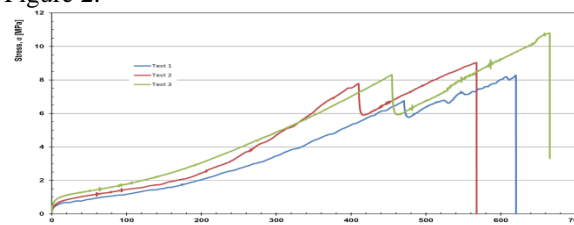


Fig.2: Stress-strain curves of electrospun PLC vascular graft with 4 mm inner diameter ( $n=3$ ).

Scaffolds were seeded with endothelial cells showing good cell adhesion followed by proliferation of the cells on the surface of the electrospun layer.

Electrospinning is well-known method for production of scaffolds for tissue engineering. To meet the requirements for small diameter vascular grafts, proper material and technology has to be used. We have showed that electrospun copolymer PLC fulfil the requirements in terms of sufficient mechanical strength and elongation at break. The scaffold also supports endothelialization of the graft that is crucial to prevent thrombosis, the most common failure of small diameter vascular grafts. Further in vivo tests are ongoing to prove the usage of such grafts.

### CONCLUSION

New material was introduced as a potential candidate for vascular tissue engineering applications. Electrospun copolymer PLC showed excellent mechanical and biological properties, the main requirements for small diameter vascular grafts.

### REFERENCES

1. Kannan R.Y. *et al.*, J. Biomed Mat Res B Appl Biomater. 74:570-81, 2005
2. Isenberg B.C. *et al.*, Circ Res 98:25-35, 2006
3. De Valence *et al.*, Biomater 33:38-47, 2012
4. Tara S *et al.*, Atherosclerosis 237:684-691, 2014.

### ACKNOWLEDGMENTS

The authors would like to thank the European Social Fund and the state budget of the Czech Republic for providing financial support to "Nanofiber materials for tissue engineering" project (Grant no: CZ.1.05/3.1.00/14.0308).

## Combination of Vinpocetine and AcSDKP for Developing Drug Eluting Stent with Anti-inflammatory Function

Seong Ho Seo<sup>1,2</sup>, Kwang-Sook Park<sup>1</sup>, Samy Olivier Gobaa<sup>1</sup>, Yoon Ki Joung<sup>1</sup>, Ik Hwan Kim<sup>2</sup>, Dong Keun Han<sup>1</sup>

<sup>1</sup>Center for Biomaterials, Korea Institute of Science and Technology, Seoul 136-791, Korea

<sup>2</sup>College of Life Sciences and Biotechnology, Korea University, Korea

[dkh@kist.re.kr](mailto:dkh@kist.re.kr)

### INTRODUCTION

Anti-inflammatory drugs have been applied to improve the function of stent, so called 'drug-eluting stents'. Many researchers reported that the reduction in neointimal hyperplasia and restenosis in stent could be accomplished by stent-based delivery of anti-immune drugs, such as sirolimus, paclitaxel and so on. However, the application of these drugs still has some major concerns.<sup>1</sup> For example, these drugs cause the endothelial toxicity to attenuate re-endothelialization, resulting in increasing stent thrombosis. In this study, we hypothesized that the combinational treatment of vinpocetine and AcSDKP inhibits the inflammatory response of endothelial cells and smooth muscle cells (SMC) without the endothelial toxicity. Additionally, it was examined the effect of this combination on macrophage infiltration and SMC proliferation. As a result, it was observed that combinational treatment of vinpocetine and AcSDKP decreased pro-inflammatory cytokines and macrophage infiltration. Also, it could reduce the SMC proliferation.

### EXPERIMENTAL METHODS

The U-937 cells and HUVECs were treated with the degradable polymer byproduct and/or vinpocetine and AcSDKP were stained with a calcein (HUVEC) and PKH26 (U-937).<sup>2,3</sup> Treated cells were rinsed with PBS solution and incubated in staining solution at 37°C for 30 min, followed by washing with PBS. The constructs were then visualized by fluorescent microscopy (U-RFL-T(CKX41), Olympus, Japan).

### RESULTS AND DISCUSSION

In the byproduct-treated sample, the significant number of U-937 cells adhered to HUVECs. While the group added to vinpocetine or AcSDKP showed the decrease in the adhesion of U-937 cells. Furthermore, the group

treated with both indicated that U-937 cells rarely adhered on HUVECs.

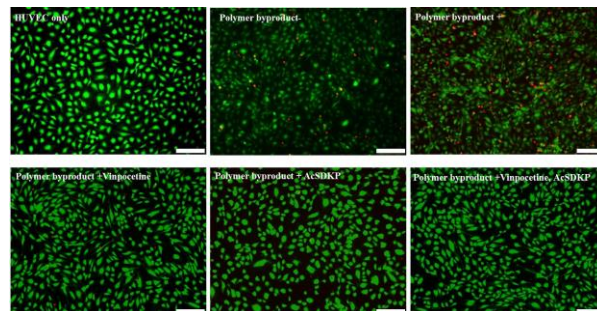


Fig. 1. Effect of vinpocetine and AcSDKP on the adhesion of U-937 cells on HUVEC.

### CONCLUSION

The significant concentration of vinpocetine was found for the inhibition of IL-6 expression and SMC proliferation, but the assurance of EC viability and proliferation. It was confirmed that vinpocetine can induce re-endothelialization, suppressing the adhesion of macrophages on EC by AcSDKP in the wound-healing process.

### REFERENCES

1. Adiguzel E. *et al.*, Vasc Med 14:73–89, 2009
2. Andrae J. *et al.*, Genes Dev 22:1276–1312, 2008
3. Bagoly E. *et al.*, Orv Hetil 148:1353–1358, 2007

### ACKNOWLEDGMENT

This research was supported by Pioneer Research Center Program (2014M3C1A3056052) through the National Research Foundation of Korea funded by the Ministry of Science, ICT & Future Planning (MSIP), Republic of Korea.



# Capture of Late Endothelial Progenitor Cell by Anti-CD146 Antibody Immobilization on Nano-filamentous Silicone-coated Stent

Sung Nam Kang<sup>1,2</sup>, Yoon Ki Joung<sup>1,2</sup>, Dong Keun Han<sup>1,2</sup>

<sup>1</sup>Center for Biomaterials, Korea Institute of Science and Technology, Seoul 136-791, Korea

<sup>2</sup>Department of Biomedical engineering, Korea University of Science and Technology, Daejeon, Korea  
[dkh@kist.re.kr](mailto:dkh@kist.re.kr)

## INTRODUCTION

Restoration of damaged endothelium might be a well-built way to prevent late stent thrombosis and restenosis. It has been reported that late endothelial progenitor cell (late EPC) can differentiate to endothelial cell and then facilitate re-endothelialization. In this study, we focused on CD146 as a target surface biomarker for late EPC capture. CD146 is a transmembrane glycoprotein that is constitutively expressed in the whole human endothelium.<sup>1</sup> Silicone nanofilament (SiNf) was modified on metal surface for increasing the amount of antibody immobilized on surface.<sup>2</sup> We demonstrated that anti-CD146 antibody (Ab)-immobilized stent can effectively capture circulating late EPCs and may restore a damaged endothelium.

## EXPERIMENTAL METHODS

SiNf surface was prepared using a trichloromethylsilane (TCMS) and modified by 3-aminopropyl triethoxysilane (APTES) for introducing the amine group as shown in Fig. 1. Morphology of SiNf surface was confirmed by SEM. SiNf, anti-CD34 Ab, and anti-CD146 Ab-immobilized surfaces were evaluated by immunofluorescence staining, scanning electron microscopy (SEM), ATR-FTIR, water contact angle, and EDX. The impact of Anti-CD146 Ab-immobilized SiNf surface on cell capture was evaluated by late EPC capture assay.

## RESULTS AND DISCUSSION

SiNf treatment changed a comparatively hydrophilic Co-Cr surface to a hydrophobic one and the SEM images showed tangled filaments with nano scale (Fig. 2A). Fluorescence staining demonstrated that anti-CD146 Ab was homogeneously covered on the surface. Capture assay exhibited that late EPCs were more significantly captured on anti-CD146 Ab-immobilized surface than bare surface and anti-CD34 Ab-immobilized one (Fig. 2B). This is probably attributed to the specific binding to CD146 marker on late EPC and larger surface area of SiNf. Early EPC do not express CD 146 but late EPC express CD 146, as mature endothelial cells. Anti-CD 146 Ab immobilized surface is able to capture more late EPCs than early

EPCs and this give rise to inducing rapid re-endothelialization to damaged endothelium lesion.

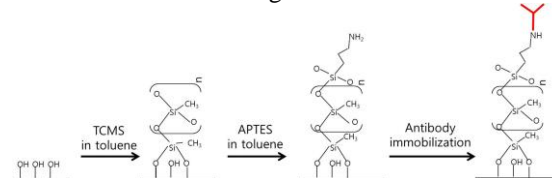


Fig. 1. Schematic procedure of antibody immobilized SiNf formation.

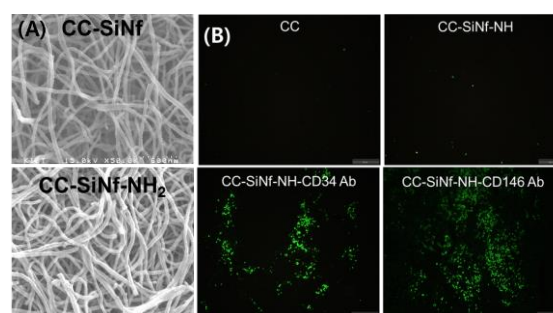


Fig. 2. (A) SEM images of SiNf on Co-Cr surface and (B) fluorescence images of late EPCs captured on modified surfaces.

## CONCLUSION

Structure of SiNf and immobilization of anti-CD146 Ab provided an effective surface for capturing specifically late EPC. Further studies are ongoing to demonstrate growth and differentiation of captured late EPC *in vitro* and their impact *in vivo*. This approach will become a promising way for preventing from restenosis and thrombosis of existing stents by accelerating re-endothelialization after stenting.

## REFERENCES

1. Bardin N. *et al.*, Blood, 98:3677-3684, 2001
2. Zimmermann J. *et al.*, Langmuir, 24:1053-1057, 2008

## ACKNOWLEDGMENT

This research was supported by the Bio & Medical Technology Development Program of the National Research Foundation (NRF) funded by the Ministry of Science, ICT & Future Planning (NRF-2014M3A9D3033887).

# Magnetic Susceptibility and Hardness of Alloys of Au and Group V Elements (Nb, Ta) for MRI Artifact-free Biomedical Applications

Kenichi Hamada, Shihoko Inui, Emi Uyama and Eiichi Honda

Institute of Health Biosciences, Tokushima University, Japan

[hamada.dent@tokushima-u.ac.jp](mailto:hamada.dent@tokushima-u.ac.jp)

## INTRODUCTION

Mismatch between the volume magnetic susceptibility ( $\chi_v$ ) of biomedical metal devices and the surrounding tissue in a human body is a major artifact in magnetic resonance imaging (MRI). The authors have developed Au–Pt–Nb alloys with  $\chi_v$  values similar to that of human tissue [approximately  $-9 \times 10^{-6}$ , (-9 ppm)] and with excellent mechanical properties<sup>1</sup>. However, the alloys exhibit insufficient deformability and improving the deformability is challenging because of the difficulty in performing a solid-solution treatment. To develop new MRI artifact-free alloys with both high strength and high deformability, a feasible solid-solution treatment is necessary. In this study, alloys of Au and group V elements (Nb and Ta) with excellent biocompatibility, were fabricated, and their  $\chi_v$ , Vickers hardness (Hv) and phase constitution were investigated.

## EXPERIMENTAL METHODS

Au–xNb (x = 4–12) and Au–yTa (y = 10–30) alloy ingots were fabricated by argon-arc-melting. The ingots were cold-rolled to a thickness of approximately 1–1.5 mm. The total rolling reduction was 50–70%. The rolled Au–Nb and Au–Ta alloy plates were homogenized at 1273 K for 20 h. Aging treatments were performed at 873 K. For all the samples, the  $\chi_v$  values were measured using a magnetic susceptibility balance; the Hv was measured under a load of 100 g for

30 s; and the phase constitution was analysed using X-ray diffractometry (XRD).

## RESULTS AND DISCUSSION

Fig. 1 shows the effect of Nb or Ta content on the  $\chi_v$  of homogenized Au–Nb or Au–Ta alloys. The  $\chi_v$  of both homogenized alloys increased linearly with increasing Nb or Ta content. The Au–6Nb and Au–15Ta alloys exhibited  $\chi_v$  values close to -9 ppm. Although the XRD profile of the Au–12Nb alloy, shown in Fig. 2, indicated the presence of a binary phase structure with Au–Nb solid-solution and Au<sub>2</sub>Nb, the linear dependence, shown in Fig. 1, did not change. In addition, the Au–8Nb alloy after aging at 873 K for 5 h showed the precipitation of Au<sub>2</sub>Nb without a significant change in  $\chi_v$ . These results suggest that the amount of Au<sub>2</sub>Nb precipitation was small and/or the  $\chi_v$  of Au<sub>2</sub>Nb was close to that of Au–Nb solid-solution. To clarify, an Au–19.1Nb alloy was fabricated and homogenized at 1323 K for 50 h. The XRD profile of the Au–19.1Nb alloy indicated clear peaks of Au<sub>2</sub>Nb with only slight peaks of Au–Nb solid-solution. Therefore, the  $\chi_v$  value of the Au–19.1Nb alloy is inferred to be equal to that of Au<sub>2</sub>Nb. Furthermore, the  $\chi_v$  value measured was -20 ppm, a value close to that of the Au–4Nb alloy, and thus, Au<sub>2</sub>Nb precipitation did not drastically change the  $\chi_v$  value of Au–Nb alloys when Nb content was less than 12%. Au–Ta alloys, where Ta content is above 20%, also indicated a binary phase structure with Au–Ta solid-solution and AuTa. This result suggests that the  $\chi_v$  value of AuTa is close to that of Au–Ta solid-solution; however, single phase AuTa was not successfully fabricated in this research.

Hv for the Au–6Nb and Au–15Ta alloys were 117 and 132, respectively, and did not increase after aging at 873 K. These results suggest that Nb and Ta are not the appropriate alloying elements to increase the Hv of Au effectively.

## CONCLUSION

Addition of Nb or Ta is not effective for increasing the Hv of Au alloy, but helps achieve the required  $\chi_v$  value to improve compatibility with human tissues, and thereby reduce MRI artifacts.

## REFERENCES

1. Uyama E. *et al.*, Acta Biomater. 9:8449–8453, 2013.

## ACKNOWLEDGMENTS

This work was financially supported by JSPS KAKENHI (21500427 and 24500528), Japan Science and Technology Agency, Tanaka Kikinzoku Research Fund and Terumo Life Science Foundation.

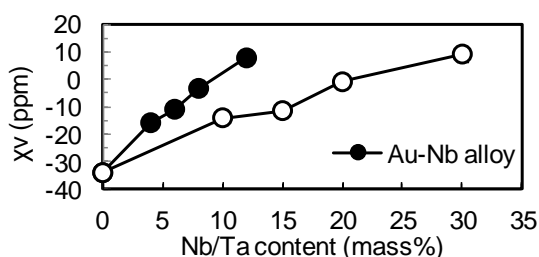


Fig. 1 Effect of Nb or Ta content on  $\chi_v$  of Au–Nb alloys and Au–Ta alloys after homogenization.

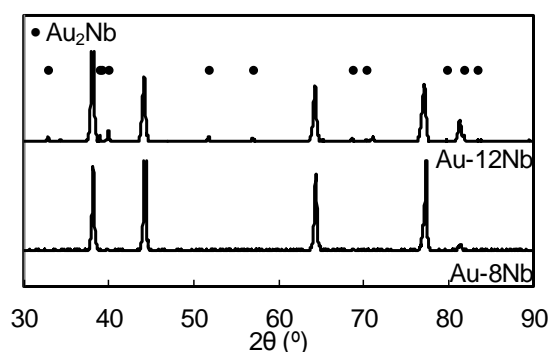


Fig. 2 XRD profiles of Au–Nb alloys after homogenization.

## Magnetic Susceptibility and Hardness of Alloys of Au and Group IV Elements (Ti, Zr) for MRI Artifact-free Biomedical Applications

Shihoko Inui, Emi Uyama, Eiichi Honda and Kenichi Hamada

Institute of Health Biosciences, Tokushima University, Japan

[c301251012@tokushima-u.ac.jp](mailto:c301251012@tokushima-u.ac.jp)

### INTRODUCTION

Mismatch between the volume magnetic susceptibilities ( $\chi_v$ ) of a biomedical metal device and the surrounding human tissue is the main cause of metal artifact in magnetic resonance imaging (MRI). The authors have developed Au–Pt–Nb alloys as candidates for MRI artifact-free alloys with  $\chi_v$  values similar to that of human tissue [approximately  $-9 \times 10^{-6}$  (-9 ppm)] and with excellent mechanical properties<sup>1</sup>. However, the alloys exhibit insufficient deformability for certain types of biomedical applications. Improving the deformability of these alloys is challenging as it is difficult to perform a solid-solution treatment on them. A feasible solid-solution treatment is required to develop new MRI artifact-free alloys with both high strength and high deformability. In this study, alloys of Au and group IV elements (Ti and Zr) that have excellent biocompatibility, were fabricated, and their  $\chi_v$ , Vickers hardness (Hv), and phase constitution were investigated.

### EXPERIMENTAL METHODS

Au–xTi (x = 0.5–5.0 mass%) and Au–yZr (y = 1.0–5.0) alloy ingots were fabricated by argon-arc-melting. The ingots were rolled to a thickness of approximately 1–1.5 mm. The total rolling reduction was 50–70%. The rolled Au–Ti and Au–Zr alloy plates were homogenized at 1273 K and 1123 K, respectively, for 20 h. Aging treatments were performed at 873 K. For all the samples, the  $\chi_v$  was measured using a magnetic susceptibility balance; the Hv was measured under a load of 100 g for 30 s; and the phase constitution was analysed using X-ray diffractometry (XRD).

### RESULTS AND DISCUSSION

Fig. 1 shows the effect of Ti content on the  $\chi_v$  of Au–Ti alloys. The  $\chi_v$  increased drastically with 0.5% Ti addition; however, with further increase in Ti content,  $\chi_v$  increased gradually. The XRD patterns showed that the precipitation of Au<sub>4</sub>Ti was enhanced with an increase in Ti content. The Au–5Ti alloy exhibited  $\chi_v$  close to -9 ppm; however, it also indicated significant embrittlement and was difficult to be rolled. Aging at 873 K for 10 min did not change the  $\chi_v$  of the alloys.

Fig. 2 shows the effect of Ti content on the Hv of Au–Ti alloys. The Hv value increased gradually with Ti content under 1% Ti, increased steeply with Ti content from 1% to 2% Ti, and decreased gradually above 2% Ti. The XRD profile of Au–Ti alloys with more than 2% Ti indicated the precipitation of Au<sub>4</sub>Ti. After aging at 873 K for 10 min, the Au–1Ti alloy exhibited a drastic increase in Hv, while the XRD profiles showed no phase constitution change. These results suggest that a small amount of Au<sub>4</sub>Ti precipitation effectively

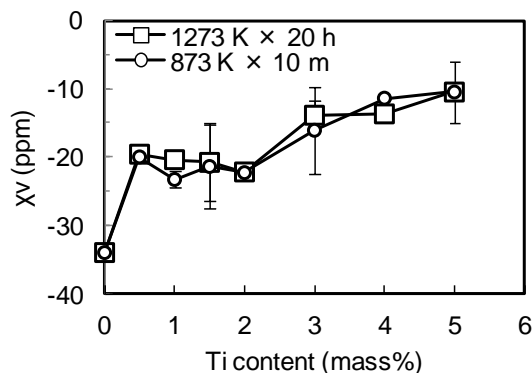


Fig.1 Effect of Ti content on  $\chi_v$  of Au–Ti alloys.

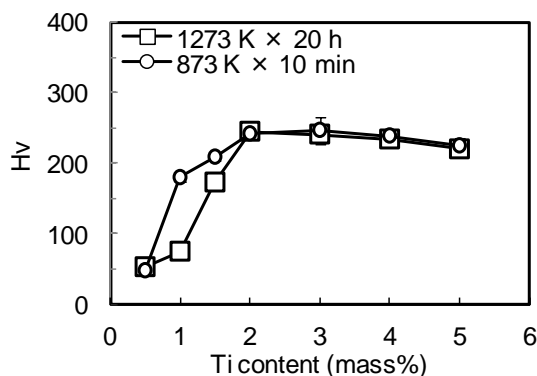


Fig. 2 Effect of Ti content on Hv of Au–Ti alloys.

increased the Hv of Au–1Ti alloy but did not change its  $\chi_v$ . The results also suggest that an increase in Au<sub>4</sub>Ti precipitation made the alloy brittle and reduced its deformability.

The Au–Zr alloys showed a similar dependence of  $\chi_v$  and Hv on Zr content. The saturated  $\chi_v$  value was smaller than that for the Au–Ti alloys and the saturated Hv value was similar to that for the Au–Ti alloys.

### CONCLUSION

A small amount of Ti or Zr addition effectively increases the Hv of an Au alloy without severe embrittlement. However, the addition of a suitable third alloying element is required to achieve the required value of  $\chi_v$ .

### REFERENCES

1. Uyama E. *et al.*, Acta Biomater. 9:8449-8453, 2013.

### ACKNOWLEDGMENTS

This work was financially supported by JSPS KAKENHI (21500427 and 24500528), Japan Science and Technology Agency, Tanaka Kikinokoku Research Fund and Terumo Life Science Foundation.



Isaiah Adekanmbi<sup>1</sup>, K. Elizabeth Tanner<sup>1</sup>, Haytham Kubba<sup>2</sup>, Helen Lu<sup>3</sup>

<sup>1</sup>Biomedical Engineering Division, School of Engineering, University of Glasgow, Glasgow, G12 8QQ, UK

<sup>2</sup>ENT Paediatric Surgery, Royal Hospital for Sick Children, Yorkhill, Glasgow, G3 8SJ, UK

<sup>3</sup>Biomedical Engineering, School of Engineering and Applied Science, Columbia University, USA

[Isaiah.adekanmbi@glasgow.ac.uk](mailto:Isaiah.adekanmbi@glasgow.ac.uk)

## INTRODUCTION

Stents provide biological support in body conduits and are useful for counteracting stenosis (constriction) in cardiovascular, gastrointestinal, urethral and airway passages<sup>1</sup>. However, the current widespread use of permanent metal stents that remain throughout the lifespan of a patient, threaten restenosis, thrombosis, or physical irritation if not surgically removed.

In infants the clinical requirement is for a stent that retains structural integrity for periods of several weeks up to many months *in vivo* during host tissue restoration<sup>2</sup> and from a materials perspective this requires an implant with appropriate mechanical and degradation characteristics.

Bioresorbable phosphate glass fibres have shown enormous potential for temporary implants and tissue repair, owing to their mechanical properties and solubility in aqueous media which can be modified by addition of various oxide compounds<sup>3,4</sup>. Further, when combined with degradable polymers the resulting glass fibre polymer composites (GFRP) become ductile allowing them to be forged into supporting scaffolds with suitable mechanical and dissolution properties. To date however, their use for stenting applications has not been investigated possibly due to major difficulties of processing these compositions into fibre form.

In this study, two phosphate glass fibre compositions containing SiO<sub>2</sub> (silica) and B<sub>2</sub>O<sub>3</sub> (Boron) were fabricated to test the hypothesis that B<sub>2</sub>O<sub>3</sub> containing phosphate glass fibres present enhanced mechanical and dissolution behaviour for use as a degradable stent.

## EXPERIMENTAL METHODS

**Glass fibres:** GF330 (Silica based) and GF331 (Boron) continuous fibre with target diameters ranging from 10–20µm were obtained (Giltch Ayrshire, UK).

**Fibre dissolution and pH study:** 200mg fibre bundles for each fibre formulation were immersed in 10ml glass vials containing phosphate buffered saline (Sigma Aldrich UK). Each sample (n=6 per formulation) was weighed (Denver Instrument) and the dissolution media pH recorded (Accument Basic AB15) before and after 3 and 7 days of incubation at 37°C. Before weighing, samples were dried in an air circulating oven at 60°C for 4 hours.

**Tensile tests:** Individual fibre filaments were placed on a paper frame (fig 2) with a gauge length of 25mm and the ends of each fibre attached to the frame using cyanoacrylate adhesive. Glass fibre diameters (n=20) were measured using optical microscopy (Zeiss Axiovert). Samples were mounted onto the specimen grips of a test machine (Instron 8841) fitted with a 10N load cell and tested at room temperature at 1mm/min. Tensile modulus and strength were calculated and Student's t-test were performed using Prism v.5

## RESULTS AND DISCUSSION

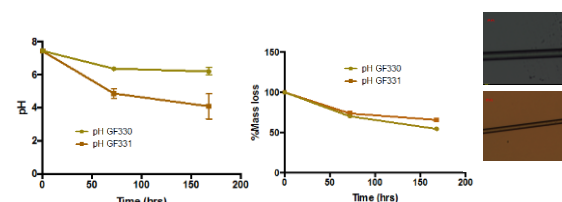


**Fig1:** Dissolution media pH (left) and % mass loss (centre) for GF330 and GF331 compositions after immersion in PBS, with light microscope images (right)

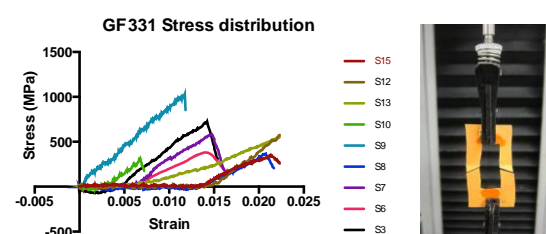


**Fig2:** Stress-strain curves for B<sub>2</sub>O<sub>3</sub> based glass fibres (left) and paper frame and mounting technique (right)

Degradation media of the boron based GF331 displayed a more dramatic decline in pH after 7 days  $4.09 \pm 0.76$  compared with GF330  $6.20 \pm 0.23$  (fig1), however a greater quantity of fibre mass was lost in the Silica based composition after 7 days of immersion in PBS. On average boron containing glass fibres demonstrated a statistically significantly higher tensile strength and tensile modulus than silica based fibres ( $p < 0.05$ ) and this maybe attributed to increased cross link density in glass fibres containing B<sub>2</sub>O<sub>3</sub> additions<sup>5</sup>.

## CONCLUSIONS

Despite creating a noticeably higher acidic environment B<sub>2</sub>O<sub>3</sub> fibres retain greater mass after days of immersion in PBS and are likely to perform with longer mechanical integrity *in vivo* than SiO<sub>2</sub> based fibres when used as part of a GFRP composite stent material.

## REFERENCES

1. Zilberman *et al* J Biomed Mat Res 74B:792-799, 2005
2. Luffy *et al* J Biom Mat Res 102A: 611-620, 2014
3. Knowles *et al* J Mat Chem 13: 2395-240, 2003
4. Sharmin *et al* J Biomater Appl 29: 639 2014
5. Shah *et al.*, Bull Mater Sci 29: 43–48, 2006

## ACKNOWLEDGMENTS

The authors would like to thank Action Medical Research and Yorkhill Children's Charity for providing financial support to this project.



## A Combined Method for Bilayered Vascular Graft Fabrication

Tamer Al Kayal<sup>1</sup>, Devid Maniglio<sup>2,3</sup>, Walter Bonani<sup>2,3</sup>, Paola Losi<sup>1</sup>, Claudio Migliaresi<sup>2,3</sup>, Giorgio Soldani<sup>1</sup>

<sup>1</sup>Institute of Clinical Physiology, National Research Council, Italy

<sup>2</sup>Department of Industrial Engineering and BIOTech Research Centre, University of Trento, Italy

<sup>3</sup>European Institute of Excellence on Tissue Engineering and Regenerative Medicine, Trento, Italy  
[giorgio.soldani@ifc.cnr.it](mailto:giorgio.soldani@ifc.cnr.it)

### INTRODUCTION

Different approaches and biomaterials have been applied to solve thrombosis and intimal hyperplasia associated with failure of small diameter grafts.

Electrospinning is a technique able to produce vascular graft with fibers in the nanometer range that resembles the extracellular matrix of native tissues, thus supporting endothelial cell attachment, alignment, proliferation and maintenance of their *in vivo* function [1, 2]. Moreover spray, phase-inversion technique was successfully employed to fabricate microporous polyurethane vascular graft able to support wall thickness cell colonization in 3D structure [3-4]. With the aim to take the advantage of both techniques we produced a bilayered polyurethane vascular graft combining electrospinning and spray technique.

### EXPERIMENTAL METHODS

A 12% (w/v) solution of Poly(ether urethane) Estane<sup>®</sup> 5714 (hereinafter PU) was prepared by dissolving the PU in a solvent mixture of tetrahydrofurane (THF), N,N-dimethylformamide (DMF) and deionized water (58/40/2, v/v/v) for electrospinning. The electrospun inner-layer of the composite graft (ID 5 mm, length 200 mm) was produced using a custom-made electrospinning apparatus equipped with a rotating cylindrical collector [5]. Electrospinning was performed using needle-to-collector distance of 22 cm, solution flow rate of 0.5 mL/h and voltage of 26kV. Electrospun fibers were deposited on a grounded stainless steel rod rotating at 125 rpm to produce a tubular mat. The process was prolonged for 2 h to obtain a 100 µm thick electrospun network.

The external layer was obtained using spray, phase-inversion method as previously described [3]. A 0.2% (w/v) PU solution was prepared by dissolving PU in THF:1,4-dioxane (DX) (1:1, v/v) added with 17% (v/v) of distilled water. The PU solution and distilled water were sprayed on the electrospun scaffold rotating at 88 rpm at a flow rate of 2 mL/min for 50 min. After fabrication, grafts were maintained for 24 h in distilled water.

For ultrastructural evaluation SEM micrographs were acquired and analyzed with ImageJ to quantify the thickness of electrospun and sprayed layers and the diameters of PU nanofibers.

A peel tests, were performed according to modified ASTM method D 903-93 with dynamometric tension/compression machine (Z1.0, Zwick/Roell Germany) equipped with a 100 N load to evaluated adhesion strengths between electrospun and sprayed layers. After the peeling test the grafts were analyzed by SEM to evaluated morphological structure.

### RESULTS AND DISCUSSION

Bilayered graft after fabrication appeared porous and without any gross defects. SEM images of the grafts evidenced different morphologies (Fig. 1A): 1) a nanofibrous inner layer with  $101 \pm 6$  µm of thicknesses; 2) a microporous external layer with  $130 \pm 13$  µm of thicknesses and a pore size measuring  $90 \pm 55$  nm (Fig. 1C); 3) an intermediate layer with a structure containing a mixing of electrospun and sprayed structures. No significant difference of electrospun layer thickness and fiber diameter was observed before and after spray deposition (Fig. 1B).

The peel test between the electrospun and sprayed layers showed a  $27 \pm 1.7$  g/mm<sup>2</sup> adhesion force.

The SEM analysis of morphological structure of electrospun surface after peel test revealed a firm adhesion of sprayed layer onto the electrospun surface of graft indicated by the presence a thin layer of the microporous structure attached to the underlining electrospun layer.

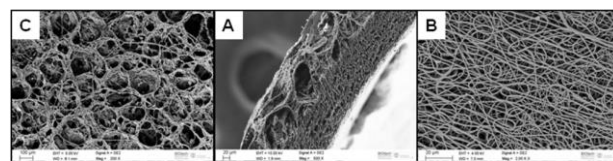


**Fig. 1.** Representative SEM images of polymeric graft. (A) cross-section of bilayered graft; (B) internal surface of the graft; (C) external surface of the graft.

### CONCLUSION

This study demonstrated the possibility to combine two different consolidated techniques to manufacture a bilayered polyurethane vascular graft with a homogeneous microporous layer firmly attached on electrospun layer with the aim to supply a provisional cell template for *in situ* tissue regeneration.

### REFERENCES

1. Bondar B, *et al.*, Biomaterials 29:561-72, 2008
2. Zonari A, *et al.*, PLoS One 7:e35422, 2012
3. Soldani G. *et al.*, Biomaterials 31:2592-605, 2010
4. Khorasani MT. *et al.*, J Biomed Mater Res A. 77:253-60, 2006
5. Bonani W. *et al.*, J. Biomed Mater Res B Appl Biomater. 96:276-86, 2011

## Circulating Cell-Capturing Technology for Rapid Neointima Formation and Excellent Patency of Acellular Vascular Grafts with 2mm ID and 30cm Length

Tetsuji Yamaoka<sup>1</sup>, Marina Kitai<sup>1,2</sup>, Maria C Munisso<sup>1</sup>, Naoki Kobayashi<sup>1,2</sup>, Shota Somekawa<sup>1</sup>,  
Yuichi Ohya<sup>2</sup>, Yoshiaki Hirano<sup>2</sup>, and Atsushi Mahara<sup>1</sup>,

<sup>1</sup>Department of Biomedical Engineering, National Cerebral and Cardiovascular Center Research Institute, JAPAN,

<sup>2</sup>Faculty of Chemistry, Materials and Bioengineering, Kansai University, Suita, Osaka, JAPAN,

[yamtet@ncvc.go.jp](mailto:yamtet@ncvc.go.jp)

### INTRODUCTION

Rapid and complete neointima formation on biomaterials is extremely important for suppressing late stent thrombosis and for high patency of the small-diameter blood vessels. We have been studying peptide-immobilization methods onto different substrate and succeeded to improve the in vitro adhesion of endothelial cells and endothelial progenitor cells on peptide-modified biomaterials surface by immobilizing REDV tetrapeptide sequence. REDV was reported as a specific sequence against  $\alpha_4\beta_1$  integrin<sup>1</sup> that is expressed by the endothelial cells and also by the circulating endothelial progenitor cells.

In the present study we tried to achieve the patency of small diameter vascular acellular grafts by using REDV-sequence immobilization technology. Small-caliber vascular grafts with the diameter less than 4 mm have not been utilized in the clinical stage because of the thrombogenic formation and rapid stenosis. Many studies on the small-caliber grafts have been carried out so far, but their size and aspect ratio was not satisfactory. We then challenged the patency of the thin and long grafts by immobilizing peptide onto the acellular tissues.

### EXPERIMENTAL METHODS

Carotid arteries of african black ostriches weighing 90–130 kg were selected as the base materials due to their straight and non-branched shape. They were trimmed, washed, packed with saline in plastic bag, and pressurized at 9800MPa for 10min to decellularize them. The treated blood vessels with the inner diameter (ID) of 2mm and the length of 20-30cm were immersed in saline containing 40 U/mL of DNase I, 20 mM MgCl<sub>2</sub>, and antibiotics for 3 days under 37°C, washed with saline, and preserved in the same medium until experimental use. The remaining DNA was quantified with DNeasy Blood & Tissue Kit, and fluorescence DNA quantification Kit.

The tissues were embedded in paraffin, sectioned, and stained with hematoxylin-eosin, Elastica van Gieson, or von Willebrand factor. The mechanical properties were tested and compared with the native arteries.

Modification peptide composed of collagen binding sequence and integrin  $\alpha_4\beta_1$  ligand (REDV) was used to immobilize REDV to the luminal surface of acellular blood vessel. A control peptide of which the collagen binding sequence was converted is also used. Acellular carotid arteries were immersed in 10 $\mu$ M peptide solution and incubated at 60°C for 1h.

The in vitro specific cell affinity of the modified surface was evaluated by seeding human endothelial cells or human endothelial progenitor cells. The number of adhering cells and their morphology was studied.

All animal experiments were conducted in accordance with the Guidelines for Animal Experiments established by the Ministry of Health, Labor, and Welfare of Japan and by the National Cerebral and Cardiovascular Center Research Institute in Japan. Goettingen minipigs were anesthetized with propofol. The left and right femoral arteries were exposed and clamped with single-use microvessel clamps. Six peptide-modified decellularized carotid arteries and three unmodified decellularized carotid arteries were transplanted in a femoral-femoral bypass manner. Blood velocity was recorded using laser Doppler flowmetry.

### RESULTS AND DISCUSSION

First of all, to evaluate the early stage thrombogenesis, the grafts were exposed to blood flow for 60 min by connecting them to a pump oxygenator, and the luminal surfaces were observed under SEM. It was revealed that the thrombus formation was greatly suppressed by the POG7G3REDV modification. This may be due to the shielding effect of the peptide against the thrombogenicity of the collagen.

Surprisingly, five POG7G3REDV-modified grafts in 6 total transplantations were patent for 3 weeks. We confirmed the presence of a von Willebrand-positive and a Vimentin-positive layer at the luminal surface without any thrombosis one week after transplantation (Figure 6b). In contrast, all unmodified grafts were occluded in a couple of days.

### CONCLUSION

The REDV peptide modification suppressed the early thrombus formation and lead to very quick neointima formation. These effects achieved the surprisingly high patency of the acellular vascular grafts with this thin and long vascular grafts, which are the clinically applicable size and aspect ratio.

### REFERENCES

1. Hubbell JA. *et al.*, Bio/Technology. 9:568-572, 1991

### ACKNOWLEDGMENTS

This work was supported by Intramural Research Fund of National Cerebral and Cardiovascular Center, and S-innovation program of Japan Science and Technology Agency (JST).



## Interaction Of Nanocomposites Containing Carbon Fillers With Different Degradation Media

Agnieszka Piegat, Zygmunt Staniszewski, Mirosława El Fray

West Pomeranian University of Technology, Polymer Institute,  
Division of Biomaterials and Microbiological Technologies, 45 Piastów Ave, Szczecin, Poland  
[apiegat@zut.edu.pl](mailto:apiegat@zut.edu.pl)

### INTRODUCTION

Polymer chemistry is the major factor determining material susceptibility to degradation. In case of biomaterials contacting with body fluids, the predominant mechanism is hydrolysis, accelerating degradation by the presence of enzymes and oxidative agents. In some applications the degradation is desirable process (e.g. absorbable sutures), while in others is main problem occurring during handling.

Polyurethane thermoplastic elastomers (TPU) are known as bio- and blood compatible, biostable materials. Their specific interaction with circulating blood is mainly connected with two-phase microdomain structure, in which domains of hard segments are dispersed in a continuous matrix of soft segments<sup>1</sup>. Depending on the chemical structure of soft segments (polyether, polyester, polycarbonate) those materials undergo hydrolytic degradation, autooxidation and environmental stress cracking<sup>2</sup>.

In this paper we analysed the influence of different degradation media on selected properties of carbon nanofillers in the polyester thermoplastic elastomer matrix (containing dimerized fatty acid (PET-DLA)), and compared to TPU medical grade material as a reference. The addition of carbon nanofiller *in situ* during the synthesis was aimed to stabilize polymer structure, by enhancing microphase separation.

### METHODS

In this work, copolymers of poly(ethylene terephthalate) and dimerized fatty acid with two different hard:soft segments ratio were evaluated, namely 40:60 and 60:40 wt%. Degradation of selected materials containing different carbon nanofillers (from 0.05 to 1 wt%): multiwall carbon nanotubes (MWCNT), carbon black (CB) and graphene (GR) was carried out in simulated body fluid prepared according to Kokubo formulation, phosphate buffer solution and oxidative solution of 20% hydrogen peroxide and cobalt chloride (0.1 M), usually used as *in vitro* oxidation medium<sup>3</sup>. The degradation was carried out for 4 weeks at 37°C. Samples were analyzed after 7, 14, 21 and 28 days in shaking incubator. Chemical structure was analysed by ATR FTIR method, additional DSC analysis was carried out in order to investigate the changes in bulk properties of degraded materials. The surface morphology of materials was analyzed with scanning electron microscope and EDX analysis. Due to the specific application of composite materials, mechanical properties were evaluated on thin film samples (0,5 mm thickness).

### RESULTS AND DISCUSSION

The changes of the chemical structure of copolymers and their composites were more noticeable for materials containing 40 wt% of hard segments. Figure 1 present FTIR spectra of neat copolymer before and after incubation in SBF.

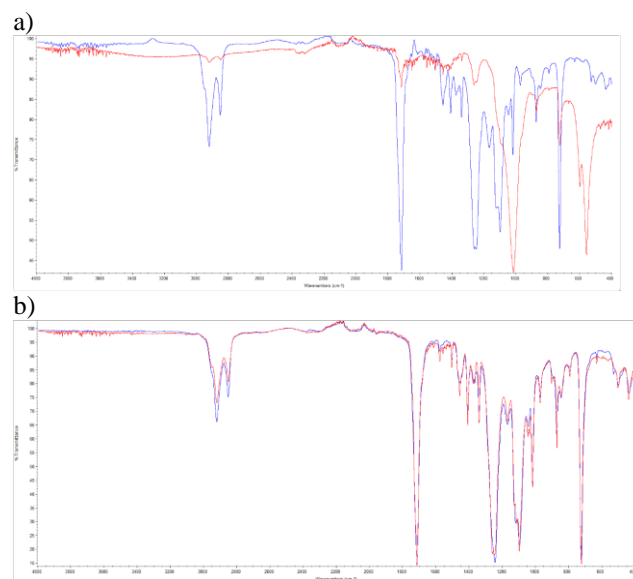


Fig.1. ATR FTIR spectra of a) 40:60, b) 60:40 PET-DLA copolymers

Similar results were found for materials with different carbon fillers - stronger changes were observed in case of 40 wt% of hard segments matrix. Thus could suggest that materials with lower content of hard segments are more susceptible to hydrolytic degradation due to the higher content of amorphous phase.

### CONCLUSIONS

PET-DLA copolymer and its composites with lower content of hard segments is more susceptible to changes in bulk properties, due to the better penetration of degradation media into the amorphous regions of polymer matrix.

### REFERENCES

1. G. Holden, et al, *Thermoplastic Elastomers*, 2<sup>nd</sup> Ed., Hanser Publishers, Munich Vienna New York, 1996
2. Chandy T., Van Hee J., Nettekoven W., Johnson J., *J Biomed Mater Res.* (2009), 89B, 314-324
3. Christenson E.M., Anderson J.M., Hiltner A. *J Biomed Mater Res.* (2009). 70A 245-255

### ACKNOWLEDGEMENTS

Financial support by research grant no: PBS1/A5/2/2012 is acknowledged.



## Scanning Electron Microscopy Assessment of the Silicon Endocardial Extracted Leads

Magdalena Ziabka<sup>1</sup>, Barbara Małecka<sup>2,3</sup>, Andrzej Ząbek<sup>2</sup>, Krzysztof Boczar<sup>2</sup>

<sup>1</sup>Department of Ceramics and Refractories, Faculty of Material Science and Ceramic, AGH-UST in Krakow, Poland

<sup>2</sup>Department of Electrophysiology, John Paul II Hospital in Krakow, Poland

<sup>3</sup>Institute of Cardiology, Jagiellonian University, Medical College in Krakow, Poland

[ziabka@agh.edu.pl](mailto:ziabka@agh.edu.pl)

### INTRODUCTION

Durability of polymer insulations applied in endocardial leads is a subject of researches during last years [1, 2, 3]. During long term insertion in human body external polymer insulation is damaged and metal wire is exposed. There are many reasons of such abrasions, however interaction between two leads, lead and pacer or insulation and metal wire are considered as the most common [1]. Leads continuously move during their normal work cycle, overlap on each other and are damaged in points of contact and bounding. Leads are removed using endovenous techniques. Very often insulation is additionally damaged during removal of leads what also makes more difficult defining the real cause of their damage. The aim of performed research is to show abrasions of insulation which appear on leads during long term insertion in human body using scanning electron microscopy and chemical analysis as confirmation methods.

### EXPERIMENTAL METHODS

The silicon leads (*Medtronic CapSureFix*) extracted by simple traction from 8 patients at the age of  $74.7 \pm 8.6$  (5 males and 3 females) were examined using optical microscopy (Nikon A2 100) and scanning electron microscopy (Nova Nano SEM 200, FEI Company). Testing have been committed with an attachment for the chemical analysis of specimens in microareas with energy dispersive x-ray spectroscopy (EDX, EDAX). The observations were carried out in low vacuum conditions in the secondary electron mode.

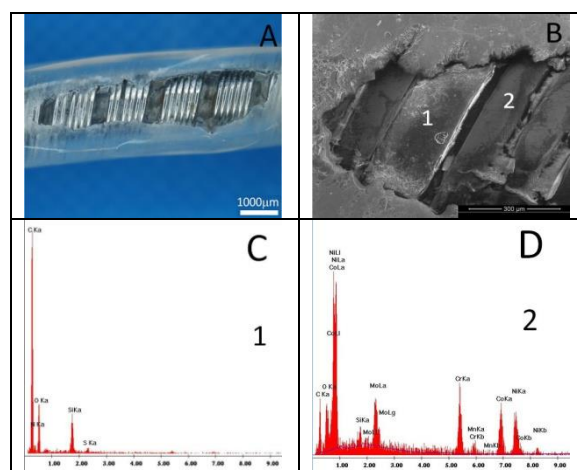
### RESULTS AND DISCUSSION

Table 1 shows optical (A) and SEM (B) microphotographs of leads surface, chemical analysis inside the abrasion on polymer surface (C) and on wire surface (D). In both pictures it is visible that outer silicone insulation is damaged. The silicon continuity is interrupted by the oval abrasion. Inside the abrasion the electrode wire is exposed.

Chemical analysis proved presence of tissue on surface of all tested polymer insulations. Moreover, analysis showed presence of tissue on internal surface of silicon insulation (1 on fig. B), which was confirmed by higher concentration of carbon (C), presence of nitrogen (N) and sulphur (S) and low signal from the silicon (Si).

Committed testing showed dependency between level of damage and period of time - the longer the lead was

implanted, the greater damage was observed. Damage were not caused during implantation or reimplantation procedures. Round shape of abrasion proved also that the polymer surface was damage during mutual overlap and abrasion of two leads.



### CONCLUSION

Combination of scanning electron microscopy and energy dispersive x-ray spectroscopy is a useful method for investigation damages on extracted leads. Both techniques are effective in distinguishing and classifying damages of polymer insulation.

### REFERENCES

1. Małecka B., et al., Kardiologia Polska. 72(10):960-8, 2014.
2. Kutarski A., et al., Pacing Clin Electrophysiol, 36:1503-1511, 2013.
3. Zabek A., et al., Pacing Clin Electrophysiol; 35:156–158, 2012.

### ACKNOWLEDGMENTS

This work was financially supported by Jagiellonian University, Medical College – as statutory research.



## Investigation into Surface Characteristics of Coronary Stents

Sarah Morgan<sup>1</sup>, Richard A. Black<sup>1</sup>, Christopher McCormick<sup>1</sup>.

<sup>1</sup>Department of Biomedical Engineering, University of Strathclyde, Scotland, UK  
[sarah.morgan@strath.ac.uk](mailto:sarah.morgan@strath.ac.uk)

### INTRODUCTION

Advanced Coronary Heart Disease (CHD) is commonly treated by insertion of a Drug-eluting Stent (DES) into a previously blocked coronary artery, helping restore blood flow to the heart. DESs are Bare Metal Stents (BMSs) that have been coated with a drug (often encased within a polymer), which is slowly released to prevent excessive cellular proliferation within the artery wall. Despite their success, DESs are not suitable for all patients and have been linked to delayed healing of the endothelial cell layer that is crucial to normal artery function.

Research efforts are now focused on the development of stents which encourage rapid endothelial cell re-growth. Surface topography has been shown to influence cell adhesion, proliferation and migration<sup>1</sup>. Additionally, surface stiffness has been shown to influence cell behaviour<sup>2</sup>. This is particularly relevant for drug eluting stents whose surfaces may exhibit variations in surface stiffness due to heterogenous distributions of drug and polymer on the surface. Conducting polymers are emerging as a potential drug-eluting stent coating<sup>3</sup> although there has been little detailed investigation of their surface topography in this context.

We investigated the surface characteristics of four well-established coronary stent types and compared the results to those obtained for a conducting polymer coating we have recently produced.

### EXPERIMENTAL METHODS

#### Surface Analyses

Atomic Force Microscopy (AFM) (Asylum Research MFP-3D, AC in air, AC160 TS cantilever, 1Hz, 5  $\mu\text{m}$ ) was used to analyse the surfaces of clinically relevant BMSs and DESs. Three stents of each type were examined (n=2 for Yukon<sup>®</sup> stent) with four random points analysed per sample. The surface topography and cantilever phase signal was recorded for each surface, from which values for Root Mean Squared Roughness ( $R_{\text{RMS}}$ ) and Surface Area (SA) were calculated.

#### Electropolymerisation

Polypyrrole coatings were produced on stainless steel wire (AISI 316L, diameter 0.2mm) by means of electropolymerisation: Potentiostatic, Voltage: 0.9V, Duration: 15-25min, Electrolyte solution: 0.1M Pyrrole, 0.1M NaSa. N=3.

### RESULTS AND DISCUSSION

Average values of  $R_{\text{RMS}}$  and SA are displayed in Table 1, demonstrating the differences in surface topography between the BMSs and DESs. Surface roughness values of the polypyrrole coating were also shown to be in line with these values. A height retrace overlaid with phase

retrace image of the surface of a Taxus<sup>®</sup> Express<sup>2</sup> stent is displayed in Figure 1, illustrating the difference in surface stiffness and height between the paclitaxel particles in blue and the polymer in red.

Table 1:  $R_{\text{RMS}}$  and SA values for surfaces of materials examined.

Sample	Average $R_{\text{RMS}} \pm \text{SD (nm)}$	Average SA $\pm \text{SD } (\mu\text{m}^2)$
Gazelle <sup>TM</sup> (BMS)	$14.39 \pm 11.24$	$25.15 \pm 0.14$
Yukon <sup>®</sup> (SES) *post drug elution	$182.02 \pm 37.04$	$28.02 \pm 0.98$
Cypher <sup>®</sup> (SES)	$34.67 \pm 34.77$	$25.20 \pm 0.34$
Taxus <sup>®</sup> Express <sup>2</sup> (PES)	$33.36 \pm 30.02$	$25.27 \pm 0.69$
PPy (0.9V, 25min)	$135.06 \pm 37.26$	$28.51 \pm 1.81$

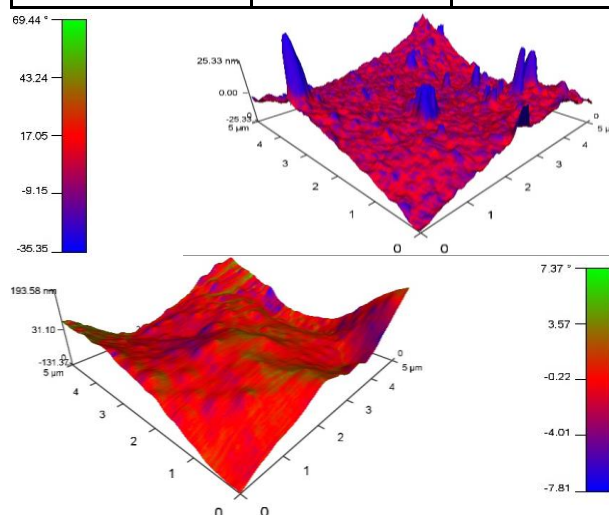


Figure 1: Representative AFM height retrace overlaid with phase retrace images (scan size 5  $\mu\text{m}$ ). Top: Taxus<sup>®</sup> Express<sup>2</sup>. Bottom: Cypher<sup>®</sup>.

### CONCLUSION

With these differences in surface characteristics, we anticipate that endothelial cells will behave differently on each stent surface, thus affecting healing following stent implantation, which is the subject of our ongoing work.

### REFERENCES

1. Chung TW. et al, Biomaterials. 24:4655-4661, 2003.
2. Yeung, T. et al. Cell Motility and the Cytoskeleton. 24-34, 2005
3. Arbizzani, C. et al, Electrochimica Acta 52: 3274-3279, 2007.

### ACKNOWLEDGMENTS

The authors would like to thank the UK Engineering & Physical Sciences Research Council (EPSRC) for providing funding for doctoral studentship to SM via the CDT in Medical Devices and Healthcare Technologies. (Grant no: EP/F50036X/1).

## Influence of Preservative on the Tensile Strength of the Tissue of Porcine Circulatory System

Alicja Stanislawska, Kinga Dawidowska

Department of Materials Science and Welding Engineering  
Technical University of Gdansk, Poland  
[alistanislawska@gmail.com](mailto:alistanislawska@gmail.com)

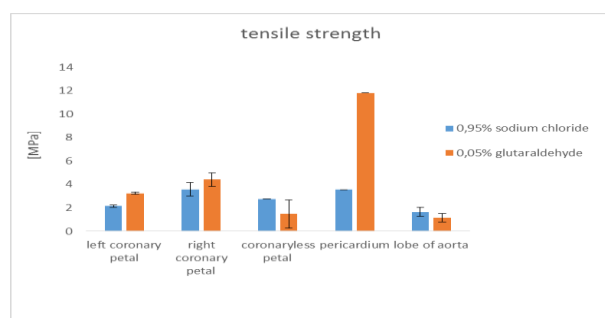
### INTRODUCTION

Currently one of the leading causes of death worldwide are heart diseases which include calcification of heart valves and vascular aneurysm. There are many biomaterials that can substitute pathologically altered tissue, however, none of them is as perfect as a native tissue. Currently, scientists are looking for new biomaterials that can be successfully implanted without exposing the patient to reoperation. We compare the tensile strength of the porcine tissues of the circulatory system that were stored in saline solution, with the same tissue-curing in a solution of glutaraldehyde. According to the literature glutaraldehyde results in the mechanical reinforcement by the binding of the so-called collagen cross-linking [1] so biological heart valve before implantation are keeping in glutaraldehyde solution. Subsequently, the tensile strength of the porcine tissues will be compared with tensile strength of Polish bionanocellulose produced by BoWil as implanting material used in cardiac surgery and vascular surgery.

### EXPERIMENTAL METHODS

We used flakes of the aortic valve (left coronary petal, right coronary petal and coronaryless petal), pericardium and porcine aortic patches (lobe). The tissues were divided into two groups. On the day of the study, all tissues were thawed and immersed for a period of about 2 hours in 0.95% sodium chloride solution. Test of the tension of the first part of the samples was carried out after the immediate removal from the sodium chloride, and the tension test of the second part was performed after keeping them in 0.05% glutaraldehyde solution for 10 min. Tensile test was carried out at the company testing machine INSTRON model 1112. Three samples of each type of material were made. Each sample came from another heart.

### RESULTS AND DISCUSSION



The studies show that the tensile strength of the left and right coronary petal and pericardium which were fixed in glutaraldehyde is characterized by higher strength properties relative to the same tissue stored in saline solution. Coronaryless petal and lobe of aorta fixed with aldehyde obtained slightly lower tensile strength values, relative to the same tissues stored in the saline, which may be due to errors resulting for example from a very fusing material and thus insufficient reagent bound collagen. The thickness of the tissue affects the binding of collagen. In the case of thinner tissue, for example pericardium, a significant increase in tensile strength was observed in comparison with the aorta, whose thickness is several times higher. In the case of application of the materials of various thickness at the same time of fixation, results consistent with expectations were obtained, because the thicker tissue requires longer time to total collagen cross-linking. The big standard deviation of the results for coronaryless petal could be due to the fact that the tissues were taken from a slaughterhouse, which does not guarantee the same conditions of rearing pigs. However, studies show that the impact of the reagent coming into contact with the test material affects its mechanical strength.

### CONCLUSION

Studies show that the impact of the reagent coming into contact with the test material affects its mechanical strength. Fixing the biological material with an aldehyde results in the mechanical reinforcement by the binding of the so-called collagen cross-linking. The results discussed in this article allow further studies on the comparison of the mechanical properties of natural tissues with bionanocellulose material. Such a material would be an interesting alternative for the currently used biomaterials in medicine.

### REFERENCES

1. Avery N.C., Sims T.J., Warkup C., Bailey A.J.: Collagen cross-linking in porcine m. longissimus lumborum: absence of a relationship with variation in texture at pork weight. *Meat Sci.*, 1996, 42, 355-369

### ACKNOWLEDGMENTS

This work has been performed within the PBS project "Preclinical studies on the possibility of the application of the genuine, Polish bionanocellulose (BNC) in regenerative medicine in terms of bioimplants in cardiac and vascular surgery", which has been financed by The National Centre for Research and Development.

## Encapsulation of Anti-inflammatory Drug into PCL Based Electrospun Fibres for Nerve Regeneration

Valentina Cirillo, Vincenzo Guarino, Annunziata Cummaro, Olimpia Oliviero, Luigi Ambrosio

Institute for Polymers, Composites and Biomaterials, Department of Chemical Sciences & Materials Technology,  
National Research Council of Italy, V.le Kennedy 54, Naples, Italy

[vincenzo.guarino@cnr.it](mailto:vincenzo.guarino@cnr.it)

### INTRODUCTION

Inflammation plays an important role in nerve regeneration strategies. Acute inflammation is the innate immune system's first line defence, intended to eliminate or segregate the foreign material. A strong inflammatory response can lead to the implant failure and disrupt nerve regeneration process. In this context, a large variety of synthetic grafts has been tested as promising solution to get fully nerve regeneration *in vivo*<sup>1</sup>. However, no matter how biocompatible a synthetic material is, the body will still give an immune response to it. Recently, several studies have remarked that active molecules (i.e., neurotrophins, antibiotics) can be efficiently incorporated in 3D scaffolds to locally hinder the inhibitory microenvironment occurring after lesion of peripheral nerve<sup>2</sup>. In particular, an anti-inflammatory drug in synthetic grafts may be locally delivered to the injury site to reduce the inflammatory response, avoiding capsule formation and cell infiltration into the lumen of conduits, so improving regeneration process.

For this purpose, in this study, Polycaprolactone (PCL) and PCL/Gelatin electrospun fibres have been prepared with and without the non-steroidal anti-inflammatory drug diclofenac sodium salt (DicNa). Electrospun fibrous scaffolds were then studied in order to evaluate the drug release profile to assess the best candidate as drug loaded electrospun grafts.

### EXPERIMENTAL METHODS

PCL and PCL/Gelatin fibres loaded with DicNa (Sigma Aldrich, Italy), were produced by electrospinning technique starting from different polymeric solutions: firstly, PCL (0.1 g/ml) and DicNa (5 mg/ml) were dissolved in 1,1,1,3,3,3 hexafluoropropanol (HFIP), secondly PCL and Gelatin (total polymer concentration 0.1 g/ml) were both mixed in HFIP with DicNa (5 mg/ml). Process parameters were changed to optimize fibres morphology. Fibrous platforms were examined by SEM/EDS, providing a complete detail on fibres size and composition.

Thermal analysis (TGA) has been performed in order to assess the inclusion of the drug. Moreover drug encapsulation and drug release profiles have been evaluated to underline the differences due to the use of mono and bicomponent systems. The drug-loaded fibrous mat was weighed and placed in PBS, incubated at 37°C and shaken. The amount of released drug, for several time intervals up to 15 days, was determined by UV-vis spectroscopy at 280 nm.

Cytotoxicity was preliminarily analysed by Alamar Blue test performed in hMSC culture via direct and indirect way.

### RESULTS AND DISCUSSION

SEM observations allowed for the correlation of final fibre morphology to process parameters set. Process parameters, such as flow rate, distance and voltage, were varied in order to identify the optimal set to obtain defect free fibres. By Image J analysis software, mean fibres diameter has found to be  $(0.12 \pm 0.02) \mu\text{m}$  and  $(0.41 \pm 0.05) \mu\text{m}$  for mono and bicomponent systems, respectively.

Moreover, in order to qualitatively verify the encapsulation of drug into the mono and bicomponent fibres, EDS spectroscopic analysis was also performed. It confirmed drug inclusion in the electrospun fibres as also showed by TGA thermograms. The encapsulation efficiency was about 50% for PCL alone and more than 80% for PCL/Gelatin.

Before reaching a plateau value, release profiles showed a strong initial burst in both cases, for the bicomponent it is strongly affected by gelatin depletion in aqueous medium while for monocomponent system it is related to the accumulation of the drug on the fibres surface. A preliminary screening of cell response until 7 days also showed a good response of hMSC in the presence of both drug loaded fibres, thus evidencing a reduction in cytotoxicity respect to the controls, namely, drug into the plate without electrospun fibers.

### CONCLUSION

PCL and bicomponent PCL/Gelatin electrospun fibres have been studied as anti-inflammatory drug release systems. Since gelatin concurs to influence the mechanism of drug release, bicomponent fibres released the drugs fairly fast and nearly completely, while monocomponent system, after an initial burst, could hold the drugs much longer. These results suggest new ideas for the fabrication of drug loaded electrospun conduits for peripheral nerve regeneration.

### REFERENCES

1. Cirillo V. *et al.*, Biomaterials. 35: 8970-82, 2014
2. Pires L. *et al.*, J. Tissue Eng. Reg. Med. 2013 doi: 10.1002/term.1792.

### ACKNOWLEDGMENTS

This work has been financially supported by PON2-00029\_3203241 (POLIFARMA) and FIRB-MERIT (RBNE08HM7T). Scanning Electron Microscopy was supported by the Transmission and Scanning Electron Microscopy Labs (LAMEST) of the National Research Council.



# Preparation of Biomedical Poly( $\epsilon$ -caprolactone) via Ring Opening Polymerization Catalyzed by *Candida antarctica* Lipase B in Ionic Liquids

Urszula Piotrowska, Marcin Sobczak, Ewa Olędzka

Medical University of Warsaw, Faculty of Pharmacy, Department of Inorganic and Analytical Chemistry, Banacha 1,  
Warsaw 02-097, Poland  
[piotrowska\\_urszula@wp.pl](mailto:piotrowska_urszula@wp.pl)

## INTRODUCTION

Enzyme catalysis has provided an environmentally friendly synthetic strategy for a variety of useful biomaterials, most of which would be difficult to produce using conventional chemical catalysts<sup>1</sup>.

Poly( $\epsilon$ -caprolactone) (PCL) is widely utilized aliphatic polyester for medical applications, such as drug delivery systems (DDS) or tissue engineering scaffolds due to its good biocompatibility and lack of toxicity. PCL has been successfully synthesized by polycondensation or by ring opening polymerization (ROP). ROP gives polyesters with a higher purity and low polydispersity, so it is the preferred route in the controlled release technology<sup>2</sup>.

A number of research topics develop an enzymatic ROP of cyclic monomers in organic solvent (e.g. toluene and heptane). Due to the toxicity of their vapor, recent literature reports suggest the possibility of using thermally stable and nonflammable ionic liquids (ILs) as the reaction medium. ILs have increasingly attracted attention as non-aqueous media for biocatalytic polymer synthesis. ILs can improve the solubility of monomers and/or polymers, provide better enzyme stability, activity and selectivity<sup>3,4</sup>.

The aim of this study was to obtain a low-molecular weight polyesters, terminated by functional groups (hydroxyl and carboxyl), with respect to their further applications as DDS. In order to this, ROP of  $\epsilon$ -caprolactone ( $\epsilon$ -CL) in the presence of non-toxic catalyst - *Candida antarctica* lipase B (CALB) in ILs media was carried out. The preliminary studies of several possible combinations of ILs anion's type, temperature and time on the polymerization process have been evaluated.

## EXPERIMENTAL METHODS

$\epsilon$ -CL, CALB and ILs were placed in 10 mL glass ampoules under an argon atmosphere. The vials were placed in a thermostated bath at predetermined temperature. After thermostated, the product was extracted with toluene and the enzyme was filtered off. Toluene was removed by evaporation in room temperature at reduced pressure.

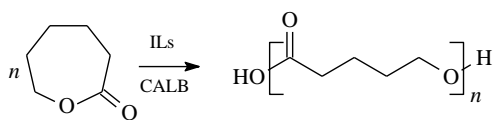


Fig.1. Ring opening polymerization of  $\epsilon$ -CL

<sup>1</sup>H NMR spectra of PCL were obtained on Varian 300 MHz spectrometer using CDCl<sub>3</sub> as a solvent. The MALDI-TOF MS spectra were performed in the linear mode on a Kompact MALDI 4 Kratos analytical spectrometer using a nitrogen gas laser and 2-[(4-hydroxyphenyl)diazenyl] benzoic acid as a matrix.

## RESULTS AND DISCUSSION

The ROP process was carried out in the presence of three ILs composed of the same cation (1-butyl-3-methylimidazolium) and three different anions (tetrafluoroborate, hexafluorophosphate, bis((trifluoromethyl)-sulfonyl)imide).

CALB has shown an activity in all types of ILs using different reactions conditions.

Polyesters with a number average molecular weight ( $M_n$ ) in the range of 1200-4200 g·mol<sup>-1</sup> were obtained.

The structure of the obtained polymers was determined by MALDI-TOF MS and spectroscopy methods. It has been found that during ROP process both linear and cyclic polymers were formed. The frequency of cycle formation is affected by both kind of ILs, temperature and reaction time. The polydispersity index (*PDI*) of the obtained polymers determined by the MALDI-TOF MS method was low and ranged from 1.03 to 1.22.

## CONCLUSION

The enzyme-catalyzed ROP of CL in ILs seems to be a promising method of the synthesis of biomedical polyester. The polymer structure was strongly dependent on ILs species, temperature and reaction time. The obtained results demonstrated that ILs offer new possibilities for solvent engineering in an enzymatic polymerization.

## REFERENCES

1. Albertsson A.C. *et al.*, Adv. Drug Deliv. Rev. 60:1077–1093, 2008
2. Sobczak M., J. Appl. Polym. Sci. 125:3602–3609, 2012
3. Yang Z. *et al.*, Enzym. Microb. Technol. 37:19–28, 2005
4. Piotrowska U. *et al.*, Molecules 20:1-23, 2015

## ACKNOWLEDGMENTS

This work was financially supported by the National Science Centre (Poland), PRELUDIUM 6 research scheme, decision No. DEC-2013/11/N/NZ7/02342, grant entitled: "Synthesis, physico-chemical and biological studies on macromolecular carriers of antimicrobial peptides".



## The Biomimetic Hydrogel Matrix for Long-term Cell Culturing

Agata Stefanek<sup>1</sup>, Tomasz Ciach<sup>2</sup>

<sup>1,2</sup>Department of Chemical and Process Engineering, Warsaw University of Technology, Poland  
[a.stefanek@ichip.pw.edu.pl](mailto:a.stefanek@ichip.pw.edu.pl)

### INTRODUCTION

Recently, there is a lack of techniques for long-term, three dimensional cell culture both in vivo and in vitro<sup>1,2</sup>. The insufficient transport rate of nutrients (glucose, oxygen) inside the 3D cell structures is the biggest obstacle for three dimensional cell culturing<sup>3</sup>. The aim of this work was to develop the method of production the biomimetic hydrogel matrix containing synthetic oxygen carrier for long-term cell culture both in vivo and in vitro. The research involves also cytotoxicity evaluation of produced material. The matrix is designed to mimic the natural originated extracellular matrix (ECM)- it forms a microcapsules of a diameter below 400  $\mu\text{m}$  with perfluorocarbon core (synthetic oxygen carrier) and alginate layer. The cells are suspended in hydrogel layer. Moreover the structure of the matrix provides free diffusion of nutrients inside the matrix and at the same time secretion of the metabolites of the encapsulated cells and immunoisolation<sup>4</sup>. The synthetic oxygen carrier in the matrix is employed to face the widely reported problem appearing in 3D cell cultures- insufficient oxygen level and occurring necrotic zones in cell aggregates<sup>5</sup>. Nowadays, development of the techniques and materials enabling long-term stable cell culture both in vitro and in vivo is a key challenge for the tissue engineering area.

### EXPERIMENTAL METHODS

#### Microcapsules production

Microcapsules were produced by the use of the encapsulator (B-395 Pro, Buchi) with concentric nozzle which enables producing core/shell structures in sterile conditions. All parameters of the process (nozzles size, liquids flow rate, gas pressure, vibration frequency, the electrode voltage) are settable, which provides good microcapsules size control. The process parameters were adjust to obtain uniform structures of define size app. 400  $\mu\text{m}$ .

#### Cytotoxicity

For cytotoxicity investigation of produced complex biomaterial, the procedure recommended in the "ISO 10993-5:2009 Biological evaluation of medical devices- Part 5: Tests for in vitro cytotoxicity" norm was applied. The MTT assay was used to evaluate the percentage of viable cells with respect to the control cell culture.

### RESULTS AND DISCUSSION

The parameters of microcapsules production process were adjust (Table 1). The process enables production uniform microcapsules of predictable diameter.

Table 1. The parameters of the microcapsules production process

Outer/inner nozzle diameter [ $\mu\text{m}$ ]	150/200
Flow rate [ml/min]	3,3
Vibration frequency [Hz]	1500
Gas pressure [mbar]	236
Diameter [ $\mu\text{m}$ ]	404,52 $\pm$ 35,74

The cytotoxicity tests proved that material has no cytotoxic potential. The viability of the L929 cells contacted with material extracts (after 24 h and 72 h of medium incubation with material) was above 70% according to the cells cultured in supplemented medium. The results of MTT assay are presented on the Figure 1.

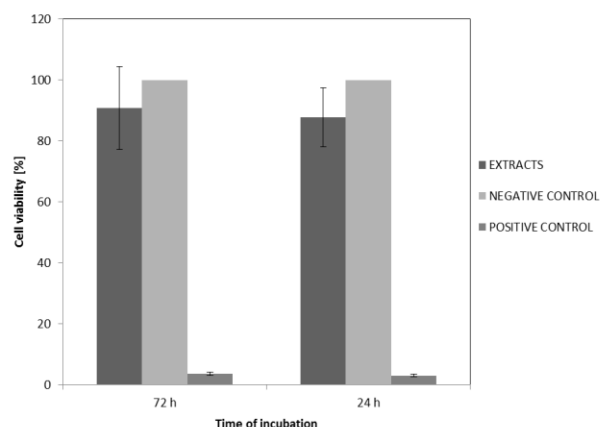


Figure 1. The MTT assay results

### CONCLUSION

The production process of uniform hydrogel microcapsules containing perfluorocarbon core was developed. The process could be employed to producing biomimetic hydrogel matrixes for long-term cell culturing both in vitro and in vivo. Moreover, the results of MTT assay proved lack of cytotoxic potential in produced microcapsules containing perfluorocarbon core.

### REFERENCES

1. Qin Zhang *et al.*, Acta Biomaterialia, 10:5-5, 2014
2. Baldino L. *et al.*, The Journal of Supercritical Fluids, 90-7, 2014
3. Zhaohui Li, Zhanfeng Cui, Biotechnology Advances, 32:2-4, 2014,
4. Kang A. *et al*, Biomaterials, 35:9-3, 2014
5. Sarwat F. *et al.*, Biotechnology and Bioengineering, , 96:1, 2007



## Microencapsulation and Nano Coating of Pancreatic Beta Cells

Niusha Nikravesh<sup>1</sup>, Gurpreet Chouhan<sup>1</sup>, Anita Ghag<sup>1</sup>, and Liam Grover<sup>1</sup>

<sup>1</sup>School of chemical engineering, University of Birmingham, UK  
[NXN372@bham.ac.uk](mailto:NXN372@bham.ac.uk)

### INTRODUCTION

Transplantation of pancreatic islets proposes a promising method for treating patients with type 1 diabetes mellitus (T1DM). It is currently, however, restricted by various problems including the shortage of donors, poor revascularization, immune rejection, and the need for life long immunosuppressive drugs. To address these issues, microencapsulation of islets has been introduced as a method to avoid host immune response by utilising a semi-permeable membrane, which provides a mechanical barrier for separating the graft from host antibodies and immune cells<sup>1</sup>. Despite significant progress being made in recent decades concerning the knowledge of microencapsulation devices, there are still several obstacles involved with the procedure. For example, relatively large number of microcapsules, and inefficiency in oxygen and nutrient diffusion due to the thickness of polymeric membrane around the cells<sup>2</sup>. In this study we aim to camouflage the surface of uniformly aggregated pseudo islets with polyelectrolyte nano coatings using the layer-by-layer (LBL) technique in order to reduce the membrane thickness around the islets, and to compare the results with traditional microencapsulated single cells.

### EXPERIMENTAL METHODS

Beta-TC-6 were cultured in Dulbecco's modified Eagle medium (DMEM) supplemented with 10% FBS, 2.5% HEPES, 1% penicillin/streptomycin, and 2.5% L-glutamine. Concave micro well arrays were developed to form uniform-sized islet spheroids. Cell survival was tested by MTT assay. As first method, cell encapsulation was conducted using encapsulator (B-390 pro) and medium viscosity alginate was cross-linked by calcium chloride. For the second encapsulation technique, cultured pseudo islets were coated with alternative layers of polycation (Poly-L-lysine) and polyanion (alginate). Furthermore, cell viability was assessed by incubating the encapsulated islets with live/dead staining in culture medium for 40mins at 37°C, and then imaged with a fluorescent microscope.

### RESULTS AND DISCUSSION

Manipulation of encapsulator parameters such as frequency, nozzle size, and pump flow rate resulted in the formation of alginate microparticles with an average diameter of <300µm (Fig.1-A). Also the result showed the effect of concave micro well on spheroid formation, demonstrating that concave micro wells more effectively generate uniform islet spheroids. The

viability of islets was assessed by staining with 5µl calcein AM, which stains live cells green, and 25µl propidium iodide, a red dye that can only permeate dead cells membrane. A high viability of coated pseudo islets was observed during the 14 day viability study (Fig.2-A, B)

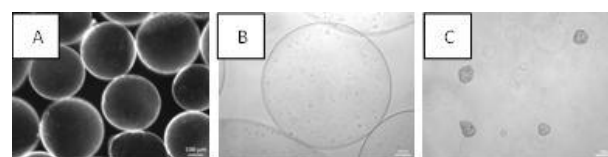


Fig 1: Morphology and viability of encapsulated cells. (A) Void alginate microparticles with average diameter of 268.63µm (frequency=2300HZ, pump flow rate=6ml/min, nozzle size=80µm). (B) Encapsulated single islet cells in alginate microsphere. (C) Pseudoislets coated with 3 bilayer of alginate-PLL.

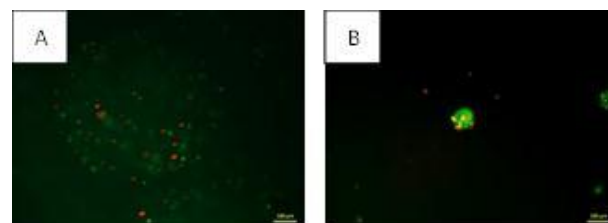


Fig 2: Cell viability assessed with live/dead staining on day 14. (A) Alginate microencapsulated islet cells. (B) Nanocoated pseudo islets.

### CONCLUSION

In this study two different approaches for encapsulation of islet cells were evaluated. Microencapsulation of islet cells, despite being studied for several years, have had issues with longevity of transplanted cells. The aim of this study is to show that coated islets produced using the LBL method have the potential to increase coverage of encapsulated cells. Minimising the capsule thickness reduces the distance for diffusion of oxygen, nutrients, and small molecules resulting in improved cell viability and functionality.

### REFERENCES

1. Langlois G.*et al.*, J.Actabiomaterial.2011
2. Esther S.*et al.*, endojournals. 32(6):827-844, 2011

## Design of a 3D Bone Cell Co-culture System Using Mineralised Alginate Microbeads

D.C. Bassett<sup>1</sup>, S. Ehnert<sup>2</sup>, A. Nüssler<sup>2</sup> and P. Sikorski<sup>1</sup>

<sup>1</sup>Department of Physics, Norwegian University of Science and Technology, Trondheim, Norway

<sup>2</sup>Seigfried Weller Institute, University of Tübingen, Germany

[david.bassett@ntnu.no](mailto:david.bassett@ntnu.no)

### INTRODUCTION

In addition to tissue engineering applications, synthetic tissue-like constructs can be used as *in vitro* models for 3D cell culture [1]. If a suitable synthetic environment that closely mimics human tissue physiology can be created, then costly and ethically questionable *in vivo* animal studies could largely be avoided. In the context of bone tissue engineering, we have already investigated this concept in a preliminary study looking into the ability of alginate beads mineralized with hydroxyapatite (HA) to support a culture of primary human osteoblasts and osteoprogenitor cells [2]. This work validated the concept of supporting osteoblast cultures and the ability to form synthetic bone like constructs using mineralized alginate. However, natural human bone undergoes continuous remodelling by a co-ordinated process involving three main cell types: bone formation is mediated by osteoblasts and osteocytes and bone resorption by osteoclasts, with all the cell types affecting each other. Imbalances in this process may cause pathological loss of bone mass as seen in conditions of delayed bone healing after fracture, osteoporosis and metabolic bone diseases. As this imbalance cannot be considered in mono-cellular systems, this represents one of the major limitations for *in vitro* testing of novel therapeutics for bone. Therefore, a primary goal of this study was to develop a co-culture of osteoblasts and osteoclasts to create a synthetic bone-like 3D platform using mineralised alginate microbeads.

### EXPERIMENTAL METHODS

Mineralised alginate hydrogel microbeads were synthesised using electrostatic extrusion as described previously [3]. SCP-1 cells were encapsulated at a concentration of  $1 \times 10^6$  cells / mL. THP-1 cells were stimulated with phorbol 12-myristate 13-acetate (PMA) for 48hrs to form adherent macrophage cells and then encapsulated in or seeded onto mineralised alginate microbeads. Co-cultures of microbeads were maintained in trans-well dishes. TRAP activity was measured after 14 days culture. Cell numbers were normalised using a resazurin assay for measuring cell metabolism.

### RESULTS AND DISCUSSION

Cells were either encapsulated in the microbeads or seeded onto the mineralised surface of the hydrogel. Mineralisation with HA was essential for cell attachment to the surface (Fig 1A). In this way binary compositions of cells could be created in 3D. In order to study the effect of co-cultures of osteoblast and osteoclast cells, microbeads with encapsulated SCP-1 pre-osteoblast cells were cultured in trans-well plates in

the presence of THP-1 osteoclast-like cells which had either been encapsulated in or seeded on mineralised alginate microbeads. Samples were cultured with and without osteoblast stimulating media. Measurements of tartrate resistant acid phosphatase (TRAP) activity, (an enzyme produced exclusively by osteoclast cells) indicated that co-culture was necessary for THP-1 cells to differentiate into osteoclast cells and this was only possible when the cells were cultured on the surface of the beads and not encapsulated within them. Addition of osteoblast differentiation medium significantly enhanced TRAP activity levels (Fig 1B).

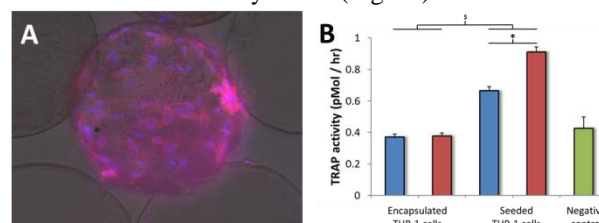


**Fig. 1. A:** Fluorescent micrograph showing SCP-1 cells adhered to a mineralised alginate microbead (actin red, nuclei blue) and not to surrounding unmineralised surfaces (grey). **B:** TRAP activity of THP-1 cells in co-culture with encapsulated SCP-1 cells after 14 days with (red) and without (blue) osteoblast differentiation media compared to negative control (green). Mann-Whitney t test \$ P = 0.002, \* P = 0.006.

### CONCLUSION

Here, previous work regarding cell attachment to mineralised hydrogels has been validated. In addition, a cell culture system to study co-cultures of cells relevant to bone biology in 3D has been developed with implications for both *in vitro* characterisation and the development of bone tissue engineering scaffolds using hydrogel-mineral composite materials. Work is now focussed on studying bone formation using this system and miniaturising the mineralised hydrogel dimensions for use in flow chambers.

### REFERENCES

1. Maltman D.J. and Przyborski S.A. Biochem. Soc. Trans. 38: 1072–1075, 2011.
2. Olderoy M.O. *et al.* J. Tiss. Eng. Regen. Med. 6: 187, 2012.
3. Xie M.L. *et al.* Acta Biomaterialia. 6(9): 3665–3675, 2010.

### ACKNOWLEDGMENTS

The authors gratefully acknowledge funding provided by the Research Council of Norway under the FRINATEK program, project no: 214607 and an IS-DAAD personal mobility grant.



## Design of Polymeric Membranes for the Encapsulation of Pancreatic Islets

Anna Cavallo<sup>1</sup>, Ugo Masullo<sup>1</sup>, Francesca Gatti<sup>2</sup>, Amilcare Barca<sup>3</sup>, Marta Madaghiele<sup>1</sup>, Alessandro Sannino<sup>1</sup>

<sup>1</sup>Department of Engineering for Innovation, University of Salento, Lecce, Italy.

<sup>2</sup>K.G. Jebsen Inflammation Research Centre, University of Oslo, Oslo, Norway.

<sup>3</sup>Division of Neuroscience and INSPE, San Raffaele Scientific Institute, Lecce, Italy.

[anna.cavallo@unisalento.it](mailto:anna.cavallo@unisalento.it)

### INTRODUCTION

Pancreatic islet transplantation is a promising strategy for the treatment of Type 1 diabetes (T1D), but the necessity of life-long systemic immunosuppression limits its clinical application. In order to protect the islet graft, several encapsulation strategies have been studied since islet transplantation became a feasible therapy, to strengthen the efficacy<sup>1</sup>. Poly(ethylene glycol) (PEG) hydrogels are one of the most widely utilized biomaterial systems, thanks to their soft tissue-like properties<sup>2</sup>. Additionally, because of their intrinsic resistance to protein adsorption and cell adhesion, PEG hydrogels seem to be the most suitable bioinert material that is ideal for use in drug delivery vehicles, blood-contacting devices, for controlled cell differentiation and cell encapsulation for transplantation<sup>3</sup>. In this work, PEGDA hydrogels were synthesized by UV crosslinking and characterized for cell encapsulation. PEGDA coating should be designed to prevent islet destruction by immune-reactive cells and antibodies, while at the same time allowing sufficient physiological exchange to prevent hypoxia, minimize the stress state of the islets and maintain a controlled glycaemic level, through proper diffusion of insulin. Macroscopic properties such as water content and compressive modulus are influenced by gel crosslinking, so we investigated how simple changes in composition of precursor solution and time of irradiation modify such important properties in the design of the coating. PEGDA hydrogels are susceptible to slow degradation *in vitro* and *in vivo*, thus hydrogel degradation properties were evaluated to understand their behaviour over time.

### EXPERIMENTAL METHODS

**Synthesis of PEGDA hydrogels.** 700Da Poly(ethylene glycol)-diacrylate was dissolved in distilled water at three different concentrations (7.5 – 10 – 15 % w/v) and a photoinitiator (Darocur® 1173) was added to the solution at 3% w/w with respect to the PEG macromer and polymerized through UV irradiation (365 nm at 2 mW cm<sup>-2</sup>) for different time lengths (1, 3, and 5 minutes). **Characterization experiments.** Swelling studies and mechanical analysis were carried out to evaluate hydrogel reticular parameters. Degradation tests were performed to study how parameters change over time. Protein release profiles were used to estimate diffusion coefficients for insulin. Cytotoxicity of the hydrogels was evaluated *in vitro* using 3T3 cell line, by means of MTT assay.

### RESULTS AND DISCUSSION

Increasing PEGDA concentration in starting polymer solution and/or UV time exposure reduced the

equilibrated swelling ratio of the hydrogels, while increased mechanical properties. This finding can be explained considering that higher crosslinking densities involve shorter mesh size of the hydrogel (Figure 1).

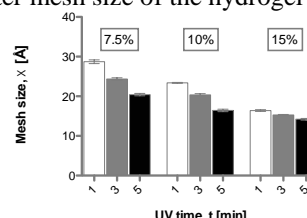


**Figure 1.** Effect of PEGDA % and UV time exposure on mesh size.

Hydrogel degradation happens through breakage of networked groups, leading to a reduced crosslink density over time and increased mesh size (Table 1).

duration	% increase of mesh size, ξ		
	PEGDA 7.5% (6 weeks)	PEGDA 10% (10 weeks)	PEGDA 15% (10 weeks)
UV 1 min	18.25±4.24	24.77±2.65	34.71±4.04
UV 3 min	27.40±3.15	22.07±4.91	32.53±3.12
UV 5 min	35.42±2.78	33.78±4.32	32.32±4.98

**Table 1.** Percentage increase of mesh size after degradation.

In islet encapsulation, it would be crucial to know how the mesh size changes over time, to evaluate which molecules can diffuse through the gel coating. Insulin release profiles gave a diffusion coefficient in the order of 10<sup>-6</sup>-10<sup>-7</sup> cm<sup>2</sup>/s. The hydrogels cytocompatibility was satisfactory, showing a slight decrease of cell viability when reducing the UV exposure time. This evidence can be explained considering that the less UV-exposed hydrogel give more unreacted polymers.

### CONCLUSION

The results obtained in this study suggest the possibility to use PEGDA hydrogels as cytocompatible coatings for islet encapsulation. Swelling ratio, mechanical properties and degradation can be conveniently and finely modulated, by controlling macromer composition and time of irradiation. Moreover, insulin diffusion within the gels is suitable for the intended application.

### REFERENCES

1. de Vos P. *et al.*, Adv Drug Deliv Rev. 67-68:15-34, 2014.
2. Nguyen K.T. *et al.*, Biomaterials. 23:4307-14, 2002.
3. Weber L.M. *et al.*, Acta Biomater. 2:1-8, 2006.

### ACKNOWLEDGMENTS

The authors acknowledge the Italian Ministry of Education, University and Research for providing partial financial support.





## Cell-Based Therapy for Targeted Treatment of Lung Injury

Sally Yunsun Kim<sup>1</sup>, Janette K. Burgess<sup>2,3</sup>, Hak-Kim Chan<sup>1</sup>, [Wojciech Chrzanowski](mailto:wojciech.chrzanowski@sydney.edu.au)<sup>1</sup>.

<sup>1</sup> Faculty of Pharmacy, The University of Sydney, Australia

<sup>2</sup> Pharmacology, School of Medical Sciences, The University of Sydney, Australia

<sup>3</sup> Respiratory Cellular and Molecular Biology, Woolcock Institute of Medical Research, The University of Sydney, Australia

[wojciech.chrzanowski@sydney.edu.au](mailto:wojciech.chrzanowski@sydney.edu.au)

### INTRODUCTION

Stem cell therapy has been increasingly used in lung diseases for various inflammatory conditions and pulmonary hypertension<sup>1,2</sup>. This expanding application does not yet include lung injury caused by burns or inhalation of smoke in fire incidents, which is known to be a leading cause of death in burn patients<sup>3</sup>. Current regimes for the treatment of inhalation injury mostly rely on the self-regeneration of the injured tissues and general treatments such as inhaled anticoagulation and oxygen therapy<sup>4</sup>. Amniotic fluid mesenchymal stem cells have been shown to have anti-inflammatory properties and also the capacity to differentiate into epithelial lung lineages<sup>5</sup>. Current cell therapies for the lungs are administered by injection and the cells are expected to reach the lungs. The current study aims to deliver the cells directly to the lungs for repair and regeneration.

### EXPERIMENTAL METHODS

Aerosolised suspensions of A549 human lung epithelial cells were used to optimise conditions of cell spraying with two devices, PennCentury MicroSprayer<sup>®</sup> Aerosoliser and LMA MiniMAD<sup>™</sup>. Cells were sprayed onto poly-L-lysine or collagen-coated plastic, gelatin 10% gel or media. A natural protein keratose extracted from Merino wool dissolved at 0.1mg/ml in media was used to explore the benefits in homing of cells. Human amniotic fluid mesenchymal stem cells (hAFMSCs) were used thereafter. To examine the survival of cells during the process of spraying, cell viability was measured using live/dead cell staining kit and live cell imaging on IncuCyte Zoom<sup>®</sup> together with cell viability assays such as alamarBlue<sup>®</sup> and Cell Counting Kit-8. All data were produced in triplicates ( $n = 3$ ) for reliability. Data were analyzed and presented as means  $\pm$  standard deviation.

### RESULTS AND DISCUSSION

Cell attachment after aerosolisation varied depending on the device used, the type of coating and hardness of the recipient surface as verified by live cell imaging and live/dead cell staining assays. At 8 hours after aerosolisation of hAFMSCs most cells recovered and attached to poly-L-lysine coated plastic after “soft landing” onto media (Fig. 1. *left*) whereas a larger proportion of cells died after being sprayed onto hard plastic (Fig. 1. *right*). The mechanical stress of the cell aerosolisation process was dependent on the device used. PennCentury MicroSprayer<sup>®</sup> Aerosoliser yielded

smaller particle size compared to LMA MiniMAD<sup>™</sup> and thus was less favourable for cell viability.

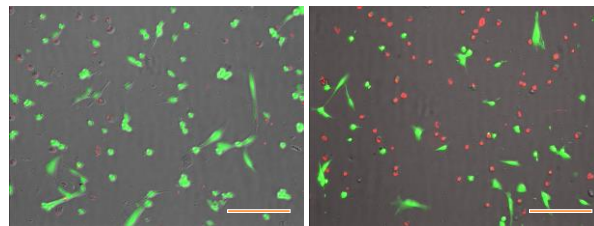


**Fig 1.** Images from a live/dead cell staining assay performed 8 hours after spraying human amniotic fluid mesenchymal stem cells onto media (*left*) and poly-L-lysine coated plastic (*right*) using LMA MiniMAD<sup>™</sup>. Green and red represent live and dead cells respectively. The type of coating and hardness of the recipient surface determines the cell viability. Scale bar represents 500  $\mu$ m.

Additional studies including cell viability assays and live cell imaging demonstrated that the cells were capable of recovering from the mechanical stress and proliferated normally after aerosolisation. In order to enhance cell homing capacity to the injured site, poly-L-lysine, collagen or keratin was used, of which collagen showed highest levels of cell attachment and proliferation. These materials also have potential to assist in the regeneration process for the lung tissues<sup>6</sup>.

### CONCLUSION

This study shows the possibility of delivering stem cells directly to the lungs for cell based therapy for the regeneration of the lung tissues. Furthermore, it has been demonstrated that the presence of keratin or collagen enhances the cell proliferation after spraying, which may have a role in regeneration of tissues after lung injury.

### REFERENCES

1. Lau AN *et al*, *Mol Ther*, 20(6):1116-30, 2012
2. Patel NM and Burger CD, *Respir Med CME*, 4(2):70-74, 2011
3. El-Helbawy RH and Ghareeb FM, *Ann Burns Fire Disasters*, 24(2):82-88, 2011
4. Dries DJ and Endorf FW, *J Trauma*, 21:31, 2013
5. Carraro G *et al*, *Stem Cells*, 26(11):2902-11, 2008
6. Kim SY *et al*, *Expert Opin Drug Deliv*, 19:1-19, 2014

### ACKNOWLEDGMENTS

The authors would like to thank the Faculty of Pharmacy, The University of Sydney for providing financial support (Faculty Innovation Challenge) to this project. The authors acknowledge Alice Hai May Wong for the preliminary work on keratin formulations.



## Development of Limonene Composed Lipid Nanocarriers of Tretinoin for Dermal Delivery

Ponwanit Charoenputtakun<sup>1,\*</sup>, Praneet Opanasopit<sup>1</sup>, Theerasak Rojanarata<sup>1</sup>, and Tanasait Ngawhirunpat<sup>1</sup>

<sup>1</sup>Faculty of Pharmacy, Silpakorn University, Nakhon Pathom, Thailand

[charoept@gmail.com](mailto:charoept@gmail.com)

### INTRODUCTION

Dermal and transdermal delivery of Tretinoin (Tr) has been used to treat acne and photodamaged skin and to manage keratinization disorders such as ichthyosis and keratosis follicularis. However, the chemical instability of Tr, the drug is unstable when exposed to heat and light. Moreover, Tr is a poorly water soluble drug<sup>1</sup>. The new-state-of-art in drug delivery is important to overcome these problems. Many researches showed the benefit of lipid nanocarriers in the dermal and transdermal applications<sup>2</sup>. Limonene (L) has been classified as a lipophilic terpene type permeation enhancer which obtained from *Citrus lemon*<sup>3</sup>. The aims of this study were to develop Limonene composed lipid nanocarriers (solid lipid nanoparticles (SLN), nanostructured lipid carriers (NLC) and nanoemulsions (NE)) to enhance the skin permeation of Tr and examined the effect of different Limonene composed lipid nanoparticles formulations (10% L-SLN, 10% L-NLC and 10% L-NE) on the physicochemical properties (size and zeta potential), drug loading, cytotoxicity, and skin permeation of Tr.

### EXPERIMENTAL METHODS

Tr-loaded 10% L-SLN, 10% L-NLC and 10% L-NE were prepared using a *de-novo* emulsification method. The dispersed phase consisted of 0.3% Tr, lipid matrix core (SLN: Cetyl palmitate, NLC-Cetyl palmitate and Oleic acids and NE: Oleic acids and Medium chain triglycerides), 10% L, Transcutol P and Butylated hydroxytoluene. Droplet size and zeta potential of Tr-loaded lipid nanocarriers were determined at 25°C by using a Zetasizer Nano ZS. The percent yield of Tr incorporated into lipid nanocarriers and the Tr content was investigated after disrupted with Propa-2-ol and analyzed by HPLC. *In vitro* skin permeation through shed snake (*Naja kaouthia*) was determined using a Franz diffusion cell with a water jacket connected to water bath at 32°C. The cytotoxicity of the nanocarriers in Normal Human Fibroblast (NHF) was evaluated based on a procedure adapted from the ISO10993-5 standard test method. Statistical significance was evaluated using a one-way-analysis of variance (ANOVA). The significance level was set at a p value < 0.05.

### RESULTS AND DISCUSSION

All Tr loaded lipid-based nanocarriers had mean size less than 200 nm (140 to 146 nm) with narrow polydispersity index (PDI). The zeta potential of particles was high and negative (-29 to -45 mV) which implied to electrostatic repulsion of lipid droplets in the system. The incorporation efficiency of Tr loaded of all formulations was higher than 80%, and Tr content was higher than 8 mg/g. This result showed all Limonene composed lipid-based nanocarriers had a high capacity

loading for lipophilic drugs. The flux of Tr from Limonene composed lipid nanocarriers was in the order of 10% L-SLN > 10% L-NLC > 10% L-NE > suspension. Furthermore, Tr cumulative at 24 h from Limonene composed lipid nanocarriers was much significant higher than suspension. The cytotoxicity level of all Limonene loaded nanocarriers was low because the IC<sub>50</sub> value was higher than 1,000 µg/ml. The result from the cytotoxicity study implies that lipid nanocarriers decrease Tr toxicity to fibroblast cells.

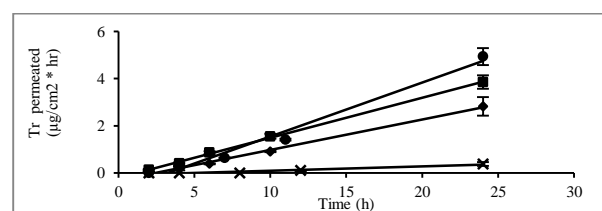


**Figure 1** The *in vitro* skin permeation of Tretinoin-loaded (●) 10% L-SLN, (■) 10% L-NLC, (◆) 10% L-NE and (X) suspension.

Formulations	IC <sub>50</sub> (µg/ml) ± SD
Tretinoin powder	350 ± 25
Tretinoin 10% Limonene-SLN	10000 ± 1000*
Tretinoin 10% Limonene -NLC	1500 ± 200*
Tretinoin 10% Limonene -NE	2500 ± 200*

**Table 1** IC<sub>50</sub> value of Tretinoin powder, Tretinoin loaded 10% L-SLN, 10% L-NLC and 10% L-NE. (\*Compared with the Tretinoin powder (p < 0.05)).

### CONCLUSION

Limonene composed SLN, NLC and NE preparations were achieved by *de-novo* emulsification method. All formulations had a size in nano-meter range with a good capacity of Tr loading. The skin permeations study showed the lipid nanocarriers can improve Tr permeation into the skin when compared to suspension formulation. Moreover, Limonene composed lipid nanocarriers also exhibited a low toxicity to NHF. From our study implied that limonene composed lipid nanocarriers were promising dermal drug carriers for Tretinoin.

### REFERENCES

1. Ascenso A. et al., AAPS PharmSciTech.12:553-563, 2011
2. Muller RH. et al., Int J Pharm. 366:170-184, 2009
3. Aqli M. et al., Drug Discovery Today. 12:1061-1067

### ACKNOWLEDGMENTS

The authors would like to acknowledge The Thailand Research Funds through the Royal Golden Jubilee Ph.D. Program (Grant No.PHD/0141/2552) and Faculty of Pharmacy, Silpakorn University, Thailand for kindly support.



## Gene Activated Matrix For Mesenchymal Stem Cells – Application To Cartilage Regeneration

Sophie Raisin<sup>1</sup>, Marc Mathieu<sup>2,3</sup>, Danièle Noël<sup>2,3</sup>, Christian Jorgensen<sup>2,3</sup>, Jean-Marie Devoisselle<sup>1</sup>, Emmanuel Belamie<sup>1,4</sup> and Marie Morille<sup>1</sup>.

<sup>1</sup>ICGM UMR5253, Equipe “Matériaux Avancés pour la Catalyse et la Santé”, Montpellier, France

<sup>2</sup>Université de Montpellier, Montpellier, France

<sup>3</sup>Inserm, U1183, Hôpital Saint-Eloi, Montpellier, France

<sup>4</sup>Ecole Pratique des Hautes Etudes, Paris, France

[sophie.raisin@univ-montp1.fr](mailto:sophie.raisin@univ-montp1.fr)

### INTRODUCTION

Gene delivery from a scaffold represents a promising approach to efficiently control stem cell fate. With this in mind, we designed an optimized tissue engineering construct for cartilage repair, based on custom made cross-linker free collagen microspheres ( $\mu$ Coll) impregnated with TGF- $\beta$ 3. This injectable biomimetic scaffold associated to mesenchymal stem cells (MSC) successfully induced a chondrocyte phenotype and the formation of neocartilage both *in vitro* and *in vivo*<sup>1</sup>. However, *in vivo* experiments suggested the late apparition of hypertrophic differentiation markers, which must be avoided for the cartilage neo-tissue to be fully functional. To maintain a mature chondrocyte phenotype, we investigate a complementary approach based on RNA interference of RunX2, a transcription factor involved in chondrocyte terminal differentiation. To ensure good transfection levels of the MSC, siRNAs were formulated into non-viral vectors: environment responsive PIC micelles<sup>2</sup>. The combination of such non viral gene vectors onto a collagen matrix, called Gene Activated Matrix, is expected to improve MSC differentiation control.

### EXPERIMENTAL METHODS

**Formulation of PIC micelles:** Double Hydrophilic Block Copolymers (DHBC) PEO<sub>x</sub>-PMAA<sub>y</sub> were formulated into micelles by polyelectrolyte complexation with either PLL or PEI. The encapsulation of siRNA into the PIC micelles was investigated as a function of loaded amount, pH, and polyacid block size. **Transfection of MSC:** Internalization of the micelles in MSC was assessed by flow cytometry, using a fluorescently labeled siRNA-TAMRA. Gene extinction efficiency of RunX2 was assessed by RT-qPCR. **Synthesis of collagen microspheres ( $\mu$ Coll):** a microfluidic set up with T-junction was used to form an emulsion between an acidic type I collagen solution and perfluorated oil. Microparticles of fibrillar collagen were obtained through a sol-gel transition induced in the aqueous droplets by vapor diffusion. **Association of micelles and microspheres:** Loading of vectors was investigated by impregnation of FITC-labelled micelles into  $\mu$ Coll and the release profile established by diffusion in PBS.

### RESULTS AND DISCUSSION

We obtained micelles with a diameter of  $60 \pm 5$  nm and a weakly positive zeta potential of  $14 \pm 2$  mV which are stable at physiological pH. To suit gene therapy applications, the pH-trigger value for micelles

dissociation and release of siRNA was chosen close to that found in endosomes (5.5), by selecting the appropriate DHBC moiety. The micelles were shown to be efficiently associated with MSC (Fig. 1) by flow cytometry. Preliminary RT-qPCR data showing a notable extinction of the targeted gene Runx2 call for further investigation. Finally, collagen microspheres with a narrow diameter distribution (mean =  $225 \pm 24$   $\mu$ m) were prepared using a custom microfluidic set-up and efficiently loaded with siRNA-micelles (Fig.2).

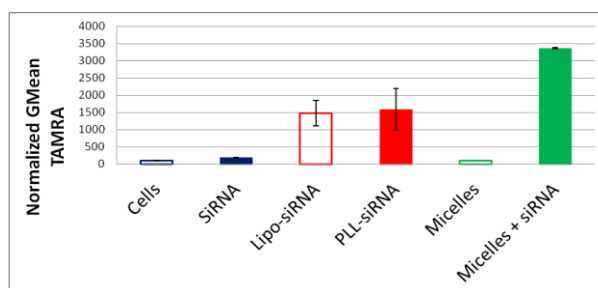


Fig. 1 Internalization of SiRNA-TAMRA into MSC (50pmol of siRNA per well, 6 well plates, 100000 cells per well)

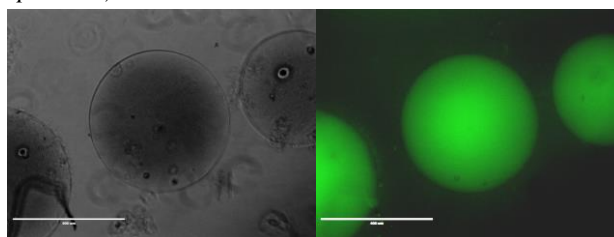


Fig.2 Association of fluorescent micelles with  $\mu$ Coll.

### CONCLUSION

Our work shows that PIC micelles can be formulated to efficiently encapsulate siRNA and disassemble at acidic (endosomal) pH. These non-viral vectors are able to deliver siRNAs inside MSCs, thereby down-regulating the hypertrophic factor Runx2. Ongoing experiments are aiming at evaluating the potential of  $\mu$ Coll to serve both as an injectable MSC carrier and as a reservoir for their long-term transfection. The latest results will be presented, notably regarding the expected improvement in transfection efficiency owing to the 3D biomimetic environment of these Gene Activated Matrices.

### REFERENCES

- <sup>1</sup>M. Mathieu et al. Eur Cell Mater, Vol28, 2014 (82-97).
- <sup>2</sup>A. Boudier et al. Drug Dev Ind Pharm, 2009; 35(8): 950–958



## Skin Penetration Enhancement of Hydrophilic Macromolecules using Microneedles Combination with Electroporation and Sonophoresis: Effect of Molecular Weight on Skin Permeation

Maleenart Petchsangai, Praneet Opanasopit, Theerasak Rojanarata, and Tanasait Ngawhirunpat

Faculty of Pharmacy, Silpakorn University, Nakhon Pathom, Thailand

[p\\_maleenart@hotmail.com](mailto:p_maleenart@hotmail.com)

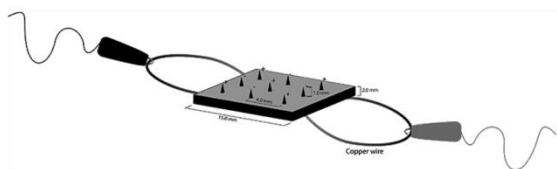
### INTRODUCTION

Limitations of transdermal drug delivery system are significantly associated with the skin's barrier function which restricts the amount of drug absorbed across the skin. As a result, physical enhancement methods such as microneedles (MN), electroporation (EP), and sonophoresis (SN), have been used to improve skin permeability. MN are micron-sized needles which can breach stratum corneum, the skin's outermost layer, to create holes big enough for the molecules to pass through. EP is the transitory structural perturbation of lipid bilayer membranes causing a rearrangement of lipid bilayer in cell membrane or in more complex structure such as stratum corneum, leading to an increase in skin permeability. SN, also known as phonophoresis, is the use of ultrasound to deliver various compounds through the skin. The three combined method, MN+EP+SN, has been shown a great effectiveness for improving skin permeation of hydrophilic macromolecules. The objective of this study was to investigate the effect of molecular weight (MW) of hydrophilic macromolecules on skin permeation using this three combined method, MN+EP+SN.

### EXPERIMENTAL METHODS

Porcine skin was used as an animal skin model in this study. 1,000  $\mu\text{m}$ -long MN+EP arrays were prepared using nine acupuncture needles (**Figure 1**). Fluorescein isothiocyanate (FITC)-dextrans with various MW; FD-4 (4 kDa), FD-20 (20 kDa), and FD-40 (40 kDa) were used as model drugs. *In vitro* skin permeation of all compounds was performed using Franz diffusion cell apparatus. First, skin was punctured with the MN+EP array using 10 N forces for 2 min. Next, 300 V of electrical current was applied to the skin using a square wave pulse generator. The MN+EP-treated skin was mounted, and 625  $\mu\text{M}$  of FD-4, FD-20, and FD-40 was instantly added to each of the diffusion cell.

(a)



(b)

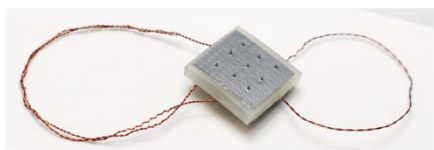


**Figure 1** A schematic diagram of the MN+EP array (a) and a homemade MN+EP array which each of needle was systematically connected by copper wire (b).

Ultrasonic energy was then applied continuously using an ultrasonic transducer for 2 min. The concentration of FD was determined using a spectrofluorophotometer.

### RESULTS AND DISCUSSION

To study the effect of MW on the macromolecular delivery through the skin treated with MN+EP+SN, the skin permeation of FD-4, FD-20, and FD-40 were investigated. The results showed that the cumulative amount of FD permeated can be ranked as follow; FD-4 > FD-20 > FD-40 (**Figure 2**). This result suggested that the higher MW of penetrant contributed to the lower skin permeation.

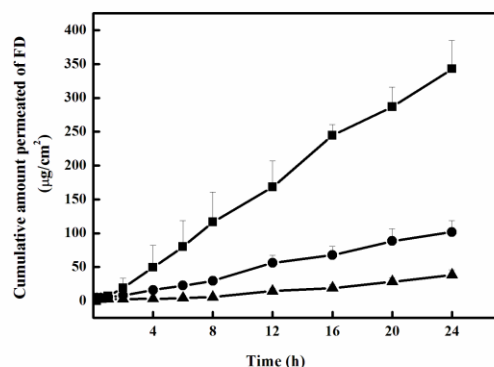


**Figure 2** *In vitro* permeation profiles of FD with various MW across porcine skin: FD-4 (■), FD-20 (●), and FD-40 (▲).

### CONCLUSION

The homemade MN+EP arrays with the length of 1,000  $\mu\text{m}$  were successfully fabricated using nine acupuncture needles. They showed the potential to deliver hydrophilic macromolecules with MW up to 40 kDa, into the skin. Nevertheless, the MW of penetrant affected the skin permeation using this three combined method. The higher MW of FD was applied, the lower skin permeability could be obtained.

### REFERENCES

1. Chen B. *et al.*, Sensor Actuat B-Chem. 145: 54–60, 2010.
2. Petchsangai M. *et al.*, Biol Pharm Bull. 37(8): 1373–1382, 2014
3. Yan K. *et al.*, Int J Pharm. 397: 77–83, 2010

### ACKNOWLEDGMENTS

The authors would like to acknowledge The Thailand Research Funds through the Royal Golden Jubilee Ph.D. Program (Grant No.PHD/0019/2553) and Faculty of Pharmacy, Silpakorn University, Thailand for kindly support.



## Poly-L-lysine Based Covalently Crosslinked Bionanocomposites with Controlled Drug Release and Cell Adhesion Properties

Minkle Jain, Kazuaki Matsumura

School of Materials Science, Japan Advanced Institute of Science and Technology, Japan

[s1340151@jaist.ac.jp](mailto:s1340151@jaist.ac.jp)

### INTRODUCTION

Engineered tissues are great substitutes for treating organ failures associated with disease, injury and degeneration<sup>1</sup>. However, challenging task is to mimic the complex cell-microenvironmental interactions to regulate the formation of functional tissue. Designing of the new biomaterials with controlled release profile and cell adhesion characteristics can be useful to precisely control cell behaviour and facilitate the formation of specific functional tissues<sup>2</sup>. In order to recapitulate the native structures various nanofillers are used with in the polymeric network. In this context injectable hydrogels are good choice with aforementioned properties. In the current study we have formulated the system based on succinylated poly-L-lysine (PLL-SA) which is chemically crosslinked using 4-arm polyethylene glycol with N-hydroxy succinimide ester (PEG-NHS). Previously, we have reported that PLL-SA is a potent cryoprotectant<sup>3</sup>. The uniqueness of this gel is that the degradation of this can be tuned from few days to months. Incorporation of synthetic clay laponite (XLG) can introduce biocompatibility. Modification of the system with nanoclay also modulates the mechanical and degradation property. Overall this hydrogel could be used for biomedical applications that require spatial control of cell adhesion and controlled release of cationic drugs.

### EXPERIMENTAL METHODS

PLL-SA was synthesised by reacting PLL aqueous solution with succinic anhydride in different mole ratios from 0-80%. This PLL-SA was then mixed with laponite and PEG-ester in appropriate amounts to formulate the hydrogel. Parameters were varied to tune the mechanical and degradation properties like concentration of the polymer, crosslinker and nanoclay. These hydrogels were analysed by XRD and ATR-IR. Dynamic mechanical analysis (DMA) was also carried out.

### RESULTS AND DISCUSSION

PLL-SA was mixed with crosslinker in various concentrations to tune the degradation profile of the system (Figure 1). Incorporation of laponite in this helps us to tailor the cell adhesion and mechanical property of the gel. Mechanical property of the gel can be tuned from 5 kPa to 25 kPa by just incorporation of nanoclay and varying the crosslinker concentration (Figure 2).

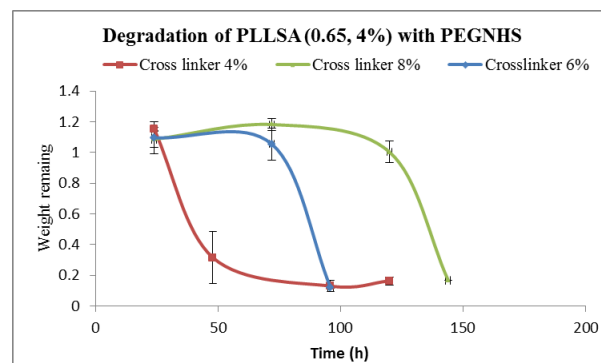


**Figure 1** Degradation profile of the gel with various crosslinker concentration.

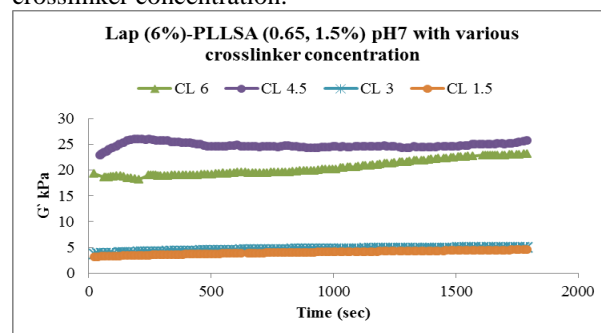


**Figure 2** Mechanical property tuning of the gel by varying crosslinker concentration after incorporation of laponite.

### CONCLUSION

The current study clearly demonstrates that covalently crosslinked PLL-SA-PEG based system exhibit tunable mechanical property and cell adhesion properties. Incorporation of nanoclay results in tough hydrogels. This system can be used as injectable hydrogels. Thus, this hydrogel enables the development of cell material platforms that can be applied and tailored to specific functions for tissue engineering and drug delivery applications.

### REFERENCES

1. Khademhosseini A. *et al.*, Biomaterials, 28:5087-5092, 2007.
2. Lutolf M.P., Nat. Mater., 8:451-453, 2009.
3. Matsumura K. *et al.*, Biomaterials, 30:4842-4849, 2009.

### ACKNOWLEDGMENTS

“The authors would like to thank the Grant-in-Aid for Young Scientists (B), MEXT, (Grant no: 25870267) for providing financial support to this project.”



## New Macromolecular Conjugates of Camptothecin - Synthesis, Characterization and *in vitro* Evaluation

Marcin Sobczak<sup>1</sup>, Ewa Olędzka<sup>1</sup>, Paweł Horeglad<sup>2</sup>, Urszula Piotrowska<sup>1</sup>, Andrzej Plichta<sup>3</sup>, Joanna Kolmas<sup>1</sup>, Grzegorz Nałęcz-Jawecki<sup>4</sup>

<sup>1</sup>Medical University of Warsaw, Faculty of Pharmacy, Department of Inorganic and Analytical Chemistry, Banacha 1, Warsaw 02-097, Poland

<sup>2</sup>University of Warsaw, Centre of New Technologies, Banacha 2c, Warsaw 02-097, Poland

<sup>3</sup>Warsaw University of Technology, Faculty of Chemistry, Chair of Polymer Chemistry and Technology, Noakowskiego 3, Warsaw 00-664, Poland

<sup>4</sup>Medical University of Warsaw, Faculty of Pharmacy, Department of Environmental Health Science, Banacha 1, 02-097 Warsaw, Poland

[marcin.sobczak@wp.pl](mailto:marcin.sobczak@wp.pl)

### INTRODUCTION

20(S)-Camptothecin (CAMPT) has been verified as a broad range of anti-cancer activity in animal models including lung, prostate, breast, colon, stomach, bladder, ovarian and melanoma cancers<sup>1,2</sup>. However, its therapeutic application is hindered by a low solubility, high toxicity and rapid inactivation through lactone ring hydrolysis at a physiological pH<sup>1,2</sup>.

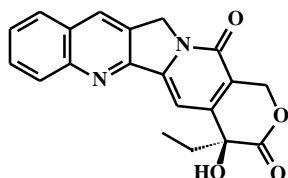


Fig. 1. 20(S)-Camptothecin

The polymeric conjugates of CAMPT could act as a transport form for this drug and enhance its biodistribution. In the past few years, the covalent conjugates of CAMPT with polymers have been developed and characterized<sup>3</sup>.

The main problem with the obtained carriers is probably owing to the not fully controlled release of CAMPT. Therefore, polymer chemists are still actively involved in the investigating of new effective drug delivery systems containing CAMPT<sup>1-3</sup>.

The aim of this study was to prepare new polyesters or poly(ester-carbonate)s conjugates containing CAMPT. The preliminary studies of the influence of polymeric chain structure on the release process of CAMPT were presented.

### EXPERIMENTAL METHODS

The polymerization of cyclic esters or carbonates were carried out under an argon atmosphere. The polymeric products were dissolved in methylene chloride and then washed with methanol and dilute hydrochloric acid.<sup>3</sup>

The toxicity tests were carried out according to procedures described in our early papers<sup>3</sup>.

Polymeric conjugates of CAMPT were synthesized using two-step methods under argon atmosphere<sup>3</sup>.

The obtained macromolecular conjugates of CAMPT were put into PBS (pH 7.4) at 37°C, and the initial UV measurement was carried out.

### RESULTS AND DISCUSSION

The macromolecular matrices were obtained by the ring-opening polymerization (ROP) of cyclic esters ( $\epsilon$ -

caprolactone, glycolide and *rac*-lactide) and cyclic carbonate (trimethylene carbonate). The ROP process was carried out in the presence of PEG as macro-co-initiators and tin (II) or gallium catalytic systems.

The cytotoxicity evaluation of the obtained polymers was studied using the luminescent bacteria *V. fischeri* and two ciliated protozoans *S. ambiguum* and *T. thermophila*. It was found that the obtained matrices were not toxic to all test bionts, both bacteria and protozoa.

In the second step of this study, the macromolecular conjugates of CAMPT were obtained. The polymers and CAMPT were coupled *via* 1,6-diisocyanatohexane. *In vitro* CAMPT release from the macromolecular conjugates was carried out in PBS buffer at 37 °C for 1-12 weeks. It has been found that many factors are influencing the release of CAMPT from the obtained macromolecular conjugates, namely the copolymers structure, co-monomer unit content in the polymer chain and  $M_n$  of macro-coinitiators.

### CONCLUSION

The obtained novel biodegradable matrixes were not toxic. The rates of CAMPT release were shown to be directly dependent on the nature of the received copolymers. The kinetic rates of CAMPT released was seen to be faster for the polymeric conjugates contained ester units as compared to those with carbonate units. The obtained results demonstrate that the polyesters or poly(ester-carbonate)s are interesting and promising materials for the controlled release of CAMPT.

### REFERENCES

1. Li Q.-Y. *et al.*, Curr. Med. Chem. 13(17):2021-2039, 2006
2. Liew S.T. *et al.*, Curr. Pharm. Design 14(11):1078-1097, 2008
3. Sobczak M. *et al.*, J. Macromol. Sci. Pure and Appl. Chem. 51:254-262, 2014

### ACKNOWLEDGMENTS

This work was financially supported by National Science Centre of Poland (OPUS-5 research scheme, grant number DEC-2013/09/B/ST5/03480 entitled: "Elaboration of anti-cancer drug implantational delivery system immobilized on polymer matrix"). P.H. thanks National Science Centre of Poland (SONATA BIS2 Programme, Grant No. DEC-2012/07/E/ST5/02860) for the financial support.



## Preparation and Therapeutic Effect of Calcium Phosphate Nano-Capsules Enclosing DNA/PEI/Hyaluronic Acid Complex for Durable Gene Expression

Tomoko Ito<sup>1,2</sup>, Yoshiyuki Koyama<sup>2</sup>, Masazumi Eriguchi<sup>2</sup>, Makoto Otsuka<sup>3</sup>

<sup>1</sup> Meiji Pharmaceutical University, Japan,

<sup>2</sup> Japan Anti-tuberculosis Association, Shin-Yamanote Hospital, Japan,

<sup>3</sup> Musashino University, Research Institute of Pharmaceutical Sciences, Japan

[tito@shinyamanote.jp](mailto:tito@shinyamanote.jp)

### INTRODUCTION

Non-viral vectors such as polycations or cationic lipids have been developed to mediate the gene transfection. Although these cationic reagents can lead to high gene expression in cultured cells, they showed very limited in vivo transfection efficiency. The complexes of plasmid DNA with these vectors usually have positive charge on their surface, which invites nonspecific interactions with blood components or cells. We found that hyaluronic acid (HA) could deposit onto the DNA/polycation (or cationic lipid) complexes to recharge their surface to negative, and effectively diminished the adverse interactions<sup>1, 2</sup>. DNA/polycation/HA ternary complex was highly biocompatible, and could be targeted to malignant cells. HA-coating also improved the transcription efficiency of the DNA complex<sup>1</sup>. Moreover, we found that the DNA/polyethyleneimine (PEI)/HA ternary complex could be freeze-dried without any cryoprotectant maintaining their gene transfection activity under precise conditions<sup>3</sup>. It enabled the preparation of very small DNA complex particles with relatively high concentration by preparing the complex at highly dilute conditions followed by condensation by lyophilizing, and rehydration with small amount of water. Small DNA/polycation/HA complexes were then prepared with plasmid DNAs coding cytokines, and were injected into tumor-bearing mice. They showed strong suppression of the tumor growth, and the small tumors completely disappeared<sup>3</sup>. In those experiments, multiple injections of the complexes were required to achieve the satisfactory therapeutic effect, and single dose rarely induced high response, probably owing to the short duration of the gene expression by such artificial vectors. Multiple injections are sometimes difficult depending on the injection site. Slow release system would, thus, be desired to get high therapeutic effect by a few times-administration.

On the other hand, calcium phosphate (CaP) such as a hydroxyapatite has been explored as biodegradable and biocompatible drug-releasing devices. In this study, we developed novel CaP nanocapsules including DNA/PEI/HA ternary complexes (CaP-DNA/PEI/HA), and their durable gene expression and anti-tumor effect were examined.

### EXPERIMENTAL METHODS

CaP-DNA/PEI/HA capsule was prepared by immersing fine pDNA/PEI/HA ternary complex particles, which had been obtained by the method described above, in 1.5 times concentrated simulated body fluid (SBF). To examine the transfection efficiency of the CaP-coated

DNA complex, CaP-DNA(GFP)/PEI/HA was prepared with plasmid coding GFP, and added to cultured B16 cells. GFP gene expression was then observed by fluorescence microscopy. Cellular uptake of the DNA complex by the cells was also examined using the complex with DNA fluorescently labeled by YOYO-1. Fluorescence intensity of GFP or YOYO-1 was evaluated by image analysis.

Tumor-bearing mice were prepared by subcutaneous inoculation of B16 cells. When the tumor size increased to 4 mm, CaP-DNA(GM-CSF)/PEI/HA, prepared with plasmid coding GM-CSF, was injected into the tumor just once, and tumor size was measured for 100 days.

### RESULTS AND DISCUSSION

SBF has a similar inorganic ion concentration to that of human blood plasma, and is supersaturated against hydroxyapatite. When a material having surface containing phosphoric acid or carboxylic acid groups are immersed in SBF, it is known that an apatite layer would be formed on it. The DNA complex surrounded by HA could also be coated by CaP layer, when the complex was mixed with 1.5-times concentrated SBF, and CaP capsule enclosing the DNA complex was obtained.

Cellular uptake of DNA/PEI/HA complex by B16 cells reached maximum 1-2 days after the addition of the complex, regardless of whether coated with CaP or not. Although uptake profile was similar, the CaP-DNA/PEI/HA showed much prolonged gene expression (>2 weeks) than that without CaP-coating.

The therapeutic effect of the slow-releasing system was then examined in tumor model mice. Durable gene expression invited much higher therapeutic efficacy, and single dose of CaP-DNA(GM-CSF)/PEI/HA completely inhibited the tumor growth in most mice.

### CONCLUSION

A CaP-encapsulated DNA complex could be obtained by immersing the hyaluronic acid-coated DNA/PEI complex in SBF. It showed highly durable gene expression. Those comprising pDNA(GM-CSF) had a significant tumor-growth suppression effect, and single injection induced complete disappearance of the tumor. DNA complex coated by CaP layer seems promising as a sustained-gene expression device.

### REFERENCES

1. Ito T. *et al.*, J. Control. Release. 112: 382-388, 2006
2. Ito T. *et al.*, J. Drug Target. 16: 276-281, 2008
3. Ito T. *et al.*, Biomaterials. 31: 2912-2918, 2010

### ACKNOWLEDGMENTS

This work was partly supported by the Japan Society for the Promotion of Science (26350533 and 23700564)



## Thermally Responsive Core-shell Nanocapsules with Independent Dual Drug Release Profiles for Combined Therapy of Osteoarthritis

Mi Lan Kang, Ji Eun Kim, Gun Il Im\*

Department of Orthopaedics, Dongguk University Ilsan Hospital, Korea

\*[gunil@duih.org](mailto:gunil@duih.org)

### INTRODUCTION

Kartogenin (KGN) is a recently characterized material that promotes the selective differentiation of mesenchymal stem cells (MSCs) into chondrocytes, thus stimulating cartilage regeneration<sup>1</sup>. Diclofenac (DCF) belongs to a class of medicines called non-steroidal anti-inflammatory drugs (NSAIDs) and helps to reduce inflammation and pain. In this study, DCF and KGN were choosing as the combined osteoarthritis (OA) therapy to induce anti-inflammatory activity and cartilage regeneration.

We developed a dual drug delivery system that can release two drugs independently by thermal responsiveness. The nanoparticles consisting of chitosan oligosaccharide (COS) and carboxyl group-terminated pluronic F127 (F127) was synthesized by covalent cross-linking. KGN was covalently conjugated to COS before the nanoparticle synthesis. DCF was encapsulated in the inner core of the nanoparticle.

The aim of this study was to (1) characterize the nanocapsules for controlled dual release by temperature change and (2) evaluate the combined therapeutic effects of the nanocapsules *in vitro*.

### EXPERIMENTAL METHODS

**Preparation of nanocapsules** Carboxylated F127 (F127-COOH) can be obtained according to the reported work with succinic acid. Conjugation of F127-COOH and KGN with COS was carried out by EDC/NHS during the nanocapsules synthesis process using emulsification/solvent evaporation method. DCF was encapsulated inside of the nanocapsules by change of wall-permeability according to temperature control. The chemical conjugation was confirmed by FTIR and <sup>1</sup>H-NMR. Size and morphology of the nanocapsules were characterized by DLS and FE-SEM, respectively.

**Controlled dual release by temperature change** *In vitro* release study of the F127-COS-KGN NCs loading DCF was carried out by temperature change. The amounts of KGN and DCF released from the NCs were determined by HPLC chromatography.

***In vitro* chondrogenic differentiation** The hBMSCs (2.5×10<sup>5</sup> cells, passage 3-5) were made by pellets and then the nanoparticles were added. After 14-21 days, pellets were analysed for DNA contents, GAG amount, and the expression of chondrogenic markers.

***In vitro* anti-inflammatory activity** After induction of inflammation with LPS in human U937 cells and primary chondrocyte, the nanoparticles were treated to the cells. The concentration of secreted IL-6 and TNF-α were determined ELISA.

### RESULTS AND DISCUSSION

**Preparation of nanocapsules** The nanocapsules are ~300 nm at 37 °C and expand to ~650 nm when cooled at 4 °C in aqueous solution. Temperature-controlled size variation was reduced according to increase of molar ratio of KGN to COS. The molar ratio of F127 to COS was increased, the range of size change according to temperature control was grown.

***In vitro* release study** While the encapsulated DCF showed burst release for 9 hours after cold shock, the conjugated KGN showed sustained release for 14 days even though temperature change. When the molar ratio of F127 decreased in the F127-COS-KGN NCs formulations, more sustained release of KGN was observed.

***In vitro* chondrogenic differentiation** While DNA levels did not change significantly, GAG per DNA content increased significantly, when exposed to nanocapsules versus no treatment or unconjugated KGN (p < 0.05). There was no significant difference whether cold shock is treated or not in nanocapsules treated groups. Safranin-O staining showed the greater intensity in the pellets treated with nanocapsules than those of pellets treated with unconjugated KGN. The gene expression of *COL2A1* and *aggrecan* increased in hBMSCs pellets exposed to unconjugated KGN and both nanocapsules for 21 days compared with those of untreated hBMSCs. In particular, nanocapsules treated pellets exposing to cold shock showed significant increases in both chondrogenic proteins compared with other pellets treated with either unconjugated KGN or nanocapsules without cold shock.

***In vitro* anti-inflammatory activity** After cold shock treatment, the nanocapsules treated chondrocyte showed rapid decrease of IL-6 secretion. A similar phenomenon was confirmed on U937 showing decrease of TNF-α.

### CONCLUSION

Both KGN and DCF were released independently from the F127-COS-KGN NCs loading DCF by temperature control. The DCF showed burst release for 6 hour respecting rapid anti-inflammatory analgesic effect, while the KGN was released sustainably and continuously from the NCs respecting effective regeneration. The F127-COS-KGN NCs loading DCF can be effective combined therapeutic for OA by thermally controlled dual drug delivery.

### REFERENCES

1. Johnson K. et al. *Sience* 336:717-21,2012

### ACKNOWLEDGMENTS

The authors would like to thank the National Research Foundation of Korea (Grant no: 2013R1A1A2062978) for providing financial support to this project.





## Combined Scaffold Composed of Hydroxyapatite/Biodegradable Polymer and Pamidronate as a Model Drug for the Therapy of Bone Tumour

Ewa Oledzka<sup>1</sup>, Marcin Sobczak<sup>1</sup>, Joanna Kolmas<sup>1</sup>, Grzegorz Nałęcz-Jawecki<sup>2</sup>

<sup>1</sup>Medical University of Warsaw, Faculty of Pharmacy, Department of Inorganic and Analytical Chemistry, Banacha 1, Warsaw 02-097, Poland

<sup>2</sup>Medical University of Warsaw, Faculty of Pharmacy, Department of Environmental Health Science, Banacha 1, 02-097 Warsaw, Poland  
[eoledzka@wum.edu.pl](mailto:eoledzka@wum.edu.pl)

### INTRODUCTION

In the last years, the tendency in the development of biomaterials for implantology indicates the growing importance of composite materials based on polymers<sup>1,2</sup>. Nonetheless, inimical mechanical properties of the polymeric materials, such as mechanical strength, Young's modulus, fracture toughness, limited their application as implants. Hydroxyapatite (HA) is known as biocompatible and bioactive material, thus was commonly used for the fabrication of highly porous, interconnected scaffolds and isotropic pore structures recently<sup>3</sup>. This material might be also applied as a coating for orthopaedic and dental implants sustaining their surface properties and the bone-implant interface leading to the improvement in its osseointegration<sup>4</sup>. Selenium is one of the essential constituents of the human diet. Furthermore, it plays a significant role in diverse metabolic processes and that it, is a constituent of selenoproteins as well as of glutathione peroxidase<sup>5</sup>. Pamidronate - alkyl-amino bisphosphonate is considered standard of care therapy for nonresectable skeletal metastases in human cancer patients<sup>6</sup>.

Therefore, the aim of this study was to develop a novel combined scaffold composed of hydroxyapatite doped with selenium ions/biodegradable polymer (linear or branched) and contained pamidronate as a model drug. We assume that the fabricated scaffolds could serve as a promising bone replacement material for patients with bone tumours or bone metastasis (jaw bone).

### EXPERIMENTAL METHODS

The polymerization of linear and branched polymers was carried out under an argon atmosphere. The polymeric products were dissolved in methylene chloride and then precipitated twice from a cold mixture hexane/diethyl ether and dried under vacuum for 72 h.

The cytotoxicity assays were carried out with the luminescent bacteria *Vibrio fischeri* and the ciliate protozoan *Spirostomum ambiguum*.

The obtained combined scaffolds for both, *in vitro* release and hydrolytic degradation studies, have been manufactured in the tablet form.

The *in vitro* release study of pamidronate was performed to measure the concentration of drug released at pH 7.00±0.05 at 37°C.

### RESULTS AND DISCUSSION

In the first step of this study, linear and branched biodegradable polymers have been synthesized and characterized. The polymerization in various molar ratio took place easily under the designated conditions.

<sup>1</sup>H and <sup>13</sup>C NMR analysis demonstrated that used initiators successfully initiated ROP of  $\epsilon$ -caprolactone and D,L-lactide. Moreover, they were effectively incorporated into macromolecule.

The combined scaffolds were manufactured in the tablets form, by a direct compression of substituted hydroxyapatite, synthesized polymer and pamidronate. It has been found that the kinetic release of drug from the scaffolds tested *in vitro*, is strongly dependent on the physicochemical properties and an average molecular weight of the polymers. Furthermore, it was well- correlated with the hydrolytic biodegradation results of the scaffolds fabricated without drug.

### CONCLUSION

A combined scaffold composed of hydroxyapatite doped with selenium ions and biodegradable polymer and containing pamidronate was successfully developed. In order to prepare biodegradable polymers, bulk ROP of  $\epsilon$ -caprolactone and D,L-lactide was carried out. The structure and physicochemical properties of the obtained products were confirmed by analytical methods. The cytotoxicity showed that the obtained polymers are not cytotoxic. *In vitro* results showed that the percentage of the released pamidronate was affected by the physicochemical properties of the synthesized polymeric matrices. Consequently, this newly developed combined scaffold might be applied as a promising material for patients with bone tumours or bone metastasis (jawbone).

### REFERENCES

1. Mano J.F. *et al.*, Comp. Sci. Technol. 64:789-817, 2004
2. Chłopek J. Composites 1:50-54, 2001
3. Son J-S. *et al.*, J. Biomed. Mat. Res. A 99A:638-647, 2011
4. Rodríguez-Valencia C. *et al.*, J. Biomed. Mat. Res. A 101A:853-861, 2013
5. Holben D.H. *et al.*, J. Am. Diet. Assoc. 99:836-843, 1999
6. Lipton A. *et al.*, Semin. Oncol. 37:S15-S29, 2010

### ACKNOWLEDGMENTS

This work was supported by the research programme (Project DEC-2011/03/D/ST5/05793 "Development and characterization of polymer-apatite composite containing selenium and bisphosphonates") of the National Science Centre of Poland.



# Poly(lactic-co-glycolic acid)-based Nanoparticles as Drug Delivery Systems for Doxycycline Hyclate and Simvastatin for the Treatment of Inflammation-caused Bone Resorption

Manuel Schweikle, Hanna Tiainen, Håvard Haugen

Department of Biomaterials/Institute of Clinical Dentistry, University of Oslo, Norway

[manuel.schweikle@odont.uio.no](mailto:manuel.schweikle@odont.uio.no)

## INTRODUCTION

Hard tissue regeneration in bone defects caused by periodontitis and periimplantitis can be challenging due to critical defect size and high risk of recurrent bacterial infections. Synthetic titanium dioxide (TiO<sub>2</sub>) scaffolds have shown to feature good osteoconductive capacities paired with high compressive strength which allows mechanical loading shortly after implantation<sup>1</sup>.

However, they are lacking the osteoinductive properties of autologous bone graft material. For that reason they should be combined with poly(lactic-co-glycolic acid) (PLGA) nanoparticles as a drug delivery system for doxycycline hyclate (DOX) which in addition it's antibiotic action has shown to feature bone growth promoting effects when presented in adequate concentrations<sup>2</sup>.

## EXPERIMENTAL METHODS

DOX-loaded PLGA nanoparticles were produced by a double-emulsion water in oil in water technique as previously described<sup>3</sup>.

Size and morphology of the fabricated particles were characterized qualitatively and quantitatively by AFM, SEM and DLS. UV-vis and FT-IR were used to characterize and quantify the encapsulated drugs. Several process modifications were investigated to manipulate particle morphology and drug diffusion during particle formation. Furthermore, the developed method was slightly adapted to produce particles loaded with the hydrophobic drug simvastatin (SIM), which has shown to have similar bone growth properties as DOX.

## RESULTS AND DISCUSSION

The introduced fabrication method was found successful for the production of smooth, spherical nanoparticles within the size range of 200 to 800 nm (see Fig. 1). Particle size and morphology could to some extent be controlled by altering different emulsification parameters.

However, maximal encapsulation efficiency (EE) for hydrophilic DOX was just below 2 %. At the same time hydrophobic SIM could be entrapped at up to 80 % EE. These findings stand in contrast to the comparatively high EEs for small hydrophilic molecules in PLGA nanoparticles reported elsewhere<sup>3</sup>.

It can be assumed that large quantities of hydrophilic DOX diffuse into the outer water phase during particle preparation due to the weak intermolecular interaction between drug and matrix. Various process

modifications were tested to decrease the loss of DOX during the fabrication process by means of accelerating polymer precipitation and retarding diffusion kinetics, but did not significantly increase the EE.

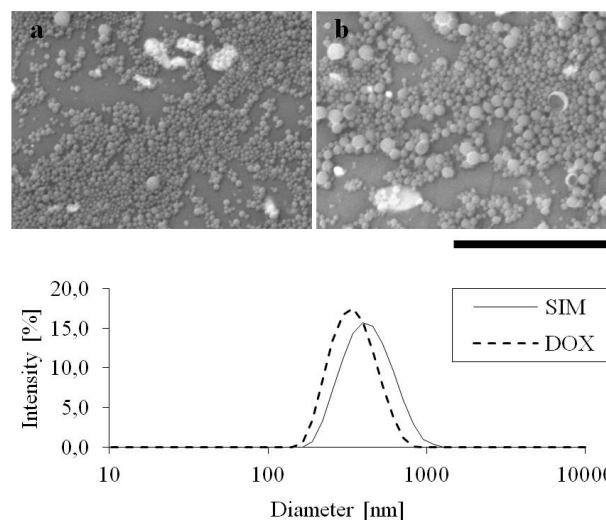


Fig. 1: SEM-images of (a) DOX- and (b) SIM-loaded PLGA nanoparticles featuring smooth, spherical shape and size distribution measured by DLS. Scale bar 10  $\mu$ m.

## CONCLUSION

No significant amounts of hydrophilic DOX could be immobilized in the produced PLGA nanoparticles. A huge discrepancy could be observed for the EE of DOX and SIM. The results question the suitability of a water based double-emulsion process for the encapsulation of small hydrophilic molecules within hydrophobic matrices.

## REFERENCES

- 1 Tiainen H. *et al.*, J Mater. Sci. Mater. Med., 21:2783-2792, 2011
- 2 Almazin S. M. *et al.*, J Periodontol. 80:999-1005, 2009
- 3 Misra R *et al.*, Nanomedicine 4: 519-530, 2009

## ACKNOWLEDGMENTS

The authors would like to thank the Research Council of Norway (grant NFR 228415) for providing financial support to this project.

## Upsalite®: Novel Mesoporous Drug Delivery System

Peng Zhang, Teresa Zardán Gómez de la Torre, Johan Forsgren, and Maria Strømme

Ångström Laboratory, Uppsala University, Uppsala, Sweden

[peng.zhang@angstrom.uu.se](mailto:peng.zhang@angstrom.uu.se)

### INTRODUCTION

Currently, poor aqueous solubility of active pharmaceutical ingredients (APIs) has been one of the most challenging issues for the pharmaceutical industry since this often results in limited oral bioavailability of these APIs which in turn limits their therapeutic effect. About 40% of newly marketed drugs have poor solubility and 80-90% of drug candidates in the R&D pipeline fail because of solubility problems. Therefore, improvement of the solubility of highly permeable but poorly soluble APIs, i.e. BCS II (Biopharmaceutics Classification System II) drugs, has been in the focus of research during the last decade.

One attractive approach to increase the aqueous solubility and thus the bioavailability of poorly soluble drugs is to formulate the poorly aqueous soluble compounds in their amorphous state since amorphous compounds generally exhibit higher apparent solubilities than the crystal form of the same substance<sup>1</sup>. However, because of their metastable nature, amorphous APIs are driven by thermodynamics to crystallise, depending on factors like the glass transition temperature ( $T_g$ ) and moisture content of the formulation. Thus, the amorphous APIs need to be stabilised in the formulation in order to prevent crystallisation.

Due to the small pore size, mesoporous structures (pores with a diameter between 2 and 50nm) have the ability to stabilize amorphous substances, which is an attractive approach to improve the solubility of drugs with poor aqueous solubility<sup>2</sup>. In the current study we aimed to investigate if Upsalite®, a mesoporous  $MgCO_3$  material, could suppress crystallisation of the BCS (Biopharmaceutics Classification System) class-II drug Ibuprofen (IBU) and hence increase the apparent solubility of the substance.

### EXPERIMENTAL METHODS

Upsalite® was synthesized as described earlier<sup>3</sup>. IBU was incorporated into the material via a soaking method and dried at 70 °C. X-ray powder diffraction (XRD), Fourier transform infrared spectroscopy,  $N_2$  sorption analysis, thermal gravimetric analysis (TGA) and differential scanning calorimetry (DSC) were employed to characterize the drug loaded material. The release of IBU was studied by the USP-II paddle method in phosphate buffer (pH=6.8) and the released concentration of IBU was monitored by UV/vis absorbance spectroscopy.

### RESULTS AND DISCUSSION

From the XRD patterns and the DSC curves (Figure 1), it could be confirmed that the IBU incorporated in Upsalite® was present in an amorphous

state demonstrating that the mesoporous structure of Upsalite® completely suppressed crystallisation of the incorporated drug.

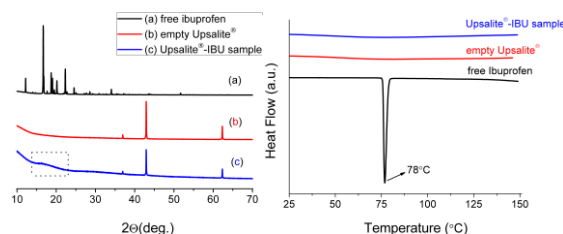


Figure 1. XRD patterns (left), DSC curves (right) for the studied samples.

The release profiles of free IBU and IBU incorporated in Upsalite® can be seen in Figure 2. Clearly, the release rate of the amorphous IBU inside the Upsalite® is more rapid than that of the free substance. The release rate of the amorphous IBU from Upsalite® is three times faster during the first 5 minutes compared to the dissolution rate of the crystalline free substance. As well, 50% of the IBU is dissolved and released from the carrier within 12 minutes while it takes 30 minutes for the free substance to reach the same level.

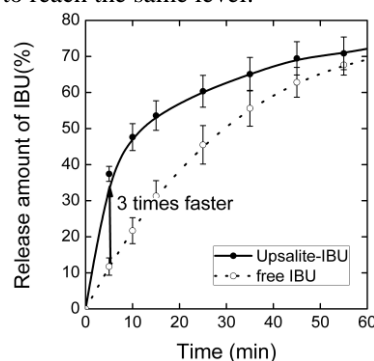


Figure 2. IBU Release Profiles.

### CONCLUSION

This work shows that the mesoporous magnesium carbonate, Upsalite®, can be used as an excipient in pharmaceutical formulations to increase the release rate and solubility of poorly soluble substances.

### REFERENCES

1. Serajuddin A.T.M. J. Pharm. Sci. 88:1058-1066, 1999.
2. Zhang P. *et al.*, Int. J. Pharm. 472:185-191, 2014
3. Forsgren J. *et al.*, Plos one: e68486, 2013

### ACKNOWLEDGMENTS

We acknowledge the funding agency Vinnova as well as the Carl Trygger Foundation and the China Scholarship Council (CSC) for financial support of the presented work.



## INTRODUCTION

Multiple clinical trials have indicated that anti-platelet treatment can reduce the likelihood of a recurrent stroke event<sup>1</sup>. Drug delivery systems (DDSs), made of biodegradable polymers, have the potential to control drug release. Electrospinning is a simple technique that can produce 3D structures capable of releasing pharmaceuticals in a controllable manner<sup>2</sup>. The main goal of this work was to study the properties of an electrospun DDS, made of polycaprolactone (PCL) and polyethylene glycol (PEG), and encapsulating acetylsalicylic acid (ASA).

## EXPERIMENTAL METHODS

All reagents and polymers were purchased from Sigma-Aldrich. The concentration of ASA in the core solution was 15 mg/ml (ASA specimens). PCL (Mn 70000 – 90000) was used in both core and shell solutions at concentrations of 150 mg/ml and 100 mg/ml, respectively. PEG (Mn 4000) was used only in the shell solution at a concentration of 50 mg/ml. Specimens without ASA encapsulated were also prepared (non-ASA specimens). Electrospinning was performed using a custom-made coaxial nozzle at an electrical field of 1 kV/cm. The flow rates of the core and shell solutions were 1 and 3 ml/h respectively. The morphology of the fibrous scaffolds was examined by scanning electron microscopy (SEM). The mechanical properties of the scaffolds were assessed under both dynamic uniaxial tensile testing and quasi-static uniaxial tensile loading to failure. The dynamic tests were conducted under 0-20% strain at 1 Hz, using a horizontal BOSE tensile testing device (LM1 Testbench), whereas the quasi-static tests were performed at a strain rate of 20 mm/min using an INSTRON tensile testing device (5967 Dual Column). Six rectangular specimens of 15 mm gauge length and 10 mm width were used for each measurement, cut along the electrospinning orientation. A thickness gauge (Quick mini, Mitutoyo) was used to measure the thickness. Both types of tests were performed at room temperature and humidity. The performance of the specimens was assessed from the recorded stress-strain data, which was used to obtain the maximum tensile stress and strain, and Young's modulus. Cytotoxicity experiments were performed according to the ISO10993-5:2009 with L929 murine fibroblasts to assess the biocompatibility of the scaffolds. A contact assay was performed in triplicates using cyanoacrylate (superglue) as the positive and collagen gel (2 mg/ml) as the negative control. Statistical analysis was performed using Origin Pro 8.5 (One-way ANOVA with post-hoc Tukey), whereas statistical significance was determined at a 0.05 level.

## RESULTS AND DISCUSSION

Morphologically, the electrospun fibres presented a smooth, cylindrical shape with random orientations and an average diameter of  $0.67 \pm 0.29 \mu\text{m}$  and  $0.49 \pm 0.10 \mu\text{m}$  for the ASA and non-ASA specimens, respectively ( $p=0.018$ ). The values of Young's modulus obtained from the quasi-static tensile tests ranged from  $68.55 \pm 15.62 \text{ MPa}$  for the non-ASA specimens to  $100.76 \pm 14.74 \text{ MPa}$  for the ASA specimens ( $p<0.05$ ). Accordingly, the values obtained from the dynamic uniaxial tests ranged from  $65.87 \pm 6.66 \text{ MPa}$  for non-ASA specimens to  $107.705 \pm 9.29 \text{ MPa}$  for the ASA specimens ( $p<0.05$ ). No statistically significant difference was found between the two testing methods ( $p>0.05$ ). Moreover, the ultimate tensile strength (UTS) was increased from  $11.32 \pm 1.93 \text{ MPa}$  for the non-ASA specimens to  $13.94 \pm 1.87 \text{ MPa}$  for the ones with ASA ( $p>0.05$ ). The maximum tensile strain values were  $0.38 \pm 0.04$  and  $0.30 \pm 0.02 \text{ mm/mm}$  for the non-ASA and ASA specimens, respectively ( $p=0.18$ ). The mechanical properties of the electrospun constructs were comparable to the mechanical properties of native tissues investigated in previous studies<sup>3</sup>. This highlights the capacity of the electrospun constructs to be tailored in terms of their mechanics to match a range of tissues for biomedical applications. Moreover, none of the specimens (with/without ASA) revealed any cytotoxic effect on the cell viability or morphology of L929 murine fibroblasts.

## CONCLUSION

The addition of ASA led to thinner fibres with significantly higher stiffness and lower ductility in comparison with fibres without ASA encapsulated. Core/shell fibre mats could be potential candidates for DDSs, used to control delivery of anti-platelet agents against recurrent stroke.

## REFERENCES

1. Sacco R.L., Diener H.C. *et al.* N Eng J Med 2008;359:1238-51
2. Szentivanyi A. *et al.* International Journal of Artificial Organs 2011;34(10):986-997
3. Morticelli L., Thomas D. *et al.* J Heart Valve Dis 2013;22(3):340-353

## ACKNOWLEDGMENTS

The authors would like to thank Ass. Prof. Dimosthenis Mavrilas for his contribution in the mechanical testing analysis. This study was partially granted (DFG EXC 62/1) by the German Research Foundation (DFG).





## Controlled Release of Acyclovir from Cytosine-modified Polymer Matrix

Katarzyna Klysik, Anna Karewicz, Aneta Pietraszek, Krzysztof Szczubiałka, Maria Nowakowska

Nanotechnology of Polymers and Biomaterials Group, Faculty of Chemistry, Jagiellonian University, Cracow, Poland  
[karewicz@chemia.uj.edu.pl](mailto:karewicz@chemia.uj.edu.pl)

### INTRODUCTION

The herpes simplex virus is one of the most frequent pathogen acquired by humans. According to the statistics, more than 50% of people are infected by that virus<sup>1</sup>. Acyclovir is a widely used antiviral agent due to of its high efficacy in the treatment of herpes simplex virus infections. Acyclovir blocks viral DNA polymerase, inhibiting replication of DNA. Its application reduces the frequency of relapses and alleviates troublesome symptoms of primary infection<sup>2</sup>. The acyclovir therapy suffers from the low solubility of the drug in aqueous media and resulting low bioavailability, short half-life (about 2.5 h) and large variability in its absorption between patients. Thus the therapy has many adverse effects and can result in neurotoxicity, urticaria, diarrhea or swoon. Therefore, it is important to find new formulations that allow for increasing the effectiveness of the drug in order to decrease the required dose and make the treatment safer.

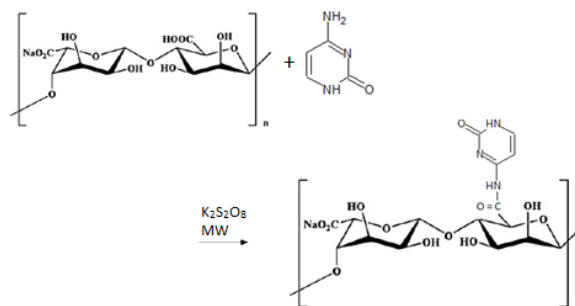
Our work aims at studying the potential use of cytosine – modified polymer matrix as a new carrier designed for acyclovir delivery. The new polymer was obtained by modifying sodium alginate, natural polysaccharide, with cytosine. It is expected that the synthesized derivative will interact specifically with guanine group present in acyclovir's structure by creating hydrogen bonds. This should increase encapsulation efficiency of the polymeric delivery system based on aforementioned derivative and allow for a better control over the release process.

### EXPERIMENTAL METHODS

The resulting derivative was obtained by using microwave irradiation. Sodium alginate, cytosine and potassium persulfate were dissolved in water, mixed thoroughly and the whole mixture was heated to 85°C prior to subjecting to microwaves. The reaction was performed at 85°C in microwave reactor for 30 min. The product was isolated from the reaction mixture by precipitation to isopropanol followed by filtration and drying. The obtained polymer was then characterized using physicochemical methods: elemental analysis, <sup>1</sup>H and <sup>13</sup>C NMR (in D<sub>2</sub>O at room temperature) spectrometry and UV/Vis spectrophotometry. The latter was performed in water at room temperature using 1 cm quartz cuvette.

### RESULTS AND DISCUSSION

Sodium alginate was modified by cytosine using microwave irradiation according to Scheme 1. The success of the reaction was first confirmed by the presence of nitrogen in the elemental analysis results.



**Scheme 1.** Reaction scheme for modification of sodium alginate with cytosine

This element is absent in the alginate structure and its presence can be associated with the introduction of cytosine into the polymeric structure of alginate. <sup>13</sup>C NMR spectrum of obtained derivative showed four signals at: 94.42, 144.52, 154.83 and 163.94 ppm which can be ascribed to the carbons of cytosine. Finally the presence of the absorption maximum at 252 nm, characteristic for acyclovir, in the UV-VIS spectrum of the synthesized derivative of alginate confirmed further the successful incorporation of the drug into the polymeric matrix. The obtained derivative was formed into microbeads using calcium ions as the cross-linking agent. Acyclovir was encapsulated into the matrix. The influence of the specific cytosine-guanine interactions on the release process was verified using unmodified alginate microbeads as a reference.

### CONCLUSION

New cytosine-modified alginate was synthesized using microwave irradiation. The physicochemical characterization of the obtained derivative was performed, including NMR spectroscopy, UV-Vis spectrophotometry and elemental analysis. All the methods confirmed the success of the modification. The obtained derivative was then used to form microbeads. Acyclovir was successfully entrapped in the polymeric matrix and the influence of the specific cytosine-guanine interactions on its release profile was demonstrated.

### REFERENCES

1. Smith J.S. *et al.*, J. Infect. Dis. 186 S3–28, 2002
2. Schuhmacher A. *et al.*, Phytomed; 10:504-510, 2003

### ACKNOWLEDGMENTS

Project operated within the Foundation for Polish Science Team Programme co-financed by the EU European Regional Development Fund, PolyMed, TEAM/2008-2/6.

# Biological Assessment of Polymeric Micelles-based Powders for Pulmonary Administration of Biopharmaceutics

Fernanda Andrade<sup>1,2</sup>, José das Neves<sup>3,4,5</sup>, Pedro Fonte<sup>5,6</sup>, Francisca Araújo<sup>4,5</sup>, Petra Gener<sup>7,8</sup>, Simó Schwartz Jr<sup>7,8</sup>, Mafalda Videira<sup>9</sup>, Domingos Ferreira<sup>1</sup>, Mireia Oliva<sup>2,8,10</sup>, Bruno Sarmiento<sup>3,4,5</sup>

<sup>1</sup>Faculty of Pharmacy, University of Porto, Portugal; <sup>2</sup>IBEC, Institute for Bioengineering of Catalonia, Spain; <sup>3</sup>INEB, Instituto de Engenharia Biomédica, Portugal; <sup>4</sup>I3S, Instituto de Investigação e Inovação em Saúde, Portugal; <sup>5</sup>CESPU, Instituto de Investigação e Formação Avançada em Ciências e Tecnologias da Saúde, Portugal; <sup>6</sup>REQUIMTE, University of Porto, Portugal; <sup>7</sup>CIBBIM, Nanomedicine, Hospital Universitari Vall d'Hebrón, Spain; <sup>8</sup>CIBER-BBN, Biomedical Research Networking Center in Bioengineering, Biomaterials and Nanomedicine, Spain; <sup>9</sup>iMed.Ulisboa, Research Institute for Medicines, Portugal; <sup>10</sup>School of Pharmacy, University of Barcelona, Spain  
[francisca.araujo@ineb.up.pt](mailto:francisca.araujo@ineb.up.pt)

## INTRODUCTION

Inhalation as a non-invasive route for systemic delivery of a variety of drugs, including biopharmaceutics, gained a new breath in the last decades<sup>1</sup>. We propose the use of amphiphilic polymers for the development of powder formulations intended for the pulmonary delivery of biopharmaceutics, using insulin as a model protein. Previously, we successfully developed and characterized insulin-loaded micelles of Soluplus® (SOL), Pluronic® F68, F108 and F127. Lyophilized micelles shown to be physically stable upon storage up to 6 months both at 4°C and 20°C, with negligible loss of the secondary structure of the protein<sup>2</sup>. This work aimed to assess the *in vitro* toxicity, pulmonary permeability, and phagocytosis by macrophages; and study the pharmacological activity and toxicity profile of formulations in diabetic animal models.

## EXPERIMENTAL METHODS

Powders obtained by freeze-drying of insulin-micelles. The geometrical particle size distribution was determined by laser diffraction and the aerodynamic diameter (*d<sub>ae</sub>*) estimated using powders' tap density. IC<sub>50</sub> and CC<sub>50</sub> values of formulation in Calu-3 and A549, and Raw 264.7 cells after 24h of contact was assessed using the MTT conversion assay and LDH leakage assay. The permeability of free and formulated insulin through alveolar and bronchial epithelium was assessed using A549 and Calu-3 cell monolayers. The uptake by THP-1 and U937 macrophages was assessed qualitatively by confocal microscopy and quantitatively by flow cytometry. *In vivo* pharmacological activity and sub-acute toxicity of formulations were assessed using streptozocin-induced diabetic male Han:Wistar rats. Insulin was administered subcutaneously as solution and endotracheally as powders and solution. Plasma glucose and insulin levels were determined at different time-points. For toxicity assessment, formulations were administered every two days during 14-days. PBS and insulin solution were used as controls. After euthanasia, blood samples were collected and bronchoalveolar lavage performed. BALF screened for toxicity markers and plasma for insulin-autoantibodies.

## RESULTS AND DISCUSSION

Formulations presented *d<sub>ae</sub>* values compatible with lung deposition (Table 1). IC<sub>50</sub> and CC<sub>50</sub> of the formulations were superior to the concentration of formulation expected in the lungs.

**Table 1.** Particle size distribution over the volume and aerodynamic diameter of insulin-based formulations (mean values ± SD, n=3).

Sample	D <sub>0.1</sub> (μm)	D <sub>0.5</sub> (μm)	D <sub>0.9</sub> (μm)	d <sub>ae</sub> (μm)
SOL:Ins	4.5±1.1	15.3±0.2	44.3±3.3	3.1±0.3
F68:Ins	9.5±4.0	39.1±19.6	328.9±221.4	13.8±8.0
F108:Ins	6.5±0.8	23.4±4.8	358.3±527.5	5.8±0.4
F127:Ins	6.7±2.0	21.6±6.3	81.9±53.7	5.6±1.4

All the formulations were partially internalized by macrophages, F127-micelles shown the lower percentage of uptake (12-13%), correlating to the small size of micelles. Pulmonary administration of insulin promoted lower hypoglycaemic effect than subcutaneous injection (Fig. 1A); however, the encapsulation of insulin increased its pharmacological availability (Fig. 1B). Additionally, no signs of inflammation and tissue damage were observed. Blood samples were negative for insulin auto-antibodies.

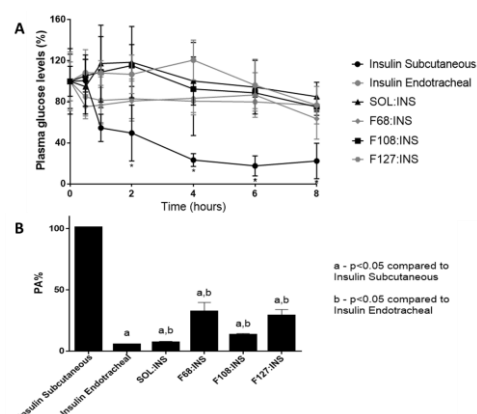


**Figure 1.** Percentage of blood glucose (A) and pharmacological availability (B) of controls and formulations (mean values ± SD, n=6).

## CONCLUSION

Powder formulations based on polymeric micelles presenting promising characteristics for the delivery of biopharmaceutics by inhalation were developed and characterized.

## REFERENCES

- Andrade F. *et al.*, Nanomedicine. 6:123-41, 2011.
- Andrade F. *et al.*, Submitted for publication.

## ACKNOWLEDGMENTS

Fundação para a Ciência e a Tecnologia, Portugal (FCT) for financial support (SFRH/BD/73062/2010). BASF for supplying the polymers, Vétoquinol for Clorketam and Abbot for the glucose meter and strips.



## Developing Stable Chitosan Microspheres for Biomedical Applications

Ewelina Kozikowska, Monika Bil, Wojciech Świąszkowski

Faculty of Materials Science and Engineering, Warsaw University of Technology, Woloska 141, 02-507 Warsaw, Poland  
mbil@inmat.pw.edu.pl

### INTRODUCTION

Creating hybrid systems for controlled drug delivery is essential for developing new forms of medicine that are more available and effective with minimal adverse event [1]. One of the forms of controlled drug delivery systems are microspheres, about 1-500  $\mu\text{m}$  in diameter, in which the medicinal substance is incorporated into the polymer matrix [2]. Microspheres are small porous single-phase polymer balls, often homogeneously gelled, with high biocompatibility and thanks to the adequately picked biodegradable polymer matrix, exhibit elongated curve of release of active substances.

In recent years the interest in research on natural polymers has dramatically increased due to their low costs, compatibility with various medicine and minimal release of organic solvents during the manufacturing of microspheres. Special attention is drawn to chitosan, (deacetylated chitin) thanks to its unique properties such as biodegradability, biocompatibility, bioactivity, and non-toxicity [3]. Production of chitosan microspheres is possible due to its ability to form gel in  $\text{pH} > 6.5$ . By adjusting the rate of deacetylation of chitin and its molecular weight one can change the size of the microspheres as well as rate of the drug release. Morphology, particle size, size distributions and efficiency of the process depend on the method and parameters of fabrication process. However the flaw of this method is low stability of the microspheres after the synthesis. This is why the aim of the study was to develop a method of producing stable chitosan microspheres with controlled particle size that can be used as a vessel for drug delivery.

### EXPERIMENTAL METHODS

Chitosan (CHN) microspheres have been obtained by emulsion polymerization with potassium tri-phosphates (TPP) and a cross-linking agent glutaraldehyde (GLT). Chitosan was dissolved in 2% acetic acid to obtain 2% polymer solution. As an emulsifier the sorbitan monooleate was used which served as a 1% oil phase. In our studies different TPP/CHN v/v ratio (1:1, 2:1 and 3:1) was used. In order to improve stability 50% of cross-linking agent glutaraldehyde has been used.

### RESULTS AND DISCUSSION

Chitosan microspheres have been obtained by emulsion polymerization, thanks to the ionic interactions between chitosan positive amino groups and potassium tri-phosphates negative phosphate ion group. In this method liquid polymer solution has been connected to organic phase by surfactant creating emulsion. Using oil phase has stopped microsphere agglomeration.

In addition, all of the obtained microspheres have been cross-linked with GLT that improved stability of the chitosan microspheres in liquid as well as after drying at room temperature.

The morphology of microspheres was characterized by SEM. Size of the particle immersed in liquid has been evaluated by laser diffraction. Best results have been obtained with volume fraction of TPP to CHN 2:1. The obtained microspheres after drying exhibit globular shape with porous internal structure (Fig. 1). They are small in diameter (10  $\mu\text{m}$ ) and show narrow size distribution (Fig.2).

The microstructures of the obtained materials have been examined by Atomic Force Microscopy and FTIR. The drug incorporation efficiency into CHN microspheres was also examined.

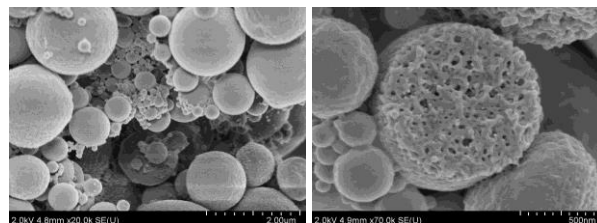


Fig.1 SEM images of the microstructure of microspheres for volume fraction of TPP to CHN 2:1

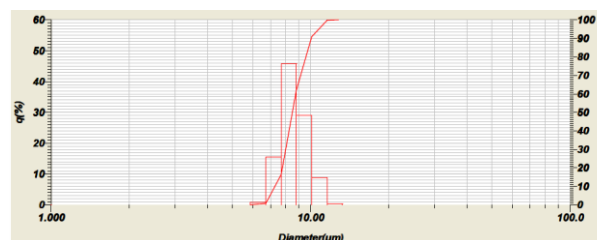


Fig.2 Particle size distribution evaluated by laser diffraction of microspheres for volume fraction of TPP to CHN 2:1

### CONCLUSION

Stable microspheres have been successfully obtained with controlled size distribution and can be used as a drug delivery vessel.

### REFERENCES

1. F. Liu et al., *J. Mater Sci: Mater Med* 18: 2215-2224, 2007
2. E. Szymańska et al., *Farm Pol*, 66(4): 238-242, 2010
3. K. Tomihata et al., *Biomaterials*, 18: 567-575, 1997

### ACKNOWLEDGMENTS

This work was financed by National Science Centre on the basis of a decision number DEC-2012/07/D/ST8/02588.



## Plasma-Grafted Intraocular Lenses for Controlled Release of Moxifloxacin

A. Paula Vieira,<sup>1</sup> Andreia F. R. Pimenta<sup>2</sup>, Patrícia Alves,<sup>1</sup> Patrícia Coimbra,<sup>1</sup> M. Helena Gil,<sup>1</sup> José L. G. C. Mata,<sup>2</sup> A. Paula Serro<sup>2,3</sup> and A. Jorge Guiomar<sup>1,4</sup>

<sup>1</sup>CIEPQPF, Departamento de Engenharia Química, Universidade de Coimbra, Portugal

<sup>2</sup>CQE, Instituto Superior Técnico, Universidade de Lisboa, Portugal

<sup>3</sup>CIEM, Instituto Superior de Ciências da Saúde Egas Moniz, Portugal

<sup>4</sup>Departamento de Ciências da Vida, Universidade de Coimbra, Portugal

[aguimar@bioq.uc.pt](mailto:aguimar@bioq.uc.pt)

### INTRODUCTION

Postoperative endophthalmitis after cataract surgery and intraocular lens (IOL) implantation is a potential blinding complication.<sup>1</sup> The most common forms of prophylaxis are topical administration of antibiotic eyedrops 1 to 3 days before and during one week after surgery, and intracameral injection immediately after surgery.<sup>2,3</sup> As eyedrops have several disadvantages, such as rapid antibiotic absorption into the bloodstream and patient-compliance problems, antibiotic-loaded IOLs have been proposed as an alternative to both eyedrops and intracameral injection,<sup>4</sup> although they are not yet commercially available. The main objective of this study was to develop efficient antibiotic release systems for the treatment of post-surgical endophthalmitis, employing moxifloxacin (MFX), a fluoroquinolone used in endophthalmitis prophylaxis,<sup>2</sup> and materials used in commercial IOLs. Surface-modification by plasma grafting was employed to alter the drug loading capacity of the discs and their release kinetics.

### EXPERIMENTAL METHODS

**Argon plasma grafting.** Poly[(2-hydroxyethyl methacrylate)-co-(methyl methacrylate)]-based discs for IOLs (from PhysiOL SA, Liège, Belgium; diameter: 5 mm) were exposed to Ar plasma for 3 min (power: 100 W; gas pressure: 0.6 mbar), were immediately immersed into a 10% (v/v) aqueous HEMA (2-hydroxyethyl methacrylate) solution containing 5 mg/mL of MFX, and were left to react for 1 h at 60 °C.

**Drug loading and release studies.** Discs were immersed into a 5 mg/mL MFX solution in Hank's Balanced Salt Solution (HBSS) for 24 or 72 h, at 4 °C. The drug release study was carried out at 37 °C, in batch, under shaking (100 rpm) in either 3 mL of HBSS, with daily periodic removal of 500 µL aliquots for MFX quantification (at 290 nm) and replacement by the same volume of HBSS, or in a microfluidic cell containing 250 µL of HBSS renovated at 0.25 µL/min, with MFX quantification by HPLC. Results were expressed as mean ± standard deviation ( $n = 3$ ).

**Discs characterization.** Characterization of the discs before and after modification was carried out by contact angle goniometry, SEM/EDX (Scanning Electron Microscopy with Energy Dispersive X-ray spectrometry), and by determination of their water swelling capacity.

### RESULTS AND DISCUSSION

Loaded discs which were plasma-grafted with PHEMA in the presence of MFX (System 14) released more MFX than unmodified loaded discs and did it for a longer period of time (20 days, at least). A disc similarly modified but reloaded with MFX after the modification (System 15) released even more MFX during the same period of time. A further increase in the amount of released drug was obtained with an unloaded disc which was plasma-grafted with PHEMA in the presence of MFX and subsequently loaded with MFX (System 17). In order to infer about the efficiency of these systems in the eye, the release study was carried out in a microfluidic cell which reproduced the hydrodynamic conditions in the eye. All three systems released MFX at a concentration above MFX's Minimum Inhibitory Concentration (MIC) for *Staphylococcus aureus*, *S. epidermidis* and *Streptococcus pneumoniae* for at least 6 days, but only System 17 released MFX for more than 10 days above the MIC, the target time period.

### CONCLUSION

Grafting of PHEMA on the discs in the presence of MFX allowed the preparation of systems which release MFX during at least 6 days above the MIC and, the best system, could sustain the release of MFX for more than 10 days above the MIC. Thus, this system is a promising option for the development of antibiotic-eluting IOLs.

### REFERENCES

- Novosad B.D. et al., Expert Rev. Ophthalmol., 5:689-698, 2010
- Braga-Mele R. et al., J. Cataract Refract. Surg. 40:2134-2142, 2014
- Packer M. et al., J. Cataract Refract. Surg. 37:1699-1714, 2011
- Lipnitzki I. et al., J. Ocul. Pharmacol. Ther. 29:414-418, 2013

### ACKNOWLEDGMENTS

The authors thank Dimitriya Bozukova (PhysiOL SA, Liège, Belgium) for the discs employed. This work was financed by FEDER funds through *Programa Operacional Factores de Competitividade – COMPETE* and by national funds (*FCT – Fundação para a Ciência e a Tecnologia*) – Project M-ERA.NET/0006/2012.





## Bioengineering of Spider Silk Protein to Modify its Affinity for Drugs

Kamil Kucharczyk<sup>1</sup>, Katarzyna Jastrzebska<sup>1,2,3</sup>, Ewelina Dondajewska<sup>1</sup>, Andrzej Mackiewicz<sup>1,3</sup>,  
Hanna Dams-Kozłowska<sup>1,3</sup>

<sup>1</sup> Chair of Medical Biotechnology, Poznan University of Medical Sciences, Poland

<sup>2</sup> NanoBioMedical Centre, Faculty of Physics, Adam Mickiewicz University, Poland

<sup>3</sup>Department of Diagnostics and Cancer Immunology, Greater Poland Cancer Centre, Poland  
[hanna.dams-kozłowska@wco.pl](mailto:hanna.dams-kozłowska@wco.pl)

### INTRODUCTION

Silk biomaterial combines superb mechanical properties, biocompatibility and biodegradability, thus it has a great potential for application in biomedical field. Moreover, silk can be processed into different morphological forms such as film, fiber, hydrogel, scaffold, capsules, and micro- and nanospheres which may serve as drug carriers. Although, spider silk is not easily accessible from nature, the genetic engineering and biotechnology production resolve the accessibility problem. The synthetic silk genes are designed. Their sequences are based on the consensus motifs of the corresponding natural equivalents<sup>1</sup>. Their further genetic modification enables the generation of bioengineered silk of altered property.

The objective of the study was to generate the bioengineered spider silk to modify its affinity for drugs, followed by studies of drug loading and release.

### EXPERIMENTAL METHODS

The bioengineered spider silk proteins were designed MS2 and EMS2. MS2 was obtained by ligation of 15 repeat units of consensus motif derived from the *N. clavipes* spidroin MaSp2, while EMS2 was based on MS2, however a glutamic acid residue was added to the each repeat unit of MS2. Bioengineered proteins were produced in *E.coli* expression system and then purified by thermal denaturation method<sup>2</sup>. To prepare silk spheres the proteins solutions were mixed with potassium phosphate<sup>3</sup> at different conditions depending on 1) concentration of potassium phosphate, 2) pH of potassium phosphate buffer, 3) concentration of silk proteins. Physical properties of the particles were characterized using scanning electron microscopy, infrared spectrometry and zeta potential measurements. The cytotoxicity of spheres was investigated by MTT assay. Two drugs mitoxantrone and etoposide were loaded into silk particles using post-loading method. The levels of drug incorporation and release profiles of drugs were studied spectrophotometrically.

### RESULTS AND DISCUSSION

Bioengineered spider silks - MS2 and EMS2 were constructed, produced and purified. Both silk variants formed spheres in conditions above a critical potassium phosphate concentration i.e. 1 and 2 M for MS2 and EMS2 protein, respectively. The type of protein and its concentration affected the size and size distribution of the obtained spheres. Zeta potential of both spheres was negative, however for spheres made of MS2 it was between -1.6 and -14mV while for EMS2 it was from -

31 to -35 mV depending on the method applied for the sphere preparation. The cytotoxicity analysis demonstrated that MS2 and EMS2 spheres were not toxic.

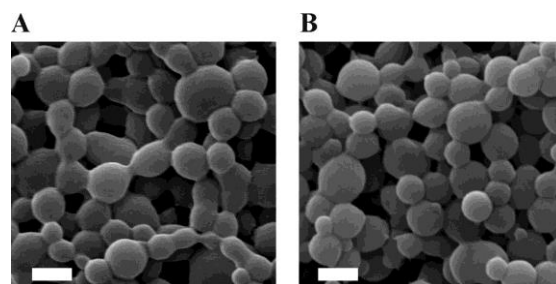


Figure 1: (A) Scanning electron image of the EMS2 and (B) MS2 spheres. Scale bars 1µm.

EMS2 spheres showed stronger affinity to positively charged mitoxantrone, while loading of neutral etoposide was similar for both silk particles. Both drugs showed a pH-dependent release profile from the particles.

### CONCLUSIONS

The genetic engineering gives a possibility to generate a new variants of bioengineered silk. By replacing, adding or/and removing a particular amino acid residue the property of bioengineered spider silk can be modified. We generated EMS2 variant of MS2 bioengineered silk protein. EMS2 retained the self-assembly property and formed spheres. By adding 15 residues of glutamic acid the, EMS2 affinity to a positively charged mitoxantrone was increased. Silk as a non-toxic and biodegradable protein polymer is an ideal biomaterial for drug delivery. By modifying the silk sequence, the affinity to drugs can be controlled.

### REFERENCES

1. Tokareva O. *et al.*, Microbial Biotechnology, 6(6):651-663, 2013
2. Dams-Kozłowska H. *et al.* J Biomed Mater Res A. 101A (2) 456-64, 2013
3. Lammel A. *et al.*, ChemSusChem. 1:413-6, 2008

### ACKNOWLEDGMENTS

KJ was supported by the International PhD Projects Programme of Foundation for Polish Science operated within the Innovative Economy Operational Programme (IE OP) 2007-2013 within European Regional Development Fund.



## Functionalized Bioengineered Spider Silk for CpG-siRNA Delivery

Anna Kozłowska<sup>1</sup>, Maciej Śmiałek<sup>1</sup>, Anna Florczak<sup>1,2,3</sup>, Andrzej Mackiewicz<sup>1,3</sup>, Marcin Kortylewski<sup>4</sup>,  
Hanna Dams-Kozłowska<sup>1,3</sup>

<sup>1</sup> Chair of Medical Biotechnology, Poznan University of Medical Sciences, Poland

<sup>2</sup> NanoBioMedical Centre, Faculty of Physics, Adam Mickiewicz University, Poland

<sup>3</sup>Department of Diagnostics and Cancer Immunology, Greater Poland Cancer Centre, Poland

<sup>4</sup> Beckman Research Institute, City of Hope National Medical Center, USA

[hanna.dams-kozłowska@wco.pl](mailto:hanna.dams-kozłowska@wco.pl)

### INTRODUCTION

Silk as a biomaterial of outstanding physico-chemical properties, biocompatible and biodegradable has great potential as a carrier of therapeutic agents. Due to the self-assembly property, silk can be processed into several morphological forms such as fibres, scaffolds, films, hydrogels, capsules and spheres. Moreover, the genetic engineering enabled the functionalization of silk by adding peptide moieties of desired attribute<sup>1</sup>. Functionalization of silk by adding nucleic acid binding domain enables development of siRNA delivery system. Efficient and specific delivery of siRNA remains a formidable challenge. Recently, the naked CpG-siRNA conjugates were used to deliver therapeutic siRNAs into target immune cells<sup>2</sup>. The CpG-STAT3siRNA conjugates showed good efficacy in preclinical tumor models<sup>3</sup>, however, further clinical translation of this strategy requires optimization for systemic delivery. Embedding siRNA into silk spheres may improve the serum stability of siRNA molecule in body fluids. The aim of this study was the development CpG-siRNA delivery system based on bioengineered spider silk functionalized with nucleic acid binding domain.

### EXPERIMENTAL METHODS

Bioengineered spider silk (MS2) was designed based on the consensus motif derived from the *N. clavipes* spidroin MaSp2. MS2 was functionalized by adding nucleic acid binding domain (KN). MS2 and hybrid KNMS2 were produced in bacterial expression system and purified using thermal denaturation method<sup>4</sup>. CpG-siRNA against oncogenic and immunosuppressive STAT3 transcription factor was used in this study<sup>3</sup>. The binding of CpG-siRNA to silk was analyzed by agarose gel electrophoresis. The silk spheres loaded with CpG-siRNA were prepared by salting out process<sup>5</sup>. For serum stability assays, the MS2KN complexes and spheres loaded with CpG-siRNA were incubated in presence of mouse serum and then analyzed in acrylamide gel. The uptake of spheres by murine macrophages was analyzed using flow cytometry and confocal microscopy.

### RESULTS AND DISCUSSION

Bioengineered spider silk MS2 and its hybrid variant MS2KN were constructed, produced and purified. CpG-siRNA efficiently bound to MS2KN in contrary to control protein MS2. The functionalization did not impede the self-assembly property of bioengineered silk, enabling the processing of MS2KN silk protein into spheres. Both complexes and spheres protected siRNA from degradation in serum. MS2KN spheres

loaded with CpG-siRNA were efficiently internalized by macrophages; both nucleic acid and silk protein were localized inside the cells.

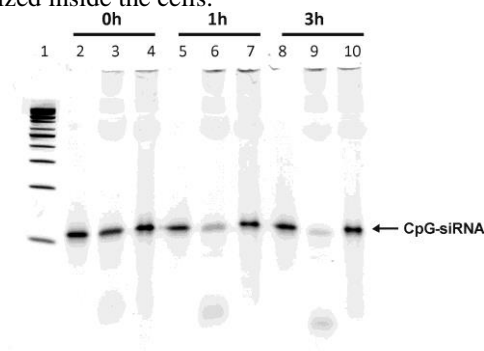


Figure 1: Analysis of the stability of CpG-siRNA-MS2KN complexes in serum. CpG-siRNA alone (3, 6, 9) or complexed with MS2KN (4, 7, 10) was incubated in 30% mouse serum for 0, 1 and 3 hours in 37° C. The control CpG-siRNA (2, 5, 8) was not treated with serum. After incubation samples were analyzed in 15% Urea-PAGE (1 - DNA ladder 50bp).

### CONCLUSION

Functionalization of silk by adding nucleic acid binding domain enabled efficient loading of CpG-siRNA into silk spheres. Silk improved the serum stability of siRNA molecule and allowed for cell-specific uptake of CpG-siRNA.

The obtained results indicated a great potential of the functionalized bioengineered spider silk for the delivery of a therapeutic nucleic acids.

### REFERENCES

1. Tokareva O. *et al.*, Microbial Biotechnology, 6(6):651-663, 2013
2. Kortylewski M. *et al.*, Nat Biotechnol. 27(10):925-32, 2009.
3. Zhang O. *et al.*, Blood 121 (8): 1304-15.
4. Dams-Kozłowska H. *et al.*, J Biomed Mater Res A. 101A (2) 456-64, 2013
5. Lammel A. *et al.*, ChemSusChem. 1:413-6, 2008

### ACKNOWLEDGMENTS

AF was supported by the International PhD Projects Programme of Foundation for Polish Science operated within the Innovative Economy Operational Programme (IE OP) 2007-2013 within European Regional Development Fund.



<sup>1</sup> Chemical and Metallurgical Engineering Faculty, Istanbul Technical University, Chemical Engineering Department, 34469, Maslak-Istanbul/TURKEY.

[ozsagiroglu@itu.edu.tr](mailto:ozsagiroglu@itu.edu.tr)

## INTRODUCTION

The encapsulation enhances the stability of drug molecules, improves the targeting properties and prolongs pharmacological activity *via* continuous local release of active molecules [1]. The aim of this study is to encapsulate, L-ascorbic acid, in biopolymers in order to obtain (i) enhancing its encapsulation efficiency (ii) increasing drug release ratio using different pH mediums. Microspheres based on polycaprolactone (PCL), polyethylene glycol (PEG), and casein (CS) is prepared by spray drying technique. Drug loaded microparticles are characterized in terms of morphology, encapsulation efficiency, and drug release. In this manner, the importance of the study is producing of a stable and effective drug encapsulation system by PCL-PEG-CS polymer mixture. First part is to define best effective drug loading terms. Final part of the study is about drug release experiments and calculation drug release ratios in different solution mediums. At the end of studies, we achieved minimum 84.05% maximum drug loading, and 68.92% drug release ratio at 9.6 pH medium. By this way, our drug loaded microparticles can be proposed as alternative or adjuvants for controlling release of L-ascorbic acid in human or animal. In particular, PCL-PEG-CS microspheres can be used for L-ascorbic acid (vitamin C) carriers.

## EXPERIMENTAL METHODS

Polymer solutions are fed to spray dryer and drying conditions are at 135 °C, 3 ml/min feed ratio.

Secondly, L-ascorbic acid in different weight ratios are loaded for microsphere which have the lowest particle diameter. L-ascorbic acid loading studies are done by indirect loading of drug to microspheres at 25 °C and 200 rpm. L-ascorbic acid contents are 5 wt%, 10 wt%, and 15 wt%, respectively.

Liquid phase is analyzed by UV at 518 nm to calculated [16-19]. Calculations in drug release step of the study are also done by UV. 0.5 mg blend/1 mL release medium (pH 2.8, 7.4, and 9.6) ratio is used.

## RESULTS AND DISCUSSION

Drug encapsulation studies are performed under three different L-ascorbic acid concentrations (5 wt%, 10 wt%, and 15 wt%) with different loading time and PCL-PEG-CS particle amounts. Figure 1 and Figure 2 indicate that how much L-ascorbic acid is encapsulated due to the time and particle amount, respectively.

Figure 1 shows drug absorbance is achieved peak value (84.05% loading efficiency) in one hour; thereafter smoothly decreased in all L-ascorbic acid solutions.

Although there is no significant difference, Figure 2 indicates that the encapsulation efficiency tended to increase from 0.5 to 2.0 mg particle/mL L-ascorbic acid solution. On the contrary, increasing weight percent of L-ascorbic acid in solution significantly increased loading rates. It changes from 49.93% to 84.05% by

PCL-PEG-CS microsphere amounts from 0.5 to 2.0 mg particle/mL solution.

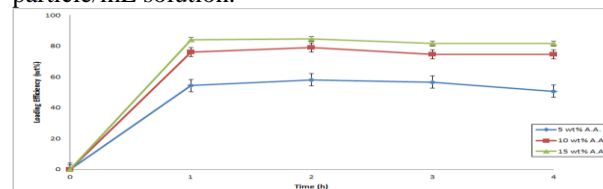


**Figure 1.** Effects of drug loading time on encapsulation of L-ascorbic acid.

It is also facts that low diameter and well distributed structure of microspheres are reasons to gain high L-ascorbic acid loading values. Thus, when highly water-soluble drugs, such as L-ascorbic acid, are encapsulated using ternary polymer blends, % encapsulations achieved are expectably high.

In-vitro release profiles of L-ascorbic acid from the microspheres produced by PCL-PEG-CS are shown in Figure 3. Experimental uncertainties in the % drug released, based on three replicates, are approximately changed from 3.4% to 5.7%.

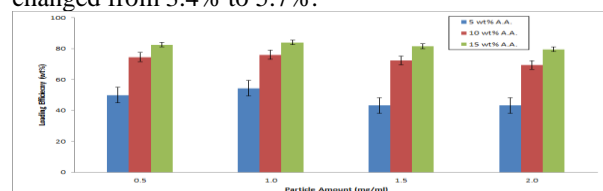


**Figure 2.** Effects of particle amount on encapsulation of L-ascorbic acid.

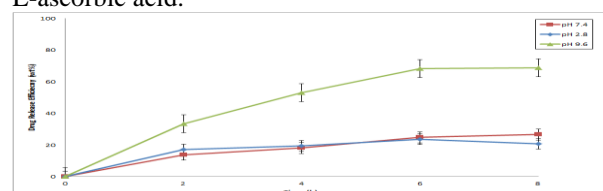


**Figure 3.** L-ascorbic acid release with different pH mediums in 8 hours.

The % drug release initially in 2 h is  $17.21 \pm 3.36$  at pH 2.8,  $13.84 \pm 3.50$  at pH 7.4 and  $33.39 \pm 5.7$  at pH 9.6. Maximum drug release ratio achieved in 6 h is  $68.21 \pm 5.7$  at pH 9.6. The results indicate that L-ascorbic acid coat in the bioblend based microspheres are easily degraded higher pH values particularly at basic scale.

## CONCLUSION

The dissolution rates of the drugs from PCL-PEG-CS microspheres are clearly improved at higher pH as compared to neutral and acidic pH values. Because of unstable and very sensitive L-ascorbic acid, producing vitamin C drugs are really difficult. Towards the aim of the study, improving the vitamin C drugs, our method provides easily procurable and effective solution.

## REFERENCES

1. Paudel A. *et al.*, Int. J. Pharmaceut. 453(1):253-284, 2013.

## Silicone Stabilized Liposomes as Novel Nanostructural Drug Carriers

Joanna Lewandowska-Lańcucka, Katarzyna Mystek, Maria Nowakowska

Faculty of Chemistry, Jagiellonian University, Poland  
[lewandow@chemia.uj.edu.pl](mailto:lewandow@chemia.uj.edu.pl)

### INTRODUCTION

Recently, there has been a growing interest in development of novel advanced drug delivery systems. In general, DDS are expected to increase therapeutical efficacy while reducing toxicity of the biologically active molecule. Liposomes – artificially constructed phospholipid vesicles are probably the most frequently studied DDS. That is due to their unique properties such as nontoxicity, biodegradability, as well as simplicity of preparation and control over the composition and size<sup>1</sup>. Unfortunately, the major problem with practical application of liposomes is related to their low stability during storage resulted from their high tendency for aggregation, degradation, and fusion leading to uncontrolled leakage of the entrapped compounds<sup>2</sup>. Various strategies have been proposed to overcome that problem. The main approaches involve optimization of the lipid composition in the membrane, adsorption of polymeric material at the liposomal surfaces<sup>3</sup>, and covalent grafting of hydrophilic polymers onto the head groups of phospholipids<sup>4</sup>. In our study we have proposed the new stabilization method of the liposomes using silicone as a protective and stabilizing agent<sup>6</sup>. Silicones are among the important biomaterials used in prosthetic devices such as implant for breast enlargement, tissue augmentation and for treatment of hydrocephalus. They exhibit interesting properties including low toxicity, low surface tension, and thermal stability in the broad range of temperatures as well as an excellent gas permeability. Thus the silicone layer will ensure high mechanical, thermal and chemical stability for the fragile liposome vesicles while not compromising biocompatibility

### EXPERIMENTAL METHODS

The cationic liposomes were obtained from egg yolk phosphatidylcholines (PC) and a cationic double-tailed surfactant, dimethyldioctadecylammonium bromide (DODAB). The surfactant was introduced to modify the surface potential of the liposomes, so the base-catalyzed polymerization/ polycondensation processes of the monomer can occur at the surface. In order to obtain the liposome dispersion of low polydispersity, the lipid vesicles were extruded through filters with 100-nm pores. 1,3,5,7-tetramethylcyclotetrasiloxane (D<sub>4</sub><sup>H</sup>) and its derivatives were employed as silicone precursors. The silicone precursors were introduced into the liposome dispersions and the polycondensation/ polymerization process was initiated by changes in pH. The stability of the obtained nanostructures were evaluated using the spectrophotometric titration with Triton X-100, measurements of zeta potential and determination of the hydrodynamic diameters (Dynamic

Light Scattering). The model hydrophilic drug, calceine was then entrapped in the nanocarriers prepared. The release of calceine molecules into the aqueous phase was monitored by fluorescence spectroscopy.

### RESULTS AND DISCUSSION

Silicone-stabilized liposomes were successfully obtained using base catalyzed polycondensation/ polymerization processes of the silicone precursors. The polycondensation process was followed by FTIR analysis of the prepared and isolated silicone materials. Depending on the type of the precursor used, the stabilized silicone layers were created on the outer side of the vesicles or in the lipid bilayer. The conditions of the synthesis were optimized in terms of the amount of the precursors used, temperatures and the pH values of the reaction. Using the silicone precursors with various numbers of the groups participating in the sol-gel reaction it was possible to obtain stable nanocarriers with the tunable permeability characteristic. They also differ in size, zeta potential and stability. The sol-gel reaction was carried out at two different pH, namely 8.5 and 10.2. The cryo-TEM micrographs proved that silicone-coated liposomes were obtained but at the higher pH, a fraction of disintegrated liposomes was also observed. The experiments with surfactant-lysis and calcein-release studies have confirmed that the silicone coated liposomes are definitely more stable than pristine cationic liposomes.

### CONCLUSION

Novel method for stabilization of liposomes by formation of silicone coating was proposed. By choosing the sol-gel reaction conditions and selection of silicone precursors it was possible to obtain the stable liposomal nanocarriers with the tunable permeability. Moreover, manipulation with the degree of silanol polymerization affects the zeta potential value of the nanocarriers resulting in reduction of their aggregation.

### REFERENCES

1. Yaroslavov AA. et.al., Adv. Colloid Interface Sci, 142, 43, 2008
2. Takeuchi H. et.al., J Controlled Release, 75, 83, 2001
3. Rinaudo M. et al., Macromol Symp, 278, 67, 2009
4. Ruyschaert T. et al., Nano Lett, 6, 2755, 2006
5. Lewandowska J. et.al., Colloid Polym Sci, 288, 37, 2010

### ACKNOWLEDGMENTS

Project operated within the Foundation for Polish Science Team Programme co-financed by the EU European Regional Development Fund, PolyMed, TEAM/2008-2/6





Damien Dupin, Pablo Casuso, Adrián Pérez-San Vicente, Natividad Diaz and Iraida Loinaz

Biomaterials Unit, Materials Department, IK4-CIDETEC, Spain,  
[ddupin@cidetec.es](mailto:ddupin@cidetec.es)

## INTRODUCTION

Efficient drug delivery is one of the most important challenges in cancer treatment<sup>1</sup>. Considerable efforts focus on the preparation of targeted vehicle to transport drugs to tumour cells.<sup>2</sup> Such delivery system requires i) good encapsulation properties, ii) efficient drug targeting/release, iii) biocompatibility and, iv) facile elimination from the body.<sup>3</sup>

Stimuli-responsive microgels, which are submicrometer-sized particles that can be swollen by change of pH, have gained growing attractions as drug delivery systems. Herein, we report the design of folic acid-functionalised microgels that can transport hydrophobic compounds to the tumour cells and release their cargo during endocytosis at lysosomal pH.

## EXPERIMENTAL METHODS

**Microgel synthesis via aqueous emulsion polymerization.** 2,2'-(diisopropylamino)ethyl methacrylate [DPA] was polymerized in water in the presence of *N*-(3-aminopropyl)-2-methylacrylamide hydrochloride (APMA) comonomer, 2-methylene-1,3,6-trioxocane (MTC), ethylene glycol diacrylate (EGDA) cross-linker, poly(ethylene glycol) ethyl ether methacrylate stabilizer (PEGMA) and ammonium persulfate (APS) initiator via aqueous emulsion polymerization at 70 °C to obtain PEGMA-PDPA particles. PDPA particles were decorated with folic acid.

**Dynamic Light Scattering (DLS) and Zeta potential** studies were carried out using Malvern Zetasizer Nano ZS on particles dispersion at 0.01 wt. % in PBS.

**PDPA particles cytotoxicity** was investigated via MTS and Live/Dead assays in the presence of HDF cells.

Cellular uptake was carried out via confocale microscopy using HeLa cell as model of cancer cells.

## RESULTS AND DISCUSSION

Lightly cross-linked PEGMA-PDPA particles of around 200 nm were obtained via aqueous emulsion polymerization.

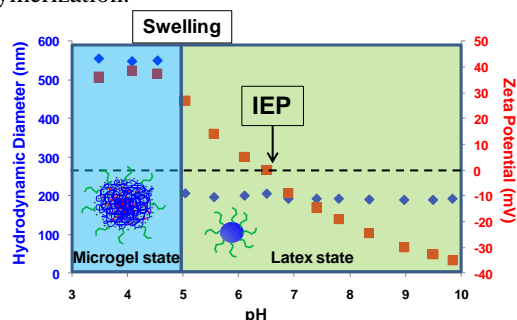


**Figure 1.** DLS (♦) and Zeta potential (■) of PEGMA-PDPA particles in function of the solution pH in PBS solution.

As judged by DLS, PEGMA-PDPA particles exhibited a latex-to-microgel transition at pH 6.5 due to the protonation of the tertiary amine of the DPA residues (**Figure 1**). This indicates that PEGMA-PDPA will swell up with water to 550 nm during the endocytosis process as originally targeted. The presence of PEGMA stabilizer is absolutely required to ensure colloidal stability in physiological conditions. Moreover, the copolymerization of MTC comonomer offered hydrolysable bonds into the particles facilitating particle degradation after 1 week in the presence of lipase at physiological conditions into shorter polymer chains easily eliminated by the kidney.

PEGMA-PDPA particles did not exhibit cytotoxicity in the presence of HDF cells (**Figure 2**). Moreover, Doxorubicin could be encapsulated into the particles and the presence of folic acid at the particle surface allowed cellular uptake by HeLa cells where DOX was efficiently released as judged by fluorescence microscopy.

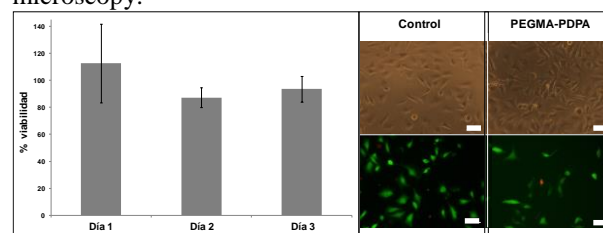


**Figure 2.** Viability (left) and Live/Dead assays (right) of HeLa cells in the presence of PEGMA-PDPA particles (50 µg L<sup>-1</sup>) after 3 days (scale bar: 100 µm).

## CONCLUSION

Stable, biodegradable and biocompatible pH-responsive microgels easily functionalised with targeting molecules were easily prepared by emulsion polymerization. Hydrophobic compounds could be encapsulated at physiological condition and efficiently released during endocytosis due to the swelling of the particles occurring at lysosomal pH.

## REFERENCES

1. Branon-Peppas, L *et al.* Adv. Drug Deliver. Rev. 64:206-212, 2012.
2. Bae, Y H *et al.* J. Control. Release 153:198-205, 2011.
3. Kost, J *et al.* Adv. Drug Deliver. Rev. 64:327-341, 2012.

## ACKNOWLEDGMENTS

The authors would like to thank the ETORTEK Program [biomaGUNE11(E11-301) and biomaGUNE12(E12-332)] for providing financial support to this project.

## Partially Oxidized Alginate Grafted with $\beta$ -CyD: A Potential Release System for Biomedical Molecules

Line Aa. Omtvedt<sup>1</sup>, Marianne Ø. Dalheim<sup>1</sup>, Thorbjørn T. Nielsen<sup>2</sup>, Kim L. Larsen<sup>2</sup>, Berit L. Strand<sup>1</sup>, and Finn L. Aachmann<sup>1</sup>

<sup>1</sup>Norwegian Biopolymer Laboratory (NOBIPOL), Department of Biotechnology, Norwegian University of Science and Technology (NTNU), Trondheim, Norway.

<sup>2</sup>Department of Chemistry and Bioscience, Aalborg University (AAU), Aalborg, Denmark.

[line.a.omtvedt@ntnu.no](mailto:line.a.omtvedt@ntnu.no)

### INTRODUCTION

Alginate is a linear polysaccharide composed of  $\beta$ -D-mannuronic acid (M) and  $\alpha$ -L-guluronic acid (G), where mainly G-blocks give alginate its ability to form a gel with divalent cations<sup>1</sup>. Cyclodextrins (CyD) consists of  $\alpha$ -(1 $\rightarrow$ 4) linked  $\alpha$ -D-glucosyl units, which have a hydrophilic exterior and a hydrophobic cavity<sup>2</sup>. This enables CyD to form inclusion complexes with various hydrophobic molecules and moieties<sup>2</sup>. The aim of this study was to combine the gel forming ability of the alginate with the capability of CyD to form inclusion complexes with hydrophobic molecules. This can potentially be used as a controlled release system of biomedically relevant molecules such as drugs, proteins and peptides.  $\beta$ -CyD has previously been grafted to the carboxyl-groups in alginate<sup>3,4</sup>. Here,  $\beta$ -CyD was grafted to partially oxidized alginate.

### EXPERIMENTAL METHODS

Alginate was grafted with  $\beta$ -CyD in three succeeding steps: High-G alginate ( $F_G = 0.68$ ) was partially oxidized with metaperiodate (step one), and the resulting aldehyde groups was thereafter bound to an alkyne linker using reductive amination (step two). Finally, the copper(I)-catalyzed azide-alkyne cycloaddition (CuAAC) click-reaction was used to covalently bind 6-O-monodeoxy-6-monoazido- $\beta$ -CyD ( $N_3$ - $\beta$ CyD) to the alkyne-substituted alginate (step three). The gelation ability of the alginate grafted with  $\beta$ -CyD was examined by the formation of calcium gel-beads composed of both high-G alginate ( $F_G = 0.68$ ) and alginate grafted with  $\beta$ -CyD. The release of a model compound, methyl orange, from the gel beads was studied and compared to release from non-grafted high-G alginate beads with and without free  $\beta$ -CyD.

### RESULTS AND DISCUSSION

The covalent binding of alginate and  $\beta$ -CyD was confirmed with <sup>1</sup>H-NMR and DOSY. Degrees of substitution (DS) for the alginate grafted with  $\beta$ -CyD were determined by <sup>1</sup>H-NMR. Gel-beads composed of both high-G alginate ( $F_G = 0.68$ ) and alginate grafted with  $\beta$ -CyD was successfully made. Alginate gel-beads incorporated with the grafted alginate showed a prolonged release of methyl orange compared to both reference beads made of non-modified alginate, and beads made of alginate mixed with non-grafted  $\beta$ -CyD (figure 1). In addition, faster dissolution of the gel-beads incorporated with the grafted alginate was observed.

The properties of the gels formed by alginate grafted with CyD can be tuned by varying the DS: The amount of immobilized  $\beta$ -CyD grafted to the alginate can be adjusted, as well as the gelation ability of the alginate due to ring opening of oxidized monomers<sup>5</sup> in the alginate chain.



**Figure 1:** Solutions coloured by methyl orange: (L) Colour of load solution (start concentration of 0.05 mg/ml methyl orange) after removal of alginate-beads, and (1-6) colour of treatment solutions after the alginate beads loaded with methyl orange was left one hour in 0.9 % (w/v) saline treatment solutions and removed. A-D denotes the alginate beads consisting of: (A) high-G alginate ( $F_G = 0.68$ ), (B) high-G alginate ( $F_G = 0.68$ ) and free  $\beta$ -CyD, (C - D) different ratios of high-G alginate ( $F_G = 0.68$ ) and alginate grafted with  $\beta$ -CyD, were beads given in C had a lower ratio of the grafted alginate compared to the beads given in D.

### CONCLUSION

Alginate was successfully grafted with  $\beta$ -CyD and retained the gelation ability. The grafted CyD gave slower release of methyl orange than alginate gels without CyD or with non-grafted CyD. Combining the gelling properties of alginate with the CyD affinity towards hydrophobic molecules allows for further tailoring of the system related to mechanical properties to obtain a controlled release system for biomedically relevant molecules.

### REFERENCES

1. Draget K. I. *et al.*, Food Polysaccharides and Their Applications, CRC Press: pp 289-334, 2006
2. Szejtli J., Chem. Rev. 95 (5), 1743-1753, 1998
3. Gomez C. G. *et al.*, Polymer, 47(26): p. 8509-8516, 2006
4. Izawa H. *et al.*, J. Mater. Chem. B 1(16):2155-2161, 2013
5. Gomez C. G. *et al.*, Carbohydr. Polym., 67(3): p. 296-304, 2007

### ACKNOWLEDGMENTS

The authors thank the MARPOL project 221576 and the Norwegian Research Council for financial support.



## Increased Cellular Uptake of Exosomes via Active Macropinocytosis Induction

Ikuhiko Nakase<sup>1</sup>, Nahoko Bailey Kobayashi<sup>2,3</sup>, Tomoka Takatani-Nakase<sup>4</sup>, Tetsuhiko Yoshida<sup>2,3</sup>

<sup>1</sup>Nanoscience and Nanotechnology Research Center, Osaka Prefecture University, Sakai, Osaka 599-8570, Japan; <sup>2</sup>Keio Advanced Research Centers (KARC), Keio University, Tsukuba, Ibaraki 300-2611, Japan; <sup>3</sup>Institute for Advanced Sciences, Toagosei Co., Ltd., Tsukuba, Ibaraki 300-2611, Japan; <sup>4</sup>Department of Pharmaceutics, School of Pharmacy and Pharmaceutical Sciences, Mukogawa Women's University, Nishinomiya, Hyogo 663-8179, Japan  
[i-nakase@21c.osakafu-u.ac.jp](mailto:i-nakase@21c.osakafu-u.ac.jp)

### INTRODUCTION

Exosomes are ~100-nm vesicles that consist of a lipid bilayer<sup>1</sup> and are secreted from various cell types. They carry bioactive molecules between cells, including microRNAs, which mediate cell functions.<sup>1</sup> Endocytosis is a major pathway for the cellular uptake of exosomes; however, the detailed internalization mechanisms are still unknown. In this research, we studied the contribution of the macropinocytosis (accompanied by actin reorganization, ruffling of the plasma membrane, and engulfment of large volumes of extracellular fluid<sup>2</sup>) to exosome uptake. We found that the active induction of macropinocytosis via stimulation of cancer-related receptors and expression of oncogenic Ras significantly increases the cellular uptake of exosomes.

### EXPERIMENTAL METHODS

HeLa cells stably expressing GFP-fused CD63 (exosome membrane marker protein) to secrete CD63-GFP-containing exosomes (CD63-GFP exosomes) were prepared by transfection with the CD63-GFP plasmid (System Biosciences) and antibiotic selection using puromycin. Secreted exosomes were isolated by Total Exosome Isolation Kit (from cell culture media) (Invitrogen) or ultracentrifugation, as previously reported.<sup>3</sup> To artificially load saporin in exosomes, CD63-GFP exosomes were mixed with saporin in PBS, prior to electroporation using a Super Electroporator NEPA21 Type II system (NEPA Genes), and unencapsulated saporin was removed by washing and filtration using Amicon Ultra Centrifugal Filters (100K device, Merck Millipore).

### RESULTS AND DISCUSSION

Endocytosis is reported to be a major pathway for the cellular uptake of exosomes; however, it has a cargo size limitation (~120 nm) for cellular uptake.<sup>4</sup> Because of this size limitation, endocytosis is considered to have low efficacy for the cellular uptake of exosomes (~100 nm). Macropinocytosis induces the engulfment of large volumes, and this pathway enables the cellular uptake of large-sized cargo (~1 µm).<sup>4</sup> The contribution of this pathway to exosomal uptake is almost unknown.

The stimulation of epidermal growth factor receptor (EGFR) by treatment with the receptor ligand EGF induces macropinocytosis signal transduction. When A431 (human epidermoid carcinoma) cells were treated with CD63-GFP exosomes (20 µg/ml) for 24 h at 37 °C, cellular uptake of the exosomes was significantly increased by the addition of EGF (i.e., cellular uptake was approximately 27-fold higher for

cells treated with 500 nM EGF than untreated cells, as analysed by a flow cytometer).

In tumour cells, the expression of the oncogenic Ras protein has been shown to induce macropinocytosis. MIA PaCa-2 (human pancreatic adenocarcinoma) cells are homozygous for the K-Ras<sup>G12C</sup> allele. As an important route of nutrient uptake, the cells induce macropinocytosis.<sup>5</sup> The relative cellular uptake of CD63-GFP exosomes (20 µg/ml) by MIA PaCa-2 or BxPC-3 (expressing wild-type K-Ras) for 24 h at 37 °C was analysed using a flow cytometer. MIA PaCa-2 cells showed superior cellular uptake efficiency of the exosomes (approximately 14-fold) relative to that of BxPC-3 cells, suggesting that increased macropinocytosis via oncogenic Ras enhances the cellular uptake efficacy of exosomes in tumour cells.

In addition, we tested the delivery of bioactive molecules by encapsulation in exosomes. Saporin is a ribosome-inactivating protein that inhibits protein synthesis and cell growth. A431 cells were treated with saporin-encapsulated exosomes (4 µg/ml of the total exosomes) for 48 h at 37 °C, prior to a WST-1 assay. For saporin-encapsulated exosomes, the addition of EGF (500 nM) resulted in significantly increased cytotoxicity compared to the absence of EGF, suggesting that macropinocytosis induction via EGF stimulation increases the cellular uptake of saporin-encapsulated exosomes and saporin bioactivity.

### CONCLUSION

In this study, we found important roles of macropinocytosis in the efficient cellular uptake of exosomes. These findings will contribute to our understanding of the biological functionality of exosomes in various cellular events (e.g., cell-to-cell communication, cancer and other diseases, and infection) under stimulated macropinocytosis conditions, and to the development of exosome-mediated delivery systems for future therapeutic and diagnostic applications.

### REFERENCES

1. Tan, A. *et al.*, Adv. Drug Deliv. Rev. 65:357–367, 2013
2. Swanson, J. A., Nat. Rev. Mol. Cell Biol. 9:639–649, 2008
3. Théry, C. *et al.*, Curr. Protoc. Cell Biol. Chapter 3, Unit 3.22, 2006
4. Conner, S. D. *et al.*, Nature 422:37–44, 2003
5. Comisso, C. *et al.*, Nature 497:633–637, 2013



## Electrospraying of Aliphatic Polyesters for Drug Delivery Systems

Aleš Šaman<sup>1</sup>, Jana Horáková<sup>1</sup>, Kateřina Pilařová<sup>1</sup>, Petr Mikeš<sup>1</sup>

<sup>1</sup>Department of Nonwovens and Nanofibrous Materials/Technical University of Liberec, Czech Republic  
[ales.saman@tul.cz](mailto:ales.saman@tul.cz)

Small diameter particles were produced by electrospraying of copolymer of poly(lactide-co-polycaprolactone), (PLC) and poly(lactic-co-glycolic acid), (PLGA). The particles were diameter about 5-20  $\mu\text{m}$ , the particles had spherical shape and irregular surface. The Particles contained small particles polyvinylalcohol (PVA) which can contain water or alcohol soluble substrates. Model substrates was rhodamine B.

### INTRODUCTION

Today, we are facing a constant search for solutions to health-related problems. Solution, which would be facilitated by the functionalization of nanofibrous materials, is targeted drug delivery systems. These mostly small polymer particles are produced may be different methods, but in recent years is gaining prominence method electrospraying. This method is suitable, because can generate small particles ( $> 20 \mu\text{m}$ ) but also below one micron<sup>1</sup>. The shape and size of the resulting particles can be influenced depending on the chosen polymer, solvent and parameters in electrospraying<sup>2</sup>. Biodegradable polymers, especially aliphatic polyesters, which can be controlled by the ratio of degradation of the individual components of the copolymer<sup>3</sup>. The whole process can be modeled truncated degradation by enzymes which catalyze the hydrolysis. Advantage electrospraying is also that it can be directly combined with electrospinning as it is in the article<sup>4</sup>. This combination can take advantage of such scaffolds are small fiber diameters, fiber orientation, size and porosity. The particles then enrich the scaffold and controlled release of active substances.

### EXPERIMENTAL METHODS

Small diameter particles were produced by electrospraying of PLC and PLGA solution. First step was preparing PVA solution, which contain active soluble substrate. PVA solution was used electrospraying technology sprayed on aluminium foil. This way prepared particles were ultrasounds disperse into PLC and PLGA solution. After follow again electrospraying. The resultant particles were combined into nanofibers scaffolds. This technology was produced on a rotating cylinder, where on one side was electrospraying needle and on the other side was the electrospinning needle. The structure was analysed by scanning electrons microscopy and image analysis.

### RESULTS AND DISCUSSION

The size of the resulting particles produced from aliphatic polyesters amounted tens of micrometres. using image analyse was measured, that PLC had  $12.06 \pm 6.69 \mu\text{m}$ , PLGA had  $13.57 \pm 7.26 \mu\text{m}$  and polyvinyl alcohol had  $272.26 \pm 167.39 \text{ nm}$ , but with fluorescence microscopy shows that the particles formed agglomerates, as seen on Fig. 2.

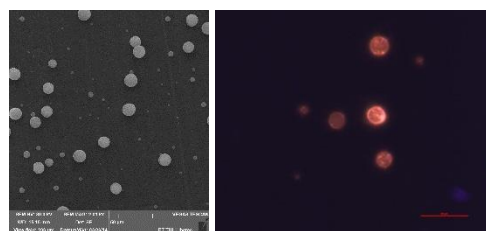


**Fig.1:** SEM photo of PLGA (left), Fluorescent microscopy photo of PLGA contain PVA agglomerates with Rhodamine B (right).

As seen of Fig. 2 can with a rotating conductive roller having a cylinder diameter 50 mm and one turn per minute, can be achieved uniformly dispersed particles in scaffold. By enzymatic degradation was found that after several days packaging PLGA and PLC started degraded. Absorption spectrophotometer recorded increasing absorbance caused rhodamine B in degradation bath.

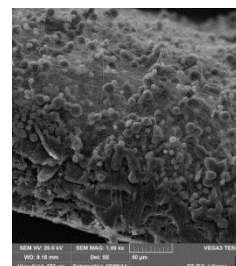


**Fig.2:** Cross section of scaffold, where is combine PCL nanofiber with PLGA Particles on paper as background material.

### CONCLUSION

New material and his combine with known materials are potential candidate for drug delivery systems in connect scaffold for tissue engineering. Electrospraying copolymer PLC and PLGA showed great control release with use lipase. Advantage this technology is big loading particles PVA and great possibilities control released active substrates. Possible disadvantage for specific applications are bigger size particles.

### REFERENCES

1. Bock, N. *et al.*, *Progress in Polymer Science*, 37(11), pp. 1510-1551, 2012
2. Jaworek, A. *et al.*, *Powder technology*, 176(1), pp. 18-35, 2007
3. Vieira, A.C. *et al.*, *Journal of the Mechanical Behaviour of Biomedical Material*, 4(3), pp. 451-460, 2011
4. Jaworek, A. *et al.*, *Journal of Electrostatics*, 67(2-3), pp.435-438, 2009

### ACKNOWLEDGMENTS

The authors would like to thank Technical university of Liberec for „students grant.



## Injectable Platforms Containing Functionalised Mesoporous Silica Nanoparticles for Controlled Release of Chemotherapeutics

A. Borzacchiello<sup>1</sup>, L. Russo<sup>1</sup>, A. Salis<sup>2</sup>, L. Medda<sup>2</sup>, M. Monduzzi,<sup>2</sup> G. D'Errico<sup>3</sup>, L. Paduano<sup>3</sup> and L. Ambrosio<sup>1,4</sup>

<sup>1</sup>Institute for Composite and Biomedical Materials IMCB-CNR, Italy

<sup>2</sup>Department of Chemical and Geological Sciences, University of Cagliari, Italy

<sup>3</sup>Department of Chemical Sciences, University of Naples "Federico II", Italy

<sup>4</sup>Department of Chemical Science and Materials Technology DCSMT- CNR, Italy

[bassunta@unina.it](mailto:bassunta@unina.it)

### INTRODUCTION

In situ-forming gels, with a phase transition temperature near to body temperature, appear particularly interesting as platforms for drug delivery applications. Being liquid at room temperature, indeed, they can be simply injected into the body but, once in place, they gelify thus allowing a time-controlled release of the active. In this context, due to their ability to undergo thermal gelation, thermosensitive amphiphilic block copolymers, namely polyethylene oxide–polypropylene oxide copolymers (pluronic PPO-PEO-PPO), have been widely used in biomedical field, particularly as a dispersing medium for drugs. However, to encapsulate hydrophobic drugs and/or to obtain a controlled release the use of a protective matrix for the drug is more convenient. To this aim Mesoporous Silica Nanoparticles (MSNs) with their highly-ordered structures having uniform but size-adjustable pores have shown high efficiency either for loading or controlled drug release<sup>1</sup>. The main target of this work is to design composite injectable *in situ* forming gels based on blends of PPO-PEO-PPO copolymers reinforced by a natural polysaccharide, hyaluronic acid (HA), and mesoporous silica nanoparticles (MSNs) functionalised with HA, as platforms for the controlled release of chemotherapeutics. The presence of the HA promotes the interaction between poloxamers blends and MSNs. Thanks to their gel nature these platforms could be potentially used to fill the cavity after tumor resection. Preliminarily, drug loading efficiency onto MSNs was optimised and *in vitro* release kinetics of a widely employed chemotherapeutic (Irinotecan) was also studied.

### EXPERIMENTAL METHODS

The dispersing medium platforms were prepared by mixing Pluronic F127 and F68 with small amounts of HA. The composition of the medium was optimised to obtain a gelification temperature ( $T_{gel}$ ) around body temperature. The medium mixture was characterised for the rheological properties and assessed for its capability of suspending efficiently MSNs.

The MSNs were synthesized and eventually functionalized with HA according to Yu et al.<sup>2</sup>, then characterized in terms of morphology, size and porous dimensions, through N<sub>2</sub> adsorption/desorption isotherms SAXS and TEM techniques<sup>3</sup>.

The first drug entrapment experiments were performed by suspending the MSNs particles in a DMSO solution of Irinotecan. Subsequently ethanol was added to promote the adsorption of Irinotecan (5 mg/ml) on the MSNs particles. After overnight stirring, the suspension was sonicated and centrifugated. The immobilized amount of the drug was determined through UV-Vis analysis ( $\lambda = 368\text{ nm}$ ) of the supernatant. Preliminary *in vitro* release experiments were performed suspending MSNs in 10 ml of release medium (PBS at

pH 7.4) at 37 °C. At scheduled time intervals, 1 ml aliquots were withdrawn and replaced with the same volume of fresh media. The aliquots were ultracentrifugated and the supernatant was analyzed through spectrophotometric analysis ( $\lambda = 368\text{ nm}$ ) to assess the content of Irinotecan.

### RESULTS AND DISCUSSION

Separate Pluronic F127 and F68 solutions do not show a gelling temperature close to the body one in the concentration range from 10 to 30% w/w (gelling temperatures higher than 40°C or lower than 25°C). By formulating Pluronic F127/F68 blends at specific concentrations, it was possible to obtain a medium with a  $T_{gel}$  close to the body temperature. The addition of low molecular weight HA at different concentrations had only a slight influence on  $T_{gel}$ , but very interestingly, improved significantly the viscoelastic properties of the final gel as determined through rheological measurements. The Irinotecan loading efficiency was optimized in terms of dissolving medium and was found to be the highest (about 5%) for the medium 50% DMSO-50% ethanol. Very promising results were obtained from the first experiments aimed to achieve stable suspensions of Irinotecan loaded MSNs in the new thermosensitive medium mixture. Stability of suspensions is very high in the gel above the  $T_{gel}$ . The main problem is related to the stability of the suspension below the sol-gel transition temperature. Indeed, below the  $T_{gel}$  the polydispersity in the size of the MSNs represents an important instability factor: the use of HA functionalized MSNs might improve the stability of the suspension also at room temperature. Work is in progress. In any case, the preliminary *in vitro* drug release experiments, simply performed with the MSNs suspended in PBS, showed that a controlled Irinotecan release occurred during about 7 days.

### CONCLUSION

Here we are presenting preliminary but very promising results aimed to build a sustained drug delivery composite platform based on pluronics, HA and MSNs, potentially useful to carry chemotherapeutic agents.

### REFERENCES

- <sup>1</sup>Jie Lu et al. Mesoporous Silica Nanoparticles as a Delivery System for Hydrophobic Anticancer Drugs. *Small* 2007, 3, No. 8, 1341 – 1346
- <sup>2</sup>Yu M. et al. Hyaluronic Acid Modified Mesoporous Silica Nanoparticles for Targeted Drug Delivery to CD44-Overexpressing Cancer Cells. *Nanoscale* 2013, 5, 178–183.
- <sup>3</sup>Salis A et al. Adsorption of Lysozyme on Hyaluronic Acid Functionalized SBA-15 Mesoporous Silica: A Possible Bioadhesive Depot System. *Langmuir* 2014, 30, 12996-13004



## Visible Light-curable, Nanoparticles Created Hydrogel for In Situ Useable Drug Delivery System

József Bakó<sup>1</sup>, Farkas Kerényi<sup>1</sup>, Edit Hrubí<sup>1</sup>, Lajos Daróczi<sup>2</sup>, Beatrix Dienes<sup>3</sup>, Csaba Hegedűs<sup>1</sup>

<sup>1</sup> Department of Biomaterials and Prosthetic Dentistry, University of Debrecen, Hungary

<sup>2</sup> Department of Solid State Physics, University of Debrecen, Hungary

<sup>3</sup> Department of Physiology, University of Debrecen, Hungary

[bako.jozsef@dental.unideb.hu](mailto:bako.jozsef@dental.unideb.hu)

### INTRODUCTION

Nanoparticles created systems have received increasing interest, because the high surface to volume ratio ensures well-tailorable properties<sup>1</sup>. The formulations in nanoparticles could reduce the risk of toxicity and the side effects of active-agents, and could increase the efficiency, specificity, and the tolerability, so the therapeutic index of different drugs<sup>2-3</sup>.

Poly-gamma-glutamic acid ( $\gamma$ -PGA) is a poly-amino acid, what is negatively charged in an aqueous solutions and it is biodegradable, edible and non-toxic<sup>4-5</sup>. The aim of this study is preparation of a light cured, so – in dentistry – an in situ practically used hydrogel system. This nanoparticles created system provides possibilities allow the tailoring of the properties such as the mechanical, swelling, and related to these the release properties.

### EXPERIMENTAL METHODS

The molecular characterizations of the modified PGAs (PGA-MNP) were accomplished by Proton Nuclear Magnetic Resonance Spectroscopy (<sup>1</sup>H NMR), and dynamic light scattering measurement (DLS) was used for the determination of hydrodynamic diameter of nanoparticles (NPs).

The NPs created hydrogels (PGA nanogel) were imaged using scanning electron microscope (SEM), and the mechanical parameters were investigated by compression tests on 2mm height, 5mm diameter cylindrical samples. The swelling experiments were carried out by immersion of hydrogels in saline-solution. The release properties were study by high-pressure liquid chromatograph (HPLC).

The biocompatibility of the PGA-nanogels was proved by Alamar Blue assays. The viability, the morphology, and the proliferation tendencies were followed by fluorescent and confocal laser scanning microscopy. Saos-2 cells were used in all of these experiments. The statistical analyses were performed by using SPSS version 17.0.

### RESULTS AND DISCUSSION

The NMR results proved that the crosslinking- and the methacrylating-reactions were successful. The resulted 10% reactive group is allowed the fast photopolymerization reaction. DLS measurements verified the nanosize ranges of the particles, average diameter was around 80 nm. The SEM micrographs of the PGA nanogels confirmed the DLS results, because the different nanoscale objects clearly visible also on broken surfaces. (Figure 1)

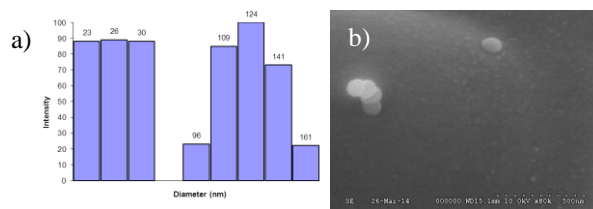


Figure 1 The size distribution of NPs according to the DLS measurements and b) SEM image of PGA nanogel

Different reticulate structures could be found in the nanogels, where the dimensions are in the nanoscale. Rigid gel could be obtained in relatively short photopolymerization time -3 min- this is the main condition for the applicability. The mechanical testing shows that the Young's modulus of nanogel  $0.927 \pm 0.433$  MPa. The swelling properties of the gels are connected to the more compact nanostructure. This is around 110% in the case of PGA-nanogel, what is less than the non-nanoparticles created hydrogel. The HPLC results show a retentive effect for the release of the ampicillin from PGA-nanogel, what can give possibilities for the control. The Alamar blue assay cannot show significant different between the cell viability of the control and the nanogel samples in 3 days period. The microscopy techniques highlighted the presence of proliferating cells after 1 week.

### CONCLUSION

Exclusively PGA nanoparticles created, in situ useable hydrogel system was demonstrated in this study. This PGA-nanogel could be suitable candidate for direct application in dentistry. The release behaviour of the nanogel could ensure a certain control possibilities for antibiotic administration, and the biocompatibility of the system was verified with various ways.

### REFERENCES

1. Gaharwar AK. *et al.*, Biotechnol Bioeng. 111:441-53, 2014
2. Hwang SR. *et al.*, Arch Pharm Res.37:24-30, 2014
3. Zhang Y. *et al.*, Adv Drug Deliv Rev. 65:104-20, 2013
4. Bajaj I *et al.*, Bioresour Technol. 102:5551-61, 2011
5. Bakó J. *et al.*, J Mater Sci Mater Med. 24:659-66, 2013

### ACKNOWLEDGMENTS

The authors would like to thank the TÁMOP-4.1.1.C-13/1/KONV-2014-0001, and the TÁMOP 4.2.4. A/2-11-1-2012-0001 'National Excellence Program' for providing financial support to this project".

## Liposomal Formulations as Treatment for Facial Erythema of Rosacea

Anca N. Cadinoiu<sup>1</sup>, Lacramioara Ochiuz<sup>2</sup>, Delia M. Rață<sup>1</sup>, Oana M. Darabă<sup>3</sup>, Vasile Burlui<sup>3</sup>, Marcel Popa<sup>1,4</sup>

<sup>1</sup>“Academician Ioan Hăulică” Research Institute, “Apollonia” University of Iași, Romania

<sup>2</sup>Faculty of Pharmacy, “Grigore T. Popa” University of Medicine and Pharmacy of Iasi, Romania

<sup>3</sup>Faculty of Dental Medicine, “Apollonia” University of Iași, Romania

<sup>4</sup>Department of Natural and Synthetic Polymers, “Gheorghe Asachi” Technical University of Iași, Romania  
[ochiuzd@yahoo.com](mailto:ochiuzd@yahoo.com)

### INTRODUCTION

Rosacea is a common and chronic disorder, characterized by flushing and persistent erythema in the central facial area<sup>1</sup>. New liposomal formulations as treatment for facial erythema of rosacea were synthesized and characterized. The *in vitro* release profile of brimonidine tartrate (BT) incorporated into two types of liposomes (MLV and LUV), dispersed in different polymeric gel matrices, was analyzed. The influence of the liposomes size and the matrices characteristics over the BT release kinetics was studied.

### EXPERIMENTAL METHODS

Liposomes were prepared by the thin film hydration method. Briefly, lipids (Phosphatidylcholine and Cholesterol) were dissolved in an appropriate volume of chloroform. The organic solvent was evaporated from the round bottom flask (250 mL) resulting in formation of a thin film on the walls of the flask. Then, the lipid film was hydrated with a solution of 6% (w/v) BT (prepared in phosphate buffer saline - PBS, pH 7.4), at 40°C. After vigorous shaking, a spontaneous formation of MLVs occurred. The dispersion was placed in a bath sonicator for 10 min at 45°C, in order to break the existing aggregates. Finally, the liposomal dispersions were incubated for 1–2 hours at a temperature above the lipid transition temperature (at 25°C) for annealing membranes structural defects. The separation of liposomes from non-encapsulated brimonidine tartrate was achieved by centrifugation. The amount of BT entrapped in the liposomes was determined by breaking them with Triton X-100. LUVs were prepared by extrusion method. A MLVs suspension was forced through a polycarbonate filter with 100 nm pore size, at 40°C, to yield liposomes having a diameter near the pore size of the filter used. Carbopol940, hydroxypropylcellulose and some poloxamers were used for gel matrix synthesis. For the preparation of new systems, in each gel matrix a certain volume of BT loaded liposomes suspension was added. The final concentration of drug in obtained formulations was 0.5% (w/w).

### RESULTS AND DISCUSSION

The mean diameter of the liposomes was determined by laser light diffractometry technique. The mean diameters measured for the vesicles used in this study were 901 nm for MLVs and 110 nm for LUVs.

The *in vitro* released amount of BT was analyzed using Franz diffusion cells. A cellulose membrane separated the donor compartment, containing the drugs loaded liposomes from the receptor compartment filled with collection medium (Phosphate buffer solution - PBS, pH 5.5, 37°C). At predetermined time points, the amount of the drug diffused across the membrane was monitored by using UV-VIS spectroscopy at specific wavelength. The BT release from different matrices has been retarded from several days to weeks after BT inclusion in LUVs and MLVs entrapped subsequently in matrices with variable composition.

The release kinetics curves shows that the composition of liposomes had no significant influence on liposomes stability.

The BT release from LUVs was slower than from MLVs. The LUV liposomes proved to be superior to MLV liposomes in terms of stability and the obtained results are consistent with other research in the field<sup>2</sup>.

The liposomes stability was greatly improved by inclusion in polymeric matrices.

*In vitro* cytotoxicity of liposomal formulations was determined on the human dermal fibroblasts cell line. Liposomal formulations were shown to be non-cytotoxic.

### CONCLUSION

Liposomes obtained in this study proved to be stable. *In vitro* tests have shown a prolonged release profile of brimonidine tartrate and therefore the liposomal formulations can be used as topical delivery systems for treatment of facial erythema of rosacea.

### REFERENCES

1. Fowler J. *et al.*, Br. J. Dermatol. 166:633-41, 2012
2. Liu H. *et al.*, Acta Pharmaceutica Sinica, 37:563-6, 2002



## Tetracycline - Loaded Chitosan/Pectin Hydrogels for the Treatment of Periodontitis

Delia M. Rață<sup>1</sup>, Anca N. Cadinoiu<sup>1</sup>, Oana Darabă<sup>1</sup>, Vasile Burlui<sup>1</sup>, Lăcrămioara Ochiuz<sup>3</sup>, Marcel Popa<sup>1, 2</sup>

<sup>1</sup>“Academician Ioan Hăulică” Research Institute, “Apollonia” University of Iași, Romania

<sup>2</sup> Department of Natural and Synthetic Polymers, “Gheorghe Asachi” Technical University of Iasi, Romania

<sup>3</sup>Faculty of Pharmacy, “Grigore T. Popa” University of Medicine and Pharmacy of Iași, Romania

[ochiuzd@yahoo.com](mailto:ochiuzd@yahoo.com)

### INTRODUCTION

Periodontal diseases are one of the common microbial infections which involve 35% of adult population in the world, that affect the gums and bones supporting the teeth and can lead to tooth loss<sup>1,2</sup>. Controlled delivery of chemotherapeutic agents within periodontal pockets can improve clinical signs of periodontitis and can prevent systemic side effects<sup>2</sup>. Hydrogels have generated great interest as biomaterial vehicle for drug delivery because many of them present excellent biocompatibility with minimal inflammatory responses. Considering this previous information, the main purpose of this study was to obtain a new type of biocompatible hydrogels based on natural polymers (chitosan and pectin) which are designed to deliver the drug into periodontal pocket, and which could present an excellent alternative for treatment of periodontitis.

### EXPERIMENTAL METHODS

#### Materials

Chitosan MMW (degree of deacetylation 91 %) and Tetracycline were purchased from Sigma Aldrich. Pectin (citrus) type USP/100 was purchased from CPKelco. Cryopreserved primary human dermal fibroblasts (HDF) cells (CO135C), Dulbecco's Modified Eagle's Medium, Fetal Bovine Serum (FBS) were purchased from Life Technologies. Penicillin, streptomycin, trypsin, non-essentials amino acids has been acquired from Antisel.

The hydrogels were prepared by complex coacervation method. The reaction took place by ionic interactions between the positively charged amino group of chitosan and negatively charged carboxyl group of pectin and offers the possibility of rapid formations of the thin films. Certain amount of chitosan was added in a lactic acid solution (1wt%) under magnetic stirring. Pectin solution has been added dropwise in chitosan aqueous solution under continuous stirring. Glycerol was added as plasticizer. Tetracycline solution was introduced in formed polyelectrolyte complex. Finally, the hydrogels were turned in the polycarbonate rectangular templates. The films were obtained after evaporation of water in an oven at  $37 \pm 0.5$  °C for 24 h. In order to remove any possible unreacted products, the films were purified by repeated washings with distilled water and then dried at room temperature for 24 h. The prepared hydrogels were analyzed from different points of view:

- FT-IR for both polymers and the hydrogels;
- Scanning electron microscopy (SEM) was used for morphology characterization;

- The swelling degree of the hydrogels in slightly alkaline aqueous medium (pH=7.2) and in artificial saliva (pH=6.75) was studied by using the gravimetric method;

- The Tetracycline release from hydrogels were performed in solutions that mimicking the biological fluids using UV-VIS spectroscopy;

- Cell viability was determined and cell number was counted with a hemocytometer.

### RESULTS AND DISCUSSION

The FT-IR spectra confirmed the interpolymeric complex formation between amino groups of chitosan and carboxyl group of pectin. Hydrogel swelling degree was caused by water penetration through diffusion within the empty pores and in the networks of the hydrogels, causing the swelling of polymer membrane. The swelling degree in artificial saliva was lower than in phosphate buffer solution (pH = 7.2). Hydrogels presented a good Tetracycline including and release capacity. The cytotoxicity of these materials was investigated on human dermal fibroblasts. Cell viability in contact with hydrogels was approximately 93% which means that the material have non-cytotoxic behavior. A slight decrease of the cells number from experimental cell cultures may be caused by the local mechanical damage as a result of the hard consistency of the material.

### CONCLUSION

In the present study, has been prepared chitosan - pectin hydrogels able to be used in the treatment of periodontitis. Hydrogels allowed a good drug release capacity of Tetracycline and showed a good cell viability.

### REFERENCES

1. Raheja I. *et al.*, Int. J. Pharm. Pharm. Sci. 5:11-16, 2013.
2. Pragati S. *et al.*, Int. J. Drug Deliv. 1:1-14, 2009.





## The Quantification of Doxorubicin and Lipids in Liposomal Doxorubicin Formulation

Jan Procek<sup>1</sup>, Maciej Łukawski<sup>1</sup>, Magdalena Przybyło<sup>1</sup>, Marek Langner<sup>1</sup>

<sup>1</sup>Faculty of the Fundamental Problems of Technology, Wrocław University of Technology, Poland  
[jan.procek@pwr.edu.pl](mailto:jan.procek@pwr.edu.pl)

### INTRODUCTION

The development of methods for the determination of active pharmaceutical ingredients (API) concentration in a drug is the main element of the documentation required for its registration. In liposomal doxorubicin (brand name: Doxil (USA), Caelyx (EU))<sup>1</sup> both lipids and doxorubicin are considered as APIs. There are numerous approaches in literature for the determination of active ingredients in liposomal doxorubicin. However, there are serious inconsistencies regarding preparation of standards for the encapsulated doxorubicin. This results with lack of a reliable data as illustrated by the low efficiency of doxorubicin recovery<sup>2</sup>. The aim of presented studies is the development of consistent and reproducible procedure, would ensure the satisfactory accuracy and precision of the quantification of doxorubicin in liposome formulation.

### EXPERIMENTAL METHODS

An HPLC-ELSD method for lipid content determination were developed and validated according to ICH Q2(R1) guidelines. Quantitative analysis of doxorubicin in liposomal form was performed using HPLC equipped with UV and Fluorescence detectors using C18 column. The reference samples of doxorubicin with lipids were prepared in a mobile phase consisting of methanol, histidine buffer, ammonium sulphate, lipid mixture and sucrose.

### RESULTS AND DISCUSSION

Data presented in table 1. summarise the results of HPLC analysis of lipids and doxorubicin quantities in Caelyx. Regardless of the type of doxorubicin reference standard used a good accuracy and precision were obtained. However, the recovery of doxorubicin always exceeded required value of 5%. The obtained results shown that free and liposomal doxorubicin are not equivalent from the analytical point of view. Conditions during and after the encapsulation process are so

complex that simple references are not sufficient. The results of lipids analysis pass the quality criteria.

Table 1. The accuracy, precision and ratio of recovery rate for doxorubicin and lipid obtained using HPLC analysis for liposomal formulation of doxorubicin.

	Method accuracy [%]	Intra-vials precision [%]	Ratio of recovery [%]
MPEG-DSPE	99.8±0.2	98.5±2.5	102.5±2.8
Doxorubicin	99.9±0.5	100.3±0.5	115 to 150

### CONCLUSION

The complex drug formulation such as liposomal doxorubicin requires dedicated methodologies for the quantification of active ingredients. Presented studies present the methodology for the quantification of lipids and encapsulated doxorubicin. Developed methodology allows for the determination of all main components of liposomal doxorubicin with accuracy satisfying standards imposed by regulatory institutions.

### REFERENCES

1. [www.ema.europa.eu](http://www.ema.europa.eu)
2. D.L. Chin et al. J. Chromatogr. B 779 (2002) 259-269

### ACKNOWLEDGMENTS

The study was supported by National Centre for Research and Development (Warsaw, Poland) grant DEMONSTRATOR+ nr WND-DEM-1-027/00.



## Lactic Acid Photocrosslinkable Adhesives to be Used as Transdermal Delivery Systems

João Santos<sup>1</sup>, Filipe Aguiar<sup>2</sup>, Fernando Cruz<sup>2</sup>, Cristina Baptista<sup>1</sup>.

<sup>1</sup>CIEPQPF-Department of Chemical Engineering, University of Coimbra, Portugal

<sup>2</sup>73100, Lda., Lisboa, Portugal

[jsantos@eq.uc.pt](mailto:jsantos@eq.uc.pt)

### INTRODUCTION

Lactic acid (LA), a 100% renewable raw material, is currently used to produce poly(lactic acid), a biodegradable/biocompatible polymer, FDA approved, with outstanding advantages over other synthetic polymers. Its properties allow a wide range of biomedical applications, though its use as a bioadhesive has not been thoroughly studied. Bioadhesives are important tools in the treatment of injured organic tissues<sup>1</sup>. Advances in adhesive science rendered their design simpler, allowing a customized thickness that improves patient comfort and increases potential for producing transdermal drug delivery systems (TDDS) with these adhesives. These systems are non-invasive, may improve therapeutic efficacy compared to conventional routes of drug administration and are ranked as patient-friendly treatments<sup>2</sup>. The pharmaceutical industry already provides transdermal drug delivery systems for hormone therapies or muscular aches treatment, as examples. In TDDS systems, known as patches, the medicine may be entrapped in the adhesive or in a layer over the film. Knowing that photo-polymerization allows a good control of film properties and fast curing rates<sup>3</sup>, in this study the performance of photocrosslinkable lactic acid adhesives as drug delivery devices was assessed.

### EXPERIMENTAL METHODS

Following a three steps process, photocrosslinkable adhesives were produced from two different lactic acid solutions upon heating at high temperatures: L-lactic acid (80%) (LA80) and lactic acid (85-90%) (LA85-90). 1,4-Butanediol (99%) was used as a co-monomer; catalysts or toxic solvents were not added. The prepolymers based on LA80 were further purified by dialysis and lyophilized to remove the residual water as well as lactic acid impurities. All LA products with OH end groups were modified with an isocyanate functional monomer, Laromer® LR 9000. Weight ratios of these reagents were in the range of 60/40 to 30/70. A low toxicity solvent, diethyl ether (99%), was used in the synthesis. In the last step different weight percentages of Irgacure® 2959, a photoinitiating agent, were added to form well defined films after UV irradiations for 2-5min. ATR-FTIR monitoring was performed to confirm the success of chemical reactions. TGA technique, surface energy measurements, *in vitro* degradation in phosphate buffer solution (PBS), water uptake in PBS, *in vitro* biocompatibility, haemocompatibility, and antimicrobial properties were assessed to characterize the synthesized materials. Drug release tests, using a

commercial drug for muscular pain, are underway to assess drug release kinetics from the bioadhesives.

### RESULTS AND DISCUSSION

The obtained membranes were transparent and highly flexible, which are major advantages for the envisaged application. These membranes were then characterized to evaluate their potential for TDDS. The swelling percentage of materials was moderate (around 20%) which means that the membranes present good hydration ability while not compromising skin adhesion. Degradation studies for 6 to 12 weeks showed a slight hydrolytic instability with a maximum weight loss of 20-30%; however the mechanical performance and chemical resistance of the films were not greatly compromised. TGA results revealed materials resistance at high temperature (> 200°C), meaning that membranes might be sterilized. Surface energy of materials ( $\gamma_s \approx 27\text{mN/m}$ ) were lower than the ones reported in the literature for skin ( $\gamma_s \approx 38\text{-}56\text{mN/m}$ ) thus, according to thermodynamic requirements<sup>2</sup>, the adhesives will adhere effectively to skin. Haemocompatibility was assessed and adhesives showed a thrombogenic character of approximately 80% and a non-haemolytic nature after a pre-incubation in PBS medium. Biocompatibility was evaluated *in vitro*: films confirmed cell viability above 85% and antimicrobial properties against *E. coli* and *S. aureus* models.

### CONCLUSION

A very simple and easy method was developed to produce biocompatible lactic acid adhesives. This method can be easily scaled up to obtain new transdermal drug delivery systems (for short or long term uses) using UV photocrosslinked materials. Drug delivery studies are the main goal of our research at the moment, and this includes using lactic acid based polymers as well as its copolymers.

### REFERENCES

1. Mohammadreza M. *et al.*, Macromol. Biosci., 13:271-288, 2013
2. Subham B. *et al.*, Int. J. Adhes. Adhes., 50:70-84, 2014
3. Jamie L. I. *et al.*, Tissue Eng., 13:2369-2385, 2007

### ACKNOWLEDGMENTS

The authors would like to thank 73100, Lda. for the financial support.



## Pitavastatin Loaded Calcium Phosphate Foams for Enhanced Mineralization and Vascularization

Kanupriya Khurana<sup>1,2,3</sup>, Jordi Guillem-Martí<sup>1,2,3</sup>, Cristina Canal<sup>1,2,3</sup>, Maria-Pau Ginebra<sup>1,2,3</sup>

<sup>1</sup> Biomaterials, Biomechanics and Tissue Engineering Group, Dept. Materials Science and Metallurgy, Technical University of Catalonia (UPC), Av. Diagonal 647, 08028 Barcelona, Spain

<sup>2</sup> Biomedical Research Networking Center in Bioengineering, Biomaterials and Nanomedicine (CIBER-BBN)

<sup>3</sup> Research Centre in NanoEngineering (CrNE), UPC

[cristina.canal@upc.edu](mailto:cristina.canal@upc.edu)

### INTRODUCTION

Bone regeneration has been investigated with different calcium phosphate materials (CaPs) incorporating biomolecules such as growth factors i.e bone morphogenetic proteins (BMPs) or drugs<sup>1</sup>. Despite their bone stimulating ability, incorporation of BMPs is questioned by the risk of serious side effects. Alternatively, several reports have indicated a therapeutic benefit of statins especially simvastatin known for neovascularization and bone formation and other benefits after incorporating with CaPs<sup>2</sup>.

In this study, an unexploited low molecular weight drug from the family of statins, Pitavastatin (PTV) in combination with CaPs has been studied with the aim of enhancing bone regeneration and vascularization. Also, the effects of PTV on physico-chemical properties of the scaffolds have been assessed.

### EXPERIMENTAL METHODS

Stability of PTV dissolved in water and phosphate buffer saline over 2 weeks at 37 °C and 4 °C, at different pH 6.5, 8 and 9.5 was measured using High performance liquid chromatography (HPLC).

Rat mesenchymal stem cells (rMSCs) and rat endothelial progenitor cells (rEPCs), were cultured in cell culture media containing PTV (1 and 0.1 µM) and the expression of some genes involved in bone regeneration (Osteocalcin, collagen type 1, BMP-2, Alkaline phosphatase, Beta actin etc.) and vascularization (VEGFA, VEGFR1, VEGFR2, eNOS etc.) was monitored by Real Time - Polymerase Chain Reaction (RT-PCR) for 72h.

Self-setting CaP foams were prepared by mechanical mixing of solid phase ( $\alpha$ - tricalcium phosphate with 2wt% hydroxyapatite) and liquid phase (10 µM PTV, 1% Tween, 10% Pluronic in MQ water) in a 0.65 L/P ratio at 1700rpm. Microstructure was assessed by optical and electronic microscopy, porosity by mercury intrusion porosimetry and He pycnometry and specific surface area by Nitrogen adsorption (BET method).

### RESULTS AND DISCUSSION

Stability studies showed PTV solutions were stable for 2 weeks in all the conditions except for 15% and 25% degradation at pH of 8 and 9.5, respectively. The presence of PTV in the cell culture enhanced the expression of genes involved in mineralization (Osteocalcin and Collagen type 1) and vascularization (VEGFA, VEGFRs), in a dose-dependent way over the course of 72h, with an overexpression for 0.1µM (Figure 1).

Characterization of the self-setting CaP foams loaded with PTV showed no differences in the microstructural or textural properties such as porosity (~78%) and interconnected porosity. This can be explained based on the low concentrations used, based on *in vitro* studies.

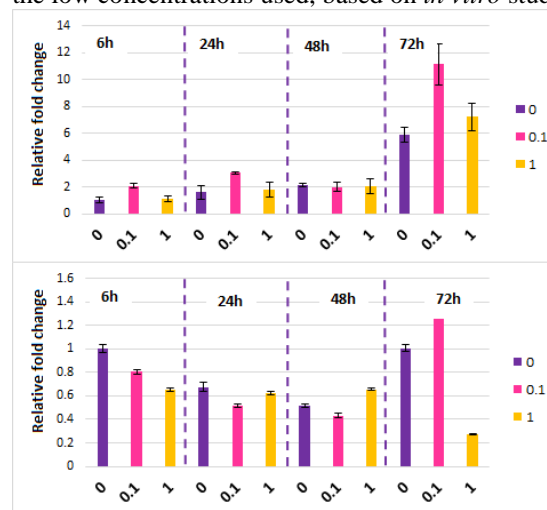


Figure 1. Gene expression of (a) Osteocalcin in rMSCs and (b) VEGFA in rEPCs in growth media with PTV (0, 0.1 and 1 µM),

### CONCLUSION

*In vitro* studies provided a new evidence of the potential of PTV to enhance bone regeneration and vascularization. Addition of PTV in the CaP foams did not interfere with the setting reaction and did not alter the microstructural and textural properties of the materials. This novel approach opens the path for further investigation of PTV-loaded CaP scaffolds as matrices for drug release experiments, which are presently in process.

### REFERENCES

1. Ginebra et al., Adv. Drug Delivery Reviews 64:1090-1110, 2012
2. Mundy et al., Curr. Pharm. Des. 7:715-736, 2001

### ACKNOWLEDGMENTS

Authors acknowledge the Spanish Government for financial support through Project MAT2012-38438-C03-01, co-funded by the EU through European Regional Development Funds, and Ramon y Cajal of CC. Support for the research of MPG was received through the "ICREA Academia" funded by the Generalitat de Catalunya.



## Stability Enhanced Gold-cross-linked Polymeric Nanocarriers

Sangmin Jeon<sup>a,b</sup>, Hong Yeol Yoon<sup>a,b</sup>, Dong Gil You<sup>a,b</sup>, Hwa Seung Han<sup>a</sup>  
Ick Chan Kwon<sup>b,c</sup>, Kwangmeyung Kim<sup>b</sup>, Jae Hyung Park<sup>a,\*</sup>

<sup>a</sup> School of Chemical Engineering, Sungkyunkwan University, Suwon 440-746, Republic of Korea

<sup>b</sup> Center for Theragnosis, Korea Institute of Science and Technology, 39-1 Hawolgok-dong, Seongbuk-gu, Seoul 136-791, Republic of Korea

<sup>c</sup> KU-KIST School, Korea University, Anam-dong, Seongbuk-gu, Seoul 136-701, Republic of Korea  
[freetama@naver.com](mailto:freetama@naver.com)

### INTRODUCTION

Polymeric nanoparticles prepared using amphiphilic polymeric derivatives has shown significant promise as carrier for imaging and therapeutic agents<sup>1</sup>. Currently, the stability of polymeric nanoparticles has been improved by covalently crosslinking using small molecule crosslinker and controlled mineralization on shell of the polymeric nanoparticles<sup>2</sup>. However, the former method utilizes toxic small molecule crosslinkers and complex crosslinking chemistry, whereas the later method is highly laborious. In this study, a new crosslinking method using gold nanoparticles as crosslinkers will be developed.

### EXPERIMENTAL METHODS

Synthesis Tertiary amine contained amphiphilic block copolymers using a versatile macroinitiator via ring opening polymerization and atom transfer radical polymerization. DOX was loaded into triblock copolymers using the simple dialysis method in dark circumstances. For the optimization of gold-crosslinking system, various molar ratio of  $\text{HAuCl}_4 \cdot 3\text{H}_2\text{O}$  was treated in contrast to tertiary amine of DOX loaded nanocarriers solution. In brief, prepared 2 mg of DOX loaded nanocarriers dissolved 2 ml of distilled water in vial and added 95 nmol (0.1 molar ratio) to 2.85  $\mu\text{mol}$  (3.0 molar ratio) of  $\text{HAuCl}_4 \cdot 3\text{H}_2\text{O}$  solution. The mixture was stirred well at 40 °C for 12 h and resulting solution was centrifuged (15000 RPM, 30 minutes) to remove any residue. Then, lyophilize to obtain gold-crosslinked nanocarriers.

### RESULTS AND DISCUSSION

As prepared triblock copolymer, DOX-loaded nanocarriers and gold crosslinked nanocarriers have a hydrodynamic radius of  $195.4 \pm 0.7$ ,  $146.2 \pm 0.84$  and  $156.0 \pm 1.629$  with a zeta potential value of  $43.1 \pm 0.46$ ,  $24.9 \pm 0.29$  and  $40.2 \pm 0.4$ .

Gold crosslinked nanocarrier was confirmed using TEM imaging (Fig. 1) and UV-Vis spectrometer.

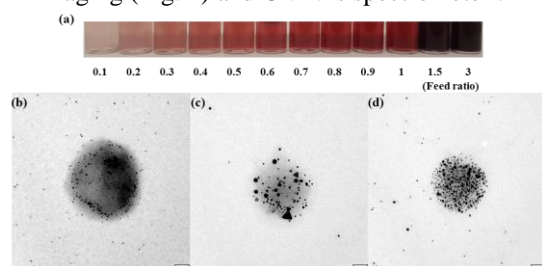


Fig.1. Images of gold crosslinked nanocarriers with various reaction conditions (a). and Transmission

electron microscopy (TEM) images of different feed ratio of  $\text{HAuCl}_4$ . 1:1 (b), 1:1.5 (c) and 1:3 (d)

In TEM image, we confirmed the reduction of  $\text{HAuCl}_4$  by tertiary amine inside nanocarriers.

One of the main advantages gold crosslinked nanocarriers is stability enhancement. The release of DOX from gold crosslinked nanocarriers was much slower than that from uncrosslinked nanocarriers (Fig. 2), which might be due to the crosslinked structure of gold crosslinked nanocarriers playing a role as the diffusion barrier.

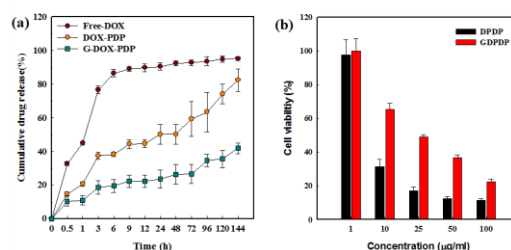


Fig. 2. *In vitro* release behavior of DOX from DOX-loaded nanocarriers and gold crosslinked nanocarriers (a) and *In vitro* cytotoxicity (b)

### CONCLUSION

In this study, we developed gold crosslinked nanocarriers by Amine induced reduction. The gold crosslinking inside nanocarriers resulted in improved stability and allowed long circulation, sustained release of loaded drug, DOX. Overall results, gold crosslinked nanocarriers might have promising potential as a drug carrier system for DOX.

### REFERENCES

1. R. Duncan. *et al.*, Nat. Rev. Drug Discov. 2;347-360, 2003
2. R.K. O'Reilly *et al*, Chem. Soc. Rev. 35;1068-1083, 2006

### ACKNOWLEDGMENTS

This work was financially supported by the Basic Science Research Programs (2012012827) of MEST



## Brushite/Alginate Microbeads for Sustained Drug Delivery

Alberto Lagazzo<sup>1</sup>, Laura Pastorino<sup>2</sup>, Noemi Frisina<sup>2</sup>, Fabrizio Barberis<sup>1</sup>, Marco Capurro<sup>1</sup>

<sup>1</sup>Department of Civil, Chemical and Environmental Engineering (DICCA), University of Genoa, Italy.

<sup>2</sup>Department of Informatics, Bioengineering, Robotics and Systems Engineering, University of Genoa, Italy.

[alberto.lagazzo@unige.it](mailto:alberto.lagazzo@unige.it)

### INTRODUCTION

Alginate is one of the most extensively studied polysaccharides and has shown great potential as drug and cell carrier<sup>1</sup>. Alginate beads can be prepared by extruding a solution of sodium alginate, containing bioactive compounds, as droplets, into a divalent crosslinking solution, such as  $\text{Ca}^{2+}$ . However, the use of alginate in drug delivery shows some drawback specifically for the release of low molecular weight molecules, since the release rate is very fast and can not be controlled or modulated<sup>2</sup>. In present work, we proposed the precipitation of brushite within alginate microdrops during alginate  $\text{CaCl}_2$  mediated crosslinking process using an encapsulation unit.

The association of microporous brushite and of biodegradable hydrogel like alginate leads to a composite material with improved mechanical properties and sustained release of encapsulated active molecules.

### EXPERIMENTAL METHODS

Composite microbeads were prepared using a commercially available air-driven droplet generator (Nisco encapsulation unit Var J30, Zurich, Switzerland). Alginate (low viscosity), 1% in ammonium phosphate monobasic, was sprayed into a  $\text{CaCl}_2$  (2% w/v) solution to gel under constant stirring using optimized instrumental parameters. A nozzle having a diameter 0.25 mm was used with a flow rate of the solution 0.2 ml/min, a pressure 100 mbar and the distance of the nozzle from the cross-linking solution was set 6 cm. A  $\text{CaCl}_2$  2% in distilled water was used as cross-linking. The composite microbeads were then washed in pure water using centrifugation at 1000 rpm for 2 minutes.

The morphology of the beads was characterized by scanning electron microscopy (SEM Hitachi 2500) and optical microscopy.

The rheological characteristics of the alginate solutions were determined using a rheometer Anton Paar MCR301, equipped with plate-cone geometry.

Mechanical properties of the microbeads (dynamic compression tests) were obtained with a homemade instrument<sup>3</sup>, consisting in a shaker, a force transducer and a laser to measure the displacement of the sample. The tests were run in the range 5-100Hz and at different pre-strains of the samples (particles).

A preliminary evaluation of the release properties of the composite microbeads was performed using model molecules, such as ibuprofen.

### RESULTS AND DISCUSSION

The alginate solution shows a rheological behaviour that can be considered Newtonian, without presence of yield stress. Morphological analysis from scanning electronic microscopy reveals particles of spherical shape with a diameter of  $50 \pm 10 \mu\text{m}$ . In comparison with the alginate microbeads produced without brushite, the surface appear more irregular and jagged, probably due to presence of brushite crystals that, trapped inside the alginate network, modify the structure of the particle and their external interface.

Mechanical tests show an increase until three times higher, of the particles stiffness, due to the brushite presence. This fact should be the cause of a more efficient behavior in the drug delivery application of these microbeads, as revealed in preliminary tests, where the composite microbeads had a more sustained release profile than alginate microbeads.

### CONCLUSION

Composite brushite-alginate microbeads showed improved mechanical properties as well as release profiles. Thus the composite material can be regarded as a promising for applications in sustained drug delivery applications.

### REFERENCES

1. C.Y. Yu et al., Int J Pharm. 357 (2008) 15-21.
2. M. Amidi et al., Adv Drug Deliv Rev. 15 (2008) 1638-1649.
3. L. Seminara et al., Sensor Act. A (2011) 169:49-58



# High Intensity Focused Ultrasound-Mediated Doxorubicin Delivery Using Thermosensitive Liposome: Induced Drug Bursting Release by Mild Hyperthermia

Wooram Um<sup>1,3</sup>, Dong Gil You<sup>2,3</sup>, Ju Eun Jeon<sup>2</sup>, Jae Hyung Park<sup>1,2,\*</sup>

<sup>1</sup> Samsung Advanced Institute for Health Sciences and Technology, Sungkyunkwan University, Republic of Korea

<sup>2</sup> School of Chemical Engineering, College of Engineering, Sungkyunkwan University, Republic of Korea

<sup>3</sup> Center for Theragnosis, Biomedical Research Institute, Korea Institute of Science and Technology, Republic of Korea  
[maniakids@skku.edu](mailto:maniakids@skku.edu)

## INTRODUCTION

High intensity focused ultrasound (HIFU), using cancer treatment for precise heating, is using as the source of focal heating for selective delivery of doxorubicin (DOX) with thermosensitive liposomes (TSLs). HIFU has been used for targeted drug release at tumour vasculature by mild hyperthermia immediately upon systemic administration of DOX bearing TSLs (DOX-TSLs). However, this single heating method (SHM) has limited on deep tissue penetration of DOX for high antitumor efficacy <sup>1,2</sup>. In an attempt to allow penetration of DOX at tumour deep tissue, the multiple heating method (MHM) has been developed. First, mild hyperthermia condition was applied by HIFU to increase vascular permeability of tumour. Second, the drug-loaded TSLs were systemically administered into the mice and selective accumulation in tumour site. Third, the mild hyperthermia was re-applied in tumour tissue to improvement drug bursting out of the cumulated TSLs. Herein, we report that the optimized timing of the hyperthermia treatment can significantly improve the antitumor efficacy.

## EXPERIMENTAL METHODS

DOX-TSLs were prepared using the ammonium sulfate gradient method as described previously [27]. The Cy5.5-labeled DOX-TSLs (Cy5.5-DOX-TSLs) were also prepared for imaging experiments, according to the procedure reported previously [28].

The HIFU parameters were optimized to maintain the temperature of tumour tissue at 42 °C (power = 20 W, frequency = 1.5 MHz, pulse repetition frequency = 15 Hz, duty cycle = 15%). Positions of about seven or eight HIFU focuses were preset on a tumour with 2.5 mm of an interval distance, and each of them was sequentially exposed by HIFU for 300 sec.

## RESULTS AND DISCUSSION

The temperature in tumour tissues where HIFU was focused reached 42 °C within 150 s, and rapidly decreased by 37 °C upon the termination of a HIFU exposure. As shown in Figure 1a for DOX-TSL with pre-heating by HIFU, the DOX amount in tumour tissues gradually increased and reached the maximum ( $9.89 \pm 1.92$  DOX  $\mu\text{g/g}$  tissue) at 6h post-injection. The beneficial effect of pre-heating on the TSL accumulation was proven by the comparison of DOX amounts in tumours at the optimal time point (Figure 1b). The *ex vivo* NIRF images of DOX in tumours were obtained. The MHM resulted in the higher DOX accumulation in tumour and significantly enhanced penetration depth compared to the other groups. It was noting that the highest anti-tumour efficacy was

observed from mice treated by MHM, which might be due to the effective delivery of DOX into the tumour tissue (Figure 2).

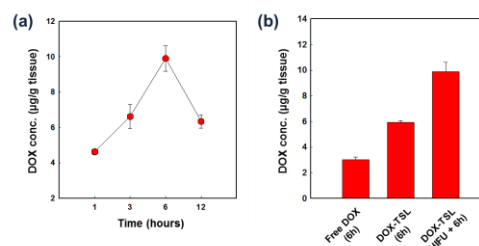


Figure 1. (a) DOX amounts in tumour tissue as a function of time after HIFU treatment. (b) The maximal amount of DOX in tumour tissue at the optimal time points.

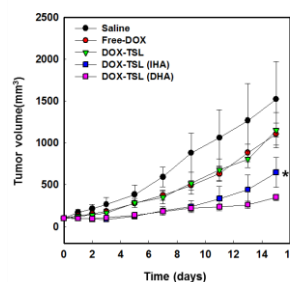


Figure 2. Antitumor efficacy of DOX-TSLs.

## CONCLUSION

In this study, we developed a new approach to improve the antitumor efficacy of DOX-TSLs using HIFU. This was followed by a burst release of a large quantity of DOX out of the TSLs accumulated within tumour tissues, triggered by post-heating of HIFU. As a consequence, our new modality of the HIFU treatment for the use of TSLs could result in higher antitumor efficacy than IHA. This new approach could be adjusted and used for various cases of cancer treatment using TSLs.

## REFERENCES

1. Allen TM et al, Adv. Drug. Del. Rev. 65;36-48, 2013.
2. Torchilin VP et al, Nat. Rev. Drug. Discov. 4;145-60, 2005.
3. Park SM et al. J Control release. 170;373-9, 2013.
4. Gasselhuber Astrid et al. PLoS One. 7;e47453, 2012.

## ACKNOWLEDGMENTS

This work was financially supported by the National R&D Program for Cancer Control (1420040) of MHW and the Basic Science Research Programs (20100027955 & 2012012827) of NRF.



## Photothermal Treatment to Remotely Control Drug Release from Plasmonic Lipogels

Francisco Martín-Saavedra<sup>1,2</sup>, Martín Prieto<sup>3,1</sup>, Manuel Arruebo<sup>3,1</sup>, Jesús Santamaría<sup>3,1</sup>, Gert Storm<sup>4</sup>, Wim Hennik<sup>4</sup>, Eduardo Ruiz-Hernández<sup>5,4</sup>, Nuria Vilaboa<sup>2,1</sup>

<sup>1</sup>Networking Center in Bioengineering, Biomaterials and Nanomedicine, CIBER-BBN, Spain

<sup>2</sup>La Paz University Hospital-IdiPAZ, Spain

<sup>3</sup>Aragon Institute of Nanoscience, Zaragoza University, Spain

<sup>4</sup>Department of Pharmaceutics, Utrecht Institute for Pharmaceutical Sciences, Utrecht University, The Netherlands

<sup>5</sup>School of Pharmacy, Royal College of Surgeons in Ireland, Ireland

[fco.martin.saavedra@gmail.com](mailto:fco.martin.saavedra@gmail.com)

### INTRODUCTION

Anticancer therapies based on liposomal drug delivery systems have the advantage of reducing toxicity to healthy tissues. Typically, release of encapsulated drugs from lipid-based carriers relies on either passive diffusion or the non-specific degradation of the lipid shell. Both mechanisms are slow and prevent cell cycle non-specific drugs such as doxorubicin (DOX) reaching effective local concentrations. In order to optimize time, location and amount of drug release, so much effort has been devoted to the development of liposomal systems capable of releasing drug in response to a specific stimulus. Examples of this are lysolipid-based thermosensitive liposomes (LTSL), which lipid membranes rapidly change structure and create pores at the gel-liquid crystal phase transition temperature ( $T_c$ ). LTSL formulation tuned for a  $T_c$  in the mild hyperthermia (HT) range of 40–42°C are very attractive carriers for chemotherapeutics as DOX, which antitumor effect is enhanced by mild HT. In this work, we incorporated DOX-loaded LTSL (DOX-LTSL) to *in situ* polymerizable fibrin hydrogels (lipogel) filled with plasmonic gold nanostructures that enable them to transduce photonic energy delivered by near-infrared (NIR) light into heat<sup>1</sup>. We tested the extent to which NIR-light of 808 nm, wavelength belonging to the “optical window” in biological tissue, can remotely control DOX release from plasmonic lipogels. Finally, we explored the therapeutic potential of this methodology in an *in vitro* model of human epithelial carcinoma.

### EXPERIMENTAL METHODS

Hollow gold nanoparticles (HGNPs) were synthesized via galvanic replacement of cobalt with gold as reported elsewhere<sup>1</sup>. DOX-LTSL with a  $T_c$  of 41.5°C were prepared as described elsewhere<sup>2</sup>. The plasmonic lipogels based in fibrin (fbn) were prepared after mixing 0.02 mg mL<sup>-1</sup> DOX-LTSL, 10 mg mL<sup>-1</sup> bovine fibrinogen, 0.01–0.05 mg mL<sup>-1</sup> HGNPs and 2 NIH units mL<sup>-1</sup> thrombin in a final volume of 1 mL of Dulbecco's Modified Eagle's Medium. Lipogels polymerized at 37°C in a CO<sub>2</sub> incubator for 1 h. The constructs were irradiated with a continuous wave NIR laser at 808 nm for 5–10 min at 33–44 mW mm<sup>-2</sup>, and then incubated at 37°C in a CO<sub>2</sub> incubator for 1–24 h. DOX release to the media was estimated by quantification of the emitted fluorescence at 590 nm, after excitation at 470 nm. Cell viability was evaluated by using the alamarBlue assay.

### RESULTS AND DISCUSSION

NIR-laser treatment of plasmonic lipogels led to a temperature increase in the construct, detected by IR thermography, which is dependent on the amount of HGNPs, the dose of photon energy delivered and the exposure time to NIR light. Temperature rises within constructs correlated with the increase in DOX concentration released to the culture medium, demonstrating the effective triggering of liposomal drug release. Close examination of irradiated plasmonic lipogels revealed the bleaching of 3-dimensional regions that faithfully matched the illuminated areas (Fig 1). This result indicates that the developed system can restrict drug release from NIR-targeted areas in the construct, also enabling temporal control of drug release. Finally, we found that NIR-controlled release of DOX from plasmonic lipogels effectively reduced the viability of HeLa cells cultures.

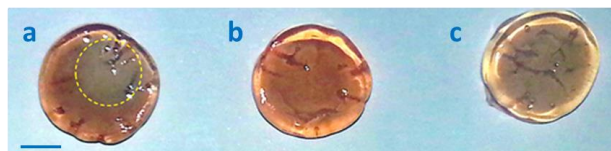


**Figure 1:** photographs of lipogels filled (a) or not (b) and (c) with HGNPs, 24 h after NIR irradiation at 44 mW mm<sup>-2</sup> for 7.5 min (a) or heat treatment at 42°C for 1 h in a thermostatically-controlled water bath (c). Scale bar= 5 mm. Dashed circle delimits area of NIR-laser influence.

### CONCLUSION

Photothermal treatment of thermosensitive plasmonic lipogels is a very attractive technology for remotely defining spatiotemporal patterns of chemotherapeutics bioavailability.

### REFERENCES

- 1-Preciado-Flores *et al.* *J Mater Chem*, **2011**, 2344–50
- 2-López-Noriega *et al.* *Adv Healthc Mater*, **2014**, 854–9

### ACKNOWLEDGMENTS

This work was supported by grant PI12/01698 from Fondo de Investigaciones Sanitarias (FIS, Spain) to NV and by grant MAT2011-24988 (MICINN) to MA. E.R.-H. is supported by the European Union FP7 under a Marie Curie Intra-European Fellowship for Career Development (Project NanoSmart).



## Determination Of Liposomal Doxorubicin Concentration In Blood By Fluorescence Spectroscopy

Maciej Łukawski<sup>1</sup>, Magdalena Przybyło<sup>1</sup>, Marek Langner<sup>1</sup>.

<sup>1</sup>Faculty of the Fundamental Problems of Technology, Wrocław University of Technology, Poland  
[maciej.lukawski@pwr.edu.pl](mailto:maciej.lukawski@pwr.edu.pl)

### INTRODUCTION

After administration, the chemotherapeutic agents are transported to the tissues by the blood in different fractions: plasma water, plasma proteins or cells. This has to be taken into consideration while determining pharmacokinetics of the drug.<sup>1</sup> The key to correctly estimate levels of given drug in blood is to account for all the fractions.

Several methods for quantification of liposomal doxorubicin in biological fluids were reported up to this day. Most of them utilize HPLC with fluorescence detectors, with complex extraction procedures, involving organic solvents, prone to errors in the final estimation of concentration.

In the present investigation we discuss main concerns during development of the method for determination of liposomal doxorubicin concentration in blood samples, using fluorescence spectroscopy.

### EXPERIMENTAL METHODS

During this study, visible light range fluorescence spectroscopy was used to carry out the experiments. Human blood samples with varying hematocrit were prepared by dilution of initial sample with serum. Samples were incubated with free and liposomal doxorubicin, and divided for hemolysis or centrifugation. Complete hemolysis was obtained, according to standard procedures, with 0.5% w/w Triton X-100 solution, and diluted in Phosphate Buffered Saline to minimise inner filter effects.

### RESULTS AND DISCUSSION

There are strong interactions between doxorubicin and blood constituents, which result in underestimation of total drug concentration. Scale of this underestimation varies from patient to patient, and is dictated by composition of blood. After centrifugation of blood with different hematocrit value, there is clear correlation between amount of blood cells and fluorescence intensity, as shown in figure 1.

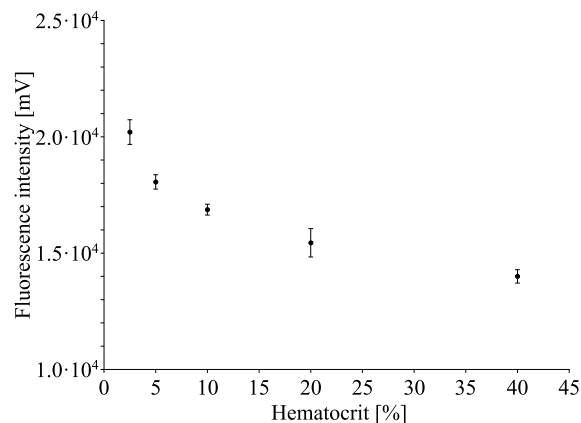


Figure 1. Fluorescence intensity of blood samples spiked with 20 µg/ml doxorubicin hydrochloride, varying in Ht. Doxorubicin fluorescence was measured in plasma, after centrifugation of blood cells.

In order to avoid consequences of interactions of drug with blood constituents, there is a possibility of hemolysis using agents such as Triton X-100. This procedure raises another major obstacle, namely release of strongly absorbing agents from blood cells, which obscure signals from the drug.

The possible solution to this problem is derivation of an equation, based on absorption spectra of hemolysed blood, to determine concentration of absorbing agents, and then correction of fluorescence intensity, to obtain final value of drug concentration.

### CONCLUSION

Measurement of the drug concentration in blood produces pharmacologically significant data about its distribution into blood cells.

Fluorescence measurements have the advantage of minimal required sample preparation, high sensitivity, and rapid collection of data. However in samples as complex as blood one has to account for multiple fluorescent and absorbing species. Carefully derived correction is crucial in development of such methods.

### REFERENCES

- Schrijvers D. Clin Pharmacokinet. 2003;42(9):779-91.

### ACKNOWLEDGMENTS

The study was supported by National Centre for Research and Development (Warsaw, Poland) grant DEMONSTRATOR+, no. WND-DEM-1-027/00.





## Capability of Polymer Ceramics Drug Delivery System

Stodolak-Zych Ewa<sup>1</sup>, Samolej Barbara<sup>1</sup>, Rapacz-Kmita Alicja<sup>2</sup>

Department of Biomaterials, Faculty of Materials Science and Ceramics, AGH – UST University of Science and Technology, Poland

Department of Department of Ceramics and Refractories, Faculty of Materials Science and Ceramics, AGH – UST University of Science and Technology, Poland  
[stodolak@agh.edu.pl](mailto:stodolak@agh.edu.pl)

### INTRODUCTION

It is well known from the literature that natural clay mineral particles like as a smectite can be used in drug delivery systems. The structure of montmorillonite (MMT) is composed of silica tetrahedral sheets layered between alumina octahedral sheets. In the interlayer positions, positively charged ions are located, which can be relatively easily exchanged by other molecules/ions during the specific intercalation process. Because of the cation exchange capacity, large specific surface area and high adsorption ability - MMT is common ingredient of organic-inorganic hybrids materials. Typical drug particles (ibuprofen, vit. B, genatmicin) or biopolymers (polysaccharides i.e. alginate, chitosan) can be used as an organic compounds for modification of the MMT structure [1]. In such systems, addition of chitosan with gel-forming properties may preface intercalation process and facilitate the drug introduction. The aim of this study was to verify the effectiveness of methods for the preparation of nanocomposite Biofuroksym drug carriers based on chitosan (CS) and montmorillonite (MMT), and the evaluation of their properties.

### EXPERIMENTAL METHODS

Intercalation of Biofuroksym (Bf, Polphrama) into montmorillonite (MMT-K10, Sigma Aldrich) was made in three different ways using: (1) pure Bf, (2) Bf dissolved in diethylamine (DEA, Sigma-Aldrich) and (3) Bf dissolved in chitosan (CS, Sigma-Aldrich). Intercalation was carried out in the two-step process, in which initial hydration of MMT (24h/60°C) was followed by the proper intercalation (7days/60°C). The modified MMT powders were lyophilized, and then examined using scanning electron microscopy (SEM/EDS), X-ray diffraction (XRD) and Zeta potential method. All types of the MMT powders were used as fillers to produce the nanocomposite samples with a medium molecular weight chitosan matrix filled with 4% wt. of the clays. Finally, the water absorption tests were performed in the culture cells medium to determine stability *in vitro* of these materials.

### RESULTS AND DISCUSSION

Microstructural observation showed differences between pure clay and clays after intercalation process. Modified MMT particles have a smaller size and irregular shape. Additionally, same spherical macromolecules were present in the interlayer space of MMT. The EDS analysis confirmed the presence of Biofuroksym (sulphur energy peak). The change in the interlayer space of the modified MMT clays was also confirmed by the XRD measurement and typical diffraction peak at  $2\Theta=8.91$  which refers to the (001)

spacing was shifted to  $2\Theta=8.85$  after intercalation. All types of the clays modified with Biofuroksym showed characteristic reflection at about  $2\Theta=6.79$  (Fig. 1.).

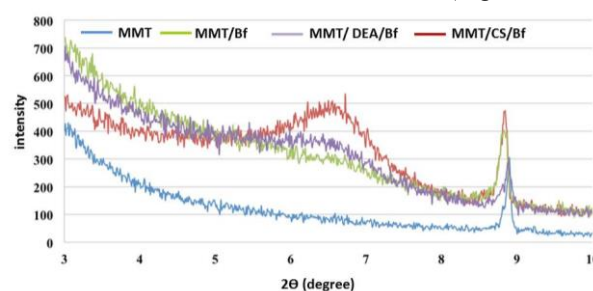


Fig. 1. XRD patterns of MMT, MMT/Bf, MMT/DEA/Bf, MMT/CS/Bf.

Intercalation process influenced also the zeta potential of MMT particles: it increased for the clay modified with chitosan (polycation) and Biofuroksym, but it decreased when pure Biofuroksym or diethylenoamine with Biofuroksym were used as modifying compounds (Tab. 1). Results of zeta potential implies also a greater dispersion in water solution (chitosan solvent), since the decrease in the negative charges of MMT increases the spacing between the layers of clay.

Table 1. Zeta potential for the MMT-based systems

Type of MMT powder	Zeta potential [eV]
MMT	-31.2±1.56
MMT/DEA/Bf	-38.6±2.18
MMT/Bf	-42.0±1.89
MMT/CS/Bf	+37.4±2.54

### CONCLUSIONS

The obtained results, even if preliminary, may however indicate, that the skilful intercalation of drug into nanofiller and homogeneous distribution of the filler in the hydrogel matrix can provide a new solution in the field of drug delivery systems.

### REFERENCES

- [1] Luo Y., *et al.*, International Journal of Biological Macromolecules, 64, 2014
- [2] Hua S. *et al.*, Drug Development and Industrial Pharmacy, 36(9): 2010

### ACKNOWLEDGMENTS

This study was performed within the framework of funding for statutory activities of AGH University of Science and Technology in Krakow, Faculty of Materials Science and Ceramics (11.11.160.617).



## Hydrolysis of Crosslinked Poly(ester anhydride) Networks in Different pH Conditions

Sanja Asikainen, Harri Korhonen and Jukka Seppälä

Research Group of Polymer Technology, School of Chemical Technology, Aalto University, Finland  
[sanja.asikainen@aalto.fi](mailto:sanja.asikainen@aalto.fi)

### INTRODUCTION

Poly(ester anhydrides) are promising materials especially for controlled drug release applications. They are surface eroding and they erode fast due to their hydrolytically labile anhydride bond. Crosslinkable poly(ester anhydrides) have been studied *in vitro* and *in vivo*, and no cytotoxicity and no or only mild inflammatory reactions in mice and rats were observed.<sup>1</sup> Since the degradation of polyanhydrides is known to be pH sensitive and they are more stable in acidic conditions<sup>2</sup>, possible application area for fast degrading poly(ester anhydrides) might be in oral drug delivery. The slow degradation of polymer matrix in acidic conditions would protect drug until it reaches the intestine.

The aim of this study was to investigate the effect of pH conditions on the hydrolysis of crosslinked poly(ester anhydride) networks. Different pH conditions simulate the pH conditions in the gastrointestinal tract.

### EXPERIMENTAL METHODS

#### Synthesis of precursors

The precursors were synthesized by a similar method to that used earlier<sup>3</sup>. In brief, the  $\epsilon$ -caprolactone based hydroxyl-terminated oligomers were synthesized in a batch reactor by using 10 mol-% pentaerythritol as a co-initiator and 0.02 mol-% Sn(II)octoate as an initiator. After polymerization, oligomers were functionalized with succinic anhydride to obtain acid-terminated oligomers. Crosslinkable precursors with labile anhydride bonds were obtained by allowing the acid-terminated oligomers to react with methacrylic anhydride. Reactions were monitored with nuclear magnetic resonance spectrometer (NMR).

#### Preparation of samples

Photoinitiator camphorquinone (1 wt-%) was mixed with the precursor until homogeneity was achieved. Teflon mould was used to obtain discs (2 mm thickness, 2 mm in diameter, 9 mg in weight). Crosslinking was carried out at room temperature by photoinitiation in visible light and post curing with blue light.

#### Molecular weight determination

The molecular weights of oligomer species were determined by room temperature size-exclusion chromatography (SEC). Chloroform was used as a solvent and eluent for polymers.

#### Gel content of crosslinked samples

Gel content was determined by immersing samples in dichloromethane for six hours. Samples were dried in vacuum overnight and weighted before ( $m_{t,0}$ ) and after ( $m_t$ ) immersion. Gel content (G) was calculated using the following equation:  $G = m_t/m_{t,0} \cdot 100\%$ .

### Hydrolysis experiment

Samples were weighted and immersed individually in 15 ml of phosphate buffer solution (pH 2.1, 6.8 and 7.4) at the temperature of 37 °C. The samples were mildly agitated at a rate of 90 strokes/min. The test specimens were removed from test tubes at different intervals and weighted after drying 24 h in vacuum at room temperature.

### RESULTS AND DISCUSSION

The molecular weights of different oligomer species as well as NMR confirmed the success of polymerization of the precursor. The gel content of the crosslinked samples was 92 %.

The mass loss of polymer samples is presented in Figure 1. Within 24 h, samples were totally eroded in pH 6.8 and 7.4, whereas in pH 2.1 the mass loss was only 6 % of initial weight. Degradation was the fastest in pH 7.4 and already small change in pH towards acidic conditions slowed the degradation down.

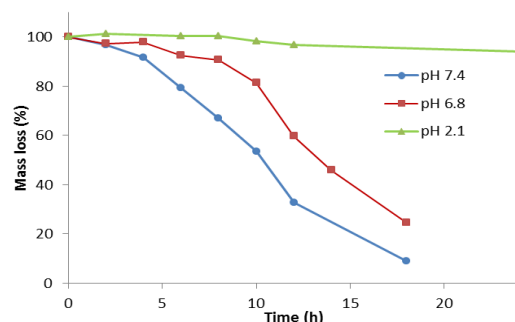


Figure 1. Mass loss of samples in different pH conditions.

### CONCLUSION

The degradation rate of poly(ester anhydride) samples is highly pH sensitive. Degradation rate is very slow at strongly acidic conditions and already a small drop in pH slows down the degradation.

### REFERENCES

1. Mönkäre J. *et al.*, J. Control. Release 146:349-355, 2010
2. Leong K. W. *et al.*, J. Biomed. Mater. Res., 19:941:955, (1985)
3. Hakala, R.A. *et al.*, Eur. Polym. J. 45:557-564 (2009)

### ACKNOWLEDGMENTS

The authors would like to thank the Academy of Finland (Grant no: 141164) and Jenny and Antti Wihuri Foundation for providing financial support to this project.



## Ceramic Scaffolds Containing Gentamicin Sulphate Loaded Poly(lactic-co-glycolic acid) Microparticles for Bone Tissue Engineering

Łucja Rumian<sup>1</sup>, Hanna Tiainen<sup>2</sup>, Urszula Posadowska<sup>1</sup>, Monika Brzychczy-Włoch<sup>3</sup>, Håvard J. Haugen<sup>2</sup>, Elżbieta Pamuła<sup>1</sup>

<sup>1</sup> AGH University of Science and Technology, Faculty of Materials Science and Ceramics, Department of Biomaterials, Poland

<sup>2</sup> University of Oslo, Institute for Clinical Dentistry, Department of Biomaterials, Norway

<sup>3</sup> Jagiellonian University, Medical College, Department of Microbiology, Poland

[lruman@agh.edu.pl](mailto:lruman@agh.edu.pl)

### INTRODUCTION

Microbial infections are responsible for a significant part of failure rate of bone filling grafts and endosseous dental implants<sup>1</sup>. In the case of reconstructing large-size bone defects a three-dimensional scaffold is needed to support the healing. Therefore a design of scaffolds assuring both mechanical support, bone tissue ingrowth and a controlled antibiotics release seems very viable for an effective, long-term clinical outcome. Titanium dioxide (TiO<sub>2</sub>) has been reported as a plausible candidate as it is biocompatible and it has the ability to directly bond to bone tissue<sup>2</sup>.

The aim of this study was to: i) modify the surface of TiO<sub>2</sub> scaffolds with poly(L-lactide-co-glycolide) (PLGA) microparticles (MPs) loaded with gentamicin sulphate (Gent); ii) evaluate *in vitro* release profile of the drug and iii) assess the bactericidal activity of the proposed system.

### EXPERIMENTAL METHODS

TiO<sub>2</sub> scaffolds were manufactured by polymer sponge replication method and sintering<sup>2,3</sup>. PLGA MPs loaded with Gent were prepared by solid/oil/water method. Gent powder was emulsified in 1.67% (w/v) PLGA (PLGA, 85:15, Mn=80 kDa) solution in dichloromethane (10 mg of Gent per 100 mg of PLGA). The primary emulsion was then introduced into an aqueous solution of 4% polyvinyl alcohol and shear stress was applied (mechanical stirring 1000 rpm). Manufactured MPs were submitted to centrifugation, multistep washing procedure and freeze-drying. Defined amounts of MPs suspended in 0.2 or 0.02% solutions of sodium alginate (Alg) were introduced on the TiO<sub>2</sub> scaffolds by drop seeding and cross-linked with 50 mM CaCl<sub>2</sub>. Six batches of scaffolds were prepared with the use of 0.2 or 0.02% Alg and containing in total 0.5, 0.75 and 1 mg of Gent. *In vitro* release study was performed in PBS by diffusion through semipermeable membrane (Zellu TransRoth, MWCO 12 kDa) and spectrophotometric quantitative analysis of Gent by orthophthaldialdehyde method<sup>4</sup>. The samples were analysed for 3 months. Kirby-Bauer method (Agar diffusion test) was applied in order to determine antimicrobial activity against *S. aureus* and *S. epidermidis*.

### RESULTS AND DISCUSSION

TiO<sub>2</sub> scaffolds were highly porous (with total porosity of 90%) with oval interconnected pores of 400 µm in size, and their microstructure was very similar to that of natural cancellous bone. The average diameter of MPs was 4.2±2.9 µm with encapsulation efficiency of 42% and loading efficiency 5.0%. SEM pictures (Figure 1) show high effectiveness of suspending MPs in sodium alginate and drop seeding procedure. Higher concentration of Alg resulted in more homogenous

distribution of MPs within the scaffolds. Results of *in vitro* release study (Figure 2) show initial burst followed by slow, sustained release of Gent for all systems. The results showed that drug release profile can be easily adjusted by amount of MPs introduced in the system. Alg concentration did not influence drug release kinetics. Microbiological tests confirmed antibacterial activity of Gent released from the TiO<sub>2</sub> scaffolds.

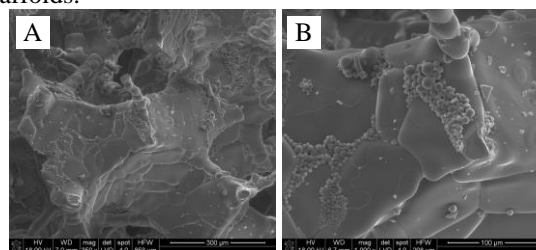


Figure 1 SEM microphotographs of TiO<sub>2</sub> scaffold containing Gent loaded PLGA MPs immobilized with 0.02% Alg (mag. 350x and 1000x)

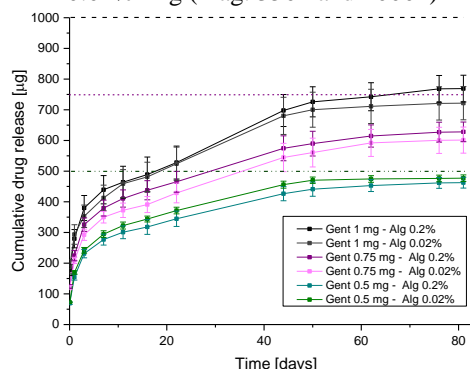


Figure 2 *In vitro* cumulative Gent release from different types of TiO<sub>2</sub> scaffolds

### CONCLUSION

The study showed that immobilization MPs loaded with Gent on TiO<sub>2</sub> scaffolds was successful; prolonged drug release was achieved and whole system exhibited antibacterial activity.

### REFERENCES

1. Paquette D. *et al.*, Dent Clin N Am, 50:361-374, 2006
2. Tiainen H. *et al.*, Acta Biomater, 8:2384-2391, 2012
3. Rumian L. *et al.*, Acta Bioeng Biomech, DOI: 10.5277/ABB-00129-2014-02
4. Posadowska U. *et al.*, Int J Pharma, 485:31-40, 2015

### ACKNOWLEDGMENTS

Polish National Science Centre (Grant no: 2013/09/N/ST8/00309) and Norwegian Research Council grant no. 228415 provided financial support to this project.

## Influence of Degradation of D,L-PLGA on the Release of Risperidone

Artur Turek<sup>1,2</sup>, Aleksandra Borecka<sup>1</sup>, Katarzyna Jelonek<sup>1</sup>, Janusz Kasperczyk<sup>1,2</sup>, Henry Janeczek<sup>1</sup>, Agata Skibińska-Zuber<sup>2</sup>, Piotr Dobrzyński<sup>1</sup>, Marcin Libera<sup>1</sup>

<sup>1</sup>Centre of Polymer and Carbon Materials, Polish Academy of Sciences, M. Curie-Skłodowskiej 34, 41-819 Zabrze, Poland

<sup>2</sup>School of Pharmacy with the Division of Laboratory Medicine in Sosnowiec, Medical University of Silesia, Katowice, Poland, Department of Biopharmacy, Jedności 8, Sosnowiec, Poland  
[borecka.alexandra@gmail.com](mailto:borecka.alexandra@gmail.com)

### INTRODUCTION

Implantable formulations with risperidone (RSP) are considered in the therapy of schizophrenia. One medical product is already available in the formulation of a long-acting injection includes microspheres composed of poly(D,L-lactide-co-glycolide) (D,L-PLGA) that must be applied every two weeks. In this medical product the main release of risperidone begins in the 3<sup>rd</sup> week, lasts from the 4<sup>th</sup> to 6<sup>th</sup> week and is accomplished within 7 weeks. This works aimed to develop delivery system which can be administered less frequently and risperidone will be released for a longer time. In this study the influence of degradation of D,L-PLGA 85:15 on RSP release and structural changes in matrices was determined.

### EXPERIMENTAL METHODS

The matrices containing RSP (10 wt-%) were obtained from D,L-PLGA 85:15 (100000 Da) by solution casting method. The D,L-PLGA was synthesized with the use of Zr(Acac)<sub>4</sub> as low toxic initiator of polymerization. Matrices with the diameter of 10 mm, thickness of 0.6273 mm ± 0.0196 (n=10) were incubated in PBS (pH 7.4) at 37°C under constant agitation. The release rate of RSP by HPLC, the composition of polymer and chain structure by NMR, thermal properties by DSC, morphology of matrices by AFM were determined.

### RESULTS AND DISCUSSION

The observations were conducted for 78 days. In this period 6163 µg ± 553 (n=10) of RSP was released, which was 91.7 % ± 0.17 of substance incorporated into matrix (Figure 1). The significant changes in release rate were observed, which resulted from degradation process. During the first 5 days 100 µg of RSP was released and the process proceeded evenly without burst effect. In the next 15 days, a gradual decrease of RSP release was noted and it turned into a phase of complete inhibition of the release in the 21<sup>th</sup> day. Resumption of release process was noted in the 41<sup>th</sup> day. This effect correlated with significant changes in copolymer. The increase of randomness was observed and decrease of the T<sub>g</sub> to 37 °C. This probably caused increase of copolymer chain mobility and improved water absorption into matrix and diffusion of drug molecules from matrix to the medium. As a result of those changes, regular and steady RSP release was observed from the day 43<sup>th</sup> to 78<sup>th</sup>.

During 78 days the NMR analysis revealed increase of content of lactidyl units from 85.0 % to 87.70% with adequate decrease of content of glycolidyl units from 15.0 to 12.3 (Table 1). An increase of average length of

lactidyl blocks from 8.99 to 9.50 was observed, whereas average length of glycolidyl blocks decreased from 1.69 to 1.30. The suppression of drug release was probably caused by increase of average length of lactidyl blocks, which may lead to crystallization and retain drug in matrix. The randomization ratio (R) increased from 0.41 to 0.60. The used copolymer had initially semi-blocky structure and became more random. The glass transition temperature (T<sub>g</sub>) of the native matrices was 54.0°C. A gradual decrease of T<sub>g</sub> to the 34.5 °C was noted. The morphologic observation revealed the changes in the surface of degraded matrices (Table 1). The native material characterized non-porous surface. However, degradation caused increase of heterogeneity of surface.

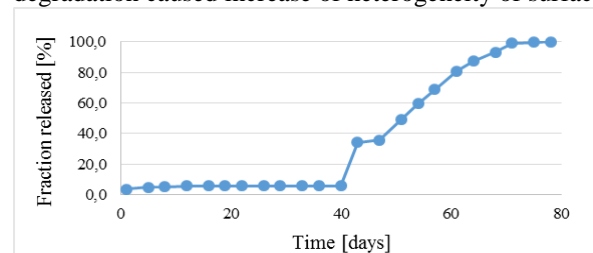


Figure 1. Fraction RSP released during the 78 days of degradation process.

Time [days]	$F_{LL}$ [%]	$F_{GG}$ [%]	$l_{LL}$	$l_{GG}$	R	$T_g$ [°C]
0	85.0	15.0	8.99	1.69	0.41	54.0
1	85.0	15.0	9.26	1.64	0.43	54.0
8	85.1	14.9	9.30	1.59	0.43	52.1
36	85.4	14.6	9.36	1.56	0.48	38.9
64	86.2	13.8	9.49	1.34	0.57	37.1
78	87.7	12.3	9.50	1.30	0.60	34.5

Table 1. The changes in structural and thermal properties during degradation.  $F_{LL}$  – mole fraction of lactidyl units;  $F_{GG}$  – mole fraction of glycolidyl units;  $l_{LL}$  - average length of lactidyl blocks;  $l_{GG}$  - average length of glycolidyl blocks; R – randomization ratio; T<sub>g</sub>- glass transition temperature.

### CONCLUSION

The degradation process significantly influences the release of RSP from D,L-PLGA matrices. Analysis of structural, thermal and morphological properties of matrices allow to develop a novel drug delivery system with for prolonged and tailored release of RSP.

### ACKNOWLEDGMENTS

This work was financially supported by the National Centre for Research and Development, RYSPCONT grant no PBS1/A7/2/20





## INTRODUCTION

Gene therapy holds great promise for treating many genetic disorders as well as cancer. Gene delivery, which introduces foreign DNA into host cells, is one of the steps necessary for gene therapy. Suitable vectors with good transfection efficiency and low cytotoxicity are essential for effective gene delivery. Since viral vectors cause safety concerns, non-viral vectors including cationic polymers are extensively investigated owing to their ease of preparation, manipulable structures, large DNA loading capability and absence of immune response<sup>1</sup>. Satisfactory transfection efficiency and good biocompatibility are two main challenges for developing successful, polymer-based vectors. Various strategies have been employed in the development of polymeric vectors for improving their ability of gene delivery at the cellular level. Among these polymers, poly(lactic-co-glycolic acid) (PLGA) is used to make biodegradable nanoparticles while poly(ethylenimine) (PEI) is applied to facilitate gene transfection but limited by its molecular weight-dependent cytotoxicity<sup>2</sup>. Poly(ethylene glycol) (PEG) modification of delivery vehicles is a proven strategy for providing shielding and ensuring long-circulation and can also serve as active sites for targeting ligand via covalent bonding. Folate is known for targeting most tumours and promotes transfection efficiency. Therefore, biodegradable copolymers with buffering capacity, hydrophilic modification and targeting ligand are promising for gene delivery with high efficiency. In this study, FOL-PEG-g-PEI-g-PLGA copolymers were synthesized and characterized as potential gene delivery vectors.

## EXPERIMENTAL METHODS

PLGA ( $M_w$ : 36kDa) with acid end group, PEI ( $M_w$ : 1.8kDa and 25kDa), PEG (COOH-PEG-NH<sub>2</sub>,  $M_w$ : 3kDa) and folic acid were used at particular molar ratios to synthesize designed copolymers through EDC/NHS amidation reaction. The chemical composition of copolymers was studied using FTIR and <sup>1</sup>H-NMR. Plasmid EGFP encoding enhanced green fluorescence protein was employed as a model gene for initial evaluation of copolymers. The morphology and structure of nanocomplexes were examined using SEM and TEM. Surface charge of freshly produced nanocomplexes was characterized using a Zetasizer. DNA condensation effect of copolymers was studied using agarose gel electrophoresis. HepG2 cells were used to evaluate the cytotoxicity of copolymers and assess their transfection efficiency.

## RESULTS AND DISCUSSION

The chemical composition of copolymers was confirmed by FTIR and <sup>1</sup>H-NMR, indicating successful synthesis of designed copolymers. SEM examination revealed that polyplexes were spherical in shape and

uniform in size (less than 200nm in diameter and with low polydispersity) (Fig. 1a). TEM results showed that a core-shell structure existed in polyplexes (Fig. 1b). Polyplexes exhibited slightly positive charge above certain N/P ratio (Fig. 2a). They were stable in aqueous solution with inappreciable aggregation for a week and could be freeze-dried and stored for further use with simple reconstitution. The surface charge of polyplexes exhibited a reversal to slightly positive with the increase in NP/pDNA ratio, indicating negatively charged DNA had been successfully encapsulated, which was also supported by the gel electrophoresis result (Fig. 2b). In the biological investigation, the amphiphilic FOL-PEG-g-PEI-g-PLGA copolymers exhibited low cytotoxicity and sufficient transfection efficiency.

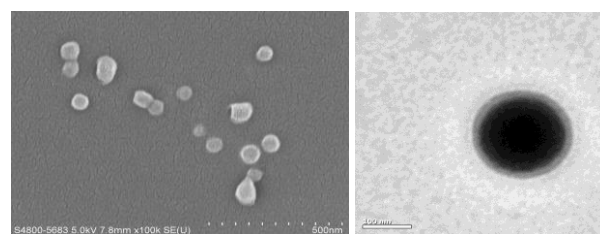


Fig. 1. a: SEM image (left) of polyplexes, b: TEM image (right) of polyplexes

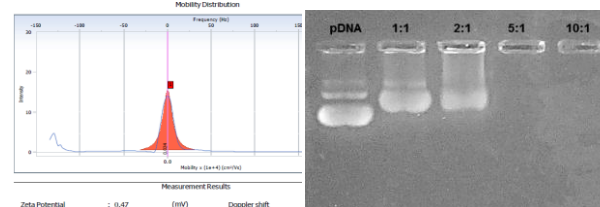


Fig. 2. a: zeta potential of polyplexes at 5:1 N/P ratio (left), b: agarose gel electrophoresis of polyplexes with different copolymers (right)

## CONCLUSION

Biodegradable FOL-PEG-g-PEI-g-PLGA copolymers with designed compositions and their polyplexes with uniform morphology, suitable particle size and designed structures were synthesized. Above certain N/P ratio, DNA was successfully encapsulated and condensed. Cytotoxicity of copolymers and transfection efficiency of polyplexes were evaluated, indicating the copolymers were promising for non-viral vectors for gene delivery.

## REFERENCES

1. He CX, *et al.*, International Journal of Pharmaceutics, 386 (1-2): 232-42, 2010
2. Wang MX, *et al.*, Journal of Materials Chemistry, 22 (13): 6038-46, 2012

## ACKNOWLEDGMENTS

This work was supported by the Hong Kong Research Grants Council via a GRF grant (7177/13E). CY.Liu thanks HKU for providing him with a PhD scholarship.



## Assessment of Drug Incorporation and Release from a Novel Coronary Stent Coating

Craig Martin McKittrick<sup>1</sup>, Simon Dixon<sup>2</sup> and Christopher McCormick<sup>1</sup>

<sup>1</sup>Biomedical Engineering, University of Strathclyde, United Kingdom

<sup>2</sup>Biomer Technology Ltd, United Kingdom

[craig.m.mckittrick@strath.ac.uk](mailto:craig.m.mckittrick@strath.ac.uk)

### INTRODUCTION

Understanding drug elution kinetics from the surface of drug eluting stents (DES) is an important tool in the development of novel designs. It is useful for testing the reliability and reproducibility of coatings, for providing insight into mechanisms of drug release and for estimation of parameters for models describing drug uptake into tissues<sup>1</sup>. Here we describe the drug elution kinetics for varying polymer to drug ratio coatings of a novel acrylic-based polymer designed to promote re-endothelialisation<sup>2</sup>.

### EXPERIMENTAL METHODS

A polymer coating, BTL *accelerate*<sup>TM</sup> AT, proprietary to Biomer Technology Ltd, was applied to the surface of glass coverslips via a standard dip-coating method. Varying AT/rapamycin(R) coating concentration and ATR ratios were assessed for release of rapamycin over a period of 28 days (n=6). Coatings are described in **Table 1**. The coverslips were immersed in 1.5 ml of release medium, phosphate buffered saline:ethanol (90:10), and were transferred to fresh release medium at regular sampling points to maintain sink conditions. The end-point of the experiment was 28 days. To determine initial drug load separate coverslips (n=2) were immersed in 1.5 ml of methanol to rapidly dissolve the rapamycin from the polymer coating. The coverslips were transferred to fresh methanol every 24 hours for 7 days. The amount of rapamycin in release medium was determined by ultraviolet spectroscopy. Comparisons were drawn between all formulations tested using 2-way ANOVA with Bonferroni post-test. Significance was considered  $P < 0.05$ .

Sample	Bottom Coat	Top Coat	Drug Load ( $\mu$ g)
1	2% AT/R (50:50)	None	32
2	2% AT/R (50:50)	2% AT	19
3	2% AT/R (50:50)	2% AT/R (50:50)	39
4	8% AT/R (80:20)	None	66
5	8% AT/R (80:20)	8% AT	62
6	8% AT/R (80:20)	8% AT/R (80:20)	149

**Table 1:** Formulations of polymer/rapamycin used to coat glass coverslips used for drug release profile determination. AT=polymer, R=rapamycin.

### RESULTS AND DISCUSSION

There cumulative amount of drug released over the 28 day period between for all formulations is shown in **Figure 1** (1vs2  $p < 0.01$ , all others  $p < 0.001$  at 28 days). The release profiles generated here are similar to those of used clinically stents, such as the ENDEAVOR stent which releases the majority of its dose within 2 weeks<sup>3</sup>. **Figure 2** shows that coatings with a higher AT/R ratio eluted drug at a significantly slower rate than the lower ratio formulations and this was most apparent in the

initial 24 hours of the release period. This finding is in line with currently used stents such as the TAXUS stent, which was coated with high and low polymer/drug ratios to yield slow and medium release drug eluting stents, respectively<sup>4</sup>. The cumulative release of initial load data is shown in **figure 3**. The higher AT/R ratio formulations eluted a significantly lower percentage during the initial 24 hours. Again these profiles are comparable to clinically available stents such as the CYPHER DES which releases around 80% of drug load after 30 days<sup>3</sup>. Formulations with a higher AT/R ratio with a drug free top coat had eluted a significantly lower amount of initial drug load by the end of the 28 day release period.

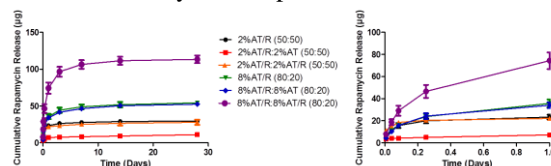


**Figure 1:** Cumulative release of rapamycin. *Right panel 24 hour period.*

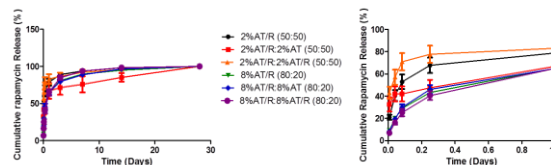


**Figure 2:** Cumulative percentage release of rapamycin. *Right panel 24 hour period.*

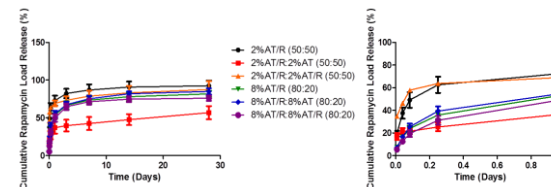


**Figure 3:** Cumulative percentage release of rapamycin initial load. *Right panel: focus on 24 hour period.*

### CONCLUSIONS

This study has demonstrated that rapamycin can be incorporated and released in clinically relevant concentrations, from a polymer designed to promote re-endothelialisation. Future in vivo studies will investigate the potential of this polymer/drug coating as an advanced stent coating.

### REFERENCES

- McGinty, S., Math. Biosci. 257:80-90, 2014
- Nickson, C.M., *et al.*, J. Biomater. Appl. 24(5):437-452, 2010.
- Martin, D.M. and Boyle, F.J. Med. Eng. Phys. 33(2), 148-163, 2011.
- Colombo, A., *et al.*, Circulation. 108(7):788-94, 2003.

### ACKNOWLEDGEMENTS

We would like to acknowledge the support of EPSRC (EP/J007242) for funding this study and Biomer Technology Ltd for providing the polymer materials.



## BMP-2 Release from Collagenous Particles

Didem Mumcuoglu<sup>1</sup>, Laura de Miguel<sup>1</sup>, Gerjo van Osch<sup>1</sup>

<sup>1</sup>Department of Orthopaedics, Erasmus University Medical Center, The Netherlands  
[z.mumcuoglu@erasmusmc.nl](mailto:z.mumcuoglu@erasmusmc.nl)

### INTRODUCTION

Development of appropriate delivery systems to regulate the release of growth factors is one of the key challenges in tissue engineering and regeneration studies<sup>1</sup>. Growth factors, especially BMPs, have a wide potential clinical application since they can mediate the bone regeneration process. In particular, BMP-2 has been used in the clinical practice delivered to the defect site adsorbed onto collagen sponges; however the high amounts of protein used have been associated to adverse effects observed<sup>2</sup>. Therefore, it is important to reduce the total dose of the protein and provide sustained delivery during the regeneration process of the bone. In this study, we produced collagenous microparticles and characterized the particles. BMP-2 was loaded to the particles the release of the protein from these particles was studied. The parameters that affect the release of the protein were studied.

### EXPERIMENTAL METHODS

Collagenous microparticles were produced by emulsification. For the release experiments particles were loaded with BMP-2 by incubating overnight with different concentrations of growth factor. Subsequently the release of BMP-2 was measured in time by rhBMP-2 ELISA development kit (Peprotech)

### RESULTS AND DISCUSSION

When BMP-2 was loaded to the microspheres and the release was measured by ELISA, a slow release of the protein has been observed in in vitro release study for

several weeks. Finally, the microspheres were degraded by collagenase thereby releasing the remaining protein fraction present in the microsphere. The release results indicate that these collagenous particles can be loaded with BMP-2 and they are suitable for the sustained delivery of these growth factors

### CONCLUSION

Collagenous particles loaded with BMP-2 demonstrated sustained release of the protein. Several factors were identified to be governing the release profile of BMP-2 from these collagenous microparticles.

### REFERENCES

1. Biondi, M., *et al.*, Adv Drug Deliv Rev 60(2): 229-242, 2008
2. Shields, L. B., *et al.*, Spine 31(5): 542-547, 2006

### ACKNOWLEDGMENTS

Authors acknowledge funding from the European Commission within the 7th Framework Programme.



## Functionalized Hydrophilic Nanogels for Endogenous Radiotherapy

Smriti Singh<sup>1</sup>, Natascha Drude<sup>1,2</sup>, Felix M. Mottaghy<sup>2</sup>, Agnieszka Morgenroth<sup>2</sup>, Martin Möller<sup>1</sup>

<sup>1</sup> DWI - Leibniz-Institute for Interactive Materials, Forckenbeckstrasse 50, D-52056 Aachen, Germany

<sup>2</sup>Department of Nuclear Medicine, RWTH Aachen University, Pauwelsstrasse 30, 52074 Aachen, Germany  
[singh@dwil.rwth-aachen.de](mailto:singh@dwil.rwth-aachen.de)

### INTRODUCTION

Most advancement in radiotherapy has been made in external beam treatments but it is still limited by the effects it induces in the surrounding healthy tissues and its limitations in patients with disseminated disease. Though endogenous radiotherapy allows a direct delivery of radiation to the tumor by means of radiolabelled antibodies, peptides, or isotopes of halogens that are organified (like radioiodine therapy of thyroid cancer), only few of these approaches are implemented in standard patient treatment since the biodistribution of these small molecules is not ideal and leads to relevant toxic doses in healthy tissue (critical organs are liver, kidneys and intestine). In order to overcome these limitations by increasing selective delivery of radiation to cancer manifestations, our approach focuses on the development of hydrophilic nanogel-carriers coupled with chelators for theranostic radioisotopes.

### EXPERIMENTAL METHODS

Nanogels were synthesized using star shaped PEG polymers with thiol functionalization; thiol chemistry was used for linking the maleimide functionalised chelator 1,4,7-triazacyclononane-1-glutaric acid-4,7-diacetic acid (NODAGA) to the polymer for radioisotope labelling, as well as for crosslinking the polymer in inverse miniemulsion to build up sub-micrometer sized nanogels.

### RESULTS AND DISCUSSION

A highly efficient and specific labelling with radioactive marker Gallium-68 was achieved in the nanogels with a radiochemical yield greater than 95% at room temperature. For in vitro studies the nanogels were additionally labelled with Alexa-Fluor 488. The studies demonstrated that the Alexa Fluor labelled nanogels were unrecognizable for monocytes. In vivo studies were performed by injection of <sup>68</sup>Ga-radiolabelled nanogels in the tail vein of male rats (n=10) and rodent  $\mu$ -PET imaging studies were done which indicated a long blood circulation of nanogels without visible accumulation in liver or spleen,

demonstrating that there was no uptake of the nanogels by the Mononuclear Phagocyte System (MPS).

### CONCLUSION

Such water swollen nano-carriers offer advantages, as their open structure barely interact with proteins and cells featuring long blood pool circulation, variability of the carrier and targeting function and responsive properties to environmental factors like enzymes, pH, ionic strength. Thus tumor targeting by the nanogels is supported by their stealth properties in combination with the enhanced permeability and retention effect (EPR effect) and is complemented by the incorporation of ligands of receptors overexpressed by tumor cells. Hence, first step in targeting results in the accumulation of the nanogels in tumor tissue by utilizing the EPR effect followed by the second step, which is targeting of tumor cells by addressing their specific surface property.

### REFERENCES

- [1] Juergen Groll, Smriti Singh, Krystyna Albrecht, Martin Moeller: J. Polym. Sci. Part A: Polym. Chem, 2009, 47, 5543.
- [2] Smriti Singh, Fuat Topuz, Kathrin Hahn, Krystyna Albrecht, Juergen Groll: Angewandte Chemie 2013, 52, 3000.
- [3] Smriti Singh, Bahar Bingoel, Agnieszka Morgenroth, Felix M. Mottaghy, Martin Moeller, Joern Schmaljohan: Macromolecular Rapid Communication 2013, 34, 562.

### ACKNOWLEDGMENTS

The authors acknowledge I<sup>3</sup>TM, RWTH Aachen for the financial support.





## Advanced Poly-( $\epsilon$ )-Lysine Dendrons as Functional Non Viral Macromolecules to Target Pancreatic $\beta$ Cells

Mariagemiliana Dessi<sup>1</sup>, Valeria Perugini, Gary Phillips and Matteo Santin

Brighton Centre for Regenerative Medicine, School of Pharmacy and Biomolecular Sciences, University of Brighton,  
UK

[M.Dessi2@brighton.ac.uk](mailto:M.Dessi2@brighton.ac.uk)

### INTRODUCTION

Type 1 diabetes mellitus is an autoimmune disorder characterized by the destruction of the insulin-producing  $\beta$  cells of pancreatic islets and high blood glucose levels. The disease results from a multitude of interactions between environmental exposures and different variant genes related to pancreatic  $\beta$  cell functions [1]. As a result, the transfection of  $\beta$  cells is providing great potential in gene therapy and diabetes therapies arena. To date, while the efficacy of viral gene vectors is indisputable, their unfavorable limitations in target-cell specificity, immunogenicity, toxicity and high costs of manufacturing, forced researchers to devise non-viral vectors [2]. In the current scenario, dendrons are emerging as challenging nano-vectors because of their unique properties such as: highly favorable branched structure, high loading ability, appropriate nanosize and targeting potentials. In order to evaluate the potency of dendrons as useful and safe non-viral vectors as therapeutics for gene delivery from bench to bedside, a full molecular design and characterization is needed. In this work, for the first time, hyperbranched dendrons have been specifically designed and characterized as *in vitro* model to predict the targeting of pancreatic cells. Cell studies were performed on MIN6 cell line that exhibit glucose-inducible insulin secretion similar to that of cultured normal mouse islet cells. They also have morphological characteristics comparable to of pancreatic  $\beta$  cells that make them a realistic model useful in the studies of the molecular mechanisms of pancreatic  $\beta$  cells.

### EXPERIMENTAL METHODS

Structurally well-defined dendrons were realized through a bottom up strategy based on a multistep sequence of coupling and deprotection reactions. The root of the dendron included an arginine moiety (R), onto which the three branching generations of lysine (G3K) were assembled. The complete molecule (RG3K) was characterised by HPLC, mass spectrometry (MS) and Fourier Transformed Infrared spectroscopy (FTIR). MIN6 cells were cultured at 37°C and 5% CO<sub>2</sub> in Dulbecco's Modified Eagle Medium (DMEM) at low glucose, with 10% (%) foetal calf serum. Cells were seeded in 24 well cell culture plates at a density of  $4.0 \times 10^4$  cells/cm<sup>2</sup> for 24 and 48 hours and mixed with increasing dendrons concentration (46, 85, 170 nmol/ml). Cell viability was assessed by Hoescht Propidium Iodide staining (HPI; Sigma, UK), while FITC labelled dendrons were used to investigate the cellular uptake.

### RESULTS AND DISCUSSION

Chemico-physical analysis confirmed the successful synthesis of hyperbranched molecules. The accurate mass measurements of MS confirmed that the actual

molecular weight matches the theoretical value (2097 m/z). The absorption bands of FTIR spectra reveal the characteristic elements present on the molecule backbone. Cell viability analysis reveals that after 24 hr in contact with dendrons, cells are viable as showed in Fig.1.

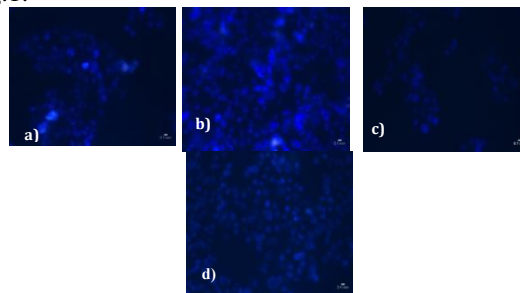


**Figure 1.** Confocal analysis of MIN6 cultured with a) 170 nmol/ml b) 85nmol/ml and c) 46 nmol/ml of RG3K dendrons and d) on tissue culture plate.

After 48hrs of exposure, cellular uptake of dendron can be detected and the FITC labeled dendron is distributed inside the nucleus (Fig.2).

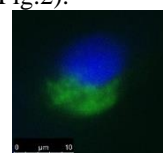


**Figure 2.** Low RG3K concentration uptake in MIN6 cells.

### CONCLUSION

This work shows a systematic study on the design of characterization of novel dendron based non-viral vectors. The innovative platform presented herein shows that dendrons can be produced in mild condition with exquisite control of composition and architecture. Cells experiments on MIN6 cell line indicate that dendron based molecules are promising as an efficient targeting model for pancreatic  $\beta$  cells. The obtained results provide support for clinical translation of non-viral vectors for gene and drug delivery applications for type 1 diabetes.

### REFERENCES

References must be numbered. Keep the same style.

1. Bottino R. *et al.*, Gene Therapy 10: 875–889, 2003
2. de Azua IR *et al.*, Proc.Nat.Acad.Sci.USA 17:7999-8004, 2010

### ACKNOWLEDGMENTS

The authors gratefully acknowledge research founding received from EC Project NEXT-Nano Engineering for Cross Tolerance (EFP Grant no.602235).

Rafał Mech, Beata Borak, Katarzyna Łuszczuk, Daniel Lewandowski, Agnieszka Baszczuk, Marek Jasierski, Jerzy Kaleta

Department of Mechanics, Materials Science and Engineering, Wrocław University of Technology,  
Smoluchowskiego 25 Str. 50-370 Wrocław, POLAND,  
[beataborak@pwr.edu.pl](mailto:beataborak@pwr.edu.pl)

## INTRODUCTION

Silica particles doped with magnetic nanoparticles and containing active substances (drugs) are seemed as an interesting materials for the biomedical applications<sup>1,2</sup>. Functionalized silica particles doped with nanoparticles of magnetic substances ( $\text{Fe}_2\text{O}_3$ ) have been obtained by the sol-gel method. To see the behavior and response of the obtained materials to external magnetic field special device was built to make a thermal induction measurements. Magnetic particles can respond to the action of alternating magnetic fields and induced thermal energy were measured in particles.

## EXPERIMENTAL METHODS

Silica particles doped with magnetic  $\text{Fe}_2\text{O}_3$  nanoparticles have been obtained by the sol-gel method. To measure the behavior and response of the obtained materials to external magnetic field special device was built (Fig.1). This device was supported on the induction of the eddy currents into conductors (silica particles with magnetic substances) by changing external magnetic field. Test stand consist on several (6 or 10) neodymium magnets, which are able to induce variable magnetic field with frequency up to 3 kHz. Induced thermal energy were measured in particles, closed into special gel capsules, by thermoelements which allow to make the temperature measurements during the experiment.

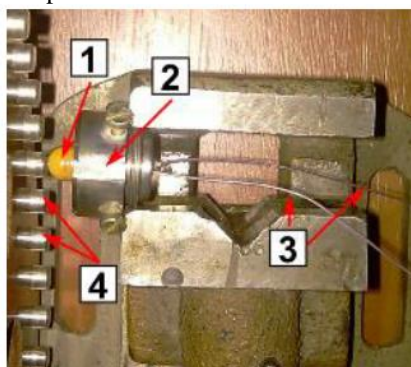


Fig. 1. Diagram of the measuring position: 1) capsules with materials, 2) handle of the capsules, 3) thermoelements, 4) neodymium magnets.

## RESULTS AND DISCUSSION

The size and morphology of silica magnetic particles were obtained using TEM (Fig. 2). Material presents the structure type core-shell and magnetic dopant are encapsulated within silica matrix, which isolates it from the environment. Simple silica particles are small, their diameter size is in the range 50-100 nm, but the presence of magnetic dopants cause that they stick

together and form bigger particles with diameter size about 250-350 nm.

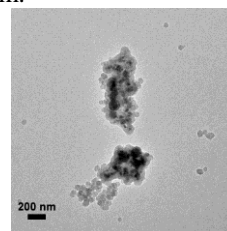


Fig. 2. TEM micrograph of the  $\text{SiO}_2/\text{Fe}_2\text{O}_3$  particles.

Excitation of the magnetic silica particles with external AC magnetic field cause induction of the thermal energy. The observed highest growth in the temperature was over 4,5 K. The results of thermal energy induction in the prepared particles were shown in Figure 3. The red line represent thermocouple placed inside the gel capsule. This thermocouple was full surrounded with the silica particles. The second thermocouple (black line) was placed on the surface of the gel capsule.

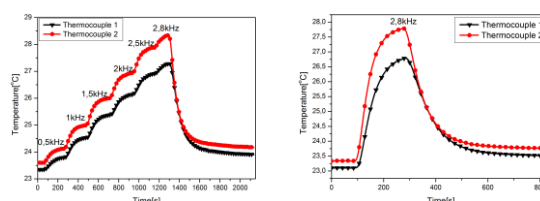


Figure 3: Temperature change of magnetic particles measured with use of thermocouples a) for different frequencies of magnetic field changes, b) for maximum frequency of magnetic field changes.

## CONCLUSION

$\text{Fe}_2\text{O}_3$  nanoparticles encapsulated into amorphous  $\text{SiO}_2$  particles were prepared by the sol-gel method. Magnetization curves confirmed the presence of ferromagnetic behavior of this material. The application of the external AC magnetic field induce thermal energy in the particles. Generated heat was immediately released to the surroundings and growth in the temperature over 4,5 K was observed.

## REFERENCES

1. Mashhadizadeh M.H. *et al.*, J Nanomed. Nanotechnol. 2012, 3:4 <http://dx.doi.org/10.4172/2157-7439.1000139>
2. Chen J.P. *et al* Int. J. Nanomedicine 2012: 7 5137

## ACKNOWLEDGMENTS

This work was partially supported by K1010/40135.

## Cell Penetrating Peptide Constructs: Novel Drug Delivery to the Eye

Felicity de Cogan<sup>1</sup>, Lisa J Hill<sup>1</sup>, Peter J Morgan-Warren<sup>1</sup>, Anna FA Peacock<sup>2</sup>, Robert AH Scott<sup>3</sup>, Ann Logan<sup>1</sup>,

<sup>1</sup>School of Clinical and Experimental Medicine, University of Birmingham, UK

<sup>2</sup>School of Chemistry, University of Birmingham, UK

<sup>3</sup>Royal Centre of Defence Medicine, Queen Elizabeth Hospital, UK

[f.decogan@bham.ac.uk](mailto:f.decogan@bham.ac.uk)

### INTRODUCTION

Age-related macular degeneration (AMD) is a major cause of blindness and is the leading cause of certified vision loss in the UK<sup>1</sup>. AMD affects the retina, the light sensing membrane at the back of the eye. In AMD the central part of the retina, the macula, degenerates causing the person to lose their central vision. AMD exists in two forms, wet and dry. Dry AMD is currently untreatable. Fortunately, the most severe form of AMD, wet AMD, is treatable by repeated injections of drugs into the back of the eye.

In wet AMD blood vessels grow from the choroid, the tissue behind the retina, into the retina. Blood vessel growth into the retina leads to swelling and bleeding, causing damage to the macula and scarring. Currently, the only method of delivering anti-VEGF drugs such as, ranibizumab or aflibercept to treat neovascularisation in AMD are by invasive intraocular injections. While the benefits of these drugs are necessary to prevent loss of vision in patients, a less invasive method of drug delivery using eye drops would prevent the associated risks of intraocular injections such as bleeding within the eye, tearing of the retinal tissues, cataracts and infection<sup>2</sup>.

In this study we present a novel cell-penetrating peptide construct (CPPC) delivery system which can allow the drugs currently used in the clinic to be delivered to the back of the eye using a topical administration of an eye drop instead of relying on invasive injections.

### EXPERIMENTAL METHODS

Peptides were synthesised using standard solid-phase peptide synthesis on a Liberty Blue peptide synthesiser. The peptides were analysed using mass spectrometry and purified using high-pressure liquid chromatography and used at a purity of >95 %. Peptide constructs were built around the drugs by vortexing for 10 seconds and incubating at room temperature. Drug delivery experiments were carried out ex-vivo in freshly enucleated porcine eyes. *In vivo* experiments were carried out in C57 mice. Mice had a three 100 µm laser burns to the choroid to model neo-vascularisation in AMD. The mice then received a single intravitreal injection of an anti-VEGF agent or cell penetrating peptide construct bound anti-VEGF drugs applied topically to the front of the eye twice daily for the duration of the experiment. Neovascularisation in the choroid was then measured using immunohistochemistry.

### RESULTS AND DISCUSSION

Ex vivo delivery into enucleated porcine eyes demonstrated that a single 60 µL drop could deliver 1.7

± 0.4 µg/mL of ranibizumab to the vitreous humour. Confocal images of immunohistochemistry on retinal wholemounts also showed the presence of ranibizumab in the retina. *In vivo* experiments showed that following laser burns to the choroid both intravitreal injection and cell-penetrating peptide construct bound anti-VEGF agents significantly reduced neovascularisation compared to controls with no significant differences between the two groups (Figure 1).

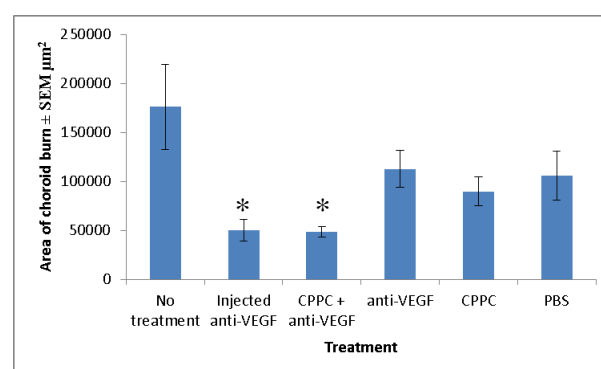


**Figure 1** Area of neovascularisation following injected and topical administration of current 'gold standard' drug. Each group shows average of 6 mice, error bars show standard error of the mean. \*p<0.05

### CONCLUSION

The pre-clinical *in vivo* data supports our hypothesis that cell-penetrating peptide constructs can be used to deliver drugs to the posterior segment of the eye via topical administration. This work has the potential to revolutionise the current treatment of diseases such as AMD, reducing the financial burden on the NHS and empowering patients.

### REFERENCES

1. Owen, Christopher G., et al. "The estimated prevalence and incidence of late stage age related macular degeneration in the UK." *British Journal of Ophthalmology* (2012): bjophthalmol-2011
2. Davis, Benjamin M., et al. "Topical delivery of Avastin to the posterior segment of the eye in vivo using Annexin A5-associated liposomes." *Small* 10.8 (2014): 1575-1584.

### ACKNOWLEDGMENTS

This work was funded by the Early Career ARVO fellowship scheme. The authors would also like to thank Professor Heping Xu and Dr Mei Chen for their invaluable advice and assistance.



## Inhibiting Pathogenous Processes by siRNA Releasing Polymer Coatings

Diane Zengerle<sup>1</sup>, Olivia König<sup>1</sup>, Christian Schlensak<sup>2</sup>, Tobias Walker<sup>2</sup>, Hans-Peter Wendel<sup>1</sup>, Andrea Nolte<sup>1</sup>

<sup>1</sup>University Department of Thoracic and Cardiovascular Surgery Clinical Research Laboratory, Eberhardt-Karls-University Tübingen, Germany

<sup>2</sup>Department of Thoracic, Cardiac, and Vascular Surgery, Tuebingen University Hospital, Germany.  
[diane.zengerle@student.uni-tuebingen.de](mailto:diane.zengerle@student.uni-tuebingen.de)

### INTRODUCTION

Although small interfering RNAs (siRNAs) have surpassed expectations *in vitro* to alter gene expression, their transfer is still the major obstacle for the *in vivo* application of RNA interference (RNAi). One important aspect for their therapeutic employment is the immobilization on implants for local delivery, such as to reduce inflammatory processes like the adhesion molecule cascade accompanied by the expansion of coronary artery stents in patients with vascular stenosis. Therefore, delivery technologies could be established for the local application of RNAi<sup>1</sup>.

Poly(lactide-co-glycolide) (PLGA) already exists as biodegradable drug eluting polymer in Drug eluting stents<sup>2</sup> but not so far in connection with siRNA delivery. We want to show the ability of PLGA coatings to release siRNA, transfect endothelial cells and induce RNA interference. From our point of view PLGAs have the ability to achieve the requirements of a appropriate siRNA delivery system which can be used in many fields of implant technologies

### EXPERIMENTAL METHODS

Three different PLGAs (PLGA 1: Resomer® RG 752 H, acid terminated, PLGA 2: PLGA Mw 50,000-75,000, ester terminated, PLGA 3: Resomer® RG 756 S, ester terminated, Sigma-Aldrich®) were used for analysis.

The ph-value change in cell medium was analysed over four weeks.

Hemocompatibility tests with PLGA coated glass slides were carried out to determine the reaction with whole blood.

For biocompatibility tests EA.hy926 cells were cultured in PLGA conditioned medium. We also tested the immune response of EA.hy926, cultivated with PLGA-siRNA coated glass slides by quantitative real-time chain reaction (qRT-PCR).

Transfection efficiency was analysed with EA.hy926 cells which were incubated with PLGA mixed with fluorescent siRNA ((f)-siRNA) coated glass slides. For that, a layer of PLGA and Lipofectamine complexed with (f)-siRNA or scrambled siRNA (SCR) was air-dried onto glass slides.

To show the functionality of siRNA knockdown after transfection in EA.hy926 and hVEC<sup>3</sup> the knockdown of ICAM-1 was quantified by flow cytometry and qRT-PCR after incubation with PLGA-siICAM or PLGA-SCR coated glass slides.

### RESULTS AND DISCUSSION

No significant pH changes and no significant decrease in viability were measured after four weeks.

The hemocompatibility assay showed no significant changes of whole blood reactions compared to control without slides.

Release and transfection of (f)-siRNA could be detected for a period of four weeks, interestingly 5.22 % new cultured cells were still transfected after this period.

Significant ICAM-1 protein knockdown of 36,03% and mRNA knockdown of 47,1 % was measured.

PLGAs are biocompatible and hemocompatible materials for drug eluting systems which is also shown by Waugh<sup>2</sup> and Szymonowicz<sup>4</sup>.

We showed that it can be used to immobilise, release and transfect functional siRNA over a long period into cells to get a knockdown of specific proteins.

Especially Resomer® RG 752 H shows the highest knockdown of ICAM-1.

### CONCLUSION

The biocompatibility and hemocompatibility together with the transfection of siRNA into cells, when they are in contact with these PLGA layers, not inducing immune response etc., makes PLGA-siRNA coatings a feasible future therapeutic application for several diseases.

### REFERENCES

- <sup>1</sup> Nolte, A., et al. (2011). "Small-interfering RNA-eluting surfaces as a novel concept for intravascular local gene silencing." *Mol Med* 17(11-12): 1213-1222.
- <sup>2</sup> Waugh, J. and A. J. Wagstaff (2004). "The paclitaxel (TAXUS)-eluting stent: a review of its use in the management of de novo coronary artery lesions." *Am J Cardiovasc Drugs* 4(4): 257-268.
- <sup>3</sup> Walker, T., et al. (2005). "Suppression of ICAM-1 in human venous endothelial cells by small interfering RNAs." *Eur J Cardiothorac Surg* 28(6): 816-820.
- <sup>4</sup> Szymonowicz, M., et al. (2014). "In vitro hemocompatibility studies of (poly(L-lactide) and poly(L-lactide-co-glycolide) as materials for bioresorbable stents manufacture." *Acta Bioeng Biomech* 16(4): 131-139.

### ACKNOWLEDGMENTS

The authors would like to thank the IZKF-Fellowship for providing financial support to this project.





# Synthesis and Characterization of Poloxamer-Based Theranostic Vehicles

Karolina Morawska<sup>1</sup>, Anna de la Fuente<sup>2</sup>, Sandra Van Vlierberghe<sup>1</sup>, Frank Roesh<sup>2</sup> and Peter Dubrue<sup>1</sup>

<sup>1</sup>Polymer Chemistry & Biomaterials Research Group, Ghent University, Belgium

<sup>2</sup>Institut für Kernchemie, Johannes Gutenberg-Universität Mainz, Germany

[karolina.morawska@ugent.be](mailto:karolina.morawska@ugent.be)

## INTRODUCTION

Despite the progress realized in the field of radiopharmaceuticals, there remains a need for effective delivery systems with prolonged circulation half-life and increased radionuclide loading capacity. Block copolymer micelles have shown to improve the payload delivery of therapeutic agents to tumours and hold great promise for passive uptake via EPR and specific uptake guided via targeting [1]. The aim of the present project is the development of molecular carriers suitable for theranostics through the modification of amphiphilic block copolymers. The synthesized polymers will enable both micelle formation as well as the incorporation of radionuclides.

## EXPERIMENTAL METHODS

In the present study, commercially available poloxamers (triblock copolymers of PEO-PPO-PEO, i.e. Pluronics) have been selected as starting materials to introduce amines [2] enabling the subsequent coupling of the chelating agent 2-(4-isothiocyanatobenzyl)-diethylenetriaminepentaacetic acid (p-SCN-Bn-DTPA) [3] (Fig. 1). The molecular carriers developed were analyzed using various techniques including NMR and IR spectroscopy for structure determination, GPC for molecular weight determination and dynamic light scattering (DLS) for micelle size evaluation. Polymers were labelled with generator produced PET nuclide Sc-44 [4]. Radiolabelling stability was tested in human serum media and in the presence of other metals (Ca<sup>2+</sup>, Fe<sup>3+</sup>, Mg<sup>2+</sup>) at 37°C for 4 h.

## RESULTS AND DISCUSSION

The IR and <sup>1</sup>H-NMR spectra indicate that the functionalization of polymers with primary amines was successful. Furthermore, SEC analysis performed excluded possible crosslinking of the polymer due to the reaction with ethylene diamine. Polymers were quantitatively labelled at room temperature within 15 min with Sc-44, showing high stability over time.

## CONCLUSION

Different Pluronics modified with primary amines serve as an excellent platform for further conjugation of various ligands, namely targeting vectors, contrast agents or chelating moieties to the polymer. Moreover, the method herein used to introduce chelating agents was successful. Therefore, we expect that the developed polymers can be used as safe and effective vehicles for theranostics.

## REFERENCES

1. Blanco E. et al., *Exp Biol Med (Maywood)* **2009**, 234: 123-13.1
2. Lu H. F. et al., *Biomaterials* **2003**, 24: 4893-4903.
3. Hoang B. et al., *Molecular Pharmaceutics* **2009**, 6: 581-592
4. Roesh F. *Current Radiopharmaceuticals*, **2012**, 5: 187-201

## ACKNOWLEDGMENTS

The research leading to these results has received funding from the People Programme (Marie Curie Actions) of the European Union's Seventh Framework Programme (FP7/2007-2013) under REA grant agreement no. PITN-GA-2012-317019 'TRACE 'n TREAT'.

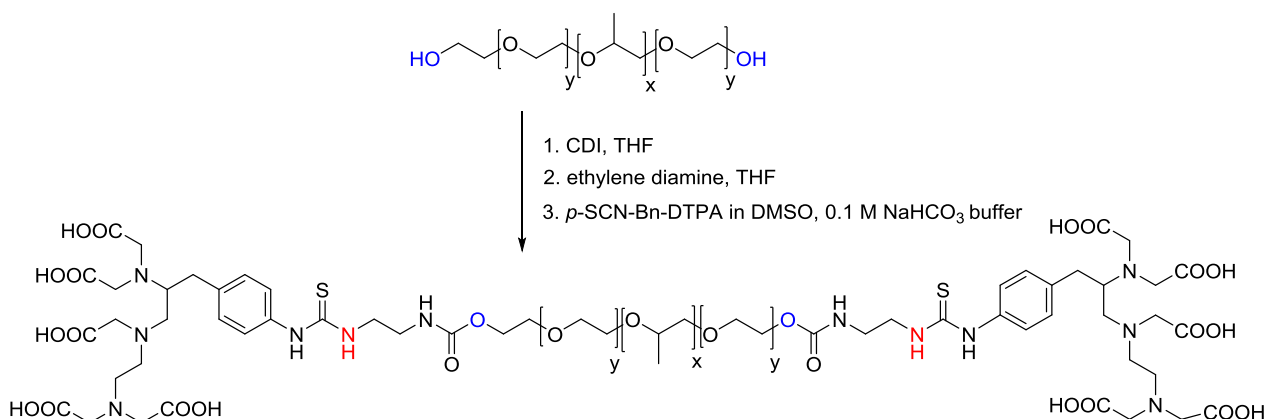


Fig. 1. Synthetic route of poloxamers modifications

## Injectable Extracellular Matrix Hydrogels as Scaffolds for Spinal Cord Injury Repair

Sarka Kubinova<sup>1</sup>, Dmitry Tukmachev<sup>1,2</sup>, Serhiy Forostyak<sup>1,2</sup>, Kristyna Zaviskova<sup>1,2</sup>, Zuzana Koci<sup>1,2</sup>, Eva Sykova<sup>1</sup>

<sup>1</sup>Institute of Experimental Medicine, AS CR, Prague, Czech Republic

<sup>2</sup>2nd Medical Faculty, Charles University, Prague, Czech Republic

[sarka.k@biomed.cas.cz](mailto:sarka.k@biomed.cas.cz)

### INTRODUCTION

Restoration of lost neuronal function after spinal cord injury (SCI) still remains a big challenge for current medicine. An important repair strategy is tissue reconstruction by bridging the SCI lesion with a supportive and stimulatory milieu that would enable axonal rewiring. Injectable extracellular matrix (ECM) derived hydrogels have been recently reported to have neurotrophic potential *in vitro*<sup>1</sup>. In this study, we evaluated the presumed neuroregenerative properties of ECM hydrogels *in vivo* in the acute model of SCI.

### EXPERIMENTAL METHODS

ECM hydrogels were prepared by decellularization of porcine spinal cord (SC) or porcine urinary bladder (UB) tissue<sup>1</sup>. *In vitro* cell growth on the surface of the hydrogels was characterized using a human umbilical cord-derived mesenchymal stem cell (hWJ-MSC) culture. Cell viability was determined after 1, 3, 7 and 14 days in culture using WST-1 reagent.

In an *in vivo* study, a hemisection was performed at the Th8 level, and hydrogels were acutely injected into the spinal cord defect and allowed to gelate *in situ* (n = 5 per group, per time point). The effects were evaluated via histological analysis and real-time qPCR at 2, 4 and 8 weeks.

### RESULTS AND DISCUSSION

Both ECM hydrogels showed comparable ability to support *in vitro* cell proliferation, which did not significantly differ from the control cell proliferation on tissue culture plastic. When injected into the spinal cord hemisection, both ECM hydrogels integrated into the host tissue and stimulated neovascularization and nervous tissue ingrowth into the lesion. No significant differences were found between SC-ECM and UB-ECM hydrogels with regards to ingrowth of neurofilaments and blood vessels in all observed time points. On the

other hand, massive infiltration of macrophages into the lesion and rapid hydrogel degradation did not prevent cyst formation, which progressively developed over 8 weeks. Gene expression analysis at 2 weeks post-SCI revealed significant down-regulation of genes related to immune response and inflammation in both hydrogel types, whereas this effect diminished at later time points. A combination of hWJ-MSC with SC-ECM did not further promote ingrowth of axons and blood vessels into the lesion, when compared with the SC-ECM hydrogel alone. Nevertheless, only a few transplanted cells were detected in the lesion after 4 weeks.

### CONCLUSION

Both ECM hydrogels modulated the innate immune response and provided the benefit of a stimulatory substrate for *in vivo* neural tissue regeneration. However, fast hydrogel degradation resulting in cyst formation might be a limiting factor for the use of ECM hydrogels in the treatment of acute SCI.

### REFERENCES

1. Medberry C.J. *et al.*, Biomaterials. 34:1033-40, 2013.

### ACKNOWLEDGMENTS

Supported by: GACR 15-01396S and MEYS of the Czech Republic under the NPU I (LO1309).



## Nerve Guidance Channels of Synthetic Biodegradable Polymers with Internal Hydrogel Scaffold of Radiation-Crosslinked Polysaccharide

Radosław A. Wach<sup>1</sup>, Jarosław Cala<sup>2</sup>, Karolina Kowalska-Ludwicka<sup>2</sup>, Charito Aranilla<sup>3</sup>, Agnieszka Adamus<sup>1</sup>,  
Alicja K. Olejnik<sup>1</sup>, Zbigniew Pasieka<sup>2</sup>, Janusz M. Rosiak<sup>1</sup>, Piotr Ulanski<sup>1</sup>

<sup>1</sup>Institute of Applied Radiation Chemistry, Lodz University of Technology, Poland

<sup>2</sup>Department of Experimental Surgery, Medical University of Lodz, Poland

<sup>3</sup>Philippine Nuclear Research Institute, Philippines

[wach@mitr.p.lodz.pl](mailto:wach@mitr.p.lodz.pl)

### INTRODUCTION

Advances surgical techniques for treating severe injuries of nerves of peripheral nervous system, when suturing of stumps is unfeasible, employ bridging. This may involve grafting of axon bundles harvested from a donor site, or application of guiding tubes. The primary function of the tubular prosthesis is to bridge a gap of discontinued nerve. Variety of formulations of biodegradable synthetic polymers offer wide range of mechanical properties and tunable degradation kinetics. Poly(trimethylene carbonate) (PTMC) is a suitable co-component to provide flexibility to poly(lactic acid) (PLA), the most utilized biodegradable synthetic polymer. Either copolymers and blends of these two components were proposed for manufacturing nerve guidance channels.[1, 2] Another strategy employs tubular structures with an internal scaffold to support mechanically regenerating nerve and be a reservoir of bioactive substances. A hydrogel matrix can be employed since its structure is characterized by random structures of interconnecting open pores. Permanent hydrogels natural polymers can be formed by chemical methods with crosslinking agents or utilizing ionizing radiation. Polysaccharides, despite general tendency for degradation, can be converted into permanent hydrogels when irradiated without additives under certain conditions. [3]

Carboxymethylchitosan (CMCS), a water-soluble biodegradable polysaccharide possesses advantageous physical, chemical and biological properties, such as low toxicity and sufficient biocompatibility to be applied as films, fibers and hydrogels in artificial bone material, drug delivery matrices or wound healing dressings.[4] Moreover, CMCS hydrogel can be synthesized by radiation methods to be applied for biomedical devices.

### EXPERIMENTAL METHODS

Carboxymethylchitosan (Kraeber GMBH & Co.) of the degree of deacetylation (DDA) 93.8% and degree of substitution (DS) 96% and viscosity-average molecular weight  $M_{\eta} = 32.5 \text{ kg mol}^{-1}$  was used. Method of tube manufacturing of poly(L-lactic acid), PLA and poly(trimethylene carbonate), PTMC was developed in our laboratory and is described elsewhere.[2] In vivo experiments on rats femoral nerve regeneration involved the hollow tubes, the tubes with CMCS hydrogel, and that including brain derives growth factor, and control group - ends suturing. Motor and sensor recovery of operated limbs, neuroma occurrence and histopathology of explanted nerves were evaluated.

### RESULTS AND DISCUSSION

Radiolysis of CMCS leads to degradation and crosslinking; the latter process predominates in concentrated solutions. Thus, irradiation of CMCS solutions of 10% and more results in formation of macroscopic hydrogel. This phenomenon was exploited for preparation of internal hydrogel matrix in nerve regeneration guides. 12% CMCS mixture with water, which formed a physical gel, was introduced into the lumen of the PTMC/PLA porous guide. Electron beam irradiation initiated crosslinking reactions to form CMCS hydrogel inside the tube, and the applied radiation dose of 25 kGy sterilized the device simultaneously. A schematic drawing of a guidance with hydrogel filling is shown along with its SEM picture in Figure 1. Biocompatibility of the produced tubes was confirmed in vitro.

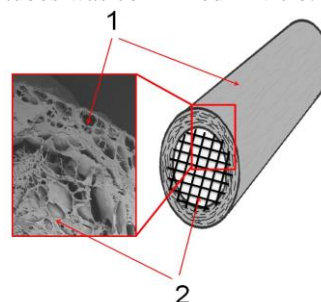


Figure 1. A schematic drawing and SEM picture of the guidance with hydrogel filling, 1 – tube wall of PTMC/PLA and 2 – CMCS hydrogel matrix.

Application of the hollow tubes, these with hydrogel, and with hydrogel infiltrated with BDNF, in rat animal model effectively supports regeneration of discontinued femoral nerves as assessed through movement and sensitive functions recovery. It prevents neuroma formation, enhances the process of nervous tissue reconstruction and reduces scar tissue formation.

### CONCLUSIONS

Manufacturing and evaluation of the guides of PLA/PTMC biodegradable polymer blend with internal CMCS hydrogels scaffold is reported. In vivo experiments gave positive results and the variation between three types of tubes will be discussed.

### REFERENCES

1. P. Pliikk, S. Malberg, A.-C. Albertsson, *Biomacromolecules*, 2009, 10, 1259.
2. R.A. Wach, A. Adamus, A.K. Olejnik, J. Dzierawska, J.M. Rosiak, *J. Appl. Polym. Sci.* 2013, 127, 2259.
3. R.A Wach, B. Rokita, N. Bartoszek, Y. Katsumura, P. Ulanski, J.M. Rosiak, *Carbohydrate Polym.* 2014, 112, 412.
4. R.A. Muzzarelli, *Carbohydrate Polym.* 1988, 8, 1.



## A Potential Advantage of Alginate and Poly(3,4-ethylenedioxythiophene): Poly(styrenesulfonate) (PEDOT:PSS) Blended for Neurite Outgrowth

Pichaya Srisuk<sup>1</sup>, Nandita Singh<sup>2</sup>, Jonathan Hanley<sup>3</sup> and Sameer Rahatekar<sup>1,2</sup>

<sup>1</sup>Advanced Composites Centre for Innovation and Science (ACCIS), University of Bristol, UK

<sup>2</sup>Centre for Nanoscience and Quantum Information (NSQI), University of Bristol, UK

<sup>3</sup>School of Biochemistry, University of Bristol, UK

[ps13010@bristol.ac.uk](mailto:ps13010@bristol.ac.uk)

### INTRODUCTION

Neural implants and stimulations are used to understand brain function and brain disorders cause by neural damage.

Alginate has a unique gelling ability which is widely leveraged in biomedical applications such as, encapsulating hydrogels for the delivery, or immobilisation of drugs, proteins or cells<sup>1,2</sup>. Conductive polymers (CPs) also play important roles in *in vivo* neural-electric platforms to increase neuron population. Poly(3,4 ethylenedioxythiophene): Poly(styrenesulfonate) (PEDOT:PSS); an aqueous solution with high conductivity and excellent cell adhesion is a popular option to employ as an organic electrochemical layer to influence and promote cell growth<sup>3</sup>.

This research aims to investigate the biocompatibility of alginate and PEDOT:PSS blended films and fibres with neurite outgrowth.

### EXPERIMENTAL METHODS

PEDOT:PSS was mixed with alginate and doped with 10 wt% of polyethylene glycol (PEG) to increase the conductivity. This solution was spun into fibres through  $\text{CaCl}_2$  (aq) (1 M), which were then subjected to heat treatment (150°C, 10 min). The properties were characterised by conductivity testing, tensile testing, and circuit stimulation.

Films were cast from high M alginate dissolved in PEDOT:PSS and other additives in different ratios. These were dried (RT, 12 h) before cross-linking with  $\text{CaCl}_2$  (aq) (50 mM) and the cell adhesion studied.

Samples were cut into small pieces and placed in 24 well plates, poly-L-lysine (PLL) was added to modify the implant surface and the wells seeded with foetal rat cortical neurons ( $10^6$  per well). The plates were observed at 7 and 14 days by live/dead cell assays under a fluorescent microscope.

### RESULTS AND DISCUSSION

Uniform fibres were continuously spun for several meters. PEG additive and heat treatment significantly increased the conductivity. However a reduction in mechanical properties was also observed in PEG mixed fibres, with a slight recovery following heat treatment. The circuit stimulations clearly showed the superior conductivity of blended fibres with added PEG and heat treatment which produced the highest light intensity (Fig 1).

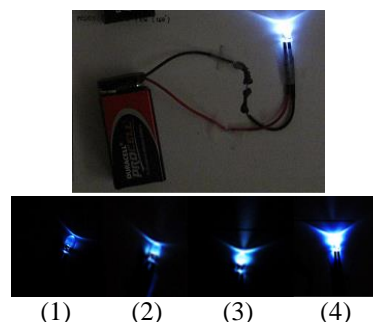


Fig.1 The LED intensity of stimulate circuits from fibres 1) Alg-PED 2) Alg-PED-heated 3) Alg-PED-PEG and 4) Alg-PED-PEG heated.

Neurons were also studied on neat alginate films, as a control point for future research (Fig 2). Composite films and fibres will be aiming to improve this level of cell growth in ongoing experiments.

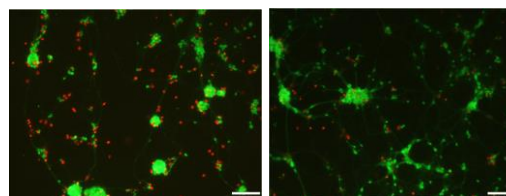


Fig.2 Fluorescent microscopy images of live (green) and dead (red) neurons growing on neat alginate films at day 7 and 14 respectively.

### CONCLUSION

Conductive alginate fibres were prepared containing PEDOT:PSS, addition of PEG and heat treatment affected their electrical conductivity and mechanical properties. Neuronal growth were observed on neat alginate films which demonstrates the ability of this materials for neurite outgrowth. These will contribute to improving the development of neural implants on composite films and fibres surface.

### REFERENCES

1. Frampton P J. *et al.*, Biomed. Mater. 6:015002, 2011
2. Matyash M. *et al.*, Tissue Eng. P. A. 18:55-66, 2012
3. Strakosas X. *et al.*, J. Mater. Chem. B. 2:2537-2545, 2014

### ACKNOWLEDGMENTS

The authors would like to acknowledge support from the Centre for Nanoscience and Quantum Information (NSQI) at University of Bristol for the access to their materials and facilities.





## Polyurethane/Poly lactide Electrospun Nonwovens for Neural Tissue Engineering

Anna Lis<sup>1</sup>, Jakub Grzesiak<sup>2</sup>, Ryszard Fryczkowski<sup>3</sup>, Dariusz Szarek<sup>4</sup>, Krzysztof Marycz<sup>2</sup>, Włodzimierz Jarmundowicz<sup>5</sup>, Jadwiga Laska<sup>1</sup>

<sup>1</sup>AGH University of Science and Technology, Faculty of Materials Science and Ceramics, Dept. of Biomaterials, Poland

<sup>2</sup>Electron Microscopy Laboratory, University of Environmental and Life Sciences, Poland

<sup>3</sup>University of Bielsko-Biala, Faculty of Materials and Environmental Sciences, Poland

<sup>4</sup>Department of Neurosurgery, Lower Silesia Specialist Hospital of T. Marciniak, Emergency Medicine Centre, Poland

<sup>5</sup>Department of Neurosurgery, Wrocław Medical University, Poland

[annal@agh.edu.pl](mailto:annal@agh.edu.pl)

### INTRODUCTION

Traumatic spinal cord and brain injuries result in long-term neurological and functional disorders, as well as death<sup>1-3</sup>. Peripheral nerve injuries may affect sensory functions and motor capabilities<sup>1</sup>. Numerous tissue engineering strategies have been evaluated for reconstruction and regeneration of the nervous system<sup>1-2</sup>. The use of biodegradable polymer scaffolds can help in the restoration of the damaged spinal cord and peripheral nerves by connecting the transected stumps and supporting the growth of nerve cells. Electrospun nonwovens are promising scaffolds for neural tissue engineering that can help the artificial environment to mimic the native extracellular matrix<sup>1-3</sup>. Additionally, scaffolds can be augmented with cells or growth factors<sup>2</sup>. Olfactory ensheathing cells which have extraordinary neurotrophic properties have been chosen for *in vitro* evaluation of the scaffolds<sup>4-5</sup>.

### EXPERIMENTAL METHODS

Polyurethane/poly lactide (PU/PLDL) nonwovens were produced via solution electrospinning as potential matrices for olfactory ensheathing cell (OEC) growth. Influence of the composition and surface morphology on proliferation of OECs was investigated. The scaffolds were composed of PU and PLDL blended at three different w/w ratios, i.e., 8/2, 6/4 and 5/5. The morphology of electrospun PU/PLDL nonwovens were studied using scanning electron microscopy (SEM). Diameter of the fibers was evaluated with image analysis software based on SEM images. The hydrophilic nature of PU/PLDL nonwovens was determined by sessile drop water contact angle measurements. The *in vitro* bioassay of the materials comprised the characterization of morphology, and determination of metabolic activity of cultured OECs. Statistical differences were presented using the Student's ten-sample t-test.

### RESULTS AND DISCUSSION

SEM images of the PU/PLDL nonwovens show fibers of microscale diameter, creating 3D architecture. It was noticed that the introduction of different amounts of flexible PU and rigid PLDL in the polymer blend resulted with creation of networks with moderately different fibrous architectures. Random oriented PU/PLDL fibers showed diameters that ranged from 20 to 900 nm. Contact angles measured for nonwovens of different compositions are noticeably different. The

viability test revealed that none of investigated substrates showed cytotoxic effect on glial cells. OECs cultured on investigated scaffolds showed differences in metabolic activity, depending on the composition of the blend. OECs showed the presence of specific GFAP in all analysed scaffolds, as well as in the control. There is presently, a growing interest in the use of olfactory ensheathing cell transplantation<sup>4,5</sup>. Lesion in the spinal cord is followed by a sequence of primary and secondary damages, e.g. proliferation of overactive astrocytes and creation of impenetrable glial scar on the stumps. The OECs have the extraordinary ability to "open" sticky scar making it penetrable for regenerating axons. It has been shown that after transplantation into human patients, OECs can positively influence repair<sup>4</sup>. However, recent data suggests that a combination, such as a scaffold seeded with OECs might be more preferable in enhancing the level of regeneration across large lesions<sup>5</sup>. Consequently, the existing challenge for researchers is to develop a scaffold that is capable of stimulating OEC proliferation and the re-growth of host tissue. Results of *in vitro* culture of OEC confirmed the potential application of the PU/PLDL nonwovens as substrates for OEC delivery and neural tissue repair.

### CONCLUSION

Our study confirms usability of novel PU/PLDL fibrous scaffolds as substrates for enhancing OECs proliferation. The scaffolds enriched with these glial cells can be implanted directly into the spinal cord or into peripheral nerves to support nerve regeneration. We find electrospinning as a promising technique for fabrication of novel PU/PLDL nonwovens.

### REFERENCES

1. Braghirolli D. I. *et al.*, Drug Discov Today 19(6):743-753, 2014
2. Elliot Donaghue I. *et al.*, J. Control. Release 190:219-277 (2014)
3. Weightman A. *et al.*, Nanomedicine: NBM 10:291-295 (2014)
4. Tabakow P. *et al.*, Cell Transplant 22:1591-1612, 2013
5. Tabakow P. *et al.*, Cell Transplant 23(12):1631-1655 (2014)

### ACKNOWLEDGMENTS

This research was financially supported by National Science Center, Poland (grants: NN 403 176540 and 2011/01/B/STB8/07795)



## Alginate-Based Hydrogels as Artificial Extracellular Matrix for Central Nervous System Regeneration

Anna Lis<sup>1</sup>, Jakub Grzesiak<sup>2</sup>, Joanna Mastalska-Popławska<sup>3</sup>, Dariusz Szarek<sup>4</sup>, Krzysztof Marycz<sup>2</sup>,  
Włodzimierz Jarmundowicz<sup>5</sup>, Jadwiga Laska<sup>1</sup>

<sup>1</sup>AGH University of Science and Technology, Faculty of Materials Science and Ceramics, Dept. of Biomaterials, Poland

<sup>2</sup>Electron Microscopy Laboratory, University of Environmental and Life Sciences, Poland

<sup>3</sup>AGH University of Science and Technology, Faculty of Materials Science and Ceramics, Poland

<sup>4</sup>Department of Neurosurgery, Lower Silesia Specialist Hospital of T. Marciniak. Emergency Medicine Centre, Poland

<sup>5</sup>Department of Neurosurgery, Wrocław Medical University, Poland

[annal@agh.edu.pl](mailto:annal@agh.edu.pl)

### INTRODUCTION

Injury to the spinal cord and brain have devastating consequences on motor, sensory and cognitive abilities<sup>1-3</sup>. A major difference between the central nervous system (CNS) and peripheral nervous system (PNS) is their regenerative capability. Peripheral nerve axons possess the ability to regenerate spontaneously in their natural environment, while CNS axons do not<sup>1-2</sup>. The difference results from different responses of the two systems to injury. Primary and secondary injuries are unique to the CNS<sup>1-2</sup>. Among other components, overactive astrocytes induce a physicochemical barrier to natural regeneration, a so-called glial scar<sup>1-2</sup>. Hindering glial scar formation after injury may be an attractive option for effective axon regrowth<sup>1</sup>. A unique population of cells, i.e. olfactory ensheathing cells (OECs) exhibit the capacity to migrate into the glial scar and promote axons regrowth, and remyelination<sup>4-5</sup>. Biomolecule/cell delivery systems have been extensively studied, and designed to stimulate endogenous repair mechanisms<sup>2-3</sup>. Biopolymers including collagen, hyaluronic acid or chitosan have been successfully used in the CNS repair, and have been found to promote axon regeneration as well as target inhibitory factors<sup>3</sup>. Hydrogels with mechanical properties comparable to these of the CNS (~2kPa) tissue can be used in place of soft nervous tissue<sup>1</sup>.

### EXPERIMENTAL METHODS

The aim of our research was to prepare and characterize alginate hydrogels in the context of neural tissue regeneration. We manipulated the conditions for external diffusion-based gelation of sodium alginate. To initiate gelation, sodium alginate sols were mixed with solutions of various concentrations of calcium chloride or calcium gluconate. Gelation rate was evaluated using rheometry methods. Microstructure of hydrogels after drying was observed using scanning electron microscopy (SEM). Viscoelastic behaviour of the ionically cross-linked alginate was verified using oscillatory shear test. Flow and viscosity curves were obtained. Rheological tests were performed at room temperature. *In vitro* tests were conducted using rat olfactory ensheathing cells isolated from the olfactory bulb. The morphology, viability and proliferation of the cells were evaluated.

### RESULTS AND DISCUSSION

Sodium alginate which is readily soluble in water can be transformed into gel by partial exchange of Na<sup>+</sup> ions for Ca<sup>2+</sup> ions. This process occurs with simultaneous crosslinking of the alginate chains, and thus rheomechanical properties of the hydrogel depend on the molar ratio of Na<sup>+</sup>/Ca<sup>2+</sup> ions. The gelation rate increases with the concentration of a parent solution of sodium alginate as well as with the concentration of Ca<sup>2+</sup> ions introduced into the parent solution. The macroscopic features of alginate hydrogels were from liquid for alginate containing small amount of Ca<sup>2+</sup> ions to dense and compact for calcium alginate gels. The SEM images showed porous structure of freeze dried gels. All aqueous sodium alginate sols exhibited shear thinning. Their viscosity increased with alginate concentration. Viscosity, complex modulus and loss angle were dependent on the concentration of parent sodium alginate sols, and the molar ratio of Na<sup>+</sup>/Ca<sup>2+</sup> ions. Varying sodium/calcium alginate compositions had significant differences in viscoelastic properties, some of them being comparable with biomechanical properties of CNS tissue. *In vitro* tests indicated that hydrogels are nontoxic, and support OECs proliferation. Injectable form of gels might be further investigated as materials for drug delivery to the CNS tissue or complementary materials to PNS tubes graft.

### CONCLUSION

The obtained results indicate that ionically cross-linked hydrogels offer a suitable viscoelastic properties and cytocompatibility, making them applicable as scaffolds for sensitive neural/glia cells cultivation and possible CNS repair. To obtain better mechanical strength, additional chemical covalent crosslinking is needed.

### REFERENCES

1. Khaing Z. Z. *et al.*, Mater. Today 17:332-340 (2014)
2. Khaing Z. Z. *et al.*, Neurosci Lett 519:103-114 (2012)
3. Elliot Donaghue J. *et al.*, J. Control. Release 190: 219-227 (2014)
4. Tabakow P. *et al.*, Cell Transplant 22:1591-1612, 2013
5. Tabakow P. *et al.*, Cell Transplant 23(12):1631-1655 (2014)

### ACKNOWLEDGMENTS

This research was financially supported by National Science Center, Poland (grant No: NN 403 176540)



## Poly Glycerol Sebacate for Use as a Neuronal Biomaterial

Dharaminder Singh, John W. Haycock, Frederik Claeyssens

Department of Materials Science & Engineering, University of Sheffield, United Kingdom

[DSingh1@Sheffield.ac.uk](mailto:DSingh1@Sheffield.ac.uk)

### INTRODUCTION

There are three main clinical approaches to aid peripheral nerve regeneration. The first is to suture the proximal and distal stumps together, but providing effective regeneration is only effective over short distances. The second approach is to use an autograft to bridge the gap, whereby an autologous nerve is harvested from elsewhere in the body, however this may result in donor site morbidity and requires additional surgery. A third approach is to use a nerve guide conduit (NGC), which can be made from natural or synthetic materials, however these are currently limited to only short gap injuries. Poly glycerol sebacate (PGS) is a polyester with interesting properties such as biodegradability and an appropriate range of moduli for biomaterials and peripheral nerve tissue engineering<sup>1</sup>. Methacrylate moieties can be attached to the PGS to create a polymer that can be cured under UV light in the presence of a photoinitiator. The methacrylated polymer (PGSm) has yet to be explored as a biomaterial. It has the beneficial material properties of the widely used PGS, whilst avoiding some of the limitations such as time taken due to thermal curing and stability of reagents in the similarly acrylated versions of the polymer<sup>2</sup>.

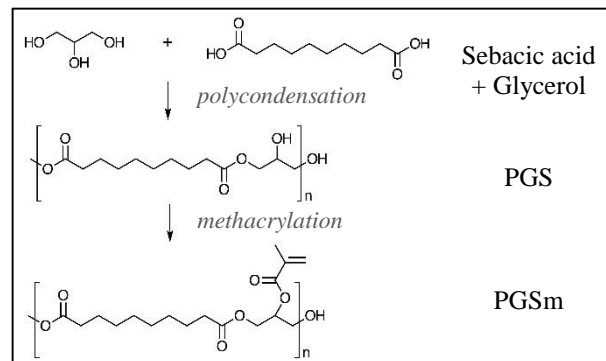


**Figure 1** - the structural formula of PGSm and the synthesis process.

### EXPERIMENTAL METHODS

PGS was synthesised by a polycondensation reaction of glycerol and sebacic acid. Methacrylate moieties were added to the PGS to create, with the addition of a photoinitiator, a photocurable material (see Fig.1). The material was characterized by GPC, FTIR, NMR, DSC, rheology, nanoindentation, mechanical analysis and goniometry. The Young's modulus of the material was varied by controlling the level of methacrylation. PGSm of varying Young's moduli were assessed by initial in vitro studies using NG108-15 neuronal cells, cultured on flat disks of PGSm, with MTT viability, live/dead analysis and immunolabelling for  $\beta$ III-tubulin / counterlabelling nuclei (DAPI), plus confocal microscopy.

### RESULTS AND DISCUSSION

Viability and live/dead assay results showed that NG108-15 neuronal cells were able to grow on PGSm without any observed toxicity. Immunolabelling for  $\beta$ III-tubulin revealed PGSm to be a good substrate for neuronal cell adhesion, spreading and neurite formation. The varied substrate modulus was shown to affect the cell survival and morphology. Young's modulus results of the material were similar to that of the native tissue. Nanoindenting results show the materials substrate modulus can be well adapted.

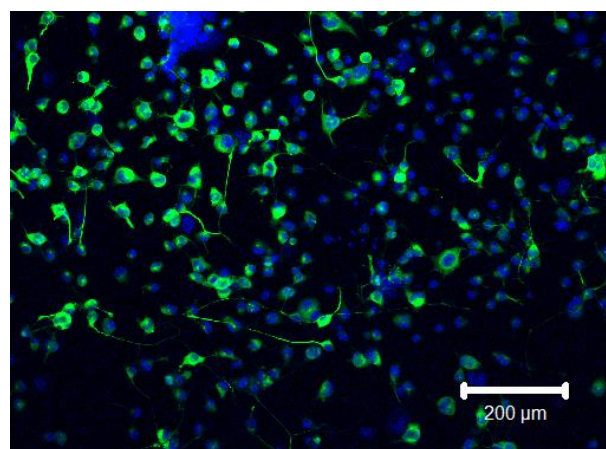


**Figure 2** - confocal image of NG108 neuronal cells differentiating on flat PGSm disks. DNA is labelled using DAPI (blue) and neuronal specific microtubules are labelled with  $\beta$ III-tubulin (green).

### CONCLUSION

PGSm is a biomaterial with potentially beneficial properties for neural regeneration, particularly as the Young's modulus can be varied from near GPa modulus to low MPa modulus levels. Initial studies have shown that it is a good substrate for supporting neuronal cell growth and differentiation in vitro. PGSm may therefore be useful as an NGC as it can be structured by UV photostereolithography techniques. PGSm has also been adapted to create 3D porous nerve guidance conduits, as it is postulated that by using a material which better replicates native nerves, it may be possible to increase the efficacy of NGCs.

### REFERENCES

1. Sundback C et al, *Biomater* 26.27: 5454-5464, 2005
2. Nijst C et al, *J. Biomacromolecules* 8.10: 3067-3073, 2007

### ACKNOWLEDGMENTS

The authors would like to thank the University of Sheffield and EPSRC for funding this project.

**INTRODUCTION**

Despite over 150 years of experience in modern surgical management of the peripheral nerve, repair of a nerve gap remains a problem and several methods have been applied by the microsurgeons in order to repair the nerve gaps, including tissue engineering technology<sup>1</sup>.

Several types of synthetic bioresorbable materials have been examined for use in the fabrication of scaffold (conduit) in neural tissue engineering<sup>2</sup> but there is still room for developing new biomaterials with suitable characteristics as well as techniques of scaffolds fabrication.

Important parameters such as surface properties, porosity, bioresorption rate and the interaction and/or communication with the external environment of the conduits have yet to be optimized. Chitosan is a biopolymer with a variety of attractive properties that present great potential for use in this area<sup>3</sup>.

Here we describe the results of an study that were undertaken to evaluate the feasibility of chitosan conduits for use as scaffolds for promoting peripheral nerve regeneration.

**EXPERIMENTAL METHODS**

A 2,5% (w/v) solution of chitosan (deacetylation degree 80%, purchased from Polymar®, Aracaju, SE, Brazil) in acetic acid 3% (w/v) was prepared by magnetic stirring. After solubilization and homogenization the chitosan solution was poured into a petri dish and submitted to solvent evaporation during 24 h at room temperature in a fume hood. The formed film was immersed in NaOH solution 1M for neutralization and subsequently rinsed in deionized water.

The water uptake of the chitosan film was calculated by the equation: water uptake (%) =  $100 \times (m_s - m_0) / m_s$ , where  $m_s$  was the mass of water swelled sample and  $m_0$  was the mass of dried sample.

The film was equilibrated in water overnight, quick frozen by immersion in liquid N<sub>2</sub> and subsequently freeze-dried using a Thermo scientific - LLI500 for at least 3 days. The dried film was cut to the desired dimensions and wrapped around a stainless steel mandrel ( $\phi=1,2$  mm or  $\neq$ ) to complete 1.5 revolutions. Chitosan solution was used to glue the end of the film. The schematic procedure is showed in figure 1.

After bonding the conduit was removed from the mold, washed, dried and stored in refrigerator, immersed in deionized water. The dimensions of the conduit were

measured with micrometer and caliper; morphological aspects of the chitosan film were photographed and observed in a scanning electron microscopy (JEOL, JSM-601 LA).



Figure 1 – Scheme of chitosan scaffold fabrication.

**RESULTS AND DISCUSSION**

The thickness of the chitosan film obtained changed from  $(92 \pm 1)$   $\mu\text{m}$  in dry state to  $(106 \pm 1)$   $\mu\text{m}$  after water swelling. The maximum water uptake of the chitosan film was  $(70 \pm 2)$  %.

Figures 2 shows the morphological aspects of the external and internal chitosan film surfaces and figure 3 shows the conduits obtained by the manufacturing technique employed in this work.

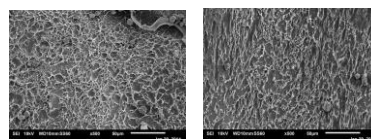


Figure 2 - SEM images of the (a) external and (b) internal surfaces of chitosan film.



Figure 3 – Chitosan conduits.

Tubes with different dimensions (diameter and length) could be easily obtained and the next step of the study involve the biological performance tests.

**CONCLUSION**

The obtained results clearly indicates that the technique used allow the fabrication of a conduit suitable to be used as a chitosan scaffold for effective peripheral nerve regeneration allowing to easily variation of the internal diameter, wall thickness and length of the conduit.

**REFERENCES**

1. Constans A. The Scientist, 21, 40-42, 2004.
2. Huang YC and Huang YY. Artificial Organs, 30-7:514-522, 2006.
3. Kim IY et al. Biotechnology Advances, 26: 1-21, 2008.

**ACKNOWLEDGMENTS**

The authors thank the PIBIC-CNPq for providing financial support to this project.



## Surface Properties of Sterilized Polyurethane/Poly lactide Films

Paulina Bednarz<sup>1</sup>, Mateusz Marzec<sup>2</sup>, Jadwiga Laska<sup>3</sup>

<sup>1</sup> State Higher Vocational School in Tarnów, Mickiewicza 8, Tarnów, Poland

<sup>2</sup> AGH University of Science and Technology, Academic Centre for Materials and Nanotechnology, Mickiewicza 30, Kraków, Poland

<sup>3</sup> AGH University of Science and Technology, Faculty of Materials Science and Ceramics, Mickiewicza 30, Kraków, Poland  
[jlaska@agh.edu.pl](mailto:jlaska@agh.edu.pl)

### INTRODUCTION

The aim of this work was to compare the influence of UV/EtOH, ethylene oxide and cold plasma sterilization on the surface properties of polyurethane/poly lactide (PU/PLA) blends, which were intended to support peripheral nerve regeneration.

### EXPERIMENTAL METHODS

Blends of polyurethane and polylactide with a weight ratio of 80/20 were fabricated. Polyurethane (PU) synthesized from hexamethylene diisocyanate and polycaprolactone, with isosorbital as a chain extender was purchased from GOY Bayer (Germany). Polylactide (PLA) consisting of 80% poly-L-lactide and 20% poly-DL-lactide was purchased from Purac (Netherlands). Water contact angle of the obtained PU/PLA films was measured using sessile drop method with Drop Shape Analysis System (DSA Mk2, Krüss, Germany). Surface roughness of the film was determined using a profilometer (Hommelwerke, Germany). Morphology of elaborated materials was evaluated using scanning electron microscopy (Nova Nano SEM 200, FEJ EUROPE Company, USA). X-ray photoelectron spectroscopic (XPS) studies were performed on PHI Versa Probe II Scanning XPS Microprobe. The materials were sterilized by low temperature hydrogen peroxide plasma (Sterrad 100S Johnson & Johnson), ethylene oxide (sterilizer Getinge), and by immersion in ethanol combined with ultraviolet radiation in a laminar chamber (Alpine).

### RESULTS AND DISCUSSION

Table 1 presents are surface atomic compositions of PU/PLA films before and after sterilization, obtained from XPS studies.

Method of sterilization	Atomic concentration [%]		
	C	O	N
before	62,5	31,2	1,8
after H <sub>2</sub> O <sub>2</sub>	67,6	29,9	1,8
after EtO	65,6	32,3	1,6
after EtOH/UV	67,4	29,1	2,1

Table 1

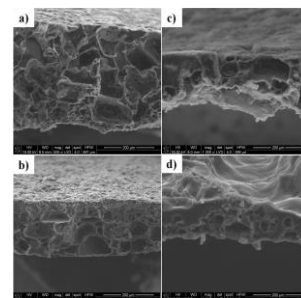
It can be seen that sterilization caused slight enrichment of the surface in carbon, while amounts of oxygen and nitrogen depended on the sterilization method. Significant changes, however, occurred in relative amounts of C-C, C-O, C=O and O-C=O groups on the surface. All sterilization methods caused oxidation of the surface resulting in the increase of C=O groups concentration. Sputtering the surface with Ar<sub>2500+</sub> proved that only the surface undergoes oxidation, and

the deeper atomic layers were not affected. Table 2 shows the results of wettability and roughness measurements of the 80/20 PU/PLA film before and after sterilization.

Method of sterilization	$\Theta$ [°]		Ra[ $\mu$ m]	
	Top	Bottom	Top	Bottom
before	83 $\pm$ 7	75 $\pm$ 5	7,3 $\pm$ 1,3	9,2 $\pm$ 0,2
after H <sub>2</sub> O <sub>2</sub>	79 $\pm$ 8	77 $\pm$ 10	6,7 $\pm$ 0,5	9,8 $\pm$ 0,7
after EtO	98 $\pm$ 6	82 $\pm$ 7	8,2 $\pm$ 0,7	12,2 $\pm$ 2,9
after EtOH/UV	78 $\pm$ 5	57 $\pm$ 6	7,2 $\pm$ 0,6	7,3 $\pm$ 0,5

Table 2

Only in case of sterilization with cold hydrogen peroxide plasma, the value of the contact angle of the top and bottom surfaces remained almost unchanged. In contrast, ethylene oxide sterilization caused that both surfaces became more hydrophobic i.e. the contact angle increased about 15% for the top surface and 8% for the bottom surface. Sterilization with ethanol and UV radiation changed the nature of the surface to more hydrophilic. Average roughness of the top surface is substantially lower than the bottom surface of the untreated blend as well as all the samples following sterilization. None of the used sterilization methods caused significant changes in the roughness of the top surfaces. All applied sterilization methods practically did not change the surface morphology except EtOH combined with UV



radiation which smoothed the surface. Figure 1 shows SEM images of cross-sections of PU/PLA films before sterilization (a), after H<sub>2</sub>O<sub>2</sub> (b), after EtO (c), and after EtOH/UV (d).

### CONCLUSION

The low temperature hydrogen peroxide plasma did not significantly change the surface of the tested blend. The sterilization with ethylene oxide caused an increase in hydrophobicity and surface roughness. A change in surface properties is most noticeable after treatment with EtOH combined with ultraviolet radiation.

### ACKNOWLEDGEMENT

This work was financially supported by National Science Center, Poland, grant # 2011/01/B/STB8/07795

## Development of Microstructured Collagen-Based Nerve Guides for Peripheral Nerve Regeneration

Hans Leemhuis<sup>1</sup>, Leon Olde Damink<sup>1</sup>, Lizette Eummelen<sup>1</sup>, Frank Schügner<sup>1</sup>, Sabien van Neerven<sup>2</sup>, Norbert Pallua<sup>2</sup>, Ahmet Bozkurt<sup>2</sup>

<sup>1</sup>Matricel GmbH, Herzogenrath, Germany

<sup>2</sup>Department of Plastic Surgery, Hand and Burn Surgery, RWTH Aachen University Hospital Aachen, Germany  
[Hans.Leemhuis@matricel.de](mailto:Hans.Leemhuis@matricel.de)

### INTRODUCTION

A variety of bioengineered nerve guides bridging the peripheral nerve defect were used experimentally and to some extent also clinically, but the clinical outcome for the treatment of larger defects is still limited. In this study we present the development of a novel two component microstructured collagen-based nerve guide from design to its first human use in a clinical study.

### EXPERIMENTAL METHODS

The novel nerve guide consists of two structural elements: An inner guiding structure for axonal regeneration “Perimaix” and a hollow outer structure replacing the epineural tube “Epimaix”, that can be sutured to the nerve ends. Both structural elements are manufactured from highly purified porcine collagen. The highly orientated Perimaix structure containing continuous, longitudinally orientated and interconnected pores is generated by a unidirectional solidification method [1]. Subsequently, the scaffolds are freeze-dried, chemically cross-linked and sterilized. The term “Neuromaix” is used to characterize the combination of Perimaix and Epimaix to bridge a peripheral nerve defect. In pre-clinical animal studies, Perimaix scaffolds without any cells and Perimaix scaffolds seeded with Schwann cells were compared against autologous nerve transplantation by bridging experimentally created supercritical defects of the sciatic nerve (2 cm) in rats.

### RESULTS AND DISCUSSION

The observed functional regeneration in this animal model initiated the design process of the Neuromaix nerve guide for human use. All essential requirements for a first clinical study were achieved and the clinical study with Neuromaix was approved and started. In this study, the medial sural nerve of patients undergoing a diagnostic nerve biopsy ( $\geq 2$  cm) is bridged by implantation of the microstructured nerve guide Neuromaix.

### CONCLUSION

Neuromaix demonstrated an improved tissue regeneration, due to the scaffold architecture which directs the cell migration and extra cellular matrix formation along the regeneration axis. So far, only a very limited number of bioengineered nerve guides have been studied successfully in humans and the step from preclinical work to a clinical application is very challenging. The Neuromaix clinical study will demonstrate the regenerative potential of this novel nerve guide.

### REFERENCES

[1] Bozkurt et al., Biomaterials 2009;30:169-1679

### ACKNOWLEDGMENTS

This study was supported by BMBF grants #0312758, #0313640, and #0315140.



## INTRODUCTION

Shape memory polymers and their composites are capable of adopting temporary shapes and recovering to the permanent shape upon an external stimulus. In recent years, SMPs have received increasing interest due to some unique advantages over other shape memory materials because of lightweight, low cost, low density, good manufacturability, high shape deformability and good biodegradability [1-2].

Biodegradable polymer composites are an emerging family within the field of smart materials and hold exciting potential as responsive biomaterials [3]. We investigated shape-memory poly(glycerol sebacate urethane) (PGSU) / cellulose nanocrystal (CNC) composites to assess their suitability as tendon specific biomaterials.

## EXPERIMENTAL METHODS

PGS pre-polymer was synthesized through the polycondensation process of equimolar amounts of glycerol and sebacic acid and crosslinking step. After polymer processing, desired amounts of the DMF solution of PGSU pre-polymer (pre-PGSU) and the CNC dioxane suspension were weighed and mixed under sonication for 30 minutes. The mixture was then cast onto a glass petri-dish to evaporate the solvent and to further crosslink the pre-PGSU into PGSU.

## RESULTS AND DISCUSSION

The presence of CNCs improved the tensile strength of PGSU, for the PGSU-CNC nanocomposite due to the strong interfacial interactions between CNCs and PGSU determined by FTIR. In addition, formation of a strong percolation network of CNCs in the matrix leads to enhancement of elastic modulus.

The incorporation of CNCs into PGSU induced the PGSU-CNC nanocomposites with shape-memory effects. The shape recovery became stable after the first three wetting-stretching drying cycles, owing to the elimination of the sample processing history and alignment of CNCs.

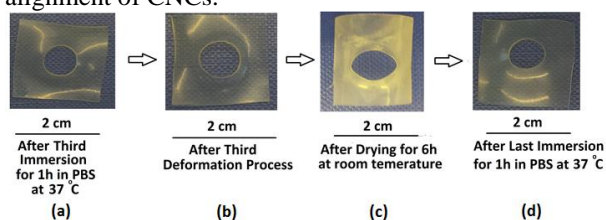


Figure 1. Water-active shape-memory effect of pre-treated composite

*In vitro* degradation results showed the PGSU nanocomposite showed the weight loss in an enzymatic PBS condition, which is lower than that for neat PGSU.

## CONCLUSION

Mechanical properties and water-responsive shape-memory performance of PGSU-CNC nanocomposites were investigated, which are dependent on the content of CNCs.

This work provides an approach to the preparation of enzymatically degradable polymer nanocomposites with water-active shape-memory that have potential for tendon regeneration.

## REFERENCES

References must be numbered. Keep the same style.

1. Chen J. *et al.*, *Materials* 7: 805-875, 2014.
2. Meng H. *et al.* *Polymer* 54: 2199-2221, 2013.
3. Xie T. *Polymer* 52: 4985-5000, 2011.

## ACKNOWLEDGMENTS

Science Foundation Ireland SIRG COFUND11/SIRG/B2135.

## Electrochemical Study of Uncemented Hip Endoprosthesis Cups

Wojciech Kajzer<sup>1</sup>, Anita Kajzer<sup>1</sup>, Ola Grzeszczuk<sup>1</sup>, Jacek Semenowicz<sup>2</sup>, Adam Mroczka<sup>2</sup>

<sup>1</sup> Department of Biomaterials and Medical Devices Engineering, Faculty of Biomedical Engineering, Silesian University of Technology, Poland

<sup>2</sup> Dr Janusz Daab Independent Public Regional Hospital of Trauma Surgery in Piekary Slaskie, Poland  
[Wojciech.Kajzer@polsl.pl](mailto:Wojciech.Kajzer@polsl.pl)

### INTRODUCTION

Due to the fact that hip endoprosthesis is a long-term implant it is important to have appropriate mechanical and tribological features, above all, to have appropriate biocompatibility which is directly connected with corrosion resistance of the implant<sup>1</sup>. Therefore, for the metal biomaterials and for implants produced from those materials, electrochemical tests are conducted in order to evaluate the influence of tissue environment and body fluids on the pitting corrosion resistance<sup>2,3,4</sup>. As is well known, products of corrosion can have a negative influence on human body and can result in metal toxicity.

### EXPERIMENTAL METHODS

In the research uncemented hip endoprosthesis cup, covered with hydroxyapatite were used: No. 1 - new and No. 2 - cup after 68 months of implantation produced from high nitrogen stainless steel Cr-Ni-Mo which chemical composition and mechanical features are compatible with recommended ISO 5832-9 standards. The research was carried out on internal (Int.) and external (Ext.) surfaces. The test of pitting corrosion resistance was carried out with the use of the VoltaLab® PGP 201 system. As a result of the tests on the basis of designated polarization curves, mean values and standard deviation (SD) of corrosion potential  $E_{corr}$ , breakdown potential  $E_b$ , repassivation potential  $E_{rp}$  and polarization resistance  $R_p$  were determined. In order to obtain additional information on physiochemical properties electrochemical impedance spectroscopy - EIS was conducted. Measurements were taken using AutoLab's PGSTAT 302N measurement system. On this basis numerical values of resistance  $R$  and capacity  $C$  of the analysed systems were determined. Impedance spectra of the tested system were presented in the form of Nyquist and Bode's diagrams. The obtained EIS spectra were interpreted after they had been adjusted according to the method of the smallest squares to the substitute electric system with error estimation 2%-6%. All electrochemical tests were carried out in Ringer's solution having a temperature  $T=37\pm1$  °C, pH = 6,9 $\pm$ 0,2.

### RESULTS AND DISCUSSION

The sample results of the corrosion test were presented in the table 1. The increase of the values of corrosion potential and polarization resistance for the cup after implantation was stated, which is a beneficial phenomenon. The EIS results prove the outcome of the potentiodynamic tests and demonstrate the presence of double oxide film of capacitive nature on the surface of the cups – fig. 1 and 2, protecting the implant from corrosion

Surface		E <sub>corr</sub> , mV	SD, mV	E <sub>b</sub> , mV	SD, mV	R <sub>p</sub> , kΩcm <sup>2</sup>	SD, kΩcm <sup>2</sup>
1	Int.	-120	±4	1230	±12	61	±10
	Ext.	-139	±53	1242	±18	23	±13
2	Int.	-24	±31	1172	±204	279	±30
	Ext.	-47	±29	1081	±108	75	±33

Table 1 Sample results of pitting corrosion resistance test

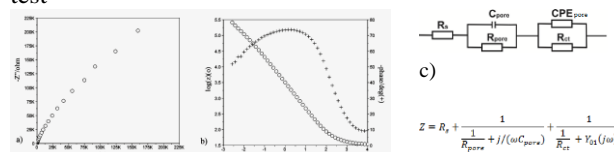


Fig. 1. Sample impedance spectra for cup No.2 int.: a) Nyquist graph, b) Bode's diagram, c) electric substitute schemes

The steel with increased content of nitrogen compatible with recommended ISO 5832-9 standards, from which the tested cups were made, has a better corrosion resistance than steel Cr-Ni-Mo compatible with ISO 5832-1 standards because characteristic for this type of steel hysteresis loop was lower on the polarization curves<sup>2,4</sup>.

### CONCLUSION

On the basis of conducted research, it can be stated that both, polished internal surface and external surface covered with hydroxyapatite, are efficient barrier protecting the implant from the influence of the body fluids and its usage does not lead to decrease of biocompatibility described by corrosion resistance and EIS in comparison with the initial state. What is more, it was observed that, despite the necessity to remove the cup caused by their loosening, no significant differences were recorded in the analysis of parameters proving their corrosion resistance and consequently, their biocompatibility.

### REFERENCES

1. Gierzyńska-Dolna M., Engineering of Biomaterials. 1:8-11, 1997
2. Kajzer A. *et al.*, Solid State Phenomena. 227:523-526, 2015
3. Walke W. *et al.*, Metalurgija. 52:371-374, 2013
4. Kajzer W. *et al.*, Przegląd Elektrotechniczny. 89: 275-27

### ACKNOWLEDGMENTS

The authors would like to thank the prof. Jan Marciniak for the opportunity to carry out research in Department of Biomaterials and Medical Devices Engineering.





## INTRODUCTION

Many biological processes depend on specific interactions between glycoproteins and lectins, including cell-cell communication, binding of toxins and pathogenic infection. Synthetic glycopolypeptides are a useful tool to investigate those processes, since they can mimic properties of glycoproteins (e.g. form secondary structures) and are relatively easy of access compared to natural glycoproteins. Glycopolypeptides can be prepared by the polymerization of glycosylated monomers or by post-polymerization glycosylation in organic solvents.<sup>1,2</sup> These methods are often restricted to monosaccharides but in most biological interactions more complex sugars are involved. A recent publication demonstrates a way with mild reaction conditions using aqueous amide coupling.<sup>3</sup> Using this approach disaccharides (e.g. maltobiose, cellobiose) were coupled to a poly-( $\alpha$ ,L-glutamic acid) scaffold and compared with the corresponding monosaccharides.

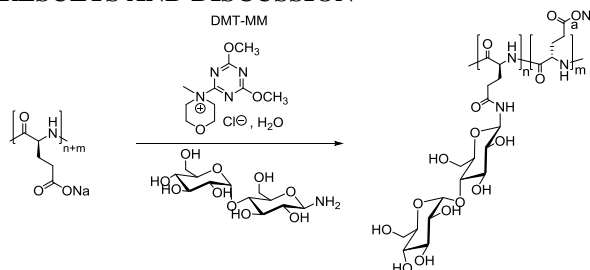
## EXPERIMENTAL METHODS

Poly( $\alpha$ ,L-glutamic acid)-precursors (PGA) were obtained by acidic hydrolysis of poly-( $\gamma$ -benzyl-L-glutamate). 1-Deoxy-1-amino saccharides were synthesized by KOCHETKOV-amination and coupled to the PGA scaffold via aqueous amide coupling with 4-(4,6-dimethoxy-1,3,5-triazin-2-yl)-4-methylmorpholinium chloride (DMT-MM).<sup>3</sup>

Secondary structures were determined via CD spectroscopy at ambient temperature.

Biological activity was tested via isothermal titration calorimetry measurements (ITC) as well as via quantitative precipitation assays with concanavalin A. The amount of precipitated ConA per glycopolypeptide was determined via UV-Vis spectroscopy.

## RESULTS AND DISCUSSION



**Scheme:** Amide-coupling of maltosylamine to PGA-Na

The sugar density on the PGA scaffold is adjustable via the amount of DMT-MM used. For maltobiose (MB) and glucose (Glu) DS up to 80 %, and for cellobiose (CB) DS up to 74 % are possible.

CD-spectroscopy revealed that the PGA scaffold shows a pH-dependent helix-coil transition close to pH 5 with a maximum helicity of 80 % at pH 3.

The glycosylated PGAs also show helix-coil transitions up to a sugar density of 64 % (MB). However, the transition point shifts with increasing amount of sugar to more acidic pH values along with a decrease in helicity. For high sugar densities no helix-coil transition could be observed. PGA-CB and PGA-Glu have a slightly higher helicity compared to PGA-MB for all tested sugar densities.

Quantitative precipitation assays were performed with PGA-MB and ConA (Figure). Both glycopolypeptides interact with the lectin and precipitate ConA.

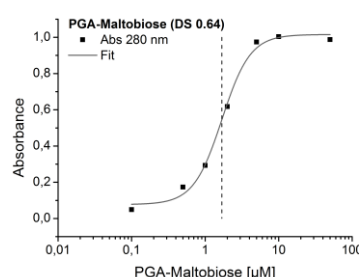


**Figure:** Quantitative Precipitation assay of PGA-MB DS 0.64

The number of ConA molecules precipitated per polymer is 3 (DS = 64 %) and 3.4 (DS = 80 %), respectively. An increase in sugar density leads to a small increase in the amount of precipitated lectin per polymer chain. PGA-MB (80 % DS) was used for ITC-measurements obtaining an equilibrium binding constant of 36 nM. This indicates affinity enhancement due to glycoside clustering.

## CONCLUSION

Well-defined, pH-responsive glycopolypeptides were prepared by post-polymerization glycosylation of poly( $\alpha$ ,L-glutamic acid) with 1-deoxy-1-amino sugars using the amide coupling agent DMT-MM in aqueous media. The glycopolypeptides showed pH-dependent helix-coil transition up to sugar densities of 64 % (CB), 62 % (Glu) and 55 % (MB), respectively. Precipitation of the lectin ConA as well as ITC measurements demonstrates biological activity.

## REFERENCES

1. Kramer J.R. *et al.*, J. Am. Chem. Soc., 132:15068–15071, 2010
2. Sun J. *et al.*, Macromolecules, 43:4445–4448, 2010
3. Mildner R. *et al.*, J. Polym. Sci. Pol. Chem., 51:3925–3931, 2013

## ACKNOWLEDGMENTS

This work was supported by the IUPAC Transnational Call in Polymer Chemistry and the German Research Foundation (DFG) (Grant: Me1057/17-1)

# Biological Properties of Oxynitrided Layers on NiTi Shape Memory Alloy Produced Under Glow Discharge Conditions

Justyna Witkowska<sup>1</sup>, Agnieszka Sowińska<sup>2</sup>, Elżbieta Czarnowska<sup>2</sup>, Tomasz Borowski<sup>1</sup>, Tadeusz Wierzchoń<sup>1</sup>

<sup>1</sup>Faculty of Materials Science and Engineering, Warsaw University of Technology, Poland

<sup>2</sup>Pathology Department, Children's Memorial Health Institute, Warsaw, Poland

[justyna.aleksandra.witkowska@gmail.com](mailto:justyna.aleksandra.witkowska@gmail.com)

## INTRODUCTION

Shape memory alloys NiTi type are becoming increasingly used in medicine due to their unique properties, such as shape memory and superelasticity. However, their high nickel content and corrosion in given circumstances [1] raises the need for surface modification in order to reduce the phenomenon of metallosis and enhance biocompatibility dedicated to particular applications. Significantly, various methods of surface engineering, which could improve a resistance for degradation and increase biocompatibility, carried out in temperature over 300°C destroy the alloy specific features [2]. Thus, low-temperature plasma oxynitriding process, similarly as nitriding [3] should offers unique possibilities to keep NiTi alloy complex properties. Preliminary studies indicated that it significantly improves the corrosion resistance of NiTi alloy [4]. Therefore, the aim of this work is to investigate the biological properties of the oxynitrided layers produced on the NiTi shape memory alloy in terms of use for bone implants.

## EXPERIMENTAL METHODS

NiTi shape memory alloy (50.8% Ni) was investigated. The glow discharge oxynitriding process was conducted at a temperature of 290°C in two stages: 30 min. of the nitriding and 15 min. of the oxidizing. Time of oxidizing was set on basis of the results of corrosion resistance investigations in Ringer solution [4]. The surface topography before and after the process was determined by SEM and AFM microscopic observation and optical profilometer use. Biocompatibility was assessed in terms of the adhesion and proliferation of osteoblast from cell line Normal Human Osteoblasts cultured on the surface of the tested samples for 2 hours (adhesion), and 24, 48 hours and 6 days (proliferation) at 37°C and tested under SEM.

## RESULTS AND DISCUSSION

The produced TiO<sub>2</sub> + TiN surface layer on NiTi alloy have increased surface roughness in comparison to NiTi alloy in initial state (Fig. 1). This was followed by a significant increase in the number of adhered osteoblasts on samples with a oxynitrided layer after 2 hours of incubation, as well as by increased cell proliferation in subsequent stages of culture (Figure 2). Osteoblasts on oxinitrided surface layers were multiform with numerous filopodia, that allowed them come into contact with each other.

The positive osteoblasts response to oxinitrided surface layer should also be considered in relation to the increased NiTi alloy corrosion resistance, which has an impact on the reduction of the metallosis effects which is

the migration of toxic nickel ions into the biological environment [4].

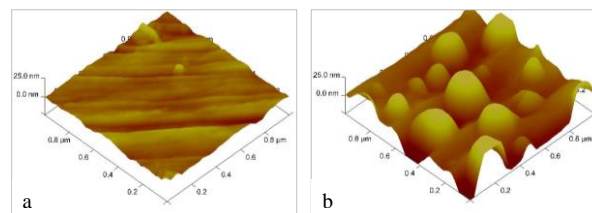


Fig.1. AFM image of the surface of NiTi alloy before (a) and after (b) oxynitriding process; area 1x1 μm.

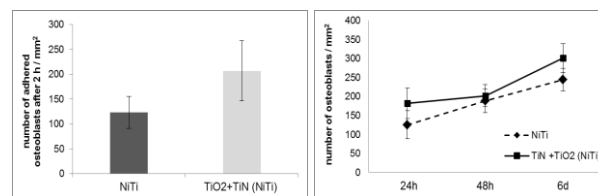


Fig. 2. Adhesion (a) and proliferation of osteoblasts (b) on NiTi alloy in the initial state and with a layer of TiO<sub>2</sub> + TiN

Our findings are consistent with known effect of the surface topography on absorption of the proteins determining both platelets adhesion and proliferation of osteoblasts [5].

## CONCLUSION

Oxynitriding under glow discharge process conducted in the temperature of 290°C enhances the biocompatibility of NiTi alloy by improving the corrosion resistance and increasing surface roughness. Therefore, this method provides the possibility of application of NiTi alloy as material for bone implants.

## REFERENCES

1. Q. Li et al., Australas Phys Eng Sci Med 33 (2010) 129-136
2. J. Lełątko et al., Solid State Phenom. 186 (2012) 259-262.
3. E. Czarnowska et al., Applied Surface Science (2014), doi:10.1016/j.apsusc.2014.07.109
4. J. Kamiński et al., Ochrona przed korozją 56, 11 (2013) 464-468
5. M. Bächle, R.J. Kohal, Clin. Oral Implants Res. 15 (2004) 683-692

## ACKNOWLEDGMENTS

This study was part of research project INNOTECH (no K1/IN1/46/157239/NCBiR/12) supported by The National Centre for Research and Development (NCBiR) and ROBIN (no POIG.02.01.00-14-05)



## Thiolated Chitosan: Biomaterial of Electrospun Nanofiber Mats for Mucoadhesive Drug Delivery

Wipada Samprasit<sup>1</sup>, Ruchadaporn Kaomongkolgit<sup>2</sup>, Prasert Akkamongkolporn<sup>1</sup>, Theerasak Rojanarata<sup>1</sup>, Tanasait Ngawhirunpat<sup>1</sup>, Praneet Opanasopit<sup>1</sup>

<sup>1</sup>Pharmaceutical Development of Green Innovations Group (PDGIG), Faculty of Pharmacy, Silpakorn University, Nakhon Pathom, 73000, Thailand

<sup>2</sup>Department of Oral Diagnosis, Faculty of Dentistry, Naresuan University, Phitsanulok, 65000, Thailand  
[swipada@hotmail.com](mailto:swipada@hotmail.com)

### INTRODUCTION

Thiolated polymers have been interested for drug delivery due to the higher mucoadhesion by the forming disulfide bonds with mucus<sup>1</sup>. The various thiolated polymers were developed and used for drug delivery<sup>2</sup>. However, there is a lack of reports that indicate the application of thiolated chitosan (CS-SH) as a nanomaterial for mucoadhesive drug delivery. Thus, this study focused on the preparation and evaluation of CS-SH nanofiber mats.

### EXPERIMENTAL METHODS

#### Synthesis of CS-SH

The CS-SH was synthesised following the previous study<sup>3</sup>. Briefly, the cysteine were activated by 150 mM EDAC and then added into chitosan (CS, MW 110 kDa, DD 0.85, Sigma-Aldrich Chemical Company, USA) solution. After stirring for 6 h, the CS-SH was isolated by dialysing and lyophilised. The amount of thiol groups on the CS-SH was determined with Ellman's reagent.

#### Preparation of electrospun nanofiber mats

CS (2% w/v) or CS-SH (2-5% w/v) was dissolved with EDTA solution at the weight ratio of CS: EDTA (2:1). The CS or CS-SH solution was mixed with 10% w/v PVA solution at weight ratios of 30:70. The solution's viscosity and conductivity were measured before preparing the nanofiber mats via the electrospinning process.

#### Morphology characterization

The morphology of nanofiber mats were examined using SEM (Camscan Mx2000, England). The diameter of nanofiber mats was determined using image analysis software (JMicroVision V.1.2.7, Switzerland).

#### Mucoadhesive study

The mucoadhesive force of the CS-SH and CS nanofiber mats onto porcine buccal mucosa was carried out by a texture analyser (TA.XT plus, UK). The nanofiber mat was attached to the mucoadhesive probe. The probe with mat was put in contact with the buccal mucosa with 3 g of force for 1 min, and the mat was then withdrawn. The force required to separate the nanofiber mats from the tissue was recorded.

### RESULTS AND DISCUSSION

The CS-SH which contained  $469.75 \pm 2.82$   $\mu\text{mol}$  thiol groups/g of polymer was successfully prepared the nanofiber mats. Fig.1 (b-e) displays the morphology and diameter of CS-SH nanofiber mats. The increased concentration of CS-SH caused the increase diameter and the appearance of beads due to the increase of viscosity and conductivity of solution.

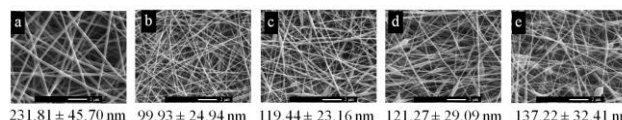


**Figure 1** SEM images and diameter of (a) 2% CS, (b) 2%, (c) 3%, (d) 4% and (e) 5% CS-SH nanofiber mats.

The mucoadhesion force of CS-SH nanofiber mats slightly increased when the concentration of CS-SH of electrospinning solution was increased (Fig.2a). This was due to the higher thiol groups to form disulphide bonds with the cysteine rich of the mucus glycoprotein. However, there were no significant differences between the concentrations of CS-SH on the mucoadhesion force. This indicated that the use of 2% CS-SH should be sufficient to improve mucoadhesion. Also, morphology of 2% CS-SH mats was smooth without the bead formation. Thus, the 2% CS-SH was the optimal concentration for nanofiber mats. Compared to 2% CS nanofiber mat, the mucoadhesive force of CS-SH mats was two times higher than CS mats (Fig. 2b).

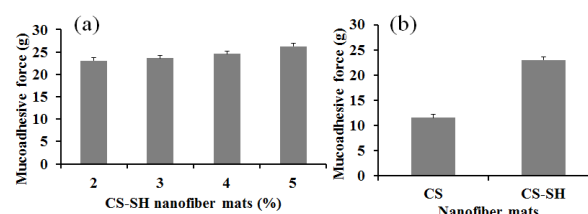


**Figure 2** Mucoadhesive forces of (a) the various concentrations of CS-SH nanofiber mats and (b) 2% CS and CS-SH nanofiber mats.

### CONCLUSION

CS-SH was successfully prepared the nanofiber mats with a smaller diameter and good mucoadhesion. Thus, CS-SH has the potential to be a material of nanofiber mats for mucoadhesive drug delivery.

### REFERENCES

1. Langoth N. *et al.*, Int. J. Pharm. 252:141–148, 2003
2. Kast C. E. *et al.*, Biomaterials. 22:2345–2352, 2001
3. Schmitz T. *et al.*, Int. J. Pharm. 347:79–85, 2008

### ACKNOWLEDGMENTS

The authors wish to thank the Commission of Higher Education (Thailand), the Thailand Research Funds through the Royal Golden Jubilee PhD Program (Grant No.PHD/0001/2553) and the Silpakorn University Research and Development Institute for financial support.



## Zwitterionic Polyampholyte as a Novel Inhibitor of Lysozyme Aggregation

Robin Rajan, Kazuaki Matsumura

School of Materials Science, Japan Advanced Institute of Science and Technology, Japan  
[robinrajan2004@gmail.com](mailto:robinrajan2004@gmail.com)

### INTRODUCTION

Protein instability in the form of protein aggregation is one of the major deterrents in the further growth of biopharmaceutics. It leads to an array of harmful effects including cellular effects like mitochondrial dysfunction, cell death, etc. and also trigger dreadful neurodegenerative diseases such as Alzheimer's Parkinson's, Prion's, Amyotrophic lateral sclerosis (ALS), etc.<sup>1</sup> Over the years, large number of organic compounds and protein engineering techniques has been employed for thermal inhibition of lysozyme aggregation with relatively good success but very high efficiencies have not been achieved yet. Polymers, especially synthetic polymers, have not been employed for such work with high efficiencies. In this report, we have developed a facile synthesis of a polyampholyte for thermal aggregation inhibition of chicken egg white lysozyme, with very high efficiency.

### EXPERIMENTAL METHODS

Poly-sulfobetaine (poly-SPB) was synthesized via reversible addition fragmentation chain transfer (RAFT) polymerization.<sup>2</sup> Polymer kinetics and control of its living nature was studied by using <sup>1</sup>H-NMR and infrared spectroscopy. Protein aggregation was observed visually, and quantitatively it was estimated using Thioflavin T. Aggregation was also observed by circular dichroism spectroscopy. The residual enzymatic activity of lysozyme was examined using gram positive cells, micrococcus lysodeikticus. Conformational states of lysozymes were also evaluated after heating by employing <sup>1</sup>H-NMR.

### RESULTS AND DISCUSSION

Lysozyme when heated in the absence of any additive displayed aggregation with 10-15 minutes whereas in the presence of poly-SPB, no aggregation was observed even after heating for an extended period of time (Fig. 1). Its efficiency was higher than its corresponding monomer also, due to more efficient interaction of polymers with proteins.

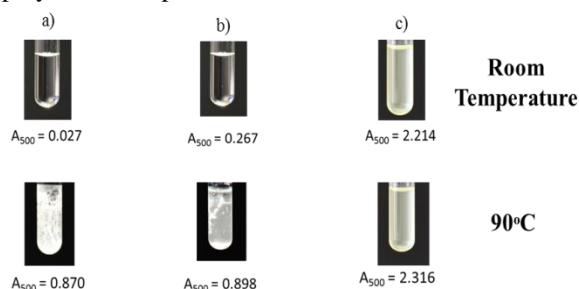


**Figure 1** Photographs of lysozyme in PBS at room temperature (top) and 90°C (bottom); a) without any additive; b) with 10% SPB; c) with poly-SPB. Numbers below indicate the absorbance value at 500nm.

Interaction between the lysozyme and the polymer was found to be electrostatic as revealed by zeta-potential measurements. Transmission electron microscopy images revealed the formation of amyloid fibrils on heating, which was then quantitatively analysed by employing Thioflavin T. The results demonstrated that poly-SPB effectively inhibits the formation of amyloid fibrils and its efficiency was found to be higher than some of the commercially available reagents also. Lysozymes retained very high enzymatic activity when heated in the presence of Poly-SPB. The study of the conformational states of lysozymes revealed that poly-SPB stabilizes the partial higher order structure of lysozyme during heating as all the amino acid residues present in the secondary structure were retained (Fig. 2), which in turn leads to the solubility of lysozyme at such elevated temperature.

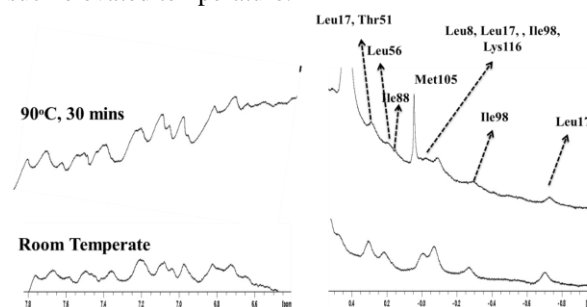


**Figure 2** <sup>1</sup>H NMR spectra of a mixture of lysozyme mixed with poly-SPB at room temperature and after heating.

### CONCLUSION

Zwitterionic polyampholytes can be employed as efficient inhibitors of thermal aggregation of lysozyme. This is the first report where a zwitterionic polyampholyte has been employed for protein aggregation inhibition. Poly-SPB stabilizes lysozymes and preserves its higher order structure. Also, the solubility of lysozyme in the presence of poly-SPB was retained even at higher temperature which led to inhibition of lysozyme aggregation. Amyloid fibril formation was also suppressed.

### REFERENCES

1. Ross C. et al., Nat. Med. 10:S10-S17, 2004.
2. Rajan R. et al., J. Biomater. Sci. Polym. Ed. 24:1767-80, 2013

### ACKNOWLEDGMENTS

"The authors would like to thank the Grant-in-Aid for Young Scientists (B), MEXT, (Grant no: 25870267) for providing financial support to this project."



## pH Dependence of Disruption of Liposomal Membranes by Artificial Lytic Peptide

Ayumi Kashiwada, Masaki Mizuno, Iori Yamane, Jun-ichi Hashimoto

Department of Applied Molecular Chemistry, Graduate School of Industrial Technology, Nihon University, Japan  
[kashiwada.ayumi@nihon-u.ac.jp](mailto:kashiwada.ayumi@nihon-u.ac.jp)

### INTRODUCTION

Lytic peptides have capability to disrupt lipid membranes. For example, melittin has a cationic C-terminal segment and a hydrophobic helical segment, and the cationic segment interacts with membranes and the hydrophobic helical segment disturbs the order of the membrane components to disrupt the membrane structure.<sup>1</sup> This bi-functional lytic activity of melittin has attracted a good deal of attention in constructing novel antibiotics. On the other hand, many scientists have been interested to design melittin-like artificial lytic peptides, because lytic peptides that respond to acidic pH can be utilized in liposomal DDS, since acidification of endosomes triggers membrane lysis to release the drugs from liposomes.

In this study, we report the design, synthesis, and characterization of an artificial lytic peptide (LP) and the novel designed pH-selective lytic peptides. Then, we discuss the results of analyses of the lytic potential of the peptide to induce leakage of liposomal contents.

### EXPERIMENTAL METHODS

**Peptide Synthesis:** The peptides with a C-terminal carboxyamide were all prepared from Fmoc solid-phase synthesis by using Fmoc-NH-SAL resin.

**Preparation of Calcein-Loaded Liposome:** Dried films of EggPC were hydrated in a calcein solution for 1 h. Then, the lipid suspension underwent the freezing-thawing process and the extrusion through a 100-nm pore sized polycarbonate filter. Non-encapsulated calcein was removed through the size exclusion chromatography column charged with a Sephadex G-25.

**Liposome Leakage Assay:** EggPC liposomes (0.2 mM) were loaded with the high concentration (90 mM) of calcein. All samples were excited at 490 nm and the emission at 530 nm was monitored for 25 min. The first 5 min of each measurement was monitored before the addition of peptide to confirm the presence of a stable baseline (0% leakage). Two  $\mu$ M of peptide was added to the sample and the calcein leakage was monitored for 20 min. To calibrate the fluorescence scale, the fluorescence intensity of calcein leaked when Triton X-100 was added to the sample was regarded as 100%.

### RESULTS AND DISCUSSION

The amino acid sequence of a typical membrane-lytic peptide (LP) is shown in Figure 1. LP has 26 amino acid residues composed of a hydrophobic helical segment (membrane interactive Leu-Ala repetitive sequence<sup>2</sup>) and a hydrophilic segment. We also designed acidic pH-selective lytic peptides (Figure 1). Our concept is to design pH-selective peptides with a hydrophobic helical segment of LP. We have replaced leucine residues with glutamic acid. This substitution is expected to cause a structural change from a

hydrophilic random coil at neutral pH to a hydrophobic  $\alpha$ -helix in an acidic pH range. This structural change would have a crucial effect on the lytic activity.



Figure 1 Amino acid sequence of artificial membrane lytic peptides used in this study.

The results of the leakage assay for characterizing pH-dependent membrane-lytic activity of designed peptides are shown in Figure 2. Acidic pH-selective membrane lysis was observed upon addition LPE3-1 to liposomes.

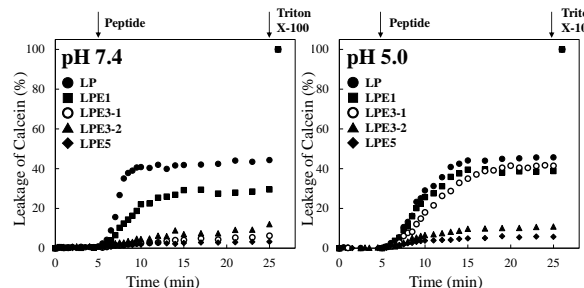


Figure 2 Kinetics of peptide induced calcein leakage.

These results indicate that replacement of three glutamic acids endows the hydrophobic segment with a suitable pH-sensitivity. Moreover, it also seems to be important to place three glutamic acids in the center of the hydrophobic segment. Thus, we consider LPE3-1 an ideal lytic peptide and a promising drug release tool for the liposomal DDS vehicle.

### CONCLUSION

We have succeeded to design and to synthesize weakly acidic pH-selective membrane-lytic peptides. Especially, LPE3-1 with a hydrophobic segment in which three leucine residues are replaced by glutamic acid ones exhibits a weakly acidic pH-controlled membrane-lytic activity. The present approach may pave the way to gain a deeper understanding of peptide-lipid interactions and their role in cell biological and pathological processes, with the potential of yielding new strategies for therapeutic applications.

### REFERENCES

1. Dempsey C. E., Biochim. Biophys. Acta 1031:143-161, 1990
2. Kashiwada A. *et al.*, Langmuir 28:2299-2305, 2012

### ACKNOWLEDGMENTS

This work was supported by JSPS KAKENHI Grant Number 24550196.



## Synthetic Biphasic Scaffold Composed of Polylactic Acid (PLA) and PLA / Bioactive Glass (G5) - Guided Vascularization Induced by Multinucleated Giant Cells

Mike Barbeck<sup>1,2</sup>, Patrick Booms<sup>1</sup>, Tiziano Serra<sup>3</sup>, Robert Sader<sup>1</sup>, Charles James Kirkpatrick<sup>2</sup>, Melba Navarro<sup>3</sup> and Shahram Ghanaati<sup>1,2</sup>

<sup>1</sup> FORM-Lab, Clinic of Oro-Maxillofacial and Plastic Surgery, Goethe University Frankfurt, Frankfurt, Germany

<sup>2</sup> Repair-Lab, Institute of Pathology, University Medical Center of the Johannes Gutenberg University, Mainz, Germany

<sup>3</sup> Department of Material Science and Metallurgy, CREB (Biomedical Engineering Research Center), Technical University of Catalonia, Barcelona, Spain  
[patrick.booms@kgu.de](mailto:patrick.booms@kgu.de)

### INTRODUCTION

The aim of the present study was the analysis of the *in vivo* (inflammatory) tissue response to a biphasic 3D-printed scaffold, combining two layers, i.e., a pure PLA component and a PLA/G5 component, with special focus on implant bed vascularization induced by multinucleated giant cells, with special focus on the bioactive glass component. Scaffolds of PLA and PLA/G5 alone were used as respective control materials. A further aim of this study was the evaluation of this model, which could assist reduction in the number of experimental animals required – in accordance with the principle of the 3Rs (Replacement, Reduction and Refinement).

### EXPERIMENTAL METHODS

For this study an established subcutaneous implantation model was used in 60 female 6-8 week-old CD-1 mice<sup>1-3</sup>. Established histological and histomorphometrical methods were applied<sup>1-3</sup>.

### RESULTS AND DISCUSSION

In addition to the pure PLA control, and the separate PLA/G5 test samples, biphasic scaffolds PLA-PLA/G5 were included. The tissue reaction to the PLA component included low numbers of multinucleated giant cells and minimal vascularization of its implant beds (Fig. 1), which suggest a mild severity of a material-related foreign body response. In contrast, the addition of G5 particles (PLA/G5) induced a tissue reaction with the involvement of higher numbers of multinucleated giant cells and also a markedly higher implant bed vascularization (Fig. 1). Furthermore, these results were substantiated in the biphasic scaffolds, as only the PLA/G5 segment showed the increased multinucleated giant cell infiltration and the correspondingly higher vascularization response.

### CONCLUSION

Bioactive glass (G5) induced an increase in the number of multinucleated giant cells and subsequently higher vascularization of the implant bed. Further studies are required to establish the influence of potential additional components, e.g. therapeutic ions on multinucleated giant cell-induced vascularization. Furthermore, the use of such biphasic scaffold represents a suitable platform to study the influence of G5 particles on the induction of multinucleated giant cells in the implant bed and subsequent vascularization. Moreover, this model could help reduce the number of experimental animals required.

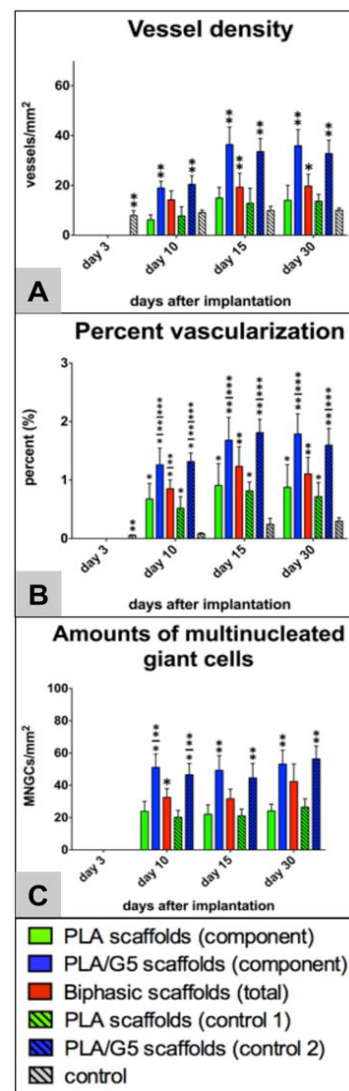


**Fig. 1** Shows the results of the histomorphometrical analyses.

### REFERENCES

- Ghanaati S. et al., M, Biomed Mater 5 (2): 25004 2010.
- Ghanaati S et al., Acta Biomater; 7 (11): 4018-28, 2011.
- Ghanaati S et al., Acta Biomater 10 (8): 3557-62, 2014.

### ACKNOWLEDGMENTS

The authors would like to thank Mrs. Verena Hoffmann and Mrs. Ulrike Hilbig for their technical assistance.



# Biosynthesis of CdS Quantum Dots by Leaf Extract of Water Minth (*Mentha aquatica* L.)

Fatih Duman<sup>1</sup>, Hakan Colak<sup>2</sup>, Fatih Dogan Koca<sup>1</sup> And Goksal Sezel<sup>3</sup>

<sup>1</sup>Erciyes University, Science Faculty, Biology Department, Kayseri, Turkey

<sup>2</sup>Cankiri Karatekin University, Science Faculty, Chemistry Department, Cankiri, Turkey

<sup>3</sup>Harran University, Science & Art Faculty, Biology Department, Sanliurfa, Turkey

[fduman@erciyes.edu.tr](mailto:fduman@erciyes.edu.tr)

## INTRODUCTION

Quantum dots are broadly used for industry and health application because of their excellent features [1, 2]. A wide range of chemical and physical methods has been used to synthesise quantum dots. However, different kind of chemical pollutants have been left to the environment. Biosynthesis of nanomaterial is determined as eco-friendly technology to reduce the toxicity of materials and amount of used chemicals. In recent years, studies focused on this topic have accelerated [3-5]. Researchers have obtained the QDs by using plant extract extracts as a source of reductants [6]. It is known that plants generate Cd-S complex to reduce the toxicity of Cd [7]. From this point of view, in this study CdS QDs (Cadmium Sulphide Quantum Dots) was obtained by the aquatic plant extract (*Mentha aquatica* L.) when reacted with a mixture of CdCl<sub>2</sub> and Na<sub>2</sub>SO<sub>3</sub>.

**Keywords:** Biosynthesis; CdS quantum dots; *Mentha aquatica*; bactericidal activity; XRD

## EXPERIMENTAL METHODS

### Synthesis of CdS QDs

In our study, CdS QDs was obtained using the method of Prasad and Jha [5]. Briefly, dried leaves (5 g) were surface cleaned with distilled water, boiled in distilled water for 20 min and filtered through Whatman No.1 filter paper. 5 ml leaf extract was added into 50 ml cadmium chloride (2 mM) solution. Sodium sulfide (50 ml, 2 mM) dissolved in deionized water was added drop wise into the solution of cadmium chloride under magnetic stirring. The mixture was mixed at 200 rpm, 30 °C for 12 h in dark condition.

### Characterization

Obtained QDs were characterized by UV-visible spectroscopy, scanning electron microscopy (SEM), X-ray diffraction (XRD), dynamic light scattering (DLS), transmission electron microscopy (TEM) and Fourier Transform Infra-Red spectroscopy (FTIR).

### Antimicrobial activity

The agar diffusion method was used for the determination of antimicrobial activities of the Cd QD's. *Escherichia coli* O157 was selected as test organism. 250 µl of *E. coli* was added into a flask containing 25 mL sterile Mueller–Hinton agar at 45 °C and poured into Petri dishes. In the agar, four equidistant holes were made and loaded with 25 µg/mL (50 µl) of the solution. Petri dish was incubated at 37 °C for 18-24 h. At the end of the period, petri dish was examined for zones of growth inhibition, and the

diameters of these zones were measured in millimeters.

## RESULTS AND DISCUSSION

UV-visible spectrum of the aqueous medium peaked between 320-360 nm corresponding to the absorbance of CdS (Fig. 1). XRD results confirmed the formation of CdS. Dynamic light scattering results showed size of CdS quantum dots are in the range of 32-52 nm (Fig 2). Zeta potential of CdS was found to be -12.9 mV (Fig. 3), so it indicates the moderate stability and dispersion. Besides, CdS QDs showed excellent bactericidal activity against pathogenic bacteria *E. coli*.

## CONCLUSION

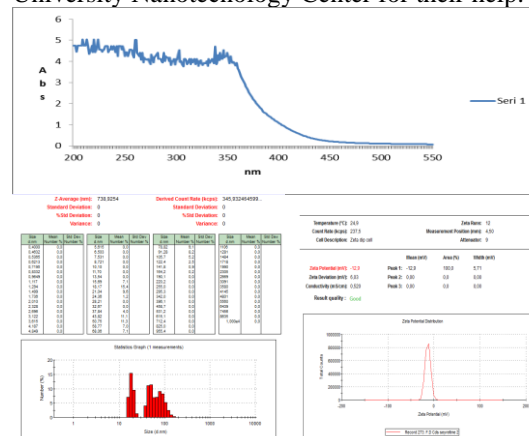
The herbal based fabrication provides an economical, green chemistry approach for production of CdS quantum dots.

## REFERENCES

1. Schröfel, A., et al., Acta Biomater. 10: 4023-4042, 2014.
2. Henglein, A. 'Chem. Rev. 89: 1861-1873, 1989.
3. Bansal, et al., J. Chem. Res. 2: 69-71, 2012.
4. Mi, C. et al., J. Biotech. 153: 125-132, 2011.
5. Prasad, K. and Jha, A.K. J. Colloid Interface Sci 342: 68-72, 2010.
6. Kharisova, O.V. et al., Trends in Biotech. 31: 240-248, 2013.
7. Salt, D., et al. Plant Physiol. 109: 1427-1433, 1995.

## ACKNOWLEDGMENTS

The authors are grateful to researchers of Erciyes University Nanotechnology Center for their help.



## Design of Multilayer Collagen-based Systems for *in situ* Drug and/or Cell Release

Diogo F.L. Rodrigues, Teresa Russo, Ugo D'Amora, Olimpia Oliviero, Antonio Gloria, Roberto De Santis, Luigi Ambrosio

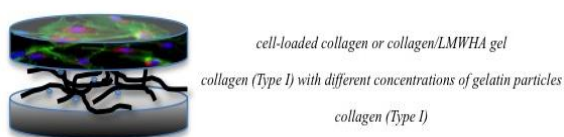
Institute of Polymers, Composites and Biomaterials, National Research Council of Italy, V. le J.F. Kennedy - Pad. 20, Mostra d'Oltremare, 80125 Naples, Italy  
[diogo.lopesrodrigues@gmail.com](mailto:diogo.lopesrodrigues@gmail.com)

### INTRODUCTION

Over the past years, hydrogel-based materials such as patches or injectable devices for *in situ* drug or cell release have been widely studied. In the treatment of cardiovascular disease (CVD)<sup>1</sup>, a natural mimic hydrogel construct should play an important role as a reservoir system to deliver multiple biomolecules to targeted ischemic sites. The aim of the present study was to propose a preliminary approach in the design of a multilayer hydrogel based on collagen/collagen–gelatin nanoparticles (GNPs)/collagen-low molecular weight hyaluronic acid (LMWHA). The viscoelastic properties, as well as the morphological/biological features of the developed systems were preliminary assessed.

### EXPERIMENTAL METHODS

Three-layer systems were suitably developed through the integration of a conventional method and an electrospray-based technique. Each system consisted of a lower collagen layer, an upper collagen or collagen-LMWHA layer, and a middle GNP-loaded collagen layer.



Schematic representation of the multilayer collagen-based system

Small amplitude oscillatory shear tests were performed on all the developed systems and the linear viscoelastic behaviour was investigated. All of the tests were carried out at a temperature of 37°C, using a rheometer (Gemini, Bohlin Instruments). The viscosity as a function of the shear rate was evaluated through steady state shear measurements at a temperature of 37°C in a wide range of shear rate (0.01 – 100 s<sup>-1</sup>). Scanning Electron Microscopy (SEM) was performed to assess the morphological features of GNPs and collagen-based networks with a great attention on the middle layer. MTT assay and further SEM analyses were also carried out on cell-laden constructs.

### RESULTS AND DISCUSSION

Results from small amplitude shear tests highlighted that the values of both dynamic moduli generally increased with frequency, and G' values were always higher than G'' ones in the frequency range investigated. A shear thinning behaviour was evidenced for all the proposed systems, as the viscosity decreased with increasing the shear rate. MTT assay provided interesting results in terms of MSC viability/proliferation. SEM analysis showed the influence of GNPs on the structural/morphological features of the collagen-based network (i.e., fibrils diameter) and the effect of collagen-LMWHA layer on cell adhesion and spreading.

### CONCLUSION

A preliminary approach in the design of patches and injectable multilayer hydrogels was proposed. The possibility to tailor the structural/morphological features and the rheological properties of the multilayer hydrogels was also highlighted. In particular, regarding the upper layer the presence of LMWHA acted as a “reinforcement”, as well as in the case of structures loaded with a specific amount of GNPs. Furthermore, the presence of collagen-LMWHA layer influenced cell adhesion and spreading.

### REFERENCES

1-Russo V., Young S., Hamilton A., Amsden B.G., Flynn L.E. Biomaterials. 35, 3956-3974, 2014.

### ACKNOWLEDGMENTS

This project has received funding from the European Union's Seventh Framework Programme for research, technological development and demonstration under grant agreement number 317304.



Michał Dziadek<sup>1</sup>, Barbara Zagrajczuk<sup>1</sup>, Kamil Karwat<sup>2</sup>, Justyna Pawlik<sup>1</sup>, Maria Łączka<sup>1</sup>, Katarzyna Cholewa-Kowalska<sup>1</sup>

<sup>1</sup>AGH University of Science and Technology, Faculty of Materials Science and Ceramics,

<sup>2</sup>AGH University of Science and Technology Faculty of Electrical Engineering, Automatics, Computer Science and Biomedical Engineering; Al. A. Mickiewicza 30, 30-059 Krakow, Poland

[cholewa@agh.edu.pl](mailto:cholewa@agh.edu.pl)

## INTRODUCTION

The standard method to produce bioactive glass is by melting a mixture of oxides, carbonates and phosphates and then quenching the molten liquid to form in most cases glass frit. Next the frit is milled to obtain powder or granules. The second way for fabricate bioglasses is the sol-gel chemical method which is based on chemical reaction: hydrolysis and polycondensations occurs in solution. These processes can be provided in the different medium: alcohol or water with different reaction catalyst and raw materials, and can affects the properties of obtained materials. In comparison to the melting sol-gel route allowed to obtain higher purity and homogeneity, and different textural parameters [1-2,4]. The present work investigated the effect of synthesis methods on the structure and properties of alkali-free bioglass. With the our best knowledge there are no in literature comparison of melted and gel-derived bioglasses with the same chemical composition, except bioactive glass 45S5, which has been studied extensively [2-3].

## EXPERIMENTAL METHODS

Alkali free glasses from the  $\text{CaO-SiO}_2\text{-P}_2\text{O}_5$  system with chemical composition  $40\text{SiO}_2$ ,  $6\text{P}_2\text{O}_5$ ,  $54\text{CaO}$  (mol%) were obtained by 1). traditional melting using chemically pure  $\text{SiO}_2$ ,  $\text{P}_2\text{O}_5$  and  $\text{CaCO}_3$  in platinum crucible at  $1500^\circ\text{C}$  – marked as A2M; 2) sol-gel method in alcohol-based solution using TEOS, TEP and  $\text{Ca}(\text{NO}_3)_2 \cdot 4\text{H}_2\text{O}$  – marked as A2; 3) sol-gel method in aqueous solution with the same raw materials marked as A2W. The obtained gels were converted to ceramic materials by multistage heat treatment up to  $800^\circ\text{C}$ . All materials were characterized by DTA analyses, Fourier transform infrared spectroscopy FTIR and X-ray diffraction XRD as well as density, porosity and BET surface area. The resulting materials were also subjected to the bioactivity evaluation in vitro conditions using acellular simulated body fluid (SBF).

## RESULTS AND DISCUSSION

FTIR spectra of melt-derived glass (A2M) shows bands characteristic of the vibrations associated to the silicate network at  $480$ ,  $760$ ,  $935$ ,  $1020\text{ cm}^{-1}$  derived from Si-O-Si bending mode, Si-O-Si stretching mode of bridging oxygen atoms between tetrahedrons, Si-O-Si stretching of non-bridging oxygen atoms Si-O-Si stretching of bridging oxygen atoms within the tetrahedron respectively. There is also occur band at  $566\text{ cm}^{-1}$  assigned to P-O bond in the  $\text{PO}_4^{3-}$  groups in amorphous calcium phosphate structures. For gel-derived glasses (A2, A2W) there are visible bands associated with silicate network structure, but the band at  $760\text{ cm}^{-1}$  is vanished, the band located at  $930\text{ cm}^{-1}$  became more intense and the maximum of the band connected with Si-O-Si vibration in  $[\text{SiO}_4]$  is shifted to

higher wavenumbers, which can suggest the formation of Si-O-P bonds. The bands in the range  $1420\text{-}1480\text{ cm}^{-1}$  indicate the presence of  $\text{CO}_3^{2-}$  groups.

According to X-ray diffractograms gel-derived glasses exhibit beginning of crystallization hydroxyapatite and calcium silicate phases while the A2M is amorphous.

As it is shown in the table the density and surface area of the samples are different, the higher density have gel glasses due to presence of crystalline phases.

Materials	Density [ $\text{g/cm}^3$ ]	BET surface area [ $\text{m}^2/\text{g}$ ]
A2M	$2,785 \pm 0,005$	$0,265 \pm 0,007$
A2	$2,924 \pm 0,006$	$38,36 \pm 0,09$
A2W	$2,939 \pm 0,007$	$59,21 \pm 0,09$

The higher surface area results from the specificity of sol-gel process. To the bioactivity SBF test melted glass was used as a polished glass plate, while the gel-derived glasses were pressed to the pellets form. After 7 day's immersion time the surface of samples were analyzed. The surface of all glasses are fully covered with calcium phosphate layer, but the its morphology are different. The A2M surface is covered by uniform, smooth coating while the layer on gel-derived glasses exhibit cauliflower - like microstructure.

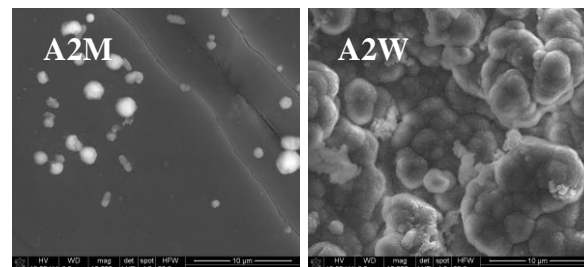


Fig. 1. Microstructure of the coating of bioactive glasses formed after immersion in SBF.

## SUMMARY

Our study demonstrate that the structure of melted glass was more polymerized then gel-derived ones. Additionally gel glasses show beginning of crystallization during heat treatment. Morphology of apatite layer formed after incubation in SBF depends on material form as well as synthesis method.

## ACKNOWLEDGMENTS

This work was supported by the Polish National Science Centre (decision no. DEC-2014/13/B/ST8/02973).

## REFERENCES

1. D. Arcos, D.C. Greenspan, M. Vallet-Regí, J. Biomed. Mater. Res. 65 (2003) 344–351,
2. P. Sepulveda, J.R. Jones, L.L. Hench, J. Biomed. Mater. Res. 61 (2002) 301–311
3. R. Siqueira, O. Peitl, E.D. Zanotto Mat. Sci.Eng. C 31 (2011) 983–991
4. A.Lucas-Girot, F.Mezahi, et al. Journal of Non-Crystalline Solids 357 (2011) 3322–3327



## Preparation of Chitosan Hydrogel Modified with Xanthan Gum

Bożena Tyliśszczak<sup>1</sup>, Katarzyna Z. Gaca<sup>1</sup>, Katarzyna Białik-Was<sup>1</sup>, Dagmara Malina<sup>2</sup>, Agnieszka Sobczak-Kupiec<sup>2</sup>

<sup>1</sup> Department of Chemistry and Technology of Polymers, Cracow University of Technology, Poland

<sup>2</sup> Institute of Inorganic Chemistry and Technology, Cracow University of Technology, Poland

[btyliszczak@chemia.pk.edu.pl](mailto:btyliszczak@chemia.pk.edu.pl)

### INTRODUCTION

Hydrogels are commonly used in medicine, pharmacy, and tissue engineering. Due to their specific features, they are generally used for production of innovative bandaging materials. The aim of this work was evaluation of the impact of the modification of the hydrogel matrix with xanthan gum on the properties and structure of polymeric superabsorbents [1-5].

### EXPERIMENTAL METHODS

The research work included synthesis of hydrogels with different contents of xanthan gum. The scope of the research included measuring their ability to swell in distilled water and other physiological solutions. Incubation studies were also performed on synthesized samples. The biological activity of the hydrogels and their structure were analysed; the latter was performed using FTIR spectroscopy.

### RESULTS AND DISCUSSION

Acrylic-chitosan matrices of hydrogels with different amount of xanthan gum were synthesized and subjected to investigation of sorptive capabilities. The results showed that the synthesized hydrogels can swell both in distilled water and a solution of physiological salt. Due to the above, they can be used as bandage materials, allowing to absorb the effusion from the wound and keep it wet to accelerate the process of healing. Additionally, incubative studies of the synthesized samples in the distilled water, Ringer solution and artificial saliva, were also carried out. The pH value of the examined solutions did not vary significantly across hydrogel samples with different content of the xanthan gum. Moreover, no sudden changes of pH were observed, which confirms the compatibility of the obtained materials with a particular environment. Biological activity of hydrogels was also determined and the results of the studies confirmed this property in all samples. In order to explore this property further, studies on the cell lines will have to be carried out. Analysis of the polymer matrix structure of the synthesized hydrogels, before and after the incubation,

was also carried out using Fourier transform infrared spectroscopy (FT-IR).

### CONCLUSION

Incubation studies and tests of biological activity confirmed that the resulting hydrogels are active, and thus may have an impact on human tissue. With respect to this, they may be used for the production of dressings, which allow gas exchange between the wound and the environment, remove exudate with toxic compounds and provide protection of newly formed tissue. In a nutshell, wound dressings made of hydrogels could accelerate the regeneration of human tissue. This is suggested by the results of this preliminary analysis and hopefully will be confirmed by further investigations of the biological activity of the obtained hydrogels using cell lines.

### REFERENCES

1. Van Vlierberghe S., Dubruel P., Schacht E., *Biomacromolecules*, 12: 1387-1408, 2011.
2. Sharma B. R., Naresh L., Dhuldhoya N. C., *Food Promotion Chronicle*, 1(5): 27-30, 2006.
3. Hoffman A.S., *Advanced Drug Delivery Reviews*, 64: 18-23, 2012.
4. Lee S., Kwon I., Park K., *Advanced Drug delivery Reviews*, 65: 17-20, 2013.
5. Feng E., Ma G., Wu Y., Wang H., *Carbohydrate Polymers*, 111: 463-468, 2014.

### ACKNOWLEDGMENTS

"The authors would like to thank the The National Centre for Research and Development (Grant no: LIDER/033/697/L-5/13/NCBR/2014) for providing financial support to this project".



## Study of Hydrogels Containing Magnetic Nanoparticles

Bożena Tylińczak<sup>1</sup>, Katarzyna Z. Gaca<sup>1</sup>, Katarzyna Bialik-Was<sup>1</sup>, Dagmara Malina<sup>2</sup>, Agnieszka Sobczak-Kupiec<sup>2</sup>

<sup>1</sup> Department of Chemistry and Technology of Polymers, Cracow University of Technology, Poland

<sup>2</sup> Institute of Inorganic Chemistry and Technology, Cracow University of Technology, Poland

[btyliszczak@chemia.pk.edu.pl](mailto:btyliszczak@chemia.pk.edu.pl)

### INTRODUCTION

Modified hydrogels have a variety of applications, including biomedical ones: they may be used for the controlled release of drugs, or for tissue engineering. Additives incorporated into the polymer structure, i.e. magnetic nanoparticles not only affect the final functionality of the material, but also can modify its properties and structure still at the synthesis stage [1-4].

### EXPERIMENTAL METHODS

The scope of the study included synthesis of acrylic hydrogels modified with magnetic nanoparticles, as well as structural analyses of the obtained hydrogel materials by means of infrared spectroscopy (FT-IR), evaluation of the surface morphology by scanning electron microscopy (SEM), research on the sorption capacity of the solutions: SBF, Ringer, Tyrode, water, 0.9% NaCl and 0.9% CaCl<sub>2</sub>, as well as degradation tests in water and simulated body fluids.

### RESULTS AND DISCUSSION

The influence of the chain length of crosslinking agents on the properties of the obtained materials was estimated. Furthermore, the study involved developing a method for obtaining hydrogel matrices containing nano-Fe<sub>2</sub>O<sub>3</sub> through photopolymerization. The absorption capacity of the obtained acrylic hydrogels was determined. Basing on the results, it was concluded that the length of the PEGDA crosslinker influences the materials' absorbency. It was also observed that the presence of nano-Fe<sub>2</sub>O<sub>3</sub> does not cause the significant decrease of swelling. The scope of the study included also the incubation studies in distilled water and simulated body fluid, which helped to determine how the hydrogel material with a given amount of magnetic nanoparticles behaves in plasma. Moreover, the structural analysis of the obtained hydrogel materials was conducted by means of infrared spectroscopy (FT-IR), which allowed to confirm the presence of the functional groups typical for this kind of material. The analysis of FT-IR spectra for the samples which had undergone incubation allowed to observe that the degradation of the obtained hydrogels containing nano-Fe<sub>2</sub>O<sub>3</sub> occurs most rapidly in the environment of Ringer's solution.

### CONCLUSION

Incubation studies in simulated body fluids and distilled water showed a change in the pH over 32 days. Modification of the polymer matrix with nano-Fe<sub>2</sub>O<sub>3</sub> significantly affects the reduction of the pH (7.5-5.0) for SBF fluid in which hydrogels crosslinked with PEGDA with  $M = 575$  and  $700$  [g / mol] were immersed. Hydrogels having greater amounts of magnetic nanoparticles yielded a pH similar to the body's natural pH (approx. 7.0). In case of Ringer's solution and distilled water, the results of the incubation test results were comparable. There was no sudden change in the pH which may adversely affect the release of the active ingredient. The addition of nano-Fe<sub>2</sub>O<sub>3</sub> is a good solution in case of biomedical applications of the received hydrogel matrices, as it influences the pH of the environment.

### REFERENCES

1. Kyung Suh S., Yuet K., Kun Hwang D., Wan Bong K., Doyle P.S., Hatton T.A., J. Am. Chem. Soc. 134: 7337–7343, 2012
2. Gao J., Zhang W., Huang P., Zhang B., Zhang X., Xu B., American Chemical Society, 130 (12): 3710-3711, 2008
3. Gao J., Gu H., Xu B., Accounts of chemical research, 42 (8): 1097-1107, 2009
4. Ramanan R.M.K., Chellamuthu P., Tang L., Nguyen K.T., Biotechnology progress, 22 (1): 118-125, 2006

### ACKNOWLEDGMENTS

"The authors would like to thank the Ministry of Science and Higher Education (Grant no: 0489/IP3/2015/73) for providing financial support to this project".



## INTRODUCTION

In this work, we have applied a novel reaction pathway based on mixed anhydrides for the synthesis of grafted-HA with photoreactive groups for cross-linking<sup>1</sup>. The method was used for the chemical modification of HA and demonstrated to be robust, cheap and easily upscalable.

## EXPERIMENTAL METHODS

Substituted benzoyl chlorides (BC) (**2**) were used to activate  $\alpha,\beta$ , unsaturated and aliphatic acids (**1**) yielding a mixed anhydride as intermediate (**3**). The *in situ* activation was successfully performed in a biphasic phase of water: organic solvent and uses a tertiary amine (**Figure 1a**). The mixed anhydride (**3**) reacts in the next step with the primary hydroxyl of HA (**Figure 2**). Using this reaction pathway HA can be esterified with several linkers of different reactivity which control the cross-linking rate (**Figure 1b**).

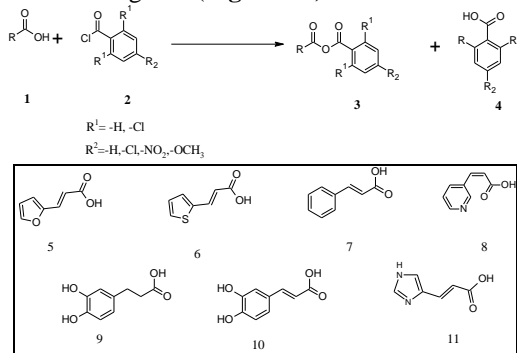


**Figure 1a.** Activation of linkers by Substituted-BC **1b**. Linkers studied in this work.

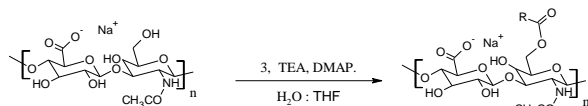


**Figure 2.** Reaction of mixed anhydride and HA

## RESULTS AND DISCUSSION

The activation of linkers (**5-11**) as depicted on Figure 2 was carried out by using 2,4,6 trichlorobenzoyl chloride (TBC), which in combination with DMAP produce acylation of primary  $-OH$  groups in HA and negligible attachment of the aromatic moiety. Benzoyl chloride (BC) a commercially available chloride is very useful from the point of view of industrial upscale due to its commercial availability and good price. Oppositely, TBC is expensive and difficult to obtain. The reaction was studied with benzoyl chloride (BC) and other activators. The reactivity of BC was found to be two times higher as compared to TBC. BC is able to produce acylation of HA even in absence of the toxic organocatalyst DMAP. In order to study the electronic effect of the substituents onto the aromatic ring some other activators were evaluated such as 4-methoxybenzoyl chloride (MBC) or 4-nitrobenzoyl chloride (NBC). The mixed anhydride (**3**) presents two

electrophilic atoms that may participate in the reaction. It is important to evaluate the reactivity of the aromatic moiety and possible grafting onto the polymeric backbone and evaluate its possible cytotoxicity. If TBC is used the nucleophilic attack have occurred exclusively on the carboxylic moiety corresponding to alkylic-carboxylic acid. Thus, the regioselectivity is controlled by steric hindrance of the chloro-substituents on the aromatic ring. Different linkers containing  $\alpha,\beta$  unsaturated bonds were tested during this development. The reaction was effective for the linkers **5,6,7,9** and **10**. On the opposite, linkers **8** and **11** characterized by the presence of a nucleophilic nitrogen atom were non-attached to the HA-backbone probably due to *N*-acylation of the linker. By a combination of steric and electronic properties, it was possible to perfectly tailor the degree of substitution (DS) and eliminate some toxic components onto the reaction feed.

In order to evaluate the feasibility of the benzoyl chloride catalysed reaction, the modified polysaccharide was enzymatically degraded and the fragments separated by chromatographic techniques (**Figure 3**). The possible cytotoxicity of active fragments (oligosaccharides) was analysed. Surprisingly, these oligosaccharides were found to increase the cell growth and were non-cytotoxic.

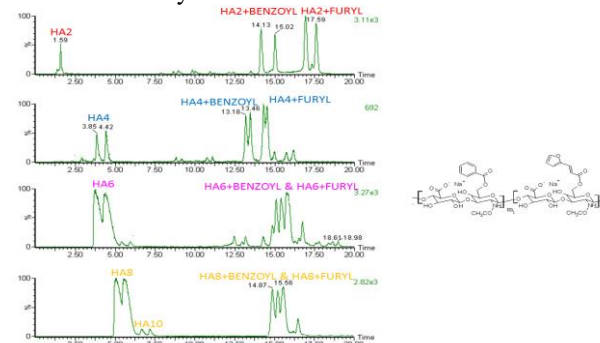


**Figure 3.** Characterization of fragments of linker **5** and benzoylation

## CONCLUSIONS

Different photo cross-linkable groups were attached to HA by mixed anhydride method. This method was found to be highly reproducible (up to 50g scale). Mixed anhydrides methodology is able to modify HA in a DS up to 45%. Additionally, the cyto-compatibility of the biomaterial was not affected after the chemical modification as demonstrated by the active fragments (degradation products). Thus, these materials have potential applications in biomedical field.

## REFERENCES

**1 a)** Patent PV 2013-914 (PCT in priority date 21.11.2013 **b)** WO2014/082609-A1

## ACKNOWLEDGMENTS

“This Project has received funding from the European Community’s Seventh Framework Programme (FP7-NMP-2013-SME-7) under grant agreement no 604450”.



## Thermoresponsive Anionic Copolymer Brush on Porous Monolithic Silica Rod For Separation of Basic Biomolecules

Kenichi Nagase<sup>1\*</sup>, Jun Kobayashi<sup>1</sup>, Akihiko Kikuchi<sup>2</sup>, Yoshikatsu Akiyama<sup>1</sup>,  
Hideko Kanazawa<sup>3</sup>, and Teruo Okano<sup>1</sup>

<sup>1</sup> Institute of Advanced Biomedical Engineering and Science, Tokyo Women's Medical University, Japan

<sup>2</sup> Department of Materials Science and Technology, Tokyo University of Science, Tokyo, Japan

<sup>3</sup> Faculty of Pharmacy, Keio University, Tokyo Japan

[nagase.kenichi@twmu.ac.jp](mailto:nagase.kenichi@twmu.ac.jp)

### INTRODUCTION

Temperature-responsive chromatography using poly(*N*-isopropylacrylamide) (PIPAAm) grafted silica beads is highly useful to control function and properties of the stationary phase for high performance liquid chromatography (HPLC) simply by changing column temperature<sup>1</sup>. In the present study, thermo-responsive anionic copolymer brushes were grafted porous monolithic silica support as an effective thermo-responsive chromatography matrices for basic biomolecules separation. Characterization of the prepared monolithic silica column was performed by observation of catechol amine and angiotensin peptides elution profiles.

### EXPERIMENTAL METHODS

((Chloromethyl)phenylethyl)trimethoxysilane (CPTMS), ATRP-initiator, was modified on monolithic silica surfaces by flowing a toluene solution containing ATRP-initiator into monolithic silica columns. IPAAm, *tert*-butylacrylate (tBA), and *tert*-butylacrylamide (tBAAm) were grafted onto monolithic-silica-rod surfaces through surface-initiated ATRP using CuCl/CuCl<sub>2</sub>/Me<sub>6</sub>TREN as an ATRP catalytic system and 2-propanol as a reaction solution at 25 °C for 4 h (Fig.1). Then, the deprotection of *tert*-butyl group was performed with methanesulfonic acid solution in dichloromethane into the columns. The prepared thermoresponsive anionic copolymer brush modified monolithic silica rod column was connected to an HPLC system and the elution behaviour of catecholamine derivatives and angiotensin peptides were observed at various temperatures.

### RESULTS AND DISCUSSION

CHN elemental analysis and GPC measurement revealed that grafted amount and grafted density of anionic copolymer on monolithic silica were 3.33 mg/m<sup>2</sup> and 0.169 chains/nm<sup>2</sup>, respectively. These indicated that large amount of anionic copolymer was grafted on monolithic silica surface through surface-initiated ATRP. Fig.2 shows temperature dependent elution profiles of catecholamine derivatives and angiotensin peptides. High resolution separation was performed at elevated temperature, because these basic analytes interacted with copolymer brush through electrostatic and hydrophobic interaction at high temperature. Additionally, copolymer modified monolithic silica exhibits remarkable short analysis time, because of the reduced diffusion pathlength of monolithic supporting materials.

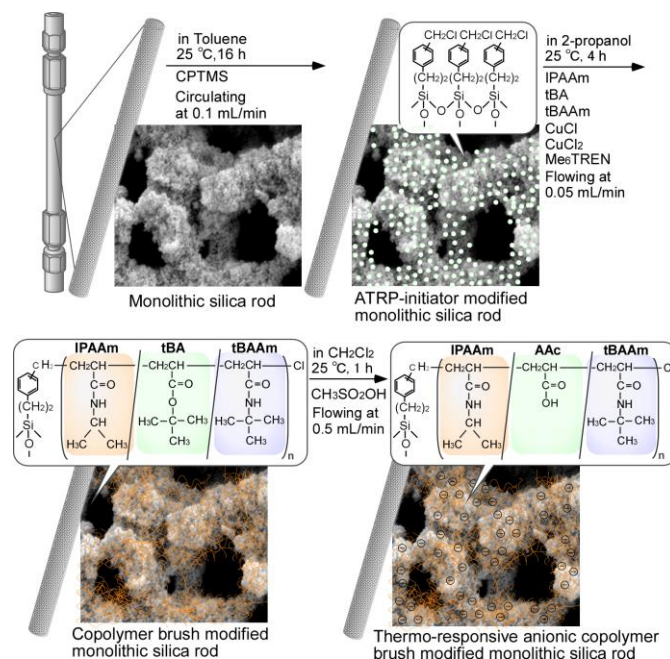


**Fig.1** Scheme of thermoresponsive anionic copolymer brush modified porous silica rod as thermoresponsive ion exchange chromatography matrices

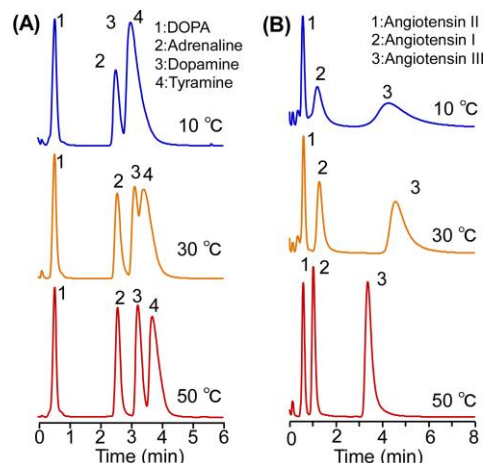


**Fig.2** Elution Profile of catechol amine and angiotensin

### CONCLUSION

Thermoresponsive anionic copolymer brush on porous monolithic silica can effectively separate basic biomolecules. Therefore, the copolymer brush modified monolithic silica would be useful as a temperature responsive chromatographic materials.

### REFERENCES

- Nagase K. *et al.*, J. Royal Soc. Interfaces, 6: S293-S303, 2009

Joanna Idaszek<sup>1\*</sup>, Monika Bil<sup>1</sup>, Wojciech Świążkowski<sup>1</sup><sup>1</sup>Faculty of Materials Science and Engineering, Warsaw University of Technology, Poland\*[joanna.idaszek@inmat.pw.edu.pl](mailto:joanna.idaszek@inmat.pw.edu.pl)

## INTRODUCTION

Biodegradable polymers with shape memory effect present exciting possibility for development of less invasive smart medical devices. The thermoresponsive effect could allow not only to reduce the size of a medical device before implantation to a human body, but also to modulate release rate of biologically active molecules in drug delivery systems. Such materials could be utilized, for example, to fabricate drug or growth factor-eluting stents. However, the release of active molecules from polymeric delivery systems might depend on many intrinsic properties of the used polymers.

The goal of the present study was to investigate release kinetics of proteins from two novel thermoresponsive block copolymers composed of caprolactone (CL) and L-lactide (LA) and to correlate them with their thermal properties, crystallinity and wettability.

## EXPERIMENTAL METHODS

The polymers were composed of blocks of CL and LA with varying lengths (5CL-10LLA, 10CL-10LLA). To study release of growth factors, we decided to use Bovine Serum Albumin (BSA) as a model protein. BSA was incorporated into the polymers at concentration of 5 wt/wt% using water in oil emulsion technique<sup>1</sup>. Thermal properties of the polymers were characterized using Differential Scanning Calorimetry (DSC) and wettability using sessile drop technique. The release study was performed in Phosphate Buffered Saline (PBS) at 37 °C for a period of 12 days. Concentration of BSA in the supernatant was measured using micro-BCA assay according to manual supplied with the kit.

## RESULTS AND DISCUSSION

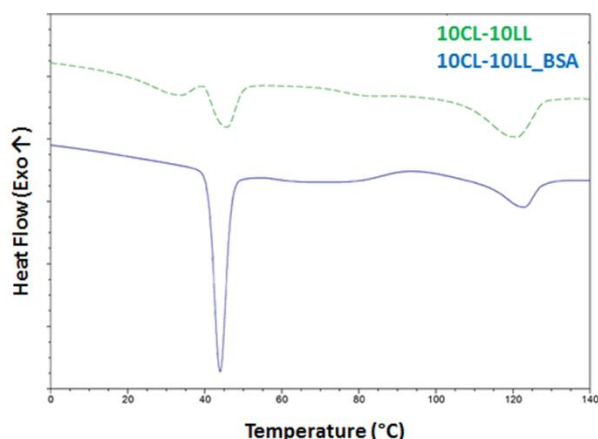


Figure 1. DSC curves of neat polymer 10CL-10LL (dashed line) and its blend with BSA (solid line).

Neat 5CL-10LL did not show a distinct melting endotherm in the CL-block range. Presence of BSA

increased crystallinity of the PCL fraction in blend 10CL-10LL\_BSA, which can be seen as a strong endothermic peak with minimum around 44°C (Figure 1). In case of 5CL-10LL\_BSA, the melting peak was much smaller and its minimum was present around 46°C.

BSA release curves are presented in Figure 2. The profiles were similar during first 24 hours of the experiment and we did not observe any burst release during that time. The release profiles started varying after 24 hours of incubation in PBS. In case of 10CL-10LL\_BSA, the release of BSA occurred in a very slow fashion, whereas 5CL-10LL\_BSA blend released the model protein at a faster rate of approximately 1% of initial load per day during first week of the experiment. This difference could arise due to lower crystallinity of the 5CL-10LL\_BSA blend and its higher hydrophilicity, both having an enhancing effect on water uptake and polymer degradation.

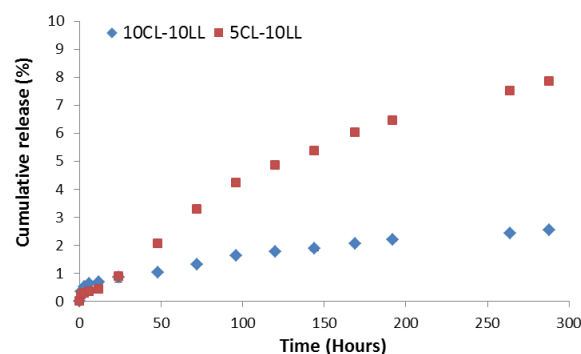


Figure 2. Profiles of BSA release from the 10CL-10LL\_BSA and 5CL-10LL\_BSA blends.

## CONCLUSION

Presence of the biologically active molecule can induce changes in the crystallinity of a material and shift the transition point of a shape memory material. We conclude, that crystallinity had bigger effect on the elution of BSA than the transition temperature. Current work focuses on investigation of BSA and growth factor release from thermoresponsive polymers with different compositions and their effect on biological response of MSC and HUVEC.

## REFERENCES

1. X. H. Zhu *et al.*, J Biomed Mater Res 89A: 411–423

## ACKNOWLEDGMENTS

The authors would like to thank the National Centre for Research and Development (Grant no. LIDER/037/673/L-4/12/NCBR/2013) for providing financial support to this project.



## Tissue-Adhesive Hydrogel for Hemostasis Comprising Water-Swellable Poly(acrylic acid)/Poly(vinylpyrrolidone) Complex

Yoshiyuki Koyama, Tomoko Ito, Shingo Yamaguchi, Yoichi Kurachi, Masazumi Eriguchi

Japan Anti-Tuberculosis Association, Shin-Yamanote Hospital, Japan

[drkoyama@vivid.ocn.ne.jp](mailto:drkoyama@vivid.ocn.ne.jp)

### INTRODUCTION

A tissue-adhesive hydrogel has been explored for medical devices such as a hemostat, adhesion barrier, wound dressing or drug release device. A film or sponge which forms an adhesive hydrogel absorbing blood or body fluid on the wet bio-tissue is useful as a hemostatic device or adhesion barrier, and some were already commercialized. Most of them are made of animal proteins such as gelatin (collagen) or fibrinogen, and risk of viral infection, bovine spongiform encephalopathy, or immunogenicity is not completely eliminated. Natural polysaccharides and their derivatives have also been utilized. However, the adhesion strength is not high, and the efficacy is limited because of their low flexibility in a dry state, and wound healing retardation properties.

We focused on a hydrogen bonding polymer complex consisting of poly(acrylic acid) (PAA), which has been known as a tissue-adhesive polymer, with poly(vinylpyrrolidone) (PVP). They are both highly safe synthetic polymers approved as pharmaceutical excipients. However, when aqueous PAA- and PVP-solutions are mixed, an insoluble precipitate soon forms. Resulting rigid gel does not swell, nor dissolve in water.

Recently, we found that solid PAA film would form a highly swollen gel by being immersed in a PVP solution. The swollen PAA/PVP complex gel was dried up to a transparent film, which could be swollen again in water to form a soft hydrogel. When it is put on a wet bio-tissue, it forms a gel absorbing body fluid, and strongly stick to it. In this study, complex-formation behavior of PAA film in PVP solution, and characteristic of the water-swallowable PAA/PVP complex was investigated. Clinical application of the tissue-adhesive hydrogel to a hemostatic agent for dental surgery was also examined.

### EXPERIMENTAL METHODS

#### Swelling behaviour of PAA film in PVP solution:

PAA solution in ethanol was poured onto a glass plate, and dried up to a film. The film on the glass was then immersed in an aqueous PVP solution to form a swollen complex gel, and changes in weight and transparency of the complex were measured.

#### Preparation of PAA/PVP complex film and sponge:

PAA solution was dried up to a clear film. PVP aqueous solution was then poured upon the PAA film to afford a swollen complex gel, which was followed by heated-air drying, or freeze-drying to give a transparent film or soft spongy sheet, respectively.

#### Swelling behaviour of PAA/PVP complex in water:

PAA/PVP complex was immersed in a buffer of pH 5 or 7, and change in weight was measured.

#### Clinical study:

Clinical study was carried out on the patients who underwent tooth extraction. PAA/PVP sponge was placed into the bleeding socket soon after the extraction, and hemostatic effect and recovery condition was observed.

### RESULTS AND DISCUSSION

#### Complex-formation behavior:

PAA film formed on a glass plate kept swelling for more than 10 hours in an aqueous PVP solution to a soft sticky hydrogel. Meanwhile, no precipitate nor clouding was observed. Swollen PAA/PVP complex hydrogel was then dried up to a transparent film. The swelling behaviour of the complex film in a buffer of pH 5 or 7 was investigated. The weight of PAA/PVP complex film in the buffer at pH 7 kept increasing for the first 100 min, and then slowly decreased. On the other hand, the film immersed in the buffer of pH 5 continued increasing in weight for more than 6 hours. Decrease in the weight in the neutral buffer would be attributed to a neutralization of the carboxyl groups of PAA, causing the dissociation of the complex to an original water-soluble polymers.

#### Clinical study:

In order to prepare the PAA/PVP complex which can be swollen rapidly, spongy PAA/PVP complex was prepared by freeze-drying the swollen hydrogel. Clinical study of the PAA/PVP complex sponge to control the bleeding after tooth extraction was performed on the patients taking anticoagulant medicine such as Bayaspirin or warfarin. The PAA/PVP sponge placed into the bleeding socket absorbed the blood, and immediately swelled to a hydrogel. It adhered to a bleeding site, and arrested the hemorrhage effectively, even in the anticoagulated patients.

### CONCLUSION

Water-swallowable PAA/PVP complex could be obtained under certain particular conditions. Excellent efficacy of the PAA/PVP complex sponge as a hemostatic device was confirmed in the clinical studies, and no adverse side effect was as yet observed.

### ACKNOWLEDGMENTS

We Thank BASF Japan Ltd, for providing PVP. This work was partly supported by The MIKIYA Science And Technology Foundation, and Golden Orchid Brothers Inc.





## An Engineered Double Network Based Composite Hydrogel for a Synthetic OOKP Skirt

Ganesh Ingavle<sup>1</sup>, Venkata Avadhanam<sup>1,2</sup>, Yishan Zheng<sup>1</sup>, Sandeep Kumar<sup>1</sup>, Christopher Liu<sup>2</sup>, Susan Sandeman<sup>1</sup>

<sup>1</sup> Biomaterials Research Group, Pharmacy and Biomolecular Sciences, University of Brighton, United Kingdom,

<sup>2</sup> Sussex Eye Hospital, Brighton, East Sussex, United Kingdom

[g.c.ingavle@brighton.ac.uk](mailto:g.c.ingavle@brighton.ac.uk)

### INTRODUCTION

In the most severe cases of corneal and ocular disease or damage, osteo-odonto-keratoprosthesis (OOKP) surgery, a specific medical procedure also known as 'tooth in eye' surgery, can be employed in order to restore the patient's vision. The whole surgery procedure involves the removal of an autologous canine tooth and adjacent bone, which is used to support a polymethylmethacrylate (PMMA) optical cylinder, subsequently implanted beneath the oculi muscle and sutured onto the cornea.<sup>1</sup> OOKP uses a biological skirt in the form of the patient's own tooth root and alveolar bone to support a PMMA optical cylinder for the prosthesis, which makes the clinical use of OOKP very demanding and expensive. Various bioactive materials and bioinert materials such as silicone, Teflon, Dacron, poly-HEMA hydrogels and titanium,<sup>2, 3</sup> have been developed for OOKP skirt substitution. However, the majority of the devices have not proven to be ideal OOKP skirt materials because they lack suitable mechanical strength, cell adhesion and cell survival. The aim of this study was to investigate a synthetic skirt material using agarose and PEGDA interpenetrating network (IPN) hydrogel for the keratoprosthesis to replace the bone-dentine composite, which is used in the OOKP.

### EXPERIMENTAL METHODS

The primary approach taken is to use interpenetrating networks (IPNs) of agarose and poly(ethylene glycol) diacrylate (PEGDA) to provide mechanical strength while supplementing the network with hydroxyapatite (HA) coated poly(lactic-co-glycolic acid) (PLGA) microspheres in order to mimic bone micro-environment and improved cellular response. In a related approach, agarose is used as a first network to encapsulate keratocytes/3T3 fibroblasts and PEGDA is used as a crosslinker with varying molecular weights (2000 and 6000 Da) and concentrations (10, 20, and 40 wt%) to create a mechanically strong IPN hydrogel in a single synthesis step.

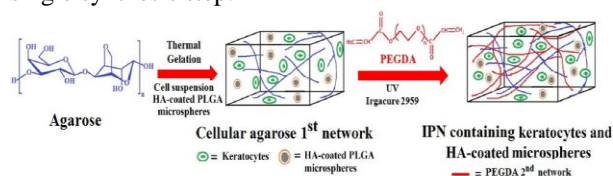


**Fig.1.** Schematic showing the formation of IPNs containing keratocytes and HA coated microspheres.

IPNs are created by encapsulating keratocytes/3T3 fibroblasts and HA coated microspheres in thermally gelling agarose, followed by soaking in a solution of PEGDA which is subsequently UV photopolymerized to form a copolymer network which interpenetrates the agarose constructs (Fig. 1). Crosslinked acellular IPN gels are made in a similar fashion but by

photopolymerizing a solution of PEGDA soaked in agarose disk without keratocytes.

### RESULTS AND DISCUSSION

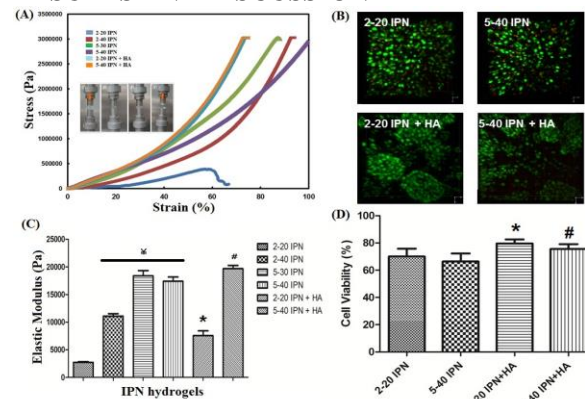


**Fig.2.** Mechanical performance and cellular behaviour of 3T3 fibroblasts encapsulated in IPN hydrogels..

The elastic moduli for IPNs with the same agarose concentration were generally greater when the 6000 molecular weight PEG-DA was used, with this difference being more pronounced with increasing PEG-DA concentration. An increased concentration of either agarose or PEG-DA led to an increase in elastic modulus (Fig. 2A and 2C). However, IPNs containing 6000 molecular weight PEG-DA and 5% agarose incorporated with HA coated microspheres (5-40IPN+HA) had a higher elastic modulus than the IPN containing 2% agarose with 40% PEGDA (2-40%IPN) and 5% agarose with 40% PEGDA (5-40%IPN).

In the absence of HA coated microspheres, cell viability drops to 65% at 1 week post-encapsulation in culture. However, by incorporating HA coated microspheres within the IPN, this low viability was rescued to 78% at 1 week post-encapsulation (Fig. 2B and 2D).

### CONCLUSION

We successfully designed and synthesized a promising new class of engineered IPN hydrogel materials with a unique combination of high mechanical strength and cyto-compatibility. Tunable mechanical strength and enhanced cell viability with HA rich micro-environment are the desirable attributes of this hybrid material system, especially when used as a potential skirt material in OOKP.

### REFERENCES

- Liu C. et al., Semin. Ophthalmol. 20:113-128, 2005
- Hicks C. et al., Surv. Ophthalmol. 42:175-189, 1997
- Iakymenko S. et al., Int. J. Ophthalmol. 6:375-380, 2013



Doriana Orbanic<sup>1</sup>, Israel González deTorre<sup>2</sup>, Javier Francisco Arias Vallejo<sup>1</sup>,  
José Carlos Rodríguez-Cabello

<sup>1</sup>G.I.R.Bioforge, University of Valladolid, Valladolid, Spain

<sup>2</sup> Technological Proteins NanoBioTechnology (TPNBT) S.L., Valladolid, Spain  
[dorbanic@bioforge.uva.es](mailto:dorbanic@bioforge.uva.es)

## INTRODUCTION

The main goal of ongoing studies in the field of biomedicine is the attainment of biomaterials that resemble as much as possible naturally occurring mechanisms and systems<sup>1</sup>. The rate of biodegradation of the employed materials is one of the major issues. We have recently designed and synthesized an elastin-like recombinamer, cleavable by enzymes involved in tissue turnover and other mechanisms of the ECM<sup>2,3</sup>. The material is chemically functionalizable for the attainment of covalently cross-linked hydrogels, whose biodegradability is naturally controlled. The overall structure contains another recombinamer, carrying an RGD cell attachment sequence.

## EXPERIMENTAL METHODS

The iterative-recursive recombinant method<sup>4</sup> has been employed for the synthesis of the gene sequence of the enzymatically cleavable recombinamer, which has been inserted in an expression plasmid. The two recombinamers of the system have been produced in *E.coli* and purified through inverse transition cycling<sup>5</sup>. After dialysis and lyophilization, the final products have been characterized by NMR, DSC, FT-IR, MALDI-TOF and HPLC. The products have been chemically functionalized at the lysine residues of the amino acid sequences by adding an azide and an activated alkyne group. A catalyst-free click chemistry reaction for the hydrogel cross-linking has been performed in an aqueous ambient at r.t.<sup>6</sup> Rheological studies have been conducted at different recombinamer concentrations. *In vitro* proteolytic hydrolysis by matrix metalloproteinases of the degradable recombinamer in solution and in the hydrogel at a concentration of 50mg/mL has been performed. Cytocompatibility, cell adhesion and proliferation in human fibroblasts HFF1 has also been evaluated.

## RESULTS AND DISCUSSION

A stimuli responsive ELR, was synthesized, produced, purified and chemically modified. The characterization of the recombinamer confirmed the expected composition. Hydrogels have been prepared through click chemistry. Rheological results gave a storage modulus value up to 4kPa at 37°C, at different recombinamer concentrations.

Therefore, an increase in concentration shows an augmentation of the mechanical properties of the scaffold.

*In vitro* enzymatic cleavage of the recombinamer in solution proved the expected fragmentation of the polypeptide chain, and also the

hydrogel degradation with enzymes has been observed in time. *In vitro* tests with human fibroblasts confirmed cytocompatibility, as well as cell adhesion and proliferation.

## CONCLUSION

The natural provenance of the material suggests high cytocompatibility, which has also been proven for the mild catalyst-free reaction applied for the hydrogel crosslinking. The novel structure confers degradability to the scaffold it composes, by enzymes which are secreted by the cells that are aimed to colonize it. Rheological results suggest that the scaffold mechanical properties can be adjusted to different applications, as the storage modulus varies with recombinamer concentration. Further characterization of the constructed scaffold, including *in vivo* studies, is necessary in the future.

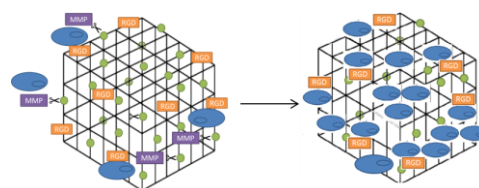


Figure 1. Scheme of the scaffold degradation by proteolytic enzymes, which brings to cell colonization and formation of new extracellular matrix

## REFERENCES

1. Van Vlierberghe et al., *Biomacromolecules* 2011, 12, 1387.
2. Sekhon, B. S. *Res Rep Biol* 2010, 1, 1.
3. Hsu, C.-W. et al., *Journal of Biomedical Materials Research Part A* 2011, 98A, 53.
4. Rodríguez-Cabello, J. C. et al., In *Nanotechnology in Regenerative Medicine*; Springer: 2012, p 17.
5. Meyer, D. E.; Chilkoti, A. In *Protein-Protein Interactions: A Molecular Cloning Manual*; Cold Spring Harbor Laboratory press: 2002, p 329.
6. González de Torre, I. et al., *Acta Biomaterialia* 2014.

## ACKNOWLEDGEMENTS

The authors would like to thank the European Union's Seventh Framework Programme for research, technological development and demonstration under grant agreement number 317304, for supporting financially this project.



Azade Yelten<sup>1</sup>, Suat Yilmaz<sup>1</sup><sup>1</sup>Department of Metallurgical and Materials Engineering, Istanbul University, Turkey  
[azade.yelten@istanbul.edu.tr](mailto:azade.yelten@istanbul.edu.tr)

## INTRODUCTION

Hydroxyapatite ( $\text{Ca}_{10}(\text{PO}_4)_6(\text{OH})_2$ , HA) is a member of the “apatite” compound family and constitutes the inorganic part of the bone which can be described as a kind of composite material composed of organic, i.e. collagen, and inorganic components<sup>1</sup>. It is an important issue to be able to produce HA powders in large amounts with controlled chemical composition and microstructure properties so that wet chemical precipitation technique is an ideal and simple way for this aim<sup>2-4</sup>. However, different apatite compounds can be obtained depending on the process parameters such as the dropping rate of the acid solution into the alkaline solution, reaction temperature, etc. and in this study, some of them were evaluated.

## EXPERIMENTAL METHODS

HA powders were obtained by the wet chemical precipitation technique by considering different process parameters such as the reaction temperature,  $\text{NH}_4\text{OH}$  addition, dropping rate of the acid solution, etc.<sup>5-7</sup> Calcium hydroxide ( $\text{Ca}(\text{OH})_2$ ) was used as the calcium source precursor while orthophosphoric acid ( $\text{H}_3\text{PO}_4$ ) as the phosphorus source precursor. The samples prepared were grouped in Table 1 and Table 2 depending on the order of precursor addition. Table 1 includes the samples that were produced by adding the phosphorus source to the calcium source and Table 2 contains the samples synthesized by calcium source addition to the phosphorus source. For every sample similar experimental sequence was followed which is composed of the stated steps respectively<sup>5,6</sup>: preparing 100 ml of 0,5M  $\text{Ca}(\text{OH})_2$  and 100 ml of 0,3M  $\text{H}_3(\text{PO}_4)$  solutions and reaction of these precursor solutions by applying continuous stirring, aging of the final solution and precipitation at room temperature, filtrating and washing the precipitation with distilled water, drying the precipitation at 110 °C for 2h and eventually heat treating the precipitation at 900 °C for 1h with 10 °C/min heating speed by using a high temperature laboratory furnace.

**Table 1.** Process parameters of the samples obtained by adding the phosphorus source to the calcium source.

Sample	Process Parameters
WCP-1	room temperature, without $\text{NH}_4\text{OH}$ addition, 4h stirring
WCP-2	room temperature, without $\text{NH}_4\text{OH}$ addition, rapid acid dropping rate
WCP-3	50-60 °C, with $\text{NH}_4\text{OH}$ addition, rapid acid dropping rate
WCP-4	50-60 °C, without $\text{NH}_4\text{OH}$ addition, rapid acid dropping rate

**Table 2.** Process parameters of the samples obtained by adding the calcium source to the phosphorus source.

Sample	Process Parameters
WCP-5	room temperature, without $\text{NH}_4\text{OH}$ addition, 3h stirring
WCP-6	60-70 °C, with $\text{NH}_4\text{OH}$ addition, 6h stirring
WCP-7	60-70 °C, without $\text{NH}_4\text{OH}$ addition, 6h stirring
WCP-8	room temperature, without $\text{NH}_4\text{OH}$ addition, 6h stirring

## RESULTS AND DISCUSSION

Crystal phases (Table 3) were determined by utilizing the X-Ray Diffraction (XRD) analysis.

**Table 3.** XRD results of the WCP-(1-8) samples.

Sample	XRD Results	Sample	XRD Results
WCP-1	HA	WCP-5	HA
WCP-2	HA	WCP-6	HA Whitlockite
WCP-3	HA	WCP-7	HA Whitlockite
WCP-4	HA Ca-deficient HA	WCP-8	HA Whitlockite

## CONCLUSION

Applying different process parameters resulted in the production of  $\text{Ca}_5(\text{PO}_4)_3(\text{OH})$  (HA, syn., PDF#09-0432) for the all experiments. However,  $\text{Ca}_3(\text{PO}_4)_2$  (Whitlockite, syn., PDF#09-0169) and  $\text{Ca}_9\text{HPO}_4(\text{PO}_4)_5\text{OH}$  (Ca-deficient HA, PDF#46-0905) phases were also detected for some of the cases during synthesis.

## REFERENCES

1. Ratner B.D. *et al.*, Biomaterials Science An Introduction to Materials in Medicine 2nd Edition, Elsevier Academic Press. New York-London, 2004.
2. Nayak A.K., Int J ChemTech Res. 2(2):903-907, 2010.
3. Afshar A. *et al.*, Mater Design. 24:197-202, 2003.
4. Saeri M. *et al.*, Mater Lett. 57:4064-4069, 2003.
5. Paz A., *et al.*, Quim. Nova. 35(9):1724-1727, 2012.
6. Salma K., *et al.*, Processing and Application of Ceramics. 4(1):45-51, 2010.
7. Garcia C., *et al.*, Key Eng Mater. 284-286:47-50, 2005.

## ACKNOWLEDGMENTS

The authors would like to thank the Research Fund (BAP) (Grant no: 37881) and Teaching Staff Training Program Office (ÖYP) of Istanbul University for providing financial support to this project.



Maziar Matloubi<sup>1</sup>, Nils Blumenthal<sup>1,2</sup> and V. Prasad Shastri<sup>1,2</sup><sup>1</sup>Institute of Macromolecular Chemistry, University of Freiburg, Germany<sup>2</sup>BIOSS - Centre for Biological Signaling Studies, University of Freiburg, Germany[maziar.matloubi@makro.uni-freiburg.de](mailto:maziar.matloubi@makro.uni-freiburg.de)

## INTRODUCTION

Polyurethane (PU) with good long-term cell and blood compatibility is highly desirable in cardiovascular applications. Most PUs currently in use were developed in early-late 1980's, however, they were not designed specifically to serve as scaffolds for vascular tissue engineering<sup>1</sup>. We have recently developed a new family of segmented polyurethanes (SPUs) possessing enhanced tunable mechanical properties<sup>2</sup> that undergoes biodegradation. In this study we report preliminary findings on degradability of SPUs in physiological condition and the cell compatibility of these surfaces to human endothelial cells.

## EXPERIMENTAL METHODS

Analytical Techniques: Differential Scanning Calorimetry (DSC) was used to determine the glass transition temperature ( $T_g$ ) of dry polymer films. Atomic Force Microscopy (AFM) was carried out on cryo fractured polymer samples to visualize phase segregation. Static water contact angle (CA) measurements were made on spun-cast polymer films at room temperature. Degradation studies were carried out polymer films in phosphate-buffered saline supplemented with sodium azide at 37 °C. The surfaces of the films were visually inspected and then imaged using scanning electron microscopy (SEM). The cellular compatibility of SPU films was assessed using human umbilical vein endothelial cells (HUVECs) and the viability was determined using MTT metabolic assay. Morphology of the cells were visualized using fluorescence microscopy after staining with FITC-Phalloidin for F-actin and DAPI nuclear stain.

## RESULTS AND DISCUSSION

SPU containing a 1:1 ratio of hydrophobic blocks and poly(L-lactic acid) (PLLA) showed a high CA of 110 ° in comparison to a CA of 83 ° for PLLA. So the high CA of 1:1 SPU could be attributed to the segregation of the hydrophobic segments to the surface due to their low surface energy. Degradation studies showed a gradual weight loss of polymer blocks without any cracks and breakage over a period of 6 months (**Figure 1**). SEM analysis revealed erosion on the surface of the polymer films with an intact bulk (**Figure 1, inset**). SPU 1:1 with 50% degradable PLLA component showed less weight loss than SPU 1:1.5 and SPU 1:2 which have 60 and 66 % PLLA in their composition respectively. This verified our design criteria that introduction of flexible hydrophobic segments could be used to both retard and control the degradation in the SPUs.

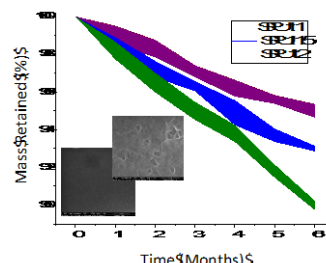


**Figure 1.** Retention of mass in SPUs as a function of time. Inset: SEMs of PSU 1:1 in two magnifications showing surface erosion.

To ascertain the suitability of these SPUs for cardiovascular applications, viability of HUVECs on SPU films of varying degradation behavior was undertaken and compared to

PLLA (Figure 2A). In general, HUVEC viability was comparable to PLLA a polymer approved by the FDA for many implantable applications. Also, qualitatively

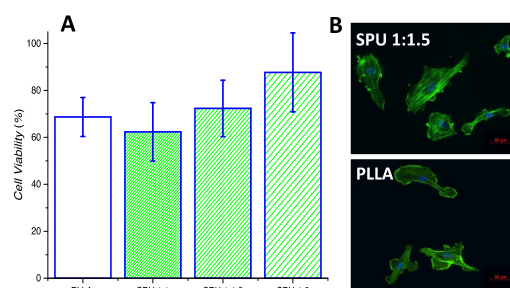


**Figure 2:** HUVEC viability on SPUs (A), and morphology (B). PLLA were used as controls for this study.

the HUVECs showed greater spreading on SPUs in comparison to PLLA (Figure 2B)

## CONCLUSION

SPUs investigated in this study exhibit tunable degradation rates in physiological conditions and show good compatibility towards HUVECs. These properties in addition to the tunability of mechanical properties<sup>2</sup> make this family of SPUs a good material class for cardiovascular applications. In ongoing studies the blood biocompatibility and fibrin adsorption of these SPUs is being assessed.

## REFERENCES

1. Zdrahala Richard J., and Ivanka J. Zdrahala, J. Biomater. Appl. 14.1 (1999)
2. Matloubi M. and Shastri V.P., ESB Talk Abstract (2015)

## ACKNOWLEDGMENTS

This study was supported by Excellence Initiative of the German federal and state government (EXC 294) and the State of Baden-Württemberg.

# Photo-responsive Fluoropolymer Coated Surface for Cell Adhesion Control

Masamichi Nakayama<sup>1</sup>, Tomonori Kanno<sup>1,2</sup>, Akihiko Kikuchi<sup>2</sup>, Teruo Okano<sup>1</sup>

<sup>1</sup> Inst. Adv. Biomed. Eng. & Sci., Tokyo Women's Medical University, Japan

<sup>2</sup> Department of Materials Science and Technology, Tokyo University of Science, Japan

[nakayama.masamichi@twmu.ac.jp](mailto:nakayama.masamichi@twmu.ac.jp)

## INTRODUCTION

Recently, active interaction control with biomolecules and cells using stimuli-responsive surfaces attracts great attention in biomedical field. In general, stimuli-responsive surfaces use hydrophilic/hydrophobic property change to regulate the interaction with bio-analytes<sup>1</sup>. On the other hand, moderately hydrophobic surfaces show high cell adhesiveness, while the strongly hydrophobic surfaces greatly reduce their cellular interaction<sup>2</sup>. We considered that the enhancement of surface hydrophobicity can be used as one of the triggers to reduce bio-related interaction. Herein, we designed a smart fluoropolymer-coated surface with showing a reversible surface hydrophobicity change derived from the photoisomerization of polymer-introducing spiropyrans moieties by light switch. Moreover, cell adhesion on photo-responsive surface was also investigated to demonstrate the possibility of reversible cell adhesion/detachment control.

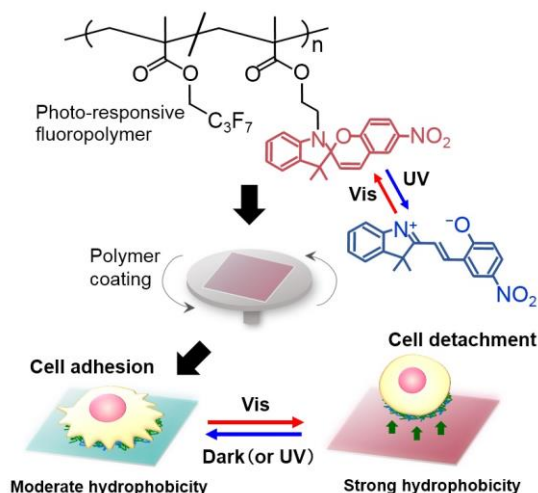


Figure 1. Schematic representation of photo-responsive fluoropolymer coated surface for cell adhesion control via light irradiation.

## EXPERIMENTAL METHODS

Poly(heptafluorobutyl methacrylate-*co*-spiropyrans methacrylate) [poly(F7MA-*co*-SpMA), monomer ratio of F7MA/SpMA: 87/13, molecular weight: 44000] was synthesized and spin-coated (1wt% polymer solution) on hydrophobic glass surface (Figure 1). The surface was characterized by ATR/FT-IR and ellipsometry. We determined surface water-wettability change after irradiating either ultraviolet (UV, 352 nm) or visible (Vis, 530 nm) light by static contact angle measurement of water droplet method. Bovine endothelial cells (BECs) were cultured on UV light-treated surface, and then the difference in cell adhesiveness was investigated between before and after visible light irradiation. In

addition, confluent cultured cells were treated by Vis-light irradiation for harvesting as a cell monolayer.

## RESULTS AND DISCUSSION

The amount of polymer and polymer layer thickness on the surfaces were 6.08  $\mu\text{g}/\text{cm}^2$  and 36.3 nm, respectively. Contact angle study showed a reversible surface wettability change via UV/Vis-light irradiation due to the photoisomerization of spiropyrans units between hydrophilic merocyanine (ME) and hydrophobic spiropyran (SP) forms (contact angles after irradiating UV- and Vis-light were of 78° and 88°, respectively).

BECs significantly adhered on the moderately hydrophobic surface with ME-forms, compared to the strongly hydrophobic surface with SP-forms. In addition, adhering cells on the moderately hydrophobic surface spontaneously detached after Vis-light irradiation probably due to the decrease in surface-cell affinity (Figure 2). Moreover, confluent cultured cells were able to be harvested as a single cell monolayer (cell sheet) with maintaining cell-cell junctions and extracellular matrix proteins via the Vis-light irradiation. These results indicate that the light-induced moderately/strongly hydrophobic surface change can be used to control cell adhesion behavior.

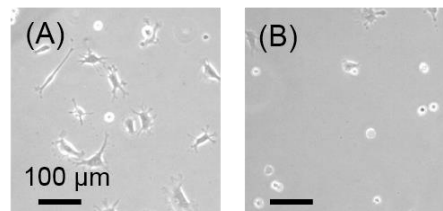


Figure 2. Phase-contrast microscopic pictures of cells on poly(F7MA-*co*-SpMA) coated surface after irradiating (A) UV- and (B) Vis-light.

## CONCLUSION

Smart surface with showing moderately/strongly hydrophobic switchable surface was designed by physical coating of spiropyran-pendant fluoropolymer. Vis-light-induced hydrophobic enhancement allowed adhering cells to detach from the surfaces. This smart surfaces would be promising tools for cell manipulation and separation in biomedical applications.

## REFERENCES

1. Nagase K. *et al.*, J. R. Soc. Interface, 6; S293–S309, 2009
2. Tamada Y. and Ikada Y., J. Biomed. Mater. Res., 28; 785–789, 1994

## ACKNOWLEDGMENTS

This study was partially supported by Grant-in-Aid for Scientific Research (B) (Grant No. 25282145) from the Ministry of Education, Culture, Sports, Science and Technology (MEXT), Japan.



# The Effect of the Vesicle Diameter on the Bending Rigidity of POPC and DOPC Lipid Bilayers

Dominik Drabik<sup>1</sup>, Magdalena Przybyło<sup>1</sup>, Marek Langner<sup>1</sup>

<sup>1</sup>Department of Biomedical Engineering, Wrocław University of Technology, Wrocław, Poland

[Dominik.drabik@pwr.edu.pl](mailto:Dominik.drabik@pwr.edu.pl)

## INTRODUCTION

Lipid bilayer, a constitutive component of any biological membrane, serves as a scaffold for many biochemical processes such as energy transfer. To understand these processes it is necessary to quantitate the lipid bilayer physical properties including its dynamics and mechanics. The elasticity of the lipid bilayer is believed to play important role in cell functioning by affecting the membrane trafficking within the cell volume whereas its dynamics influences a range of processes in different time scales. The membrane bending is quantitated by coefficient defined by W. Helfrich<sup>1</sup> model. The bending rigidity coefficient can be measured by quantitation thermal fluctuations of the lipid bilayer model.

## EXPERIMENTAL METHODS

The thermal fluctuations of the lipid bilayer can be used for the determination of the bending coefficient. In the methods the thermal fluctuations are quantitated based on a series of microscopic images of lipid membrane model ("flicker noise spectroscopy"). 1200 images of fluorescently labelled liposomes equatorial cross-sections are collected using fluorescence confocal microscopy (Zeiss LSM 510 Meta with 40x water immerse objective). Images were acquired at a rate of 7 frames per second. The acquired microscopic images are numerically analyzed according to well established methodologies; average-based method<sup>2</sup> or the statistical method<sup>3</sup>.

## RESULTS AND DISCUSSION

In presented studies the bending rigidity of lipid bilayers formed from DOPC or POPC lipids were measured. The typical image of fluorescently labelled liposome is presented on Figure 1. To identify contour of vesicle the self-written C++ software with OpenCV library was used. Obtained images were used to identify and quantitate thermal fluctuations, which have been next fitted to mechanical model. All calculations have been carried out with MATLAB software.

At least 8 vesicles were measured and analyzed to confirm possible correlation. The correlation of bending rigidity coefficient with liposome diameter was better than  $R^2=0,80$ . The correlation between bending rigidity of DOPC and POPC membranes and diameters of vesicles is presented on Figure 2 and Figure 3, respectively.

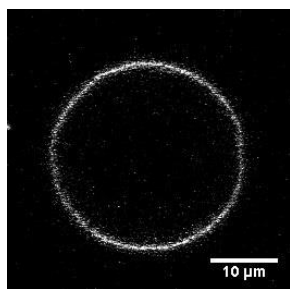


Figure 1. The typical image of DOPC vesicle cross-section.

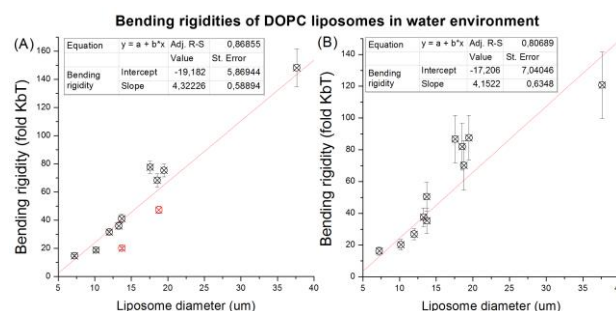


Figure 2. The dependence of the bending rigidity of DOPC membrane in water on vesicle diameter. Panel A and Panel B present data obtained when vesicle contour was analyzed using average-based method and statistical method, respectively.

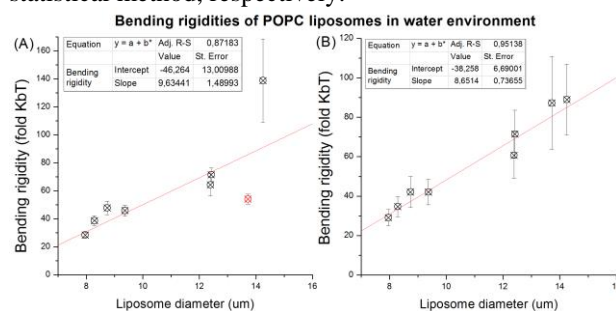


Figure 3. The dependence of the bending rigidity of POPC membrane in water on vesicle diameter. Panel A and Panel B present data obtained when vesicle contour was analyzed using average-based method and statistical method, respectively.

## CONCLUSION

Presented results show, for the first time, that the bending rigidity coefficient determined with the "flickering noise technique" depends on size of lipid vesicles. The effect is significant; the value of the bending rigidity coefficient rises by almost an order of magnitude when vesicle diameters differ only by factor of two.

## REFERENCES

1. Helfrich, W., Elastic Properties of Lipid Bilayers: Theory and Possible Experiments. *Z. Naturforsch.*, 1973. 28(c): p. 693-703,
2. Facon, J.F., et al., Bending elasticity and thermal fluctuations of lipid membranes. Theoretical and experimental requirements. *J. Phys. France*, 1989. 50: p. 389-414,
3. Meleard, P., et al., Advantages of statistical analysis of giant vesicle flickering for bending elasticity measurements. *Eur Biophys J.E.*, 2011. 34(116): p. 1-14.

## ACKNOWLEDGMENTS

This work was supported by DEMONSTRATOR+ grant UOD-DEM-1-027/001.

Youn-Mook Lim<sup>1\*</sup>, Young Min Shin<sup>1</sup>, Jong-Seok Park<sup>1</sup>, Hui-Jeong Gwon<sup>1</sup>, Sung In Jeong<sup>1</sup>, Sohyoun Lee<sup>2</sup>

<sup>1</sup>Research division for industry and environment, Advanced radiation technology institute, Korea atomic energy research institute, Jeongeup-si, Jeollabuk-do, Korea

<sup>2</sup>Department of Prosthodontics, Pusan national university, Korea  
[ymlim71@kaeri.re.kr](mailto:ymlim71@kaeri.re.kr)

## INTRODUCTION

Recently, numerous efforts to develop an ideal scaffold mimicking a native extracellular matrix (ECM) have been conducted using a variety of materials and techniques. In particular, hydrogel has been designed to provide a specific site or three-dimensional space for cells to regenerate damaged tissue. However, some hydrogels have exhibited different microenvironments without fibrous architectures similar to a collagen presented by ECM, and the structural discrepancy might hinder the development of artificial tissues or organs. In this report, we developed fibrous particles (FP), which can act as collagen fibrils in the ECM, and investigated the influence of FP on the encapsulated hMSC behavior in the hydrogel.

## EXPERIMENTAL METHODS

A PLLA sheet was fabricated through electrospinning, which was fragmented into the FP by aminolysis under shear stress.<sup>1</sup> For the functionalization, acrylic acid was grafted onto the FP under gamma-ray exposure,<sup>2</sup> and subsequently RGD peptide was conjugated through the induced carboxyl groups by EDC chemistry. RGD-FP and hMSC were mixed in the alginate solution, which was cross-linked by Ca<sup>2+</sup> ions. The cellular responses in the hydrogel were investigated with metabolic activity measurement, immunofluorescent staining, and an ALP assay for osteogenic differentiation.

## RESULTS AND DISCUSSION

The mean length of FP was  $28.9 \pm 6.6 \mu\text{m}$ , and  $177.2 \pm 18.9 \text{ nmol/mg}$  of the RGD peptide was conjugated. The RGD-FP was homogeneously distributed in the hydrogel. Gelation behaviors and mechanical property of the hydrogel were affected by the RGD-FP incorporation. Gelation time was delayed in a RGD-FP concentration dependent manner, and storage or loss modulus was significantly increased due to the loaded RGD-FP. The RGD-FP loaded hydrogel improved the viability of the cells for 14 days, in which the metabolic activity of the cells was approximately 1.5-times higher than those in other hydrogels. Consistent results for cell viability were identified with Live/Dead staining. In hydrogel, the cells could bind to the RGD-FP, and presented spatial spreading morphology in 3D. Furthermore, those bindings facilitated osteogenic

differentiation and mineralization under constant differentiation induction.

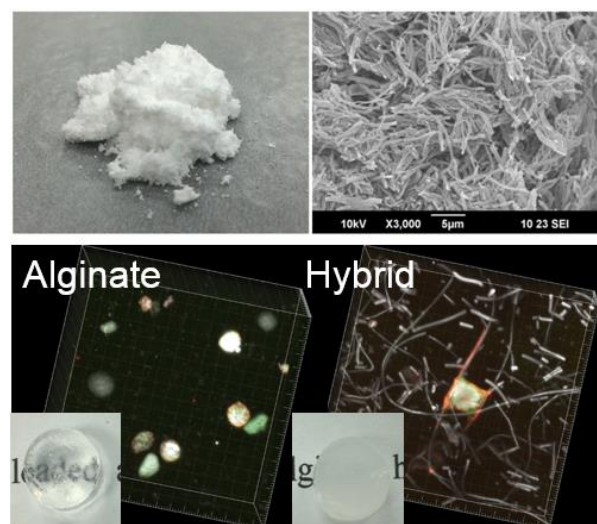


Fig. 1. RGD-FP loaded hydrogel and cell spreading in 3D

## CONCLUSION

Our hybrid hydrogel containing RGD-FP concomitantly presents structural and biochemical cues for regulating cell behaviors. In a 3D hydrogel, the cells successfully bound to the particles, and displayed spatial spreading morphology. The bindings could improve the viability and differentiation of the cells. Therefore, our strategy to append the fibrous particles in the hydrogel can be a novel tool to improve the cell survival in 3D.

## REFERENCES

1. T. G. Kim *et al.*, Macromol. Rapid Commun., 29:1231-1236, 2008
2. Y. M. Shin, *et al.*, Biomacromolecules, 9(7):1772-1781, 2008

## ACKNOWLEDGMENTS

This work was supported by National Research Foundation of Korea (NRF) grant funded by the Korea government (MSIP). (2012M2A2A6013196)

Monika Bil<sup>1\*</sup>, Natalia Wojas<sup>1</sup>, Marcin Heljak<sup>1</sup>, Joanna Idaszek<sup>1</sup>, Wojciech Świąszkowski<sup>1</sup>

<sup>1</sup>Faculty of Materials Science and Engineering, Warsaw University of Technology, Poland  
[mbil@inmat.pw.edu.pl](mailto:mbil@inmat.pw.edu.pl)

## INTRODUCTION

The multifunctional polymers that integrate shape-memory capability and biodegradability present enormous opportunities for the design of next generation, resorbable less invasive smart medical implants, tissue scaffolds and medical devices [1,2].

Shape memory polymers (SMPs) with thermo-responsive memory effect could utilize the difference between the ambient temperature and the temperature of the human body, as the stimulus that activate shape changing. The intrinsic mechanism for shape memory behaviour in thermal responsive SMPs is the reversible freezing and activation of polymeric chain motion in the switching segments below and above the transition temperature ( $T_{trans}$ ), respectively. The transition temperature ( $T_{trans}$ ) is either a glass transition temperature ( $T_g$ ), or a melting temperature ( $T_m$ ). The previous data [3] indicate that sharp transitions with narrow range of transition temperature and fully shape recovery exhibit SMPs with crystalline switching segments and fully cross-linked network. However, it should be noted that in case covalently cross-linked polymers limited number of processing methods could be utilized for fabrication of three-dimensional porous scaffolds.

Therefore, in order to intensify the transfer of research results to medical practice additional research in terms of technology optimization is required. The aim of the presented research is to develop thermoplastic biodegradable polymers with thermo-responsive shape memory effect in a narrow temperature range close to the physiological range.

## EXPERIMENTAL METHODS

Poly(lactide) (PLA) and polycaprolactone (PCL) were blended in solvent with different weight ratios. Polyurethanes based on caprolactone (CL) and lactide (LA) oligomers were synthesized in one-shot process using 1,6-hexamethylene diisocyanate (HMDI) as a coupling agent and dibutyltin dilaurate as the catalyst. Chemical structure of the materials were analysed by FTIR spectroscopy. Transition temperature – melting temperature ( $T_m$ ) and crystallinity were analysed by differential scanning calorimetry (DSC). The storage modulus of samples and shape memory effect were determined using a dynamic mechanical analyser (DMA). The shape recovery ratio  $R_r$  and the fixity ratio  $R_f$  were calculated based on DMA measurement. *In vitro* biocompatibility test with L929 cell line were also performed.

## RESULTS AND DISCUSSION

A series of biodegradable PCL/PLA blends and LA/CL-based urethanes with various compositions were obtained. The DSC results revealed that transition temperature can be more effectively modulated at urethane systems than at blends (Fig.1). Additionally, quantitative assessment of the shape memory performance through strain-controlled shape memory cycles verified that blends exhibited shape-fixing ratio in the range of 76-96% and shape recovery ratio from 50 to 100% whereas LA/CL-urethanes demonstrated  $R_f$  and  $R_r$  in the range of 79-99 % and 83-100%, respectively.

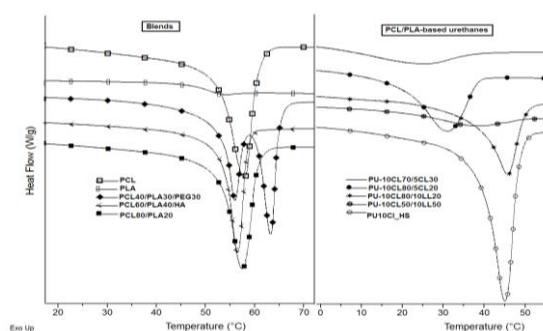


Fig. 1 DSC thermograms of PCL/PLA blends and PCL/PLA –based urethanes

These results indicate that the transition temperature ( $T_{trans}$ ) of the CL/LA-urethanes can be tailored for shape restoration when inserted in the human body without external heat source.

## CONCLUSION

A series of thermoplastic LA/CL-urethane materials with shape-memory properties based on biodegradable switching segments were designed. This kind of materials may have great potential as self-fitting tissue scaffolds and implants.

## REFERENCES

1. Huang W.M. *et al*, Adv.Drug Deliv. Rev. 65;4;515-535,2012,
2. Wishke Ch, *et.al.*, Journal of Controlled Release 138: 243-250, 2009
3. S. Pandini *et al.* Polymer 53: 1915-1924, 2012

## ACKNOWLEDGMENTS

“The authors would like to thank the National Centre for Research and Development (Grant no: LIDER/037/673/L-4/12/NCBR/2013) for providing financial support to this project”.

## Towards an Embedded Integrated Measurement System for the In Vitro Monitoring of Biomedical Impedance Related to Fibrosis Phenomenon

Mehdi Terosiet<sup>1</sup>, Aymeric Histace<sup>1</sup>, Olivier Romain<sup>1</sup>, Michel Boissière<sup>2</sup>, Sabrina Kellouche<sup>2</sup>, Franck Carreiras<sup>2</sup>, Emmanuel Pauthe<sup>2</sup>

<sup>1</sup>ETIS, ENSEA, University of Cergy-Pontoise, CNRS, Cergy, France

<sup>2</sup>ERRMECe, University of Cergy-Pontoise, France

[emmanuel.pauthe@u-cergy.fr](mailto:emmanuel.pauthe@u-cergy.fr)

### INTRODUCTION

Nowadays science and technology have deep involvement in the development of embedded systems for health to achieve the wireless monitoring of different physiological parameters. Nevertheless, a natural response of the immunity system to the implantation of such devices within the human body is the fibrosis phenomenon consisting in an abnormal proliferation of the surrounding cells in order to isolate the electronic device considered as an unnatural intrusion. Currently, the compensation of fibrosis phenomenon represents a veritable challenge for future embedded system. Fibrosis can damage the embedded system by surrounding this one, making it suboptimal or non-functional. We investigate here the possibility of directly monitoring the fibrosis proliferation in the surroundings area of the implant in order to control and regulate its functioning.

### EXPERIMENTAL METHODS

The study of fibrosis induced by an implanted medical device can be studied by the impedance measurement of the interface between the cells and the electrode of the device<sup>1</sup>. More precisely, a comparative study of electrical and biological parameters collected along the time will allow identifying an electrical marker of fibrosis development, used for establishing a systematic monitoring method. Main principle of bioimpedance measurement is to submit the living tissue to a small AC electrical current (less than 20 $\mu$ A) and to extract from the response the changes in magnitude and phase shift so that to obtain a complex impedance diagram. Scan of a wide frequency range is of primary benefits for a more interesting characterization of the usual electrical cell model of fig. 1.

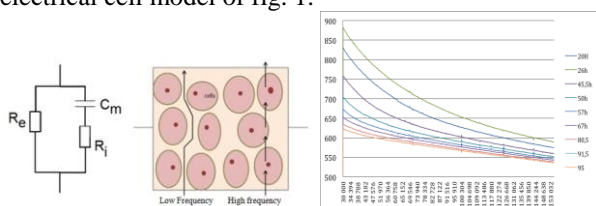


Fig. 1. Left: Frequency flow through cell membrane. Right: Example of Impedance Diagram obtained with the designed measurement circuits (in vitro conditions)

Taking into account the specificities of electrical model of figure 1, and the constraints imposed by a wireless embedded monitoring of impedance changes, we propose an adapted architecture based on the most recent technology and in accordance with a use in a culture chamber for instance. The embedded system for wireless impedance measurement is composed of a Mbed NXP LPC 1768 microcontroller, a AD5933 impedance converter chip<sup>2</sup>, a Xbee wireless

communication module and finally a Sensor/Electrode module.

In order to acquire impedance from the biological material, the AD5933 device excites the medium, with a frequency ranging from 10 Hz to 100 kHz, and gets the response. For each frequency step, the chip samples the response. After the frequency sweep is complete, a DFT is processed internally and returns the real and imaginary parts of the measured impedance for each frequency. These real and imaginary data are then transferred to an external PC Controller via the Xbee protocol. Cortex M0 processor allows to parametrize and drive all the devices and master the whole acquisition / transmission sequence.

### RESULTS AND DISCUSSION

The measuring system was experienced for different resistors. The results are summarized in Table 1.

Tab. 1 Measured resistances for system validation

Rtest ( $\Omega$ )	Real (Hexa)	Imaginary (Hexa)	Admittance magnitude (w/o SF)	Calculated Resistance
560	CEB2	ECB2	13555	716
1000	E36F	EFA3	8428	1152
4700	F8DF	FC37	2066	4700
10000	FBF3	004D	1034	9392

A non-zero value for the imaginary components was expected since the AD5933 operates with known intrinsic phase drift. For a resistor of 560  $\Omega$ , the difference between the resistor under test and the calculated one is large. Actually, the AD5933 datasheet defines its operating range from 1 k $\Omega$  to 1 M $\Omega$  [2]. For the three other values, the maximal relative error is of 15.2% when the mean one is about 7.1%.

### CONCLUSION

As a proof of feasibility, we demonstrate on simple use case that the proposed architecture makes possible an automatic, accurate and secure transmission of impedance data. This is the first step for an in vitro systematic use of the device in the context of an in-vitro monitoring of cell proliferation (see figure 2 for illustration of first results), tentatively related to the fibrosis phenomenon, but also, at a longer term for the designed of a complete in-vivo system to be used in real-leaving condition.

### REFERENCES

- [1] Angelo Rottigni, "Electronical instrumentation for impedance measurement on biosamples", PhD Thesis, 26-mar-2012, Politecnico di Milano, 2011
- [2] Texas Instruments, "1 MSPS, 12-Bit Impedance Converter, Network Analyser", AD5933 Datasheet [Revision E, 2013]



## Preparation of Beetosan

Bożena Tylińczak<sup>1</sup>, Katarzyna Z. Gaca<sup>1</sup>, Katarzyna Bialik-Was<sup>1</sup>, Dagmara Malina<sup>2</sup>, Agnieszka Sobczak-Kupiec<sup>2</sup>

<sup>1</sup> Department of Chemistry and Technology of Polymers, Cracow University of Technology, Poland

<sup>2</sup> Institute of Inorganic Chemistry and Technology, Cracow University of Technology, Poland

[asobczak@chemia.pk.edu.pl](mailto:asobczak@chemia.pk.edu.pl)

### INTRODUCTION

Chitin and chitosan are widely used in cosmetics, biotechnology and biomedicine. They are commonly used in preparation of hydrogel dressings, as they belong to a group of substances which accelerate the wound healing process. Great interest in these polysaccharides is primarily due to their properties, which include: biocompatibility, biodegradability, bacteriostatic properties, non-toxicity, good adsorption, very good mechanical strength and bioadhesion [1-4]. Chitosan which is derived from bees' exoskeletons is called Beetosan®.

### EXPERIMENTAL METHODS

The aim was to obtain Beetosan® - chitosan from exoskeletons (armours) of bees. Typically extraction of chitin from armour of the bees is carried out in the following manner: dead bees are crushed, then proteins and calcium carbide are removed chemically. Enzymatic deacetylation of chitin is an interesting alternative to the chemical process. Thin and soft bees' armours are well suited for the mild conditions of the process, which generates significantly less waste than conventional chemical process. Enzymatic modification also allows to carry out the process under controlled conditions, which would enable the production of Beetosan with a predetermined degree of acetylation.

### RESULTS AND DISCUSSION

Proteins were successfully removed using a weak solution of sodium hydroxide (1-10%) at a high temperature (85-110 °C). Liners were then chopped and deprived of calcium carbide, which was carried out by treatment with a weak solution of hydrochloric acid (1-10%) at room temperature. Physicochemical properties of the chitin naturally depend on the parameters of the extraction. The most influential parameters are: temperature, concentrations of used chemicals, the time of their operation and the concentration and size of armours. The basic parameters which characterize chitin are the degree of polymerization, deacetylation and purity. When chitin is soluble in weak acids, then we can speak of chitosan, which is formed when chitin is reacted with a strong solution of sodium hydroxide (NaOH) (> 40%) at a high temperature (90-120 °C). Such a "violent" reaction on chitin is its deacetylation, resulting in the removal of acetyl groups (-CH<sub>3</sub>) from

the amine groups (-NH<sub>2</sub>), forming a soluble product - chitosan. It is believed that at least 65% of acetyl groups should be removed from any chitin polymer to obtain a soluble product. The degree of deacetylation is dependent on the reaction time, temperature and concentration of NaOH

### CONCLUSION

The problem which is aimed to be solved within the project, is utilization of dead bees. Once every few years every beekeeper must replace the bee hives, and thus get rid of the old degenerate units. As a result, such an exchange produces waste in the form of dead bees which have to be disposed of. Often these wastes are incinerated in an uncontrolled manner or ground and served as food for farmed fish. Preparation of chitosan from bees' exoskeletons (armours) solves the utilization problem of these dead insects while giving high quality product for biomedical applications, especially wound dressings.

### REFERENCES

References must be numbered. Keep the same style.

1. Kumar M.N.V.R., Reactive and Functional Polymers, 46: 1-27, 2000
2. Alsarra I., International Journal of Biological Macromolecules, 45: 16-21, 2009
3. Silva C.L., Pereira J.C., Ramalho A., Pais A.A.C.C., Sousa J.J.S., Journal of Membrane Science, 320: 268-279, 2008
4. Tajik H., Moradi M., Rohani S.M.R., Erfani A.M., Jalali F.S.S., Molecules, 13: 1263-1274, 2008

### ACKNOWLEDGMENTS

"The authors would like to thank the The National Centre for Research and Development (Grant no: LIDER/033/697/L-5/13/NCBR/2014) for providing financial support to this project".



## Preparation of Chitosan Hydrogel Modified with *Salvia Officinalis*

Bożena Tylińczak<sup>1</sup>, Katarzyna Z. Gaca<sup>1</sup>, Katarzyna Białik-Was<sup>1</sup>, Dagmara Malina<sup>2</sup>, [Agnieszka Sobczak-Kupiec](mailto:asobczak@chemia.pk.edu.pl)<sup>2</sup>

<sup>1</sup> Department of Chemistry and Technology of Polymers, Cracow University of Technology, Poland

<sup>2</sup> Institute of Inorganic Chemistry and Technology, Cracow University of Technology, Poland  
[asobczak@chemia.pk.edu.pl](mailto:asobczak@chemia.pk.edu.pl)

### INTRODUCTION

Hydrogels prepared from chitosan due to their high biocompatibility and biodegradability are increasingly often used in many areas of medicine and pharmacy. These materials can absorb and retain up to thousand times more water than their dry weight, which is why they are mainly used as wound dressings. The aim of this study was to obtain chitosan-based hydrogels and then to modify them with *salvia officinalis* extracts [1-5].

### EXPERIMENTAL METHODS

The scope of the research included measuring the swelling ability of the obtained hydrogels in various liquids: distilled water, sodium chloride and magnesium dichloride. Moreover, incubation studies were conducted in a number of solutions, such as distilled water, sodium chloride, Ringer's and Tyrode fluids. The biological activity was investigated with the addition of a solution of potassium chromate. Additionally, the structure of the samples was investigated by means of identification of several characteristic functional groups. This study was performed using Fourier transform infrared spectroscopy (FTIR).

### RESULTS AND DISCUSSION

In the initial stage of the research hydrogels containing different amounts of chitosan were synthesized using a UV lamp. Then samples were subjected to a swelling test in distilled water and 0,9 % solution sodium chloride and magnesium dichloride, which showed that the greatest sorptive capacity is exhibited in distilled water. The obtained hydrogels were also subjected to incubation tests in distilled water, 0,9 % NaCl solution, Ringer's solution and Tyrode fluid for a period of two weeks. In each of the solutions with an increase of pH value was observed. High biological activity was revealed by a very fast decolorization of a KMnO<sub>4</sub> solution. Finally the hydrogels were analysed using Fourier transform infrared spectroscopy (ATR-FTIR). For this purpose, the samples were placed on a diamond

and the measurement was possible due to incidence of the light beam on the inner surface of the hydrogels. This analysis allowed a detailed description of the spectrum, which contained characteristic vibrations of functional groups of the polymers.

### CONCLUSION

Basing on the incubation and biological activity studies, it can be stated that all obtained hydrogels containing different amount of chitosan exhibit high activity. This is due to the use of organic compounds such as chitosan and *salvia officinalis* as substrates. These materials are very promising and may be used in the treatment of diabetic wounds and burns.

### REFERENCES

1. Hoffman A.S., Advanced Drug Delivery Reviews, 64: 18-23, 2012.
2. Bhattarai, N., Gunn, J., Zhang, M., Advanced Drug Delivery Reviews, 62: 83-99, 2010.
3. Van Vlierberghe S., Dubruel P., Schacht E., Biomacromolecules, 12: 1387-1408, 2011.
4. Lee S., Kwon I., Park K., Advanced Drug delivery Reviews, 65: 17-20, 2013.
5. Feng E., Ma G., Wu Y., Wang H., Carbohydrate Polymers, 111: 463-468, 2014.

### ACKNOWLEDGMENTS

"The authors would like to thank the The National Centre for Research and Development (Grant no: LIDER/033/697/L-5/13/NCBR/2014) for providing financial support to this project".



Anna Mikulska<sup>1</sup>, Joanna Filipowska<sup>2</sup>, Agnieszka Iwanowska<sup>1</sup>, Anna Osyczka<sup>2</sup>, Maria Nowakowska<sup>1</sup>  
and Krzysztof Szczubiałka<sup>1</sup>

<sup>1</sup>Faculty of Chemistry, Jagiellonian University, Poland

<sup>2</sup>Department of Biology and Cell Imaging, Jagiellonian University, Poland  
[szczubia@chemia.uj.edu.pl](mailto:szczubia@chemia.uj.edu.pl)

## INTRODUCTION

The light-responsive polymers are a group of polymers whose structure and/or properties change in response to the absorbed light<sup>1</sup>. These properties include chemical reactivity, conductivity, refractivity, photochromism, etc. A special group of photoresponsive polymers are polymeric photosensitizers which do not change upon light absorption but may induce chemical reactions in other molecules present in their surroundings. Most of light-responsive polymers are of industrial and technological interest, while their biomedical uses are still infrequent. Here, we describe the applications of light-responsive polymers for the preparation of functional biomedical materials.

## RESULTS AND DISCUSSION

We have applied light-responsive polymers to obtain three different types of materials.

### 1. Molecularly photoimprinted hybrid polymer-silicagel materials for the selective adsorption of adenine compounds of biomedical interest.

We obtained a series of thymine-containing synthetic polymers to form LbL ultrathin multilayers on silicagel microspheres. Thymine forms dimers when excited with UV light, so irradiation of the multilayers with UV light results in the multilayer photocrosslinking. Thymine binds to adenine, a complementary nucleobase, via hydrogen bonds so the latter is adsorbed on the surface coated with a thymine-containing multilayer.

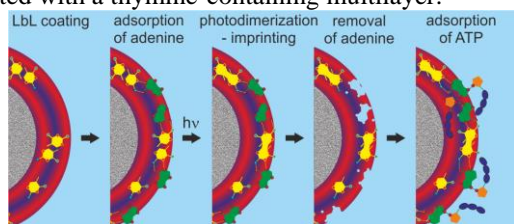


**Figure 1. A scheme showing the principle of the preparation of ATP-photoimprinted microspheres.**

Therefore, adenine or compounds containing adenine functionalities could be photoimprinted in the polymeric multilayer by adsorption of adenine followed by UV irradiation (see Figure 1). Photoimprinting resulted in increased selectivity of adsorption of adenine<sup>2</sup>, adenosine<sup>3</sup> and ATP<sup>4</sup> vs other nucleobases, nucleosides and nucleotides, respectively. These materials are of interest as adsorbents of adenine compounds which are biochemical markers of some pathologies, e.g. cancer. Importantly, the same principle can be applied to obtain adsorbents for compounds of other nucleobases.

### 2. Photocrosslinkable cell culture supports for culturing human mesenchymal stem cells (hMSCs).

We have prepared cell culture supports in the form of ultrathin LbL multilayers obtained from anionic

polysaccharides such as pectin,  $\iota$ -carrageenan, heparin, hyaluronic acid and chondroitin sulfate and photoactive cationic diazo-resin. Irradiation of the supports resulted in the photocrosslinking of the multilayers and their increased resistance against solvents. The supports obtained using pectin were found to induce osteogenic response in human mesenchymal stem cells<sup>5</sup>, while those obtained from  $\iota$ -carrageenan significantly accelerated the growth of hMSCs<sup>6</sup>.

### 3. Insulin-functionalized osteoinductive cell culture supports

Insulin could be photoimmobilized on the surface of the LbL multilayer cell culture support obtained from pectin and diazo-resin<sup>7</sup>. This was achieved by UV irradiation of the support immersed in the insulin solution resulting in the reaction of diazo-resin with insulin (Figure 2). It was found that the effect of immobilized insulin on the proliferation of cultured hMSCs and its osteoinductivity differs significantly from those of dissolved insulin. Moreover, osteogenic activities of insulin and rhBMP-2 protein were found to be additive.

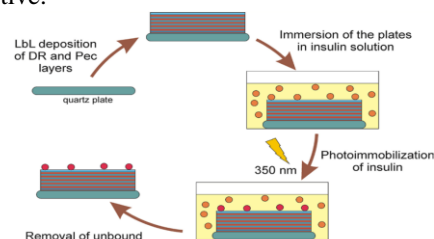


**Figure 2. Fabrication of insulin-functionalized cell culture supports.**

## CONCLUSION

The light-responsive polymers are very attractive for preparation of smart functional biomedical materials.

## REFERENCES

1. Schnabel W. *Polymers and light*. Wiley-VCH, 2007
2. Wybrańska K *et al. Chem.Mater.* **2010**, 22, 5392.
3. Mikulska A *et al. Eur.Polym.J.* **2014**, 59, 230.
4. Plewa A *et al. J.Med.Chem.* **2012**, 55, 8712.
5. Plewa A *et al. Eur.Polym.J* **2011**, 47, 1503.
6. Mikulska A *et al. Cell Prolif.* **2014**, 47, 516.
7. Mikulska A *et al. Front.Chem.* **2015**, 117.

## ACKNOWLEDGMENTS

Polish National Science Centre grants UMO-2011/03/B/ST5/01559, UMO-2012/05/N/ST5/01495 and Foundation for Polish Science grant co-financed by the EU European Regional Development Fund, PolyMed, TEAM/2008-2/6 are acknowledged

# Hyaluronic Acid Modified as $\alpha,\beta$ -Unsaturated Aldehyde - Biopolymer Suitable for Tissue Engineering and Drug Delivery

Radovan Buffa<sup>1</sup>, Ivana Basarabová<sup>1</sup>, Petra Šedová<sup>1</sup>, Martina Dvořáková<sup>1</sup>, Lucie Wolfová<sup>1</sup>, Vladimír Velebný<sup>1</sup>.

<sup>1</sup>Department of Chemical Modification, Contipro Biotech, Czech Republic

[buffa@contipro.cz](mailto:buffa@contipro.cz)

## INTRODUCTION

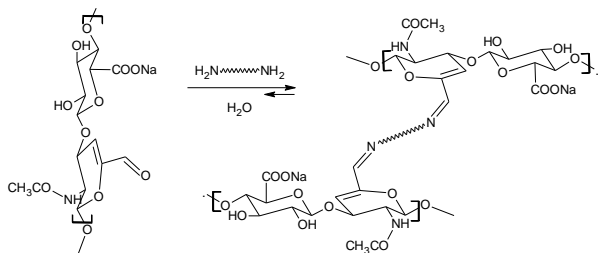
Hyaluronic acid modified with an aldehyde group has been extensively used for various medical and tissue engineering applications<sup>1</sup>. The main advantage of aldehyde moieties is their ability to react with a wide range of amino compounds at physiological conditions. This presentation describes an application of a unique HA-aldehyde derivative  $\alpha,\beta$ -unsaturated-6(GlcNAc)-oxo HA ( $\Delta$ HA-CHO) for preparation of cross-linked materials.

## EXPERIMENTAL METHODS

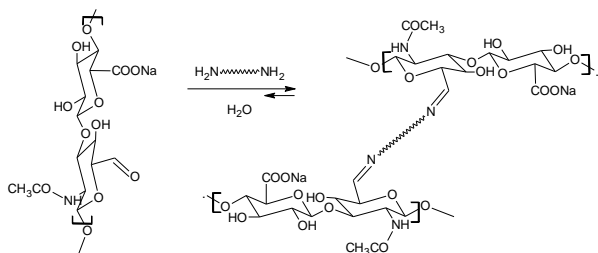
$\Delta$ HA-CHO and deacetylated HA were prepared from the native HA according to previously described procedures<sup>1</sup>. Hydrogel samples were prepared by mixing and a thorough homogenization of both components (solution of HA derivative in PBS and solution of linker in PBS). The samples were always left to mature for 240 minutes at room temperature, thereafter a homogenous transparent gel is formed. All samples were of the same proportions and were measured at constant laboratory conditions (temperature, pressure, humidity).

## RESULTS AND DISCUSSION

Crosslinking of  $\Delta$ HA-CHO is based on the condensation reaction of amino and aldehyde groups. Reaction is reversible and pH dependent (Scheme1). Several parameters have been investigated in order to prepare hydrogels with suitable mechanical properties. The most important are follows: structure of the linker, the ratio (molar amount of amino groups / molar amount of aldehyde groups) and concentration of polymer in solution have been studied in details.



Scheme1. Crosslinking of  $\Delta$ HA-CHO



Scheme2. Crosslinking of HA-CHO

Materials prepared from  $\Delta$ HA-CHO and HA-CHO (Scheme2) showed significantly different mechanical properties (Table 1) and *in vivo* stability.

Nr.	Compressive Young's modulus (kPa)	Compressive stress at Break (kPa)	Modulus of Toughness (J/m <sup>3</sup> )	Storage modulus (Pa)	Shear loss angle $\delta$ (°)
1	0.844	382.06	29690	160	2.36
2	0.482	309.29	19488	55	10.3

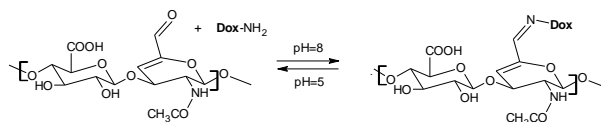
Table1.

Material Nr1. - 3% solution of  $\Delta$ HA-CHO in PBS and 3% solution of deacetylated hyaluronan in PBS)

Material Nr2. - 3% solution of HA-CHO in PBS and 3% solution of deacetylated hyaluronan in PBS)

Results demonstrate the advantageousness of the use of the  $\Delta$ HA-CHO compared to the saturated HA-CHO with regard to the preparation of more rigid and more tenacious (better crosslinked) materials suitable for tissue engineering.

Another possible application of  $\Delta$ HA-CHO is pH-responsible attachment of biologically active amines e. g. doxorubicin (Scheme2).



Scheme 2. pH-dependent attachment of doxorubicin on  $\Delta$ HA-CHO

Detailed NMR study showed that equilibrium is shifted in the area of pH values, that is very promising for potential *in vivo* applications.

## CONCLUSION

Several parameters of crosslinking reaction were successfully tested and their influence on the final mechanical properties and *in vivo* stability has been investigated. Results showed that prepared cross-linked hydrogels are fully biocompatible so  $\Delta$ HA-CHO has great potential for applications in tissue engineering, drug delivery and regenerative medicine<sup>1</sup>.

## REFERENCES

1. Buffa R., Šedová P. *et al.*: CZ 304512 (2014)
2. Collins M.N., Birkinshaw C.: Carbohydrate polymers 92, 2013, 1262-79.

## ACKNOWLEDGMENTS

Authors would like to acknowledge to Contipro Group a.s for financial support.



# Gelatin Methacrylamide: Poly(Ethylene Glycol) Composite Hydrogels with Tunable Mechanical Properties to Control Mesenchymal Stromal Cell Differentiation

Jeroen Rouwkema<sup>1,2,3</sup>, Ajaykumar Vishwakarma<sup>1,2</sup>, Ali Khademhosseini<sup>1,2</sup>

<sup>1</sup> Department of Medicine, Center for Biomedical Engineering, Brigham and Women's Hospital, Harvard Medical School, Cambridge, Massachusetts, USA

<sup>2</sup> Harvard-MIT Division of Health Sciences and Technology, Massachusetts Institute of Technology, Cambridge, Massachusetts, USA

<sup>3</sup> Department of Biomechanical Engineering, MIRA Institute for Biomedical Technology and Technical Medicine, University of Twente, Enschede, The Netherlands  
[j.rouwkema@utwente.nl](mailto:j.rouwkema@utwente.nl)

## INTRODUCTION

It is well known that the differentiation of mesenchymal stromal cells (MSCs) can be controlled by adapting the mechanical properties of the matrix in which the cells reside<sup>1</sup>. For this purpose, we have developed a photocrosslinkable hydrogel platform consisting of gelatin methacrylamide (GelMA) and poly(ethylene glycol) dimethacrylate (PEGDMA).

In this study, the concentration of GelMA remained constant at 5% w/v in order to have a constant availability of bioactive sites for cell attachment. The concentration of PEGDMA was varied between 0% and 15% w/v, resulting in a range of hydrogel stiffness.

## EXPERIMENTAL METHODS

### HYDROGEL PREPARATION

PEGDMA and lyophilized GelMA were mixed into DPBS with 0.5% (w/v) 2-hydroxy-1(4-(hydroxyethoxy)phenyl)-2-methyl-1-propanone (Irgacure 2959; CIBA Chemicals) at 80°C until completely dissolved. Five percent (w/v) GelMA was mixed with 0%, 2.5%, 5%, 7.5%, 10%, or 15% (w/v) PEGDA. Prepolymer was pipetted between two glass slides separated by a 600µm spacer and exposed to 6.9mW/cm<sup>2</sup> UV light (360–480 nm) for 30 s.

### HYDROGEL ANALYSIS

Hydrogels were swollen in DPBS for 1 hour, after which a 6mm Ø biopsy punch was used to generate samples with a reproducible shape and size. For pore size analysis, samples were freeze dried, coated with a thin gold layer, and analyzed using a scanning electron microscope. Average pore size was determined using image-J. Mechanical properties were determined using an Instron mechanical tester. The compressive modulus was recorded at a compression of 10%

## RESULTS AND DISCUSSION

The addition of low amounts of PEGDMA resulted in a decrease of hydrogel compressive modulus (see fig1) and an increase in the hydrogel pore size (see fig2). Further increasing the amount of added PEGDMA resulted in an increase of the compressive modulus and a decrease in the hydrogel pore size.

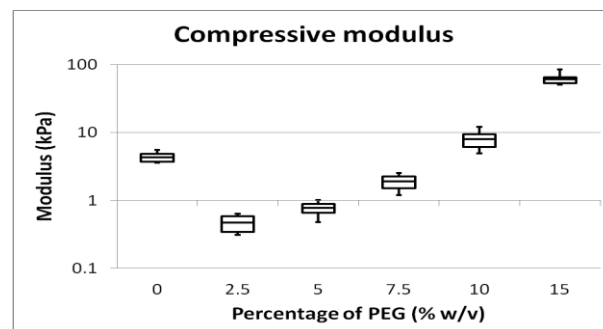


**Fig1** Box-and-whisker plot showing the compressive modulus of hydrogels with different amounts of PEGDMA (n=10 from two separate experiments).

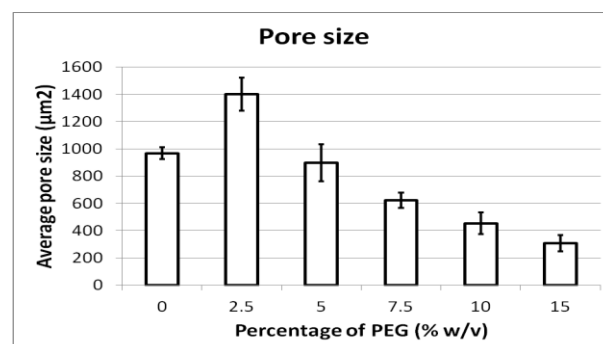


**Fig2** Average pore size of dehydrated hydrogels with different amounts of PEGDMA (n=4, average value and standard deviation shown).

## CONCLUSION

We have developed and analyzed a hydrogel system which allows us to make hydrogels with mechanical properties ranging from the sub-1 kPa to the 100 kPa range. This range is hypothesized to be adequate to direct the differentiation of MSC towards different tissue types, including osteogenic and neural cells<sup>2</sup>. Future studies will explore the differentiation of MSCs in these hydrogels.

## REFERENCES

- Huebsch N. *et al.*, Nature Mat. 9: 518-526, 2010
- Engler AJ. *et al.*, Cell 126: 677-689, 2006

## ACKNOWLEDGMENTS

The research leading to these results has received funding from the People Programme (Marie Curie Actions) of the European Union's Seventh Framework Programme (FP7/2007-2013) under REA grant agreement n°622294.



# Toxic Chemical Crosslinker-free Chitosan Cryosponge for Cartilage Tissue Engineering

Takayuki Takei, Hiroki Yoshitomi, Kohei Fukumoto, Yoshihiro Ozuno, Masahiro Yoshida

Department of Chemical Engineering, Graduate School of Science and Engineering, Kagoshima University, Japan  
[takei@cen.kagoshima-u.ac.jp](mailto:takei@cen.kagoshima-u.ac.jp)

## INTRODUCTION

Principal function of articular cartilage is to reduce friction between bones and allow load distribution in articulation. Because the tissue is devoid of blood vessels, its self-repairing capacity is extremely limited. Development of tissue engineering has enabled us to regenerate damaged cartilage using porous scaffolds. To date, many natural and synthetic polymers have been utilized as scaffold materials.

Chitosan is an aminopolysaccharide present in fungal cell walls and exoskeletons of arthropods such as insects and crabs. The biocompatible and biodegradable natural polymer has been widely utilized as a scaffold material for cartilage regeneration because it has a similar structure to glucosaminoglycans that is a main component of cartilage. However, conventional chitosan porous scaffolds are prepared using toxic chemicals (chemical crosslinkers, polymerization initiators and salts). We previously developed a novel chitosan sponge containing no additives<sup>1,2</sup>. The sponge is formed only by freeze-thawing an aqueous solution with dissolved chitosan-gluconic acid conjugate (CG). We showed that the CG cryosponge (CG-sponge) accelerated wound healing<sup>1,2</sup>.

In this study, we applied the CG-sponge to cartilage tissue engineering. Proliferation of articular chondrocytes and their production of glucosaminoglycan in the CG-sponges were compared with those in CG cryosponges crosslinked by glutaraldehyde (CG/G-sponge).

## EXPERIMENTAL METHODS

CG was prepared according to our previous report<sup>1</sup>. The number of incorporated gluconic acid per 100 glucosamine units of chitosan were 12. CG was first dissolved in HCl solution (pH 4.0). The pH of the polymer solution was adjusted to 7.0 by adding a NaOH solution. The final concentration of CG was 2% (w/v). A 0.2 ml aliquot of the solution was poured into a vial and frozen at -30°C. After 12 h, it was stood at room temperature for 2 h for thawing. CG/G-sponge were prepared by freeze-thawing of a CG aqueous solution containing 0.5% glutaraldehyde. The CG- and CG/G-sponges were immersed 70% (w/v) ethanol solution for 2 h for sterilization and rinsed with culture media for removal of ethanol and unreacted glutaraldehyde. Bovine articular chondrocytes suspended in culture media (0.15 ml) were seeded in the sponges ( $4.4 \times 10^5$  cells/sponge). After 3 and 7 days of cultivation at 37°C, amounts of glucosaminoglycan and DNA in the sponges were determined.

Data are presented as mean  $\pm$  standard deviation. Statistical differences between two groups were analyzed using the two-tailed Student's unpaired *t*-test.

## RESULTS AND DISCUSSION

CG-sponges had porous structure as shown in Figure 1 (a). Pore size of the sponge was  $136 \pm 46 \mu\text{m}$ . Much difference was not observed between pore size of the CG- and CG/G-sponges. We confirmed that the CG-sponges were barely degraded in culture media for more than 7 days although they were not chemically crosslinked (data not shown). Bovine articular chondrocytes proliferated faster in CG-sponges than in CG/G-sponges (Figure 1 (b)). Furthermore, production rate of glucosaminoglycan by the chondrocytes was higher in CG-sponges than in CG/G-sponges (Figure 1 (c)). These results show that importance of use of toxic chemical crosslinker-free chitosan scaffold for cartilage tissue engineering.

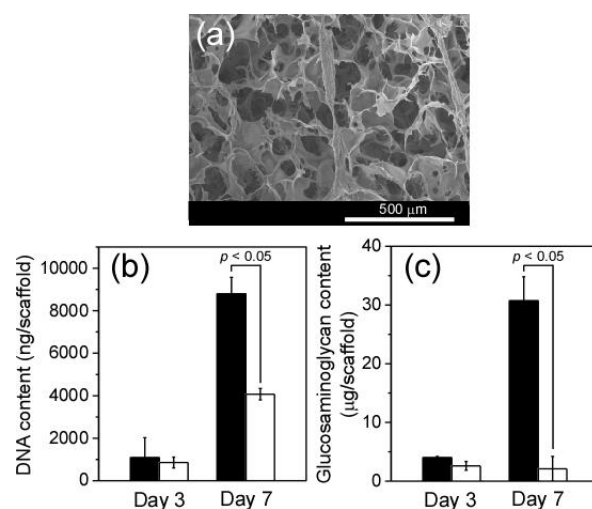


Figure 1. (a) Scanning electron microscope image of CG-sponge. (b, c) DNA (b) and glucosaminoglycan contents (c) of CG-sponges (closed bars) and CG/G-sponges (open bars).

## CONCLUSION

Proliferation rate of chondrocytes and production rate of glucosaminoglycan were higher in CG-sponges than in CG/G-sponges. These results show that the toxic chemical crosslinker-free CG cryosponges possess a great potential as a scaffold for cartilage tissue engineering.

## REFERENCES

1. Takei T. *et al.*, Acta Biomater. 8:686-693, 2012
2. Takei T. *et al.*, J. Mater. Sci. Mater. Med. 24:2479-2487, 2013

## ACKNOWLEDGMENTS

This research was partially supported by the Adaptable and Seamless Technology Transfer Program through Target-driven R&D, Japan Science and Technology Agency (AS262Z00651P).



## INTRODUCTION

The development of innovative systems optimized for the controlled release of bioactive species represents a true challenge in biomaterial science. Biomaterials systems dealing with the release of molecules (such as drugs, growth factors, enzymes...) include several mechanisms, as burst effect, kinetic of release, and kinetic of degradation, which may be tuned to regulate the biologic effects. Self-assembled systems represent interesting way to control the release of active molecules like growth factors<sup>1</sup>. The reversible interactions implied in the self-assembled systems can be used in a first time for the retention of the molecules, and in a second time for their delivery. The liberation can be tune by specific physicochemical conditions (pH, temperature, ionic strength). Using self-assembled technique, we propose in this study the development of a core-shell innovative system of respectively albumin (+ the active specie) and chitosan. The release is controlled by enzymatic degradation of the chitosan capping layer using  $\alpha$ -amylase loaded into the particles. The release is activated and modulated at physiological temperature condition.

## EXPERIMENTAL METHODS

Core-shell nanoparticles are prepared by desolvation technique<sup>2</sup> using method previously described by Li<sup>3</sup>. Briefly, the nanoparticles are obtained by electrostatic interaction between negatively charged core-protein and positively charged shell-glucosamine. Core-protein is constituted by Bovine Serum Albumin (BSA, 1%<sub>w</sub>) and  $\alpha$ -amylase (pH9) by desolvation step with dropwise pure ethanol (BSA nanoparticles). The influence of the pH for the BSA solution on the size and zeta ( $\zeta$ ) potential of the nanoparticles are investigated at pH3, 5, 7 and 9. Finally, the complete core-shell nanoparticles are obtained adding BSA nanoparticles suspension in chitosan solution in excess (0.1%<sub>w</sub> in 1%<sub>v</sub> acetic acid, pH5.5). The thickness of the shell, constituted by chitosan coating, is evaluated in function of the chitosan concentration at 0.05, 0.07 and 0.1%<sub>w</sub>. Yield and protein/chitosan ratios are evaluated and the protein release is studied at 10, 19 and 37°C in PBS medium.

## RESULTS AND DISCUSSION

Whatever the pH of the BSA solution, the size of the BSA core is constant. However, the size of the global nanoparticles with chitosan decreases with the pH. Comparatively, the  $\zeta$  potential of the nanoparticles decreases with the pH probably due to chitosan adsorption decreasing on the BSA nanoparticles. Consequently, the protein/chitosan ratios increase with the pH. Oppositely, the size of the nanoparticles increases with the chitosan concentrations (Figure 1. a) The Figure 1. b. confirms the protein/chitosan ratios decreasing with chitosan concentrations. The increase

of the  $\zeta$  potential is proportional to the quantity of chitosan present around the particles.

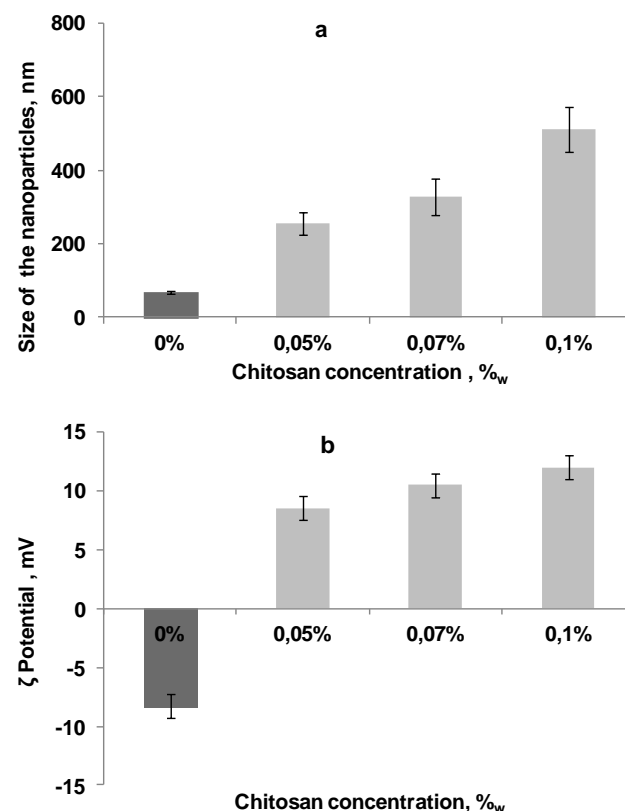


**Figure 1.** Influence of the chitosan concentration (shell) on the size (a) and the  $\zeta$  potential of the nanoparticles (core-shell) (b). The 0%<sub>w</sub> chitosan concentration represents BSA nanoparticles (core) before chitosan adsorption.

Kinetic studies of the release of the protein loaded within the core shows that without  $\alpha$ -amylase very few deliveries is evident compared to those with the enzyme. We also demonstrate the ability to optimized and control the release from the nanoparticles with the temperature. 37°C appears as ideal to promote the delivery.

## CONCLUSION

In the next step we propose to use our innovative system to confine specific bioactive species (as growth factor) within the BSA core. The relative small size of these confined systems and their versatility, due to the nature of the different molecules used for their preparation, open the door to multiple applications as in hydrogels or thin films-based biomaterials.

## REFERENCES

1. Eun J C. *et al.*, Tissue Engineering. 19(23-24): 2664-2673, 2013
2. Marty J. *et al.*, Pharm Acta Helv. 53: 17-23, 1978
3. Li L. *et al.*, Biomaterials. 37: 218-229, 2015

## PFKFB3-Expression Pattern Distinguishes Between Induced-Pluripotent Stem Cells and Cancer-Stem Cells

Artur Cieślak-Pobuda<sup>1,2,3</sup> Mayur Vilas Jain<sup>1,3</sup>, Gunnar Kratz<sup>3,4,5</sup>, Joanna Rzeszowska-Wolny<sup>2</sup>, Saeid Ghavami<sup>6</sup>,  
Emilia Wiecheć<sup>1,3</sup>

<sup>1</sup> Department of Clinical and Experimental Medicine (IKE), Division of Cell Biology, Linköping University, 58185 Linköping, Sweden

<sup>2</sup> Biosystems Group, Institute of Automatic Control, Silesian University of Technology, Akademicka 16, 44-100 Gliwice, Poland

<sup>3</sup> Integrative Regenerative Medicine Center (IGEN), Linköping University, 58185 Linköping, Sweden

<sup>4</sup> Experimental Plastic Surgery, IKE, Linköping University, 58185 Linköping, Sweden

<sup>5</sup> Department of Plastic Surgery, County of Östergötland, Linköping, Sweden

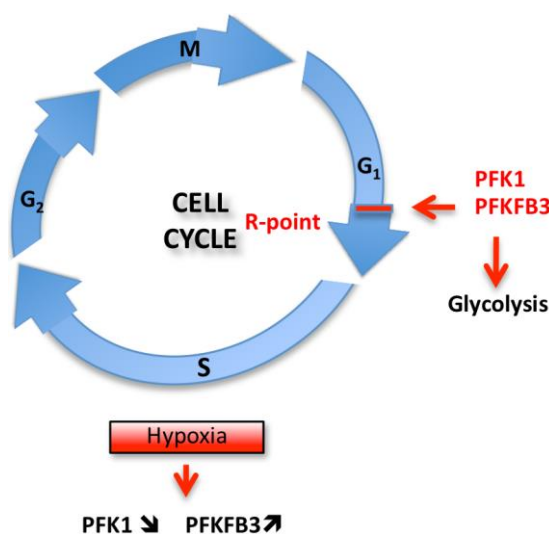
<sup>6</sup> Department of Human Anatomy and Cell Science, University of Manitoba, Manitoba, Canada

[Emilia.wiehec@liu.se](mailto:Emilia.wiehec@liu.se)

Various studies have revealed phenotypic similarity between the induced-pluripotent stem cells (iPS) and cancer stem cells (CSCs). Both iPS and CSCs are fast proliferating cells with high propensity to form tumors, suggesting that molecular mechanisms of cell cycle regulation may be similar. In this work we compare the restriction (R) point-governed regulation of the cell cycle progression in different cellular systems (iPS, cancer, CSCs and normal cells) based on the expression profile of PFKFB3 and PFK1.

Our study reveals that cancer- and iPS when cultured under hypoxic conditions alter expressions of PFKFB3

and PFK1 so that the expression levels of both molecules resemble that found in CSCs. Moreover, we also observed cell type-related differences in response to PFKFB3 inhibition. Present study provides a new insight into the molecular mechanism of cell cycle regulation in various types of cells, especially CSCs and cancer cells. Possibility to distinguish CSCs from cancer- and iPS by PFKFB3 and PFK1 expression improves the chance for clinical application of stem cell-based therapies, for more precise detection of cancer stem cells.





## Extracellular Vesicles From Induced Pluripotent Stem Cells: A Promising Source of Cell-based Therapy

Marta Adamiak<sup>1</sup>, Sylwia Bobis-Wozowicz<sup>1</sup>, Elżbieta Karnas<sup>1</sup>, Michał Sarna<sup>2</sup>, Zbigniew Madeja<sup>1</sup>, Ewa Zuba-Surma<sup>1,\*</sup>

<sup>1</sup>Department of Cell Biology, Faculty of Biochemistry, Biophysics and Biotechnology, Jagiellonian University, Poland

<sup>2</sup>Department of Biophysics, Faculty of Biochemistry, Biophysics and Biotechnology; Laboratory of Imaging and Atomic Force Spectroscopy, Malopolska Centre of Biotechnology, Jagiellonian University, Poland

\* [ewa.zuba-surma@uj.edu.pl](mailto:ewa.zuba-surma@uj.edu.pl)

### INTRODUCTION

Nano-sized extracellular vesicles (EVs) released by various cell types participate in physiological and pathological processes and have potential applications in diagnostics or therapeutics<sup>1</sup>. EVs originate from their donor cells either by shedding from the plasma membrane or as exosomes through secretion from late endosomal compartments<sup>2</sup>. Such cell-derived membranous vesicles contain bioactive molecules and can be detected in cell culture-conditioned medium where they may function as vehicles for intercellular communication. Although EVs from several stem cell (SC) populations including e.g. murine mesenchymal SCs<sup>3</sup>, embryonic SCs<sup>4</sup> and endothelial progenitor cells<sup>5</sup> have been already studied, the phenotypical and biological characteristics of EVs derived from murine induced pluripotent stem cells (iPSCs) has not been investigated yet. Thus, in this study, we characterized the morphology, size and molecular composition of murine EVs from iPSCs.

### EXPERIMENTAL METHODS

EVs were collected by differential centrifugation of conditioned media harvested from the serum-free and feeder-free culture of murine iPSCs obtained in our laboratory *via* genetic reprogramming. Atomic force microscopy (AFM) in liquid environment and dynamic light scattering (DLS) were used to reveal the morphology and size of EVs. Western blot and high-sensitivity flow cytometry analyses for EV markers were performed to confirm the presence of EVs in the samples. The level of transcripts related to pluripotency, angio- and cardiomyogenesis (e.g. Oct4, Nanog, Gata4) in iPSC-derived EVs and their parental cells was compared by real-time RT-PCR method. High-throughput approaches such as mass spectrometry-based proteomics and microRNA (miRNA) profiling are being currently used to further evaluate the molecular composition of miPSC-EVs.

### RESULTS AND DISCUSSION

AFM and DLS analyses showed that miPSC-EV samples contain homogenous spherical vesicles with the vast majority <100 nm in size. We established that miPS-EVs are rich in mRNAs, miRNAs and proteins carried by their donor cells. We also evaluated the

expression of selected exosomal markers in iPSC-EVs, including CD9, CD63 and CD81. Our preliminary data demonstrated that EVs derived from miPSCs may represent natural nanocarriers of genetic material to target cells.

### CONCLUSION

This study brings novel insights on EVs released by pluripotent stem cells and provides a reference for further studies of unmodified or engineered EVs and their synthetic mimics as potential therapeutic tools for tissue regeneration. Moreover, we optimized harvesting of EVs from serum-free and feeder-free cultures of murine iPSCs that may be further used for studying their potential regenerative capacity in murine models of ischemic tissue injury including limb ischemia and acute myocardial infarction that is currently ongoing. Thus, EVs derived from pluripotent SCs may be promising as highly bioactive, acellular carriers in a wide variety of biomedical applications including tissue regeneration.

### REFERENCES

1. EL Andaloussi S. *et al.*, Nat. Rev. Drug Discov. 12:347-357, 2013
2. Kowal J. *et al.*, Curr. Opin. Cell Biol. 29:116-25, 2014
3. He J. *et al.*, Nephrology 17:493-500, 2012
4. Ratajczak J. *et al.*, Leukemia 20:847-856, 2006
5. Deregibus M.C. *et al.*, Blood 110:2440-2448, 2007

### ACKNOWLEDGMENTS

This study was supported by TEAM-2012/9-6 grant from the Foundation for Polish Science (FNP) to EZS and in part by POIG.01.01.02-00-109/09 project. The authors would also like to thank Malopolska Centre of Biotechnology for access to AFM.



## New Concept Of Stem Cells Differentiation - Graphene-Based Substrate As A Promising Tool In Biomedical Applications

Małgorzata Sekuła<sup>1,2</sup>, Magdalena Baran<sup>3</sup>, Katarzyna Kmiotek<sup>1</sup>, Joanna Jagiełło<sup>3</sup>, Elżbieta Karnas<sup>1</sup>, Zbigniew Madeja<sup>1</sup>, Ludwika Lipińska<sup>3</sup>, Ewa Zuba-Surma<sup>1,\*</sup>

<sup>1</sup> Department of Cell Biology, Faculty of Biochemistry, Biophysics and Biotechnology, Jagiellonian University, Krakow, Poland

<sup>2</sup> Malopolska Centre of Biotechnology, Jagiellonian University, Krakow, Poland

<sup>3</sup> Institute of Electronic Materials Technology, Department of Chemical Technologies, Warsaw, Poland

\*correspondence: [ewa.zuba-surma@uj.edu.pl](mailto:ewa.zuba-surma@uj.edu.pl), presenting author: [malgorzata.sekula@uj.edu.pl](mailto:malgorzata.sekula@uj.edu.pl)

### INTRODUCTION

Regenerative medicine, combining biomaterials and stem cells is an innovative field in biomedical sciences. As stem cells are unique cell type possessing the ability to self-renewal and differentiation toward different types of specialized cells, their utilization is one of the greatest hopes of contemporary medicine. Together with biomaterials support, they are promising tools which can stimulate repair of injured tissue, directly by differentiation, or more likely due to paracrine effects and remodeling of extracellular environment. Recently, there has been great focus on mesenchymal stem cells (MSC) utilization in medical applications, resulted from their low immunogenicity that makes them suitable for transplantation with low risk of the rejection. Importantly, MSC can be easily isolated from various tissues including umbilical cord Wharton's jelly (UC), cord blood (CB), bone marrow or adipose tissue. However, it was shown, that UC-MSCs occurred to have significant advantages, as their collection is noninvasive and obtained cells display improved proliferative capacity and wider differentiation potential, comparing to non-neonatal sources. Nevertheless, there are still several limitations of stem cell utilization, like effectiveness of their directed differentiation or engraftment.

### EXPERIMENTAL METHODS

To challenge these expectations we develop innovative concept of stem cell utilization in association with biocompatible composites. In this study, we used graphene-oxide (GO) scaffolds for stem cell-related applications. Graphene is two dimensional (2D) single layer of carbon atoms which have been investigated in a broad range of scientific areas e.g. biosensing, prevention of bacterial infections, photothermal therapy, drug delivery, electrical cell stimulation or skeletal tissue engineering. Importantly, bio-functionalization of graphene sheets improves their biocompatibility, solubility and selectivity.

In current study we examined an influence of graphene-based substrate on UC-MSC physiology. GO was prepared from graphite according to the Marcano method. We tested different flake size, thickness and type of solvent (aqueous or alcohol) to determine the most effective graphene suspension for stem cell growth and differentiation. To investigate the effect of

graphene-based substrate on the behavior of UC-MSC, we analyzed morphology, proliferation capacity and migratory activity of cells cultured on GO scaffolds. Next, we employed flow cytometry to evaluate cells viability and apoptosis. Furthermore, we analyzed spontaneous and cardiomyocyte-directed differentiation of UC-MSC seeded on graphene-based substrate.

### RESULTS AND DISCUSSION

Our data revealed that GO is non-toxic culture substrate for UC-MSC. GO had no influence on UC-MSC proliferation potential. Moreover, we did not observe GO cytotoxicity, the number of apoptotic cells, measured after 48 h or 96 h of culture, was similar to control cells. Microscopic analysis of cells demonstrated, that GO can stimulate elongation of UC-MSC in a flake size-dependent manner. We observed that thicker and larger layers of GO flakes promoted elongated morphology of cells. On the other hand, GO-modified substrate had no significant influence on the UC-MSC migration, comparing to cells cultured in standard conditions. However, analysis of cells trajectories revealed, that GO flakes dissolved in ethanol slightly increased the speed of cell movement. We hypothesized, that this phenomenon may be associated with more uniform and smooth coating layer of GO flakes. Furthermore, our preliminary findings indicate that graphene derivatives stimulate UC-MSC differentiation toward cardiomyocytes. After 10 days of UC-MSC culture in cardiac medium, we observed changes of cell morphology toward more elongated cells. Importantly, real-time PCR analysis revealed, that there was higher upregulation of cardiomyocyte differentiation markers GATA-4 and VE-cadherin on mRNA level, comparing to cells without GO.

### CONCLUSION

Further studies are required to analyze the impact of combining stem cells and graphene-based nanomaterials in cardiomyocyte differentiation. However, we believe that they could provide a promising tools for tissue engineering in medical applications.

### ACKNOWLEDGMENTS

This study was supported by N N302 1773 38 grant from Ministry of Polish Science and Higher Education (MNiSW) to EZS and in part by POIG.01.01.02-00-109/09 project.



# Mesenchymal Stem Cell Culture Evaluation by CVD Graphene-transferred PDMS Substrates

Masahito Ban<sup>1</sup>, Hiroki Sunada<sup>1</sup>, Masatou Ishihara<sup>2</sup> Masataka Hasegawa<sup>2</sup>

<sup>1</sup>Environmental Symbiotic System Major, Nippon Institute of Technology, Japan

<sup>2</sup>Nanotube Research Center, National Institute of Advanced Industrial Science and Technology (AIST), Japan

[ban@nit.ac.jp](mailto:ban@nit.ac.jp)

## INTRODUCTION

Cell scaffolds are important techniques for regenerative medicine to reproduce biological tissues, and have been actively studied in the world. Meanwhile, the application of nano carbon materials with nanostructure to the scaffolds remains to be unknown, and it has been a significant subject to clarify the effects of particularly the nm scale structure on cellular behaviors. Our group reported that flat graphene sheet attached on scaffold substrate promoted the proliferation of mouse myoblast cell (C2C12). In this study, the effects of graphene sheet on the proliferation and shape change of human mesenchymal stem cells were investigated.

## EXPERIMENTAL METHODS

Three kinds of scaffold substrates (Gr01, Gr02 and Gr03) were obtained by transferring graphene sheets deposited on copper foils by a large-area surface wave plasma (SWP) CVD<sup>1</sup> and microwave plasma CVD<sup>2</sup>, on PDMS (polydimethylsiloxane) flat plates. Oxygen plasma was irradiated on Gr01, Gr02 and Gr03 to obtain Gr01O<sub>2</sub>, Gr02O<sub>2</sub> and Gr03O<sub>2</sub>, respectively. Mesenchymal stem cells (hMSC: Lonza, PT-2501) were cultured on the substrates with MSCGM medium (Lonza, PT-3001) for 3 days, and observed the nuclei and F-actins stained by phalloidin and DAPI, respectively. The surfaces of the substrates were observed using confocal laser microscope (CLM) and evaluated with Raman spectroscopy. In addition, contact angle was measured for the surfaces.

## RESULTS AND DISCUSSION

Raman results showed that a few up to 10 layers of graphene were attached on the fabricated substrate surfaces. The CLM observation results indicated that three kinds of substrates had the different surface structures. Gr03 and Gr03O<sub>2</sub> were confirmed to have flat surfaces, indicating that graphene sheets were almost uniformly attached all over the surfaces. As for Gr01 and Gr01O<sub>2</sub>, the graphene sheets with a number of cracks on the surfaces were overspread. The graphene sheets of Gr02 and Gr02O<sub>2</sub> were exfoliated in fragments from the surface and curled to be in fibrous form. It was found that the oxygen plasma irradiated substrates showed lower contact angles, about 80 °, than non-irradiated ones, about 120 °.

As shown in Fig. 1, using the observation images of the nuclei and F-actins obtained by a fluorescence microscope, (a) the number of cells on the substrates and (b) the average area of one cell were calculated. The cells on Gr02 increased up to 1.3 times compared to the PDMS flat plates without graphene. More, it was

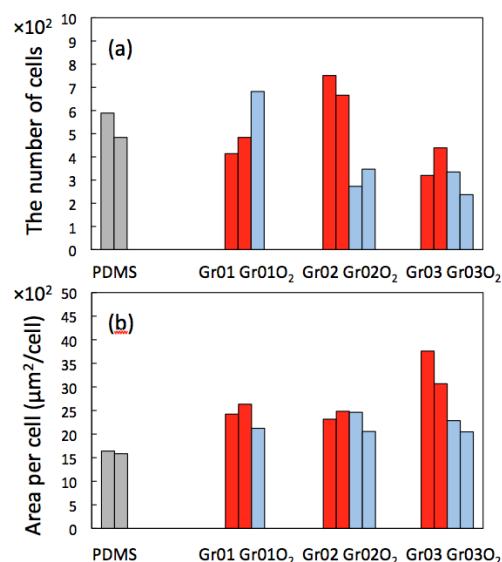


Fig. 1 Cell number and area obtained from the cell nuclei and F-actins stained images

found that the cells on the graphene-attached substrates had larger areas than the PDMS, and in particular the cells of Gr03 were about 2 times bigger than ones of PDMS. These results implied that the existence of graphene had the ability to promote the cell proliferation and enlargement, and the surface microstructure of attached graphene sheets affected cellular adhesion, division and stretching.

## CONCLUSION

The PDMS substrates transferred the graphene sheets prepared by the CVD methods were used as the scaffolds for human mesenchymal stem cells. The cells on PDMS substrates with graphene in fibrous form on the surfaces increased more compared to the flat PDMS. Moreover, the cells on the overspread flat graphene-attached PDMS substrates stretched and grew more than the PDMS.

## REFERENCES

1. J. Kim, M. Ishihara, Y. Koga, K. Tsugawa, M. Hasegawa, S. Iijima, *Appl. Phys. Lett.*, 98, 091502 (2011).
2. R. Kato, K. Tsugawa, Y. Okigawa, M. Ishihara, T. Yamada, M. Hasegawa, *CARBON*, 77, 823 (2014).
3. H. Sunada, M. Ishihara, M. Hasegawa, M. Ban, *Recent Progress in Graphene Research (RPGR)*, Tokyo, 214 (2013).



# Very Small Embryonic-Like Stem Cells are Activated by Acute Tissue Injury In Vivo and Participate in Regeneration of Ischemic Tissue

Anna Labedz-Maslowska<sup>1</sup>, Elzbieta Kamycka<sup>1</sup>, Tomasz Brzozowski<sup>2</sup>, Mariusz Z. Ratajczak<sup>3</sup>, Zbigniew Madeja<sup>1</sup>, and Ewa K. Zuba-Surma<sup>1</sup>

<sup>1</sup>Department of Cell Biology, Faculty of Biochemistry, Biophysics and Biotechnology, Jagiellonian University, Krakow, Poland

<sup>2</sup>Department of Physiology, Jagiellonian University Medical College, Krakow, Poland

<sup>3</sup>Stem Cell Biology Institute, University of Louisville, Louisville, KY, USA

Very small embryonic-like stem cells (VSELs) were identified as rare quiescent population of nonhematopoietic cells in adult murine and human tissues including bone marrow (BM). During tissue injury, BM-derived VSELs are mobilized into peripheral blood (PB). Moreover, these primitive stem cells can participate in heart repair after injection into infarcted myocardium by enhancing tissue perfusion and angiogenesis.

In this study, we examined if acute tissue injury may stimulate both proliferation of quiescent VSELs in BM and their mobilization into PB *in vivo*. We also investigated genetic status of VSELs following tissue injury including expression of genes controlling their proliferation. The other goal was to evaluate regenerative potential of VSELs injected into ischemic tissues in murine model of limb ischemia (LI) *in vivo*.

Thus, C57BL/6 mice underwent LI by permanent proximal femoral artery occlusion. Mice were administrated with BrdU and scarified at 2, 7, 14 and 28 days following LI. The presence of proliferating (BrdU<sup>+</sup>): VSELs (Sca-1<sup>+</sup>/Lin<sup>-</sup>/CD45<sup>-</sup>), endothelial progenitor cells (EPCs; Flk-1<sup>+</sup>/Sca-1<sup>+</sup>/Lin<sup>-</sup>/CD45<sup>-dim</sup>) and hematopoietic stem/progenitor cells (HSPCs; Sca-1<sup>+</sup>/Lin<sup>-</sup>/CD45<sup>+</sup>) in PB and BM was evaluated by flow

cytometry and ImageStream system. The expression of genes related to the presence of VSELs and EPCs was examined by real-time PCR. Moreover, we examined the change in secretion of angiogenesis-related proteins in plasma. Then, GFP VSELs sorted from ischemic and non-ischemic mice were injected into site of injured tissue in WT mice at 2d following LI. At 2, 7, 14 and 28days post transplantation, blood flow were measured by Laser Doppler System. Paraffin-embedded ischemic tissue sections were analyzed for GFP VSELs presence and formation of new blood vessels.

We found that the number of proliferating VSELs and EPCs was significantly increased in BM tissue and circulating in PB of ischemic mice at 7d post injury. Elevated number of BrdU<sup>+</sup> VSELs was accompanied with change in expression of genes guiding their proliferation. Moreover, changes in secretion of selected angiogenesis- related proteins may stimulate activation and proliferation of VSELs. Importantly, VSELs injected into ischemic tissues enhance the improvement in tissue perfusion and blood flow recovery by formation of new blood vessels. The data indicates vast impact of acute injury on activation of VSELs proliferation *in vivo* and possibility of their application for tissue regeneration.





## Human Adipose Stem Cells on Ti-6Al-4V Alloy with Various Surface Modifications

Nikola Krocilova<sup>1</sup>, Lucie Bacakova<sup>1</sup>, Martin Parizek<sup>1</sup>, Jana Havlikova<sup>1</sup>, Hooman Motarjemi<sup>2</sup>, Martin Molitor<sup>2</sup>, Roman Gabor<sup>3</sup>

<sup>1</sup>Institute of Physiology, Academy of Sciences of the Czech Republic, Prague, Czech Republic

<sup>2</sup>Department of Plastic Surgery, Bulovka Hospital in Prague, Czech Republic

<sup>3</sup>Division of Laboratories and Testing, Chemical and Radio-Isotopes Laboratory, VUHZ Joint-Stock Company, Dobruška, Czech Republic  
[n.kroci@seznam.cz](mailto:n.kroci@seznam.cz)

### INTRODUCTION

Adipose-derived stem cells (ASCs) are of great importance for regenerative medicine, including bone tissue engineering, thanks to their abundance in the body and less invasive methods of their isolation [1]. Liposuction is widely used method for obtaining ASCs, and the way in which it's done can affect the number, viability, growth and differentiation of the isolated cells. Nowadays, studies on the interaction of stem cells with artificial materials are very important for construction of tissue replacements, because these cells have a higher growth potential than conventionally used differentiated cells. In addition, stem cells are able to differentiate in many cell types and to produce growth factors by a paracrine manner, which stimulate the tissue regeneration [2].

### EXPERIMENTAL METHODS

In the first part of our study, we compared the properties of ASCs obtained from a patient (43 years old woman) by liposuction under lower and higher negative pressure, i.e. -200 mmHg and -700 mmHg, respectively. For each pressure, 10 ml of lipoaspirate was taken, and the ASCs were isolated by a method described earlier [3]. Briefly, the lipoaspirate was repeatedly rinsed in the phosphate-buffered saline, digested by 0.1 % collagenase type I (1 h and 37 °C), centrifuged, filtered through a cell filter (Cell Strainer, 100 µm, BD Falcon, USA) and seeded into polystyrene culture flasks (25 cm<sup>2</sup>, TPP, Switzerland) in the amount of 0.16 ml of the original lipoaspirate per cm<sup>2</sup>.

In the second part of our study, we focused on the adhesion and growth of ASCs (obtained from the patient in the first experiment) on Ti-6Al-4V alloy, currently used for the bone implants in clinical practice. The alloy samples were modified by different surface treatments, namely grit blasting and tarnishing (sample A), grinding to the roughness of  $R_a = 0.2$  µm (sample B) and grinding to the roughness of  $R_a = 0.08$  µm, followed by grit blasting and polishing (sample C). All these modifications were performed on samples with  $R_a = 0.28$  (control sample K). ASCs were seeded on the samples in the 2<sup>nd</sup> passage (~5700 cells per cm<sup>2</sup>).

### RESULTS AND DISCUSSION

In the first experiment we found that the higher negative pressure during liposuction was more suitable for obtaining of ASCs because of a higher number of the isolated cells and their faster proliferation. Five days after seeding, the ASCs obtained under high pressure reached a population density of ~63 000 cells/cm<sup>2</sup>, while in the cells obtained under low pressure, it was only ~40 000 cells/cm<sup>2</sup>. The differences in the cell

growth also persisted in passaged cells and after freezing and thawing of cells.

In the second experiment, we found that on day 1 after seeding, the spreading area was the largest in ASCs on A and K samples (1060-1310 µm<sup>2</sup>), and the smallest on B samples (730-820 µm<sup>2</sup>). However, on day 3, the cells on B samples reached the highest population density, which could be explained by an appropriate wettability and polarity of B samples. Nevertheless, on day 7, the cell numbers of A, B and C samples evened out and were significantly higher than on K samples. At the same time, the population densities of cells obtained under high pressure reached significantly higher population densities. These cells were mainly spindle-shaped, while the cells isolated under low pressure were mostly polygonal (**Fig. 1**). Experiments on the osteogenic differentiation of ASCs, measured by concentrations of collagen I, alkaline phosphatase and osteocalcin, are in progress.

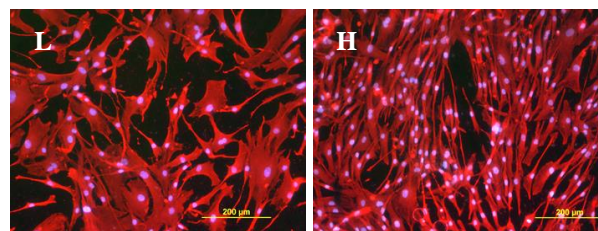


**Fig. 1.** Human adipose-derived stem cells obtained by liposuction under low (L) and high (H) pressure in 7-day-old cultures on Ti-6Al-4V samples modified with grit blasting and tarnishing (group A). Stained with Hoechst 33258 (cell nuclei) and Texas Red C<sub>2</sub>-Maleimide (cell membrane and cytoplasm). Olympus IX 51 microscope, DP 70 digital camera, bar=200 µm.

### CONCLUSION

The adipose-derived stem cells obtained by high pressure liposuction were isolated in a larger quantity, grew faster. All tested surface modifications of Ti-6Al-4V samples enhanced the colonization of the alloy with the stem cells.

### REFERENCES

1. Zhang Y *et al.*: ScientificWorldJournal 2012: 793823, 2012.
2. Hassan WU *et al.*: Wound Repair Regen 22: 313-325, 2014.
3. Estes BT *et al.*: Nat Protoc 5: 1294-311, 2010.

### ACKNOWLEDGMENTS

The authors would like to thank the Grant Agency (P108/12/G108) and the Technological Agency (TA04011214) of the Czech Republic for providing financial support for this project.



## Genome Editing of HLA Locus Using Zinc Finger Nucleases

Ken-ichi Tezuka<sup>1</sup>, Shunji Chikusa<sup>1</sup>, Shota Ishii<sup>1</sup>, Ken Sugiyama<sup>2</sup>, Tomoko Kawaguchi-Takeda<sup>2</sup>

<sup>1</sup>Department of Tissue and Organ Development, Gifu University, Japan

<sup>2</sup>Department of Oral Surgery, Gifu University, Japan

[tezuka@gifu-u.ac.jp](mailto:tezuka@gifu-u.ac.jp)

### INTRODUCTION

Human dental pulp cells (DPCs) are present in the cell population isolated from dental pulp tissues<sup>1</sup>. We reported that viral introduction of four transcription factors (*OCT3/4*, *SOX2*, *KLF4*, and *c-MYC*) can reprogram DPCs into induced pluripotent stem (iPS) cells, which closely resemble embryonic stem cells<sup>2</sup>. However, establishing quality-controlled iPS cell lines from a large number of individual patients is not easy and validation of them requires considerable time and cost.

Human leukocyte antigen (HLA) plays an important role in rejection of tissues and cells transplanted from allogenic donors. In recent days, tissue transplantation is conducted without complete matching of HLA because of shortage of the donors. Instead of matching HLA types, immunosuppressants are frequently used to prevent immune reaction both host to graft and graft to host directions; however, when the immune system function is suppressed, there is an increased susceptibility to infectious diseases and cancers.

To solve this problem, usage of HLA haplotype-homo (HHH) donors has been considered in iPS cell therapy<sup>3</sup>. HHH donors have a couple of identical HLA gene sets, resulting in presentation of HLA molecules half in the variation. Therefore, iPS cells derived from HHH donors are expected to be successfully transplanted to many patients with less possibility of rejection. However, it is not easy to obtain sufficient number of HHH donors to cover major part of Japanese population because of their rarity.

In this study, we tried to generate iPS cells, phenotypically similar to HHH cells, by directly modulating HLA loci of non-HHH cells with Zinc Finger Nucleases (ZFNs).

### EXPERIMENTAL METHODS

We designed 4 pair of ZFNs targeting exon2 or 3 of HLA-A02:01 gene by aid of SIGMA. Expression plasmids were introduced into DP144 cells with HLA type of HLA-A\*02, 33;B\*44, -;DRB1\*13, -. Cells were stained with an anti HLA-A02 specific monoclonal antibody, and subjected to cell sorting. PCR primers

were designed to amplify exon2 and 3 of HLA-A gene. iPS cells were generated by introducing 4 Yamanaka's factor using Sendai virus vector system.

### RESULTS AND DISCUSSION

After introduction of each pair of ZFNs, 1% to 5% cells became immunologically negative for HLA-A02. After expanding these cells, genomic DNA was prepared and HLA-A locus was sequenced. Among 63 sequences of HLA-A02, 17 (27%) contained in-del mutations. On the other hand no such mutations were found in 12 HLA-A33 sequences.

Then, we introduced Yamanaka's factors into HLA-A02 negative cells and established several iPS cell clones. One of the clones showed mutated HLA-A locus showing a mosaic structure of HLA-A02 and A33.

These results indicate that HLA locus can be modulated by subtype specific ZFNs. Targeted cells enriched using subtype specific antibodies could be subjected to derivation of iPS cells.

### CONCLUSION

Combination of HLA subtype specific ZFNs and monoclonal antibodies can be used to generate genetically designed HHH-like cells.

### REFERENCES

1. Takeda T. *et al.*, 87, 676-681, 2008
2. Tamaoki N. *et al.*, 89, 773-778, 2010
3. Okita, K. *et al.*, 8, 409-412, 2011

### ACKNOWLEDGMENTS

This work was supported by JST Yamanaka iPS Cell Project, JSPS KAKENHI Grant Numbers 12855208 and 14512576.



## Human Mesenchymal Stem Cells Expansion under Xeno-Free Conditions for Regenerative Therapies

Cimino M<sup>1,2,3</sup>, Bauman E<sup>1,2,3</sup>, Gonçalves RM<sup>1,2</sup>, Belda F<sup>4</sup>, Barrias CC<sup>1,2</sup>, Martins MCL<sup>1,2,4</sup>

<sup>1</sup>I3S, Instituto de Investigação e Inovação em Saúde, Universidade do Porto (UP), Portugal

<sup>2</sup>INEB - Instituto de Engenharia Biomédica, UP, Portugal

<sup>3</sup> Faculdade de Engenharia, UP, Portugal

<sup>4</sup>Virology Section, Viral Safety Division, Research and Development, Bioscience Industrial Group, GRIFOLS. Parets del Vallés, Barcelona, Spain.

<sup>5</sup>ICBAS — Instituto de Ciências Biomédicas Abel Salazar, UP, Portugal

[maura.cimino@ineb.up.pt](mailto:maura.cimino@ineb.up.pt)

### INTRODUCTION

In the new era of regenerative medicine, human mesenchymal stem cells (hMSC) have generated great interest mainly because of their multidifferentiation potential and immunomodulatory role<sup>1</sup>. MSCs can be derived from different tissues but bone marrow is the most common although containing a relatively low frequency of hMSC, decreasing with the donor age<sup>2</sup>.

For cellular therapies, high cell numbers are required thus cells must be expanded *ex vivo*. Most of the current protocols make use of fetal bovine serum (FBS) as nutrient-rich supplement. However, several regulatory guidelines encourage novel xeno-free alternatives to define safer and standardized protocols for hMSC expansion. A new pharmaceutical-grade Cell Culture Supplement medium (SCC), derived from industrial human plasma pools, was recently described as a potential candidate for xeno-free supplementation of hMSC expansion media<sup>3</sup>. The behaviour of attachment-dependent cells, such as hMSC, is mediated not only by soluble factors present in the medium, but also by cell adhesive components that adsorb to the culture surface<sup>4</sup>. This work aims to evaluate the effect of different soluble and adsorbed bioactive factors in hMSC growth under xeno-free conditions in SCC supplemented medium.

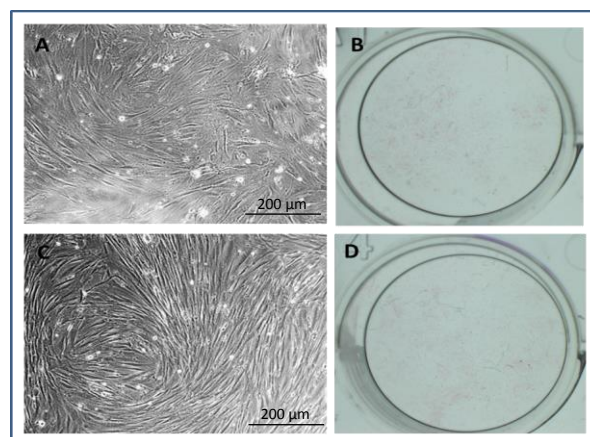
### EXPERIMENTAL METHODS

BM-derived hMSC (Lonza) were plated at (3000 cells/cm<sup>2</sup>) in 24 well tissue culture polystyrene (TCPS) plates and cultured in media supplemented with 10% v/v SCC (Grifols) or 10% FBS (Hyclone). To analyse the effect of exogenously added adsorbed factors, plates were pre-coated with different xeno-free coatings before culture. To assess the effect of soluble factors, medium was supplemented with different human recombinant growth factors, alone or in combination. At days 1, 3, 7, 10 and 14 cell metabolic activity was assayed by Resazurin assay, while cells morphology was monitored through phase contrast optical microscopy. Finally, the maintenance of cells undifferentiated state was checked by Oil Red (adipogenesis), Alcian Blue (chondrogenesis) and ALP (osteogenic) staining.

### RESULTS AND DISCUSSION

While xeno-free coatings improve initial cell adhesion and preserve cell morphology, do not significantly

improve cell growth comparing to the animal-derived serum supplemented medium. The addition of human recombinant growth factors alone to the medium also did not show any improvement, but when used simultaneously these growth factors led to a substantial increase in metabolic activity levels, suggesting a synergistic role. This effect was further improved with the use of xeno-free coating. Also, cells maintained an undifferentiated state along 14 days in culture, implying the possibility to expand hMSC in animal – free condition for a safer use in regenerative medicine therapies.



A and B: hMSC morphology and ALP staining after 14 days culture on xeno free coating, FBS containing medium (animal-derived condition). C and D: hMSC morphology and ALP staining after 14 days culture on xeno free coating, SCC + GF containing medium (xeno-free condition). On xeno-free conditions hMSC appear well spread and keep undifferentiated state.

### CONCLUSION

SCC can be a potential candidate for cell culture supplement in xeno-free hMSC expansion.

### REFERENCES

1. Caplan AI, et al. Cell Stem Cell, 2011, 9(1):11.
2. Shigeno Y, et al. J Bone Joint Surg Br. 1995, 77(1):139.
3. Diez JM, et al. Stem Cell Res Ther. 2015, 13;6(1):28.
4. Barrias CC, et al. Biomaterials. 2009, 30:307.

### ACKNOWLEDGMENTS

This project is part of a Marie Curie Initial Training Network - European Industrial Doctorate (ITN-EID) IB2 (317052), and has been funded under the European Community 7th Framework Programme project”.

Yaser Greish<sup>1</sup>, Abdel-Hamid Mourad<sup>2</sup>, Nuha Attia<sup>3</sup><sup>1</sup>Department of Chemistry, College of Science,<sup>2</sup>Department of Mechanical Engineering, College of Engineering,

United Arab Emirates University, Al Ain, UAE

[y.afifi@uaeu.ac.ae](mailto:y.afifi@uaeu.ac.ae)

## INTRODUCTION

Hard tissues are natural composites of inorganic (hydroxyapatite; HAP), and organic (collagen) components. The interlocking between the collagen nanofibers and the HAP nanocrystals growing on them provides the well known unique mechanical stability of hard tissues<sup>1</sup>. In case of partial fractures; bone or dental cements are often used. A widely used polymer; polymethyl-methacrylate (PMMA), has been long applied in this regard<sup>2</sup>. However, this polymer is classified as a bioinert material that can be accepted by the human body without having a positive interaction; bioactivity, with the surrounding tissues. Therefore, attempts have been done to introduce more bioactive bone/dental cements to replace PMMA.

Gypsum has been always considered a bioresorbable material and has wide scope of biomedical applications. In fact, gypsum is one of the first known biomaterials to be introduced to augment broken hard tissues<sup>3</sup>. However, gypsum as a calcium sulfate is characterized by its fast resorption after implantation, which may lead to limited stability of the cement after use. In addition, its chemical composition is different from that of the mineral components in hard tissues; HAP. Due to these concerns, a bioactive calcium silicate; known as wollastonite, has been considered to be added to gypsum to improve its bioactivity. Wollastonite is relatively more stable than gypsum in the body and is known to bond to the surrounding bone tissue through the formation of bone apatite-like layers on its surfaces after implantation<sup>4</sup>.

## EXPERIMENTAL METHODS

The current study investigates the formation of a composite of gypsum and wollastonite at weight percentages of 1, 5, and 10%. Three types of wollastonites; varying in their degree of crystallinity were used in the study. Powder mixtures of a gypsum precursor; Plaster of Paris (POP) and wollastonite were well blended prior to reactions with water. The effect of using as-received wollastonite fibers or those treated in acidic media on the setting reactions, phase composition, morphology, mechanical properties and the preliminary *in vitro* performance of the produced composites were studied. Phase composition and morphology were investigated by XRD, FT-IR, TGA, and SEM techniques. Both tensile and compressive strengths of the composites were measured. Preliminary *in vitro* performance tests were carried out in simulated body fluids and were followed by studying the variations of concentrations of certain ions in the solutions and morphology of the SBF-treated

composites after soaking for up to 14 days in these solutions.

## RESULTS AND DISCUSSION

Results showed an overall enhancement in the bioactivity of the composites as a result of the addition of wollastonites; both as-received and acid-treated. A slight decrease in the mechanical properties of the composites was observed with the addition of wollastonite fibers. Phase composition of the composites indicated no interference of wollastonite with the formation of gypsum. The advantages of the currently studied composites are, therefore, the enhancement of the bioactivity and the ability to control the biodegradation of the composite by controlling the proportion of POP in the original powder mixture of the reactants.

## CONCLUSION

Gypsum composites containing various types of wollastonite fibers were investigated for their mechanical and preliminary *in vitro* performance. Despite the fact that no significant improvement of the mechanical properties of the formed composites was observed, a pronounced improvement of the bioactivity of the composites was shown. Deposition of Hap from SBF media was observed on the prepared composites, indicating their potential for application as bone and dental cements with improved bioactivity.

## REFERENCES

1. Buckwalter JA *et al*, Instr Course Lect. 45:371-86, 1996
2. Rohmiller MT *et al*, The Spine Journal, 2: 255–2602, 2002
3. Orsini G *et al*, J. Biomed. Mater. Res. Part B: Appl. Biomater. 68B: 199–208, 2004
4. Liu X *et al*, Biomed and Pharmacotherapy. 62: 526–529, 2008

## ACKNOWLEDGMENTS

“The authors would like to thank the Research Funding provided by the Office of Graduate Studies at UAEU towards the completion of this MSc research work of Ms. Nuha Attia”.





## Functionalization of Hydrogels for Cells Encapsulation

Noverraz François<sup>1</sup>, Solène Passemard<sup>1</sup>, Virginia Crivelli<sup>1</sup>, Françoise Borcard<sup>1</sup>, Redouan Mahou<sup>1</sup>, Sandrine Gerber<sup>1</sup>\*, Christine Wandrey<sup>1</sup>\*

<sup>1</sup> EPFL Lausanne, Switzerland  
[francois.noverraz@epfl.ch](mailto:francois.noverraz@epfl.ch)

### INTRODUCTION

The progress of medical therapies, which rely on the transplantation of microencapsulated cells has been widely investigated and has shown high potential to enter the clinics as treatment option for various types of diseases<sup>1</sup>.

However due to inflammatory response of the organism, one of the major challenges of cell encapsulation remains long term cell viability *in vivo*. Formation of fibrosis around the capsules prevents efficient diffusion of nutrients and results in cell asphyxiation<sup>2</sup>.

However, studies demonstrated that regular injection of anti-inflammatory drugs increases long term viability<sup>3</sup> but also lead to a loss of interest for using encapsulated cells as it requires constant medical intervention.

In order to improve the long term cell viability while avoiding recurrent medical interventions, the goal of this project is to produce modified PEG-grafted alginate hydrogels<sup>4</sup> conjugated to small anti-inflammatory molecules (fibroblast activation protein  $\alpha$  (FAP- $\alpha$ ) inhibitor). These molecules could interact with the surrounding of the capsule and limit formation of fibrosis in order to improve long term cell viability.

### EXPERIMENTAL METHODS

A convergent synthetic pathway was developed to produce Gly-Pro derivatives as inhibitors of FAP- $\alpha$  for further conjugation to alginate based hydrogels. A maleimide moiety was envisaged as anchoring group to thiol containing hydrogels.

Characterisation of synthetic intermediates and final products was done *via* nuclear magnetic resonance on a Bruker-ARX-400 spectrometer (400 MHz) (<sup>1</sup>H & <sup>13</sup>C). Precise mass (*m/z*) were obtained on a Nermag R-10-10C spectrometer. Infrared analysis were performed on a JASCO FT/IR 4100 spectrometer.

### RESULTS AND DISCUSSION

Coupling of building blocks **1** and **2** afforded the core of the inhibitor of FAP- $\alpha$ , which was further derivatized with a maleimide containing linker.

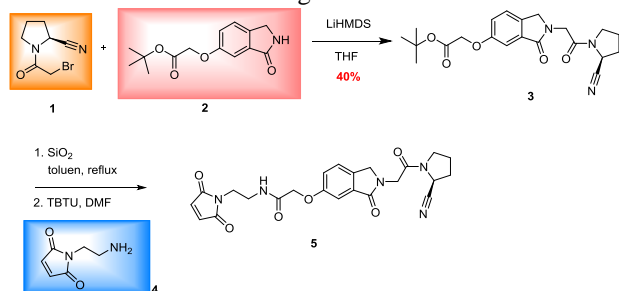


Fig 1: Synthetic strategy

Using the reactivity of maleimide moiety, the modified FAP- $\alpha$  inhibitor (**5**) was then linked to a thiol group available on PEG-grafted alginate derivatives (fig 2).

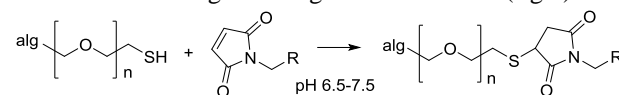


Fig 2: Functionalization of alg-based hydrogels

The effect of the modification of alg-based microspheres with anti-inflammatory molecules will be evaluated *in vitro* and in mice models.

### CONCLUSION

The improvement of biocompatibility and long term cell functionality remains a crucial challenge to further develop microencapsulated cells as therapy products. The modification of encapsulating hydrogels with anti-inflammatory agents, either covalently linked or co-encapsulated, might result in important benefit for the patient by reducing medical intervention. The functionalization strategy reported here can be applied to a large range of other active molecules presenting anti-inflammatory activities.

### REFERENCES

1. Rokstad, A. M. A., Lacik, I., de Vos, P. & Strand, B. L. *Advanced Drug Delivery Reviews* **67–68**, 111–130 (2014).
2. Říhová, B. *Advanced Drug Delivery Reviews* **42**, 65–80 (2000).
3. Ichii, H. & Ricordi, C. *Journal of Hepato-Biliary-Pancreatic Surgery* **16**, 101–112 (2009).
4. R. Mahou, G. Kollarikova, C. Gonelle-Gispert, R. Meier, F. Schmitt, N.M. Tran, M. Dufresne, I. Altimari, I. Lacik, L. Bühler, L. Juillerat-Jeanneret, C. Legallais, C. Wandrey, *Macromol. Symp.*, **2013**, 329, 49-57

### ACKNOWLEDGMENTS

The SNSF (205321-116397/1, 205320\_130572/1, 205321\_141286/1), the CTI (138041.1 PFLS-LS) and BÜCHI Labortechnik AG, Switzerland supported this research.

## The Comparison of Wettability and Surface Energy of Biomaterials and Bone Tissue

Anita Kajzer<sup>1</sup>, Wojciech Kajzer<sup>1</sup>, Ewa Kieruzel<sup>1</sup>

<sup>1</sup>Department of Biomaterials and Medical Devices Engineering, Silesian University of Technology,  
ul. Generała Charlesa de Gaulle'a 72, 44-800 Zabrze

[anita.kajzer@polsl.pl](mailto:anita.kajzer@polsl.pl)

### INTRODUCTION

The surface layer of the biomaterial used in implants is constantly exposed to the activity of biological environment. The interaction between the surface layer of the product and the body is determined by many factors such as wettability and surface energy (SEP). Testing wettability and surface energy (SEP) gives us opportunity to predict the level of interaction between the material and the body. The high value of surface energy correlates with good protein adsorption and as a consequence, cells adhesion. In case of the low value of SEP we experience opposite effect<sup>1,2</sup>. Therefore, in order to predict those effects, the influence of biomaterial surface modifications on wettability as well as surface energy were analyzed. In addition, the same evaluation was conducted for the surface of the bone tissue.

### EXPERIMENTAL METHODS

In order to test wettability and surface energy, steel CrNiMo, titanium alloy Ti6Al4V, polyurethane, fresh and dry beef bones were selected. The surface of the steel and titanium alloy were grinded with 120 and 800 abrasive paper. Next, they were polished and passivated. In addition, the surface of the steel was covered with carbon layer and sol-gel. To determine the wettability of the surface on the selected samples we analyzed contact angles and surface energy (SEP) with the Owens-Wendt method. Contact angle measurements were performed using two liquids: distilled water and diiodomethane. Measurement of liquid drops and diiodomethane deposited onto surfaces of the specimens was made at room temperature on a test bench consisting of a SURFTENS UNIVERSAL manual goniometer manufactured by OEG and computer with Surftens 4.5 software for the analysis of the recorded drops' image. 5 drops of distilled water and diiodomethane were applied onto the surface of each sample, each with a capacity of 1.5  $\mu$ l. The measurement began 20 seconds after the application of the drops. The duration of a single measurement was 60 seconds with a sampling rate of 1 Hz. Next, the measured values of wetting angles were presented as mean values with a standard deviation

### RESULTS AND DISCUSSION

The results of the research are presented on the Fig. 1. It was stated that the surface of the steel CrNiMo sample covered with sol-gel presented values of contact angle and surface energy comparable to fresh beef bone. The increase of the surface wettability for substrate made of steel CrNiMo was observed for a sample with sol-gel layer. In case of titanium alloy Ti6Al4V substrate, the

highest value of wettability was observed on the surface grained with 800 abrasive paper, whereas the lowest value – on the polished surface. Among all the analysed samples the highest value of contact angle was observed on the surface of polyurethane, which proves its hydrophilic properties.

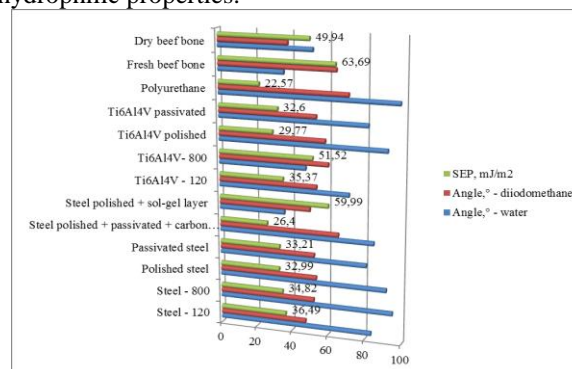


Fig. 1. Surface energy (SEP) and contact angles of selected materials

For various purposes, various properties of surface layer are desired. Thus, for log-term implants (eg. endoprosthesis) it is required to create opportunity for the best possible osteosynthesis, which helps to stabilize endoprosthesis properly in the bone. With such property correlates good surface wettability and therefore, hydrophilicity and higher value of surface energy. On the other hand, in case of dialysis devices or elements of artificial heart valves it is required they don't integrate with tissues or body fluids. Therefore, materials of low wettability and consequently, lower surface energy are required<sup>1,3,4</sup>.

### CONCLUSION

On the basis of carried research and obtained results it can be stated that surface layer modification has a significant influence on wettability and the value of surface energy.

### REFERENCES

1. Liber-Kneć *et al.*: Poli. w Med. 44:29-37, 2014
2. Sobieska S. *et al.*: Aktualne Problemy Biomechaniki. 7:153-156, 2013
3. Sobolewska E. *et al.*: Protetyka Stomatologiczna. 6:401-406, 2009
4. Lim J. *et al.*, Biomat. 29:1776-1784, 2008

### ACKNOWLEDGMENTS

The authors would like to thank prof. Jan Marciniak for the opportunity to carry out research in The Department of Biomaterials and Medical Devices Engineering.

## INTRODUCTION

The aim of this study is to combine the chemotactic activities of the trace elements copper and zinc with inorganic surface modification already successful in bone applications. In this combination chemotactic signals from released Cu ions are intended to provoke enhanced vascularization (demonstrated *in vivo* for amounts in the ng scale<sup>1</sup>) while released Zn ions recruit circulating bone forming cells to the site of surgery. Calcium phosphate phases (CPP) which are widely used in the field of bone surgery are utilized as a carrier for the selected trace elements in order to i) provide osteoconductive surfaces and ii) to allow fine tuning of immobilized amounts and release kinetics of the deposited trace elements.

## EXPERIMENTAL METHODS

Depositions of brushite were performed by using electrolytes composed of 83.5 mM  $\text{Ca}(\text{NO}_3)_2$  and 50 mM  $\text{NH}_4\text{H}_2\text{PO}_4$  (pH 4.0) with or without additional  $\text{Cu}(\text{NO}_3)_2$  or  $\text{Zn}(\text{NO}_3)_2$  in different concentrations. Electrochemically assisted depositions (ECAD) were carried out at 30°C applying a current density of  $-0.5 \text{ mA/cm}^2$  for 40 min. Sandblasted and additionally acid etched c.p.Ti discs were used as substrates.

The obtained coatings were characterized by i) scanning electron microscopy (SEM) with a DSM 982 Gemini combined with energy dispersive X-ray spectroscopy (EDX), ii) chemical analysis of calcium, phosphate, and zinc content in the layers following their dissolution in 0.1 N nitric acid with photometric assays and of copper content with atomic absorption spectroscopy.

## RESULTS AND DISCUSSION

Zinc and copper ions were added to the electrolytes in the range from 0.05 mM to 0.3 mM. Depending on the concentration this resulted in  $1.5 \pm 0.9 - 7.8 \pm 0.5 \text{ } \mu\text{g/cm}^2$  deposited Zn or  $5.9 \pm 0.7 - 31.7 \pm 2.9 \text{ } \mu\text{g/cm}^2$  Cu, respectively. The corresponding amounts of brushite were  $3150 \pm 200 \text{ } \mu\text{g/cm}^2$  irrespective of the added trace metal concentration.

Depositions of CPP in presence of Cu or Zn resulted in separate phases of brushite plates and Cu and Zn species, respectively (Fig. 1). EDX-mapping revealed isolated spots of copper structures within the brushite layers (Fig. 1a). This was in contrast to co-depositions under conditions which result in hydroxyapatite (HAp) layers, where the copper is homogeneously distributed throughout the HAp mineral coating<sup>2</sup>. The occurrence of dendritic structures in case of Cu indicates the partial reduction to Cu(I) and the subsequent formation of  $\text{Cu}_2\text{O}$  crystals. Further reduction to elemental copper is unlikely under the applied electrochemical conditions.

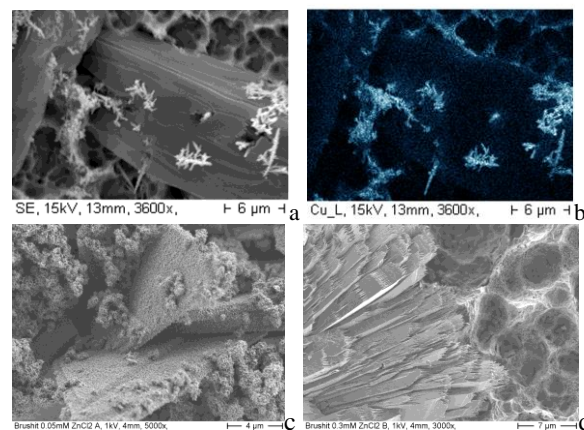


Fig. 1 SEM images of co-deposited trace element species within brushite layers on top of titanium surfaces: a) for 0.3 mM Cu, b) Cu mapping for 0.3 mM Cu, c) for 0.05 mM Zn and d) for 0.3 mM Zn in the respective electrolytes.

For the lowest applied concentration of added Zn (0.05 mM) Zn containing species homogeneously decorated the brushite plates. Increasing the concentration of zinc resulted in increased amounts of Zn in the deposited layers as well as changes in the morphology of the brushite plates (Fig. 1d).

## CONCLUSION

It was shown that copper and zinc can be co-deposited together with calcium phosphates onto metallic implant materials by means of electrochemically assisted deposition with only minor changes in general structure and amount of the deposited calcium phosphate. The relative amount of copper (or zinc) to calcium is tunable in a wide range. Current investigations focus on quantification of ion release in serum protein containing solutions and on improving retention of the trace metals within the coatings by other included components like chitosan.

The pro-angiogenic stimulation of human umbilical vein endothelial cells (HUVECs) by released copper ions is currently being studied with 2D and 3D angiogenic assays. For the chemotactic action of zinc the migration of human mesenchymal stromal cells (hMSC) will be analyzed.

## REFERENCES

1. Barralet J. et al., *Tissue Engineering* 15: 1601-1609, 2009
2. Wolf-Brandstetter C. et al., *J Biomed Mat Res B* 102: 160-172, 2014

## ACKNOWLEDGMENTS

The authors would like to thank the German Research Foundation (Grant no: WO 1903/2-1) for providing financial support to this project.

## Surface Properties of Chitosan Mixtures with Hyaluronic Acid and Collagen as Materials Designed for Biomedical Applications

Alina Sionkowska<sup>1</sup>, Katarzyna Lewandowska<sup>1</sup>, Sylwia Grabska<sup>1</sup>

<sup>1</sup>Department of Chemistry of Biomaterials and Cosmetics, Faculty of Chemistry, Nicolaus Copernicus University in Toruń, Poland  
[as@chem.umk.pl](mailto:as@chem.umk.pl)

### INTRODUCTION

Manufacturing of new functional and structural materials from natural renewable and degradable materials has attracted much attention. Natural polysaccharides are the right candidates due to their unique structures and properties<sup>1-3</sup>.

In this paper, mixtures composed of chitosan (Ch) with hyaluronic acid (HA) and collagen (Coll) at different component ratio have been prepared as material designed for different applications e.g. biomedical applications.

The purpose of the present work was the preparation and evaluation of the physico-chemical properties of chitosan mixture with hyaluronic acid and collagen, using the tapping-mode atomic force microscopy and by means of contact angle measurements.

### EXPERIMENTAL METHODS

Hyaluronic acid (HA) is a commercial polymer from Aldrich Company with a viscosity average molecular weight of  $1.8 \times 10^6$ . Chitosan (Ch) sample has a degree of deacetylation of 78% with a viscosity average molecular weight of  $0.59 \times 10^6$ . Collagen (Coll) was extracted in our laboratory from rat tail tendon. Chitosan and HA mixture was prepared by mixing of two solutions in 50/50 weight ratio. Collagen was added in the ratio 10% based on the mixture.

The measurements of contact angles ( $\Theta$ ) by the sessile drop method were performed at the room temperature using the DSA10 goniometer of Krüss GmbH (Germany), equipped with software for the drop shape analysis. The droplets of probe liquid (high purity, volume of  $3 \mu\text{l}$ ) were deposited on studied surface by a microsyringe. Each value of contact angle is an average of 10 measurements.

AFM imaging in the tapping mode and ambient conditions was done using a multimode scanning probe microscope with a Nanoscope IIIa controller (Digital Instruments Santa Barbara, CA). Surface images, using scan widths ranging from  $1 \mu\text{m}$  to  $10 \mu\text{m}$ , with a scan rate of 1.97 Hz were acquired at fixed resolution ( $512 \times 512$  data points). The AFM images were obtained for different sample places and the most typical areas are presented.

### RESULTS AND DISCUSSION

The surface properties of chitosan mixtures films were observed using atomic force microscopy. The examples of AFM images of chitosan, Ch/HA and Ch/HA/Coll mixtures are shown in Figure 1. The AFM images show difference in surface properties films for the homopolymers and their mixtures.

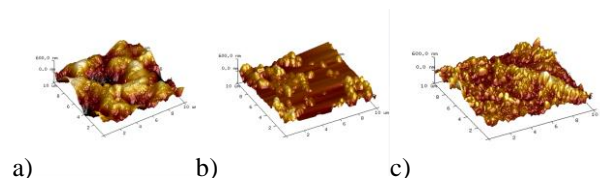


Fig. 1. AFM images of the surface of chitosan film and films made of chitosan mixtures: a) Ch, b) Ch/HA, c) Ch/HA/Coll.

Table 1

Values of contact angles (deg) for Ch and its mixtures

Sample	contact angle (°) G	contact angle (°) D
Ch	$65.7 \pm 0.8$	$55.7 \pm 0.7$
Ch/HA	$67.9 \pm 0.8$	$57.7 \pm 0.6$
Ch/HA/Coll	$55.4 \pm 1.5$	$66.7 \pm 1.2$

As it can be observed (Table 1), the surfaces of chitosan film and its mixtures were rather hydrophobic. The lowest value of glycerol contact angles is found for Ch/HA/Coll mixture, which suggests that this surface is the most hydrophilic.

The obtained results suggested that there was existence of the strong interactions between polymeric components.

### CONCLUSION

The study of mixtures by AFM showed a completely different morphology when compared with pure components. This may indicate a strong interaction between the polymeric components. Moreover, it was found that the surfaces of pure components and their blends had similar values of contact angles. The exception is the Ch/HA/Coll mixture. Summarizing, the structure and surface properties of investigated mixtures depend on the mixture composition and on the used solvent.

### REFERENCES

1. Sionkowska A. Prog. Polym. Sci. 36:1254-1276, 2011.
2. Sionkowska A. et al., J. Mol. Liq. 198:354-357, 2014.
3. Lewandowska K. Appl. Surf. Sci. 263:115-123, 2012.

### ACKNOWLEDGMENTS

The authors would like to thank the Research Frontiers Programme (NCN, Poland, Grant no: UMO-2013/11/B/ST8/04444) for providing financial support to this project.



## Alendronate Self assembling Monolayers. A Bioactive Bonding Agent on Titanium Surfaces

Luis Rojo<sup>1</sup>, Borzo Gharibi<sup>1</sup>, Sanjukta Deb<sup>1</sup>

<sup>1</sup> Division of Tissue Engineering & Biophotonics King's College London Dental Institute. United Kingdom.  
[luis.rojo\\_del\\_olmo@kcl.ac.uk](mailto:luis.rojo_del_olmo@kcl.ac.uk)

### INTRODUCTION

Ti6Al4V alloy is commonly used for manufacture of dental and orthopaedic implants because their biocompatibility, corrosion resistance, low modulus and good fatigue strengths, among other desirable properties. However different approaches have been investigated such as air blasting, acid etching, sol-gel and chemical treatments in order to obtain titanium implants grafted with extracellular matrix compounds with enhanced biological and chemical surface properties.

Bisphosphonates are a well-known class of osseointegrative drugs used in osteoporosis therapy with the ability to form self-assembled monolayers (SAMs) on titanium surfaces<sup>1</sup>. However, conventional methodologies for preparing these SAMs need the use of organic solvents that impede the widespread use of these materials as medical devices. This study presents an investigation of modification of Ti6Al4V alloy by chemisorption of alendronate SAMs from aqueous solutions with the capability to induce differentiation of human mesenchymal stem cells (hMSC) into bone cell phenotypes and promoting *in vitro* bone formation.

### EXPERIMENTAL METHODS

Alendronate SAMs formation onto alkali etched Ti6Al4V discs were carried out by solvent casting surface from alendronate aqueous solution and evaporation followed by gently washing with DI water and isopropanol. Control and treated discs were studied by contact angle measurements and surface free energy was calculated. SEM microscopy accompanied by energy dispersive X-ray analysis (EDX) (Hitachi S3500N) was used to obtain high resolution imaging and composition. Surface chemistry was further determined by RAMAN spectroscopy (Renishaw) and X-ray photoelectron spectroscopy (XPS, Kratos). Cell viability and osseointegrative capacity of alendronate SAMs were studied *in vitro* by assessing the expression of differentiation markers by hMSC cultured onto the treated discs.

### RESULTS AND DISCUSSION

Alendronate SAMs on Ti6Al4V have been effectively prepared from aqueous solution. Modified surfaces showed higher wettability than the native titanium alloy, with a regular surface topography and tailored surface chemistry. XPS analysis revealed that an effective Ti-O-P mode of bonding is created between the metal oxide surface and the phosphate residue of alendronate leading to the formation of homogenous drug distribution along the surface. hMSC cultured onto treated Ti6Al4V surfaces showed similar cell attachment capacity and proliferation rate than those observed for non-treated surfaces. However significant differences were found in the expression of skeletal markers ALP, osteopontin, RUNx2 and BMP compared to controls showing a clear differentiation of hMSC into skeletal cell phenotypes.

### CONCLUSION

Alendronate SAM formation from aqueous solution onto Ti6Al4V surfaces constitutes a simple approach to anchor bisphosphonates on titanium medical implants with enhanced osseointegration capacity. In addition the presence of free amino pendant groups of the alendronate SAM allows further surface modification permitting to act as bonding agent of further bioactive molecules such as hyaluronic acid, collagen and other surrounding extracellular matrix compounds.

### REFERENCES

1. Xuanyong L. et al., Mat Sci and Eng. R 47:49-121, 2004

### ACKNOWLEDGMENTS

We gratefully acknowledge Robbie Mac Lister and Prof Brian Meenan from University of Ulster and Prof Francis Hughes from King's College University for their kind advice on XPS and Cell studies.

"This work has been funded from EU FP7 Marie Curie Actions (PIEF-GA2013-622280)".

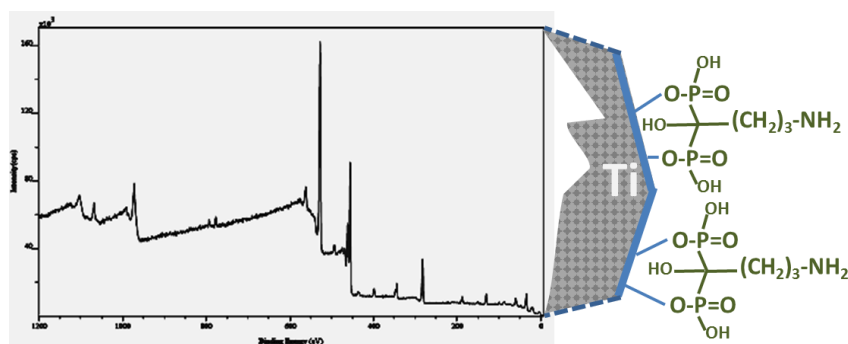


**Figure 1.** XPS surface analysis and schematic representation of the alendronate based SAMs on Ti6Al4V surfaces.

<sup>1</sup>Institute of Metallurgy and Materials Science; Polish Academy of Sciences, 25 Reymonta Street, 30-059 Cracow, Poland

<sup>2</sup>JOANNEUM RESEARCH- Materials- Institute for Surface Technologies and Photonics; Leobner Strasse 94; 8712 Niklasdorf, Austria  
[l.major@imim.pl](mailto:l.major@imim.pl)

## INTRODUCTION

Around the foreign body in a blood vessel, neointima is formed. To prevent this process metallic materials which are placed in the blood vessel, are usually modified. The new, smart coatings have the ability to both extend the life of structures and to provide additional functionalities to coated systems<sup>1</sup>. The paper describes the innovative, nano-composite, Cr/CrN+[Cr/ a-C:H implanted by metallic nanocrystals] coatings development which connects tribological protection together with increased biocompatibility in comparison with metallic substrates.

## EXPERIMENTAL METHODS

Thin films were fabricated by a hybrid Pulsed Laser Deposition technique<sup>2</sup>. Three types of coatings were investigated (Table 1).

Number	Description
1	Cr/CrN+[DLC (8 bilayer)]
2	Cr/CrN+[Cr-DLC/DLC (32 bilayer)]
3	Cr/CrN+[Cr-DLC/DLC (8 bilayer)]

The coatings were subjected under the analysis in the biomechanical system optimized to test the direct contact with a human whole blood<sup>3</sup>. The study considered physiological conditions, mainly related to the temperature and humidity and the frequency of cyclic deformation of the artificial vessel into which the tested sample was introduced (Fig. 1).

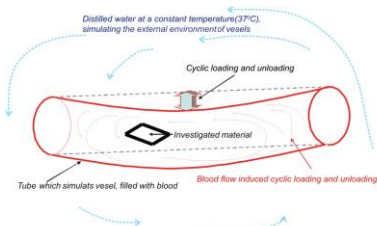


Fig. 1. Scheme of the bio-mimetic biological test.

The test was performed using electrodynamic tensile machine MTS Acumen equipped with bio- chamber. Blood above the investigated surface was examined by flow cytometry. Attached blood cells were examined by confocal laser scanning microscopy (CLSM) using Zeiss Exciter 5 instrument. Complex microstructure characterization of investigated coatings was performed by means of transmission electron microscopy techniques (TEM) using TECNAI G<sup>2</sup> F20 (200kV) FEG microscope.

## RESULTS AND DISCUSSION

The microstructure characterization was performed at the cross- section (Fig. 1).

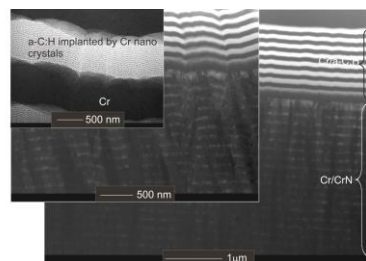


Fig. 2. Microstructure characterization of investigated coatings performed by TEM technique.

The applied coating showed slight improvement of the haemocompatibility compared to pure titanium (Fig. 3).

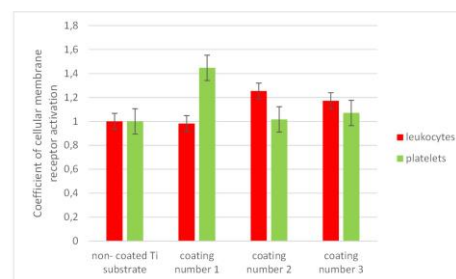


Fig. 3. Haemocompatibility test results

The coating number 3 showed an immune response similar in nature to the coagulation cascade, which may indicate that the coating from the haemocompatible point of view exhibits properties intermediate between 1 and 2.

## CONCLUSION

- Investigated coatings were built of two parts, the inner Cr/CrN and the outer part (DLC)
- The bio- mimetic, biological investigation showed slight improvement of the haemocompatibility in the coated titanium substrate to pure titanium

## REFERENCES

1. Majot L. *et al.*, RSC Adv. 5 : 9405–9415, 2015
2. Lackner J.M., Surf. Coat. Technol. 200: 1439–1444, 2005
3. Major R., J. Mater Sci: Mater. Med. 24: 725–733, 2013

## ACKNOWLEDGMENTS

The authors would like to thank the National Science Centre (pol. NCN), for providing financial support to the following projects:

- Research Project Number: 2012/06/M/ST8/00408
- Research Project Number: 2012/07/B/ST8/03396

## Novel Silicon-enriched Bioactive Coatings for Titanium Implants

Amanda Bartkowiak<sup>1</sup>, Katarzyna Suchanek<sup>1</sup>, Barbara Szaraniec<sup>2</sup>, Marta Marszałek<sup>1</sup>

<sup>1</sup>The Henryk Niewodniczański Institute of Nuclear Physics, Polish Academy of Sciences, Poland

<sup>2</sup>Department of Biomaterials, The University of Science and Technology AGH, Poland

[amanda.bartkowiak@ifj.edu.pl](mailto:amanda.bartkowiak@ifj.edu.pl)

**Silicon-enriched bioactive coatings were successfully produced on modified titanium substrates using hydrothermal method. The coatings were investigated for their chemical and phase composition, morphology, adhesion, thermal stability and bioactivity *in vitro*.**

### INTRODUCTION

In order to promote osseointegration at the implant-tissue interface, hydroxyapatite (HAp) has been used to coat the femoral stem of hip prosthesis. Among different deposition techniques, hydrothermal method was found to produce highly crystalline and uniform HAp coatings on titanium, dealing with complex shapes typical for orthopedic implants<sup>1</sup>. At the level of synthesis it is possible to introduce silicon, as it was found that bone mineralization requires the smallest amount of this element<sup>2</sup>. Silicon was also found to promote collagen type I synthesis and osteoblast differentiation<sup>3</sup>. It was shown to play an essential role in metabolic processes involving normal bone and cartilage formation<sup>4</sup>. In the following study the novel silicon-enriched bioactive coatings were synthesized and investigated for their potential to enhance biocompatibility of titanium implants.

### EXPERIMENTAL METHODS

The hydrothermal synthesis was performed on titanium plates of 10x10 mm previously undergone chemical and thermal treatment. The deposition process was carried out in an autoclave from stock solution containing: calcium salt hydrate, diammonium phosphate, calcium chelating agent and soluble source of silicon. Accordingly to expected wt% substitution of silicon in the HAp lattice, three kinds of samples were prepared with 0,2wt%, 0,8wt% and 1,5wt% of silicon. After the synthesis samples were left to dry and subsequently heated at 700°C, 850°C and 1000°C for adhesion improvement and thermal stability evaluation. The morphology and structure of as prepared specimens were characterized using XRD, SEM, EDX, FTIR and Raman techniques. Changes in surface morphology were examined after incubation in SBF and PBS solutions.

### RESULTS AND DISCUSSION

High crystallinity of HAp coating for implantation applications is desirable since low crystallinity accelerates the speed of dissolution of the HAp films in the living body, causing the disappearance of coatings that bond to bone tissue at an early stage after implantation. The XRD and spectroscopic analysis confirmed the existence of well crystallized HAp in the prepared specimens. The microstructure of synthesized

coatings, showed as an example on SEM image in Fig.1, demonstrates an interesting combination of HAp crystals and micro- and nano-sized spherical particles, likely of amorphous silica, deposited simultaneously during the hydrothermal process. As HAp is itself recognized to be an osteoconductive material, recent studies done on nanoparticle form of silica showed that it mediates potent anti-osteoclastogenic activities on monocytes and stimulates osteoblast differentiation<sup>5</sup>. XRD calculations on changes in the values of lattice parameters of HAp with increasing silicon content imply that the silicon has also replaced phosphorous in the crystal lattice of HAp. It has been reported that silicon-substituted HAp has enhanced bioactivity *in vitro*<sup>6</sup> rather than its pure form.

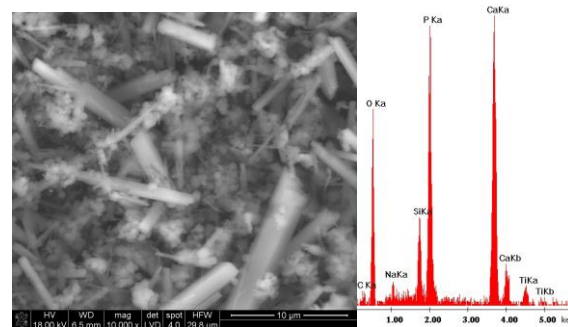


Fig. 1. SEM image and EDX spectrum of silicon-enriched coating with 0,8wt% of silicon in the HAp lattice.

### CONCLUSION

Hydrothermal synthesis followed by a thermal treatment resulted in crack-free, dense and durable silicon-enriched films. Biological activity was observed for each sample. The as-prepared coatings are promising for applications in the area of bioactive surface modification for titanium based implants. The technique should be extended to metal substrates of varying shapes, such as mesh, porous, or tubular geometry.

### REFERENCES

1. Liu D. *et al.*, Surf. Coat. Tech. 205:3975-3986,2011
2. Seaborn C.D. *et al.*, Biol. Trace Elem. Res. 42:151-164, 1994
3. Reffit D.M. *et al.*, Bone 32: 35-127,2003
4. Carlise E., J. Nutr. 110:55-1046,1979
5. Beck G. R. Jr. *et al.*, Nanomed.: Nanotech. Biol. Med. 8:793-803, 2012
6. Thian E.G. *et al.*, Biomaterials 27:2692-2698,2006

## Composite Sol-gel Bioactive Glass/Chitosan Coatings Deposited on Ti13Zr13Nb Alloy

Dawid Jugowiec<sup>1</sup>, Katarzyna Cholewa-Kowalska<sup>2</sup>, Michał Dziadek<sup>2</sup>, Łukasz Cieniek<sup>1</sup>, Tomasz Moskalewicz<sup>1</sup>

<sup>1</sup>AGH University of Science and Technology, Faculty of Metals Engineering and Industrial Computer Science,  
Al. A. Mickiewicza 30, 30-059 Kraków, Poland

<sup>2</sup>AGH University of Science and Technology, Faculty of Materials Science and Ceramics,  
Al. A. Mickiewicza 30, 30-059 Kraków, Poland  
[jugowiec@agh.edu.pl](mailto:jugowiec@agh.edu.pl)

### INTRODUCTION

The rising demand for enhanced and stable adhesion between rigid, metallic implants and host tissue requires improvement of surface properties of these biomedical devices<sup>1</sup>. The composite sol-gel bioactive glass/chitosan coatings have been utilized for this particular purpose. Bioactive glasses are materials which quickly react with physiological fluids, forming hydroxyapatite layers on the surface and connect strongly with hard and soft tissues through cellular activity<sup>2</sup>. Chitosan is a natural cationic polysaccharide, which due to its adequate properties such as biocompatibility, biodegradability and antimicrobial properties has found its use in many biomedical applications<sup>3</sup>. One of the most efficient technique used for deposition of the composite coatings is electrophoretic deposition (EPD). This is due to its simplicity, versatility, low cost and high coating uniformity. The aim of this study was surface modification of Ti13Zr13Nb alloy by electrophoretic deposition of bioactive glass/chitosan coatings as well as characterization of microstructure of coated alloy.

### EXPERIMENTAL METHODS

Near- $\beta$  Ti13Zr13Nb titanium alloy was used as substrate material for coatings deposition. The coatings were deposited by EPD. Dilute solution of sol-gel bioactive glass (1.5 g/l) and chitosan (2 g/l) in a mixture of distilled water and 0.5 vol. % acetic acid and 50 vol. % ethanol was prepared by magnetic stirring at room temperature for 72 hours. The EPD was carried out in a two-electrode cell, under constant voltage conditions in the range of 8-30 V. Deposition time was varied in the range of 1-5 minutes and the distance between electrodes in the EPD cells was 10 mm. A titanium alloy, bioactive glass and coating microstructure were investigated by scanning- and transmission electron microscopy (SEM, TEM).

### RESULTS AND DISCUSSION

Ti13Zr13Nb alloy microstructure was mainly composed of  $\alpha'$  (hexagonal close-packed; hcp) laths in  $\beta$  (body-centered cubic; bcc) grains. Sporadically, a fine  $\alpha''$  laths (orthorhombic, Cmc<sub>2</sub>m space group) also could be observed. It was found during EPD that both, the chitosan molecules and bioglass particles were positively charged in the deposit used. The most homogeneous and continuous coatings were deposited using solution of bioactive glass (2 g/l) and chitosan (2 g/l) in a mixture of distilled water and 0.5 vol. % of acetic acid as well as 50 vol. % of ethanol at the voltage of 10 V during 4 minutes. The coating microstructure consisted of bioglass particles (diameter up to 4.5  $\mu$ m) homogeneously embedded in the chitosan matrix. The

chemical composition of sol-gel bioglass was 54 mol % CaO, 40 mol % SiO<sub>2</sub> and 6 mol% P<sub>2</sub>O<sub>5</sub><sup>4</sup>. SEM-EDS microanalyses confirmed the presence of Ca, Si, P and oxygen in the coating.

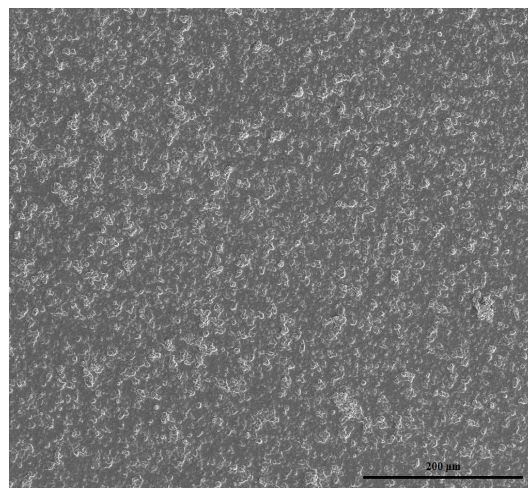


Fig. 1. Microstructure of as-deposited bioactive glass/chitosan coating on near- $\beta$  Ti13Zr13Nb alloy, SEM plan-view, secondary electron image

Due to micrometric particles size the surface topography of the coating exhibited high surface development.

### SUMMARY

The composite, sol-gel bioactive glass/chitosan coating has been successfully deposited by EPD technique on the near- $\beta$  Ti13Zr13Nb alloy. The coating was homogeneous and was composed of bioglass particles embedded in chitosan matrix. Further, optimization of EPD parameters as well as detailed investigation of microstructure and properties of the coated alloy are in progress.

### REFERENCES

1. Pishbin F. *et al.*, Surf. Coat. Tech. 205:5260-5268, 2011
2. Zhitomirsky D. *et al.*, J. Mater. Process. Technol. 209:1853-1860, 2009
3. Sun F. *et al.*, J. Mater. Process. Technol. 209:1597-1606, 2009
4. Łączka M. *et al.* J. Mol. Str. 511-512:223-231, 1999

### ACKNOWLEDGMENTS

This work was supported by the Polish National Science Centre (decision no. DEC-2013/09/B/ST8/00145).





## Deposition and Characterisation of Microporous Sol-gel Bioactive Glass/PEEK 704 Coating on Near- $\beta$ Titanium Alloy

Anita Sak, Łukasz Cieniek, Katarzyna Cholewa-Kowalska, Agnieszka Radziszewska, Marcin Kot, Alicja Łukaszczyk, Tomasz Moskalewicz

AGH University of Science and Technology, Al. A. Mickiewicza 30, 30-059 Kraków, Poland  
[anisak@agh.edu.pl](mailto:anisak@agh.edu.pl)

### INTRODUCTION

An effective technique of deposition of the porous composite coatings for biomedical applications is electrophoretic deposition (EPD). EPD is based on the movement of the colloidal particles in a suspension under the influence of an electric field and the deposition of particles on the oppositely charged electrode<sup>1</sup>.

PEEK is a polymer which exhibits good mechanical properties, including low coefficient of friction and non-toxicity<sup>2</sup>. Bioactive glass particles are added to PEEK, because they facilitate the knitting of bone tissue. Therefore, this coating is advantageous in medical application. The aims of the present work were:

- to produce microporous, good quality sol-gel bioactive glass/PEEK 704 coating on near- $\beta$  Ti13Zr13Nb alloy by EPD,
- to characterise the microstructure and selected properties of coated alloy.

### EXPERIMENTAL METHODS

A near- $\beta$  Ti13Zr13Nb alloy was used as a substrate material. A calcium-rich glass with a composition (in mol %) of 54 CaO, 40 SiO<sub>2</sub>, 6 P<sub>2</sub>O<sub>5</sub> produced by a sol-gel method was applied as a bioactive coatings component<sup>3</sup>. Bioactive glass/PEEK 704 coating was deposited on titanium alloy by EPD. The EPD was performed at a constant voltage in a range of 30-80 V. Deposition time was 2 minutes. The distance between electrodes was 5 mm. The coated specimen was heat treated at temperature of 355 °C during 20 minutes.

The microstructure of the coating components and the coatings was investigated by scanning electron microscopy (SEM) and X-ray diffractometry (XRD). The coatings adhesion to the alloy was investigated by means of micro-scratch test method. The corrosion resistance of uncoated and coated alloy was studied in the Ringer's solution at 37 °C. Measurements were performed for pH equal 7.4 and in deaerated solutions using electrochemical techniques.

### RESULTS AND DISCUSSION

The microstructure of the sol-gel glass used for EPD was characterised by XRD and SEM. XRD analysis revealed the presence of Ca<sub>5</sub>(PO<sub>4</sub>)<sub>3</sub>(OH) (hexagonal primitive; hp) and CaSiO<sub>3</sub> (triclinic primitive; tp) phases. The particles size evaluated from SEM images was up to 40  $\mu$ m. During EPD, both the glass and the PEEK particles in suspension were positively charged and they moved towards the cathode under the applied electric field. The best quality, homogeneous coatings were achieved for suspension containing PEEK, bioactive glass and citric acid in ethanol at 50 V during 2 minutes. SEM investigation revealed that the coating

was highly porous with pores diameter up to 35  $\mu$ m (Fig. 1). The coating had an uniform thickness approx. of 35  $\mu$ m. SEM-EDS microanalyses confirmed the occurrence of glass particles containing Ca, Si, P and oxygen embedded in the PEEK matrix.

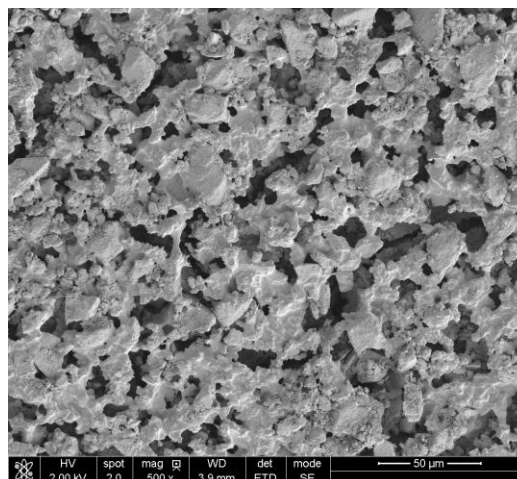


Fig. 1. Microstructure of the sol-gel glass/PEEK 704 coating on Ti13Zr13Nb titanium alloy. SEM plan-view

It was found that the coating exhibit sufficient (for non-tribological applications) adhesion to the titanium alloy substrate. No cohesive cracks were observed during micro-scratch test. First adhesive cracks were observed after scratching with a load of 8 N.

Both uncoated- and coated alloys have good corrosion resistance in neutral Ringer's solution, however the coated alloy exhibits slightly better resistance to corrosion than uncoated one.

### SUMMARY

This work shows that EPD is very useful technique to deposit fairly uniform, well-adhered and microporous composite sol-gel glass/PEEK 704 coatings on near- $\beta$  titanium alloy.

The coated alloy exhibited a good corrosion resistance in Ringer's solution.

### REFERENCES

1. Corni I. *et al.*, J. Eur. Ceram. Soc. 28:1353-1367, 2008
2. Wang C. *et al.*, Surf. Coat. Tech. 173:271-275, 2003
3. Pamuła E. *et al.*, Ann. Biomed. Eng. 39:2114-2129, 2011

### ACKNOWLEDGMENTS

This work was supported by the Polish National Science Centre (decision no. DEC-2013/09/B/ST8/00145).

## Influence of PEEK 704 Coating on Tribological Properties of Ti13Zr13Nb Alloy

Anita Sak<sup>1</sup>, Sławomir Zimowski<sup>2</sup>, Marcin Kot<sup>2</sup>, Beata Dubiel<sup>1</sup>, Tomasz Moskalewicz<sup>1</sup>

<sup>1</sup>AGH University of Science and Technology, Faculty of Metals Engineering and Industrial Computer Science,  
Al. A. Mickiewicza 30, 30-059 Kraków, Poland

<sup>2</sup>AGH University of Science and Technology, Faculty of Mechanical Engineering and Robotics,  
Al. A. Mickiewicza 30, 30-059 Kraków, Poland  
[anisak@agh.edu.pl](mailto:anisak@agh.edu.pl)

### INTRODUCTION

Titanium alloys due to their unique properties are widely used in medical application<sup>1</sup>. A near- $\beta$  Ti13Zr13Nb alloy is designed for bone implants. However, its use in applications involving friction and wear is limited due to the relatively low hardness and poor tribological properties. Therefore, it is important to improve tribological properties of this alloy by surface engineering. A very promising coating material for improvement of tribological properties of metallic materials is polyetheretherketone (PEEK). PEEK is a semicrystalline, thermoplastic polymer, which is popular in the biomedical application. It exhibits high strength, excellent tribological properties, high hardness and toughness<sup>2,3</sup>. A very prospective technique for deposition of PEEK coating on titanium alloys is electrophoretic deposition (EPD)<sup>1</sup>. The aim of this work was application of PEEK 704 coating on Ti13Zr13Nb alloy by EPD and investigation microstructure as well as tribological properties of the baseline and coated alloy.

### EXPERIMENTAL METHODS

A polymer PEEK 704 coating was electrophoretically deposited on the near- $\beta$  Ti13Zr13Nb titanium alloy substrate. Suspension of PEEK powder in ethanol was used for coatings deposition. The EPD was performed at a constant voltage in the range of 70-90 V and deposition time equal to 60 s. The distance between the cathode and counter electrode was 10 mm. Post deposition heat treatment was performed at temperature of 355 °C for 30 minutes.

A microstructure of the alloy and the coating was characterized by scanning- and transmission electron microscopy (SEM, TEM). The adhesion of the coating to the titanium alloy was investigated by means of micro-scratch test method.

Hardness and Young's modulus were measured by instrumented indentation tests using a Vickers indenter. The friction and wear properties of the baseline and coated alloy were evaluated using a ball-on-disk apparatus at unlubricated contact. Alumina balls of 6 mm in diameter were used as the counter body.

### RESULTS AND DISCUSSION

Microstructure of the substrate material consisted of  $\alpha'$  laths (hexagonal close-packed; hcp) in  $\beta$  grains (body-centered cubic; bcc). Sporadically, a fine  $\alpha''$  laths (orthorhombic, Cmc<sub>2</sub>m space group) was also identified by selected area electron diffraction. The grain size of  $\beta$  ranged from 20  $\mu$ m to 60  $\mu$ m. During EPD the PEEK particles were negatively charged in the suspension. The best deposition conditions for PEEK coatings on

titanium alloy were obtained applying a constant voltage of 92 V and the deposition time of 60 seconds. SEM investigation revealed that the as-deposited and subsequently annealed PEEK coating was homogeneous. The coating thickness was about 70  $\mu$ m. It was found during micro-scratch test that PEEK 704 coating after annealing exhibited very good adhesion to the substrate material. The critical load was equal about 25 N. Hardness and Young's modulus of the alloy were measured as  $3 \pm 0.2$  GPa and  $89 \pm 2$  GPa, respectively. The coating hardness was measured as  $0.26 \pm 0.03$  GPa, while Young's modulus as  $4.7 \pm 0.3$  GPa. The coating essentially improved the frictional wear resistance of the titanium alloy (Fig. 1). Coated alloy exhibited much better wear resistance than that of the uncoated one.

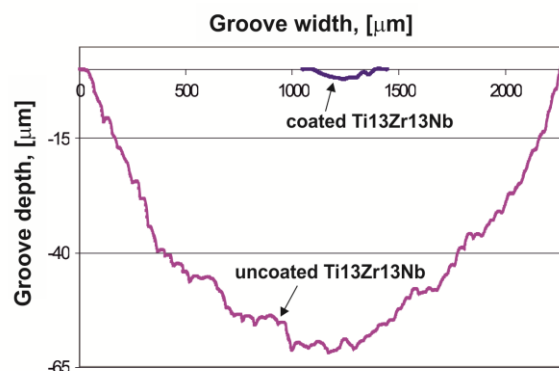


Fig. 1. Frictional wear resistance of the PEEK 704 coating on Ti13Zr13Nb alloy compared with the wear of uncoated alloy

### SUMMARY

Homogeneous polymer PEEK 704 coating was successfully deposited on Ti13Zr13Nb alloy by EPD. It was found that the coating exhibited very good adhesion to the titanium alloy substrate and essentially improved the alloy wear resistance.

### REFERENCES

1. Moskalewicz T. *et al.*, Appl. Surf. Sci. 273:62-67, 2013
2. Corni I. *et al.*, Surf. Coat. Tech. 203:1349-1359, 2009
3. Clavijo S. *et al.*, J. Appl. Polym. Sci. 40953:1-6, 2014

### ACKNOWLEDGMENTS

This work was supported by the Polish National Science Centre (decision no. DEC-2013/09/B/ST8/00145).

A part of this study (tribological tests) was supported by the AGH-UST (project nr 11.11.110.293).



## Influence of Electrophoretic Deposition Parameters on Chitosan Coatings Quality

Dawid Jugowiec, Tomasz Moskalewicz

AGH University of Science and Technology, Faculty of Metals Engineering and Industrial Computer Science,  
Al. A. Mickiewicza 30, 30-059 Kraków, Poland

[jugowiec@agh.edu.pl](mailto:jugowiec@agh.edu.pl)

### INTRODUCTION

Titanium and its alloys are extensively used as suitable dental and orthopaedic implants in biomedical engineering<sup>1</sup>. Ti13Zr13Nb alloy exhibits low Young's modulus (below 100 GPa), good corrosion resistance and sufficient biocompatibility<sup>2</sup>. In order to further improve bone cell adhesion to the surfaces of the titanium alloy implant, the biodegradable polymers coating might be applied. Among different methods exploited for such coatings, electrophoretic deposition (EPD) is especially attractive. This is due to its ability to deposit uniform polymer coatings with controlled properties on complex-shaped and porous microstructure<sup>3</sup>. Chitosan is one of the most promising natural biopolymer, which due to its biocompatibility, biodegradability and non-toxicity has found significant interest in biomedical applications<sup>4</sup>. The aim of this work was detailed investigation of electrophoresis parameters for deposition of uniform, good quality chitosan coating on near- $\beta$  Ti13Zr13Nb alloy.

### EXPERIMENTAL METHODS

Near- $\beta$  Ti13Zr13Nb alloy was used as a substrate material for EPD of chitosan coatings. Dilute solution of chitosan (0.5 g/l) in a mixture of distilled water and 1 vol. % acetic acid as well as 9 dilute solutions of different concentrations of chitosan (0.5 g/l, 1 g/l, 2 g/l) in a mixture of distilled water, 50 vol. % ethanol and different vol. % of acetic acid (0.5%, 1% and 2%) were prepared by magnetic stirring at room temperature for 24-72 hours and later used for EPD. The EPD was carried out under constant voltage conditions in the range of 8-30 V. Deposition time was varied in the range of 1-5 minutes. The distance between electrodes in the EPD cells was 10 mm. Zeta potential of the solutions was measured by Zetasizer Nano ZS90 of Malvern Instruments Ltd. The coatings quality was evaluated by visual inspection and scanning electron microscopy (SEM) observations.

### RESULTS AND DISCUSSION

Electrophoretic mobility of suspended molecules in solution is one of the main driving forces of EPD and significantly affects the uniformity of as-deposited coatings. In our work the greatest value of electrophoretic mobility was achieved for solution of chitosan (2 g/l) in a mixture of distilled water and 0.5 vol. % of acetic acid and 50 vol. % of ethanol (Fig. 1). During EPD a voltage and deposition time were determined in order to obtain homogeneous coatings. The most homogeneous and continuous coatings were deposited at the constant voltage of 10 V and deposition time 4 minutes. It was also investigated, that addition of ethanol to chitosan suspension reduces H<sub>2</sub> bubbles formation and thus gas evolution during EPD, which

resulted in more homogenous chitosan coatings. Similar effect on the H<sub>2</sub> bubbles formation had an electrophoretic voltage value during EPD. If the voltage was higher than 10 V the H<sub>2</sub> bubbles formation was very intensive. On the other hand if the voltage value was lower than 10 V the coating was only partially deposited on the substrate surface.

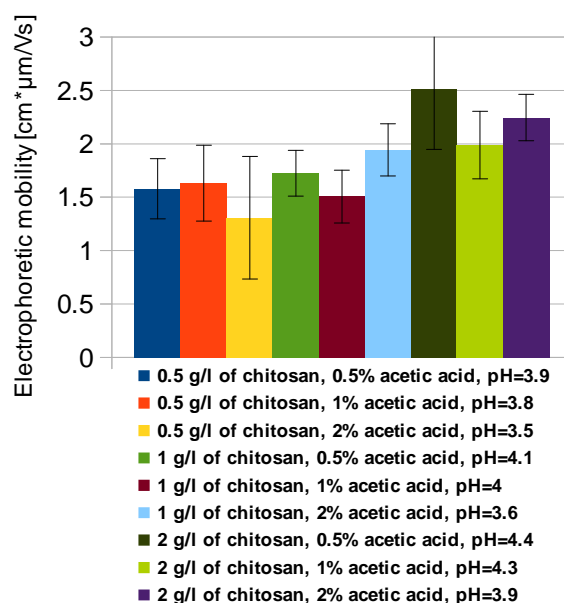


Fig. 1. Electrophoretic mobility of different colloidal solutions used for EPD

### CONCLUSION

The adequate solution composition and EPD parameters were selected for EPD of good quality chitosan coatings on Ti13Zr13Nb alloy. It was established that the uniformity of the as-deposited chitosan coating is highly dependent on solution composition, EPD voltage and time. Further, microstructure and properties characterization of the coated alloy as well as biocompatibility analysis are in progress.

### REFERENCES

1. Ordikhani F. *et al.*, Appl. Surf. Sci. 317:56-66, 2014
2. Simka W. *et al.*, Appl. Surf. Sci. 279:317-323, 2013
3. Pishbin F. *et al.*, Acta Biomater. 9:7469-7479, 2013
4. Łosiewicz B. *et al.*, Solid State Phenom. 203-204:212-215, 2013

### ACKNOWLEDGMENTS

This work was supported by the Polish National Science Centre (decision no. DEC-2013/09/B/ST8/00145).



# Surface Modification of Ti-Nb-Sn Alloy Controlling OCP Precipitation by Electron Cyclotron Resonance Plasma Oxidation

Hiroshi Masumoto<sup>1</sup>, Mayumi Oikawa<sup>2</sup>, Yusuke Orii<sup>2</sup>, Takahisa Anada<sup>2</sup>, Osamu Suzuki<sup>2</sup> and Keiichi Sasaki<sup>2</sup>

<sup>1</sup>Frontier Research Institute for Interdisciplinary Sciences (FRIS), Tohoku University, Japan

<sup>2</sup>Graduate School of Dentistry, Tohoku University, Japan

[hiromasu@fris.tohoku.ac.jp](mailto:hiromasu@fris.tohoku.ac.jp)

## INTRODUCTION

Commercially pure titanium (cp-Ti) and titanium alloys are widely used in various types of implants in orthopaedic and dental fields, because they have the greatest biocompatibility with bone among the metallic biomaterials. Ti-Nb-Sn alloy (Ti-35mass%Nb-7.9mass%Sn alloy) is a novel  $\beta$ -type Ti alloy with a 40 GPa Young's modulus, which is similar to that of human cortical bone (30 GPa)<sup>[1]</sup>. It is known that the biocompatibility of Ti will change with the condition of the surface oxide (titania: TiO<sub>2</sub>) film of implant Ti alloy. Electron cyclotron resonance (ECR) plasma is high-active plasma, and high-quality crystalline films can be obtained at low temperature for short time. ECR plasma oxidation is effective surface modification of metal Ti for biocompatibilities, which became clearly in previous study<sup>[2]</sup>. Our previous studies indicated that implantation of octacalcium phosphate [ $\text{Ca}_8\text{H}_2(\text{PO}_4)_6 \cdot 5\text{H}_2\text{O}$ , OCP] was efficiently enhanced bone regeneration compared to HAp<sup>[3]</sup>. In the present study, TiO<sub>2</sub> films were deposited on Ti-Nb-Sn alloy by ECR plasma oxidation, and the effect of oxidation conditions on structure and precipitation behaviour of OCP were investigated.

## EXPERIMENTAL METHODS

ECR plasma apparatus was used for oxidation of Ti-Nb-Sn alloy surface ( $8\Phi \times 1.0 \text{ mm}^3$ ). A magnetic field ( $8.75 \times 10^{-2} \text{ T}$ ) was applied to the plasma chamber to satisfy the ECR condition. The oxygen gas pressure during ECR oxidation was set to 0.003-1.5 Pa and the oxidation time was set to 1.8 ks. The microwave power was 900 W. An infrared lamp was used for controlling the substrate temperature in the range from room temperature (RT) to 600 °C.

The structure and morphology of the films were characterized by X-ray diffraction analysis (XRD) and

optical and scanning electron microscopy (SEM). OCP was precipitated in phosphate-buffered solution on TiO<sub>2</sub> film deposited Ti substrate<sup>[3]</sup>. The calcification ability was estimated by weighing the substrate before and after the immersion.

## RESULTS AND DISCUSSION

Figure 1 shows XRD patterns of the substrates oxidized by ECR plasma at various temperatures and after calcification. Crystalline rutile-type TiO<sub>2</sub> films were obtained above 500 °C. The ECR plasma was effective to prepare crystallized TiO<sub>2</sub> films at low temperatures. Mixtures of OCP and dicalcium phosphate dihydrate (DCPD) peaks were observed after calcification.

Fig. 2 shows macroscopic images of calcium phosphate deposits formed on the Ti-Nb-Sn alloy substrate after ECR plasma oxidation at 400°C. Whole surface was covered by many flocculent precipitates of calcium phosphate. The amount of OCP and DCPD after calcification increased with increasing total pressure ( $P_T$ ) from  $3.3 \times 10^{-3}$  -  $1.5 \times 10^{-2}$  Pa, and showed the maximum at  $P_T = 1.5 \times 10^{-2}$  Pa.

Fig. 3 shows the effect of the oxidation temperature and time on calcium phosphate deposition onto the substrate surfaces. The amount of calcium phosphate deposition was maximized at 600°C, 60 min.

It was suggested that ECR plasma oxidation method is effective surface modification for the Ti-Nb-Sn alloy, because of their calcification ability.

## Reference

1. S. Hanada, *et al. Inter. Cong. Ser.* (2005), **1284**: 239.
2. Y. Orii, *et al. J. Biomed. Mat. Res. Part B, Appl. Biomater.*, (2010) **93**(2):476.
3. O. Suzuki, *et al. Biomaterials* (2006) **27**: 2671

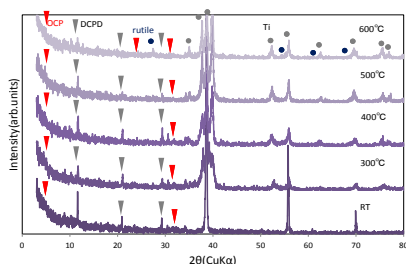


Figure 1 XRD patterns of the surfaces of Ti-Nb-Sn alloys oxidized by ECR plasma and after calcification.

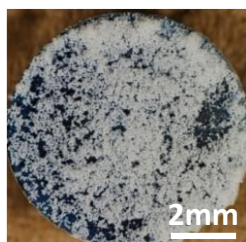


Figure 2 Macroscopic images of calcium phosphate deposits on the substrate after ECR plasma oxidation at 400°C.

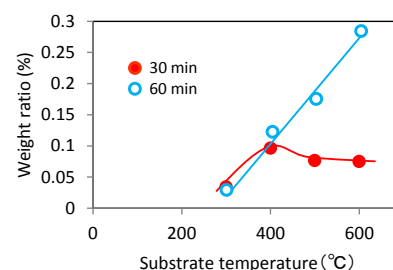


Figure 3 Amount of calcium phosphate deposits estimated by the weight ratio at different substrate temperatures.



## Influence of Purified ECM Components on Corneal Epithelial Cells Cultivated on Silk Fibroin

Thomas A. Hogerheyde<sup>1,2</sup>, Shuko Suzuki<sup>2</sup>, Sally-Anne Stephenson<sup>1</sup>, Damien G. Harkin<sup>1,2</sup>  
 Laura J. Bray<sup>1,2</sup>, Neil A. Richardson<sup>1,2</sup>

<sup>1</sup>School of Biomedical Sciences, Queensland University of Technology, Australia

<sup>2</sup>Queensland Eye Institute, Queensland University of Technology, Australia

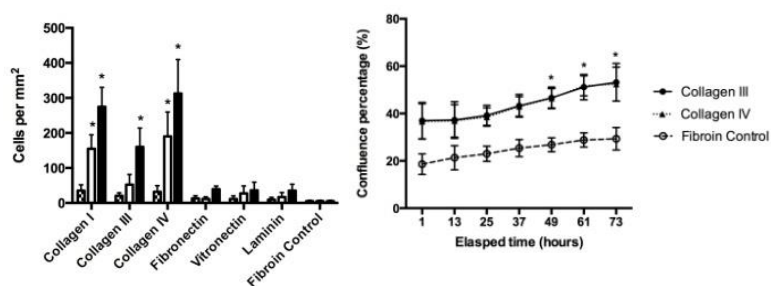
[thomas.hogerheyde@gmail.com](mailto:thomas.hogerheyde@gmail.com)

### INTRODUCTION

A transparent and avascular cornea is essential for healthy vision. Due to the high failure rate of cadaveric-donor corneal-limbal transplants, a range of biomaterials have been explored as potential scaffolds for cultivated autologous limbal epithelial transplants. One material that demonstrates significant potential for this role is the silk protein fibroin. Membranes prepared from *Bombyx mori* silk fibroin demonstrate attractive properties of tensile strength, biodegradability, and transparency that make them an excellent candidate scaffold material for corneal-limbal epithelial cells. The ability of fibroin-based membranes to support the attachment and growth of human limbal epithelial (HLE) cells has been reported by our group<sup>1</sup>. The limbus contains a population of stem cells responsible for regenerating the corneal epithelium. While these findings represent a significant advance in the application of fibroin biomaterials, the performance of fibroin for generating corneal epithelial equivalents does not yet match that of amniotic membrane that is widely utilised for this purpose. Elsewhere, others have modified fibroin substrata with biological materials that mimic the native environment of the cells to be implanted<sup>2</sup>. Previous studies by our group demonstrated that coating of fibroin films with collagen IV significantly improved attachment and growth of human corneal endothelial cells<sup>3</sup>. It has also been reported that vitronectin coating of therapeutic contact lenses encourages corneal epithelial migration during wound healing<sup>4</sup>. In the current study, selected extracellular matrix (ECM) components were shown to promote changes in morphology, attachment and spreading of corneal/limbal epithelial cells cultured on fibroin films. Findings such as these offer the potential to assist those seeking to develop improved strategies to yield functional corneal constructs

### EXPERIMENTAL METHODS

**Corneal epithelial cell attachment:** Attachment of transformed human corneal epithelial (HCE-T; n=4) and primary HLE cells (n=5) seeded onto fibroin-coated films treated with selected ECM components (0.2, 1 and 5 µg/mL) was determined after 90 min. HLE phenotype was assessed by performing immunohistochemistry for p63. **Corneal epithelial cell morphology and confluency:** HCE-T (n=4) and primary HLE cells (n=3) were seeded onto fibroin films coated with selected ECM components (5 µg/mL). Cultures were then assessed for changes in cell morphology or confluency after 1 or 73 h, respectively.



### RESULTS AND DISCUSSION

Figure 1 shows HCE-T cell attachment to *Bombyx mori* fibroin films coated with selected ECM components. Statistical analysis by two way ANOVA revealed a significant (\* =  $P < 0.05$ ) increase in cell attachment in response to coating with collagen I, III or IV. Collagen III coating was also found to significantly increase rates of HLE cell attachment to fibroin for the majority of primary donors. Figure 2 shows changes in HCE-T cell confluency on ECM-treated *Bombyx mori* fibroin-coated films. It was demonstrated that significantly higher (\* =  $P < 0.05$ ) levels of confluency were achieved on fibroin films coated with collagen III or IV after 49 hours. Coating of fibroin with collagen I, III, IV or fibronectin also induced significant changes in cell morphology which were consistent with re-epithelialisation.

### CONCLUSION

Results indicate that coating of fibroin films with selected ECM components substantially improved specific cellular processes crucial for corneal re-epithelialisation. In particular, collagen-coating of fibroin was found to dramatically increase HCE-T cell attachment and confluency while also promoting changes in cell morphology. Increased attachment of primary HLE cells in response to coating of fibroin with collagen III was also observed, however, further optimisation is required to improve donor consistency.

### REFERENCES

1. Bray, L. J. *et al.*, *Biomaterials*. 32(22): 5086-5091, 2011
2. Yeo, I. S. *et al.*, *Biomacromolecules*. 9(4): 1106-1116, 2008
3. Madden, P. W. *et al.*, *Biomaterials*. 32(17): 4076-4084, 2011
4. Chow, S. *et al.*, *Investigative ophthalmology & visual science*. 55(10): 6590-6600, 2014

## Change in Mechanical Performance of Biomedical Titanium Alloys Subjected to Mechanical Surface Modifications

Toshikazu Akahori<sup>1</sup>, Yurie Oguchi<sup>2</sup>, Tomokazu Hattori<sup>1</sup> and Hisao Fukui<sup>3</sup>

<sup>1</sup>Faculty of Science and Technology, Meijo University, Japan

<sup>2</sup>Graduate School of Science and Technology, Meijo University, Japan

<sup>3</sup>School of Dentistry, Aichi-Gakuin University, Japan

[akahori@meijo-u.ac.jp](mailto:akahori@meijo-u.ac.jp)

### INTRODUCTION

Beta-type Ti-29Nb-13Ta-4.6Zr (TNTZ) was recently developed as a representative biomedical Ti alloy. As-solutionized TNTZ has a low elastic modulus less than 60 GPa close to that of cortical bone along with very low cytotoxicity and good bone biocompatibility. Solution treatment and aging (STA) is a typical heat treatment for improving the mechanical properties of beta-type Ti alloys. However, STA also drastically increases the elastic modulus. Therefore, this study investigated the effects of fine particle bombarding, which is one of shot peening processes, on the mechanical properties of TNTZ subjected to more severe thermomechanical treatment in order to maintain a relatively low elastic modulus. The bone contact characteristics of TNTZ samples subjected to surface modification and cancellous bone were also compared.

### EXPERIMENTAL METHODS

This study used cold-swaged TNTZ bars (working ratio: around 94%), which was designated as TNTZ<sub>SW</sub>. TNTZ<sub>SW</sub> was solutionized at 1063 K for 3.6 ks in a vacuum followed by water quenching (WQ); it was designated as TNTZ<sub>ST</sub>. Some samples of TNTZ<sub>SW</sub> were aged at 573 to 723 K in under aging conditions. Mechanical surface modification by a fine particle bombarding (FPB) machine was applied to some samples of TNTZ<sub>SW</sub>, TNTZ<sub>ST</sub> and aged TNTZ<sub>SW</sub>; these specimens were designated as TNTZ<sub>SW</sub>/FPB, TNTZ<sub>ST</sub>/FPB and aged TNTZ<sub>SW</sub>/FPB, respectively. Optical microscopy (OM), scanning electron microscopy (SEM), and X-ray diffraction (XRD) spectroscopy were carried out on each specimen to evaluate the microstructure. The Vickers hardness elastic modulus and the tensile and fatigue properties were investigated for each specimen to examine the mechanical properties. For the bone contact characteristics, some cylinder-type samples of TNTZ<sub>SW</sub>/FPB and TNTZ<sub>SW</sub> with mirror and as-machined surfaces were implanted into the femurs of Japanese white rabbits. All samples were extracted 12 weeks after implantation. The bone contacts were evaluated by image analysis.

### RESULTS AND DISCUSSION

Figure 1 shows Vickers hardness and Young's modulus profiles from very edge of samples of TNTZ<sub>SW</sub> and TNTZ<sub>SW</sub>/FPB to around 300  $\mu\text{m}$  in depth on TNTZ<sub>SW</sub>/FPB and TNTZ<sub>ST</sub>/FPB. The Vickers hardness of the very edges for TNTZ<sub>SW</sub>/FPB and TNTZ<sub>ST</sub>/FPB showed the highest value, which is Hv 270 and Hv 235, respectively), and it tends to decrease drastically as a

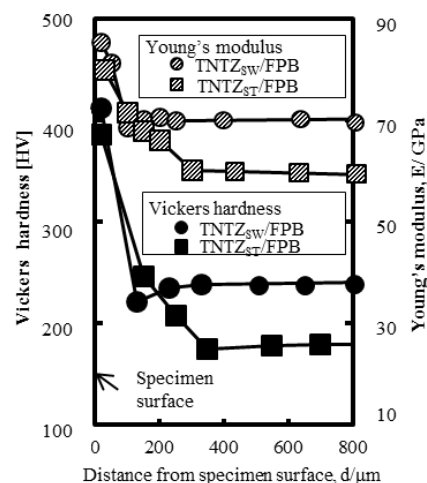


Fig. 1 Vickers hardness and Young's modulus profiles of TNTZ<sub>SW</sub>/FPB and TNTZ<sub>ST</sub>/FPB.

function of distance from the surface to a depth of around 20  $\mu\text{m}$ . The trend of change in Young's modulus is almost similar to that of Vickers hardness.

The fatigue strength of TNTZ<sub>SW</sub>/FPB increased, especially in the high cycle fatigue life region. The fatigue limit of TNTZ<sub>SW</sub>/FPB was around 400 MPa and around 100 MPa higher than that of TNTZ<sub>SW</sub>. The Vickers hardness near the surface of the TNTZ<sub>SW</sub>/m-SP specimen was around 200 Hv higher than that at the center of specimen, as noted above. As a result, the effect of residual compressive stress by FPB was marked in the high cycle fatigue life region.

In animal tests, TNTZ<sub>SW</sub>/FPB had the highest bone contact ratio among the three kinds of sample, although the bone formation ratios of the three were almost the same.

### CONCLUSIONS

- (1) The Vickers hardness of cold-swaged TNTZ subjected to fine particle bombarding was increased significantly within 20  $\mu\text{m}$  from the very edge of the specimen surface.
- (2) The fatigue strength of TNTZ<sub>SW</sub> subjected to fine particle bombarding increased in the high cycle fatigue life region only. The fatigue limit was around 400 MPa.
- (3) The bone contact ratio of TNTZ subjected to fine particle bombarding was better than that of TNTZ with the mirror surface.

### REFERENCES

1. T. Akahori, M. Niinomi, H. Fukui, and A. Suzuki: Materials Transactions, Vol. 45, No. 5 (2004), 1540-1548.

## Evaluation of the Possibilities of Affecting the Interspike Structural-osteoconductive Potential of Additively Manufactured Prototypes of the Multispiked Connecting Scaffold for Hip Resurfacing Arthroplasty Endoprostheses

Ryszard Uklejewski<sup>1,2</sup>, Mariusz Winiński<sup>1,2</sup>, Piotr Rogala<sup>3</sup>, Adam Patalas<sup>2</sup>

<sup>1</sup>Department of Medical Bioengineering Fundamentals, Institute of Technology, Casimir the Great University, Poland

<sup>2</sup>Laboratory of Medical Biomaterials and Bioprocess Engineering, Department of Process Engineering, Institute of Technology and Chemical Engineering, Poznan University of Technology, Poland

<sup>3</sup>Department of Spine Surgery, Oncologic Orthopaedics and Traumatology, Poznan University of Medical Sciences, Poland  
[winiński@ukw.ukw.pl](mailto:winiński@ukw.ukw.pl)

### INTRODUCTION

In case of porous coated long-stem endoprostheses the porostructural-osteoconductive properties of their porous coatings outer layers can be described by the poroaccessibility parameters set<sup>1</sup> and determined using the methodology<sup>2</sup> worked out in our research team for quantitative evaluation of the structural-osteoconductive potential of porous coatings outer layers. To determine such potential in case of the multispiked connecting scaffold (MSC-Scaffold), which is the essential innovation in the fixation technique of the components of the resurfacing arthroplasty (RA) endoprostheses<sup>3-5</sup>, the analogous structural analysis of its interspike space – regarding to the expected requirements of its pro-osteoconduction functionality and its proper successive osteointegration with the periarticular trabecular bone tissue – can be performed. The major purpose of this work is the examination of the prototypes of the MSC-Scaffold manufactured in the Selective Laser Melting (SLM) technology and the evaluation of the possibilities to affect its interspike structural-osteoconductive potential.

### EXPERIMENTAL METHODS

The confocal scanning of the SLM manufactured MSC-Scaffold of the THRA endoprosthesis prototype<sup>5</sup> was performed, and followed by the essential structural examination of the MSC-Scaffold specimens representing the fragments of various variants of the MSC-Scaffold of both components of the THRA endoprosthesis prototype. These variants were designed to investigate the aspects of possible affecting their interspike structural-osteoconductive potential. In CAD models of the two designed series of the MSC-Scaffold fragments there was assumed the specific modification of geometrical properties of their spikes to impact the interspike structural-osteoconductive potential of the MSC-Scaffold by the change of the nominal height of the spikes (1<sup>st</sup> series) and, independently, by the change of spikes' shape (2<sup>nd</sup> series). The verification of the assumed in particular CAD models effect was examined in the corresponding SLM manufactured MSC-Scaffold variants.

### RESULTS AND DISCUSSION

The values of the effective height of the MSC-Scaffold's spikes in the SLM manufactured prototype of THRA endoprosthesis were significantly lower (by 48%±9% for the femoral component and by 51%±9% for the acetabular component) in relation to the

effective height of their geometrical equivalents in the corresponding CAD models. This significantly reduces, in case of the SLM manufactured prototypes, the expected interspike structural-osteoconductive potential of the MSC-Scaffold, assumed in their CAD models. The change the geometrical shape of the MSC-Scaffold's spikes without change of its nominal height applied in CAD models of the 2<sup>nd</sup> series of specimens can affect the interspike structural-osteoconductive potential of the SLM manufactured MSC-Scaffold by the circa 20% increase of the effective height of its spikes in relation to the initial variant.

### CONCLUSIONS

Being aware of the appearing technological limitations of the SLM technology, which is determined among others by the powder grain size distribution or the applied laser beam properties, the necessary modification in the CAD model design of the MSC-Scaffold, taking into account the adjustments of the technological limitations, have to be considered. The most favourable effect of the possible affecting the interspike structural-osteoconductive potential of the MSC-Scaffold can be obtained by the combined modification of its spikes design in the CAD model, which includes the extension of the spikes nominal height with the simultaneous modification of its geometrical shape in the CAD model. This allows achieving the effective height of the MSC-Scaffold's spikes in the SLM manufactured prototype at the same level as designed and expected from the CAD model of the original prototype.

### REFERENCES

1. Uklejewski R. *et al.*, Metrology MS. 15:215-226, 2008.
2. Uklejewski R. *et al.*, Metrology MS. 20:427-438, 2013.
3. Uklejewski R. *et al.*, Eng. Biomat. 12(87):2-6, 2009.
4. Uklejewski R. *et al.*, Acta Bioeng. Biomech. 11(2):65-70, 2009.
5. Uklejewski R. *et al.*, Rapid Prototyping J. 17(1):76-85, 2011.

### ACKNOWLEDGMENTS

The work supported by the Polish Ministry of Science in the Research Project no. NN518412638: "The thermochemical surface modification of preprototypes of the minimally invasive hip RA endoprostheses and porous intraosseous implants" (Head: R. Uklejewski).



## Thin Nanostructured RF-magnetron Sputter-deposited Hydroxyapatite Coatings on Metals

Roman Surmenev<sup>1,2</sup>, Maria Surmeneva<sup>1</sup>, Irina Selezneva<sup>3</sup>, Matthias Eppler<sup>4</sup>

<sup>1</sup>Theoretical and Experimental Physics Department, Tomsk Polytechnic University, Russia

<sup>2</sup>Fraunhofer Institute for Interfacial Engineering and Biotechnology IGB, Germany

<sup>3</sup>Institute of Theoretical and Experimental Biophysics, Pushchino, Russia

<sup>4</sup>University of Duisburg-Essen, Essen, Germany

[rsurmenev@gmail.com](mailto:rsurmenev@gmail.com)

### INTRODUCTION

Surface modification of biomedical materials is one of the most important objectives of research this time. Therefore, different surface modification strategies should be investigated. This study reports on application of radio-frequency (RF) magnetron sputtering to prepare thin CaP-based coatings on the surface of permanent (Ti, NiTi) or biodegradable (Mg-based) metallic substrates.

### EXPERIMENTAL METHODS

Pure hydroxyapatite (HA) and silicon-containing HA coatings with the content of silicon 0.5 and 1.72 mol were deposited by a conventional RF magnetron sputtering set-up operated in high vacuum conditions. Details on the coating deposition regimes can be found elsewhere [1,2]. Different thicknesses of the coatings up to 1500 nm were obtained. The physico-chemical properties of the biocomposites were studied by TEM, SEM, EDS, and XRD. Wettability, contact angle hysteresis, nanohardness and adhesion strength, corrosion resistance were also measured, together with biological *in vitro* tests. Cross-sections of the specimens were prepared by FIB to study the microstructure of the coatings by TEM.

### RESULTS AND DISCUSSION

The CaP coating homogeneously covered the entire surface of the substrates. In all cases, a single phase coating of HA was prepared. The coating deposition process resulted in a slight increase of the surface roughness and in nano-scale grains, generating an amorphous layer at the substrate/coating interface and inducing the growth of a columnar grain structure perpendicular to the substrate surface. A microstructural analysis of the film showed that the grain size and crystallinity increased with increasing deposition time. In the case of NiTi substrates, a significant decrease of the Ni release rate compare to the bare substrate was observed [2]. Nanoindentation tests demonstrated that all HA coatings had an increased surface hardness on both the micro- and nanoscale. The films significantly enhanced the wear resistance of this resorbable alloy. The nanostructured HA-based coatings were not cytotoxic, as proven by *in vitro* assays using primary dental pulp stem cells (DPS) and mouse fibroblast NCTC clone L929 cells. HA coatings with different thicknesses stimulated cells to attach, proliferate and form mineralized nodules on the surface better than uncoated substrates (Fig. 1). Potentiodynamic

polarization tests indicated that the corrosion current density ( $I_{corr}$ ) of the 1500-nm thick HA coated AZ31 magnesium alloy substrate was significantly lower ( $9.2 \cdot 10^{-7}$  A/cm<sup>2</sup>) compared with to the uncoated alloy substrate. Thus, the nanocrystalline HA coating can increase the corrosion resistance of AZ31 magnesium alloy ( $I_{corr}=1.3 \cdot 10^{-5}$  A/cm<sup>2</sup>), and such coated magnesium alloys have a good potential for biomedical applications.

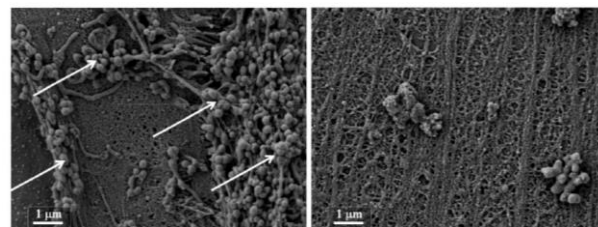


Fig. 1. SEM images of the mineralized matrix synthesized by DPS cells cultured on a 440 nm thick CaP coating (left) and on uncoated titanium (right). The signs of mineralization are marked by arrows (left) [1].

### CONCLUSION

RF magnetron sputtering is a versatile technique to prepare nanostructured CaP-based coatings on the surface of biodegradable and permanent implants. The corrosion resistance of the magnesium-based alloys can be improved by RF magnetron sputter deposited nanocrystalline CaP coatings. The bias applied during the deposition of HA coating resulted in a decrease of the grain and crystallite size of the film having a positive effect on the mechanical properties of the biocomposites. The potentiodynamic polarization test demonstrated that a 1500-nm thick nanocrystalline HA coating significantly improved the corrosion resistance of the bare AZ31 magnesium alloy. HA coatings with different thicknesses stimulated cells to attach, proliferate and form mineralized nodules on the surface better than uncoated substrates.

### REFERENCES

- <sup>1</sup> M.A. Surmeneva, R.A. Surmenev, *et al.* Appl Surf Sci 317:172-180, 2014.
- <sup>2</sup> R.A. Surmenev, M.A. Ryabtseva, M. Eppler *et al.* J Mater Sci: Mater Med 21:1233-1239, 2010.

### ACKNOWLEDGMENTS

The authors would like to thank the RFBR (14-08-31027 mol-a, 15-08-08652), the Russian President's Stipend SP-6664.2013.4, MK-485.2014, NAUKA #11.1359.2014/K for providing financial support to this project.





## Electrochemical Immobilisation of Doxycycline on Titanium Surfaces

Sebastian Geissler, Hanna Tiainen, Håvard Haugen

Department of Biomaterials, Institute of Clinical Dentistry, University of Oslo, Norway  
[sebastian.geissler@odont.uio.no](mailto:sebastian.geissler@odont.uio.no)

### INTRODUCTION

Cathodic polarisation has been used to bind doxycycline to implant surfaces aiming at infection control and stimulation of bone formation<sup>1</sup>. It was hypothesised that the molecule binds covalently to a complex layer of hydrogen and oxygen created on the metal surface during the polarisation process. However, the exact binding mechanisms and their effect on short- and long-term availability of doxycycline still remain poorly understood.

### EXPERIMENTAL METHODS

The extent of adsorbed doxycycline on mirror-polished titanium coins that were cathodically polarised for 3 h with a current density of 1 mA/cm<sup>2</sup> in 2 M sodium acetate buffer at pH 3 was examined. Doxycycline hyclate was added to the buffer with a concentration of 1 mg/ml. After polarisation, the coins were thoroughly rinsed with deionised water and dried with nitrogen gas. Surface topography was analysed by AFM. Characterisation of the surface chemistry was done by XPS. Furthermore, the presence of doxycycline was evaluated using diffuse reflectance FTIR and fluorescence microscopy. Following this, the coins were immersed in DI water for 10 h and the analyses were repeated.

### RESULTS AND DISCUSSION

The doxycycline coated coins showed a significant increase in nano-roughness compared to the polished coins. Reduction of the substrate XPS signal and increase of the carbon and nitrogen signal confirmed the presence of an organic layer on the surface. Bands characteristic for doxycycline were seen in the infrared spectra. In addition, the build-up of a fluorescent film was observed. After immersion in DI water, the roughness had decreased and the morphology of the surface had changed significantly (Fig. 1). Increased substrate signals as well as decreased carbon and nitrogen signals were detected. The characteristic infrared bands were weakened and fluorescence had disappeared completely. This indicates that a fraction of the biomolecules is only weakly attached to the titanium surface.

### CONCLUSION

An adsorbed layer of doxycycline was found to be present after the polarisation process. This layer could be easily removed by immersion in water and thus only short-term effects of the antibiotic can be expected. The remaining lower substrate signal and increased carbon signal indicate that there still is organic material attached to the surface. The nature of this material, the

way it is bound to the surface and the potential release of it will be further explored.

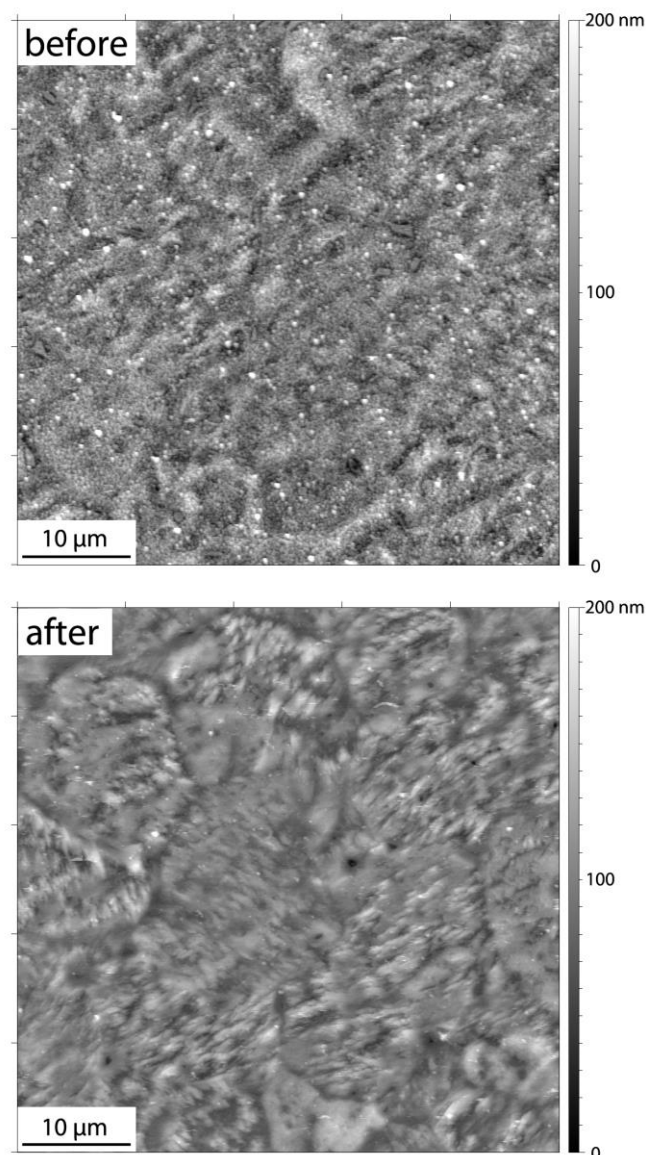


Fig. 1: AFM images of the doxycycline coated surface before (top) and after immersion (bottom).

### REFERENCES

1. Walter M.S. *et al.*, Dental Materials 30:200-214, 2014

### ACKNOWLEDGMENTS

This study was supported by the Research Council of Norway (Grant no: NFR 230258).

## INTRODUCTION

In a recent study by Johnson and Johnson, it has been observed and revealed that 40% of the artificial articular joints fail within five years of its implantation<sup>1</sup>. Failures of these orthopaedic implants are extensively credited towards the wear particles generated by the implant material itself. The wear debris generated within the prosthetic joints initiate a cascade of tissue responses, leading to osteolysis and results in the loosening of implants. Immense research efforts are contributed to improve the biocompatibility and longevity of the prosthetic joints by engineering the implant materials and its tribological properties. The present study is based on a markedly different view point to the problem; instead of developing a wear resistant material for implants, we aim to reduce the wear by administering lubricants to prosthetic joints. This approach would be synonymous to the work on lubricin<sup>2</sup> (a natural Mucin-like macromolecule secreted by the synovial membranes surrounding the joints, regulates the synovial homeostasis, eliminates any friction in the joints, protect the cartilage surfaces and also inhibits synovial cell overgrowth<sup>3</sup>) in the natural synovial joints. Our work is primarily on the recently developed polymeric lubricant additives that are water-soluble and claimed to improve anti-friction and anti-wear properties of a various engineering materials, including metal alloys, polymers, ceramics etc. We created injectable lubricant comprising of water-soluble polymers in aqueous solutions and are specifically targeted to lubricate and reduce the wear production from ultrahigh molecular weight polyethylene (UHMWPE) materials. As a proof of concept, first set of experiments were conducted to challenge the lubricating efficacy and/or mechanism in the model synovial fluids, serum. The in-vitro cytotoxicity tests of the screened lubricants are also analyzed and discussed.

## EXPERIMENTAL METHODS

Pin-on-disk tribometry was employed to assess the lubricating capabilities of injectable lubricants for the sliding contacts between UHMWPE and CoCrMo tribo-pair. Injectable lubricants were formulated by dissolving commercial amphiphilic triblock copolymers, PEO-PPO-PEO (Pluronics), especially "F127", "F108", "P105" and "F68" in aqueous solution (1 mM HEPES). For comparison, various biopolymers, including hyaluronic acid (HA), bovine submaxillary mucin (BSM), bovine serum albumin (BSA) and alginic acid (AA) were tested as lubricant additives. Influence of temperature, longevity, composition of model synovial fluid (serum) and aging of implants were also tested as control parameters. In-vitro cytotoxicity tests were attributed by analyzing the cell morphology and standard MTT assay on murine fibroblast (L929 fibroblasts) and murine osteoblast (MC3T3). Free

prostaglandin-E<sub>2</sub> (PGE<sub>2</sub>) on the cell are estimated by ELISA as a correlation of the immune response stimulated by bone lysis (*experiment in progress*)<sup>4</sup>.

## RESULTS AND DISCUSSION

All lubricants exhibited immediate reduction in the coefficient of friction (COF) upon injecting into serum while sliding between CoCrMo pin and UHMWPE disk as tribo-pair (Fig 1). This reduction was proportional to the concentration of lubricant additives. While the influence of temperature (22° C vs. 37° C) on the tribometry was insignificant, lubricant additives were equally effective on both aged and damaged UHMWPE and CoCrMo materials<sup>4</sup>. In model synovial fluid, 3.5 mg/ml hyaluronic acid was added along with serum to further emulate real synovial fluid. However, the efficacy on the reduction of friction coefficient was retarded. While the homo-polymeric lubricant additives were effective in reducing the friction forces (less extent when compared to amphiphilic copolymers), none of the biopolymers tested showed any lubrication<sup>4</sup>. In-vitro cytotoxicity, as observed from both cell morphology and MTT assay, showed that hydrophilic copolymers F127 and F108 are more favorable for the cell viability (Fig 2)<sup>4</sup>. Analysis of free PGE<sub>2</sub> on the cells as a correlation of immune response due to bone lysis would be discussed (*experiment in progress*)<sup>4</sup>.

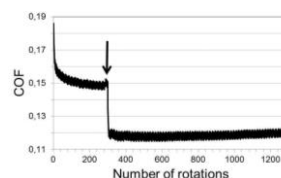


**Fig 1:** Graph showing the effect of COF when F127 copolymer was injected (arrow) into the serum solution at 300 rotations<sup>4</sup>.

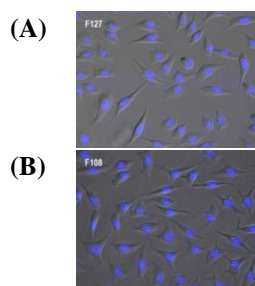


**Fig 2:** (A) and (B) are slides showing good morphology of viable L929 fibroblast cells after exposure to F127 and F108 copolymers respectively for seven days.

## REFERENCES

1. Meier, Barry. "Maker Aware of 40% Failure in Hip Implant - NYTimes.com"; 22 January 2013.
2. Musumeci G. OA Anatomy 1;2.
3. Schumacher BL, *et al.*, Arch Biochem Biophys 311:144–152, 1994.
4. Rishikesan S, *et al.*, (*manuscript in preparation*)

## ACKNOWLEDGMENTS

"The authors are thankful to ERC starting grant (project no: 261152) for providing financial support".

# pH Triggered Aggregation of Structurally Disordered Proline-Rich Polypeptide

Hanna Tiainen<sup>1</sup>, Sebastian Geißler<sup>1</sup>, Reidar Lund<sup>2</sup>, Håvard J. Haugen<sup>1</sup>

<sup>1</sup>Department of Biomaterials, University of Oslo, Norway

<sup>2</sup>Department of Chemistry, University of Oslo, Norway

[hanna.tiainen@odont.uio.no](mailto:hanna.tiainen@odont.uio.no)

## INTRODUCTION

Unfolded, structurally disordered, proline-rich regions of natural proteins such as collagen, amelogenin, and ameloblastin have recently been found to play an important role in biomineralisation.<sup>1</sup> Short synthetic peptides that mimic the disordered regions of such proteins may therefore be bound onto biomaterial surfaces to stimulate bone formation and regeneration in vivo. Since the function and bioactivity of these peptides is likely to be strongly linked to their lack of well-defined three-dimensional structure, it is important to understand the behaviour of such biomolecules when dissolved in aqueous media.

## EXPERIMENTAL METHODS

The structure of two dissolved synthetic proline-rich polypeptides (Table 1) that have previously shown potential in inducing bone mineralisation of both osteoblast-like cells and mesenchymal stem cells<sup>2</sup> were examined.

Table 1: Amino acid sequence of the two examined proline-rich polypeptides.

Peptide	Sequence
P2	PLV PSQ PLV PSQ PLV PSQ PQP PLP P
P5	PLV PSS PLV PCC PLV PCC PSP PLP P

These polypeptides were dissolved in either TRIS-buffered saline (pH 6-12) or sodium acetate buffer (pH 3-5.5) at 5 mg/ml concentration and their structure was analysed with small-angle X-ray scattering (bioSAXS; BM29 beamline, ESRF, Grenoble). In order to evaluate chain conformation and the size and shape of the peptide aggregates, both model-independent analysis (IFT, Guinier) and geometrical body modelling were performed. Circular dichroism spectroscopy (CD) was used to characterise the secondary structures of the polypeptides at three different pH: 5, 7.5, and 9.

## RESULTS AND DISCUSSION

While P2 maintained its disordered random coil -like structure throughout the tested pH range (pH 3-12), P5 formed aggregates at high pH (pH 8-12) as shown in Fig. 1. Radius of gyration nearly doubled and over tenfold increase in the calculated molecular weight was observed in this pH region, indicating that several polypeptide chains clustered together into nanoparticles whose scattering profile best fitted a geometrical scatter model for a triaxial ellipsoidal structure. However, no formation of specific secondary structures within these polypeptide aggregates was observed at pH 9.

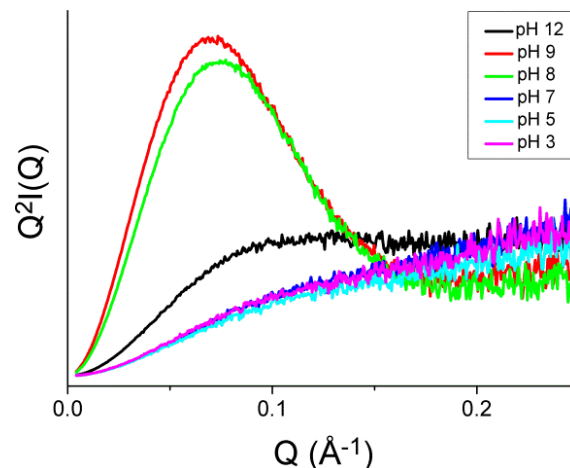


Fig. 1: Kratky plots reveal the pH dependent assembly of P5 to elongated globular structures

The main difference between the two examined proline-rich polypeptides P2 and P5 is the presence of cysteine (C) in the amino acid sequence of P5. Cysteine being the only amino acid that contains a thiol group (-SH), the observed aggregation at high pH may be explained by the formation of disulphide bonds (-S-S-) which link several polypeptide chains together as the thiol groups of the cysteines become deprotonated with increasing pH ( $pK_{a_{thiol}} = 8.3$ ). Consequently, the disordered polypeptide chains assemble together forming elongated covalently bound clusters that were observed as the characteristic increase in the scatter intensity.

## CONCLUSION

Aggregation of the polypeptide chains was not observed within physiological pH range, and it is therefore not expected to influence the bioactivity of the molecule. However, such pH dependent change in peptide characteristic must be taken into account when choosing the appropriate processing conditions for binding the disordered peptides onto biomaterial surfaces.

## REFERENCES

1. Kalmar L. *et al.*, Bone 51:528-34, 2012
2. Rubert M. *et al.*, J Biomater Tissue Eng 1:198-209, 2011

## ACKNOWLEDGMENTS

This study was financially supported by Research Council of Norway (grant no. 231530) and European Synchrotron Radiation Facility.





# Stability of Oxygen Plasma Treatment of Parylene C Biomedical Coating

Monika Gołda-Cępa<sup>1</sup>, K. Engvall<sup>2</sup>, A. Kotarba<sup>1</sup>

<sup>1</sup>Faculty of Chemistry/Jagiellonian University, Krakow, Poland,

<sup>2</sup>Department of Chemical Engineering and Technology/KTH Royal Institute of Technology, Stockholm, Sweden.

[golda@chemia.uj.edu.pl](mailto:golda@chemia.uj.edu.pl)

The effect of oxygen plasma treatment of parylene C on its thermal stability and surface properties was evaluated using thermogravimetric analysis (TG/DTA) and contact angle measurement, respectively. The influence of oxygen plasma treatment depends strongly on operation parameters set ( $pO_2 = 0.2$  mbar,  $t=10$  min,  $P=50$  W). The bulk thermal stability of parylene C, remained unaffected even after overexposure to oxygen plasma. The hydrophilicity of the treated samples was constant only for the first hours after the plasma exposure.

## INTRODUCTION

Parylene C has previously been proven to be an excellent anticorrosive coating<sup>1</sup>. Continuous, dense, thin films on metallic substrates, produced by chemical vapour deposition (CVD), exhibit excellent mechanical properties and low permeability to water. For example, a 8  $\mu$ m layer creates an effective and protective barrier for heavy metal ion release, as well as implant surface corrosion in the body. Moreover, the parylene surface can be functionalized via oxygen plasma treatment, forming specific chemical surface groups<sup>2,3</sup>. The oxygen plasma technique offers the possibility of changing the chemical composition and properties of a surface, and thus the overall performance of the material. The oxygen-containing groups, formed on the surface ( $-C-OH$ ,  $-C=O$ ,  $-COOH$ ), changing the surface properties into hydrophilic, and at the same time provide with adsorption centres for drug molecules. However, oxygen plasma modification and insertion of oxygen into the polymer chain, beneficial for its biocompatibility, may influence the thermal stability of parylene C. This is a critical parameter, since steam sterilization procedure, carried out at  $T = 121^\circ C$ , and hence the polymer has to be stable well above this temperature.

## EXPERIMENTAL METHODS

Parylene C films were prepared by CVD technique (provided by ParaTech Coating Scandinavia AB). In order to modify the parylene C surface, the oxygen plasma treatment was carried out using a Diener electronic Femto plasma system. Thermogravimetric analysis (TG/DTA) were performed with the use of the TG/DTA Mettler-Toledo apparatus. The experiments were carried out in the temperature range  $30-600^\circ C$ , with a heating rate of  $6.5^\circ C/min$  and an Ar flow of  $50\text{ cm}^3/min$ .

## RESULTS AND DISCUSSION

Typical changes of  $T_{melt}$  (grey plot) and water contact angle (blue plot) evolution in time are shown in Fig. 1. The general trend in  $T_{melt}$ , as a function of plasma exposure time, can be observed for the unmodified and oxygen plasma modified samples (grey plot). The  $T_{melt}$

of oxygen plasma modified parylene C remain essentially stable until the plasma exposure time reaches 5 min. After longer exposure times to plasma,  $T_{melt}$  of the samples shifts to a higher temperature. After 30 min of oxygen plasma exposure, the  $T_{melt}$  is significantly higher:  $300.7^\circ C$ . These values are in line with the XRD results and indicate a clear substantial bulk changes in the polymer structure upon longer plasma treatment. However, the  $T_{melt}$  of oxygen plasma modified parylene C, is still at a significantly higher range of temperatures, compared to the steam sterilization temperature. The aging of plasma treatment was evaluated by water contact angle ( $\theta_w$ ) measurements. 24h after the treatment, a recovery of the hydrophobicity is observed. However, still after 21 days, the obtained contact  $\theta_w$  is approx.  $50^\circ$ , which implies a significantly more hydrophilic surface compared to the unmodified parylene C ( $\theta_w \approx 90^\circ$ ).

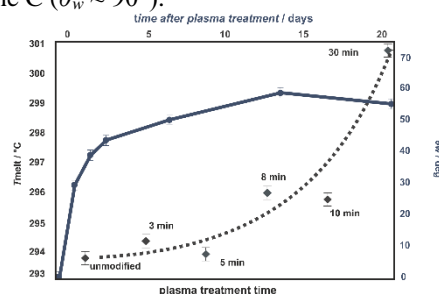


Fig. 1 The general trend in  $T_{melt}$  of parylene C as a function of plasma exposure time (grey) and the plasma treatment aging process presented by the means of  $\theta_w$  (blue)

## CONCLUSION

The influence of oxygen plasma treatment on the properties of parylene C depends strongly on the time of exposure to oxygen reactive species. Overexposure to oxygen plasma alters significantly the bulk properties of parylene C, shifting the melting point temperature. Although adverse bulk changes, the thermal stability of treated parylene C remains similar to the unmodified one. Therefore, the functionality in a biomedical application context will remain unaffected. Moreover, the water contact angle measurements imply that a biomedical application of oxygen plasma modified parylene C, should take place before 48h after the plasma exposure.

## REFERENCES

1. Cieřlik M. *et al.*, Mater Sci Eng C 32:31-35, 2012
2. Gołda M. *et al.*, Mater Sci Eng C 33:4221-4227, 2013
3. Gołda-Cępa M. *et al.*, RSC Adv 4:26240-26243, 2014

## ACKNOWLEDGMENTS

The authors would like to thank the Polish National Science Centre decision number DEC-2012/05/N/ST8/ for providing financial support to this project





# Synthesis and Characterization of Thermo-sensitive Poloxamer 407/Chitosan-Functionalized Carbon Nanotubes Hydrogel

Jun Ou<sup>1</sup>, Li Zhen<sup>2</sup>, Jin-Min Zhao<sup>2</sup>, Qing H. Qin<sup>3</sup>, Zbigniew H. Stachurski<sup>3</sup>.

<sup>1</sup>Biomaterials group/Materials Science and Engineering College, Guilin University of Technology, China

<sup>2</sup>Translation Medicine Research and Development Center, Guangxi Medical University, China

<sup>3</sup> Research School of Engineering, Australian National University, Canberra, Australia

[glouj@hotmail.com](mailto:glouj@hotmail.com)

## INTRODUCTION

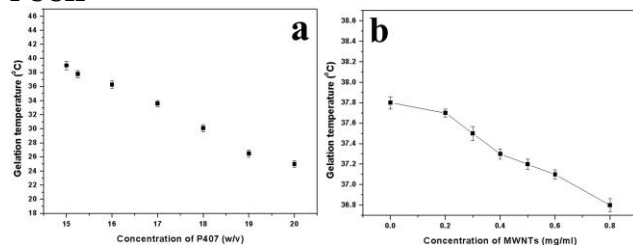
There has been enormous interest in the area of thermo-sensitive hydrogels for drug delivery<sup>1</sup>. It is noted that chitosan(CS) is biocompatible, biodegradable, antibacterial and low toxicity. Pluronic P407 is a typical commercial thermo-sensitive hydrogels, which has potential application in experimental medicine. But the drawback of P407 hydrogels are their weak mechanical strength and being easily eroded<sup>2</sup>. Thus, how to increase the mechanical strength and enhance the anti-erosion of the P407 hydrogel is important for biomedical applications of the bio-materials<sup>3</sup>. This paper reports modifications of thermo-sensitive carbon nanotubes hydrogel with soluble multi-walled carbon nanotubes (CNTs).

## EXPERIMENTAL METHODS

In this work, Poloxamer 407 and chitosan (degree of N-deacetylation (80~95%)) were purchased from Sinopharm Chemical Reagent CO., Ltd., China. CS solution (0.2 % w/v) used in this study was prepared by weighing the CS in a solution of acetic acid 0.5% (v/w). A pre-determined amount of MWNTs were dissolved in the poloxamer 407/chitosan hydrogel(PCH), which was chosen for optimum composing by measuring the gelation temperature of PCH. Statistical analysis of the data was performed via one-way analysis of variance (ANOVA) using origin software; a value of  $p < 0.05$  was considered significant ( $n = 3$ ).

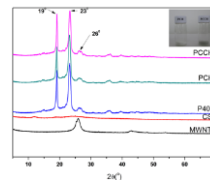
## RESULTS AND DISCUSSION

### 3.1 Critical gelation temperature of PCH and PCCH

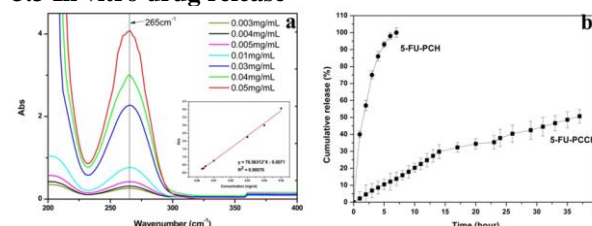


The gelation temperature of PCH and PCCH: (a) Critical gelation temperature of PCH with different content of P407; (b) Critical gelation temperature of PCCH with different content of MWNTs.

### 3.2 The interactions occurred between the P407 and CS during the preparation of PCH

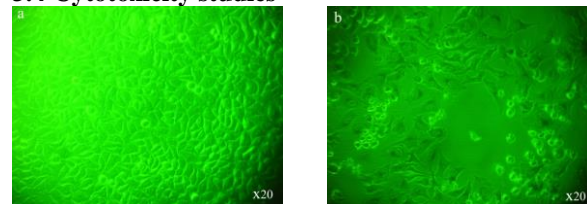


### 3.3 In vitro drug release



The UV-vis absorption spectrum of 5-FU in water, (lower right of Fig a) the standard curve of 5-FU in water at 265 nm<sup>-1</sup>, (b) the release profile for the 5-FU from the 5-FU-PCH and 5-FU-PCCH

### 3.4 Cytotoxicity studies



Optical in vitro bioimaging of hepatoma cell line smmc 7721 cells incubated with 25 µg / mL PCCH-NPs (a) and MWNTs-NPs (b) for 24 h

## CONCLUSION

The thermo-sensitive carbon nanotubes hydrogel was found to significantly improve the solubility and biocompatibility of the MWNTs in aqueous media. The experimental results show that the MWNTs can improve the drug release life and delay the degradation of poloxamer407/chitosan. The thermo-sensitive poloxamer 407/chitosan-functionalized carbon nanotube hydrogels are promising materials for drug delivery and further investigation of MWNTs is under way for enabling the new material to function as a novel drug delivery platform.

## REFERENCES

- Jeong B. et al., Adv. Drug. Deliver. Rev., 64, 154, 2012.
- Wei H., et al., Prog. Polym. Sci., 34, 893, 2009.
- Zhang Y., et al., ACS nano, 4, 3181, 2010.

## ACKNOWLEDGMENTS

The authors would like to thank the National Natural Science Foundation of China (Grant no: 51362006) for providing financial support to this project.



Milena Supernak-Marczewska<sup>1</sup>, Agnieszka Ossowska<sup>1</sup>, Paulina Strąkowska<sup>2</sup>, Tomasz Seramak<sup>1</sup>, Andrzej Zieliński<sup>1</sup>

<sup>1</sup>Department of Engineering Materials and Bonding, Faculty of Mechanical Engineering, Gdańsk University of Technology, Poland

<sup>2</sup>Department/Research Institute, Gdańsk University of Technology, Poland  
[milsuper@pg.gda.pl](mailto:milsuper@pg.gda.pl)

**The present study is concerned on development of the technology for obtaining the nanotubular oxide layers on porous titanium alloy Ti13Nb13Zr followed by deposition of phosphate coating by electrochemical method.**

## INTRODUCTION

Titanium and its alloys are currently widely used for load-bearing implants, such as hip joint endoprosthesis. They possess a very good strength, high corrosion resistance, and they are biocompatible [1]. Despite the improvement of biomaterials and technologies for their production, about 15-25% of metal implants is degraded after 15 years of use [2,3]. Such negative behavior is associated with an inappropriate (too weak) bond of the bone and implant. There is a need for such modification, which will increase the biological activity on the interface implant - environment of tissues and body fluids [3].

## EXPERIMENTAL METHODS

Tests were carried on porous samples (Fig. 1) made of titanium alloy Ti-13Nb-13Zr. The samples were polished with grinding papers, No. 2500 as the last, and washed in an ultrasonic cleaner in three different reagents - acetone, 2-propanol and distilled water. The prepared samples were subjected to electrochemical oxidation in the 1M H<sub>3</sub>PO<sub>4</sub> + 0.3% wt. HF environment, during 30 min, at a voltage of 20 V.

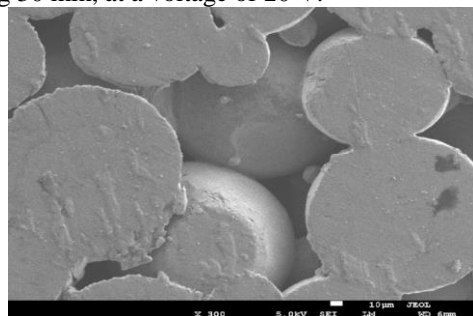


Fig. 1. Surface top view (SEM) of porous sample made of titanium alloy Ti13Nb13Zr

## RESULTS AND DISCUSSION

The microscopic examinations of anodized specimen was performed with the SEM, JEOL JSM-7600F (EDS) at the University of Zielona Góra. The results are presented in Fig. 2 after anodizing process.

The obtained results are an evidence that this ternary and biphasic porous alloy can be successfully oxidized electrochemically to nanotubular structure. The length of nanotubes can be adjusted by mainly change in time. The drastic change in voltage may result in disappearance of nanotubular structure, change in

temperature – in an increase in porosity or decrease in crystallinity. The colonies of nanotubes may vary depending on the phase composition of the substrate but this effect seems relatively small.

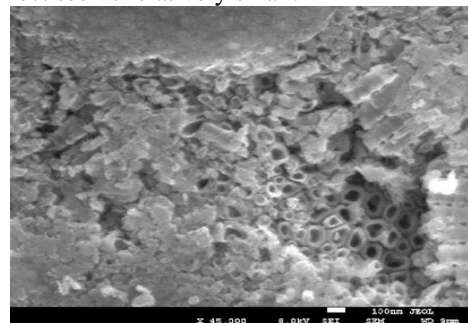


Fig. 2. Surface top view (SEM) of nanotubular oxide layer formed in 1M H<sub>3</sub>PO<sub>4</sub> + 0.3% HF, and temperature 20°C for:30 min

## CONCLUSION

- Titanium alloy here studied is susceptible to produce nanotubular titanium oxide layer
- The presence of nanotubular oxide layers with internal diameter ranging from 20 to 100 nm is observed. The resulting nanotubes have dimensions able to facilitate an adhesion of hydroxyapatite and / or osteoblasts to the metallic implant
- Formation of nanotubes on the surface of two-phase alloy is a complex process, determined by the crystallisation of the acid solution in presence of fluorides

## REFERENCES

- 1.J. Marciniak: *Biomaterials*, Silesian Technical University Publishing House, Gliwice 2002
- 2.Seramak T., Serbiński W., Zieliński A.: Formation of porous structure of the metallic materials used on bone implants.Solid State Phenom. 183 (2012) 155-162.
- 3.Ossowska A., Zieliński A., Supernak M.: Preparation of nano-tubular oxide layers on titanium alloy Ti13Nb13Zr. Eng. Biomater. 14 (2011) 66-68.

## ACKNOWLEDGMENTS

The authors would like to thank National Science Centre (Grant No. 02909) for providing financial support to this project. The project was financed by the National Science Centre awarded on the basis of the decision number DEC-2012/05/N/ST8/02909.

## Low Temperature Atomic Layer Deposition Technology for Low Thermal Resistance Polymer Surface Modification

Li-Chun Wang<sup>1</sup>, Hsin-Chih Lin<sup>1,\*</sup>, Kai-Chiang Yang<sup>2</sup>, Miin-Jang Chen<sup>1</sup>, Yin-Yi Han<sup>3,4</sup>

<sup>1</sup>Department of Materials Science and Engineering, National Taiwan University, Taipei, Taiwan.

<sup>2</sup>School of Dental Technology, Taipei Medical University, Taipei, Taiwan.

<sup>3</sup>Department of Traumatology, National Taiwan University Hospital, Taipei, Taiwan.

<sup>4</sup>Department of Surgery, National Taiwan University Hospital, Taipei, Taiwan.

[hclinntu@ntu.edu.tw](mailto:hclinntu@ntu.edu.tw)

### INTRODUCTION

Atomic layer deposition (ALD), a technique which has widely used in semiconductor industry, can deposit high quality nanoscale films with a uniform thickness. Recently, some research groups develop a low temperature ALD technique which can be applied in low thermal resistance substrates such as polymers [1]. Thus, ALD technology is used in surface modification of medical grade polymer in this study.

### EXPERIMENTAL METHODS

Poly(vinyl chloride) (PVC, raw material of cannula in daily practice) was used as a substrate and ultrasonically cleaned with deionized water before study.  $\text{Al}(\text{CH}_3)_3$  was reacted with water vapour (thermal mode) or/and oxygen plasma (plasma mode) to form a thin  $\text{Al}_2\text{O}_3$  film on PVC substrates using a low-temperature ALD technique. Prepared  $\text{Al}_2\text{O}_3$ -coated PVA and un-treated PVA samples were characterized.

### RESULTS AND DISCUSSION

The surface morphology and water contact angle of thermal mode and plasma mode  $\text{Al}_2\text{O}_3$ -coated PVC samples were shown in Fig. 1 to Fig. 3. A highly uniform thin  $\text{Al}_2\text{O}_3$  layer was successfully grown on the PVC substrates by difference mode deposition, but the surface roughness is widely discrepancy with each other and raw PVC. That mean we can tune the biological response on PVC materials in difference application. It possible to form “wavy surface” or “non-uniform surface” when polymer substrate used ALD process, which is due to PVC has a porous surface that the interstitial space between individual molecules. Furthermore, the precursor was diffuse into the bulk of the polymer matrix, the reaction will occurred efficiently at or near the surface of the polymer plate and  $\text{Al}_2\text{O}_3$  clusters will be formed [2]. The hydrophobic surface, which improves protein absorption on the substrates.

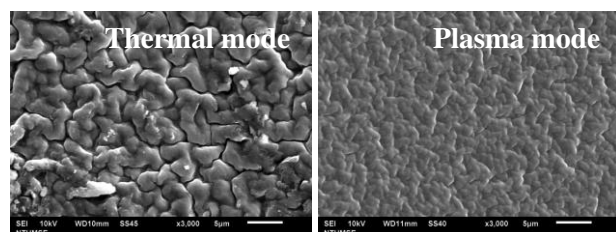


Fig. 1: Surface morphology of  $\text{Al}_2\text{O}_3$ -coated PVC substrates with thermal mode and plasma mode deposition.

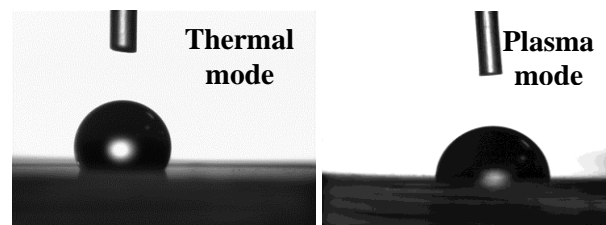


Fig. 2: Wettability of  $\text{Al}_2\text{O}_3$ -coated PVC substrates with thermal mode and plasma mode deposition.

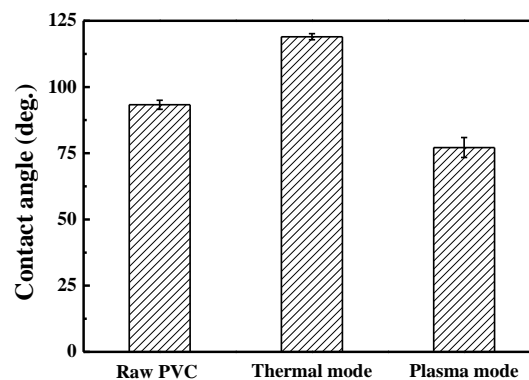


Fig. 3: Contact angle of un-treated PVC and  $\text{Al}_2\text{O}_3$ -coated PVC substrates with thermal mode and plasma mode deposition.

### CONCLUSION

A highly uniform thin  $\text{Al}_2\text{O}_3$  layer was successfully grown on the PVC substrates. This surface modification approach makes PVC surface more hydrophobic or hydrophilic. Albumin films also prevent platelet adhesion, and may decrease the formation of thrombosis. This study reveals surface modification using ALD technology can improve the hemocompatibility of PVC. ALD technology may also be applied to modify other biomaterials.

### REFERENCES

1. Wilson C., *et al.*, Chemistry of materials. 17:5625-5634, 2005
2. Liang X., *et al.*, Journal of the American Ceramic Society. 90:57-63, 2007.

### ACKNOWLEDGMENTS

This study was supported by Ministry of Science and Technology under grant number 101-2325-B-002-013 and 103-2218-E-002-028.



Paulina Trzaskowska<sup>1</sup>, Marta Trzebińska<sup>1</sup>, Aleksandra Poniatowska<sup>1</sup>, Tomasz Ciach<sup>1</sup>

<sup>1</sup>Faculty of Chemical and Process Engineering, Warsaw University of Technology, Poland  
[p.trzaskowska@ichip.pw.edu.pl](mailto:p.trzaskowska@ichip.pw.edu.pl)

## INTRODUCTION

Stainless steel (SS) 316L is often used for medical applications, e.g. for fabrication of stents or artificial valves. However, these life-saving devices have negative long-term influence on tissues of a patient. Adsorption of platelets and leukocytes leads to formation of blood clots and inflammation<sup>1</sup>. Also, steel releases toxic ions (e.g. Cr or Ni); in case of stents there is also a problem of restenosis<sup>2</sup>. Many approaches<sup>3</sup> has been undertaken to solve these problems, however none of them seems to be good enough. Coating the surface of steel with biocompatible layer is expected to minimize harmful effects by isolating it from blood components and other tissues and thus prolonging the lifetime of a steel device. In present paper we propose a novel method of SS coating which appears to give satisfactory results.

## EXPERIMENTAL METHODS

In this work we propose a method of electrochemical SS 316L surface coating with a) phospholipids from soy lecithin and b) polymers such as poly(glycol dimethacrylate) (PEGDMA). We use flat SS 316L discs (Ø14mm) because we consider it be a comfortable model of an SS object.

### SS 316L coating

We applied electrochemical method of coating. The aqueous solution contained a) phospholipids and b) PEGDMA as main component. DC power supply was used as a power source. Several physicochemical parameters vital for the process of coating, such as pH, time of coating, main compound concentration, current density, were altered.

### Analysis of coatings

The dependence of obtained coatings quality on altered process parameters was investigated. Coatings homogeneity was studied with the use of infrared spectroscopy (FTIR-ATR) and electron microscopy (SEM). Roughness of the layers ( $R_a$ ) was determined (optical profilometry).

## RESULTS AND DISCUSSION

Both phospholipid and PEGDMA coatings seem to be present on the whole surface of coated SS discs, which has been determined thanks to FTIR-ATR and SEM techniques. SEM indicated that thickness of coatings depends on process time and component concentration. First trials revealed that calculated  $R_a$  fits in the range assigned by other authors<sup>4</sup>. However, the roughness needs to be further minimized to decrease the risk of blood clotting. It has to be highlighted that there is no sufficient data available in existing body of literature to fully compare gained results with other authors' observations. Most suitable process parameters have

been selected, yet the research is still being conducted. Selected materials are going to be further studied to determine their influence on blood in static conditions (analysis of coagulation parameters) and cytotoxic properties (e.g. MTT in vitro test).

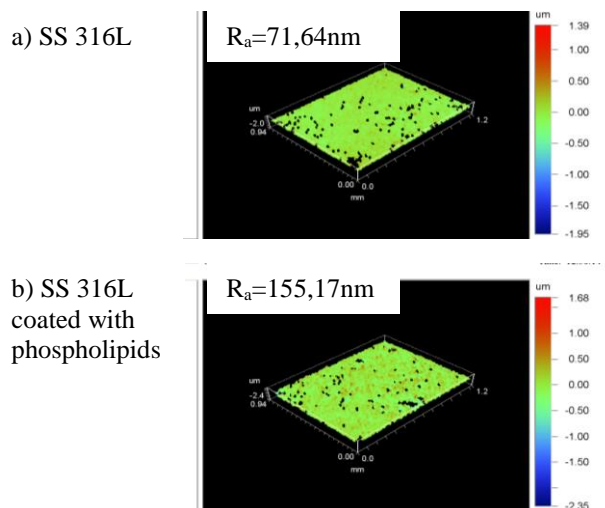


Fig. 1. An example of obtained profilometric 3d plots showing roughness of a) SS 316L and b) SS 316L coated with phospholipids. Calculated  $R_a$  given.

## CONCLUSION

It has been proven that it is possible to obtain a phospholipid or polymer coating on SS 316L surface through a not yet reported method utilizing electrochemical processes. The method is fast and cheap, hence it could be considered as an alternative for already proposed methods. It could possibly be applicable for objects of complex shape such as stents. The procedure is promising, thus we are still working on it.

## REFERENCES

1. Vasilis G. *et al.*, Anal Bioanal Chem 384: 65–72, 2006
2. Haidopoulos M, *et al.*, J Mater Sci: Mater Med 17:647–657, 2006
3. Sydow-Plum G *et al.*, Mater Sci Tech 24:1127-1143, 2008
4. Willumeit R. *et al.*, Mat.-wiss. u. Werkstofftech 34:1084-1093, 2003

## ACKNOWLEDGMENTS

The authors would like to thank National Science Centre Poland (Grant no: 2013/11/N/ST8/00636) for providing financial support to this project.



## INTRODUCTION

Surface modification techniques are currently extensively applied in wide variety of biomaterials, i.e. ferrous and non-ferrous alloys, ceramics and polymers. The use of ferrous alloys in medical applications is still a concern due to their questionable corrosion and wear resistance. To extent their biocompatibility and maximize performance, diffusion layers and coatings are applied to the surface. Unfortunately, there is relatively little data concerning martensitic stainless steels and their surface modification in biomedical applications. As shown in previous studies, low-temperature plasma nitriding (LTN), successfully used in industry for over 30 years, can lead even to deterioration of corrosion resistance of AISI 440B martensitic stainless steel<sup>1</sup>.

The aim of the study was to evaluate the effect of TiN, DLC and LTN surface modification on biofunctional properties, i.e. corrosion resistance and wear, of AISI 440B martensitic stainless steel.

## EXPERIMENTAL METHODS

Material has been divided in following groups:

- I. reference I, heat treated in 250°C,
- II. reference II, heat treated in 500°C,
- III. LTN diffusion layer modified, 390°C, 50% H : 50% N,
- IV. DLC modified
- V. TiN modified.

Electrochemical corrosion studies were carried out in 0,9% NaCl<sub>aq</sub> using potentiostat-galvanostat (PGP-201, Radiometer). A conventional three-electrode system was used. Corrosion potential ( $E_{corr}$ ), corrosion current ( $i_{corr}$ ) (Tafel method) and pitting potential ( $E_p$ ) were determined. Open circuit potential ( $E_{ocp}$ ) was monitored for 2 hours of immersion.

Wear tests were performed on a disc-on-plate tribometer working in a reversing movement mode of a frequency of 1 Hz with given initial gap between working surfaces. 0,9% NaCl<sub>aq</sub> solution was used as lubricant.

The post-test samples pit and surface morphology were studied by scanning electron microscopy (SEM – S-3000N, Hitachi), confocal laser scanning microscopy (CLSM – LEXT OLS 4000, Olympus) and energy-dispersive X-ray analyser (EDX).

## RESULTS AND DISCUSSION

### Corrosion resistance

Both  $E_{ocp}$  observations and anodic polarization tests suggest that DLC layers have the most beneficial impact on corrosion resistance of AISI 440B amongst all applied layers. In comparison with reference, TiN and LTN treated material, DLC application results in significant shift of  $E_{ocp}$  and  $E_{corr}$  towards noble values,

as well as in two orders of magnitude lower  $i_{corr}$ . This may be due to low porosity and high density of DLC layers<sup>2</sup>. TiN layers did not affect significantly corrosion resistance of considered steel. As some authors claim, the titanium nitride layers are porous<sup>3,4</sup> and water-penetrable<sup>4,5</sup>. Due to that, they do not limit the aqueous solutions contact with metals.

The worst performance in corrosion tests amongst all modified samples exhibited the LTN modified ones. Not only  $E_{corr}$  and  $i_{corr}$  values were not far different from the reference ones, but also visible even with the unaided eye corrosion pits occurred. Due to that, LTN samples were not considered in wear tests.

### Wear resistance

Wear studies indicated that DLC layers are characterized by low friction coefficient value (average  $\mu = 0,03$ ), which remained stable during whole 2 h test. On the contrary, friction coefficient of TiN-modified samples rose each time until the end of the test, to reach even the redoubled value of DLC  $\mu$ . What is the most important, modified samples fulfilled its task as anti-wear layers. Unlike the reference material, DLC and TiN modified samples indicated no measurable wear. It should however be noted that there are noted cases of TiN spalling from martensitic stainless steels<sup>6</sup>.

## CONCLUSION

Experiments performed on reference and surface modified AISI 440B martensitic stainless steel show that the best biofunctional properties are exhibited by DLC-modified material. Deposition of DLC layer results in significant reduction of corrosion and wear rate. In the future it will be necessary to perform further analyses in martensitic stainless steels surface modification techniques.

## REFERENCES

1. Łepicka M. *et al.*, Acta Mechanica et Automatica 7:155-159, 2013
2. Kim H. G. *et al.*, Diam. Relat. Mater. 14:35-41, 2005
3. He C. *et al.*, Appl. Surf. Sci. 276:667-671, 2013
4. Subramanian B. *et al.*, Mater. Lett. 62:1727-1730, 2008
5. Liu C. *et al.*, Surf. Coat. Tech. 200:4011-4016, 2006
6. Wang L. *et al.*, Surf. Coat. Tech. 205:1599-1605, 2010

## ACKNOWLEDGMENTS

This scientific work was supported by the Faculty of Mechanical Engineering, Białystok University of Technology, project No MB/WM/13/2014.



## An Electrically Conducting Composite Scaffold for Bone Tissue Engineering

Izabella Rajzer<sup>1</sup>, Monika Rom<sup>2</sup>, Elżbieta Menaszek<sup>3</sup>.

<sup>1</sup>Department of Mechanical Engineering Fundamentals, ATH - University of Bielsko-Biała, Poland

<sup>2</sup>Institute of Textile Engineering and Polymer Materials, ATH-University of Bielsko-Biała, Poland

<sup>3</sup>Department of Cytobiology, Collegium Medicum, UJ Jagiellonian University, Poland

[irajzer@ath.bielsko.pl](mailto:irajzer@ath.bielsko.pl)

### INTRODUCTION

Recent developments in bio-interface engineering have shown that inkjet printing is a promising method for surface modification as it allows for noncontact layer-by-layer accurate deposition of conductive particles on the surface, however it requires the careful preparation of stable in time inks of appropriate viscosity and suitable ability to drying after deposition<sup>1</sup>. The non-contact mode of the operation reduces cross-contamination between samples and that is why inkjet printing has become the technique of choice for the functionalization of biomaterials<sup>2</sup>. The current drop-on-demand (DOD) inkjet printing technology allows the generation of accurate patterns on various substances using a layer by layer deposition with ink droplets of a few picolitres. Inks can be composed of soluble or well dispersed and stable in time particles, including conductive polymers or biomolecules. In case of piezoelectric nozzles, the process can be done at room temperature which is beneficial for temperature-sensitive materials, so that the functionality of the immobilized substance can be maintained. The conductive polymers (e.g. polyaniline (PANI)) possesses many interesting properties that make them attractive materials for variety of applications. They have electrical properties similar to semiconductors and metals while their mechanical properties are similar to conventional polymers<sup>3</sup>. These materials have been considered for biomedical applications because of their physical, electrical, and biocompatibility characteristics<sup>4</sup>. Furthermore, conducting polymer structures can also be fabricated with inkjet printer. Combining electrospun, biodegradable scaffolds with conductive polymers would enable us to stimulate a multitude of cellular functions, including attachment, proliferation, migration, and differentiation through a modulation of electrical stimuli to the cell.

### EXPERIMENTAL METHODS

Conductive polymer (polyaniline) were deposited on the surface of various electrospun composite membranes (PCL, PLA, gelatin modified with hydroxyapatite, bioglass and osteogenon) using piezoelectric material printer DMP-2831. Determination of the electrical properties of materials was done basing on the electrochemical impedance spectroscopy measurements (EIS). The complex structure of the obtained scaffolds and their chemistry were characterized using SEM, FTIR, and WAXD. The scaffolds were also characterized in terms of their

porosity, mechanical properties and bioactivity, as well as by in-vitro cellular tests using NHOst cells.

### RESULTS AND DISCUSSION

In the current paper we have proposed a method to obtain a novel composite scaffolds for bone tissue engineering. Two techniques, namely electrospinning and inkjet printing processes, were used to fabricate bioactive scaffolds which provide an electrically conductive environment for cells.

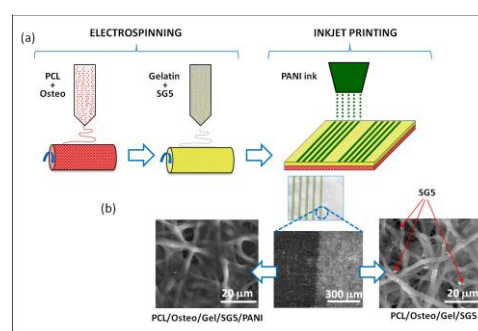


Fig. 1. (a) Scheme of the scaffold preparation process. (b) SEM images of the electrospun scaffold after inkjet printing<sup>5</sup>.

### CONCLUSION

Our research is initially aimed at fabricating scaffolds for improved cell-material interactions. Conductive PANI micropatterns were successfully inkjet printed on electrospun scaffolds. Presence of PANI did not affect apatite formation in SBF fluid. Cells proliferation was observed both on PANI modified and non-modified surface of scaffold.

### REFERENCES

1. Zheng Q. *et al.*, Analytical Biochemistry 2011;410:171-176.
2. Khan MS. *et al.* Colloids and Surfaces B: Biointerfaces 2010;75(2),441-777.
3. Shin S. *et al.*, Microelectronics Reliability 2011;51:437-444.
4. Mabrook MF *et al.* Sensors and Actuators B: Chemical 2006;115(1):547-551.
5. Rajzer, I. *et al.* Materials Letters 2015;138:60-63.

### ACKNOWLEDGMENTS

The authors would like to thank the Polish Ministry of Science and Higher Education (project Iuventus Plus: IP2012 033372) for providing financial support to this project.

# Biocomposite Materials Based on Poly(Butylene Succinate) with Modified Hemp Fibers

Zoe Terzopoulou<sup>1</sup>, Vasileios Nikolaidis<sup>1</sup>, Konstantinos Triantafyllidis<sup>1</sup>, Dimitrios Bikiaris<sup>1</sup>

<sup>1</sup> Department of Chemistry, Aristotle University of Thessaloniki, Greece  
[dbic@chem.auth.gr](mailto:dbic@chem.auth.gr)

## INTRODUCTION

Nowadays, the use of natural fibers to reinforce polymers in order to improve their properties is widespread. Biocomposite materials are increasingly used in various sectors such as automotive, medicine and manufacturing. There is a particular class of biocomposite materials wherein a biodegradable polymeric matrix is reinforced with natural fibers, and such materials are called green biocomposite materials and they represent a growing field in polymer science<sup>1</sup>.

Aliphatic polyesters such as poly(butylene succinate) (PBSu) have intriguing properties, including biodegradability and non-toxic hydrolysis products. One of the main problems with polymer-natural fiber composites is the low interfacial adhesion due to the hydrophilicity of the fibers and the hydrophobicity of most polyesters.

The primary method for enhancing the interaction between the fiber and the matrix is the surface modification of the fiber. The addition of binders on the fibers surface and/or compatibilizers in the polymeric matrix, leads to good compatibility between the cellulosic fibers and the nonpolar polymeric matrices<sup>2</sup>. In the present work citric acid was used to modify hemp fibers in order to increase the mechanical performance of PBSu/hemp composites.

## EXPERIMENTAL METHODS

Hemp fibers have been modified by 2 different ways: first by the use of NaOH and with a combination of NaOH treatment and citric acid addition. Thus, two series of PBSu composites have been prepared, with the two different modifications of the fibers. The fiber content was 20, 30 and 50wt%. The composites have been prepared by melt blending, using a twin screw co-rotating extruder, followed by their physicochemical characterization. Mechanical properties were studied by measuring the tensile and impact strength as well as their rate of biodegradation by enzymatic hydrolysis and degradation in soil. The dispersion and adhesion were studied with scanning electron microscopy (SEM). Interactions between the matrix and the fibers was also studied with FTIR spectroscopy.

## RESULTS AND DISCUSSION

Washing with NaOH removed the excess of waxes and hemi-cellulose from the surface of hemp fibers, and the remaining cellulose can react with citric acid in high temperature during melt mixing. The cellulosic hydroxyl groups combined with citric acid anhydride form an ester linkage and introduced carboxyl groups to the natural fiber, thus providing more polar groups available for the creation of hydrogen bonds with the polymer. The reaction of the modification is presented in Fig. 1.

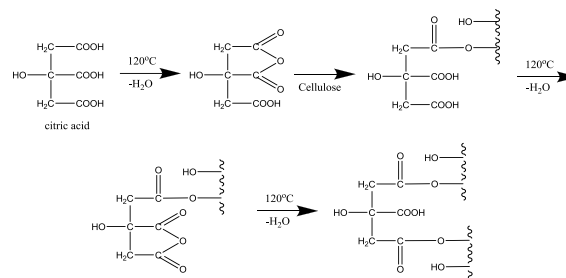


Figure 1: Thermochemical reaction of hemp cellulose with citric acid

SEM micrographs of the modified fibers revealed a smoother and cleaner surface, due to the efficient removal of waxes and hemi-cellulose. Stronger OH peaks in the FTIR spectra suggest the exposure of cellulose that can induce stronger interactions with the polymeric matrix. XRD diffractograms reveal increased crystallinity in the modified fibers, consistent with the removal of amorphous components of the fibers during the modification. The composite materials with hemp fibers modified with citric acid exhibited improved mechanical properties and interfacial adhesion, due to the large number of hydroxyls and carboxyl groups on the fillers surface. The presence of hemp fibers caused great rates of biodegradability in the composite materials, as was revealed after enzymatic hydrolysis and soil burial for several days.

## CONCLUSION

The modification of hemp fibers led to more sites available for hydrogen bonding with PBSu polymeric matrix. Thus, stronger interactions are taking place enhancing the interfacial adhesion between the different materials. As the result these composites have improved mechanical properties compared with unmodified fibers.

## REFERENCES

1. Summerscales J. et al., Composites Part A 41:1329–1335, 2010
2. Mehan L. et al., Compos Sci Technol. 60:1013-1026, 2000

**ACKNOWLEDGMENTS** The present research has been co-funded by European Union- European Regional Development Fund and Greek Ministry of Education/GGET- EYDE-ETAK through program ESPA 2007-2013 / EPAN II / Action “Bilateral R&T Cooperation Greece-China 2012-2014” (project 12CHN322).



## Impact of Sterilisation in Ethylene Oxide on Electrochemical Characteristics of Drawn Steel Wires Used as Urological Guidewires

Joanna Przondziona<sup>1</sup>, Witold Walke<sup>2</sup>, Marek Tkocz<sup>1</sup>

<sup>1</sup>Institute of Technology Metals, Silesian University of Technology, Poland

<sup>2</sup>Department of Biomaterials and Medical Engineering Devices, Silesian University of Technology, Poland  
[joanna.przondziona@polsl.pl](mailto:joanna.przondziona@polsl.pl)

### INTRODUCTION

Guidewires are used for proper insertion of catheters, endoscopes or stents during urological treatment<sup>1</sup>. They should feature high resistance to electrochemical corrosion in the environment of tissues and body fluids<sup>2,3</sup>. Guidewires after their production are subject to sterilisation aimed at getting rid of all microorganisms. The purpose of this study is to evaluate the impact of surface modification and sterilisation in ethylene oxide on electrochemical characteristics of wires made of stainless steel X10CrNi 18-8 used as urological guidewires.

### EXPERIMENTAL METHODS

Wires made of steel X10CrNi 18-8 after cold drawing were used for the tests. Wire surface was modified, in turn, by means of electrochemical polishing and chemical passivation. Resistance to electrochemical corrosion was evaluated on the ground of potentiodynamic tests with application of VoltaLab PGP201 system by Radiometer. EIS was performed with application of measurement system Auto Lab PGSTAT 302N equipped with FRA2 module. Tests were performed in the environment of artificial urine at the temperature of  $T = 37\text{ }^{\circ}\text{C}$ <sup>2,4,5</sup>.

### RESULTS AND DISCUSSION

Potentiodynamic tests results (mean measurement values of 5 measurements) are presented in Table 1.

Table 1. Potentiodynamic tests results

Type of surface	$E_{\text{corr}}$ , mV	$E_b$ , mV	$R_p$ , $\text{k}\Omega\text{ cm}^2$
Polished*	-84	+331	294
Passivated*	+44	+412	1390
Polished**	+67	+483	1070
Passivated**	+84	+757	2600

\*wires prior to sterilisation

\*\*wires after sterilisation in ethylene oxide

Analysis of experimentally determined impedance spectra of corrosion systems was made with application of electric equivalent systems presented in Fig. 1. The best matching of model spectra to impedance spectra determined experimentally in the solution of artificial urine for wires prior to sterilisation was provided by a simple model of oxide layer (it consisted of a parallel CPE connected with the resistance of ion transition through phase boundary: electrode –  $R_{\text{ct}}$  solution and resistance at high frequencies, that may be attributed to the resistance of electrolyte  $R_s$ ). Whereas, for samples after sterilisation, the best matching of impedance spectra was obtained through application of electric equivalent system that consisted of two consecutive parallel systems of CPE connected with resistance of transition and resistance at high

frequencies –  $R_s$ . In addition,  $R_{\text{pore}}$  means resistance of electrolyte in the porous layer, and  $\text{CPE}_{\text{pore}}$  capacity of the surface zone of material with high degree of surface development (porous)<sup>6</sup>.

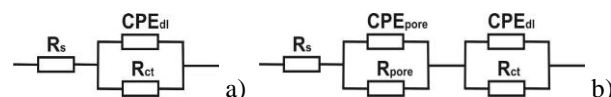


Fig. 1. Models of electric equivalent system for wires prior to sterilisation (a) and after sterilisation (b)

On the ground of obtained equivalent circuit diagrams, electrical values were determined; they are presented in Table 2. Results obtained in impedance tests confirmed favourable impact of sterilisation process in ethylene oxide. Increase of resistance of ion  $R_{\text{ct}}$  transition was observed, irrespective of the way of surface preparation, which is a favourable phenomenon and improves resistance of the material to electrochemical corrosion.

Table 2. Results of impedance tests

Type of surface	$R_{\text{pore}}$ , $\text{k}\Omega\text{ cm}^2$	$\text{CPE}_{\text{pore}}$		$R_s$ , $\text{k}\Omega\text{ cm}^2$	$\text{CPE}_{\text{dl}}$	
		$Y_{02}$	$n_2$		$Y_{01}$	$n_1$
Polished*	-	-	-	1060	$0.7621\text{E-}4$	0.85
Passivated*	-	-	-	5900	$0.1981\text{E-}4$	0.90
Polished**	992	$0.1086\text{E-}2$	0.60	1280	$0.3391\text{E-}3$	0.93
Passivated**	722	$0.2006\text{E-}3$	0.79	11430	$0.1363\text{E-}4$	0.86

\*wires prior to sterilisation

\*\*wires after sterilisation in ethylene oxide

### CONCLUSION

On the ground of performed corrosion tests it was proved that chemical passivation and sterilisation in ethylene oxide have favourable impact on corrosion resistance of wires made of stainless steel X10CrNi 18-8. Passive layer created on the surface of wire protects the alloy from impact of corrosion environment in a more efficient way and secures proper bio-tolerance of steel wires used in urology. Chemical passivation is surface modification treatment useful for creation of a barrier layer protecting steel from influence of artificial urine.

### REFERENCES

- Przondziona J. *et al.*, Eng. Biomater. 77-80:107-109, 2008
- Walke W. *et al.*, Acta Bioeng. Biomech. 3:93-99, 2012
- Walke W. *et al.*, Metalurgija 3:371-374, 2013
- Kajzer W. *et al.*, Int. J. Microstruct. Mater. Prop. 2:188-201, 2007
- Przondziona J. *et al.*, Metalurgija 50: 201-204, 2011
- Łosiewicz B. *et al.*, Ochr. przed Kor.. 11:49-54, 2003



## Photopolymerisation Preparation of Chitosan Hydrogel Containing Iron (II, III) Oxide Nanoparticles

Bożena Tylińczak<sup>1</sup>, Katarzyna Z. Gaca<sup>1</sup>, Katarzyna Bialik-Was<sup>1</sup>, Dagmara Malina<sup>2</sup>, Agnieszka Sobczak-Kupiec<sup>2</sup>

<sup>1</sup> Department of Chemistry and Technology of Polymers, Cracow University of Technology, Poland

<sup>2</sup> Institute of Inorganic Chemistry and Technology, Cracow University of Technology, Poland

[kgaca@chemia.pk.edu.pl](mailto:kgaca@chemia.pk.edu.pl)

### INTRODUCTION

Hydrogels are a class of cross-linked polymers and due to their three-dimensional structure and hydrophilic nature, they can absorb large quantities of water. These materials have high physical, chemical and mechanical stability in the swollen state. Water absorbance of the hydrogels can range from ten up to a thousand percent of its own volume. Chitosan is a polymer containing a primary amine group and two free hydroxyl groups on each molecule of glucose. The purpose of the study was to obtain polymeric hydrogels based on chitosan with the addition of iron (II,III) oxide nanoparticles by means of photopolymerization, and then to investigate their properties.

### EXPERIMENTAL METHODS

Hydrogels with different amounts of a crosslinking agent - diacrylate poly(ethylene glycol) (PEGDA) - and photoinitiator were synthesized by direct ultraviolet (UV) photopolymerization. Subsequently, the following investigations were carried out: sorptive ability in distilled water and different solutions, incubation studies in water and simulated body fluids (Ringer's solution and SBF). Incubation studies were also performed on the synthesized samples. Biological activity and structure analysis were performed on the polymer matrix using FT-IR spectroscopy.

### RESULTS AND DISCUSSION

The research covered synthesis of the polymer matrix with addition of iron (II,III) oxide nanoparticles, physicochemical tests and in vitro incubation research. A decrease in water absorption was observed in samples with an increasing amount of added crosslinking agent. Moreover, the type of solution in which the sample was immersed, also influenced the results. The lowest absorption occurred in a solution of  $\text{MgCl}_2 \cdot 6\text{H}_2\text{O}$ . Analysis of the polymer matrix structure of the synthesized hydrogels, before and after the incubation, was also carried out using Fourier transform infrared spectroscopy (FT-IR).

By using systems sensitive to magnetic fields, various treatments can be more effective, thus use of oxide iron (II,III) nanoparticles may assist a better and faster delivery of the drug into the tissue.

### CONCLUSION

Hydrogels containing nanoparticles of iron (II, III) oxide can be used in many medical applications. Use of materials containing such metal oxides may be useful, for example, in dressings applied to the affected part of the body and subjected to a magnetic field to enhance the therapeutical effect. Additionally the generated heat will act beneficially.

### REFERENCES

References must be numbered. Keep the same style.

1. Van Vlierberghe S., Dubruel P., Schacht E., *Biomacromolecules*, 12: 1387-1408, 2011.
2. Sharma B. R., Naresh L., Dhuldhoya N. C., *Food Promotion Chronicle*, 1(5): 27-30, 2006.
3. Hoffman A.S., *Advanced Drug Delivery Reviews*, 64: 18-23, 2012.
4. Lee S., Kwon I., Park K., *Advanced Drug delivery Reviews*, 65: 17-20, 2013.
5. Feng E., Ma G., Wu Y., Wang H., *Carbohydrate Polymers*, 111: 463-468, 2014.

### ACKNOWLEDGMENTS

"The authors would like to thank the The National Centre for Research and Development (Grant no: LIDER/033/697/L-5/13/NCBR/2014) for providing financial support to this project".



## Change in Mechanical Strength of Newly Developed Ti-Cr System Alloy Subjected to Heat Treatments and Surface Modification Processing

Kentaro Niwa<sup>1</sup>, Toshikazu Akahori<sup>2</sup>, Tomokazu Hattori<sup>2</sup>, Mitsuo Niinomi<sup>3</sup> and Masaaki Nakai<sup>3</sup>

<sup>1</sup>Graduate School of Science and Technology, Meijo University, Japan

<sup>2</sup>Faculty of Science and Technology, Meijo University, Japan

<sup>3</sup>Faculty of Science and Technology, Tohoku University, Japan

[110425241@ccalumni.meijo-u.ac.jp](mailto:110425241@ccalumni.meijo-u.ac.jp)

### INTRODUCTION

In recent years, a relatively low elastic modulus of around 30 GPa nearly equal to the bone has been demanded on the metallic biomaterial. However, in the case of the application with the spinal fixture, the metallic material needs a relatively high elastic modulus in order to suppress the spring back during deformation process. Therefore, the control of the elastic modulus by stress-induced transformation on newly developed biomedical  $\beta$ -type Ti-Cr system alloy has been proposed by preset authors. During the local plastic deformation, the elastic modulus rises locally by the precipitation of  $\omega$  phase.

Therefore, the change in the mechanical properties of Ti-Cr system alloy for the spinal fixture subjected to heat treatments and surface modification processing was investigated in this study.

### EXPERIMENTAL METHODS

Materials used in this study were hot forged Ti-12Cr ( $\phi$ : around 3.0 mm) and Ti-29Nb-13Ta-4.6Zr alloy ( $\phi$ : around 3.0 mm) bars. Ti-12Cr and Ti-29Nb-13Ta-4.6Zr (TNTZ) were solutionized at 1003 K and 1063 K for 3.6 ks in a vacuum followed by water quenching (WQ), respectively. Both solutionized alloys are designated as Ti-12Cr<sub>ST</sub> and TNTZ<sub>ST</sub>. Some Ti-12Cr<sub>ST</sub> were subjected to aging treatment (AT) at 573 K, 673 K and 723 K. Aged Ti-12Cr<sub>ST</sub> was classified by aging temperature (e.g. Ti-12Cr<sub>AT573K</sub>). Surface modification used by fine particle bombarding (FPB) was done on the specimen surface of Ti-12Cr<sub>ST</sub> at a pressure of 0.6 MPa for 0.3 to 0.6ks, which is designated as e.g. Ti-12Cr<sub>ST</sub>/FPB<sub>0.3ks</sub>.

For the evaluation of microstructures, the optical microscope (OM), and the X-ray diffraction (XRD) spectroscopy were carried out on each specimen. For the mechanical properties, Vickers hardness and tensile properties were investigated on each specimen.

### RESULTS AND DISCUSSION

Figure 1 shows the profiles of HV and elastic modulus ranging from very edge of the specimen surface to the center of cross-section of Ti-12Cr<sub>ST</sub>/FPB<sub>0.3ks</sub>. The change in HV and elastic modulus shows almost the same trend each other. Each HV (elastic modulus) of very edge of specimen surface and the center is 354 HV (104 GPa) and 354 HV (80 GPa), respectively. Therefore, HV and elastic modulus is increased by around 15 % and 30 % through FPB.

Figure 2 shows XRD profiles of Ti-12Cr<sub>ST</sub> and Ti-12Cr<sub>ST</sub>/FPB<sub>0.3ks</sub>. The XRD profile of Ti-12Cr<sub>ST</sub>/FPB<sub>0.3ks</sub> shows the stress-induced  $\omega$  phase.

From these results, an increase in HV and elastic

modulus near the specimen surface mainly is attributed to the precipitation of  $\omega$  phase and work hardening, which is enhanced by  $\omega$  phase through FPB.

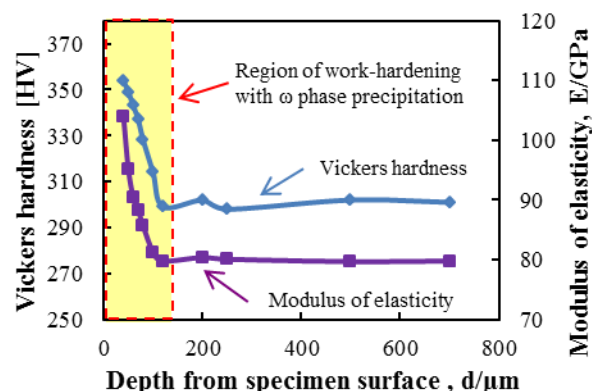


Fig. 1 Vickers hardness and elastic modulus profiles of Ti-12Cr<sub>ST</sub>/FPB<sub>0.3ks</sub>

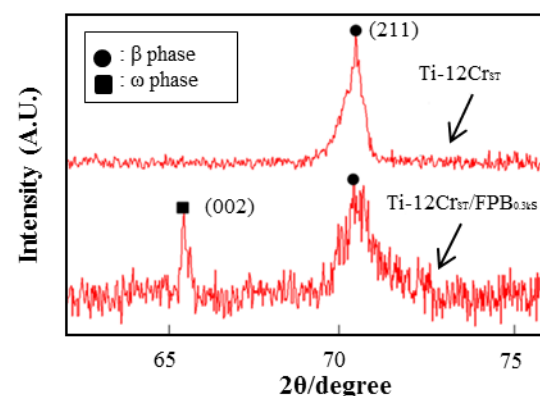


Fig. 2 XRD profiles of Ti-12Cr<sub>ST</sub> and Ti-12Cr<sub>ST</sub>/FPB<sub>0.3ks</sub>

### CONCLUSIONS

- 1) Precipitation of stress-induced  $\omega$  phase was confirmed on Ti-12Cr through FPB.
- 2) An increase in HV and elastic modulus near the specimen surface was attributed to the precipitation of  $\omega$  phase and work hardening, which was enhanced by  $\omega$  phase on Ti-12Cr through FPB.

### REFERENCE

- 1) X. Zhao, M. Niinomi, M. Nakai, G. Miyamoto, T. Furuhashi, J. Japan Inst. Acta Biomaterialia 7 (2011) 3230-3236.

## High Mechanical Functionalization of Biomedical Ti Alloys Subjected to Air Oxidation Processing

Yoshiki Tsujimura<sup>1</sup>, Toshikazu Akahori<sup>2</sup>, and Tomokazu Hattori<sup>2</sup>

<sup>1</sup>Graduate School of Science and Technology, Meijo University, Japan

<sup>2</sup>Faculty of Science and Technology, Meijo University, Japan

[110434044@calumni.meijo-u.ac.jp](mailto:110434044@calumni.meijo-u.ac.jp)

### INTRODUCTION

Recently, Ti alloys are getting great attention as metallic biomedical material,  $\beta$ -type Ti-29Nb-13Ta-4.6Zr alloy (TNTZ) with high biocompatibility and low elastic modulus similar to the cortical bone around 30 GPa has been developed in Japan.

Surface modification processing for metals is mainly applied for improvement in the wear resistance by the formation of hardened layer on the surface. Air oxidation processing (OX)<sup>1)</sup> is one of the simple methods for obtaining the hardened layer. In this study, the mechanical properties of TNTZ and  $\alpha+\beta$ -type Ti-6Al-4V (Ti64) as a comparison material subjected to OX under various conditions were investigated. In addition, the change in mechanical properties of TNTZ and Ti64 subjected to fine particle bombarding (FPB) were also done for improving those more.

### EXPERIMENTAL METHODS

Materials used in this study were TNTZ and Ti64 respectively. TNTZ was solutionized at 1063 K for 3.6 ks in a vacuum followed by water quenching (WQ), which is designed as TNTZ/ST. Ti64 was used in anneal condition. Some samples were conducted with OX at 873 K for 3.6 ks, 10.8 ks and 21.6 ks followed by air cooling (AC). Those are classified by the holding time (e.g. TNTZ/OX 3.6 ks). FPB with high speed steel particles less than 150 $\mu$ m in diameter was applied to some TNTZ/OX and Ti64/OX (e.g. TNTZ/OX 3.6 ks+FPB). Optical microscopy (OM) and X-ray diffraction (XRD) spectroscopy were carried out on each specimen to evaluate the microstructure. Vickers hardness, and tensile and fatigue properties were investigated for each specimen to evaluate the mechanical properties.

### RESULTS AND DISCUSSION

Figure 1 shows Vickers hardness profiles from very edge of specimen surface to subsurface in depth around 100  $\mu$ m of TNTZ/OX and TNTZ/OX+FPB. Vickers hardness near the specimen surface of TNTZ/OX is around 300 Hv higher than that of the subsurface near center of cross section. Vickers hardness increases remarkably with the holding time for OX. On the other hand, Vickers hardness of all TNTZ/OX+FPB increase by around 60 Hv as compared to that of TNTZ/OX. 0.2% proof stress and tensile strength of TNTZ/OX 3.6 ks was slightly higher than those of TNTZ/ST while the elongation showed a reverse trend. According to an increase in the holding time of OX, both 0.2% proof stress and tensile strength rose due to mainly solid solution hardening and formation of oxide layer. On the other hand, a decrease in elongation was due to easily

crack initiation in the oxide layer. 0.2% proof stress and tensile strength of TNTZ/OX+FPB were slightly higher than those of TNTZ/OX while the elongation was also slightly reduced. These trends of TNTZ were almost similar to Ti64. From these results, it needs to investigate the optimization of OX condition with relatively short holding time because of poor balance of tensile properties in OX condition with long holding time.

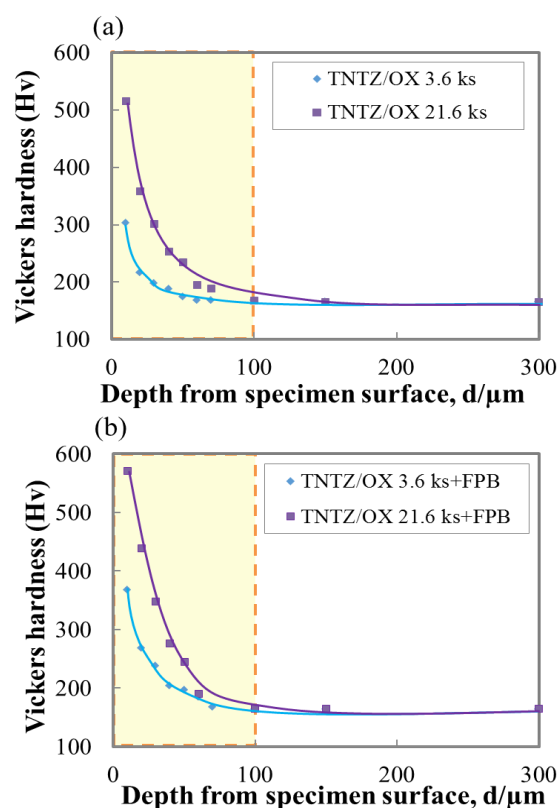


Fig. 1 Vickers hardness profiles of (a) TNTZ/OX and (b) TNTZ/OX+FPB.

### CONCLUSIONS

- 1) Vickers hardness near the specimen surface of TNTZ/OX 21.6 ks and TNTZ/OX 21.6 ks+FPB showed the maximum value (Hv 516 and 571).
- 2) 0.2% proof stress and tensile strength of TNTZ/OX and Ti64/OX was slightly increased with an increase in holding time of OX.

### REFERENCES

- 1) M. Niinomi, T. Akahori, S. Nakamura, H. Fukui, A. Suzuki, Tetsu-to-Hagane, 88(2002), pp. 567-574



# Surface Modification Layer and Mechanical Properties of Biomedical Titanium Alloys Subjected to HAp Fine Particle Bombarding

Akinori Ban<sup>1</sup>, Toshikazu Akahori<sup>2</sup>, Tomokazu Hattori<sup>2</sup>, Koichiro Nambu<sup>3</sup>, Shoichi Kikuchi<sup>4</sup>

<sup>1</sup>Graduate School of Science and Technology, Meijo University, Japan

<sup>2</sup>Faculty of Science and Technology, Meijo University, Japan

<sup>3</sup>Dept. of Mechanical Engineering, Suzuka National College of Technology, Japan

<sup>4</sup>Dept. of Mechanical Engineering, Kobe University, Japan

[110434061@ccalumni.meijo-u.ac.jp](mailto:110434061@ccalumni.meijo-u.ac.jp)

## INTRODUCTION

Newly developed  $\beta$ -type Ti-29Nb-13Ta-4.6Zr (TNTZ) is one of representative biomedical Ti alloys with high biocompatibility and a relatively low elastic modulus around 60 GPa close to that of cortical bone<sup>1)</sup>. However, TNTZ doesn't show the direct contact with the bone while biomedical ceramics such as hydroxyapatite (HAp) easily contacts with that. Therefore, the formation of bioactive layer on the surface of TNTZ and the change in mechanical properties of TNTZ by HAp fine particle bombarding were investigated in this study.

## EXPERIMENTAL METHODS

Materials used in this study were TNTZ subjected to a solution treatment (ST) at 1063 K for 3.6 ks in a vacuum followed by water quenching (WQ), which are designated as TNTZ<sub>ST</sub>. Some samples were subjected to aging treatment at 673 K for 1.2 ks after ST, which are designated as TNTZ<sub>AT673 K</sub>. Surface modification by HAp fine particle bombarding (HAp FPB) for 10 and 20s was conducted with all samples as mentioned above, which are designated as TNTZ<sub>ST</sub>/HAp and TNTZ<sub>AT</sub>/HAp, respectively. Annealed Ti-6Al-4V was used as a comparison material (Ti64<sub>annealed</sub>). Ti64<sub>annealed</sub> was also subjected to HAp FPB in the same condition for TNTZ, which is designated as Ti64/HAp. Optical microscopy (OM), scanning electron microscopy (SEM), and X-ray diffraction (XRD) spectroscopy were carried out on each specimen to evaluate the microstructure. Vickers hardness (HV) and fatigue tests were performed to examine the mechanical properties.

## RESULTS AND DISCUSSION

HV of TNTZ<sub>ST</sub>/HAp for 10 and 20s, TNTZ<sub>AT</sub>/HAp for 10 and 20s and Ti64/HAp for 10 and 20s increased slightly near the specimen surface as compared with that of TNTZ<sub>ST</sub>, TNTZ<sub>AT673 K</sub> and Ti64<sub>annealed</sub>. HV profile of TNTZ<sub>ST</sub>/HAp for 10s and TNTZ<sub>ST</sub>/HAp for 20s as representatively shown in Fig. 1 have a hardened region of HV from the specimen surface to around 100 $\mu$ m in depth. The increased value of HV on TNTZ<sub>ST</sub>/HAp is around 30 HV higher as compared to that of TNTZ<sub>ST</sub>. According to an increase in treatment time for FPB, the thickness of harden layer increases

slightly. Figure 2 shows S-N curves obtained from fatigue tests on TNTZ<sub>ST</sub> and TNTZ<sub>ST</sub>/HAp for 20s. The fatigue strength of TNTZ<sub>ST</sub>/HAp for 20s increases in the high cycle fatigue life region. The fatigue limit of TNTZ<sub>ST</sub>/HAp for 20s is around 300 MPa and around 60 MPa higher than that of TNTZ<sub>ST</sub>. HV near specimen surface on TNTZ<sub>ST</sub>/HAp for 20s was around 40 HV higher than that of center of specimen as mentioned above. As a result, it is considered that the effect of residual compressive stress by HAp FPB occurred in high cycle fatigue life region.

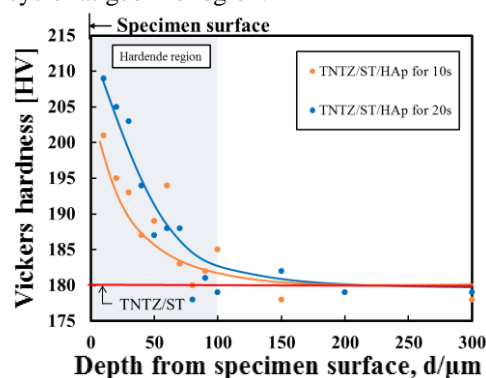


Fig.1 HV profiles of TNTZ<sub>ST</sub>, TNTZ<sub>ST</sub>/HAp for 10 and 20s

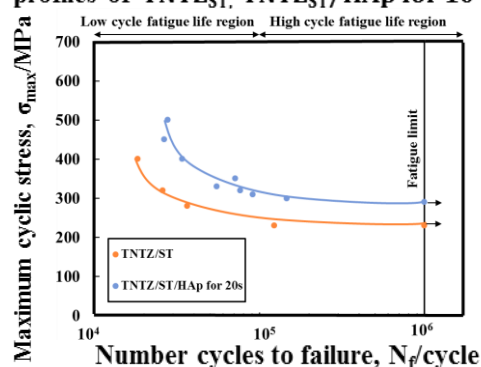


Fig.2 S-N curves of TNTZ<sub>ST</sub> and TNTZ<sub>ST</sub>/HAp for 20s

## CONCLUSION

- (1) HV of TNTZ<sub>ST</sub> subjected to HAp FPB showed the maximum value in very edge of specimen surface. In particular, HV near the specimen surface of TNTZ<sub>ST</sub>/HAp 20s increased by around 30HV as compared to that of TNTZ<sub>ST</sub>.
- (2) Fatigue strength of TNTZ<sub>ST</sub> subjected to HAp FPB increased in high cycle fatigue life region. The fatigue limit was around 300 MPa.

## REFERENCES

- 1). M. Niinomi: Metall. Mater. Trans. A, 33A(2002), pp.477-486



## Development of New Polymer-Liposome Complexes of Poly(acrylic acid) for Controlled Drug Delivery

Patrícia Alves<sup>1</sup>, Manuela Carnevalheiro<sup>2</sup>, M. Manuela Gaspar<sup>2</sup>, J.F.J. Coelho<sup>3</sup>, M. Eugénia Cruz<sup>2</sup>, M.H. Gil<sup>1</sup>, P.N. Simões<sup>1</sup>

<sup>1</sup>CIEPQPF, Department of Chemical Engineering, University of Coimbra, Portugal

<sup>2</sup>Research Institute for Medicines (iMed.Ulisboa), Faculty of Pharmacy, University of Lisbon, Portugal

<sup>3</sup>CEMUC, Department of Chemical Engineering, University of Coimbra, Portugal

[palves@eq.uc.pt](mailto:palves@eq.uc.pt)

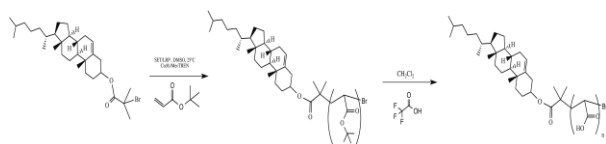
### INTRODUCTION

Liposomes are self-assembled vesicular lipidic bilayers surrounding aqueous compartments. As Drug Delivery Systems (DDS), they are able to circumvent cell barriers, allow the incorporation and protection of hydrophilic and lipophilic drugs, and facilitate their release for effective target delivery. Many efforts have been made to further enhance the properties of liposomes. Its surface modification by polymeric materials is a remarkable example<sup>1</sup>.

The key idea is to gather in the same amphiphilic polymeric entity two crucial attributes: caging capabilities (for liposome stabilization) and high degree of functionalization (for polymer structural response to pH and/or temperature stimuli)<sup>2</sup>. The development of new polymers to be used in polymer-liposome complexes (PLC) is crucial in these systems. In this regard, the tailored synthesis of macromolecules based on control/living radical polymerization (C/LRP) method is a suitable approach<sup>3</sup>. In particular, ATRP is very well established for different families of monomers<sup>4</sup>, and has several advantages over other methods, such as mild work conditions, fast kinetics, and very high tolerance to different functionalities<sup>4</sup>.

### EXPERIMENTAL METHODS

**Polymer synthesis:** In this work, cholesterol (CHO) was used to anchor the polymer into liposome. The synthesis started with the esterification of the OH-end group of CHO with bromocarboxylic acids, yielding an initiator structure<sup>5,6</sup>. CHO-Br initiator was later used for the ATRP of tert-butyl acrylate (tBA) with Cu(0) and Me<sub>6</sub>-TREN in dimethylsulfoxide (DMSO) at 25 °C. The tBA units of CHO-PtBA were then deprotected with trifluoroacetic acid (TFA) in CH<sub>2</sub>Cl<sub>2</sub> to form CHO-PAA (Scheme 1). ATRP method of synthesis is much simpler than other C/LRP methods and uses mild conditions of polymerization along with a rigorous control of the polymer properties (viz. molecular weight).



**Scheme 1:** Schematic illustration of the synthesis of CHO-PAA.

**PAA caged liposomes:** The liposome formulation DMPC:DMPG (50:5) was selected and CHO-PAA polymer was incorporated into the liposomal bilayer to obtain polymer-incorporated liposomes (PIL). Then, PILs were crosslinked using the COOH groups from PAA with a diamine in order to obtain polymer

liposomes complexes (PLCs). To assess the PCL efficacy to encapsulate an active drug, BSA was used to load the liposomes and several PLC parameters were evaluated. The cytotoxicity of PLC systems was determined for THP-1 cell line using the MTS assay.

### RESULTS AND DISCUSSION

The chemical structure of the obtained polymer was analysed by NMR and FTIR spectroscopies. Gel permeation chromatography (GPC) was used to determine the number-average molecular weight ( $M_n$ ) and dispersity ( $\bar{D} = M_w/M_n$ ). The good control over the polymer synthesis achieved by the ATRP method could be supported by the results ( $\bar{D} \approx 1$ ).

The results from calorimetric and zeta-potential studies demonstrated that cholesterol is inserted in the hydrophobic moiety of PIL (more negative surface charge and an enthalpy reduction in comparison to the formulation without polymer). The crosslinking of PAA in the PLC formulation was confirmed by FTIR and TEM studies. The same studies confirmed that the PLC parameters and membrane rigidity were not affected by the entrapment of BSA. Finally, none of the formulations tested revealed signs of *in vitro* toxicity after 24 h of incubation.

### CONCLUSION

These studies have established that PAA with a CHO end-group obtained by ATRP was successfully incorporated in a DMPC:DMPG liposomal membrane, which allowed to achieve PLC with high degrees of reticulation, non-toxic, and competent to incorporate active molecules.

### REFERENCES

1. Paasonen L. *et al.*, Bioconjug. Chem. 18:2131, 2007
2. Drummond D.C. *et al.*, Prog. Lipid Res. 39:409, 2000
3. Matyjaszewski K. *et al.*, Chem. Rev. 101:2921, 2001
4. Guliasvili T. *et al.*, Chem. Eur. J. 18:4607, 2012
5. Alves P., *et al.*, Colloids Surf. B. 104:254, 2013
6. Alves P., *et al.*, Colloids Surf. B. 123:446, 2014

### ACKNOWLEDGMENTS

The present study was supported by FCT (Fundação para a Ciência e a Tecnologia) R&D Projects (REF: PTDC/EQU-EPR/099226/2008). PA would like to thank FCT (Grant no: SFRH/BPD/69410/2010) for her postdoctoral fellow. NMR data was obtained at the NMR Laboratory of the Coimbra Chemistry Centre ([www.nmrccc.uc.pt](http://www.nmrccc.uc.pt)), Universidade de Coimbra, supported in part by grant REEQ/481/QUI/2006 from FCT, POCI-2010 and FEDER, Portugal.

# Magnetron Sputtering of Modular Targets for the Deposition of Silver-doped Titanium Coatings

Tobias Schmitz<sup>1,2</sup>, Franziska Warmuth<sup>1</sup>, Jürgen Groll<sup>1</sup>, Uwe Gbureck<sup>1</sup>, Claus Moseke<sup>1</sup>

<sup>1</sup>Department for Functional Materials in Medicine and Dentistry, University of Würzburg, Germany

<sup>2</sup>Institute of Tissue Engineering and Regenerative Medicine, University of Würzburg, Germany

[claus.moseke@fmz.uni-wuerzburg.de](mailto:claus.moseke@fmz.uni-wuerzburg.de)

Silver-doped Ti films were produced using a single magnetron sputtering source equipped with a titanium target with implemented silver modules under variation of bias voltage and substrate temperature. The Ti(Ag) films were characterized regarding their morphology, contact angle, phase composition, silver content and distribution as well as the elution of Ag<sup>+</sup> ions into cell culture medium.

## INTRODUCTION

Physical vapor deposition (PVD) is a common method to generate hard implant coatings, e.g. for abrasion-resistant or antimicrobial surface properties. The latter are realized in the binary system Ti-Ag by simultaneous vaporization using both magnetron sputtering and arc vaporization of single component targets. Here we simplified this process by developing modular Ti/Ag targets for an easy and precise variation of the silver content in magnetron-sputtered Ti(Ag) coatings.

## EXPERIMENTAL METHODS

Conventional disc-shaped titanium targets were modified with circular concentrated holes (5 mm in diameter) which were filled with silver nuggets by means of spot-welding. It was possible to change the silver fraction in the coating by either altering the number of holes filled with Ag or by varying the deposition parameters such as applied substrate bias (up to 200 V) and substrate temperature (up to 500 °C). X-ray diffraction (XRD) was used to examine the crystal structure of the generated films.

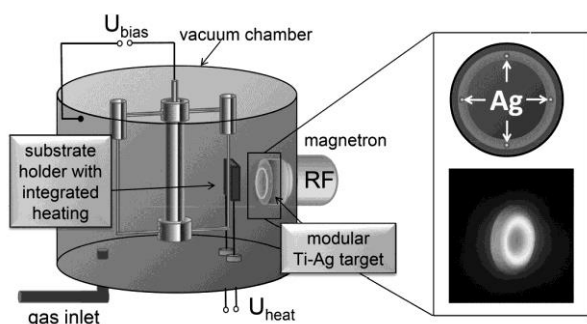


Figure 1: PVD setup with modular target.

The silver content of the coatings and the elution of silver into cell culture medium were quantified by inductively coupled mass spectrometry (ICP-MS). The morphology of the coating was investigated with scanning electron microscopy (SEM) and focused ion beam (FIB).

## RESULTS AND DISCUSSION

SEM pictures (Figure 2) showed that substrate heating during film deposition led to an even and dense surface layer, an effect that was even enforced by applying a negative substrate bias voltage. This was also reflected in decreased surface roughness. XRD confirmed the deposition of both Ti and Ag. ICP-MS showed a clear correlation between the applied sputtering parameters and the silver content of the coatings. Additional elution measurements using ICP-MS revealed that the elution kinetics of silver could be strongly influenced by variation of the sputter conditions.

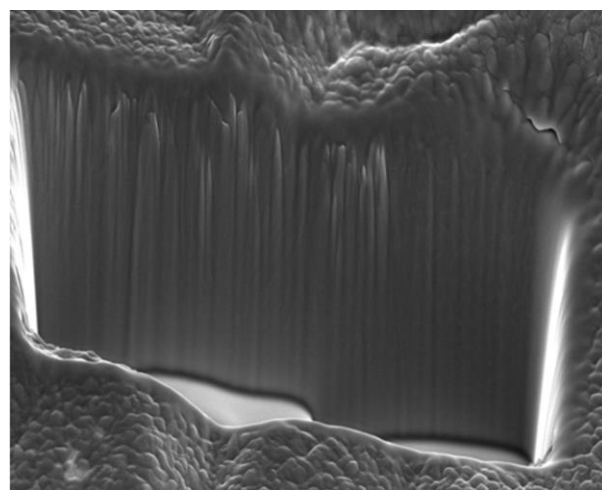


Figure 2: SEM image of a FIB cut through a Ti(Ag) film deposited with 400 W sputtering power and a substrate temperature of 500 °C.

## CONCLUSION

Modular targets are easy to build, very flexible in their material configuration and were successfully used to deposit Ti(Ag) films. The properties of the films can be adjusted by variation of the coating parameters such as the applied bias voltage, sputtering power, and substrate temperature. In particular, the Ag content of the films and the amount of eluted silver could be influenced by coating parameters.

## REFERENCES

1. Schmitz *et al.*, Mater. Sci. Eng. 44:126-131, 2014

## ACKNOWLEDGMENTS

The authors wish to thank the Deutsche Forschungsgemeinschaft for their financial support (DFG Gb1/13-2).

## Co-localization of RGD and PHSRN Peptides on Titanium to Guide Stem Cell Behaviour and Enhance Implant Osteointegration

Roberta Fraioli<sup>1,2,3</sup>, José María Manero<sup>1,2</sup>, Javier Gil<sup>1,2</sup>, Carlos Mas-Moruno<sup>1,2,3</sup>

<sup>1</sup>Biomaterials, Biomechanics and Tissue Engineering Group, Department of Materials Science and Metallurgical Engineering, Technical University of Catalonia (UPC), Spain

<sup>2</sup>Biomedical Research Networking Centre in Bioengineering, Biomaterials and Nanomedicine (CIBER-BBN), Campus Río Ebro, Spain

<sup>3</sup>Centre for Research in NanoEngineering (CRNE), Universitat Politècnica de Catalunya, Spain  
[carles.mas.moruno@upc.edu](mailto:carles.mas.moruno@upc.edu)

### INTRODUCTION

Controlling the interface between the implant and the surrounding tissue is of paramount importance to ensure the success of implantable devices. Adverse body reactions to the implant, such as fibrous encapsulation, can be avoided by accurately tuning the properties of the synthetic material surface. For this purpose, one approach, which is explored in this study, is to chemically functionalize the surface with bioactive molecules, capable of binding cell receptors and thereby influencing cell behaviour<sup>1</sup>. Specifically, the aim of our modification is to guide the response of human mesenchymal stem cells (hMSCs), enhancing adhesion, growth and differentiation into the osteoblastic lineage. Following a biomimetic approach, the two fibronectin sequences RGD and PHSRN have been chosen as bioactive moieties of our double-branched ligand (fig. 1). This recently synthesized peptidic platform<sup>2</sup> guarantees the co-presentation of the motifs, which are known to synergically bind integrin  $\alpha 5\beta 1$ <sup>3</sup>, a key receptor in osteogenesis<sup>4</sup>.

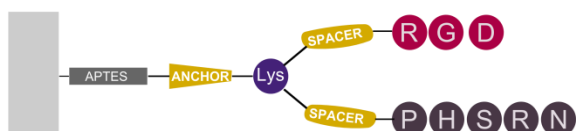


**Fig 2.** Schematic representation of the dual ligand for the co-presentation of RGD and PHSRN sequences.

### EXPERIMENTAL METHODS

The divalent platform was covalently immobilized on smooth mirror-like commercially pure Ti (grade 2) via silanization with 3-(aminopropyl)-triethoxysilane (APTES). The physicochemical properties of the surface were studied with contact angle measurement, white light interferometry, AFM and XPS.

The response of hMSCs was analyzed by means of immunofluorescence, proliferation and differentiation studies. These included evaluation of calcium deposits formation by Alizarin Red staining method, analysis of ALP expression via enzymatic-assay, and gene expression by RT-PCR.

One-way ANOVA with Tukey post-hoc analysis was used to detect significant differences.

### RESULTS AND DISCUSSION

The immobilization of the dual ligand significantly increased the adhesive capacity of the metallic surface: the number of cells attached and their projected area were significantly increased compared to the control (fig. 2). Proliferation of cells was efficiently supported

by the synthetic ligand at all time points. Analysis of calcium deposits, ALP activity and gene expression revealed that the branched ligand is able to support the differentiation into the osteoblastic lineage. This study provides further evidence that an accurate choice and controlled presentation of peptidic ligands is crucial to design bioactive coatings and significantly improve the biological performance of an implantable material.

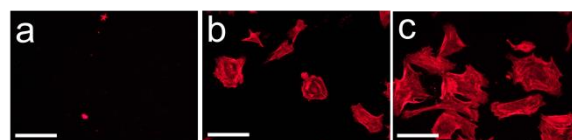


**Fig 1.** Actin immunostaining of the uncoated (a), RGD-functionalized (b), and RGD/PHSRN dual ligand-functionalized (c) Ti disks. Bar 500  $\mu\text{m}$  in (a), 200  $\mu\text{m}$  in (b) and (c).

### CONCLUSION

The covalent immobilization method was proved efficient to stably anchor the peptidic ligand to the metallic surface. Stem cells attached and spread to a higher extent on the surfaces coated with the dual biomolecule, displaying a polygonal shape, which is associated to the differentiation into bone-forming cells. The analysis of gene expression, ALP activity and calcium deposits also confirmed that the simultaneous co-presentation of the RGD and PHSRN motifs is able to stimulate the differentiation of stem cells into osteoblasts. Hence, our functionalization strategy constitutes a promising and versatile approach to guide stem cells behaviour by tailoring surface anchored ligands.

### REFERENCES

1. Maia F. R. *et al.*, Acta Biomater. 9:8773-8789, 2013
2. Mas-Moruno C. *et al.*, ACS Appl. Mater. Interfaces. 6:6525-6536, 2014
3. Aota S. *et al.*, J. Biol. Chem. 269:24756-24761, 1994
4. Martino M. M. *et al.*, Biomaterials 30:1089-1097, 2009

### ACKNOWLEDGMENTS

RF and CMM thank the Generalitat de Catalunya and the Government of Spain for financial support (SGR2009 1039, MAT2012-30706). CMM also thanks the European Commission (FP7-PEOPLE-2012-CIG).

Toshiki Miyazaki<sup>1</sup>, Chisato Matsunami<sup>1</sup> and Yuki Shirosaki<sup>2</sup><sup>1</sup> Graduate School of Life Science and Systems Engineering, Kyushu Institute of Technology, Japan<sup>2</sup> Frontier Research Academy for Young Researchers, Kyushu Institute of Technology, Japan[tmiya@life.kyutech.ac.jp](mailto:tmiya@life.kyutech.ac.jp)

## INTRODUCTION

When a backbone disease is treated with an operation, there is a method to fix the backbone with a medical appliance. Polyetheretherketone (PEEK) is popularly used for such an appliance. The advantage of PEEK is high strength and high biocompatibility. In addition, composites of PEEK and carbon are also expected as novel medical devices with enhanced mechanical properties. However, such PEEK-based materials cannot combine with bone tissue. Tight bone integration of PEEK medical devices is necessary for long-term stability *in vivo*.

It is reported that formation of bone-like apatite on artificial materials in body environment through chemical reaction with body fluid is essential requirement for exhibiting bone-bonding ability, i.e. bioactivity [1]. Although several techniques including sulfuric acid treatment [2] and incorporation of sol-gel-derived CaO-SiO<sub>2</sub> powders [3] have been attempted, such modification is not applied for the PEEK-carbon composites.

In the present study, we attempted various acid treatments and subsequent incorporation of Ca<sup>2+</sup> to provide with the apatite-forming ability on the composites. After the treatment, we evaluated their apatite formation ability *in vitro* by soaking the modified composites in simulated body fluid (SBF).

## EXPERIMENTAL METHODS

The PEEK-carbon composite disks with 10 mm in diameter and 1.2 mm in thickness were soaked in 5 mL of concentrated sulfuric acid (97 wt%) at 20°C for 1 min or 5 mL of concentrated acetic acid at 20°C for 24 h. After the treatment, they were soaked in 30 mL of 1 M-CaCl<sub>2</sub> solution at 36.5°C for 24 h and subsequently 30 mL of SBF at 36.5°C for 14 days.

Surface structural changes were characterized by scanning electron microscopic (SEM) observation attached with energy-dispersive X-ray (EDX) spectroscopy, Fourier-transform infrared spectroscopy (FT-IR) and contact angle measurement.

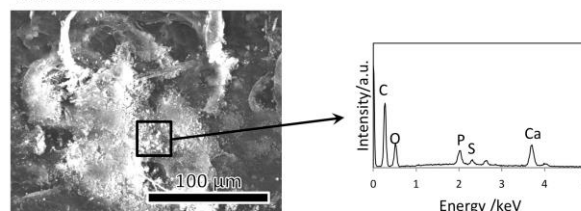
## RESULTS AND DISCUSSION

Sulfonic group was formed on the PEEK surfaces and morphology of the PEEK changed into porous structure after the sulfuric acid treatment. On the other hand, obvious change in chemical structure was not detected in FT-IR spectra after the acetic acid treatment, although contact angle decreased by the treatment. This means that top surface of the composite would become more hydrophilic by the treatment. Fig. 1 shows SEM photographs and EDX spectra of the surfaces of PEEK-

carbon composites treated with sulfuric and acetic acid, followed by CaCl<sub>2</sub> treatment and soaking in SBF for 14 d. Fine particles containing Ca and P were observed for the sulfuric acid treatment, but such particles were hardly observed for the acetic acid treatment.

The sulfonic groups formed on the PEEK-carbon composites would act site for the heterogeneous apatite nucleation. In addition, it was found that sulfonic groups were formed even on pure carbon plates after the sulfuric acid treatment. They would also contribute to the apatite formation.

### Sulfuric acid treatment



### Acetic acid treatment

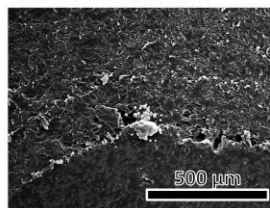


**Fig. 1** SEM photographs and EDX spectra of the surfaces of PEEK-carbon composites treated with sulfuric and acetic acid, followed by CaCl<sub>2</sub> treatment and soaking in SBF for 14 d.

## CONCLUSION

It was found that chemical surface modification using sulfuric acid was effective for providing PEEK-carbon composites with apatite-forming ability. This type of treatment would be effective for development of PEEK-based biomaterials by immobilization of various biological molecules.

## REFERENCES

1. Kokubo T. *et al.*, Biomaterials 24: 2161-75, 2003
2. Zhao Y. *et al.*, Biomaterials 34:9264-9277, 2013
3. Kim I *et al.*, J. Biomater. Appl. 24: 105-118, 2009

## ACKNOWLEDGMENTS

This work was supported by research grant program "Medtronic Japan External Research Institute".



# Controlled Growth of Smooth Muscle Cells to Provide Biomaterial with Blood Vessel-like Properties

Aldona Mzyk<sup>1</sup>, Roman Major<sup>1</sup>, Jan Marczak<sup>2</sup>, Bogusław Major<sup>1</sup>

<sup>1</sup>Institute of Metallurgy and Materials Science, Polish Academy of Sciences, Poland

<sup>2</sup>Laser Technology Division/Institute of Optoelectronics, Military University of Technology, Poland  
[aldonamzyk@gmail.com](mailto:aldonamzyk@gmail.com)

## INTRODUCTION

Nowadays, the hemocompatibility improvement of blood contacting material is aimed at vessel wall structure reconstruction on its surface.<sup>1</sup> The most recent studies focus on cells interacting with flat scaffolds. However, in blood vessels smooth muscle cells are found covering a highly curved surface.<sup>2</sup> It raises a fundamental question how surface curvature may determine cells behavior. This study was aimed at showing the mechanism of smooth muscle cells adhesion, morphology and function control in response to surface patterning.

## EXPERIMENTAL METHODS

The substrate surface was covered with 500 nm a-C:H:Si coating by physical vapor deposition method. Then, the laser interference lithography technique was used to form channel-like patterns of 32  $\mu\text{m}$  diameter with the 25  $\mu\text{m}$  inter-channel distance. Patterns were prepared in two depth variants, as consist of 5  $\mu\text{m}$  and 15  $\mu\text{m}$  sections (Fig. 2A) or 30  $\mu\text{m}$  (Fig. 2B) on the entire length of channel. After patterns formation, the 24 bilayer poly-L-lysine/hyaluronic acid (PLL/HA) films were deposited. Changes in coating microstructure after patterning were investigated by the transmission electron microscopy (TEM), whereas surface topography and cells response was analyzed by the confocal laser microscopy (CLSM) technique.

## RESULTS AND DISCUSSION

The analysis of TEM images confirmed microstructure inhomogeneity in the area of patterns (Fig. 1). The deformation around pattern was smaller for deeper channels. Selected area electron diffraction (SAED) pattern revealed the change of the crystal size.

The relation between surface topography and smooth muscle cells preferences during migration and spreading on the a-C:H:S surface was found. On the flat surface the migration and settlement was not oriented similarly to other researchers observation.<sup>2</sup> It has been shown that channel depth of 5  $\mu\text{m}$  also did not promote oriented cells growth. Moreover, cells were able to growing on the all surface area, including channels' bottom. Contrary, cells alignment was observed on 15  $\mu\text{m}$  and 30  $\mu\text{m}$  pattern depth variants. Surface coverage by polyelectrolyte films had an beneficial influence on cellular behavior. It was found that PLL/HA films promoted intercellular connections formation between smooth muscle cells from the opposite sides of channel.



Fig.1. Microstructure and SAED patterns of unmodified (A) and modified (B) channel surface area.

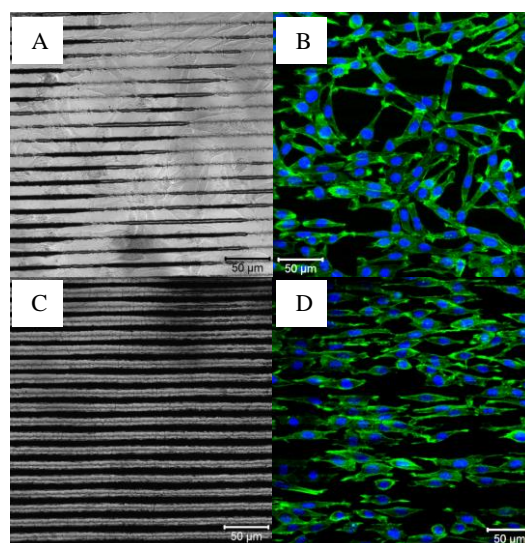


Fig.2. Surface topography (A,C) and (B,D) smooth muscle cells growth on the patterned surface.

## CONCLUSION

Among investigated patterns, channels of deepness above 15  $\mu\text{m}$  and inter-channel distance of 25  $\mu\text{m}$  facilitate directed cells culture *in vitro* analogous to the orientation of blood vessel wall's smooth muscle cells. Modification of patterned surface by PLL/HA film enhanced intercellular connections formation across the channels.

## REFERENCES

1. Major R. *et al.*, Bull. Pol. Acad. Sci. 60:337-342, 2012
2. Hu J. *et al.*, PLOS ONE, 9(8):9405-9415, 2014

## ACKNOWLEDGMENTS

The research was financially supported by the Project No. POKL.04.01.00-00-004/10 and Project No. 2011/03/D/ST8/04103 "Self-assembling, biomimetic porous scaffolds in terms of inhibiting the activation of the coagulation system" of the Polish National Center of Science.

Alina Vladescu<sup>1</sup>, Mihaela Dinu<sup>1,2</sup>, Mariana Braic<sup>1</sup>, Mihai Balaceanu<sup>1</sup>, Viorel Braic<sup>1</sup>

<sup>1</sup>National Institute for Optoelectronics (INOE2000), Romania

<sup>2</sup>University Politehnica of Bucharest, Romania

[alinava@inoe.ro](mailto:alinava@inoe.ro)

## INTRODUCTION

Cr-based nitrides or oxynitrides with silicon addition were found to typically consist of crystalline CrN or CrON and amorphous SiN<sub>x</sub> phases<sup>1</sup>. It was also shown that CrNO presented better biocompatibility and corrosion resistance as compared with nitrides<sup>2</sup>.

For this work, three types of novel multilayers were prepared by cathodic arc technique in order to increase the mechanical properties of CoCr alloy used in biological applications.

## EXPERIMENTAL METHODS

CoCr alloy discs (25 mm diameter) were used as substrates for the multilayer coatings with different structures: Cr/CrSi/CrSiN/CrSiON; CrSi/CrSiN/CrSiON; CrSiN/CrSiON. An example of a multilayer system is shown in Fig. 1.

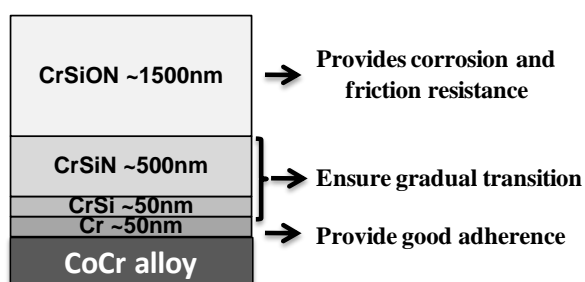


Fig. 1. Architecture of the multilayer coatings

The phase composition and crystallographic structure of the coatings were determined using X-ray diffraction. A comparison between the hardness and tribological properties (friction, wear) of the coatings was performed. Tribological tests were conducted using a ball-on-disc tribometer (3N load, 1500 m sliding distance). After the sliding tests, a surface profilometer was used to measure the wear tracks profiles in order to determine the worn out volume and thereafter the wear rate of the uncoated and coated CoCr samples. The surface morphology and elemental composition of the wear tracks were carried out by scanning electron microscope (equipped with an energy dispersive X-ray spectroscope).

## RESULTS AND DISCUSSION

XRD patterns revealed face-centered cubic (FCC) structures, with (200) preferred orientations. This orientation is indicative of the surface energy dominance.

All coatings exhibited similar hardness values (~14 GPa), higher than the CoCr substrate (~4 GPa).

The evolution of the friction coefficient ( $\mu$ ) as a function of sliding distance (Fig. 2) showed an improved friction behaviour for the samples with the adhesion layer. Cr/CrSi/CrSiN/CrSiON also exhibited the lowest wear rate after 1500m sliding distance under a constant normal load of 3N. SEM results showed that for the coatings which displayed lower friction coefficients as compared with the uncoated CoCr sample, more flat surfaces are formed at the contact area.

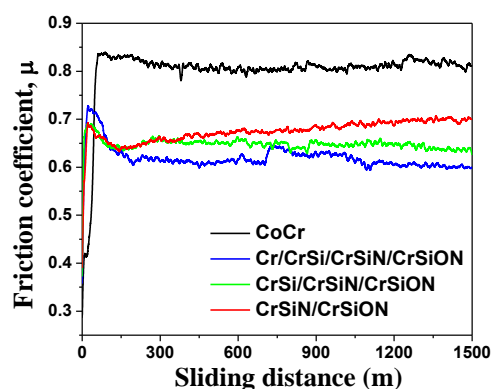


Fig. 2. Evolution of friction coefficient as a function of sliding distance

## CONCLUSION

The main conclusion is that the Cr-based multilayer coatings improved significantly the hardness and tribological characteristics of the CoCr alloy. Among the coatings, the Cr/CrSi/CrSiN/CrSiON system exhibited the highest hardness and the best friction and wear performance.

## REFERENCES

1. Martinez E. *et al.*, Surf. Coat. Technol. 180 – 181:570–574, 2004
2. Wierzchoń T. *et al.*, Surf. Coat. Technol. 21: 274–279, 2000

## ACKNOWLEDGMENTS

“This work was supported by Partnerships in priority areas program - PN II, developed with support from ANCS, CNDI - UEFISCDI, project no. 175/02.07.2012 (Coat4Dent)”.

## Dual Modal Superparamagnetic Iron Oxide Nanoparticles with Surface Attached Gadolinium Complexes

Witold Prendota<sup>1</sup>, Agnieszka Szpak<sup>2</sup>, Sylwia Fiejdasz<sup>2</sup>, Tomasz Strączek<sup>1</sup>, Kamil Goc<sup>1</sup>, Czesław Kapusta<sup>1</sup>, Janusz Szmyd<sup>3</sup>, Maria Nowakowska<sup>2</sup>, Szczepan Zapotoczny<sup>2</sup>

<sup>1</sup>Department of Solid State Physics, Faculty of Physics and Applied Computer Science, AGH University of Science and Technology, Poland

<sup>2</sup>Nanotechnology of Polymers and Biomaterials Group, Department of Physical Chemistry and Electrochemistry Faculty of Chemistry, Jagiellonian University, Poland

<sup>3</sup>Faculty of Energy and Fuels, AGH University of Science and Technology, Poland  
[Witold.Prendota@fis.agh.edu.pl](mailto:Witold.Prendota@fis.agh.edu.pl)

### INTRODUCTION

Magnetic resonance imaging technique plays a very important role in medical diagnostic<sup>1,2</sup>. In order to improve quality of this kind of research it is necessary to use contrast agents which have influence on protons relaxation times. This work describe synthesis and physicochemical properties of biocompatible magnetic nanoparticles (superparamagnetic iron oxide nanoparticles, in brief: SPIONs) which shorten  $T_1$  and  $T_2$  proton NMR relaxation times. The materials obtained exhibit an advantage over commonly used MRI contrast agents (shortening usually one type of relaxation time  $T_1$  or  $T_2$ ) which implies their name: dual modal MRI contrast agents.

### EXPERIMENTAL

Dual modal nanoparticle agents consisting of maghemite magnetic and protective coatings of ionic chitosan with gadolinium complex have been synthesized. Three types of preparation methods of those materials were proposed. They differ from each other in the way the gadolinium ions were introduced into the coating layer: SPION-Gd (ACh-GdDTPA) involves covalent and SPION-Gd (electrostatic) electrostatic Gd-complex attachment. The properties of materials obtained were investigated with several methods e.g.: nuclear magnetic resonance (NMR), X-ray fluorescence (XRF), transmission electron microscopy (TEM), vibrating sample magnetometry (VSM), FTIR spectroscopy and dynamic light scattering (DLS).

### RESULTS AND DISCUSSION

Physiochemical measurements allowed us to determine the following properties of SPIONs: DLS (hydrodynamic diameters: ca. 100 nm and Zeta potential), VSM (SPION-Gd (ACh-GdDTPA) exhibit superparamagnetic behaviour and a high saturation magnetisation) and XRF (confirmed gadolinium contents in the material synthesized). NMR studies show a linear dependence of  $1/T_1$  and  $1/T_2$  relaxation rates versus nanoparticle concentrations. This allowed us to derive the respective relaxivities:  $r_1$  and  $r_2$ . Their values obtained for SPION-Gd (ACh-GdDTPA) and SPION-Gd (electrostatic) are outstanding when compared to commercial contrast agents: FeREX<sup>TM</sup> and Ocean (table 1).

Sample name	$r_1$ (mM <sup>-1</sup> s <sup>-1</sup> )	$r_2$ (mM <sup>-1</sup> s <sup>-1</sup> )
SPION-Gd (ACh-GdDTPA)	36.0 ± 0.9	361.4 ± 4.3
SPION-Gd (electrostatic)	53.7 ± 1.1	375.5 ± 9.7
SPION-CCh	46.5 ± 2.8	282 ± 21
Ocean	23.5 ± 0.9	93.8 ± 1.9
FeREX <sup>TM</sup>	33.1 ± 1.3	160.1 ± 6.6

Table 1 show  $r_1$ ,  $r_2$  relaxivities values of all samples.

These results imply that dual modal MRI contrast agents synthesized and studied in this work exhibit better properties than single positive or negative agents.

### CONCLUSION

The dual modal agents obtained exhibit an outstanding relaxivity (high values of  $r_1$  and  $r_2$ ) and a very good long-term stability. Presence of gadolinium atoms in polymer layer influences magnetic properties of nanoparticles. The method of synthesis used in this work enables us to: change the type of (SPIONs) coating polymer and precisely control the distance between core and gadolinium complex. The nanoparticle materials presented can be considered as effective contrast agents for low-field MRI scanners.

### REFERENCES

1. Gupta AK. *et al.*, Synthesis and surface engineering of iron oxide nanoparticles for biomedical applications. *Biomaterials* 26:3996–4021, 2005
2. Laurent S. *et al.*, Magnetic iron oxide nanoparticles: synthesis, stabilization, vectorization, physicochemical characterizations, and biological applications. *Chem Rev* 108:2064–2110, 2008

### ACKNOWLEDGMENTS

This work was supported by the European Union from the resources of the European Regional Development Fund under the Innovative Economy Programme (grant coordinated by JCET-UJ, No. POIG.01. 01.02-00-69/09). Partial support from National Science Centre, Poland, Project No. 2012/07/B/ST8/03109 is acknowledged.



## On the Cytocompatibility of Ti6Al4V Thermally Oxidized by Means of Laser Shock Processing

Lara Crespo<sup>1,2</sup>, Margarita Hierro-Oliva<sup>3,2</sup>, Sandra Barriuso<sup>4</sup>, Virginia Vadillo-Rodríguez<sup>3,2</sup>, M<sup>a</sup> Ángeles Montealegre<sup>5</sup>, Laura Saldaña<sup>1,2</sup>, Enrique Gomez-Barrena<sup>6</sup>, José Luis González-Carrasco<sup>4,2</sup>, María Luisa González-Martín<sup>3,2</sup>, Nuria Vilaboa<sup>1,2</sup>

<sup>1</sup>Hospital Universitario La Paz-IdiPAZ, Spain

<sup>2</sup>CIBER de Bioingeniería, Biomateriales y Nanomedicina (CIBER-BBN), Spain

<sup>3</sup>Departamento de Física Aplicada, Universidad de Extremadura, Spain

<sup>4</sup>Centro Nacional de Investigaciones Metalúrgicas, CENIM-CSIC, Spain

<sup>5</sup>Centro Tecnológico AIMEN, Centro de Aplicaciones Láser, Spain

<sup>6</sup>Departamento de Cirugía, Universidad Autónoma de Madrid, Spain

[nuria.vilaboa@salud.madrid.org](mailto:nuria.vilaboa@salud.madrid.org)

### INTRODUCTION

Ti6Al4V alloy (Ti64) is the metallic biomaterial most widely used for the fabrication of orthopaedic implants. The interaction of the alloy with physiological fluids affects the stability of the passive outer layer that provides corrosion resistance. Technologies to produce outer layers resilient to chemical attack include thermal oxidation in air, which generates thick rutile layers on Ti64 surfaces<sup>1</sup>. However, the full component has to be subjected to treatment, which may cause thermal stability loss of the alloy microstructure.

Laser shock processing (LP) is a technology in which metallic surfaces are irradiated with short and intensive laser pulses. The net effect is the development of compressive residual stresses that improve fatigue strength<sup>2</sup>. Interestingly, LP is suitable for treating local areas of a component. For biomedical applications, LP cannot use sacrificial layers as they may lead to toxicity due to surface contamination. In the absence of ablative coatings, thermal rise at the surface during laser focusing is extremely high, which may oxidize the alloy surface. The changes that experience the Ti64 surface treated by means of LP without protective coating and the interactions of bone cells with the treated alloy, not addressed to date, were studied in this work.

### EXPERIMENTAL METHODS

Discs of Ti6Al4V ELI (extra low interstitial) alloy were irradiated with a Q-switched Nd-YAG laser working in fundamental harmonic at 1.6 J/pulse and producing pulses of 10 ns. Samples were irradiated at a density of 421 pulses cm<sup>-2</sup>. Samples polished to get a mirror-like finish were used as control. Surface characterization included scanning electron microscopy (SEM), X-ray diffraction, atomic force microscopy, X-ray photoelectron spectroscopy and time of flight secondary ion mass spectrometry analyses. Human mesenchymal stem cells (hMSC) and primary cultures of human osteoblasts (hOB) were used for cytocompatibility studies. Cell adhesion was examined by spectral confocal microscopy and SEM. For immunostaining, cells were stained with specific antibodies for paxillin, p-FAK Y397 and fibronectin. To visualize actin filaments, cells were stained with phalloidine-TRITC. p-FAK Y397 levels were quantified in protein extracts using a specific immunoassay kit. Cell viability was assessed using the alamarBlue assay. The degree of cell

layer maturation was investigated in cells cultured in osteogenic medium, by means of Alizarin Red staining and determination of alkaline phosphatase (ALP) activity.

### RESULTS AND DISCUSSION

Due to the temperature rise during LP, melting and ablation generate a waved surface with roughness values at the submicron scale that can be recognized by cells. A small percentage of metastable TiO was detected in the treated surface. In addition to Al-OH, not detectable in the untreated alloy, the outer surface layer of the treated alloy contains higher amounts of Ti<sub>2</sub>O<sub>3</sub>. The oxide layer and oxygen diffusion zone in the treated surface is several microns thick. Cells adopt a stretched morphology on the treated alloy and exhibit a great number of filopodia. Only some minor colocalization of paxillin and p-FAK Y397 with actin fibers are observed in the attachment sites. Morphometric analysis indicates that focal adhesion length decreases in cells cultured in the treated alloy. Intracellular p-FAK Y397 levels are lower than in cells incubated on the untreated alloy. Despite quality of adhesion is deeply affected in the LP-treated Ti64 surface, the rate of cell attachment is identical than in the untreated surface. Cell viability and organization of extracellular fibronectin matrix are also as in the untreated alloy. Moreover, the degree of cell mineralization and ALP activity in cells cultured in treated Ti64 are higher than in the untreated alloy.

### CONCLUSION

Ti64 surface thermally oxidized by means of LP allows the proliferation of hMSC and hOB, and enhances the osteoblastic maturation of hMSC as well as the lineage-specific activities of terminally differentiated hOB.

### REFERENCES

1. Browne M. et al. Biomaterials 15:894-8, 1994.
2. Ashley S. Mech. Eng. 120:12, 1998.

### ACKNOWLEDGMENTS

This work was supported by grants PI12/01698 (FIS, Spain), S2013/MIT-2862 (Comunidad de Madrid, Spain), MAT2009-14695-C04-01-02-04, MAT2012-37736-C05-03-05 (MINECO, Spain), GR10149 (Junta de Extremadura, Spain) and fellowship BES-2010-034989 (MINECO) to LC.





## Cell Adhesion to Plasma Treated and Fluorinated Collagen Surfaces

Ina Prade, Frauke Junghans, Michael Meyer

Collagen / Leather / Biopolymers, Forschungsinstitut für Leder und Kunststoffbahnen, Germany  
[ina.prade@filkfreiberg.de](mailto:ina.prade@filkfreiberg.de)

### INTRODUCTION

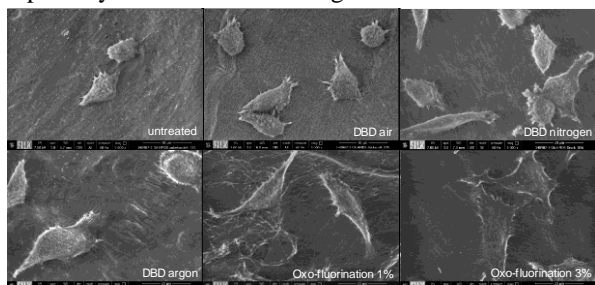
Cell adhesion to biomaterials, implant surfaces and tissue engineering scaffolds is essential for the formation of tissues *in vitro* and *in vivo*. Especially cell adhesion to extracellular matrix proteins like collagen influences cellular morphology, proliferation and differentiation<sup>1</sup>. In this study, collagen coatings and foils were functionalized with atmospheric plasma and gaseous fluorine, respectively, to investigate effects of a modified surface chemistry on cell adhesion.

### EXPERIMENTAL METHODS

Plasma activation was performed as a dielectric-barrier discharge (DBD) in the presence of the process gases air, nitrogen or argon. The fluorination took place in a reaction chamber, which was filled with a fluorine/nitrogen mixture (ratio 10 : 90) and air.

### RESULTS AND DISCUSSION

Cell cultivation on functionalized collagen surfaces revealed two effects. Oxo-fluorination and plasma treatment resulted in an increase in cellular adhesion and elevated cell density after three days of cultivation. Spreading area of the cells was remarkably increased especially for fluorinated collagen surfaces.



Contact angle measurements showed significant improvement of surface wettability and a decrease in

surface energy after plasma treatment. Fluorinated surfaces however revealed only weak changes, indicating that improved cell adhesion can not be explained with hydrophilic surface properties. Interestingly, X-ray photoelectron spectroscopy (XPS) analyses indicate changes in the elemental composition of treated collagen. Oxygen and nitrogen content was increased upon plasma treatment and fluor atoms were found in the surface of oxo-fluorinated samples.

The thermal stability of collagen was not affected as observed by differential scanning calorimetry (DSC).

Increased cellular adhesion to fluorinated surfaces is not affected by topography of the surface, because no differences could be observed with scanning electron microscopy (SEM).

Ongoing studies with chemical derivatisation of the treated collagen surface will further help to identify differences in chemical composition of the surface. So far the reason for the improved cellular adhesion is unknown and new surface sensitive methods are required to explain these observations.

### CONCLUSION

By now, the results demonstrate that it is possible to influence cell adhesion to collagen in a biocompatible way without the use of solvents. Plasma techniques and fluorination could thereby improve the properties of collagen and increase its applicability.

### REFERENCES

1. Boudreau and Jones, Biochem J. 339:481-488, 1999

### ACKNOWLEDGMENTS

The authors gratefully acknowledge the support provided by the German national BMWi / AiF program Innokom-Ost Marktforschung (MF120182).

## Enhancement of Osseconductivity of Ti Based Alloy by Bioactive Calcium Phosphate Coatings

Cosmin Cotrut (Mihai)<sup>1</sup>, Irina Titorencu<sup>2</sup>, Adrian Kiss<sup>3</sup>, Mihai Tarcolea<sup>1</sup>, Florin Miculescu<sup>1</sup>,  
Diana Vranceanu (Maria)<sup>1</sup>, Alina Vladescu<sup>3</sup>

<sup>1</sup>University Politehnica of Bucharest, Romania

<sup>2</sup>Department of Regenerative Medicine, Institute of Cellular Biology and Pathology "Nicolae Simionescu", Romania

<sup>3</sup>National Institute for Optoelectronics-INOE2000, Romania

[cosmin.cotrut@upb.ro](mailto:cosmin.cotrut@upb.ro)

### INTRODUCTION

Hydroxyapatite (HAP) ceramics belong to a class of calcium phosphate-based materials, which have been widely used as coating on titanium medical implants in order to improve bone fixation and thus increasing the lifetime of the implant<sup>1-3</sup>. The aim of the study is to evaluate the influence of the substrate temperature on the characteristics of HAP coatings prepared by RF magnetron sputtering. It was reported that the HAP coatings with the best bioactivity properties could be obtained by controlling the morphology, surface roughness, and crystallinity of the coatings<sup>3</sup>.

### EXPERIMENTAL METHODS

As substrates, Si wafers (100) and Ti based alloy discs (10 mm diameter) were used. The coatings were prepared using a RF magnetron unit equipped with one cathode made of HAP (1 inch diameter, 99.9 % purity, Kurt Lesker Ltd). The deposition parameters were: the base pressure =  $1.3 \times 10^{-4}$  Pa, Ar working pressure =  $6.6 \times 10^{-1}$  Pa, target power fed = 50 W, substrate bias voltages = -60 V, substrate temperature = 400, 500, 600, 700, 800°C, deposition time = 360 min.

The element composition was carried out using a Scanning Electron Microscope coupled with Energy Dispersive Spectroscopy. Crystalline structure, phase composition and texture were determined by means of X-ray diffractometer (XRD). The surface morphologies were evaluated by Atomic Force Microscope (AFM), on  $10 \times 10 \mu\text{m}^2$  area. The corrosion behaviour of the coatings was evaluated in Fusayama artificial saliva solution at 37°C, according to the ASTM standard G 59 - 97 (reapproved 2003). Viability of MG63 cells was measured by the MTT (3-(4,5-dimethylthiazol-2-yl)-2,5 diphenyl tetrazolium bromide) assay. MG 63 human osteosarcoma cells were cultured in Dulbecco's modified Eagle's medium (DMEM) with 10% inactivated fetal bovine serum (FBS) supplemented with 1% penicillin, streptomycin and neomycin (Sigma). The  $25 \times 10^3$  cells/cm<sup>2</sup> were seeded and cultured for 3, 5 and 7 days on studied samples.

### RESULTS AND DISCUSSION

EDS analysis of the coatings reveals that all samples exhibited the Ca/P ratios in the range 1.67 – 1.81. The Ca/P ratios of the HAP prepared at 600 °C and at 700 °C are close to 1.67, which corresponds to a stoichiometric HAP. All the coatings exhibit a (002) texture, which is a common for the HAP coatings deposited by RF magnetron sputtering technique. The HAP prepared at 400 °C show two peaks: (002) and (202). The increase in temperature leads to the occurrence of new diffraction peaks (corresponding to planes (200), (222),

(213) and (004). The SEM analysis indicates that the morphology of the HAP coatings deposited at 400 and 500°C are very smooth with a few visible particles. For the HAP prepared at substrate temperatures ranged from 600 to 800°C, some spherical in-growths appear.

The roughness of the coatings increases with increasing substrate temperature. At low temperature, an enlarged boundary grains are observable. The increase of the substrate temperature leads to the decrease in corrosion current density, indicating an enhancement of the corrosion resistance. Regarding the polarization resistance, note that this increase with substrate temperature and all the coatings have much higher polarization resistance than the uncoated alloy. First of all, it can be seen that all the coatings improve the biocompatibility of the Ti based alloy, independent on the days of culture. Comparing the coatings, after 1 day, no significant changes in cell viability were observed. After 5 days, the cell viability of the coatings increased by increasing the substrate temperatures (Fig.1).

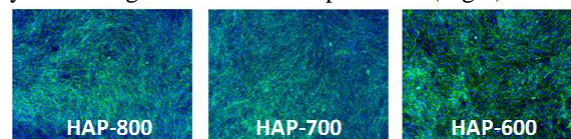


Fig. 1. Actin cytoskeletal organization and nuclear staining of the osteosarcoma cell growth on the investigated surfaces after 5 days (blue-nuclei; green - F-actin fibres)

### CONCLUSION

The results showed that all of the coatings exhibited uniformly growth and that the increasing substrate temperature induced an increase in the crystallinity of the prepared coatings. Corrosion performance of the coatings was improved with the increase of the substrate temperature from 400°C to 800°C. Furthermore, all of the coatings support the attachment and growth of the osteosarcoma cells with regard to the in vitro test findings.

### REFERENCES

1. Stan G.E. *et al.*, Optoelectron. Adv. Mat. 11: 1132–1138, 2009
2. Toque J. A. *et al.*, J. Mech. Behav. Biomat. 3: 324–330, 2010
3. Surmenev R.A. Surf. Coat. Technol. 206: 2035–2056, 2012

### ACKNOWLEDGMENTS

“This work was supported by Partnerships in priority areas program - PN II, developed with support from ANCS, CNDI - UEFISCDI, project no. 212/01.07.2014 (Osseopromote)”.



## Permanent Implant Surfaces Equipped With the Cell Adhesive Plasma Polymer Film PPAAM

Birgit Finke<sup>1</sup>, Henrike Rebl<sup>2</sup>, Uwe Walschus<sup>3</sup>, Michael Schlosser<sup>3</sup>, Carolin Gabler<sup>4</sup>, Carmen Zietz<sup>4</sup>, Rainer Bader<sup>4</sup>, Klaus-Dieter Weltmann<sup>1</sup>, Barbara Nebe<sup>2</sup>

<sup>1</sup>Leibniz Institute for Plasma Science and Technology (INP), Greifswald, Germany

<sup>2</sup>Department of Cell Biology and <sup>4</sup>Department of Orthopedics, Rostock University Medical Center, Rostock,

<sup>3</sup>Department of Medical Biochemistry and Molecular Biology, University Medical Center Greifswald, Germany  
[schlosse@uni-greifswald.de](mailto:schlosse@uni-greifswald.de)

### INTRODUCTION

The rapid cellular acceptance of the implant surface by the surrounding tissue is the crucial factor for the ingrowth in the bone. The aim is the fast and successful osseointegration by improved initial interactions of the titanium surface with bone regenerating osteoblasts. These interactions may be supported by additional bioactive coatings.

Gas-discharge plasma processes are successfully applied for the modification of titanium surfaces. Physico-chemical surface properties like roughness, cleanness, and also chemical coatings determine the cellular acceptance *in vitro* and *in vivo*. The cell adhesion via integrins but also additional adhesion mechanisms via hyaluronan play a key role in the very first encounter with the biomaterial. A new surface functionalization strategy was developed by stimulating the electrostatic immobilization [1,2]. The deposition of plasma polymerized allylamine (PPAAm) leads to the desired surface properties. Furthermore, the knowledge of long term stability, sterizability of such plasma polymer coatings is essential for the use of implants. Besides *in vitro* studies especially *in vivo* investigations show no inflammatory response and an enhanced surface adhesion capacity of these nitrogen containing plasma polymers.

### EXPERIMENTAL METHODS

**Implants and film preparation.** Polished discs and platelets (1-3 cm; 5x5x1cm) from chemically pure Ti-6Al-4V\_P were used as substrates. They were coated with 50–100 nm thin PPAAM films applying low-pressure microwave discharge plasma [1]. Film properties were analyzed by XPS, FT-IR (IRRAS), water contact angle, and surface energy, after film deposition,  $\gamma$ -sterilization and aging.

***In vitro* study.** Human osteoblasts (MG-63 cells) were cultured on the samples in serum-free DMEM [1]. Adhesion and cell cycle phases were calculated by flow cytometry. Spreading and actin cytoskeleton were visualized by confocal microscopy.

***In vivo* study.** The biocompatibility was studied after intramuscular implantation of untreated Ti6Al4V and PPAAM-coated platelets in male LEWIS rats. The inflammatory tissue response was analysed after 7, 14, and 56 days [3].

Custom-made implants were used for the determination of the bone-to-implant contact BIC by  $\mu$ CT [4].

### RESULTS AND DISCUSSION

Closed pinhole-free PPAAM films resistant to hydrolysis and delamination were detected. Advantageous medium hydrophilicity exists.

The density of primary amino groups is at about 2-3 %. It could be shown that not only primary amino groups but also other nitrogen-functional groups as e.g. acid amides or imides play a role for initial cell functions. PPAAM aging processes are not relevant for cell response during one year's storage. Gamma sterilization has no influence on film and also cell adhesion [5].

The positively charged surfaces improve impressively adhesion and spreading of MG-63 osteoblastic cells as initial cellular effect. The PPAAM film enables the cells to literally melt into the structure of the titanium alloy substrate.

No local inflammation processes could be observed.

Implants with PPAAM coating revealed a clear but not significant increase of the bone-to-implant contact BIC (58.5%) compared to uncoated titanium surfaces [4].

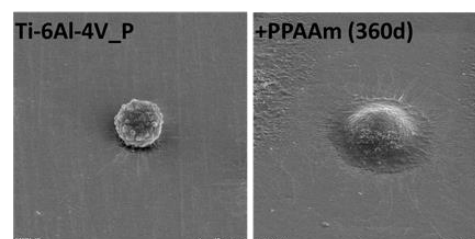


**Figure 1:** Morphology (SEM) of MG-63 cells (after 30 min) on a PPAAM surface stored for 360 d. (magnification 2000x, 45°, DSM 960A, Carl Zeiss; bar = 10 µm)

### CONCLUSION

Although the bioactivation of material surfaces with immobilized proteins and peptides is an established method, our results demonstrate that functionalization of Ti-6Al-4V\_P alone with positively charged nitrogen functional groups carrying plasma polymer films is sufficient enough to improve initial steps of the cellular contact to the material surface significantly.

It could be shown that also other N-functional groups as e.g. acid amides or imides seem to play an important role for initial cell functions as well.

*In vivo* results demonstrate that PPAAM films are biocompatible; local inflammatory reactions do not exist. An increase of BIC could be verified.

### REFERENCES

- [1] Finke B. *et al.* Biomaterials 28:4521-4534, 2007.
- [2] Rebl H. *et al.* Adv. Biomat. 12/8:356-364, 2010.
- [3] Hoene A. *et al.* Acta Biomat. 6:676-683, 2010.
- [4] Gabler C. *et al.* IJMS. 15:2454-2464, 2014.
- [5] Finke B. *et al.* Langmuir 30:13914-24, 2014.

### ACKNOWLEDGMENTS

The study was supported by the Federal Ministry of Education & Research in the Campus PlasmaMed (project PlasmaImp).



## Structure and Biological Response of Multi-layers Deposited on NiTi Shape Memory Alloy

Tomasz Goryczka<sup>1</sup>, Karolina Dudek<sup>1</sup>, Agnieszka Szurko<sup>2</sup>, Beata Świeczko-Żurek<sup>3</sup>

<sup>1</sup>Department of Informatics and Materials Science, Institute of Materials Science, University of Silesia, Poland

<sup>2</sup>Department of Mathematics, Physics and Chemistry, Institute of Physics, University of Silesia, Poland

<sup>3</sup>Department of Materials and Welding Engineering, Faculty of Mechanical Engineering, Gdansk University of Technology, Poland

[tomasz.goryczka@us.edu.pl](mailto:tomasz.goryczka@us.edu.pl)

### INTRODUCTION

The NiTi shape memory alloy has been known from its medical applications<sup>1</sup>. However, relatively long time of its being in the human body environment can cause corrosion as well as migration of nickel ions. Nickel is known from its toxicity. In order to reserve unique shape memory properties of the NiTi alloys for medicine, the surface can be modified with layers, coatings or/and covers. Covering NiTi alloy with multi-layers leads to improvement of its functionality as a material for medical implants.

### EXPERIMENTAL METHODS

Rectangular samples (8mm x 5mm) of commercial NiTi shape memory alloy (49.4at%Ti and 50.6at.%Ni) was used as a matrix for multi-layers deposition. First, polished samples were subjected to oxidizing or nitriding/oxidizing. Next, a hydroxyapatite layer was deposited. Samples were sintered at temperature ranged from 400°C to 800°C and sintering time from 5 minutes to 2 hours. Finally, they were divided into two groups. One group was subjected for studies of the biodegradation in bacteria environment whereas second for fibroblast growing.

### RESULTS AND DISCUSSION

#### Structure of multi-layer deposited on NiTi

The microscopy observations shown that the structure, on the cross section of the layers, is in a nanoscale. Following steps in layer deposition, first the TiN and then the TiO<sub>2</sub> layer was formed on surface of the NiTi alloy. An average thickness of the layer was 26 nm and 32 nm for the TiN and the TiO<sub>2</sub> phase, respectively. Roughnesses of top of the surface varied in the range of several nanometers. On the top of the TiN/TiO<sub>2</sub> layer the hydroxyapatite was deposited with use of electrophoresis. The thickness of the HAp layer was about 2µm. Dependently on the HAp sintering temperature, the roughness of the top layer increased from 5nm to 170 nm.

#### Cytotoxicity of the deposited multi-layers

Experiments were done with use of normal human dermal fibroblasts (NHDF). The cells were growing in the culture medium DMEM/F12. The cell growth was determined from the number of cells, adhesion as well as their morphology after 24, 48, 72, 96 hours from the seeding. The surviving fraction was determined in reference to the control group of cells.

After 24 hours the oxidized surface show comparable degree of cell growth to the control group. Surface covered with sintered the HAp was covered by the fibroblast in lower density than control group. However,

they were growing in colonies and their morphology were not correctly developed. Extending time of cell growth up to 96 hours brought improvement of the fibroblast adhesion. Also, cell morphology got improved and higher number of the correctly developed cells was observed. The lowest proliferation of the cells and their low amount was observed for the surface sintered at 800°C. Surfaces sintered at temperatures between 500°C and 700°C revealed similar properties to the control group. However, number of the cells was lower than one observed on the oxidized surface.

#### Bacteria adhesion and composite biodegradation

Resistivity of the NiTi alloy covered with multi-layers against bacteria adhesion and biodegradation in bacterial environment was carried out with use of bacteria mixture consisted of: "Staphylococcus aureus", "Staphylococcus epidermidis", "Enterococcus faecalis", "Enterobacter cloacae" and "Pseudomonas aeruginosa". Samples were deeped in bacterial solution for 1, 3 and 6 months at 38°C. Covered NiTi without its sintering as well as after HAp sintered at temperature up to 600°C revealed good adhesion for bacteria, biofilm formation and pitting effect event for short time immersion. Increase of the sintering temperature above 700°C improved resistivity for bacteria adhesion as well as a biodegradation of the composite. Even for long time immersion (6 months) no effects of bacteria activity on sample surface was observed.

### CONCLUSION

Reassuming all received results it can be found, that the NiTi shape memory alloy after surface modification, done with deposited multi-layer, improves its properties as potential material for implant application. Multi-layers consisted of titanium nitride, titanium oxide as well as hydroxyapatite sintered at temperatures between 700°C - 800°C are beneficial for the fibroblast growing. Moreover, they can create effective barrier against bacteria adhesion.

### REFERENCES

1. Yoneyama T., Miyazaki S., "Shape Memory Alloys for Biomedical Applications", Woodhead Pub. (2008)

### ACKNOWLEDGMENTS

The authors like to thank professor T. Wierzchoń (University of Technology, Faculty of Materials Science and Engineering) for sample nitriding/oxidizing done by glow discharge technique.

The studies were financially supported from the project N N507 230540 funded by The National Science Centre (NCN).





## Electrochemical Properties of CrSi-based Oxynitrides Deposited on NiCr and CoCr Dental Alloys

Mihai Tarcolea<sup>1</sup>, Mihaela Dinu<sup>1,2</sup>, Ana Gherghilescu (Iulia)<sup>1</sup>, Diana Vranceanu (Maria)<sup>1</sup>,  
Raluca Comaneanu (Monica)<sup>3</sup>, Cosmin Cotrut (Mihai)<sup>1</sup>

<sup>1</sup>University Politehnica of Bucharest, Romania

<sup>2</sup>National Institute for Optoelectronics-INOE2000, Romania

<sup>3</sup>Faculty of Dental Medicine, Titu Maiorescu University of Bucharest, Romania

[mihai.tarcolea@upb.ro](mailto:mihai.tarcolea@upb.ro)

### INTRODUCTION

Chromium nitride and oxynitride layers showed good corrosion resistance and biocompatibility properties<sup>1,2</sup>. For this reason, this type of coatings could be successfully applied in biomedical field, where the action of the corrosive body environment on the used biomaterials could be reduced.

In this study, CrSi-based oxynitrides with protective properties were developed by cathodic arc method. Since the obtained coatings are intended to be used as interlayers between ceramic and metallic components of dental restorations, their electrochemical behaviour in artificial saliva was analysed.

### EXPERIMENTAL METHODS

NiCr and CoCr dental alloy discs with 12 mm diameter were obtained by casting in an induction furnace. 150  $\mu\text{m}$  alumina particles were used for sandblasting of the experimental samples. CrSi-based oxynitrides were deposited on NiCr and CoCr discs using cathodic arc technique in an  $\text{N}_2/\text{N}_2 + \text{O}_2$  mixed reactive atmosphere. The obtained coatings have different grading structures and a total thickness of 2  $\mu\text{m}$ .

Protective properties of the coatings were analyzed by potentiodynamic polarization technique in artificial saliva at 37°C. Pt counter electrode, SCE reference electrode and a working electrode with 1  $\text{cm}^2$  exposed area were used. After the OCP was monitored during 60 min immersion time, the potentiodynamic curves were plotted from -1 V to 1.5V vs. SCE (0.166 mV/s scanning rate) and the main electrochemical parameters were determined ( $E_{\text{corr}}$  - corrosion potential,  $i_{\text{corr}}$  - corrosion current density,  $R_p$  - polarisation resistance).

The surface roughness before and after the electrochemical evaluation was measured using a stylus surface profilometer and the surface morphology was determined by a scanning electron microscope.

### RESULTS AND DISCUSSION

Before electrochemical tests, the Cr-based oxynitrides exhibited a surface roughness between 1.5 and 2  $\mu\text{m}$  as a function of substrate. SEM investigations showed that the obtained coatings have a compact surface without defects.

After 60 min immersion in artificial saliva all the tested coatings exhibited more electropositive potential values as compared with the substrates, indicating a higher corrosion resistance. Among them, the coatings deposited on NiCr alloy showed a higher tendency to form passive films after only ~ 60 s immersion.

The electrochemical parameters also demonstrated the protective behaviour of the CrSi-based oxynitride coatings. The type of the substrate used influenced the

corrosion resistance of the coatings. Thus, the use of NiCr as a substrate resulted in lower values of the  $E_{\text{corr}}$  and  $i_{\text{corr}}$ . The best electrochemical behaviour was exhibited by the CrSi/CrSiN/CrSiON coating, deposited both on NiCr and CoCr.

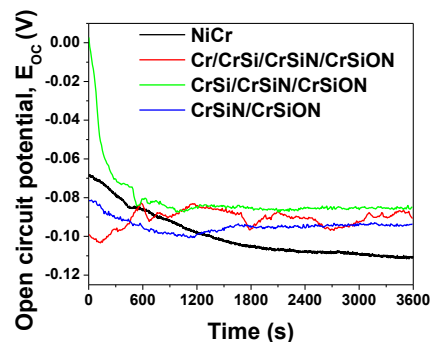


Fig. 1. Open circuit potential of CrSi-based oxynitride coatings deposited on NiCr alloy

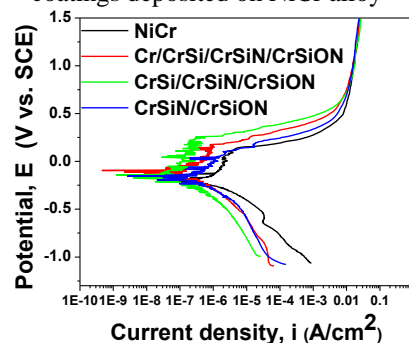


Fig. 2. Potentiodynamic polarisation curves of CrSi-based oxynitride coatings deposited on NiCr alloy

### CONCLUSION

The experimental results showed that CrSi-based oxynitrides with different grading structures deposited on NiCr and CoCr dental alloys by cathodic arc technique improved the corrosion resistance of the substrates. Among them, the CrSi/CrSiN/CrSiON coating exhibited the most electropositive  $E_{\text{OC}}$  values, the lowest corrosion current density and the highest polarisation resistance, irrespective of the substrate type.

### REFERENCES

1. Wierchoń T. *et al.*, Surf. Coat. Technol. 21: 274–279, 2000
2. Lai D. *et al.*, J. Mater. Res. 26: 3020-3031, 2011

### ACKNOWLEDGMENTS

“This work was supported by Partnerships in priority areas program - PN II, developed with support from ANCS, CNDI - UEFISCDI, project no. 175/02.07.2012 (Coat4Dent)”.



## Dynamics of Motion and Agglomeration of Magnetic Nanoparticles in Suspensions under Applied Magnetic Field

Kamil Goc<sup>1</sup>, Tomasz Strączek<sup>1</sup>, Jakub Jurczyk<sup>1</sup>, Witold Prendota<sup>1</sup>, Czesław Kapusta<sup>1</sup>, Agnieszka Szpak<sup>2</sup>, Szczepan Zapotoczny<sup>2</sup>, Maria Nowakowska<sup>2</sup>, Janusz Szmyd<sup>3</sup> and Stanisław Rumian<sup>4</sup>

<sup>1</sup>Department of Solid State Physics, Faculty of Physics Applied Computer Science, AGH University of Science and Technology, Poland

<sup>2</sup>Nanotechnology of Polymers and Biomaterials Group, Department of Physical Chemistry and Electrochemistry Faculty of Chemistry, Jagiellonian University, Poland

<sup>3</sup>Faculty of Energy and Fuels, AGH University of Science and Technology, Poland

<sup>4</sup>Interuniversity Center For The New Techniques and Medical Technologies (UJCM, AGH, PK, AWF), Poland

[Kamil.Goc@fis.agh.edu.pl](mailto:Kamil.Goc@fis.agh.edu.pl)

### INTRODUCTION

Study of dynamics of magnetic nanoparticles (MNPs) is an attractive field of research due to possible applications e.g. in medicine. The knowledge about motion, aggregation and aligning of MNPs is very important when considering bioimaging, drug delivery and magnetic hyperthermia. Presence of interparticle magnetic forces leads to formation of aggregates. They form chain-like structures when interacting with external magnetic field, and undergo displacement when the magnetic field is inhomogeneous.

### EXPERIMENTAL METHODS

Computer simulations of movements of magnetic nanoparticles were carried out at various magnetic field strength (0.0 – 0.4 T) and its gradient (0 - 100 MT/m) in fluids of different density and viscosity (water, glycerine, propanol, liquid epoxy resin) and their results have been verified experimentally. Simulations were taking into account the gravity, buoyancy, and magnetic forces and solving Newton equations for each particle. In the experiments suspensions of magnetic micro- and nanoparticles dispersed in liquid at zero and nonzero applied field have been obtained and observed with optical microscope and SEM/TEM. The images of obtained structures are used for generation of distributions of particles position, concentration and distances between them. The degree of structural anisotropy has been estimated for different samples using Mean Intercept Length and Line Fraction Deviation methods for both simulations and experiment data to compare the quality of final structures formed by magnetic particles. Temperature dependences of the AC susceptibility have been measured for the suspensions of magnetic nanoparticles at the range 4 K – 330 K, i.e. in the solidified and liquid states.

### RESULTS AND DISCUSSION

Computer simulations show an increase in particle dynamics with growing magnetic field. The resultant structures are characterized by longer chains and higher speed of particle displacement. An average spacing between the closest neighbour, which can serve as a measure of the number of aggregated particles, was calculated. It decreases with elapsing time and saturates at nonzero value, which means that there are still some grains not connected to chains. For higher field the

saturation value is an order of magnitude lower than for simulations performed without applied magnetic field.

In the system simulated at no external magnetic field chains combine into closed loops. Magnetic moments of particles form a closed structure due to magnetic interactions between grains. Average velocity of particle translational motion is limited by drag force caused by fluid viscosity. It is the highest in propanol and water but causes that particles collide at relatively high velocity and energy and aggregates are destroyed. In more dense and viscous glycerol and resin the structures formed are more stable – the energy of high speed particles after collision is dissipated by friction.

The results of AC magnetic susceptibility measurements for various frequencies of the alternating field have been analysed. From a step-like change of the real and imaginary susceptibility values the contributions related to Brownian motions have been derived and compared with the predictions obtained from simulations at zero constant magnetic field.

### CONCLUSION

A combined computational and experimental study of dynamics of magnetic nanoparticles reveals a complex character of their behaviour at zero and nonzero DC and AC magnetic fields. It includes occurrence of a pulse-like force of considerable magnitude that can be exerted on adjacent particles or e.g. biological cells. Possible applications of the results in medical therapy (ultrasound, AC magnetic field hyperthermia) and diagnostics (MRI) are discussed.

### REFERENCES

1. Ly H. et al., J. Comp. Phys., 155:160–177, 1999
2. Li H, J. Intel. Mat. Syst. Str. 16:653-658, 2005
3. Badiei A. et al., Phys. Eng. Sci. Med. 29:48-53, 2006

### ACKNOWLEDGMENTS

The work was supported by the National Science Centre, Poland, Project No. 2012/07/B/ST8/03109. Partial support from the European Union from the resources of the European Regional Development Fund under the Innovative Economy Programme (grant coordinated by JCET-UJ, No. POIG.01. 01.02-00-69/09) is acknowledged.



<sup>1</sup>Department of Biomaterials, Faculty of Materials Science and Ceramics, AGH – University of Science and Technology, Krakow

<sup>2</sup>Faculty of Materials Science and Engineering, Warsaw University of Technology, Warsaw  
[afrazcek@agh.edu.pl](mailto:afrazcek@agh.edu.pl)

## INTRODUCTION

For several years, interest in nanomaterials, especially carbon nanomaterials, has been increasing in the fields of biology and medicine. Bearing in mind a number of the unusual properties of these materials such as their electrical and mechanical properties, as well as the possibility of modifying their surfaces using chemical and biological substances, gives those involved with them hope for nerve tissue regeneration and stimulation<sup>1,2</sup>. Nanomaterials deposited on the surface of different traditional materials such as metal may serve as a kind of protective coating on standard metal electrodes, such as those used in deep brain stimulation (DBS), to protect them from increased proliferation of glial cells and glial scar formation that affects the transfer of electrical impulses from the electrode to the tissue. In order to analyze the effects of nanomaterials on nerve cells, the physicochemical properties of these nanomaterials, the properties of coatings made from these materials on the surfaces of metallic substrates, and also the interaction at the interface of metal-carbon nanomaterials should be understood in detail. The physicochemical analysis is the first stage of research of carbon nanomaterials coatings for their potential application in nerve cells regeneration and stimulation.

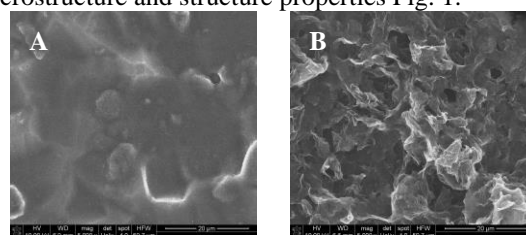
## EXPERIMENTAL METHODS

Two types of multi walled carbon nanotubes (MWCNTs) differing in kind of chemical groups on their surface and one kind of graphene were selected to the experiments. One of the MWCNTs have carboxyl (-COOH) and one hydroxyl (-OH) groups. Nanomaterials were deposited by an electrophoretic deposition (EPD) method on titanium substrates, which was prepared in an appropriate way to ensure good adhesion of MWCNTs and hybride (combination MWCNTs and graphene) coatings. For this purpose titanium substrates were chemically etched in two types of solution; in 5% HF solution and in mixture of concentrated HF:HNO<sub>3</sub> acids. During EPD process two parameters were optimized such as deposition time and voltage value. Carbon nanomaterials coatings on titanium were subject to a detailed assessment: the integrity of the carbon coating's bonding to the substrate, the continuity and thickness of the coatings, their morphology, microstructure and structural properties. For these investigations several methods such as SEM, TEM, AFM, FTIR and Raman spectroscopy were used.

## RESULTS AND DISCUSSION

Our investigations demonstrated that thickness, homogeneity, integrity of carbon coatings to titanium

substrates strongly depend on duration of the EPD process and voltage value. Also types of chemically etched of titanium substrates have big impact for coating adhesion. The physicochemical properties such as wettability and surface energy, which are very important from the point of view of the cellular response, strongly depend on functional groups on MWCNTs surface. The presence of graphene in MWCNTs coatings influence their morphology, microstructure and structure properties Fig. 1.



Figures 1 presents SEM morphology of carbon nanomaterials coatings containing only MWCNTs (A) and MWCNTs with graphene (B) (hybrid coating). The presence of several percent of graphene in MWCNT-based coatings also improves their adhesion to the titanium substrates.

## CONCLUSION

An exists several parameters such as time deposition of carbon nanomaterials, presence of functional groups on MWCNTs surface, voltage value and presence of another type of nanocarbon such as graphene which have significant impact on carbon nanomaterials coatings deposited on titanium surface. By optimizing the EPD process conditions it is possible to obtained carbon nanomaterials coatings which could be used as a potential substrates for nerve cells stimulation and regeneration.

## REFERENCES

1. Fraczek-Szczypta A., Mater. Sci. Eng., C. 34: 35–49, 2014
2. Cellot G, *et al.* Nat. Nanotechnol. 4:126-133, 2009

## ACKNOWLEDGMENTS

The authors would like to thank the National Science Centre (Grant no: UMO-2013/11/D/ST8/03272) for providing financial support to this project.

## INTRODUCTION

Stainless steel (SS) 316L has been applied in medicine for fabrication of implantable devices such like stents or artificial valves. The surface of steel induces dangerous biochemical events such like blood clotting<sup>1</sup> and thus superficial coating is demanded. Surface pre-treatment is an obligatory initial step of SS 316L surface modification since the surface naturally presents oxides layer that needs to be removed in order to provide proper adhesion between organic layer and metal<sup>2</sup>. In existing body of literature there are several methods of SS 316L pre-treatment reported. Nevertheless, we state that provided data are not sufficient and there are still many controversies among this subject. In present work we focused on comparing the usability of two different methods of oxides layer removal as the initial step of SS 316L surface coating.

## EXPERIMENTAL METHODS

In this work we applied two methods of SS 316L pre-treatment: a) electropolishing and b) mechanical polishing. We use flat SS 316L discs (ø14mm) as we consider it be a comfortable model of an SS object.

### *Electropolishing of SS 316L surface*

Electropolishing bath consisted of H<sub>3</sub>PO<sub>4</sub> (60% v/v), H<sub>2</sub>SO<sub>4</sub> (35% v/v) and triethanolamine (5% v/v). We studied the influence of time of the process, temperature and current density. Samples were then cleaned and dried.

### *Mechanical polishing of SS 316L surface*

Different methods were applied, such as grinding with abrasive paper of different gradation and polishing with a polish past. Samples were then cleaned and dried.

### *Analysis of coatings*

Obtained surfaces quality was investigated with the use of infrared spectroscopy (FTIR-ATR) and electron microscopy (SEM). Roughness of the layers (R<sub>a</sub>) was determined (optical profilometry).

## RESULTS AND DISCUSSION

### *Electropolishing of SS 316L surface*

Unlike the authors<sup>3</sup> who studied electropolishing process we found that this actual combination of process parameters does not lead to obtain smooth SS 316L surface. Current density, temperature and polishing time need to be carefully selected to avoid breaches and irregularities. For 55°C and 15 min we achieved the smoothest surface with no traces of oxides, nevertheless further studies revealed that such “mirror-like” surface precludes organic layer deposition in the next step of SS 316L surface modification, which was not clearly pointed out by other authors.

### *Mechanical polishing of SS 316L surface*

We found that this is the easiest and the fastest way to both remove the oxides and standardize all samples' surface. However, after the pre-treatment the surfaces presented relatively high roughness (e.g. R<sub>a</sub> = 173nm). High roughness value of the surface of a blood-contacting material needs to be avoided since it could increase the risk of thrombosis. Thus, further study concerning the effect on blood is demanded. So far, very few authors<sup>4</sup> have undertaken such detailed research and more data is still needed. Also, it has to be remembered that mechanical polishing cannot be applied for stents pre-treatment.

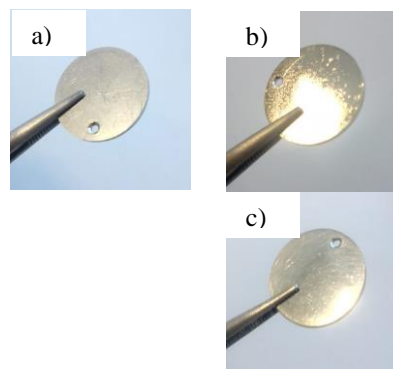


Fig. 1. The appearance of SS 316L surface: a) untreated, b) electrochemically polished, c) mechanically polished

## CONCLUSION

Although we present rather basic study, we believe that it would help to select a proper method of metallic surface pre-treatment since the majority of authors focus on the stage on coating and not on the stage of preparing the surface. So far, we state that mechanical polishing gives better results than electrochemical polishing. In case of stents, other method could be applicable, such like acidic etching.

## REFERENCES

1. Ratner B.D., *et al.*, Annu Rev Biomed Eng 6:41–75, 2004
2. Haidopoulos M, *et al.*, J Mater Sci: Mater Med 17:647–657, 2006
3. Łyczkowska, E., *et al.*, Przem Chem 92:1364–1366, 2013
4. Mileret, V., *et al.*, J Biomed Mater Res Part B: Appl Biomater 00B:001–012, 2014

## ACKNOWLEDGMENTS

The authors would like to thank National Science Centre Poland (Grant no: 2013/11/N/ST8/00636) for providing financial support to this project.



Tobias Schmitz<sup>1</sup>, Maren Jannasch<sup>1</sup>, Tobias Weigel<sup>1</sup>, Sabine Gaetzner<sup>1</sup>, Jan Hansmann<sup>1</sup>

<sup>1</sup>University Hospital Wuerzburg, Junior Research Group ETface, Chair of Tissue Engineering and Regenerative Medicine, Roentgenring 11, 97070 Wuerzburg  
[Tobias.Schmitz@uni-wuerzburg.de](mailto:Tobias.Schmitz@uni-wuerzburg.de)

## INTRODUCTION

Current cardiac electrodes limit the lifetime of pacemakers. Approximately one percent of the energy that is available in a battery of current cardiac pacemakers is used for the regular stimulation of cardiomyocytes. More than half of the stored energy is lost by leakage currents and at the interfaces between pacemaker and tissue – the electrodes that are implanted at the heart muscle.

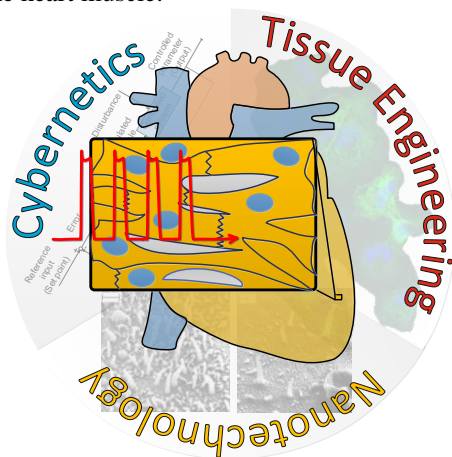


FIGURE 1: To optimize the electrode-tissue interaction, interdisciplinary methods are employed. The approach includes Cybernetics, Nanotechnology and Tissue Engineering.

The implantation of an electrode induces the migration of immune cells from the vasculature to the electrode surface [1]. After an acute inflammation, macrophages stimulate cells from the connective tissue such as fibroblasts to migrate to the implant via chemokines. The macrophages and fibroblasts form a two-layered fibrous capsule that insulates the electrode from the body, and increases the electric resistance [2]. By controlling the foreign body reaction, the lifetime of the battery/ pacemaker could be extended.

## EXPERIMENTAL METHODS

The aim of the project is to realize seamless electronic-tissue interfaces for efficient electronic-tissue communication. Therefore, methods of Cybernetics, Nanotechnology and Tissue Engineering are employed (see Figure 1).

## RESULTS AND DISCUSSION

By generating nano- and microstructured electrode surfaces, the cell-material interaction is controlled to modulate immunological reactions. To analyze the cellular crosstalk that results in encapsulation of the implant, computational modelling is performed. Additionally, the distribution of the electric potential at a given nanostructured surface is investigated by simulations prior to experimental studies.

## CONCLUSION

Based on methods of tissue engineering, an in vitro model will be developed as a standardized test platform for the characterization of the generated electrodes. These test systems will fulfill the electrophysiological properties of myocardial tissue. Furthermore, the foreign body reaction will be included to study the integration of a nanostructured electrode.

## REFERENCES

- [1] Franz, S., et al., Immune responses to implants - A review of the implications for the design of immunomodulatory biomaterials. *Biomaterials*, 2011. 32(28): p. 6692-6709.
- [2] Ratner, B.D., Reducing capsular thickness and enhancing angiogenesis around implant drug release systems. *J Control Release*, 2002. 78(1-3): p. 211-

## ACKNOWLEDGMENTS

The authors would like to thank the Bundesministerium für Bildung und Forschung (BMBF) for providing financial support to this project.

## Improvement of Bioactivity of Vanadium-Free Titanium Alloy using Plasma Electrolytic Oxidation

Maciej Sowa<sup>1</sup>, Magdalena Piotrowska<sup>1</sup>, Magdalena Widziołek<sup>2</sup>, Grzegorz Dercz<sup>3</sup>, Grzegorz Tylko<sup>2</sup>, Tadeusz Gorewoda<sup>4</sup>, Anna M. Osyczka<sup>2</sup>, Wojciech Simka<sup>1</sup>

<sup>1</sup>Faculty of Chemistry, Silesian University of Technology, Poland

<sup>2</sup>Faculty of Biology and Earth Sciences, Jagiellonian University, Poland

<sup>3</sup>Institute of Materials Science, University of Silesia, Poland

<sup>4</sup>Institute of Non-Ferrous Metals, Poland

[maciej.sowa@polsl.pl](mailto:maciej.sowa@polsl.pl)

### INTRODUCTION

Concerns regarding cytotoxic properties of vanadium and possible neurotoxicity of aluminium were raised years ago<sup>1</sup>, which led to the belief that a substitute for notoriously applied Ti-6Al-4V alloy needs to be devised. One of such candidate alloys for this purpose is Ti-13Nb-13Zr alloy, which not only exhibits higher corrosion resistance in physiological fluids compared to that of Ti-6Al-4V<sup>2</sup> but also has a notably lower elastic modulus<sup>3</sup>. The latter has a significant effect on stress shielding of the load bearing elements of orthopaedic implants.

Nevertheless, attempts to improve surface properties of this alloy are still made as they play a key role in the overall response of the host organism upon implantation<sup>4</sup>.

Plasma electrolytic oxidation (PEO) is an electrochemical technique of surface modification of valve metals (capable of growing insulating passive oxide layers). The metallic surfaces treated by PEO are porous and enriched with electrolyte species present in anodising baths<sup>5</sup>. By introducing bio-elements (such as Ca and P) into oxide layers bioactivity of the surface can be enhanced<sup>6</sup>.

This work is concerned with surface modification of Ti-13Nb-13Zr alloy by PEO process in Ca containing electrolytes.

### EXPERIMENTAL METHODS

Disc-shaped samples (diameter = 8 mm) of Ti-13Nb-13Zr alloy (BIMO metals) after electropolishing were subjected to anodising (Kikusui, 800H DC power supply) at constant current density in calcium formate and calcium lactate solutions with different concentration at voltages of 200 and 400 V.

The resulting coatings were characterised by a large gamut of experimental techniques: SEM/EDX (Hitachi S-3400N /Thermo Noran), AFM (NanoScope E, Digital Instruments), XRD (X-Pert Philips PW 3040/60), XPS (PHI 5700, Physical Electronics) and XRF (ZSX Primus, Rigaku). Bioactivity was assessed by the use of SBF soaking and biological studies using adult human bone marrow derived mesenchymal stem cells (hBMSC).

### RESULTS AND DISCUSSION

The results of SEM/EDX investigations have shown that surface morphology was highly influenced by the anodising voltage and electrolyte composition. Rougher

and more porous surfaces were obtained at higher concentrations of calcium salts and higher voltages. The incorporation of calcium into the oxide layer was the most significant in the case of 1 M Ca(HCOO)<sub>2</sub> electrolyte solution.

Rutile and anatase TiO<sub>2</sub> phases were identified in the oxide layers. Calcium was present in the form of calcium oxide and calcium carbonates as was determined by XPS. Additionally, it was found Ca was uniformly distributed within the oxide layers. The coating obtained from 0.1 M calcium lactate solution was additionally enriched with the salt in the unchanged form (Ca(C<sub>2</sub>H<sub>4</sub>OHCOO)<sub>2</sub>).

SBF soaking tests showed that no calcium phosphates were precipitated after 4 weeks. However some crystallites of CaO were observed. Their number increased slightly after each week of immersion.

hBMSC cultures has shown that the anodised surfaces are suitable for proliferation of the cells. The most notable seems to be the surface obtained after anodising in a 0.1 M calcium lactate solution as stem cells colonise the surface and form a 3-D structures. Moreover, Col 1 mRNA gene expression determined for this sample was approximately 20-fold higher compared to the electropolished Ti alloy sample.

### CONCLUSION

Authors proposed a method of surface modification of vanadium-free Ti-13Nb-13Zr alloy which consisted of electropolishing and plasma electrolytic oxidation of the alloy in calcium formate and calcium lactate solutions. The examinations have shown that the procedure has a positive effect on the overall bioactivity of Ti-13Nb-13Zr alloy.

### REFERENCES

1. David A. *et al.* J Appl Biomater 6:109, 1995
2. Khan M.A. *et al.* Biomaterials 20:631, 1999
3. Geetha M. *et al.* Prog Mater Sci 54:397, 2009
4. Cooper L.F. J Prosthet Dent 84:522, 2000
5. Yerokhin A.L. *et al.* Surf Coat Tech 122:73, 1999
6. Campbell A.A. Mater Today 6:26, 2003

### ACKNOWLEDGMENTS

This work was supported by the Polish Ministry of Science and Education under research project nos. IP 2012 0459 72 (Wojciech Simka) and 2011/01/B/NZ4/00664 (Anna M. Osyczka).



Eva Jablonská<sup>1\*</sup>, Penelope M. Tsimbouri<sup>2</sup>, Jaroslav Fojt<sup>3</sup>, Matthew J. Dalby<sup>2</sup>, Jan Lipov<sup>1</sup>, Tomáš Ruml<sup>1</sup>

<sup>1</sup>Department of Biochemistry and Microbiology, University of Chemistry and Technology, Prague, Czech Republic

<sup>2</sup>Centre for Cell Engineering, Institute of Molecular, Cell and Systems Biology, University of Glasgow, Scotland, UK

<sup>3</sup>Department of Metallic materials and Corrosion Engineering, University of Chemistry and Technology, Prague, Czech Republic

[eva.jablonska@vscht.cz](mailto:eva.jablonska@vscht.cz)

## INTRODUCTION

Titanium and its alloys have been widely used for permanent orthopaedic implants; however, they are considered as bioinert, which means that fibrous layer is often formed on the implant-bone interface. For better integration of the implant that could accelerate healing and prolong lifespan of the implant, material surfaces can be modified in various ways. It has been shown that nanotopography influences cell adhesion and differentiation<sup>1</sup>. Anodic oxidation in appropriate electrolytes<sup>2</sup> is a method which can be used for scale-up nanopatterning of metallic materials. Specific parameters of the nanotubes and their influence on the cell growth have been extensively studied recently. Interestingly, various authors obtained contradictory results when performing *in vitro* tests with TiO<sub>2</sub> nanotubes (diameter 15 – 100 nm) using mesenchymal stem cells (MSCs)<sup>3,4</sup>.

Our aim was to perform *in vitro* tests with nanotubular surfaces on commercial titanium alloy and to study the influence of the nanostructure on the adhesion, growth and differentiation of human bone marrow-derived MSCs.

## EXPERIMENTAL METHODS

Cylindrical discs of Ti-6Al-4V alloy with nanotubes (50 nm and 100 nm in diameter) were used. Polished discs of the same alloy served as a control. Human bone marrow-derived MSCs were seeded onto the surfaces at a density of 5,000 cells·cm<sup>-2</sup>. After three days, cells were fixed, permeabilized and stained with DAPI, phalloidin-FITC and immunostained for vinculin (primary anti-vinculin antibody, secondary biotinylated antibody, TexasRed-streptavidin). Images were taken at 10x magnification using epifluorescence microscope Olympus BX51. Samples were subsequently processed for electron microscopy according to a standard protocol and analysed by FEI Quanta 200F ESEM.

## RESULTS AND DISCUSSION

Our previous experiments with Saos-2 cell line showed no differences in cell numbers on nanostructures compared to control (unpublished data). However, we observed decreased adhesion of human bone marrow derived MSCs after 3 days of growth on the surfaces. Also the cell shape area was smaller compared to control (Fig. 1, A, C, E). These observations suggest potential change in cell phenotype that may subsequently lead to reduction in fibrogenesis. We also detected less filopodia compared to control (Fig. 1 B, D, F), which could imply decreased cell motility.

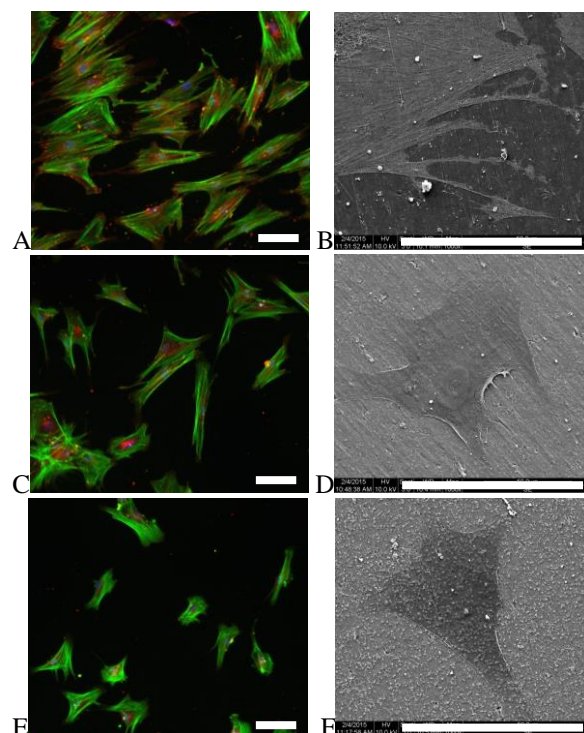


Fig. 1 Human bone marrow derived MSCs on Ti-alloy samples (A, B – flat control, C, D – nanotubes 50 nm, E, F - nanotubes 100 nm in diameter) after 3 days of growth. Green – actin, red – vinculin, blue – nuclei. Scale bar equals to 100 µm.

## CONCLUSION

Surface nanotubular structures on Ti-alloy altered cell adhesion and morphology. Determination of markers of differentiation and stemness by immunofluorescence microscopy and also at mRNA level using qPCR will follow in order to uncover the cell responses to the surfaces.

## REFERENCES

1. Dalby M.J. *et al.*, Nature Mater. 13:558-569, 2014
2. Regonini D. *et al.*, Mater. Sci. Eng., R. 74:377-406, 2013
3. Park J. *et al.*, Nano Lett. 7:1686-1691, 2007
4. Oh S. *et al.*, P Natl Acad Sci USA, 106:2130-2135, 2009

## ACKNOWLEDGMENTS

Financial support from specific university research (MSMT No 20/2015) and the Technology Agency of the CR (project no. TE01020390).

E. Diana Giol<sup>1</sup>, Sandra Van Vlierberghe<sup>1,2</sup> and Peter Dubruel<sup>1</sup><sup>1</sup>Polymer Chemistry and Biomaterials Research (PBM) Group, Ghent University, Belgium;<sup>2</sup>Brussels Photonics Team, Vrije Universiteit Brussel, Belgium[elenadiana.giol@ugent.be](mailto:elenadiana.giol@ugent.be)

## INTRODUCTION

The excellent bulk properties of poly(ethylene terephthalate) (PET) including mechanical strength and chemical resistance, propelled it as one of the few materials considered suitable for long-term cardiovascular applications. However, its poor surface properties negatively influence its biological performance (e.g. haemo- and biocompatibility) and represent the major drawback of pristine PET.

To date, a wide variety of surface modification strategies (physical and/or chemical) has been pursued to improve the surface properties of PET. Physical strategies generally result in low stability coatings or imply the use of toxic substance (e.g. glutaraldehyde) in order to increase their stability<sup>1</sup>. Chemical approaches provide a more stable coating. In the latter case, the outer layer is generally functionalized with alcohols, carboxylic acids, amines, etc., that are further used as anchoring points for the covalent coupling of proteins, anti-inflammatory agents (e.g. gamoxilicin, amikacin) or anti-coagulants (e.g. heparin). The main drawback is the need for complex procedures which demand time-consuming protocols under harsh chemical conditions and often compromise the mechanical properties of PET. Consequently, novel concepts are required in this field. In the present study, we propose the covalent immobilization of gelatin on PET *via* two different surface functionalization strategies: 1) the use of a perfluoro aromatic succinimide ester and 2) dopamine. A comparative study between thus-modified PET surfaces was initiated in an attempt to identify the most promising protocol. Gelatin has been selected due to its non-toxic nature, biodegradability, low price and cell-interactive properties<sup>2</sup>.

## EXPERIMENTAL METHODS

A two-step surface modification strategy was applied to PET. The surface of PET was functionalized with 4-azido-2,3,5,6-tetrafluorobenzoic acid, succinimidyl ester (AFB) by UV-C treatment (15 min, 254 nm) and gelatin type B (GelB, 5w%) was subsequently immobilized. In parallel, a dopamine-based coating procedure<sup>3</sup> was used to facilitate the GelB coating (5w%) to become immobilized.

An in depth study of the gelatin-modified PET surfaces was pursued. The surface morphology was assessed by atomic force microscopy (AFM) and scanning electron microscopy (SEM), the coating composition and homogeneity was verified by X-ray photoelectron spectroscopy (XPS) and static contact angle (SCA) measurements, while the coating stability was analyzed *via* radiolabelling experiments.

## RESULTS AND DISCUSSION

For both strategies, the appearance of a distinctive peak in the XPS spectra characteristic for N (10 to 12 at%) together with a sharp decrease in hydrophobicity ( $SCA_{PET} = 73^\circ C$ ,  $SCA_{PET-GelB} \sim 50^\circ C$ ) confirmed the successful immobilization of GelB on PET. Although no distinct differences were observed between the chemical compositions of the final gelatin coated surfaces *via* the two above-mentioned functionalization methods, AFM indicated the presence of different morphologies and roughness profiles (see Figure 1).

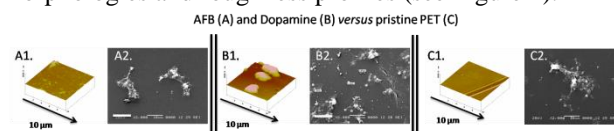


**Figure 1.** AFM profile images of gelatin modified PET immobilized *via* AFB strategy (A1), dopamine (B1) and pristine PET (C1); SEM images showing platelet adhesion on gelatin modified PET (A2, B2 and C2). The Z scale for AFM is 3600nm and the scale bars for the SEM images are 10  $\mu m$ , and.

A roughness value being a 7-fold lower was noticed for the AFB-based strategy compared with the dopamine methodology ( $R_{RMS, AFB} = 18 \text{ nm}$ ,  $R_{RMS, dopamine} = 132 \text{ nm}$  for a scan size  $10 \times 10 \mu m^2$ ). As expected, platelet activation slightly increased with surface roughness, but, overall, it was much lower than for pristine PET.

## CONCLUSION

The main aim of the present work was to compare two different surface modification strategies adequate to obtain a stable/durable protein coating on PET for cardiovascular applications. Both AFB and dopamine based approaches successfully facilitate the covalent immobilization of GelB, but strategy-specific surface morphologies were noticed. Preliminary platelet adhesion tests indicated a superior behavior of modified surfaces compared with pristine PET. Future perspectives include the transition of the surface modification strategies from 2D to 3D tubular structures which can be inserted into veins.

## REFERENCES

1. Chen H. *et al.*, Prog Polym Sci. 33(11):1059-1087, 2008;
2. Van Vlierberghe S. *et al.*, Polymers 3(1):114-130, 2011;
3. Haeshin L. *et al.*, Science. 318:426-430, 2007;

## ACKNOWLEDGMENTS

The authors would like to thank Ghent University and the Research Foundation Flanders (FWO) for the financial support.



# The Influence of NiTi-Alloy Surface Passivation on Biofilm Formation by *Desulfovibrio desulfuricans* Bacteria

Beata Cwalina<sup>1</sup>, Weronika Dec<sup>2</sup>, Joanna Michalska<sup>3</sup>, Marzena Jawoska-Kik<sup>4</sup>, Wojciech Simka<sup>5</sup>

<sup>1,2</sup>Department of Environmental Biotechnology, Silesian University of Technology, Poland

<sup>3</sup>Institute of Materials Sciences, Silesian University of Technology, Poland

<sup>4</sup>Department of Biopharmacy, Medical University Of Silesia, Division Of Pharmacy, Poland

<sup>5</sup>Department of Inorganic, Analytical Chemistry and Electrochemistry, Silesian University of Technology, Poland

[beata.cwalina@polsl.pl](mailto:beata.cwalina@polsl.pl)

## INTRODUCTION

NiTi alloys are widely used for many purposes including medical and technical applications. Metabolic activity of sulphate-reducing bacteria (SRB) such as *Desulfovibrio desulfuricans* species may lead to corrosion of various metals<sup>1</sup>. It has been demonstrated that also titanium and its alloys may corrode in the presence of these bacteria strains<sup>2,3</sup>. In this study, the influence of the NiTi-alloy surface passivation on the biofilm formation by *D. desulfuricans* bacteria in the presence of artificial saliva or inflammatory saliva has been investigated.

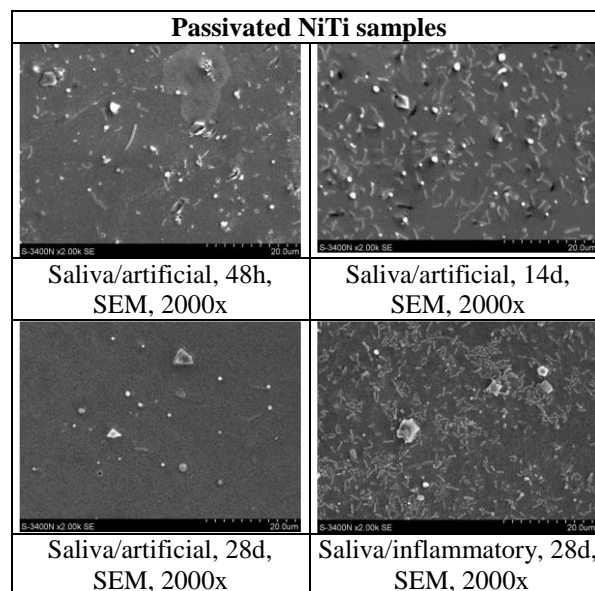
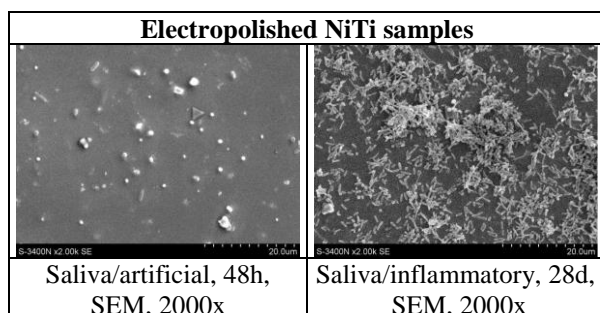
## EXPERIMENTAL METHODS

The samples of NiTi were electropolished or passivated, then cleaned in ethanol in an ultrasonic bath, air dried, and sterilized at 180°C. The sterile samples were placed into tubes containing the artificial or inflammatory saliva and then were inoculated with bacteria *Desulfovibrio desulfuricans* (standard soil strain DSM and two wild intestinal strains). As control samples, the sterile systems without bacteria were used. The tubes were incubated at 30°C under anaerobic conditions. Biofilm formation was studied after 48 hours and after 7, 14, 28 days of samples' incubation, using following methods: assay of protein concentration in a medium, extraction of extracellular polymeric substances (EPS), and examination of bacterial biofilms using scanning electron microscope (SEM) analysis.

## RESULTS AND DISCUSSION

Table 1 presents examples of biofilms formed by DSM strain in artificial or inflammatory saliva on a surface of the NiTi electropolished or passivated samples.

Table 1. Growth of *D. desulfuricans* DSM strain on surface of the NiTi-alloy samples (electropolished or passivated), submerged in artificial or inflammatory saliva.



Diversity between intensity of biofilms formation by *D. desulfuricans* on the NiTi samples surface was due to the alloy surface state (electropolished or passivated) as well as to character of artificial saliva. Inflammatory state of saliva proved to be especially important factor promoting the bacteria growth on NiTi surface, also after its passivation.

## CONCLUSION

It has been demonstrated that *D. desulfuricans* can form biofilms in the presence of both artificial and inflammatory saliva on the NiTi alloy surface, even when it was passivated. However, inhibition of the biofilm growth on passivated surface of alloy was observed after 28 days, whereas the mature biofilm was formed during this time on the NiTi samples immersed in inflammatory saliva.

## REFERENCES

1. Dzierżewicz Z. *et al.*, Res. Microbiol. 148:785-793, 1997.
2. Rao T. *et al.*, Corros. Sci. 47:1071-1084, 2005.
3. Cwalina B. *et al.*, Solid State Phenom. 227:302-305, 2015.

## ACKNOWLEDGMENTS

This work was supported by the research project No N N518 291940 (Polish National Science Center), using equipment purchased in the project "BIO-FARMA" Silesia. Centre for Biotechnology, Bioengineering and Bioinformatics", co-financed by ERDF OP IG, 2007-2013.



# Dynamics of Biofilm Formation by *Desulfovibrio desulfuricans* Bacteria on Grinded Surface of NiTi-Alloy

Beata Cwalina<sup>1</sup>, Weronika Dec<sup>2</sup>, Joanna Michalska<sup>3</sup>, Marzena Jawoska-Kik<sup>4</sup>, Wojciech Simka<sup>5</sup>

<sup>1,2</sup>Department of Environmental Biotechnology, Silesian University of Technology, Poland

<sup>3</sup>Institute of Materials Sciences, Silesian University of Technology, Poland

<sup>4</sup>Department of Biopharmacy, Medical University Of Silesia, Division Of Pharmacy, Poland

<sup>5</sup>Department of Inorganic, Analytical Chemistry and Electrochemistry, Silesian University of Technology, Poland

[beata.cwalina@polsl.pl](mailto:beata.cwalina@polsl.pl)

## INTRODUCTION

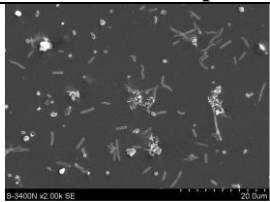
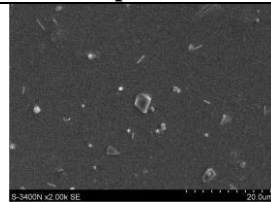
Titanium and its alloys possess exceptional corrosion resistance in various aggressive environments including mouth. For that reason, they are also used as orthodontic alloys<sup>1</sup>. For example, the nickel-titanium (NiTi) alloys are applied in the endodontic instruments in form of super-elastic wires for root canal treatment. Among many other, the sulphate-reducing bacteria (SRB) can be present in mouth, mainly in tooth plaque and cavities<sup>2</sup>. SRB such as *Desulfovibrio desulfuricans* species may be responsible for corrosion of many metals, including titanium and its alloys<sup>2-4</sup>. The aim of this study was to investigate the dynamics of *D. desulfuricans* growth on grinded surface of NiTi-alloy in solution of artificial saliva, also with the inflammatory state.

## EXPERIMENTAL METHODS

The NiTi samples were electropolished or grinded, then cleaned in ethanol in an ultrasonic bath, air dried, and sterilized at 180°C. The sterile samples were placed into tubes containing the artificial or inflammatory saliva and then were inoculated with bacteria *D. desulfuricans* (standard soil strain DSM and two wild intestinal strains: DV/A, DV/B). As control samples, the sterile systems without bacteria were used. The tubes were incubated at 30°C under anaerobic conditions. Biofilm formation was studied after 24 and 48 hours, and after 7, 14 and 28 days of samples' incubation, using following methods: assay of protein concentration in a medium, extraction of extracellular polymeric substances (EPS), and examination of bacterial biofilms using scanning electron microscope (SEM) analysis.

## RESULTS AND DISCUSSION

Table 1. Dynamics of growth of *D. desulfuricans* biofilm (DV/A strain) on surface of the NiTi-alloy samples (electropolished or grinded), submerged in artificial or inflammatory saliva.

Electropolished NiTi samples	
	
Saliva/inflammatory, 24h, SEM, 2000x	Saliva/artificial, 28d, SEM, 2000x

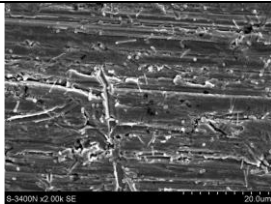
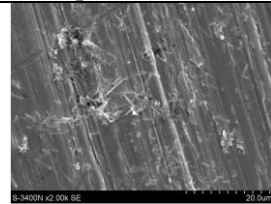
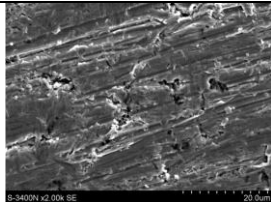
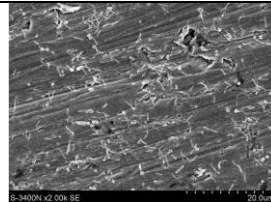
Grinded NiTi samples	
	
Saliva/inflammatory, 24h, SEM, 2000x	Saliva/inflammatory, 48h, SEM, 2000x
	
Saliva/inflammatory, 14d, SEM, 2000x	Saliva/artificial, 28d, SEM, 2000x

Table 1 presents examples of biofilms formed on the NiTi-alloy surfaces (electropolished or grinded) after incubation with *D. desulfuricans* strain DV/A, in the solutions of artificial or inflammatory saliva.

## CONCLUSION

It has been demonstrated that *D. desulfuricans* can form biofilms on the NiTi alloy surface in the presence of both artificial and inflammatory saliva. However, scratches present on the surface of grinded samples have stimulated the bacteria settlement on alloy surface, and thus induced the biofilm formation. The biofilm growth on the NiTi grinded samples was affected by both the surface roughness as well as the inflammatory state of saliva.

## REFERENCES

1. Papadopoulou K., Eliades T. Aust. Orthod. J. 25:63-75, 2009.
2. Chaturvedi T., Upadhyay S. Indian J. Dent. Res. 21:275-284, 2010.
3. Kameda T. *et al.*, Dental Mat. J. 33:1-9, 2014.
4. Rodrigues D. *et al.*, Materials. 6:5258-5274, 2013.

## ACKNOWLEDGMENTS

This work was supported by the research project Nr N 518 291940 (Polish National Science Center), using equipment purchased in the project "BIO-FARMA Silesia. Centre for Biotechnology, Bioengineering and Bioinformatics", co-financed by ERDF OP IG, 2007-2013.

## An Electrically Conductive Non-Woven Web Made of Microfibrous Poly(L-lactic acid) and Poly(3,4-ethylenedioxythiophene)

Xufeng Niu<sup>1,2</sup>, Mahmoud Rouabhia<sup>4</sup>, Nicolas Chiffot<sup>2,4</sup>, Martin W. King<sup>3,5</sup>, [Ze Zhang](mailto:ze.zhang@chg.ulaval.ca)<sup>2</sup>

<sup>1</sup> Key Laboratory for Biomechanics and Mechanobiology of Ministry of Education, School of Biological Science & Medical Engineering, Beihang University, Beijing, China.

<sup>2</sup> Department of Surgery, Faculty of Medicine, Laval University; Division of Regenerative Medicine, CHU Research Center of Quebec, Quebec, QC, Canada

<sup>3</sup> College of Textiles, North Carolina State University, Raleigh, NC, USA

<sup>4</sup> Oral Ecology Research Group, Faculty of Dentistry, Laval University, Quebec, QC, Canada

<sup>5</sup> College of Textiles, Donghua University, Shanghai, China

[ze.zhang@chg.ulaval.ca](mailto:ze.zhang@chg.ulaval.ca)

### INTRODUCTION

As an emerging biomaterial, PEDOT has proven to be electrically more stable than polypyrrole (PPy). However, in most biomedical related studies, PEDOT was electrochemically polymerized on metal electrodes, which is ideal for sensors but not suitable for tissue regeneration. Electrospun nanofibres made of PEDOT and poly(lactide-co-glycolide), polycaprolactone and chitosan have also been explored. Conductive mat made of electrospun nanofibres normally have pores too small for cell penetration, and also contain rather high percentage of the non-biodegradable conductive polymer because it is bulk rather than surface modification. This study was to present a new conductive nonwoven textile fabric made of biodegradable PLLA and a very thin layer of PEDOT, and to show that the resulting 3D material was electrically stable, easy for cell penetration and retained its textile structure and flexible properties. Such a conductive and largely biodegradable scaffold is easily prepared and would be useful in biomedical applications where a conductive, flexible and fibrous scaffold is needed.

### EXPERIMENTAL METHODS

A thermoplastic fibre grade PLLA resin was heated to 240 °C and melt spun through a spunbond machine. By cooling the web on the moving collector belt a continuous spunbond fabric containing microfibres was produced. The nonwoven PLLA fabric was thoroughly washed to eliminate all chemical residuals left from the manufacturing process. To synthesize the polymer, the PLLA fabric was first immersed in a series of concentrations of EDOT solution in methanol to absorb monomers. Then, FeCl<sub>3</sub> dissolved in deionized water was introduced dropwise onto the EDOT-adsorbed PLLA fabrics to trigger an oxidative polymerization. The polymerisation continued at room temperature for 24h. Finally, the PEDOT-coated PLLA fabrics were thoroughly washed in a solution of MeOH:H<sub>2</sub>O (50:50) to eliminate all residual FeCl<sub>3</sub> and FeCl<sub>2</sub>, and then dried, firstly at 37 °C in a hot air oven, and then in a vacuum oven overnight at room temperature. The surface morphology, surface chemistry and wettability, mechanical property, electrical conductivity and stability were analyzed. Cytotoxicity was tested using human skin fibroblasts. Preliminary experiment was performed to test the feasibility of stimulating cells by

using such conducting scaffold.

### RESULTS AND DISCUSSION

When monomer concentration increased from 0.10 to 0.25 mol/L, the surface resistivity of the fabric decreased dramatically from 49.4 KΩ/square to 0.4 KΩ/square. Further increases in EDOT concentration up to 1.0 mol/L did not significantly affect the surface resistivity. Therefore the optimal concentration in polymerization was found to be 0.25 mol/L. The PEDOT coated fabric appeared dark in color but with no significant change in surface morphology under both optical and scanning electron microscopes, meaning a very thin layer of PEDOT on the microfibers. X-ray photoelectron spectroscopy and water wettability measurements revealed a surface property mixed of PLLA and PEDOT. Thermal analysis showed that the polymerization process did not significantly affect the crystalline structures of the fibres but increased material phase separation. Electrical stability test demonstrated that the PEDOT coated fabric had superior stability than the PPy coated fabric. Cytotoxicity experiment showed that the PEDOT-coated fabric was not toxic to human skin fibroblasts, and supported cell growth as the non-coated fabric did. Finally, the ES activated fibroblasts showed slightly higher proliferation than the controls, showing that this new type of conductive fabric is suitable to mediate ES to cultured cells.

### CONCLUSION

A two-step surface polymerization process was successfully developed to prepare a new type of conductive scaffold based on biodegradable nonwoven web. The fabric web was rendered conductive with other properties not significantly affected. This conductive web can be used as scaffold for cell growth and to mediate ES to the cells.

### ACKNOWLEDGMENTS

This work was supported by the Canadian Institutes of Health Research, the Natural Sciences and Engineering Research Council of Canada, and the Fonds de la recherche en santé du Québec. The first author was supported by The National Natural Science Foundation of China (No. 31470915).





## Electroless Deposition of Calcium-Phosphate Coatings on Ti6Al4V and Their Biological Response

Ena A. Aguilar-Reyes, Benito Jacinto-Díaz, Carlos A. León-Patiño

Instituto de Investigación en Metalurgia y Materiales, Universidad Michoacana de San Nicolás de Hidalgo, México  
[aareyes@umich.mx](mailto:aareyes@umich.mx)

### INTRODUCTION

Titanium implants have relatively low density, high strength and good processability. The surface of such implants exhibits bioactivity, which can be controlled through the titanium oxide layer that forms [1]. In the case of the metal structure with a fine-grained dispersed, the bioactivity can be increased simply through an intense plastic deformation [2]. The application of synthetic calcium phosphate is the most effective way for surface modification, as it provides an osseointegration of metal implant with bone tissue. Calcium phosphate is the main mineral component of bone tissue and the presence of several components of calcium phosphate in the coating provides the possibility to control the biochemical activity through changes to the composition of the phase [3]. This work is aimed at obtaining Ca-P coatings on Ti6Al4V substrates by an autocatalytic route in order to increase the osteoconductivity through biochemical and surface modification.

### EXPERIMENTAL METHODS

Rectangular substrates of dimensions of 10 mm x 10 mm x 1.6 mm were cut from an annealed plate of Ti6Al4V alloy (Titanium Industries, USA) of 1.6 mm in thickness. The samples were pre-treated in an alkali solution of NaOH 5 M for 24 h. Autocatalytic bath solutions of a 1.2 Ca/P molar ratio were prepared through the dissolution of appropriate amounts of  $\text{CaCl}_2$ ,  $\text{NaH}_2\text{PO}_2$ , and  $\text{C}_4\text{H}_4\text{Na}_2\text{O}_4 \cdot 6\text{H}_2\text{O}$  in distilled water. Electroless deposition experiments were carried out at different pH (5.5 and 6.0), temperatures (80 to 90°C) and times (60 and 180 min). After coating, the samples were characterized by FE-SEM, AFM, XRD, and IR spectroscopy.

### RESULTS AND DISCUSSION

The SEM micrographs in Figure 1 show the morphology of the Ca-P coating formed on the Ti6Al4V substrate after being immersed in the autocatalytic bath for a period of 480 minutes (8 hours) at pH 5.5 and at a 80 °C. As it can be seen, these deposits consist of small particles and the substrate is coated on most of its surface.

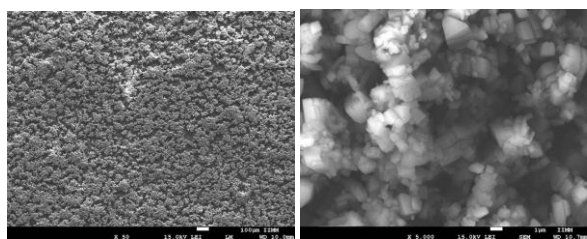


**Fig. 1.** SEM micrographs of Ca/P coatings on Ti6Al4V substrate obtained at 80°C, pH of 5.5 and 480 min of immersion time at 50x and 5000x, respectively.

Figure 2 shows the Ca/P coated surface after immersion in cell media for a period of 6 days. According to the results of cell culture, the obtained coatings showed no cytotoxicity and attachment of cells on the surface.

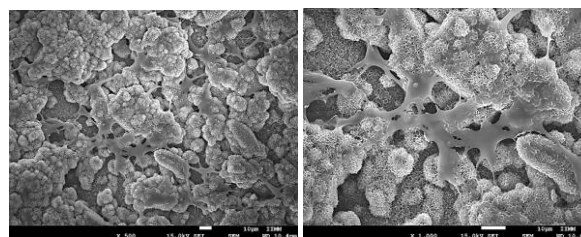


**Fig. 2.** SEM micrographs Ca/P coated-Ti6Al4V substrates after 6 days immersion in MC3T3-E1 preosteoblast subclone 4 cells media at 250x and 1000x, respectively.

### CONCLUSION

The obtained results indicated that it was possible the complete coating of the metallic surface (Ti6Al4V) with a Ca/P layer (100 µm in thickness) after 480 min of immersion in autocatalytic solutions. The morphology and microstructure of Ca/P coatings were directly affected by the different processing conditions such as pH, temperature and time.

Furthermore, calcium phosphate coatings were cytocompatible since adhesion of MC3T3-E1 preosteoblast subclone 4 cells was observed.

### REFERENCES

1. Ellingen J.E., *Biomaterials*. 12:593-596, 1991
2. Valiev R.Z. *et al.*, *Nanotechnologies in Russia* 3:593-601, 2008
3. Barinov S.M., *Russian Chemical Reviews* 279:13-29, 2010

### ACKNOWLEDGMENTS

The authors would like to thank CONACYT (Grant no. CB-2013-C01-222262) and UMSNH (Grant no. CIC-2014-2015-108681) for providing financial support to this project.



## Microhardness of the Polylactide Sheets Modified by Laser

Magdalena Tomanik<sup>1</sup>, Bogusz Stępak<sup>2</sup>, Jarosław Filipiak<sup>1</sup>, Arkadiusz Antończak<sup>3</sup>,  
Krzysztof Abramski<sup>3</sup>, Celina Pezowicz<sup>1</sup>

<sup>1</sup> Department of Biomedical Engineering, Mechatronics and Theory of Mechanisms, Faculty of Mechanical Engineering

<sup>2</sup> Faculty of Microsystem Electronics and Photonics,

<sup>3</sup> Laser & Fiber Electronics Group, Faculty of Electronics,

Wrocław University of Technology, Poland

[magdalena.tomanik@pwr.edu.pl](mailto:magdalena.tomanik@pwr.edu.pl)

### INTRODUCTION

Bioresorbable polymers are the interesting class of materials used for medical devices such as implants and scaffolds<sup>1</sup>. Due to the chemical characteristic those materials does not cause any inflammation in the human body as degrade to non-toxic products<sup>2</sup>. The polymers like polylactide (PLA), polycaprolactone (PCL) poly(lactic-co-glycolic acid) (PLGA) and theirs copolymers are worldwide approved for clinical application and been the subject of many investigations<sup>2,3</sup>.

Despite the growing use of polylactide, there are still unsolved issues regarding the chemical and mechanical properties of the material due to manufacture process.

During the technological processes leading to a product substrate is subjected to a series of actions which could affect the chemical properties of thus changing the mechanical properties.

Shaping polymeric sheets with thickness under 400 microns mechanically can be problematic and not accurate. The use of laser to form the polymer could be the answer in order to obtain good accuracy especially in small objects.

Laser beam has an optical power concentrated to a small area with enough energy to cause the ablation of polymer and in the result cut it. When use under ablation threshold can modify the surface of material by partly degradation.

The aim of the study was to investigate the differences in mechanical properties by defining microhardness of the polylactide sheets exposed to laser light.

### EXPERIMENTAL METHODS

The polymer sheets having a thickness of 340 microns were extruded from commercial medical poly(L-lactide) (Evonic, RESOMER®). Mechanical properties were determined for modified chemical composition of polymer surface by KrF (248 nm) excimer laser. The samples were prepared by irradiation of 5 x 5 mm fragments with increasing number of pulses with same fluence.

Regarding the sheets thickness the method used to characterized specimens was Vickers hardness test method, conducted on microindenter CSM Micro Combi Tester.

During the indentation the force and depth of the penetration are measure, the microhardness HV is calculated as a ratio of the Fi to the lateral surface area of the impression left by the Vickers indenter.

### RESULTS AND DISCUSSION

Conducted studies show that the irradiation of poly(L-lactide) below ablation threshold by the KrF excimer changes the mechanical properties of the surface significant. With the increasing number of irritation pulses on unit of area the polymer become more degraded therefore the decrease of the structure integrity was observed.

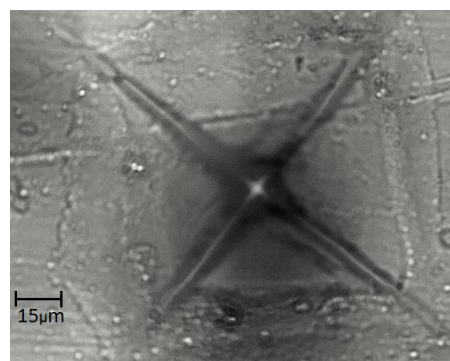


Fig.1. Impression left by the Vickers indenter on non-irradiated PLLA, magnification 200x

### CONCLUSION

Application of the laser technique may be the solution for precise shaping of the thin polymer layers for usage as a medical devices. It should however be noticed that the cutting edges arising are affected by laser beam causing ablation. The hardness of used in experiment poly(L-lactide) changes for different laser beam parameters. Thus linking the mechanical properties with characteristic of the laser beam will be relevant for manufacturing process.

### REFERENCES

1. Hutmacher, D. W., Scaffolds in tissue engineering bone and cartilage," *Biomaterials* 21(24): 2529-2543, 2000.
2. Schnabel, W., Polymer degradation: principles and practical applications, Munich: Hanser, Vol. 131, 1981.
3. Bogusz Stępak *et.al*: Degradation of poly(L-lactide) under KrF excimer laser treatment, *Polym. Degrad. Stab.* 110: 156-164, 2014.

### ACKNOWLEDGMENTS

The authors would like to thank the National Science Centre for providing financial support to research project no: UMO- 2013/09/B/ST8/02423



## The Metal Implants Covered with Hydroxyapatite Coatings and Nanometals Supplements

Beata Świczko-Żurek

Gdansk University of Technology, Faculty of Mechanical Engineering, Narutowicza str.11/12, 80-233 Gdansk, Poland  
[bswiczko@wp.pl](mailto:bswiczko@wp.pl)

### INTRODUCTION

Silver was known for its antibacterial properties as long ago as in antiquity. The Greeks covered their plates and mugs with silver to prevent spread of diseases, they also put silver coins into jugs of water to prolong the duration of the liquid. Greek children were given silver spoons to suck to prevent them from getting ill. In the 90 of the 20<sup>th</sup> century scientists discovered that people with insufficient amount of silver in their bodies are frequently subjected to virus, bacteria and other illnesses. However too much silver introduced into the body may result in necrosis of the liver tissues [1].

### EXPERIMENTAL METHODS

The first research was conducted on specimens covered with nanosilver. The specimens were dipped into the bacteria liquids containing 5 most aggressive bacteria occurring in human body. It was shown by the microscope examinations performed 6 months later, the bacteria didn't form any biofilm. Only separated bacteria were attached to the surface.

The further experiments were followed on the metallic specimens (titanium and titanium alloys) deposited with hydroxyapatite coatings by an use of electrophoretic method, at different voltage and time. Afterwards the nanometals (nanosilver and nanocopper) were implemented into the hydroxyapatite coatings.

The future research is planned to be carried out on cytotoxicity and osteoblast adhesion to the biomaterials. The biological research will be performed in vivo on animals.

### CONCLUSION

To reduce unfavourable phenomena occurring after introducing an implant into human body various modifications of the surface are suggested. Such modifications may have significant impact on biocompatibility of metallic materials. The nanosilver and nanocopper layers are considered most biocompatible. Those layers prevent bacteria from forming the biofilm.

### REFERENCES

[1] Bugla-Płoskońska G., Oleszkiewicz A.: The biological activity of silver and its application in medicine.

<http://ag123.pl/Biologiczna-aktywnosc-srebra-i-jego-zastosowanie-w-medycynie.html>



## Zinc Oxide and Titanium Dioxide-Chitosan Nanocomposites for UV-light Protection

Anna Regiel-Futyr<sup>1</sup>, Małgorzata Kus-Liśkiewicz<sup>2</sup>, Szymon Wojtyła<sup>1</sup>, Grażyna Stochel<sup>1</sup>, Wojciech Macyk<sup>1</sup>

<sup>1</sup>Faculty of Chemistry, Jagiellonian University in Kraków, Poland

<sup>2</sup>Faculty of Biotechnology, Biotechnology Centre for Applied and Fundamental Sciences, University of Rzeszów, Poland  
[anna.regiel@uj.edu.pl](mailto:anna.regiel@uj.edu.pl)

### INTRODUCTION

Due to the UVA and UVB light absorption semiconducting metal oxides nanoparticles (NPs), *e.g.* zinc oxide (ZnO) or titanium dioxide (TiO<sub>2</sub>), are the main components of sunscreen lotions<sup>1</sup>. Their main task is ultraviolet irradiation absorption, reflection and scattering. However, the most important concern in the use of oxides NPs as protective component of suntan lotions is Reactive Oxygen Species generation (ROS) and resulting toxicity. Several efforts are undertaken in order to minimize the photoactivity and thus cytotoxicity of ZnO/TiO<sub>2</sub> materials. Usually deactivation is achieved through their surface chemical modifications with polymers or addition of antioxidants<sup>2</sup>. Herein, we present nanocomposite materials with quenched photoactivity based on zinc and titanium oxide nanoparticles, surface-modified with chitosan (CS).

### EXPERIMENTAL METHODS

Two grades of commercially available ZnO-NPs and TiO<sub>2</sub>-NPs, varying in the average particle size, were utilized in our studies. Chitosan with medium average molecular weight was chosen for semiconductors modification (~1300 kDa). Chitosan modified ZnO/TiO<sub>2</sub>-NPs were prepared by ionic-gelation technique with sodium tripolyphosphate (TPP) as a cross-linking agent. Physicochemical characterization of the materials was conducted with application of several techniques. The average hydrodynamic diameter and zeta potential before and after surface modification were measured by Dynamic Light Scattering technique (DLS). Scanning Electron Microscopy (SEM) was used for materials morphology visualization. Chemical composition and sample purity was assessed *via* Energy Dispersive Spectroscopy (EDS). X-Ray diffraction measurements were performed to determine the crystalline pattern of ZnO/TiO<sub>2</sub>-NPs. The chitosan presence on NPs surface was confirmed by IR- spectra measurements. The UV light absorption ability was confirmed *via* collecting the reflectance spectra. In order to check the photocatalytic activity of the composites degradation processes of Azure B, bovine serum albumin and  $\alpha$ -terpinene was monitored. For all materials the photocurrents generation was measured. Moreover, the antibacterial activity against Gram-positive (*Staphylococcus aureus*) and Gram-negative bacteria (*Escherichia coli*) was evaluated by colony-forming capability test. The potential cytotoxicity of materials was tested by MTT assay on human keratinocyte cell line (HaCaT).

### RESULTS AND DISCUSSION

The polymer layer on the ZnO and TiO<sub>2</sub> grains aggregates was observed as round and smooth shapes on SEM micrographs. Also DLS measurements and IR spectra confirmed chitosan presence on NPs surface. Modification of semiconductor nanoparticles with chitosan did not block the UV light absorption ability of materials. A significant decrease in ZnO/TiO<sub>2</sub> photocatalytic activity after chitosan modification in connection with a considerable inhibition of photo-induced charge transfer processes make nanocomposites a perfect protective agent in biomedical field. What is more, chitosan modified materials were recognized as efficient antibacterial agents against both tested bacterial strains: *Staphylococcus aureus* *Escherichia coli*. Simultaneously, no cytotoxic effect towards HaCaT cell line was confirmed.

### CONCLUSION

Our studies focused on developing new nanocomposites with potential biomedical application based on zinc oxide and titanium dioxide NPs and biocompatible, antibacterial polymer-chitosan. The preserved UV light absorption ability and blanked photocatalytic activity towards selected substrates confirms materials photoprotective properties. Moreover, materials did not generate reactive oxygen species such as singlet oxygen. Furthermore, a complete photocurrents quenching for chitosan modified oxides was obtained, which confirms the lack of photoactivity. Presented materials resolve the problem of risks associated with semiconductor nanoparticles utilization as the active ingredient of sunscreen formulations.

### REFERENCES

1. Buchalska M. *et al.*, J. Photochem. Photobiol., A 213:158-163, 2011
2. Lee W.A. *et al.*, Chem. Commun.45:4815-4817, 2007

### ACKNOWLEDGMENTS

The authors would like to thank IDEAS PLUS project (grant No. IdP2012000362) for providing financial support to this project.



Agnieszka Witecka<sup>1,2</sup>, Akiko Yamamoto<sup>1</sup>, Wojciech Swieszkowski<sup>2</sup><sup>1</sup> International Center for Materials Nanoarchitectonics, National Institute for Materials Science (NIMS), Japan<sup>2</sup> Faculty of Material Science and Engineering, Warsaw University of Technology, Poland[agnieszka.witecka@inmat.pw.edu.pl](mailto:agnieszka.witecka@inmat.pw.edu.pl)

## INTRODUCTION

Mg alloys are promising materials for orthopaedic biodegradable devices due to their biocompatibility, low density and a high mechanical strength, but corrosion rate of Mg and its alloys currently available is still too high. One of the methods to improve their initial corrosion resistance and cytocompatibility is polymer coatings<sup>1),2)</sup>. However, details of the relation between coating properties and their improvement remain unclear. In this study, the improvement of cytocompatibility and corrosion resistance of ZM21 alloy was conducted by spin-coating of different biodegradable polymers. The effect of polymer structures on their coating properties as well as their improvement of substrate corrosion resistance and cytocompatibility was investigated.

## EXPERIMENTAL METHODS

Cast ZM21 alloy (2.0 wt% Zn and 0.98 wt% Mn) was used in this study. Samples (10x5x1.5mm) were polished using SiC papers up to #600 in ethanol. Then, 2% (w/v) chloroform solution of poly(lactic-co-glycolic) acid [PLGA], poly-L-lactide (PLLA), poly(3-hydroxybutyrate) [PHB] or poly(3-hydroxybutyrate-co-3-hydroxyvalerate) [PHBV] was spin-coated on both sides of the samples. These samples are abbreviated as PLGA, PLLA, PHB, and PHBV, respectively. Static water contact angle (WCA) was measured at 2000 msec after the contact of a water droplet to the sample surface. Prior to cell culture, samples were sterilized with ethylene oxide gas (EOG).

For WST-1 assay, human osteosarcoma cell line (SaOS-2) was inoculated at a density of 4000 cells/ml in 27.5 ml of Dulbecco's Modified Eagle Minimum Essential Medium supplemented with 10% (v/v) fetal bovine serum, abbreviated as D-MEM+10%FBS, and was incubated under cell culture condition (37°C, 5% CO<sub>2</sub>) for 1, 4 and 7 days. For calcification and alkaline phosphatase (ALP) tests, SaOS-2 was inoculated at a density of 10 000 cells/ml in 27.5 ml of D-MEM+10% FBS and incubated under cell culture condition for 7 days. Then, culture medium was replaced into a "osteogenic medium", which was D-MEM+10%FBS supplemented with 0.5 mM  $\beta$ -glycerophosphate, 50  $\mu$ g/mL L-ascorbic acid and 1% (v/v) antibiotic solution [penicillin (5000IU/mL) and streptomycin (5000  $\mu$ g/mL)]. Then, samples were additionally incubated for 7 and 14 days with exchange of the osteogenic medium every 7 days. Degradation of the substrate during cell culture was examined by quantification of released Mg<sup>2+</sup> ions.

## RESULTS AND DISCUSSION

Polymer coating increased the hydrophobicity of the ZM21 substrate surface. PHB and PHBV, which have relatively hydrophobic moieties, showed relatively high WCA around 80° whereas PLGA and PLLA showed those around 74°. The WCA of ZM21 substrate was around 62°. The thickness of the coated layer is around 0.20, 0.28, and 0.18  $\mu$ m for PLLA, PHB, and PHBV, respectively, whereas that of PLGA was 0.12  $\mu$ m. This may be due to the much lower molecular weight of PLGA than those of other polymers.

PLLA, PHB and PHBV coatings successfully improved cell growth during 7 days of incubation and suppressed the Mg<sup>2+</sup> ion release, while PLGA has no significant impact on corrosion suppression. This is probably because of thinner coating of PLGA as described above, as well as its relatively high degradation ratio.

The samples coated with PLLA, PHB and PHBV have much larger calcified area than PLGA or ZM21 substrate after 2 weeks of incubation in the osteogenic medium. The results of ALP tests after 1 week of incubation in osteogenic medium agreed with this trend. After 2 weeks, however, ALP activities decreased for PLLA, PHB and PHBV, whereas they increased for ZM21 substrate and PLGA coated samples. This suggests that SaOS-2 on the former samples differentiated into the next phase of bone formation process. PLLA, PHB and PHBV encourage higher cell growth and faster functionality.

## CONCLUSION

The polymeric coatings modified the physicochemical properties of ZM21 alloy surface, which contributes to improve its biocompatibility. During cell culture, PLLA, PHB, PHBV coatings successfully reduced the Mg<sup>2+</sup> release, while PLGA had no impact on the corrosion suppression. This is probably due to the smaller molecular weight, thinner coating thickness and faster degradation of PLGA. The successful reduction of substrate corrosion by the three polymers contributed to improve cell growth and cell functionality. It is also found that higher cell growth in the early stage of incubation is important to support faster and higher cell functionality in the later stage.

## REFERENCES

1. L. Xu L., et al., Colloids Surf. B, 93: 67-74. 2012
2. Witecka A. et al., Magnesium Technology 2014, TMS, Wiley, New Jersey (2014). pp.375-380.

## ACKNOWLEDGMENTS

This work was supported by the statutory work: WIM PW in Poland-NIMS in Japan, Joint Graduate Program.





# Influence of Plasma Nitriding Process on Multi-Layer Coatings Produced by MW CVD Technique for Hip Prosthesis Applications

Agnieszka Kyzioł<sup>1</sup>, Łukasz Kaczmarek<sup>2</sup>, Marek Klich<sup>2</sup>, Karol Kyzioł<sup>3</sup>

<sup>1</sup>Faculty of Chemistry, Jagiellonian University, Poland

<sup>2</sup>Institute of Materials Science and Engineering, Łódź University of Technology, Poland

<sup>3</sup>Faculty of Materials Science and Ceramics, AGH University of Science and Technology, Poland

[kyziol@chemia.uj.edu.pl](mailto:kyziol@chemia.uj.edu.pl)

## INTRODUCTION

Implantation, especially total hip replacement is a serious surgery to human body, for that reason there is a need to improve biocompatibility and osseointegration of material of which implants are made *e.g.* titanium alloys<sup>1</sup>. Diamond-like Carbon (DLC) coatings has been developed in order to improve parameters important from biological application point of view.

Noteworthy, such properties as modulus of elasticity and residual stress may cause unfavourable stress distribution at the substrate-coating interface. There is possibilities to reduce these disadvantages by intermediate layer deposition or by doping with silicon<sup>2</sup> and nitrogen<sup>3</sup> atoms with plasmochemical methods application.

In this work multilayer, nitrogen doped coatings based on carbon and silicon deposition by Microwave Plasma Assisted Chemical Vapour Deposition method were studied.

## EXPERIMENTAL METHODS

Samples of 3 mm thickness made from two titanium alloys: Grade2 (10mm dia.) and Ti6Al7Nb (14mm dia.) were mechanically polished to achieve mirror-like surfaces. Then surface modification in Plasma Assisted Chemical Vapour Deposition (PA CVD) vacuum system, equipped with microwave (2.45 GHz) antenna was performed. Two processes varying depending on the substrate pre-functionalization with plasma nitriding process were studied (Figure 1).

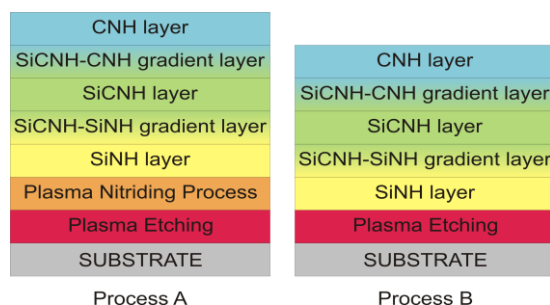


Figure 1. Scheme of the applied plasma processes.

Structure characterization (in various atomic scale) of the resulting coatings by SEM, AFM and spectroscopic methods (FT-IR, Raman) was carrying out. Hardness and modulus of elasticity were determined by nanoINDENTER® G200 (Agilent technologies, USA) with continuous stiffness measurement. Preliminary biological study *in vitro* was performed: (i) cytotoxicity towards human osteosarcoma MG-63 cell line was evaluated by MTT assay and (ii) level of Ti and Al ions

release in cell culture media was detected by ICP-MS technique.

## RESULTS AND DISCUSSION

MW PA CVD process application resulted in obtaining of coatings with relatively low hardness ( $3.2 \pm 0.4$  GPa) for Ti6Al7Nb sample after process B (Figure 2). While in case of process A, increase of surface hardness for Ti-Grade2 sample to value of  $3.7 \pm 0.4$  GPa was achieved.

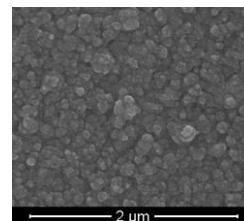


Figure 2. Microstructure of Ti6Al7Nb sample after process B application.

Sample	Hardness GPa	
	Ti-Grade2	Ti6Al7Nb
Reference	$3.38 \pm 0.1$	$4.79 \pm 0.2$
After process A	$3.70 \pm 0.4$	$4.31 \pm 0.2$
After process B	$3.23 \pm 0.4$	$3.20 \pm 0.4$

Table 1. Hardness values for the obtained coatings.

The tendency to increase of hardness by plasma nitriding process application was observed (Table 1). The resulting values of hardness are probably connected with their non-dense and columnar structure, which is characteristic for MW PA CVD coating method application<sup>4</sup>.

## CONCLUSION

This investigation resulted in successful two novel deposition layers. Multi-layer deposition after only plasma etching without plasma nitriding process assures better osseointegration, biocompatibility, metal ions diffusion barrier (antimetabolism properties) and lower Young modulus. Nano-metric structure of the resulting coatings was correlated with hardness distribution obtained by nanoindentation method. Influence of plasma nitriding process on hardness parameters was observed.

## REFERENCES

- Green G. et al., Orthopaedics & Trauma, 2014
- Damasceno J.C. Surf. & Coat. Techn. 133-134:247-252:2000.
- Dwivedi N. Mat. Chem. & Phys. 130:775-785:2011
- Tong W. et al., Mat. Sci. & Eng. C 43:135-144, 2014

## Topographic Nanostructures for the Regulation of Cell Adhesion

Patrick Elter<sup>1,3</sup>, Thomas Weihe<sup>2</sup>, Jan Gimsa<sup>2</sup>, Ulrich Beck<sup>3</sup>

<sup>1</sup>Department of Hospital and Clinical Engineering, Environmental and Biotechnology (KMUB), Technische Hochschule Mittelhessen, University of Applied Sciences, Germany

<sup>2</sup>Chair of Biophysics, Department of Biology, University of Rostock, Germany

<sup>3</sup>Interface Research Group, Institute for Electronic Appliances and Circuits, University of Rostock, Germany  
[patrick.elter@kmub.thm.de](mailto:patrick.elter@kmub.thm.de)

### INTRODUCTION

One of the challenges in biomaterials research is the functionalization of implant surfaces to adjust their biocompatibility for specific applications. A relatively new approach is the use of topographic nanostructures for the regulation of cell adhesion. However, the solid-liquid interface between a biomaterial and the adjacent tissue is complex and cell adhesion is regulated by many factors such as the electrochemical double layer, protein adsorption and the interaction of cell-surface receptors with the adsorbed proteins<sup>1</sup>. As a consequence, nanostructured functionalizations are frequently developed by the “*trial and error*” method. For a more systematic tailoring of nanostructured functionalizations a detailed knowledge of the interplay between material properties, protein adsorption and cell adhesion is required. In the presented study, this interplay was examined in detail by analysing the influence of a periodically grooved nanostructure on the initial adhesion of L929 fibroblasts at different fibronectin concentrations.

### EXPERIMENTAL METHODS

Periodically grooved nanostructures with 90 nm groove and summit widths and groove depths of 120 nm were fabricated on silicon wafers using interference lithography (AMO GmbH, Aachen, Germany)<sup>2,3</sup>. The substrates were incubated with 0 µg/ml, 5 µg/ml and 25 µg/ml bovine fibronectin<sup>2,3</sup>. The local protein density and conformation was characterized using single-molecule force spectroscopy (SMFS)<sup>2</sup>. The interpretation of the experiments was supported by computer simulations in which numerical field calculation methods were combined with Brownian Dynamics and a simple mechanism for protein adsorption on topographic nanostructures was derived<sup>4</sup>. Moreover, the cell adhesion strength of L929 fibroblasts was observed by single-cell force spectroscopy (SCFS) and the results were correlated with the results from the protein adsorption<sup>3</sup>.

### RESULTS AND DISCUSSION

Cell adhesion to the nanostructure was compared with that to a similarly treated planar reference using single-cell force spectroscopy. The adhesion strength of L929 fibroblasts to the bare nanostructure (without fibronectin) was lower ( $79\% \pm 13\%$ ) than to the planar substrate, which we attribute to a reduced contact area<sup>3</sup>.

After pre-incubation with a low fibronectin concentration (5 µg/ml) the adhesion strengths to both surfaces (nanostructured and planar) increased, with adhesion strength on the nanostructure outweighing that of the planar substrate by  $133\% \pm 14\%$ <sup>3</sup>. At a high fibronectin concentration (25 µg/ml) the adhesion strengths further increased on both surfaces and showed wide variations<sup>3</sup>.

The comparison of the results from the SCFS and SMFS experiments suggest that the enhanced cell adhesion at the low fibronectin concentration (5 µg/ml) was caused by an increased amount of protein per surface area on the nanostructure as well as an associated higher rate of native proteins<sup>3</sup>. This interpretation is supported by the computer simulations that demonstrate that the interplay of van der Waals- and electrostatic forces lead to a locally increased protein concentration on a grooved nanostructure<sup>4</sup>.

### CONCLUSION

This study demonstrates that the adhesion strength of L929 fibroblasts can be influenced by a topographic nanostructure and that the exact effect of the nanostructure depends on the fibronectin concentration.

### REFERENCES

1. Lord, M. *et al.*, Nano Today 5:66-78, 2010.
2. Elter P. *et al.*, Colloids Surf. B 89:139-146, 2012.
3. Elter P. *et al.*, Colloids Surf. B 95:82-89, 2012.
4. Elter P. *et al.*, Langmuir 27:8767-8775, 2011.

### ACKNOWLEDGMENTS

We thank Dr. Sebastian Bühler for helpful discussions and for assistance in cell culture. Funding from the Deutsche Forschungsgemeinschaft DFG (Graduate School “welisa” 1505/1 and project BE 2362/2-2) is gratefully acknowledged.



## The Effect of TiN and DLC Surface Modification on Wear of AISI 440B Martensitic Stainless Steel Surgical Drill Bits

Magdalena Łepicka, Małgorzata Grądzka-Dahlke

Department of Materials and Biomedical Engineering, Faculty of Mechanical Engineering, Białystok University of Technology, Poland  
[magdalena.lepicka@gmail.com](mailto:magdalena.lepicka@gmail.com)

### INTRODUCTION

Development in modern invasive surgery is highly dependent on surgical instruments performance, understood as long-term efficiency, arising i.e. from high resistance to wear and corrosion. Taking into consideration complexity, manufacturing costs and diversity of contemporary surgical instruments, it is an issue of great significance to provide reliable and durable medical devices<sup>1,2</sup>. In order to improve their ease of handling, resistance to wear and corrosion and stability in variable environmental conditions, surface modification techniques are applied. There are numerous reports considering research into improvement of surgical instruments' reliability and durability, especially drills, by the means of anti-wear layers deposition<sup>1,3,4</sup>.

Instruments designed to contact with bone tissue, e.g. saws, drills, chisels, are one of the most exposed to tribological wear medical devices. As early as after only few operational procedures their geometry changes, pre-sharpened edges round, sometimes even material chipping is noticeable<sup>5,6</sup>. As a consequence, it may cause problems with their handling, or even contribute to generating far too high temperatures during drilling, what results in bone necrosis<sup>7</sup>.

The aim of the study was to evaluate the effect of TiN and DLC surface modification on wear of AISI 440B martensitic stainless steel surgical drill bits.

### EXPERIMENTAL METHODS

Commercial surgical drill bits (AISI 440B stainless surgical steel) were chosen as research material. Cutting surgical instruments were divided in following groups (Figure 1):

- I. reference, heat treated in 250°C,
- II. DLC modified
- III. TiN modified.



Figure 1. Drill bits for field-testing

In order to evaluate effectiveness of modified and non-modified drill bits, study was carried out on cutting efforts when drilling porcine cortical bone. Tests were performed on a specially designed test stand, consisting of bench drill equipped with force sensor and force transducer, and a computer, on which friction torque changes during drilling were recorded. Femoral and

shin bones were picked up fresh from a local butchery and were prepared a few days after 10-months old piglets were sacrificed. 40 holes were made with each bit. Total cutting depth of each bit was approx.  $160 \times 10^{-6}$  m. After drilling, change of teeth geometry was measured on FALCON QC 3-axis non-contact video measuring machine.

### RESULTS AND DISCUSSION

No direct correlation between the number of drilled holes and drilling time or axial torque has been observed, as one would expect. This might be caused by heterogeneity of bone tissue. Uneven surface of the porcine bone could lead to the observed during experiment drill run-out. Performed studies were of comparative nature and in this respect obtained results can be considered reliable. Nevertheless, certain relationships and differences between the non-modified and modified drills were observed. The non-modified cutting tool was characterized by shorter cutting times and lower average friction forces during drilling. In comparison, the modified drills, especially the TiN one, was characterized by a significantly longer single-hole cutting time, higher frictional forces and additional heating of the tool. However, it had no significant effect on tool wear. The use of anti-wear layers has improved wear resistance of considered tools.

### CONCLUSION

Experimental procedure performed on reference and surface modified AISI 440B martensitic stainless steel drill bits shows that deposition of anti-wear layers improves wear resistance of surgical cutting tools. In the future it will be necessary to perform further analyses in surgical drill bits wear mechanisms.

### REFERENCES

1. Biel-Gołaska M. *et al.*, Prace Instytutu Odlewnictwa 48:29-38, 2008
2. Marciniak J. *et al.*, PE 4:179-186, 2006
3. Dearnaley G. *et al.*, Surf. Coat. Tech. 200:2518-2524, 2005
4. Marciniak J. *et al.*, JAMME 20:259-262, 2007
5. Paszenda Z. *et al.*, AMSE 36:103-109, 2009
6. Gierżyńska-Dolna M. *et al.*, Eng. Biomat. 7:102-106, 2004
7. Basiaga M. *et al.*, Acta Bioeng. Biomech. 13:29-36, 2011

### ACKNOWLEDGMENTS

This scientific work was supported by the Faculty of Mechanical Engineering, Białystok University of Technology, project No MB/WM/13/2014.

## INTRODUCTION

Controlling material-tissue interaction with respect to tissue mechanics, physiological environment and biochemical signaling is likely to be beneficial to achieve guided reorganization of impaired tissue.

To fulfill these requirements we developed a toolbox of macromeres that can be cross-copolymerized into constructs with tunable hydrophilicity, swelling, biodegradability and mechanics. Copolymerization with monomethacrylated PEG (PEGMA) allowed for covalent surface modification with functional molecules.

In order to rationalize material development and surface design of 3D constructs, we processed the toolbox components into films as an analytical platform.

Film hydrophilicity and presentation of functional groups were assessed by static water contact angle and quantification of a covalently bound dye with a fluorescence plate reader. Cell adhesion onto films was determined where RGD-peptide modified films were employed as a proof of principle for functional film modification.

## EXPERIMENTAL METHODS

Films were cross-polymerized onto glass-disks bearing MA-silane layer using thermally controlled radical polymerization reactions with benzoylperoxide and 2-(4-dimethyl-aminophenyl)-ethanol as initiator/accelerator system. The films consisted of core molecules (T134, T170, T450) which are trivalent alcohols with different degrees of ethoxylation and thus molecular weights. These are flanked by lactic acid (LA) side chains of variable block length (LA2, LA4, LA6). This macromer platform can further be modified using PEGMAs and methoxyPEGMAs (mPEGMA). PEGMAs anchoring in the film surface, provided a free hydroxyl group to be modified by succinic anhydride and activated by dicyclohexyl-carbodiimide and N-hydroxy-succinimide. Density of functional groups present at the surface was determined by the immobilization of 5-((aminopentyl)thiouredyl)-fluorescein (Fcad). Hydrophilicity of films composed of pure macromeres and those containing 20% (m/m) PEG<sub>1000</sub>MA was systematically determined by measuring the static water contact angle. Saos-2 adhesion was characterized for the same compositions. A choice of materials was additionally functionalized with GRGDS peptide to check for positive effects on cell adhesion.

## RESULTS AND DISCUSSION

Static water contact angles of films consisting of pure macromers exhibited strong differences depending on the core molecule. T134 cores – without ethoxylation – were the most hydrophobic materials with contact

angles of approximately 60°. The degree of ethoxylation had the biggest impact on hydrophilicity as it led to a cut down of the contact angle to 35° for the most hydrophilic macromer 450LA2. By cross-copolymerization of the macromers with 20% PEG<sub>1000</sub>MA, the hydrophilicity of the films increased leading to contact angles in the range of 50°.

The usage of different anchoring groups (PEG<sub>526</sub>MA and PEG<sub>1000</sub>MA) gave the opportunity to tether adjustable amounts of Fcad in the range of up to 1 nmol/cm<sup>2</sup> onto films of the macromer T450LA2 when reaction batches consisted of 50% PEGMA.

Hydrophobic macromers, such as T134LA6, showed low analyte immobilization capacity which was limited to a range of pmol/cm<sup>2</sup> inspite of high PEG chain density. To improve their immobilization capacity, shorter mPEGMAs were cross-copolymerized with PEGMAs into the macromer films as mPEGs are known to foster brush-like structures on surfaces<sup>1</sup>. In order to limit the total amount of PEG in the films, detailed studies on mixing ratios of PEGMA and mPEGMA with T134LA6 and T450LA2 revealed that compositions with 20% of the PEGMA and 10% of the filler mPEGMA were sufficient to increase the immobilizing capacity by factor two to five depending on the macromer.

Adhesion experiments with Saos-2 cells showed just little differences in the number of attached cells between the macromers but a strong decrease in cell number for all formulations when 20% PEG<sub>1000</sub>MA were incorporated with the least cell numbers on films based on T450LA6. By functionalizing this material with GRGDS peptide, cell numbers exceeded those of all other formulation displaying the success of this surface functionalization concept.

## CONCLUSION

We engineered surfaces from a toolbox of biodegradable macromers that can be cross-copolymerized with PEGMA to functional films. The surface properties, namely hydrophilicity, immobilization capacity and cell adhesion were controlled by molecular weight of macromers and cross-copolymerization with PEGMAs. Relevant effects on cellular response were shown by immobilization of RGD peptides.

## REFERENCES

1. Chen H. *et al.*, Colloids and Surfaces B:Biointerfaces 61:237-243, 2008

## ACKNOWLEDGMENTS

The authors thank the German Research Council (DFG SFB/Transregio 67) for financial support.





## Tribocorrosion of Ca-P Doped TiO<sub>2</sub> Nanotubes

Ana Caroline Crema de Almeida, Carlos A. H. Laurindo, Paulo Soares

Polytechnic School, Mechanical Engineering Department, Pontificia Universidade Católica do Paraná,  
Brazil

[ana.crema@pucpr.edu.br](mailto:ana.crema@pucpr.edu.br)

### INTRODUCTION

The improvement of the interface between bone and implant have been of particular interest in dental and orthopedic implant research. Titanium has been used in dentistry for more than five decades but there still ongoing research to improve the surface properties of the material in order to improve the molecular interactions, cellular response and thereby, osseointegration [1]. Tribocorrosion can be defined as a degradation phenomenon of material surfaces subjected to the combined action of mechanical loading and corrosion attack caused by the environment. Usually the dental implants undergo micro-movements under loading mastication when exposed to a biological aggressive environment, causing fretting corrosion [3]. TiO<sub>2</sub> nanotubes array give completely new types of interactions between implant surfaces and cells because the surface area is increased and the surface topography can be modified to resemble native bone tissue. The aim of this work was to evaluate the influence of the annealing treatment at different temperatures in the surface and tribocorrosion properties of TiO<sub>2</sub> nanotubes.

### EXPERIMENTAL METHODS

Samples with 30 x 20 x 1 mm were polished with SiC abrasive papers of #320, #600, #800, #1200 and colloidal silica. Then, they were cleaned ultrasonically in acetone, alcohol and rinsed in deionized water. The anodization was performed in a two-electrode configuration with Ti plate as working electrode and platinum foil as the counter electrode. The samples were anodized potentiostatically with 60 V, in an electrolyte containing calcium, phosphorous and fluoride ions. The TiO<sub>2</sub> nanotube layer morphology and crystalline phase were evaluated by scanning electron microscopy and X-ray diffraction measurements

respectively. The tribocorrosion evaluation was carried out using a linear reciprocating ball on flat tribometer with a three electrode electrochemical cell coupled to potentiostat.

### RESULTS AND DISCUSSION

The results show that the amount of rutile crystalline phase increases with annealing temperature improving the tribocorrosion resistance, producing though several cracks in the oxide layer due to elastic mismatch between the oxide layer and substrate.

### CONCLUSIONS

The tribocorrosion of TiO<sub>2</sub> nanotubes is influenced by the crystalline phase.

### REFERENCES

1. Mutlu Özcan and Christoph Hämmerle, Titanium as a Reconstruction and Implant Material in Dentistry: Advantages and Pitfalls, *Materials* 2012, 5, 1528-1545; doi:10.3390/ma5091528
2. M. T.Mathew, P. Srinivasa Pai, R. Pourzal, A. Fischer, and M. A.Wimmer, Significance of Tribocorrosion in Biomedical Applications: Overview and Current Status, *Advances in Tribology* 2009, Article ID 250986, 1-12, doi:10.1155/2009/250986.
3. Karla S. Brammer, Christine J. Frandsen and Sungho Jin, TiO<sub>2</sub> nanotubes for bone regeneration, *Trends in Biotechnology* June 2012, Vol. 30, No. 6, doi:10.1016/j.tibtech.2012.02.005.

## Adsorption Reaction of L-cysteine on the Au Nanoparticle Precovered with PC Molecules

Chie Tsukada<sup>1,2</sup>, Takuma Tsuji<sup>2</sup>, Koichi Matsuo<sup>3</sup>, Toyokazu Nomoto<sup>4</sup>, Takaaki Murai<sup>5</sup>, Toyonari Yagi<sup>6</sup>, Toshiaki Ohta<sup>6</sup>, Hirofumi Nameki<sup>5</sup>, Satoshi Ogawa<sup>2,4</sup>, Tomoko Yoshida<sup>1,4</sup>, Shinya Yagi<sup>1,3,4,6</sup>

<sup>1</sup>EcoTopia Science Institute, Nagoya University, Japan,

<sup>2</sup>Graduate School of Engineering, Nagoya University, Japan

<sup>3</sup>Hiroshima Synchrotron Radiation Center, Hiroshima University, Japan

<sup>4</sup>Aichi Synchrotron Radiation Center, Aichi Science & Technology Foundation, Japan

<sup>5</sup>Aichi Center for Industry and Science Technology, Aichi Prefecture, Japan

<sup>6</sup>The SR Center, Ritsumeikan University, Japan

[tsukada.chie@e.mbox.nagoya-u.ac.jp](mailto:tsukada.chie@e.mbox.nagoya-u.ac.jp)

### INTRODUCTION

Gold nanoparticles (AuNPs) are taken notice of the uses of the hyperthermia for cancer cell in medical field<sup>1</sup>. The AuNPs should have the biocompatibility. We have decided to fabricate the AuNPs colloidal solution without several reagents, which have a possibility of low biocompatibility. In addition, we propose a hypothesis that if the biomolecule is not easy to adsorb on the AuNPs surface, the NPs have higher biocompatibility. In our previous study, we have revealed that the phosphatidylcholine (PC) molecule adsorbs on the Au material surface at hydrophilic group<sup>2</sup>. The PC molecule constitutes the biological membrane and has the hydrocarbon chain of the hydrophobic group. Y. Sato *et al.* have reported that the molecules with the hydrocarbon chain can possess the ordered state by the intermolecular force between hydrocarbon chains<sup>3</sup>. Thus, one of purposes in this study is to fabricate the AuNPs covered by phosphatidylcholine (PC). Subsequently, the other purpose is to reveal the adsorption reaction between L-cysteine and the AuNPs with/without the PC membrane because the L-cysteine has adsorbed rapidly on the AuNPs surface at thiol group (-SH)<sup>4</sup>.

### EXPERIMENTAL METHODS

The AuNPs colloidal solution was fabricated by the solution plasma method<sup>4</sup>. The solution plasma method used two materials only, which are gold rods and NaCl aqueous solution. The DPPC dissolved in milli-Q water. The DPPC aqueous solution was kept at 45 °C and was added into the AuNPs colloidal solution. The precipitate, which was the PC covered AuNPs, was produced and rinsed several times with the milli-Q water. The rinsed precipitate and the L-cysteine powder were mixed in aqueous solution. After promoting the adsorption reaction, the precipitate was rinsed with the milli-Q water again. This sample is described as Cysteine/DPPC/AuNPs. As the reference sample, the L-cysteine powder was added into the AuNPs aqueous solution and the occurred precipitate was rinsed with the milli-Q water. This sample is called as Cysteine/AuNPs. Infrared spectroscopy (IR) and S K-edge near-edge X-ray absorption fine structure (NEXAFS) measurements for those precipitates were carried out at the SR center BL-15 and AichiSR BL6N1 with He-path system, respectively.

### RESULTS AND DISCUSSION

Taking into account of the results of IR measurement,

not shown here, we suppose the DPPC molecules cover around the AuNPs surface with ordered state by the intermolecular force between the hydrocarbon chains of DPPC on NPs. Figure 1 shows the S K-edge NEXAFS spectra for Cysteine/AuNPs and Cysteine/DPPC/AuNPs under water environment. The peak intensity at 2470.0 eV corresponds the amount of atomic S on the AuNPs surface. The atomic S occurs by dissociating both S-H and S-C bonds of the L-cysteine adsorbed on AuNPs. Thus, we think that the L-cysteine molecule is not easy to adsorb on the AuNPs surface of DPPC/AuNPs compared to the non-covered AuNPs.

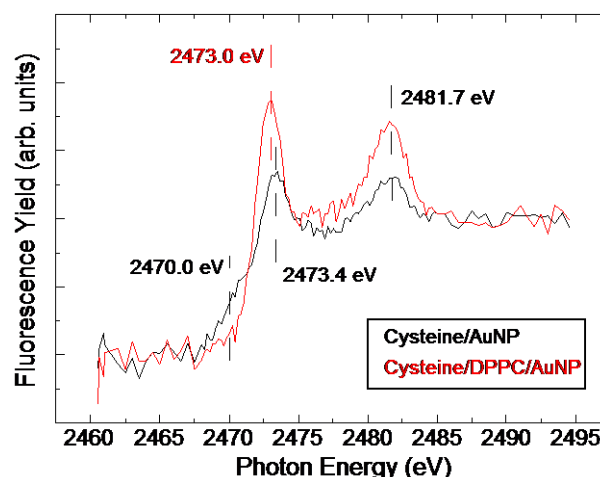


Figure 1. S K-edge NEXAFS spectra for Cysteine/AuNPs and Cysteine/DPPC/AuNPs.

### CONCLUSION

We have fabricated the AuNPs covered by DPPC membrane with ordered state. We think that the L-cysteine is not easy to adsorb on the AuNPs surface of DPPC/AuNPs compared to the non-covered AuNPs.

### REFERENCES

1. Huang H.-C. *et al.*, ACS Nano 4:2892-2900, 2010
2. Tsukada C. *et al.*, IOP Conf. Series: Mater. Sci. Eng. 76:012001 1-9, 2015
3. Sato Y. *et al.*, Bull. Chem. Soc. Jpn. 67:21-25, 1994
4. Tsukada C. *et al.*, e-J. Surf. Sci. Nanotech. 11:18-24, 2013

### ACKNOWLEDGMENTS

The authors would like to thank the JSPS Research Fellowship for Young Scientists (No. 253655) for providing financial support. This work was performed under the approvals AichiSR and the SR center.



# Sol-Gel Siloxane-Gelatine Coatings for Improving Titanium's Osseointegration: Synthesis, Characterization and Biological Assessment

María Martínez-Ibañez<sup>1</sup>, Yong Mao<sup>2</sup>, Julio Suay<sup>3</sup>, Mariló Gurruchaga<sup>1</sup>, Isabel Goñi<sup>1</sup>, Joachim Kohn<sup>2</sup>

<sup>1</sup>Polymer Science-Technology Department, Faculty of Chemistry of San Sebastian, UPV/EHU, Spain

<sup>2</sup>New Jersey Center for Biomaterials, Rutgers University, New Jersey (USA)

<sup>3</sup>Jaime I University, Castellón, UJI, Spain

[maria.martinezi@ehu.es](mailto:maria.martinezi@ehu.es)

## INTRODUCTION

The use of titanium screws in implant therapy is highly predictable and successful. However, there are certain risk factors such as smoking, disease and periodontitis, which can predispose individuals to lower rates of success and to failure of the implant treatment<sup>1</sup>. In this context there is a great interest in finding new surface to promote bone formation and accelerate the osseointegration process. There is an increasing number of works that shows the beneficial effect of silicon containing biomaterials, such enhancing bioactivity and regulation of osteoblast proliferation and gene expression<sup>2</sup>. Moreover, their dissolution products have been proved to stimulate collagen type I synthesis and enhance osteoblast differentiation<sup>3</sup>. Furthermore, gelatine was selected because of its cell adhesion ability and osteoregenerative properties.

The aim of this work is to design new siloxane-gelatine coatings through the sol-gel process with tailored properties for titanium dental implants. For that, the effect and behaviour of different alkoxysilane precursors were evaluated in order to control the surface chemistry and the silicon release rate. This parameters and their influence on cell attachment and differentiation were studied.

## EXPERIMENTAL METHODS

**Synthesis:** Hybrids were prepared via sol-gel, using HCl 0.1M as catalyst, with methyltrimethoxysilane (MTMOS), 3-glycidypropyl trimethoxysilane (GPTMS) and tetraethoxysilane (TEOS). Different matrixes are called M:T and M:G:T. Hybrids synthesized with the incorporation of 0.9% by weight of gelatine are M:T\_0.9% and M:G:T\_0.9%. Titanium discs were coated with the different hybrids and a heat treatment of 80 °C for 2hours was applied.

**Chemical characterization:** <sup>29</sup>Si—NMR in liquid and solid states were used to follow the kinetics of the reaction and to study the cross-linking degree of the resulting materials, respectively. Since hydrophobicity/hydrophilicity has an important influence on protein and cell adhesion, coatings' contact angle measurements were performed.

**In vitro silicon release quantification:** The dissolution properties of films were determined by immersing them in PBS at 37 °C, and measuring the Si released at different time points using an inductively coupled plasma mass spectrometer (ICP-MS).

**Biological evaluation:** hMSC were seeded onto coated titanium surfaces. After 24 hr, the cell adhesion to these surfaces was quantified by a DNA quantification kit (PicoGreen assay kit). Finally, the osteogenic differentiation of hMSC on hybrids was evaluated at 7 and 14 days in the presence or absence of osteogenic induction. The relative gene expression of osteogenic markers (RunX2, ALP and BGLAP) was analyzed using quantitative polymerase chain reaction (qPCR).

## RESULTS AND DISCUSSION

Homogenous, transparent and crack-free coatings were obtained. <sup>29</sup>Si-NMR confirmed the siloxane network formation, as well as the presence of silanol groups in the surface, which are important in the bone formation process. The degradation rate was tailored with the incorporation of different silicon precursors and gelatine in the matrix, as was reflected by silicon quantification assay. The incorporation of the epoxy group through the addition of GPTMS resulted in a higher cell adhesion. Silicon released from the coatings promoted higher osteogenic differentiation of hMSC compared to titanium. This was proved by the earlier gene expression.

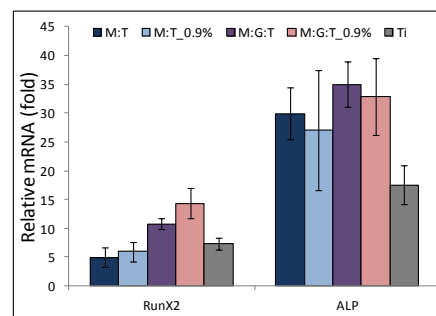


Figure 1. RunX2 and ALP gene expression after 14 days.

## CONCLUSION

The results of this study are encouraging for the use of siloxane-gelatine hybrids as bioresorbable and osteoinductive coatings for dental implants. Moreover they can have a potential application for patients with poor bone regenerative properties. Further investigation will be done to assess their behaviour *in vivo*.

## REFERENCES

1. Klokkevold P.R. *et al.*, Int. J. Oral Maxillofac. Implants 22:173-202, 2007
2. Kim E. *et al.*, Biol. Trace Elem. Res. 152:105-112, 2013
3. Reffit D.M. *et al.*, Bone 32:172-135, 2003



Daniel Ibegbu<sup>1</sup>, Eugen Barbu<sup>1</sup>, and John Tsibouklis<sup>1</sup><sup>1</sup>School of Pharmacy and Biomedical Sciences, University of Portsmouth, UK[madu.ibegbu@myport.ac.uk](mailto:madu.ibegbu@myport.ac.uk)

## INTRODUCTION

One of the major problems in drug delivery to the brain is the difficulty of transporting therapeutic entities across the blood-brain barrier (BBB). Consequently, the treatment of many brain-associated disorders through conventional delivery strategies is of limited value.<sup>1</sup>

It has been suggested that nanoparticles of poly(alkyl cyanoacrylate) (PACA) with dextran may be capable of transporting actives across the BBB. Poly(butyl cyanoacrylate) nanoparticles coated with Polysorbate 80 are biodegradable carriers that have been demonstrated to facilitate the delivery of drugs and peptides across the BBB.<sup>2,3,4</sup>

This study is aimed towards the formulation of amphiphilic nanocarriers from alkyl cyanoacrylate and a functionalised dextran for improved therapeutic delivery to the brain. Work to date has involved the derivatisation of dextran with alkyl glycidyl ethers (alkyl glycerol has been shown to aid the transport of particles to the brain)<sup>5</sup> and their subsequent formulation with PACA nanoparticles

## EXPERIMENTAL METHODS

Functionalised dextran and poly (ethyl 2-cyanoacrylate) nanoparticles were prepared in two steps: grafting of the aliphatic chain of alkyl glycerol to dextran (and product characterisation using FTIR, which was followed by anionic polymerisation<sup>1</sup> with ethyl 2-cyanoacrylate

## RESULTS AND DISCUSSION

The successful synthesis of functionalised dextran was consistent with FTIR spectroscopy data: the grafting of alkyl glycerol chains resulted in the formation of a new secondary alcohol. The band at 1012 cm<sup>-1</sup> is assigned to the vibrational mode of C–O. In crystalline dextran, two absorption peaks at 851 and at 914 cm<sup>-1</sup> were observed, respectively assigned to (C–C) and (C–H) bending modes. It has been proposed that the absorption bands in the spectral range between 1200 and 1500 cm<sup>-1</sup> are mainly due to CH deformation vibrations and (COH) bending vibrations<sup>6</sup>. The bands at 2921 cm<sup>-1</sup> and at 3215 cm<sup>-1</sup> are respectively consistent with (C–H) and (O–H) stretching vibrations.

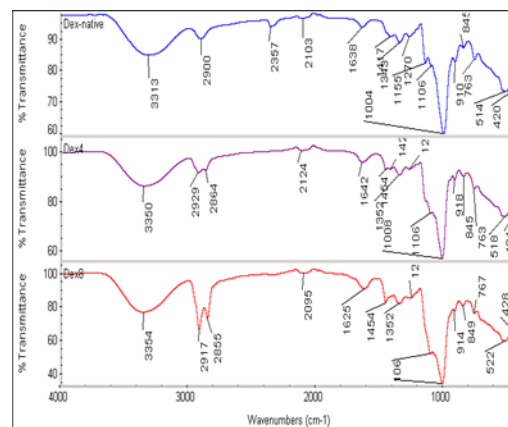


Fig. 1 FTIR spectrum of functionalised and non-functionalised dextran

## CONCLUSION

Anionic polymerisation of ethyl 2-cyanoacrylate with functionalised dextran and native dextran respectively, showed that polymerisation of ethyl 2-cyanoacrylate with functionalised dextran resulted in nanoparticles with lower polydispersity index and higher zeta potential when compared to non-functionalised dextran, which indicates that functionalization of dextran results in an improved nanoparticle formulation.

## REFERENCES

1. Kreuter J *et al.*, *Pharma Res.* 20: 409-416, 2003
2. Wohlfart S, *et al.*, *J. Controlled Release.*;161:264-273, 2012
3. Alyautdin RN *et al.*, *Pharma. Res.*14:325-8, 1997
4. Kreuter J *et al.*, *Brain Res.*; 674:171-4, 1995
5. Erdlenbruch, B *et al.*, *British J Pharmacol.* 140: 1201-1210, 2003
6. Gil EC *et al.*, *European J.Pharma and Biopharma* 68:319-29, 2008

## ACKNOWLEDGMENTS

Authors would like to acknowledge TETFUND-Nigeria for financial support for this study.



## TiO<sub>2</sub> Mesoporous Layers of Tunable Chemical Composition and Morphology

Paolo Canepa<sup>1</sup>, Sureeporn Uttiya<sup>1</sup>, Ilaria Solano<sup>1</sup>, Gianluca Gemme<sup>2</sup>, Ranieri Rolandi<sup>1</sup>, Maurizio Canepa<sup>1</sup>, Ornella Cavalleri<sup>1</sup>

<sup>1</sup>Department of Physics, University of Genova, Italy

<sup>2</sup>INFN, Genova Unit, Italy

[canepap@fisica.unige.it](mailto:canepap@fisica.unige.it)

### INTRODUCTION

Titanium and its alloys are widely investigated for the development of biocompatible dental and orthopedic implants thanks to their good mechanical properties and their good resistance to corrosion due to the presence of a stable oxide layer<sup>1</sup>. With the aim of developing implantable devices, an accurate control of the surface device is needed since the surface structural properties modulate the bio-integration process. In particular, incorporation of calcium phosphates into the titanium oxide matrix can represent a viable strategy to promote osseointegration<sup>2</sup>. We investigated the growth of titanium oxide layers prepared by electrochemical anodization in order to correlate the growth conditions with the resulting surface layer structure and composition.

### EXPERIMENTAL METHODS

Mechanically polished titanium sheets were electrochemically oxidized by anodic spark deposition (ASD) in three electrolytes: sulphuric acid solution, phosphoric acid solution and in a solution containing both calcium (stabilized by complexation with EDTA) and phosphate ions<sup>3</sup>. Anodization voltages were varied in the range 100V – 250V. Oxidized samples were thoroughly rinsed with Milli-Q water and dried.

The morphology and chemical composition of the TiO<sub>2</sub> layers were analysed by Tapping Mode Atomic Force Microscopy (TM-AFM), Scanning Electron Microscopy (SEM) and X-Ray Photoemission Spectroscopy (XPS). Oxide layer thickness was evaluated by cross-section SEM and AFM analysis.

### RESULTS AND DISCUSSION

Titanium dioxide layers grown by ASD in all the three investigated electrolytes are characterized by a mesoporous structure. Fig 1 shows typical AFM images of TiO<sub>2</sub> layers grown in sulphuric acid at two different anodizing potentials.

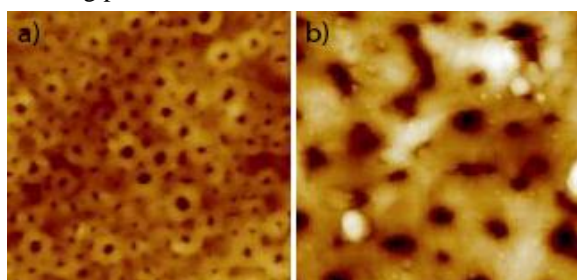
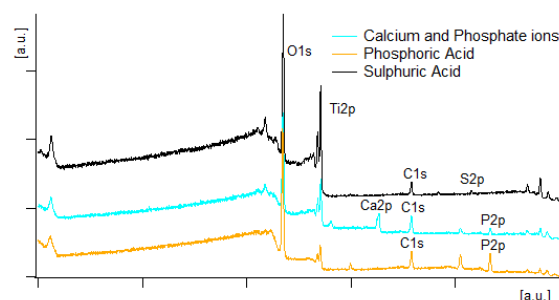


Fig. 1. AFM images (5µm x 5µm) of TiO<sub>2</sub> surfaces prepared by ASD in a sulphuric acid electrolyte at (a) 150V, (b) 200V.

From the analysis of the profile of AFM images it turns out that increasing the anodization potential results in an increase of the pore diameter and depth, from a few hundreds nanometers to more than one micron, depending from the electrolyte.

The thickness of the oxide layer was evaluated by SEM and AFM sectional analysis. The data indicates a layer thickness ranging from 1 to 8 µm depending on the electrolyte and anodization potential.

The chemical analysis of the sample surfaces has been carried out by XPS measurements. Figure 2 shows the XPS survey spectra of titanium after anodization in the three electrolytes. Peaks corresponding to Ti, O and C are present in all the spectra. P peaks can be observed in the spectra of Ti oxidized in phosphoric acid solution while both P and Ca signals can be detected from the analysis of samples anodized in the solution containing



calcium and phosphate ions.

Fig. 2. XPS survey spectra of Ti samples oxidised in electrolytes containing: (light blue) calcium and phosphate ions, (yellow) phosphoric acid, (black) sulphuric acid.

### CONCLUSION

By tuning the anodic oxidation conditions it is possible to tailor the TiO<sub>2</sub> surface morphology and to include specific chemical species in the oxide matrix. ASD is therefore a viable strategy for biomaterial development.

### REFERENCES

1. D.M. Brunette *et al.* Eds, Titanium in Medicine, Springer-Verlag, Berlin Heidelberg GmbH, 2001
2. Y.L. Chang *et al.*, Journal of Biomedical Materials and Research, 52 (2000) 270-278
3. V.M. Frauchiger *et al.*, Biomaterials, 25 (2004) 593-606

### ACKNOWLEDGMENTS

The authors would like to thank Genoa University for financial support and Dr. M. Salerno (IIT, Genova) for helpful discussions.

## Surface Modification by a Catalyst Free Covalent Layer-by-Layer Approach of Clickable Elastin-Like Recombinamers

I. González de Torre<sup>1,2</sup>, L. Quintanilla<sup>1</sup>, M. Alonso<sup>1</sup>, J. Carlos Rodríguez-Cabello<sup>1</sup>

<sup>1</sup>BIOFORGE, CIBER-BBN, Centro I+D, Universidad de Valladolid, Paseo Belén 11, 47011, Valladolid, Spain.

<sup>2</sup>TECHNICAL PROTEINS NANOBIO TECHNOLOGY (TPNBT S.L.) Paseo Belén 9 A, 47011, Valladolid,  
[igonzalez@bioforge.uva.es](mailto:igonzalez@bioforge.uva.es)

### INTRODUCTION

To improve the success ratio of the implant integration the Layer by Layer (LbL) technology is a good candidate, because it is an easy approach to perform a consecutive self-assembly of layers of at least two distinct materials onto substrates<sup>1</sup>.

Recently, our group has developed a new family of hydrogels based on the crosslinking of at least two modified bioactive Elastin-like recombinamers through a catalyst free click reaction (ELR-CFCGs)<sup>2</sup>. In this work these materials will be applied in the LbL technique to surface modification with the idea of combining the control and efficiency of the LbL approach with the stability and robustness of the covalent bonding.

### EXPERIMENTAL METHODS

Several substrates, polystyrene, titanium, glass and PS beads as simple surface systems were modified. In addition, a more complex structure, such as a coronary stent was also coated to get a continuous layer that helps to its integration after implantation. Two methodologies were employed. The first approach consists in consecutive immersions of the substrate inside two different ELRs clickable solutions, in such a way to the first solution will react forming a covalent bond with the second ELR solution (till 5 immersions on each solution). The first layer is adhered to the plasma activated substrate by electrostatic interactions. In the second approach, an additional washing step was introduced after each layer deposition. In this way, the thickness and topography of the LbL structure can be controlled.

### RESULTS AND DISCUSSION

Microscopy (optic, florescence, and SEM) offers us a first sight of the coating effectiveness, showing a good covering from the first layer where the surface topography is covered to the fifth layer, where a thicker, soft and continuous ELR click layer covers completely the substrate irregularities.

FTIR and XPS results evidence the variation at atomic level of the superficial layers of the surfaces. A clear evolution from the typical spectra of each substrate to the specific spectra of the ELRs can be observed in the results from both techniques.

Contact angles values underscore the variation of the surface hydrophobicity before and after the plasma cleaning and after the ELR-click layers deposition. Rising till contact angles values around 100°, which means a substantial increase in the surface hydrophobicity for the samples.

According to the AFM results, a good and complete covering of the substrates was observed. Substrates were covered by layers that provide a completely different nano-topography than the general aspect of the

bare substrates. Moreover, the mechanical properties change yielding lower Young's modulus with each new layer. Thus, the surface mechanical properties of the system can be controlled by the number of layer used to form them

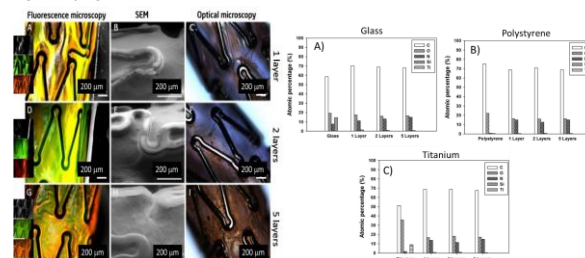


Figure 1. Fluorescence, SEM) and optical micrographs of coronary stents after the LbL process. And Evolution of the atomic percentage on the outer surface as function of the number of layers

We show an alternative catalyst free click covalent LbL method based on catalyst free click chemistry applied to ELRs. This originate a completely cytocompatible technology to biofunctionalize surfaces. Short times and mild conditions are adequate for cell encapsulation applications, combining cells and materials in the same LbL approach, which are currently being evaluated in our laboratory..

### CONCLUSION

In this work, structures, as simple as flat pieces or as complicated as 3D metallic grids, made of several materials, have been biofunctionalized by LbL techniques by using clickable ELRs and without the need of any other molecules. The use of an ELR having a bioactive sequence as RGD will improve the cell adhesion to these functionalized surfaces. Moreover, any other peptide domains that can be incorporated to the ELR backbone can be also used under this same approach.

### REFERENCES

- (1) Costa, R. R.; Mano, J. F. Chemical Society Reviews 2014, 43, 3453.
- (2) González de Torre, I.; Santos, M.; Quintanilla, L.; Testera, A.; Alonso, M.; Rodríguez Cabello, J. C. Acta Biomaterialia 2014, 10, 2495

### ACKNOWLEDGMENTS

We acknowledge financial support from the EU through the European regional development fund (ERDF) NMP3-LA-2011-263363, HEALTH-F4-2011-278557, PITN-GA-2012-317304, from the MINECO (MAT-2010-15982, MAT2010-15310, PRI-PIBAR-2011-1403 and MAT2012-38043-C02-01), the JCyL (projects VA152A12-2, VA244U13 and VA155A12-2), the CIBER-BBN, and the JCyL and the Instituto de Salud Carlos III under the "Network Center of Regenerative Medicine and Cellular Therapy.

# Paired Cyclodextrin Polyelectrolytes Multilayer Coatings onto a Textile Support for Prolonged Drug Delivery of Model Molecules

Jatupol Junthip<sup>1</sup>, Nicolas Tabary<sup>1</sup>, Bernard Martel<sup>1</sup>, Laurent Leclercq<sup>2</sup>, Feng Chai<sup>3</sup>, Nicolas Blanchemain<sup>3</sup>

<sup>1</sup>Unité Matériaux et Transformations (UMET) UMR CNRS 8207, University of Lille, France

<sup>2</sup>Université Montpellier, Institut des Biomolécules Max Mousseron (IBMM) UMR CNRS

<sup>3</sup>INSERM U 1008, Controlled Drug Delivery Systems and Biomaterials, Lille, France

[nicolas.tabary@univ-lille1.fr](mailto:nicolas.tabary@univ-lille1.fr)

## INTRODUCTION

Surface modification of biomaterial devices is commonly used to reduce the risk of infection. Polyelectrolyte multilayer (PEM) coatings have become an original way to functionalize these surfaces by immobilizing drugs or active molecules in multilayer films according to the Layer-by-Layer technique (LbL) [1]. In these kinds of system, cyclodextrin polymers (polyCD) can be especially used to embed hydrophobic drug with preserved activity. The present work focus on a PEM system based on two oppositely charged cyclodextrin polyelectrolytes and applied to a textile substrate for drug delivery of model molecules. After optimization, the cytocompatibility, drug release and antibacterial activity of multilayer assemblies were assessed.

## EXPERIMENTAL METHODS

The virgin textile PET (PET, 65 g.m<sup>-2</sup>) samples were preliminary functionalized by *pad-dry-cure* process to obtain negative charges on the surface [2]. The weight gain of this anionic layer was fixed at 6 and 20% wt (respectively 1.6 and 6.5  $\mu\text{mol}$  of COOH/cm<sup>2</sup> of textile). The build-up of the multilayer assembly was monitored in situ by Optical Waveguide Lightmode Spectroscopy (OWLS) on the one hand and was assessed by gravimetry on the other hand when applied onto the textile substrate. The dip-coating process used for the LbL build-up was performed at room temperature with both positive and negative CD polyelectrolytes solutions in water at their natural pH, synthesized according the method of Junthip and al. [3] (the positive polyEPG-CD-X was prepared by reacting  $\beta\text{CD}$  with epichlorohydrin (EP) in presence of glycidyltrimethylammonium chloride (GTMAC, X= molar ratio GTMAC/CD was 1 or 10) and the negative polyCTR-CD was prepared by reacting  $\beta\text{CD}$  with citric acid (CTR) in presence of sodium hypophosphite as catalyst). The incorporation of 4-tert-butyl benzoic acid (TBBA) as drug model molecule was carrying out by dipping the textile into polyCTR-CD/TBBA and polyEPG-CD-X solutions. The release of TBBA was determined by UV-visible spectroscopy at 235 nm. The cytocompatibility of the modified textile was evaluated with epithelial cells (L132) according to the ISO 10993-5 standards. The antibacterial activity was determined by the time-dependent bacterial reduction (Kill Time) on *Staphylococcus aureus*, CIP224 and *Escherichia coli* K12.

## RESULTS AND DISCUSSION

The weight gain of assembly changed with both the nature of polyEPG-CD-X and thermofixed layer of polyCTR-CD. A better LbL deposition was found with the polyEPG-CD-10 even in 6 or 20% thermofixed layer used, and it was proportional to the amount of COOH groups of the thermofixed layer (Figure 1). Incorporation of TBBA disturbed slightly the build-up of the LbL system. A sustained release of TBBA until 7 days was also obtained particularly in 20%-polyEPG-CD-10 system. This system also exhibited a better intrinsic antibacterial activity against *S.aureus* and *E.coli*.

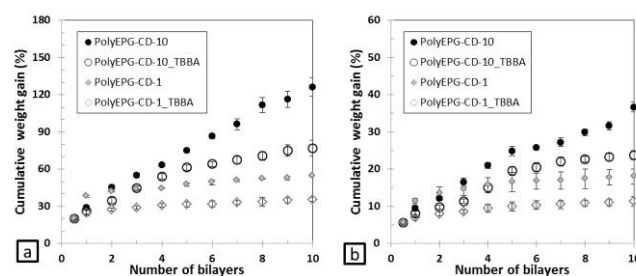


Figure 1: Evolution of cumulative weight gain of the textile with the number of bilayers of the PEM coating based on polyEPG-CD-X and polyCTR-CD in presence or in absence of TBBA. The textile samples were preliminarily treated by thermofixation corresponding to weight increases of (a) 6% of polyCTR-CD and (b) 20% of polyCTR-CD.

## CONCLUSION

We demonstrated the possibility to control the reservoir properties and the sustainability of the antibacterial activity through the extent of the multilayer deposition onto the PET support. The next steps should focus on the loading of various drugs with polyvalent therapeutic activity.

## REFERENCES

- [1]Decher et al, *Thin Solid Films*, 210-211, Part 2(0), 831-835, 1992
- [2]Martin et al, *Carbohydrate Polymers*, 93, 718-730, 2013
- [3]Junthip et al, *Carbohydrate Polymers*, 126, 156-167, 2015

## ACKNOWLEDGMENTS

Thanks to the Royal Thai Government Scholarship allocated upon the Ministry of Science and Technology who supported this work to the first author.



## Spatial Arrangements of Carboxylate-Derived Ti6Al4V Alloy for Medical Applications

Abraham Rodríguez-Cano<sup>1,2</sup>, Anna Zdziennicka<sup>3</sup>, Margarita Hierro-Oliva<sup>1,2</sup>, Maria Luisa González-Martín<sup>1,2</sup>, Reyes Babiano<sup>4</sup>, Pedro Cintas<sup>4</sup>, Bronisław Jańczuk<sup>3</sup>

<sup>1</sup>Dept. of Applied Physics, Univ. of Extremadura, Badajoz, Spain

<sup>2</sup>Networking Research Center on Bioengineering, Biomaterials and Nanomedicine (CIBER-BBN)

<sup>3</sup>Dept. of Interfacial Phenomena, Maria Curie-Skłodowska University, Lublin, Poland

<sup>4</sup>Dept. of Organics and Inorganics Chemistry, Univ. of Extremadura, Badajoz, Spain

[margahierro@unex.es](mailto:margahierro@unex.es)

## INTRODUCTION

Microbial infection is probably the most detrimental side complication after orthopedic surgery. Moreover, the overuse and misuse of antibiotics have led to increasing resistance to these drugs. For these reasons, the research in this field is focus on the surface modification of biomaterials in order to achieve a high effective inhibition of bacterial colonization. To this end, we have modified the Ti6Al4V alloy surface with several antibacterial compounds such as carboxylic acids, with promising results [1, 2]. Herein, we report the structural characterization of carboxylate-derived Ti6Al4V for medical applications.

## EXPERIMENTAL METHODS

**Contact angle analyses.** A contact angle goniometer DO4224Mk1 (KRÜSS GmbH) was used. Droplets of pure water (4  $\mu$ L, 100  $\mu$ L min<sup>-1</sup>), diiodomethane (2  $\mu$ L, 50  $\mu$ L min<sup>-1</sup>) and formamide (4  $\mu$ L, 100  $\mu$ L min<sup>-1</sup>) were gently deposited on the surfaces and measured at room temperature (20 °C). Left and right contact angles for each drop were measured with Drop Shape Analysis 3 (DSA3) software implemented with Tangent 2 method. At least two drops of each liquid on at least two different samples were analysed. **Surface preparation.** The coated-Ti6Al4V disks (ELI grade 23, DKSH Ltd (SWZ)) were prepared under the optimal conditions previously reported by our group [1,2]. In brief, the disks were polished, etched in piranha solution (H<sub>2</sub>SO<sub>4</sub>:H<sub>2</sub>O<sub>2</sub> 1:1, 30 min, 45 °C), amino-silanized (aminopropyltrimethoxysilane 1M, 6 h) and cross-linked (24 h, 120 °C). Then, the disks were reacted with sorbic (0.156 M, 52 h, 60 °C) or benzoic (1 M, 24 h, 60 °C) acids solutions yielding ammonium-salts. Cleaning steps in ultrasonic bath after each treatment were set.

## RESULTS

Table 1 shows surface free energy and components for polished (PO), silanized (SL, after 1 min) and treated with sorbic (SR) or benzoic acids (BZ) Ti6Al4V alloy, what were analysed by using the van Oss model (1).

$$\gamma_{SL} = \gamma_S + \gamma_L - 2(\gamma_S^{LW} \gamma_L^{LW})^{1/2} - 2(\gamma_S^+ \gamma_L^-)^{1/2} - 2(\gamma_S^- \gamma_L^+)^{1/2} \quad (1)$$

Table 1. Surface free energy of coated and polished Ti6Al4V alloy.

Sample	Surface free energy (value $\pm$ SD) (mJ m <sup>-2</sup> )			
	$\gamma_S^{LW}$	$\gamma_S^-$	$\gamma_S^+$	$\gamma_S$
PO	39 $\pm$ 1	8 $\pm$ 1	1.3 $\pm$ 0.3	45 $\pm$ 1
SL*	41 $\pm$ 1	2.2 $\pm$ 0.3	0.20 $\pm$ 0.05	42 $\pm$ 1
SR	41 $\pm$ 1	18 $\pm$ 2	2.7 $\pm$ 0.4	55 $\pm$ 1
BZ	40.6 $\pm$ 0.8	4 $\pm$ 2	0.5 $\pm$ 0.2	43.2 $\pm$ 0.9

## DISCUSSION & CONCLUSIONS

Lifshitz-van der Waals component ( $\gamma_S^{LW}$ ), electron-donor ( $\gamma_S^-$ ) and electron-acceptor ( $\gamma_S^+$ ) parameters, and also surface free energy ( $\gamma_S$ ) were used to unveil the functional group oriented toward the external layer. High values of  $\gamma_S^-$  and  $\gamma_S^+$  demonstrate the presence of –COOH, instead low values are according with the phenyl group (Figure 1).

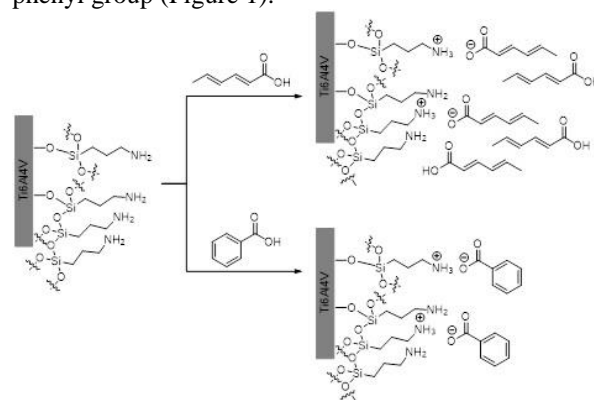


Fig. 1: Structural arrangements of Ti6Al4V alloy surfaces derived via ammonium-salt formation.

**REFERENCES:** <sup>1</sup>A. Rodríguez-Cano et al. (2013) *Colloid and Surfaces B: Biointerfaces* **106**:248-257. <sup>2</sup>A. Rodríguez-Cano A. et al., *Surface and Coatings Technology* (2014) **245**:66–73.

**ACKNOWLEDGEMENTS:** Authors are grateful to Consejería de Economía, Ciencia e Innovación, Junta de Extremadura and FEDER (GR10049) and to Ministerio de Ciencia e Innovación (MAT2009-14695-C04-01 and BES-2010-033417) and Ministerio de Economía y Competitividad (EEBB-14-1-09051).



# Structural Characterization of Silver-Organic Complexes on Ti6Al4V

Rodríguez-Cano, A.<sup>1,2</sup>, Zdziennicka, A.<sup>3</sup>, González-Martín, M.L.<sup>1,2</sup>, Cintas, P.<sup>4</sup>, Babiano, R.<sup>4</sup>,  
Fernández-Calderón, M.C.<sup>2,5</sup>, Jańczuk, B.<sup>3</sup>

<sup>1</sup>Dept. of Applied Physics, Univ. of Extremadura, Badajoz, Spain

<sup>2</sup>Networking Research Center on Bioengineering, Biomaterials and Nanomedicine (CIBER-BBN)

<sup>3</sup>Dept. of Interfacial Phenomena, Faculty of Chemistry, Maria Curie-Skłodowska University, Lublin, Poland

<sup>4</sup>Dept. of Organic and Inorganic Chemistry, Univ. of Extremadura, Badajoz, Spain

<sup>5</sup>Dept. of Biomedical Sciences, Univ. of Extremadura, Badajoz, Spain

[mlglez@unex.es](mailto:mlglez@unex.es)

## INTRODUCTION

Biocompatible materials such as Titanium and related alloys are commonly used in the replacement of human hard tissues due to their adequate properties. However, bacterial colonization is one of the most important reasons of their failure that used to imply subsequent surgeries. In order to prevent bacterial adhesion and proliferation, many approaches have been proposed, searching also to enhance the biocompatibility of the material. In this line, we have modified the Ti6Al4V alloy surface with several antibacterial compounds such as carboxylic acids, aldehydes, antibiotics, etc. via their anchoring to a broad and well-defined poly(aminosiloxane) network [1,2]. Herein, we present the structural characterization of silver-mediated complexes with organic compounds on Ti6Al4V alloy surface, which have showed promising result in the inhibition of the bacterial adhesion.

## EXPERIMENTAL METHODS

### Surface preparation

The coated-Ti6Al4V disks (ELI grade 23, DKSH Ltd (SWZ)) were prepared under the optimal conditions previously reported by our group [1,2]. In brief, the disks were polished to a mirror finish, etched in piranha solution (H<sub>2</sub>SO<sub>4</sub>:H<sub>2</sub>O<sub>2</sub> 1:1, 30 min, 45 °C), amino-silanized (aminopropyltrimethoxysilane 1M, 6 h) and cross-linked (24 h, 120 °C) for stabilizing the coating. Then, the disks were reacted with silver acetate (1.8 mM, 48 h, 60 °C), and silver-containing surfaces were treated with sorbic (0.156 M, 72 h, 25 °C) or benzoic (1 M, 24 h, 25 °C) acids solutions yielding the silver-organic complexes. Cleaning steps in ultrasonic bath after each treatment were set. Polished disks were used as control.

### Contact angle analyses

A contact angle goniometer DO4224Mk1 (KRÜSS GmbH) was used. Droplets of pure water (4 µL, 100 µL min<sup>-1</sup>), diiodomethane (2 µL, 50 µL min<sup>-1</sup>) and formamide (4 µL, 100 µL min<sup>-1</sup>) were gently deposited on the surfaces and measured at room temperature (20 °C). Left and right contact angles for each drop were measured with Drop Shape Analysis 3 (DSA3) software implemented with Tangent 2 method. At least two drops of each liquid on at least two samples were analyzed.

## RESULTS AND DISCUSSION

Surface free energy ( $\gamma_s$ ) of polished (PO), silanized (SL), silver-derived (Ag), and complexed with sorbic (Ag-SR) or benzoic acids (Ag-BZ) Ti6Al4V alloy were

analysed by using the van Oss model. Lifshitz-van der Waals ( $\gamma_s^{LW}$ ) and acid-base ( $\gamma_s^{AB}$ ), as well as the electron-donor ( $\gamma_s^-$ ) and electron-acceptor ( $\gamma_s^+$ ) parameters were evaluated and the total surface free energy determined (Table 1).

Table 1. Surface free energy, components and parameters for modified Ti6Al4V surfaces.

Sample	Surface free energy (value $\pm$ SD) (mJ m <sup>-2</sup> )				
	$\gamma_s^{LW}$	$\gamma_s^{AB}$	$\gamma_s^-$	$\gamma_s^+$	$\gamma_s$
PO	39 $\pm$ 1	6 $\pm$ 1	8 $\pm$ 1	1.3 $\pm$ 0.3	45 $\pm$ 1
SL*	41 $\pm$ 1	1 $\pm$ 1	2.2 $\pm$ 0.3	0.20 $\pm$ 0.05	42 $\pm$ 1
Ag	40 $\pm$ 2	1 $\pm$ 2	2 $\pm$ 2	0.1 $\pm$ 0.4	41 $\pm$ 4
Ag-SR	43 $\pm$ 1	5 $\pm$ 1	7 $\pm$ 3	1.2 $\pm$ 0.2	48 $\pm$ 2
Ag-BZ	44.6 $\pm$ 0.9	3 $\pm$ 2	2 $\pm$ 1	0.8 $\pm$ 0.1	47 $\pm$ 2

All the surface treatments promote values of the Lifshitz-van der Waals component close to 40 mJ m<sup>-2</sup>, being higher for surfaces containing silver complexes. The acid-base component presents a high variability depending on the functional group that results oriented toward the external layer. Polar groups, such as those containing oxygen atoms do increase these values, while apolar substituent like phenyl lead to a significant decrease. The prevalent binding of such groups determines the hydrophobicity-hydrophilicity balance of these highly functionalized surfaces. Finally, the differences in the solid-surface free energy of these samples show high variation in their properties depending on the existence of polar or apolar groups.

## CONCLUSION

Contact angle goniometry show excellent results in order to determine the polar or apolar groups oriented to the external layer.

## REFERENCES

- Rodríguez Cano A. *et al.*, Colloid and Surfaces B: Biointerfaces 106:248-257, 2013.
- Rodríguez-Cano A. *et al.*, Surface and Coatings Technology 245:66–73, 2014.

## ACKNOWLEDGMENTS

The authors are grateful to Consejería de Economía, Ciencia e Innovación, Junta de Extremadura and FEDER by economical support (GR10049) and to Ministerio de Ciencia e Innovación (MAT2009-14695-C04-01 and BES-2010-033417) and Ministerio de Economía y Competitividad (EEBB-14-1-09051).



# Pulse Current Cathodic Deposition of Hydroxyapatite on Type 316L Stainless Steel

Sayaka Miyabe<sup>1</sup>, Naoya Asakura, Takuya Nakao and Shinji Fujimoto

Division of Materials and Manufacturing Science, Graduate School of Engineering, Osaka University, Japan  
[miyabe@mat.eng.osaka-u.ac.jp](mailto:miyabe@mat.eng.osaka-u.ac.jp)

## INTRODUCTION

HAp (Hydroxyapatite ( $\text{Ca}_{10}(\text{PO}_4)_6(\text{OH})_2$ )-coating has been examined to improve biocompatibility of metals and alloys applied as biomaterials. Plasma spraying, which is commonly used technique for producing HAp coatings on metallic implants, is hard to control the composition and structure of the HAp due to high-temperature during process. Moreover, it is a line-of-sight process. In contrast, cathodic deposition has advantages such as low-temperature process, ability to deposit on complex surface and low cost<sup>1</sup>. In the cathodic deposition process, HAp is not directly deposited by cathodic reaction. The reduction of water actually occurs as electrochemical reaction which induces local pH increase, then solubility of HAp decreases, resulting in HAp deposition. At the same time,  $\text{H}_2$  evolution leads to poor adherence of the HAp. One possible approach to improve adhesion of HAp is to employ pulse cathodic current<sup>2</sup>, because the pulse parameters such as pulse on and off time influence  $\text{H}_2$  evolution and pH changes. In the present study, the authors examined to form HAp coating on type 316L stainless steel by the pulse current cathodic deposition, then characterized the HAp layer with field emission-type scanning electron microscopy (FE-SEM) with energy-dispersive spectroscopy (EDS), X-ray diffraction (XRD) and fourier transform infrared (FT-IR) spectroscopy.

## EXPERIMENTAL METHODS

Material examined was type 316L stainless steel, the composition is as follow: Cr: 17.35, Ni: 12.18, Mo: 2.07, Mn: 1.20, Si: 0.63, P: 0.030, C: 0.011, S: 0.001, Fe: Bal. (wt%). The material was cut into square specimens with dimensions of 10 mm x 10 mm x 1 mm. The samples were polished with SiC abrasive paper up to #2000 and mirror-finished with 0.3, 0.03  $\mu\text{m}$  alumina powder, then ultrasonically cleaned in acetone and ethanol, followed by rinsing with deionized water and dried at room temperature. Electrochemical treatments were carried out in the solution containing 1.67 mM  $\text{K}_2\text{HPO}_4$ , 2.5 mM  $\text{CaCl}_2 \cdot 2\text{H}_2\text{O}$  and 138mM NaCl using a three-electrode electrochemical cell with a platinum counter electrode and Ag/AgCl as the reference electrode. The applied current densities were -100 mA/cm<sup>2</sup> and 0 mA/cm<sup>2</sup>, modulated as square wave, with various parameters ( $t_{\text{on}}$ : pulse on time and  $t_{\text{off}}$ : pulse off time).

## RESULTS AND DISCUSSION

Figure 1 shows SEM images of the depositions on type 316L stainless steels formed by constant current and various pulse currents. Regardless of the methods of current application, needle-like depositions were

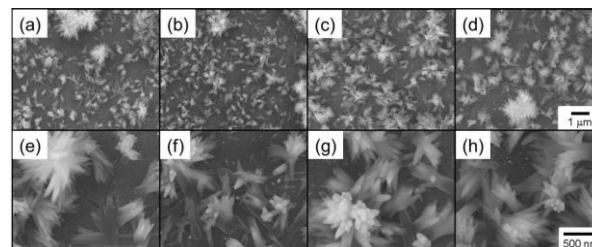


Fig. 1 SEM images of deposits formed on type 316L stainless steel by constant current ((a), (e)) and pulse current cathodic deposition of  $t_{\text{on}}-t_{\text{off}} = 2-4$  ms ((b), (f)), 20-40 ms ((c), (g)) and 200-400 ms ((d), (h)) at 100 mA/cm<sup>2</sup> for 30 min. (a)-(d) low magnification and (e)-(h) high magnification.

observed. The depositions were identified as carbonate containing apatite by XRD and FT-IR analysis. The deposition formed by constant current was more aggregated than that formed by pulse currents. Focusing on the effect of pulse parameter, the deposition formed by pulse current of  $t_{\text{on}}-t_{\text{off}} = 20-40$  ms coated more widely than that formed by pulse current of  $t_{\text{on}}-t_{\text{off}} = 2-4$  ms and 200-400 ms. Furthermore, the amount of the deposition formed by pulse current of  $t_{\text{on}}-t_{\text{off}} = 20-40$  ms was larger than that of that formed by pulse current of  $t_{\text{on}}-t_{\text{off}} = 2-4$  ms and 200-400 ms. These results suggest that the effectiveness of the pulse current for the cathodic deposition of hydroxyapatite and to set appropriate pulse parameter can increase the deposition amount and reduce the aggregation of apatite.

## CONCLUSIONS

The pulse current cathodic deposition was examined for deposition of HAp on type 316L stainless steel, and the following conclusions are obtained:

1. Needle-like depositions were observed on the substrates applied both constant current and pulse current. The depositions were identified as carbonate containing HAp.
2. Appropriate pulse current can increase the amount of deposition and suppress the aggregation of apatite.

## REFERENCE

1. Redepenning J. et al., Chem. Mater. 2:625-627, 1990
2. Blackwood D. J. et al., Mater. Sci. Eng. C 30:561-565, 2010

## ACKNOWLEDGMENT

This study was supported by the Grant-in-Aid for Young Scientists (B) (Project No. 25870410) from the Japan Society for the Promotion of Science.

## Evaluation of Biomaterials Modified by UV Nanosecond Nd:YVO<sub>4</sub> Laser. Effects on Cell Viability

E.F. Burguera<sup>1,2</sup>, M.P. Fiorucci<sup>3</sup>, L. Gato-Calvo<sup>2</sup>, J. Magalhães<sup>1,2</sup>, A.J. López<sup>3</sup>, S. Pozo-António<sup>3</sup>, F.J. Blanco<sup>2</sup>, A. Ramil<sup>3</sup>

<sup>1</sup>Ciber de Bioingeniería, Biomateriales y Nanomedicina (CIBER-BBN).

<sup>2</sup>Grupo de Bioingeniería Tisular y Terapia Celular (GBTTC-CHUAC), Servicio de Reumatología, Instituto de Investigación Biomédica de A Coruña (INIBIC), Complejo Hospitalario Universitario de A Coruña (CHUAC), SERGAS, Universidade da Coruña, 15006 A Coruña, Spain

<sup>3</sup>Laboratorio de Aplicacións Industriais do Láser, Centro de Investigacións Tecnolóxicas (CIT), Departamento de Enxeñaría Industrial II, Escola Politécnica Superior, Universidade de Coruña, Campus Ferrol, 15403 Ferrol, Spain

[Joana.cristina.silva.magalhaes@sergas.es](mailto:Joana.cristina.silva.magalhaes@sergas.es)

### INTRODUCTION

The performance of implant materials depends on their composition and bulk physical properties, but also, critically on their surface properties. Surface topography mediates cellular response at the implant/surrounding tissue interface<sup>1</sup>. Laser micro-machining is an emerging surface modification strategy that allows precisely controlled processing to obtain diverse textures on implantable metallic surfaces<sup>2</sup>.

### EXPERIMENTAL METHODS

Laser surface modification, by means of a UV nanosecond Nd:YVO<sub>4</sub> laser structuring, was conducted on two typical implant materials, stainless steel 316L and titanium alloy Ti6Al4V, to create different surface patterns and densities. In particular, two configurations were designed: a matrix of pits and a series of parallel grooves were machined into the surfaces, with different spacing, 50, 75 and 100  $\mu\text{m}$ . Surfaces were characterized with optical and scanning electron microscopy. Topographic characterization was also performed with a profilometer.

To study the effects of the topographic changes on cell behaviour we performed a viability assay with human bone derived cells (HBCs) isolated from trabecular bone by explant culture. Cells were seeded ( $10^4$ /sample) on the differently texturized metal surfaces. Differences in viability were quantified with the alamarBlue® method. A cleaning protocol was optimized to eliminate all organic residual matter to reuse the metallic surfaces in subsequent experiments.

### RESULTS AND DISCUSSION

Laser micromachining resulted in two distinct types of topographies, a matrix of pits and a distribution of parallel grooves. Spacing separating features was either 50, 75 or 100  $\mu\text{m}$ , which were achieved with high precision and reproducibility.

Cellular origin was checked by means of immunofluorescence of alkaline phosphatase and collagen type I, confirming an osteoblastic phenotype. Cells attached and were viable on all the surfaces tested, but we found differences in cell viability due to the different laser treatments. First, all laser treatments slightly reduced cell viability with respect to the untreated control samples. Cell viability was also slightly lower in the stainless steel samples with respect

to Ti6Al4V samples. Cells generally preferred the pit morphology to the grooves, and the larger the distance between the features the better, i.e. P100 was better than P50.

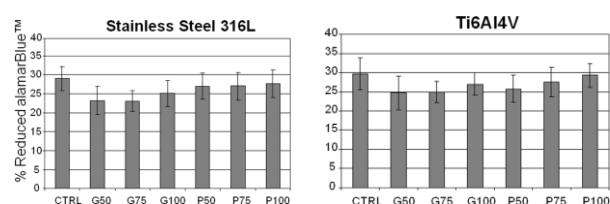


Fig. 1 Osteoblast viability as a function of surface topography; matrix of pits (P), grooves (G).

Further experiments will be performed to evaluate other cell parameters, in particular those relevant to cell adhesion and osteoblasts-like phenotype maintenance. The developed cleaning procedure, that included a plasma cleaning step, satisfactorily removed all organic matter from the biometal surfaces, as shown by carbon elemental (EDX) surface analysis.

### CONCLUSIONS

Surface microstructuring resulted in differences in cell viability. Ti6Al4V with a matrix of pits and 100  $\mu\text{m}$  exhibited the best results. The cleaning protocol was appropriate to eliminate residual matter from the surfaces.

These results indicate the potential of UV nanosecond laser treatment as a relevant tool to precisely modify implant surface micro-structuring and influence cell behaviour.

### REFERENCES

1. Jäger M. *et al.*, J. Biomed. Biotechnol. (8):69036, 2007
2. Kurella A. *et al.*, J. Biomater Appl. 20:5-50, 2005.

### ACKNOWLEDGMENTS

EF Burguera and J Magalhães thank CIBER-BBN and the Galician Network of Biomaterials (R2014/033) for their financial support. CIBER-BBN is a Spanish National Initiative of ISCIII. We thank the patients from the Traumatology and Rheumatology Services of the CHUAC that donated tissue for this study. MP Fiorucci would like to thank A Tempo project for the research contract.



Alexey Klymov<sup>1</sup>, Remco Doodkorte<sup>1</sup>, John A Jansen<sup>1</sup>, X Frank Walboomers<sup>1</sup>

<sup>1</sup>Radboud University Medical Center, Department Biomaterials, Nijmegen, The Netherlands

[Alexey.Klymov@radboudumc.nl](mailto:Alexey.Klymov@radboudumc.nl)

## INTRODUCTION

Adherent cells have the intrinsic property of binding, and reacting to the topographical features of their microenvironment. Such mechanisms are nowadays exploited for design of artificial surfaces controlling cell-behavior *in vitro*. We studied the cellular ability to recognize and to display preferential migration between different patterns. Furthermore, we evaluated the contribution of focal adhesions to the observed behavior.

## EXPERIMENTAL METHODS

For the experiments a multi-patterned culturing substrate (submicron and nanometric grooves/squares) was utilized. The individual patterned fields of 500x500µm<sup>2</sup> were enclosed by a smooth surface, allowing migrating cells to experience interfaces of patterns. It was hypothesized that cells with preference for a pattern would mostly enter the topographical field, while staying on the smooth surface in case of repulsion (Figure 1). Cell lines with differences in the expression

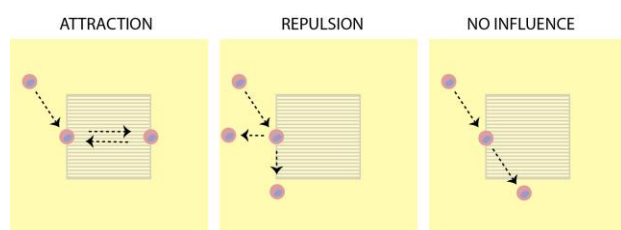


**Figure 1:** Theoretical model for cell-preferential migration on a multi-topographical substrate.

level of the focal adhesion dynamic regulating metalloproteinase MT1-MMP were cultured on the substrates over a period of 48 hours. The recorded time-lapse micrographs were analyzed for the cellular preference migration behavior. In the last part of the study the cell-line displaying the strongest pattern-loving behavior was co-cultured with cells that preferred the smooth surfaces to see the separation ability of the multi-patterned surface.

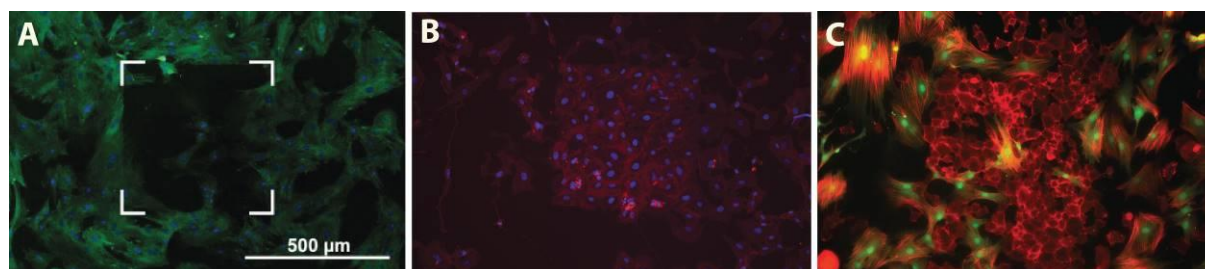


**Figure 2:** Topographical control over cell-repelling or attraction of a surface. A) Nano-sized squares can be used to avoid the interaction of the surface with primary mesenchymal cells B) Same pattern can be used for the attraction of a mineralizing osteoblast cell line. C) Simultaneously seeded mesenchymal and osteoblast cells are separated by the topography (from our own data, in progress for publication; A from Klymov et al. Acta biomaterialia 2015. B and C Manuscript in preparation)

## RESULTS AND DISCUSSION

In our results, we found a clear correlation between MT1-MMP expression and cellular behavior on patterns. The more dynamic the focal adhesions were, the more the cells tended to enter topographical fields, remain, and proliferate, slowly leading to filling up of the field (Figure 2). Moreover, cells with contrasting properties could be separated during co-culture on the multi-patterned surface.

## CONCLUSION

Cells feature a pattern recognition mechanism, which is mediated by focal adhesions. The here found mechanisms can be utilized during the design of various surfaces for the means of tissue regeneration. Moreover, it can deliver *in vitro* methods for separation of cells in co-culture models.

## REFERENCES

1. Klymov A, Prodanov L, Lamers E, Jansen JA, Walboomers XF. Understanding the role of nano-topography on the surface of a bone-implant. *Biomater Sci-Uk* 2013;1:135-51.
2. Klymov A, Bronkhorst EM, Te Riet J, Jansen JA, Walboomers XF. Bone marrow-derived mesenchymal cells feature selective migration behavior on submicro- and nano-dimensional multi-patterned substrates. *Acta biomaterialia* 2015.

## ACKNOWLEDGMENTS

This work was supported by a grant from the Dutch government to the Netherlands Institute for Regenerative Medicine (NIRM, grant No. FES0908). We also thank Dr. Katarina Wolf from the Radboud Institute for Molecular Life Sciences for the kind provision of the cell-lines.



## Innovative Nanostructured Medical Devices - A Risk of Nanoparticles Release

Laëtitia Salou<sup>1,2,3</sup>, Engin Vrana<sup>4,5</sup>, Anne Piscitelli<sup>6</sup>, Pierre Layrolle<sup>1</sup>, Guy Louarn<sup>2</sup>, Valérie Dumay<sup>3</sup>

<sup>1</sup> Inserm U957, Lab. Pathophysiology of bone resorption, University of Nantes, France

<sup>2</sup> CNRS –Institut des Matériaux, Nantes, France

<sup>3</sup> Biomedical Tissues, Nantes, France

<sup>4</sup> Inserm U1121, Biomatériaux et Bioingénierie, Strasbourg, France

<sup>5</sup> Protip Medical, Strasbourg, France.

<sup>6</sup> Subatech, Nantes, France.

[laetitia.salou@univ-nantes.fr](mailto:laetitia.salou@univ-nantes.fr)

### INTRODUCTION

Titanium and its alloys are commonly used for medical applications because of their good mechanical properties and biocompatibility. The surface properties of titanium implants are key factors for rapid and stable bone tissue integration. Micro-rough surfaces are commonly prepared by grit-blasting and acid-etching. However, proteins and cells interact with implant surfaces in the nanometer range. During this last decade, titania nanotubes have attracted interest because of their favourable bone tissue integration by a phenomenon of mechano-transduction (1). Although bacterial infection are the most severe and devastating complication, scientifics also discover the presence of nano-particles around failing implants. The aim of the study is to realise a nano-bioactive surface on tracheal prosthesis and determine it adhesion onto the titanium substrate and the release of particles.

### EXPERIMENTAL METHODS

Titanium Commercially Pure (cp) prothesis were treated using an anodization process to form titania nanotubes. After rinsing, an annealing treatment was performed at 500°C for 2h. Surface morphology was investigated by FEG-SEM. Chemical and physical property were characterized by means of EDS, XPS, RAMAN and XRD analysis. Nanotubes adhesion were measured by scratch test and nanotribology assay. Prothesis were immersed in buffer solution in order to measure any nanoparticle release by using Laser Induced Breakdown Detection (LIBD). Data were statistically analyzed for significance using Mann-Whitney and Kruskal-Wallis statistical tests (p-value<0.05).

### RESULTS AND DISCUSSION

SEM observations showed a regular nanotubular surface with pores of 30 nm in diameter. EDS and XPS analysis reveals the migration of fluoride from the electrolyte into the newly formed oxide layer. It has been observed that the quantity of fluoride decreased with heat treatment due to the evaporation of TiF<sub>4</sub>. LIBD analysis reveals the presence of nanoparticle detached from the surface. Particules release was also observed in the water bath of the rinsing step. [TiF<sub>6</sub>]<sup>2-</sup> species are the main cause of this weak adhesion due to its solubility in water. These results were confirmed by scratch test analysis, for which we obtain a critical value of only 25 mN. Nanotribology assay also show a weak surface behaviour under wear and delamination are observed by individual nanotubes, by agregats or by plates.

### CONCLUSION

Nanostructured surface have been widely published to give promising biological results for biomedical application. However this study reveal weak mechanical properties of the oxide layer. Moreover nanoparticles released from this innovative surface and could be a risk to implants failure. Particules emissions is a current top as a new European regulation will take place this year regarding the incorporation of nanomaterials in medical devices.

### REFERENCES

1. Bacakova L. *et al.*, J. Biotechnology. Adv. 29:739-767, 2011

### ACKNOWLEDGMENTS

The authors would like to acknowledge the National Association of Research and Technology (ANRT) for providing financial support to the PhD thesis of LS.



## Chitosan Nanofibers for Peripheral Nerve Applications

Cristiana R. Carvalho<sup>1,2</sup>, Albino Martins<sup>1,2</sup>, Nuno M. Neves<sup>1,2</sup>, Rui L. Reis<sup>1,2</sup>, Joaquim M. Oliveira<sup>1,2</sup>

<sup>1</sup> 3B's Research Group - Biomaterials, Biodegradables and Biomimetics, University of Minho, Headquarters of the European Institute of Excellence on Tissue Engineering and Regenerative Medicine, AvePark, 4806-909 Taipas, Guimarães, Portugal

<sup>2</sup> ICVS/3B's - PT Government Associate Laboratory, Braga/Guimarães, Portugal  
[miguel.oliveira@dep.uminho.pt](mailto:miguel.oliveira@dep.uminho.pt)

### INTRODUCTION

The clinical gold standard for bridging peripheral nerve gaps of critical length is the transplantation of autologous nerve tissue, which is harvested from sensory nerves of the same patient<sup>1</sup>. In general, autologous nerve grafts provide optimal guidance cues for regenerating nerve fibers, such as peripheral glia cells and Schwann cells (SCs). They do not only produce regeneration-promoting factors but also line their basal laminae up to the so-called bands of Bungner, the guiding tubes within the distal nerve segments<sup>2</sup>. Undoubtedly, the use of autologous nerve tissue leads to loss of sensation at the site of harvest and the functional outcome after its utilization is described to range from extremely poor to satisfying. As an alternative to this, tubulisation strategies, using biomaterials, have been performed<sup>3-5</sup>. However, so far the results have been quite disappointing. To tackle this, new biomaterials have been developed that can easily be modified to provide an optimized environment for peripheral nerve regeneration and qualify as substitutes for autologous nerve grafts. Chitosan is among the biodegradable polymers that demonstrate good properties for neural tissue engineering<sup>6</sup>. It is an attractive material to produce as an inner guidance of nerve conduits, because it can easily be blended with other materials or be processed in different ways provide guiding and structural cues supporting axonal growth<sup>7</sup>.

### EXPERIMENTAL METHODS

Chitosan (CS) powders from Altakitin (Portugal) were supplied and its cytotoxicity was assessed. Using these biomedical grade powders, biodegradable scaffolds were developed to support neuronal regeneration using the electrospinning technique to produce nanofibers from chitosan solutions. Random and aligned nanofibers were produced and characterized, using techniques such as Fourier Transform Infrared Spectroscopy (FTIR), Scanning Electron Microscopy (SEM), Atomic Force Microscopy (AFM), Differential Scanning Calorimetry (DSC) and Contact Angle. *In vitro* tests to characterize L929 cells viability (MTS assay) and proliferation (DNA quantification) on nanofibers scaffold were performed.

### RESULTS AND DISCUSSION

Medical grade CS powders were found to be non-cytotoxic. To produce a mesh of random chitosan fibers with no beads or other defects, a 5% chitosan solution in trifluoroacetic-acid and dichloromethane as solvents, in the proportion of 70:30 was used. The produced

nanofibers are super hydrophilic, defect-free and have an average diameter of  $184 \pm 36$  nm. Yarns of aligned chitosan fibers were obtained using two blades placed in line set up, with the exact same conditions used to obtain random nanofibers. Cell viability and proliferation increased over time showing this is a suitable substrate for cell adhesion.

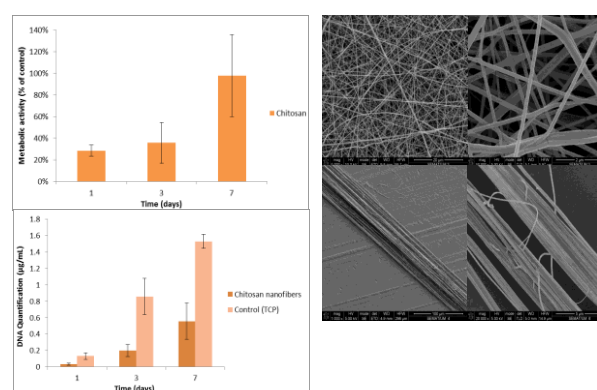


Figure 1 – Random and aligned nanofibers were produced. L929 cells adhere and proliferate up to 7 days.

### CONCLUSION

After physico-chemical analyses, was shown that the fibers produced did not undergo any relevant chemical modification after processing. Biological assays indicated that the scaffold is non-cytotoxic and allowed cellular proliferation over time. Therefore, it can be concluded that the scaffold can find promising applications in peripheral nerve regeneration, specifically as guiding luminal filler.

### REFERENCES

1. Ray WZ, et al. Experimental neurology. 2010 May;223(1):
2. Pfister BJ, et al. Critical reviews in biomedical engineering. 2011;39(2)
3. Oliveira JT, et al. Frontiers in neuroanatomy. 2014;8(111)
4. Wang Z, et al. American journal of translational research. 2014;6(4)
5. Konofaos P, et al. Journal of reconstructive microsurgery. 2013 Mar;29(3)
6. Haastert-Talini K, et al. Biomaterials. 2013 Dec;34(38)
7. Wrobel S, et al. Tissue engineering Part A. 2014 Sep;20(17-18):

### ACKNOWLEDGMENTS

The authors would like to thank the EC funded Biohybrid project (Biohybrid Templates for peripheral nerve regeneration, grant agreement number 278612) The certified medical grade chitosan used for all tests was supplied by Altakitin S.A. (Lisboa, Portugal).



## The Concurrent-Electrospinning of Polylactide and Gelatine Fibres as a Way of Obtaining Advanced Hybrid Materials

Anna Magiera<sup>1</sup>, Stanisław Błazewicz<sup>1</sup>

<sup>1</sup>Faculty of Materials Science and Ceramics, Department of Biomaterials, AGH University of Science and Technology, Poland

[asocha@agh.edu.pl](mailto:asocha@agh.edu.pl)

### INTRODUCTION

During the electrospinning (ES) process fibrous form of a material (mainly polymer) is obtained from its liquid state<sup>1</sup>. Nanocomposite fibres can be produced due to functionalisation of a polymer precursor with nanoconstituents. Electrospun fibrous structures have already been applied in numerous fields<sup>2-4</sup>, which makes this technique extremely versatile and worth further developing. The concurrent electrospinning (co-ES) technique is a modification of the standard ES method in which more than one jet is simultaneously generated from multiple polymer sources<sup>5</sup>.

This work focuses on the obtaining of the individual poly(lactic acid) (PLA) and gelatine (GEL) fibres via ES technique and the composite PLA/GEL material by co-ES method. The fibrous samples were analysed using scanning electron microscopy (SEM).

### EXPERIMENTAL METHODS

#### MATERIALS

To obtain polymeric fibres the PLA (Ingeo™ Biopolymer 3251D) and GEL (POCH, analytical grade) were used. As solvents dichloromethane (DCM) (POCH, analytical grade), N,N-dimethylformamide (DMF) (POCH, analytical grade) and concentrated (99,5-99,9 %) acetic acid (CH<sub>3</sub>COOH) (POCH, analytical grade) were used. The PLA solution in the concentration of 15 % (wt/v) was prepared in mixed solvents DCM, DMF 3:1 (wt:wt)<sup>6</sup>. The GEL (in the concentration of 20 % (wt/v)) was dissolved in concentrated acetic acid<sup>7</sup>.

#### ELECTROSPINNING PROCESS

The ES experiments were conducted using a device constructed at the Department of Biomaterials, AGH-UST. A 10 ml syringe, ended with a needle having a diameter of 0,9 mm, was loaded with the polymer solution. The voltage of 12 kV was applied between the needle tip and the collector, moving grounded roller covered with an aluminium foil. The tip-to-collector distance was 3 cm. The electrospinning processing conditions were determined in previous experiments<sup>6,7</sup>.

#### SCANNING ELECTRON MICROSCOPE ANALYSIS

The samples obtained were coated with gold and analysed using scanning electron microscope, SEM (JROL 5400 microscope with EDS analyser).

### RESULTS AND DISCUSSION

Individual PLA and GEL fibres have been obtained using the ES experimental setup constructed at the AGH University of Science and Technology. Nanofibre diameters and porosity of the resulting fibrous samples were determined from the SEM images. The

microphotographs FIG. 1A-1B illustrate the extent of porosity between the nanofibres of nonuniform fibre distribution. The microstructure of samples is characterized by high amount of interconnected open pores up to 95 %, and the pore sizes were in micron scale. A slight variation in fibre diameter distribution was found.

Hybrid PLA/GEL structure has been obtained as it is shown in FIG. 1C. An interaction between the two simultaneously generated jets results in an increasing nanofibre-to-nanofibre contact and decreasing sample porosity.

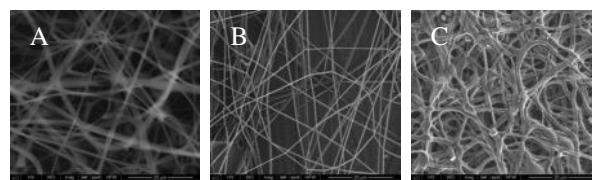


FIG. 1. SEM images of (A) PLA, (B) GEL, and (C) PLA/GEL fibres. Scale bars 20 μm.

### CONCLUSION

The aim of this work was to obtain the hybrid polylactide (PLA) and gelatine (GEL) fibrous structure via the concurrent electrospinning (co-ES) technique. The experiments performed proved the possibility of manufacturing polymeric fibres under relatively low voltage conditions (12 kV) using a simple, laboratory scale device. The co-electrospun composite of PLA/GEL has been successfully obtained. Further functionalisation of the hybrid polymeric structure should be performed in the future as it constitutes a promising path towards the manufacture of specialised multifunctional materials.

### REFERENCES

1. A. Frenot *et al.*, Curr. Opin. Colloid Interface Sci. 8:64-75, 2003
2. Chigome S. *et al.*, Anal. Chim. Acta 706:25-36, 2011
3. Balamurugan R. *et al.*, Membranes 1:232-248, 2011
4. Inagaki M. *et al.*, Adv. Mater. 24:2547-2566, 2012
5. Ladd M.R. *et al.*, Biomaterials 32:1549-1559, 2011
6. Socha A. *et al.*, Engineering of Biomaterials 115:12-17, 2012
7. Magiera A. *et al.*, Engineering of Biomaterials 121:6-12, 2013

### ACKNOWLEDGMENTS

The authors would like to thank the National Science Centre (Poland), Grant no: 2013/11/N/ST8/01169, for providing financial support to this project.

## Bone Marrow MSC Systemic Administration for *in vivo* IVD Regeneration

C. Cunha<sup>1,2</sup>, M.I. Almeida<sup>1,2</sup>, C.R. Almeida<sup>1,2</sup>, S. Lamas<sup>1,3</sup>, A.M. Silva<sup>1,2,4</sup>, M. Molinos<sup>1,2,4</sup>, C.L. Pereira<sup>1,2,4</sup>, G.Q. Teixeira<sup>1,2,4</sup>, S.G. Santos<sup>1,2</sup>, R.M. Gonçalves<sup>1,2</sup>, M.A. Barbosa<sup>1,2,4</sup>

<sup>1</sup>Instituto de Investigação e Inovação em Saúde, Universidade do Porto, Portugal

<sup>2</sup>INEB - Instituto de Engenharia Biomédica, Microenvironments for NewTherapies Group, University of Porto, Portugal

<sup>3</sup>IBMC - Instituto de Biologia Molecular e Celular, University of Porto, Portugal

<sup>4</sup>ICBAS, Department of Regenerative Medicine, University of Porto, Portugal

[carla.cunha@ineb.up.pt](mailto:carla.cunha@ineb.up.pt)

### INTRODUCTION

Cell therapies for IVD regeneration presently rely on transplantation of IVD cells or stem cells directly to the lesion site. Still, the harsh IVD environment given by low irrigation and high mechanical stress, poses problems to cell administration and survival. Our approach, instead, explores tissue regeneration via endogenous cell migration and/or signalling to the lesion site. MSCs have been shown to induce regenerative features in the IVD and MSC trafficking to the lesioned IVD has been shown in organ culture and *in vivo*.

### EXPERIMENTAL METHODS

In this study, we administered allogeneic bone marrow MSCs intravenously into a rat IVD lesion model, which has been previously developed in the lab by caudal needle puncture. Allogeneic dermal fibroblast transplantation has been performed in parallel. We have quantified parameters of degeneration and herniation within the IVD by radiological (X-rays), histological (Safranin staining and IHC) and gene expression analysis (qPCR), 2 weeks after transplantation. Analysis of the systemic immune response has also been quantified by cytometry.

### RESULTS AND DISCUSSION

Percentage of disc height index and histological grading score indicate a less degenerative phenotype within the IVD for the MSCs transplanted group. Moreover, this group has significantly less herniation. Gene expression analysis indicates no alteration in the main ECM components (Coll1, Coll2 and Aggrecan) at 2 weeks post-lesion for the transplanted groups, while showing a significant upregulation in these genes in the control lesion group. The results for the systemic immune response associated with MSC transplantation seem to indicate an immunosuppressive effect in the MSCs transplanted animals. Also, we found an increase in B lymphocytes and a decrease in T lymphocytes in the blood, associated with the lesion.

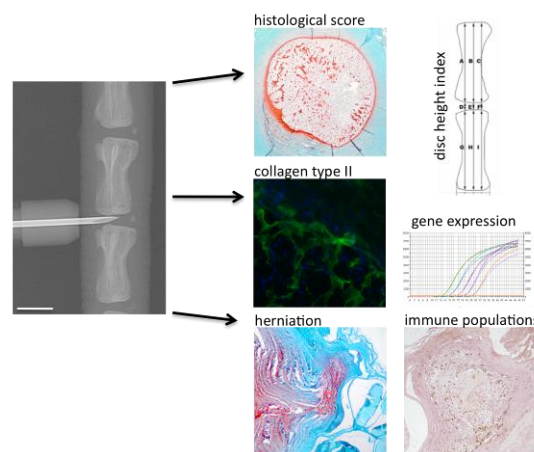


Figure 1 IVD injury model created by 21-G needle puncture, with analysis of IVD degeneration performed 2 weeks after MSC systemic transplantation by measurement of disc height index, histological grading score, determination of hernia volume, quantification of ECM components and immune populations present in the hernia site. Scale bar: 5 mm.

### CONCLUSION

Overall, our results seem to indicate a positive effect of systemically transplanted MSCs on *in situ* IVD regeneration.

### REFERENCES

- Sakai et al, 2015. Nat. Rev. Rheumatol
- Sakai et al, 2015. The Spine Journal
- Illien-Jünger et al, 2012. Spine
- Han et al., 2008. Spine

### ACKNOWLEDGMENTS

Financial support was provided by Portuguese funds through FCT – Fundação para a Ciência e a Tecnologia in the framework of project UID/BIM/04293/2013 and through Fellowship SFRH/BDP/87071/2012 to Carla Cunha.



## Evaluation of the Efficiency of Mechanical Agitation Method in Heart Decellularization Process

Ana Paula Brandão<sup>1</sup>, Jonathas Haniel<sup>1</sup>, Betânia Soares<sup>1</sup>, Rosana Cruz<sup>1</sup>, Marcos Pinotti<sup>1</sup>.

<sup>1</sup>Department of Mechanical Engineering, Engineering School, Federal University of Minas Gerais, Brazil  
[jonathashaniel@hotmail.com](mailto:jonathashaniel@hotmail.com)

### INTRODUCTION

Cardiac transplantation has been shown continuous growth in Brazil<sup>1</sup>. However, lack of a good immune-suppression, inability to monitoring and control rejection, and the donor shortage has prompted to looking for new alternative approaches as cell transplantation, gene therapy and tissue engineering<sup>2</sup>.

Decellularized tissues have been successfully used in a variety of tissue to application in regenerative medicine. More recently decellularized organs have been utilized as the first stages to organ engineering<sup>3</sup>. The aim of decellularization process is isolate the extracellular matrix (ECM) from the organ without its loss, damage, or disruption, while removing completely the cellular components<sup>4,5</sup>. The ECM can be used for subsequent repopulation with new contractile, vascular muscle tissue<sup>6</sup>. This bioartificial tissue could be generate fewer effects in immune response.

Thus, the objective of this study was to evaluate the efficiency of the chemical method already proposed in the literature, using an alternative method to immersion with mechanic agitation.

### EXPERIMENTAL METHODS

Heart chicken was used in a decellularization pilot assay. Entire cold heart were weighed, measured and fixed on a support through the aorta and immersed in a beaker. The chemical method by perfusion has been proposed by Weymann *et. al.*<sup>7</sup> and consists in the use of phosphate-buffered solution (PBS) 1X and 4% p/v sodium dodecyl sulfate (SDS) in PBS. In this study, mechanical agitation was used for delivering the decellularization agents without temperature control. The structure was placed on a magnetic stirrer and initially immersed with PBS 1X to remove the coagulated blood and tissue debris. After, the organ was immersed in 4% p/v SDS with PBS 1X for 12 hours. During this process, every three hours, the hearts were immersed in PBS 1x for 15 minutes in order to remove residual substances. The final washing step after SDS treatment included immersion with PBS 1X for another 24 hours to remove remnant detergents and cell debris. At the end of assay the heart was cut and observed visually.

### PARTIAL RESULTS AND DISCUSSION

After 3 hours was possible to observe the start of decellularization process. This process was more pronounced and faster in the upper region of the heart where the tissue is thin. After 6 hours of washed, the atrial region and mainly blood vessels showed whitish,

translucent and more pronounced at the final of decellularization process. The ventricular region became more clearer than natural color but there was remaining muscle tissue after 37 hours. The heart increased its weight and size compared to initial condition. The aorta supported the heart's weight during all decellularization process without disrupt. After the cut was possible to see only an external decellularized layer in the heart lower region. Ventricles are thicker than atria. So, the cellular removal using the proposed method was inefficient in those regions. .

The mechanical agitation method showed inefficient to deliver the decellularization agents in a heart when compared to perfusion described by Weymann *et. al.*,<sup>7</sup> probably because chemical and controlled mechanical methods together are necessary to complete lysis and remotion of the cellular debris.

### PARTIAL CONCLUSIONS AND PERSPECTIVES

The method used in this assay was not enough to completely decellularization of the heart. Therefore, the use of a vascular network for fluid movement in the organ can be an alternative to increase the efficiency of the decellularization process in complex tissues.

The next steps in this study include quantitative and histologic analysis, tension and deformation mechanical tests, and temperature control using perfusion methods.

### REFERENCES

1. Brazilian Registry of Transplant - Brazilian Association of Organ Transplantation. Year XX, number 3. January / September 2014, 2014.
2. Murphy S.V. and Atala A., *Bioessays*, 35 (3), 163–172, 2013.
3. Gilbert, T. W., *Journal of Cellular Biochemistry*, 113:2217- 2222, 2012.
4. Gilbert *et al.*, *Biomaterials* 27:3675–3683, 2006.
5. Crapo *et al.*, *Biomaterials* 32:3233–3243, 2011.
6. Galvez-Monton C. *et. al.*, *Rev. Esp. Cardiol.* 66: 391-399, 2013.
7. Weymann A. *et. al.*, *Circ. J.* 75:852–860, 2011.

### ACKNOWLEDGMENTS

The authors would like to thank the Department of Mechanical Engineering of UFMG and CAPES (Coordination for the Improvement of Higher Education Personnel) for providing financial support to this project.



# Vascularization of Biphasic Calcium Phosphate Biomaterials: Correlation with Monocyte Pre-seeding, but not with Foreign Body Giant Cell Reaction or Granule Size

Barbeck M<sup>1,2</sup>, Dard M<sup>3</sup>, Kokkinopoulou M<sup>4</sup>, Markl J<sup>4</sup>, Booms P<sup>2</sup>, Sader RA<sup>2</sup>, Kirkpatrick CJ<sup>1</sup> and Ghanaati S<sup>1,2</sup>

<sup>1</sup> Institute of Pathology, Repair-Lab, University Medical Center of the Johannes Gutenberg University, Mainz, Germany

<sup>2</sup> Department for Oral, Cranio-Maxillofacial and Facial Plastic Surgery, FORM-Lab, Medical Center of the Goethe University, Frankfurt am Main, Germany

<sup>3</sup> Department of Periodontology and Implant Dentistry, New York University, New York, USA

<sup>4</sup> Institute for Zoology, Johannes Gutenberg University, Mainz, Germany

[mike.barbeck@kgu.de](mailto:mike.barbeck@kgu.de)

## INTRODUCTION

The present study analyzes the influence of granule size of two biphasic bone substitutes (BoneCeramic® 400-700 µm and 500-1000 µm, Fig. 1) on the induction of multinucleated giant cells (MNGCs) and implant bed vascularization in a subcutaneous implantation model in rats. Furthermore, cellular degradation mechanisms were studied by transmission electron microscopy (TEM), and the influence of the addition of (human) monocytes to both materials and its impact on the tissue reactions were analyzed in immunodeficient mice.

## EXPERIMENTAL METHODS

To conduct this study an established subcutaneous implantation model was used in 61 female 6-8 week-old Wistar rats and 12 female 5-week-old SCID mice<sup>1</sup>.

Primary monocytes were isolated from the peripheral blood of two donors from whole blood donations in accordance with ethical approval in cooperation with the Transfusion Center of the University Medical Center Mainz. Furthermore, established histological methods, i.e., specialized (immuno-) histochemical staining methods, and histomorphometrical methods were applied<sup>1</sup>. For TEM analysis previously described methods were used<sup>2</sup>.

## RESULTS AND DISCUSSION

Both materials induced tissue reactions involving primarily mononuclear cells and only small numbers of MNGCs (Fig. 1). Higher numbers of MNGCs were detected in the group with small granules starting on day 30, while higher vascularization was observed only at day 10 in this group. Thus, no correlation between the occurrence of MNGCs and the implant bed vascularization was found.

TEM analysis revealed that both mono- and multinucleated cells were involved in the phagocytosis of material, exhibiting typical subcellular elements of this process. The MNGCs were identified as foreign body giant cells in this analysis by a lack of typical osteoclastic organelles. The analysis of the size of phagocytized particles showed no differences between the two groups.

The added human monocytes were detectable either as mononuclear cells or as (components of chimeric) MNGCs within both groups without an increase in the total number of MNGCs, but with increased vascularization.

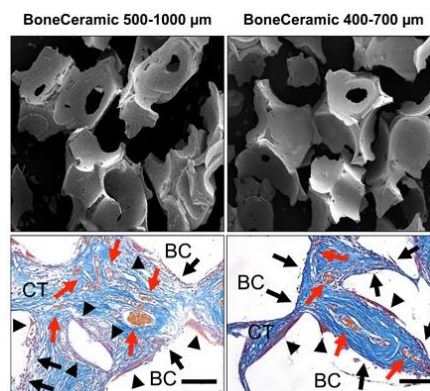


**Fig. 1.** SEM images of the both biphasic bone substitutes (upper row) and histological images of the tissue reaction to the materials (BC) at day 10 (red arrows = vessels, black arrows = mononuclear cells, arrowheads = MNGCs, CT = connective tissue) (lower row).

## CONCLUSION

The results show that synthetic materials can induce tissue reactions similar to those of some xenogeneic materials, leading to a need to determine their “ideal” physical characteristics<sup>3</sup>. The results also raise the question of the differentiation of material-induced MNGCs and their induction especially in the context of the “inflammatory” tissue reaction to biomaterials. Finally, the addition of monocytes to biomaterials is shown to increase implant bed vascularization. Thus, monocyte addition provides a basis for a new tissue regeneration concept.

## REFERENCES

1. Ghanaati S *et al.*, Biomaterials 32 (32): 8150-60, 2011.
2. Kokkinopoulou M *et al.*, PLoS One 9 (6): e101078, 2014.
3. Barbeck M. *et al.*, Ann Maxillofac Surg Jul-Dec; 4 (2): 150-7, 2014.

## ACKNOWLEDGMENTS

The authors would like to thank Ms. Ulrike Hilbig and Mr. Mykhaylo Reshetnykov for their technical assistance. This research was funded by the ITI International Team for Implantology (ITI Research Grant No. 601\_2008).



## Design and Development of Device for Decellularization Process of Heart

Jonathas Haniel<sup>1</sup>, Ana Paula Brandão<sup>1</sup>, Betânia Soares<sup>1</sup>, Rosana Cruz<sup>1</sup>, Marcos Vale<sup>1</sup>, Marcos Pinotti<sup>1</sup>.

<sup>1</sup> Bioengineering Laboratory/Department of Mechanical Engineering, Universidade Federal de Minas Gerais, Brazil  
[jonathashaniel@hotmail.com](mailto:jonathashaniel@hotmail.com)

### INTRODUCTION

Heart diseases are leading causes of death in developed countries. The total organ transplantation is most commonly used procedure for end-stage of heart failure; however the treatment is limited by the shortage of donors and the antigenicity of the transplanted organ which may lead to rejection frames<sup>1</sup>.

Therefore, the field of tissue engineering has great potential in the search for new transplant strategies for a better quality of life.

A serious difficulty of tissue engineering is the creation of scaffolds that can be used for the development of complex three-dimensional tissue or even whole organs<sup>2</sup>. One solution would be to use the extracellular matrix (ECM) from own organ that you want to transplant performing its decellularization. In this process, occurs the withdrawal and lysis of the cellular materials, creating a bioartificial scaffold<sup>3</sup>.

Among the challenges of decellularization is to build a device capable of allowing the complete removal of cellular debris with perfusion trials covering all regions of the organ without affecting the structural capacity of the ECM<sup>4</sup>. The aim of this work is to design and develop the decellularization equipment to provide the necessary conditions for this process.

### EXPERIMENTAL METHODS

The design and construction of this equipment must meet the needs of perfusion and heart fixing.

The perfusion allows the transport of decellularization solution and remove cellular debris from the tissues<sup>5</sup>. To date, our group has conducted tests with decellularization protocol to lift all the needs of the equipment. The perfusion is designed to occur with the action of a positive displacement pump with rollers, which has continuous flow with little vibration.

The fixation of the heart will be made through structures which will cannulate its two large vessels, connecting it to the product cover, and also allowing the perfusion which will occur mainly via these vessels. Thus, following the isolated heart perfusion method of Langendorff<sup>6</sup>, this may also facilitate the subsequent repopulation and maintenance *in vitro* of the ECM.

Another strategy used will be submerge the organ in the solution, using the buoyant force to help support, reducing the tension strainer in the aorta and vena cava, and to facilitate the decellularization in the epicardium.

### PARTIAL RESULTS

We considered, during development, the possibility of controlling the pressure and flow of perfusion, whereas they are determined by the pipe diameter and the rotational speed of the rollers. The flow capacity ranges from 30 to 3000 ml / min.

Moreover, before starting the circulation in the organ, the solution will go through a heat exchanger, enabling that the temperature of decellularization can be controlled to meet the many existing decellularization protocols.

A filter will also be added to the system to minimize the effect of particles that can hinder the circulation.

### PERSPECTIVES

The next steps are the construction of the entire sustaining and fixing system. It is expected that the equipment can help in the study of characterization and improvement of the decellularization process, apart from allow futures adaptations to the process of recellularization and use in different organs.

### REFERENCES

1. Morimoto T, *et al.*, Circ. J 74: 1059–1066, 2010
2. Gálvez-Montón C. *et al.*, Rev Esp Cardiol 66(5):391-399, 2013
3. Gilbert T.W. *et al.*, Biomaterials 27 3675–3683, 2006
4. Weymann A. *et al.*, Circ. J 75: 852–860, 2011
5. Thomas W. G., Journal of Cellular Biochemistry 113:2217–2222, 2012
6. Langendorff O., Pflügers Arch 61: 291 – 332, 1895

### ACKNOWLEDGMENTS

The authors would like to thank the Department of Mechanical Engineering of UFMG and CAPES (Coordination for the Improvement of Higher Education Personnel) for providing financial support to this project.



## Mechanical Properties of Chitosan/Collagen Composites Modified by Sodium Alginate

Alina Sionkowska<sup>1</sup>, Beata Kaczmarek<sup>1</sup>, Marta Michalska<sup>1</sup>

<sup>1</sup>Department of Chemistry of Biomaterials and Cosmetics, Faculty of Chemistry, Nicolaus Copernicus University in Toruń, Poland  
[as@chem.umk.pl](mailto:as@chem.umk.pl)

### INTRODUCTION

Biodegradability, biocompatibility and bioactivity are the most important properties of natural polymers through which they play an important role in medicine, pharmacy and tissue engineering<sup>1</sup>. Collagen and chitosan are natural polymers widely used in tissue engineering. They are resorbable with a high biocompatibility and stability to foster the tissue regeneration<sup>2,3,4</sup>. Chitosan is polysaccharide derived by deacetylation of chitin<sup>5</sup>. Collagen is the most abundant protein in animals. It is the main component of connective tissue, tendon and skin<sup>4</sup>. Collagen extracted from natural sources sometimes does not have mechanical properties required for several biomedical applications. To improve the mechanical properties of collagen scaffolds, other natural polymers or cross-linking agents have to be added<sup>6,7</sup>. In this study to the mixtures of collagen and chitosan the cross-linking agent, sodium alginate was added and mechanical properties were studied.

### EXPERIMENTAL METHODS

Chitosan (CTS) sample has a degree of deacetylation of 78% with a viscosity average molecular weight of  $0.59 \times 10^6$ . Collagen (Coll) was extracted in our laboratory from rat tail tendon. Chitosan and collagen mixtures were prepared by mixing two solutions in weight ratio 50/50. Sodium alginate as a 1% solution in 0.1 M acetic acid was added as a cross-linking agent in weight ratios 2 and 5%. To obtain total miscibility few drops of 2M hydrochloric acid were added. Hydrochloric acid did not change the final pH of the mixture. Solutions were mixed and put into a polystyrene container, frozen at -80°C, then the frozen mixtures were lyophilized at -55°C and 5Pa for 48h (ALPHA 1-2LD plus, CHRIST, Germany). Samples with pure chitosan, collagen and their mixtures were left as control samples. Mechanical properties were measured by mechanical testing machine (Z.05, Zwick/Roell, Germany). Samples were located between two discs and pressed. All measurements were carried at room temperature and humidity.

### RESULTS AND DISCUSSION

Compressive modulus and the tensile strength for chitosan/collagen composites with and without sodium alginate are shown in Table 1. Sodium alginate was used in two concentrations of 2 and 5 %. The properties of materials were compared. The highest compressive modulus and tensile strength was observed for chitosan's scaffolds. The scaffold made of collagen had

compressive modulus almost four times lower than pure chitosan scaffolds. Young modulus for composites mixture of collagen and chitosan was medial compared to collagen and chitosan separately. However, the tensile strength for chitosan/collagen composites was much lower than for scaffolds made of chitosan and/or collagen. The addition of 5% of sodium alginate to chitosan/collagen mixture led to the increase of Young modulus. The addition of 2% of sodium alginate was not sufficient to improve mechanical properties of chitosan/collagen composite and even led to the decrease of Young modulus.

Specimen	E <sub>mod</sub> [kPa]	F <sub>max</sub> [kPa]
CTS	4.93±0.70	12.88±0.47
Coll	1.27±0.87	5.59±0.90
CTS/Coll	2.43±0.16	1.19±0.43
CTS/Coll/2SA	1.89±0.29	1.12±0.26
CTS/Coll/5SA	3.03±0.60	1.23±0.09

Table 1. Compressive modulus (E<sub>mod</sub>) and tensile strength (F<sub>max</sub>) for chitosan/collagen (CTS/Coll) composites in 3D structure with 2% (CTS/Coll/2SA) and 5% (CTS/Coll/5SA) of sodium alginate.

### CONCLUSION

Mechanical properties of new materials based on the blends of chitosan and collagen can be modified by the addition of sodium alginate. The addition of 2% of sodium alginate causes decrease in Young modulus and tensile strength in 3-D chitosan/collagen scaffolds. The addition of 5% of sodium alginate can lead to material with improved mechanical properties.

### REFERENCES

1. Sionkowska A. *et al.*, J. Mol. Liq. 198:354–357, 2014
2. Gu Z. *et al.*, Int. J. Biol. Macromol. 58:121–126, 2013
3. Sionkowska A. *et al.*, J. Mol. Liq. 199:318–323, 2014
4. Sionkowska A. *et al.*, Int. J. Biol. Macromol. 52:250–259, 2013
5. Kucukgulmez A. *et al.*, J. Polym. Environ. 20:431–437, 2012
6. Sang L. *et al.*, Carbohydr. Polym. 82: 1264–1270, 2010
7. Fan L. *et al.*, Carbohydr. Polym. 93:380–385, 2013

### ACKNOWLEDGMENTS

The authors would like to thank the Research Frontiers Programme (NCN, Poland, Grant no: UMO-2013/11/B/ST8/04444) for providing financial support to this project.





## Biophysical, Biochemical and Biological Tools for Tendon Repair and Regeneration

D Gaspar, K Spanoudes, A Satyam, P Kumar, D Cigognini, A Pandit, DI Zeugolis\*

Network of Excellence for Functional Biomaterials (NFB)  
National University of Ireland Galway (NUI Galway), Galway, Ireland  
[dimitrios.zeugolis@nuigalway.ie](mailto:dimitrios.zeugolis@nuigalway.ie)

### INTRODUCTION

Advancements in engineering and cell biology have led to the development of advanced therapy medicinal products (ATMPs). Such approaches often require removal of cells from their optimal tissue context and propagation in a far from physiological *in vitro* microenvironment to attain suitable numbers. However, bereft of their optimal *in vivo* niche, cells perform poorly, lose their functionality and with it their therapeutic potential. To this end, research efforts have been directed towards reconstruction of more functional *in vitro* microenvironments by modulating biophysical (e.g. surface topography, macromolecular crowding), biochemical (e.g. oxygen tension) and biological (e.g. growth factor supplementation, gene transfection) cues to maintain permanently differentiated cell phenotype and to direct stem cells towards specific lineage (1-4).

### EXPERIMENTAL METHODS

Herein, the influence of macromolecular crowding on tenogenic phenotype maintenance and the potential of anisotropic scaffolds (extruded collagen fibres and electro-spun polymeric fibres) on differentiation of other cell populations towards tenogenic lineage were assessed.

### RESULTS AND DISCUSSION

Macromolecular crowding, the addition of inert macromolecules in the culture media, effectively emulates the dense *in vivo* extracellular space, resulting in amplified deposition of extracellular matrix (ECM) *in vitro* and subsequent production of cohesive and rich in tissue specific ECM living substitutes.

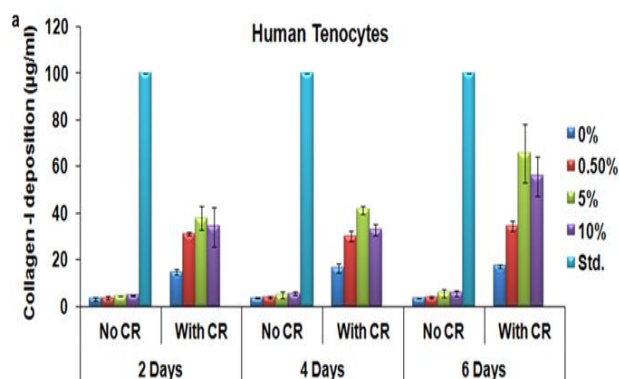


**Figure 1a:** Densitometric analysis of SDS-PAGE demonstrated that human tenocytes in the presence of macromolecular crowders (75µg/ml carrageenan; CR) deposited the highest ( $p < 0.0001$ ) amount of collagen I

after 6 days at 5% FBS. Standard (STD): 100µg/ml collagen type I.

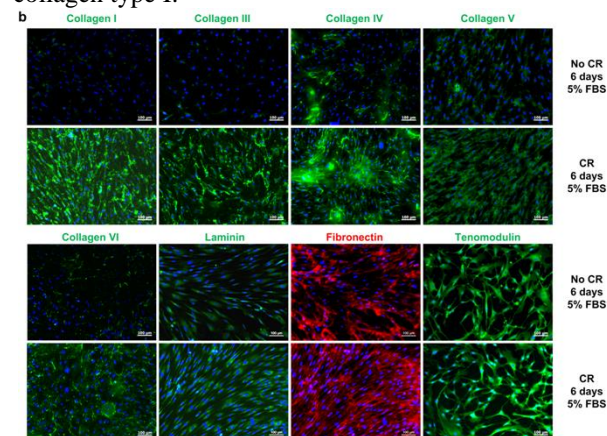


**Figure 1b:** The addition of carrageenan (CR) in human tenocyte culture results in tenogenic phenotype maintenance and enhanced tendon-specific matrix deposition, even in the presence of low serum.

### FUTURE WORK & CONCLUSION

Preliminary *in vitro* data indicate that anisotropic collagen fibres induce differentiation of non-tendon permanently differentiated cells towards tenogenic lineage. Overall, *in vitro* microenvironment modulators will allow us overcome current bottlenecks in *ex vivo* cell culture and consequently enable clinical translation and commercialisation of cell-based therapies.

### REFERENCES

1. Gaspar D, Spanoudes K, Holladay C, Pandit A, Zeugolis D. Adv Drug Deliv Rev. In Press
2. Spanoudes K, Gaspar D, Pandit A, Zeugolis DI. Trends Biotechnol. 32, 474, 2014
3. Satyam A, Kumar P, Fan X, Gorelov A, Rochev Y, Joshi L, Peinado H, Lyden D, Thomas B, Rodriguez B, Raghunath M, Pandit A, Zeugolis D. Adv Mater. 26, 3024, 2014
4. Cigognini D, Lomas A, Kumar P, Satyam A, English A, Azeem A, Pandit A, Zeugolis D. Drug Discov Today. 18, 1099, 2013

### ACKNOWLEDGMENTS

The authors would like to acknowledge: EU FP7 Marie Curie, IAPP, Tendon Regeneration; EU FP7, NMP, Green Nano Mesh; Science Foundation Ireland; Health Research Board; Irish Research Council; Enterprise Ireland.

### DISCLOSURES

The authors declare no conflict of interest.

# Adhesion/Proliferation of Cells on TiO<sub>2</sub> under UV Irradiation

Masato Ueda<sup>1</sup>, Yasuka Yoshida<sup>1</sup>, Masahiko Ikeda<sup>1</sup>, Aira Matsugaki<sup>2</sup> and Takayoshi Nakano<sup>2</sup>

<sup>1</sup>Faculty of Chemistry, Materials and Bioengineering, Kansai University, Japan

<sup>2</sup>Division of Materials and Manufacturing Science, Graduate School of Engineering, Osaka University, Japan  
[m-ueda@kansai-u.ac.jp](mailto:m-ueda@kansai-u.ac.jp)

## INTRODUCTION

Anatase-type TiO<sub>2</sub> is an n-type semiconductor with an energy band gap of  $E_g=3.2$  eV, which displays a relatively high photocatalytic activity under light irradiation at wavelengths of  $\lambda < 380$  nm and has high chemical stability. In addition, TiO<sub>2</sub> is known to absorb water on its surface, resulting in the formation of hydroxide groups. When an n-type semiconductor is immersed in an aqueous solution, an up-hill potential gradient is produced towards the surface in the conduction and the valence bands. Under ultraviolet (UV) irradiation, electrons and holes are formed in the conduction and the valence band, respectively. These photogenerated charges are then spatially separated by the potential gradient.

The purpose of this work was to investigate the adhesion/proliferation behaviour of cells under UV irradiation on TiO<sub>2</sub> showing the characteristic surface reaction mentioned above.

## EXPERIMENTAL METHODS

Anatase-type TiO<sub>2</sub> film was synthesised on commercial purity Ti disks ( $\phi 6 \times 2$  mm) by the combined chemical-hydrothermal treatment<sup>1</sup>.

Primary osteoblasts, isolated from new-born mouse calvariae, were used in this study. The cells were seeded at  $2.5 \times 10^3$  cells/well on specimens in 96-well microplates and then incubated at 37 °C for 4-72 h in a controlled humidified 5% CO<sub>2</sub> atmosphere. During the incubation, the UV irradiation with a centred wavelength of  $\lambda=365$  nm was applied intermittently for 1 h just after the seeding and every 24 hours. In addition, continuous UV irradiation was also examined.

After the incubations, the cells on the samples were stained with 5% Giemsa staining and observed by optical microscope. The number of cells was also evaluated by the WST assay. In addition, fluorescence imaging was also performed in order to investigate the number and the placement of desmosomes.

## RESULTS AND DISCUSSION

Basically the number of cells monotonically increased with incubation periods on both Ti and TiO<sub>2</sub> under darkness. In contrast, the cells decreased in 4 h-incubation under continuous UV irradiation. The decrease on the TiO<sub>2</sub> was statistically significant. Direct UV irradiation is known to damage to the cells. In this case, the cells might be additionally received some sort of stimulus from the surface of TiO<sub>2</sub>. The number of desmosomes was decreased by the UV irradiation. In the incubation for 72 h, most cells dead without proliferation regardless of the samples.

Figure 1 shows optical density of cells, measured by the WST, on Ti and TiO<sub>2</sub> after 4 h-incubation with 1 h-UV irradiation at the initial stage. Cells decreased in the

wells without samples under UV irradiation. In contrast, the numbers of cells increased on Ti and TiO<sub>2</sub> even in the UV irradiation. The increase on TiO<sub>2</sub> with the UV was statistically significant. The formation of Ti-OH groups on the TiO<sub>2</sub> seems to be facilitated by the UV irradiation. As a result, adhesion of cells to the samples might be improved. Actually the cells could be confirmed to spread their pseudopods (Fig. 2).

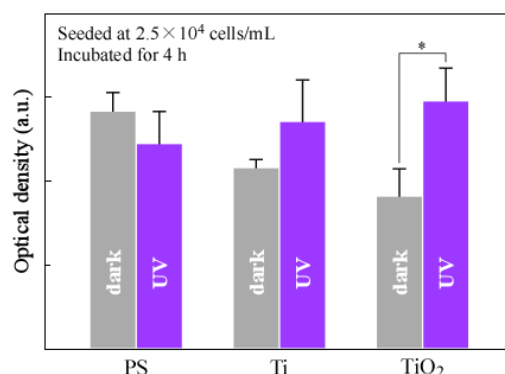


Figure 1 Adhesion of cells on pure Ti or TiO<sub>2</sub> under darkness or UV irradiation. PS indicates that without samples. \*:  $p < 0.01$  in Student *t*-test.

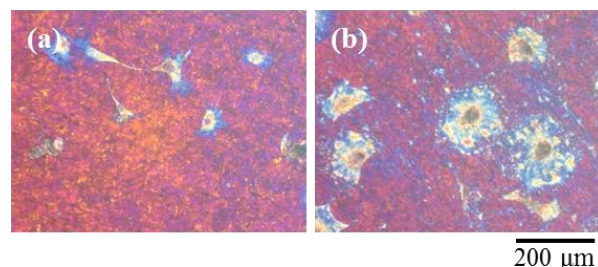


Figure 2 Morphology of cells, incubated for 4 h, on TiO<sub>2</sub> under darkness (a) or under intermittent UV irradiation (b).

## CONCLUSION

The intermittent UV irradiation might promote the adhesion of cells on TiO<sub>2</sub>. This must be closely related to functional groups on the TiO<sub>2</sub> induced by the photochemical reaction.

## REFERENCES

1. Ueda M. *et al.*, Mater. Trans. 49:1706-1709, 2008

## ACKNOWLEDGMENTS

The authors would like to thank the Ministry of Education, Culture, Sports, Science and Technology (MEXT), Grants-in-Aid for Scientific Research (Grant no: 22760546, 24656420) for providing financial support to this project.

Rouhollah Mehdinavaz Aghdam<sup>1,2</sup>, Seyed Hossein Ahmadi Tafti<sup>2</sup><sup>1</sup>Nanotechnology Department, Engineering Research Institute, Tehran, Iran<sup>2</sup>Tehran Heart Research Center, Tehran University of Medical Sciences, Tehran, Iran[mehdinavaz@aut.ac.ir](mailto:mehdinavaz@aut.ac.ir)

## INTRODUCTION

Cardiac tissue engineering has emerged as a promising approach to replace or support an infarcted cardiac tissue and thus may hold a great potential to treat and save the lives of patients with heart diseases. The development of scaffold for biografts for the repair of myocardial tissue is particularly challenging but holds great potential. Electrospinning is one of the most effective methods for providing new, bio-mimicking natural matrices. The aim of this research is to develop poly ( $\epsilon$ -caprolactone) and Sodium Alginate, blended nanofibrous scaffolds as a patch for cardiac tissue-engineering applications [1,2].

## EXPERIMENTAL METHODS

The polymer solution with concentration of 10 wt% was prepared by dissolving PCL and Alginate with a weight ratio of 70:30 in acetic acid and stirred for 24 hr at room temperature. The solution was electrospun from a 5ml syringe with a needle diameter of 0.49 mm and mass flow rate of 1 ml/h. The properties of PCL/ Alginate nanofibrous patches were measured by SEM, FTIR and contact angle measurement, while the in vitro biodegradability of the nanofibrous patches were determined by measuring their weight loss when immersed in phosphate-buffered saline (PBS), pH 7.2, at 37 °C. on.

The adhesion and proliferation cardiac progenitor cells were assessed on patches cut into 7 mm diameter circles. The prepared scaffolds were sterilized under UV light overnight and  $5 \times 10^4$  cells were seeded. After 3days the adhered cell morphologies were observed by SEM.

## RESULTS AND DISCUSSION

PCL/ Sodium Alginate blend nanofibers have average diameters of  $350 \pm 73$  nm vs.  $150 \pm 40$  for pure PCL (Fig.1a&b). Although the PCL nanofiber was hydrophobic (CA= $110 \pm 5^\circ$ ), the presence of Sodium Alginate significantly improved the water affinity, such as the water contact angle (CA=  $60 \pm 4^\circ$ ). It was also found that the biodegradability rate of PCL/ Sodium Alginate blend nanofibers was faster than the pure PCL nanofiber (Fig.2). Finally, SEM observation of cell culture (Fig.3) showed that PCL/ Alginate nanofibrous patches support adherence and monolayer growth of cardiac progenitor cells.

## CONCLUSION

We produced PCL/ Sodium Alginate nanofibrous patches and showed that they allowed efficient cardiac

cells adhesion. Therefore, novel electrospun Sodium Alginate and PCL blend to be a biomaterial may provide the development of contractile myocardial patch in cardiac tissue engineering.

## REFERENCES

1. Prabhakaran M. P. *et al.*, Mater. Sci. Eng. C31, 503–513, 2011.
2. Gaetani R. *et al.*, Biomaterials. 33, 1782–1790, 2012.

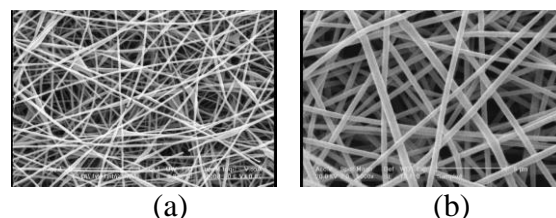


Fig.1: (a) Electrospun PCL nanofiber scaffold (b) PCL/ Sodium Alginate nanofiber scaffold

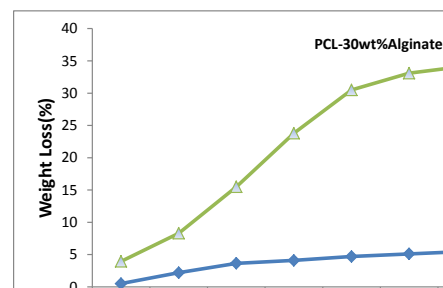


Fig. 2: Weight loss (%) of PCL/Alginate blend nanofibers: (a) pure PCL, (b) PCL/Alginate (70/30) blend nanofibers.

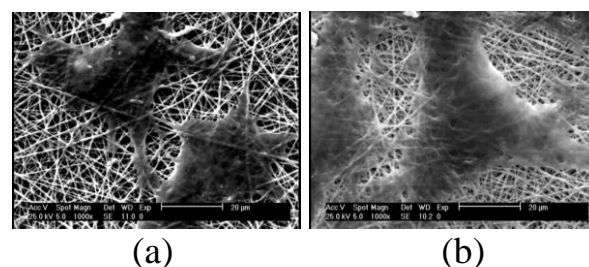


Fig 3: Morphology of cardiac progenitor cells on (a) PCL, (b) PCL:Alginate (70:30) nanofibrous scaffolds after six days of cell culture.



## Biofunctional Microassemblies Based on an Exopolysaccharide Produced by a Deep-Sea Hydrothermal Bacterium for Tissue Engineering Applications

Agata Zykwinska,<sup>1</sup> Mélanie Marquis,<sup>2</sup> Corinne Sinquin,<sup>1</sup> Jacqueline Ratiskol,<sup>1</sup> Stéphane Cuenot,<sup>3</sup> Denis Renard<sup>2</sup> and Sylvia Collic-Jouault<sup>1</sup>

<sup>1</sup>Ifremer, EM<sup>3</sup>B Laboratoire des Ecosystèmes Microbiens et Molécules Marines pour les Biotechnologies, Nantes, France

<sup>2</sup>INRA, UR1268 Biopolymères Interactions Assemblages, Nantes, France

<sup>3</sup>Institut des Matériaux Jean Rouxel (IMN), Université de Nantes, CNRS UMR 6502, Nantes, France

[Agata.Zykwinska@ifremer.fr](mailto:Agata.Zykwinska@ifremer.fr)

### INTRODUCTION

Microencapsulation presents not only an interesting way to protect active compounds against external degradation, but also offers a controlled release of encapsulated compounds, thus enhancing their bioavailability. Natural polysaccharides have emerged as promising materials for delivery system conception due to their biocompatibility and biodegradability, as well as their broad range of mechanical properties. In this context, an exopolysaccharide (EPS) secreted by a deep-sea hydrothermal bacterium *Vibrio diabolicus*<sup>1</sup> was used to elaborate biofunctional microassemblies using microfluidic technology. Microfluidic manipulates fluidic flows on microscale and provides a new means to generate monodispersed droplets<sup>2</sup>. In order to evaluate the potential of microassemblies formed as delivery systems, encapsulation of a model protein was assessed.

### EXPERIMENTAL METHODS

HE800 EPS was produced by *Vibrio diabolicus* hydrothermal bacterium by the fermentation process<sup>1</sup>. Native high molecular weight (HMW) HE800 EPS was firstly depolymerized to obtain low molecular weight (LMW) derivatives (DR). HPSEC-MALS was used to determine the molecular weight,  $M_w$  of the derivatives obtained. Gel formation was set in the presence of different divalent cations. Microfluidic flow-focusing devices (FFD) were used to structure HE800 DR into microassemblies. Two-channels FFD device was designed to produce microfibrils, whereas three-channels FFD device was elaborated to obtain microparticles. Fluorescein isothiocyanate labelled bovine serum albumin (BSA-FITC) encapsulation within HE800 microassemblies was then assessed. BSA-FITC release from microassemblies was studied in PBS, HEPES, MES and DMEM media at 37°C. The amount of released protein was analysed by fluorescence spectroscopy.

### RESULTS AND DISCUSSION

In the present study, microfluidic technology was used for the first time to structure HE800 EPS into microparticles and microfibrils. HE800 EPS displays an interesting glycosaminoglycan (GAG)-like structure close to hyaluronan<sup>3</sup> and was previously shown to promote both collagen structuring and extracellular matrix settle by dermal fibroblasts<sup>4</sup>. This natural EPS can thus be considered as an innovative GAG-like compound to design biomaterials for tissue engineering and repair. In the first step, the ability of cross-linking

between carboxylic groups of polysaccharide glucuronic acids and divalent cations, which leads to gel formation, was assessed. To promote the cross-linking, native HMW HE800 EPS ( $>10^6$  g/mol) was firstly depolymerized and two LMW derivatives of 100 000 g/mol and 300 000 g/mol were obtained. Both LMW derivatives were only able to gel in the presence of copper cations. In the next step, microfluidic devices were used to structure HE800 DR into functional microassemblies. Two-channel FFD device was designed to produce microfibrils, whereas three-channel FFD device was elaborated to obtain microparticles. Both microassemblies were shown to be stable in copper solution. It was assessed that the morphology of microparticles formed depends on the polysaccharide concentration and its molecular weight. The potential application of the microassemblies formed in the controlled release of active compounds by encapsulation of a model protein, BSA-FITC, was evaluated. Encapsulation using microfluidic devices is highly advantageous since all active compound is integrated within microassemblies formed. BSA-FITC was successfully microencapsulated within both microassemblies. The protein release was studied in different buffers and culture media. It was observed that even if microassemblies were progressively destructured during incubation, the quantity of protein released was low most likely due to the interaction with the polysaccharide.

### CONCLUSION

In the present work, HE800 bacterial EPS from marine origin having GAG-like properties was shown to be able to form microassemblies such as microfibrils and microparticles through the cross-linking with copper ions. The use of these microassemblies as controlled release systems was assessed. The microencapsulation of active compounds and their progressive release within hydrogel scaffolds used for bone and cartilage engineering will now be investigated.

### REFERENCES

1. Raguénès *et al.*, Int. J. Syst. Bacteriol. 47:989-995, 1997
2. Lorenceau *et al.*, Phys. Fluids 18:097103, 2006
3. Rougeaux *et al.*, Water Res. 31:1171-1179, 1997
4. Senni *et al.*, Mar. Drugs 11:1351-1369, 2013

### ACKNOWLEDGMENTS

We would like to thank J. Davy for her technical assistance in confocal and SEM microscopy.





## INTRODUCTION

The regeneration of the central nervous system (CNS) is one of the major challenges that the regenerative medicine faces nowadays. In order to promote *in vitro* neural cell regeneration, the use of artificial substrates may provide support for the neural cell growth and axon regeneration<sup>1</sup>. Membranes of biodegradable and biocompatible polymers have been proven as promising substrates to promote cell adhesion and proliferation<sup>2</sup>. In our previous work<sup>2</sup>, flat Poly( $\epsilon$ -caprolactone) (PCL) membranes with adequate morphology to allow neuronal tissue growth have been fabricated by phase inversion. Additionally, the scaffolds should present high nutrient transport properties to favor cell proliferation and tissue regeneration in a bioreactor. Therefore, in this work, the transport properties of those PCL membranes will be evaluated.

## EXPERIMENTAL METHODS

PCL membranes were prepared by phase inversion, following the procedure previously reported<sup>2</sup>. The coagulation baths were either ethanol (PCL/EtOH) or isopropanol (PCL/IPA).

The clean water flux (CWF) of PCL membranes during 8 hours was measured at a constant transmembrane pressure of 0.4 bars, using a cross-flow configuration system. Cross-sectional SEM images were performed to evaluate the membrane thickness ( $\delta$ ) and morphology before and after the CWF experiments.

The significance of the statistical difference of the water flux at steady state and the thickness of the PCL/EtOH and PCL/IPA membranes was analyzed by t-Student method ( $p < 0.05$ , with  $n \geq 3$ ).

## RESULTS AND DISCUSSION

Figure 1 shows the change in water flux with the time during the cross-flow water transport experiment. The steady state, reached after 5 hours of experiment, showed similar average CWF values ( $J_w^{ss}$ ) of 66 and 55  $\text{L} \cdot \text{m}^{-2} \cdot \text{h}^{-1}$ , for PCL/EtOH and PCL/IPA membranes, respectively.

The CWF decline between the initial and steady state conditions was about a 97%. This phenomenon might be attributed to membrane compaction<sup>3</sup>, caused by the pressure applied during CWF experiments, which would produce the reduction of the effective porosity of the membrane. In order to evaluate this theory, SEM images before and after CWF experiments were performed (Figure 2). The SEM images did not show significant difference in membrane thickness or in porous morphology before and after CWF experiments. According to the mechanical properties of PCL membranes previously reported<sup>4</sup>, this effect could be explained because at 0.4 bars the PCL membranes were under the elastic region, and therefore the compaction

would not be permanent once the load was removed.

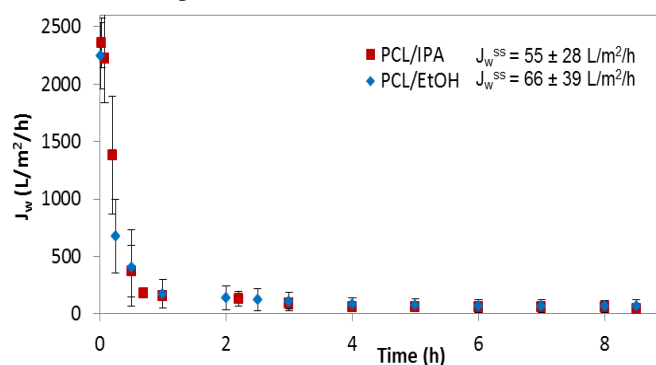


Figure 1. Change of CWF ( $J_w$ ) with time of PCL/EtOH and PCL/IPA membranes at 0.4 bar.

	Before CWF experiment (x1000, scale bar 10 $\mu\text{m}$ )	After CWF experiment (x250, scale bar 20 $\mu\text{m}$ )
PCL/EtOH		
	$\delta$ ( $\mu\text{m}$ ) = $100.44 \pm 0.04$	$\delta$ ( $\mu\text{m}$ ) = $104.95 \pm 4.75$
PCL/IPA		
	$\delta$ ( $\mu\text{m}$ ) = $105.23 \pm 0.18$	$\delta$ ( $\mu\text{m}$ ) = $108.75 \pm 8.15$

Figure 2. Cross-sectional SEM images and thickness ( $\delta$ ) of PCL/EtOH and PCL/IPA membranes before and after CWF experiments.

## CONCLUSION

Flat PCL/EtOH and PCL/IPA membranes fabricated by phase inversion present high porosity expecting important transport properties. However, the CWF decline with time, attributed to reversible membrane compaction, limits the actual transport properties at steady state. Currently, research under conduction focuses on the improvement of the mechanical stability of the PCL membranes working under pressure in a bioreactor.

## REFERENCES

- Orive G. *et al.*, Nat. Rev. Neurosci. 10: 682-692, 2009
- Diban N. *et al.*, Curr. Top. Med. Chem. 14(23): 2743-2749, 2014
- Wang Y. *et al.*, Tissue Eng. 16: 281-289, 2010
- Diban N. *et al.*, J. Membr. Sci. 438: 29-37, 2013

## *In situ* Forming and H<sub>2</sub>O<sub>2</sub>-generating Gelatin Hydrogels via Glucose Oxidase- and Horseradish Peroxidase-catalyzed Reaction

Bae Young Kim, Jin Woo Bae, Yunki Lee, Dong Hwan Oh, Ki Dong Park

Department of Molecular Science and Technology, Ajou University, Suwon, Korea  
[kdp@ajou.ac.kr](mailto:kdp@ajou.ac.kr)

### INTRODUCTION

A horseradish peroxidase (HRP)-catalyzed crosslinking reaction has recently received much attention as a promising approach to developing *in situ* forming hydrogels suitable for cell delivery<sup>1</sup>. As both HRP and H<sub>2</sub>O<sub>2</sub> greatly contribute to control of the degree and density of crosslinking, each role in designing *in situ* forming hydrogels has been well identified. In addition, H<sub>2</sub>O<sub>2</sub> plays a pivot role in a wide range of biological and processes, including aging, signaling, immune reactions, cancer development, wound healing, and serve as a marker for numerous diseases<sup>2</sup>. Therefore, generation of low levels of continuous oxidative stress (H<sub>2</sub>O<sub>2</sub>) is hypothesized to support wound healing. In this study, gelatin-based hydrogels were first prepared using the co-enzymatic cross-linking, and their physicochemical properties such as gelation time and elastic modulus, H<sub>2</sub>O<sub>2</sub> generation were investigated by varying HRP, GOx and glucose.

### EXPERIMENTAL METHODS

The gelatin-poly(ethylene glycol)-tyramine (GPT) conjugate was synthesized by conjugating tyramine to gelatin backbone using the PEG as a hydrophilic linker. The gelatin-based hydrogel were prepared in the presence of HRP, GOx and glucose as shown Fig. 1. We indirectly supplied H<sub>2</sub>O<sub>2</sub> to the HRP-catalyzed hydrogelation system using GOx as an oxidoreductase that catalyzes the oxidation of glucose to H<sub>2</sub>O<sub>2</sub> and glucono-*d*-lactone. The gelation time and mechanical properties were investigated with different GOx and glucose concentration. *In vitro* cell studies were carried out to evaluate the effect of contained GOx on cell viability and proliferation. Furthermore, we employed this material as an *in vitro* continuously H<sub>2</sub>O<sub>2</sub> generating hydrogel.

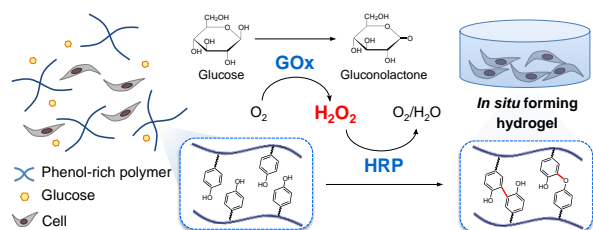


Figure 1. Schematic representation of *in situ* forming hydrogels via HRP- and GOx-mediated reaction.

### RESULTS AND DISCUSSION

The gelatin-based hydrogels were successfully prepared and the mechanical strength of the hydrogels was fairly well controlled by changing the glucose concentration (2-20 kPa). The gelation times decreased from around 600 s to 30 s with increasing GOx concentration from 1 U/mL to 100 U/mL. On the other hand, the gelation

times were relatively independent of HRP concentration but dependent on GOx concentration. In previous research, the gelation time slightly increased from 18 to 30 s, when H<sub>2</sub>O<sub>2</sub> concentration increased from 4 to 12 mM, which might result from the HRP oxidation to an inactivated form by excess H<sub>2</sub>O<sub>2</sub><sup>3</sup>. In contrast, GOx-mediated hydrogelation system did not show HRP activity loss due to the normal H<sub>2</sub>O<sub>2</sub> concentrations. The H<sub>2</sub>O<sub>2</sub> generation rate and amount were determined by varying the concentration of GOx and glucose in the hydrogels. As shown in Fig. 2, higher concentration of GOx in the hydrogels would lead to increasing H<sub>2</sub>O<sub>2</sub> production rate. These data show that the production of H<sub>2</sub>O<sub>2</sub> is tunable over concentration glucose, allowing them to act as dependent adjustment parameter to produce the desired dose.

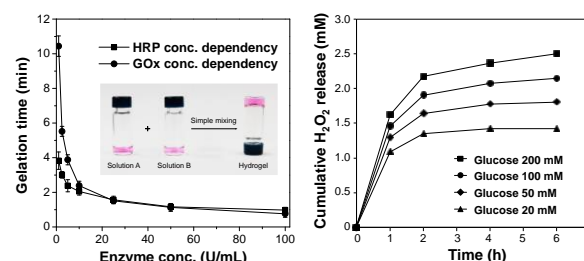


Figure 2. Gelation time of GPT hydrogels as a function of catalyst concentration and cumulative H<sub>2</sub>O<sub>2</sub> release with different glucose concentration in hydrogels.

### CONCLUSION

*In situ* cross-linked gelatin hydrogels via HRP- and GOx-catalyzed reaction have been developed as H<sub>2</sub>O<sub>2</sub>-generating materials. The physico-chemical properties of the hydrogels could be controlled by varying the concentration of HRP, GOx, and glucose. Furthermore, this system can be dynamically tuned to provide constant generation of H<sub>2</sub>O<sub>2</sub> at a desired physiologic rate. The obtained results demonstrated that the *in situ* forming and H<sub>2</sub>O<sub>2</sub>-generating gelatin hydrogels via HRP- and GOx-catalyzed reaction have great potential for biomedical applications.

### REFERENCES

- Teixeira LS. *et al.*, Biomaterials 33:1281-2190, 2012
- Garland SP. *et al.*, Biomaterials 35:1762-1770, 2014
- Sakai S. *et al.*, RSC Adv. 2:1502-1507, 2012

### ACKNOWLEDGMENTS

This work was supported by Basic Science Research Program through the National Research Foundation of Korea (NRF) grant funded by the Ministry of Science, ICT & Future Planning (NRF2012R1A2A2A06046885) and the Ministry of Education (NRF-2009-0093826).

## Controlling Macro-porosity in Hydrogels with Sacrificial Fibers Prepared from Melt Electrospinning Writing

Jodie N. Haigh<sup>1</sup>, Ya-Mi Chuang<sup>1</sup>, Brooke Farrugia<sup>2</sup>, Richard Hoogenboom<sup>3</sup>, Paul Dalton<sup>4</sup>, Tim R. Dargaville<sup>1</sup>

<sup>1</sup>Chemistry, Physics and Mechanical Engineering, Science and Engineering Faculty,  
Queensland University of Technology, Australia

<sup>2</sup>Graduate School of Biomedical Engineering, Faculty of Engineering, UNSW, Australia

<sup>3</sup>Supramolecular Chemistry Group, Department of Organic and Macromolecular Chemistry, Ghent University, Belgium

<sup>4</sup>Department for Functional Materials in Medicine and Dentistry, Universität Würzburg, Germany

[jodie.haigh@hdr.qut.edu.au](mailto:jodie.haigh@hdr.qut.edu.au)

### INTRODUCTION

Melt electrospinning writing (MEW) is an additive manufacturing (3D printing) process that enables polymer fibers to be accurately placed with a translating collector.<sup>1, 2</sup> Compared with traditional solution electrospinning, MEW offers high control over fiber disposition as well as fiber diameter. MEW provides a printing method with high degree of tunability to achieve the desired 3D pattern.

In the past, sacrificial materials have been used to produce 3D porous hydrogels with pore dimensions between 6 and 1000  $\mu\text{m}$ , but below 20  $\mu\text{m}$  the channels start to lose their precision.<sup>3, 4</sup> For example, sacrificial 2D gelatin fibers with features as small as 6  $\mu\text{m}$  tend to swell during embedding leading to poor reproduction of the fibers.<sup>5</sup> MEW produces fibers typically around 5-12  $\mu\text{m}$  which we hypothesize could fill the gap of low micron 3D printed pores with high fidelity.

Poly(2-alkyl-2-oxazoline) (PAOx) hydrogels are biocompatible, can be functionalised via end groups and side chains and can be synthesised in facile, biological relevant crosslinking conditions. Thus making PAOx hydrogels an ideal candidate material to demonstrate the utility of fiber templating using MEW scaffolds.<sup>6, 7</sup>

### EXPERIMENTAL METHODS

Sacrificial polycaprolactone (PCL) scaffolds were produced using MEW, whereby scaffold fibers were deposited onto a computer-programmed x-y stage as collector.<sup>2</sup> The PCL melt was electrospun onto the stage at a distance of 15 mm from needle tip to collector using a flow rate of 20  $\mu\text{L/hr}$  and 11.7 kV potential.

Hydrogels were formed around pre-printed 3D PCL scaffolds, by submersion of the scaffold into precursor solutions, or by printing onto pre-produced hydrogels, before addition of extra precursor solution. Crosslinking of PEtOx-ButenOx copolymers was achieved by using Irgacure 2959 as and dithiolthreitol (DTT) as crosslinker, using UV irradiation.<sup>6</sup>

Washing with or without sonication of the 3D constructs was done in acetone/water, until complete dissolution of the scaffolds occurred.

### RESULTS AND DISCUSSION

MEW was used to successfully print PCL scaffolds as templates to engineer the microenvironment of PAOx hydrogels. The MEW scaffolds directly influenced the pore architecture of the resulting hydrogels, which can be seen in the images of Figure 1 and Figure 2.

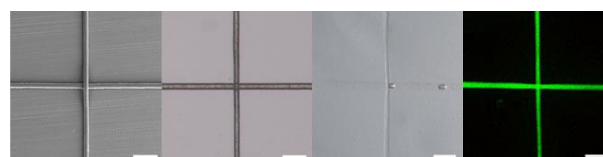


**Figure 1.** Left to right: SEM of MEW printed PCL fibers, optical microscopy (OM) of fibers embedded in gel, OM of partial leached fibers showing channels, confocal microscopy of channels backfilled with fluorescent probe. Scale bar = 100  $\mu\text{m}$



**Figure 2.** Left to right: SEM of MEW printed 3D PCL scaffold, OM of leached scaffold showing channels, confocal microscopy of channels backfilled with fluorescent probe. Scale bar = 100  $\mu\text{m}$

### CONCLUSION

The work has demonstrated the addition of controlled porosity to hydrogels via MEW for the first time. Such materials may have use in 3D microfluidics, tissue engineering (as cell guides or for improving nutrient transport) and soft machines.

### REFERENCES

1. Brown TD *et al.*, Adv Mater, 23: 5651-5657, 2011
2. Farrugia BL *et al.*, Biofabrication, 5: 025001, 2013
3. Kolesky DB *et al.*, Adv Mater, 26: 3124-3130, 2014
4. Wu W *et al.*, Adv Mater, 23: H178-183, 2011
5. Golden AP *et al.*, Lab Chip, 7: 720-725, 2007
6. Dargaville TR *et al.*, Macromol Rapid Commun, 33: 1695-1700, 2012
7. Hoogenboom R, Angew Chem Int Ed Engl, 48: 7978-7994, 2009

### ACKNOWLEDGMENTS

The authors would like to thank Queensland University of Technology for JNH's scholarship and for providing financial support to this project.



## INTRODUCTION

Reconstruction of bone defects caused by trauma or surgical resectioning of a bone tumor is a major issue in orthopedic surgery. Due to the fact that the natural bones contain mainly collagen and hydroxyapatite, calcium phosphate ceramics (CaP) with addition of collagen (Col) are widely used in bone regeneration<sup>1</sup>. Collagen is the common protein (about 30% of the human body) and it is found in most of the animal connective tissues<sup>2</sup>. To improve a physical properties of the collagen biomaterials, especially resistance of degradation and mechanical properties, the crosslinking is used. Different chemical and physical crosslinking methods are used for crosslinking of collagen materials<sup>3</sup>.

This paper is focused on the development of a novel Col/CaP composites using a new method. This study explores the effect of the different crosslinking method on the mechanical properties of Col/CaP scaffolds.

## EXPERIMENTAL METHODS

Collagen suspension with concentrations 2% (w/w) was prepared from lyophilized collagen in deionized water using an IKA disintegrator<sup>4</sup>. Col/CaP scaffold were created by deposition of calcium phosphate within collagen matrix in two steps using freeze-drying process before immersing samples in calcium solution. To improve a physical properties of prepared scaffolds crosslinking with carbodiimide (EDC/NHS) and dehydrothermal treatment (DHT) was used.

Compression tests were performed for dry, lyophilized scaffolds as well as for scaffolds soaked in PBS (pH 7.4) during testing. The presented values are the average values calculated from five measurements. All testing was carried out using a mechanical testing machine (Z.05, Zwick/Roell, Germany) at room temperature.

## RESULTS AND DISCUSSION

Mechanical properties of Col/CaP scaffolds were presented in Figure 1.

DHT and EDC/NHS crosslinking improved the mechanical properties of samples. Compressive modulus ( $E_c$ ) increased from 1155 kPa for non-crosslinked Col/CaP samples to 1960 kPa for DHT crosslinked samples.

In conditions of full hydration the materials become more elastic, as indicated by decrease of the value of compressive modulus. Compression test performed for the samples soaked in PBS during the test showed that

the  $E_c$  of DHT or EDC/NHS crosslinked samples were higher in comparison with non-crosslinked Col/CaP samples.

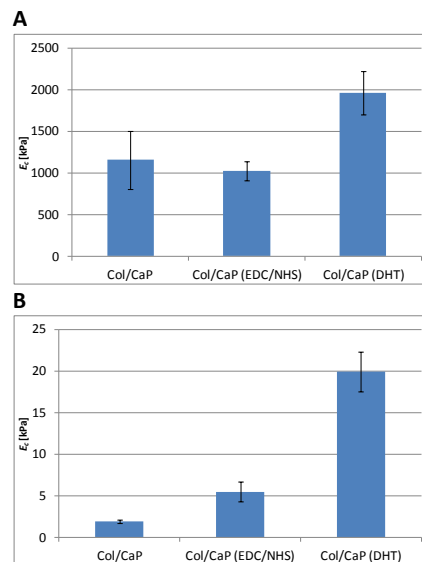


Fig. 1. Compressive modulus [ $E_c$ ] of scaffolds obtained by calcium phosphate precipitation within collagen matrix and crosslinked by two different methods: a) dry scaffold, b) scaffold soaked in PBS

## CONCLUSION

Col/CaP scaffolds were successfully produced by the precipitation method. After freeze-drying process, the samples exhibited 3D porosity structure. EDC/NHS and DHT as crosslinking agents lead to an increase of mechanical properties of Col/CaP scaffolds. In conditions of full hydration the materials become more elastic. This is caused by the high swelling capacity and porosity structure of Col/CaP scaffolds.

## REFERENCES

1. Li Z. *et al.*, J Artif Organs. 14:163–170, 2011
2. Prockop D.J. Matrix Biol. 16:519–528, 1998
3. Yahyouché A. *et al.*, Acta Biomater. 7:278–286, 2011
4. Sionkowska A. *et al.*, Int. J. Biol. Macromol. 52: 250–259, 2013

## ACKNOWLEDGMENTS

Financial support from the National Science Centre (NCN, Poland) Grant No UMO-2013/11/B/ST8/04444 is gratefully acknowledged.



## Chitosan Solution as the Effective Liquid Phase for Composite-type Bone Cements

Joanna Czechowska, Aneta Zima, Dominika Siek, Anna Ślósarczyk

Department of Ceramics and Refractories, AGH University of Science and Technology, 30 Mickiewicza Av. 30-059, Krakow, Poland  
[jczech@agh.edu.pl](mailto:jczech@agh.edu.pl)

### INTRODUCTION

Calcium phosphate bone cements (CPCs) are a family of chemically bonded materials, composed of powder and liquid phase which when mixed together create a mouldable paste. After introduction into the bone defect it sets *in situ* filling tightly the void<sup>1</sup>. The main advantages of CPCs include excellent biocompatibility, low setting temperature and mouldability. In order to improve some properties of CPCs such as: mechanical strength, injectability or resorption rate the composite bone cements with the inorganic (calcium sulphate, magnesium phosphates, calcium carbonate) or/and organic (alginate, sodium hyaluronate) additives were developed<sup>2-3</sup>. In the present studies calcium sulphate was used as a rapidly resorbable component of chemically bonded materials. Furthermore, chitosan was applied as the CPCs constituent due to its biocompatibility as well as the antibacterial and antifungal activity<sup>4</sup>. A number of studies regarding chemically bonded materials on the basis of calcium phosphate have already been conducted. Nevertheless still some substantial understandings of these composite-type cements in terms of their setting chemistry and physicochemical properties need to be gained.

### EXPERIMENTAL METHODS

Chemically bonded biomaterials consisting of calcium sulphate, hydroxyapatite doped with titanium ions (TiHA) and chitosan were developed. A raw TiHA as well as the heat treated TiHA powders were applied. Initial powder batches composed of 60wt% of calcium sulphate hemihydrate and 40wt.% of raw (THCS-1) and calcined TiHA (THCS-2, THCS-3). Chitosan was introduced into the materials with the liquid phase as the 1% wt. chitosan solution in acetic acid. Setting times of cement pastes were determined using Gillmore needles. Physicochemical properties of the set cement bodies, namely: phase composition (XRD, D-2 Phaser, Bruker), compressive strength (Universal Testing machine, Instron) as well as microstructure (SEM) and porosity (MIP, Auto Pore IV, Micromeritics) were determined. The results were presented as mean  $\pm$  standard deviation (S.D.).

### RESULTS AND DISCUSSION

All developed implant materials possessed excellent handling properties. Results of XRD studies revealed that after setting cements THCS-1 and THCS-2 composed of hydroxyapatite and calcium sulphate dihydrate. Material THCS-3 consisted also of non-fully hydrated calcium sulphate as well as perovskite ( $\text{CaTiO}_3$ ) and  $\alpha$ TCP, which were products of TiHA

thermal decomposition. The setting time values remained between 6 – 23 min - initial and 7 - 69 min - final. The set cement bodies consisted of both platelet-like and needle-like crystals of calcium sulphate. Hydroxyapatite was mainly present in the form of agglomerates embedded in calcium sulphate matrix (Fig.1).

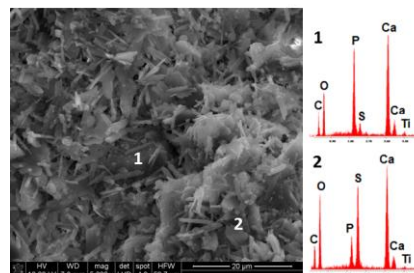


Fig.1. SEM micrograph of the set cement body and EDS results.

The mechanical strength of the materials was close to the cancellous bone and ranged from 2MPa to 9MPa. Porosimetric studies revealed that all of the composites were characterized by bimodal pore size distribution. The open porosity of set cement bodies remained between 46-52 vol.%.

### CONCLUSION

The cement pastes as well as the hardened bodies properties were evaluated. The properties of developed THCS-1 and THCS-2 composites are acceptable from the medical point of view and allow to suppose that the above materials may be use in non-load bearing areas. Material THCS-3 need to be excluded from the further *in vitro* experiments. The results of conducted researches imply that chitosan solution in acetic acid may serve as the effective liquid phase of bone cements on the basis of calcium phosphate and calcium sulphate. Further *in vitro* and *in vivo* studies need to be done to confirm biocompatibility of the materials.

### REFERENCES

1. Brown W.E., Chow L.C., J.Dent. Res. 62: 672,1983
2. Pijocha D. *et.al.*, JAMME. 49[2]: 204-029, 2011
3. Kai D. *et.al.* J. Mater. Sci. 20:1595–1602, 2009
4. Dash M. *et al* Prog. Polym. Sci. 36: 981-1014,2011

### ACKNOWLEDGMENTS

The work was supported by Faculty of Materials Science and Ceramics AGH - University of Science and Technology (2015) no 11.11.160.617.

Dominika Siek, Joanna Czechowska, Aneta Zima, Anna Ślósarczyk

Faculty of Materials Science and Ceramics, AGH University of Science and Technology, 30 Mickiewicza Av., 30-059 Krakow, Poland  
[siek@agh.edu.pl](mailto:siek@agh.edu.pl)

## INTRODUCTION

Calcium phosphates (CaPs) such as hydroxyapatite (HA) and  $\beta$ -tricalcium phosphate ( $\beta$ -TCP) are widely used in hard tissue replacement because of their excellent biological properties. The interesting alternative for high-temperature calcium phosphate ceramics are calcium phosphate cements (CPCs) which are not only biocompatible but also mouldable and self-setting<sup>1</sup>. Nevertheless, these materials have also some drawbacks which limit their clinical use. Their disadvantages include: relatively slow setting reaction, lack of macroporosity and low mechanical strength. Furthermore CPCs degrade at very low rates which are not optimal for bone regeneration. Combining a stable hydroxyapatite with more soluble  $\alpha$ -tricalcium phosphate or calcium sulphate (resorbability: CS >>  $\alpha$ -TCP > HA) may lead to development of materials with gradual resorption<sup>2-5</sup>. The aim of the study was to develop and evaluate the new implant materials based on calcium phosphates and calcium sulphate.

## EXPERIMENTAL METHODS

Hydroxyapatite was synthesized by the wet chemical method and then calcined above 700°C (HA/c). Powder phase was prepared by mixing HA/c with  $\alpha$ -tricalcium phosphate ( $\alpha$ -TCP) or calcium sulphate (CS). Calcium sulphate and  $\alpha$ -tricalcium phosphate were the setting components in the studied cement-type materials. Distilled water, chitosan, methylcellulose and alginate solutions served as the liquid phases. Liquid to powder ratio (L/P) was adjusted for each material. The phase composition (XRD, Bruker), initial (I) and final (F) setting times (Gillmore Needles), open porosity (Auto Pore IV, Micromeritics) and compressive strength (Instron 3345) were checked. The chemical stability and bioactivity were evaluated *in vitro*.

Table 1 Initial composition of the cements.

Material	Powder phase	Liquid phase	L/P [g/g]
A	CS, HA/c	distilled water	0.54
B		chitosan solution	
C	$\alpha$ -TCP, HA/c	methylcellulose solution	0.50
D		alginate solution	

## RESULTS AND DISCUSSION

Cements based on CS showed shorter setting times. They set from  $3 \pm 1$  (I) to  $14 \pm 1$  (F) min, while cements with  $\alpha$ -TCP set from  $10 \pm 1$  (I) to  $30 \pm 1$  (F) min. Material B revealed the highest ( $9.4 \pm 1$  MPa), while

material D the lowest ( $2.7 \pm 0.6$  MPa) compressive strength. Developed cements (Fig. 1) exhibit a bimodal pore size distribution (open porosity: ~50 vol.%) with pores below 1.4  $\mu$ m (A and B) and 0.5  $\mu$ m (C and D).

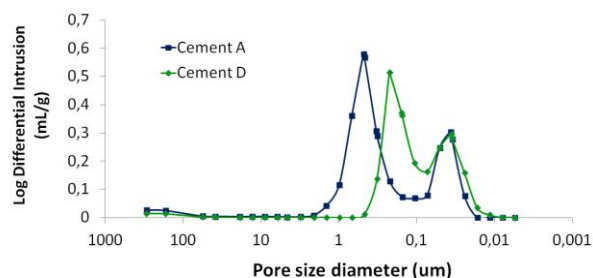


Fig. 1 Pore size distribution curve of cement A and D.

*In vitro* studies revealed that materials with calcium sulphate (A and B) are potentially more degradable than those with  $\alpha$ -tricalcium phosphate (C and D). SEM observations showed that, as soon as after 7 days of incubation in simulated body fluid (SBF), surfaces of tested materials were covered by the cauliflower-like CaPs structures what indicates on their bioactivity. Implant materials based on calcium sulfate (A and B) and  $\alpha$ -TCP (C and D) varied in the morphologies of apatite layers on their surfaces after soaking in SBF. The reason of observed differences is a higher susceptibility of calcium sulphate to both disintegration and biodegradation.

## CONCLUSION

New biodegradable and bioactive materials based on calcined hydroxyapatite and  $\alpha$ -tricalcium phosphate or calcium sulphate were developed. The impact of the setting component ( $\alpha$ -TCP or CS) on the physicochemical properties of the final products was confirmed. It was found that the resorption rate of hydroxyapatite based materials can be controlled by the addition of appropriate amount of more soluble and resorbable phase.

## REFERENCES

1. Brown W., J Am Ceram Soc. 352-379, 1986
2. Khashaba R. *et al.*, Int J Biomater. 2010
3. Wang X. *et al.*, Biomaterials. 22:2247-2255, 2001
4. Moreau J. *et al.*, Biomaterials. 30:2675-2682, 2009
5. Ooms E. *et al.*, J Biomed Mater Res. 61:9-18, 2002

## ACKNOWLEDGMENTS

The work of the first author has been supported by the Polish National Science Centre funds allocated with the decision DEC-2013/09/N/ST8/04171.

## Effect of Liquid Phase on the Basic Properties of Chemically Bonded Material

Joanna Czechowska, Dominika Siek, Aneta Zima, Anna Ślósarczyk

Department of Ceramics and Refractories, AGH University of Science and Technology, 30 Mickiewicza Av. 30-059, Krakow, Poland  
[jczech@agh.edu.pl](mailto:jczech@agh.edu.pl)

### INTRODUCTION

Calcium phosphate cements (CPCs) are mouldable bone grafting materials with exceptional biocompatibility and the ability to adapt to the shape and size of bone defect<sup>1</sup>. These chemically bonded materials are widely applied in surgical procedures that require augmentation of the bone tissue in non-load bearing areas. In the recent years, the increasing attention has been paid to  $\alpha$ -tricalcium phosphate ( $\alpha$ -TCP) as the constituent of CPCs due to its self-setting properties and ability to hydrolyze to calcium-deficient hydroxyapatite (CDHA), which is very similar to the mineral phase of bone<sup>2,3</sup>. The main goal of this work was to study the effect of liquid phase on the physicochemical properties of calcium phosphate bone cement on the basis of  $\alpha$ -tricalcium phosphate.

### EXPERIMENTAL METHODS

In the present studies the powder phase of CPCs consisted of  $\alpha$ -TCP synthesized via wet chemical method. Methylcellulose and chitosan solutions were applied as the liquid phases. Initial (I) and final (F) setting times of the cement pastes were determined with Gillmore needles. The phase composition of the hardened cement bodies was characterized using XRD method (D2Phaser, Bruker) and the compressive strength measurements were conducted (Universal Testing Machine, Instron). The open porosity of the final materials was evaluated by mercury porosimetry (AutoPoreIV, Micromeritics). The chemical stability as well as the bioactive potential of developed materials *in vitro* was evaluated via pH, ionic conductivity as well as ICP-OES measurements. Their bioactive potential was assessed on the basis of SEM observations and EDS studies after different periods of immersion in SBF.

### RESULTS AND DISCUSSION

The new, surgically handy bone substitutes on the basis of  $\alpha$ -tricalcium phosphate were developed. The initial  $\alpha$ -TCP powder was obtained using the wet chemical method. The results of XRD measurement revealed that the hardened cement bodies consisted of various amount of  $\alpha$ -TCP and HA phases. It was demonstrated that the final phase composition of materials depended on the type of applied liquid phase. Cement prepared with the use of methylcellulose solution contained higher amount of hydroxyapatite. Initial (I) and final (F) setting times of the cement pastes differed in the range of 4-32 min (I) and 9-77 min (F). All examined materials were characterized by a bimodal pore size distribution however they differed in the range of pore sizes (5nm - 0,67  $\mu$ m). Open porosity of the chemically

bonded material was similar for all investigated compositions (40vol.% - 46vol.%) regardless of the liquid phase. Mechanical strength depended on the kind of liquid. The highest compressive strength was noticed for cement obtained by mixing  $\alpha$ -TCP powder with methylcellulose solution ( $16 \pm 3$  MPa). The results of pH and ionic conductivity measurements demonstrated that the developed materials were chemically stable. The thick, apatite-like films exhibiting the typical cauliflower like morphology were formed on the surfaces of all cement samples (Fig.1).

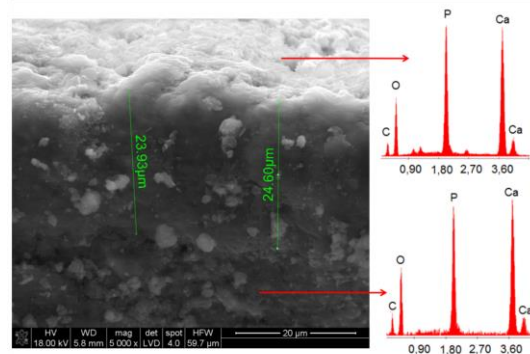


Fig.1. SEM micrograph and EDS of apatite layer on the cement sample after 7 days of incubation in SBF.

### CONCLUSION

The obtained results proved that calcium phosphate bone cement on the basis of  $\alpha$ -TCP has the potential to be applied for bone augmentation. It was confirmed that the physicochemical properties of cement paste and final material depended on the nature of the liquid phase.

### REFERENCES

1. Brown W.E., Chow L.C., J. Dent. Res. 62: 672,1983
2. Böhner M. *et al.*, Acta Biomater, 5: 3524-3535,2009
3. Pina S. *et al.*, Acta Biomater, 5: 1233-1240,2009

### ACKNOWLEDGMENTS

The work was supported by Faculty of Materials Science and Ceramics AGH - University of Science and Technology (2015) no 11.11.160.617.

# Cement-type Implant Material Based on Ca and Mg Phosphates with Adjustable Setting Time and Improved Resorption

Aneta Zima, Joanna Czechowska, Dominika Siek, Anna Ślósarczyk

Department of Ceramics and Refractories, AGH University of Science and Technology, 30 Mickiewicza Av. 30-059, Krakow, Poland  
[azima@agh.edu.pl](mailto:azima@agh.edu.pl)

## INTRODUCTION

To overcome the main disadvantages of prefabricated bioceramics and obtain superior handling properties a new generation of calcium phosphate biomaterials has been developed, namely calcium phosphate bone cements (CPCs)<sup>1</sup>. It has been more than thirty years since Brown and Chow<sup>2</sup> developed first calcium phosphate bone cement and now many commercial products are available on the market<sup>3</sup> however their properties are of different complaints. Undoubtedly too slow resorption not adjust to the resorption rate of bone tissue is one of the main CPCs drawbacks. Furthermore, initial and final setting times, rheological properties of cement pastes as well as the cohesion and mechanical strength after setting often need to be improved<sup>4,5</sup>. Preparation a new bone cement, based on calcium and magnesium phosphates was the main goal of this study. Designed material would combine the advantages of both: the calcium phosphate (brushite cement - fast resorption in the body) and magnesium phosphate (struvite cement - high mechanical strength).

## EXPERIMENTAL METHODS

The powder phase was produced by the selection and combination of the following powders: high reactive  $\alpha$ -tricalcium phosphate, calcium carbonate, magnesium phosphate and ammonium dihydrogen phosphate. As the liquid phases distilled water, 0.5wt.% methylcellulose solutions and 1.0wt.% sodium alginate solution were used. Setting times of cement pastes were determined using Gillmore needles. Physicochemical properties of the obtained material like: phase composition (XRD, D-2 Phaser, Bruker), porosity (Mercury Intrusion Porosimetry, Auto Pore IV, Micromeritics) microstructure (SEM) and compressive strength (Universal testing machine, Instron) were determined. The chemical stability *in vitro* was evaluated by the measurements of changes in pH of simulated body fluid (SBF) and ionic conductivity of distilled water during the samples incubation at 37°C (Pol-Eko).

## RESULTS AND DISCUSSION

The setting time of the developed cement ranged from 6 min (initial setting time) to 28.5 min (final setting time). In the phase composition of the hardened bodies two dominant phases, namely brushite (57-68 wt.%) and struvite (21-39 wt.%) were observed. XRD analysis showed the presence of a small amount of hydroxyapatite (up to 6 wt.%) and trace amounts of other phases, such as hannayite or biphosphammite. The open porosity of the tested materials was in the range

from 34.8 to 37.0 vol.%. Microscopic observations after incubation in SBF confirmed the bioactive potential of the developed cement-type material. After soaking in SBF the apatite layer on the surface of cement samples was observed (Fig.1).

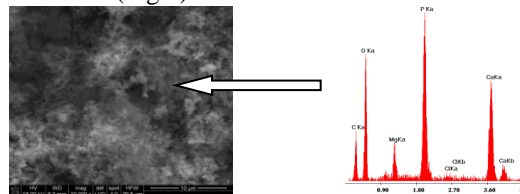


Fig.1. SEM and EDS studies of struvite-brushite cement after soaking in SBF.

The compressive strength increased from the value 10 MPa (for samples where distilled water was applied) to approximately 16 MPa (for samples with sodium alginate solution as the liquid phase) (Fig.2).

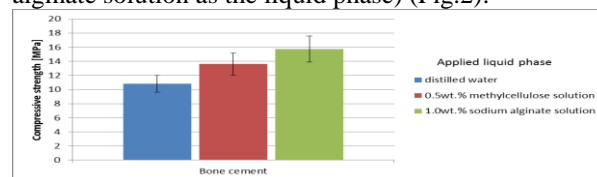


Fig.2. Mechanical strength of developed struvite-brushite cement.

The developed bone cement on the basis of calcium and magnesium phosphates had a high chemical stability. After 28 days of incubation in SBF, pH of the solution around the samples was in the range of 7.35 - 7.15 i.e. remained close to the biological conditions.

## CONCLUSION

The setting process as well as the phase composition and mechanical strength of hardened cement strongly depended on the kind of liquid applied for paste preparation. The 1wt.% sodium alginate solution was found to be the most favorable liquid phase. The high chemical stability and bioactivity of the new struvite-brushite cement were confirmed. The final evaluation will be possible after further research, including biological studies.

## REFERENCES

1. Kokubo T. Woodhead Publishing Limited, England, 2008
2. Brown W.E., Chow L.C., J.Dent. Res. 62: 672,1983
3. R.Z. LeGeros, et al. J. Mater. Med. 14 (2003) 201-209.
4. Perez R., Kim H., Ginebra M., J Tissue Eng. (2012) 1-20.
5. Engstrand, J., Persson, C., Engqvist, H., Biomater, 3(4), (2013) e27249. doi:10.4161/biom.27249

## ACKNOWLEDGMENTS

The work was supported by Faculty of Materials Science and Ceramics AGH - University of Science and Technology (2015) - Project no. 11.11.160.617.



# Modified Citrus Pectin and Silk Fibroin Based Scaffolds for Bone Tissue Engineering Applications

Sibel Atao<sup>1</sup>, Dilek Keskin<sup>1,2,4</sup>, Akin Akdağ<sup>3</sup>, Ayşen Tezcaner<sup>\*1,2,4</sup>

Departments of <sup>1</sup>Biomedical Engineering., <sup>2</sup>Engineering Sciences, <sup>3</sup>Chemistry  
Middle East Technical University, Ankara, Turkey

<sup>4</sup>BIOMATEN Center of Excellence in Biomaterials and Tissue Engineering, Middle East Technical University, Ankara, Turkey

[tezcaner@metu.edu.tr](mailto:tezcaner@metu.edu.tr)

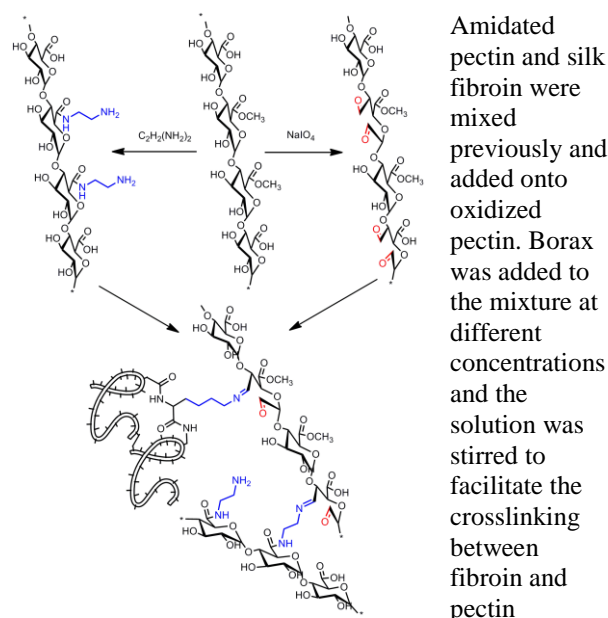
**The present work deals with development of scaffolds with silk fibroin, and modified citrus pectin, by periodate oxidation and amidation.**

## INTRODUCTION

Natural polymers are gaining interest in biomedical applications like in developing proper scaffolds since they are biocompatible materials with good mechanical properties that have already many roles in biochemical pathways<sup>1</sup>. The objective of this study was to 3D porous scaffolds by crosslinking silk fibroin (SF) and citrus pectin (PEC) in the presence of sodium tetra borate (borax). Pectin was oxidized and amidated individually and reacted with silk fibroin to prepare the cross-linked hydrogel which was obtained by Schiff's base reaction between aldehyde groups of oxidized pectin and amino groups of fibroin and amidated pectin blend.

## EXPERIMENTAL METHODS

Silk fibroin solution was extracted from *Bombyx mori* cocoons as given in study<sup>2</sup>. Citrus pectin was oxidized with sodium periodate as given in literature<sup>3</sup>. The amidation was executed from methyl ester units of citrus pectin chain by reacting with ethylenediamine.



## RESULTS AND DISCUSSION

FTIR-ATR analyses confirmed the chemical modifications of pectin. Degradation profiles of scaffolds were assessed to compare the crosslinking efficiency of the different borax concentration and in

vitro stability of the scaffolds. Silk fibroin-oxidized pectin and amidated pectin (O.PEC:A-PEC:SF) based scaffolds mixed with CaCl<sub>2</sub> and 0.015 M borax prior to molding had lower weight loss after 1 week incubation and highest water uptake. SEM analyses revealed that scaffolds had porous internal structures, with a polymer layer on surface.

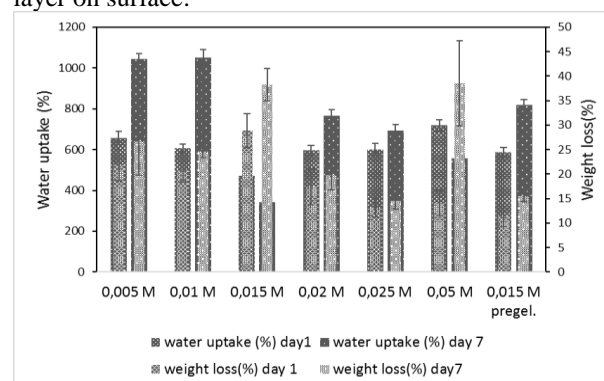


**Figure 1** The comparison of water uptake (%) and weight loss (%) values of scaffolds crosslinked with different borax concentrations.

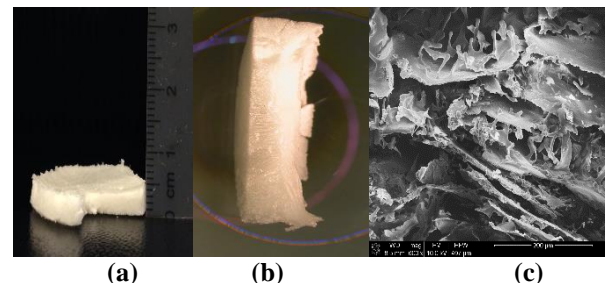


**Figure 2** The macroscopic images of scaffolds (a) thickness, (b) lateral view, (c) SEM image of scaffold prepared with 0.015 M borax and CaCl<sub>2</sub> which were treated with methanol after freeze drying (c) scale bar: 200 µm.

## CONCLUSION

Among all experimental groups the scaffolds crosslinked with 0.015 M borax and treated with methanol and calcium chloride retained structural stability with the lowest weight loses among all groups and high water uptake values. In vitro cell culture studies are being conducted for evaluating the biocompatibility of the scaffolds

## REFERENCES

- Smith G. et al., J. Biomech. 2:5-11, 2011
- Mandal, B. B. & Kundu, S. C. *Biotechnol. Bioeng.* 99, 1482-9 (2008).
- Gupta B et al., *Carbohydr Polym.*;98:1160-5.(2013)

## ACKNOWLEDGEMENTS

The authors thank METU BAP-07-02-2013-001 for providing financial support to this project.

## Fabrication Methods of Porous Biomaterials for Dental and Orthopedic Applications Using the Selective Laser Sintering Technique

Żaneta Anna Mierzejewska<sup>1</sup>, Jarosław Sidun<sup>2</sup>, Bartłomiej Wonsewicz<sup>3</sup>

<sup>1-3</sup> Faculty of Mechanical Engineering, Białystok University of Technology, Poland  
[a.mierzejewska@doktoranci.pb.edu.pl](mailto:a.mierzejewska@doktoranci.pb.edu.pl)

### INTRODUCTION

Metallic biomaterials, e.g. titanium and its alloys, are widely used in medical applications due to their biocompatibility, high strength and good corrosion resistance<sup>1</sup>. Porous biomaterials are used for dental and orthopedic implant manufacturing, because they allow to achieve the mechanical properties closer to the human bone and to improve the osseointegration process<sup>2</sup>. Porous surface improves mechanical interlocking between the implant biomaterial and the surrounding natural tissue, providing greater mechanical stability at this critical interface<sup>3</sup>. The most common technique used to create porosity in biomaterial are salt leaching, gas foaming, phase separation, freeze-drying and selective laser sintering<sup>4</sup>. Technological parameters of the SLS process are considered to be the key determinant of achieving the desired structural features and mechanical properties of materials. This paper defines the relationship between selected parameters of laser, structure and mechanical properties of implant elements made from titanium alloy (Ti-6Al-4V).

### EXPERIMENTAL METHODS

Samples were produced on the machine EOSINT M280 using SLS technology. For this purpose, a titanium alloy Ti-6Al-4V, characterized by such features as low weight, high specific strength, Young's modulus lower than other metallic biomaterials, very good corrosion resistance in the environment and high biotolerance tissue was used. Powder with a grain size of about 30 microns was used in the production process. Four series of ten element samples for testing the tensile strength (Very\_weak, Weak, Middle, Strong), of the size and shape conforming with the PN-EN ISO 6892-1 and four series of five element samples of cylindrical shape for structure research have been produced. Samples were sintered in a high vacuum environment, with presence of argon and limited to 0.1% oxygen content, which provided restricted surface reactivity of the titanium compound. Factors that differed each manufacturing process of the samples were settings parameters of the laser. Each series was sintered with the same laser power but with various powder surface scanning speed.

### RESULTS AND DISCUSSION

On the basis of fracture structures observed by electron microscope, it can be concluded that samples manufactured at a higher speed laser scanning are characterized by a higher porosity. This results from too short beam interaction with the powder layer. Strength

analysis of the tested samples showed that mechanical properties of obtained values are within the limits established by the manufacturer of the material. The differences are minimal and may be caused by other conditions prevailing within the process chamber, including low power laser. The exception, however, is the last series of samples (Strong), whose tensile strength reaches a value between the Weak and the Middle series of samples. The results do not differ from each other to a large extent, but may be the basis for determining the impact of technological parameters on mechanical properties of tested subjects.

Table 1 A comparison of the strength parameters for samples made by SL

Sample	A [%]	E [GPa]	Rm [MPa]
Very_weak	8,72	122,0	1137,8
Weak	9,45	119,4	1124,4
Middle	10,77	103,2	1104,6
Strong	10,98	101,9	1115

### CONCLUSION

Analysis of obtained results enables to conclude that modification of technological parameters of sintering process allows to change the properties of obtained element, depending on the requirements of the product. Appropriate selection of settings for laser and atmosphere in the working chamber is the key factor to achieve satisfactory results in the SLS technology applications.

### REFERENCES

1. Dabrowski B. *et al.*, Highly porous titanium scaffolds for orthopaedic applications. J Biomed Mater Res B Appl Biomater, 95(1): 53 – 61, 2010
2. Ryan G., *et al.*, Fabrication methods of porous metals for use in orthopaedic applications. Biomaterials, 27(13):2651 – 70, 2006
3. Matassi F. *et al.*, Porous metal for orthopaedics implants. Clin Cases Miner Bone Metab, 10(2): 111–115, 2013
4. Savalani M. M. *et al.*, Fabrication of porous bioactive structures using the selective laser sintering technique. J Engineering in Medicine, vol. 221: 873 – 886, 2007

### ACKNOWLEDGMENTS

This scientific work was supported by the Faculty of Mechanical Engineering, Białystok University of Technology, project No MB/WM/14/2014.



# Mechanical Properties and Degradation of a Co(poly-lactide- $\epsilon$ -caprolactone) Braided Scaffold for ACL Tissue Engineering

Blandine Landrieu, Cédric Laurent, Rachid Rahouadj

Biomechanics/LEMTA, UMR 7563 CNRS  
University of Lorraine, France  
2, avenue de la forêt de Haye, 54500 Vandoeuvre-les-Nancy  
[blandise.landrieu@univ-lorraine.fr](mailto:blandise.landrieu@univ-lorraine.fr)

## INTRODUCTION

Anterior crutiate ligament (ACL) tissue engineering would be an interesting alternative to current procedures which requires harvesting part of a healthy ligament. This last decade there has been a lot of research on appropriate materials for ACL reconstruction<sup>1</sup>. Among them, our group developed and characterized a braided scaffold in co(poly-lactide- $\epsilon$ -caprolactone)<sup>2</sup>.

The crucial point is tissue engineering is to be sure that the cells make new extracellular matrix (ECM) quickly enough to compensate the weakening of the biodegradable scaffold. Thus, studying both the degradation of the material and the growth and influence of cells is paramount<sup>3</sup>.

In the present contribution, we use a custom bioreactor<sup>4</sup> in order to study the evolution of the mechanical properties of seeded and non-seeded braided scaffolds in co(poly-lactide- $\epsilon$ -caprolactone) under physiological like mechanical stress.

## EXPERIMENTAL METHODS

First, the braided scaffold are checked for signs of cyclical creep after a week immersed in water at 37°C and subject to a mechanical stress routine aimed at mimicking the ACL loading of a recovering patient. Then the modification of the mechanical properties of scaffolds immersed in a liquid media at 37°C over the course of a four months period of time are characterized from tensile tests, and compared to the properties of seeded scaffolds cultivated in the cyclical bioreactor. During these experiments, the following parameters are checked: the evolution of the mass of the scaffolds; the pH of the surrounding liquid; and the health and differentiation of the pluripotent cells. Several imaging techniques are used to study both the geometrical evolution of the braided scaffold and the morphology and growth of cells.

## RESULTS AND DISCUSSION

Preliminary observations clearly confirmed cellular adhesion and proliferation on the scaffold as a result of 28-days static culture, and also after 3 days of dynamic culture in our custom bioreactor (Figure 1).

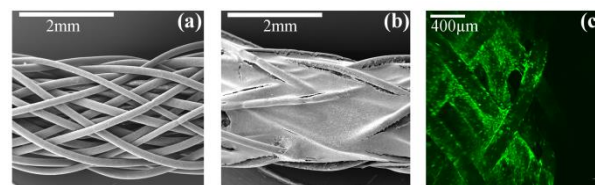


**Figure 1** Images issued from scanning electron microscopy at (a) Day 3 of culture (b) Day 28 of culture. Image issue from macroconfocal microscopy (c), at Day 3 of culture in the bioreactor and seeded with 600,000 cells.

Tensile tests were performed on different scaffold configurations (Figure 2) and confirm that the scaffold mimic the native ligament mechanical properties for the strains it endures.

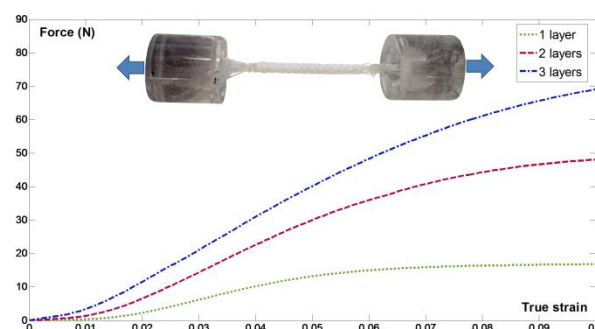


**Figure 2** Curve linking force and true strain when the scaffold is made of increasing numbers of braided layers.

## CONCLUSION

The progressive transition between scaffold degradation and tissue regeneration is studied in the present contribution. The PLCL braided scaffold as well as the bioreactor system are clearly adapted to the formation of a neo-tissue. We bring new data concerning the evolution of such a substitute that help to evaluate its clinical relevance.

## REFERENCES

1. Leong, N. L., et al. *J. Biomed. Mater. Res. A* **102**, 1614–1624 (2014).
2. Laurent, C. P. et al. *J. Mech. Behav. Biomed. Mater.* **12**, 184–196 (2012).
3. Yeo, A., et al. *J. Biomed. Mater. Res. A* **84A**, 208–218 (2008).
4. Laurent, C. P. et al. *Processes* **2**, 167–179 (2014).

## ACKNOWLEDGMENTS

This research project was funded by Université de Lorraine, the French research agency CNRS and national subsidies.



## Sulfation of Textile Chitosan Scaffolds enhances Adhesion, Proliferation and osteogenic Differentiation of Human Bone Marrow Stromal Cells

Christiane Heinemann<sup>1</sup>, Susanne Höhne<sup>2</sup>, Annette Breier<sup>2</sup>, Frank Simon<sup>2</sup>, Hans-Peter Wiesmann<sup>1</sup>, Thomas Hanke<sup>1</sup>

<sup>1</sup>Max Bergmann Center of Biomaterials and Institute of Materials Science,  
Technische Universität Dresden, Dresden, Germany

<sup>2</sup>Leibniz-Institut für Polymerforschung Dresden e.V., Dresden, Germany  
[thomas.hanke@tu-dresden.de](mailto:thomas.hanke@tu-dresden.de)

### INTRODUCTION

Tissue engineering of bone is still a field of growing interest in biomaterials research. Owing to a valuable profile of materials properties regarding processing and biocompatibility the polysaccharide chitosan is an excellent candidate for hard tissue substitution<sup>1</sup>. Since scaffold processing using spinning techniques is still established, future development focuses on chemical modification in order to improve materials properties or enhance biocompatibility. The present study reports on the assessment of several methods for sulfation and demonstration of remarkably positive effects on the activity of human mesenchymal stem cells (hMSC).

### EXPERIMENTAL METHODS

Chitosan (Heppe Medical Chitosan GmbH Halle/Germany), was spun to threads (Institute of Textile Machinery and High Performance Material Technology/TU Dresden) and embroidered to scaffolds. Sulfation was achieved by treating scaffolds with sulphur trioxide dimethylformamide complex (DMF/SO<sub>3</sub>) or chlorethan sulfonic acid (CLESA) or sulphur trioxide pyridine complex (Pyr/SO<sub>3</sub>), each optionally combined with chemical cross-linking using Genipin (GP)<sup>2</sup>. HMSC, isolated from human bone marrow, were transferred onto chitosan samples and cultivated in  $\alpha$ -MEM<sup>3</sup>. Osteogenic differentiation was induced by supplementation of 50  $\mu$ M ascorbate, 5 mM  $\beta$ -glycerophosphate and 10 nM dexamethasone after 3 days. Activity of lactate dehydrogenase (LDH) was determined to evaluate cell proliferation, relative activity of alkaline phosphatase served as indicator for differentiation, both evaluated after 1, 7, and 14 days of cultivation. All experiments were performed at least in triplicate. Confocal laser scanning microscopy (cLSM) with DAPI-stained cell nuclei and AlexaFluor 488-stained cell actin was applied for qualitative analysis of cell behaviour on chitosan samples.

### RESULTS AND DISCUSSION

Chitosan fibers with polypropylene using as an inert support fiber were processed to samples fitting exactly in 48-well plates. Seeding efficiency levelled out at 70-80% whereas solely cells attached directly to scaffolds where used for analysis. In general, all sulfation methods result in enhanced proliferation and enhanced osteogenic differentiation. During cultivation, Pyr/SO<sub>3</sub> scaffolds turned out to provide the best conditions in both of the disciplines (Fig. 1). After 14 days proliferation rate was about factor 2.5 compared to day

1 and factor 6 compared to non-modified control sample (GP). The ALP level was remarkably enhanced already on day 7 and about 3.5 times higher compared to GP. Results were confirmed by cLSM demonstrating that cells did not attach to PP thread, but formed a dense layer of spread actin skeletons completely covering the blue-appearing chitosan fibers (Fig. 1).

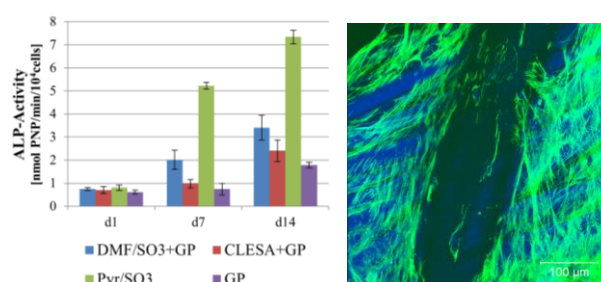


Fig. 1: Relative ALP activity of osteogenically differentiating hMSC cultivated on chemically modified chitosan scaffolds (left) and 3D reconstruction from cLSM image stacks showing nuclei (blue) and actin (green) on blue appearing fibers of Pyr/SO<sub>3</sub> chitosan.

### CONCLUSION

The results confirm sulfation to be a valuable method to enhance the biocompatibility of chitosan scaffolds. However, the results also highlight the importance of identifying the most suitable method for sulfation and also related processes like chemical cross-linking and washing. In the present study with pyridine/SO<sub>3</sub> a protocol was designed which resulted in remarkably enhanced performance in terms of proliferation of hMSC and differentiation into osteoblasts. Further experiments will include the differentiation of human monocytes into osteoclasts and co-cultivation of both cell lineages in order to investigate bone remodelling processes on the modified chitosan scaffolds.

### REFERENCES

1. Heinemann C. et al., *Eur Cell Mater* 19:96-106, 2010
2. Hoehne S. et al., *Macromol Symp* 346, 66-72, 2014
3. Heinemann C. et al., *Biomacromolecules* 10:1305-10, 2009

### ACKNOWLEDGMENTS

The authors would like to thank Deutsche Forschungsgemeinschaft (DFG) (Grant no: HA 5284/2-1) for financial support.



## Reconstruction of a Dog Mandibular Resection Defect by Octacalcium Phosphate Collagen Composite

Tadashi Kawai<sup>1</sup>, Keiko Matsui<sup>1</sup>, Yushi Ezoe<sup>1</sup>, Yuji Tanuma<sup>1</sup>, Hidenori Tanaka<sup>2</sup>, Fumihiko Kajii<sup>2,3</sup>,  
Atsushi Iwai<sup>2</sup>, Tetsu Takahashi<sup>1</sup>, Osamu Suzuki<sup>4</sup>, Shinji Kamakura<sup>3</sup>

<sup>1</sup>Division of Oral and Maxillofacial Surgery, Tohoku University Graduate School of Dentistry, Japan

<sup>2</sup>TOYOBO CO., LTD, Japan.

<sup>3</sup>Division of Bone Regenerative Engineering, Tohoku University Graduate School of Biomedical Engineering, Japan

<sup>4</sup>Division of Craniofacial Function Engineering, Tohoku University Graduate School of Dentistry, Japan

[email: ta-shi@dent.tohoku.ac.jp](mailto:ta-shi@dent.tohoku.ac.jp)

### INTRODUCTION

Synthetic octacalcium phosphate (OCP) has become recognized as a highly osteoconductive bone substitute material based on *in vitro* and *vivo* studies <sup>1, 2</sup>. OCP enhances osteoblastic cell differentiation *in vitro* in a dose-dependent manner <sup>3</sup>. Furthermore, the dose-dependent stimulatory capacity of OCP was confirmed *in vivo* implantation with collagen matrix in rat critical sized calvaria defect <sup>4</sup>. OCP has higher solubility than be-ta tricalcium phosphate (be-ta TCP) therefore more resorbable than be-ta TCP *in vivo* <sup>5</sup>. It has been shown that OCP combined with collagen (OCP/Collagen) facilitates bone regeneration in comparison with OCP itself <sup>6</sup>. The osteoconductivity of OCP/Collagen has been demonstrated also in critical-sized bone defect at calvaria of dog <sup>7</sup>. After that, we examined the effect of OCP/Collagen on alveolar bone regeneration in human small bone defect and confirmed the healing at the defect <sup>8</sup>. In this study, we investigated bone regeneration in mandibular resection defect of dog by OCP/Collagen.

### EXPERIMENTAL METHODS

OCP was prepared according to a method of synthesis by mixing calcium and phosphate solution <sup>1</sup>. Particle size of OCP was 300 – 500 µm in diameter. OCP/Collagen was prepared from pepsin-digested atelocollagen isolated from the porcine dermis and OCP. OCP/Collagen was molded in the shape of a disc, 9 mm diameter, and 1 mm thick. Eighteen-months-old male beagle dogs were used in this study. The principles of laboratory animal care, as well as national laws, were followed. All procedures were approved by the Animal Research Committee of Tohoku University. Under general anesthesia, an incision was made along the inferior border of mandible. Skin, muscle and periosteum were ablated from mandible. Then we performed bone resection at left side mandible, the defect width was 15 mm that was a critical-size defect <sup>9</sup>. The mandible defect was kept by titanium plates and screws. After the defect was filled with OCP/Collagen discs, flap was repositioned and sutured. After that, we examined the bone generation by radiographically until 3 months.

### RESULTS AND DISCUSSION

Just after operation, the radiopacity was not marked because that of OCP/Collagen was very low. However, the radiopacity was observed in the defect at 1 month. The radiopacity increased and expanded at 3 months and both margins of bone defect was connected with hard tissue. Our results indicated that OCP/Collagen could make bone a bridge in mandibular resection defect. We will examine the specimens more by histologically in next time.

### CONCLUSION

In this study, it was demonstrated that OCP/Collagen could have a possibility as a bone substitute material at large bone defect.

### REFERENCES

1. Suzuki O. *et al.*, Tohoku J Exp Med 164: 37-50, 1991.
2. Suzuki O. *et al.*, Biomaterials 27: 2671-2681, 2006.
3. Anada T. *et al.*, Tissue Eng Part A 14: 965-978, 2008.
4. Kawai T. *et al.*, Tissue Eng Part A 15: 23-32, 2009.
5. Kamakura S. *et al.*, J Biomed Mater Res B 59: 29-34, 2002.
6. Kamakura S. *et al.*, J Biomed Mater Res B 79: 210-217, 2006
7. Kawai T. *et al.*, Clin Implant Dent Relat Res 13: 112-123, 2011.
8. Kawai T. *et al.*, Tissue Eng Part A 20: 1336-1341, 2014.
9. Jin-Young Huh. *et al.*, Oral Surg Oral Med Oral Pathol Oral Radiol. 100: 296-301, 2005.

### ACKNOWLEDGMENTS

“The authors would like to thank the Research Frontiers Programme (Grant: Knowledge based Medical Device Cluster / Miyagi Area) for providing financial support to this project”.



## The Biological Evaluation of Ultra-fine Titanium with Improved Mechanical Strength for Tissue Engineering

Lucie Ostrovska<sup>1</sup>, Lucie Vistejnova<sup>1</sup>, Jan Dzugan<sup>2</sup>, Egor Ukraintsev<sup>3</sup>, Dana Kubies<sup>4</sup>, Milena Kralickova<sup>1</sup>, Marie Hubalek Kalbacova<sup>1</sup>

<sup>1</sup>Biomedical Center of Medical Faculty in Pilsen, Charles University in Prague, Pilsen, Czech Republic

<sup>2</sup>Comtes FHT a.s., Dobruška, Czech Republic

<sup>3</sup>Institute of Physics, Academy of Sciences of the Czech Republic, Prague, Czech Republic

<sup>4</sup>Institute of Macromolecular Chemistry, Academy of Sciences of the Czech Republic, Prague, Czech Republic

[Lucie.Ostrovsky@lfp.cuni.cz](mailto:Lucie.Ostrovsky@lfp.cuni.cz)

### INTRODUCTION

Titanium (Ti)-based implants are one of the most widely used implantable devices due to their superior mechanical properties and the stability in a physiological conditions<sup>1</sup>. New approaches in Ti fabrication, especially grain refinement<sup>2</sup>, and modification of the Ti surface roughness at the micro- and nano-scales provides a lot of possibilities leading to improvement of mechanical strength, durability and biological features of Ti<sup>3</sup>.

The aim of our work was to evaluate the cytocompatibility of a commercially pure Ti (CP Ti, Grade 2) with the ultra-fine grain size of the bulk material and mechanically treated surface which provides an enhanced mechanical strength to the material. Due to intended future utilization of the material in dental and orthopaedic implantology experiments were conducted with appropriate human cell types – osteoblasts and mesenchymal stem cells.

### EXPERIMENTAL METHODS

The bulk Ti with 3 different grain sizes (1, 4.6 and 30 µm in diameter) was formed by the equal channel angular extrusion (ECAP-CONFORM). Subsequently, the surface was modified by polishing with a diamond paste (RMS 5-12 nm) or by grinding with an abrasive grinding paper 1200 (RMS 270 nm), resulting in a higher surface hydrophilicity. Cell line of human osteoblast-like cells (SAOS-2) and human mesenchymal stem cells (MSC) were used throughout all experiments. Evaluated parameters for cytocompatibility assessment were: a) cell number on Ti, b) cell area, c) metabolic activity of cells and d) cell morphology. Evaluations were performed after 2 and 48h of cultivation of cells on Ti samples, metabolic activity was measured only at the time point of 48h. Tissue culture polystyrene plastic (PS) was used as a control material. Presented data were derived from at least two independent experiments in doublets. Nonparametric Wilcoxon matched-pairs test was used for determining significant differences between the datasets from Ti samples and PS control. ANOVA was used for comparison of Ti samples to each other.

### RESULTS AND DISCUSSION

In the early phase of adhesion (2h), both cell types adhered onto Ti in a higher rate than onto PS control, while the cell area was comparable on both Ti and PS material. However, after 48 hours number of cells differs between the cell types – SAOS-2 still showed a significantly higher cell number on Ti than on PS yet

number of MSC on Ti was significantly lowered when compared to PS. Surprisingly, the cell area of all cell types was significantly smaller on Ti after 48 hours of cultivation. The metabolic activity of cells on Ti was mostly comparable with the activity of cells cultivated on PS. Comparing the cell types to each other, higher values of metabolic activity were detected for SAOS-2. Morphology of cells and formation of cell adhesion plaques was different depending on the surface treatment of Ti.

Presented results showed that primary adhesion (2h) of SAOS-2 and MSC on Ti is increased. Additionally, high proliferation and metabolic activity of SAOS-2 cells after 48h indicate that experimental Ti material enhance the growth of osteoblasts. Although proliferation of MSC after 48h was slightly decreased they remained metabolically active. Interestingly, cell area for both cell types did not increase so rapidly during time in comparison to PS control. Different cell morphology and arrangement and shape of focal adhesions confirmed that surface treatment has an influence on cell attachment and spreading<sup>4</sup>.

### CONCLUSION

Experimental Ti material with the specific ultra-fine grain size and surface topography can positively influence adhesion and growth of particular cell types, especially osteoblasts, which is very important for this type of Ti further application in dentistry and orthopaedics.

### REFERENCES

1. Plecko M. *et al.*, BMC Musculoskelet Disord. 13, 2012
2. Greger M. *et al.*, Nanocon, 2nd International Conference:502-507, 2010
3. Mishnaevsky L. *et al.*, Mater. Sci. Eng. R-Rep. 81:1-19, 2014
4. Chen X.Y. *et al.*, Adv. Eng. Mater. 14(5):B216-B223, 2012

### ACKNOWLEDGMENTS

This work was supported by the project CZ.1.05/2.1.00/03.0076 of European Regional Development Fund, project PRVOUK-P24/LF1/3 of First Faculty of Medicine and by the programme of support and co-operation of companies and universities in the Pilsen region “Plzeňské vouchery”.



## The Effect of Alendronate-Loaded Polycaprolactone Scaffolds for the Enhancement of Osteogenic Differentiation *in vitro* and Bone Regeneration *in vivo*

Kwang-Won Park, Sung-Eun Kim, Young-Pil Youn, and Hae-Ryong Song

Rare Diseases Institute  
Korea University Guro Hospital  
Department of Orthopaedic Surgery  
[kwpark77@gmail.com](mailto:kwpark77@gmail.com)

### INTRODUCTION

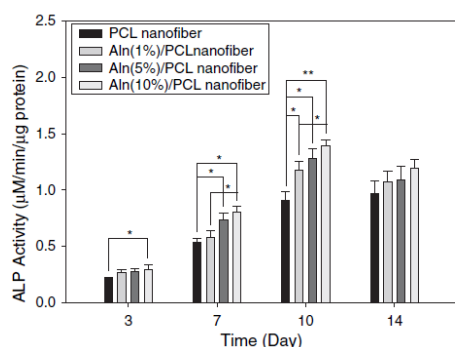
The purpose of the study was to investigate the effect of Alendronate (Aln)-loaded Polycaprolactone (PCL) scaffolds for the osteogenic differentiation *in vitro* and bone formation *in vivo*.

### EXPERIMENTAL METHODS

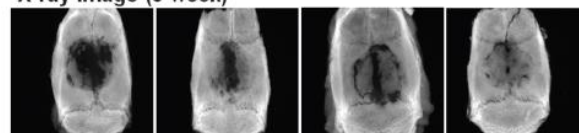
Aln/PCL scaffolds were prepared by using a Rapid Prototyping System (RPS). The characterizations of Aln/PCL were evaluated by scanning electron microscopy (SEM) and thermogravimetric analysis (TGA). The osteogenic effect of culturing adipose-derived stem cells (ADSCs) on Aln-loaded PCL nanofibrous scaffolds were evaluated by examining alkaline phosphatase (ALP) activity, calcium content, and expression of osteogenic differentiation genes *in vitro*. The capacity of Aln/PCL nanofibrous scaffolds to regenerate new bone was studied in a rat calvarial defect model *in vivo*. *In vivo* study was evaluated by radiography (X-ray), micro-computed tomography (micro-CT), and histological analysis.

### RESULTS AND DISCUSSION

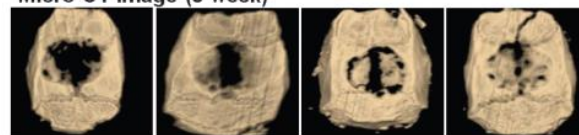
The 10% Aln/PCL nanofibrous scaffolds showed more ALP activity, mineralization, and osteocalcin and osteopontin mRNA than the 1% or 5% Aln/PCL nanofibrous scaffolds. At 8 weeks after implantation, Aln/PCL scaffolds had a positive effect on bone formation and matrix formation by the results of X-ray, micro-CT, and histological analysis.



X-ray image (8 week)



Micro-CT image (8 week)



PCL Aln(1%)/PCL Aln(5%)/PCL Aln(10%)/PCL

### CONCLUSION

These results suggested that Aln/PCL nanofibrous scaffolds enhanced the osteogenic differentiation of ADSCs *in vitro* as well as bone formation *in vivo* compared with PCL scaffolds.

### REFERENCES

1. Kolambkar YM. et al., Biomaterials 32:65-74,2011
2. Kusamori K. et al., J Bone Miner Res 25:2582-91,2010
3. Duque G. and Rivas D., J Bone Miner Res 22:1603-11,2007
4. Wang Y. et al., J Biomater Sci Polym Ed 21:1227-38,2010
5. Zuk PA. et al., Tissue Eng 7:211-28,2001

### ACKNOWLEDGEMENTS

This study was supported by a grant of the Korea Health Technology R&D project, Ministry of Health and Welfare, Republic of Korea (HI1C0388 & HI13C1501).

## New Fibrin-Polymer Interpenetrating Networks: a Potential Support for Human Skin Construct

Véronique Larreta Garde<sup>1</sup>, Marie Deneufchatel<sup>1,2</sup>, Laurent Bidault<sup>1,2</sup>, Mathilde Hindié<sup>1</sup>, Cédric Vancaeyzeele<sup>2</sup>, Odile Fichet<sup>2</sup>

<sup>1</sup>Department of Life Sciences, ERRMECE, Cergy-Pontoise University, France

<sup>2</sup>Department of Chelmsitry, LPPI Cergy-Pontoise University, France

[veronique.larreta-garde@u-cergy.fr](mailto:veronique.larreta-garde@u-cergy.fr)

### INTRODUCTION

Fibrin hydrogels show promising biological properties for clinical applications in tissue engineering; however, they are not easily handled<sup>1</sup> when synthesized at the physiological concentration. To confer it good mechanical properties a fibrin network was entrapped inside interpenetrating polymer networks (IPN) architecture<sup>2</sup>. A co-network was synthesized by copolymerization of serum albumin (SA) - a protein conferring the network biodegradability - and PVA (polyvinyl alcohol) - a synthetic polymer giving the network rigidity - both modified with methacrylate functions. PVA-SA co-network were then associated with fibrin gel inside IPNs through a one pot - one shot process.

Their mechanical properties were evaluated by rheological measurements. Their biodegradability through enzyme hydrolysis was followed and the hydrolysis rate related to the protein content. Finally, fibroblast viability and growth on (2D) and inside (3D) the different IPNs were examined to demonstrate their biocompatibility.

### EXPERIMENTAL METHODS

**IPNs** were synthesized as follows: PVA and/or SA (total concentration 100 mg), both bearing methacrylate groups were mixed with 5 mg fibrinogen and a photoinitiator all dissolved in 1 mL buffer pH 7.4 containing CaCl<sub>2</sub> and NaCl, then thrombin was added. The biomaterial mechanical properties were characterized by rheology.

**Cell behavior** was followed using human fibroblasts. Viability tests were performed; nuclei, cytoskeleton and extracellular matrix components were stained and observed by CSLM.

### RESULTS AND DISCUSSION

#### *Synthesis and properties of the different IPNs*

While the co-network was carried out by free radical photopolymerization, the fibrin gel was synthesized by the enzymatic hydrolysis of fibrinogen by thrombin. Different IPNs were synthesized varying the PVA/SA ratio. The *in situ* synthesis of PVA<sub>100</sub>/Fb<sub>5</sub>, PVA<sub>50</sub>SA<sub>50</sub>/Fb<sub>5</sub> and SA<sub>100</sub>/Fb<sub>5</sub> IPNs has been developed. In each case, a solid material was obtained after 15 min and the addition of any synthetic co-network to a fibrin gel leads to a large increase in storage modulus (G') from 8 to 40 fold.

**Biodegradability** : The biodegradability of IPNs was then measured by incubation in a concentrated protease solution. Both the macroscopic appearance and the

degradation kinetics were followed. As suspected, the PVA<sub>100</sub>/Fb<sub>5</sub> IPN was not degraded by the protease while the degradation rate increased with the total protein concentration. Moreover, the hydrolysis process follows a Michaelis -Menten kinetics, indicating that the diffusion of the protease is not limited inside the solid material. These results show that controlling the protein total concentration allows tuning the IPN degradability.

**Cell viability:** Viability of cells in contact with the materials has been measured. Cells survived but did not proliferate on PVA<sub>100</sub> /Fb<sub>5</sub> IPN. Contrarily, the introduction of SA into the network allowed fibroblasts to proliferate up to total recovery of the material surface. Fibroblast cells at the surface of the IPNs also secrete and mature the extracellular matrix biomacromolecules (fibronectin, hyaluronic acid, collagens) and they are able to structure them into fibers (fibronectin, collagen I).

Fibroblast were then entrapped inside the biomaterial and 3D culture performed. Cell viability was higher than 90% after 5 weeks and the IPN network was significantly remodelled by the encapsulated fibroblasts. Development of long fibroblast pseudopodia was observed during cell culture accompanied by a significant synthesis of type I collagen, hyaluronic acid and fibronectin by the encapsulated cells. No contraction of the material was observed after cell culture.

### CONCLUSION

These co-network IPNs are the first ones to be potentially biodegradable through tunable fragmentation, then elimination. They also exhibit the unique feature for a protein-based biomaterial of being non-retractable when used as support for fibroblast culture. The materials are biocompatible and appear as excellent supports for 2D- and 3- cell culture. They present good potentiality as supports for skin construct.

### REFERENCES

1. Ahmed *et al.* Tissue Eng Part B Rev;14:199–215, 2008.
2. Bidault *et al.* Biomacromolecules, 14: 3870-3879, 2013

### ACKNOWLEDGMENTS

The authors would like to thank the French National Agency for Research (ANR-13-TECS-014) and Direction Générale de l'Armement (DGA) of France for providing financial support to this project.





## A New Light Comes up in the World of Periodontal Therapy- P11 Peptides and their *in vitro* Evaluation on Human Hard and Soft Tissue Cells

Franziska Koch<sup>1</sup>, Uwe Pieleš<sup>1</sup>, Stephanie Mathes<sup>2</sup>, Ursula Graf<sup>2</sup>

<sup>1</sup>Institute for Chemistry and Bioanalytics, University of Applied Sciences, Switzerland

<sup>2</sup>Life Science and Facility Management, ICBC, ZHAW, Switzerland

[Franziska.koch@fhnw.ch](mailto:Franziska.koch@fhnw.ch)

### INTRODUCTION

Beside caries, periodontitis is also a very common degenerative disease affecting at least every second to third people is suffering once on this disease. It is characterized by a microbial alteration which leads to a inflammation resulting in the degradation of alveolar bone, root cementum and periodontal ligament. If the progressive destruction of these different tissues left untreated, it results to a tooth loss. A new treatment strategy uses different kinds of material which were placed in a defect area where progenitor/stem cells from neighbouring tissues can be recruited for in situ regeneration<sup>1</sup>. In the present study newly synthesized peptides were produced to form hydrogels which could be applied through an injection in a periodontal defect without a surgery. The peptides, called P11-4 and P11-8, consist of 11 amino acids which could be triggered by pH and salt concentration to form beta-sheet structures. Furthermore these beta sheet structures are able to form higher ordered structures like fibrils and fibres leading to a 3D network that serve as extracellular matrix (ECM).

### EXPERIMENTAL METHODS

To evaluate the characteristics of self-assembling peptides like P11-4 and P11-8, quartz crystal microbalance with dissipation monitoring (QCM-D) measurements were performed. Furthermore cell attachment and proliferation were studied using osteosarcoma cell line SAOS-2 and human primary periodontal fibroblast (hPDLF) in combination with different peptide hydrogels, at concentrations of 15, 20 and 30 mg/ml after 24h, 48h and 96h, respectively.

### RESULTS AND DISCUSSION

The viscoelastic properties of the different peptide hydrogels and the time which they need to build up, depend on the peptide sequence and their self-assembling behaviour. Furthermore as demonstrated in Figure 1, cell attachment and cell proliferation are directly depending on the net-charge of the peptide as well as on the viscoelastic properties. For example SAOS cells showed a higher cell attachment and proliferation rate on P11-4 hydrogels (Figure 1D), which are characterized by a negative net charge and a low viscoelasticity, than on P11-8 hydrogels (Figure 1C), known to have a positive net-charge with a higher viscoelasticity. On contrary hPDLF cells showed less attachment and proliferation if they were incubated on P11-4 hydrogels (Figure 1B) than on P11-8 hydrogels (Figure 1A). These results goes ahead with the different

phenotypes of the cells as e.g. for hPDLF are well spreaded on P11-8 hydrogels (Figure 1A), whereas on P11-4 hydrogels, hPDLF seem to be more roundish in shape and not well spreaded.

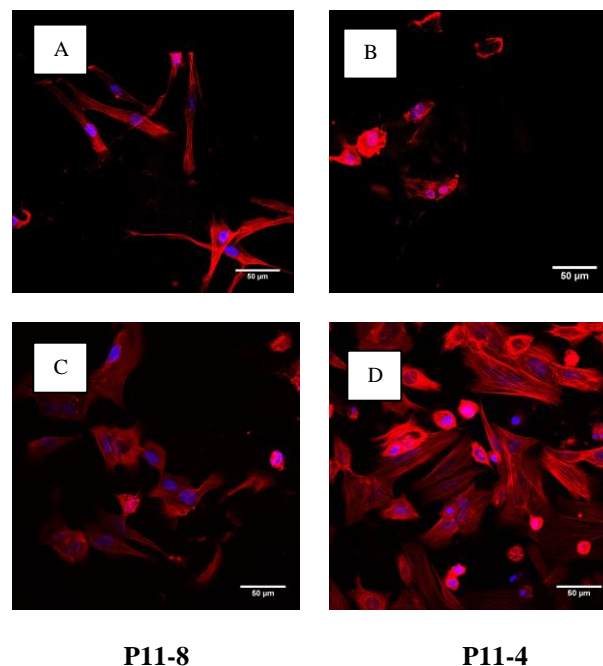


**Figure 1** show cell attachment of PDLF (1A, 1B) and SAOS (1C, 1D) on P11-8 (Figure 1A,C) and on P11-4 (Figure 1B,D) after 24 hours at a concentration of 6.35 mM. PDLF cells were stained with DAPI and TRITC-conjugated Phalloidin. A magnification of 40x was used in the study.

### CONCLUSION

It could be demonstrated that in consideration of the specific characteristics of the natural microenvironment like e.g. soft connective tissue for hPDLF, provide a possible scaffold where cells are able to attach, spread and proliferate into newly tissue. Therefore P11-peptides could be used as a new treatment strategy in periodontal therapy.

### REFERENCES

<sup>1</sup> L. Shue et al. (2012) in *Biomatter* 2:4, 271 – 277

### ACKNOWLEDGMENT

Credentis AG (M.Hug and D.Lysek) is gratefully acknowledged for supporting the project

## Evaluation of Bone Formation Using Solid Freeform Fabrication-based PCL/PLGA Scaffolds Containing Bone Morphogenetic Protein-2

Sung-Eun Kim, Kwang-Won Park, Young-Pil Youn, and Hae-Ryong Song

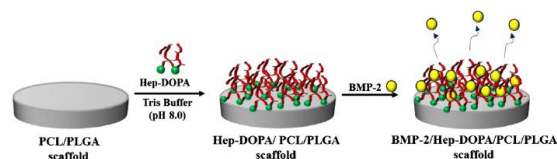
Rare Diseases Institute  
Korea University Medical Center, Guro Hospital  
Department of Orthopaedic Surgery  
[sekim10@korea.ac.kr](mailto:sekim10@korea.ac.kr)

### INTRODUCTION

The aim of this study was to develop novel polycaprolactone/polylactic-co-glycolic acid (PCL/PLGA) scaffolds with a heparin-dopamine (Hep-DOPA) conjugate for controlled release of bone morphogenetic protein-2 (BMP-2) to enhance osteoblast activity *in vitro* and also bone formation *in vivo*.

### EXPERIMENTAL METHODS

PCL/PLGA scaffolds were prepared by a solid freeform fabrication method. The PCL/PLGA scaffolds were functionalized with Hep-DOPA and then BMP-2 was sequentially coated onto the Hep-DOPA/PCL/PLGA scaffolds. The characterization and surface elemental composition of all scaffolds were evaluated by scanning electron microscope and x-ray photoelectron spectroscopy. The osteoblast activities on all scaffolds were assessed by cell proliferation, alkaline phosphatase (ALP) activity and calcium deposition *in vitro*. To demonstrate bone formation *in vivo*, plain radiograph, micro-computed tomography (micro-CT) evaluation and histological studies were performed after the implantation of all scaffolds on a rat femur defect. Hep-DOPA/PCL/PLGA had more controlled release of BMP-2, which was quantified by enzyme-linked immunosorbent assay, compared with Hep/PCL/PLGA.



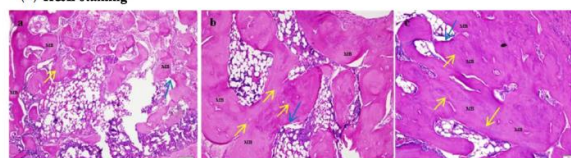
	PCL/PLGA	Hep/PCL/PLGA	Hep-DOPA/ PCL/PLGA
Carbon (%)	71.6	68.8	64.7
Oxygen (%)	28.4	26	30.9
Nitrogen (%)	0	4.7	3.7
Sulfur (%)	0	0.5	0.7

### RESULTS AND DISCUSSION

The *in vitro* results showed that osteoblast-like cells (MG-63 cells) grown on BMP-2/Hep-DOPA/PCL/PLGA had significantly enhanced ALP activity and calcium deposition compared with those on BMP-2/Hep/PCL/PLGA and PCL/PLGA. In addition, the plain radiograph, micro-CT evaluation and histological studies demonstrated that the implanted

BMP-2/Hep-DOPA/PCL/PLGA on rat femur had more bone formation than BMP-2/Hep/PCL/PLGA and PCL/PLGA *in vivo*.

(A) H&E staining



(B) Tri chrome staining



### CONCLUSION

This study suggested that a BMP-2-eluting Hep-DOPA/PCL/PLGA scaffold system would be a good and promising platform to develop the next generation of scaffolds for regenerating bone defects in the field of orthopedics.

### REFERENCES

1. Cook D. et al., J Bone Joint Surg Am 77:734-50, 1995
2. Kim E. et al., J Biomed Sci 15:771-7, 2008
3. Shields B. et al., Spine 31:542-7, 2006
4. Kim Y. et al., Tissue Eng A 16:2229-36, 2010
5. Lee W. et al., Biomaterials 32:744-52, 2011

### ACKNOWLEDGEMENTS

This study was supported by a grant of the Korea Health Technology R&D project, Ministry of Health and Welfare, Republic of Korea (HI11C0388 & HI13C1501).

## Chitin Nanofibers as Structural and Functional Units in Genipin-cross-linked Chitosan Foams for Regenerative Nanomedicine

Veronica Zubillaga<sup>1§</sup>, Asier Salaberria<sup>2§</sup>, Jalel Labidi<sup>2</sup>, Susana Fernandes<sup>2</sup>, Ana Alonso-Varona<sup>1</sup>, Teodoro Palomares<sup>1</sup>,

<sup>1</sup>Faculty of Medicine UPV/EHU, Leioa, Biskay, Spain

<sup>2</sup>Polytechnic School UPV/EHU, Donostia, Gipuzkoa, Spain

<sup>§</sup>The authors contributed equally to this work

[Teodoro.Palomares@ehu.es](mailto:Teodoro.Palomares@ehu.es)

### INTRODUCTION

Chitosan (CS) and chitin nanofibers (CHNF) have become the focus of interest in biomedical research for tissue engineering, due to their structural properties such as mechanical strength and low density and functional properties like biocompatibility, antimicrobial activity and biodegradability<sup>1-3</sup>.

We have recently developed novel foams based on CS as matrix, CHNF as functional nanofibers and genipin (G) as a natural cross-linker. The aim of this study is to evaluate the potential of the foams (GCS:CHNF) in terms of cell response for its application in osteoarticular damage.

### EXPERIMENTAL METHODS

Genipin-cross-linked foams based on CS and CHNF were prepared by freeze-drying processing method. First, three different compositions (CS:CHNF = 1:2; 1:1 and 1:0.5) were prepared by dispersing the CHNF in a GCS solution. Then the samples were frozen at -20 °C for 72 h and lyophilized. The ensuing foams were characterized in terms of physicochemical and mechanical properties and cell response. We used murine fibroblasts L929 (according to ISO 10993-12) to determine biomaterials cytotoxicity (MTT assay), cell adhesion (SEM) and cell viability (Live/Dead). Statistical significance was determined by ANOVA test.

### RESULTS AND DISCUSSION

The ensuing foams showed to be stable with a high and interconnected porosity morphology (pore diameter ranging from 90 µm for GCS up to 300 µm for GCS/CHNF = 1:2 foams). In addition, the introduction of CHNF induced a significant increase on mechanical properties. The Young modulus jumped from 200 to 900 kPa for GCS and GCS:CHNF = 1:2 foams, respectively.

None of the biomaterials exhibit cytotoxic effect in the murine fibroblasts. However, the foam GCS:CHNF = 1:0.5 showed higher proliferation rate than GCS:CHNF = 1:1 and 1:2 foams compared to the control at 24, 48 and 72 h.

Regarding cell adhesion, L929 cell line attached properly onto the three biomaterials. Nonetheless, as occurs with proliferation, at 72 hours, the foam GCS:CHNF=1:0.5 presented higher adherent cells than the materials with 1:1 and 1:2 proportions (Figure 1).

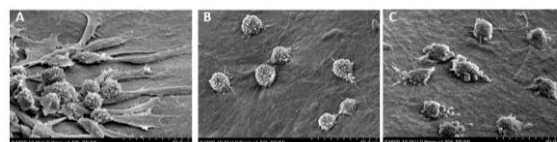


**Figure 1:** Cell adhesion of L929 on material GCS:CHNF = 1.0.5 (A), GCS:CHNF = 1:1 (B) and GCS:CHNF= 1:2 (C) at 72h.

With respect to cell viability, murine fibroblasts were able to proliferate and adhere not only to the surface but also inside the foam porous within 7 days (Figure 2).

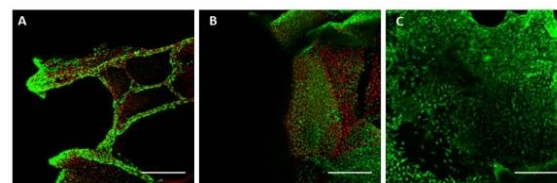


**Figure 2:** Viability of L929 on material GCS:CHNF = 1.0.5 (A), GCS:CHNF = 1:1 (B) and GCS:CHNF= 1:2 (C) at 7 days. The scale bar represents 100 µm.

### CONCLUSION

1. The cell response characterization of the three foams revealed optimal cell proliferation and adhesion, so these materials have high potential application to repair osteoarticular damage.
2. The foam GCS:CHNF = 1:0.5 showed to be more appropriate than GCS:CHNF = 1:1 and 1:2 concentrations.
3. The data showed that the final properties of the foams can be controlled by the content of CHNF incorporated in the GCS matrix.

### REFERENCES

1. Salaberria A, et al. Carbohydr Polym. 2015; 286–291
2. Takeshi I, et al. BioMed Res Int. 2014;2014:786892
3. Jayakumar R, et al. Int. J. Mol. Sci. 2011; 12:1876-1887.

### ACKNOWLEDGMENTS

Fundación Jesus Gangoiti Barrera.

### DISCLOSURES

Authors declare no competing financial interests.



## Effect of Solvent Type on Material Properties of Solution-cast Poly( $\epsilon$ -caprolactone) Films

M. Dziadek<sup>1</sup>, B. Zagrajczuk<sup>1</sup>, K. Cholewa-Kowalska<sup>1</sup>

<sup>1</sup> Department of Glass Technology and Amorphous Coatings, Faculty of Materials Science and Ceramics, AGH University of Science and Technology, 30 Mickiewicza Ave., 30-059 Krakow, Poland, [dziadek@agh.edu.pl](mailto:dziadek@agh.edu.pl)

### INTRODUCTION

One of the material, which is used to produce a three-dimensional highly porous scaffolds for bone tissue engineering is poly( $\epsilon$ -caprolactone) (PCL). PCL is slowly degrading polymer and highly compatible with osteoblasts, hence, it may be suitable for long-term bone implant applications<sup>1</sup>.

Before a material can be considered for use as a scaffold, its surface properties must be first properly characterised and optimised. Films are often used for this purpose in biomaterials research<sup>2,3</sup>.

It is currently well recognized that behaviour of cells in contact with biomaterials depends on the several material parameters. According to recent works<sup>2,4</sup> the cellular adhesion and proliferation of cells are influenced by the crystallinity of polymer materials. The crystallinity of polymer matrix affects also the material bioactivity<sup>5</sup> and also degradation kinetics<sup>1</sup>. Furthermore, the properties of material surface such as topography and wettability are factors controlling cell adhesion, proliferation, migration, phenotype maintenance and intracellular signalling<sup>2,3</sup>.

### EXPERIMENTAL METHODS

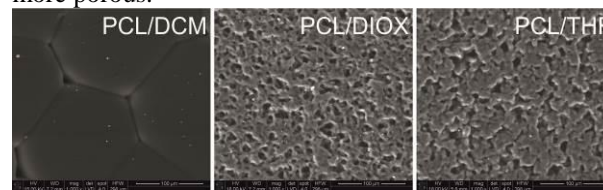
PCL films were prepared by solution-casting method using three different solvents: dichloromethane (DCM), 1,4-dioxane (DIOX) and tetrahydrofuran (THF). The surface of the films in contact with glass Petri dish and exposed to the gas phase was denoted the GS and AS surface, respectively. Both surfaces of films were characterised in terms of surface properties: morphology (SEM), roughness (contact profilometer), wettability (contact angle goniometer). Also tensile strength, Young's modulus and crystallinity (DSC) of films were evaluated.

### RESULTS AND DISCUSSION

The results showed that the use of various solvents affected the surface properties such as morphology, topography, wettability; matrix crystallinity and also mechanical behaviour of the PCL films.

Figure shows the AS surface morphology of the solution cast PCL films. The surface of the DCM cast was rough with visible discontinuous spherule-like aggregations (diameters from 120 to 180  $\mu\text{m}$ ) present on the entire surface of the film. The aggregations were partially connected together, resulting in irregular pores on the surface. PCL films cast from DIOX exhibited rough and highly porous surface morphologies comprised numerous irregular filamentous PCL aggregations. As with DCM, the surface of the THF cast PCL film was made up of fused spherule-like aggregates (diameters from 5 to 20  $\mu\text{m}$ ). However, in

contrast to PCL film cast from DCM, the surface was more porous.



Furthermore, results show that opposite surfaces (GS and AS) of the same films differed in studied surface parameters. The use of various solvents influences both the overall crystallization process – degree of crystallinity and the morphology as well as surface area, and roughness of the PCL films.

### CONCLUSION

The results indicate the possibility to use different solvents to obtain polymer films with various, but controlled, surface and mechanical properties as well as degree of crystallinity. It could be useful to control of other material properties such as degradation rate, bioactivity and also cellular response.

### REFERENCES

1. Chouzouri G., Xanthos M. In vitro bioactivity and degradation of polycaprolactone composites containing silicate fillers. *Acta Biomater* 2007;3(5):745-56.
2. Washburn N.R. *et al.* High-throughput investigation of osteoblast response to polymer crystallinity: Influence of nanometer-scale roughness on proliferation. *Biomaterials* 2004;25(7-8):1215-24.
3. Gümüşderelioglu M. *et al.* Comparison of epithelial and fibroblastic cell behavior on nano/micro-topographic PCL membranes produced by crystallinity control. *J Colloid Interf Sci* 2011;358(2):444-53.
4. Wang S. *et al.* The roles of matrix polymer crystallinity and hydroxyapatite nanoparticles in modulating material properties of photo-crosslinked composites and bone marrow stromal cell responses. *Biomaterials* 2009;30(20):3359-70.
5. Tamjid E. *et al.* Effect of particle size on the in vitro bioactivity, hydrophilicity and mechanical properties of bioactive glass-reinforced polycaprolactone composites. *Mater Sci Eng C* 2011;31(7):1526-33.

### ACKNOWLEDGMENTS

This work was supported by the Polish National Science Centre Grant No. DEC-2014/13/B/ST8/02973 and the Polish Ministry for Science and Higher Education, AGH University of Science and Technology, Faculty of Material Science and Ceramics Grant No. 11.11.160.365.





## Materials Determinants of Biological Activity of New Polymer-Based Composites Modified by Gel-Derived Bioglasses

B. Zagrajczuk<sup>1</sup>, M. Dziadek<sup>1</sup>, J. Pawlik<sup>1</sup>, J. Filipowska<sup>2</sup>, A. Bryła<sup>2</sup>, K. Cholewa-Kowalska<sup>1</sup>, A.M. Osyczka<sup>2</sup>, M. Łączka<sup>1</sup>

<sup>1</sup>Dept. of Glass Technology and Amorphous Coatings, Fac. of Mat. Sci. and Ceramics, AGH University of Science and Technology, Mickiewicza Ave. 30, 30-059 Krakow, Poland; <sup>2</sup>Dept. of Cell Biology and Imaging, Fac. of Biology and Earth Sciences, Jagiellonian University, Ingardena 6, 30-060 Krakow, Poland

[b.zagrajczuk@gmail.com](mailto:b.zagrajczuk@gmail.com)

### INTRODUCTION

Ceramic materials called bioglasses are characterized by the ability to create permanent and stable bond with bone tissue, and can stimulate the bone tissue to faster regeneration. Bioglasses can be obtained by melting method or sol-gel process. Gel-derived bioglasses show higher bioactivity than melted ones due to high surface area and lower temperature processing resulting in retaining SiOH groups on the surface<sup>1</sup>. Incorporation of gel-derived bioactive glass into a polymer creates possibility of obtaining the new composites with controlled biological activity as well as other useful properties<sup>2</sup>. In our research assumed that chemical composition of gel-derived bioglasses used as composites modifiers is primarily responsible for both the creation *in vitro* of surface HAp layer in simulated body fluid SBF indicating the bioactivity and the cellular response being a result of a contact of cells with biomaterials.

### EXPERIMENTAL METHODS

Several gel-derived biomaterials of CaO-SiO<sub>2</sub> and CaO-SiO<sub>2</sub>-P<sub>2</sub>O<sub>5</sub> systems differing from each other in the ratio of CaO:SiO<sub>2</sub> were produced in the form of powders. The molar ratio of CaO:SiO<sub>2</sub> in CaO-SiO<sub>2</sub> and CaO-SiO<sub>2</sub>-P<sub>2</sub>O<sub>5</sub> gel-derived bioglasses was: 1:4; 2:3; 1:1; 3:2. These powders were incorporated into polymer PLGA matrix in order to obtain 2D composites (foils) by solvent casting method. The various CaO:SiO<sub>2</sub> ratio determines the type of created by Si anions groups Q<sup>n</sup> (n - number of bridging oxygen ions in Si nearest environment) and it was examined by <sup>29</sup>Si MAS NMR. For produced composites, the *in vitro* test in simulated body fluid SBF was conducted in order to estimate the bioactive properties by determination of the structure of surface layer forming during contact with SBF using SEM/EDAX, XRD and FTIR methods. Moreover, the series of biological *in vitro* tests, designed to assess the stimulation of osteogenesis by composite biomaterials, were carried out. Cells cultured on experimental materials analyzed for the cellular level and activity of liver-bone-kindly alkaline phosphatase (ALP) which increases markedly at early stages of osteoblast differentiation. In addition, expression levels of several osteogenic markers that include both osteogenic transcription factors and bone-like tissue extracellular matrix proteins were evaluated in cells grown on experimental biomaterials.

### RESULTS AND DISCUSSION

All of gels were transparent and after heat treatment up to the temperature 800°C transformed to the white powder. The <sup>29</sup>Si MAS NMR spectra show that by

decreasing of SiO<sub>2</sub> content in gel-derived materials the network de-polymerisation was observed which is evidenced by increase in intensities of Q<sup>2</sup> and Q<sup>3</sup> species derived from Si-units with two (Q<sup>2</sup>) and one (Q<sup>3</sup>) non-bridging oxygen ions<sup>3</sup>. The glass with the highest concentration of CaO is invert glass and there are also present Q<sup>1</sup> groups (3 non-bridging oxygen ions). Disrupted network structure results in higher solubility and the same time faster Ca/P rich layer formation during immersion in simulated body fluid.

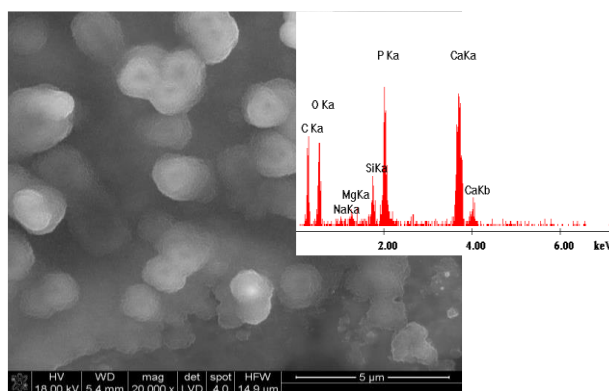


Fig. 1. Microstructure of bioactive invert glass/PLGA composites after immersion in SBF for 7 days.

Biological tests indicated that chemical composition of gel-derived bio-glasses determines biological activity of composite materials although there is no simple correlation between CaO:SiO<sub>2</sub> ratio and cell behaviour stimulated by biomaterials ALP-activity levels of cells and ability to promote both osteoblast and osteoclast formation were higher on biomaterials with higher CaO:SiO<sub>2</sub> ratio while silica-rich bioglasses enhanced cells proliferation and osteoinductive properties.

### SUMMARY

**Our study confirmed thesis that chemical composition of gel-derived bioglasses used as composite modifiers affects the bioactivity and osteoinductivity of composites.**

### REFERENCES

1. L.L. Hench, J.K. West, Life Chem. Rep. 13 (1996) 187–241.
2. E. Pamula *et al.* Ann. Biomed. Eng., Vol. 39, No. 8, (2011), 2114–2129.
3. I. Elgayar, A.E. Aliev, A.R. Boccaccini, R.G. Hill, J. Non-Cryst. Solids 351 (2005) 173–183.

### ACKNOWLEDGMENTS

This work was supported by the Polish National Science Centre (decision No. DEC-2014/13/B/ST8/02973).



## Pulp–Dentin Complex Regeneration by Boron Doped Biomimetic Nano Hydroxyapatite Coated Chitosan Scaffolds

Farzin Asghari Sana<sup>1</sup>, Gokce Kaynak<sup>2</sup>, Merve Capkin Yurtsever<sup>2</sup>, Ekin O. Tuncay<sup>2</sup>, Arlin Kiremitci<sup>1,3</sup>  
Menemse Gumusderelioglu<sup>1,2</sup>

<sup>1</sup>Department of Nanotechnology and Nanomedicine, Hacettepe University, Turkey

<sup>2</sup>Department of Chemical Engineering and Bioengineering, Hacettepe University, Turkey

<sup>3</sup>Department of Restorative Dentistry, Hacettepe University, Turkey

[farzin\\_sana@yahoo.com](mailto:farzin_sana@yahoo.com)

### INTRODUCTION

Human dental pulp stem cells (hDPSCs) are multipotent mesenchymal stem cells found in the teeth and constitute a readily source of stem cells. There are a few studies reporting that boron derivatives promote bone and teeth growth *in vivo* and *in vitro*. Our hypothesis was fabricating boron (B) doped nano hydroxyapatite coated chitosan (Ch/B-nHAp) scaffolds, using biomimetic method supported by microwave energy in order to promote odontogenic differentiation of hDPSCs and pulp-dentin complex regeneration.

### EXPERIMENTAL METHODS

In this study, hDPSCs were isolated from third molars of healthy female individuals (aged 16-25) with enzymatic digestion. Freeze-drying method was used to fabricate porous chitosan scaffolds<sup>1</sup>. Biomimetic nHAp and B-nHAp coating procedure with 10xSBF like solution were applied to scaffolds<sup>2</sup>. In addition, to improve cell attachment, fibronectin (Fn) immobilized to the scaffolds. Cells were seeded into Ch, Ch+Fn, Ch/nHAp+Fn and Ch/B-nHAp+Fn scaffolds (2mm x 9mm). Then, the bioactivity of scaffolds was investigated. Suspension of hDPSCs at a concentration of  $1.2 \times 10^5$  cells/scaffold were cultured with odontogenic/osteogenic differentiation medium ( $\alpha$ -MEM containing 15% (v/v) FBS, 10 mM  $\beta$ -glycerol phosphate, 50  $\mu$ g/mL ascorbic acid and dexamethasone  $10^{-8}$ M) up to 21 days under static conditions. Cell viability and proliferation were analyzed by PrestoBlue<sup>®</sup> assay. SEM analysis was carried out for morphological observation. Expression level of odontogenic differentiation markers (ALP, collagen-I, RUNX2, osteocalcin and osteopontin) were determined using RT-PCR.

### RESULTS AND DISCUSSION

SEM images of hDPSCs seeded on Ch, Ch+Fn, Ch/nHAp+Fn and Ch/B-nHAp+Fn scaffolds after 14 days are presented in Fig. 1. The results showed that, chitosan scaffolds (Fig.1a) were not able to support attachment and spreading of hDPSCs as we expected. Certainly, much more hDPSCs were shown on Ch/B-nHAp+Fn scaffolds when compared to Ch/nHAp+Fn scaffolds (Fig. 1c and d). It is obvious that hDPSCs attached, spread and grew well on Ch/B-nHAp+Fn scaffolds. Also PrestoBlue<sup>®</sup> analysis indicated that the presence of boron enhanced the cell attachment and proliferation (Data not shown). In addition the results obtained from RT-PCR analysis

showed that odontogenic differentiation of hDPSCs was better on Ch/B-nHAp+Fn scaffolds than that of hDPSCs on the other scaffolds (Data not shown).

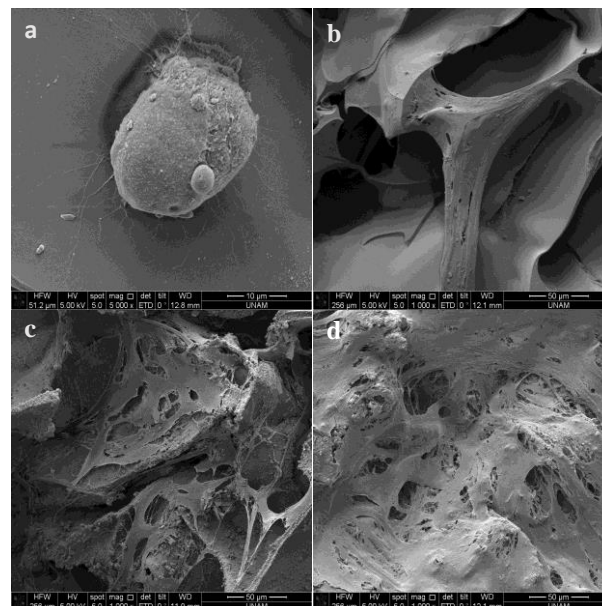


**Fig. 1:** SEM images of hDPSCs after 14 day cell culture period on a) Ch 5000x; b) Ch+Fn 1000x; c) Ch/nHAp+Fn 1000x and d) Ch/B-nHAp+Fn 1000x; scaffolds.

### CONCLUSION

In conclusion, it was determined that B enhances proliferation and odontogenic differentiation of hDPSCs and Ch/B-nHAp+Fn scaffold could be considered as a potential scaffold for dental tissue engineering applications. For the first time, we have identified that, Fn immobilized Ch/B-nHAp scaffolds with optimized surface modification improve adhesion and proliferation of hDPSCs and therefore they have interesting potential for *in vivo* transplantation

### REFERENCES

1. Tıgılı R S. *et al.*, Int J Biol Macromol. 43: 2-121, 2008
2. Demirtas T T. *et al.*, Mater Sci Eng C 49: 713–719, 2015

### ACKNOWLEDGEMENT

The authors would like to thank Turkish Scientific and Research Council (Grant no: 114S755) for providing financial support to this project.

## Humoral Immune Response against Poly(L-lactide-co-D/L-lactide) after Implantation in Rats

Uwe Walschus<sup>1</sup>, Silke Lucke<sup>1</sup>, Andreas Hoene<sup>2</sup>, Maciej Patrzyk<sup>2</sup>, Matthias Schnabelrauch<sup>3</sup>, Michael Schlosser<sup>1\*</sup>

<sup>1</sup>Department of Medical Biochemistry and Molecular Biology, University Medical Center Greifswald, Germany

<sup>2</sup>Department of Surgery, University Medical Center Greifswald, Germany

<sup>3</sup>INNOVENT e. V., Biomaterials Department, Jena, Germany

\*schlosse@uni-greifswald.de

### INTRODUCTION

Poly(L-lactide-co-D/L-lactide) (PLA), a synthetic biodegradable polymer, can be used to produce matrices which are structurally similar to the extracellular matrix and could thus be suitable for tissue engineering purposes. An *in vivo* study demonstrated that the inflammatory tissue response following implantation of electrospun PLA meshes was strictly localized to the implant site and declined from an acute to a chronic phase<sup>1</sup>, further illustrating their potential applicability. However, implanted biomaterials might also cause systemic immunological reactions initiated by the different inflammatory and immune cells involved in the local cellular response, such as macrophages in their role as antigen-presenting cells as well as T and B lymphocytes. In previous studies, we could demonstrate the occurrence of specific IgG antibodies against several synthetic polymers such as polyurethane and cellulose acetate<sup>2</sup> or polyester<sup>3-5</sup>. Therefore, the aim of the present study was to examine the immunogenicity of PLA following repeated implantation by detection of specific antibodies in rats.

### EXPERIMENTAL METHODS

**In vivo study.** Male Lewis rats (n=4) received one piece (5×5 mm) of an electrospun PLA mesh<sup>1</sup> implanted into their neck musculature. After 14 and 28 days, additional implantations were performed after removal of the previous implants. Blood was collected before the first implantation and in weekly intervals until day 56.

**Antibody detection.** Anti-PLA IgG and IgM antibodies were detected using a PLA particle suspension as assay target. Unspecific binding was blocked with BSA. Diluted serum samples were incubated with the particle suspension in microplates with V-shaped wells. Following stringent washing by repeated centrifugation/resuspension, particles were incubated with anti-rat IgG- or IgM-specific peroxidase conjugates. After washing, the particles were resuspended in chromogenic solution and transferred into a flat-bottom microplate. Following addition of sulphuric acid, optical density was measured at 490/630 nm wavelength.

### RESULTS AND DISCUSSION

After the first two implantations, no anti-PLA IgG or IgM antibodies were detectable in any animal. Only after the third implantation, an anti-PLA IgG and IgM response was observed in 3/4 rats, respectively. This is in accordance with a previous study in which single implantation of vascular grafts with a PLA-containing coating did not elicit coating-specific antibodies<sup>5</sup>. However, these results for PLA differ from previous experiments with polyester as anti-polyester antibodies

were detected in rats already after the first implantation and further boosted by additional implantations<sup>3</sup>. The anti-PLA IgG response was not as pronounced as for polyester, indicating a lower immunogenic potential for PLA. Furthermore, extent and duration of antibody formation was not uniform among individual animals. The animal with the highest IgM level remained negative for IgG antibodies, and the only animal without IgM antibodies had the second-highest IgG response. Furthermore, the anti-PLA IgG and IgM response was generally short-lived.

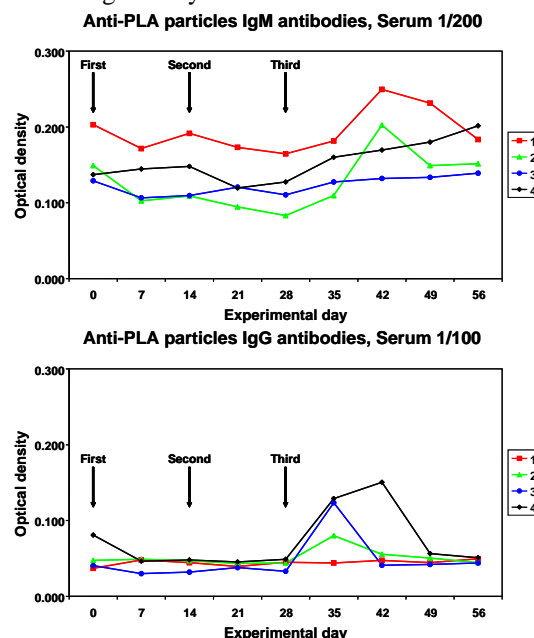


**Figure 1:** Time course of anti-PLA IgM and IgG antibodies after repeated implantation of electrospun PLA meshes into 4 individual rats. Arrows indicate implantation time points.

### CONCLUSION

Repeated implantations of the resorbable polymer PLA induced a moderate and transient anti-PLA IgG and IgM response with a broad individual variability. While these results indicate a low immunogenicity of PLA compared to other investigated polymers, they should be kept in mind for its clinical application.

### REFERENCES

1. Schnabelrauch M. *et al.*, Int J Polymer Sci 6:439784, 2014
2. Ziegler M. *et al.*, Biomaterials 15:859, 1994
3. Schlosser M. *et al.*, J Biomed Mater Res 61:450, 2002
4. Wilhelm L. *et al.*, J Biomed Mater Res A 83:104, 2007
5. Walschus U. *et al.*, J Mater Sci Mater Med, 19:1595, 2008

### ACKNOWLEDGMENTS

The study was supported by the Federal Ministry of Education & Research in the Campus PlasmaMed (project PlasmaImp).





Andrada Serafim<sup>1</sup>, Sergiu Cecoltan<sup>1</sup>, Eugeniu Vasile<sup>2</sup>, Izabela-Cristina Stancu<sup>1</sup>

<sup>1</sup>Advanced Polymer Materials Group, University Politehnica of Bucharest, Romania

<sup>2</sup>METAV Research and Development, Romania

[andrada.serafim@gmail.com](mailto:andrada.serafim@gmail.com)

## INTRODUCTION

Hybrid natural-synthetic polymeric biomaterials are intensively studied for tissue regeneration. We developed various hydrogels based on gelatin – poly(vinylpyrrolidone) (G-PVP) that could be assembled into scaffolds with personalized architecture and controlled functionality for skin grafts applications. Freeze-dried hydrogel layers and mats of electrospun submicronic fibers have been obtained.

## EXPERIMENTAL METHODS

**Hydrogel synthesis.** A first type of hydrogel consists in bicomponent polymer systems with various compositions (G:PVP 6:1, 3:1, 2:1). The polymer solutions were prepared by direct dissolution in distilled water followed by semi-interpenetrated polymer network generation, as reported elsewhere<sup>1</sup>. The total solid content (T%) was adjusted to 20 and 30%, respectively. Porous membranes were generated by freeze-drying, after crosslinking the protein with glutaric aldehyde. Porous mats of submicronic fibers were obtained using a modular electrospinning set-up developed by our team. All the membranes were characterized with respect to their affinity for simulated physiologic aqueous media relevant for the target application (including swelling kinetics, equilibrium water content - EWC and dehydration kinetics), capacity to generate porous scaffolds through freeze-drying, tensile behavior of the hydrated samples (using a Brookfield CT3 texture analyzer equipped with a dual grip assembly TA-DGA), dynamic oscillatory measurements on fully hydrated samples (using a stress controlled rheometer Kinexus Pro, Malvern). In addition, morphology examination was performed using Scanning Electron Microscopy (SEM): QUANTA INSPECT F SEM device equipped with a field emission gun with a 1.2 nm resolution.

## RESULTS AND DISCUSSION

The synthesized materials reach the maximum swelling relatively fast (< 6 hours) the composition being the main factor to control this behavior. Increasing the content of synthetic polymer (while T is constant) leads to faster swelling; decreasing PVP leads to an increase of the dehydration rate probably due to the formation of denser networks. Accordingly, the elasticity of the resulting bicomponent materials is also strongly influenced by (i) the G:PVP ratio (augmenting G leads to less elastic hydrogels) and (ii) T% (higher T values decrease the elasticity of the membranes). The mechanical properties are consistent with the results of

the study regarding the affinity for simulated physiologic aqueous media.

It was confirmed that porous scaffolds with various thickness, porosity and pores' architecture can be obtained. Figure 1 is relevant with this respect. In addition, the porous membranes can be combined with the mats of electrospun submicronic oriented or random fibers.

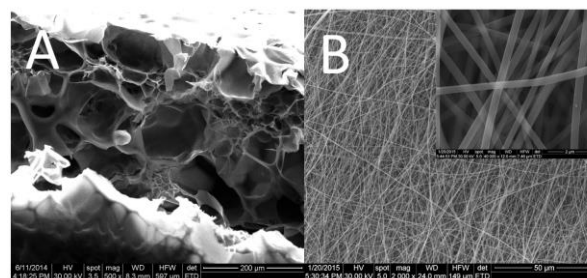


Fig.1 shows the morphology of A - cross-section of a porous hydrogel membrane G-PVP (T=30%), B – mat of electrospun G submicronic fibers

## CONCLUSION

Porous membranes and mats of electrospun fibers based on G-PVP and G, respectively, were obtained. The synthesized materials can be assembled into multilayer scaffolds with personalized architecture and tunable functionality for skin grafts applications. The mechanical and morphostructural properties of the obtained hydrogels can be easily tailored through the composition of the initial polymer solutions. The ratio between the natural and synthetic polymer and the total solid content value have a strong influence on the overall behavior of the hydrogels, allowing the control of the properties to the best possible outcome for skin graft applications.

## REFERENCES

1. Serafim A. *et al.*, Key Eng. Mat. in press, 2015

## ACKNOWLEDGMENTS

The work has been funded by the Sectorial Operational Programme Human Resources Development 2007-2013 of the Ministry of European Funds through the Financial Agreement POSDRU/159/1.5/S/132397. Also the authors would like to acknowledge the financial support from the National project PCCA Grant no: 201/2014, ZettaSkin.



Carlos A. Fernandez<sup>2</sup>, Cristian A. Martinez<sup>2</sup>, Andrés Ozols<sup>2</sup>, Dagnija Loca<sup>1</sup>, Miguel O. Prado<sup>3</sup>, Daniel Olmedo<sup>4</sup>

<sup>1</sup>Riga Biomaterials Innovations and Development Centre of Riga Technical University, Latvia

<sup>2</sup>Institute of Biomedical Engineering, Buenos Aires University, Argentina

<sup>3</sup>Group of Nuclear Materials, Bariloche Atomic Centre, Argentina

<sup>4</sup>Pathological Anatomy Cathedra, Buenos Aires University, Argentina

[dagnija.loca@rtu.lv](mailto:dagnija.loca@rtu.lv)

## INTRODUCTION

The aim of this development is to optimize a bone substitute for use in tissue engineering. This is achieved through the combination of three phases in a biocomposite (BCO), in which each is reabsorbed in the site of implantation and replaced by autologous bone (patient's own). The inorganic phases are composed of irregular particles (150-300 microns) obtained by milling and sieving of a biphasic bioceramic (BC) of hydroxyapatite (HA of bovine origin) with 40 % (wt.)  $\beta$ -tricalcium phosphate ( $\beta$ -TCP, obtained by wet chemical synthesis) and Bioglass (BG) (45SiO<sub>2</sub>-24,5CaO-24,5Na<sub>2</sub>O-6P<sub>2</sub>O<sub>5</sub>, in % wt.). Instead, the biological matrix consists mainly of collagen extracted from Wharton's jelly (WJ), obtained from human umbilical cords, subject to proprietary physical and chemical processes.

## EXPERIMENTAL METHODS

The BC is produced by mixture of HA and  $\beta$ -TCP (< 45 $\mu$ m) and moulding by gelcasting with albumin in aqueous solutions, drying and sintering at 1200°C for 2 hours. The BG is obtained from the mixture of the oxides, melting at 1350°C and cast onto metal. Each phase and BCO is subjected to studies by electron microscopy an energy dispersive energy, X-ray diffraction and infrared spectrometry.

The histological chrono-dynamics of tissue response to BCO is evaluated, using the experimental model of *laminar implant*<sup>1</sup> in Wistar rats (n = 40) from the time of implantation up to 60 days. The BCO shaped as micro-implants (1 x 6 x 0.5 mm<sup>3</sup>), was implanted in both tibias. Euthanasia of animals was performed by overdose of anaesthesia at T0, T1h, T24h, T7D, T14d, T30d and T60d of post- implementation times. The tibias were resected and fixed in 10% formalin, were radiographed, and demineralised, obtaining histological sections stained with HE.

## RESULTS AND DISCUSSION

BCO provided an adequate biocompatibility at different evaluated times. From the first hour (T1h-T24h) good hydrophilic, surrounded with abundant erythrocytes and the subsequent clot formation at the site of implantation were observed. At 7 days (T7D) formation of granulation tissue with abundant fibroblasts was observed. From T14d bone tissue formation around BC and BG particles, interconnected through bone bridges, and was identified. Bone tissue was reticular after 14 days (T14) and laminar like after 30 days (T30 and T60) (Fig.1).

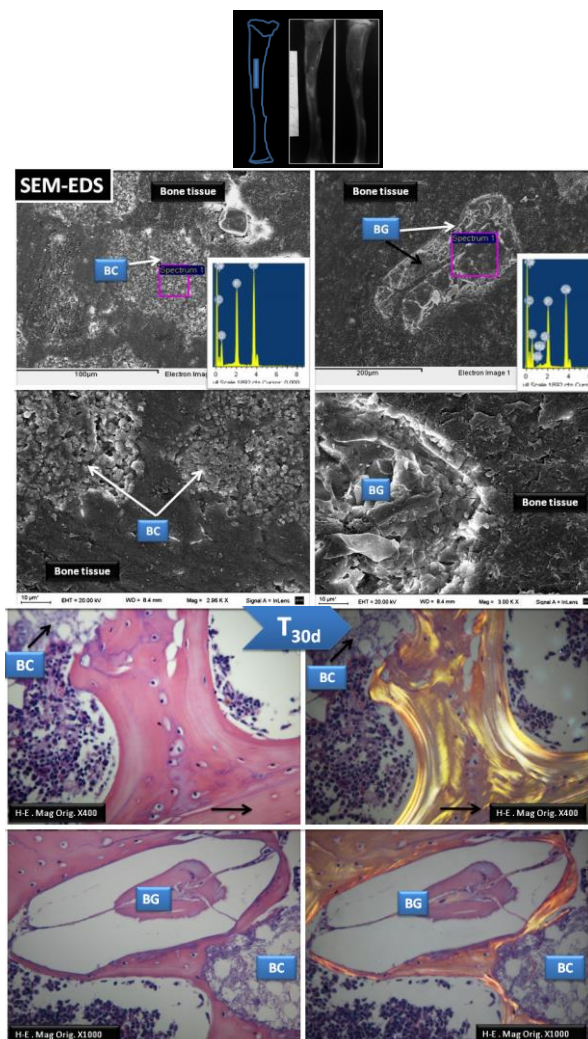


Fig. 1: Radiography at first hour and after 30 days of implanted BCO (top) in SEM images (middle) and histological section study (bottom).

## CONCLUSION

The new BCO synthesized and characterized, used as scaffold for bone tissue engineering is highly biocompatible. It allows the formation of laminar bone interconnecting BG and BC particles, making it suitable for potential clinical application in implant and maxillofacial surgeries, which have begun in several Institutes.

## REFERENCES

1. Cabrini *et al.*, G. Bot. Ital., 127, 835–837.1993.

## ACKNOWLEDGMENTS

This research was mainly funded by Dr. A. Ozols and C. A. Fernández.

# **Porcine-based Collagen Membranes and Matrices Induce Different Tissue Reaction Depending on Origin: Vascularization and Inflammatory Response in Preclinical and Clinical Studies**

Shahram Ghanaati<sup>1,2</sup>; Mike Barbeck<sup>1,2</sup>; Jonas Lorenz<sup>1</sup>; Patrick Booms<sup>1</sup>; Robert A Sader<sup>1</sup>; C James Kirkpatrick<sup>2</sup>

<sup>1</sup> FORM-Lab, Department for Oral, Cranio-Maxillofacial and Facial Plastic Surgery, Medical Center of the Goethe University Frankfurt, Germany

<sup>2</sup> REPAIR-Lab, Institute of Pathology, Johannes Gutenberg University Mainz, Germany  
[shahram.ghanaati@kgu.de](mailto:shahram.ghanaati@kgu.de)

## **INTRODUCTION**

The aim of the present study was to assess the vascularization and cellular reaction to five different collagen-based materials after their application either in human or animal tissue. The focus was on material integration, degree of degradation, transmembranous vascularization and the inflammatory cell types involved in the tissue reaction.

## **EXPERIMENTAL METHODS**

The five different collagen materials in this study were used for socket preservation, lateral augmentation and vestibuloplasty in humans. The same materials were histologically assessed in wild-type mice over a time period of 60 days (Fig. 1). Biopsies of these materials have been excised, processed and investigated histologically with special focus on material stability, vascularization and induction of a multinucleated giant cell triggered foreign body reaction using established histological and histomorphometrical methods<sup>1-3</sup>. Analysis of variance and subsequent LSD post-hoc statistical tests were employed to study significance.

## **RESULTS AND DISCUSSION**

The histological analysis showed distinct differences concerning the cellular reactions to the different collagen membranes depending on material-specific characteristics and processing techniques (Fig. 1). Cellular reactions consisted of either mononuclear cells (e.g. macrophages) with absence of a foreign-body-reaction or, alternatively, multinucleated giant cell-triggered granulation tissue, and were observed for the materials in both species (Fig. 1). These two different tissue reactions significantly influenced the material stability and premature degradation.

## **CONCLUSION**

In periodontology and implantology collagen-based membranes serve as versatile barriers, which should separate different tissues and cell types involved in the healing process regarding the process of the Guided Tissue Regeneration (GTR). For clinical application of collagen membranes a detailed knowledge of the cells involved in the tissue response to materials is of great importance. These cells, either mononuclear or multinucleated cells can significantly influence material stability and integration. The latter two parameters have distinct influence on the clinical outcome and successful application of collagen membranes.

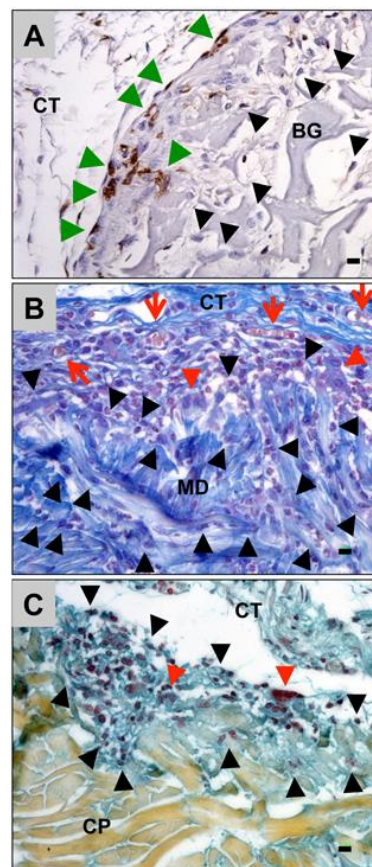


**Fig. 1** shows exemplarily the different tissue reactions to three collagen membranes (A: Bio-Gide (BG), B: Mucoderm (MD), C: Collprotect (CP)) at day 15 within the subcutaneous connective tissue (CT). Thus, the BG membrane induced a mild tissue reaction based on mononuclear cells such as macrophages (green arrowheads) and other cells (black arrow heads), while multinucleated giant cells (red arrowheads) were involved in the tissue reactions to the other two membranes. Mononuclear cells are shown as black arrowheads (red arrows in B = vessels).

## **REFERENCES**

1. Ghanaati S. *et al.*, Biomed Mater, 6 (1): 015010, 2011
2. Ghanaati S., Acta Biomater, 8 (8): 3061-72, 2012
3. Barbeck M. *et al.*, J Oral Implantol., 2014

## **ACKNOWLEDGMENTS**

The authors would like to thank Ms. Ulrike Hilbig, Mrs. Verena Hoffmann and Mr. Mykhaylo Reshetnykov for their technical assistance.

## Cultivation of Mesenchymal Stem Cells on Collagen-based Scaffolds Cross-linked by EDC/NHS or Genipin

Pavla Sauerova<sup>1</sup>, Martina Verdanova<sup>2,3</sup>, Tomas Suchy<sup>4</sup>, Monika Supova<sup>4</sup>, Sarka Ryglova<sup>4</sup>, Margit Zaloudkova<sup>4</sup>, Zbynek Sucharda<sup>4</sup>, Marie Hubalek Kalbacova<sup>1,3,5</sup>

<sup>1</sup>Biomedical Centre, Faculty of Medicine in Pilsen, Charles University in Prague, alej Svobody 1655/76, Pilsen – Severní Předměstí, 323 00, Czech Republic

<sup>2</sup>Department of Genetics and Microbiology, Faculty of Science, Charles University in Prague, Albertov 6, Prague 2, 128 43, Czech Republic

<sup>3</sup>Institute of Inherited Metabolic Disorders, 1<sup>st</sup> Faculty of Medicine, Charles University in Prague, Ke Karlovu 2, Prague 2, 128 08, Czech Republic

<sup>4</sup>Department of Composites and Carbon Materials, Institute of Rock Structure and Mechanics, Academy of Sciences of the Czech Republic, V Holešovičkách 41, Prague 8, 182 09, Czech Republic

<sup>5</sup>Department of Histology and Embryology, Faculty of Medicine in Pilsen, Charles University in Prague, Karlovarská 48, Pilsen, 301 66, Czech Republic  
[pavla.sauerova@gmail.com](mailto:pavla.sauerova@gmail.com)

### INTRODUCTION

Interactions of human mesenchymal stem cells (hMSCs) with collagen-based scaffolds were studied with the aim of bone surgery application. The scaffolds should imitate an extracellular bone matrix and support hMSCs adhesion, proliferation and their osteogenic differentiation. The scaffolds should degrade after appropriate time. Collagen-based scaffolds are widely researched due to collagen positive effect on many cell types, its lattice-like organization ability and biocompatibility<sup>1</sup>. However, the fast biodegradation rate and the low mechanical strength of the untreated collagen very often complicate *in vitro* and *in vivo* applications<sup>2</sup>. The stability of collagen scaffolds can be enhanced by cross-linking. Thus, in this study, various cross-linking agents were used, e.g. genipin<sup>3</sup>, EDC/NHS/EtOH or EDC/NHS/PBS<sup>4,5</sup>.

### EXPERIMENTAL METHODS

The cell metabolic activity (Cell Titer 96 Aqueous One Solution Cell Proliferation Assay, MTS, Promega, USA) of the cells cultivated in scaffolds infusions (cytotoxicity determination), the metabolic activity of cells seeded on scaffolds, number of cells adhered on scaffolds and fluorescent visualization of cell/scaffold interactions (nuclei and actin were stained) were determined. All procedures were performed after short (48 h) and long (168 h) cell cultivation. Tissue culture treated polystyrene (PS) (TPP, Switzerland) was used as a positive control. hMSCs were isolated from a bone marrow blood of three healthy donors to simulate a stem cell variability naturally occurred among individuals.

### RESULTS AND DISCUSSION

Composite scaffolds (consisting of natural collagen as matrix, poly(DL-lactide) electrospun nanofibers, calcium phosphate as dispersed filler supplemented by sodium hyaluronate) cross-linked by EDC/NHS/EtOH, EDC/NHS/PBS or genipin, were tested *in vitro*. The scaffold infusions were tested to check a releasing of any cytotoxic agents from individual scaffolds to cultivation medium. After 48 h, the metabolic activities of hMSCs cultivated in all three scaffolds infusions were comparable and slightly higher than the PS control. After 168 h, the metabolic activities of the cells

treated by genipin and EDC/NHS/EtOH cross-linked scaffolds infusions remained similar as after 48 h. However, the metabolic activity of hMSCs treated by EDC/NHS/PBS cross-linked scaffold infusion markedly decreased to 83 % of PS control. Metabolic activity of the cells seeded on scaffolds was almost comparable among all three scaffolds in both incubation times. The value reached cca. 50 % of the control cells. The reduced cell adherence on the scaffolds in comparison to the control cells seeded on PS surface was predicted due to the different character of both surfaces. Fluorescent visualization determined the cell ability to adhere on all tested scaffolds. After 48 h, hMSCs on the genipin cross-linked scaffold revealed the best morphology and symmetric distribution. Interestingly, after 168 h, cells on all scaffolds were similarly organized with comparable appearance. Thus, the genipin cross-linked scaffold provided the best conditions for cells after both 48h and 168h cultivation time. In addition, it maintained constant mechanical properties in contrast to the rest of cross-linked scaffolds.

### CONCLUSION

It could be concluded that the genipin cross-linked scaffold is the best one with ideal mechanical and biological properties for subsequent *in vitro* 3D analyses and *in vivo* experiments.

### REFERENCES

1. Glowacki J. *et al.*, Biopolymers. 89:338–44, 2008
2. Rault I. *et al.*, J. Mater. Sci. Mater. Med. 7:215–21, 1996
3. Chen Y-S. *et al.*, Biomaterials. 26:3911–8, 2005
4. Chang J-Y. *et al.*, Macromol. Biosci. 7:500–7, 2007
5. Ma L. *et al.*, Biomaterials. 25:2997–3004, 2004

### ACKNOWLEDGMENTS

This work was supported by grants of Charles University in Prague: project ED2.1.00/03.0076 from European Regional Development Fund (ERDF) and SVV 260 047; project PRVOUK-P24/LF1/3 and grant SVV-2014-260081. We gratefully acknowledge the financial support provided for our work by the long-term conceptual development research organisation under project no. RVO: 67985891.





## Remineralization of Demineralized Bone Matrix in Critical Size Cranial Defects in Rats: a Six Months Follow-up Study

<sup>1,2</sup> Dénes B. Horváthy, <sup>3</sup> Dora Polsek, <sup>1</sup> Gabriella Vác, <sup>1</sup> István Hornyák, <sup>1,2</sup> Zsombor Lacza

<sup>1</sup> Tissue Engineering Laboratory, Semmelweis University, Budapest, Hungary.

<sup>2</sup> Lacerta Technologies GmbH, Krems an der Donau, Austria

<sup>3</sup> School of Medicine, Zagreb University, Zagreb, Croatia

[zsombor.lacza@lacertatech.com](mailto:zsombor.lacza@lacertatech.com)

### INTRODUCTION

The key drawback of using demineralized bone matrix (DBM) is its low initial mechanical stability due to the severe depletion of mineral content. Although the ingrowth of new bone undoubtedly restores the mechanical strength of the DBM-filled bone defect, it is not known whether this restoration ever gets complete or if there is a residual depletion in some elements. In the present study we investigated the long term regeneration of DBM in a critical size bone defect model and investigated the remineralization after six months.

any of these minerals, it induces a faster and more complete regeneration process.

### ACKNOWLEDGMENTS

Sponsored by a research grant to Semmelweis University from Lacerta Technologies GmbH

### DISCLOSURES

Dr. Lacza is founder and CEO and Dr. Hornyák is an employee of Lacerta Technologies GmbH, which holds a pending patent of the technology.

### MATERIALS AND METHODS

Critical size bone defects were created in the cranium of male Wistar rats which were filled with DBM or left empty as negative controls. In vivo bone formation was monitored with computed tomography after 11, 19 and 26 weeks postoperatively. After 6 months, parietal bone pieces were harvested and subjected to microCT. Images from the CT scan were analyzed to determine bone density. Circular region of interest (ROI) was set on the 11th postoperative week for every defect. Reference points were used to set the same ROI at each time point. Area of the remaining bone defect was measured from the CT scans. Mineral content was determined with inductively coupled plasma optical emission spectrophotometer (ICP-OES) analysis.

### RESULTS

After 11 weeks the DBM-filled bone defects were completely closed, while empty defects were still open. Bone density of the DBM-treated group increased significantly while the controls remained unchanged. Quantitative analysis by microCT confirmed the in vivo results, bone volume / tissue volume was significantly lower in the controls than in the DBM group. The demineralization procedure depleted the key minerals of the bone to a very low level, in case of Calcium it was below 1%. Sulphur and several micro-elements such as Fe and Cu were unaffected by demineralization, indicating that the protein volume of DBM is largely intact. Six months after implantation Ca, P, Na, Mg, Zn, and Cr contents were completely restored to the normal level, while K, Sr and Mn were only partially restored.

### DISCUSSION AND CONCLUSIONS

The remineralization process of DBM is largely complete by the 6th month after implantation in terms of bone density, structure and key mineral levels. Although DBM does not provide sufficient sources for





## Development of a Bioactive and Biodegradable Poly( $\epsilon$ -Caprolactone)-Based Prosthetic Ligament

Géraldine Rohman<sup>1,2</sup>, Amélie Auge<sup>1,2</sup>, Gabriela Radu-Bostan<sup>1,2</sup>, Roger Guillard<sup>3</sup>, Bernard Brulez<sup>3</sup>, Véronique Migonney<sup>1,2</sup>

<sup>1</sup>Université Paris 13, Sorbonne Paris Cité, CSPBAT, F-93430, Villetaneuse, France.

<sup>2</sup>CNRS, UMR 7244, F-93430, Villetaneuse, France

<sup>3</sup>Société LARS, 5 rue de la Fontaine, 21560 Arc-sur-Tille, France

[veronique.migonney@univ-paris13.fr](mailto:veronique.migonney@univ-paris13.fr)

### INTRODUCTION

Current therapies for anterior cruciate ligament (ACL) injuries are transplants, and for very specific cases, the use of artificial prostheses designed from poly(ethylene terephthalate) (PET) fibers. In particular, data from short to medium term follow-up studies supports the ongoing use of the Ligament Augmentation and Reconstruction System LARS<sup>TM</sup> as a safe surgical technique with low complication rate<sup>1</sup>. Besides, to enhance the interaction of the LARS ligament with fibroblasts and osteoblasts, a radical graft polymerisation of polystyrene sodium sulfonate (PNaSS) onto PET had been developed<sup>2</sup>. Indeed, PNaSS grafting allowed a stronger fibroblast adhesion, a better cell spreading, a more homogeneous cell distribution over the material surface, and an increase in the cell collagen secretion<sup>2,3</sup>. Moreover, PNaSS grafting enhanced ALP secretion in osteoblasts, had a positively significant impact on the *in vitro* mineralisation, as well as enhanced direct ligament-to-bone contact with a decrease of fibrous scar tissue at the bone/ligament interface<sup>4</sup>.

Lately, ACL reconstruction using connective tissue engineering has emerged and recent researches focus on the development of biodegradable structures that could allow graft functioning while enhancing host integration. Based on the results obtained with the bioactive LARS system, our work aims to develop a bioactive and biodegradable prosthetic ligament based on poly( $\epsilon$ -caprolactone) (PCL) fibers grafted with PNaSS. The present study brings out the graft polymerization of PNaSS onto PCL fibers by different processes.

### EXPERIMENTAL METHODS

PURASORB PCL fibers were supplied by Luxilon and used after scouring. PCL-based constructs were developed by associating 20 fibers of 10 cm length. PCL constructs were activated by 2 different processes and thereafter immersed in styrene sodium sulfonate (NaSS) solution allowing the polymerization to occur up to 17 hours for process 1 and 60 minutes for process 2.

After washing to remove the ungrafted NaSS, the evidence of PNaSS grafting was provided by a colorimetric method, elemental analyses and infrared spectroscopy. SEC, DSC and SEM analyses as well as tensile tests were carried out to characterize the PCL construct before and after PNaSS grafting.

### RESULTS AND DISCUSSION

For different grafting processes, the PNaSS grafting was obtained in a very homogeneous way over the fiber-based constructs. The grafting density increased with the polymerization time as shown in Figure 1; however, the process 2 was faster than process 1.

Characterization of PCL constructs before and after PNaSS grafting did not reveal any variation in the molecular weights and characteristic temperatures of PCL, neither in fiber diameter and mechanical properties of the construct.

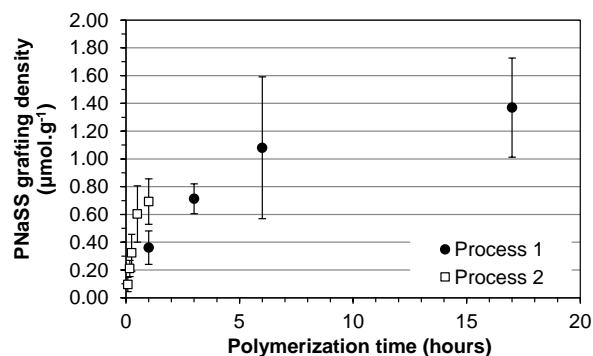


Figure 1: Concentration of grafted pNaSS on PCL constructs as a function of polymerization time.

### CONCLUSION

Our work brings out two easy and versatile ways of immobilizing bioactive PNaSS onto PCL fibers through 2 different activating processes. This can provide a new generation of scaffolds which could be “biointegrable” and be used for ligament tissue regeneration. For further investigation, it is necessary to investigate the cell response *in vitro* and *in vivo*.

### REFERENCES

1. Newman S.D.S. *et al.*, Int. Orthop. 37:321-326, 2013.
2. Ciobanu M. *et al.*, Biomacromolecules 7:755-760, 2006.
3. Viateau V. *et al.*, IRBM 32:118-122, 2011.
4. Vaquette C. *et al.*, Biomaterials 34:7048-7063, 2013.

### ACKNOWLEDGMENTS

The authors would like to thank the National Association for Research and Technology (ANRT) and LARS Society for the CIFRE contract and financial support granted to Amélie Auge. The authors also thank Luxilon Industries NV for providing the PCL fibers.



## Dental Caries: Biomimetic Mineralization Model Development

Lucy Kind<sup>1</sup>, Christian Mangeng<sup>2</sup>, Sabrina Stevanovic<sup>1</sup>, Benjamin Bellon<sup>2</sup>, Stefan Winkler<sup>2</sup>, Iwona Dziadowiec<sup>3</sup>, Hans Deyhle<sup>3</sup>, Bert Müller<sup>3</sup>, Uwe Pielels<sup>1</sup>

<sup>1</sup>Life Sciences/Institute for Chemistry and Bioanalytics, University of Applied Sciences and Arts Northwestern Switzerland (FHNW), Switzerland

<sup>2</sup>Nanotechnology/Institute of Chemistry, University of Basel, Switzerland

<sup>3</sup>Biomaterials Science Center (BMC), University of Basel, Switzerland

[lucy.kind@fhnw.ch](mailto:lucy.kind@fhnw.ch)

### INTRODUCTION

Dental Caries is one of the most prevalent chronic diseases worldwide with significant impacts on global healthcare systems<sup>1</sup>.

Commonly, carious attacks start off with sub-surface demineralization by acid secretion from bacteria. Arresting the process in early stage is crucial to avoid cavitation of the surface resulting in costly tooth restoration and replacement. Therefore non-invasive, regenerative methods to treat early caries in tooth enamel are drawing more and more attention.

Biomimetic mineralization is a very promising method. It is induced by a peptide (P11-4) which self-assembles into a supramolecular fibrillar 3D network that triggers the nucleation of de-novo hydroxyapatite<sup>2</sup>. Previous studies showed a significant increase of remineralization in artificial induced early caries lesions confirming in-vivo results<sup>3</sup>.

Additionally and due to the limited availability and great structural variety of human teeth a bioceramic tooth model (BTM) was developed mimicking natural human dental enamel. This study should facilitate the possibility to establish enamel-like and dentin-like BTM as a standardized test system for further studies in caries treatment by biomimetic mineralization.

### EXPERIMENTAL METHODS

#### De-/Remineralization of natural human tooth

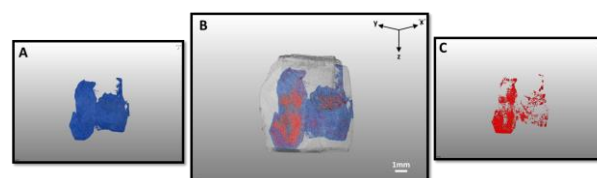
Artificial sub-surface lesions on human enamel were induced by incubation in acidic demineralization buffer. P11-4 was directly applied on sub-surface lesion and the tooth was subsequently incubated in saliva simulating remineralization buffer for 2 weeks. The remineralization state was analyzed by micro-computed tomography ( $\mu$ CT).

#### Bioceramic tooth model (BTM)

BTMs are based on mixtures of hydroxyapatite and porosifying agent (porosifier) and the ratio reflects the degree of porosity and density of BTMs. The mixtures were pressed into tablets and sintered at 1250°C. The models were characterized by  $\mu$ CT, scanning electron microscopy (SEM) and Brunauer-Emmett-Teller (BET) in order to compare them with human dental enamel.

### RESULTS AND DISCUSSION

Fig. 1B shows an overlaid 3D image reconstructed from  $\mu$ CT data of an artificial lesion in human enamel tooth slice.



The overlay includes the lesion demineralized before peptide treatment (A) and the lesion remineralized (C). By comparing the results an increase of density was clearly visible after 2 weeks incubation in remineralization buffer.

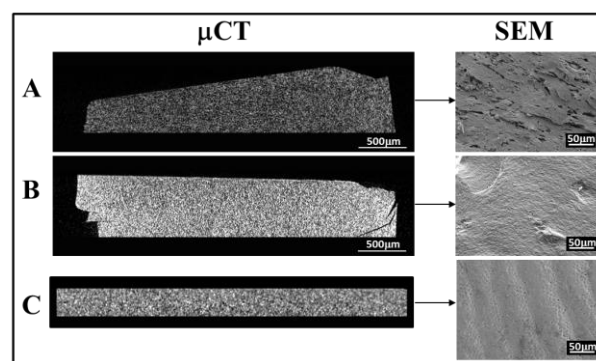


Fig. 2 presents  $\mu$ CT images of BTMs with different ratio of hydroxyapatite (HA) and porosifier (P) (A-80(HA):20(P) w% and B-100(HA) w%) and the corresponding SEM images of interface. C represents human enamel slice as a reference.

BTMs could be successfully produced comparable with human enamel concerning density and surface.

### CONCLUSION

Diffusion of self-assembling peptide into carious lesions of human teeth and their remineralization demonstrates the non-invasive regeneration potential of the peptide P11-4.

Mixing porosifier with hydroxyapatite powder, compressing the mixture and sintering, showed a comparable structure to enamel useful for further research.

### REFERENCES

1. Bagramian R. A. *et al.*, Am. J. of Dent. 21:3-8, 2009
2. Kirham J. *et al.*, J. Dent. Res. 86:426-430, 2007
3. Brunton P. *et al.*, Br. Dent. J. 215:4, E6, 2013

### ACKNOWLEDGMENTS

The authors would like to thank Swiss-Nanoscience Institute (SNI) and Swiss National Science Foundation (SNSF) (project no 144617) for providing financial support to this project.



## Glycomer™ 631 in Tendon Tissue Engineering: an Old Material in New Ventures

Kyriakos Spanoudes,<sup>1</sup> Geoffrey Hanley<sup>1</sup>, Yves Bayon,<sup>2</sup> Abhay Pandit,<sup>1</sup> Dimitrios I Zeugolis,<sup>1</sup>

<sup>1</sup>Network of Excellence in Functional Biomaterials, National University of Ireland, Galway, Ireland

<sup>2</sup>Covidien - Sofradim Production, Trevoux, France

[dimitrios.zeugolis@nuigalway.ie](mailto:dimitrios.zeugolis@nuigalway.ie)

### INTRODUCTION

Tendon tissue engineering is becoming increasingly important, as current surgical treatment modalities based on tissue grafts and non-degradable polymers have numerous drawbacks, including (inter-species) disease transmission, foreign body response and scar tissue formation. Although electro-spun scaffolds based on biodegradable polymers have demonstrated promising results in both *in vitro* and *in vivo* setting, long-term implantation studies indicate suboptimal mechanical resilience [1-3]. Herein, we hypothesise that Glycomer™ 631, composed of 60% glycolide, 26% trimethylene carbonate and 14% dioxanone will maintain tenogenic phenotype *in vitro* and promote functional repair and regeneration *in vivo*.

### EXPERIMENTAL METHODS

Glycomer™ 631 was dissolved in hexafluoro-isopropanol (HFIP) at 100mg/ml concentration. Using a rotating collector (1400 RPM) anisotropic electro-spun fibres were produced. Human patellar tendon tenocytes were expanded up to passage 3 in DMEM media, supplemented with 10% foetal bovine serum and 1% penicillin / streptomycin. 50,000 cells / cm<sup>2</sup> were subsequently cultured for up to 5 days. Fibre orientation was assessed with Scanning Electron Microscopy (SEM). The influence of electro-spun fibres on cell viability and metabolic activity was assessed using Live/Dead® and alamarBlue® assays respectively. Cell morphometric analysis was carried out using DAPI and rhodamine conjugated phalloidin and subsequent image analysis (ImageJ).

### RESULTS AND DISCUSSION

**Figure 1:** Collector rotation speed of 1400 RPM resulted in anisotropically orientated (>80% axial alignment) Glycomer™ 631 electro-spun fibres.

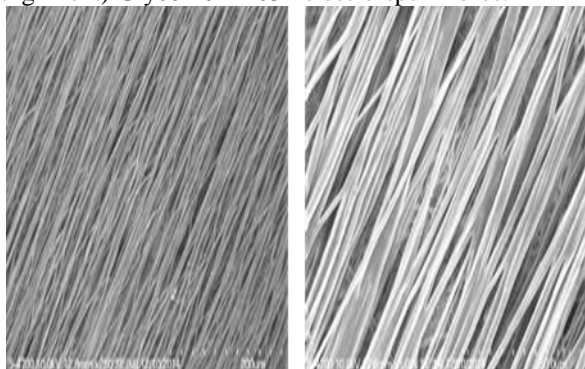


**Figure 2:** Tenocytes remain viable & metabolically active up to 5 days in culture.

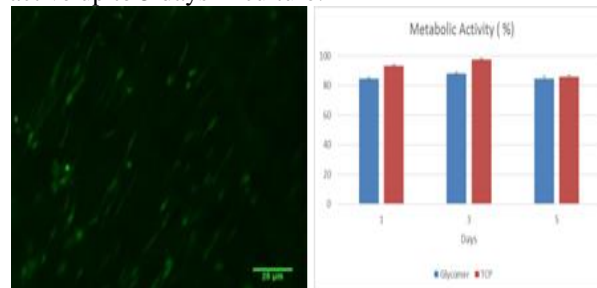
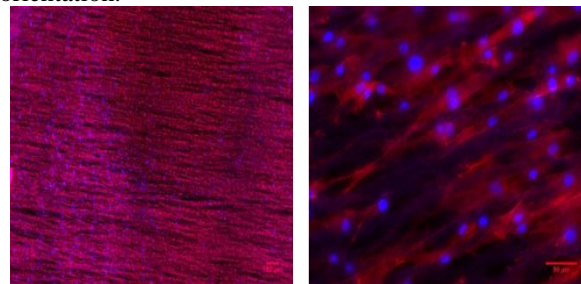


**Figure 3:** DAPI (blue) and rhodamine conjugated phalloidin (red) staining indicates bidirectional nuclei and cytoskeleton orientation, parallel to the scaffold orientation.



### CONCLUSION

These preliminary *in vitro* data indicate that anisotropic electro-spun Glycomer™ 631 scaffolds provide a suitable microenvironment for tenocyte growth. Further mechanical analysis, protein and gene assays and *in vivo* studies are under way.

### REFERENCES

- Spanoudes K. et al Trends Biotechnol, 32: 472-482, 2014.
- Abbah S.A. et al, Stem Cell Res Ther, 5: 1-9, 2014.
- Gaspar D. et al, Adv Drug Deliv Rev, In Press

### ACKNOWLEDGMENTS

The authors would like to acknowledge Irish Research Council and College of Engineering and Informatics for financial support. KS, GH, AP and DIZ have no conflict of interest. YB is an employee of Covidien.

## Efficacy of Platelet Rich Plasma in Treatment of Plantar Fasciopathy

Lukasz Nagraba<sup>1</sup>, Tomasz Mitek<sup>1</sup>, Jarosław Deszczyński<sup>1</sup>, Artur Stolarczyk<sup>1</sup>

<sup>1</sup>Orthopaedics and Rehabilitation Department II Medical Faculty, Medical University of Warsaw, Poland  
[nagraba@gmail.com](mailto:nagraba@gmail.com)

### INTRODUCTION

Plantar fascia is a strong, connective tissue structure with its proximal insertion in calcaneal tuberosity and distal ends on bases of distal phalanges of all toes. Fasciopathy is one of the most common causes of pain problems in this area in adults. It is estimated that such patients constitute about 1% of people seeking help of orthopedic surgeon. In plantar fasciopathy chronic, regional inflammation and remodeling process lead to collagen necrosis, angiofibroblastic hyperplasia and calcification of extracellular matrix.

PRP (Platelet Rich Plasma) is an autologous concentrate of blood platelets in low volume of plasma. Platelets release seven basic growth factors responsible for tissue healing process (three isoforms of PDGF, TGF- $\beta$ , TGF- $\beta$ 2, VEGF and EGF). Previous studies showed synergistic action of several growth factors in PRP and their optimal ratios to enhance the healing. Taking into consideration degenerative nature of fasciopathy, the use of platelet rich plasma in treatment of this illness should be justified and efficient.

### EXPERIMENTAL METHODS

The aim of the study was to assess the efficacy of platelet rich plasma treatment in patients with plantar fasciopathy.

The study included 30 patients diagnosed with plantar fasciopathy, verified by ultrasound or MRI examination. All patient included in the study had suffered heel pain for at least 6 month prior to inclusion and underwent extensive physical therapy for at least 3 months without satisfactory result.

Study protocol included autologous PRP injection and following physiotherapy. Investigators evaluated patients quality of life and pain symptoms by means of: visual analog scale, EQ-5D questionnaire and Foot Function Index. Biodex Balance System was utilized to acquire data for objective evaluation.

### RESULTS AND DISCUSSION

The treatment, carried out by following study protocol, resulted in significant pain reduction and increase in health related quality of life. The majority of patients also improved their score in balance and fall risk tests during the final evaluation.

### CONCLUSION

Single injection of autologous platelet rich plasma followed by carefully planned physical therapy is an efficient treatment option for patients with chronic plantar fasciopathy. Currently the investigators carry out further studies to compare the efficacy of presented protocol to other widely spread treatment methods such as TOPAZ and ESWT.

### REFERENCES

1. Barrett S, Erredge S. Growth factors for chronic plantar fasciitis. *Podiatry Today*. 2004;17:37–42.
2. Lemont H, Ammirati KM, Usen N. Plantar fasciitis: a degenerative process (fasciosis) without inflammation. *J Am Podiatr Med Assoc*. 2003;93(3):234–237
3. Schepsis AA, Leach RE, Gorzyca J. Plantar fasciitis. Etiology, treatment, surgical results, and review of the literature. *Clin Orthop Relat Res*. 1991;266:185–196
4. Gill LH. Plantar Fasciitis. Diagnosis and Conservative Management. *J Am Acad Orthop Surg*. 1997;5(2):109–117





## Development and Characterisation of a Decellularised Porcine Mitral Valve Scaffold

Sofia Andriopoulou<sup>1</sup>, Lucrezia Morticelli<sup>1</sup>, Michael Harder<sup>2</sup>, Andres Hilfiker<sup>1</sup>, Igor Tudorache<sup>1</sup>, Sergei Cebotari<sup>1</sup>, Axel Haverich<sup>1</sup>, Sotirios Korossis<sup>1</sup>

<sup>1</sup>Dept. of Cardiothoracic, Transplantation and Vascular Surgery, Hannover Medical School, Germany

<sup>2</sup>Corlife, Hannover, Germany

[andriopoulou.sofia@mh-hannover.de](mailto:andriopoulou.sofia@mh-hannover.de)

### INTRODUCTION

Valvular heart disease represents a common disorder that causes significant morbidity and mortality rates worldwide. Current surgical approaches include the replacement of the diseased valve with a mechanical or a bioprosthetic valve. Nevertheless, these valve replacements have severe drawbacks, such as the necessity for chronic anti-coagulation therapy with the mechanical valves<sup>1</sup>, and the limited durability of the bioprosthetic valves<sup>2</sup>. Tissue engineered heart valves (TEHV) have emerged as a promising solution for heart valve replacement<sup>3</sup>.

The aim of this work was to develop and characterise a decellularised mitral valve scaffold suitable for mitral valve replacement.

### EXPERIMENTAL METHODS

Whole mitral valves (MVs) from 6 month old German Landrace pigs were harvested under sterile conditions. The valves were disinfected, placed in hypotonic buffer and treated with 0.5% Triton X-100 for 24h and 0.5% SDS for a further 24h. The valves were washed extensively and finally sterilised with 0.1% peracetic acid. Radial sections comprising annulus, leaflet, chordae tendinae, and papillary muscle were analysed histologically by H&E, DAPI, Elastica van Gieson and Masson's trichrome. The presence of the  $\alpha$ -gal epitope was assessed by immunohistochemistry. Tissue sections were visualized using standard bright-field microscopy and fluorescence microscopy (Nikon Eclipse TE300).

The biocompatibility of the decellularised valves was assessed using contact and extract cytotoxicity assays to examine any potential cytotoxic effects of the decellularisation method.

### RESULTS AND DISCUSSION

H&E and DAPI staining revealed that the decellularised MV components, including the leaflets, papillary muscles, chordate and annulus were free of cells and cell nuclei. The treatment resulted in a decrease of the  $\alpha$ -gal epitope (Fig. 1A, B), whereas it preserved the histoarchitectural integrity of the MV tissue (Fig.2A-D).

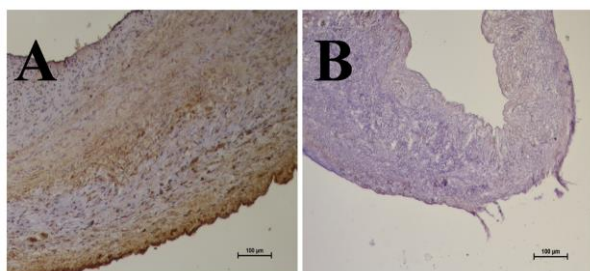


Figure 1: Alpha-gal staining of native (A) and decellularised (B) leaflet.

Moreover, the produced scaffold was not cytotoxic, as indicated by the contact and extract cytotoxicity assessment.

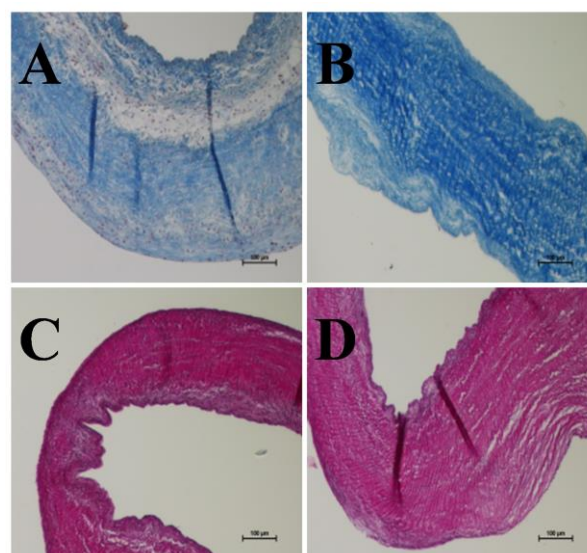


Figure 2: Masson's trichrome and van Gieson staining of native (A,C) and decellularised leaflet (B,D).

### CONCLUSION

A protocol that effectively removed cells, whilst grossly maintaining the MV histoarchitecture and was developed. The problem with the presence of  $\alpha$ -gal could be potentially overcome by the use of whole MVs from either  $\alpha$ -gal-knockout or human donors. The decellularised whole MV scaffolds did not show any cytotoxic effects on the cell viability of L929 murine fibroblasts.

Future work will focus on the optimisation of the decellularisation protocol in terms of the  $\alpha$ -gal removal, as well as on further assessing the decellularised scaffolds in terms of DNA removal and biomechanical and hydrodynamic assessment.

### REFERENCES

- 1.Crapo PM. *et al.*, Biomaterials 2011;32(12):3233–43
- 2.Gilbert TW. *et al.*, Biomaterials 2006;27(19):3675–83
- 3.Vorotnikova E. *et al.*, Matrix Biol 2010;29(8):690–700

### ACKNOWLEDGMENTS

This research was funded by the People Programme (Marie Curie Actions) of the European Union's Seventh Framework Programme FP7/2007-2013/ under REA grant agreement n° 317512.

R. De Santis<sup>1</sup>, A. Ronca<sup>1</sup>, S. Ronca<sup>2</sup>, G. Forte<sup>2</sup>, U. D'Amora<sup>1</sup>, A. Gloria<sup>1</sup>, T. Russo<sup>1</sup>, L. Ambrosio<sup>1,3</sup>

<sup>1</sup> Institute of Polymers, Composites and Biomaterials - National Research Council of Italy, Mostra d'Oltremare, V.le J.F. Kennedy 54 - Pad.20, 80125 Naples, Italy.

<sup>2</sup>Department of Materials, Holywell Park Loughborough University, Leicestershire, UK, LE11 3TU

<sup>3</sup> Department of Chemical Science and Materials Technology – National Research Council of Italy, P.le Aldo Moro, 7 - 00185 Rome, Italy  
[rosantis@unina.it](mailto:rosantis@unina.it)

## INTRODUCTION

Rapid Prototyping technologies are increasingly demonstrating the great potential for fabricating biocompatible 3D structures with precise control of the micro- and macro-scale characteristics<sup>1,2</sup>. Despite it being the first commercialized RP technology, the use of Stereolithography (SL) in Tissue Engineering has not been significantly explored, probably due to the lack of commercially available implantable or biocompatible materials<sup>3</sup>. An ideal scaffold design should be able to provide the necessary properties to satisfy simultaneously the biological and mechanical requirements for optimal bone tissue regeneration<sup>4</sup>. Stereolithography is able to reproduce with high resolution 3D complex structures that can simultaneously control the external shape anatomically matching the bone defect and creating a well-defined internal structure to enhance an optimum vascularization and then bone reconstruction. In this work, a novel divinyl-fumarate-Polycaprolactone (VPCLF) has been synthesized using Sn-free catalyst in order to realize refined 3D scaffolds for bone tissue regeneration.

## EXPERIMENTAL METHODS

In this work, a Sn-free catalyst has been used for the ROP of  $\epsilon$ -Caprolactone (CL) with a high monomers conversion at room temperature, with hydroxyethyl vinyl ether (HEVE) as both initiator and photo-curable functional group. Following the synthesis of the vinyl-terminated PCL (VPLC), its reaction with fumaryl chloride (FuCl) results in chains containing photocrosslinkable vinyl units at both ends and in the middle of the chain in order to obtain a divinyl-fumarate-PCL (VPCLF). Networks were formed from VPCLF-F by UV irradiation (365 nm) using Lucirin TPO as a biocompatible initiator, Orasol Orange G as dye and N-Vinyl-2-pyrrolidone (NVP) as reactive solvent (Figure 1).

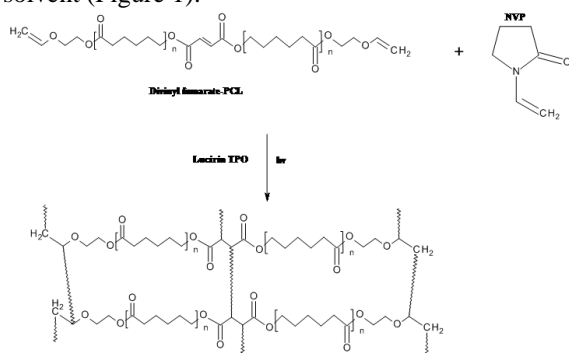


Figure 1: proposed structures of photo-crosslinked VPCL-F/NVP using Lucirin TPO as photoinitiator.

## RESULTS AND DISCUSSION

The resulting polymer was characterized by its specific molecular weights, functional end groups and transition temperatures, using several techniques including Rheometry, Nuclear Magnetic Resonance (NMR), Fourier Transformed Infrared Spectroscopy (FTIR), Differential Scanning PhotoCalorimetry (DPC) and Differential Scanning Calorimetry (DSC). Photo crosslinked disk-shaped specimens (diameter 6 mm) of VPCLF/NVP were seeded with human mesenchymal stem cells (hMSCs) to assess biocompatibility. Mathematically defined porous structures with Gyroid architecture were prepared using the VPCLF/NVP resin. SEM images show structures with an open pore and fully interconnected architecture, allowing cell seeding and proliferation (Figure 2).

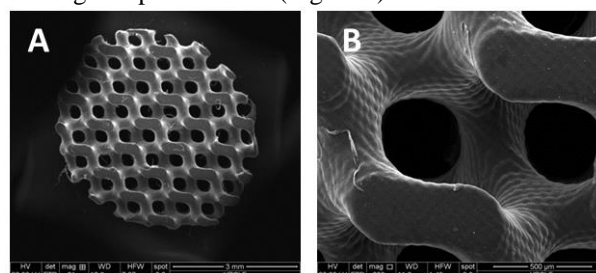


Figure 2: SEM images of Gyroid structure at different magnifications (scale bars represent respectively (A) 3 mm and (B) 500  $\mu$ m)

## CONCLUSION

The major objective of this study was to create biocompatible PCL scaffolds with a controlled internal structure for bone tissue engineering. Results proved that it is possible to obtain mathematically refined scaffolds with a homogeneous micro architecture by stereolithography technique using VPCLF/NVP photocurable resin.

## REFERENCES

1. Kim K. et al, *Tissue Engineering: part B*, 2010, 16(5): 523-539.
2. Gloria A. et al, *Journal of Applied Biomaterials and Biomechanics*, 2009, 7(3): 141-152.
3. Ronca A. et al, *Acta Biomaterialia*, 2013, 9(4):5989-96.
4. Hollister S. J. *Nat Mater*, 2005, 4, 518-524.

## ACKNOWLEDGMENTS

The authors would like to thank MAGISTER project (NMP3-LA-2008-214685), and FIRB MERIT project (GAE: P0000570) for providing financial support.

## Scaffolds for the Bone Tissue Engineering Combining Micro and Nano Fibres

Jakub Erben<sup>1</sup>, Kateřina Pilařová<sup>1</sup>, Filip Sanetrník, Jiří Chvojka<sup>1,2</sup>, Jana Horáková<sup>1</sup>, Lenka Blažková<sup>1</sup>, Eva Košťáková<sup>1</sup>, Jiří Havlíček<sup>1</sup>, Petr Mikeš<sup>1</sup>, David Lukáš<sup>1</sup>, Věra Jenčová<sup>1</sup>, Martin Pelc<sup>1</sup>

<sup>1</sup>Department of Nonwovens and Nanofibrous Materials, Technical University of Liberec, Technical University of Liberec, <sup>2</sup>Center for Nanomaterials, Advanced Technologies and Innovation, Technical University of Liberec  
[pelc.martin@gmail.com](mailto:pelc.martin@gmail.com)

### INTRODUCTION

Bone TE scaffolds have to fulfill some basic requirements. They are typically made of porous biodegradable materials which structure has to allow osteoprogenitor cells migrate into inner structure of scaffold followed by their proliferation and matrix formation. Incorporation of biologically active molecules can facilitate regeneration process and is also of special interest in bone TE.

The meltblown is a nonwoven technology, which produce fine fibers (1-5µm). Structurally the meltblown materials are destined to be the bone or knee cartilage scaffold for their diameter of fibers, random orientation of fibers, three-dimensional structure, high porosity, optimal pore size etc. Electrospinning is generally well known technology for polymer nanofibrous materials production with respect to application in medicine and tissue engineering.

### EXPERIMENTAL METHODS

**Scaffold fabrication:** Solution of PCL in chloroform/ethanol was prepared for electrospinning. The production equipment set-up consisting of meltblow and needle-less electrospinning ("all in one"). The study compare materials: i) meltblown material (M) and ii) meltblown material combining with electrospun fibers (ME). Dry scaffolds were characterized in term of morphology by a scanning electron microscopy. The biocompatibility of the material, cell proliferation and migration was tested *in vitro*.

**In-vitro culture of MG-63 osteoblasts:** human osteoblasts (MG63) were maintained in EMEM with 10% FBS and 1% ATB. Cells were maintained in a incubator (37 °C/5% CO<sub>2</sub>).

**Sample preparation, cell seeding:** from prepared layers were cutted discs (diameter 15mm, thickness 5mm) which were sterilized (70% Et-OH, 30min) and washed in PBS (pH7.4) prior the cell seeding. MG63 cells were seeded 1\*10<sup>5</sup> cells per sample.

**MTT assay for the cell proliferation:** Cell proliferation was monitored after 1, 3, 7, 14 and 21 days by MTT assay. Samples were incubated in solution of MTT in sample medium (EMEM) for 3 hours at 37 °C/5% CO<sub>2</sub>. Absorbance of the formazane solution was measured at 570 nm (reference at 650nm).

**Microscopy analysis (SEM and fluorescence):** After 1, 3, 7 and 14 days of cell seeding, the cell-cultured scaffolds were processed for microscopy analysis. **SEM:** the scaffolds were fixed by 2.5% glutaraldehyde and dehydrated with upgrading concentrations of Et-OH. Samples were analysed by scanning electron microscope (Tescan, VEGA3 SB easy probe).

**Fluorescence microscopy:** The cells were fixed in frozen methanol and stained with propidium iodide. The layers were analyzed using fluorescence microscope (NICON Eclipse Ti-E)

### RESULTS AND DISCUSSION

Morphology characteristics were studied by SEM visualization of the produced fibrous structures (Fig. 1.).

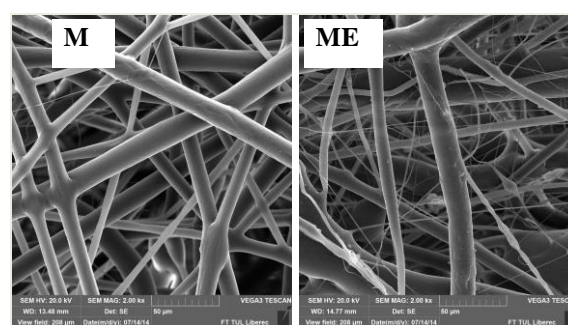


Fig 1: scaffold morphology observed by SEM for four tested materials – meltblown material (M); meltblown material combining with electrospun fibers (ME), scale bar is 50µm.

*In vitro* tests reveal similar rates of adhered MG-63 osteoblasts in all kinds of tested materials. However from the 7<sup>th</sup> day after cell seeding the significant differences in the cell proliferation rates had been observed. Osteoblasts on samples containing electrospun fibers (ME) showed significant increase in proliferation. Microscopy also confirms osteoblasts proliferation into the inner structure of the materials with the significantly higher rate in materials containing nanofibers (ME).

### CONCLUSION

Good porosity of tested materials allows osteoblasts to proliferate into the sample inner structure with the significant contribution of nanofibers content to the cell proliferation rate.

### REFERENCES

Erben, J. at all.: "The combination of meltblown and electrospinning for bone tissue engineering", *Materials Letters*, 143(2015)172-176.

### ACKNOWLEDGMENTS

This research was supported by the project "Nanofiber materials for tissue engeneering" reg. No. CZ.1.05/3.1.00/14.0308, which is co-financed by the European Social Fund and the state budget of the Czech Republic.



## Biophysical, Biochemical and Biological Properties of Nano-textured Collagen Fibres

Anna Sorushanova<sup>1</sup>, Anne Maria Mullen<sup>2</sup>, Abhay Pandit<sup>1</sup>, Dimitrios Zeugolis<sup>1</sup>

<sup>1</sup> Network of Excellence for Functional Biomaterials, National University of Ireland, Galway,

<sup>2</sup> Teagasc, Food Research Centre, Ireland

[abhay.pandit@nuigalway.ie](mailto:abhay.pandit@nuigalway.ie)

### INTRODUCTION

Through self-assembly, macromolecules with chemical complementarity form supramolecular structures, which are held together by weak bonds. Thus, exogenous cross-links are required to produce stable constructs. Specifically in collagen-based scaffolds, chemical, physical and biological cross-linking methods are under investigation to control the biophysical, biochemical and biological properties of the produced devices (1-3). However, biological and physical methods are not suitable for load-bearing tissues, due to the weak-induced stability. Chemical stabilisation methodologies are associated with foreign body response. Although the potential of multi-functional poly(ethylene glycol) systems as stabilisation and functionalisation agents for collagen hydrogels / sponges has been shown (4, 5), it is still unclear whether such agents can induce proportional stability to traditional cross-linking methods, without associated cytotoxicity. Herein, we hypothesise that 4-star poly(ethylene glycol) ether tetrasuccinimidyl glutarate (PEG) can produce cytocompatible collagen fibres with biophysical, biochemical and biological properties, superior to customarily used chemical approaches.

### EXPERIMENTAL METHODS

Collagen fibres were fabricated and cross-linked with PEG, carbodiimide (EDC/NHS) and glutaraldehyde (GTA) based on established protocols (1-3). Non-cross-linked fibres (NXL) acted as control. Structural characteristics were assessed with Scanning Electron Microscopy (SEM). Thermal stability was assessed with Differential Scanning Calorimetry (DSC). The extent of cross-linking was assessed with ninhydrin / collagenase assays. Mechanical properties were assessed with tensile testing. *In vitro* cytocompatibility was assessed with human skin fibroblasts.

### RESULTS AND DISCUSSION

**Fig. 1:** SEM analysis revealed that only PEG stabilised fibres maintained the anisotropic nano-texture surface topography, induced by the fibrillar substructure.

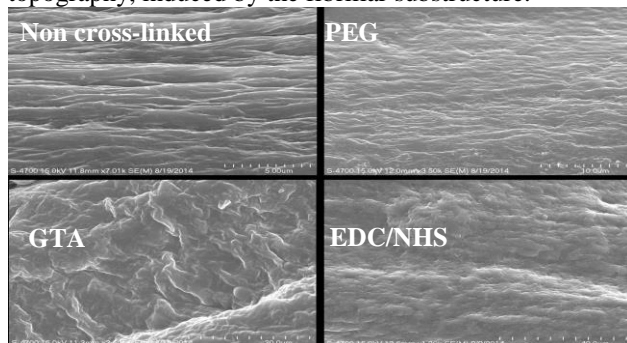


**Fig. 2:** Ninhydrin assay revealed that GTA had the lowest amount of free amines, followed by PEG and EDC/NHS.

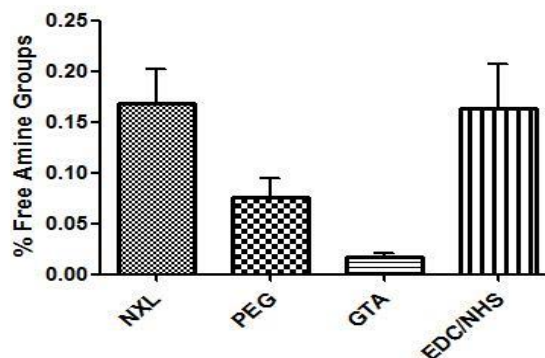


**Table 1:** DSC analysis indicated that PEG induced similar thermal stability to GTA fixation and higher than EDC/NHS stabilised fibres (n=5).

Sample	Peak (C)	Onset (C)	Heat J/g
NXL	43.91 ±1.04	40.67 ±1.25	-4.16 ±6.1
PEG	77.78 ±8.25	75.78 ±9.13	-16.19 ±21.88
GTA	74.52 ±0.76	71.64 ±1.24	-4.53 ±2.04
EDC/NHS	60.68 ±4.41	55.59 ±3.27	-6.22 ±10.3

### CONCLUSION

Stabilisation of collagen fibres with PEG maintained the surface anisotropic nano-texture appearance, responsible for cell attachment and growth. Further, PEG induced stabilisation efficiency, as judged by ninhydrin and DSA analysis, similar to traditional chemical (GTA and EDC / NHS) approaches. Mechanical and biological analyses are under way.

### REFERENCES

- Zeugolis, D. I., et al. J Biomed Mater Res A, 89: 895-908, 2009
- Zeugolis, D.I., et al. J Biomed Mater Res A, 92: 1310-1320, 2010
- Zeugolis, D.I., et al. Mater Sc Eng C, 30: 190-195, 2010
- Collin, E., et al., Biomaterials, 32: 2862-2870, 2011
- Ward, J., et al., Biomacromolecules, 11: 3093-3101, 2010

### ACKNOWLEDGMENTS

ReValueProtein Research Project (Exploration of Irish meat processing streams for Recovery of high Value Protein based ingredients for food and non-food uses, Grant Award No. 11/F/043) is supported by the Department of Agriculture, Food and the Marine (DAFM) under the National Development Plan 2007–2013 funded by the Irish Government.





## Multifactorial Approaches on Cell Phenotype Maintenance and Function

Christina N M Ryan<sup>1</sup>, Manus J Biggs<sup>1</sup>, Abhay Pandit<sup>1</sup>, Dimitrios I Zeugolis<sup>1</sup>

<sup>1</sup>Network of Excellence for Functional Biomaterials, National University of Ireland Galway, Ireland

Corresponding Author: [dimitrios.zeugolis@nuigalway.ie](mailto:dimitrios.zeugolis@nuigalway.ie)

### INTRODUCTION

Cell-based therapies require removal of cells from their optimal *in vivo* tissue context and propagation *in vitro* to attain suitable number. However, bereft of their optimal tissue niche, cells lose their phenotype and function. To this end, biophysical, biochemical and biological strategies are at the forefront of scientific and technological research and innovation (1, 2). Biophysical properties, such as surface topography and substrate stiffness, have been shown to maintain permanently differentiated cell phenotype and to direct stem cells towards specific lineage (3, 4). Herein, we assess simultaneously the influence of topographical features and substrate rigidity on permanently differentiated cell phenotype and on stem cell lineage commitment.

### EXPERIMENTAL METHODS

PDMS substrates with varying ratios of monomer to curing agent (1:1, 5:1, 10:1, and 20:1) were fabricated based on established protocols. Grooved substrates were created using a silanated wafer with groove dimensions of  $2\mu\text{m} \times 2\mu\text{m} \times 2\mu\text{m}$ ; planar control groups were created using flat glass. The aforementioned PDMS solutions were poured onto the wafer/glass and cured at  $200^\circ\text{C}$ . X-ray Photoelectron Spectroscopy (XPS) was used to determine the elemental composition of the substrates. Atomic Force Microscopy (AFM) and Scanning Electron Microscopy were used to assess the topographical features of the substrates. Dynamic Mechanical Analysis (DMA) was used to determine the mechanical properties of the substrates. The simultaneous effect of surface topography / substrate rigidity on cell phenotype and function was assessed using human permanently differentiated cells and various morphometric and gene / protein assays.

### RESULTS AND DISCUSSION

**Figure 1:** XPS analysis showed that surface composition did not change as a function of monomer to curing agent ratio.

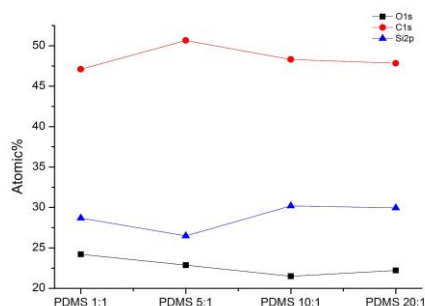


**Figure 2:** AFM analysis revealed that topographical features were not maintained at soft PDMS substrates.

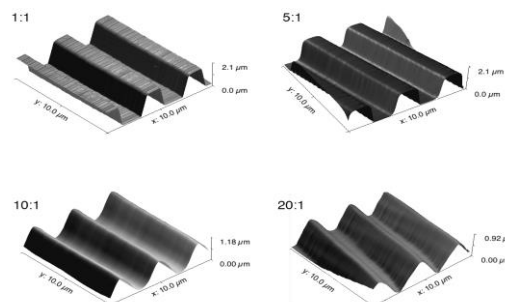
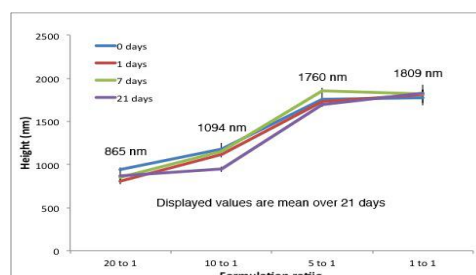


**Figure 3:** The more rigid PDMS substrates retained their topographical features for up to 21 days.



### CONCLUSION

The softer substrates did not retain their topographical features. Preliminary *in vitro* data indicate that surface topography and substrate stiffness play crucial role in determining cell fate, with substrate stiffness overwhelming surface topography.

### REFERENCES

- Spanoudes K, Gaspar D, Pandit A, Zeugolis DI. Trends Biotechnol. 2014; 32 (9): 474-482.
- Cigognini D, Lomas A, Kumar P, Satyam A, English A, Azeem A, Pandit A, Zeugolis D. Drug Discov Today. 2013; 18 (21-22): 1099-1108.
- Murphy WL, McDevitt TC, Engler AJ. Nat Mater. 2014;13 (6): 547-557.
- Azeem A, English A, Kumar A, Satyam A, Biggs M, Jones E, Tripathi B, Basu N, Henkel J, Vaquette C, Rooney N, Riley G, O'Riordan A, Cross G, Ivanovski S, Hutmacher D, Pandit A, Zeugolis D. Nanomedicine (Future in Medicine), In Press

### ACKNOWLEDGMENTS

The research has received funding from the European Union Seventh Framework Programme (FP7/2007-2013) under grant agreement n° 263289 (Green Nano Mesh).

## Stimulating Cellular Response via Cross-linking in Tissue Engineering Scaffolds

Kendell M. Pawelec<sup>1</sup>, Gloria Ramírez-Rodríguez<sup>2</sup>, Monica Sandri<sup>2</sup>, Simone Sprio<sup>2</sup>, Suzan van Dongen<sup>1</sup>, Bas Kluijtmans<sup>1</sup>

<sup>1</sup>FUJIFILM Europe B.V., Tilburg, Netherlands

<sup>2</sup>Institute of Science and Technology for Ceramics, Faenza, Italy

[kendell\\_pawelec@fujifilm.eu](mailto:kendell_pawelec@fujifilm.eu)

### INTRODUCTION

The mechanical properties of tissue engineering scaffolds are known to be an import signal for cell differentiation and metabolism<sup>1-2</sup>. As the most widespread method of stabilizing the mechanical properties of tissue engineering scaffolds, cross-linking has a profound effect on mechanical properties and swelling. Many cross-linking methods have been reported in the literature to stabilize biological polymers<sup>3</sup>. However, while the cytotoxic effects of cross-linking agents have been discussed, as well as their influence on scaffold mechanics, potential changes in cell behaviour with cross-linking have rarely been investigated<sup>4</sup>. It has already been shown that mesenchymal stem cells preferentially differentiate into bone like lineages as the stiffness of their substrate increases<sup>2</sup>. Therefore, it was hypothesized that through careful consideration of cross-linker, stem cell differentiation and mineralization could be induced for bone tissue engineering.

### EXPERIMENTAL METHODS

Linear scaffolds were created from synthetic collagen-like peptide (SCP), Figure 1. According to van Bortel et al<sup>5</sup>, to create linear structures ice was nucleated at the base of a cylindrical mold and allowed to grow upwards, resulting in linear channels of between 350–400 µm in diameter. Scaffolds were cross-linked by various cross-linking methods. Murine mesenchymal stem cells (mMSCs) were seeded onto the scaffolds and the mineralization was evaluated after two weeks *in vitro*.

### RESULTS AND DISCUSSION

No changes in the structure of the scaffolds were observed using the different cross-linking methods. In contrast, large differences in the mechanical properties were noted. Scaffold elasticity strongly depended on the cross-linking method.

The linear SCP scaffolds were able to support cell growth and infiltration throughout the entire pore volume, regardless of cross-linker, Figure 1. The cell response was sensitive to the cross-linking. While little attention is generally given to the cross-linker once cytocompatibility is demonstrated, these results show that it is an important factor in the final outcome of tissue engineering scaffolds.

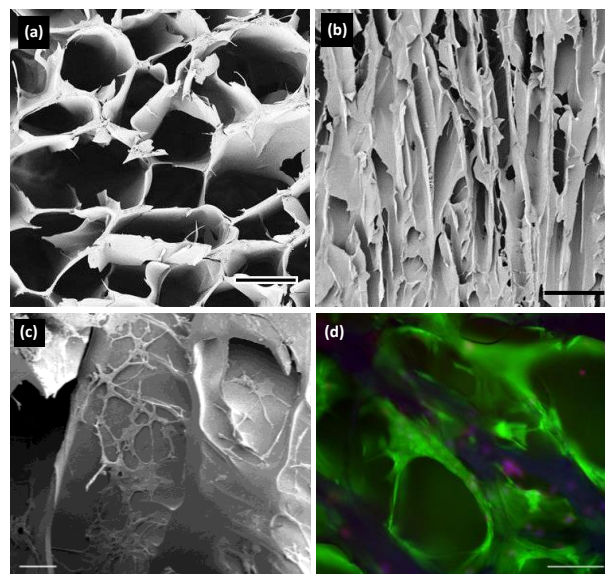


Figure 1. Scaffolds were anisotropic, as seen via scanning electron microscopy (SEM) in the (a) transverse (b) longitudinal direction. Cells could attach and proliferate, (a) SEM in the longitudinal direction and (b) live/dead fluorescent staining (green: live, red: dead, blue: nucleus). Scale bars: (a) 300 µm (b) 1 mm, (c-d) 100 µm.

### CONCLUSION

Cross-linking has a significant effect on the mechanical properties of tissue engineering scaffolds. Cell response is sensitive to these changes, as demonstrated in this study, using mMSCs. Cross-linking does more than just stabilize tissue engineering scaffolds, but can affect the functional outcome of the repair by altering mechanical properties and cellular response.

### REFERENCES

1. Wu S. *et al.*, Mater. Sci.Eng. R. 80:1-36, 2014.
2. Engler A.J. *et al.*, Cell 126:677–689, 2006.
3. Rault I. *et al.*, J Mater Sci: Mater Med.7:215-21, 1996.
4. Koegh *et al.*, Bone 44:S253–S338, 2009.
5. van Bortel, H.*et al.*, WO2013/068722

### ACKNOWLEDGMENTS

The research leading to these results has received funding from the European Union Seventh Framework Programme FP7/2007-2013 under grant agreement n° 607051.

## Control over Anisotropic Permeability in Aligned Tissue Engineering Scaffolds

Kendell M. Pawelec<sup>1</sup>, Huib van Boxtel<sup>1</sup>, Bas Kluijtmans<sup>1</sup>

<sup>1</sup>FUJIFILM Europe B.V., Tilburg, Netherlands  
[kendell\\_pawelec@fujifilm.eu](mailto:kendell_pawelec@fujifilm.eu)

### INTRODUCTION

For bone tissue engineering, the optimization of scaffold structure has a large impact on the final outcome of tissue regeneration. Scaffolds must encourage cell and nutrient diffusion while maintaining adequate mechanical properties<sup>1</sup>. For bone tissue engineering, a pore size of 200-400  $\mu\text{m}$  and interconnections above 100  $\mu\text{m}$  have been shown to aid bone formation and capillary innervation<sup>1-4</sup>. Anisotropic pore architectures can also impact tissue regeneration, and aligned scaffolds appear to encourage the growth of an organized lamellar bone rather than the woven bone, which is formed in equiaxed structures<sup>3</sup>. Unlike the traditional measures of scaffold structure, permeability is sensitive to all scaffold features and additionally, has a direct link to the diffusion of nutrients<sup>5</sup>. However, there is little information on how permeability relates to traditional measures of scaffold architecture or how this metric can be tailored. It was hypothesized that permeability could be controlled in anisotropic scaffolds, offering researchers a better functional measure of scaffold architecture.

### EXPERIMENTAL METHODS

Aligned scaffolds were created from synthetic collagen-like peptide (SCP) as described by van Boxtel<sup>6</sup>. To create linear structures, ice was nucleated at the base of a cylindrical mold and the temperature was raised to allow ice to grow upwards at a set freezing temperature and freezing slope. Pore size was measured via SEM micrographs at the base and top of the scaffolds and permeability was tested in the longitudinal and transverse direction using a falling head method<sup>5</sup>.

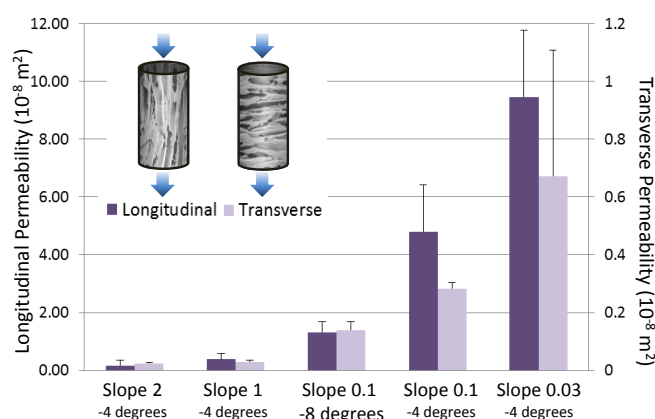


Figure 1. Scaffold permeability was anisotropic. In both the longitudinal and transverse direction, shown schematically in the inset, the permeability was affected by the freezing protocol. (average  $\pm$  standard deviation)

### RESULTS AND DISCUSSION

By varying the set freezing temperature and the freezing slope, the pore size of the linear scaffolds was controlled. With decreasing set freezing temperature and increasing freezing slope, the pore size decreased significantly. The pore size ranged from 85  $\mu\text{m}$  to 650  $\mu\text{m}$ . Decreasing the set freezing temperature from led to a decrease in pore size of around 200  $\mu\text{m}$ .

It was found that the permeability of linear scaffolds was proportional to the scaffold pore size, both in the transverse and longitudinal direction. As the pore size was affected by the way in which ice grew in the aqueous solution, the permeability was also dependent on the freezing protocol, Figure 1. However, in the transverse direction, the permeability was an order of magnitude lower than in the longitudinal direction.

The scaffold structure formed during ice-templating techniques is dependent on ice growth within an aqueous slurry. With decreases in the freezing slope, the ice had a longer time to grow and anneal, resulting in larger pores. As the size of the pores increased, the ease of fluid movement through the scaffold also increased, which would have a significant effect on the diffusion of nutrients and growth factors *in vivo*. This study demonstrates that the parameters used to form scaffold structure can also be used to tailor scaffold permeability.

### CONCLUSION

It has been demonstrated that scaffold permeability has a direct relationship to the pore size of the scaffold. By controlling the freezing protocol, the permeability can be tailored for optimal performance in tissue engineering and regenerative medicine applications.

### REFERENCES

1. Tsuruga E *et al.*, J. Biochem. 121:317-324, 1997.
2. Murphy C *et al.*, Biomaterials 31:461-466, 2010.
3. Correia C *et al.*, Acta Biomater. 8:2483-92, 2012.
4. Jones AC *et al.*, Biomaterials 30:1440-51, 2009.
5. Pennella F *et al.*, Ann Biomed Eng. 41:2027-41, 2013.
6. van Boxtel, H. *et al.*, WO2013/068722

### ACKNOWLEDGMENTS

The research leading to these results has received funding from the European Union Seventh Framework Programme FP7/2007-2013 under grant agreement n° 607051.

# Biocompatibility of Dental Pulp Stem Cells onto PLA Scaffolds Synthesized by Air Jet Spinning Technique

José Luis Suárez-Franco<sup>1</sup>, N Vargas-Becerril<sup>1</sup>, L Téllez-Jurado<sup>2</sup>, O Alvarez-Fregoso<sup>3</sup>, M Hipólito-García<sup>3</sup>, JA Fernández-Pedrero<sup>1</sup>, MA Álvarez-Pérez<sup>1</sup>

<sup>1</sup>Laboratorio de Bioingeniería de Tejidos; DEPeI, Facultad de Odontología, UNAM, 04510, México DF, México.

<sup>2</sup>Departamento de Ingeniería Metalúrgica y de Materiales E.S.I.Q.I.E-I.P.N, 07738, México DF, México.

<sup>3</sup>Instituto de Investigaciones en Materiales, UNAM, 04510, México DF, México.

## INTRODUCTION

Tissue engineering is a novel approach and it is major goal is to regenerate tissue lost by trauma and disease and this regeneration strategy is supported by three factors: cells, molecular signalling and scaffolds<sup>1</sup>. Periodontitis is an infection caused by accumulation of dental plaque onto the tooth surface and leading to the tooth lost through destruction of the attachment apparatus and tooth-supporting structures affecting the quality of life of the patients<sup>2</sup>. Periodontal regeneration therapy is based on arrest periodontal disease progression and trying to recovering the tissue structures destroyed during the periodontal phases. Osseous grafting and guided tissue regeneration are the two techniques goals used for periodontal regeneration. Recently the synthesis of fibres scaffold open a new strategy for understanding the applications on the periodontal regeneration because the scaffold could be similar to the extracellular fibrous matrix of the tissue. The aim of the study is to evaluated the poly-lactic acid fibre scaffold synthesized by air jet spinning and evaluated the biological response of dental pulp stem cells, in order to intent to replace tissue lost by periodontitis disease<sup>3</sup>.

## EXPERIMENTAL METHODS

A commercially available airbrushed was used to fabricate nanofiber scaffolds. Nanofiber scaffolds were airbrushed from a solution containing 10 % of poly lactic acid (W/V) dissolved in a 90% chloroform, 10% ethanol (V/V) solution. Scaffold porosity, fibre diameter and interaction cell-scaffold were evaluate by SEM. Chemical stability of PLA scaffold was evaluated by FTIR and RAMAN. In order to determinate if the nanofiber airbrushed scaffold shows better biological properties in comparison with PLA film, adhesion, proliferation and mineralization assays were performed cultured dental pulp stem cells.

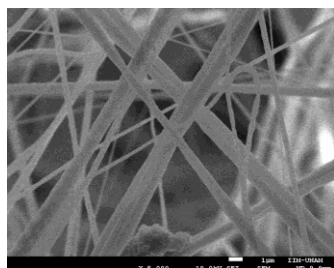


Figure 1. SEM image of PLA nanofiber scaffold.

## RESULTS AND DISCUSSION

SEM images show random nanofiber architecture of the scaffold with an average of 250 and 500 nm diameter of the fibre. Dental pulp stem cells show a better attachment when places onto the scaffold in comparison with film scaffold.

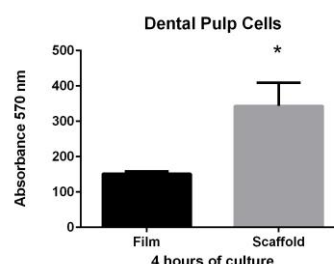


Figure 2. Dental pulp cells show significant differences in cell attachment.

## CONCLUSION

Air jet spinning is a novel technique that allows to fabricate nanofiber scaffolds faster, easier and saver way. Moreover dental pulp stem cells showed better biological response like attached and proliferation when comparing with thin film scaffold. This nanofiber scaffold open the possibility to use as biomaterial for periodontal tissue regeneration therapy.

## REFERENCES

1. Alberto Di Martino, Liliana Liverani, Alberto Rainer, Giuseppe Salvatore, Marcella Trombett, Vincenzo Denaro. Electrospun scaffolds for bone tissue engineering. *Musculoskelet Sur* (2011) 9569-80.
2. M. Cenk Haytac, Onur Ozcelik, Angelo Mariotti. Periodontal disease in men. *Periodontology* 2000, Vol. 61 2013, 252-265.
3. P. Mark Bartol, Yin Xiao, S. Petter Lyngstaadas, Michael L. Paine, Malcom L. Snead. Principles and Applications of Cell Delivery Systems For Periodontal Regeneration. *Periodontology* 2000, Vol. 41, 2006, 123135

## ACKNOWLEDGMENTS

The authors want to thanks to PROMEP programme for PhD scholarship PROMEP/103.5/10/5701 (UV-555) to JLSF and UNAM-DGAPA for postdoctoral scholarship supporting to NVB. This research were financially supported by funds from the UNAM-DGAPA: PAPIIT project IN213912 and PAPIIT project IN210815.



## Characterization of Cellulose/Hydroxyapatite Scaffolds for Bone Tissue Engineering

Jolanta Liesiene<sup>1</sup>, Odeta Baniukaitiene<sup>1</sup>, Povilas Daugela<sup>2</sup>, Arturas Stumbras<sup>2</sup>,  
Mindaugas Pranskunas<sup>2</sup>, Gintaras Juodzbaly<sup>2</sup>

<sup>1</sup>Department of Polymer Chemistry and Technology, Kaunas University of Technology, Lithuania

<sup>2</sup>Department of Oral and Maxillofacial Surgery, Lithuanian University of Health Sciences, Lithuania  
[jolanta.liesiene@ktu.lt](mailto:jolanta.liesiene@ktu.lt)

### INTRODUCTION

The development of polymer based three-dimensional scaffolds is one of the current challenges in bone tissue engineering. The porous structure of such scaffolds should be precisely designed as it is related with cell adhesion, proliferation, differentiation and vascularization. The permeable pore network with micro and macro pores is also required for nutrient delivery to bone cells and waste exchange [1].

In this work the morphology as well as sorption properties of the cellulose/hydroxyapatite scaffolds were evaluated.

### EXPERIMENTAL METHODS

For the morphological characterisation of the obtained scaffolds scanning electron microscopy (Quanta 200 FEG, FEI Company, Netherlands) and micro-computed tomography  $\mu$ CT40 (Scanco Medical AG, Switzerland) were used.

Water retention of the scaffolds was determined gravimetrically using the phosphate buffer solution, pH 7.4. Glucose diffusion within the scaffolds was evaluated using a „side-by-side” cell. The amount of diffused glucose was determined by means of the phenol-sulfuric acid method.

### RESULTS AND DISCUSSION

There are many studies reporting variety of techniques for the fabrication of a desired structure, including freeze-drying (lyophilization), electrospinning, solvent casting/particulate leaching, gas foaming, phase separation, rapid prototyping (stereolithography, selective laser sintering, fused deposition modelling, three-dimensional printing) or even combinations of them [2]. In this work lyophilization was chosen to create highly porous cellulose/hydroxyapatite scaffolds with an optimal pore size required for successful bone regeneration. It was found that a porous structure of the scaffold depended on the solvent in its discontinuous phase prior the drying process. Changing the solvent in the discontinuous phase the morphology of the lyophilized matrix varied from macroporous to dense. The matrix of the desired morphology with micro and macro pores was obtained by lyophilization of the composite which was filled with the ethanol solution in water. The porosity of the scaffolds varied from 65 to 72%, when microhydroxyapatite ( $\mu$ HA) and nanohydroxyapatite (nHA) were used, respectively.

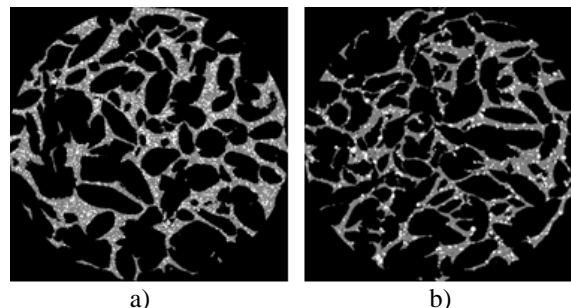


Fig. 1. 2D image of the scaffolds: a) cellulose/ $\mu$ HA and b) cellulose/nHA.

The average size of the pores was 490  $\mu$ m and 540  $\mu$ m of cellulose/nHA and cellulose/ $\mu$ HA, respectively.

The water retention experiment showed that cellulose/nHA and cellulose/ $\mu$ HA composites could absorb large quantities of water (303–405%). This property substantiates high hydrophilicity of the scaffolds, which reveals biocompatibility with biological systems.

It is important to note that both scaffolds were permeable to the glucose solution. After 24 h, the concentration of glucose was approximately equal in both chambers, revealing that the structure of cellulose-based scaffolds was suitable for the transport of nutrients.

### CONCLUSION

The morphology of the prepared scaffolds for bone tissue engineering meets the requirements of materials which are implanted in the bone defect. The porosity of the scaffolds varied from 65 to 72% when microhydroxyapatite and nanohydroxyapatite were used, respectively. The cellulose/hydroxyapatite scaffold showed a permeable pore network for glucose thus revealing its suitability for fast diffusion of nutrients and metabolites.

### REFERENCES

- Porter J.R., Ruckh T.T., Popat K.C. Biotechnol. Progr. 25:1539–1560,2009
- Lu T., Li Y., Chen T. Int. J. Nanomedicine.8:337–350, 2013.

### ACKNOWLEDGMENTS

The authors would like to thank the Research Council of Lithuania (Grant no: MIP-019/2014) for providing financial support to this project.

## Effect of Different Nanoparticles on the Mechanical and Biological Properties of Poly( $\epsilon$ -caprolactone): A Comparative Study

Maria Nearantzi<sup>1</sup>, Iro Koliakou<sup>2</sup>, Dimitrios Bikiaris<sup>1</sup>

<sup>1</sup> Department of Chemistry, Aristotle University of Thessaloniki, Greece

<sup>2</sup> Department of Biology, Aristotle University of Thessaloniki, Greece.

[marinera002@gmail.com](mailto:marinera002@gmail.com)

### INTRODUCTION

PCL is a good bone scaffold material because it can take several years to degrade *in vivo* and is biocompatible, relatively inexpensive, and available in large quantities. However, there are a few problems when considering the practical use of PCL for tissue engineering. PCL lacks bioactivity, so that when used in bone tissue engineering, the new bone tissue cannot bond tightly to the polymer surface. Therefore, it is important to incorporate reinforcing fillers into PCL matrix in order to result in a promising combination of bioactivity, biodegradability, and strength<sup>1</sup>. This comparative study aims to investigate the synergistic effect of different additives on mechanical and biological properties of PCL scaffolds.

### EXPERIMENTAL METHODS

In the present study, PCL biocomposites containing 2.5 wt% of either fumed silica nanoparticles (SiO<sub>2</sub>), multi-walled carbon nanotubes (MWCNTs), montmorillonite (MMT) or modified montmorillonite (MMT15A) were prepared by melt mixing in a Haake-Buchler Reomixer at 110°C at 50 rpm for 10 min. Films of the samples were received using a hydraulic press, at 100°C. Measurements of the tensile mechanical properties of the prepared nanocomposites were performed on an Instron 3344 dynamometer, in accordance with ASTM D63. Enzymatic hydrolysis was studied in aqueous solutions containing 0.025% w/v of *Pseudomonas cepacia* lipase, at 37°C and pH=7.8. Contact angle measurements were carried out by the sessile drop method using a Krüss DSA 100 apparatus. After ultrasonic cleaning in acetone and rinsing with distilled water, all the samples were soaked in a simulated body fluid (SBF) for 14 and 28 days in order to assess their bioactivity. Furthermore cell culture studies were performed using Mesenchymal stem cells derived from Wharton Jelly. DMEM supplemented with 10% FBS and 1% penicillin-streptomycin was used to culture MSC's. Proliferation and morphology of MSC's on the scaffolds was observed using fluorescence microscopy, Scanning and Transmission Electron Microscopy. Cell viability on the scaffolds was measured using MTT (3-(4,5-dimethylthiazol-2-yl)-2,5-diphenyltetrazolium bromide) assay.

### RESULTS AND DISCUSSION

Concerning the mechanical properties, all stress-strain curves exhibited the same pattern, which is similar to the one of neat PCL. Except in the sample containing

MMT15A, due to the plasticizing effect of the montmorillonite's organic modifier<sup>2</sup>, for all the other samples a small increase was observed in the Young's modulus, reaching a maximum improvement of 19% for the sample containing SiO<sub>2</sub> (Table 1). Enzymatic hydrolysis rates of the nanocomposites were significantly different from those of neat polyester. PCL showed the fastest enzymatic degradation among the tested samples, while PCL/nanocomposites showed a slower rate. Additionally, due to the addition of nanoparticles all nanocomposites have higher hydrophilicity than neat PCL and present much lower contact angles. This fact affected on the biocompatibility of the samples as the metabolic activity of the cells differentiated on the tested surfaces.

**Table 1.** Mechanical properties of PCL and its nanocomposites.

Sample	Strength at Yield (MPa)	Strength at break (MPa)	Elongation at break (%)	Young's Modulus (MPa)
PCL-neat	19.5 ± 0.3	22.7 ± 0.8	567 ± 24	282 ± 10
PCL-MMT 15A 2.5% w/w	18.5 ± 1.1	20.6 ± 0.6	479 ± 29	283 ± 16
PCL-MMT 2.5% w/w	18.1 ± 0.7	20.7 ± 0.4	481 ± 6	290 ± 20
PP-SiO <sub>2</sub> 2.5% w/w	20.9 ± 0.7	19.8 ± 1.6	460 ± 21	336 ± 27
PCL-MWCNTs 2.5% w/w	20.4 ± 1.0	19.3 ± 1.9	367 ± 60	317 ± 30

### CONCLUSION

A series of nanocomposites based on the biodegradable PCL matrix were prepared by adding Cloisite®Na+ (pristine MMT), Cloisite®15A (organomodified MMT), fumed silica nanoparticles (SiO<sub>2</sub>), or MWCNTs. The composites were characterized with respect to their biological and mechanical properties. Both biocompatibility and mechanical properties were found to depend on the filler type.

### REFERENCES

References must be numbered. Keep the same style.

1. Armentano I. *et al.*, Polym Degrad Stab 95:2126-2146, 2010
2. Xie W. *et al.*, Polym Eng Sci 43:214-222, 2003



## Rheology of Alginate Gels Containing Modified Alginate: Gels with Tunable Properties

Marianne Ø. Dalheim<sup>1\*</sup>, Line Aa. Omtvedt<sup>1\*</sup>, Finn L. Achmann<sup>1</sup> and Berit L. Strand<sup>1</sup>.

<sup>1</sup>Norwegian Biopolymer Laboratory (NOBIPOL), Department of Biotechnology, Norwegian University of Science and Technology (NTNU), Trondheim, Norway. \* Contributed equally to this work.

[line.a.omtvedt@ntnu.no](mailto:line.a.omtvedt@ntnu.no)

### INTRODUCTION

Alginate is a relevant biopolymer for tissue engineering applications due to its ability to form a gel at close to physiological conditions, and its biological inertness. However, the alginate can be made biologically active through grafting of bioactive molecules<sup>1</sup>. The biopolymer is a linear polysaccharide composed of  $\beta$ -D-mannuronic acid (M) and  $\alpha$ -L-guluronic acid (G), where mainly G-blocks give alginate its ability to form a gel with divalent cations<sup>2</sup>. The mechanical properties of the alginate gel can be designed by enzymatic<sup>3</sup> and chemical<sup>4</sup> modifications of the alginate. In this study, gels of alginate with a high G-content mixed with partially oxidized alginate were made, and mechanical properties were determined.

### EXPERIMENTAL METHODS

Alginate was partially oxidized with metaperiodate according to literature<sup>5</sup> and established protocols in our laboratories. Alginate gels composed of different ratios of high-G alginate ( $F_G = 0.68$ ) and partially oxidized alginate of varying oxidation degrees ( $P_0$ ) were made by internal gelation with  $\text{CaCO}_3$  and GDL as previously described<sup>6</sup>. Reference gels were made with high-G alginate ( $F_G = 0.68$ ). The Young's modulus, force and compression at rupture and syneresis were measured for the gels.

### RESULTS AND DISCUSSION

The Young's modulus measured for the gel cylinders made of both high-G alginate ( $F_G = 0.68$ ) and partially oxidized alginate showed an overall decrease in gel strength with increasing amount of partially oxidized alginate incorporated in the gel. A decrease in gel strength was also observed when increasing the oxidation degree of the modified alginate mixed in the gels. However, the gels largely retained their Young's modulus when 25% of the gelling alginate was substituted with oxidized material. The gels all disrupted at a compression of approximately 60% of the gel height, but the force needed to rupture varied from  $37.2 \pm 2.3$  N for the reference gel to  $2.8 \pm 0.6$  N for a gel of 100% oxidized material with a degree of oxidation of 8%. The results concur with the expectation that partially oxidized alginate would give gels with reduced mechanical properties compared to gels consisting only of high-G alginate<sup>4,7</sup>: The ring opening of oxidized monomers is expected to perturb the gelling sequences of the alginate. This is possibly due to smaller G-block length<sup>7,8</sup>, as the oxidation reaction of alginate favors oxidation of G-units<sup>9</sup>. In addition, the oxidized monomers can give higher flexibility of the alginate chain<sup>10</sup>, which can also influence the gelling properties of the alginate.

The syneresis of the gels containing partially oxidized alginate was slightly reduced compared to the reference gels. The syneresis of alginate gels is shown to depend on the composition of the alginate<sup>11</sup>. Possibly, the difference in syneresis of the gels seen in this experiment can be caused by change of the length of G-blocks or of the MG-blocks. This will result in destabilization of gelling segments<sup>4,7,11</sup>, and thus the alginate gel network. Future studies will focus on measuring the mechanical properties of gels containing both high-G alginate and partially oxidized alginate covalently bound with biomedical relevant ligands.

### CONCLUSION

The mechanical properties of the alginate gels were reduced with the introduction of alginate with varying compositions of partially oxidized alginate, however the Young's modulus was maintained at high values for mixtures of alginate with 25% oxidized material. Hence, the mechanical properties may be tuned with the mixing in of oxidized material, giving the potential to design alginate gels with desired strength and e.g. bioactivity when the oxidized material is further modified with bioactive ligands.

### REFERENCES

1. Rowley J.A. *et al.*, *Biomaterials*, 20(1): p. 45-53, 1999
2. Draget K. I. *et al.*, *Food Polysaccharides and Their Applications*, CRC Press: pp 289-334, 2006
3. Mørch Y. A. *et al.*, *Biomacromolecules*, 9(9):2360-8, 2008
4. Kristiansen K. *et al.*, *Carbohydr. Polym.*, 77(4): 725-735, 2009
5. Smidsrød O. and Painter T., *Carbohydr. Res.*, 26(1): p. 125-132, 1973
6. Draget K. I. *et al.*, *Appl. Microbiol. Biotechnol.*, 31(1): p. 79-83, 1989
7. Gomez C. G. *et al.*, *Carbohydr. Polym.*, 67(3):296-304, 2007
8. Draget K. I. *et al.*, *Hydrobiologia*, **261**: p. 563-569, 1993
9. Painter T. and B. Larsen, *Acta Chem. Scand.*, 24(3): p. 813, 1970
10. Vold I. M. *et al.*, *Biomacromolecules*, 7(7): p.2136-46, 2006
11. Donati I. *et al.*, *Biomacromolecules*, 6(2): 1031-40, 2005

### ACKNOWLEDGMENTS

The authors thank the MARPOL project 221576 and the Norwegian Research Council for financial support.



## Quality and Quantity of Growth Factors Released from Processed Bone Matrix

Katarzyna Włodarczyk<sup>1,2</sup>, Ilona Kalaszczyńska<sup>1,2</sup>, Artur Kamiński<sup>3</sup>, Małgorzata Lewandowska-Szumieł<sup>1,2</sup>

<sup>1</sup> Department of Histology and Embryology, Centre for Biostructure Research, Medical University of Warsaw, Poland

<sup>2</sup> Centre for Preclinical Research and Technology, Poland

<sup>3</sup> Department of Transplantology & Central Tissue Bank, Medical University of Warsaw, Poland

[katarzyna.wlodarczyk@wum.edu.pl](mailto:katarzyna.wlodarczyk@wum.edu.pl)

### INTRODUCTION

Demineralized bone matrix (DBM) is a widely used allogenic graft with osteoconductive and osteoinductive properties that promote bone regeneration. Material is rich in potent proteinaceous components stimulating osteogenesis like growth factors, e.g. bone morphogenetic proteins. Diverse array of DBM-containing composite products<sup>1</sup>, as well as deep-frozen bone grafts<sup>2</sup> for clinical applications, are available from tissue banks and commercial companies. However, differences in DBM preparation and processing methods are reported and can impact properties and clinical performance<sup>1</sup>.

In this study, we investigate the level of pro-osteogenic factors passively released from mineralized and demineralized bone matrix granules and powders – a waste product of bone matrix processing.

### EXPERIMENTAL METHODS

Tested bone materials were provided by the Department of Transplantology & Central Tissue Bank in Warsaw. Initially, all bone samples were defatted, optionally decalcified (demineralized), milled and sterilized. Samples were classified into two categories. Group I included granules, which are ready to use bone grafts derived from donor 1, while group II contained milling waste products - bone powders derived from donor 2. Following samples were subjected to GF quantification:

#### Group I

1. Demineralized bone matrix granules (DBM)
2. Mineralized bone matrix granules (MBM)

#### Group II

1. Demineralized bone powder (DBP)
2. Mineralized bone powder (MBP)

200 milligrams of each material were incubated in 1 ml of Dulbecco's Modified Eagle Medium in 37°C for 24 hours. Samples were centrifuged and supernatants were collected. Using the ELISA method, in all samples following growth factors were quantified: BMP-7, TGF- $\beta$ 1, FGF-2 and VEGF (R&D Systems).

### RESULTS AND DISCUSSION

Our results for group I indicate that decalcification of bone resulted in the release of significant amounts of BMP-7, TGF- $\beta$ 1 and VEGF with undetectable amounts of FGF-2, while mineralized granules released significant amounts of FGF-2 and undetectable level of BMP-7 and TGF- $\beta$ 1. For samples from group II we observed significant release of BMP-7 from demineralized powders and VEGF from mineralized. Our approach of passive extraction and the following measurement of released factors allows to estimate their real availability in the graft site. It differs from methodology based on enzymatic or chemical extraction of proteins trapped in DBM and frequently used by others<sup>3</sup>.

### CONCLUSION

Our results demonstrate that powders – a waste product of bone graft preparation can be an attractive source of growth factors, especially VEGF and BMP-7. Additionally, we are showing, that the process of decalcification completely eliminated FGF-2 from the granules. It demonstrates that methods of DBM processing have significant impact on quality and quantity of released factors.

### REFERENCES

1. Gruskin E. *et al.*, Adv Drug Deliv Rev 64:1063–1077, 2012
2. Kamiński A. *et al.*, Czas. Stomatol. LX 9:601-610, 2007
3. Wildemann B. *et al.*, Cell Tissue Bank 8:107–114, 2007

### ACKNOWLEDGMENTS

This work was supported by National Centre for Research and Development grant NR13-0008-10/2010. The authors have no conflict of interest.





## Modulation of Cell Microenvironments with Oxygen Tension and Macromolecular Crowding: A Multifactorial Approach Towards *In Vitro* Organogenesis

Abhigyan Satyam<sup>1</sup>, Pramod Kumar<sup>1</sup>, Diana Gaspar<sup>1</sup>, Abhay Pandit<sup>1</sup> and Dimitrios Zeugolis<sup>1</sup>

<sup>1</sup>Network of Excellence for Functional Biomaterials (NFB), National University of Ireland, Galway, Ireland

[diana.alves.gaspar@gmail.com](mailto:diana.alves.gaspar@gmail.com)

### INTRODUCTION

Advancements in tissue engineering have enabled the development of scaffold-free substitutes; a technology termed *Tissue Engineering by Self-Assembly*<sup>1</sup>. Despite efficacious *in vitro* and *in vivo* results, very few products have been commercialised, primarily due to prolonged time required to develop an implantable device<sup>2,3</sup>. It has been demonstrated that macromolecular crowding (MMC)<sup>4,5</sup> and low oxygen tension<sup>6,7</sup> enhances deposition of extracellular matrix (ECM). Here, we assessed the potential of combining MMC technology with low oxygen tension.

### EXPERIMENTAL METHODS

Human skin fibroblasts (WS-1) were cultured under various MMC conditions [dextran sulphate (DxS); Ficoll™ (FC) & carrageenan (CR)] in a range of foetal bovine serum (FBS), human serum (HS) concentrations (0.0-10%) and oxygen tension (0.5%, 2%, 20%). ECM deposition was assessed by SDS-PAGE, immunocytochemistry (ICC), atomic force microscopy (AFM), scanning electron microscopy (SEM) and mass-spectrometry (MS). The influence of crowders on cell morphology, cell viability and metabolic activity were evaluated using phase-contrast microscopy, Live/Dead® and alamarBlue® assays respectively. NIPAM based thermo-responsive polymers were developed to facilitate detachment of ECM-rich cell-sheets.

### RESULTS AND DISCUSSION

**Figure 1:** Densitometry of SDS-PAGE demonstrated that MMC significantly increase type I collagen deposition ( $p < 0.0001$ ) at all tested serum concentrations (maximum deposition was in 2 days & 0.5% FBS or HS).

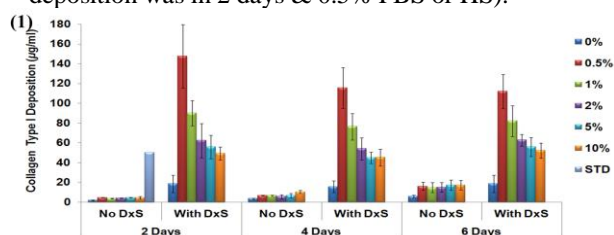


**Figure 2:** ICC, AFM and SEM further confirmed enhanced deposition of fibrillar ECM in presence of MMC.

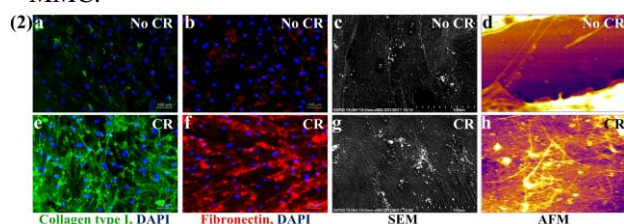


**Figure 3:** Thermo-responsive pNIPAAm failed to produce intact cell-sheets, whilst coating with 65% NIPAM / 35% N-tert-butylacrylamide facilitated detachment of intact ECM-rich cell sheets.

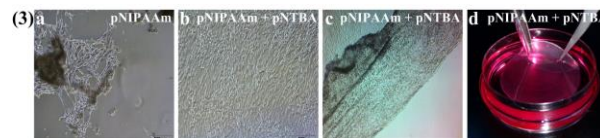


**Figure 4:** Complementary ICC for MS validation confirmed the enhanced deposition of collagens (I, III, IV, V, VI) and other ECM molecules (laminin, fibronectin, hyaluronic acid, decorin, lysyl oxidase), without changing other tested proteins.

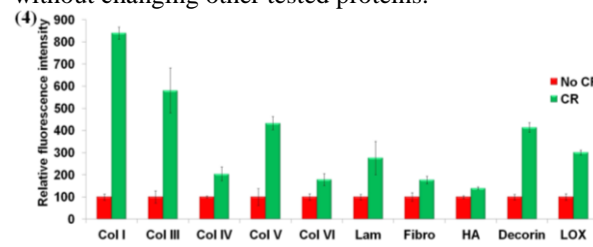
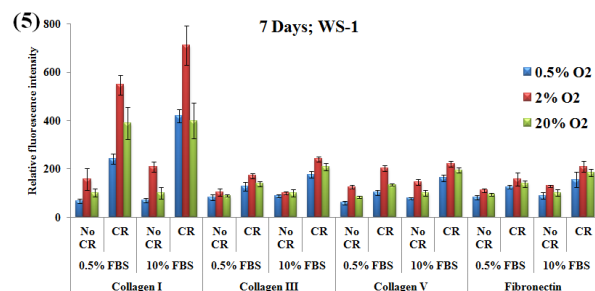


**Figure 5:** Relative fluorescence intensity measurement for ICC demonstrated that MMC with 2% oxygen supply significantly increase collagen-I, III, V and fibronectin deposition ( $p < 0.001$ ) at all tested serum concentrations.



### CONCLUSION

Modulation of the *in vitro* microenvironment with polydispersed MMC and low oxygen tension enhances ECM deposition, even under low serum supply.

### REFERENCES

1. Peck M *et al.*, Materials Today, 14: 218-24, 2011
2. L'Heureux N *et al.*, Nat Med, 12: 361-65, 2006
3. Vrana N *et al.*, IOVS, 49: 5325-31, 2008
4. Satyam A *et al.*, Adv Mater, 26: 3024-34, 2014
5. Kumar P *et al.*, Tissue Eng Part C, 2014 (in press)
6. Simon MC *et al.*, Nat Rev Mol Cell Biol, 9:285-96, 2008
7. Falanga V *et al.*, J Cell Physiol, 191: 42-50, 2002

### ACKNOWLEDGMENTS

Science Foundation Ireland (09/RFP/ENM2483 & 07/IN1/B031) for financial support.



## INTRODUCTION

Collagen type II is the most abundant constituents of cartilage extracellular matrix (ECM), Chondroitin Sulphate (CS) is the main and most abundant glycosaminoglycans in cartilage ECM. Cartilage scaffolds containing collagen II and Chondroitin Sulphate have been formed and characterised widely in the field of cartilage tissue engineering. EDC-NHS crosslinking have been investigated in several studies as the chemical method for improving the mechanical properties of scaffolds<sup>1</sup>. To date, the majority of collagen scaffolds were produced from insoluble naturally fibrillar collagen whilst atelocollagens (monomeric collagen devoid of telopeptide) have been used in only a few studies<sup>2</sup>. Telopeptide elicit antigenicity and atelocollagen has the advantage of not being antigenic due to excluding (not comprising) telopeptide in their structure<sup>3</sup>. In this study, cartilage scaffolds is fabricated from reconstituted fibrillar atelocollagen (type II) crosslinked to CS via EDC-NHS reagents.

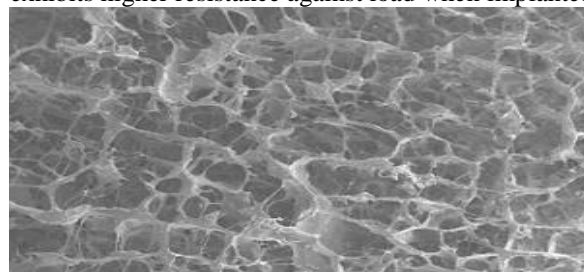
## MATERIALS AND METHOD

Reconstituted fibrillar collagen type II has been produced by fibrillogenesis of Type II atelocollagen monomers extracted from foetal calf cartilage in lyophilized form. Chondroitin sulphate A from bovine trachea was supplied by Sigma-Aldrich. In order for fibrillogenesis to occur, 1% w/w atelocollagen solution in acetic acid is mixed with TBS and placed in 37°C oven for 8hrs. Atomic force microscopy (AFM) and TEM images of the fibrils confirmed the formation of collagen fibrils. Reconstituted fibrillar collagen solution is then centrifuged and washed to remove TBS, subsequently CS is added to collagen followed by EDC-NHS crosslinking process. EDC-NHS molar ratio of 2:1 has been used. Rheology studies of the collagen solution, Fourier Transform Infrared (FTIR) spectroscopies, Scanning Electron Microscopy (SEM), mechanical testing, dissolution study and cell culturing have been performed to assess the effect of crosslinking on scaffold properties.

## RESULTS AND DISCUSSION:

Rheology results of Crosslinked Collagen-CS solution illustrate higher viscosity, loss modulus and storage modulus compared to those of Collagen II only solution. It shows that addition of CS and also crosslinking improves the visco-elastic behaviour of collagen solution which subsequently influences the pore structure and mechanical stiffness of the scaffolds. Results of cell culturing on crosslinked Collagen-CS scaffolds and Collagen only scaffolds exhibited much higher cell proliferation on crosslinked scaffolds compared to uncrosslinked collagen only scaffold. This could be due to the higher mechanical integrity of scaffolds in cell culture media, as it was observed that the collagen only scaffolds were dissolved and lost in media rapidly.

Moreover, CS could have stimulatory influence on cell growth. Histology analysis and FTIR results both showed the presence of CS in crosslinked scaffolds which ensures the covalent attachment of CS to collagen. Collagen only scaffolds dissolve and disintegrate in TBS in couple of hours; however dissolution studies exhibits that crosslinked scaffolds were stable in TBS for the period of four weeks. The pore size decreases by crosslinking but they are still in an appropriate range for cell infiltration and growth. The most significant advantage of crosslinked scaffold is their improved mechanical stability which enhances cell growth and exhibits higher resistance against load when implanted.



SEM image of Crosslinked Collagen-CS Scaffold

## CONCLUSION

The use of afibrillar collagen type II initially and creating fibrillar collagen and its further attachment to CS for cartilage scaffolds showed promising results as it can closely mimic the native cartilage structure. Enhanced mechanical properties and cell culture results confirmed the advantage of this scaffold to naturally fibrillar collagen or uncrosslinked reconstituted collagen II scaffolds.

## REFERENCES

1. Cao H, Xu S. EDC/NHS-crosslinked type II collagen-chondroitin sulfate scaffold: Characterization and in vitro evaluation. *J Mater Sci Mater Med.* 2008;19(2):567-575.
2. Tamaddon M, Walton R, Brand D, Czernuszka J. Characterisation of freeze-dried type II collagen and chondroitin sulfate scaffolds. *J Mater Sci Mater Med.* 2013;24(5):1153-1165.
3. Lynn A, Yannas I, Bonfield W. Antigenicity and immunogenicity of collagen. *Journal of Biomedical Materials Research Part B: Applied Biomaterials.* 2004;71(2):343-354.

## Collagen Hydrogels Cross-linked by Squaric Acid

Joanna Skopinska-Wisniewska<sup>1</sup>, Anna Bajek<sup>2</sup>, Malgorzata Maj<sup>2</sup>, Marta Ziegler-Borowska<sup>1</sup>, Alina Sionkowska<sup>1</sup>

<sup>1</sup>Biopolymer Research Group, Faculty of Chemistry, Nicolaus Copernicus University in Torun, Torun, Poland

<sup>2</sup>Collegium Medicum, Nicolaus Copernicus University in Torun, Karłowicza 24, 85-092 Bydgoszcz, Poland

[joanna@chem.umk.pl](mailto:joanna@chem.umk.pl)

### INTRODUCTION

Hydrogels are a class of materials widely used in medicine for many years. Proteins, such as collagen, due to the presence of a large number of functional groups are easily wettable by polar solvents and can create hydrogels. The supramolecular network capable to swelling is created by cross-linking of the biopolymers using various reagents [1,2]. Many cross-linking agents has been tested for last years, however, researchers still are looking for a new, more secure reactants. Squaric acid, 3,4-dihydroxy 3-cyclobutene 1,2- dione, is a very strong acid, which possess flat and rigid structure. Due to the presence of two carboxyl groups the squaric acid willingly reacts with amino groups of collagen [3]. The main purpose of this study was to investigate the influence of addition of squaric acid on the chemical, physical and biological properties of collagen materials.

### EXPERIMENTAL METHODS

The collagen type I was extracted from rat tail tendons and 1% solution in 0.1 M acetic acid was prepared. The samples were cross-linked by the addition of 5%, 10% and 20% of squaric acid. The mixtures of all reagents were incubated 30 min on magnetic stirrer and then dialyzed against deionized water.

### RESULTS AND DISCUSSION

The FTIR spectra show that the collagen structure is not changed by cross-linking by squaric acid. Although the mechanical properties of the collagen material deteriorate, the temperature of thermal denaturation of collagen increases after cross-linking, what indicates that the protein network was created. The lyophilized collagen gels exhibit porous structure and the pore size decreases with the higher addition of squaric acid. Also

the swelling ability is lower after the cross-linking. The in vitro study demonstrates that the materials are attractive for 3T3 cells.

### CONCLUSION

The addition of squaric acid causes formation of cross-linking bonds in the collagen materials. The changes of physicochemical properties of the material are typical for cross-linking process, except mechanical properties – it requires further experiments. However, the results let us to conclude that squaric acid is a suitable cross-linker for protein materials.

### REFERENCES

1. Slaughter B. V. *et al.*, Adv. Mater. 3307:3329-21, 2009
2. Wallace D.G. *et al.*, Adv. Drug Deliver. Rev. 1631:1649-55, 2003
3. Korkmaz U. *et al.*, Struct. Chem. 1249:1259-22, 2011

### ACKNOWLEDGMENTS

The authors would like to thank the National Science Centre (NCN, Poland, Grant no: UMO-2011/03/D/ST8/04600) for providing financial support to this project.



## Synthesis and Characterization of Biodegradable Genipin-cross-Linked Chitosan Scaffold for Bone Tissue Engineering

Simona Dimida<sup>1</sup>, Vincenzo De Benedictis<sup>1</sup>, Nadia Cancelli<sup>1</sup>, Francesca Gervaso<sup>1</sup>, Francesca Scalera<sup>1</sup>, Barbara Palazzo<sup>1,2</sup>, Christian Demitri<sup>1</sup>, Alessandro Sannino<sup>1</sup>

<sup>1</sup>Department of Engineering for Innovation, University of Salento, Lecce, Italy

<sup>2</sup>Ghimas S.p.A., c/o Ditech S.c.a.r.l., Lecce, Italy

[simona.dimida@unisalento.it](mailto:simona.dimida@unisalento.it)

### INTRODUCTION

Bone regeneration by autogenous cell transplantation is one of the most promising techniques in orthopedic surgery. This technique would eliminate problems of donor site scarcity, immune rejection and pathogen transfer. Several materials have been developed and analyzed to be used to this purpose. Chitosan has been widely used for its capacity to promote growth and mineral rich matrix deposition by osteoblasts in culture<sup>1</sup>. In addition, chitosan is biocompatible, biodegradable and can be manufactured into porous structures. In this study we report on the preparation and characterization of an innovative scaffold made starting from chitosan cross-linked with genipin, a natural extract of *Gardenia Jasminoides Ellis*<sup>2</sup>.

### EXPERIMENTAL METHODS

Chitosan scaffolds were prepared by freeze-drying technique. Chitosan solutions (medium Mw, 75% DD, Sigma Aldrich) were prepared by suspending 1.5 g of chitosan in 100 ml of acetic acid 0.1M in a glass flask and stirred for 6 hours at 4°C till complete dissolution. Afterwards, genipin was added to solution and stirred for another hour. Batches with different genipin concentrations were prepared in order to obtain samples with different degrees of cross-linking and properties. In particular, two different concentrations of genipin were used: 0.25 M and 0.50 M. The resulting mixture, GN1 (0.25 M genipin) and GN2 (0.50 M genipin), were poured into round moulds and thermal treated at 37°C for 30h in order to activate the crosslinking reaction. Afterward GN1 and GN2 hydrogels were frozen at -40 °C (freezing rate of 1°C/min) then lyophilized. Samples with 6 mm diameter and 2 mm thickness were obtained by cutting the obtained dry samples by means of a surgical punch (biopsy punch – Kai Medical BB-807). The morphological, physicochemical, and mechanical properties of materials have been evaluated and performed by means SEM analysis, degradation, swelling and compression tests. Furthermore, preliminary biological analysis by using human osteosarcoma cells (MG63) to estimate the cytocompatibility of scaffolds at two different cross-linking degree were performed by means MTT assay.

### RESULTS AND DISCUSSION

The chitosan-genipin scaffolds developed in this study presents great potentiality for applications in tissue engineering. The SEM images proves that the freeze-drying method allow to obtain a highly interconnected porosity, with pores at different shape and diameter, according to the different genipin concentration and cross-linking degree. GN1 presents round shape pores

with diameter ranging between 20-150 µm, while GN2 hexagonal pores, ranging 20-300 µm. The porosity looks isotropic in both the samples. The macrostructure of GN1 and GN2 scaffold is presented in Fig. 1.

Effects of cross-linking degree on degradation kinetics and swelling ability of the scaffolds were also measured, as well as their mechanical properties in compression. The *in vitro* degradation tests conducted both in PBS and PBS with lysozyme, showed a gradual dissolution of the scaffolds over time, but maintaining their integrity even after 28 days of incubation. GN1 samples show faster degradation kinetics than GN2 ones in both solutions. The results of the swelling test at 24h in PBS are likewise bound to the degree of cross-linking and show that GN1 scaffolds are more able to fluid uptake. The compression tests showed that as the cross-linking degree increases, a decrease in the mechanical strength is produced at low strain values.

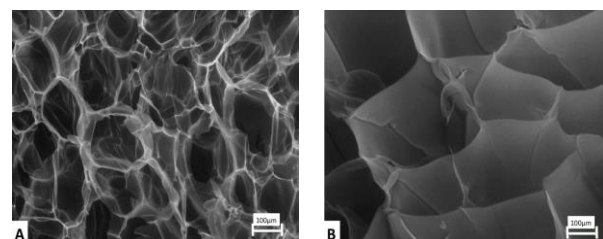


Fig.1 SEM images of GN1 chitosan-genipin scaffold (A) and GN2 one (B).

The biological tests performed in EMEM supplemented of FBS (10%), penicillin (100 U/mL) and streptomycin (100 mg/mL) demonstrated that the cell proliferation increases with time during the *in vitro* culture period, suggesting that the materials are nontoxic, not affecting the cell proliferation and showed good biocompatibility profile. No proliferation difference was found between GN1 and GN2 scaffold at every time points.

### CONCLUSION

This study has demonstrated the possibility to generate a novel cross-linked chitosan scaffold with an highly interconnected and homogeneous structure. Porosity in the range of about 20 µm to 300 µm is in agreement with the dimensional characteristics required for the scaffolds used in bone regeneration applications. The degradation profile, in combination with swelling and mechanical values, confirms their suitability in the field of bone tissue regeneration.

### REFERENCES

1. Rochet N. *et al.*, Biomaterials. 30(26):4260-7, 2009
2. Muzzarelli RAA., Carbohydrate Polymer. 77(1):1-9, 2009



## Towards the Regeneration of Gastric Epithelium Using a Tissue Engineering Approach

Yaser E. Greish<sup>1</sup>, Sunitha Polikkot<sup>1,2</sup>, Sneha Ann Thomas<sup>1,2</sup>, Abdel Hamid I. Mourad<sup>3</sup>, Sherif Karam<sup>2</sup>

<sup>1</sup>Department of Chemistry, College of Science,

<sup>2</sup>Department of Anatomy, College of Medicine and Health Sciences

<sup>3</sup>Department of Mechanical Engineering, College of Engineering,  
United Arab Emirates University, Al Ain, UAE

[y.afifi@uaeu.ac.ae](mailto:y.afifi@uaeu.ac.ae)

### INTRODUCTION

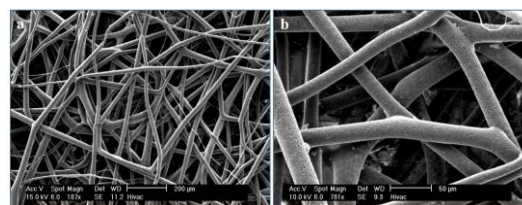
Various approaches have been considered to treat damaged gastric epithelium due to gastric ulcer and/or following the removal of cancer. Epithelial stem cells drive perpetual renewal of glandular cells secreting mucus, acid, pepsinogen, and various hormones or peptides. Little is known about the differentiation program and self-renewal of these stem cells. A recently established immortalized mouse gastric stem (mGS) cell line with features of undifferentiated morphology<sup>1</sup> (2) and expressing stem cell-specific markers: Notch3, DCAMK11 and Oct4 (3,4) represents a useful tool to study these rare cells<sup>2,3</sup>. Recent developments in regenerative medicine and tissue engineering could provide possibilities for improving the quality of life following gastrectomy. Differentiation of epithelial stem cells into any or all of these stomach cells upon culture on previously tailored scaffold is expected to provide an alternative modality for the treatment of damaged gastric epithelium. This study investigates the potential differentiation of mouse gastric stem cells (mGS) upon culture in a 3D culture system at different pH values. Three types (nonporous, microporous, and fibrous) of polycaprolactone (PCL) scaffolds were tested for the growth and differentiation of mGS cells at various normal and acidic pH values.

### EXPERIMENTAL METHODS

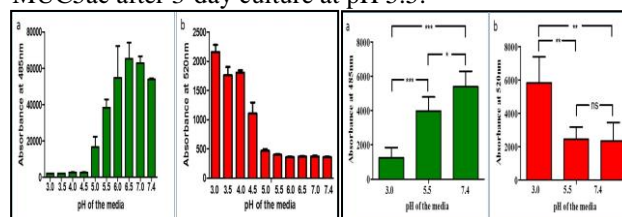
Polycaprolactone (PCL) scaffolds; non-porous, microporous, and microfibrous, were fabricated and characterized using scanning electron microscopy (SEM) and mechanical testing. The mGS cells were initially seeded on PCL scaffolds and allowed to grow for up to 3 days. Upon screening and based on cell viability results, microfibrous PCL scaffolds were seeded with mGS cells for up to 12 days. Cell growth and differentiation were monitored using PicoGreen assay of DNA quantification, SEM and lectin-/immunocytochemistry, and quantitative RT-PCR. In addition, the viability of mGS cells grown onto 3D scaffolds using RPMI media at pH ranging from 3 to 7.4 was tested using Calcein and Propidium iodide assays. The wound-healing method was used to examine the effects of acidic pH on mGS cell migration.

### RESULTS AND DISCUSSION

SEM features and mechanical properties of the scaffolds revealed similarities with connective tissue elements of the stomach wall.



A change in the number and size of the cells with time was observed suggesting their differentiation. Analysis of cryosections of scaffolds containing cells probed with N-acetyl-D-glucosamine-specific lectin and anti-trefoil factor 2 antibodies indicated that within 9 days of culture, around 50% of the mGS cells differentiated into mucous neck cells. Lower pH values decreased cells viability, while no significant change in viability was observed at pH  $\geq 5.5$ . In addition, RT-PCR revealed upregulation (3 folds) of mucous cell-specific gene, MUC5ac after 3-day culture at pH 5.5.



### CONCLUSION

Microfibrous PCL scaffolds support not only growth of mGS cells, but also their differentiation into mucus-secreting cells, showing their potential in stomach tissue engineering. Acidic pH value of culture media around 5.5-6.0 modulate the mGS cells proliferation program and speed up their differentiation into mucous cells.

### REFERENCES

1. Farook VS *et al*, Cell Prolif. 41:310-20, 2008.
2. Giannakis M *et al*, The Spine Journal, J Biol Chem. 281:11292-300, 2006.
3. Al-Marzooqee FY *et al*, . Int J Oncol. 41:1733-43, 2012

### ACKNOWLEDGMENTS

"The authors would like to thank the Research Funding provided by the National Research Foundation and the Office of Research and Graduate Studies at UAEU towards the completion of this work".

Daria Chernobrovkina<sup>1</sup>, Ekaterina I. Shishatskaya<sup>1,2</sup>, Egor V. Proskurin<sup>3</sup>, Victor I. Lazarenko<sup>3</sup>

<sup>1</sup>Institute of Fundamental Biology and Biotechnology, Siberian Federal University, Russia

<sup>2</sup>Laboratory of Chemoautotrophic Biosynthesis, Institute of Biophysics Siberian Branch of RAS, Russia

<sup>3</sup>Krasnoyarsk Regional Ophthalmological Hospital named after Prof. P.G. Makarov, Russia  
[namtuda@ya.ru](mailto:namtuda@ya.ru)

## INTRODUCTION

Tissue engineering is a promising approach for reconstructing damaged tissues and organs. Polytetrafluoroethylene (PTFE) is a synthetic material which confers non-biodegradability due to its highly crystalline nature. PTFE is widely used in medical implants due to a combination of mechanical performance, corrosion resistance and biocompatibility<sup>1</sup>. However, the use of this polymer as scaffolds for tissue engineering is often limited because of the poor retention of cells on its hydrophobic surface<sup>2</sup>.

Another group of materials which attracts interest as scaffolds is polyhydroxyalkanoates (PHAs)<sup>3</sup>. They are a family of biopolymers of microbial origin possessing excellent biocompatibility and biodegradability, and a wide range of physical and mechanical properties<sup>4</sup>. PHAs promote cell attachment and they can combine with different groups of materials including polymers, ceramics, and metals.

To overcome the limitations of PTFE, a composite scaffold was developed. The aim of this study was to investigate whether composite polytetrafluoroethylene/polyhydroxyalkanoate scaffolds promote cell attachment and proliferation.

## EXPERIMENTAL METHODS

PTFE porous plates were coated with poly(3-hydroxybutyrate) to create composite scaffolds with the method of dip coating. In order to study the ability of scaffolds to promote cell attachment we seeded them with fibroblasts NIH 3T3. The tissue culture polystyrene (TCPS) was used as a positive control. Cell viability was assessed by fluorescent microscopy using LIVE/DEAD staining (Molecular Probes) 24, 72, 168 hours after seeding. To investigate cell proliferation, MTT test was performed 24, 72, 168 hours after seeding.

## RESULTS AND DISCUSSION

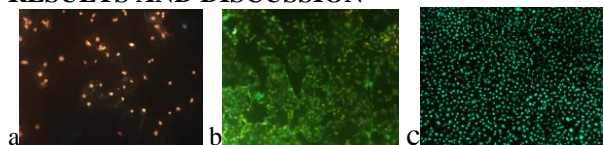


Figure 1. Cell viability after 7 days of culture on uncoated (a), coated (b) scaffolds and control tissue culture polystyrene (c) with LIVE/DEAD staining.

Cell viability was reduced after the cultivation on PTFE scaffolds. The number of cells adhered on the composite scaffolds was not significantly different when compared to the cell number on TCPS. Thus, coated scaffolds seem to provide the good adhesion of cells.

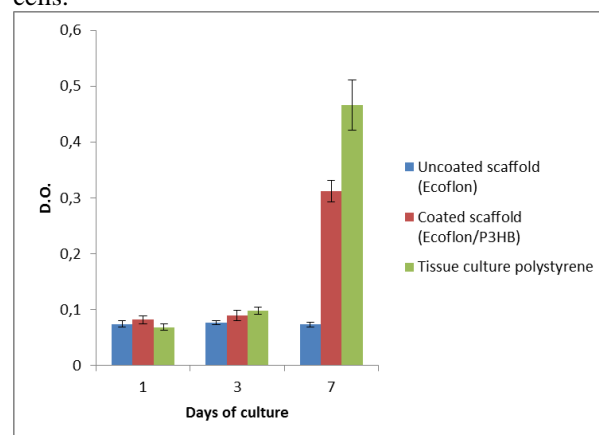


Figure 2. MTT assay for NIH 3T3 on scaffolds.

The obtained results in MTT test after 3 and 7 days of culture show consistent cell proliferation. Comparing the composite and PTFE scaffold, the cell viability and proliferation was improved by hydrophilic PHA-coating. However, the number of metabolically active cells on both, PTFE and composite scaffolds was lower compared to that of polystyrene seven days after seeding; on the composite scaffolds it was about 3 times higher than on PTFE.

## CONCLUSION

We have developed a new approach to increase cell attachment to PTFE porous scaffolds coating it with PHAs to scaffold artificial tissues.

## REFERENCES

1. Shao H.-J. *et al.*, Artificial Organs. 33(4):309–317, 2009
2. Hollweck T. *et al.*, Biomed. Mater. 5 065004, 2010
3. Williams S. F. *et al.*, in Biopolymers. 4:91–128, 2002
4. Volova T.G. *et al.*, J Mater Sci Mater Med. 15(6): 719-728, 2004

## ACKNOWLEDGMENTS

The authors would like to thank the Laboratory of New Biomaterials of the SibFU's Institute of Fundamental Biology and Biotechnology for providing poly(3-hydroxybutyrate) BIOPLASTOTAN for this work.

Malika Ould Aklouche<sup>1</sup>, Kerstin Gritsch<sup>1</sup>, Brigitte Grosgeat<sup>1</sup>, Jérôme Sohier<sup>2</sup>.<sup>1</sup> Laboratory for Multimaterials and Interfaces, UMR CNRS 5615, Faculty of Odontology, Lyon, France,<sup>2</sup> Laboratory of Tissue Biology and Therapeutic Engineering (LBTI), UMR CNRS 5305, Lyon, France,[jerome.sohier@ibcp.fr](mailto:jerome.sohier@ibcp.fr)

## INTRODUCTION

Dental implants represent the most reliable and long lasting therapeutic solution for tooth loss. However, peri-implantitis, an inflammatory disease mainly caused by bacterial infection and which induces a slow and gradual destruction of the implant supportive tissues, results in implant loss within 12 months in about 20% of the patient<sup>1</sup>. Healing of the peri-implant tissue is a slow process resulting in a scar tissue of lower quality, which lacks periodontal ligament and specific tissue fiber orientation in the peri-implant mucosa. Such inadequate healed tissue accounts for its sensitivity to bacterial invasion.

If biodegradable synthetic polymers (polyesters) shaped as dense or nanofibrillar membranes for guided tissue regeneration have been developed in the context of periodontal diseases, their fast resorption rate are likely to allow early wound healing, but not to provide efficient mechanical behaviour supporting tissue maturation. Furthermore, no biomaterial which would allow efficient cellular colonization has been proposed as scaffold for tissue regeneration among peri-implantitis therapeutics. Interestingly, jet-spraying, a method based on polymer diffraction by airflow, has recently been described as a successful way to create highly porous polycaprolactone (PCL) nanofibrillar scaffolds that allow extensive cell colonisation and tissue formation, unlike electrospinning<sup>2</sup>.

With this consideration in mind, we hypothesized that such open nanofibrillar structures composed of different biodegradable polymers, and therefore of distinct mechanical behaviours over time, would allow to enhance the quality of peri-implant scar tissue while providing improved handling and controlled shrinkage around the implant.

To investigate these hypotheses, we developed composite nanofibrillar matrices containing different ratio of PCL and poly(lactic-co-glycolic acid) (PLGA) nanofibers using the versatile jet-spraying approach, and evaluated their structural, mechanical, shrinkage and degradation properties.

## EXPERIMENTAL METHODS

Parameters to create PLGA (50/50, MW 153000 g/mol) nanofibers by jet-spraying were investigated with a 3<sup>4</sup> factorial design. Composite nanofibrillar matrices were obtained by concomitantly jet-spraying PCL (MW 80000 g/mol) and PLGA on the same collection point with two distinct setups. Modulation of each polymer in the nanofibrillar composite was achieved by selective shielding and ratio determined by selective PLGA dissolution in DMSO. Structure of the resulting matrices was characterized by SEM, mechanical properties by tensile testing and degradation by 3 weeks incubation in PBS at 37°C. Porosity and shrinkage in PBS, at RT, were determined by direct measurements.

## RESULTS AND DISCUSSION

Production of PLGA nanofibrillar matrices by jet-spraying was straight forward, controlled, highly productive (0.9 to 21 mm/hour thick) and resulted in high porosity (93 to 98%). Microscopically, PLGA nanofibers were smooth and homogeneous (Fig. 1A), with median diameters that could be adjusted from 0.24 to 1.43  $\mu$ m by increasing polymer concentration. Composite matrices of PLGA and PCL nanofibers (diameter 600 nm) were similarly easily produced. The nanofibers from each polymer were intimately entangled in porous structures while their respective structure and diameter was retained (Fig. 1B).

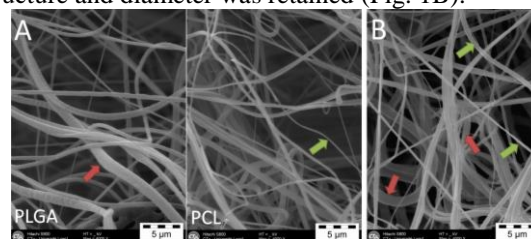


Fig. 1. PLGA (red arrows) and PCL (green arrows) jet-sprayed nanofibers (A) and resulting composite (B).

The ratio of each polymer could be adjusted at will, which resulted in fine modulation of the composite properties. Young's modulus showed a sharp and tuneable increase as compared to PCL and PLGA matrices alone (up to 2 and 4 fold respectively) (Fig. 2) while ultimate tensile strength followed the same trend, possibly due to a decrease of overall porosity by arrangement of smaller PCL fibers between PLGA's. By increasing PCL ratio, shrinkage of the composite matrices during incubation could as well be improved in a controlled fashion.

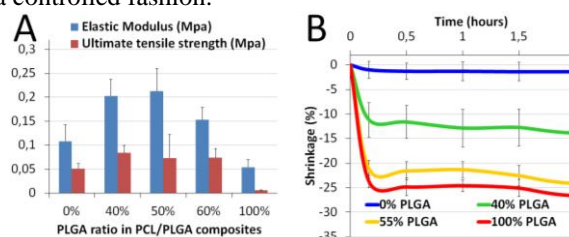


Fig. 2. Effect of composite PLGA ratio on mechanical properties(A) and shrinkage over incubation (B).

## CONCLUSION

Overall, these results present a simple and efficient approach, based on jet-spraying, to create composite nanofibrillar matrices of controlled and improved properties. Ongoing degradation experiments will further determine the selective modulation of mechanical properties over time.

## REFERENCES

- Derks J and Tomasi C. J. Clin. Periodont. 2014.
- Sohier J, Corre P, et al. Tiss. Eng. Part C, Methods. 20(4), 285-96, 2014.





Valeria Baronti<sup>1</sup>, Alberto Lagazzo<sup>2</sup>, Fabrizio Barberis, Marco Capurro, Rodolfo Repetto

Department of Civil, Chemical and Environmental Engineering (DICCA), University of Genoa, Italy.

<sup>1</sup>[valeria.barontidu.unige.it](mailto:valeria.barontidu.unige.it), <sup>2</sup>[alberto.lagazzo@unige.it](mailto:alberto.lagazzo@unige.it)

## INTRODUCTION

Liver diseases and cirrhosis deteriorate microcirculation; liver cirrhosis is the most common cause of death in men and in women in Europe and USA<sup>1</sup> and this condition is largely associated with primary liver cancer. An artificial material<sup>2</sup> that simulates the liver from the point of view of mechanical properties was produced to perform mechanical measurements and to test theoretical models. These materials, made of polyurethane, are porous and have the mechanical characteristics (elasticity and visco-elasticity) similar to those of the liver tissue. They were subjected to perfusion tests with different flow rate (0-78 ml/min) and their hydrodynamic behaviour was found to be similar to that of the liver. The next step, to be discussed in this work, is to perform compression experiments in perfusion at different pressures to evaluate the poroelastic behaviour of these materials.

## EXPERIMENTAL METHODS

Mechanical measurements were made through indentation tests using a testing machine with a maximum load of 500 N (Zwick/Roell Z0.5) with the experimental set up shown in Fig.1. The samples, perfused with water, were compressed with different values of the inlet pressure from 0 to 10 cmH<sub>2</sub>O (step of 2 cmH<sub>2</sub>O) to study the poroelastic behaviour in the undrained condition.

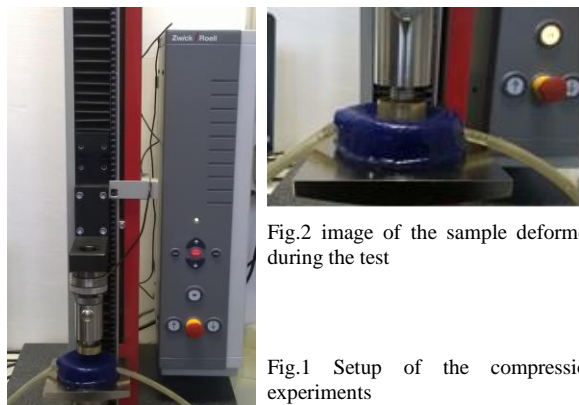


Fig.2 image of the sample deformed during the test

Fig.1 Setup of the compression experiments

The inlet tube was connected to a reservoir with water, which was initially positioned at the same height of the sample's inlet tube ( $p=0$  cmH<sub>2</sub>O) and for each test was lifted of 2 cm; the outlet tube was closed. The load was applied to the sample through a cylindrical indenter of 35 mm diameter. This method permits to neglect the change of shape of the sample during the deformation; it was positioned in the centre of the sample to avoid boundary effects. The values obtained were processed using a relationship between force and displacement<sup>3</sup> from which the Elastic Modulus can be calculated by the following expression:

$$E = \frac{2(1-\nu)}{3\pi(1+\nu)} \frac{F h^3}{\delta a^4} \quad (1.1)$$

where  $\nu$  is the Poisson coefficient (in this case it is considered equal to 0.2),  $F$  is the applied force,  $\delta$  the vertical displacement,  $h$  the actual height of the sample and  $a$  the radius of the indenter. In all tests the maximum deformation of the samples was 10% of its height. The preload velocity was 50 mm/min and the initial preload was 0.05 N.

## RESULTS AND DISCUSSION

The Elastic Modulus of the tested samples increase with pressure as shown in Fig.3; there is a little decrease of this value during the test at an inlet pressure of 6 cmH<sub>2</sub>O (0.6 kPa) and this seems to be a poroelastic feature of the material.

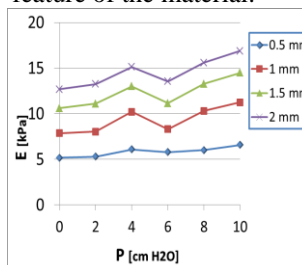


Fig.3 Elastic modulus vs. pressure for different values of compression

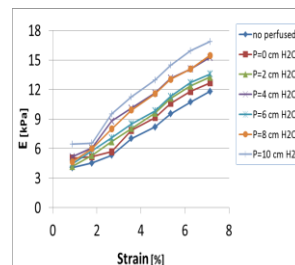


Fig.4 Elastic modulus vs. strain for different values of pressure

The value of the elastic modulus increases with strain (Fig.3) in the whole range of the applied pressures. As it is possible to see from the plot, the modulus at very low strain is quite similar to that of a healthy liver<sup>4</sup> (about 5 kPa).

The second step of this work is to explain these results with an analytical model of a poroelastic material.

## CONCLUSION

These materials subjected to indentation tests show that the elastic modulus increases with the pressure and the deformation. They reflect properly the behaviour of the liver and it will be necessary to make further experiments to make quantitative assessments.

## REFERENCES

1. M. Pinzani et al., J. Hepatology, 42 22-36 (2005).
2. A. Lagazzo, V. Baronti et al., AMBA Gent (2014).
3. F. Yang et al., Mech. Mat., 30 275-286 (1998).
4. G. Badino, F. Corradi et al., ESB Madrid (2013).

## ACKNOWLEDGMENTS

The authors would like to thank Ing. M. Gavi and Ing. M. Berta of the company BASF Polyurethane Italy SpA.



## Effects of Strontium on Physicochemical and Biological Properties of Hydroxyapatite Gel Materials for Periodontal Tissue Regeneration

<sup>1</sup>M. G. Raucci, <sup>1</sup>Daniela Giugliano, <sup>2</sup>M.A. Alvarez-Perez, <sup>3</sup>C. Demitri, <sup>3</sup>V.M. De Benedictis and <sup>1,4</sup>Luigi Ambrosio

<sup>1</sup>Institute of Polymers, Composites and Biomaterials – National Research Council of Italy. Mostra d'Oltremare Pad.20 - Viale Kennedy 54, 80125- Naples, Italy

<sup>2</sup>Tissue Bioengineering Laboratory; DEPeI, Faculty of Dentistry, National Autonomous University of Mexico; 04510, Mexico DF, Mexico

<sup>3</sup>Department of Engineering for Innovation, University of Salento, Via Monteroni, 73100 Lecce, Italy

<sup>4</sup>Department of Chemicals Science and Materials Technology, National Research Council of Italy (DSCTM-CNR), P.le Aldo Moro 7, 00185 – Rome, Italy

[mariagrazia.raucci@cnr.it](mailto:mariagrazia.raucci@cnr.it)

### INTRODUCTION

Hydroxyapatite  $[\text{Ca}_{10}(\text{PO}_4)_6(\text{OH})_2]$ , HA] is a primary constituent of vertebral animal's hard tissues and synthetic HAP has attracted attention due to its utility in the fields of bioceramics, catalyst, adsorbent, and so on. Because of the high stability and flexibility of the apatitic structure, a great number of substitutions, both cationic and anionic are possible.  $\text{Ca}^{2+}$  ion sites can be replaced by various divalent cations including  $\text{Sr}^{2+}$ ,  $\text{Ba}^{2+}$ ,  $\text{Pb}^{2+}$ ,  $\text{Cd}^{2+}$ ,  $\text{Mg}^{2+}$ , etc. In recent times, strontium hydroxyapatite  $\text{Sr}_{10}(\text{PO}_4)_6(\text{OH})_2$  (Sr-HAP) has received enormous attention of researchers because of its crystallochemical similarity to calcium hydroxyapatite. In particular, an increasing interest in strontium incorporation into biomaterials for hard tissue repair is justified by the growing evidence of its beneficial effect on bone [1]. Strontium is present in the mineral phase of bone, mainly in the regions of high metabolic turnover. *In vitro*, it increases the number of osteoblasts and reduces the number and activity of osteoclasts; *in vivo*, it inhibits bone resorption and improves bone formation. Strontium can replace calcium in the HA structure for the whole range of compositions, inducing a linear variation in the lattice constants. This study reported an evaluation of the substitution effect of strontium-modified hydroxyapatite gels (Sr-HA) on physicochemical, morphological and biological properties of hydroxyapatite materials prepared by sol-gel approach for periodontal tissue regeneration.

### EXPERIMENTAL METHODS

Sr-HA gels containing 5 - 10 - 15 and 20 mol %  $\text{Ca}^{2+}$  replaced by  $\text{Sr}^{2+}$  were synthesized at room temperature by using calcium nitrate tetrahydrated  $\text{Ca}(\text{NO}_3)_2 \cdot 4\text{H}_2\text{O}$  and di-ammonium hydrogen phosphate  $(\text{NH}_4)_2\text{HPO}_4$  as precursors and using water as solvent. Strontium nitrate  $\text{Sr}(\text{NO}_3)_2$  was dissolved in water and used to replace  $\text{Ca}^{2+}$  ions. The chemical composition of Sr-HA and the effect of strontium on viscosity properties have been evaluated by physicochemical (FTIR, XRD) and rheological analysis (rheometer ARES). The morphology of the materials was characterized by using SEM and TEM microscopy. Furthermore, biological tests were performed to estimate the effect of strontium on cellular behaviour by using human periodontal ligament cell.

### RESULTS AND DISCUSSION

A preliminary investigation showed a difference in the gelification time of the biomaterials prepared at different Sr concentration. In particular, gels prepared at 0, 5 and 10 mol% of Sr reached a final setting after 1hr

of stirring at 40°C. Meanwhile, the gels prepared at 15 and 20 mol% of Sr showed a slight delay, their gelation time was achieved after 2-3 hrs. This different behaviour probably is due by the ionic substitutions in the crystallographic sites of the hydroxyapatite lattice that generally cause changes in the values of the cell parameters dependent on the different sizes and amount of the ions, which are directly or indirectly responsible for the gelification time and for the general features of the material. In fact, TEM analysis demonstrated that in 10 and 20mol% Sr-doped HA the particles were changed in size than hydroxyapatite (l:  $40 \pm 2.7\text{nm}$ ; Ø:  $10 \pm 1.6\text{nm}$ ), in fact a length of  $40 \pm 2.7\text{nm}$  and diameter of  $10 \pm 1.6\text{nm}$  were detected. Moreover, the structural analysis of the powders of hydroxyapatite (HA) and hydroxyapatite doped with strontium 15mol% (HA-15Sr), done by X-ray diffraction, allowed us to identify the hexagonal hydroxyapatite crystalline phase. From the microstructural analysis we have found that 15mol%Sr doping reduces the domain size along all crystallographic directions while expanding the cell volume. The respond of periodontal ligament cells cultured onto the Sr-doped HA showed that material is not cytotoxic and have good biocompatibility. The potential of differentiation of periodontal ligament cells were evaluated by expression of bone related molecules by gene expression and our results showed that Sr-HA material have good potential for therapeutic application on periodontal defects where bone is need to be regenerated.

### CONCLUSION

The strontium incorporated in the hydroxyapatite structure decreases the domain size along all crystallographic directions with some effects on physicochemical and rheological properties. Moreover, the gel materials with strontium show better osteogenic differentiation by the expression of specific gene markers. This work confirms the ability of the hydroxyapatite modified Sr materials resulted in a solid gel to show good osteogenic properties for periodontal tissue regeneration.

### REFERENCES

[1] M.G. Raucci, D. Giugliano, M.A. Alvarez-Perez, L. Ambrosio. J Mater Sci: Mater Med (2015) 26(2):5436 DOI: 10.1007/s10856.

### ACKNOWLEDGMENTS

This study was supported through funds provided by the PNR-CNR Aging Program 2012-2014, UNAM-DGAPA: PAPIIT Project IN210815. The authors also thank Mrs. S. Zeppetelli for facilitating biological analysis and Cristina Del Barone for TEM analysis.



## Osteoblast Response to Novel Zinc and Silicon Co-substituted Hydroxyapatite

Robert J. Friederichs<sup>1</sup>, [Helen F. Chappell](mailto:Helen.chappell@mrc-hnr.cam.ac.uk)<sup>2</sup>, David V. Shepherd<sup>1</sup>, Roger A. Brooks<sup>3</sup>, Serena M. Best<sup>1</sup>

<sup>1</sup>Department of Materials Science & Metallurgy, University of Cambridge, UK

<sup>2</sup>MRC Human Nutrition Research Unit, University of Cambridge, UK

<sup>3</sup>Orthopaedic Research Unit, Addenbrooke's Hospital Cambridge, UK

[Helen.chappell@mrc-hnr.cam.ac.uk](mailto:Helen.chappell@mrc-hnr.cam.ac.uk)

### INTRODUCTION

The chemical similarity of synthetic hydroxyapatite  $\text{Ca}_{10}(\text{PO}_4)_6(\text{OH})_2$  (HA) and natural bone mineral has led to its use as a bone grafting material, both in phase-pure and substituted forms. A particularly successful substitution in HA-based orthopaedic materials is silicon, which plays an important role in connective tissue health<sup>1, 2</sup>. Silicate substitution limits are typically ~2 wt% Si before phase decomposition occurs with heat-treatment. Equally, while high levels of zinc are known to be cytotoxic<sup>3</sup>, low substitution levels in calcium phosphates have been investigated for their potential to stimulate bone formation, act as an anti-microbial and, slow osteoclast (OC) resorption. Therefore, we have synthesised and characterized a doubly substituted material, ZnSiHA, at various concentrations of Si and Zn in an attempt to combine several desirable characteristics of singly substituted HAs.

These materials were characterized using XRD, FTIR and XRF. The objective of the work presented here was to assess whether the materials could support the growth of primary human osteoblasts (hOB). Osteoblast growth and Collagen type I production were all measured on ZnSiHA discs and singly substituted controls with similar Zn and Si concentrations. Additionally, staining for mineral nodule growth was carried out after 21 days.

### EXPERIMENTAL METHODS

hOBs were isolated from minced trabecular bone, expanded until confluent, and then passaged. Samples were seeded at a density of 200 cells.mm<sup>-2</sup> or 14,540 hOBs per HA disc. A Cyquant cell proliferation kit (C7026, Molecular Probes, Invitrogen, Life Technologies, Paisley, UK) was used to determine the cell number at 21 days.

Type I collagen synthesis was measured by immunoblotting medium aspirates taken at 7, 14 and 21 days.

Twenty four hours prior to termination of cell culture medium containing 9  $\mu\text{gml}^{-2}$  was added to label mineral. At termination, the cells were fixed with 4% paraformaldehyde for 10 minutes and rinsed with 1X PBS. The samples were mounted with Vectashield containing DAPI and imaged using a fluorescence microscope to assess mineral nodule formation.

### RESULTS AND DISCUSSION

Both ZnHA and the higher Zn and Si concentration ZnSiHA sample showed significantly ( $p < 0.05$ ) more cells compared to HA, as shown in Figure 1.

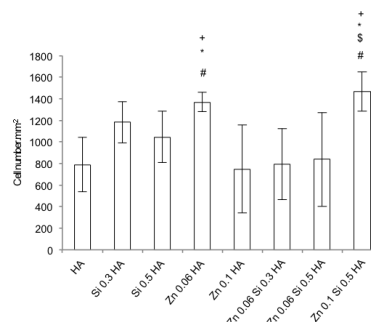


**Figure 1. Cell numbers on co-substituted and singly substituted control HA discs at day 21 (# indicates a significant difference with HA,  $p < 0.05$ ).**

Collagen I synthesis was significantly ( $p < 0.05$ ) increased on SiHA, ZnHA and ZnSiHA with high amounts of Si, at day 14 compared to phase-pure HA. Physiological mineral formation was observed on each sample after 21 days despite the lack of supplemental glucocorticoids and  $\beta$ -glycerophosphate.

### CONCLUSION

This study showed that newly developed ZnSiHA materials could support the growth of primary hOBs isolated from human tissue for up to 21 days *in vitro*. hOBs showed signs of differentiation and produced new mineral deposits on all samples. These results pave the way for testing the anti-microbial efficacy of ZnSiHA, which could be used to deliver a higher amount of Zn to combat bacterial infections, while retaining a desirable OB response.

### REFERENCES

1. Carlisle E.M., Science. 178:619-21, 1972
2. Jugdaohsingh R. et. al., Bone Reports, 1: 9-15, 2015
3. Yamaguchi M. et al., Biochem. Pharmacol., 36:4007-12, 1987

### ACKNOWLEDGMENTS

This work was supported by a NSFGRFP grant (DGE-1042796) (RJF) and a Cambridge International Scholarship (RJF). Thanks to Rakesh Rajan for isolating primary human OBs and Dr. John Wardale for assisting with COL I immunoblotting.



## Incorporation of the Chondroitin Sulfate into Collagen Scaffolds to Create a Biomimetic Niche with Neurally Committed Human Induced Pluripotent Stem Cells

Krystyna Pietrucha<sup>1</sup>, Marzena Zychowicz<sup>2</sup>, Justyna Augustyniak<sup>2</sup>, Martyna Podobinska<sup>2</sup>, Leonora Buzanska<sup>2</sup>

<sup>1</sup> Department of Material and Commodity Sciences and Textile Metrology, Lodz University of Technology, Lodz, Poland

<sup>2</sup> Stem Cell Bioengineering Laboratory, Mossakowski Medical Research Centre, Polish Academy of Sciences, Warsaw, Poland

[krystyna.pietrucha@p.lodz.pl](mailto:krystyna.pietrucha@p.lodz.pl)

### INTRODUCTION

The capability of the central nervous system (CNS) to regenerate and development crucially depends on the mutual interaction of the neural stem cells with the biomimetic microenvironment (scaffold) resembling a natural stem cell niche. In the existing state of knowledge, there is no clinically effective therapy for CNS regeneration [1,2]. The bi-component collagen-chondroitin sulfate (Col-CS) scaffold can possess very poor biological activity or be very bioactive depending on detailed structural features.

### EXPERIMENTAL METHODS

In this *in vitro* study, human induced pluripotent (iPS) stem cells committed to neural precursors were seeded into a biochemical highly standardized 3D porous collagen (Col) scaffold with covalently immobilized chondroitin sulfate (CS). Building up “biomimetic” microenvironment Col-CS sponge-like scaffold was based on two stage process: multiple freeze-drying followed by carbodiimide modification.

### RESULTS AND DISCUSSION

Of particular importance was spectroscopy (FTIR) observation that the collagen triple helix was preserved during bond-forming between Col and CS. Moreover, these scaffolds had average pore diameter of 31 µm and

relatively large surface area per pore volume. This scaffold has low autofluorescence and allows for proper visualization of immunostained experimental cells. The human induced pluripotent cells neurally *committed* (nestin positive) easily adhere to the surface of the scaffold and acquire markers of neuronal (β-tubulin III) and glial (GFAP, GalC, PDGFRα) cell population.

### CONCLUSION

Such results indicate feasibility of Col-CS scaffolds as “niche-like” microenvironment for human iPS-derived neural stem cells.

### REFERENCES

1. Vink R. *et al.*, Neurotherapeutics 7:1-2, 2010.
2. He J. *et al.*, Front. Mat. Sci. 6:1-25, 2012.

### ACKNOWLEDGMENTS

This work is supported by National Science Centre via Grant No DEC-2011/03/B/ST8/05867.



## Hybrid Scaffolds of Collagen Modified by Dialdehyde Cellulose with iPS-derived Neural Precursor Cells

Krystyna Pietrucha<sup>1</sup>, Marzena Zychowicz<sup>2</sup>, Justyna Augustyniak<sup>2</sup>, Martyna Podobinska<sup>2</sup>, Leonora Buzanska<sup>2</sup>

<sup>1</sup> Department of Material and Commodity Sciences and Textile Metrology, Lodz University of Technology, Lodz, Poland

<sup>2</sup> Stem Cell Bioengineering Laboratory, Mossakowski Medical Research Centre, Polish Academy of Sciences, Warsaw, Poland

[krystyna.pietrucha@p.lodz.pl](mailto:krystyna.pietrucha@p.lodz.pl)

### INTRODUCTION

Nowadays, the important approach towards neural tissue engineering involves the *in vitro* culturing of stem cells on biodegradable and bioactive collagen (Col) scaffold to form hybrid tissue-like structure feasible for implantation into the injured site of brain or spinal cord. Such scaffold must have especially stable micro-architecture and biophysical properties. The main focus of our previous studies was the enhancing the functional properties of collagen by cross-linking using carbodiimide [1,2].

### EXPERIMENTAL METHODS

In this study we are interested in activation of collagen with biocompatible 2,3 dialdehyde cellulose (DAC). Synthesis of scaffold was done in three steps: (i) preparation of 2,3 DAC, (ii) construction of 3D collagen sponge, (iii) modification of sponge by solution of DAC and lyophilization. Collagen scaffolds modified by DAC were seeded with induced pluripotent stem cells.

### RESULTS AND DISCUSSION

The results obtained suggest that intermolecular cross-links occur primarily between the free amine groups of collagen macromolecules and aldehyde groups in DAC. Of particular importance was spectroscopy examination that only small changes in the absorption ratio  $A_{1235}$  to  $A_{1450}$   $\text{cm}^{-1}$  was observed that unambiguously indicate that secondary structure of triple helix of collagen not altered significantly. An extremely important feature of collagen cross-linked by DAC is fact that scaffold is occupied by a size pore regime of 20-160  $\mu\text{m}$ . Some

rheological properties of scaffold which play an essential role in cell fate will also be presented and discussed. Col-DAC scaffolds were seeded with induced pluripotent stem cell-derived neural precursors which adhere in a good manner and differentiated into more advanced phenotypes expressing neuronal (b-tubulin III, Map2, Doublecortin) and glial (GFAP, GalC, PDGFRa) markers.

### CONCLUSION

Collagen modified by dialdehyde scaffolds may serve as the carriers for the specific population of neuronal cells.

### REFERENCES

1. Pietrucha K. *et al.*, IFMBE 45 (2014) 549-552. DOI: 10.1007/978-3-319-11128-5\_137.
2. Zychowicz M. *et al.*, Folia Neuropathologica 52:371-372, 2014.

### ACKNOWLEDGMENTS

This work is supported by National Science Centre via Grant No DEC-2011/03/B/ST8/05867.





## Study of Poly(lactic acid) Hybrid Systems for Preparation of Interconnected Porous Scaffolds

Ioanna-Georgia Athanasoulia, Maria Kanidi, Petroula A. Tarantili

Polymer Technology Lab., School of Chemical Engineering, National Technical University of Athens, Greece  
[taran@chemeng.ntua.gr](mailto:taran@chemeng.ntua.gr)

### INTRODUCTION

Poly lactic acid (PLA) is one of the most widely used materials in biomedical applications due to its interesting characteristics, such as tuneable mechanical properties, degradation into natural metabolites and biocompatibility<sup>1</sup>. However, the brittleness and degradation rate of PLA, as well as its inherent hydrophobicity have limited its applications<sup>2</sup>. To overcome these problems, chemical modification as well as the use of amphiphilic mixtures have been investigated. Since poly(ethylene glycol) (PEG) is known to be miscible with PLA in the amorphous phase, it has been utilized as a component to be blended with PLA. PEG is a hydrophilic polymer widely used in the field of biomedicine, due to its lack of toxicity, good biocompatibility and elimination from the human body when its molecular weight is low. PLA/PEG blends vary from completely miscible to partially miscible, depending on the PEG concentration.

Scaffolds for tissue engineering should have a specific three dimensional shape, appropriate pore size, high porosity and pore interconnectivity to achieve better nutrient transport and cell migration. Also, they should possess sufficient mechanical strength to provide the necessary physical support for tissue reconstruction. Available techniques for fabricating polymer porous scaffolds, such as solvent casting, particle leaching, gas foaming, electrostatic spinning, freeze drying and phase separation have already been widely used<sup>3</sup>.

In this work, PEG/PLA blends were studied and the salt leaching technique was applied in order to obtain a porous PLA with interconnected cells. Combination of inorganic (NaCl) and organic (PEG) porogens in particulate leaching method were also examined.

### EXPERIMENTAL METHODS

PLLA (Resomer - L210 Boehringer Ingelheim) and PEG ( $M_w=3000$  g/mol, Merck) blends, with various PEG concentrations (20, 30 and 50%) were prepared by dissolution in dichloromethane using sonication for 15 min. The obtained films were characterized by differential scanning calorimetry (DSC) and thermogravimetric analysis. PEG/PLLA films were immersed in deionized water for removal of water soluble PEG. In PLA and PEG/PLLA systems, sieved NaCl (200-300  $\mu$ m particle sizes) was added and salt leaching by immersion in deionized water was studied. Optical and Scanning Electron Microscopy (SEM) were used for observation of the obtained material morphologies.

### RESULTS AND DISCUSSION

DSC analysis of PEG/PLLA blends revealed that the presence of PEG enhances the crystallization of PLLA

phase, whereas a decrease in the crystallization ability of PEG was recorded. Minor decrease in melting temperatures of both phases was observed.

Sample PEG/PLLA	$T_{m,PEG}$ (°C)	$T_{m,PLLA}$ (°C)
PLLA	-	181.2
20/80	43.1	178.5
30/70	59.0	179.6
50/50	61.2	178.0
PEG	61.0	173.9

Table 1. DSC results of PEG/PLLA blends.

Thermogravimetric analysis of PLLA/PEG gave two stages of thermal degradation: the low temperatures area corresponds to PLA and that at the higher temperatures area corresponds to PEG degradation. The presence of PEG shifts the onset of PLA thermal degradation to lower temperatures, whereas no significant effect in the degradation rate of PEG phase in the blend was observed.

PEG/PLLA w/w	$T_{onset}$ (°C)	$T_{peak,PLLA}$ (°C)	$T_{peak,PEG}$ (°C)
PLLA	336.6	360.3	-
20/80	304.1	347.8	392.2
30/70	298.4	338.3	397.1
50/50	279.6	317.1	401.1
PEG	384.0	-	402.9

Table 1. TGA results of PEG/PLLA blends.

### CONCLUSION

The incorporation of PEG in PLA matrices decreases the thermal stability of PLA phase, whereas no significant changes can be recorded for that of the PEG phase. The presence of PEG enhances the crystallization ability in PLLA phase, whereas that of PEG was lower, in comparison with respective pure polymers. The formation of porous PLLA scaffolds is expected to proceed via the NaCl particles leaching method and the interconnectivity of pores might be improved by the combined action of the polymeric porogen of PEG.

### REFERENCES

1. Tarantili P.A. In Biodegradable Polymers: Processing, Degradation and Applications, Nova Science Publ., 2011
2. Stephansson S.N. *et al.*, Biomaterials 23:2527-2534, 2002
3. Okamoto M., John B., Progr Polym Sci 38:1487-1503, 2013



Michał Wojański<sup>1</sup>, Małgorzata Bieniak<sup>1</sup>, Tomasz Ciach<sup>1</sup>

<sup>1</sup>BioMedical Engineering Laboratory, Department of Biotechnology and Bioprocess Engineering, Faculty of Chemical and Process Engineering, Warsaw University of Technology, Poland

[m.wojasinski@ichip.pw.edu.pl](mailto:m.wojasinski@ichip.pw.edu.pl)

## INTRODUCTION

Nanofibrous materials are commonly applied in the field of biomedical engineering due to their properties: high area to volume ratio, fiber diameter corresponding to natural extra cellular matrix, suitable mechanical properties, etc. However, stable and efficient production of high amount of the nanofibers remains challenging. Thus, researchers proposed combination of common technologies - electrospinning and meltblowing – known as solution blow spinning (SBS)<sup>1</sup>. In present work we investigated possibilities to design nanofibrous product of SBS for tissue engineering applications by controlling process parameters.

## EXPERIMENTAL METHODS

Solution blow spinning technique was applied for polyurethane nanofibers production. Briefly, the system contains concentric nozzle: inner for polymer solution flow, outer for air flow; compressor and syringe pump. Details are described in our previous work<sup>2</sup>. Solutions of three concentrations of polyurethane (PU, Elastollan 1185A, BASF, Germany) were prepared: 4, 6 and 8% w/w in tetrahydrofuran (THF).

Rheological properties of the solutions were investigated in Rheotest 2.1 (VEB MLW, Germany). Resulting nanofibers diameters, morphology, alignment, and cell culture evaluation were made based on scanning electron microscope (SEM, Phenom™, Phenom World) images. Porosity of materials was measured by gravimetric technique. For wettability measurements DSA 100 goniometer (Krüss, Germany) was used, and for single nanofiber wettability calculations the meta-stable Cassie Baxter equation was applied. Cytotoxicity and proliferation analysis were made based on ISO 10993-5 standard, with MTT assay on L929 fibroblasts cell line cultures. Investigation of cells migration through the nanofibrous material was conducted in confocal microscope (LSM 880, Zeiss, Germany), with AlexaFluor 488 Phalloidin staining of L929 filaments.

## RESULTS AND DISCUSSION

Flow curves for all concentrations present the rheological properties of investigated polymer solutions. In figure 1 we present the dependence of average fiber diameter in function of process parameters (solution concentration, air pressure). Nanofibers size varies from about 100nm to about 800nm. Alignment of the nanofibers within the material depends on collector rotational speed, and porosity of the material on nozzle-collector distance. Wettability measurement shows slight hydrophobic properties of non-woven material,

but calculations for single fiber indicate the hydrophilic properties. MTT assay shows both, cytotoxicity evaluation and proliferation of the L929 fibroblasts on the materials. PU nanofibers exhibit nontoxic property, allowing cells to migrate through the material's pores – effect illustrated by confocal microscopy.

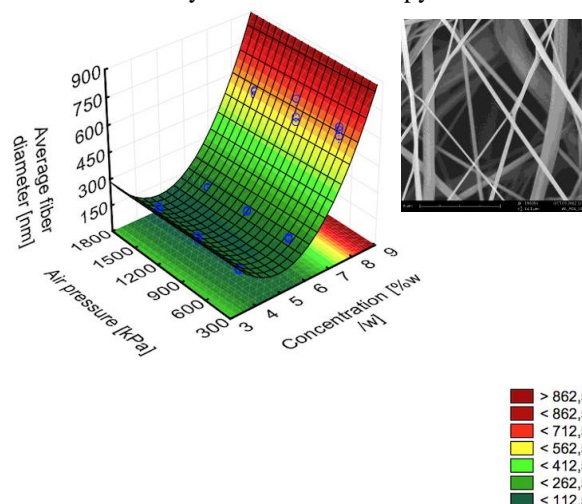


Figure 1. Average nanofibers diameter in function of applied air pressure and polymer concentration; SEM insert, scale-bar 6μm

Presented results indicate the importance of processing parameters control for production of proper nanofibrous biomaterial from polyurethane for tissue engineering applications by solution blow spinning. Additionally, the investigation of cells behavior, not only on the surface of the biomaterial, shows the importance of designing the internal structure of solution blow spun nanofibers.

## CONCLUSION

Solution blow spun polyurethane nanofibers with potential application in the field of biomedicine exhibit proper physical and biological properties, when the production process is consciously controlled. The resulting biomaterial promotes cells migration on the surface and within the material structure, lacks cytotoxicity and promotes proliferation of cells.

## REFERENCES

1. Medeiros E.S. *et al.*, J. Appl. Polym. Sci. 133:2322-2330, 2009
2. Wojański M. *et al.*, Pol. J. Chem. Technol. 16;2:43-50, 2014

## Integration of Biphasic Calcium Phosphate Bioceramics Mixed with Autologous Mesenchymal Cells in Osteoporotic Rabbit's Jaw

Aleksandrs Grishulonoks<sup>1</sup>, Inese Chakstina<sup>2</sup>, Arvids Jakovlevs<sup>3</sup>, Vita Zalite<sup>4</sup>, Ilze Salma<sup>1</sup>, Andrejs Skagers<sup>1</sup>, Vadims Klimecs<sup>1</sup>

<sup>1</sup>Department of Oral and Maxillofacial Surgery/Riga Stradins university, Latvia

<sup>2</sup>Laboratory of biodosimetry and bioanalytical methods/University of Latvia, Latvia

<sup>3</sup>Department<sup>e</sup> of Pathology/Riga Stradins university, Latvia

<sup>4</sup>Rudolfs Cimdins Riga Center for development and innovation of Biomaterials/Riga Technical university, Latvia  
[aleksandrs.gr@gmail.com](mailto:aleksandrs.gr@gmail.com)

### INTRODUCTION

Bone tissue engineering using biphasic calcium phosphate bioceramics as scaffold saturated by autologous mesenchymal cells in autologous environment of host living organism as bioreactor is one challenge for substitution of autologous bone grafting [1-2]. Role of autologous mesenchymal cells for biologisation of inorganic bone substitutes to improve their osteogenic properties is contradictory between healthy bone and compromised bone and environments. The fate of transplanted mesenchymal cells is discussed between new bone formation [3-4] and early death with release of some osteotrophic growth factors [5] and mediators for cell recruitments remains unknown.

### EXPERIMENTAL METHODS

Experimental osteoporosis was induced in 8 2,5 years female rabbits by ovariectomy and 1 mg/kg of methylprednisolone daily for 8 weeks. On 4 animal the holes was created in bouth angles of lower jaw; on the left side filled with a biphasic calcium phosphate bioceramics (HAP/TCP 90/10) granules; on the right side the same granules mixed with autologous fat tissue-derived mesenchymal cells. The two control groups each had 2 rabbits – with the analagous defect of osteoporotic jaw bone without bioceramics and without of any defect. After 3 months bone samples for Hem/Eoz staining and mBiotin-streptavidin method for immunohistochemical detection of collagen I, osteonectin and osteopontin were prepared. Semi-quantitative counting method was used for quantification of relative frequency of immunohistochemically detected tissue degrading collagen I, osteonectin and osteopontin. Relative frequency of the collagen I type, osteonectin, osteopontin was analyzed in three visual fields of a single section. The diameter of the visual field was 1.8 mm when the enlargement was 100x, or the diameter the visual field was 0.9 mm when the enlargement was 200x. No collagen I type, osteonectin or osteopontin positive cells in the visual field were marked -, rare positive cells were marked 0/+, few positive cells +, moderate ++, numerous +++, a lot of positive collagen I, ON and OP cells were marked ++++.

### RESULTS AND DISCUSSION

Evaluation of histological slices stained with hem/eoz revealed different response of host tissue around implanted Hap/TCP granules. In healthy bone granules

mainly were embeded in new formed bone, but in osteoporotic bone surrounded by fibrous tissue layer more thick in samples where mesenchymal cells were added.

Table 1. Average expression of collagen I, ON and OP in osteoporotic jaw bone defects.

<i>Osteoporotic jaw bone defect</i>	<i>collagen I type</i>	<i>ON</i>	<i>OP</i>
<i>Defect without filling</i>	+++	++	++
<i>Filled with HAP/TCP 90/10 granules</i>	++++	++++	+++
<i>Filled with HAP/TCP granules and mesenchymal cells</i>	+++	+++	+++

### CONCLUSION

Integration of HAP/TCP granules in defect of osteoporotic rabbit jaw is through encapsulation by fibrous tissue while in healthy bone osseointegration occurs. The addition of autologous mesenchymal cells resulted in more thick capsule without significant influence on collagen I expression, ON or OP. No signs of inflammation were detected.

### REFERENCES

- 1.Cheng L. *et al.*, Osteoinduction of calcium phosphate biomaterials in small animals. *Mater Sci Eng C Mater Biol Appl.* 33:1254-60, 2013
2. Fellah B.H. *et al.*, Osteogenicity of biphasic calcium phosphate ceramics and bone autograft in a goat model. *Biomaterials.* 29:1177-88, 2008
- 3.Cowan C. *et al.*, Adipose-derived adult stromal cells heal critical-size mouse calvarian defects *Nat Biotechnol* 22:560-67, 2004
- 4.Taub P.J. *et al.*, Bioengineering of calvaria with adult stem cells *Plast Reconstr Surg* 123:1178-85, 2009
- 5.Corre P. *et al.*, Determining a clinically strategy for bone tissue engineering : an all-in-one” study in nude mice *PLOS One*8:e81599, 2013

### ACKNOWLEDGMENTS

The presented work was supported by Latvian State Research program's activity 4.5 "New materials and technologies for evaluation and substitution of biological tissue "



## Evaluation of Graphene Based Composite Films for Biomedical Applications

C. Demitri<sup>1</sup>, M.G. Raucci<sup>2</sup>, A. Moscatello<sup>1</sup>, D. Giugliano<sup>2</sup>, V.M. De Benedictis<sup>1</sup>, A. Sannino<sup>1</sup>, L. Ambrosio<sup>3</sup>

<sup>1</sup>Department of Engineering for Innovation, University of Salento, Via Monteroni, 73100 Lecce, Italy.

<sup>2</sup>Institute of Polymers, Composites and Biomaterials – National Research Council of Italy. Mostra d'Oltremare Pad.20 - Viale Kennedy 54, 80125- Naples, Italy.

<sup>3</sup>Department of Chemicals Science and Materials Technology, National Research Council of Italy (DSCTM-CNR), P.le Aldo Moro 7, 00185 – Rome, Italy.

[christian.demitri@unisalento.it](mailto:christian.demitri@unisalento.it)

### INTRODUCTION

Graphene is a flat monolayer of carbon atoms tightly packed into a two-dimensional (2D) honeycomb lattice and is a basic building block for graphitic materials of all other dimensionalities with unique physical, chemical, and mechanical properties. Graphene and graphene oxide (GO) layers have become a hotspot so far and have been actively investigated to build new composite materials. It has been shown that graphene induces no obvious toxic effects *in vivo* [1]. It possesses the large aspect ratio, high mechanical strength, and superior electrical conductivity and the presence of abundant epoxide, hydroxyl and carboxylic groups on the GO basal plane could provide enormous reactive sites for chemical interactions. Thus, it has been regarded as an important component for making various functional composite materials.

In this work, we present the results of the applications of graphene and GO in biomedical application with focus on regenerative applications. Different mixtures of both graphene and GO with chitosan at different ratios were prepared in sheet-like structure in order to characterize the synergic combination of the composite materials.

### EXPERIMENTAL METHODS

Expandable graphite flakes (GIC), intercalated with a mixture of sulfuric acid and nitric acid, were obtained from Anthracite Industries (EG 3772). A content of 3.5 wt% of intercalate was reported on the technical data sheet. GIC, after a rapid heating at 700°C for 2 min, is transformed in expanded graphite (EG) characterized by a volume of about 250 cm<sup>3</sup>/g and a carbon content of about 99.5%. EG flakes were further disaggregated by sonication in water, acetone and chitosan solutions leading to expanded and sonicated graphene stacks (EGS) [2]. Graphene oxide (GO) was then produced by using the Hummer's method. EGS were characterized with X-ray diffraction (XRD) and dynamic light scattering (DLS). GO solutions were characterized with X-ray photoelectron spectroscopy (XPS) and Raman Spectroscopy. The rheological properties of Graphene and GO-chitosan mixtures were characterized with a rotational rheometer. The mechanical properties of the Graphene-Chitosan and GO-chitosan composite films were evaluated in comparison with those of pure chitosan samples. The cell morphology and cell spreading pattern interaction of human Mesenchymal Stem Cell (hMSC) onto composite materials sonicated at different time was evaluated by confocal laser scanning microscopy (LSM 510, CarlZeiss).

The biocompatibility of graphene/chitosan composite

films was checked *in vitro* by alamar blue colorimetric assay.

### RESULTS AND DISCUSSION

XRD and DLS analyses showed a time dependence particles dimensions. In particular longer sonication times lead to a lower particle dimension. A higher degree of exfoliation was achieved when EGS were further sonicated in presence of chitosan. Both XPS and Raman spectroscopy show an excellent conversion of EGS to GO. The morphology analysis by Transmission Electron Microscopy (TEM) confirmed a good exfoliation of graphene.

The cell adhesion result showed that the cell can adhere to and develop on the graphene/chitosan composite films, indicating that the composite films have good biocompatibility. Furthermore, according to the data it can be found that the number of hMSCs increases with time during the *in vitro* culture period; suggesting that the materials are nontoxic, not affecting the cell proliferation and showed good biocompatibility.

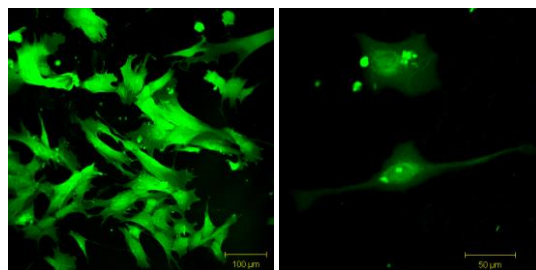


**Fig.1: Confocal microscopy of hMSC cultured on composite films after sonication treatment (8hours).**

### CONCLUSION

In this study, we have proposed a new technique for a direct exfoliation of graphite with chitosan allowing to obtain graphene flakes in a polymer matrix. The combination of this technique with Hummer's method allowing to obtain chitosan-graphene oxide composite films. The new composite materials may have wide range of potential applications, e.g. for conducting composites, optoelectronic, and in biological or medical research.

### REFERENCES

1. Kim J, *et al.*, J. Am. Chem. Soc, 132:8180–8186, 2010.
2. Corcione Esposito C, *et al.*, Polymer Eng & Science, 53(3): 531–539, 2013



## ***In Situ* Investigation of Chemical Composition, Morphology, Gelling and Mineralisation Kinetics in Hydrogel/Mineral Composites**

Sindre H. Bjørnøy<sup>1</sup>, David C. Bassett<sup>1</sup>, Stefan Mandaric<sup>1</sup>, Pawel Sikorski<sup>1</sup>

<sup>1</sup>Department of Physics, Norwegian University of Science and Technology, Norway

[sindre.bjornoy@ntnu.no](mailto:sindre.bjornoy@ntnu.no)

### **INTRODUCTION**

Due to its complex architecture at different length scales, the hierarchical structure of bone is not easily replicated in the laboratory. One strategy to overcome this obstacle when engineering synthetic bone tissue scaffolds is to provide a simpler material which inherent or implanted cells can remodel into natural bone. We have previously developed an alginate-calcium phosphate (CaP) composite material which shows good potential in this regard<sup>1</sup>. We envisage the formation of constructs which include beads, fibres and/or films with different mineral phases, content or mineralising potential, and the possibility to co-culture different cell types, such as osteoblasts and osteoclasts, in order to provide a synthetic matrix to stimulate remodelling of the composite and the formation of new bone.

The goal of this study was to develop *in situ* tools to study temporally and spatially resolved gel formation and mineralization of hydrogels simultaneously using a range of physicochemical characterization techniques.

### **EXPERIMENTAL METHODS**

The flow cell consisted of a microscope slide and a cover slip separated by a polymer film. A 10  $\mu$ L drop of alginate containing various concentrations (0 to 1 M) of sodium phosphate was placed between the slides creating a thin disc.  $\text{CaCl}_2$  gelling solution (50 mM to 1 M) was then introduced into the cell to initiate gelling and mineral formation.

Gelling kinetics, mineral formation, and local pH evolution were monitored using optical microscopy (Olympus IX70) and confocal microscopy (Leica SP5/SP8) of fluorescently labelled alginate and pH-sensitive fluorescent dyes.

To monitor the chemical composition of the mineral phases, Raman microscopy was used (Renishaw InVia Reflex Spectrometer System equipped with 532 nm and 785 nm lasers).

A selection of flow cell experiments were quenched during the gelling process by submerging the sample into acetone pre-cooled with liquid  $\text{N}_2$  and critical point dried (Emitech K850) before imaging with a SEM (Hitachi S-5500 S(T)EM).

### **RESULTS AND DISCUSSION**

The thin disc of hydrogel simulated the cross-section of a bead or a fibre and allowed us to follow gelling and mineralisation under different initial conditions. Freezing the samples in the process of gelling followed by critical point drying enabled us to study the mineral distribution and morphology with high resolution SEM-imaging at chosen time points after gelling had been initialized.

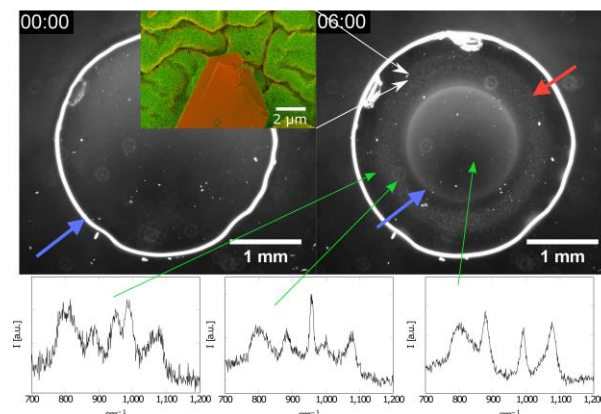


**Figure 1:** Optical microscopy images before and during gelling/mineralising. The blue arrows indicate the gelling front, the red arrow indicates a belt of minerals following the gelling front, and the green arrows show the position of spatially resolved Raman spectra. **Inset:** SEM-image of DCPD-crystal in an alginate matrix.

Figure 1 shows optical phase contrast images of a gelling sample with accompanying Raman-spectra of different positions on the sample. The inset is a density-dependent colour SEM-image, where the red channel is the BSE-signal and green channel is the SE-signal. This technique generates a larger contrast between the gel matrix and the denser mineral. The Raman-scattering technique could detect non-crystalline precipitates as well as spatially resolve the different phases that formed. In addition this approach, along with pH changes detected by fluorescence (data not shown), allowed *in situ* monitoring of mineral phase transformation, which occur in composites prepared with this method.

### **CONCLUSION**

We have developed a system which enables simultaneous study of spatially and temporally resolved gelling kinetics and crystallisation of hydrogel-mineral composite materials. The system is compatible with a range of physicochemical and optical characterization techniques. Results from these experiments can be compared with theoretical models and will be used to improve understanding of crystallisation processes and gelling kinetics of hydrogel-mineral composite materials.

### **REFERENCES**

1. Xie M., *et al.*, *Acta Biomaterialia* 6:3665-3675, 2010.

### **ACKNOWLEDGMENTS**

We acknowledge the Research Council of Norway for financial support (FRINATEK project 214607).

## Fabrication of co-Axial Electrospinning Nanofibrous Mats for Bone Tissue Engineering

Katarzyna Zalewska-Wierzbicka<sup>1</sup>, Joanna Idaszek<sup>1</sup>, Ewa Kijeńska<sup>1</sup>, Manfred Zinn<sup>2</sup>, Wojciech Swieszkowski<sup>1</sup>

<sup>1</sup>Faculty of Materials Science and Engineering, Materials Design Division, Warsaw University of Technology, Woloska 141, Warsaw 02-507, Poland

<sup>2</sup>Life Technologies, University of Applied Sciences Western Switzerland, Route du Rawyl 47/CH-1950 Sion, Switzerland

[katarzyna.wierzbicka@inmat.pw.edu.pl](mailto:katarzyna.wierzbicka@inmat.pw.edu.pl)

### INTRODUCTION

Electrospinning is a versatile technique which enables fibers production from nano to micro size. Production of the fibers can be obtained not only by single needle electrospinning but also by co-axial spinning of two separate solutions. From polymers solution to the electrospun mats with adequate parameters such as voltage, solution concentration, needle to collector distance single fibers and core-shell fibers are produced<sup>1</sup>. Biomedical purposes of electrospun fibers require specific conditions. The fibers should be biocompatible, bioactive and biodegradable. Several materials have been used to fabricate fibers. In our studies we have used novel polyhydroxyalcanoates polymer obtained from biomass and as an additives the protein was incorporated<sup>2</sup>. This material is of the high potential for tissue engineering due to its degradation ratio and non-toxic product hydrolysis (R)-3-hydroxybutyric acid which is a normal constituent of human blood. The main goal for tissue engineering is to design scaffold which can ideally mimic native Extracellular Matrix (ECM). The aim of the studie was to prepare core-shell and single fibers with controlled release of model protein and material cell response to the obtained fibers.

### EXPERIMENTAL METHODS

Electrospun mats were produced using electrospinning with single needle and co-axial method. Nanofibrous mats were analyzed using Scanning Electron Microscopy (SEM) and Confocal Laser Scanning Microscopy (CLSM). Mechanical properties of electrospun fibrous membranes were investigated with electromechanical testing machine. Water contact angle measurements were determined to obtain wettability of produced fiber mats. The cytotoxicity effect of nanofibrous mats was examined. Additionally ATR-FTIR spectrum was recorded. The amount of released protein was evaluated using spectrophotometer UV-Vis. The human Mesenchymal Stem Cells (hMSC) were seeded on the prepared fibers.

### RESULTS AND DISCUSSION

Optimization of electrospinning parameters allowed for proper fiber preparation. By varying different parameters including feeding-rate, polymer concentration and other important parameters for core-shell (CLSM micrographs (Fig. 1)) and single fibers preparation the scaffolds were obtained. The obtained scaffolds can be used in bone tissue engineering with fibers diameters in the range up to 900nm. The ideal scaffold should possess ideal structure mimicking ECM that is why fibers were produced by random electrospinning.

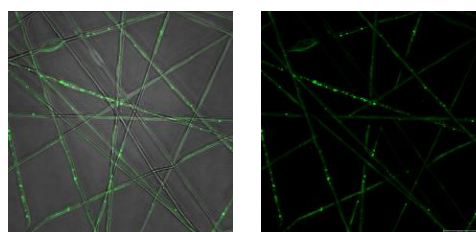


Figure 1. CLSM images of electrospun co-axial nanofibers with FITC-BSA (fluorescein conjugate -bovine serum albumin) in core.

### CONCLUSION

Our studies present the controlled release profiles of the model protein from co-axial and single polyhydroxyalcanoates fibers and its influence to Human Mesenchymal Stem Cells (hMSC) response to the obtained materials. Fibers morphology and designed properties of the obtained material is suitable for bone tissue engineering.

### REFERENCES

1. Kijeńska E. *et al.*, J Biomed Mater Res B Appl Biomater. 100(4):1093-102, 2012
2. Idaszek, J. *et al.*, Mater Sci Eng C Mater Biol Appl. 33(7):4352-60, 2013

### ACKNOWLEDGMENTS

This work was financed by National Science Centre on the basis of a decision number DEC-2011/01/M/ST8/07742.

## Crystal Structure of Calcium Carbonates Influence Osteoclasts Stimulation – Potential Importance of Similarity to the Bone Mineral

Malgorzata Kolodziejczyk<sup>1,2</sup>, Zbigniew Jaegermann<sup>3</sup>, Jaroslaw Sadlo<sup>4</sup>, Malgorzata Lewandowska-Szumiel<sup>1,2</sup>.

<sup>1</sup>Department of Histology and Embryology, Centre for Biostructure Research, Medical University of Warsaw, Poland

<sup>2</sup>Centre for Preclinical Research and Technology, Warsaw, Poland

<sup>3</sup>Institute of Ceramics and Building Materials, Warsaw, Poland

<sup>4</sup>Institute of Nuclear Chemistry and Technology, Warsaw, Poland

[malgorzata.kolodziejczyk@wum.edu.pl](mailto:malgorzata.kolodziejczyk@wum.edu.pl)

### INTRODUCTION

Among the ceramic materials used in bone reconstructive surgery, calcium carbonates are of interest. Not only aragonite – which is the most widely investigated  $\text{CaCO}_3$ , but also calcite, can be taken into account as bone supporting ceramic. Interestingly, although those materials are identical in their chemistry, the difference of the crystallographic form results in different response to the ionizing irradiation – often used for sterilization of medical devices. As revealed by the electron paramagnetic resonance (EPR), radiation sterilization of aragonite induced the presence of a stable signal assigned to the  $\text{CO}_2^-$  – characteristic for bone mineral<sup>1</sup>. In contrast, there are no such paramagnetic centers registered after irradiation of calcite. Since this signal is characteristic for bone mineral we wondered if this phenomenon may be connected with biological activity of the materials. In particular, we focused on the differentiation and maturation of human osteoclasts in contact with both the materials, because these are the cells responsible for involving ceramic substitutes in bone remodeling.

### EXPERIMENTAL METHODS

Two different crystallographic forms of calcium carbonate, i.e. aragonite or calcite were added in the form of a powder to the culture of human osteoclast precursors (Lonza). Both quantitative and qualitative analysis was performed on day 7, 11 and 21. Morphological analysis was based on Tartrate-resistant acid phosphatase staining (TRAP), as well as on Scanning Electron Microscopy examination and time-laps observation. TRAP5b was measured by ELISA and concentration of calcium ions in the supernatants was determined in a colorimetric assay. The EPR analysis both before and after cell culture was performed.

### RESULTS AND DISCUSSION

All the results indicated that aragonite (material exhibiting a bone-like paramagnetic signal after irradiation) have significantly stronger impact on differentiation and maturation of osteoclasts precursors as compared to calcite (material with no  $\text{CO}_2^-$  signal after irradiation). Particularly, in the presence of aragonite powder there were more TRAP-positive multinucleated cells (optical microscopy), which were organized earlier in the culture (time-laps) and finally visible as giant cells in SEM (Fig. 1). It was accompanied by the higher amount of TRAP5b, which is considered as a marker of osteoclasts, in all time

points. Also, the higher concentration of calcium ions in supernatants indicates the more advanced degradation of aragonite as compared to the calcite, which shows the higher osteoclasts activity. Decreasing  $\text{CO}_2^-$  signal in aragonite during the culture additionally confirms its degradation.

The more efficient stimulation of osteoclasts by aragonite as compared to calcite may have some impact on bone remodeling in the presence of  $\text{CaCO}_3$ -based bone substitutes

### CONCLUSION

We demonstrate that osteoclasts differentiation and maturation *in vitro* in the presence of calcium carbonate depends on the crystallographic form of the material. It is more advanced in contact with aragonite, which express the EPR signal characteristic for bone mineral after irradiation, than with calcite, which do not have such a signal.

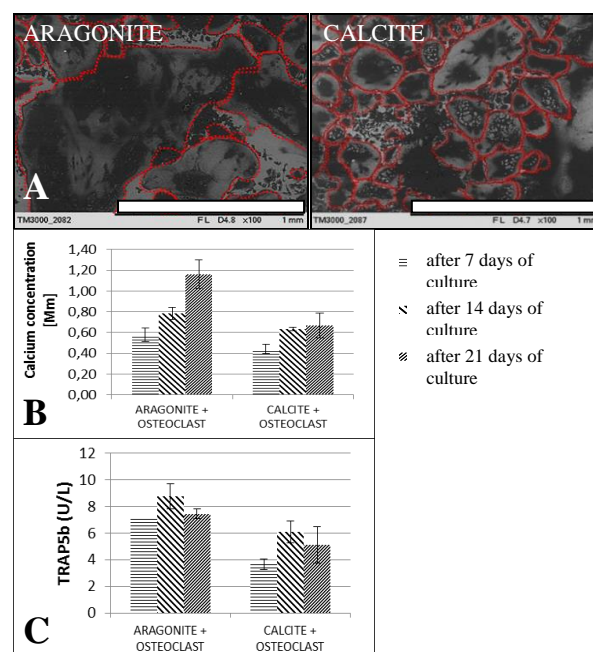


Fig. 1. SEM images of osteoclast after 21 days of culture (A); Concentration of calcium ions (B) and production of TRAP5b in supernatant (C) after 7, 11 and 21 days of osteoclast culture; scale bar, 1mm.

### REFERENCES

1. L. M. de Oliveira et al., Radiation Physics and Chemistry, 61, 485-487, 2001

## Shark Collagen/hydroxyapatite scaffolds Envisaging Biomedical Applications

Gabriela S. Diogo<sup>1,2</sup>, Estefania López<sup>3</sup>, Pio González<sup>3</sup>, Julia Serra<sup>3</sup>,  
Ricardo I. Pérez-Martín<sup>4</sup>, Carmen G. Sotelo<sup>4</sup>, Tiago H. Silva<sup>1,2</sup>, Joana Moreira-Silva<sup>1,2</sup>, Rui L. Reis<sup>1,2</sup>

<sup>1</sup> 3B's Research Group - Biomaterials, Biodegradables and Biomimetics, University of Minho,  
Headquarters of the European Institute of Excellence on Tissue Engineering and Regenerative Medicine,  
AvePark, 4805-017 Barco, Guimarães, Portugal

<sup>2</sup> ICVS/3B's - PT Government Associate Laboratory, Braga/Guimarães, Portugal

<sup>3</sup> New Materials Group, Applied Physics Dpt, Institute of Biomedical Research of Vigo (IBIV), University of Vigo,  
Campus Lagoas-Marcosende, 36310 Vigo, Spain

<sup>4</sup> Instituto de Investigaciones Marinas (CSIC), Eduardo Cabello 6, 36208 Vigo, Spain  
[joana.silva@dep.uminho.pt](mailto:joana.silva@dep.uminho.pt)

### INTRODUCTION

Apatite materials in the form of hydroxyapatite (HA) are very demanded in bone tissue engineering for repairing, replacing or regenerating defects in human bones or teeth due to the similarity in mineral composition. To respond to the current demands in orthopedical and dental repairing of bone defects, new biological sources of HA are being investigated. One of these sources is the shark tooth, which is an abundant by-product of enormous interest. In addition, it is also known that besides hydroxyapatite, shark tooth contains other bioceramic, called fluorapatite, exhibiting improved mechanical properties with respect to HA as a greater stiffness, higher elastic modulus and greater hardness(1).

### EXPERIMENTAL METHODS

Type I collagen was isolated from *Prionace glauca* skin as previously described(2). Apatite granules were obtained through pyrolysis (950°C, 12h) of shark teeth (*Isurus oxyrinchus*, *P. glauca*), followed by a ball milling and sieving processes. Scaffolds with different formulations (collagen:hydroxyapatite ratios of 100:0, 70:30, 50:50, 30:70), were prepared with in situ crosslinking followed by freeze-drying, evaluating two crosslinkers (HMDI and EDC/NHS). Hydroxyapatite grain sizes were 20-63 µm. To evaluate scaffolds stability, structures of each condition were incubated in culture medium for up to 15 days. Bioactivity of the scaffolds was evaluated by immersion in Simulated Body Fluid (SBF) and evaluating the formation of new calcium phosphates by SEM and micro-CT morphological analysis. Mechanical properties were evaluated by compression tests. Cytotoxicity evaluation was performed, addressing cell metabolic activity (MTS assay) and cell proliferation (DNA quantification). The most promising scaffolds in terms of stability, pore size, interconnectivity and bioactivity were chosen for human adipose derived stem cells (hASC) cell seeding, and their ability to promote the differentiation into osteoblast-like cells was evaluated.

### RESULTS AND DISCUSSION

An homogeneously distribution of hydroxyapatite granules into the scaffold structure were confirmed by SEM and micro-CT analysis. Crosslinking of collagen was shown to be more effective with EDC/NHS, producing stable scaffolds in culture medium up to 15 days. Depending on the crosslinking conditions, different porosities, interconnectivities, and mechanical properties were achieved. Scaffolds crosslinked with EDC/NHS were the ones showing less cytotoxicity, being the ones chosen for the assessment of hASCs differentiation.

### CONCLUSION

- Possibility to obtain collagen/apatite composite scaffolds, by valorisation of marine by-products, with an homogeneous distribution of apatite particles;
- Incorporation of apatite particles into the collagen matrix contributed to increase the scaffold stability;
- Mean pore size of these collagen/apatite scaffolds was in the proper range for bone tissue engineering;
- Lower cytotoxicity was demonstrated for EDC/NHS crosslinked scaffolds;
- Scaffolds crosslinked with 12.5% EDC/NHS promoted higher mineralization and their morphological features (pore size, porosity and interconnectivity) make them the best candidate for cell differentiation studies.

### REFERENCES

1. Enax, J. *et al.*, Journal of structural biology 178, 290-299, 2012
2. Fernandes-Silva, S. *et al.*, Macromolecular bioscience 13, 1621-1631, 2013

### ACKNOWLEDGMENTS

Funding from POCTEP Project 0687\_NOVOMAR\_1\_P, Atlantic Area Transnational Cooperation Programme Project MARMED (2011-1/164) and FP7 project POLARIS (REGPOT-CT2012-316331). JMS thank FCT for the Post-Doctoral fellowship financed by POPH/FSE (SFRH/BPD/70230/2010).





Sina Rößler<sup>1</sup>, Christiane Heinemann<sup>1</sup>, Thomas Hanke<sup>1</sup><sup>1</sup>Max Bergmann Center of Biomaterials and Institute of Materials Science,  
Technische Universität Dresden, Dresden, Germany[Sina.Roessler@tu-dresden.de](mailto:Sina.Roessler@tu-dresden.de)

## INTRODUCTION

Implantation of bone graft material into the human body causes a cascade of processes on enzymatic and cellular level. Once implanted, biomaterial gets in contact with blood and leads to the adsorption of proteins. Inflammatory foreign body reaction starts with an acute sterile inflammatory response and changes into a chronic fibrotic response. Macrophages and their precursor cells, monocytes, play a key role in innate immunity. They recognize and attach foreign objects as well as they secrete inflammatory mediators for initiating inflammation<sup>1</sup>.

Recent studies presented the direction of macrophage polarization into pro-inflammatory M1 or anti-inflammatory M2 by engineering morphology of material surface. Particular surface structures in range of micrometer polarize macrophages in the direction of M2 that promotes healing<sup>2</sup>.

The present study refers on macrophage polarization cultured on triphasic silica/collagen/calcium phosphate xerogels.

## EXPERIMENTAL METHODS

Xerogels were produced by sol-gel-process. Tetraethoxysilane (TEOS) was hydrolysed to orthosilicic acid and mixed with a homogenous suspension of fibrillar bovine collagen and a calcium phosphate phase. Calcium phosphate phase was used in defined amount and size ranges. After atmospheric drying of the intermediate hydrogel a xerogel resulted. Surfaces of the samples were investigated using scanning electron microscopy.

Monocytes, isolated from human buffy coats, were matured and polarized into activated macrophages. For maturation basic medium (Dulbecco's MEM alpha modification containing fetal bovine serum, human serum and penicillin/streptomycin) was supplemented by macrophage-colony stimulating factor (M-CSF) was used. Polarization on 2D was performed using basic medium supplemented by interferon- $\gamma$  (IFN- $\gamma$ ) with day five until day seven for M1 direction and supplemented by interleukin-4 (IL-4) for M2 direction. For polarization studies on 3D basic medium was only supplemented by M-CSF. Light microscopy and

confocal laser scanning microscopy (cLSM) was applied for qualitative analysis of cell behaviour.

## RESULTS AND DISCUSSION

By the help of cytokine supported maturation as well as polarization of human monocytes into macrophages, morphology, phenotype and expression of typical M1 or M2 specific proteins were evaluated on 2D (polystyrene) as basis for the cultivation on 3D. Surface structuring of composites based on silica, collagen and calcium phosphate phase influences polarization of human macrophages *in vitro*. First results suggest the hypothesis that larger patterns support M2 phenotype, small patterns promote M1. The results are in accordance with previous studies of Bartneck *et al.*<sup>2</sup>, Garg *et al.*<sup>3</sup> and Paul *et al.*<sup>4</sup> concerning the possibility of modulating macrophage phenotype by surface morphology. So, inflammatory potency of a biomaterial could be influenced by modification of its topography and thus biocompatibility of the implant could be affected<sup>4</sup>.

## CONCLUSION

Controlling immune response affected by macrophages could be a step further in improvement of implant compatibility. The study demonstrated that promoting macrophages with pro- or anti-inflammatory response can be directed by modifying surface topography. Mechanisms which are involved in molecular events of controlling macrophage phenotype by topography are still not known.

## REFERENCES

1. Ma Q. *et al.*, Biomaterials 35:9853-9867, 2014
2. Bartneck M. *et al.*, Acta Biomater. 6:3864-3872, 2010
3. Garg K. *et al.*, Biomaterials 34:4439-4451, 2013
4. Paul N. *et al.*, Biomaterials 29:4056-4064, 2008

## ACKNOWLEDGMENTS

The authors would like to thank Deutsche Forschungsgemeinschaft (DFG) (Collaborative Research Centre TRR79-M03) for financial support.



# Linear Polyglycerol Derivatives with Adjustable LCST and Good Biocompatibility

Daniel Stöbener<sup>1</sup>, Silke Heinen<sup>1</sup>, Tobias Becherer<sup>1</sup>, Qiang Wei<sup>1</sup>, Rainer Haag<sup>1</sup>, Marie Weinhart<sup>1</sup>

<sup>1</sup>Institute of Chemistry and Biochemistry, Freie Universität Berlin, Takustr. 3, 14195 Berlin, Germany  
[daniel.stoebener@fu-berlin.de](mailto:daniel.stoebener@fu-berlin.de)

## INTRODUCTION

Thermoresponsive polymers are of essential relevance for numerous applications in tissue engineering and regenerative medicine (TERM)<sup>1</sup>. Due to their reversible switchability from a hydrophilic to a hydrophobic state by a convenient temperature trigger, these smart materials are of particular importance in the field of cell sheet engineering<sup>2-3</sup>. The key concept of this technique is the attachment and growth of cells on substrates, which have been surface modified with thermoresponsive polymers, at 37°C under standard cell culture conditions. Controlled detachment of confluent grown cell sheets is accomplished by simply cooling below the lower critical solution temperature (LCST) of the thermoresponsive polymer coating<sup>4</sup>. The state of the art coating is based on extensively studied poly(*N*-isopropylacrylamide) (PNIPAAm) which is commercially available on cell culture dishes (UpCell™)<sup>5-7</sup>. However, PNIPAAm coated surfaces suffer from limited biocompatibility. Polymer coatings that have been recently designed to overcome these drawbacks are based on oligo(ethylene glycol) methacrylates (OEGMA)<sup>8-9</sup>.

In this study, we evaluate linear copolymers based on glycerol as a potent alternative to currently applied thermoresponsive materials for cell culture<sup>10</sup>.

## EXPERIMENTAL METHODS

Thermoresponsive poly(glycidyl ethers) were synthesized by anionic ring opening copolymerization (AROP) of glycidyl methyl ether (GME) and ethyl glycidyl ether (EGE) with adjustable comonomer ratios, molecular weights and narrow PDIs ( $\leq 1.2$ ). The cloud points (CP) of the copolymers were determined by turbidimetry measurements ( $\lambda=500\text{nm}$ ) in phosphate buffered saline (PBS, pH 7.4) and cell culture medium (DMEM) with 10% fetal calf serum. NIH/3T3 mouse fibroblast viability was assessed by fluorescent live/dead staining of a harvested cell sheet from thermoresponsive polymer coated gold substrates.

## RESULTS AND DISCUSSION

In our study we synthesized statistical thermoresponsive copolymers using AROP (Fig. 1A). By varying the molar ratios of the monomers GME and EGE we were able to finely tune the CPs of the corresponding polymers by simply adjusting the hydrophobicity of the copolymer side chains.

GME/EGE	0:1	1:5	2:3
CP (PBS)	18.7±0.3°C	23.5±0.3°C	32.8±0.2°C
CP (DMEM)	18.8±0.4°C	25.2±0.5°C	32.6±0.1°C

The cloud points of polymers with varying GME/EGE ratio (0:1, 1:5, 2:3) are given in Table 1 at a

concentration of 0.5 mM in the presence (DMEM) and absence (PBS) of proteins. Turbidity curves demonstrated a very sharp phase transition during multiple heating and cooling cycles as well as negligible hysteresis. Only very small differences in CP temperatures are observed from measurements in the presence and absence of proteins indicating no significant interaction of proteins with the polymers below the LCST.

We further immobilized self-assembled monolayers (SAMs) of these copolymers on gold substrates. Fibroblasts easily attach and grow on these thermoresponsive coatings above the respective LCST of the copolymer and detach spontaneously by simply lowering the temperature. Live/dead staining reveals excellent viability, which provides evidence for the biocompatibility of these switchable surfaces (Fig 1B).

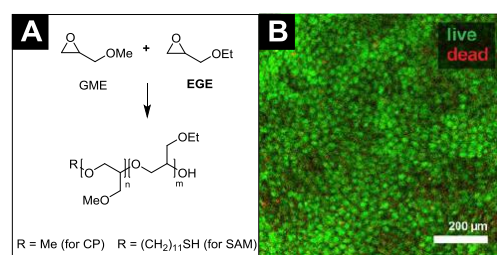


**Figure 1.** (A) Structure of thermoresponsive polyglycidyl ethers. (B) Viability of fibroblasts in a confluent cell sheet grown and harvested on/from a copolymer coated gold substrate using a live/dead assay.

## CONCLUSION

Due to their finely adjustable LCST and their good biocompatibility, thermoresponsive poly(glycidyl ethers) are promising candidates for the application in cell-sheet engineering.

## REFERENCES

1. Langer R. *et al.*, Science 260:920-926, 1993
2. Yamato M. *et al.*, Mater. Today 7(5):42-47, 2004
3. Matsuda N. *et al.*, Adv. Mater. 19:3089-3099, 2007
4. Roy D. *et al.*, Chem. Soc. Rev. 42:7214-7243, 2013
5. Schild H. G., Prog. Polym. Sci. 17:163-249, 1992
6. da Silva R. M. P. *et al.*, Trends Biotechnol. 25(12):577, 2007
7. Kobayashi J. *et al.*, React. Funct. Polym. 73:939-944, 2013
8. Wischerhoff E. *et al.*, Angew. Chem. Int. Ed. 47:5666-5668, 2008
9. Uhlig K. *et al.*, Polymers 6:1164-1177, 2014
10. Weinhart M. *et al.*, Chem. Commun. 47:1553-1555, 2011

## ACKNOWLEDGMENTS

We would like to thank the BMBF (13N13523) for providing financial support to this project.



## Long-term Propagation of Cells in 3D Culture Effects Cell Morphology and Behaviour

Alisha Chhatwal<sup>1</sup>, Stefan Przyborski<sup>1,2</sup>

<sup>1</sup>School of Biological and Biomedical Sciences, Durham University, Durham, UK

<sup>2</sup>Reinnervate Limited, NETPark Incubator, Sedgefield, UK

[stefan.przyborski@durham.ac.uk](mailto:stefan.przyborski@durham.ac.uk)

### INTRODUCTION

Conventionally cells are grown and passaged in 2D. However, 2D growth substrates force cells to flatten and lose their characteristic morphology (Fig 1). Thus, the artificial nature of 2D culture can produce physiologically irrelevant observations of cell behaviour. Using commercially available porous polystyrene Alvetex® Strata scaffolds, a method has been developed to propagate cells continually in 3D, allowing for an observation of the long-term adaptation cells undergo when placed in an *in vivo*-like environment. This is a fundamental question in cell biology and understanding the adaptation process will help elucidate tissue formation. We hypothesise that changes in focal adhesion signalling networks lead to cytoskeletal reorganisation and down-stream perturbation in gene expression, directly linking a more tissue-like morphology to more physiological cell behaviour.

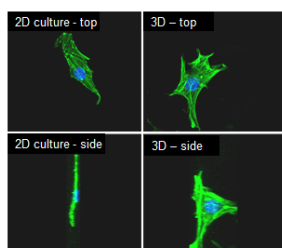


Fig. 1. Cells show a more 3D tissue-like morphology when grown in 3D culture, compared to their 2D counterparts, as indicated by a change in cytoskeletal F-actin staining.

### EXPERIMENTAL METHODS

Using a conventional cell line such as HepG2 hepatocytes, were seeded onto Alvetex® Strata 6-well membranes (5x10<sup>5</sup>) and grown for 5 days in 3D culture. Cells were removed, counted, re-suspended and plated again onto fresh inserts every 5 days. This process was conducted in parallel with HepG2 cells maintained in 2D culture. The phenotype of cells passaged in 2D and 3D was analysed. Data are presented as mean ± SEM.

### RESULTS

Cells maintained in 3D culture adopted rounder morphologies than their 2D counterparts (Fig 2A); this increase in circularity is maintained when cells are re-introduced into 2D, indicating that changes are hard-wired into cells, allowing for priming to 3D culture. This was shown by introducing 2D and 3D maintained cells into a 3D cell-suspension aggregate model (Figs 2B and 2C). 2D and 3D adapted cells behave differently: 3D primed cells show markedly reduced expression of phosphorylated FAK (pFAK) (a key molecule in cell-ECM signalling and indirectly involved in control of cell shape) (Fig 2D).

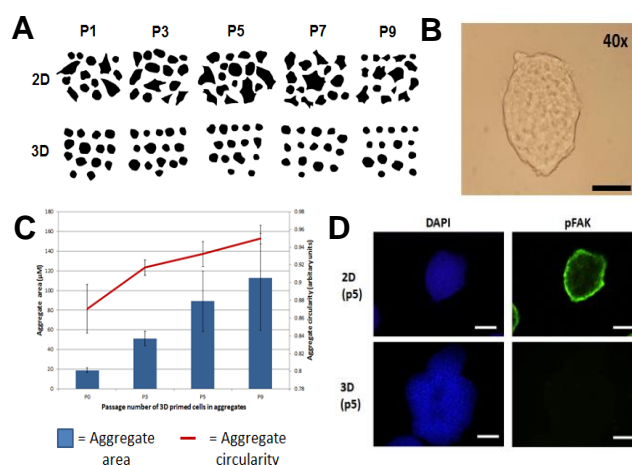


Fig. 2. Cells on Alvetex® Strata adapt to the 3D micro-environment when continually maintained in 3D culture. Cytoskeletal reorganization over the adaptation period allows cells to acquire a rounder 3D phenotype (A). Cells become primed to 3D culture environments (B,C), and show differences in FAK signalling (D).

### DISCUSSION & CONCLUSIONS:

Cells primed for 3D growth maintained morphologies that more closely resemble primary tissue. The reduction in pFAK in 3D appears to be due to a switch in signalling pathway brought about by the change in physical microenvironment. Differences seen in aggregates grown from 2D and 3D primed cells are possibly due to changes in cell adhesion and cell-ECM signalling, a hypothesis supported by the change in pFAK expression which correlates with lower levels in real tissues. Further work into this pathway will show how cells adapt to 3D culture. Such mechanisms are fundamental to understanding tissue formation.

In conclusion, we have developed technology that enables cells to continually be propagated in 3D culture. We have demonstrated how cells adapt to these environmental changes and acquire a more 3D architecture that results in important molecular changes within the cells. We propose to develop this technology further to routinely propagate cells in 3D culture so that they are primed ready for subsequent analysis in 3D in vitro models and transplantation. This will have important implications for enhancing the predictive accuracy of in vitro assays and priming cells for transplantation in tissue engineering applications.

### ACKNOWLEDGMENTS

The authors would like to thank the BBSRC and the CASE partner, Reinnervate Limited, for providing financial support to this project.

## Electrospinning of a Chitosan Based Artificial GAG for Tissue Engineering Application

Safa Ouerghemmi<sup>1</sup>, Stéphanie Degoutin<sup>1</sup>, Nicolas Tabary<sup>1</sup>, Frédéric Cazaux<sup>1</sup>, Ludovic Janus, Feng Chai<sup>2</sup>, Nicolas Blanchemain<sup>2</sup>, and Bernard Martel<sup>1</sup>

<sup>1</sup>Unité Matériaux et Transformations (UMET) UMR CNRS 8207, University of Lille, France

<sup>2</sup>INSERM U1008, Controlled Drug Delivery Systems and Biomaterials, University of Lille, France

[safa.ouergemmi@ed.univ-lille1.fr](mailto:safa.ouergemmi@ed.univ-lille1.fr)

### INTRODUCTION

Glucosaminoglycans (GAGs) are polysaccharides of the extracellular matrix that play an important role in the proliferation and the differentiation of cells. Therefore, GAGs are often used as scaffolds for tissue engineering applications. Among the artificial scaffold elaboration processes, electrospinning is one of the most convenient approaches as the obtained nanofibrous mats mimic the structure of the extracellular matrix. As GAGs such as chondroitin sulphate, hyaluronic acid and heparin carry sulphate, aminosulfate, carboxylic groups, we imagined the concept of an artificial GAG, based on chitosan (CHT), whose amino groups were partially substituted by a disulfonated benzyl group (CHT2S) [1]. CHT2S was firstly characterized by FTIR and NMR, and then electrospun mixed with the minimal necessary polyethylenoxyde (PEO) ratio.

### EXPERIMENTAL METHODS

**Synthesis of CHT2S:** CHT (5g) was dissolved in 500 ml of 0.5% of aqueous solution of acetic acid. Methanol (650 ml) was added to the chitosan solution. Sodium cyanoborohydride (NaBH<sub>3</sub>CN) (10g) was dissolved in the solution under vigorous stirring and after 3 min aldehyde (4-formyl-1,3-benzenedisulfonic acid, disodium salt dissolved in 150ml of water was added. The resulting precipitate was filtered and washed with water and dried, yielding a powder [1].

**Electrospinning:** 7.6wt% of CHT2S/Polyethylene oxide (PEO) mixtures with different ratios (5/5, 6/4 and 7/3 (w/w)) were dissolved in 0.05M of NaOH aqueous solution. The solution was spun with a flow rate of 0.3ml/h using a syringe pump applying a voltage ranging from 10 to 20kV. The tip to-collector (grounded aluminium foil) distance was varied from 20 to 25 cm. The temperature and the relative humidity in the chamber were set at 20°C and 30%, respectively.

**Crosslinking:** The electrospun mats were exposed to glutaraldehyde (GA) vapour for 24h and then rinsed with water.

**Characterizations:** The chemical composition and the quantification of the degree of substitution of the glucosamine units of CHT were evaluated by Fourier Transform Infrared Spectroscopy (Perkin Elmer Spectrum one FTIR-ATR instrument) and <sup>1</sup>H NMR. The morphology of the chrome sprayed nanofibres was observed with a scanning electronic microscopy (Hitachi S-4700 SEM) operating with an acceleration voltage of 5 kV.

### RESULTS AND DISCUSSION

The chemical structure of the CHT-2S is represented in figure1.

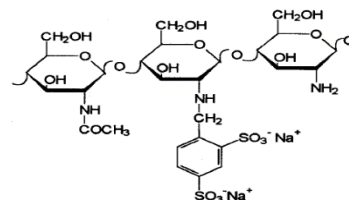


Figure 1:  
Chemical  
structure of  
CHT2S

The CHT2S structure was confirmed by FTIR thanks to the new bands relative to sulfonic acid hydrates at 2400-2000 cm<sup>-1</sup> and 1230-1235 cm<sup>-1</sup>, and to substituted benzene groups below 800 cm<sup>-1</sup>. NMR spectrum evidenced the presence of the grafted aromatic substituent through peaks appearing above 7ppm and signals integrations revealed a degree of substitution of the CHT glucosamine repeat units in the range of 66.5%.

Nanofibres with bulbs were obtained (fig 2c) for the weight ratio CHT2S/PEO 7/3, therefore it was necessary to lower this ratio down to 6/4 and 5/5 to obtain perfect nanofibres (fig 2a-b)).

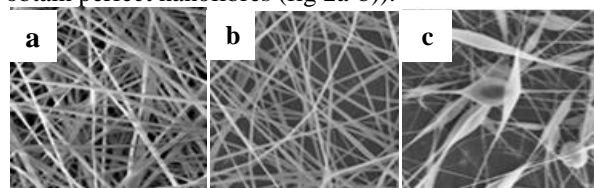


Figure 2: SEM observations of nanofibres obtained with different CHT-2S/PEO mass ratio a) 5/5 b) 6/4 c) 7/3

Furthermore, the electrospinning process parameters were investigated. It was observed that the increase of the tip to-collector distance from 20cm to 25cm allow to obtain bulb-free nanofibres. We noticed, that the greater the flow rate, the more polydispersed nanofibres diameters we obtained.

SEM analysis displayed that GA crosslinking improved the stability of the electrospun mats as the nanofibrous structure resisted to a prolonged stay in water and in PBS buffer (pH7.4). Cytocompatibility study and cell proliferation tests with fibroblasts NIH3T3 are now in progress in order to evaluate the biological properties of our obtained membranes and will inform on the relevance of this concept of CHT based artificial GAG.

### CONCLUSION

Stable and defect-free nanofibres were obtained by electrospinning of an artificial GAG, synthesized after chitosan modification, mixed with PEO. The obtained membranes are a suitable candidate for tissue engineering application.

### REFERENCES

[1] Martel *et al.*, *J Appl Polym Sci*, 59, 647-654 (1996)

### ACKNOWLEDGMENTS

The authors acknowledge University of Lille 1, region Nord-Pas-de-Calais and Federation Chevreul for their financial support.



## Electrospun Piezoelectric P(VDF-TrFE) Scaffolds and the Effect of Electrical Stimulation for Tendon Tissue Regeneration

Gemma Orpella-Aceret<sup>1</sup>, Marc A. Fernandez-Yague<sup>1</sup>, Matteo Palma<sup>2</sup>, Dimitrios Zeugolis<sup>1</sup>, Abhay Pandit<sup>1</sup> and Manus J. P. Biggs<sup>1</sup>

<sup>1</sup> Network of Excellence for Functional Biomaterials (NFB), National University of Ireland Galway

<sup>2</sup>Department of Chemistry, School of Biological and Chemical Sciences, Queen Mary, London

[gemma.orpella@gmail.com](mailto:gemma.orpella@gmail.com)

### INTRODUCTION

Tendon regeneration remains an important challenge in the field of tissue engineering. Up until recently, materials scientists have concentrated upon the physical characteristics of scaffolds (modulus, strength, stiffness), and more recently on chemistry and nanotopographical modification which can perturb or enhance cellular adhesion<sup>1</sup>.

Piezoelectric materials are promising as they can exploit the loading capacity of tendon tissue to produce stimulating current for tendon regeneration. Evidence is gathering on the complexity of the tendon electromechanical environment, and in particular collagen mediated streaming potentials and electric fields<sup>2</sup>. Polyvinylidene Fluoride Trifluoroethylene P(VDF-TrFE) is a polymer ferroelectric material that has piezoelectric properties that can be used to stimulate tendon tissue regeneration through electrical outputs. These scaffolds were assessed for piezoelectricity and compatibility with human dermal fibroblasts (HDF) and human primary tenocyte cells (HPT).

### EXPERIMENTAL METHODS

P(VDF-TrFE) was dissolved in DMF/Acetone and electrospun into fine fibers by varying the voltage, mandrel rotation speed and the distance between tip and collector with a constant flow rate. The scaffold morphology was studied by Field Emission Scanning Electron Microscopy (FESEM) and the electrical properties in response to cyclic loading were assessed with piezoresponse force microscopy (PFM).

HDF were used for optimization process and seeded onto the scaffolds for 1, 3 and 7 days under static and dynamic loading conditions and glass was used as main control. The cell viability of the cells was assessed by cell nuclei counting, and the metabolic activity of the cells was assessed by alamarBlue<sup>®</sup> assay. The analysis of focal adhesion formation was performed via vinculin labelling and samples were also stained for actin using rhodamine phalloidin and DAPI for nucleus. The alignment of the cells in the scaffolds was assessed using fluorescence images. Subsequent genomic profiling via RT-PCR to assess cell adhesion and phenotype maintenance, respectively with Human Primary Tenocytes was also conducted.

### RESULTS AND DISCUSSION

By varying the electrospinning parameters, it was possible to produced nanofibers with similar dimensions as collagen fibers and what is more, high aligned fibers. Furthermore the electrical output of the scaffold in response to mechanical loading was demonstrated with PFM. Finally, cytocompatibility studies showed high cell viability and alamarBlue<sup>®</sup> assay showed no difference in cell metabolic activity over all time points relative to control. Moreover, the cells growth parallel to the direction of the fibers showing high alignment.

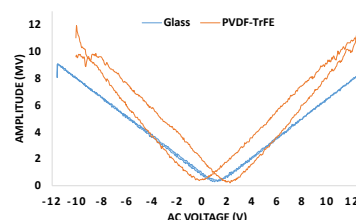


Fig. 1- Characteristic hysteresis loop (butterfly loop) indicating ferroelectricity in PVDF-TrFE fibers.

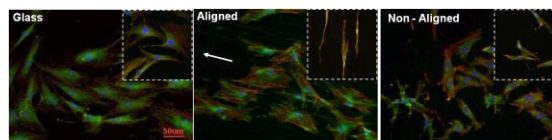


Fig. 2 – Human dermal fibroblasts cultured on glass, P(VDF-TrFE) aligned and non-aligned scaffolds, showing the alignment of the cells parallel to the direction of the fibers.

### CONCLUSION

P(VDF-TrFE) demonstrate a piezoelectric response has a positive effect on cell adhesion. Moreover, high cell viability and no cell toxicity were confirmed by Live and Dead<sup>®</sup> assay. The scaffolds induced cellular alignment and promoted cell attachment.

### REFERENCES

1. Lomas AJ. *et al.*, Advanced Drug Delivery Reviews In press, 2014.
2. Minary-Jolandan M. *et al.*, Nanotechnology 20: 085706, 2011.

### ACKNOWLEDGMENT

Science Foundation of Ireland SIRG COFUND11/SIRG/B2135

## Highly Porous Silica Aerogel-Based Bioactive Composite Materials as Potential Scaffolds for Bone Regeneration

Farkas Kerényi<sup>1</sup>, Andrea Kuttor<sup>1</sup>, István Tombácz<sup>1</sup>, Ágnes Baráthné Szabó<sup>1</sup>, István Lázár<sup>2</sup>, Csaba Hegedűs<sup>1</sup>

<sup>1</sup> Faculty of Dentistry, Department of Prosthetic Dentistry and Biomaterials, University of Debrecen, Hungary

<sup>2</sup> Faculty of Science, Department of Inorganic and Analytical Chemistry, University of Debrecen, Hungary  
[kerenyi.farkas@dentel.unideb.hu](mailto:kerenyi.farkas@dentel.unideb.hu)

### INTRODUCTION

Improving materials for bone regeneration are needed in medicine including prosthetic dentistry. Ameliorating biodegradable and bioactive materials supporting bone regeneration could satisfy this demand.<sup>1</sup>

Aerogels are used, among others, as tissue engineering materials.<sup>2</sup> Calcium phosphates, such as hydroxiapatite (HA) and  $\beta$ -tricalcium phosphate ( $\beta$ TP) have been described as bioactive and osteoinductive materials.<sup>3</sup>

SAOS-2 is a widely used and well characterized osteosarcoma derived cell line for in vitro osteoblast differentiation studies.<sup>4,5</sup>

The aim of this study was to examine newly developed aerogel-based composite materials if they are suitable for bone regeneration.

### EXPERIMENTAL METHODS

Highly porous composite materials made of  $\beta$ TP and/or HA, combined with silica based aerogel, was developed.<sup>6</sup> Five different ratio of  $\beta$ TP and HA was used to prepare this aerogel composite as follows: 100%  $\beta$ TP, 75%  $\beta$ TP and 25% HA, 50%  $\beta$ TP and 50% HA, 25%  $\beta$ TP and 75% HA, 100% HA.

SAOS-2 cells were seeded on the composites' surface. The differentiation of SAOS-2 cells to osteoblast were examined by laser scanning microscopy, qRT-PCR and western blot after 1, 2 and 3 weeks.

### RESULTS AND DISCUSSION

Five differently synthesized aerogel composite materials were used. Confocal imaging and gene expression analyses showed osteoblastic differentiation: collagen I and bone sialoprotein were

secreted and some of the measured osteoblast-differentiation specific gene expression (Runx2, BMP-2, osterix, osteopontin) were changed.

In a preliminary experiment, aerogel composite put into rat femur showed early signs of osteointegration.

Our result suggest that these aerogel-based composite materials are able to trigger differentiating of SAOS-2 cells to osteoblast.

### CONCLUSION

According to the results of our experiments, these aerogel composite materials could be used as a scaffold material for bone regeneration in dentistry.

### REFERENCES

1. Tan L. *et al.*, J. Mater. Sci. Technol. 29: 503-513, 2013
2. Bernik D. L., Recent Pat Nanotechnol. 1:186-92, 2007
3. Al-Sanabani J. S. *et al.*, Int. J. Biomater. 2013: 876132, 2013
4. Ayobian-Markazi N. *et al.*, Dent. Res. J. (Isfahan) 9: 86-92, 2012
5. Czekanska E. M. *et al.*, Eur. Cell. Mater. 24:1-17, 2012
6. Kuttor *et al.*, Front. Mater. Sci. 8:46-52, 2014

### ACKNOWLEDGMENTS

The authors would like to thank the European Union (Grant No.: TAMOP-4.1.1C-13/1/KONV-2014-0001) for providing financial support to this project.

# Fabrication and Evaluation of $\beta$ -TCP/ZrO<sub>2</sub>-Doped-Phosphate Bioglass Scaffolds for Bone Tissue Engineering

Ena A. Aguilar-Reyes<sup>1</sup>, Criseida Ruiz-Aguilar<sup>1</sup>, Carlos A. León-Patiño<sup>1</sup>, Ana E. Higareda-Mendoza<sup>2</sup>

<sup>1</sup>Instituto de Investigación en Metalurgia y Materiales, Universidad Michoacana de San Nicolás de Hidalgo, México

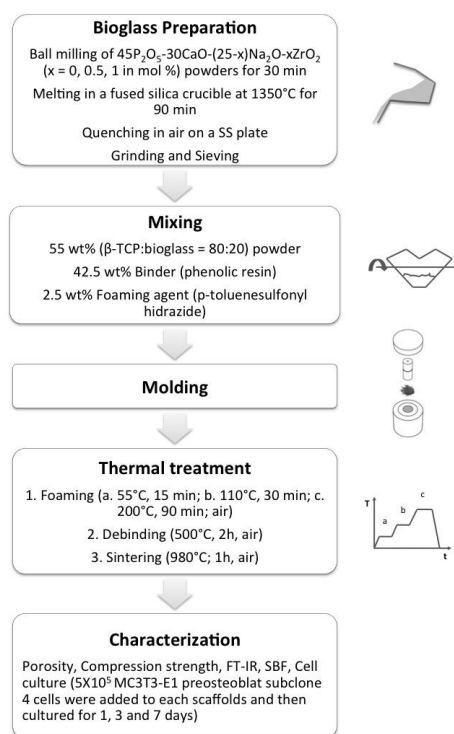
<sup>2</sup>Facultad de Ciencias Médicas y Biológicas, Universidad Michoacana de San Nicolás de Hidalgo, México

[aareyes@umich.mx](mailto:aareyes@umich.mx)

## INTRODUCTION

Scaffolds are an excellent alternative to regenerate bones; for this purpose they have to fulfill requirements such as biocompatibility, osteoconductivity, porosity, mechanical properties, controlled degradation, and formability. Beta-tricalcium phosphate ( $\beta$ -TCP) ceramics are biocompatible and osteoconductive materials that offer a chemical environment and a surface conducive to new bone formation. These are brittle materials and have low fracture resistance. Thus, it is necessary to add reinforcement materials to improve their properties.<sup>1-3</sup>

## EXPERIMENTAL METHODS



## RESULTS AND DISCUSSION

As-sintered scaffolds are presented in Table 1.

**Table 1.** Properties for sintered TCP/bioglass scaffolds.

Scaffold	Porosity (%)	Compression Strength (MPa)
SZ0 (0% ZrO <sub>2</sub> )	68-73	0.6
SZ0.5 (0.5% ZrO <sub>2</sub> )	75-86	1.4
SZ1.0 (1% ZrO <sub>2</sub> )	72-85	2

After immersion of scaffolds in SBF, FT-IR technique corroborated the main groups of HA phase at values of 1382, 1214 y 452 cm<sup>-1</sup> characteristic of CO<sub>3</sub><sup>2-</sup>, 3422 cm<sup>-1</sup> corresponding to OH<sup>-</sup> and 900-1200 cm<sup>-1</sup> corresponding to PO<sub>4</sub><sup>3-</sup>. HA phase can be also observed in the SEM images at 7 days of immersion in SBF, Fig. 1 (b), (d) and (f).

Cell adhesion and interaction with the scaffold surface of MC3T3-E1 preosteoblast subclone 4 cells 3 days is observed in Fig. 1 (a), (c), and (e).

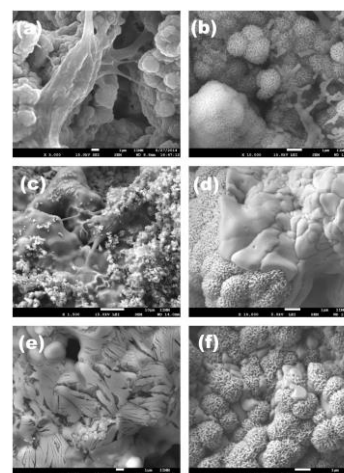


**Fig. 1.** SEM images from as-sintered scaffolds after in vitro acellular and cellular tests.

## CONCLUSION

Beta-tricalcium phosphate mixed with ZrO<sub>2</sub>-doped phosphate bioglass seems to be a promising material for bone tissue engineering applications because of their physical and mechanical properties and biological response.

## REFERENCES

1. Cai, S. et al., *J Mater Sci.*; 20: 351-358, 2009.
2. Lou T. et al., *Int J Biol Macromol.*; 69C: 464-470, 2014.
3. Dorozhkin S V. *Biomaterials.*; 31(7): 1465-1485, 2010.
4. Ebrahimi M. et al., *J Biomed Mater Res A.* 100(9): 2260-2268, 2012.

## ACKNOWLEDGMENT

The authors would like to thank CONACYT (Grant no. CB-2013-C01-222262) and UMSNH (Grant no. CIC-2014-2015-108681) for providing financial support to this project.

## Biocompatibility Study of Polylactide Composites with Iron Oxide Nanoparticles

Katarzyna Nowicka<sup>1</sup>, Anna Wiecheć<sup>2</sup>, Marta Błażewicz<sup>1</sup>

<sup>1</sup>AGH-University of Science and Technology, Faculty of Material Science and Ceramic, Department of Biomaterials, Krakow, Poland

<sup>2</sup>The Henryk Niewodniczanski Institute of Nuclear Physics, Polish Academy of Sciences, Krakow, Poland  
[nowicka@agh.edu.pl](mailto:nowicka@agh.edu.pl)

### INTRODUCTION

Magnetite nanoparticles ( $\text{Fe}_3\text{O}_4$ ) due to their physico-chemical properties currently belong to the most interesting materials considered for applications in medicine and biotechnology. The magnetic nanoparticles possess very low toxicity on the living cells [1]. They are used, among others, to enhance contrast in magnetic resonance imaging (MRI), in drug delivering system, in diagnosis and treatment of tumours [2,3,4]. Magnetite can also be used to modify polymer matrix of implantation materials. This work demonstrates an assessment of thermal and surface properties and also degradation process of composite materials consist of polylactide matrix and 0,5%wt magnetite nanoparticles. Biological tests were performed in MG63 cell cultures

### EXPERIMENTAL METHODS

The influence of added nano-size magnetite nanoparticles on polymer matrix were studied with differential scanning calorimetry (DSC). Composite was incubated in distilled water and artificial biological environment. During incubation measurements of pH and fluid conductivity were performed. The composites surface wettability was studied by measuring the contact angle (static drop method). Free surface energy was determined by Owens–Wendt method using double distilled UHQ water and diiodomethane. The roughness was measured using a static profilometer with ceramic head.

### RESULTS AND DISCUSSION

Thermal analysis confirmed that there were not significant differences between properties magnetite nanocomposites and pure polymer. We noticed slight increase of crystallinity degree (Table 1).

Table 1: Degree of crystallinity for polymer and its composite.

Parametr	PLA	PLA/0,5% $\text{Fe}_3\text{O}_4$
$W_c$ [%]	14,16	15,01

The magnetite addition to PLA does not significantly affect the change of the contact angle (wettability of

materials surface and also the surface tension. The roughness profile for the pure polymer was under 0,2  $\mu\text{m}$ , and the composite value increased to approx. 0,5  $\mu\text{m}$ . We noted slight differences in the values of both the contact angle and the surface roughness for different side of the sample. The pure polymers and composites incubation in water and artificial biological environment by six weeks revealed influence of the materials on the pH and conductivity of the medium. However, the biological study indicated no cytotoxicity effect of polymers and their composites.

### CONCLUSION

The addition of magnetite to the polymer matrix may give new properties. In our study addition of magnetite slightly changed properties of the composite such as surface properties, magnetic, mechanical or biological. We demonstrate that composites with 0,5%wt magnetite nanoparticles are comparatively little better surface properties. Also stable conditions during cell culture confirmed that applied materials can be successfully used as implants. The biological study confirm the materials have no cytotoxic properties. We conclude that polylactide modified with magnetite is biocompatible material.

### REFERENCES

1. M.E. Kafayati *et al.*, Iran J Biotech., 11, 1-13, 2013.
2. Y. Xin *et al.*, J. Magnetism and Mag. Mat., 381, 21-27, 2015
3. S. Sasikala *et al.*, Powder Tech., 266, 321- ,2014.
4. H. Jian-Yuan *et al.*, Ceramics Int., 41, 2399-2410, 2014

### ACKNOWLEDGMENTS

This work was financed from statutory works of AGH (No 11.11.160.616)





## In Situ Patterning of Collagen by Laser-Assisted Bioprinting Guides HUVECs Alignment and Promotes the Creation of Capillary-Like Structures

Olivia Kérourédan<sup>1,2</sup>, Jérôme Kalisky<sup>1</sup>, Murielle Rémy<sup>1</sup>, Emeline Pagès<sup>1</sup>, Joëlle Amédée<sup>1</sup>, Jean-Christophe Fricain<sup>1,2</sup>, Sylvain Catros<sup>1,2</sup>, Raphaël Devillard<sup>1,2</sup>

<sup>1</sup>INSERM, U1026 BioTis, University Bordeaux, Bordeaux F-33076, France

<sup>2</sup>Faculty of Dentistry, University Bordeaux, 16-20 Cours de la Marne, Bordeaux F-33076, France

[fricainj@aol.com](mailto:fricainj@aol.com)

### INTRODUCTION

Development of microvasculature and microcirculation is critical for bone tissue engineering<sup>1</sup>. To resolve the issue of a reduced vascular component, the reproduction of local microenvironment and the organization of cells are regarded as ultimate goals<sup>2</sup>. In biofabrication, parallel to inkjet printing and pressure-operated mechanical extruders, the Laser-Assisted Bioprinting (LAB) is an alternative method for the assembly and micropatterning of biomaterials and cells<sup>3</sup>. This technology allows fabrication of 2 and 3 dimensional tissue engineering constructs<sup>4</sup>. The objective of this work was to pattern Human Umbilical Vein Endothelial Cells (HUVEC) by seeding them on collagen patterns obtained by LAB, in order to promote the creation of tailor-made capillary-like structures with small diameter up to 30  $\mu\text{m}$ .

### EXPERIMENTAL METHODS

The LAB workstation used in this study comprised an infra-red laser ( $\lambda=1064$  nm, 30 ns), focused on a quartz ribbon that was coated with a thin absorbing layer of gold (60 nm) and a 30  $\mu\text{m}$  layer of collagen. This system was used to print collagen type I lines on agarose. HUVECs, obtained from cord blood, were seeded on these collagen patterns. The viability of cells, cytoskeleton and tubular organization were assessed by immunofluorescence at 2h, 24h, 48h and 72h.

### RESULTS AND DISCUSSION

The patterning of HUVECs in collagen was achieved with dimensions of 10mm length and width from 30 to 200  $\mu\text{m}$ .

Figures 1A and 1B show that HUVECs were adherent to collagen patterns after 2 hours in culture, and that morphology of the cells changed after 24 hours, respectively.

Figures 1C and 1D reveal respectively that the patterns were preserved after 48 hours and that HUVECs formed capillary-like structures after 72 hours. Diameter of the structure decreases during the process of cell organization and leads to small capillary-like structure. These results imply that LAB allows printing of collagen with micrometric resolution and organizing HUVECs when seeded on these collagen patterns.

Capillary-like structures can then be created on other hydrogels and will be included in 3D structures in order to promote angiogenesis.

### CONCLUSION

This study demonstrates that LAB is a relevant method for micropatterning HUVECs with an indirect method and is adapted to promote the creation of vascular-like structures and to control their distribution. Moreover, other applications could be developed, namely in neurogenesis.

### REFERENCES

1. Santos MI *et al.*, Macromol Biosci. 10(1):12-27, 2010
2. Anderson DE *et al.*, Ann Biomed Eng. 39(9):2329-45, 2011
3. Guillemot F. *et al.*, Acta Biomater. 6(7):2494-500, 2010
4. Guillotin B. *et al.*, Trends Biotechnol. 29(4):183-90, 2011

### ACKNOWLEDGMENTS

The authors would like to thank the IFRO for providing financial support to this project.

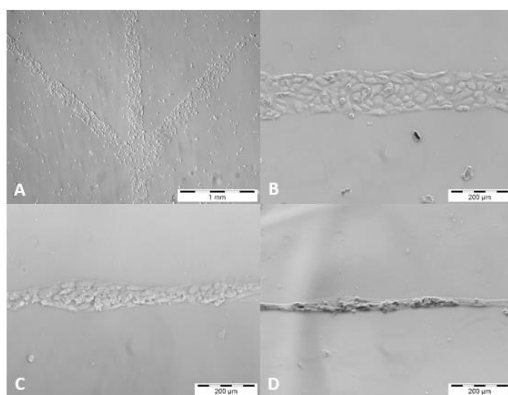


Fig.1. HUVECs seeded on collagen type I patterned by LAB: (A) 2h post-seeding (B) 24h post-seeding (C) 48h post-seeding (D) 72h post-seeding

Liga Stipniece<sup>1</sup>, Kristine Salma-Ancane<sup>1</sup>, Dagnija Loca<sup>2</sup><sup>1</sup> Institute of General Chemical Engineering, Riga Technical University, Latvia<sup>2</sup> Rudolfs Cimdins Riga Biomaterials Innovations and Development Centre, Riga Technical University, Latvia[Liga.Stipniece@rtu.lv](mailto:Liga.Stipniece@rtu.lv)

## INTRODUCTION

The focus of this work is to understand the influence of Sr ions on the physicochemical properties of resorbable biphasic calcium phosphate (BCP) bioceramics composed of a controlled mixture of hydroxyapatite (HAp) and  $\beta$ -tricalcium phosphate ( $\beta$ -TCP) with special emphasis toward degradation. It has been established that HAp and  $\beta$ -TCP differ in degradation rates.  $\beta$ -TCP shows good ability to biodegrade up to 10-20 times faster than HAp, but in an unpredictable manner, so it may not provide solid scaffolding for new bone formation<sup>1,2</sup>. However, BCP is able to gradually degrade, leaving room for natural bone<sup>3</sup>.

In this work, at constant Ca/P ratio, we have varied Sr content and studied physicochemical properties and degradation behaviour of those compositions.

## EXPERIMENTAL METHODS

Calcium deficient hydroxyapatite (CDHAp) powders containing various amounts of Sr were synthesized through neutralization route. Starting suspensions of  $\text{Ca}(\text{OH})_2$  and/or  $\text{Sr}(\text{OH})_2$  were prepared of CaO and/or SrO, and deionised  $\text{H}_2\text{O}$  by “lime slaking” process followed by homogenization in planetary ball mill. Aqueous solution of 2 M  $\text{H}_3\text{PO}_4$  was added to starting suspensions at a slow addition rate ( $\sim 1$  ml/min). Synthesis temperature was maintained constant at 45 °C. Precipitates were left overnight to mature, filtered and dried at 105 °C for  $\sim 24$  h.

Obtained powders were uniaxially pressed ( $p=15$  kN) in cylindrical pellets ( $\varnothing$  20 mm) and sintered in air atmosphere at 1150 °C for 2 h.

Phase compositions of the CDHAp powders, pure BCP and Sr-containing BCP (Sr-BCP) were determined by X-ray diffraction analysis (XRD). Specific surface area (SSA) of the CDHAp powders was determined by BET method using nitrogen ( $\text{N}_2$ ) as an adsorbate. The bioceramics were examined using field emission scanning electron microscopy (FE-SEM) with incorporated energy dispersive X-ray spectroscopy (EDS) for microstructure and chemical analysis, respectively.

For degradation experiments the bioceramics were placed in polystyrene bottles containing Tris-HCl buffer solution. The bottles with the bioceramics and Tris-HCl were maintained at 37 °C for 3, 7, 21 and 28 days, respectively. Microstructural degradation in Tris-HCl was also observed as a function of time. The chemical dissolution of each bioceramic composition was measured by its release of Ca ions into a buffered solution.

## RESULTS AND DISCUSSION

In the case of Sr-containing CDHAp, the XRD peaks were found to be broader and less intense when compared to pure system (Fig. 1). This indicates the reduced crystallinity and size of the Sr-containing CDHAp crystallites due to partial substitution of Ca by Sr. Moreover, XRD analysis confirmed the formation of BCP with different HAp and  $\beta$ -TCP ratios after sintering at 1150 °C depending upon the Sr content.

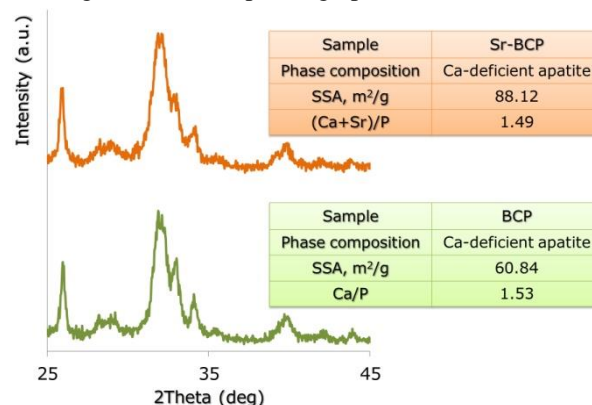


Fig.1. XRD patterns of pure (green) and Sr-containing (orange) CDHAp powders

*In vitro* degradation tests showed that BCP bioceramics containing Sr is associated with higher degradation and dissolution than pure CaP with the same phase composition.

## CONCLUSION

The results proved that the phase composition of HAp and  $\beta$ -TCP in the prepared bioceramics is dependent on the initial Ca deficiency of the precursor powders. The presence of Sr reduced the nucleation and growth rate of CDHAp crystals when compared to pure system. Results showed that resorbable characteristics of BCP can be tailored by adding Sr.

## REFERENCES

1. Wiltfang J., *et al.* J. Biomed. Mater. Res. Appl. Biomater. 63:115–121, 2002
2. Yuan H., *et al.* J. Mater. Sci.: Mater. Med. 12:7-13, 2001
3. Li Z.Y. *et al.*, Biomaterials 28:1452-1460, 2007

## ACKNOWLEDGMENTS

This work has been supported by the EuroNanoMed II JTC2014 project „PhOtocrosslinked hydrogels for guided periodontal TissUe REgeneration” (POStURE).

Lenka Kohutová<sup>1,2</sup>, Lucie Wolfová<sup>1</sup>, Martin Pravda<sup>1</sup>, Ivana Ščigalková<sup>1</sup>, Julie Bystroňová<sup>1</sup>, Vladimír Velebný<sup>1</sup>

<sup>1</sup>Contipro Biotech s.r.o., Dolní Dobrouč, Czech Republic

<sup>2</sup>Brno University of Technology, Faculty of Chemistry, Purkyňova 464/118, Brno, Czech Republic

[Lenka.Kohutova@contipro.com](mailto:Lenka.Kohutova@contipro.com)

## INTRODUCTION

One of promising application of hyaluronan (HA) is a development of hydrogel-based materials for use in biomedicine or tissue engineering.

In our previous work we presented new designed hyaluronan-tyramine derivatives (HA-TA), which are capable to form covalently crosslinked hydrogels with addition of horseradish peroxidase (HRP).<sup>1</sup> In this work crosslink reaction is initiated by highly diluted H<sub>2</sub>O<sub>2</sub> or enzymatic generated H<sub>2</sub>O<sub>2</sub>. We designed two systems of H<sub>2</sub>O<sub>2</sub> generators which led to hydrogelation of HA-TA solution. First system used H<sub>2</sub>O<sub>2</sub> generated by reaction of glucose (Glu) catalysed by glucose oxidase (GOx) and the second system used galactose (Ga) catalysed by galactose oxidase (GaO). Advantages and disadvantages of these three systems are evaluated in this work.

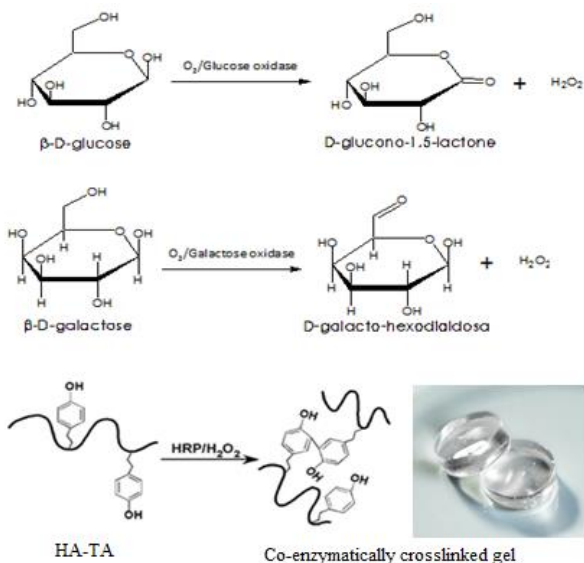


**Figure 1** Schemes of H<sub>2</sub>O<sub>2</sub> generation which led to hydrogelation of HA-TA solution.

## EXPERIMENTAL METHODS

Influence of enzymes concentrations (HRP, GaO, GOx) on gelation time and mechanical properties has been studied. The gel point (GP) was measured as the time at which the elastic moduli  $G'$  and viscose moduli  $G''$  were equal. Cross over point was determined at 37 °C. Following parameters were evaluated for hydrogel

mechanical properties: Young's modulus, compressive stress at breaking point and toughness. Measuring of mechanical properties has been repeated 3 times with variability  $\pm 10\%$ .

## RESULTS AND DISCUSSION

In situ forming hydrogels present a valuable system for cell or drug delivery in the field of regenerative medicine. For proper cell proliferation, it is necessary to ensure sufficient mechanical strength of hydrogels. Rapid gel formation prevents undesirable leakage of delivered material out of implantation, which could be used to fill out defects e.g. to regenerate articular cartilage or bone. HRP mediated crosslink of HA-TA derivatives initiated by addition of highly diluted H<sub>2</sub>O<sub>2</sub> leads to formation of hydrogels with desirable properties. The system allows preparation of hydrogels with wide range of mechanical properties from soft, viscous, tough to hard gels, which can be used as cell scaffolds.

The system of Glu-GOx is a promising approach for preparation in situ crosslinkable HA-TA hydrogels, mainly because gelation can occur in contact with human blood. Gelation rate ranges from slow to fast, depending mainly on the enzyme activity (HRP and GOx). This system is suitable for preparation of injectable acellular hydrogels.

Ga-GaO system is more suitable for prolongation of gelation, therefore in most cases also leads to preparation of soft hydrogels. HA-TA hydrogels are prepared by non-cytotoxic reaction that marks them as appropriate for the cell cultivation.

## CONCLUSION

All presented systems are suitable for preparation of biocompatible HA-TA hydrogels with range of mechanical properties from soft to hard and kinetics of gelation from few seconds to minutes. Hydrogels are suitable for in situ gelation and according to the system they could be acellular or contain appropriate cells. All these aspects predispose these materials for use in tissue engineering and regenerative medicine.

## REFERENCES

1. Wolfova L et. al., WO/2013/127374, 2013.

## Graphene-based Tissue Engineering Scaffolds Prepared by 3D Printing

Harri Korhonen, Le Hoang Sinh, Nguyen Dang Luong, Jukka Seppälä

Research Group of Polymer Technology, Aalto University, Finland

[harri.korhonen@aalto.fi](mailto:harri.korhonen@aalto.fi)

### INTRODUCTION

Graphene, a two dimensional monoatomic thick building block of a carbon allotrope, has received world-wide attention due to its exceptional properties.<sup>1</sup> In order to fully utilize and further explore new functions of graphene, a number of methods have been developed for fabricating 3D graphene foams. 3D graphene architectures not only have the inherent properties of graphene, but can also exhibit improved functions such as light weight, high porosity, large surface area, high electrical conductivity, and stable mechanical property.<sup>2</sup> As demonstrated in recent studies for mesenchymal<sup>3</sup> and neural<sup>4</sup> stem cells, graphene foams are promising candidates also as tissue engineering scaffolds.

The aim of this study was to investigate the suitability of stereolithography for the fabrication of graphene-based 3D architectures. Tissue engineering scaffolds could thus combine the designed 3D architecture with exceptional inherent properties of graphene.

### EXPERIMENTAL METHODS

Photocrosslinkable resin was prepared by dispersing 1 wt-% of graphene oxide with SLA resin (PIC100, Envisiontec). 3D structures were fabricated by a self-made projection stereolithography. Fabrications were carried out by using light intensity of 1100  $\mu\text{W}/\text{cm}^2$ , layer thickness of 30  $\mu\text{m}$ , and curing time of 7s for each layer. The dimensions of the samples were 10\*10\*4 mm. The designed scaffold model had a gyroid-like pore architecture and porosity of 50 %. After printings the 3D composites were pyrolysed under nitrogen to decompose and evaporate the crosslinked polymer and to convert graphene oxide to reduced graphene oxide (r-GO). In pyrolysis the temperature was stepwise raised up to 500°C during 10 hours.

### RESULTS AND DISCUSSION

Well-controlled 3D structures were obtained with the used fabrication parameters. As seen in figure 1, the prepared scaffolds closely followed the structure of the designed mode. In printed samples the graphene oxide flakes were found to be uniformly dispersed throughout the polymer matrix.

The xy dimensions of the original sample were 10\*10 mm, while after pyrolysis the same dimensions were about 2\*2 mm. Although pyrolysis of polymer matrix caused considerable shrinking, the r-GO scaffold had the similar pore structure as in the original scaffold. Shrinking is obviously due to the small 1 wt-% content of GO used in photocrosslinkable resin. In addition to GO content, shrinking ratio is probably affected by the used sample dimensions and the pore structure.

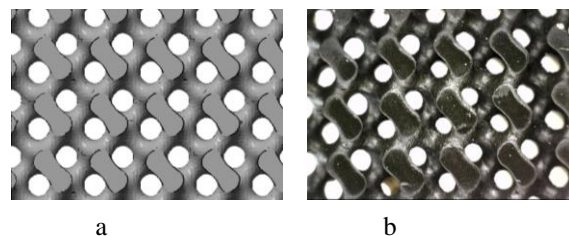


Figure 1. a) 3D-model, b) printed scaffold

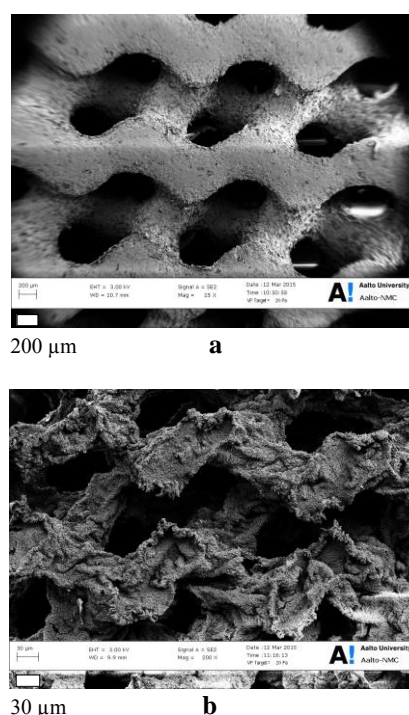


Figure 2. Scaffold a) before, b) after pyrolysis

### CONCLUSION

The results of this study show that stereolithography can be used for the fabrication of graphene-based 3D composites that can be further pyrolysed to reduced graphene oxide scaffolds.

### REFERENCES

1. Singh. *et al.*, Progress in Mater. Sci. 56:1178, 2011
2. Li. *et al.*, Nanoscale. 4:5549, 2012
3. Crowder. *et al.*, Nanoscale 5:4171, 2013
4. Li. *et al.*, Sci Rep. 3:1604, 2011

### ACKNOWLEDGMENTS

The authors would like to thank the Academy of Finland (Grant no: 272725) for providing financial support to this project.





## Decidual Mesenchymal Stem Cells and Ceramic-Based Graft Substitutes as Constructs for Bone Tissue Engineering

Gema Vallés<sup>1,2</sup>, Fátima Bensiamar<sup>2,1</sup>, Laura Saldaña<sup>1,2</sup>, Ana Flores de la Cal<sup>3</sup>, Almudena de Laiglesia<sup>4</sup>, Rosa M. Gonzalo-Daganzo<sup>4</sup>, Jose Cordero<sup>5,6</sup>, Nuria Vilaboa<sup>1,2</sup>, Enrique Gómez-Barrena<sup>1,6</sup>

<sup>1</sup>Hospital Universitario La Paz-IdiPAZ, Spain

<sup>2</sup>CIBER de Bioingeniería, Biomateriales y Nanomedicina (CIBER-BBN), Spain

<sup>3</sup>Instituto de Investigación Hospital 12 de Octubre, Spain

<sup>4</sup>Hospital Universitario Puerta de Hierro-Majadahonda, Spain

<sup>5</sup>Hospital Universitario La Princesa, Spain

<sup>6</sup>Departamento de Cirugía, Universidad Autónoma de Madrid, Spain

[gema.valles@salud.madrid.org](mailto:gema.valles@salud.madrid.org)

### INTRODUCTION

Cell-based therapies are promising new therapeutic approaches for bone regenerative medicine. The combination of mesenchymal stem cells (MSCs) and bone-graft substitutes offers an advanced strategy for the manufacture of restorative constructs for pathologically altered bone tissues<sup>1</sup>. Due to limitations associated to autologous cellular sources, alternative allogeneic sources have been considered. Human decidua-derived MSCs (hDMSCs) have several advantages (accessible tissue source, ethical aspects, high cell yielding...) over those obtained from human bone marrow (hBMSCs) and are attractive alternatives for tissue engineering purposes<sup>2</sup>. The healing and regeneration process induced by these therapies depends critically upon the MSCs response to the local microenvironment provided by cell-cell, cell-material and soluble factor-mediated interactions. Synthetic porous ceramic biomaterials based in tricalcium-phosphate ( $\beta$ -TCP) and hydroxyapatite (HA) are frequently used in clinical practice due to their biocompatibility, bioactivity and osteoconductive properties. Many studies have addressed the behaviour of BMSCs seeded on calcium phosphate scaffolds but there is very limited information about the growth, osteogenic potential or production of growth- and bone-related soluble factors of hDMSCs. Our study aimed to evaluate the in vitro viability and secretory profile of specific bioactive factors of hDMSCs seeded on calcium-phosphate  $\beta$ -TCP- and HA- based materials. For comparison purposes, hBMSCs and primary human osteoblasts (hOB) were also investigated.

### EXPERIMENTAL METHODS

hDMSCs of maternal origin were isolated from the extra-embryonic decidual membranes in full term human pregnancies and characterized at phenotypic and functional level. hBMSCs were isolated from bone-marrow aspirates obtained from the iliac crest of patients during orthopaedic surgical procedures. Primary hOB derived from osteoarthritic patients undergoing knee arthroplasty were also used. All procedures involving human cells were approved by the corresponding Ethical Committees. Cells were seeded on commercial Polybone ( $\beta$ -TCP-based; Kyungwon Medical Co., Ltd., Seoul, Korea) and commercial

Engipore (HA-based; Finceramica, Faenza, Italy) in block type and shaped in 100 mm<sup>3</sup> pieces. Cells were then seeded on materials and incubated for different time points up to 28 days. Culture medium was changed every 3 days. Metabolic activity was monitored using the Alamar Blue assay and soluble factors levels in culture media were quantified using the CBA Flex Set System (BD Biosciences) and ELISA kits.

### RESULTS AND DISCUSSION

hDMSCs, hBMSCs and hOB were able to adhere and grow on both calcium-phosphate-based materials. Independently of their origin, cells adhered and exhibited a higher growth capability on HA- than on  $\beta$ -TCP-based material. Levels of bioactive factors in culture media were quantified after 7 and 14 days of incubation. Compared to hOB, hDMSCs and hBMSCs released lower levels of IL-6, MCP-1 and VEGF. Secretion profile of these soluble mediators over time was dependent on the cell type and scaffold employed. In general, DMSCs showed good degree of reproducibility, interpreted as similar levels of release, in experiments performed at different cell passages that was not observed for BMSCs. MCP-1 and VEGF release from hDMSCs or hBMSCs after 14 days did not increase after 7 days in culture. However, IL-6 levels in  $\beta$ -TCP/ or HA/hDMSCs derived-culture media increased with time, an effect that was not observed in BMSCs. After 14 days in culture, hDMSCs released higher VEGF levels in HA constructs than in  $\beta$ -TCP-based substrates.

### CONCLUSION

To date, our data suggest that h-DMSCs in combination with commercial HA is a promising strategy for the development of constructs with applications in bone tissue engineering.

### REFERENCES

1. Gómez-Barrena E. *et al.*, Bone 70: 93-101, 2015
2. Kanematsu D. *et al.*, Differentiation. 82:77-88, 2011.

### ACKNOWLEDGMENTS

This work was supported by grant SAF 2012-40149-C02-01 (MINECO, Spain) y and grant AP117862013 (Fundación Mutua Madrileña).



## Characterization of Human Neural Networks Cultured on Hydrogel Matrix

Tiina Joki<sup>1</sup>, Laura Ylä-Outinen<sup>1</sup>, Susanna Narkilahti<sup>1</sup>

<sup>1</sup>NeuroGroup/BioMediTech, University of Tampere, Finland  
[tiina.joki@uta.fi](mailto:tiina.joki@uta.fi)

### INTRODUCTION

In future, cell transplantation therapies and sophisticated 3D tissue models could offer clinically relevant treatments or diagnostic tools for patients having currently incurable neural deficits. In both cases, modelling and craft applications, biomaterials can be utilized as extra cellular matrix (ECM) mimicking substance. This artificial ECM serves as supportive growth matrix for the cells and as backbone of 3D cell-material construct. The demands for the optimal biomaterial are quite similar both *in vitro* and *in vivo*. Material needs to be non-harmful, easy to handle and support cell growth and survival. In stem cell based applications it is also desirable that the biomaterial could guide cell differentiation and maturation into desired cell types. Both chemical and physiological properties of the material are important<sup>1,2</sup>. In neural applications the hydrogels are most prominent, due to their properties that are similar as properties of native nervous system ECM<sup>2</sup>.

### EXPERIMENTAL METHODS

Human neural cells were obtained from human pluripotent stem cells by using growth factor based suspension differentiation method. Pre-differentiated immature neural cells were plated on 1) top of the hydrogels, 2) inside the hydrogels, and 3) under the hydrogels. Laminin protein coating was used as positive 2D growth control, non-coated cell culture plastic as negative control and PuraMatrix (BD Bionciences) as positive 3D growth control. Cells were cultured up to 4 weeks in the hydrogel matrix before analysis. The cultures were characterized using fluorescence based viability analysis, immunocytochemical stainings, time-lapse monitoring, confocal imaging and network level electrophysiological measurements (Micro electrode array, MEA).

### RESULTS AND DISCUSSION

Long term culturing of cells was successful either under or on top of the hydrogels (2D cultures) and embedded

inside the hydrogels (3D cultures). Cell viability on 2D cultures either on top of hydrogel surfaces or under the hydrogel block, was similar compared to positive 2D growth control. Viability in 3D cultures was also similar when compared to positive 3D control but lower in both cases when compared to 2D cultures. Hydrogel as growth matrix was able to support neural cell maturation both in 2D and 3D when comparing protein expression using immunocytochemistry.

Based on published literature it seems that human neural cells are more demanding when it comes to artificial ECM if compared to rodent primary neural cells. Finding suitable growth matrix for the neural networks is first step towards functional *in vivo* mimicking 3D cultures. Here we describe testing of one material with promising properties.

### CONCLUSION

According to our *in vitro* results the studied hydrogel was suitable culturing matrix for human neural cells due to it was able to support the neural cell viability, maturation and network formation in long term cultures.

### REFERENCES

1. Gelain, F., et al., PLoS One 1, e119, 2006
2. Thonhoff, J. et al., Brain Res. 42–51, 2008

### ACKNOWLEDGMENTS

We acknowledge for financial support: Finnish Funding Agency for Innovation (Human Spare Parts project), Finnish cultural foundation, Doctoral Programme in Biomedicine and Biotechnology and Paulo Foundation.



## Functionally Graded Hybrid Scaffolds for Osteo-Chondral Defect Repair: Osteogenic Differentiation of Human Placenta-Derived Cells (hPDC)

Valentina Spoldi<sup>1</sup>, Gabriela Kmicik<sup>1</sup>, Silvia De Munari<sup>1</sup>, Patrizia Bonassi Signoroni<sup>1</sup>, Roberta Gentilini<sup>2</sup>, Antonietta Silini<sup>1</sup>, Silvia Farè<sup>2,3</sup>, Ornella Parolini<sup>1</sup>

<sup>1</sup>Centro di Ricerca E. Menni, Fondazione Poliambulanza-Istituto Ospedaliero, Brescia, Italy

<sup>2</sup>Department of Chemistry, Materials and Chemical Engineering "G. Natta", Politecnico di Milano, Italy

<sup>3</sup>INSTM Local Unit Politecnico di Milano, Italy

[silvia.fare@polimi.it](mailto:silvia.fare@polimi.it)

### INTRODUCTION

The aim of this study is to evaluate *in vitro* an engineered construct constituted by hPDC populations encapsulated in pectin gels, interpenetrated in a CaPs/PU foam (namely: a functionally-graded hybrid, FGHY) scaffold, for osteogenic purposes<sup>1</sup>.

*In vitro* characterization was performed to assess the potential of the previously optimized FGHY scaffold to support growth and osteogenic differentiation of different hPDC populations when loaded inside the FGHY scaffold via pectin gels.

### EXPERIMENTAL METHODS

Functionally graded CaPs/PU scaffolds were prepared as described in Ref.1<sup>1</sup>. Human placentas (n ≥ 10) were obtained from healthy woman after delivery and processed immediately<sup>2</sup>. Phenotype and morphology of hPDCs were assessed as previously described<sup>3</sup>.

The study of hPDCs *in vitro* differentiation toward the osteogenic lineage was performed as follows: 1) cells seeded in tissue culture plastic plates (as previously described<sup>3</sup>) and 2) cells loaded in pectin gels injected into the FGHY scaffold. hPDC populations were cultured at different time points (at least 1, 2, 3 weeks) to set up and optimize the culture protocol. Alamar Blue assay was used to assess cell viability. Cell colonization and morphology onto the FGHY scaffolds were evaluated by SEM. Cytochemical staining with Alizarin Red was used to assess osteoblast differentiation.

### RESULTS AND DISCUSSION

hPDC demonstrated the ability to differentiate toward the osteogenic lineage *in vitro*, as demonstrated by the presence of calcium deposits detected by cytochemical staining (Fig 1).

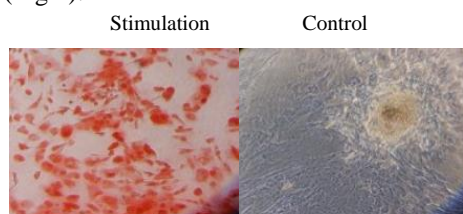


Figure 1. Cytochemical staining using Alizarin Red

The proliferation of hPDCs encapsulated in pectin gel interpenetrated into FGHY scaffolds increased over time (Fig 2). Good cell adhesion was observed at 10 days post seeding: hPDCs formed cell extensions, bridging parts of the walls of the pores of FGHY scaffold, as shown by SEM (Fig 3a). At day 17, above

the cell layer, a high deposition of inorganic phase was observed inside the FGHY scaffold (Fig 3b).

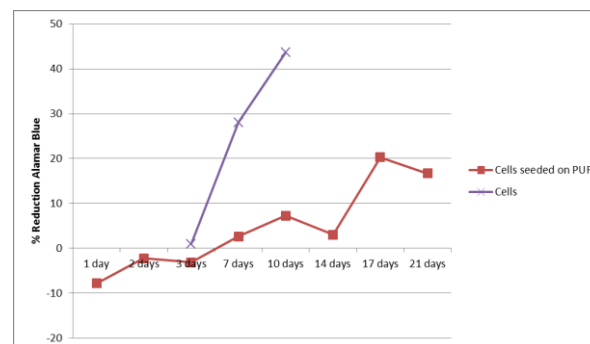


Figure 2. Alamar blue assay performed on hPDCs encapsulated in pectin gel and seeded into the FGHY scaffold, compared to the control (cells)

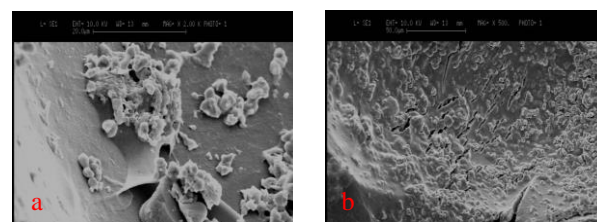


Figure 3. SEM images of hPDCs seeded on FGHY scaffold: 10 (a) and 17 days (b) after seeding

### CONCLUSION

The ability of novel functionally graded CaPs/PU (FGHY) scaffolds to stimulate cell adhesion and proliferation and to support differentiation of hPDCs make these scaffolds excellent candidates for an use in bone regeneration. Differentiation of hPDCs into chondrocytes is now under evaluation to verify the potential of the scaffold for osteo-chondral defect repair.

### REFERENCES

1. Farè S. *et al.*, abstract submitted to the ESB 2015
2. Rossi *et al.*, PLoS One. 7(10):e46956.2012.
3. Soncini *et al.*, J Tissue Eng Regen Med. 1(4):296-305, 2007.

### ACKNOWLEDGMENTS

The authors would like thank Fondazione Poliambulanza-Istituto Ospedaliero, Brescia (Italy) and the Cariplo Foundation (Grant n.2012-0842) for their support.

## Synthesis and Characterization of Hydroxyapatite/Polyvinyl Alcohol Nanocomposite Hydrogels

Marta Branka<sup>1</sup>, Dagnija Loca<sup>1</sup>, Marina Sokolova<sup>1</sup>, Agnese Pura<sup>1</sup>.

<sup>1</sup>Rudolfs Cimdins Riga Biomaterials Innovations and Development Centre of Riga Technical University, Latvia  
[dagnija.loc@rtu.lv](mailto:dagnija.loc@rtu.lv)

### INTRODUCTION

Synthesis of materials that mimic the natural bone have become an objective of many research groups. Mimicking the natural bone composition, where the ratio of inorganic to organic phase is high, still is a challenge. It is well known that hydroxyapatite (HAp) is widely used in hard tissue regeneration due to its biocompatibility, bioactivity and osteoconductive properties. However the poor mechanical properties (brittleness and low plasticity) of HAp biomaterials limit their application<sup>1</sup>, thus new materials with improved properties are prospected. Introducing a polymer component into the HAp in order to form an organic-inorganic nanocomposite is a method most commonly used to overcome the mechanical weakness of HAp. Among biodegradable and biocompatible polymers, polyvinyl alcohol (PVA) has attracted attention for cartilage and orthopaedic applications<sup>2</sup>.

The aim of the current study was to combine biological properties of hydroxyapatite with high plasticity of polyvinyl alcohol and *in-situ* develop mineralization method that leads to high affinity integration of HAp particles inside the PVA hydrogel. HAp/PVA hydrogels with Ca/P molar ratio of 1,67 and 1,50 were obtained and characterized.

### EXPERIMENTAL METHODS

The HAp nanoparticles were synthesized *in situ* in the 5% PVA aqueous solution. Briefly, Ca(OH)<sub>2</sub> solution was added to the PVA and stirred for 1 hour. 2M H<sub>3</sub>PO<sub>4</sub> was then added drop wise to the reaction media until Ca/P molar ratio of 1,67 and 1,50 were reached. Finally, reaction media was matured for 12h and five freeze-thaw cycles were applied to obtain the hydrogels. In each cycle samples were frozen at -24°C for 12h and then thawed at room temperature for 12h. Obtained samples were freeze-dried and characterized using X-ray diffraction, scanning electron microscopy (SEM) and Fourier transform infrared spectroscopy.

### RESULTS AND DISCUSSION

Obtained results showed that it was possible to synthesize PVA/HAp composites where inorganic to organic phase ratio was 50:50wt%. Moreover, it was possible to vary the Ca/P molar ratio from 1,67 to 1,50 in the final nanocomposite. It was also found that the

number of freeze-thaw cycles for the hydrogel preparation depended on the Ca/P molar ratio. SEM studies revealed that the HAp particles were dispersed throughout the PVA matrix (Fig.1. A) and porous hydroxyapatite/polyvinyl alcohol nanocomposites can be prepared (Fig 1. B) with pore size ranging from 2-80 µm.

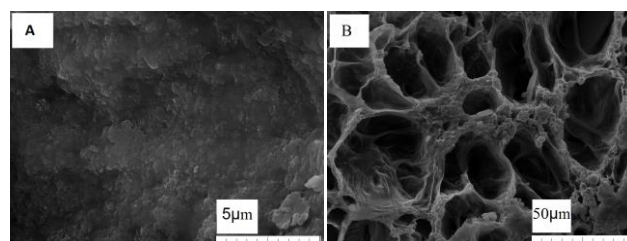


Fig. 1. SEM microphotographs of: A) HAp particles distributed in the PVA matrix; B) cross section of HAp/PVA nanocomposite.

### CONCLUSION

Current research has shown that nanocomposites with high inorganic to organic phase ratio as well as Ca/P molar ratio of 1,67 and 1,50 can be obtained by simple chemical route. The interconnected pore structure indicates that such composites can be promising materials for the cell ingrowth and can be good candidates in bone tissue regeneration.

### REFERENCES

1. Rajkumar M. *et al.*, J. Eng. Sci. Technol. 6:2437-2444, 2010
2. Baker M. I. *et al.*, J. Biomed. Mater. Res. B. 5:1451-1457, 212

### ACKNOWLEDGMENTS

This work has been supported by the National Research Programme No. 2014.10-4/VPP-3/21 "Multifunctional Materials and composites, photonicS and nanotechnology (IMIS<sup>2</sup>)" Project No. 4 "Nanomaterials and nanotechnologies for medical applications".



# Synthesis and Characterization of Chitosan-Modified Montmorillonite Nanoparticles for Tissue Engineering Applications

Zahra Rezvani, Masoud Mozafari

Bioengineering Research Group, Nanotechnology and Advanced Materials Department, Materials and Energy Research Center (MERC), P.O. Box 14155-4777, Tehran, Iran

[rezvani.rz@gmail.com](mailto:rezvani.rz@gmail.com)

## INTRODUCTION

During the last years, clay/polymer nanocomposites have received a significant attention as they can combine the structure and physico-chemical properties of organic and inorganic materials<sup>1</sup>. Modifying clays with biopolymers such as chitosan can be utilized to prepare polymer/clay nanocomposites for bio-applications<sup>2-4</sup>. Intercalants could increase interlayer distance of the clay. In modification process, intercalants should have opposite charge with clay surface to occur ionic exchange reaction between intercalants and clay layers<sup>5-7</sup>. Chitosan is a cationic biopolymer that was used to modify montmorillonite with negative charge<sup>5-6</sup>. In this study, bio-modified nanoclay was obtained by chitosan intercalation. Chitosan is a crystalline polysaccharide which is obtained by deacetylation of chitin, the second most abundant natural polymer<sup>6</sup>. Chitosan has been one of the most attractive biopolymers due to its remarkable properties such as; biocompatibility, biodegradability and antibacterial activity<sup>4-6</sup>. Polymer/clay nanocomposites are widely used in various fields such as; medical, drug delivery, wound healing and tissue engineering<sup>7</sup>. This study aims to incorporate chitosan molecules in the multilayer structure of montmorillonite nanoparticles and examine the antibacterial properties for tissue engineering applications.

## EXPERIMENTAL METHODS

### Materials

Chitosan with medium molecular weight was obtained from Sigma-Aldrich (Germany). Acetic acid (AA) was purchased from Merck (Germany). The montmorillonite -type clay utilized for this research supplied by Rockwood from USA.

### Preparation of chitosan/ montmorillonite nanoparticles

One gram of montmorillonite powder was dispersed in deionized water under magnetic stirring and two gram of chitosan powder was separately dissolved in 1% v/v acetic acid aqueous solution with the same condition. Then, chitosan solution was slowly added to montmorillonite solution. After the heat treatment, the mixture solution was centrifuged and washed with distilled water.

## RESULTS AND DISCUSSION

The interlayer expansion or d-spacing of unmodified montmorillonite and chitosan/ montmorillonite nanocomposite were determined by x-ray diffraction (XRD). As shown in Fig.1 XRD patterns demonstrated that peaks of montmorillonite and chitosan/ montmorillonite was at  $2\theta = 7.8^\circ$  (d-spacing=1.128 nm) and  $2\theta=3.7^\circ$  (d-spacing= 2.365 nm), respectively.

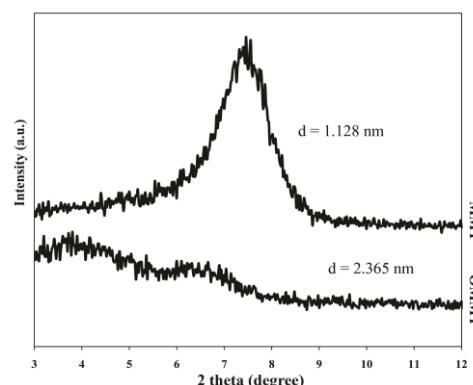


Figure 1: XRD patterns of montmorillonite and chitosan/ montmorillonite.

The XRD data was confirmed that chitosan molecular chains incorporated between the interlayer of montmorillonite by an ionic exchange reaction. In addition, the antibacterial properties of the modified nanoparticles indicated that the incorporation of chitosan molecules effectively induce a significant antibacterial properties which is useful for tissue engineering applications.

## CONCLUSION

The intercalation of chitosan biopolymer into montmorillonite, through ionic exchange method, resulted in polymer/clay nanocomposite which can be used in range of applications particularly in biomedicine. Intercalating chitosan molecular chains between montmorillonite layers increased the d-spacing which was shown by XRD data. The antibacterial results suggested that the modified nanoparticles can be used as an antibacterial agent for tissue engineering applications.

## REFERENCES

1. Babul Reddy A. *et al.*, J. Carbohydrate Polymers. 122:230-236,2015.
2. Oliveira M.J. *et al.*, J. Radiation Physics and Chemistry. 94:194-198, 2014.
3. Lavorgna M. *et al.*, J. Carbohydrate Polymers. 102:385-392, 2014.
4. Ling Y. *et al.*, J. Industrial Crops and Products. 51:470-479, 2013.
5. Salcedo I. *et al.*, J. Applied Clay Science. 55:131-137,2012.
6. Pillai C.K.S. *et al.*, J. Progress in polymer science. 34(7):641-678,2009.
7. Zare Y. *et al.*, J. Applied Clay Science. 105: 66-70, 2015.

## INTRODUCTION

During the last decade, fabrication of nanofibrous scaffolds has gained a great deal of attention due to their high potential of mimicking extracellular matrix (ECM) <sup>1</sup>. Nanofibers provide high aspect ratio, high interconnected porosity and low density which are essential factors for increasing cell adhesion leading to enhanced cellular migration, differentiation and proliferation<sup>2-3</sup>. Among different methods electrospinning is promising and progressive technique to fabricate nanofibers<sup>4</sup>. In addition, this method makes it possible to produce nanofibrous scaffolds from different categories of non-polymeric materials, natural and synthetic polymers <sup>5-6</sup>. Preparation of nanofibrous scaffolds by electrospinning of polymer blends has specific properties which can be used in biomedical applications<sup>3-4</sup>. This paper reports a study to fabricate chitosan/PVA nanofibrous scaffolds by electrospinning method. Chitosan is a polysaccharide derived by deacetylation of chitin. It has different biological properties including: biodegradability, biocompatibility and antibacterial activity<sup>4-6</sup>. As well, PVA is a non-toxic, hydrophilic, and biocompatible material that has also been used for tissue engineering applications<sup>3-6</sup>. In this study, different amounts of chitosan were added as a polymeric blend into the structure of PVA nanofibrous scaffolds to observe the changes associated with this blending process on the physic-chemical characteristics of the final scaffolds.

## EXPERIMENTAL METHODS

### Materials

Chitosan with medium molecular weight was purchased from Sigma-Aldrich (Germany). PVA with average molecular weight and acetic acid (AA) was obtained from Merck (Germany).

### Preparation of chitosan/PVA nanofibers

PVA was dissolved in distilled water at a concentration of 5 wt% and chitosan was dissolved in 90 % acetic acid at a concentration of 3 wt%. The PVA solution 5 wt% was mixed with the chitosan solution 3 wt% at a weight ratio of chitosan/PVA (20/80). For electrospinning process the solutions were fed into the syringe pump, the applied voltage was 20kv, the feeding rate and the tip to collector distance was set at 0.02 mm/min and 10cm, respectively.

## RESULTS AND DISCUSSION

The morphology and microstructure of nanofibers were evaluated by scanning electron microscopy (SEM). As shown in Fig.1 in chitosan / PVA blend (weight ratio 20/80), the average fiber diameter was found to be  $79.85 \pm 21.21$  nm while in PVA and chitosan alone, the average fiber diameter was  $173.7 \pm 24.52$  nm and  $97.41 \pm 25.22$  nm, respectively.

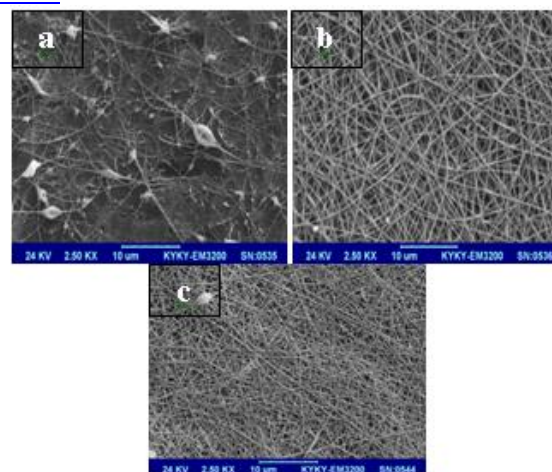


Figure 1: SEM micrograph of the electrospun nanofibers. a)chitosan, b)PVA, c)chitosan/PVA(20/80)

In Fig.1 (a) droplets and beads are diffused on the surface and fibers are scarcely noticeable. While in chitosan/PVA (20/80) blend Fig.1(c) uniform and thin fibers are observed. The chitosan-containing scaffolds were used for *in vitro* cell culture, and they were found to exhibit the most balanced properties to meet the basic required specifications for tissue engineering applications. It was demonstrated that the addition of chitosan to the PVA scaffolds enhanced the differentiation and proliferation of the cells compared to PVA nanofibrous scaffolds and acted as a positive cue to support neurite outgrowth, indicating that the addition of chitosan to the PVA scaffolds is a promising polymeric blend suitable for tissue regeneration.

## CONCLUSION

In this study, chitosan/PVA nanofibrous scaffolds were produced by electrospinning method. Chitosan/PVA ratio of 20/80 was recognized as the optimum ratio for fabrication of nanofibrous scaffolds with uniform morphologies and minimum beads and defects which can be utilized in a variety of fields such as; medical, drug delivery, wound healing and tissue engineering.

## REFERENCES

1. Mishra S.K. *et al.*, J. Carbohydrate polymers. 121: 37-48, 2015.
2. Santos C. *et al.*, J. Carbohydrate polymers. 99:584-592, 2014.
3. Hadipour-Goudarzi E. *et al.*, J. Carbohydrate polymers. 113: 231-239, 2014.
4. Anitha A. *et al.*, J. Progress in Polymer Science. 39(9):1644-1667, 2014.
5. Chahal S. *et al.*, J. Procedia Engineering. 53: 683-688, 2013.
6. Sambudi N.S. *et al.*, J. Composites Science and Technology. 106:76-84, 2015.

Alberto Ballardini<sup>1</sup>, Andrea Ruffini<sup>1</sup>, Simone Sprio<sup>1</sup>, Anna Tampieri<sup>1</sup>.

<sup>1</sup>Institute of Science and Technology for Ceramics, National Research Council, Faenza, Italy  
[alberto.ballardini@istec.cnr.it](mailto:alberto.ballardini@istec.cnr.it)

## INTRODUCTION

The regeneration of critical size bone defects requires the use of implants/scaffolds able to instruct cells towards new bone formation by the release of suitable chemical signals. In this respect, hydroxyapatite phases (HA) endowed with low crystal order and multiple substitutions of calcium and/or phosphate with ions relevant for the regeneration processes (e.g.: magnesium, carbonate) are elective biomaterials for bone healing due to their high mimicry with the composition of newly formed bone.

Multiple substitutions with biologically-competent ion amounts can provide synergistic effects towards improved efficiency in bone regeneration. Moreover, nowadays interest is raising for the effect of ions with specific antibacterial effect, to be exploited in bioactive and osteointegrative coatings that may greatly improve the performance of metallic implants that very often undergo early failure due to the formation of biofilms.

In this respect the substitution of Calcium ion with Zinc in the HA lattice has recently attracted a lot of attention for its effect as substituting ion into the HA lattice due to their antibacterial properties.

Besides, Gallium is considered very promising for antibacterial activity but its effect when used as doping ion in biomimetic hydroxyapatite has not yet been thoroughly investigated. In this respect the present paper reports the synthesis of a new apatite containing both Mg and CO<sub>3</sub> ions as well as gallium ions in amount that can be suitable for exhibiting antibacterial effect.

## EXPERIMENTAL METHODS

New biomimetic HA phases with multiple ion substitutions were synthesized as nano-powders by the simultaneous dropping of H<sub>3</sub>PO<sub>4</sub> and NaHCO<sub>3</sub> in a stirred suspension of Ca(OH)<sub>2</sub>, MgCl<sub>2</sub> and Ga(NO<sub>3</sub>)<sub>3</sub> or Zn(NO<sub>3</sub>)<sub>2</sub> at the temperature of 40°C.

At the end of the synthesis the solution was stirred for 2h and left overnight for maturation. Then the product was washed 3 times with fresh water and dried in a ventilated oven at 40°C.

The as-synthesized materials were analyzed by X-Ray Diffraction (XRD), ICP-OES, Fourier Transform Infra-Red spectroscopy (FTIR), Thermo-Gravimetric Analysis (TGA).

## RESULTS AND DISCUSSION

The XRD analysis shows that all synthesized powder are composed by only low-crystallinity hydroxyapatite phase without the presence of any other calcium phosphate phase and exhibiting nanosize, as evaluated by both SEM and Scherrer equation. The elemental analysis by ICP and XRD analysis both confirmed the incorporation of the foreign ions in the HA lattice.

Together with TGA, used for the determination of carbonate, ICP shows that in respect of a high Ca/P ratio, the ratio of total cations/anions is always lower than 1,67 and this ratio is closer to natural bone.

The FTIR and TGA analyses reported qualitatively and quantitatively the effective carbonation in B position (i.e. substituting PO<sub>4</sub><sup>3-</sup> in the HA lattice).

## CONCLUSION

Various multi-substituted HA powders also containing Zn and/or Ga ions were successfully synthesized and characterized. These powders have Mg<sup>2+</sup> ions substituting Ca<sup>2+</sup> in biologically-competent amounts (i.e. Mg<sup>2+</sup>: 1-10 mol% and CO<sub>3</sub><sup>2-</sup>: 5-20 mol%).

The presence of Zn<sup>2+</sup> or Ga<sup>3+</sup> in the amount of 1-10 mol% and 1-5 mol%, respectively, have been determined and we have proved that, as the doping with Zn<sup>2+</sup> and Ga<sup>3+</sup> is competitive with the entering of Mg<sup>2+</sup>, the anionic substitution with CO<sub>3</sub><sup>2-</sup> results not affected.

These preliminary results encourage to further investigation to assess the actual antibacterial effect of these new materials and to test them as coatings for metallic implants/protheses.

## REFERENCES

1. Kawamura H. *et al.*, J. Biomed. Mat. Res., 50:2-184-190, 2000
2. Thian E., *et al.*, J. Mat. Sci. Mater. Med., 24:2-437-445, 2013
3. Verron E., *et al.*, Br. J. Pharmacol., 159-1681-1692, 2010
4. Bernstein L., Pharmacol. Rev., 50:4-665-682, 1998

## ACKNOWLEDGMENTS

The authors would like to thank the Fondazione del Monte di Bologna e Ravenna for providing financial support to this project.



Żaneta Anna Mierzejewska<sup>1</sup>,

<sup>1</sup> Faculty of Mechanical Engineering, Białystok University of Technology, Poland  
[a.mierzejewska@doktoranci.pb.edu.pl](mailto:a.mierzejewska@doktoranci.pb.edu.pl)

## INTRODUCTION

In modern implantology special attention is paid to a long-standing problem of rapid degradation and progressive dysfunction implants. The cause of reoperation is mostly lack of proper interaction between bone tissue and the implant [4]. Appropriate combination of the two most important factors: the implant surface, the type of intermediate layer and the proper relation between implant deformation and bone tissue should allow to obtain the optimal solution to the problem of the bone and implant interface interactions [5]. The aim of this paper is theoretical analysis and the evaluation of biomechanical and biochemical conditions for the proper formation of the outer layer and the structure of the implant.

Modern implantology is dominated by components made from metallic materials. Because of structural role of bone, most commonly in the manufacture of implants metallic biomaterials was used [1]. Most willingly titanium alloys and austenitic steels are used. Alloys of aluminum and vanadium as documented cases of dissolution of Al and V, while it has been proven that Al affects on the development of Alzheimer's disease, and V is characterized by high cytotoxicity. In the new alloys generation included those having a lower modulus of elasticity and greater biotolerance, it is worth mentioning also highly biocompatible and osteoconductive [5]. Research on the quality of implants alloys of these metals is being conducted.

Condition for obtaining osseointegration of the bone implant is the formation of a hematoma, and it is converted into fibrous tissue. To osseointegration occurred it should be retained certain conditions, among others, the relative relationship of deformability and avoiding stress shielding in the surrounding the implant bone tissue as well as biocompatibility. Proper relationship of deformability is obtained by appropriate selection of the mutual stiffness (modulus of elasticity, shape cross-sectional geometry). Consequently with the occurrence of the phenomenon of bone remodeling - to adapt the structure of the bone to the current state of stress (Wolff's law), it is important that the size of the stresses after implantation was not different significantly from the state before the implantation [1]. In the case of the strong connection of the implant and bone, can be assumed that both materials are subject to the same deformation.

The ideal implant should have a modulus similar to the bone module, and occupy not greater area than the replaced tissue [3]. Currently the material that minimizes or would obviate the problem of stress-shielding is looking for. On the other hand, too large susceptibility of placed in medullary canal implant causes the existence of significant shear stresses in the boundary

layer, which destroys fresh tissue structure. As a result of the large difference in the deformability of the implant and bone it comes between them to micromovements. If these movements exceeding 100  $\mu\text{m}$  it may results in proliferation of connective tissue instead of the desired bone tissue leading to impaired mechanical stability. Moreover, they become the cause of the destruction of the fiber network and the new blood vessels [2]. The strength of the connection between the bone and the biomaterial should be close to the strength of the bone tissue. Today it is one of the weakest links in implantation.

## CONCLUSION

There are no documented studies that have shown clearly how to solve this problem. The analysis shows, however, that one of the conditions of use of hydroxyapatite is to reduce the hardness and brittleness. Conducted a study on the activation of collagen making hydroxyapatite structure similar to bone structure. The alternative seemed to be a layer of nanocrystalline diamond. Unfortunately, the diamond is too hard and too little resistant to abrasion. The analysis shows that the optimum solution would be implant made of titanium alloys containing Ta, and Nb-coated titanium oxide with the shaping of the open pores with appropriate sizes depending on the type of implant and the bone tissue quality. The hope are layers applied with sol-gel method, involving hydroxyapatite or metal oxides. As a result, the layers are obtained with greater flexibility and reduces the susceptibility to brittle fracture layer. Research follow in the direction of interaction studies on samples and tests shear strength, stretching and bending.

## REFERENCES

1. Będziński R., Biomechanika Inżynierska. Zagadnienia Wybrane, Wrocław, Oficyna Wydawnicza Politechniki Wrocławskiej, 1997.
2. Będziński R., Relacje Tkanka-Implant, Inżynieria Biomateriałów, 2002.
3. Kutz M., Standard Handbook Of Biomedical Engineering And Design, Usa, The McGraw-Hill Companies, 2008.
4. Marciniak J., Biomateriały, Gliwice, Wyd. Politechniki Śl. 2002
5. Pillai C., Sharma C., Biointegration: an Introduction, Biointegration of Medical Implant Materials: Science and Design, 2010

## ACKNOWLEDGMENTS

This scientific work was supported by the Faculty of Mechanical Engineering, Białystok University of Technology, project No MB/WM/14/2014.





## Treatment of Osteonecrosis of Femoral Head (ONFH) with Co-transplantation of Adipose-Derived Stromal Cells and Bone Marrow Stromal Cells in Minipig Model

Woo-Lam Jo<sup>1</sup>, Mi Lan Kang<sup>2</sup>, Ji Eun Kim<sup>2</sup>, Eun Ah Kim<sup>2</sup>, Soon-Yong Kwon<sup>3</sup>, Gun-Il Im<sup>2</sup>

<sup>1</sup> Department of Orthopaedic Surgery, Seoul National University Bundang Hospital,  
Seoul National University College of Medicine, South Korea

<sup>2</sup> Department of Orthopedics, Dongguk University Ilsan Hospital, Goyang, South Korea

<sup>3</sup> Department of Orthopaedic Surgery, St. Mary's Hospital,  
The Catholic University of Korea, Seoul, South Korea

[jis25@naver.com](mailto:jis25@naver.com)

### INTRODUCTION

Osteonecrosis of femoral head (ONFH) is irreversible disease which treatment is almost depending on total joint replacement. The synergistic effect by co-transplantation of adipose-derived stromal cells (ASCs) in enhancing the osteogenic differentiation of bone marrow stromal cells (BMSCs) proved in critical sized calvarial defect model of rat in our previous study<sup>1</sup>. The purpose of this study was to evaluate the effect of co-transplanted ASCs and BMSCs at the ratio of 0.5 to 1 to heal the osteonecrotic lesion created in the minipig.

### EXPERIMENTAL METHOD

Six female minipigs (age: 23 to 25 months, weight: 55 kg) were used in this study. We made ONFH model on both hips of minipig with surgical procedures. Also we harvest bone marrow and adipose tissue. In laboratory, ASCs and BMSCs were co-cultures and transplanted to ONFH portion of minipig sealing with fibrin glue. In control hip, we only sealing with fibrin glue.

After transplantation of cells, we checked x-ray every 4 weeks. At 12 weeks, we sacrificed all the animals. The femoral heads were harvested and examined grossly. The specimen underwent computed tomography and histological examination.

### RESULTS AND DISCUSSION

In the results of x-rays and CT, defect of cells transplantation group was complete healed up with new bone tissue while control group had unfilled bone defect. Histological findings also corroborated the radiological findings. In the cell transplantation group, great number of regenerated trabecular bone rimmed with abundant osteoblast. In the control group, the lesion was principally filled with fibrotic or fatty tissue

### CONCLUSION

We observed very rapid and good quality osteogenesis in combined ASCs and BMSCs implantation group compared with control group.

### REFERENCES

1. KI Kim, S Park, GI Im, J. Biomaterials, 35, 4792 (2014).



## Bioengineering of Mandibular Reconstruction in Cancer Surgery

Camille Ehret<sup>1</sup>, Thomas Sagardoy<sup>1</sup>, Rachida Aid<sup>3</sup>, Robin Siadous<sup>1</sup>, Reine Bareille<sup>1</sup>, Damien Le Nihouanen<sup>1</sup>, Jérôme Kalisky<sup>1</sup>, Stanislas Pechev<sup>2</sup>, Leatitia Etienne<sup>2</sup>, Didier Letourneur<sup>3</sup>, Jean-Christophe Fricain<sup>1</sup>, Erwan De Monès<sup>1</sup>, Joëlle Amedee<sup>1</sup>

<sup>1</sup>Inserm U1026, Tissue Bio-engineering, Bordeaux University, Bordeaux, France

<sup>2</sup>ICMCB, Bordeaux University, Bordeaux, France

<sup>3</sup>Inserm U1148- LVTS, Paris 13 University, Paris, France

[camille.ehret@inserm.fr](mailto:camille.ehret@inserm.fr)

### INTRODUCTION

Worldwide 500,000 cases of head and neck cancer are diagnosed each year<sup>1</sup>. After carcinologic surgery, the reconstruction of the mandible is often required. The technique of reconstruction described by Masquelet with the induced membranes is one of the strategies, but still exhibits limitations in an oncological context. The aim of our project is to develop an injectable osteoinductive and osteoconductive composite polymer composed of doped strontium hydroxyapatite (HA) dispersed within a polysaccharide-based scaffold<sup>2</sup> to fill the induced membrane instead of autologous bone. The aim of this work is 1) to synthesize and characterize HA doped by strontium with different ratios of strontium (Sr); 2) associate these nanoparticles with polysaccharide-based scaffolds, 3) analyze *in vitro* the cellular responses of mesenchymal stem cells (MSC) and progenitor endothelial cells (PEC) seeded within this matrix and then, 4) evaluate the fate of this composite polymer subcutaneously in mice.

### EXPERIMENTAL METHODS

**Synthesis of HA or Sr-doped HA:** HA was synthesized by wet chemical precipitation at 40 or 90°C. Different ratios of HA/Sr were tested (8 and 50 % w/w). **Characterization of HA or Sr-doped HA:** X-ray diffraction (XRD), Inductively Coupled Plasma (ICP) and Transmission Electronic Microscopy (TEM) were used to characterize the HA particles. **Cell culture and matrices seeding:** MSC were isolated from human bone marrow stromal cells according to our previous work<sup>2</sup> and PEC were obtained from human umbilical cord blood according to our previous work<sup>3</sup>. **MSC and PEC behaviour within the 3D scaffold:** After 7 and 14 days, Live/Dead Assay was used to confirm the viability of cells cultured within the composite polymer. Bone markers (runx2, ALP, OCN) and endothelial cells markers (CD31, VE-cadherin, vWF) were analyzed and quantified by quantitative polymerase chain reaction (qPCR). **Non osseous implantation of composite matrices in mice (subcutaneously):** Matrices were inserted into subcutaneous pockets in the dorsum of 12-week-old Balb/c mice. After 15 and 30 days samples were collected and analysed by micro-CT and histologically. **Micro-computed tomography (micro-CT):** Micro-CT was performed *ex vivo* and cross sectional slices were reconstructed (resolution: 14 µm, software: Microview). **Histological procedure:** Fixed samples

were decalcified, dehydrated and paraffin-embedded. Sections were then stained with Masson's Trichrome.

### RESULTS AND DISCUSSION

TEM analyses of HA particles revealed that whatever the temperature, HA forms aggregates constituted by 50 to 150 nm particles. Live/Dead Assay confirmed the cells viability of MSC and PEC cultured within 3D scaffold after 14 days of culture. HA particles were then dispersed at different ratios within the polysaccharide and analyzed by ESEM and ICP. Preliminary *in vivo* data (**Fig.1**) suggest that the composite polymer developed with a final ratio of 1.4% (w/v) of Sr within the matrix is able to stimulate tissue mineralization (**Fig.1A**), once implanted in ectopic site. Histological analyses confirmed the presence of osteoid structures within the implant (**Fig.1B**). Controls were performed using the polysaccharides based scaffold polymer (PUDNA) alone and using the scaffold supplemented with undoped HA (PUDNA-HA).

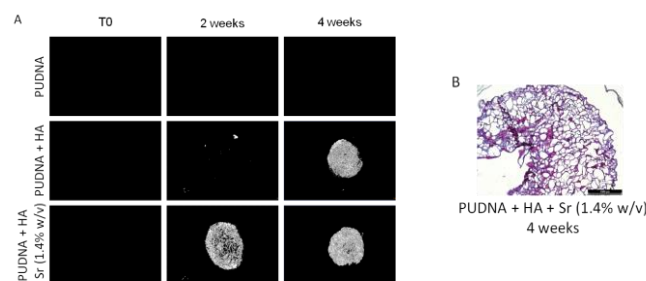


**Fig. 1**

### CONCLUSION

In conclusion, the use of osteoinductive composite scaffold doped with Sr could be an alternative of the autografts supplemented with BMP2 for the regeneration of large bone defects in a carcinological context.

### REFERENCES

1. Ligier K. *et al.*, Rev. Stomatol. Chir. Maxillofac. 112:164-71, 2011
2. Fricain JC. *et al.*, J. Biomaterials 34:2947-59, 2013
3. Thebaud NB *et al.*, J. Tissue Eng. Regen. Med. 4(6):473-84. 2010

### ACKNOWLEDGMENTS

The authors would like to thank the Fondation pour la Recherche Médicale for providing financial support to this project.



## iPS-Derived Neural Cells in a 3D Collagen Scaffold as a Tool for Investigating Interrelations Between Biomaterials and Nerve Tissue

Marzena Zychowicz<sup>1,2\*</sup>, Jose Luis Gerardo Nava<sup>3\*</sup>, Krystyna Pietrucha<sup>4</sup>, Hanna Winiarska<sup>1,2</sup>, Martyna Podobińska<sup>1,2</sup>, Gary Brook<sup>3\*</sup>, Leonora Buzańska<sup>1,2\*</sup>

<sup>1</sup> Stem Cell Bioengineering Unit, Mossakowski Medical Research Centre, Polish Academy of Sciences, Warsaw, Poland

<sup>2</sup> Department of Biotechnology, Wrocław Research Centre EIT+, Wrocław, Poland

<sup>3</sup> Institute for Neuropathology, RWTH Aachen University, Aachen, Germany

<sup>4</sup> Department of Material and Commodity Sciences and Textile Metrology, Lodz University of Technology, Lodz, Poland

\* Equally contributing authors

[mzychowicz@imdik.pan.pl](mailto:mzychowicz@imdik.pan.pl)

### INTRODUCTION

Induced pluripotent stem (iPS) cells present great promise for future applications in personalized regenerative medicine, since they can be obtained from any adult tissues. On the other hand providing 3D biomaterial-based microenvironmental conditions, has proved to have protective and supportive functions for transplanted stem cells. We are currently investigating the mutual relationship between a collagen scaffold seeded with human iPS cells (or their committed progeny) and organotypic slice cultured neural tissue derived from the central nervous or dissociated peripheral nervous system neurons. For this purpose, collagen scaffolds seeded with iPS-derived neural cells were co-cultured with organotypic spinal cord slices or dorsal root ganglion explants. This system can be used to investigate aspects of CNS neuroregeneration by assessing cell developmental processes such as migration and neuronal outgrowth in 3D ex-vivo scenarios.

### EXPERIMENTAL METHODS

The porous, 3D collagen scaffolds were made from porcine collagen using a lyophilisation technique<sup>1</sup> and modified by carbodiimide cross-linking to provide appropriate thermal and mechanical properties. Prior to cell seeding, scaffolds were functionalized by incubation in a laminin-containing solution for 2h. A human iPS cell line was obtained from CD34+ cells of human cord blood using seven episomally expressed vectors (Oct4, Sox2, Klf4, c-Myc, Nanog, Lin28, and SV40 T) (Gibco). iPS cells were neurally committed according to Yan et al.<sup>2</sup> and further differentiated and seeded onto the laminin-functionalised modified collagen scaffolds. Such hybrid cell-scaffold preparations were co-cultured with organotypic spinal cord slices<sup>3</sup> or dorsal root ganglion (DRG) neurons for investigation of cell migration between the nervous tissues and the scaffold for up to 2 weeks culture. In order to track or identify the iPS-derived, neurally differentiated cells, green fluorescent CMFDA tracer or alternatively the anti-human mitochondria antibodies were used.

### RESULTS AND DISCUSSION

The iPS cells in serum-free and feeder-free culture conditions presented the markers of pluripotency (Oct4, Sox2, Nanog) while upon the neural differentiation

acquired nestin,  $\beta$ -tubulin III, MAP-2, Dcx, GFAP, GalC and PDGFR $\alpha$ , as revealed by immunocytochemical and RT-PCR analyses.

Seeding 3D collagen scaffolds with undifferentiated, iPS cells resulted with low cell attachment, limited viability, and limited differentiation, while iPS-derived neural stem cell (NSC) populations colonized the scaffold in a well defined manner. NSC progenitors adhered to the collagen scaffolds without losing differentiation markers, but did not show signs of migration. Moreover, laminin-functionalization of the scaffold enhanced neurite outgrowth from dissociated DRG neurons into the biomaterial. When scaffolds and iPS-derived cells hybrids were co-cultured with rat organotypic spinal cord (OSC) slices, migration of slice-derived cells into the scaffold was observed while there was no migration of human NSC from the scaffold into the tissue explant. This may be due to strong adhesive interactions between the iPS-derived cells and the supporting biomaterial niche.

### CONCLUSION

The highly porous collagen scaffolds/cell hybrids used in this study are suitable for testing mutual interactions between human iPS (and neurally committed iPS-derived cells) and organotypic CNS slices or dissociated PNS neurons. The uni-directional migration from the spinal cord organotypic slice into the biomimetic cell-seeded scaffold should be further investigated for exploitation in a range of tissue engineering and regenerative medicine applications.

### REFERENCES

1. Pietrucha K. *Med & Biol Eng & Comp (JIFMBE)* 14: 3369-3372, 2007.
2. Yan Y. *et al Stem Cells Transl Med.* 2(11):862-70, 2013.
3. Gerardo-Nava J. *et al Biomaterials* 35(14):4288-96, 2014.

### ACKNOWLEDGMENTS

The research was supported by Wrocław Research Centre EIT+ under the project „Biotechnologies and advanced medical technologies” – BioMed (POIG.01.01.02-02-003/08) financed from the European Regional Development Fund (Operational Programme Innovative Economy, 1.1.2)”; and statutory funds to MMRC.



Anna Magiera<sup>1</sup>, Joanna Konko<sup>1</sup>, Jaroslaw Markowski<sup>2</sup>, Jan Pilch<sup>2</sup>, Elzbieta Menaszek<sup>3</sup>, Marta Blazewicz<sup>1</sup>

<sup>1</sup>Department of Biomaterials, Faculty of Materials Science and Ceramics, AGH-University of Science and Technology, Krakow, Poland

<sup>2</sup>Laryngology Department, Medical University of Silesia, Katowice, Poland

<sup>3</sup>Collegium Medicum, Jagiellonian University, Krakow, Poland

[asocha@agh.edu.pl](mailto:asocha@agh.edu.pl)

## INTRODUCTION

Biomimetic nanofibers are becoming more and more popular for manufacturing tissue engineering scaffolds. Such types of materials offer new concepts and methods to design nano-biomimetic tissue Extracellular Matrix. At present, the ECM in a body is essentially constructed by nanofibrous network containing protein and glycosaminoglycans, with a diameter ranging from 50 to 300 nm<sup>1,2</sup>. An optimal scaffold should mimic the native ECM. It was already proved that the scaffold consisted from nanofibrous structure has improved the application of tissue engineering scaffolds to bone, cartilage, cardiovascular and nervous tissue regeneration with less scars<sup>3</sup>. Numerous findings support the hypothesis that fibrous carbon components can act as chondrogenic materials<sup>4</sup>. The carbonaceous materials, including carbon fibers and carbon nanotubes were successfully applied in the treatment of cartilage defects. The work describes experiments, results and selected characteristics of ex-PAN carbon nanofibers in the form of thin mesh as potential materials to support cartilage cell growth at nano scale.

## EXPERIMENTAL METHODS

A polyacrylonitrile copolymer consisting of 93-94 wt % acrylonitrile, 5-6 wt % methyl methacrylate and 1 wt % sodium allylsulfonate (Mavilon, Hungary) was used as carbon nanofiber precursor, and N,N-dimethylformamide (DMF) (POCH, Poland) as the polymer solvent. Spinning solutions were prepared by dissolving polyacrylonitrile powder in a determined amount to obtain a solution of the desired concentration. The PAN nanofibers were spun using a laboratory electrospinning set-up. Mechanical properties (tensile strength and elastic modulus) of samples prepared in the form thin mesh were determined in tensile uniaxial mode using Zwick testing machine model 1435. Prior to carbonization, PAN nanofibers were preliminarily oxidized in air followed by heat treatment up to 1000°C. To characterize the surface morphology of the nanofibers before and after carbonization, a scanning electron microscope (SEM; Nova Nanos 200, FEI COMPANY EUROPE) was used. The samples obtained were studied to determine fiber diameters and porosity of the resulting mesh samples. The contact angle of samples was measured by sessile drop method using an automatic drop shape analysis system DSA 10Mk2 (Kruss, Germany). Cytotoxicity of carbon fibrous samples was determined by indirect and direct contact cytotoxicity tests in accordance to EN-ISO 10993.

## RESULTS AND DISCUSSION

The fibrous material microstructure was visualized by SEM as shown in Fig.1. Depending on the processing parameters various samples were obtained and analyzed.

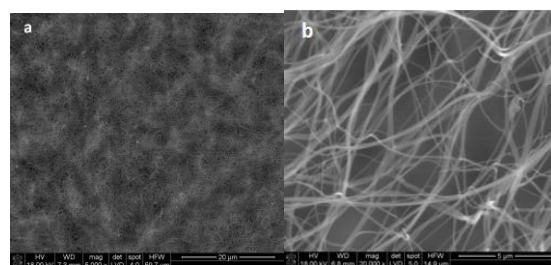


Fig. 1 SEM microphotographs of a) PAN nanofibers and b) ex-PAN carbon nanofibers

Results of the study demonstrated the increased elastic modulus and strength with a greater surface density of fibrous structure and its preferred nanofiber orientation (anisotropy). Carbon nanofibrous materials have been tested in contact with normal human cells chondroblasts. In vitro cytotoxicity and cell viability showed a high biocompatibility of the materials studied.

## CONCLUSION

By changing the processing parameters during electrospinning it was possible to change properties and microstructure parameters of fibrous mesh including nanofibers diameter, pores size, total porosity and preferred orientation of single nanofibers of mesh-based scaffolds. The results indicate that carbon fibrous samples differing in their microstructure perform good biocompatibility in contact with human chondrocytes and provide structures which seem to be promising as scaffolds to regenerate defective cartilage. Tunable mechanical properties of nanofibrous samples indicate the need for further study of such materials to optimize their properties for cartilage engineering scaffolds.

## REFERENCES

1. Xiumei M. *et al.*, JFBI. 6:225-235, 2013
2. Yoshimoto H. *et al.*, Biomaterials. 24:2077-2082, 2003
3. Markowski J. *et al.*, J. Nanomater. 2015:564087, 2015
4. Webster T.J., *et al.*, Nanotechnology. 15:48-54, 2004

## ACKNOWLEDGMENTS

The authors would like to thank the National Science Centre, Poland (project no: 2014/13/B/ST8/01195) for providing financial support to this project.



## Collagen and Carboxymethyl Cellulose Bilayers for Skin Tissue Repair

Cemile Kilic Bektas<sup>1,2,6</sup>, Ilgin Kimiz<sup>4</sup>, Aylin Sendemir Urkmez<sup>4,5</sup>, Vasif Hasirci<sup>1,2,6</sup> and Nesrin Hasirci<sup>2,3,6</sup>

Departments of <sup>1</sup>Biological Sciences, <sup>2</sup>Biotechnology and <sup>3</sup>Chemistry, Middle East Technical University, Ankara, Turkey

Department of <sup>4</sup>Bioengineering and <sup>5</sup>Biomedical Technologies, Ege University, Izmir, Turkey

<sup>6</sup>BIOMATEN- Center of Excellence in Biomaterials and Tissue Engineering, METU, Ankara, Turkey

[cemile.kilic@metu.edu.tr](mailto:cemile.kilic@metu.edu.tr)

### INTRODUCTION

Skin is the largest and critically important organ of the body that serves as a physical barrier to the outside world, takes role in controlling the body temperature and hydration levels<sup>1</sup>. When these functions are damaged due to burns, diseases or other skin problems, wounded area become very susceptible to the bacterial infection which may result in extensive tissue loss. In such extreme cases routine applications cannot help to tissue restoration and regeneration. As alternatives, tissue engineering approaches are promising solutions. However, design of a bi-layer matrix having both the dermis and epidermis layers with proper functionality is still challenging<sup>2</sup>.

In this current study, a bilayer skin model was produced to mimic the natural organization of the skin. Thin layer collagen foams with small pores and suitable degradation rate will serve as the epidermis layer, which would enable oxygen permeability and prevent microbial infection. Sodium carboxymethyl cellulose (NaCMC) foams having larger pores and high water retention capacity are aimed to form the dermis layer, which would keep the hydration levels in required ranges and be scaffold for the cells to attach and proliferate for regeneration of the skin. To mimic the skin, human keratinocytes and dermal fibroblasts are loaded to the bilayer scaffolds.

### EXPERIMENTAL METHODS

Collagen solution was prepared in acetic acid, frozen at -80°C and lyophilized. Foams were crosslinked by dehydrothermal treatment (DHT) at 140°C for 24 h, and/or *via* glutaraldehyde (Glu) treatment. NaCMC solutions were prepared in distilled water and lyophilized and crosslinked with epichlorohydrin and by DHT at 140°C for 3 h. All samples were examined with stereomicroscope and SEM. *In situ* degradation profiles were studied by incubating the samples in PBS (pH 7.4) for two weeks. Enzymatic degradation of the collagen foams was also studied by incubating in Collagenase Type II (0.1 mg/mL in PBS pH 7.4) for 3 h at 37°C. At predetermined time points, the samples were taken out, lyophilized and weighed. Material loss was determined gravimetrically. Swelling of the NaCMC foams were determined after incubating in PBS pH 7.4 for 24 h, at 37°C. Weights of the samples were recorded in dry and swollen form. For the tests of biocompatibility, human keratinocytes (HS2) were seeded in the epidermis (collagen) layer, and human dermal fibroblasts (Detroit 551) were seeded in the dermis (NaCMC) layer with different seeding protocols. Cell attachment, proliferation and distribution within the scaffolds were examined.

### RESULTS AND DISCUSSION

SEM and stereomicroscopy images showed that NaCMC-5 (prepared from 5% solution) foams prepared at -80°C and -20°C yielded sheet like or circular pores, respectively (Figure 1A and B). *In situ* degradation profiles of all NaCMC foams were similar ( $p \leq 0.05$ ), where they lost about 35% of their initial weights after 14 days of incubation in PBS. For this reason, NaCMC-5 foams frozen at -20°C were chosen for the rest of the study to prepare bilayers. Bilayer structures were prepared by combining NaCMC-5 foams at bottom and collagen foams at top (Figure 1C). Collagen foams were highly stable *in situ* and against Collagenase type II enzyme and more than 80% of their initial weights remained after two weeks and 3 h of incubations, respectively. Cell culture and co-culture studies revealed that with earlier seeding of keratinocytes and subsequent seeding of dermal fibroblasts, it was possible to maintain the cellularized bi-layered skin like structure for up to 14 days.

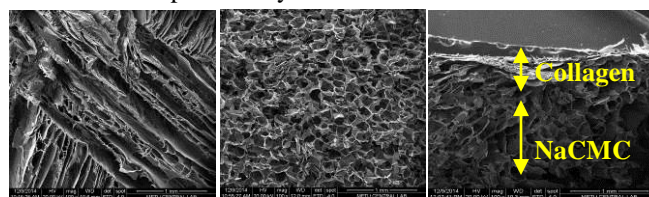


**Figure 1:** SEM images. A) Frozen at -80°C, B) Frozen at -20°C, and C) Collagen and NaCMC-5 bilayer.

### CONCLUSION

Collagen foams with small pores and demonstrating certain stability in *in situ* PBS media as well as for enzymatic degradation were obtained to serve as the epidermis layer of the skin. NaCMC-5 foams that have uniform and interconnected pores and appropriate stability *in situ* were used as dermis layer. High water retention capacity of NaCMC-5 foams was suitable for hydration needs of the dermis layer. For the construction of the bilayer skin structures, the results are promising.

### REFERENCES

- 1-Brohem, C. A. et al. *Pigment Cell Melanoma Res* 24(1): 35-50 (2011).
- 2-Metcalf, A. D. and M. W. *J R Soc Interface* 4(14): 413-437 (2007).

### ACKNOWLEDGMENTS

Authors acknowledge the support by TUBİTAK through the 1002 project 213 M 651; TUBİTAK for the BİDEP 2211 Scholarship for C.K. and the Turkish Ministry of Development for the establishment of BIOMATEN.

# *In Vitro* Studies of novel PLDA/Mg Composites Processed by Injection Moulding

Sandra C. Cifuentes<sup>1,2</sup>, Marcela Lieblich<sup>1</sup>, Rosario Benavente<sup>2</sup>, José Luis González-Carrasco<sup>1,3</sup>

<sup>1</sup>Centro Nacional de Investigaciones Metalúrgicas, CENIM-CSIC, Spain

<sup>2</sup>Instituto de Ciencia y Tecnología de Polímeros, ICTP-CSIC, Spain

<sup>3</sup>Centro de Investigación Biomédica en red de Bioingeniería, Biomateriales y Nanomedicina, CIBER-BBN, Spain  
[scifuentes@cenim.csic.es](mailto:scifuentes@cenim.csic.es)

## INTRODUCTION

The development of radically new materials for biodegradable and bioresorbable implants in bone repair seeks to overcome the disadvantages implicit in the use of permanent implants. The challenge is to produce a material that is suitable to be replaced by mature bone without transient loss of mechanical support. Biodegradable polymers and magnesium (Mg) alloys have played an important role writing the history of resorbable implants. Very recently, a novel approach has emerged that consists on the development of polymer/Mg<sup>1</sup> composites as new bioresorbable materials for temporary medical applications.

This work elucidates the degradation behaviour of PLDA/Mg composites processed by injection moulding. Their degradation mechanism, morphological changes and mechanical performance under *in vitro* test conditions are studied. The effect of the crystallinity degree of polymeric matrix and Mg content on the degradation behaviour of these novel composites is also evidenced.

## EXPERIMENTAL METHODS

PLDA/Mg composites with 0.2 and 1 wt % of Mg content were manufactured by injection moulding. Two types of materials were studied: As injected samples (Q), which are amorphous materials with a very low crystallinity degree ( $f_c \approx 0.10$ ), and thermally treated samples (TT), which are materials subjected under a thermal treatment at  $125 \pm 1$  °C for 1 hour that yields a crystallinity degree close to 0.45.

The degradation behaviour of PLDA/Mg composites was followed by measuring the hydrogen release, pH evolution, mass variation and water accumulation during 3 weeks. Morphological changes were followed by optical microscopy. The change in mechanical properties was measured under compression tests before and after *in vitro* testing.

## RESULTS AND DISCUSSION

Hydrogen evolution rate is larger for materials with a higher crystalline degree and with higher amount of Mg (Fig 1). The higher hydrogen release and mass loss of crystalline composites in comparison with amorphous ones could be due to the non-uniform distribution of water within the semi-crystalline matrix. The preferential diffusion of water through the amorphous domains can induce a localized corrosion on Mg particles that enhances their degradation rate.

The pH of the immersion media that simulates the physiological environment remains neutral throughout the test.

Mg degradation takes place prior degradation of the polymeric matrix. Mg particles at the surface react with immersion media faster than particles localized at composite's core. The strength retention properties of the composites are highly dependent on the crystallinity degree of the polymeric matrix. After 3 weeks, amorphous composites show 100% strength retention, whereas thermally treated composites lost 20% of stiffness and 15% of compressive strength.

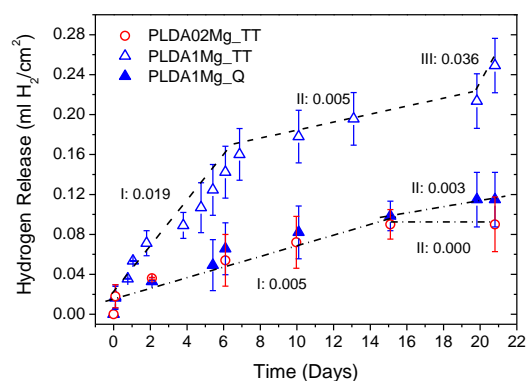


Fig 1. Accumulated amount of hydrogen released as a function of immersion time in PBS

## CONCLUSION

PLDA/Mg composites present controllable degradation rates that can be customized through polymeric matrix crystallinity or Mg particles content. Considering the *in vitro* results, these novel materials have great potential to be used as future materials for biodegradable implants.

## REFERENCES

1. S.C. Cifuentes et al (2012) *Mater Lett* **74**:239-42.

## ACKNOWLEDGMENTS

This work was supported by grants MAT2012-37736-C05-01-05 (MINECO, Spain). S.C. Cifuentes is supported by a European Social Fund for JAE-I3P Grant (CSIC). Special thanks are due to Amalia San Román and Jesús Chao (CENIM) for technical assistant.

# Quantification of Cell Migration on Culture Substrates —the Effect of the Surrounding Cells on Direction of Chondrocyte Migration—

Yotaro Nakane<sup>1</sup>, Kumpei Sano<sup>1</sup>, Kenji Isshiki<sup>1</sup>, Akihisa Otaka<sup>1</sup>, Kazuya Takahashi<sup>1</sup>, Katsura Kojima<sup>2</sup>, Yasushi Tamada<sup>3</sup> and Naohide Tomita<sup>1</sup>

<sup>1</sup> Graduate school of Engineering, Kyoto University, Japan

<sup>2</sup> National Institute of Agrobiological Sciences, Japan

<sup>3</sup> Faculty of Textile Science and Technology, Shinshu University, Japan

[nakane.youtarou.36w@st.kyoto-u.ac.jp](mailto:nakane.youtarou.36w@st.kyoto-u.ac.jp)

## INTRODUCTION

The cell–substrate interaction is known to play an important role in spatio-temporal behavior of cells such as migration. The cell migration is essential for various biological processes including wound healing and tissue formation, immune response. However, there are only a few studies to investigate multi-cellular motility. In this study, we proposed a new method to quantify the effect of surrounding cells on direction of cell migration using chondrocyte migration on fibroin and ProNectin substrate as an example.

## EXPERIMENTAL METHODS

Chondrocytes harvested from rabbit joint were seeded on fibroin coated plates and ProNectin coated plates, and time-lapse phase contrast images were acquired during a 24-hour culture ( $n = 6$  for fibroin and  $n = 5$  for ProNectin). Every cell was tracked manually, and position data of each cell was measured. The effect of the nearest cell position on direction of migration was evaluated by *direction index*, which is the cosine of the angle between velocity vector and the relative position vector of the nearest cell (Fig.1). *Direction index* was stratified into six classes by the distance from the nearest cell to distinguish taxis from other phenomena. *Direction index* more than 65  $\mu\text{m}$  away from the nearest cells was stratified by the contact. Welch's t-test was performed for *direction index* in each class with a significance level of 0.05.

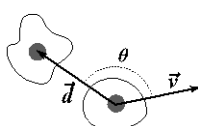
$$\text{direction index} = \frac{\vec{d} \cdot \vec{v}}{|\vec{d}| |\vec{v}|} = \cos\theta$$


Fig.1 Mathematical explanation and schematic drawing of *direction index*.

## RESULTS AND DISCUSSION

The cells less than 52  $\mu\text{m}$  away from the nearest cells on fibroin had higher *direction index* than that of ProNectin (Fig.2). Conversely the cells more than 65  $\mu\text{m}$  away from the nearest cells on fibroin had lower *direction index* than that of ProNectin (Fig.2). The *direction index* was different between the cells with the nearest cells in 65–78  $\mu\text{m}$  without contact on fibroin and those on ProNectin (Fig.3). This may suggest that some kind of taxis on chondrocyte migration may exist. One possible explanation for this interaction is the chemotaxis. Some growth factors and cytokines are reported to induce chondrocyte migration<sup>1</sup>. Another possibility is the influence of cell traces. For example, *P. aeruginosa* is reported to use its traces for the

guidance cues<sup>2</sup>. As chondrocytes produce cell traces composed of actin and integrin as they migrate<sup>3</sup>, there is a possibility that chondrocytes use traces on their migration.

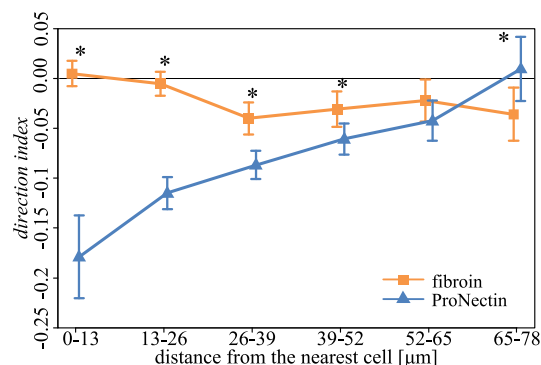


Fig.2 *Direction index* stratified by the distance from the nearest cells. (\*:  $p < 0.05$  by Welch's t-test)

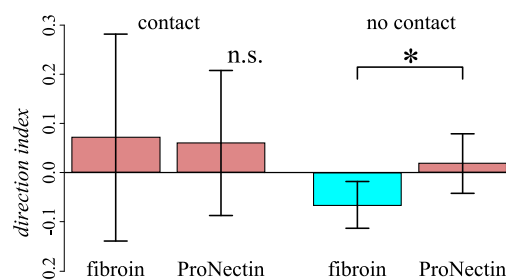


Fig.3 *Direction index* more than 65  $\mu\text{m}$  away from the nearest cells stratified by the contacts. (\*:  $p < 0.05$  by Welch's t-test)

## CONCLUSION

We proposed *direction index* to quantify the effect of surrounding cells on direction of cell migration, and used it to analyze chondrocyte migration on fibroin and ProNectin substrate. From this analysis, we suggest the existence of taxis on chondrocyte migration.

## REFERENCES

1. Mishima Y. *et al.*, J. Orthop. Res. 26:1407-1412, 2008
2. Zhao K. *et al.*, Nature 497:388-391, 2013
3. Hillgärtner M. *et al.*, Materialwiss. Werkst. 30:783-792, 1999

## ACKNOWLEDGMENTS

This work was supported by the Health and Labour Sciences Research Grant, Japan.



## Quantification of Cell Migration on Culture Substrates —Proposal of New Parameters for Co-Migration—

Hirota<sup>1</sup> Nakamura<sup>1</sup>, Kumpei Sano<sup>1</sup>, Akihisa Otake<sup>1</sup>, Kazuya Takahashi<sup>1</sup>, Yotaro Nakane<sup>1</sup>,  
Oki Shimizu<sup>1</sup>, Katsura Kojima<sup>2</sup>, Yasushi Tamada<sup>3</sup> and Naohide Tomita<sup>1</sup>

<sup>1</sup>Graduate school of Engineering, Kyoto University, Japan

<sup>2</sup>National Institute of Agrobiological Sciences, Japan

<sup>3</sup> Faculty of Textile Science and Technology, Shinshu University, Japan

[nakamura.hirota.24m@st.kyoto-u.ac.jp](mailto:nakamura.hirota.24m@st.kyoto-u.ac.jp)

### INTRODUCTION

In recent years, autologous cell implantation has gotten a lot of attention as cartilage repairing treatments. It has been reported that chondrocytes cultured in the silk fibroin sponge form cell aggregation and synthesize cartilage matrices without dedifferentiation<sup>1</sup>, but so far the mechanism of aggregation has not been clarified yet. In this study, the cell migrations are classified by the cell distance, and the relationship between migration speed and direction of the cell migration was investigated.

### EXPERIMENTAL METHODS

The chondrocytes harvested from joints of 4-week-old Japanese white rabbits were once subcultured and were seeded on culture dishes coated with fibroin substrate and with ProNectin substrate. The chondrocyte migration was observed with time-lapse microscopy for 24 hour (n=6 for fibroin, n=5 for ProNectin), and the position of each cell was acquired manually. We analyze this position data using *field direction method*<sup>2</sup>, which is a new analysis method explained as following; a certain cell are focused on and relative position vector ( $\mathbf{d}$ ), velocity vector ( $\mathbf{v}$ ) of other cells toward the focused cell and their crossing angle ( $\theta$ ) are calculated (Fig.1-a), and repeat the same process focusing on the other cells (Fig.1-b). Two kinds of velocity, absolute and relative velocity, were applied to velocity vector. These data acquired here were classified into four classes by the relative distance ( $|d|$ ).

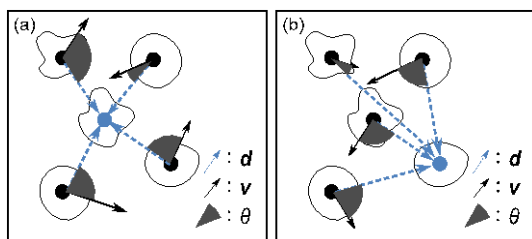


Fig.1 Schematic drawing of *field direction method*.

### RESULTS AND DISCUSSION

As shown in Fig.2, the regression coefficients of migration speed against direction were negative in the distance in 0–20  $\mu\text{m}$  class on both substrates. We called this phenomenon ‘*negative speed polarization*’<sup>3</sup> where the cell approaching speed is higher than that repulsing speed.

In comparison of absolute speed with relative speed, the average relative migration speed on fibroin was reduced by the cell distance. This may suggest co-migration of cells on fibroin substrate. There was a possibility that

this co-migration behavior on fibroin substrate promoted cell aggregation. In previous research, ProNectin substrate tends to show higher cell-substratum adhesive force than that of fibroin substrate<sup>4</sup>. Taking the above into consideration, different behaviors of the chondrocytes on two substrates were thought to be causally related to different adhesive force.

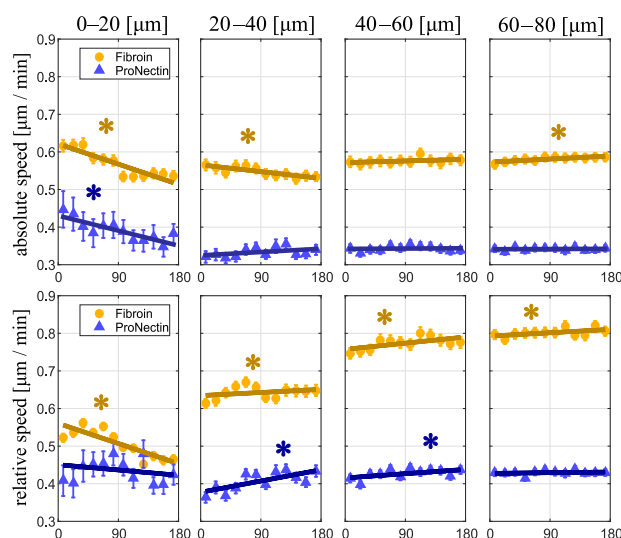


Fig.2 Classified chondrocytes' average migration speed and regression line on fibroin and ProNectin. (Error bars represent 95% confidential intervals. \*:  $p < 0.05$  of regression coefficients by t-test)

### CONCLUSION

The ‘*negative speed polarization*’ where the cell approaching speed is higher than that repulsing speed, was observed by *field direction method* on fibroin and ProNectin substrate. And co-migration behavior of the cells, where the averaged relative migration speed was reduced by the cell distance, was also observed on fibroin substrate.

### REFERENCES

1. Kawakami M. *et al.*, Biomed.Mater.Eng. 21:53-61, 2011
2. Sano K., master thesis, Kyoto University, Kyoto, Japan, 2015 (Japanese)
3. Nakane Y., graduation thesis, Kyoto University, Kyoto, Japan, 2014 (Japanese)
4. Kambe Y. *et al.*, Biomaterials. 31:7503-7511, 2010

### ACKNOWLEDGMENTS

This work was supported by the Health and Labour Sciences Research Grant, Japan.



## Wet Spun Scaffolds of PHA-PLA Blend for Bone Tissue Engineering

Ayşe Selcen Alagoz<sup>1</sup>, Jose Carlos Rodriguez-Cabello<sup>5</sup>, Nesrin Hasirci<sup>2,3,4</sup>, Vasif Hasirci<sup>1,2,4</sup>

Depts. of <sup>1</sup>Biological Sciences, <sup>2</sup>Biotechnology, <sup>3</sup>Chemistry, METU, Turkey

<sup>4</sup>BIOMATEN, Center of Excellence in Biomaterials and Tissue Engineering, METU, Turkey, <sup>5</sup>Department of Condensed Material, Universidad de Valladolid, Spain  
[selcen.alagoz@metu.edu.tr](mailto:selcen.alagoz@metu.edu.tr)

### INTRODUCTION

Bone defects related with trauma, aging, diseases, tumors, and nonunion fractures increasingly create health problems. Each year, over 6.2 million bone fractures happen in the U.S. and 10% of them do not properly heal because of delayed union or non-union. Also, osteoporosis currently affects 10 million people and this is estimated to increase to 14 million by 2020<sup>1</sup>. Wet spinning is a simple approach that, does not require elaborate equipment and its products have pores and gaps that are randomly distributed and not uniform in size.

In this study, a poly(3-hydroxyalkanoate)-poly(lactic acid) (PHA-PLA) blend was used to fabricate a wet spun scaffold for use in bone tissue engineering. An elastin like recombinamer (ELR) with REDV sequences specific for endothelial cells<sup>2</sup> was introduced to the scaffold to make it attractive for endothelial cells so that it can be vascularized as needed in a thick implant which otherwise cannot maintain the viability of the cells that have penetrated deep into the scaffold.

### EXPERIMENTAL METHODS

PHA-PLA scaffolds were produced by wet spinning, mechanical properties were measured under compression, and fiber morphology and porosity were determined by SEM and micro CT. Scaffold chemistry was modified by exposing to oxygen plasma and contact angles were determined with a goniometer. After oxygen plasma treatment, surface of the fibers was coated with ELR by dip coating technique. Staining with Toluidine Blue and FTIR-ATR analysis were used to show the protein presence on the surface.

### RESULTS AND DISCUSSION

Average fiber diameter of the scaffolds was measured with NIH imageJ program as 100  $\mu\text{m}$ .  $\mu\text{-CT}$  images showed well defined, interconnected 3D structure with a porosity of approximately 77% (Figure 1).

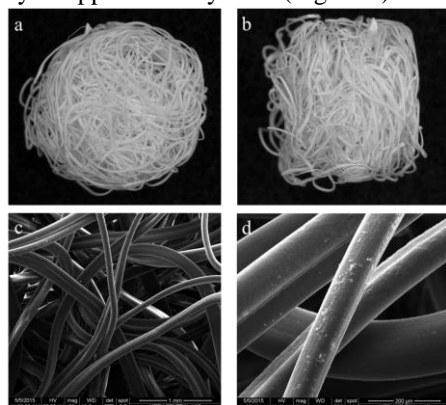


**Figure 1:** Microscopic images of PHA-PLA scaffolds. Stereomicroscope (a) top, and (b) side views of scaffold. SEM micrographs (c) top view (scale bar: 1 mm), and (d) top view at higher magnification fibers (scale bar: 200  $\mu\text{m}$ ).

The ultimate compressive strength of the dry scaffolds under compression (5 mm/min) found to be  $1.25 \pm 0.10$  (MPa). This result indicated that PHA-PLA wet spun scaffolds are too soft for cortical bone and compact bone. The contact angle of the PHA-PLA films decreased from  $83^\circ$  to  $63^\circ$  after oxygen plasma treatment ( $p \leq 0.05$ ) indicating that the wettability of PHA-PLA blend was improved. Blue stains on the surface of ELR attached PHA-PLA films were observed after treatment with Toluidine Blue. FTIR-ATR showed that upon treatment with  $\text{O}_2$  plasma new peaks at around  $1530\text{ cm}^{-1}$  and  $1650\text{ cm}^{-1}$  were observed due to stretching of the carbonyl groups. After ELR attachment, these peaks became more intense. This was probably due to the amide I and amide II groups of ELR attached onto the PHA-PLA film<sup>3</sup>.

### CONCLUSION

The results of this study indicated that wet spinning technique could be used to obtain highly porous fiber mesh scaffolds from PHA-PLA blend. Compression test results showed that samples could more suitable for use non load bearing application. Plasma modification made the PHA-PLA surfaces more hydrophobic when compared with untreated PHA-PLA scaffolds and therefore they are more suitable for bone tissue engineering.

### REFERENCES

1. Fu et al., Materials Science and Engineering. C, 31(7), 1245-1256, 2011.
2. Garcia et al., Tissue Engineering. 15(4): 887-899, 2009.
3. Serrano et al., Biophysical Journal. 93:2429-2435, 2007.

### ACKNOWLEDGMENTS

The authors would like to thank METU (BAP-06-11-2013-014), BIOMATEN and the Ministry of Development Turkey for financial support.

## Bone Formation in a Rat Tibial Defect Model Using Carboxymethyl Cellulose/BioC/Bone Morphogenic Protein-2 Hybrid Materials

Young-Pil Yun<sup>1</sup>, Sang-Heon Song<sup>2</sup>, Hak-Jun Kim<sup>1</sup>, Kyeongsoon Park<sup>3</sup>, Sung Eun Kim<sup>1</sup>, Hae-Ryong Song<sup>1</sup>.

<sup>1</sup>Department of Orthopedic Surgery and Rare Diseases Institute, Korea University Medical College, Korea

<sup>2</sup>Department of Orthopedic Surgery, Myongji Hospital, Korea

<sup>3</sup>Division of Bio-imaging, Chuncheon Center, Korea Basic Science Institute, Korea

[ofeel0479@korea.ac.kr](mailto:ofeel0479@korea.ac.kr)

### INTRODUCTION

Hydroxyapatite (HAp) and calcium phosphate (CaP) have been successfully used as bone graft materials for the regeneration of bone defects due to their physical and chemical properties and their structural similarity to natural bone. CaP-based materials possess bioactive, biocompatible, and osteoconductive properties. CaP-based materials have been approved by the Food and Drug Administration (FDA) for clinical applications in the fields of dental and orthopedic surgery <sup>1</sup>.

On the basis of these results, we hypothesized that a CMC-based hydrogel containing BioC (biphasic calcium phosphate (BCP); tricalcium phosphate (TCP): hydroxyapatite (HAp) = 70:30) and bone morphogenic proteins-2 (BMP-2) would promote greater bone formation in a rat tibial defect model than would a CMC-based hydrogel containing BioC without BMP-2<sup>2</sup>.

### EXPERIMENTAL METHODS

**Animal study.** Eight-week-old Sprague-Dawley rats (Orient Bio Co., Seongnam City, Korea) were used for the in vivo evaluation of CMC/BioC, CMC/BioC/BMP-2 (0.1 mg), and CMC/BioC/BMP-2 (0.5 mg) groups.

**Plain Radiographs & Microcomputed Tomography (Micro-CT) Evaluation.** At 4 and 8 weeks after injection, samples were fixed in 3.7% paraformaldehyde solution. Radiographs of the specimens were obtained with a plain radiograph apparatus (In Vivo DXS 4000 Pro System, Carestream Health, Rochester, NY, USA), bone volume was obtained with a micro-CT system (Albira II Imaging System, Carestream Health). The CT image analysis was performed with a bone analyzer (Molecular Imaging Analysis software; Carestream Health Inc., Woodbridge, VA, USA).

**Histological Study.** The specimens were retrieved at 4 and 8 weeks. After decalcification, the samples were embedded in paraffin. The tissues were cross-sectioned at an 8  $\mu$ m thickness in the longitudinal parallel direction and stained with hematoxylin and eosin (H&E) and Masson's trichrome staining.

**Statistical Analysis.** Data are presented as mean  $\pm$  standard deviation. Statistical comparisons were carried out via one-way analysis of variance using Systat software (Chicago, IL, USA). Differences were considered statistically significant at  $*P < 0.05$  and  $**P < 0.001$ .

### RESULTS AND DISCUSSION

At 4 weeks after surgery, the plain radiographs revealed no mineralization at the defect area for the CMC/BioC group but slight mineralization for the CMC/BioC/BMP-2 (0.1 mg) and CMC/BioC/BMP-2

(0.5 mg) groups. At 8 weeks after surgery, both the CMC/BioC/BMP-2 (0.1 mg) and CMC/BioC/BMP-2 (0.5 mg) groups showed much more mineralization than did the CMC/BioC group. All three groups showed much greater mineralization at 8 weeks than at 4 weeks.

	BV/TV(%)		Tb.Th(mm)	
	4 week	8 week	4 week	8 week
CMC/Bio-C	36.22 $\pm$ 1.29	44.89 $\pm$ 2.24	32.91 $\pm$ 4.25	34.42 $\pm$ 4.05
BMP-2(0.1mg)/CMC/Bio-C	39.24 $\pm$ 1.19	*52.27 $\pm$ 3.16	*42.06 $\pm$ 3.27	*45.10 $\pm$ 2.06
BMP-2(0.5mg)/CMC/Bio-C	**48.53 $\pm$ 1.25	**67.46 $\pm$ 3.0	*51.13 $\pm$ 2.78	**66.08 $\pm$ 4.14

Table 1. Bone formation and bone remodelling. BV: Bone volume, TV: Total volume, Tb.Th: Trabecular thickness.

Our results suggest that CMC/BioC/BMP-2 hybrid materials induce greater bone formation at an earlier stage through release of BMP-2 than CMC/BioC hybrid materials. However, our in vivo study has some limitations. For example, long-term evaluation greater than 8 weeks is needed to compare the quality and architecture of new bone formation between control and implanted groups. More comprehensive analyses that include the histology and angiogenesis of new bone and biomechanical testing are needed. Finally, the effects of long-term release of BMP-2 require further investigation.

### CONCLUSION

CMC/BioC/BMP-2 (0.5 mg) hybrid materials implanted in a rat tibial defect model led to greater bone formation than did CMC/BioC and CMC/BioC/BMP-2 (0.1 mg) hybrid materials. Thus, CMC/BioC/BMP-2 hybrid materials may be useful in an injectable substrate for the clinical application of the regeneration of bone defects in the orthopedic field.

### REFERENCES

1. LeGeros R. Z., Chem. Rev. 108:4742-4753, 2008.
2. Arosarena O. A. and Puleo D., Arch. Facial Plastic Surg. 9:242-247, 2007.

### ACKNOWLEDGMENTS

This study was supported by a Grant from the Korea Healthcare Technology R&D Project, Ministry of Health and Welfare, Republic of Korea (HI11C0388).



## Acellular Periodontal Ligament Matrix for Artificial Tooth Implant

Naoko Nakamura<sup>1</sup>, Tsuyoshi Kimura<sup>1</sup>, Ai Ito<sup>1</sup>, Toshiya Fujisato<sup>2</sup>, Takashi Tsuji<sup>3</sup>, Akio Kishida<sup>1</sup>.

<sup>1</sup>Institute of Biomaterials and Bioengineering, Tokyo Medical and Dental University, Japan

<sup>2</sup>Faculty of Engineering, Osaka Institute of Technology, Japan

<sup>3</sup>Center for Development Biology, RIKEN, Japan

[nakamura.nmbme@tmd.ac.jp](mailto:nakamura.nmbme@tmd.ac.jp)

### INTRODUCTION

Dental implant has become a major treatment for lack of teeth. As the implant is inserted to alveolar bone directly, it lacks periodontal ligament (PDL) that can be got the feeling such as chewiness and firmness of foods and can prevent the infection. Moreover, in the case of the decreasing the alveolar bone for supporting the implant, the enlargement of bone is needed before or at the same time of implant treatment. Here, we investigated the reconstruction of the unit of periodontal tissue, including the alveolar bone, PDL matrix, and artificial tooth, as a novel treatment for periodontal tissue, expecting to implant it into the lack of alveolar bone. In this study, we prepared the decellularized mandible bone remained the PDL matrix and evaluated the reconstruction of the unit of periodontal tissue using artificial tooth, focusing the adhesion of PDL matrix and artificial tooth.

### EXPERIMENTAL METHODS

The units of mandible bone with molar were harvested from mouse. They were treated by high hydrostatic pressure and washed in order to remove the cells from tissue<sup>1)</sup>. After additional treatment of detergent, the molar were pulled out from the decellularized units. The decellularization was evaluated by H-E staining and DNA quantitation. For *in vitro* and *in vivo* study, PDL fibroblasts were harvested from rat PDL. The cells were seeded on the decellularized PDL matrix that was remained on the decellularized alveolar bone. After seeding of rat PDL fibroblasts to decellularized PDL matrix, they were implanted under the renal capsule of rats. As a model of artificial molar, molars that were obtained from decellularized units were used. They were demineralized and recalcified by alternate immersion of CaCl<sub>2</sub> in Tris-HCl and Na<sub>2</sub>HPO<sub>4</sub> solution<sup>2)</sup>. The recalcified molars were inserted to recellularized PDL matrix on decellularized mandible bone *in vitro*. They were implanted under the renal capsule of rats for three weeks. The adhesion of recalcified molar and decellularized PDL matrix were evaluated by H-E staining.

### RESULTS AND DISCUSSION

The units of mandible bone with molar were decellularized by high hydrostatic pressure treatment. In the case of the molar was pulled out from the mandible bone, the PDL matrix was usually attached on the molar. On the other hand, by detergent treatment before the pulling out the molars, the PDL matrix was

maintained on the mandible bone after molar extraction. In order to evaluate the recellularization of decellularized PDL matrix by PDL fibroblasts, the cells were seeded on the decellularized PDL matrix. The PDL fibroblasts were observed not only on but also inside the decellularized PDL matrix, although the orientation of the cells were not similar to original tissue. The decellularized mandible bones with PDL matrix were implanted under the renal capsule of rats after seeding the PDL fibroblasts. Three weeks after implantation, they were not observed the inflammation and absorption under renal capsule. Many cells were observed in decellularized PDL matrix. Moreover, the orientations of the cells in PDL matrix were similar to original, indicating the cells oriented along the collagen fiber of PDL matrix.

As a model of artificial molar, we here used the molars that were pulled out from decellularized mandible bones in order to fit the decellularized mandible bones. The molars were demineralized and recalcified by alternate immersion treatment. The observation of scanning electron microscope showed that the surfaces of recalcified molar were covered with calcium phosphate. The recalcified molar was inserted to decellularized mandible bone, and they were implanted under the renal capsule of rat. The artificial molars were adhered to PDL matrix on decellularized mandible bone. It indicated that the artificial tooth was able to adhere to the decellularized mandible bone by recellularization of the decellularized PDL matrix. Moreover, this result shows the surface characteristics of artificial tooth for adhesion to PDL matrix. For a future work, the artificial tooth that has an appropriate shape prepared by CAD/CAM would be needed surface modification to induce the adhesion to PDL matrix.

### CONCLUSION

Decellularized mandible bone with PDL matrix could reconstruct the unit of periodontal tissue using artificial tooth model. It suggested that it would become a novel treatment for periodontitis and mandible bone defect.

### REFERENCES

- 1 Nakamura N. et al. Advanced Biomedical Engineering 2013;2:95-100.
- 2 Taguchi T. et al. Biomaterials 2002;22:53-58.

### ACKNOWLEDGMENTS

This work was supported by Grant-in-Aid Scientific Research (A) and (B).



Karel Výborný<sup>1,2</sup>, Zuzana Kočí<sup>1,2</sup>, Oleg Lunov<sup>3</sup>, Eva Syková<sup>1,2</sup>, Šárka Kubinová<sup>1</sup>

<sup>1</sup>Institute of Experimental Medicine, AS CR, Prague, Czech Republic

<sup>2</sup> Department of Neuroscience, 2nd Medical Faculty, Charles University, Prague, Czech Republic

<sup>3</sup> Institute of Physics, AS CR, Prague, Czech Republic

[karel.vyborny@biomed.cas.cz](mailto:karel.vyborny@biomed.cas.cz)

## INTRODUCTION

Extracellular matrix (ECM) scaffolds prepared by tissue decellularization preserve the composition, mechanical integrity, and biological activity of the native ECM. While ECM scaffolds are commonly used for various tissue reconstructions, including skin, muscles, bone, cartilage, trachea, lung or heart, there is little evidence of their use in CNS tissue reconstruction. The aim of this study is to prepare injectable ECM hydrogels from CNS and non-CNS tissues and compare their physical, biochemical and biological properties in vitro.

## EXPERIMENTAL METHODS

Four types of ECM hydrogels were prepared by the decellularization of porcine brain (BM), porcine spinal cord (SCM), porcine urinary bladder (UBM) and human umbilical cord (WJM)<sup>1</sup>. All materials were characterized in terms of their residual DNA concentration as well as their collagen and glycosaminoglycans content. The morphologies and mechanical properties of the hydrogels were characterized by scanning electron microscope (SEM), atomic force microscopy (AFM) and rheometry. The viability and migration of MSCs isolated from bone marrow (BM MSCs), adipose tissue (ASCs) and Wharton jelly (WJ MSCs) were evaluated using a WST assay and xCELLigence system. The neurotrophic properties of ECM hydrogels were assessed on dorsal root ganglion (DRG) explant cultures.

## RESULTS AND DISCUSSION

All ECM hydrogels showed a three-dimensional porous fibrillar structure (Fig.1). In terms of composition, WJM hydrogels contained the highest concentration of sulphated glycosaminoglycans and collagen.

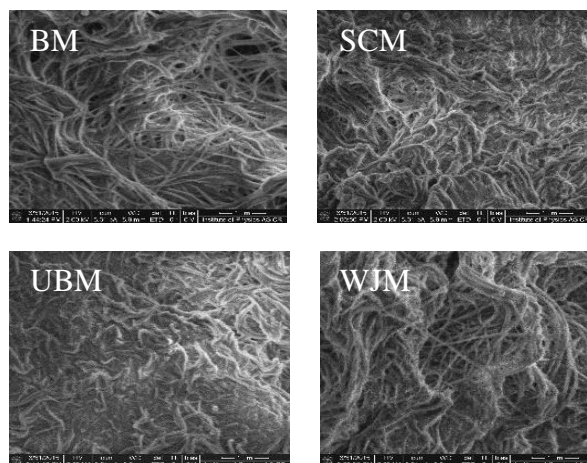


Fig. 1. SEM images of ECM hydrogels from porcine brain (BM), spinal cord (SCM) and urinary bladder (UBM) and human umbilical cord (WJM).

## CONCLUSION

All types of ECM hydrogels promoted the proliferation and migration of hMSCs. Moreover, all types of ECM also promoted massive neurite sprouting out of DRG explants.

## REFERENCES

1. Medberry C. J., Crapo P. M., Siu B. F., Carruthers C. A., Wolf M. T., Nagarkar S. P., Agrawal V., Jones K. E., Kelly J., Johnson S. A., Velankar S. S., Watkins S. C., Modo M., Badylak S. F.: *Biomaterials* 34(4), 1033 (2013).

## ACKNOWLEDGMENTS

This project was supported by GAUK 1846214, , GAČR 15-01396S, LO1309 of the MEYS CR.



## A Novel Human Plasma-Derived Medium Supplement for Xeno-Free Culture of hMSC

Ewa Bauman<sup>1,2,3,4</sup>, Cristina C. Barrias<sup>1,2</sup>, Arantxa Blázquez<sup>1,2,3,4</sup>, José M Diez<sup>4</sup>, Rodrigo Gajardo<sup>4</sup>, Salvador Grancha<sup>4</sup>

<sup>1</sup>I3S, Instituto de Investigação e Inovação em Saúde, Universidade do Porto (UP)

<sup>2</sup>INEB – Instituto de Engenharia Biomédica, UP, Portugal

<sup>3</sup>Faculdade de Engenharia, UP, Portugal

<sup>4</sup>Research&Development Biologics Industrial Group, Grifols, Parets del Vallès, Barcelona, Spain

[ewa.bauman@ineb.up.pt](mailto:ewa.bauman@ineb.up.pt)

### INTRODUCTION

Mesenchymal stromal cells (MSC) – are currently a focus of many intense studies worldwide, aiming on both defining their nature and developing cell-based therapies for regenerative medicine (1). The constantly increasing use of human MSC (hMSC) in clinical trials calls for the development of robust, reproducible and, most importantly, safe methods for the expansion of these cells. Fetal bovine serum (FBS), despite many disadvantages such as its high variability between batches and ill-defined composition, still remains widespread applied as a medium supplement for hMSC cultures (2,3). SCC (supplement for cell culture) is a novel xeno-free cell culture supplement under development at Grifols that supports the growth of hMSC and several other cell lines (4). SCC is obtained from well-controlled human plasma starting material through Cohn-Oncley industrial plasma fractionation and manufactured under GMP rules.

### EXPERIMENTAL METHODS

hMSC of different origin (bone marrow, umbilical cord and adipose tissue) were purchased from commercial suppliers (Lonza and Promocell); furthermore non-commercial bone marrow-hMSC from 28-year old male donor were obtained from blood bank. Cells were cultured in home-made xeno-free media formulations supplemented with SCC for several passages and then characterized. Cell viability and cell yield were assessed with an automated cell counter. Immunofluorescence staining was used to qualitatively determine hMSC-characteristic cell markers. hMSC were further brought under adipogenic, osteogenic, chondrogenic and neurogenic differentiation. Differentiation was assessed by observation of cell morphology changes and by specific staining procedures. In addition, SCC was tested as a supplement for cryopreservation medium for hMSC.

### RESULTS AND DISCUSSION

The hMSC cultured in media supplemented with SCC maintained correct morphology and the expression of a set of characteristic surface markers. They were positive for CD29, CD44, CD90, CD105, CD146, CD166, and Stro-1, whereas they were negative for CD14 and CD19. hMSC cultured in SCC-supplemented media were characterized by an elongated, spindle-shaped morphology. The growth rates of hMSC cultured in xeno-free formulations were in general comparable to the ones observed in non xeno-free media – either commercial or home-prepared.

In SCC-supplemented media the growth of umbilical cord-hMSC was faster than BM-MSC and AT-MSC, which confirms the well-described high proliferation potential of neonatal MSCs. Moreover, their potential to differentiate into adipogenic, osteogenic, chondrogenic and neurogenic lines was preserved. Figure 1 shows AT-MSC brought under respective differentiation assays. The results of the present study imply that SCC possesses a high potential as a supplement for hMSC xeno-free culture media.

### CONCLUSION

hMSC were successfully expanded in SCC-supplemented xeno-free media formulations while maintaining their phenotype and differentiation potential. SCC can be considered a potential candidate for cell culture supplement in advanced cell therapies.

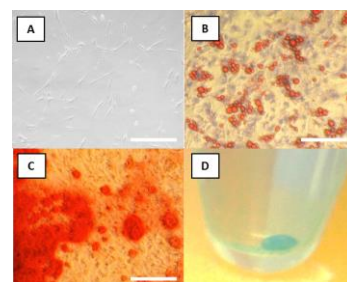


Figure 1. Morphology and differentiation potential of AT-MSCs cultured in SCC-supplemented media: A. Cell morphology, B. Adipogenesis, C. Osteogenesis, D. Chondrogenesis. (Scale bars correspond to 200  $\mu$ m)

### REFERENCES

1. Nombela-Arrieta C et al., Nature Reviews Molecular Cell Biology 2011 12(2):126–131.
2. Tekkotte Ch et al., Stem Cells International 2011:504723.
3. Bernardo ME et al., Journal of Cellular Physiology 2007 211: 121–130.
4. Diez JM et al., Stem cell research and therapy 2015 Mar 13;6(1):28.

### ACKNOWLEDGMENTS

The project is a part of a Marie Curie Initial Training Network - European Industrial Doctorate (ITN-EID) IB2 (317052), and has been funded under the European Community 7th Framework Programme. The authors gratefully acknowledge the collaboration of Daniel Casals, Laura Gómez, Judith Luque and Eduard Sala (R&D Biologics Industrial Group, Grifols).



## ***In vitro* Hemolysis Assay and Platelet Aggregation Test of PEG Hydrogels for Tissue Engineering Applications**

Alondra Escudero-Castellanos<sup>1,2</sup>, Jaime Flores-Estrada<sup>3</sup>, Victoria Domínguez-García<sup>1</sup>, Blanca Elí Ocampo-García<sup>4</sup>,  
Miriam V. Flores-Merino<sup>1</sup>

<sup>1</sup>Research Center in Medical Sciences, Autonomous University of the State of Mexico (UAEM), México, <sup>2</sup>School of Medicine, UAEM, Mexico, <sup>3</sup>School of Chemistry, UAEM, México

<sup>4</sup>ININ, National Institute of Nuclear Research, México.

[mv.flores.merino@gmail.com](mailto:mv.flores.merino@gmail.com)

### **INTRODUCTION**

Biocompatibility is an essential characteristic that all biomaterials must have for their use in the field of tissue engineering<sup>1</sup>. One type of widely used biomaterials are hydrogels matrices, however their preparation involves mixing of various additives, which increase the risk of inducing cytotoxicity<sup>2</sup>. Hemocompatibility tests are important because they allow to evaluate the potential damage of blood cells due to its exposure to biomaterials<sup>3</sup>. Therefore, in this study three different hydrogels based on Polyethylene glycol (PEG) were studied.

### **EXPERIMENTAL METHODS**

PEG-chitosan, PEG-arm, and PEG-4000 hydrogels were embedded in blood samples from healthy volunteers. Subsequently, they were evaluated under the following *in vitro* hemocompatibility studies: hemolysis assay and platelet aggregation in blood samples of healthy volunteers, according to ISO 10 993-4 (1992). The authors certify that all research was done under full compliance with the Helsinki Declaration (2013).

### **RESULTS AND DISCUSSION**

Qualitative evidence of hemolysis was negative in samples that were in contact with the polymeric biomaterials. In the quantitative study it was found that all hydrogels exhibited less than 5% hemolysis. The higher hemolysis value was 1.72% in samples that were in contact with PEG-arm hydrogel (Fig. 1). In the study of platelet aggregation cells displayed a very similar morphology compared with the negative control and agglomerates were not observed (Fig. 2).

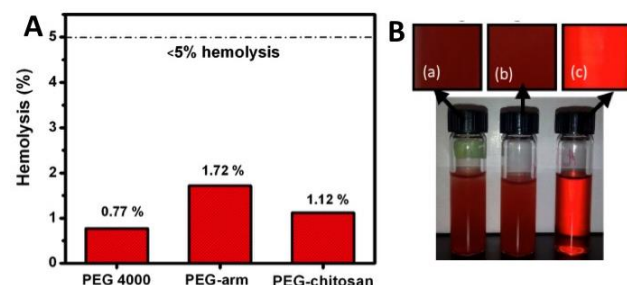


Fig.1. Direct *in vitro* hemolysis assay based on ISO 10993-4 (1992). A) Quantitative evaluation: 5% of human red blood cells (RBC) were incubated in direct contact with PEG hydrogel samples (60 min, 37 °C). The average absorbance of the positive control (+C) is considered as 100% hemolysis and the average absorbance of the negative control (-C) is considered as 0%, for each sample (n=3, *t* test: *p*<0.05). B) Qualitative assessment. Each tube contains 5% of RBC and (a) PEG hydrogel sample (b) isotonic saline solution (-C) and (c) distilled water (+C).

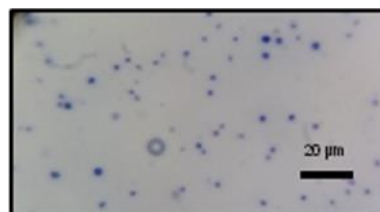


Fig 2. Micrograph of wright-stained platelet rich plasma (PRP) smear. Human platelets were in direct contact with PEG-chitosan hydrogel showing non-aggregated and rounded platelet. It indicates the absence of platelet activity (wright staining)

PEG has the characteristic of reducing cell adhesion<sup>4</sup>, this characteristic make it an excellent biocompatible material. In this study PEG-arm showed the higher percentage of hemolysis in direct contact with blood cells, this could be due to the additives used in the synthesis process. Although, the results showed that all PEG hydrogels guarantee a percentage of hemolysis below five and can be considered compatible with RBC.

### **CONCLUSIONS**

Studies showed that PEG based biomaterials are hemocompatible as they do not damage erythrocytes or platelets in the conditions studied, therefore PEG hydrogels have promising potential for their use in tissue engineering. Finally, it is necessary to expand studies evaluating blood cells in direct contact with PEG hydrogels and generate studies to study leukocyte behaviour in direct contact with PEG biomaterials.

### **REFERENCES**

- Atala A, Lanza R, Thomson J, Nerem R. Principles of Regenerative Medicine. Canada: Academic Press, Elsevier. Canada; 2011
- Franco RA, Min Y, Yang H, Lee B. J Biomater Appl., 27(5): 605-615, 2011
- Motlagh D, Yang J, Lui KY, Webb AR, Ameer GA. Biomaterials, 27: 4315 – 4324, 2006
- Balakrishnan B, Kumar DS, Yoshida Y, Jayakrishnan A. Biomaterials, 26: 3495–3502, 2005

### **ACKNOWLEDGMENTS**

The authors would like to thank the project UAEM 3890/2015FS and CONACYT for providing financial support to this project.

## Elastin-like Recombinamer and Allogeneic Mesenchymal Stem Cells for repair of Rotator Cuff Injury in Infrapinatus Tendon Rabbit Animal Model

Alessandra Girotti<sup>1</sup>, Matilde Alonso<sup>1</sup>, Arturo Ibañez<sup>1</sup>, José María Trigueros Larrea<sup>2</sup>, Aurelio Vega Castrillo<sup>2</sup>, Ana Sánchez García<sup>3</sup>, Ángel Luis Gato<sup>4</sup>, Francisco J. Santos Martín<sup>5</sup>, Jose Carlos Rodríguez-Cabello<sup>1</sup>

<sup>1</sup>Bioforge Res. Group, CIBER-BBN, University of Valladolid, Paseo Belén 19, Spain

<sup>2</sup>Hospital Clínico Universitario de Valladolid, Spain

<sup>3</sup>IBGM Institute University of Valladolid, Spain

<sup>4</sup>Anatomy and Radiology Department University of Valladolid, Spain

<sup>5</sup>E.T.S.I.I University of Valladolid, Spain

[agirotti@bioforge.uva.es](mailto:agirotti@bioforge.uva.es)

### INTRODUCTION

Shoulder pain is the third most common musculoskeletal pathology, the rotator cuff injury affects more than 40% of patients over 60 years and causes disabling pain and loss of shoulder functionality<sup>1</sup>. Despite the recent improvements and advances in the surgery, there remains a failure rate of between 20% and 70%. To obtain the tendon repair augmentation new treatment strategies are directed to reinforce the mechanical properties and the biological healing capacity by implanting matrices, although the currently in use cause inflammatory reaction<sup>2</sup>. In this study we employed a modified version of an advanced matrix that has been demonstrating high efficiency as bioactive support<sup>3</sup> in regenerative medicine. It belongs to a family of (ELRs) the Elastin-like recombinamers with high mechanical performance designed as injectable thermogelling systems<sup>4</sup>. The matrix was co-injected with rabbit bone marrow mesenchymal stem cells (rMSCs), under physiological conditions to evaluate the effect of cell therapy on the tendon pathology.

### EXPERIMENTAL METHODS

ELRs were produced by DNA recombinant techniques and *E. coli* biosynthesis. Rabbit mesenchymal stem cells (rMSCs) were obtained from rabbit bone marrow and BrdU stained. New Zealand rabbits with critical defect in the infrapinatus tendon were randomly allocated into 3 groups (negative control, treated with ELRs matrix, treated with ELRs matrix and rMSCs). At 4 and 16 weeks the animals were sacrificed and their tendons removed to perform biomechanical tests and immunohistochemical analysis.

### RESULTS AND DISCUSSION

This study describes the use of injectable thermogelling scaffold whose applicability is focused specifically on regenerative medicine. The scaffold generated "in situ" under physiological condition was assayed in combination or not with rMSCs for an artificial matrix that improved tendon repair capacity. The results at 4 and 16 weeks were compared with which obtained adding ELR matrix and with the normal healing process the after injury of the infrapinatus tendon in rabbits.

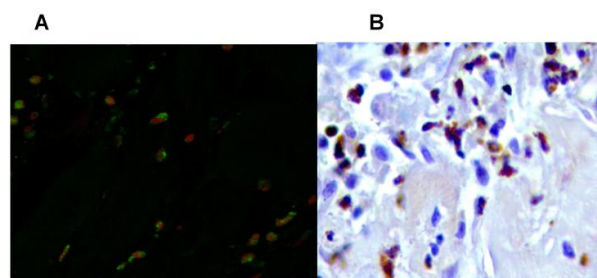


Fig. Showed the BRdU stained rMSCs and the ELR matrix after 1 month in the rabbit tendon implantation.

In this work we observed a stronger and more physiological infrapinatus tendon repair using allogeneic rabbit mesenchymal stem cells in combination with an innovative ELRs thermogelling scaffold.

### CONCLUSION

The thermo-gelling property of the ELRs matrix has greatly facilitated the surgical technique as it is easier to handle (for injection), especially when used arthroscopically. The effects of adding rMSCs embedded in a matrix of ELR for the tendon suture repair of the infrapinatus tendon has been studied in New Zealand rabbits. The rMSCs showed a high proliferation rate in the ELRs matrix when implanted in the tendons and a reinforced structural was obtained as was proved through the biomechanical, histological and immunohistochemical assays.

### REFERENCES

References must be numbered. Keep the same style.

1. Vitale MA *et al.*, J. Should Elbow surg.16:181-7, 2007.
2. Ricchetti ET *et al.*, J.Should Elbow surg; 21: 251-5, 2012.
3. PCT/ES2010/070084
4. Girotti A *et al.*, Adv Healthc Mat in press 2015

### ACKNOWLEDGMENTS

The authors would like to thank the MINECO MAT2012-38043, the CIBER-BBN and the Castilla y Leon "Consejería de Sanidad" for providing financial support to this project.

Jason Bolderson<sup>1</sup>, Maggie Cusack<sup>2</sup>, Matthew Dalby<sup>3</sup> and Huabing Yin<sup>1</sup>

<sup>1</sup> University of Glasgow, Division of Biomedical Engineering, Glasgow, Scotland

<sup>2</sup> University of Glasgow, Division of Geographical and Earth Sciences, Glasgow, Scotland

<sup>3</sup> University of Glasgow, Division of Centre for Cell Engineering, Glasgow, Scotland  
[j.bolderson.1@research.gla.ac.uk](mailto:j.bolderson.1@research.gla.ac.uk)

## INTRODUCTION

Increasing activity and popularity in extreme sports is causing more injuries within the population and those requiring transplants often outlive the transplants [1]. With limited supply of both autograft (the gold standard) and allografts, an alternative is required that can replace damaged bones, leading to advances required to scaffolds and stem cells [2]. Ideal cell scaffolds require excellent biocompatibility and biodegradability, as well as sufficient porosity for transport of nutrients and waste. They should also have the ability to be moulded into different sizes and shapes [3]. One problem with current alginate scaffolds is the low viability of cells growing on the scaffolds [4]. The scaffold design that is proposed here is a way around this problem which involves the use of biodegradable strontium cross-linked alginate microfibers, made into porous scaffold structures to promote cell growth and potentially for the use of directing stem cell growth in tissue engineering.

The aim of the project is to create porous structured microfiber with tunable stiffness to promote targeted cell differentiation.

## EXPERIMENTAL METHODS

1.8% Alginate solution used to create microfibers by using a microfluidic device with a flow focusing T-junction combined with a narrow focal aperture to allow the formation of microbubbles within the microfibers. Microbubbles created with the use of N<sub>2</sub> and the microfibers gelled in a 0.1 M strontium chloride (SrCl<sub>2</sub>) solution.

Stiffness of the alginate microfibers was measured via nanoindentation using atomic force microscopy (AFM). The internal structure of the microfibers was characterised using scanning electron microscopy (SEM).

## RESULTS AND DISCUSSION

It was found that the stiffness of the fibres can be modulated with the inclusion of microbubbles. The stiffness ranges seen in the microfibers are from 65 mN/m for a plain microfiber, down to 30 mN/m for the largest diameter microbubble of 320 µm.

SEM analysis of the microfibers shows that the microfibers are highly porous (figure 1).

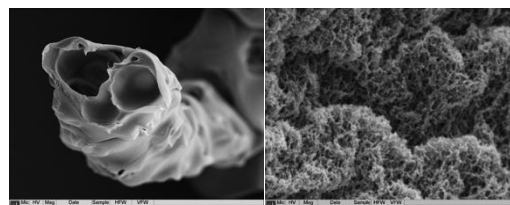


Figure 1: Shows the SEM of microbubbled microfibers. Left shows the voids created during the gelation process of the microfibers. Right shows the porous matrix of the microfiber.

MG63 human osteosarcoma cells were seeded upon the fibres and incubated for several days. It was found MG63 cells adhered and grew on the microbubbled regions but die on the plain regions (figure 2), suggesting the softer bubble regions may promote cell spreading and hence growth.

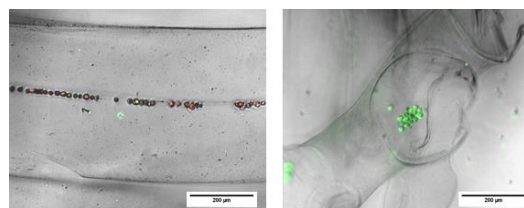


Figure 2: shows MG 63 cells stained with calcein AM and ethidium homodimer 1 (live/dead stain) after culture on fibers for 5 days. Cells stain red (dead) on plain microfiber (left) and green (alive) on microbubble microfibers (right).

## CONCLUSION

We have created highly porous alginate based scaffolds with the inclusion of microbubbles. The inclusion of microbubbles allows modulation of regions of stiffness to promote cell adhesion and proliferation on the surface.

## REFERENCES

- [1] Crawford, R. W. and Murray, D. W., *Annals of the Rheumatic Diseases* **56** (1997), p. 455.
- [2] Crowley, C., et al. *Current Stem Cell Research and Therapy* **8** (2012), p. 243.
- [3] Doaga, I. O., et al. *Journal of Biological Physics* **34** (2008), p. 495.
- [4] Chan, B. P. and Leong, K. W. *European Spine*

## ACKNOWLEDGMENTS

The supervisors and respective labs. Peter Chung and Margaret Mullen for SEM. JWNC and finally EPSRC for funding the project.



## Gradiently Mineralised Polysaccharide Hydrogels for the Treatment of Osteochondral Lesions

Krzysztof Pietryga<sup>1,2</sup>, Katarzyna Reczyńska<sup>1</sup>, Jonas Wengenroth<sup>2</sup>, Håvard Haugen<sup>2</sup>, Elżbieta Pamuła<sup>1</sup>

<sup>1</sup> Department of Biomaterials, Faculty of Materials Science and Ceramics  
AGH University of Science and Technology, Poland

<sup>2</sup> Department of Biomaterials, University of Oslo, Norway  
[pietryga@agh.edu.pl](mailto:pietryga@agh.edu.pl)

### INTRODUCTION

In order to obtain biphasic scaffold for osteochondral lesions treatment combining two types of materials differing in structure and mechanical properties is required: the first one intended to replace bone tissue, while the second one of hyaline cartilage. Producing stable connection between them is a great challenge<sup>1</sup>. The aim of this study was to assess possibility of fabrication of hydrogel osteochondral plug with gradually changing level of mineralization. This approach can eliminate delamination occurring between two types of materials: with and without mineral phase. Further advantages of using hydrogels in this application are: biocompatibility, biodegradability, high water content and close fitting to implantation site<sup>2</sup>.

### EXPERIMENTAL METHODS

In the experiments polysaccharide gels containing 0.7% gellan gum (GG), 2.5 mg/ml alkaline phosphatase (ALP) and 0.03% CaCl<sub>2</sub> were used. After casting and gelation the samples were enzymatically mineralized by incubation in 0.1 M calcium glycerophosphate (CaGP) for 3 days. Enzymatic activity of ALP led to creation of inorganic orthophosphate group from CaGP and precipitation of the minerals inside the structure of polysaccharide hydrogel matrix<sup>3</sup>. To obtain gradient of mineralization, it was required to limit above mentioned reaction to only one part of the gel. This was achieved by closing the sample in a container that provided access to mineralization solution only from one side. Progress in mineralization was assessed by dry mass percentage measurement. Chemical composition in different parts of the material was measured by SEM/EDX method. Young's modulus and topography of native gels in aqueous environment were measured by atomic force microscopy (AFM, MFP 3D; Asylum Research, Santa Barbara, USA). Force-distance curves and Young's modulus maps were collected as well. Biological response to the produced samples was assessed in contact with osteoblast-like MG-63 cells. Viability, proliferation and morphology of the cells were assessed by Alamar Blue and live-dead tests.

### RESULTS AND DISCUSSION

Thanks to proposed method it was possible to produce mineralization gradient across the hydrogel material. This gradient was stronger in the samples with higher ALP concentration.

AFM measurements revealed that mineralized part was significantly stiffer than non-modified part of GG gel

(0.8 kPa and 32 kPa, respectively). Stiffness maps showed that mineralization was inhomogeneous at the nanoscale. The depth on which mineralized phase was formed did not exceed 2 mm due to CaGP diffusion limitation inside mineralized "outer part". Formed mineral phase prevented ALP release outside the gel thus provided preferable conditions to form higher mineralization gradient.

Differences in mineral phase concentration and stiffness between two phases were correlated with biological response of MG-63 cells. Sharp transitions of cell number and morphology were noted at the interface: non-mineralized – mineralized part of GG. Basically cells adhered and proliferated better on mineralized side of the gel, exhibited higher viability and had morphology of those growing on control tissue culture polystyrene (TCPS).

### CONCLUSION

Presented approach based on preventing substrate diffusion into deeper parts of the material seems to be one of the easiest production methods of gradiently mineralized hydrogels. This method preserves continuity of hydrogel matrix therefore eliminates delamination that may occur when two different types of materials are connected. Thanks to the blockage of ALP diffusion by inorganic precipitates it is possible to obtain strong transition between two phases of resulting material. However most notable limitation is that such method does not provide possibility to form thicker mineral phase. Biological response of osteoblast-like cell was considerably better on mineralized side of the samples.

### REFERENCES

1. Sherwood, J.K. et al., 2002. A three-dimensional osteochondral composite scaffold for articular cartilage repair. *Biomaterials*, 23(24), pp.4739–4751.
2. M.M. Stevens, *Biomaterials for bone tissue engineering*. *Materials Today*, 11(5): p. 18–25, 2008.
3. Douglas, T.E. et al., 2012. Enzymatic mineralization of hydrogels for bone tissue engineering by incorporation of alkaline phosphatase. *Macromolecular Bioscience*, 12(8), pp.1077–1089.

### ACKNOWLEDGMENTS

Financial support was provided from FSS-EEA grant.



Zbigniew Jaegermann<sup>1</sup>, Zdzisław Wiśniewski<sup>1</sup>, Artur Oziębło<sup>1</sup>, Robert Michalik<sup>2</sup>

<sup>1</sup>Institute of Ceramics and Building Materials, Department of Ceramic Technology, Warsaw, Poland

<sup>2</sup>ROBOCAM, Warsaw, Poland

[z.jaegermann@icimb.pl](mailto:z.jaegermann@icimb.pl)

## INTRODUCTION

In modern dental prosthetics, a special emphasis is put on the aesthetics of the reconstruction of both dental cavities, as well as permanent prosthetic restorations<sup>1</sup>. Translucency of the material of which the construction of prosthetic restoration is made is very important for their appearance, and thus for the ability to reproduce natural teeth by artificial crowns<sup>2</sup>.

The issue is important because in recent years the biggest effort of prosthetic materials producers is directed to improve the aesthetic qualities of dental restorations, which mainly depend on the optical properties of materials used<sup>3</sup>.

The objectives of the study described in the article consisted in comparing optical characteristics of selected Y-TZP materials used for manufacturing of permanent prosthetic restorations using CAD/CAM methods, as well as an attempt to determine the relationship between translucency and selected physical properties and microstructure of Y-TZP ceramics.

## EXPERIMENTAL METHODS

Comparative studies were based on the following zirconia ceramics: TZ and Zpex (Tosoh), N-100 (Saint Gobain), Prettau (Zirconzahn), CH (Jiazuo Wein) and TI (Treibacher AG) from which disc-like test samples ( $\phi 20\text{mm}$ ) were prepared in accordance with the manufacturer's instructions. The apparent density of the materials were determined by hydrostatic weighing. The evaluation of translucency and color was carried out by spectrophotometric method. Observation of microstructure was performed by scanning electron microscope with field emission. The grain size distribution of zirconia ceramics was verified by stereological method and the equivalent grains diameter  $E(d_2)$  was determined by planimetric method using computer image analysis.

## RESULTS AND DISCUSSION

Test results of apparent density showed that Zpex, CH, and TI materials were characterized by densities  $6,09 \div 6,10 \text{ g/cm}^3$ , which is a good standard in the group of Y-TZP ceramics<sup>4</sup>. The group of materials characterized by lower density ( $6,04 \div 6,07$ ) consist of TZ, N100 and Prettau ceramics.

Observations with the use of scanning electron microscope, showed significant differences in the microstructure what indicate differences in homogeneity of each material. The most dense materials (Zpex, Prettau), are characterized by a homogeneous microstructure without visible molding errors. A characteristic feature of the microstructure of TZ material consists of a large amount of small pores

(less than  $1\mu\text{m}$ ) occurring uniformly in the sample volume. In the case of TI the presence of large amount of isomorphic  $3 \div 5\mu\text{m}$  size pores and the lack of small pores of less than  $1\mu\text{m}$  has been observed. N100 is the least dense of all the materials tested. Many large pores of various shapes and sizes greater than  $30\mu\text{m}$  are present in its volume. Pores with sizes up to  $40\mu\text{m}$ , in the form of cracks and crevices, straight and branched can be observed as well.

On the basis of microscopic images of polished and etched cross sections of tested materials it can be concluded that all Y-TZP ceramics are characterized by fine-grained microstructure of varying size and isomorphic-shape grains. Excessively grown grains and grains of elongated shape have not been spotted. Equivalent grains diameter  $E(d_2)$  of tested materials comprises between  $0,19\mu\text{m}$  and  $0,87\mu\text{m}$ , depending mainly on the temperature of sintering.

Translucency of tested ceramics comprises between  $9,6 \div 31,9\%$ . Higher values correspond to materials of higher apparent density ( $6,09 \div 6,10 \text{ g/cm}^3$ ). Prettau material is an exception, as its density is not high ( $6,07 \text{ g/cm}^3$ ), but its translucency matched the best materials of all the ones tested.

## CONCLUSION

Based on the survey it may be concluded that the number of pores has a high influence on translucency of the material. Among the materials with similar density, these with a greater number of fine pores show lower translucency than the ones that had been well-sintered, but not that strongly compacted in the molding process. No relationship between translucency and grains size of Y-TZP ceramics has been observed.

The possible explanation of relationship between properties of Prettau ceramics, which combines high translucency and homogeneous microstructure with low apparent density, is complex. We might suppose that small amounts of substances of lower specific gravity, were added to chemically pure zirconia powder, and that altered the material's microstructure and optical performance.

## REFERENCES

1. Holand W. *et al.*, J. Eur. Ceram. Soc. 29: 1291-1297, 2009
2. Kumagai N. *et al.*, J. Dent. 41: e87-e92, 2012
3. Denry I. *et al.*, Dent. Mater., 24: 299-307, 2008
4. Kelly J.R. *et al.*, Dent. Mater., 24: 289-298, 2008

## ACKNOWLEDGMENTS

The authors would like to thank the Institute of Ceramics and Building Materials in Warsaw for providing financial support to this project



## The Implementation of a Novel Process for the Preparation of Colored Zirconia Blocks for Dental Prosthetics

Zbigniew Jaegermann<sup>1</sup>, Zdzisław Wiśniewski<sup>1</sup>, Artur Oziębło<sup>1</sup>, Robert Michalik<sup>2</sup>

<sup>1</sup>Institute of Ceramics and Building Materials, Department of Ceramic Technology, Warsaw, Poland

<sup>2</sup>ROBOCAM, Warsaw, Poland

[z.jaegermann@icimb.pl](mailto:z.jaegermann@icimb.pl)

### INTRODUCTION

Common methods of preparation of colored zirconia substructures in dental prosthetics consist in the addition of pigments to the batch composition of ceramic material or in staining by impregnating biscuit sintered constructions by colored solutions<sup>1,2</sup>. Opinions of dental prosthetists as well as previous research have shown that staining by impregnating does not provide sufficient uniformity of color, because staining procedure and physical properties of the colored material have a too strong impact on color reproducibility<sup>3</sup>. Therefore an alternative method of preparing a wide range of homogeneously colored zirconia blocks was sought. It was considered that coloring ready to press zirconia powders can lead to the fulfillment of established requirements.

The aim of the work described in the paper was to develop and implement an innovative system of staining zirconia powders as well as to prepare colored zirconia blocks of Vita scale (A1, A2, A3, A3.5 shades).

### EXPERIMENTAL METHODS

Ready to press zirconia powders produced by Jiazuo Wein company and the coloring liquid in the form of aqueous solutions with different concentrations of  $\text{Fe}^{+3}$  and  $\text{Cr}^{+3}$  were used for the study. Staining process was carried out in a rotary unit, and the coloring liquid that watered the powders during the process of mixing, was sprayed through a special nozzle. Tests of spraying were carried out using nozzles which differ by inside diameters. A number of liquids were prepared with different concentrations of coloring ions ( $\text{Fe}^{+3}$ ,  $\text{Cr}^{+3}$ ). Colored powders were used for isostatic forming of test samples as well as CAD/CAM zirconia blocks that were fired at the temperature of 1500°C.

In order to evaluate the color of sintered samples the visual method (comparison with the color of the VITA scale) and determination of the values of color parameters (spectrophotometer) were applied. The impact of consecutive stages of staining (humidification, mixing, drying) on the powder properties, and particularly on agglomeration and destruction of granules was assessed by measuring the size distribution using laser diffraction method and observations its morphology using stereoscopic microscope. Quality of sintered zirconia material was evaluated on the basis of apparent density tests by hydrostatic weighing method and strength measurements by three-point bending test.

The study aimed not only to confirm the possibility of effective dying zirconia powders by coloring liquids, but was also a step towards the implementation of this technology into the production of colored zirconia blocks. For this purpose, a series of model blocks, made of colored zirconia powder and sent them to the prosthetic company - Robocam. Using CNC machine (milling machine Robomill 5), a series of model substructures in the form of a three-point bridgework were cut from the discs.

### RESULTS AND DISCUSSION

Apparent density tests showed that with increasing content of the pigment lowers the value of the apparent density from 6,10 g/cm<sup>3</sup> for not colored material and A1 shade to 6,07 g/cm<sup>3</sup> for A3.5 shade.

The results of size distribution analysis for starting powder and for selected samples of colored ones indicate that the average size of the granules is higher for colored powders. This may prove that the coloring process results in a slight agglomeration (clumping) of granules, especially the finest silt fraction. The presence of agglomerates of granules in colored powders is also confirmed by observations granules morphology in stereomicroscope. The staining time had a considerable influence on the agglomeration and destruction of the granules during mixing.

Coloring the powders by solutions based on ferric chloride causes a reduction in the bending strength of sintered zirconia materials, whereas the use of ammonium ferric oxalate does not affect the strength.

### CONCLUSION

Both the ability of the material to machining and the color uniformity after firing as well as other material properties were positively rated by manufacturer. Now the Robocam company as a producer of zirconia blocks offers the colored ones, which are very popular among the dental laboratories for manufacturing fixed dental restorations using CAD/CAM techniques.

### REFERENCES

1. Denry I. *et al.*, Dent. Mater. 24: 299-307, 2008
2. Wen N. *et al.*, Key Eng. Mater. 368-372: 1255-1257, 2008
3. Jaegermann Z. *et al.*, Szkło i Ceramika, 63, 1: 34-41, 2012

### ACKNOWLEDGMENTS

The authors would like to thank the Institute of Ceramics and Building Materials in Warsaw for providing financial support to this project



### 3D Printing of Artificial Nerve-Guides may be Clinically Effective and may Bring Ethical Benefit

Antonio Merolli, Paolo Scialabba D'Amico

Gemelli Medical School, The Catholic University in Rome, Italy

[antonio.merolli@gmail.com](mailto:antonio.merolli@gmail.com)

#### INTRODUCTION

In 2006 a new concept of nerve-guide was proposed, termed "NeuroBox", which is flat, double-halved, not-degradable and rigid, and allows the use of cyanoacrylic glues instead of stitches [1,2]. The physical characteristics of the NeuroBox guide are quite different from traditional nerve-guides which are, basically, empty cylindrical conduits where the regenerating nerve can find protection and guidance [3]. "NeuroBox" was made of poly-methyl-metacrylate (PMMA) and its performance was compared with the well-known treated-collagen cylindrical shaped guides (TCC).

#### EXPERIMENTAL METHODS

In 2008 an off-the-shelf 3D printer was used to produce NeuroBox guides made of Poly-Lactic Acid. In 2009 a small number of 3D printed guides was implanted in the same Wistar Rat sciatic nerve model, as the "NeuroBox" and TCC. Analysis was performed by visible light microscopy (VLM) and transmission electron microscopy (TEM).

#### RESULTS AND DISCUSSION

Physical characteristics of nerve-guides can correlate with the effectiveness of regeneration and we found an effective nerve-regeneration in the 3D printed guides as well.

At that time we found that having implanted a 3D printed nerve-guide was of little relevance. We did not follow this route as far as traditional CAM machining of the PMMA was not more expensive or cumbersome than 3D printing. However, we underestimated that a possible translation into clinical practice in Humans could necessitate a strategic requirement: namely to provide a vast combination of diameters and lengths for the guides. We later discovered, while practicing with already CE-FDA approved guides in Humans [4], that it could be useful to have nerve-guides whose diameter increases with a step of 0.5 mm (from 2.0 to 7.0 mm) or whose length increases with steps not longer than 2.0 mm. These needs are presently satisfied by having industrial firms providing a set of diameters which increase of 1.0 mm on the average (even some 0.5 mm is available) and always having a maximum length (generally 25.0 or 30.0 mm) which can be trimmed during surgery. However, these are not the only requests. Sometimes particular architecture should be desirable like, for example, one-entry two-exit guides. Sometimes bented guides could be useful. None of all these clinical requests are technically demanding but they collectively bring to unacceptable raise in costs. Furthermore, even in the case that a whole kit of diameters and lengths would

be provided (at a reasonable cost), the questions remains about the waste for public Hospitals to buy artifacts that may not find an application; so it will be likely that the less common measures of the guides should be discharged after their expiry date.



Fig. 1: 3D printed artificial nerve-guides (l=14mm).

#### CONCLUSIONS

In our opinion, by demonstrating that 3D printing of artificial nerve-guide can be clinically effective and economically competitive we can certainly advocate to translate this technology into the operating room. In addition, we see as an ethical benefit that such technology will envisage two major advantages: *first*-a nearly tailor made guide can be produced for every occasion and; *second*-no unutilized guide in storage will be discharged when expired; actually the old concept of needing a relevant stock of guides in storage will be replaced by the new one of having the guides produced on demand.

#### REFERENCES

- 1-Merolli A, et Al. In-vivo regeneration of rat sciatic nerve in a double-halved stitch-less guide: a pilot-study. **Microsurgery** 2009;29(4):310-318
- 2-Merolli A, et Al. In vivo study of ethyl-2-cyanoacrylate applied in direct contact with nerves regenerating in a novel nerve-guide. **J Mater Sci Mater Med** 2010;21(6):1979-1987
- 3-Ijkema-Paassen J, et Al. Transection of peripheral nerves, bridging strategies and effect evaluation. **Biomaterials** 2004;25(9):1583-1592
- 4-Meek MF, Coert JH. US Food and Drug Administration/Conformit Europe-approved absorbable nerve conduits for clinical repair of peripheral and cranial nerves. **Ann Plast Surg** 2008;60(1):110-11



## Implementation and Commercialization Process of the New Polish Extracorporeal Ventricular Assist Device

Małgorzata Gonsior<sup>1</sup>, Roman Kustosz<sup>1</sup>, Artur Kapis<sup>1</sup>, Agnieszka Szuber<sup>1</sup>, Paweł Jurkowski<sup>2</sup>, Zenon Narojek<sup>2</sup>

<sup>1</sup>Artificial Heart Laboratory (AH Lab), Foundation for Cardiac Surgery Development (FCSD), Poland

<sup>2</sup> WADIM PLAST Narojek SP. J., Poland

[gosiag@frk.pl](mailto:gosiag@frk.pl)

### INTRODUCTION

The innovative extracorporeal pulsatile ventricular assist device, called ReligaHeart EXT<sup>1,2</sup> (Fig.1), has been developed in Poland, as the new generation of POLVAD device, used in over 300 patients with the longest assistance duration over one year.

The following improvements of ReligaHeart EXT (70ml pump) were applied in order to increase its safety and reliability: optimized blood chamber construction, new low profile membrane system, original Polish tilting disc valves called Moll valves<sup>3,4</sup>, special cannulas protection system. The pump is made of innovative biocompatible polyurethane with modified surface structure (Bionate II, DSM Biomedical, USA). The modern manufacturing process has to be developed, utilizing advanced injection and lamination technology, as well as an automatized assembling. The special Technological Department of AH Lab. FCSD<sup>5</sup> was established (including clean room) for the ReligaHeart EXT production development.

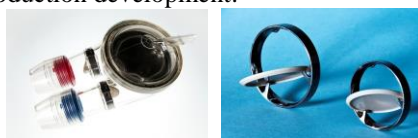


Fig.1. ReligaHeart EXT blood pump, Moll valves

### EXPERIMENTAL METHODS

The advanced injection process of ReligaHeart EXT polyurethane hard elements (Fig.2.) was developed in WADIM PLAST Narojek Sp.J. The technology upscale was implemented: the optimization of injection molding process in the clean-room conditions, in order to achieve the best surface material properties, just after injection process, without any further post-processing for surface modification.



Fig.2. ReligaHeart EXT polyurethane hard elements

The polyurethane soft elements (0,3mm thick pump membranes) lamination process and complete pump assembly technology were developed in AH Lab FCSD (Fig.3.), utilizing original innovative automatized technological stands and specialized technological equipment: molds, holders, and actuators.

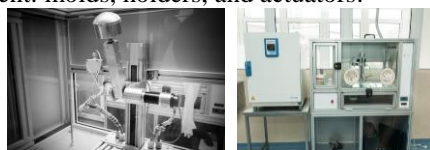


Fig.2. Technological stands in AH Lab FCSD

The Moll tilting disc valve consists of titanium ring and polymer disc. The precise valve elements numerically controlled machining (5 axis milling) was developed in WADIM PLAST. The special polishing technology was developed in order to obtain the titanium and polymer surface roughness allowing the elements to have proper contact with blood ( $R_a < 0,08\mu m$ ).

The special automatized assembling technology was developed by AH Lab FCSD, for valve assembling and mounting it within the ReligaHeart EXT pump. ETO sterilization process of the final product was validated.

### RESULTS AND DISCUSSION

ReligaHeart EXT pump production in compliance with ISO 13485 standard was established. Production process includes: blood pump's and valve's elements manufacturing, incoming elements quality control, valve assembling and qualification tests, blood pump manufacturing, quality control and examination for final medical product, and it's sterilization. Over 50 blood pumps were manufactured for pre-clinical and clinical study. System safety was confirmed during in vitro and long term in vivo trials. The prototype clinical parts were manufactured and utilized in the 1<sup>st</sup> phase of clinical study. The first 2 clinical applications confirmed ReligaHeart EXT's safety and proper manufacturing technology.

### CONCLUSION

The ReligaHeart EXT system has been introduced to the routine production, and the II phase of clinical trials is performed, in order to confirm the system effectiveness, CE certification and introduce to the market.

### REFERENCES

1. A.Kapis, *et al.*, ISBN 978-83-63310-12-7 (2013): 23-77
2. K.Janiczak *et al.*, ISBN 978-83-63310-12-7 (2013): 155-189
3. A.Szuber, *et al.*, ISBN 978-83-63310-12-7 (2013): 129-154
4. M.Gawlikowski, *et al.*, Int J Artif Organs (2014), 37 (8): 609 – 643, P25, pp. 613
5. M.Gonsior, *et al.*, ISBN 978-83-63310-12-7 (2013): 582-602

### ACKNOWLEDGMENTS

The authors would like to thank the National Centre for Research and Development and Minister of Health (Polish Artificial Heart programme) for providing financial support to this project.

## Evaluation of Angiogenic Effect of Drug-Loaded Poly (DL-Lactic Acid) Porous Matrix Film for Wound Dressing Application by CAM Assay

Sasiprapa Chitrattha<sup>1\*</sup>, Thawatchai Phaechemud<sup>1</sup>

<sup>1</sup>Department of Pharmaceutical Technology, Faculty of Pharmacy, Silpakorn University, Nakhon Pathom, Thailand  
[sasi\\_toey@hotmail.com](mailto:sasi_toey@hotmail.com)

### INTRODUCTION

Poly (DL-lactic acid) (PLA) has been developed into the porous matrix film for wound dressing materials owing to its biodegradable and biocompatible abilities. Because of the outstanding properties of polyethylene glycol (PEG) which are essential for biomedical applications, PEG 400 was intently added into the structure to induce the pore interconnectivity of PLA matrix films<sup>1</sup>. Metronidazole (MZ) and gentamicin sulphate (GS) were incorporated into developed films for antimicrobial activities of these wound dressings. However, angiogenesis plays an important role during wound healing process in order to bring the nutrients and oxygen to the regenerating tissue<sup>2</sup>. The aim of this study was to investigate the morphology of prepared drug-loaded PLA porous matrix films and their angiogenic activity using chick chorio-allantoic membrane (CAM) model.

### EXPERIMENTAL METHOD

#### Preparation of drug-loaded porous matrix films

MZ 3% or GS 15% of polymer were loaded into the porous PLA matrix film, namely PPMZ and PPGS, respectively. Firstly, the drug was dissolved in PEG 400 (150% of polymer), then the obtained solution was mixed into PLA in dichloromethane solution (15%w/w). The mixtures were poured into the glass plate, placed at -20 °C for 24 h and dried in an oven at 60 °C for 24 h.

#### Morphology characterization

The morphology of the films was determined using scanning electron microscope (SEM) (Maxim 200 Camscan, Cambridge, England) with the BEI mode. The samples were sputter coated with gold before examination. SEM micrographs were obtained at an acceleration voltage of 15 kV.

#### In ovo angiogenesis test by CAM assay

*In ovo* method was performed as the method described previously<sup>3</sup> with some modifications. Briefly, the fertilized chicken eggs were incubated in a humidified incubator at 37 °C for 9 days. After incubation, small round window at the wide end was created. Subsequently, the disc of sample (diameter = 6 mm) was placed on the CAM surface. The open window was then sealed using parafilm. The chick embryos were then incubated for 3 days before observing the results. The amount of GS in PPGS discs were about 900 µg/disc, and MZ in PPMZ discs were about 180 µg/disc. Approximately 10 embryos per sample were used. Angiogenesis activity of the tested substances was scored as the following 4 levels<sup>4</sup>:

Score 0 = no blood vessel response to the tested substance

Score 1 = little response is observed; some large microvessels incline to the tested substance

Score 2 = moderate response is observed; the large microvessels certainly incline to the tested substance

Score 3 = strong response is observed; the large microvessels certainly incline to the tested substance and exhibit spoke wheel pattern

### RESULTS AND DISCUSSION

The morphology of PPGS and PPMZ films (Fig. 1b and 1c, respectively) displayed the porous structure that drug particles were inserted into the pore. However, PLA porous film without the drug (PPEG) showed only the porous structure (Fig. 1a). This indicated that drug loading into the PLA porous matrix film was successfully. The CAM assay of all of samples was shown in Table 1. The surrounding blood vessels of the positive control (asiaticoside 320 µg) disc (Ac) score was indicated as 2.25±0.5. However, average angiogenesis score of plain PLA film (PLA), PPEG, PPGS and PPMZ were similar to negative control (PBS pH 7.4). Therefore, they did not induce angiogenesis on the chicken embryo because a positive response of about 0.33±0.5 of the eggs was usually observed in negative control and was considered as background angiogenesis. Corresponding to previous research, GS did not promote angiogenesis<sup>5</sup>.

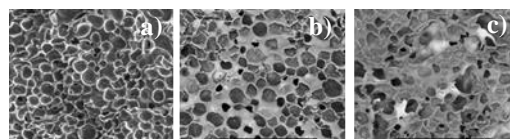


**Figure 1** SEM micrographs using BEI mode (x200) of cross section of films a) PPEG, b) PPGS and c) PPMZ.

**Table 1** Summary of CAM assay of samples detailing the total number of the used embryos, the dead embryos, the unable to be evaluated embryos (N/E), evaluable embryos and average angiogenesis score.

Sample	Total	Dead	N/E	Evaluable	Average score
PBS	10	1	-	9	0.33±0.5
Ac	10	1	1	8	2.25±0.5
PLA	10	4	-	6	0.33±0.5
PPEG	10	2	1	7	0.29±0.5
PPGS	10	3	1	6	0.33±0.5
PPMZ	10	1	1	8	0.50±0.5

### CONCLUSION

MZ or GS-loaded PLA porous matrix films was successfully prepared in this study. Nevertheless, they did not induce an angiogenesis by CAM assay. This result demonstrated that they had no angiogenic property.

### REFERENCES

- Chitrattha S. *et al.*, Key. Eng. Mat. 545:57-62, 2013
- Perng C. K. *et al.*, J. Surg. Res. 168(1):9-15, 2011
- Zwadlo-Klarwasser G. *et al.*, J. Mater. Sci-Mater. M. 12:195-199, 2001
- Ponce M. L. *et al.*, Curr. Protoc. Cell. Biol. 18:19.5.1-19.5.6, 2003
- Hu G. Proc. Natl. Acad. Sci. USA. 95:9791-9795, 1998

### ACKNOWLEDGMENTS

This research work was kindly supported by The Thailand Research Fund via The Royal Golden Jubilee Ph.D. Program (Grant No. PHD/0141/2552) and Faculty of Pharmacy, Silpakorn University, Thailand.



## Bilayered Scaffolds Incorporated with Gold Nanoparticles: Fabrication, Characterization and Toxicological Evaluation as Potential Skin Substitutes

Ömer Aktürk<sup>1</sup>, Dilek Keskin<sup>12</sup>

<sup>1</sup>Engineering Sciences, Middle East Technical University, Turkey

<sup>2</sup>BIOMATEN, Center of Excellence in Biomaterials and Tissue Engineering, Middle East Technical University, Turkey  
[dkeskin@metu.edu.tr](mailto:dkeskin@metu.edu.tr)

### INTRODUCTION

Scaffolds in bilayered structure are widely used in skin tissue regenerative medicine<sup>1</sup>. Gold nanoparticles (AuNPs) recently gained an increased interest especially in tissue engineering applications<sup>2, 3</sup>. In this study, collagen/sericin film was combined with lyophilized collagen sponge to form the bilayered collagen based scaffolds (BLCS). AuNPs were synthesized and loaded into BLCS (BLCS-Au). Bilayered scaffolds were also cross-linked with glutaraldehyde (GTA) to form BLCS-X and BLCS-AuX.

### EXPERIMENTAL METHODS

AuNPs were synthesized with citrate reduction method and characterized with TEM. The effect of GTA and AuNPs on scaffold physicochemical properties (morphology, water swelling, oxygen permeability, water vapour transmission rate, aqueous and enzymatic stability, mechanical properties), in vitro biocompatibility (ISO 10993-5 extract cytotoxicity on L-929 fibroblast, adhesion and proliferation of L-929 fibroblast) and toxicological effects (ISO 10993-10 skin sensitization closed-patch test, ISO 10993-10 animal intradermal reactivity test and ISO 10993-3- OECD 471 bacterial reverse mutation test) were investigated.

### RESULTS AND DISCUSSION

Synthesized AuNPs demonstrated uniform particle size and mostly spherical shape (Figure 1).

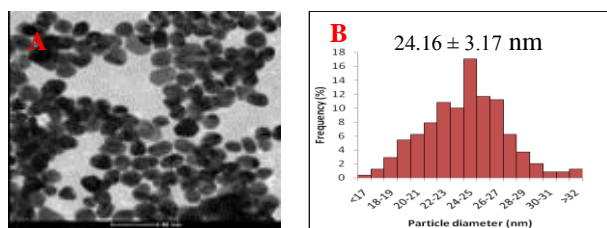


**Figure 1.** Morphological evaluation of AuNPs: (A) TEM images of synthesized AuNPs, (B) particle size distribution analysis with histogram

Cross-linking decreased the hydrolytic and enzymatic degradation of scaffolds prominently. AuNPs seemed to increase the resistance against both hydrolytic and enzymatic degradation in long term incubation period. Cross-linking had increasing effect on water swelling of scaffolds, but AuNPs had no distinct influence. All the scaffolds had similar (about 1300 gr/m<sup>2</sup>/day) water vapor transmission rates and also excellent oxygen permeability, which was thought to be mainly controlled by collagen/sericin film layer. Tensile strength of BLCS increased with either cross-linking or AuNPs incorporation. AuNPs incorporation made the

scaffolds more brittle with high elastic modulus and low elongation at break.

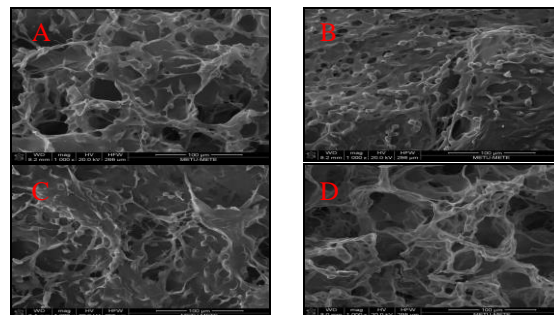


**Figure 2.** SEM micrographs showing L929 fibroblasts proliferated on (A) BLCS, (B) BLCS-Au (C) BLCS-X and (D) BLCS-AuX groups in 3 days of incubation period.

The synthesized AuNPs at different concentrations (5, 10 and 20 ppm) and all the scaffold extracts were biocompatible (cell viability > 85%) according to cytotoxicity studies on L-929 cells. Cell seeding tests showed that, L-929 cells and keratinocytes attached and gained their natural morphology in 1 day and proliferated on the scaffolds during 3 days incubation period according to SEM analysis (Figure 2). Finally, the scaffold group containing all the possible toxic components, AuNPs and glutaraldehyde (BLCS-AuX) was confirmed to have no adverse skin reactions (intradermal irritation and skin sensitization), and no genotoxicity.

### CONCLUSION

The results signified that all the scaffolds fabricated in this study have good physicochemical properties and were safe toxicologically to be used as a promising skin substitute. Especially BLCS-AuX group could be a very promising material in skin tissue engineering applications

### REFERENCES

1. Biedermann T. et al., Eur. J. Pediatr. Surg. 23:375–82, 2013.
2. Labala S. et al., Mol Pharm, 2015.
3. Silveira P.C. et al., Mater. Sci. Eng. C. Mater. Biol. Appl. 44:380–5, 2014.

### ACKNOWLEDGMENTS

This investigation was financially supported by the Scientific and Technological Research Council of Turkey, TUBITAK (Project no: 111M810 and 2120189). All toxicological tests were conducted by biocompatibility group in Hacettepe University, Faculty of Pharmacy Department of Pharmacology.





## Sulfated Glycosaminoglycan Derivatives Affect the Bioactivity of Angiogenic Growth Factors

Linda Huebner<sup>1</sup>, Vera Hintze<sup>1</sup>, Stephanie Moeller<sup>2</sup>, Matthias Schnabelrauch<sup>2</sup> and Dieter Scharnweber<sup>1</sup>

<sup>1</sup>Institute of Materials Science, Max Bergmann Center of Biomaterials, Technische Universität Dresden, Germany

<sup>2</sup>Biomaterials Department, INNOVENT e.V. Jena, Germany

[Linda.Huebner@tu-dresden.de](mailto:Linda.Huebner@tu-dresden.de)

### INTRODUCTION

Sulfated hyaluronan (sHA) and chondroitin sulfate (sCS) derivatives are promising candidates for functional biomaterials since their sulfate groups modulate the binding of growth factors, thereby influencing their biological profile. The interaction of different glycosaminoglycan (GAG) derivatives with several growth factors like BMP-2/4 and TGF- $\beta$ 1 has previously been reported. These studies demonstrated that GAGs not only bind to these mediators in a sulfation- and carbohydrate backbone-dependent manner but also influence their interaction with receptors and therefore their bioactivity [1-3].

Angiogenic growth factors, like vascular endothelial (VEGF) and basic fibroblast growth factor (bFGF) play an important role during wound healing, since they both stimulate angiogenesis and in addition bFGF promotes skeletal muscle function and regeneration [4, 5].

Heparin is known to distinctly regulate VEGF and bFGF signalling by altering their interaction with the respective receptors [5, 6]. Hence we hypothesize that VEGF and bFGF interaction with different GAG derivatives influences their bioactivity depending on sulfation and carbohydrate backbone.

This might lead to important implications for the use of GAG derivatives as part of biomaterials for controlling angiogenesis during wound healing in health compromised patients.

### EXPERIMENTAL METHODS

The interaction of VEGF and bFGF with different sHA and CS derivatives was determined via surface plasmon resonance (SPR) using a BIACORE<sup>TM</sup> T100. VEGF or bFGF were immobilized onto a CM3<sup>TM</sup> sensor chip surface and different concentrations of solute sHA and CS derivatives were injected to reveal their binding strength. Additionally, ELISA experiments with immobilized GAG derivatives were performed to validate the SPR results. The influence of GAG derivatives on the capability of growth factors to bind to their respective receptors was again investigated by SPR, while the consequences of the GAG/growth factor interaction on bioactivity were studied in cell-based bioassays. Here the growth factors were pre-incubated with different GAG concentrations and added to the cells (e.g. mouse myofibroblast cell line C2C12 for bFGF). The growth factor-stimulated cell proliferation in the presence of the GAGs was determined via the lactate dehydrogenase (LDH) activity of the cells.

### RESULTS AND DISCUSSION

The binding strength of GAG derivatives to bFGF was clearly depending on sulfation degree and carbohydrate

backbone (Figure 1). For VEGF, however, this was less clear since low sulfated sHA (sHA1) and high sulfated CS (sCS3) showed a comparable binding strength. The different molecular geometries in the carbohydrate backbone of the GAGs might render the respective sulfated groups to interact differently. This is further emphasized in investigations with TGF- $\beta$ 1 where naturally sulfated heparin demonstrated a comparable binding strength to sCS3, even though it has a lower degree of sulfation [2]. Beside the GAG derivatives the structure of the growth factor might play a role for the interaction as well.

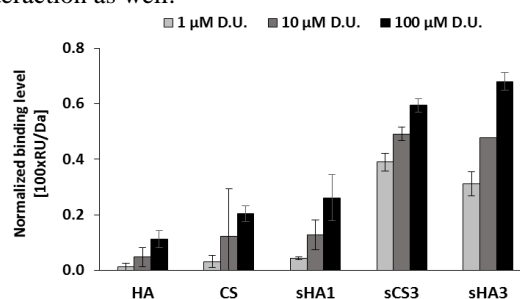


Fig. 1: Ranking of binding levels for the interaction of GAG derivatives with bFGF by SPR analysis at 37°C. D.U. = disaccharide units

The binding of growth factors to their respective receptors was modulated in the presence of GAG derivatives which implies an altered biological profile.

This could be verified in cell-based bioassays, since the presence of GAGs affected the growth factor-stimulated proliferation of the cells.

### CONCLUSION

The results imply that sulfated GAGs are promising candidates to be included in biomaterials or biomaterial coatings for controlling angiogenic and therefore healing processes.

### REFERENCES

- Hintze V. *et al.*, *Biomacromolecules* 10:3290-3297, 2009
- Hintze V. *et al.*, *Acta Biomater.* 8:2144-2152, 2012
- Hintze V *et al.*, *Biomacromolecules* 15:3083-3092, 2014
- Suhardja A. *et al.*, *Micros. Res. Tech.* 60:70-75, 2003
- Sangaj N. *et al.*, *Biomacromolecules* 11:3294-3300, 2010
- Ito N. *et al.*, *Angiogenesis* 3:159-166, 1999

### ACKNOWLEDGMENTS

The authors acknowledge financial support by the DFG [SFB Transregio 67, projects A2 and A3].





## Electrospun Fibrous Scaffolds for Wound Dressing of Mucous Membranes

Gerlind Schneider<sup>1</sup>, Ralf Wyrwa<sup>2</sup>, Sibylle Voigt<sup>1</sup>, Katja Otto<sup>1</sup>, Matthias Schnabelrauch<sup>2</sup>

<sup>1</sup> Department of Otorhinolaryngology/Jena University Hospital, Jena, Germany

<sup>2</sup> INNOVENT e.V. Technologieentwicklung, Jena, Germany

[gerlind.schneider@med.uni-jena.de](mailto:gerlind.schneider@med.uni-jena.de)

### INTRODUCTION

Wounds in mucous membranes, such as the nasal and oral mucosa, have to heal without wound covering so far, due to limited access and the lack of required fixation. This often leads to crust formation, wound infection, and delayed healing.

Therefore, electrospun wound dressings were developed and tested to ensure fixation and haemostasis, protect the wound from infection and mechanical stress, and allow undisturbed healing for mucous membranes. Electrospun fibrous scaffolds made of biocompatible materials (e.g. polylactide) were developed and produced for the application as a wound dressing. For special requirements, the polymeric fibers can be loaded with active ingredients in a wide concentration range<sup>1</sup>.

### EXPERIMENTAL METHODS

The electrospinning of the scaffolds made of poly(L-lactide-co-D,L-lactide) (70/30, Resomer® 708) was carried out using commercial electrospinning machine E-Spintronic (Erich Huber GmbH, Gernlinden, Germany) under adapted process conditions.

Mechanical properties of pure and loaded electrospun scaffolds were tested, as well as their properties with regard to handling, sterilization, and drug release. Biocompatibility and cytotoxicity were tested using WST1 und LDH test on MC-3T3 and MRC-5 cells.

In a first animal study, pure scaffolds as well as scaffolds loaded with styptics (tranexamic acid, 20 %, or epinephrine, 10 % + 4 % cysteine), sterilized by gamma radiation, were tested for haemostatic effects and biocompatibility. 9 NZW rabbits underwent rhinotomy and a small artificial defect of nasal mucosa on both sides of the septum. On one side, a scaffold was used to cover the defect. After four weeks, the septum with the scaffold was explanted and examined after histological preparation.

### RESULTS AND DISCUSSION

The electrospun fibrous scaffolds showed good mechanical properties with small differences between loaded and unloaded fibers. Scaffolds made of pure polylactide fibers showed higher tensile strength, whereas drug-loaded scaffolds showed better adhesion to the moist mucosa.

Pure fiber mats as well as the scaffolds loaded with tranexamic acid are biocompatible. Epinephrine-loaded scaffolds showed higher cytotoxic effects (Fig. 1).

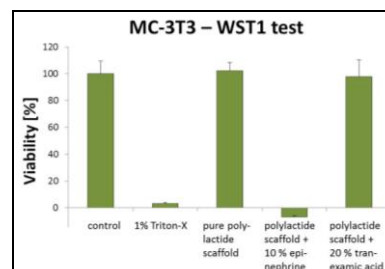


Fig. 1: Cell viability in WST 1 test on MC-3T3 cells (mouse); after 24 h, elution test.

The ongoing animal study gives reason to expect positive results with high effectiveness and good tolerability of the electrospun scaffolds.

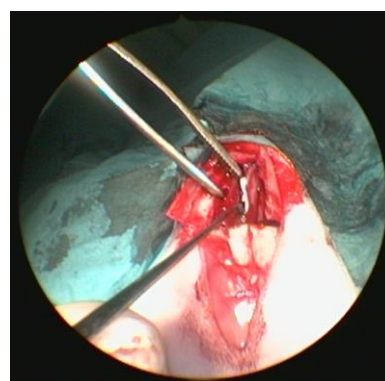


Fig. 2: A scaffold is placed at the septum nasi (NZWR).

### CONCLUSION

The described problems of wound healing can be significantly improved using electrospun fibrous scaffolds. Extra healing time due to postsurgical complications can be shortened, and postoperative care can be reduced. In addition to the application in head and neck area, there is a large application potential in a variety of medical fields.

### REFERENCES

1. Kluger PJ *et al.*, J Mater Sci Mater Med. 21:9, 2010

### ACKNOWLEDGMENTS

The authors would like to thank the German Ministry of Economics (BMW, ZIM grant no. KF2022431SB2) for providing financial support to this project.

## Impact of Biomimetic 3D Microenvironments on Macrophage Polarization

Katja Franke<sup>1</sup>, Liv Kalbitzer<sup>1</sup>, Jiranuwat Sapudom<sup>1</sup>, Sandra Franz<sup>2</sup> and Tilo Pompe<sup>1\*</sup>

<sup>1\*</sup>Institute of Biochemistry, Faculty of Biosciences, Pharmacy and Psychology, Universität Leipzig, Germany,

<sup>2</sup>Department of Dermatology, Venerology and Allergology, Universität Leipzig, Germany

[tilo.pompe@uni-leipzig.de](mailto:tilo.pompe@uni-leipzig.de)

### INTRODUCTION

Cues of the extracellular matrix are considered to tightly control the polarization of macrophages along inflammatory versus regulatory pathways during wound healing. While *in vivo* studies do not allow for high-resolution in-depth analysis, *in vitro* systems frequently lack important physiological cues of the microenvironment like 3D matrices and controlled stiffness.

In our *in vitro* approach, we precisely control fibrillar architecture, stiffness and glycosaminoglycan (GAG) content of 3D biomimetic matrices namely reconstituted fibrillar networks based on collagen and fibrin. We are interested whether and in which context biophysical and biomolecular network properties influence macrophage polarization and how they can be implemented in the design of biomaterials scaffolds to support wound healing. In this context we ask how permanent and directional the polarization of macrophages between so-called M1 and M2 phenotypes in inflammatory and regulatory stages of wound healing occur.

### EXPERIMENTAL METHODS

3D fibrillar networks of either collagen I or fibrin were reconstituted with defined topology, elasticity and thickness. Network topology and elasticity is controlled by biopolymer concentration, pH of buffer during preparation and network cross-linking. Automated image analysis reveal diameter, density and distribution of network pores and fibrils.<sup>1</sup> Network elasticity was measured by colloidal probe spectroscopy. Using active-ester chemistry the networks were functionalized with GAG namely hyaluronan (HA) with varying degree of sulfation. HA content was quantified by fluorimetry and ELISA. Monocytes from human peripheral blood (CD14 depletion) were either cultivated and differentiated directly in the matrices or cultivated after pre-differentiation into inflammatory and wound healing phenotypes by granulocyte macrophage colony-stimulating factor (GM-CSF) and macrophage colony-stimulating factor (M-CSF), respectively. After cultivation of macrophages on different matrices the cells were activated by lipopolysaccharide and analyzed for expression levels of IL10, IL12 and CD206 by immunofluorescence and ELISA to characterize macrophage polarization by the IL10/IL12 ratio. Cell migration and differentiation was analysed within the 3D context of the biomimetic matrices using time-lapse microscopy. Automated image analysis revealed single cell trajectories, migration pattern, speed and morphology.

### RESULTS AND DISCUSSION

Biomimetic 3D collagen I and fibrin networks could be engineered with a defined topology and mechanics. Pore size and Young's moduli were controlled in a range of 5 to 15 µm and 20 Pa to 500 Pa. Stable covalent binding of hyaluronan and sulfated hyaluronan within the 3D networks was up to 10% mass content of GAG per collagen matrix. Fibrillar networks of fibrin exhibited a pore size in a range of 1 to 4 µm and Young's moduli between 200 and 800 Pa.

Depending on the collagen network stiffness and HA functionalization we observe an enhanced level of IL10/IL12 expression ratio on stiff networks (0.03 to 0.12) while introduction of HA reduces the IL10/IL12 ratio (0.12 to 0.05) analysed by ELISA of cell culture supernatant. Much lower IL10/IL12 ratios were found on controls of 2D environments on tissue culture plastics indicating the importance of 3D biomimetic environments for physiologically relevant studies. These observations were verified by immunofluorescent staining of intracellular IL10 and IL12 inside the matrices. IL10 and IL12 levels were found much higher in fibrin scaffolds in comparison to collagen scaffolds accomplished by significantly higher IL10/IL12 ratios (0.57). These observations suggest a support of a regulatory phenotype of macrophages in stiffer 3D environments, a regulatory function of GAG functionalization and a strong support of regulatory phenotypes in fibrin environments.

Single cell tracking experiments inside the scaffolds support the above findings on macrophages polarization showing a higher migratory activity and morphological polarization for regulatory phenotypes. An ongoing study on genotypic characterization of macrophages will substantiate the current results.

### CONCLUSION

Our studies demonstrated the importance of analysing macrophage behaviour in topologically and mechanically biomimetic 3D microenvironments in order to gain physiologically relevant results. Matrix stiffness, GAG modification and matrix composition were found to control macrophage polarization into a regulatory phenotype.

### REFERENCES

1. Franke K. *et al.*, Acta Biomaterialia 10:2693 (2014).

### ACKNOWLEDGMENTS

The authors thank EFRE, ESF 'European Social Funds' and Free State of Saxony (SAB 100144684, SAB 100140482) and Deutsche Forschungsgemeinschaft (SFB-TR67/B3 and B10, INST 268/293-1 FUGG) for financial support



## Surface Modification of Chitosan Hydrogels

Bożena Tylińczak<sup>1</sup>, Katarzyna Z. Gaca<sup>1</sup>, Katarzyna Białik-Was<sup>1</sup>, Dagmara Malina<sup>2</sup>, Agnieszka Sobczak-Kupiec<sup>2</sup>

<sup>1</sup> Department of Chemistry and Technology of Polymers, Cracow University of Technology, Poland

<sup>2</sup> Institute of Inorganic Chemistry and Technology, Cracow University of Technology, Poland

[kgaca@chemia.pk.edu.pl](mailto:kgaca@chemia.pk.edu.pl)

### INTRODUCTION

Materials which are used for medical applications but which are not drugs, are called biomaterials. Often these are intended for the manufacture of components for internal use to assist diseased organs and tissues, and with a predetermined time to be replaced. Biomaterials can include groups such as metals, bioceramics, glass, polymers and composite materials [1-3]. The aim of this study was to obtain a hydrogel material based on acrylic acid and chitosan modified with hydroxyapatite.

### EXPERIMENTAL METHODS

Hydrogel material with acrylic acid/chitosan matrix modified with hydroxyapatite was prepared and its properties were investigated. Investigation included 30-days incubation, oxidation, swelling research, chemical structure identification using IR spectroscopy and SEM imaging of the material's surface.

### RESULTS AND DISCUSSION

The research covered synthesis of the polymer matrix with addition of hydroxyapatite, physicochemical tests and in vitro incubation research. It was stated that the synthesized hydrogels are swelling both in distilled water and a solution of physiological salt. Additionally incubative studies of the synthesized samples were carried out in the following liquids: distilled water, Ringer solution and artificial saliva. The pH value of the solutions during the incubation period did not show significant differences among the hydrogel samples with a different hydroxyapatite content. Moreover, no rapid or significant changes of pH were observed, which confirms the compatibility of collected material with a particular environment. During the research, the biological activity of hydrogels was determined. The studies showed that the obtained exhibit this property. However, more advanced research, such as on the cell lines, is required to examine further the biological

activity of these materials. Analysis of the polymer matrix structure of the synthesized hydrogels, before and after the incubation, was also carried out using Fourier transform infrared spectroscopy (FT-IR).

### CONCLUSION

On the basis of the collected test results it can be concluded that modification of the surface characteristics of hydrogels with hydroxyapatite is possible, and can be done so to improve its compatibility with the components of the bone. This will allow to tailor the properties of the hydrogel materials for tissue engineering applications, especially in the process of bone regeneration.

### REFERENCES

1. Zhao W., Jin X., Cong Y., Liu Y., Fu J., Journal of Chemistry Technology and Biotechnology, 88: 327-339, 2013,
2. Agnihotri S., Kulkarni V., Kulkarni A., Aminabhavi T, Journal of Applied Polymer Science, 102: 3255-3258, 2006
3. Castro S., Paulin E. „Is chitosan a new panacea? Areas of application”, InTech, 2012

### ACKNOWLEDGMENTS

“The authors would like to thank the The National Centre for Research and Development (Grant no: LIDER/033/697/L-5/13/NCBR/2014) for providing financial support to this project”.



Stacy Morgado<sup>1</sup>, João Santos<sup>1</sup>, T. Correia<sup>2</sup>, I. Correia<sup>2</sup>, Cristina Baptista<sup>1</sup>, M. H. Gil<sup>1</sup>, Paula Ferreira<sup>1</sup>

<sup>1</sup>Department of Chemical Engineering, University of Coimbra, Portugal

<sup>2</sup>CICS-UBI, Universidade da Beira Interior, Covilhã, Portugal

[pferreira@eq.uc.pt](mailto:pferreira@eq.uc.pt)

## INTRODUCTION

Traditional methods of wound closure are suturing and stapling, but they are associated with pain, wound infection and low aesthetic results. As a result of these shortcomings, medical tissue adhesives are considered an attractive alternative since, besides wound closure, they can accomplish other tasks, such as haemostasis and the ability of sealing air leakages. The most used surgical glues nowadays are the fibrin based adhesives [1] and cyanoacrylates [2]. Fibrin based adhesives present several problems, e.g. immunogenicity and risk of blood transmission diseases such as HIV and BSE. Cyanoacrylates have been reported to degrade in aqueous media to produce formaldehyde, which causes inflammation and has got carcinogenicity potential. Other options are now being considered, and among them, photopolymerizable/photocrosslinkable adhesives are the most promising. UV curable adhesives offer major advantages, such as fast-curing rate, control of the polymerization heat evolution, superior control over the final properties of the material and are ideal for application to weakened and diseased tissue.

## EXPERIMENTAL METHODS

Photocrosslinkable biodegradable bioadhesives based on a low molecular weight poly(caprolactone diol) (PCL) and poly(lactic acid) (PLA) were developed and tested as a possible bioadhesives. PLA and PCL were modified with a recently developed compound from BASF: Laromer® 9000 (Lr9000). Lr9000 is an isocyanate-functional, unsaturated acrylic ester resin, based on allophanated hexamethylene diisocyanate. Its isocyanate groups may easily react with compounds containing hydroxylic groups (creating urethane linkages), such as the case of PLA and PCL, in order to obtain macromers with carbon-carbon double bonds (C=C). The accomplishment of this chemical modification was confirmed by Attenuated Total Reflectance – Fourier Transform Infrared Spectroscopy (ATR-FTIR) by detection of the typical bands of the urethane groups. C=C bonds were then crosslinked using Iracure® 2959 by BASF as the photoinitiating agent. Crosslinking was achieved by UV irradiation for the period of 120s for the PLA macromers and 30s for the PCL macromers. After these time frames, flexible, uniform and well defined films were obtained. These were then further characterized, by swelling capacity evaluation, morphologic analysis by scanning electronic microscopy (SEM), hydrolytic degradation *in vitro*, determination of surface energy by contact angle measurements as well as thermal characterization TGA and DMTA). Blood compatibility studies were performed including thrombosis and determination of haemolytic potential. Finally, biocompatibility using

human dermal fibroblasts (hFib) and antibacterial activity of the materials were evaluated *in vitro*.

## RESULTS AND DISCUSSION

PCL and PLA bioadhesives were characterized by swelling evaluation and the percentage of the materials swelling was low, indicating that volume increase *in situ* will not be significant and damage to the surrounding tissues will not occur.

The biodegradation of the samples was performed in PBS and low percentages of weight loss were registered after 6 weeks with a maximum of nearly 20%. The results obtained for surface free energies ( $\gamma_s$  PLA  $\approx$  40mN/m and  $\gamma_s$  PCL  $\approx$  30mN/m) were lower than the ones reported for skin ( $\gamma_s \approx$  38-56mN/m) and blood ( $\gamma_s \approx$  47mN/m). Therefore, we may suggest that once films are formed over any of these surfaces, they won't slough off easily since adhesion forces will be significant. Haemocompatibility studies were performed, and both thrombosis and haemolytic potential were evaluated. Thrombosis percentages obtained for PCL bioadhesives were around 90% and close to 80% for PLA bioadhesives meaning that both surfaces present thrombogenic character. The haemolytic potential of the synthesized materials was also evaluated, and results showed that it could be classified as slightly haemolytic when in direct contact with blood. However, this haemolysis was eliminated when the samples were subjected to the extraction with PBS solution (indirect contact). This result does not mean, however that this material cannot have a clinical application, since as already reported, values of haemolysis are within acceptable limits. Cell culture *in vitro* studies showed that the materials are biocompatible and in the case of PLA based materials they also present antibacterial activity.

## CONCLUSION

PLA and PCL were modified with a new compound from Lr9000 and films were obtained by UV irradiation induced crosslinking. Their overall performance during characterization indicates that they may be promising materials as bioadhesives.

## REFERENCES

1. Kotzampassi K., *et al.*, Surgery 157:79-86, 2015
2. Singer A., *et al.*, Am. J. Emerg. Med. 26:490-496, 2008

## ACKNOWLEDGMENTS

The authors would like to thank FCT for the financial support to P. Ferreira (SFRH/BPD/86338/2012).





## Hybrid Dressing of Highly Absorbent Polyurethane Foam and PVA Nano Fiber with Adipose-derived Stem Cell promotes Wound Healing

Ho Yun Chung<sup>1</sup>, Hyung Min Sung<sup>1</sup>, Eun Jung Oh<sup>1</sup>, Tae Jung Kim<sup>1</sup>, Jin Hyun Choi<sup>2</sup>

<sup>1</sup>Department of Plastic & Reconstructive Surgery, School of Medicine, Kyungpook National University, Korea

<sup>2</sup>Department of Advanced Materials Science and Engineering, Kyungpook National University, Korea  
[hy-chung@knu.ac.kr](mailto:hy-chung@knu.ac.kr)

### INTRODUCTION

Stem cells are spotlighted as an attractive method to replace conventional treatment method in the regenerative medicine field. Adipose-derived stem cells (ADSCs) are also a member of the pluripotent cells. Although adipose-derived stem cells have the potentials to be used for damaged tissues in various ways, few researches have dealt with the effects of ADSCs on wound healing. Absorption degree is important factors in the wound healing process. Moreover, polyurethane (PU) is frequently used wound dressings because of its good barrier properties, oxygen permeability and higher absorption degree. Therefore, in this present study, we investigated the effect and usability of adipose-derived stem cell seeded on Poly vinyl alcohol (PVA) nano web fiber and newly developed PU foam, which has high absorption degree, hybrid dressing material on wound healing.

### EXPERIMENTAL METHODS

The number of rats (Sprague-Dewley rats) used in this experiment was forty. Four round (diameter 2cm) surgical wounds were created bilaterally on the dorsum of the white rat's trunk and were assigned into 4 groups by each dressing materials: Group A, as the control group, was dressed with sterilized gauze, Group B with PVA nano web fiber-PU foam hybrid dressing material, Group C with ADSCs seeded PVA nano web fiber-PU foam hybrid dressing material, Group D with the dressing material named Medifoam™, which is commercially available. Each group was compared with gross findings at periodic times and both histological and biochemical test were conducted for each time.

### RESULTS AND DISCUSSION

In surgical wounds, Group C showed statistically higher contraction rate, higher epithelization rate and higher wound healing rate (Fig.1). In a histological aspect, on 14th day after wound formation, more thick and dense epithelial layer was observed in Group C (Fig.2). Moreover, more regular and thick alignment of collagen fibers was also observed in the same period. In Western blot, on 14th day after wound formation, the expression of TGF-β1, VEGF and Laminin α-3 was detected to be relatively strong in Group C (Fig.3).

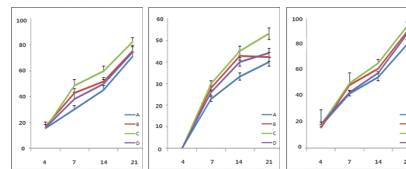


Fig. 1. The mean percentage of the wound contraction rate (left), epithelization rate (center), healing rate (right) according to processing time of each group.

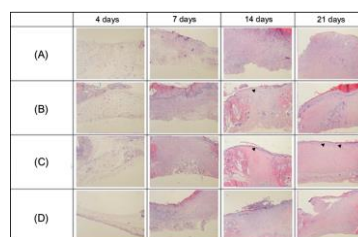


Fig. 2. Histological finding of post-wound tissues stained with hematoxylin and eosin stain (x100).

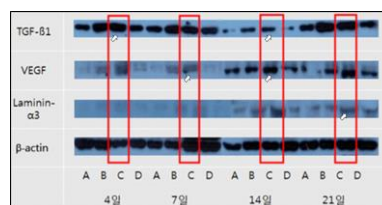


Fig 3. The expression pattern of TGF-β1, VEGF, laminin α-3 protein using western blots in the surgical wound.

### CONCLUSION

This study suggest that adipose-derived stem cell seeded on PU dressing foam which has highly absorbent degree dressing material induces stable reepithelization, angiogenesis and collagen fiber synthesis in the wound healing process. Given this, it is considered as an effective biological dressing material, as well as an innovative invention that can replace existing dressing materials with.

### REFERENCES

1. Hardig KG. *et al.*, BMJ. 324:160-3, 2002
2. Kim WS. *et al.*, J. Dermato. Sci. 48:15-24, 2007
3. Lächli S. *et al.*, Dermatology. 227:361-6, 2013

### ACKNOWLEDGMENTS

This research was supported by a grant of the Korea Health Technology R&D Project through the Korea Health Industry Development Institute (KHIDI), funded by the Ministry of Health & Welfare, Republic of Korea (grant number: HI14C3309).

## Antimicrobial Activity of Silver Nanoparticles Incorporated in a Cryogel Matrix

Matthew Illsley<sup>1</sup>, Cressida Bower<sup>1</sup>, Akhmetova Alma<sup>2</sup>, Gulsim Kulsharova<sup>3</sup>, Timur Saliev<sup>4</sup>, Nurgozhin Talgat<sup>2</sup>, Sergey Mikhalevsky<sup>1,3</sup>

<sup>1</sup>School of Pharmacy and Biomolecular Sciences, University of Brighton, United Kingdom

<sup>2</sup>Laboratory of Experimental and Clinical Pharmacology and Pharmacy/National Laboratory Astana, Nazarbayev University, Kazakhstan

<sup>3</sup>School of Engineering, Nazarbayev University, Kazakhstan

<sup>4</sup>Laboratory of Translational Medicine and Life Sciences Technologies/National Laboratory Astana, Nazarbayev University, Kazakhstan  
[alma.akhmetova@nu.edu.kz](mailto:alma.akhmetova@nu.edu.kz)

### INTRODUCTION

Hospital acquired infections are a major financial and societal burden with high mortality, morbidity and cost. Such infections are caused by a number of pathogenic and opportunistic bacteria, many of which are resistant to front line antibiotics. To combat their emergence and spread, new approaches have been developed such as adding biocides to wound dressings and surgical implants, but have met with limited success. We proposed an innovative technology capable of improving the clinical outcomes associated with bacterial infection of skin, deep wounds and surgical implants. This approach will exploit the ability of silver nanoparticles (NPs)<sup>1</sup> to produce antibacterial radicals and reactive compounds. To begin with, antimicrobial activity of NPs and cytotoxicity of materials were tested.

### EXPERIMENTAL METHODS

Silver nanoparticles have been synthesized using sodium borohydride reduction of silver nitrate. For the synthesis of the scaffold, silver nanoparticles were added to acrylamide and N,N'-Methylenebisacrylamide solution. The mixture was placed into a cryobath at -20°C. After 5 hours it was moved to freezer at -20°C for 12 hours.

To test antimicrobial effect, method of agar well diffusion was used. Briefly, small wells were cut in the agar medium, which was previously cultured with *Staphylococcus aureus*. Cryogel alone and cryogel with NPs were cut and placed in the wells. After incubation at 37°C for 24 hours, zone of inhibition was measured. Morphological studies were carried out using SEM. For cytotoxicity studies MTT assay was used. Cytotoxicity of cryogels, NPs, and cryogels with nanoparticles were tested. All experiments were carried in triplicates.

### RESULTS AND DISCUSSION

Polymerization of acrylamide and N,N'-methylenebisacrylamide eliminates toxicity of cryogels. Cryogels are sponge-like materials with medium to large pore sizes. The prepared cryogels were elastic, wet, and the colour was white. Upon drying, cryogel solidified and lost its properties. However, due to its property of shape memory, addition of water brought back the initial shape and characteristics. Nanoparticles were successfully incorporated into the pore walls of the cryogels according to SEM images.

Agar well diffusion method is based on the diffusion of NPs through the semi-solid agar growth medium to inhibit the growth of potentially sensitive microorganisms. The assessment of antibacterial activity of NPs within the cryogel demonstrated good inhibition zone of *S.aureus* by silver NPs within the cryogel matrix. Thus, silver NPs were not blocked by the cryogel and are available for interaction with the surrounding environment. Cytotoxicity experiments demonstrated no toxicity either by cryogels or NPs or both.

### CONCLUSION

Acrylamide cryogel and nanoparticles were successfully fabricated and fused together. The prepared novel combination demonstrated good properties for use in wound healing: good adsorption, moist environment, no toxicity, and good antimicrobial effect. Our future work will be focused on application of microwaves to NPs in a controlled regime and pulsed motion, studying effect of microwaves on antimicrobial activity of NPs and formation of free radicals.

### REFERENCES

1. Solomon S. D. *et al.*, J. Chem. Educ. 84,322–325, 2007

### ACKNOWLEDGMENTS

The work was funded by the grant of the Ministry of Education and Science of the Republic of Kazakhstan, 'Nanoparticle based wound dressings with microwave-enhanced antimicrobial function' (2013-2015/ N 698).



## Design of a Functional Degradable Wound Dressing for Acute Injuries

Beren Sen, Ayse Buse Ozdabak, Alper Tunga Akarsubasi, Fatma Nese Kok

Molecular Biology-Genetics and Biotechnology Programme, Istanbul Technical University, Turkey

[sen.beren@gmail.com](mailto:sen.beren@gmail.com)

[aysebuse@hotmail.com](mailto:aysebuse@hotmail.com)

### INTRODUCTION

The aim of this study is to design a degradable wound dressing with double functionality using naturally derived polymers like chitosan and gelatin. Chitosan is chosen for its well-known superior properties in wound healing applications. Existing systems generally contain only one functionality, mostly an antimicrobial agent, and the agent was directly incorporated into the wound dressing matrix. In addition, pain management is not included in the design.

In this study, we proposed a wound dressing which is designed both to alleviate the pain of the patient during the treatment and to protect the wound from infections. For this purpose, ibuprofen and gentamicin encapsulated in type A and B gelatin microspheres will be incorporated into the chitosan matrix. Gelatin with different isoelectric points was chosen to tune the release behavior of the drugs, especially the antibiotic, at different pH conditions of a clean or infected wound.

### EXPERIMENTAL METHODS

1%, 2% and 3% (w/v) of chitosan was dissolved in 0.1 M acetic acid to prepare chitosan sponges. Chitosan solutions were frozen overnight at  $-20^{\circ}\text{C}$  or  $-80^{\circ}\text{C}$  and the samples were freeze-dried for 24 hours. Characterization of chitosan sponges was performed via scanning electron microscope (SEM). Gelatin microspheres were prepared by using water-in-oil emulsion technique adapted from the literature<sup>1</sup>.

### RESULTS AND DISCUSSION

Freezing conditions had considerable effect on the structure of chitosan sponges (Figure 1). The ones which were frozen at  $-20^{\circ}\text{C}$  had more porous structure than the others. Thickness and uniformity of the sponges, and freeze drying conditions were also optimized (data not shown).

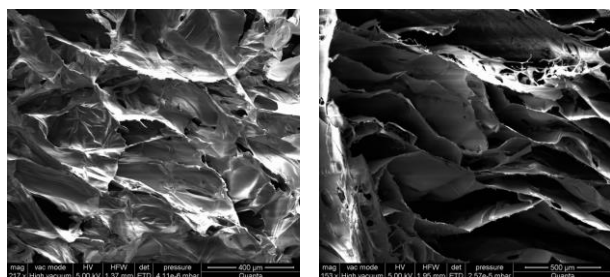


Figure 1: SEM images of the chitosan sponges after freeze drying (left, at  $-20^{\circ}\text{C}$ ; right at  $-80^{\circ}\text{C}$ )

Before the encapsulation of the drugs, the preparation conditions were optimized by unloaded microspheres. Size distribution studies showed that although the majority of the microspheres were within  $20\text{--}30\text{ }\mu\text{m}$  for both types, size range laid between  $15\text{--}40\text{ }\mu\text{m}$  for Type B gelatin while this value was  $20\text{--}60\text{ }\mu\text{m}$  for Type A (Figure 2).

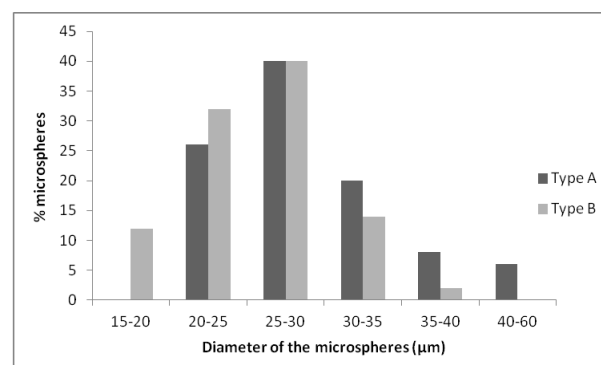


Figure 2: Size distribution of Type A and B gelatin microspheres

Swelling studies showed that Type B but not Type A gelatin microspheres swell at pH:8. Basic pH indicates infectious wound so antibiotic encapsulation will be done using those microspheres to trigger an increase in the release rate during infection.

### CONCLUSION

Swelling behavior of the Type B gelatin microspheres could be suitable to tune the release of gentamicin depending on the infectious state of the wound. Pain management drug (ibuprofen), on the other hand, should be designed not to be affected from the pH of the wound. After the optimization of the release behavior of both drugs (on-going studies), incorporation of the microspheres to the chitosan matrix will be performed.

### REFERENCES

1. P.S. Gungor-Ozkerim et al, J. Biomedical Mat. Res.: Part A 102(6):1897–1908, 2014

### ACKNOWLEDGMENTS

The authors would like to thank The Scientific and Technological Research Council of Turkey (Grant no: 114M870) for providing financial support to this project.

## Design of a Functional Degradable Wound Dressing System for Effective Pain Relief

Beren Sen, Ayse Buse Ozdabak, Fatma Nese Kok

Molecular Biology-Genetics and Biotechnology Programme, Istanbul Technical University, Turkey  
[sen.beren@gmail.com](mailto:sen.beren@gmail.com)

### INTRODUCTION

In this study, we proposed a wound dressing which is designed to alleviate the pain of the patient during the treatment. For this purpose, ibuprofen encapsulated in type A gelatin microspheres will be prepared and incorporated into the chitosan sponges. Chitosan was chosen because of its superior properties in wound healing systems. Although different bioactive materials (antibiotics, growth factors, silver etc.) can be used to increase the functionality of the wound dressing systems, only one active agent is generally incorporated into the matrix for the existing systems. Additionally, pain management is not included in the design.

### EXPERIMENTAL METHODS

Gelatin microspheres were prepared by using water-in-oil emulsion technique adapted from the literature<sup>1</sup>. Ibuprofen solution (1 mg/mL) was added to gelatin solution to obtain loaded microspheres. Microspheres were crosslinked with 5% and 7.5% glutaraldehyde (GTA) solutions overnight. Release studies were carried out in pH: 4.5 and 8.0 buffers.

Chitosan (low viscosity from shrimp, medium MW) solutions were prepared at different concentrations in 0.1 M acetic acid (1%, 2% and 3% (w/v)). They were frozen overnight at -20°C and the samples were freeze-dried for 24 hours. Characterization of chitosan sponges was performed via scanning electron microscope (SEM).

### RESULTS AND DISCUSSION

Release studies showed that a burst release at the first 24 h was observed in all cases that were followed by slow release (Figure 1).

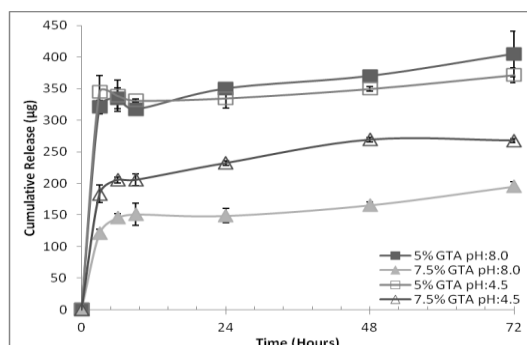


**Figure 1:** Release profiles of gelatin microspheres in pH 4.5 and 8.0 buffers

Depending on the presence/absence/stage of infection, pH of the wound would vary from normal acidic (pH=5) to basic (infectious wound, pH=8) so the system

for the pain management drug should be designed so that the release would not be affected to a great extent from the pH of the wound. For this purpose, ibuprofen was loaded into Type A gelatin microspheres with an isoelectric point of 6-9. The release study showed that microspheres crosslinked with 5% GTA had high burst release which was not depended on pH while higher crosslinking affected both rate and pH dependence of the drug release.

SEM micrographs showed that increase in the chitosan concentration resulted in more dense sponge structures (Figure 2).

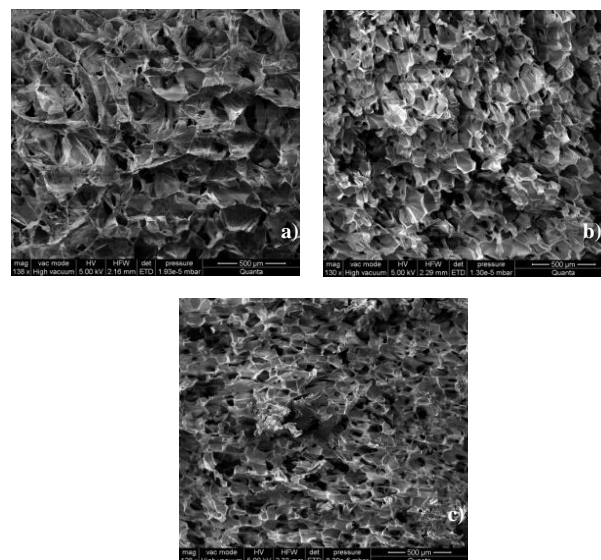


**Figure 2:** SEM micrographs of the chitosan sponges with different concentrations a)1% b)2% c)3%

### CONCLUSION

Release behavior of ibuprofen from Type A gelatin microspheres in different pH conditions was found to be dependent on crosslinking degree. Further optimization will be done to obtain microcapsules with better release profile, and then the microspheres will be incorporated into the chitosan sponge for further characterization.

### REFERENCES

1. P.S. Gungor-Ozkerim et al, J. Biomedical Mat. Res.: Part A 102(6):1897–1908, 2014

### ACKNOWLEDGMENTS

The authors would like to thank The Scientific and Technological Research Council of Turkey (Grant no: 114M870) for providing financial support to this project.



## Dental Lessons from the Past: Ultrastructure of Teeth from Recent and Extinct Sharks, Plesiosaurs and Dinosaurs

Alwina Lübke,<sup>1</sup> Joachim Enax,<sup>1</sup> Oleg Prymak,<sup>1</sup> Helge Fabritius,<sup>2</sup> Dierk Raabe,<sup>2</sup> and Matthias Eppele<sup>1,\*</sup>

<sup>1</sup> Institute of Inorganic Chemistry and Center for Nanointegration Duisburg-Essen (CeNIDE), University of Duisburg-Essen, Universitätsstr. 5-7, 45117 Essen, Germany

<sup>2</sup> Microstructure Physics and Alloy Design, Max-Planck-Institut für Eisenforschung, Max-Planck-Str. 1, 40237 Düsseldorf, Germany

[alwina.luebke@uni-due.de](mailto:alwina.luebke@uni-due.de)

### INTRODUCTION:

Teeth represent the hardest tissue in most living vertebrates, including mammals, having been designed for tearing and cutting (1). Their excellent mechanical properties arise from their delicate ultrastructure, typically with highly mineralized enamel on the outside and the softer, more bone-like dentin on the inside. Mammals (including humans), amphibia and most bony fish use calcium phosphate as tooth mineral (2). The most common tooth mineral is hydroxyapatite with some carbonate substitutions on phosphate positions, the so-called dahllite (3). A notable exception are sharks which use fluoroapatite as tooth mineral (4). We have shown that teeth of recent sharks contain fluoroapatite only in enameloid but not in dentin (5). Here we report on a comprehensive study of teeth of fossilized sharks and dinosaurs where the ultrastructure and their chemical composition were analyzed in detail.

### EXPERIMENTAL METHODS:

Teeth of the extinct shark species *Squalicorax pristodontus*, *Palaeocarchorodon orientalis*, *Otodus obliquus*, *Carcharocles angustidens*, *Carcharocles megalodon*, *Isurus hastalis* as well as of the dinosaur species *Spinosaurus maroccanus*, *Carcharodontosaurus saharicus*, and the extinct marine reptiles *Plesiosaurus mauretanicus* and *Mosasaurus beaugei* were analyzed using scanning electron microscopy, X-ray powder-diffraction with Rietveld-refinement for structural analysis and elemental analysis for chemical composition. The results have been compared to the structure and chemical composition of the recent great white shark *Carcharodon carcharias*.

### RESULTS AND DISCUSSION:

The elemental analysis showed a fluoride content in all fossil shark teeth that was close to that of stoichiometric fluoroapatite, in dentin and enameloid, respectively (Fig. 1). X-ray powder-diffraction identified the crystal phase as apatite. The ultrastructure of the teeth was extraordinarily well preserved; the individual bundles and crystallites can be seen in the SEM-images (Fig. 2). In contrast to the recent shark tooth both, dentin and enameloid, were microcrystalline, whereas in *C. carcharias* only enameloid was microcrystalline, dentin was nanocrystalline. Another difference was the calcium content and with it the degree of mineralization. It was higher in dentin of the fossil teeth than in the recent great white shark. The reason is the decomposition of the organic matrix during the fossilization. The ultrastructural organization of the dinosaur teeth and plesiosaur resembles to those of crocodiles (6), but the individual crystallites in the

enameloid resemble those occurring in shark tooth enameloid.

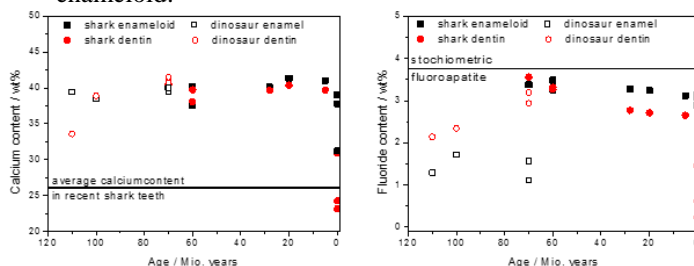


**Fig. 1:** Correlation between calcium and fluoride content and the age of the fossilized teeth.

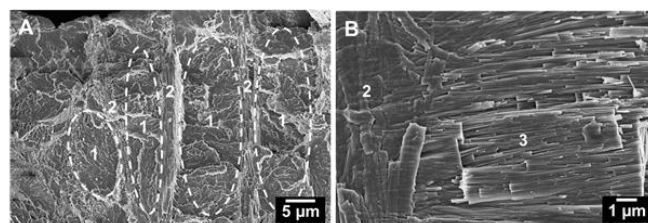


**Fig. 2:** SEM-images of the enameloid of *C. angustidens*.

### CONCLUSION:

We have shown that the ultrastructure of fossil shark teeth is comparable to that of recent sharks, irrespective to the age of the fossil. All fossil teeth, from sharks as well as from plesiosaurs and dinosaurs, contained high amounts of fluoride.

### ACKNOWLEDGMENT:

We thank the Deutsche Forschungsgemeinschaft (DFG) for generous support within the priority program 1420. We thank Mrs. Carola Fischer for helping during the sample preparation.

1. M. F. Teaford, M. M. Smith, M. W. J. Ferguson, *Development, function and evolution of teeth*. Cambridge University Press, Cambridge (2000).
2. H. A. Lowenstam, S. Weiner, *On biomineralization*. Oxford University Press, New York (1989).
3. R. Z. LeGeros, in *Hydroxyapatite and related materials*, P. W. Brown, B. Constantz, Eds. CRC Press, Boca Raton (1994).
4. L. B. Whitenack, D. C. Simkins Jr., P. J. Motta, *J. Morphol.* **272**, 169-179 (2011).
5. J. Enax, O. Prymak, D. Raabe, M. Eppele, *J. Struct. Biol.* **178**, 290-299 (2012).
6. J. Enax, H. O. Fabritius, A. Rack, O. Prymak, D. Raabe, M. Eppele, *J. Struct. Biol.* **184**, 155-163 (2013).



## Testing Stress Relaxation Process of a Pig's Skin

Aneta Liber-Kneć, Sylwia Łagan

Division of Experimental Mechanics and Biomechanics, Faculty of Mechanical Engineering,  
Cracow University of Technology, Poland  
[aliber@pk.edu.pl](mailto:aliber@pk.edu.pl)

### INTRODUCTION

The mechanical properties of a pig's skin which is used as the human skin substitute in the studies carried out in vitro are important for a number of applications, including surgery and biomechanics [1, 2]. In this study, uniaxial tensile test and stress relaxation tests were performed with swine skin samples in two different directions to study the effects of fibre direction on stress relaxation process.

### EXPERIMENTAL METHODS

The samples were taken from the dorsal region of a pig in two directions with respect to the long axis of the pig's body: parallel, perpendicular. All samples had the same dimensions: the length 100 mm and the width 10 mm. The average thickness was equal to  $2.2 \pm 0.2$  mm. The mechanical properties under static tension (modulus of elasticity, tensile strength) and relaxation tests were determined with the use of the MTS Insight 50 testing machine. The samples were mounted using flat clamps and they were extended at the speed of 5 mm/minute. The measurement base of the sample was 50 mm. With stress relaxation tests, each sample (3 for every test) was preloaded with 2 N and then loaded to different strains (5, 10, 15%) to observe its effects on stress relaxing over time.

### RESULTS AND DISCUSSION

In figures 1 and 2 stress relaxation curves for tested skin samples were shown over a 1500 second period. For the strains 5% and 10%, both for parallel and perpendicular samples the trend of relaxation curves is similar. For the strain 15% rapid relaxation can be observed at the beginning over a 500 second period and then the trend of stress relaxation become comparable to the strains 5% and 10%.

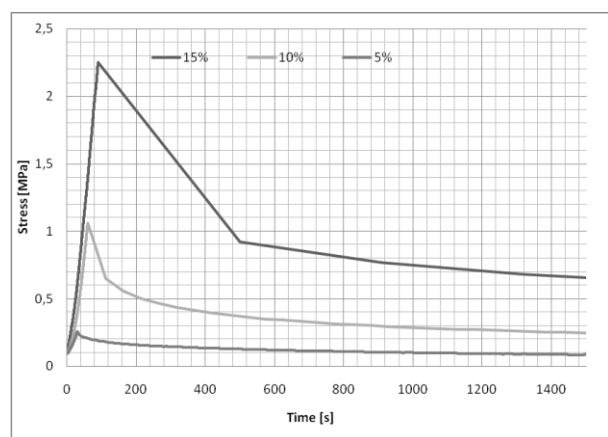


Fig. 1. Relaxation curves for perpendicular samples

For the same level of strain, the time of achieving initial stress was the same: for 5% - 30 s, for 10% - 60 s, for 15% - 90s.

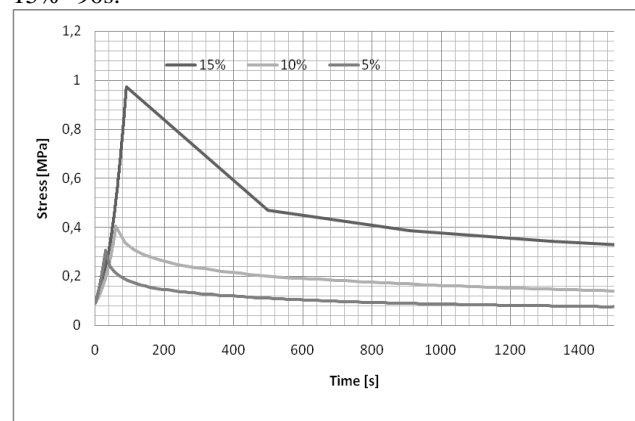


Fig. 2. Relaxation curves for parallel samples

Both parallel and perpendicular samples were tested till time decreased below the value of prestress. For parallel samples both the time of relaxation and decreased below the value of prestress is lower than for perpendicular samples (Table 1).

Direction of sample	Strain [%]	Initial stress [MPa]	Time of decreasing stress below value of prestress [s]	Relaxation time [s]
perpendicular	5%	0,3	1 329,4	100
parallel	5%	0,3	849,4	95
perpendicular	10%	1,1	8 508,1	150
parallel	10%	0,4	3 823,3	110
perpendicular	15%	2,3	61 939,7	1600
parallel	15%	1,0	25 894,9	1000

Table 1. Results of stress relaxation tests

### CONCLUSION

The obtained results can be used for the modelling of stress relaxation behaviour based on QLV theory with the reduced relaxation function [3].

### REFERENCES

1. Corr D.T. *et al.*, Wound Repair and Regeneration, 250-259, 17, 2009
2. Meyer W. *et al.*, Polish Journal of Veterinary Sciences, 17-28, 6(1), 2003
3. Liu Z. *et al.*, Journal of Biomedical & Pharmaceutical Engineering, 22-28, 2008

## Relationship between Solution Treatment and Mechanical Properties of Newly Developed Ag-Pd-Cu-Au System Alloy

Yushi Hoshiya<sup>1</sup>, Toshikazu Akahori<sup>2</sup>, Tomokazu Hattori<sup>2</sup>, Hisao Fukui<sup>3</sup>

<sup>1</sup>Graduate School of Science and Technology, Meijo University, Japan

<sup>2</sup>Faculty of Science and Technology, Meijo University, Japan

<sup>3</sup>Dental School, Aichi-Gakuin University, Japan

[143434029@ccalumni.meijo-u.ac.jp](mailto:143434029@ccalumni.meijo-u.ac.jp)

### INTRODUCTION

Silver alloy is one of semi-precious alloys for dental prosthesis, which has been applied remarkably in Japanese dental field. Ag-20Pd-17.7Cu-12Au alloy (G12) with Cu/Ag ratio of 0.367, which was newly developed for commercial dental silver alloy, shows a unique hardening mechanism after a simple solution treatment (ST) at relatively high temperature as well as traditionally applied Ag-20Pd-14.5Cu-12Au alloy (S12) with Cu/Ag ratio of 0.284<sup>1</sup>. However, the relationship between ST at various temperatures and the mechanical strength of G12 has not been investigated fully. Therefore, the relationship between ST and mechanical properties of G12 after ST at various temperatures was investigated systematically in this study.

### EXPERIMENTAL METHODS

Materials used in this study were hot-rolled plates of Ag-20Pd-17.7Cu-12Au alloy (G12) and Ag-20Pd-14.5Cu-12Au alloy (S12). All samples were conducted with the solution treatment (ST) at 1023~1173 K for 3.6 ks in an Ar gas atmosphere followed by water quenching (WQ). Hereafter, the samples of G12 and S12 subjected to ST were designated by using temperature. (e.g. G12/1123 K). In addition, some samples subjected to aging treatment (AT) at 673 K for 1.2 ks in a vacuum followed by air cooling after ST (G12/AT673 K).

Back-scattering electron (BSE) images from a scanning electron microscope (SEM) and elemental mapping by a wavelength dispersive X-rays spectrometer (WDS) were used for the observation of microstructures and the identification of phase constitutions. The Vickers hardness (HV) and tensile tests were performed to evaluate the mechanical strength. The corrosion potential was measured in a 3 mass% NaCl solution to evaluate the corrosion resistance.

### RESULTS AND DISCUSSION

Figure 1 shows the microstructures of G12/1173 K and G12/AT673 K. G12/1173 K is composed of three kinds of phases with Ag-rich  $\alpha_2$  phase (white area), Cu-rich  $\alpha_1$  phase (gray area) and  $\beta$  phase (black area) of Pd-Cu intermetallic compound. Although nominal melting point of G12 is around 1233 K, the high Cu concentration area like  $\alpha_1$  phase is partially dissolved and then the  $\alpha_1$  and  $\beta$  phases reprecipitate during cooling. On the other hand, the microstructure of the G12/AT673 K was composed of two kinds of phases with  $\alpha_2$  and  $\beta$  phases, which is a typical microstructure of AT after ST.

Figure 2 shows the Vickers hardness of as-received G12 and S12, and those subjected to each heat treatment.

The Vickers hardness of G12/1173 K and G12/AT673 K were almost the same value each other. It is considered that the Vickers hardness increases remarkably by the precipitation of some meta stable  $\beta'$  phases of the coherency in  $\alpha_2$  phases<sup>1</sup>. The Vickers hardness of G12 subjected to ST at relatively high temperature of 1173 K is identical to that of the same alloy subjected to typical age-hardening.

The corrosion potential of G12 changed drastically with the temperature of ST. The potential may have been increased by the decrease in the volume fraction of the  $\alpha_1$  phase with relatively high Cu content.

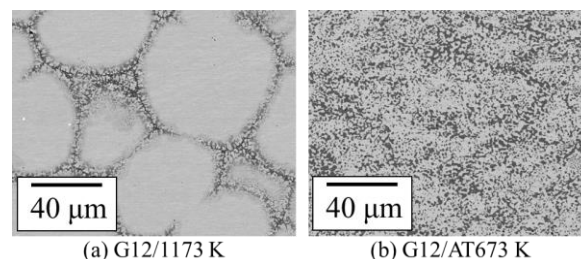


Fig. 1 BSE images of G12/1173 K and G12/AT673 K.

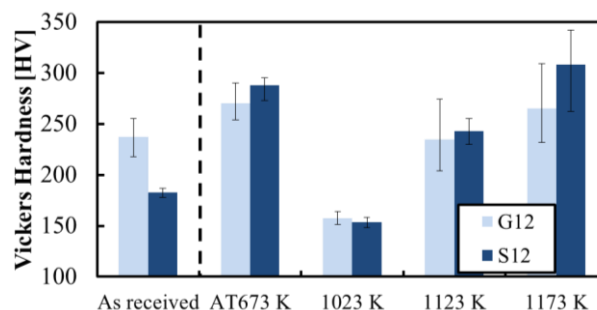


Fig. 2 Vickers hardness of as-received G12 and S12, and those subjected to each heat treatment.

### CONCLUSIONS

- 1) Microstructure of G12 subjected to ST at relatively high temperature of 1173 K was composed of three kinds of phases with  $\alpha_2$ ,  $\alpha_1$  and  $\beta$  phases, and had partially dissolved at around high Cu concentration area.
- 2) Vickers hardness of G12 subjected to ST as mentioned above was identical to that of the same alloy subjected to typical age-hardening.

### REFERENCE

- 1) T. Akahori, M. Niinomi, M. Nakai, H. Tsutsumi, T. Kanno, Y.H. Kim, H. Fukui, J. Japan Inst. Metals, 74(2010), pp. 337-344

Torbjørn Knarvang, Hilde M. Kopperud and Jan T. Samuelsen

Nordic Institute of Dental Materials, Oslo, Norway  
[tok@niom.no](mailto:tok@niom.no)

## INTRODUCTION

Resin-based restorative materials are widely used in dentistry. In general, the resin part of these materials consists of a mixture of methacrylate monomers that are polymerized *in situ* with a blue light initiated free-radical polymerization mechanism. The polymerization process is never complete, and unpolymerized monomer may be released after curing. The resin composition is a parameter influencing polymerization (degree of conversion; DC), material properties and toxic potential.

2-[3-(2H-Benzotriazol-2-yl)-4-hydroxyphenyl]ethyl methacrylate (UV090) is a mono-methacrylate monomer used in several commercial materials such as contact lenses and as UV-absorbant in polymer industry. It has been used in small amounts in resin-based filling material. In this study we aimed to characterize physical properties and toxic potential of resin-based dental composites containing different amounts of the triazol-monomer.

## EXPERIMENTAL METHODS

Experimental dental composites containing 70 % inorganic filler, 12.5-15.0 % bisphenol A glycidyl methacrylate (BisGMA), 12.5-15.0 % triethylene glycol dimethacrylate (TEGDMA), 0-5 % UV090 and initiator components were prepared. The composites (2 mm thick) were cured for 20 seconds with blue light irradiation before the tests.

The degree of conversion (DC) was determined using FTIR and ATR-method directly after irradiation and at 3 h. Relation between aliphatic and aromatic double bond absorbance was used as a measurement to calculate the DC. Flexural strength was determined according to ISO 4049<sup>1</sup> with a Lloyds LRX testing machine. Leakage of unreacted monomer was measured in extracts from cured specimens incubated for 24 h in ethanol/water (75/25 vol/vol) at 37 °C using gas-chromatography.

Toxic potential of UV090 was determined by the MTT test (ISO 10993-5<sup>2</sup>). Briefly, L929 cells (a fibroblast cell line) was exposed to UV090 (0-200 µM) for 24 h. After exposure, MTT was added to the cell culture. The formation of purple coloured formazan after incubation was measured as absorbance at 570 nm and used to indicate viability.

## RESULTS AND DISCUSSION

There were no differences in DC (78 % at 3 h) with different triazol-monomer contents in the composites. This may be due to the relatively small amounts of the triazol-monomer (0-5%) in the composites. However, a decreased MPa value in flexural strength and an increase in monomer release were observed with increasing UV090-content. This suggests the formation of a less complete polymer network using the mono-methacrylate.

The MTT test showed a dose-dependent decrease of viability in the L929 cells. The MTT test yields a relative number of living cells. Hence, both cell death and decreased cell growth may be the cause of this finding. Further studies supplementing the MTT data is currently in progress and will be presented.

Results summarized:

- Addition of UV090 to the resin reduced the flexural strength of the composite
- UV090 is released from cured composites
- UV090 has a toxic potential *in vitro*

## CONCLUSION

In summary, this study showed that increased amounts of the triazol-monomer negatively influenced the measured properties of the experimental composites.

## REFERENCES

1. ISO 4049:2009 Dentistry – Polymer-based restorative materials. International Organization for Standardization, Geneva, 2009.
2. ISO 10993-5:2009 Biological evaluation of medical devices -- Part 5: Tests for in vitro cytotoxicity. International Organization for Standardization, Geneva, 2009.

## ACKNOWLEDGMENTS

The authors would like to thank Anne Wesmann and Hanne Wellendorf for excellent technical assistance.





## Structures of Chosen Degradation Byproducts Originating from Alkali Treatment of Hyaluronan Oligosaccharides

Ondřej Kotland<sup>1</sup>, Petra Lišková<sup>1</sup>, Daniela Šmejkalová<sup>1</sup>, Martina Hermannová<sup>1</sup>, Marek Kuzma<sup>2</sup>, Radovan Buffa<sup>3</sup>, Kristina Nešporová<sup>3</sup>, Tereza Šílová<sup>1</sup> and Vladimír Velebný<sup>4</sup>

<sup>1</sup>Contipro Pharma, Dolní Dobrouč 401, 561 02 Dolní Dobrouč, Czech Republic

<sup>2</sup>Laboratory of Molecular Structure Characterization, Institute of Microbiology, Academy of Sciences of the Czech Republic, Vídeňská 1083, 142 20 Prague, Czech Republic

<sup>3</sup>Contipro Biotech, s.r.o. Dolní Dobrouč 401, 561 02 Dolní Dobrouč, Czech Republic

<sup>4</sup>Contipro Group s.r.o. Dolní Dobrouč 401, 561 02 Dolní Dobrouč, Czech Republic

[ondrej.kotland@contipro.com](mailto:ondrej.kotland@contipro.com)

### INTRODUCTION

Alkali degradation is widely applied for elimination of N-acetylglucosamine from the reducing end of hyaluronan oligosaccharides. However, besides the main  $\beta$ -elimination reaction, there are further side and consecutive reactions proceeding, leading to formation of mixture of degradation byproducts. These byproducts could be potentially harmful similarly as the byproducts originating from acidic hydrolysis<sup>1</sup>. Thus, it is vital to identify structures and to describe basic cytotoxic characteristics of these byproducts.

### EXPERIMENTAL METHODS

The mixture after alkali degradation of HA4<sup>AN</sup> was pre-fractionated on the gel column. The later eluting band was then chromatographed on the reversed phase and degradation byproducts were isolated in milligram quantities. Structures of the purified degradation byproducts were then elucidated using NMR and MS/MS approaches.

### RESULTS AND DISCUSSION

Our results show that during alkali treatment of hyaluronan oligosaccharides, besides the major expected odd-numbered oligosaccharide and isomers of  $\Delta$ -N-acetylglucosamine described previously<sup>2</sup>, a rich mixture of further byproducts origins in a wide concentration span. These include shorter than expected

oligosaccharides, dehydrated and deacetylated oligosaccharides or several yet undescribed furan-like structures.

Some of these byproducts showed cytotoxic properties on 3T3 mouse fibroblasts and can therefore be potentially harmful. Hence, it is vital to provide satisfactory purification of all hyaluronan-based products prepared by alkali treatment and monitor the residual concentrations of these byproducts in final preparations.

### CONCLUSION

During the alkali degradation of hyaluronan oligosaccharide some yet undescribed reaction byproducts are formed, besides the expected main products. These can be comparatively nontoxic, but also strongly cytotoxic on mouse fibroblasts. Therefore it is vital to purify the coveted alkali degradation products properly and to monitor the residual levels of harmful byproducts in oligosaccharide preparations.

### REFERENCES

1. Šmejkalová D. *et al.*, *Carbohydrate Polymers* 88:1425-34, 2012
2. Blundell C.D. and Almond A., *Analytical Biochemistry* 353:236-47, 2006



Sam'an Malik Masudi<sup>1</sup>, Ninin Sukminingrum<sup>1</sup><sup>1</sup>School of Dental Sciences, Universiti Sains Malaysia, 16150 Kubang Kerian, Kelantan, Malaysia  
[sam@usm.my](mailto:sam@usm.my)

## INTRODUCTION

Teeth restored using composite resins are especially prone to this phenomenon due to stress generated within the tooth-restoration interface following resin contraction during polymerization, known as polymerization shrinkage. Thereby, both shrinkage and quality of the bond seem to be responsible for the degradation of marginal adaptation [1]. Microleakage is strongly controlled by marginal adaptation and is thought to be one of the major disadvantages of resin composite restorations. Amalgam surface corrosion and deposition of oxides improves marginal auto-sealing over time. In contrast to composite resins, amalgam is dimensionally stable. Sandwich technique was proposed as an effective technique as a means for pulpal protection from the acid-etch and a mechanism for sealing the cavity in the absence of good dentin adhesion. SDR<sup>®</sup>/Smart Dentine Replacement is the first bulk fill composite, simplifies the procedure for placing adhesive posterior composite fillings, even in extended class II cavities [2]. The aim of this study is to compare materials-composite resin interface characterization on nano glass ionomer, silver amalgam and dentin replacement materials in the proximal box of open sandwich combined with composite resin restorations in class II cavities by using SEM.

## EXPERIMENTAL METHODS

Cavities were prepared in 45-extracted first permanent maxillary with carbide bur. Mesio-occlusal (MO) box-like cavities (3 mm width x 1.5 mm depth) with gingival margins ended 1mm below CEJ were prepared and filled in each tooth. The teeth selected were non carious, without any restoration or cracks. The teeth were divided randomly into 3 groups of 15 teeth. The prepared cavities were filled in open sandwich technique as follows: Group I: RMGI/resin modified glass ionomer Ketac N100 nanoionomer (3M-ESPE); Group II: Silver Amalgam/ Silverfil<sup>®</sup> with Panavia F amalgam bonding (Kuraray); Group III: SDR<sup>®</sup>/Smart Dentine Replacement (Dentsply). The composite used was Filtek Z350 XT (3M-ESPE). Dental tissues were etched with 37% phosphoric acid and a Scotchbond<sup>™</sup> Universal Adhesive bonding agent (3M-ESPE) was applied and cured. The gingival increment in the open sandwich as well as the first composite increment for the composite fillings was 2 mm thick. The restored teeth were thermocycled between 5° to 55° C with 30 second dwell time for 500 cycles to stimulate the temperature changes under clinical conditions. Teeth were longitudinally broken mesio-distally. Specimens were then metalized with fine gold overlay using gold sputter machine (Leica EM SCD005, Germany).

The specimens were photographed at different sections and evaluated for gap present, if any, between base materials and resin composite/CR using SEM (FEI Quanta FEG 450) at 250 magnifications. Adaptation was evaluated at the following interfaces: Nanoionomer-composite resin (A); silver amalgam/ Silverfil<sup>®</sup>-composite resin (B) and SDR<sup>®</sup>-composite resin (C). Microleakage was evaluated by means gap between materials and CR.

## RESULTS AND DISCUSSION

The mean gap between the two materials in group A was highest 3.84µm followed by group B 2.72µm, then by group C showed least mean gap 2.05µm. At 5% probability level, mean gap of group A was higher than all the other groups, but no significant difference was observed between mean gap of group A and group B and group C.

Group	No. of samples	Mean gap (µm)	Range (µm)	S.D.
A	15	3.84*	6.84	1.43
B	15	2.72*	5.29	1.37
C	15	2.05*	4.48	1.32

Table 1 showed gap measured between test materials and composite resin.

\* Indicate no significant difference ( $p > 0.05$ ).

Although the bonding mechanism between amalgam and composite has not yet been completely explained, Silverfil<sup>®</sup>/CR interface exhibited similar microleakage gap compared with Ketac nanoionomer/CR and SDR<sup>®</sup> dentin replacement material/CR.

## CONCLUSION

Since Silverfil<sup>®</sup>/CR interface exhibited similar microleakage scores than nanoionomer/CR and SDR<sup>®</sup>/CR, sandwich restorations can be considered as a biological and aesthetic alternative to conventional Class II composite or amalgam restorations.

## REFERENCES

1. Mickenautsch S. Research gaps identified during systematic reviews of clinical trials: glass-ionomer cements. BMC Oral Health.12(1):18-29, 2012
2. Pfefferkorn, F. What is smart dentin replacement? [www.dentistry.co.uk](http://www.dentistry.co.uk). 68, 2013

## ACKNOWLEDGMENTS

The authors would like to thank the short-term Grant USM (Grant no: 304/PPSG/61311039) for providing financial support to this project.



## Microleakage in Open-Sandwich Class II Dental Restorations

Sam'an Malik Masudi<sup>1</sup>, Ninin Sukminingrum<sup>1</sup>

<sup>1</sup>School of Dental Sciences, Universiti Sains Malaysia, 16150 Kubang Kerian, Kelantan, Malaysia  
[sam@usm.my](mailto:sam@usm.my)

### INTRODUCTION

One of the key functions of a dental restoration is to seal the exposed dentin from the oral environment, to prevent pulpal damage and further decay. Therefore, the microleakage at the tooth-restorative interface is a major concern influencing the clinical longevity of the restorations. The integrity and durability of the marginal seal has always been of prime concern in the investigation of dental restorative materials performance. In order to overcome the inherent composites disadvantages such as the polymerisation shrinkage and the weaker adhesion at the composite-dentin interfaces several solutions were proposed. The step-by-step incremental technique, transparent matrices, reflecting wedges and improved adhesive systems solved only partially these problems. The technique, so-called "Sandwich" as an effective technique for both anterior and posterior resin based restorations. The open-sandwich technique was proposed, which consists in a gingival layer of another class of material prior to resin composite insertion in class II cavities [1]. The aim of the present study is to assess the microleakage between different restorative materials and the dentine gingival margin used in the open sandwich technique in class II cavities.

### EXPERIMENTAL METHODS

Forty upper permanent premolar teeth were used and class II box-like cavities (3 mm width x 1.5 mm depth) with gingival margins ended 1mm below CEJ were prepared and filled in each tooth. The teeth were randomly divided into four groups each containing ten teeth. The prepared cavities were filled as follows: Group I: Silver Amalgam/Silverfil® with Panavia F amalgam bonding (Kuraray) + CR/composite resin; Group II: RMGI/resin modified glass ionomer Ketac N100 nanoionomer (3M-ESPE) + CR; Group III: GI/glass ionomer conventional Fuji II™ (GC Corp) + CR and Group IV: full composite filling using incremental technique. The composite used was Filtek Z350 XT (3M-ESPE). Dental tissues were etched with 37% phosphoric acid and a Scotchbond™ Universal Adhesive bonding agent (3M-ESPE) was applied and cured. The gingival increment in the open sandwich technique as well as the first composite increment for the composite fillings was 2 mm thick. The specimens were thermocycled between 5° to 55° C with 30 second dwell time for 500 cycles. The samples were then immersed in 0.5% Rhodamine B dye for 10 hours and were sectioned longitudinally. Dye penetration at the gingival margin was quantified under confocal laser scanning microscopy/CLSM (Leica, TCS SP2) at 10x magnification.

Data were analyzed using the Mann-Whitney tests and Kruskal-Wallis with a *P* value of  $\leq 0.05$  was considered statistically significant.

### RESULTS AND DISCUSSION

For the dentin-material Kruskal-Wallis test showed statistically significant differences among groups ( $p < 0.05$ ,  $\alpha = 0.0177$ ). The mean gap widths and standard deviations ( $\mu\text{m}$ ) obtained from each experimental group between dentin and the materials tested are shown in Table 1.

Group	Mean gap width ( $\mu\text{m}$ )
1. Silverfil® with Panavia F amalgam bonding + CR	$4.6 \pm 2.2^*$
2. Ketac N100 nanoionomer RMGI + CR	$5.2 \pm 2.7^*$
3. Conventional Fuji II™ GIC+ CR	$20.6 \pm 6.9$
4. Full CR Filtek Z350 XT	$3.8 \pm 2.1^*$

Table 1 show the mean gap widths and SD ( $\mu\text{m}$ ) obtained from each experimental group between dentin and the materials tested.

\* Indicate no significant difference ( $p > 0.05$ ).

The least microleakage between dentin-material interfaces was obtained using composite resin, but the results showed that there was not any statistically significant difference of microgaps in the interfaces between Z350XT® composites with Silverfil® and Ketac N100 nanoionomer (Groups 1, 2 and 4), while conventional glass ionomer (Group 3) exhibited the contrary.

### CONCLUSION

Nanohybrid composite resin Filtek Z350 XT®, Silverfil® amalgam and resin modified nanoionomer Ketac N100 restorative materials were produced similar results in microleakage between dentin-material interfaces at gingival margin of class II open-sandwich restorations. All materials used in this study were not able to totally eliminate microleakage on dentin.

### REFERENCES

1. Kirsten GA. *et al.* Effect of open-sandwich vs. adhesive restorative techniques on enamel and dentine demineralization: an in situ study. J Dent. 41(10):872-80. doi: 10.1016/j.jdent.2013.07.003. Epub, 2013.

### ACKNOWLEDGMENTS

The authors would like to thank the short-term Grant USM (Grant no: 304/PPSG/61311039) for providing financial support to this project.



## Microscopy Analysis of Cement-Enamel Junction in Teeth

Urszula Stachewicz<sup>1</sup>, Wojciech Kożuch<sup>2</sup> and Aleksandra Czyrska-Filemonowicz<sup>1</sup>

<sup>1</sup>International Centre of Electron Microscopy for Materials Science, Faculty of Metals Engineering and Industrial Computer Science, AGH University of Science and Technology, Kraków, Poland

<sup>2</sup>Dental Practise, 2Th, Kraków, Poland

[ustachew@agh.edu.pl](mailto:ustachew@agh.edu.pl)

### INTRODUCTION

Teeth sensitivity is one of great interests in clinical research, therefore cement-enamel junction in teeth has become recently a well studied area. Simply, the cement-enamel junction is the boundary between enamel on tooth crown and cement, which covers the root of the tooth. It is also called in the literature cemento-enamel junction (CEJ). Cementum is an essential mineralized dental tissue, importantly it is cementing the principal collagen fibres of periodontal ligament and enamel is a protective coating on the crown.<sup>1</sup> There are three types of CEJ, including: a) overlap, in which cementum overlaps enamel and is called coronal cementum; b) abutment, cementum butts with enamel; and (c) gap, a finite space between cementum and enamel, as shown in Figure 1.

CEJ is one of the major area where tooth external resorption can start. This process is destructive in nature and can lead to the loss of your tooth without special treatment. In case of no treatment, the tooth loss is inevitable.<sup>2</sup>

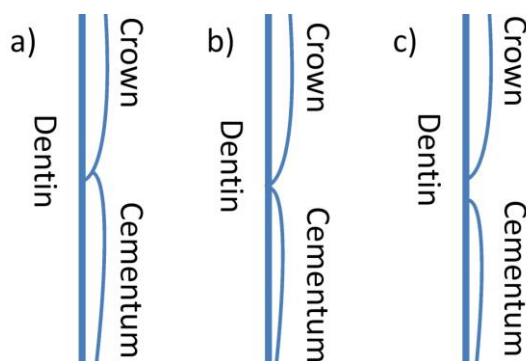


**Figure 1.** Schematic drawing of CEJ types: a) overlap, b) abutment, and (c) gap, a finite space, between cementum and enamel.

### EXPERIMENTAL METHODS

Several teeth samples were extracted from the patient with suspicion of root resorption. The sample teeth were obtained directly from the dental clinic. The carefully extracted teeth were cleaned at the final stage with dental bleaching agents. Scanning electron microscopy

(SEM, Merlin Gemini II, ZEISS) with EDX detector, Quantax 800 (Bruker) microanalysis system and EBSD detector, Quantax CrystAlign 400 (Bruker) microanalysis system was used to localize the cement-enamel junction and perform the chemical analysis.

### RESULTS AND DISCUSSION

We have demonstrated that the SEM can be used to investigate the cemento-enamel junction in tooth to image the gap between cement and enamel in teeth. Moreover, we have not observed any damaging effect of using dental bleaching agents during the samples preparation.

The empty space between the mentioned junction was observed and analyzed on the individual tooth surface. The teeth with the gap, schematically shown in Figure 1c), were cervical region where the tooth resorption process was present.

Scanning electron microscopy can be used as method to verify the resorption process on tooth for the medical diagnosis. The understanding of the teeth resorption process through the microscopy analysis allow to adjust treatment to the patient.

### SUMMARY

Scanning electron microscopy analysis of teeth resorption is able to provide depth analysis of changes at cement-enamel junction that is linked with the chemical analysis at the sub-micron level.

The thorough analysis of the early stages of resorption on teeth can be detected and lead to precise diagnosis and higher chance of successful dental treatment. Within this research we have shown that scanning electron microscopy may assist the clinician in diagnosis of the cause of teeth resorption process.

### REFERENCES

1. I. Roa, M. del Sol and J. Cuevas, *Int J Morphol*, 2013, 31, 894-898.
2. M. Astekar, P. Kaur, N. Dhakar and J. Singh, *J Forensic Dent Sci*, 2014, 6, 86-91.



## Influence of Precipitation Conditions on Cytocompatibility of Hydroxyapatite Substrates

Sophie C. Cox<sup>1\*</sup>, Parastoo Jamshidi<sup>2</sup>, Richard L. Williams<sup>1</sup>, Liam M. Grover<sup>1</sup> and Kajal K. Mallick<sup>3</sup>

<sup>1</sup>School of Chemical Engineering, University of Birmingham, UK,

<sup>2</sup>School of Materials and Metallurgy, University of Birmingham, UK

<sup>3</sup>WMG, University of Warwick, UK

[s.c.cox@bham.ac.uk](mailto:s.c.cox@bham.ac.uk)

### INTRODUCTION

Hydroxyapatite [ $\text{Ca}_{10}(\text{PO}_4)_6(\text{OH})_2$  - (HA)] exhibits chemical and crystallographic similarity to bone mineral. Due to this likeness significant research has been performed to develop preparation methods of HA. Aqueous precipitation is the most common technique used to synthesise HA since the use of low reaction temperatures ( $<100^\circ\text{C}$ ) combined with relatively cheap raw materials results in minimal operating costs. The high scalability of this methodology also makes it attractive for industrial use.

Despite much research being conducted concerning synthesis of CaPs, such as HA, relatively few authors have combined the knowledge of material properties and biological performance. Typically, it is more common to assess only the in-vitro/in-vivo performance of the end product and as such often the effects of chemical variations of the raw material are overlooked. The objective of this study is to investigate the effect of pH, temperature, solute concentration and solvent system on a range of physiochemical characteristics and to perform a number of in-vitro tests to determine any variations in biological performance. Concurrent analysis of HA substrates using a range of characterisation methods contributes to the established knowledge in this field and supported the observed differences in the viability and proliferation of MC3T3 cells assessed by live/dead and MTT assays.

### EXPERIMENTAL METHODS

HA was formed using a precipitation technique previously reported by the authors [1]. Table 1 summarises the varied precipitation conditions used.

Sample	Parameter	Parameter Value
AP01	pH	10 (adjusted)
AP02		11 (adjusted)
AP03		10 (controlled)
AP04		11 (controlled)
AP05	Solute concentration	0.1M (Ca reagent)
AP06	Temperature	$70^\circ\text{C}$
AP07	Ethanolamine	5wt%
AP08	Toluene	60%
AP09	Ethanolamine and Toluene	5wt%, 60%

Table 1: Precipitation conditions

Physiochemical properties of HA powders were characterised using XRD, FTIR, SEM, TEM, DTA-TGA, BET surface area and zeta potential. Cytocompatibility of HA substrates was assessed using a live/dead assay and the rate of MC3T3 cell proliferation was quantitatively distinguished using an MTT assay for up to 7 days.

### RESULTS AND DISCUSSION

XRD patterns for all samples were matched to HA (09-432) with no presence of secondary phases. Analysis of the molecular structure via FTIR revealed the presence of vibrations associated with  $\text{HPO}_4^{2-}$ . AP01 was also shown to exhibit bands corresponding to a PO stretch associated with DCPD. The morphology of powders visualised by SEM exposed a high degree of agglomeration that was prevalent throughout samples. Crystallites of AP01 were observed to exhibit a needle-like morphology, known to be typical of precipitated HA and synonymous with biological equivalents, with an average length and width of  $32.8 \pm 10.1\text{nm}$  and  $5.7 \pm 1.2\text{nm}$ , respectively.

Thermal studies using DTA-TGA highlighted key temperature regions associated with weight loss:  $<200^\circ\text{C}$  (all),  $200 - 300^\circ\text{C}$  (AP01 and AP03),  $250 - 700^\circ\text{C}$  (all), and  $700 - 800^\circ\text{C}$  (all except AP01 and AP06). Weight loss between these temperatures were attributed to: loss of non-bound surface water, dehydration of DCPD to DCPA, dehydration of  $\text{HPO}_4^{2-}$  to  $\text{P}_2\text{O}_7^{4-}$ , and transformation of  $\beta\text{-Ca}_2\text{P}_2\text{O}_7$  to HA and  $\beta\text{-TCP}$ , respectively. Promisingly the surface area of AP06, AP08 and AP09 powders were shown to be larger than other samples.

The zeta potential of both AP01 and AP06, measured in DI at  $25^\circ\text{C}$ , were positive compared to all other samples that exhibited varying degrees of negativity.

Interestingly, corresponding fluorescence micrographs collected up to 7 days of culture using a live/dead assay illustrated the death of the entire cell population after 1 and 3 days, respectively. MTT results further highlighted a significant variation in the proliferation of MC3T3 cells seeded onto HA substrates prepared under different synthesis conditions. Specifically the low crystallinity of powders prepared in a solvent system containing Toluene was attributed to the 200% increase in the proliferative rate of cells between 1 and 7 days compared with AP02.

### CONCLUSION

This work establishes that changes to precipitation conditions cannot be deemed trivial since they may determine the cytocompatibility of HA and the proliferative rate of cells.

### REFERENCES

1. Cox S. C. *et al.*, J. Maters Sci: Maters in Med, 2013

### ACKNOWLEDGMENTS

The authors would like to thank the Warwick Chancellor's scholarship and the Institute of Advanced Study at the University of Warwick for providing financial support to this project.



## Characterisation of Bioresorbable Composite Performance for Validation of New On-Line Process Monitoring Technology

Mark Billham<sup>1</sup>, Darren Whitaker<sup>2</sup>, Marion McAfee<sup>2</sup>, Nicholas Dunne<sup>1</sup>, Fraser Buchanan<sup>1</sup>

<sup>1</sup>School of Mechanical Engineering and Aerospace, Queens University Belfast

<sup>2</sup>Centre for Precision Engineering, Materials & Manufacturing, Institute of Technology, Sligo, Ireland  
[n.dunne@qub.ac.uk](mailto:n.dunne@qub.ac.uk)

### INTRODUCTION

There is an increasing interest in the biomedical field to create implantable medical devices to provide a temporary mechanical function for use inside the human body. In many of these applications bioresorbable polymer composites using PLLA with  $\beta$ -TCP, are increasingly being used due to their biocompatibility, biodegradability and mechanical strength.<sup>1,3</sup> These medical devices can be manufactured using conventional plastics processing methods such as injection moulding and extrusion, however there is great need to understand and control the process due to a lack of knowledge on the influence of processing on material properties. With the addition of biocompatible additives there is also a requirement to be able to predict the quality and level of dispersion within the polymer matrix. On-line UV-Vis spectroscopy has been shown to monitor the quality of fillers in polymers. This can eliminate time consuming and costly post-process evaluation of additive dispersion. The aim of this work was to identify process and performance relationships of PLLA/ $\beta$ -TCP composites with respect to melt-extrusion conditions. This is part of a wider study into on-line process monitoring of bioresorbable polymers as used in the medical industry.

### EXPERIMENTAL

In this study  $\beta$ -TCP particles at 5, 15 and 30  $\mu$ m were compounded at 10, 20 & 30 wt% with poly(L,D)-lactide copolymer in a twin-screw extruder at temperatures of 200°C, 220°C and 240°C; a constant screw speed of 300rpm and constant throughput of 33g/min. The material was extruded through a strip die with an a UV-Vis probe mounted onto the die. The UV-Vis spectra in the wavelength range 290 - 990 nm were recorded through the 1mm path length and collected for each variant for evaluation of the readings. Multi-variate analysis was carried out on the spectra at each temperature and particle size. Extruded samples were collected and analysed by SEM, DSC, TGA and mechanical testing.

### RESULTS AND DISCUSSION

On-line UV-Vis spectroscopy was used to confirm the particle size and loading of the  $\beta$ -TCP filler. Multivariate analysis of the UV-Vis spectra consistently classified the data of the main principle components into particle size (fig. 1).

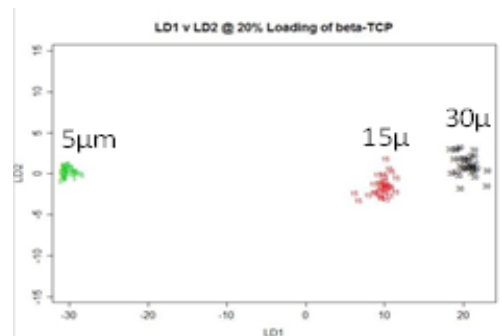


Figure 1. Analysis of UV-Vis spectra of 20 %-TCP/PLA shows consistency of grouping the spectral components into particle size.

The particle size and loading of the  $\beta$ -TCP influenced the rheological and tensile properties of the poly(L,D)-lactide copolymer/ $\beta$ -TCP composite. The smaller particle size of 5  $\mu$ m showed greater reduction in the tensile strain and tensile strength as the % loading increased. (fig. 2) as well as a greater increase in the modulus of the composite.

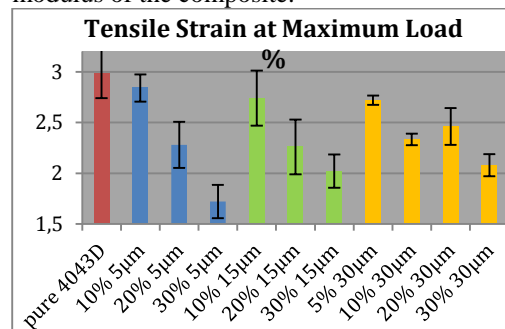


Figure 2. Tensile strain of PLLA/  $\beta$ -TCP samples.

### CONCLUSION

These results show that final properties of the PLLA/  $\beta$ -TCP composite are highly influenced by the particle size and loading. UV-Vis spectroscopy can be used on-line to monitor the final product and this can be utilised as a valuable tool for quality control in an application where consistent performance is of paramount importance.

### REFERENCES

1. Damadzadeh, B., J Mater Sci Mater Med. 2010 21(9):2523-31.
2. Rezwan, K., Biomaterials 27, 2006, 3413-3431.
3. Alig I., Meas. Sci. Technol. 21, 2010, 19

### ACKNOWLEDGEMENTS

This research leading to these results has received funding from EU FP7 managed by the REA [http://ec.europa.eu/research/rea\(FP7/2007-2013\)](http://ec.europa.eu/research/rea(FP7/2007-2013)) under agreement FP7-SME-2012.



## Silica Nanoparticles Stability in Model Biological Media

Beata Borak<sup>1</sup>, Błażej Pożniak<sup>2</sup>, Rafał Wiglus<sup>3</sup>, Robert Pązik<sup>3</sup>

<sup>1</sup>Department of Mechanics, Materials Science and Engineering, Wrocław University of Technology, POLAND

<sup>2</sup>Department of Biochemistry, Pharmacology and Toxicology, Faculty of Veterinary Medicine  
Wrocław University of Environmental and Life Sciences, POLAND

<sup>3</sup>Institute of Low Temperature and Structure Research, Polish Academy of Science, Wrocław, POLAND  
[beataborak@pwr.edu.pl](mailto:beataborak@pwr.edu.pl)

### INTRODUCTION

Silica nanoparticles have attracted attention in biomedical fields due to their safe history, good biocompatibility and biodegradability, and easily tunable surface functionality. They have been used extensively for various applications including photothermal therapy, photodynamic therapy, magnetic resonance imaging, peptide delivery, and gene delivery<sup>1</sup>. The application of the nanoparticles is influenced by their dispersion stability in different media. Characteristics of nanoparticles may be affected by the chemistry of the surrounding and the presence of inorganic and biological moieties, so understanding of their behavior in specific environments is important<sup>2</sup>. The interaction of silica nanoparticles with proteins plays a key role in modern biotechnology and in the biomedical field.

### EXPERIMENTAL METHODS

Silica nanoparticles were synthesized by the sol-gel process using Stöber method<sup>3</sup> (SN1 and SN2) and in different way, in the water-based solution of cyclohexane and arginine (SN3). In both types of synthesis tetraethoxysilane (TEOS) or tetramethoxysilane (TMOS) were used as silica precursors. Size and stability of the silica nanoparticles in different biological media: water, bicarbonate buffering system RPMI-1640 (RPMI) and mixture of RPMI and FBS (fetal bovine serum) were examined by the dynamic light scattering (DLS) measurements (Malvern Zeta Nanosizer). The shape and size of the presented nanoparticles were also determined by transmission electron microscopy (TEM).

### RESULTS AND DISCUSSION

Obtained materials consist of silica nanoparticles with the size about 20-30 nm. TEM images of the materials are presented in the Fig. 1.

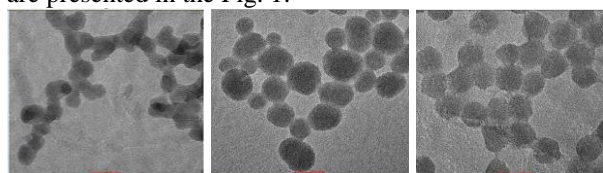


**Fig. 1.** TEM images of the silica nanoparticles: SN1, SN2 and SN3 respectively. The scale bar is 20 nm for all images.

When nanoparticles enter a biological fluid, proteins and other molecules bind to their surface leading to a formation of a dynamic protein or ion layer that defines

the biological identity of the particles. Size of the presented silica nanoparticles in different biological media are presented in the Table 1. Nanoparticles SN1 are the most resistant and show weak response to all types of biological media. The second particles SN2 show tendency to agglomeration in all researched fluids. Particles SN3 aggregate only in RPMI solution which has high ionic strength. This fact agrees with results obtained from the zeta potential measurements. Particles with small value of zeta potential are less stable and have tendency to agglomeration.

method \ probe	SN1	SN2	SN3
TEM [nm]	20	20-30	20
DLS (H <sub>2</sub> O) [nm]	46	136	41
DLS (RPMI) [nm]	50	166	490
DLS (RPMI-FBS) [nm]	87	164	95
Zeta potential (H <sub>2</sub> O)	- 45	- 45	-32
Zeta potential (NaCl)	- 28	- 28	- 6

Tab. 1. Size of the SiO<sub>2</sub> in different biological media.

We have also examined the stability of the silica nanoparticles in RPMI and RPMI+FBS versus time. SN1 and SN2 show small tendency to agglomeration in both media. After initial growth, the particle size are almost at the same level during the time of 240 minutes because of the FBS presence what stabilize nanoparticles against further agglomeration, even when the RPMI is added. SN3 nanoparticles in the RPMI agglomerate to the microparticles but they are stabilized by proteins in the RPMI+FBS fluids.

### CONCLUSION

Synthesis method, ionic strength and biological molecules can change the properties of silica nanoparticles and affect their biological effects. The proposed approach may be a useful tool in the preliminary prediction of nanoparticles behaviour in biological fluids and interpretation of toxicological results. Such knowledge is crucial for estimation of stability of the potential nanocarrier systems intended for use.

### REFERENCES

1. Yu T. *et al.*, ACS Nano 5 (7), 5717, 2011
2. Izak-Nau E. *et al.*, Particle and fibre toxicology, 10(1), 56, 2013
3. Stöber W. *et al.*, J. Colloid Interf. Sci. 26, 62, 1968

### ACKNOWLEDGMENTS

This work was supported by S40135/W10.



## Direct Contact Cytotoxicity Evaluation of Three Different Tricalcium Silicate Cements Used in Dentistry – An in Vitro Study

Sivaprakash Rajasekharan<sup>1</sup>, Heidi Declercq<sup>2</sup>, David Schaubroeck<sup>3</sup>, Peter De Coster<sup>4</sup>, Luc Martens<sup>1</sup>

<sup>1</sup>Department of Paediatric Dentistry & Special Care, PAECOMEDIS research cluster, Ghent University, UZ Ghent, 1P8, De Pintelaan 185, 9000 Ghent, Belgium.

<sup>2</sup> Department of Basic Medical Science–Tissue Engineering Group, Ghent University, De Pintelaan 185 (6B3), B-9000 Ghent, Belgium

<sup>3</sup> Centre for Microsystems Technology, imec, Department of Electronics and Information Systems, Faculty of Engineering and Architecture, Ghent University, Ghent, Belgium.

<sup>4</sup> Oral Biology, Dental School, Ghent University, Ghent, Belgium

[sivaprakash.rajasekharan@ugent.be](mailto:sivaprakash.rajasekharan@ugent.be)

### INTRODUCTION

Hydraulic calcium silicate cements are bioactive materials showing a dynamic interaction with dentine and pulp tissue interface<sup>1</sup>. Biodentine™, Pro Root® mineral trioxide aggregate (MTA) and MedCem® MTA are three such hydraulic tricalcium silicate cements used in the field of dentistry. Materials used in endodontics should preferably be biocompatible. This is particularly desirable when they are placed in direct contact with living tissue such as in pulp capping, perforation repair or when used as a retrograde filling<sup>2</sup>. To promote healing and restoration of the function of the tooth, dental materials should either stimulate repair or be biologically neutral.

The purpose of this study was to evaluate in vitro cytotoxicity of three different commercially available dental materials (tricalcium silicate cements) using MG-63 osteoblast cells.

### EXPERIMENTAL METHODS

Biodentine™, Pro Root® MTA and MedCem® MTA were mixed according to manufacturer's instructions. Thirty disks, 5mm in diameter and 1 mm in height were made per material and allowed to set in a sterile environment. All samples were subjected to ultraviolet radiation for one hour. One half of the samples were randomly chosen and subjected to overnight extraction in medium.

Light optic profilometry, Energy dispersive x-ray analysis (EDX) and scanning electron microscopy (SEM) were used to assess surface topography, homogeneity and reproducibility of the samples used respectively.

MG63 osteoblast-like cells originally isolated from a human osteosarcoma, were used.  $1 \times 10^5$  cells were first seeded onto a 24-well plate and samples were placed on top of a monolayer cell culture. Live/death was evaluated by confocal microscopy using calcein-AM/propidium iodide staining. Cell viability and proliferation were assessed using the MTT assay. Direct contact cytotoxicity tests after 24 hours were performed with and without overnight extraction in medium.

Based on the ISO 10993-5, all tests were performed in triplicate. Statistical analysis was performed by ANOVA and post-hoc Tukey's tests. The level of significance was set at 0.05.

### RESULTS AND DISCUSSION

Biodentine™, Pro Root® MTA and MedCem® MTA showed crystalline, uneven surface topography. Surface roughness of all the three materials used were comparable.

After overnight extraction in medium, all the three materials exhibited statistically similar cell viability ( $p > 0.005$ ). Without extraction, Biodentine™ showed significant reduction in cell viability when compared to control group ( $p = 0.004$ ), Pro Root® MTA ( $p = 0.001$ ) and MedCem® MTA ( $p = 0.001$ ). Live/death assay images using calcein-AM/propidium iodide staining were in correlation with the MTT assay. In all the three cements, cell viability was increased when the samples were placed in contact with the cells after overnight extraction in medium.

Various studies report decreases in the viability of cells cultured in vitro in the presence of tricalcium silicate based biomaterials. The variation in the quantity of calcium hydroxide released may be responsible for the varying cell viability. Calcium hydroxide release may cause the denaturation of proteins in the medium and pH fluctuations which affect cell viability<sup>3</sup>.

### CONCLUSION

Our findings indicate that media conditioned with Biodentine™, Pro Root® mineral trioxide aggregate (MTA) and MedCem® MTA may modify the viability and proliferation of cells.

### REFERENCES

1. Gandolfi MG. *et al.*, Int Endod J. 44: 938-49, 2011
2. Zhou H. *et al.*, J Endod. 39: 478-83, 2013
3. Perard M. *et al.*, J Mater Sci: Mater Med. 24: 1527-34, 2013





## Gene Expression Profiling and Molecular Signalling of Dental Pulp Cells in Response to Tricalcium Silicate Cements: A Systematic Review

Elanagai Rathinam<sup>1</sup>, Sivaprakash Rajasekharan<sup>1</sup>, Ravi Teja Chitturi<sup>2</sup>, Luc Martens<sup>1</sup>, Peter De Coster<sup>3</sup>

<sup>1</sup>Department of Paediatric Dentistry & Special Care, PAECOMEDIS research cluster, Ghent University, UZ Ghent, 1P8, De Pintelaan 185, 9000 Ghent, Belgium.

<sup>2</sup> Department of Oral Pathology, SIBAR Institute of Dental Sciences, Guntur, Andhra Pradesh, India

<sup>3</sup> Oral Biology, Dental School, Ghent University, Ghent, Belgium

[elanagai.rathinam@ugent.be](mailto:elanagai.rathinam@ugent.be)

### INTRODUCTION

Tricalcium silicate cements refer to a group of hydraulic cements with tri- and di- calcium silicates as their dominant ingredient, which react with water to form calcium silicate hydrate and calcium hydroxide. Application of these cements is abundantly being recommended for vital pulp therapy, and over the past decade, a field of research has emerged focusing on modification or development of newer tricalcium silicate cements that could overcome the shortcomings of their predecessors and increase their clinical efficiency. Signalling molecules and responding dental pulp stem cells are the two main control keys of dentin regeneration/dentinogenesis<sup>1</sup>.

The aim of this study was to present a systematic review investigating the gene expression of various dental pulp cells in response to different variants of tricalcium silicate cements. The systematic review question was: *'what are the gene or molecular expressions induced by tricalcium silicate cements when they interact with dental pulp cells?'*

### EXPERIMENTAL METHODS

A systematic search of the literature was performed by two independent reviewers followed by article selection and data extraction. The Gwets AC1 inter rater reliability coefficient for screening data was calculated as 97.35% (95% confidence interval; 0.96 – 0.99). Studies analysing all sorts of dental pulp cells (DPCs) and any variant of tri-calcium silicate cement either as the experimental or as the control group were included.

Study design, type of cells, source of cells, variant of tricalcium silicate cement, inhibitors used, techniques used for analysis, duration, staining, up-regulated/ down-regulated genes, genes and pathways expressed, molecular signalling, mineralization effect, statistics used and any significant/ non-significant results were extracted from each selected manuscript to piloted, pre-defined data extraction sheets. Evidence tables based on the included studies, provided the framework to assess data for further analysis.

### RESULTS AND DISCUSSION

A total of 39 articles were included in the review. Among the included studies, ProRoot® MTA was the most commonly used tricalcium silicate cement variant. The ERK-MAPK pathway was the most commonly activated pathway to be identified and similarly DSPP, OCN, DMP-1, ALP, BSP, OPN, COL 1 and Runx2 were the most commonly expressed genes in that order of frequency.

Biodentine™, Bioaggregate™ and MTA stimulate the osteogenic/odontogenic capacity of DPCs by proliferation, angiogenesis and biomineralization through activation of the ERK 1/2, Nuclear factor E2 related factor-2 (Nrf-2), p38, JNK MAPK, p42/p44 MAPK, NF-κB and FGFR pathways. When DPCs are placed into direct contact with tricalcium silicate cements, they show higher levels of gene activation, which in turn could translate into more effective pulpal repair and faster and more predictable formation of reparative dentin.

### CONCLUSION

Osteogenicity and dentinogenicity are highly desirable properties for any endodontic/regenerative cement. These properties have been adequately demonstrated in calcium-silicate cements in the literature. The bioactive properties of calcium-silicate cements combined with biointeractivity, biocompatibility, bioinductivity and osteoconductivity are responsible for the continuously expanding number of clinical applications of these cements in biomedical tissue engineering<sup>2</sup>.

Although tremendous progress has been made in understanding the molecular biology that controls the mechanism of action of calcium-silicate cements, the exact mechanism remains unclear and, consequently, a subject of future research.

### REFERENCES

1. Zanini M. *et al.*, J Endod. 38: 1220-26, 2012
2. Eid AA. *et al.*, Acta biomaterialia. 10: 3327-34, 2014



# Porous Ca-deficient Hydroxyapatite/Biodegradable Polymer Composites

Marina Sokolova<sup>1</sup>, Janis Locs<sup>1</sup>, Aleksandrs Mirosnikovs<sup>1</sup>

<sup>1</sup>Rudolfs Cimdins Riga Biomaterials Innovations and Development Centre,  
Riga Technical University, Riga, Latvia;  
[marina.sokolova@rtu.lv](mailto:marina.sokolova@rtu.lv)

## INTRODUCTION

Natural bone is a complex composite, mainly constituted of biological apatite and molecules of collagen. The natural composite material should combine the strength and stiffness of an inorganic compound with flexibility, toughness and resorbability of an organic phase. Osteoconductivity and load-bearing capability of a scaffold are controlled by the scaffold architecture (pore size, shape, interconnectivity) and by the biomaterial that is used in the construction. Ca-deficient hydroxyapatite (CaP) has been used as bone substitutes and bone-filling materials, due to excellent biocompatibility, osteoconductivity, bone-bonding properties. Polylactic acid (PLA) is a thermoplastic, biodegradable, biocompatible, synthetic polymer with high strength and modulus<sup>2</sup>. It can be easily processed into shapes such as screws, pins and plates for orthopedic applications, and fabricated into scaffolds for replacement and regeneration of tissues. The combination of calcium phosphate compounds and polylactide are expected to take advantages of both materials to obtain optimal scaffold for bone tissue engineering, since it possesses the fundamental characteristics such as bioactivity, biomechanical similarity, processability, and biodegradability. It also can reduce acidity of degradation products of the polylactide<sup>1</sup>.

## EXPERIMENTAL METHODS

Ca-deficient calcium phosphate was obtained via wet precipitation reaction using calcium oxide and orthophosphoric acid, as described in literature<sup>2</sup>. Biodegradable polymer and calcium phosphate composites with composition 20 wt% PLA / 80 wt% CaP and 30 wt% PLA / 70 wt% CaP were manufactured using novel liquid/solid suspension technology. Prepared CaP/PLA composite were mixed with a pore forming agent and formed into a cylinder by a pressing method. Particle size of pore forming agent was in the range from 100 µm to 300 µm. Mass proportions of all materials used in the preparation process are shown in Table 1.

Table 1. List of sample compositions

PLA/CaP composition, wt%	PLA-CaP/pore formed agent composition, wt%
20 PLA/80 CaP	60/40
	50/50
	40/60
30 PLA/70 CaP	60/40
	50/50
	40/60

Fourier-transform infrared spectroscopy (FT-IR) was used to determine the various functional groups in the

composite samples. X-ray diffractometry (XRD) was used to analyse phase composition of obtained calcium phosphates and biodegradable polymer composite samples. Archimedes method was used for the determination of samples porosity<sup>3</sup>. Compressive strength of fabricated CaP/PLA composites was measured at ambient temperature. The crosshead was run at 0.05 mm/min.

## RESULTS AND DISCUSSION

Compressive strength and open porosity of prepared samples is shown in Fig.1. For 30PLA/70 CaP porosity increases from 37% to 59%, but compressive strength decreases from 3,2 MPa to 1,2 MPa. For 20PLA/80CaP porosity increases from 39% to 61% and compressive strength decreases from 2,9 MPa to 0,3 MPa. Varying amount of pore forming agent in the range from 40 wt% to 60 wt%, open porosity increased from 37% to 60%.

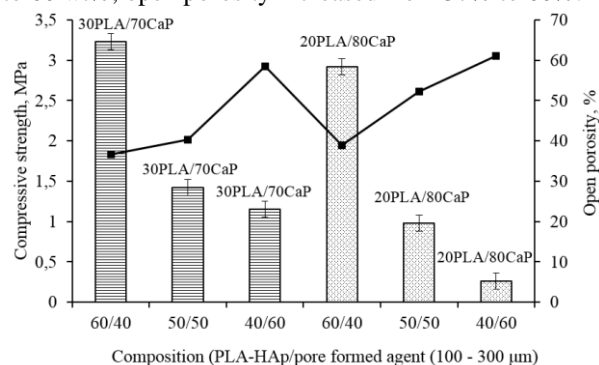


Fig. 1 Compressive strength and open porosity of prepared samples

## CONCLUSION

The porosity of composite scaffold has a noticeable effect on its compressive strength. The scaffolds exhibit minimal compressive strength, with the maximal porosity. By reducing mass fraction of pore formed agent in composite for 20wt%, open porosity is decreasing for 20 % also, but compressive strength increases 3 times for 30PLA/70 CaP composite and 6 times for 20PLA/80CaP composite.

## REFERENCES

1. Wagoner J. A.J. *et al.*, Acta Biomater. 7:16-30, 2011.
2. Sokolova M. *et al.*, Key Eng Mater. 604:216-219, 2014.
3. Locs J. *et al.*, J Eur Ceram Soc. 33:3437-3443, 2013.

## ACKNOWLEDGMENTS

This work has been supported by the M-ERA.NET within the project "Tough, Strong and Resorbable Orthopaedic Implants" (GoIMPLANT).



## Modulation of A $\beta$ (25-35) Conformation: Curcumin and Curcumin Derivatives Effects

Anna Maria D'Ursi<sup>1</sup>, Manuela Rodriguez<sup>1</sup>, Maria Carrano<sup>1</sup>, Manuela Grimaldi<sup>1</sup>, Rosario Randino<sup>1</sup>

<sup>1</sup>Department of Pharmacy, University of Salerno, Italy

[dursi@unisa.it](mailto:dursi@unisa.it)

### INTRODUCTION

Neuritic plaques, the hallmark of Alzheimer's disease (AD), are primarily composed of  $\beta$ -amyloid peptides A $\beta$ (1-40) and A $\beta$ (1-42).<sup>1</sup> A $\beta$ (25-35) represents the biologically active region of A $\beta$ , as it includes the shortest fragment capable of forming large  $\beta$ -sheet aggregates.<sup>2</sup>

Extracts from the rhizome of *Curcuma longa* (Turmeric), has been used for treatment and prevention of certain pathologies, in Chinese medicine, due to its numerous biological activities including antioxidant, antiproliferative, neuroprotective and memory-enhancing activities.<sup>3-5</sup> Curcumin and curcumin derivatives were also proved to inhibit amyloid  $\beta$  peptide A $\beta$  (1-40) and A $\beta$  (1-42) fibril formation.<sup>5-8</sup>. Curcuma extract is a mixture of curcumin and its derivatives shown in Figure 1. Increasing evidence show that the single curcumin derivatives contribute in different, specific way to the final biological effect of curcuma extracts.<sup>8-9</sup>

Aim of our research is to evaluate the effect of curcumin and its derivatives **1-7** to modify the conformation of A $\beta$  (25-35). Accordingly we purified the single curcumin derivatives by HPLC and carried out an extensive spectroscopic investigation, in liposome systems composed of 1,2-Dioleoyl-sn-glycero-3-phosphocholine (DOPC), 1,2-dioleoyl-sn-glycero-3-[phospho-*rac*-(1-glycerol)] (DOPG) and DOPC/DOPG (90/10).

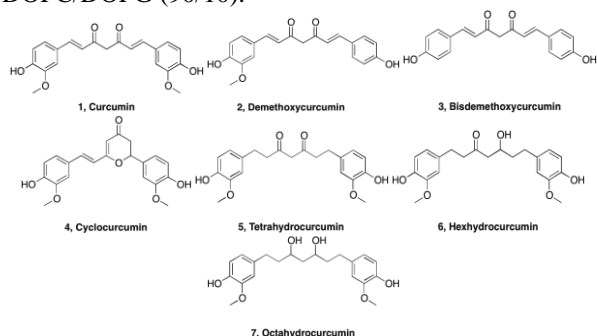


**Figure 1.** Structures of curcuminoids and its derivatives.

### EXPERIMENTAL METHODS

High performance liquid chromatography system (Waters 486 Tunable Absorbance Detector and Varian 9012 pump) with variable wavelength detector was used for analysis and purification of extract of *Curcuma longa*. NMR spectra for full characterization of compounds were recorded on a 300 MHz. High-resolution Mass Spectrometry (HRMS) were recorded on a high resolution mass spectrometer equipped by electrospray (ESI) and nanospray sources, and a quadrupole-time of flight hybrid analyser, coupled with capillary UPLC system (Q-TOF Premier/nanoAquity, Waters) in positive mode, and either protonated molecular ions [M+H]<sup>+</sup> were used for empirical formula confirmation, unless otherwise stated. Circular

dichroism measurements were performed on a JASCO J-810 spectropolarimeter (Jasco, Cremella, Italy) equipped with a thermostated cell holder, using a quartz cell with a 1.0-mm path length. Spectra were collected over the wavelength range from 260–190 nm with a bandwidth of 2.0 nm and a time constant of 8 s.

### RESULTS AND DISCUSSION

CD spectra of A $\beta$ (25-35) (100  $\mu$ M solution), assumes 93-94% of random coil conformation in DOPC and in DOPC/DOPG vesicles; in DOPG vesicles, the prevalence of  $\alpha$ -helix is evident. Circular dichroism spectra recorded after the addition of compounds **1-7** indicate that some of these compounds modify A $\beta$ (25-35) secondary structures. This effect is different in relation to the phospholipid content: evident conformational perturbations are observable in particular in DOPG vesicles. In these conditions the presence of the curcumin derivatives **4** and **5** induces alterations of the CD spectra corresponding to modification of the A $\beta$ (25-35) conformation. These compounds induce similar effects even in the presence of A $\beta$ (25-35) aggregates.

### CONCLUSION

Study of A $\beta$ (25-35) structure in membrane mimetic DOPC and DOPG vesicles show that the secondary structure of this peptide varies in response to the specific composition of phospholipids. In these conditions the single constituents of curcuma evidence peculiar ability to affect the secondary structure of A $\beta$ (25-35). These data suggest that the full biological activity of curcuma extracts critically depends on its composition and therefore on the conditions that favor the specific mixture of *Curcuma* extracts.

### REFERENCES

1. Walsh D.M *et al.*, Neuron 44 181-193, 2004
2. D'Ursi A.M. *et al.* J. Med. Chem. 47 4231-4238, 2004
3. Ahmed T. *et al.*, Pharma- col Biochem Behav 91:554–559, 2009
4. Hamaguchi *et al.*, CNS Neurosci Ther 16:285–297, 2010
5. Narasingappa *et al.*, Biochem Biophys Res Commun 424:691–696, 2012
6. Y. Porat, A *et al.*, Chemical Biology & Drug Design 67, 27-37, 2006
7. F. Re *et al.*, Current Medicinal Chemistry 17 2990-3006, 2010
8. K. Ono *et al.*, Journal of Neuroscience Research 75, 742-750, 2004
9. Yanagisawa D *et al.*, Biomaterials. 31(14) 4179-85. 2010

### ACKNOWLEDGMENTS

“The authors would like to thank the INDENA for providing financial support to this project”.

Katarzyna Gorazda<sup>1</sup>, Ipsita Roy<sup>2</sup>, Agnieszka Makara<sup>1</sup><sup>1</sup>Department of Chemical Engineering and Technology, Cracow University of Technology, Poland<sup>2</sup>Department of Life Sciences, Faculty of Science and Technology, University of Westminster, UK.[gorazda@chemia.pk.edu.pl](mailto:gorazda@chemia.pk.edu.pl)

## INTRODUCTION

Caring for the environment and reducing the adverse effects of the use of common fertilizers such as soil acidification, the introduction of excessive amounts of heavy metals, salinity and over-fertilization of plants causes considerable interest in efficient fertilizers of controlled release, coated with biodegradable polymers. Polymer-coated or encapsulated controlled-release fertilizers can cause an environmental problem since undesirable residues of the coating material may accumulate in the fields. PHAs as a water-insoluble polyesters characterized by a non-toxicity and biodegradability under both aerobic and anaerobic conditions are relevant materials for coating and encapsulation of fertilizers<sup>1,2</sup>. Moreover PHAs can be produced from renewable raw materials what enables the creation of waste management systems in a closed cycle and is consistent with sustainable development<sup>3</sup>.

## EXPERIMENTAL METHODS

In the ongoing research at Cracow University of Technology using the ashes after thermal processing of sewage sludge as alternative raw material, different phosphate fertilizer were produced: liquids and solids in the form of P and NP fertilizers originating from renewable sources.

Using PHAs: poly(3-hydroxybutyrate), poly(3-hydroxyoctanoate) and their mixtures as a coating and encapsulating agent, biodegradable slow released fertilizers were produced in the form of microspheres and coated granules. The production of PHB using *B. cereus* SPV, obtained from the University of Westminster culture collection, was carried out in 20 L fermenters using modified Kannan and Rehacek medium. Medium chain length, mcl-PHA production was carried out in 72L fermenter using *P. mendocina* in MSM media.

Microstructural studies of the surface topography of the products were carried out. Microspheres and coated granules of fertilisers were investigated for nutrient release according to standard EN 13266:2001: Slow-release fertilizers. Structure, size, specific surface area and other properties of granules and microspheres were investigated.

## RESULTS AND DISCUSSION

Figure 1 show surface morphology of the calcium phosphate fertiliser (MCP) coated with mixture of P(3HB) with 10, 20, 50% of P(3HO) and microspheres

with encapsulated MCP solution with the same polyester composition.

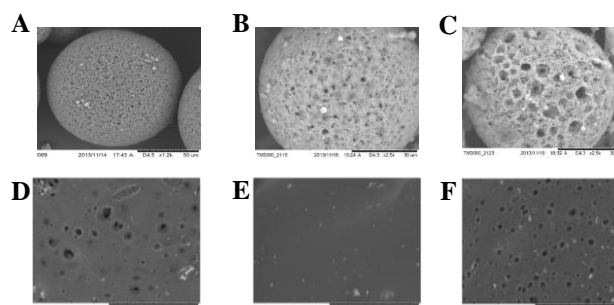


Fig.1. (SEM) of microspheres (A-C) and coated fertiliser granules (D-F): (A) and (D) 10% P(3HO) 90% P(3HB); (B) and (E) 20% P(3HO), 80% P(3HB); (C) and (F) 50% P(3HO), 50% P(3HB);

Phosphorus release from fertilisers coated with 20% mixture of P(3HO) with P(3HB) meets EN13266:2001 standard requirements. After 72h phosphorus cumulative release was only 25%. The profile of cumulative release of phosphorus from P(3HB)/P(3HO) microspheres is seen to be bimodal, with an initial burst release followed by controlled continuous release.

## CONCLUSION

It was confirmed that PHAs as a coating for solid fertilizers or encapsulating agent for liquid one's have a very good potential in future use. Moreover, the combination of biopolymers derived from waste with the fertilizers produced from waste materials will contribute to the creation of entirely new fertilizer products in the market with potentially lower costs of production and compatible with the expectations of the European market for fertilizers.

## REFERENCES

1. Rai R. *et al.*, J. Mater. Sci. Eng. 72(3):29-47, 2011
2. Keshavarz T. *et al.*, Curr. Opin. Biotechnol. 13:321–326, 2010
3. Sukan A. *et al.*, J. Biomat. Nanobiotech. 5(4):229-240, 2014

## ACKNOWLEDGMENTS

This study was supported by NCBiR by the research grant PBS/A1/2012, European Union through the European Social Fund within Cracow University of Technology development program - top quality teaching for the prospective Polish engineers; University of the 21st century” project (contract no.UDA-POKL.04.01.01-00-029/10-00



## Comparative Study of Mechanical Properties of the Selected Bioresorbable Thread Used in Orthopedics

Magdalena Tomanik<sup>1</sup>, Sylwia Szotek<sup>1</sup>, Anna Nikodem<sup>1</sup>

Department of Biomedical Engineering, Mechatronics and Theory of Mechanisms  
Wrocław University of Technology, Poland  
[magdalena.tomanik@pwr.edu.pl](mailto:magdalena.tomanik@pwr.edu.pl)

### INTRODUCTION

Surgical sutures are used to close wounds and post-traumatic surgery. They are used to ease and speed up the healing process. Surgical sutures play a very role in the surgery, and they should have adequate physicochemical properties<sup>1</sup>.

Sutures are characterized by set of parameters that make it easier for the physician to select the appropriate suture to type, location and advance of tissue healing. Improper selection can lead to abnormal tissue adhesion and its infection. Therefore, researchers continue to develop and analyze new materials striving to ensure the best possible functionality while minimizing detrimental effects. In addition, analysis of the process of absorption of the thread makes it possible to assume that resorption will occur in a given environment

The main aim of this study was to determine mechanical properties of surgical sutures composed of bioresorbable materials in various stages of resorption and to determine speed of resorption.

### EXPERIMENTAL METHODS

The material consisted of five resorbable sutures – four of synthetic origin (Biosyn<sup>TM</sup>, Caprosyn<sup>TM</sup>, Polysorb<sup>TM</sup>, PDS<sup>TM</sup> II) and one of natural origin (Catgut<sup>TM</sup>). Sutures differed in total resorption time and the structure (monofilamentne and multifilamentne). For each type of suture at least 5 samples were prepared, each 30cm long. The material was chosen in such a way that the diameters of all suture samples were similar.

The first experiment carried out was to measure geometric parameters of each suture using a stereoscopic microscope SteREO Discovery V20 Zeiss®. For each sample we have measured the diameter in several places, calculated the average diameter and measured the weight. Afterwards samples were placed in a container of saline solution (following PN-EN ISO 10993 guidelines). Containers were then placed in a laboratory oven at 37C. For next 2 months, every 7 days one sample was removed from each container and tested. Uniaxial tension tests were carried out using a testing machine MTS Synergie 100®. Samples were mounted in the machine using dedicated holders placed 50cm apart. Tensile speed was constant and equal to 30 mm/min. Based on the experiments several mechanical parameters were estimated – breaking force, extension at break, stiffness coefficient, tensile strength strain at break and Young's modulus.

### RESULTS AND DISCUSSION

Stress-strain characteristics obtained before incubation for five types of the sutures are presented in Figure 1. Differences in shapes for each suture type can be clearly seen on this basis one can observe differences in the

shapes of the curves. They were close to the sutures Caprosyn<sup>TM</sup>, Biosyn<sup>TM</sup> and PDS<sup>TM</sup> II, Catgut. Figure 1 presents that the maximum stress values ranged from about 250MPa to 800MPa, and the maximum value of extension of the sample ranged from approximately 50 to 150%.

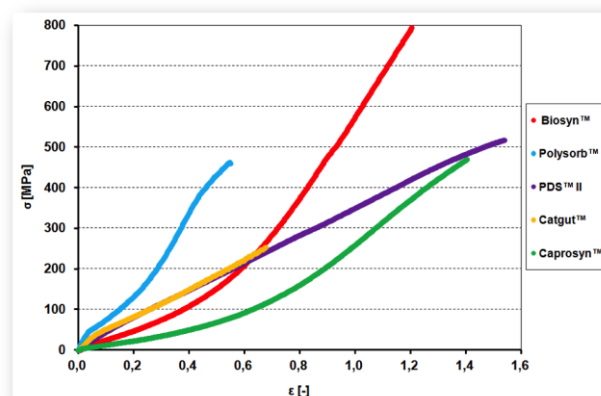


Fig. 1. Stress-strain characteristics obtained in the uniaxial tensile resorbable thread

Fastest resorption among analyzed sutures types was observed for Caprosyn<sup>TM</sup> and Polysorb<sup>TM</sup>. The values of all the mechanical parameters measured decreased with incubation time. The only exception was the PDS<sup>TM</sup> II for which stiffness increased with incubation time.

### CONCLUSION

Based on these results, it was possible to compare mechanical parameters of different types of surgical sutures and to determine the relationship between the parameters and bioresorption stage. This study is a source of valuable information on how bioresorption affects suture's properties, this relation is not fully known at the moment<sup>4</sup>.

### REFERENCES

1. Pillai C.K.S., *et al.*, Review Paper: Absorbable Polymeric Surgical Sutures: Chemistry, Production, Properties, Biodegradability, and Performance. *J Biomater Appl.* 25(4): 291-366, 2010.
2. Tiyek İ., *et al.*, Comparison of physical properties of sutures in medical liquids. *International Journal of the Physical Sciences.* 6(8): 2158-2168, 2011.
3. Khiste S.V., *et al.*, Evaluation of tensile strength of surgical synthetic absorbable suture materials: an in vitro study. *J Periodontal Implant Sci.* 43(3): 130–135, 2013.
4. Najibi S., *et al.*, Material Properties of Common Suture Materials in Orthopaedic Surgery. *The Iowa Orthopaedic Journal.* 30: 84–88, 2010

# Influence of Processing Methods on Biological Behaviour of Polylactide and Its Composites

Anna Morawska-Chochół<sup>1</sup>, Jan Chłopek<sup>1</sup>, Danuta Paluch<sup>2</sup>

<sup>1</sup> Department of Biomaterials, Faculty of Materials Science and Ceramics, AGH University of Science and Technology, Krakow, Poland

<sup>2</sup> Department of Experimental Surgery and Biomaterials Research, Faculty of Dentistry, Wrocław Medical University, Wrocław, Poland  
[morawska@agh.edu.pl](mailto:morawska@agh.edu.pl)

## INTRODUCTION

The biological properties of polymer materials strongly depend on many factors, such as the phase composition, the structure (degree of crystallinity), the microstructure and the surface properties (roughness, wettability)<sup>1</sup>. Yet these characteristics can undergo significant changes as a result of processing of polymer materials and their composites, due to the exposure to high temperature, pressure and a solvent<sup>2</sup>. In the presented paper, the influence of the PLDLA polymer's processing and its composites with TCP on the proliferation and vitality of the cells was examined. These dependences were combined with the changes in the surface and structural properties of the tested materials as a result of their processing.

## EXPERIMENTAL METHODS

The  $\beta$ -tricalcium phosphate (TCP, Fluka, Germany) was used as the filler of the PLA matrix (PLDLA: 70% L/30% DL). Two methods of polymer processing were used: injection moulding (W) and hot compression of prepress (R). The injection moulding was performed at 160°C in a screw injection moulding machine. The hot compression methods included casting polymer films from the PLDLA or PLDLA+TCP solution in  $\text{CH}_2\text{Cl}_2$  and next cutting out the correct shape and hot compressing of the prepress (120°C, 110 kPa/cm<sup>2</sup>). The thermal stability and wettability of the samples were measured. The cytotoxicity tests were performed in Laboratory Cell, Department of Histology and Embryology, Wrocław Medical University according to PN-EN ISO 10993-5 Part 5: Tests for *in vitro* cytotoxicity'. The tests were conducted by the direct contact method on mouse fibroblasts 3T3/Balb.

## RESULTS AND DISCUSSION

In the cytotoxicity test on the samples made of polymers PLDLA „0”, PLDLA (R) and PLDLA (W), we did not state any agglutination, vacuolization, separation from the substrate or lysis of the cell membranes. The highest proliferation of the cells, at all the test times, was stated for the cultures with the non-processed polymer PLDLA „0” (Fig.1a). Both processing methods had their effect on the worsening of the cell proliferation. In all the cultures with the tested samples the percentage of dead cells was identical (Tab.1). The differences in proliferation between the non-processed polymer and that after the processing can be connected with the influence of processing on the structural and surface properties of the tested materials. Both the injection moulding and the hot compression caused a slight increase of the crystallinity degree of the polymer, as a result of the high temperature of processing, which is favourable for the ordering of the

structure and the creation of small crystalline areas. Processing also decreases the hydrophilicity of the surface, which significantly impairs cell proliferation (Tab.2).

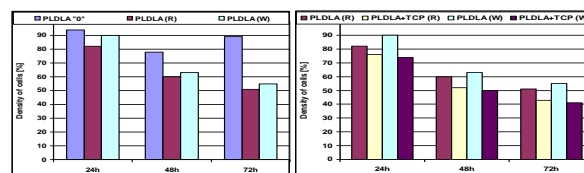


**Fig.1.** Proliferation of mouse fibroblasts 3T3 Balb in cultures with (a) PLDLA and (b) PLDLA+TCP as compared to the control culture.

**Tab. 1.** Evaluation of cytotoxicity of biomaterials.

Culture	Time - 24 h		Time - 48 h		Time - 72 h	
	dead cells %	cyto-toxicity	dead cells %	cyto-toxicity	dead cells %	cyto-toxicity
Control culture	0	0	0	0	2	0
PLDLA „0”	0	0	0	0	2	0
PLDLA (R)	0	0	0	0	2	0
PLDLA (W)	0	0	0	0	2	0
PLDLA+TCP (R)	0	0	2	0	5	0
PLDLA+TCP (W)	0	0	3	0	5	0

**Tab. 2.** Contact angle of tested materials.

Material	PLDLA „0”	PLDLA (R)	PLDLA (W)	PLDLA+TCP (R)	PLDLA+TCP (W)
$\Phi$ [°]	54,4±3,6	82,0±1,9	84,3±1,9	59,4±4,0	79,8±4,4

For PLDLA+TCP(R) and PLDLA+TCP(W), the cell proliferation was lower than in the polymer cultures without TCP (Fig.1b). After 48 and 72h, we stated a higher percentage of dead cells, as compared to the control cultures and the polymer cultures without TCP. The worsening of these properties was more significant for PLDLA+TCP(W) with regard to PLDLA(W) than in the case of the hot-compressed samples. These changes also correlate with the hydrophilicity of materials. For PLDLA+TCP(R) the surface hydrophilicity does not undergo any significant change as compared to PLDLA „0”, although an increase of the contact angle for PLDLA+TCP(W) is clearly seen (Tab.2).

## CONCLUSION

The non-processed polymer showed better biological properties than after processing. The technique of polymer processing had only a slight influence on the cytotoxicity of the materials. A significant effect of the surface and structural properties on the cell proliferation was observed.

## REFERENCES

1. Vert M. *et al.*, J. Mater. Sci. Mater. in Med. 3:432-446, 1992
2. Lima L. *et al.*, Progress in Polym. Sci. 33:820-52, 2008

## ACKNOWLEDGMENTS

This research was financially supported by the research project: PARP No 5.23.160.254 in cooperation with Medgal Company.



Kamil Dudziński<sup>1</sup>, Robert Kańtoch<sup>2</sup>, Karol Gryń<sup>3</sup><sup>1,3</sup>Department of Biomaterials, Faculty of Material Science and Ceramics, AGH University of Science and Technology, Krakow, Poland<sup>2</sup>Faculty of Mechanical Engineering and Robotics, AGH University of Science and Technology, Krakow, Poland  
[ka.dudziński@gmail.com](mailto:ka.dudziński@gmail.com)

## INTRODUCTION

Internal fixation using miniplates is a common technique for stabilising bone fragments in maxillofacial fractures and osteotomies [1]. In this research the stability of a model fixation during uniaxial tensile test was analysed using finite element method (FEA). The comparison between FEA and actual tensile test was conducted to learn about utility of FEA in biomedical engineering and the nature of a miniplate's cracking process.

## EXPERIMENTAL METHODS

The miniplate was made of medical grade poly(L-lactide PLLA (Purasorb® PL38, Purac). Injection moulding was applied to form samples (T=200°C) (Fig.1).



Figure 1. Tested miniplate made of PL38

### Finite element method

FEA was accomplished with ABAQUS CAE software. It was used to determine how geometry of the miniplate affects its destruction. Owing to the two existing planes of symmetry the model was simplified to 1/4 of its original size to make the analysis easier and quicker (Fig.2).

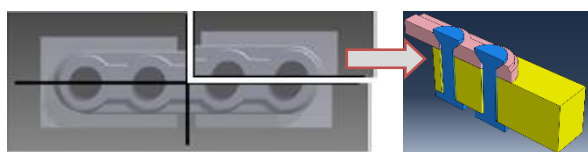


Figure 2. Analysed fixation model and its simplification.

The simulation was divided in three parts, respectively:

- 1) determination of boundary conditions;
- 2) simplification of the screws tightening;
- 3) static extension of the joint.

### Tensile test

To compare and verify the results of the simulation an uniaxial tensile strength test was performed. The miniplate was attached to the base with metallic screws. Various values of the tightening torque were applied (80% and 60% of  $M_{max}$ ).

## RESULTS AND DISCUSSION

### Finite element method

FEA simulations showed the layout of stress concentration. Based on these maps, analysis of the deformation process up to decohesion were done (Fig.3a).

### Tensile test

Tensile tests revealed the influence of a tightening torque values on the deformation process of the miniplates. The best results were obtained for a 60% of  $M_{max}$ . The miniplate broke in the same spot as it was indicated by FEA (Fig.3b).

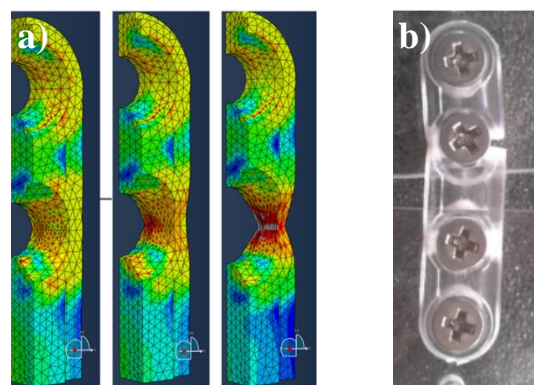


Figure 3. a) Visualisation of tensile test simulation. Progression of the necking within next three steps during elongation; b) miniplate after actual test

## CONCLUSION

The simulation and the actual tensile test were compared. It showed that simulation can help engineers to understand what happens inside of the tested sample. Investigating the mechanical aspects of resorbable miniplates used for bone fixation is a very important issue. They are more brittle than metal plates, so there is a greater possibility of their destruction during or after implantation.

## REFERENCES

1. Keung Chow L. *et al.*: Oral and Maxillofacial Surgery 16:224-233, 2004
2. B. Szaraniec, K. Gryń, T. Szponder *et al.* Engineering of Biomaterials 125: 30-36, 2014

## ACKNOWLEDGMENTS

This research was financially supported by the research project No: 5.23.160.254 financed by the Ministry of Science and Higher Education with cooperation with MEDGAL Company.

## Water Loss of Surface Treated Glass-Ionomer Cements

Elizabeth Bent<sup>1</sup>, John Nicholson<sup>1</sup>.

<sup>1</sup>Applied Physics/School of Sports, Health and Applied Sciences, St Mary's University, England  
[lizzy.bent@stmarys.ac.uk](mailto:lizzy.bent@stmarys.ac.uk)

### INTRODUCTION

Glass-ionomer cements (GICs) are dental restorative materials that have a high susceptibility to water loss in the early stages of setting, as a result of the water that is used and made in the acid-base reaction<sup>1</sup>.

The water present in GICs has been found in two states: 'tightly bound' and 'loosely bound' the distinction between these types of water is whether water is removed from the GIC in a desiccating environment or with a high temperature<sup>2</sup>. 'Superficial water' is another state found in GICs which is seen 'to arise from a small loss from the surface water'<sup>3</sup>. The use of surface protection for GICs has been employed in research to understand water movement in the cement system; it was found the use of varnishes, emollients and light-activated bonding resin were effective in limiting water movement<sup>4, 5</sup>. In this research four treatments are used on GICs surfaces for 24 hours before being transferred to a desiccating environment to ascertain how surface treatment affects water loss in modern Type II.1 GICs<sup>1</sup>.

### EXPERIMENTAL METHODS

Three brands of commercial GICs; AquaCem (DENTSPLY), Fuji IX GP Extra (GC Corporation) and Ketac Molar Aplicap (3M ESPE) were used for the experiments. The first cement was hand mixed with distilled water and the remaining cements were capsules; each GIC was made by following the manufacturer's instructions then placed in a silicone rubber mould between two glass slides. The specimens were disc shaped with dimensions of 5mm in diameter by 1mm depth. Once made the specimens were transferred to an incubator for 10 minutes at 37°C to further harden. The surface treatments were applied to each brand, the treatments utilised were: desiccation over concentrated sulphuric acid, 5ml distilled water, no treatment (control) and Vaseline. Treatments were applied for 24 hours then transferred to a desiccator over concentrated sulphuric acid for six weeks; the loss in mass was recorded weekly.

### RESULTS AND DISCUSSION

Table 1 Greatest % Water Loss of surface treated GICs.  
 Key: Week 3 - a, Week 4 - b, Week 5 - c, Week 6 - d

	<i>Vaseline</i>	<i>No Treatment</i>	<i>Desiccator</i>	<i>Water</i>
AquaCem	12.99% <sub>d</sub>	15.58% <sup>a</sup>	16.36% <sub>d</sub>	14.96% <sub>c</sub>
Fuji IX GP Extra	7.04% <sup>a</sup>	8.94% <sup>c</sup>	8.96% <sup>b</sup>	8.46% <sup>c</sup>
Ketac Molar Aplicap	6.03% <sup>c</sup>	7.47% <sup>c</sup>	7.53% <sup>c</sup>	10.49% <sub>c</sub>

Table 1 show the greatest percentage water loss calculated during the six week experiment, it was found that this loss occurred at a variety times for each treatment yet was quite similar within brands. Previously GICs were found to loose between 18-28% of water under desiccation<sup>6</sup>; whilst these results have shown that even specimens under desiccation for the entire experiment lost less water than was once expected. In regards to the treatments used Vaseline offered the best protection as it had the lowest percentage water loss for each brand and Ketac Molar Aplicap lost the least amount of water and took up to five weeks to reach this loss. This data implies that there was a greater ratio of 'tightly bound' water to 'loosely bound' water in Ketac Molar Aplicap, as less water was available to be removed by desiccation over the period of the experiment.

### CONCLUSION

It was found that the treatment of Fuji IX GP Extra and Ketac Molar Aplicap with Vaseline for 24 hours was effective in reducing the amount of water lost from the material over the entire experiment. However it has yet to be found how the application of this treatment affects strength.

### REFERENCES

1. Mount, G. J (2002). An Atlas of Glass-Ionomer Cements. 3rd ed. London: Martin Dunitz Ltd. 2,13
2. Wilson, A. *et al.*, Br. Polym. J., 7:279-296,1975
3. Nicholson, J. *et al.*, J Mater Sci: Mater Med., 19:1723-1727, 2008
4. Earl, M. *et al.*, Aus. Dent J., 30(4):298-301, 1985
5. Earl, M. *et al.* Aus. Dent J., 34(4):326-329, 1989
6. Prosser, H. *et al.* J. Chem. Technol. Biotechnol., 29:69-87,1979





## Imaging of In-vitro Plaque Removed From Titanium Using Cavitation

Emilia Pecheva<sup>1,2\*</sup>, Nina Vyas<sup>1,3</sup>, Judith Brown<sup>4</sup>, Gareth J. Price<sup>4</sup>, Rachel Sammons<sup>1</sup> and Damien Walmsley<sup>1</sup>

<sup>1</sup> School of Dentistry, University of Birmingham, Birmingham, United Kingdom

<sup>2</sup> Institute of Solid State Physics, Bulgarian Academy of Sciences, Sofia, Bulgaria

<sup>3</sup> Physical Sciences of Imaging for Biomedical Sciences (PSIBS), University of Birmingham, Birmingham, United Kingdom

<sup>4</sup> Department of Chemistry, University of Bath, Bath, United Kingdom

\*[e.v.pecheva@bham.ac.uk](mailto:e.v.pecheva@bham.ac.uk)

### INTRODUCTION

Bacterial biofilms, also known as plaque, form on teeth and dental implants, and may lead to dental caries, periodontal disease with tooth loss, serious infections or implant failure. Biofilms also mineralise, forming calculus that is removed mechanically by clinicians using the chipping action of a dental scaler.

Ultrasonic scalers are used in dentistry for plaque and calculus removal due to their efficiency and greater comfort for the patient than hand instruments. Another advantage is the generation of cavitation within the water flow over the dental tip, which increases the cleaning efficiency<sup>1</sup>. Our objective was to investigate, image and quantify the disruption of bacterial biofilms on titanium by piezoelectric dental scaler tips.

### EXPERIMENTAL METHODS

Biofilms were grown in-vitro on titanium disks in a bioreactor by *Serratia* (NCIMB40259) bacterial model system and *Streptococcus mutans* oral bacterium. *Serratia* is capable of forming biofilm on various surfaces, as well as mineralising it to calcium deficient hydroxyapatite that chemically resembles calculus<sup>2</sup>. A Satelec ultrasonic dental scaler with water irrigation of the tip was used to disrupt the dehydrated biofilms for 30 seconds at fixed power setting giving a tip displacement of 15µm. Three tips with different shape (fig. 1)



**Fig.1** Design of the tips chosen for the study. The free end of the tip is placed parallel to the biofilm during the disruption. The threaded end of the tip is attached to a handpiece.

were applied with their front side parallel to the biofilm and tip end facing down. Two positions along the tips length, the tip end (A in fig. 1) and the tip curved side

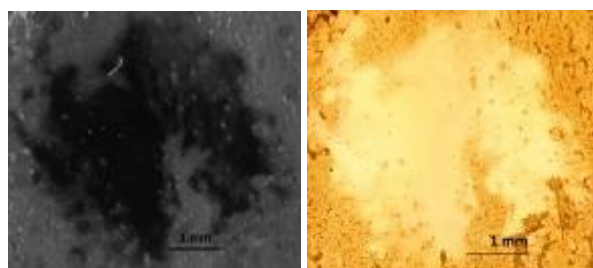


**Fig.2** Images of the disrupted biofilm, obtained by Nikon camera (left) and optical microscope (right).

(B), where previous work has demonstrated cavitation were chosen to approach the biofilms. The removal was visualised by SEM, white light interferometry, optical microscopy, high-speed camera (figs. 2 and 3) and quantified using image analysis.

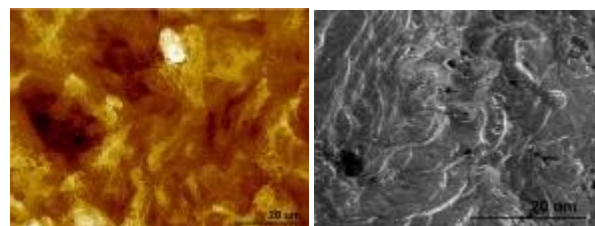


**Fig.3** Disrupted biofilm imaged by white light interferometry (left) and SEM (right).

### RESULTS AND DISCUSSION

An area of disruption on both *Serratia* and *Streptococcus mutans* biofilms occurred when the tip-biofilm distance was set at 40 µm to avoid direct mechanical action of the tip (figs. 2, 3). The disruption efficacy of the cavitation decreased at a higher tip-plaque distance (1 mm). The most effective removal occurred with the thinnest tip. The effect of the disruption varied with the position of the cavitation along the tip length. SEM revealed bacteria still present in the cleaned area but not as many as before the scaling. This might be due to the roughness of the titanium surface making it difficult to be completely cleaned by the scaler as well as to the much higher adhesion, which the biofilm layer adjacent to the material surface has. High speed camera imaging reveals the detachment of large biofilm flakes while the scaler tip is vibrating within the water flow.

### CONCLUSION

We have imaged how cavitation around ultrasonic tips might be used for the non-contact disruption of biofilms. Tip shape, tip-biofilm distance and position of cavitation along the tip length have all influenced the biofilm removal with the scaler.

### REFERENCES

- Walmsley AD. *et al.*, Clin. Oral. Invest. 17:1227–1234, 2013
- Medina Ledo H. *et al.*, J. Mater. Sci. Mater. Med. 19:3419–3427, 2008

### ACKNOWLEDGMENTS

The work was funded by EPSRC Grant № EP/J014060.

## Degradation Processes of Ti6Al4V Alloy by Fretting and Fretting-Corrosion

Marcin Klekotka<sup>1</sup>, Jan Ryszard Dąbrowski<sup>1</sup>

<sup>1</sup>Department of Materials and Biomedical Engineering,  
Białystok University of Technology Wiejska 45C, 15-351 Białystok, Poland  
[j.dabrowski@pb.edu.pl](mailto:j.dabrowski@pb.edu.pl)

### INTRODUCTION

High biofunctionality of titanium and its' alloys enabled it to be one of the most promising groups of metallic biomaterials used for elements of bone surgery and prosthodontics<sup>1,2</sup>. Relatively low modulus of elasticity, good corrosion resistance, high biocompatibility are characteristics undoubtedly required among modern biomaterials. Essential downside of titanium alloys is their low tribological resistance and the presence of toxic additions of aluminium and vanadium (alloys of Ti-Al-V group)<sup>3</sup>. As a result of degradation of the elements of kinematic bounds, particularly exposed to processes of fretting and fretting-corrosion, ions of aluminium and vanadium are released to the organism. They may block the regeneration of nerve cells, as well as cause many diseases, inflammations, or even, when influencing for a long period of time, carcinogenic changes<sup>4</sup>. Considering high friction and wear, their usage is limited, and incompetent adjustment to exploiting conditions may be a cause to a decrease of exploitation durability of medical constructions. Better cognition of mechanisms of destruction of biomaterials is a crucial issue, which will directly contribute to an increase of medical comfort of patients.

### EXPERIMENTAL METHODS

Titanium alloy Ti6Al4V was subjected to fretting and fretting-corrosion tests. Friction couples operated in configurations metal-metal and metal-alumina ceramic. Tests were carried out in the conditions of dry friction and simulated oral cavity environment (saliva and its substitutes based on phosphate buffer). The processes of fretting and fretting-corrosion were conducted with the use of own construction pin-on-disc fretting tester combined with potentiostat VoltaLab21. Authorial method of examination was determined by a standard PN-EN ISO 10993-15:2009. Observations of sample surfaces were carried out using a Hitachi S-3000N (SEM) scanning electron microscope and a LEXT OLS4000 confocal microscope with capability of 3D imaging. Investigations of morphology and surface structure allowed to determine volume loss of material.

### RESULTS AND DISCUSSION

Fretting and fretting-corrosion tests were started by a friction force measurement. Received figures were used to calculate friction coefficients. Positive influence of lubricants on reduction of motion resistance and wear of was observed. Natural saliva presents the most profitable tribological characteristics. Potentiodynamic tests of fretting-corrosion have shown strong influence of fraction on corrosion processes. Polarisation curves

present characteristic ragged course, which evidences constant deterioration and renovation of boundary layers. In the case of adsorption oxide layers it is an unwanted phenomenon leading to an intensification of material wear.

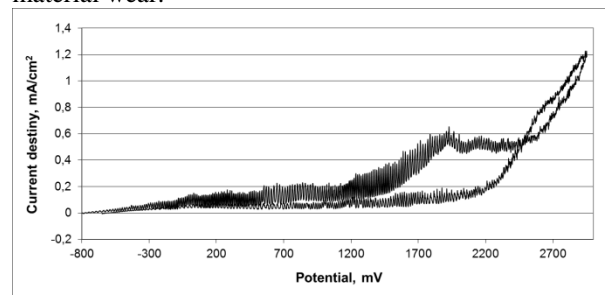


Fig. 1. Anode polarisation curve in the saliva environment during fretting

### CONCLUSION

The results of the studies confirmed the high susceptibility of titanium alloy Ti6Al4V to wear as a result of fretting and fretting-corrosion. A clear influence of fretting on corrosion processes was observed. Application of lubricants such as saliva and its substitutes leads to reduce friction and tribological wear in various degrees. This is caused by formation of adhesive boundary layers on the alloy surface, which were built from organic components of used lubricants. Binding energy and adhesive abilities of biofilm may determine the efficiency of its performance.

### REFERENCES

1. Hansen D.C, The Electrochemical Society Interface 17:31-34, 2008.
2. Martin E. *et al.*, Tribology International 43:918-924, 2011.
3. Bronzino J.D, ed. The Biomedical Engineering HandBook, Second Edition. Boca Raton: CRC Press LLC, 2000.
4. Gunnar F, ed. Handbook on the Toxicology of Metals, Third Edition. Elsevier, 2007.

### ACKNOWLEDGMENTS

The paper was accomplished with financial support within the framework of research project S/WM/1/14

## INTRODUCTION

Enamel demineralization and gingival inflammation are common side effects during orthodontic treatment with fixed appliances<sup>1</sup>. Surface free energy (SFE) and surface roughness (SR) are important surface characteristics for biofilm formation around teeth<sup>2</sup>. The purpose of this study was to investigate the effects of surface characteristics of orthodontic adhesives on the multi-species biofilm.

## EXPERIMENTAL METHODS

Thirteen strains of bacteria (*Streptococcus mutans* ATCC 700610, *Streptococcus sanguinis* CCUG 17826, *Streptococcus sobrinus* ATCC 27607, *Streptococcus salivarius* CCUG 50207, *Lactobacillus rhamnosus* ATCC 7469, *Veillonella dispar* KCOM 1864, *Actinomyces naeslundii* KCOM 1472, *Streptococcus oralis* ATCC 9811, *Neisseria subflava* ATCC 49275, *Fusobacterium nucleatum* ATCC 10953, *Prevotella nigrescens* ATCC 33563, *Porphyromonas gingivalis* KCOM 2797, and *Aggregatibacter actinomycetemcomitans* ATCC 43718) were used to simulate biofilm formation in the oral cavity. The multi-species biofilms were grown in the CDC biofilm reactor (BioSurface Technologies, Bozeman, MT, USA). The lid of reactor supports eight independent rods which can house three removable coupons. Three orthodontic adhesives – composite (Transbond XT, TX), compomer (Transbond Plus, TP) and resin-modified glass ionomer cement (Multi-Cure, MC) (3M Unitek, Monrovia, CA, USA) – were selected to prepare coupons. Six disk-shaped coupons of each adhesive were prepared with a diameter of 12.7 mm and thickness of 3.0 mm. BMMUG medium<sup>3</sup> was used to cultivate multi-species biofilms. Three coupons of each adhesive from a reactor rod were collected at the following time points: at day 1 (T1), day 4 (T2), and day 7 (T3). Bacterial chromosomal DNAs were extracted after biofilms were detached from the coupons. Total bacteria, two cariogenic bacteria (*S. mutans* and *S. sobrinus*) and two periodontal pathogens (*P. gingivalis* and *A. actinomycetemcomitans*) were quantified using real-time PCR. Each analysis was independently repeated five times.

SR and SFE characteristics were investigated for the orthodontic adhesives using a confocal laser scanning microscopy and sessile drop method, respectively. Each analysis was repeated five times for each of three specimens.

Repeated measures analysis of variance (ANOVA) was used to determine the time-related differences in the bacterial amounts with respect to adhesive type. Kruskal-Wallis test was used to determine the differences in surface characteristics among the 3

groups. For all analyses,  $\alpha < 0.05$  was considered statistically significant.

## RESULTS AND DISCUSSION

Adhesion of total bacteria and cariogenic streptococci bacteria (*S. mutans* and *S. sobrinus*) to orthodontic adhesives significantly increased between days 1 and 4, but there was no significant difference between days 4 and 7 ( $T1 < T2 = T3$ ). Adhesion of *P. gingivalis* and *A. actinomycetemcomitans* to orthodontic adhesives significantly decreased at day 7 ( $T1 = T2 > T3$ ).

There were no significant differences in adhesion of total bacteria among adhesives ( $TX = TP = MC$ ). *S. mutans* and *S. sobrinus* adhered to MC higher than other adhesives ( $TX = TP < MC$ ). However, the amounts of *A. actinomycetemcomitans* and *P. gingivalis* did not show significant differences between the three adhesives ( $TX = TP = MC$ ).

There were significant differences in surface characteristics among the adhesives. The order of SR was, from the lowest to highest, TX, TP, and MC. However, SFE showed different trends and TP had the greatest SFE followed by MC and TX ( $TX < MC < TP$ ). Considering that MC showed the higher adhesion of cariogenic bacteria and had higher SR than other adhesives, this study suggests that the effects of SR on bacterial adhesion would be more prominent than those of SFE, specifically on cariogenic streptococci. In contrast, periodontal pathogens may not be significantly influenced by surface characteristics.

## CONCLUSION

1. Resin-modified glass ionomer cement showed higher SR than composite and compomer.
2. Adhesion of total bacteria and cariogenic bacteria to orthodontic adhesives significantly increased at T2, while that of periodontal pathogens decreased at T3.
3. Cariogenic bacteria adhered to resin-modified glass ionomer higher than to composite and compomer. However, adhesion of periodontal pathogens was not significantly influenced by the adhesive type.
4. The effects of the SR on adhesion of cariogenic streptococci may be more prominent than those of the SFE.

## REFERENCES

1. Ren Y. *et al.*, Clin Oral Investig. 18:1711-18, 2014
2. Quirynen M *et al.*, J Clin Periodontol. 17:138-44, 1990
3. Shu M *et al.*, Infect Immun. 71: 7188-92, 2003

## ACKNOWLEDGMENTS

The authors would like to thank 3M Unitek for kindly supplying their materials.



## Hydrazide Modified Dextran as Scavengers for Carbonylated proteins

Ming Gao<sup>1</sup>, Tobias Larsson<sup>1,2</sup> and Tim Bowden<sup>3</sup>

<sup>1</sup>Department of Clinical Science, Intervention and Technology, Karolinska Institutet, Sweden

<sup>2</sup>Department of Nephrology, Karolinska University Hospital, Stockholm, Sweden

<sup>3</sup>Department of Chemistry– Ångström Laboratory, Uppsala University, Sweden

[ming.gao@kemi.uu.se](mailto:ming.gao@kemi.uu.se)

### INTRODUCTION

Reactive oxidative species (ROS) that damage components of cells including proteins, lipids and DNA have been linked to various diseases<sup>1</sup>. When cell membrane is attacked by radicals, lipid peroxidation products (LPOs) are formed. They are often unsaturated aldehydes of great reactivity and with potential to oxidise proteins, producing carbonylated proteins. Oxidised proteins are dysfunctional and a hypothesis is that they are an underlying cause of oxidative stress related diseases, e.g. atherosclerosis. Endogenous nucleophilic molecules such as carnosine or synthetic analogues, so-called aldehyde scavengers, have shown great potential in removing ROS or LPOs including but not limited to acrolein, and carbonyl proteins<sup>2,3</sup>.

In this paper we present hydrazide modified dextran molecules as scavengers for products of oxidative stress. They were applied to scavenge the acrolein modified BSA in buffer. The capability of protecting cells against carbonyls toxicity was also investigated.

### EXPERIMENTAL METHODS

#### Preparation of hydrazide modified dextran

Schematic chemical reaction was shown in Figure 1.

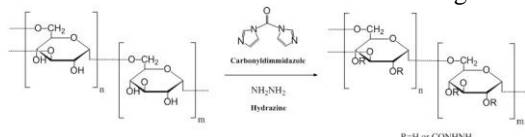


**Figure 1.** Synthesis of hydrazide modified dextran.

#### Colorimetric characterization of scavenging effects

Protein samples were treated with 2,4-dinitrophenyl hydrazine (DNPH) in dark and then precipitated by cold trichloroacetic acid buffer. The pellet was washed by ethanol/ethyl acetate before dispersing in urea-PBS buffer and observed by UV-Vis spectroscopy at 370nm.

#### Cell viability and cytotoxicity

Mouse myoblast cells (C2C12) were incubated for 24h after adding sample solutions with modified BSA with or w/o added scavenger. The cells were washed with buffer and stained by alamar blue solution. Absorbance was measured at 570nm by microplate reader.

#### Protein gel electrophoresis

All protein samples were diluted to 1 mg/ml by PBS buffer for gel electrophoresis after loading 10μl protein samples in each of wells.

### RESULTS AND DISCUSSION

Hydrazide modified dextran samples with different substitution ratio were denoted as L1 and L2 (Mw=40000, 20 and 52 hydrazide groups per 100 glucose units), H1 and H2 (Mw=100000, 17 and 57

hydrazide groups per 100 glucose units). Un-modified dextran (Mw=40000) was defined as L0.

The scavenging effects were considered for factors including different types and amount of scavengers, and different concentration of acrolein modified BSA (Figure 2A). Figure 2B described the capability of hydrazide modified dextran protecting C2C12 cells against toxicity of acrolein handled BSA. Protein gel electrophoresis was also utilized to investigate the scavenging effects (Figure 3).

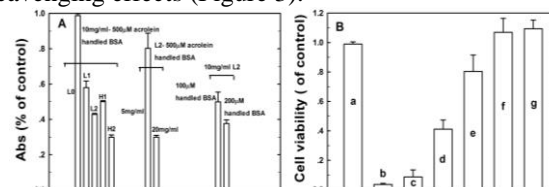


**Figure 2.** Scavenging effects on acrolein handled BSA. A) UV-Vis absorbance of different acrolein concentration handled BSA after different amount or different types of dextrans. B) Cell viability of C2C12 cells after incubation for 24hs with 10mg/ml L2 (a), 3mg/ml

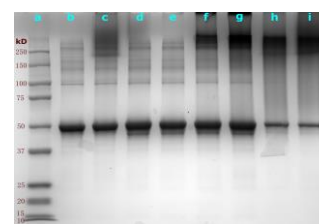


**Figure 3.** Gel electrophoresis of protein markers (a), fresh BSA (b), fresh BSA-10mg/ml L2 (c), 500μM acrolein handled BSA (d), and 500μM acrolein handled BSA with 10mg/ml L0 (e), 1mg/ml L2 (f), 2mg/ml L2 (g), 5mg/ml L2 (h) and 2mg/ml H2 (i).

Higher hydrazide substitution ratio and Mw of dextran with higher amounts were always equivalent with higher scavenging effects on carbonyl proteins. Hydrazide modified dextran could protect the cells against the toxicity of protein carbonyls by the reaction between hydrazide and carbonyl groups. The Mw of BSA samples was increased by the reaction between protein carbonyls and hydrazide modified dextrans leading to the darker band in the higher Mw areas.

### CONCLUSION

Hydrazide modified dextran was synthesized for scavenging carbonyl proteins in PBS buffer. It was observed that high Mw of hydrazide modified dextran with high substitution ratio could achieve best effects on scavenging carbonyl proteins and protecting cells against their toxicity. The proposed samples have the potential to be utilized as scavengers for oxidative stress.

### REFERENCES

1. Burcham, P. C. *et al.* J. Biochem. Mole Toxi. 15: 309-316, 2001.
2. Guiotto, A., *et al.* J. of Medicinal Chem. 48: 6156-6161, 2005.
3. Burcham, P. C. *et al.* Mole Phar. 69: 1056-1065, 2006.



## Preparation of Substituted Hydroxyapatite for Tooth Enamel Remineralization

Vita Zalite<sup>1</sup>, Janis Locs<sup>1</sup>

<sup>1</sup> Rudolfs Cimdins Riga Biomaterials Innovations and Development Centre, Riga Technical University, Riga, Latvia  
[vita.zalite@rtu.lv](mailto:vita.zalite@rtu.lv)

### INTRODUCTION

Hydroxyapatite (HAp) is the most frequently used mineral form for biomedical application among apatite mineral family, due to its chemical relevance to hard tissue of mammals. Chemical and structural modification of HAp have a great interest among materials scientists, practitioners of medicine and dentists. In the last decade, calcium phosphate have been studied extensively for tooth remineralization, i.e., for caries preventive purpose<sup>1</sup>. Strontium (Sr) and fluorine (F) co-substituted hydroxyapatite (SrFHAp) could be a good candidate for tooth enamel remineralization due to HAp structural similarity to mineral part of enamel, a long known anti-caries effect of fluorine<sup>2</sup> and a potential of strontium as dentin desensitising agent<sup>3</sup>. Therefore it is challenging to obtain partly co-substituted HAp with desired amount of fluorine and strontium in the apatite structure, moreover so far synthesis application of SrFHAp has not been researched for dental application.

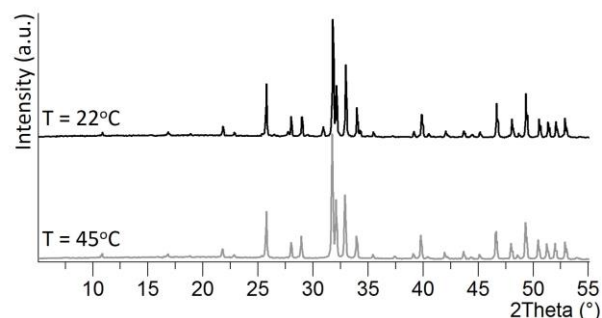
### EXPERIMENTAL METHODS

SrFHAp powder was synthesized through a wet precipitation method. Chosen reagents ( $\text{Ca}(\text{NO}_3)_2 \cdot 4\text{H}_2\text{O}$ ,  $\text{Sr}(\text{NO}_3)_2$ ,  $\text{NH}_4\text{F}$  and  $(\text{NH}_4)_2\text{HPO}_4$ ) were provided by Sigma-Aldrich.  $\text{NH}_4\text{F}$  and  $(\text{NH}_4)_2\text{HPO}_4$  were dissolved in the deionized water to prepare 0.03 M solution and afterwards added dropwise into the 0.05 M solution obtained from  $\text{Ca}(\text{NO}_3)_2 \cdot 4\text{H}_2\text{O}$  and  $\text{Sr}(\text{NO}_3)_2$  as  $\text{Ca}^{2+}$  and  $\text{Sr}^{2+}$  ion sources. The amounts of reagents were selected to gain solution with (Ca, Sr)/P molar ratio of 1.67. Synthesis was carried out at the ambient temperature and 45°C under continuous stirring. During precipitation reaction,  $\text{NH}_4\text{OH}$  (26 wt%) was used to adjust pH of suspension between 9-9.5 till the end pH remains in the range from 9.1 to 9.5. Obtained precipitates were left overnight, afterwards centrifuged and washed threefold with deionized water, followed by drying at 105°C. Dried products were sintered in at 1000 °C for 1 h. Fourier transform infrared spectrometry (FT-IR) and X-ray diffraction (XRD) were applied for chemical and phase analyses of SrFHAp. The morphology of the powder crystallites was observed using a field emission scanning electron microscope (FE-SEM) and presence of Sr and F were confirmed by EDS analysis.

### RESULTS AND DISCUSSION

X-ray diffraction pattern of as-synthesized SrFHAp powders showed maximum at 25.8° 2θ and a set of broader peaks around the HAp characteristic regions from 31° to 34.5° 2θ, from 38.4° to 40.9° 2θ. The nature of XRD pattern indicated SrFHAp powders with low crystallinity. Figure below revealed phase composition

of SrFHAp powders after sintering at 1000°C for 1h. The peaks at 30.93° and 34.23° 2θ in black pattern indicated presence of β-tricalcium phosphate phase, which means that obtained SrFHAp synthesized at 22°C was calcium deficient HAp, while powder synthesized at 45°C (grey pattern) showed only HAp phase.



FT-IR spectra of as-synthesized SrFHAp, indicating physically attracted  $\text{H}_2\text{O}$  presence with broad absorbance bands between 3650-3200  $\text{cm}^{-1}$  and 1890-1600  $\text{cm}^{-1}$ . The characteristic bands of  $[\text{PO}_4]$  group were located at 1200-920, 600 and 570  $\text{cm}^{-1}$ , but existence of  $[\text{HPO}_4]$  group was confirmed with peak around 880  $\text{cm}^{-1}$  in SrFHAp powder obtained at 22°C, indicating calcium deficient HAp, that agrees with XRD data. Characteristic  $\text{OH}^-$  band of HAp structure existing at 3570  $\text{cm}^{-1}$  shifted to the lower wavenumber value 3546  $\text{cm}^{-1}$  due to  $\text{OH} \dots \text{F}$  bonding appearance in apatite structure in both products. EDS analysis showed 0.62±0.10 at% of Sr and 1.42±0.80 at% of F presence in the SrFHAp powder (T=22°C), and 0.85±0.07 at% of Sr and 1.81±0.43 at% of F in the SrFHAp powder (T=45°C). FE-SEM analyse revealed nanosized, rod-like morphology of obtained SrFHAp crystallites.

### CONCLUSION

SrFHAp powders were successfully obtained *via* wet precipitation synthesis method. The phase composition and element substitution level in SrFHAp powders was dependent on synthesis temperature. Future work will be devoted to evaluation *in vitro* of enamel remineralization efficiency of SrFHAp for caries preventive purpose.

### REFERENCES

1. Ryu S. *et al.*, Bull. Korean Chem. Soc. 30(4):887-890, 2009
2. Reynolds EC., Aust. Dent. J. 53(3):268-273, 2008
3. Mantzourani M., J. Dent. 41(4):S3-17, 2013

### ACKNOWLEDGMENTS

This work has been supported by the EuroNanoMed II JTC2014 project „PhOtocrosslinked hydrogels for guided periodontal Tissue REgeneration” (POsTURE).



## Shape and Surface Chemistry Effects on the Cytotoxicity and Cellular Uptake of Metallic Nanorods and Nanospheres

Pelagie Favi<sup>1</sup>, Mariana Morales<sup>2</sup>, Paul Elliot<sup>3</sup>, Alejandro Restrepo<sup>4</sup>, Ming Gao<sup>5</sup>, Hanchen Huang<sup>6</sup>, Juan Pavon<sup>4</sup> and Thomas Webster<sup>1,7</sup>

<sup>1</sup>Department of Chemical Engineering, Northeastern University, Boston, MA, USA

<sup>2</sup>School of Medicine, University of Antioquia, Medellín, Antioquia, Colombia

<sup>3</sup>Department of Mechanical Engineering, University of Connecticut, Storrs, CT, USA;

<sup>4</sup>Group of Advanced Biomaterials and Regenerative Medicine – BAMR, Bioengineering Programme, University of Antioquia, Medellín, Colombia

<sup>5</sup>Department of Pharmaceutical Sciences, School of Pharmacy, Bouvé College of Health Sciences, Northeastern University, Boston, MA USA;

<sup>6</sup>Department of Mechanical and Industrial Engineering, Northeastern University, Boston, MA, USA;

<sup>7</sup>Center of Excellence for Advanced Materials Research, King Abdulaziz University, Jeddah, Saudi Arabia.

[juan.pavon@udea.edu.co](mailto:juan.pavon@udea.edu.co)

### INTRODUCTION

Metallic nanoparticles (materials with at least one dimension at scales of 1-100 nm) such as gold and silver have shown promise for current and future medical applications due to their enhanced total surface area to volume ratio<sup>1</sup>, ability to penetrate tissues and cells, deliver therapeutic drugs and genes, and respond to IR and other wavelengths of light to assist in disease diagnosis. In this study, rod-shaped silver nanorods (AgNRs) and gold nanorods (AuNRs) were fabricated by electron beam physical vapor deposition (EBPVD) and their cytotoxicity towards human skin fibroblasts were assessed and compared to sphere-shaped silver nanospheres (AgNSs) and gold nanospheres (AuNSs).

### EXPERIMENTAL METHODS

**Materials.** Nanospheres of silver with a diameter of 40 nm and at a stock concentration of 0.02 mg/mL; gold with a diameter of 60 nm and at a stock concentration of 0.05 mg/mL (Sigma-Aldrich, St. Louis, MO); Dulbecco's Modified Eagle Medium (DMEM), penicillin/streptomycin (P/S), acetone, and methanol (Sigma-Aldrich), Cacodylate buffered, glutaraldehyde, cacodylate buffer, osmium tetroxide, uranyl acetate, and lead citrate; Silicon wafers (Nova Wafers, Flower Mound, TX); Primary human dermal fibroblast cells (ATTC# CCL-110); Fetal bovine serum, FBS (Hyclone, Logan, UT); Promega CellTiter 96® Aqueous Non-Radioactive Proliferation (MTS) assays (Fisher Scientific, Pittsburgh, PA). **Growth of silver and gold nanorods.** Metallic nanorods of gold and silver were produced using EBPVD<sup>2</sup>. The substrates used were silicon {100} wafers with a diameter of 76.2 mm. **Characterization and cells evaluation.** The morphology features were analysed by SEM. The absorption spectra of the nanorods and nanospheres were collected on a SpectraMax M3® spectrophotometer (Molecular Devices, Sunnyvale, CA). Nanorods and nanospheres were each mixed at 1:1 v/v with cell culture media.

### RESULTS AND DISCUSSION

The morphology of the AgNRs and AuNRs fabricated by EBPVD, and the commercially obtained AgNSs and AuNSs, were assessed by SEM and are illustrated in Fig. 1. The top view SEM images of the AgNRs and AuNRs as grown on silicon substrates confirmed the successful synthesis of rod-shaped silver and gold nanostructures using the EBPVD system.

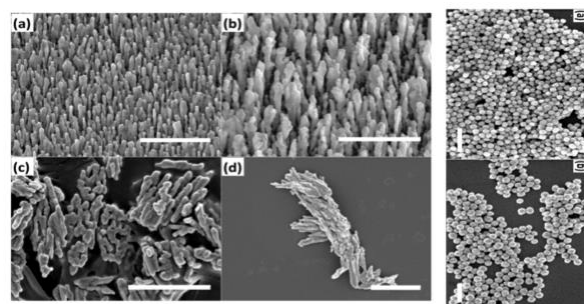


**Figure 1.** SEM images (100 nm) of metallic nanorods grown by the electron beam physical vapor deposition system. SEM images of (a) AgNS and (b) AuNS.

### CONCLUSION

This study has demonstrated that the surface chemistry, size and shape of citrate-capped spherically shaped nanoparticles (silver and gold) and PVD grown rod-shaped nanoparticles (silver and gold) can be controlled and influenced the toxicity of fibroblast cells.

### REFERENCES

1. Sonavane G. et al., Colloids Surf B Biointerfaces. 66(2):274-80, 2008.

### ACKNOWLEDGMENTS

This study was supported by Northeastern University. Dr. Pelagie Favi is grateful for Northeastern Fellowship Program (sponsored by NSF Grant #0811170).

# Chitosan-Based Hydrogels Modified with Silk Fibres for Cartilage Tissue Regeneration

Magdalena Kozioł, Kinga Pielichowska, Jan Chłopek

Department of Biomaterials, Faculty of Materials Science and Ceramics, AGH University of Science and Technology, Poland  
[mkoziol@agh.edu.pl](mailto:mkoziol@agh.edu.pl)

## INTRODUCTION

Chitosan (CS) has a number of useful properties such as biocompatibility, non-toxicity and bioactivity and is often used in biomedical applications<sup>1</sup>. One of the most important features of chitosan is its ability to create hydrogels<sup>2</sup>. Despite many desired properties of natural polymers, they have also some disadvantages such as low mechanical strength<sup>3</sup>. Because of low flexibility and brittleness of the chitosan, short silk fibres (SF) have been applied<sup>4</sup>. Recently, growing interest in silk fibers biomedical applications can be observed, due to their high tensile strength, flexibility, stability to heat and humidity, biocompatibility and high permeability to oxygen<sup>5,6</sup>. Structural proteins constituting silk fibers are biocompatible and biodegradable, hence they may be used to form hydrogels based on natural polymers<sup>6</sup>.

The aim of this work was to design chitosan-based hydrogels modified with silk fibres that can be used for cartilage tissue regeneration.

## EXPERIMENTAL METHODS

Chitosan with a molecular weight of 600,000 - 800,000 and sodium tripolyphosphate (TPP) were purchased from Acros Organic. Laponite® RDS was purchased from Rockwood Additives (USA). Silk fibers were from Jedwab Polski sp. z o.o. Milanówek, Poland. Lactic acid was purchased from AVANTOR. In the first step, Laponite dispersion was made. The Laponite was dispersed in 5% lactic acid solution using magnetic stirrer for 0,5 h, and then chitosan was added. The chitosan/Laponite system was stirred for 0,5 h. In the last stage various amount (0; 0,06; 0,13; 0,17 wt. %) of short silk fibers (SF) were introduced to chitosan/Laponite system. The obtained hydrogels were poured into a Petri dish and samples were dried at room temperature for one day, and next under vacuum for seven days. In the next step, the obtained samples were characterized using differential scanning calorimetry (DSC), Fourier transform infrared spectroscopy (FT-IR) and scanning electron microscopy (SEM) methods.

## RESULTS AND DISCUSSION

Results of DSC investigations are presented in Table 1 and in Fig. 1. As it can be seen with increase of SF content in the hydrogel, the glass temperature ( $T_g$ ) of obtained composites also increases.

Table 1. Thermal properties of CS/Laponite/SF systems.

SF content [%]	$T_g$ [°C]	Delta Cp [J/g·K]
0.00	117.95	0.101
0.06	125.28	0.041
0.13	126.62	0.007
0.17	127.46	0.057

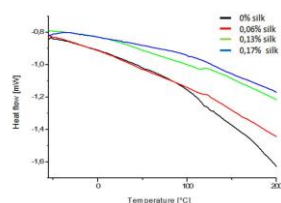


Fig. 1. DSC curves of chitosan hydrogels modified with SF.

In FTIR spectra of investigated samples, the absorption bands of amides I, II and III can be seen – Tab. 2 and Fig. 2. For CS/Laponite/SF system, some characteristic absorption bands were shifted to lower wavenumbers in comparison to the pure chitosan hydrogel that suggests changes in hydrogen interactions in obtained systems.

Table 2. Descriptions of absorption bands of CS/Laponite/SF systems.

CS/Laponite Wavenumber [cm <sup>-1</sup> ]	CS/Laponite/0.06% SF Wavenumber [cm <sup>-1</sup> ]	CS/Laponite/0.17% SF Wavenumber [cm <sup>-1</sup> ]	Absorption bands
1740	1730	1738	C=O
1616	1618	1618	N-H (amides I)
1462	1462	1462	CH <sub>2</sub> , CH <sub>3</sub>
1417	1414	1416	C-N (amides I)
1321	1319	1319	C-O
1281	1281	1279	C-O-C
1126	1126	1126	C-O-C
1092	1092	1092	Si-O-Si
1005	1005	1005	Si-O-Si
866	866	864	C-O-C
777	777	777	C-O-C
652	654	652	band characteristic for Laponite

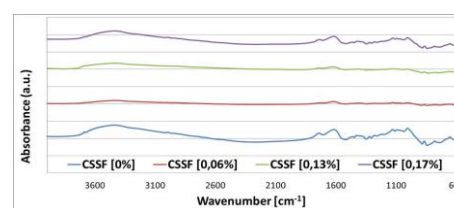


Fig. 2. FTIR spectra of CS/Laponite/SF systems.

Also some changes in microstructure in CS/Laponite/SF systems have been observed - Fig. 3.

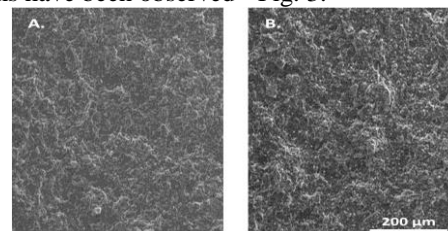


Fig. 3. SEM microphotographs: (A) CS/Laponite system (B) CS/Laponite system modified with 0.21% SF.

## CONCLUSIONS

Chitosan hydrogels modified with short SF were obtained. Modification of chitosan hydrogels with SF leads to increase of glass temperature of chitosan. Some changes in microstructure can be also observed.

## REFERENCES

1. C.K.S. Pillai, Willi Paul, Chandra P. Sharma, Chitin and chitosan polymers, Progress in Polymer Science, 2009, 7, 641–678.
2. P. Schexnailder, G. Schmidt, Nanocomposite polymer hydrogels, Colloid and Polymer Science, 2009, 1, 1–11.
3. Q. Jin, P. Schexnailder, AK. Gaharwar, G. Schmidt, Silicate Cross-Linked Bio-Nanocomposite Hydrogels from PEO and Chitosan, 2009, 10, 1028–1035.
4. L. Noble, A.I. Gray, L. Sadiq, I.F. Uchebu, A non-covalently crosslinked chitosan based hydrogel, Int. J. Pharm., 1999, 192, 173–182.
5. GH. Altman, F. Diaz, C. Jakuba, Caroline Jakuba, T. Calabro, RL. Horan, J. Chen, H. Lu, J. Richmond, DL. Kaplan, Silk-based biomaterials, Biomaterials 2003, 24, 401–416.
6. N. Minoura, S. Aiba, Y. Gotoh, M. Tsukada, Y. Imai, Attachment and growth of cultured fibroblast cells on silk protein matrices. J. Biomed. Mater. Res., 1995, 29, 1215–1221.

## ACKNOWLEDGMENTS

This work was financed by statute fund of Faculty of Materials Science and Ceramics AGH-UST under contract No.11.11.160.616.



## Stable Pluronic Gel Formation by Incorporating Graphene Oxide

Da-Ae Won, Manse Kim, Giyoong Tae

School of Materials Science and Engineering, Gwangju Institute of Science and Technology, Korea  
[gytae@gist.ac.kr](mailto:gytae@gist.ac.kr)

### INTRODUCTION

Injectable hydrogels are useful for drug delivery, tissue engineering, and other biomedical applications. Aqueous solution of Pluronic shows a thermos-sensitive sol-gel transition and can be applied as an injectable hydrogel system since it is a solution at a low temperature but quickly converted to a gel state at a body temperature<sup>1</sup>. However, since it is a lyotropic transition, the gel state is not stable in an open environment, thus it shows a very fast dissolution upon injection, which limits its practical application *in vivo*. Various reports have attempted to enhance the stability of pluronic gel *in vivo*, mostly via post-crosslinking after injection by using chemically modified pluronic<sup>2</sup>. In this study, we reported that the addition of a small amount of graphene oxide (GO) can greatly enhance the stability of pluronic hydrogel in an open environment, and demonstrated the application of this system as an injectable and stable gel *in vivo*<sup>3</sup>.

### EXPERIMENTAL METHODS

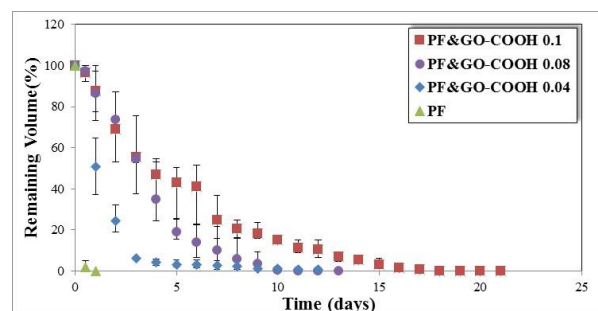
To an aqueous solution (200  $\mu$ l) of 17 wt % Pluronic F127 (PEO100 PPO65 PEO100, MW 12.6 kDa) at 4 °C, 0.04, 0.08, or 0.1 wt% carboxylated GO was added. Then, the gel was formed by increasing temperature to 37 °C. Then, 5 ml of a release buffer (PBS with 2 mM% sodium azide) was added and kept in a shaking incubator at 37°C and 100 rpm. Then, the *in vitro* degradation rates of the hydrogels were measured by measuring the remaining volume of the hydrogel daily with the exchange of the whole release buffer.

*In vivo* stability and biocompatibility of the hydrogels were studied using male BALB/c mice (8 weeks old). All animals were handled in accordance with the guidelines of the Animal Care and Use Committee of GIST. Hydrogels were prepared as a sol state by lowering temperature to 4°C and injected subcutaneously at the back of mice using a syringe with a 22G needle. The sizes of injected hydrogels were monitored at 1 day, 1 week, 2 weeks, and 8 weeks. And, histochemical staining was done to characterize the biocompatibility of the hydrogels.

### RESULTS AND DISCUSSION

As expected, hydrogel made of 17wt % of pluronic was dissolved very fast; the gel phase disappeared mostly at day 1. In contrast, by adding GO, the stability of the hydrogel was greatly improved. Also, by increasing GO from 0.04 to 0.1 wt%, the stability of gel phase was

improved systematically. So, the addition of small amounts of GO could provide the long lasting gel.



By subcutaneous injecting a sol state of the solution at 4°C, the gel was formed immediately. And, the gel with 0.1 wt % GO lasted very long; ~ 80 % of the gel was remained in one month. So, the dissolution rate of GO-containing gel was much slower *in vivo* than *in vitro*, whereas the gel formed by pluronic alone disappeared completely in 1 day. No severe inflammation was observed in all cases, supporting acceptable biocompatibility of the present system.

### CONCLUSION

A simple addition of GO could greatly enhance the stability of a physical gel system, pluronic solution, and it was possible to apply as an injectable gel *in vivo*. The present results demonstrated that the addition of GO not only increases the mechanical properties of materials, but also can enhance the thermodynamic stability of physical gel systems.

### REFERENCES

1. Mortensen G, Pedersen JS, *Macromolecules* 26:805-812, 1993.
2. Lee S-Y, Tae G, *J. Control Release* 119:313-319, 2007.
3. Won D-A, Kim M, Tae G, *Colloids. Surf. B Biointerfaces* 128:515-521, 2015.

### ACKNOWLEDGMENTS

Partial financial supports were provided by the Basic Science Research Program, NRF, MEST (2013R1A2A2A03068802), Korea, and by the "GIST-Caltech Research Collaboration Project" through a grant provided by GIST, Korea..





# Nanotoxicity Studies of Nanodiamond on 2D and Magnetically Bioprinted 3D Scaffold-free Liver Model

Dipesh Khanal, Dong Fu, Iqbal Ramzan, Wojciech Chrzanowski

Faculty of Pharmacy, The University of Sydney, Australia

[dipesh.khanal@sydney.edu.au](mailto:dipesh.khanal@sydney.edu.au)

## INTRODUCTION

Among classes of nanoparticles developed as drug carriers, nanodiamond (NDs) has been gaining attention owing to its biocompatibility, easy functionalization, chemical stability, high thermal conductivity, and favourable optical properties<sup>1</sup>. New classes of NDs (Ray NDs) were recently produced based on laser ablation techniques. The NDs produced by this technique have higher purity index, diamond phase content and fewer purification steps<sup>2</sup>. However, novel properties and safety of these materials and their impact on biological processes are still largely unknown and need further investigation.

Current approach for nanotoxicity study relies on the use of two-dimensional cell culture models, which have severe limitation due to lack of “biomimicry” and do not provide robust scientific evidence of nanoparticle effects *in vivo*.

3D scaffold-free magnetically bioprinted liver model mimic complexity and functionality of tissues and may serve as a platform to study effect of nanomaterials on healthy and diseased tissues<sup>3</sup>. Here we demonstrate the applicability of 3D scaffold-free liver model to interrogate toxicity of NDs.

## EXPERIMENTAL METHODS

Fao Cells were used to prepare both (i) 2D monolayer cell culture model ( $2 \times 10^3$  cells per 200  $\mu$ L Dulbecco's Modified Eagle's Medium (DMEM) in a 96 well plate) and (ii) 3D scaffold-free model ( $1 \times 10^5$  cells per 300  $\mu$ L of DMEM in an ultralow adhering 96 well plate). 3D tissue model was generated by magnetic levitation (Figure 1 a and b). Nanotoxicity was assessed using real-time cell imaging up to 7 days (cell growth rate and morphology), viability (live/dead assay) on day 7, vitality assay (alamarBlue®) on day 2, 4 and 7 and 3D-spheroid ‘dot’ assay (where rate of change in area of each spheroids were monitored using a mobile based device over the period of 24 h). In both the models concentrations of NDs used were 10, 25, 50 and 100  $\mu$ g.mL<sup>-1</sup>. To examine the distribution of NDs in 2D and 3D structures and microtomed tissue sections scanning electron microscopy based on gatan back scattered electron, Lorentz contact resonance microscopy and nanoIR spectroscopy were used.

## RESULTS AND DISCUSSION

NDs was found to reduce the metabolic activity of the cells in 2D possibly associated with genotoxic effect of oxidized nanodiamonds and this effect was time-dependent (time-dependent NDs uptake) as metabolic activity of cells was seen to be significantly reduced in comparison to the control after 4 days of nanoparticle exposure. Interestingly, above a threshold concentration of 18.63  $\mu$ g.mL<sup>-1</sup>, cells had similar metabolic activity irrespective of increase in concentration (Figure 1 (e)).

It may be suggested that cells could not uptake NDs above this threshold value. On the contrary, toxic effect of NDs was observed within 24 h in the 3D model as indicated by significant differences ( $p < 0.05$ ) in rate of change in the area of spheroids, which may be related to reduced metabolic activity and cell death owing to toxic effect of NDs (Figure 1(d)). Under such condition, higher contraction of spheroid corresponds to lower toxic effect whereas dilation indicates toxicity. However, above the concentration of 25  $\mu$ g.mL<sup>-1</sup>, no significant differences ( $p > 0.05$ ) in the rate of contraction of spheroids was observed indicating uptake threshold.

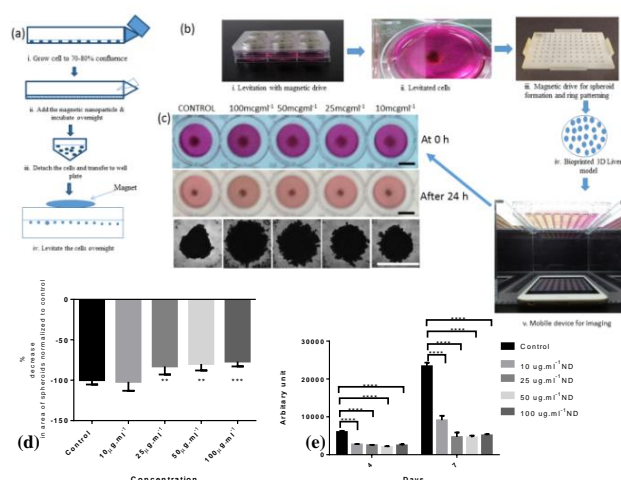


**Figure 1** Toxicity studies of NDs in 2D and 3D model; (a) schematic chart for magnetization and levitation of cells; (b) magnetic levitation of the cells and bio printing of 3D Spheroids; (c) bio patterned 3D spheroids at 0 time and after 24 h of treatment with NDs, (image from mobile device; upper two panel) (scale bar = 5 mm), brightfield images of the spheroids after 24 h of treatment (lower panel) (Scale bar = 300  $\mu$ m); (d) graph showing the percentage change in area of spheroid over the treatment period; with the increase in concentration rate of change in area decreased. \*\*\* indicates significant difference from control ( $p < 0.05$ ); (e) metabolic activity results (alamarBlue® assay) on the monolayer culture treated with NDs; with the increase in concentration, metabolic activity was found to be reduced based on duration of exposure; \*\*\*\* indicates highly significant difference from control ( $p < 0.05$ ).

## CONCLUSION

Results of cell growth, viability, vitality as well as quantitative measurements of morphologic changes of 3D models after exposure to increasing concentration of NDs indicate that NDs have toxicity above the threshold concentration of  $\sim 20$   $\mu$ g.mL<sup>-1</sup>. 3D model was able to detect the toxic effect within 24 h of treatment in comparison to 2D where longer incubation (4 days) was required indicating its higher sensitivity. Thus, 3D spheroid based assay may be a useful tool for high throughput screening of nanotoxicity.

## REFERENCES

1. Ajima, K., et al., Acs Nano, 2(10): 2057 2064, 2008
2. Zousman, B., Google Patents, 2012
3. Timm, D.M., et al., Scientific reports, 3(3000): 1-8, 2013

## Investigation of a Novel Bioresorbable Polymer Coated Drug-Eluting Scaffold

Tamara Mahmood<sup>1</sup>, David Scurr<sup>1</sup>, Nial Bullett<sup>2</sup>, Kadem Al-Lamee<sup>2</sup>, Morgan R. Alexander<sup>1</sup>, and Clive J. Roberts<sup>1</sup>

<sup>1</sup>Laboratory of Biophysics and Surface Analysis, School of Pharmacy, The University of Nottingham, NG7 2RD, UK, <sup>2</sup>Arterius Ltd, Bradford, BD7 1DP, UK, [Paxtm1@nottingham.ac.uk](mailto:Paxtm1@nottingham.ac.uk)

### INTRODUCTION

A stent is a medical device designed to function as a permanent or non-permanent internal scaffold to increase the diameter of the lumen of a blood vessel. Drug eluting stents have revolutionised the treatment of coronary artery disease<sup>1</sup>. Drug eluting stents have been approved for use in humans since 2002 and yet the drug release mechanism and uptake into the arterial wall are relatively poorly understood<sup>2</sup>. The first bioresorbable drug eluting scaffold (Abbott ABSORB) was introduced in 2011. In this study, a polymeric stent with novel mechanical property stent [patent W02014/045068A1] for treating coronary artery disease was characterised using Scanning electron microscopy (SEM), Atomic force microscopy (AFM) and time-of-flight secondary ion mass spectrometry (ToF-SIMS).

### EXPERIMENTAL METHODS

Using a spray-coating, sirolimus/P<sub>DLLA</sub> was coated onto the surface of a bioresorbable P<sub>L</sub>LA scaffold by Arterius Ltd. A Philips XL30 SEM and AFM FastScan (BrukerNano) were used to study the surface morphology of stents exposed to dissolution media for 0, 11 and 14 weeks. ToF-SIMS investigation was carried out on flattened luminal and abluminal sections of the scaffold. ToF-SIMS depth profiling utilised a ION-ToF-SIMS IV instrument using 10KeV Ar<sub>2500</sub><sup>+</sup> for sputtering and 10KeV Bi<sub>3</sub><sup>+</sup> for analysis.

### RESULTS AND DISCUSSION

Key functions of this device is to be a fully bioresorbable and give controlled release of a drug (sirolimus) from a polymeric coating layer. SEM (Fig.1) and AFM (Fig.2) images show that the coating layer appeared homogenous on coating (albeit with some evidence of nanoscale structures in the AFM) but became heterogeneous on dissolution. The three-dimensional distribution of sirolimus in P<sub>DLLA</sub> as a function of elution time was achieved by ToF-SIMS imaging and depth profiling (Fig.3) clearly showing the loss of drug from the coating.

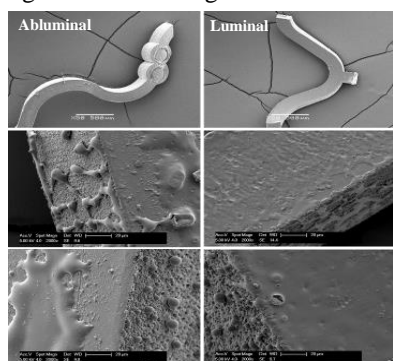
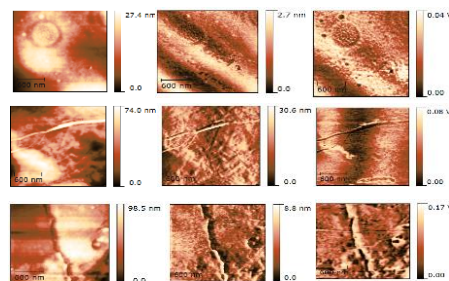
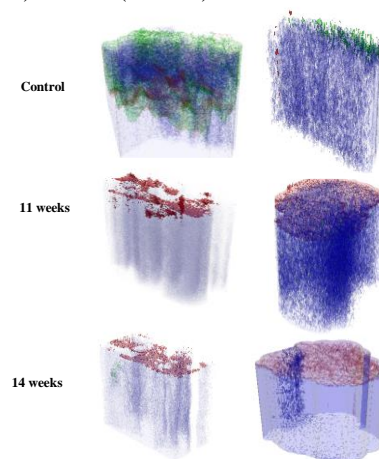


Figure 1. SEM images of bioresorbable drug-polymer coated scaffolds. A drug-polymer control (top), 11 (centre) and 14(bottom) weeks eluted scaffolds.



**Figure2.** AFM images for 2x2μm area of topography (left), deformation (centre) and adhesion (right) of the abluminal side of a drug/polymer control (top), 11 (centre) and 14 (bottom) weeks eluted scaffolds.



**Figure 3.** 3D images taken from an abluminal and luminal areas of control and eluted stent. The 3D images are iso-surface overlay of Na<sup>+</sup> (red), sirolimus (green), and P<sub>DLLA</sub> (blue).

### CONCLUSIONS

The morphology and chemical composition of a novel bioresorbable drug eluting scaffold has been characterised at the nano and micro-scale. SEM and AFM revealed that the P<sub>DLLA</sub> coating presents a heterogeneous surface on dissolution. Distinctive fragments of the drug and polymers were used to monitor the spatial distribution of the drug with ToF-SIMS. Molecular depth profiling of coatings on scaffold is shown to be feasible and that 3D molecular compositional information was obtained.

### REFERENCES

1. Zhang et al., *Medical Devices: Evidence and Research*. 2013.
2. McGinty et al., *Mathematical Medicine and Biology*. 2013.

### ACKNOWLEDGMENTS

The authors would like to thank the BBSRC and Arterius for providing financial support to this project.

## In Vitro Degradation Study of Calcium Phosphate Glass-Ceramic Exhibiting Angiogenic Properties

Anna Matras<sup>1</sup>, Agata Roguska<sup>2</sup>, Małgorzata Lewandowska<sup>1</sup>, Marc Batista<sup>3</sup>, Elisabeth Engel<sup>3</sup>, Oscar Castano<sup>3</sup>

<sup>1</sup>Faculty of Materials Science and Engineering, Warsaw University of Technology (WUT), Warsaw, Poland

<sup>2</sup>Institute of Physical Chemistry, Polish Academy of Sciences, Warsaw, Poland

<sup>3</sup>Institute for Bioengineering of Catalonia (IBEC), Barcelona, Spain

[aankam@gmail.com](mailto:aankam@gmail.com)

### INTRODUCTION

Nowadays, scaffolds used in tissue engineering application not only have to meet the stringent requirements of biocompatibility and biodegradability but should as well stimulate natural regeneration process of the body. In the case of bone tissue regeneration, ability to trigger new blood vessel formation is essential for proper reconstruction of the tissue as the vessels provide regenerating tissues with oxygen and nutrients. It has been demonstrated that calcium ions, present in calcium phosphate glass-ceramic, exhibit angiogenic properties and help in faster and proper bone concretion process [1-5]. Therefore, comprehensive understanding of degradation process of calcium phosphate glass-ceramic is a matter of great importance.

### EXPERIMENTAL METHODS

In the present study, detailed characteristic of calcium phosphate glass-ceramic in the system of  $P_2O_5 - CaO - Na_2O - TiO_2$  was performed in order to evaluate changes occurred during degradation process of CaP glass-ceramic – ceramic scaffolds in SBF solution. Glasses with different calcinations temperatures were investigated. Morphology of tested materials in initial state and after degradation test was determined using scanning electron microscopy (SEM). Energy-dispersive X – ray spectroscopy (EDS) and Fourier transform infrared spectroscopy (FTIR) techniques were used to evaluate the changes in chemical composition of examined materials. For initial evaluation of the biocompatibility of CaP glass-ceramic, protein adsorption test was performed with Bovine Serum Albumin (BSA) as a model protein.

### RESULTS AND DISCUSSION

SEM observations revealed that the materials possess porous microstructure with round shape pores and there were no significant changes in internal architecture between glass-ceramic produced with different temperature of calcinations. After incubation in SBF solution, shapes of pores change from round to elongated. In addition, the sample surface was covered with precipitations from SBF solution in flower-like shapes. Thin film on the samples was detected as well. EDS results revealed that after degradation additional elements such as chlorine, potassium and magnesium were detected which precipitate from SBF solution. As far as FTIR results are concerned, it has been revealed that chemical composition after incubation in SBF solution changed in comparison to initial state and additional picks corresponding to the P-O and P=O bonding occurred. The picks related to phosphate

groups correlate with newly formed precipitations from SBF solution that settled on the glass-ceramic surface. Protein adsorption test revealed that BSA adsorbed to the surface of CaP glass-ceramic as pick at  $1658\text{ cm}^{-1}$  corresponding to amide I has been observed which indicate biocompatibility of this materials.

### CONCLUSION

The significant changes in morphology and chemical composition of analyzed materials after degradation test has been observed. Numerous particles in the shape of flower-like precipitation from SBF solution has been detected and identify as phosphate compounds attached to glass-ceramic surface. Preliminary biocompatibility test revealed ability to bond proteins on the surface of the tested material. Therefore, calcium phosphate glass-ceramic in the system of  $P_2O_5 - CaO - Na_2O - TiO_2$  is appeared to be promising candidate for bone tissue reconstruction supporting the natural process of regeneration.

### REFERENCES

- [1] A. G. Dias, J. M. S. Skakle, I.R. Gibson, M. A. Lopes, J.D. Santos, *Journal of Non-Crystalline Solids* 351 (2005) 810–817
- [2] M. Navarro, M.P. Ginebra, J.A. Planell, C.C. Barrias, M.A. Barbosa, *Acta Biomaterialia* 1 (2005) 411–419
- [3] A.G. Dias, M.A. Lopes, I.R. Gibson, J.D. Santos, *Journal of Non-Crystalline Solids* 330 (2003) 81–89
- [4] M. C. Harris, S. del Valle, Emilie Hentges, P. Bleuet, D. Lacroix, J. A. Planell, *Biomaterials* 28 (2007) 4429–4438
- [5] M. Navarro, S. del Valle, S. Martinez, S. Zeppetelli, L. Ambrosio, J. A. Planell, M. P. Ginebra, *Biomaterials* 25 (2004) 4233–4241

### ACKNOWLEDGMENTS

This work was supported by European Union ERANET EuroNanoMed initiative within project “nAngioFrac - Angiogenic nanostructured materials for non-consolidating bone fractures”.





## Potential for Bio-Inspired Eggshell-derived Hydroxyapatite/Collagen Scaffolds for Osteochondral Tissue Engineering

Cristian Parisi<sup>1,2</sup>, Luca Salvatore<sup>2</sup>, Neelam Gurav<sup>1</sup>, Sanosh Kunjalukkal Padmanabhan<sup>2</sup>, Francesca Gervaso<sup>2</sup>, Marta Madaghiele<sup>2</sup>, Antonio Licciulli<sup>2</sup>, Alessandro Sannino<sup>2</sup>, Lucy Di Silvio<sup>1</sup>

<sup>1</sup>Tissue Engineering & Biophotonic Division, King's College London, United Kingdom

<sup>2</sup>Department of Engineering for Innovation, University of Salento, Lecce, Italy

[cristian.c.parisi@kcl.ac.uk](mailto:cristian.c.parisi@kcl.ac.uk)

### INTRODUCTION

Bio-inspired materials are synthetic materials whose structure, properties or function mimic those of natural materials or living matter. In this study, collagen (Coll) scaffolds reinforced by eggshell-derived nano-hydroxyapatite (nHAp) have been developed for potential use in osteochondral defects. Such defects can arise from trauma, degeneration or age-related diseases and they remain a major clinical challenge due to the limited repair capacity of the articular cartilage due to its avascularity<sup>1</sup>. Tissue engineering plays a key role in the development of improved strategies for osteochondral regeneration, providing engineered extracellular matrices that support, lead and promote new tissue regeneration<sup>2</sup>. nHAp/Coll scaffolds were characterized physicochemically to verify their chemical composition and mechanical properties. Furthermore, they were seeded with primary human mesenchymal stem cells (hMSCs) and examined for differentiation towards osteogenic and chondrogenic lineages for a period of 28 days.

### EXPERIMENTAL METHODS

**Scaffolds synthesis** Bovine type I collagen was used as a collagen source. Hydrated calcium oxide (from hen eggshell), and phosphoric acid were used for nHAp synthesis. nHAp/Coll porous scaffolds were fabricated by freeze-drying. Three different weight ratios were analysed: 0/100 (A), 30/70 (B) and 50/50 (C).

**Physicochemical analysis** X-ray diffraction and FT-IR spectroscopy were used to verify, respectively, phase and chemical composition of the composite scaffolds. Mechanical properties were evaluated by uniaxial unconfined compression tests in cell culture media.

**Biological analysis** Scaffolds were seeded with primary hMSCs. After seeding, cells were conditioned to induce terminal differentiation in osteo- or chondrogenic differentiation conditions. Cell proliferation (AlamarBlue™) and viability (Live and dead®) were analysed after 1,3,7,14,21 and 28 days. The morphology of cells on the scaffolds was evaluated using SEM analyses. Immunostaining was used to confirm terminal differentiation of cells after 28 days.

**Statistical analysis** Statistical significance was determined using One- and Two-Way ANOVA ( $p < 0.05$ , Kruskal-Wallis and Tukey's tests).

### RESULTS AND DISCUSSION

**Physicochemical properties** XRD and FT-IR analyses confirmed that scaffolds were composed of collagen and HAp, and both materials were chemically integrated with each other. Compression tests showed

improved mechanical properties with the increase of the HAp content.

**Biological response** AlamarBlue assay showed that both in osteogenic and chondrogenic conditions cell proliferation in the 30/70 and 50/50 nHAp/Coll scaffolds was significantly higher than the 0/100 (Fig. 1). Live and dead staining confirmed good cell viability for the scaffolds up to 28 days. Immunostaining showed good results both in osteo- and chondrogenic conditions after 28 days.

The scanning electron micrographs show that after 28 days in chondrogenic medium the cells had more processes compared to the cells after 28 days in osteogenic medium (Fig. 2). The cells appeared larger and more "active" and had good cell to cell interaction with adjacent cells.

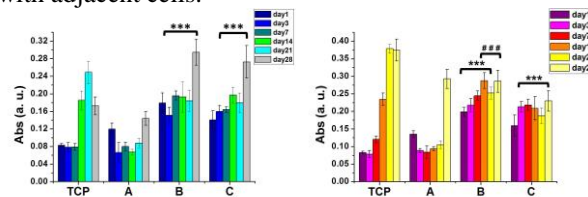


**Fig. 1:** Cell proliferation in osteogenic (left) and chondrogenic (right) conditions. Statistical significance: \* 0/100 vs. 30/70, 50/50; # 30/70 vs. 50/50;  $p < 0.001$ .

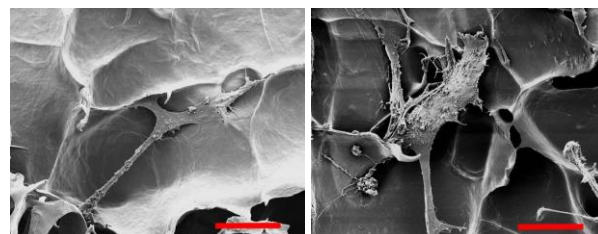


**Fig. 2:** SEM images of two hMSCs after 28 days in osteogenic (left) and chondrogenic (right) condition. Scale bar 30 μm.

### CONCLUSION

nHAp/Coll scaffolds were biocompatible and were able to support stem cells and allow differentiation towards specific lineages. Scaffolds with a high HAp content showed better biological properties in the osteogenic environment. On the other hand, scaffolds with a lower HAp content showed a much better biological response in the chondrogenic environment. Further investigations are ongoing, however, these materials show potential for applications in osteochondral tissue engineering.

### REFERENCES

1. Zhang T. *et al.*, Biomaterials. 38:72-85, 2015
2. Nukavarapu S. *et al.*, Biotech. Adv. 31:706-21, 2013



## Biomimetic Scaffolds Based on Biopolymers and Calcium Phosphates for Bone Tissue Engineering

Liliana Verestiuc, Florina Ivan, Maria Butnaru

Faculty of Medical Bioengineering, 'Grigore T. Popa' University of Medicine and Pharmacy, Iasi, Romania

[liliana.verestiuc@bioinginerie.ro](mailto:liliana.verestiuc@bioinginerie.ro)

### INTRODUCTION

Although the preferred treatment for restoring bone defects is autologous bones grafting some limits are associated with it: morbidity associated with the bone-graft donor site and limited quantity or quality of autologous-bone graft material [1]. An alternative therapeutic technique is tissue engineered bone [2]. Not only the combination of biomaterials but also the morphology of the scaffold, characterised by a highly interconnected, 3D pore network as well as tailored surface characteristics, determine the suitability of the scaffold. For bone tissue engineering, pore size >100  $\mu\text{m}$  are desirable, as well as high pore interconnectivity, in order to facilitate the attachment and proliferation of cells, the ingrowth of new tissue and vascularisation.

This study presents the synthesis and characterization of scaffolds based on collagen(Col), chitosan (Cs), sodium hyaluronate (Hya) and calcium phosphates (CP), obtained by using a biomimetic method. Collagen provides structural and mechanical support to tissues and organs and fulfils biomechanical functions in bone, cartilage, skin, tendon, and ligament [3]. Freeze-dried chitosan sponges have shown the ability to support osteoblast growth and deposition of mineralized matrix [4]. Hyaluronic acid has several advantages as a biomaterial like as: excellent physical properties and chemical structure that can modulate the biological interactions; the biopolymer acts locally and in combination at the fracture site to promote healing by stimulating tissue formation. The novelty of our work is represented by the biomimetic co-precipitation method of CP in the biopolymeric mixture, used to obtain calcium phosphate crystals similar to the natural process of bone formation.

### EXPERIMENTAL METHODS

By precipitation of CP from its precursors ( $\text{Ca}(\text{NO}_3)_2$  and  $\text{NaH}_2\text{PO}_4$ ) on the mixture of collagen, chitosan and hyaluronic acid, in presence of  $\text{NH}_4\text{OH}$ , biomimetic composites scaffolds were obtained. The materials were maintained at room temperature for 24 hours and than they were purified (extensively washed with distilled water) and freeze-dried. Scanning electron microscopy (SEM) and Fourier transformed infrared spectroscopy (FTIR), X-ray photoelectron spectroscopy (XPS) and X-ray diffraction (XRD) were used to characterize the structure and the morphology of the scaffolds.

The simulated fluids retention in composites was evaluated in phosphate buffer and the PBS retention degree was calculated. In vitro enzymatic degradation study was performed in the phosphate buffer solution (pH 7.2), in the presence of collagenase or lysozyme at the temperature of 37 °C.

The *in vitro* cytotoxicity studies were performed on osteoblasts and STEM cells.

### RESULTS AND DISCUSSION

FTIR, SEM(Fig.1) and XPS data confirmed the forming of CP, onto biopolymeric matrix. The results obtained indicate that the major inorganic phase is represented by hydroxyapatite and these composites present a lower enzymatic degradation which facilitates an *in vitro* degradation control.

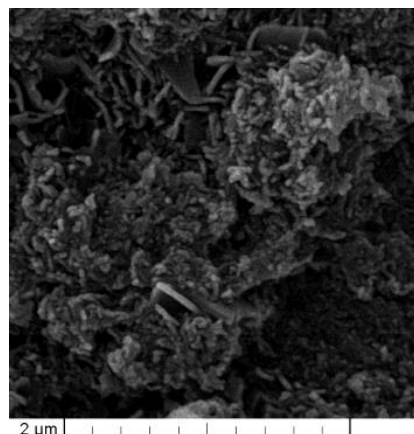


Fig.1. SEM data of CP-Col-Cs-Hya scaffold

The scaffolds are interacting with PBS at physiological pH and the PBS retention is strictly connected with the scaffolds three-dimensional porous structure. The *in vitro* biocompatibility studies have showed that the osteoblasts and STEM cells are viable in the studied cultures.

### CONCLUSION

The obtained results confirmed that biocompatible scaffolds based on collagen, chitosan, sodium hyaluronate and calcium phosphates have been obtained using a co-precipitation biomimetic method. The chemical composition of the scaffolds, their morphology, a good interaction with simulated body fluids and the non cytotoxic effect indicate that these scaffolds are suitable for bone tissue engineering.

### REFERENCES

1. Cama G., Calcium phosphate cements for bone regeneration, in: P. Dubruel, S. Van Vlierberghe (Eds.), Biomaterials for Bone Regeneration, Woodhead Publishing, 2014;
2. Sajesh K.M. *et al.*, Int J. Biol. Macromol. 62:465-471, 2013;
3. Chew K.K. *et al.*, J. Mech. Beh. Biomed. Mater. 4:331-339, 2011;
4. Seol Y.J. *et al.*, Biotechnol. Letters 26:1037-1041, 2004.

### ACKNOWLEDGMENTS

This work was financially supported by the Romanian Ministry of Education and Research; grant PN-II-PT-PCCA-2013-4-2287- MAGBIOTISS.

## Porosity Related Mechanical Response of Calcium Phosphate Bone Cements

D.E. Mouzakis<sup>1</sup>, S.P. Zaoutsos<sup>1</sup>, S. Rokidi<sup>2</sup>, N.Bouropoulos<sup>2</sup>

<sup>1</sup>\*Laboratory of Advanced Materials and Constructions, Department of Mechanical Engineering, Technological Educational Institute of Thessaly, GR 41110-Larissa, Hellas,

<sup>2</sup> Department of Materials Science, University of Patras, Rion 26500, Patras, Greece

[mouzakis@teilar.gr](mailto:mouzakis@teilar.gr)

### INTRODUCTION

Calcium phosphate (CaP) cements are used as bone substitutes and they have the advantages of injectability and in situ hardening in comparison with other implants such as ceramics. The main objective of the current study as part of an overall project for the development of new CaP bone cements is the study of calcium phosphate cements with enhanced mechanical properties. In spite the good biological properties of CaP based biocements they are usually plagued by low inherent mechanical properties. Porosity on the other hand promotes the osteoblast cell anchoring and proliferation but also reduces mechanical properties.

### EXPERIMENTAL

For the preparation of  $\alpha$ -TCP powder, equimolar quantities of calcium carbonate and calcium pyrophosphate ball milled and next the mixture was placed in alumina crucible, dried at 80 °C, placed in a furnace at 1300 °C for 12 hours and rapidly quenched on a metallic surface. The resulted material was crushed in the ball mill. The cement powder was mixed with 4 % w/v  $\text{Na}_2\text{HPO}_4$  solution in an agate mortar at a powder/liquid ratio of 0.32. Albumin and gelatin incorporated in the liquid phase of the cement were used as foaming agents. A stable foam was formed after mechanically stirring and next the powder was mixed with the foam to form the paste which was moulded in 6 mm x 12 mm cylindrical moulds. The specimens remained in 100 % humidity for 12 hours and were then removed from the mould and placed at 37 °C in a polyethylene vial containing 60 ml of Ringer solution for 14 days for hardening. Mechanical properties of these materials were determined in compressive mode at 0.5 mm/min crosshead speed. Porosity was calculated by the Ishikawa-Asaoka relation [J. Biomed. Mater. Res. 29, 1537 (1995)].

### RESULTS AND DISCUSSION

It can be seen from the compressive properties presented in Table 1 and Figure 2 below of the  $\alpha$ -TCP based porous bone cements that their mechanical properties are comparable to those of the human bones (e.g. cortical bone), making them candidates for implants in bone deficiencies.

Additive Percentage [%]	Compressive Strength [MPa]		Porosity as Calculated [%]	
	Albumin	Gelatine	Albumin	Gelatine
0	29,24	37,99	33,30	29,45
1	24,33	30,7	36,00	32,58
5	14,9	16,97	43,21	41,30
10	4,27	6,34	61,59	55,78

Table 1. Typical Compressive properties of the porous bone cements studied.

These properties remain high at foaming agents up to 5wt% added in solution. Representative SEM images showing the morphological characteristics of the porous hardened cements are shown below in Figure 1 below.

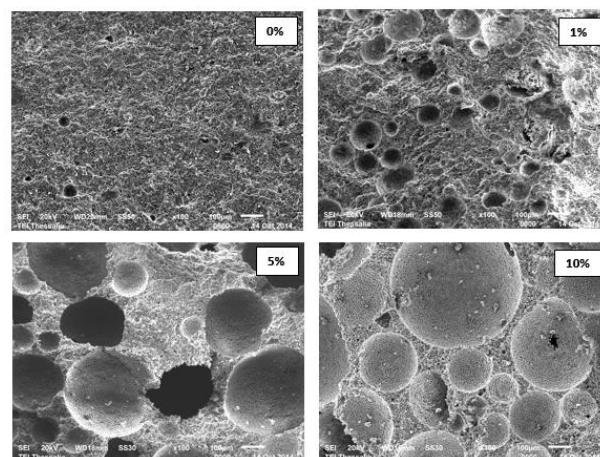


Figure 1. Representative SEM images from the porous calcium phosphate specimens tested as a function of albumin content.

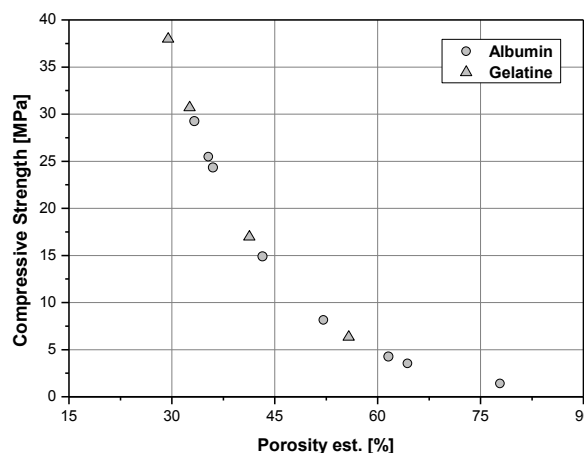


Figure 2. Compressive Strength as a function of specimen porosity.

### CONCLUSION

It was shown that it is feasible to produce porous bone cements based on  $\alpha$ -TCP and foaming agents with satisfactory biomechanical compressive properties.

### ACKNOWLEDGMENTS

The authors would like to thank the European Union and Greek national funds through the Operational Program "Education and Lifelong Learning" of the National Strategic Reference Framework (NSRF) - Research Funding Program: THALES. (Grant no: MIS 379380) for providing financial support to this project.

Liliana Verestiuc, Lacramioara Lungoci, Vera Balan, Maria Butnaru, Ovidiu Bredetean

Faculty of Medical Bioengineering, 'Grigore T. Popa' University of Medicine and Pharmacy, Iasi, Romania  
[liliana.verestiuc@bioinginerie.ro](mailto:liliana.verestiuc@bioinginerie.ro)

## INTRODUCTION

A promising therapy for diseases associated with increased production of reactive oxygen species (ROS), such as hypertension, ischemia, myocardial infarction and restenosis, involve the antioxidant enzymes. The efficiency of enzyme is dependent on the ability to achieve therapeutically adequate levels at the site of ROS-mediated injury [1]. Enzymes immobilization on superparamagnetic iron oxide nanoparticles (SPIONs) can increase efficiency and limit adverse effects of thermal and proteolysis degradation [2]. In this paper, with the aim to design such enzyme-immobilized SPIONs (enzySPIONs), catalase and superoxide dismutase (SOD) have been used as targeted therapeutic agents. These enzymes contain active centers with coordinated metals, which decompose superoxide anion and hydrogen peroxide, respectively, the most important reactive oxygen species [3]. For modulation the enzySPIONs efficiency the following parameters of the immobilization process were studied: the enzyme type, the ratio enzyme/SPIONs and enzyme conformation.

## EXPERIMENTAL METHODS

Functionalized SPIONs with antioxidant enzymes have been obtained by Catalase/SOD immobilization through direct reaction onto SPIONs based on magnetite, coated with functional synthetic polymer (copolymer of maleic anhydride). Briefly, 5 mg enzyme was dissolved in 20 mL phosphate buffer saline (PBS), at pH=8.00 and then poured within a suspension of SPIONs (100 mg nanoparticles dispersed in 30 mL PBS, pH=8.00, 0.05 M) and slowly mechanically stirred for 24 h. The particles have been collected from suspension through magnetic separation, purified by repeated washes with PBS (2x) and deionised water (3x) and finally freeze-dried. For modulation the enzySPIONs efficiency the immobilization parameters were studied: the enzyme type and the ratio enzyme/ SPIONs.

## RESULTS AND DISCUSSION

FT-IR data, dynamic light scattering evaluation of the zeta potential and hydrodynamic particle mean diameter confirmed the enzymes immobilization onto SPIONs. The enzySPIONs dimensions vary from 400nm for catalase immobilization to 1µm for SOD immobilization (Table 1).

The particles morphology was studied by scanning electron microscopy and suggests that the obtained enzySPIONs interact during the drying process and some clusters are formed (Figure 1).

The MTT assay revealed the citocompatibility of the enzyme-immobilized SPIONs and the hemocompatibility data indicated no interference of the enzySPIONs with blood coagulation system.

Enzymatic activity of magnetic particles has been

determined indirect by NTB-methionine-riboflavin (in the case of superoxide dismutase) and direct, with H<sub>2</sub>O<sub>2</sub> (for catalase). EnzySPIONs preserve an enzymatic activity which is dependent of the magnetic particles concentration, the enzyme nature and biological molecule conformation onto magnetic particle.

Table1. SPIONs dimension and Zeta Potential

SPIONs	Hidrodynamic diameter(nm)	Zeta Potential(mV)
Pure SPIONs	330±0.32	-20 ± 0.15
Catalase-SPIONs	432±3.12	-17 ± 0.39
SOD-SPIONs	970±0.27	-22 ± 0.32

data are presented as means ±standard deviation for n=3

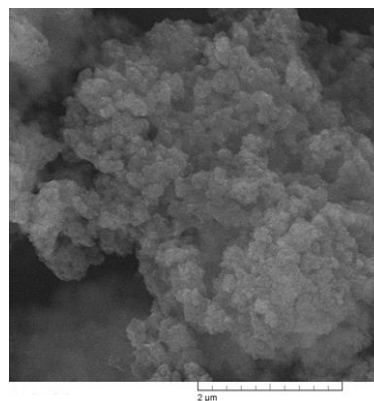


Figure 1. SEM morphology of SOD-SPIONs

From the magnetization data was observed that the residual magnetization and the coercive force were zero, and there was no magnetic hysteresis loop. The lack of hysteresis is one of the criteria requirements for the identification of the particles as superparamagnetic.

## CONCLUSION

A new type of functionalized superparamagnetic nanoparticles has been obtained by SOD/catalase immobilization onto SPIONs. Functionalized SPIONs are characterized by good magnetic properties, are biocompatible and exhibits enzymatic activity which recommend them in cardiovascular applications.

## REFERENCES

- 1.Wattanapitayakul S.K. *et al.*, Pharmacol Ther., 89:187-206, 2001.
2. Netto C.G.C.M. *et al.*, J. Mol. Catal. B: Enzym., 86:71-92, 2013.
- 3.Chorny M. *et al.*, J Control Rel., 17:146-144, 2010.

## ACKNOWLEDGMENTS

This work was financially supported by the Romanian Ministry of Education and Research; grant PN II- PT-PCCA-2011-3.2-0428 - INTERBIORES.



## Regeneration the Urethral with Collagen Scaffold in Stricture Urethral Induced the Heat

Christian Acevedo-García<sup>1,4</sup>, Jorge Jaspersen<sup>4</sup>, Guillermo Soria<sup>4</sup>, Luis Molina<sup>1</sup>, Jaime Sanchez<sup>1</sup>, Saulo Mendoza<sup>1</sup>, Jorge García<sup>1</sup>, Benjamin León-Mancilla.<sup>2</sup> Piña-Barba C.<sup>3</sup> Gutierrez-Reyes G.<sup>1</sup>

1) Laboratory HIPAM, Unit of Medicine Experimental, School of Medicine, UNAM. Hospital General of México, México City.

2) Department of surgery, School of Medicina, UNAM. México City.

3) Institut of Investigation in Material, UNAM, México City

4) Department of Urology, Hospital General of México, México City

[c.acevedo.uro@gmail.com](mailto:c.acevedo.uro@gmail.com) and [christianacevedogarcia@gmail.com](mailto:christianacevedogarcia@gmail.com)

## INTRODUCTION

The urethral stenosis is a disease caused by inflammatory conditions secondary by traumatic processes, infectious, iatrogenic or surgical procedures. Different therapeutic options has been used that the internal urethrotomy, terminal urethroplasty, the urethroplasty using buccal mucosa, colon, foreskin flaps and other grafts<sup>1, 2</sup>. However, the results are not always favorable. We initiated the development of a therapeutic approach using a biomaterial obtained from osseous matrix (Nukbone®) in urethral its heals the dog.

## EXPERIMENTAL METHOD

Cylindrical implants of collagen type 1 were obtained from osseous matrix (Nukbone®), with appropriate measures to replace a portion of 3 cm of the urethra in stricture induced by heat in the group 1 and three dog Sham in the group 2. between 6 and 8 years of age. The animals were sacrificed after 350, 360 and 370 days of implantation. The implanted segments were removed to perform histological studies of the regenerated tissues. The histological samples were fixed in formalin and were embedded in paraffin for cutting techniques, were used Hematoxylin-Eosin, Masson staining and Cytokeratin 7 and 20. MMP2, MMP 9, Colagenasa I and IV, were used to aid in the identification of normal and abnormal epithelial cells and residues of the Nukbone®. Also the evaluated whit uretroscopy and Magnetic Resonance (fig.1), with suitable permeability in the urethral.

## RESULTS AND DISCUSSION

In the surfaces of the urothelial implants, cell proliferation were observed for all cases, the cells were layered whose number increased with time, these were healthy urothelial cells. It was observed that the collagen cylinders were degraded the rest was healthy urethral tissue, with the permeability and low fibrosis in the Magnetic Resonance. Was maintained until complete resorption. There normal cell proliferation was proportional to the time of implantation with healthy cells. Also the form and function of the urethral stricture induced the heat.



Fig.1. Urethroscopy and permeability of the Scaffold. Arrow red. Urothelial over the implant.

## CONCLUSIONS

Collagen cylinders tested are a possible therapeutic solution for stricture the urethral in the model experimental, the use in human is the option in that diseases the urethral and ureter.

## KEYWORDS

Collagen Scaffold, Urethral stricture induced, regeneration, Nukbone®

## REFERENCES

1. Barbagli G. J Urol. (2005) 174: 955-7.
2. Andrew E. Urol Clin Am (2006) 33: 1-12.

## AKCNOWLEDGES

-Thank to DGAPA-UNAM for financial support through projects: IT 104011, to Biocriss SA de CV for providing us bone matrix implants to obtain the scaffolds. And MVZ. Camacho.



Richard M. Langford<sup>1</sup>, Jonathan Earl<sup>2</sup> and John J. Melcholsky<sup>3</sup>.

<sup>1</sup>Cavendish Laboratory, University of Cambridge, UK

<sup>2</sup>GSK Consumer Healthcare, Weybridge, UK

<sup>3</sup>Materials Science & Engineering Department, University of Florida, USA  
[rml42@cam.ac.uk](mailto:rml42@cam.ac.uk)

## INTRODUCTION

*In situ* nanoindentation in a scanning electron microscope (SEM) enables site specific loading and the discontinuities in the loading and unloading curves to be associated with the discrete events such as fracture onset or delamination. Here, we report on the use of *in situ* nanoindentation to study the mechanical properties of demineralised dentine and enamel after treatment with a sodium calcium phosphosilicate bioactive glass (45S5, supplied by GSK). To aid the mechanical analysis, a focused ion beam (FIB) system has been used to micromachine mechanical test structures such as coupons, bridges and cantilevers and to make site specific cross-sections to obtain sub surface information such as the depth of occlusion of the tubules.

## EXPERIMENTAL METHODS

Ten 2 mm thick tooth slices prepared from ethically acquired sound human molars were etched in 0.5% citric acid for 30 seconds. After washing the demineralised slices were cleaved in two and one half immersed in 50 ml of artificial saliva (AS) containing 10 mg of the calcium sodium phosphosilicate bioactive glass (the treated samples) and the remaining halves were immersed in only AS for 2 hours (the untreated samples). The samples were then dried and a FIB/SEM tool was used to micro machine mechanical test structures into both the dentine and the enamel and to make site specific cross sections for SEM and TEM.

## RESULTS AND DISCUSSION

EM analysis showed that a platelet hydroxyapatite-like crystalline layer occurred both on the surface and into the tubules and that the demineralised dentine zone was

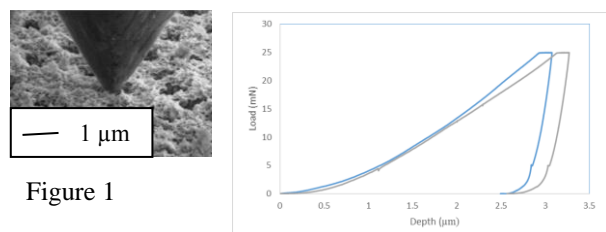


Figure 1

remineralised. Figure 1, above shows a SE image of a site specific loading of a treated sample and corresponding load-displacement curves. The average hardness of the intertubular dentine of the treated samples was 1.2 GPa and the untreated samples was 0.8 GPa. The hardness and mechanical response was found to vary with distance from the bioactive glass particles that were adhered to the surface of the samples.

Site specific FIB cross-sectioning close to the indents enabled the orientation of the tubules, their degree/depth of occlusion and the degree of remineralisation to be correlated with the load curves.

Figure 2, below shows a FIB machined bridge in a treated sample during loading by a flat punch and the corresponding load-displacement curve. The FIB

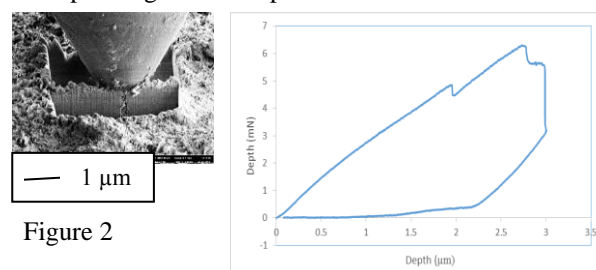


Figure 2

milling was used to select an area that contained a single occluded tubule which ran perpendicular to the surface to enable the fracturing of the formed material to be correlated to the load curves and to simplify the analysis. The fracturing was found to occur through occluding material and not at the interfaces to the peritubular dentine.

Figure 3 below shows a FIB machined enamel coupon prior to being loaded and the corresponding load-

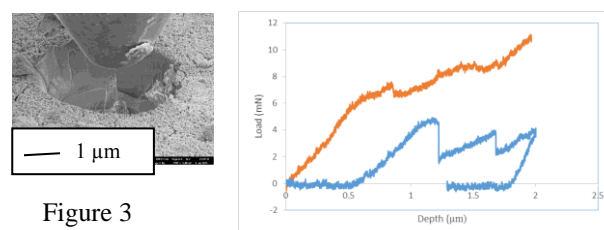


Figure 3

displacement curves of treated and untreated enamel pillars. The untreated enamel was observed to undergo more fracturing than the treated enamel pillars. EM analysis showed that in the treated enamel the etched inter prisms regions were bridged by hydroxyapatite-like crystalline material which can partly explain the differences in mechanical response.

## CONCLUSION

The work has shown how the use of FIB micro machining, site specific FIB cross-sectioning with *in situ* nanoindentation is a very powerful combination to aid understanding the micromechanics of treated dentine and enamel.

## Effect of Crystallinity of Carbonated Hydroxyapatite on Bone Repair

Suelen Sartoretto<sup>1</sup>, Marcelo Uzeda<sup>1</sup>, Adriana Alves<sup>1</sup>, Rodrigo Resende<sup>1</sup>, José Calasans-Maia<sup>1</sup>, Mônica Calasans-Maia<sup>1</sup>, Alexandre Rossi<sup>2</sup>, José Mauro Granjeiro<sup>1,3</sup>

<sup>1</sup>Dentistry School/Biotechnology applied Laboratory, Fluminense Federal University, Brazil

<sup>2</sup>CBPF - Brazilian Center for Research in Physics, Brazil

<sup>3</sup>INMETRO - National Institute of Metrology, Quality and Technology, Brazil

[alex.mrossi@gmail.com](mailto:alex.mrossi@gmail.com)

### INTRODUCTION

Carbonated hydroxyapatite (CHA) is the main mineral component of bone and a potential bone substitute for orthopedic/maxillofacial surgery<sup>1,2</sup>. In this work we synthesized CHA samples (carbonate occupying phosphate sites) with different crystallinity and dissolution rate. Samples were characterized from the point of view of phase composition and stoichiometry, carbonate sites, crystallite long and short range order, crystal morphology and crystal size, surface structure, specific surface area, pore distribution and *in vitro* dissolution rate. The *in vivo* behavior of CHA samples with low, medium and high crystallinity were evaluated in order to check the inflammatory response and bone repair efficiency of each CHA.

### EXPERIMENTAL METHODS

Nanostructured CHAs containing 6-wt% CO<sub>3</sub> in phosphate sites (B type CHA) were synthesized by a wet precipitation method at 5°C (CHA5), 37°C (CH37) and 90°C (CH90) and pH=11. Samples were analyzed by X-ray diffraction (XRD), X-ray fluorescence (XRF), Fourier Transform Infrared (FTIR), Scanning and Transmission Electron Microscopy (SEM, TEM, HRTEM, XDS), thermogravimetric analysis (TGA), X-ray photoelectron spectroscopy (XPS) and Physisorption techniques. Biological evaluations were conducted using microspheres (425-600µm) of nanostructured-CHA. Subcutaneous tissue analysis, 75-Balb/C mice were randomly divided in groups of 5 animals to evaluate the local biological effects 1, 3 and 9 weeks after implantation, comparing to sham-group, according to the scoring system established in the ISO 10993-6:2007. Similarly, 72-Wistar rats (n=5, 4, 12 and 24 weeks) were used for a critical-size-calvaria-defect treated with biomaterials and cloth. These samples were processed for light microscopy and polarized light microscopy to evaluate new bone formation through histomorphometric analysis

### RESULTS AND DISCUSSION

Physico-chemical analyses showed that the decrease of the synthesis temperature induced disorder in CHA structure and decrease in the particle size, specific surface area, pore size and *in vitro* dissolution rate. Sample synthesized at 5 °C was predominantly amorphous with a high, *in vivo*, biodegradation rate while the one synthesized at 90 °C was crystalline. The inflammatory potential was also evaluated from the perspective of the capacity of the materials to attract mast cells. The CHAs did not induce a

significant increase in the number of mast cells compared to the sham group, in contrast to HA. No groups showed signs of fibrosis around the biomaterial. On the contrary, intense cellularity was observed without necrosis suggestive of the attempt to absorb the material. Together, the data obtained from the tissue response to the CHs indicates that they are biocompatible are bioabsorbable, particularly CHA5 and CHA37. In calvaria defect, CHA37 exhibited the highest resorption ( $p < 0.05$ ) and together with cHA 5°C led to greatest new bone formation (ANOVA, Kruskal-Wallis, Dunn's,  $p < 0.05$ ), Fig.1.

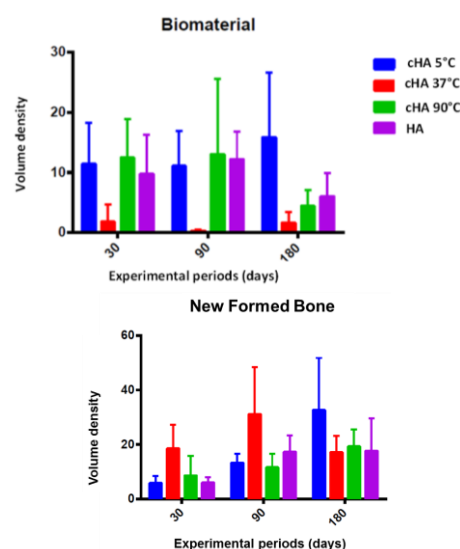


**Figure 3.** (A) Volume density of newly formed bone and (B) biomaterial 30, 90 and 180 days post-implantation.

### CONCLUSION

Carbonate substitution improves biological behavior of hydroxyapatite. However, crystallinity and degradation rate of CHA must be adjusted to optimize bone repair.

### REFERENCES

1. Hasegawa M. *et al.*, J. Bone Joint. Surg. Br 85:142-147, 2003
2. Wang G., J Bone Joint Surg Br. 92:320-325, 2010

### ACKNOWLEDGMENTS

The authors would like to thank the FAPERJ for providing financial support to this Project.

## Production of HA Scaffolds via Conversion of 3D Printed Gypsum Structures

Alan C.S. Dantas<sup>1</sup>, Andrea V. Ferraz<sup>1</sup>, Amanda A. Barbosa<sup>1</sup>, Debora Scalabrin<sup>2,3</sup>, Márcio C. Fredel<sup>3</sup>, Jens Günster<sup>2</sup>, Cynthia M. Gomes<sup>2</sup>

<sup>1</sup> Department of Materials Science /Federal University Vale do Sao Francisco, Brazil

<sup>2</sup>Department of Materials Engineering/BAM Federal Institute for Materials Research and Testing, Germany

<sup>3</sup>Department of Materials Engineering, Federal University of Santa Catarina, Brazil

[alan.dantas@univasf.edu.br](mailto:alan.dantas@univasf.edu.br)

### INTRODUCTION

Additive manufacturing (AM) technologies allow the creation of 3D structures by direct conversion of the patient data into implantable scaffolds of a specific material system. Porous ceramic bodies obtained by this method have better mechanical strengths than porous structures obtained by other technologies as replica-SSV, foaming, etc. However, most of the AM technologies for ceramics produce a green body, which requires debinding and sintering at high temperatures in order to achieve adequate mechanical properties<sup>1</sup>.

Gypsum can be used as raw material for the production of HA<sup>2</sup>. The conversion of solid porous gypsum scaffolds on HA scaffolds<sup>3</sup> presents a great advantage due to formation of HA at temperatures of approximately 100°C, without the need of further thermal treatment. It results in a low crystalline structure considered to be bioresorbable<sup>4</sup>.

The aim of this work is the production of HA porous scaffolds with controlled porosity and high dimensional precision using hydrothermal conversion of gypsum scaffolds produced by 3D printing.

### EXPERIMENTAL METHODS

Gypsum hemihydrate powder ( $\text{CaSO}_4 \cdot 0.5\text{H}_2\text{O}$ , P.A: Merck, Germany) was granulated in a spray drier (B290 – Büchi Switzerland) using 5%-masse of PVB (B-79, Butvar, Eastman, USA) as binder. The printable granules were used to produce cylindrical structures with a diameter of 18 mm and a height of 1.9 mm in a 3D Printing machine (RX Series, Prometal, Germany).

The porous gypsum structures were submersed in 200 mL of  $(\text{NH}_4)_2\text{HPO}_4$  solution ( $0.5 \text{ mol.L}^{-1}$ ) at a temperature of 100°C at different reaction times to convert into HA. The pH of the medium was adjusted to 9 by addition of  $\text{NH}_4\text{OH}$  solution ( $6.0 \text{ mol.L}^{-1}$ ). At the end of the reaction time, the blocks were washed in deionized water until reaching neutral pH and then dried in an oven at 50°C for approximately 4 hours.

The scaffolds were characterized before and after conversion by Electron Microscopy (SEM) using Energy Dispersive Spectroscopy (EDS) and X-Ray Diffraction.

### RESULTS AND DISCUSSION

The gypsum structures produced by 3D print showed enough mechanical properties to permit their handling and conversion into HA. The produced scaffolds can be observed in Fig.1. These structures presented a geometrical density of  $0.82 \pm 0.04 \text{ g/cm}^3$  that can be related to a porosity of  $68.1 \pm 2.0 \%$ . After conversion a

slightly increase of the porosity is expected to occur due to changing of the crystal structure.

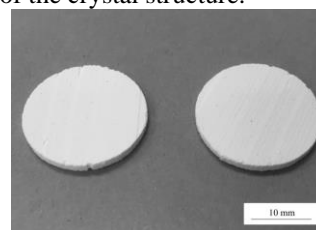


Fig. 1. Gypsum samples produced by 3D printing.

The XRD patterns before and after 12 hours conversion are showed in Fig. 2, where a total conversion of the Gypsum in HA can be verified. The maximum intensities peaks of gypsum at  $2\theta = 11.63^\circ$  and  $20.70^\circ$  are not present on the patterns of the samples after conversion.

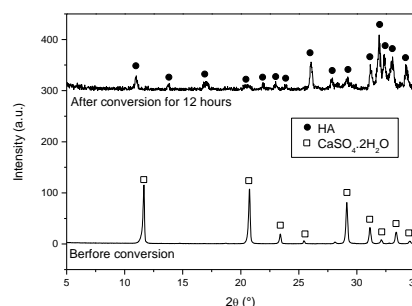


Fig. 2. XRD Patterns of the samples before and after conversion for 12 h.

### CONCLUSION

HA scaffolds were produced by chemical conversion of 3D printed gypsum structures. A reaction time of 12 hours was enough to promote a complete formation of single phase HA.

### REFERENCES

1. Gildenhaar, R. et al., Key Eng. Mater. 493-494:849-854, 2012
2. Furuta, S., et al., J. Mater. Chem. 8: 2803-2806, 1998.
3. Barbosa, A.A, et al., Mater. Res. 17:39-44, 2014
4. Legeros, R.Z. and Legeros, J.P., Key Eng. Mater. 3:240-242, 2003

### ACKNOWLEDGMENTS

The authors would like to thank the CAPES - Brazil (Grant no: 24886/2013-1) for providing financial support to this project.



## Repeatability of Surgical Implantation of Biomaterials. Radiological Analysis of a-TCP Localization in Critical Sized Femoral Metaphysis Defect in Rabbits

Nikolaos Papaioannou<sup>1</sup>, Triantafillos Papadopoulos<sup>2</sup>, Christos Zafeiris<sup>1</sup>, Nikitas Schizas<sup>1</sup>, Aikaterini – Anna Neri<sup>1</sup>,  
Cleopatra Nacopoulos<sup>1</sup>, Ismini Donta<sup>1</sup>

<sup>1</sup>Laboratory for the Research of the Musculoskeletal System (LRMS), Faculty of Medicine, University of Athens, Athens, Greece

<sup>2</sup>Department of Biomaterials, Dental School, University of Athens, Athens, Greece  
[npapaioan@med.uoa.gr](mailto:npapaioan@med.uoa.gr)

### INTRODUCTION

Accuracy and high repeatability of experimental surgical implantation technique is one of the major factors in the study of biomaterials. High repeatability allows the extraction of homogenous characteristics and secure results while reduces the sample size and the cost of the study. The aim of this study was the topographical assessment of a-TCP implantation in a femoral metaphysis rabbit model by using radiological signs and anatomic landmarks [1,2].

### EXPERIMENTAL METHODS

Twenty-four New Zealand White Rabbits were divided in two groups. All specimens underwent plain / facial radiographs and a computer-assisted topographic numeric division of each distal femur was conducted. In the first group a-tcp was implanted in the femoral metaphysis based only on anatomic landmarks. In the second group, a-tcp was implanted in the femoral metaphysis based on pre-operative radiologic evaluation combined with anatomic landmarks. Post-operative radiographic localization result of a-tcp was compared between the two groups

### RESULTS AND DISCUSSION

The second group, with the preoperative radiographic marking assistance, had higher rate of a-tcp coverage (statistically significant) of the targeted area compared with the first group. More specifically, the first group presented 80% a-tcp coverage while the second group 90% based on pre-operative planning.

The size of the rabbit as well as the presence of preoperative radiological assessment affected the direction (towards diaphysis) of the critical size defect and the distribution of the a-tcp which was injected. The second group had smaller peri-operative complications and smaller incision size .

The New Zealand White Rabbits are ideal experimental model for the study of filling bone defects. Skeletal maturation occurs in the species with the closure of the epiphyseal plates at the age of about 6 (six) months. Among experimental models, the KNZ have significant advantages such as the rate of bone turnover, the stability, the experimental reproducibility, ease hosting , small size and relative low cost [3,4,5].

The femoral metaphysis of the rabbits was chosen due to specific anatomical and cortico-cancellous characteristics which may affect the

histomorphometric analysis. The high repeatability of this anatomic site ensures these characteristics of the environment which hosts the biomaterial.

### CONCLUSION

The combination of pre-operative radiographic assessment and the anatomic landmarks provides higher rates of experimental repeatability and accuracy in the implantation of a-tcp.

### REFERENCES

1. Digital radiography. A comparison with modern conventional imaging. *Postgrad Med J* 2006;82:425–428
2. A Standard Surgical Protocol for a Rabbit Ulnar Osteotomy Model . *Scand. J. Lab. Anim. Sci.* 2006 Vol. 33 No. 2
3. To what degree is digital imaging reliable? Validation of femoral neck shaft angle measurement in the era of picture archiving and communication systems. *The British Journal of Radiology*, 84 (2011), 375–379
4. The influence of alendronate on osseointegration of nanotreated dental implants in New Zealand rabbits. *Clin. Oral Impl. Res.* 23, 2012; 659–666
5. Accurate scaling of digital radiographs of the pelvis . *J Bone Joint Surg [Br]* 2006;88-B:1508-12.

### ACKNOWLEDGMENTS

The authors would like to thank the European Union and Greek national funds through the Operational Program "Education and Lifelong Learning" of the National Strategic Reference Framework (NSRF) - Research Funding Program: THALES. (Grant no: MIS 379380) for providing financial support to this project. Also they want to thank Associate Professor Nikolaos Bouropoulos for providing the selfdeveloped implantive experimental ceramic material.





Antonio Tilocca<sup>1</sup><sup>1</sup>Department of Chemistry, University College London, United Kingdom  
[a.tilocca@ucl.ac.uk](mailto:a.tilocca@ucl.ac.uk)

## INTRODUCTION

The initial stages following contact between a bioactive glass and a biological aqueous host play a key role in starting the chain of processes ending in the dissolution of soluble species that trigger tissue regeneration and interfacial bonding. The central interaction of the glass with water results in rapid exchange between alkali ions and protons and formation of a silica-rich layer. Whereas the formation of this layer on highly bioactive glasses such as 45S5 is established<sup>1</sup>, its structural properties and mechanism of formation are less understood. A fundamental understanding of these issues can be gained through atomistic simulations.<sup>2</sup> In the past years, we have been using simulations to rationalise the behaviour of bioactive glasses at a fundamental level, from identifying new structural features of the bulk glass beyond the network connectivity that may help in predicting its bioactivity<sup>3,4</sup> to explicitly modelling the Bioglass/water interaction at the surface<sup>5</sup> and in the bulk,<sup>6</sup> to unveiling the effect of hydration on glasses for radiotherapy.<sup>7</sup> Here the target is shifted on an ion-exchanged bioactive glass, and on the effect of Na<sup>+</sup>/H<sup>+</sup> exchange on the structural features of the alkali-depleted glass.<sup>8</sup> The simulations provide a high-resolution picture of the structural evolution of the glass during this stage.

## EXPERIMENTAL METHODS

Systems of composition Na<sub>0.49-z</sub> Ca<sub>0.27</sub> P<sub>0.05</sub> Si<sub>0.46</sub> O<sub>1.56-z</sub> (OH)<sub>z</sub> with z=0, 0.1, 0.3 and 0.49 (z=0 corresponds to 45S5) were modelled, reproducing the gradual replacement of all Na<sup>+</sup> content by H<sup>+</sup> via increasing OH contents incorporated in the structure. A randomly-generated structure of ca. 3000 atoms was relaxed by thermal annealing via Molecular Dynamics (MD) simulations with a shell-model forcefield.<sup>7,8</sup> For each composition, the structural analysis was carried out on a final room-temperature MD trajectory.

## RESULTS AND DISCUSSION

The models provide a clear view of the way in which hydroxyl groups created upon alkali release are distributed and affect the glass structure. Whereas it is often assumed that the exchanged protons are found in Si-OH bonds, the simulations reveal a significant amount of OH groups not bonded to Si, but stabilised within cages of modifier (mostly Ca) ions. These “free-OH” species have been previously identified in silicate glasses and melts<sup>6,9</sup> at low hydration levels, which agrees with the present finding that their fraction decreases with increasing Na<sup>+</sup>/H<sup>+</sup> substitution (z): in Figure 1, we observe a transition from a structure with predominance of free OH at low z, to a structure where the dominant OH type is bonded to Si, at high z.

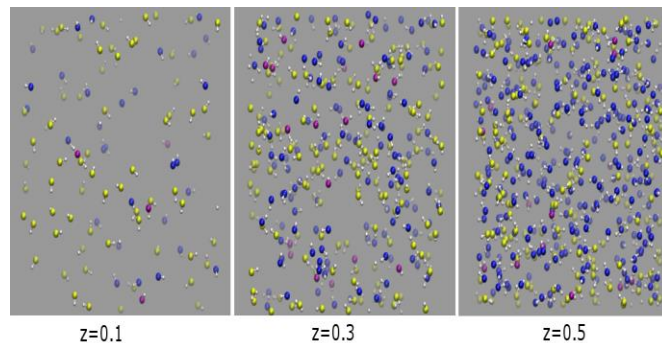


Figure 1: Free (yellow) and Si-bonded (blue) OH distribution across the Na<sup>+</sup>/H<sup>+</sup>-exchanged glass structures.

The analysis also highlights an increased connectivity of the silicate network upon gradual OH incorporation via Na<sup>+</sup>/H<sup>+</sup> exchange. This effect reflects the presence of free OH groups that preferentially attract Ca<sup>2+</sup> ions, removing them from NBOs bonded to Si atoms, which are thus led to repolymerise by forming new Si-O-Si bridges via Si-O...Si cross-linking in order to satisfy their oxygen coordination.<sup>8</sup>

## CONCLUSION

MD simulations suggest a direct, free OH-mediated mechanism for the formation of a repolymerised silica-rich network following Na<sup>+</sup>/H<sup>+</sup> exchange in 45S5 Bioglass, which can be alternative or complementary to the mechanism generally proposed. As the latter becomes more likely at higher Na<sup>+</sup>/H<sup>+</sup> exchange levels, a gradual transition between the two mechanisms could be envisaged as Na leaching proceeds and the silica gel layer is created.

## REFERENCES

- 1 Kim, Clark & Hench, *J. Non-Cryst. Solids*, 1989, **113**, 195
- 2 Tilocca, *J. Mater. Chem.*, 2011, **21**, 12660
- 3 Tilocca & Cormack, *J. Phys. Chem. B*, 2007, **111**, 14256
- 4 Christie & Tilocca, *J. Mater. Chem.* 2012, **22**, 12023
- 5 Tilocca & Cormack, *ACS Appl. Mater. Interfaces*, 2009, **1**, 1324
- 6 Berardo, Corno, Cormack, Ugliengo & Tilocca, *RSC Advances*, 2014, **4**, 36425
- 7 Malik & Tilocca, *J. Phys. Chem. B*, 2013, **117**, 14518
- 8 Tilocca, *Phys. Chem. Chem. Phys.* 2015, **17**, 2696
- 9 Kohn, Dupree & Smith, *Geochim. Cosmochim. Acta*, 1989, **53**, 2925

## ACKNOWLEDGMENT

Financial support from the UK's Royal Society (URF) is gratefully acknowledged.



# Physical and Mechanical Characterization of Hybrid Scaffolds Based on $\beta$ -TCP and Collagen

Isadora Deschamps<sup>1</sup>, Gabriel Magrin<sup>2</sup>, Aguedo Aragoes<sup>2</sup>, César Benfatti<sup>2</sup>, Ricardo Magini<sup>2</sup>, Júlio Souza<sup>2</sup>, Márcio Fredel<sup>1</sup>

<sup>1</sup> CERMAT, Department of Mechanical Engineering, Federal University Santa Catarina (UFSC), Florianópolis, Brazil

<sup>2</sup> CEPID, Department of Dentistry, Federal University of Santa Catarina (UFSC), Florianópolis, Brazil

[julio.c.m.souza@ufsc.br](mailto:julio.c.m.souza@ufsc.br)

## INTRODUCTION

Nowadays, scaffolds are used in several fields of tissue regeneration including dentistry. Their 3D shape stimulates growth, migration and differentiation of human cells for the reparation of the desire tissue. Successful scaffolds follow requirements, such as: possessing interconnected pores of proper size to allow the integration and vascularization of the tissue; controlled biointegration and biodegradability; surface that induces proliferation, differentiation and coupling of cells; adequate mechanical properties; and viability to be manufactured into specific shapes and sizes [1]. The aim of this study was to characterize hybrid scaffolds of  $\beta$ -TCP and collagen in their physical and mechanical properties.

## EXPERIMENTAL METHODS

The synthesis of  $\beta$ -TCP powders was based on the well-known route shown in Figure 1.

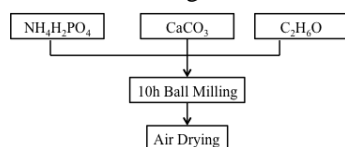


Figure 1: Route for synthesis of  $\beta$ -TCP.

After milling, a thermal treatment was performed to decompose the carbonate and nitrates, and to dehydrate the material [2]. Scaffolds were obtained by replica method, in which a sponge made of polyurethane was immersed in a ceramic suspension in order to cover its structure. Then, the pattern was compressed to remove the excess of suspension. As a result, the porous structure was covered by a uniform layer of ceramic slurry. Samples were thereafter submitted to thermal treatment in order to remove the polymer and sinter the ceramic. Collagen coating was then performed. The characterization of materials was carried out by X-ray diffraction and SEM-EDS. Scaffolds underwent compression test for mechanical assessment.

## RESULTS AND DISCUSSION

X-ray diffraction and SEM analyses revealed appropriate surface and composition of the material.

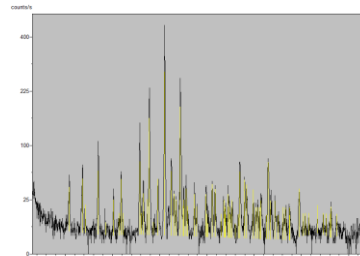


Figure 2: X-Ray diffraction of  $\beta$ -TCP.

Coated scaffolds presented better mechanical properties in comparison with non-coated samples.

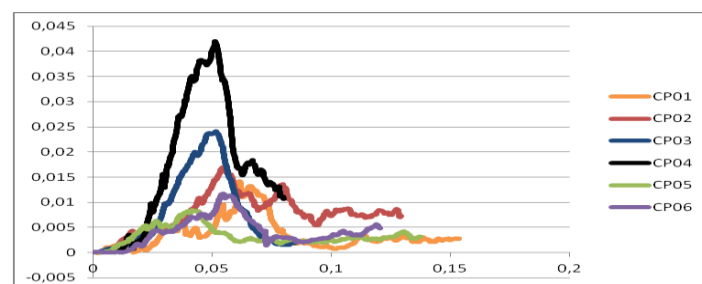


Figure 3: Compression test result.

## CONCLUSION

Within the limitations of this study, it can be concluded that coating  $\beta$ -TCP scaffolds with a biodegradable polymers as collagen is an advantageous method to increase mechanical resistance in porous ceramic materials.

## REFERENCES

1. SACHLOS E, CZERNUSZKA JT. *European Cells & Materials*, 2940, 2003
2. CORRÊA, UR, *Síntese do mineral  $\beta$ -trifosfato de cálcio para uso em Biomateriais*, 2008
3. Philippart, A *et al.* *Expert Rev. Med. Devices* Early online, 1–19, 2014

## Combined Effect of Magnesia and Zirconia on the Bioactivity of Calcium Silicate Ceramics at C/S ratio Less Than Unity

Emad Ewais<sup>1</sup>, Amira Amin<sup>1</sup>, Yasser Ahmed<sup>1</sup>, Eman Ashor<sup>2</sup>, Ulrike Hess<sup>3</sup>, Kuroschi Rezwan<sup>3</sup>

<sup>1</sup> Refractory & Ceramic Materials Division (RCMD), Advanced Materials Department, Central Metallurgical R&D Institute (CMRDI), P.O. Box 87, Helwan, 11421 Cairo, Egypt

<sup>2</sup> Chemical Engineering Department, Faculty of Engineering, El-Minia University, El-Minia, Egypt

<sup>3</sup> Advanced Ceramics, University of Bremen, Am Biologischen Garten 2, 28359 Bremen, Germany

[dr\\_ewais@hotmail.com](mailto:dr_ewais@hotmail.com)

### INTRODUCTION

In recent years, CaO-SiO<sub>2</sub> based ceramics are categorized as bioactive ceramic materials. They have been regarded as potential candidates for artificial bone due to their excellent bone bioactivity and biocompatibility. They need only to improve their mechanical properties to use as implants under heavy loads. This paper describes the effect of magnesia in the presence of zirconia on the bioactivity, microstructure and physico-mechanical properties of calcium silicate composition adjusted at calcia/silica ratio (C/S) of 0.5.

### EXPERIMENTAL METHODS

A mixture from calcium carbonate and silica was conducted at C/S of 0.5. 20 wt. % of magnesia and 5-25wt. % of ZrO<sub>2</sub> were added. The batch with 20 wt.% MgO without ZrO<sub>2</sub> termed master batch (MB), and batches containing ZrO<sub>2</sub> termed "MBZ5", "MBZ15" and "MBZ25" for 5, 15 and 25 wt. %, respectively. Each mixture was planetary ball mill mixed in ethanol, dried, formed and fired at a temperature of 1325± 5°C. Phase composition, FE-SEM, and physico-mechanical properties in terms of apparent porosity, bulk density, linear shrinkage, Vickers hardness and fracture toughness of the fired specimens were determined and explained. The in vitro bioactivities of these specimens were investigated by analysis of their abilities to form apatite in the simulated body fluid (SBF) for a short time (7days) using SEM-EDS.

### RESULTS AND DISCUSSION

The findings indicated that the surface of the MBZ5 and MBZ15 specimens are completely covered by hydroxyapatite (HA) typical to "cauliflower"

morphology, while the MBZ25 specimens revealed the beginning of HA formation but its surface did not completely cover. The differences among the results were rationalized based on the phase composition. Vickers hardness and fracture toughness of the specimens of highly promised bioactivity are given in Table 1.

Table (1) Vickers hardness and fracture toughness of highly promised bioactivity specimens

Composition	Hardness (GPa)	Fracture toughness K <sub>IC</sub> , MPa.m <sup>1/2</sup>
MBZ5	2.32	1.8
MBZ15	2.57	1.5

### CONCLUSION

The properties of specimens of highly promised bioactivity are similar to the properties of human cortical bone. Consequently, these composites might be used as a bone implant materials.



## Lanyu Minipig is a Better Model System for Studying Wound Healing

Ting-Yung Kuo<sup>1,2</sup>, Ming-Jen Lin<sup>1</sup>, Lih-Ren Chen<sup>2</sup>, Lynn L.H. Huang<sup>1,3,4</sup>

<sup>1</sup>Institute of Biotechnology/College of Bioscience and Biotechnology, National Cheng Kung University, Taiwan

<sup>2</sup>Livestock Research Institute/Council of Agriculture, Executive Yuan, Taiwan

<sup>3</sup>Institute of Clinical Medicine/College of Medicine, National Cheng Kung University, Taiwan

<sup>4</sup>Research Center of Excellence in Regenerative Medicine, National Cheng Kung University, Taiwan

[lynn@mail.ncku.edu.tw](mailto:lynn@mail.ncku.edu.tw)

### INTRODUCTION

Developing therapeutic approaches to treat wounds requires the selection of a suitable animal model that resembles human skin conditions. This study aimed to compare the skin wound healing features of Taiwanese Lanyu mini-pigs (TLY) with those of the domestic pig (Landrace, which is a well-known skin wound animal model) for evaluating whether TLY can be used to develop a wound healing animal model. Physiological parameters were measured, and skin growth rate was determined by measuring the changes in the size of tattoos drawn on the dorsal skin of pigs as a percentage of skin expansion of the original tattooed area. Contraction and re-epithelialization of full-thickness wounds were monitored histologically as well as by measuring the margin area and open wound area during healing.

### EXPERIMENTAL METHODS

Castrated male Taiwanese Lanyu mini-pigs (age: 7, 9, 16, and 40 weeks) from Taitung Animal Propagation Station and domestic Landrace pigs (age: 7 and 8 weeks) from the Genetic and Breeding Division of the Livestock Research Institute were used in this study. All animal care and operation procedures were performed according to the regulations of the Council of Agriculture, Executive Yuan Livestock Research Laboratory Animal review board. The skins on the dorsal side of the pigs were shaved and sterilized following anesthesia. The full-thickness excision wounds were created using a scalpel by removing the epidermis and dermis to a depth up to the subcutaneous fat layer.

### RESULTS AND DISCUSSION

The results indicated that, unlike Landrace pigs, TLY are relatively smaller in size and have a lower body weight; further, there was a linear correlation between skin growth and animal age up to maturity. Full-thickness wounds contracted remarkably during the first 5 weeks of healing in both strains irrespective of age. In >16-week-old TLY, wounds larger than 5×5 cm<sup>2</sup> showed a stable healing profile, overcoming the impact of skin growth on wound size expansion. The histological results also revealed similar healing and remodeling patterns between the two strains. Our findings suggested that 16-week-old TLY are optimally suitable for skin wound studies because they are easy to handle due to their smaller size and stable wound healing features. Skin wound model developed using TLY might be economically feasible for wound drug

screening and investigating healing profiles.

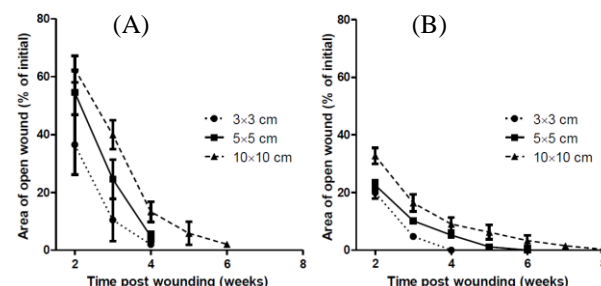


Figure 1. Profiles of wound re-epithelialization at the indicated breed and ages. Wounds were created on (A) 8-wks-old Landrace, (B) 9-wks-old TLY.

The wound healing profiles of Landrace and TLY pigs were determined at different growth stages by creating full-thickness wounds on the dorsal side of 8-week-old Landrace pigs and of 9-, 16-, and 40-week-old TLY. In TLY, the time to complete re-epithelialization did not differ according to age and wound sizes, and all smaller wounds closed within 4 to 5 weeks post wounding, whereas the larger wounds required more than 6 weeks for wound closure.

### CONCLUSION

In conclusion, compared to domestic pigs, Landrace pigs, the TLY mature earlier, have a smaller body size and bodyweight, show stable increases in physiological growth parameters, including body weight, body length, and abdominal circumference. Thus, TLY are favored for laboratory experiments. We highlight the main physiological properties of Taiwanese Lanyu mini-pig skin compared with those of domestic pig skin. The morphological features, skin growth profile, stable wound healing profile during wound contraction, re-epithelialization potential, and histological findings for the TLY obtained in this study might serve as the basis for future researches on using this breed as excision wound healing models. Taken together, our findings suggest that Taiwanese Lanyu mini-pigs can be used for developing skin wound healing animal models.

### ACKNOWLEDGMENTS

This work was supported by grants from the National Science Council (MOST102-2622-M-006-002-CC2, CZ-20-18-146-103), and the Council of Agriculture (101AS-2.1.1-LI-L1(6)) in Taiwan.





## Scanning Electron Microscope in Evaluation of Biomedical Materials – Own Experiences

Jacek Składzień, Agnieszka Wiatr, Katarzyna Zagórska-Świeży, Maciej Wiatr

Otolaryngology Department, Jagiellonian University, Poland

[jacek.skladzien@uj.edu.pl](mailto:jacek.skladzien@uj.edu.pl)

### INTRODUCTION

The limitation of development in surgery is possibility of reconstruction required after resection of pathologic tissues. Use of own patients' tissues in reconstruction is very often difficult or impossible. Therefore many studies to find alternative ways of reconstruction with artificial materials are undertaken. Biomedical materials are widely used in the surgery. They are used in organs' reconstruction (as prostheses) and in typical suturing of the surgical wounds (tapes, drainage)<sup>1</sup>. Stability in contact with patients' tissues and lack of allergic reaction with no rejection of the prostheses are of the greatest importance for biomedical materials.

### EXPERIMENTAL METHODS

Analysis of biomedical materials used in otolaryngology was performed with the scanning electron microscope (SEM). Biomedical materials obtained during surgery were compared with their sterile analogues. Changes in structure as a result of contact with patients' tissues were studied. Surgical sutures, prostheses for reconstruction of the ossicular chain in the middle ear, silastic removed from the nasal cavity that supported mucous membrane after septoplasty and latex as dressing material in the nose were taken into consideration.

### RESULTS AND DISCUSSION

Bacterial biofilm (known better than fungal one) is a three-dimensional structure that contains microcolonizations (aggregation of bacterial cells), that adheres to organic as well as inorganic surfaces (e.g. all sutures, prostheses used in reconstructions). Scanning electron microscope revealed features of biofilm on the surfaces of biomedical materials obtained from otolaryngological sites. Relationship between period of exposition and range of growth of the biofilm on analyzed surfaces was observed.

### CONCLUSION

The growth of bacterial biofilm on artificial biomedical materials is frequently observed. The stability and protection against rejection of artificial materials requires resistance to bacterial growth. This observation leads to necessity of additional modification of biomedical materials surfaces with bacteriostatic components due to decreasing or elimination of inflammation in the closest neighborhood of the used artificial prostheses or implants.

### REFERENCES

1. Undas A, Siudut J, Ząbczyk M. SEM skaningowy mikroskop elektronowy. CX News 2014;49:3.
2. Laura Munteanu E, Spielman I, Biais N. Analyzing bacterial movements on surfaces. Methods Cell Biol. 2015;125:453-69.

### ACKNOWLEDGMENTS

The present results are not overlapping any of our earlier work and co-authors of this paper revealed no conflict of interest.



Laurence Padiolleau<sup>a,\*</sup>, Laurent Plawinski<sup>a</sup>, Gaëtan Laroche<sup>b,c</sup>, Marie-Christine Durrieu<sup>a</sup>

<sup>a</sup>Institute of Chemistry & Biology of Membranes & Nanoobjects (CBMN UMR 5248, CNRS), Bordeaux University, European Institute of Chemistry and Biology, 33607 Pessac, France

<sup>b</sup>Laboratoire d'Ingénierie de Surface (LIS), Département de Génie des Mines, de la Métallurgie et des Matériaux, Centre de Recherche sur les Matériaux Avancés (CERMA), Université Laval, Québec, Canada

<sup>c</sup>Centre de Recherche du Centre Hospitalier Universitaire de Québec (CRCHUQ), Hôpital St-François d'Assise, Québec, Canada

[laurence.padiolleau@u-bordeaux.fr](mailto:laurence.padiolleau@u-bordeaux.fr)

## INTRODUCTION

Mature osteoblasts are the cells responsible for bone formation and are derived from precursor osteoblasts. However, mechanisms that control this differentiation are poorly understood. In fact, unlike the majority of organs in the body, which are composed of “soft” tissues from which cells can easily be isolated and studied, the “hard” mineralized tissue of bone has made it difficult to study bone cells function. **The objective of our research program is the development of a smart and bioactive material, which can mimic the native bone extracellular matrix (ECM), and enable the understanding of their impact on the differentiation of mesenchymal stem cell (MSC).**

For this purpose, bioactive molecules were grafted onto the surface of polyethylene terephthalate (PET) in order to induce an osteogenic differentiation of MSC. Our objective is to control the spatial organization of these bioactive molecules on the surface at the micro and/or nanoscale, therefore mimicking bone ECM<sup>1</sup>.

Two different active biomolecules were used. On one hand, a RGD-containing (Arg-Gly-Asp) peptide which was selected to promote cell adhesion. On the other hand, the RKIPKASSVPTELSAISMLYL sequence from the BMP-2 (Bone Morphogenetic Protein-2), previously identified in Durrieu's group<sup>2</sup> was chosen due to its ability to promote bone differentiation while co-immobilized with RGD on PET surfaces.

## EXPERIMENTAL METHODS

In order to design the above-mentioned material, PET surfaces were modified according to the method described by Chollet et al<sup>3</sup>. First, materials were modified to generate COOH functionalities onto PET surfaces, by hydrolysis and oxidation of the material. Then, materials were immersed in a solution containing 1-Éthyl-3-(3-diméthylaminopropyl)carbodiimide (EDC) (0.2 M) + N-Hydroxysuccinimide (NHS) (0.1 M) + 4-Morpholineethanesulfonic acid (MES) (0.1 M) in order to activate the surface for peptide immobilization. Fluorescent peptides were used to characterize the homogenous functionalization of PET using fluorescence microscopy. All the samples were analysed with XPS, AFM. The amount of COOH grafted onto the film was determined using the toluidine blue-O method.

## RESULTS

Preliminary results have been obtained for homogenous surfaces by using the toluidine blue-O (TBO) method. COOH densities obtained for “PET Native”, “PET-Oxidized”, “PET-NHS” and “PET-GRGDSPC” are, respectively, 5, 32, 10, 24 pmol/mm<sup>2</sup>.

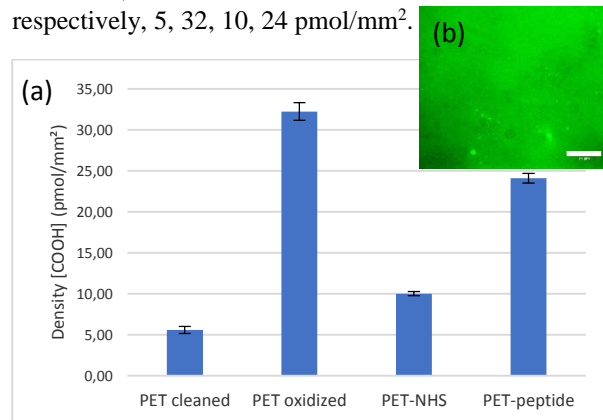


Figure 1 – (a) [COOH] densities obtained by toluidine blue staining and (b) fluorescent image of surface grafted with fluorescent peptides GRGDSK-FITC (scale bar: 25 µm).

These results show a rather low surface density of COOH moieties onto PET surfaces, while a 6-fold increase is observed after material hydrolysis and oxidation. The decrease in COOH surface concentration observed after conversion of acidic groups into activated esters and peptide immobilization confirmed successful grafting of these biomolecules. These results were further confirmed by XPS (not shown). In addition, the surface grafting of the aforementioned peptides labeled with fluorescent markers allowed measuring a steady fluorescent signal throughout the PET surface sample, therefore confirming peptide homogeneous grafting.

## CONCLUSION

Further works will focus first, on the evaluation of the impact of homogeneous bioactive surface on MSC differentiation and then on the patterning of both RGD or/and BMP-2 mimetic peptide according to predetermined micro and nanopatterns to promote the differentiation of MSC.

<sup>1</sup>L Hench, & J. Polak, Science, 2002; 295(5557): 1014-1017.

<sup>2</sup>O Zouani, L Rami, Y Lei, & MC Durrieu, Biology open, 2013; BIO20134986.

<sup>3</sup>C Chollet, C Chanseau, B Brouillaud, & MC Durrieu, Biomolecular engineering, 2007, 24, 5:477-482.



## Textile-based Silk Scaffolds for Bone Tissue Engineering Applications

Viviana Ribeiro<sup>1,2</sup>, Alain Morais<sup>1,2</sup>, Vitor M. Correlo<sup>1,2</sup>, Alexandra P. Marques<sup>1,2</sup>, Ana Ribeiro<sup>3</sup>, Carla Silva<sup>3</sup>, Nuno Durães<sup>3</sup>, Graça Bonifácio<sup>4</sup>, Rui Sousa<sup>1,2</sup>, Joaquim M. Oliveira<sup>1,2</sup>, Rui L. Reis<sup>1,2</sup> and Ana L. Oliveira<sup>1,2,5</sup>

<sup>1</sup>3B's Research Group—Biomaterials, Biodegradables and Biomimetics, University of Minho, Headquarters of the European Institute of Excellence on Tissue Engineering and Regenerative Medicine, AvePark, Guimarães, Portugal; <sup>2</sup>ICVS/3B's - PT Government Associate Laboratory, Braga/Guimarães, Portugal; <sup>3</sup>CeNTI, Centre for Nanotechnology and Smart Materials, V.N. Famalicão, Portugal; <sup>4</sup>CITEVE, Technological Center for Textile and Clothing Industry, V.N. Famalicão, Portugal; <sup>5</sup>CBQF—Center for Biotechnology and Fine Chemistry, Portuguese Catholic University, Porto, Portugal.

[aloliveira@porto.ucp.pt](mailto:aloliveira@porto.ucp.pt)

### INTRODUCTION

Scaffolds developed for bone tissue engineering (TE) need to facilitate and promote cell adhesion, proliferation and neo-tissue formation. They must possess specific properties to allow the new tissue to integrate with the material, without inducing any inflammatory response<sup>1</sup>. The intra-architectural scaffold geometry, porosity, scaffold material and surface area play important roles in this process<sup>2</sup>. Several polymeric systems (natural and/or synthetic) and processing methods have been proposed to develop the “ideal” scaffold for bone TE. However, so far the proposed strategies do not fulfil all the requirements for effective bone regeneration. Textile-based technologies constitute an innovative alternative for the production of 3D structures for bone TE applications, offering a superior control over scaffolds' design, manufacturing and reproducibility<sup>3</sup>. Silk fibroin (SF) derived from silkworm *Bombyx mori* has already proved to be a good biomaterial for bone TE applications<sup>4</sup>. SF-based structures offer impressive mechanical properties, biodegradability, biocompatibility and stability, which meets the basic requirements for the design of structures for bone regeneration applications<sup>5</sup>.

### EXPERIMENTAL METHODS

In this work we describe for the first time the processing of natural silk yarns into 3D scaffolds, combining standard knitting fabrics spaced by a monofilament of polyethylene terephthalate (PET). A comparative study is established using a stable polymeric system made entirely of PET. The obtained knitted spacer constructs were described in terms of morphology and mechanical properties. An *in vitro* biological assay was performed to evaluate the potential of the developed structures to support human Adipose-derived Stem Cells (hASCs) adhesion, proliferation and osteogenic differentiation. Cells were cultured over 28 days in standard basal and osteogenic conditions and evaluated through different quantitative (DNA, ALP, Calcium, RT-PCR) and qualitative (SEM, Alizarin Red, immunocytochemistry) assays. The *in vivo* biocompatibility of the textile materials was assessed by subcutaneous implantation in mice model. After 2 and 4 weeks of implantation the explants were collected and the obtained slides were stained with hematoxylin and eosin (H&E).

### RESULTS AND DISCUSSION

The cross-sections of the developed spacer textile constructs reveal a significant increase of the scaffolds three-dimensionality induced by the PET monofilament (Figure 1a). The hASCs seeded onto the spacer textile scaffolds were able to attach, spread, proliferate and differentiate, both in osteogenic and basal conditions (Figure 1b). Great evidences of ECM mineralization were observed, also penetrating and colonizing the PET monofilament (Figure 1a). The preliminary *in vivo* results revealed that the implanted scaffolds allowed tissue ingrowth, without inducing any acute inflammatory reaction (Figure 1c).

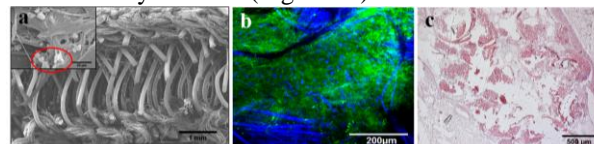


**Figure 1**—SF textile scaffolds seeded with hASCs and cultured for 28 days in osteogenic medium: (a) SEM micrographs from a cross-section and top view perspective. The red circle indicates mineralization nodules; (b) Confocal micrographs, nuclei stained in blue and Col I in green. (c) H&E staining of a SF textile scaffold in the explant, after implantation for 2 weeks.

### CONCLUSION

In this study, innovative 3D biotextile scaffolds able to support cell adhesion, proliferation and osteogenesis were successfully developed. Furthermore, these scaffolds allowed the new tissue formation and integration within the material, when subcutaneously implanted in mice. Thus, the proposed textile-based scaffolds can be promising candidates for bone TE applications such as the craniomaxillofacial complex<sup>6</sup>.

### REFERENCES

1. Burg K. *et al.*, *Biomaterials*. 21(23):2347-2359, 2000
2. Salgado J. *et al.*, *Macromol Biosci*. 4(8):743-765, 2004
3. Sumanasinghe R. *et al.*, *Research Journal of Textile and Apparel*. 9(3):80-90, 2005
4. Kundu B. *et al.*, *Adv Drug Deliver Rev*. 65(4):457-470, 2013
5. Yan L-P. *et al.*, *J Bioact Compat Pol*. 28(5):439-452
6. Liu G. *et al.*, *Biomaterials*. 34(11):2655-2664

### ACKNOWLEDGMENTS

Portuguese Foundation for Science and Technology (FCT) for the project TISSUE2TISSUE (PTDC/CTM/105703/2008). Investigator FCT program IF/00423/2012 and IF/00411/2013 are also greatly acknowledged.

## Impact of the Micro-scale Distribution of RGD/BMP-2 Peptides on hMSCs Osteogenesis

Ibrahim Bilem<sup>1,2,3</sup>, Pascale Chevallier<sup>1</sup>, Laurent Plawinski<sup>2</sup>, Eli Sone<sup>3</sup>, Marie-Christine Durrieu<sup>2\*</sup>, Gaétan Laroche<sup>1\*</sup>

<sup>1</sup>Deprt of Min. Met. Mater, Lab of surface engineering/RC-CHUQ, Laval university, Canada

<sup>2\*</sup> Institute of Chemistry & Biology of Membranes & Nanoobjects (UMR5248 CBMN), Bordeaux University, France

<sup>3</sup>Deprt of Mater.Sci.Eng, Institute of Biomaterials and Biomedical Engineering, University of Toronto, Canada

[ibrahim.bilem.1@ulaval.ca](mailto:ibrahim.bilem.1@ulaval.ca)

### INTRODUCTION

Nowadays, several protocols are proposed to induce the osteogenesis (new bone tissue formation) in order to regenerate or replace bone tissue when it is severely damaged. Unfortunately, producing clinically relevant volumes of bone with adequate stiffness to support load bearing functions in large defects remains the major drawback of the current approaches<sup>1</sup>. Indeed, this is mainly due to the lack of understanding of the osteogenesis mechanism *in vivo*. Accordingly, this project attempts to clarify these signalling pathways triggered during the response of stem cells to their osteoinductive microenvironment<sup>1</sup>. The original approach of this project consists in mimicking the extracellular matrix (ECM) of mesenchymal stem cells (MSCs) by grafting and micropatterning specific peptides on model biomaterial surfaces. Indeed, surface microstructuration, which somewhat mimics the ECM component organization, was demonstrated in several instances to improve cell adhesion, and even differentiation<sup>2</sup>. The peptides to be micropatterned are the RGD and BMP-2 mimetic peptides, which were selected for their ability to respectively induce the adhesion and the differentiation of MSCs into mature osteoblasts, able to synthesize a mineralized ECM<sup>3</sup>. In addition, it was shown that this combination of peptides increases the expression of RUNX2 (osteogenic marker), as opposed to the sole grafting of BMP-2 peptide<sup>3</sup>.

### EXPERIMENTAL METHODS

Glass slides were first functionalized using an amine-terminated silane. Then, the RGD and BMP-2 mimetic peptides were grafted through SMPB crosslinker. These two peptides were grafted as micropatterns by using photolithography. The designed micropatterns corresponded to square, rectangle or triangle with a constant surface area of 50  $\mu\text{m}^2$ . The surface chemistry and topography of the material were assessed using X-ray Photoelectron Spectroscopy (XPS) and Atomic Force Microscopy (AFM). Micropattern visualization and peptides surface concentration were achieved using fluorescent peptides RGD-TAMRA and BMP-2-FITC.

### RESULTS AND DISCUSSION

XPS survey analysis (Table 1) evidenced the grafting efficiency after each step of peptides grafting. On one hand, we noticed the appearance of nitrogen on aminated glass surfaces, which remains almost constant

after peptide grafting. Simultaneously, the silicon detection (substrate) decreased after each step of grafting. On the other hand, high resolution C1s XPS spectra clearly confirmed the immobilization of both peptides since the amount of amide bonds significantly increased from 1.1% on aminated glass to 7.6% and 8% on RGD and BMP-2 grafted surfaces, respectively.

Table 1: Surface composition determined by XPS

%	C	N	Si	288.4 eV : NH-C=O
SiO <sub>2</sub>	5.9	-	23.9	-
NH <sub>2</sub> -glass	58.5	8.7	8.4	1.1
RGD grafted	65.5	7.3	5.3	7.6
BMP2 grafted	62.8	8.8	5.1	8.0

The surface concentration of RGD-TAMRA and BMP FITC peptides, based on fluorescence measurements, was  $0.53 \pm 0.01$  and  $0.73 \pm 0.02$  Pmole/ $\text{mm}^2$ , respectively. Finally, peptide micropatterning was confirmed by fluorescence microscopy using fluorescent peptides. Indeed, the spatial distribution of the two peptides with the different geometries (rectangle, square, and triangles) was clearly evidenced and precisely defined (Fig. 1).

### CONCLUSION

Designing a biomimetic microenvironment onto biomaterial surfaces seems to be a promising tool to study the biological response of stem cells to their microenvironment. Indeed, understanding the mechanism of bone tissue regeneration may greatly help to induce osteogenesis by drawing relevant *in vitro* models capable to precisely direct stem cell towards specific lineages. Our preliminary surface characterization results evidenced efficient peptide grafting as well as surface microstructuring. Future works will assess the effect of peptide micropatterning on human MSCs commitment and differentiation.

### REFERENCES

1. Locke M. *et al.*, J. Stem Cells. 404-411, 2011
2. Kilian K-A. *et al.*, J. PNAS. 11, 4872-4877, 2010
3. Zouani O-F. *et al.*, J. Biol Open. 29, 872-81, 2013

### ACKNOWLEDGMENTS

The authors would like to thank the NSERC Create Program in Regenerative Medicine for providing financial support to this project.

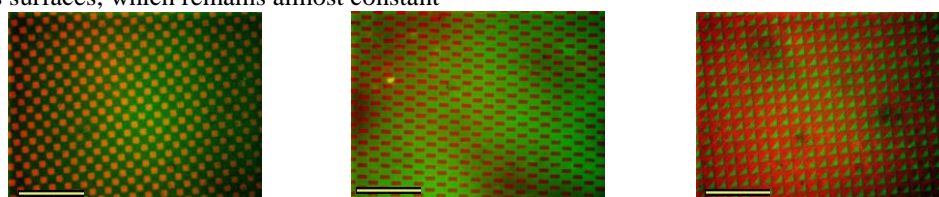


**Figure1:** Fluorescent images of peptides micropatterns grafted on borosilicate glass surfaces: RGD-TAMRA/BMP 2-FITC. Scale bar 50 $\mu\text{m}$



## Controllable Synthesis and Characterization of Multifunctional Poly(Lactic-co-Glycolic Acid) Nanoparticles for Tissue Engineering Applications

Masoud Mozafari<sup>1</sup>, Katayoun Nazemi<sup>2</sup>, Fathollah Moztarzadeh<sup>2</sup>

<sup>1</sup>Bioengineering Research Group, Nanotechnology and Advanced Materials Department, Materials and Energy Research Center (MERC), P.O. Box 14155-4777, Tehran, Iran

<sup>2</sup>Biomaterials Group, Faculty of Biomedical Engineering (Center of Excellence), Amirkabir University of Technology, P.O. Box 15875-4413, Tehran, Iran

[mozafari.masoud@gmail.com](mailto:mozafari.masoud@gmail.com)

### INTRODUCTION

Natural vitamin E has been frequently utilized for multiple pharmaceutical applications, demonstrating its positive effects as an emulsifier [1]. The potential health benefits of vitamin E supplementation were suggested in the 1950s [2]. An extensive attention has been paid on the antioxidant nature and free radical scavenging properties of vitamin E, due to the rapidly growing awareness of the physiological and toxic effects of free radicals in human diseases [3]. As mentioned earlier, PLGA NPs have been frequently prepared by using chemical emulsifiers such as PVA, which has showed side effects and problems. In this study, the effects of using natural vitamin E as an emulsifier for the synthesis of PLGA NPs have been studied. These combined techniques comprise three major steps as preparing an organic solvent, dispersing the organic solvent into an aqueous solution, and evaporating the volatile solvent. In addition, the cell response of the synthesized NPs has been tested by the MTT assay using osteoblast cells, as an important cell models for bone tissue engineering, in different dosages and time intervals.

### EXPERIMENTAL METHODS

The PLGA NPs were prepared by a one-step oil-in-water emulsion and solvent evaporation techniques. PLGA (50:50, Resomer-RG 503H; Boehringer Ingelheim) was dissolved in 1 mL of dichloromethane. Then, 50 mg of PLGA in dichloromethane was added into 50 mL of the dispersing phase including 0.02% sodium chloride (NaCl) and vitamin E (472.75 g/mol, Merck co.) aqueous solution (0.12%, 0.18%, 0.22% and 0.26%) under moderate magnetic stirring. The formed emulsion was then stirred on a magnetic stirrer plate at room temperature for 2 h to evaporate dichloromethane (DCM). The synthesized NPs were not necessarily required to be washed for removing the emulsifier.

### RESULTS AND DISCUSSION

Tissue engineering scaffolds can locally release biomolecules and accelerate bone ingrowth to the treated bone defects [4]. This allows for custom grafts to be designed as localized delivery systems. The homogenous distribution of the nanoparticles on the surface of porous scaffolds increases their surface area. As can be seen in the SEM micrographs provided in Fig. 1, the addition of vitamin E as the emulsifier to the PLGA nanoparticles resulted smaller particles in the

range of nanometers (ranging from 30 to 60 nanometers) for the sample containing 0.6 % vitamin E. The cellular activity of the nanoparticles showed to be nontoxic and without any sign of toxicity, suggesting that vitamin E can be used as an effective emulsifier. The main advantage of this system is that the vitamin E molecules are not required to be washed after the formation of the nanoparticles.

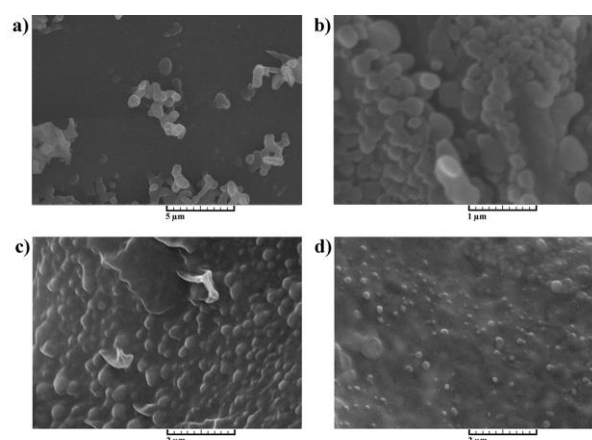


**Figure 4.** SEM micrographs of the synthesised samples containing NaCl and a) 0.12, b) 0.18, c) 0.22, d) 0.26 w/v % vitamin E

### CONCLUSION

In conclusion, this study suggested the use of vitamin E as an effective emulsifier in the formation of PLGA nanoparticles. It was shown that by further addition of emulsifier into the system, the nanoparticles became smaller in the range of nanometers, which is useful for incorporating in tissue engineering applications when the delivery of biological molecules and drugs is necessary in the defected sites.

### REFERENCES

1. Brindley G.W. *et al.*, Philos. Mag. Lett. 12:505-512, 1965.
2. Tsai M.T. *et al.*, J. Euro. Ceram. Soc. 23:1283-1291, 2003.
3. Guo C. *et al.*, Mater. Lett. 74:197-199, 2012.
4. M. Mozafari, *et al.*, Mater. Sci. Eng: C, 50:117-123, 2015.
4. K. Nazemi, *et al.*, Mater. Lett. 138: 16-20, 2015.

Sina Moztarzadeh<sup>1</sup>, Fuzhan Rahmanian<sup>1</sup>, Fathollah Moztarzadeh<sup>1</sup>, Masoud Mozafari<sup>2</sup><sup>1</sup>Biomaterials Group, Faculty of Biomedical Engineering (Center of Excellence), Amirkabir University of Technology, P.O. Box 15875-4413, Tehran, Iran<sup>2</sup>Bioengineering Research Group, Nanotechnology and Advanced Materials Department, Materials and Energy Research Center (MERC), P.O. Box 14155-4777, Tehran, Iran  
[mozafari.masoud@gmail.com](mailto:mozafari.masoud@gmail.com)

## INTRODUCTION

There have been several attempts for the incorporation of bioactive nanoparticles into polymeric scaffolds to enhance the physico-chemical and biological response prior transplantation.

Among different bioactive ceramics, nanocrystalline forsterite (NF) is a crystalline form of magnesium silicate with the chemical formula  $Mg_2SiO_4$ .<sup>1</sup> The vast advantages of this material have made it interesting in a wide range of applications especially for bone tissue engineering applications.<sup>2</sup>

In this research, using ice-NF hybrid particles as porogens and coating carriers to finish the NF coating and the scaffold fabrication at a time, the porous poly (L-lactide-co- $\beta$ -malic acid) (PLMA) scaffolds with NF coating was directly fabricated by a combined technique using porogen leaching and freeze drying methods.

## EXPERIMENTAL METHODS

The ice-NF hybrid particles have been prepared according to a recently published work by Guo *et al.*<sup>3</sup> Briefly, the NF particles were milled, sieved and pre-cooled at  $-20^\circ\text{C}$ . The ice particles were separated into the desired size range (about  $300\ \mu\text{m}$ ) using standard sieves and added to the NF particles to form a mixture of ice particles and NF particles (with a ratio of 10 to 1 mg). The mixture was immersed in liquid nitrogen to fabricate ice-NF hybrid particles. The prepared particles were arranged in the mold to form a template for the porous scaffold in the next step.

## RESULTS AND DISCUSSION

It is known that by applying effective coatings on the surface of composites, a relatively higher strength and stiffness to weight ratios could be obtained. On the other hand, they could show better durability, fatigue behaviour and dimensional stability.<sup>4</sup> Fig. 1 shows the load displacement curves of the uncoated and coated scaffolds. The areas below the curves are a measure of the fracture (the energy required to fracture the sample, obtained from the area under the load-displacement curve normalized by the samples' cross-sectional area). According to this figure, the fracture energy for the coated scaffold was higher than the uncoated sample.

In addition, no significant difference was seen in LDH activity of the both PLMA and NF-coated PLMA scaffolds at three time points compared with control, indicating non-cytotoxicity effects of the scaffolds on the cells. Although spreading and expansion of the cells on the NF-coated PLMA scaffolds seems to be more

than PLMA scaffold, the cells were actively attached to the surface of both type of scaffolds. All the results obtained from *in vitro* biologic response indicated that NF coating had a promising effect on the biocompatibility of the scaffolds.

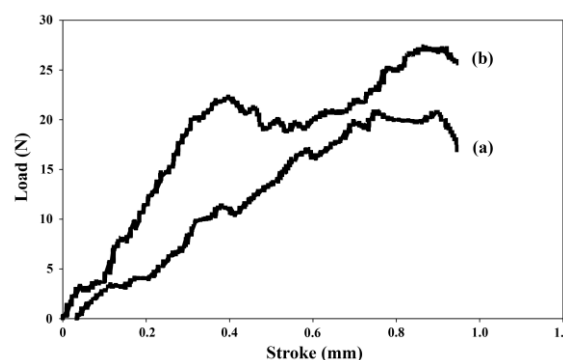


**Figure 4.** Load displacement curves of (a) the prepared uncoated, and (b) NF-coated PLMA scaffolds

## CONCLUSION

In this study, the phase-pure NF was successfully synthesized by the sol-gel low temperature process. The crystallite size of synthesized powders was in the range of 10-20 nm. Then, NF-coated porous PLMA scaffolds were fabricated by porogen leaching method combined with the pressure seepage and freeze-drying method. The obtained results confirmed the existence of the NF coating on the surface of the scaffolds, which is suitable for tissue engineering applications. The BMSCs spread and attached actively on both PLMA and NF-coated PLMA scaffolds. Furthermore, MTT and LDH specific activity tests indicated that NF coating could remarkably increase the biocompatibility *in vitro*.

## REFERENCES

1. Brindley G.W. *et al.*, Philos. Mag. Lett. 12:505-512, 1965.
2. Tsai M.T. *et al.*, J. Euro. Ceram. Soc. 23:1283-1291, 2003.
3. Guo C. *et al.*, Mater. Lett. 74:197-199, 2012.
4. M. Mozafari, *et al.*, Mater. Sci. Eng: C, 50:117-123, 2015

## ACKNOWLEDGMENTS

The authors would like to thank Amirkabir University of Technology and Materials and Energy Research Centre (MERC) for providing support to this project.

## Organ Decellularization: Design and Construction of a Device for Obtaining 3D Scaffolds, The Beginning of Bioartificial Organs in México

Héctor Martínez-Hernández<sup>1</sup>, Benjamín León Mancilla<sup>2</sup>, María-Cristina Piña-Barba<sup>1</sup>

1. Instituto de Investigaciones en Materiales, Laboratorio de Biomateriales, Universidad Nacional Autónoma de México, Ciudad Universitaria, Circuito Exterior s/n, Coyoacán, C.P. 04510, México D.F.

2. Facultad de Medicina, Depto. De Cirugía, Universidad Nacional Autónoma de México, Ciudad Universitaria, s/n, Coyoacán, C.P. 04510, México D.F.

[crispina99@gmail.com](mailto:crispina99@gmail.com)

### ABSTRACT

Tissue engineering has as main objective to obtain a suitable 3D scaffold; this can be obtained by decellularization organ from a donor who is functionalized by placing the patient's stem cells. The general objective of this research is to obtain 3D scaffolds by decellularization<sup>[1]</sup> of porcine organs; this implies removing total cells of the organ with the perfusion of different solutions through the vascular system in the organ, leaving intact the supporting structure called Extracellular Matrix (MEC), the main composition is collagen, elastin and other signaling proteins, preserving the essential architecture of each organ<sup>[2]</sup>. The decellularization process is performed on a device, designed and built in the laboratory specifically for this purpose named Bio-MEC, this guarantees obtaining the extracellular matrix, without damaging or changing its composition. Subsequently, this structure will provide support for the cells of the recipient patient; the future goal is to obtain a fully functional bioartificial organ.

### EXPERIMENTAL METHODS

A device was built and the appropriate parameters for optimal organ decellularization by perfusion, were determined. The key to the success of the process is the design of an air trap, this piece is critical because the presence of air in the capillaries of the organ causes inefficient decellularization. The organs are treated with a pH 7.4 saline solution to remove blood then decellularized with a detergent-based solution<sup>[3]</sup>. Scaffolds are studied with Histology, IR and SEM.

### RESULTS AND DISCUSSION

The first attempt of the decellularization process was to mimic the blood flow reported in the literature for each organ; however these values were clearly higher due to rupture of the organ. Based on that, the initial flow was decreased in 50% allowing decellularization. The time required for the decellularization is related to the intrinsic characteristics of the organ to be processed, which can range from a few hours to several days. The infrared pattern shows the presence of collagen because their characteristic bands are observed: amide A  $3290\text{cm}^{-1}$ , amide B  $2975\text{cm}^{-1}$ , amide I  $1533\text{cm}^{-1}$ , amide II  $1552\text{cm}^{-1}$ , and amide III  $1402\text{cm}^{-1}$ .

The structure of each organ is maintained after decellularization process and it is confirmed by the SEM images.

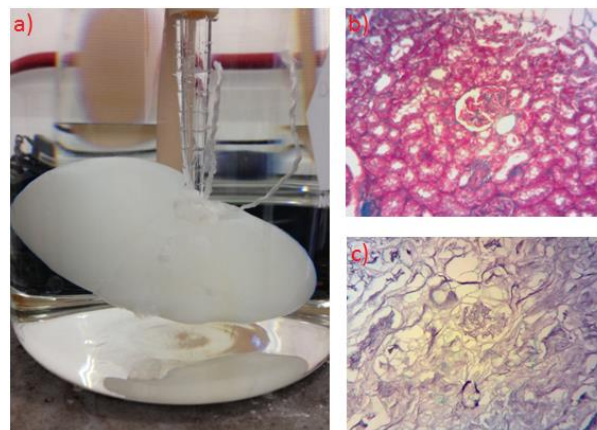


Fig. 1 The image shows a) the kidney decellularization, histological examination, Masson's trichrome, of b) native kidney, b) acellular kidney.

### CONCLUSIONS

Using the Bio-MEC device it can be obtained 3D scaffolds for organ regeneration which maintain the desirable characteristics of the extracellular matrix. This device allows the processing of any organ that has vasculature; this device may also decellularized from one to three organs at once.

### REFERENCES

- <sup>1</sup> Harald C. Ott et al., Decellularized scaffolds as a platform for bioengineered organs. *Current Opinion Organ Transplant* 2014, 19:145-152.
- <sup>2</sup> Giuseppe Orlando et al., Discarded human kidneys as a source of ECM Scaffold For Kidney Regeneration technologies. *Biomaterials* 2013, 34:5915-5925.
- <sup>3</sup> Stephen F. Badylak et al., An overview of tissue and whole organ decellularization processes

### ACKNOWLEDGES:

The authors would like to thank the PAPIIT program for the financial support through the IG100114 project, CONACyT through project 214128. To Sergio Serrano Guzmán, Verónica Rodríguez Mata, Damaris Cabrero Palomino, Miguel Ángel Martínez Canseco, for their technical support.

# Special Sessions





## Young Scientists Forum

Sunday, 30<sup>th</sup> August

13:00 – 17:00

Hall 2



### “From Creative Thinking Towards Product Commercialization: The Complete Value Chain”

**Organizers:**

Sandra Van Vlierberghe, Lorenzo Moroni, Giuseppe Cama, Anna Finne Wistrand, Izabela Stancu

**Supported by:**

Young Scientists Forum @ ESB

The YSF workshop in Kraków, Poland will aim to cover the entire value chain ranging from idea creation towards commercialization of a developed product.

**Programme:**

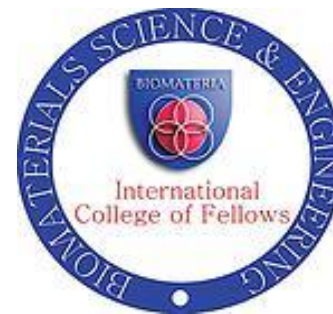
- 13:00 Prof. Abhay Pandit**, National University of Ireland, Galway, Ireland  
*“Creative Thinking – How to Come up with New Ideas”*
- 13:35 Prof. Fabrizio Barberis**, University of Genoa, Italy  
*“How to Get Money to Work out your Idea”*
- 14:10 Prof. Paul Santerre**, University of Toronto, Canada  
*“You Received Funding – What’s Next – How to Survive in Research Land”*
- 14:45** Coffee break
- 15:15 Prof. Joachim Kohn**, The New Jersey Center for Biomaterials, United States  
*“How to Advance Research Results Towards the Development of a Medical Product”*
- 15:50 Dr. Lechosław F. Ciupik**, LfC-Medical, Poland  
*“R&D in Creation of Bio-Engineering Product; Researcher Responsibility”*
- 16:25 Panel discussion**

In addition to PhD students, the workshop will also focus on topics relevant for post-doctoral researchers as well as PIs. The workshop will be closed with a round table discussion during which delegates can share their opinion and exchange ideas to create an excellent networking opportunity.



## Special Fellows Session

Monday, 31<sup>st</sup> August  
16:00 – 17:45  
Hall 1



### **ICF-BSE Fellows Session, ESB-Krakow 2015**

#### **“Biomaterials education is not ready for the challenges of the future”**

**Speakers:** David Grainger, Dietmar Hutmacher, Kristi Anseth, Laura Poole-Warren,  
Kathleen Elizabeth Tanner, Lynne Jones

**Moderator:** Joachim Kohn

The “Special Fellows Session” is organized by the International College of Fellows of Biomaterials Science and Engineering (IUS-BSE). Special Fellows Sessions explore important and sometimes controversial topics. A group of six prominent Fellows will highlight the perceived strengths and weaknesses of the way most universities educate and train the next generation of biomaterials scientists. Three Fellows will argue in favor of the current status of biomaterials education, while three other Fellows will provide provocative and stimulating arguments highlighting the weaknesses of current biomaterials education. One key point of the debate will be an exploration to which extent the careers of young scientists are impacted by a lack of skills needed to translate laboratory research into products within an industrial setting. Another key point relates to the fact that current biomaterials education prioritizes breadth over depth, producing “generalists” who are not well-trained in any one field. The changing job market for biomaterials scientists (especially at the PhD level), and global challenges and perspectives will also be discussed. Together, the six presenters will provide the audience with a deep and multifaceted understanding of the strength and weaknesses of the way many young biomaterials scientists are educated and prepared for their careers. Special Fellows Sessions are designed to be interactive: the audience will have an opportunity to participate in the debate and will vote on the issues. Previous “Special Fellows Sessions” examined the utility of animal experiments (WBC Amsterdam, 2008), explored whether we will ever be able to regenerate a complete human arm (WBC Chengdu, 2012), looked at the tension between basic research and translational research (ESB Liverpool, 2014) and the competition between material science approaches and biology-based approaches in developing the next generation of regenerative therapies (US Society for Biomaterials, Charlotte NC, 2015).

---

The International College of Fellows- Biomaterials Science & Engineering (**ICF-BSE**) was established in April 1992 after the constituent biomaterials societies of the World Biomaterials Congress, now the International Union of Societies – Biomaterials Science and Engineering (**IUS-BSE**), recognized the need for the public recognition of those of their members who have gained a status of excellent professional standing and high achievements in the field of biomaterials science and engineering. The ICF-BSE is chaired by Joachim Kohn, PhD, FBSE.



## Session Agenda:

### **“Biomaterials education is not ready for the challenges of the future”**

Agree with statement- Laura Poole-Warren, Lynne Jones, Dietmar Hutmacher

Disagree with statement Kristi Anseth, David Grainger, Liz Tanner

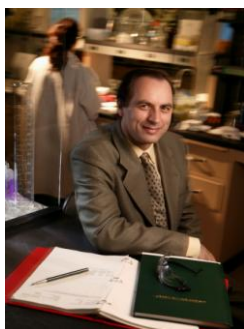
(See the following pages for Participants' Biosketches)

### **Moderator:**

Joachim Kohn, Ph.D., FBSE

Director, the New Jersey Center for Biomaterials

Board of Governors Professor, Rutgers, the State University of New Jersey



**Joachim Kohn**, is a Board of Governors Professor at Rutgers University and honorary professor at Sichuan University, China. Professor Kohn's research interests focus on the development of new biomaterials. He pioneered the use of combinatorial and computational methods for the optimization of biomaterials for specific medical applications. He is mostly known for his seminal work on "pseudo-poly(amino acid)s"- a new class of polymers that combine the non-toxicity of individual amino acids with the strength and processability of high-quality engineering plastics. Medical devices using these materials have been implanted in more than 50,000 patients, and several new products are in pre-clinical development.

In 1997, Kohn founded the New Jersey Center for Biomaterials, which has grown into a collaborative network spanning 25 institutions, and 40 laboratories located in countries across the entire globe. He has raised about \$100M in research funding at Rutgers and helped companies to raise about \$200M in private capital for the development of his technologies. In 2008, Kohn became the Principle Investigator and Director of the Rutgers-Cleveland Clinic Consortium of the Armed Forces Institute of Regenerative Medicine (RCCC-AFIRM). In this position, Kohn oversees approximately \$60 million of funding from the Department of Defense, with the goal to develop innovative new therapies for catastrophic injuries.

The New Jersey Center for Biomaterials  
145 Bevier Road, Piscataway, NJ 08854  
kohn@rutgers.edu

## David Grainger, Ph.D, FBSE

George S. and Dolores Doré Eccles Presidential Endowed Chair in Pharmaceutics/Pharmaceutical Chemistry,  
Professor of Pharmaceutical Chemistry, Professor of Bioengineering, University of Utah



**David W. Grainger** is a *University Distinguished Professor* and *George S. and Dolores Doré Eccles Presidential Endowed Chair in Pharmaceutics and Pharmaceutical Chemistry*, and *Professor of Bioengineering* at the University of Utah, USA. Grainger's research focuses on improving drug delivery methods, implanted medical device and diagnostics performance, and nanomaterials toxicity. Grainger has published 185 research papers and 23 book chapters on biomaterials innovation in medicine and biotechnology, and novel surface and diagnostics chemistry. He has won research awards, including the *2013 Excellence in Surface Science Award* (Surfaces in Biomaterials Foundation), the *2007 Clemson Award for Basic Research* (Society for Biomaterials), and the 2005 American Pharmaceutical Research and Manufacturer's

Association's award for "*Excellence in Pharmaceutics*". Grainger served as Chair of the several of NIH's prominent review panels and also featured in the award-winning National Institutes of Health's *Center for Scientific Review Mock Study Section* professional instructional video October, 2009 (posted to <http://www.youtube.com/watch?v=HMO3HoLJuJY>). He is a co-founder of 4 biomedical start-up companies, and serves on scientific advisory board positions for several others. He advises major multi-national EU research projects and several major international interdisciplinary biomedical research centers. Grainger has won numerous teaching awards and has provided over 350 invited lectures globally.

University of Utah - Health Sciences Campus  
301 Skaggs; 190D BPRB  
Salt Lake City, Utah 84112  
[david.grainger@utah.edu](mailto:david.grainger@utah.edu)

---

## Kristi S. Anseth, Ph.D., FBSE

Distinguished Professor, Tisone Professor, Associate Professor of Surgery, and  
Howard Hughes Medical Institute Investigator



Kristi S. Anseth was trained in the field of chemical engineering and earned her B.S. degree from Purdue University in 1992 and her Ph.D. degree from the University of Colorado in 1994. She then conducted post-doctoral research under the guidance of Bob Langer at MIT as an NIH fellow. Dr. Anseth is presently a Howard Hughes Medical Institute Investigator and Distinguished Professor at the University of Colorado at Boulder. Her research interests lie at the interface between biology and engineering where she designs new biomaterials for applications in drug delivery and regenerative medicine. Dr. Anseth's research group has published over 280 publications in peer-reviewed journals and presented over 250 invited lectures in the fields of biomaterials and tissue engineering. She was the first engineer to be named a Howard Hughes Medical Institute Investigator. She has also received the distinguished Alan T. Waterman Award from the NSF. Dr. Anseth is an elected member of the

National Academy of Engineering (2009), the National Academy of Medicine (2009), and the National Academy of Sciences (2013). She is a dedicated teacher, who has received four University Awards related to her teaching, as well as the American Society for Engineering Education's Curtis W. McGraw Award. Dr. Anseth is a Fellow of the American Association for the Advancement of Science, the American Institute for Medical and Biological Engineering, the Materials Research Society, and was newly elected by IUSBE as fellow of Biomaterial Science and Engineering (2015). She serves on the editorial boards or as associate editor of *Biomacromolecules*, *Journal of Biomedical Materials Research — Part A*, *Acta Biomaterialia*, *Progress in Materials Science*, and *Biotechnology & Bioengineering*.

University of Colorado Boulder, College of Engineering  
596 UCB, Boulder, CO 80309-0596  
[kristi.anseth@colorado.edu](mailto:kristi.anseth@colorado.edu)





### **Dietmar W. Hutmacher, Ph.D, FBSE**

Professor and Chair of Regenerative Medicine at the Institute of Health and Biomedical Innovation (IHBI),  
Queensland University of Technology



**Dietmar W. Hutmacher** is Professor and Chair of Regenerative Medicine at the Institute of Health and Biomedical Innovation (IHBI), Queensland University of Technology, where he leads the Regenerative Medicine Group, a multidisciplinary team of researchers including engineers, cell biologists, polymer chemists, clinicians, and veterinary surgeons. His work on scaffold design and fabrication via 3D printing has created a number of new research directions and has resulted in thousands of subsequent papers, making this process one of the most commonly used in the field today. Professor Hutmacher has also pioneered a number of scaffolding approaches to engineer bone, cartilage, skin and breast tissue engineering. As a result of this unique combination of expertise and experience, he is one of the few academics to take a holistic bone-engineering concept from fundamental research to clinical application.

Importantly, this research translation has led to the treatment of a large number of patients. Professor Hutmacher has recently pioneered a highly innovative way of using tissue engineering technologies developed in his lab for cancer research. He is leading an emerging area of research in which tumours are engineered in vitro with physiological properties that can be used to study cancer biology in a highly controlled manner or test the efficacy of new drugs.

Queensland University of Technology  
2 George Street, Brisbane QLD 4000, Australia  
[dietmar.hutmacher@qut.edu.au](mailto:dietmar.hutmacher@qut.edu.au)

---

### **Laura Poole-Warren, Ph.D., UNSW, FBSE, FAIMBE**

Pro Vice-Chancellor (Research Training) and Dean of Graduate Research, The University of South Wales



**Laura Poole-Warren** is a Professor in Biomedical Engineering at The University of New South Wales (UNSW Australia). Her research group focuses on incorporating functional biological molecules into hydrogels and electroactive polymers for application to medical devices. Specific interests are in cell and drug delivery in neural and cardiovascular applications. She has published over 110 papers and has had grant funding of approximately \$4 million over the past 10 years. She has also held appointments as visiting research professor at Rutgers University in the USA and as a preclinical scientist in the biomedical industry working on development of implantable devices including wound dressings and embolic agents for cancer treatment. For 10 years up to 2012, she was a member of the Australian

Commonwealth Government statutory Advisory Committee on Medical Devices which advises the Therapeutic Goods Administration on the safety of medical devices. Laura is also the Pro-Vice Chancellor (Research Training) & Dean of Graduate Research at UNSW Australia. In these roles she has responsibility for graduate research education, researcher development and early career and postgraduate researchers. Laura is currently one of the two IUSBSE delegates for the Australasian Biomaterials and Tissue Engineering Society. Her other roles include being an Associate Editor of the journal *Biomaterials* and an advisory board member of the Bionic Vision Australia Consortium.

The University of New South Wales  
UNSW Sydney NSW 2052 Australia  
[L.Poolewarren@unsw.edu.au](mailto:L.Poolewarren@unsw.edu.au)

## **Kathleen Elizabeth (Liz) Tanner, Ph.D., FBSE, DPhil, FEAMBES, FEng, FRSE**

Professor of Biomedical Materials, University of Glasgow



**Liz Tanner** has been Professor of Biomedical Materials at the University of Glasgow since 2007, held a similar position at Queen Mary University of London (1998-2007) and was in the IRC in Biomedical Materials (1991-2001). Her research is on bioactive bone replacement and augmentation composites and bone biomechanics.

Her interests in the training of biomedical engineers and biomaterials scientists started at Queen Mary, the first university in the UK to offer degrees in Biomaterials. She started the Intercalated BSc in Clinical Materials at Queen Mary, where medical and dental students take a year out of their degree to study biomaterials and their clinical application. She developed and ran the first undergraduate degree in Biomedical Engineering in Scotland at Glasgow until July 2015. This five year enhanced undergraduate Master of Engineering degree started with 23 students in 2010, had its first MEng graduates in 2015 and now has over 150 students. Liz was one of the few non-US based academics invited to the Second Whitaker Foundation Engineering Education Summit (2005).

She was elected FBSE in 2004, a Fellow of the Royal Academy of Engineering (FEng) in 2006 and Fellow of both the Royal Society of Edinburgh (FRSE) and the European Alliance of Medical and Biological Engineering and Science (FEAMBES) in 2015.

University of Glasgow, School of Engineering  
R471 Level 4, Biomedical Engineering, James Watt Building South, Glasgow G12 8QQ  
Elizabeth.Tanner@glasgow.ac.uk

---

## **Lynne C. Jones, Ph.D., M.S., FBSE**

Director, Center for Osteonecrosis Research and Education

Associate Professor of Orthopaedic Surgery, Johns Hopkins University School of Medicine



**Lynne C. Jones**, is an Associate Professor of Orthopaedic Surgery with a joint appointment in Materials Science & Engineering at the Johns Hopkins University. She serves as the Director of the JHU Clinical Research Group for Hip & Knee Surgery; the Director of Resident Research for JHU Orthopaedic Surgery; and the Director of the JHU Center for Osteonecrosis Research and Education. She is a member of numerous prestigious national and international societies including the SFB, the ORS, AAOS, the Hip Society, and the RMBS. She is the current President of ARCO-International and the Secretary-Treasurer of the National Osteonecrosis Foundation. She is a past President of the Society

For Biomaterials USA and is a current SFB representative to the ISUBSE. She has received numerous national and international recognitions including the SFB Award for Service (2015), and election as a Fellow of the International Union of Societies - Biomaterials Science and Engineering and a Fellow of the American Institute for Medical and Biological Engineering.

Dr. Jones has over 37 years of research experience in orthopaedics involving basic science and clinical science. She has published over 130 peer-reviewed publications and has been the keynote speaker at international meetings speaking on her research areas of interest – osteonecrosis, total joint arthroplasty (knee; hip), and bone grafting.

Johns Hopkins Orthopaedic Surgery  
A663/Bayview  
4940 Eastern Avenue  
Baltimore, MD 21224-2780  
Ljones3@jhmi.edu



## Translational Research Symposium



Tuesday, 1<sup>st</sup> September

10:00 – 11:00

11:30 – 13:00

16:45 – 18:30

Hall 1

### **“Innovating in the Medical Device Industry – Challenges & Opportunities”**

**Organizers:**

Yves Bayon, Marc Bohner, David Eglin, Geoff Richards, Dimitrios Zeugolis

**Supported by:**

DSM Biomedical, Netherlands

Innovation and product development in the medical device industry have largely been technology driven in the last decades. Advancements have been often rapid and significant. Today’s solutions, particularly biomaterial implants, have reached high standards and state of the art treatment generally supports acceptable return to daily activities and quality of life, in the vast majority of mild cases.

Today’s product development occurs in a more complex environment, with multiple stakeholders involved. Each of these stakeholders can have different and sometimes conflicting requirements and expectations. While technological innovation may still be the driving force behind new product developments, in many cases it is not a sufficient justification.

Innovation in the medical device industry can take many forms. From an entrepreneurship perspective, it does not require inventing something completely new; it can simply involve applying an existing idea in a new way or to a new situation. Innovation includes i) Rapid cadence of market release of new devices or services, ii) Scientific communication on company’s products and key opinion leaders (KOL) support, iii) Clinical education of care providers, iv) Skilled communication channels & v) Brand equity or the value of the brand name, the five pillars of success in medical devices business.

Innovation is greatly influenced by the customer, i.e., at the same time, all major healthcare stakeholders, the patients, but also the care providers and payers, who can all influence real-world health care decision making. Putting on the market innovating products also depends on the fulfillment of regulatory requirements, guaranteeing the safety and efficacy of any market approved products. This is a crucial bottleneck for a biomaterial based device and therapy which will be specifically addressed this year though lecturers from regulatory consultants and industry describing the processes (e.g. 510K, PMA, combination product...) toward market approval. The customer and the unending changing regulatory environment represent both innovation challenges and opportunities for medical device industries.

The key driver of innovation is the value of your medical device solutions which should offer optimal efficacy, showing a proven ease of use, satisfying for users, with the greatest safety profile and at the most acceptable cost. And, innovation should also lead to, economically viable and technically feasible projects, delivering, at the end, desirable products for the customer.

For an innovative idea to reach successfully the market place, its success, the innovation process throughout its entire lifecycle should not be driven exclusively by the company, but should fully incorporate the influence of the patient needs, the clinical feedback, the regulatory and reimbursement environment and, finally, the science and technology contribution of academic partners.

The ESB 2015 Translational Research Symposium will focus on **“Innovating in the Medical Device Industry – Challenges & Opportunities”**. It will include invited lectures from the medical device innovation stakeholders, i.e. medical device industry, academic translational centres, customers and medical device regulatory experts.

The Translational Research Symposium will also offer open sessions for sharing translational research initiatives both from academia and industry.

This event will be of interest to a wide audience from large medical device producers to academics and entrepreneurs and promoters of biomaterial technologies for medical applications. The program includes significant time for networking during coffee breaks, lunch and is also synchronized with other ESB2015 sessions throughout the day allowing the delegates to view other interesting lectures during the event.



## Special Sessions

### Session 1 (10.00-11.00)

#### **Invited Speakers:**

**(TRS1) Philip Procter**, Medical Device Industry Consultant, France

*“Clinical Needs Based Biomaterial Strategy: Reducing the Risk that Innovation is “Lost in Translation” in Products for Poor Quality Bone”*

**(TRS2) Nils Reimers**, Manager R&D, Global Funding & Reimbursement, Stryker Trauma & Extremities, Germany

*“Best Practice for Registration Trials of Biodegradable Implants”*

**(TRS3) Xiang Zhang**, Lucideon Ltd., Royal Society Industry Fellow at University of Cambridge, UK

*“New Concept of Hybrid Polymer Composites for Implant Applications”*

**(TRS4) Ipsita Roy**, University of Westminster, London, UK

*“Novel Biodegradable and Biocompatible Polymers for Medical Applications”*

### Session 2 (11.30-13.00)

#### **Invited Speakers:**

**(TRS5) Jan Weber**, Sr Research Fellow, Corporate Research, Boston Scientific Corporation, USA

*“Insights into Collaboration and Innovation for Early Stage Medical Device Development”*

**(TRS6) Jens Thies**, Director Science and Innovation, DSM Biomedical, Netherlands

*“From Biomaterials Supplier to Device Development Partner – Supporting Medical Device Companies in De-Risking Medical Products”*

**(TRS7) Herbert De Breuck**, Manager R&D, Luxilon, Wijnegem, Belgium

*“Next Generation of Fibers for Medical Devices: Biopolymers and Functionalized Coatings”*

### Session 3 (16.45-18.30)

#### **Oral Presentations of Candidates for Translational Research Award:**

**(116) Antoine Alves**, NAMSA, Chasse/Rhône, France

*“FTIR Microscopy Contribution for Comprehension of Poly-L-Lactic Acid (PLA) Degradation Mechanisms”*

**(117) Mikhail Durymanov**, Institute of Gene Biology of the RAS, Russia

*“Possible Approach to Improve Systemic Gene Delivery to Tumour Using Polyplex Nanoparticles”*

**(118) Beata Butruk-Raszeja**, Warsaw University of Technology, Poland

*“Endothelialization of Polyurethanes: Immobilization of REDV Peptide”*

**(119) Inês Gonçalves**, INEB - Instituto de Engenharia Biomédica, Universidade do Porto, Portugal

*“Helicobacter Pylori-Binding Small Chitosan Microparticles that Penetrate Gastric Mucosa”*

**(120) Stephen Swioklo**, Institute for Genetic Medicine, Newcastle University, United Kingdom

*“Leaving Cells Out in the Cold: Hydrogel Encapsulation for the Improved Hypothermic Preservation of Stem Cells”*

**(121) Daniel Rodriguez**, Technical University of Catalonia (UPC-BarcelonaTECH), Barcelona, Spain

*“Antibacterial Coatings on Titanium Surfaces: a Comparison Study Between In Vitro Single-species and Multispecies Biofilm”*

**(122) Elisabeth Engel**, Institute for Bioengineering of Catalonia (IBEC), Barcelona, Spain

*“The Proangiogenic Potential of a Novel Poly(Lactic) Based Composite Membrane for Guided Bone Regeneration”*





## **Clinical Needs Based Biomaterial Strategy: Reducing the Risk that Innovation is “Lost in Translation” in Products for Poor Quality Bone**

Philip Procter

Medical Device Industry Consultant, 01220 Divonne les Bains, France  
[consultphilipprocter@gmail.com](mailto:consultphilipprocter@gmail.com)

### **INTRODUCTION**

The gap between unmet clinical needs and biomaterials qualified to meet these needs is widening. Clinicians are increasingly reluctant to use what they consider clinically unproven biomaterials products<sup>1</sup>. High end biomaterials products such as BMP's are now being phased out and the commercial resources necessary to qualify new innovative biomaterials are now scarce as there are now very few independent biomaterials makers of any significant size today. The larger medical device companies are increasingly focused on acquisition of biomaterials rather than developing their own products. The biomaterials developers are often caught in a paradox. If a biomaterial is not novel it will not attract investment, if it is novel (eg needs a new claim approval) it will also not attract investment. In any case without prospective clinical studies that prove a measurable benefit both reimbursement agencies and hospitals are increasingly reluctant to accept “novel” biomaterials. So with all these factors combining it becomes more likely that innovation does not make it through to an end product as investors/developers seek to minimise project risks. So what strategies could enable innovation in biomaterials in spite of these factors?

### **A CLINICAL NEEDS LEAD BIOMATERIALS STRATEGY**

Many biomaterials that are on sale today come from a technology lead approach. That is to say that an available technology is adapted to fit a broader and broader range of user needs, eventually risking going “off-label”. In the author’s opinion this is largely what happened with calcium phosphate cements. In the 30 years since CaP’s were introduced there have been many hundreds of CaP projects (author’s estimate) all aiming to be non-load bearing void fillers. Less than 10 of these products make up 80% of the market volume today and only two of these are available with enhanced claims (antibiotic, screw augmentation in EU markets only). Yet it is clear from the off-label use reported for CaP cements that there are clinically unmet needs. Examples are: load sharing/bearing applications, adding bone quality enhancement, or infection control measures via drugs. The author proposes the following to increase the success rate of translation of innovative biomaterials projects into clinically valued treatments.

- 1) First and foremost an evidence based approach is mandatory, starting with well-defined unmet clinical needs, ideally from prospective randomised studies.
- 2) Selection of technologies based on the unmet needs rather than making a technology fit the application.
- 3) A focus on indication specific biomaterials, as different anatomic locations and clinical conditions have different requirements.

- 4) Definition of intraoperative handling/clinical site delivery as part of the user needs
- 5) Making an assessment of the reimbursement potential at the beginning of the project.
- 6) Early determination that clinical outcome studies are needed/not needed to prove a clinical advantage.

### **ILLUSTRATIVE CASE STUDIES**

#### **1: Commercialisation of a premix CaP cement**

This project began with the unmet needs of ease of mixing and delivery together with stop start functionality. This case study shows proof of concept through to commercial realisation (CE mark) of an integrated cement mixing, delivery and implant system, iN3 (Celgentek Ltd).

#### **2: Development of an injectable cement minimising vascular impact in a bone void environment**

This unmet need resulted from the post market surveillance observation that CaP cements compromised the vascular recovery in femoral neck fractures<sup>2</sup>. The root cause was suggested to be the presence of CaP cement in the fracture line. Two approaches were pursued 1) Literature research suggested that hydrogels combined with nanoparticulate calcium and antiporotic drugs such as zoledronic acid might be effective, even when injected into the fracture line. 2) Design cement/selection of a cement that does not extrude into the fracture site or beyond. A group<sup>3</sup> has evaluated a number of cements to determine their suitability for use in the femoral neck with regard to this extrusive/intrusive behaviour. This case study reports proof of concept for both pathways.

### **CONCLUDING COMMENTS:**

The last three decades have seen many innovations in biomaterials research but few of these have succeeded in becoming mainstream as part of clinically valued treatments. Evidence based design of biomaterials is a way to change this whilst challenging to put into practice but in the author’s opinion this is essential if we are to increase the successful translation of innovative biomaterials projects into clinically valued treatments.

### **REFERENCES**

1. Kurien, T *et al.* Bone graft substitutes currently available in orthopaedic practice. The evidence for their use. The Bone and Joint Journal; Vol. 95-B, No. 5, 2013:2. Mattsson, P., Resorbable bone cement for augmentation of hip fracture. Doctoral Thesis University of Uppsala, ISBN: 91-554-6271-5, 2005. 3) Russell, T *et al* The Problem of Fracture Fixation Augmentation and Description of a Novel Technique and Implant for Femoral Neck Stabilization Cements. Techniques in Orthopaedics, Volume 30, No 1, 2015.



**Best Practice for Registration Trials of Biodegradable Implants**

Nils Reimers

Stryker Trauma GmbH, Kiel, Germany  
[Nils.Reimers@STRYKER.com](mailto:Nils.Reimers@STRYKER.com)

**SUMMARY**

Prospective clinical study shows the safety, efficacy, and resorption characteristics of an ultrasonically inserted bioresorbable pin after four years.

**INTRODUCTION**

Corrective osteotomies for treatment of Hallux Valgus are among the most prevalent procedures in foot and ankle surgery. Various treatment options have shown to be safe and effective. Bioresorbable implants may be preferred to avoid metallic implant removal and reduce the burden on the healthcare system. The aim of this study was to assess the safety, efficacy, and resorption characteristics of an ultrasonically inserted bioresorbable pin.

**PATIENTS & METHODS**

30 consecutive patients with a moderate Hallux Valgus deformity were treated with a polylactide co-polymer pin that was selectively liquefied by ultrasonic energy allowing it to flow into cancellous bone and solidifying immediately, resulting in a stable construct. Patients went through a clinical and radiographical evaluation. MRI scans were obtained at 3, 12, 24, 36, and 48 months post index procedure. Clinical outcome was measured by the EQ-5D at one year.

**RESULTS**

25 patients were included for final MRI evaluation at 48 months. All osteotomies healed without adverse reaction. The implant was still visible on MRI at 36 months in all subjects but was completely resorbed in 14 patients at 48 months, with a partially iso-intense signal detectable in the cavity that was left by the resorbed implant. The remaining patients showed advanced signs of degradation at this point in time.

**CONCLUSION**

The long-term MRI follow-up showed full degradation of the bioresorbable implant and partially to fully remodeled bone after 4 years in the majority of patients. Reducing metallic implant removal by substituting bioresorbable implants appears to be beneficial both financially and clinically.



## **New Concept of Hybrid Polymer Composites for Implant Applications**

Xiang Zhang

Lucideon Ltd. UK

Royal Society Industry Fellow at University of Cambridge

Coordinator, Reinforced Bioresorbable Biomaterials for Therapeutic Drug Eluting Stents REBIOSTENT,  
EU FP7 Project

Coordinator, Drug-Free Antibacterial Hybrid Biopolymers for Medical Applications HyMedPoly,  
Horizon 2020 Project

Novel Biodegradable and Biocompatible Polymers for Medical Applications

[Xiang.Zhang@lucideon.com](mailto:Xiang.Zhang@lucideon.com)

This presentation will introduce new concept on development of hybrid polymer composites for industrial applications. It will report the outcomes from a large European project involving over 14 organisations on development of new polymer hybrids, i.e. reinforced and resorbable polymer hybrids for medical applications. The presentation will cover the following points:

- New concepts of hybrid polymer composites;
- New technology for synthesis of nanoporous silica and nano phosphate bioresorbable glass for develop polymer hybrids;
- Introduction of design and development methods hybrid polymer composites i.e blends of organic and inorganic nano-materials
- Introduction of therapeutic polymer hybrids: drug-loaded bioresorbable nanoglass and polymer hybrids
- Therapeutic reinforced bioresorbable polymer hybrids for medical implants

## **Novel Biodegradable and Biocompatible Polymers for Medical Applications**

Ipsita Roy

Reader, Faculty of Science and Technology, University of Westminster, London, UK  
Scientific Coordinator, Reinforced Bioresorbable Biomaterials for Therapeutic Drug Eluting Stents REBIOSTENT,  
EU FP7 Project

Scientific Coordinator, Drug-Free Antibacterial Hybrid Biopolymers for Medical Applications HyMedPoly,  
Horizon 2020 Project

[I.Roy01@westminster.ac.uk](mailto:I.Roy01@westminster.ac.uk)

This presentation will discuss the development of novel Biopolymers, both natural and synthetic with potential for application in a range of different medical applications.

Currently there is a huge need for novel and innovative polymers of medical grade for use in the fast evolving areas such as tissue engineering, controlled and targeted drug delivery, biodegradable implants including biodegradable stents and nerve conduits. These polymers need to be biocompatible, have mechanical properties suitable for the particular application, have controllable degradation rate and have suitable surface properties and microstructure to support the regeneration of tissue via optimal cell attachment, proliferation, infiltration, and vascularisation.

These wide ranging properties can be acquired by production of polymers using various synthetic routes and also efficient utilisation of a range of different known natural polymers. In addition, novel physical and chemical functionalization of the polymers can be used to make them much more effective. Finally, processing of such polymers to produce suitable microstructure in 2D and 3D constructs can be used to enhance their suitability for a wide range of medical applications.

All these aspects of the development of novel Biopolymers for use in medical applications will be elaborated in this presentation.





## Insights into Collaboration and Innovation for Early Stage Medical Device Development

David Knapp

Boston Scientific Corporation, USA

[David.Knapp@bsci.com](mailto:David.Knapp@bsci.com)

### INTRODUCTION

Large medical device companies have traditionally benefitted from internal organic growth supplemented by a healthy startup environment fueled by venture. In recent years, it has become more important than ever to innovate internally with significant changes in the funding, regulatory, reimbursement and healthcare system dynamics.

Collaboration has been a cornerstone of the culture of innovation at Boston Scientific. Taking lessons from across academia, medicine and industry, we will describe the ways in which we conduct exploratory development, collaborate internally and externally, leading to connections that are critical in this multi-disciplinary field. Over the years, we have learned that the principles that are important for creating an open and creative culture are consistent with this collaborative mindset. We will describe those key principles that we feel most reflect the culture at Boston Scientific and are critical for nurturing and translating successful early stage development to solutions that can benefit patients.



**From Biomaterials Supplier to Device Development Partner – Supporting Medical Device Companies  
in de-Risking Medical Products**

Jens C. Thies

DSM Biomedical, The Netherlands

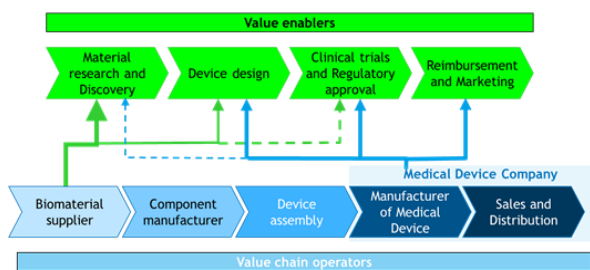
jens.thies@dsm.com

## INTRODUCTION

There are several methods and strategies by which organisation with biomaterials competences such as academic labs, small medium sized companies or large corporations can engage in the medical device industry.

The primary difference in these strategies is determined by the chosen position of the organisation in the supply (value) chain, see figure 1.

**Figure 1.** Medical device industry value chain depicting both value enablers and value chain operators.



Moving from raw (bio)material supplier to component manufacturer all the way to medical device assembler takes an organisation closer and closer to the end point of the chain which is ultimately the patient. This implies more value but also more regulatory complexity, particularly with respect to the assessment of benefit vs. risk.

In this paper we will give examples of various DSM offerings to the medical device field and show how different positions in the chain demand different levels of regulatory understanding and support of the final product. Of primary importance in all fields is the concept of risk management

## METHODS

Three product offerings are described. The first being a raw biomaterial (thermoplastic polyurethanes).

The second a medical device component (Dyneema Purity® UHMWPE fiber). The third a fully developed medical device solution (cartilage repair device). The regulatory requirements, essential biocompatibility testing as well as examples of pre-clinical translation studies and clinical studies will be discussed.

## RESULTS AND DISCUSSION

As a supplier of a raw biomaterials (thermoplastic polyurethanes), the regulatory focus is mainly with respect to biocompatibility and biostability testing and chemistry & manufacturing controls (e.g. supply chain, validations) and end product shelf life. These chapters are contained within the materials master file. Certain raw materials may also be subject to adjunct requirements such as chemical controls law.

For a medical device component (e.g. Dyneema Purity) naturally biocompatibility, biostability and CMC are still extremely relevant but here functional requirement resulting from the risk management relating to the intended use of the component become a critical aspect. These issues are the responsibility of the ‘legal’ manufacturer, i.e. the organisation who owns the regulatory approval. Therefore by effectively anticipating these risk aspects, component manufacturers can create added value for the medical device company ultimately putting the component to use.

For a fully developed medical device solution (cartilage repair device) all of the above as well as the Design Dossier detailing design history, verification and validation are critical aspects and again relate to risk management processes. For medical device development in the EU the Medical Device Directive is the leading regulatory requirement.

## CONCLUSION

Risk management is critical in mastering the regulatory requirement at various points in the business chain. This is best achieved through intimacy with the final clinical use thereby essentially mitigating risk in the final application not only for end-user (clinicians), but also for the marketing entity and most importantly for patients.

## REFERENCES

ISO 13485:2012 Medical devices - Quality management systems - Requirements for regulatory purposes

ISO 14971:2007 Medical devices - Application of risk management to medical devices

ISO 10993-1:2009 Biological evaluation of medical devices - Part 1: Evaluation and testing within a risk management process

**Next Generation of Fibers for Medical Devices: Biopolymers and Functionalized Coatings**

Herbert De Breuck

Luxilon Industries NV, Vosveld 11L, B-2110 Wijnegemvidien, Belgium

[Herbert.Debreuck@luxilon.be](mailto:Herbert.Debreuck@luxilon.be)

**INTRODUCTION**

The Belgian filament manufacturer, Luxilon, is since many years a leading company in the production of specialty yarns for medical applications, such as surgical sutures for wound care and yarns for all different types of implants (hernia mesh, cardiovascular surgery, orthopaedic surgery, etc.)

In the Surgical mesh industry, there is a structural shift ongoing from completely non-absorbable mesh, via semi-absorbable, hybrid structures towards completely absorbable meshes. Compared to the non-absorbable materials, the new absorbable materials have the following benefits: improved biocompatibility, lower rejection and infection, added functions (anti-bacterial, anti-fouling, etc.). Due to the absorption, a secondary surgery is avoided, with a serious benefit, as well for the patient as for the health service costs. Materials involved are PLLA, PGA, PGLA, PCL, PLCA, etc.

On top of the development of the basic polymeric yarns, Luxilon and its partners developed a unique method to apply coatings of biomaterials on yarns and implants to give an extra benefit to polymers: better acceptance of the implant, faster / better healing and lower infection risk.

The development of all these new yarns is a multi-disciplinary cooperation between polymer suppliers, textile companies and medical device manufacturers. With a strong support of RTD centers and Universities, financing governments (EU) and controlling bodies like NAMSA, FDA,...

Luxilon participates in 3 EU funded projects for medical applications (Green Nano Mesh, Colcomp and ASCaffolds). The aim is to develop a new generation of functionalized textile based implants. Examples of products developed in these projects are anti-bacterial yarns (other than silver technology), protein and poly-saccharide coated yarns for implants and wound care, yarns for scaffolds and stem cell therapy,

As Colcomp and Green Nano Mesh come to a conclusion, the results of the project will be shown as well as a look at the further steps to industrialization. Luxilon is also working together directly with other industrial partners to develop new products. This is done in bi-lateral, strictly confidential collaboration. The presentation explains that with a good interaction, understanding and cooperation between research and industry, the EU is still on top for developing new and innovative products

**REFERENCES**

1. Green Nano Mesh, FP7 EU funded research project
2. Colcomp, Matera+ EU funded research project
3. ASCaffolds, Eurotransbio EU funded research project



## Surface Charge for Biomaterial Characterization

Tuesday, 1<sup>st</sup> September

11:30 – 13:00

Hall 4B



### Speakers:

Dr. Christine Körner, Anton Paar GmbH, Graz, Austria

Dr. Martina Lorenzetti, Jožef Stefan Institute, Ljubljana, Slovenia

### Sponsored by:

Anton Paar, Austria

### Programme:

11:30

#### **(SCh1) Zeta Potential for Biomaterial Surface Characterization**

Christine Körner, Thomas Luxbacher

*Anton Paar GmbH, Graz, Austria*

12:15

#### **(SCh2) TiO<sub>2</sub>-Coated Ti-Alloys for Body Implants & Surface Charge: Expectations on the Bio-Response**

Martina Lorenzetti, Mukta Kulkarni, Aleš Iglič, Thomas Luxbacher, Spomenka Kobe, Saša Novak

*Jožef Stefan Institute, Ljubljana, Slovenia*

The session “Surface Charge for Biomaterial Characterization” focuses on the role of zeta potential analysis as a surface sensitive technique for the characterization of biomaterial surfaces. The zeta potential is an interfacial parameter which describes the charge that a surface assumes when it gets in contact with a liquid. As the zeta potential is sensitive to the outermost surface layer, it furthermore enables time-resolved adsorption studies of biological compounds on solid surfaces. It thus combines the clear visualization of the interaction between biomaterials and their environment with the validation of the chemistry of the adsorbed layer. This enables the optimization of solid surface properties of biomaterials.

The surface charge of solid materials is best assessed by means of zeta potential analysis performed directly at the solid/water interface using the streaming potential technique. Zeta potential analysis is applicable to all classes of materials used for biomaterial applications, i.e. metals, polymers and ceramics.

The first part of the session introduces the basic principles and benefits of zeta potential analysis. The state-of-the-art instrument for zeta potential analysis on solids, SurPASS Elektrokinetic Analyzer, will be presented. Together with its wide range of measuring cells, SurPASS allows for the analysis of biomaterial samples of different shape and geometry over a wide pH range and at different electrolyte compositions.

The second part of the session focuses on recent research on modified titanium-based substrates (TiO<sub>2</sub>-coated by nanocrystals or nanotubes) used for hard tissue replacement. Influences of the topography of the surface (roughness and size of nanostructures), the substrate nature, and the material behaviour in contact with different biologically relevant electrolytic solutions on the surface charge are discussed. The information obtained by zeta potential analysis allowed for a better understanding of the behavior of such coatings in physiological conditions.

The session “Surface Charge for Biomaterial Characterization” is interesting for scientists and researchers searching for a direct method for biomaterial/environment interface analysis and a state-of-the-art technique for solid surface analysis to successfully promote the development of biomaterials.



## Zeta Potential for Biomaterial Surface Characterization

Christine Körner<sup>1</sup>, Thomas Luxbacher<sup>1</sup>

<sup>1</sup>Material Characterization, Anton Paar GmbH, Austria  
[christine.koerner@anton-paar.com](mailto:christine.koerner@anton-paar.com)

### INTRODUCTION

The present work deals with the role of zeta potential analysis as a surface sensitive technique for the characterization of biomaterial surfaces. The zeta potential is an interfacial parameter which describes the charge a surface assumes when it gets in contact with a liquid. As the zeta potential is sensitive to the outermost surface layer, it is also suited to monitor adsorption processes, thus contributing to the understanding of e.g. protein-biomaterial interaction.

Zeta potential analysis is applicable to all classes of materials used for biomaterial applications, i.e. metals, polymers and ceramics.

The work presented here focuses on titanium and adsorption of bovine serum albumin on titanium surfaces.

### EXPERIMENTAL METHODS

Zeta potential analysis of various materials was performed with SurPASS Electrokinetic Analyzer using the streaming potential technique.

If a surface is brought in contact with an aqueous electrolyte solution, charges are formed at the solid-liquid interface. Upon streaming the electrolyte solution across the sample surface, the charge compensating ions are sheared off their equilibrium position. The charge separation generates an electrical potential difference: the streaming potential.<sup>1</sup>

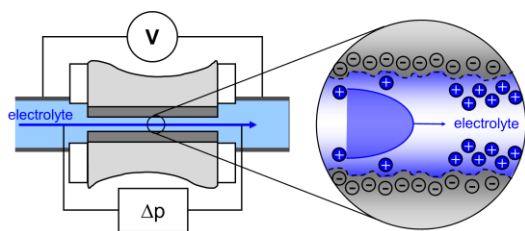


Fig. 1: Measuring principle of zeta potential on solid surfaces.

### RESULTS AND DISCUSSION

The zeta potential strongly depends on the parameters of the electrolyte solution, such as pH value, conductivity or additive concentration. The pH value where the zeta potential is 0 mV and a charge reversal takes place is called isoelectric point (IEP) and describes the chemistry of a surface.

Fig. 2 shows the pH dependence of zeta potential for titanium (IEP at pH 4.2) as well as a glass surface (IEP at pH 3) in phosphate buffered saline. After adsorption of albumin to the surface of the material the IEP is shifted to pH 4.7, which corresponds to the IEP of

albumin in solution<sup>2</sup>. This result implies that the material surface is completely covered with the protein.

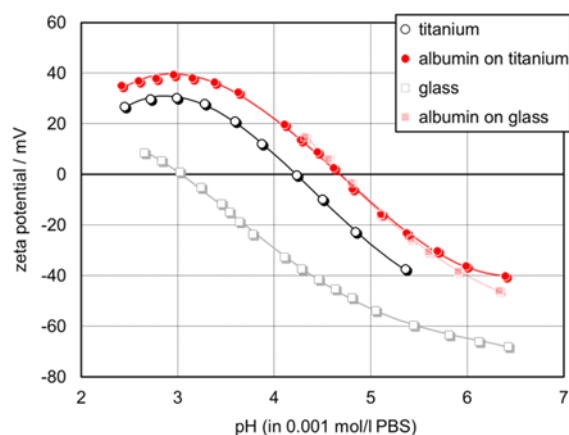


Fig. 2: pH dependence of zeta potential for titanium (IEP 4.2) and glass (IEP 3.0) in PBS buffer, also in the presence of albumin (IEP 4.7).

Being sensitive to the outermost surface layer of a material, the zeta potential is also used to assess adsorption processes<sup>3</sup> of biological compounds in real time. The adsorption kinetics of albumin on titanium indicates an initial fast protein attachment and a subsequent slower rearrangement on the solid surface, depending on the pre-treatment of the titanium surface.

### CONCLUSION

The zeta potential serves as an indicator for surface charge at the interface of a solid and a liquid. Zeta potential analysis thus provides information on the surface chemistry of biomaterials.

Zeta potential analysis furthermore allows for the clear visualization of the interaction of biomaterials with their environment. It combines the real-time measurement of adsorption kinetics with the validation of the chemistry of the adsorbed layer. This enables the optimization of solid surface properties of biomaterials.

### REFERENCES

1. Werner C. *et al.*, J. Biomater. Sci. Polymer Edn. 7:61-76, 1995
2. Müller C. *et al.*, Langmuir, 26:4136-4141, 2010
3. Norde W. *et al.*, J. Colloid Interface Sci. 139:169-176, 1990

## TiO<sub>2</sub>-Coated Ti-Alloys for Body Implants & Surface Charge: Expectations on the Bio-Response

Martina Lorenzetti<sup>1</sup>, Mukta Kulkarni<sup>2</sup>, Aleš Iglič<sup>2</sup>, Thomas Luxbacher<sup>3</sup>, Spomenka Kobe<sup>1,4</sup>, Saša Novak<sup>1,4</sup>

<sup>1</sup>Department of Nanostructured Materials, Jožef Stefan Institute, Ljubljana, Slovenia

<sup>2</sup>Laboratory of Biophysics, Faculty of Electrical Engineering, University of Ljubljana, Ljubljana, Slovenia

<sup>3</sup>Anton Paar GmbH, Graz, Austria

<sup>4</sup>Jožef Stefan International Postgraduate School, Ljubljana, Slovenia

[martina.lorenzetti@ijs.si](mailto:martina.lorenzetti@ijs.si)

### INTRODUCTION

The physico-chemical properties of a biomaterial surface are considered the key factors for the design of body implants. In fact, they are responsible for the interactions with the surrounding tissues and, influencing the “race for the surface” between cells and bacteria<sup>1</sup>, they affect the following acceptance of the implant.

The most studied surface characteristics concern the wetting degree and the roughness, either at the micro- or nano-scale. Besides, the assessment of the solid surface charge becomes fundamental when the adsorption of certain ions and proteins from the body fluids and the on a body implant is considered.

Streaming potential represents a reliable method to evaluate the surface charge by determining the zeta potential (ZP) at the interface between the material and the fluid around<sup>2</sup>.

Thus, the purpose of this work was to assess measurements of zeta potential of modified titanium-based substrates used for hard tissue replacement. The surface modification concerned the synthesis of titanium dioxide (TiO<sub>2</sub>) nanostructured coatings, with the function of protecting and enhancing the properties of the bare Ti-substrate.

Several parameters were taken into consideration during the streaming potential measurements, such as the topography of the surface (roughness and size of nanostructures), the influence of the substrate nature, and the material behaviour in contact with different, biologically relevant electrolytic solutions.

### EXPERIMENTAL METHODS

A series of different nanostructured TiO<sub>2</sub>-coatings was produced. The synthesis of fully-dense and stable nanocrystalline TiO<sub>2</sub>-anatase coatings was performed by hydrothermal treatment (HT) of different Ti-based alloys for bone implants<sup>3</sup>. The formation of TiO<sub>2</sub>-nanotubes (NTs) and TiO<sub>2</sub>-nanopore structures within Ti-substrates (different diameter and length) was achieved by electrochemical anodization (EA)<sup>4</sup>.

The obtained nanostructured surfaces were analysed in terms of morphology by scanning electron microscopy (SEM), wettability by sessile drop contact angle, and roughness by atomic force microscopy (AFM).

The zeta potential of not treated (NT) and both HT and EA titanium substrates was determined by the streaming current technique, using a SurPASS electrokinetic analyzer (Anton Paar GmbH). Titration curves were carried out in potassium chloride (KCl), phosphate buffer saline (PBS) and artificial saliva, at different

ionic strengths, to determine the ZP dependence on the pH and the isoelectric point (IEP) of the materials.

### RESULTS AND DISCUSSION

The physico-chemical characterization of the TiO<sub>2</sub>-coating properties in terms of morphology, wettability and roughness was performed prior any streaming potential measurement, in order to correlate the surface properties to the surface charge.

The streaming potential analysis revealed that all the surfaces (NT, HT, EA) were negatively charged at physiological pH (7.4) in the used electrolytic solutions, even though in a different extent. In particular, significant differences were noticed when the TiO<sub>2</sub> nanostructured coatings were compared to the bare Ti-substrates. In the case of HT coatings, both the ZP values and the IEP were influenced by the morphology, nanoporosity and conductive character of the TiO<sub>2</sub> nanocrystals<sup>2,5</sup>; in the case of nanotubular structures, ZP and IEP were mostly affected by the NT diameter and the NT curvature on the top<sup>4</sup>. Such behaviour among the substrates was even more highlighted when the electrolytic solutions were switched; this was mainly due to the different ions involved and their adsorption/interaction with the surfaces.

### CONCLUSION

Streaming potential analysis represents a valuable method to evaluate the surface charge behaviour of modified-titanium surfaces (namely, TiO<sub>2</sub>-coated by nanocrystals or nanotubes). The obtained information can help to better deduce the behaviour of such coatings in physiological conditions.

### REFERENCES

1. Gristina AG., Science. 237:1588-95, 1987.
2. Lorenzetti M. *et al.*, J Mater Sci - Mater Med. In press.
3. Lorenzetti M. *et al.* ACS Appl Mater Interfaces. 7:1644–51, 2015.
4. Kulkarni M. *et al.* Colloids Surf B. 129: 47–53, 2015.
5. Lorenzetti M. *et al.* Biomed Mater. Under 2<sup>nd</sup> revision.

### ACKNOWLEDGMENTS

The authors would like to acknowledge the European Commission within the framework of the FP7-ITN network BioTiNet (FP7-PEOPLE-2010-ITN-264635) and the Slovenian Research Agency (ARRS) (grants No. P2-0232, P3-0388, J1-6728) for the financial support.



## Science for Industry: Bioresorbable Materials for Medical Applications

Wednesday, 2<sup>nd</sup> September

9:30 – 11:00

11:30 – 13:00

16:45 – 17:45

Hall 4B



### Organizers:

Xiang Zhang, Ipsita Roy, Kadem Al-Lamee, Stuart Maclachlan, Maria Joao Barros, Nial Bullett, Mark Taylor

### Supported by:

- ReBioStent project, grant agreement n° 604251 from the European Union's Seventh Programme for research, technological development and demonstration (FP7)
- ARTERIUS, United Kingdom

### Chairs:

Dr Xiang Zhang, *Principal Consultant, Lucideon Limited, and Royal Society Industry Fellow at University of Cambridge*  
Dr Ipsita Roy, *Reader, Head of Applied Biotechnology Research Group, Department of Life Sciences, Faculty of Science and Technology, University of Westminster*

Materials for medical applications take many forms, from metallic to synthetic and natural polymers, composites and materials of biological origin. The ultimate goal of an implantable device is for it to be unrecognised by the body, to allow for stable long term lifetime of the device. One strategy for this is for the devices to be bioresorbable – to disappear after their initial function is no longer needed as healing has occurred. Permanent implants may cause complications many years after initial healing has occurred and their presence in the body is no longer necessary.

Bioresorbable materials have applications in a wide range of medical indications, such as sutures, coronary and peripheral vascular scaffolds, bone pins and anchors, tissue fixation screws, drug delivery coatings and microspheres and surgical meshes and matrices. The bioresorbable materials may include polymers, metals, ceramics, glasses, composites and materials of biological origin such as natural collagen, and may allow for drug elution and delivery as well as performing a mechanical function.

Bioresorbable sutures have been available for over 40 years, yet recent innovations have expanded the market for bioresorbable implants to include cardiovascular, orthopaedic and general surgery. This has demanded increased performance from polymers, with increased strength and control over degradation being necessary.

Lead Researchers from the ReBioStent project and invited speakers will focus on novel and commercially applicable research and product development work on bioresorbable materials and medical devices.

A series of presentations will cover various aspects of materials development, product design and commercialisation.

### Programme:

#### Session 1 (9.30-11.00)

**9:30 Welcome and Introduction: Dr Xiang Zhang, Dr Ipsita Roy**

**9:50 Dr Kadem Al Lamee, Arterius Limited**

*"Commercial needs for bioresorbable materials, transfer from laboratory and barriers and gaps in the technology"*

**10:15 Prof. Oskar Hoffmann, University of Vienna**

*"Production and evaluation platforms for preclinical assessment of novel biomaterials for non-healing bone lesions"*

**10:40 Dr Ipsita Roy, University of Westminster**

*"Bioresorbable Systems: Polymers and Metals"*



## Special Sessions

### Session 2 (11.30-13.00)

- 11:30 Prof. Aldo R. Boccaccini**, University of Erlangen-Nuremberg  
*"Bioresorbable Systems: The Role of Inorganic Fillers in Composites"*
- 11:50 Dr Iban Quintana, IK4 - Tekniker**  
*"Bioresorbable Systems: The Role of Surface Functionalisation"*
- 12:10 Prof. Atul Bhaskar**, University of Southampton  
*"Bioresorbable Systems: The Role of Modelling and Simulation in Performance Assessment of Bio-Structures and Implants"*
- 12:30 Dr Gianluca Giavaresi**, Istituto Ortopedico Rizzoli, Bologna  
*"Bioresorbable Systems: The Role of Preclinical Testing"*
- 12:50 Bioresorbable Systems: Discussion**
- 13:00 Lunch including networking and posters**

### Session 3 (16:45 – 17:45)

- 16:45 Welcome back and overview of morning's proceedings: Dr Xiang Zhang, Dr Ipsita Roy**
- 16:55 Elena Boccardi**, University of Erlangen-Nuremberg  
**Zein Azhari**, Cambridge University  
*"Research into Bioresorbable Systems"*
- 17:15 Panel discussion and overview of proceedings with speakers from the Bioresorbable System Session**

---

#### **Keynote 1:**

**Commercial needs for bioresorbable materials, transfer from laboratory and barriers and gaps in the technology.**

**Dr Kadem Al Lamee, Arterius Limited**

A variety of bioresorbable materials exist for medical applications, including polymers and metals. The real-world commercial requirements for these include sufficient mechanical strength, degradation period, biocompatibility and safe degradation products. In addition, regulatory and quality requirements demand careful control of the raw materials and a high burden of proof for bench testing, biocompatibility, pre-clinical and clinical evidence.

#### **Keynote 2:**

**Production and evaluation platforms for preclinical assessment of novel biomaterials for non-healing bone lesions.**

**Prof. Oskar Hoffmann, University of Vienna**

Development and transfer from laboratory to commercial application from the perspective of InnovaBone, which is focussed on optimally performing bio-inspired biomaterials mimicking the natural physiological processes underlying bone repair of non-healing bone lesions

#### **Polymers and Metals.**

**Dr Ipsita Roy, University of Westminster**

Biodegradable polymers and metals are core materials essential for the development of resorbable medical structures and devices. The currently available biodegradable polymers and metals include both synthetic polymers (e.g. PLA, PLLA, PLGA, PCL) and natural polymers, including bacteria derived polymers (e.g. collagen, gelatin, alginate, polyhydroxyalkanoates and  $\gamma$ -polyglutamic acid) and Magnesium. The availability of such a wide range of polymers and metals has widened the possible areas of medical applications, heralding an exciting new era of innovative smart functional materials.

#### **The role of inorganic fillers in composites.**

**Prof Aldo R. Boccaccini, University of Erlangen-Nuremberg**

Inorganic fillers in composite materials for biomedical applications cover a broad range of bioactive ceramics, e.g. CaP and HA particles, bioactive glasses (BG), bioinert oxides, e.g. TiO<sub>2</sub>, as well as antibacterial components, e.g. Ag, ZnO, and functional inclusions, e.g. carbon nanotubes. In addition, inorganic fillers exhibiting mesoporous structure, e.g. silicate BG, can enhance the biological performance of the composite by imparting controlled drug delivery properties.

#### **The role of surface functionalisation.**

**Dr Iban Quintana, IK4 - Tekniker**

Rapid re-endothelialization of the arterial wall and the inner surface of the stent are critical for the prevention of the main causes of in-stent restenosis or thrombosis. In combination with biochemical modifications, physical modifications of this surface can be applied to recruit endothelial cells (ECs), to support their adhesion, proliferation and migration. In this talk, physical and biochemical technologies used during the RebioStent project will be described, as well as the results obtained in terms of ECs behavior.





### **The role of modelling and simulation in performance assessment of bio-structures and implants.**

**Professor Atul Bhaskar, University of Southampton**

The prediction of the performance of implants and bio-structures under mechanical stress is required in a wide range of applications such as scaffolds, orthopedic implants, and stents—before carrying out expensive laboratory as well as in-vivo tests, which may or may not involve animals and humans. This is particularly critical for bioresorbable implants and structures. With advances in computational stress analysis, such as the Finite Element Analysis, it is now possible to assess the stiffness and strength of such structures in-silico with increased confidence. Examples of lattice bio-structures and expandable stents will be taken up to illustrate the methodology.

### **The Role of Preclinical Testing.**

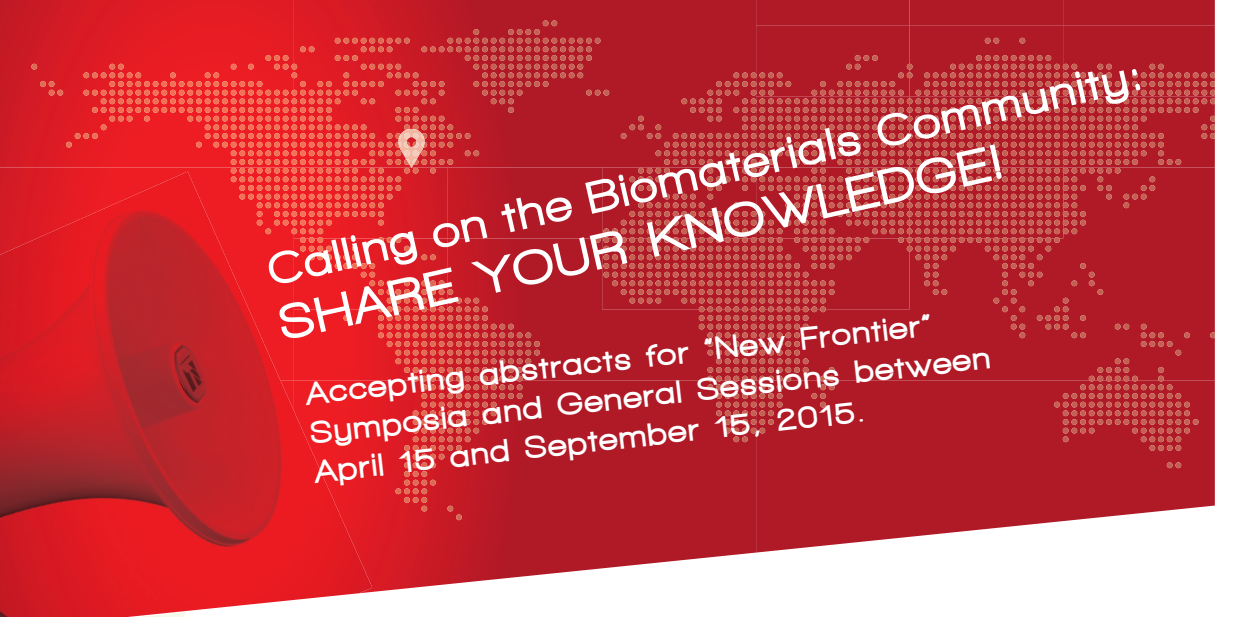
**Dr Gianluca Giavaresi, Istituto Ortopedico Rizzoli, Bologna**

As stated in ISO 10993-1, the selection and evaluation of any material or device intended for use in humans requires a structured programme of assessment that is an extend evaluation of different physico-chemical and biological aspects, such as biocompatibility, toxicology, degradation and mechanical function, giving assurance that the final product will perform as intended and be safe for human use. Preclinical in vitro and in vivo testing is part of this structured programme with the aim to evaluate the biological response of tested material or device.

### **Research into Bioresorbable Systems:**

- **Elena Boccardi, University of Erlangen-Nuremberg**
  - Mesoporous silica particles as drug carriers in drug delivery systems have been explored for the better controlled release of drugs due to their high surface areas, well-defined pore structures and tuneable pore sizes. In this study, bioresorbable mesoporous silica particles have been used as inorganic filler into biodegradable polymers to develop biocomposites which could improve the surface hydrophilicity, mechanical stability and drug delivery capability.
- **Zein Azhari, Cambridge University**
  - This work investigates novel di-block copolymers consisting of Poly-Ethylene Glycol (PEG) and a larger PLLA block of constant molecular weight. The study focuses on the degradation behaviour of the materials and how varying the molecular weight of the PEG component could regulate this to suit certain applications.

The event will be of interest to a wide audience of biomaterials scientists and engineers, including medical device manufacturers and academics. The programme will include a discussion and Q&A panel.



Calling on the Biomaterials Community:  
**SHARE YOUR KNOWLEDGE!**

Accepting abstracts for "New Frontier"  
Symposia and General Sessions between  
April 15 and September 15, 2015.

The WBC 2016 will host the worldwide biomaterials community to define the next phase of biomaterials development between May 17-22, 2016 in Montréal, Canada.

We seek innovative biomaterials, new paradigms and emerging methodological approaches to chart the future of biomaterials science and engineering. We are providing a stimulating cosmopolitan venue for multidisciplinary research to germinate breakthrough ideas and share the translational activity in clinical and industrial development. Engage the biomaterials community with your scientific and engineering endeavours to make an impact!

**Submit Your Abstracts at: [WBC2016.org](http://WBC2016.org)**

#### GENERAL SESSIONS:

Biomaterials and Host Response

Biomaterials in Therapeutic and  
Diagnostic Delivery

Building Blocks

Functional Biomaterials

Innovation in Fabrication

Mechanics and Modelling

Regenerative Medicine

Surfaces and Interfaces

Tissue Engineering

#### NEW FRONTIER SYMPOSIA:

The final list of "New Frontier" Symposia is available at [WBC2016.org](http://WBC2016.org).



10<sup>th</sup> World Biomaterials Congress  
May 17-22, 2016 | Montréal, Canada

Join the global  
biomaterials  
community online!



@WBCmtl

#Biomaterials16



Organizing  
Committee  
Hellenic Society  
for Biomaterials

[www.esb2017.org](http://www.esb2017.org)



# ESB 2017

## September 4-8, 2017

Megaron Athens International Conference Centre

### *Save the Date*

**PCO CONVIN S.A.**

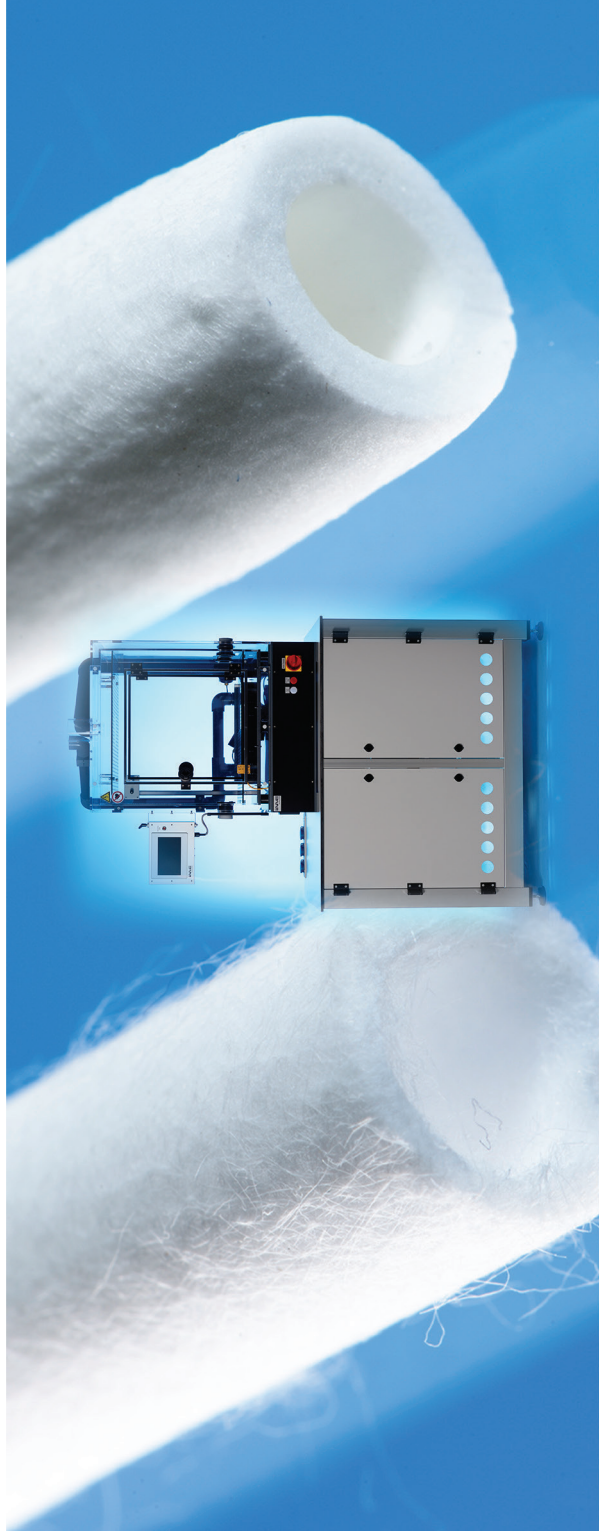
Organizing Secretariat  
PCO CONVIN S.A. 29 Kosta Varnali St.  
15233, Chalandri Athens, Greece  
T: +30 210 6833600 F: +30 210 6847700  
E: [congress@pco-convin.gr](mailto:congress@pco-convin.gr) W: [www.pco-convin.gr](http://www.pco-convin.gr)

#### Important dates

On-line registration opens:  
On-line abstract submission opens:  
Abstract Submission deadline:  
Notification to authors:  
Early-bird registration deadline:

1 December 2016  
1 December 2016  
31 March 2017  
20 May 2017  
31 May 2017

## Electrospinning equipment and technology



**Your partner in medical device development and production**



